ODICAL
ol 31
1961

UNIVERSITY OF CALIFORNIA, SAN DIEGO
SCRIPPS INSTITUTION OF OCEANOGRAPHY

CONTRIBUTIONS

VOLUME 31
1961

LIBRARY
OCT 1 1962
FISH & WILDLIFE SERVICE

THE UNIVERSITY LIBRARY
UNIVERSITY OF CALIFORNIA, SAN DIEGO
SCRIPPS INSTITUTION OF OCEANOGRAPHY
La Jolla, California

LIBRARY
BUREAU OF COMMERCIAL FISHERIES
U. S. FISH AND WILDLIFE SERVICE
P. O. BOX 3830
HONOLULU 12, HAWAII

PERIODICAL
CALIF. UNIV.
S.I.O.
CONTRIBUTIONS
1961
(v. 31)

DATE OF MAGAZINE	BORROWER'S NAME	TIME

PERIODICAL
CALIF. UNIV.
S. I. O.
CONTRIBUTIONS
1961
VOL. 31

LIBRARY
BUREAU OF COMMERCIAL FISHERIES
U. S. FISH AND WILDLIFE SERVICE
P. O. BOX 3830
HONOLULU 12, HAWAII

UNIVERSITY OF CALIFORNIA, SAN DIEGO
SCRIPPS INSTITUTION OF OCEANOGRAPHY

CONTRIBUTIONS

VOLUME 31

1961

3074

This volume contains contributions from the Scripps Institution of Oceanography which have appeared in publications other than *Bulletin of the Scripps Institution of Oceanography.*

THE UNIVERSITY LIBRARY
UNIVERSITY OF CALIFORNIA, SAN DIEGO
SCRIPPS INSTITUTION OF OCEANOGRAPHY
La Jolla, California
1962

UNIVERSITY OF CALIFORNIA, SAN DIEGO
SCRIPPS INSTITUTION OF OCEANOGRAPHY
CONTRIBUTIONS, NEW SERIES
VOLUME 31, 1961

NUMERICAL INDEX

Contrib. Number		Page Number
1228	GOLDBERG, EDWARD D. Determination of opal in marine sediments. Journal of Marine Research, v. 17, 1958. pp. 178-182	1
1229	JOHNSON, MARTIN W. Observations on inshore plankton collected during summer 1957 at Point Barrow, Alaska. Journal of Marine Research, v. 17, 1958. pp. 272-281	7
1230	ARTHUR, ROBERT S. Variation in sea temperature off La Jolla. Journal of Geophysical Research, v. 65, no. 12, December 1960. pp. 4081-4086	19
1231	WOOSTER, WARREN S. and BRUCE A. TAFT. On the reliability of field measurements of temperature and salinity in the ocean. Journal of Marine Research, v. 17, 1958. pp. 552-566	25
1232	FOLSOM, THEODORE R. and GOVINDARAJU J. MOHANRAO. Trend of caesium-137 in the effluent of a large city. Nature, v. 188, no. 4755, December 17, 1960. pp. 979-982	41
1233	SWEENEY, BEATRICE M. The photosynthetic rhythm in single cells of *Gonyaulax polyedra*. Cold Spring Harbor Symposia on Quantitative Biology, v. 25, 1960. pp. 145-148	49
1234	BODEN, BRIAN P. Euphausiacea. In "McGraw-Hill Encyclopedia of Science and Technology," 1960. v. 5, p. 108	*
1235	KREJSA, RICHARD J. The eastern, tropical Pacific fishes of the genus *Blenniolus*, including a new island endemic. Copeia, no. 4, December 30, 1960. pp. 322-336	54
1236	KNAUSS, JOHN A. The structure of the Pacific equatorial countercurrent. Journal of Geophysical Research, v. 66, no. 1, January 1961. pp. 143-155	69
1237	NEUSHUL, MICHAEL. Diving in Antarctic waters. Polar Record, v. 10, no. 67, January 1961. pp. 353-358	83
1238	TYLER, JOHN E. Sun-altitude effect on the distribution of underwater light. Limnology and Oceanography, v. 6, no. 1, January 1961. pp. 24-25	89
1239	BIEN, GEORGE S., NORRIS W. RAKESTRAW, and HANS E. SUESS. Radiocarbon concentration in Pacific Ocean water. Tellus, v. 12, no. 4, 1960. pp. 436-443	91
1240	ENRIGHT, JAMES T. Pressure sensitivity of an amphipod. Science, v. 133, no. 3455, March 17, 1961. pp. 758-760	101

*Not available for exchange

Contrib. Number		Page Number
1241	GOLDBERG, EDWARD D. Chemical and mineralogical aspects of deep-sea sediments. Physics and Chemistry of the Earth, v. 4, 1961. pp. 281-302	105
1242	RUDNICK, PHILIP. Likelihood detection of small signals in stationary noise. Journal of Applied Physics, v. 32, no. 2, February 1961. pp. 140-143	127
1243	CLENDENNING, KENNETH A. Photochemical activity of isolated chloroplasts (Hill reactions). Handbuch der Pflanzenphysiologie, v. 5, pt. 1, 1960. pp. 736-772	*
1244	CROMWELL, TOWNSEND. Pycnoclines created by mixing in an aquarium tank. Journal of Marine Research, v. 18, no. 2, October 30, 1960. pp. 73-82	131
1245	COX, CHARLES S. Measurements of slopes of high-frequency wind waves. Journal of Marine Research, v. 16, no. 3, October 15, 1958. pp. 199-225	141
1246	COX, CHARLES S. Comments on Dr. Phillip's paper. Journal of Marine Research, v. 16, no. 3, October 15, 1958. pp. 241-245	169
1247	ALVARINO, ANGELES. Two new chaeognaths from the Pacific. Pacific Science, v. 15, no. 1, January 1961. pp. 67-77	175
1248	BOYD, CARL M. The larval stages of *Pleuroncodes planipes* Stimpson (Crustacea, Decapoda, Galatheidae). Biological Bulletin, v. 118, no. 1, February 1960. pp. 17-30	187
1249	RUSNAK, GENE A. Sediments of Laguna Madre, Texas. In "Recent Sediments, Northwest Gulf of Mexico, 1951-1958," edited by F. P. Shepard, F. B Phlegar, and T. H. van Andel. American Association of Petroleum Geologists, 1960. pp. 153-196	*
1250	HERTLEIN, LEO G. and EDWIN C. ALLISON. Species of the genus *Cypraea* from Clipperton Island. Veliger, v. 2, no. 4, April 1, 1960. pp. 94-95	202
1251	GROVES, GORDON W. and WALTER H. MUNK. A note on tidal friction. Journal of Marine Research, v. 17, 1958. pp. 199-214	205
1252	SWEENEY, BEATRICE M. and J. WOODLAND HASTINGS. Effects of temperature upon diurnal rhythms. Cold Spring Harbor Symposia on Quantitative Biology, v. 25, 1960. pp. 87-104	221
1253	FRY, JOHN C. and RUSSELL W. RAITT. Sound velocities at the surface of deep sea sediments. Journal of Geophysical Research, v. 66, no. 2, February 1961. pp. 589-597	239
1254	JOHNSON, MARTIN W. Calanoida. In "McGraw-Hill Encyclopedia of Science and Technology," 1960. v. 2, pp. 392-393	*
1255	JOHNSON, MARTIN W. Copepoda. In "McGraw-Hill Encyclopedia of Science and Technology," 1960. v. 2, pp. 462-463	*

*Not available for exchange

Contrib. Number		Page Number
1256	TYLER, JOHN E. Radiance distribution as a function of depth in an underwater environment. SIO Bulletin, v. 7, no. 5, 1960. pp. 363-412	*
1257	LIMBAUGH, CONRAD. Life-history and ecologic notes on the black croaker. California Fish and Game, v. 47, no. 2, April 1961. pp. 163-174	249
1258	TYLER, JOHN E. Observed and computed path radiance in the underwater light field. Journal of Marine Research, v. 18, no. 3, November 30, 1960. pp. 157-167	261
1259	PATTULLO, JUNE G. Seasonal variation in sea level in the Pacific Ocean during the International Geophysical Year, 1957-1958. Journal of Marine Research, v. 18, no. 3, November 30, 1960. pp. 168-184	273
1260	PATTULLO, JUNE G. Sea level fluctuations. In "McGraw-Hill Encyclopedia of Science and Technology," 1960. v. 12, pp. 95-98	*
1261	MORIARTY, JAMES R. Submarine archeology. Science of Man, v. 1, no. 4, June 1961. p. 134	291
1262	MORIARTY, JAMES R., GEORGINA C. PEYTON and PRISCILLA W. FIELD. Prehistory sites in the San Diego coastal area. Science of Man, v. 1, no. 4, June 1961. pp. 116-119	293
1263	RAKESTRAW, NORRIS W. Particulate matter in the oxygen-minimum layer. Journal of Marine Research, v. 17, 1958. pp. 429-431	299
1264	JENSEN, DAVID. Cardioregulation in an aneural heart. Comparative Biochemistry and Physiology, v. 2, 1961. pp. 181-201	303
1265	KELLY, ARTHUR L. and DAVID JENSEN. Chronic aortitis in the California sea-lion, *Zalophus californianus*. Nature, v. 186, no. 4726, May 28, 1960. p. 731	325
1266	REID, JOSEPH L., JR. On the temperature, salinity, and density differences between the Atlantic and Pacific oceans in the upper kilometre. Deep-Sea Research, v. 7, 1961. pp. 265-275	327
1267	SACKETT, WILLIAM M. Protactinium-231 content of ocean water and sediments. Science, v. 132, no. 3441, December 9, 1960. pp. 1761-1762	339
1268	SHEPARD, FRANCIS P. Recent sediment studies, 1955-1959. In "Symposium Bibliography of Recent Works in Sedimentology." International Association of Sedimentology. Paris, Technip, 1960. pp. 9-27	341
1269	ARRHENIUS, GUSTAF O. S. Pelagic sediments. In "The Sea, Ideas and Observations," edited by E. D. Goldberg and others. New York, Interscience (probable date of publication, 1962)	*
1270	MENARD, HENRY W. Some rates of regional erosion. Journal of Geology, v. 69, no. 2, March 1961. pp. 154-161	361
1271	BUZZATI-TRAVERSO, ADRIANO A. and WARREN H. SCHMIDT. An experiment in the design of a scientific conference. Experientia, v. 14, no. 6, 1958. p. 231	371

*Not available for exchange

Contrib. Number | Page Number

1272 BUZZATI-TRAVERSO, ADRIANO A. Paper chromatography in relation to genetics and taxonomy. In "New Approaches in Cell Biology," edited by P. M. B. Walker. New York, Academic, 1960. pp. 95-123 375

1273 HOLMES, ROBERT W. and JAMES M. SNODGRASS. A multiple-detector irradiance meter and electronic depth-sensing unit for use in biological oceanography. Journal of Marine Research, v. 19, no. 1, March 15, 1961. pp. 40-56 405

1274 ROBINSON, MARGARET K. Comparison of Norpac temperature sections with average BT sections along the same tracks. Journal of Marine Research, v. 19, no. 1, 1961. pp. 21-27 421

1275 BRAMLETTE, MILTON N. and FRANK R. SULLIVAN. Coccolithophorids and related nannoplankton of the early Tertiary in California. Micropaleontology, v. 7, no. 2, April 1961. pp. 129-188 429

1276 ARRHENIUS, GUSTAF O. S. Geological record on the ocean floor. In "Oceanography." Washington, D. C., American Association for the Advancement of Science, 1961. pp. 129-148 475

1277 BRAMLETTE, MILTON N. Pelagic sediments. In "Oceanography" Washington, D. C., American Association for the Advancement of Science, 1961. pp. 345-366 495

1278 FISHER, ROBERT L. Middle America trench: topography and structure. Geological Society of America. Bulletin, v. 72, no. 5, May 1961. pp. 703-720 515

1279 SHOR, GEORGE G., JR. and ROBERT L. FISHER. Middle America trench: seismic-refraction studies. Geological Society of America. Bulletin, v. 72, no. 5, May 1961. pp. 721-730 533

1280 RIEDEL, WILLIAM R. and HELEN P. FOREMAN. Type specimens of North American paleozoic radiolaria. Journal of Paleontology, v. 35, no. 3, May 1961. pp. 628-632 543

1281 BERNER, LEO D. and JOSEPH L. REID, JR. On the response to changing temperature of the temperature-limited plankter *Doliolum denticulatum* Quoy and Gaimard 1835. Limnology and Oceanography, v. 6, no. 2, April 1961. pp. 205-215 549

1282 WOOSTER, WARREN S. Yearly changes in the Peru current. Limnology and Oceanography, v. 6, no. 2, April 1961. pp. 222-226 561

1283 ENRIGHT, JAMES T. Lunar orientation of *Orchestoidea corniculata* Stout (amphipoda). Biological Bulletin, v. 120, no. 2, April 1961. pp. 148-156 567

1284 LIMBAUGH, CONRAD. Observations on the California sea otter. Journal of Mammalogy, v. 42, no. 2, May 1961. pp. 271-273 577

1285 HEMMINGSEN, EDVARD A. and PER F. SCHOLANDER. Specific transport of oxygen through hemoglobin solutions. Science, v. 132, no. 3437, November 11, 1960. pp. 1379-1381 581

Contrib. Number		Page Number
1286	SHEPARD, FRANCIS P. and RUTH YOUNG. Distinguishing between beach and dune sands. Journal of Sedimentary Petrology, v. 31, no. 2, June 1961. pp. 196-214	585
1287	LEIGHTON, DAVID L. Observations of the effect of diet on shell coloration in the red abalone, *Haliotis rufescens* Swainson. Veliger, v. 4, no. 1, July 1, 1961. pp. 29-32	605
1288	HASSAN, EL SAYED MOHAMED. Fluctuations in the atmospheric inertia: 1873-1950. Meteorological Monographs, v. 4, no. 24, December 1960. 40p.	609
1289	BRADSHAW, JOHN S. Laboratory experiments on the ecology of foraminifera. Contributions from the Cushman Foundation for Foraminiferal Research, v. 12, pt. 3, July 1961. pp. 87-106	649
1290	SNODGRASS, JAMES M. A telemetering oceanographic current meter. Fall Instrument-Automation Conference and Exhibit, New York City, New York, September 26-30, 1960. Preprint No. 62-NY60. 9p.	669
1291	CHOW, TSAIHWA J. and EDWARD D. GOLDBERG. On the marine geochemistry of barium. Geochimica et Cosmochimica Acta, v. 20, 1960. pp. 192-198	679
1292	KRAUSE, DALE C. Geology of the sea floor east of Guadalupe Island. Deep-Sea Research, v. 8, no. 1, June 1961. pp. 28-38	687
1293	ROSENBLATT, RICHARD H. A new pearlfish (family Carapidae) from the Gulf of California. Biological Society of Washington. Proceedings, v. 74, August 11, 1961. pp. 207-212	699
1294	NORTH, WHEELER J. Life-span of the fronds of the giant kelp, *Macrocystis pyrifera*. Nature, v. 190, no. 4782, June 24, 1961. pp. 1214-1215	705
1295	SWEENEY, BEATRICE M. and FRANCIS T. HAXO. Persistence of a diurnal rhythm in photosynthesis in enucleated *Acetabularia*. Phycological News Bulletin, v. 14, no. 2, July 1961. p. 11	709
1296	RAKESTRAW, NORRIS W. The chemist in oceanography. ICSU Review, v. 3, no. 4, October 1961. pp. 164-169	711
1297	SHEPARD, FRANCIS P. Sea level rise during the past 20,000 years. Zeitschrift für Geomorphologie, supplement to v. 3, 1961. pp. 30-35	719
1298	CRAIG, HARMON. Standard for reporting concentrations of deuterium and oxygen-18 in natural waters. Science, v. 133, no. 3467, June 9, 1961. pp 1833-1834	727
1299	CRAIG, HARMON. Isotopic variations in meteoric waters. Science, v. 133, no. 3465, May 26, 1961. pp. 1702-1703	729
1300	HASSAN, EL SAYED MOHAMED. Power from the sea. American Society of Civil Engineers. Proceedings. Journal of the Power Division, July 1961. pp. 2850-2857	731

Contrib. Number		Page Number
1301	SNODGRASS, JAMES M. Long-range outlook for oceanographic telemetering. Instrument Society of America. Fall Instrument-Automation Conference and Exhibit, Los Angeles, California. September 11-15, 1961. Preprint No. 221-LO-61. 5p.	739
1302	KAMPA, ELIZABETH M. Daylight penetration measurements in three oceans. International Union of Geodesy and Geophysics. International Association of Physical Oceanography. Symposium on Radiant Energy in the Sea. Helsinki, 4-5 August 1960. Monograph No. 10, June 1961. pp. 91-95	745
1303	BODEN, BRIAN P. Twilight irradiance in the sea. International Union of Geodesy and Geophysics. International Association of Physical Oceanography. Symposium on Radiant Energy in the Sea. Helsinki, 4-5 August 1960. Monograph No. 10, June 1961. pp. 96-101	751
1304	JOHNSON, MARTIN W. On zooplankton of some Arctic coastal lagoons of northwestern Alaska, with description of a new species of *Eurytemora.* Pacific Science, v. 15, no. 3, July 1961. pp. 251-262	773
1305	BODEN, BRIAN P. *Euphausiacea* (Crustacea) from tropical West Africa. Atlantide Report No. 6, May 20, 1961. pp. 251-262	773
1306	CRAIG, HARMON and DEVENDRA LAL. The production rate of natural tritium. Tellus, v. 13, no. 1, 1961. pp. 85-105	785
1307	BODEN, BRIAN P., ELIZABETH M. KAMPA and BERNARD C. ABBOTT. Photoreception of a planktonic crustacean in relation to light penetration in the sea. Progress in Photobiology, Proceedings of the Third International Congress on Photobiology, Finsen Memorial Congress, Copenhagen, July 31-August 5, 1960. pp. 189-196	807
1308	ECKART, CARL H. Internal waves in the ocean. Physics of Fluids, v. 4, no. 7, July 1961. pp. 791-799	815
1309	WISNER, ROBERT L. Evidence of a northward movement of stocks of the Pacific sardine based on the number of vertebrae. California Cooperative Oceanic Fisheries Investigations. Reports, v. 8, 1 July 1959-30 June 1960. pp. 75-82	825
1310	CRAIG, HARMON. Mass-spectrometer analyses of radiocarbon standards. Radiocarbon, v. 3, 1961. pp. 1-31	833
1311	RODEN, GUNNAR I. and JOSEPH L. REID, JR. Sea surface temperature, radiation, and wind anomalies in the North Pacific Ocean. Records of Oceanographic Works in Japan, v. 6, no. 1, March 1961. pp. 36-52	837
1312	RODEN, GUNNAR I. On nonseasonal temperature and salinity variations along the west coast of the United States and Canada. California Cooperative Oceanic Fisheries Investigations. Reports, v. 8, 1 July 1959-30 June 1960. pp. 95-119	855

Contrib. Number — Page Number

1313 BLACKBURN, MAURICE. Fisheries oceanography in Europe. California Cooperative Oceanic Fisheries Investigations. Reports, v. 8, 1 July 1959-30 June 1960. pp. 33-39 881

1314 PILSON, MICHAEL E. Q. and PETER B. TAYLOR. Hole drilling by octopus. Science, v. 134, no. 3487, October 27, 1961. pp. 1366-1368 889

1315 VACQUIER, VICTOR, ARTHUR D. RAFF and ROBERT E. WARREN. Horizontal displacements in the floor of the northeastern Pacific Ocean. Geological Society of America. Bulletin, v. 72, no. 8, August 1961. pp. 1251-1258 891

1316 MASON, RONALD G. and ARTHUR D. RAFF. Magnetic survey off the west coast of North America, 32° N. latitude to 42° N. latitude. Geological Society of America. Bulletin, v. 72, no. 8, August 1961. pp. 1259-1266 899

1317 WYLLIE, JOHN G. The water masses of Sebastian Vizcaino Bay. California Cooperative Oceanic Fisheries Investigations. Reports, v. 8, 1 July 1959-30 June 1960. pp. 83-93 907

1318 WOOSTER, WARREN S. Fisheries oceanography. California Cooperative Oceanic Fisheries Investigations. Reports, v. 8, 1 July 1959-30 June 1960. pp. 73-74 919

1319 TYLER, JOHN E. Scattering properties of distilled and natural waters. Limnology and Oceanography, v. 6, no. 4, October 1961. pp. 451-456 921

1320 TYLER, JOHN E. Measurement of the scattering properties of hydrosols. Optical Society of America. Journal, v. 51, no. 11, November 1961. pp. 1289-1293 927

1321 CURRAY, JOSEPH R. Late quaternary sea level: a discussion. Geological Society of America. Bulletin, v. 72, no. 11, November 1961. pp. 1707-1712 933

1322 TYLER, JOHN E. *In situ* detection and estimation of chlorophyll and other pigments in the ocean. National Academy of Sciences. Proceedings, v. 47, no. 11, November 1961. pp. 1726-1733 939

1323 LANCE, JAMES R. A distributional list of Southern California opisthobranchs. Veliger, v. 4, no. 2, October 1, 1961. pp. 64-69 948

1324 SNODGRASS, JAMES M. Some recent developments in oceanographic instrumentation. International Union of Geodesy and Geophysics. International Association of Physical Oceanography. Symposium on Radiant Energy in the Sea. Helsinki, 4-5 August 1960. Monograph No. 10, June 1961. pp. 83-91 955

1325 PREISENDORFER, RUDOLPH W. Application of radiative transfer theory to light measurements in the sea. International Union of Geodesy and Geophysics. International Association of Physical Oceanography. Symposium on Radiant Energy in the Sea. Helsinki, 4-5 August 1960. Monograph No. 10, June 1961. pp. 11-30 965

Contrib. Number | Page Number

1326 TYLER, JOHN E. On the measurement of the scattering function of the sea. International Union of Geodesy and Geophysics. International Association of Physical Oceanography. Symposium on Radiant Energy in the Sea. Helsinki, 4-5 August 1960. Monograph No. 10, June 1961. pp. 40-45 985

1327 GOLDBERG, EDWARD D. Chemistry in the oceans. *In* Oceanography. Washington, D. C., American Association for the Advancement of Science, 1961. pp. 583-597 993

1328 FOX, DENIS L. Coloration of animals. *In* Encyclopedia of the Biological Sciences, edited by Peter Gray. New York, Reinhold, 1961. pp. 254-261 1008

1329 ZoBELL, CLAUDE E. Marine bacteria. *In* Encyclopedia of the Biological Sciences, edited by Peter Gray. New York, Reinhold, 1961. pp. 593-595 1016

1330 HAXO, FRANCIS T. and BEATRICE M. SWEENEY. Bioluminescence. *In* Encyclopedia of the Biological Sciences, edited by Peter Gray. New York, Reinhold, 1961. pp. 150-151 1019

1331 CLARKE, WILLIAM D. A giant specimen of *Gnathophausia ingens* (Dohrn, 1870) (Mysidacea) and remarks on the asymmetry of the paragnaths in the suborder Lophogastrida. Crustaceana, v. 2, pt. 4, 1961. pp. 313-324 1021

1332 MUNK, WALTER H. and EL SAYED MOHAMED HASSAN. Atmospheric excitation of the earth's wobble. Geophysical Journal, v. 4, 1961. pp. 339-358 1033

1333 LIMBAUGH, CONRAD, HARRY PEDERSON and FENNER A. CHACE, JR. Shrimps that clean fishes. Bulletin of Marine Science of the Gulf and Caribbean, v. 11, no. 2, June 1961. pp. 237-257 1053

1334 HUBBS, CARL L. Isolating mechanisms in the speciation of fishes. *In* Vertebrate Speciation, a University of Texas symposium, 1961. pp. 5-23 1075

1335 SHUMWAY, GEORGE A., CARL L. HUBBS and JAMES R. MORIARTY. Scripps Estates site, San Diego, California: a La Jolla site dated 5460-7370 years before the present. New York Academy of Sciences. Annals, v. 93, art. 3, December 4, 1961. pp. 37-132 1095

1336 HUBBS, CARL L. The marine vertebrates of the outer coast. *In* Symposium: the biogeography of Baja California and adjacent seas—Part II. Marine Biotas. Systematic Zoology, v. 9, nos. 3 & 4, September-December 1960. pp. 134-147 1187

1137 CHOW, TSAIWHA J. and C. C. PATTERSON. On the primordial lead of the Canyon Diablo meteorite. Geokhimiya, no. 12, 1961. pp. 1124-1125 1201

Contrib. Number		Page Number
✓ 1138	RODEN, GUNNAR I. On the wind-driven circulation in the Gulf of Tehuantepec and its effect upon surface temperatures. Geofisica Internacional, v. 1, no. 3, July 1961. pp. 55-72	1203
1339	RAFF, ARTHUR D. and RONALD G. MASON. Magnetic survey off the west coast of North America, 40° N. latitude to 52° N. latitude. Geological Society of America. Bulletin, v. 72, no. 8, August 1961. pp. 1267-1270	1225
1340	SCHAEFER, MILNER B. Some fundamental aspects of marine ecology in relation to radioactive wastes. Health Physics, v. 6, 1961. pp. 97-102	1229

UNIVERSITY OF CALIFORNIA, SAN DIEGO
SCRIPPS INSTITUTION OF OCEANOGRAPHY
CONTRIBUTIONS, NEW SERIES
VOLUME 31, 1961

AUTHOR INDEX

	Number Contrib.	Page Number
ABBOTT, BERNARD C.		
(with Brian P. Boden and Elizabeth M. Kampa) Photoreception of a planktonic crustacean in relation to light penetration in the sea	1307	807
ALLISON, EDWIN C.		
(with Leo G. Hertlein) Species of the genus *Cypraea* from Clipperton Island	1250	202
ALVARINO, ANGELES		
Two new chaetognaths from the Pacific	1247	175
ARRHENIUS, GUSTAF O. S.		
Geological record on the ocean floor	1276	475
Pelagic sediments	1269	*
ARTHUR, ROBERT S.		
Variation in sea temperature off La Jolla	1230	19
BERNER, LEO D.		
(with Joseph L. Reid, Jr.) On the response to changing temperature of the temperature-limited plankter *Doliolum denticulatum* Quoy and Gaimard 1835	1281	549
BIEN, GEORGE S.		
(with Norris W. Rakestraw and Hans E. Seuss) Radiocarbon concentration in Pacific Ocean water	1239	91
BLACKBURN, MAURICE		
Fisheries oceanography in Europe	1313	881
BODEN, BRIAN P.		
Euphausiacea	1234	*
Euphausiacea (Crustacea) from tropical West Africa	1305	773
(with Elizabeth M. Kampa and Bernard C. Abbott) Photoreception of a planktonic crustacean in relation to light penetration in the sea	1307	807
Twilight irradiance in the sea	1303	751
BOYD, CARL M.		
The larval stages of *Pleuroncodes planipes* Stimpson (Crustacea, Decapoda, Galatheidae)	1248	187

*Not available for exchange

	Number Contrib.	Page Number
BRADSHAW, JOHN S.		
Laboratory experiments on the ecology of foraminifera	1289	649
BRAMLETTE, MILTON N.		
(with Frank R. Sullivan) Coccolithophorids and related nannoplankton of the early Tertiary in California	1275	429
Pelagic sediments	1277	495
BUZZATI-TRAVERSO, ADRIANO A.		
(with Warren H. Schmidt) An experiment in the design of a scientific conference	1271	371
Paper chromatography in relation to genetics and taxonomy	1272	375
CHACE, FENNER A., JR.		
(with Conrad Limbaugh and Harry Pederson) Shrimps that clean fishes	1333	1053
CHOW, TSAIHWA J.		
(with Edward D. Goldberg) On the marine geochemistry of barium	1291	679
(with C. C. Patterson) On the primordial lead of the Canyon Diablo meteorite	1337	1201
CLARKE, WILLIAM D.		
A giant specimen of *Gnathophausia ingens* (Dohrn, 1870) (Mysidacea) and remarks on the asymmetry of the paragnaths in the suborder Lophogastrida	1331	1021
CLENDENNING, KENNETH A.		
Photochemical activity of isolated chloroplasts (Hill reactions)	1243	*
COX, CHARLES S.		
Comments on Dr. Phillip's paper	1246	169
Measurements of slopes of high-frequency wind waves	1245	141
CRAIG, HARMON		
Isotopic variations in meteoric waters	1299	729
Mass-spectrometer analyses of radiocarbon standards	1310	833
(with Devendra Lal) The production rate of natural tritium	1306	785
Standard for reporting concentrations of deuterium and oxygen-18 in natural waters	1298	727
CROMWELL, TOWNSEND		
Pycnoclines created by mixing in an aquarium tank	1244	131
CURRAY, JOSEPH R.		
Late quaternary sea level: a discussion	1321	933
ECKART, CARL H.		
Internal waves in the ocean	1308	815
ENRIGHT, JAMES T.		
Lunar orientation of *Orchestoidea corniculata* Stout (Amphipoda)	1283	567
Pressure sensitivity of an amphipod	1240	101
FIELD, PRISCILLA W.		
(with James R. Moriarty and Georgina C. Peyton) Prehistory sites in the San Diego coastal area	1262	293

*Not available for exchange

	Contrib. Number	Page Number
FISHER, ROBERT L.		
(with George G. Shor, Jr.) Middle America trench: seismic-refraction studies	1279	533
Middle America trench: topography and structure	1278	515
FOLSOM, THEODORE R.		
(with Govindaraju J. Mohanrao) Trend of caesium-137 in the effluent of a large city	1232	41
FOREMAN, HELEN P.		
(with William R. Riedel) Type specimens of North American paleozoic radiolaria	1280	543
FOX, DENIS L.		
Coloration of animals	1328	1008
FRY, JOHN C.		
(with Russell W. Raitt) Sound velocities at the surface of deep sea sediments	1253	239
GOLDBERG, EDWARD D.		
Chemical and mineralogical aspects of deep-sea sediments	1241	105
Chemistry in the oceans	1327	993
Determination of opal in marine sediments	1228	1
On the marine geochemistry of barium	1291	679
GROVES, GORDON W.		
(with Walter H. Munk) A note on tidal friction	1251	205
HASSAN, EL SAYED MOHAMED		
(with Walter H. Munk) Atmospheric excitation of the earth's wobble	1332	1033
Fluctuations in the atmospheric inertia: 1873-1950	1288	609
Power from the sea	1300	731
HASTINGS, J. WOODLAND		
(with Beatrice M. Sweeney) Effects of temperature upon diurnal rhythms	1252	221
HAXO, FRANCIS T.		
(with Beatrice M. Sweeney) Bioluminescence	1330	1019
(with Beatrice M. Sweeney) Persistence of a diurnal rhythm in photosynthesis in enucleated *Acetabularia*	1295	709
HEMMINGSEN, EDVARD A.		
(with Per F. Scholander) Specific transport of oxygen through hemoglobin solutions	1285	581
HERTLEIN, LEO G.		
(with Edwin C. Allison) Species of the genus *Cypraea* from Clipperton Island	1250	202
HOLMES, ROBERT W.		
(with James M. Snodgrass) A multiple-detector irradiance meter and electronic depth-sensing unit for use in biological oceanography	1273	405

	Contrib. Number	Page Number
HUBBS, CARL L.		
Isolating mechanisms in the speciation of fishes	1334	1075
The marine vertebrates of the outer coast	1336	1187
(with George A. Shumway and James R. Moriarty) Scripps Estates site, San Diego, California: A La Jolla site dated 5460-7370 years before the present	1335	1095
JENSEN, DAVID		
Cardioregulation in an aneural heart	1264	303
(with Arthur L. Kelly) Chronic aortitis in the California sea-lion, *Zalophus californianus*	1265	325
JOHNSON, MARTIN W.		
Calanoida	1254	*
Copepoda	1255	*
Observations on inshore plankton collected during summer 1957 at Point Barrow, Alaska	1229	7
On zooplankton of some Arctic coastal lagoons of northwestern Alaska, with description of a new species of *Eurytemora*	1304	759
KAMPA, ELIZABETH M.		
Daylight penetration measurements in three oceans	1302	745
(wilth Brian P. Boden and Bernard C. Abbott) Photo-reception of a plankton crustacean in relation to light penetration in the sea	1307	807
KELLY, ARTHUR L.		
(with David Jensen) Chronic aortitis in the California sea-lion, *Zalophus californianus*	1265	325
KNAUSS, JOHN A.		
The structure of the Pacific equatorial counter-current	1236	69
KRAUSE, DALE C.		
Geology of the sea floor east of Guadalupe Island	1292	687
KREJSA, RICHARD J.		
The eastern, tropical Pacific fishes of the genus *Blenniolus*, including a new island endemic	1235	54
LAL, DEVENDRA		
(with Harmon Craig) The production rate of natural tritium	1306	785
LANCE, JAMES R.		
A distributional list of Southern California opisthobranchs	1323	948
LEIGHTON, DAVID L.		
Observations of the effect of diet on shell coloration in the red abalone, *Haliotis rufescens* Swainson	1287	605
LIMBAUGH, CONRAD		
Life-history and ecologic notes on the black croaker	1257	249
Observations on the California sea otter	1284	577
Shrimps that clean fishes	1333	1053

*Not available for exchange

	Contrib. Number	Page Number
MASON, RONALD G.		
(with Arthur D. Raff) Magnetic survey off the west coast of North America, 32° N. latitude to 42° N. latitude	1316	899
(with Arthur D. Raff) Magnetic survey off the west coast of North America, 40° N. latitude to 52° N. latitude	1339	1225
MENARD, HENRY W.		
Some rates of regional erosion	1270	361
MOHANRAO, GOVINDARAJU J.		
(with Theodore R. Folsom) Trend of caesium-137 in the effluent of a large city	1232	41
MORIARTY, JAMES R.		
(with Georgina C. Peyton and Priscilla W. Field) Prehistory sites in the San Diego coastal area	1262	293
(with George A. Shumway and Carl L. Hubbs) Scripps Estates site, San Diego, California: A La Jolla site dated 5460-7370 years before the present	1335	1095
Submarine archeology	1261	291
MUNK, WALTER H.		
(with El Sayed Mohamed Hassan) Atmospheric excitation of the earth's wobble	1332	1033
(with Gordon W. Groves) A note on tidal friction	1251	205
NEUSHUL, MICHAEL		
Diving in Antarctic waters	1237	83
NORTH, WHEELER J.		
Life-span of the fronds of the giant kelp, *Macrocystis pyrifera*	1294	705
PATTERSON, C. C.		
(with Tsaiwha J. Chow) On the primordial lead in the Canyon Diablo meteorite	1337	1201
PATTULLO, JUNE G.		
Sea level fluctuations	1260	*
Seasonal variation in sea level in the Pacific Ocean during the International Geophysical Year, 1957-1958	1259	273
PEDERSON, HARRY		
(with Conrad Limbaugh and Fenner A. Chace, Jr.) Shrimps that clean fishes	1333	1053
PEYTON, GEORGINA C.		
(with James R. Moriarty and Priscilla W. Field) Pre-history sites in the San Diego coastal area	1262	293
PILSON, MICHAEL E. Q.		
(with Peter B. Taylor) Hole drilling by octopus	1314	889
PREISENDORFER, RUDOLPH W.		
Application of radioactive transfer theory to light measurements in the sea	1325	965

*Not available for exchange

	Contrib. Number	Page Number
RAFF, ARTHUR D.		
(with Victor Vacquier and Robert E. Warren) Horizontal displacements in the floor of the northeastern Pacific Ocean	1315	891
(with Ronald G. Mason) Magnetic survey off the west coast of North America, 32° N. latitude to 42° N. latitude	1316	899
(with Ronald G. Mason) Magnetic survey off the west coast of North America, 40° N. latitude to 52° N. latitude	1339	1225
RAITT, RUSSELL W.		
(with John C. Fry) Sound velocities at the surface of deep sea sediments	1253	239
RAKESTRAW, NORRIS W.		
The chemist in oceanography	1296	711
Particulate matter in the oxygen-minimum layer	1263	299
(with George S. Bien and Hans E. Suess) Radiocarbon concentration in Pacific Ocean water	1239	91
REID, JOSEPH L., JR.		
(with Leo D. Burner) On the response to changing temperature of the temperature-limited plankter *Doliolum denticulatum* Quoy and Gaimard 1835	1281	549
On the temperature, salinity, and density differences between the Atlantic and Pacific oceans in the upper kilometre	1266	327
(with Gunnar I. Roden) Sea surface temperature, radiation, and wind anomalies in the North Pacific Ocean	1311	837
RIEDEL, WILLIAM R.		
(with Helen P. Foreman) Type specimens of North Atlantic paleozoic radiolaria	1280	543
ROBINSON, MARGARET K.		
Comparison of Norpac temperature sections with average BT sections along the same tracks	1274	421
RODEN, GUNNAR I.		
On nonseasonal temperature and salinity variations along the west coast of the United States and Canada	1312	855
On the wind-driven circulation in the Gulf of Tehuantepec and its effect upon surface temperatures	1338	1203
(with Joseph L. Reid, Jr.) Sea surface temperature, radiation, and wind anomalies in the North Pacific Ocean	1311	837
ROSENBLATT, RICHARD H.		
A new pearlfish (family Carapidae) from the Gulf of California	1293	699
RUDNICK, PHILIP		
Likelihood detection of small signals in stationary noise	1242	127
RUSNAK, GENE A.		
Sediments of Laguna Madre, Texas	1249	*
SACKETT, WILLIAM M.		
Protactinium-231 content of ocean water and sediments	1267	339

*Not available for exchange

	Contrib. Number	Page Number
SCHAEFER, MILNER B.		
Some fundamental aspects of marine ecology in relation to radioactive wastes	1340	1229
SCHMIDT, WARREN H.		
(with Adriano A. Buzzati-Traverso) An experiment in the design of a scientific conference	1271	371
SCHOLANDER, PER F.		
(with Edvard A. Hemmingsen) Specific transport of oxygen through hemoglobin solutions	1285	581
SHEPARD, FRANCIS P.		
(with Ruth Young) Distinguishing between beach and dune sands	1286	585
Recent sediment studies, 1955-1959	1268	341
Sea level rise during the past 20,000 years	1297	719
SHOR, GEORGE G., JR.		
(with Robert L. Fisher) Middle America trench: seismic-refraction studies	1279	533
SHUMWAY, GEORGE A.		
(with Carl L. Hubbs and James R. Moriarty) Scripps Estates site, San Diego, California: a La Jolla site dated 5460-7370 years before the present	1335	1095
SNODGRASS, JAMES M.		
Long-range outlook for oceanographic telemetering	1301	739
(with Robert W. Holmes) A multiple-detector irradiance meter and electronic depth-sensing unit for use in biological oceanography	1273	405
Some recent developments in oceanographic instrumentation	1324	955
A telemetering oceanographic current meter	1290	669
SUESS, HANS E.		
(with George S. Bien and Norris W. Rakestraw) Radiocarbon concentration in Pacific Ocean water	1239	91
SULLIVAN, FRANK R.		
(with Milton N. Bramlette) Coccolithophorids and related nannoplankton of the early Tertiary in California	1275	429
SWEENEY, BEATRICE M.		
(with Francis T. Haxo) Bioluminescence	1330	1019
(with J. Woodland Hastings) Effects of temperature upon diurnal rhythms	1252	221
(with Francis T. Haxo) Persistence of a diurnal rhythm in photosynthesis in enucleated *Acetabularia*	1295	709
The photosynthetic rhythm in single cells of *Gonyaulax polyedra*	1233	49
TAFT, BRUCE A.		
(with Warren S. Wooster) On the reliability of field measurements of temperature and salinity in the ocean	1231	25

Contrib. Number Page Number

TAYLOR, PETER B.
(with Michael E. Q. Pilson) Hole drilling by octopus 1314 889

TYLER, JOHN E.
In situ detection and estimation of chlorophyll and other pigments in the ocean 1322 939
Measurement of the scattering properties of hydrosols 1320 927
Observed and computed path radiance in the underwater light field 1258 261
On the measurement of the scattering function of the sea 1326 985
Radiance distribution as a function of depth in an underwater environment 1256 *
Scattering properties of distilled and natural waters 1319 921
Sun-altitude effect on the distribution of underwater light 1238 89

VACQUIER, VICTOR
(with Arthur D. Raff and Robert E. Warren) Horizontal displacements in the floor of the northeastern Pacific Ocean 1315 891

WARREN, ROBERT E.
(with Victor Vacquier and Arthur D. Raff) Horizontal displacements in the floor of the northeastern Pacific Ocean 1315 891

WISNER, ROBERT L.
Evidence of a northward movement of stocks of the Pacific sardine based on the number of vertebrae 1309 825

WOOSTER, WARREN S.
Fisheries oceanography 1318 919
(with Bruce A. Taft) On the reliability of field measurements of temperature and salinity in the ocean 1231 25
Yearly changes in the Peru current 1282 561

WYLLIE, JOHN G.
The water masses of Sebastian Vizcaino Bay 1317 907

YOUNG, RUTH
(with Francis P. Shepard) Distinguishing between beach and dune sands 1286 585

ZoBELL, CLAUDE E.
Marine bacteria 1329 1016

*Not available for exchange

REPRINT FROM JOURNAL OF MARINE RESEARCH, VOLUME 17, 1958
pp.178-182.

(1)

DETERMINATION OF OPAL IN MARINE SEDIMENTS

By

EDWARD D. GOLDBERG

Scripps Institution of Oceanography
University of California
La Jolla, California

ABSTRACT

The opal contents of recent marine sediments are ascertained by conversion of the opal to crystobalite by heating and by a subsequent quantitative x-ray diffraction analysis of the crystobalite. An opal stratigraphy is evident in Bering Sea deposits. Further, the opal concentrations appear to be covariant with barium, an element previously suggested as indicative of biological productivity in overlying water masses.

INTRODUCTION

One of the principal constituents in some marine sediments is opal, a highly disordered form of silicon dioxide, which generally contains less than 12 % water. This opal originates in the plant and animal life of the sea as frustules of diatoms or as skeletal remains of such organisms as radiolaria and sponges. There is no evidence for the inorganic deposition of opal in the marine environment. Although siliceous oozes and siliceous muds are defined in terms of the amount of opal present, there have been no direct methods of assay other than that of visual estimation. This situation prompted a survey of possible analytical techniques. Professor William D. Johns of Washington University, St. Louis, suggested converting the opal to crystobalite by heating and carrying through a quantitative x-ray diffraction analysis of the crystobalite. This paper covers preliminary results of experiments that consider such a method.

EXPERIMENTAL

General Method. A calcium carbonate-free marine sediment sample of 0.5–1.5 g, ground to a fine powder (100–200 mesh), was placed in a platinum crucible and heated at 900° C for four hours. The height of the resultant 4.04 *Å* diffraction peak of crystobalite was determined on a Norelco X-Ray Diffraction Spectrometer at 35 *KV*

Contribution from the Scripps Institution of Oceanography, New Series, 1228
Reproduced by Permission

and 20 *MA*, using copper K_α radiation. In order to secure the most reproducible results, known amounts of opal (10 and 20 $^0/_0$ by weight) were added to a second and third sample respectively, and these samples were then heated simultaneously; peak height determinations were subsequently made. The opal content of the sample was found from the best fit to the following equations, where x is the original percentage of opal in the sediment, k a proportionality factor, and P_n the intensity of the 4.04 Å line obtained in samples with an added percentage n of crystobalite:

$$\begin{aligned} &\text{(a)} \qquad x = k\,P_0\,, \\ &\text{(b)} \qquad x + 10 = k\,P_{10}\,, \\ &\text{(c)} \qquad x + 20 = k\,P_{20}\,. \end{aligned}$$

Note 1. Opal standards. Sponge spicules, obtained from live animals taken from Mission Bay, San Diego, California, constituted the primary opal standard. The sponges, treated with a mixture of one part nitric and one part perchloric acid, were heated to a temperature approaching the boiling point of the mixture to destroy the organic phases and subsequently cooled. The residue of spicules was washed repeatedly with distilled water, dried and ground to a 100–200 mesh powder.

Note 2. The temperature of 900° C and the heating time of four hours were arrived at empirically. Typical conversion data are given in Table I for diatomaceous earth from the Monterey formation at Palos Verdes, California.

TABLE I. EFFECT OF TEMPERATURE AND TIME OF HEATING ON THE CONVERSION OF OPAL TO CRYSTOBALITE

Heating-Time (hrs)	*Heating Temperature (° C)*	*Peak Height of Crystobalite (arbitrary units)*
1	800	5
2	800	5
4	800	13
1	900	28
2	900	28
4	900	31
8	900	30
	Untreated Control	0

Note 3. Inasmuch as calcium carbonate and silicon dioxide interact at the heating temperature to form the calcium silicate woll-

astonite, samples containing calcium carbonate were initially washed with 0.01 N hydrochloric acid, rinsed with distilled water, and dried before heating.

Note 4. Heating to or above 1000° produced glassy materials, and the resultant diffraction intensity of crystobalite was not as high as at 900° C and was not in general reproducible.

TABLE II. TYPICAL OPAL RUNS ON A SEDIMENT SAMPLE. SAMPLE FROM BERING SEA, CHINOOK 9 CORE SCRAPINGS

(a)	$x = k\,23$	(a–b)	$k = 10/23 = 0.43$
(b)	$x + 10 = k\,46$	(a–c)	$k = 20/43.5 = 0.46$
(c)	$x + 20 = k\,66.5$	(b–c)	$k = 10/20.5 = 0.49$
	Average k = 0.46		Percent opal in sample is 11 %.

Note 5. In the initial work, uric acid was added to the samples (following heating) as an internal standard. However, this technique was abandoned in favor of the "use of incremental amounts of opal as internal standards" because it was found that the amount of

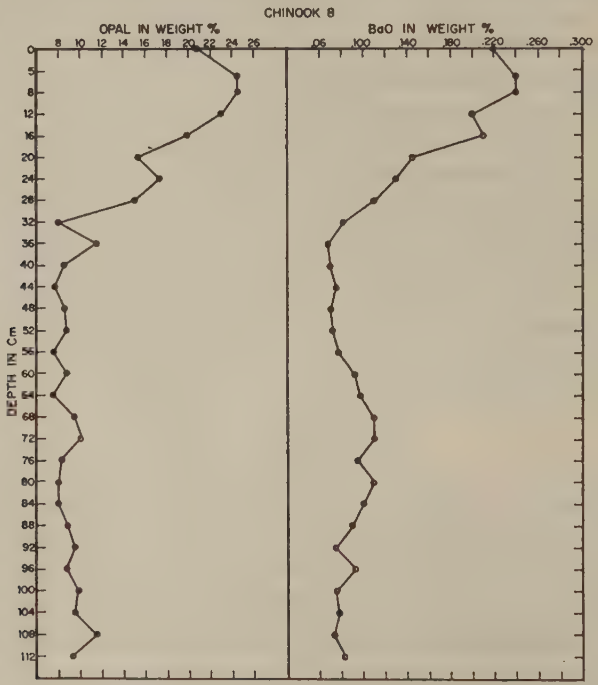

Figure 1. Opal and barium oxide concentrations in Chinook 8, from Lat. 53°01.5′ N, Long. 176°15.0′ W at a depth of 3660 m.

(4)

conversion was a function of any previous chemical treatments the samples had received. Washing with HCl, NH_4Cl or distilled water reduced the intensity of the resultant crystobalite peak and/or broadened the peak. These disturbances, introduced by such washings, were eliminated by introduction of the "incremental opal" to the samples before washing.

Note 6. The reproducibility of the results appears to be of the order of ± 10 $^0/_0$. Table II gives illustrative data on a typical set of replicate runs. The lower limit of detection was 2 $^0/_0$ opal.

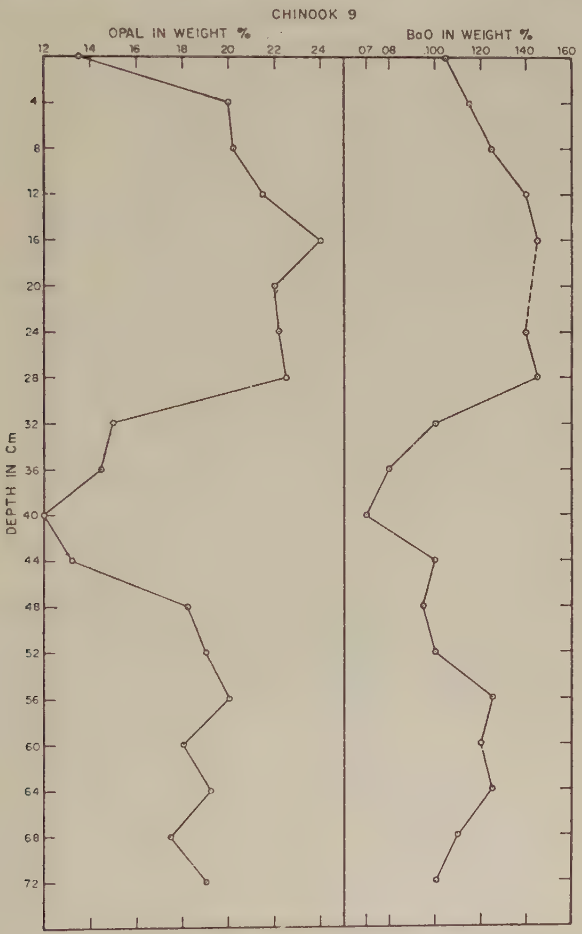

Figure 2. Opal and barium oxide concentrations in Chinook 9, from Lat. 52°25.2′ N, Long. 176°24.5′ W at a depth of 3440 m.

RESULTS

The depth distribution of opal in a pair of diatomaceous sediment cores from the Bering Sea, Chinook 8 and Chinook 9, is shown in Figs. 1 and 2. In both cores, obtained not far from one another, an opal stratigraphy appears. There is a marked decrease of opal with depth, with values of 20 % by weight at the surface and of 10–15 % at about 30 cm. In Chinook 9 there is a clear increase again at about 48 cm. The significance of such concentration changes is not as yet understood.

Of interest, however, is the possibility of a relationship between the opal, presumed to represent in these cores a measure of the biogenous contribution to the sediment, and barium, an element believed to be related to the productivity of an area (Goldberg and Arrhenius, 1958). Figs. 1 and 2 clearly demonstrate the covariance between barium and opal. The barium values were determined by emission spectroscopy (Goldberg and Arrhenius, 1958).

Since concentrations of barium are markedly higher in pelagic sediments below productive oceanic areas than in either the calcareous or siliceous parts or in the dried organic phases of the marine biosphere, barium is probably accumulated in deep sea deposits through chemical reactions involving organic debris. High barium contents are associated with both siliceous and calcareous deposits. One possibility may be the release of high concentrations of sulphate ion, resulting from oxidation of organically bound sulphur, in such deposits with a consequential precipitation of barium sulphate (Arrhenius, 1959).

REFERENCES

Arrhenius, G. O. S.
1959. Sedimentation on the ocean floor, *in*, Researches in geochemistry. (Ed., P. H. Abelson). John Wiley & Sons, New York. 511 pp.

Goldberg, E. D. and G. O. S. Arrhenius
1958. Chemistry of Pacific pelagic sediments. Geochim. Cosmochim. Acta, *13*: 153–212.

(6)

REPRINT FROM JOURNAL OF MARINE RESEARCH, VOLUME 17, 1958
pp.272-281.

(7)

OBSERVATIONS ON INSHORE PLANKTON COLLECTED DURING SUMMER 1957 AT POINT BARROW, ALASKA[1]

By

MARTIN W. JOHNSON

Scripps Institution of Oceanography
University of California,
La Jolla, California

ABSTRACT

Analyses of 34 net tows, collected July 16 to August 16, 1957 to depths of about 66 m, were concerned mainly with the microplankton. The concentration of plankton varied greatly while the composition remained quite uniform. *Acartia longiremis, Oithona similis* and *Pseudocalanus minutus* were the most abundant copepods. Other species of Calanoida recorded include *Acartia clausi*, especially in Nuwuk Pond; *Calanus finmarchicus*; *C. hyperboreus*; *Centropages mcmurrichi*; *Epilabidocera amphitrites*; *Eurytemora herdmani*; and *Tortanus discaudatus*. The presence of nauplii and early copepodid stages of *E. amphitrites* and *T. discaudatus* are of interest in demonstrating some reproduction by these more southerly forms on the Arctic coast and in pointing to a tenuous faunal connection of the east and west coast populations of *T. discaudatus*.

The macroplankton, especially *Limacina helicina, Clione limicina* and *Thysanoessa raschii*, were most conspicuous following heavy on-shore winds bringing in ice.

The temporary zooplankton consisted mainly of pelecypod, gastropod, annelid, barnacle, echinoderm and brachyuran larvae. Clypeasteroid plutei were common, although benthic adults have not been reported from the immediate area. Fish larvae were rare.

Results from culturing of copepods up to August 15 show that single isolated females of *Cyclops* from Imikpuk Lake are capable of producing a minimum of three successive broods without additional fertilization over the period.

INTRODUCTION

A brief study was made of the general character of inshore marine plankton in the Point Barrow area of Alaska from July 16 to August 16, 1957. Although ice conditions permitted sampling only within five miles of shore, this study supplements studies of offshore plank-

---

[1] Contribution from Scripps Institution of Oceanography, New Series. Research performed in connection with oceanographic investigations under contract No. ONR-206. no. 1229.

Reproduced by Permission

ton from collections made by the ice breaker USS BURTON ISLAND on two extensive cruises in the summers of 1950 and 1951 (Johnson, 1956). Previously the inshore plankton of Alaskan seas along the Arctic coast of North America had been studied to some extent in a preliminary survey by the Canadian Arctic Expedition 1913–18 (Willey, 1920). The early marine investigations of the Arctic Research Laboratory, concerned mainly with the benthic fauna, included primarily gross analyses of only the large plankton forms (MacGinitie, 1955).

The present report concerns particularly the microplankton, especially some of the copepoda and larvae of benthic invertebrates.

The collections comprise: 25 net tows taken just off the Arctic Research Laboratory, a few miles west of Point Barrow and seaward to about four miles, depending upon ice conditions; five tows from Eluitkak Pass just east of Point Barrow; and four tows from Nuwuk Pond. This somewhat brackish pond, about 250 m in length and about 6 m deep, is isolated from the sea by a gravel and permafrost barrier near the Point. The sampling was done with both fine (No. 20 mesh) and medium (Nos. 4 and 8 mesh) bolting silk nets towed horizontally at the surface or obliquely and vertically from depths up to about 30 m.

RESULTS

The characteristic percentage composition of plankton, as shown by several typical hauls, is given in Table I.

COPEPOD PLANKTON. The concentration of plankton varied greatly, but the composition remained quite uniform, with but few genera and species. Usually some harpacticoids occurred but these were not identified or counted. Two species of copepods, *Acartia longiremis* (Lilljeborg) and *Oithona similis* Claus were numerically the dominant forms (Table I). Nauplii of these genera were also the most numerous observed. It was expected that *Acartia clausi* Giesbrecht, a more strongly neritic species than other Acartias, would be more abundant than it was, but a careful examination of 25 or more adult females from each tow showed only a few specimens, except in collections from Nuwuk Pond, where it was the only *Acartia* found. The abundance of *A. longiremis* is of special interest in light of its small penetration in numbers and area into the Beaufort Sea, as shown by the USS BURTON ISLAND collections, in which no *Acartia* occurred in the Beaufort Sea except as a diminishing extension from the Chukchi Sea population and as scattered individuals near shore.

Among the copepods occurring only rarely or in small numbers in the collections are the following:

Calanus finmarchicus (Gunnerus), a cosmopolitan species, was usually represented by only scattered specimens, nearly all in early copepodid stages. Some large *Calanus* nauplii, probably this species, occurred commonly. The scarcity of *Calanus* species and the absence of other forms such as *Metridia longa* (Lubbock) and *Microcalanus pygmaeus* (G. O. Sars), all of which are common offshore, further demonstrates that in this area as elsewhere there is a clear distinction between inshore and offshore pelagic environment, each favoring its characteristic fauna. However, offshore forms do penetrate close to the coast when the water is deep, as shown by an oblique tow with a 1-meter net (No. 30 mesh gritgauze with apertures of approximately 0.65 mm) from the bottom at 66 m aboard the IVIK on August 8 about four miles from shore. In this tow 53 *Calanus finmarchicus* (including adult females and copepodids III, IV and V) and one *Calanus hyperboreus* Krøyer were taken. A surface tow of undetermined length taken at the same station with a $^1/_2$-meter net contained many neritic forms (Table I).

Centropages mcmurrichi Willey 1920 was consistently present, but in only small numbers. There is some doubt as to the proper name of this species. In describing the species, Willey included no figures. But reference to the figures given by McMurrich (1916), who listed the species with some doubt as *Centropages hamatus* (Lilljeborg), and to the figures by Mori (1937) for *Centropages abdominalis* Sato (1913), indicates that *mcmurrichi* and *abdominalis* are synonymous. Should further study of Sato's description show this to be so, his species name must be used.

Epilabidocera amphitrites (McMurrich) was found in five tows, one of which was in Eluitkak Pass. Usually the species was found only in the readily recognizable nauplius stage (Johnson, 1934). But several adult females and males were also captured in a $^1/_2$-meter net on August 8 about four miles offshore. This species, originally described from the west coast of Vancouver Island, is at times abundant in Puget Sound and is reported also from San Francisco Bay (Esterly, 1924). It was found in small numbers in neritic waters of the Bering Sea and off Cape Lisbourn, Alaska. In 1950 it was also found near Point Barrow, but the present record is its farthest eastward known penetration along the Arctic coast. Its absence from the east coast of North America suggests that, even though it is capable of penetrating into the Arctic Ocean to a distance just east of Point Barrow and is even able to reproduce to some degree there, still it has not been able to negotiate the remainder of the Arctic coast to become established as an endemic form of the West Atlantic. In this respect it contrasts sharply with *Tortanus discaudatus.*

Eurytemora herdmani Thompson and Scott is a small neritic and brackish water species. In the coastal collections it usually occurred sparsely as scattered individuals. However, in one surface haul three to four miles offshore it was common, the males outnumbering the females by about 30 to 1. Nauplii were also present in small numbers.

In Nuwuk Pond this species was present in large numbers, being numerically the dominant crustacean in the pond, where it was actively reproducing. In contrast to the coastal collections, about 65 $^0/_0$ of the adults were females, most of which carried egg sacs. All developmental stages were present, nauplii and copepodids being especially numerous.

Nuwuk Pond has been studied previously by Mohr (1953) who has reported a salinity of 24.5 $^0/_{00}$ for July 1952. How constant this salinity remains is apparently not known, but the pond is said to be reached at times by ocean waves during autumnal storms. In studying the life of the pond, Mohr was concerned with only the larger animals, *Mysis relicta* Loven, two gammaridean amphipods and an enchytraeid worm. To the crustaceans inhabiting the pond can now be added the copepods *Eurytemora herdmani*, *E. canadensis* and *Acartia clausi*, and, among unidentified copepods, a cyclopoid and an harpacticoid. Ostracods and tintinnids also occurred. The only living vegetation found by Mohr was an algal film on the gravel in shallow water. The present study shows a good crop of phytoplankton consisting of a small species of the diatom *Chaetoceras.* The extent to which the composition of this fauna and flora changes may depend upon the extent of renewal of water from the sea together with its load of euryhaline organisms.

Pseudocalanus minutus (Krøyer) is the third most abundant copepod encountered at coastal stations, where it was present in all samples. The numbers counted are probably minimal because exact identification is difficult, especially in subadult stages, so it is likely

TABLE I. PERCENTAGE COMPOSITION OF TYPICAL INSHORE MICROPLANKTON AT POINT BARROW, ALASKA, JULY AND AUGUST 1957

Location	*Eluitkak Pass*	*Off Arctic Research Laboratory*					*Av. % Copepods Only*
Date	*July 22*	*July 24*	*Aug. 1*	*Aug. 2*	*Aug. 8*	*Aug. 14*	
Type of Net and Haul	*40 cm # 8 mesh surface*	*40 cm # 8 mesh surface*	*40 cm # 8 mesh surface*	*40 cm # 8 mesh oblique 30–0 m.*	*$^{1}/_{2}$-m # 4 mesh surface*	*$^{1}/_{2}$-m # 4 mesh oblique 10–0 m.*	
Acartia clausi	+		+			+	+
Acartia longiremis	32.0	53.2	13.8	23.2	51.0	4.8	37.3
Calanus finmarchicus	+	+	+	+			+
Centropages mcmurrichi	0.4	0.6	0.3	0.5	0.2	+	0.5
Epilabidocera amphitrites							
nauplii	+			+	+		+
copepodid				+	+		+
adult					+		+
Eurytemora herdmani					0.4	+	+
Oithona similis	15.6	13.8	28.4	24.8	28.0	21.9	33.3
Pseudocalanus minutus	+	1.9	4.3	2.0	3.0	+	3.4
Tortanus discaudatus							
nauplii		+					+
copepodid II		+					+
copepodid IV			+				+
adult		+			+		+
Copepod nauplii	15.2	10.6	19.1	17.7	4.0	6.1	16.7
Copepod spp.	17.2	3.3	16.1	8.5	0.4	1.2	10.0
Amphipods (Gammaridean)	+	+	+	+			
Barnacle nauplii		0.6	0.5	7.5	5.0	29.0	
– cyprids	+	+	+	1.9	+	+	
Brachyuran zoea	+		+	+	+	+	
Macruran larvae		+					
Evadne		+				+	
Podon	0.4	0.7	0.5		+	7.3	
Gastropod larvae	2.5	3.2	4.3	3.9	1.0	5.1	
Lamellibranch larvae	2.5	7.4	1.5	2.7	3.0	20.8	
Clione limacina	0.1	0.1	+	+		+	
Limacina helicina	0.1	+	+	0.2		+	

+ Present singly or in small numbers.

TABLE I (continued).

Location	*Eluitkak Pass*	*Off Arctic Research Laboratory*					*Av. °/₀ Copepods Only*
Date	*July 22*	*July 24*	*Aug. 1*	*Aug. 2*	*Aug. 8*	*Aug. 14*	
Type of Net and Haul	*40 cm #8 mesh surface*	*40 cm #8 mesh surface*	*40 cm #8 mesh surface*	*40 cm #8 mesh oblique 30–0 m.*	*½-m #4 mesh surface*	*½-m #4 mesh oblique 10–0 m.*	
Annelid larvae	8.2	0.9	9.3	4.1	0.4	2.0	
Sagitta	0.8	3.4	+	0.8		+	
Rotifers	3.3	0.3	1.5	+	3.0	1.4	
Bipinnaria larvae				+			
Echinoplutei	1.6	+	+	2.2	0.4	0.5	
Ophioplutei		+	0.5	0.2			
Cyphonautes larva						+	
Oikopleura					+		

+ Present singly or in small numbers.

to enter preponderantly into enumeration of unidentified copepods. It is widespread in Arctic and sub-Arctic seas.

Tortanus discaudatus (Thompson and Scott) was present in five tows, two of which were in Eluitkak Pass. In the August 8 tow off the Arctic Research Laboratory, about 30 adult males were caught, but in the other tows combined, only one nauplius, three copepodids (II, III, IV) and one adult male were found. No floating egg cases were observed. In 1951, some egg cases were found and one specimen was taken at each of three adjacent stations off the Coleville River. From these data it seems clear that *Tortanus discaudatus* is able to reproduce to a limited extent in the region of Point Barrow and for some distance to the east.

This species, inhabiting both the east and west coasts of Canada and the United States, is often abundant in coastal waters. On the west coast it ranges southward to La Jolla, California. Few plankton observations are available along the Arctic coast, but doubtless there is or has been at times a more or less tenuous connection between the east and west coast populations. How complete or persistent this connection may be is an interesting question. The transport with water currents appears to be from west to east along the coast of the Beaufort Sea. With respect to its northern limits on the east coast, the species is not mentioned by Fontaine (1955) in three summer surveys of copepods in Ungava Bay. Willey (1931) has reported it in only small numbers from Richmond Gulf and James Bay in Hudson Bay.

Miscellaneous Plankton. Conspicuous in the macroplankton were *Limacina helicina* and *Clione limacina* which, while usually occurring only as scattered individuals in the tows, were on one occasion blown in with the ice and formed extensive windrows on the beach. Also among the zooplankton stranded on the beach were considerable numbers of the euphausiid *Thysanoessa raschii* (M. Sars) and ctenophores, probably *Mertensia*, which was numerous in Eluitkak Pass on July 16. At this time the copepod plankton in Eluitkak Pass was unusually sparse, likely as a result of predation by the ctenophores. Young *Sagitta* (4 to 10 mm) occurred regularly but never in abundance.

An important part of the neritic population was the temporary plankton found at all stations out to the edge of the ice. This plankton consisted mainly of larvae of bottom-living invertebrates, especially larval pelecypods, gastropods, annelids, barnacles and echinoderms together with a good number of decapod larvae, particularly brachyuran zoea. A small number of ascidian tadpole larvae were observed, and a single specimen of the bryozoan cyphonautes larva was caught. The advanced stage of growth of many of the invertebrate larvae indicates that reproduction was well under way before the survey was begun. Fish larvae were exceedingly rare.

The echinoderm larvae that occurred most commonly were clypeasteroid plutei. These were similar if not identical to the larva of the sand dollar *Dendraster excentricus* (Eschscholtz), judging from the structure of the calcareous rods supporting the arms (Johnson and Johnson, 1950). The postoral rods are fenestrated in characteristic clypeasteroid fashion (Mortensen, 1921). The presence of these larvae is interesting, in part because, in the benthic survey of the area, MacGinitie (1955) found only one echinoid, *i. e.*, *Strongylocentrotus drobachiensis*, a species with a recognizably different larva. The present observation would indicate that a considerable sand dollar population may be expected in some adjacent sandy bottom environment that has not been examined. It is probable that among the as yet unidentified larvae there may still be others that are indexes to unreported local adults or to transport of larvae from the more southernly Alaskan coastal areas along the Bering and Chukchi seas.

The occurrence of so many planktonic larvae of the benthos is of some significance in that it implies sub-Arctic conditions at Point Barrow with respect to the life history of many of the invertebrates; however, an analysis has not been made of the precentage of bottom invertebrates that have a life cycle involving pelagic larvae. This would be an important consideration. Specific or generic identification of most larvae was not attempted, but several types of larvae indicating taxonomic differences were noted. In the high Arctic of East Greenland only 5 % of the bottom invertebrates produce pelagic larvae, but these few may be quantitatively the most common (Thorson, 1950). From this brief study it was also impossible to arrive at any conclusion as to whether the planktonic life was a relatively short one compared with that of the same or related species in more temperate waters. Here again a flow of water mainly from the Alaskan coastal area of the Chukchi Sea rather than through the Beaufort Sea must have an ameliorating effect that is favorable to planktotrophic pelagic larvae.

As supplementary work, especially when ice conditions were unfavorable in the sea, samples of gravid females of *Eurytemora herdmani* from Nuwuk Pond and of a cyclopoid from Imikpuk Lake (fresh water) were isolated in culture dishes. These cultures were kept at the laboratory in an unheated room where temperatures remained near that of the natural environment. No food was added other than detrital material from the habitats. This may have been inadequate food for egg production and for growth of the developing stages. The adult specimens, however, survived in most instances from two to four weeks, when the experiments were terminated. The objective in these experiments was to gain some preliminary information relative to the fecundity of Arctic copepods.

Results from the culturing of these copepods up to August 15 show that single isolated females of *Cyclops* from Imikpuk Lake are capable of producing at least three successive broods of active nauplii without additional fertilization during the period. The resulting larvae of these broods grew slowly and survived rarely beyond the second naupliar stage. However, in one culture they reached the first copepodid stage in a minimum of 15 days after the eggs hatched on July 24. By August 15, when the animals were preserved, they had all reached the second copepodid stage.

(15)

The *Eurytemora herdmani* did not perform as well as the above mentioned specimens. Each female produced only one brood in captivity but, as with *Cyclops*, it is not possible to know how many, if any, broods had been produced before isolation. Most of the larvae died within ten days, but a few reached the second naupliar stage.

A study of the external morphology of the naupliar stages of *Eurytemora* from plankton collections made in the lagoon will be published elsewhere.

REFERENCES

ESTERLY, C. O.
1924. The free-swimming copepoda of San Francisco Bay. Univ. Calif. Publ. Zool., *26* (5): 81–229.

FONTAINE, MARION
1955. The planktonic copepods (Calanoida, Cyclopoida, Monstrilloida) of Ungava Bay, with special reference to the biology of *Pseudocalanus minutus* and *Calanus finmarchicus*. J. Fish. Res. Bd. Can., *12* (6): 858–898.

JOHNSON, M. W.
1934. The developmental stages of the copepod *Epilabidocera amphitrites* (McMurrich). Biol. Bull. Woods Hole, *67* (3): 466–483.
1956. The plankton of the Beaufort and Chukchi Sea areas of the Arctic and its relation to the hydrography. Tech. Pap. Arctic Inst. N. Amer., No. 1; 32 pp.

JOHNSON, M. W. AND L. T. JOHNSON
1950. Early life history and larval development of some Puget Sound Echinoderms. Studies Honoring Trevor Kincaid. University of Washington Press, Seattle; pp. 73–153.

MACGINITIE, G. E.
1955. Distribution and ecology of the marine invertebrates of Point Barrow, Alaska. Smithson. misc. Coll., *128* (9): 1–153.

MCMURRICH, J. P.
1916. Notes on plankton of British Columbia Coast. Trans. roy. Soc. Canada, (3) *10* (4): 75–89.

MOHR, J. L.
1953. Some observations on Arctic crustaceans and their associates: notes on the fauna of Nuwuk Pond, Point Barrow. Stanford Univ. Publ. Biol., *11*: 14–18.

MORI, TAKAMOCHI
1937. The pelagic copepoda from the neighboring waters of Japan. Yokendo Company, Tokyo. 150 pp.

MORTENSEN, TH.
1921. Studies of the development and larval forms of echinoderms. Copenhagen, G. E. C. Gad, pp. 1–261.

SATO, T.

1913. Pelagic copepods. No. 1. Rep. Fish. Res. Hokkaido Fish. exp. St. 79 pp. (In Japanese).

THORSON, GUNNAR

1950. Reproductive and larval ecology of marine bottom invertebrates. Biol. Rev., *25*: 1–45.

WILLEY, A. A.

1920. Report of the Canadian Arctic Expedition, 1913–18. Vol. 7, Crustacea. Part K. Marine Copepoda, pp. 1–46 k.

1931. Biological and oceanographic conditions in Hudson Bay. 4. Hudson Bay copepod plankton. Contr. Canadian Biol., N.S. *6* (25): 485–493.

(18)

JOURNAL OF GEOPHYSICAL RESEARCH VOLUME 65, NO. 12 DECEMBER 1960
pp.4081-4086.

Variation in Sea Temperature off La Jolla

ROBERT S. ARTHUR

Scripps Institution of Oceanography
University of California
La Jolla, California

Abstract. Hour-to-hour and seasonal changes in temperature were measured by bathythermograph at 32°52'30"N, 117°16'50"W during the IGY period. The temperature-depth traces for 21 series, each extending over 6 to 9 hours, show important hour-to-hour variations at all seasons as a result of internal waves. The median value of the ranges in mean temperature from surface to 100 meters for the 21 series is 0.8°C. The corresponding sampling error in charts of relative topography of the sea surface is about ±1 centimeter. Longer-term variations result from horizontal and vertical (upwelling) advection as well as local heating and cooling.

Introduction. As a part of the oceanographic program during the recent International Geophysical Year, observations of sea level were initiated over a network of island observatories and coastal stations in the Pacific [*Pattullo*, in press]. Observations of temperature and salinity were also made every two weeks to permit calculation of changes in the *steric* level which is determined from the vertical distribution of density by application of the hydrostatic equation. The writer undertook to monitor the field procedures and performance of equipment by occupying a station off La Jolla every few weeks. A by-product of the observations is information on the variation of temperature in the area and on the significance of a single temperature trace from a bathythermograph (BT). The recorded variations in temperature, particularly the hour-to-hour changes, are considered in the present paper. The relation of the observations to changes in sea level will be discussed elsewhere [*Pattullo*, in press].

Methods. Some notes on the instrumentation and procedures are given to indicate the accuracy of the measurements and the feasibility of obtaining hydrographic observations in coastal areas from a small skiff with light-weight equipment.

Two standard (135 m) BT's and two deep (270 m) BT's were used for the temperature measurements. The original new standard instrument was lost on October 7, 1958, when the wire parted. Replacement was made with a reconditioned instrument. The first deep instrument was replaced after October 28, 1958, because of indications that the bellows was beginning to deteriorate.

Checks were made on the temperature readings from the BT's by simultaneous lowerings of two BT's, by simultaneous lowerings of a BT and the temperature element of an electrical resistance thermometer, and by comparisons between BT's and a mercury thermometer in a stirred bath in the laboratory. The results indicated that with the usual calibration procedure [*LaFond*, 1951] the absolute accuracy of the BT readings could not be guaranteed to better than ±0.4°C. Corrections have been applied from the laboratory checks in an attempt to maintain the temperatures reported here to an accuracy of ±0.2°C. Results are better with respect to reproducibility. Identifiable features on traces from repeated lowerings on the same day show a precision of about ±0.1°C. It is to be emphasized that these instruments were handled much more carefully than is possible in ordinary shipboard use.

The customary reading of the bucket thermometer was made in conjunction with each lowering of a BT for calibration purposes [*LaFond*, 1951]. On a number of occasions the temperature at a depth of 1 to 2 m was more than 0.5°C lower than the temperature at the depth of 20 to 30 cm, as determined with the bucket thermometer suspended from a cork float. The effect was naturally most pronounced on relatively calm, clear days during the early afternoon. The recording of the thin, warm layer at the surface is usually obscured on the BT trace by the temperature variations which occur when

(19)

Contributions from the Scripps Institution of Oceanography, New Series, 1230
Reproduced by Permission

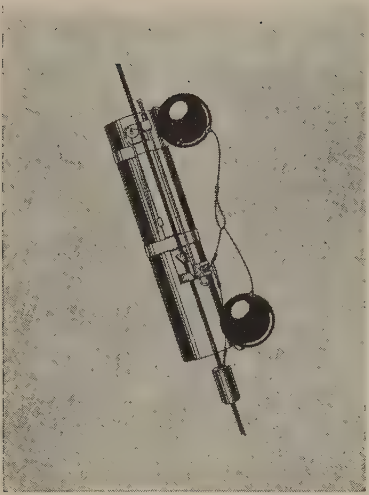

Fig. 1. Sketch of water sampler.

the instrument is put in and taken out of the water. An erroneous calibration comparison may frequently result because the tendency is to assume that the deeper isothermal layer extends to the depth at which temperature is measured with the bucket thermometer. When observations are made from a skiff the difficulty may be eliminated by holding the BT over the side and allowing the temperature element to equilibrate with water at a depth of 20 to 30 cm before the stylus is released. The observation is then made and the stylus is lifted before the BT is taken out of the water. With a sharp stylus and gold-plated slides it was routinely possible to obtain a thin, unobscured trace at the surface.

A check was made on the depths recorded by the BT's. The wire was marked with nylon thread at the maximum depths to which the standard and deep BT's were to be lowered. The wire angle was maintained at less than 10° as estimated visually. The depth recorded by the standard BT was always within ±2 m of wire length at 135 m. The depth element of the deep BT did not remain so accurate. After 15 lowerings the trace showed a depth of less than zero at the surface and a depth greater than the wire length at 245 m. The recorded depth interval from the top to the bottom of the trace was 5 to 10 m too great, and the results indicated deterioration of the bellows. A replacement BT performed satisfactorily for the subsequent lowerings.

The plastic water samplers (Fig. 1) were designed by J. D. Frautschy as a modification of a sampler described by *Van Dorn* [1956] The salinities of some water samples collected below 135 m appeared to be anomalously low, and it seemed probable that the sampler was exchanging water during the return to the surface. The hollow ball closures had been provided with a vent, so that the pressure inside the ball could equalize with the pressure outside. Comparison samples were taken at 135 and 245 m with the plastic bottles before and after an additional vent of ⅛-inch diameter was provided. Samples were also collected with a Nansen bottle. The results showed that the original vent was adequate at collected below 135 m after the enlarged vents were provided are reported. It was also found that the plastic tubing in the samplers could get out of round and the seat at the ends for the ball closure could become worn. It is necessary to take routine comparative samples with these collectors and a Nansen bottle at the maximum depth.

In a check on the titrations, salinities of duplicate samples from the same bottle and from closely spaced bottles (1- to 2-meter interval) agreed within ±0.04 per mil. All samples were collected at depths determined by measured lengths marked on the wire, and the wire angles were small enough so that sample depths are accurate to within about 2 per cent.

Observations. The station was located 2.3 km from shore on the axis of La Jolla Canyon (32°52′30″N, 117°16′50″W), where depth was about 300 m. On station the standard BT and a water sampler were lowered to 135 m with three additional samplers attached between the surface and the BT. Six to eight subsequent lowerings of the BT without samplers were made at intervals of about an hour. On many days one or two additional sets of water samples were collected. When the deep BT was available it was used immediately after the first lowering of the standard BT, and water samples were collected below 135 m. A second lowering of the deep BT was made on some days.

Observations were made on 26 days between August 1, 1957, and March 31, 1959. All the bathythermograms were read and curves of temperature against depth and salinity against depth were drawn for each day. A selection of 18 of the 26 days has been made, and the curves for

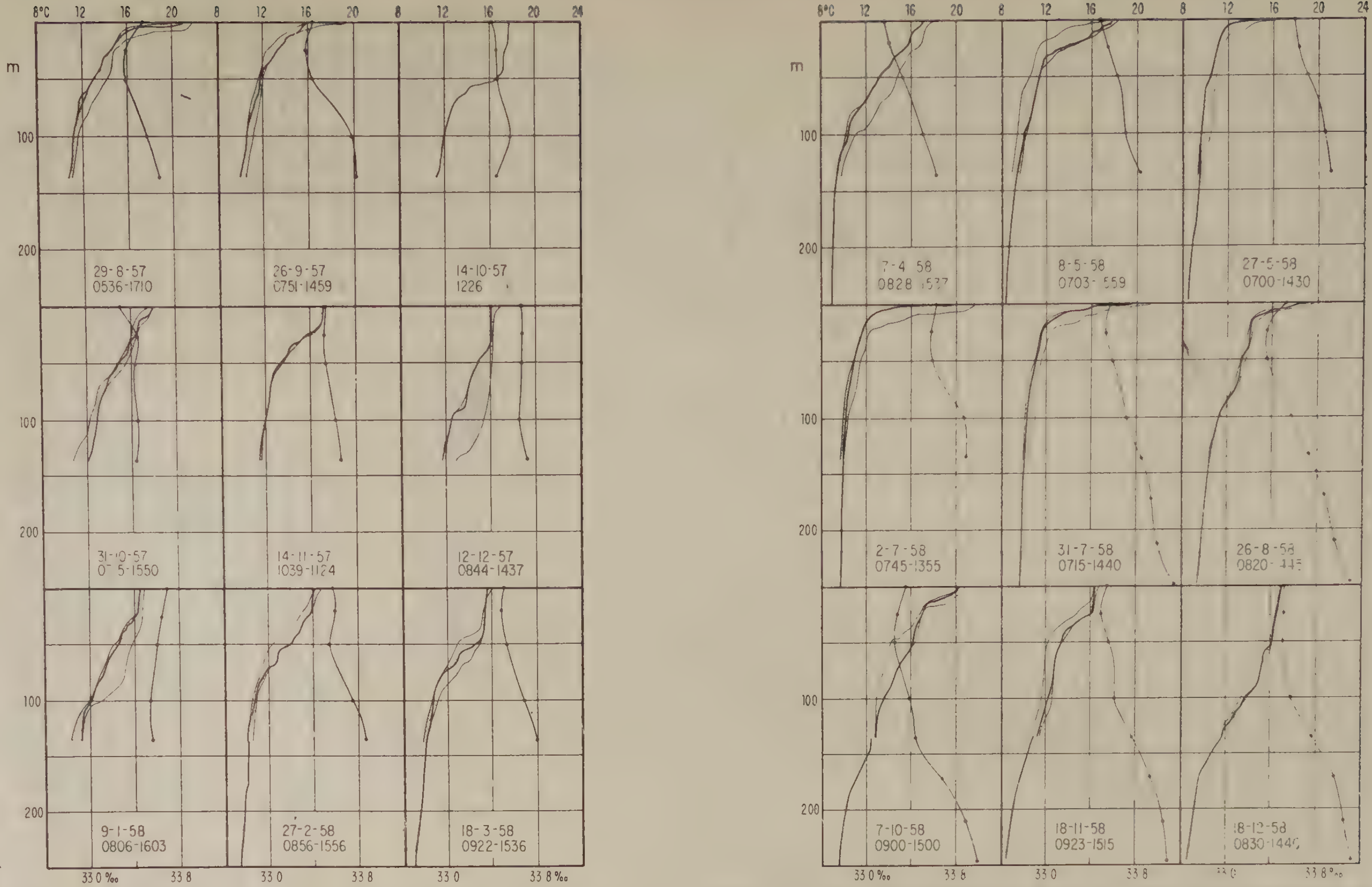

Fig. 2. Temperature (heavy line) and salinity (thin line with points) as functions of depth. The shaded area shows the range of temperature from additional BT lowerings between the times (PST) indicated below the date.

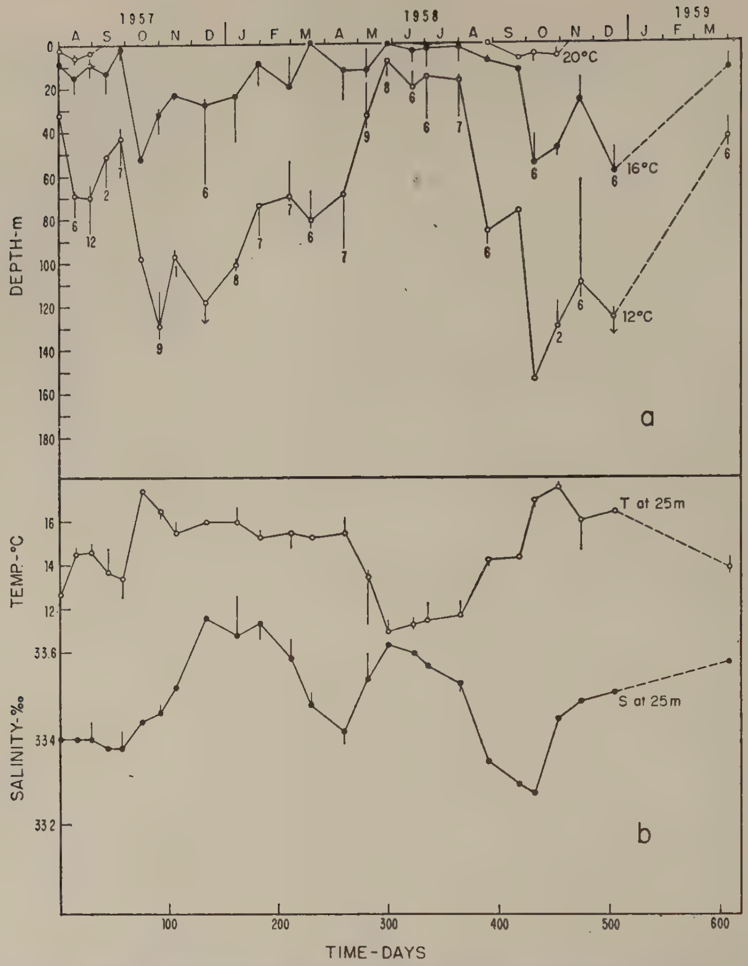

Fig. 3. (*a*) Depth of isotherms as a function of time from a single BT on each day. Vertical lines show range of depth from additional BT's extending over the number of hours indicated (to nearest hour). (*b*) Temperature and salinity at 25 meters as functions of time. Vertical lines show range of variation. In the case of salinity, only one or two additional samples were taken on each of 10 days.

these representative days are shown in Figure 2. In general, the temperature curve to 135 m has been taken from the first lowering of the standard BT on the day. The shaded area shows the range of temperature from subsequent lowerings on the same day. The curve below 135 m is taken from the first lowering of the deep BT. The two curves do not always match at 135 m because of the difference in time (about 30 minutes) and errors in the measurement. The shape of each curve was drawn to follow the actual BT trace in all major features. Salinities from the samples corresponding to the temperature curves were plotted and curves dra
through the points.

Points which represent the depths of particul
isotherms have been plotted in Figure 3*a* fro
a single BT lowering for each day. Vertical lin
through the points indicate the range of dep
variation for each isotherm as obtained from a
ditional BT lowerings for the same day. T
temperature at 25 m from a single lowering a
the range for each day are shown in Figure
Salinity at 25 m is also represented with t
range for those days when additional water sa
ples were collected.

TABLE 1. Range of Variation in Temperature (°C) at Standard Depths

Depth, m	Min	Max	25%	50%	75%
Surface	0.2	2.2	0.5	0.7	1.2
10	0.2	3.9	0.4	1.0	2.0
20	0.2	3.4	0.4	0.6	1.0
30	0.2	1.8	0.4	0.5	0.8
50	0.3	2.1	0.5	0.7	1.3
75	0.2	2.1	0.5	0.8	1.2
100	0.2	2.9	0.4	0.5	0.8
$\overline{\Delta T}_{0-100}$	0.5	1.6	0.6	0.8	1.2

Discussion. Important hour-to-hour variations in temperatures were present at all seasons during the months of observations. These short-term variations are considered to be associated primarily with internal waves. Such waves have been observed [*Reid*, 1956; *Leipper*, 1955; *Arthur*, 1954] or are now being observed [*LaFond*, 1960] off the California coast. The range of vertical movement of three isotherms (12°, 16°, 20°C) is shown in Figure 3*a*. The extreme occurred on November 18, 1958, when the depth of the 12°C isotherm ranged from 63 to 117 m. The inadequacy of a sample consisting of a single temperature trace is apparent.

The variations in temperature at standard depths from surface to 100 m are summarized in Table 1. The basis for the summary consists of 21 intervals of time during each of which the series of BT observations extended over 6 to 9 hours. During 17 of the 21 intervals the observations extended over 6 to 7 hours. The minimum range is 0.2°C and the maximum is 3.9°C. Inspection of the individual BT traces has shown that greater ranges tend to occur where the vertical temperature gradient is greater. These reported values are undoubtedly less than the total ranges of variation produced by the internal waves. The energy in internal waves is distributed from periods of minutes to many hours, but tidal periods are very prominent in the records [*Reid*, 1956: *Arthur*, 1954]. Hourly observations over intervals of at least 12 hours are required to cover the full range of temperature variation.

The influence of the temperature variations on the relative topography of the sea surface may be estimated from entries in the last row in Table 1. Let ΔT denote the difference between the minimum and maximum temperatures at any depth during one of the BT series. The mean value of $\overline{\Delta T}$ between the surface and 100 m, denoted by $\overline{\Delta T}_{0-100}$, has been determined for each of the 21 series. Some 50 per cent of the series have a mean difference greater than 0.8°C and 25 per cent greater than 1.2°C. An approximate value of the coefficient of thermal expansion of sea water is $0.0002/°C^{-1}$ and the corresponding variation in height of the surface relative to 100 m is 1.6 and 2.4 cm, respectively. These values are probably an underestimate of the variation in height of the sea surface for three reasons: (1) the BT series have not extended over complete tidal periods, (2) the temperature oscillations extend below 100 m, and (3) salinity tends to increase with depth and would add to the variation. The variations are comparable to those found by *Reid* [1956]. They may be regarded as representing the sampling error which exists when stations occupied at different times are used in constructing a chart of relative topography [*Wooster and Taft*, in press]. In view of the magnitude of about 2 cm for the range, the use of a contour interval of 2 cm or less in such charts for the waters off California is certainly inappropriate. Various factors enter into the determination of contour interval, but these results on short-term variation suggest that perhaps 5 cm is a permissible minimum interval

The location of the station over a submarine canyon raises the question whether the observed temperature variations are representative. The curves of temperature and salinity with depth at the IGY station are similar to corresponding curves at a station about 25 km to the west which was occupied seven times during the IGY period. Internal wave activity in much more shallow water close to shore has been shown to be similar with or without the presence of a canyon [*Arthur*, 1954]. It is, therefore, believed that the observed variations are representative of the area off the California coast, particularly in view of *Reid's* [1956] similar results north of Point Conception.

Some longer-term variations, e.g. seasonal, which have been discussed previously [*e.g.*, *Reid, Roden, and Wyllie*, 1958], may be noted in Figures 2 and 3:

1. During the fall months, the temperature and salinity at depths below about 25 m show an increase, with the cumulative effect reaching

a maximum in December. The seasonal inshore countercurrent is important in introducing warmer, more saline southern water at these depths.

2. A more transient variation occurred in October 1957 (Fig. 2, Oct. 14, 1957). A single observation was made within a few hours of the passage of a front which was preceded by relatively strong southerly winds and followed by westerly winds. Warmer water from offshore apparently flooded the water column to a depth of 50 m. For nearshore stations, the onshore movement of surface water is of at least occasional importance during the fall season.

3. Below the surface, e.g. at a depth of 25 m, the lowest temperatures occur in May, June, and July (note Fig. 3, especially). The greater salinity of the cold water suggests the influence of late spring and early summer upwelling at the station.

Acknowledgments. This paper represents the results of research carried out by the Scripps Institution of Oceanography, University of California, under contract with the Office of Naval Research and an IGY grant through the National Science Foundation. Reproduction in whole or in part is permitted for any purpose of the United States Government. The author is indebted to Earl D. Murray for his assistance with all of the observations. Helmuth Sandstrom assisted with the analysis. The scientific program for the IGY observations of sea level was developed by June G. Pattullo and Jeffrey D. Frautschy.

References

Arthur, R. S., Oscillations in sea temperature at Scripps and Oceanside Piers, *Deep-Sea Research, 2,* 107–121, 1954.

LaFond, E. C., Processing oceanographic data, *U. S. Navy Hydrograph. Office Publ. 614,* Washington, D. C., 1951.

LaFond, E. C., Isotherm follower (abstract), *J. Geophys. Research, 65,* 2505–2506, 1960.

Leipper, D. F., Sea temperature variations associated with tidal currents in stratified shallow water over an irregular bottom, *J. Marine Research, Sears Foundation, 14,* 234–252, 1955.

Pattullo, J. G., Seasonal variation in sea level in the Pacific Ocean during the International Geophysical Year, 1957–1958. *J. Marine Research, Sears Foundation,* in press.

Reid, J. L., Observations of internal tides in October 1950, *Trans. Am. Geophys. Union, 37,* 278–286, 1956.

Reid, J. L., Jr., G. I. Roden, and J. G. Wyllie, Studies of the California Current System, *Marine Research Comm., Calif. Cooperative Oceanic Fisheries Invest., Progr. Rept., 1 July 1956 to 1 January 1958,* The State Printer, Sacramento, 1958.

Van Dorn, W. G., Large-volume water samplers, *Trans. Am. Geophys. Union, 37,* 682–684, 1956.

Wooster, W. S., and B. A. Taft, On the reliability of field measurements of temperature and salinity in the ocean. *J. Marine Research, Sears Foundation, 17,* in press.

(Manuscript received July 28, 1960.)

REPRINT FROM JOURNAL OF MARINE RESEARCH, VOLUME 17, 1958
pp.552-566.

(25)

ON THE RELIABILITY OF FIELD MEASUREMENTS OF TEMPERATURE AND SALINITY IN THE OCEAN[1]

By

WARREN S. WOOSTER AND BRUCE A. TAFT

Scripps Institution of Oceanography, University of California
La Jolla, California

ABSTRACT

In order to evaluate the reliability of recent field measurements of temperature and salinity we have followed the behavior of certain pairs of reversing thermometers through many reversals and have examined the distribution of closely spaced measurements of temperature and salinity at intermediate depths. The errors of measurement are comparable to those of the classical expeditions and are small with respect to sampling and other errors in the upper layers of the ocean. The effect of measurement errors on computed values of specific volume anomaly, of geopotential anomaly, and of geostrophic current speed was examined.

INTRODUCTION

Subsurface measurements of temperature and salinity are usually used by oceanographers to describe the distributions of these properties, to characterize water masses, and to derive the field of mass in the sea. From the field of mass, by means of hydrostatic computations and the geostrophic equation, it is possible to compute a measure of the field of velocity. The accuracy with which the field of velocity is known depends among other things on the accuracy of the measurements of temperature and salinity employed.

It is often assumed by oceanographers that all temperature measurements with reversing thermometers are accurate to within 0.01° and that salinity measurements have errors not greater than 0.02 ‰ (for example, see Sverdrup, *et al.*, 1942: 349, 54). Such estimates of error are based in part on laboratory studies of precision and accuracy, but generally they are derived from studies made in connection with the major expeditions of the late 1920s (such as METEOR, SNELLIUS and CARNEGIE).

---

[1] This paper represents results of research supported by the Office of Naval Research and by the U.S. Bureau of Commercial Fisheries. Contribution from Scripps Institution of Oceanography, New Series. 1231.

Reproduced by Permission

Now that the collection and processing of large quantities of oceanographic data have become well established routines, it is possible that different quality standards may pertain. To what extent has accuracy been sacrificed to obtain detailed coverage in space and time? To answer this we have attempted a realistic evaluation of the reliability of some recent field measurements of temperature and salinity.

TEMPERATURE

It is common practice in oceanography to measure subsurface temperature by means of protected reversing thermometers; often two such thermometers are used at a given depth. After application of an index correction and a correction for expansion of the mercury column as the thermometer warms up, the resulting corrected temperatures are averaged to obtain the accepted *in situ* temperature. Such replicate measurements have been used to estimate errors in temperature measurements, for example by Böhnecke (1932) for METEOR observations and by Hamaker (1941) for those of SNELLIUS. The latter paper includes a summary of Böhnecke's study along with a useful general discussion of the sources and treatment of errors.

Both Böhnecke and Hamaker computed standard deviations of differences between paired thermometers on the assumption that all came from a single population. In our study it was possible to follow various pairs of thermometers through many reversals so that the data from each given pair represents a single population. With this approach it is possible to separate the variance into its random and systematic components.

The temperature measurements analysed in this paper were made for the most part with thermometers of American and German manufacture which had been calibrated at the Scripps Institution within two years of the time of use. Pairs of thermometers were chosen from the records of two long Scripps expeditions (DOWNWIND in 1957–58 and SHELLBACK in 1952) and of two shorter operations of the Marine Life Research program (Cruises 5704S and 5704H, both in 1957). The only criterion for choosing a pair of thermometers was that a large number of reversals be available (from 31 to 103 reversals were available for the pairs used). For each pair the difference between the corrected readings of the left and right thermometer (d_i) was calculated for the i^{th} reversal:

TABLE I. ESTIMATES OF TEMPERATURE MEASUREMENT ERRORS FROM ANALYSIS OF PAIRED THERMOMETER REVERSALS

Thermometer Pair	$\bar{d}$ (° *C*)	$s^2_{wp} \times 10^4$ (° C^2)	$s^2_0 \times 10^4$ (° C^2)	$s^2_s \times 10^4$ (° C^2)	*n*
DOWNWIND					
1	0.009	2.2	1.9	0.3	35
2	0.003	1.9	1.8	0.1	44
3	0.013	2.5	1.7	0.8	43
4	0.017	3.6	2.2	1.4	41
5	0.014	2.2	1.2	0.9	42
6	0.029	4.8	0.4	4.3	43
7	0.013	2.8	1.9	0.9	43
8	0.022	2.9	0.5	2.4	54
11	0.006	0.9	0.7	0.2	80
14	0.014	1.5	0.6	0.9	79
15	0.022	3.5	1.1	2.4	31
16	0.002	0.6	0.6	0.0	54
17	0.002	0.5	0.4	0.0	75
18	0.019	2.6	0.8	1.8	59
5704 S					
36	0.005	1.4	1.3	0.1	34
35	0.005	4.7	4.6	0.1	56
13	0.001	2.8	2.9	0.0	60
17	0.008	1.9	1.6	0.3	60
47	0.021	2.6	0.5	2.1	53
5704 H					
3	0.003	2.4	2.4	0.0	68
19	0.015	2.0	0.9	1.1	61
4	0.005	3.3	3.2	0.1	59
12	0.007	0.8	0.5	0.3	67
7	0.018	3.1	1.4	1.6	69
SHELLBACK					
29	0.008	3.0	2.7	0.3	93
35	0.008	3.0	2.7	0.3	92
96	0.014	1.9	0.9	0.9	103
94	0.012	1.5	0.9	0.7	102
79	0.023	4.8	2.1	2.8	103
101	0.017	1.9	0.4	1.5	101
26	0.009	2.5	2.2	0.4	56
89	0.008	0.7	0.5	0.3	99
Over-all Average	0.012	2.4	1.5	0.9	—

$\bar{d}$ is mean difference, s^2_{wp} the estimate of within-pair variance, s^2_0 the estimate of variance of random error, s^2_s the estimate of variance of systematic error, and *n* the number of reversals used.

$$d_i = (t_L - t_R)_i .$$

Averages of differences ($\bar{d}$) for n reversals of the various pairs are listed in Table I.

If there were no systematic difference between the thermometers of a pair, then the average of differences would be zero. However, in most cases (85 $^0/_0$) the mean difference is significantly different from zero at the 5 $^0/_0$ level of significance, the grand mean difference being 0.012° with a range from 0.001 to 0.030°. The source of this systematic difference between thermometers presumably lies in their calibration or in a shift in zero point. On the average this relative systematic error will underestimate the true systematic error (since the true temperature is unknown). The data suggest that differences between paired thermometers are commonly as great as 0.01° and that the average systematic error of a single thermometer is at least 0.005°.

The variance of the two corrected readings from a pair of thermometers averaged over a large number of reversals provides a good estimate of the within-pair variance, σ^2_{wp}, through use of the equation[2]

$$s^2_{wp} = \frac{\sum_1^n d_i^2}{2n} .$$

This variance is equal to the sum of a systematic component, σ^2_s, and of a random component, σ^2_0. The relative contributions of these two components can be determined since the random component can be estimated[3]. The readings of the two thermometers of a pair are independent, and the variance of the difference in corrected readings, d_i, is

$$\sigma^2_{d_i} = \sigma^2_L + \sigma^2_R .$$

Then the average random component of variance of a given thermometer is

$$\sigma^2_0 = \sigma^2_{d_i}/2 ;$$

$\sigma^2_{d_i}$ can be estimated by

$$s^2_{d_i} = \sum_{i=1}^{n} \frac{(d_i - \bar{d})^2}{n-1} .$$

---

[2] The equation for the weighted average of a set of variances, each of which is calculated from two observations.

[3] The systematic component can also be estimated directly, since $s^2_s = \bar{d}^2/2$.

Total within-pair variance and variances of the random and systematic components are listed for 32 pairs of thermometers (Table I). In terms of standard deviation, the over-all estimates of total, random and systematic errors of single thermometer readings average 0.016°, 0.012° and 0.010° respectively.

Errors in reversing thermometer temperature measurements may also be estimated by using data from special hydrographic casts with closely spaced Nansen bottles. Such casts have frequently been made to intermediate depths in order to check the pressure calibrations of unprotected thermometers. In certain cases the slope of the temperature-depth curve is sufficiently constant that a regression line may be fitted to the data. Residuals from this line may then be interpreted as the sum of random and systematic errors on the assumption that in the particular situation the relation is truly linear. Strictly speaking, this assumption is never completely valid, and this method presumably overestimates the error (since the residuals contain a component due to the nonlinear trend). In the statistical model, errors in relative depth are considered small in relation to the temperature errors.

Of the large number of special casts taken during the last ten years at the Scripps Institution of Oceanography, only a few were found to be suitably linear for analysis. On these casts, thermometer separation ranged from 2 to 25 m; in the summary of results (Table II) the casts with 25 m spacing are listed separately from those with separations of 2 to 10 m since there appeared to be a significant difference between the two groups[4]. The square root of the weighted average of estimates for closely spaced thermometers is 0.020° (with a range of 0.012° to 0.030°) whereas that for casts with 25 m spacing is 0.027°. The former value is considered a more valid estimate since, in the case of the widely spaced thermometers, the casts cover such a vertical distance that the assumption of linearity is less justifiable.

In summary these studies lead to the following conclusions. The standard deviation of random error of a single thermometer is 0.012°. This random error is superposed on a systematic error, the standard deviation of which is 0.010°. The upper limit of combined errors of a single thermometer is estimated by a standard deviation

---

[4] Note that each thermometer reading has been considered independent, although there were usually two thermometers at each depth.

TABLE II. ESTIMATES OF TEMPERATURE MEASUREMENT ERRORS FROM ANALYSIS OF CLOSELY SPACED OBSERVATIONS

Cruise	*Depth Range* (*m*)	*Spacing* (*m*)	s_{zT} (° *C*)	*n*
5404 F	502–520	2	0.013	19
H-36	893–933	5	0.014	11
C-35	884–910	3	0.019	16
B-33 (a)	921–945	2	0.014	22
B-33 (b)	956–976	2	0.016	23
B-35	943–963	2	0.018	19
Y-32	1240–1264	3	0.014	17
B-20	921–945	2	0.027	18
B-19	953–1008	5	0.013	16
C-19 (a)	985–1035	5	0.020	18
C-19 (b)	989–1039	5	0.018	18
5404 F	503–521	2	0.012	19
Q-4	479–528	5	0.021	18
5807 S	405–478	10	0.029	15
5807 B	425–521	9	0.018	22
5807 O	424–573	10	0.030	31
C-21 (a)	815–935	25	0.017	12
C-21 (b)	765–951	25	0.027	18
H-25	785–981	25	0.022	17
C-25	781–1001	25	0.029	16
B-25	780–1003	25	0.019	18
C-27	818–995	25	0.014	13
C-24 (a)	655–879	25	0.038	18
C-24 (b)	668–887	25	0.031	19
H-24	640–852	25	0.023	14
H-24	758–1004	25	0.019	21
H-23	670–998	25	0.032	23
H-23	779–926	25	0.019	14
B-23	752–975	25	0.023	18
C-23 (a)	646–981	25	0.028	28
C-23 (b)	693–1011	25	0.035	28
C-22	762–1004	25	0.026	21
C-22	676–898	25	0.027	19
B-22	703–1022	25	0.021	26

s_{zT} is standard error of regression, and *n* the number of observations used.

of 0.020° (from the analysis of closely spaced thermometers) and the lower limit by 0.016° (from the analysis of within-pair variance).

These estimates of error in temperature measurements are comparable to those made by other authors. In Hamaker's (1941) summary of METEOR and SNELLIUS observations, standard errors of a single observation range from 0.008 to 0.012° depending on the type of thermometer used (compared to our value of 0.016°). The estimated standard deviation of systematic error for SNELLIUS observations is 0.007° (compared to our value of 0.010°). From table I of Thomsen's (1937) discussion of DANA observations, we have computed the standard deviation of combined errors to be 0.015° (compared to our value of 0.016°). Sverdrup's (1944) discussion of CARNEGIE data does not contain estimates in a form comparable with ours, except that his grand mean difference between paired thermometers seems to be essentially the same as ours (about 0.012°).

All of the above estimates refer to errors of a single thermometer reading. When a temperature measurement is obtained by averaging the corrected readings of two thermometers, the standard deviation is reduced by the factor $1/\sqrt{2}$. Our results show that the 95 % confidence limits of random errors for a two-thermometer average are ±0.017°.

SALINITY

Duplicate chlorinity titrations conventionally run on sea water samples are not sufficiently independent to be used in an analysis of errors. Laboratory tests of precision, where a skilled operator carries out carefully replicated analyses, will presumably lead to a smaller estimate of error than is valid for more heterogeneous field data. It is possible to obtain some idea of the magnitude of errors in such data if we refer to the same special hydrographic casts with closely spaced Nansen bottles used above in the analysis of temperature errors; however, compared to the temperature data there were fewer casts with reliable salinity values, and, since only one salinity resulting from a duplicate titration is assigned to each sampling depth, only half as many observations were available from each cast. As before, casts were selected on which salinity appeared to change with depth in linear fashion, and residuals from the regression line were computed. The results are summarized in Table III.

The estimates of standard deviation for the various casts range from 0.005 to 0.032 ‰, and the square root of the weighted average of the estimated variances is 0.018 ‰. On the assumption that deviations are normally distributed, the 95 % probability limits are estimated by ± 0.036 $^0/_{00}$. This error estimate is considered an upper limit, since the deviations presumably include a component due to the nonlinearity of the salinity-depth relationship.

There are few estimates of error in the literature with which our results can be compared. Based on statistical analysis of results obtained by skilled operators in a shore based laboratory, Strickland (1958) has reported 95 $^0/_0$ confidence limits as ± 0.017 $^0/_{00}$, implying a standard deviation of 0.0085 $^0/_{00}$. Hardon's (1941) summary of SNELLIUS and METEOR observations has assumed that duplicate analyses of single samples are completely independent; thus his estimates, expressed as standard deviation in salinity units, namely 0.008 $^0/_{00}$ for SNELLIUS and 0.021 $^0/_{00}$ for METEOR, are presumably low.

TABLE III. ESTIMATES OF SALINITY MEASUREMENTS ERRORS FROM ANALYSIS OF CLOSELY SPACED OBSERVATIONS

Cruise	*Depth Range* (*m*)	*Spacing* (*m*)	s_{zS} ($^0/_{00}$)	*n*
5810 H	529–679	10	0.012	17
5811 P	483–612	10	0.022	14
5807 O	415–573	10	0.005	16
5807 S	405–551	8	0.029	17
5810 P	449–597	10	0.017	16
5807 B	469–538	9	0.014	9
B-20	921–985	5	0.021	15
B-33 (a)	956–976	2	0.032	15
B-33 (b)	921–945	2	0.030	10
H-36	888–933	5	0.016	11
C-35	881–910	3	0.014	15
C-19	955–1035	5	0.017	15
H-35	946–973	3	0.010	15
B-35	943–963	2	0.023	11
5810 S	342–568	10	0.017	23

s_{zS} is standard error of regression, and *n* the number of observations used.

An estimate more analagous to ours comes from comparison of shipboard analyses of 18 SNELLIUS samples with later replicate analyses by T. G. Thompson using the Volhard method (Hardon, 1941). Since the Volhard method is known to be more accurate than the usual Mohr titration, it is not unreasonable to assume that

Thompson's values represent the true salinity; in salinity units, his results were on the average 0.009 ‰ low, with a standard deviation of 0.023 ‰.

SAMPLING AND OTHER ERRORS

The estimates of error discussed above refer only to measurements at given depths in the sea. The depths themselves, which are derived from measurements with reversing thermometers, may be in error. Hamaker (1941) has estimated a standard error of depth determination of 4 m at all depths. A more recent study, by Whitney (1957), suggests that below 1000 m an accuracy of about 0.5 % can be expected; at lesser depths the percentage error may be greater.

It is possible to use our estimate of error in temperature measurement to calculate the associated error in thermometric depth determination. Thermometric depth, D, is computed from the equation

$$D = \frac{10 \Delta t}{Q \varrho_m},$$

where Δt is the difference between temperature indicated by the unprotected thermometer and the true *in situ* temperature, Q is the pressure coefficient of the unprotected thermometer in °C/kg/cm², and ϱ_m is the mean density of the water column above the level of reversal in gm/cm³. The variance of D equals

$$\sigma_D^2 = \left(\frac{10 \Delta t}{Q \varrho_m}\right)^2 (v_Q^2 + v_{\Delta t}^2),$$

where v_Q^2 and $v_{\Delta t}^2$ represent the relative variances of Q and Δt respectively.

If Q is known exactly, it can be shown that random errors in thermometric depth resulting from errors in temperature measurement alone (using two protected thermometers and one unprotected thermometer at a depth) is ± 4 m (two standard deviations) regardless of depth. If, as Whitney (1957) suggests, the pressure factor, Q, is accurate within ± 0.0001 °C/kg/cm² (we assume that this is one standard deviation), random errors in depth determination increase slightly with depth, being about ± 7 m at 3000 m. If Q is a function of temperature or pressure rather than of a constant, the use of a constant value will introduce a systematic error.

(34)

In the upper 100 m or so, where vertical gradients are greatest, determination of depth may be somewhat more accurate, since it is based on wire angle and wire length rather than on unprotected thermometer measurements. In the thermocline, where the vertical temperature gradient may be as great as 0.5 °/m, a one meter depth error causes a 0.5° temperature error; the same depth error in a strong halocline ($2\ ^{0}/_{00}$ in 50 m) causes a salinity error of $0.04\ ^{0}/_{00}$. At a depth of several thousand meters, where the vertical temperature gradient is about 0.002 °/m, a 5 m depth error leads to a temperature error of only 0.01°; at such depths salinity gradients are so small that depth errors have a negligible effect on salinity measurement.

Interpolation errors are introduced whenever values are assigned to depths other than those of measurement. These errors are difficult to estimate, because they depend not only on the relation between the vertical spacing of observations and the shape of the depth distribution or characteristic curve of the property in question but also on the interpolation method employed. Such methods range from objective linear, logarithmic or parabolic interpolations to subjective analyses of characteristic curves based on data from neighboring stations. Without knowing the true vertical distribution of a property, *i. e.*, the function which interpolation is being used to approximate, it is hard to evaluate errors thus introduced. It is unlikely, however, that the interpolation errors are smaller than those of the original measurements.

The interpolation error can be considered a sampling error in space. Sampling "errors" in time occur when a measurement is assumed to represent conditions over a period of time longer than that required for the measurement. The magnitude of error depends both on the time interval assumed and on the rate of change of the property in question. Such errors must vary considerably from place to place; an estimate of their magnitude can be obtained from time series data such as those from anchor stations.

Seiwell (1939), in an analysis of an eight-day anchor station in the western Sargasso Sea, found that the rate of change of temperature at various standard depths was greatest at those depths where the maximum vertical temperature gradient occurred. In the summer thermocline (at 100 m) an average daily range of 0.9° was observed; in the lower part of the permanent thermocline (at 1000 m) the average daily range was 1.2°. Hamaker (1941), in an examination of data from four anchor stations in the East Indian Archipelago, has reported standard deviations "due to internal waves" of 1.15° at 100 m (in the thermocline), decreasing to 0.12° at 800 m; similar calculations by Hamaker, using data from nine METEOR anchor stations, showed a standard deviation of 1.2° at 25 m, decreasing to 0.01° at 1200 m.

We have examined data from two eight-day anchor stations (70.90 and 70.130) which were taken in October 1950 in the region of the California Current. Reid (1956), in a study of these data, found no sign of any periodic phenomena with periods up to 27 hours, although on an anchor station farther inshore he found evidence of internal waves of semidiurnal period. (The presence of prominent periodicities makes statistical treatment difficult because measurements taken at constant time intervals cannot then be considered independent. Of course, even the absence of obvious periodicity does not guarantee that the data are not autocorrelated).

At both stations, oscillations with apparent periods longer than 27 hours were often present in the upper few hundred meters. These long oscillations can be considered trends; the "random" deviation from the trend, as estimated by the variate-difference method (Kendall, 1948: 387), is an indication of error introduced by assuming that a given measurement represents some period up to a day. Deviations from an eight-day mean, on the other hand, are indicative of error introduced by assuming that a given measurement represents a period of up to a week. At or below the depth where these two deviations are the same, no trend is apparent.

Standard deviations of temperature and salinity at selected depths at these two stations, with and without trend, are summarized in Table IV. Note that measurement, interpolation and depth errors are included in these deviations and that below 300 m the estimates are less reliable than those above 300 m, since only a fourth as many observations were available. Near the surface, where the largest vertical gradients occur, large changes (1–2° in temperature, 0.1 $^0/_{00}$ in salinity) take place. At greater depths the daily and weekly deviations are much smaller, although they can be greater than those of measurement alone even at 500 and 1000 m. These results are not substantially different from those of Hamaker's analysis in the East Indian Archipelago mentioned earlier. In regions with small vertical gradients or less pronounced vertical oscillations one would expect small changes with time.

(36)

DYNAMIC CALCULATIONS

For a general description of distributions of temperature, salinity or density, the various errors discussed above are of little significance. Only at great depths is it likely that measurement errors will be critical for descriptive purposes. However, when temperature and salinity distributions are used for computing density parameters and horizontal pressure gradients, then measurement, sampling, and other errors can be important. The effect of sampling errors due to vertical oscillations, discussed by Seiwell (1939), Reid (1956) and others, will not be treated further here.

We have examined the effect of measurement and depth errors on the calculation of geopotential anomaly and geostrophic current speeds. Geopotential anomaly, ΔD, is determined from an approximation of the integral

$$\Delta D = \int_0^p \delta\, dp \doteq \sum_i (\bar{\delta} \Delta p)_i ,$$

TABLE IV. Examples of Time Sampling Errors from Analysis of two Eight-Day Anchor Stations

Depth (*m*)	$^{s}T^{\circ}$ *w/trend*	$^{s}T^{\circ}$ *w/o trend*	$^{s}S^{\circ}/_{\circ\circ}$ *w/trend*	$^{s}S^{\circ}/_{\circ\circ}$ *w/o trend*
Station 70.130				
30	0.13	0.08	0.08	0.06
50	1.17	1.12	0.12	0.10
75	0.67	0.57	0.10	0.08
150	0.34	0.21	0.09	0.08
300	0.13	0.11	0.03	—
500	0.16	—	0.05	—
1000	0.04	—	0.09	—
Station 70.90				
30	2.18	1.61	0.07	0.04
50	0.79	0.57	0.14	0.09
75	0.23	0.16	0.14	0.09
150	0.07	—	0.04	—
300	0.05	—	0.02	—
500	0.11	—	0.02	—
1000	0.05	—	0.02	—

s is estimate of standard deviation from eight-day mean (*w/trend*) or with trend removed (*w/o trend*). Down to 300 m, 60–64 observations were available for each station; below 300 m, 14–16 observations were used.

and the variance of geopotential anomaly is

$$\sigma^2_{\Delta D} = \sum_i (\Delta p_i)^2 \sigma^2_{\delta_i}.$$

The variance of specific volume anomaly at a given depth, $\sigma^2_{\delta_i}$, consists of two principal terms

$$\sigma^2_{\delta_i} \doteq \sigma^2_e + \sigma^2_z \left(\frac{\partial \delta}{\partial z}\right)^2,$$

where σ^2_e is the variance of measurement errors and $\sigma^2_z\ (\partial \delta / \partial z)^2$ the variance of depth errors. As an approximation, the terms are additive, since the first is primarily salinity dependent, the second primarily temperature dependent.

From our analysis of temperature and salinity measurement errors, the value of the first term can be computed, since the standard deviation of specific volume anomaly due to such errors (assumed here to be 0.01° in temperature and 0.015 $^0/_{00}$ in salinity) is approximately 1.5 cl/T (centiliters per metric ton, or 10^{-5} cm^3/g)[5]. This is dominated by salinity measurement errors, the effect of temperature measurement errors being an order of magnitude smaller. Below the surface layer the second term is much smaller than the first; even with an extremely large vertical gradient at depth (for example, 0.24 cl/T/m at 700–800 m for ATLANTIS St. 5203), it is an order of magnitude smaller. Near the surface, although $\partial \delta / \partial z$ may be large, the layer for which this is true is relatively thin (*i.e.*, Δp is small) and the depth error is small, so that $\sigma^2_{\Delta D}$ can be approximated by

$$\sigma^2_{\Delta D} \doteq \tfrac{1}{2} \sigma^2_e \sum_i (\Delta p_i)^2.$$

Since measurement errors do not vary significantly with depth, the variance of geopotential anomaly is quite sensitive to the number of pressure intervals used in the integration. For example, between the surface and 1000 *db*, $\sum (\Delta p_i)^2$ for one layer 1000 m thick is 10^3 times greater than that for a thousand layers 1 m thick. If one uses the so-called "standard" depth intervals (Sverdrup, *et al.*, 1942: 357), the standard error in geopotential anomaly (0 over 1000 *db*) is 0.004 dyn m. The standard error of the difference in geopotential anomaly (0 over 1000 db) between two stations is 0.0056 dyn m.

---

[5] This computation assumes the validity of the temperature-chlorinity-density relationship used in oceanographic tables (LaFond, 1951).

Thus one can say that the measurement error of this difference is ± 0.011 dyn m (two standard deviations); for a pair of stations at 30° of latitude separated by 100 km, the resulting error in geostrophic current speed is ± 1.5 cm/sec.

SUMMARY

By observing various pairs of thermometers through many reversals and by examining the scatter of data on temperature-depth curves where observation points were closely spaced, we have obtained estimates of the measurement errors in temperature data obtained in the field. These estimates, expressed as standard deviations for averages of two thermometer readings, are as follows:

total error	0.014°	upper limit, from temperature-depth curves
	0.011°	from paired thermometer analysis
random error	0.009°	
systematic error	0.007°	

An upper limit of measurement error in salinity data from the field, obtained from an analysis of salinity-depth curves, is 0.018 $^0/_{00}$ (standard deviation). Both temperature and salinity measurement errors as thus estimated are not significantly different from comparable estimates by previous investigators.

In the upper layers of the ocean other errors may be significantly greater than those of measurement. This is particularly true in the upper few hundred meters where vertical gradients of temperature and salinity are usually large. Here sampling errors due to vertical oscillations and errors resulting from uncertainty in depth determination may be as large as 1 to 2° and 0.1 $^0/_{00}$. At greater depths, where vertical gradients are small, such errors are comparable to measurement errors.

The effect of salinity measurement errors on the determination of specific volume anomaly is much greater than that of temperature errors and amounts to a standard deviation of about 1.5 cl/T. The resulting standard deviation of geopotential anomaly (0 over 1000 db) for a station on which standard depth intervals are used is 0.004 dyn m. The measurement error of the difference between two such stations is ± 0.011 dyn m (two standard deviations), and at 30° latitude and 100 km separation, the corresponding error in geostrophic current speed is ± 1.5 cm/sec.

REFERENCES

Böhnecke, Günther

1932. Die Temperaturmessung an der Oberfläche und in der Tiefe. Meteor Rep., *4* (1): 199–244.

Hamaker, H. C.

1941. The oceanographic instruments and the accuracy of the temperature observations. Snellius Rep., *2* (1): 1–45.

Hardon, H. J.

1941. The determination of chlorine and oxygen content. Snellius Rep., *2* (1): 46–54.

Kendall, M. G.

1948. The advanced theory of statistics. Volume II. Charles Griffin. London. 521 pp.

LaFond, E. C.

1951. Processing oceanographic data. Publ. U.S. Navy Hydrogr. Off., No. 614; 114 pp.

Reid, jr. J. L.

1956. Observations of internal tides in October, 1950. Trans. Amer. geophys. Un., *37*: 278–286.

Seiwell, H. R.

1939. The effect of short period variations of temperature and salinity on calculations in dynamic oceanography. Pap. phys. Oceanogr., *7* (3); 32 pp.

Strickland, J. D. H.

1958. Standard methods of seawater analyses. MS Rep. Fish. Res. Bd., Canada, (Ser. No. 18) *1*; 143 pp.

Sverdrup, H. U., M. W. Johnson and R. H. Fleming

1942. The oceans, their physics, chemistry and general biology. Prentice Hall, Inc., New York. 1087 pp.

Sverdrup, H. U.

1944. Subsurface temperatures. Carnegie Rep., *1–A*: 5–10.

Thomsen, Helge

1937. Hydrographical observations made during the Dana Expedition 1928–30. Introduction. Dana Rep., No. 12.

Whitney, jr. G. G.

1957. Factors affecting the accuracy of thermometric depth determination. J. Cons. int. Explor. Mer, *22*: 167–173.

(40)

(*Reprinted from Nature, Vol.* 188, *No.* 4755, *pp.* 979-982,
December 17, 1960)

TREND OF CÆSIUM-137 IN THE EFFLUENT OF A LARGE CITY*

By Dr. T. R. FOLSOM
Scripps Institution of Oceanography, La Jolla, California
AND
Dr. G. J. MOHANRAO
California Institute of Technology, Pasadena, California

THE oceanographer is concerned with the mechanisms controlling the dispersion of materials in the ocean. For this reason, the progress of fall-out radioactivity in the ocean has been studied for several years at the Scripps Institution; recently special consideration has been given to contributions coming from terrestrial run-off. Several radioactivities in sewage flowing from a large coastal city were monitored at the treatment plant for more than two years. Cæsium-137 was followed in detail; this fission product has useful tagging properties; it emits a penetrating, easily detectable γ-ray, and decays relatively slowly.

Detailed off-shore mapping has not yet been done; however, the average and peak outputs from the city have been recorded over a period of 21 months, permitting estimates of the influence on coastal waters. The character and trend of the concentration, and comparisons with reported contamination of human food by fall-out, point to an unexpected source for the cæsium-137 observed in the sewage. Not a great deal is known about the chemical behaviour of this nuclide, at very low concentrations and in complex systems, so that the partition observed for cæsium in the plant should be of general interest.

We were fortunate in being permitted to make measurements throughout the Hyperion Treatment Plant of the City of Los Angeles. This modern installation is situated on the seashore 120 miles north of the Scripps Institution; it collects sanitary sewage from a large city centred about 30 miles inland; and disposes the treated material mainly through outfall pipes extending as far as 7 miles into the open sea where the depth is about 200 ft. Very little storm water enters this system.

---

* Substance of a paper read in part at the meeting of the International Association of Physical Oceanography, Helsinki, Finland, on August 5, 1960.

Contributions from the Scripps Institution of Oceanography, New Series, 1232
Reproduced by Permission

For about ten years, until June 1, 1960, the treatment included primary settling, aeration with activated sludge, final settling, digestion of primary and activated sludge, followed by the filtering, washing and drying of part of the digested solids to produce a stable dry fertilizer that was sold as soil conditioner. After this date a change was made in the treatment scheme, so that routine drying of large amounts of fertilizer was stopped.

Investigation at the plant consisted of: (1) sampling continuously and in detail at one point in the system; (2) sampling also at several points during a given short period, preferably when the input character was not changing rapidly. While it was available, the commercial fertilizer was used in the continuous monitoring; it was convenient, and because cæsium is greatly enriched by treatment up to this point, extremely small changes in input concentration could be deduced. These samples were assayed after being composited daily for periods of 3–5 days. Most of the other specimens used for establishing partition ratios were liquids, some of them very dilute. All were reduced to dryness at the plant in 40-gallon soup kettles heated with steam.

Assaying was done at the Scripps Institution by exposure of a sodium iodide scintillator crystal to the radiation from a relatively large specimen, one weighing about 200–400 grams. With a modern multichannel gamma-ray spectrometer a specimen may be analysed within a few minutes for one or more gamma-emitting nuclides, even when their concentrations are very low. Usually no wet preparation whatever was undertaken; however, specimens were assayed in plastic containers under uniform conditions, so that accurate comparisons with standard specimens could be made. The laboratory at Scripps had already developed a spectrometer accessory[1] permitting the rapid comparison of measurements with a library of background measurements and measurements of standard specimens all stored in digital form on magnetic tape loops.

In passing, it will be mentioned that the sewage had less radioactivity than was anticipated; no concentration was observed even approaching a recognized tolerance-level. Nevertheless, the natural background from the uranium and thorium families almost always was surpassed by one or more man-made activities. Iodine-131 appeared in nearly every input specimen as might be expected from its use in medicine;[*] cobalt-60 repeatedly appeared in easily measurable amounts. Relative to the concentration of cæsium-137, the concentrations of both zirconium-95 and ruthenium-106 were extremely deficient when

(42)

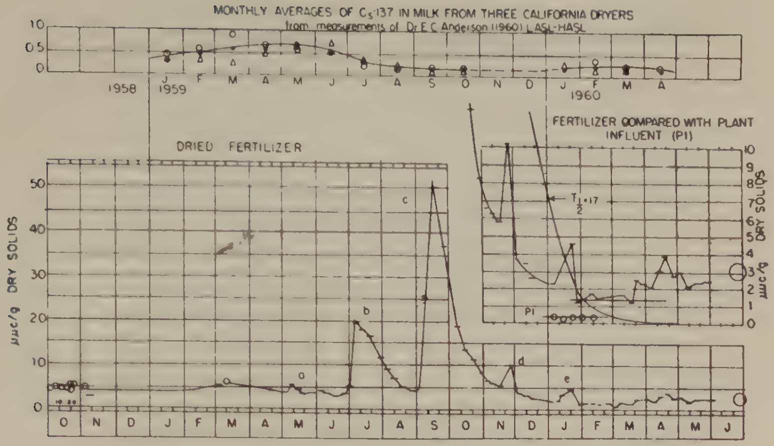

Fig. 1. Trend of cæsium-137 in the sewage treatment plant compared with the trend in milk. All ordinates are micromicrocuries per gm. of dried solids. Inset illustrates that batch inputs probably contributed little during comparisons early in 1960

compared with the ratios observed in rainfall for this period. Details concerning these and other activities will be reported elsewhere.

Monitoring radiocæsium in digested material has several practical advantages; but because of the long dwell of material in digesters, the information is not contemporary, and some input detail is lost entirely. Fig. 1 shows the trend of cæsium-137 concentration over 21 months derived from 75 composited samples of digested fertilizer. The large peaks attenuate at a rate consistent with what is known about the purging-rate of these digesters. Actually a battery of digester units is used at Hyperion; nevertheless, their performance might be approximated roughly by a model having a single tank into which a daily input is suddenly injected and mixed thoroughly followed by the withdrawal of an equal amount, about one-thirtieth of the whole. It can be shown that this model would purge itself after a sudden excessive input to half-peak-concentration in about 21 days. The actual measured initial slopes of the two larger peaks correspond to a half-purging time T of about 17 days.

In spite of the large batch inputs, it appears from Fig. 1 that the input concentration varies only slowly much of the time and follows an easily measurable basic trend. It required roughly four months for attenuation of the largest batch, but ultimately this reached insignificance. An inset is shown in Fig. 1 magnifying the data for the first three months of 1960, and an exponential curve having half-value of

Table 1. COMPARISON OF INFLUENT AND FERTILIZER CONCENTRATIONS

Collection date of composite sample (5-day period ending)	Concentration of ^{137}Cs ($\mu\mu$c. per gm., dry)
Dry fertilizer (after long digestion)	
January 27, 1960	1·2
February 2	1·4
,, 10	1·8
,, 17	1·5
,, 24	1·6
March 2	0·7
,, 9	1·8
Fertilizer average	1·4
Influent (composited 5 days and dried)	
January 6, 1960	0·39
,, 15	0·22
,, 22	0·48
,, 29	0·19
February 12	0·32
Influent average	0·32

17 days has been added to it to illustrate that the largest peak and later smaller ones probably have become greatly attenuated during the period when input concentrations were compared with average concentrations in the digested material. These comparative measurements are plotted in the inset of Fig. 1 and listed in Table 1. From these roughly steady-state conditions we can derive ratios that should approximate fixed characteristics of the plant. Table 1 indicates that the incoming cæsium-137 is enriched after digestion by a factor of about 1·4/0·32 or 4·4 (on a dry basis).

It can be concluded from these measurements that the concentration of cæsium-137 in the sewage coming into the plant fell slowly over 21 months from about 1·1 to about 0·32 μμc. per dry gram; this corresponds to a change from 1·4 to 0·4 μμc. per litre.

Now it can be appreciated why direct monitoring was not carried out. No satisfactory chemical precipitation had been developed; boiling down all specimens in barrel-sized amounts would have been expensive; and the spectacular enrichment in the digested material was attractive. For example, raw sewage having 0·4 μμc. per litre of cæsium-137 produces dried fertilizer having 1,400 μμc. per dry kgm.

Obviously the large peaks in Fig. 1 arose from batch inputs. But no technical or medical practice has been discovered that would explain the slowly varying basic concentration-level. When measurements were made of representative samples from the city's major water supplies it was found that this source, too, was deficient. The average value measured for the fresh drinking water was only 0·025 μμc. per litre; this corresponds to only about

0·02 μμc. per gm. of sewage (having 1,250 p.p.m. total solids), so that fresh water could contribute only about 6 per cent of the cæsium-137 observed in the sewage.

Anderson[4] has considered in some detail the available reports concerning U.S. national dietary habits, and by introducing values of cæsium-137 found in foods, he has ventured a rough estimate of the amount of cæsium-137 that was daily ingested per person in 1956. There are several reasons for concluding that the value he derived, about 50 μμc. per day per person, would become no smaller if it could be corrected by deriving it from data pertaining to the spring of this year. If this value is tentatively accepted, and also if the estimates are taken that 2·8 million people contribute to a system carrying 250 million gallons per day and 1,250 p.p.m. total solids, then a possible daily input of cæsium is discovered that is much larger than could come through drinking water. In fact these, apparently conservative, values provide for roughly one-third of the average cæsium observed in sewage early this year. To this, of course, must be added a contribution from garbage now frequently disposed of through kitchen grinders in this community.

No attempt will be made to balance the budget precisely, but use here of a 1956 fall-out contamination value needs some justification. After 1956 world-wide fall-out increased in rate ; later it decreased[5]. During the period of these investigations at Hyperion the concentration of cæsium-137 in dried milk from three nearby milk-sheds varied as shown at the top of Fig. 1. Milk is reported to be the largest contributor of cæsium-137 in diet, and the concentrations in dried milk reported for the spring of 1960 are not strikingly different from those reported for 1956. Between these dates there were higher levels in almost every food ; and almost every food in practice experiences a lag before it is delivered and consumed. There is also a substantial lag that occurs between input and output of cæsium in the human system[4,6]. It would therefore appear necessary to correlate sewage concentrations not with contemporary food contaminations but with concentrations measured in foods produced several months earlier. Because of these circumstances, it appears quite possible that the basic trend of cæsium-137 in the Hyperion sewage could be controlled almost entirely by fall-out cæsium entering through human food.

In many circumstances cæsium behaves chemically and biologically like potassium, an essential tissue constituent ; nevertheless there are several biological systems reported where a clear distinction

Table 2. Cæsium-137 to Potassium Ratio in Raw Sewage and Fertilizer

Date of collection	Fertilizer			Date of collection	Raw sewage		
	^{137}Cs μμc./gm.	K(total) gm./gm.	Cs/K μμc./gm.		^{137}Cs μμc./gm.	K(total) gm./gm.	Cs/K μμc./gm.
January 27, 1960	1·2	0·003	400	January 6, 1960	0·39	0·024	16
February 2	1·4	0·003	470	,, 15	0·22	0·031	7
,, 10	1·8	0·002	900	,, 22	0·48	0·029	17
,, 17	1·5	0·003	500	,, 29	0·19	0·012	16
,, 24	1·6	0·002	800	February 12	0·32	0·020	16
March 2	0·7	0·001	700				
,, 9	1·8	0·003	600				
Average	1·4	0·002	620		0·32	0·023	14

is made between these two elements. In some cases, the discrimination has been observed to be against the intake of cæsium and in favour of potassium; for example, plants are reported to discriminate strongly against radiocæsium in taking the two elements up from the soil.

Concentration and digestion of sewage depends largely on metabolic processes, and much of the final solid material has been synthesized by micro-organisms. Therefore, it was not anticipated that cæsium would become strongly concentrated in the solid digested fraction relative to potassium. Table 2 indicates that cæsium-137 is enriched relative to potassium by forty-fold during the reduction of sewage to digested, dried fertilizer. This aspect is being studied further.

Although it appears that the sewage system studied can collect the minute traces of fall-out cæsium passing through in human food, the effect on the sea cannot be great. This is because surface sea waters have caught and have failed to dissipate downward such large amounts of fall-out that the concentration of cæsium-137 persists at levels not far below what is seen in average sewage. Measurements[2] made of the cæsium-137 concentration in the local surface sea water early this year by us, gave an average of about 0·1 μμc. per litre. This should be compared with the value of 0·4 μμc. per litre representing the average concentration in the Hyperion sewage at the same period.

It is useful to compare average concentrations in this manner, but it should be pointed out that even in specimens taken from nearby points in the open sea the concentration may vary by more than 50 per cent. Smaller average concentrations were measured[2,3] in local coastal waters than in waters far off this coast; and Yamagata[7] has reported the average concentration for 1959 Japanese coastal water of 0·38 μμc. per litre, or essentially what has been observed in Hyperion sewage.

Even the peak concentrations observed at this plant should cause no alarm. From plant characteristics, it may be estimated that the largest peak in Fig. 1 corresponds to a batch input of about 0·4 curie. However, the sewage travels on the average 30 miles to the plant and is not likely to pass through in much less than one day, and the 250 million gallons of water put through in one day would dilute this to an average concentration of only $3{\cdot}7 \times 10^{-7}$ μc./ml. This falls far below the value of 2×10^{-5} μc./ml. now accepted as maximum permissible concentration for this particular isotope in water that is to be drunk continually by humans.

From these investigations something has been

(47)

learned concerning the behaviour of radiocæsium in a large modern sewage disposal plant, and useful conclusions can be drawn concerning the probable influence on the downstream environment. It can be seen, for example, that the original objective of following the local dispersal of sewage by the ocean can be attained only if the most sensitive and refined methods are applied. It appears, too, that suitable monitoring of the gamma-ray activities in sewage systems might provide additional safeguards to the public against misuse of the radioactive materials that are becoming more and more common in research, medicine and in industry.

This work was supported by the United States Atomic Energy Commission under Contract No. *AT*(11-1)-34, sponsored by Dr. A. B. Joseph, and made use of facilities supplied by the United States Office of Naval Research under Contract *Nonr*-233(34), sponsored by Dr. William Thaler. We are particularly indebted to Prof. J. E. McKee of the California Institute of Technology for consultations, and wish to acknowledge the co-operation of the professional staff of the Bureau of Sanitation of the City of Los Angeles, especially N. B. Hume, R. D. Bargman, J. M. Parkes, G. A. Betz, W. F. Garber, and C. G. Gunnerson. We are grateful to Dr. E. C. Anderson for supplying before publication the values for dried milk seen in Fig. 1.

[1] Folsom, T. R., and Cramer, R. A., Scripps Inst. Interim Tech. Rep. (1958).

[2] Folsom, T. R., Mohanrao, G. J., and Winchell, Perrin, *Nature*, **187**, 480 (1960).

[3] Mohanrao, G. J., and Folsom, T. R. (submitted to *Anal. Chem.*, 1960).

[4] Anderson, E. C., Schuch, R. R., Fisher, W. R., and Langham, Wright, *Science*, **125**, 1273 (1957).

[5] Langham, Wright, and Anderson, E. C., Hearings, Joint Committee on Atomic Energy, **2**, 1067 (1959).

[6] McNeill, K. G., and Green, R. M., *Canad. J. Phys.*, **37**, 528 (1959).

[7] Yamagata, N., *Nature*, **184**, 113 (1960).

Printed in Great Britain by Fisher, Knight & Co., Ltd., St. Albans.

(48)

Reprinted from Cold Spring Harbor Symposia on Quantitative Biology
Volume XXV, 1960
Printed in U.S.A.
pp.145-148.

The Photosynthetic Rhythm in Single Cells of *Gonyaulax polyedra*

Beatrice M. Sweeney

University of California, La Jolla, California

Many biological rhythms disappear in continuous bright light. As examples of such behavior may be cited the rhythm in leaf movement in *Phaseolus* [1], that of phototaxis in *Euglena* [2], the rhythm of carbon dioxide evolution in *Bryophyllum* [3], and that of activity in the spider beetle *Ptinus* [4]. Diurnal rhythms are usually measured in many cells simultaneously, either in multicellular plants and animals or in populations of unicellular organisms. From such measurements it is difficult to distinguish whether the loss of rhythmicity of the assemblage of cells arises from the lack of rhythmicity in every cell or from a loss of synchrony between cells, each of which continues its rhythmic behavior. That rhythmicity is lost in continuous light is suggested by the constant small size of the nuclei found in the epidermal cells of *Vicia faba* grown in continuous light [5]. The nuclei of plants grown in alternating light and darkness show small but recognizable diurnal variations in volume.

The most direct method for distinguishing between the two alternative causes for the disappearance of a rhythm in cell populations is the study of rhythmicity in a single cell. Cells of the unicellular dinoflagellate *Gonyaulax polyedra* seemed well adapted for this purpose. This organism shows a diurnal rhythm in luminescence [6, 7], cell division [8], and photosynthesis [9]. All of these rhythms disappear in cell suspensions exposed to continuous bright light, although under these conditions growth continues unimpeded.

Bright light inhibits luminescence so that measurements of light production by a single cell would not reveal an underlying rhythm. Cell division may be observed in single cells in capillary tubes. In alternating light and darkness, these isolated cells divide at or close to dawn, and their generation times are thus even multiples of 24 hours. Cells grown in bright light, however, do not divide at predictable intervals, and their generation times were thus difficult to measure. It could be determined, however, that at least ⅓ to ½ of the generation times of these cells in bright light were not even multiples of 21–25 hour periods. A loss of rhythmicity was thus strongly suggested.

There remained the possibility of detecting a rhythm in photosynthesis in a single cell in bright light. An oxygen production of about 1 mμl O_2 per hour per cell was predicted from measurements of the photosynthesis of cell suspensions by conventional techniques.

A microrespirometer of adequate sensitivity has been developed by Scholander, Claff, and Sveinsson [10, 11]. This method involves the use of a reference diver, the gas bubble of which is kept constant in volume. For the present study, this technique was adapted to measure oxygen evolution by the use of evacuated rather than oxygenated solutions. Only cells from recently-inoculated rapidly-growing cultures were used. The cell, bathed in nutrient solution containing 0.02M $NaHCO_3$, was illuminated with incandescent light. The temperature was 26 ± 0.02°C. That the method gave satisfactory data may be seen from Fig. 1.

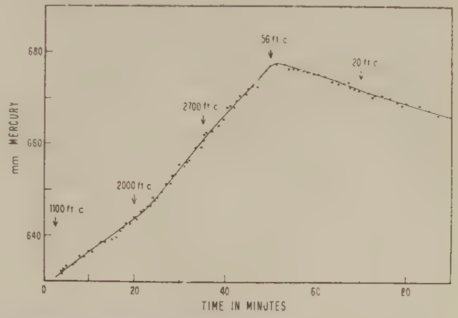

Figure 1. Pressure changes in the reference diver microrespirometer containing a single *Gonyaulax polyedra*. The cell, in nutrient solution with 0.02M sodium bicarbonate at 26°C., was irradiated with an incandescent beam, the intensity of which was changed at the arrows. The cell is from a culture in alternating light and darkness (12L:12D, dawn being 30 min. prior to 0 time on the abscissa). The factor for converting mm. pressure to mμl. O_2 is 0.032.

In cell suspensions of *Gonyaulax*, a rhythm in photosynthesis could only be demonstrated when the measurements of carbon fixation were made in bright light [9, 12]. Thus it was concluded that the photosynthetic capacity, rather than the efficiency of the photochemical step, changes in relationship to the phase of the endogenous cycle. Cell suspensions in alternating light and darkness or in continuous dim light both showed this rhythm in photosynthetic capacity, although cells in bright continuous light did not.

Before undertaking a study of single cells growing in continuous bright light, it seemed desirable to show

Contributions from the Scripps Institution of Oceanography, New Series, 1233

Reproduced by Permission

that rhythmic changes in the photosynthetic capacity of one cell could be demonstrated by the reference diver technique. Consequently, cells growing in alternating light and darkness (12L:12D) were used in a series of experiments. The rate of oxygen evolution with saturating light was measured at different times subsequent to mounting the cell in the respirometer. A series of saturation curves for the same cell (Fig. 2) showed that the photosynthesis at low light intensities continued at a constant rate for at least 14 hours, while a large change in the value at light saturation with time of day could be observed. The true rate of oxygen evolution was calculated by applying a respiratory correction obtained by extrapolation to zero light intensity, since the reference diver cannot be observed in darkness.

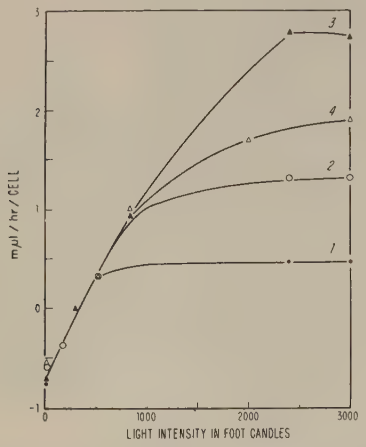

FIGURE 2. The net oxygen production of a single *Gonyaulax polyedra* at different light intensities measured at 4 different times in the diurnal cycle using the same cell: curve 1, dawn to 1 hr. after dawn; curve 2, 1 to 3 hrs. after dawn; curve 3, 3 to 4 hrs. after dawn; curve 4, 10½ to 11 hrs. after dawn.

Measurements with one cell could not be continued for longer than 14 hours because of a loss of photosynthetic activity at low as well as at high light intensities. The survival of the cell within the respirometer was not prolonged by the presence of antibiotics (penicillin G and streptomycin, 50 mg. per l. each). In order that measurements span the whole 24 hours, experiments were begun at different times. The resulting composite curve (Fig. 3) shows one cycle of the rhythm of photosynthetic capacity. The rhythm was also detected in one cell cultured in continuous light of low intensity (Fig. 4). The observations depicted in Figs. 2, 3, and 4 demonstrate that a rhythm can be detected in a single cell by the reference diver technique.

When the oxygen production of a cell cultured in continuous bright light (800–1000 ft. c.) was measured (Fig. 5), no cyclic changes in photosynthetic capacity were observed. The oxygen production in bright light

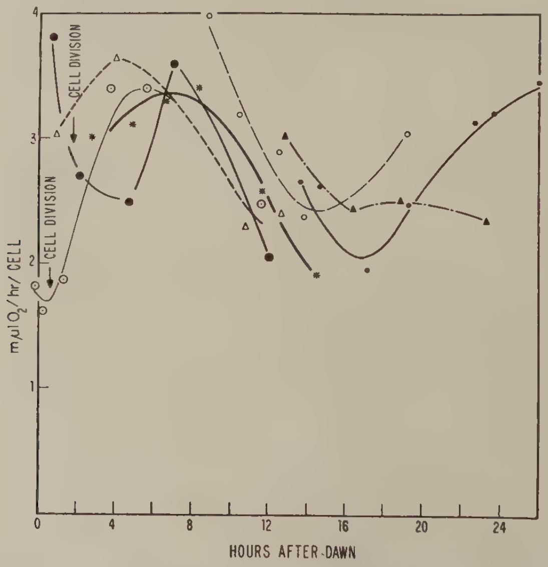

FIGURE 3. The rhythm in photosynthetic capacity (the oxygen production at saturating light intensity corrected for respiration) of single cells of *Gonyaulax polyedra* from alternating light and darkness (12L:12D, dawn is at 0 time on the abscissa). Each curve represents the measurements from one cell.

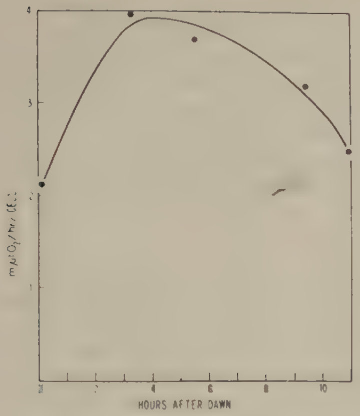

FIGURE 4. The rhythm in the photosynthetic capacity in a single cell of *Gonyaulax polyedra* from a culture in continuous light of low intensity (50 ft. c.). The subjective dawn is at 0 on the abscissa.

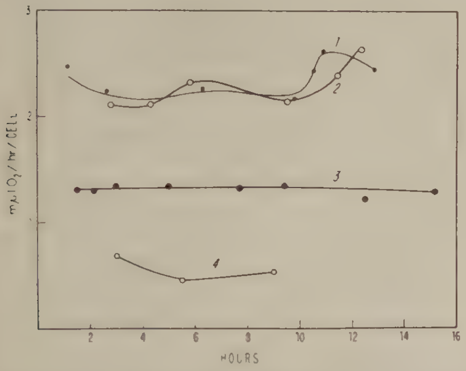

FIGURE 5. The photosynthetic capacity in four isolated cells of *Gonyaulax polyedra* from cultures in continuous bright light (800 ft. c.). Cell number 2 divided 24–31 hours after time zero; cell number 4 divided 23 hours prior to time zero.

was comparable to the lowest values obtained with cells from alternating light and darkness. Cell division in cell number 4 took place 24 hours prior to the beginning of measurements and thus this cell should have been in the "day" [8] or high phase of photosynthetic capacity, were a rhythm present. Furthermore, at least a portion of the measurements of cell number 2 (Fig. 5) should have fallen within the day phase, since this cell divided between 24 and 31 hours after the beginning of measurements.

Thus it seems clear that in *Gonyaulax polyedra* in bright continuous light, the rhythm in photosynthetic capacity is absent, and the lack of apparent rhythm in cell populations is a true reflection of the behavior of each cell, not the result of asynchrony.

ACKNOWLEDGEMENTS

The author wishes to thank Dr. P. F. Scholander for his encouragement and interest in these studies.

Studies reported here have been supported by a grant from the National Science Foundation.

REFERENCES

1. BÜNNING, E. 1931. Untersuchungen über die autonomen tagesperiodischen Bewegungen der Primärblätter von *Phaseolus multiflorus*. Jb. wiss. Bot., *75:* 439–489.
2. BRUCE, V. G., and C. S. PITTENDRIGH. 1956. Temperature independence in a unicellular "clock." Proc. Nat. Acad. Sci. U. S., *42:* 676–682.
3. WILKINS, M. B. 1959. An endogenous rhythm in the rate of carbon dioxide output of *Bryophyllum*. I. Some preliminary experiments. J. Exper. Bot., *10:* 377–390.
4. BENTLEY, E. W., D. L. GUNN, and D. W. EWER. 1941. The biology and behaviour of *Ptinus tectus* Boie (Coleptera, Ptinidae), a pest of stored products. I. The daily rhythm of locomotory activity, especially in relation to light and temperature. J. Exper. Biol., *18:* 182–195.
5. WASSERMANN, L. 1959. Die Auslösung endogentagesperiodischer Vorgänge bei Pflanzen durch einmalige Reize. Planta, *53:* 647–669.
6. SWEENEY, B. M., and J. W. HASTINGS. 1957. Characteristics of the diurnal rhythm of luminescence in *Gonyaulax polyedra*. J. Cell. Comp. Physiol., *49:* 115–128.
7. HASTINGS, J. W., and B. M. SWEENEY. 1958. A persistent diurnal rhythm of luminescence in *Gonyaulax polyedra*. Biol. Bull., *115:* 440–458.
8. SWEENEY, B. M., and J. W. HASTINGS. 1958. Rhythmic cell division in populations of *Gonyaulax polyedra*. J. Protozool., *5:* 217–224.
9. HASTINGS, J. W., and L. ASTRACHAN. 1959. A diurnal rhythm of photosynthesis. Fed. Proc., *18:* 65.
10. SCHOLANDER, P. F., C. L. CLAFF, and S. L. SVEINSSON. 1952. Respiratory studies of single cells. I. Methods. Biol. Bull., *102:* 157–177.
11. SCHOLANDER, P. F., H. LEIVESTAD, and G. SUNDNES. 1958. Cycling in the oxygen consumption of cleaving eggs. Exper. Cell. Res., *15:* 505–511.
12. HASTINGS, J. W. 1959. Unicellular clocks. Ann. Rev. Microbiol., *13:* 297–309.

DISCUSSION

SOLLBERGER: During the discussion of this lecture another point was raised of considerable interest, namely whether relations may exist between phase differences and frequencies? Of course, one would think that the study of phase differences presupposes a constant frequency. But, if so, one forgets that two different biological curves are never quite equal in shape, and that this may actually induce a shift in phase between the curves during one single cycle.

If, now, we assume that external influences bring different curves together in time (timing) and that endogenous rhythms will, at an average, increase the phase difference, we may use this to find out how and when the external influences act.

KRIS: Dr. Mercer's plea for the presentation of raw scores such as the full scatter of points for a given sample of data drawn in preference to—or, as well as—a smoothing function that appears as a mere line approximating a "trend"; Dr. Harker's reminder that it is necessary to distinguish between discrete and continuous functions when discussing biological events; and Dr. Sollberger's slide, demonstrating that when the time-course of fluctuation in cyclically changing variables is studied, there are sections of least scatter about certain points in time that characterize the period—all point to the necessity of distinguishing between two approaches to the investigation of cyclical phenomena—both in the elucidation of cycles and their experimental manipulation. The first is based on the deductive theoretical analysis of postulated time- and process-functions, for which the mathematical and physical (e.g., electronic) model builders seek examples in nature; the second is the approach of the naturalist, who gathers empirical observations which he classifies, and from which he induces patterns of re-relations; and where a temporal pattern of variation occurs repeatedly, he is interested either in controlling it, or in its investigation per se, if it can be experimentally manipulated. In both cases, he has to account for statistical variation in his data; and for the sake of parsimony, he may wish to make use of already existing mathematical formulations that can be applied to the quantification of his data. As long as these "borrowed" methods are used merely to classify and clarify the presentation of collected data, they serve their purpose, if they "fit." If, however, assumptions made by the mathematicians who derived the functional models in a different physical context are extended for use in the new context of their biological application, then a true meeting of minds between naturalist and functional symbolist must occur if confusing misconceptions or over-generalizations are to be avoided.

Schmitt: While I believe that many of us have a clear idea of the relationship between phase shift and frequency variation nomenclatures for describing rhythmic processes of somewhat irregular periodicity as encountered in studies of circadian biological rhythms, it is perhaps worthwhile to examine this relationship specifically and to emphasize that these nomenclatures are fully interchangeable and that the choice of one over the other is dictated primarily by the mathematical model of oscillation that the author has in mind.

If he thinks of the rhythmic process as originating in an intrinsic or extrinsic oscillator of constant frequency which passes on its signal to an overt manifestation through a series of delaying or modifying processes, then he will probably utilize the phase shift nomenclature. If he thinks of the oscillation as being autonomous and essentially free running but controlled or modulated by environmental parameters, then he will probably utilize the variable frequency nomenclature.

Note for example that a steady 12 cycle per second sinusoidal oscillation can be exactly described as a 10 cycle/second oscillation that is suffering a constantly increasing forward phase shift of 4π radians or 720° per second. It is similarly possible to describe any oscillation which ranges repeatedly back and forth between equal positive and negative extremes as a pure sine wave which is suffering frequency modulation or phase shift so long as the function does not reverse itself except at the maxima. The phase or frequency shifts may of course be so bizarre and irregular as to make the usage a mere formality, but the representation is possible and unambiguous. If amplitude is admitted to be variable, then there is real additional ambiguity for a particular change in value of the function could in many cases be caused by amplitude, phase or frequency shift.

As Dr. Klotter has so clearly pointed out in his lecture, it is important to distinguish between the two very different uses of the term phase in analysis of oscillations. "Phase" when used in describing the motion of the unit vector in the reference circle of the usual mathematical model for simple harmonic oscillation is a continually increasing quantity which gains 2π radians or 360 degrees during each cycle. System phase, which is what most biologists care about, is the deviation from this reference vector of the vector describing the system at a particular time. While system phase and phase shifts can properly be stated in terms of time rather than angular measures, it should be carefully stated, when this is done, on what basic period or frequency the time shift is based as the statement might otherwise be ambiguous. Usually it is meaningless to ask whether a given shift is really due to change of frequency or of phase but this can be a meaningful question when experimental data is being tested for conformity with one or another mathematical or biophysical model.

(53)

Reprinted from COPEIA, 1960, No. 4, pp. 322–336, December 30
Printed in U. S. A.

The Eastern, Tropical Pacific Fishes of the Genus *Blenniolus,* including a New Island Endemic[1]

Richard J. Krejsa[2]

THE present study grew out of an attempt to identify the eastern Pacific blenniid material in the Fish Collection of the Department of Zoology at the University of California, Los Angeles (UCLA). The collection contained a number of specimens of *Blenniolus* from the Revillagigedo Islands which appeared to differ in some respects from the only described species, *B. brevipinnis* (Günther). A preliminary comparison revealed that while the mainland and island populations agreed in most meristic characters, they differed markedly in color pattern and size. It soon became obvious that the apparent differences could not be fully evaluated without a consideration of the ontogeny of the color pattern. The rich collections at UCLA contained good numbers of larvae and adults of both groups. These allowed the ontogeny of both proportions and color pattern to be determined with confidence. This study indicated that the latter differ throughout life and that the mainland and Revillagigedo populations are specifically distinct (Figs. 1–4). In addition, it has been apparent for some time that several enigmatic blenniid species and genera were based on growth stages of *B. brevipinnis* and therefore must be synonymized with that species. In order to document these alterations in blenniid taxonomy, *B. brevipinnis* is herein redescribed on the basis of a large number of specimens, representing the various stages of its life history.

Acknowledgments.—I wish to thank the following persons for making available specimens in their care: Dr. George S. Myers and Miss Margaret H. Storey of the Natural History Museum of Stanford University (SU); Dr. W. I. Follett and Mrs. Lillian J. Dempster of the California Academy of Sciences (CAS); Dr. Casimir C. Lindsey and Mr. J. Donald McPhail of the University of British Columbia (BC); and Mr. Wayne J. Baldwin of UCLA. Thanks are due to Dr. Ethelwynn Trewavas and Mr. G. Palmer of the British Museum (Natural History) (BMNH) for examining and providing me with information on the type specimens of *B. brevipinnis.* I am indebted to Dr. H. R. MacMillan for providing me with the opportunity to obtain life color notes on the new form while aboard the 1960 cruise of the "Marijean" to the Revillagigedo Islands. Mr. James E. Rupert, of Scripps Institution of Oceanography, took the photographs that appear in the text. To Dr. Boyd W. Walker, of UCLA, and Dr. Carl L. Hubbs, of Scripps Institution of Oceanography (SIO), my most sincere thanks for their valuable suggestions and critical reviews of the final manuscript. Finally, it is a pleasure to acknowledge the invaluable assistance of Dr. Richard H. Rosenblatt, of Scripps Institution of Oceanography, for his constructive criticism and frequent assistance and direction throughout the preparation of this manuscript.

Terminology and Methods

The term prejuvenile, used herein, is adopted as proposed by Hubbs (1958), "to cover a diversity of more or less strikingly—often bizarrely—modified pelagic life history stages, of various marine fishes, that are not appropriately termed either postlarval or juvenile."

In addition to the abbreviations listed in the acknowledgments, the following are used

---

[1] Contributions from the Scripps Institution of Oceanography, New Series. 1235

[2] Present address: Institute of Fisheries, University of British Columbia, Vancouver 8, Canada.

Reproduced by Permission

in the synonymy: ANSP, Academy of Natural Sciences of Philadelphia; CNHM, Chicago Natural History Museum; and USNM, United States National Museum.

With the exception of the following, all counts and measurements were taken in accordance with the methods of Hubbs and Lagler (1958):

The last ray of dorsal and anal fins.—Radiographs reveal that in *Blenniolus*, *Hypsoblennius*, and *Homesthes*, the last ray has its own basal element and is therefore counted independently of the penultimate ray.

Caudal rays.—Radiographs reveal that in *Blenniolus*, *Hypsoblennius*, and *Homesthes*, two dorsal unbranched rays and two ventral unbranched rays, in addition to the branched caudal rays, articulate with the hypural. Therefore, the number of principal rays is defined for these genera as the number of branched rays plus four (for this is the obvious count). In Table 2 the principal rays are given as dorsal plus (+) ventral.

Body depth.—Taken from a point immediately behind the base of the first dorsal spine to the angle between the outer pelvic base and the body wall.

Length of pelvic fin.—Taken from the inner pelvic base, i.e., between the fourth rays, to the tip of the longest ray.

Abdominal length.—Taken from the inner pelvic base to the anterior rim of the anus.

Measurements of the least bony interorbital width were made by drying the area with air and then were read to within 0.025 mm. accuracy with an ocular micrometer. All other measurements were measured to within 0.1 mm. with break-arm dividers with one flat point and one needle point.

The measurements of the sexes have been combined, since, except in respect to the length of the orbital cirri, I have found no significant morphometric differences between males and females.

THE GENERA OF BLENNIINAE IN THE EASTERN TROPICAL PACIFIC

Blenniolus is one of three genera of the subfamily Blenniinae into which the species of the eastern tropical Pacific appear to be most satisfactorily classified, in accordance with the characters outlined in the following key. A further discussion of these genera is included in the account of *Blenniolus brevipinnis*.

Other blenniine genera, much in need of revision, occur in western South America south of the tropics. The three species of the Californian fauna are referred to *Hypsoblennius*.

Key to the Genera of Blenniinae in the Eastern Tropical Pacific

1a.—Pelvic rays I, 3; vertebrae 33–37. Margin of dorsal fin entire or slightly notched; dorsal rays XII (XI–XIII), 17 (15–19); anal rays II, 18 (16–20); lateral line ranging from incomplete to complete . . . . *Hypsoblennius*

1b.—Pelvic rays I, 4; vertebrae 29–32.

  2a. Dorsal fin with a shallow notch between the spinous and soft portions; dorsal rays XII (XI–XIII), 16 (15–17); anal rays II, 17 (15–19); lateral line complete, or nearly so, extending at least to middle of soft dorsal fin; vertebrae 32 (counted for *H. caulopus* only). . . . . . . *Homesthes*[3]

  2b. Dorsal fin deeply notched; dorsal rays XII (XI–XIII), 12 (11–13); anal rays II, 14 (12–15); lateral line incomplete, never extending beyond first dorsal soft-ray; vertebrae 29–31 . . . . *Blenniolus*

GENUS *Blenniolus* JORDAN AND EVERMANN

Figs. 5–6

Blenniolus.—Jordan and Evermann, 1898: 2386 (diagnosis, as subgenus; type *Blennius brevipinnis* Günther, 1861).

The body is short, stocky and moderately compressed. The head is blunt. The snout is rounded in prejuveniles, but steep to nearly vertical in juveniles and adults. In prejuveniles a broad supraocular bony plate, which decreases abruptly in width at metamorphosis (Fig. 10), interrupts the lateral outline of the head just before the eye (Fig. 8). The mouth is small and horizontal: the maxillary ends under the anterior margin of the pupil in prejuveniles, but extends as far as the rear margin of the orbit in adults. The fixed, subequal, incisiform teeth are in a single series, with no canines. The united gill membranes form a slight fold across the isthmus. The gill openings are restricted to the sides and are slightly larger than the base of the pectoral. Prejuveniles have one or no strong preopercular spine; juveniles and adults have none and the rear margin of the preopercle is smooth and broadly rounded. There are 12 or, occasionally, 13 preoperculomandibular pores or sets of pores, usually with 1 to 3, but never more than 5, paired sets. The 2 to 5 slender supraorbital cirri arise from a com-

---

[3] Includes *Homesthes paytensis* (Steindachner, 1876), n. comb.

(55)

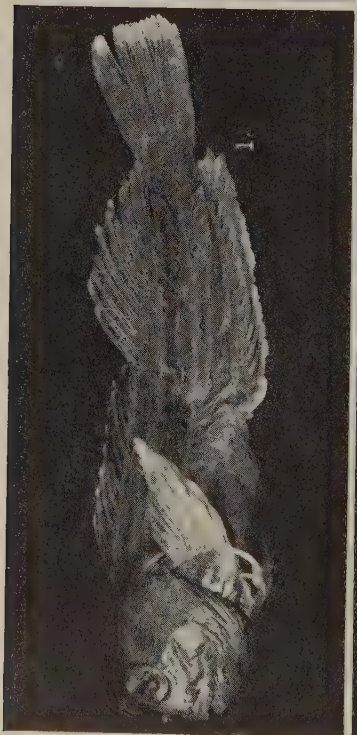

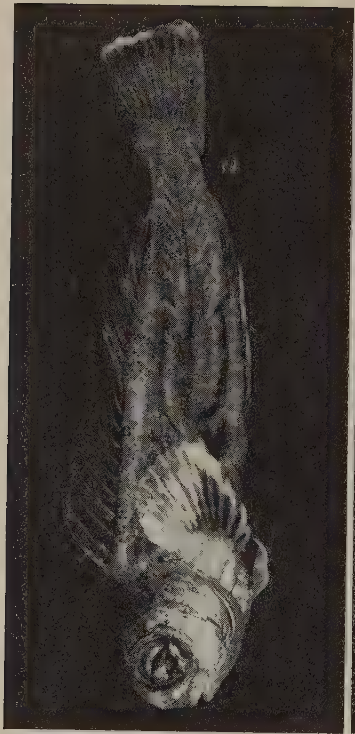

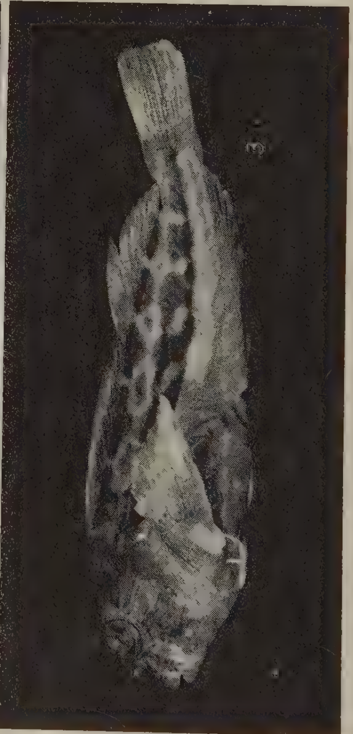

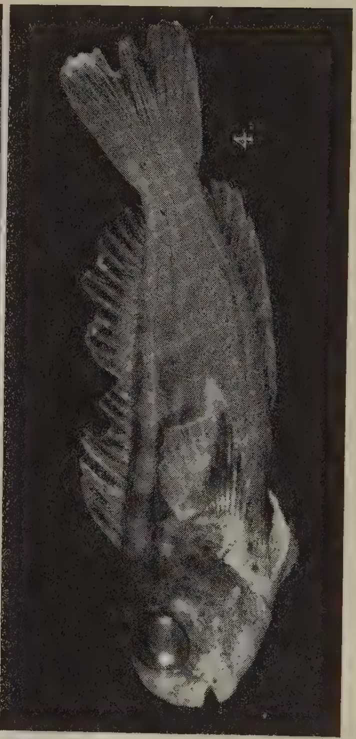

Fig. 1. *Blenniolus proteus*, holotype, USNM 179306, a 26.4 mm. male.
Fig. 2. *Blenniolus proteus*, paratype, SU 53152, a 19.8 mm. prejuvenile.
Fig. 3. *Blenniolus brevipinnis*, SIO 59-225, a 31.0 mm. female.
Fig. 4. *Blenniolus brevipinnis*, UCLA 56-356, a 16.0 mm. prejuvenile.

(56)

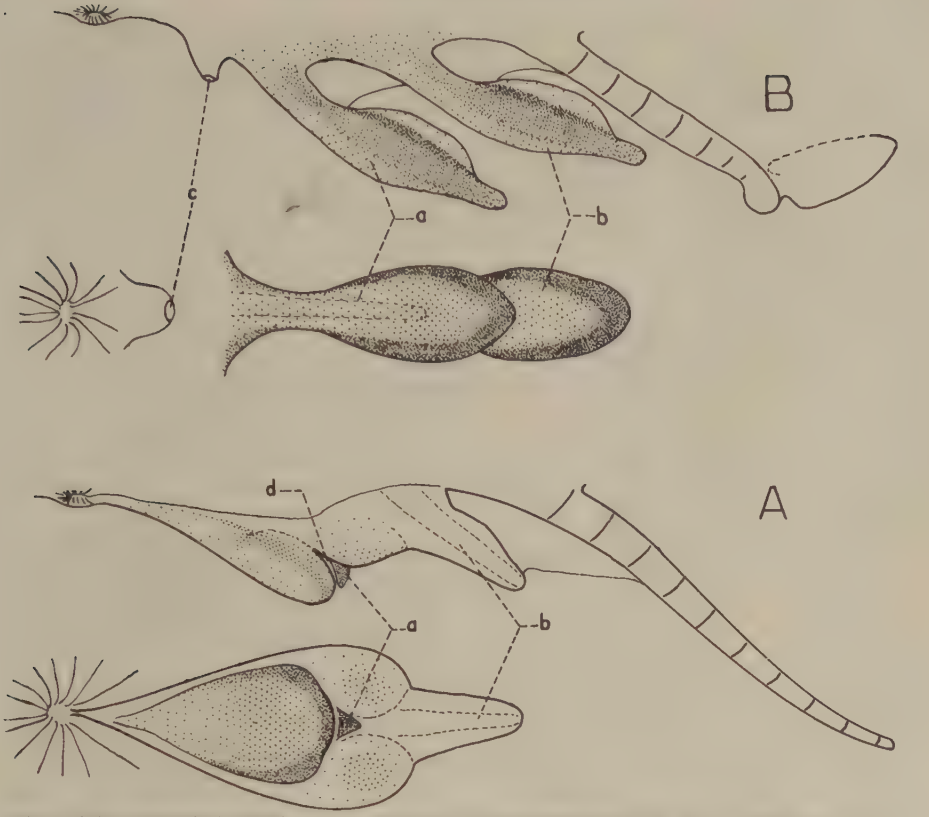

Fig. 5. The urogenital papillae and anal spines of *Blenniolus* showing the sexual dimorphism exhibited by (A) females and (B) males: a, first anal spine; b, second anal spine; c, urogenital pore of male; d, urogenital opening of female.

mon base; the outermost cirrus is thrice as long as the inner cirri and is longer in mature males than in females. The anterior nostril is a low tube surmounted by a narial flap about as long as the space between the anterior and posterior nostrils.

The dorsal fin is short and continuous; its origin is slightly in advance of the upper edge of the gill slit; there is a distinct, relatively deep notch between the low spinous portion and the higher soft portion; dorsal rays XII (XI–XIII), 12 (11–13).

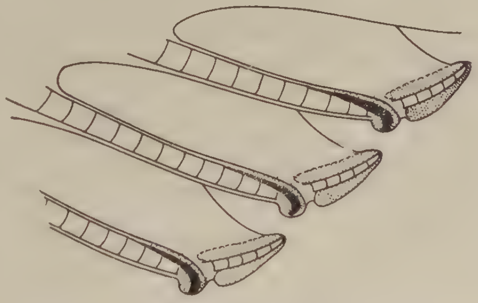

Fig. 6. Anal soft-rays of *Blenniolus* showing the fleshy bulbs and the posteriorly directed tabs which occur only in mature males.

The anal fin is narrow; the soft-rays increase in length posteriorly, and the eleventh or twelfth ray is longest. The interradial membranes are shallowly incised, leaving the distal third of each ray free. A low membranous keel extends along each side of the basal two-thirds of each soft-ray. The anal spines are short. In males, the sub-equal spines are half as long as the first soft-ray, and a broad fleshy keel develops at the tip and on either side of the distal third of each spine. In mature males this keel forms a smooth, non-convolute, spatulate pad (Fig. 5). In females the first spine is about one-fourth and the second spine one-third as

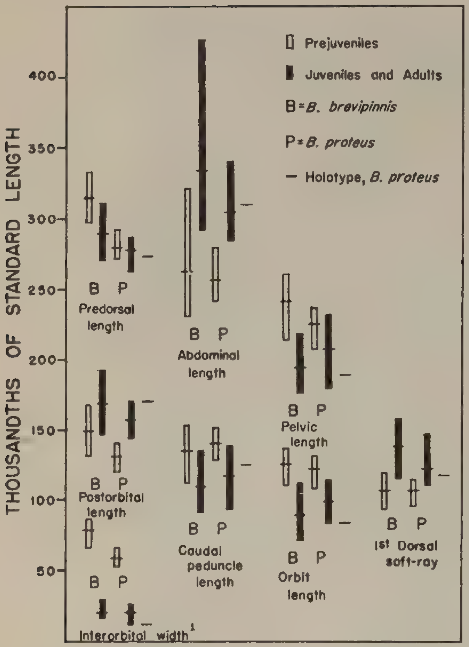

Fig. 7. Ranges and means of allometric proportional measurements comparing prejuveniles with juveniles and adults of both species of *Blenniolus*. The solid and hollow bars represent the ranges and the horizontal dashes represent the means. The number of specimens (N) in each group is as follows: *B. brevipinnis* prejuveniles (26), juveniles and adults (25); *B. proteus* prejuveniles (12), juveniles and adults (15). For the interorbital width of *B. brevipinnis* only, N = 21 for prejuveniles, and N = 13 for juveniles and adults.

long as the first soft-ray. In prejuveniles, and juvenile and adult males, both anal spines are visible. In juvenile and adult females, however, the first spine is almost completely enfolded by the urogenital papilla and, except for the tip, cannot be seen without dissection (Fig. 5). In mature males the tips of the anal rays are swollen. On the rays, distal to the insertion of the interradial membrane, low lateral keels terminate in a fleshy bulb. Distal to the bulb, the investing membrane of the ray is thickened to form a posteriorly directed tab (Fig. 6).

In prejuveniles the anus is followed posteriorly by another small pore, around which the urogenital papilla will form. In males, this papilla is developed as a blunt tube, but in females the tube expands laterally and posteriorly to form a hood over the tip of the first anal spine. Swollen ridges develop around the base of the first anal spine and enfold all but the tip (Fig. 5).

The narrowly rounded pectoral fin has 14 (13–15) rays; the tenth (rarely ninth) ray is the longest. As in prejuveniles of species in related genera the lower half of the pectoral is boldly covered with black or brown chromatophores. There is a Y-shaped black chromatophore immediately behind the base of each anal spine and soft-ray, and, in larger prejuveniles, another at the junction of the anal membrane and the caudal peduncle. As in related genera, the bold pectoral pigmentation and the specks at the base of the anal rays are lost at metamorphosis. The pelvic fins are inserted slightly in advance of the base of the pectorals; rays I, 4; the anal fin is low; rays II, 14 (12–15). The caudal fin is free from the dorsal and anal; its outline is truncate to slightly emarginate in prejuveniles and convex in adults; the procurrent caudal rays number 7 to 11 dorsally, and 6 to 9 ventrally. The incomplete lateral line never extends beyond the first dorsal soft-ray. The vertebrae number 29 to 31. In prejuveniles, never more than 6 saddle-like bars develop across the back. Scales are lacking and the skin is smooth.

The two known species of *Blenniolus* are contrasted in Table 1.

Blenniolus proteus, *sp. nov.*

Figs. 1, 3, 7, 9–10

Scartella atrimana (misidentification).—Clark, 1936:393 (Isla Socorro material only).

The comparison of the species of the genus (Table 1) furnishes a diagnosis of *B. proteus*. Counts and proportional measurements of

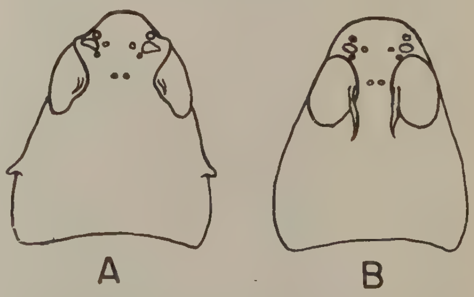

Fig. 8. Dorsal aspect of the head of *B. brevipinnis* showing the decrease in interorbital width and the loss of preopercular spines during metamorphosis. Notice the positions of the anterior and posterior nostrils, and the sensory pores. A, 15.3 mm. prejuvenile; B, 16.0 mm. juvenile. Except for the loss of preopercular spines (which are not present in *B. proteus*), the changes illustrated are typical of both species.

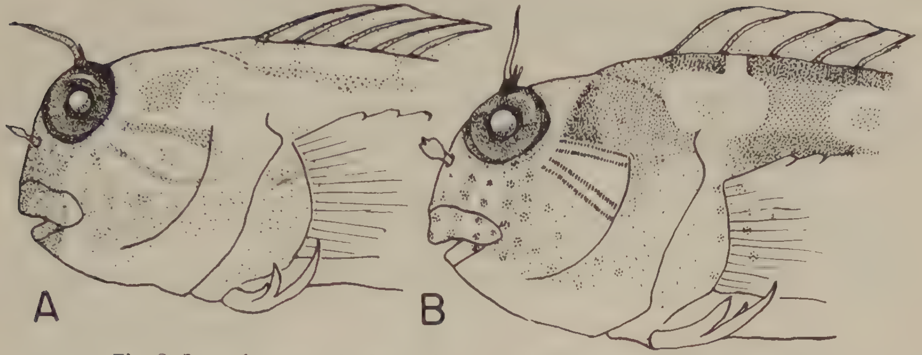

Fig. 9. Lateral aspect of adults of *B. proteus* (A) and *B. brevipinnis* (B).

the two species are presented in Table 2 and in Fig. 7.

Comparisons

Numerous characters distinguish *B. proteus* from its cognate, *B. brevipinnis* (Tables 1 and 2). The physiognomy of both species differs at all ages (Figs. 1–4, 9). *B. proteus* also has certain features in common with species of the allied genera *Homesthes* and *Hypsoblennius.* In addition to the characters given in the generic key, *B. proteus* differs from *Homesthes caulopus* Gilbert in that *caulopus* has a nearly complete lateral line, numerous multibranched lateral-line and head pores, and a stalked supraorbital tentacle with many branches. *H. caulopus* is more robust than *B. proteus* and is a much larger species, attaining a length of four inches. In the adult stage, *B. proteus* may be immediately separated from the various species of adult *Hypsoblennius* by its smaller size, and by its more robust appearance, which is correlated with the lesser number of vertebrae, 30 to 31, as contrasted with 33 to 37. Furthermore, no adult *Hypsoblennius* has a similar color pattern, and none [except *H. gentilis* (Girard)] has a single large orbital tentacle (in that species, however, the trailing edge of the tentacle is partly fimbriate). Prejuveniles of *Hypsoblennius,* while possessing a color pattern very similar to that of *B. proteus,* are at once distinguishable by having three (rarely two) preopercular spines as compared to none in *B. proteus.* By careful examination it is possible even in prejuveniles to detect the generic distinction in number of pelvic rays (I, 4 in *Blenniolus,* I, 3 in *Hypsoblennius*).

Like some other insular endemics among marine fishes (Carl L. Hubbs, personal communication), *B. proteus* seems to have become reduced in certain characters (though an hypothesis of primary simplicity is not readily excluded). It is definitely a smaller fish, with weaker texture and simpler coloration, with fewer dorsal saddles. It seldom develops even a trace of the preopercular spine. It has fewer and simpler supraorbital tentacles, and a simpler narial flap. Fewer of the preoperculomandibular pores are paired.

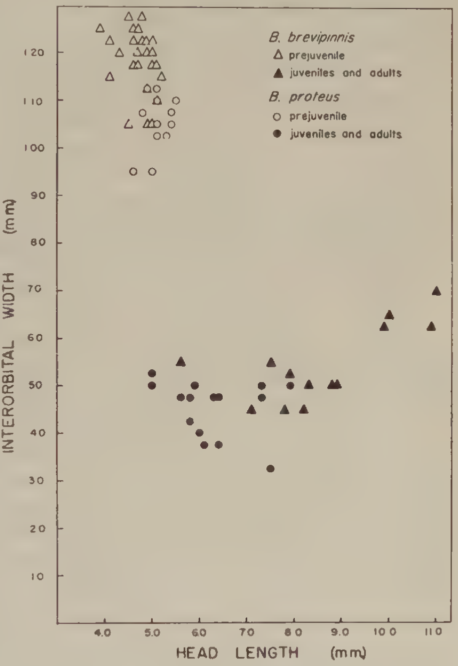

Fig. 10. Plot of absolute measurements showing the sharp decrease in interorbital width during metamorphosis in *Blenniolus.*

Table 1. Some Distinguishing Characters of the Species of *Blenniolus*

Character	*B. proteus*	*B. brevipinnis*
Range	Islas Revillagigedo	Golfo de California to Perú
Greatest standard length	Under 30 mm.	To 40 mm.
Supraorbital tentacles	Two, evenly peppered with melanophores	Three to five, clear except for basal black ring
Procurrent caudal rays	8–11 above, 7–9 below	7–9 above, 6–8 below
Vertebrae	30–31	29–30
Preopercular spines in prejuveniles	None, or one vestigial[1]	One, short, flat, blunt spine[2] at the angle, rarely with vestigial second[3]
Dorsal saddles in prejuveniles (full complement)	Five	Six
Peritoneum in adults	Clear	Black or brown
Black dots on body behind pectoral fin in adults	Three to 10	None
Body color of adult (in alcohol)	Very light; lateral and dorsolateral stripes narrow and faint, almost vestigial. No chain-like interspaces on body	Darker; lateral and dorsolateral stripes broad and dark. Chain-like interspaces on body between stripes
Number of paired preoperculomandibular pores	1 or rarely 2	2 or 3, rarely 4 or 5
Anterior narial flap	A slender filament never with projections	Lanceolate, occasionally with blunt, terminal projections
Lateral line terminates	Above the midline between tenth and eleventh dorsal spines	On the midline under or just in front of first dorsal soft-ray
In juveniles and adults the maxillary ends between verticals from	Midpoint of eye and hind margin of pupil	Hind margin of pupil and rear margin of orbit
Lower margin of eye in prejuveniles	Opposite seventh to ninth pectoral ray	Opposite fifth or sixth pectoral ray
Lower margin of eye in juveniles and adults	Opposite or above third pectoral ray	Opposite or above first pectoral ray

[1] In one specimen (17.1 mm., UCLA 55-136), a vestigial spine is present on each side at the angle.

[2] In the smallest specimen of *B. brevipinnis* (11.5 mm., UCLA 58-352), this spine is long and sharp and is contained almost three times in the length of the head. In larger prejuveniles, the spine decreases in length and becomes flatter and blunter.

[3] Rarely there is a second vestigial spine on the ventral margin of the preopercle, just anterior to the spine at the angle.

Only in the greater number of procurrent caudal rays and vertebrae does *B. proteus* tend to exceed. In coloration, in the shorter and more rounded head, and in the more slender body, *B. proteus* appears to diverge less in ontogeny than does *B. brevipinnis.*

Color in Alcohol

Prejuveniles.—The chromatophores in most specimens are dispersed and brown; occasionally they are contracted, and then appear as black dots. The ground color of the prejuvenile is light cream-yellow. When viewed from above, a deep-lying layer of giant brown chromatophores forms a crescentic saddle over the midbrain. The occiput is superficially covered by a less dense layer of brown chromatophores that extend ventrally to the upper edge of the opercle. A few brown chromatophores are scattered on the lower half of the cheek, on the opercle, along the suborbital and preorbital, and on the

Table 2. Meristic Counts and Proportional Measurements of the Two Species of *Blenniolus*

	B. brevipinnis	*B. proteus*	
	Mean (range)	Mean (Range)	Holotype
Counts:			
Dorsal spines	12.0 (11–13)	12.0 (11–12)	12
Dorsal soft-rays	11.9 (11–13)	12.2 (12–13)	12
Anal spines	2.0 ...	2.0 ...	2
Anal soft-rays	13.9 (12–14)	14.1 (14–15)	14
Pectoral rays	14.0 (13–15)	14.0 (13–15)	13
Pelvic spines	1.0 ...	...	1
Pelvic soft-rays	4.0 ...	4.0 ...	4
Caudal rays:			
Principal	7 + 6 ...	7 + 6 ...	7 + 6
Procurrent (dorsal)	7.7 (7–9)	9.0 (8–11)	9
Procurrent (ventral)	7.1 (6–8)	8.3 (7–9)	8
Vertebrae	29.8 (29–30)	30.6 (30–31)	31
Measurements:			
Standard length, mm	11.5–39.6	17.0–28.5	26.4
Head length	307 (282–326)	287 (265–306)	284
Body depth	267 (228–298)	233 (216–260)	231
Snout length	102 (81–120)	91 (80–102)	91
Upper jaw length	101 (83–126)	92 (74–117)	91
Longest pectoral ray	263 (221–296)	264 (241–286)	254
Caudal peduncle depth	100 (87–120)	89 (78–108)	79
Second dorsal spine	132 (95–165)	129 (112–147)	132
Penultimate dorsal spine	61 (33–80)	60 (38–72)	72
Last dorsal spine	39 (28–53)	30 (21–43)	23

Measurements are expressed in thousandths of the standard length. The numbers of specimens in the samples are as follows, for *B. brevipinnis* and *B. proteus*, respectively, are 77 and 29 for dorsal, anal, pectoral, and pelvicray counts; 35 and 29 for caudal-ray counts; 9 each for vertebrae, and 51 and 27 for all measurements.

snout. The interorbital space and the lips are lightly sprinkled with punctate black and brown chromatophores. The chin and throat are immaculate.

Five bars of brown chromatophores develop across the back (Fig. 2). In the largest prejuvenile at hand (19.8 mm., UCLA 55-128), and in another specimen intermediate in size (18.1 mm., UCLA 55-152), all five bars are present. The first four bars extend ventrally to the midline, but the fifth (peduncular) bar is dorsal only and does not extend onto the sides. In the smallest specimen at hand (17.0 mm., UCLA 53-45), only four dorsal bars are present and these do not extend ventrally. No smaller specimens are available for comparison but it may be assumed that in this species, as in *B. brevipinnis,* the bars appear anteriorly at first and successively develop posteriad with increase in age.

Juveniles and adults.—The following condition, although transient, seems more significant than the loss of the bolder pectoral pigmentation at metamorphosis. The areas formerly covered by vertical bars in prejuveniles gradually become free of brown chromatophores and the deep integument of each area takes on the appearance of a faint, but distinguishable, pale orange bar. This may be an artifact of preservation since the bars closely approximate the limits set by the brown chromatophores in the prejuvenile. The cream-yellow spaces between the orange bars become superficially covered by punctate black chromatophores. As growth proceeds, these chromatophores outline flat dorsolateral hexagons, each of which is connected to the dorsal base by two short vertical lines and to the midline by two ventrally divergent lines. In addition, each interspace has a thin horizontal line of black on the midline. In the adult the upper base of each hexagon traverses the orange bars both anteriorly and posteriorly to form a thin, ragged, dorsolateral stripe, which extends from the base of the last dorsal ray to a point on the occiput approximately one pupil diameter ventral and anterior to the dorsal insertion. Likewise, the chromatophores on the midline traverse the orange bars to form a broken horizontal line that extends from the caudal peduncle to the tip of the opercular flap. One apparently transitional specimen (17.8 mm., UCLA 55-152), lacks the bold pectoral pigmentation, retains vestiges of the vertical brown bars of the prejuvenile, and possesses the beginnings of the juvenile pattern as described above.

The pectoral base is peppered with punctate black chromatophores, as are the lowermost six pectoral rays. Three to 10 giant black contracted chromatophores, not present in the prejuvenile, appear in the deep integument of the axilla.

The network of giant brown chromatophores that saddled the occiput of the prejuvenile appears as punctate black chromatophores in the juvenile. Two characteristic bands of black radiate from the orbit. The upper band is horizontal or sub-horizontal and extends from the mid-orbit, across the cheek, and onto the opercle. The second band is curved and extends from the orbit to the preopercular margin at an angle of about 25° below the horizontal. A third diffuse band occasionally extends across the cheek at an angle of about 60° below the horizontal. In juveniles the opercle and the chin, and in mature specimens the throat as well, are peppered with black. The rim of the orbit, the interorbital area, the snout, the lips, and the suborbitals and preorbitals are similarly peppered, but several, scattered, unpigmented blotches give the face a piebald appearance. The anterior nostril is lightly dusted, and the orbital tentacle is heavily dusted with black (Fig. 9A).

The entire spinous dorsal fin is dusted with black. The distal third to half of the soft dorsal is likewise dusted with black, but the basal portion is clear. The basal third of the anal fin is clear, the medial third is dusted with black, and the distal third is white. The caudal base and the margin of the caudal fin are dusted with black and each caudal ray is edged with black, but the remainder of the fin is clear.

COLOR IN LIFE

The following notes were taken from three adult males (BC 60-255) three hours after capture and preservation at Caleta Grayson. The basic ground color of the head is olive-green. The wide postorbital bar that radiates across the cheek is rusty-orange but a scattering of irridescent blue-white dots gives it a pinkish cast when viewed in strong sunlight. The bar is bordered above and below by a narrow, irridescent blue-white ray. The half-crescent mark behind the eye and above the cheek is blue-black. The chin, lips and throat are light, olive-green. The spots on the chin, snout and suborbital, which, in preserved specimens, give the face a piebald appearance, are actually arranged in distinctive bands radiating from the orbit. These spots and those on the cheek and opercle are olive-orange and have a golden cast when viewed in strong sunlight. The supraorbital tentacles and the anterior nostrils are orange and peppered with brown.

The iris is rusty-orange except for a ring of irridescent blue-white which borders the pupil. A blue-white slash crosses the outer base of the pectoral fin. The interradial membranes of the pectoral fin are clear. The radial membranes are peppered with black but more boldly on the lower six rays. The dorsal fin is light olive-green and is dusted with black more densely on the spinous than on the soft dorsal. The anal fin is light olive, blending into dark olive-brown at the middle and then into white at the tips. The base of the caudal fin is light olive, blending into pale yellow at the distal third and the distal margin is clear.

A series of five, dark, olive-brown bars cross the back and extend saddle-like down to the midline of the body. The first saddle extends under the first four dorsal spines; the second is located under the sixth to ninth spines; the third extends from under the ultimate dorsal spine to the first four dorsal soft-rays; the fourth extends from the seventh to the penultimate ray; and the fifth is located on the caudal peduncle. In two of the specimens at hand the first and the second saddles are contiguous and, when viewed dorsally, appear as a tongue-like projection from the first to the ninth spines. An irregular, flesh-colored, dorsolateral stripe bisects the lateral wings of the first three, and occasionally the fourth, saddles. Irregular, dark olive-brown blotches fill part of the flesh-colored interspaces between the saddles. In addition, an irregular series of irridescent blue-white spots is found in the interspaces and along the midline of the body. The ventral half of the body is flesh-colored and peppered with black.

DISTRIBUTION

Range.—All known specimens were taken about the Revillagigedo Islands, to which *B. proteus* is apparently confined. According to Dr. Richard H. Rosenblatt (personal communication), this is the only blenniid known to be endemic to any of the islands of the eastern tropical Pacific. *B. brevipinnis,* on the other hand, ranges along the Pacific Coast of the Americas from México to Perú and, in addition, to the Galapagos and Cocos Islands. *B. proteus* has never been taken on the mainland, although the distance separating Clarion and Socorro Islands is almost as great as that which separates Socorro from the mainland. Furthermore, Clarion and Socorro are separated by deep water. It is probable, therefore, that the factors which restrict *B. proteus* to its insular habitat are ecological and that its insularity is not a mere product of distance.

Material examined.—A total of 32 specimens from 14 collections. Place names in the Revillagigedo Archipelago conform to those suggested by Richards and Brattstrom (1959).

Holotype.—USNM 179306 (formerly UCLA 55-152), a male 26.4 mm. in standard length, from the north edge of Caleta Binner on Isla Socorro, of the Revillagigedo Archipelago, México: depth of water, to 5 feet; bottom coral heads and larva: predominant vegetation, species of *Ralfsia, Dictyosphaera,* and *Neomeris;* water temperature, 76° F.; collected May 1, 1955, by Richard H. Rosenblatt and Bayard H. Brattstrom.

The 24 paratypes include 9 (USNM 179305), 17.8–22.6 mm. long, collected with the holotype and the following additional specimens from Caleta Binner on Isla Socorro: BMNH 1959. 8. 10. 1 (formerly UCLA 53-350), 1 (24.4 mm.); and CAS 21219 (formerly UCLA 55-126), 1 (19.0), and UCLA 53-49, 1 (21.0), from rocky area east of landing place; still others from Isla Socorro are: SU 53151 (formerly UCLA 55-156), from front of point marking southwest end of next cove north of Caleta Binner, 3 (20.6–26.5); SIO 58-142, Bahia Braithwaite, 1 (26.5); BC 57-152, Bahia Braithwaite, 1 (17.9); and BC 57-158, Caleta Grayson, 1 (28.5).

Six paratypes came from other islands in the Revillagigedo group: CNHM 62774 (formerly UCLA 53-45), from the southeast side of San Benedicto, 2 (17.0–17.6); and SU 53152 (formerly UCLA 55-128), ¼ mile west of Roca Partida, 4 (18.3–19.8).

Four additional specimens, not designated as paratypes, came from Isla Clarion, of the Revillagigedo group: UCLA 55-136, from anchorage at southeast end of island, 2 (17.1–17.5); UCLA 59-153, no other data, 1 (17.0).

Three specimens, recently collected at Isla Socorro, were not designated as paratypes: BC 60-255, Caleta Grayson, about 50 feet west of the water hole, 3 (25.7–26.3).

Etymology.—In Greek mythology Proteus was a sea-god, Neptune's herdsman, whose distinguishing characteristic was the faculty of assuming different shapes. The name is applied to *B. proteus* in allusion to the changes that occur during the metamorphosis of this and other blenniines.

Blenniolus brevipinnis (Günther)

Figs. 2, 4, 7–10.

Blennius brevipinnis.—Günther, 1861a:373 (original description; "West Coast of Central America"); 1861b:226 (description; "Sandwich Islands" and "West Coast of Central America"); 1869:389 (Central America). Steindachner, 1876:84, pl. 8 (description; Navidad, near Mazatlan). Günther, 1877:194 (description, "West Coast of Isthmus of Panama and Sandwich Islands"). Boulenger, 1899:8 (St. Helena Bay, Ecuador).

Isesthes brevipinnis.—Jordan and Gilbert, 1883:108 (Mazatlán).

Hypsoblennius brevipinnis. — Jordan and Evermann, 1898:2390 (description; synonymy; Mazatlán to Panamá; type of subgenus *Blenniolus*). Gilbert and Starks, 1904:193 (Panamá Bay). Meek and Hildebrand, 1928:946 (description; Chame Point, Panamá).

Scartella brevipinnis.—Hubbs, 1927:365 (generic reference and synonymy). Jordan, Evermann, and Clark, 1930: 461 (synonymy; Mazatlán to Panamá).

Homesthes brevipinnis.—Norman, 1943: 803 (generic reference).

Blenniolus brevipinnis.—Fowler, 1944: 229 and 298 (description and synonymy; north of Galápagos, at 4° 53′ N., 81° 31′ W.; Playa Muerto, Panamá); Ricker, 1959:12 (Las Tres Marías, México).

Syntypes.—BMNH 1855. 9. 19. 751 and 1861.8. 13. 17.

Hypsoblennius striatus (not of Steindachner). —Fowler, 1919:128 (Panamá City, Panamá).

Spinoblennius spiniger.—Herre, 1935:435 (orignial description, Eden Island, Galapagos Islands); 1936:399, fig. 39 (description: same material).

Holotype.—CNHM 17395.

Scartella atrimana.—Clark, 1936:393–4 (original description; Albemarle (Isabela) Island, Galápagos Islands, and one paratype, from Banderas Bay, México).

Holotype.—CAS 3988. Paratypes.—CAS 5498 and CAS 21220.

Spinoblennius actesoma.—Fowler, 1944:232, 251, and 401, fig. 248 (original description; Playa Muerto, Panamá; Bahía Santelmo, Isla del Rey, Islas Perlas, Panamá: Isla María Madre, Islas Tres Marías, (México).

Types.—ANSP 70086 and 70087.

The characters of this species are presented in the account of the genus, in the figures, and in Tables 1 and 2.

NOMENCLATURAL HISTORY

As outlined in the preceding synonymy, the species *brevipinnis* was first referred to the then very inclusive genus *Blennius,* which has now been much divided, as by Norman (1943). It was next referred to the rather speciose New World genus *Hypsoblennius* and its synonym *Isesthes.* Hubbs, misinterpreting the character of the gill membranes, referred the species in 1927 to the Western Atlantic genus *Scartella.* Norman, in 1953, referred it to *Homesthes,* with which, as indicated in the key above, it shares several characters, though a combination of other characters seems to warrant generic separation, especially now that two species are referable to each genus. *Blenniolus* was first recognized as a genus by Fowler in 1944, but the same author, as well as Herre, 1935, and Clark, 1936, described the prejuveniles of *B. brevipinnis* under two other generic and three specific names. This species has apparently only once been misidentified as a species (*Hypsoblennius striatus*) of another genus.

COLOR IN ALCOHOL

Prejuveniles.—The ground color is light cream-yellow. When viewed from above, a deep-lying layer of giant brown chromatophores forms a crescentic saddle over the midbrain. The occiput is superficially covered by a less dense layer of brown chromatophores that extend laterally over the preopercle and opercle and under the eye. A small patch on the preopercle, just behind the lower half of the eye, is free of chromatophores. A narrow diffuse band of brown chromatophores radiates from the anterior corner of the orbit across the maxillary and onto the lower lip just before the angle of the gape. There is a scattering of chromatophores on the upper lip. The snout and chin are immaculate, except for a narrow, black-brown chromatophore located in the deep integument of the chin at the symphysis.

Six saddle-like bars of brown chromatophores develop across the back (Fig. 4). These appear anteriorly at first and successively posteriad with increase in age. In the smallest specimens at hand (11.5 mm., SIO 58-352; 11.7 mm., UCLA 54-293), only the faint beginnings of the first bar are present. In a slightly larger specimen (13.5 mm., UCLA 54-293), there are one and one-half bars. At 14 mm., two bars are visible; only in the largest prejuveniles (16.1 mm., UCLA 56-358), are all six bars present. With increase in size, the saddles become angular, roughly hourglass-shaped bars, which extend ventrally to the midline. The resultant interspace between the bars is hexagonal and light cream-yellow.

Juveniles and adults.—In contrast to the condition in *B. proteus,* the pigment pattern of the prejuvenile is intensified in the juvenile, and fully expressed in the adult. The entire body is overlaid with punctate black and brown chromatophores. The small light patch on the upper cheek of the prejuvenile is developed in the adult as a broad, pearly-white band, which extends from the orbit to the preopercular margin at an angle of approximately 25 to 30° below the horizontal. The upper and lower margin of this band are each bordered by a double set of thin brown lines. A characteristic half-crescent of black pigment is developed just behind the eye above the cheek (Fig. 9B).

The occipital saddle of the prejuvenile is expressed to varying degrees in the adult. In some it appears as a slightly darker, shaded area; in others, as a very dark saddle overlaid by a honeycomb of thin white lines. The preorbital band is most pronounced in adults. The opercle, the lower half of the cheek, the suborbital, preorbital, snout and upper lip are peppered with brown spots, each approximately as large as the posterior nostril. In some individuals there are similar spots on the pectoral base and on the upper sides above the pectoral. In some specimens the spots appear to radiate in bands from the orbit, but in others, the spotting is more dense, and a honeycomb pattern may be formed. The base of the orbital tentacle is ringed with black, but the individual cirri are immaculate, as is the anterior nostril. The dusky chin and throat region is crossed by a broad, lightly pigmented X, which is obvious in juveniles but rather diffuse in adults.

In adults the hourglass-shaped bars are contiguous, or nearly so, so that a dark-brown dorsolateral stripe is formed along the base of the dorsal fin and a dark lateral stripe just above the midline. The hexagonal, cream-yellow interspaces of the prejuvenile become more oval with age. Since in adults the ends of these interspaces are nearly contiguous, a light chain-like stripe is formed between the darker lateral stripes. A spot of brown in the center of each oval interspace accentuates this chain-like appearance. The lower dark lateral stripe usually includes five or six cream-yellow spots in its course but it may be partially or completely interrupted.

The spinous dorsal is clear, but dusted with melanophores, more densely basally than distally. The soft dorsal fin is similar in color, but is lighter. The caudal fin is mostly clear, but lightly peppered with black at the base. The anal fin has a light basal band, a characteristic thin, dark, medial band, and a very light distal band.

Color in Life

The following notes were taken from two live females at Cabo San Lucas (SIO 59-223). The basic ground color of the head is olive-brown. The wide postorbital bar that radiates across the cheek is bright lemon-yellow. This bar is bordered above and below by a narrow, brown-edged, pearly-white ray. The occipital saddle forms a honeycomb of brick-red or orange spots, each bordered by blue-violet. The half-crescent mark behind the eye and above the cheek is blue-black. The chin and lips are lemon-yellow. The spots on the chin are brown, and those on the snout, preorbital, suborbital, cheek, and opercle are brick-red to brown. The supraorbital tentacle is ringed with black at the base and the individual cirri are yellow-white. A powder-blue crescent lies immediately behind the base of the tentacle. The anterior nostril is brick-red.

Six equally spaced dark-orange bars radiate from the margin of the pupil, across the light-orange iris. The lower five or six pectoral rays are olive, the upper rays clear. The dorsal fin is clear olive-brown basally and orange distally. The anal fin is cream-orange at the base, blending into dark brown in the middle and then into white at the tips. The base of the caudal fin is clear and the tips are orange. The lateral stripes on the body are chocolate-brown, with creamy-tan interspaces. The center spots in the interspaces are brick-red to brown. The ventral half of the body is creamy-tan.

Distribution

Range.—From Guaymas and Punta Pescadero, in the Gulf of California, to Cabo Blanco, Perú; and Galápagos and Cocos islands.

The provenance of the type specimens of *Blennius brevipinnis* has long been in doubt. Günther (1861b:226) listed two specimens, as follows: "a. Sandwich Islands. From the Haslar Collection." and "b. West Coast of Central America. Collected by Captain Dow."

I have personally examined the "Sandwich [Hawaiian] Islands" specimen, BMNH 1855. 9. 19. 751. It is 33.7 mm. in standard length and, although slightly faded, agrees well with all the meristic, proportional, and phenotypic characteristics given in Tables 1 and 2. Although the specimen is undoubtedly *Blenniolus brevipinnis*, its Sandwich Islands locality is presumably erroneous, as Jordan and Evermann (1898:2391, 1905:504) and Strasburg (1956:243) have indicated.

In a parallel case, Günther (1864:157), listed a siluroid, *Arius dasycephalus*, from the Sandwich Islands, "From the Haslar Collection." In this case, as in that of *B. brevipinnis*, it has been suggested (Jordan and Evermann, 1905:130, and Meek and Hildebrand, 1923:106) that the Sandwich Islands locality of *Galeichthys dasycephalus* (Günther) is in error.

Even Günther (1869:382) had his doubts about the scientific value of the Haslar Hospital collections: "In the second place I have to mention Dr. Seemann, who as naturalist attached to the expedition of the Herald, brought to England a collection of Central American fishes. These, as I have mentioned above, were originally deposited in the collection of the Haslar Hospital, but no record as regards the origin of the specimens was kept, so that most of them are lost for the purpose of this Memoir."

In a final attempt to establish the validity

(65)

of the Sandwich Islands locality of *B. brevipinnis,* I searched through the narrative of the voyage of the "Herald." Indeed, the "Herald" did visit the Sandwich Islands on three different occasions, but only as a stopover point on its way to or from the Arctic (Seemann, 1853). I was unable to find an account of any fish collecting done during this part of the voyage. However, Richardson (1854) does allude to some fish collecting done by Drs. Seemann and Goodbridge in the Galápagos Islands. It is not unlikely that the "Sandwich Islands" specimen of *B. brevipinnis* was taken by these men while the "Herald" was in the Galápagos area.

Mr. G. Palmer, of the British Museum, has kindly re-examined the specimen collected by Captain Dow. It is 40 mm. in standard length and the fin-ray counts are in agreement with the ranges given in Table 2. The specimen likewise fits all the distinguishing characteristics as summarized in Table 1. According to G. Palmer (personal communication), this specimen is listed in the register of the British Museum as being from Panamá. Why Günther first recorded it as being merely from the "West Coast of Central America" is a moot question.

On the basis of the foregoing information, the Panamanian specimen, BMNH 1861. 8. 13. 17, is selected as the lectotype of *Blenniolus brevipinnis.*

Material examined.—A total of 217 specimens from 43 collections.

México, Cape region, Baja California Sur.—SIO 59-223, Bahía San Lucas, about 100 yards north of sand beach near tip of Cabo San Lucas, 2 (16.2–17.3 mm. in standard length); SIO 59-210, Bahía San Lucas, 300 yards south of cannery pier, 7 (19.7–36.7); SU 18765, Bahía San Lucas, southwest end, 8 (24.5–32.3); SU 18926, Bahía San Lucas, south side, 600 yards from tip of Cabo San Lucas, 12 (20.3–37.9); SIO 59-225, about one-third mile south of Punta Pescadero, just south of fisherman's camp, 30 (15.5–37.5); SU 47791, northeast corner of Bahía de los Muertos, 2 (15.5–15.8).

México, Golfo de California, eastern shore.—UCLA 51-10, Sonora, Punta San Guillermo, 1 (35.5); UCLA 51-29, Sinaloa, south tip of Isla Lobos, Islas Venados group, near Mazatlán, 2 (27.7–30.7); UCLA 51-54, Sinaloa, isthmus (shoreward side) of Isla Venados, 1 (18.7).

Mexico, Islas Tres Marías.—BC 54-76, Isla Magdalena, 2 (14.8–17.0); BC 57-163, Isla Magdalena, 1 (16.1); BC 57-171, Isla Magdalena, 3 (15.6–16.8); UCLA 56-358, Isla Cleopha, southeast side, 20 (14.2–16.1).

México, Nayarit.—UCLA 58-5, south edge of small point inside larger point at Chacala, 3 (16.0–24.0); UCLA 58-11, three-fourths mile south of point forming the south end of Ensenada Chacala, 1 (19.7); CAS 21220 Banderas Bay, 1 (ca. 16.0), paratype of *Scartella atrimana* Clark.

México, Colima.—UCLA 56-232, west end of Playa de Santiago, about 10 miles northwest of Manzanillo, 14 (13.5–33.3); UCLA 56-230, Playa de Santiago, in vicinity of rocks near Hotel Auita, 7 miles northwest of Manzanillo, 3 (32.2–35.1); UCLA 56-231, Ensenada Carrizal, across bay from Manzanillo, 4 (22.7–27.5).

México, Guerrero.—UCLA 52-112, Puerto del Marques, near Acapulco, 1 (31.2); UCLA 53-190, same locality, 1 (24.9); UCLA 52-119, Acapulco Harbor, 1 (15.2); UCLA 56-17, Playa las Pulgas (El Farallon), 1 (26.5).

Costa Rica.—SIO 58-352, 25 miles west of Cabo Velas, 1 (11.5); UCLA 49-463, 10 miles west of Punta Quepas, 1 (20.4).

Costa Rica, Isla del Coco.—UCLA 56-211, 2 (15.4–15.9).

Panamá.—UCLA 53-31, vicinity of Isla Jicarita, from dugout canoe awash, 1 (17.4); UCLA 51-248, Golfo de Panamá, Isla Montuosa, 4 (14.1–14.6); UCLA 56-304, Golfo de Panamá, taken from floating log, 7 (16.5–33.9); UCLA 55-241, Bahía Panamá, 1 (35.4); SU 6929, Bahía Panamá ?, 1 (17.4).

Colombia.—UCLA 54-304, 25 miles west of Cabo Marzo, 1 (14.4); UCLA 54-332, upper Colombia bank, 1 (14.9).

Ecuador.—SIO 52-20, north-northeast of Cabo San Francisco, 4 (31.4–39.6).

Ecuador, Islas Galápagos.—SU 37576, Isla Seymour, south side, 1 (30.8); UCLA 54-293, Isla Isabela (Albemarle), 5 to 10 miles south of Punta Cristóbal, 2 (11.7–13.5); SIO 51-53, Isla Fernandina (Narborough), Punta Mangle, 1 (34 +, smashed specimen); SU 24423, Eden Island, 4 (14.9–16.0) cotypes of *Spinoblennius spiniger* Herre; CAS 3988, Isla Isabela (Albemarle), off Vilamil, about submerged light, 1 (16.0), holotype of *Scartella atrimana* Clark; CAS 5498, same location as holotype, 56 (ca. 14.0–16.0), paratypes of *S. atrimana* Clark.

Perú, Cabo Blanco.—BC 56-139, 3 (15.5–16.6); BC 56-140, 2 (15.9–16.4); BC 56-158, 1 (13.9).

REMARKS ON THE LIFE HISTORY AND HABITAT OF THE SPECIES OF *Blenniolus*

The prejuveniles of the two species of *Blenniolus*, as well as, so far as known, all species of the closely allied genera *Homesthes* and *Hypsoblennius*, are pelagic in habit. Presumably, as Hubbs (1958:283) suggested for analagous prejuveniles of other marine fishes, their "metamorphosis seems to be triggered by shore conditions, whenever they happen to be encountered." Transformation occurs rapidly and widely, with the result that, within species, prejuveniles overlap juveniles in size (Fig. 10). Breder (1949) found that, when placed in an aquarium, the pelagic larvae of *Acanthurus coeruleus* immediately sought the shelter of shells and began their metamorphosis. He suggested that the young of the species continue to grow and to delay metamorphosis until the currents chance to carry them over a suitable substrate inshore. They then transform immediately into a miniature adult. This theory accounts well for the taxonomic enigma of having larval forms overlapping adults in size. The overlap in *Blenniolus* (Fig. 10) is not as great as in *A. coeruleus*, but Breder's explanation seems applicable.

After metamorphosis, the juvenile settles to the bottom, usually on a substrate of large granitic or volcanic rocks, or coral heads. Apparently, however, *B. brevipinnis* can live in the absence of these habitats, since seven juvenile to adult specimens were taken from a floating log in the Golfo de Panamá (UCLA 56-304). Fowler (1944:295) reported on one 30 mm. adult that was taken when "About 15 miles north of this station [north of Galapagos, 4° 53′ N., 81° 31′ W.] the ship was stopped and the skiff launched. Some small fishes were collected from underneath floating logs." Another specimen (17.4 mm., UCLA 53-31) was taken from a dugout canoe floating in the vicinity of Isla Jicarita, Panamá. Meek and Hildebrand (1928:946), mentioned that their specimens "were taken from old submerged wood, in which they appear to inhabit the crevices, and the burrows of the shipworm."

While skin-diving at Cabo San Lucas and Punta Pescadero, I have observed several individuals of *B. brevipinnis* resting in empty shells of barnacles (*Balanus* sp.), which were attached to the vertical sides of large granitic rocks. Usually, only the head projected from the barnacle shell, but the fish could be readily identified by the bright lemon-yellow cheek bar and the yellow-white supraorbital tentacles, which wave in the surge. Between swells at low water, the retreats were occasionally exposed completely to the air. The fish remained in the shell during these times.

Presumably, like some species of *Hypsoblennius*, and other related genera, the species of *Blenniolus* deposit the eggs within a shell or crevice, where they are guarded by the male.

Ripe females of *B. proteus* have been taken from February through May; collections from other seasons are not available. Ripe females of *B. brevipinnis* have been collected in October (Manzanillo and Costa Rica); in January (Chacala, Isla Lobos, and Punta San Guillermo, México); in February (Panamá); and in March (Cabo San Lucas, Acapulco, and Panamá). Collections are scarce during the midsummer months. The available data suggest that *B. brevipinnis*, at least, may spawn the year around.

Although there is a marked difference in maximum size, there appears to be no significant difference between the species of *Blenniolus* in size at maturity. Both species mature very soon after metamorphosis. Among 30 females of *B. brevipinnis* examined, the smallest sexually mature specimen (UCLA 55-152) was 19.5 mm. long. This specimen retains vestiges of the prejuvenile body pattern and appears to have recently transformed.

Two specimens of *B. proteus* have been collected during an apparent metamorphosis. Both show characters that are primarily juvenile, but they also retain vestiges of the prejuvenile. In one of these (UCLA 59-153), the interorbital width, postorbital length, orbit length, abdominal length, and the length of the first dorsal soft-ray all fall within the range of proportions of the juvenile and adult. However, the color pattern and the lengths of the pelvic fin and the caudal peduncle are typically prejuvenile. This 17.0-mm. specimen is 1.6 mm. shorter than the largest prejuvenile of *B. proteus*. Its sex is indeterminable. The other specimen (UCLA 55-152) is 17.8 mm. in standard length and it is definitely a male. Its orbit length, interorbital width, and abdominal length all fall within the range of proportions of juveniles and adults. However, other characters such as the postorbital length, the length of the caudal peduncle, and the pelvic length, are intermediate between the ranges of proportions of prejuveniles and juveniles. In addition, as stated in the description, this specimen retains vestiges of the vertical brown bars of the prejuvenile and shows the beginnings of the juvenile color pattern. On the basis of the available data, *B. proteus,* although a definitely smaller species than its congener, *B. brevipinnis,* appears to have a more protracted larval life.

Literature Cited

Boulenger, George A. 1899. Viaggo del Dr. Enrico Festa nell'Ecuador e regioni vicine. *Boll. Mus. Zool. e Anat. Comp. Univ. Torino 14 (335):1–8.*

Breder, Charles M. 1949. The taxonomy of post-larval stages of *Acanthurus hepatus. Copeia 1949 (4):296–7.*

Clark, H. Walton. 1936. The Templeton Crocker Expedition of the California Academy of Sciences, 1932. New and noteworthy fishes. *Proc. Calif. Acad. Sci. (4) 21 (29):383–96.*

Fowler, Henry W. 1919. Notes on tropical American fishes. *Proc. Acad. Nat. Sci. Phila. 1919:128–55.*

———. 1944. Results of the Fifth George Vanderbilt Expedition (1941) (Bahamas, Caribbean Sea, Panamá, Galápagos Archipelago and Mexican Pacific Islands). The fishes. *Acad. Nat. Sci. Phila. Monograph 6: 57–583.*

Gilbert, Charles H., and Edwin C. Starks. 1904. The fishes of Panama Bay. *Mem. Calif. Acad. Sci. 4:1–304.*

Günther, Albert C. L. G. 1861a. On a collection of fishes sent by Capt. Dow from the Pacific Coast of Central America. *Proc. Zool. Soc. London 1861:370–6.*

——— 1861b. . . . Acanthopterygian Fishes. . . . *Cat. Fishes Brit. Mus. 3:1–583.*

——— 1864. . . . Physostomi, . . . *Cat. Fishes Brit. Mus. 5:1–455.*

——— 1869. An account of the fishes of the states of Central America, based on collections made by Capt. J. M. Dow, F. Godman, Esq., and O. Salvin, Esq. *Trans. Zool. Soc. London 6:377–494.*

——— 1877. Andrew Garrett's "Fische der Südsee." *Jour. Mus. Godeffroy, 13:169–216.*

Herre, Albert W. 1935. New fishes obtained by the Crane Pacific Expedition. *Field Mus. Nat. Hist. Zool. Ser. 18(12):383–438.*

——— 1936. Fishes of the Crane Pacific Expedition. *Field Mus. Nat. Hist. Zool. Ser. 21: 1–472.*

Hubbs, Carl L. 1927. Notes on the blennioid fishes of Western North America. *Pap. Mich. Acad. Sci. Arts and Letters 7(1926):351–94.*

——— 1958. *Dikellorhynchus* and *Kanazawaichthys*: nominal fish genera interpreted as based on prejuveniles of *Malacanthus* and *Antennarius,* respectively. *Copeia, 1958 (4):282–5.*

——— and Karl F. Lagler. 1958. Fishes of the Great Lakes Region. *Bull. Cranbrook Inst. Sci. 26:1–213.*

Jordan, David S. and Barton W. Evermann. 1898. The fishes of North and Middle America. *Part III. Bull. U. S. Nat. Mus. 47:2183–3136.*

——— 1905. The aquatic resources of the Hawaiian Islands. Part 1. The shore fishes. *Bull. U. S. Fish. Comm. 23 (1903):1–574.*

——— and H. Walton Clark. 1930. Check list of the fishes and fishlike vertebrates of North and Middle America north of the northern boundary of Venezuela and Colombia. *Rep. U. S. Comm. Fish. for 1928, pt. 2: 1–670.*

——— and Charles H. Gilbert. 1883. List of fishes collected at Mazatlan, Mexico, by Charles H. Gilbert. *Bull. U. S. Fish Comm. 2 (1882): 105–8.*

Meek, Seth E., and Samuel F. Hildebrand. 1923. The marine fishes of Panama, *Part 1. Field Mus. Nat. Hist. Zool. Ser. 15: 1–330.*

——— 1928. The marine fishes of Panama, *Part 3. Field Mus. Nat. Hist. Zool. Ser. 15:709–1045.*

Norman, John R. 1943. Notes on the blennioid fishes. A provisional synopsis of the genera of the family Blenniidae. *Ann. and Mag. Nat. Hist. (11) 10:793–812.*

Randall, John E. 1956. A revision of the surgeon fish genus *Acanthurus. Pacific Sci. 10:159–235.*

Richards, Adrian F., and Bayard H. Brattstrom. 1959. Bibliography, cartography, discovery, and exploration of The Islas Revillagigedo. *Proc. Calif. Acad. Sci. (4) 29:315–60.*

Richardson, John. 1854. The zoology of the voyage of H. M. S. Herald. Vertebrals, including fossil mammals. *L. Reeve, London 1854.*

Ricker, Karl E. 1959. Mexican shore and pelagic fishes collected . . . during the 1957 cruise of the "Marijean." *Inst. Fish. Univ. British Columbia, Mus. Contr. No. 3:1–18.*

Seemann, Berthold C. 1853. Narrative of the voyage of H. M. S. Herald during the years 1845–51, under the command of Captain Henry Kellett. *Reeve and Co. London 1853, 2 vols.*

Steindachner, Franz. 1876. Ichthyologische Beiträge (III). *Sitz. Akad. Wiss. Wien, 72, Abt. 1:29–96. (reprint pp. 1–68).*

Strasburg, Donald W. 1956. Notes on the blennioid fishes of Hawaii with descriptions of two new species. *Pacific Sci. 10: 241–67.*

Institute of Fisheries, University of British Columbia, Vancouver 8, Canada.

Journal of Geophysical Research Volume 66, No. 1 January 1961
pp.143-155.

The Structure of the Pacific Equatorial Countercurrent[1]

John A. Knauss

Scripps Institution of Oceanography
La Jolla, California

Abstract. The Pacific equatorial countercurrent flows from west to east across the entire Pacific, a few hundred miles north of the equator. The velocity structure of this current in the eastern Pacific has been studied on three cruises during the period 1955–1959; in this paper the results of the work are summarized. (1) The most unusual observation concerns the variation in transport. In August 1958 the transport was in excess of 60 × 10^6m^3/sec. Eleven months later it was nearly zero. (2) Direct current measurements indicate that the current is in approximate geostrophic balance. (3) There is some indication of an Ekman drift current superimposed on the geostrophic current at the surface. (4) There is considerable day-to-day variation in the surface current. The mean speed of the surface current (in the region studied) increases to the east and the rms variation of the surface current increases as the mean speed increases.

Introduction. The Pacific equatorial countercurrent flows from west to east across the entire Pacific, a few hundred miles north of the equator. It is relatively narrow, 300 to 500 kilometers wide, and it separates the broader, westward-flowing north and south equatorial currents. As such, it acts as a boundary between the great current gyres of the North and South Pacific. The countercurrent is part of the wind-driven circulation, and its presence is accounted for in the theories of wind-driven circulation [*Sverdrup*, 1947; *Reid*, 1948; *Munk*, 1950; and others]. On three recent cruises (Eastropic: Oct.-Dec. 1955, Doldrums: Aug.-Sept. 1958, Dorado: July-Aug. 1959) this current has been studied using Swallow current floats, a modified Roberts current meter, free-floating parachute drogues, and the GEK (Geomagnetic Electrokinetograph), as well as the classical technique of calculating the geostrophic currents from standard hydrographic data. This report summarizes these measurements.

It has been known for a great many years [see, for instance, *Puls*, 1895] that the Pacific equatorial countercurrent does not have the same strength at all seasons of the year and at all longitudes. The measurements reported here were all made between 105°W and 120°W and during those seasons when the countercurrent is thought to be well developed. All the instrumentation and techniques used in making these measurements have been described previously (Roberts meter: *Knauss* [1960]; neutral bouyant floats: *Swallow* [1955]; GEK: *Von Arx* [1950], *Longuet-Higgins, Stern and Stommel* [1954], *Knauss and Reid* [1957]; parachute drogues: *Volkmann, Knauss, and Vine* [1956]).

The mean flow of the countercurrent. The water in the region of the countercurrent in the eastern Pacific is characterized by a well-mixed surface layer, 30 to 100 meters thick, below which there is a sharp thermocline in which the temperature drops about 10° in 30 meters. Thus, the water immediately beneath the mixed layer is very stable.

Although the entire equatorial region is characterized by this high-stability layer, there are regional differences in its intensity. Highest values seem to occur in the vicinity of the equatorial countercurrent; hence, there are higher values in the northern hemisphere than in the southern. There are higher values in the eastern Pacific than in the central and western Pacific (Fig. 1). A similar situation occurs in the Atlantic [*Defant*, 1936]. In the Pacific the maximum stability appears to be at the northern edge of the countercurrent, which is also the zone of minimum mixed layer depth.

Measurements made with an 'electronic bathythermograph' attached to the Roberts current meter have shown that the thermocline layer includes a rapid decrease in velocity (Fig. 2); however, the maximum velocity is usually not at the surface but near the middle

---

[1] Contribution from the Scripps Institution of Oceanography, New Series, 1236

Reproduced by Permission

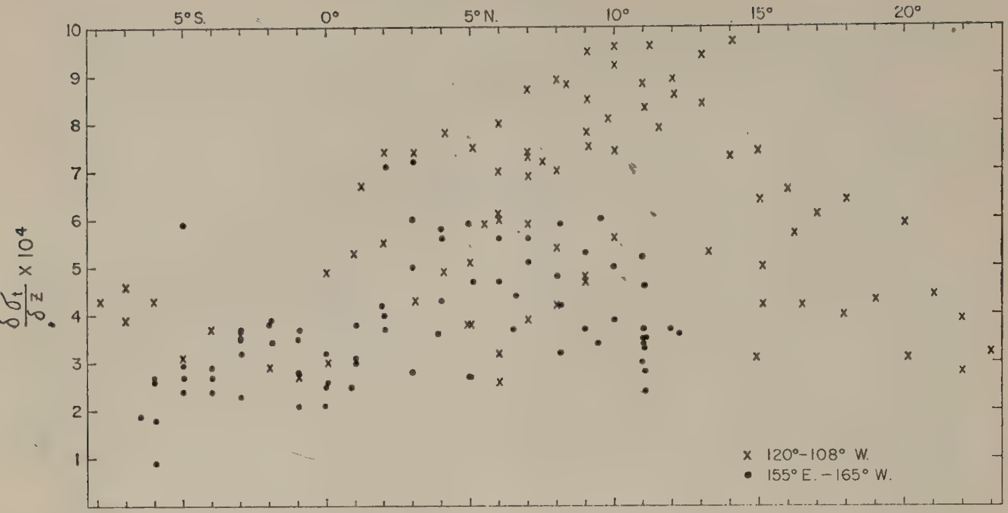

Fig. 1. Density gradient values versus latitude in the eastern tropical Pacific. Values are the average over the first 50 meters below the mixed layer.

of the mixed layer. This feature and the marked velocity shear associated with the thermocline have been known for many years from geostrophic calculations, and they are clearly indicated on the geostrophic velocity profile based on hydrographic observations made near the time of the Roberts meter lowerings (Fig. 3). The fact that the geostrophic currents are less than the velocities based on averaging eleven sets of Roberts meter observations can perhaps be explained by the fact that the geostrophic current is an average for the entire width of the current whereas the Roberts meter measurements were made near the center of the current. However, in another section other data are presented which suggest that in this region of the countercurrent, the geostrophic currents are systematically less than the actual currents.

The velocity shear $(\partial u/\partial z)$ in the countercurrent was 8×10^{-3}/sec, averaged over 50 meters, and is very similar to the value reported by *Montgomery* [1939] in the equatorial countercurrent of the North Atlantic, based on geostrophic calculations. These shears are not as high as those found at the equator in the Cromwell current, where the mean value was 22×10^{-3}/sec for the region above the core and 12×10^{-3}/sec for the zone beneath the core.

A criterion for the maintenance of vertical turbulence is for

$$Ri < A_z/K_z$$

where Ri is the Richardson number and A_z and K_z are the coefficients of vertical eddy diffusivity of momentum and heat, respectively [see, for instance, *Proudman*, 1953, p. 101]. The Richardson number is nondimensional and defined by

$$Ri = g(\partial\rho/\partial z)/\rho(\partial u/\partial z)^2$$

where g is gravity and ρ is density. The data from the Roberts meter lowerings and the hydrographic stations have been used to calculate values of shear, vertical density gradient, and the Richardson number for both the countercurrent and the Cromwell current (Fig. 4, Table 1). The Richardson numbers in the Cromwell current are considerably smaller than those in the countercurrent. The difference is evidence that the ratio A_z/K_z is greater in the countercurrent than in the Cromwell current; and, although the ratio A_z/K_z may be unity in the Cromwell current, it must be greater than 12 in the countercurrent. *Ellison* [1957] suggested that the so-called flux Richardson number $(K_z/A_z)Ri$ is always less than 0.15. If so, the ratio of A_z/K_z is greater than 80 for the countercurrent and greater than 5–10 for the Cromwell current. Regardless of the exact value of the ratio, however, the difference in the distribution of salt, oxygen, and phosphate is strong evidence that the coefficient of vertical eddy diffusion in the Cromwell current is much greater than that in the thermocline of the countercurrent. In the former, salt, oxygen, and phosphate appear to be well mixed throughout the current; in the latter there appears to be little mixing of these properties through the thermocline [*Wooster and Cromwell*, 1958; *Knauss*, 1960].

Short-period changes in the surface velocity. The velocity in the countercurrent is not steady. Successive crossings using the GEK have indicated that the surface current pattern can change markedly over periods of a few days. During one 10-day period the countercurrent appeared to go through two cycles of velocity change (Fig. 5). These variations are believed to be indicative of real changes in the flow and not merely a measure of the displacement of the current. In none of the crossings of the countercurrent has there been any evidence of its having the 'shingled' structure reported for the Gulf Stream [*Fuglister*, 1955].

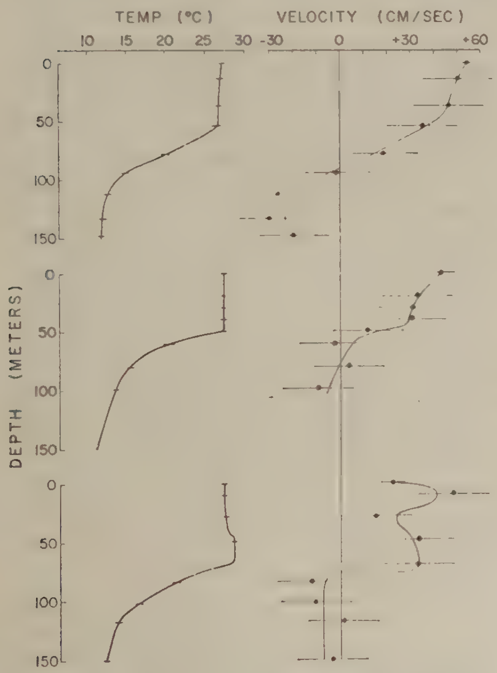

Fig. 2. Comparison of simultaneous velocity and temperature profiles through the countercurrent made by attaching an electronic bathythermograph to the Roberts meter. The BT recorded continuously. The instruments were stopped at different depths (noted by dots on the temperature profile), and current observations were made. The uncertainty of any given current observation (15 cm/sec) is noted. Surface observations were made with drogues and have a smaller uncertainty (5 cm/sec).

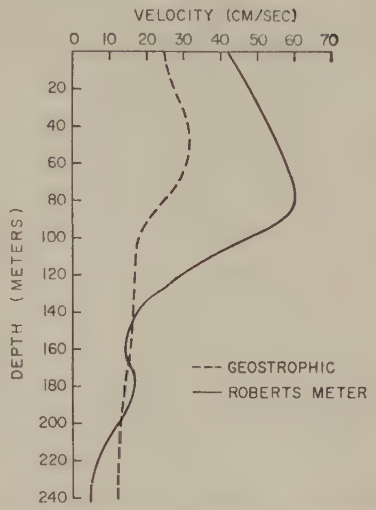

Fig. 3. The mean profile of current versus depth in the countercurrent. This profile is an average of eleven Roberts meter lowerings in the countercurrent at 7°52′N, 107°30′W, during the period August 11–27, 1958.

The Roberts meter data suggest that, at any given time, all the water in the mixed layer is flowing in approximately the same direction; that is, if the surface current is flowing southeast, all the water in the mixed layer is flowing southeast. However, it is emphasized that the

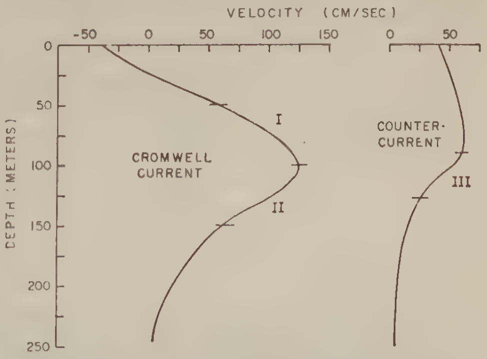

Fig. 4. Schematic current profiles of the Cromwell current and the countercurrent indicating the positions relative to the currents at which the stability data given in Table 1 were calculated.

TABLE 1. Values of Shear, Stability, and Richardson Number for the Cromwell Current (I and II) and the Countercurrent (III)

Current Zone*	$\partial u/\partial z$, sec^{-1}	$1/\rho \times \partial\rho/\partial z$, cm^{-1}	Ri
I	22×10^{-3}	3.5×10^{-7}	0.7
II	12	2.0	1.4
III	8	7.5	12

* Current zones defined in Figure 4.

data support this statement in only a general way. The motion in the mixed layer is turbulent, and the precision of the Roberts meter is limited (the standard error may be as much as 15 cm/sec [*Knauss*, 1960]). The data are not adequate to answer such questions as, is the average direction of the flow of water at all depths the same at any given time, or is there more or less variation from the mean eastward flow as one descends through the mixed layer?

Another way of measuring the irregular motion is to take continuous GEK observations around a drifting drogue. This was done during one brief, 11-hour period in the countercurrent. The mean current as measured by the drift of the drogue was nearly identical with the average of the 31 GEK observations. The rms variation from the mean was 10 cm/sec, 27 per cent of the mean velocity (Fig. 6). The distribution of individual observations suggests that the irregular motion consisted of a clockwise rotation around the mean.

A major portion of one cruise, Doldrums, was devoted to a study of the irregular motion connected with the countercurrent. This was done by stationing ships along the countercurrent and making continuous surface current measurements with the GEK. Measurements were made at seven positions along the eastern end of the countercurrent between 90°W and 109°W (1140) miles. Each station was occupied from 5 to 14 days, during which 300 to 500 surface current observations were made with the GEK. (A square jog pattern was run. Each measurement took 20–40 minutes to complete.) It was hoped that a fairly detailed study of the irregular motion of the surface current, carried out simultaneously at several points along the current, would indicate something about the nature of this variation. Analysis of these data is not complete, but one of the results that has appeared is that the magnitude of the irregular

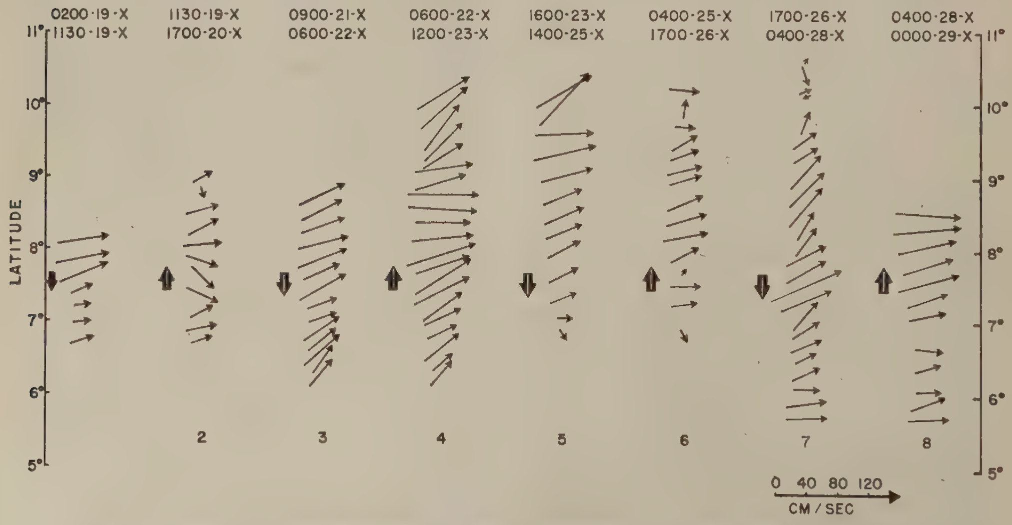

Fig. 5. Surface velocities as recorded by the GEK on successive crossings of the counter-current between 111–115°W during the period October 19–28, 1955. The heavy arrows give the direction the ship was heading on each crossing. The current appeared to be weaker on the second crossing, October 19–20, than on the first, but was strong again two days later on the fourth crossing. It began to diminish and was fairly weak on the sixth crossing, October 25–26, but appeared to be reaching a peak again on the last and foreshortened crossing, October 28.

motion appears to be roughly proportional to the mean speed of the current. The instantaneous velocity at a point **V** can be divided into a mean flow $\bar{\mathbf{V}}$ plus an irregular component **V′**:

$$\mathbf{V} = \bar{\mathbf{V}} + \mathbf{V}'$$

$$\bar{\mathbf{V}} = \frac{1}{T}\int_0^T \mathbf{V}\,dt$$

$$\langle V' \rangle = \overline{[(V')^2]^{1/2}}$$

All the GEK measurements at one location were averaged to get the mean, and a vector subtraction of the mean from the individual observations yields the irregular component **V′**.

The data indicate that both the mean velocity and the turbulent velocity increase toward the east, and that the turbulent velocity component is half to two-thirds of the mean velocity (Table 2). The fact that the mean velocity is increasing downstream does not necessarily imply, however, that the total kinetic energy of the current is increasing downstream. As was previously noted, the speed of the current is rather constant through the mixed layer and drops rapidly through the thermocline (Figs. 2 and 3). The depth of the mixed layer (h) shallows to the east from about 85 meters at 110°W to 15 meters at 90°W, and the product $\rho\bar{V}^2h/2$, which is a fair estimate of the mean kinetic energy in a unit water column, although not constant for the seven stations (Table 2), does not show any tendency to increase downstream.

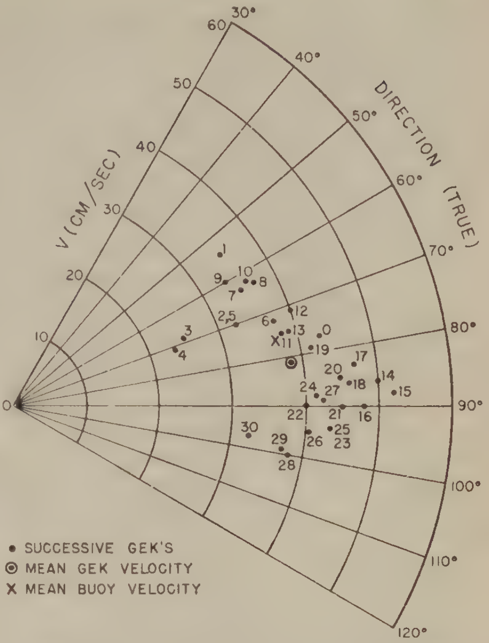

Fig. 6. Comparison of successive surface current observations with a GEK made in the vicinity of a drifting buoy during an 11½-hour period (from star sight to star sight) the evening of October 30–31, 1955. The average velocity of the buoy and the mean of the GEK measurements are also shown.

The GEK does not measure current directly but rather the electrical potential between two electrodes which are towed behind the ship and are in contact with the water. Water velocity is calculated by an application of Faraday's law of electromotive force. The calculation is only approximate, but under most circumstances it gives reasonable results in the open ocean. (For a discussion of the theory of the GEK see *Longuet-Higgins, Stern, and Stommel* [1954]; its use and

TABLE 2. Estimates of Turbulent Velocity along the Countercurrent as Measured by the GEK ($T = \rho V^2/2$)

Ship	Position		Dates of Station	No. of Obs.	$\bar{V}$,		$\langle V' \rangle$, cm/sec	$\langle V' \rangle/V$	h, meters	Th, ergs/cm²
	N	W			cm/sec	dir. toward				
Baird,	7°50′	109°00′	July 19–25	300	39	132	21	0.56	84	$12 \times 10^{+4}$
Horizon	7°52′	107°29′	July 19–25	345	30	120	19	0.63	81	7
Baird	7°40′	106°30′	Aug. 14–24	541	32	090	23	0.73	70	7
Stranger	7°49′	106°30′	July 21–26	283	39	132	23	0.58	72	11
Stranger	7°48′	103°52′	Aug. 15–23	456	50	095	19	0.37	54	13
Horizon	7°40′	92°30′	Aug. 10–22	570	58	107	41	0.69	22	7
Tono	7°40′	90°00′	Aug. 10–24	394	68	071	40	0.59	13	6

applicability at sea are discussed by *von Arx* [1950] and *Knauss and Reid* [1957]).

It is likely that the turbulent component is somewhat less than that given in Table 2. Any random variation in electrode potential, such as might result from magnetic storms, uncompensated polarization of the electrodes, etc., would cause a greater variation from the mean than that generated by changes in the velocity field alone. However, it is difficult to imagine an error term that would be proportional to the velocity, and it seems unlikely that any subsequent correction of the values given in Table 2 could appreciably change the primary result, that the turbulent component increases as the mean velocity increases.

A comparison of velocity measurements and geostrophic calculation. To a first approximation the countercurrent is in geostrophic equilibrium. That is, for the meridional plane all terms in the equation of motion,

$$\frac{\partial v}{\partial t} + u\frac{\partial v}{\partial x} + v\frac{\partial v}{\partial y} + w\frac{\partial v}{\partial z} = -\alpha\frac{\partial p}{\partial y} - uf$$
$$+ \alpha A_V\frac{\partial^2 v}{\partial z^2} + \alpha A_H\left(\frac{\partial^2 v}{\partial x^2} + \frac{\partial^2 v}{\partial y^2}\right)$$

can be neglected except the pressure term and the Coriolis term,

$$-\alpha\frac{\partial p}{\partial y} = uf$$

where u, v, and w are the velocity components in the x (east), y (north), and z (up) direction, A_V and A_H are coefficients of vertical and horizontal eddy viscosity, p is pressure, and $f = 2\omega \sin\varphi$ where ω is the angular velocity of the earth and φ the latitude. Using the geostrophic equation, others have described such features as the

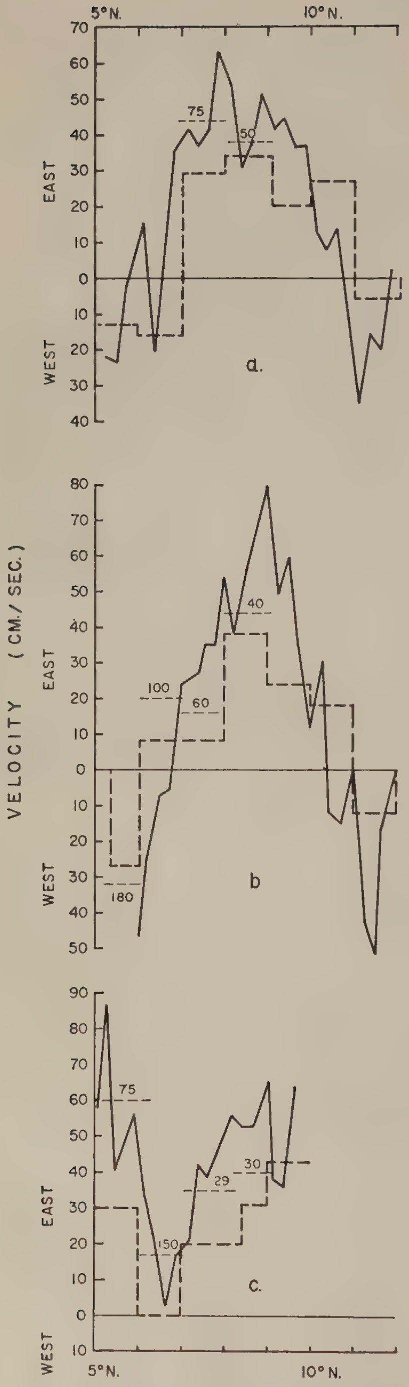

Fig. 7. A comparison of the east-west component of the surface velocity as determined by the GEK with the geostrophic current as determined from hydrographic stations made concurrently. The GEK components are point observations. The geostrophic currents are shown in horizontal lines running between the successive hydrographic stations. If the hydrographic data showed a subsurface current appreciably stronger than the surface current, this current is shown by a dashed line. The depth of this current in meters is noted. Pertinent data concerning these crossings are as follows: (*a*) 120°W, Oct. 8–11, 1955; (*b*) 116°W, Oct. 8–11, 1955; (*c*) 108°W, Aug. 18–20, 1958. Note that crossings (*a*) and (*b*) were made simultaneously.

decrease in velocity in the thermocline and the tendency for the maximum velocity to occur near the middle of the mixed layer (Figs. 2 and 3) [*Sverdrup*, 1932; *Jerlov*, 1956; *Austin, Stroup, and Rinkel*, 1956; and others].

From a comparison of individual sections it would appear that the short-period changes in the surface currents as measured by the GEK are also approximately geostrophic (Fig. 7). There are not enough sections of simultaneous GEK and hydrographic station measurements to be certain that this is so, but the three available sections suggest that this is the case. This agreement is most striking in the 1958 crossing, during which both the GEK measurements and the geostrophic calculations showed a bifurcation in the current. A more elaborate observational program (with continual hydrographic sections and GEK or other direct current measurements) will be required, however, before this point can be determined.

In three sections in Figure 7, the GEK velocity is 20 to 50 per cent greater than the geostrophic velocity. The calculation of surface velocity from the GEK measurement gives a value that is too low, unless a correction is applied. This correction is very small in the countercurrent and is ignored. The GEK velocity should, therefore, be equal to or less than the geostrophic velocity, assuming that all measurements are correct and that the current is entirely geostrophic. Furthermore, the average of the Roberts meter measurements also gives a higher velocity than the geostrophic calculations.

One possible explanation for this difference is that the actual flow in the countercurrent includes an Ekman transport in addition to the geostrophic current. The wind south of 10°N in these longitudes is usually from the south (Beaufort 3 or 4), and, as the following order-of-magnitude calculations indicate, it is possible that the countercurrent flow in the mixed layer is a combination of geostrophic current plus Ekman wind drift.

We add the vertical eddy viscosity term to the geostrophic equation

$$uf = -\alpha \frac{\partial p}{\partial y} + \alpha A_V \frac{\partial^2 v}{\partial z^2}$$

and then integrate from the surface to the bottom of the mixed layer h,

$$\bar{u}f = -\alpha \overline{\frac{\partial p}{\partial y}} + \alpha[(\tau_y)_0 - (\tau_y)_h]/h$$

where $(\tau_y)_0$ is wind stress. If we assume $(\tau_y)_h$ to be zero, then

$$\bar{u}f = -\alpha \overline{\frac{\partial p}{\partial y}} + \frac{\alpha}{h}(\tau_y)_0$$

For the value of $(\tau_y)_0$ of 1 dyne/cm^2 and $h = 50$ meters, the wind stress term is 2×10^{-4} cm/sec^2. The measured horizontal pressure gradient is about -6×10^{-4} cm/sec^2. Therefore, the current necessary to balance the last equation should be, in this case, a third greater than the observed 'geostrophic current.'

Observations of the countercurrent beneath the thermocline. Measurements at depths greater than 300 m were made with Swallow neutral bouyant current floats on two of the cruises (Tables 3 and 4). The picture of the countercurrent below the thermocline depicted by these measurements is not simple. In 1958, all the floats (5) in the region 300–700 m went eastward at speeds of 13–19 cm/sec. The two floats at

TABLE 3. Swallow Current Float Observations during Doldrums Cruise (1958)

Position					Velocity,	
N	W	Date	Depth, meters	Hrs. Tracked	cm/sec	toward
7°52′	107°30′	Aug. 12	375 ± 205	7.6	18.6 ± 1.7	080° ± 5°
		Aug. 14	440 ± 200	4.8	13.2 ± 2.7	116° ± 12°
		Aug. 26	440 ± 170	14.0	16.6 ± 0.9	080° ± 3°
		Aug. 16	595 ± 125	16.0	17.5 ± 0.7	085° ± 2°
		Aug. 15	685 ± 190	11.0	19.3 ± 1.1	100° ± 3°
		Aug. 18	1000 ± 220	7.3	9.0 ± 1.7	129° ± 10°
		Aug. 17	1570 ± 215	15.0	6.5 ± 1.0	088° ± 8°

TABLE 4. Swallow Current Float Observations during Dorado Cruise (1959)

Position		Date	Depth, meters	Hrs. Tracked	Velocity,	
N	W				cm/sec	toward
15°08′	120°02′	July 12	720 ± 270	57	2.5 ± 0.2	183° ± 6°
		July 13	2140 ± 440	38	1.2 ± 0.3	150° ± 17°
14°54′	120°00′	Aug. 13	620 ± 130	37	<3.0	...
		Aug. 14	1030 ± 90	21	<3.0	...
11°32′	119°56′	Aug. 10	610 ± 120	24	7.2 ± 0.5	283° ± 5°
		Aug. 10	1130 ± 190	19	6.7 ± 0.7	284° ± 6°
		Aug. 11	1560 ± 210	25	2.6 ± 0.5	238° ± 12°
10°00′	120°00′	Aug. 6	720 ± 190	20	6.8 ± 0.6	102° ± 6°
		Aug. 5	740 ± 170	7	4.8 ± 1.8	123° ± 24°
		Aug. 6	830 ± 150	35	5.9 ± 0.4	090° ± 4°
9°02′	120°01′	July 17	3130 ± 540	19	4.6 ± 0.7	340° ± 10°
8°58′	120°06′	Aug. 4	205 ± 120	6.5	13.0 ± 1.9	070° ± 11°
		Aug. 4	410 ± 180	18	4.4 ± 0.7	090° ± 10°
		Aug. 3	1600 ± 330	22	5.2 ± 0.6	132° ± 7°
8°29′	120°09′	July 29	630 ± 50	5.3	4.4 ± 2.3	272° ± 34°
7°30′	120°00′	July 23	640 ± 60	7.4	6.5 ± 1.7	295° ± 16°
		July 20	500 ± 230	40	6.6 ± 0.3	270° ± 3°
		July 20	820 ± 190	8.5	17.0 ± 1.5	273° ± 6°
		July 20	1170 ± 310	49	4.3 ± 0.3	300° ± 4°
		July 21	1720 ± 300	31	4.7 ± 0.4	004° ± 5°
		July 21	2730 ± 440	21	5.6 ± 0.6	030° ± 7°
5°32′	120°05′	July 25	530 ± 140	28	7.0 ± 0.4	285° ± 4°
		July 27	810 ± 220	19	3.4 ± 0.7	314° ± 12°
		July 26	1070 ± 270	43	5.3 ± 0.3	268° ± 3°
		July 26	1130 ± 600	5.2	9.8 ± 2.4	302° ± 16°
5°31′	120°04′	July 24	550 ± 220	18	3.1 ± 0.7	285° ± 14°

depths of 1000 m and 1500 m went generally eastward at speeds of 5–10 cm/sec (Table 3). As reported by *Knauss and Pepin* [1959], there appeared to be as much eastward transport below the thermocline as above. They speculated that if the width of this subthermocline countercurrent were as great as the surface countercurrent, the estimated transport of the Pacific equatorial countercurrent would have to be revised upwards from 30 × 10⁶ to 60 × 10⁶ m³/sec.

These measurements were made, however, at only one point in the countercurrent. The Dorado Cruise of July-August 1959 was designed to get a realistic estimate of the transport in the countercurrent. A series of buoys were anchored in the countercurrent and on either side of it, along 120°W; and some 26 neutral buoyant floats were tracked successfully at depths between 300 and 3000 meters (Table 4). Any time a float went more than 5 cm/sec in the areas north or south of the countercurrent, it went to the west, as might be expected, since the surface water on either side of the countercurrent flows westward. The measurements in the countercurrent itself show a markedly different regime from that found the previous year. Only the floats in the northern half of the countercurrent below 300 m (8°58′N and 10°00′N) showed an eastward movement, and these currents were not 15 cm/sec, as was found the previous year, but 4–7 cm/sec (except float VIII-D, which was almost in the thermocline). The floats in the southern half of the countercurrent below 300 m went west. The large eastward transport below the thermocline of the previous year was completely missing.

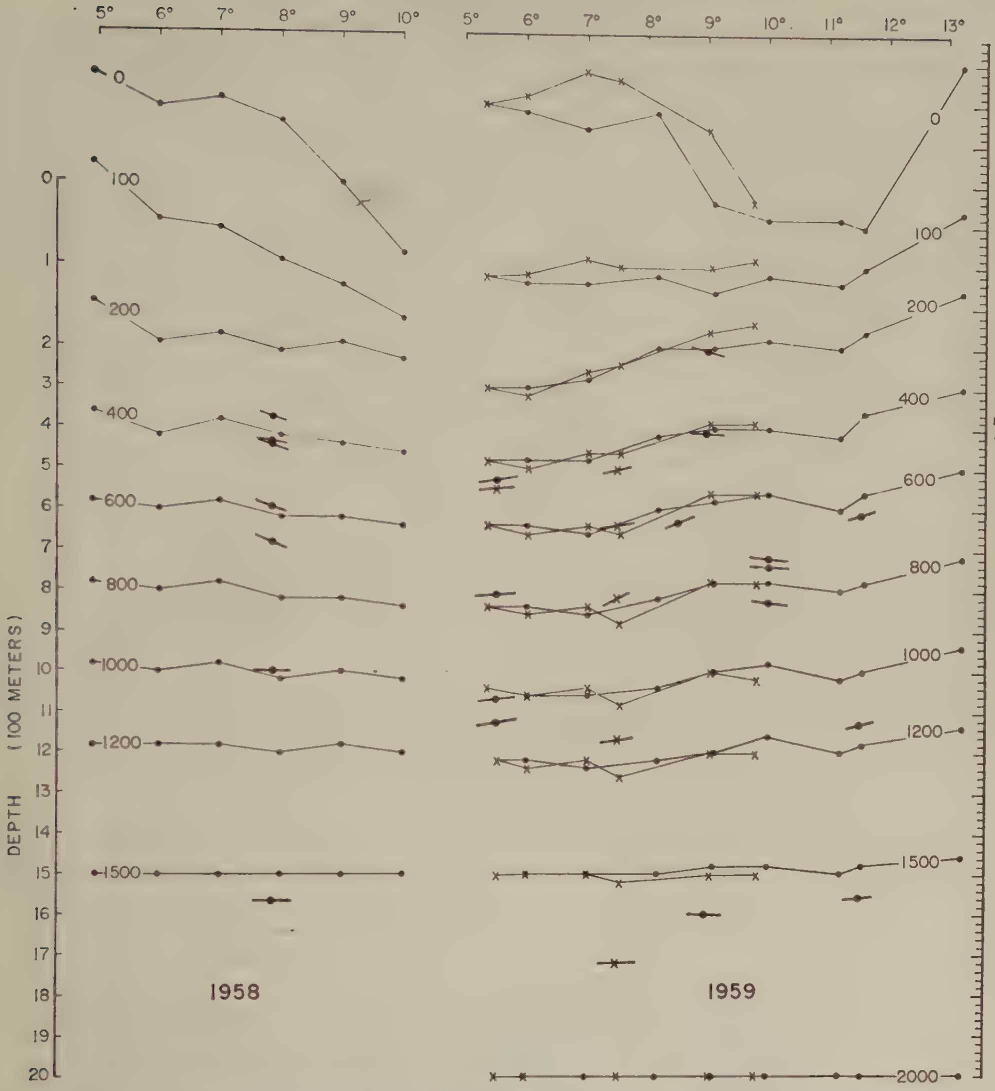

Fig. 8. A comparison of geostrophic currents with the current observations made with Swallow floats (see text for procedure used.) In 1959, when stations were occupied on both the outgoing and return sections, the differences are noted. Lines connect stations in chronological order.

Apparently the currents in the region below the thermocline are also in approximate geostrophic balance, although the horizontal pressure gradients in this region are so weak that it is difficult to measure them with sufficient accuracy. Since the primary data for this comparison are velocity measurements from Swallow floats and pressure gradients from hydrographic stations, the observations have been plotted in two ways for easier comparison. In Figure 8 the Swallow float data have been transformed into pressure gradients; in Figure 9 the mean pressure gradients have been translated into current profiles.

For geostrophic measurements, the comparison of horizontal pressure gradients is simply a plot of dynamic height (relative to 1500 m in 1958 and 2000 m in 1959) at selected depths for all the hydrographic stations occupied (Fig. 8).

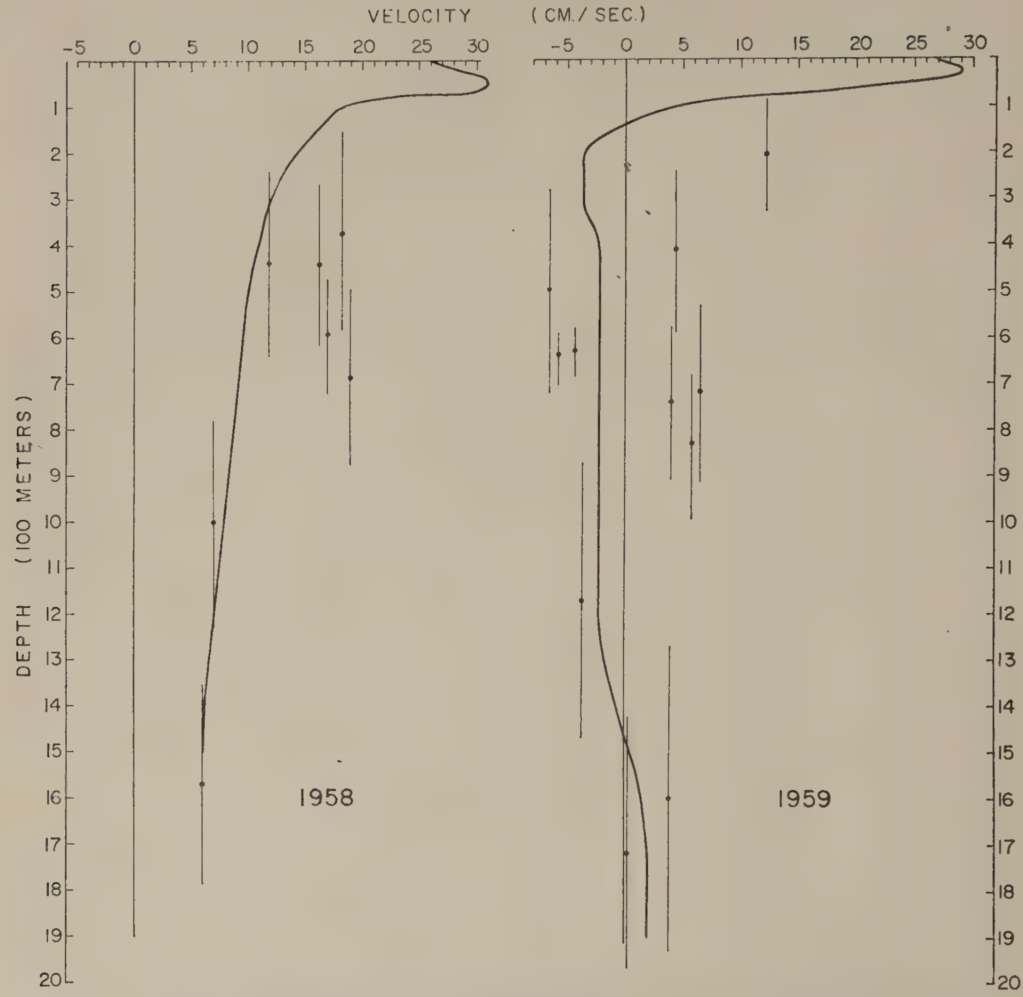

Fig. 9. Velocity profiles used in the transport calculations. In both cases the hydrographic stations used were those which seemed to define the north and south edges of the countercurrent. In 1958 these stations were at 10°N and 4°55′N, and in 1959 they were at 10°N and 7°N. The zonal component of velocity measurements made with Swallow current floats are shown as dots. The uncertainty in the depth of the floats is indicated by the vertical lines. With respect to the 1959 data (Table 4), only those observations made between 7–10°N are plotted.

To compare these gradients with the Swallow float measurements, the zonal components were calculated for the velocities listed in Tables 3 and 4. These values were graphed in order to estimate the current speed at the reference level. The value adopted for the 1958 observations was 6 cm/sec to the east at 1500 m. The 1959 data include more observations and at different locations and the defining of the velocity at the reference level of 2000 m is not obvious. The following were adopted: 1 cm/sec south of 8.5°, 3 cm/sec between 9° and 10.5°, 0 north of 11°. All speeds are eastward components. The appropriate reference velocities were subtracted from the zonal components. The resulting speed was transformed into a pressure gradient by the geostrophic equation.

The greatest difficulty in the measurement of weak horizontal pressure gradients is that there is a variation in density as a function of depth at a given place over periods of a few hours to a few days caused by small-scale changes in the current structure, by internal waves, or by other effects. Changes of 1 to 2 dynamic centimeters at the same location on successive days are the rule rather than the exception. In particular, there is a scatter of points in the plot of dynamic height anomaly versus latitude for the 1959 section, for which measurements were made on the run south as well as on the return run north (Fig. 8). However, the scatter is not so great that one cannot clearly see the reversal in pressure gradient at depth in the 1959 data and the absence of such a reversal in the 1958 data. Furthermore, the required pressure gradients for the velocities observed with the Swallow floats (assuming that these currents were in geostrophic equilibrium) are not very different from the observed pressure gradients (Figs. 8 and 9).

The fact that the flow beneath the thermocline is in approximate geostrophic balance is perhaps not surprising. For a velocity of 5 cm/sec, the Coriolis term at 8°N is 1×10^{-4} cm/sec^2. Geostrophic balance was approximately achieved near the equator in the Cromwell current when both the pressure gradient term and the Coriolis term had values of $1\text{–}2 \times 10^{-4}$ cm/sec^2 [*Knauss*, 1960]. Because the velocities and shears were so much greater in the Cromwell current, it might be expected that the inertial and frictional terms would be correspondingly greater in the Cromwell current than in the deep countercurrent. Therefore, if geostrophic balance is achieved in the former, it is most likely to be found in the latter also.

There are now two examples of geostrophic balance in which the pressure force terms are of the order of $1\text{–}2 \times 10^{-4}$ dynes/gram. One is for a high-velocity, high-shear current (the Cromwell current); the other is for a low-velocity current (the deep countercurrent). Since there appears to be a first-order balance between the pressure and Coriolis terms in these two dissimilar cases, and since there is no reason to believe that these examples represent atypical oceanic situations, it seems likely that for open ocean conditions (and below the immediate surface layer), the frictional terms in the cross-current component of the equation of motion can be expected to be less than 10^{-4} dynes/gram.

Since there is good agreement between the observed and the geostrophic currents, it would seem reasonable to believe that calculation of geostrophic transports for the 1958 and 1959 sections would prove meaningful. The difficulty, of course, is that the transport calculation is very sensitive to the choice of the 'layer of no motion.' A small change in these 'reference velocities' creates a large change in the east-west transport. Geostrophic velocities were calculated with reference to the deepest level at which bottles were placed, and the calculated velocity curve was made to fit the current measurements made with the Swallow floats. An eastward current of 6 cm/sec at 1500 m was used for the 1958 profile and an eastward current of 2 cm/sec at 2000 m was used for the 1959 profile (Fig. 9). Transport T is found by

$$T = L \int_0^z u \, dz ,$$

where L is the distance between the hydrographic stations used in calculating u. In 1959, the net transport was nearly zero ($T = 7.4 \times 10^6$ m^3/sec to the east above 125 m and $T = 9.6 \times 10^6$ m^3/sec to the west between 125 and 1500 m). In 1958, the transport above 1500 m was 88×10^6 m^3/sec. As an indication of how sensitive such transport values are to the choice of reference velocity, $T = 63 \times 10^6$ m^3/sec and 38×10^6 m^3/sec, if the velocity at 1500 m is assumed to be 3 cm/sec and 0, respectively. Although the exact numbers are certainly questionable, the basic conclusion is not. In August 1958, the transport above 1500 m was very high, probably more than 60×10^6 m^3/sec. Eleven months later, in July 1959, the small eastward transport above 125 m was balanced by the westward flow below, and as a result there was little, if any, net eastward transport above 1500 m.

Of the various results reported in this paper, the significance of these transport calculations is probably the most interesting. The countercurrent has usually been thought of as a shallow current confined to the zone above the thermocline. It may be that the circulation between 150 and 1500 m in this region is not part of the wind-driven circulation and moves independently of it. If this is the case, these results suggest that at times there are transports in the 'intermediate water' of the equatorial Pacific which are of the same magnitude as that found in the wind-driven circulation. However, there is nothing in the theories of *Montgomery and*

Palmén [1940], *Sverdrup* [1947], or *Munk* [1950] that limit the countercurrent to the surface layer. Large fluctuations in the Florida current continue to be reported [*Wertheim*, 1954; *Stommel*, 1957, 1959]. Such large changes in transport may be the rule rather than the exception in the wind-driven circulation. If so, an understanding of these variations is one of the most challenging problems in oceanography today.

Summary. 1. Measurements made with an 'electronic bathythermograph' attached to the Roberts current meter showed that the current speed dropped very rapidly through the thermocline. The speed in the mixed layer was fairly constant, with the maximum occurring somewhat below the surface. These observations are consistent with geostrophic calculations.

2. Calculations of current shear from observations with the Roberts meter, as lowered through the thermocline, were compared with previous observations in the Cromwell current. The shear in the countercurrent (8×10^{-3}/sec) is about half that of the Cromwell current. The Richardson number for the countercurrent is 12, as compared with less than 1 for the Cromwell current.

3. The surface velocity of the countercurrent can vary markedly from day to day. Averaging several hundred continuous GEK observations at each of seven stations along the countercurrent showed that the turbulent component of the current is proportional to the mean current; that is, as the mean velocity increases, the turbulent velocity increases also. This turbulent component may be as much as half to two-thirds of that of the mean current.

4. In general, the velocity of the countercurrent as measured by the GEK is greater than the geostrophic velocity. The winds in this region are usually from the south, and it is suggested that there is an 'Ekman current' superimposed upon the geostrophic current.

5. There were marked differences in the flow below the thermocline (300–1500 m) during the summer of 1958 and 1959, as measured by Swallow current floats. In both years this deep flow appeared to be in approximate geostrophic balance, even though the forces involved were often no more than $1\text{–}2 \times 10^{-4}$ dynes/gram. Transport calculations over 1500 meters were made for these two years. The transport in 1958 was in excess of 60×10^6 m³/sec. In 1959 the transport was about 1×10^6 m³/sec.

Acknowledgments. This work was supported by the Office of Naval Research and the National Science Foundation. Some of it was carried out as part of the United States oceanographic program of the IGY and IGC.

REFERENCES

Austin, T. S., E. D. Stroup, and M. O. Rinkel, Variation in the equatorial counter-current in the central Pacific. *Trans. Am. Geophys. Union, 37*, 558–564, 1956.

Defant, A., Die Troposphäre, Deutsche Atlantische Exped., *Meteor*, 1925–27, Wiss. Erg. Bd. VI, Teil 1, 289–411, 1936.

Ellison, T. H., Turbulent transport of heat and momentum from an infinite rough plane, *J. Fluid Mech., 2*, 456–466, 1957.

Fuglister, F. C., Alternative analysis of current surveys, *Deep-Sea Research, 2*, 213–229, 1955.

Jerlov, N. G., The equatorial currents in the Pacific Ocean, *Repts. of the Swedish Deep-Sea Expedition 1947–1948, vol. III, Physics and Chem. No. 6*, Göteborg, 129–154, 1956.

Knauss, J. A., Measurements of the Cromwell Current, *Deep-Sea Research, 6*, 265–286, 1960.

Knauss, J. A., and R. Pepin, Measurements of the Pacific equatorial countercurrent. *Nature, 183*, 380, 1959.

Knauss, J. A., and J. L. Reid, The effect of cable design on the accuracy of the GEK, *Trans. Am. Geophys. Union, 38*, 320–325, 1957.

Longuet-Higgins, M. S., M. E. Stern, and H. Stommel, The electrical field induced by ocean currents and waves with applications to the method of towed electrodes, *Papers Phys. Oceanog. Meteorol., Mass. Inst. Technol. and Woods Hole Oceanog. Inst., 13* (1), 37 pp., 1954.

Montgomery, R. B., Ein Versuch, den vertikalen und seitlichen Austausch in der Tiefe der Sprungschicht im äquatorialen Atlantischen Ozean zu bestimmen, *Ann. Hydrog. Marit. Meteorol., 67*, 242–246, 1939.

Montgomery, R. B., and E. Palmén, Contribution to the question of the Equatorial Countercurrent. *J. Marine Research, Sears Foundation, 2*, 112–133, 1940.

Munk, W. H., On the wind-driven ocean circulation, *J. Meteorol., 7*, 79–93, 1950.

Proudman, J., *Dynamical Oceanography*, John Wiley & Sons, New York, 409 pp., 1953.

Puls, C., Oberflächentemperaturen und strömungsverhältnisse des Aequatorialgürtels des Stillen Ozeans, doctoral dissertation, Universität Marburg, 38 pp., 1895.

Reid, R. O., The equatorial currents of the eastern Pacific as maintained by the stress of the wind. *J. Marine Research, Sears Foundation, 7*, 6–14, 1948.

Stommel, H., Florida Straits transport, 1952–1956, *Bull. Marine Science of the Gulf and Caribbean, 7*, 252–254, 1957.

Stommel, H., Florida Straits transport, June 1956–

July 1958, *Bull. Marine Sci. of the Gulf and Caribbean, 9*, 222–223, 1959.

Sverdrup, H. V., Arbeider i luft-og havforskning, *Beretninger fra Chr. Michelsens Inst. Videnskap og Andsfrihet, 2*, 1–20, 1932.

Sverdrup, H. V., Wind-driven currents in a baroclinic ocean; with application to the equatorial currents of the eastern Pacific, *Proc. Natl. Acad. Sci. U. S., 33*, 318–326, 1947.

Swallow, J. C., A neutral-buoyancy float for measuring deep currents, *Deep-Sea Research, 3*, 74–81, 1955.

Taylor, G. I., Internal waves and turbulence in a fluid of variable density, *Conseil Perm. Intern. p. l'Explor. de la Mer., Rappt. et Proc. Verb, 76*, 35–43, 1931.

Volkmann, G., J. Knauss, and A. Vine, The use of parachute drogues in the measurement of subsurface ocean currents, *Trans. Am. Geophys. Union, 37*, 573–577, 1956.

Von Arx, W. S., An electromagnetic method for measuring the velocities of ocean currents from a ship underway. *Papers in Phys. Oceanog. and Meteorol., Mass. Inst. Technol. and Woods Hole Oceanog. Inst., 11* (3), 62 pp., 1950.

Wertheim, G. K., Studies of the electrical potential between Key West, Florida, and Havana, Cuba. *Trans. Am. Geophys. Union, 35*, 872–882, 1954.

Wooster, W. S., and T. Cromwell, An oceanographic description of the eastern tropical Pacific, *Bull. Scripps Inst. Oceanog. Univ. Calif., 7*, 169–281, 1958.

(Manuscript received August 22, 1960.)

Reprinted from THE POLAR RECORD, Volume 10, Number 67, January 1961
pp. 353-358.

DIVING IN ANTARCTIC WATERS

BY M. NEUSHUL*

[MS. received 22 July 1960.]

CONTENTS

Introduction . . . . page 353
Areas visited 354
Diving equipment and techniques . . . . page 354
Collections and observations . 357

Introduction

The traditional methods of studying the marine biology of any coastline almost always involve the collection of plants and animals when the shore is exposed by the fluctuation of the tides. In the Antarctic, however, intertidal collecting is generally impossible due to the continuous abrasive action of floating ice, which scours this zone clean. Further difficulties are encountered in areas where fast ice extends out directly into the water, leaving no intertidal zone exposed. Thus our knowledge of the marine plants and animals of the Antarctic has been obtained largely through the use of the dredge. Skottsberg,[1] in 1906, provided the first indication that there was, below the action of the ice, a rich growth of large marine algae. Unfortunately the bulk of his collections were lost when the *Antarctic*, the ship of the ill-fated Swedish Antarctic Expedition, 1901–03, was crushed and sunk by pack ice.

This is an account of an attempt to find out if it was feasible to use diving equipment for making repeated dives in Antarctic regions in order to study the ecology and species composition of this reputedly rich area; also to find out if a selective collection of the little-known plants and animals characteristic of the Antarctic sublittoral could be made by hand.

These studies were aided by a contract between the United States Office of Naval Research and the Scripps Institution of Oceanography of the University of California. The trip was made possible by the generous invitation of the Argentine Navy, whose facilities and ships were used during the course of these investigations. Close co-operation, equipment and assistance was provided at all times.

The companionship of Lieutenant R. O. Dains, U.S.N. and Teniente de Corbeta Juan Carlos Carosella during the diving activities and during the strenuous and often unpleasant overland trips to diving localities was greatly appreciated. One cannot emphasize too greatly the necessity for complete confidence in one's diving companions under the unusual diving conditions to be met in Antarctic waters.

---

* Department of Botany, University of Washington.

Contributions from the Scripps Institution of Oceanography, New Series, 1237
Reproduced by Permission

Areas visited

Sailing from Ushuaia, Tierra del Fuego, on the Argentine icebreaker, *General San Martin*, on 1 January 1958, we crossed Drake Passage in good conditions and were left at "Teniente Camara", on Half Moon Island in the South Shetland Islands. It was here that a large part of the test diving was done. During the first few days we were confined to the huts by strong winds and snow that made diving both out of the question and hideous in prospect. With more pleasant weather we began to test various combinations and types of equipment. After the initial testing period lasting about one week, we began overland trips to various parts of the island where dives were made from the shore. During the latter part of January we were taken on the *Chiriguano* to temporary Argentine summer stations on King George Island. Dives were made also at Harmony Cove and Deception Island. On 4 February we boarded the *Bahia Aguierre* and visited Hope Bay, the Melchior Islands and the continental base "Almirante Brown" at Paradise Harbour. Dives were made in all of these localities.

During a total of 71 days spent in the Antarctic, thirty-three dives were made in water ranging in temperature from 1° C. (34° F.) to as low as −1·5° C. (29·5° F.). Although repeated short dives were made, the longest continuous period spent in the water was slightly over one hour. Dives were made to depths down to 20 m.

Diving equipment and techniques

The diving equipment included both "dry"- and "wet"-type exposure suits with full hood protection, gloves, mittens, boots, face plates, different types of fins, depth gauges and other standard diving equipment. In addition a small portable air compressor, compressed air tanks, and demand type regulators were taken. The Argentine Navy supplied heavy-duty constant-volume diving suits, compressed air tanks, and self-contained oxygen rebreathing units.

The short working time made it necessary to find the most efficient combination of equipment as quickly as possible so that observations and collections could be made. Thus certain articles of equipment were discarded after limited use, and no concerted efforts were made to assess the relative merits and demerits of each individual article of equipment thoroughly. Some, such as face plates and fins, depend upon the individual who is diving.

Protective clothing. Two types of "dry" suits were used, a regulation United States Navy "dry" suit with seals at waist, neck and wrists, and the Cousteau "Constant Volume" suit with seals at the neck and wrists. The United States Navy suit and undergarment combination is the same as that described and illustrated by Fain.[2] The Cousteau "Constant Volume" suit used is of heavier rubber. Both "dry" suits suffered from similar disadvantages, they were cumbersome to put on, and if a leak occurred in the water, it was difficult for the diver to re-adjust the suit himself. With both the "dry" suits, punctures and cuts on ice and stones were experienced during the course of working

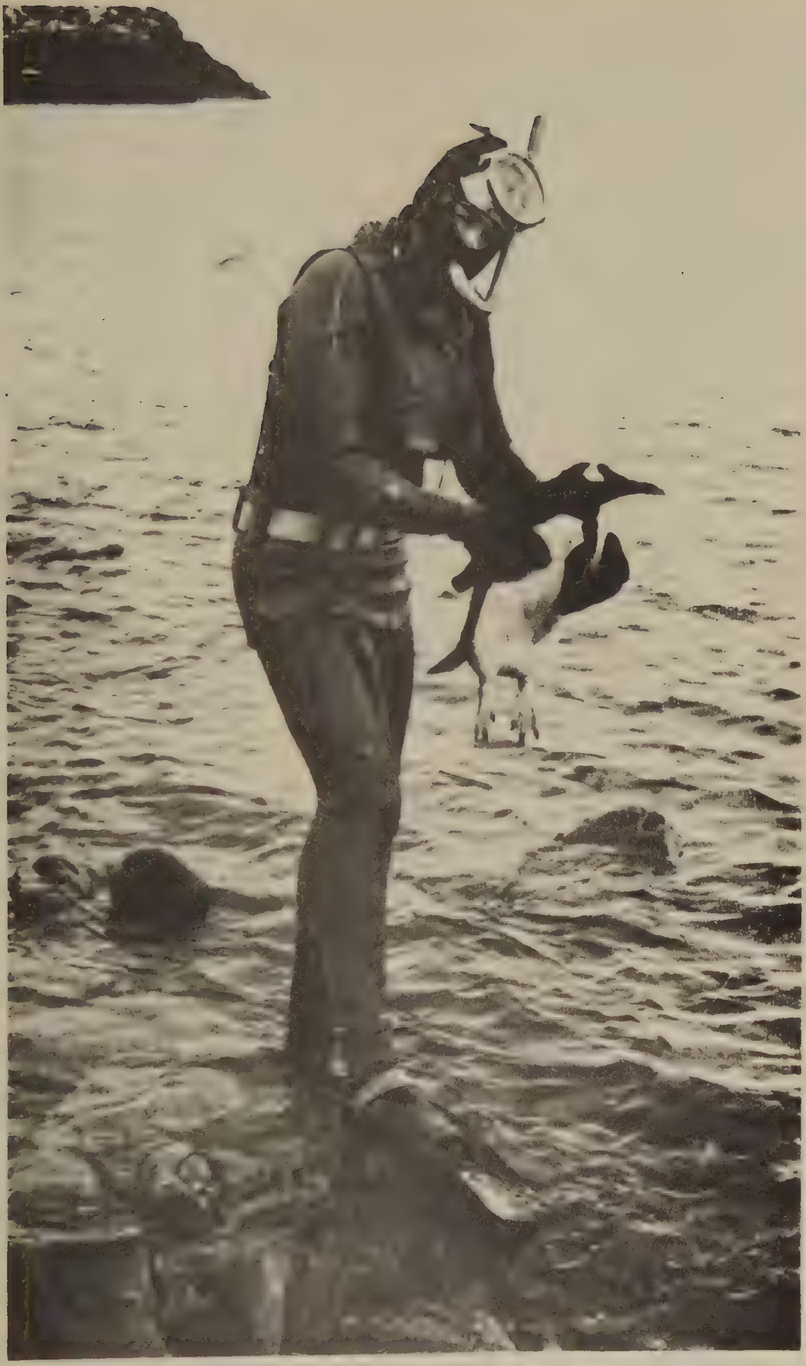

Foam neoprene "wet" suit and diving apparatus used in Antarctic waters

Photograph by M. Neushul

(*Facing p.* 354)

dives. The "dry" suits also somewhat restricted the swimmer's arms and legs while in the water, slowing his speed; as activity generates warmth, this feature is important. For long periods in the water, however, where one is not able to swim vigorously, the "dry" suit with several layers of insulating underwear is superior to the "wet" suit.

Two types of foam-neoprene "wet" suits were used with great success, and ultimately all of the diving was done with this type. Both strip reinforced and non-reinforced suits were tried, of different thicknesses of neoprene ($\frac{3}{8}$ in. and $\frac{5}{16}$ in.); both provided protection, the thicker being the more comfortable. The suits were individually tailored, as the fit under these conditions was found to be very important. Short trousers were inferior to long ones that came high around the chest. Reinforced knee pads protected the suit against cuts from ice. Reinforcing under the arms was useful as one tends to use the arms a great deal in cold water, especially when free-diving from the surface. It was found that one could stay longer in the water if one swam continuously, possibly due to the generation of heat by such activity. Any leak in the suits results in immediate termination of a dive; the rapid entry of water into the suit being an extremely uncomfortable, if not painful, experience.

The "wet" suit had the advantage that it could be worn with relative comfort while travelling over-land to the diving location, or for long periods in a small boat. This type of diving suit can also be worn comfortably under other clothing such as a parka. "Wet" suits were worn for as long as six hours on several occasions.

The biggest problem with both the "dry" and "wet" type of protective clothing is keeping the head, hands and feet warm, so considerable attention was given to the choice of gloves, mittens, hoods, face-plates, boots and fins. The exposure of any part of the body to direct contact with the water must be avoided. Water entering a wet suit is initially cold, but is soon warmed by the body; as long as it does not circulate within the suit, allowing more water to enter, the diver is perfectly comfortable.

In order to remain submerged, full covering of the face is necessary. When a full face-plate is used with the breathing apparatus, the normal types of open face hood can be used. However, if the ordinary face-plate is used, an extension of the hood to cover the lower face is needed. (See photograph on p. 354, where the face-plate is shown pulled out of position.) A small hole in the hood over the mouth can be stretched and the snorkel, or demand valve mouthpiece, inserted. The face-plate fits against the skin and the hood fits over it. Either saliva or a small amount of water inside the face-plate was found to be adequate to prevent fogging. The full face hood was used, and worked well even when it was worn over the open-faced dry suit hood.

Protection for the hands used with the "dry" suits was provided either by rubber gloves with suitable woollen gloves underneath, or by mittens, made from foam neoprene, that could be used with either type of suit. The "wet" suit mittens were best when there was ample room inside them, any tightness that impeded circulation, even slightly, was found to be uncomfortable.

With both mittens and boots of the "wet" suit a long cuff was found to be desirable, as this prevented water circulation and heat loss. The long overlap of the leg or sleeve is far better than a tight encircling of the wrist or ankle.

The feet were very difficult to keep warm, mainly because the swimming fins were worn outside the "dry" or "wet" suit boots. To secure the fins, a certain degree of tightness is necessary; thus, even though the boot is loose, some constriction can be expected from the fin straps. The most comfortable boot and fin combination is shown in the photograph where the fin is "shoe-like" and its position on the foot is governed by uniform pressure around the foot, rather than a tight strap around the heel, or a tight fit around the ball of the foot.

Breathing apparatus. The underwater breathing apparatus employed was of two kinds: the usual compressed air tanks with air demand valves, and the Pirelli self-contained closed circuit type. No difficulties were encountered with either. As oxygen is a usual medical supply, it was easy to re-charge the oxygen cylinders of the closed-circuit apparatus.

Scientific apparatus. Among the scientific and other diving equipment used were depth gauges, compasses, an underwater movie camera, light meter, and a galvanometer and barrier-type photronic cell used for measuring the penetration of light into water. Also used regularly were more usual types of apparatus such as matt-surface plastic for underwater writing, collecting knives and bags. All of these things worked well under Antarctic conditions and no difficulties were noted that would not have occurred in warmer waters.

Safety precautions. Preoccupation with one's physical safety during any diving activities is a serious limiting factor in the amount of work that can be accomplished. Experience with the equipment to be used and familiarity with the techniques of systematic observation and collection are even more important under the unusual conditions present in the Antarctic. All diving was done in pairs, one diver carrying out the necessary work while the other stayed very near him, according to a pre-arranged plan. A deflated life jacket was worn with all combinations of diving equipment; it could be inflated by pulling a cord which opened a small carbon dioxide cylinder. In all of the dives made from the shore, an observer was posted with a shrill warning whistle in case Leopard Seals, or other large marine mammals, were seen. Only on two occasions was it necessary to leave the water for this reason. When dives were made from small boats, observers watched the surface bubbles closely.

No dives were made under solid ice, but on several occasions they were made in brash, or loose growlers, and around stranded icebergs. When diving around ice, it is necessary to exercise great care, since protective clothing can be damaged by the sharp edges of freshly broken pieces. The presence of ice on the surface may hamper swimming and can knock off a face-plate or catch on projecting equipment. Larger pieces, moving in the surge near shore, can severely bruise a swimmer, particularly when he is entering or leaving the water. Entering or leaving the water from the shore is much less hazardous if the swimmer refrains from walking on the bottom and keeps on top of the ice as much as possible. Some types of ice are more dangerous than others; of these, clear "growler" ice seemed to be the sharpest when broken by surf action. If it was necessary to mount larger pieces of ice in order to reach shore, it was found advisable to keep off the hands and knees as much as possible and to find smooth hand-holds with which to pull oneself over the ice on one's stomach. In order to prevent them catching on the ice, the weights on the belt were kept at the side of the body, and the knife in the small of the back.

Collections and observations

The foam neoprene "wet" suit and snorkel was used for a great deal of the collecting and plants and animals were collected to a depth of 30 ft. in this way. Freedom from encumbrance made it possible to swim along the shore examining the bottom for favourable collecting areas, or unusual associations of organisms.

Collecting animals and plants underwater presented no special problems. The mittens used made it rather difficult to pick up small plants or animals, however, with the aid of a short knife, most small specimens could be dislodged and scooped into a small collecting bag. In deeper water, surface ice limited visibility and hampered collecting; in such cases, rocks were brought back to the surface and examined for smaller plants and animals. The extreme clarity of the water generally made collections and observations both pleasurable and easy. In some areas, near large active glaciers, more opaque waters were noted.

Observations of ice action on the sea floor, and its influence on the plants and animals, were made. Larger icebergs had the greatest effect on the sea floor where it was composed of mobile material; they were observed gouging hollows or trenches of considerable size.

Antarctic marine algal growth is rich. At depths in these waters below the influence of ice action, and within the range of light penetration, marine algae flourish and apparently do not have to contend with the low salinity which is said to deter algal growth on certain Arctic coasts.[5]

The use of the dredge by Skottsberg[1,3] and Gain[4] provided the first indication of the abundance of marine animals and plants bordering the Antarctic. However, the nature of the bottom in many areas was such that the dredge merely skipped over the surface of the rocks or became caught between them. Skottsberg[3] stated that the only reliable way of obtaining an accurate idea of the plants and animals growing in Antarctic waters is through the use of a bathysphere or by diving. This certainly seems to be true, for many plants were found growing only in areas not accessible to the dredge. The large size of some of the plants[6] also makes dredging difficult.

Incidental observations were made on the diving habits of penguins and the activities of fish and invertebrate animals. Molluscs such as the limpet, *Nacella polaris*, were ubiquitous and easily collected. Chitons were also found on the sides and beneath rocks. Fish, mostly *Notothenia corriceps*, were few but easily collected since they moved away only when touched or otherwise disturbed. Even though these animals live under conditions of constant low temperatures, no sluggishness was noted in their activities. Penguins in the water were inquisitive, and in one case came near enough to be seen underwater. The extreme speed and manœuvrability of these birds underwater is striking when compared with their activities on land.

The observations and collections made during the course of the diving activities were of a preliminary and exploratory nature. It is hoped that, with the study of the specimens and data obtained, a more complete account can be given of the abundant life found in the Antarctic sublittoral, and that the experience gained will be valuable for future studies of marine biology.

References

[1] C. Skottsberg. Observations on the vegetation of the Antarctic sea. *Botaniska studier tillägnade F.R. Kjellman*, Uppsala, 1906, p. 254–64.

[2] F. D. Fane. Skin diving in polar waters. *Polar Record*, Vol. 9, No. 62, 1959, p. 433–35.

[3] C. Skottsberg. Communities of marine algae in Sub-antarctic and Antarctic waters. *Kungliga Svenska Vetenskapscrokademiens Handlingar*, Series 3, Vol. 19, No. 4, 1941, p. 1–92.

[4] L. Gain. *La Flora algologique des régions antarctiques et subantarctiques.* Paris, 1912.

[5] J. L. Mohr, N. J. Wilimovsky *and* E. Y. Dawson. An Arctic Alaskan kelp bed. *Arctic*, Vol. 10, No. 1, 1957, p. 45–52.

[6] C. Skottsberg *and* M. Neushul. Phyllogigas and Himanthothalus, Antarctic phaeophyceae. *Botanica Marina*, International review for seaweed research and utilization. (In the Press.)

Made in United States of America
Reprinted from Limnology and Oceanography
Vol. 6, No. 1, January, 1961
pp. 24–25

SUN–ALTITUDE EFFECT ON THE DISTRIBUTION OF UNDERWATER LIGHT

J. E. Tyler

Scripps Institution of Oceanography, University of California

ABSTRACT

Skylighting which is symmetrical about the zenith generates a light vector diagram which is symmetrical about the vertical axis. When the sun departs from a position of symmetry the light vector diagrams become distorted. The extent of this distortion can to some extent be predicted from a knowledge of the scattering and reflecting properties of the water. The method of prediction is explained.

In homogeneous water, at a fixed depth, the distribution of light with azimuth angle in the horizontal plane will of course depend on the sun's altitude in the sky. If the sun is exactly at the zenith in a clear sky the light vector diagram for the horizontal plane will be a circle, that is, the magnitude of the flux will be a constant for all azimuths. If the sun were just below the horizon and the sky were clear, one would also expect that the horizontal light vector diagram would approach a circle of somewhat smaller magnitude than in the previous case. A truly circular light vector diagram would result in the latter case if the sky-dome exhibited a constant gradient from zenith to horizon at all azimuths, but this is not the case at sunset.

In between sunset and zenith-sun the horizontal light vector diagram is known to be pseudo-elliptical in shape (Johnson and Liljequist 1938; Whitney 1941; Sasaki *et al.* 1958). Thus, as the sun moves from the zenith to the horizon, the horizontal light vector diagram must stretch into a pseudo ellipse, attaining a maximum major axis at some intermediate sun angle and then shrink back again to a near circular shape at sunset.

Experimental data have recently been obtained by Sasaki and his co-workers (Sasaki *et al.* 1958) which demonstrate this sequence of changes in the horizontal light vector diagram.

The phenomena can be explained and the sun angle for maximum distortion of the light vector diagram can be predicted from fundamental hydro-optical considerations. There are two major factors which govern the shape of the horizontal light vector diagram. The first of these is intimately associated with the scattering function of the water. From Figure 1 it can be seen that as the sun sets and the angle of incidence, i, increases to 90°, the angle of refraction, r, increases to 48.6°, while θ (or $90° - r$), decreases to 41.4°. Considering only the collimated light from the sun, the objective lens of the instrument, which is pointed horizontally, will face more and more into the forward lobe of the scattering from this collimated beam as the sun sets. The reading obtained will therefore increase more or less proportionately to the scattering function of the water and if nothing intervened would reach a maximum at sunset.

However, as i increases, the reflection of the air–water surface increases in accord-

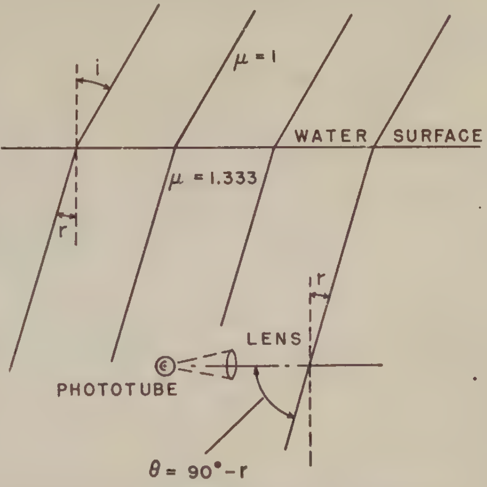

FIG. 1. Diagram illustrating the relationship between the scattering function of the water and the magnitude of the horizontal light vector in the direction of the sun.

Contributions from the Scripps Institution of Oceanography, New Series, 1238
Reproduced by Permission

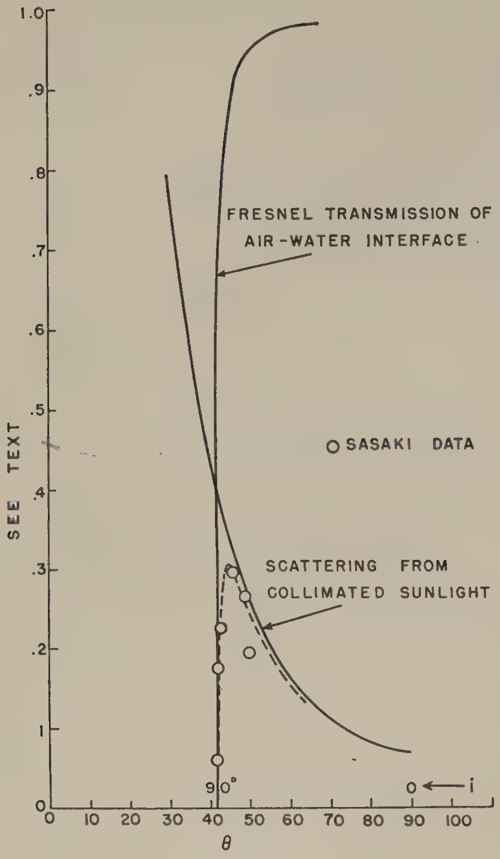

FIG. 2. Graphical illustration of the effect of scattering and of Fresnel transmission on the magnitude of the horizontal light vector in the direction of the sun.

ance with Fresnel's equations and the flux transmitted through the boundary decreases, finally reaching zero at $i = 90°$. The two effects are illustrated in Figure 2.[1] The Fresnel transmission data are plotted from 0 to 100% on the ordinate. The scattering function curve is taken from measurements of a water sample having an attenuation coefficient of 0.302/m, and a total scattering coefficient of 0.148/m. The directional scattering from the sun's collimated beam is assumed to be proportional to the shape of this scattering curve but the magnitude of the flux measured would be influenced by the depth at which measurements were made and by the volume of water involved. In the present problem Sasaki has measured the magnitude of the scattering and the scattering curve in Figure 2 is placed to conform with his maximum reading.

The horizontal flux measured in the direction of the sun as a function of i or θ will evidently be proportional to the product of these two curves, illustrated in Figure 2 by the dashed line.

From Figure 2 the maximum distension of the horizontal light vector diagram will occur when the sun is 70° from the zenith. The maximum distension reported by Sasaki occurred when the sun's angle from the zenith was 67.5°. Sasaki's normalized data are plotted in Figure 2 as circled points. In plotting these points the flux in the direction opposite to the sun has been subtracted since for normalized data this portion of the flux is not affected by the position of the sun.

This same phenomena should of course be observable at other angles than horizontal, and should be greatly exaggerated for observation angles less than 48° from the zenith.

REFERENCES

JOHNSON, N. G., AND G. LILJEQUIST. 1938. On the angular distribution of submarine daylight and on the total submarine illumination. Svenska Hydrografisk—Biologiska Kommissionens Skrifter, N. S., **14**: 3–15.

WHITNEY, L. V. 1941. The angular distribution of characteristic diffuse light in natural water. J. Mar. Res., **4**: 122–131.

SASAKI, T., S. WATANABE, G. OSHIBA, AND N. OKAMI. 1958. Measurements of angular distribution of submarine daylight by means of a new instrument. Oceanogr. Soc. Japan, **14**(2): 1–6.

---

[1] The Fresnel computations are here based on a flat interface. A roughened surface would no doubt alter the figures to some extent as would any change from the assumed scattering function of the water.

Särtryck ur Tellus nr 4, 1960

Tellus, v.12, no.4,
1960. pp.436-443.

(91)

Radiocarbon Concentration in Pacific Ocean Water

By G. S. BIEN, N. W. RAKESTRAW, and H. E. SUESS,

Scripps Institution of Oceanography, University of California, La Jolla

(Manuscript received April 26, 1960)

Abstract

Results of C^{14} determinations in surface water from the Pacific were in agreement with those reported by Rafter and Fergusson. However, abnormal C^{14} concentrations seem to exist locally, for which no oceanographic explanation can be given. It seems premature to draw conclusions from existing determinations as to the rate of increase of C^{14} in surface ocean water resulting from the uptake of C^{14} produced in the atmosphere by atomic bombs.

Samples from a constant depth of about 3,500 meters show a C^{14} content decreasing from south to north. This decrease may be attributed to radioactive decay of C^{14} during the time of migration. From this the northward component of the rate of water movement of about 0.06 cm/sec can be calculated. The C^{13} determinations, for the purpose of correcting the C^{14} values for isotope fractionation effects, were found to be remarkably consistent, although made on reburned acetylene.

Introduction

The C^{14} content of the bicarbonate of ocean water is of twofold interest: First, it offers a valuable method for the study of isotope exchange and transfer of carbon dioxide between the atmosphere and the ocean. Second, it can be used as a new tool in oceanography for the study of the movement of deep ocean water and the mixing of water masses. The rate of transfer of CO_2 from the atmosphere into the oceans was first discussed in the light of the C^{14} distribution by REVELLE and SUESS (1957), and independently by ARNOLD and ANDERSON (1957). An order of magnitude of about ten years was derived by these authors for the residence time of CO_2 in the atmosphere before it gets dissolved in the oceans. Subsequently several others, CRAIG (1957), FERGUSSON (1958), BOLIN and ERIKSSON (1959), attempted to establish a more precise figure for this residence time. All these considerations were based on the measurement of two empirical quantities: the apparent C^{14} age of ocean water, and the effect of industrial coal combustion on the specific activity of atmospheric CO_2. But the data up until now have been scarce, the observed effects of small magnitude, and there has been uncertainty about such things as the size of the so-called geochemical carbon reservoirs (such as the terrestrial biosphere). However these data are treated, the calculated residence time can scarcely be very accurate. But the addition of artificial radiocarbon to the atmosphere by bomb explosions during the years from 1954 to 1958 will offer a much better opportunity to determine the accurate residence time and the geochemical pathway of CO_2 than the previous data afforded. A further discussion of this problem will therefore not be indulged in. Much more reliable answers will result from the combination of the data reported here with future observations during the coming decade. This paper will therefore be limited to the consideration of the use of radiocarbon as a means of following water movements.

Part of our data were obtained from samples collected during the International Geophysical

Contributions from the Scripps Institution of Oceanography, New Series, 1239

Reproduced by Permission

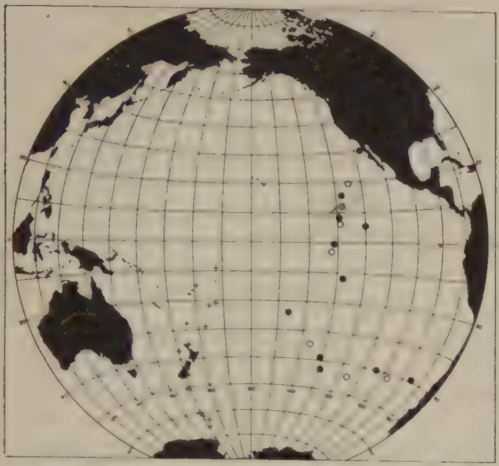

Fig. 1. Locations of sampling stations. Circles denote places where samples were taken by the Scripps Institution. Open circles indicate surface water; solid circles are deep water samples or profiles. Crosses show locations from which samples were analyzed by the New Zealand Institute for Nuclear Science.

Year for the study of secular variations (see Figure 1). During the next few years the C^{14} activity of surface water will undoubtedly increase continuously, as a result of bomb-produced C^{14} in the atmosphere. Measurements made at this laboratory and at the Institute for Nuclear Science in New Zealand will be a useful basis for future study of this problem in the Pacific Area.

The question of normalization presents a serious problem in the comparison of data from different laboratories. The oxalic acid standard distributed by the National Bureau of Standards is now used widely. In order to correct for isotope fractionation effects, results are normalized to a δC^{13} of -25 per mil relative to the Chicago PDB standard (CRAIG, 1957 a). The Lamont normalization, which we have adopted, uses this correction as well as a factor of 0.95 times the δC^{14} of the oxalic acid standard (BROECKER and WALTON, BROECKER and OLSON, 1959).[1]

Sampling and measurements

On the Downwind Expedition of the International Geophysical Year, six surface samples and ten samples from deep water were collected and the carbon dioxide extracted and processed directly on shipboard. The samples for the profiles were collected with the same sampling equipment but stored in 50-gallon steel drums and processed on shore shortly after the return of the ships. The Atlantic samples, obtained from Dr. John Lyman, were in the form of barium carbonate and were collected and processed in a different manner.

The water samples were taken in a sampler of approximately 50-gallon capacity constructed in the Special Developments Shop of the Scripps Institution of Oceanography under the direction of Mr. J. D. Frautschy. The sampler consisted of a stainless steel barrel about five and one-half feet long and fifteen inches in diameter, closed at each end by stainless steel flanges sealed with soft plastic gasket material. When closed, the end flanges were held together in place by a strong steel spring in the axis of the barrel. The flanges could be opened by a detachable "cocking" lever and held open about five inches from the ends of the barrel by a tripping mechanism which would be released by a messenger. When lifted inboard, the water sample was transferred as quickly as possible through a rubber hose into a "process tank" on deck built from a 50-gallon glass-lined hot water heater, and filled with nitrogen gas before the transfer to avoid contact with the carbon dioxide of the air. The tank was fitted with a tightly bolted top plate with lead-in tubes for the addition of acid and the inflow and exit of nitrogen gas to flush out the liberated carbon dioxide. Two liters of concentrated HCl was added to each charge of the tank, and nitrogen was passed in through a coarse diffusion head at a rate of from one to four liters per minute, and finally led into an absorption bottle through a sintered-glass diffuser. The process tank was warmed with heating coils to a temperature of 40 to 50° C, under which conditions it was ascertained that all the CO_2 in the water was liberated and absorbed in a minimum of four hours. Twice this time or more was used in routine runs.

The carbon dioxide in the nitrogen stream was absorbed in one liter of concentrated ammonia solution saturated with barium chloride. We believe that absorption in ammonium hydroxide solution is much faster than in alkali hydroxide, and that the use of ammonium hydroxide represents a real improvement over techniques used elsewhere. The one-liter bottle, containing the remaining solution and the precipitated barium carbonate, was tightly stoppered and returned to the laboratory. This method proved very satisfactory, in spite of the fact that the precipitation of solid $BaCO_3$ on the diffuser head generally made its replacement necessary at least once during a run. Completion of the absorption could always be verified, however, by replacing the absorption bottle with a fresh one and observing whether precipitation of barium carbonate continued or not. In the absorption of the CO_2 from some of the later samples, strontium chloride was substituted for barium chloride. In any case, the strontium or barium carbonate was reduced with magnesium metal to the carbide, which was then hydrolyzed to acetylene.

---

[1] It should be pointed out that the reference C^{14} in the oxalic acid standard is *not* corrected for any deviation of its δC^{13} from the chosen standard value of -25 per mil. The δC^{13} of the oxalic acid standard is actually -18.65 ± 0.13 per mil relative to the PDB standard (Private communication of Toshiko K. Mayeda to J. R. Arnold). In case of deviation from this value, due to isotope fractionation in the laboratory, the δC^{14} measured for the standard should be corrected accordingly.

Hydrochloric rather than sulfuric acid was used for acidification with the thought that it would interfere less with the subsequent determination of radium. In five liters of each sample, after the removal of carbon dioxide, barium sulfate was precipitated by the addition of barium chloride. This precipitate, carrying with it the radium, was washed and separated by decantation and returned for the determination of radium.

The deep samples for the C^{14} measurements were all taken from depths of about 3,500 meters. In each case a Nansen bottle was suspended about five meters below the sampler in such a way that the bottle, with its protected and unprotected thermometers, was tripped when the large sampler closed. From these thermometer readings the depth was accurately determined in the standard manner.

With one exception, the surface samples were obtained through the ship's salt-water pumping system, which operates without diffusing air into the water. One water sample was obtained from mid-depth, 400 meters.

The La Jolla Radiocarbon Laboratory uses the method developed at the U.S. Geological Survey in Washington (SUESS, 1954) in which acetylene serves as the counting gas. The C^{14} counting was done in a special low-level counter developed by HOUTERMANS and OESCHGER (1958) and manufactured in the instrument shop of the Physikalisches Institut, University of Bern, Switzerland. This counter showed a background of less than two counts per minute at one atmosphere and a sensitive volume of about 1.7 liters. Total counting time for each sample was several days.

Discussion of results

The results of the measurements are given in Table 1, 2 and 3, and shown in Figure 2. They contain two remarkable features: (1) the occurrence of abnormal surface water concentrations of C^{14}; and (2) a distinct, regular increase in the apparent age of deep water from south to north.

Surface water samples. Careful measurements in the laboratory of the Institute for Nuclear Science, New Zealand (RAFTER and FERGUSSON, 1957; FERGUSSON, 1958) have shown that the activity of the surface water in the South Pacific decreases from lower toward higher latitudes along with decreasing stability of the thermocline. Values more than 150 per mil below the equilibrium value are found beyond the Antarctic convergence. Considering the uncertainty in the calibration and the experimental errors of about one per cent, our results agree very satisfactorily with the New Zealand findings. In comparing results we have assumed a difference between the New Zealand and Lamont normalizations of -61 per mil. In a few cases, however, there is considerable deviation from the general trends. One abnormal sample was found by Rafter and Fergusson (BURLING and GARNER, 1959) with an activity of more than three per cent below the expected, and the investigators attribute this deviation to chemical effects from storage in a steel drum. We believe that in our case such an explanation of the deviations is highly improbable. Along the La Jolla coast and in offshore areas varying ΔC^{14} values ranging from -50 to about -80 per mil have been obtained. These variations can be explained by upwelling water along the California coast. It is well known that such upwelling results in great differences in the local properties of surface water at different times and locations. The vertical circulation and mixing of surface

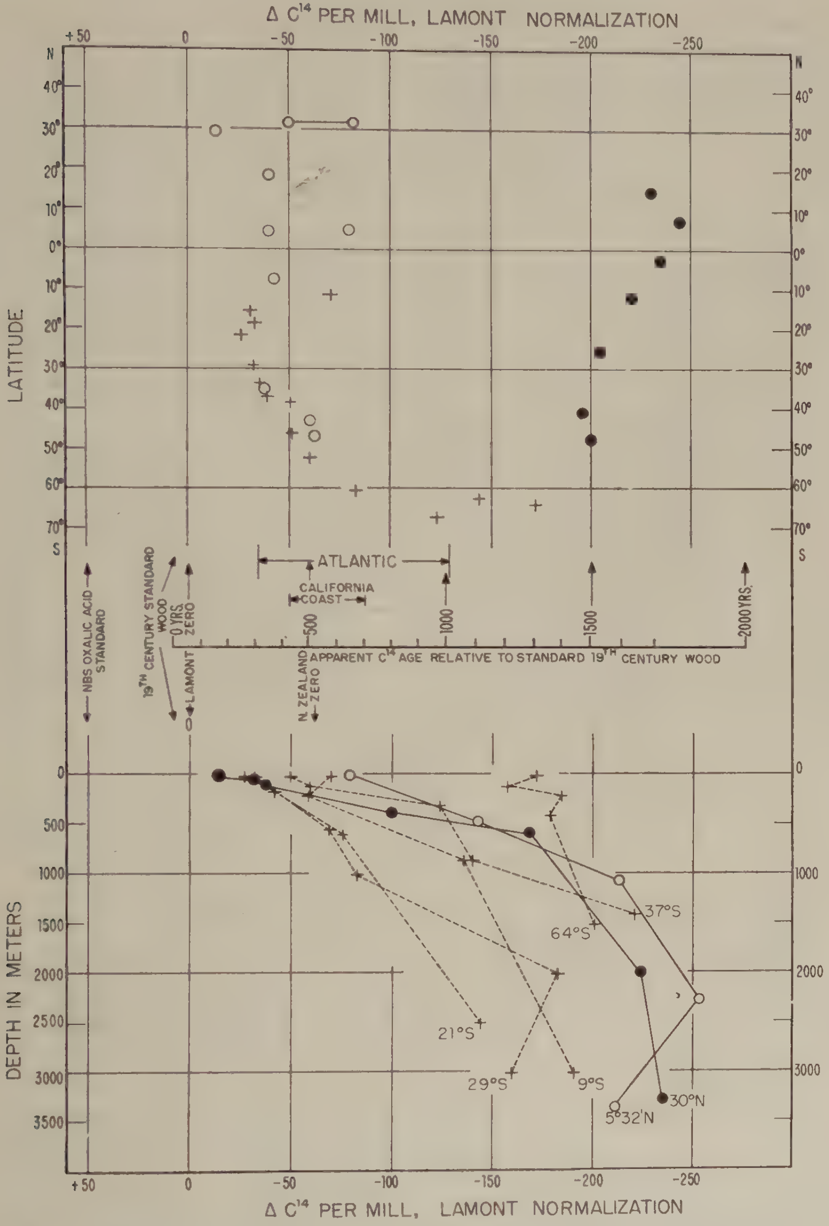

Fig. 2. Upper part: ΔC^{14} plotted as a function of latitude for surface water samples (open circles indicate La Jolla measurements, crosses New Zealand measurements), and for samples from approximately 3,500 m. depth (solid circles).

Middle part: Normalization and the conversion of ΔC^{14} to apparent ages is indicated. All values, except that for the NBS oxalic acid standard, are normalized to a δC^{13} of —25°/oo relative to the Chicago PDB standard.

Lower part: ΔC^{14} as a function of depth. Crosses indicate New Zealand measurements. Open circles show results on samples collected by J. A. Knauss, and solid circles by J. E. Reid.

Table 1. IGY downwind expedition[1]

Collector: N. W. Rakestraw
Dates of Collection: October through December 1958
C^{13} measurements: P. Eberhardt in laboratory of H. C. Urey

LJ No.	Field No.	Latitude	Longitude	Depth meters	Salinity ‰	O_2 (l/l)	T °C	δC^{13} per mil PDB Standard (± 0.2 ‰)	ΔC^{14} in per mil (± 8 ‰) Lamont Normalization
58	2	19° 35′ N	125° W	0	34.69	4.82	24.4	—0.5	—40
62	6	5° N	130° W	0	34.40	4.65	28.0	—0.1	—40
66	8	7° ′ S	132° W	0	34.68	4.88	26.7	—1.0	—42
68	11	34° 50′ S	135° 53′ W	0	35.05	5.64	17.7	—0.4	—38
90	14	46° 30′ S	116° W	0		6.78	9.2	—0.7	—60
93	16	42° 43′ S	96° W	0		6.64	11.5	—0.6	—62
60	4	11° N	128° 31′ W	400	34.65	0.13	10.9	—1.5	—103
59	3	14° 58′ N	127° 31′ W	2987	34.69	2.73	1.66	—1.2	—230
61	5	7° 08′ N	129° 16′ W	3508	34.69	3.43	1.48	—1.4	—243
63	7	2° 08′ S	131° 27′ W	3473	34.69	3.48	1.52	—1.3	—235
57	9	14° 29′ S	135° 30′ W	3449	34.69	3.73	1.58	—1.8	—220
67	10	25° S	145° W	3560	34.65	4.05	1.54	—2.9	—204
69	12	40° 35′ S	132° 10′ W	3500	34.67	4.00	1.50	—1.2	—195
88	13	46° 46′ S	123° 53′ W	3550	34.69	4.03	1.62	—2.0	—200
91	15	40° 37′ S	103° 20′ W	3500	34.67	4.10	1.85	—2.5	—180
94	17	39° 33′ S	84° 10′ W	3500		4.15	1.46	—1.9	—196

[1] The values for ΔC^{14} given here differ slightly from those previously reported (Rakestraw, Oeschger and Suess (1959) Preprints, International Oceanographic Congress, p. 440). They are calculated with a revised calibration.

Table 2. Samples from La Jolla beach or offshore

LJ No.	Material	δC^{13} ‰ PDB	ΔC^{14} ‰ ± 10	Date of Collection
86	Shells, collected alive (mytilus Californianus), La Jolla Shores	—8.3	—85	1953
48	Vellela velella, SW of Farallon Islands	—23	—82	15 April 1957
70	Kelp (Macrocystis pyrifern)	—16	—70	8 July 1957
65	Red Tide (Gonyaulax)	—18	—60	18 August 1958
97	Shells, collected alive (mytilus Californianus), La Jolla Shores	+ 0.6	—37	February 1959
127	Carbonate from Pier Water	— 2.3	—88	4 August 1959

water with that from lower depths results in variations in the C^{14} activity of surface water as well as in other characteristics, such as temperature. One measurement (LJ 149) gave an abnormally high value for which we have no explanation.

As FERGUSSON'S results show (1959) one must be cautious in interpreting increases in the C^{14} activity of surface water as a consequence of uptake of bomb C^{14} from the atmosphere. Many measurements will be necessary to determine the rate of this uptake.

Deep water samples. The C^{14} concentration of a particular deep water sample may be influenced by the following factors:

1) The degree of equilibration between the CO_2 in the water and that in the atmosphere, provided the water mass can be regarded as a

Table 3. Profiles

Collector	Dates of Coll.	C^{13} done by	LJ No.	Field No.	Latitude	Longitude	Depth Meters	Salinity ‰	O_2 (ml/liter)	T °C	δC^{13} (PDB) ‰	ΔC^{14} Lamont Normalization
John A. Knauss	July, 27, 28, 1959	R. Bowen (H.C. Urey Laboratory)	146	1	5° 32′ N	120° 05′ W	10	33.50	4.45	27.5	—1.22	—79
			140	2	»	»	485	34.67	0.25	7.88	—2.51	—143
			147	3	»	»	1080	34.63	0.94	4.12	—1.81	—213
			139	4	8° 29′ N	120° 09′ W	2280	34.70	2.34	1.97	—1.66	—253
			137	5	»	»	3370	34.70	3.25	1.58	—0.74	—211
Joseph Reid	October 14, 1959	S. Epstein, Cal Tech	149	1	30° 04′ N	118° 02′ W	10	33.48	5.13	19.30	+1.9	—13
			150	2	»	»	75	33.44	5.70	15.85	+1.0	—32
			151	3	»	»	120	33.48	5.12	13.40	+0.2	—38
			152	4	»	»	390	33.16	0.90	6.60	—1.9	—100
			153	5	»	»	600	34.35	0.32	5.21	—6.0	—169
			154	6	»	»	2000	34.66	—	2.00	—1.6	—238
			158	7	»	»	3300	34.67	2.30	1.60	+0.3	—235
Atlantic samples submitted by John Lyman	July 8, 9, 1957	P. Eberhardt (H. C. Urey Laboratory)	123	878	27° 34′ N	59° 38′ W	25	36.42	4.94	25.72	—0.2	—33
			124	879	»	»	3163	34.87	6.21	2.75	—2.0	—115
			125	880	»	»	5944	34.85	—	2.13	—1.9	—140

closed system. If not, then the water mass must be considered as a sum of components, each with a different history.

2) The time since such equilibration occurred, during which radioactive decay has taken place.

3) Oxidation of particulate or dissolved organic matter. Settling of particulate organic matter from the ocean surface and subsequent oxidation will add younger carbon and decrease the apparent radiocarbon age. Evidence of such a process may possibly be obtained from the O_2 distribution in the water.

4) Redissolving of carbonaceous sediments from the ocean bottom. Geological evidence indicates that such processes are in general too slow to affect C^{14} concentrations.

The Pacific deep water obtained its C^{14} through exchange with the atmosphere south of the Antarctic convergence below 60° S. latitude, or through admixture of surface water from lower latitudes. New Zealand measurements show that exchange is incomplete and the water masses sink with a ΔC^{14} of about -150 or less (apparent C^{14} age of 1,200 to 1,500 years). Our measurements show a further increase in apparent age of 200 to 300 years as the water moves toward the equator. This age difference may well indicate the true travel time of the water mass. At the same time a decrease in O_2 occurs that can be attributed to oxidation of organic matter. Assuming that this organic matter reached the deep water by sedimentation from the surface and is correspondingly high in C^{14}, this addition of younger carbon to the dissolved bicarbonate will make the radiocarbon age of the water appear too young. Sea water contains about 2.3 millimol per liter of carbon in the form of bicarbonate. On its way from 40° S to 15° N the water loses about 1.3 milliliters or 0.055 millimol of oxygen, equivalent to about 4.2 % of the carbon present. The carbon added by oxidation of organic matter may be about 20 per cent higher in C^{14} and therefore may increase the C^{14} concentration of the water mass by $0.042 \times 20\% = 0.84\%$. This corresponds to a decrease in the apparent age of about 100 years. Figure 2 shows that the difference in the apparent C^{14} age for the samples from around 3,500 meters depth between 40° S and 15° N was found to be between 200 and 300 years. If the oxygen in this water mass was consumed by organic carbon from the surface, then the true travel time of the water would be about 100 years longer. Assuming that effects from other processes, such as the dissolving of particulate inorganic carbonate, are unimportant, then we can estimate the travel time for 55 ° of latitude (6,100 km) as 300 ± 100 years. This corresponds to an average northward component of the velocity of the water of 0.06 ± 0.02 cm/sec.

Our evidence leads us to expect that radiocarbon studies will be more valuable in explaining water movements in the Pacific than in the Atlantic, where conditions are apparently more complicated.

Profiles. The variation of the C^{14} concentration as a function of depth in the Pacific was investigated at two stations. The samples from one station were collected by Dr. John Knauss on the Doldrums Expedition of the Scripps Institution of Oceanography; those of the other station by Mr. Joseph Reid on another cruise. In both cases the seawater samples were brought ashore in 55-gallon drums and processed at La Jolla. The results obtained show a more regular depth dependence than those obtained by the New Zealand laboratory. The C^{14} concentration was found to decrease almost linearly with depth down to about 1,000 meters and from there downwards to remain almost constant (Figure 2). One profile showed evidence for a C^{14} minimum at a depth of about 2,000 meters. Until the occurrence of this at other stations is verified, speculation as to its significance is scarcely profitable.

C^{13} *results.* The mass spectroscopic C^{13} determinations carried out by Dr. Samuel Epstein and Mrs. Iren Vidzuinas at the California Institute of Technology, and in Dr. Urey's laboratory at La Jolla by Dr. Peter Eberhardt and Dr. Robert Bowen, are remarkably consistent. They show a relatively small spread, much smaller than that found at the Lamont laboratory (BROECKER, TUCEK, and OLSON, 1959) in samples from the Atlantic. Also, their variations follow qualitatively the expectation that the C^{13} should show lower values at depths where oxidation of organic matter may have taken place, than at the surface where photosynthesis predominates. The lowest C^{13} value observed (LJ 153) is in a sample which comes from a depth near that of the oxygen minimum. However, it should be noted that the C^{13} determinations were made on reburned acetylene, and that small isotope fractionations in the laboratory during extraction of CO_2 and preparation of acetylene cannot be excluded.

Acknowledgments

We are grateful to Dr. Samuel Epstein and Mrs. Vidzuinas, Dr. Peter Eberhardt and Dr. Robert Bowen for making C^{13} determinations in their mass spectrometers. We appreciate the help of Mr. J. D. Frautschy in the design and construction of the water sampler, the cooperation of Dr. John Knauss and Mr. Joseph Reid in securing samples and in giving valuable comments, and the cooperation of Dr. John Lyman in furnishing samples from the Atlantic. The counter used was brought to the C^{14} laboratory from the University of Bern by Dr. Hans Oeschger, who remained for three months and carried out the installation and calibration and participated in the laboratory work connected with the counting of the majority of the IGY samples. Technical assistance in the Radiocarbon Laboratory was provided by Mrs. Paula Sandoval, and on shipboard by Mr. Lee Waterman. The collection and processing of the samples was provided from funds for the International Geophysical Year and by the Office of Naval Research. Determination of the C^{14} was done under Contract AT (11-1)-34, Project 40 with the Atomic Energy Commission.

REFERENCES

ARNOLD, J. R. and ANDERSON, E. C., 1957: The Distribution of C-14 in Nature. *Tellus* **9**, pp. 28—32.

BOLIN and ERICSON

BROECKER, W. S. and WALTON, A., 1959: Radiocarbon From Nuclear Tests, *Science* **130**, p. 309.

BROECKER, W. S., TUCEK, C. S. and OLWON, E. A., 1959: Radiocarbon Analysis of Oceanic CO_2, *International Journal of Applied Radiation and Isotopes.*

BURLING, R. W. and GARNER, D. M., 1959: A Section of ^{14}C Activities of Sea Water Between 9° S and 60° S in the Southwest Pacific Ocean, *N.Z. Journal Geology and Geophysics*, **2**, p. 799.

CRAIG, H., 1957: The Natural Distribution of Radiocarbon and the Exchange Time of Carbon Dioxide Between Atmosphere and Sea, *Tellus* **9**, pp. 1—17.

—, 1957: Isotopic Standards for Carbon and Oxygen and Correction Factors for Mass-Spectrometric Analysis of Carbon Dioxide, *Geochim. et Cosmochim Acta*, **12**, p. 133.

FERGUSSON, G. J., 1958: Reduction of atmospheric Radiocarbon Concentration by Fossil Fuel Carbon. Dioxide and the Mean Life of Carbon Dioxide in the Atmosphere, *Proceedings Royal Society*, **A234**, pp. 561—74.

HONTERMANS, F. G. and OESCHGER, H., 1958: A Special Low-Level Counter, *Helvetica Physica Acta*, **31**, p. 117.

RAFTER, T. A. and FERGUSSON, G. J., 1900: Atmospheric Radiocarbon as a Tracer in Geophysical Circulation Problems, *N.Z. Journal of Science and Technology*, **B38.**

REVELLE, R. and SUESS, H. E., 1957: Carbon Dioxide Exchange Beetwen Atmosphere and Ocean and the Question of an Increase of Atmospheric CO_2 during the Past Decade., *Tellus*, **9**, pp. 18—27.

SUESS, H. E., 1954: Natural Radiocarbon Measurements by Acetylene Counting., *Science*, **120**, pp. 5—6.

PRINTED IN SWEDEN
ESSELTE, STHLM 61

(99)

Reprinted from Science, March 17, 1961, Vol. 133, No. 3455, pages 758-760

Pressure Sensitivity of an Amphipod

Abstract. The responses of an intertidal amphipod indicate an ability to perceive rapid pressure changes of less than 0.01 atm. The interaction of rate of change of pressure and total difference in pressure implies a rapid accommodation as well as a threshold. Evidence suggests that the sensory mechanism may not involve compressibility of a gas.

It has long been recognized that changes in hydrostatic pressure, in the range of hundreds of atmospheres, can have marked, and often lethal, effects on organisms (*1*). Recently, Hardy and Bainbridge (*2*) described controlled experiments in which decapod larvae slowly swam upward after much smaller increases of hydrostatic pressure: 500 to 2000 mb (*3*). The response continued for more than an hour. Two other recent papers have claimed that planktonic invertebrates, including representatives of several phyla, may be sensitive to changes in hydrostatic pressure as small as 10 mb. Knight-Jones and Qasim (*4*) described a "negative geotaxis" associated with pressure increase, and a general decrease in activity associated with pressure decrease. Baylor and Smith (*5*) stated that the organisms they examined swam upward the appropriate distance to compensate for pressure increase, and downward to compensate for pressure decrease. Neither of these reports described the experimental methods used to determine the presumed thresholds.

This preliminary report (*6*) deals with the brief but sharp increase in activity shown by a benthic intertidal amphipod, *Synchelidium* n. sp. (*7*), in response to small changes in hydrostatic pressure. The experimental equipment consisted of: a 250-cm^3 observation flask, containing about 300 amphipods, attached to a 50-cm^3 syringe by 6 m of 3-mm (inside diameter) plastic tubing, the entire system being filled with seawater, except for a 5-cm^3 airspace in the flask; a transducer-type pressure gauge (Statham model PM 6 TC, ± 1 lb/in.^{2} full range) connected directly to the flask by a glass Y-tube; a 30-cy/sec amplifying recorder (Gilson Medical Electronics, "Mini-polygraph") with one pen connected to the transducer and a second pen to an event-recording line leading from near the flask. The observation chamber, pressure gauge, and an observer were in a room where a high noise level was maintained; the recorder and the syringe through which pressure changes were applied were in a separate, adjacent room. The observer thus had no auditory or visual cue to the timing of pressure changes, other than the behavior of the animals. The large number of amphipods was used in order to allow more precise differentiation between the normal, average activity pattern of the animals and the increased activity associated with pressure changes.

Pressure on the system was changed either by placing (or removing) small weights on a platform atop the syringe plunger, producing an almost instantaneous pressure change; or by mechanically raising the open syringe up an inclined ramp at a rate that could be adjusted as desired. The air space in the flask is not essential to the response of the amphipods; they reacted similarly when the system was completely filled with water. It did serve, however, to considerably cushion the pressure change, eliminating large overshoot and rebound with the first method, and producing a much smoother pressure record with the second method.

The observer was notified that a recording had been started; at sometime within the next 60 seconds, the timing being determined by a number selected from a table of random numbers, the operator changed the pressure on the system. When, and if, the observer noted a marked change in the behavior of the amphipods, his signal depressed the event-recording pen of the recorder.

Several considerations make it appear unlikely that the observed response was due to a pressure-correlated sound stimulus: (i) The behavior of the animals when subjected to a wide variety of shock and noise stimuli, in the absence of pressure changes, indicates that this species is relatively unresponsive to all sounds tested, including loud, strong blows on the syringe. (ii) The absence of the air space in the experimental system, which should have altered the sound transmissive characteristics, had no noticeable effect on the response. (iii) The same type of response was obtained when the open syringe was raised carefully by hand, either with or without the airspace in the flask, a procedure presumably avoiding any high-frequency mechanical shocks associated with other methods. (iv) There is no known mechanical peculiarity of the system which could account for a sound stimulus present during prolonged linear pressure increases and absent during briefer increases (Table 1).

Table 1. Responses to slow, linear pressure increases: av. rate, 2.8 mb/sec (2.6 to 3.1); percentage of time at atmospheric pressure, 61 and 77; three "spontaneous activity" records. For ΔP, ΔP_T, and T, see Fig. 1*B*.

ΔP (mb)		Responses		T (sec)	
Av.	Range	Positive	None	Av.	Range
		Large increases (final $\Delta P > 35$ mb)			
41.8*	27–51*	19	1	14.4	9.4–17.7
		Small increases (final $\Delta P < 25$ mb)			
18.7	18–21	0	19		

* ΔP_T

The system has been carefully examined for the possibility of some pressure-correlated visual cue to the animals; none has been found.

The most evident response to pressure change is the sudden onset of a rapid scrambling and darting by the amphipods, which are otherwise far less active, predominantly resting on the bottom of the flask. The reaction occurs whether the pressure is increased or decreased, but is much stronger after pressure increase. With slow rates of pressure increase, the sudden burst of activity is preceded by a brief reduction of the slight normal movements of the animals. This decreased activity is less easily discerned, however, and the criterion for pressure response will here be restricted to the sudden pronounced increased activity. Rough estimates of the duration of increased activity associated with pressure change ranged from about 5 seconds for an increase of 10 mb, to about 15 seconds for an increase of 100 mb.

Small bursts of spontaneous activity occasionally occurred in the observation flask; signals denoting an apparent response to pressure at a time prior to

Table 2. Threshold for observable reaction to rapid pressure increases: t, 0.6–0.9 sec; percentage of time at atmospheric pressure, 86 and 92; one "spontaneous activity" record. For ΔP, T, and t, see Fig. 1*A*.

ΔP (mb)	Responses		T (sec)	
	Positive	None	Av.	Range
	Initial threshold			
6–8	6	4	1.7	1.0–2.3
8–15	5	1	1.3	1.0–1.7
15–20	4	0	1.1	1.1–1.2
	Final threshold			
6–8	0	5		
8–10	1	4	2.0	
10–15	8	4	1.9	1.5–3.0
15–20	5	0	1.6	1.4–1.8

Contributions from the Scripps Institution of Oceanography, New Series, 1240

Reproduced by Permission

the actual pressure change were designated as "spontaneous activity" records. These errors were made only when dealing with the weak responses near threshold level. Rapid pressure changes of more than 30 mb are associated with such an emphatic response that it cannot be confused with spontaneous activity. The decision that there has been a "sudden increase in activity" is, of course, subjective; the precision in timing relative to the randomly timed pressure changes, the reproducibility of results, and the low frequency of "spontaneous activity" records suggest, however, that activity changes associated with pressure changes are great enough to provide an objective basis for study of the phenomenon.

Pressure increases during the "active" phase of the animal's endogenous tidal rhythm (*8*) result in some increase in the number of upward-swimming animals, after the rapid scrambling on the bottom of the flask, a result similar to the "negative geotaxis" referred to by Knight-Jones and Qasim (*4*). This feature is not conspicuous during the "inactive" phase of the rhythm, even with large pressure increases, and has not been observed after pressure decreases at any time. Those animals which swim upward rise a distance of only 2 to 5 cm, regardless of the magnitude of the pressure increase; these benthic amphipods do not appropriately "compensate" in the manner described by Baylor and Smith (*5*) for planktonic organisms.

Tracings from typical experimental records are shown in Fig. 1. More than 50 experiments have been conducted with rapid pressure changes of 25 to 50 mb (Fig. 1*A*) with 100 percent positive responses and no "spontaneous activity" records.

Tables 1 and 2 summarize a representative set of experiments with pressure increase performed on 13 September 1960 from 9 A.M. to 1 P.M. during the "inactive" phase of the amphipod's tidal rhythm. The same group of animals was used throughout, with a minimum of a 1-minute interval between trials. The initial threshold experiments of Table 2 preceded the experiments in Table 1; the final threshold experiments followed them. The initial pressure, in all cases, was atmospheric ± 10 mb. The percentage of recorded time at atmospheric pressure is an index of the time during which "spontaneous activity" records were possible. Any responses to stimuli not associated with pressure changes would be expected to be distributed more or less evenly over the entire period of observation.

Table 2 indicates that the initial threshold for observable reaction was at least as low as 7.0 mb. Similar experiments with other freshly collected animals have shown positive responses down to a pressure increase of 5.1 mb. As a determination based on an overt reaction, this value should be regarded as only an estimated upper limit of true threshold.

Table 2 also indicates that the threshold to rapid pressure changes had increased during the experiments, to a value greater than 8.0 mb, but less than 15.0 mb. The increase in apparent threshold may be related to sensory fatigue from the intervening series of larger pressure increases. Control experiments indicated that reduced oxygen tension and other factors associated only with the experimental confinement did not measurably increase threshold.

Table 1 indicates that the response of the amphipods is dependent on both the total change and the rate of change of pressure. The large and small pressure increases of this series were presented in a random sequence. At a rate of change of about 2.8 mb/sec, an accumulated pressure difference of 18 to 21 mb did not evoke the response ("small increases"), compared with positive responses to less than 10 mb given rapidly (Table 2). The same rate (2.8 mb/sec), continued for 10 seconds or more, reproducibly induced response ("large increases"). The nature of the interaction of rate of change of pressure with total change of pressure is similar, at least superficially, to the properties of other better-known sensory systems.

The time between the start of pressure increase and the observation of a response (*T*) has a far greater range in Table 1 than in Table 2. In part, this is due to the fact that there was a significant trend ($p < .001$) for the value of *T* to increase during the course of the experiments. The trend may be another aspect of the sensory fatigue suggested by a comparison of initial and final thresholds (Table 2). In addition to this trend, however, the timing of *sequential* positive responses was also less precise than with rapid pressure changes. The difference in the value of *T* for successive responses averages 2.4 seconds (ignoring sign), which is greater than the entire range in Table 2. With slow pressure changes, interindividual variability in both the threshold pressure difference and the accommodation rate could contribute to a less sharp and coordinated response in a population; these factors would not alter the timing of initial response to rapid pressure changes.

While a gas-containing organ seems the most likely basis for a pressure-responsive sensory mechanism, there is, so far, no evidence for the presence of such an organ: (i) Extensive micro-

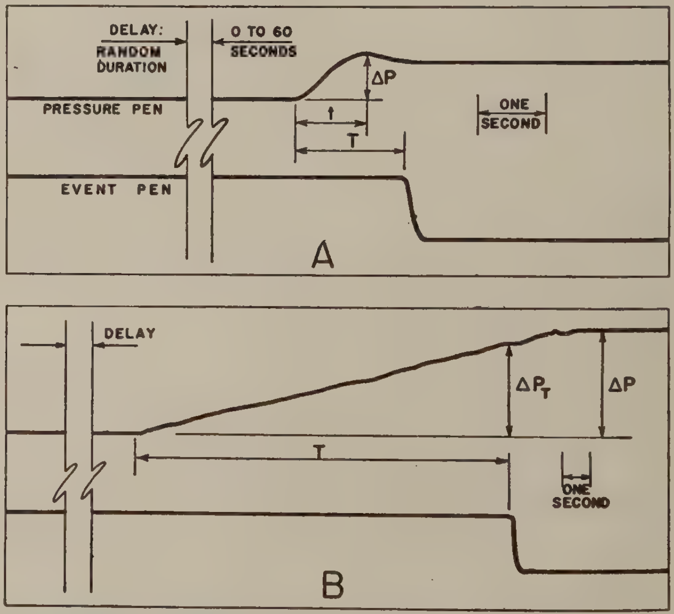

Fig. 1. Tracings of records from typical experiments. *A*, rapid pressure change; *B*, slower, linear rate of change. Symbols as used in Table 1.

scopic examination of the animals has not revealed any visible gas bubble. (ii) Upon evacuation of a flask of amphipods in sea water, any gas contained in a flexible organ might be expected to greatly expand and thus increase the buoyancy of the animals, but no change in buoyancy was observed on evacuation. (iii) After the animals were maintained at several atmospheres (about 4000 mb) for 10 minutes, they showed an activity response to pressure increases of as little as 30 mb above the 4000-mb level, even though one might expect a marked reduction in the size of a contained gas bubble, due to both compression and solution of the gas in the animal's tissue fluids, with probably an accompanying larger loss in sensitivity to pressure changes than that observed.

J. T. Enright
Scripps Institution of Oceanography,
La Jolla, California

References and Notes

1. P. Regnard, *Compt. rend. soc. biol.* **37**, 510 (1885); U. Ebbecke, *Arch. ges. Physiol. Pflüger's* **236**, 648 (1935).
2. A. C. Hardy and R. Bainbridge, *Nature* **167**, 354 (1951).
3. One millibar equals 1000 dy/cm^2 and is approximately equivalent to the pressure exerted by a column of seawater 1 cm high. One atmosphere equals 1.0132 bars.
4. E. W. Knight-Jones and S. Z. Qasim, *Nature* **175**, 941 (1955).
5. E. R. Baylor and F. E. Smith, "Recent advances in invertebrate physiology," *Univ. Oregon Publs. (1957)*, p. 31.
6. This work was performed during the tenure of a National Science Foundation predoctoral fellowship. Experimental work was supported by National Science Foundation grant No. G-7141 to Dr. E. W. Fager. I wish to express my sincere thanks to my scientific adviser, Dr. E. W. Fager, for much helpful discussion and encouragement with the work. Thanks are also due to Richard Ford and Nancy Enright for their time as observers and operators in the experimental work, to Frank Snodgrass and James Snodgrass for help with instrumentation, to Dr. Robert Arthur for a helpful discussion of methods, and to a large number of other friends for valuable comments and discussions.
7. This small oedicerotid amphipod, which is abundant on the intertidal beach at Scripps Institution of Oceanography, La Jolla, California, was identified by Dr. Clarence Shoemaker (deceased) and will be formally described by Dr. Thomas E. Bowman in a forthcoming monograph on the genus. It differs from two other undescribed species of the genus found in the La Jolla area in the following conspicuous morphological characters: the first and second antennae of the mature male are roughly 80 and 95 percent, respectively, of the length of the cephalothorax; those of the female are roughly 45 percent each; comparable values for the other two species are about 50 and 220 percent for the male and 35 percent each for the female. The second and third uropods, in both sexes, are roughly 65 and 35 percent, respectively, of the length of the first uropod, compared with 80 and 65 percent for the other two species. The bulk of the adult population of this species is in the uprush zone of the beach at La Jolla; of the other two species, which are much less abundant, one ranges from low intertidal to depths of about 3 m, and the second is usually taken deeper than 5 m.
8. J. T. Enright, *Cold Spring Harbor Symposia in Quant. Biol.* **25**, 487 (1960).

12 October 1960

Reprinted from "Physics and Chemistry of the Earth
[illegible]"

PERGAMON PRESS
OXFORD · LONDON · NEW YORK · PARIS
1961 pp.281-302.
Printed by the Pitman Press, Bath, Somerset

8

CHEMICAL AND MINERALOGICAL ASPECTS OF DEEP-SEA SEDIMENTS

By Edward D. Goldberg
Scripps Institution of Oceanography, University of California, La Jolla, California

Keys to phenomena which occurred on the surface of the earth are sought in studies of the chemistry and mineralogy of sediments from the deep-sea floor. Climate, vulcanism, and the paths of ocean water currents are but a few examples of activities that may well be logged in pelagic deposits. Recently, emphasis has been placed on the calcareous deposits with impetus being provided by the isotopic geology of carbon and oxygen. The problems of paleo-temperatures and paleo-productivity in the marine environment have been dealt with most successfully (a summary of this work may be found in Arrhenius, 1959).

The deep-sea deposits are especially attractive on a number of counts. First of all, the total length of the column of unconsolidated sediments is small; in the Pacific the first major change in travel times of seismic waves occurs at a depth of the order of hundreds of meters (Raitt, 1956). Although up to the present only a surface layer of tens of meters has been cored and but a modest penetration into the Cretaceous has been made, there is every hope that within a few years all levels of the pelagic column will have been explored. Secondly, most of the recovered samples from the deep-sea floor appear to be relatively undisturbed. Some alterations in the depositional record are evident and are apparently due to near-bottom currents, earthquakes, or bottom organisms or combinations of any of the three, but, as will be pointed out in the text, we are now in a position to estimate in many cases the degree of disordering quantitatively. Finally, the various minerals that make up the deposits are small in number, compared to their terrestrial or near-shore counterparts, and can often be unambiguously traced to the geosphere in which they were formed. This circumstance can provide a ready entry into investigations of the mechanisms of formation and modes of transport of individual components of the deposit.

Present day researches have for the most part left the descriptive stage; two related areas of work appear quite rewarding—geochronology and the authigenic minerals. The potential radioactive clocks for the pelagic deposits cover essentially the entire span of geologic time. However, their full utilization awaits more information on the chemistry and mineralogy of the solid phases of the deep-sea floor. Also, present laboratory work on the synthesis and analysis of authigenic minerals is already yielding significant information on oceanic conditions in the past accompanying their formation. This paper will attempt to take stock of recently acquired knowledge, and the accompanying problems, emphasizing by way of examples the non-calcareous pelagic sediments of the Pacific Ocean.

Contributions from the Scripps Institution of Oceanography, New Series, 1241

Reproduced by Permission

GENERAL CONSIDERATIONS

The chemical characteristics of pelagic sediments are distinct from those of the sediments of the coastal marine and continental environments. The unique feature of deep-sea accumulations is the enrichment of such metals as manganese, nickel, copper, cobalt and lead. These elements are primarily associated with the ferromanganese minerals, a group of layer lattice compounds composed principally of oxides of manganese and iron. `In general there is a close association between the gross chemical composition of a given sediment and the minerals present, and it is on this basis that a satisfactory introduction into the chemistry of pelagic deposits can be made.

Figure 1 gives the ratios of elemental abundances in Pacific pelagic sediments to those of igneous rocks. It is quite evident that the major rock-forming elements, Si, Al, Fe, Ti, Mg, Ca, Na and K are neither enriched nor depleted on an over-all basis in the oceanic deposits as compared to the crustal rocks of the earth.*

The marked accumulation of boron in marine sediments, first pointed out by GOLDSCHMIDT and PETERS (1932), is related to the high boron content of sea-water. Whereas non-marine argillaceous sediments contain about 5 to 50 p.p.m. of boron, those of the oceanic environment are around an order of magnitude higher. The major part of the boron is strongly bound in the authigenic minerals (GOLDBERG and ARRHENIUS, 1958) and quite probably proxies for silicon in the tetrahedral sheets of the clays.

Deposits from given areas can often be characterized by slight, but evident, modifications in their chemical makeup compared to the norms shown in Fig. 1. For example, the titanium content is normally similar to that of igneous rocks, but in areas subjected to volcanic influences of a basaltic nature, the titanium contents rise quite significantly. Whereas most sediments have a titanium content of the order of a half per cent, the deposits north of the Hawaiian Islands assay 1 to 2½ per cent. In clays having no volcanic contributions, titanium occurs in probably authigenic anatase (also rutile, whose origin is as yet unknown) and is also structurally bound in iron minerals (GOLDBERG and ARRHENIUS, 1958).

The importance of pelagic sediments, which may be defined as those with characters not strongly influenced by nearby land masses as distinguished from the generally largely terrigenous deposits of the continental slope and shelf, in the major sedimentary cycle has been evaluated many times with a range of all possible answers. At one end of the spectrum is the hypothesis of GOLDSCHMIDT (1954) who believed the regions of deposition are mainly the continental areas, and the pelagic regions are relatively unimportant. He assumed, as have subsequent investigators, that, for all practical purposes, the weathered surface materials of the earth eventually end up as solid or dissolved phases in the oceans. He concludes that the average thickness of sediments is 638 m over the surface of the earth distributed among the shales and sandstones (585 m), limestones (38 m) and dolomites (15 m).

---

* The data in Fig. 1 are based on chemical analyses of *untreated* pelagic sediments, i.e. no attempt was made to remove the pore solution contained in the solid phases. Ordinarily, the samples are freed of water by drying at 110 °C subsequent to analyses. Early workers attempted to remove the sea salts from their samples, but in the light of present knowledge of the ion-exchange and sorbtion properties of minerals, it is very difficult to conceive of a washing technique which would solely remove the dissolved salts from the sample without altering the composition of the solid phases.

Kuenen (1950) calculated that the mass of deep-sea clays accounts for over 50 per cent of the sediments with a ratio of red clay, blue mud and globigerina ooze of 8:2:1 and that the total mass of pelagic and hemipelagic sediments is three times the mass of the continental and epicontinental sediments. Goldberg and Arrhenius (1958) in their balance sheet accounting for the weathering of igneous rocks to sediments and dissolved substances in sea-water compute that around 13 per cent of the total amount of sediments has entered the pelagic areas. For every square centimeter of earth's surface, they find 185 kg/cm^2 of igneous rock eroded to form 23 kg/cm^2 of pelagic clay, 8·5 kg/cm^2 of globigerina ooze and limestone and finally 145 kg/cm^2 of shales and sandstones.

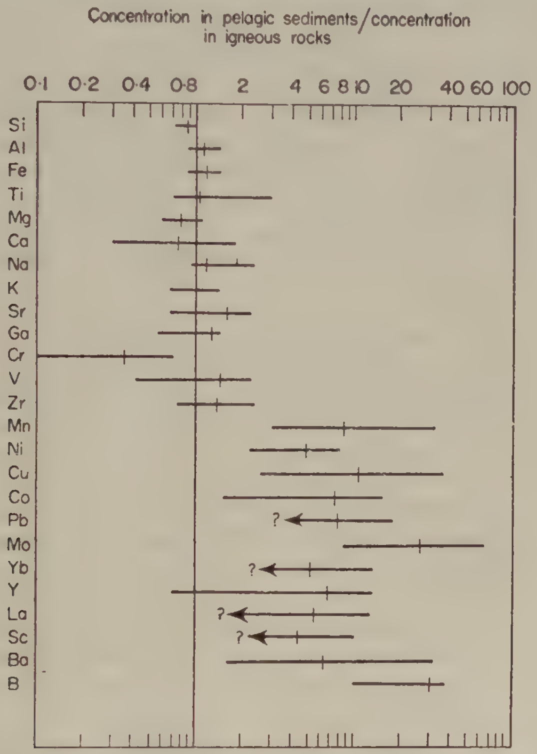

Fig. 1. Ratios of average elemental abundances in Pacific pelagic sediments and igneous rocks. Ranges are indicated by the lengths of the horizontal lines, and modes by a short vertical line. (From Goldberg and Arrhenius, 1958.)

Such results are unsatisfying. First of all, the figures one obtains by such geochemical balance computations are not in agreement with field measurements on the relative percentages of types of sedimentary rocks. Whether the discrepancies arise from the deficiencies in either or both methods is not clear. Also, there is a rather large region of cloudiness surrounding many entries in such bookkeeping. It is normally assumed that the ultimate sources of sediments are the weathering products from the continents, although a number of authors have pointed out that the pyroclastics and the substances derived from their decomposition may contribute significantly to deep-sea deposits. It is very difficult to weigh such effects at the present time. In addition, as previously pointed out, our sampling of the pelagic deposits is inadequate. RAITT'S (1956) value of a few hundred meters depth of an unconsolidated layer can be compared with values of the order of meters or tens of meters for typical depths of recovered samples. Radical changes in the types of sediment between the Tertiary and Quaternary have been observed (GOLDBERG and ARRHENIUS, 1958) and, depending upon the weighting, either group of samples can strongly influence the calculated average composition of pelagic sediments.

Possibly, the role of pelagic sediments in the major sedimentary cycle can best be approached by considerations of the reactivities of the elements in sea-water with respect to the formation or incorporation into solid phases. A quantitative consideration of this problem may be found by studying the average residence times, expressed in years, that an element spends in the sea before precipitation to the ocean floor. BARTH (1952) calculated such numbers on the basis of the amount of element delivered to the oceans per year by the rivers, defining

$$t = \frac{\text{amount of element in the sea in grammes}}{\text{supply in grammes per year}}$$

Using published values of the average composition of river water and the influx of river waters into the ocean per year he arrived at the values in Table 1.

Table 1. *Residence Times of Elements in the Oceans*

Element	Amount in oceans (g)	Residence time (years)	
		Goldberg and Arrhenius	Barth
Na	$1{\cdot}5 \times 10^{22}$	$2{\cdot}6 \times 10^{8}$	$2{\cdot}1 \times 10^{8}$
Mg	$1{\cdot}8 \times 10^{21}$	$4{\cdot}5 \times 10^{7}$	$2{\cdot}2 \times 10^{7}$
Li	$2{\cdot}8 \times 10^{17}$	2.2×10^{7}	
Sr	$9{\cdot}8 \times 10^{18}$	$1{\cdot}6 \times 10^{7}$	
K	$5{\cdot}3 \times 10^{20}$	$1{\cdot}1 \times 10^{7}$	$1{\cdot}0 \times 10^{7}$
Ca	$5{\cdot}6 \times 10^{20}$	$8{\cdot}0 \times 10^{6}$	$1{\cdot}0 \times 10^{6}$
U	$5{\cdot}2 \times 10^{15}$	$6{\cdot}5 \times 10^{5}$	
Zn	$1{\cdot}4 \times 10^{16}$	$1{\cdot}8 \times 10^{5}$	
Cu	$5{\cdot}2 \times 10^{15}$	$6{\cdot}5 \times 10^{4}$	
Co	$7{\cdot}0 \times 10^{14}$	$1{\cdot}8 \times 10^{4}$	
Si	$5{\cdot}2 \times 10^{18}$	$1{\cdot}0 \times 10^{4}$	$3{\cdot}5 \times 10^{4}$
Mn	$1{\cdot}4 \times 10^{15}$	$7{\cdot}0 \times 10^{3}$	
Th	$< 2{\cdot}8 \times 10^{13}$	$< 1{\cdot}4 \times 10^{3}$	
Ti	$1{\cdot}4 \times 10^{15}$	$1{\cdot}6 \times 10^{2}$	
Al	$1{\cdot}4 \times 10^{16}$	$1{\cdot}0 \times 10^{2}$	

On the basis of their geochemical balance sheets, GOLDBERG and ARRHENIUS (1958) computed the residence times on the amounts of elements precipitating to the ocean floor where

$$t = \frac{\text{amount of element in the sea in grammes}}{\text{amount sedimented per year}}$$

Their values, also given in Table 1, show a remarkable agreement with those of Barth. There are many assumptions involved in the derivation of these numbers. A steady state system is assumed and the mixing times of the waters containing the introduced elements (or the waters which have lost elements) are taken as short compared to the residence times. The residence times of the order of hundreds of years, of elements such as iron, titanium and aluminum, are of the same order as the mixing times of the oceans. Such elements can either be highly reactive or can enter the oceans as solid phases and rapidly fall to the ocean floor. Probably much of the silicon and aluminum in deep-sea deposits enters as solid phases (see Section on lithogenous components). Such residence times cannot be taken too seriously. On the other hand, ARNOLD (1958) and KOCZY (personal communication) have pointed out another condition to be fulfilled, that the supply per year or the amount sedimented per year has not changed in times of the order of $3t$. Thus, one might question the significance of the sodium residence time which is probably about an order of magnitude smaller than the age of the oceans.

Elements enriched in pelagic sediments, such as manganese, cobalt, nickel and zinc, all have short residence times, probably coming about from their incorporation into such hydrogenous and biogenous phases as ferromanganese minerals and skeletal debris of fish. Their enrichment in pelagic sediments, about a factor of ten over surface rocks, also results in their impoverishment in sea-water, all of these elements being in highly undersaturated states (Table 2; GOLDBERG, 1958). Similarly, barium, possibly removed by excess sulphate produced by the combustion of organic material in the sediment deposit site, is also enriched in pelagic sediments and enjoys but a short residence time in the oceans.

Table 2. Comparison of Observed Concentrations of some Trace Elements in Sea-water with those Concentrations calculated upon the basis of their most Insoluble Compound (GOLDBERG, 1958)

Ion	Observed concentration in oceans	Calculated limiting concentration	Limiting compound
Mn^{++}	4×10^{-8}	$\sim 10^{-5}$	$MnCO_3$
Ni^{++}	4×10^{-8}	$\sim 10^{-3}$	$Ni(OH)_2$
Co^{++}	$\sim 10^{-8}$	$\sim 10^{-6} - 10^{-7}$	$CoCO_3$
Zn^{++}	2×10^{-7}	$\sim 10^{-4}$	$ZnCO_3$
Cu^{++}	6×10^{-8}	$\sim 10^{-4}$	$CuCO_3$

SOURCES OF THE SEDIMENT COMPONENTS

Lithogenous components. Those solid phases in the sediments include the substances resistant either to chemical or mechanical weathering, or both, which originate from the earth's lithosphere. Such minerals as quartz, mica, feldspar, augite and hornblende, as well as volcanic debris, constitute the more obvious members in the group, although certain of the clay minerals may have initially formed on the continents.*

Volcanic ash horizons have been observed in a number of areas. BRAMLETTE and BRADLEY (1940) used two silicic volcanic ash zones to establish a stratigraphy in Atlantic sediments, while MELLIS (1954) has made preliminary attempts at defining stratigraphic levels in the Eastern Mediterranean on the basis of the refractive index of volcanic glass fragments. In the Cape Verde Basin, RADCZEWSKI (1937b) found the sediments to be extraordinarily rich in volcanic material derived from the Cape Verde Islands. Up to 45 per cent of the non-calcareous portions of the deposits consist of volcanic augite. Increased amounts of feldspar, augite and hornblende accompany deposits of volcanic glass in the Pacific (REVELLE, BRAMLETTE, ARRHENIUS and GOLDBERG, 1955). Quantitative studies on the relative contributions to oceanic deposits of such volcanic material, are lacking.

The transport of atmospheric dusts to oceanic areas was initially recorded in the twelfth century by the Arabian geographer Edrisi (RADCZEWSKI, 1937a). Radczewski further notes the rather common occurrence of dust falls which have been observed as far as one thousand sea miles from the coastline. The dusts furthest from land, composed of fine-grained clays, are reddish due to the preferential loss of the larger yellow quartz grains which give the dusts, closer to the continents, a more buff-colored tinge. The particles consist of quartz, clay, calcite, iron oxides, feldspars with minor quantities of green hornblende, biotite, tourmaline, garnet, epidote, titanite, rutile and zircon.

Such dusts stimulated RADCZEWSKI (1937a) to find a quantitative measure for terrestrial contributions to the deep-sea deposits. Inasmuch as the most probable source for some of the non-volcanic material in the Cape Verde basin was the Sahara Desert, a search was made for an indicator, characteristic of this arid area. Quartz grains, coated with a red-brown hematite, proved to be diagnostic of the desert material. These particles, the so-called "Wüstenquarz," constituted between 3·1 and 39 per cent of the total quartz in the 10–50 μ size range and between 5 and 22 per cent in the 5·5–10 μ size range. The percentage decreased in these deposits further from the shore and the highest values were found in the inshore coarse fractions. Finally, the Wüstenquarz was found in all samples of the last glacial and interglacial states.

In the Pacific REX and GOLDBERG (1958 and some unpublished data) made quantitative analyses of quartz in surface sediment samples and found a marked latitudinal dependence with maximum concentrations around 30° N and, somewhat less distinctly, around 35° S (Fig. 2).

These results are reported on a calcium carbonate-free basis. The quartz particles occur in the deposits as chips and shards and are well sorted with maximum concentrations between 1 and 20 μ. The Stoke's law settling times of approximately 2 years for 10 μ particles to cover 4000 m, coupled with the observation that the highest quartz concentrations in the mid-latitudes were in deposits furthest from land, suggested modes of transport other than by water currents. In addition it is difficult to fit the observed latitudinal variations with any observed circulations of Pacific waters.

---

* The distinction between detrital and authigenic minerals, for example the clays, is not clearcut. For example, a clay mineral particle, derived from the continents, may undergo partial changes in its structure while passing through the hydrosphere to the ocean floor. Boron, much more abundant in the oceans than in terrestrial waters, may well enter the clay structure or additions to the already existing minerals, resulting in higher contents of boron in marine clays. (See GOLDBERG and ARRHENIUS, 1958, for a review of the boron problem.) This problem in the extreme reverts to the classical conundrum of the sock, which is repeatedly darned until none of the original material is left. Is this a new sock or not?

Several lines of evidence pointed to the atmospheric transportation of the quartz and to a relationship of the observed distribution in sediments to the exposed arid land areas, i.e. the deserts of the world are the primary sources of this mineral in the sediments (Fig. 2). The atmospheric wind fluxes in the troposphere, the presumed transporting agent, are zonal and are consistent with the latitudinal distribution. The authors found quartz in the intestines of filter-feeding pelagic organisms living in the surface waters of the mid-Pacific ocean. The observed size distribution of quartz is similar to that observed in atmospheric fallouts. Finally, quartz has been repeatedly reported as a main constituent of atmospheric dusts.

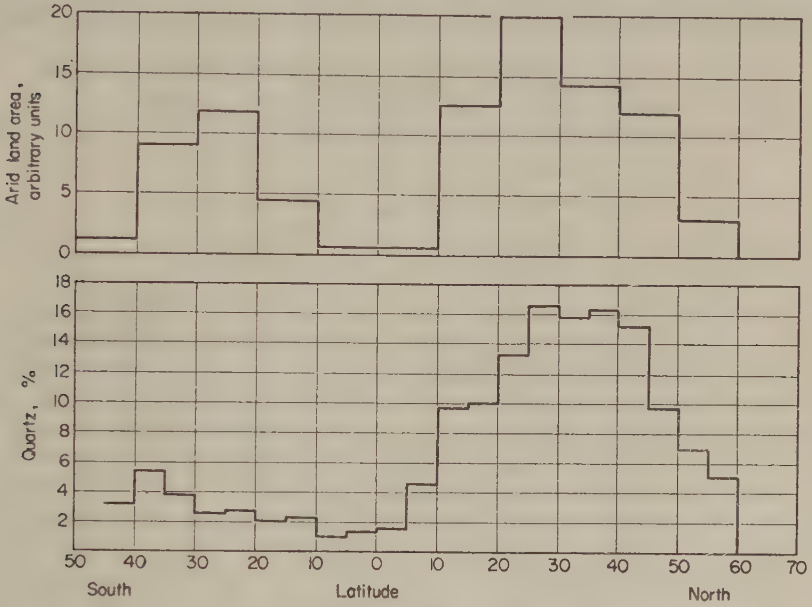

Fig. 2. The quartz contents of Pacific pelagic sediments (on a calcium carbonate-free basis) and the arid land areas of the world as a function of latitude.

Goldberg and Rex also observed that the longer cores from the ocean floor displayed a marked decrease going from the recent to the older strata. It was suggested that the changes indicate a major climatic shift that occurred sometime during the Late Tertiary.

Cosmogenous components. In 1876 Murray first called attention to certain spherical particles in deep-sea sediments, having a highly magnetic nature (a rather detailed account of his work may be found in MURRAY and RENARD, 1891). They seldom exceed 0·2 mm in diameter and were more commonly found in the 30–60 μ size range. The spherules generally have a nucleus and a crust; the former is metallic iron while the shell is magnetite. The metallic phase directed Murray to consider a relationship with iron meteorites and an extra-terrestrial origin for these spherules. The presence of the oxidized coating was attributed to the combustion of the iron nucleus while passing through the earth's atmosphere.*

Some eighty years later chemical confirmation of the deduction of Murray was made in several laboratories (SMALES, MAPPER and WOOD, 1958; CASTAING and FREDRIKSSON, 1958; and HECHT and PATZAIC, 1957). These groups of workers attempted to compare the rather unique composition of iron meteorites with the spherules. Typical results, as given in Table 3, indicate that the copper, cobalt and nickel concentrations in these two materials are remarkably similar.

Table 3. *Some Elemental Ratios in Deep-sea Spherules and Iron Meteorites* (SMALES, MAPPER and WOOD, 1958)

	Ni/Cu	Ni/Co	Cu/Co	Ni/Fe
Magnetic spherules	~1400; ~1100	17; 13	0·012; 0·012	~0·08; ~0·13
Iron meteorites	210–1650	7·3–43·4	0·013–0·069	0·06–0·17

These spherules have been gathered *in situ* by the use of magnetic rakes (BRUUN, LANGER and PAULY, 1955) and in the laboratory by the use of magnetic separators (LAEVASTU and MELLIS, 1955; PETTERSSON and FREDERIKSSON, 1958). Besides the metallic spherules, other magnetic materials have been collected including some reniform slag-like particles consisting of a silicate ground mass with magnetite crystals, some irregular pieces of metal, and spherules containing no metal (BRUUN *et al.*, *op. cit.*). Some of the siliceous matter bears resemblances to stony meteorites, but definitive work on possible cosmic origins of such particles remains to be done.

PETTERSSON and FREDRIKSSON (1958) made quantitative measurements on the numbers of spherules larger than 30 μ in a group of deep-sea cores. They pointed out that the contributions of particles with diameters under 30 μ, particles difficult to count and easy to overlook, were not significant to the total weight of the spherules. The numbers of counted spherules per kilogram of salt- and carbonate-free sediment varies in the units of hundreds and thousands and a typical depth distribution of spherules is given in Fig. 3. From results in other cores which had higher concentrations of spherules in the upper layers, Pettersson and Fredriksson suggest that the frequency of such spherules deposited in recent times has been higher than in the past. Further, on the basis of ionium–radium chronology for the rate of accumulation of pelagic sediments, they calculate the total accruement of spherules to the earth's surface to be of the order of 2500–5000 metric tons annually.

Biogenous components. The three principal solid phases in pelagic sediments arising from living matter in the sea are calcium phosphates, calcium carbonates and silicon dioxide. These three substances make up in large part the skeletal building blocks of the plants and animals.

---

* This conclusion was experimentally verified by CASTAING and FREDRICKSSON (1958) who found that the content of nickel, cobalt and iron were in similar concentrations in both the shell and metallic core.

Biogenous apatite consists primarily of the skeletal debris of fish in the sediments. ARRHENIUS, BRAMLETTE and PICCIOTTO (1957) and ARRHENIUS and KORKISCH (unpublished manuscript) have examined material from the late Pleistocene to Recent and found that it contained not only very high contents of uranium and thorium but also 0·6–1·5 per cent of zinc, 0·1–0·5 per cent of copper, 0·05–0·15 per cent of tin and 0·03–0·10 per cent of lead. These workers separated the organic phases from the inorganic phosphate matrix and demonstrated that the rare earth elements, most of the strontium and barium occur in the apatite structure, whereas the organic phases were host to the zinc, tin, lead, titanium, copper and silver and much of the magnesium, aluminum chromium and nickel. There were no significant differences in these elementa, contents between the Recent and Tertiary strata.

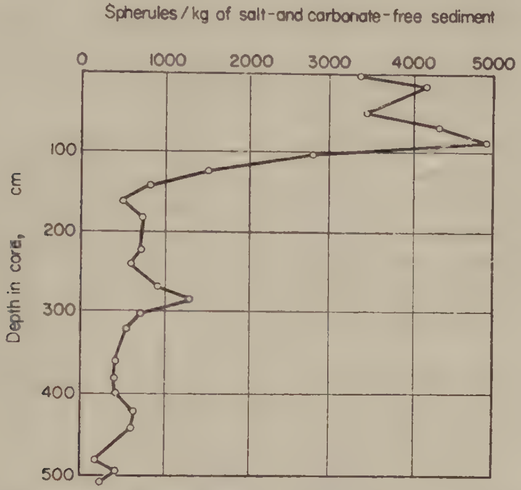

Fig. 3. The number of cosmic spherules, per kg of salt- and carbonate-free sediment from Swedish Deep Sea Core 90, 3° 21′ S; 174° 12′ W; 4830 m. (From PETTERSSON and FREDERIKSSON, 1958.)

Analyses of fish bones taken from living organisms did not reveal high concentrations of any of the above cited metals. The accumulation of the metals appears to take place subsequent to the death of the organisms and apparently at the surface of the sedimentary deposits.

BOWIE and ATKIN (1956) reported high amounts of thorium and uranium in the skeletal remains of Devonian fish. The thorium occurs principally in the organic matter while the uranium is concentrated in the apatite structure.

The calcium carbonate deposits on the deep-sea floor stem mainly from Foraminifera, Coccolithophoridae and pteropods. The carbonate content of sediments in general decreases in amount with increasing depths of the superficial water layer. In the Pacific, for example, at 2000 m the carbonate content of sediments is of the order of 60 per cent; at 4000 m, 40 per cent; and 5000 m, 15 per cent and disappearing somewhere after 5500 m (REVELLE *et al.*, 1955). The calcium carbonate content of pelagic sediments can range from zero to nearly one hundred per cent.

Opal, a highly disordered form of silicon dioxide, generally contains less than 12 per cent water and comes to the sea floor as the frustules of diatoms, a unicellular group of marine plant life, or the skeletal remains of such organisms as Radiolaria and sponges. There is no evidence for the inorganic deposition of opal in the marine environment.

Associated with the high amounts of biogenous phases in certain deposits is the element barium. GOLDBERG (1959, in press) has indicated a covariance between this alkaline earth and the opal content of a pair of diatomacous cores from the Bering Sea. The barium concentrations rose to values of 0·25 per cent in levels containing 20 per cent or so of opal, while barium itself could not be detected (less than 0·005 per cent) in the pure separated diatom frustules.

REVELLE (1944) has commented upon the high contents of barium in deep-sea sediments, especially the enrichment in the globigerina oozes (pelagic sediments with over 30 per cent by weight of calcium carbonate in the form of foraminiferal tests).

GOLDBERG and ARRHENIUS (1958) have extended this observation by measuring the barium/clay mineral ratio across the equatorial zone of high organic productivity. The ratio was twenty times higher under the remarkably fertile zone of the equatorial divergence (10° N to 10° S) than at higher northerly or southerly latitudes. In such deposits the absolute barium concentration rose to values of one per cent or even higher. As in the case of the opal skeletal remains, there is practically no barium in the calcite of Foraminifera and Coccolithophoridae.

Inasmuch as unusual concentrations of barium are associated with biogenous solid phases that do not contain barium, it appears profitable to seek out an accumulation mechanism involving the non-skeletal living matter. Perhaps, as ARRHENIUS (1959) suggests, the combustion of the organic matter on the sea floor by oxygen results in the release of additional sulphate ion to the surrounding sea-water. If the supply of sulphate ion is sufficient, the precipitation of barium sulphate in the form of barite can occur. Barite is apparently one of the principal forms of barium in the pelagic deposits (GOLDBERG and ARRHENIUS, 1958).

Hydrogenous minerals. The ferromanganese minerals represent the most nearly unique, and for possibly this reason, the most studied of the marine authigenic minerals. They exist in the form of nodular concretions, the so-called manganese nodules which range in size from millimeters to about a meter, coatings, and as components of the unconsolidated sediments. The two principal metals, iron and manganese, are normally present in similar amounts, although, less generally, either of these two elements can be dominant. They are found on both ocean floors and normally occur in localities where the total rate of accumulation of the sediments is low. MENARD and SHIPEK (1958) estimate that about 20–50 per cent of the deep-sea floor in the Southwestern Pacific is covered with the manganese nodules, from studies of photographs of the deep-sea floor and of the occurrence of nodules in cores. Such phases as phillipsite, barite and fish debris, which are diluted in rapidly amassing deposits tend to accompany the ferromanganese minerals.

The ferromanganese minerals act as hosts for a suite of elements, including copper, nickel, cobalt, zinc, lead and the rare earths, which can attain concentrations up to values around one per cent (Table 4; GOLDBERG, 1954; GOLDBERG

Table 4. Chemical Composition of Manganese Nodules with respect to some Heavy Metals

Element	Range (per cent)
Fe	6·2–20
Mn	11–24
Ni	0·16–1·1
Co	0·01–0·7
Cu	0·17–1·8
Th	0·0020–0·0130
Pb	0·0500–0·2500

and ARRHENIUS, 1958). These guest metals which are enriched in the ferromanganese minerals, as well as the manganese, all exist in sea-water in a highly undersaturated condition (GOLDBERG, 1958) and their assimilation by these minerals has been postulated to account at least in part for this situation.

The unique chemical composition, unlike that of any terrestrial mineral, has strongly established the authigenic character of the ferromanganese accumulations. Further support comes from the lead isotopic analyses of CHOW and PATTERSON (1959). These authors point out that the distinctive values of the radiogenic lead isotopes strongly suggest a derivation of the lead in manganese nodules from dissolved species in sea-water.

Structural investigations by BUSER and GRÜTTER (1956; see also GRÜTTER and BUSER, 1957) indicates an irregular pile of quasi-two-dimensional layers. Common to all of the nodules are layers of MnO_2. Sandwiched between the manganese dioxide layers is an irregular in-between layer consisting mainly of the hydrated hydroxides of manganous or ferric ions. In nodules with amounts of iron, greater than can be accommodated in the in-between layer, the mineral goethite appears. Buser and Grütter point out that some of the iron can also be built into the MnO_2 layers through the isomorphous exchange of Mn^{+4} by Fe^{+3}.

The nodular materials possess rather high specific surface areas, ranging from 6 to 190 m^2/g (BUSER and GRÜTTER, *op. cit.*). By coupling this observation with the ability of other polyvalent cations to substitute in the disordered layer the high concentrations of accessory metals in the ferromanganese minerals can be explained.

On the basis that the radium in manganese nodules is unsupported, PETTERSSON (1943) and VON BUTTLAR and HOUTERMANS (1950) derived values of 1 mm/10^3 years for the rates of accretion. However, on the basis of the unusually high amounts of thorium in the nodules (from 30 to over 100 p.p.m., GOLDBERG and PICCIOTTO, 1955), GOLDBERG and ARRHENIUS (1958) suggest that these results may be much too high in that much of the radium may be ionium-supported. If all of the radium is ionium-supported, that is the extreme case, the rate of deposition given above is too high by a factor of 50, the ratio of the half-life of ionium (80,000 years) to that of radium (1600 years). GOLDBERG and KOIDE (unpublished data) found ionium/thorium ratios of over 30 in a surface layer of the Horizon nodule (40° 14′ N and 155° 15′ W, recovered from a depth of 5500 m) which was removed by lightly going over the surface with a dental drill. Directly below this layer the ratio dropped to values near 5, possibly substantiating the postulated lower growth rate or indicating a discontinuous deposition. The concentric layered structure of most nodules probably results from periods of relatively rapid accumulation followed by intervals of little growth.

The rather exotic nature of these minerals has inspired a number of speculations as to their mode of formation. The earlier workers were more concerned with the immediate origin of the elements, rather than any physicochemical considerations, and such sources of manganese as Foraminifera, volcanic debris, sub-surface springs, etc. Both biochemical and inorganic mechanisms to deposit the manganese and iron oxides were invoked.

A satisfactory hypothesis must not only account for the observation that iron, as well as manganese, is markedly enriched in these accretions but also for the evidence that, whereas manganese is in a divalent dissolved state in sea-water, in the ferromanganese minerals it is mainly tetravalent. The only non-biological species in the ocean capable of oxidizing manganese is oxygen and the reaction

$$2OH^- + Mn^{++} + \tfrac{1}{2}O_2 = MnO_2 + H_2O$$

has a free energy of $-$ 9 kcal at 25 °C, at a pH of 8, a manganous ion concentration of 10^{-9} M and a partial pressure of oxygen of 0·25 atm. These concentrations are all similar to those in near-bottom sea-water; the near-bottom temperature is 0 °C. Since tetravalent manganese is not found in sea-water, it is apparent a surface is necessary for the reaction. The well known catalytic properties of iron oxide surfaces suggest the association of such material in the formation of the nodules. Iron exists in the oceans dominantly in an insoluble form, partly colloidal. The accumulation of iron oxides, possibly by some type of electrodeposition, results in the formation on the sea floor of the initial surface. The accretion of manganese leads to the formation of the ferromanganese minerals, the scavenging of the high charge density ions in sea-water by the forming in-between layer, and the formation of a new surface of iron–manganese which can be the site of further oxidation and further accumulation of the metallic oxides.

The authigenic zeolite of the deep-sea floor, a phillipsite mineral, not only accompanies and possesses similar abundances to the ferromanganese minerals, but is certainly as puzzling with respect to occurrence and mode of formation. The highest surface concentrations of phillipsitic minerals in the Pacific occur in the southern regions where values between 5 and 20 per cent by weight in the dried sediments are common. Phillipsite is quite rare at the surface in the equatorial regions (10° N to 10° S) and becomes abundant in the North Pacific in the Mid-Pac mountain vicinity west of Hawaii. Even though it is quite often found in association with those substances which in high concentrations reflect low rates of deposition, apatite, barite and the ferromanganese minerals, the highest surface concentration, on a calcium carbonate-free basis, was found at Downwind BG 38 station (29° 43′ S; 142° 23′ W, depth 4420 m) with a value of 40 per cent, but there was 21 per cent of calcium carbonate in the sample; other calcareous deposits in these regions may have high amounts of phillipsite. These results do not coincide with the observations of Murray and Renard who report this zeolite "as occurring most abundantly in red clays, more rarely in radiolarian oozes, and still more rarely in globigerina oozes". Rarely do siliceous organic remains coexist in deposit with phillipsite, and, where they do, they are heavily corroded (REIDEL, personal communication).

The phillipsite microliths are apparently at least as ubiquitous as the ferromanganese minerals, but their influence on the gross composition of pelagic sediments is less felt because their composition is more similar to that of crustal rocks. Semi-quantitative analyses made by the author on a marine phillipsite gave: Si, 25·0 per cent; Al, 8·8 per cent; Mg, 0·04 per cent; Ca, 0·21 per cent; K, 5·1 per cent; Na, 5·5 per cent; Ti, 0·02 per cent and P, 0·09 per cent. These values may be compared with the literature composition range of $KCa_3Si_9Al_7O_{32}.12H_2O$–$K_3CaSi_{11}Al_5O_{32}.12H_2O$ (WINCHELL, 1951, p. 343). Evidently, the high Si/Al ratio in the marine form accounts for the increased alkali metal/alkaline earth ratio. These results are comparable to those of MURRAY and RENARD (*op. cit.*) who found the high sodium values, but also high iron values, quite clearly contamination resulting from a surface coating which the authors cite was not removed prior to analysis.

The remarkable water capacities, ion-exchange and molecular sieve properties, characteristic of zeolites, are reflected in the behaviour of the phillipsite-rich behavior. Samples from these areas contain unusual amounts of those large cations, such as barium and radium, which can be accommodated in the cavities and channels of these open network minerals (GOLDBERG and ARRHENIUS, 1958).

Only limited studies on the clay minerals of the pelagic marine environment have been made and this state of affairs probably results from the difficulties in analysing these poorly crystalized, and in many cases, mixed layer materials. GRIM (1953) has surveyed the literature in the field and concludes that many of the reported determinations suffer on the basis of inadequate or incomplete analytical data. He favors only those analyses made by a combination of X-ray diffraction, differential thermal and chemical methods. On the basis of such results some agreement on the types of clay minerals encountered on the ocean floor can be reached. In the following discussion, an attempt has been made to use those results that conform, or nearly so, to Grim's criteria.

The ubiquitous clay mineral is illite, defined by its 10 Å reflection and its non-swelling character under ethylene glycol treatment. ZEN (1957) found it to be the most common mineral in samples off the coast of Peru and Chile, a result also reported by GRIM, DIETZ and BRADLEY (1949) in samples from the Gulf of California and from the Pacific Ocean off the California coast and by DIETZ (reported in GRIM, 1953) in 39 samples collected from the various oceans of the world. In the last cited work, illite was dominant in 23 of the samples. CORRENS (1937) apparently found this mica-like mineral in South Atlantic deposits.

The reports on a 7 Å kaolinite-type mineral indicate a non-uniform distribution. Zen finds it to be the second most common clay, while MURRAY and HARRISON (1956) find its presence questionable in sediments in the Gulf of Mexico (Sigsbee deep and environs). Correns found it predominant in some of his samples, while it was the major mineral in 9 of the 39 world-wide samples of Dietz. Grim, Dietz and Bradley found it in their Pacific investigations.

Montmorillonite, as given by a basal spacing around 15 Å which swells to around 17 Å, upon ethylene glycol treatment and collapses to around 10 Å on heating to temperatures above 200 °C, is found by Murray and Harrison to be the principal clay mineral member, and approximately twice as abundant as chlorite and illite in their samples. Montmorillonite is scarce or absent in the spectra given by Zen, Dietz and Grim and co-workers. Correns found it in relatively limited areas near sites of basic volcanic activity.

Chlorite, designated by a 14 Å periodicity which is unaltered by glycolation or heat treatment, apparently improved its interlayer organization with depth in the Gulf of Mexico deposits investigated by Murray and Harrison; Zen, as did other workers, found it to be scarce.

No systematic treatment of the origin or sources of these clay minerals has yet been presented. ARRHENIUS (1954) suggests an authigenic origin for some of these aluminosilicates while Zen emphasizes the devitrification of volcanic glasses in his studies. REX and GOLDBERG (1958) estimate that in the mid-latitudes of the North Pacific a large portion of the clays arise from their terrestrial counterparts that have been transported by the winds to the pelagic areas.

GEOCHRONOLOGIES

Developments in obtaining ages in sedimentary minerals have been occurring at highly accelerated rates in the last few years. In the 1940s only the ionium–radium method was available for studying the rates of sedimentation in the deep sea and it is now for the most part discredited. Today, a number of techniques, covering the entire span of geologic time, are at the disposal of the marine scientist (Table 5); some of these have already been applied to the pelagic environment.

Table 5. Principal Geochronologies, based on Radioactive Decay, applicable to Marine Sediments

Method	Half-lives of significant isotopes (years)	Dating range (years)
Ionium–thorium	^{230}Th $8{\cdot}0 \times 10^4$	10,000–400,000
Beryllium–10	^{10}Be $2{\cdot}7 \times 10^6$	10^5–10^7
Rubidium–strontium	^{87}Rb 5×10^{10}	10^7–10^{10}
Potassium–argon	^{40}K $1{\cdot}2 \times 10^{10}$*	10^6–10^{10}
Radio-carbon	^{14}C 5600	500–30,000
Ionium–radium	^{226}Ra 1600; also ^{230}Th	500–400,000

* Half-life for decay to argon-40.

Certain requirements must be fulfilled in the utilization of a given method to a particular sediment. First of all, the entire sample, or a separable component of it, must contain in sufficient amounts the nuclides to be assayed, and in certain cases, be free of other. For example, the application of the strontium–rubidium technique demands the sample have appreciable (say a few per cent) rubidium and essentially no strontium.

Secondly, the depth or time interval in the sedimentary column that is mixed or stirred must be small in relationship to the dating range. Preliminary results in the author's laboratory indicate that the pelagic clays in the Pacific can be mixed over at least 10 cm levels or times of hundreds of thousands of years. Hence, the radio-carbon method would not be expected to provide a reliable timetable in such deposits.

Finally, there are restrictions relating to the origin of the various components of the deposit. For example, lithogenous minerals high in potassium, say certain feldspars, could not be present in significant amounts in sediments that were subjected to potassium–argon analyses. For any derivable ages would include the age of formation of the non-authigenic feldspars.

The following paragraphs briefly survey the various radioactive time-clocks that have been used or appear promising in work on pelagic sediments. A number of techniques have been purposely omitted for a variety of reasons. The times involved in pelagic sedimentation appear to be much too long for tritium dating. Methods based on the natural β-radioactivities of ^{187}Re and ^{176}Lu were not considered due to the fact that concentrations of either of these two elements by marine deposits is unknown and their terrestrial abundances are extremely low. Lead–lead, uranium–lead and thorium–lead methodologies were neglected because of the complex non-equilibrium problems in authigenic mineral formation. Radioactive decay relationships involving other members of the uranium and thorium radioactive series such as actinium and protoactinium are promising. But since they all resemble in certain aspects the ionium–thorium method and since no actual applications of such nuclides have been published, such geochronologies have not been considered.

Ionium–thorium chronology. The method of ionium–thorium chronology (PICCIOTTO and WILGAIN, 1954) is based upon the simultaneous removal of ionium (^{230}Th, $t\frac{1}{2} = 80{,}000$ years, a member of the ^{238}U radioactive series) and thorium (^{232}Th, $t\frac{1}{2} = 1{\cdot}4 \times 10^{10}$ years) from the overlying sea-water to one or more of the mineral components of the sediments. In theory such a technique should cover a time span of about 4 half-lives of ionium, or 360,000 years.

A number of assumptions and prerequisites govern the validity of the method. First of all, the Io/Th ratio in the water adjacent to the sediment has to remain constant over the time intervals to be measured. Secondly, the ionium and thorium should be in the same chemical forms in sea-water. Since thorium exists in aqueous solution only in the + 4 state under normal conditions, and since any non-equilibrium forms of ionium formed following the decay of its parent have times of the order of thousands of years to become the more stable ionic species, at the present time there is little question concerning this assumption. Any uranium-supported ionium should be insignificantly small or subtracted from the total ionium. Finally, the analysed materials cannot contain any detrital materials, of continental or volcanic origin, which contain significant amounts of either of these isotopes of thorium. Inasmuch as the lithogenous fractions of the deposits are usually of a high chemical resistance to attack, preferential dissolution of the sample can eliminate difficulties associated with the presence of such minerals (GOLDBERG and KOIDE, 1958).

Russian investigators (BARANOV and KUZMINA, 1958a; 1958b; see also STARIK *et al.*, 1958) conducted analyses on these thorium isotopes in a series of scooped bottom samples and cores from the Pacific and Indian Oceans. They found that in general the ionium was nearly completely supported in the near coastal regions, but in areas distant from the coast there can be one to two orders of magnitude more unsupported than uranium-supported ionium. Computed rates of sedimentation of marine sediments on the basis of this technique were 1–3 cm/1000 years for the border regions of the Pacific and 0·5–0·63 years/cm for the solids of the Indian Ocean. These workers made no attempts at partial dissolution of the sediment samples to eliminate contributions of lithogenous thorium.

GOLDBERG and KOIDE (1958) have applied ionium/thorium chronology to a series of samples from the Eastern Pacific Ocean and have noted exponential decreases in the ratios in most of the cores they analysed. The samples were dissolved in concentrated hydrochloric acid and the residues of quartz, feldspars and other resistant minerals were discarded. Several cores showed no significant ratio decrease with depth. This situation may result from either a lack of deposition of solids or a loss or disturbance in the upper sections of the sample during shipboard handling. Table 6 gives a not unusual depth distribution of the ionium/thorium ratio for a Southeastern Pacific deposit. These results give a rate of accumulation for the levels below 10 cm of 0·3 mm/10^3 years and a mixing zone of about 10 cm from the surface.

Table 6. The Depth Distribution of the ionium/thorium Ratio in Downwind HG 49 *taken* 14 *December* 1957 *at* 42° 02′ *S;* 98° 01′ *W; Depth* 4350 *m*

Depth in core (cm)	Io/Th in disintegrations of Io per disintegration of Th
0–2	37
2–4	32
4–6	36
6–8	28
8–10	28
10–12	17
12–14	6·5
14–16	2·5
16–18	2·5
18–20	1·7

The surface ratios were observed to fall into two distinct groups: a set in the region between the Aleutian Islands and Hawaii with values of the Io/Th ratio, in units of disintegrations of Io per disintegration of Th per unit time, averaging about 15 and a second group in the region between longitude 120° and 140° W and latitude 40° N and 40° S with ratios varying about 35.

These results can be interpreted on the basis that the deep-oceanic water masses, which are in contact with the sediment surfaces, furnish these isotopes. The ionium arises principally from the uranium in sea-water, while the thorium must have as its ultimate source the weathered materials of the lithosphere. Since the residence time of uranium is of the order of a million years, a time in which it is conceivable the world oceans become mixed, the rate of production of ionium per year can be assumed constant. The rate of introduction of thorium, on the other hand, because of the short residence time of thorium, under a thousand years, determines the value of the ratio. Thus, in the Atlantic, with a more rapid circulation of waters, a smaller ocean with a greater amount of run-off, should have a higher thorium input per unit time and hence a lower value of the ratio. This is actually observed and typical Atlantic surface values range between 8 and 12. The North Pacific which receives a greater input of river waters than the South Pacific shows surface values intermediate to the Atlantic and Southeastern Pacific.

A similar situation exists with the distribution of lead isotopes in the sediments of the Pacific (Chow and Patterson, 1959). The radiogenic isotopes, ^{206}Pb, ^{207}Pb and ^{208}Pb were all enriched relative to ^{204}Pb going from the Northwest to the Southeast Pacific. The residence time of lead in the oceans is probably ten times that of thorium, of the order of 10^4 years.

Beryllium-10. This isotope of beryllium has a half-life of 2·7 million years and is produced throughout the atmosphere, principally the upper levels, by cosmic ray interactions with the gaseous atoms. This nuclide holds a certain fascination for the marine geochemist inasmuch as it was first discovered in pelagic sediments (Arnold, 1956; Goel *et al.*, 1957). On the basis that sedimentation rates have remained constant over the time intervals considered, Goel *et al.* (*op. cit.*) obtained a value of 5·5 mm per thousand years for the accumulation rate for some Pacific cores taken from a depth of 5200 m at 4° 04′ S and 152° 53′ W. These workers also used absolute disintegration rates of ^{10}Be, implicitly assuming the beryllium deposition equals the average global production rate. There remains the possibility that different oceanic water masses contain dissimilar amounts of stable beryllium, giving rise to differing specific activities of ^{10}Be. Merrill *et al.* (1959) delimited this by showing that samples from the Atlantic and Pacific had beryllium contents between 2·0 and 3·0 p.p.m. with an over-all average of 2·6.

Table 7. The ^{10}Be *and* Io/Th *in Capricorn* 50 *BG1.* ^{10}Be *values* (*from* Merrill *et al.*, 1959)

Depth in core (cm)	^{10}Be (d.p.m. × 5/g)	Depth in core (cm)	Io/Th
0–12	$61 \pm 3 \times 10^{-3}$	0–5	39·8
12–24	$1·3 \pm 0·3$	5–12	32·0
24–36	$-0·5 \pm 0·5$	12·5–18	5·2
36–48	$1·6 \pm 0·4$	18–24	5·9
48–60	$7·7 \pm 0·4$	24–29	3·1
		29–36	1·4
		36–48	2·2
		48–60	1·6

Arnold and his co-workers have made detailed analyses on a number of cores for the ^{10}Be concentration. Several have shown erratic values with depth indicating probable disturbances in the core. A core from the near-equatorial Pacific (Capricorn 50 BG1, 14° 55′ N; 124° 12′ W; depth of 4270 m) had a remarkably high activity at the surface, followed by a rapid drop in the subsequent levels (Table 7). Goldberg and Koide ran the ionium/thorium on cuts from the same core and obtained similar results, a sharp fall-off in activity after 12 cm. This discontinuity may reflect a change from a more rapid to a slower sedimentation rate. The time interval is at least one-third of a million years from the ionium/thorium values. The reliability of any ages on the basis of the ^{10}Be values, at the present are certainly questionable. First of all, the constancy of the production or the flux of ^{10}Be to the oceans over the time periods of millions of years has not been established. Again, the composition of the core with respect to its various components may have changed with depth. MERRILL *et al.* (*op. cit.*) found stable beryllium lower in phillipsite and higher in some ferromanganese minerals as compared to the above-cited gross sediment average. No quantitative analyses on the various mineral components of this core were made. Compositional changes or variations in the ^{10}Be flux may account, in part, for the quite disturbing high value at 48–60 cm. Again, we know little about disturbances in the continuity of deposition.

It is of interest to note that GOLDBERG and KOIDE (1958) made Io/Th determinations on a duplicate core taken in the same general area. In this case there was almost a continual deposition to a depth of 24 cm indicating a quite different history of accumulation with a sedimentation rate of about one mm/thousand years over this interval.

Rubidium–strontium. Rubidium-87 is naturally radioactive and constitutes 27·85 per cent of natural rubidium. It has a half-life of five billion years, decaying to strontium-87 which is a minor strontium isotope (7·02 per cent). There are two general applications of this decay scheme to geochronology. The first involves the parent-daughter relationships in rubidium-rich, strontium-poor minerals. The total rubidium and ^{87}Sr contents are determined, corrections are made for any naturally occurring strontium, and an age determined from the radioactive decay equations. Secondly, one can postulate that the relative ^{87}Sr content in the strontium of the oceans has systematically changed over geologic times with the introduction of radiogenic strontium from the decay of rubidium. Here the certainly justifiable assumption of continuity and uniformity in the major sedimentary cycle is made.

Ages derived from direct measurements of rubidium and ^{87}Sr have been obtained for glauconite, a clay mineral with a hydrous mica structure (HURLEY *et al.*, 1958a; 1958b). Where simultaneous potassium–argon measurements have been made, it appears at the present time that the strontium–rubidium results are not nearly as consistent and have larger errors. Although glauconites form in the shelf and slope but not the pelagic areas, the possibility of applying this method to components of the deep-sea sediments looks favorable. The zeolite phillipsite, in a single sample analysed by the author, gave potassium values of around 5 per cent and calcium values of a few tenths of a per cent. Since the pairs, potassium and rubidium and calcium and strontium, have similar behaviors in the major sedimentary cycle, one *a priori* predicts a high rubidium–low strontium mineral. Further, the zeolites are rather readily separated from sediment samples of size-density bases.

EWALD, GARBE and NEY (1956) have calculated the ages of some marine strontianites, celestite and limestones by the second method. All of these materials are rubidium-poor. They were able to assign ages over periods of greater than 100 million years and these results showed excellent agreement with values obtained by other means. This technique will undoubtedly enjoy a great popularity when pelagic sediments of the Mesozoic are recovered from the pelagic environment.

Potassium–argon. Potassium-40 (a minor isotope of potassium) decays to argon-40, the principal isotope of argon (99·6 per cent of atmospheric argon) and calcium-40. As universally applied, the potassium content and the ^{40}A content of minerals, suitable for dating, are determined to derive an "age". The 1·2 billion year half-life, with the potentiality of obtaining ages of one million years or possibly less, has made this technique extremely attractive. It has been applied to certain igneous minerals and sedimentary silvites with considerable success and quite recently (LIPSON, 1958; see also CURTIS and REYNOLDS, 1958) to glauconites. As in the case of rubidium–strontium, phillipsites appear to be the most suitable of the pelagic deposit components for attempted dating.

Radio-carbon. Ages of depths in the sedimentary carpet up to 30,000 years or so have been readily determined by assaying Foraminifera tests for carbon-14 ($t\frac{1}{2}$ = 5600 years) (see for example BROECKER, TUREKIAN and HEEZEN, 1958; EMILIANI, 1955). The rate of clay accumulation is simultaneously determined, if the clay contents of the various samples are known. The possibility of applying this technique to calcium carbonate-free clays exists in the utilization of the organic carbon, often present in amounts in the neighborhood of a per cent or so.

Ionium–radium. PETTERSSON (1937) indicated that the thorium isotopes have a very short residence time in sea-water, probably being precipitated by metallic hydroxides, notably iron. Ionium, ^{230}Th, is a daughter in the ^{238}U series, and the parent of radium-226. Utilizing the growth relationship of radium to its parent ionium, PIGGOT and URRY (1942) were able to obtain rates of accumulation of marine sediments.

However, most subsequent determination of the radium concentration with depth, as well as many published by Piggot and Urry, did not correspond to the theoretical curve in which radium grows into a maximum concentration and then decays with the half-life of its parent ionium. Instead of a single maximum, often many were found (KRÖLL, 1954). Kröll sought explanations for these anomalies by denying one of the basic assumptions of the method, that the amounts of ionium accumulated in the sediments per unit time are constant, and by considering what factors govern the distribution of radium in sediments. He suggests that changes in the concentration of uranium, in sea-water, the primary source of ionium, brought about through variations in conditions in the major sedimentary cycle, may have occurred.

Secondly, Kröll points out that changes in the *total* rate of deposition influence the distribution of radium. Other methods of determining the rates of accumulation substantiate marked changes in the total rates of deposition.

Finally, he indicated it was necessary to take into account any diffusion of radium or ionium from the sites at which they became a part of the sediment. ARRENHIUS and GOLDBERG (1955) made an attempt to study the localization of radium in the different phases of pelagic clays. Their results indicated that radium, derived from ionium, is redistributed by diffusion through the interstitial water and that the zeolite phillipsite readily accommodated such radium in its structure. In a typical clay core from the Pacific (Capricorn 23 HG, 16° 58′ S; 161° 35′ W; depth 5140 m) a second maximum appeared which corresponded to a maximum in the phillipsite content. Radio-autographs of α-particles emitted from phillipsite crystals gave a high proportion of multi-branched stars, strongly suggesting radium, which gives birth to two short-lived α-emitters, as the primary source of the tracks.

KOCZY (reported by PETTERSSON, 1955) finds the radium content of abyssal waters higher than waters of intermediate depths. He attributes this finding to the diffusion of radium, produced in the upper layers of the sediment, to the bottom waters where aided by turbulence it distributes itself in the water mass. These ideas are reinforced by the observation that radium is in excess by a factor of 6 in sea-water with respect to presumed equilibrium amounts of ionium (KOCZY, PICCIOTTO, POULAERT and WILGAIN, 1957).

All measurements of rates of accumulation of pelagic clays, because of the above results, become suspect on the basis of the migration of radium from its deposition site. In fact, future applications of this technique in pelagic clays will depend upon the finding of a mineral that has the properties of accommodating thorium isotopes in great preference to radium and of maintaining all of the ionium-supported radium.

REFERENCES

ARRHENIUS G. (1954) Significance of carbonate stratification in pelagic deposits. *Bull. Geol. Soc. Amer.* **65**, 1228–1229.

ARRHENIUS G. (1959) Sedimentation on the Ocean Floor. (1959) *Researches in Geochemistry* (Edited by Abelson, P. H.) John Wiley, New York. 1–24.

ARRHENIUS G., BRAMLETTE M. N. and PICCIOTTO E. (1957) Localization of radioactive and stable heavy nuclides in ocean sediments. *Nature, London* **180**, 85–86.

ARRHENIUS G. and GOLDBERG E. D. (1955) Distribution of radioactivity in pelagic clays. *Tellus* **7**, 226–231.

ARNOLD J. R. (1956) Beryllium-10 produced by cosmic rays. *Science* **124**, 584.

ARNOLD J. R. (1958) Trace elements and transport rates in the ocean. *Second United International Conference on the Peaceful Uses of Atomic Energy, Geneva, Proceedings*, **18**, 344–346.

BARANOV V. I. and KUZMINA L. A. (1958a) Radiochemical analyses of deep-sea sediments in connection with the determination of the rate of sediment accumulation. *Radioisotopes in Scientific Research.* Edited by Exterman, R. C., pp. 601–618. Pergamon Press, London.

BARANOV V. I. and KUZMINA L. A. (1958b) The rate of silt deposition in the Indian Ocean. *Geochemistry* (*English Translation published by The Geochemical Society*) 131–140.

BARTH T. F. W. (1952) *Theoretical Petrology.* Wiley, New York.

BOWIE S. and ATKIN D. (1956) An unusually radioactive fish from Thurso, Scotland. *Nature, London* **177**, 487.

BRAMLETTE M. N. and BRADLEY W. H. (1940) Geology and biology of North Atlantic Deep-sea cores between Newfoundland and Ireland. Part 1. Lithology and geologic interpretation. *U.S. Geol. Survey Prof. Paper 196A.*

BROECKER W. S., TUREKIAN K. K. and HEEZEN B. C. (1958) The relation of deep-sea sedimentation rates to variations in climate. *Amer. J. Sci.* **256**, 503–517.

BRUUN A. F., LANGER E. and PAULY H. (1955) Magnetic particles found by raking the deep-sea bottom. *Deep-Sea Res.* **2**, 230–246.

BUSER W. and GRÜTTER A. (1956) Über die Natur der Manganknollen. *Schweiz. Min. Petrogr. Mitt.* **36**, 49–62.

VON BUTTLAR H. and HOUTERMANS F. G. (1950) Photographic determination of the activity in manganese nodules of deep-sea origin. *Naturwiss.* **37**, 400–401.

CASTAING R. and FREDRIKSSON K. (1958) Analyses of cosmic spherules with an X-ray microanalyser. *Geochim. et Cosmoch. Acta* **14**, 114–117.

CHOW T. J. and PATTERSON C. C. (1959) Lead isotopes in manganese nodules. *Geochim. et Cosmoch. Acta* **17**, 21–31.

CORRENS C. W. (1937) Die Sedimente des äquatorialen Atlantischen Ozeans. *Wiss. Ergebn. Dtsch. Atlant. Exped. Meteor 1925–1927 3, part 3.*

CURTIS G. H. and REYNOLDS J. H. (1958) Notes on the potassium–argon dating of igneous rocks. *Bull. Geol. Soc. Amer.* **69**, 151–160.

EMILIANI E. (1955) Pleistocene temperatures. *J. Geol.* **63**, 538–578.

EWALD H., GARBE S. and NEY P. (1956) Die Isotopen-Zusammensetzung von Strontium aus Meerwasser und aus Rubidium–armen Gesteinen. *Zeit. Naturf.* **11a**, 521–522.

GOEL P. S., KHARKAR D. P., LAL D., NARSAPPAYA N., PETERS B. and YATIRAJAM V. (1957) The beryllium-10 concentration in deep-sea sediments. *Deep-Sea Res.* **4**, 202–210.

GOLDBERG E. D. (1954) Marine Geochemistry I. *J. Geol.* **62**, 249–265.

GOLDBERG E. D. (1958) The processes regulating the composition of sea-water. *J. Chem. Educ.* **35**, 116–119.

GOLDBERG E. D. (1959) The determination of opal in marine sediments. *J. Mar. Res.* In press.

GOLDBERG E. D. and ARRHENIUS G. (1958) Chemistry of Pacific pelagic sediments. *Geochim. et Cosmoch. Acta* **13**, 153–212.

GOLDBERG E. D. and PICCIOTTO E. (1955) Thorium determinations in manganese nodules. *Science* 613–614.

GOLDBERG E. D. and KOIDE M. (1958) Ionium–thorium chronology in deep-sea sediments of the Pacific. *Science* **128**, 1003.

GOLDSCHMIDT V. M. (1954) *Geochemistry*. Oxford Univ. Press, London.

GOLDSCHMIDT V. M. and PETERS CL. (1932) Zur Geochemie des Bors. *Nachr. Ges. Wiss. Gottingen* **27**, 402.

GRIM R. E. (1953) *Clay Mineralogy*. McGraw-Hill, New York.

GRIM R. E., DIETZ R. S. and BRADLEY W. F. (1949) Clay mineral composition of some sediments from the Pacific Ocean of the California coast and the Gulf of California. *Bull. Geol. Soc. Amer.* **60**, 1785–1808.

GRÜTTER A. and BUSER W. (1957) Untersuchungen an Mangansedimenten. *Chimia* **11**, 132–133.

HECHT F. and PATZAIC R. (1957). Quoted by SMALES, MAPPER and WOOD (1958) *Astronautic Acta* **3**, 47.

HURLEY P. M. *et al.* (1958a, and b). Fifth and Sixth Annual Progress Reports, U.S. Atomic Energy Commission.

KOCZY F. F., PICCIOTTO E., POULAERT G. and WILGAIN S. (1957) Mesure des isotopes du thorium dans l'eau de mer. *Geochim. et Cosmoch. Acta* **11**, 103–129.

KRÖLL V. S. (1954) On the age-determination in deep-sea sediments by radium measurements. *Deep-Sea Res.* **1**, 211–215 (1954).

KUENEN PH. (1950) *Marine Geology*. Wiley, New York.

LAEVASTU T. and MELLIS O. (1955) Extra-terrestrial material in deep-sea sediments. *Trans. Amer. Geophys. Un.* **36**, 385–389.

LIPSON J. (1958) Potassium–argon dating of sedimentary rocks. *Bull. Geol. Soc. Amer.* **69**, 139–150.

MELLIS O. (1954) Volcanic ash-horizons in deep-sea sediments from the Eastern Mediterranean. *Deep-Sea Res.* **2**, 89–92.

MENARD H. W. and SHIPEK C. J. (1958) Surface concentrations of manganese nodules. *Nature, Lond.* **182**, 1156–1158.

MERRILL J. R., LYDEN E. F. X., HONDA M., ARNOLD J. R. (1959) The sedimentary geochemistry of the beryllium isotopes. Manuscript submitted to *Geochim. et Cosmoch. Acta.*

MURRAY H. H. and HARRISON J. L. (1956) Clay mineral composition of recent sediments from Sigsbee Deep. *J. Sediment. Petrol* **26**, 363–368.

MURRAY J. and RENARD A. F. (1891) Report on deep-sea deposits based on the specimens collected during the voyage of the H.M.S. *Challenger* in the years 1872–76. *Challenger Reports*, p. 525, Longmans, London.

PETTERSSON H. (1943) Manganese nodules and the chronology of the ocean floor. *Medd. Oceanogr. Inst. Göteborg*. **B2**, 1–39.

PETTERSSON H. (1937) Das Verhältnis Thorium zu Uran in den Gesteinen und im Meer. *Anz. Öst. Akad. Wiss.* Nr. 16.

PETTERSSON H. (1955) Manganese nodules and oceanic radium. *Deep-Sea Res.* Suppl. to Vol. **3**, 335–345.

PETTERSSON H. and FREDRIKSSON K. (1958) Magnetic spherules in deep-sea deposits. *Pacif. Sci.* **12**, 71–81.

PICCIOTTO E. and WILGAIN S. (1954) Thorium determinations in deep-sea sediments. *Nature, Lond.* **173**, 632.

PIGGOT C. S. and URRY W. D. (1942) Time relations in ocean sediments. *Bull. Geol. Soc. Amer.* **53**, 1187.

RADCZEWSKI O. E. (1937a) Eolian deposits in marine sediments. *Recent Marine Sediments* (Edited by Parker Trask), pp. 496–502.

RADCZEWSKI O. E. (1937b) Die Mineral fazia der Sedimente des Kapverden-Beckens. *Wiss. Ergebn. Dtsch. Atlant. Exped. Meteor* 1925–1927 3, part 3, 262–277.

RAITT, R. W. (1956) Seismic-refraction studies of the Pacific Ocean Basin I. *Bull. Geol. Soc. Amer.* **67**, 1623–1639.

REVELLE R. (1944) Marine bottom samples collected in the Pacific Ocean by the Carnegie on its seventh Cruise. *Carnegie Inst. of Washington*, Publ. 556.

REVELLE R., BRAMLETTE M., ARRHENIUS G. and GOLDBERG E. D. (1955) Pelagic sediments of the Pacific. *Geol. Soc. Amer. Special Paper 62*, 221–236.

REX R. W. and GOLDBERG E. D. (1958) Quartz contents of pelagic sediments of the Pacific Ocean. *Tellus* **10**, 153–159.

SMALES A. A., MAPPER D. and WOOD A. J. (1958) Radioactivation analysis of "cosmic" and other magnetic spherules. *Geochim. et Cosmoch. Acta* **13**, 123–126.

STARIK I. E., KUZNETSOV Y., GRASHCHENKO S. M. and FRENKLIKH M. S. (1958) The ionium method of determination of age of marine sediments. *Geochemistry* (*English Translation published by the Geochemical Society*) 1–15.

WINCHELL A. N. (1951) *Elements of Optical Mineralogy*. Part II. Descriptions of Minerals. John Wiley, New York.

ZEN E.-AN (1957) Preliminary report on the mineralogy and petrology of some marine bottom samples off the coast of Peru and Chile. *Amer. Min.* **42**, 889–903.

Reprinted from JOURNAL OF APPLIED PHYSICS, Vol. 32, No. 2, 140–143, February, 1961
Copyright 1961 by the American Institute of Physics
Printed in U. S. A.

Likelihood Detection of Small Signals in Stationary Noise*

PHILIP RUDNICK
University of California, La Jolla Marine Physical Laboratory of the Scripps Institution of Oceanography, San Diego, California

(Received May 5, 1960)

An approximation to the likelihood ratio which may be used in detecting a small signal in stationary noise is derived. The result contains only low-order moments of the signal and only stationary properties of the noise; hence it is applicable without change of form to any sufficiently long observation period. In the Gaussian case, with the signal also stationary and both signal and noise power spectra continuous, the result represents passage through a linear Eckart filter, followed by square law detection and equal-weight smoothing.

I. INTRODUCTION

A SIMPLE example will illustrate the problem of detection to be treated here. Suppose a receiver of underwater sound to furnish a continuously varying output voltage. Let a sample of this output of duration T be called an observation. Presented with a single observation, an observer judges whether the observation arose from noise alone or whether a signal from some source of a specified class contributed to the observation in question.

A statistical doctrine of great power and generality is available to guide such judgments.[1] Exploitation of this general theory by application to practically important cases has only begun. This paper is concerned particularly with the case when the underlying statistics is not Gaussian. Only limited progress is achieved on this problem, but additional results on the Gaussian case are also obtained.

The physical detection problem stated above is made mathematical as follows. The observation is represented by a finite set of instantaneous voltage values, $x_i (1 \leqq i \leqq K)$ which are equally spaced in time, at intervals $\tau_0 = T/K$, and are regarded as the components of a vector $\mathbf{x}$ which locates a point in K-dimensional observation space. Two known probability density distributions in the observation space are postulated: $f(\mathbf{x})$ for an ensemble of observations representing noise, and $f'(\mathbf{x})$ for another ensemble representing signal and noise. The problem is then to decide from which of the two ensembles a given observation came. The solution has the form of a two-part division of the observation space; all observations in one part are judged to be noise, and all in the other are adjudged signal and noise. The problem is trivial unless the two distributions overlap. When they do, errors in judgment will occur, and the problem here considered is to minimize the errors of one kind or the other, or a linear combination of the two. This purpose is accomplished by choosing contours of the likelihood ratio,

$$L(\mathbf{x}) = f'(\mathbf{x})/f(\mathbf{x}),$$

as the form of partition.[1] The corresponding decision rule is that an observation $\mathbf{x}$ will be judged to be signal and noise when and only when $L(\mathbf{x}) > Q$, a constant.

At this point, application of the theory can be seen to involve two quite separate parts. One is the employment of actually available statistical information on signal and noise to determine the form of the function $L(\mathbf{x})$. The second is the choice of the threshold Q and the prediction of consequent performance of the system. Only the first of these will be dealt with here.

II. CALCULATION OF THE LIKELIHOOD RATIO FOR SMALL SIGNALS

We now make assumptions which permit the distribution $f'(\mathbf{x})$ to be calculated as a perturbation of the distribution $f(\mathbf{x})$. The signal is taken as small, additive, and statistically independent of the noise. We write

$$\mathbf{x} = \mathbf{n} + \mathbf{s}$$

and

$$x_i = n_i + s_i,$$

when $\mathbf{x}$ is a signal and noise observation and $\mathbf{n}$ and $\mathbf{s}$ are its noise and signal parts, respectively. The unit of measure in which x_i, n_i, and s_i are expressed is chosen so as to make the root mean square value of n_i (averaged over all i and with a weight $f(\mathbf{n})$ over all observations of the noise ensemble) equal to unity. Each value of s_i is then a ratio of instantaneous signal voltage to rms noise voltage. $F(\mathbf{s})$ will represent the known cumulative distribution function of the signal. We then have

$$f'(\mathbf{x}) = \int f(\mathbf{x} - \mathbf{s}) dF(\mathbf{s}), \tag{1}$$

the integration extending throughout the observation space.

It is now assumed that $f(\mathbf{x} - \mathbf{s})$ has a Taylor series expansion about $\mathbf{x}$, and that $f(\mathbf{x})$ is smooth enough and the s_i almost always small enough to warrant use of

---

* This work represents one of the results of research carried out under contract with the Office of Naval Research.

[1] J. Neyman and E. S. Pearson, Phil. Trans. Roy Soc. London Ser. A, 231, 289 (1933). For an exposition of application to detection and recent literature references to the subject, cf. W. W. Peterson, T. G. Birdsall, and W. C. Fox, IRE Trans. PG, 171 (1954).

Reproduced by Permission

this expansion in Eq. (1). In this way we reach

$$L(\mathbf{x})-1=\frac{1}{f(\mathbf{x})}\left[-\sum_i\frac{\partial f(\mathbf{x})}{\partial x_i}\langle s_i\rangle_{\mathrm{av}}+\frac{1}{2}\sum_i\sum_j\frac{\partial^2 f(\mathbf{x})}{\partial x_i\partial x_j}\langle s_is_j\rangle_{\mathrm{av}}+\cdots\right] \tag{2}$$

$$=\sum_i y_i\langle s_i\rangle_{\mathrm{av}}+\tfrac{1}{2}\sum_i\sum_j(y_iy_j+z_{ij})\langle s_is_j\rangle_{\mathrm{av}}+\cdots, \tag{3}$$

with

$$\left.\begin{aligned} y_i&=-\frac{\partial}{\partial x_i}\log f(\mathbf{x})\\ z_{ij}&=\frac{\partial^2}{\partial x_i\partial x_j}\log f(\mathbf{x})\end{aligned}\right\} \tag{4}$$

$$\langle s_i\rangle_{\mathrm{av}}=\int s_idF(\mathbf{s}),\quad \langle s_is_j\rangle_{\mathrm{av}}=\int s_is_jdF(\mathbf{s}). \tag{5}$$

Equation (3) is a useful form of the result when $f(\mathbf{x})$ is Gaussian, since in this case the z_{ij} are absolute constants and hence trivial. In other, near-Gaussian cases, the z_{ij} may be of secondary importance. The first part of the right member of Eq. (2) or (3) is of course a cross-correlation with an expected form of signal, which is a familiar detection procedure.

III. APPLICATION TO STATIONARY NOISE

We now restrict attention to the case where the noise is a stationary process, and the observation time is in a certain sense long. We first introduce conditional probability distributions:

$$c_i(x_i;\,\mathbf{x}_i)\equiv f(\mathbf{x})\Big/\int f(\mathbf{x})dx_i$$

is the distribution function for a particular component x_i of the observation, subject to fixed values for all other components x_j, $(j\neq i)$, which are symbolized by the vector $\mathbf{x}_i$. Similarly, with $i\neq j$,

$$c_{ij}(x_i,\,x_j;\,\mathbf{x}_{ij})\equiv f(\mathbf{x})\Big/\int\int f(\mathbf{x})dx_idx_j$$

is the joint distribution of x_i and x_j conditioned on fixed values of x_k, $(k\neq i,\,k\neq j)$, which are denoted by $\mathbf{x}_{ij}$. Clearly, log c_i and log c_{ij} may replace log f in Eqs. (4), since they differ from it by quantities independent of the variable of differentiation.

We now assign the noise a quasi-Markoff property which is physically plausible. It is supposed that $c_i(x_i;\,\mathbf{x}_i)$ depends in fact not importantly on all x_j with $j\neq i$, but only on these x for which $0<|j-i|\leqq M$, denoted by ${}_M\mathbf{x}_i$, the dependence on all other $x_j(|j-i|>M)$ being either rigorously lacking[2] or negligible. The interval measured by M may be called a coherence time; we suppose the observation time to be long in comparison, $K\gg M$. For all i satisfying $M<i\leqq K-M$, ${}_M\mathbf{x}_i$ is wholly included in $\mathbf{x}$. We will refer to this restriction on i as the neglect of end effects, and henceforth will consider all summations on i to be so restricted. Consequently, the c_i will have a common functional form because of the stationarity of the noise; hence we write

$$c_i(x_i;\,\mathbf{x}_i)\cong C(x_i;\,{}_M\mathbf{x}_i). \tag{6}$$

In a corresponding way,

$$c_i\,(x_i,x_j;\,\mathbf{x}_{ij})\cong C_{i-j}(x_i,x_j;\,{}_M\mathbf{x}_i,{}_M\mathbf{x}_j), \tag{7}$$

and whenever $|i-j|>M$,

$$C_{i-j}(x_i,x_j;\,{}_M\mathbf{x}_i,{}_M\mathbf{x}_j)\cong C(x_i;\,{}_M\mathbf{x}_i)C(x_j;\,{}_M\mathbf{x}_j). \tag{8}$$

The use of Eqs. (6) and (7) in Eqs. (4) gives

$$\left.\begin{aligned} y_i&=-\frac{\partial}{\partial x_i}\log C(x_i;\,{}_M\mathbf{x}_i)\\ z_{ii}&=\frac{\partial^2}{\partial x_i^2}\log C(x_i;\,{}_M\mathbf{x}_i)\end{aligned}\right\} \tag{9}$$

and

$$z_{ji}=z_{ij}=\frac{\partial}{\partial x_i\partial x_j}\log C_{i-j}(x_i,\,x_j;\,{}_M\mathbf{x}_i,\,{}_M\mathbf{x}_j). \tag{10}$$

Because of Eq. (8), $z_{ij}\cong 0$ when $|i-j|>M$.

We are now able to allow the observation time T and K to be variables which need not be specified at the outset of the calculation. Subject to the hypotheses already made, and with neglect of end effects, we regard the x_i as an unending sequence of observation components produced in real time as K increases. Through Eqs. (9), the y_i and z_{ii} are also unending sequences generated by the x_i with a lag of M steps; the z_{ij} are similarly an M-fold sequence determined by Eq. (10). The remaining reference to observation size in Eq. (3) is in the signal moments $\langle s_i\rangle_{\mathrm{av}}$ and $\langle s_is_j\rangle_{\mathrm{av}}$. If the signal is also a stationary process, with $\langle s_i\rangle_{\mathrm{av}}=0$ and $\langle s_is_j\rangle_{\mathrm{av}}=R_{j-i}$, $R_k\cong 0$ for $|k|>L$, $L\ll K$, Eq. (3) becomes

$$L(\mathbf{x})-1=\tfrac{1}{2}\sum_i\left[\sum_{k=-L}^{+L}(y_iy_{i+k}+z_{i,i+k})R_k\right], \tag{11}$$

with the y_i and z_{ij} determined by Eqs. (9) and (10). The range of summation on i is supposed great enough to permit neglect of end effects generated by L as well as by M.

The observation time enters Eq. (11) only through the summation limits on i. Three different cases may be distinguished in physical application:

---

[2] This is the Markoff case. Specifically, in this case $(x_{i-M},\,x_{i-M+1},\,\cdots x_{i-1})$ form the ith member of an M-component stationary discrete Markoff process. See J. L. Doob, Ann. Math. Statist. 15, 229 (1944).

(1) Both upper and lower limits on i are fixed. This is the simple situation of one decision based on one observation.

(2) The lower limit on i is fixed; the upper limit continuously increases, giving a continually changing likelihood ratio, based on a growing accumulation of data.

(3) Both limits on i increase together. The likelihood ratio again continually changes, now based on the data contained in a running time interval of fixed extent.

The third case is the common one in many applications, and is the one considered in the following section.

IV. GAUSSIAN CASE

For Gaussian noise, $\log f(\mathbf{x})$ is quadratic, and the y_i given by Eq. (4) are linear in the observation components x_i. We now consider the corresponding situation for the stationary noise process independent of sample limits, as contemplated in Eq. (9).

The correlation matrix of the noise process is doubly infinite and has the form $\rho_{ij} \equiv \rho_{i-j}$, with $\rho_k = \rho_{-k}$. The periodic power spectrum, assumed continuous, is

$$N(f) = \sum_{n=-\infty}^{\infty} \rho_n \cos 2\pi n \tau_0 f. \tag{12}$$

If $1/N(f)$ is also a permissible power spectrum, it too will have a Fourier series representation:

$$1/N(f) = \sum_{n=-\infty}^{\infty} a_n \cos 2\pi n \tau_0 f. \tag{13}$$

If the expansion in Eq. (13) exists, and if $|\rho_n|$ and $|a_n|$ have convergent sums, the matrix a_{i-j} is easily shown to be the reciprocal of the moment matrix ρ_{i-j} by multiplying Eqs. (12) and (13) together. The expansion in Eq. (13) will not exist if $N(f)$ vanishes over any finite frequency interval, as is the case for band-limited Gaussian noise sampled at a rate above Nyquist. The writer does not know that ρ_{i-j} must fail to have a reciprocal in this case, but if this is indeed true, the hypothesis of limited coherence will also fail. This may be an "unrealistic" aspect of band-limited Gaussian noise. Slepian has discussed a similar point.[3]

The Gaussian distribution functions C and C_k will be constructed from the matrix a_{i-j}. For the Gaussian case, we replace Eq. (9) by

$$y_i = \sum_{j=-\infty}^{\infty} a_j x_{i-j}, \tag{14}$$

in which the summation range, though shown infinite for formal reasons, is supposed for practical purposes to be limited to a finite range $|j| \leq M$. The z_{ij} will, as previously mentioned, be constants and hence trivial. By inserting Eq. (14) in Eq. (11) and rearranging the order of summations as the neglect of end effects permits, one obtains

$$L(\mathbf{x}) - 1 = \tfrac{1}{2} \textstyle\sum_l \sum_i x_i x_{i+l} \sum_k A_{l-k} R_k, \tag{15}$$

where

$$A_i = \sum_{j=-\infty}^{\infty} a_{i+j} a_j$$

and $A_i \cong 0$ for $|i| > 2M$.

We may regard the linear operation in Eq. (14) as the action of a formal filter with the symmetrical (and hence only approximately realizable) impulse response a_i. The power transmission of this filter is $1/N^2(f)$, and the corresponding correlation function is A_i. The sum $\sum_k A_{l-k} R_k$ in Eq. (15) is then recognized as the correlation function of the Eckart[4] filter, whose power transmission is $S(f)/N^2(f)$ when $S(f)$ is the power spectrum of the sampled signal.[5] The right-hand member of Eq. (15) corresponds to the steady-state procedure of filtering the x_i with the Eckart filter, squaring, and then accumulating or averaging with uniform weighting. Eckart arrived at this same process as optimum for detection in the Gaussian case by signal-to-noise considerations, following an *a priori* choice of a square-law detector as part of the process. The present result shows that the square-law detector is not arbitrary, but in fact required in approximating the likelihood ratio.

V. CONCLUDING REMARKS

The problem dealt with in this paper may be called the steady-state likelihood ratio calculation. The most general solution achieved, embodied in Eqs. (3), (9), and (10), is an approximation which involves only stationary statistics of the noise, is unaffected by the particular choice of observation period, and is appropriate to any sufficiently long period. The ultimate objective is to discover how observable non-Gaussian characteristics of noise encountered in a practical detection problem should influence the design of a detection receiver. The functions C and C_i are in principle approximately observable, but may contain so many variables that immediate practical progress seems to call for much further approximation and simplification. On the mathematical side, further discussion of the property of limited coherence time may be of interest, as would a development, parallel to the present one, which employs a continuous time parameter and is hence free of reference to any sampling scheme.

---

[3] D. Slepian, I.R.E. Trans. on Inform. Theory **IT-4**, 65 (1958).

[4] C. Eckart, University of California, Marine Physical Laboratory of Scripps Institution of Oceanography, SIO Ref. 52-11 (1952).

[5] Presumably the same result could be derived from Middleton [D. Middleton, IRE Trans. on Inform. Theory **IT-3**, 36 (1957), Eqs. (19a), (22), and (23)] by (a) supposing the signal to be small compared to noise, (b) replacing the finite matrices by infinite ones, and (c) introducing, as here, an hypothesis of limited coherence time which makes the near-diagonal matrix elements the important ones.

The most immediately useful, though secondary, result is considered to be the Gaussian case. In spite of the considerable literature, in which the present result is no doubt implicit, to the author's knowledge it has not been previously shown that the steady-state likelihood receiver for a small stationary signal in stationary Gaussian noise, when both have continuous power spectra, is a linear Eckart filter followed by square-law detection and equal-weight smoothing.

ACKNOWLEDGMENTS

The author is indebted to both Carl Eckart and T. G. Birdsall for stimulating discussions.

Reprinted from the Journal of Marine
Research, v.18, no.2, October 30, 1960.
pp.73-82.

PYCNOCLINES CREATED BY MIXING IN AN AQUARIUM TANK

By

TOWNSEND CROMWELL

Inter-American Tropical Tuna Commission
Scripps Institution of Oceanography

Foreword

The experiments described in this paper were carried out by the author before his death in an airplane crash near Guadalajara, Mexico, 2 June 1958. We had planned to collaborate in studying the results from the standpoint of possible model similarity between events in the experimental tank and in the ocean, possibly repeating some of the experiments or devising new ones. But I was unable to find many of the pertinent numerical data in Mr. Cromwell's files.

It was the general opinion of our colleagues that Mr. Cromwell's interesting experiments had shed considerable light on the problem of thermocline formation and that a qualitative description would be of value even without a detailed discussion of the results. Fortunately, Mr. Cromwell had finished writing a preliminary draft and had prepared several figures. The present article consists entirely of that draft, with few minor changes by myself.

Considering the possibility of performing further experiments on pycnocline formation, Mr. Cromwell and I agreed that the initial linear density gradient herein used was probably an unnessary complication; the fluid above the pycnocline was shown to be sensibly homogeneous, and apparently only a thin layer of fluid immediately below participates in the process at any given time. Rouse and Dodu (1955), using the simpler initial state of two homogeneous layers, kept the pycnocline in the same relative position by allowing water to flow into the lower layer and out of the upper. It would be even simpler to eliminate the flow and allow the pycnocline to descend during the experiment. Then a thorough investigation of the effects of all parameters influencing the experiment, including mesh size, agitation frequency and amplitude, distance from mesh to pycnocline, etc., would be enlightening. Or, it might be possible to devise parameters that come closer to de-

Contributions from the Scripps Institution of Oceanography, New Series, 1244
Reproduced by Permission

scribing the turbulence introduced than those mentioned, thus facilitating comparison with an ocean where there is no oscillating mesh.

The loss of Townsend Cromwell was a great loss to the science of the oceans. It is hoped that others may be inspired to undertake model studies of thermocline behaviour, in which he had such an enthusiastic interest.

Gordon W. Groves

Instituto de Geofísica Universidad Nacional Autónoma de Mexico.

ABSTRACT

Experiments here reported show that a vertical density gradient can be concentrated in a small aquarium tank by simple agitation immediately below the fluid surface with a mesh. A pycnocline, which is immediately formed, descends rapidly at first and then more and more slowly as its distance from the source of turbulence increases. An explanation for pycnocline descent is suggested. Fluid particles which move upward from the region of the pycnocline are rapidly deformed and mixed throughout the upper layer whereas fluid particles which move downward into the quiet layer below are buoyed upward intact. Thus the upper layer increases in thickness at the expense of the lower layer, *i.e.*, mixing across the pycnocline is one-way.

The sequence of events in the tank agrees with the hypothesis that pycnoclines in the ocean can be formed as a result of turbulence produced at the sea surface by wind. However, since these experiments were not properly scaled and since the turbulence spectrum in the ocean is undoubtedly dissimilar from that in the aquarium tank, our results are only suggestive and do not incontestably verify this hypothesis.

Introduction. Thermoclines are among the most striking features of the ocean's thermal structure. Since the effect of salt on density in the open ocean is generally small, the thermocline is a layer through which the vertical density gradient is large relative to overlying and underlying gradients; *i. e.*, the thermocline is also a "pycnocline".

Knowledge of pycnocline formation and maintenance is summarized in a report of the Chesapeake Bay Institute of the Johns Hopkins University (Pollak, 1954). Qualitative explanations of the phenomenon appear in a number of publications (Sverdrup, *et al.*, 1942; Schule, *et al.*, 1952; Anonymous, 1946). Presumably wind stress on the sea surface produces stirring and mixing downward to a limited depth. The layer affected is rendered nearly homogeneous, but below the region of effective mixing the vertical density gradient remains essentially unaffected. In between is a thin layer of sharp transition. In this way an initial vertical gradient, perhaps established by warming near the sea surface, is modified only by redistribution of mass in a vertical column, thereby "creating" a pycnocline.

Purposes of Experiment. Experiments were performed in a small tank to ascertain whether or not a pycnocline could be formed by introducing turbulent energy near the surface and possibly to gain insight into the mechanism of pycnocline formation and maintenance. Although the results were affirmative, it will be pointed out below that there are objections to drawing an analogy to events as they occur in the ocean.

Equipment and Experimental Procedure. A small rectangular aquarium tank, 27 × 17 cm and 19 cm deep, was used. A rectangular one-quarter inch galvanized iron mesh (hardware cloth) was cut to fit snugly into the tank. The mesh, with appropriate linkages to an electric motor, was driven up and down in regular oscillatory motion near the surface. This equipment is illustrated in Fig. 1.

The density structure desired initially was a linear increase with depth from top to bottom of tank. A clear mixture of roughly half sea water and half distilled water was diluted with dyed sea water in four proportions. It was found most practical to introduce the lightest (least colored) mixture into the tank first. Successively denser (more deeply colored) mixtures were then introduced near the bottom through a siphon. Sharp interfaces, visible because of the dye and because of refraction of light from a source behind the tank, tended to develop between successive mixtures. However, sharp gradients could be smoothed out by waving the nozzle up and down across the interfaces during siphoning. It was impossible to avoid all sharp vertical density gradients, but those which remained after siphoning could be "mixed away" by means of a small piece of hardware cloth on the end of a pencil. Establishing the initial gradient in the tank was the most difficult part of the whole experimental procedure, but by these crude methods a gradual increase in density with depth could be obtained (Fig. 2, curve A; Fig. 4).

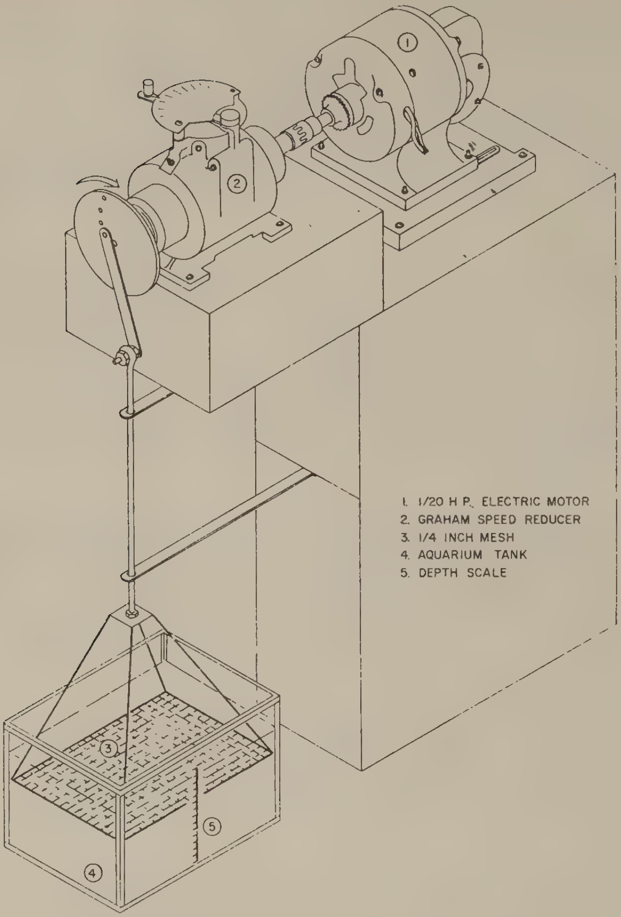
①
②
③
④
⑤
1. 1/20 H P. ELECTRIC MOTOR
2. GRAHAM SPEED REDUCER
3. 1/4 INCH MESH
4. AQUARIUM TANK
5. DEPTH SCALE

Figure 1. Experimental apparatus.

The experimental procedure was to agitate the fluid near its surface, the mesh describing simple harmonic motion over a 2.5 cm range of depth. From time to time the motor was stopped and, after all visible movement of the fluid had ceased, samples were drawn with a volumetric syringe and titrated. Titration and temperature measurements in the tank were to an accuracy allowing the determination of density to 0.1 in σ_t.

Sampling depth was read from a scale pasted to the tank and zeroed at the water surface before any samples were drawn. "Adjusted depth" enters because withdrawal of the samples lowered the fluid surface appreciably during the experiments. Adjustments were made according to the formula, $z_a = [z_s - (h_i - h_n)]\,[h_i/h_n]$, where z_a is "adjusted depth", h_i is water depth at start of the experiment, h_n is water depth at start of sampling run, and z_s is reading from depth scale.

During agitation by the mesh, the tank was checked visually to see that no "large scale" circulation was set up, *i.e.*, that there were no circulation cells which seemed to be bounded by the walls of the tank. When this happened, as it sometimes did, the fluid to a considerable depth would overturn, producing a homogeneous layer very quickly. However, when a mesh was obtained that was manufactured with reasonable precision, when it filled the tank snugly, and when it was nearly level, the motion appeared to result only from the irregular "turbulent" elements produced by the mesh grid, free of the influence of lateral boundaries.

Results. Results of a typical experiment appear in Fig. 2. A homogeneous surface layer is created by the stirring and mixing produced by the mesh. Immediately below, a sharp pycnocline appears. The vertical gradient in this pycnocline is greater than that which existed anywhere in the tank before agitation was begun. With the passage of time the pycnocline descends, rapidly at first but then more and more slowly as the distance from the mesh increases.

There are some further qualitative observations of tank experiments that can be mentioned. If the mesh is oscillated close to the bottom of the tank, a pycnocline forms above the mesh and gradually ascends. If the mesh is oscillated through an intermediate depth, pycnoclines form both above and below, rising and descending respectively. Thus, the position at which turbulent energy is introduced is important in determining the modification of the density structure that will occur.

Pycnoclines can be destroyed, or at least diminished in intensity, as well as created by the mixing. If, during an experiment, the frequency of mesh oscillation is increased suddenly, then turbulent elements penetrate into the lower stratum. As a result the gradient in the pycnocline becomes diminished. If the mesh is allowed to continue oscillating at this new, higher frequency, a new sharp pycnocline will form at some greater depth in the tank.

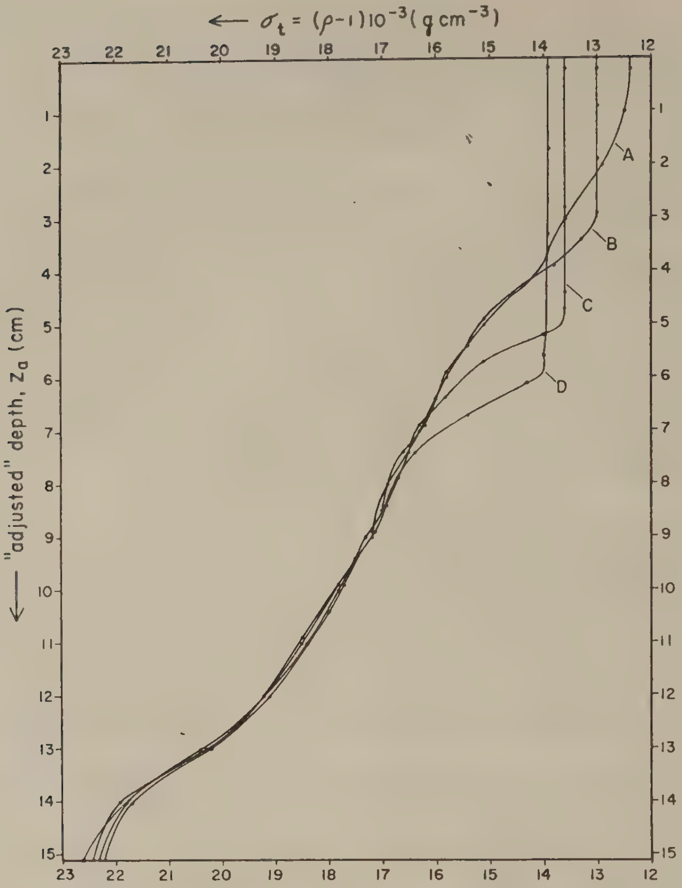

Figure 2. Successive density profiles in tank during an experiment; Curve A represents initial profile, curves B, C, and D occurring at later times.

Pycnocline Formation. Turbulence over the range of the mesh is so extreme that a mixed layer, bounded below by an interface, is formed with the first thrust. This occurrence defies any useful interpretation. At the same time, however, fluid elements are impelled downward by the mesh, interspersed by upward elements (Fig. 3a). Their spacing is uniform and equal to the grid size of the agitating mesh. Across the interfaces separating these elements of differing density, molecular diffusion is favored. Those downward elements which penetrate most deeply into the undisturbed fluid below are buoyed upward, intact, before any appreciable mixing takes place. At an intermediate level, somewhat above the level to which extreme downward elements penetrate, an interface gradually appears. The quantitative aspects of these events, *e.g.*, the depth and rapidity of pycnocline formation, depend on the original density structure, on the fundamental dimensions of the mesh, and on the frequency; but qualitatively it seems that the development of a mixed surface layer and a subjacent stable layer may occur when stirring is induced by any means whatever. For example, when the surface of the tank is cooled by suspending a sheet of dry ice just above it, roughly the same series of events takes place. But in this case other factors determine the size and spacing of the fluid filaments.

Once formed, the pycnocline maintains its identity and progresses downward. The interface is in irregular wave-like motion, and it separates the turbulent surface layer from the stable fluid below, which is quiet (Fig. 3b). This abrupt change in the state of motion across the interface can be seen during the experiment by sprinkling ashes from above, which, as they sink, describe irregular and varied paths downward until they pass the interface. Thereafter the particles sink slowly, straight downward. The predominant wave length of the wavy interface is now greater than it was just after the first few thrusts of the mesh, and apparently it is unrelated to the grid

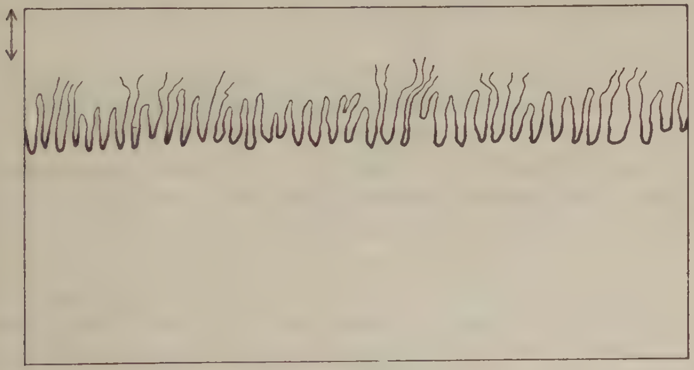

a.

Figure 3a. Initial appearance of interface after first thrust of mesh.

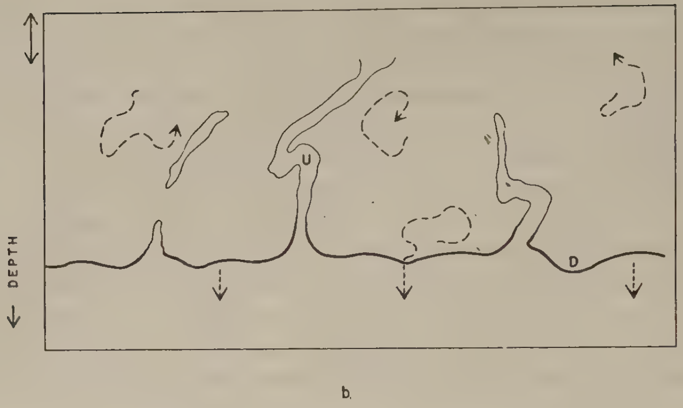

Figure 3b. Subsequent appearance of interface.

size. Segments of typical paths are illustrated in Fig. 3b by dashed arrows.

The explanation for descent of the pycnocline is as follows: Downward directed fluid elements at the interface (*e.g.*, at D) enter a quiet environment and are buoyed upward, intact. Upward directed elements (*e.g.*, at *U*) enter a turbulent environment where they are deformed and mixed quickly throughout the surface layer. Thus the mixing, or entrainment, is one way, and the surface layer thickens at the expense of the lower layer, so that the pycnocline must gradually descend. Fig. 4 illustrates the varying rate of descent of the pycnocline.

Rouse and Dodu (1955) performed experiments with equipment basically similar to that described here. They began their experiments with a two-layered system of fresh and saline waters. They found that turbulence induced in the upper layer by a mesh was restricted to the upper layer, with entrainment from the layer below, an occurrence which our experiments have duplicated.

Analogy to Events in the Ocean. There is a striking similarity between events in the tank and those occurring in the ocean during increased winds. Francis and Stommel (1953), using data from weather ships, have shown that the oceanic thermocline descends during a gale. The author analyzed these same data in greater detail and found that (1) the surface layer becomes more nearly

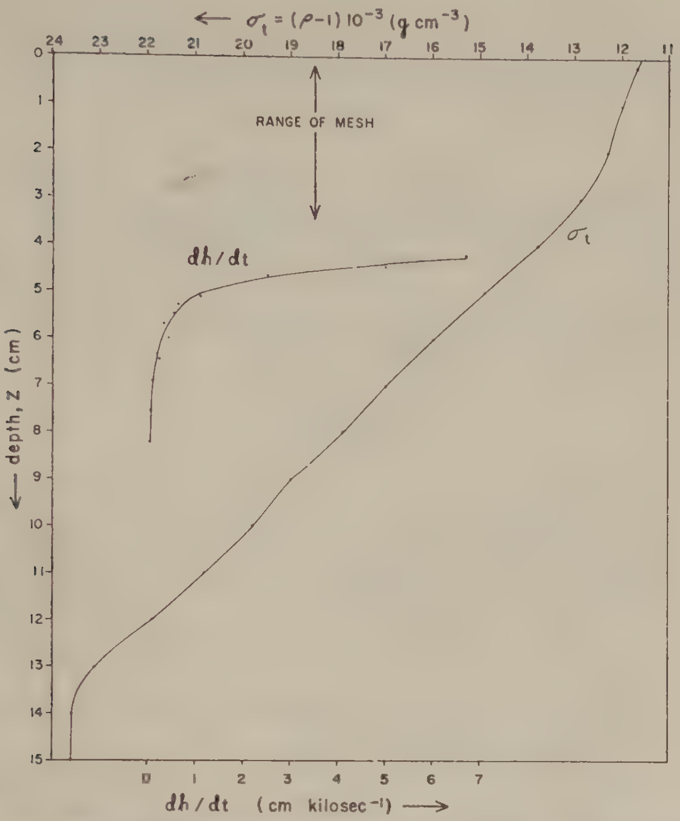

Figure 4. Diagram showing initial density profile and region of agitation ("range of mesh") as a function of distance from surface as well as the rate of pycnocline descent as a function of pycnocline depth, for a particular experiment.

isothermal (as measured by the BT), (2) the temperature gradient in the upper part of the thermocline becomes more intense, and (3) the separation between surface layer and thermal layer becomes sharper. An example of this series of events has been shown by Cromwell and Reid (1956: Fig. 6). This series of events can also be seen here in Fig. 2.

It has been suggested (by Carl Eckart) that the turbulence spectra in the tank and in the ocean are dissimilar and that this dissimilarity may be critical. The turbulent energy introduced into the tank by the mesh lies within the dissipative range of the spectrum, whereas in the ocean there may be relatively little turbulent energy concentrated at such small scale. Thus, even when properly scaled model experiments are performed, results cannot be applied to the ocean with certainty until more is known of the spectrum of ocean turbulence.

Acknowledgements. The author is grateful for the interest and help of Dr. Wilhelm Brandhorst in setting up and carrying out the experiments. The advice and comments of Dr. Ray Montgomery, Dr. Carl Eckart and Dr. Warren Wooster have been very helpful. This work was partially supported through Research Support Shops by the Office of Naval Research.

REFERENCES

ANONYMOUS
1946. The application of oceanography to subsurface warfare. Summ. Tech. Rep. NDRC, *6A*, Div. 6.
CROMWELL, TOWNSEND and J. L. REID, JR.
1956. A study of oceanic fronts. Tellus, *8* (1): 94–101.
FRANCIS, J. R. D. and HENRY STOMMEL
1953. How much does a gale mix the surface layers of the ocean? Quart. J. R. met. Soc., *79*: 534–536.
POLLAK, M. J.
1954. Notes from the conference on the thermocline of 25–27 May, 1953. Chesapeake Bay Institute, Ref. 54–2.
ROUSE, H. and J. DODU
1955. Diffusion turbulente a travers une discontinuite de densite. Houille blanche, Aug.–Sept., No. 4: 522–532.
SCHULE, J. J., *et al.*
1952. Effects of weather upon the thermal structure of the ocean. U.S. Navy Hydrographic Office, Misc. 15360.
SVERDRUP, H. U., M. W. JOHNSON and R. H. FLEMING
1942. The Oceans. Prentice Hall, Inc., New York. 1087 pp.

Reprinted from the Journal of Marine
Research, v.16, no.3, October 15, 1958.
pp.199-225.

MEASUREMENTS OF SLOPES OF HIGH-FREQUENCY WIND WAVES[1]

By

CHARLES S. COX

University of California
Scripps Institution of Oceanography
La Jolla, California

ABSTRACT

Water-surface slopes due to wind waves have been measured in a laboratory wind-wave tunnel. In all measurements, nonlinear effects are important for high-frequency wind waves; nonlinear effects noted are: increase of phase velocity due to finite amplitude of gravity waves, trapping of ripples on the leading slope of gravity wavelets, and limitation of slopes after the explosive growth of waves beyond a critical fetch.

The mean square water-surface slope observed in the tunnel showed a complicated behavior as a function of wind speed. The slope increases rapidly above a sharply defined minimum wind speed for wave generation; the minimum wind speed decreases with increasing fetch. There is no large effect of air-water temperature difference.

The frequency spectrum of slopes shows (for light winds) two peaks separated by a minimum near the frequency corresponding to waves of minimum-phase velocity. As the wind increases, the frequency difference between peaks tends to increase.

Measurements at three frequencies have shown changes of phase velocities of ripples as a function of wind speed that amount to as much as 30% of the theoretical phase velocity appropriate to still water and no wind; much smaller changes are noted for gravity waves. In general, the highest velocities are associated with the strongest winds.

Comparisons with Jeffreys' (1924–25) and Phillips' (1957) theories of wave generation show disagreements at short fetches.

1. INTRODUCTION

The friction of wind blowing over the sea presents an unusually difficult subject to discuss because the roughness of the surface is not

---

[1] Contribution from Scripps Institution of Oceanography, New Series. 1245

This article by Dr. Cox and the one by Dr. Phillips which follows, both pertinent to the same area of interest, were submitted at approximately the same time, and since it is the policy of this Journal to encourage discussion, I asked each author if he would be willing to prepare a constructive comment on the other's article. Both authors gladly agreed to my proposal, and the Comments which appear after each article resulted. To each author, many thanks.

Y. H. Olsen

Reproduced by Permission

only caused by but is the cause of the pattern of flow in the air above the surface and in the water beneath. There have been several attempts to deduce properties of the large roughness elements (ocean waves) from various *ad hoc* hypotheses concerning the nature of the interactions between wind and water, but no great success has attended these efforts. (See Ursell, 1956; 216–248, for a discussion of these attempts and their limitations.) It is with the hope of finding some of the effective forces that a study has been made of the smallest roughness elements on the sea surface: high-frequency waves and ripples.

The first problem is to describe in some way, statistical or otherwise, typical shapes of the sea surface and to find how this shape changes with time. In representing the shape of the water surface, it has been found convenient to use the *slope* of the water surface rather than the more usual *elevation from mean water level* as the parameter to be studied. This is done because high-frequency waves, although of low elevation, have large slopes. It also turns out that rather simple apparatus can be used to detect slopes of the water surface.

Suppose that the elevation of the water surface is $z(x, y)$, where the horizontal axes x, y are directed toward the mean direction of the wind and cross wind, respectively. Then

$$s_x \equiv \frac{\partial z}{\partial x}, \quad s_y \equiv \frac{\partial z}{\partial y}$$

represent the up-down wind and cross-wind components of slope, respectively. In the experiments to be described below, the principal emphasis has been laid upon measurements of the up-down wind component of slope in time and space.

2. APPARATUS

Wind waves were produced in a wind-water tunnel (Fig. 1). A centrifugal blower driven by a ¾-hp motor draws air at speeds up to 12 m sec^{-1} through the tunnel. Observations of waves are made through any of the glass ports by means of the photocell telescopes illustrated in large scale. For measurements at a single point on the water surface, a single telescope is used; for simultaneous measurements at two points, two telescopes are used.

The optical principle upon which slopes are measured is that of refraction of light at the air-water interface. Consider a bundle of rays which passes through the pinhole and terminates on the sensitive surface of the photocell. Since the telescope is focussed on the water surface, all of the rays must have passed through, and been refracted at, a small spot on the water surface. The region of origin of rays on the "wedge" (cross-section indicated at 8, Fig. 1) then depends primarily on the up- or down-wind component of tilt of the water surface at this spot. The wedge was so constructed that its transmission of light varied linearly from almost nil at the thick end to almost unity at the thin end. Hence brightness of light entering the photocell was proportional to the up-down wind component of slope of the water surface. By rotating the wedge 90° around a vertical axis, the cross-wind component of slope could be measured.

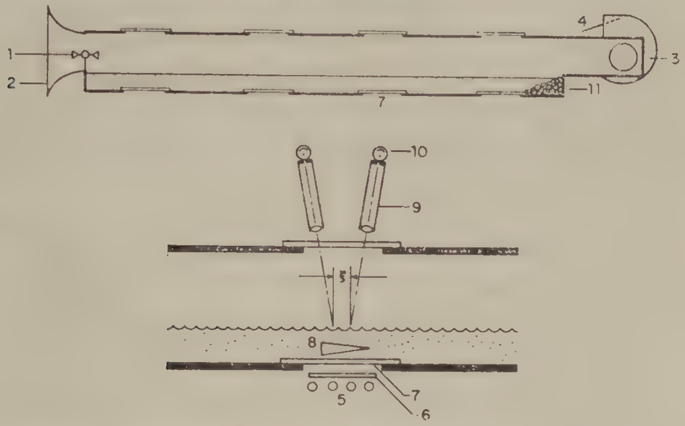

Figure 1. Wind and water tunnel for measurements of slopes of waves generated by wind. The stippled area in the lower third of the tank indicates water. The cross-sectional area of the air passage is 26.3 by 26.3 cm. The dimensions of the water channel are: 14 cm (depth), 26.3 cm (breadth), 6.1 m (length). Numerals refer to the following details: 1, cup anemometer; 2, entrance nozzle; 3, suction centrifugal fan; 4, damper for controlling wind speed; 11, gravel beach for absorbing waves. On an enlarged scale are shown: 5, light source composed of four cylindrical incandescent light bulbs operated on direct current; 6, diffusing glass; 7, plate glass windows (top and bottom of tank); 8, hollow wedge filled with inky water (placed directly upon or beneath lower plate glass window but here shown raised for clarity); 9, telescope tube which focusses an image of water surface on a pinhole directly in front of photocell; 10, photocell.

There are a number of features of this technique which make it less than ideal. The most serious fault is that the brightness registered by the phototube is affected to some extent by the elevation of the water surface above the wedge; for example, as the crest of a large wave comes into the field of view, the rate of change of brightness with respect to slope is increased above its mean value because rays traced back from the water surface have a longer than average distance to travel between wedge and water surface. Thus the effect is a change of scale between slopes measured near the crest of waves and near the troughs. It can be shown that the change of scale is to the mean scale as the change of depth of water is to the mean depth from water surface to wedge. At the highest wind speeds (12 m sec^{-1}) one may estimate the changes of scale as ±20% of the mean scale; at lower wind speeds the changes become rapidly smaller so that at 8 m sec^{-1} the changes of scale are estimated at ±5%.

Second, for angles of slope greater in magnitude than 40°, the brightness is not linearly related to slope. For angles less than 40° the maximum departure from linearity is found to be about 5%.

Third, the brightness depends slightly on *cross-wind* components of slope as well as on the intended (up/down-wind) component. This effect is expected to be negligible compared to the larger errors mentioned above.

A final difficulty is brought about by scattered light which enters the photocell and causes spurious signals (generally of lower frequency than the intended signal); this is reduced by painting the interior of the photocell telescope tubes dull black.

The wind speed in the tank was measured by a cup anemometer in the entrance nozzle. It was calibrated by comparison with a propeller vane anemometer with a National Bureau of Standards calibration. The position of the anemometer in a section where the air flow is uniform ensures that it measures the *mean flow* through the tunnel.

Measurements of air temperature, wet bulb temperature, and water temperature were made adjacent to the anemometer by mercury-in-glass thermometers.

Surface tension measurements *in situ* were made with a De Nouy ring tensiometer only when the air blower was not operating. Some attention was paid to the question of surface films on the water, since these are known to affect wave generation markedly (see Keulegan, 1951; Van Dorn, 1953; Cox and Munk, 1954). It was found that, by continuous draining through an overflow trough at the lee end of the tank, the surface could be kept clean. This was confirmed by measurements of surface tension. Without draining, the surface film would be compressed to the lee end of the tank by strong winds; when the wind ceased it would then expand rapidly in a few seconds over the entire tank. With continuous draining, the process of reformation of the surface film took several minutes.

2.1 Wave Length Response of System. The finite dimensions of the spot on the water through which all rays pass on their way to the photocell form a "low-pass" filter to the signal. Slopes due to waves of length much less than the diameter of the spot are not effective in causing variations of brightness on the photocell; conversely, slopes due to waves much longer than the diameter of the spot are properly recorded.

The size of the spot on the water is determined by three factors: (1) size of pinhole in telescope divided by magnification ratio between object and image; (2) degree of malfocussing (caused by rise and fall of waves); (3) perfection of lens in telescope. These factors were estimated separately. For observations of mean square slope (Section 3.1), the effective spot size was 2.0 mm in diameter. An improved lens system was used for observations of the frequency spectrum of slopes; the effective spot diameter was 0.7 mm.

Suppose that the spot radius is r_0 and that all light transmitted through the spot contributes equally to the signal. Suppose further that a wave of slope $s = s_0 \cos (kx - \omega t)$ crosses the field of view centered at $r = x \cos \theta = 0$ in an arbitrary direction x and that the brightness is proportional to s plus a constant. Then the photocell current is proportional to a constant plus

$$\int_0^{r_0} \int_{-\pi}^{\pi} s_0 \cos (kr \cos \theta - \omega t)\, r\, dr\, d\theta = 2\pi \int^{r_0} s_0 r J_0(kr)\, dr \cos \omega t$$
$$= \text{const}\ s_0 \frac{J_1(kr_0)}{kr_0} \cos \omega t \ ,$$

where J_0 and J_1 are Bessel's functions in standard notation. The mean square output is therefore proportional to $\left[2 \frac{J_1(kr_0)}{kr_0} \right]^2$. This quantity lies between 1.00 and 0.90 for wave lengths $\lambda = 2\pi/k > 6.8\, r_0$. For $\lambda = 1.7\, r_0$ the output vanishes, and for smaller wave lengths the output remains always below .017. For values $2r_0 = 2.0$, 0.7 mm as above, the wave length of 90% response is $\lambda = 6.8$, 2.4 mm. These correspond (according to the usual theory of infinitesimal waves on still water) to frequencies of 42, 190 cps.

2.2 Calibration. A rectangular block of lucite supported on a horizontal axle, with its upper surface just above water level, is used to calibrate the slope-measuring system. When the block is rotated about its axle, the phototube registers a change of light intensity as though the water surface were tilted. In practice the lucite block is oscillated by a motor through a 24-degree arc and the phototube output is recorded.

2.3 Measurements of Phase Velocities. Here two photocell pickups are used. One is fixed while the other is mounted on a movable carriage so that the distance, ξ (Fig. 1), which separates the two fields of

TABLE I

Fetch (*m*)	*Temperature* (°*C*)		*Wind speed* (*m sec*$^{-1}$)	*Mean square slope*
	Air	*Water*		
1.47	23.8	22.1	4.18	0.0186
	24.2	21.8	5.63	0.0358
	24.4	21.8	2.99	0.00115
	24.6	21.7	6.83	0.0440
	24.5	21.7	7.90	0.0458
	24.7	21.6	9.29	0.0483
	25.0	21.4	10.40	0.0508
	23.9	21.3	12.17	0.0733
	24.0	21.6	4.92	0.0268
2.14	22.2	19.9	4.69	0.0332
	22.0	19.8	3.88	0.0256
	23.4	19.8	3.49	0.0176
	23.4	19.9	2.39	0.0000
	—	—	3.13	0.0126
	23.4	20.0	4.25	0.0286
	22.2	19.6	12.12	0.0885
	23.4	19.6	11.67	0.0772
	22.1	19.8	9.34	0.0598
	21.9	19.1	10.52	0.0622
	—	—	10.94	0.0670
	23.8	19.3	8.65	0.0585
	—	—	7.84	0.0564
	—	—	6.99	0.0522
	22.2	—	6.07	0.0439
	23.7	19.7	5.42	0.0381
	—	—	4.57	0.0281
3.20	—	—	12.04	0.0836
	23.0	—	11.78	0.0796
	—	—	11.45	0.0752
	23.3	—	10.86	0.0679
	23.3	—	10.25	0.0587
	23.2	—	9.48	0.0571
	23.8	—	8.20	0.0535
	23.6	—	7.57	0.0500
	23.7	—	7.07	0.0491
	23.8	—	6.43	0.0471
	23.9	—	5.22	0.0383
	23.6	—	5.99	0.0456
	—	—	4.73	0.0347
	24.2	—	4.44	0.0364
	24.0	20.6	3.79	0.0262
	23.7	19.9	3.11	0.0165
	24.6	20.0	2.73	0.00724
	22.8	20.1	2.39	0.00096
	—	—	2.28	0.00161

(146)

view can be varied. The electrical output signals are sent first through two narrow-band electrical filters tuned as nearly as possible to the same frequency and then to a correlator which measures the mean product of the filtered signals. The correlation shows a nearly sinusoidal variation as ξ is varied. The wavelength of the sinusoidal variation is the apparent wavelength of the water waves having the same frequency as the filters. The apparent wavelength needs correction for the fact that the direction of propagation of the waves is not always parallel to ξ. The corrected wavelength multiplied by the frequency of the filtered disturbance yields the phase velocity.

3. LABORATORY MEASUREMENTS

3.1 Mean Square Slope. Mean square slopes were measured by passing the electrical output from a single photocell telescope to a squaring and averaging circuit. Data, recorded for three fetches (Fig. 2; Table I), show that below a certain wind speed, U_0, the mean square slope is extremely small; above this speed, however, the mean square slope increases very rapidly with wind speed at first, then more slowly, and finally more rapidly again. The magnitude of U_0, defined by extrapolating the mean square slope curve linearly to the abscissa, varies with fetch as shown in Table II.

TABLE II

Fetch (m)	U_0 *(m sec⁻¹)*
1.47	2.9
2.14	2.5
3.20	2.3

Using data from the three fetches, one can get a rough idea of the change of mean square slope with fetch. In Fig. 3 the data shown as circled points have been found from intersections of the freehand curves in Fig. 2 with lines of constant wind velocity. Although these data are sparse, they suggest that there is a sharply defined *critical fetch* for winds in the range 2.4 to 3.2 m sec^{-1}, above which the mean square slope increases rapidly from a very low value.

An attempt was made to find a variation of mean square slope with changes of air-water temperature difference. The tank water temperature was varied by heating and cooling while the air temperature was uncontrolled. The data are summarized in Table III. Here $\langle s_x^2 \rangle$ is reported relative to its value under "normal" conditions (group 2 in Table III). All measurements were made at a fetch of 2.14 m.

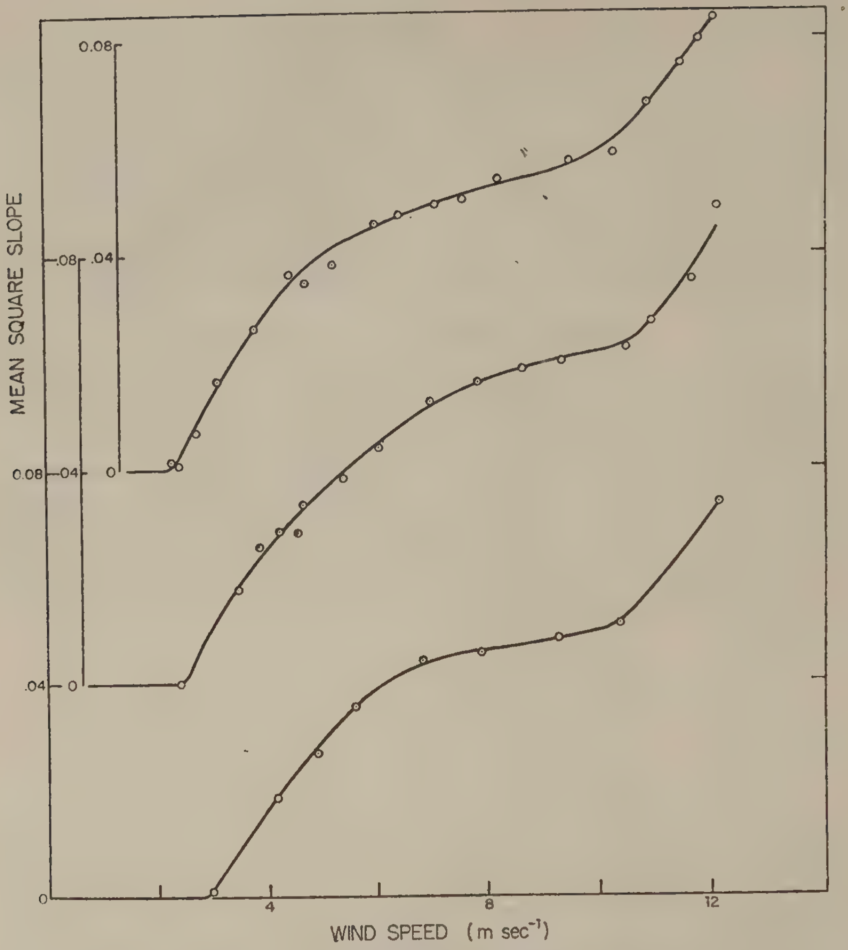

Figure 2. Mean square value (⟨ s_x^2 ⟩) of up/down-wind slope component as a function of wind speed. The three curves refer to fetches of 3.20 m (upper curve), 2.14 m (middle), and 1.47 m (lower). The curves have been separated vertically for clarity.

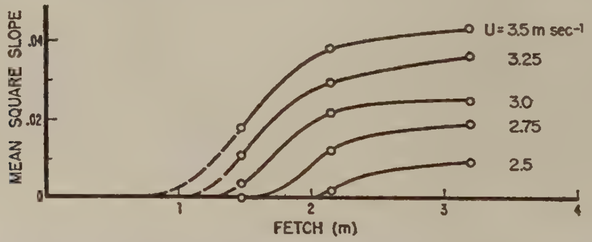

Figure 3. Relation of mean square water surface slopes to fetch for various wind speeds, *U*. The circled points have been estimated by reading off selected values of the smooth curves shown in Fig 2. The dotted lines are extrapolated.

TABLE III

Group	*Wind speed*	*Temperatures (°C)*			*Relative mean*
		Air		*Water*	
	($m\ sec^{-1}$)	*Wet bulb*	*Dry bulb*		*square slope*
1	4.52	22.1	25.0	29.5	1.04
(hot)	7.73	21.8	26.6	29.5	0.93
	11.71	22.0	26.2	29.2	0.98
2	4.54	20.8	25.6	22.3	1.00
(normal)	7.69	—	—	—	1.00
	11.79	21.0	25.1	22.2	1.00
3	4.68	20.1	25.6	14.9	1.17
(cold)	7.90	20.0	25.6	15.5	0.94
	11.67	20.0	24.9	20.4	1.05
4	4.52	—	—	9.4	1.01
(very cold)	7.76	19.2	24.4	8.9	0.84
	11.69	19.0	24.6	10.0	0.85

From these observations no consistent change of mean square slope with water temperature is apparent.

3.2 Frequency Spectrum of Slope. The signal at 2.14 m fetch from a single phototube telescope, recorded on magnetic tape and played back at a speed 37.5 times higher than the recorded speed, was analyzed on a spectrum analyzer of the analogue type (Fig. 4). Calibration of the analyzer was carried out by impressing on the same tape a "white noise" (*i.e.*, a signal of uniform spectral intensity) produced by the shot effect in a multiplier phototube exposed to steady light. By comparing the spectrum of the white noise with sine-wave signals passed through the same system, it was found that the multiplier phototube output yielded a uniform spectral intensity (within the probable error of measurement, ± ½ db) from high frequencies down to 1 cps. Schwantes *et al.* (1956) have demonstrated with greater precision that some multiplier phototubes yield a uniform noise intensity above 1 cps.

Calibration in terms of real units of slope was performed as indicated in Section 2.2.

The frequency analyzer consists of 30 band-pass filters spaced one-third octave apart (frequency ratio between bands = 1.23). The effective width of each filter band is also one-third octave. Each datum reported by the analyzer is then proportional to the total spectral intensity integrated over the band passed by one filter.

The input to the spectrum analyzer is composed of two parts: (1) a noise spectrum compounded of multiplier phototube shot noise and stray electrical pickup (mostly 60 cps noise introduced in the analyzer which shows up as a peak at 60/37.5 cps = 1.7 cps in Fig. 4) and (2) signal proportional to the spectrum of s_x. The shot noise is "white" and hence can easily be removed if its intensity is known at any frequency. The observations at low wind speed (3.2 m sec^{-1}) show a high-frequency tail from 170 to 540 cps of uniform intensity. It is assumed that this is the photomultiplier noise and that the same noise

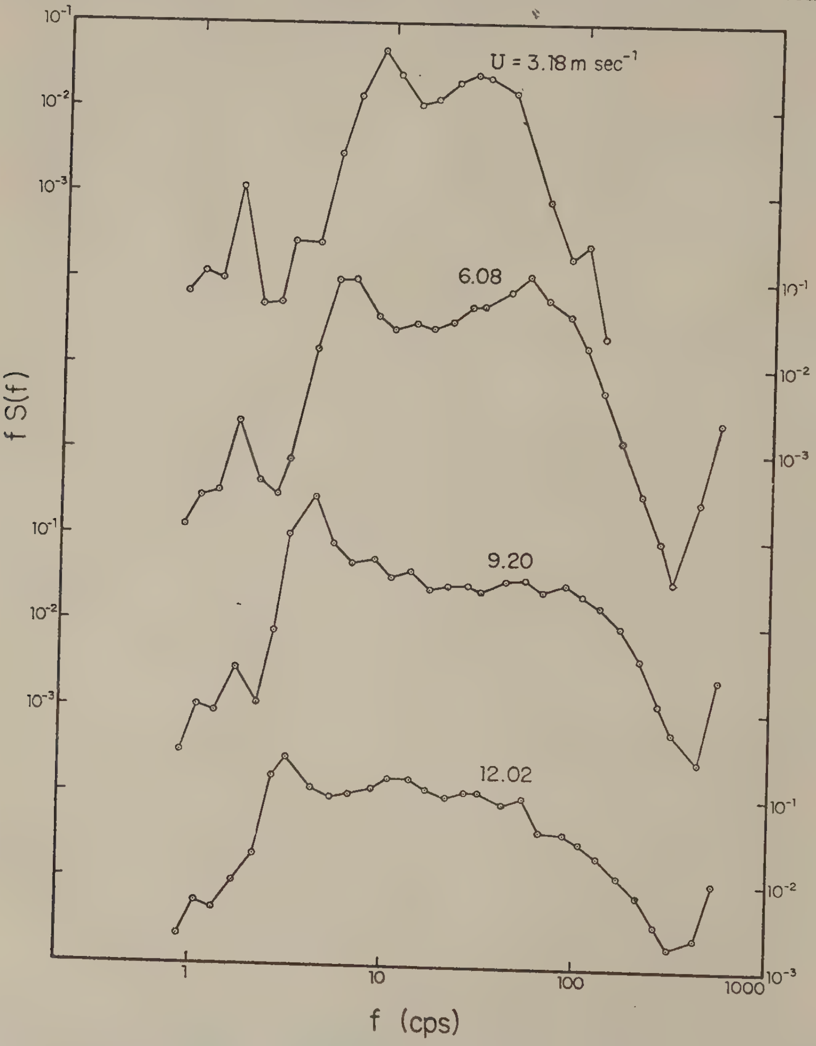

Figure 4. Slope spectrum times frequency, $fS(f)$, of up- and down-wind slopes as a function of frequency, f, for four wind speeds U as shown. The fetch was 2.14 m.

level occurs for each of the spectra at all frequencies; accordingly, this source of noise has been subtracted from all spectra shown in Fig. 4. Some features of doubtful authenticity still remain. The rise of spectral intensity shown by the three lower curves beyond 300 cps is probably not real. It may be caused by imperfect frequency calibration of the magnetic tape at frequencies where large corrections are necessary or by nonlinear recording of slopes larger than tangent 40°.

The spectral intensity, S, is the contribution to mean square slope by waves in a unit frequency band:

$$\langle s_x^2 \rangle = \int_0^\infty S(f)\, df. \tag{1}$$

Since s_x is dimensionless, the dimensions of $S(f)$ are $(\text{cps})^{-1}$.

The observations show that $S(f)$ tends to decrease with increasing frequency. Accordingly, it is clearer to plot $f\, S(f)$, since this quantity gives equal importance to high- and low-frequency waves (Fig. 4). By transforming eq. (1) to the form

$$\langle s_x^2 \rangle = \int_0^\infty f\, S(f)\, d(\ln f),$$

one sees that $f\ S(f)$ is the spectral intensity referred to the *relative* frequency band $\delta(\ln f) = \delta f/f$.

As a check on the spectra, mean square slopes calculated by integrating each spectrum are compared below with those observed directly (Section 3.1):

Wind speed (*m sec*$^{-1}$)	*Mean square slope from spectrum*	*Mean square slope observed directly*
3.2	1.32×10^{-2}	1.36×10^{-2}
6.1	5.18	4.56
9.2	6.21	6.00
12.0	12.6	8.26

The agreement is satisfactory except at the highest wind speed. The causes of the poor agreement here are not entirely clear. Part of the difference can be accounted for by consideration of the poor lens system (Section 2.1) used to measure mean square slope, but this can hardly account for the whole effect.

3.3 Phase Velocity. Phase velocities were measured for three frequencies of waves: 6.6, 37, and 104 cps by the method outlined in Section 2.3. The data are summarized in Table IV. In columns 5–8, f_0 and Q are respectively the center frequencies and quality factors of the filters. The effective f_0 (column 9) is intermediate between f_0 for each filter and is used together with the corrected wave lengths to compute the phase velocity. Estimations of apparent wave length, λ, and the remaining quantities are described below. Corrections to the apparent wave length (column 11) have to be made for the fact that all wave velocities are not parallel to the axis of the tank. If all wave directions are within a small angular spread of the axis of the tank, it can be shown that the true wave length, λ_0 (column 16), is related to the apparent wave length, λ, by a reduction factor F, (column 15) according to

$$\lambda_0 = \lambda F, \tag{2}$$

where

$$F = 1 - \tfrac{1}{2}(\sigma_y^2/\sigma_x^2). \tag{3}$$

Here σ_x and σ_y are rms filter outputs when the wedge (Fig. 1) is oriented to respond to slopes up-down wind and cross wind, respectively.

If the angular spread of wave directions, $2\theta_0$, is appreciable compared to

$$\left(\frac{10}{\pi^2}\frac{\lambda_0^2}{\xi_m^2}\right)^{1/3},$$

where ξ_m is the maximum separation of the photocell telescopes, then the foregoing method is no longer accurate. It is now necessary to know not only the value of σ_y^2/σ_x^2 but also the directional distribution

TABLE IV.

Date	*Temperature*			*Filters*					*Wind*	
1956	*Air* °*C*	*Wet* °*C*	*Water* °*C*	*No. 1* f_0 (*cps*)	*Q*	*No. 2* f_0 (*cps*)	*Q*	*Effective* f_0 (*cps*)	*speed* (*m/sec*)	λ (*cm*)
1	2	3	4	5	6	7	8	9	10	11
Oct. 24–26				36.1	19	36.1	16	36.1	3.69	.853 ±.008
Oct. 29				36.85	22	36.90	19	36.87	9.22	1.007 ±.043
Oct. 29–30				36.9		36.9		36.9	5.48	.838 ±.005
Oct. 30				36.9		36.9		36.9	7.28	.901 ±.037
Oct. 31				37.07	16.5	36.75	19.5	36.95	11.46	.958 ±.064
Nov. 8				6.53	25.5	6.53	36	6.53	5.48	4.971 ±.011
Nov. 8–9				6.53	25.5	6.53	36	6.53	6.55	5.15 ±.15
Nov. 12–13	24.4		20.1	6.57	34	6.62	41	6.60	8.83	5.23 ±.25
Nov. 13	23.9	16.7	18.9	6.57	34	6.62	41	6.60	3.90	5.08 ±.16
Nov. 15	22.6	15.4	16.6	6.87	31	6.88	41	6.88	11.89	
Nov. 21–26	22.8	16.4	18.8	103.63	200	103.63	100	103.63	5.82	.373 ±.006
Nov. 27	25	15.1	20.0	104.3	115	104.0	54	104.2	4.32	.330 ±.013
	26.8	16.5	19.4							
Nov. 28	23.9	15.0	21.1	104.2	130	104.8	50	104.4	7.33	.384 ±.013
Nov. 29	23.9	14.6	21.6	104.2	130	104.3	50	104.2	9.32	.417 ±.009
	26.6	16.8	19.0							
Nov. 29	24.3	16.4	20.6	104.2	130	104.3	50	104.2	11.70	.437 ±.049
			19.2							

of the waves. Since results do not depend critically on this distribution, it has been assumed in the subsequent analysis that the directional spectrum of wave *elevations* is fan-shaped, *i.e.*, the spectral intensity (at the frequency of observation) is uniform for wave directions less than θ_0 (measured with respect to the axis of the tank) and is zero for wave directions larger than θ_0. With this assumption it can be shown that the correlation between two pickups separated by a distance ξ will be proportional to

$$G(\xi)\ [A \cos x + B \sin x], \tag{4}$$

where

$$x = \frac{2\pi\xi}{\lambda_0}; \quad A = \sqrt{\frac{\pi}{x}}\, C\left(\theta_0\sqrt{\frac{x}{\pi}}\right) + \sqrt{\frac{\pi}{x^3}}\, S\left(\theta_0\sqrt{\frac{x}{\pi}}\right) - \frac{\theta_0}{x} \sin\left(\frac{x\theta_0^2}{2}\right);$$

$$B = \sqrt{\frac{\pi}{x}}\, S\left(\theta_0\sqrt{\frac{x}{\pi}}\right) - \sqrt{\frac{\pi}{x^3}}\, C\left(\theta_0\sqrt{\frac{x}{\pi}}\right) + \frac{\theta_0}{x} \cos\left(\frac{x\theta_0^2}{2}\right);$$

C, S are Fresnel's integrals, $C(u) + iS(u) = \int_0^u \exp\left(\tfrac{1}{2}i\pi t^2\right) dt$; and G is a slowly varying factor which depends on the Q of the filters and on the accuracy with which one can associate a single wave length with waves of one frequency. In deriving the formula, the assumption has been made that $\theta_0^2 \ll 1$.

TABLE IV (cont.)

N 12	$N_{1/e}$ 13	θ_0 (*radians*) 14	F 15	λ_0 (*cm*) 16	c (*cm sec*$^{-1}$) 17	c_0 (*cm sec*$^{-1}$) 18	$c - c_0$ (*cm sec*$^{-1}$) 19
8	>4	.26 ±.15	.989 ±.010	.844 ±.012	30.5 ±0.4	26.2 ±.5	+ 4.3 ±0.6
4	>2	.17 ±.04	.9952 ±.0024	.959 ±.043	36.4 ±1.6	25.3 ±.5	+11.1 ±1.7
8	3½	.21 ±.02	.9927 ±.0014	.832 ±.005	30.7 ±0.2	26.4 ±.5	+ 4.3 ±0.5
7	3	.19 ±.03	.9940 ±.0018	.896 ±.037	33.2 ±1.4	25.8 ±.5	+ 7.4 ±1.5
5	2½	.21 ±.04	.9927 ±.0028	.952 ±.064	35.2 ±2.4	25.4 ±.5	+ 9.8 ±2.4
3	>3	.52 ±.05	.958 ±.009	4.76 ±.011	31.0 ±0.3	28.9 ±.02	+ 2.1 ±0.3
5	3	.71 ±.07	.924 ±.008	4.76 ±.15	31.1 ±1.0	28.9 ±.02	+ 2.2 ±1.0
4	3	1.02 ±.10	.902 ±.001	4.72 ±.23	31.2 ±1.5	28.8 ±.02	+ 2.4 ±1.5
5	4	1.08 ±.11	.905 ±.001	4.60 ±.14	30.4 ±0.9	28.5 ±.02	+ 1.8 ±0.9
1	<1	1.29 ±.13	.88 ±.01				
13	8	.65 ±.08	.957 ±.006	.357 ±.006	37.0 ±0.6	37.0 ±.24	0.0 ±0.6
9	>6	.67 ±.13	.945 ±.013	.312 ±.013	32.5 ±1.4	39.5 ±.24	− 7.0 ±1.4
14	6	.72 ±.09	.956 ±.008	.367 ±.013	38.3 ±1.4	36.9 ±.24	+ 1.4 ±1.4
10	3	1.10 ±.08	.925 ±.002	.386 ±.008	40.2 ±0.8	35.9 ±.24	+ 4.3 ±0.8
6	3	1.36 ±.10	.911 ±.001	.398 ±.045	41.5 ±4.7	35.3 ±.24	± 5.2 ±4.7

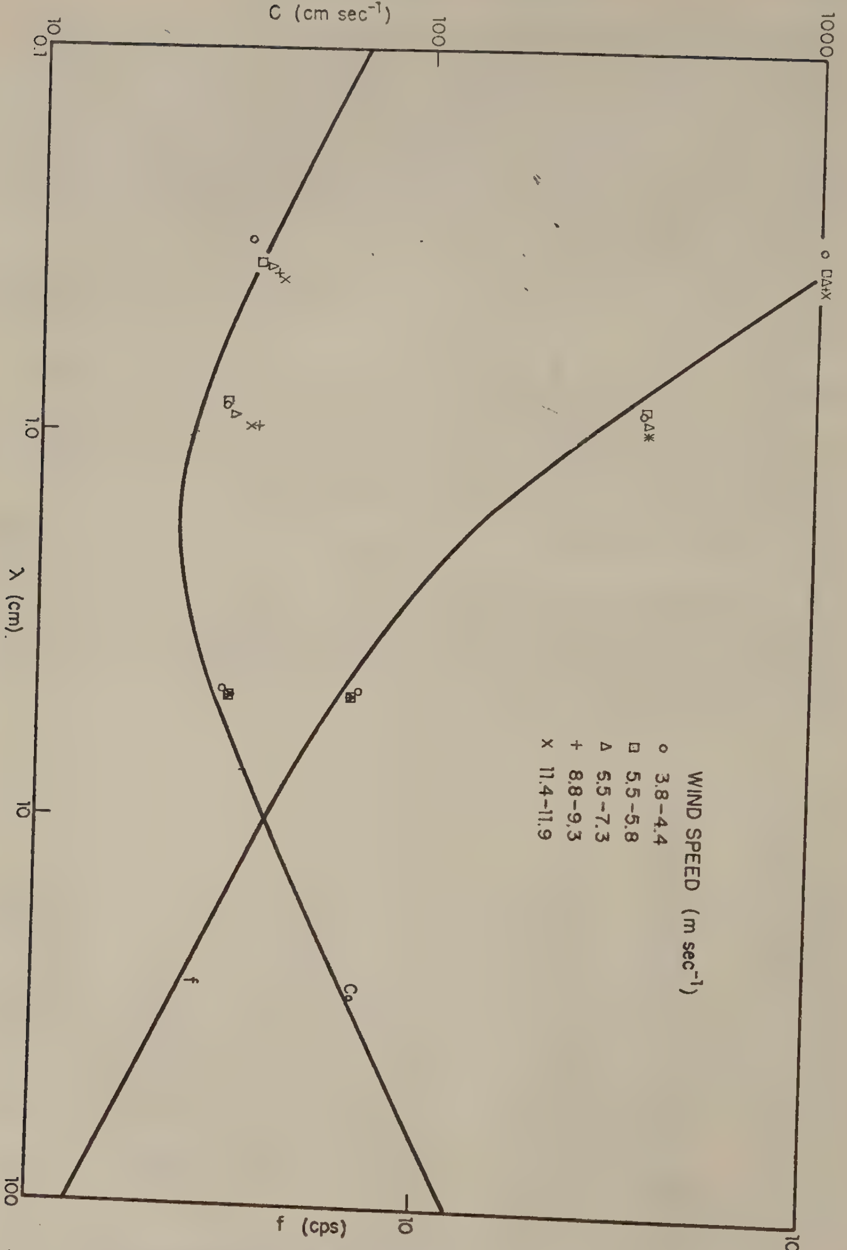

Figure 5. The theoretical phase velocity, c_0, and frequency, f, for waves on still water in the absence of wind. The observational data are indicated by points which correspond to the wind speeds shown.

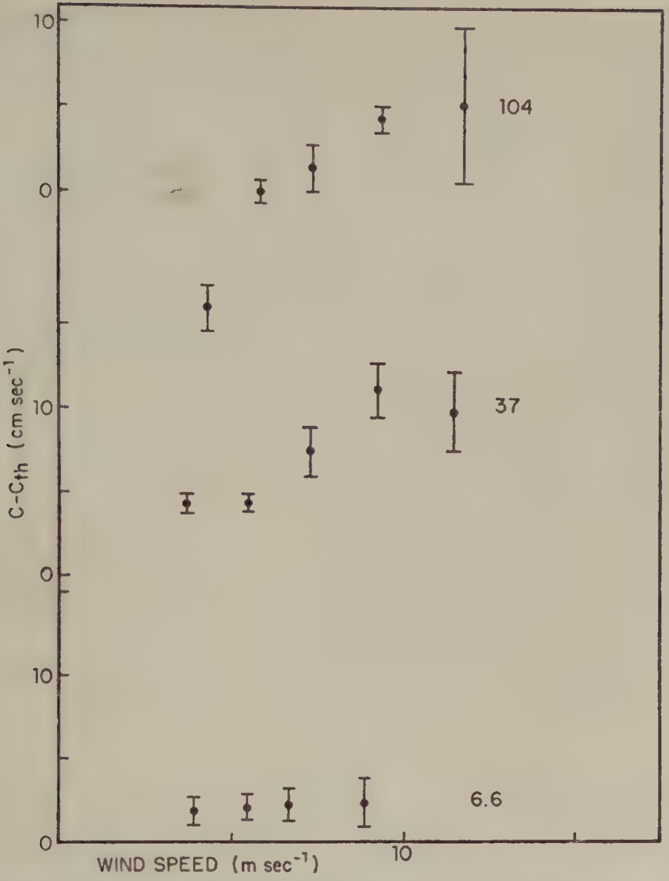

Figure 6. The difference between observed and theoretical phase velocities as a function of wind speed. The three graphs refer to three frequencies (in cps) of waves as noted on the right.

The half-beam width, θ_0, can be found from σ_y/σ_x according to a formula derived by Cox and Munk (1954).

In finding the apparent wave length, λ, the procedure has been to find the successive phototube separations, ξ_n, at which the correlation reverses sign. From a plot of ξ_n vs n, a least square analysis yields λ as well as an estimate of its standard error (see Table IV). Similar plots were made from the theoretical eq. (4) for suitable values of θ_0. From a least square analysis of these plots, one gets a factor F which can be used (eq. 2) to correct the apparent wave length.

Entered in columns 12 and 13 are the total number, N, of changes in sign of the correlation as well as an estimate of the ordinal number, $N_{1/3}$, of the zero crossing (reckoned from zero separation) at which the *amplitude* of the correlation curve has dropped to one third of its initial value. $N_{1/3}$ permits an estimate of the factor $G(\xi)$, eq. (4), a discussion of which is postponed until Section 4.

The half-beam width, θ_0 (column 14), is estimated together with its standard error from a measurement of σ_y/σ_x (data not shown). Then, from the quantities N and λ, one can estimate ξ_m by $\xi_m \approx \lambda N/2$ and evaluate the criterion for the applicability of eq. (3). Using eq. (3) or (4), whichever is suitable, one finds F (column 15) together with its standard error. Fortunately the correction factor is always close to unity and its uncertainty is generally of negligible importance for the corrected wave length, λ_0 (column 16). In column 17, c is the phase velocity (and standard error) computed from $c = \lambda_0$ times (effective f_0). In column 18 c_0 is the theoretical phase velocity for free waves on still water without wind (Lamb, 1945: 459, eq. 2). Comparison of theoretical and observed quantities is shown in Fig. 5. In computing c_0 it has been assumed that the surface tension corresponded to the temperature measured by the wet bulb thermometer. Because of the uncertainty of this estimate, there is an uncertainty in c_0. No measurements of wet bulb temperature were made on 24–31 October, and here the temperature is estimated at 16 ± 4°C.

The quantity $c - c_0$ (column 19) shows the difference between the observed phase velocity and c_0. The same quantity is plotted in Fig. 6.

4. DISCUSSION

Measurements of mean square slope may be compared with measurements made in the open sea (Cox and Munk, 1954). Measurements of wind speed in the tank represent average speed throughout the air channel; it may be estimated that the level at which this speed is reached in the boundary layer next to the water is 4 to 8 cm above mean water level. Hence, oceanic measurements of wind speeds made at a height of 12.5 m must be reduced by a large and uncertain correction factor before a useful comparison can be made. I assume the factor is

$$ln\left[\left(\frac{6.0}{0.1}\right) \Big/ \left(\frac{1.25 \text{ x } 10^4}{0.1}\right)\right] = 2.2 \;;$$

this assumes (1) a logarithmic velocity profile near the water in both tank and ocean, (2) an effective height of wind observation in the tank of 6 cm, and (3) a roughness length in both the tank and ocean of 0.1 cm. Ocean measurements reduced in this way show a linear increase of mean square of the up-down wind component of slope with wind speed from zero at no wind to a value of .044 at a wind speed of 6.3 m sec^{-1}. Tank measurements showed that a mean square slope of .044 was reached at wind speeds of 6.4, 6.1, and 6.0 m sec^{-1} at fetches of 1.5, 2.1, and 3.2 m respectively. With due regard to the uncertainty of comparing wind speeds between tank and ocean, it appears that the mean square slope at 6 m sec^{-1} wind speed will not markedly increase beyond a fetch of 3 m. This is confirmed by the shape of the curves showing mean square slope as a function of fetch (Fig. 3). It appears that, regardless of the mechanism responsible for the explosive growth of waves just beyond the critical fetch, nonlinear effects rapidly set in to limit the slopes at fetches slightly greater than 3 m. On the other hand, it is clear that, for wind speeds lower than 6 m sec^{-1}, oceanic measurements showed appreciable mean square slopes at wind speeds below the critical speed for the tank. This fact indicates that the critical wind speed decreases to a low value for the long fetches encountered in the open sea.[2]

Curves showing the growth of mean square slope with fetch (Fig. 3) may shed some light on the question of the initial generation of waves. According to Jeffreys' (1924–25) "sheltering" theory, the wave amplitude should, in the initial stages, increase exponentially down wind. If this were indeed the case, then observations of very small mean square slope at the critical fetch and rapid growth down-wind imply that waves must be extremely small at the up-wind end of the tank. This was not in fact the case. On viewing objects reflected in the surface, it appeared that there was more wave motion here than at a point just short of the critical fetch (but still so small as to be unmeasurable by the slope apparatus). These small waves at short fetches were probably caused by vibration of the tank and by fluctuating pressures set up by turbulence in the air stream as it flowed around the anemometer at the mouth of the wind channel and over a 1- or 2-cm lip (designed to keep waves from splashing water out at the up-wind end of the water channel). One concludes that there is not an exponential growth of waves at short fetches.

In contrast to Jeffreys' development, in which the air pressure fluctuations are coupled to the already existing waves, Phillips (1957) has developed a theory of wave generation based on a model in which the pressure fluctuations are completely independent of the waves. The theory has been worked out for unlimited fetches and finite duration of winds only. However, Phillips makes the remark that waves generated by steady winds at a small fetch are likely to be similar to those described by his theory at a short time after the sudden onset of wind. If this correspondence is valid, Phillips' calculation of the directional distribution of the waves should be comparable to wave measurements in the tank. According to Phillips' result, practically all of the waves of frequency f and wavelength λ will make an angle θ_1 with the wind where

---

[2] The waves generated at these low wind speeds are probably gravity waves; *cf* Fig. 2 in "Comments on Dr. Phillip's Paper" (J. Mar. Res., *16*(3): 241-245).

$$|\theta_1| = \cos^{-1}\frac{c(f)}{U_\lambda}, \tag{5}$$

c is the phase velocity of the waves, and U_λ is the "convection velocity" of the turbulent pressure fluctuations: that is, the average speed at which pressure fluctuations of wave length λ are drawn over the water. It seems plausible to assume, with Phillips, that U_λ is the mean wind velocity at a height $\lambda/2\pi$ above mean water level.

This result contrasts with the assumption made in the analysis of phase velocities (Section 3.3) that waves were found at *every* angle to the wind within the fan-shaped beam $|\theta| \leqslant \theta_0$. Measurements of the ratio of mean square filtered slope components, σ_y^2/σ_x^2, cannot distinguish between the two directional patterns of waves; but they do permit a check of eq. (5). In Table V, for waves at $f = 6.6$ cps, estimates of θ_1 from eq. (5) are compared with estimates based on the measurement of σ_y/σ_x according to $\tan\theta_1 = \sigma_y/\sigma_x$.

TABLE V

Mean wind speed (*cm sec*$^{-1}$)	λ_0 (*cm*)	*c* (*cm sec*$^{-1}$)	$U\lambda$ (*cm sec*$^{-1}$)	θ_1 (*Eq. 5*)	$\theta_1 = \tan^{-1}(\sigma_y/\sigma_x)$
1	2	3	4	5	6
548	4.76	31	402, 120	86°, 75°	17° ± 2°
655	4.76	31	471, 144	86°, 78°	23° ± 2°
893	4.72	31	648, 194	87°, 81°	32° ± 3°
390	4.60	30	286, 86	84°, 69°	39° ± 3°

The first three columns of Table V are taken from Table IV. In column 4, the two values of U_λ have been estimated by calculating the mean wind speed at a height $2\pi/\lambda_0$ above the water, assuming a logarithmic velocity profile near the water, with a roughness length of ⅓ mm and 3 mm respectively. These are representative limits within which the value of z_0 is likely to lie according to measurements in the open sea (Hay, 1955). The two values of U_λ so derived lead to two values of θ_1 (eq. 5) shown in column 5. The value derived from observation of σ_y/σ_x is shown in column 6.

The uncertainty in U_λ is very large; consequently, one must regard the values of θ_1 calculated by eq. (5) as rough estimates. Nevertheless, it is difficult to see how the observed values of σ_y/σ_x can be reconciled with eq. (5). It is concluded that waves do not run at the angle θ_1 to the wind shown by eq. (5), and this suggests that the hypothesis adopted by Phillips is not correct for the initial generation of waves.

Direct cathode-ray oscillograph recordings of slope at 2.14 m fetch are shown in Figs. 7–9. In Fig. 7, one sees clearly that for each wind speed there are two preferred frequency bands of activity; this

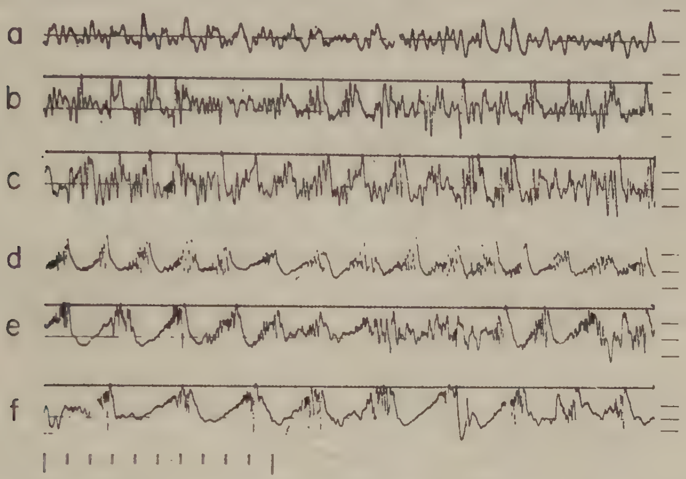

7

Figure 7. Records of up- and down-wind slope component, s_x, as a function of time for various wind speeds in m sec^{-1} as follows: (a) 3.0; (b) 4.8; (c) 6.1; (d) 8.5; (e) 9.5; and (f) 11.5. (A record at 7.1 m sec^{-1} is shown in Fig. 7b). The slope scale (vertical) is shown by three horizontal dashes to the right of each trace. The separation between dashes is 0.50 in slope. An upward deflection of the trace refers to a water surface element whose up-wind edge is higher than the down-wind edge. The time scale (horizontal) is shown at the bottom of the figure by large marks at one-second intervals and small marks indicating tenths of seconds. Time increases to the right.

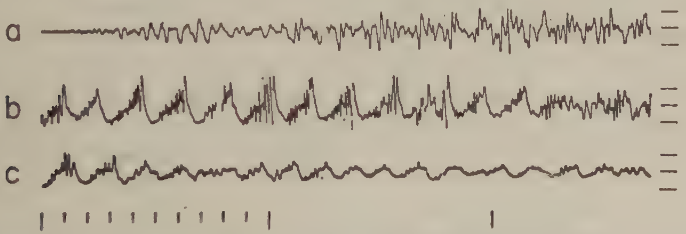

8

Figure 8. (a) Initial generation of waves; (b) waves in equilibrium with the wind; (c) decay of waves after blower is turned off. These records show up- and down-wind slope (vertical) vs. time (horizontal) as in Fig. 6. The wind speed and fetch are 7.1 m sec^{-1} and 2.14 m, respectively.

is shown also by the frequency spectra (Fig. 4). As the wind speed increases, the low-frequency band tends to low frequencies while the high-frequency band broadens and extends into high frequencies. The dip in the spectrum at low wind speed between the two bands occurs at the frequency of minimum-phase velocity (Figs. 4, 5). Consequently the changes of spectra are such as to keep both bands of activity moving at a speed proportional to the wind.

For winds greater than about 7 m sec^{-1} a new effect becomes important: high-frequency ripples become associated with the *leading slopes* of low-frequency wavelets, *i.e.*, the region down wind of a crest but up wind of the preceding trough (Figs. 7d, e, f; 8b).

Munk (1955) has given two alternative explanations for similar observations in the ocean. According to the first, it is stated that the only stable position for ripples is on the leading slope of a wavelet because the orbital velocity of the wavelet creates a zone of convergence which sweeps ripples onto the leading slope. Some computations of the relative positions of ripples of various length to be expected with this hypothesis are given by Munk. It is thought that these computations are in error because they are based on equating ripple *phase* velocity to the combination of phase and orbital velocity of the underlying wavelet. Since the energy moves with the *group* velocity, it is felt that the correct computation should equate the ripple *group* velocity to the combination of phase and orbital velocity of the wavelet. Qualitatively both computations lead to the same result: that the short ripples should precede the long ones.

Munk's second explanation is based on intermittent generation of ripples by a moving pressure disturbance of short duration. This leads (according to a generalization of the well known solution of the "fish-line" problem) to a dispersive ripple train in front of the moving pressure. Munk associates the pressure disturbance with some (unknown) process located near the crest of wavelets.

From the rather irregular records shown in Figs. 7 and 8, it seems impossible to deduce which of these processes is operative. Accordingly some records were made of wavelets artificially generated by a plunger (Fig. 9). These also show the characteristic ripple trains on the leading slopes of wavelets even though the plunger supplied energy only at the wavelet frequency. It may be that ripples were generated because there was a finite spread of direction of the wavelets; where two crests intersected, there was a momentary nonlinear interaction which gave rise to the ripples.

The rather regular appearance of ripples on the records of Fig. 9 permits not only a rough estimate of the period of individual ripples but comparison with Munk's hypotheses as well. The result is that plots of position of ripple vs ripple frequency are consistent with Munk's first hypothesis (as modified for equality of ripple group velocity to wavelet phase plus orbital velocity).

It seems likely then that the energy of the ripples is trapped on the leading slope of wavelets by convergence due to the distribution of the orbital velocity in that position. The possibility of trapping in this manner requires that the magnitude of the difference between the phase velocity of the wavelets and the group velocity of the ripples be not greater than the maximum orbital velocity of the wavelets. To a considerable extent this possibility is, therefore, an artifact of the wave tank used in these experiments, because the fetch is sufficient to allow the generation of wavelets with large orbital velocities but is not long enough to permit development of wavelets of high phase velocity. In the open sea, where a sharp spectral peak of low-velocity wavelets is not to be expected, one expects that trapping of ripples will not be such a noticeable and persistent phenomenon. Some evidence on this point is shown in Fig. 14; in the left-hand photograph only a few ripples appear to be trapped on the leading (top) slopes of wavelets about 50 cm long; in the right-hand photograph the whole surface appears uniformly covered with ripples.

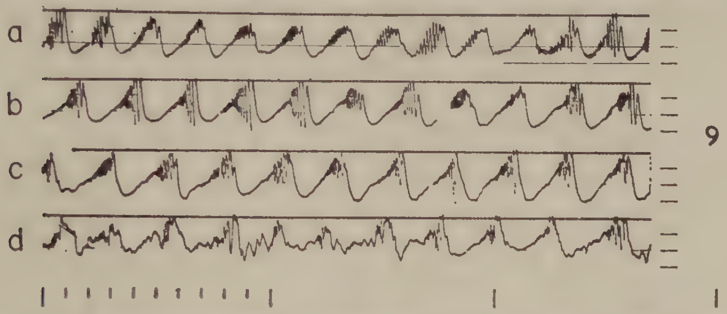

Figure 9. Up- and down-wind slope of plunger-generated waves: (a) without wind; (b) with 2.8 m sec^{-1} wind; (c) with 9.0 m sec^{-1} wind; (d) with 11.6 m sec^{-1} wind. The horizontal and vertical scales are similar to those of Fig. 6. The distance from plunger to recording pickup and the effective fetch was 0.6 m.

Also shown in Fig. 9 are records of plunger-generated waves as modified by winds (Fig. 9b, c, d). The effects of wind appear to be an increase in the average energy and frequency of ripples. The increase of energy may be due to generation by wind. The change of frequency suggests that the relation between frequency and group velocity of ripples is altered by the effects of wind in such a way that only high frequency ripples can keep up with the wavelets.

Measurements show pronounced changes of phase velocity (Section 3.3) with wind speed. There are four factors which are of the appropriate order of magnitude to be of importance. They are (1) finite amplitude of waves, (2) effects of orbital velocity of low-frequency wavelets, (3) water currents, and (4) dynamic effects of wind.

The theory of finite amplitude capillary-gravity waves has been initiated by Sekerzh-Zenkovich (1956). The velocity, c, of waves of constant form is given in the following form to the third order:

$$c^2 = c_0^2 + \Delta(\lambda, \epsilon^2);$$

here c_0 is the velocity of infinitesimal waves, Δ is a function of wave length λ and ϵ, a parameter (which tends in the limit of infinitesimal amplitude to the maximum slope of the wave). The equation is equivalent to the following expression, correct to the third order in ϵ:

$$c = c_0\left(1 + \tfrac{1}{2}\frac{\Delta}{c_0^2}\right). \tag{6}$$

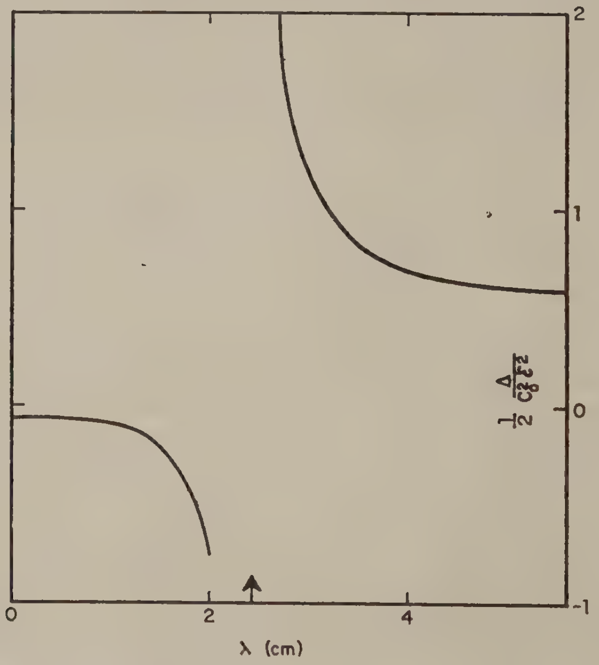

Figure 10. Effects of finite amplitude on wave velocity as a function of wave length, λ. The quantity $\frac{1}{2}\frac{\Delta}{c_0^2\epsilon^2}$ is defined in eq. (5), Section 4. The curve is not valid at the wave length indicated by the arrow.

The quantity $\frac{1}{2}[\Delta/(c_0^2\epsilon^2)]$ is shown in Fig. 10. Certain assumptions in the derivation make the solution invalid when the wave length is such that n capillary waves have the same length as one gravity wave. The wave length where $n = 2$ is indicated in the figure by an arrow.

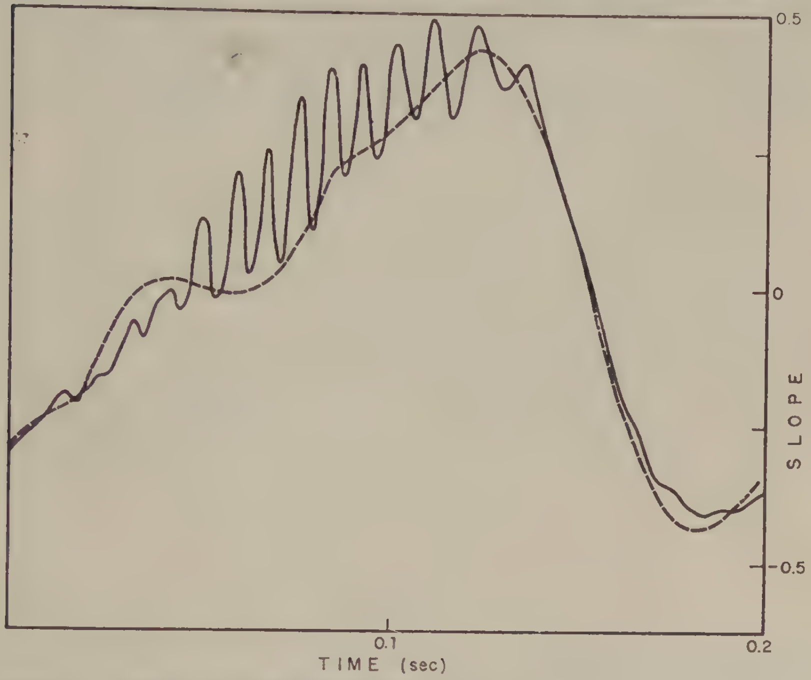

Figure 11. Comparison of plunger-generated wave (solid line) (see Fig. 8a) with slope profile predicted by finite amplitude theory of Sekerzh-Zenkovich (dashed line).

For $\lambda > 3$ cm, the value of $\frac{1}{2}[\Delta/(c_0^2\epsilon^2)]$ is positive and tends to the limit $\frac{1}{2}$ as $\lambda \rightarrow \infty$. Hence the phase velocity approaches $c_0(1 + \frac{1}{2}\epsilon^2)$. It is clear that waves of length $\lambda > 3$ cm behave substantially like finite amplitude gravity waves according to Stokes' solution. On the other hand, if $\lambda < 1$ cm, the effect of finite amplitude on the phase velocity is markedly reduced and reversed in sign.

Measurements at 6.6 cps ($\lambda = 4.7$ cm, $c_0 = 28.9$ cm sec^{-1}, wind speeds from 3.9 to 8.8 m sec^{-1}) give $c/c_0 = 1.075 \pm .010$ (Table III). Taking $\frac{1}{2}[\Delta/(c_0^2\epsilon^2)] = 0.62$ from Fig. 10 and $\frac{1}{2}\Delta/c_0^2 = c/c_0 - 1 = .075 \pm .010$, one finds $\epsilon = .35 \pm .05$. To find the value of maximum slope to which this value of ϵ corresponds, it is necessary to fit some wave profiles to the Sekerzh-Zenkovich wave profile formula. One wave from Fig. 9a has been so fitted (Fig. 11). The best fit was for

(163)

$\epsilon = 0.33$, $\lambda = 7.0$ cm. (The wiggles on the computed profile are probably the result of pushing the third order theory beyond its limits of validity.) The maximum slope of the observed wave was about 0.42. One estimates then that wavelets with maximum slopes of 0.42 will have a value of ϵ sufficiently large to account for the observed increase of phase velocity. But this is a fairly representative slope for waves near 6.6 cps at the wind speeds where phase velocities were measured. In conclusion, the increase of phase velocity at 6.6 cps for moderate winds is probably the effect of finite amplitude.

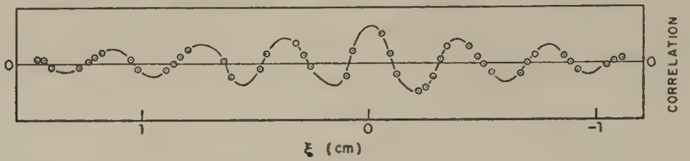

Figure 12. Correlogram of slopes measured at two points a distance ξ apart. Measurements from 28 November; f_s = 104 cps, wind speed = 7.3 m sec^{-1}.

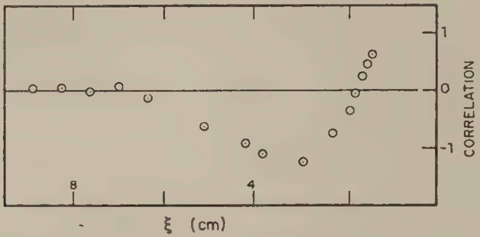

Figure 13. Correlogram of slopes at two points a distance ξ apart. Data from 15 November; f_s = 6.9 cps, wind speed = 11.9 m sec^{-1}.

Phase velocities of 37 and 104 cps waves will scarcely be affected by their finite amplitude according to Sekerzh-Zenkovich's theory, but it can be shown that the other three factors will be effective. Unfortunately it does not now appear possible to disentangle the effects.

Measurements of phase velocity gave as a by-product an estimation of the degree to which one can associate a single wave length with a single frequency of wave. According to the usual theory of infinitesimal waves, those of a single frequency would have an accurately defined wavelength. The effect of waves running in a beam of directions on the correlogram of slopes measured at two points is to reduce, for large ξ, the amplitude of the oscillations of the correlation rather slowly. This reduction is shown by factors A and B of eq. (4), Section 3.3. The effect is rather well illustrated by Fig. 12.

Most correlograms showed a much more rapid decrease of amplitude as ξ was increased, and the effect could *not* have been caused by the directional beam of waves. An extreme example is shown in Fig. 13 where the decrease of amplitude was so great that it was not possible to measure an apparent wave length at all.

A variation in wave length for waves of a single frequency can be caused by variation of any of the factors which alter phase velocity or by processes of generation and decay. The latter can be illustrated by a simple model. Suppose the slope component due to a narrow range of frequencies of waves can be represented by

$$s(x, t) = \Sigma_i\, g(x - x_i) f\,[x - x_i - v(t - t_i)] \cos[k(x - ct)],$$

where $f(x)$ is a slowly varying function compared to $\cos(kx)$ and $g(x)$. The parameters x_i, t_i indicate the general location and epoch of a single train of waves, $f(x - vt)$ represents the motion of the envelope at group velocity, v, and $g(x)$ represents processes of generation and decay. There are two extreme cases to consider· (1) the individual trains are generated completely at random so that x_i, t_i are independent and random variables; (2) the successive trains overlap in a regular fashion so that the sum represents a periodic function of time. In the first case the correlation of slopes at two points a distance ξ apart becomes

$$< s(x, t)\, s(x + \xi, t) > \; = G(\xi) \cos (k\xi),$$

where

$$G(\xi) = \int_{-\infty}^{\infty} g(x)\, g(x + \xi)\, dx$$

is a measure of the distance traversed by a single wave train; in the second case, the correlation is proportional to $\cos k\xi$.

The first example is representative of random generation of waves while the second represents generation which is locked in phase with the already existing waves. To this extent they represent two theoretical models proposed respectively by Eckart (1953) and Phillips (1957) on the one hand and by Jeffreys (1924, 1925) on the other.

The measurements of $N_{1/3}$ (Table IV; Section 3.3) can therefore yield some estimates of $G(\xi)$ provided variations of phase velocity (see above) are negligible.

In the present data it is not possible to rule out the effects of variations of phase velocity. The values of $N_{1/3}$ must then be regarded as lower limits on the distance (measured in wave lengths) of travel of a single randomly generated wave train. They do not yield any information on nonrandom generation processes.

Measurements showed that $N_{1/3}$ was surprisingly small. In only four out of 15 measurements was $N_{1/3}$ larger than three. The largest values are associated with low winds.

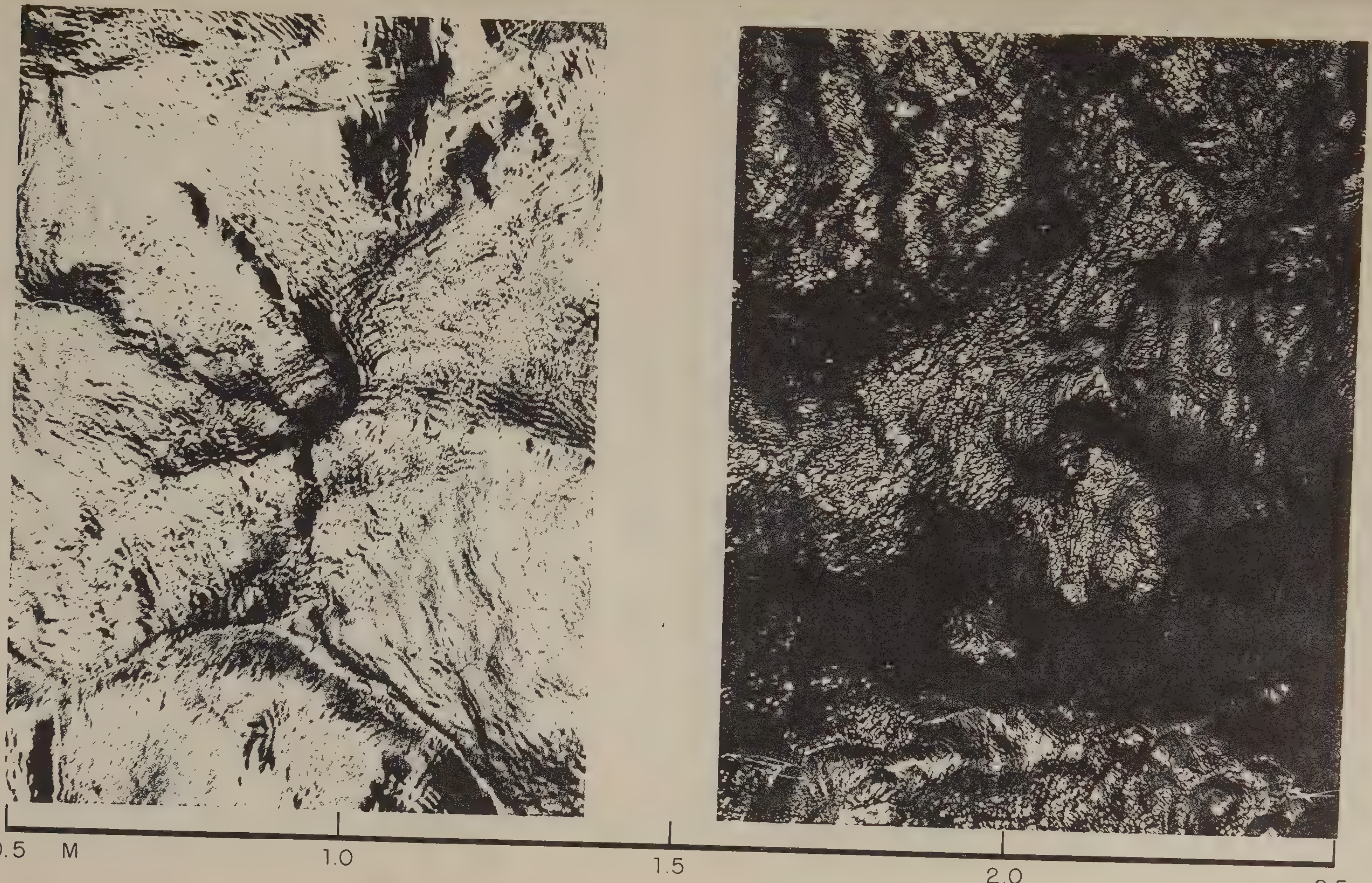

Figure 14. Photographs of the sea surface made from Scripps pier 29 March 1956. Wind speed was 6.5 m sec-1 measured 12 m above sea level. The pronounced white dots on one photograph are reflections of the sun. The other photograph was exposed when the sun was covered with a cloud; the tiny white dots are reflections of a gas-discharge lamp supported 10 m above sea level. The scale indicates distances in meters. In these photographs the wind was blowing from an offshore direction, hence the fetch was almost unlimited. Some of the larger gravity wave motions shown may be due to reflections from piles supporting the pier, but it was clear to the eye that the ripples were driven by the wind towards the pier.

5. ACKNOWLEDGMENTS

The experimental work reported here has been aided by many people, but particular thanks are due F. Peterson, F. Snodgrass, and P. Teller. J. Zimmerman kindly made the spectrum analyses; G. Groves pointed out Sekerzh-Zenkovich's paper and translated it; and M. DeSelle helped with many computations. W. Munk's advice and encouragement is gratefully acknowledged.

REFERENCES

Cox, Charles and Walter Munk
1954. Statistics of the sea surface derived from sun glitter. J. Mar. Res., *13:* 198-227.
Eckart, Carl
1953. The generation of wind waves on a water surface. J. appl. Phys., *24:* 1485-1494.
Hay, J. S.
1955. Some observations of air flow over the sea. Quart. J. R. met. Soc., *81:* 307–319.
Jeffreys, Harold
1924–25. On the formation of water waves by wind. Proc. roy. Soc., (A) *107:* 189–206; *110,* 341–347.
Keulegan, G. H.
1951. Wind tides in small closed channels. J. Res. Nat. Bur. Stand., *46:* 358–381.
Lamb, Horace
1945. *Hydrodynamics*, 6th edition. Dover Publications, New York. 738 pp.
Munk, Walter
1955. High frequency spectrum of ocean waves. J. Mar. Res., *14:* 302–314.
Phillips, O. M.
1957. On the generation of waves by turbulent wind. J. fluid Mech., *2:* 417–445.
Schwantes, R. C., H. J. Hannam and A. van der Ziel
1956. Flicker noise in secondary emission tubes and multiplier phototubes. J. app. Phys., *27:* 573–577.
Sekerzh-Zenkovich, Y. I.
1956. On the theory of stationary capillary waves of finite amplitude on the surface of a heavy fluid. Dokl. Akad. Nauk., *109:* 913–918.
Ursell, Fritz
1956. Wave generation by wind, in *Surveys in Mechanics*. Cambridge University Press. 475 pp.
Van Dorn, W. G.
1953. Wind stress on an artificial pond. J. Mar. Res., *12:* 249–276.

Reprinted from the Journal of
Marine Research, v.16, no.3,
October 15, 1958. pp.241-245.

COMMENTS ON DR. PHILLIP'S PAPER[1]

By

CHARLES S. COX

Dr. Phillips (1958) has found evidence to support his "resonance" theory of wave generation in the wave directionality measurements computed from the Stereo Wave Observation Project data (S.W.O.P., 1957). On the other hand, my observation of 5 cm wavelength waves in a wind and water tunnel (Cox, 1958) showed that the waves did not have the directionality predicted by Phillips. These observations are not necessarily contradictory since different processes may control the growth of 5 cm waves in the tank and of waves 40 m and longer considered by Phillips in the ocean. The inability to settle this point is due to a serious lack of knowledge of the pressure fluctuations in the air stream—a lack which Dr. Phillips has rightfully emphasized to experimentalists.

Phillips (1958: fig. 1) has interpreted the peaks in the directional spectra deduced from S.W.O.P. data in terms of his resonance mechanism; however, another possibility needs examination: that waves are generated predominantly in the direction of the wind but that the wind direction fluctuates. This possibility gains some weight when one examines the original sections from which Phillips' fig. 1 is abstracted. Phillips has omitted one section, $\kappa = .074\ \text{m}^{-1}$, $\lambda = 85$ m, and this is shown here as Fig. 1 and may be labeled b' because it belongs in the sequence between b and c of Phillips' fig. 1. There are two features on this section which call for attention.

First, a peak centered at an azimuth of $-45°$ is not explained by the resonance mechanism since these waves are traveling faster than the wind. One gets the impression, on comparing a, b, b', and c, that this peak is connected with the left-hand peak in d, e, f, and g. If so, there is no definite trend to the azimuth of this peak since the peak tends to move to the right in the sequence a, b, and b', while it moves to the left in c, d, e, f, and g.

Second, note in Fig. 1 the peak centered at an azimuth of 60°. A similar feature exists on all of the original sections corresponding to a–f, but Phillips does not indicate this peak, presumably because one of the authors of S.W.O.P. considered that it was due to swell from a distant source. On the other hand, another author states "For the

---

[1] Contribution from Scripps Institution of Oceanography, New Series. 1246

Reproduced by Permission

entire period [of five days preceeding the stereo-photographs] there appears to have been little or no possibility of a contribution to the waves at the ship by wind fields in other parts of the North Atlantic. Therefore, the ship was essentially in the generating area at all times and no swell should be recorded." This statement and the observations that the spectral peak has a rather broad azimuth and frequency range suggest that the generation is local.

Weather maps from S.W.O.P. (fig. 10.3) show: 1) that wind directions were highly variable for a period of 12 to 42 hours before stereo-photographs were taken; 2) that wind observations to the west of the stereo observation point showed strong westerly winds from 42 to 36 hours before the stereo-photo time; 3) that lack of information prevents determining whether these winds persisted until 28 hours before stereo-photographs were exposed. If they did, then waves of 85 m wavelength, traveling at their group velocity, would reach the photograph area in time. These waves would arrive from an azimuth of about −90°; owing to an indeterminacy of 180°, these waves would appear on the directionality sections at an azimuth of +90°. One can therefore identify the observed peak in this way, although identification is not certain. What then of the peaks discussed by Phillips? I believe there is a possibility that they can be interpreted in a similar way and that the wind observations are certainly not sufficient to rule out this possibility.

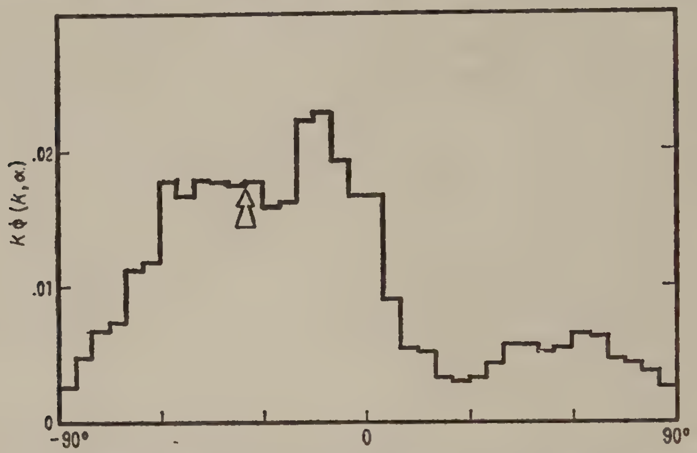

Figure 1. The angular variation of ocean waves of wavelength 85 m according to measurements by S.W.O.P. The ordinate is proportional to the estimated spectral density, the abscissa is the azimuth of the direction of the waves measured in degrees eastward of true north. The estimated wind direction is indicated by arrow and establishes the origin $\alpha = 0$ of Phillips' fig. 1.

The considerations above suggest that definitive experiments must be designed to measure not only the parameters of the turbulence in the wind stream but also the large-scale meteorological effects of variable wind direction.

In the second part of his paper Phillips has found new data (also from S.W.O.P.) which support his dimensional arguments for an "equilibrium" range in the wave spectrum where the frequency spectrum has the form

$$\Phi(\omega) \sim \beta g^2 \omega^{-5} ,$$

with $\beta = 7.4 \times 10^{-3}$, independent of wind speed. The notation follows Phillips' usage. The dimensional argument is independent of any theory of wave generation. It is gratifying to find that experimental data now supply information down to much lower frequencies than those available earlier (due to Burling).

Wind and wave tank observations (Cox, 1958: fig. 4) suggest that the equilibrium range is limited at the high-frequency end by a sharp cut-off at an angular frequency of $\omega_1 = 85 \text{ sec}^{-1}$, independent of wind speed, followed by a capillary spectral peak for still higher frequency waves.

The contribution of capillary waves to the mean square slope in the open sea can be estimated with the help of the expression for the equilibrium spectral density. Let σ^2, σ_1^2 be the contributions of all waves and of gravity waves respectively to the mean square slope. By a known formula

$$\sigma_1^2 = \int_0^{\omega_1} \kappa^2 \Phi(\omega)\, d\omega .$$

Because of the factor κ^2, the contribution by long waves to the integrand is minor. Consequently it should be possible to replace the spectrum function by its equilibrium expression, provided one starts the integration at a suitable lower limit ω_0. From many studies it seems plausible that the lower limit should be taken such that the longest waves run at a speed nearly equal to U, the wind speed measured at "anemometer level." This gives

$$\omega_0 = cg/U,$$

where $c \doteq 1$. Taking the appropriate gravity wave formula for κ, one finds

$$\sigma_1^2 = \int_{\omega_2}^{\omega_1} \beta \omega^{-1}\, d\omega = \beta \ln \left(\frac{\omega_1 U}{cg} \right).$$

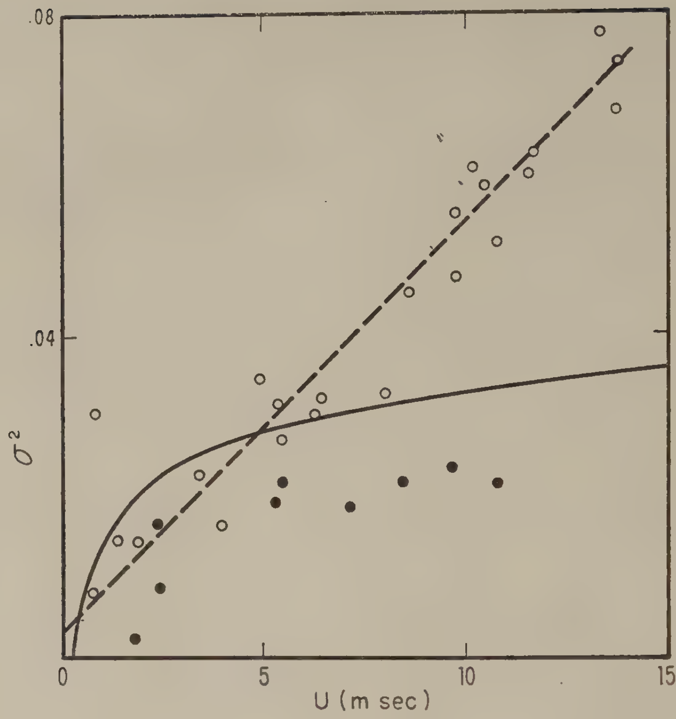

Figure 2. Mean square slope, σ^2, vs. wind speed U measured 41 feet above sea level according to Cox and Munk (1954). The open circles represent measurements over clean water surfaces; the solid circles, measurements over water covered with an oil slick. The dashed curve is a least square fit to the open circles; the solid curve represents σ_1^2, the contribution to mean square slopes by gravity waves according to Phillips' form of the equilibrium spectrum. The difference $\sigma^2 - \sigma_1^2$ must represent the contribution by capillary waves.

Fig. 2 compares σ_1^2 (computed with $c = 1$) with σ^2 as measured in the open sea (Cox and Munk, 1954). If $c = ½$ or 2, the computed curve would be moved up or down by only .005. For winds below 4 m $\sec^{-1}$, the computed value of σ_1^2 lies above σ^2. Since this is an impossibility, one concludes that the equilibrium waves are not fully developed at such low winds. It is only for winds above 6 m $\sec^{-1}$ that the curve for σ_1^2 falls significantly below the one for σ^2 and that an appreciable contribution from capillaries can occur. Observations of mean square slope where the ocean was covered by an oil slick fit into this picture well because detailed estimates (Cox and Munk, 1954) indicate that all capillaries and some of the gravity waves should be removed by such a slick; therefore the mean square slope in a slick should be slightly less than σ_1^2, as is indeed found. Observations in the wind and wave tank are also consistent with a rapid growth of capillaries for winds above a critical windspeed. (The speed measured in the tank was 2.5 m sec^{-1}; see Cox, 1958: table II; the windspeed measured at an anemometer level of 40 feet would have been approximately 5.5 m sec^{-1}.)

Conclusions of this commentary are:

First, additional experiments are necessary before directional properties of ocean waves become known. In this work it will be necessary to pay particular attention to large-scale fluctuations of wind direction over the generating area.

Second, the form of the equilibrium spectrum proposed and verified by Dr. Phillips is at harmony with measurements of water slopes both with and without oil slicks. An indirect calculation based on comparison of the analytical form of the equilibrium spectrum with observations of slopes in the open sea suggests that capillary waves become important only for winds above 6 m sec^{-1}.

REFERENCES

Cox, Charles and Walter Munk

1954. Statistics of the sea surface derived from sun glitter. J. Mar. Res., *13:* 198–227.

Cox, Charles

1958. Measurements of slopes of high frequency wind waves. J. Mar. Res., *16:* 199–225.

Phillips, O. M.

1958. On some properties of the spectrum of wind-generated ocean waves. J. Mar. Res., *16:* 231–240.

Stereo Wave Observation Project

1957. The directional spectrum of a wind generated sea. Research Division, College of Engineering, New York University. 267 pp.

Reprinted from PACIFIC SCIENCE, *vol. XV, no. 1, January, 1961*
pp.67-77.

Two New Chaetognaths from the Pacific

ANGELES ALVARIÑO[1]

THE PRESENT PAPER deals with two species of chaetognaths observed when working on the distribution of this group in California waters, and on their relation to the hydrographic conditions of the area. The material was collected by the California Cooperative Oceanic Fisheries Investigations (CalCOFI) off the coast of California, a project sponsored by the Marine Research Committee of the State of California.

Acknowledgments. I wish to thank Dr. M. W. Johnson, who has given me a great deal of valuable advice and many helpful suggestions during the preparation of this paper, and who has also corrected the typescript and provided space for me in the Marine Invertebrates Department to carry out my work on zooplankton. I am also greatly indebted to Dr. R. Revelle and Professor J. D. Issacs for their interest in providing an opportunity for me to work and continue my research at this Institution. I also offer my sincere thanks to Gail Holden Theilacker for doing the drawings contained in this paper.

Sagitta bierii n. sp.

The body is rigid and slender, retaining its cylindrical shape. It is transparent, so that the ovaries are easily seen and the gut appears as a dark straight line along the body. The small head is attached to a long narrow neck which gradually broadens out into the body, which is widest at the level of the ovaries. The shape

TABLE 1

MEASUREMENTS OF *Sagitta bierii* n. sp.

NUMBER OF SPECIMENS	TOTAL LENGTH, MM.	TAIL LENGTH, MM.		OVARY LENGTH, MM.		HOOKS		ANTERIOR TEETH		POSTERIOR TEETH	
		Median	Range	Median	Range	Mode	Range	Mode	Range	Mode	Range
2	17.0	3.5		3.5	(3.0–4.0)	6		6			(14–16)
6	16.0	3.2	(3.0–3.5)	2.5	(1.3–4.5)	6		6	(6–8)	14	(12–16)
18	15.0	3.08	(3.0–3.5)	2.4	(0.5–4.5)	6	(5–6)	6	(6–7)	14	(12–18)
7	14.5	3.01	(3.0–3.5)	2.6	(1.0–4.0)	6	(5–6)	6	(6–7)	14	(12–16)
30	14.0	3.0	(3.0–3.2)	2.37	(1.0–4.0)	6	(6–7)	6	(6–8)	14	(12–18)
33	13.5	2.9	(2.8–3.5)	1.9	(1.0–4.0)	6	(6–7)	6	(6–8)	14	(12–18)
42	13.0	2.8	(2.5–3.5)	2.0	(1.0–4.0)	6	(6–7)	6	(6–8)	14	(12–18)
29	12.5	2.7	(2.5–3.0)	1.3	(0.8–3.0)	6	(6–7)	6	(6–7)	14	(12–18)
40	12.0	2.78	(2.2–3.0)	1.7	(0.5–2.4)	6	(6–7)	6	(5–8)	12	(12–18)
26	11.5	2.6	(2.5–2.9)	0.9	(0.2–2.0)	6	(6–7)	6	(5–6)	12	(12–14)
29	11.0	2.6	(2.2–2.8)	0.7	(0.0–2.0)	6	(6–7)	6	(4–7)	12	(10–16)
23	10.5	2.3	(2.2–2.6)	0.3	(0.0–1.0)	6	(6–7)	6	(4–6)	12	(10–14)
20	10.0	2.29	(2.0–2.5)	0.14	(0.0–1.2)	6	(6–7)	4	(4–6)	10	(10–12)
14	9.5	2.1	(2.0–2.5)	0.16	(0.0–0.5)	6	(6–7)	4	(3–6)	10	(10–13)
18	9.0	2.1	(2.0–2.4)			6	(6–7)	4	(3–6)	10	(8–12)
10	8.5	2.08	(2.0–2.2)			6	(6–7)	4	(3–5)	10	(8–12)
11	8.0	2.0	(1.9–2.2)			6	(6–7)	4	(3–4)	10	(10–14)
7	7.5	1.77	(1.7–2.0)			6	(6–7)	4	(3–5)	10	(8–10)
6	7.0	1.75	(1.6–2.0)			6	(6–7)	3	(3–4)	10	(8–10)
5	6.5	1.72	(1.6–1.8)			6	(6–)	3	(3–4)	8	(8–10)
3	6.0	1.6	(1.5–1.7)			6	(6–7)	3	(3–4)	8	(2–10)
1	5.0	1.8				7		3		6	

---

[1] Scripps Institution of Oceanography, University of California, La Jolla, California. Manuscript received July 22, 1959.

Contributions from the Scripps Institution of Oceanography, New Series, 1247 (175)
Reproduced by Permission

of the body resembles *Sagitta decipiens* Fowler. That species, however, is more transparent and flaccid and differs in the position of the fins and in having hooks without serrations.

The anterior fins begin at the level of the posterior end of the ventral ganglion. They broaden at their posterior end and are without a rayless zone.

The posterior fins begin at a short distance from the posterior end of the anterior fins and end at the level of the seminal vesicles. They are somewhat roundly triangular in shape and about the same or slightly longer than the anterior fins. They are broadest behind the tail septum, but their greatest length lies in the trunk region. They do not have a rayless zone (Fig. 1*a*).

The head is small, slightly elongated in the longitudinal axis, and thus differs from *S. decipiens* Fowler, which has a larger head (Fig. 1*b*).

The hooks have strong serrations as in other species of the "*serratodentata* group." The serrations are very conspicuous with low magnifications (Fig. 1*c*).

The eye pigment forms a kidney-shaped body which in the long axis is one-half the width of the eye, with the longitudinal diameter longer than the transverse (Fig. 1*d*).

The collarette is small.

The seminal vesicles are triangular to pear shape and not very conspicuous. The species is not as protandric as most chaetognaths (Figs. 2*a*, *b*, 3*a*). In about 60,000 specimens studied, less than a dozen appeared with the seminal vesicles well developed or undamaged. The seminal vesicles do not touch the tail fin.

The ovaries are long, fine tubes; when mature they reach to the posterior end or the middle of the anterior fins. The right ovary is usually shorter. Viewed laterally, the alternated position of the ovulae is clearly seen (Fig. 3*b*).

The number of ovulae in mature specimens is from 30 to 48.

LENGTH: In a well-mixed population the most abundant size is 12–14 mm. In April, 1958, from Monterey northwards, the prevailing size was from 14 mm. to 17 mm. The northern specimens all had stronger bodies and those from 13 to 15 mm. in length were mostly immature (Fig. 4).

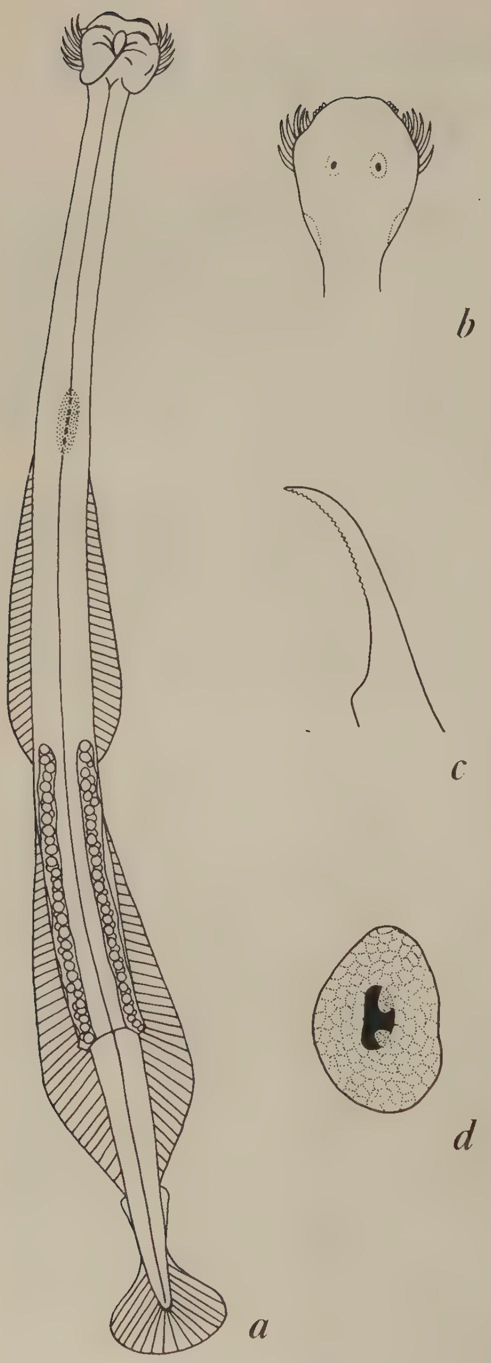

FIG. 1. *Sagitta bierii. a,* Ventral view; *b,* dorsal view; *c,* hook; *d,* left eye.

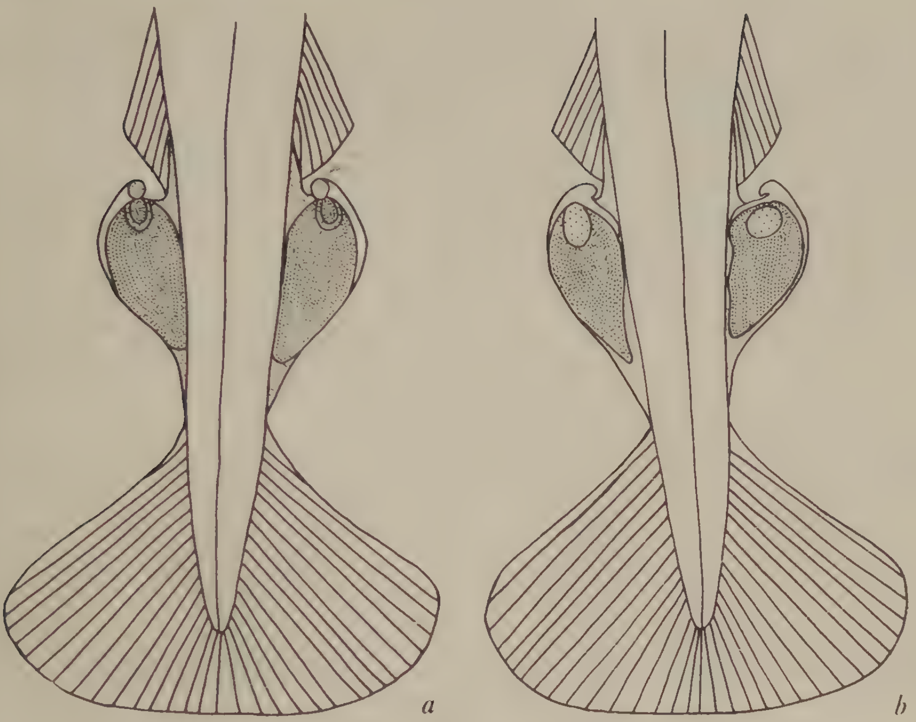

FIG. 2. *Sagitta bierii. a,* Seminal vesicles, dorsal view; *b,* ventral view.

Immature specimens 16 mm. long with almost no trace of ovaries were found. Others were observed with ovaries 1.0–1.5 mm. in length. A summary of measurements is given in Table 1.

DISTRIBUTION: The species was recorded by R. Bieri (1957) in Peruvian waters, from collections of the Transpacific Expedition, and from Cape Blanco to Punta Eugenia (Baja California) (Bieri, 1959). It was found in the CalCOFI collections of April, 1958, from Cape Mendocino, the northern limit of the sampling, down to the southern part of Baja California, as well as in the plankton samples from Peruvian waters taken by the Consejo de Investigaciones Hidrográficas del Perú in February and April, 1958.

S. bierii is found mainly from 100 to 580 mi. offshore, and hence it is not coastal in habitat.

RELATIONSHIPS: The shape of the seminal vesicles in the various forms of the "*serratodentata* group" is discussed by Ritter-Zahony, 1911*b*; Tokioka, 1939, 1940; Thomson, 1947; and Furnestin, 1953, 1957. In the present report, based on material from the Pacific and the Atlantic, the differences observed are given in Figures 5, 6, and 7 to compare with Figures 2 and 3.

S. serratodentata tasmanica reported by Tokioka (1959) apparently is *S. bierii* n. sp. for the following reasons:

He says that *S. selkirki* Fagetti, from Chilean waters "resembles most closely *tasmanica* in the appearance of the seminal vesicles." This is true and the species are certainly synonymous. The characteristic of the seminal vesicles as well as the other specific characters are identical for both. The anterior part of the seminal vesicles in both *S. serratodentata tasmanica* Thomson and *S. selkirki* Fagetti have numerous short, soft protuberances (Fig. 6). This being true, *S. serratodentata tasmanica* cannot possibly be the species Tokioka describes (1959). The seminal vesicles which Tokioka (1959, fig. 7, p. 368) illustrated and described as belonging to *S. serratodentata tasmanica* Thomson, differ from the descriptions and figures of the seminal vesicles for this species as given by Thomson (1947) and Furnestin (1957), and for *S. selkirki* by Fagetti (1958). *S. bierii* n. sp., recorded from the same area where Tokioka (1959) reports *S. serratodentata tasmanica,* has seminal vesicles with one prominence at the anterior end (Fig. 2*a, b*) as figured by Tokioka for *S. serratodentata tasmanica.*

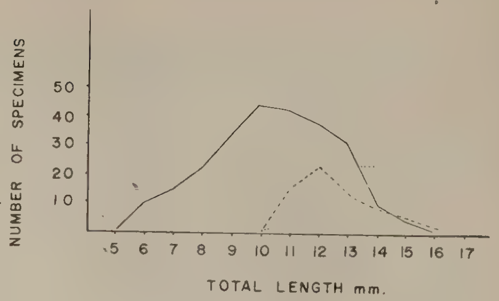

FIG. 4. *Sagitta bierii.* Distribution of size in relation to the sexual stages, April 1958. Stage I, ——; Stage II, -----; Stage III, ...

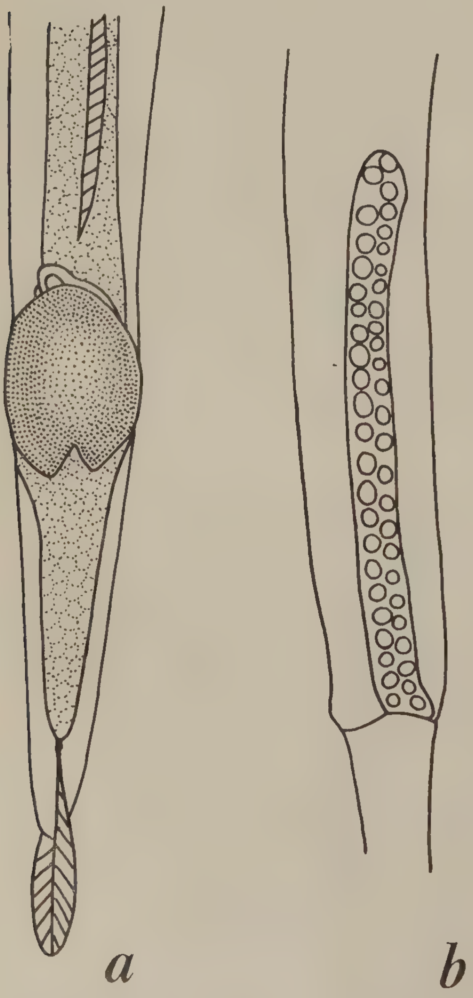

FIG. 3. *Sagitta bierii. a,* Seminal vesicles, lateral view; *b,* ovary, lateral view.

Tokioka's (1959, fig. 12, p. 372) figure of the left seminal vesicle for ? *S. serratodentata atlantica* does not agree with his own description of the seminal vesicles for this species (Tokioka, 1940, p. 373 and fig. 7d, p. 374) nor with that given by Furnestin (1957, fig. 53, p. 150). The seminal vesicle which Tokioka (1959) describes as belonging to ? *S. serratodentata atlantica* agrees with his drawing for *S. serratodentata tasmanica* in the same paper.

In revising the chaetognaths of the "*serratodentata* group" from both the Atlantic and Pacific, it was easy to separate specimens belonging to the different species. Since the characteristics for each species appear constant with no characteristics in common among the different species except for the serrations on the hooks, each one can be considered to rank as a species. The fact that each one of these species typifies different masses of water offers additional evidence for considering each one a good species. A revision of the name of each species appears at the top of each column in Table 2.

Named after Dr. Robert Bieri, who recorded it in his work as *Sagitta* sp. in the "*serratodentata* group."

HOLOTYPE: USNM no. 29919.

PARATYPES: USNM no. 29920.

TABLE 2

PRINCIPAL DIFFERENTIAL CHARACTERISTICS OF THE "*Serratodentata* GROUP"

	S. serratodentata Krohn 1853 *S. serratodentata atlantica* Tokioka 1940, Thomson 1947, Furnestin 1953, 1957	*S. pseudoserratodentata* Tokioka 1939	*S. pacifica* Tokioka *S. serratodentata pacifica*, Tokioka 1940, Thomson 1947, Furnestin 1953, 1957	*S. tasmanica* Thomson *S. serratodentata tasmanica* Thomson 1947, Furnestin 1953, 1957 *S. selkirki* Fagetti 1958	*S. bierii* n. sp.
Total length, mature, mm.	10–13	7–10	12–14	15–20	14–17
% tail	23–26	26–29	23–26	22–26	20.5–23.3
Body shape	Same width from head to tail septum.	Same.	Same.	Same.	Neck region long, thin. Body widest at ovary region.
Collarette	Well apparent.	Smaller than in *S. serratodentata.*	As in *S. pseudoserratodentata.*	As in *S. serratodentata.*	Very small, if present.
Posterior fins	Long, rounded. About same length on tail as on trunk. At level of tail, septum begins rayless zone which extends over anterior part of fin.	Long, rounded, more on tail than trunk. Very close to posterior fins. Internal portion of fins on trunk is rayless.	As in *S. pseudoserratodentata.* Very close to anterior fins. No rayless zone.	Continuous with anterior fins by extremely narrow connexion, not visible with low power 10× and in badly preserved specimens. More on tail than trunk. Rayless zone begins at level of first third of tail extending over anterior part of fin as in *S. serratodentata.*	Triangular, rounded, more on trunk than tail. No rayless zone.
Seminal vesicles	Separated from tail fin, close to posterior fins. Two prominences at anterior lateral corner. Thickening of collarette tissue in front of anterior end. Markedly protandric.	Close to posterior end of posterior fins and at longer distance from tail fin. One prominence at lateral anterior corner and small teeth at anterior end. Protandric.	Oval with thickening frothy tissue. 5–10 chitinous teeth at anterior end. Protandric.	Close to posterior fins, separated from tail fin. Numerous short protuberances at anterior end. Notable thickening in front and behind vesicle. Markedly protandric.	Pear shape. One prominence and no soft protuberances as in *S. tasmanica.*
Ovaries	Long tubes extending to anterior end of anterior fins. Ovulae small and in one row.	Fine tubes extending to anterior end of ventral ganglion. Ovulae large for size of specimens, arranged in one row.	Very fine tubes, extending up to neck. Ovulae in one row.	Long tubes extending to ventral ganglion. Ovulae in two rows.	Fine tubes extending to posterior end of anterior fins. Ovulae in two rows.

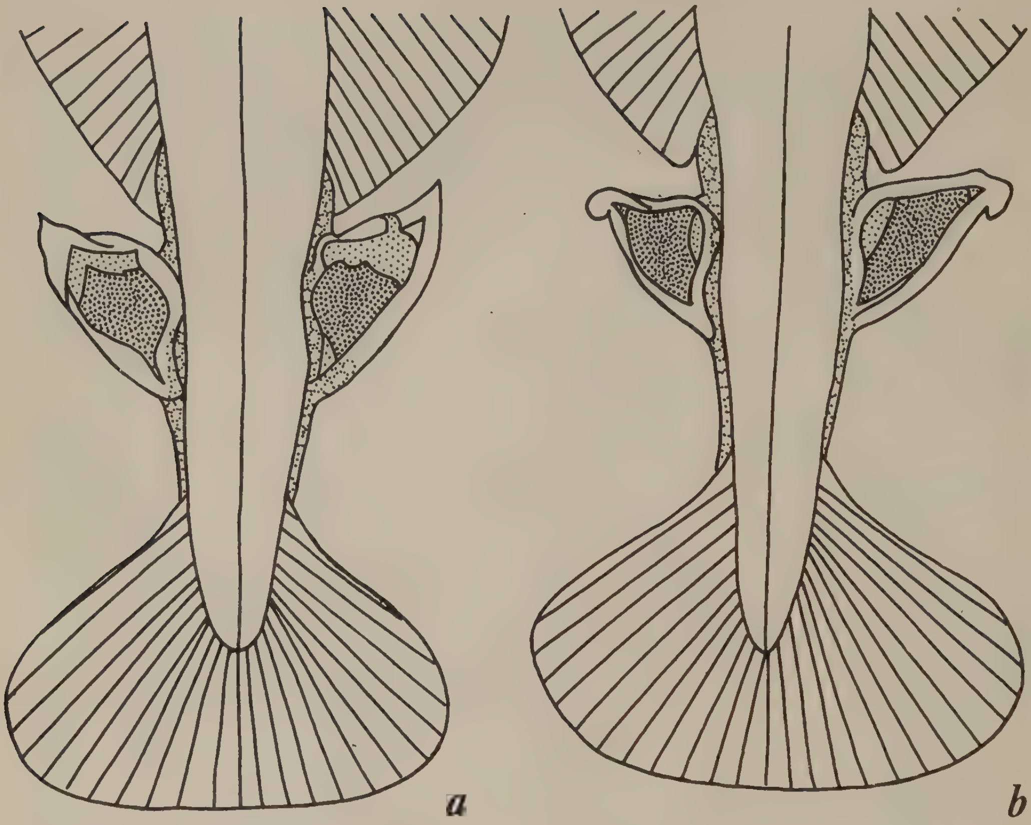

FIG. 5. *Sagitta pseudoserratodentata* Tokioka, seminal vesicles, two phases observed.

Sagitta euneritica n. sp.

The body is very translucent, almost transparent as in *Sagitta setosa* Müller; however, the larger specimens which mature at a size over 13 mm. in length appear less transparent. The body is uniform in width, narrowing at the head and at the tail ends. The rather poorly marked neck region is filled by a collarette. Viewed dorsoventrally on a dark background, the gut appears as a narrow white line extending from the head down to the body as in *S. setosa.*

The anterior fins do not reach the ventral ganglion. They are wider at the posterior end and have no rayless zone.

The posterior fins lie more on the trunk than on the tail. They are longer than the anterior fins, broadest behind the level of the tail septum, and they end touching the seminal vesicles. They are without a rayless zone (Fig. 8*a*).

The head is somewhat square and regular in size.

The eye pigment is gathered into a rather perfect square with several clear spots which differ in position and shape from those of *S. setosa* and *S. euxina* Moltschanoff (Furnestin, 1958) (Fig. 8*c*, *d*).

The collarette is well developed with the characteristic structure of round cells in a network.

The sensorial cells are spread all over the body as they are in *S. setosa* and *S. friderici* Ritter-Zahony.

The seminal vesicles are in contact with the tail fin and with the posterior fins. They are not very prominent, being small and similar to

TABLE 3

MEASUREMENTS OF *Sagitta euneritica* n. sp.

NUMBER OF SPECIMENS	TOTAL LENGTH, MM.	TAIL LENGTH, MM.		OVARY LENGTH, MM.		HOOKS		ANTERIOR TEETH		POSTERIOR TEETH	
		Median	Range	Median	Range	Mode	Range	Mode	Range	Mode	Range
2	15.5	3.2	(3.0–3.4)	2.0	(2.0–2.0)	7–9		6–8		14–16	
7	15.0	3.2	(3.0–3.4)	1.6	(1.0–2.2)	8	(8–9)	6	(5–7)	14	(10–16)
7	14.5	3.1	(3.0–3.2)	1.3	(1.0–2.5)	8	(7–9)	6	(5–7)	12	(12–16)
30	14.0	2.9	(2.5–3.2)	1.59	(1.0–2.3)	8	(7–8)	6	(6–7)	14	(10–16)
34	13.5	2.8	(2.5–3.0)	1.52	(1.0–2.0)	8	(7–9)	6	(4–7)	12	(10–16)
54	13.0	2.58	(2.5–3.2)	1.5	(0.4–3.0)	8	(7–9)	6	(5–7)	12	(10–16)
16	12.5	2.6	(2.5–3.0)	1.2	(0.6–2.6)	8	(7–8)	6	(5–6)	12	(10–12)
44	12.0	2.7	(2.3–3.0)	1.2	(0.0–2.5)	8	(7–9)	6	(4–7)	12	(10–16)
16	11.5	2.6	(2.3–2.6)	0.8	(0.3–2.0)	8	(7–8)	6	(4–7)	12	(10–12)
15	11.0	2.2	(2.0–2.6)	0.66	(0.3–1.3)	8	(7–8)	6	(4–6)	10	(10–14)
10	10.5	2.05	(2.0–2.3)	0.56	(0.3–1.0)	8	(6–8)	6	(4–6)	10	(10–12)
9	10.0	2.0	(2.0–2.2)	0.54	(0.3–1.1)	8	(7–8)	6	(4–6)	10	(10–12)
7	9.5	1.9	(1.8–2.0)	0.41	(0.2–0.7)	8	(7–8)	6	(3–6)	10	(8–12)
6	9.0	1.8	(1.6–2.0)	0.25	(0.1–0.4)	8	(7–8)	4	(2–6)	8	(6–12)
7	8.5	1.8	(1.5–2.0)	0.2	(0.1–0.3)	8	(7–8)	4	(3–6)	8	(8–10)
6	8.0	1.7	(1.5–2.0)	0.18	(0.1–0.3)	8	(7–8)	3	(3–6)	8	(8–10)
6	7.5	1.7	(1.5–2.0)	0.1	(0.1–0.2)	8	(7–8)	3	(3–5)	8	(8–10)
4	7.0	1.6	(1.4–1.9)	0.1	(0.1–0.2)	8	(7–8)	3	(3–5)	8	(8–10)
5	6.5	1.4	(1.3–1.5)	0.1	(0.1–0.2)	8	(7–8)	3	(2–4)	8	(6– 8)
5	6.0	1.4	(1.3–1.5)	0.1		8	(7–8)	3	(2–4)	7	(7– 8)
2	5.0	1.2	(1.2–1.3)			7			(2–3)		(6– 8)
1	4.5	1.2				8		2		6	
1	4.0	0.9				7		2		6	

TABLE 4

PRINCIPAL DIFFERENTIAL CHARACTERISTICS OF FORMS CLOSELY RELATED TO *Sagitta euneritica* n. sp.

	S. setosa Müller	*S. friderici* Ritter-Zahony	*S. euneritica* n. sp.
Total length, mm., mature	10–14	10–15	10.5–15.5
% tail	16–21.7	22.6–27	19–22
Anterior fins	Begin somewhat behind ventral ganglion.	Begin at posterior end of ventral ganglion.	Begin a small distance behind posterior end of ventral ganglion.
Posterior fins	More on trunk than tail, and end at seminal vesicles.	More on tail than trunk, and extend to seminal vesicles.	More on trunk than tail, and extend to seminal vesicles.
Collarette	Very small.	Noticeable.	Well developed.
Seminal vesicles	Far from tail fin and close to posterior end of posterior fins.	Touching both tail fin and posterior fins.	Touching both tail fin and posterior fins.
Ovaries	Short, extend to anterior end of posterior fins. Ovulae large and in small numbers.	Extend forward of anterior end of posterior fins. Ovulae regular in size and numerous.	Short, extend to anterior end of posterior fins. Ovulae small, filling ovaries.

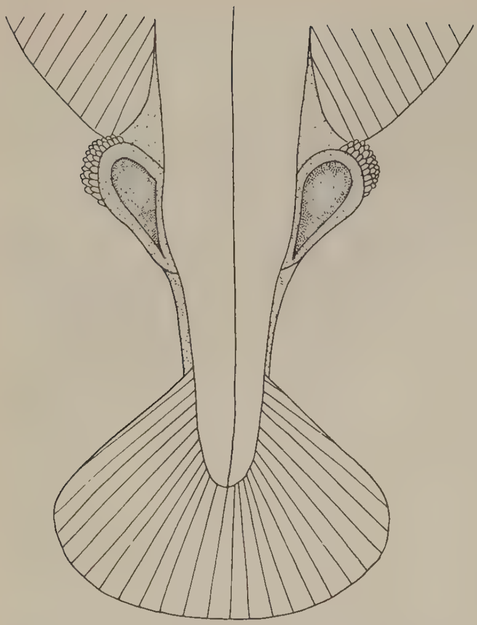

FIG. 6. *Sagitta tasmanica* Thomson, seminal vesicles, ventral view.

those of *S. neglecta* Aida (Fig. 9), and they belong to the "*bedoti*-type" (Tokioka, 1939). To compare the seminal vesicles of *S. euneritica* n. sp. with those of *S. friderici* Ritter-Zahony, see Tokioka, 1955, and Furnestin, 1953 and 1957; and to compare with *S. setosa* Müller see Furnestin, 1958.

The ovaries almost fill the width of the body and extend up to the anterior end of the posterior fins. The ovulae are not as large as those in *S. setosa* and they completely fill the ovaries.

The ecology of this species is very similar to *S. setosa* and *S. friderici* which are also found in coastal waters. In the California region *S. euneritica* n. sp. appears in large numbers (thousands per sample) in the neritic areas. In some places they are carried offshore by local superficial currents or eddies. In these cases the total number per haul gradually decreases as the distance from shore increases.

Table 3 gives the meristic characters and armature formulae.

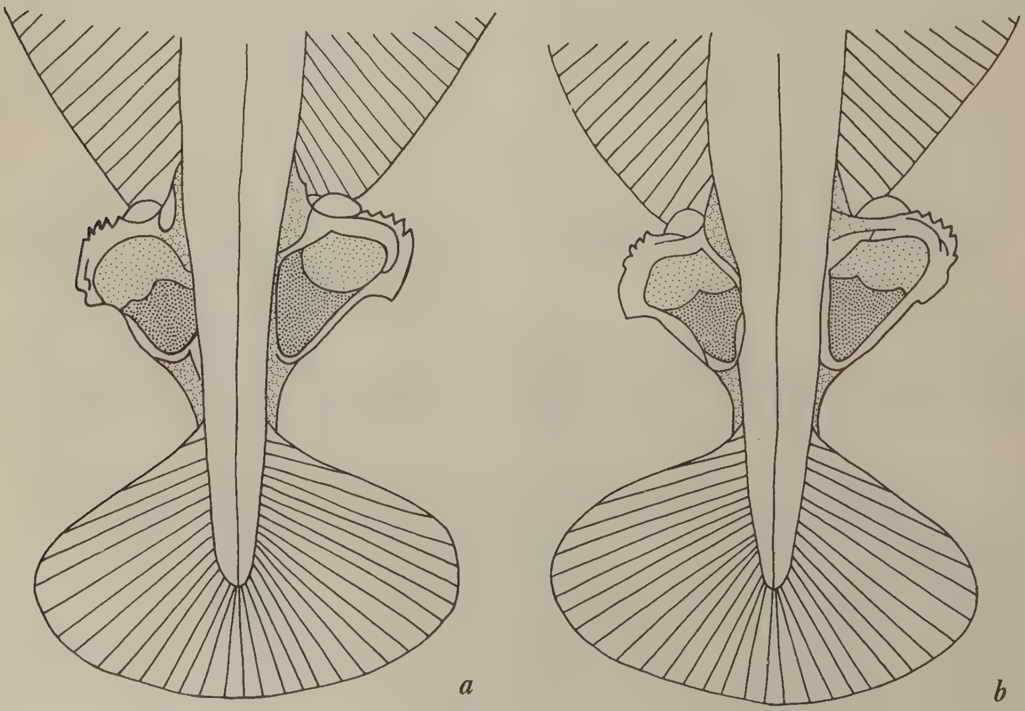

FIG. 7. *Sagitta pacifica* Tokioka. *a*, Seminal vesicles, dorsal view; *b*, ventral view.

It appears that *S. euneritica* n. sp. is closely related to *S. setosa* Müller and *S. friderici* Ritter-Zahony, but there are several points of difference as shown in Table 4 and Figure 10.

DISTRIBUTION: In the collections studied, CalCOFI cruises 5405 and 5804, it occurred close to shore from Cape Mendocino to Punta Eugenia in Baja California. Dr. Fager of the Scripps Institution collected some specimens using a hand-operated dredge net, when diving off the Tijuana River mouth (June, 1958) at a 50-ft. depth and also south of Scripps Pier (August, 1958) at 20- and 26-ft. depths.

Bieri (1957 and 1959) recorded this species as *S. friderici* ? in the same area along the coasts of North America extending south to the waters of Peru and Chile.

HOLOTYPE: USNM no. 29917.
PARATYPES: USNM no. 29918.

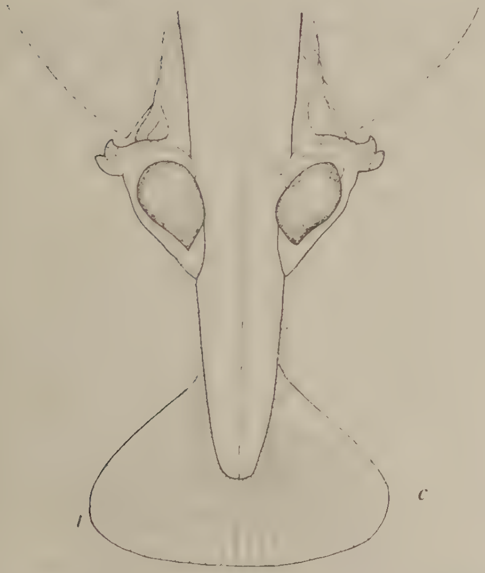

FIG. 7*c*. *Sagitta serratodentata* Krohn, seminal vesicles, dorsal view.

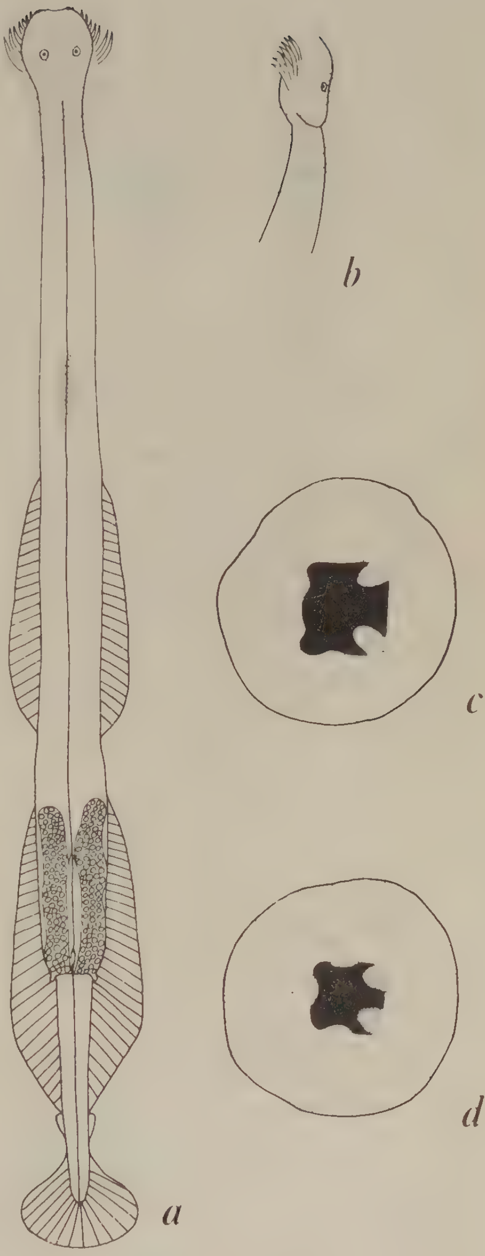

FIG. 8. *Sagitta euneritica*. *a*, Dorsal view; *b*, lateral view; *c*, left eye, mature specimen; *d*, left eye, immature specimen.

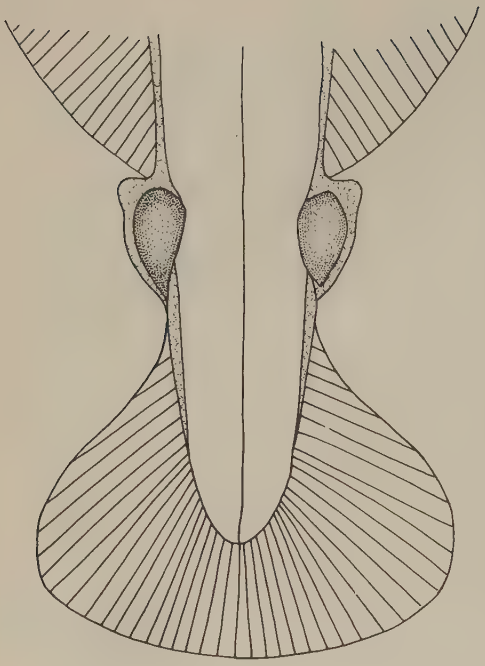

FIG. 9. *Sagitta euneritica,* seminal vesicles, dorsal view.

REFERENCES

BIERI, R. 1957. The Chaetognath fauna off Peru in 1941. Pacif. Sci. 11(3).

——— 1959. Distribution of the planktonic Chaetognatha and their relationship to the Pacific water masses. Limnol. Oceanogr. 4(1).

FAGETTI GUAITA, ELDA. 1958. Quetognato nuevo procedente del Archipiélago de Juán Fernández. Rev. Biol. Marina, Univ. Chile 8(1, 2, 3).

FAURE, M. L. 1953. Contribution à l'étude morphologique et biologique de deux Chaetognathes des eaux Atlantiques du Maroc: *S. friderici* Ritter-Zahony et *S. bipunctata* Quoy et Gaimard. Vie et Milieu 3(1).

FRASER, J. H. 1952. The Chaetognatha and other zooplankton of Scottish area and their value as biological indicators of hydrographical conditions. Scottish Home Dept. Mar. Res. (2).

FURNESTIN, M. L. 1953. Contribution à l'étude morphologique, biologique et systematique de *S. serratodentata* Krohn des eaux Atlantiques du Maroc. Bull. Inst. Oceanogr. Monaco (1025).

——— 1957. Chaetognathes et zooplancton du secteur Atlantique Marocain. Revue des Travaux de l'Institut des Pêches Maritimes 21(1, 2).

——— 1958. Les variationes morphologiques de *S. setosa* Müller et ses rapports avec deux especes voisines. Rev. Trav. Inst. Pêches Marit. 22(2).

RITTER-ZAHONY, R. 1911*a*. Revision des Chätognathen. Dtsch. SüdpolExped. 1901–1903. 12 Zool. 5(1).

——— 1911*b*. Die Chätognathen der Plankton Expedition. Plankton Exped. Humbolt Stiftung, 2 H.e.

ROSE, M., and M. HAMON. 1953. Nouvelle note complementaire sur les Chétognaths de la Baie d'Alger. Bull. Soc. Hist. Nat. Afr. N. 44 (5–6).

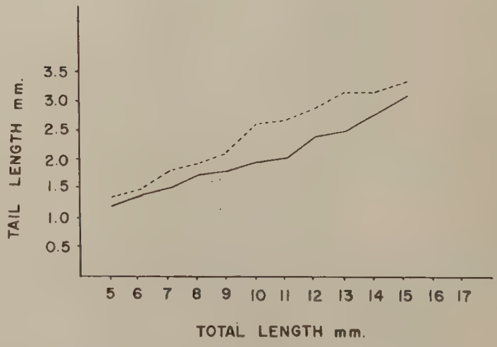

FIG. 10. Relation of total length to tail length. *S. euneritica,* ——; *S. friderici,* -----; *S. setosa,* ..... According to records of Ritter-Zahony, 1911*a*, Faure, 1953, Tokioka, 1955, and Furnestin, 1958, for *Sagitta friderici* Ritter-Zahony. Furnestin, 1958, and Ritter-Zahony, 1911*b*, for *Sagitta setosa* Müller.

THOMSON, J. M. 1947. The Chaetognatha of South-Eastern Australia. Coun. Sci. Industr. Res. (14).

TOKIOKA, T. 1939. Chaetognatha collected chiefly from the bays of Sagami and Suruga with some notes on the shape and the structure of seminal vesicles. Rec. Oceanogr. Wks. Jap. 10(2).

——— 1940. A small collection of Chaetognaths from the coasts of New South Wales. Aust. Mus. Rec. 20(6).

——— 1955. Notes on some Chaetognaths from the Gulf of Mexico. Bull. Mar. Sci. Gulf Caribbean 5(1).

——— 1959. Observations on the taxonomy and distribution of Chaetognaths of the North Pacific. Seto Mar. Biol. Lab. 7(3).

(185)

Reprinted from the Biological Bulletin,
v.118, no.1, February 1960. pp.17-30.

THE LARVAL STAGES OF PLEURONCODES PLANIPES STIMPSON (CRUSTACEA, DECAPODA, GALATHEIDAE)

CARL M. BOYD

Scripps Institution of Oceanography,[1] *University of California, La Jolla, California*

The zoeal larval stages of a galatheid crab were found in large numbers (up to 42,000/1000 m.^{3}) in plankton tows taken at several stations of the Marine Life Research program of the California Cooperative Oceanic Fisheries Investigations near Magdalena Bay, Baja California, Mexico. Since these unknown larvae were found in an area where the galatheid *Pleuroncodes planipes* was extremely abundant, it seemed likely that they were the zoeal stages of that species.

METHODS

The larvae were tentatively identified as *P. planipes.* This identification was later confirmed by two methods: (1) the first larval stages were hatched from the eggs of the adult *P. planipes,* (2) one specimen of the fifth larval stage was caught in the process of molting to the juvenile stage, and this juvenile could be identified as *P. planipes.* Several attempts were made to follow the succession of larval molts in the laboratory. Hatching the larvae from the egg was relatively easy, and was achieved by several methods. However, no larvae survived longer than eight days, and all died before they had molted once. Plunger jars and still-water aquaria were used with variations of temperature, aeration and food (*Platymonas, Chlamydomonas* and Coccolithophores). The plunger jar method and a procedure described briefly by Ray (1958; p. 501), involving rotating flasks, apparently failed because of the constant vigorous tumbling of the larvae.

Adult females carrying eggs have been found in the plankton from December through March. Gravid females kept in the laboratory hatched larvae during most of that period and the same is probably true of females in nature. As larvae of all stages are found in the plankton from January to July, it has proved impossible to determine rates of development.

DESCRIPTION OF THE LARVAE

Stage I (Figure 35)

First antenna (Fig. 1). This appendage has a long, unsegmented base with two distal branches. These, the exopodite and endopodite, are continuous with the base. The former bears six setae, the latter, a long plumose spine.

Second antenna (Fig. 6). The antenna consists of a base, continuing into a long medial prickly spine, and a scale. The scale bears about eight plumose setae and is continued as an apical spine, prickly at the terminal end. On the

---

[1] Contribution from the Scripps Institution of Oceanography, New Series, 1248

Reproduced by Permission

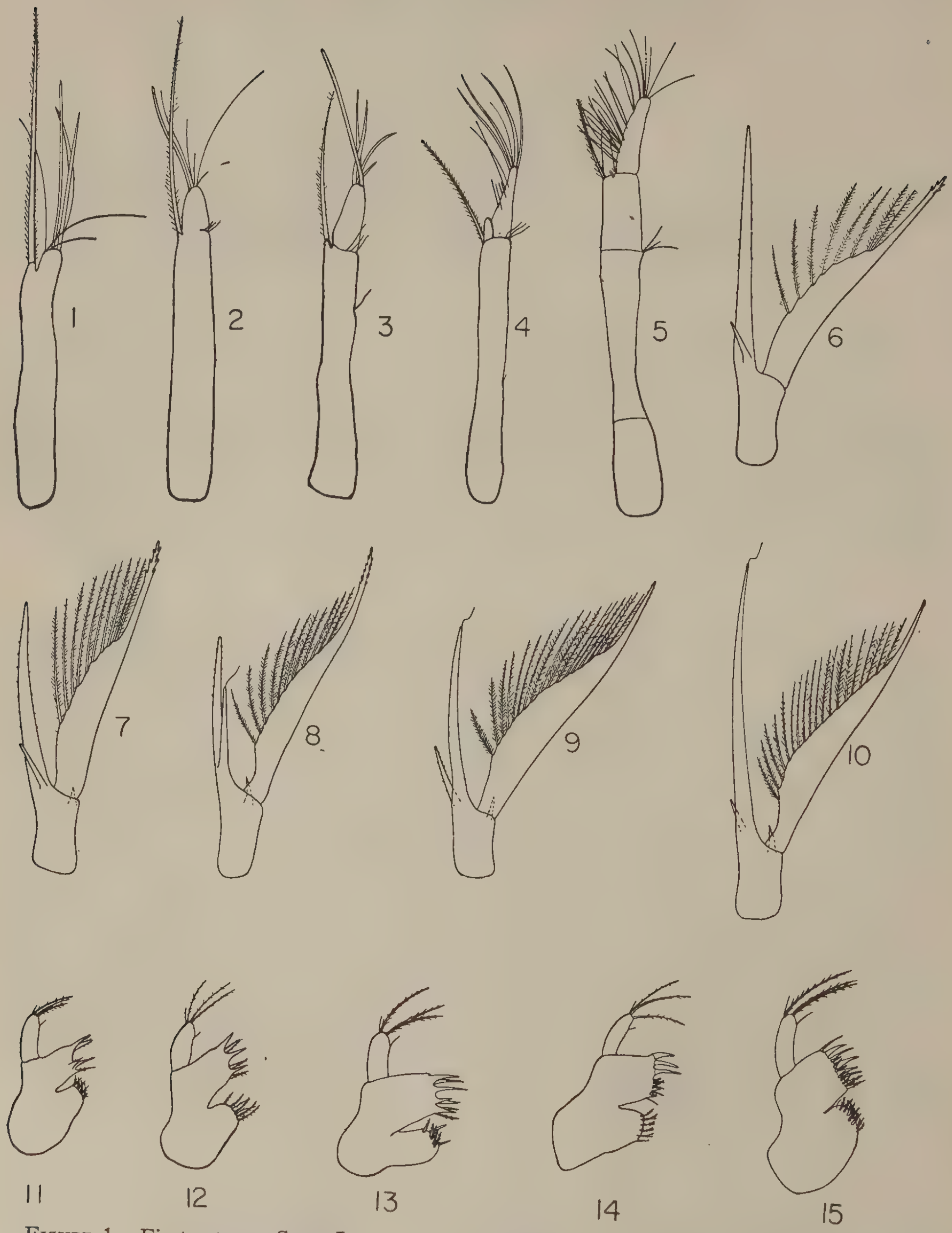

Figure 1. First antenna, Stage I.
Figure 2. First antenna, Stage II.
Figure 3. First antenna, Stage III.
Figure 4. First antenna, Stage IV.
Figure 5. First antenna, Stage V.
Figure 6. Second antenna, Stage I.
Figure 7. Second antenna, Stage II.
Figure 8. Second antenna, Stage III.
Figure 9. Second antenna, Stage IV.
Figure 10. Second antenna, Stage V.
Figure 11. First maxilla, Stage I.
Figure 12. First maxilla, Stage II.
Figure 13. First maxilla, Stage III.
Figure 14. First maxilla, Stage IV.
Figure 15. First maxilla, Stage V.

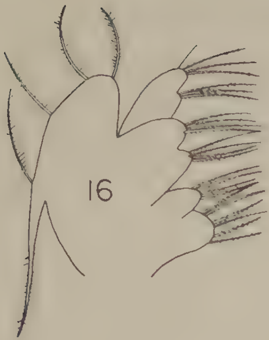

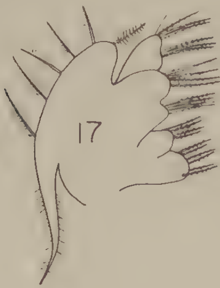

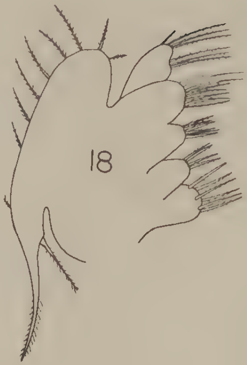

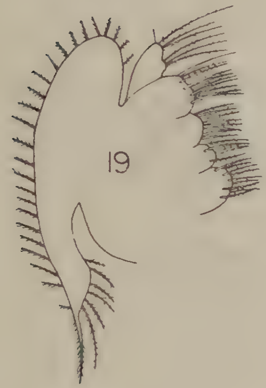

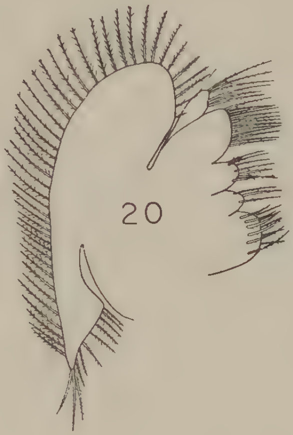

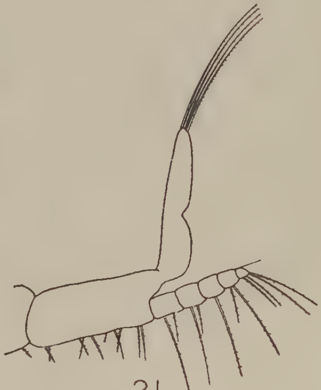

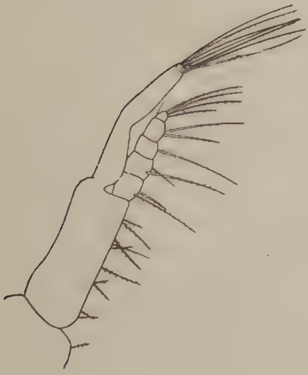

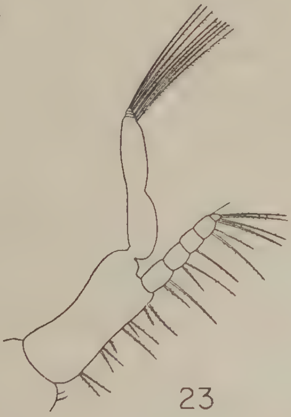

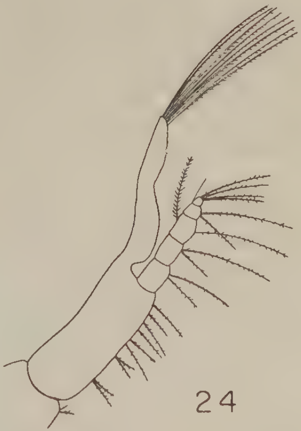

FIGURE 16. Second maxilla, Stage I.
FIGURE 17. Second maxilla, Stage II.
FIGURE 18. Second maxilla, Stage III.
FIGURE 19. Second maxilla, Stage IV.
FIGURE 20. Second maxilla, Stage V.

FIGURE 21. First maxilliped, Stage I.
FIGURE 22. First maxilliped, Stage II.
FIGURE 23. First maxilliped, Stage III.
FIGURE 24. First maxilliped, Stage IV and V.

dorsal side of the inner flagellum is a smooth spine which, though small in this stage, increases in size in later stages.

Mandible. The mandible is a simple toothed process lacking a palp.

First maxilla (Fig. 11). The endopodite is a simple unjointed structure bearing three spinose setae and two smooth setae. The endopodite does not change in number of setae but only in size in the next four stages. The exopodite is split into a basipodite and a coxopodite. These generally add setae in the later stages. In Stage I, the basipodite bears five heavy setae. The coxopodite has seven setae.

Second maxilla (Fig. 16). As in the endopodite of the first maxilla, the endopodite of the second maxilla does not change the number of setae in any of the stages. Terminally on the endopodite there are four setae; three spinose and one naked. A group of three spinose setae is located subterminally. The basipodite lobes each bear four spinose setae, as does the distal lobe of the coxopodite. The proximal lobe of the latter carries six spinose setae. The scaphognathite carries only four plumose setae along its margin. Its posterior end is produced into a long plumose projection.

First maxilliped (Fig. 21). The maxilliped is well developed in the first larval stage. The appendage consists of a coxopodite with one seta on its interior margin, an unsegmented basipodite, an endopodite with five segments, and an exopodite with two indistinct segments. The basipodite has ten spinose setae on its interior margin. There are four setae terminally on the exopodite. The five segments of the endopodite each bear spinose setae, but in differing numbers. The fourth, second, and first segments have two setae, and the third but one seta. There is also one fine, smooth seta coming off from the joint of the distal (fifth) segment.

Second maxilliped (Fig. 25). The second maxilliped has much the same structure as the first. The endopodite of the second maxilliped, however, has only four segments; the third is elongated. The coxopodite has no setae; the basipodite has three spinose setae. The terminal (fourth) segment of the endopodite has four spinose setae and one fine, smooth seta. There are four setae terminally on the exopodite.

Third maxilliped (Fig. 29). The third maxilliped is rudimentary in Stage I; it lacks setae and is poorly developed in musculature. The appendage consists only of a basipodite and an exopodite; the endopodite is not present.

Abdominal segments. There are five segments, plus the telson in Stages I and II.

Telson (Fig. 36). The telson of the first larval stage has seven projections on each side. The first (outermost) is a spinose extension of the telson, and is unjointed at its base. This spine has 6–10 thorns distally. The second projection is a fine, hair-like, plumose seta. The next five are similar in that they are all plumose setae. In addition to the plumes, each seta carries thorns on its inner and outer margins.

Along the posterior margin of the telson between the plumose setae, several small thorns occur. In Stage I larvae there are usually one to three thorns between each of the inner five setae. Generally the number of thorns increases between the setae more medially located, so that there are usually two to three thorns between setae #6 and #7. In the medial cleft of the telson; one to three thorns

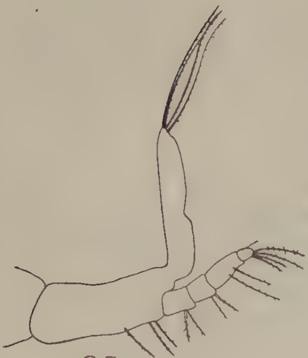

25

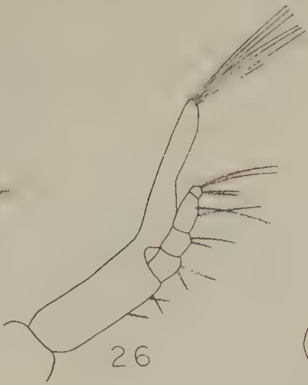

26

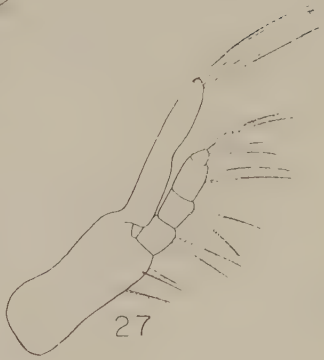

27

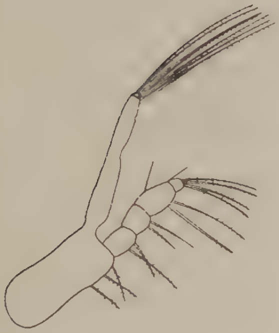

28

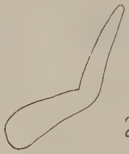

29

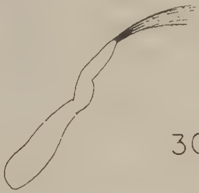

30

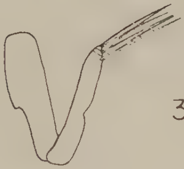

31

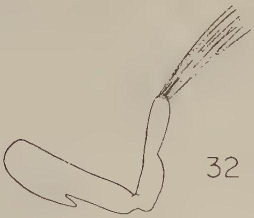

32

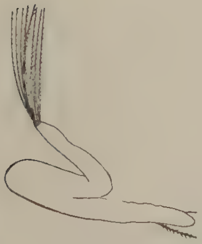

33

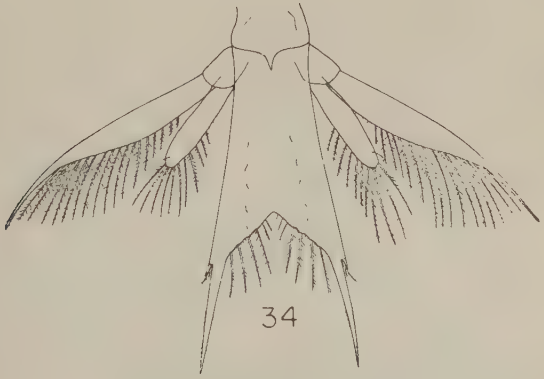

34

FIGURE 25. Second maxilliped, Stage I.
FIGURE 26. Second maxilliped, Stage II.
FIGURE 27. Second maxilliped, Stage III and IV.
FIGURE 28. Second maxilliped, Stage V.
FIGURE 29. Third maxilliped, Stage I.
FIGURE 30. Third maxilliped, Stage II.
FIGURE 31. Third maxilliped, Stage III.
FIGURE 32. Third maxilliped, Stage IV.
FIGURE 33. Third maxilliped, Stage V.
FIGURE 34. Telson, Stage IV.

may occur on each side. A tuft of short fine hairs occurs further medially. Each tuft is composed of seven to ten hairs. The numbers of these thorns and hairs are variable and are seldom identical between the right and left halves of the telson of any individual.

Stage II (Figure 37)

First antenna (Fig. 2). This appendage is much the same as in Stage I, but here three small hairs appear toward the distal end of the base. These hairs are on the location of an ultimate segmentation appearing fully in Stage III.

Second antenna (Fig. 7). The antennal scale has gained two more plumose setae, giving it usually ten. A new spine has appeared on the ventral side of the base. This spine is not segmented from the base, but is common with it.

Mandible. No change from Stage II.

First maxilla (Fig. 12). A seta has been added to the basipodite. The coxopodite has remained unchanged.

Second maxilla (Fig. 17). The endopodite, basipodite and coxopodite are unchanged. The scaphognathite has added two marginal setae, giving a total of six.

First maxilliped (Fig. 22). There are now seven terminal setae on the exopodite.

Second maxilliped (Fig. 26). There are now seven terminal setae on the exopodite.

Third maxilliped (Fig. 30). This appears to have become a functional organ; its musculature has developed and there are six setae on the terminal end of the exopodite.

Telson (Fig. 38). The primary change in the telson of Stage II larvae is the addition of one plumose seta, increasing the number of projections to eight. In this stage, however, the third projection does not have thorns on its margins, but only plumes.

The arrangement of thorns occurring between setae is similar to that of Stage I. In Stage II, however, there are neither hairs nor thorns in the medial cleft.

Stage III (Figure 39)

First antenna (Fig. 3). The segmentation initiated in Stage II has been completed, setting the exopodite off from the base. Three hairs originate at the joint. A hair appears on the exterior lateral margin of the base. The combined length of the new terminal segment and the setae is longer than the spine of the endopodite.

Second antenna (Fig. 8). The antennal scale now usually has 11 setae. The spine on the inner flagellum has increased in length and now has a terminal hair.

Mandible. No change.

First maxilla (Fig. 13). The basipodite has eight setae, an increase of two setae over Stage II. The coxopodite is unchanged.

Second maxilla (Fig. 18). The distal lobe of the basipodite now has seven setae. The proximal lobe has six. The coxopodite is unchanged. The exterior margin of the scaphognathite now has nine setae, plus one seta located on the interior margin of the posterior end.

First maxilliped (Fig. 23). There are now eight setae on the exopodite.

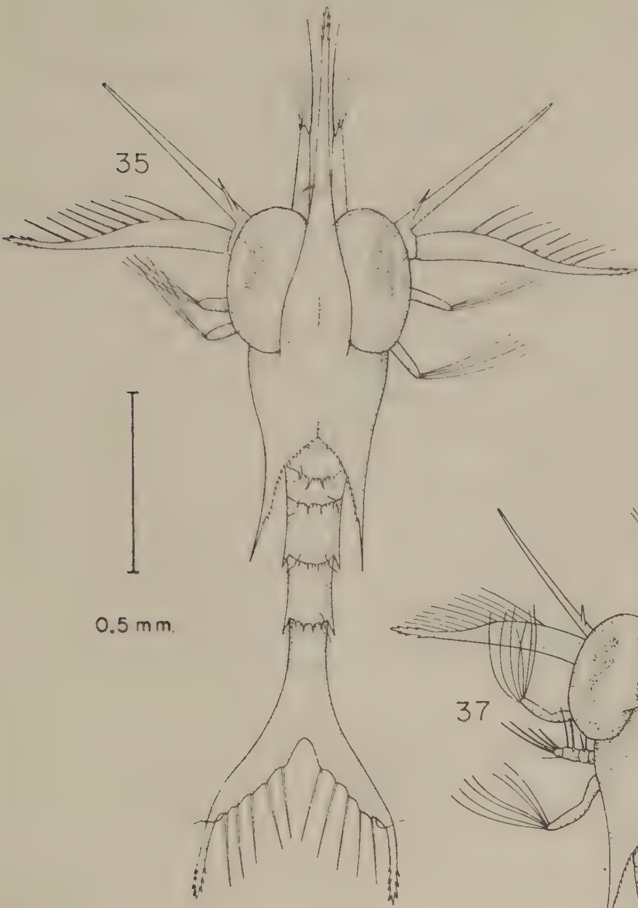

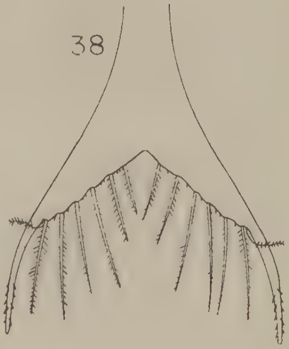

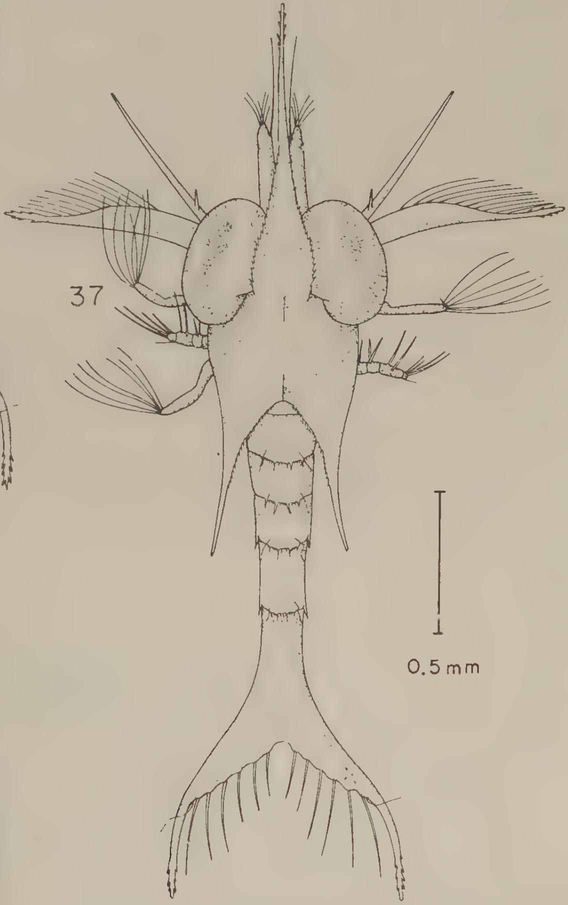

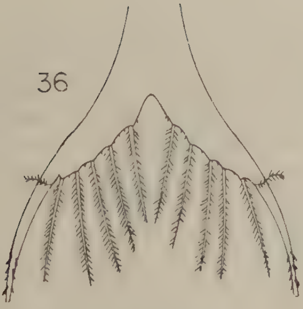

FIGURE 35. Larva, Stage I.
FIGURE 36. Telson, Stage I.

FIGURE 37. Larva, Stage II.
FIGURE 38. Telson, Stage II.

Second maxilliped (Fig. 27). The exopodite has added one terminal seta, giving a total of eight.

Third maxilliped (Fig. 31). The only change in the third maxilliped is the development of a small bud on the basipodite.

Abdominal segments. There are six segments, plus the telson in Stages III, IV and V.

Telson (Fig. 40). The changes in the telson between Stages II and III are radical. There are typically now nine projections on each half of the telson. The first (outermost) is a short naked spinose extension of the body of the telson. The second is a plumose hair-like seta. The third is a short heavy plumose seta. The fourth is the major projection of the telson; it is an extension of the telson and is not jointed at its base. It is covered on its interior and exterior margins by many small thorns. The fifth through the eighth projections are plumose setae bearing thorns on their lateral margins. The ninth projection is a small plumose seta lacking thorns. This innermost seta is not always present. It may be lacking on one or both sides of the telson.

Thorns are found abundantly between the fourth through the eighth projections. Between projections #4 and #5, zero to three thorns may occur. Usually three to five thorns are found between each of the fifth through eighth projections. Between the eighth projection and the medial line up to four hairs may be present, in addition to the ninth projection. The occurrence of these hairs is erratic.

On the dorsal surface of the telson, two pairs of very fine setae are found. The posterior pair is near the base of the seventh projection. The second pair is in line with the first pair, but anterior to it.

Uropods. The inner uropods are present only as poorly developed plates; they carry no setae. The outer uropods have from 8 to 11 plumose setae. The setae do not carry thorns. Their number is variable and may differ between the right and left sides. The tip of the outer uropod is not produced in an extended spine, but is short and naked. Small accessory setae commonly occur on the ventral surface of the outer uropod. These are not at the margin but are based somewhat anteriorly of the posterior margin. Generally there are two on each uropod, one between setae #1 and #2 (counting from the distal end) and the second between setae #4 and #5.

Stage IV (Figure 41)

First antenna (Fig. 4). The exopodite has gained three pairs of setae along its inner margin. In addition, the endopodite has developed a joint at its base.

Second antenna (Fig. 9). The scale usually now has 17 plumose setae. The spine on the inner flagellum has now increased in length so that it is much longer than the flagellum.

Mandible. The mandible at this stage has a small bud on the anterior margin which will become a palp in Stage V.

First maxilla (Fig. 14). The basipodite has 11 setae. The coxopodite has 10–11 spinose setae.

Second maxilla (Fig. 19). The lobes of the basipodite and coxopodite have added setae, but their absolute numbers are variable. The exterior margin of the scaphognathite now has about 25 setae; the posterior interior margin has six setae.

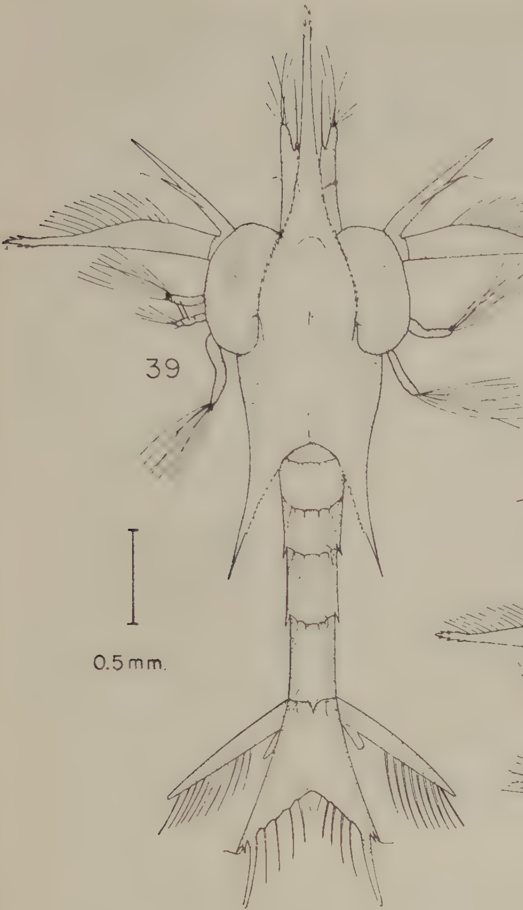

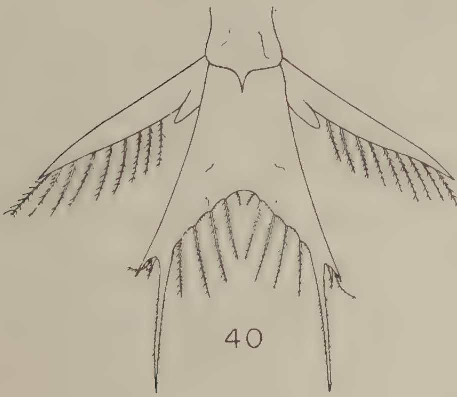

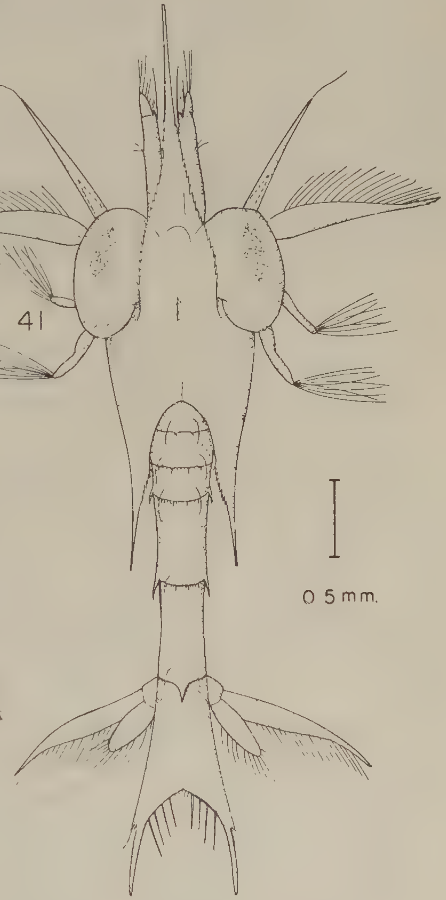

Figure 39. Larva, Stage III.
Figure 40. Telson, Stage III.
Figure 41. Larva, Stage IV.

First maxilliped (Fig. 24). The only change from Stage II and III is in the addition of a plumose seta on the exterior margin of the third segment of the endopodite.

Second maxilliped (Fig. 27). No change from Stage III.

Third maxilliped (Fig. 32). The exopodite has added two setae, giving now a total of eight. The bud on the basipodite has somewhat increased in size from Stage III, but is still rudimentary.

Thoracic legs. Thoracic legs are not visible on Stage IV larvae from a lateral view. They are present, however, as poorly developed appendages under the carapace.

Telson (Fig. 34). The telson in this stage is similar in aspect to that in Stage III, but it has added several plumose setae. The total number of projections may vary from 10 to 12, with the deletions occurring in the innermost setae; *i.e.,* setae #11 and #12 may individually or both be absent. Typically there are 11 projections. Setae #9, #10, #11, and #12 are plumose but do not bear thorns. Projection #1 appears to be jointed and is no longer common with the body of the telson.

On the dorsal surface of the telson there are now five pairs of fine, hair-like setae. Three pairs have been added anteriorly to those present in Stage III.

Uropods. Inner uropod: this now has from 10 to 17 plumose setae. Three tufts of hairs occur medially from the innermost seta. A fine, hair-like accessory seta is found on the dorsal surface of the distal end of the inner uropod. Outer uropod: the extremity of this branch is now extended as a long spine bearing many thorns along its lateral margins. From 13 to 21 plumose setae are present on the posterior margin of this branch. Several fine hairs are found medially of the innermost seta. Four accessory setae are again found on the ventral surface of the outer uropod. These commonly occur between setae #1 and #2, #4 and #5, #9 and #10, and #14 and #15, starting from the outer seta.

Stage V (Figures 42–44)

First antenna (Fig. 5). The exopodite has added more medial setae, bringing the total to about 22. The endopodite has elongated, but is still shorter than the exopodite. The base now appears to be very lightly segmented into three parts.

Second antenna (Fig. 10). The number of plumose setae on the scale has increased to usually 19. The inner flagellum is reduced to a very small size and the spine which formerly grew upon it is as long as the antennal scale.

Mandible. The palp on the anterior margin is well developed, though unsegmented.

First maxilla (Fig. 15). The basipodite has about 15 setae and the coxopodite has about 13 setae.

Second maxilla (Fig. 20). The basipodite and coxopodite have added setae. The scaphognathite now has about 43 plumose setae on its exterior margin. Its posterior interior margin now has eight setae. The extreme posterior spine has been replaced by three plumose setae.

First maxilliped (Fig. 24). Unchanged from Stage IV.

Second maxilliped (Fig. 28). The only change from Stage III and IV is in the addition of a smooth seta on the exterior margin of the third segment of the endopodite.

Third maxilliped (Fig. 33). At this stage the endopodite appears. However, it is soft, poorly musculatured and unsegmented. On its interior margin is a plumose seta and on its exterior margin, distally, is a fine smooth seta.

Thoracic legs. The thoracic legs are easily visible in a lateral view of the Stage V larvae. The first is chelate, the fifth is quite small and hidden behind the fourth leg.

Pleopods. There are now four pairs of unequally bifid pleopods present.

Telson (Fig. 43). The telson of this stage has reached its full development and variability of spine count is reduced. There are now commonly 12 projections. Of the inner eight projections, only #5 through #8 have thorns as well as plumes on their margins. One to five thorns are found on the margins of the telson between each of projections #4 through #9. No thorns are found medially of the ninth projection, but up to three hairs may occur between each of the setae between the ninth projection and the medial line. The five pairs of fine dorsal accessory setae of Stage IV are unchanged in Stage V.

Uropods. Inner branch: the inner branch now has from 18 to 21 plumose setae. Several hairs are found medially of the innermost setae. The fine setae occurring on the dorsal surface of the distal tip of the inner uropod in Stage IV is still found in this stage. Outer branch: the characteristic form of the outer uropod has not changed from that of Stage IV. The tip of the uropod is still drawn out as a spine and still bears thorns on its lateral margins. In this stage there are from 20 to 23 plumose setae on the posterior margins of the outer uropods. Fine, accessory setae occur ventrally between #1 and #2, #4 and #5, #9 and #10, and #14 and #15.

THE LARVAL STAGES

The five larval stages may be separated by the following key:

A. Uropods absent

1. The posterior margin of the telson has five plumose setae on each side; the third maxilliped is rudimentary. *STAGE I*
2. The telson has six plumose setae on each side; the third maxilliped is functional. *STAGE II*

B. Uropods present

1. The inner uropods are naked; pleopods are absent. *STAGE III*
2. The inner uropods have setae; pleopods are absent. *STAGE IV*
3. Pleopods are present. *STAGE V*

The sizes (total lengths) of the larvae in each stage were as follows (range and mean):

Stage	Minimum	Mean	Maximum	Number measured
I	2.6 mm.	2.7 mm.	2.8 mm.	8
II	3.1	3.4	3.6	8
III	4.1	4.6	5.0	7
IV	5.3	5.7	6.5	11
V	7.2	7.6	7.8	11

All the larvae measured and figured were from the Magdalena Bay area.

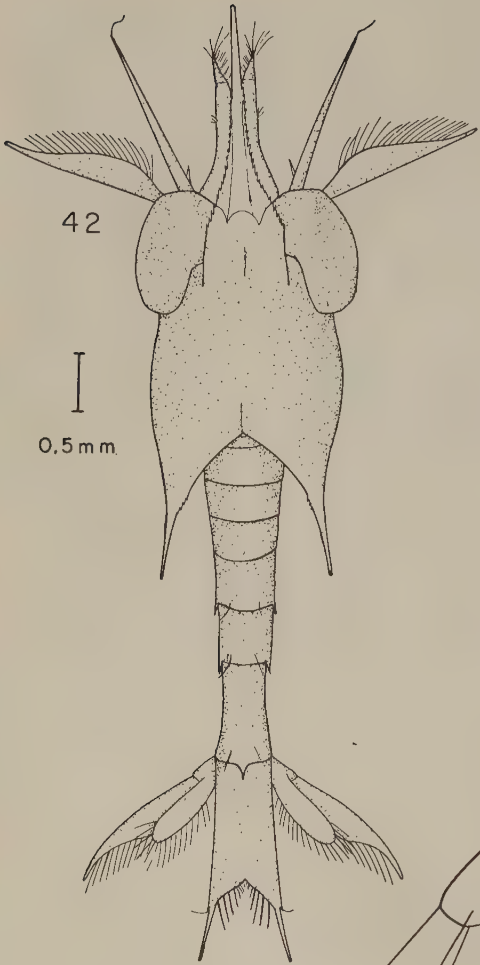

42

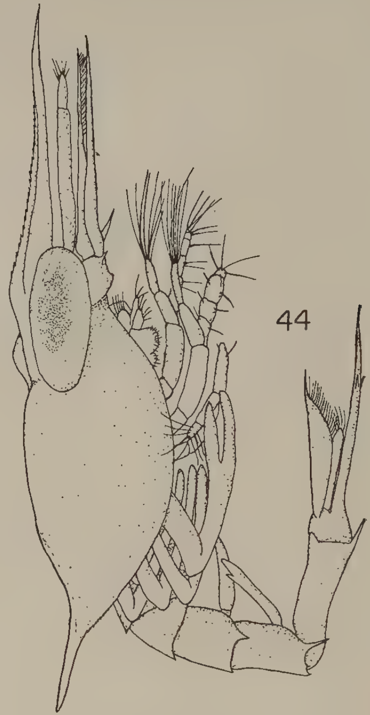

44

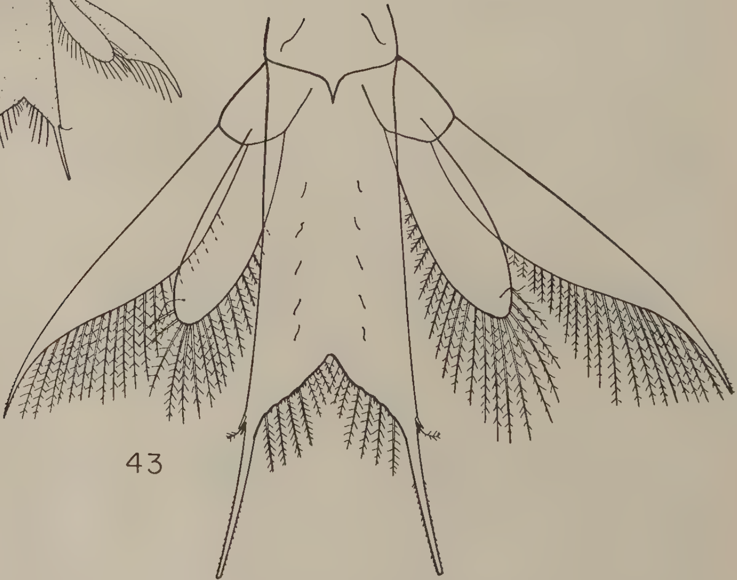

43

Figure 42. Larva, Stage V.
Figure 43. Telson, Stage V.
Figure 44. Larva, Stage V.

Lebour (1930) notes that *Galathea dispersa* may omit either Stage IV or V, but that there are usually five stages. It is not known if all *P. planipes* larvae pass through each of the five stages before molting to the juvenile stage; one or more stages may be by-passed. However, the measurements given above indicate that this is infrequent.

DISCUSSION

All except one of the developmental features of *Munida* and *Galathea* larvae as described by Lebour (1930; p. 177) are also found in *P. planipes:* the pleopods do not appear as small knobs in the third stage in *P. planipes,* but appear without previous indication in the fifth stage. *Pleuroncodes* larvae share the following traits with larvae of *Munida,* but not with those of *Galathea:* the endopod of the first maxilla has only one segment; in Stages I and II the lateral-most spine of the telson of both *Munida* and *Pleuroncodes* is longer than any of the posterior margin on the telson; a large dorsal spine occurs on the posterior margin of the sixth abdominal segment in Stages III, IV and V. *Pleuroncodes* thus appears to be more closely related to *Munida* than to *Galathea.*

The larval stages of five species of the genus *Munida* have been described. G. O. Sars described the larvae of *M. sarsi* Brinkman in 1889. Johan Huus (1934) found that these were morphologically identical with the larvae of *M. tenuimana* M. Sars, with the exception of some minute hairs in the medial cleft of the telson. Lebour (1930) described the larval stages of *M. rugosa* (Fabricius) and later (1931) set up a key to distinguish the galatheid larvae of the Plymouth area. *M. rugosa* is, however, the only species of the genus *Munida* covered by this key. (Lebour described the larvae as *M. banffica;* Zariquiey (1952), however, has synonymized this species with *M. rugosa.*) Rayner (1935) described five larval stages of *M. gregaria* (Fabricius) and *M. subrugosa* (White) but was unable to distinguish the larvae of the two species. The adults of these two species are limited to the southern hemisphere and along the Eastern Pacific they do not occur north of 41° 30′ S. (Matthews, 1932; p. 470).

Larvae of *Pleuroncodes planipes* can be easily distinguished from the described larvae of European munids by the aciculate second antennae and the elongated postero-lateral spines of the carapace of the latter. They are, however, very much like the larvae of the New World munids described by Rayner (1935). The chief difference is the lack of serration on the lateral margins of the rostrum of the larvae of *M. gregaria* and *M. subrugosa.* The rostrum of each of the stages of *P. planipes,* except the first, is strongly serrated. The fifth stage of the *Munida* species has some serration on its rostrum, but not to the degree found in *P. planipes.* Rostral serration probably will not hold good in the future as a valid characteristic setting off the genus *Pleuroncodes,* for Gurney (1942; p. 255) mentions an unidentified galatheid larva from Bermuda which had a serrated rostrum. No species of *Pleuroncodes* is known from that area.

Both Huus (1934) and Lebour (1930, 1931) use color and arrangement of pigmented areas as an aid to specific identification. All color fades, however, from specimens kept longer than a few weeks in either alcohol or formalin. No color pattern was noted in *P. planipes* for that reason.

The area off Magdalena Bay (24° 40′ N., 112° W.) appears to be peculiar as far as *P. planipes* larvae are concerned. Within a 50-mile radius of this bay, densities up to 42,000/1000 m.^{3} have been observed and are not uncommon. Outside this area, but well within the usual distributional area of adult *P. planipes*, the larvae, as sampled with a meter net from 140 m. to the surface, have an average density of 5/1000 m.^{3} (based on 22 tows taken between January and July; range 0–26/1000 m.^{3}). On this evidence it would appear that the Magdalena Bay area is a center of breeding. This is somewhat unusual in that adults are considered epi-pelagic and are distributed over a very wide range, from about 16° N. to 36° N. and from the littoral to several hundred miles off-shore.

The author wants to express his thanks to Dr. Martin W. Johnson for the help he has given me in this study. The author is also grateful for the assistance of Dr. E. W. Fager and Mrs. Margaret K. Riedel in criticism and preparation of this paper.

SUMMARY

The larval stages of a galatheid decapod crustacean, *Pleuroncodes planipes*, have been identified, described and figured. There are five stages. First stage larvae were hatched from eggs carried by adults; no larvae molted under laboratory conditions. Larval morphology indicates that the genus *Pleuroncodes* is more closely allied to the genus *Munida* than to *Galathea*. The larvae occur in high densities (42,000/1000 m.^{8}) in the region of Magdalena Bay, Baja California, Mexico.

LITERATURE CITED

GURNEY, ROBERT, 1942. Larvae of Decapod Crustacea. 306 pp. The Ray Society, London.

HUUS, JOHAN, 1934. Zur morphologisch-systematischen und biologischen Kenntnis der nordischen *Munida*-Larven (Crustacea Decapoda). *Bergens Museums Arsbok, Naturvidenskapelig rekke*, **1934**: 1–32.

LEBOUR, MARIE V., 1930. The larvae of the Plymouth Galatheidae. I. *Munida banffica, Galathea strigosa* and *Galathea dispersa*. *J. Mar. Biol. Assoc.*, **17**: 175–188.

LEBOUR, MARIE V., 1931. The larvae of the Plymouth Galatheidae. II. *Galathea squamifera* and *Galathea intermedia*. *J. Mar. Biol. Assoc.*, **17**: 385–390.

MATTHEWS, L. HARRISON, 1932. Lobster-krill; anomuran crustacea that are the food of whales. *Discovery Reports*, **5**: 467–484.

RAY, D. L., 1958. Some marine invertebrates useful for genetic research. In: Perspectives in Marine Biology, edited by A. A. Buzzati-Traverso, pp. 497–512.

RAYNER, G. W., 1935. The Falkland species of the crustacean genus *Munida*. *Discovery Reports*, **10**: 209–245.

SARS, G. O., 1889. Bidrag til Kundskaben om Decapodernes Forvandlinger II. *Lithodes—Eupagurus, Spiropagurus—Galathodes—Galathea—Munida—Porcellana—(Nephrops)*. *Archiv. for Mathematik og Naturvidenskab*, 13, 1889–1890: 132–201.

ZARIQUIEY ALVAREZ, RICARDO, 1952. Estudio de los especies Europea, del Gen. *Munida* Leach 1818. *Eos; Revista Espanola de Entomologia*, **28**: 143–231.

pp.94-95.

SPECIES OF THE GENUS CYPRAEA FROM CLIPPERTON ISLAND

by
Leo G. Hertlein
Associate Curator, Department of Geology, California Academy of Sciences

and
Edwin C. Allison
Museum Paleontologist, University of California Museum of Paleontology

(Plate 22)

The composition of the molluskan fauna of Clipperton Island is remarkable for its mixture of West American and Indo-Pacific elements.

In a recent number of this quarterly, Allison (1959) discussed the habitat of the species of Conus found living on this atoll. Empty shells of three additional species, Conus brunneus Wood, C. gradatus Mawe, and C. tessulatus Born also have been taken there. The present paper is based primarily upon material collected during Scripps Institution of Oceanography Expeditions of 1956 and 1958 to Clipperton Island.

The species of Cypraea are a colorful and conspicuous element of the shallow water fauna in tropical waters. Twelve species and subspecies are here listed from Clipperton Island: the identification of two is doubtful and the identification of one species recorded earlier from the island may be open to question. All are Indo-Pacific species except two, Cypraea albuginosa and C. isabella mexicana, which live in tropical west American waters.

We wish to acknowledge the aid of Mr. Ray Summers who checked the identifications of the species which follow:

Cypraea albuginosa Gray. Live specimens rare, taken at edge of reef-flat; fresh shells from reef-flat and among coral debris to a depth of 10 meters; beachworn shells on all beaches but especially common on north and west sides of the island where shells of C. isabella mexicana are relatively uncommon.

Cypraea arenosa Linnaeus. A single worn specimen from the beach on the north side of the island.

Cypraea caput-serpentis Linnaeus. Fresh shells from the beach on the north side of the island.

Cypraea depressa Gray. Worn shells from the beach.

Cypraea helvola Linnaeus. Worn shells fairly common on the beach on the north and west sides of the island.

Cypraea isabella Linnaeus. Recorded from Clipperton Island by Hertlein and Emerson (1953). Identified as C. isabella mexicana by R. Summers (oral communication).

Cypraea isabella mexicana Stearns.

(202)

Contributions from the Scripps Institution of Oceanography, New Series, 1250
Reproduced by Permission

Two live specimens from the reef-flat on the north side of the island and one from a depth of 10 meters. Fresh shells fairly common on the north and west sides of the island; abundant worn shells all around the island. Largest specimen is 52 mm. long, 30 mm. wide, convexity, 25.5 mm.

Cypraea maculifera Schilder (= *C. reticulata* Martyn). A single worn shell on the beach-flat on the north side of the island.

Cypraea moneta Linnaeus. (Plate 22, Figure 1) Worn shells on all sides of the island, especially in areas protected from violent waves.

Cypraea moneta Linnaeus, elongate variety. (Plate 22, Figure 2) Chalky shells on the shelf side of the lagoon at depths of approximately 10 meters, in coral sand, associated with paired valves of *Codakia* in sand between remnants of coral ridges.

Cypraea scurra Gmelin. Fresh as well as worn shells on the rocky beaches.

Cypraea teres Gmelin. Fresh as well as worn shells on the rocky beaches.

Cypraea cf. *C. vitellus* Linnaeus. Single worn specimen from the beach-flat on the north side of the island.

LITERATURE CITED.

Allison, E. C.
1959. Distribution of *Conus* on Clipperton Island. *The Veliger*, Vol. 1, No. 4, pp. 32-35.

Hertlein, L. G., and Emerson, W. K.
1953. Mollusks from Clipperton Island (eastern Pacific) with the description of a new species of gastropod. San Diego Soc. Nat. Hist., Transactions, Vol. 11, No. 13, pp. 345-364, pls. 26-27.

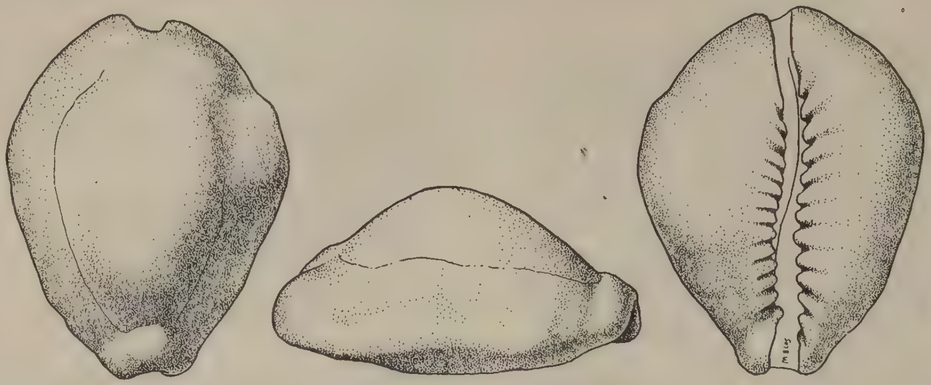

Figure 1. *Cypraea moneta* Linnaeus; Hypotype 37726, Univ. Calif. Mus. Paleon. Type Coll., Loc. B-4237. Clipperton Island, living. x 2

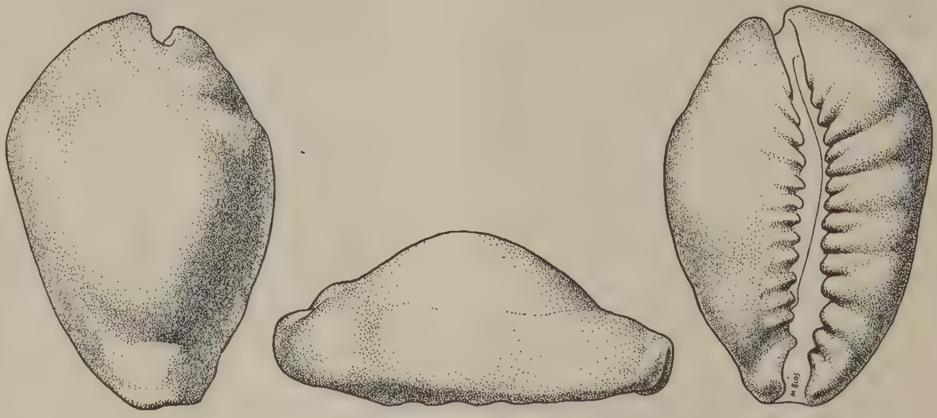

Figure 2. *Cypraea moneta* Linnaeus. Hypotype 37727, Univ. Calif. Mus. Paleon. Type Coll., Loc. B-6098. Clipperton Lagoon, dead. x 2

Reprinted from the Journal of Marine
Research, v.17, 1958. pp.199-214.

A NOTE ON TIDAL FRICTION[1]

By

GORDON GROVES[1a] AND WALTER MUNK

Scripps Institution of Oceanography
La Jolla, California

ABSTRACT

The Moon's gravitational torque on the ocean tide has been computed on the basis of Dietrich's cotidal charts. The result is -4.5×10^{23} dynes cm as compared to Heiskanen's (1921) value of -2.9×10^{23} dynes cm based on Sterneck's (1920) charts. Both values are subject to great uncertainty. The observed deceleration of the Moon implies a torque of $(-3.9 \pm 1.0) \times 10^{23}$ dyne cm, which is consistent with both foregoing calculations. It is concluded that the deceleration of the Moon's orbital motion and the associated deceleration of the Earth's rotation *may* be due to oceanic tidal dissipation. The solar decelerating torque is estimated at 0.31 times that of the lunar torque. The forces associated with the decelerating tidal torque give rise to a minute steady oceanic circulation.

INTRODUCTION

The observed position of the Sun and Moon do not agree precisely with their ephemerides. The discrepancies are due to (1) variations in the rate of rotation of the Earth and (2) variations in the orbital motion of the Moon over and above those included in the ephemerides. From simultaneous observations of the discrepancies in longitude of the Moon and Sun (or Moon and Mercury), the two effects can be separated according to Murray's (1957) scheme. Observations since 1680 indicate a constant deceleration[2] in the Moon's orbital motion by $11''.2$ century^{-2} (in addition to the $6''.1$ century^{-2} accel-

---

[1] Contribution from the Scripps Institution of Oceanography, New Series. We are indebted to the National Science Foundation for support of this study. #1251

[1a] Present address: Instituto de Geofísica, Universidad Nacional Autónoma de México, México, D. F.

[2] If the Moon's motion is referred to a time standard based on the Earth's rotation (such as a sundial), the velocity, angular and linear, does in fact increase. If it is referred to an "absolute" time standard, the motion is decelerated. The term "secular acceleration" used in astronomic literature refers to the former concept. The present discussion refers all acceleratious, etc. to absolute time.

eration due to planetary perturbations allowed for in the ephemerides). The modern value for the deceleration is not inconsistent with discrepancies inferred from Babylonian eclipses and other ancient observations (Munk and MacDonald, 1960).

The only theory that has been advanced to account for the anomalous lunar deceleration is that it is associated with tides on the Earth (Jeffreys, 1952: chap. 8). The astronomic evidence can give no information as to whether the atmosphere, the oceans or the bodily tides may be responsible. Atmospheric tides are rather well determined from barograms at many weather stations; however, the resulting lunar[3] torque is too small by a factor of 100 to account for the lunar deceleration. Bodily tides could be responsible if they lagged by 1° with respect to their equilibrium configuration (Munk and MacDonald, 1960), but this value is too small to be checked against measurements of Earth tides with gravimeters. Indirect evidence based on the anelastic properties of the solid Earth indicate that the bodily tide may be an important factor, but apparently not the principal factor. This leaves the ocean tide. The observations are barely good enough to make a rough estimate possible. The existence of steady tidal stresses and of a resulting westward oceanic drift, first mentioned by Hertz (1883), was subsequently discussed by G. H. Darwin (1898: 276). New observations conducted in southern oceans during the International Geophysical Year should lead to a substantial improvement in this estimate.

TIDAL FORCE AND TORQUE

Let ψ designate the tide-producing potential. This can be written as a sum of three groups of terms (see, for example, Doodson, 1921),

$$\begin{aligned}
\psi_S &= -\tfrac{1}{2} B \frac{gr^2}{a} \sin^2\theta \sum_S C_i \cos(\sigma_i t + \varepsilon_i + 2\varphi) \\
\psi_D &= -\tfrac{1}{2} B \frac{gr^2}{a} \sin 2\theta \sum_D C_i \cos(\sigma_i t + \varepsilon_i + \varphi) \qquad (1) \\
\psi_L &= -\tfrac{1}{2} B \frac{gr^2}{a} (\tfrac{1}{2} - \tfrac{3}{2}\cos^2\theta) \sum_L C_i \cos(\sigma_i t + \varepsilon_i),
\end{aligned}$$

---

[3] This lunar atmospheric torque must not be confused with a thermally induced solar atmospheric torque that is much larger and of opposite sign.

corresponding to the semidiurnal, diurnal, and long-period constituents, respectively. Here

$$B = \frac{3}{2}\frac{M}{E}\frac{a^3}{D^3} = 0.843 \times 10^{-7}$$

is a dimensionless constant, M the mass of the Moon, E the mass of the Earth, a the Earth's radius, D^{-1} the mean inverse distance of the Moon, r the distance from the Earth centroid, θ the colatitude, φ the east longitude, C_i the constituent coefficients, σ_i the frequencies, and ε_i the epochs depending on the time origin.

Eq. (1) includes only potentials of degree two; higher harmonics, proportional to higher powers of a/D, have been neglected. Both lunar or solar terms are to be included in the expansion.

The force per unit mass, $F = -\nabla\psi$, can be considered as constant from the (tidally disturbed) sea surface ($z = \eta$) to the sea bottom ($z = -h$). The total force per unit area on a water column equals

$$\boldsymbol{\tau} = \varrho\, \boldsymbol{F}(\theta, \varphi; t)\, [\eta\, (\theta, \varphi; t) + h\, (\theta, \varphi)]\,,$$

where ϱ is water density, assumed constant. The time-average of this stress equals

$$\bar{\boldsymbol{\tau}} = \varrho\, \overline{\boldsymbol{F}\eta} \tag{3}$$

plus a term $h\varrho\overline{\boldsymbol{F}}$, causing a permanent tidal deformation which is customarily absorbed in the gravity field. The quantity $\bar{\boldsymbol{\tau}}$ as defined by (3) will be referred to as the *steady tidal stress.*

Strictly speaking, the time-average should be taken for each mass particle following its tidal trajectory. Actually, we have taken time-averages in fixed columns. It turns out that the steady tidal stress is distributed vertically depending on the vertical distribution of the tidal current. In a frictionless homogeneous ocean the tidal current, and hence the steady tidal forces, would be uniform from top to bottom.

The tidal elevation above mean sea level can be expanded in a form similar to (1), with the components

$$\begin{aligned}
\eta_S &= \sum_S H_i \cos\,(\sigma_i t + \varepsilon_i + 2\varphi - \varkappa_i) \\
\eta_D &= \sum_D H_i \cos\,(\sigma_i t + \varepsilon_i + \varphi - \varkappa_i) \qquad (4) \\
\eta_L &= \sum_L H_i \cos\,(\sigma_i t + \varepsilon_i - \varkappa_i)\,,
\end{aligned}$$

where H_i and $\varkappa_i$ are empirical functions of θ, φ, to be determined from tide data. The essential feature is that the σ_i's are the same in (1) and (4); this follows because the response of the sea surface to the tide-producing force $\boldsymbol{F}$ contains the same frequencies as $\boldsymbol{F}$. The ε_i's are the same by appropriate definitions of $\varkappa_i$. In the product (3) of the summations, common frequencies have non-zero means. We note that $\boldsymbol{F}$ can be precisely computed for any geographic position according to (1); in the case of η we must depend on interpolation between widely separated tide stations. Combining (1), (3) and (4) we find that the steady tidal stress $\bar{\tau}$ has the components

$$\begin{aligned}\bar{\tau}_\theta &= B\varrho g\left[\tfrac{1}{4}\sin 2\theta \sum_S C_i H_i \cos\varkappa_i + \tfrac{1}{2}\cos 2\theta \sum_D C_i H_i \cos\varkappa_i \right.\\ &\qquad\left. - \tfrac{3}{8}\sin 2\theta \sum_L C_i H_i \cos\varkappa_i\right]\\ \bar{\tau}_\varphi &= B\varrho g\left[-\tfrac{1}{2}\sin\theta \sum_S C_i H_i \sin\varkappa_i - \tfrac{1}{2}\cos\theta \sum_D C_i H_i \sin\varkappa_i\right] \qquad (5)\\ \bar{\tau}_r &= B\varrho g\left[\tfrac{1}{2}\sin^2\theta \sum_S C_i H_i \cos\varkappa_i + \tfrac{1}{2}\sin 2\theta \sum_D C_i H_i \cos\varkappa_i \right.\\ &\qquad\left. + \left(\tfrac{1}{4} - \tfrac{3}{4}\cos^2\theta\right) \sum_L C_i H_i \cos\varkappa_i\right].\end{aligned}$$

The *steady tidal torque* about the Earth's axis of rotation is

$$\bar{N} = a^3 \int_{\text{oceans}} \bar{\tau}_\varphi \sin^2\theta \, d\theta \, d\varphi. \qquad (6)$$

In passing, let us consider the significance of the other torque components, $\bar{L}$, $\bar{M}$. If the Earth had finite strength, these components would lead to a minute permanent displacement of the pole of rotation. If, on the other hand, the Earth were to yield as a fluid to prolonged stress, no matter how minute, polar wandering would result. Eventually the pole would reach a position (if any) for which $\bar{L}$ and $\bar{M}$ are zero. The trouble with this intriguing hypothesis for polar wandering is that the torques involved are small, $\bar{L}$ and $\bar{M}$ being of the same order as $\bar{N}$, 10^{23} dyne cm. The distribution of continents and oceans, if isostatically balanced, are associated with a torque of the order of 10^{30} dyne cm (Munk and MacDonald, 1960: chap. 12). It should be remembered that the time-average was taken relative to geographical co-ordinates, and hence these components rotate with the Earth. If the time-average were to be taken relative to a nonrotating system, the steady torque components $\bar{L}$ and $\bar{M}$ would be fixed in space and would cause a slight anomaly in the Earth's precession rate. The reader can find a discussion in Darwin's works (for example, see Darwin, 1898).

EVALUATION FROM COTIDAL CHARTS

We assume that the cotidal contours ($\varkappa_\iota$ = constant) are identical for all semidiurnal constituents and that the co-range charts differ, one from another, by a constant factor equal to the ratio of the corresponding equilibrium tides. Thus

$$\begin{aligned} \varkappa_\iota(\theta,\varphi) &= \varkappa_S(\theta,\varphi) \\ H_\iota(\theta,\varphi) &= \frac{C_\iota}{C_S} H_S(\theta,\varphi) \end{aligned} \tag{7}$$

for each of the semidiurnal constituents. The subscript $_S$ refers to an important semidiurnal constituent for which satisfactory cotidal charts are available. Eq. (7) is essentially the "inference" method for evaluating the lesser constituents from short tide records. Similar relations are assumed for diurnal and long-period constituents, but application to the long-period components is doubtful (see section on long-period tides). The errors inherent in the approximation (7) are smaller than those associated with existing cotidal charts.

With this scheme, the only summations to be performed are of the type

$$\lambda_S = \sum_S C_\iota^2; \tag{8}$$

and similarly for λ_D, λ_L. Eq. (5) can then be written

$$\bar{\tau}_0 = B\varrho g\left[\frac{1}{4}\frac{\lambda_S}{C_S}\sin 2\theta\,(H_S\cos\varkappa_S) + \frac{1}{2}\frac{\lambda_D}{C_D}\cos 2\theta\,(H_D\cos\varkappa_D) - \frac{3}{8}\frac{\lambda_L}{C_L}\sin 2\theta\,(H_L\cos\varkappa_L)\right]$$

$$\bar{\tau}_\varphi = B\varrho g\left[-\frac{1}{2}\frac{\lambda_S}{C_S}\sin\theta\,(H_S\sin\varkappa_S)-\frac{1}{2}\frac{\lambda_D}{C_D}\cos\theta\,(H_D\sin\varkappa_D)\right] \tag{9}$$

$$\bar{\tau}_r = B\varrho g\left[\frac{1}{2}\frac{\lambda_S}{C_S}\sin^2\theta\,(H_S\cos\varkappa_S)+\frac{1}{2}\frac{\lambda_D}{C_D}\sin 2\theta\,(H_D\cos\varkappa_D)\right.$$
$$\left.+\frac{\lambda_L}{C_L}\left(\frac{1}{4}-\frac{3}{4}\cos^2\theta\right)(H_L\cos\varkappa_L)\right].$$

Values of H_S and H_D have been interpolated for every ten degree square of the oceans from Dietrich's (1944) chart of the tidal range of the constituents M_2 and K_1, respectively. Values of $\varkappa_S$ and $\varkappa_D$ were read off Dietrich's cotidal charts for the same two constituents. Accordingly, we take $C_S = 0.9085$ and $C_D = 0.5305$, corresponding to these two constituents. The interpolated values are tabulated in the Appendix. The combined lunar and solar horizontal tidal stress is illustrated in Fig. 1.

THE DARWIN DEVELOPMENT

In order to use the more familiar tidal constituents from Darwin's development (see for example, Shureman, 1941), we would have to allow for their slowly varying amplitude over the Moon's nodal cycle. This is done by introducing the node factor $f_i(t)$ for each constituent. The only modification required is that λ must be written

$$\lambda_S = \sum_S \overline{f_i^2}\, C_i^2; \tag{10}$$

and similarly for λ_D and λ_L. The mean values of f_i^2 can be calculated by using eqs. (65) through (80), (206), (215), (227), (235), and the formula at top of page 156 in Shureman (1941). The values are as follows:

Constituent	f
Mf	1.172
MSf, $2SM$, MS, M_2, N_2, $2N_2$, ν_2, λ_2, μ_2	1.0014
Ssa, Sa, P_1, S_2, R_2, T_2	1.0000[4]
K_1	1.0188
O_1, Q_1, $2Q_1$, ϱ_1, σ_1	1.0356
J_1, MP_1, SO_1, χ_1, θ_1	1.0402

[4] The node factors of the purely solar constituents have the constant value unity.

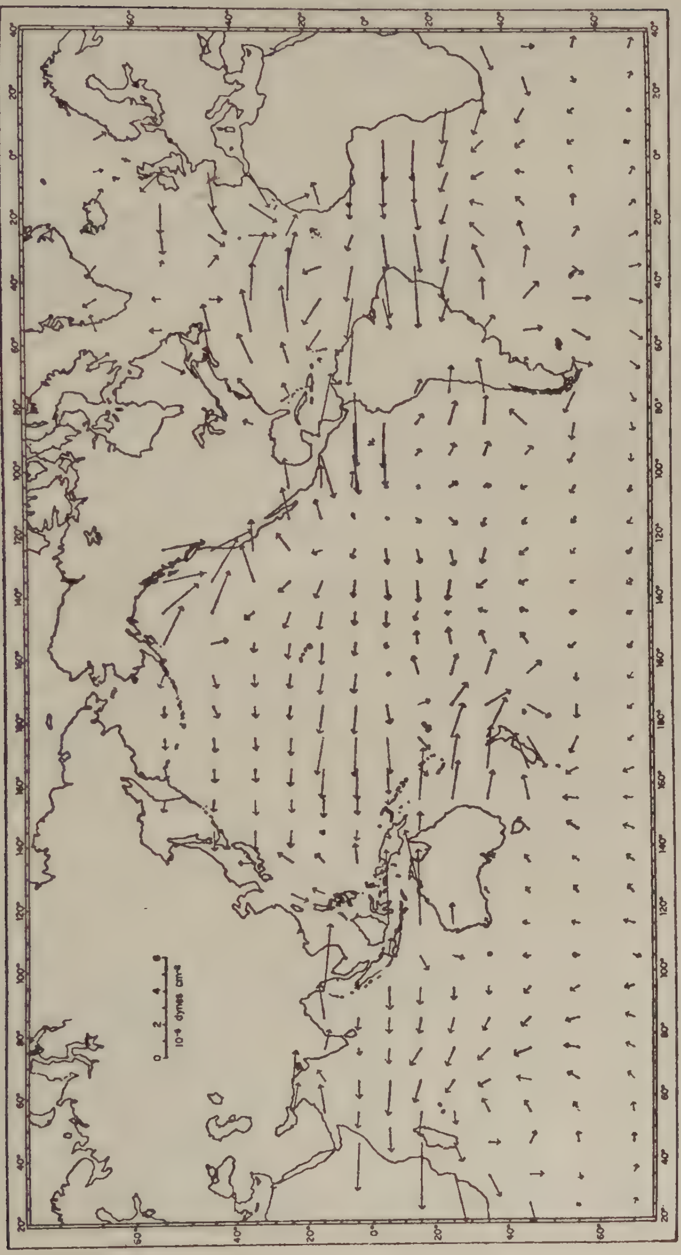
0 2 4 6
10⁻⁴ dynes cm⁻²
60°
40°
20°
0°
20°
40°
60°
20°
40°
60°
80°
100°
120°
140°
160°
180°

Figure 1. Horizontal component of the steady tidal stress from semidiurnal tides. The vectors are drawn from the center of each 10° square for which the stress could be computed.

Constituent	f
OO_1, KQ_1	1.421
M_1	2.574[5, 6]
K_2	1.0876
L_2	1.002[5]
KJ_2	1.192

There is difficulty in separating the lunar from the solar effects with Darwin's development owing to the presence of lunisolar constituents, especially K_1, and we shall not have further recourse to it.

SEPARATION OF LUNAR AND SOLAR EFFECTS

The separation of lunar and solar effects is somewhat arbitrary. The ambiguity arises with respect to such constituents for which lunar and solar contributions have identical frequencies. Thus far in the development, such constituents have been lumped into a single term.

The principal reason for considering separately the lunar and solar effects is that we may wish to evaluate the reaction of the steady tidal stress on the orbits of the Moon and Sun. In particular, an anomalous secular deceleration of the Moon has been observed and attributed to tidal friction. Accordingly we define the lunar effect as the Moon's gravitational action on the *actual* tidal bulge resulting from the combined action of the Sun and Moon; similarly we consider as the solar contribution the solar gravitational action on the combined bulge.

For the general case we need to reinterpret (8) by writing

$$\lambda_S = \sum_S C_i C_i'; \tag{11}$$

and similarly for the diurnal and long-period constituents. Here C_i' is the sum of the coefficients having the frequency σ_i. This procedure is possible because the arguments are identical for lunar and solar equilibrium constituents having the same frequency. The lunar contribution to λ is given by summing (11) over the lunar constituents etc. Thus the lunar and solar contributions are given by

---

[5] The values for L_2 and M_1 are difficult to calculate from theory and were evaluated by averaging the squares of 93 consecutive mean yearly values (approximately 5 nodal cycles), from 1850 through 1942, of the node factors given by Shureman (1941: table 14).

[6] The large value of M_1 is to be used with Darwin's miscomputed value of C(M_1) of 0.0209. (The theoretical value is 0.0317.)

$$\lambda_{S☾} = \sum_{S☾} C_{t☾}(C_{t☾} + C_{t\odot}), \quad \lambda_{S\odot} = \sum_{S\odot} C_{t\odot}(C_{t☾} + C_{t\odot}) \qquad (12)$$

respectively; and similarly for λ_D, λ_L, with the understanding that for purely lunar constituents $C_{t☾} = C_t$, $C_{t\odot} = 0$, for purely solar constituents $C_{t\odot} = C_t$, $C_{t☾} = 0$, whereas for luni-solar constituents $C_{t☾} + C_{t\odot} = C_t$. Note that

$$\lambda_S = \lambda_{S☾} + \lambda_{S\odot} = \sum_S C_t^2, \quad \lambda_D = \ldots, \quad \lambda_L = \ldots.$$

The summations have been carried out by using Doodson's expansion. The results are

	λ_S	λ_D	λ_L
Lunar	0.888	0.353	0.041
Solar	0.222	0.120	0.005
Total	1.110	0.473	0.046
Lunar/solar	4.00	2.94	8.2

The lunar to solar ratios are not those of the square of the equilibrium heights. These values give a rough idea of the contribution of the three species to $\bar{\tau}$.

THE LONG-PERIOD TIDES

Eq. (7) is not a valid approximation for the long-period tides. Frequencies are widely separated, and the annual and semi-annual terms are predominantly of meteorological origin[7]. Moreover the seasonal tides are largely steric over most of the oceans; that is, the variation in sea level is associated with a change in the specific volume of the water column. Only the variable mass per unit area contributes to $\bar{\tau}$.

In all events, the contribution from long-period tides is relatively small. The component $\bar{\tau}_\varphi$ (and consequently $\bar{N}$) is not influenced at all by long-period tides.

[7] The meteorological contribution to the S_1- and S_2-tides has a small effect on $\bar{\tau}$ and has been neglected.

THE STEADY TIDAL STRESS

Fig. 1 shows the horizontal component of $\bar{\tau}$ arising from semidiurnal tides only. A predominance of westward stresses is apparent. These act in the sense required to decelerate the Earth's angular velocity. An equivalent chart for diurnal tides (not presented here) has the same general appearance, but the stresses are roughly one-fourth of the semidiurnal stresses. The existence of steady tidal stresses and of a resulting westward oceanic drift has been discussed by Darwin (1898: 276).

TABLE I. Tidal Torque on the Earth in Units of 10^{23} Dyne cm

	Heiskanen's Lunar Semid.	*Lunar*			*Solar*			*Total*
		Semid.	*Diurnal*	*Total*	*Semid.*	*Diurnal*	*Total*	
Pacific								
+	3.5	2.7	0.0	2.7	0.7	0.0	0.7	3.4
—	*–5.4*	*–4.0*	*–0.8*	*–4.8*	*–1.0*	*–0.3*	*–1.2*	*–6.0*
Total	–1.9	–1.3	–0.8	–2.1	–0.3	–0.3	–0.5	–2.6
Atlantic								
+	1.7	1.6	0.1	1.7	0.3	0.0	0.3	2.0
—	*–2.5*	*–3.0*	*–0.1*	*–3.1*	*–0.7*	*0.0*	*–0.7*	*–3.8*
Total	–0.8	–1.4	0.0	–1.4	–0.4	0.0	–0.4	–1.8
Indian								
+	2.3	1.3	0.1	1.4	0.3	0.0	0.3	1.7
—	*–2.5*	*–2.1*	*–0.3*	*–2.4*	*–0.6*	*–0.1*	*–0.7*	*–3.1*
Total	–0.2	–0.8	–0.2	–1.0	–0.3	–0.1	–0.4	–1.4
Grand Total	–2.9	–3.5	–1.0	–4.5	–1.0	–0.4	–1.3	–5.8

The irrotational component of the stress field would result in a steady distortion of the sea surface relative to the geoid by the order 10^{-4} cm. There is no associated circulation. The rotational component of the stress field causes a steady circulation and surface displacement. We might make an estimate by analogy to the steady wind-driven circulation. Typical wind stresses are of the order of several dynes cm^{-2}, or 10^5 times the steady tidal stresses. In the western boundary zone, where the currents are strongest, the observed transport per unit width is of the order 10^7 $\text{cm}^2\ \text{sec}^{-1}$ and is concentrated near the surface. The maximum surface displacement is about 10^2 cm. Accordingly, we might expect the steady tidal transport and the surface displacement to be 10^2 cm^2 sec^{-1} and 10^{-3} cm, respectively. If the velocity is distributed uniformly from top to bottom, its maximum might attain 10^{-3} cm sec^{-1}. This is altogether negligible. Observed steady deep currents in the western boundary zone are of the order of one cm sec^{-1} (Swallow and Worthington, 1957). Away from the western boundary zone, the steady currents are probably an order of magnitude less.

In this calculation we have not allowed for distortion of the sea bottom. Such a distortion arises directly from the tide-generating force as well as from the variable load of the ocean tide. The load correction would be difficult to apply, if at all possible; one would have to evaluate the contribution of the ocean tide to the spherical surface harmonic of second degree (as a function of time), and apply the appropriate Love numbers (Munk and MacDonald, 1960). In related geophysical problems such corrections have been of the order of 20 to 30 °/₀.

THE STEADY TIDAL TORQUE

Table I summarizes the torque calculation. Integration (6) was carried out separately for the Sun and Moon, for semidiurnal and diurnal tides, and for the three major oceans. For each of these 12 calculations the positive and negative contributions to the torque integral were evaluated separately, as shown. In general the positive and negative contributions are of the same order, which implies a considerable uncertainty in the sum. It is encouraging that in each of the 12 instances the sum is negative or zero.

Our results for the lunar semidiurnal tide agree well with Heiskanen's (1921) calculation. He neglected the lunar diurnal effect, which we find to be only one fourth of the total lunar effect. The combined lunar torque of $-4.5 \times 10^{+23}$ dyne cm is to be compared with the value $-3.9 \times 10^{+23}$ inferred from the astronomically observed deceleration of the Moon. The agreement is better than we have any right to expect. The chief uncertainty has to do with the poorly known tidal amplitudes in the open sea.

In a similar manner, solar torque must be associated with a deceleration of the Sun's motion around the Earth, but because of the large mass and distance of the Sun, this effect is far too small to be observed.

APPENDIX. VALUES OF H AND $\varkappa$, DEDUCED FROM DIETRICH'S CATIDAL CHARTS, WHICH WERE USED
SQUARE INDICATED BY CO-ORDINATES OF ITS MIDPOINT. THE FOUR VALUES FOR EACH

	5E	15E	25E	35E	45E	55E	65E	75E	85E	95E	105E	115E	125E	135E	145E	155E	165E
75N	35	30	40	—	—	—	—	—	—	—	—	—	—	—	—	—	—
	010	030	050	—	—	—	—	—	—	—	—	—	—	—	—	—	—
	05	06	06	—	—	—	—	—	—	—	—	—	—	—	—	—	—
	155	195	205	—	—	—	—	—	—	—	—	—	—	—	—	—	—
65N	40	—	—	—	—	—	—	—	—	—	—	—	—	—	—	—	—
	330	—	—	—	—	—	—	—	—	—	—	—	—	—	—	—	—
	10	—	—	—	—	—	—	—	—	—	—	—	—	—	—	—	—
	175	—	—	—	—	—	—	—	—	—	—	—	—	—	—	—	—
55N	—	—	—	—	—	—	—	—	—	—	—	—	—	—	—	20	20
	—	—	—	—	—	—	—	—	—	—	—	—	—	—	—	100	075
	—	—	—	—	—	—	—	—	—	—	—	—	—	—	—	30	30
	—	—	—	—	—	—	—	—	—	—	—	—	—	—	—	155	145
45N	—	—	—	—	—	—	—	—	—	—	—	—	—	—	30	15	20
	—	—	—	—	—	—	—	—	—	—	—	—	—	—	090	095	085
	—	—	—	—	—	—	—	—	—	—	—	—	—	—	30	30	28
	—	—	—	—	—	—	—	—	—	—	—	—	—	—	165	145	125
35N	—	—	—	—	—	—	—	—	—	—	—	—	—	50	30	20	15
	—	—	—	—	—	—	—	—	—	—	—	—	—	180	090	085	090
	—	—	—	—	—	—	—	—	—	—	—	—	—	22	22	20	20
	—	—	—	—	—	—	—	—	—	—	—	—	—	185	165	160	145
25N	—	—	—	—	—	40	40	—	—	—	—	50	50	40	20	15	20
	—	—	—	—	—	290	280	—	—	—	—	170	190	195	110	090	095
	—	—	—	—	—	45	45	—	—	—	—	20	20	18	18	16	14
	—	—	—	—	—	055	065	—	—	—	—	205	215	205	190	185	180
15N	—	—	—	—	40	40	35	30	45	80	—	—	50	40	15	20	35
	—	—	—	—	210	235	200	310	245	290	—	—	185	195	170	095	100
	—	—	—	—	35	39	35	30	12	11	—	—	15	15	16	14	10
	—	—	—	—	045	055	065	045	355	005	—	—	215	210	205	205	210
05N	55	—	—	—	60	35	20	20	20	30	—	—	50	40	20	15	35
	110	—	—	—	115	120	070	015	140	190	—	—	180	210	150	095	105
	10	—	—	—	28	28	20	10	08	08	—	—	15	15	17	16	10
	005	—	—	—	045	055	055	045	325	305	—	—	215	215	215	215	225
05S	45	45	—	—	80	50	45	25	20	25	40	75	—	—	10	05	30
	095	105	—	—	110	115	060	040	070	105	210	290	—	—	110	100	115
	10	08	—	—	18	20	10	02	04	10	20	20	—	—	25	24	15
	025	040	—	—	045	055	085	075	250	245	245	255	—	—	195	205	220

in the Computations. The Values Represent a Sort of Subjective Average over the Ten Degree Square are Arranged in the Following Order: H, k for M_2; H, k for K_1

175E	175W	165W	155W	145W	135W	125W	115W	105W	95W	85W	75W	65W	55W	45W	35W	25W	15W	5W
—	—	—	—	—	—	—	—	—	—	65	45	45	45	—	—	40	40	40
—	—	—	—	—	—	—	—	—	—	280	300	310	315	—	—	310	000	090
—	—	—	—	—	—	—	—	—	—	35	35	35	35	—	—	05	05	05
—	—	—	—	—	—	—	—	—	—	155	165	160	155	—	—	095	105	115
20	20	20	—	—	—	—	—	—	—	—	—	45	45	40	40	40	40	25
110	130	150	—	—	—	—	—	—	—	—	—	330	250	150	130	190	060	350
40	40	40	—	—	—	—	—	—	—	—	—	25	25	10	10	07	05	07
175	185	195	—	—	—	—	—	—	—	—	—	125	125	105	095	090	100	115
20	20	25	90	100	100	100	—	—	—	—	—	60	30	20	10	35	55	60
085	090	120	300	325	350	350	—	—	—	—	—	020	180	180	290	080	090	140
35	40	40	40	40	40	40	—	—	—	—	—	15	15	08	05	04	10	10
155	155	145	115	110	110	115	—	—	—	—	—	115	115	100	085	080	080	115
20	20	20	35	80	90	100	—	—	—	—	60	55	45	25	25	40	60	60
080	060	070	350	300	310	340	—	—	—	—	230	260	250	000	320	025	050	080
27	30	35	36	36	37	35	—	—	—	—	06	07	07	05	04	05	07	07
125	105	090	085	090	100	115	—	—	—	—	105	115	110	090	070	055	055	065
15	15	15	10	25	60	40	40	—	—	20	40	50	60	50	60	65	70	60
085	085	085	105	160	240	265	270	—	—	190	210	230	250	275	310	000	020	050
23	23	25	26	29	31	32	31	—	—	07	05	05	05	03	04	05	06	06
125	095	075	080	085	090	095	095	—	—	125	120	120	125	105	040	030	030	050
20	15	15	20	25	35	40	45	40	—	—	20	30	60	65	50	40	65	—
095	100	100	110	130	160	210	240	250	—	—	215	230	250	275	300	320	350	—
15	17	17	16	18	20	18	18	17	10	10	09	07	05	04	04	06	06	—
150	105	075	080	080	085	085	080	065	290	275	135	145	170	205	305	345	000	—
45	35	25	25	25	35	40	35	25	80	80	—	05	65	85	75	40	40	—
110	115	120	115	130	150	175	220	270	040	310	—	230	160	160	175	190	220	—
09	10	10	10	10	11	13	15	16	16	10	10	10	05	04	04	05	05	—
205	155	075	080	080	085	075	055	045	015	005	180	165	190	215	275	315	345	—
50	45	30	15	15	25	30	20	20	75	85	85	—	80	90	90	65	60	55
120	135	140	130	115	135	165	195	300	035	065	100	—	130	150	155	165	180	110
08	08	07	05	05	06	08	10	12	13	13	13	—	05	08	05	05	10	12
235	225	165	085	075	075	035	015	355	340	335	345	—	215	225	265	305	335	355
55	45	30	05	15	25	25	20	10	35	50	—	—	—	100	90	60	35	40
130	155	180	050	085	125	150	180	180	095	085	—	—	—	160	140	140	155	105
09	07	05	02	02	04	05	07	08	09	11	—	—	—	08	05	05	07	10
235	245	240	235	275	315	315	305	315	325	320	—	—	—	225	265	290	330	355

APPENDIX

	5E	15E	25E	35E	45E	55E	65E	75E	85E	95E	105E	115E	125E	135E	145E	155E	165E
15S	45	45	—	80	80	30	45	30	20	20	35	90	100	—	20	60	40
	085	095	—	115	090	070	035	040	060	095	150	275	310	—	260	250	170
	06	06	—	05	12	10	07	05	05	10	18	22	22	—	40	27	18
	055	060	—	035	055	085	155	205	230	245	255	265	305	—	175	180	205
25S	40	45	—	70	35	15	30	30	20	15	15	25	—	—	—	60	45
	055	070	—	120	140	110	030	045	060	090	170	280	—	—	—	250	250
	05	05	—	03	05	04	04	04	05	09	17	20	—	—	—	22	15
	095	090	—	275	135	155	195	210	145	245	255	280	—	—	—	155	175
35S	30	40	50	40	25	20	25	30	20	10	05	10	10	15	25	40	60
	030	060	095	130	180	320	015	030	050	075	210	310	320	330	350	250	260
	04	05	05	05	04	03	04	04	06	10	15	17	19	20	13	16	10
	125	135	175	175	180	190	205	220	240	260	295	315	350	015	055	120	130
45S	20	25	30	25	20	20	30	40	20	15	10	10	10	15	30	40	65
	025	055	110	180	240	305	350	015	035	040	360	350	310	315	325	290	300
	05	04	04	04	04	04	04	05	08	12	17	20	20	20	08	07	06
	115	135	155	170	200	235	255	275	295	305	320	330	345	005	035	095	115
55S	10	05	10	20	20	20	30	35	30	20	15	15	15	15	30	35	30
	025	055	110	250	280	310	335	355	010	020	360	350	310	320	330	355	020
	07	06	05	04	04	04	05	07	10	14	20	22	25	26	14	10	10
	080	075	025	260	295	315	320	330	330	335	335	345	355	005	025	030	030
65S	15	15	15	20	20	20	25	25	25	20	20	20	20	20	30	30	25
	240	230	245	260	270	280	315	340	350	010	165	350	315	325	340	360	020
	08	07	06	04	05	05	07	10	13	16	20	23	25	28	30	20	17
	035	015	005	345	335	345	350	355	360	005	360	355	360	005	005	010	015
75S	—	—	—	—	—	—	—	—	—	—	—	—	—	—	—	—	20
	—	—	—	—	—	—	—	—	—	—	—	—	—	—	—	—	000
	—	—	—	—	—	—	—	—	—	—	—	—	—	—	—	—	20
	—	—	—	—	—	—	—	—	—	—	—	—	—	—	—	—	015

(continued)

175E	175W	165W	155W	145W	135W	125W	115W	105W	95W	85W	75W	65W	55W	45W	35W	25W	15W	5W
50	50	30	15	15	25	20	10	10	20	30	30	—	—	—	75	50	35	35
165	185	220	290	035	100	135	160	180	200	200	210	—	—	—	105	120	125	090
10	06	05	04	03	04	05	06	07	09	10	14	—	—	—	04	03	02	05
220	240	255	265	275	285	295	305	315	305	310	315	—	—	—	195	185	120	065
55	55	30	20	15	25	20	20	20	20	35	35	—	—	35	45	40	30	30
230	210	235	290	010	070	120	160	195	220	235	255	—	—	050	060	060	050	050
08	06	04	03	03	03	04	07	08	10	11	11	—	—	06	05	04	04	04
210	245	260	275	280	285	295	305	315	320	325	325	—	—	130	135	130	125	120
70	60	40	20	15	20	20	10	10	20	40	50	—	30	30	40	35	30	25
230	200	240	305	355	025	065	120	190	240	265	285	—	220	275	310	330	350	015
07	05	04	04	04	05	05	08	12	12	13	13	—	03	04	04	04	05	05
205	260	275	280	285	295	300	305	315	325	325	335	—	115	105	100	105	105	115
65	55	35	20	15	15	15	10	10	20	40	40	05	40	40	35	25	20	15
130	160	210	310	350	020	035	055	015	220	325	340	230	185	220	260	295	325	355
05	05	05	05	05	07	08	12	15	16	16	15	10	05	05	04	05	05	06
355	280	280	290	295	300	310	315	320	335	340	350	295	050	065	075	080	090	100
35	25	15	15	10	10	10	10	15	20	40	45	45	45	40	25	20	20	15
060	090	090	040	010	025	040	050	060	050	050	060	170	155	180	145	240	270	300
08	07	08	09	11	12	14	17	18	19	20	20	18	12	08	05	06	06	07
335	305	300	295	300	310	315	320	335	345	000	015	025	035	045	055	065	065	075
20	15	15	15	15	15	15	15	15	20	20	25	30	40	35	30	25	20	20
035	040	060	050	035	040	045	060	075	090	105	120	140	145	165	190	205	225	240
16	16	17	17	18	19	21	24	26	27	28	30	30	15	12	10	09	08	08
355	335	330	315	320	320	325	335	345	350	000	005	000	000	005	015	025	030	035
15	10	10	10	10	10	10	10	10	10	15	—	—	30	20	25	20	20	—
025	040	045	050	050	050	060	070	085	095	115	—	—	140	155	175	195	210	—
19	19	19	20	20	22	24	26	28	30	30	—	—	15	14	12	10	09	—
015	020	015	355	350	345	350	355	000	005	010	—	—	355	000	005	010	015	—

Both lunar and solar torques contribute appreciably to the deceleration of the Earth's rotation. The total value is

$$\frac{\bar{N}}{I} = \frac{-5.8 \times 10^{23}}{.81 \times 10^{45}} = -7.1 \times 10^{-22} \quad \text{rad} \quad \text{sec}^{-2},$$

where I is the Earth's principal moment of inertia. This is of the same order as the observed deceleration since Egyptian times. An exact comparison is impossible because of much larger effects arising from variations in the Earth's moment of inertia.

REFERENCES

DARWIN, G. H.
1898. The Tides. John Murray, London, 378 pp.

DIETRICH, GUENTER
1944. Die Gezeiten des Weltmeeres als geographische Erscheinung. Z. Ges. Erdk. Berlin.

DOODSON, A. T.
1921. The harmonic development of the tide-generating potential. Proc. roy. Soc., (A) *100*: 305–329.

HEISKANEN, W. A.
1921. Über den Einfluss der Gezeiten auf die Säkuläre Acceleration des Mondes. Ann. Acad. Sci. fenn., (A) *18*: 1–84.

HERTZ, HEINRICH
1883. Über die kontinuierlichen Ströme, welche die fluterrengende Wirkung der Gestirne im Meere veranlassen muss. Verh. physik. Ges., Berlin.

JEFFREYS, HAROLD
1952. The Earth. Cambridge University Press. 392 pp.

MUNK, WALTER AND GORDON MACDONALD
1960. The rotation of the earth: a geophysical discussion. Cambridge University Press. 301 pp.

MURRAY, C.
1957. The secular acceleration of the moon, and the lunar tidal couple. Mon. Not. R. astr. Soc., *117*: 478.

SHUREMAN, PAUL
1941. Manual of harmonic analysis and prediction of tides. Spec. Publ. U.S. Cst. Geod. Surv., 98; 317 pp.

STERNECK, R. V.
1920. Die Gezeiten der Ozeane. SB. Akad. Wiss. Wien, Abt. IIa *129*: 131–150.

SWALLOW, JOHN AND V. W. WORTHINGTON
1957. Measurements of deep currents in the western North Atlantic. *Nature*, London, *179*: 1183–84.

Reprinted from COLD SPRING HARBOR SYMPOSIA ON QUANTITATIVE BIOLOGY
Volume XXV, 1960
Printed in U.S.A.

pp.87-104.

Effects of Temperature upon Diurnal Rhythms

BEATRICE M. SWEENEY AND J. WOODLAND HASTINGS

University of California, La Jolla, California and University of Illinois, Urbana, Illinois

INTRODUCTION

The phenomenon of temperature-independence has probably been the most important single factor in sparking the interest of scientists in the problem of biological rhythms. From observations which only fifteen years ago might have been considered curious and interesting, but trivial, there has emerged a generalization of prime importance concerning the regulation in time of physiological and biochemical processes. The generalization has gained an enormously greater impact through its statement in the form that organisms possess biological clocks—the subject of this symposium.

The realization of the unique implication and importance of the temperature-independent period of biological rhythms emerged rapidly in the early 1950's. The concept of the biological clock developed, at least in part, as Pittendrigh and Bruce [1] suggested in their review, from the work of Kramer [2] on time-compensated sun orientation of birds. But it was certainly Pittendrigh's [3] elegant paper on *Drosophila* which first convincingly formulated the clock generalization with regard to persistent daily rhythms; and it was in this paper that the problem of temperature-independence was first fully and forcefully placed in what we now consider to be its proper perspective. Subsequently, there rapidly evolved an appreciation for the view that rhythms are a manifestation of time-measuring, for which temperature-independence is clearly of great functional importance.

We do not suggest that these questions had not been previously considered and appreciated, for they surely had been. But the orientation and emphasis had been different. It had previously concerned simply whether persistent daily rhythms—i.e., rhythms which persist under apparently constant conditions—were endogenous or exogenous.

This was Bünning's primary concern in his excellent paper of 1931 [4], where he concluded that there was an endogenous mechanism, which he likened to a "clock," which had a metabolic nature, since it "ran faster" at higher temperatures. He significantly noted, however, that the change in rate was relatively small compared to other metabolic processes—even those of a rhythmic nature. He marshalled many other pertinent experiments to support his thesis of an endogenous mechanism.

Again, Brown and Webb [5] were concerned primarily with this aspect of the problem in their now famous study of *Uca* color change. They reported *complete* temperature independence in the period of the rhythm and reasoned that it was difficult to unconditionally assert that the mechanism was wholly endogenous, since "one seeks in vain for descriptions of a biological (temperature-compensating) mechanism (and) . . . even with the existence of such a one it is difficult to credit it with sufficient precision . . ."

Let us just introduce here a reminder to the effect that the generalization of the temperature-independent biological clock has not yet yielded any solutions to the basic problem of mechanism. It has made the task and prospect of solution more exciting and more compelling, and it has, hopefully, served to direct our efforts along more fruitful lines; but we are still a long way from a complete understanding of the problem.

Within the range of temperatures where a particular organism survives, the rate of any particular process is usually greater at higher than at lower temperatures. As is well known, this may be attributed to increases in the rates of chemical reactions involved. Since temperature is, in fact, a measure of the kinetic energy of molecules, it follows that molecules, upon possessing a greater energy, collide more frequently and, therefore, the reaction rate is greater.

Before proceeding to consider the effects of temperature upon diurnal rhythms, the more general situations might be briefly mentioned. In the typical case (Fig. 1), the relation is a logarithmic one in the region where rate is increasing with temperature. The slope of this function is a constant, characteristic of the system. This is essentially another way of expressing the Q_{10}. It is apparent that a system where the rate decreases with increasing temperature would have a slope with a negative value in the log plot; and that a completely temperature-independent system would have a slope with the value zero.

We should also note here that the occurrence of an optimum temperature may be attributed, at least in many instances, to thermal inactivation of enzymes, and that the precise temperature range at which this occurs may vary widely. In contrast to β-galactosidase (Fig. 1), some enzymes are unstable at room temperature, while others require boiling for inactivation.

The effect of temperature upon the rate of heart beat is included to draw attention to the well-known fact that rhythmic processes of this kind are highly

Contributions from the Scripps Institution of Oceanography, New Series, 1252

Reproduced by Permission

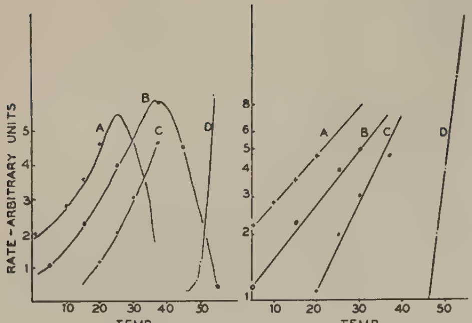

FIGURE 1 *A–D*. Effect of temperature (in degrees centigrade upon abscissa) upon several rates, expressed in arbitrary units on the ordinate. (*A*) Intensity of bioluminescence in cell free extract of *Gonyaulax polyedra* (after Hastings and Sweeney), [59]. (*B*) Rate of hydrolysis of ortho-nitrophenyl-β-galactoside by the enzyme β-galactosidase from a constitutive mutant of *E. coli* (from a class experiment). Note that the apparent temperature optimum is different from that in *A*. (*C*) Rate of heartbeat of the rat at temperatures indicated (from Spector), [60]. (*D*) Rate of heat denaturation of the enzyme β-galactosidase as used in *B* (from a class experiment). Note that the rate of this process is increased greatly with a relatively small increase in temperature.

On the graph at the right we have plotted the log of the rate for each of the processes as a function of temperature.

temperature-dependent, in homeothermic, as well as in poikilothermic organisms.

Many possibilities have been considered to explain the phenomenon of temperature independence [1]. The only one which has received any substantial experimental support is that of temperature-compensation. While the details are not known, it is clear from the examples in Fig. 1 that an appropriately coupled physico-chemical mechanism could exhibit essential temperature-independence. Thus the rate of one of the processes could be decreasing and that of another increasing such that their net coupled output was constant.

Various other possibilities, such as feedback control via the regulation of enzyme activity, are possible [6].

The likelihood of a temperature-compensation mechanism gains strong support from the fact that Q_{10} values of less than 1.0 have been reported [7, 6]. A compensation mechanism might be inaccurate in either direction.

The concept of a biological mechanism stands in contrast to the opinion that the phenomenon is of such an extraordinary nature that it defies understanding on physiological and biochemical grounds (see quote above, from Brown and Webb) [5, 8].

Our discussion of temperature effects upon biological rhythms will be divided into two major sections. The first will consider effects of temperature upon the steady state, i.e., excluding effects which may be attributed to temperature changes. In the second, we will consider the effects of temperature changes, pulses, cycles, and the like.

TEMPERATURE AND THE STEADY STATE

A. EFFECTS UPON THE FREE-RUNNING PERIOD

The generalization concerning temperature-independence in biological clocks should not be misunderstood. The temperature-independent aspect refers to the lack of large differences in the free-running period of a rhythm when the organism is maintained under constant conditions, but at different temperatures.

In reviewing the studies, we consider the fact that better results may be expected where a good assay method was available, and particularly where the course of a rhythm could be observed continuously, or at least frequently. Of course, some biological materials may be preferable for a certain kind of experiment and others for another kind, so that selection of material need not be dictated by this single criterion.

There are other aspects of experimental procedure which need mention. First, it is important to be able to follow the rhythm for several days after any temperature change, so as to avoid transient effects of temperature [3].

Also, it may be very important that the same organism or organisms not be repeatedly used for assay when the observational methods involve a marked change in conditions—particularly turning a light on or off. The reason for this is apparent from the interesting observations of Bruce and Pittendrigh [9]. They found that a test light for 15 minutes, occurring exactly every two hours, acted as a signal and caused the period of the rhythm to be fixed at exactly 24 hours.

Finally, it is important that diurnal fluctuations in temperature be excluded, even small ones. The entraining effect of temperature cycles has been demonstrated (see later).

In Fig. 2 we show records reproduced from Bünning [4], which we consider to be the first well-conceived experiments of this type. If the points which we have marked are taken as maxima, then it is clear that the period is shorter at higher temperatures, but, as Bünning noted, the Q_{10} is not large. From about 40 periods each, the average values given in Table I were calculated.

It is apparent that the *Phaseolus* rhythm does not exhibit smooth sinusoidal curves, and the variance was found to be large. Leinweber [10] especially noted this in his exhaustive re-investigation of this problem, and his figure, summarizing experiments with more than 1000 leaves, gives a direct indication of the extent of this variation (Fig. 3). No large effect upon period was noted in these experiments (Table I), and Bünning's earlier results were attributed to the fact

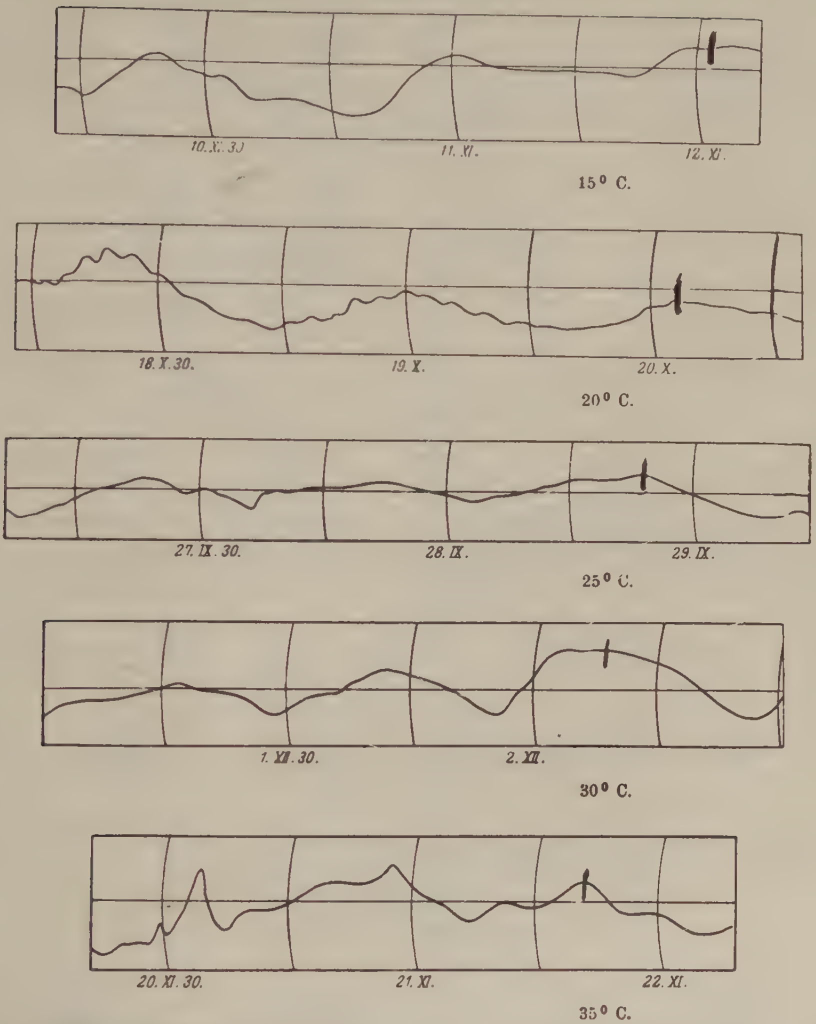

FIGURE 2. Recordings of endogenous rhythm of leaf movements in *Phaseolus* at constant but different temperatures in darkness. All plants were grown at 20°C. and transferred to the new temperature at the time the recordings shown were begun (from Bünning, 1931–32), [4].

that the first period after a temperature change may show an apparent temperature dependence, as Pittendrigh had demonstrated in the *Drosophila* eclosion rhythm. This supposition was directly verified [10].

Went [11] has recently contested Leinweber's conclusion and has reported experiments which he interprets to show a relatively large effect of temperature upon the period, more like Bünning's original finding. We find it difficult to conclude from Went's data that his two experiments are unambiguous, particularly in view of Leinweber's demonstration of the enormous variability of the system. In addition, Went has not eliminated the possible transient effects of the temperature shift.

In 1929 Beling [12] described a time-sense in the bee, and in 1932 Wahl [13] published his classical study on the effect of temperature on this time-sense. This experiment was carried out for only one day after changing the temperature, and for reasons already discussed, we might discredit the experiment if

TABLE I. EFFECTS OF TEMPERATURE UPON PERIOD OF DAILY RHYTHMS

Organism	Rhythm	Temperature	Period in Hours	Q_{10}	Reference
Phaseolus multiflorus (bean)	leaf movement *DD*	15°	29.7	1.3	Bünning, 1931 [4]
		20°	27.0		
		25°	23.7		
		30°	22.0		
		35°	19.0		
	DD	15°	28.3 ± 0.4	1.01	Leinweber, 1956 [10]
		20°	28.0 ± 0.4		
		25°	28.0 ± 1.0		
		14°	30.5	1.2–1.3	Went, 1959 [11]
		23°	23.1 ± 0.5		
Avena coleoptile (oat)	growth rate *DD*	15–17°	ca. 24	ca. 1.0	Ball and Dyke, 1954 [44]
		20–25°	ca. 24		
	DD	26–28°	ca. 24		
Helianthus (sunflower)	exudation 10 ft. c. continuous light	15°	ca. 25	1.1	Grossenbacher, 1939 [19]
		30°	ca. 22		
Cestrum nocturnum (night blooming jasmine)	flower opening 500 ft. c. continuous light	17°	27		Overland, 1960 [45]
		14°	31		
	DD	23°	24.7		
Euglena gracilis (flagellate)	phototaxis *DD* and test light	16.7°	26.2	1.01–1.1	Bruce and Pittendrigh, 1956 [9]
		23°	23.5		
		26°	23.8		
		33°	23.2		
Oedogonium cardiacum (alga)	sporulation	17.5°	20	0.8	Bühnemann, 1955 [7]
		25°	22		
		27.5°	25		
Gonyaulax polyedra (marine dinoflagellate)	bioluminescence (induced flashing) in dim light	15.9°	22.5	0.85	Hastings and Sweeney, 1957 [6]
		19°	23.0		
		21°	24.4		
		22°	25.3		
		26.6°	26.8		
		32°	25.5		
	bioluminescence (spontaneous glow) *DD*	18°	22.9	0.9	Sweeney and Hastings, 1958 [23], Hastings and Sweeney, 1959 [22]
		20°	23.3		
		25°	24.7		
	cell division	18.5°	23.9	0.85	Sweeney and Hastings, 1958 [23]
		25°	25.4		
Pilobolus mold (Phycomycete)	sporulation	15°	36	1.3	Schmidle, 1951 [30]
	DD	20°	24	1.5	Uebelmesser, 1954 [31]
		25°	24		
		25°	27		
Neurospora (bread mold)	zonation of growth in dim red light	24°	22 ± 1.5	1.03	Pittendrigh, Bruce, Rosensweig, and Rubin, 1959 [25]
		31°	21.7 ± 1.8		

TABLE I. (*Concluded*)

Organism	Rhythm	Temperature	Period in Hours	Q_{10}	Reference
Paramecium (ciliate)	mating *DD*	17° 25° 29.5°	22–23 22–23 22–23	ca. 1.0	Ehret, 1959 [24]
Cavernularia obesa (sea pen)	expansion and contraction of colony *DD*	30° 20° 10°	ca. 24 ca. 24 some at 24 some at 48		Mori, 1960 [46]
Cambarus (crayfish)	eye-pigment migration	7° 21°	ca. 24 ca. 24	ca. 1.0	Welsh, 1941 [47]
Uca pugnax (fiddler crab)	color change (both black and white chromatophores, studied separately) in dim light	26° 16° 6°	24 24 24	1.0	Brown and Webb, 1948 [5]
Bee	time sense feeding activity	23° 32°	ca. 24 ca. 24	ca. 1.0	Wahl, 1932 [13]
	DD	18–35°	24 (stated)	ca. 1.0	Kalmus, 1934 [14]
Grasshopper	hatching	22° → 11°	24 → 72	3.0	Kalmus, 1938 [16]
Drosophila sp. (fruit fly)	eclosion *DD*	10° 20° 30°	30 24 22	1.1–1.25	Bünning, 1935–36 [18]
D. pseudoobscura (fruit fly)	eclosion *DD*	16° 21° 26°	24.5 24.0 24.0	1.02	Pittendrigh, 1954 [3]
Periplaneta americana (cockroach)	activity in dim light	18° 19–20° 22–23° 27–28° 29° 31°	24–25 24.4 ± 0.1 24.5 ± 0.1 25.0 ± 0.3 25.8 ± 0.7 24–27		Bünning, 1958 [48]
Lacerta sicula (lizard)	activity	16° 25° 35°	25.05 ± .413 24.38 ± .071 24.55 ± .16	1.02	Hoffmann, 1957 [49] and personal communication, 1960
MAMMALS					
Myotis lucifugus (bat) *Eptesicus fuscus* (bat)	activity *DD*	10°–22° and 37° for several days		1.04 1.07	Rawson, 1956, 1959 [50, 51]
Mesocricetus auratus (hamster)	activity *DD*	15° for 3 hrs.		1.1	Rawson, 1956, 1959 [50, 51]
Peromycus (deer mouse)	activity *DD*	between 20° and 37° for 5–8 hr.		1.1–1.4	Rawson, 1956, 1959 [50, 51]
Myotis lucifucus and *Eptesicus fuscus* (bats)	body temperature *DD*	3°–10°C.	(winter bats) 23½–27½ (summer bats) 19–24		Menaker, 1959 [52] Menaker, 1960 [53]

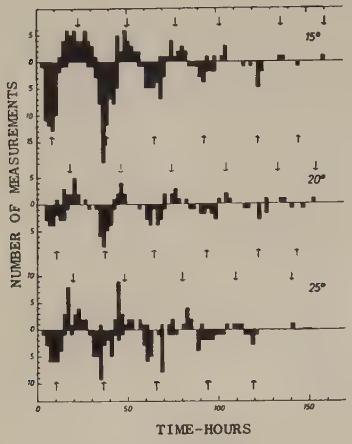

FIGURE 3. Plots of data obtained in experiments on the rhythm of leaf movement in *Phaseolus* similar to those shown in Fig. 2 but with plants grown at the experimental temperature. Many measurements were made, and on the ordinate are the numbers of cases in which the maxima and minima occurred at the times shown on the abscissa (grouped into classes of 2 hours). The spread thus shows that there is a great variance in the time at which maxima and minima occur in different plants (after Leinweber, 1956), [10].

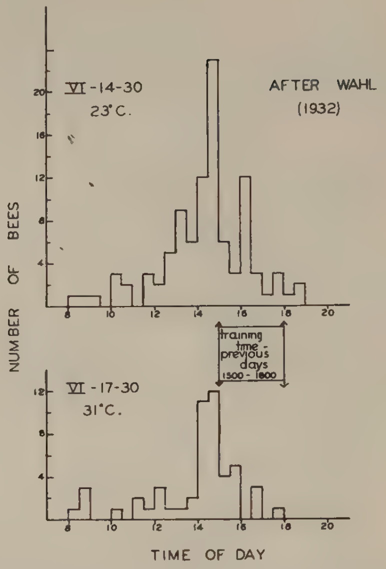

FIGURE 4. This illustrates the lack of a marked effect of temperature upon the time sense of bees. Trained to feed at a particular time of day, they return on the subsequent day without additional light-dark cues, even at different temperatures (after Wahl, 1932), [13].

the time-sense had been modified. But, in fact, it was not (Fig. 4).

A year or two later, Kalmus [14] also studied the bee time-sense and stated that he too found it to be temperature independent between 18° and 35°C. However, he could not agree with Wahl's conclusion that metabolism could not explain rhythms and found that pulses of cold (5–7°C.) or high temperatures (40°C.) will delay or hasten, respectively, the time when feeding activity occurs. Renner [15] has recently confirmed this.

Kalmus [16], intent on pursuing the endogenous vs. exogenous question, was convinced that an examination of the temperature relations in a wide variety of organisms would give support to the endogenous thesis. In the grasshopper he studied a rhythm of egg-hatching and found a large effect of temperature. In constant darkness at 22°C., a natural period of about 24 hours was evident; by then lowering the temperature to 11°C., the period was apparently about 72 hours. The free-running period was again apparent after the temperature was raised.

In 1935 Kalmus [17] stated that the rhythm in *Drosophila* also exhibited dependence on temperature, and Bünning [18] reported that the effect of temperature upon the free-running period (Table I) showed a Q_{10} of about 1.2.

Pittendrigh's [3] reinvestigation of the *Drosophila* eclosion rhythm illustrated the essential temperature independence of the steady state system (Fig. 5). With organisms kept at different temperatures on light-dark regimes, the rhythms exhibit free-running periods very close to 24 hours after being transferred to the dark. However, an important demonstration was that it was necessary to maintain them in a light-dark regime at the different temperatures. With cultures raised at one temperature (26°C.), transferred to the dark, and then transferred to another temperature (16°C.), the rhythm exhibits remarkable transients (Fig. 6) where there occurs a "temporary temperature-dependent error." But this error is subsequently largely corrected. A notable aspect of this, of course, is that correction occurs in darkness without light-dark cues.

Grossenbacher's report in 1939 [19] of temperature-independence in the diurnal period of the exudation rhythm in *Helianthus* apparently attracted relatively little interest. From his curves we can estimate that there was actually a slight temperature effect (Table I). But after the work of Brown and Webb in 1948 [5], a strong interest in the field became more and more evident.

In Fig. 7 we have reproduced the data of Brown and Webb for the effect of temperature upon the *Uca* rhythm during the first six days after the temperature change, and in Fig. 8, the data obtained after 2, 3, and

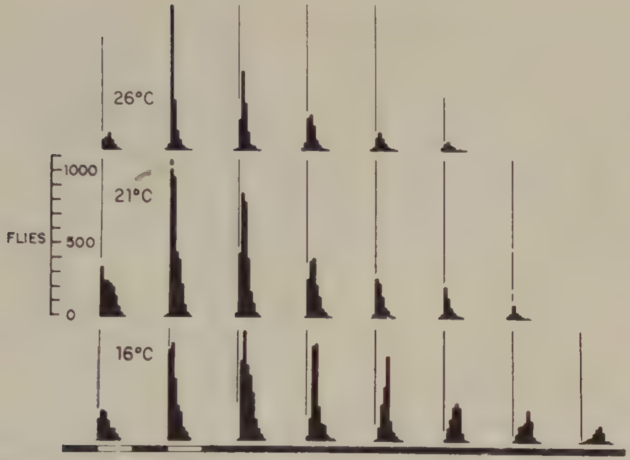

Figure 5. Temperature independence in the persistent rhythm of eclosion in *Drosophila pseudoobscura*. The cultures were raised at each of the three temperatures and transferred to constant darkness prior to the third peak of eclosion. The persistence of the rhythm is evident, and at 16°C. the period is slightly longer, about 24½ hours (after Pittendrigh, 1954), [3].

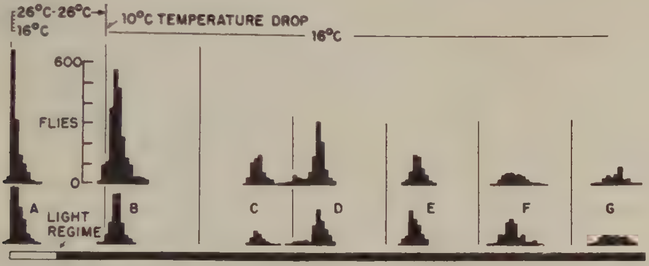

Figure 6. Experiment similar to Fig. 5 except that the flies were raised at 26°C. and transferred to constant darkness and subsequently (about 12 hours later) subjected to a 10° drop in temperature. There is a transient disturbance (peak C is delayed) before the culture resumes its free-running period with a phase shift of about 3 hours. The two cultures are replicates (after Pittendrigh, 1954), [3].

4 weeks at these temperatures. Note that the rhythm does not persist at 6°C.

This case stands out as the only one where the period is reported to be completely independent of temperature over a 20° range [20]. In view of this, and especially since the period was exactly 24 hours, with the phase fixed to the normal day-night relationship found in nature, we feel that additional studies on this system could yield valuable information. This is particularly desirable in view of the fact that Webb, Brown, and Sandeen [21] reported in 1954 that under certain circumstances the free-running period of the rhythm was found to be different from 24 hours.

It would be useful to have the effect of temperature upon this latter system in *Uca* examined. For, in fact, experiments concerned with the effect of temperature upon period are difficult to interpret when the period is exactly 24 hours. In such cases, one is naturally concerned with the possibility that exogenous entraining agents might have been involved.

From 1954 to the present there have appeared one or more papers yearly reporting temperature independence in diurnal rhythms in a variety of different organisms. Those which are not discussed in the text are listed in Table I.

Bühnemann's elegant study on *Oedogonium* in 1955 [7] demonstrated for the first time that a slight temperature dependence could be "in the opposite direction." That is, increasing the temperature was found to result in an apparent slowing of the clock, so that the Q_{10} was estimated at 0.8.

The study by Bruce and Pittendrigh [9] on the

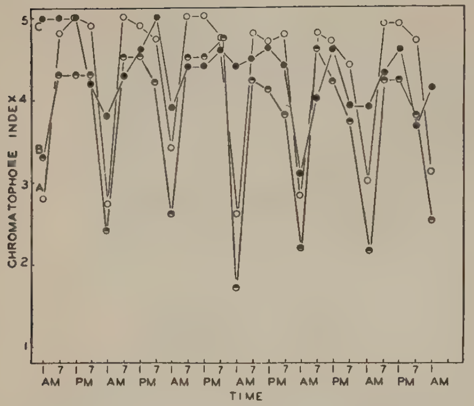

FIGURE 7. Rhythm in color change in *Uca* at 26°C. (*A*) 16°C. (*B*) and 6°C. (*C*) shown here is due to the dispersion and contraction of the white chromatophores. The rhythm retains its usual pattern where the concentration of the pigment is greatest, and the animal is lightest in color at night. Ordinate values are chromatophore stages assigned by visual estimation (after Brown and Webb, 1948), [5].

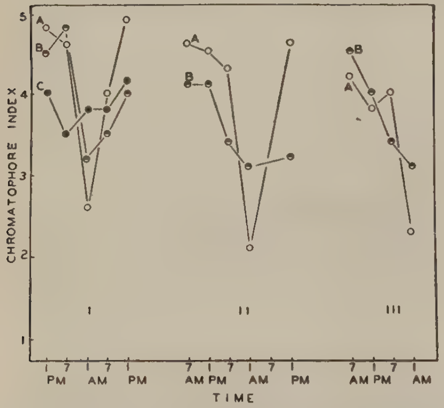

FIGURE 8. Subsequent measurements of the rhythm of color change in *Uca,* as in Fig. 7 after 2, 3, and 4 weeks at temperatures indicated. Even after 4 weeks, the maximum concentration of the pigment occurs at night, both at 26° and at 16°C. The rhythm does *not* persist at 6°C. (after Brown and Webb, 1948), [5].

phototactic rhythm of *Euglena* significantly demonstrated that a unicellular form exhibited a phenomenon of persistent rhythmicity. It was shown to exhibit several characteristic features of daily rhythms, including the most diagnostic and crucial one, i.e., temperature-independence (Fig. 9).

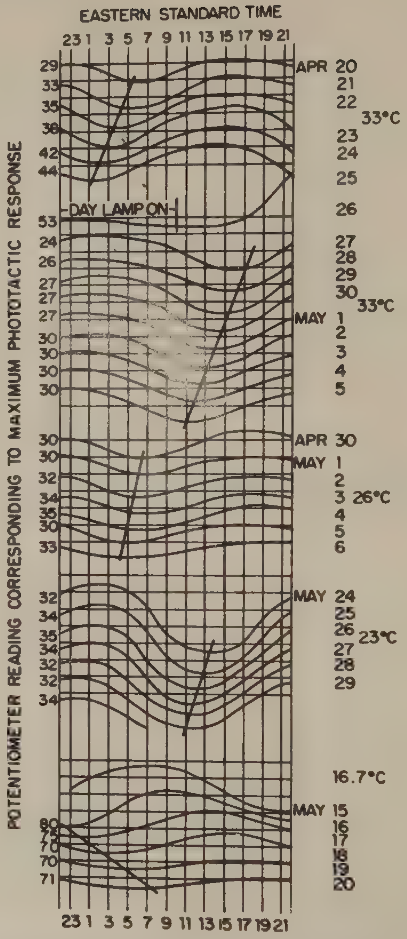

FIGURE 9. The temperature-independence of the rhythm of phototaxis in *Euglena gracilis.* Curves for each day are drawn through successive potentiometer readings, corresponding to the maximum phototactic response recorded each time the test light is on. The ordinate shows the relative levels of the potentiometer readings on successive days. The inclined lines passing through the minimum points on the response curves illustrate the slight departure of the natural period from 24 hours and form the basis for the estimate of the period at different temperatures. Twelve hours of the day lamp light were used on May 25 and 26 to shift the phase of the rhythm as indicated (after Bruce and Pittendrigh, 1956), [9].

Temperature was found to have a similar effect upon each of three rhythms studied in the marine dinoflagellate *Gonyaulax polyedra* [6], [22], [23]. This is another instance where a Q_{10} of less than 1.0 was found (Fig. 10), and it was interpreted as an overcompensation

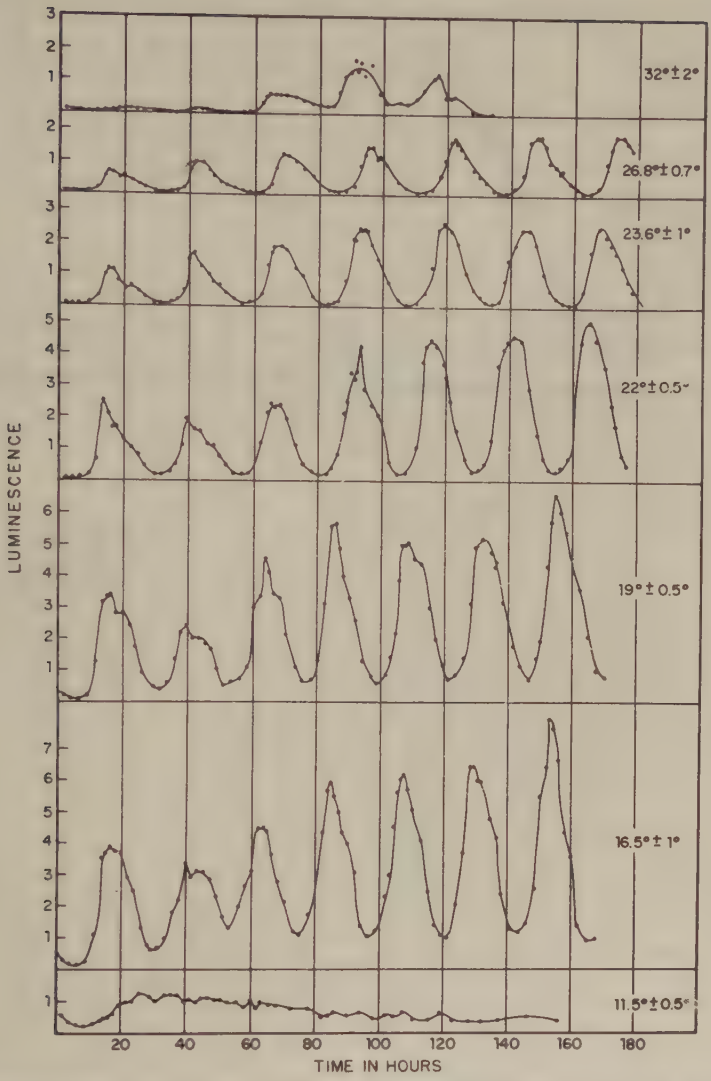

FIGURE 10. Characteristics of the rhythm of luminescence in *Gonyaulax polyedra* at different temperatures. The cells were kept at 22°C. in *LD* conditions prior to the beginning of the experiment shown in the graph. At that time the cells were transferred from the dark at 22°C. to the various temperatures all in dim light (100 ft. c.) and left in these conditions throughout the experiment. The luminescence of the cells was determined approximately every 2 hours (after Hastings and Sweeney, 1957), [6].

by a relatively imprecise temperature regulation mechanism. The magnitude of the effect is not small (Q_{10} = 0.85). Since the different rhythms have the same Q_{10} (Table I), it may be inferred that separate physiological processes may be subject to the same controlling mechanism.

Rhythms in several additional organisms have been shown to exhibit temperature independence, including the mating reaction in the ciliate *Paramecium* [24], and zonation in the growth of *Neurospora* [25], (Fig. 11 and 12).

It has thus been demonstrated unequivocally in

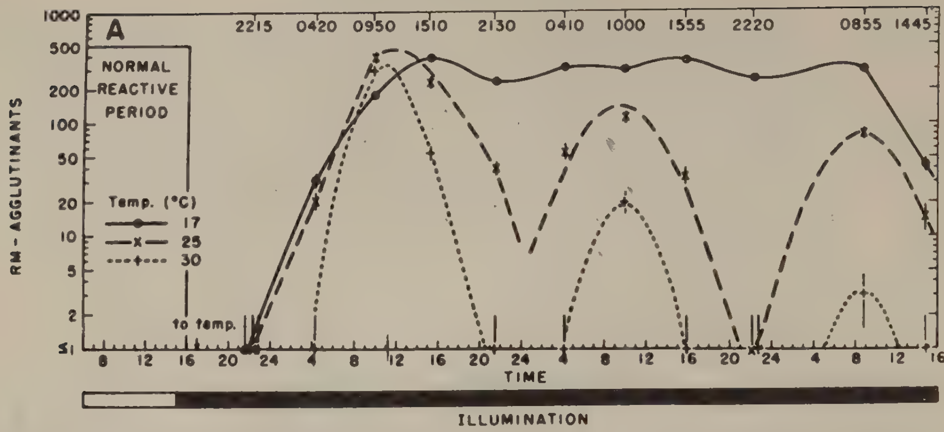

FIGURE 11. The mating reaction in *Paramecium* at the temperatures indicated in constant darkness. Rhythmicity at 17°C. is not pronounced (after Ehret, 1959), [24].

several cases that periods of biological rhythms are only slightly dependent upon the ambient temperature.

B. EFFECTS UPON THE FORM OF RHYTHMS

As is readily apparent from experiments which we have illustrated, there may be large differences with temperature in the shape or form of the curves which describe the rhythm. In several cases it is clearly apparent that at lower temperature the amplitude of the overt rhythm may be reduced, as in the phototactic response of *Euglena* (Fig. 9).

An opposite effect is observed in the overt rhythm of luminescence in *Gonyaulax* (Fig. 10), where the amount of light emitted decreases with increasing temperature over the range 16–32°C. The interpretation of this phenomenon is not clear, but it is very striking. It may, in fact, be related to the mechanism of temperature compensation.

The activity rhythm in snakes, recently investigated by Heckrotte [26], shows a most unusual and interesting temperature effect (Fig. 13). In alternating light and darkness (12L:12D) at a temperature of 21°C., the snakes were most active toward the middle of the day, 4–5 hours after dawn. At increasingly higher temperatures there develops a minimum in the activity during the middle of the day, with two maxima, one around dawn and one in the late afternoon. At still higher temperatures the activity maximum around dawn becomes more pronounced.

The adaptive importance of this is clear enough. At each temperature the activity is maximal at a time of day when temperature would be expected to be optimum for activity.

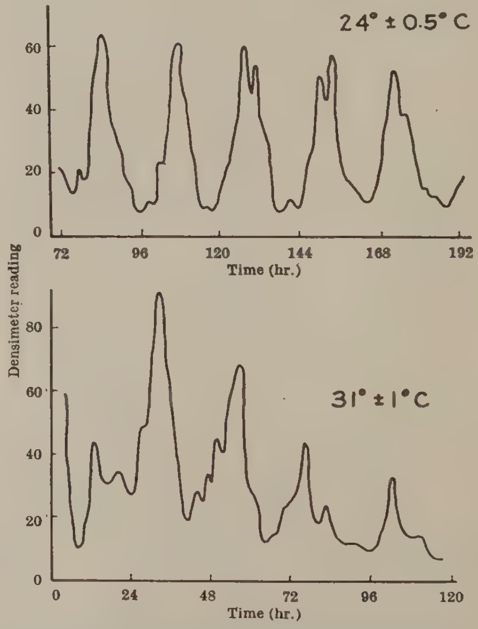

FIGURE 12. The rhythmicity in the density of the production of mycelium in *Neurospora crassa* growing along a race-tube, at two different temperatures, in continuous dim red light (after Pittendrigh, Bruce, Rosensweig, and Rubin, 1959), [25].

TEMPERATURE CHANGES AND PHASE

The question to which we can now immediately direct our attention is, can a temperature change act as a time cue or signal so as to determine phase?

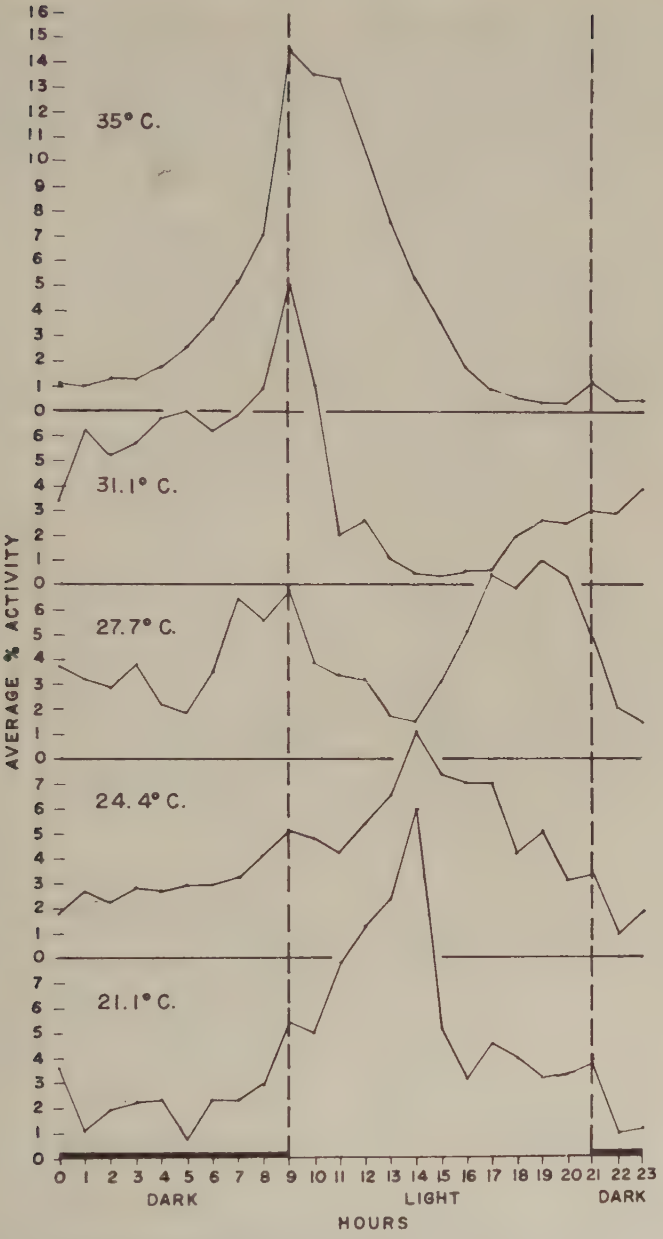

Figure 13. The activity of a garter snake, *Thamnophis radix radix*, in alternating light and darkness at different temperatures. Note the marked daytime bimodal shape of the activity curve at 27.7°C. in contrast to the single midday peak at 21.1°C. and the single peak at dawn at 35°C. (after Heckrotte, 1960), [26].

The answer is definitely yes. There are several viewpoints from which one can consider the problem. We will attempt to bring together the large number of often complex and certainly diverse experiments which are concerned with temperature effects and to group them expressly to answer this question. Where more convenient, relevant experiments are summarized in Table II.

A. TEMPERATURE CYCLES

Just as rhythms have phase determined by the daily light-dark cycle, so they can be similarly entrained to temperature cycles. This was reported in 1929 by Stern and Bünning [27] in experiments where they reversed the phase of the *Phaseolus* rhythm in the dark by a cycle having its maximum temperature at night.

TABLE II. NON-STEADY-STATE TEMPERATURE EFFECTS

Organism	Rhythm	Description of Temperature Changes	Effects of Temperature Changes	Reference
A. LOW TEMPERATURE EXPOSURES				
Phaseolus (bean)	Leaf movement	Low temperature (10°) (continuous)	Irregular and shorter periods	Bünning and Tazawa, 1957 [54]
	Leaf movement	Low temperature (0°C.) for several hours	Phase delayed by equal number of hours but compensation occurs later	Leinweber, 1956 [10]
Avena (oat)		4°C. for 6, 11, and 16 hrs.	Phase delay of about this amount but compensation at next peak	Ball and Dyke, 1957 [42]
Oedogonium (alga)	Sporulation	6-hr. treatment at −5°C. at various times in cycle	Phase delay of 6 hrs. or less depending upon time in cycle	Bünning and Ruddat, 1960 [38]
		12-hr. treatment at 0°C.	Phase delay of 8 hrs. or less dependent upon time in cycle	Ruddat, personal communication, 1960
Talitrus (amphipod)	Sun orientation	4–6°C. temperature pulse for 18 hrs.	No effect on phase	Pardi and Grassi, 1955 [55]
Uca (crab)	Color change	0–3°C. treatment for 6 hrs.	6-hr. phase delay	Brown and Webb, 1948 [5]
	Color change	5°C. cold treatment for 2 hrs.	Less than 2-hr. phase delay	Webb *et al.*, 1953 [36]
	Color change	9.5°C. treatment for 12 hrs.	Phase delay of 5 hrs. or less, depending upon time in cycle	Stephens, 1957 [37]
Bee	Time sense	5–7°C. cold treatment for several hours	Delays peak	Kalmus, 1933–34 [14]
	Time sense	4–5°C. cold treatment for 5¾ hrs.	3-hr. delay in peak. No study of phase dependence	Renner, 1957 [15]
B. TEMPERATURE CYCLES				
Phaseolus (bean)	Leaf movement	Temperature cycle reversed—high temp. at night	With plants kept in dark phase of rhythm changed by 12 hrs.	Stern and Bünning, 1929 [27]
Tomato	—	Temperature cycle introduced in plants grown in constant light	Prevents leaf damage which occurs in absence of environmental diurnal periodicity	Hillman, 1956 [34]
Euglena (flagellate)	Phototaxis	Temperature cycle phase varied with respect to light-dark cycle	Cycle modified by temperature cycle	Bruce; and Pittendrigh, this volume [56]
Oedogonium (alga)	Sporulation	24-hr. cycle, 2.5°C. difference	Entrains so that phase is determined by temperature	Bühnemann, 1955 [7]
		Non-24-hr. cycle	Entrains at 18 hrs. but not at 12 or 30 hr. cycles	
Pilobolus (mold)	Sporulation	Cycle 12 hrs. at 21°C.: 12 hrs. at 25°C. in dark.	Restores rhythm in dark	Schmidle, 1951 [30]
	Sporulation	Warming 5°C. or more 1 hr. every 12 hrs.	Entrains to cycle, which persists for about 24 hrs. in constant conditions, after which free-running period is regained	Uebelmesser, 1954 [31]
Drosophila (fruitfly)	Eclosion	Temperature cycle	Entrains	Pittendrigh, 1954 [3]
Drosophila	Eclosion	Temperature cycle along with light-dark cycle relative phase varied	Time of eclosion modified by imposed temperature cycle	Pittendrigh, 1958 [33]
Periplaneta (cockroach)	Activity	24-hr. temperature cycle	Prevents loss of rhythm in constant dark	Cloudsley-Thompson, 1953 [29]
Leucophaea (cockroach)	Running activity	24-hr. sinusoidal change 19°–29°	Phase entrained. Phase shift maintained in subsequent *DD*. Onset of activity coincides with max. of temp. cycle	Roberts, 1959 [32]
Ptinus (spider beetle)	Activity	Temperature cycle	Restores rhythm lost in continuous light	Bentley, Gunn, and Ewer, 1941 [28]
Glaucomys volans (flying squirrel)	Locomotor activity	Cycle: 4 animals *DD* 15°C. for several weeks—12 hr. (25°C.): 12 hr. (15°C.) *DD* for 46 days until onset of activity for 3 of 4 animals spanned both temperature transitions—*DD* 20°C. for several weeks	Activity cycle frequency persists unchanged. Apparent synchronization to cool period in 3 animals shown to be suppression of activity during warm period rather than entrainment	DeCoursey, 1959, 1960 [57, 58]

Table II. (*Cont'd*)

C. PULSES OR STEPS AT MODERATE TEMPERATURES

Phaseolus (bean)	Leaf movement	1 hr. raising temperature 5°C. with plants where rhythm has died out. *DD*	Rhythm initiated again without any light stimulus	Bünning, 1931–32 [4]
Pilobolus (mold)	Sporulation	Raising temperature from 21° to 25°C. in *DD* with arrhythmic organisms	Initiates rhythmicity	Schmidle, 1951 [30]
Paramecium (ciliate)	Mating	Temperature changed from 25° to 29.5°C. in continuous darkness	Cycle-dependent phase advance (maximum 12 hrs.) if temperature change is made at end of non-reactive phase	Ehret, 1959 [24]
Talitrus (amphipod)	Sun orientation	Exposure to high temperature (35–37°C.) for 18 hrs.	Phase advance of 5–6 hrs.	Pardi and Grassi, 1955 [54]
		4–6°C. for 18 hrs.	No effect	
Drosophila (fruitfly)	Eclosion	4-hr. increase of temp. from 16° to 26°C. and back upon arrhythmic cultures raised and kept in dark	24-hr. rhythm initiated without any light signal whatever	Pittendrigh, 1954 [3]
Drosophila	Eclosion	Temperature lowered from 26° to 16°C.	One long period following reduction in temperature, then very short period; little net change in phase	Pittendrigh, Bruce, and Kaus, 1958 [40]
Leucophaea and *Byrsotria* (cockroaches)	Running activity	Pulse from 25 → 12° → 25°C. Lower temperature maintained for periods of 12 hrs. and 48 hrs. In both cases pulses were staggered to cover all times of cycle. Animals kept in *DD*	Phase of rhythm reset. New phase directly related to time of temperature treatment. Time of onset of activity coincides with time of rising temperature. Change in period always observed subsequent to pulse	Roberts, 1959 [32]
Glaucomys volans (flying squirrel)	Locomotor activity	Single perturbations: 4 animals *DD* (20°C.) given single ½ hr. perturbations at 3–12 day intervals (20°C. → 15°C.)	No shift in phase of activity onset at any point in activity cycle	DeCoursey, 1959 [57. 58]

Bühnemann's [7] study of the sporulation rhythm in *Oedogonium* has demonstrated two additional points relative to temperature cycles. First, that the rhythm may be entrained by the relatively small day-night differentials of 2.5°C. (Fig. 14). Second, that rhythms could be entrained to non-24-hour temperature cycles. A cycle with an 18-hour period (9 hours high; 9 hours low) was effective (Fig. 15), indicating that the limits of entrainment are wide. A 12-hour cycle (6:6) entrained to a 24-hour rhythm, with a maximum every other cycle, while a 30-hour cycle was not effective in entraining.

There are other examples of the effects of temperature cycles. The activity rhythm in the spider beetle *Ptinus*, lost in continuous light, was regained in the presence of a temperature cycle [28]. In *Periplaneta* the presence of temperature cycles prevented the loss of the rhythm in continuous darkness, although such cycles could not reinstate rhythmicity once it had disappeared [29]. In *Pilobolus*, it has been shown that one hour exposures to somewhat higher or lower temperatures repeated at intervals can regulate the rhythm in sporulation, which then was observed to continue at the entraining frequency for several cycles in constant conditions, after which the free-running period was reinstated [30, 31]. Roberts [32] has also studied the effects of temperature cycles in the cockroach,

Of particular interest are the studies by Pittendrigh and Bruce [33, 1] concerned with the interaction of light and temperature cycles. One of their figures is reproduced in Fig. 16, where the eclosion rhythm was studied under conditions where the phase angle between the light and temperature cycle was systematically varied. The result illustrates that light entrains more strongly than does temperature and that there are excluded times for eclosion. Note the sharp difference in eclosion time between the culture where the minimum temperature was at the end of the light period and the one where it was at the beginning of the dark period. Experiments of this nature with *Euglena* and the cockroach [32, 56] have also been carried out.

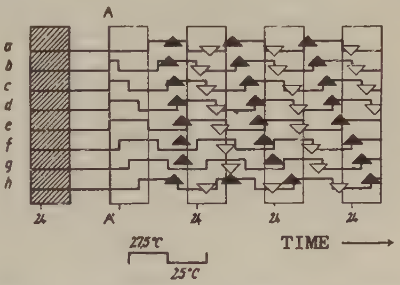

Figure 14. The sporulation rhythm in *Oedogonium cardiacum* in continuous light with 2.5°C. temperature cycles (12 hours 27.5°C.:12 hours 25° C.) as indicated by the horizontal lines *a–h*. Maxima in sporulation are indicated by ▲ and minima by ▽. Entrainment to the temperature cycles is evident (after Bühnemann, 1955), [7].

While it has been generally believed that many if not most organisms grow and divide normally in constant conditions of light and temperature, this may not be so. The leaves of the tomato, for example, have been

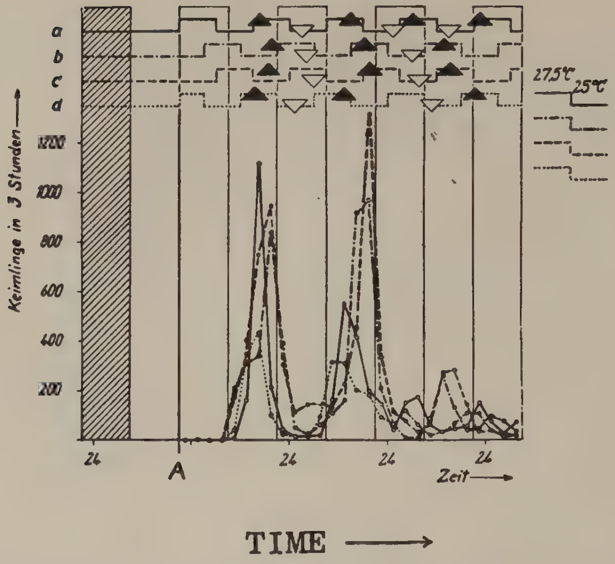

FIGURE 15. Experiments on the sporulation rhythm of *Oedogonium* similar to those of Fig. 14 but with a temperature cycle of 9 hours' high temperature (27.5°C.), 9 hours' low temperature (25°C.). The actual number of spores is plotted in the lower part of the figure. Entrainment to this temperature cycle is also evident (after Bühnemann, 1955), [7].

shown in several studies to suffer damage under constant conditions [34]. In Hillman's study, he found marked damage to tomato leaves kept in constant light and at constant temperatures, ranging from 14° to 30°C. As expected, it was found that no damage occurred with the introduction of a light-dark cycle. But Hillman also found that a 24-hour temperature cycle could prevent injury. Dividing the day into periods of 16 and 8 hours, it was found that temperature cycles of 26°:10°, 20°:30°, and 30°:17° respectively would prevent damage.

Thus, the often-expressed view that there exist light-loving and dark-loving (photophil and scotophil) phases is not supported. But rather the view is favored that the clock must be in operation for proper function.

B. TEMPERATURE PULSES AND PERTURBATIONS

As we have already noted from the experiments of Pittendrigh (Fig. 6), a single change in the temperature has a marked effect upon the rhythm. It is now clear that we can generalize: a *single* temperature change, either of the step or pulse type, can effectively perturb the phase of the oscillator or clock in motion. There have been many experiments demonstrating this.

But let us note here that the question in most of the earlier experiments was directed towards the endogenous-exogenous question. The matter concerned whether or not a temperature pulse would either stop or slow the motion of the presumed "metabolic clock." With the oscillator model of Pittendrigh and Bruce [1], the question has been oriented differently—namely, can a temperature shift or pulse change the phase of a clock in motion?

It is useful and necessary to retain both of these two points of view, for the oscillator analogy includes the possibility that there are temperature limits beyond which the oscillator principles are no longer applicable—or that perhaps the clock is stopped [35]. At very low temperatures, in the neighborhood of 0° C., rhythmicity is characteristically no longer observed. In *Uca* it was reported that the clock was stopped for precisely the length of the low temperature treatment [5], but in more extensive studies with *Uca* [36, 37], it has not been found that this rule always holds. Rather it has been found that the effect depends markedly upon the time in the cycle when cold is administered.

Other investigators, using a variety of organisms, have substantiated the conclusion that the magnitude and kind of the response to extreme cold are variable and depend on the phase when administered (Table II). Bünning and Ruddat [38] showed this with *Oedogonium*. Bünning has reported that in *Periplaneta* the temperature-sensitive half of the cycle begins in the second half of the light phase and is most sensitive just at the beginning of the dark phase. With the lizard (Hoffmann, personal communication) the maximum effect of a low temperature (1–3°C.) shock is found at a time of maximum activity. Other cases are tabulated.

We want to distinguish the above from experiments where temperature pulses or steps are administered in ranges where the rhythm operates normally. As we have seen in experiments of this sort, there have been observed major phase disturbances which are substantially corrected for in a striking way (Fig. 6, 17). In both *Drosophila* [3] and in *Phaseolus* [10, 32], this has been well documented.

Again the effect is markedly dependent upon phase, as illustrated in experiments of Pittendrigh (Fig. 17). It is significant to note that the temperature shift generates peaks which occur about 40 hours after the drop, i.e., an apparent resetting phased to the time of the temperature change; but that by the next peak this has been corrected. Still it is significant to note that some final phase shift does occur.

The phenomenon whereby non-repeated temperature pulses can "initiate" and phase-determine a rhythm in arrhythmic systems merits special discussion. Bünning [4] noted that in *Phaseolus* plants, where the rhythm had died down, it could be initiated again by increasing the temperature by 5° for 1 hour. Pittendrigh [3] noted that a 4-hour pulse of increased temperature (16°-26°-16°C.) induced a 24-hour rhythm in arrhythmic cultures raised in constant darkness. A temperature pulse is therefore comparable to the action of light in this regard.

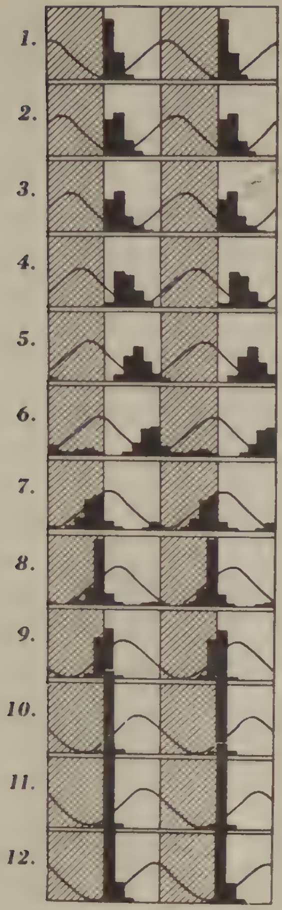

FIGURE 16. The rhythm of eclosion in *Drosophila* in alternating light and darkness and a 16° temperature cycle (26°–10°C.), the phase of which in different cultures is systematically varied so as to span the whole cycle. The dark periods are represented by cross hatching; the temperature cycle by the sinusoidal line; and the number of flies emerging by black bars. Note that light entrains more strongly than does the temperature cycle (after Pittendrigh, 1958), [33].

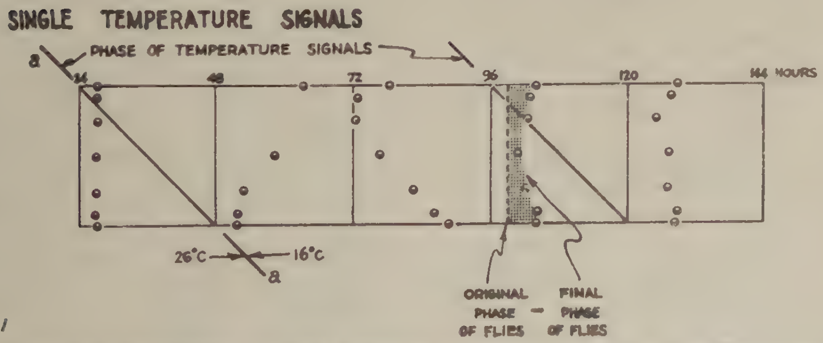

FIGURE 17. The eclosion of *Drosophila* following a change of temperature in constant darkness. The cultures had been at 26°C. and on a light-dark cycle, the last dawn of which corresponds to hour zero. The temperature was dropped to 16°C. at different times as shown by the heavy diagonal line (a–a) between hours 24 and 48. The times at which maxima in eclosion occurred are shown by the symbols (O). (After Pittendrigh, Bruce, and Kaus, 1958, [40].)

In considering the mechanism whereby single perturbations determine phase and apparently "initiate" rhythmicity in arrhythmic systems, Pittendrigh [3, 40, 41] has noted two alternative explanations:

"(1) Clocks (oscillatory mechanisms) in the flies were inherited at rest and set in motion by the unrepeated stimulation;

(2) Clocks were inherited in motion with the phase of individuals at random to that of solar day, so that the population as such manifested a net aperiodicity until the single stimulus served to synchronize the phase of individuals."

The second hypothesis, that "clocks" are all in motion and are phased by the stimulus, was favored largely on the basis of some elegant experiments in which the initiation of a rhythm by a single stimulus was compared to the expected synchronization. Bünning also [39] has discussed these alternatives and has favored the second, as have Ball and Dyke [42].

However, from the data available, this second alternative might be logically excluded if the effect of a temperature pulse upon the phase of clocks in motion is similar to the effect of a temperature step (Fig. 17). Following a spectacular but temporary phase disturbance (transient), the phase returns to its original position. If all clocks were out of phase prior to the temperature shock, they would not be synchronized by it.

This conclusion was forthcoming—but not yet adequately documented—in experiments where the cell division rhythm in *Gonyaulax* has been studied. In rhythmic cultures the time between cell divisions is either 24 hours, 48 hours, or a higher multiple of 24 hours for any particular cell. In arrhythmic cultures grown in constant bright light, no such periodicity was observed. From studies of the photosynthesis rhythm in *Gonyaulax*, similar conclusions have been obtained [43].

Acknowledgement

The previously unpublished studies cited in this paper have been supported in part by grants from the National Science Foundation.

REFERENCES

1. Pittendrigh, C. S., and V. G. Bruce. 1957. An oscillator model for biological clocks. pp. 75–109. *Rhythmic and Synthetic Processes in Growth*, ed. Rudnick. Princeton: Princeton University Press.
2. Kramer, G. 1952. Experiments on bird orientation. Ibis, *94:* 265–285.
3. Pittendrigh, C. S. 1954. On temperature independence in the clock system controlling emergence time in *Drosophila*. Proc. Nat. Acad. Sci. U. S., *40:* 1018–1029.
4. Bünning, E. 1931. Untersuchungen über die autonomen tagesperiodischen Bewegungen der Primärblatter von *Phaseolus multiflorus*. Jahrb. Wiss. Bot., *75:* 439–480.
5. Brown, F. A., Jr., and H. M. Webb. 1948. Temperature relations of an endogenous daily rhythmicity in the fiddler crab, *Uca*. Physiol. Zool., *21:* 371–381.
6. Hastings, J. W., and B. M. Sweeney. 1957. On the mechanism of temperature independence in a biological clock. Proc. Nat. Acad. Sci. U. S., *43:* 804–811.
7. Bühnemann, F. 1955. Das endodiurnale System der *Oedogoniumzelle*. III. Über den Temperatureinfluss. Zeit. Naturforsch., *10b:* 305–310.
8. Brown, F. A. 1957. Biological chronometry. Amer. Nat., *91:* 129–133.
9. Bruce, V. G., and C. S. Pittendrigh. 1956. Temperature independence in a unicellular "clock." Proc. Nat. Acad. Sci. U. S., *42:* 676–682.
10. Leinweber, F. J. 1956. Über die Temperaturabhängigkeit der Periodenlänge bei der endogenen Tagesrhythmik von *Phaseolus*. Zeit. f. Bot., *44:* 337–364.
11. Went, F. W. 1959. The periodic aspect of photoperiodism and thermoperiodicity. pp. 551–564. *Photoperiodism and Related Phenomena in Plants and Animals*, ed. Withrow. Washington: A.A.A.S.
12. Beling, I. 1929. Über das Zeitgedächtnis der Bienen. Z. vergl. Physiol., *9:* 259–338.
13. Wahl, O. 1932. Neue Untersuchungen über das Zeitgedächtnis der Bienen. Zeit. vergl. Physiol., *16:* 529–589.
14. Kalmus, H. 1934. Über die Nature des Zeitgedächtnisses der Bienen. Zeit. f. vergl. Physiol., *20:* 405–419.
15. Renner, M. 1957. Neue Versuche über den Zeitsinn der Honigbiene. Zeit. f. vergl. Physiol., *40:* 85–118.
16. Kalmus, H. 1938. Tagesperiodische verlaufende Vorgänge an der Stabheuschrecke (*Dixippus morosus*) und ihre experimentelle Beeinflussung. Zeit. f. vergl. Physiol., *25:* 494–508.
17. ——. 1935. Periodizität und Autochronie (Ideochronie) als zeitregelnde Eigenschaften der Organismen. Biol. Gen., *11:* 93–114.
18. Bünning, E. 1935. Zur Kentnis der endogenen Tagesrhythmik bei Insekten und bei Pflanzen. Ber. deutsch. bot. Ges., *53:* 594–623.
19. Grossenbacher, K. A. 1939. Autonomic cycle of rate of exudation of plants. Amer. J. Bot., *26:* 107–109.
20. Brown, F. A. 1959. Living clocks. Science, *130:* 1535–1544.
21. Webb, H. M., F. A. Brown, and M. I. Sandeen. 1954. A modification in the frequency of the persistent daily rhythm of the fiddler crab. Anat. Rec., *120:* 796.
22. Hastings, J. W., and B. M. Sweeney. 1959. The *Gonyaulax* clock. pp. 567–584. *Photoperiodism and Related Phenomena in Plants and Animals*, ed. Withrow. Washington: A.A.A.S.
23. Sweeney, B. M., and J. W. Hastings. 1958. Rhythmic cell division in populations of *Gonyaulax polyedra*. J. Protozool., *5:* 217–224.
24. Ehret, C. F. 1959. Photobiology and biochemistry of circadian rhythms in non-photosynthesizing cells. Fed. Proc., *18:* 1232–1240.
25. Pittendrigh, C. S., V. G. Bruce, N. S. Rosensweig, and M. L. Rubin. 1959. A biological clock in *Neurospora*. Nature, *184:* 169–170.
26. Heckrotte, C. 1960. The effect of environmental factors on the locomotory activity of the Plains garter snake (*Thamnophis radix radix*). Ph.D. Thesis, University of Illinois.

27. Stern, K., and E. Bünning. 1929. Über die Tagesperiodischen Bewegungen der Primärblätter von *Phaseolus multiflorus*. I. Der Einfluss der Temperatur auf die Bewegungen. Ber. deutsch. bot. Ges., *47:* 565–584.
28. Bentley, E. W., D. L. Gunn, and D. W. Ewer. 1941. The biology and behavior of *Ptinus tectus* Boie. (Coleoptera, Ptinidae) a pest of stored products. I. The daily rhythm of locomotory activity, especially in relation to light and temperature. J. Exper. Biol., *18:* 182–195.
29. Cloudsley-Thompson, J. L. 1953. LXIX—Studies in diurnal rhythms. III. Photoperiodism in the cockroach *Periplaneta americana* (L). Ann. Mag. Nat. Hist. Ser. 12, *6:* 705–712.
30. Schmidle, A. 1951. Die Tagesperiodizität der asexuellen Reproduktion von *Pilobolus sphaerosporus*. Arch. f. Mikrobiol., *16:* 80–100.
31. Uebelmesser, E. R. 1954. Über den endonomen Tagesrhythmus der Sporangienträgerbildung von *Pilobolus*. Arch. f. Mikrobiol., *20:* 1–33.
32. Roberts, S. K. 1959. Circadian activity rhythm in cockroaches. Ph.D. Thesis, Princeton University.
33. Pittendrigh, C. S. 1958. Perspectives in the study of biological clocks. pp. 239–268. *Perspectives in Marine Biology*, ed. A. A. Buzzati-Traverso. Berkeley and Los Angeles: University of California Press.
34. Hillman, W. S. 1956. Injury of tomato plants by continuous light and unfavorable photoperiodic cycles. Amer. J. Bot., *43:* 89–96.
35. Bünning, E. 1959. Physiological mechanism and biological importance of the endogenous diurnal periodicity in plants and animals. pp. 507–530. *Photoperiodism and Related Phenomena in Plants and Animals*, ed. Withrow. Washington: A.A.A.S.
36. Webb, H. M., M. F. Bennett, R. C. Graves, and G. C. Stephens, 1953. Relationship between time of day and inhibiting influence of low temperature on the diurnal chromatophore rhythm of *Uca*. Biol. Bull., *105:* 386–387.
37. Stephens, G. C. 1957. Influence of temperature fluctuations on the diurnal melanophore rhythm of the fiddler crab *Uca*. Physiol. Zool., *30:* 55–69.
38. Bünning, E., and M. Ruddat. 1960. Weitere Experimente zur Deutung der physiologischen Uhr als Kippschwingungssystem. Zeit. f. Naturf., (in press).
39. Bünning, E. 1957. Endogenous diurnal cycles of activity in plants. pp. 111–126. *Rhythmic and Synthetic Processes in Growth*, ed. Rudnick. Princeton: Princeton University Press.
40. Pittendrigh, C. S., V. G. Bruce, and P. Kaus. 1958. On the significance of transients in daily rhythms. Proc. Nat. Acad. Sci. U. S., *44:* 965–973.
41. Pittendrigh, C. S., and V. G. Bruce. 1959. Daily rhythms as coupled oscillator systems and their relation to thermoperiodism and photoperiodism. pp. 475–505. *Photoperiodism and Related Phenomena in Plants and Animals*, ed. Withrow. Washington: A.A.A.S.
42. Ball, N. G., and I. J. Dyke. 1957. The effects of decapitation, lack of oxygen, and low temperature on the endogenous 24-hour rhythm in the growth-rate of the *Avena* coleoptile. J. Exper. Bot., *8:* 323–338.
43. Sweeney, B. M. 1960. Cold Spring Harbor Symp. on Quant. Biol. Vol. 25.
44. Ball, N. G., and I. J. Dyke. 1954. An endogenous 24-hour rhythm in the growth rate of the *Avena* coleoptile. J. Exper. Bot., *5:* 421–433.
45. Overland, L. 1960. Endogenous rhythm in opening and odor of flowers of *Cestrum nocturnum*. Amer. J. Bot., *47:* 378–382.
46. Mori, S. 1960. Cold Spring Harbor Symp. on Quant. Biol. Vol. 25.
47. Welsh, J. H. 1941. The sinus glands and twenty-four hour cycles of retinal pigment migration in crayfish. J. Exper. Zool., *86:* 35–49.
48. Bünning, E. 1958. Über den Temperatureinfluss auf die endogene Tagesrhythmik, besonders bei *Periplaneta americana*. Biol. Zbl., *77:* 141–152.
49. Hoffmann, K. 1957. Über den Einfluss der Temperatur auf die Tagesperiodik bei einem Poikilothermen. Naturwiss., *44:* 358.
50. Rawson, K. S. 1956. Homing behavior and endogenous activity rhythms. Ph.D. Thesis, Harvard University, Cambridge.
51. ——. 1959. Experimental modification of mammalian endogenous activity rhythms. pp. 791–800. *Photoperiodism and Related Phenomena in Plants and Animals*, ed. Withrow. Washington: A.A.A.S.
52. Menaker, M. 1959. Endogenous rhythms of body temperature in hibernating bats. Nature, *184:* 1251–1252.
53. ——. 1960. Cold Spring Harbor Symp. on Quant. Biol. Vol. 25.
54. Bünning, E., and M. Tazawa. 1957. Über den Temperatureinfluss auf die endogene Tagesrhythmik bei *Phaseolus*. Planta, *50:* 107–121.
55. Pardi, L., and M. Grassi. 1955. Experimental modification of direction-finding in *Talitrus saltator* (Montagu) and *Talorchestia deshayesei* (Aud.) (Crustaceae-Amphipoda). Experimentia, *11:* 202–205.
56. Bruce, V. G.; and C. S. Pittendrigh. 1960. Cold Spring Harbor Symp. on Quant. Biol. Vol. 25.
57. De Coursey, P. 1960. Ph.D. Thesis, University of Wisconsin, Madison.
58. —— 1960. Cold Spring Harbor Symp. on Quant. Biol. Vol. 25.
59. Hastings, J. W., and B. M. Sweeney. 1957. The luminescent reaction in extracts of the marine dinoflagellate, *Gonyaulax polyedra*. J. Cell Comp. Physiol., *49:* 209–226.
60. *Handbook of Biological Data*, ed. W. S. Spector. 1956. Philadelphia: W. B. Saunders and Co.

DISCUSSION

Harker: May I put in a plea for not regarding continuous and discontinuous processes in the same way?

When considering transients which are produced by a light or temperature perturbation it is, I think, important to remember that in the results obtained by measuring eclosion of *Drosophila* each dot represents something which has happened to one fly. When there are two successive peaks of eclosion, these represent animals which are likely to have received the signal at very different stages in their development. In particular when a temperature signal has been given, this may affect one stage in the process of molting much more than another. The first peak of eclosion may represent animals which were ready to molt, but which were prevented from doing so by the decrease in temperature; the second peak may include animals also affected by a temperature change which affected their ability to pupate. Another peak may represent animals which were larvae or eggs at the time of the stimulus and which were completely unaffected. The transients may result from the effect of temperature on a non-periodic function.

PITTENDRIGH: The possibility that the temperature-induced transients may result from temperature acting on a non-periodic process has been carefully considered. I believe the analysis of Fig. 6 in my paper, and the similar effects noted for Fig. 1A raise, at least, serious difficulties for this view. I personally can see no "non-periodic process" approach that will accommodate either these effects or the other details of the shape of the transient curves in Fig. 1A. Finally, the results summarized in Figs. 4 and 5 nearly demand, as I discussed, the assumption of a distinct temperature sensitive oscillation.

HASTINGS: I want to have clarified a point in connection with Dr. Hillman's study, where the introduction of a temperature cycle prevented leaf damage in tomatoes kept in constant light. The Earhart Laboratory procedure for changing temperature involved, I believe, moving plants from one temperature room to another by way of a hallway of different light intensity. Although it might have seemed unnecessary at that time, it now is clear that control plants moved in and out through the hallway without temperature change should have been included. Might the prevention of injury have been caused by this daily light [illegible].

Would Dr. Went be willing to comment on this?

WENT: Hillman's work has been repeated, e.g., by Kristoffersen, who moved his plants rapidly between temperature conditions. It was also found that only with temperature fluctuations of more than 4° a response was elicited. Therefore, the mechanism of moving plants in the Earhart Laboratory was presumably not the reason for the response Hillman observed.

BÜNNING: To the question of positive and negative temperature coefficients: two different temperature effects are involved. On the one hand, there is the influence of temperature on the time required for the system to get from one maximum through a minimum to the next maximum. If we measure this, for which purpose we are to work with normal medium temperatures, we mostly find temperature coefficients between 1.0 and 1.1. On the other hand, with extreme low or also sometimes with extreme high temperatures, another effect becomes evident. The system is no longer actually going through the whole way. To speak in terms of relaxation oscillations, the phase of tension is interrupted before the extreme tension of the system is reached. These interruptions occur in many cases of suppressed respiration, not only with extreme high or low temperatures. Respiratory poisons have the same effect. Thus under the influence of low temperatures (mostly between 0 and 10°C.), before the oscillation is stopped at all, very short periods appear, as mentioned in the opening address. This fact is responsible for the negative temperature coefficients which may be 0.8 or even less.

SWEENEY: This may be the case in *Phaseolus* where short periods appear only at quite low temperatures. In *Oedogonium* and in *Gonyaulax* where the length of the period increases with increasing temperature over the whole physiologic range I do not think the low Q_{10} can be explained in this way. I would like to emphasize again that the occurrence of Q_{10} values less than 1.0 is strong evidence for the view that low Q_{10} values reflect an inaccurate temperature compensation mechanism.

BÜNNING: To the question of Dr. Went, how the data on rather low temperature coefficients fit into my older observations showing Q_{10} values of 1.2 in *Phaseolus*, and into a similar Q_{10} in his experiments with plants developing under the influence of light-dark cycles with different total length, deviating more or less from the 24 hour period: the first part of the question has been answered by Dr. Sweeney. In those older experiments the transient periods were not excluded from the calculations. To the second part of the question it may be mentioned that the cycles, as we know, to a certain extent can adjust themselves to a light-dark period deviating from the 24-hour period by as much as ±5 hours. This ability to get adjusted to longer or shorter periods is, as also is known, different with higher or lower temperatures. This may be one of the reasons for the facts observed by Dr. Went.

ASCHOFF: As just mentioned by Pittendrigh, speaking of temperature independence can be misleading. Therefore, why not speak of dependence and say how much and what directions. This seems not only more correct but also more important.

SWEENEY: Yes, of course. This would be very fine and it is certainly unambiguous. But as I pointed out in my paper, the use of the term temperature-independence has been very useful as a way to get the idea across and to get it across quickly. But as we also pointed out in the paper, its meaning should not be misunderstood. I think any term you try to use will be misunderstood by some, and you should try to minimize this.

SOLLBERGER: If several individuals are kept simultaneously at constant external temperature, their own bodies will heat the room against the thermostat. In this way they will in their vicinity evoke a rhythm parallel to their spontaneous periodicity, and they will furthermore exert influence on each other, co-ordinating their spontaneous rhythms.

JOURNAL OF GEOPHYSICAL RESEARCH VOLUME 66, NO. 2 FEBRUARY 1961
pp.589-597

Sound Velocities at the Surface of Deep Sea Sediments[1]

JOHN C. FRY AND RUSSELL W. RAITT

Marine Physical Laboratory
Scripps Institution of Oceanography
University of California
La Jolla, California

Abstract. A study of the initial amplitude of reflection of explosive sound from the sea floor in the Pacific has shown many cases in which the amplitude decreases with increasing angle of incidence and becomes negative at angles of about 74° to 80°. If the sediment can be treated as a fluid, the angle of phase change gives a measure of the sound velocity in sediments at the sea floor. Throughout most of the Pacific, velocities average about 2 per cent less than the bottom water velocity. At some stations, notably those in the Chilean and Aleutian trenches, in the Hawaiian deep, and off the western coast of the United States, sediment velocities were found to be higher than the sound velocity in the overlying water, suggesting the effect of turbidity-current deposits in these areas. Illustrations of these two types of reflection from the sea floor are presented.

Introduction. Seismic records obtained primarily for the study of the crustal structure of the earth beneath the sea are also useful in investigating certain of the physical characteristics of deep sea sediments. Numerous seismic refraction records obtained on Scripps Institution of Oceanography expeditions throughout the Pacific Ocean [*Raitt*, 1952, 1956] show a systematic change in the amplitude of first motion of the first bottom-reflected arrival with increasing angle of incidence. In most cases the amplitude of first motion decreases and becomes negative at large angles of incidence, indicating the widespread existence in the Pacific of a sediment layer of lower sound velocity than that of the overlying water and providing quantitative determinations of *in situ* velocities at the surface of deep sea sediments. Previously, *Hersey, Officer, Johnson, and Bergstrom* [1952] observed a single frequency forerunner to the RSR arrival at distances greater than 35 to 40 miles which they inferred could be due to a low-velocity sediment layer. More recently the constant frequency forerunner was observed by *Katz and Ewing* [1956], who reached similar conclusions. This phenomenon is only rarely observed in the Pacific, however. From sound reflection measurements northwest of Bermuda, *Officer* [1955] considered the changes in reflected energy and travel times with range and frequency and concluded that sediment velocities were less than bottom water velocities. *Shumway* [1956, 1960], *Laughton* [1957], and *Sutton, Berckheimer, and Nafe* [1957] have in some cases measured in the laboratory low sound velocities in samples of deep sea sediments obtained from representative areas of deposition in the Atlantic and Pacific oceans. In the present study the first motion of the bottom reflection is used to indicate the distribution of this low-velocity layer in the deep Pacific and to measure the magnitude of the sound velocities associated with such a layer.

Reflection of sound from the sea floor. From *Rayleigh* [1945, p. 81], the amplitude reflection coefficient R for plane waves reflected from a plane boundary between two fluids of densities ρ_1 and ρ_2 and sound velocities c_1 and c_2 is

$$R = \frac{\rho_2 \cos \theta_i - \rho_1(n^2 - \sin^2 \theta_i)^{1/2}}{\rho_2 \cos \theta_i + \rho_1(n^2 - \sin^2 \theta_i)^{1/2}} \qquad (1)$$

where $n = c_1/c_2$ is the index of refraction and θ_i is the angle of incidence of the plane wave at the fluid boundary. For $c_2 < c_1$ the reflection coefficient decreases from normal incidence to 0 at an angle of incidence

$$\theta_i = \theta_I = \text{ctn}^{-1} \left[\frac{1 - n^{-2}}{(\rho_2 c_2/\rho_1 c_1)^2 - 1} \right]^{1/2} \qquad (2)$$

Sound transmitted through the deep ocean (layer 1) is reflected from the sedimentary layer

---

[1] Contribution from the Scripps Institution of Oceanography, New Series. 1253

Reproduced by Permission

(layer 2) at the ocean floor. At the angle of intromission θ_I, all sound energy is admitted to the lower fluid; none is reflected. For $\theta_i > \theta_I$ the reflected wave is reversed in phase by 180° with respect to the incident wave, and the amplitude coefficient increases rapidly to a value of 1 at $\theta_i = 90°$.

When $c_2 > c_1$, the reflection coefficient R increases from the value at normal incidence to 1 at an angle of incidence,

$$\theta_i = \theta_c = \sin^{-1} c_1/c_2 \qquad (3)$$

For angles of incidence greater than the critical angle, θ_c, the reflected wave is changed in phase from 0° at θ_c to 180° at $\theta_i = 90°$; the reflection coefficient remains unity for $\theta_i > \theta_c$, and total reflection of the incident sound occurs within this range.

Equations 1 and 2 would be modified in the case of a solid lower layer; however, the available evidence indicates that, owing to high porosities, the rigidity of deep sea sediments is probably small ($\mu < 10^9$ dynes cm^{-2}) [*Hamilton*, 1956, 1959] and in this case the change in R is small and has been neglected.

Interpretation of reflection data. The seismic refraction stations selected for this study are widely distributed throughout the Pacific Ocean (Fig. 1). Individual seismic records from each of these stations have been examined to determine the change in the characteristics of the first bottom-reflected signal with increasing range.

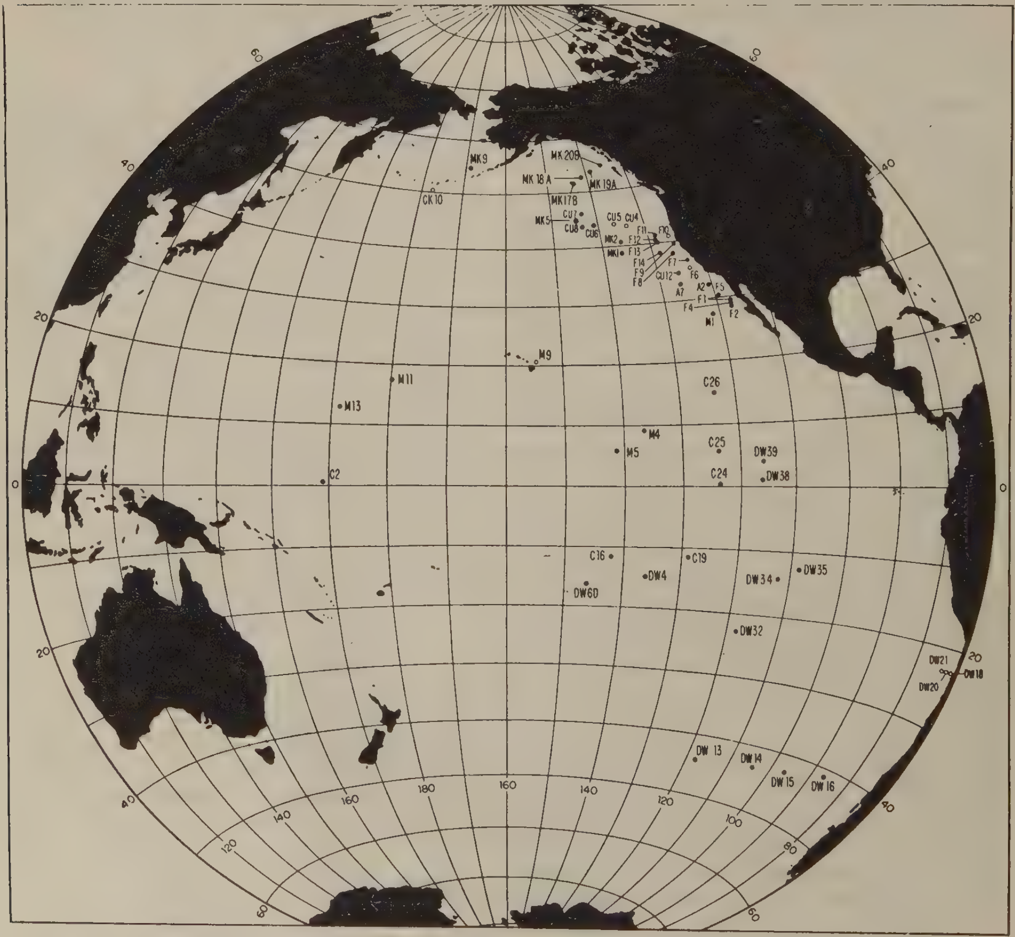
60
60
40
40
20
20
0
0
20
20
40
40
60
60
180
160
140
120
100
80
160
140
120
MK9
CK10
MK 20B
MK 18A
MK 19A
MK17B
MK5
CU7
CU8
CU6
CU5
CU4
MK2
MK1
F11
F10
F12
F13
F14
F9
F8
F7
CU12
F6
A7
A2
F5
F1
F4
F2
M1
M9
M11
M13
C26
M4
M5
C25
DW39
C24
DW38
C2
C16
C19
DW4
DW60
DW34
DW35
DW32
DW21
DW18
DW20
DW 13
DW 14
DW 15
DW 16

Fig. 1. Distribution of seismic refraction stations in the Pacific used to investigate the sound velocity of deep sea sediments. Black dots indicate $c_1/c_2 > 1$; open circles indicate $c_1/c_2 < 1$.

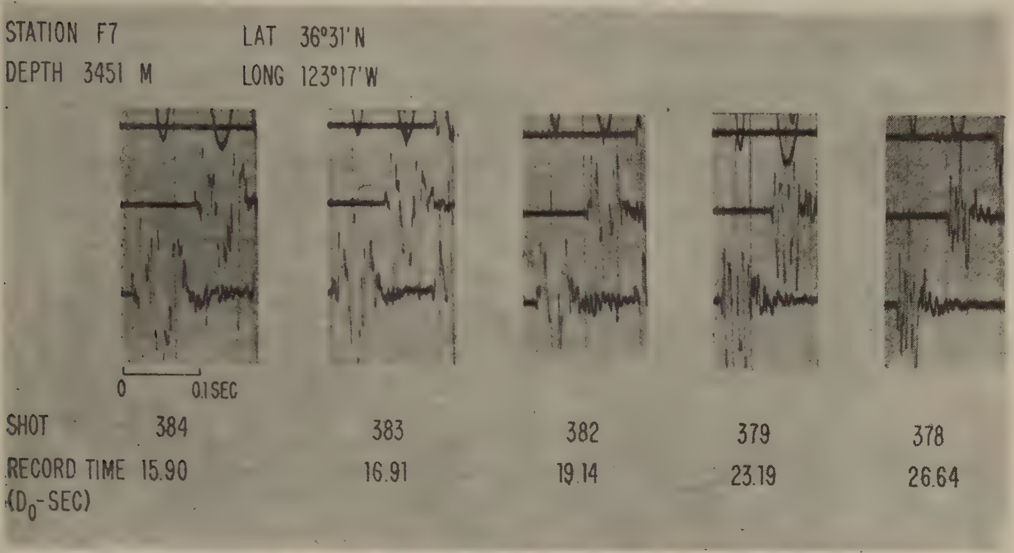

Fig. 2. Illustration of change in the direction of initial motion between shots 383 and 382 at Station F 7. This indicates a lower sound velocity in the sediment than in the overlying water.

Frequently at ranges between 21 and 35 km, depending on the water depth, a change in phase of π, that is a change of the direction of first motion, is observed on the intermediate-frequency channel (30 to 200 cps). Several shots in the vicinity of the phase change are illustrated for station F 7 in Figure 2. When a phase reversal is observed in a shot sequence, indicating $c_1 > c_2$, θ_i is determined, and the calculation of sediment velocity follows from equation 2, assuming a reasonable value of sediment density. At some stations a change in the direction of first motion is not observed, indicating $c_1 < c_2$; in these cases the amplitude of first motion may be used to estimate the critical angle and an approximation of the sediment velocity is given by equation 3.

Ray path calculations. The basis of determining the angle of intromission of a sound ray at the ocean floor is the sound-velocity profile calculated from serial measurement of temperature and salinity at a seismic station. Although sound velocity usually changes only a few per cent with depth, at large angles of incidence refraction can cause significant deviations of ray paths from the usual straight line approximation. To simplify the calculations but still partially account for the effect of refraction, we have adopted an approximation of the sound velocity profile suggested by *Brekhovskikh* [1949] (Fig. 3). In this approximation it is assumed that the velocity profile beneath the mixed layer consists of two layers, the upper one of constant velocity and the lower of constant velocity gradient, 0.018 sec^{-1}. The approximate velocity is fitted to the observed values near the bottom, and the assumed constant velocity is adjusted to give the same sounding velocity as that calculated from the true velocity function. From this simplified velocity function, the angle of incidence θ_i is easily calculated as a function of the direct wave travel time or of the reflected wave travel time. A similar calculation based on the true velocity function is laborious.

The accuracy of this approximate method has been evaluated for one station. A comparison of θ_i obtained by the approximate method with a more accurate computer calculation based on the sound velocity profile at station *Cusp* 12 shows a difference of less than 1°.

Sediment and water density. One of the major uncertainties in the application of equation 2 to determine the *in situ* velocity of deep sea sediments is that of the sediment density *in situ*. The recent measurements by *Shumway* [1960] of the density of deep sea sediments representative of several depositional environments in the Pacific show for nine sediment samples, two consisting of calcareous ooze and the remainder consisting of silt and clay in various gradations,

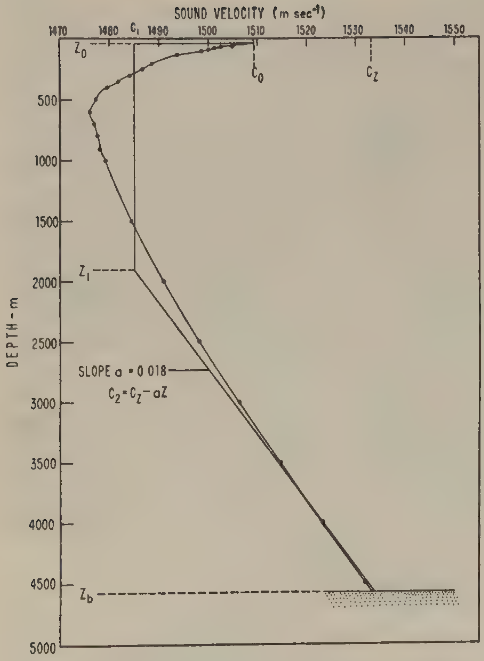

Fig. 3. The observed sound velocity profile at station Cusp 12 and an approximation showing necessary values for ray path calculations.

a range of values from 1.30 to 1.50 g cm^{-3}. We have used his mean value, 1.40 g cm^{-3}, for sediment density. These values are lower than those reported for Atlantic deep sea sediments by *Laughton* [1957] and *Sutton, Berckheimer, and Nafe* [1957]. The mean densities for six of Laughton's samples and twenty of Sutton's samples were 1.60 and 1.61 g cm^{-3}, respectively; however, the latter density, according to Sutton, is more typical of sea mount and turbidity current deposits than of the sea floor. The mean density of bottom water, 1.0277 g cm^{-3}, has been calculated from standard tables [*Kuwahara*, 1939] from temperature and salinity data for each seismic station.

Discussion of results. The records of 56 seismic stations have been examined in this study; those stations for which the sediment velocity has been calculated are listed in Table 1, and the remaining stations for which a qualitative determination of the sediment velocity has been made are listed in Table 2. The last two columns of Table 1 give the sediment velocity both with reference to a single value of c_1 for comparison, and the *in situ* value. At most stations two profiles were made, one toward and the other away from the receiving ship, which permitted independent determinations of the sediment velocity in a station area. These data show quite good agreement. Small differences of between 1 and 4 m sec^{-1} are found for all stations except two, MK 2 and MK 15, located in topographically rough areas characterized by abyssal hills (Hurley, unpublished manuscript, SIO Ref. 60-7, 1960) where the differences are found to be 15 and 9 m sec^{-1}, respectively. Whether such differences are the result of spurious topographic effects or a change in sediment characteristics over relatively short horizontal distances cannot be estimated with certainty owing to limitations in the experimental method. The effect of a systematic change in depth along a profile between the first bottom reflection point and receiving ship may be introduced in the determination of θ_i; however, since for the stations of Table 1 this effect is small compared with other probable errors discussed below, it has been neglected and we have assumed reflection from a plane horizontal surface.

Other sources of error in the determination of sediment velocity are the shot distance of phase reversal, the angle of incidence obtained from the approximate sound velocity profile, and the sediment density. Assuming probable errors of 1.5 km, 1.5°, and 0.1 g cm^{-3}, respectively, the separate resultant errors in sediment velocity are ±6, ±7, and ±12 m sec^{-1}. The independence of errors permits use of the error equation [see, for example, *Worthing and Geffner*, 1943, p. 213] yielding a probable error in sediment velocity of 15 m sec^{-1}. Since the differences in c_2 for the two profiles at a single station are in most cases much lower than this, this error is probably too high but nevertheless is useful in indicating the magnitude of the error arising from these sources.

The results of laboratory measurements by *Laughton* [1957], *Shumway* [1960], and *Sutton, Berckheimer and Nafe* [1957] of the sound velocities in deep sea sediments are useful for comparison with our results (Table 3). The sediment velocities listed in Table 1 have been recalculated with reference to a sound velocity of 1522 m sec^{-1}, the velocity of sound in sea water of temperature 21°C, salinity 35 parts per million.

The sound velocities for deep sea clays are

TABLE 1. Summary of Calculated Sediment Velocities

Station	Lat. (N)	Long. (W)	Depth, meters	Record Time, sec	θ_I	c_1/c_2	c_2*	c_2†
F 1	29°08′	117°34′	3598	S_1 16.52	76.23	1.024	1494	1481
F 2	28°33′	117°20′	3598	S_1 16.41	76.10	1.024	1494	1481
F 4	28°59′	117°29′	3598	S_1 16.61	76.35	1.024	1494	1482
				16.09	75.70	1.026	1492	1479
F 5	30°43′	119°46′	3943	S_1 16.99	75.44	1.027	1490	1484
				17.27	75.78	1.026	1492	1485
F 6	35°09′	123°16′	4071	...	...	0.9537	1604	1597
F 7	36°31′	123°17′	3451	D_0 18.94	80.40	1.012	1512	1497
				18.39	79.90	1.013	1510	1495
F 8	37°28′	125°51′	4365	S_1 18.81	76.05	1.025	1493	1494
				18.58	75.75	1.026	1492	1493
F 10	41°01′	125°56′	3113	...	...	0.9455	1618	1596
MK 1	38°54′	136°10′	4972	S_1 19.49	74.45	1.030	1486	1497
				19.99	75.17	1.028	1489	1500
MK 2	40°18′	136°15′	4611	S_1 22.12	79.24	1.015	1508	1513
				19.23	76.05	1.025	1493	1498
MK 5	45°02′	144°27′	4701	S_1 20.56	76.90	1.022	1497	1504
				19.02	75.00	1.028	1488	1495
A 2	32°28′	120°34′	3772	D_0 15.59	75.58	1.026	1491	1482
A 7	32°59′	125°56′	4394	D_0 18.20	76.66	1.022	1496	1498
				18.76	77.30	1.020	1499	1500
DW 39	4°08′	115°46′	4163	D_0 16.04	74.55	1.030	1486	1482
CU 12	34°29′	126°02′	4583	D_0 19.75	77.10	1.021	1498	1502
M 5	5°51′	141°51′	4811	D_0 17.31	74.36	1.031	1485	1593
				16.77	73.65	1.033	1481	1489

* For c_1 1530 m $\sec^{-1}$.

† In situ sediment velocity.

consistent with the other values given; the velocities of calcareous ooze, however, apparently represent a lower limit for the other three sets. According to the emulsion theory of *Wood* [1941, p. 361] in which lattice nonrigidity was assumed, a lower limit for sound velocity in sediments is predicted to be about 3 per cent less than that in water. *Shumway* [1960] has shown that deviations from Wood's theory, caused by the effect of sediment rigidity and compressibility, are less than 1 per cent for sediment porosities greater than 0.45. Hence the theory is considered to be valid for deep sea sediments where the porosity is usually greater than 0.6 [*Hamilton*, 1959]. Within the limit of probable error our calculated sediment velocities are in agreement with those predicted by the emulsion theory.

The typical occurrence of the low-velocity sediment layer throughout the Pacific Ocean basin is shown in Figure 1. Observed exceptions to this are confined to stations in the Chilean and Aleutian trenches at the edges of the basin (DW 18, 20, 21; CK 10), one in the Hawaiian deep (M 9), near which the submarine slopes average 11° [*Hamilton*, 1957], two at the base of the continental slope of the western United States (F 6, F 10), and two near the region of abyssal hills north of the Mendocino escarpment (CU 4, CU 5). The records obtained at these stations are distinctly different from the other records studied; as θ_i increases, the amplitude of first motion increases until θ_c is reached, which can be seen in the sequence of shot records from station F 10 shown in Figure 4.

For two stations which illustrate the two types of reflection, calculated values of the reflection coefficient R and the graphs of equation 1 are shown in Figures 5 and 6. In the calculation of the reflection coefficient, R is assumed to be proportional to the amplitude of initial motion, the travel time of the first bottom-reflected arrival, the 2/3 power of the charge weight in pounds, and the square root of the coefficient

TABLE 2. Qualitative Determination of Sediment Velocities for Seismic Stations in Figure 1

Station	Latitude	Longitude	Sediment Sound Velocity	Sea Depth, meters
F 9	39°13′N	125°03′W	$c_2 < c_1$	3248
F 11	41°16′N	128°30′W	$c_2 < c_1$	3156
F 12	40°31′N	128°24′W	$c_2 < c_1$	3222
F 13	40°04′N	128°11′W	$c_2 < c_1$	4510
F 14	38°34′N	128°00′W	$c_2 < c_1$	4681
MK 9	54°45′N	168°16′W	$c_2 < c_1$	1939
MK 17B	51°32′N	144°40′W	$c_2 < c_1$	4219
MK 18A	52°32′N	141°45′W	$c_2 < c_1$	3776
MK 19A	53°02′N	139°20′W	$c_2 < c_1$	3596
MK 20B	54°04′N	135°29′W	$c_2 < c_1$	2653
DW 4	14°59′S	136°02′W	$c_2 < c_1$	4492
DW 6D	16°08′S	146°15′W	$c_2 < c_1$	1301
DW 13	44°27′S	117°45′W	$c_2 < c_1$	2685
DW 14	43°45′S	104°28′W	$c_2 < c_1$	3786
DW 15	42°44′S	96°06′W	$c_2 < c_1$	4565
DW 16	41°05′S	86°39′W	$c_2 < c_1$	3304
DW 18	23°18′S	70°53′W	$c_2 > c_1$	3097
DW 20	23°18′S	71°22′W	$c_2 > c_1$	7386
DW 21	23°29′S	72°59′W	$c_2 > c_1$	3736
DW 32	23°18′S	117°49′W	$c_2 < c_1$	3039
DW 34	14°44′S	112°11′W	$c_2 < c_1$	3096
DW 35	13°31′S	108°31′W	$c_2 < c_1$	3462
DW 38	1°27′N	116°13′W	$c_2 < c_1$	3825
M 1	27°24′N	121°35′W	$c_2 < c_1$	4176
M 4	9°38′N	136°19′W	$c_2 < c_1$	4804
M 9	20°26′N	154°54′W	$c_2 > c_1$	5199
M 11	17°20′N	179°58′W	$c_2 < c_1$	4929
M 13	12°39′N	172°10′E	$c_2 < c_1$	5547
C 2	00°47′N	169°11′E	$c_2 < c_1$	4414
C 16	11°20′S	142°25′W	$c_2 < c_1$	4590
C 19	11°46′S	128°57′W	$c_2 < c_1$	4073
C 24	00°11′N	123°26′W	$c_2 < c_1$	4463
C 25	5°47′N	123°59′W	$c_2 < c_1$	4264
C 26	14°58′N	124°12′W	$c_2 < c_1$	4393
CU 4	43°00′N	134°27′W	$c_2 > c_1$	3872
CU 5	43°45′N	137°06′W	$c_2 > c_1$	4026
CU 6	43°58′N	140°38′W	$c_2 < c_1$	4304
CU 7	45°34′N	143°11′W	$c_2 < c_1$	4550
CU 8	43°49′N	143°07′W	$c_2 < c_1$	4234
CK 10	50°19′N	177°39′W	$c_2 > c_1$	7308

of refraction. The amplitude of initial motion and the travel time of the first bottom-reflected arrival are obtained from the seismic record. The amplitude of initial motion is proportional to the sound pressure received at the listening hydrophone [*Raitt*, 1952]. The travel time of the first bottom-reflected arrival is used to establish the inverse square spreading loss between the shot and the receiving hydrophone.

Similarity laws applied to explosive sound sources show that the energy spectrum for the frequency range of interest varies as the 4/3 power of the charge weight in pounds; hence, the amplitude reflection coefficient varies as the 2/3 power of the charge weight. The coefficient of refraction is proportional to the change in sound intensity relative to the intensity determined for inverse square spreading. The refraction coefficient, which is significant in value at large angles of incidence is determined from ray path calculations according to the approximate sound velocity structure. For these stations, sound refraction reduces the sound intensity at the receiving hydrophone at large angles of

TABLE 3. Comparison of Laboratory Measurements of Sediment Velocities and In Situ Velocities Corrected for Laboratory Conditions

Sediment type	Velocities, km sec^{-1}			
	Shumway	Sutton	Laughton	This study†
Pelagic clay or terrigenous sediments*	1.49–1.60	1.49–1.57	1.47–1.54	1.47–1.61
Calcareous ooze	1.49–1.52	1.48–2.37	1.54–1.63	1.47–1.48

* Sediment with less than 30 per cent calcium carbonate.

† DW39 and M5 assumed calcareous ooze [*Revelle, Bramlette, Arrhenius and Goldberg*, 1955]; remainder pelagic clay or terrigenous sediments.

incidence. An arbitrary reference level is chosen so that the theoretical and calculated values of R are in agreement at normal incidence. In Figure 5 a sediment density of 1.4 g cm^{-3} and the water/sediment velocity ratio given in Table 1 have been used with equation 1; in Figure 6 a higher density, 1.6 g cm^{-3}, more representative of the values reported by *Sutton, Berckheimer, and Nafe* [1957] for turbidity current deposits, was introduced and the water/sediment velocity ratio was determined from the critical angle using equation 3. The decrease in R at large angles of incidence is probably due to the change in pulse shape beyond the critical angle described by *Arons and Yennie* [1950].

The two observed types of reflection from the sea floor are not necessarily inconsistent with the results of *Mackenzie* [1960], who noted, 'The ratio of the velocities determined by the fit of the theoretical curves indicated that $c_2/c_1 > 1$ for all the cases although for two of the three bottoms it might have been expected that the ratio would be less than unity.' The present method accounts only for the energy reflected from the sediment surface; sound energy is also reflected from sub-bottom layers or refracted

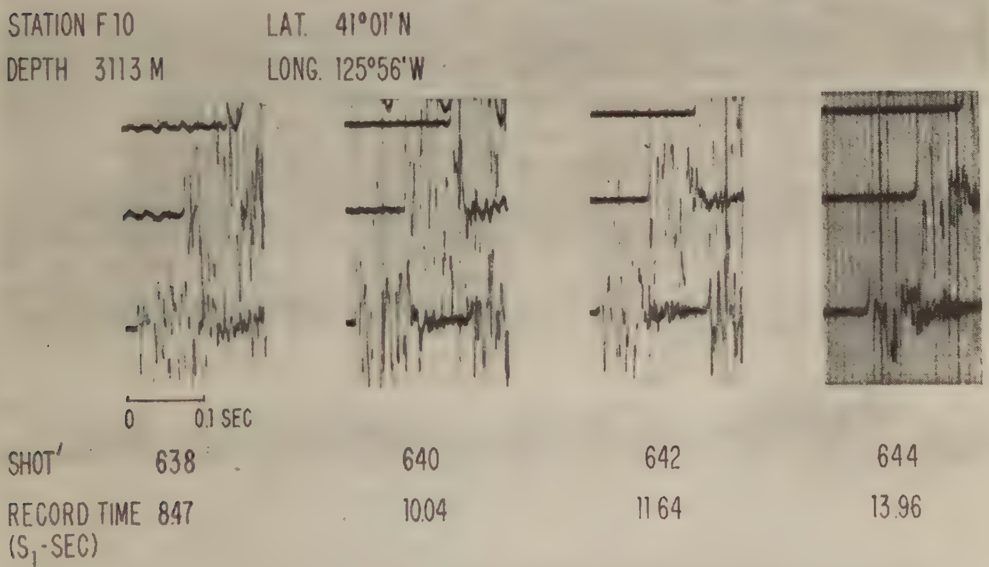

Fig. 4. Increase in the amplitude of initial motion with increasing angle of incidence at station F 10, indicating high sediment velocities relative to water.

upward owing to a positive velocity gradient within the sediment layer, as observed by *Hill* [1952], which may easily obscure the one type of reflection (Fig. 5), particularly at angles of incidence near the angle of intromission. This is a more probable explanation than the change in sediment velocity with higher frequencies [*Officer*, 1955], since *Laughton* [1957] has shown that the sound frequency must be increased to the megacycle range to obtain even a 1 per cent change in sound velocity.

Conclusions. The sediment velocities determined in this study are in good agreement with experimental determinations of the sound velocities of unconsolidated sediment samples in the laboratory. From this we conclude that this method provides a direct and useful means for investigating *in situ* sediment velocities, and hence, the reflective characteristics and nature of deep sea sediments. Throughout most of the Pacific, sound velocities average about 2 per cent less than the bottom water velocity, causing relatively high reflection losses of sound energy. Those few stations at which the low-velocity sediment layer was not observed were all in areas believed to be receiving turbidity current deposits capable of increasing the sediment velocity. However, the sparse distribution of deep sea stations does not exclude the possibility that high velocities occur elsewhere in volcanic deposits or in authigenic manganese crusts. The available evidence indicates that coarse sands can be deposited in deep ocean basins where these are not barred by submarine topography [*Menard*, 1959]. From this we would expect that, owing to the absence of oceanic trenches in the Atlantic, the low-velocity sediment layer is less extensive there than in the Pacific.

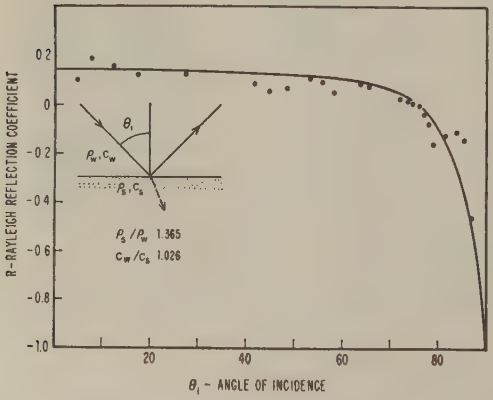

Fig. 5. Rayleigh reflection coefficient and calculated sediment reflection coefficients for various angles of incidence, station F 5.

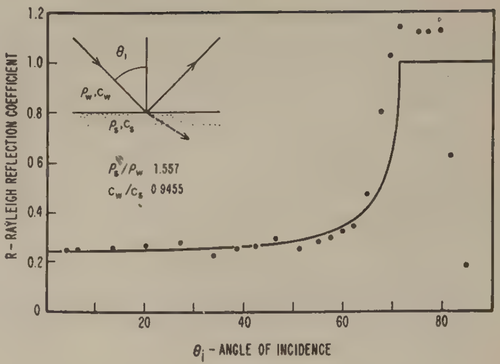

Fig. 6. Rayleigh reflection coefficient and calculated sediment reflection coefficients for various angles of incidence, station F 10.

Acknowledgments. The seismic refraction records used in this study have been made on many expeditions and therefore it is not possible to mention personally all those who have been helpful to us. However, we wish to acknowledge the cooperation and assistance of the officers and men of U.S.S. *Epcer* 857, R.V. *Horizon*, R.V. *Baird*, R.V. *Stranger*, and R.V. *H. M. Smith*, the members of the firing and recording groups, and Gloria J. Slack and Wanda R. Willson, who have helped in many ways with the records. One of us (JCF) was supported by the Office of Naval Research and the U. S. Navy Postgraduate School. The remainder of the work was supported by the Office of Naval Research and the Bureau of Ships of the Navy Department under contracts Nobsr 43356 and 72512, Nonr 2216(01) and 2216(05) with the University of California. We wish to thank Dr. F. N. Spiess and Dr. G. G. Shor, Jr., for critically reading the manuscript.

REFERENCES

Arons, A. B., and D. R. Yennie, Phase distortion of acoustic pulses obliquely reflected from a medium of higher sound velocity, *J. Acoust. Soc. Am.*, *22*, 231–237, 1950.

Brekhovskikh, L. M., The propagation of sound in an underwater sound channel, *Doklady Akad. Nauk SSSR*, *69*, 157–160, 1949.

Hamilton, E. L., Low sound velocities in high porosity sediments, *J. Acoust. Soc. Am.*, *28*, 16–19, 1956.

Hamilton, E. L., Marine geology of the southern

Hawaiian Ridge, *Bull. Geol. Soc. Am.*, *68*, 1011–1026, 1957.

Hamilton, E. L., Thickness and consolidation of deep sea sediments, *Bull. Geol. Soc. Am.*, *70*, 1399–1424, 1959.

Hersey, J. B., C. B. Officer, H. R. Johnson, and S. Bergstrom, Seismic refraction observations north of the Brownson deep, *Bull. Seism. Soc. Am.*, *42*, 291–306, 1952.

Hill, M. N., Seismic refraction shooting in an area of the Eastern Atlantic, *Phil. Trans. Roy. Soc. London A*, *244*, 561–596, 1952.

Katz, S., and M. Ewing, Seismic refraction measurements in the Atlantic Ocean, 7, Atlantic Ocean basin, west of Bermuda, *Bull. Geol. Soc. Am.*, *67*, 475–510, 1956.

Kuwahara, S. Velocity of sound in sea water and calculation of the velocity for use in sonic soundings, *Hydrograph. Rev.*, *16*, 123–140, 1939.

Laughton, A. S., Sound propagation in compacted ocean sediments, *Geophysics*, *22*, 233–260, 1957.

Mackenzie, K. V., Reflection of sound from coastal bottoms, *J. Acoust. Soc. Am.*, *32*, 221–231, 1960.

Menard, H. W., Geology of the Pacific sea floor, *Experientia*, *15*, 205–213, 1959.

Officer, C. B., A deep sea seismic reflection profile, *Geophysics*, *20*, 270–282, 1955.

Raitt, R. W., Geophysical measurements, *Symposium on Oceanog. Instrumentation*, Natl. Research Council Natl. Acad. Sci. U. S., 70–84, 1952.

Raitt, R. W., Seismic refraction studies of the Pacific Ocean basin, *Bull. Geol. Soc. Am.*, *67*, 1623–1640, 1956.

Lord Rayleigh, *The Theory of Sound*, Vol. II, Reprinted, Dover, New York, 504 pp., 1945.

Revelle, R. R., M. N. Bramlette, G. Arrhenius, and E. D. Goldberg, Pelagic sediments of the Pacific, 221–236 in *Crust of the Earth*, edited by A. Poldervaart, *Geol. Soc. Am. Spec. Paper 62*, 762 pp., 1955.

Shumway, G., A resonant chamber method for sound velocity and attenuation measurements in sediments, *Geophysics*, *21*, 305–319, 1956.

Shumway, G., Sound speed and absorption studies of marine sediments by a resonance method, *Geophysics*, *25*, 451–467, 1960.

Sutton, G. H., H. Berckheimer, and J. E. Nafe, Physical analysis of deep sea sediments, *Geophysics*, *22*, 779–812, 1957.

Wood, A. B., *A Textbook of Sound*, G. Bell and Sons, London, 578 pp., 1941.

Worthing, A. G., and J. Geffner, *Treatment of Experimental Data*, Wiley, New York, 342 pp., 1943.

(Manuscript received August 22, 1960; revised November 7, 1960.)

REPRINT FROM

CALIFORNIA FISH and GAME

"CONSERVATION OF WILDLIFE THROUGH EDUCATION"

VOLUME 47 APRIL, 1961 NUMBER 2

pp.163-174

LIFE-HISTORY AND ECOLOGIC NOTES ON THE BLACK CROAKER[1]

CONRAD LIMBAUGH
Scripps Institution of Oceanography,
University of California, La Jolla

INTRODUCTION

The black croaker, *Cheilotrema saturnum* (Girard) belongs to the Sciaenidae, a fish family containing many important food, game, and bait species in tropical and temperate regions around the world. The croakers are largely confined to shallow waters over sandy and muddy bottoms, chiefly along continental shores; only a few live around coral or rock, about tropical islands or in fresh waters. The family is most abundantly developed along the tropical shores of the eastern Pacific and the Californian species are outliers of that rich fauna.

Eight kinds of croaker are native to California (two others, in recent years, have been successfully introduced into Salton Sea). The largest of the eight, the white seabass, *Cynoscion nobilis* (Ayres), attains a weight of over 70 pounds and is important to commercial and sport fishermen alike. The smallest, the queenfish, *Seriphus politus* Ayres, is utilized almost exclusively for bait. The five other native sciaenids of California are: spotfin croaker, *Roncador stearnsii* (Steindachner); white croaker, *Genyonemus lineatus* (Ayres); yellowfin croaker, *Umbrina roncador* Jordan and Gilbert; California corvina, *Menticirrhus undulatus* (Girard), and shortfin corvina, *Cynoscion parvipinnis* (Ayres). A ninth species, *Sciaena thompsoni* Hubbs, was once recognized, but recently has been shown to have been based on a young yellowfin croaker and thus is not valid (Carl L. Hubbs, personal communication).

Except for the black croaker and the shortfin corvina, all native Californian sciaenids are commonly captured and are familiar to most fishermen in southern California, where, within the state, several of the species are largely confined. The lack of familiarity with the short-

---

[1] Contribution from the Scripps Institution of Oceanography, New Series. 1257
Preparation of this manuscript was aided by the Conrad Limbaugh Memorial Fund and by a grant from the Permanent Science Fund of the American Academy of Arts and Sciences.

Editorial Note.—This report, based on a manuscript prepared by the author prior to his death, has been revised and brought up-to-date by Howard M. Feder, Hartnell College, Salinas, California. Carl L. Hubbs, under whom Conrad Limbaugh worked as a graduate student, and John E. Fitch assisted in the preparation of the final draft.

Conrad Limbaugh, chief diving officer at Scripps Institution of Oceanography and one of the world's foremost underwater naturalists, had been working on numerous and diverse research projects before he met an untimely death in a diving accident in the Mediterranean on March 20, 1960. Many of his projects, including this paper, were left unfinished. However, because of the extensive field notes and photographic records he maintained, it is anticipated that the results of most of these studies can be assembled and eventually published so the vast wealth of his accumulated knowledge will not be lost.

(249)

fin corvina is readily explained, because only on rare occasions and in small numbers, during the present century, has it visited our shores from the south. The black croaker, however, as the present study shows, is relatively abundant in southern California; it has kept out of the fishing public's eye by reason of its retiring habits.

During recent years, with the advent and development of SCUBA diving which has increasingly been applied to scientific research under water, the secretive habits of the black croaker have been revealed, and its life history has been elucidated. Bits of information have been pieced together until now a relatively connected account of its life ways can be formulated. This knowledge has accrued primarily as a result of countless hours of underwater observation at all seasons, over a period of more than 12 years. It has been supplemented by observations, over a two-year period, of young individuals in aquaria at the Scripps Institution of Oceanography (particularly of one very young individual whose daily progress and color transformation was closely followed).

Most of the diving was done at Point Dume, Santa Catalina Island, Newport Beach, Laguna Beach and La Jolla, in California, and at the Coronado Islands, Ensenada and Playa María Bay, Baja California. During the course of the investigation, specimens were collected at Newport Beach, Corona Del Mar, La Jolla and Ensenada.

Without such knowledge as has been acquired, intelligent management of the resource, should it become desirable or necessary, would not be possible.

DISTRIBUTION

The distribution of the black croaker has been variously stated by different authors, as follows:

> "Santa Barbara southward" (Jordan and Gilbert, 1881b).
>
> "Pacific Coast, north to Point Concepcion" (Jordan and Gilbert, 1883).
>
> "Coast of Southern California, north to Santa Barbara" (Jordan and Eigenmann, 1889).
>
> "Coast of Southern California, from Santa Barbara to Cerros Island" (Jordan and Evermann, 1898).
>
> "Santa Barbara south to the Gulf of California" (Starks and Morris, 1907).
>
> ". . . has not been reported north of Santa Barbara. Its range extends southward along the coast of Lower California" (Starks, 1919).
>
> "Santa Barbara to Cerros Island" (Ulrey and Greeley, 1928).
>
> "Point Conception to Cerros Island on the coast of Lower California" (Walford, 1931).
>
> "Gulf of California to Santa Barbara" (Barnhart, 1936).
>
> "Coast of California and west coast of Mexico, from Point Conception southward into the Gulf of California" (Skogsberg, 1939).
>
> "Point Conception south along the Mexican coast and into the Gulf of California" (Roedel, 1948 and 1953).
>
> "Santa Barbara to Cape San Lucas, and into Gulf of California" (Cannon, 1953).
>
> "Costa de California desde Punta Concepcion hasta el Golfo de California" (Berdegué A., 1956).

(250)

Specific locality records are given as follows:

"San Diego", or "San Diego Bay" (Girard, 1858; Günther, 1860; Steindachner, 1879; Smith, 1883; Jordan and Gilbert, 1880, 1881a; Eigenmann, 1892; Eigenmann and Eigenmann, 1892; Starks and Morris, 1907).

"San Pedro" (Jordan and Gilbert, 1881b; Eigenmann and Eigenmann, 1892; Craig, 1926, 1928).

"Santa Barbara" (Jordan and Gilbert, 1881b; Eigenmann and Eigenmann, 1892).

"Gulf of California" (Albatross Station 3026 . . .) (Starks and Morris, 1907).

"Newport" and "Laguna" (Metz, 1912).

"Venice" (Ulrey and Greeley, 1928).

Specimens in the Scripps Institution of Oceanography collection were taken at and near La Jolla, Mission Bay and San Diego Bay, in California, and in Todos Santos, Playa María and Turtle bays, and at Lagoon Head, in Baja California. John E. Fitch (personal communication) indicates there are no reliable reports of black croakers south of Santa María Bay, Baja California.

The range of the species, according to present indications, extends from the Santa Barbara Channel in California (near Pt. Conception) to Santa María Bay in southwestern Baja California. The inclusion of the Gulf of California in the range has rested on two specimens collected by the *ALBATROSS* on March 25, 1889, at Lat. 31° 22′ 00″ N., Long. 114° 07′ 45″ W., near the head of the Gulf. A comparison of these with the two cotypes of *Amblodon saturnus* Girard (1858) disclosed differences that seem to indicate the form occurring in the upper part of the Gulf is either specifically or subspecifically distinct. The only other member of the genus *Cheilotrema* is a very similar form in Peru, namely *Cheilotrema fasciata* Tschudi (1845), the type species of the genus (Carl L. Hubbs, personal communication).

The California species has been referred successively to the genera *Amblodon, Rhinoscion, Corvina, Sciaena* and finally *Cheilotrema,* where it may rest pending the much needed revision of the eastern Pacific sciaenids (Carl L. Hubbs, personal communication).

IMPORTANCE AND ABUNDANCE

Earlier authors rated the black croaker a food fish of some importance (Jordan and Eigenmann, 1886; Jordan and Evermann, 1898; Walford, 1931; Hiyama, 1937; and others). It was reported abundant in San Diego Bay by Eigenmann (1892), and the "Chinese croaker," as it was called, was commonly caught there in the first decade of this century (Carl L. Hubbs, personal communication). Metz (1912) stated that it was common at Newport and Laguna.

Although later authors (Skogsberg, 1939; Roedel, 1948, 1953; and others) have regarded it as rather rare, diving observations have revealed it is fairly common and black croakers do occur rather frequently in the spear fisherman's catch. Very likely, however, the species was more abundant in former years. Pollution may have played an important role in limiting their numbers, especially in San Diego Bay and in the metropolitan district about Los Angeles. Part of the decrease, however, may be attributable to a change in fishing gear: the large beach seines formerly used to supply the fresh fish market probably were much more effective than the gear currently used for catching them.

HABITAT

The habitat of the black croaker has been reported as the open coast, bays, sloughs and fairly deep water (Skogsberg, 1939; Roedel, 1948, 1953). In the present study, adults were observed only along open rocky coasts, although a few juveniles were seen near rocks in the entrance to Newport Bay. The adults generally have been associated with rocks, and most were in fair-sized rock caves or dark crevices, but in murky water several schools were noted 8 to 10 feet off the bottom in patches of ribbon kelp, *Egregia laevigata* Setchell. The aggregations in the caves were often so dense that a single thrust with a spear would impale one or two small adults. Occasionally during the summer some adults, displaying the juvenile striped color pattern described below, were observed over sand patches among the shallow reefs. (It should be kept in mind, however, that diving was heavily concentrated in rocky areas).

Although adult black croakers usually live in water 10 to 50 feet deep, they have been observed on rare occasions as deep as 150 feet and as shallow as four. Their center of abundance is at approximately 21 feet. Their rarity in deeper waters, in the areas of observation, may have been due to lack of suitable rock crevices or caves there.

In more turbid waters, as in the coastal bays where they have been seined and trawled in considerable numbers, black croakers are apparently much less restricted to rocky retreats (Carl L. Hubbs, personal communication).

The young, to a standard length of about 88 mm. (3.5 inches) are concentrated at a depth of about 8 to 10 feet, and range from 4 to 18.

APPEARANCE AND HABITS OF THE ADULTS

The adults are easily approached in caves and tunnels 10 to 50 feet below the surface, where their deep brown or black color renders them almost invisible to the human eye. Outside the caves and tunnels they are in almost constant motion, and when approached promptly seek shelter among the rocks.

Their ability to change color has given rise to several unauthorized common names, such as blue fish (Craig, 1928), black perch (Walford, 1931; Craig, 1926), black bass and blue bass (Craig, 1926; Walford, 1931; Roedel, 1948, 1953), striped croaker, and blue croaker. A number of distinct color patterns have been observed in adults. The coloration developed in the caves is dark brown, at times with a faint dark band across the anterior back. This band is said to fade with age (Starks, 1919), and to become more distinct at night (Barnhart, 1936). Except for cream-colored spots, the night pattern (Figure 1) is essentially the same as that displayed in caves during daylight. A light tan color, without the band, may be displayed in clear, open water, whereas a striped pattern is assumed over sand patches, especially by juveniles.

The striped pattern provides good protection on the sand. The longitudinal stripes against a background of ripple marks render them almost invisible to the human eye at a distance of 15 feet. The assumption of the striped pattern by the adult may also be related to breeding. Any sand-colored or light-colored fish is difficult to see against

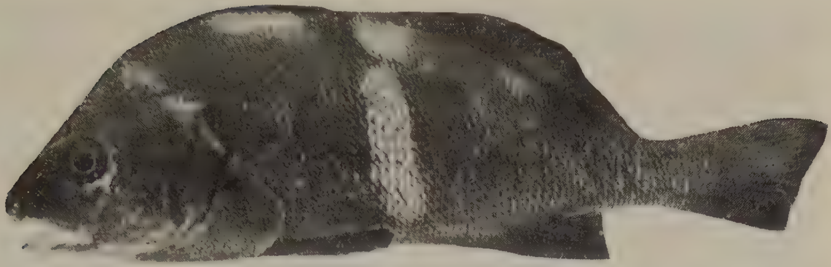

FIGURE 1. A live adult black croaker, *Cheilotrema saturnum*, exhibiting the nocturnal color pattern. *Photograph by Conrad Limbaugh.*

a sand background, but the stripes blend so well with the parallel sand-level marks at the bases of rocks, to which the fish retreat when frightened, as to increase markedly the concealing effect. Striped individuals seldom or never retreat into caves or rock crevices, whereas dark or tan-colored ones always do. A striped fish turns dark when speared. Black croakers when brought to the surface may appear bluish or olive. On the upper parts of the fish, the scale bases have a coppery luster becoming whiter on the lower parts.

FOOD

Black croakers have been reported to eat small crabs and shrimps (Skogsberg, 1939). The present study indicates they feed exclusively on crustaceans, and mainly on rock-dwelling crabs such as the lumpy crab, *Paraxanthias taylori* Stimpson and young moss-covered crabs, *Loxorhynchus crispatus* Stimpson. The lumpy crab seems to be favored. Red-and-white shrimp, *Hippolysmata californica* Stimpson, and various amphipods, are also consumed. In general, the black croaker is nocturnal in its feeding and other behavior.

SPAWNING

Spawning takes place in the late spring and early summer (Skogsberg, 1939). Plankton tows over the breeding grounds of San Diego Bay from May through August (Eigenmann, 1892) and at La Jolla in the summer have yielded collections of their eggs. A striped female speared in August had ripe ovaries. Juveniles have been taken only in August, September and October.

Clusters of striped adult black croakers mixed with aggregations of striped and barred adults of the California sargo, *Anisotremus davidsoni* (Steindachner) have been observed early in July, in shallow water over sand patches near rocks. The almost constant motion of these fish, repeatedly covering the same area, seemed to represent breeding behavior.

Eigenmann (1892) reported that black croakers emit croaking sounds during the breeding season. Croaking or drumming noises apparently produced by black croakers have been detected at the entrance to Newport Bay, but were not correlated with spawning behavior.

Eigenmann further indicated that males entered San Diego Bay in January and February, and that ripe males were taken there in March

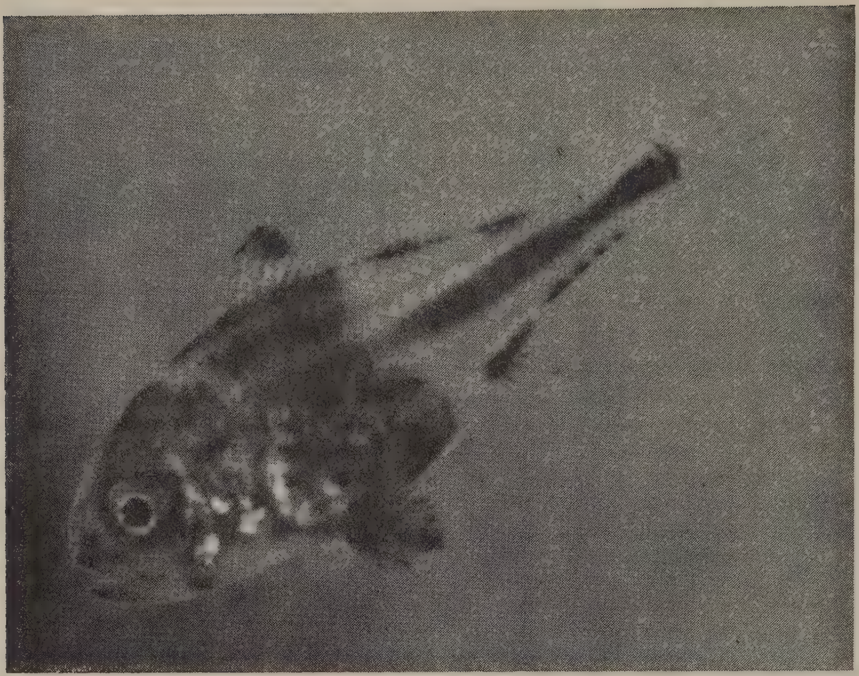

FIGURE 2. A black croaker 14 mm. in standard length collected September 6, 1950, the smallest specimen obtained during the investigation. *Photograph by Conrad Limbaugh.*

and ripe females in April and May. Possibly due to the more rapid increase of temperatures in the bays, breeding occurs earlier there than along the open coast.

The tiny, colorless eggs, 0.78 mm. in diameter, resemble those of the diamond turbot, *Hypsopsetta guttulata* (Girard). They are pelagic and drift with the currents until they hatch. They are reported to hatch within 18 to 48 hours (Eigenmann, 1892).

CHANGES IN COLORATION AND GROWTH OF THE YOUNG

The smallest black croaker taken during this study was slightly shorter than 14 mm. in standard length when photographed six days after capture (Figure 2). It was caught on September 6 at a depth of about 10 feet near a rocky reef, within 18 inches above the sand bottom. It was swimming at the rear of a school of striped black croaker, California sargo and California salema, *Xenistius californiensis* (Steindachner), juveniles. Some adult black croakers also were included.

This young fish, which was estimated to be from four to six weeks old, differed markedly from the other juveniles and the adult black croakers in the school. The lips, top of the head, opercle and trunk back to the soft dorsal were black, except for a light-tan blotch on top of the head in front of the eye and another blotch on the nape. The underside of the head and body in advance of the pelvic fins was translucent tan. The posterior half of the fish was transparent, except for some prominent black markings. An intensely black median stripe, as wide as the eye, extended from its origin, slightly before the vertical through the anus, backward to the midline of the caudal peduncle. Following a constriction on the peduncle, the band broadened into an inky-black rather oblong blotch. This blotch was almost completely separated by a vertical light streak from a narrow blackish crescent at the extreme base of the caudal rays. Other black marks on the body comprised two linear spots at the base of the dorsal soft-rays, and a similar spot at the base of the anal rays. This latter was

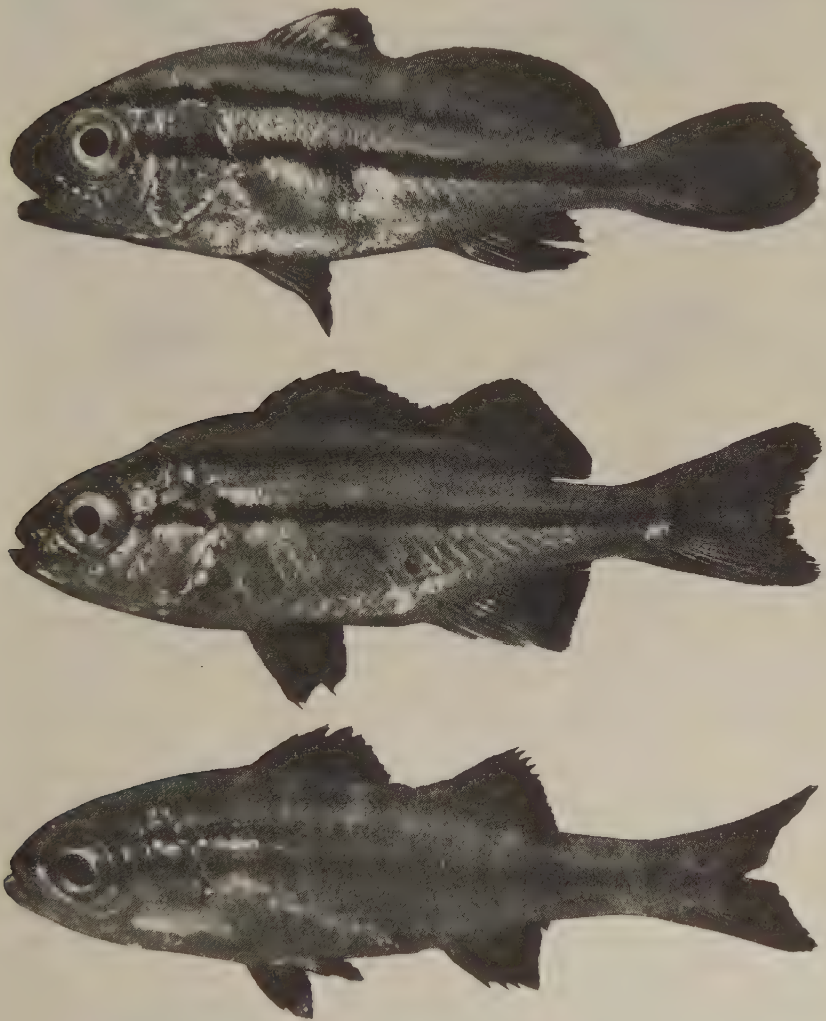

FIGURE 3. (Top.) The 14 mm. juvenile (Figure 2) after six weeks growth in an aquarium; standard length now 25 mm. The downward-curved anterior pelvic ray is typical for juvenile black croakers and apparently is of some sensory significance. (Center.) Juvenile California sargo, *Anisotremus davidsoni,* collected October 17, 1950 and photographed October 24, 1950. (Bottom.) Juvenile California salema, *Xenistius californiensis,* collected September 6, 1950; photographed October 24, 1950. Note the striking similarities in the juvenile color patterns of the three species, all of which school together. *Photographs by Conrad Limbaugh.*

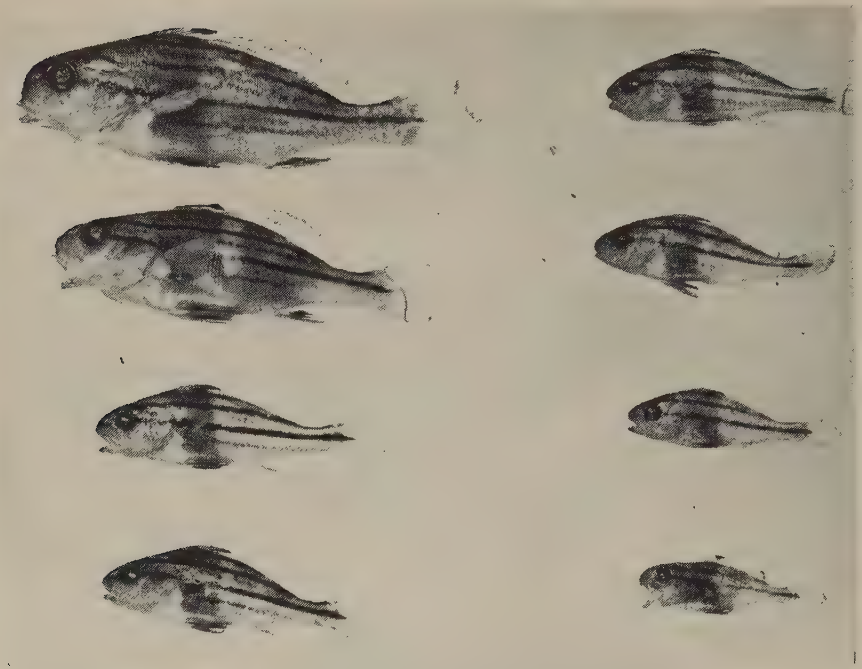

FIGURE 4. A series of juvenile black croakers, collected August 30, 1950, exhibiting the colorational changes that occur with increasing size (24 to 58 mm. in standard length). *Photograph by Conrad Limbaugh.*

in line with about four not completely separated spots on the ventral edge of the caudal peduncle.

The pelvics, pectorals and tip of the spinous dorsal were black. The anal fin carried a few dusky specks anteriorly, chiefly along its base. The lower two-thirds of the spinous dorsal was whitish, somewhat speckled, darkening to gray at the base. The soft dorsal and caudal were indistinctly speckled outward. The pupil was black, the iris gray. The black lining of the body cavity showed through the flesh.

It was maintained alive in an aerated aquarium supplied with running sea water. For the first few weeks it was fed live brine shrimp, which it ate regularly. As it grew, this diet was supplemented by mussel (*Mytilus* sp.), fish and chopped liver. In six weeks it grew to a length of 25 mm. and had assumed the juvenile color pattern. It now swam closer to the bottom of the aquarium.

At this 25 mm. size (Figure 3, top) it bore three black stripes, each much narrower than the eye. One, originated on the snout, extended through the eye, and continued, along the midline of the sides, to the base of the caudal fin. A slightly narrower stripe began above the eye and extended to the top of the caudal peduncle. The third and uppermost stripe roughly paralleled the dorsal contour from a point just above and behind the eye to the front of the soft dorsal. The background color was silvery-gray. The fins were colored much as at the

14 mm. stage, except for the slight yellowish color in the caudal and a clearing of the pectorals; the anterior pelvic rays had become silvery and elongated, with a downward curve at the tip. Presumably this modification of the pelvic fin has some sensory significance, for at this size black croakers begin to swim close to the sand.

Another pattern (Figure 4), superimposed when fish at this size become sick, frightened or preserved, is normally exhibited at night. The nocturnal coloration is a modification of the pattern characterizing the 14-mm. stage day and night. The principal feature is a vertical brown bar four-fifths as wide as the head at the base of the first dorsal fin, narrowing downward to half this width at the abdomen.

By the time they reach the length of 32 mm., black croakers have developed a fourth lengthwise stripe, below the other three. It extends from the pectoral fin to the lower edge of the caudal peduncle, where it continues to the tail fin.

At 38 mm. the nocturnal pattern is modified by two additional bars, which at their origin along the base of the soft dorsal are half as wide as the head is long. These bars fade out near the midline of the body.

By the time the young attain a length of 50 mm. the two posterior bars have become fused and cover the entire posterior half of the fish, with the exception of a whitish spot at the base of the soft dorsal fin. The fish now appears to be dark-brown, with a light band below the front of the soft dorsal. The lengthwise stripes are still readily discernible through this color pattern, and somewhat interrupted dusky stripes have become interpolated between the main blacker stripes.

When they attain a standard length of about 120 mm. (nearly five inches), black croakers become much darker, but retain the light bar at night. This seems to be the same light bar that is exhibited by adults at night (Figure 1).

The juvenile color pattern is so different from that of the adults it led to the erection of a nominal species, *Corvina jacobi* (Steindachner, 1879). In a parallel situation, Hubbs and Walker (1951) showed that the strongly striped young of *Elattarchus archidium* (Jordan and Gilbert), which superficially resemble young black croakers, had been described as *Odontoscion australis* Meek and Hildebrand.

HABITS OF THE YOUNG

Under natural conditions juvenile black croakers 14 to 50 mm. in standard length school together with the young California sargo and California salema (Figure 3, center and bottom). All three have remarkably similar striped color patterns (Steindachner, 1879, commented on such parallel color patterns).

Once formed, such a school or aggregation is maintained near the base of a rock, over sand bottom, in water 4 to 18 feet deep, along the open coast just beyond the surf. The rocks obviously afford protection from the surge. Within the somewhat lenticular-shaped school the individuals are 6 to 10 inches apart, and all face directly into the constantly reversing surge. Those schools observed did not shift their position more than 10 feet during an entire season. Within the school, however, the species, size and number of fish fluctuated from day to day.

As they become larger, black croakers break away from the main school and retire to caves and crevices. Half-grown individuals 88 to 150 mm. long tend to lead a solitary existence. Single fish about 150 mm. (six inches) long are not uncommon in crevices. They do not maintain schools in particular recesses, but seem to wander freely among crevices or caves.

SIZE AND AGE

According to Skogsberg (1939) black croakers mature at a standard length of about 22 cm. (8.7 inches). Observations made somewhat incidentally throughout the year suggest that at this size they are two or three years old and are schooling with larger adults, usually in caves and dark crevices.

On mature fish, most of the scales examined had been regenerated, but a few readable ones almost always could be found. Scales from a female 10.5 inches long had four distinct annuli. The ear bones (otoliths) of a female 11.25 inches in total length showed five winter rings and those from a fish 14.0 inches in total length (sex not determined) had 20 (John E. Fitch, personal communication).

Black croakers were reported by Jordan and Gilbert (1881), perhaps not as a result of definite measurements, to attain the length of 18 inches. Lengths to 15 inches have been indicated by other writers (Jordan and Evermann, 1898; Starks, 1919; Walford, 1931; Barnhart, 1936; Roedel, 1948, 1953). The largest adults observed in the course of diving were an estimated 14 inches long, but the largest ones collected measured only slightly more than 11. The California State Fisheries Laboratory has a record of a female 14.25 inches in total length (11.5 inches standard), weighing 1 pound, 9 ounces, that was taken off Seal Beach on March 10, 1959 (John E. Fitch, personal communication).

METHODS OF CAPTURE

Black croakers have been taken with gill nets, round-haul nets, hook and line, and beach seines (Walford, 1931); and by using lampara nets (Skogsberg, 1939) and set lines (Roedel, 1948, 1953). Some have been killed by explosives (Fitch and Young, 1948), and others have been taken by spear fishermen. During this investigation specimens were collected by angling, by diving with spears and small hand nets, and by using rotenone.

IMPORTANCE

The black croaker is probably more abundant than the highly-prized California corbina, but is seldom taken by either commercial fishermen or anglers. It is not as large as some of the other California croakers, but is quite palatable and potentially valuable as a food fish.

Since 1933 it has been illegal to sell black croakers (Roedel, 1948). They are taken only incidentally by commercial fishermen. As a result of their present scarcity in bays, their retiring habits on the open coast and their comparatively small size, it is doubtful that a successful commercial fishery could be established, even if their sale were legalized.

SUMMARY

Many features in the life history and ecology of the black croaker, *Cheilotrema saturnum* (one of the eight native sciaenids of California) have been elucidated through underwater observations, rearing in aquaria and literature review.

The species ranges from the Santa Barbara Channel (about Pt. Conception) in California to Santa Maria Bay, Baja California. Related forms occur in the Gulf of California and off Peru. Adults have been reported from bays and sloughs as well as the open coast, but were observed only while diving along rocky coasts, in water 4 to 150 feet deep, with their abundance centering at about 21 feet. They are generally very retiring in habits, chiefly frequenting caves and crevices. Juveniles, smaller than 88 mm. (3.5 inches) in standard length, were noted in depths of 4 to 18 feet with a concentration at about 9.

Adult black croakers undergo changes in coloration of apparent adaptational significance. The nocturnal pattern is distinct from the diurnal. The coloration changes remarkably between the attainment of standard lengths of 14 to 120 mm. The juveniles strikingly resemble the young of the California sargo, *Anisotremus davidsoni,* and the California salema, *Xenistius californiensis,* and the young of these three species school together.

Black croakers appear to feed exclusively on crustaceans. They mature at a standard length of about 22 cm. (9 inches) and spawn in late spring and early summer. A total length of 18 inches has been attributed to the species but most authors give the maximum size as 15 inches. The largest ones observed in diving were estimated to be 14 inches long. A 14.25-inch female checked by the Department of Fish and Game weighed slightly more than a pound and a half.

Published statements indicate black croakers were formerly more abundant, especially in non-polluted bays. They have been regarded as now rare, but diving observations disclosed considerable abundance. The black croaker is a palatable food fish, but the development of any considerable fishery for it seems unlikely.

REFERENCES

Barnhart, Percy Spencer
1936. Marine fishes of southern California. Berkeley, Univ. Calif. Press, iv + 209 pp.

Berdegué A., Julio
1956. Peces de importancia commercial en la costa nor-occidental de México. Secretaría de Marina, Dir. Gen. Pesca e Industrias Conexas, 345 pp.

Canon, Raymond
1953. How to fish the Pacific coast. A manual for salt water fishermen. Menlo Park, Lane Publ. Co., xi + 337 pp.

Craig, Joe A.
1926. Common names of commercial fishes. Calif. Fish and Game, vol. 11, no. 4, p. 185.
/ 1928. Untangling the names of fishes. Calif. Fish and Game, vol. 14, no. 2, pp. 168-169.

Eigenmann, Carl H.
1892. The fishes of San Diego, California. U. S. Nat. Mus., Proc., vol. 15, pp. 123-178.

Eigenmann, Carl H., and Rosa S. Eigenmann
1892. A catalogue of the fishes of the Pacific coast of America north of Cerros Island. New York Acad. Sci., Ann., vol. 6, no. 6, pp. 349-358.

(259)

Fitch, John E., and Parke H. Young
1948. Use and effect of explosives in California coastal waters. Calif. Fish and Game, vol. 34, no. 2, pp. 53-69.

Girard, Charles
1858. Fishes. General report upon the zoology of the several Pacific Railroad Routes, part IV. U. S. Pac., R. R. Surv., 10, pp. 1-400.

Günther, Albert
1860. Catalogue of the Acanthopterygian fishes in the collection of the British Museum. London, vol. 2, xxi + 548 pp.

Hiyama, Yosio
1937. Marine fishes of the Pacific coast of Mexico. The Nissan Fisheries Institute, Odawara, Japan, 75 pp. + 102 pls.

Hubbs, Carl L., and Boyd W. Walker
1951. *Odontoscion australis*, the juvenile stage of *Elattarchus archidium*, a Panamaic sciaenid fish. Copeia, no. 3, pp. 205-207.

Jordan, David Starr, and Carl H. Eigenmann
1889. A review of the Sciaenidae of America and Europe, U. S. Comm. Fish., Rept., pp. 343-451.

Jordan, David Starr, and Barton W. Evermann
1898. The fishes of North and Middle America. U. S. Nat. Mus., Bull. 47, pt. 2, pp. i-xxx, 1241-2183.

Jordan, David Starr, and Charles H. Gilbert
1880. Notes on a collection of fishes from San Diego, California. U. S. Nat. Mus., Proc., vol. 3, pp. 23-34.
1881a. List of the fishes of the Pacific Coast of the United States, with a table showing the distribution of the species. U. S. Nat. Mus., Proc., vol. 3, pp. 452-458.
1881b. Notes on the fishes of the Pacific coast of the United States. U. S. Nat. Mus., Proc., vol. 4, pp. 29-70.
1883. Synopsis of the fishes of North America. U. S. Nat. Mus., Bull., vol. 16, pp. i-lvi, 1-1018.

Metz, Charles W.
1912. The fishes of Laguna Beach, California, I. Laguna Mar. Lab., Ann. Rept., vol. 1, pp. 19-66.

Roedel, Phil M.
1948. Common marine fishes of California. Calif. Div. Fish and Game, Fish Bull. 68, 153 pp.
1953. Common ocean fishes of the California coast. Calif. Dept. Fish and Game, Fish Bull. 91, 184 pp.

Skogsberg, Tage
1939. The fishes of the family Sciaenidae (croakers) of California. Calif. Div. Fish and Game, Fish Bull. 54, pp. 1-62.

Smith, Rosa
1885. The fishes of San Diego, California. A revision of the list of the fishes made November 5, 1880. West American Scientist, vol. 1, no. 7, pp. 45-47.

Starks, Edwin C.
1919. The fishes of the croaker family (Sciaenidae) of California. Calif. Fish and Game, vol. 5, no. 1, pp. 13-20.

Starks, Edwin Chapin, and Earl Leonard Morris
1907. The marine fishes of southern California. Univ. Calif. Publ. Zool., vol. 3, No. 11, pp. 159-251.

Steindachner, Franz
1879. Ichythyologische Beitrage (VIII). Sitz. K. Akad. Wiss. Wien., Abth. 1, vol. 80, pp. 119-191.

Ulrey, Albert B., and Paul O. Greeley
1928. A list of the marine fishes (Teleostei) of Southern California with their distribution, So. Calif. Acad. Sci., Bull., vol. 27, pp. 1-53.

Walford, Lionel A.
1931. Handbook of common commercial and game fishes of California. Calif. Div. Fish and Game, Fish Bull. 28, 181 pp.

o

38991 4-61 900 *printed in* CALIFORNIA STATE PRINTING OFFICE

(260)

Reprinted from the Journal of Marine
Research, v.18, no.3, November 30, 1960.
pp.157-167.

OBSERVED AND COMPUTED PATH RADIANCE IN THE UNDERWATER LIGHT FIELD

By

J. E. TYLER

Scripps Institution of Oceanography
University of California
La Jolla, California

ABSTRACT

This paper presents experimental data on changes in underwater radiance in zenith and nadir directions as a function of depth for both overcast and clear sunny lighting conditions at the surface. The equation developed by Preisendorfer (1957) to describe path radiance along any path is then used to predict observed changes, and predicted results are compared with the observed data.

INTRODUCTION

Recently Preisendorfer (1959) published theoretical proof of the existence of characteristic diffuse light in natural waters. This proof formalizes the early conjectures of Jerlov and Liljequist (1938), Whitney (1941a, 1941b), *et al.*, which were based on experimental data obtained by Jerlov in the Baltic and by Whitney in Wisconsin lakes and in the Atlantic Ocean near Woods Hole, Massachusetts.

The concept of characteristic diffuse light, or asymptotic radiance distribution as it has more recently been called, sometimes requires drastic changes in the distribution of radiance as a function of depth. Highlights in this distribution must be attenuated and dark areas must be filled in with space light. Jerlov (1951) has estimated that these changes are completed at about 300 m in the ocean while Tyler's (1960) data have shown that the changes are nearly complete at 60 m in the water of Lake Pend Oreille. Attempts to study these changes by measuring downward, upward, and horizontal "illumination" (Poole, 1945) have apparently not been successful, probably due to the integrating characteristics of the optical collector used. Jerlov and Liljequist (1938) and Jerlov (1951), however, have given comparative radiance data at 5 m and 15 m which show attenuation in the sun's direction as well as an increase in "vertical intensity"

Contributions from the Scripps Institution of Oceanography, New Series, 1258

Reproduced by Permission

with depth. Whitney's (1941b) radiance data at three depths (3 m, 6 m, 9 m) have also demonstrated attenuation in the direction of the sun and a progressive increase in "light intensity" in the vertical direction as depth increases; his data are especially interesting because they demonstrate that the rate of change of the zenith radiance ("light intensity") with depth is decreasing. More detailed measurements with monochromatic light (Tyler, 1958), made at depths of 2.5 cm, 3 m and 6 m, demonstrate the complex nature of changes in radiance that are taking place in the upper layers of the ocean.

The theoretical treatment of radiative transfer in hydrosols, worked out by Preisendorfer, has contributed greatly to a clear understanding of the physical nature of radiative transfer in a multiple scattering and absorbing hydrosol (nonisotropic). The theory can be used to predict changes in radiance along a fixed path of sight underwater.

This paper presents monochromatic data for fixed paths of sight, illuminated by constant sky conditions, over a depth range from c. 0.6 to c. 60 m. The equation for path radiance will be given from Preisendorfer (1957) and the observed radiances will be compared with those obtained by computation.

EXPERIMENTAL

A radiance measuring device (Tyler, *et al.*, 1959) having a solid angle of acceptance of 6.6° was oriented vertically and lowered into optically deep homogeneous water. The water involved in this experiment is described in detail by Tyler (1960). For the bandwidth under consideration the total attenuation coefficient α was 0.442/m, the diffuse attenuation coefficient at 29 m was $K = 0.169$/m, and the absorption coefffcient was $a = 0.117$/m. Since the transfer of radiant energy within a hydrosol depends on physical factors only, not on chemical or biological considerations, the data presented here can be applied equally well to any hydrosol having physical properties which are identical with those of the water used in this research. For example, the water found by Nielsen and Jensen (1957) at their Station 109 in the South Atlantic off Angola is apparently very similar to the water described here. A Wratten No. 45 filter combined with the sensitivity of the multiplier-phototube itself limited the half-bandwidth to about 64 mμ with peak value at 480 mμ. Radiance

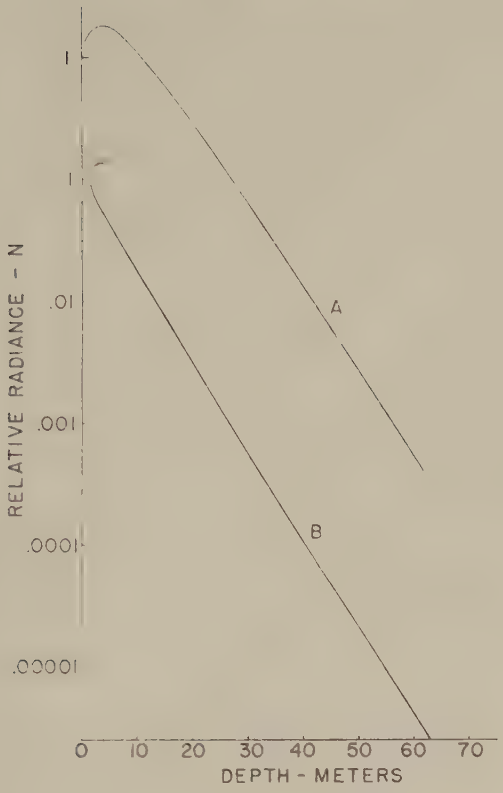

Figure 1. Observed data for zenith (Curve A) and nadir (Curve B) path radiance as a function of depth for a clear sunny day, sun altitude 56.6°.

measurements were obtained in the zenith and nadir directions simultaneously.

Observed data for zenith and nadir directions on a clear sunny day with sun altitude of 56.6° are shown in Fig. 1. Referring to Curve A, if the thickness of the water film between the measuring device and the surface could be made zero, then the instrument would measure the radiance of the zenith sky. As the instrument is submerged the radiance in the zenith direction increases because the increase in light due to scattering along the path is greater than the decrease in light due to attenuation along the same path. At 3.7 m these two effects just balance each other, with the result that

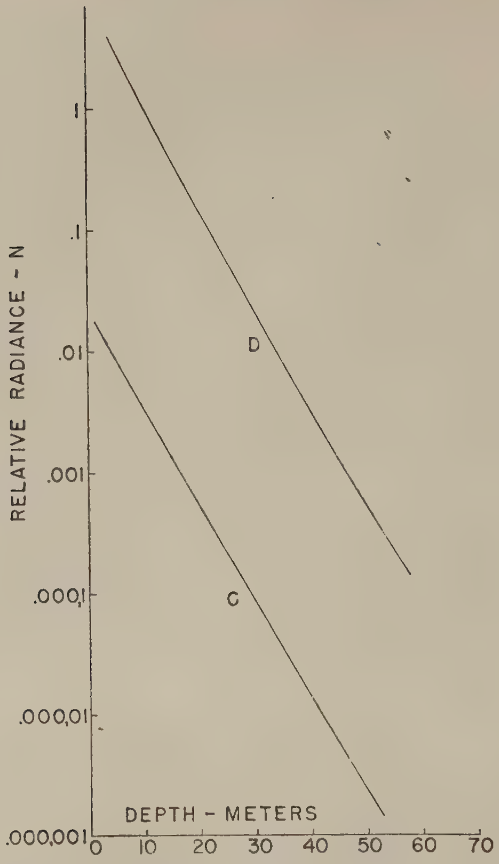

Figure 2. Observed data for zenith (Curve D) and nadir (Curve C) path radiance as a function of depth on an overcast day.

the slope of the curve at this depth is zero. Below 3.7 m the negative slope of the curve, which at any point is equal to the instantaneous value of the attenuation coefficient for radiance (radiance k value), is increasing and is in fact approaching the asymptotic value, k_{00}, discussed by Preisendorfer (1959).

In the nadir direction (Curve B), with the measuring device at the surface, the reading is at first influenced by the back scattering of the sun's rays, which is indicated in Curve B by its initially high slope. This effect is quickly lost. As depth increases the negative

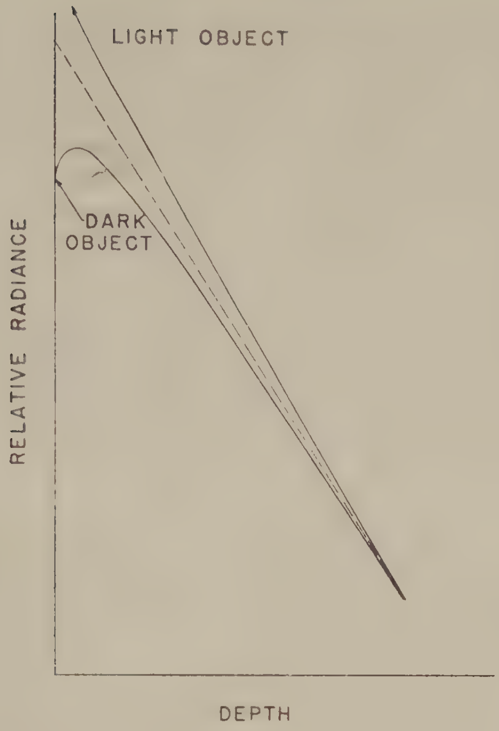

Figure 3. Radiance data adjusted at about 60 m to illustrate the relative radiance attenuation of a dark object and a light object by the same water. The intersection of the dashed straight line with the ordinate gives the object radiance which would be attenuated linearly for all depths.

slope of the nadir curve decreases, again approaching k_{00} as an asymptotic value.

When the slopes of the two curves in Fig. 1 are compared critically at 60 m they are found to differ slightly. This means that the region of asymptotic distribution (Preisendorfer, 1959) was not reached in this experiment.

Experimental data of this same kind, obtained under an overcast sky, are shown in Fig. 2. In this case both nadir (Curve C) and zenith (Curve D) radiance readings yield relatively high slopes at the surface, with the slopes of both curves decreasing with depth.

In Fig. 3 the zenith readings for the two lighting conditions have been adjusted to have the same radiance value at about 60 m. Thus

(265)

Fig. 3 can be used to represent a situation (in homogeneous water) in which a dark object and a light object both appear in the initial radiance distribution for the scene. The directions in which these objects occur are not specified, nor is the initial depth. From Fig. 3 the general principle of radiance attenuation can be seen at a glance; radiances with magnitudes that are relatively too large to conform with the asymptotic radiance distribution are attenuated rapidly whereas those with magnitudes that are relatively too small are attenuated slowly, or even enhanced. The net effect of this process is to inexorably return the distribution to its asymptotic shape. It follows that there must be a value of radiance which will be attenuated lineary over all depths. Its magnitude will depend on the values of α and s for the hydrosol. It is approximated in Fig. 3 by the intersection of the dashed line with the ordinate. The slope of the dashed straight line is of course equal to k_{00}.

THEORETICAL PREDICTIONS

Preisendorfer (1957) has developed a general equation to describe the path radiance along any path as a function of its length:

$$N_r(Z,\theta,\varphi) = N_0(Z,\theta,\varphi)\, e^{-\alpha r} + \frac{N_*(Z,\theta,\varphi)}{\alpha + K\cos\theta}\left[1 - e^{-(\alpha - K\cos\theta) r}\right]. \quad (1)$$

In this equation $N_r(Z, \theta, \varphi)$ is the radiance of a path observed in the direction θ, φ, from a depth Z. The first term on the right is the transmitted radiance from the source (*e. g.*, a patch of zenith sky). The second term represents the space light which accumulates in the path by processes of scattering and attenuation.

$N_0(Z_t, \theta, \varphi)$ is the inherent radiance of the source at depth Z_t observed in the direction θ, φ;
α is the total attenuation coefficient of the hydrosol;
r is the length of the path;
$N_*(Z, \theta, \varphi)$ is the path function in the direction θ, φ from depth Z (*i.e.*, the radiance per unit length along the line of sight, which is generated by the scattered light only);
K is the diffuse attenuation function;
θ is the angle between the verticle and the direction of the path; and
φ is the azimuth angle.

For a path of sight directed at the zenith, the angles θ and $\varphi = 0°$ and $\cos\theta = 1$. $N_0(Z_t, \theta, \varphi)$ can be interpreted as the radiance of the zenith sky (N_0) as seen from just below the water, and the path length, r, becomes equal to depth Z. Introducing these conditions into (1) and dropping the parenthetical notation for θ and φ, we have the expression

$$N(Z) = N_0 e^{-\alpha Z} + \frac{N_*(Z)}{\alpha - K}\left(1 - e^{-(\alpha-K)Z}\right), \tag{2}$$

which should predict Curve A of Fig. 1 and Curve D of Fig. 2.

For a path of sight directed downward, $\theta = 180°$, $\cos\theta = -1$, $\varphi = 0°$, $N_0 = 0$ (*i.e.*, the bottom is so far away that only space light needs to be considered) and $r = 00$.

Substituting these conditions into (1) and simplyfying yields

$$N(Z) = \frac{N_*(Z)}{\alpha + K}. \tag{3}$$

This equation should predict Curves B and C of Figs. 1 and 2 respectively.

During the experiment described here, all of the unknowns of (2) and (3) were measured except $N_*(Z)$. In order to compute $N(Z)$ as a function of Z from (2) and (3) it is necessary to first evaluate $N_*(Z)$. The following methods were used.

Method 1. One procedure for evaluating $N_*(Z)$ is based on the fact that $N_*(Z)$ is generated by scattering and is thus diffuse light which will be transmitted exponentially in accordance with

$$N_*(Z) = N_*(0)\, e^{-KZ}. \tag{4}$$

A single value of $N_*(Z)$ can be computed from experimental data by means of (2), and from this $N_*(0)$ can be determined by using (4). The resulting value of $N_*(0)$ can now be substituted into (2) to give

$$N(Z) = N_0 e^{-\alpha Z} + \frac{N_*(0)\, e^{-KZ}}{\alpha - K}\left(1 - e^{-(\alpha-K)Z}\right), \tag{5}$$

which can be used to compute $N(Z)$ as a function of Z over the depth range.

Method 2. Using the form of the equation of transfer for radiance given by Preisendorfer (1959), we have

$$\frac{dN(Z,\theta,\varphi)}{dr} = -\alpha N(Z,\theta,\varphi) + N_*(Z,\theta,\varphi); \tag{6}$$

we again apply the conditions for vertical measurements, *i.e.*, $r = Z$, $\theta = \varphi = 0$ to obtain

$$\frac{dN(Z)}{dr} = -\alpha N(Z) + N_*(Z). \tag{7}$$

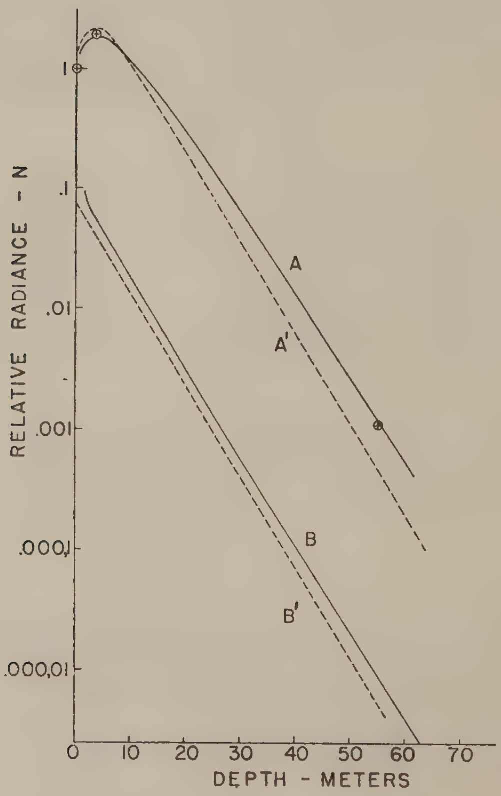

Figure 4. Comparison of observed (A) and computed (A′) values of the zenith path radiance and of the observed (B) and computed (B′) values of the nadir path radiance for clear sunny lighting conditions.

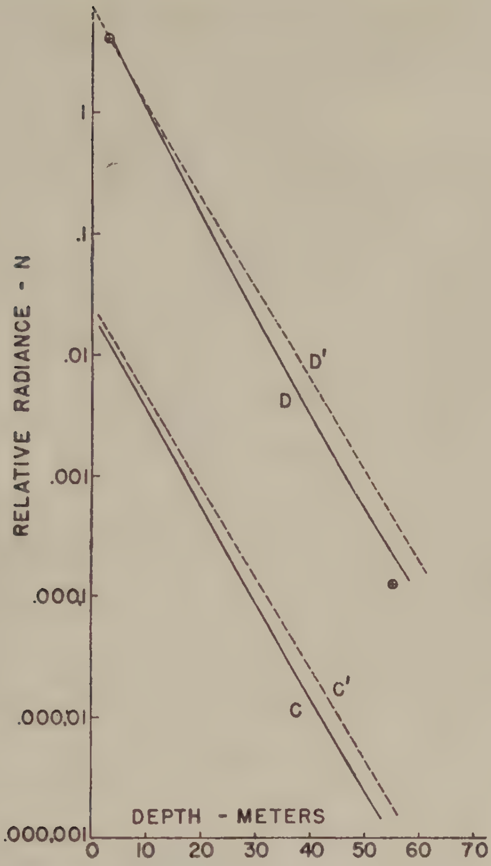

Figure 5. Comparison of observed (D) and computed (D′) values of the zenith path radiance and of the observed (C) and computed (C′) values of the nadir path radiance for overcast lighting conditions.

In the zenith data for the clear sunny day, $[dN(Z)]/dr$ is 0 at Z = 3.7 m. Thus N_* can be computed for this depth from

$$N_*(3.7\text{ m}) = \alpha N(3.7\text{ m}). \tag{8}$$

Using observed values of α, K, Z, N_0, and $N(Z)$, a series of points were computed giving the predicted zenith and nadir radiance as a function of depth. These points have been plotted to give curves A′, B′, C′, D′ in Figs. 4 and 5. Fig. 4 compares the results of the computation with observed values obtained on a clear sunny day; Fig. 5 compares the results of computation with observed data for an overcast day.

DISCUSSION

The differences in slope between observed and computed curves is believed to be the result of small inaccuracies in the measurement of α and K. For example, an average experimental value of K was used in the computations whereas theory calls for the asymptotic value. If a value of K closer to the asymptotic value had been used, then the computed zenith curves would have been much closer to the observed curves. Several points have been computed with an extrapolated value of K for the asymptotic value. These points, plotted and circled in Figs. 4 and 5, indicate the result that might have been obtained if the asymptotic value of K could have been measured.

The curves shown in Figs. 1, 2, 4 and 5 are on the same relative basis and can be intercompared. From Curves A and D it can be seen that, although there was generally less light in the water on the overcast day, the radiance from the zenith direction was actually greater on the overcast day down to a depth of about 10 m.

The approach to asymptotic radiance distribution can be seen in a number of ways. In both Fig. 1 and Fig. 2 the slopes of the zenith and nadir curves are approaching a constant value (k_{00}). Also, the ratio of zenith to nadir radiance ($\log N_{\text{zenith}} - \log N_{\text{nadir}}$) is approaching the same constant value for both the clear sunny day and for the overcast day.

The lack of dependence of the shape of the asymptotic radiance distribution on the surface lighting is seen in the facts that the slopes of the curves for the sunny day are approaching those for the overcast day and that the ratio of zenith to nadir radiance approaches the same value (approx. 30) for both days.

This comparison of observed and computed path radiance is one of a series of experiments designed to validate the nonisotropic, multiple scattering theory of Preisendorfer and to prove methods for measuring the specified water properties. In general the results of these experiments have consistently demonstrated the validity of this theory and have indicated its usefulness in handling problems relating to underwater light.

REFERENCES

Jerlov (Johnson), N. G.

1951. Optical studies of ocean waters. Rep. Swedish Deep-sea Exped., 1947–1948. 3, Physics and Chemistry No. 1: 1–59.

Jerlov (Johnson), N. G. and Gösta Liljequist

1938. On the angular distribution of submarine daylight and on the total submarine illumination. Svenska hydrograf.-biol. Komm. Skr., N.S. Hydrogr., *14*: 3–15.

Nielsen, E. Steemann and E. Aabye Jensen

1957. Primary oceanic production. The autotrophic production of organic matter in the oceans. Galathea Rep., Sci. Res. Danish Deep-sea Exped. 1950–52, *1*: 49–136 (see p. 65).

Poole, H. H.

1945. The angular distribution of submarine daylight in deep water. Sci. Proc. R. Dublin Soc., *24*: 29–42.

Preisendorfer, R. W.

1957. Model for radiance distribution in natural hydrosols. Visibility Lab., Scripps Inst. Oceanogr., SIO Ref. 58–42: 1–15.

1959. Theoretical proof of the existence of characteristic diffuse light in natural waters. J. Mar. Res., *18*: 1–9.

Tyler, J. E.

1958. Comparison of light distribution above and below water, J. Mar. Res., *16*: 96–99.

1960. Radiance distribution as a function of depth in an underwater environment. Bull. Scripps Inst. Oceanogr., *7* (5): 363–412.

Tyler, J. E., W. H. Richardson and R. W. Holmes

1959. Method of obtaining the optical properties of large bodies of water. J. geophys. Res., *64*: 667–673.

Whitney, L. V.

1941a. The angular distribution of characteristic diffuse light in natural waters. J. Mar. Res., *4*: 122–131.

1941b. A general law of diminuation of light intensity in natural waters and the percentage of diffuse light at different depths. J. opt. Soc. Amer., *31*: 714–722.

(271)

REPRINT FROM JOURNAL OF MARINE RESEARCH, VOLUME 18, 3, 1960
pp.168-184

(273)

SEASONAL VARIATION IN SEA LEVEL IN THE PACIFIC OCEAN DURING THE INTERNATIONAL GEOPHYSICAL YEAR, 1957-1958[1]

BY

JUNE G. PATTULLO[2]

Scripps Institution of Oceanography
University of California
La Jolla, California

ABSTRACT

Seasonal variations in sea level derived from IGY measurements are described and compared with those previously published. These measurements confirm the earlier descriptions, which were based on observations from gauges attached mostly to continental coastlines. That is, in low latitudes in each hemisphere, sea level is high at the end of summer. There is a zonal band of high sea level from about the Equator to 40° N in September while in comparable southern latitudes sea level is low. Furthermore, north of 40° N there is a distinct change of phase; sea levels all around the Gulf of Alaska and the Aleutians are highest in December.

The following new information has resulted from the improved distribution of samples. First, sea level variations in the South Pacific are measurably smaller than those in the North Pacific. Second, the seasonal variation is appreciably larger near the continents than in the central oceanic regions of the northern hemisphere; this effect is virtually absent in the southern hemisphere. Finally, the December maxima found earlier in the Gulf of Alaska are now known to be far more widely distributed than previously thought.

In December, sea level is high from Bering Strait south to the central South Pacific and low nearer the coasts from Mexico to Chile and from southern Japan to Australia. Similar contours, but of opposite sign, appear in June.

Introduction. During the recent International Geophysical Year a widespread effort was made to extend and to improve the network of tide gauges over the oceans, with the primary aim of improving our understanding of seasonal variations in the elevation of the sea. The necessity for international co-operation and for at least a full

---

[1] Contribution from the Scripps Institution of Oceanography, New Series. 1259

[2] Present address: Department of Oceanography, Oregon State College, Corvallis, Oregon.

Reproduced by Permission

year's observations is obvious. Fortunately, workable instruments (tide gauges) were readily available. More significant, though, is the fact that work done just prior to the start of the Year (Lisitzin, 1955; Pattullo, *et al.*, 1955) indicated that the seasonal variation in sea level is sufficiently coherent over large areas in the ocean so that a grid, even of widely separated locations, could be expected to yield interpretable results. The principal difficulty in previous investigations had been the vast lack of data in midocean; tide gauges, like their human operators, are clustered principally along the coastlines of the more scientifically advanced nations of the world. To remedy this defect, we went to the islands. This paper describes results of these sea level measurements in the Pacific Ocean.

Locations of Observations. The Pacific Ocean contains several thousand islands, but by far the larger number of these are never visited by ships and are only occasionally touched by yachts, fishing boats, or other small craft. Operation of a scientific station in such a spot is difficult logistically, and expensive, and it is usually trying on the morale of the personnel who man it unless resident observers can be found. Therefore, wherever possible, inhabited islands, not impossibly cut off from normal transportation and communication facilities, were selected.

In the North Pacific, the U.S. Coast and Geodetic Survey has established a comprehensive and permanent network of tide gauge stations. There are unfortunate gaps in the grid, principally because there are no suitable islands in the north-central and eastern portions of the North Pacific Ocean. South of the Equator, island control is divided among many nations and here new gauges were installed for the IGY by Chile, France, Australia and New Zealand. At a few points installations were made by the Scripps Institution, for the United States, with the co-operation of the authorities and inhabitants.

Data from all gauges used in this paper are listed in Table I, and station locations are illustrated in Fig. 1.

Instrumentation and Operation of Stations. The difficulties of supply and supervision demanded that the instrument be reliable and simple, relatively easy to install and maintain, and operable by a

TABLE I. Station Locations and Monthl

No.	*Place*	*Latitude*	*Longitude*	*Operator*	*Years*	*Zon*
–	Ugolnyi	63° 02′ N	179° 25′ E	USSR	1945–54	–
C033	Yuzhno Kurilsk	44° 01′ N	145° 52′ E	UGGI	IGY	–
B070	Attu	52° 50′ N	173° 12′ E	USCGS	IGY	1
B100	Adak	51° 52′ N	176° 39′ W	USCGS	IGY	1
B056	Unalaska	53° 53′ N	166° 32′ W	UGGI	IGY	–
B015	Kodiak	57° 43′ N	152° 31′ W	USCGS	IGY	1
–	Sitka	57° 03′ N	135° 20′ W	USCGS	IGY	1
–	Crescent City	41° 45′ N	124° 12′ W	USCGS	IGY	1
–	San Francisco	37° 48′ N	122° 28′ W	USCGS	IGY	–
C407	La Jolla	32° 52′ N	117° 15′ W	USCGS	IGY	–
C240	Ensenada	31° 51′ N	116° 38′ W	UGGI	IGY	–
C271	La Paz	24° 10′ N	110° 21′ W	UGGI	IGY	4
C294	Mazatlan	23° 12′ N	106° 25′ W	UGGI	IGY	4
C295	Socorro I.	18° 44′ N	110° 01′ W	UGGI	IGY	–
C272	Manzanillo	19° 03′ N	104° 20′ W	UGGI	IGY	4
C305	Acapulco	16° 50′ N	099° 55′ W	UGGI	IGY	4
C307	Salina Cruz	16° 10′ N	095° 12′ W	UGGI	IGY	4
46	Balboa	08° 58′ N	79° 34′ W	PMRS	1909–46	4
47(1)	Talara	04° 35′ S	81° 17′ W	PMRS	1942–50	–
47(2)	Matarani	17° 00′ S	72° 07′ W	PMRS	1941–50	7
47(3)	Valparaiso	33° 01′ S	71° 38′ W	PMRS	1941–47	7
48	Puerto Montt	41° 29′ S	72° 58′ W	PMRS	1942–46	–
C937	Juan Fernandez	33° 33′ S	78° 47′ W	Chile	IGY	7
E712	Easter	27° 09′ S	109° 29′ W	Chile	IGY	6
C945	Rurutu	22° 27′ S	151° 20′ W	France	IGY	–
E739	Takaroa	14° 40′ S	145° 05′ W	France	IGY	–
–	Taiohae	08° 55′ S	140° 06′ W	France	IGY	6
52	Samoa	14° 17′ S	170° 41′ W	PMRS	1949–51	–
E467	Christmas	01° 57′ N	157° 28′ W	USCGS	IGY	3
E585	Fanning	03° 54′ N	159° 24′ W	SIO/UK	IGY	3
E574	Palmyra	05° 52′ N	162° 06′ W	SIO	IGY	3
E728	Arorae	02° 37′ S	176° 50′ E	SIO/UK	IGY	3
E620	Ocean	00° 53′ S	169° 35′ E	SIO/UK	IGY	3
E569	Kwajalein	08° 44′ N	167° 44′ E	USCGS	IGY	–
E563	Eniwetok	11° 22′ N	162° 21′ E	USCGS	IGY	2
E605	Moen	07° 27′ N	151° 51′ E	USCGS	IGY	–
E606	Koror	07° 20′ N	134° 28′ E	Japan	1925–33 1936–38	2
E556	Guam	13° 26′ N	144° 39′ E	USCGS	IGY	2
E534	Wake	19° 17′ N	166° 37′ E	USCGS	IGY	–
E545	Johnston	16° 45′ N	169° 31′ W	USCGS	IGY	3

Deviations from Mean Sea Level (cm)

J	*F*	*M*	*A*	*M*	*J*	*J*	*A*	*S*	*O*	*N*	*D*
+1	−1	−10	−12	−8	−12	−3	+2	+5	+11	+17	+12
+4	−3	0	−7	−2	+2	+3	+4	+5	−1	−3	−2
+4	+3	+2	−2	0	−8	−8	−2	0	+2	+6	+8
+12	+10	−2	−5	0	−9	−7	−6	0	−2	+2	+2
−10	−9	+2	−2	0	+2	−3	−3	+4	+1	+7	+12
+19	+17	−9	−6	−10	−14	−8	−2	+2	+2	+6	+7
+24	+21	−8	−6	−11	−18	−16	−6	−5	+2	+9	+17
+15	+26	+2	−6	−12	−8	−8	0	−4	+1	−4	+3
0	+13	+3	−3	−7	−5	−3	−1	+3	+2	−4	+1
+2	−3	−5	−8	−9	−7	+1	+7	+8	+7	+3	+5
−3	−6	−8	−8	−7	−2	+2	+7	+8	+9	+6	+3
−8	−12	−13	−13	−5	−2	+8	+13	+16	+11	+8	−1
−8	−13	−15	−17	−3	+3	+13	+11	+20	+1	−8	−1
−7	−6	−3	−1	+5	+4	0	−3	+10	+5	0	−4
−2	−10	−12	−15	−2	+2	+11	+8	+11	+3	+3	+2
−2	−8	−10	−10	0	+3	+11	+7	+7	−1	+2	0
−7	−9	−9	−1	+4	+10	+10	+9	+8	−2	−3	−10
−8	−18	−18	−11	+2	+7	+6	+5	+8	+11	+9	+6
+4	+6	+4	+3	+2	+2	0	−3	−5	−5	−5	−4
+4	+3	+4	+2	+4	0	−2	−4	−5	−4	−2	0
+3	+2	+3	+2	0	+2	−1	−1	−4	−5	−3	+1
−1	−4	−2	−2	+2	+2	+2	+2	+2	−4	+1	+2
+1	+6	+4	+6	0	+1	+10	−3	−6	−11	−5	−3
+2	+3	+3	+3	+2	−2	0	−1	−3	−3	−2	+3
+8	+8	+1	+5	+6	+3	−4	−2	−6	−10	−3	−4
0	+7	+6	+3	+2	−2	0	−2	−2	−5	0	−1
+3	+2	+3	+1	+1	−2	−1	−1	−2	−2	−2	+2
−2	+2	+4	+3	+3	−2	−3	−4	−2	−1	−1	+1
+3	0	−5	−6	−4	−7	−2	0	0	+4	+7	+12
0	−1	−5	−10	−14	−8	−1	+5	+8	+9	+6	+16
+1	−6	−7	−7	−8	−6	+1	+5	+20	0	+9	+3
−4	−2	+1	−1	−2	−2	0	+2	+5	+3	+3	−2
0	−7	−7	−3	−2	−2	0	+1	+2	+6	+7	+6
−15	−3	+4	+8	+5	+2	+4	+5	+3	+2	−5	−11
−13	−7	−5	−5	+4	+5	+7	+7	+5	+1	−1	−3
−16	−8	+2	+10	+11	+7	+2	+1	+1	−2	−6	−5
−15	−15	−6	−1	−1	+4	+8	+10	+8	+9	+4	−4
−6	−3	−4	−1	−1	−4	+10	+11	+7	+3	−1	−7
−9	−8	+2	+6	−12	−2	+2	+13	+4	+1	+5	+2
+1	−1	−7	−7	−7	−16	−4	+9	+11	+7	+13	+1

(cont.)

TABLE I. STATION LOCATIONS AND MONTHLY

No.	*Place*	*Latitude*	*Longitude*	*Operator*	*Years*	*Zone*
C288	Hilo	19° 44′N	155° 03′W	USCGS	IGY	3
C278	Honolulu	21° 18′N	157° 52′W	USCGS	IGY	3
C282	Kahului	20° 45′N	156° 28′W	USCGS	IGY	3
C408	Mokuoloe	21° 26′N	157° 47′W	USCGS	IGY	3
C275	Nawiliwili	21° 58′N	159° 21′W	USCGS	IGY	3
C262	Midway	28° 13′N	177° 22′W	USCGS	IGY	3
–	Hanasaki	43° 17′N	145° 35′E	UGGI	IGY	–
C178	Aburatsubo	35° 09′N	139° 37′E	UGGI	IGY	2
E499	Naze	28° 23′N	129° 30′E	UGGI	IGY	2
62	Takao	22° 37′N	120° 16′E	PMRS	1904–43	2
E552	Manila	14° 35′N	120° 58′E	UGGI	IGY	2
E607	Davao	07° 05′N	125° 38′E	UGGI	IGY	–
58a	Menado	01° 32′N	124° 50′E	PMRS	1927–31	–
55(1)	Port Moresby	09° 26′S	147° 06′E	PMRS	1939–40	5
55(2)	Guadalcanal	09° 25′S	159° 59′E	PMRS	1947–49	5
–	Cairns	16° 55′S	145° 43′E	UGGI	IGY	5
–	Townsville	19° 20′S	146° 50′E	UGGI	IGY	5
–	Gladstone	23° 53′S	151° 12′E	UGGI	IGY	5
–	Coff's Harbour	30° 20′S	153° 00′E	UGGI	IGY	–
–	Camp Cove	33° 53′S	151° 15′E	UGGI	IGY	–
C929	Lord Howe I.	31° 31′S	159° 07′E	UGGI	IGY	–
–	Williamstown	37° 52′S	144° 58′E	UGGI	IGY	–
–	Cape Sorrell	42° 13′S	145° 13′E	UGGI	IGY	–
70	Auckland	36° 51′S	174° 49′E	PMRS	1917–19,1921–23, 1937,1941	5
71	Bluff	46° 35′S	168° 22′E	PMRS	1917–22	–

TABLE I.

Number When available, the number designated by Comité Spécial de l'Année Géophysique Internationale has been used to identify the station. Stations for which data have been taken from Pattullo, *et al.* (1955) are given the number assigned to the station group by these workers. Several times an additional number is added in parentheses to distinguish between different members of the same station group. In some cases neither CSAGI nor PMRS numbers apply.

Place Name of city or island at which each tide guage was located.

Operators The operator or source of data are identified as follows:

USSR: data collected by Russian workers; transmitted to Scripps Institution by personal communication.

USCGS: stations operated by United States Coast and Geodetic Survey. Data obtained through World Data Center (A) Oceanography, A & M College of Texas.

PMRS: Data taken directly from Pattullo, *et al.*, 1955.

Chile: IGY stations operated by the National IGY Committee of Chile. Data transmitted to Scripps by the Chilean IGY Committee.

DEVIATIONS FROM MEAN SEA LEVEL (cm) (cont.)

J	*F*	*M*	*A*	*M*	*J*	*J*	*A*	*S*	*O*	*N*	*D*
− 8	− 5	+ 1	− 7	− 2	0	− 1	+ 4	+ 5	+ 7	+ 2	+ 1
− 9	− 2	− 1	− 7	− 4	− 4	+ 3	+ 5	+ 5	+ 6	+ 6	+ 2
− 9	− 2	− 2	− 6	− 3	− 1	+ 1	+ 4	+ 7	+ 6	+ 6	+ 2
− 6	− 2	+ 1	− 8	− 3	− 5	+ 3	+ 5	+ 5	+ 7	+ 5	+ 3
− 8	− 5	− 4	− 2	− 1	− 6	+ 1	+ 1	+ 9	+ 8	+ 9	+ 3
+11	+12	− 9	−15	− 3	− 5	− 7	+ 1	+ 7	+ 5	+ 1	− 1
+ 4	− 2	+ 2	− 4	− 1	− 2	+ 1	+ 2	+ 4	− 1	− 3	0
− 8	− 6	− 6	−11	− 2	+ 6	+ 6	+ 1	+ 8	+ 6	+ 5	+ 1
−14	−17	−20	−16	+ 3	+ 7	+17	+16	+18	+ 9	+ 3	− 6
−13	−11	− 7	− 4	0	+ 5	+10	+13	+11	+ 7	0	−10
−12	−11	− 8	− 5	− 1	+ 6	+10	+12	+17	+ 4	− 4	− 9
− 6	− 3	− 3	+ 1	+ 4	+ 8	+ 8	+ 6	+ 5	+ 1	− 2	−18
+ 1	− 1	+ 3	+ 4	+ 1	0	+ 1	− 3	− 5	− 2	− 1	+ 2
0	+ 3	+10	+10	+10	+11	− 5	−12	− 5	−10	− 6	− 6
− 4	− 2	+ 3	+ 8	+10	0	− 5	− 4	− 2	− 1	0	− 3
− 4	+ 4	+10	+21	+ 4	+ 5	− 7	− 6	− 9	− 6	− 8	− 4
− 4	+ 9	+13	+26	+ 5	0	− 8	− 7	−10	−10	− 8	− 3
− 2	+ 7	+ 9	+14	0	+ 7	− 3	− 5	− 9	−11	− 5	− 1
−12	− 6	+ 6	+ 9	+13	+ 2	+ 6	− 2	+ 1	− 2	−10	− 3
− 6	+ 1	+10	+ 5	+12	+ 3	+ 1	− 9	− 8	− 3	− 5	− 2
− 5	− 2	+23	+16	+11	−22	− 8	− 8	−13	− 7	+ 6	+11
−18	− 4	+ 1	+ 2	+12	+ 2	+ 6	− 3	− 2	+ 1	+ 3	− 1
− 8	− 9	− 3	− 7	+23	+ 8	+11	− 4	− 3	− 2	− 1	− 5
+ 2	0	+ 3	+ 2	+ 4	+ 5	0	− 2	− 5	− 3	− 5	− 1
− 5	+ 1	+ 6	+ 3	+ 1	− 2	− 2	− 2	− 4	+ 2	0	+ 2

EXPLANATIONS

	France:	IGY stations operated by National IGY Committee of France, in part with equipment and assistance from Scripps Institution. Data obtained directly from French IGY Officers in French Polynesia.
	SIO/UK:	stations operated by Scripps Institution personnel or island resident in co-operation with National IGY Committee of the United Kingdom.
	Japan:	stations operated by Japan; data provided by Japanese Hydrographic Department.
	UGGI:	Monthly means published by Union Géodesique et Geophysique Internationale.
Years	Indicates the years during which observations were taken. IGY means 1957 and/or 1958.	
Zone	Area of ocean in which gauge is located; if gauge is close to a boundary between zones, no number appears in this column. See Fig. 5 and the discussion of this figure in text.	
J, F, M etc.	Monthly mean sea level minus annual mean sea level at the gauge, in centimeters. This quantity is referred to in the text as the "deviation."	

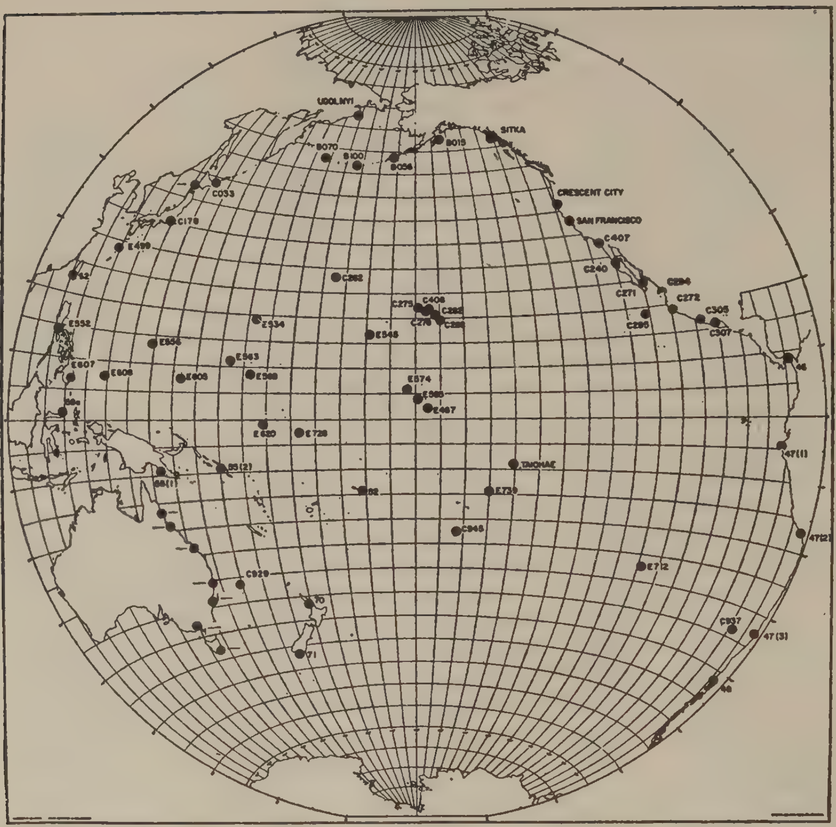
UGOLNYI
B070
B100
B056
B019
SITKA
C033
C178
E499
62
C262
CRESCENT CITY
SAN FRANCISCO
C407
C240
C294
C271
C272
C295
C305
C307
C275
C408
C282
C276
C288
E552
E534
E548
E556
E563
E607
E608
E605
E588
E574
E585
E467
38a
E620
E728
46
47(1)
55(2)
55(1)
TAIOHAE
62
E739
C945
47(2)
C929
E712
70
71
C937
47(3)
48

Figure 1. Locations of tide gauges that provided data used in this study. See Table I for identification.

semiskilled observer. Further, the data had to be such that, with reasonable care, they could be referred to a constant datum (reference level) throughout the observational period. Standard tide gauges, such as those used by the Coast Survey (Crouse-Hinds Instrument Co., or D. Ballauf and Co., manufacturers), or water level recorders made by Leupold and Stevens, Inc. filled these requirements, and both were used at various locations.

Operation was provided by local residents whenever possible. When this was not feasible, special technicians were maintained on the islands, at least until residents could be trained. In almost all cases the observers donated all or part of their efforts generously without reimbursement. This and the exceptionally high level of international co-operation achieved were the deciding factors in making the observational program a success. Details of the trials and ingenuity of the operators at each station are impressive and they will be included in a mimeographed data report.[3]

Results. The seasonal deviation of sea level from its annual mean is illustrated in Fig. 2 by four quarterly contour charts. Wherever available, values from the IGY data are used for these charts; most of the values are from this period. Where IGY data have not become available or are lacking, data from earlier years have been used, but these instances are few. The problems raised by this combination of IGY and non-IGY data will be mentioned later.

Let us look first at the chart centered around September (Fig. 2a). Note particularly the unbroken zone of higher-than-average sea level across the entire ocean from Asia to North America and from near the Equator to about 45° N. Zero deviation lines run east-west nearly along the Equator and on a line slightly northwest-southeast at 45° to 55° N. Outside of this band, *i.e.*, north of 50° N and south of the Equator, all deviations are negative. There is a slight indication of another zero deviation line to the south of the sampled region: Puerto Montt, Chile, at 40° S, has a slight positive value, and gauges on New Zealand and southern Australia show only small negative values.

In addition to this principal feature we note that the coastal deviations, at least in the northern hemisphere, are a little larger than those out at sea. We have a band of high sea level from Japan to North America, but the level tilts up as the coastal edges are approached. Note also that the deviations in the southern hemisphere are generally smaller than those in the northern and that the near-shore deviations here are not particularly larger than those offshore.

We can make nearly the same remarks about the chart for March (Fig. 2c) as we did for the September one, except that now the areas that had positive deviations had negative ones, etc. The two pictures are nearly mirror images of each other.

When we turn to the remaining pair of charts we find an immediate difference. Again the deviations are appreciable, but instead of east-west contours the isolines run largely north-south. For example,

---

[3] Island Observatories, Pacific, available from World Data Center (A), Oceanography, A. and M. College of Texas.

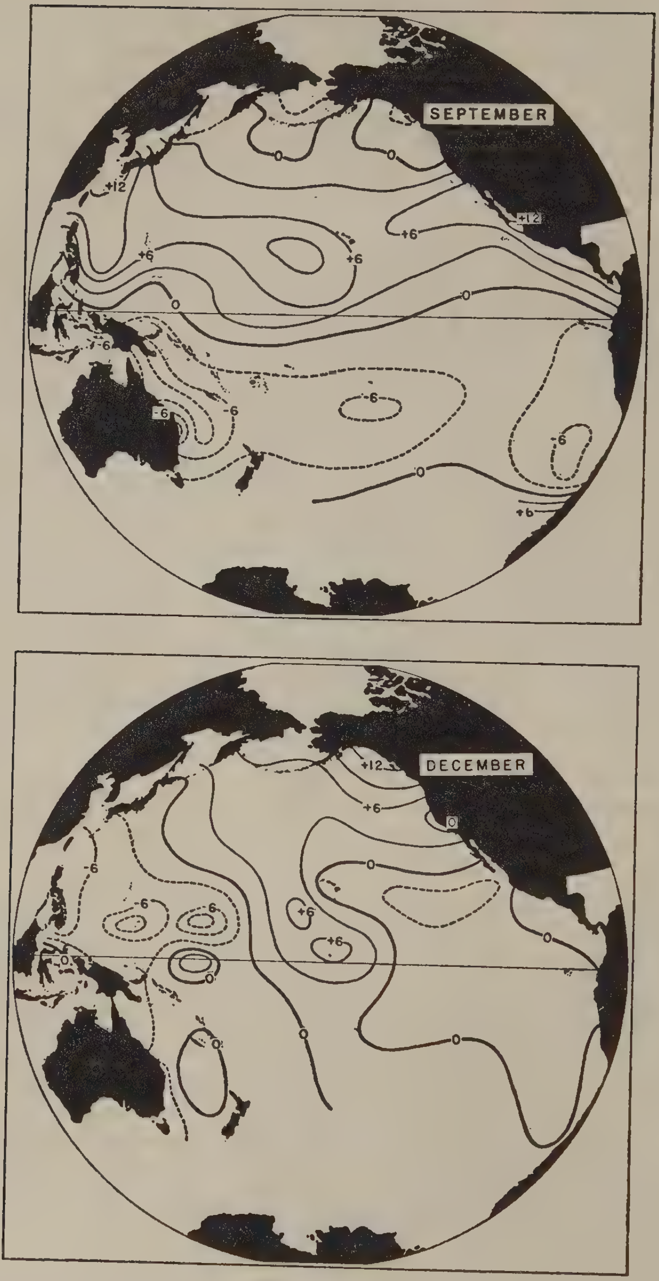
SEPTEMBER
+12
0
0
+12
+6
+6
+6
0
0
-6
-6
-6
-6
-6
0
+6
DECEMBER
+12
+6
0
0
-6
-6
-6
+6
+6
0
0
0
0
0
0

Figure 2. Deviations from mean annual sea level, by quarters, drawn for an average of all values in: (a) August, September, October; (b) November, December, January; (c) February, March,

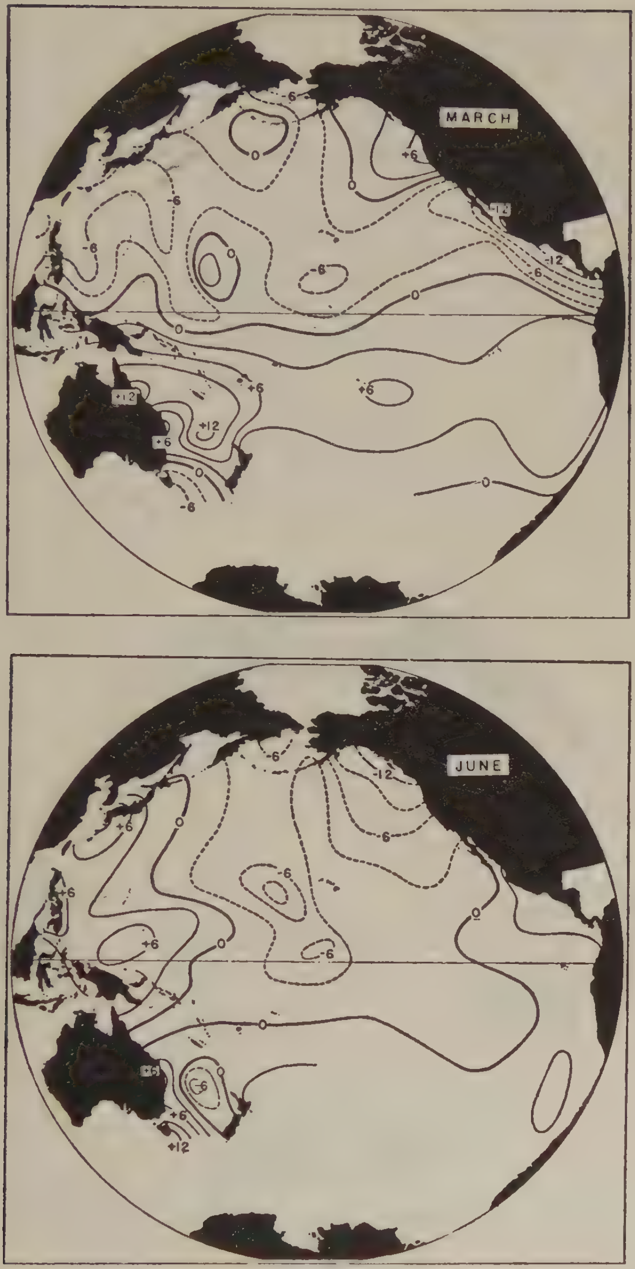
MARCH
-6
0
+6
0
-12
-6
-6
0
-6
-12
-6
0
0
+6
+6
+12
+12
+6
0
-6
0
JUNE
-6
-12
+6
0
6
-6
+6
0
0
+6
-6
0
+6
-6
+6
+12

April; (d) May, June, July. Contour interval, 2 cm. Light solid lines indicate positive deviations (higher than annual mean); dashed lines negative deviations; heavy solid lines zero deviations.

in November, December, and January the largest positive deviation is found along the shores of the Gulf of Alaska while a strong ridge of high sea level sweeps southward across the Line Islands and into the southern hemisphere. At the same time, off the continental coasts, sea level is low in both hemispheres. The oceanic maximum and offshore minima are all particularly well marked just north of the Equator. In the southern hemisphere the western boundary of the area of positive deviation seems poorly delineated; two isolated areas of higher-than-average sea level appear, one in the Tasman Sea and one to the north of it near the Equator.

The June picture (Fig. 2d) shows the same pattern as the December one, but again there is a reversal of sign, with the December negative areas taking on positive values six months later.

We are left with essentially two patterns, one of which we can call the September-March oscillation, the other the December-June oscillation. The nodal, or zero, lines of these two patterns are shown in Fig. 3. These lines are drawn at the average positions of the zero

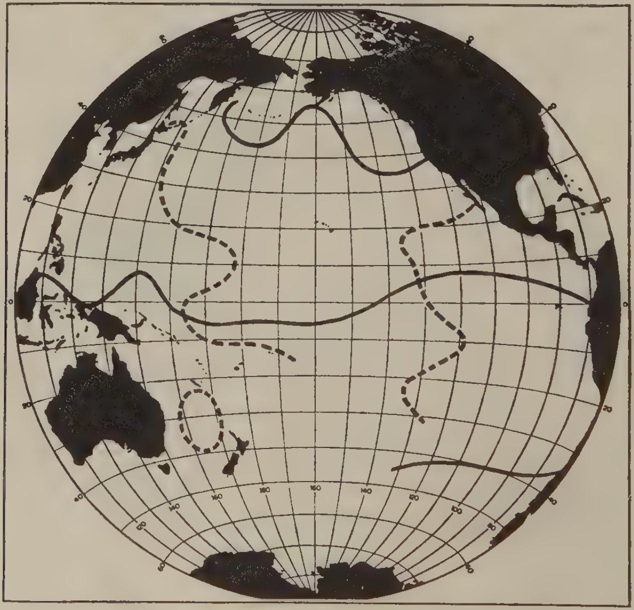

Figure 3. Zero deviations. Solid lines indicate zero deviations on September and March charts; dashed lines represent zero deviations on December and June charts.

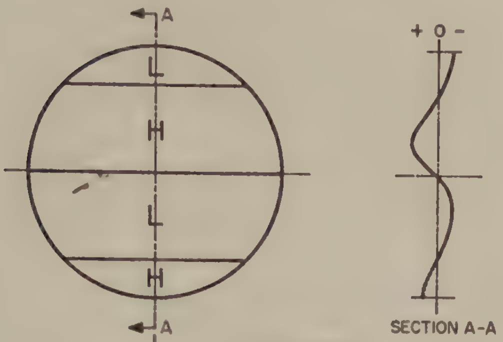

(a) SEPTEMBER

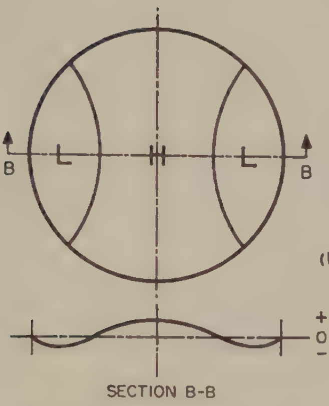

(b) DECEMBER

Figure 4. Schematic representation of seasonal variation in sea level. (a) September plan and elevation section looking from the east; (b) December plan and elevation section looking from the south.

lines of Fig. 2, and although their general positions and trends can be considered determined, obviously the details cannot be given much credence. For example, evidence given by Hamon and Stacey (manuscript) indicates that the change of phase between the Australian coast and the central Tasman Sea is real. However, since it is based on data from only one tide gauge located on Lord Howe Island, we will omit it from the present discussion.

Simplified schematic representations of the September and December patterns are shown in Fig. 4. These would serve equally well for March and June, respectively, if the high areas (H) were replaced by low areas (L) and vice versa. They include only the most basic

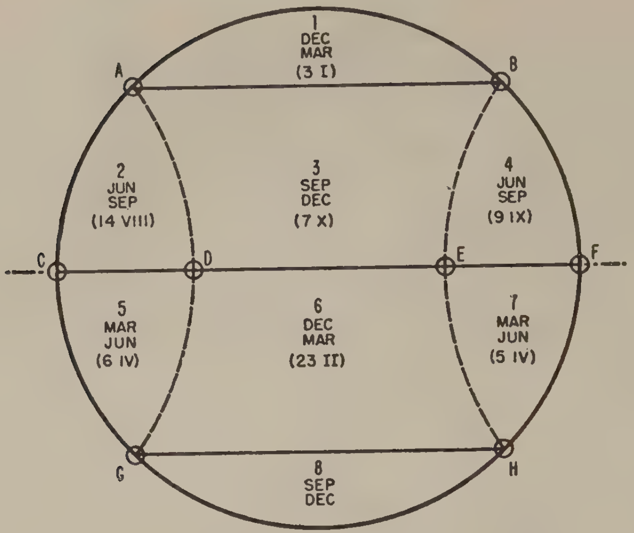

Figure 5. Schematic summary. Solid lines represent zero deviations in September; dashed lines zero deviations in December. For discussion of lettered points, etc., see text.

features of the quarterly patterns, *i.e.*, in September there are east-west zero lines along the Equator and at 45°N and 45°S; in December there are two nearly longitudinal zero lines and two zero points on the Equator at the coastlines.

These zero lines are combined in Fig. 5, which is the schematic representation of Fig. 3. According to this model there are eight nodal points, lettered A to H, where the deviation in sea level is zero during *all four quarters of the year*. Also, since the equinoctial nodal line on the Equator bisects the solstitial nodal lines, the model ocean is divided into eight zones, two each of four possible kinds. Sea level is high in both December and March in zones 1 and 6, high in June and in September in zones 2 and 4, etc. The two quarters of high level are always successive, of course, according to our postulate that where sea level is high in one quarter it is low two quarters later. The quarters of high level are indicated by the names of the months lettered in each zone; the earlier of the two is given on top. We say, for example, December to March, *not* March to December.

We can examine the usefulness of this model as a description of the variations in two ways: (1) verification of the nodal points, and (2) comparison of the expected time of maximum with the observed time.

As one can see from Fig. 3 and from examination of the charts in Fig. 2, the nodal points can be located, but only approximately. Variations are low at all seasons along the coast of Kamchatka (point A) and along California (point B). A zero line lies near the Equator south of the Philippines on all four charts (point C) while point F is identified nearly as well by an intersection of a zero line and the coast of South America at Ecuador on three of the charts. In every season a zero line intersects the Equator just north of Guadalcanal (point D), and another intersection occurs between 140° W and 120° W (point E). A line twenty degress of longitude in extent can hardly be considered a point, but there are no islands near the Equator between 90° W and 150° W to help us locate the

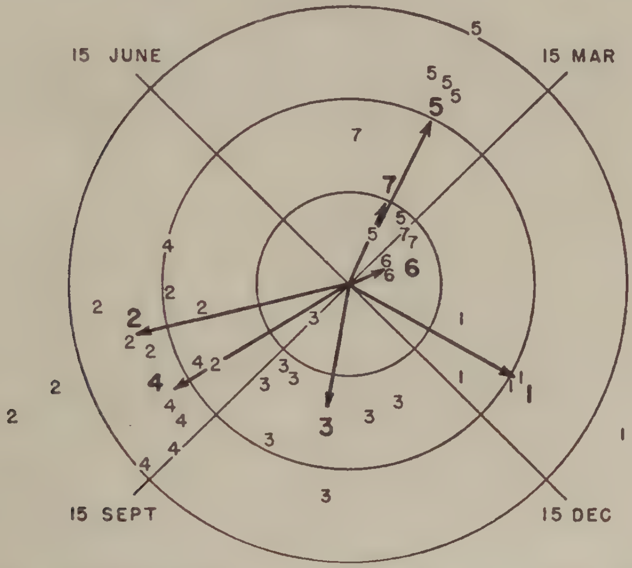

Figure 6. Phase and amplitude of the annual term for all localities within each zone. Date of maximum is given by angular position: 15 March at top right, 15 June at top left, etc. Amplitude is indicated by distance from center; the concentric circles show amplitudes of 5, 10 and 15 cm. Each small number represents one locality within the zone indicated, excepting Hawaii, where all five gauge results were averaged before the harmonic analysis was made. Vectors show mean phase and amplitude for all localities within the zone (vector mean); the zone to which each applies is indicated by the large number placed near the end of the vector.

intersection more accurately. Points G and H can be neither determined nor rejected with the present distribution of data.

Harmonic analyses of the data from each gauge lying within the zones were made, zones being delineated according to Fig. 3. Gauges lying on or near nodal lines were omitted; zone numbers as assigned are given in Table I. The vector mean date of maximum for the annual term for each zone is shown in parentheses in Fig. 5 and plotted as a vector in Fig. 6. From Fig. 5 we see that the time of maximum so computed lies within the expected months in all seven zones where data were available. Fig. 6 illustrates the fact that not only the vector means but the individual station vectors as well agree with the expected times of maxima. We conclude that the schematic model is an adequate if not complete summary of the seasonal sea level variations in the Pacific Ocean during the IGY.

This simple model has certain obvious weaknesses. The nodal lines drawn from the data are by no means as simple as those on our circular ocean, nor is the Pacific circular. The December midocean ridge actually has two maxima, one near Alaska and the other around the Line Islands. Also, the hemispherical asymmetry of the variations has been neglected. However, further refinements of the model are probably not feasible at this time.

Representativeness of Results. One may reasonably ask if a short time-series such as that of the 18-month IGY period is sufficient for determination of the principal features of the average seasonal variation. A further uncertainty is introduced by the fact that many of the IGY installations were made under somewhat unfavorable conditions, so that some of the data cannot be considered as reliable as those from well established gauges operated by experienced personnel. For example, at Arorae Island it was not possible to take staff readings, therefore we have found it necessary to assume that the position of the chart paper does not change appreciably and that all readings refer to "chart zero". This is the worst situation, for all other stations have comparative staff readings, though on occasion parts of the records are missing and other difficulties have occurred.

An estimate of the representativeness of the IGY data may be obtained from the five samples shown in Fig. 7, each representing a different zone among the eight illustrated in Fig. 5. There is by no means exact agreement; month-to-month changes are appreciable and sometimes erratic, and the range of heights observed at each

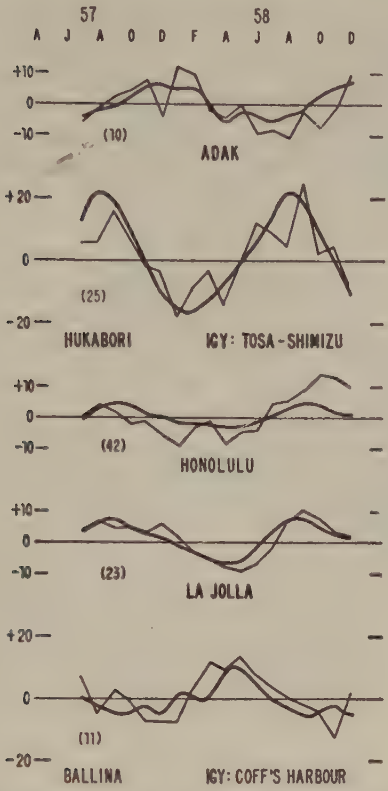

Figure 7. Comparison of IGY results with long-term means at five localities. Light solid lines show monthly mean deviations (cm) during IGY; heavy lines show long-term monthly means. The figures in parentheses indicate the number of years used in finding the long-term mean.

location is larger during the IGY than when long-term monthly means are compared. However, these differences are exactly what one expects when measuring climatological variables for only one year, and we can see that the phase and amplitude relationships among the stations were much the same during the IGY as they were found to be from the long-term means. This implies that combination of and comparison of data from different years is probably permissible, and we can state with some confidence that the patterns shown in Fig. 2 are typical of the average seasonal variations in sea level although neither the details nor the relative slopes indicated should be given any credence.

Causes of Observed Variations. The September-March oscillation has been described and discussed previously in some detail (Pattullo, *et al.*, 1955); at least in lower latitudes it is closely related to seasonal changes in the density of the water column. This close relationship does not in itself constitute an explanation of either the recorded or the steric oscillation, nor does it identify the forces that must be operative to maintain the variable slopes associated with these oscillations.

Lisitzin and Pattullo (manuscript) have found that both the September-March and December-June oscillations are isostatic in the open ocean (total pressure at great depth does not vary). In low latitudes the principal factor is the steric term whereas in high latitudes atmospheric pressure plays the dominant role. However, the large deviations along some coastlines are apparently not isostatic and an additional explanation must be sought; it probably lies in the relationships between sea slopes on the one hand and the effects of winds and nonisostatic currents on the other.

Acknowledgment. This description has been made possible through the efforts of many individuals, particularly Mr. J. D. Frautschy and Mrs. Elizabeth Parker, without whom the great amount of co-ordination and co-operation could not have been achieved. To all I am grateful for the generous help.

REFERENCES

HAMON, B. V. AND F. D. STACEY

Sea levels around Australia during the International Geophysical Year. Austr. J. Mar. Freshw. Res.

LISITZIN, EUGÉNIE

1955. Les variations annuelles du niveau des océans. Bull. Inf. COEC, VII (6): 235–250.

LISITZIN, EUGÉNIE AND JUNE G. PATTULLO

The principal factors influencing the seasonal oscillation in sea level. Manuscript.

PATTULLO, JUNE, WALTER MUNK, ROGER REVELLE AND ELIZABETH STRONG

1955. The seasonal oscillation in sea level. J. Mar. Res., *14* (1): 88–155.

UGGI, UNION GÉODESIQUE ET GÉOPHYSIQUE INTERNATIONALE

1959. Monthly and annual mean heights of sea level for the period of the International Geophysical Year (1957 to 1958) and unpublished data for earlier years. Publ. sci. Ass. Océanogr. phys., No. 20. 65 pp.

(290)

Reprinted from Science of Man, v.1, no.4
June 1961. p.134

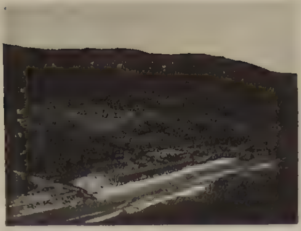

SUBMARINE ARCHEOLOGY

During the last few years a new field of anthropology has come into being. Scientists of Scripps Institution of Oceanography (University of California, La Jolla, California) and the San Diego Science Foundation have been in the forefront of its development. This new field is submarine or underwater archeology.

Due to the recession (melting) of the glaciers after the last (fourth) glacial period, sufficient water was produced to raise the shorelines of our continent a great distance. The last recession of the glaciers took place after Man had found his home in North America. Quite naturally many made their homes along those old shorelines for the same reasons that men today often live on the seacoasts. Today, remains of those cultures are to be found offshore along the continental shelf.

It is difficult to say who was the first to make this discovery, but the greatest amount of credit is due to divers from the Scripps Institution of Oceanography. Shortly after the aqualung was introduced to personnel at the University of California at La Jolla, the divers began recovering large numbers of small stone mortars at depths ranging from a few feet to a hundred feet offshore near La Jolla Beach and Tennis Club. It was some time before it was recognized that this rather small area represented an archeological site

The first recoveries of artifacts consisted of only the stone mortars because they were easily recognized. Little effort was made to recover anything else. As the attention of persons trained in archeology was attracted by this phenomenon the situation changed. Slowly the observers began recovering various types of lithic material, curiously grooved ovid cobbles, numerous bifaced and unifaced manos, an occasional chopper showing some retouching on the edges, and large matates fairly deeply bowled, made from beach rock slabs averaging from 30 to 40 pounds. In addition, four very large mortars made from either sandstone or granite boulders, weighing 60 to 80 pounds, were recovered.

This area since has produced over 3,000 of the small stone mortars. The quantity of material, all lithic in ntaure, unquestionably represents an underwater archeological site. Further investigations along the coast have turned up other material at Solano Beach, Cardiff, Encinitas, Oceanside, and as far north as Santa Barbara. Southward from La Jolla recoveries have been made at Bird Rock, Pacific Beach, Ocean Beach, and San Ysidro. Some variance in the technological abilities of the cultures in these places has been noted.

In the report which the San Diego Science Foundation is preparing, the hypothesis of the advance of the sea level due to the recession of the glaciers mentioned above is corroborated by radiocarbon datings. According to the most recent findings the last recession of the glaciers took place at a period from ten to fifteen thousand years ago. Sea level advance has been graphed (based on carbon dating from core samples from around the world) to show that sea level stood forty or more feet lower along the California coast seven to eight thousand years ago. The landward sites carbon date between five and seven thousand years for our oldest known culture. The advance of sea level eroded away and possibly assorted the nonperishable material by current and wave action. The area in the San Diego region has been reasonably stable geologically from that period to the present, discounting emergence and submergence.

There are, of course, many problems in dealing with the subject of underwater archeology and scientists realize that they are just beginning. The San Diego Science Foundation researchers hope that others having additional information will contact them and exchange ideas, photographs, and data.

Full investigation of even a few of these sites requires a great amount of work and cooperation from many people. The research promises to be of great importance in increasing our knowledge of prehistory and will also reward the student with the thrill of underwater discovery.

James R. Moriarty
Scripps Institution of Oceanography
University of California, La Jolla, Calif.

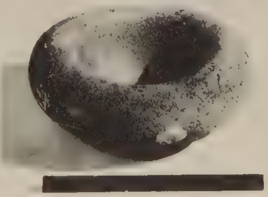

Contributions from the Scripps Institution of Oceanography, New Series, 1261

Reproduced by Permission

Reprinted from Science of Man,
v.1, no.4, June 1961. pp.116-119.

PREHISTORY SITES in the SAN DIEGO COASTAL AREA

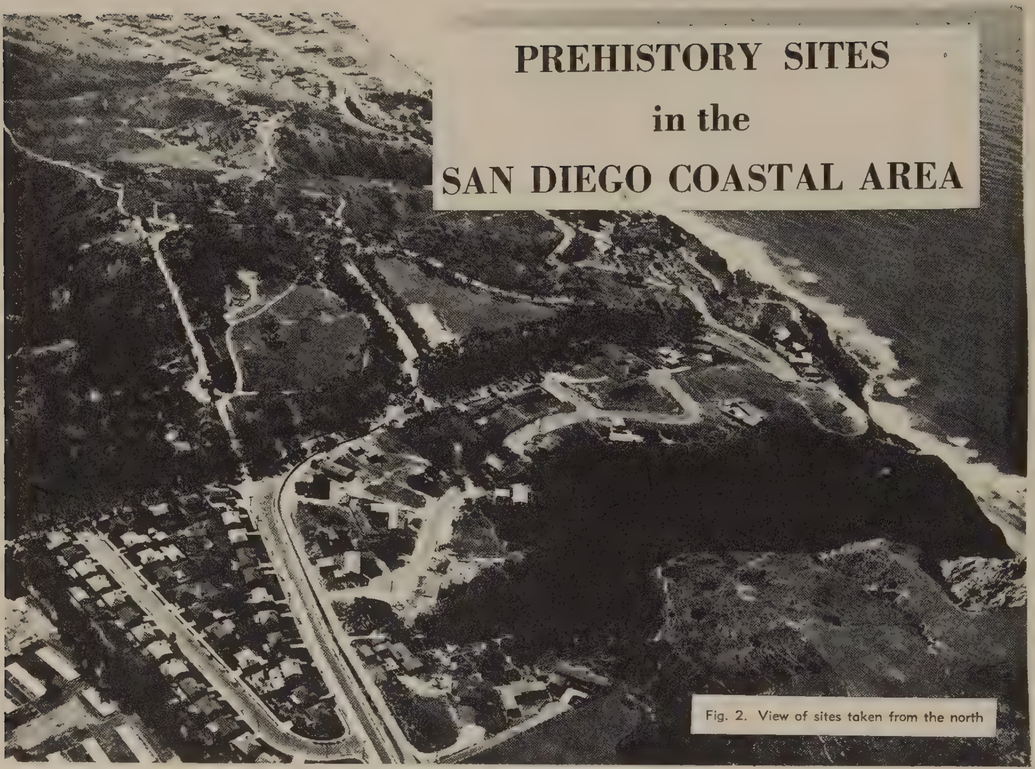
Fig. 2. View of sites taken from the north

By James R. Moriarty, Georgina Peyton, and Priscilla Field*

Until the beginning of the twentieth century, the occupation of North America by man was considered to be a rather recent event. Early anthropological work in the United States was based on the assumption that the ancestors of the present-day Indian had arrived two or three thousand years ago. From time to time fragments of evidence pointing to a much greater antiquity were recovered. In one or two cases, for example, artifacts were discovered in close association with the remains of prehistoric animals, such as the mammoth and Taylor's bison. By and large most of this evidence was discounted, and in some cases was patently ignored.

Since many of the finds were discovered accidentally, by amateurs or by people with no scientific training, such an attitude is understandable. In the majority of cases, these materials had been removed from the site and presented by the finders to universities or museums for identification. As there was no documentation and seldom any witness who had observed the material *in situ*, it was impossible to accept many of the discoveries as evidence of the existence of man long before the generally accepted dates.

The settling of the westernmost states brought about an increase in the anthropological work in that area. More field work was done, and more discoveries were made and reported. As additional information was accumulated, the American anthropologist began to realize that an error had been made in earlier chronology. Since anthropology is better defined as an art rather than an exact science, much of our present-day knowledge of the subject is due to the efforts of men in other fields, particularly geology and chemistry.

The chemist has given us the materials necessary to prepare and preserve archeological finds such as leather, basketry and other perishable materials. Utilization of these methods by archeologists allows us, in many cases, to remove extraneous matter which often surrounds perishable substances such as bone, leaving it unharmed. Perhaps the greatest tool we have received from the chemist is the radiocarbon dating method developed by Dr. W. T. Libbey of the University of California at Berkeley. Carbon-14 dates now have established an antiquity for the North American Indian that previously had been only conjectured.

The first chronologies available were those established by the field geologists. The end of the last glacial advance has been established in time reasonably well. It is from the period of approximately ten to fifteen thousand years ago that the geologist dates the Holocene, that is, the time interval from the end of the Pleistocene to the present. The great glaciers held within their confines tremendous quantities of water. As a consequence, sea level was much lower during periods of glacial advance than it is now. Graphs

---

*Archaeon Society, La Jolla, California.

Contributions from the Scripps Institution of Oceanography, New Series, 1262 Reproduced by Permission

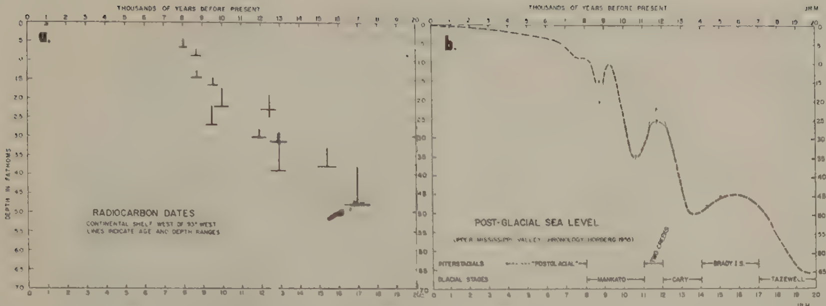

Fig. 1. Post-glacial sea level changes (after Curray, 1959).

have been constructed (Fig. 1) which show that about 7000 years ago sea level was very near the present-day six-fathom contour. Quite simply this means that scores of acres of what was once shore line are presently below sea level to a depth of 36 feet. The earliest occupants inhabited this shore line.

The La Jolla Indian

In the fall of 1958, a group of persons at Scripps Institution of Oceanography, University of California, La Jolla, California, began a series of investigations on a site near the Institution (Fig. 2). This site had been known for many years. During World War II, considerable work was done on it by Malcolm J. Rogers, former curator of the San Diego Museum of Man. As a consequence of the construction of an army camp in the area, numerous finds were made, including 33 burials. Due to the unusually crude lithic industry discovered, it was realized at the time that this culture possibly represented a very early occupation.

Since Mr. Rogers' discovery, numerous other investigators have become interested in the culture, and the name La Jolla has been applied to distinguish it from the more recent historical Indian occupation. From time to time other burials were recovered from the site along with some artifact material, but these were accidental discoveries and primarily arose from the construction of the Scripps Estates, a housing development. Little of value was recovered during this period. In the fall of 1958 a burial was discovered in excellent condition at Scripps Estates, and it was decided to make a complete investigation (Moriarty, Shumway and Warren, *Archaeological Survey, Annual Report*, 1958-1959, University of California, Los Angeles).

A number of additional burials was discovered on unoccupied lots adjoining the original find. With the consent of the owners a series of trenches was dug, and several burials were sculptured in place and preserved in concrete enclosures (Fig. 3). Because the property on which the burials were discovered is privately owned, the preservation in place, of a few La Jolla burials will allow interested persons to observe these remains under their original conditions. Credit for this unique idea is due primarily to the hard work and efforts of Dr. George Shumway who is owner of part of the property upon which the burials lie.

One of the burials, No. 14 (Fig. 4), the Archaean Society removed in a block and then sculptured. It may now be seen as one of the semipermanent exhibits in the Scripps Aquarium-Museum. Along with the burial, the Society has added a representative collection of La Jolla artifacts (Fig. 5).

Scripps Estates Site 1 is only a segment of a much larger site. The Archaean Society decided to continue work on that part of the site which is University of California property. Site UCLJ-M-1 is located at a point where there are no buildings now and where none are contemplated in the near future (Fig. 2). A reconnaissance showed the area to be the least disturbed part of the over-all site. Investigation indicated that only tentative attempts at dry farming had occurred off and on over the last 40 years. Surface evidence showed plowing to a depth of approximately eight inches, which left the greatest depth of the midden undisturbed.

Samples of shell material (*Mytilus californianus*) were taken from site UCLJ-M-1 and Scripps Estates Site 1. The radiocarbon laboratory at Scripps Institution of Oceanography, headed by Dr. Hans E. Suess, returned a date of 6370 ± 170 years B.P. for the lowest level in UCLJ-M-1. At Scripps Estates dates were 5000 for the surface, 6900 for the middle, and 7000 ± 200 years B.P. for the bottom.

It was decided that we would continue our work at UCLJ-M-1 directing our attention primarily to a collection of the artifacts and a study of the probable living conditions of the La Jolla Indian. The history of the area revealed that approximately ten years ago two burials were removed from the site (files of the *San Diego Union*). After surveying and mapping the area, these two burials were plotted into the grid and were numbered 1 and 2. Having made all of our preliminary preparations, we were then ready to proceed with a formal excavation.

In the spring of 1959 actual work began. It was necessary to conduct most of the work during week-ends, as the members of the Society are otherwise employed during the week. The midden in

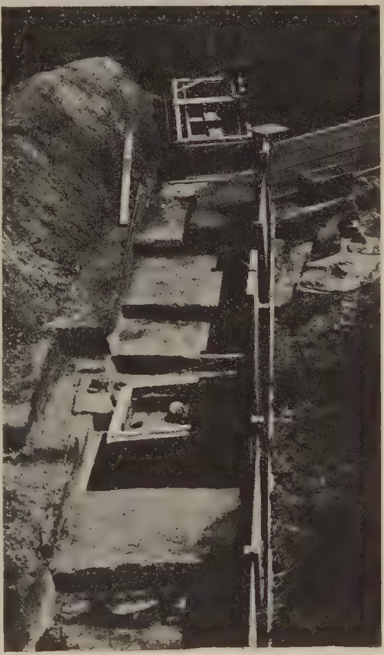

Fig. 3. Exposed burial in finished concrete frame, lower left.

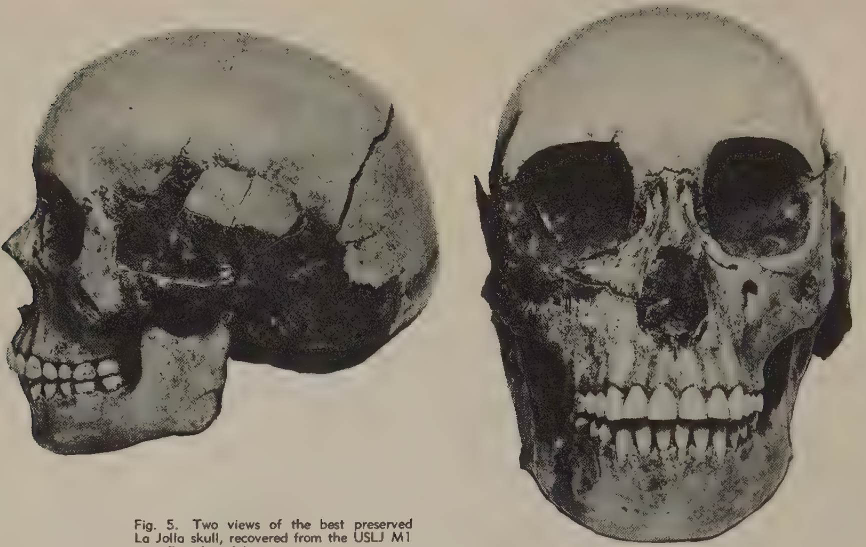

Fig. 5. Two views of the best preserved La Jolla skull, recovered from the USLJ M1 site. Female, adult.

UCLJ-M-1 is distinguished by a dark black topsoil which reaches an average depth of one meter. Quantities of shell material are found throughout the soil with the greatest abundance lying at the lowest levels and decreasing in abundance toward the surface. Great quantities of broken stone are found throughout.

Conversations with old San Diego residents described how 20 years ago it was possible to pick up complete artifacts such as metates and manos and occasional projectile points from the surface. Unfortunately, UCLJ-M-1, like most of the coastal sites, had been completely scavenged by the time formal investigations were started. Even so, a careful reconnaissance of the surface still produces a few manos and pieces of metates. Because of the crudity of the La Jolla lithic industry, such things as scrapers and hammer stones usually are passed over by the casual pot-hunter. They still can be collected in fair quantity by the trained observer.

Since the surface has been disturbed by plowing, the material gathered from it has simply been collected, catalogued and classified. As the archeologist investigates a site, he is always careful to note the depth and position placement of artifacts within it. In the case of material which has been disturbed and is no longer in its original position, classification by typology is about all that can be gained.

As the digging proceeded below the plowed surface, we began to build a picture of the general conditions of life among the La Jolla Indians. Here were the ashes of his fires; here he had placed an ellipse of heavy beach cobbles; here had been tossed the pieces of a broken metate, no longer useful. How did this man fit into the total picture of the age-old migrations?

Although many questions remain, by careful examination of the evidence we now have sufficient information to draw a preliminary and somewhat tentative picture of the coastal occupation at La Jolla from a period of about 7000 B.P. to around 4000 B.P.

The question that arises again and again concerns the origin of the La Jolla Indian. Where did he come from and who preceded him? Occasional evidence has appeared suggesting a previous occupation. By the time the La Jolla Indians were occupying UCLJ-M-1, man already had migrated to the southernmost regions of the western hemisphere. Cave evidence in South America has been carbon-dated as old as 8000 years. We must therefore consider that man had previously reached and then passed beyond the California coastal region. It is reasonable therefore to assume that the coastal region of California was occupied for a long time before the La Jolla came. Who these people were and what they were like remains to be uncovered.

We know that in the first stages of La Jolla occupation the Indian was primarily dependent upon the ocean for sustenance. The greatest abundance of shell and fishbone material appears in the lowest levels of the site. From this we can draw a number of conclusions. The shell material consists entirely of a fauna whose natural environment is near-shore and lagoonal. As there is no evidence of offshore fauna in the site, we can say with some assurance that he had no method of fishing or food-gathering at any great distance offshore. This would seem to eliminate anything except simple boat-building such as raft or reed-boat construction as a cultural trait.

All of the encampments known at this time are located near canyons and sloughs which still contain, or at least in the near past did contain, fresh water. The greatest obstacle to investigations along this line is the advance of sea level in the period extending from approximately 15,000 years ago to the present. As we have seen, tremendous areas of what was once coast are now submerged beneath the sea. This means that occupation of the coast and evidence of it must be sought in most cases below present sea level.

There is no evidence of pottery in the La Jolla culture and as a consequence water must have been carried in some basketlike container or skin. As very little animal bone is found in the early levels and there is little increase in the upper level, particularly in coastal sites, the elimination of carrying devices made of skin seems reasonable. The historical precedent of basket-making of high qual-

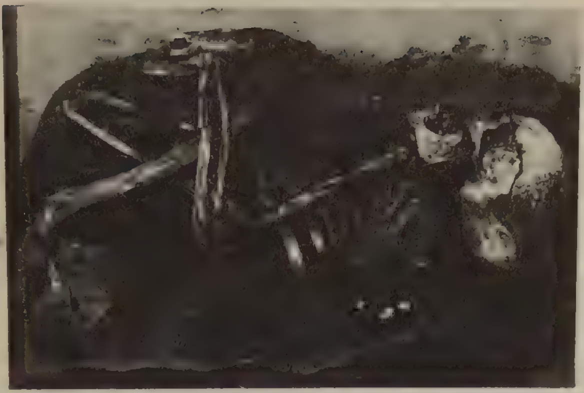

Fig. 4. Burial 14, Scripps Estates Site No. 1. Note caliche forming cast of original depression along side.

ity is well established for Indians of the San Diego area. The Channel Island peoples also used basketry and because, in UCLJ-M-1, tar-coated rock and shell receptacles containing natural tar have been found, the investigator might tentatively make the assumption that tarred basketry was used.

It is felt that there has been a tendency to overstress the simplicity, i.e. crudity, of the lithic industry of La Jolla. It should be pointed out, we feel, that stone artifacts of an equally poor manufacture have been found not only in cultures of great antiquity but were still used by some peoples in quite recent times. Therefore the crudity of the artifacts should play no part in suggesting an even greater antiquity for La Jolla, but should only assist in identifying the La Jolla typologically in the San Diego area.

The use of the fire-hardened wooden point both for projectiles and spears, is not uncommon along the California coast. Such a point dated 4000 years B.P. has been recovered recently from La Brea and dated at Scripps radiocarbon laboratory (personal communication, Dr. Carl Hubbs). Very little trade material is found in UCLJ-M-1. This would tend to indicate very little communication between the La Jolla and other groups during this period of occupation, thereby eliminating, perhaps, a necessity for weapons or other more specially developed stone tools.

It is hoped that in some areas the record of this earlier occupation still may be above sea level. Investigations of the Channel Islands by Phil Orr of the Santa Barbara Museum, and others are turning up such evidence. A great deal of work remains to be done.

An archeological site should be viewed as a crudely written page of history. It is the duty of the scientist to read between the lines of this page whenever possible. In one sense the archeologist is the detective of history. Clues to the story of the past are found in what he sees. It is his duty to put forward his interpretation after the laboratory and field work are completed.

There is a definite romantic side to any archeological investigation. As the layers of earth are meticulously removed, a story slowly unfolds. The burial of a child and the few small treasures enclosed with it, signifying a mother's sorrow; the crippled, aged warrior encased in his last garment of earth, surrounded by his tools and weapons with the charms that gave him victory in battle or success in the hunt; these are the romantic aspects. Each of these finds adds a minute word or phrase to prehistory. It is our hope that through further work we may add a few footnotes to the page of prehistory concerned with the California coastal Indians.

GLOSSARY

Midden. A refuse heap, usually used for many generations. May be of different types such as, kitchen midden, shell midden, etc. A shell midden is the kind referred to in this article.

Sculptured. The dirt is dug out around bones or artifacts leaving them set out in high relief for better photography.

Fig. 6. Some of the more typical examples of the La Jolla lithic materials

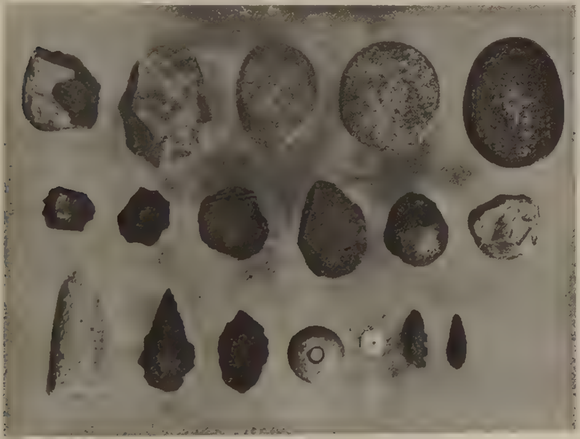

Reprinted from the Journal of
Marine Research, v.17, 1958.
pp.429-431.

PARTICULATE MATTER IN THE OXYGEN-MINIMUM LAYER[1]

By

NORRIS W. RAKESTRAW

Scripps Institution of Oceanography
La Jolla, California

In view of the interest in oxygen distribution in the ocean, it seems advisable to bring to light some observations which were made in the 1930's but which were never published. Some of these data were collected at the same time as those previously reported by Rakestraw and Carritt (1948).

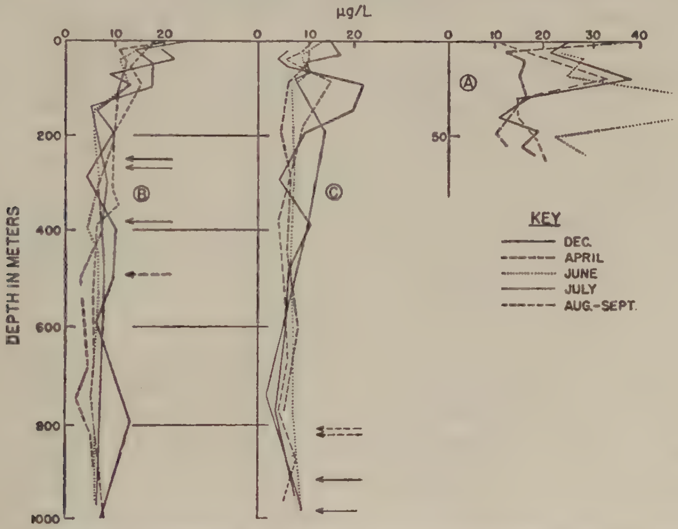

Figure 1. Particulate nitrogen in micrograms per liter at Sts. A, B and C, during 1937–38. Arrows indicate levels of oxygen minimum.

Water samples were collected five times during 1937–38 from three key stations: St. A, on the Continental Shelf about 30 mi SE of Montauk Point (Lat. 49°40′ N; Long. 71°45′ W); St. B, in the slope water northwest of the current of the Gulf Stream (Lat. 39°00′ N; Long. 70°40′ W); St. C, in the Sargasso Sea southeast of

---

[1] Contribution from Scripps Institution of Oceanography, New Series. 1263.

Reproduced by Permission

the Gulf Stream (Lat. 35°30′ N; Long. 67°30′ W). Samples were taken during 1939 also at Sts. B and C.

Determinations of "particulate-nitrogen" were made by a method previously described (von Brand, 1935). While these analytical results are in terms of micrograms of nitrogen in particulate matter contained in one liter of water, they afford at least a relative comparison of the content of total organic particulate matter in the water. Results are shown in Figs. 1 and 2.

It is scarcely necessary to indulge here in a general discussion of the origin of the oxygen-poor layer, since past and current views on this question have been adequately summarized by Richards (1957). Many factors undoubtedly contribute to this phenomenon, including: vertical distribution and origin of oxidizable organic matter, relative rates of sinking and of oxidation, velocities of horizontal and vertical advection, coefficients of eddy diffusion,

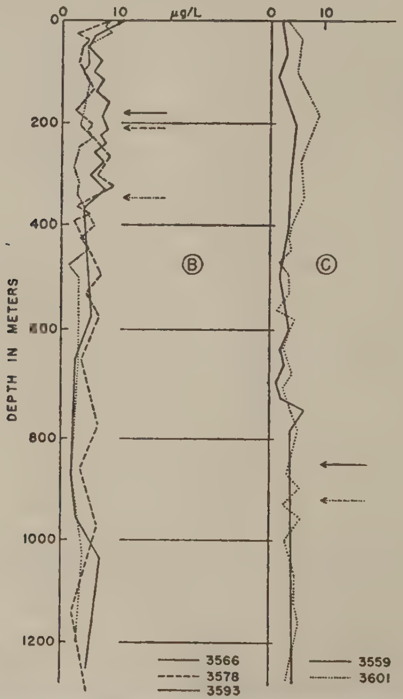

Figure 2. Particulate nitrogen in micrograms per liter at Sts. B and C, during 1939 Arrows indicate levels of oxygen minimum. Numbers correspond to Atlantis stations

(300)

variation of rate of oxidation with temperature, pressure and oxygen concentration, etc. In fact, the very nature of the determinative factors will doubtless vary from place to place.

Several of the theoretical pictures which have been proposed (Seiwell, 1938; Wattenberg, 1939) postulate an accumulation of organic particulate matter at the level of greatest stability, near the bottom of the thermocline, and it has been supposed that this is important in determining the depth of the oxygen-minimum zone. However, inspection of Figs. 1 and 2 shows no such relation. Obviously the vertical distribution of particulate matter is irregular but, although it seems to be more abundant near the surface, there is certainly no indication of any accumulation in the zone of low oxygen.

Jerlov (1953) has also determined the vertical distribution of particulate matter (organic plus inorganic) by an entirely different method, and while his results occasionally show a higher concentration in the low-oxygen zone, there are as many cases in which the reverse is true.

Apparently we must abandon any conception that particulate matter accumulates in the oxygen-minimum zone.

REFERENCES

Jerlov, N. G.

1953. Particle distribution in the ocean. Rep. Swedish Deep-Sea Exped. III, Phys.-Chem. No. 3: 73–97.

Rakestraw, N. W. and D. E. Carritt

1948. Some seasonal chemical changes in the open ocean. J. Mar. Res., *1*: 362–369.

Richards, F. A.

1957. Oxygen in the oceans, *in*, Treatise on marine ecology and paleo-ecology. (Edit., J. W. Hedgpeth). Geol. Soc. Amer., New York. Vol. 1, Chap. 9.

Seiwell, H. R. and G. E.

1938. The sinking of decomposing plankton in sea water and its relationship to oxygen consumption and phosphorus liberation. Proc. Amer. phil. Soc., *78*: 465–481.

von Brand, Theodor

1935. Methods for the determination of nitrogen and carbon in small amounts of plankton. Biol. Bull. Woods Hole, *69*: 221.

Wattenberg, Hermann

1939. Die Entstehung des Sauerstoffarmen Zwischenschicht im Ozean. Ann. Hydrogr., Berl., *5*: 247–266.

(301)

Comp. Biochem. Physiol., 1961, *Vol.* 2, *pp.* 181 *to* 201. *Pergamon Press Ltd., London. Printed in Great Britain*

CARDIOREGULATION IN AN ANEURAL HEART*

D. JENSEN

Division of Marine Biology, Scripps Institution of Oceanography, University of California,
La Jolla, California

(*Received* 14 *October* 1960)

Abstract—1. The aneural branchial heart of the California hagfish (*Eptatretus stoutii*) was used in these experiments. The evidence indicates that the myocardium of this species possesses a pressure-sensitive, diffuse, myocardial pacemaker.

2. Electron microscopic studies have revealed in the heart of this species heretofore undescribed atypical subendothelial cells which strongly resemble secretory cells.

3. Biochemical studies, in extension of earlier work, indicate that pacemaker activity is linked to a small-molecule metabolite found in the heart (but not in the liver). This cardioaccelerator substance is not species specific, but it will exert its effect on the hearts of frog and mussel as well as on that of the hagfish.

4. It is suggested that there may be a relationship between the atypical cells and the cardioaccelerator material.

5. It is concluded that cardioregulation in the aneural branchial heart of the hagfish is accomplished by two major factors: tension as governed by venous return and a biochemical factor produced in the heart.

INTRODUCTION

CARDIOREGULATION presupposes that the normal myocardium is able to adapt itself to the circulatory demands imposed upon it by the organism. Two factors are of prime importance in this regard: first, the stroke volume; and, second, the rate at which the heart beats.

The stroke volume, or volume of blood expelled from the heart per contraction, is dependent upon the venous return to the heart. Consequently, and within definite limits, an increased diastolic filling precedes a greater stroke volume on the part of the myocardium. This general statement is usually referred to as "Starling's law of the heart" (1918). Actually, however, the foundation for such a concept was laid some years earlier by the work of Frank (1895).

The heart rate at a given moment is the resultant of many factors impinging upon the myocardium. Among these are temperature, nervous influences from higher centers (accelerator and/or depressor), inherent rhythmicity, endogenous metabolism and humoral influences imparted by the blood itself. Another condition of extreme importance with regard to heart rate (as well as to stroke volume) is the degree of stretch to which the cardiac muscle is subjected during diastole, whether from internal or external sources. The relevance of this latter factor to the present study is such that it will be considered in some detail.

---

* This work was carried out during the tenure of a Fellowship-Grant from the San Diego County Heart Association, to which grateful acknowledgement is made. Contribution from the Scripps Institution of Oceanography, New Series. 1264

Reproduced by Permission

Using the neurogenic adult *Limulus* heart Carlson (1904a,b) found an augmentation of the rate when external tension was applied to this organ. Even more pronounced acceleration was found when the filling pressure was increased by introduction of fluid into the lumen of the heart (Carlson, 1907). However, if the ganglion was removed, such an acceleration failed to occur in either case. Unfortunately, he did not report similar experiments on the non-innervated myogenic *Limulus* embryo heart (Carlson & Meek, 1908). Carlson also reported experiments dealing with the effects of tension on the heart rates of various crustaceans and molluscs (1904b, 1906), notably studies using the myocardium of the giant California slug *Ariolimax*. In addition to extending his *Limulus* studies to this species he found that increased intraventricular pressure actually induced a beat in fatigued hearts which again ceased when the perfusion fluid was withdrawn.

Recently Blinks (1956) working with the dog and rabbit, Pathak using the frog, rabbit, dog, rat and guinea pig (1957, 1958a,b) and Keatinge on the rabbit, tortoise and frog (1959a,b) independently found that an increase in heart rate could be elicited by increased external tension and/or internal filling pressure.

The foregoing studies indicate clearly that myocardial distension, especially of the right atrium, is effective *per se*, in producing cardioacceleration in a wide variety of species. Based on his studies using the neurogenic *Limulus* heart, Carlson suggested (1907) that tension would mediate its acceleratory effect in the heart (regardless of species) via stimulation of intracardiac nerves, rather than by direct action on the muscle, a view still held today.

A critical test of this hypothesis would rest upon experiments performed on an aneural heart.

Almost 60 years ago Greene discovered that the branchial (or systemic) heart of the adult California hagfish is aneural (1902a,b). Subsequent work has confirmed this observation (Carlson, 1904c; Fänge & Östlund, 1954; Augustinsson *et al.*, 1956; Jensen, 1958; Results section 4). In the conclusion to his paper on the hagfish, Greene stated: "Any regulation of the heart's action must depend upon the conditions which affect the muscle directly, i.e., tension, nutrition, etc. The volume and pressure of the blood coming to the heart and the changes in the pressure upon the internal organs produced by the ever-varying movements of the plastic body of the animal are the factors that must have a decided influence on the hagfish heart."

Throughout the course of earlier studies by the writer (Jensen, 1957, 1958) pertaining to certain physiological and biochemical aspects of the hagfish heart, as well as others to be reported here, it was repeatedly observed that the isolated hearts accelerated for several minutes following the mechanical disturbance attendant upon lavage of the chamber with medium of the same composition and temperature. It was also noted that manipulation of the heart during the dissection sometimes accelerated the beat. Investigation of these casual observations followed under more controlled experimental conditions. The data to be presented indicate that increase in the rate of the branchial heart of the hagfish is in part dependent upon the diastolic volume: hence one factor governing cardioacceleration in this non-innervated but spontaneously contractile organ is the action of a pressure-sensitive myocardial pacemaker. Data are also presented which suggest that this aspect of cardioregulation is related to the operation of a biochemical mechanism.

MATERIALS AND METHODS

Two species of animals were employed for this investigation: California hagfish, *Eptatretus stoutii* (= *Polistotrema stoutii*) and grassfrogs (*Rana pipiens*).

The hagfish were collected by the method and at the locality previously described (Jensen, 1959). Mature specimens of both sexes were employed; no differences were noted in their cardiac activity. After collection, the animals were kept at about 10°C in well-aerated sea water which was changed frequently. It was unnecessary to feed them, as they remain thus in excellent condition for over 5 months in the laboratory; however, the experiments here reported were conducted within 2–3 months after collecting the animals. Specimens collected throughout the year showed no evident seasonal differences in their myocardial activity.

The grassfrogs came from a commercial dealer in Oshkosh, Wisconsin. All males were specially selected for pregnancy tests. (Average length: 7·4 cm nose to crotch; weight: 31 g.) They too were kept at 10°C, but were used within a week or so after arrival.

The hagfish hearts were prepared for recording as follows: the animal was grasped by the head with a hemostat, and the brain crushed. Another hemostat was clamped on the caudal fin and the fish stretched out on a board. A midline incision revealed the liver: the anterior lobe was deflected, exposing the branchial heart and ventral aorta. A thread was placed about the aorta and later attached to the strain gage for recording. Another thread, containing a small loop, was then securely tied about the atrioventricular junction or the cardinal veins to secure the heart to a glass hook in a constant temperature chamber. Generally, only the ventricle was used. Never did the atrioventricular ligature induce an interruption of the ventricular rhythm.

The frogs were pithed, the heart exposed, and a thread sutured into the ventricular apex. A second thread with the small loop described above was secured about the aortic trunks near their bifurcation just anterior to the truncus arteriosus. Thus, atrial and ventricular contractions were both recorded.

After placement of the threads, the hearts were rapidly excised and placed in the constant temperature chamber controlled to within ± 0·1°C and calibrated to 10·0 ml. Artificial sea water (Jensen, 1958) was used for the hagfish studies (pH 5·8) and Ringer's solution (Prosser, 1952) without glucose (pH 7·2) for the frog hearts. All media, extracts, etc. were made with glass-distilled water. The media were gassed continuously with 95% $O_2+5\%$ CO_2 in all studies, and the temperature maintained at 15°C, except where otherwise noted (Table 1). Under these conditions, the frog hearts could be maintained routinely *in vitro* at a steady spontaneous rhythm without internal perfusion for 4 hr or longer, whereas the hagfish preparation would beat for over 18 hr. Before the start of any experiment, the heart was allowed to "equilibrate" in the apparatus for at least half an hour; if spontaneous irregularities in the beat occurred during this interval, the heart was discarded.

Before the addition to the chamber of any solution, its pH and temperature were carefully adjusted, and a volume of fluid equivalent to that being added was removed so that the final volume in all cases was 10·0 ml. When the additives were washed out of the chamber, a minimum of 100 ml of appropriate medium at the same temperature was used to effect this lavage.

(305)

Isotonic contractions were recorded by placing a weak spring in series with the thread from the heart to a Model G7A Statham transducer. After suitable amplification (Brush universal D.C. amplifier) the tension developed by each contraction was recorded on one channel of a Brush two-channel oscillograph. Silver–silver chloride electrodes contained in small glass tubes filled with saline solution were placed directly on each side of the ventricular base to record the spontaneous action potentials (electrocardiographs). This position was chosen arbitrarily as it interfered least with the movement of either heart or electrodes during systole, and permitted reasonably consistent results from different preparations. The actual configuration of the potentials would, however, vary somewhat depending upon the exact placement of the electrodes on the epicardial surface. These potentials were amplified (Brush high gain D.C. amplifier) and recorded simultaneously with the myogram on the adjacent channel of the oscillograph. This latter instrument was equipped with a timing device to give signals at 1 sec intervals which were recorded at the bottom of the chart at the same time as the other data. The oscillograph was equipped with six speeds, enabling continuous recording during a given experiment at chart rates up to 12·5 cm/sec. Thus, action potential, tension developed and heart rate could be recorded and the individual cardiac cycles expanded or compressed on the graph in time as required for a given study.

Each preparation served as its own control; where possible, several observations were made on the same heart. No attempt is made to report absolute values, but rather comparative figures relating control and experimental findings in the same preparation. However, a number of similar experiments were conducted on different heart preparations; the exact number is summarized under Results.

For the distension studies, a cannula was constructed from the shank of a 27 gage hypodermic needle connected to a 0·25 ml tuberculin syringe by a fine polyethylene catheter (i.d., 0·015 in. × o.d., 0·043 in.). The needle was inserted into the lumen of the hagfish ventricle through the aorta, and its tip gently forced past the ventriculoaortic valve during systole so that it was placed in the ventricular lumen. In the frog, the cannula was inserted directly into the ventricular cavity through the apex and secured in place by a tight mass ligature which also served, in both hagfish and frog, to connect the heart with the strain gage.

A Grass stimulator was used where indicated, and the artificial stimuli were delivered through silver–silver chloride electrodes in direct contact with the epicardial surface.

For routine histological examination, the hearts were fixed by perfusion with Bouin's fluid and stained with hematoxylin and eosin after paraffin imbedding and sectioning at 6 μ. Ventricles for electron microscope study were cut at approximately 0·05 μ or less after osmium fixation. No special staining techniques were employed. An RCA electron microscope was used for examination and photography.

The tissue extracts were prepared as follows: After collection of a large number of hagfish, the branchial hearts were dissected from the animals and freed of excess fat and connective tissue. After blotting on Whatman No. 1 filter paper, the still-beating hearts were frozen immediately and pooled in a jar chilled by a dry ice–acetone bath. They remained frozen until subjected to lyophilization, usually within 2 or 3 days. The dried tissue was then thoroughly ground in a mortar, and the coarse reddish brown hagfish heart powder stored in tightly sealed jars at −5°C until needed for extraction. Ten lots of this material were thus prepared, representing the myocardia from over 4000 fish. The powder retained its biological activity even when stored for periods of up to 1 year before extraction.

Hagfish liver powder and rabbit heart powder were similarly prepared for extraction from the respective tissues after thorough exsanguination.

Hagfish heart extract (HHE) was prepared by placing a weighed quantity of the powder in a mortar and thoroughly triturating with a known volume of appropriate solvent. This was usually the medium in which the succeeding experiment was to be conducted, or glass-distilled water if further manipulations were to be carried out on the extract. (In general, 0·1 g of powder was treated with 1·0 ml of solvent.) The system was then subjected to centrifugation at 5000 rev/min for 20 min. Following such treatment, the material was separated into three sharply-defined layers; an upper fatty zone, a clear reddish middle area and a firmly-packed pellet of tissue-detritus at the bottom. The clear middle layer was carefully removed to the exclusion of the other areas, and is termed HHE. Hagfish liver and rabbit heart extracts were similarly prepared.

Further experimental treatment of the HHE is dealt with fully where appropriate (see Results).

Hematocrits were obtained by taking blood samples in capillary tubes from the hagfish ventral aorta immediately anterior to the heart, the tubes were sealed at one end and centrifuged for 15 min at 5000 rev/min.

The following drugs were used in this study: α-epinephrine-bi-tartrate from the California Corporation for Biochemical Research, Los Angeles, 63; Isuprel hydrochloride (Isoproterenol hydrochloride) from the Winthrop Laboratories, New York 18, N.Y.

RESULTS

1. *Distension studies*

Large adult hagfish of similar size were selected for these experiments so that the results might be comparable. The average length of the animals was 39 cm and the average weight 72 g. The isolated, spontaneously beating ventricle was selected for cannulation as it was possible to obtain preparations without leaks under controlled conditions in which known volumes of saline solution could be

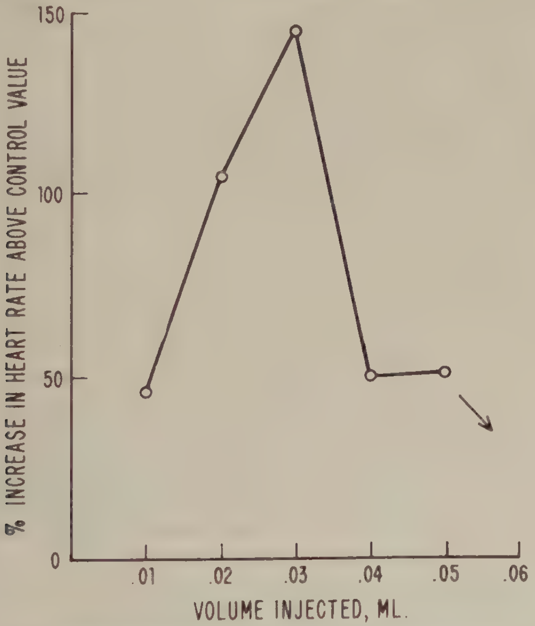

FIG. 1. Each point represents the average value of five observations. Ten ventricular preparations were used. Arrow at 0·05 ml on abscissa indicates that neither electrocardiographs nor myograms were detectable at higher injection volumes.

introduced and withdrawn at will. In all, seventy-one observations of this sort were carried out, using different volumes of fluid. A total of twenty-seven hagfish ventricular preparations were included in this group of experiments. Of these, twenty-three (85 per cent) responded to an increase in intraventricular volume by an increase in rate, not force, of the beat. Four ventricles failed completely to alter their rhythm for no accountable reason.

Fig. 1 indicates the increase in rate above the control level plotted against the volume of saline injected. Although the rates of the individual hearts varied widely from experiment to experiment and in the same preparation during the course of several studies, it may be seen from the graph that, over a narrow volume range in hearts from fish in the size range indicated, the percent change in rate is approximately proportional to the volume injected. The response to distension occurred almost immediately; it was sustained until the excess fluid was withdrawn, at which point the rate gradually returned to its control value. This usually occurred in about 2–3 min and was a consistent finding (see Fig. 2).

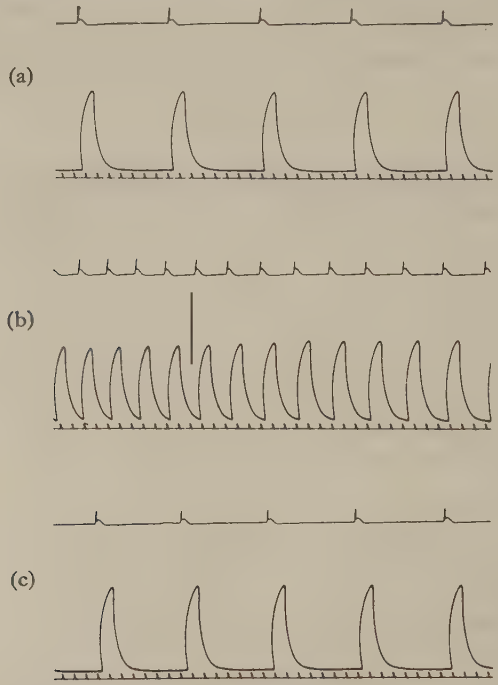

FIG. 2. Effect of mechanical distension on the isolated spontaneously beating hagfish ventricle. (a) Control record, rate = 8 beats/min. (b) Rate at approximately 30 sec after injecting 0·03 ml of saline = 30 beats/min. At mark, fluid was withdrawn. Note gradual slowing and slight positive force increase. (c) 3 min after (b). Rate = 8 beats/min.

In all figures, the upper trace of each chart segment indicates the spontaneous action potential, the middle record is the myogram, and the bottom record is the time signal at 1 sec intervals.

It was repeatedly noted that the introduction of volumes of about 0·04 ml or greater caused the rate decrease recorded in Fig. 1 except when hearts from larger fish (about 50 cm in length) were used. In addition, a consistent decrease in the force of the beat was observed upon ventricular distension regardless of volume injected in these studies.

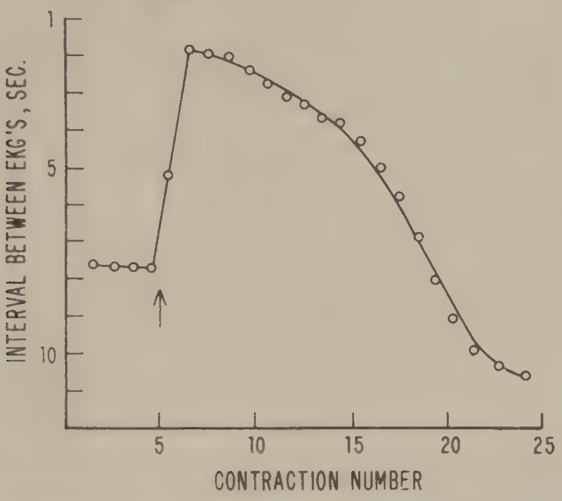

FIG. 3. Isolated spontaneously beating hagfish ventricle with small puncture to permit fluid to escape. At arrow, 0·01 ml of saline was injected. Total elapsed time from contraction 1 to 24 was 132 sec.

The phenomenon of cardioacceleration produced by stretching the myocardium was by no means limited to the ventricular cannulation experiments. For example, injection of 1·5 ml of saline into the portal vein of several large specimens *in situ* induced a rate change in the systemic heart from about 34 to 44 per minute. In addition, a slight tension induced by stretching the isolated heart between pairs of forceps caused a rate increase as did manipulation of the thread and aspiration of a small bit of epicardium into the tip of the electrodes during their adjustment *in vitro*. Another method found successful in producing cardioacceleration *in situ* was "milking" the blood toward the heart from the posterior cardinal and portal veins by gently stroking these vessels simultaneously in a posteroanterior direction with a finger.

In six preparations, the ventricular epicardia were punctured to impart a very slight leak to the system; thus, a small quantity of medium could be introduced during diastole which would be expelled during the succeeding systoles. By pulsatile injections of 0·01 or 0·02 ml of saline during the diastolic interval, it was found possible approximately to double the control rate for as long as the injections were continued, deceleration occurring as the perfusion was stopped. The tension had to be maintained for several seconds, otherwise acceleration would not occur. A single very rapid stretch produced no effect on the rate.

As controls, two spontaneously beating frog hearts were cannulated (*vide supra*) and Ringer's solution introduced at volumes ranging from 0·01 to 0·08 ml in steps of 0·01 or 0·02 ml. Absolutely no rate effect was obtained in twelve trials; however, a clear-cut and definite increase in force of the contractions was obtained repeatedly in both preparations. Within limits, this force increase was related to the volume of fluid introduced.

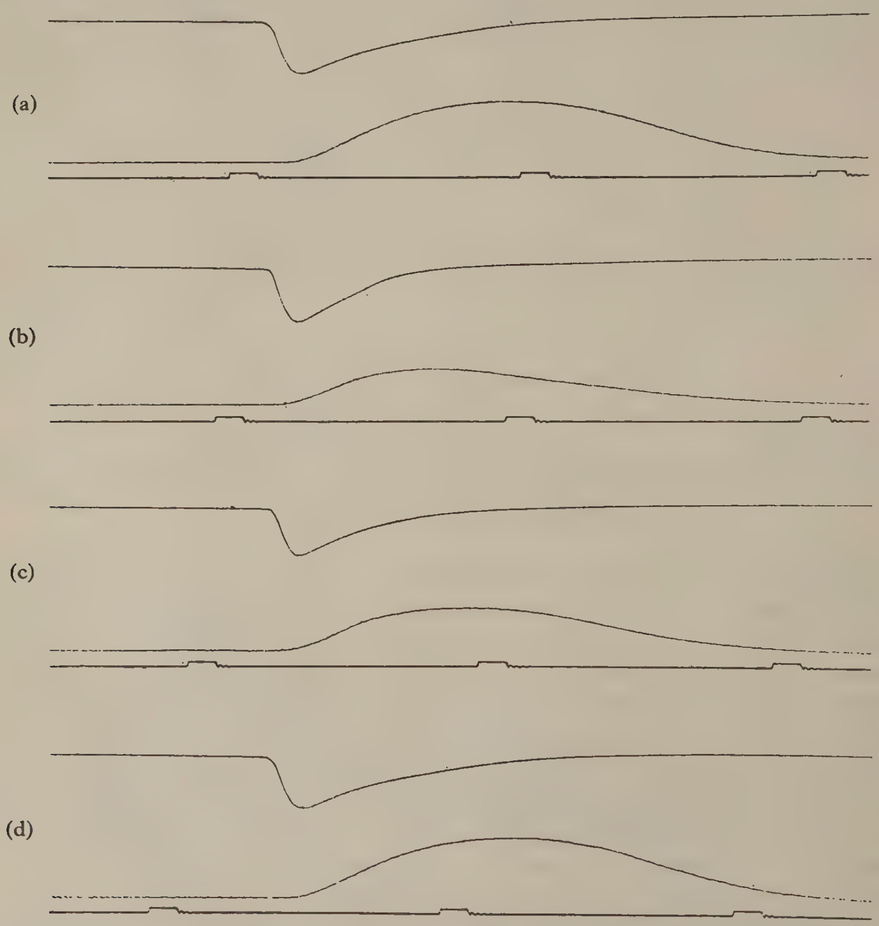

FIG. 4. High-speed records of several contractions of a spontaneously beating hagfish ventricle (punctured) before and after mechanical stretch. (a) Control contraction. (b) Contraction immediately following introduction of 0·03 ml of saline. (c) Fifth contraction after introduction of saline. (d) Tenth contraction after introduction of saline. Note the decreased force of the contraction in (b) and (c).

Fig. 3 illustrates a time-curve of acceleration and deceleration during and after distension of a hagfish ventricle which, as previously described, had a small puncture in the epicardium to permit the fluid to escape. As the rate during this experiment was changing, the time interval between the start of successive EKG's is plotted on the ordinate, and this figure is placed at the midpoint of successive contractions on the abscissa. This curve was obtained from one of three similar experiments performed on this ventricle; it illustrates the rapid acceleration followed by the gradual decline in rate as the fluid is expelled. The final rate was somewhat lower than the control value. This figure qualitatively rather than quantitatively exemplifies a fact observed three times in one heart and also in several other preparations.

Fig. 4 shows a series of contractions obtained when the oscillograph was running at 12·5 cm/sec in order to study in more detail the individual cardiac cycles. Taking the sharp downstroke on the EKG as the depolarization phase, this was markedly accelerated immediately following the introduction of 0·03 ml of saline. The average time for this interval derived from several control observations was 104 msec, while the comparable figure for the three successive contractions after distension was 88 msec, or a decrease of about 15 per cent. Similarly, the latent period of systole was reduced from 82 to 72 msec for the same contractions (−12 per cent). The contraction phase declined about 11 per cent, whereas the relaxation phase remained about the same. It is also worthy of remark that once again a decrease in force of the contraction was observed.

2. *The effect of temperature on the rate of the branchial heart*

The results in this section are summarized in Table 1. The average rates of the systemic heart in thirty fish of both sexes were found to be 16/min at 13°C and 30/min at 26°C. Thus, the rate approximately doubles for this 13° rise in temperature. Studies *in vitro* indicated that the entire branchial heart beats at a somewhat faster rate than the isolated ventricle alone. It is interesting to note that the branchial heart beats at a somewhat faster rate when first isolated than *in situ*. This probably reflects in part mechanical effects resulting from setting up the preparation as well as the slight external tension under which the organ is placed for recording. A number of observations on the rate of the spontaneously beating isolated frog heart are included in Table 1 for comparative purposes. Generally the heart of this species beats at a much higher rate at 15°C than did the branchial heart of the hagfish.

In a series of hagfish heart observations, the heater in the water bath was shut off while the refrigeration unit continued to run, allowing the temperature in the chamber to descend gradually toward 0°C. At about 1°C the rate was much reduced (about 3–4 beats/min), but usually the contractions remained strong and regular. Conversely, as the temperature was permitted to approach or exceed 30°C, the beat generally weakened and became erratic. Consequently, it appears that the myocardial function of these animals is in part dependent upon rather low temperatures, a fact borne out by the observation that the hagfish will not survive long in aquaria at temperatures substantially exceeding 20°C. This also is of interest in relation to the general habitat of these Cyclostomes since in Southern California they occur in much deeper waters than in the Northern latitudes, although the temperatures in the two areas are approximately the same.

TABLE 1—EFFECT OF TEMPERATURE ON THE RATE OF THE HAGFISH BRANCHIAL HEART

Group	Species	Sex	Preparation*	No. of animals	Temp. (°C)	Heart rate† (beats/min)
1	*E. stoutii*	Mixed	Branchial heart *in situ*	30 30	13 26	16 ± 0·73 30 ± 1·85
2	*E. stoutii*	♂	Branchial heart *in situ*	18 18	13 26	15 ± 0·886 30 ± 2·10
3	*E. stoutii*	♀	Branchial heart *in situ*	12 12	13 26	18 ± 3·37 31 ± 2·16
4	*E. stoutii*	Mixed	Isolated branchial heart	20	15	26 ± 1·35
			Isolated ventricle of branchial heart	20	15	16 ± 0·684
5	*R. pipiens*	♂	Isolated heart	33	15	37 ± 1·13

* Groups 1, 2 and 3: the fish were pinned to a board and a small ventrolateral incision made on the left side revealing the branchial heart: the rate was counted three times for each fish at each temperature by three independent observers. These closely agreeing rates were averaged, and used in the Table. Groups 2 and 3 represent Group 1 separated according to sex. There is no significant difference between the rates of each sex at either temperature (*t*-Test). The rates for Groups 4 and 5 were obtained directly from the oscillograph record about 10 min after the preparation was set up.

† Including standard error of the mean.

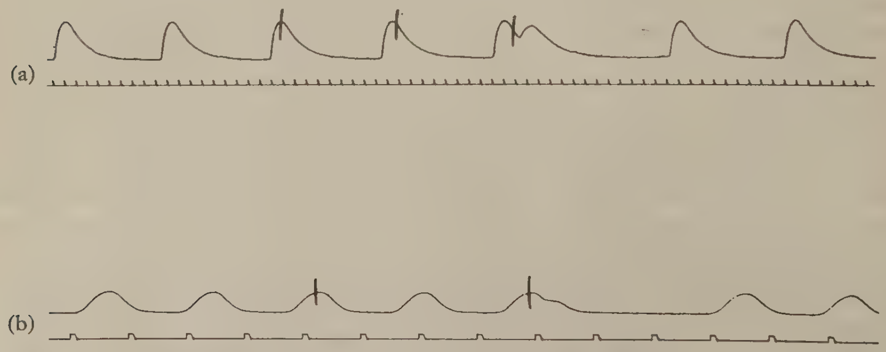

FIG. 5. (a) Determination of refractory period of hagfish ventricle. Single square wave pulses (150 V, 2 msec duration) were delivered at points indicated by vertical bars on myograms. No electrocardiographs were recorded. (b) Frog ventricle for comparative purposes. Stimuli applied as above. Note that in (b) the recording chart speed was somewhat faster. Time signal, 1 sec in both cases.

3. *Electrical stimulation of the hagfish ventricle*

Five isolated hagfish ventricles were employed for these studies; two frog hearts served as controls. Fig. 5(a) illustrates the fact that in no case could an extrasystole be induced until the heart was well into diastole, indicating that the refractory period in these organs is quite long. This observation was repeatedly confirmed in all preparations, and usually the heart failed to respond until much further in diastole than illustrated in the figure. (See also Fig. 6.) By contrast, Fig. 4(b) shows that under similar conditions, stimulation of the frog ventricle at about the peak of its contraction resulted in an extrasystole and compensatory pause. This was a consistent finding in the frog heart.

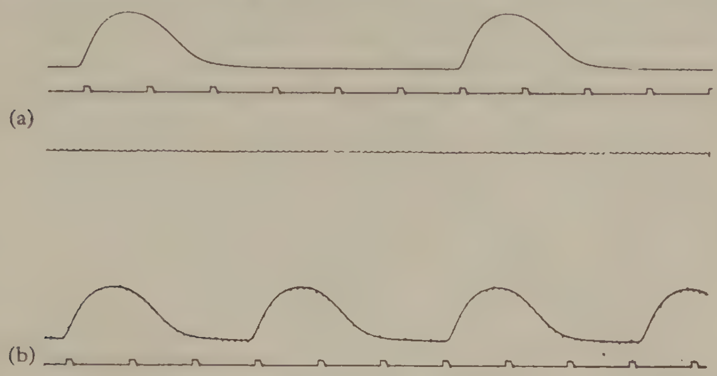

FIG. 6. Effect of artificial stimulation on the rate of a spontaneously beating hagfish ventricle. (a) Control rate = 12 beats/min. Signal magnet trace omitted from top of this chart. (b) Stimulated at a rate of 10/sec, at 100 V with 2 msec square wave pulses. Rate during stimulation = 24 beats/min. (Third trace from top is of signal magnet indicating when stimuli were applied.)

Attempts to induce quiescence in the hagfish ventricle by atrioventricular ligation in order to study the staircase phenomenon failed completely as did low temperature. In a non-beating frog ventricle (Stannius' ligature number 2) the staircase effect could be readily produced. The threshold voltages for inducing ventricular extrasystoles in the hagfish were consistently higher than in the frog. However, a wide range of voltages were tested on each preparation, and levels much higher than threshold were used.

Attempts to stimulate the hagfish ventricle with currents of 100 V (2 msec square wave pulses) applied at rates of 30/min, 10/sec or 50/sec, produced an acceleration of the rate; however, as tested, no stimulus was effective until late in diastole as with the single pulses (see Fig. 6).

4. *Histological studies on the hagfish heart*

The microscopic anatomy of the hagfish ventricle presents a number of unusual features which are of sufficient importance to warrant their inclusion here. Although an earlier paper mentioned the lack of neural elements in the myocardium (Augustinsson *et al.*, 1956), no photographs were published, nor was the histology of this organ presented in any detail. The following discussion, however, is concerned primarily with those anatomical details which are relevant to a better understanding of the physiological and biochemical data presented in the other sections of Results.

Sections of hagfish branchial hearts stained with hematoxylin and eosin revealed that these organs are invested in a clear-cut pericardium. The epicardial layer was very thin (about three cells thick), and stained very deeply. Under lower magnifications, the myocardium of both auricle and ventricle was extremely diffuse and trabecular in appearance; the structure of the former was far thinner and more delicate-appearing than that of the latter chamber. Study of these slides under an oil immersion lens disclosed typically striated myofibrils, fusiform in shape and imbedded in large quantities of sarcoplasm. There was no evidence of blood vessels to denote a coronary system; however, the general paucity of muscle fibers and the extremely spongy character of the myocardial elements indicate that nourishment of the heart may be readily accomplished by diffusion from the venous blood passing through the chambers. Collagenous connective tissue was quite sparse. The endothelial cells possessed relatively large elongated nuclei; their cytoplasm was flattened and closely invested the strands of muscle fibers, which possessed few nuclei.

Electron microscope studies demonstrated several other interesting details of the fine structure of the hagfish ventricle. Fig. 7 illustrates a longitudinal section of this organ. At the left is a thin sheet of endothelial cytoplasm. Note the irregular size and relative scarcity of the myofibrillae and the numerous mitochondria scattered about in the sarcoplasm. Neither capillaries nor connective tissue are evident. Neural elements were not observed in confirmation of earlier findings. No sarcolemma is present.

Fig. 8 shows an interesting and atypical form of cell which was found scattered throughout the myocardium, always in a subendothelial position, but never found imbedded in the myocardial substance proper. The densely packed, dark-appearing granules were a consistent finding, and the presence of these "secretory" cells taken in conjunction with some of the biochemical data (Results section 5) lend credence to the suggestion that the hagfish heart may possess an endocrine as well as pulsatile function. Subsequent to the discovery with the electron microscope of these atypical structures distributed in random fashion throughout the myocardium, a careful re-examination of the stained sections under an oil immersion lens revealed that they can be distinguished by this means also (but only with great difficulty) from the other myocardial elements. Consequently, it is not surprising that these structures have not been reported heretofore. It is possible, however, that these cells could be revealed more easily by the use of special staining techniques.

5. *Biochemical studies on hagfish heart extracts*

The experiments included in this section represent a number of preliminary investigations dealing with the nature of the cardioactive material reported

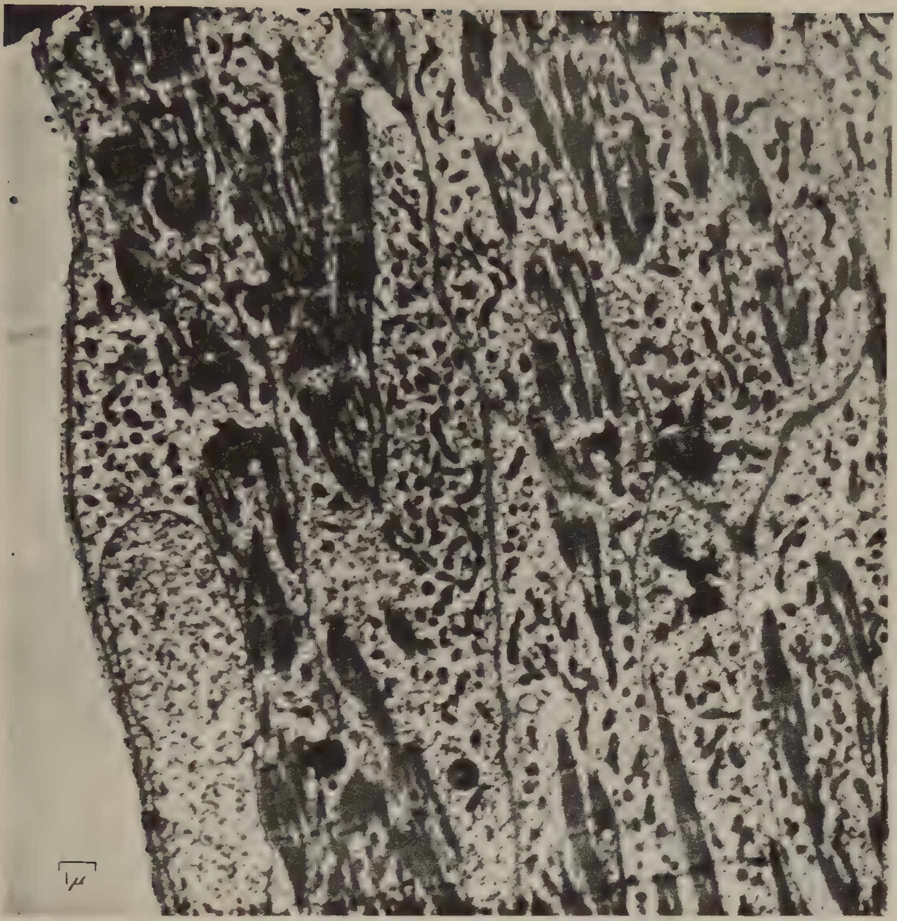

FIG. 7. Electron photomicrograph of longitudinal section of hagfish ventricle. Endothelial sheet at left. Large black marks are fixation artifacts. (× 4680).

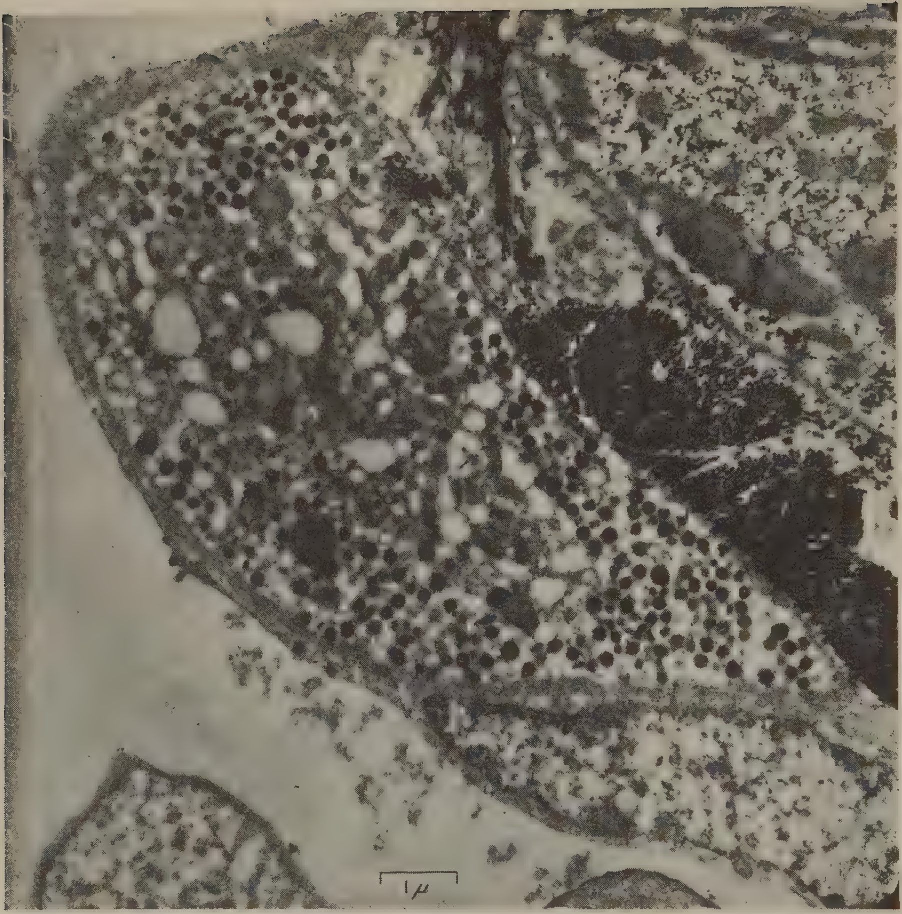

FIG. 8. Electron photomicrograph of hagfish ventricle. At lower right, nucleus of endothelial cell with its thin cytoplasmic layer. In center of field and in a subendothelial location, is an atypical "secretory" cell filled with dark-appearing granules of an unknown nature. The large dark mass above the endothelial cell nucleus on the right is a collagen bundle. Muscle cells may be faintly seen at the upper right. (× 9600).

earlier in crude saline extracts of the systemic heart of the hagfish (Jensen, 1958). The positive chronotropic response of the isolated spontaneously beating frog heart was chosen for bioassay of the extracts, as it was repeatedly observed that these preparations, after a short equilibration period *in vitro*, would accelerate markedly if extracts containing the active material were added to the chamber*.

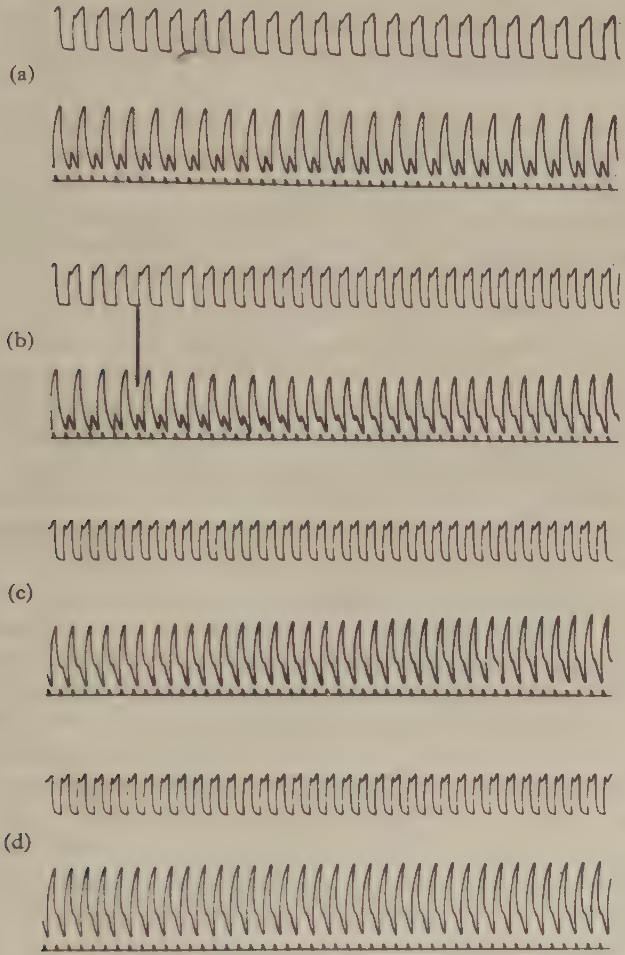

FIG. 9. The effect of HHE on the isolated spontaneously beating heart of the frog. The small peaks on the myogram are auricular and the large peaks ventricular systoles. The action potential was recorded only from the ventricle. (a) Control record. (b) At vertical bar, HHE was added to the chamber. Note progressive rate increase, fusion of atrial and ventricular contraction, and apparent force increase due to this fusion. (c) and (d) are continuations of the record from (b).

---

* This is in distinct contrast to hagfish hearts, which were unresponsive unless isolated for some hours prior to testing. The frog heart, then, affords a distinct advantage for bioassay in this respect.

If, however, the extract was inactivated by preliminary treatment (*vide infra*) the heartbeat rate remained unchanged. Each assay was carried out a minimum of three times, on at least two different hearts.

It should be re-emphasized that in every experiment the pH, temperature, and the volume of the additives were carefully adjusted to that of the Ringer's solution prior to introduction to the test heart, and the final volume was always 10·0 ml.

The experiments here reported were carried out on thirty-one isolated spontaneously beating frog hearts. Every heart served as its own control, and in most instances a number of experiments could be conducted on the same preparation after washing followed by a suitable re-equilibration period.

Fig. 9 illustrates the typical effect of untreated HHE on an isolated frog heart. The control rate was 30 beats/min; 1·5 min after addition of 1·0 ml of HHE (representing the aqueous extract derived from 0·1 g of hagfish heart powder), the rate had accelerated to 44 beats/min and it remained unchanged until the chamber was washed, 26 min after the extract had been added. After washing, the rate gradually returned to the control value in about 10 min. Note that as the rate accelerates, there is a definite fusion of the auricular systole with the ventricular contraction, indicating a decreased atrioventricular conduction time. That this finding is real rather than a recording artifact was revealed by high-speed records which show a definite decrease in the atrioventricular peak to peak distance of the contraction phases. No positive force increase is evident here save that produced by fusion of the systolic phases of both chambers, although such a response was elicited by HHE in several experiments. These findings were confirmed fifteen times on as many preparations using extracts prepared from different lots of hagfish heart powder. It is worthy of comment that acceleration usually took several minutes to reach a maximum, which was then sustained until the chamber was washed; in one study this exceeded 1 hr after the extract was introduced. It is also noteworthy that the return of the rhythm to the control rate was usually quite gradual and occasionally several hundred millilitres of Ringer's solution were required to bring about this reversion. An increasingly greater rate response could be elicited when the concentration of HHE in the chamber was increased by successive additions; however, the data are far from adequate to attempt quantitative treatment at this time.

Neither hagfish liver extracts nor rabbit heart extracts derived from the exsanguinated lyophilized organs in a fashion identical to the preparation of HHE produced the slightest effect on the chronotropism of the frog heart, even though HHE was effective in the same preparations (four each). This despite the fact that both the hagfish liver and rabbit heart extracts represented the soluble material derived from up to five times the mass of tissue (0·5 g) used for the HHE (0·1 g). Aside from the inherent interest of these results, they also serve as tissue extract controls on the other studies.

A quantity of hagfish heart powder of known cardiac activity was ashed in a crucible heated to redness, cooled, taken up in a small volume of Ringer's solution, and the pH adjusted with N-HCl. The product was completely inactive in the frog heart.

Earlier reported results on the effects of heating the HHE were inconclusive (Jensen, 1958). Consequently, a quantity of HHE was prepared in Ringer's solution as described in Methods and placed into several heat-resistant 15 ml polyethylene centrifuge tubes: one lot was untreated and served as the control; the remaining batches of HHE were placed in a boiling water bath for 10, 20 and 40 min respectively. After cooling, centrifugation removed the protein coagulum and the clear straw-colored supernate was bioassayed. All fractions save the one heated for 40 min exerted a positive chronotropic effect, indicating that the cardioactive material is relatively thermostable. Here, too, it was noted that the atrioventricular interval decreased. Typical bioassay records were quite similar to Fig. 9.

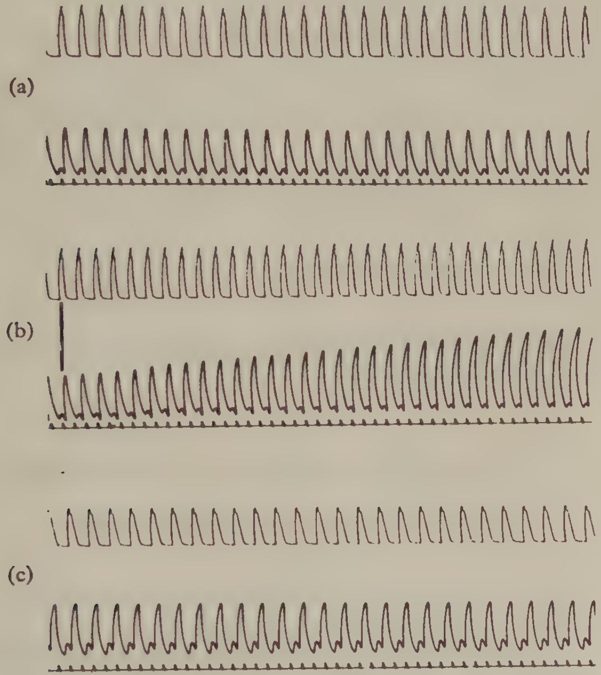

FIG. 10. The effect of α-epinephrine bitartrate (10^{-4} g/ml) on the isolated spontaneously beating frog heart. Compare with Fig. 9. (a) Control rate = 36 beats/min. (b) At mark indicated, epinephrine was added to chamber. Rate in 30 sec = 42 beats/min. Note lack of fusion of atrial and ventricular contractions, marked increase in force of contractions. 6 min after adding the epinephrine, rate = 42 beats/min, but force of beat was markedly less. (c) 10 min after adding the epinephrine, the rate had returned to the control value. The chamber was not washed during this interval.

Another preparation of HHE in distilled water was divided into two portions. The control extract was stored in the cold room (5°C), while the remaining material was dialysed in cellophane tubing against three 3 l. changes of distilled water with constant stirring at 5°C for 44 hr. After lyophilization and resolution of the residue in Ringer's it was found that the dialysed material was completely inactive, whereas the control extract produced a marked cardioaccelerator effect.

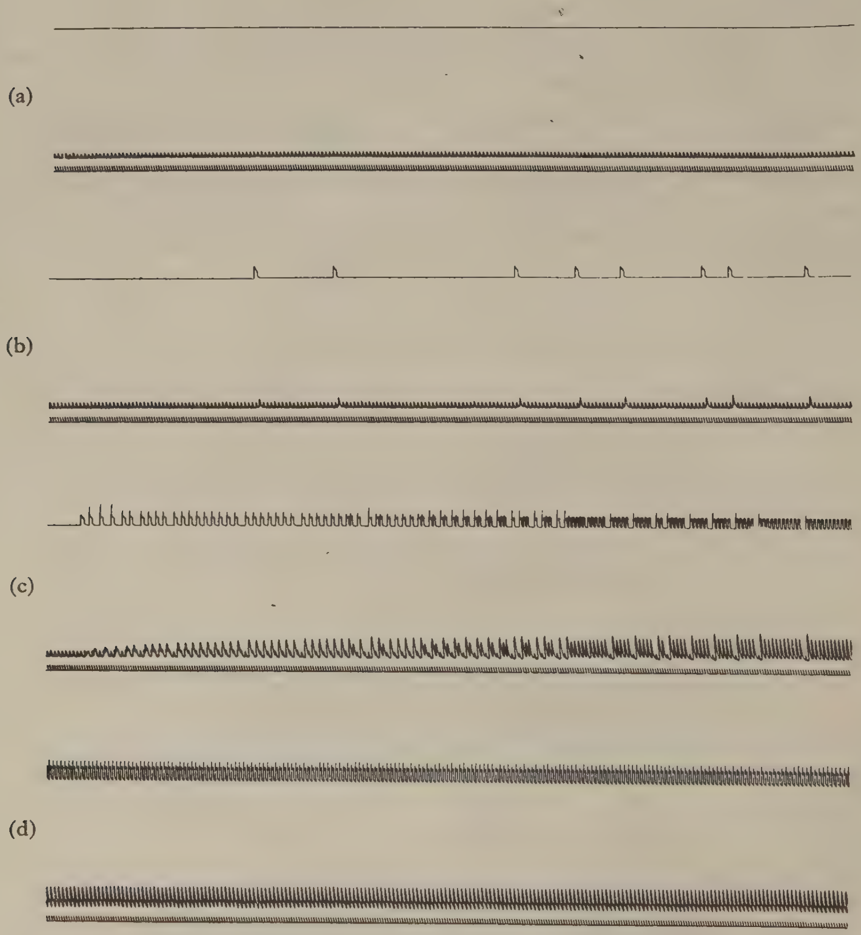

FIG. 11. The effect of HHE on a frog heart with spontaneous total atrioventricular block. (a) Total AV block which had been in effect for 40 min. Note absence of ventricular action potentials. (b) 15 min after placing 1·0 ml HHE in chamber. Occasional ventricular contractions are evident. (c) 5 min after introduction of 1·0 ml additional HHE (20 min from first application of material). Progressively better rhythm is evident from left to right. (d) 1 hr after first application of HHE. The preparation was not washed or otherwise disturbed during this interval.

As the hagfish systemic heart is known to contain a relatively high concentration of catecholamines (Augustinsson *et al.*, 1956), it was conceivable that the effect on the frog heart was due to these compounds. Therefore a series of frog hearts was tested for comparative purposes with various concentrations of α-epinephrine bitartrate to determine its effect on these preparations under the present experimental conditions. The concentration range employed was 10^{-4}, 5×10^{-5}, 10^{-5} and 10^{-6} g of the salt per millilitre. Fig. 10 shows the rapid response to 10^{-4} epinephrine. No atrioventricular fusion occurred. The response to this drug was quite rapid, the maximum ino- and chronotropic effect being reached in about 30 sec and the preparation returned to slightly below its control rate and force spontaneously in 10 min without washing. These findings were consistent at this higher dosage level in four hearts; however, the response to the lower concentration was consistently erratic or non-existent. Briefly, then, the effect of epinephrine in the frog heart was quite irregular in occurrence and evanescent in nature in sharp contrast to the results obtained with HHE on these preparations.

An interesting effect of HHE on the isolated frog heart is recorded in Fig. 11. It was noted in about 60 per cent of the preparations that after repeated treatment with drugs or extracts and subsequent washings, progressive atrioventricular block occurred spontaneously, and finally the ventricle ceased beating entirely except, in some cases, for an occasional contraction; the auricles under these conditions usually maintained an excellent beat. Once this condition developed, it generally did not revert spontaneously; in fact it usually persisted until the run was terminated after several hours. The effect of HHE (from 0·2 g tissue) on this condition is recorded in the figure together with the details of the experiment. Neither epinephrine in the aforementioned doses nor isoproterenol ($0{\cdot}25 \times$, $0{\cdot}50 \times$ and $0{\cdot}75 \times 10^{-5}$ g/ml) exerted the slightest effect on this heart block save for a slight rate effect on the auricular contractions. As the auricles were beating normally when the HHE was added under these conditions, it is evident that these experiments provide additional evidence that HHE facilitates atrioventricular conduction.

6. *Miscellaneous observations*

In this section are included a number of studies, general in nature, which enlarge upon certain aspects of the general cardiovascular physiology of the hagfish.

1. The average blood pH in the ventral aorta (seventeen specimens) was found to be 7·70 ± 0·112 (including standard error of the mean).

2. The hematocrit obtained from aortic blood samples (nineteen fish, mostly duplicate determinations) was 24 ± 1·8 per cent packed red cells (including standard error of the mean).

3. Average branchial heart weight for ten fish of both sexes (average size: 38·7 cm, 58 g) was 0·146 g or 0·25 per cent of the body weight. This finding is consistent with the earlier report that sluggish fish tend to have a much lower proportion of cardiac tissue to body weight than do more active species (Brown, 1957).

4. During the entire course of this work to date approximately 9000 fish were dissected. Of these, four branchial hearts were found in which the ventricle was dark purple (instead of the usual pink colour), very firm to the touch, and they exhibited not the slightest trace of a pulsation. It was also noted in these specimens that the atria were somewhat dilated and beat normally. Thus, it appears that the systemic ventricle is not essential to survival, since in all other respects these fish appeared to be of normal vigor until this defect was noted upon sacrifice.

5. Three fish were subjected to extirpation of the neurogenic (Greene, 1899) caudal heart by complete ablation of the posterior several centimetres of the caudal fin containing

(319)

this organ. 3 weeks later these animals appeared in quite good condition, save for the handicap in swimming occasioned by the loss of the tail-fin. The caudal heart, then, is not an essential organ to survival. The wounds were clean at sacrifice and some healing, albeit slight, was evident.

6. The aforementioned experiments led to another observation of some interest. It was repeatedly noticed, during the routine dissections of the hearts, that clotting of the blood was erratic in its occurrence either *in situ* or otherwise, and when clot formation did occur the resultant mass was very soft and quite friable. When the caudal hearts were removed and the fish returned to sea water for observation, the wounds bled quite freely, and clot formation occurred only on the bottom of the container rather than at the more useful locus in the injured region. It was then observed that the animals secreted masses of slime. This material then became entangled in the wound and bleeding stopped. When the slime was removed, bleeding resumed until the mass of slime was replaced by further secretion. It is therefore suggested that the abundant capacity of these animals to produce this viscous and tenacious material perhaps may serve to protect the fish from excessive hemorrhage.

7. Three hagfish were placed in a bucket containing the medium adopted for the isolated hearts. After remaining for 60 days in this artificial sea water, which was changed weekly or more often, all of the animals were alive and in apparently good condition. At this point, the fish were sacrificed and recordings made of the spontaneous branchial heartbeat. In each of these preparations, the contractions became irregular a short time after isolation, a finding perhaps attributable to the absence of trace elements normally present in natural sea water. This interpretation is even more creditable when one considers that hagfish are normally in ionic balance with sea water (McFarland & Munz, 1958).

8. In five unanesthetized specimens the blood pressure was obtained directly by cannulation of the ventral aorta immediately anterior to the pair of branchial arteries nearest the heart. The average value obtained was 38 mm of blood (range 25–49 mm) in these fish at 20°C. Although these values are rather crude, they are included here to illustrate the low arterial blood pressure found in these fish. This observation is consistent with the fact that the blood merely flows when an artery is severed, and is not ejected in spurts as would occur under a higher pressure.

DISCUSSION AND CONCLUSIONS

There is now definite evidence for the operation of at least two major factors governing cardioregulation in the aneural branchial heart of the hagfish, factors which Greene (1902a) many years ago suggested would be of importance in this regard. These are: degree of stretch of the myocardium and biochemical (or humoral) influences. A third element, of minor significance to the animal considering the relative stability of its natural habitat, is the effect of temperature on the myocardium.

It has been demonstrated in several ways, both *in situ* and *in vitro* that either the entire hagfish heart or the ventricle alone will accelerate when distended slightly, hence it obviously possesses a pressure-sensitive pacemaker. This heart has given no indication of contracting with greater force when the diastolic filling is increased, as might have been expected on the basis of Frank's (1895) and Starling's (1918) work. On the contrary, as the intraventricular volume is increased. the force of the contraction was found actually to decrease, and this was a consistent observation.

Since the heart of the adult hagfish is aneural, the accelerator mechanism undoubtedly resides within the myocardium. This is not to imply, however, that an empty hagfish heart or even minute fragments taken from either auricle or ventricle fail to contract spontaneously in the absence of external stretch; on the contrary, even the fragments exhibit an amazing degree of rhythmicity, indicating a very diffuse origin of pacemaker activity. This second conclusion pertaining to the pacemaker in these organs is substantiated by applying a tight atrioventricular ligature. This procedure never produced cessation, or even a transient interruption, of the beat in the auricle or the ventricle; the latter chamber merely beats at a slower rate after the ligature is applied (*vide infra*).

As higher filling pressure or increased mechanical tension also will exert a cardioaccelerator effect on the hearts of arthropods, molluscs, amphibians and mammals as well as in the hagfish, it appears that such a mechanism may be quite widespread throughout the animal kingdom. The hagfish heart is, however, aneural indicating that intracardiac nerve influences as mediators in producing this accelerator effect may be considered as not essential in all species.

If one considers from the standpoint of phylogeny, the extremely primitive biological status of the hagfish in relation to the other chordates, it is interesting to consider the possibility that both myogenic automaticity coupled with a pressure-sensitive accelerator mechanism may represent a very primitive evolutionary development. In this connexion it is noteworthy that the embryonic *Limulus* myocardium exhibits myogenic automaticity, a property which is lost in favor of complete neural control as the cardiac ganglia develop (Carlson & Meek, 1908).

Pharmacologically, the hagfish heart is quite unresponsive to a number of drugs and other compounds, especially acetylcholine and the catecholamines (Fänge & Östlund, 1954; Augustinsson *et al.*, 1956; Jensen, 1957, 1958). However, there is present in the hagfish heart (but not in the liver) a markedly cardioactive material. This substance is not species specific in its action, but also is effective in molluscan (Jensen, 1958) and frog hearts as well as the isolated hypodynamic hagfish heart. In regard to the latter preparation, it may be suggested that the inefficacy of the HHE on freshly isolated hagfish hearts is due to the presence of optimal quantities of the material. During the experiment this is gradually metabolized and/or leached out of the heart, thus rendering it more sensitive to later additions of HHE.

The cardioactive substance derived from hagfish myocardia is not merely cardioaccelerator in the frog but reduces atrioventricular conduction time in that species and will even reverse total atrioventricular block; this point warrants further study.

Regarding the identity of the cardioactive material, little can be stated at present except in general terms. The substance does not appear to be epinephrine. Available data indicate that it is a water-soluble, relatively thermo-stable small molecule. It is apparently not a mineral, protein or lipid. Detailed studies are underway at present toward isolating and characterizing the cardioactive substance.

Two facts are of interest at this point: the liver, the only other large organ in the hagfish body save the gut and muscle mass, possesses no demonstrable cardioaccelerator activity; second, the heart possesses atypical "secretory" cells. It is at this stage suggestive, if nothing more. It is possible that the hagfish heart may have an endocrine as well as pulsatile function in these primitive animals, and that these atypical cells, located as they are throughout the myocardium, may serve as local "pacemakers" which liberate their secretion upon stretch and concomitant permeability changes.

A brief word regarding the metabolism of the hagfish heart is relevant. Rybak & Boivinet (1959) working on the branchial hearts of the European hagfish or slime eel (*Myxine glutinosa*) found that the auricle : ventricle ratio of O_2 consumption in these animals was 1·75 : 1. In the present study, the ratio of heart rate of the entire isolated heart to that of the isolated ventricle alone was 1·63 : 1. (Data from Table 1.) These figures are in surprisingly good agreement, considering the wide differences in technique and even of genera of the fish employed. However, these facts suggest that in the hagfish heart, as in other species, there is a definite metabolic gradient from auricle to ventricle, levels in the former being higher than in the latter, and although this Cyclostome has an extremely high degree of automaticity in all parts of its heart, the graded metabolic rate serves to coordinate its function.

Acknowledgements—The author's sincere thanks are due to the following people for their generous contributions to this work:

Professor Daniel C. Pease, Department of Anatomy, School of Medicine, University of California at Los Angeles for the excellent electron photomicrographs, assistance in their interpretation and permission to reproduce them here.

Dr. Lewis A. Palmer, La Jolla Clinical Laboratories, La Jolla, California for preparation of the hematoxylin and eosin sections.

Messrs. Charles J. Zilis, James Maggert and Gerald Scholl for their invaluable technical assistance.

Professors Denis L. Fox, Carl L. Hubbs, Paul R. Saunders and Per F. Scholander for their valuable criticism of the manuscript and their helpful discussions during the course of this work.

Mrs. Elizabeth S. Jensen and Miss Peggy McNally for their continued interest and assistance in preparing the manuscript.

Captain Robert C. Newbegin and the entire crew of the Research Vessel T-441 deserve especial mention for their unfailing patience and cooperation during the numerous (and sometimes extended!) collecting trips during which the hagfish used in this study were obtained.

REFERENCES

Augustinsson K. B., Fänge R., Johnels A. & Östlund E. (1956) Histological, physiological and biochemical studies on the heart of two Cyclostomes, hagfish (*Myxine*) and lamprey (*Lampetra*). *J. Physiol.* **131**, 257–276.

Blinks J. R. (1956) Positive chronotropic effect of increasing right atrial pressure in the isolated mammalian heart. *Amer. J. Physiol.* **186**, 299–303.

Brown M. E., ed. (1957) *The Physiology of Fishes*, Vol. I, pp. 81–108. Academic Press, New York.

Carlson A. J. (1904a) The nervous origin of the heart-beat in *Limulus*, and the nervous nature of co-ordination or conduction in the heart. *Amer. J. Physiol.* **12**, 67–74.

Carlson A. J. (1904b) Further evidence of the nervous origin of the heart-beat in *Limulus. Amer. J. Physiol.* **12**, 471–498.

Carlson A. J. (1904c) Contributions to the physiology of the heart of the California hagfish (*Bdellostoma dombeyi*). *Z. Allg. Physiol.* **4**, 259–288.

Carlson A. J. (1906) Comparative physiology of the invertebrate heart—V. The heart rhythm under normal and experimental conditions. *Amer. J. Physiol.* **16**, 47–66.

Carlson A. J. (1907) On the mechanism of the stimulating action of tension on the heart. *Amer. J. Physiol.* **18**, 149–155.

Carlson A. J. & Meek W. J. (1908) On the mechanism of the embryonic heart rhythm in *Limulus. Amer. J. Physiol.* **21**, 1–10.

Fänge R. & Östlund E. (1954) The effects of adrenaline, noradrenaline, tyramine and other drugs on the isolated heart from marine vertebrates and a cephalopod (*Eledone cirrosa*). *Acta Zool., Stockh.* **35**, 289–305.

Frank O. (1895) Zur Dynamik des Herzmuskels. *Z. Biol.* **32**, 370–447. (Translated by Chapman C. B. & Wasserman E. (1959) *Amer. Heart J.* **58**, 282–317, 467–478).

Greene C. W. (1899) Contributions to the physiology of the California hagfish, *Polistotrema stouti*—I. The anatomy and physiology of the caudal heart. *Amer. J. Physiol.* **3**, 366–382.

Greene C. W. (1902a) Contributions to the physiology of the California hagfish, *Polistotrema stouti*—II. The absence of regulative nerves for the systemic heart. *Amer. J. Physiol.* **6**, 318–324.

Greene C. W. (1902b) Notes on the physiology of the circulatory system of the California hagfish, *Polistotrema stouti. Amer. J. Physiol.* **6**, xii.

Jensen D. (1957) Role of acetylcholine in cardiac automatism. *Fed. Proc.* **16**, 291.

Jensen D. (1958) Some observations on cardiac automatism in certain animals. *J. Gen. Physiol.* **42**, 289–302.

Jensen D. (1959) Albinism in the California hagfish, *Eptatretus stoutii. Science* **130**, 798.

Keatinge W. R. (1959a) The effect of increased filling pressure on the rate of beating and on atrioventricular conduction in the heart. *J. Physiol.* **145**, 46P.

Keatinge W. R. (1959b) The effects of increased filling pressure on rhythmicity and atrioventricular conduction in isolated hearts. *J. Physiol.* **149**, 193–208.

McFarland W. N. & Munz F. W. (1958) A re-examination of the osmotic properties of the Pacific hagfish, *Polistotrema stouti. Biol. Bull., Woods Hole* **114**, 348–356.

Pathak C. L. (1957) The influence of stretch stimuli on the chronotropic response of the frog's isolated whole heart and its individual chambers. *Indian J. Med. Sci.* **11**, 808–812.

Pathak C. L. (1958a) Effect of stretch on formation and conduction of electrical impulses in the isolated sinoauricular chamber of frog's heart. *Amer. J. Physiol.* **192**, 111–113.

Pathak C. L. (1958b) Effects of changes in intraluminal pressure on inotropic and chronotropic responses of isolated mammalian hearts. *Amer. J. Physiol.* **194**, 197–199.

Prosser C. L. (1952) *Comparative Animal Physiology*, p. 95. Saunders, Philadelphia.

Rybak B. & Boivinet P. (1959) Caractères biochimiques du cœur branchial de *Myxine glutinosa. C. R. Acad. Sci., Paris* **249**, 2231–2233.

Starling E. H. (1918) *The Law of the Heart*. Linacre Lecture, London.

(*Reprinted from Nature, Vol.* 186, *No.* 4726, *p.* 731 *only,*
May 28, 1960)

Chronic Aortitis in the California Sea-lion, *Zalophus californianus**

DURING a long-term study on the general biology of the California sea-lion, *Zalophus californianus* (Lesson), it became evident that degenerative diseases associated with ageing are very common in this species. Therefore, a study of the heart and aorta was undertaken.

Circulatory disease in captive pinnipeds has been extensively studied by Fox[1] over a number of years. His findings included arteriosclerosis with typical medial involvement as well as myocarditis. Of the ten pathological specimens he found during this work, no indication was given of the genus and species involved ; all animals were grouped under the order Pinnipedia.

The present study deals with lesions in the aorta of three mature bull sea-lions and is the first report of such pathology in this species to be found in a wild population. The hearts of seventy animals of both sexes were taken at random for study from a total collection of some two hundred specimens ; these were obtained over the past two and a half years from islands off the coast of Baja California, Mexico. The collection area ranged from Los Coronados Islands (lat., 32° 26′ N. ; long., 117° 16′ W.) to Cabo San Lucas, the extreme southern tip of Baja California (lat. 22° 45′ N. ; long. 110° 00′ W.). All three of the abnormal individuals were secured on Los Coronados Islands, where most of the males were collected.

As soon as possible after killing, the hearts were removed leaving several inches of aorta attached : after rinsing in water, the tissue was preserved in 10 per cent formalin for later examination. The aortas were screened for visible lesions. Of the three specimens exhibiting gross pathology, two were sent to two separate laboratories for section and independent histopathological study ; the third was retained and examined by us. The three diagnoses were identical. The sections were stained with hæmatoxylin and eosin. No gross myocardial disease was evident in any case.

Using the Liebermann–Burchard reaction on ether

---

* Contributions from the Scripps Institution of Oceanography, of the University of California. New Series. 1265

Reproduced by Permission

extracts of the finely ground material, samples from the pathological areas revealed a considerably higher cholesterol content than samples of the tissue from apparently normal adjacent regions.

Grossly, the intimal surface of the arteries contained numerous punctate elevations which, in the most extreme case, resembled tree bark. Approximately 10 per cent of the intimal surface was involved and the affected areas ranged in width from 0·1 to 1·5 cm.

Microscopically, the sections of aorta revealed extensive active aortitis, while other areas showed healing. The intima itself was not involved ; rather there was, in the foci of the active areas, an extensive inflammatory reaction in the media, extending from the subintima to the adventitia. The disease process involved destruction of elastic tissue about the blood vessels and an infiltration of plasma cells, macrophages and lymphocytes. A secondary fibrosis in the subintimal areas overlaid the zones of aortitis. The healed areas contained abnormally large blood vessels surrounded by small amounts of scar tissue.

In many respects the condition found in these sea-lions resembles the aortic lesions found in chronic human syphilis, although the etiology of the disease in these animals is unknown.

The work was accomplished while the senior author served as a research assistant of the Institute of Marine Resources at the University of California and while the junior author held a fellowship-grant from the San Diego County Heart Association, to which grateful acknowledgment is made. The work was made possible by the effective co-operation of the Mexican Government.

Our sincere thanks are due to Dr. Lewis A. Palmer, La Jolla Clinical Laboratory, and Dr. Findlay E. Russell, College of Medical Evangelists, Los Angeles, for their kindness in the preparation and diagnosis of the sections.

ARTHUR L. KELLY
DAVID JENSEN

Scripps Institution of Oceanography,
La Jolla,
California.

Fox, H., *Amer. J. Med. Sci.*, 159, 821 (1920); *Trans. Coll. Phys., Philadelphia*, 3rd Ser., 43, 130 (1921); "Diseases in Captive Wild Animals and Birds", 70 (J. B. Lippincott Co., Philadelphia, 1923).

Printed in Great Britain by Fisher, Knight & Co., Ltd., St. Albans.

Deep-Sea Research, 1961, Vol. 7, pp. 265 to 275. Pergamon Press Ltd., London. Printed in Great Britain

On the temperature, salinity, and density differences between the Atlantic and Pacific oceans in the upper kilometre*

JOSEPH L. REID, JR.
Scripps Institution of Oceanography

(*Received* 26 *May* 1960)

Abstract—The surface of the Pacific Ocean stands about 40 cm higher than the Atlantic Ocean with respect to the 1000-decibar surface, and the North Atlantic and North Pacific stand respectively about 14 and 17 cm higher than the South Atlantic and Pacific. The North Atlantic is warmest and saltiest, the South Atlantic is coldest and densest, and the North Pacific is least dense and least salty.

The extreme values in temperature and salinity of the North Atlantic are probably related to the formation of the deep water there, which carries away from the upper layer the cold water of relatively low salinity. If this water spreads into the South Atlantic at depth and is replaced with warm saline surface water from the South Atlantic via the South Equatorial Current and the Gulf Stream, then the South Atlantic should be substantially cooler and less salty.

The difference in density and sea level of the Atlantic and Pacific oceans may stem from the difference in latitude of the southern tips of America, Africa, and Australia, and the constriction of the west wind drift at Drake Strait. Only the densest surface waters of the Pacific pass through to the Atlantic, while lighter waters from lower latitudes of the South Atlantic pass eastward south of Africa. Further, the constriction of the flow by Drake Strait may result in a higher sea level on the Pacific side through the effect of *Windstau* (MONTGOMERY, 1938).

The density difference between the southern and northern oceans may be partly a consequence of the west wind drift around Antarctica. This is the greatest current of all oceans. Its flow is approximately geostrophically balanced and the surface slopes down to the south. The northern west wind drifts are not so strong, are at lower latitudes, and the high latitude flow is westward with slope upward to the north.

These differences are not confined to the upper thousand metres. The average density difference between the Atlantic and the Pacific from the surface to the bottom is about 17×10^{-5} g/cm^3. Referred to some deep surface such as 4000 decibars, the Pacific stands about 68 cm higher than the Atlantic.

INTRODUCTION

IN COMPUTING the geopotential at the sea surface with respect to the 1000-decibar surface in the Pacific, one arrives at values much higher than those for the corresponding latitudes of the Atlantic Ocean that were computed by DEFANT (1941). These differences must stem from differences in temperature and salinity. In the present paper the author has sought to locate the areas and levels of extreme difference. It seems worthwhile also to point out that certain features and processes in the ocean are consonant with the formation or the maintenance of these differences. The study of these features and processes might have led, and in some cases has led, to previous speculations that differences of this nature might exist.

THE DATA

Temperature and salinity data were read from various atlases. The *Meteor* Atlases (WÜST and DEFANT, 1936 ; BÖHNECKE, 1936) were used for the Atlantic. For the

---

*Contribution from the Scripps Institution of Oceanography, New Series. 1266

Reproduced by Permission

Pacific the works of SCHOTT (1935), MUROMTSEV* (1958) and the NORPAC ATLAS (1960) were used. For surface temperatures the months of August and February were chosen for the northern and southern hemispheres, respectively, but since the salinity data in northern summer were more numerous and the seasonal variation is relatively small, BÖHNECKE'S chart for June–July–August was used for the Atlantic and SCHOTT'S chart for northern summer was used for the Pacific.

Table 1. The area over which the averages were taken.

Latitude	*North Atlantic*		*North Pacific*		*South Atlantic*		*South Pacific*	
	from	*to*	*from*	*to*	*from*	*to*	*from*	*to*
55–60	35W	10W	155W	140W	60W	20E	145E	75W
50–55	50	10	160E	135	60	20	145	75
45–50	50	5	155	130	60	20	145	75
40–45	60	10	145	125	60	20	150	75
35–40	75	10	140	125	60	20	150	75
30–35	75	10	125	120	50	15	155	75
25–30	75	15	125	115	50	15	155	70
20–25	75	15	125	115	40	10	150	70
15–20	60	15	120	100	35	10	150	80
10–15	60	15	120	100	35	10	150	80
5–10	50	15	130	80	35	10	150	80
0–5	50	10E	130	80	35	10	150	80

Average values were estimated by eye in areas five degrees on a side in the Atlantic and North Pacific. South of 20 °N in the Pacific averages were taken from areas ten degrees on a side. The five-degree areas were then combined into ten-degree areas and all were expressed as the averages in ten-degree zones of latitude for each ocean.

The levels chosen were 0, 200, 400, 600 and 1000 metres. These are of course not adequate to make good vertical averages but they serve to describe the levels and zones of greatest differences.

The density was obtained in two ways. For each latitudinal zone at each level the average temperature and salinity were used to calculate σ_t (Tables 2 and 3) which is defined as $(\rho_{s,t,0} - 1)\,1000$ where $\rho_{s,t,0}$ is the density in g/cm³ of water of the appropriate temperature and salinity but at a pressure of one atmosphere. Since the coefficient of thermal expansion increases with temperature, density computed from an average of two temperatures will be greater than the average of the densities at the two temperatures. Values of σ_t as tabulated are too large by amounts up to 0·20. Greatest errors will occur where the maximum temperature and its range are both high ; that is, at the surface in the tropics. These particular values are included so that the densities at the various zones and depths may be compared. At each of the five depths the mean value of σ_t in each ocean has been calculated (Table 3) but no vertical averages of σ_t were calculated.

The other method of obtaining density was to convert the computed geopotential distance from the zero- to the 1000-decibar surface to average specific volume and

---

*It is not Muromtsev's tabulated averages which are used here, but the charts in his atlas (1958, Appendix II). Since the Atlantic values were to be estimated by eye from charts it was thought best to use the same method, with the same number of depths, in the Pacific. Muromtsev has used all of the material available to him in 1954 and has prepared averages by Marsden squares, by depth, and by month (1958, Appendix I). His tables are far more detailed and inclusive than those prepared here, and if similar tables were available for the Atlantic a more detailed comparison could be made.

Table 2. Average temperature, salinity, and σ_t by ten-degree bands by depth. (The means listed are the depth-integrals of the tabulated values, divided by 1000 metres. σ_t is computed at each level and latitude from the tabulated salinity and temperature).

A. Atlantic

	50°–60 °N			40°–50 °N			30°–40 °N			20°–30 °N		
	T,°C	S,‰	σ_t	T,°C	S,‰	σ_t	T,°C	S,‰	σ_t	T,°C	S,‰	σ_t
0	11·06	35·04	26·82	18·04	34·94	25·24	25·17	36·43	24·36	26·52	36·79	24·24
200	6·56	35·06	27·56	11·47	35·49	27·08	17·13	36·27	26·48	18·76	36·56	26·30
400	6·36	35·06	27·58	10·16	35·39	27·25	14·99	36·06	26·82	15·30	36·07	26·75
600	5·41	35·03	27·67	8·79	35·30	27·41	13·02	35·64	26·90	10·94	35·63	27·29
1000	4·35	34·97	27·75	5·33	35·18	27·80	8·17	35·37	27·57	6·74	35·09	27·55
Mean	6·18	35·03		9·83	35·30		14·48	35·88		14·09	35·91	

	10°–20 °N			0°–10 °N			0°–10 °S			10°–20 °S		
0	26·92	35·84	23·40	24·53	34·96	24·06	26·70	35·89	23·51	24·68	36·76	24·80
200	15·58	36·10	26·72	12·40	35·21	26·69	12·45	35·19	26·67	14·24	35·43	26·49
400	11·03	35·28	27·01	8·40	34·76	27·05	8·32	34·74	27·04	8·70	34·73	26·98
600	8·14	34·96	27·24	6·05	34·59	27·24	5·49	34·51	27·25	5·55	34·42	27·18
1000	5·30	34·85	27·55	4·56	34·65	27·45	4·05	34·59	27·48	3·70	34·54	27·47
Mean	11·52	35·32		9·34	34·80		9·28	34·85		9·46	34·94	

	20°–30 °S			30°–40 °S			40°–50 °S			50°–60 °S		
0	23·79	36·14	24·59	20·73	35·37	24·87	10·85	(34·28)	26·26	3·15	(33·89)	(27·01)
200	15·20	35·49	26·34	13·06	35·16	26·52	5·46	34·24	27·04	1·26	34·33	27·52
400	10·76	34·92	26·78	9·91	34·83	26·85	3·75	34·21	27·21	1·71	34·55	27·66
600	6·71	34·53	27·11	6·27	34·47	27·11	2·97	34·24	27·30	1·61	(34·64)	27·74
1000	3·50	34·44	27·41	3·40	34·28	27·29	2·66	34·41	27·45	(0·40)	34·68	27·85
Mean	10·28	34·94		9·23	34·73		4·35	34·27		1·47	34·49	

B. Pacific

	50°–60 °N			40°–50 °N			30°–40 °N			20°–30 °N		
	T,°C	S,‰	σ_t	T,°C	S,‰	σ_t	T,°C	S,‰	σ_t	T,°C	S,‰	σ_t
0	10·01	32·63	25·12	14·61	33·03	24·56	23·07	34·28	23·39	25·45	34·98	23·21
200	4·24	33·85	26·87	5·77	33·82	26·68	12·69	34·23	25·87	16·26	34·65	25·44
400	3·80	34·10	27·11	4·60	34·00	27·05	9·10	34·23	26·53	11·04	34·30	26·24
600	3·54	34·26	27·26	3·83	34·16	27·16	5·88	34·09	26·87	6·99	34·18	26·80
1000	2·82	34·42	27·45	3·01	34·37	27·40	3·62	34·31	27·29	3·90	34·41	27·34
Mean	4·24	34·02		5·29	33·99		9·15	34·21		10·88	34·42	

	10°–20 °N			0°–10 °N			0°–10 °S			10°–20 °S		
0	27·06	34·42	22·30	27·24	34·26	22·11	26·54	35·16	23·01	26·43	35·60	23·37
200	15·70	34·73	25·63	12·90	34·84	26·31	16·50	35·25	26·07	19·60	35·59	25·34
400	9·30	34·46	26·66	9·10	34·71	26·89	10·10	34·73	26·75	10·90	34·77	26·63
600	6·50	34·45	27·07	6·90	34·61	27·14	7·10	34·61	27·11	7·00	34·58	27·11
1000	4·40	34·54	27·40	4·70	34·57	27·39	4·60	34·54	27·38	4·20	34·52	27·41
Mean	10·54	34·52		10·13	34·63		11·02	34·80		11·68	34·91	

	20°–30 °S			30°–40 °S			40°–50 °S			50°–60 °S		
0	24·12	35·61	24·08	19·83	35·06	24·86	13·50	34·39	25·84	7·03	33·96	26·62
200	17·90	35·42	25·64	12·10	34·91	26·52	7·90	34·59	26·98	4·80	34·41	27·25
400	11·50	34·70	26·47	8·60	34·60	26·89	6·70	34·42	27·04	3·80	34·24	27·22
600	7·20	34·47	26·98	6·90	34·42	27·10	6·20	34·37	27·05	3·60	34·34	27·32
1000	4·60	34·43	27·28	4·70	34·38	27·24	4·50	34·37	27·25	2·90	34·43	27·46
Mean	11·37	34·81		9·13	34·61		7·03	34·43		4·08	34·31	

then to average density. Charts of this quantity (the depth integral of the specific volume) were available for both the Atlantic (DEFANT, 1941, BEILAGE XIV) and for the Pacific* (REID, manuscript in preparation), and the horizontal averages were obtained in a similar manner to that used for the salinity and temperature. Both the Atlantic and the Pacific charts of geopotential contain materials from all months of the year and from many different years. They show the same tendency for high-latitude observations to be made in summer and low-latitude observations throughout the year.

Table 3. Average temperature, salinity, and σ_t *by depth. The relative width of the ocean in each zone was taken into account in calculating these values from those in Table 2. These values of* σ_t *were also calculated from Table 2, not from the adjacent temperature and salinity in this table. The means listed below each column are the depth-integrals of the tabulated values divided by* 1000 *metres.*

	Temperature °C			*Salinity, ‰*			σ_t		
Depth	*North Atlantic*	*North Pacific*	Δ	*North Atlantic*	*North Pacific*	Δ	*North Atlantic*	*North Pacific*	Δ
0	23·30	23·80	− 0·50	35·84	34·26	+ 1·58	24·27	22·88	+ 1·39
200	16·30	13·20	+ 3·10	35·91	34·56	+ 1·35	26·68	25·97	+ 0·71
400	11·72	8·91	+ 2·81	35·48	34·38	+ 1·10	26·98	26·65	+ 0·33
600	9·31	6·26	+ 3·05	35·19	34·36	+ 0·83	27·23	27·01	+ 0·22
1000	5·99	4·09	+ 1·90	35·00	34·47	+ 0·53	27·54	27·37	+ 0·17
Mean	11·78	9·58	+ 2·20	35·42	34·42	+ 1·00	26·84	26·39	+ 0·45
	South Atlantic	*South Pacific*	Δ	*South Atlantic*	*South Pacific*	Δ	*South Atlantic*	*South Pacific*	Δ
0	19·25	20·91	− 1·66	35·48	35·06	+ 0·42	24·98	24·50	+ 0·48
200	10·91	14·00	− 3·09	34·98	35·03	− 0·05	26·72	26·18	+ 0·54
400	7·54	9·01	− 1·47	34·67	34·61	+ 0·06	27·05	26·80	+ 0·25
600	4·95	6·50	− 1·55	34·45	34·48	− 0·03	27·25	27·08	+ 0·17
1000	3·15	4·31	− 1·16	34·48	34·45	+ 0·03	27·48	27·34	+ 0·14
Mean	7·73	9·51	− 1·78	34·71	34·67	+ 0·04	26·92	26·64	+ 0·28

The area over which the averages were taken (Table I) excludes the Caribbean Sea and the Gulf of Mexico because the *Meteor* Atlas did not include them. The latitudes above 60° were left out partly because of the sparseness of the data and partly because in the far north the two oceans are not really comparable in depth or in circulation.

LIMITATIONS

Averages of this sort could best be made by some form of machine data processing in which more data and data at closer depth intervals could be used. Since temperature and salinity data for standard levels such as 10, 25, 50, 75, 100, and 150 metres were not available in the form of charts for the Atlantic, these levels were not included for the Pacific either. As a test of the sort of errors in the mean that might result from a linear interpolation from zero to 200 metres the area from 150° to 160 °W longitude was examined again by ten-degree zones from 0° to 60 °N, including data at 25, 50, 100, and 150 metres. In the average from 0 to 1000 metres no changes greater

---

*The materials used in preparing the Pacific chart include 1750 stations. A listing of the stations and a station pattern will be included when the chart is published.

Table 4. Average temperature, salinity, density ($\rho_{s,t,p}$), and geopotential anomaly (at the sea surface with respect to the 1000-decibar surface) by latitudinal bands. In computing the means the relative width of the ocean in each zone was taken into account. The density was computed from the geopotential anomaly, which had been calculated from individual stations, not from the σ_t averages of Table 2. Both density and geopotential are tabulated, since the latter may be used directly to estimate variations of sea level with respect to the 1000-decibar surface.

	Temperature, °C			Salinity, ‰			Density, g/cm³			Geopotential Anomaly (dynamic metres)		
Latitude	Atlantic	Pacific	△	Atlantic	Pacific	△	Atlantic	Pacific	△	Atlantic	Pacific	△
50°–60 °N	6·18	4·24	1·94	35·03	34·02	1·01	1·02986	1·02935	51	0·60	1·08	– 0·48
40°–50 °N	9·83	5·29	4·54	35·30	33·99	1·31	1·02946	1·02923	23	0·98	1·20	– 0·22
30°–40° N	14·48	9·15	5·33	35·88	34·21	1·67	1·02911	1·02876	35	1·31	1·65	– 0·34
20°–30 °N	14·09	10·88	3·21	35·91	34·42	1·49	1·02903	1·02846	57	1·38	1·92	– 0·54
10°–20 °N	11·52	10·54	0·98	35·32	34·52	0·80	1·02907	1·02862	45	1·35	1·77	– 0·42
0°–10 °N	9·34	10·13	– 0·79	34·80	34·63	0·17	1·02911	1·02872	39	1·32	1·68	– 0·36
Mean	11·78	9·58	2·20	35·42	34·42	1·00	1·02915	1·02872	43	1·27	1·68	– 0·41
0°–10 °S	9·28	11·02	– 1·74	34·85	34·80	0·05	1·02917	1·02872	45	1·25	1·68	– 0·43
10°–20 °S	9·46	11·68	– 2·22	34·94	34·91	0·03	1·02913	1·02862	51	1·29	1·77	– 0·48
20°–30 °S	10·28	11·37	– 1·09	34·94	34·81	0·13	1·02907	1·02873	34	1·35	1·67	– 0·32
30°–40 °S	9·23	9·13	0·10	34·73	34·61	0·12	1·02913	1·02899	14	1·29	1·42	– 0·13
40°–50 °S	4·35	7·03	– 2·68	34·27	34·43	–0·16	1·02951	1·02923	28	0·93	1·20	– 0·27
50°–60 °S	1·47	4·08	– 2·61	34·49	34·31	0·18	1·02997	1·02959	38	0·50	0·86	– 0·36
Mean	7·73	9·51	– 1·78	34·71	34·67	0·04	1·02930	1·02889	41	1·13	1·51	– 0·38

than 0·10‰ were found in salinity. In temperature, however, systematic changes resulted from the nature of the thermal structure. Values too high by as much as 0·37 °C were found north of 20 °N, and values too low by 0·21 °C and 0·54 °C in the areas from 10° to 20 °N and 0° to 10 °N, respectively. This last error is a consequence of the great thickness of the mixed layer between the Equatorial Current and Countercurrent. A similar thermal feature is found in the corresponding latitudes of the Atlantic on *Meteor* stations 213, 258, 259, 261 and 297.

Since temperature data from the summer season were used in all oceans the errors may tend to cancel each other when differences are taken by latitude. In any case the horizontal averages (Tables 2 and 3) are unaffected by this sort of error, and the differences of temperature (Table 4) are in all but one case large compared with the maximum error found. The temperature anomalies of the two Atlantic oceans are large compared with the maximum error (Table 5). The Pacific anomalies are very small and cannot be much increased by the systematic errors found in the test area.

Table 5. Average temperature, salinity, density ($\rho_{s,t,p}$) *and geopotential anomaly (at the sea surface with respect to the* 1000*-decibar surface) of the upper kilometre of the Atlantic and Pacific oceans between* 60° *N and* 60 °*S latitude, and the deviations from the average in four areas. Both density and geopotential are tabulated, since the latter may be used directly to estimate variations of sea level with respect to the* 1000*-decibar surface.*

		T,°C	S,‰	$\rho_{s,t,p}$ g/cm³	*Geopotential Anomaly (dynamic metres)*
Mean		9·55	34.70	1·02894	1·47
Atlantic	*North*	+ 2·23	+ 0·72	$+ 21 \times 10^{-5}$	− 0·20
	South	− 1·82	− 0·01	$+ 36 \times 10^{-5}$	− 0·34
	Mean	+ 0·03	+ 0·32	$+ 30 \times 10^{-5}$	− 0·28
Pacific	*North*	+ 0·03	− 0·28	$- 22 \times 10^{-5}$	+ 0·21
	South	− 0·04	− 0·03	$- 04 \times 10^{-5}$	+ 0·04
	Mean	− 0·01	− 0·15	$- 13 \times 10^{-5}$	+ 0·12
Mean of North Atlantic and North Pacific		+ 0·68	+ 0·02	$- 09 \times 10^{-5}$	+ 0·09
Mean of South Atlantic and South Pacific		− 0·58	− 0·02	$+ 07 \times 10^{-5}$	− 0·07

Calculations of the geopotential anomaly (from which, in turn, density was calculated) were made for individual stations using data from about 16 depth intervals. These results are undoubtedly more accurate than the temperature and salinity averages over depth. They may suffer somewhat through the inadequate knowledge of the equation of state of sea water (ECKART, 1958 ; 1959). R. O. REID'S (1959) examination of the problem suggests that errors in the pressure dependent terms, which are the most inaccurately known, should result in negligibly small errors in the differences in the upper thousand metres. Probably the density differences found here are gross enough to remain relatively unchanged after refinement of the equation of state, but this limitation must be kept in mind.

THE RESULTS

Over the greater part of the Atlantic and Pacific oceans (Table 1) the temperature and salinity have been averaged at various depths in each zone (Table 2) and by depth (Table 3) and by zone (Table 4) for each ocean, and the average values for the various oceans have been compared (Table 5). In each table the appropriate values of σ_t, density, or geopotential have been included.

With respect to the 1000-decibar surface the Pacific Ocean stands 40 cm higher than the Atlantic, and the North Pacific and North Atlantic stand, respectively, 17 and 14 cm higher than the South Pacific and South Atlantic (Table 5). The North Atlantic is warmest and saltiest, the South Atlantic is coldest and densest, and the North Pacific is least dense and least salty.

In the upper thousand metres the South Atlantic's high density is the result of its low temperature. This may be partly the consequence of the ratio of high-latitude to low-latitude area there. The low density of the North Pacific is the result of its low salinity. The North Atlantic, although the warmest of the oceans in its upper thousand metres, is denser than the mean because of its great salt content.

The effect of the ratio of high-to-low latitude area is not present in the averaging in Table 4, where it is seen that the North Atlantic is warmer at every latitude than the South Atlantic and is the warmest of all oceans at latitudes above 20°. It is most saline at all latitudes above 10°. The South Atlantic is densest at all latitudes. The North Pacific is least saline at all latitudes and is at no latitude denser than any other ocean.

DISCUSSION

Some of these simple results were among the earliest findings in physical oceanography, yet they have received remarkably little attention. Von BOGUSLAWSKI (1884) refers to the results of the *Challenger*, *Tuscarora*, and *Gazelle* measurements, which indicate (Von BOGUSLAWSKI, 1884, p. 250, my translation) ‘ Between the upper water layer influenced by radiation, which reaches a depth of 110 to 160 m, and a depth of 2750 m or 1500 fathoms, all the water of the North Atlantic is warmer than the water of the South Atlantic at the same depth and latitude.’ (The data he compares extend from 42 °N to 42 °S in the Atlantic and do not reach below 2750 m). He writes also (p. 310, my translation) ‘ The water of the North Pacific is in its total mass colder than that of the North Atlantic ’ and ‘ The water of the South Pacific is to 1300 m (about 700 fathoms) depth warmer than the South Atlantic, beneath this depth colder.’

KRÜMMEL (1907) calculated mean values of temperature for the separate oceans. Since his values of temperature are for the total volume of the ocean (p. 495) they are not directly comparable to the results of this paper. He finds, however, that the North Atlantic is warmest (except for the North Indian Ocean), the South Atlantic is coldest, and the North and South Pacific are about equal and intermediate. He does not make vertical averages of salinity but his tabulations at various depths (p. 337) indicate that in the upper kilometre the North Atlantic is saltiest, the North Pacific least salty, and the South Atlantic and South Pacific about equal.

SEA LEVEL AND DENSITY

Levelling surveys (RAPPLEYE, 1932) indicate that along the Pacific Coast of the United States mean sea level is about 50 cm higher than along the Atlantic Coast, and that across the Panama Canal Zone 'mean sea level at Balboa along the Pacific Coast is about 3/4 foot higher than mean sea level on the Atlantic Coast' (U.S.C.G.S., personal communication). SVERDRUP *et al.* (1942, p. 459) speculated that 'this difference may perhaps be related to the lower average density of the Pacific water.' It is possible that this speculation was made also in the light of the *Carnegie* data (FLEMING *et al.*, 1945), with which SVERDRUP was working at that time and which he might have compared with DEFANT'S (1941) chart.

Of processes which might contribute to the difference, or the maintenance of the difference, in density and sea level between the Atlantic and Pacific oceans, two can be mentioned. One is related to the difference in the southern limits of South America (56 °S), Africa (35 °S) and Australia (44 °S). The other is related to the constriction of the west wind drift around Antarctica by Drake Strait.

As a consequence of the first, the water from only the southernmost one-fifth of the South Pacific passes through Drake Strait, while the southern half of the South Atlantic may flow eastward into the Indian Ocean. In southern summer the average surface density (σ_t) between 50° and 60 °S in the Pacific is 26·62 (Table 2). In the South Atlantic the average σ_t of the zones between 30° and 40°, 40° and 50°, and 50° and 60 °S are 24·87, 26·26, and 27·01, respectively. The South Atlantic may lose surface water of an average σ_t of about 26·05 and gain water of about 26·62 from the Pacific. The South Pacific may lose water of about 26·62 to the Atlantic and gain water from the Indian Ocean south of 44° S whose average surface σ_t between 45° and 60 °S is about 26·25 in southern summer according to SCHOTT (1935). This is about the same as for the zone between 40° and 60 °S in the Pacific.

The other process is best stated by quoting from MONTGOMERY (1938) who writes (p. 170, second footnote), 'Imagine a canal encircling the earth in the zone of westerly winds, and let there be a constriction at one part of the canal ; sea level would be higher at the western end of this constriction than at the eastern end due to *Windstau*. This is essentially the case in the Southern Ocean and the constriction occurs at Drake Strait, sea level being higher on the Pacific side and lower on the Atlantic side (presumably!), accounting for the probable fact that the Pacific Ocean is generally at a higher level than the Atlantic.' He then cites the U.S.C.G.S. measurements of different sea level on the Atlantic and Pacific coasts of the United States.

Some part of the north-south difference in density and sea level might have been expected as a consequence of the difference in circulation. Given the observed distribution of the surface currents of the oceans, and assuming approximate geostrophic equilibrium, one might expect that the average sea level in the regions of the west wind drifts might be lower in the southern hemisphere than in the northern. The flow around Antarctica is stronger and is eastward everywhere except in part of the Weddell Sea. For the flow to be in geostrophic balance a steep slope downward to the south must exist, with the slope proportional to the velocity and to the sine of the latitude. The northern west wind drifts (North Pacific and North Atlantic Currents) are not so strong and occur at lower latitudes. Westward flow occurs at higher latitudes (Alaska Current and East Greenland Current) with slopes upward to the North.

The highest values of temperature and salinity are found in the North Atlantic Ocean. Although the extremely warm and saline waters (about 12 °C and 38‰) of the Mediterranean undoubtedly contribute to the high values of the upper kilometre

(334)

of the North Atlantic, the effect is lessened by their high density, which causes them to sink very rapidly as they mix. Little direct evidence of their presence is seen on the horizontal distributions of salinity and temperature above 800 metres (Wüst and Defant, 1936), and the effect of the Mediterranean water is most apparent over large areas on the charts at 1500 and 1750 metres. Wüst (1935, Tabelle 19) estimates the Mediterranean water at $36-\frac{1}{4}$ °N $6-\frac{3}{4}$ °W to be at 600 to 700 metres and to be of 11·9 °C and 36·5 ‰. The σ_t of such water is 27·82 and it is more dense than the average at 1000 metres in the zone 30°– 40 °N (Table II). The horizontal charts indicate that in the upper thousand metres the water of high density originates at higher latitude than the Straits of Gibraltar.

A process which has quite different effects in the North Pacific and the North Atlantic is the sinking of surface water in winter. Only intermediate water of low salinity is formed in the North Pacific while much saltier deep water is formed in the North Atlantic. The North Pacific thus retains within the upper thousand metres of the subtropical anticyclonic gyre the product of the precipitation and cooling of its high latitudes. The analogous water is eliminated from the upper thousand metres of the North Atlantic when it sinks to depths greater than 2000 metres. The difference is a consequence of the low salinity at the surface in high latitudes in the North Pacific (32·63‰) which limits the surface density to about 1·02609 g/cm^3 (Table 2) and the high salinity at the surface in the high latitude Atlantic (35·04‰) which permits the surface density to rise above 1·02775 g/cm^3 over large areas in winter. The surface water of the North Pacific thus remains in the upper thousand metres, while part of the surface water of the North Atlantic sinks to more than 2000 metres, forming the North Atlantic Deep Water and removing a large part of the precipitation from the surface.

The North Atlantic Deep Water extends southward and supplies a great part of the water in the South Atlantic. Since South Atlantic surface water flows from the South Equatorial Current along the north coast of South America, the South Atlantic contributes a part of its warm water to the North Atlantic. This, in turn, accounts in part for the low temperature of the South Atlantic.

Another important consideration is the temperature of the surface water entering and leaving the South Atlantic in the west wind drift. In a like manner to that used for the density it can be estimated that in southern summer the average temperature of the incoming surface water is not more than 7 °C, while the outgoing water ranges from 3·2° to 21 °C, with a mean of about 9·7 °C.

The surface water passing Drake Strait is only about 34‰ in salinity while the average between Africa and 60 °S is about 34·40‰. That passing between Australia and 60 °S is about 34·40‰ (Schott, 1935). If other effects could be neglected one would expect the South Atlantic to be less saline than the South Pacific, but this is clearly not the case (Table V).

THE DIFFERENCES AT GREATER DEPTHS

Montgomery (1958), Cochrane (1958), and Pollak (1958) have computed the mean potential temperature, salinity, and potential specific volume anomaly of the Atlantic, Pacific, and Indian oceans, respectively, and Montgomery's work combines the results for the world ocean. These figures, which are for the total volume of the ocean, indicate that the potential specific volume anomaly of the Atlantic is less than that of the Pacific by 17×10^{-5} cm³/g. This may be taken roughly as a density difference of 17×10^{-5} g/cm³, with the Atlantic being heavier. This is about half the difference in density in the upper kilometre, and implies, as might be expected, that the density differences decrease with depth. However, it implies also that the deeper densities are also greater in the Atlantic, that the 1000-decibar surface also stands higher in the Pacific, and that with respect to some deep pressure surface, such as 4000 decibars, the Pacific sea surface must stand 68 cm higher than the Atlantic.

MONTGOMERY (1958) finds the average potential temperature (from the surface to the bottom) to be 0·37 °C higher in the Atlantic than the Pacific. This is greater than the difference in the upper thousand metres and implies that the differences increase at greater depths. A comparison of the charts of WÜST and DEFANT (1936) and MUROMTSEV (1958) confirms this. MONTGOMERY finds the salinity to be greater in the Atlantic by 0·28‰ This is less than in the upper thousand metres.

For the Pacific Ocean COCHRANE (1958) has calculated the average potential temperature (again from the surface to the bottom) and found the North and South Pacific to differ by only 0·02 °C. He finds the salinity of the South Pacific to be 0·05‰ higher than the North Pacific. This is about one-fifth of the difference in the upper thousand metres and implies that the deeper salinities are not significantly different. He finds the potential specific volume anomaly to be 5×10^{-5} cm³/g higher in the North Pacific. If this is taken to represent roughly a density difference of 5×10^{-5} g/cm³, with the North Pacific lighter, then it is about a third of the difference in the upper thousand metres and implies that the density differences extend somewhat deeper.

Acknowledgment—The author wishes to express his appreciation to Prof. R. B. MONTGOMERY, Prof. J. D. ISAACS, and Prof. R. S. ARTHUR for various discussions and suggestions. This work was supported by the Marine Life Research Program, the Scripps Institution of Oceanography's component of the California Co-operative Oceanic Fisheries Investigations, a project sponsored by the Marine Research Committee of the State of California.

REFERENCES

BÖHNECKE G. (1936) Atlas zu : Temperatur, Salzgehalt und Dichte an der Oberfläche des Atlantischen Ozeans. Deutschen Atlantischen Exped., *Meteor* 1925–1927. *Wiss. Ergeb.*, **5**, Atlas, Beilagen I–LXXIV.

COCHRANE J. D. (1958) The frequency distribution of water characteristics in the Pacific Ocean. *Deep-Sea Res.* **5**, 111–127.

DEFANT A. (1941) Die relative Topographie einzelnar Druckflachen im Atlantischen Ozean. Deutschen Atlantischen Exped., *Meteor* 1925–1927, *Wiss. Ergeb.*, **6**, (2), 183–190, Beilagen I–XVIII.

ECKART C. (1958) The equation of state of water and sea water at low temperatures and pressures. *Amer. J. Sc.*, **256** (4), 225–240.

ECKART C. (1959) On the need for a revision of the equation of state of sea water. Conference on Physical and Chemical Properties of Sea Water, Easton, Maryland, Sept. 4–5, 1958, *Nat. Acad. Sci.—Nat. Res. Council Publication* **600**, 156–165.

FLEMING J. A., ENNIS C. C., SVERDRUP H. U., SEATON S. L. and HENDRIX W. C. (1945) Observations and results in physical oceanography. Scientific results of cruise VII of the *Carnegie* during 1928–1929 under command of Captain J. P. Ault. *Oceanography*, **1** B, 315 pp.

KRÜMMEL O. (1907) Die räumlichen, chemischen und physikalischen Verhältnisse des Meeres, Handbuch der Ozenographie, Band **1**, 526 pp., Stuttgart.

MONTGOMERY R. B. (1938) Fluctuations in monthly sea-level on eastern U.S. coast as related to dynamics of western North Atlantic Ocean. *J. Mar. Res.*, **1** (2), 165–185.

MONTGOMERY R. B. (1958) Water characteristics of Atlantic Ocean and of world ocean. *Deep-Sea Res.* **5**, 134–148.

MUROMTSEV A. M. (1958) Osnovnye Cherty Gidrologie Tikhogo Okeana. (Principal features of the Hydrology of the Pacific Ocean) 632 pp. Appendix II (bound separately) Atlas of Vertical Sections and Maps of Temperature, Salinity, and Oxygen Content. 124 pp., Leningrad (in Russian).

NORPAC Committee (1960) *Oceanic Observations of the Pacific*: 1955, the NORPAC Atlas, Univ. of Calif. and Univ. of Tokyo Press, Berkeley and Tokyo, 123 plates.

POLLAK M. (1958) Frequency distribution of potential temperatures and salinities in the Indian Ocean. *Deep-Sea Res.* **5**, 128–133.

RAPPLEYE H. S. (1932) Further study of the variation of mean sea level from a level surface. Geodetic Operation in the United States 1927–1929. U.S.C.G.S. SP. PUB. **166**, 21–23.

REID R. O. (1959) Influence of some errors in the equation of state or in observations on geostropic currents. Conference on Physical and Chemical Properties of Sea Water, Easton, Maryland, Sept. 4–5, 1958, *Nat. Acad. Sci.–Nat. Res. Council Publication* **600**, 10–29.

SCHOTT G. (1935) *Geographie des Indischen und Stillen Ozeans.* Hamburg. 413 pp., 37 charts, 114 figs.

SVERDRUP H. U., JOHNSON M. W. and FLEMING R. H. (1942) *The Oceans, their physics, chemistry, and general biology.* 1087 pp. Prentice-Hall, New York.

VON BOGUSLAWSKI G. (1884) Räumliche, physikalische und chemische Beschaffenheit der Ozeans, Handbuch der Ozeanographie, Band **I**, 400 pp., Stuttgart.

WÜST G. and DEFANT A. (1936) Atlas zur Schichtung und Zirkulation des Atlantischen Ozeans. Schnitte und Karten von Temperatur, Salzgehalt und Dichte. Deutschen Atlantischen Exped., *Meteor* 1925–1927. *Wiss. Ergeb.*, **6**, Atlas, Beilagen I–CIII.

WÜST G. (1935) Die Stratosphare. Deutschen Atlantischen Exped., *Meteor* 1925–1927. *Wiss. Ergeb.* **6**, (1) (2), 288 pp.

Printed in Great Britain by The Salisbury Press Ltd., Publicity House, Wilton Road, Salisbury Wilts. (27336)

Reprinted from SCIENCE, December 9, 1960, Vol. 132, No. 3441, pages 1761-1762

Protactinium-231 Content of Ocean Water and Sediments

Abstract. By means of a direct method for determining the nuclide protactinium-231, a deficiency in ocean water was found to be accompanied by unsupported Pa^{231} in ocean sediments. Protactinium-ionium ratios obtained for a surface and a deep section in the same equatorial core yielded apparent ages which were in agreement with predicted ages.

In the past, workers (*1*) set maximum concentration limits for Pa^{231} in ocean water by determining an upper limit for Th^{227} and then assuming that Th^{227}, Ac^{227} and Pa^{231} were in secular equilibrium. Since the half-life of 27.7 years gives ample time for solvation and precipitation processes to act selectively on Ac^{227} and effect a separation of it from its parent Pa^{231}, I thought that a direct determination of Pa^{231} in ocean water was necessary.

The procedure, a modification of one developed by Potratz and Bonner (*2*), was as follows. A known activity of Pa^{233} (a beta emitter which results from the decay of Th^{233} produced by the thermal neutron irradiation of Th^{232}), Fe^{3+} solution, and acid were added to portions of ocean water filtered through Whatman 41H paper. Naturally occurring Pa^{231} and the added Pa^{233} were concentrated by co-precipitation with $Fe(OH)_3$ upon the addition of NH_4OH and then separated from the iron by two co-precipitations on $ZrO(IO_3)_2$ from 4*M* HNO_3 solutions. Further purification of the protactinium isotopes was obtained by their extraction from a 6*M* HCl solution into diisobutylcarbinol. After washing the organic phase with several portions of 6*M* HCl, protactinium was back-extracted into a dilute HF solution which was washed with several portions of fresh diisobutylcarbinol and evaporated to dryness on a platinum plate. After these operations, the yield of protactinium was determined by comparing the Pa^{233} beta activity with that of an aliquot of the original tracer solution mounted and counted in the same manner. Counts of the total alpha activity gave a measure of Pa^{231}, since this is the only naturally occurring alpha-emitting isotope of protactinium.

Table 1. Protactinium-231 content of New Brunswick Laboratories AEC counter calibration sample, which contained 0.5 percent of uranium.

Sample size (g)	Yield (%)	Pa^{231}(disintegration/min)	
		Experimental	Theoretical
0.200	96 ± 4	31.6 ± 1.3	33.8
0.200	75 ± 3	28.3 ± 1.1	33.8
0.400	66 ± 2	65.0 ± 2.0	67.6
0.400	80 ± 2	64.5 ± 2.0	67.6

Table 2. Protactinium-231 content of ocean water.

Sample	Tracer yield	Total alpha activity corrected for yield and geometry (disintegration/min)
Reagent blank	72 ± 3	0.22 ± 0.06
No. 1, 76 lit.	57 ± 2	0.22 ± 0.08
No. 2, 76 lit.	36 ± 1	0.24 ± 0.10

Table 3. Protactinium content of deep-sea sediments. Ppm, parts per million; *A*, activity.

Core No.	$CaCO_3$* (%)	Total uranium (ppm)	Pa^{231} uranium equivalents† (ppm)	Th^{230} uranium equivalents (ppm)	$A_{Th^{230}}/A_{Pa^{231}}$	Apparent age (yr)
			Scripps			
Capricorn 33HG 1 cm	86		342 ± 17			
Capricorn 42HG 0 cm	85		447 ± 33			
Capricorn 50HG 0 cm	76		123 ± 9			
			Swedish deep-sea expedition			
Core 61, surface	65	1.5	216 ± 11	86 ± 9	9 ± 1	(0 ± 10) × 1000
Core 61, 161 cm	87		133 ± 30			
Core 61, 232–240 cm	67	1.0	86 ± 9	111 ± 11	28 ± 4	(95 ± 13) × 1000

* Cores with a high calcium carbonate content and thus with a comparatively high rate of deposition were selected for analysis in order to minimize the effect of mixing by organisms at the sediment surface on the resolution of time (*4, 5*). Protactinium and ionium values are listed on a carbonate-free basis. † Uranium equivalents are defined as that concentration of uranium which is necessary to support the protactinium or ionium activity found, or both.

For sediments, 2-g samples were digested with H_2SO_4 and addition of HF was repeated until no silica remained. After the last traces of HF had been removed by fuming with H_2SO_4, the solution was cooled and diluted, and the procedure described above was followed, starting with the precipitation of $Fe(OH)_3$.

In order to test the validity of the foregoing methods, several Pa^{231} determinations were made on material which had a known amount of uranium and the equilibrium quantity of daughter elements. The results are listed in Table 1. There is rather good agreement between experimental and theoretical values, and the experimental alpha activity did not change with time—a finding which indicated the absence of short-lived radioactive species or long-lived species with short-lived daughter elements.

On the assumption that the foregoing procedures are valid, determinations were made on two 76-lit. samples of Pacific Ocean water collected from the end of the pier of the Scripps Institution of Oceanography at La Jolla, Calif., and the results in Table 2 were obtained.

It appears that one may safely state that the Pa^{231} alpha activity in 76 lit. of ocean water is less than 0.2 disintegration/min, which is less than 3 percent of the amount which could be in equilibrium with a uranium content of 3 μg/lit. (*3*).

The deficiency of Pa^{231} in ocean water indicates that Pa^{231} is removed as it is formed from the radioactive decay of U^{235} in a time much shorter than its half-life; this behavior is similar to that of ionium (Th^{230}). Therefore, as in the case of ionium, one may expect to find quantities of unsupported protactinium in ocean sediments. This was experimentally verified for the six samples listed in Table 3.

The data indicate that there is unsupported Pa^{231} in the top layers of equatorial Pacific deep-sea sediments and that there is also the expected decrease with depth. Apparent protactinium-ionium ages for the two sections for which ionium values were obtained agree with estimates based on productivity studies and extrapolated C^{14} ages (*4*). Protactinium-ionium dating promises to be a valuable tool in the geochronological study of deep-sea sediments (*6*).

WILLIAM M. SACKETT*
Scripps Institution of Oceanography,
La Jolla, California

References and Notes

1. F. F. Koczy, E. Picciotto, G. Poulaert, S. Wilgain, *Geochim. et Cosmochim. Acta* **11**, 103 (1957); W. M. Sackett, H. A. Potratz, E. D. Goldberg, *Science* **128**, 204 (1958).
2. H. A. Potratz and N. A. Bonner, *U.S. Atomic Energy Comm. Rept. No. La-1721* (1958).
3. M. Nakaneshi, *Bull. Chem. Soc. Japan* **24**, 36 (1951).
4. G. Arrhenius, *Report of the Swedish Deep-Sea Expedition* (Royal Society of Arts and Sciences, Göteborg, 1952), vol. 5.
5. ———, *Researches in Geochemistry*, P. H. Abelson, Ed. (Wiley, New York, 1959), p. 22.
6. This is a Scripps Institution of Oceanography contribution, new series. The research was carried out under contract with the U.S. Atomic Energy Commission [contract No. AT (11-1)-34, project 44], whose support is gratefully acknowledged. I am indebted to Dr. Gustaf Arrhenius for making this work possible through his invaluable advice and encouragement, and I also acknowledge the personal communications of Dr. Edward D. Goldberg and Dr. Hans Korkisch regarding the ionium and the uranium analyses, respectively. Some of the equipment and materials were kindly furnished by Dr. James R. Arnold and Dr. William H. Thomas, and I wish to express my gratitude for this help.

† Present address: Pan American Petroleum Corp., Tulsa, Okla.

14 July 1960

Reproduced by Permission

Reprinted from SYMPOSIUM BIBLIOGRAPHY OF
[illegible] WORKS IN SEDIMENTOLOGY
International Association of Sedimentology
Published TECHNIP, Paris, 1960
pp.9-27.

RECENT SEDIMENT STUDIES, 1955-1959(¹)

---

f. p. shepard
Scripps Institution of Oceanography, University of California
La Jolla, California.

INTRODUCTION

The past four years have seen a great increase in the study of modern marine sediments whereas studies of modern continental sediments have not received as much attention. The importance of recent sediment studies has long been realized by geologists but it is only in the last few years that any major effort has been made to satisfy this need. Since World War II a vast amount of oceanographic study has been made by the major marine laboratories. Most of this, however, has not contributed very much towards the understanding of conditions of deposition of ancient sediments because of the emphasis on the deep oceans. Although locally there are indications that ancient sediments were deposited in deep troughs, it is probable that most of them were deposited under shallow water conditions and virtually none in true ocean basins.

The first concerted investigation of shallow water sediments on a relatively large scale was initiated in 1951 at *Scripps Institution of Oceanography* by the *American Petroleum Institute.* A. P. I. Project 51 was first developed to study the sediments along the northwestern margin of the Gulf of Mexico and is now being continued as an investigation of the Gulf of California. American petroleum companies have also sponsored studies of coral reefs and other environments of calcareous deposition. Considerable study has been made by the field laboratories of the major oil companies of portions of the Gulf of Mexico not covered by A. P. I. 51. The *Royal Dutch Shell Organization* has supported the marine sediment studies of the *Universities of Groningen and Wageningen* in the Orinoco Delta and Trinidad Island area. The *U. S. Geological Survey* has made extensive studies of the sediments in the coral islands of the Pacific. The relatively deep basins off the southern California coast have been investigated by the *Hancock Foundation* with many interesting results which can be related to the Tertiary oil bearing sediments of the California area. Extensive studies by the Soviet geologists have covered sediments in the seas surrounding the Soviet Union. Almost all of this Soviet work, however, has been published in Russian and almost no translations into English are available although some works have been translated into French and German. The Germans have made many local studies of sediments, particularly in the Baltic and the North Sea and both the French and the Germans have investigated sediments in the Mediterranean. The Dutch have investigated the extensive tidal inlets along their coasts and have compared results with ancient sediments. Sediments from many other areas have been studied as will be indicated in the discussion to follow.

(¹) The writer wishes to acknowledge the helpful suggestions particularly concerning European literature given by Tj. H. van Andel.

Contributions from the Scripps Institution of Oceanography, New Series, 1268
Reproduced by Permission

During the past four years a series of volumes have appeared which contain synopsis on recent as well as ancient sediments. These include *Habitat of Oil* edited by WEEKS (1958), the two volumes of the *Treatise on Marine Ecology and Paleoecology* edited respectively by HEDGPETH (1957) and LADD (1957), *Finding Ancient Shorelines* edited by HOUGH and MENARD (1955), *Colloque de Sédimentologie* published by *Institut Français du Pétrole* (1957), and *Die Heutigen Meere* which appeared in the *Geologische Rundschau* (1958).

Estuaries and Lagoons.

In discussing the recent sediment studies in the past four years it seems advisable to separate the investigations into depositional environments although some overlap cannot be avoided. The first part of the important new volume on *Stratigraphy* by DUNBAR and RODGERS (1958) used a similar approach. The embayments along the coasts of the world constitute a distinctive depositional environment because they are areas in which the development of waves is considerably hampered by the short fetch of the wind. Also most of them represent good settling basins because of the absence of strong currents, except for the tidal currents which are largely confined to the bay mouths. There are various types of embayments. The deep elongate structural types such as the Gulf of California require special treatment and will be considered under another heading. The two other most common types are the *lagoons* which are roughly parallel to the coast and form behind barriers, particularly sand islands, and *estuaries*, most of which are developed by drowning of river valleys. The latter may or may not have sand barriers protecting their mouths. The lagoons and estuaries of the Texas coast (fig. 1) have been given very extensive sediment studies (see SHEPARD and MOORE, 1955 ; INMAN and CHAMBERLAIN, 1955 ; SHEPARD and RUSNAK, 1957, and RUSNAK, in press). Almost the entire Texas coast is bordered by barrier islands and most of the rivers enter estuaries. Exceptions exist at the Rio Grande, the Brazos, and the Colorado where these large rivers have filled or largely filled both the estuaries and lagoons in their vicinity.

The Texas bays are small, few being more than ten miles across, and the estuaries reach a maximum length of about 25 miles whereas the lagoons extend for about 100 miles in the case of Laguna Madre to the south, although the middle portion of this lagoon is now free from water except under conditions of strong southerly winds. These bays are shallow, 5 meters being the maximum depth aside from some tidal inlets where the depths are slightly greater. All of the bays are shoaling and the rate averages about one foot per century so that they should soon become filled unless sea level rises or the land sinks at a much more rapid rate than is now taking place.

Climatically the Texas bays are influenced by the semiaridity to the south and the humid conditions to the north. As a result the northern bays are being filled largely by stream deposits whereas the Laguna Madre to the south has no appreciable entering stream and little runoff. On the other hand the Laguna Madre receives much wind-blown material from the dunes of the barrier island because these dunes have little vegetation. The net result is that sediments are largely silt and clay in the northern lagoons and largely sand in the south. There are, however, clay sediments in a deep estuary of the Laguna Madre and the northern bays have some sandy sediments mixed with considerable clay near their inlets. Because of the bottom churning of organisms stratification is poor in the northern bays, except locally near the river mouths. Stratification is more pronounced in the Laguna Madre partly because of an algal mat which forms on the shallow flats and causes a stagnant anaerobic condition in the underlying sediments and hence is inhospitable to bottom scavengers. The climate also results in great differences in salinity between the north and the south. The northern bays have a low salinity except near the inlets and there is a low salinity in the central bays during unusual draughts. The southern lagoon has a salinity considerably in excess of the Gulf

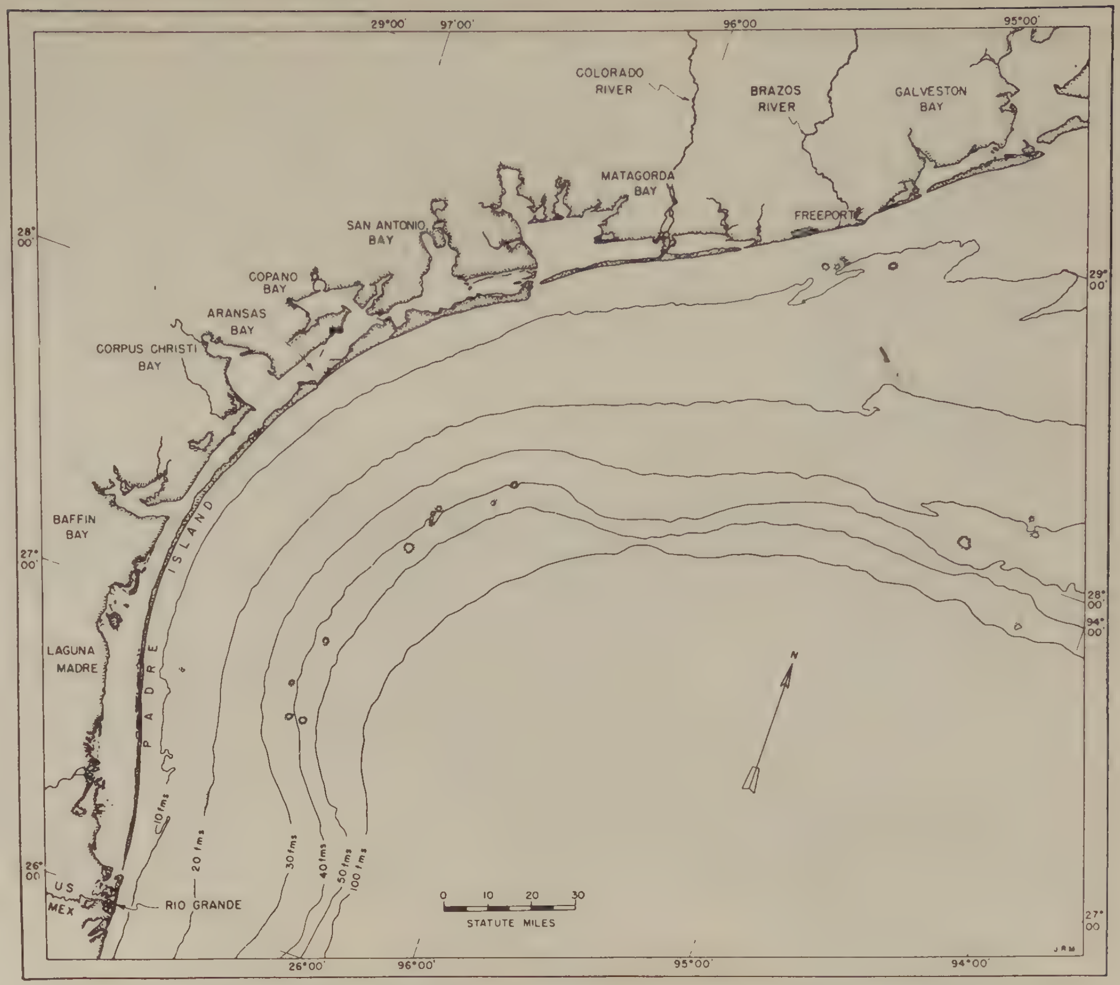
29°00'
97°00'
96°00
95°00'
COLORADO RIVER
BRAZOS RIVER
GALVESTON BAY
MATAGORDA BAY
FREEPORT
SAN ANTONIO BAY
COPANO BAY
ARANSAS BAY
CORPUS CHRISTI BAY
BAFFIN BAY
LAGUNA MADRE
PADRE ISLAND
US
MEX
RIO GRANDE
28° 00'
27° 00'
26° 00
29° 00'
28° 00'
94° 00'
27° 00
10 fms
20 fms
30 fms
40 fms
50 fms
100 fms
N
0
10
20
30
STATUTE MILES
26°00'
96°00'
95°00'
94°00'
JRM

Figure 1 showing the bays along the Texas coast which were investigated in A. P. I. Project 51 and the general nature of the adjacent continental shelf, with the offshore banks indicated by stippling.

of Mexico. This hypersaline condition combined with warm summer temperatures results in the formation of calcareous deposits, presumably of a chemical nature. The sand grains are often coated with lime and oolites are forming in the shallow central portions along the shore. Gypsum is found locally at a small distance below the floor of the lagoon. The lower salinities in the northern bays are favorable for the formation of oyster reefs, another type of calcareous deposit.

Along the California coast the estuaries are described by STEWART (1958) as much sandier than most of the Texas bays due to the introduction of sand by the intermittent rivers. He showed the contrast between sediments introduced from the ocean, those of the lagoon, and those of river origin. STEWART observed the changes in sedimentation in a lagoon which resulted from the seasonal opening and closing of the entrance. From a study of the marshlands at Newport Bay, California, STEVENSON (1956) concluded that fossils are likely to be missing on the fine-grained sediments of the marsh and tidal flat deposits due to the low pH which produces solution, but are more common in the coarser sediments. He found a high organic content in these marshes.

The *Wadden* or tidal flat bays of Holland have been extensively studied by Dutch geologists (see especially VAN STRAATEN, 1954; VAN STRAATEN and KUENEN, 1957). Here, because of the large tidal ranges, conditions differ considerably from the Gulf of Mexico bays where tides are small. The tides bring great quantities of sediments in from the North Sea so that the Wadden sediments are actually derived from outside rather than from the Rhine River which might have been supposed to be the source. The sediments grow from coarse on the outside and in the tidal channels to fine on the inside both on the flats (except in the center which is sand) and in the marshes bordering the flats. Stratification is least disturbed by boring organisms in the tidal channels and most in the marshes, where roots also are destructive to layering. Another interesting study from the Holland coast was the investigation of the sediments of the Zuyder Zee (WIGGERS, 1955). This shallow bay was artificially drained in 1942.

Warnboro Sound in southwest Australia (CARRIGY, 1956) has another type of bay deposit. It is primarily calcareous. As in the Wadden deposits and in the Texas bays the sediments grow finer towards the mainland, although in Warnboro Sound there is no appreciable mainland source. The sediments are introduced by wave and tidal erosion of the islands and shoals along the outside of the Sound. The coarser sediments occur in shallow water in the outer sound and consist of shell fragments and Foraminifera along with small amounts of quartz. Inside, in the deeper water, the sediment is a lime mud and contains a relatively high content of organic material.

The muddy sediments of Villefranche Bay along the Riviera coast of France (BOURCART, 1957) are also predominantly calcareous although much of the calcareous material is detrital and derived from the erosion of the neighboring Alps. Triturated shells supply much of the mud. In a small basin near the head of the bay the mud is black showing poor circulation. According to LALOU (1954) a surface film of spheroidal calcium carbonate is precipitated as the result of sulphate reducing bacteria which are operative in the area. Experiments by LALOU have produced such precipitation under laboratory conditions.

An unusual type of deposit occurs in Florida Bay (GINSBURG, 1956). The bottom is predominantly limestone but in localities where grass has grown up from the bottom the shifting lime muds derived largely from the Florida Keys are anchored and mud banks form. Where these grow to the surface, mangroves develop forming a peat covering over the lime substrate.

The coastal lagoons of Abijan on the Ivory coast of Africa are described by DEBYSER (1955). He found euxinic conditions during the dry season. The drillings preparatory to developing a port have shown that the soft muds of the deeper parts of the bays are often underlain by hard sand and laterally the soft mud changes rapidly into sand. The sand is generally related to areas where there are tidal or river currents. The muds are high in organic content, partly from vegetation and partly phytoplankton.

Additional information concerning shallow embayments can be found in the *Treatise on Marine Ecology* (HEDGPETH, 1957 ; LADD, 1957). In general this information refers to the biology and to the conditions of the water but these have a large influence on the nature of sediments. The ecological conditions of lagoons and estuaries are described by EMERY, STEVENSON, and HEDGPETH (1957). The low salinity Baltic Sea is discussed by SEGERSTRALE (1957). An ecological discussion of Lake Maracaibo, which is an embayment along the north coast of South America, is given by REDFIELD (1958), who describes the soft black mud with strong H_2S smell which is underlain by an equally soft blue mud a few inches below the surface (¹). There is not sufficient oxygen to oxidize the large quantity of organic matter so that the area might be a highly favorable site for future oil accumulation.

Barrier Island Deposits.

The sandy barrier islands (often referred to in the past as *offshore bars*) have commonly been considered as ephemeral developments which form on coasts of emergence (JOHNSON, 1919, p. 386) and hence they have been given little attention as an important petroleum source in ancient sediments, although BASS (1934) has considered that many shoestring sands of Pennsylvanian age were of barrier origin. The studies along the Texas coast (SHEPARD and MOORE, 1955 ; SHEPARD, in press), on the other hand, have shown that barrier islands have formed during the relative subsidence which accompanied the rise in sea level at the end of the last glacial epoch. If this is correct, the barriers are more likely to have been incorporated into ancient sediments. In size the barriers are often several mile wide and scores or even hundreds of miles in length. The islands are very common along lowland coasts of the world and usually separate areas in which muddy sediments are being deposited. Hence, they may become good stratigraphic traps for future oil deposits.

The Texas barrier islands have been extensively studied and many borings have been made into them. The sediments are largely sand. On the Gulf side the sands of the beach are well sorted and the dune belt inside is very similar in sediment characteristics. The two facies can be distinguished best by a slightly greater rounding in the dune sands than in the beach sands and a slightly higher content of silt in the dunes. Where the stratification of the dunes is preserved (McKEE, 1957) the dunes could easily be distinguished by their cross-bedding although the stratification in island borings is rarely seen. In general the shell content is higher in the beach sands except locally where a shell concentration is found in the dunes due to deflation of sand leaving larger shell fragments. Inside the dune tract on many barrier islands there are broad barrier flats containing many ponds and channels. Often these flats extend as a convexity into the lagoon, being due to the delta-building along overwash channels. Such overwashes accompany storm tides particularly during hurricanes, even if the storm center is hundreds of miles distant. The sediments of the barrier flats are distinguished from the other barrier island environments by their higher content of silt and clay. They have numerous calcareous aggregates, apparently the result of the evaporation during low water which precipitates the lime. Also the pollen content was found to be considerably higher than in other environments along the Texas coast (WILSON and LE BLANC, 1954). The stratification is usually horizontal and is plainly visible in the sides of artificial cuts across the higher portions of the flats. There are many channels crossing the barrier islands, some of them occupied only during storm tides. Deposits in these inlets are largely sand where they are open, but when the seaward end becomes closed by a bar, muddy sediments are introduced from the bays. The faunas of the

---

(¹) According to Tj. H. VAN ANDEL (personal communication) a revisit of the area two years later failed to find the oxygen deficiency or the black mud, suggesting this may have been a temporary development.

inlets include a mixture of marine and lagoonal species. The lagoon side of many barrier islands has another but narrower beach, often with more shells than on the Gulf side.

The borings into the Texas barriers have revealed a thickness of sand sediments up to at least 20 meters. In a few places the Pleistocene *Beaumont Clay* is exposed in the barriers, but ordinarily the Pleistocene is deeply buried. The sands are largely of a facies which is comparable to the barrier island deposits. Fortunately, it is relatively easy to distinguish continental shelf sands because of the marked contrast in sand sizes from those of the beaches. The finding of barrier deposits to a depth of 20 meters indicates that the barriers have grown upward during a submergence. Since Carbon 14 has indicated that shells of a barrier facies found at 15 meters have an age of 6,500 years it seems probable that at least this barrier was growing upward during the last part of the post-glacial sea level rise (SHEPARD and SUESS, 1955 ; SHEPARD, in press).

A study of the grain orientation in the barrier island by CURRAY (1956) has shown that the preferred direction is transverse to the islands on the beaches as would be expected from the nature of wave action. Around the ends of the islands, on the other hand, the orientation may conform to the shape of the island as the result of current action.

A discussion of old barriers now found above water in Surinam is presented by VAN DER EYK (1957).

Delta Deposits.

The deposits formed in and around deltas have been studied more completely in recent years than have those of any other environment. Particular attention has been paid to the deltas of the Mississippi, the Orinoco, the Rhone, and the Fraser. The importance of delta studies is suggested by the fact that today the great bulk of sediments carried to the sea or into lakes is being deposited in or near deltas. Yet the literature concerning facies of ancient sediments includes few references to the deltas of the past. This leads to the suspicion that ancient deltas have often been overlooked, being confused with flood plain deposits on the one hand and undifferentiated neritic deposits on the other.

The subaerial portion of the Mississippi Delta has been studied for many years by the geologists of *Louisiana State University* (see especially RUSSELL, 1936 ; FISK, 1944, 1952). Recent studies have been conducted by the *Engineer Corps, U. S. Army* (KOLB, 1958), by the *Louisiana Institute of Coastal Studies* (TREADWELL, 1955 ; MORGAN, 1955), and by the geologists of the *Humble Oil Company* (FISK and MCFARLAN, 1955). The principal studies of the marine facies of the delta have been made by *American Petroleum Institute* Project 51 (SHEPARD, 1956 ; SCRUTON, 1955 ; INMAN and CHAMBERLAIN, 1955 ; SCRUTON, 1956 ; PHLEGER, 1955 ; PARKER, 1956 ; LANKFORD, 1959, and SHEPARD and LANKFORD, 1959). A notable attempt to reconstruct the Pleistocene history of the delta has come from the study of the borings made near the end of Southwest Pass (AKERS and HOLCK, 1957).

Examination of the old charts has shown the considerable changes which have taken place during the last century in the land outlines of the delta and in the surrounding water depths (SHEPARD, 1955). The greatest growth of land has occurred around Main Pass and in the bay northeast of South Pass (fig. 2). Here as the result of artificial crevassing new deltas have built forward between eight and ten miles during a period of about 70 years. On the other hand, portions of the delta which were cut off from a main source have sunk to depths of three meters or more. Beyond the principal passes the water is shoaling at a rate of about one foot (0.3 m) a year due to the forward building of the slopes. These slopes which are rarely steeper than one percent are cut by numerous submarine gullies, believed to be due to landslides (SHEPARD, 1955 ; TERZAGHI, 1957).

The sediment facies can best be divided into topset, foreset, and bottomset beds although the

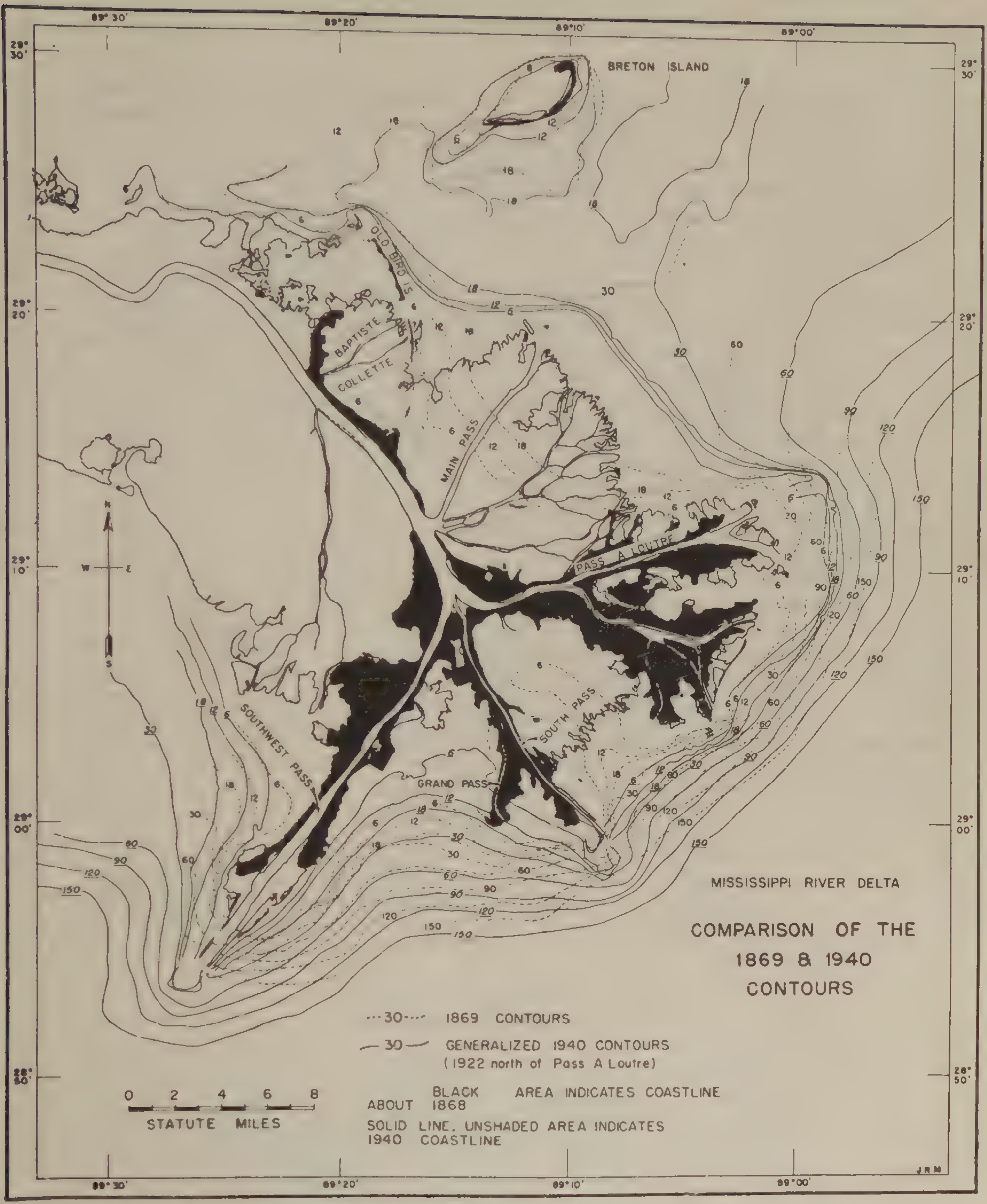
MISSISSIPPI RIVER DELTA
COMPARISON OF THE 1869 & 1940 CONTOURS
···30···· 1869 CONTOURS
—30— GENERALIZED 1940 CONTOURS (1922 north of Pass A Loutre)
BLACK AREA INDICATES COASTLINE ABOUT 1868
SOLID LINE, UNSHADED AREA INDICATES 1940 COASTLINE
0 2 4 6 8
STATUTE MILES
BRETON ISLAND
OLD BIRD IS.
BAPTISTE
COLLETTE
MAIN PASS
PASS A LOUTRE
SOUTH PASS
SOUTHWEST PASS
GRAND PASS
N
W
E
S
89° 30'
89°20'
89°10'
89°00'
29° 30'
29° 20'
29° 10'
29° 00'
28° 50'
JRM

Figure 2 showing growth of the Mississippi Delta since 1869 and depth changes. Since the 1869 soundings were not sufficiently detailed to show submarine gullies, the 1940 contours were generalized for comparative purposes.

angle of the foreset bed deposition is far lower than in typical textbook illustrations as is also true in most other large marine deltas. The topset beds include the subaerial channel, levee, and marsh deposits and the marine delta front platforms (also called bars) and the interdistributary bays. Some disagreement is found between the results reported by Fisk and McFarlan (1955) and those of the A. P. I. Project 51 (Shepard and Lankford, 1959). The former refer to « sand » fingers built forward with the advance of the bars at the mouths of the passes and they assume that the 65 meter thicknesses of sand found in some of the birdfoot delta borings represent these bars although some settling has occurred since deposition. The A. P. I. studies make such an explanation difficult to understand because the present day bars or platform deposits are only partially sand and the sand becomes negligible on the slopes below depths of three meters in contrast to the 65 meters of sand in the borings. The supposed clay wedges reported by Fisk and referring to the interdistributary bays were found by the A. P. I. studies to differ only slightly in grain size from the bar deposits. Almost all of these topset beds are nicely laminated as shown by numerous cores. The lamination virtually disappears in the foreset slope deposits and stratification of any type is rare in both foreset and bottomset beds. Because of slower deposition and because of higher salinity in the water, the organisms in the sediments become much more numerous with distance from the subaerial delta. All of the Mississippi delta deposits are characterized by relatively high contents of wood fibers, aggregates (mostly orange in color), and mica. In this way the coarse fraction of the delta deposits differs notably from those of other environments along the Gulf Coast. The Foraminifera are also very distinctive, particularly in the river mouths where they are introduced by salt water wedges coming in under the river water. Some confusion in the stratigraphy is caused by the upthrust of mud lumps forming islands and intersecting the delta front platforms. Sediments deposited at considerably greater depths than now exist are brought to the surface (Morgan, 1955).

The largest distributary of the Mississippi River is the Atchafalaya. This river enters Grand Lake to the west of the main delta where it is rapidly building a delta so that soon the lake will be filled and the river will be entering directly into the Gulf. At present much of the finer sediment goes right through the lake and, coming out into Atchafalaya Bay, continues into the open Gulf where it is building a delta that is entirely submarine (Thompson, 1955). Old surveys show that this delta-building has caused a shoaling during a 45-year period of as much as two meters. The top of the delta is horizontal and hence is in the nature of a topset bed. The principal growth is seaward of this flat surface where the bottom drops from three to seven meters in four nautical miles, a slope much gentler than those off the Mississippi. This slope must be interpreted as the foreset although it is inclined only about one meter in 1500.

The submarine portion of the Brazos Delta, which is building out into the Gulf along the Texas coast, has been studied by Nienaber (1958). He found again that the topset beds are laminated sand, silt, and clay. The foreset beds are deposited on a one degree slope and grade from fine sand into clay whereas the bottomset beds, largely clay, represent very slow deposition mixed with reworked Pleistocene material. He makes good use of the size parameters particularly the modality in interpreting the sediment history.

The Orinoco Delta and vicinity also has been studied intensively in recent years. Many of these studies are only available in oil company reports but the cooperative investigation of *Dutch Royal Shell* and the *University of Groningen* constituting the « Orinoco Shelf Expedition » has resulted in some outstanding reports, particularly on the marine facies of this great delta (van Andel and Postma, 1954 ; Nota, 1958 ; other information comes from Kidwell and Hunt, 1958). The marginal sediments of the Orinoco show many features similar to those of the Mississippi. The same barren sediments are found directly off the stream mouths, absolutely barren in this case. The lamination of the sediments is largely confined to the shallow water topset facies. The delta deposits overlap on old Pleistocene of the outer shelf as is true to the east of the Mississippi Delta. The study of the heavy minerals shows distinctive suites coming from the Orinoco and from other sources. This establishes that sand from the river is only carried out to 5 meters and the sand sediments beyond have a different source. In the Gulf of Paria VAN ANDEL has separated the sources of the sediments by the minerals which have at least three sources. The action of the strong Equatorial current in preventing modern deposition on the outer shelf off the main delta is indicated. In the southeast entrance to the Gulf of Paria the sands are now believed to be post-Pleistocene transgressive (Tj. H. VAN ANDEL, personal communication).

The Rhone Delta has been the subject of a number of recent investigations (KRUIT, 1955 ; DUBOUL-RAZAVET, 1956 ; DUBOUL-RAZAVET and KRUIT, 1957 ; VAN ANDEL, 1955 ; VAN STRAATEN, 1959). KRUIT has shown the history of the advance of the delta since about 3,500 B. C. The delta has advanced by the building of beach ridges and by crevassing which has formed new distributaries. He found poorly sorted coarse sediments at the river mouths where rapid deposition is taking place. Slow deposition beyond the delta produced by wave action causes much better sorting. He found a stable beach west of the delta which he believes to have been present for the past 5,500 years. VAN STRAATEN (1959) sounded the foreset slope of the delta and found small valleys present similar to but smaller than those of the Mississippi. VAN ANDEL (1955) found the heavy minerals had unstable hornblende and pyroxene-hornblende suites which he had also found characterizing the Rhine and Orinoco. He considers them to be typical « products of vast source areas of complex petrographic, tectonic, and climatic nature, which do not reflect the true proportion of sedimentary igneous and metamorphic rocks in the source » (VAN ANDEL, in press). The submarine Fraser Delta is being studied by the writer in collaboration with W. H. MATTHEWS. Preliminary results show that although the delta is being built into a fiord it has many features in common with the deltas built into more open bodies of water. There is a narrow platform in front of the river mouths representing the submerged portion of the topset beds. The foreset slope beyond is steeper than that of most deltas built into the open ocean, having a slope of three percent. In front of the principal pass there are several small valleys which like those of other marine delta fronts give out part way down the slope and are bordered by hummocks indicative of landsliding. The lamination of the topset beds virtually gives out on the foreset slope. The sediments vary from silty clays off the inactive portion of the delta to the north to silty sands in the more actively growing delta to the south. The Sénégal delta has been studied by TRICARD (1956). He discusses the special effects of a delta formed by an intermittent river in a region of migratory bars and dunes.

Continental Shelf Deposits.

Widely divergent views have been held concerning the continental shelf as a depositional environment. On the one hand the shelf has been considered as one of the principal sites in which ancient sediments were deposited and on the other it has been considered as a nondepositional environment. Recent studies seem to show that many parts of the present shelves are receiving little sediment whereas other areas are building up at an appreciable rate and are underlain by great thicknesses of sediments, a large portion of which are essentially shelf sediments.

The shelves of the northern Gulf of Mexico have been given the greatest attention of any in the world. The principal work on these shelves has been by A. P. I. Project 51 (CURRAY, 1959, and in press). Areas of active deposition have been found off the principal rivers with accumulations of six meters or more since the major portion of sea level rise at the end of the last glacial stage, that is, in about 10,000 years. These deposits, consisting of poorly stratified silty clays, overlap into weathered Pleistocene and transgressive basal sand deposits, some of the latter being dated by

Carbon 14 as 8,000 to 17,000 years old. The source of many of these old deposits, according to VAN ANDEL (in press), can be identified by their heavy minerals which relate them to the major rivers. Many of the older deposits are predominantly sands with abundant shells. These sands occur both as sheet sands which have been spread widely over the shelf partly under present day conditions, and as shoestring sands which represent old barrier islands formely existing on the shelf when the sea level was low. Both the old and recent sediments of the shelf are characterized by their content of glauconite and echinoids which are very scarce in the bays. The outer shelf deposits are further distinguished by their relatively high content of planktonic Foraminifera. The study by CURRAY has made use of grain size modes to trace the history and origin of the sediments. The sedimentation is complicated by calcareous covered hills due at least in part to the pushing up of salt domes around the edge of the shelf west of the Mississippi Delta (PARKER and CURRAY, 1956 ; LANKFORD and CURRAY, 1957). These hills are partly covered with calcareous algae, mostly Lithothamnion. These deposits supply sediments to the surrounding flat portion of the shelf giving them an unusually high content of calcareous debris.

To the east of the Mississipi Delta beyond the belt of deltaic sediments the shelf is largely covered with quartz sand (J. D. LUDWICK, personal communication ; GOULD and STEWARD, 1955). Exceptions are found in the Mississippi Sound and in the bays where muddy sediments exist. The sand is clearly derived from the southern Appalachians rather than the Mississippi River. Also, near the outer part of the shelf, hills are found with calcareous sediments somewhat comparable to those to the west of the delta. LUDWICK and WALTON (1957) have made extensive studies of these mounds and are of the opinion that they represent old coral and algal reefs formed when the sea level was lower than at present. A similar opinion is expressed by NOTA (1958) for the hills off the Orinoco delta. Going south along the Florida coast the quartz sand mixed with shells is found only near the shore. Beyond, according to GOULD and STEWART (1955), there are shell sands with little quartz, then a zone of algal sands, an oolite sand, and finally a foraminiferal sand with a high silt content at and beyond the break in slope at the shelf edge. In general deposition on this west Florida shelf appears to be small. Rock is found at many places. Coral reefs grow in patches on the shelf especially to the south. The oolite sand is quite clearly a remnant of earlier low sea level and presumably represents a condition of greater salinity, perhaps the result of barriers along the outer edge. An old barrier island is reported at about 100 fathoms along the outer shelf (JORDAN and STEWARD, 1959).

The continental shelf sediments off southern California have been studied particularly by EMERY (1954). Information has also come from the work of MOORE (1954). The sediment patterns indicate large areas where sediments are either relic or residual. Also there are areas where shell banks or accumulations of Foraminifera constitute the principal sediment. There are a few places where the sediment grades outward from coarse at the shore to fine at the outer edge. Many alternations are found although most of them are due to the antiquity of the outer sediments. The use of a Sonoprobe (MOORE, 1957) has shown that rather appreciable thicknesses of unconsolidated sediment are found locally on the southern California shelf. In some places these profiles show that terraces have been blanketed by recent sediment. The ripple marks of the inner California shelf have been studied by INMAN (1957) who found that the wave length varied directly with the grain size. He found the largest and least dense material in the ripple crests.

Along the coast of Lower California (Baja California) there are several comparatively wide shelves. These have been studied by EMERY and his students (1957). Todos Santos Bay has a protected environment because of the off-lying islands. The sediments show a fairly complete gradation from the long beach extending south of Ensenada out into the canyon head, changing from sand near shore to silty clay in the canyon. Apparently this canyon is being filled with fine sediment rather than maintained, by landslides and turbidity currents, as are many other canyons. The organic content also shows a progressive increase outward to the canyon floor. The Foraminifera (WALTON, 1955) have an interesting series of facies also related to the distance from the shore. However, out beyond the islands rock bottom is found along with gravel and ripple-marked sand.

The continental shelf off the east coast of India has been studied locally (MAHADEVAN and RAO, 1954). Off Vizagapatam they found terrigenous sediments extending out to 55 meters with sand along the shore and muddy sediments outside, but beyond 55 meters the sediment coarsens and a shell sand is found with bands of oolite somewhat like those off western Florida.

The shelf off Trinidad Island and the Paria Peninsula was studied by KOLDEWIJN (1958) as a part of the report on the Dutch Orinoco Shelf Expedition referred to above. He found active deposition of muddy sediments (pelites) occurring off both sides of the entrance to the Gulf of Paria whereas to the west off Paria Peninsula there is a reworking of Pleistocene and Holocene (Recent) calcareous sediments (calcarenites). To the east of Trinidad essentially the same conditions exist except that there are areas where coral reefs are growing on the shelf and other forms of calcarenite deposition are taking place. Carbon 14 dates from the cores provided evidence of reworking of older calcareous sands. Carbon 14 dates also showed that a decreasing rate of sedimentation has taken place as the result of rising sea level. The shelf to the south described by NOTA (1958) and referred to previously has many features simular to those described by CURRAY (1959) off the Texas coast.

Sediments in Elongate Basins.

A paper by KUENEN (1957) refers to the importance of a depositional source coming predominantly from one end of elongate basins. He gives as examples the Gulf of California, the Persian Gulf, the Caspian Sea, and the Bay of Bengal. Each of these basins which run north and south have a major contributing sediment source from the north. It could perhaps be questioned whether the Bay of Bengal should be included as it is more oval than elongate ; there is, however, no doubt of the northern source of the bulk of the basin sediment. On the other hand, the Gulf of California, now being studied by a group at the Scripps Institution, partly supported by A. P. I. 51, appears to receive fully as much sediment from the sides as the head, at least at present because of the cutting off of the bulk of the Colorado River drainage by the various dams. Even before the building of the dams it seems likely that the sediments filling the Gulf from the north were deposited largely north of Tiburon and Angel de la Guarda islands (150 miles from the head) and the sediments along the rest of the Gulf were and are still derived from the considerable streams coming in on the east side from Sonora. These streams are building great deltas and fans, and the sediments may have in places covered the fault scarps on the east side of the Gulf (RUSNAK, 1959). In addition sediments are contributed to the basin by turbidity currents from the west sides.

The Persian Gulf receives its principal source of sediment from the Tigris and Euphrates (EMERY, 1956). These sediments are largely muddy. Another source exists in the Arabian deserts which contribute fine sands by eolian action. To the south, especially on the west side, there are extensive areas of calcareous sediment. These have been studied locally by HOUBOLT (1957). He found rounded calcarenites near shore at the Qatar Peninsula and more angular, finer calcarenites farther out. Approaching the deeper central parts of the Gulf the terrigenous sediments are mingled with some calcarenites from the west. According to R. A. BRAMKAMP (personal communication) local growing reefs exist off Dhahran, a little north of the Qatar Peninsula, where winter temperatures recorded by the *Arabian American Oil Company* frequently go below 60° F (15.5° C), and as low as 52° F (11° C) for short intervals

Deep Marginal Basins.

An area of considerable importance to stratigraphic studies is located off the southern California coast where the continental borderland has basins ranging in depth up to 1,400 fathoms (2,600 meters). These basins have been shown previously to be equivalent to the Tertiary basins of the Los Angeles and Ventura areas. Extensive exploration of the present day basins has been conducted by the scientists of the *Hancock Foundation* (Emery and Rittenberg, 1952 ; Orr and Emery, 1956 ; Emery, 1958 ; Orr, Emery and Grady, 1958). Turbidity current deposits have been found in most of these basins. These consist of sand layers interbedded with the basin silty-clays. Large fans are found at the mouths of the submarine canyons. Also attributed to turbidity current action are some gray muddy layers in Santa Barbara Basin which are very low in Foraminifera and coarser than the typical green muds of the basin. These gray layers are lower in nitrogen and pheophytin presumably because of rapid deposition. On the other hand, the green layers underlying the gray are especially high in nitrogen and pheophytin because of the protecting cover of the supposed turbidity current deposits. Santa Barbara Basin has the only present day California basin deposits that are well stratified, apparently because here alone low oxygen content of the poorly aerated bottom waters prevents development of bottom churning organisms. Pheophytin, the source of the major porphyrins in crude oil, is more consistent in content below the surface of the deep outer basins but the highest quantities are found in Santa Barbara Basin.

The Black Sea has been extensively studied by the Russians. The results of their studies are summarized in English in two recent articles appearing respectively in the *Treatise on Marine Ecology*, and in *Habitat of Oil* (Caspers, 1957 ; Smirnow, 1958) although the latter lacks references. An earlier excellent review was written by von Raupach (1952). Somewhat conflicting maps of the sediments are found in these sources. The article by Caspers stresses the ecological, hydrobiological, and hydrochemical aspects of the sea. Much of the information comes from Strakov (1947). The problem of the effect of the H_2S layer and of the resulting lifeless zone of the deep portions on the deep basin sediments is discussed. These sediments have a high calcium carbonate content in the central part of the eastern and western basins, with white marly layers alternating with dark clayey sapropelitic layers. There seems to be some uncertainty about whether there are extensive black clays in the basin. The cores show that the basin sediments are stratified, with sapropelitic clays underlying the gray clays indicating a change in condition at what Strakov considers to be about 2,500 years ago. Rates of sedimentation according to Arkhangelsky and Strakov (1938) average 0.5 mm/year for the entire sea.

The deep basin of the Gulf of Mexico has been studied by the geologists at *Lamont Geological Observatory* (Ewing, et al., 1958). Their cores are used as a basis for the hypothesis that during the lowered sea level of the ice age sediments were carried down the Mississippi submarine trough building a cone beneath and an abyssal plain in the Sigsbee Deep. Turbidity current origin of a gray silt is inferred because in contrast to the overlying layer it contains no burrowing except near the top, a size-sorting of foraminiferal tests, a decreasing sediment grade upward in the layer, and reworked Neogene material. On the south side of the Sigsbee Deep cores contain breccias of calcarenites derived apparently from the slides or turbidity currents that have occurred on the steep escarpment extending down from the calcareous Campeche Shelf. On the other hand, Greenman and Le Blanc (1956) concluded that the three foot layer of sand found in the Sigsbee Deep by the *Woods Hole Oceanographic Institution* was not a turbidity current deposit since it was not graded but indicated great fault movements during the Pleistocene. This suggestion seems to have been adequately answered by the *Lamont Laboratory* studies (EWING, et al., 1958). Furthermore, analyses made by *Scripps Institution* from the sand layer indicated that it was graded.

Cores from the Deep Ocean Basins.

In addition to the many new reports on deep sea sand layers in the ocean basins (see ERICSON, et al., 1955 ; LOCHER, 1952 ; REVELLE, et al., 1955) a new concept of the importance of deep sea sedimentation along the continental margins has come from the discovery of numerous fans along the margins of both the Atlantic and the Pacific (MENARD, 1955 ; HEEZEN, 1959). These are apparently built by the movement of sediments down the submarine canyons. Enormous quantities of sediment seem to have been transported in this fashion, presumably by a combination of sliding and turbidity currents. Because of the presence of many sand layers in the fans it is clearly possible that ancient deposits of this type now found as sedimentary rocks on the continents may not have been recognized as deep sea deposits. Considerable progress has been made in the identification of Pleistocene glacial stages in the deep sea cores (ERICSON and WOLLIN, 1956 ; EMILIANI, 1958 ; ERICSON, et al., in press) and in the correlation of these horizons between cores. In the Pacific, cores have shown that over wide areas Tertiary formations are at or near the surface (RIEDEL, 1952).

Coral Reef Studies.

Several notable reports have appeared concerning the sediments of coral reefs. Professional Paper 260 of the *U. S. Geological Survey*, is perhars the most complete study ever made of recent reefs. Section A of this report by EMERY, TRACEY and LADD (1954) gives a description of the principal atolls in the Marshall Islands with especial emphasis on Bikini and Eniwetok. A section of the reefs shows a Lithothamnion ridge at the outer border of the reef flats, inside which is a coral-algal zone, then a smooth surface of dead reef covered with a mat of Foraminifera, and then the island consisting largely of coral rubble built up by the waves. The lagoons contain a reef flat, then a ring of broken coral and Foraminifera, and a central zone consisting largely of Hallimeda, but having also numerous coral knolls rising steeply from the floor. The nature of deposits in the lagoons and on the outer slopes of the atolls has served as a basis for the interpretation of the long cores made into Eniwetok atoll and studied largely by LADD et al., (1953, 1958). The reports by NEWELL on the Bahamas (1955) and on Raroia in the Tuamotus (1956) have added much new information on the organisms of the reef and, like the Marshall Island reports, have involved considerable diving operations. The study of the giant ripples in the Bahamas is equally enlightening. Work by the *University of Miami*, partly supported by A. P. I. Project 51, has given a clear picture of the reef zonation outside the Florida Keys (GINSBURG, 1956). The constituents of each zone have been calculated by GINSBURG and provide useful data in recognizing back reef, outer reef, and fore reef deposits in ancient coral formations.

The investigations of McKEE (1958) on Kapingamarangi Atoll have shown that the deeper atolls may have a central zone with lime mud. This consists largely of aragonite needles with only about ten percent of calcite Foraminifera. Since the surrounding deposits in shoaler water are calcite, the presumption is that the aragonite represents chemical precipitation.

The modification of the coral reefs of Djakarta Bay in historical times is well documented in a paper by VERSTAPPEN (1953). He shows that the changes in the monsoon circulation are largely responsible for the changes in the reefs and discusses also the effect of the change of position of a river mouth on the reefs.

Conclusion.

In the foregoing review of the studies of modern sediments an attempt has been made to refer briefly to the investigations which have seemed to be the most pertinent to stratigraphic problems. No doubt many important papers have been omitted because of language barriers or because they were not available to the present writer. It can be assumed also that overemphasis has been placed on the work which the writer was thoroughly familiar. In any case it is evident that much new information has become available in the last four years. Making use of this should facilitate the interpretation of ancient sedimentary formations. It is to be hoped that the information may also serve to correct erroneous interpretations made in the past on the basis of too few data. On the other hand, it should be realized that the study of modern sediments has only begun. Only a very small portion of the seas of the world have been sampled and too few of the samples have had adequate study. There is an infinite amount of work yet to be done. When one realizes the revolutionary effect of the recent discovery of the significance of turbidity current deposits alone, it can well be imagined how many more important discoveries lie ahead.

BIBLIOGRAPHY

AKERS (W. H.) and HOLCK (A. J. J.), 1957. — Pleistocene beds near the edge of the continental shelf, southeastern Louisiana. *Bull. Geol. Soc. Amer.*, **68**, 983-992.

ARKHANGELSKY (A. D.) and STRAKHOV (N. M.), 1938. — Geological structure and developmental history of the Black Sea. *Moscow-Leningrad, Academiia Nauk.*

BASS (N. W.), 1934. — Origin of the Bartlesville Shoestring Sands. *Bull. Amer. Assoc. Petrol. Geol.*, **18**, 1313-1345.

BOURCART (J.), 1957. — Géologie sous-marine de la baie de Villefranche. *Ann. Inst Océan.*, **33**, 3, 137-200.

CARRIGY (M. A.), 1956. — Organic Sedimentation in Warnbro Sound, Western Australia. *Journ. Sed. Petrol.*, **26**, 3, 228-239.

CASPERS (H.), 1957. — Black Sea and the Sea of Azov, in : *Treatise on Marine Ecology and Paleoecology*, **1**, *Ecology. Geol. Soc. Amer. Memoir* 67, 801-889.

CLOUD (P. E.) Jr., BLACKMAN (P. D.) and SISLER (F. D.), 1957. — Calcium carbonate deposition west of Andros Island, Bahamas (abs.). *Soc. Econ. Paleontol. and Mineralog.* (31st Ann. Meeting, St. Louis), 51-58.

—, SCHMIDT (R. G.) and BURKE (H. W.), 1956. — Geology of Saipan Mariana Islands, part 1 : General geology. *U. S. Geol. Surv. Prof. Paper* 280-A, 1-126.

CURRAY (J. R.), 1956. — Dimensional grain orientation studies of Recent coastal sands. *Bull. Amer. Assoc. Petrol. Geol.*, **40**, 10, 2440-2456.

CURRAY (J. R.), 1959. — Sediments and history of the Holocene transgression, continental shelf, Northwest Gulf of Mexico. *Ph. D. Thesis, University of California.*

— in presse « The continental shelf », from « Recent Sediments : Northwestern Gulf of Mexico », edited by F. P. SHEPARD, F. B. PHLEGER and Tj. H. VAN ANDEL, to be published by *Amer. Assoc. Petrol. Geol.*

DAETWYLER (C. C.) and KIDWELL (A. L.), 1959. — The Gulf of Batabano, a modern carbonate basin. *Fifth World Petroleum Congress, Section* I, *Paper* 1, 20 p.

DEBYSER (J.), 1955. — Etude sédimentologique du système lagunaire d'Abidjan (Côte d'Ivoire). *Rev. Inst. Français du Pétrole*, **X**, 5, 319-334.

DUBOUL-RAZAVET (G.), 1956. — Contribution à l'étude géologique et sédimentologique du delta du Rhône. *Mémoire de la Société Géologique de France, nouv. sér.*, 76, 234.

— and KRUIT (C.), 1957. — Sédimentologie du delta du Rhône. *Rev. Inst. Français du Pétrole*, **XII**, 4, 399-410.

DUNBAR (C. O.) and RODGERS (J.), 1957. — Principles of Stratigraphy. *John Wiley and Sons, Inc., New York*, 356 p.

EMERY (K. O.), 1954. — Some characteristics of southern California sediments. *Jour. Sed. Petrol.*, **24**, 1, 50-59.

— 1956. — Sediments and water of Persian Gulf. *Bull. Amer. Assoc. Petrol. Geol.*, **40**, 10, 2354-2383.

— 1958. — Southern California Basins, in : *Habitat of Oil*, a symposium. *Amer. Assoc. Petrol. Geol., Tulsa, Oklahoma*, 955-967.

— Gorsline (D. S.), Uchupi (E.) and Terry (R. D.), 1957. — Sediments of three bays of Baja California : Sebastian Viscaino, San Cristobal, and Todos Santos. *Jour. Sed. Petrol.*, **27**, 2, 95-115.

— and Rittenberg (S. C.), 1952. — Early diagenesis of California basin sediments in relation to origin of oil. *Bull. Amer. Assoc. Petrol. Geol.*, **36**, 5, 735-806.

— Stevenson (R. E.) and Hedgpeth (J. W.), 1957. — Estuaries and lagoons, in : *Treatise on Marine Ecology and Paleoecology*, **1**, *Ecology. Geol. Soc. Amer. Memoir* 67, 673-749.

— Tracey (J. I.), Jr. and Ladd (H. S.), 1954. — Geology of Bikini and nearby atolls, Part 1, Geology. *U. S. Geol. Surv. Prof. Paper* 260-A, 265.

Emiliani (C.), 1958. — Paleotemperature analysis of core 280 and Pleistocene correlations. *Jour. of Geol.*, **66**, 3, 264-275.

Ericson (D. B.), Ewing (M)., Heezen (B. C.) and Wollin (G.), 1955. — Sediment deposition in the deep Atlantic, in : *The Crust of the Earth, Geol. Soc. Amer. Spec. Paper* 62, 205-220.

— Ewing (M.), Wollin (G.) and Heezen (B. C.) (in press). — Twohundred and twenty-one Atlantic deep-sea cores. *Geol. Soc. Amer.*

— and Wollin (G.), 1956. — Micropaleontological and isotopic determinations of Pleistocene climates. *Micropaleontology*, **2**, 3, 257-270.

Ewing (M.), Ericson (D. B.) and Heezen (B. C.), 1958. — Sediments and topography of the Gulf of Mexico, in : *Habitat of Oil*, a symposium. *Amer. Assoc. Petrol. Geol., Tulsa, Oklahoma*, 995-1053.

Fisk (H. N.), 1944. — Geological investigation of the alluvial valley of the Lower Mississippi River. *Mississippi River Commission*, 78 p.

— 1952. — Geological investigation of the Atchafalaya Basin and the problem of Mississippi River diversion. *Mississipi River Commission*, 78.

— and McFarlan (E.), Jr., 1955. — Late Quaternary deltaic deposits of the Mississippi River, in : *The Crust of the Earth. Geol. Soc. Amer. Spec. Paper* 62, 279-302.

Folk (R. L.) and Ward (W. C.), 1957. — Brazos River bar : a study in the significance of grain size parameters. *Journ. Sed. Petrol.*, **27**, 1, 3-26.

Geologische Rundschau, 1958. — Die Heutigen Meere, **47**, Part 1, 24-249.

Ginsburg (R. N.), 1956. — Environmental relationships of grain size and constituent particles in some south Florida carbonate sediments. *Bull. Amer. Assoc. Petrol. Geol.*, **40**, 10, 2384-2427.

— 1957. — Early diagenesis and lithification of shallow water carbonate sediments in South Florida. *Soc. Econ. Paleont. and Mineral. Spec. Publ.*, 5, 80-100.

— and Lowenstam (H. A.), 1958. — The influence of marine bottom communities on the depositional environment of sediments. *Journ. of Geol.*, **66**, 3, 310-318.

Gould (H. R.) and Stewart (R. H.), 1955. — Continental terrace sediments in the northeastern Gulf of Mexico, in : *Finding Ancient Shorelines, Soc. Econ. Paleont. and Mineral. Spec. Publ.*, 3, 2-20.

Greenman (N. N.) and Leblanc (R. J.), 1956. — Recent marine sediments and environments of northwest Gulf of Mexico. *Bull. Amer. Assoc. Petrol. Geol.*, **40**, 5, 813-847.

Grim (R. E.) and Johns (W. D.), 1955. — Clay mineral investigation of sediments in the northern Gulf of Mexico. *2nd Nat'l. Conf. on Clays and Clay Minerals, Nat'l. Res. Council*, 81-103.

Hedgpeth (J. W.), 1957, editor. — *Treatise on Marine Ecology and Paleoecology*, **1**. *Ecology. Geol. Soc. Amer. Memoir* 67, 1296. p.

Heezen (B. C.), Tharp (M.) and Ewing (M.), 1959. — The floors of the oceans ; I. The North Atlantic. *Geol. Soc. Amer. Spec. Paper* 65, 122 p.

Houbolt (J. J. H. C.), 1957. — Surface sediments of the Persian Gulf near the Qatar Peninsula. *Mouton and Co, La Haye.*

Hough (J. L.) and Menard (H. W.), editors, 1955. — In : *Finding Ancient Shorelines, Soc. Econ. Paleont. and Minerals. Spec. Publ.*, 3, 129 p.

Inman (D. L.) and Chamberlain (T. K.), 1955. — Particle-size distribution in nearshore sediments, in : *Finding Ancient Shorelines. Soc. Econ. Paleont. and Mineral Spec. Publ.*, 3, 99-105.

— 1957. — Wave-generated ripples in nearshore sands. *Beach Erosion Board, Tech. Mem.* 100, 42 p.

Institut Français du Pétrole, 1957. — Colloque de Sedimentologie, 511 p.

Johnson (D. W.), 1919. — Shore Processes and Shoreline Development. *John Wiley and Sons, New York*, 584 p.

Jordan (G. F.) and Stewart (H. B.), Jr. — Continental slope off southwest Florida. *Bull. Amer. Assoc. Petrol. Geol.*, **43**, 5, 974-991.

Kidwell (A. L.) and Hunt (J. M.), 1958. — Migration of oil in Recent sediments of Pedernales, Venezuela, in : *Habitat of Oil*, a symposium. *Amer. Assoc. Petrol. Geol., Tulsa, Oklahoma*, 790-817.

Kolb (C. R.), 1958. — Geological investigation of the Mississippi River-Gulf outlet channel. *U. S. Army Engineer Waterways Experiment Station, Vicksburg, Miss., Misc. Paper*, 3-259, 22.

— and van Lopik (J. R.)., 1958. — Geology of the Mississippi River deltaic plain, Southeastern Louisiana. *U. S. Army Engineer Waterways Experiment Station, Vicksburg, Miss., Tech. Rept.*, 3-483, 120 p.

Koldewjin (B. W.), 1958. — Sediments of the Paria-Trinidad Shelf, Reports of the Orinoco Shelf Expedition, **III.** *Mouton and Co., Den Haag*, 109 p.

Kruit (C.), 1955. — Sediments of the Rhone Delta : Grain size and microfauna. *Rijkuniversiteit te Groningen, Mouton and Co.*, 141 p.

Kuenen (Ph. H.), 1957. — Longitudinal filling of oblong sedimentary basins. *Geologisch Mijnbouwkundig Genootschap*, Proc. XVIII, pp, 189-195.

Ladd (H. S.), editor 1957. — Treatise on Marine Ecology and Paleocology, **2**, Paleoecology. *Geol. Soc. Amer. Memoir* 67, 1077 p.

— 1958. — Fossil land shells from western Pacific atolls. *Journ. Paleont.*, **32**, 1, 183-198.

— Ingerson (E.), Townsend (R. C.), Russell (M) and Stephenson (H. K.), 1953. — Drilling on Eniwetok Atoll, Marshall Islands. *Bull. Amer. Assoc. Petrol. Geol.*, **37**, 10, 2257-2280.

Lalou (Claude), 1954. — Sur les formes cristallines observées dans les voiles calcaires formées par cultures bactériennes à partir des vases noires de Villefranche-sur-mer (Alpes-Maritimes). *C. R. Acad. Sci.* **238**, 2329-2330.

Lankford (R. R.), 1959. — Distribution and ecology of Foraminifera from the east Mississippi Delta margin. *Amer. Assoc. Petrol. Geol.*

— and Curray (J. R.), 1957. — Mid-Tertiary rock outcrop on continental shelf, Northwest Gulf of Mexico. *Amer. Assoc. Petrol. Geol.*, **41**, 9, 2113-2117.

Locher (F. W.), 1952. — Kurzer Bericht die sedimentpetrographische Untersuchung zweier Lotkerne der Albatross-Expedtion. *Heidelberger Beitrage zur Mineralogie und Petrographie*, **3**, 193-218.

Ludwick (J. C.) and Walton (W. R.), 1957. — Shelf-edge, calcareous prominences in northeastern Gulf of Mexico. *Bull. Amer. Assoc. Petrol. Geol.*, **41**, 2054-2101.

Mahadevan (C) and Rao (M. Poornachandra), 1954. — Study of ocean floor sediments off the east coast of India. *Andhra Univ. Memoirs in Oceanography*, **1**, 1-35.

McKee (E. D.), 1957. — Primary structures in some Recent Sediments. *Bull. Amer. Assoc. Petrol. Geol.*, **41**, 8, 1704-1747.

— 1958. — Geology of Kapingamarangi Atoll, Caroline Islands. *Bull. Geol. Soc. Amer.*, **69**, 241-278.

Menard (H. W.) Jr., 1955. — Deep-sea channels, topography, and sedimentation. *Bull. Amer. Assoc. Petrol. Geol.*, **39**, 2, 236-255.

Moore (D. G.), 1954. — Submarine geology of San Pedro Shelf. *Jour. Sed. Petrol.*, **24**, 3, 162-181.

— 1957. — Acoustic sounding of Quaternary marine sediments off Point Loma, California. *U. S. Navy Electronics Lab., San Diego, Research. Rept.*, 815, 17 p.

Morgan (J. P.), 1955. — A geographical and geological study of the Louisiana coast with emphasis upon establishment of the historic shoreline. *Coastal Studies Inst., Louisiana State University.*

Newell (N. D.), 1955. — Bahamian platforms. *Geol. Soc. Amer., Spec. Paper* 62, 303-316.

— 1956. — Geological reconnaissance of Raroia (Kon Tiki) Atoll, Tuamotu Archipelago. *Bull. Amer. Mus. Natural History*, **109**, Art. 3, 315-372.

Nienaber (J. H.), 1958. — Shallow marine sediments offshore from the Brazos River, Texas. *Ph. D. Thesis, The University of Texas*, 181 p.

Nota (D. J. G.), 1958. — Sediments of the western Guiana shelf, Reports of the Orinoco Shelf Expedition, **II**. *H. Veenman en Zonen, Wageningen*, 98 p.

Orr (W. L.) and Emery (K. O.), 1956. — Composition of organic matter in marine sediments : preliminary data on hydrocarbon distribution in basins off southern California. *Bull. Geol. Soc. Amer.*, **67**, 1247-1258.

— Emery (K. O.) and Grady (J. R.), 1958. — Preservation of chlorophyll derivatives in sediments off southern California. *Bull. Amer. Assoc. of Petrol. Geol.*, **42**, 5, 925-962.

Parker (R. H.), 1956. — Macro-invertebrate assemblages as indicators of sedimentary environments in East Mississippi Delta region. *Bull. Amer. Assoc. Petrol. Geol.*, **40**, 2, 295-376.

— and Curray (J. R.), 1956. — Fauna and bathymetry of banks on continental shelf, Northwest Gulf of Mexico. *Bull. Amer. Assoc. Petrol. Geol.*, **40**, 10, 2428-2439.

Phleger (F. B.), 1955. — Ecology of Foraminifera in southeastern Mississippi Delta area. *Bull. Amer. Assoc. Petrol. Geol.*, **39**, 5 712-752.

Raupach (F.) von, 1952. — Die rezente sedimentation im Schwarzen Meer, im Kaspi und im Aral und ihre Gesetzmassigkeiten. *Zeitsch. Geologie Jahrgang* 1, *Heft* 1, 78-132.

Redfield (A. C.), 1958. — Preludes to the entrapment of organic matter in the sediments of Lake Maracaibo, in : *Habitat of Oil*, a symposium. *Amer. Assoc. Petrol. Geol., Tulsa, Oklahoma*, 968-981.

Revelle (R. R.), Bramlette (M.), Arrhenius (G.) and Goldberg (E. D.), 1955. — Pelagic sediments of the Pacific, in : *The Crust of the Earth. Geol. Soc. Amer. Spec. Paper* 62, 221-235.

Riedel (W. R.), 1952. — Tertiary Radiolaria in western Pacific sediments. *Göteborgs Kungl. Vetenskaps och Vitterhets-Samhalles Handlingar*, Ser. B, Band **6**, 3, 1-21.

— 1959. — *Amer. Petrol. Inst. Research Project* 51, *Progress Rept*. XXXIII.

Rusnak (G. A.). — Laguna Madre, from « Recent Sediments : Northwestern Gulf of Mexico », edited by F. P. Shepard, F. B. Phleger and Tj. H. van Andel, to be published by *Amer. Assoc. Petrol. Geol.* (in press).

Russell (R. J.), 1936. — Physiography of lower Mississippi River delta. *Louisiana Geol. Survey Bull.*, 8, 3-199.

Scruton (P. C.), 1956. — Oceanography of Mississippi Delta sedimentary environments. *Bull. Amer. Assoc. Petrol. Geol.*, **40**, 12, 2864-2952.

Segerstrale (S. G.), 1957. — Baltic Sea, in : *Treatise on Marine Ecology and Paleoecology*, **1**, *Ecology. Geol. Soc. Amer. Memoir* 67, 751-800.

Shepard (F. P.), 1955. — Delta-front valleys bordering the Mississippi distributaries. *Bull. Geol. Soc. Amer.*, **66**, 12, 1489-1498.

— 1956. — Marginal Sediments of Mississippi Delta. *Bull. Amer. Assoc. Petrol. Geol.*, **40**, 11, 2537-2623.

— Barrier Islands, from « Recent Sediments : Northwestern Gulf of Mexico », edited by F. P. Shepard, F. B. Phleger and Tj. H. van Andel, to be published by *Amer. Assoc. Petrol. Geol.* (in press).

— and Curray (J. R.). — Rise of sea level along the northwest Gulf of Mexico, edited by F. P. Shepard, F. B. Phleger, and Tj. H. van Andel, to be published by *Amer. Assoc. Petrol. Geol.* (in press).

— and Lankford (R. R.), 1959. — Sedimentary facies from shallow borings in the lower Mississippi Delta. *Amer. Assoc. Petrol. Geol.*

— and Moore (D. G.), 1955. — Central Texas coast sedimentation : characteristics of sedimentary environment, recent history and diagenesis. *Bull. Amer. Assoc. Petrol. Geol.*, **39**, 8, 1463-1593.

— and Rusnak (G. A.), 1957. — Texas bay sediments. *Inst. of Marine Science*, **IV**, 2, 5-13.

Shepard (F. P.) and Suess (H. E.), 1956. — Rate of postglacial rise of sea level. *Science*, **123**, 3207, 1082-1083.

Smirnow (L. P.), 1958. — Black Sea Basin, in : *Habitat of Oil*, a symposium. *Amer. Assoc. Petrol. Geol., Tulsa, Oklahoma*, 982-994.

Stevenson (R. E.), 1956. — The marshlands at Newport Bay, California. *Ph. D. thesis, Univ. of Southern California*.

Stewart (H. B.) Jr., 1958. — Sedimentary reflections of depositional environment in San Miguel Lagoon, Baja California, Mexico. *Bull. Amer. Assoc. Petrol. Geol.*, **42**, 11, 2567-2618.

Strakhov (N. M.), 1947. — Zur Erkenntnis der Gesetzmässigkeiten und des Mechanismus der marinen Sedimentation. I. Schwarzes Meer. *Izv. Akad. Nauk SSSR, geol.*, ser. 2.

Terzaghi (K.), 1956. — Varieties of submarine slope failures. *Proc. 8th Texas Conf. on Soil Mechanics and Foundation Engineering, Spec. Publ.* 29, *Bur. of Eng. Res., Univ. of Texas*, 41 p.

Thompson (W. C.), 1955. — Sandless coastal terrain of the Atchafalaya Bay area, Louisiana, in : *Finding Ancient Shorelines. Soc. Econ. Paleont. and Mineral. Spec. Paper* 3, 52-76.

Treadwell (R. C.), 1955. — Trafficability and navigability of delta-type coasts, trafficability and navigability of Louisiana coastal marshes : sedimentology and ecology of southeast coastal Louisiana. *Louisiana State Univ. Tech. Rept.* 6, 78 p.

Tricart (J.), 1956. — Aspects géomorphologiques du delta du Sénégal. *Revue de Géomorphologie Dynamique*, 5-6, 65-86.

van Andel (Tj. H.), 1955. — Sediments of the Rhône Delta ; II, Sources and deposition of heavy minerals. *K. Nederl. Geol.-Mijnb. Gen., Verh., Geol. Ser.*, 15, 3, 515-556.

van Andel (Tj. H.). — Sources of sediments, from « Recent Sediments : Northwestern Gulf of Mexico », edited by F. P. Shepard, F. B. Phleger and Tj. H. van Andel, to be published by *Amer. Assoc. Petrol. Geol.* (in press).

— and Postma (H.), 1954. — Recent sediments of the Gulf of Paria. *Reports of Orinoco Shelf Expedition*, **I**, *North-Holland Publishing Co., Amsterdam*, 245 p.

van der Eyk (J. J.), 1957. — Reconnaissance soil survey in northern Surinam. *Wageningen*, 99 p.

van Straaten (L. M. J. U.), 1954. — Composisition and structure of recent marine sediments in the Netherlands. *Leidse Geol. Med.*, XIX, 1-110.

— 1959. — Littoral and submarine morphology of the Rhone Delta. *Second Coastal Geography Conference held at Louisiana State Univ.*, 233-264.

— and Kuenen (Ph. H.), 1957. — Accumulation of fine grained sediments in the Dutch Wadden Sea. *Geologie en Mijnbouw* (*NW. Ser*), 19ᵉ *Jaargang*, 329-354.

Verstappen (H. Th.), 1953. — Djakarta Bay. *Thesis Utrecht*.

Walton (W. R.), 1955. Ecology of living benthonic Foraminifera, Todos Santos Bay, Baja California. *Jour. Paleont.*, **29**, 952-1018.

Weeks (L. W.), editor, 1958. — *Habitat of Oil*, a symposium. *Amer. Assoc. Petrol. Geol., Tulsa, Oklahoma*, 1384 p.

Wiggers (A. J.), 1955. — De wording van het Noordoostpoldergebied. *Thesis Amsterdam Tjeenk Willink, Zwolle*, 216 p.

Wilson (L. R.) and Le Blanc (A. E.), 1954. — Microorganism studies in the Rockport, Texas, area. *Amer. Petrol. Inst. Research Project* 51, *Progress Rept.*, XI, 24-35.

DISCUSSION

David B. Ericson (¹).

Reviewed evidence for rapid filling of the Sigsbee Deep, Gulf of Mexico by sediments, mostly from the Mississippi Delta transported by turbidity currents. Probably the most cogent evidence is the complete absence of characteristic graded layers in cores taken on the tops of low hills, about 100 meters above the general level of the nearly featureless Sigsbee Plain.

These cores from the Sigsbee Deep prove beyond reasonable doubt that the depth of water in the middle of the Gulf has remained essentially as it is now continuously during the past several hundred thousand years.

That deposition of the graded layers of the abyssal plain, must have been deposited under conditions very similar to those of the present time. The only plausible explanation is deposition by turbidity currents.

This is further supported by the topographical control of the distribution of these graded layers.

Bruce C. Heezen (¹).

I would like to draw attention to two problems of deep sea marine geology which bear on paleocology and paleogeography. Dr. Shepard has discussed several examples of subaerial deltas. The pleistocene Mississippi river had a submarine delta. The modern Congo and Magdalena rivers have submarine deltas. Turbidity currents occurring at about 50 per century a retransporting sands, leaves and wood, gravels, silts and clays to deep water. These deposits have built up tremendous natural levee systems.

The other problem that I wish to mention concerns an anaerobic basin off Venezuela. The Cariaco Trench was formed in the Pleistocene when the entrance of marine waters was restricted. Now when there is no subaerial silt on the north side of the trench we find the basin anaerobic. This modern sediment strongly resembles the Laguna Fm. of Venezuela which is a major source bed of oil. The Cariaco trench seems to be a modern oil basin in the process of formation.

Henry F. Nelson (²).

A brief review of the Research Laboratories Recent Sediments research program was presented. The area being investigated is located on the north west of the Gulf of Mexico and covers 1 000 sq. ml. In this area 8 000 samples have been collected by means of gravity core barrels and dredges ; now long cores are being obtained by means of rotary coring rigs.

Three scientists are working on the project : a geologist, a micropaleontologist and a marine biologist. The distribution of sediments, the microfauna (living and dead) and the macrofauna (living and dead) are being mapped. Environmental interpretations are being checked by means of C^{14} dating to determine the sequence of geologic events.

Bert C. Aschenbrenner (³)

Various studies of recent sediments in various parts of the world have defined environmental criteria for numerous environments by different means. This information is dispersed throughout the international literature and using this information is difficult because of the fact that :

a) the same environments are defined by different criteria ;

b) the same environments is called different things in different studies ;

c) different environments are called the same name in different studies, etc.

A preliminary standardization of terms and environmental criteria is suggested which should pull together the results of the studies of recent depositional provinces which have been studied all over the world.

G. W. Hodgson (⁴).

Question : What is the present state of knowledge of recent sediments of arctic waters ?

Gordon A. Young (⁵).

1) You mentioned that the grains of dune sand were much more rounded than those of beach sands. Are there any such parameters like roundness or skewness that could determine the sands of the lagoonal side of a sand bar from that on the open sea side ?

2) What are the forams found in the mangrove environment ?

F. G. Lines (⁶)

Question : Are the rounder dune sands derived from the adjacent beaches ? Do you suggest

---

(¹) Lamont Geological Observatory. Palisades. N. Y.

(²) Magnolia Petroleum Co. Field Research Laboratory, Dallas. Texas. U. S. A.

(³) Autometric Corp. Paramount Bldg., Times Square, New-York. N. Y.

(⁴) Research council of Alberta, Edmonton, Alberta. Canada.

(⁵) Mene Grande Oil Co. Venezuela.

(⁶) Calif. Stud. Co. Calgary. Canada.

these sands have been rounded during such a short transportation ?

Have you been able to artificially start a turbidity current and subsequently photograph its movements ?

« Yes, the rounder dune sands are derived from the beaches. They were not rounded during transportation but the wind selected rounder grains. »

« Attempts to start turbidity currents have so far been unsussessful. Dynamite charges dropped to the floor of a canyon did not start a current reaching the recorders down canyon a few hundred yards. Scuba diving has started small currents, but they have not extended very far according to E. C. Buffington. »

John C. Griffiths.

1. General Statement.

It is necessary to differentiate compositional characteristics from size features ; a sediment may be composed of (1) coarse fossil fragments, (2) medium to fine-grained quartz sand and (3) a very fine sand or silt of zircons. Upon sieving such a sediment there would be three « sizes » of different composition all of which may be hydraulically equivalent, i.e. imply the same sedimentational environmental conditions.

On a different scale the sediments of the Carioca trough, while resembling those of a trough off the Californian coast in terms of « sand-lime-silt-shale » terminology may well be very different ; the Carioca sediments are probably high rank graywackes, those of the Californian area, arkoses. Again, confusion of gross lithology and apparent grain size, is inadequate to appraise the exact petrographic nature of the different sediments.

2. In reply to a question on where sedimentation of quartz sands (« quartzites ») is taking place at present :

According to P. D. Krynine, the western shelf coast of Australia possesses the main pre-requisites — a topographically low « shield » source of peneplain type and an area of deposition of flat shallow sea ; this implies « quartzite-carbonate » sedimentation analogous to the Ordovician-Cambrian sediments of Central Pennsylvania.

(360)

SOME RATES OF REGIONAL EROSION

H. W. MENARD

Reprinted for private circulation from
THE JOURNAL OF GEOLOGY
Vol. 69, No. 2, March 1961
Copyright 1961 by the University of Chicago
PRINTED IN U.S.A.

pp.154-161

(361)

SOME RATES OF REGIONAL EROSION[1]

H. W. MENARD[2]

ABSTRACT

Past and present rates of regional erosion are calculated for the Appalachian, Mississippi, and Himalayan regions. The present rate of erosion of the Mississippi region is about the same as the average rate during the last 150×10^6 years. The average rate of erosion of the Appalachian region during the last 125×10^6 years is 7.8 times as fast as at present. The average rate of erosion of the Himalaya region during the past 40×10^6 years is only 0.02 of the present rate. The fastest average rate observed is about 20 cm/10^3 years, obtained in the Himalaya region for the past 40×10^6 years and also in the Rocky Mountain region for the 40×10^6 years of Upper Cretaceous time.

The proportion of sediment permanently lost from the continents to abyssal plains is: Appalachian region, 17 per cent; Mississippi region, 8 per cent; and Himalaya region, possibly 49 per cent. Losses of these magnitudes cannot have occurred during much of the geological past.

INTRODUCTION

An average rate of regional erosion for a particular time interval can be determined if the following are known: the area of the source region, the volume of deposits derived from the source region, and the duration of the erosion. Closed systems exist where the drainage from a well-defined highland is the only quantitatively significant source of sediment deposited in a continental terrace and an adjoining continental rise and abyssal plain. The bathymetry and sediment thickness in various places in three such systems are known well enough so that rates of erosion for certain periods can be calculated and the fraction of material deposited in different topographic provinces can be distinguished.

Present rates of regional erosion can be calculated from the sediment load of rivers. The present and past rates of erosion in a given area can be compared, but any conclusions drawn have the same limitations as other comparisons of a single measurement and an average of several measurements which are not individually known. The present rate, for example, may be twice the average past rate and yet lie within the range of values which has been averaged. Geologically, erosion may alternate locally with deposition, and erosion, when it occurs, would be much more rapid than the average would indicate. However, deposition and reworking in sedimentary basins outside the source region have no effect on the calculations.

MEASUREMENTS AND CALCULATIONS

APPALACHIAN REGION

The source region is taken as the part of the Appalachian Mountains from Alabama to Newfoundland which drains to the Atlantic Ocean. The sediments derived from this source are taken as the sedimentary rocks forming the emerged and submerged continental terrace plus the relatively unlithified sediments of the continental rise and of the Sohm, Hatteras, and Nares abyssal plains in the North American basin of the Atlantic.

The area of the Appalachian Mountains is taken from the Geologic Map of North America, published by the Geological Society of America in 1946. It is assumed that the source area now under the Gulf of St. Lawrence was ordinarily exposed to erosion. The area is 1.0×10^6 km.^{2} (table 1).

The volume of the emerged and submerged continental terrace off the source region can be calculated with some assurance from the seismic observations at sea by Maurice Ewing and his collaborators. Plate 26 in Heezen *et al.* (1959) provides summary cross sections of the terrace on a uniform scale. Correcting for the angle of the profiles to the regional trend and interpolating between profiles, the "unconsolidated" and

---

[1] Contribution from the Scripps Institution of Oceanography, New Series. Manuscript received May 27, 1960. 1270

[2] University of California Institute of Marine Resources and Scripps Institution of Oceanography, La Jolla, California.

(362)

"consolidated" sedimentary rocks have a volume of 2.3×10^6 km.^{3}.

The continental rise may be defined as the gently sloping province between the base of the continental slope and any abyssal plains. Volume of the rise can be calculated from the same profiles of Heezen *et al.* which are used for the continental terrace. A minor element of uncertainty is introduced in attempting to separate the terrace and the rise on subsurface profiles. The volume of unconsolidated and consolidated sedimentary rock in the continental rise is 4.2×10^6 km.^{3}.

The sediments underlying the Hatteras and Nares abyssal plains are derived ultimately from the Appalachian source region because they slope downward from the region. Most of the sediment of the Sohm abyssal plain comes from the same source, but a minor fraction has a separate source to the northeast (Heezen *et al.*, 1954, fig. 3). The area of the abyssal plains on plate 20 of Heezen *et al.* (1959), taking 50° W. longitude as the eastern boundary of the Sohm plain, is 1.3×10^6 km.^{2}. The thickness of sediment at representative localities in the plain ranges between 0.68–1.65 km. (Katz and Ewing, 1956). Some of the sediment under the plain is of pelagic origin and should be subtracted to give a remainder transported by turbidity currents from the ultimate Appalachian source. The proportion of pelagic sediment probably can be neglected for the present purposes (Menard, 1960). Seismic methods introduce a much greater uncertainty in measuring the thickness of a thin layer of sediment on the deep-sea floor because of the possibility of undetected thin layers of higher-velocity material at the base of the sediment. A thickness of 1 km. for the whole area of the abyssal plain seems reasonable, even though it certainly thins toward the edges. The volume of the abyssal plains is 1.3×10^6 km.^{3}.

TABLE 1

PAST AND PRESENT RATES OF DENUDATION

1 Region	2 Area Denuded (10^6 km^2)	3 Time* (10^6 yr.)	4 Volume Deposits (10^6 km.^{3})	5 Denudation (km.)	6 Past Rate (cm/10^3 yr)	7 Present Rate† (cm/10^3 yr)	8 Ratio: 6/7
Appalachian	1.0	125	7.8	7.8	6.2	0.8	7.8
Mississippi	3.2 (1.6)‡	150	11.1	6.9	4.6	4.2	1.1
Himalaya	1.0	40	8.5	8.5	21	100	0.2
Rocky Mt. (L. Cret.)§	0.8	25	0.6	0.7	3	.....	...
Rocky Mt. (U. Cret.)§	<0.4	40	2.2	>4.8	12–20	.....	...

* Geological Names Committee, 1958, U.S. Geol. Survey.

† Suspended load of rivers.

‡ Area denuded in past.

§ Gilluly (1949).

The total volume of sediments derived from the Appalachian source is 7.8×10^6 km.^{3}. This is taken to be the volume of rock eroded—on the assumption that the pore space of the sediments is at least no greater than the volume of material lost from the system by solution. Sediments deposited in the continental terrace are Lower Cretaceous or younger so that the period of erosion and deposition of interest here is about 125×10^6 years. The total denudation is 7.8 km., and the rate is 6.2 cm/10^3 years.

MISSISSIPPI REGION

From the volume of sediment in the Gulf Coast, Gilluly (1955) and Jacobs *et al.* (1959), among others, have calculated the rate of erosion of the Mississippi drainage basin. The rate is recalculated here because seismic stations in the Gulf of Mexico (Ewing *et al.*, 1955) permit more accurate estimates of the volume of sediment offshore. Seismic stations do not indicate age, and the entire post-Triassic period of deposition must be considered as a unit.

The drainage basin of the Mississippi River north of the Gulf embayment has an area of 3.2×10^6 km.^{2}. However, much of this basin is covered with Cretaceous and Tertiary sediment. The area of erosion of Triassic or older rocks is roughly half the whole basin.

The volume of sedimentary rock from the edge of the Gulf embayment to the shore line and from Texas to Alabama inclusive is 4.6×10^6 km.^{3} (Murray, 1952; Colle *et al.*, 1952). Areas and thicknesses of offshore provinces are available from Ewing *et al.* (1955, fig. 1; 1959, figs. 6–8). The volume of the submerged continental terrace is 4.4×10^6 km.^{3}. It is noteworthy that this volume is several times larger than was assumed in previous calculations which were made before Ewing's stations were published. The total volume of the emerged and submerged continental terrace is 9.0×10^6 km.^{3}. The Cretaceous sediments of the high plains are neglected here because they were derived from outside the source area under consideration. In any event the volume is small.

The continental rise off the Gulf Coast and the Gulf of Mexico abyssal plain have an ultimate source in the Mississippi drainage basin. The plain, grading outward from the so-called "Mississippi cone," has had negligible contributions of sediment from any source but the Mississippi River. Off the west coast of Florida, for example, the plain slopes downward toward the continental slope and is filling in embayments (submarine canyons) from the west. The continental rise and abyssal plain have an area of 3.4×10^5 km.^{2}. Thickness of the rise is 7.5 km. and of the abyssal plain, 5.0 km. These values are derived from single localities and are subject to confirmation in other places. The abyssal-plain thickness may be larger than the average for other oceans because the plain is ponded unlike most abyssal plains which slope downward to a feather edge. Accepting both values as representative of whole provinces, the volume of the rise and plain is 2.1×10^6 km.^{3}.

The total volume of sediments derived from the Mississippi source region is 11.1×10^6 km.^{3}. The sedimentary rocks of the continental terrace which are considered here are Jurassic or younger, and the age is 150×10^6 years. The total denudation is 6.9 km., and the rate of erosion is 4.6 cm/10^3 years. This rate compares with 1.2 cm/10^3 years for the same time interval, on the assumption that the entire Mississippi River basin has been eroded uniformly in post-Triassic time and that there is less sediment offshore than appears to exist (Jacobs *et al.*, 1959). Gilluly (1955) calculates 2.5 cm/10^3 years for Cenozoic deposits, using slightly different assumptions from those stated here.

HIMALAYAS

The erosion, transportation, deposition system of the Himalayas–Indian plains–Indian Ocean is completely contained with regard to detritus, and, although the marine part of the system is not well known, it can be analyzed in the same way as the Appalachian and Mississippi valley systems. With a very high and vigorously eroded source, this system provides a marked contrast to the others. The Ganges and Brahmaputra rivers drain the eastern Himalayas and deposit part of their load in the Gangetic plain; the remainder escapes from the continent and is deposited in the continental rise and the Bengal abyssal plain. The Indus River drains the western Himalayas and deposits sediment both in the Indus plain and also offshore.

The source region drained by the Indus, Ganges, and Brahmaputra rivers has an area of 1.0×10^6 km.^{2}.

The area of the sedimentary deposits of the Indo-Gangetic plain is 0.8×10^6 km.^{2} (Krishnan, 1956). Thickness of Oligocene to recent sedimentary rocks in the region is now known because of vigorous exploration for oil, but most of the results are not released. Drilling in the middle of the Indus plain was still in Siwalik beds at a depth of 4 km., and several other holes were drilled to similar depths, although the formations reached were not published (Hotchkiss, 1959). According to Krishnan (1956), geodetic data indicate an average thickness of 2–3 km. of sediment under the plain, and seismic stations in the Ganges delta show 0.7 km. of alluvium and a basement at 5–6 km. depth. It appears that 3 km. is a reasonable average thickness for the post-Eocene sediments of the plain. The volume of sediments is 2.4 × 10^6 km.^{3}. The area of the submerged continental terrace off the Indus and Ganges rivers is roughly 0.45 × 10^6 km.^{2} as measured on plate 10, volume 2, of the Morskoi Atlas of 1953. Thickness of the submerged continental terrace is unknown, but the thickness of sediment in the Ganges Delta suggests that 4 km. is reasonable. The volume of the submerged terrace is 1.8 × 10^6 km.^{3}, and the total volume of sediments from the edge of the source region to the base of the continental slope is 4.2 × 10^6 km.^{3}.

The abyssal plains south of India are known from only a few echograms, older spot soundings, and two seimic refraction stations; however, the data are consistent internally and with what is known of other areas of the deep-sea floor off large rivers (Dietz, 1953; Menard, 1959). The Bengal abyssal plain slopes downward from the Ganges Delta to at least 5° S. latitude, and it appears to continue to about 15° S. latitude and possibly beyond. The existence of an abyssal plain off the Indus River is not confirmed by modern echograms known to the writer, but it is indicated by spot soundings, many of excellent quality. The total area of the abyssal plains is estimated at 4.2 × 10^6 km.^{2}. Two seismic stations at about 84° W. longitude and 2° to 4° S. latitude show sediment thicknesses of 1.1 km. and at least 1.8 km. (Gaskell *et al.*, 1958). An average thickness of 1.0 km. for the abyssal plains seems conservative. The volume according to these estimates is 4.2 × 10^6 km.^{3}.

The total volume of sediments derived from the Himalaya source region since the Late Eocene uplift is 8.5 × 10^6 km.^{3}. The erosion is 8.5 km. in 40 × 10^6 years or an average of 21 cm/10^3 years. Within the accuracy of the estimates, this is the same rate as the 20 cm/10^3 years for 40 × 10^6 years given by the data of Gilluly (1949) for the Rocky Mountains in Upper Cretaceous time if his assumptions are modified so that the detrital limestone which bypassed the depositional basin roughly equaled the volcanic debris added to the basin from sources other than erosion.

PAST AND PRESENT RATES OF EROSION

Present rates of erosion can be determined by measuring the bed and suspended load and the dissolved material in rivers draining an area. Quantitatively the bed load is negligible compared to the suspended load at the mouths of large rivers. The dissolved load is not measured in most rivers, but it may exceed the suspended load where chemical weathering predominates. It is completely neglected in the present comparisons of rates of erosion at different times. The absolute rates determined from transportation and deposition of particulate matter alone are too low by a factor of about 10 per cent on the average (Gilluly, 1955), but the ratios of past and present rates are not necessarily affected.

The present rate of erosion of the Appalachian source region in the United States, considering suspended material alone, is 0.8 cm/10^3 years (Dole and Stabler, 1909). The average for the whole region is somewhat less because a significant fraction of the source region now lies under the Gulf of St. Lawrence and is not being eroded. The average rate of erosion for the last 125 × 10^6 years, as indicated by the sediments deposited in that time, is 6.2 cm/10^3 years. The ratio of past to present rate is 7.8, and this does not appear unreasonable considering that the Appalachian Mountains of the past probably had much more relief from time to time than they do now.

The drainage basin of the Mississippi River is being eroded at a rate of 4.2 cm/10^3 years considering only suspended solids (Fisk *et al.*, 1954). The average rate of erosion for the past 150 × 10^6 years is 4.6 cm/10^3 years for half the basin, and the ratio of past to present erosion is about 1. Gilluly (1955) calculates a volume of deposits for Cenozoic time which can be converted into an average rate of 2.5 cm/10^3 years. He states that the present to past ratio is $\frac{1}{3}$, but

(365)

this calculation appears to be in error unless a very low density of sedimentary rock is assumed. For a density of 2.6 gm/cm³, the ratio is 0.6, using Gilluly's data on the volume of Cenozoic sediment and the suspended load he cites. Probably the ratio for the past 60×10^6 years would be closer to 1 if the volume of Cenozoic sedimentary rock seaward of the area considered by Gilluly could be separated from the Mesozoic rocks in the great thicknesses revealed by seismic stations. In any event, the present calculations tend to strengthen Gilluly's conclusion that the rate of erosion in the Mississippi source region is not substantially different from what it was in the past.

The present rate of erosion of the Himalaya Mountains is exceptionally large, and the Indus, Ganges, and Brahmaputra rivers are heavily laden with silt during the monsoon season. Much of modern knowledge of irrigation hydraulics was developed through the notable efforts of engineers in India combating the deposition of the silt in reservoirs and canals.

Silt loads of two tributaries of the Indus have been studied recently (Khosla, 1953). The Sutlej River at the Bakra reservoir site in Punjab has a drainage basin of 5.6×10^4 km.² and an average rate of erosion of 21 cm/10³ years. The Beas River at the Balchu reservoir site, also in Punjab, has a drainage area of 0.8×10^4 km.² and a rate of erosion of 30 cm/10³ years. These appear to be unusually low rates for the region. The Indus River and the western tributaries of the Ganges River drain roughly 0.4×10^6 km.² of the Himalayas, and contributions of sediment from other source regions are relatively unimportant. Lyell (1875) cites measurements by Everest in 1831–32 at Ghazipur, 500 miles from the mouth of the Ganges River, which give a suspended load of 3.4×10^{14} gms/year. For the Indus River, Buckley (1905) measured 3.2×10^{14} gm. of suspended load during the 100 days of a monsoon flood period. All measurements in northern India show that the silt load other than in the monsoon season is a trivial fraction of the whole, and Buckley's figures may be taken as the annual transport. Combining the transport for the Indus and the western Ganges gives a rate of regional erosion of 62 cm/10³ years.

The eastern Himalayas have higher relief and more rainfall than the western part, and erosion is correspondingly rapid. The great Sapt Kosi River in Uttar Pradesh drains an area of 5.9×10^4 km.² in the center of the Himalayas. The rate of regional erosion is 100 cm/10³ years, according to an average of the silt-load measurements at Barakshetra during a three year period (Khosla, 1953). The range of values for individual years is 80–130 cm/10³ years. Measurements of silt loads of rivers in the eastern Himalayas are not known to the writer. However, Lyell estimates that the silt load of the Brahmaputra River is about five times as great as the load of the Ganges at Ghazipur, or roughly $1\text{–}2 \times 10^{15}$ gm. per year. This is equivalent to a rate of regional erosion of 70–140 cm/10³ years. Considering the measurements for the Sapt Kosi River, it is probable that the average rate of erosion of the eastern Himalayas exceeds 100 cm/10³ years; and the average rate for the whole Himalaya range is roughly 100 cm/10³ years.

The rate of erosion of the Himalayas for the past 40×10^6 years is 21 cm/10³ years. Compared to a present rate of 100 cm/10³ years, the past to present ratio is about 0.2. The calculated past rate may tend toward a maximum because of the estimated large volume of little-known abyssal plains. Consequently, the present rate is much greater than during most of Tertiary time.

The pattern that emerges from this analysis of rates of erosion in different places and at different times seems relatively simple. Where mountains are high and rainfall is abundant, erosion is rapid; and these circumstances may occur at any time. In the Himalayan region erosion is more rapid now than in the past, but in the Appalachian region the reverse is true. The rate of erosion of the Rocky Mountains must also vary in time, but this effect is masked in the Mississippi drainage system because of the relatively constant rate of erosion of a very large central plain. For the Mississippi region the rate of erosion has not varied significantly for 150 × 10^6 years, and this may be characteristic of regions of low plains. In low, flat regions the only important variable affecting erosion rates is rainfall, and even a twofold change in rate requires a major change in climate. In mountainous regions, however, the rise of a range produces both steep slopes and increased rainfall because of the orographic effect, and many-fold changes in erosion result without any change in climate.

LOSS OF CONTINENTAL MATERIAL TO OCEAN BASINS

Continental rises and abyssal plains are deposited by turbidity currents which spread out for distances as great as 1,000 km. from the base of the continental slope. All this material is at least temporarily lost from the continents, and part of it seems lost forever. Table 2 indicates the quantities of sediment deposited in continental basins, emerged and submerged continental terraces, continental rises, and abyssal plains. The percentage of detrital sediment transported beyond the continental slope is: Appalachian region, 71 per cent; Mississippi region, 19 per cent; Himalaya region, 51 per cent. The existence of unfilled sediment traps between a source area and the deep sea determines whether any sediment escapes from the continent. At one extreme is the central California region where only a very narrow continental shelf separates the Coast Ranges from the deep sea, and almost all the sediment eroded is lost from the continent (Menard, 1960). At the other extreme, the sediment eroded from the Rocky Mountains in Upper Cretaceous time was deposited in an adjacent shallow marine basin, and hardly any was lost from the continent.

TABLE 2

AMOUNT OF SEDIMENT IN DIFFERENT PROVINCES

1 Region	2 Volume Deposits (10^6 km.^{3})	3 Continent and Continental Terrace	4 Continental Rise	5 Abyssal Plains	6 Ratio: 5/2
Appalachian.......	7.8	2.3	4.2	1.3	0.17
Mississippi........	11.1	9.0	1.2	0.9	0.08
Himalaya..........	8.5	4.2	0.1	4.2	0.49

Sediment deposited near the margins of a continent later may possibly become incorporated into an enlarged continent (Wilson, 1951) or may possibly be returned to the continental mass by subcrustal convection (Gilluly, 1955). Consequently, the only material definitely and permanently lost to the continents may be the fraction in abyssal plains. The amount lost to abyssal plains is: Appalachian region, 17 per cent; Mississippi region, 8 per cent; Himalaya region, 49 per cent. The striking difference between the fraction of sediment in the combined continental rise and abyssal plain off the Appalachian region, and in the abyssal plain alone reflects the existence of a deep-filled trench under the present continental rise (Heezen *et al.*, 1959). Allowing for the areas of the various regions, the average irreversible loss from the continents to abyssal plains is 18 per cent. Compounded through geological time by the recycling of sediment in continental basins, this rate of loss would inevitably displace a large part of the continents into the ocean basins. It seems evident that at most times in the past almost all sediment was trapped before it could spread across the deep-sea floor. This agrees with the observation that almost all abyssal plains are distributed only where they are not barred from the deep sea by existing sediment traps of Mesozoic and Cenozoic age. Older abyssal plains which might have been formed by the spread of turbidity currents prior to the formation of existing traps have not been found, with the possible exception of a region in the Gulf of Alaska.

The reasons for the increased loss of continental sediment to the deep sea during the last 10^8 years may be complex, but the rate of sedimentation at the continental margins probably is an important factor. If sedimentation is slow, basins may deepen as rapidly as they are filled, and sediment is not lost to the deep sea. Sedimentation is a function of rate of erosion but also of area of the source region. If the continents are larger than in the past, a constant rate of erosion would produce more sediment. An increase in the average rate of erosion would have the same effect. In either case the change need not be large. The shallow-water environment of deposition in most geosynclines shows that structural basins commonly are almost full. A very small increase in sedimentation might cause sediment to bypass the geosyncline and reach the deep-sea floor.

CONCLUSIONS

Present rates of erosion range through two orders of magnitude, and past rates for periods of 10^7–10^8 years range through one order of magnitude. Consequently, worldwide average rates cannot be established from these data with the small sample available.

Whether present rates of erosion are the same as in the geological past as proposed by Gilluly (1949, 1955) is not determined from data on erosion alone. If mountain-building is random, in time the rate of erosion of the whole world may be relatively constant when averaged for periods of 10^7–10^8 years. The large lowlands may have a relatively constant rate of erosion, and rapid erosion of a smaller mountain range at one time and place would be balanced by a similar mountain range at another time and place. If mountain-building is periodic, this argument does not hold.

ACKNOWLEDGMENTS.—The writer is indebted to A. E. J. Engel and D. T. Griggs for reading the manuscript and for helpful criticism. The study was made while the writer was on leave of absence at the California Institute of Technology.

REFERENCES CITED

BUCKLEY, R. B., 1905, The irrigation works of India: London, E. and F. N. Spon, Ltd., 336 p.

COLLE, J., *et al.*, 1952, Sedimetary volumes in Gulf Coastal Plain of United States and Mexico, Pt. IV. Volume of Mesozoic and Cenozoic sediments in Western Gulf coastal plain: Geol. Soc. America Bull., v. 63, p. 1193–1200.

DIETZ, R. S., 1953, Possible deep-sea turbidity-current channels in the Indian Ocean: Geol. Soc. America Bull., v. 64, p. 375–378.

DOLE, R. B., and STABLER, H., 1909, Denudation: U.S. Geol. Survey Water-Supply Paper 234, p. 78–93.

EWING, M., WORZEL, J. L., ERICSON, D. B., and HEEZEN, B. C., 1955, Geophysical and geological investigations in the Gulf of Mexico, Pt. I: Geophysics, v. 20, p. 1–18.

FISK, H. N., MCFARLAN, E., JR., KOLB, C. R., and WILBERT, L. J., JR., 1954. Sedimentary framework of the modern Mississippi delta: Jour. Sed. Petrology, v. 61, p. 877–892.

GASKELL, T. F., HILL, M. N., and SWALLOW, J. C., 1958, Seismic measurements made by H. M. S. Challenger in the Atlantic, Pacific and Indian Oceans and in the Mediterranean Sea, 1950–53: Phil. Trans. Royal Soc. London, Ser. A, v. 251, p. 23–83.

GILLULY, J., 1949, The distribution of mountain building in geologic time: Geol. Soc. America Bull., v. 60, p. 561–590.

——— 1955, Geologic contrasts between continents and ocean basins, p. 7–18. *In* POLDERVAART, A., (ed.), Crust of the earth: Geol. Soc. America Special Paper 62, 762 p.

HEEZEN, B. C., EWING, M., and ERICSON, D. B., 1954, Reconnaissance survey of the abyssal plain south of Newfoundland: Deep-Sea Research, v. 2, p. 122–133.

———, THARP, M., and EWING, M., 1959, The floors of the oceans, Pt. I. The North Atlantic: Geol. Soc. America Special Paper 65, 122 p.

HOTCHKISS, H., 1959, Petroleum developments in Middle East and adjacent countries in 1958: Bull. Am. Assoc. Petroleum Geol., v. 43, p. 1676–1713.

JACOBS, J. A., RUSSELL, R. D., and WILSON, J. T., 1959, Physics and geology: New York, McGraw-Hill Book Co., Inc., 424 p.

KATZ, S., and EWING, M., 1956, Seismic-refraction

(368)

measurements in the Atlantic Ocean. Pt. VII: Atlantic Ocean Basin, west of Bermuda: Geol. Soc. America Bull., v. 67, p. 475–510.

KHOSLA, A. N., 1953, Silting of reservoirs: Central Board of Irrigation and Power of India, Pub. 51, 206 p.

KRISHNAN, M. S., 1956, Geology of India and Burma: Madras, Higgenbothams (Private) Ltd., 555 p.

LYELL, C., 1873, Principles of geology, v. 1, 11th ed.: New York, D. Appleton and Co., 671 p.

MENARD, H. W., 1959, Distribution et origine des zones plates abyssales, p. 95–108. *In* La Topographie et la géologie des profondeurs océaniques: Colloq. Internat., Centre Nat. Recher. Sci., v. 83.

——— 1960, Possible pre-Pleistocene deep-sea fans off central California: Geol. Soc. America Bull., v. 71, p. 1271–1278.

MURRAY, G. E., 1952, Sedimentary volumes in Gulf Coastal Plain of United States and Mexico, Pt. III. Volume of Mesozoic and Cenozoic sediments in Central Gulf coastal plain: Geol. Soc. America Bull., v. 63, p. 1177–1192.

WILSON, J. T., 1951, On the growth of continents: Papers and Proc. Royal Soc. Tasmania, 1950, p. 85–111.

(369)

Separatum
EXPERIENTIA
BIRKHÄUSER VERLAG, BASEL, SCHWEIZ
Vol. XIV/6, 1958 – pag. 231

CONSTRUCTIONES

An Experiment in the Design of a Scientific Conference

The purpose of this note is to report on a conference design that differed somewhat from the traditional plan of scientific meetings, and on its possible value for similar scientific conferences.

As science progresses, as the number of scientists increases and as scientists become more specialized, the problem of communication among scholars becomes more and more pronounced. The large scientific conventions and the international congresses that several decades ago provided an adequate form for technical discussion are no longer performing this function because of the tremendous increase in the number of participants and of the ensuing limitations of time. For the last twenty years or so symposia, i.e., scientific meetings with limited attendance and with only invited speakers, have been used more frequently because of the advantages offered by bringing together a relatively small number of specialized scientists. The climate of such gatherings is more conducive to a high level of technical discussions than the larger and more heterogeneous scientific congresses. When, however, the symposium has a relatively large number of participants and their primary interests are diverse, a problem of communication arises. One such problem was faced by the organizers of the international symposium on 'Perspectives in Marine Biology', held at the Scripps Institution of Oceanography of the University of California at La Jolla, California.

The primary purpose of this conference was that of identifying those areas of investigation that could be

Contributions from the Scripps Institution of Oceanography, New Series, 1271
Reproduced by Permission

most profitably attacked at the experimental level in the field of marine biology. For this aim it appeared necessary to invite a number of biologists representing a wide range of specialized interests, such as marine and non-marine ecologists, physiologists, microbiologists, biochemists, etiologists, geneticists and evolutionists. The actual participation was as follows: 47 invited participants, 131 observers; 14 nations were represented. In developing the conference design, the planners considered the following problems which were inherent in the nature of the symposium: (1) the difficulty of communication between specialists in the different scientific fields represented; (2) language problems because of the different nationalities represented; (3) the tendency of some scientists to focus on single areas of research rather than on broad problems of the total field; (4) the reluctance of some scientists to explore unfamiliar grounds in the presence of their colleagues; and (5) the tendency of specialists in a particular field of science to seek out and converse with colleagues from the same field rather than from other disciplines.

In one respect this conference was like many other symposia: scientists were invited to prepare papers in advance and read them at the meeting; each formal presentation was followed by a discussion of the issues raised by the speaker, to which all the attendants, invited and observers, were free to participate. However, in order to provide a setting in which interdisciplinary thinking could better take place and where new areas of research might be found, this particular symposium included another element: the 'Idea Group'. Six such groups, consisting of eight or nine invited participants, plus a discussion leader and a recorder, met periodically throughout the conference. Each 'Idea Group' included scientists from the different fields represented at the conference. These heterogeneous groups met every noon for lunch and several other times during the symposium. Their stated purpose was that of dealing with the broad question around which the entire symposium was built: What are now the most promising areas of experimental research in the field of marine biology? The 'Idea Groups' were instructed to use the formal presentations as background and as a springboard for discussing this general problem. The discussion leaders and recorders of each 'Idea Group' were members of the staff of the host Institution. A week prior to the conference, these leaders and recorders met to be oriented to the conference design, the purpose of the 'Idea Groups', methods to get them under way, and the roles the leaders and the recorders were expected to play. The recorders prepared a written summary of the subjects discussed during each working session of the groups; the highlights of these discussions were also reported to all the members of the symposium at the final session by a panel including one person from each 'Idea Group'.

At the end of the conference each participant was asked to fill out an evaluation form in which questions were asked about the value of this conference design.

In spite of some doubts expressed at the beginning of the conference about the value of the 'Idea Group', the participants at the end expressed general satisfaction with this experience and felt that this kind of conference design would be useful in other scientific conferences of this type. The planned heterogeneity of the groups appeared to be useful and appreciated in that it provided a fine opportunity for participants in the conference to become better acquainted with colleagues from other disciplines. Probably the term 'Idea Group' was not very fortunate; a more appropriate name might be adopted in future conferences. A thorough orientation of the leadership (leader and recorder) prior to the conference appears essential for the success of this technique. That this design has a definite value in symposia of this kind follows also from the fact that one of the participants used it successfully in the organization of another scientific conference held in France last summer.

A. A. Buzzati-Traverso*
and W. H. Schmidt

Scripps Institution of Oceanography, La Jolla, California and Department of Conferences and Special Activities, University of California, Los Angeles, May 9, 1957.

---

* Gegenwärtige Adresse: Istituto di Genetica, Pavia.

Reprinted from :
New Approaches in Cell Biology
P. M. B. Walker, Editor
Academic Press Inc., 1960 p. 95-123

PAPER CHROMATOGRAPHY IN RELATION TO GENETICS AND TAXONOMY

A. A. Buzzati-Traverso

Istituto di Genetica, Università di Pavia, Pavia, Italy

and

Scripps Institution of Oceanography, University of California,
La Jolla, California

Summary

Paper-partition chromatography has been applied successfully to the study of some genetic and taxonomic problems in animals, plants and micro-organisms. A survey is presented of the main results so far obtained in this area of investigation, and some original data pertaining to the subject are submitted. The relationships between this evidence and those resulting from the use of other biochemical and immunological techniques are discussed and analyzed in terms of their significance for genetics, physiology and taxonomy. The potentialities of the paper-chromatographic method are discussed and an outline of further investigations aiming at the solution of some genetic and taxonomic problems is presented.

I. Introduction

Because of its simplicity, versatility and cheapness, the technique of paper partition chromatography has been effectively used in many kinds of biological investigation since the publication of "Qualitative analysis of proteins: a partition chromatographic method using paper" by R. Consden, A. H. Gordon and A. J. P. Martin in 1944 [19]. In the course of the last few years this technique has been applied successfully to the analysis of some genetic and taxonomic problems and what follows is an attempt to present a survey of these investigations.

The technique of paper partition chromatography consists basically of a few simple operations. A small drop of the solution containing the substances to be separated is applied to a strip of filter paper a short distance from one end, and allowed to dry. The end of the strip filter paper nearest to the dried spot is then soaked with the devel-

Contributions from the Scripps Institution of Oceanography, New Series, 1272
Reproduced by Permission

oping solution. By capillary action the solvent will flow along the strip and down through its length. In so doing it will remove molecules of the different substances contained in the spot at speeds which are typical for each particular substance and each particular solvent. After a certain time and after the front of the solvent has travelled down the paper, each substance will have moved a characteristic distance, proportional to its speed of movement, from its original position. The relative speeds of the various substances can be measured by calculating the ratios between the distances moved by each spot and the distance covered by the front of the solvent, measured also from the original position. This ratio is called the R_F value of that substance. In this way, for any one solvent each separated substance can be distinguished by its R_F value and by its peculiar chemical properties. Thus, if the original spot was composed of a mixture of amino-acids, e.g., arginine, α-alanine, and leucine, and if a solution of butanol and acetic acid was allowed to flow in the filter paper strip, and after removal from the jar where the partition took place and drying of the paper, then one can identify the three substances by: (1) visualizing them by spraying the paper with a ninhydrin solution which by reacting with the amino-acids will produce coloured spots on the paper, and (2) by measuring the R_F value which will be about 0.19 for arginine, 0.39 for α -alanine and 0.72 for leucine. If one applies one spot of the substance to be analyzed near one corner of a square paper and allows one solvent to flow first in one direction, and then another solvent to flow at right-angles better resolution than with one-dimensional runs can be obtained. With this technique, very small quantities of chemical compounds can be detected, of the order of a microgram or less, and one can thus analyze very small amounts of mixtures.

Very extensive and detailed descriptions of this technique and its modifications, and of the various sets of solvents and developing substances which can be used for the analysis of many organic and inorganic molecules are given in the many laboratory manuals now available [6, 7, 9, 14, 20, 110]. I will therefore refer the reader to these for more technical data.

I wish to stress, however, that this method represents a wonderful tool for biologists who have not available the complicated apparatus that characterizes a modern biochemical laboratory. Only the following were needed to obtain many of the very interesting results to be discussed here: samples of the organisms to be investigated, a few solvents, some filter paper, a few jars or simple cabinets, a drying oven and an ultraviolet lamp.

For the study of genetic and taxonomic problems the technique was further simplified by directly applying onto the filter paper without previous chemical manipulations, either whole organisms such as *Drosophila* or parts of them [62] or bits of tissues of larger animals and plants [12]. After these are squashed on the paper and dried they are subjected to partition chromatography. Care should be taken to use solvents appropriate for the separation of the substances present, avoiding if possible the interference of salts and proteins and other disturbing products. This simple and crude technique has given remarkably interesting results, notwithstanding the horror manifested at times by professional biochemists. The relative merits of more or less elaborate techniques of analysis will be discussed in the concluding section of this paper.

II. Paper Chromatography in Genetic Research

Paper partition chromatography has become so widely used in biochemical research that by now there are few experiments in which the biochemist does not use it. This holds true also for biochemical genetics: accordingly there are already innumerable papers in this field in which the author mentions using this technique for the identification of previously known chemical compounds. No attempt will be made here to review such instances. The present survey will focus attention only on those contributions in which the technique of paper chromatography has been used as a tool in genetic research, i.e., either to reveal new aspects of the action of the genetic material or to elucidate previously less well understood physiological and biochemical processes controlled by the genotype.

1. *Drosophila melanogaster*

The paper by Hadorn and Mitchell [62] on "Properties of mutants of *Drosophila melanogaster* and changes during development as revealed by paper chromatography" opened this field of investigation. By conducting paper chromatographic analysis of eggs, larvae, pupae and adult individuals or of their various body sections and organs of *Drosophila*, these two authors discovered a number of chemically unidentified substances having constant and typical R_F values. These could be seen under ultraviolet light by their fluorescence or as coloured spots when the chromatograms were developed with ninhydrin (triketohydrindene hydrate) and were found to vary in number or amount in different tissues at different ages and in different genotypes. These substances, to which preliminary conventional names were given, were later studied chemically in greater detail and in some instances their structure was determined.

The main results obtained by Hadorn and Mitchell can be summarized as follows. (1) During development from the egg to the adult fly, major changes occur in the type and amount of ninhydrin-positive substances; (2) Fluorescing substances change also remarkably during development, as shown in Fig. 1 taken from the paper under review; (3) Very clear-cut differences are apparent in the fluorescent patterns of males and females; (4) Differences in both groups of substances are found regularly in different organs; (5) Mutants affecting the eye

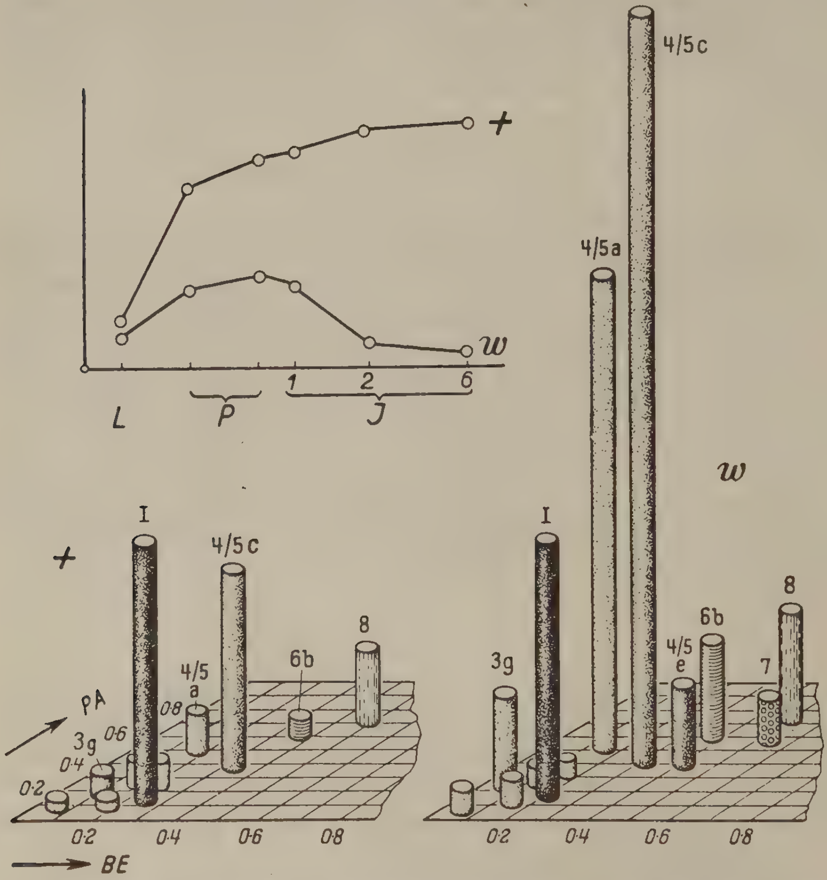

Fig. 1. Biochemical differences between normal genotypes (+) and the white mutant (*w*) of *Drosophila melanogaster*. The curves represent the mean quantities of isoxanthopterine present in males of different developmental stage; L, larvae before metamorphosis; P, younger and older pupae; J, 1, 2, 6 imagoes one, two and six days after hatching. The diagrams with the columns show the set of fluorescent substances found in corresponding quantities of meconial excrements, for + (left) and *w* (right). Distribution with R_F values in two-dimensional chromatograms developed in n-propanol-ammonia (PA) and butanol-acetic acid (BE). The heights of the columns indicate the relative quantities as measured fluorometrically (from Hadorn, 57).

colour of the adult fly differ markedly in fluorescent substances; (6) No difference was found in the fluorescent patterns of mutants having different body colours; (7) The chromatograms of larvae of the lethal genotype *ltr* (lethal-*translucida*) showed the presence of many more amino-acids and peptides than the normal control.

These observations were later expanded by various authors. Thus, while the writer [12] confirmed the differences in the fluorescent chromatograms of the two sexes, Fox [44] found that normal males from an isogenic strain possess seven ultraviolet-fluorescent or absorbing substances not observed in normal females; while these possess two fluorescent or absorbing substances not observed in males, ten additional such substances are common to both sexes. Fox showed also that while the two sexes also possess 19 amino-acids, and four unidentified ninhydrin-positive substances, normal males also possess a peptide, referred to as the "sex-peptide" which is not observed in normal females. According to this author the chromatographic differences between males and females cannot be attributed to the Y-chromosome. Very recently Kaplan, Holden and Hochman [75] demonstrated the occurrence of about twice as much free methionine in ethanol extracts of *Drosophila* females than in males.

Expanding their own investigations E. Hadorn and H. K. Mitchell [53, 57] as well as other research workers collected in recent years a large number of data which well substantiate the other observations summarized above. Some of the fluorescing substances have been identified as pteridines [28, 30, 31, 39, 40, 41, 42, 54, 55, 91, 111, 112, 113, 114, 115, 116, 117]. A quantitative study of these substances made possible a better understanding of the formation of the eye pigments of *Drosophila*. These are composed of two groups: the so-called brown and red pigments. While the origin and the first steps in the biosynthesis of the former group were already fairly well understood before the introduction of paper chromatography only this technique has made it possible recently to distinguish and identify the action of mutants which block the last steps in the synthesis of ommochromes. These mutants could not be distinguished by means of feeding experiments and transplantation tests. The red pigment complex is a complicated mixture, whose components are difficult to separate and chemically unstable. For this reason they could not be investigated by ordinary chemical procedures. As late as 1951 no clues were available for understanding the chemical constitution of the red pigments.

When the problem was approached in a different manner, making use of paper chromatography, rapid progress occurred; it was shown that the mutant *sepia* contained a much greater quantity of a yellow pigment than the wild type. Since this mutant does not produce any of the red pigments, the assumption was made that this yellow pigment might be an intermediate in their synthesis or might be closely related to them. Forrest and Mitchell [39, 40, 41] succeeded in obtaining the yellow pigment in crystalline form and in sufficient quantity for further chemical study. In this way they reached the conclusion that the isolated substance was a pteridine, called pteridine-s having the following structure:

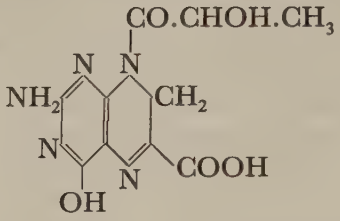

Viscontini, Karrer, Hadorn and others have subsequently isolated several fluorescent substances from *Drosophila* and identified them as pteridines [111]. Three components of the red pigment were also isolated [113] and identified, thus proving the occurrence of a pteridin nucleus in their molecules, which by oxidation or after alkaline hydrolysis gave a common product, 6-carboxy-pteridinic acid. They are: drosopteridine, neodrosopteridine and isodrosopteridine.

By a simple procedure of two-dimensional chromatography the behaviour of the components of the red pigment in mutants affecting eye colour of *Drosophila* has recently been studied in this laboratory (Baglioni, unpublished results). Thus it was shown that there were two more pteridines, which possessed chromatographic and electrophoretic characteristics and ultraviolet spectra similar to those of drosopterine and isodrosopterine, but which could be distinguished from these two substances by their different R_F values using a 20% KCl solution as solvent. The three major components isolated by Viscontini were found to be present in constant ratios also in those mutants which possess an amount of red pigment much smaller than the wild type, while the two new pteridines isolated by Baglioni behave independently from the other components of this group.

On the basis of the extensive investigations of Hadorn and his group on several mutants affecting eye colour the conclusion was reached that each mutation influences the number of different substances in the organism in a specific way, thus determining a pleiotropic action of the gene at the biochemical level [54, 60, 61, 62, 63, 64, 66].

Striking variations in the occurrence of certain fluorescent substances were also observed in the course of development. Fig. 1 shows how the amount of isoxanthopterine varies in wild type flies and in white-eyed ones, and the difference between the corresponding fluorescent patterns in the excretion products of the two genotypes, which is revealed by chromatographic analysis of the meconium deposited by the flies after emerging from the pupa [61]. A paper by Danneel and Zimmermann [24] on the distribution of fluorescent substances in the course of development of several eye colour mutant strains brings further evidence on the pleiotropic effects at the biochemical level of the genes involved. Further detailed data on differences in the concentration of several pteridines measured fluorometrically in the wild type, the *sepia* and *white* mutants and their combinations, showed that the chemical effects of the factors *se* and *w* are of a genuine locus-specific nature [23, less 122].

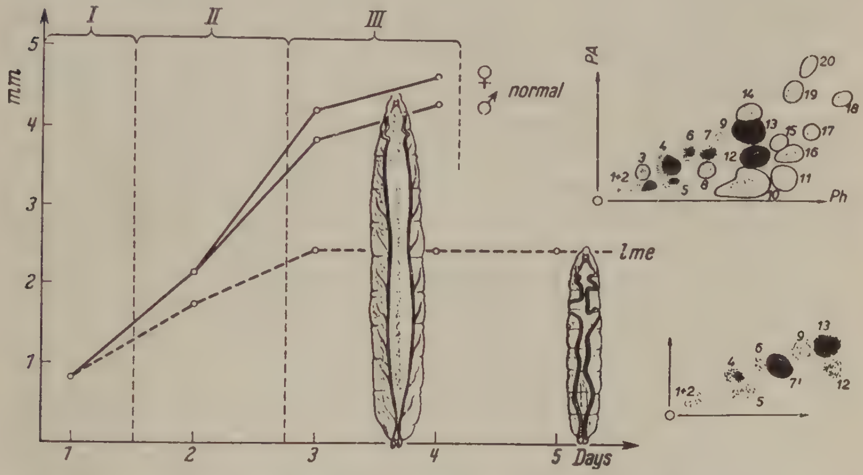

Fig. 2. Growth curves of normal and lethal meander larvae (*lme*) and content of amino-acids, peptides and amides in body extracts of the two genotypes, as revealed in two-dimensional paper chromatograms. Above, the normal; below, the *lme* pattern. The solvents used were n-propanol-ammonia (PA). 1+2, 5, 8: peptides, 3: aspartic acid, 4: glutamic acid, 6: serine, 7: glycine, 9: threonine, 10: lysine, 11: arginine, 12: glutamine, 13 and 15: α- and β- alanine, 14: tyrosine, 16: histidine, 17: γ-amino butyric acid, 18: proline, 19: valine, 20: leucine and isoleucine. The substances missing in *lme* but present in normals are encircled. Note the accumulation of glycine (7!) in *lme*, (from Hadorn, 57).

The work on the effects of lethal genes was also extended. Not only was the case of the lethal-*translucida* analyzed further [16, 65, 109] but also the lethal-*meander* mutant (*lme*) provided more evidence for the interference in the protein metabolism produced by these lethal genes [18, 56]. Fig. 2 illustrates this latter case.

As soon as the first results of their investigations were announced by Hadorn and Mitchell, it appeared of interest to check whether this technique could be used for the investigation of other genetic problems.

Thus the writer [11, 12] attempted to find out whether different genotypes could be distinguished at the paper chromatographic level when their phenotypes were indistinguishable or when mutant phenotypes differed from the wild type in some morphological trait, i.e., when the end product of the mutated gene by which it can be recognized was of a less obvious chemical nature than in the series of mutants studied by Hadorn and Mitchell which affected eye or body colours.

The main results of my investigations can be summarized as follows. (1) Extensive tests on the constancy of results were carried out on a large number of chromatograms obtained from single flies belonging to many different strains, and proved that while, during the first days of adult life, the fluorescent patterns undergo appreciable change, after the tenth day they become constant. Feeding experiments with different strains of yeasts, with moulds and also a comparison between flies grown on a medium containing live yeast and on a completely synthetic medium (unpublished results of the author) proved that the biochemical patterns obtained by this procedure are highly independent of dietary and environmental conditions. (2) Comparison between four unrelated wild type strains showed that these possessed appreciably different fluorescent patterns under ultraviolet, but were identical when the ninhydrin-positive substances were compared. (3) Comparison of the ninhydrin-positive patterns obtained from various *Drosophila melanogaster* strains did not show any appreciable difference. (4) Comparison of a series of several dozen chromatographic patterns obtained from single individuals of a laboratory strain (Oregon-R) and of a highly inbred line derived from it revealed that in the latter the individual variability was much smaller than in the former and that, correspondingly, the inbred strain has much more sharply clear-cut spots than the mass cultured strain. (5) Each of 15 mutant strains gave distinctive fluorescent patterns, except for the striking difference in the fluorescent spots which distinguishes the sexes, a remarkable parallelism of results is to be found when comparing the patterns of females and males of the same mutant strain. (6) Analysis of the chromatographic patterns of special strains in which the *forked* and the *giant* mutations had been introduced into a common genetic background allowed us to conclude that the biochemical specifity as revealed by this procedure falls under the control of a single genetic locus. (7) Individuals heterozygous for completely recessive genes gave, in every case, a chromatographic pattern which differed from that of their wild homozygous parent as well as from that of the parental homozygous recessive. (8) In three cases, maternal effects were evident in the chromatograms of hybrids between wild and mutant strains.

These results, which were obtained while working at the University of California, Berkeley and La Jolla, were later confirmed by further unpublished work carried out in this laboratory. Other authors also obtained similar results. Thus Fox [43, 46] found that there are no appreciable differences in the ninhydrin-positive patterns obtained from one wild type and a dozen strains containing various combinations of the *lozenge* pseudoalleles. Goldschmidt [48] observed differences in the fluorescent patterns of two wild type laboratory strains and the *eyeless*^{2} mutant. By repeated backcrossing to the two wild type strains this author showed that after five generations the fluorescent pattern of the eyeless flies could not be distinguished from that of the normal strains with which they shared a common genetic background. These data, however, do not seem at variance with the conclusions reported above concerning the biochemical specificity determined by singly gene differences. The fact that different wild type strains possess different chromatographic patterns indicate clearly that their biochemical phenotype, as revealed by this technique, is controlled by many genes, and this is also indicated by the differences found between individuals derived from highly inbred and mass cultured strains. The overriding effect of the *forked* and *giant* mutants over the common genetic background which we have just discussed may not always occur. The facts observed by Goldschmidt could then be ascribed to the overriding action of the genetic background of the two chosen strains over the *eyeless*^{2} mutant. It should also be noted that while this author studied the chromatograms obtained from adult heads, mine were obtained from the flies abdomens and thoraxes.

During the larval stage, Koref and Brncic [79] found clear and constant biochemical differences as revealed by ninhydrin-positive substances between individuals belonging to two different strains each of them homozygous for two recessive genes. Larvae with tumours did not differ in their chromatographic pattern from that of their parental strains.

Differences between wild type strains were recently confirmed by Robertson and Forrest [99] who compared the content of isoxanthopterin in mass cultured strains in inbred lines and in their crosses. They came to the conclusion that the amount of this substance is controlled by many genes.

By an analysis of the chromatograms of eggs of *Drosophila* obtained from reciprocal crosses between wild type and *vermillion* mutant flies Graf [49] showed that the amount of kinurenin present is determined by the genotype of the mother and is independent of the genotype of the egg.

Hadorn [58] has determined the amount of drosopterines present in transplanted and host eyes of *Drosophila*, and has found that a wild type pupa is self sufficient for the synthesis of the red eye pigments required for at least 10 eyes.

Hoenigsberg and Castiglioni [71, 72, 73] report that the chromatographic fluorescent patterns of inbred flies show a greater variability during the ageing process of the adult than mass cultured flies. The results appear at variance with those reported by the writer (see point 4, page 102). On the fact that the comparison was made by these workers between mass cultured strains with the *cardinal* mutant and inbred strains with wild type eyes, does not seem to warrant their conclusion, since the *cardinal* mutant is known to affect drastically the metabolism of tryptophan.

The identification of heterozygotes for recessive genes by means of chromatography has been attempted by Kikkawa [76] but he failed to obtain results consistent with those I had previously reported. Further investigations on this point carried out in this laboratory using both uni-dimensional and two-dimensional chromatograms confirmed my original data. A very recent paper by Ziegler-Günder [122] has further evidence to show that, indeed, recessive genes can be identified when in heterozygous conditions, by the effect they exert on the biochemical make up of the organism, even though no difference appears at the phenotypic level.

2. *Other insects*

The interest of the results obtained on *Drosophila melanogaster* prompted research on other species. While more detailed data about the chromatographic patterns of different species of the genus *Drosophila* will be reported in section III of this paper, it is worthwhile to mention here that all species studied by Rasmussen [95, 96] presented clear differences between males and females in the fluorescent substances. While this also proved to be the case for the pupae of *Aedes aegypti* [100] several other insects belonging to *Diptera Culicidae* did not show any sexual dimorphism at the chromatographic level.

In a series of papers on the meal moth *Ephestia kühniella* Hadorn and Kühn and coworkers [37, 59, 60, 80, 81, 82] found that in this species also there is a widespread phenomenon of biochemical pleiotropy, as previously found in *Drosophila*. It was found that a single gene mutation may alter the biochemical constitution of every organ of the individual in a very distinctive way, according to the local biochemical and physiological conditions and structure in different cell systems which build up a body. Fig. 3 illustrates some of the findings on this species.

Laven and Chen [83] working on a lethal mutant of the mosquito *Culex pipiens* discovered facts very similar to those found in the two lethal mutants of the fruit fly, which we have discussed. In this case also, the action of the mutation consists of an interference with the protein metabolism of the larva. The ninhydrin-positive chromatograms

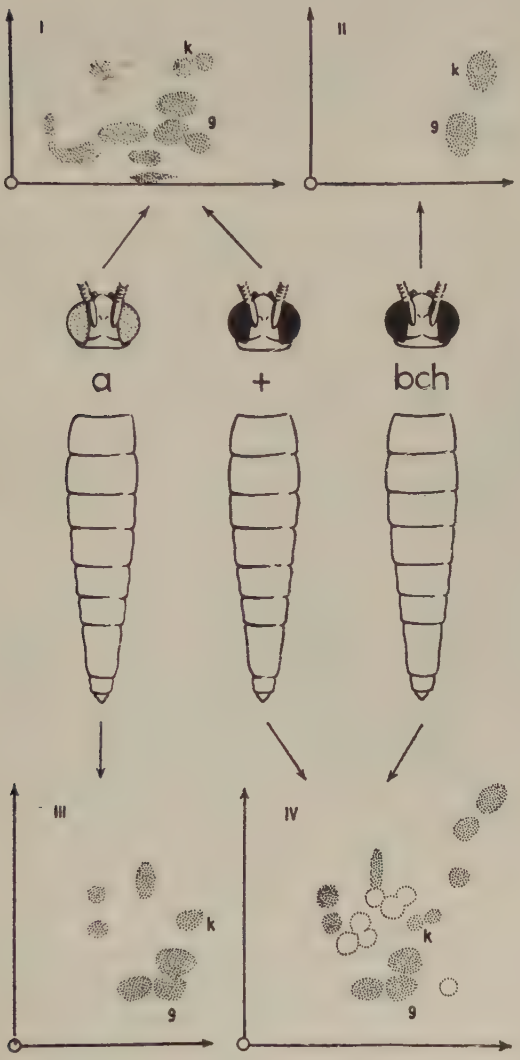

Fig. 3. Organ specificity of biochemical pleiotropy in three genotypes of *Ephestia kühniella*, *a*, + and *bch*. The diagrams above the heads show the set of fluorescent substances present in eyes as revealed by two-dimensional paper chromatograms (I for *a* and +; II for *bch*). Below we see the inventory of substances present in abdomes (III for *a*; IV for + and *bch*). The letters near two fluorescent spots indicate isoxanthopterine (g) and 2-amino-6-oxypterine (k). (from Hadorn, 57).

of methanol extracts of the wild and of the mutant strains show a very marked decrease in the number and amount of amino-acids and peptides in the latter as compared to the former.

A preliminary report by Kikkawa, Ogito and Fujito [77] report that the paper chromatographic analysis of extracts from eggs of wild type and mutant strains of *Bombyx mori* and also of *Drosophila melanogaster* eggs has made possible the identification of metallic complex salts directly connected with the formation of pigments.

3. *Protozoa*

As yet, there are only two short reports on unicellular animals. In both instances acid hydrolysates of cells were subjected to paper chromatography and only ninhydrin-positive patterns were studied. While Butzel and Martin [10] did not find any qualitative difference in the amino-acids content of different stocks, mating types and serotypes of *Paramecium aurelia* (quantitative studies are announced but the results are not yet known), Finley and Williams [38] found clear cut differences in the sexual and asexual forms of the ciliate *Vorticella microstoma*: the former showed 15 bands in the one-dimensional chromatograms and the latter only 10.

4. *Plants*

Very little information is available on plants also, although the technique of paper chromatography has been widely utilized for the identification of certain chemical compounds in some species [e.g., 52, 68, 93] and also in some mutants of *Antirrhinum majus* by Schütte, Langenbeck and Böhme [103]. Buzzati-Traverso has shown [11, 12] that ninhydrin-positive as well as fluorescent patterns obtained from plant tissues, such as root tips, leaves and anthers made a distinction possible between homozygous wild types and heterozygotes for a recessive gene in tomato and in the muskmelon *Cucumis melo* (see Fig. 4).

5. *Man*

The technique of paper chromatography has been recently used for the study of problems of human inheritance and the results are indeed encouraging. Most research workers have focused their attention on the study of amino-acid excretions, because these can be directly assayed by this technique in body fluids such as urine and saliva and because there are large variations between individuals in amino acid excretion.

In the case of cystinuria, a clinical and hereditary condition first recognized over a century ago by the discovery of a renal calculus of unusual composition, the use of paper chromatography has led to a complete reorientation of research. In a paper which can be considered as the first contribution of paper chromatography to genetic investigations, Dent [33, 34] showed how the study of urine by this method could yield precious information. Dent and coworkers [33, 34, 35, 36] showed that cystinuria should be regarded as capable of being broken down into at least two distinct entities: (1) the classical type with a tendency to cystine stone formation and characterized by the excretion in the urine of excessive amounts of cystine, lysine and arginine; (2) a generalized aminoaciduria, corresponding to Lygnac's disease or Fanconi syndrome, with cystine also present as one of the several amino-acids excreted in excess. A third condition in which recessive cystine excretion takes place is Wilson's disease (hepatolenticular degeneration) [35]. The standard tests, for cystine in the urine would permit a discrimination between these distinct pathological conditions, while paper chromatography has made possible the acquisition of this new knowledge.

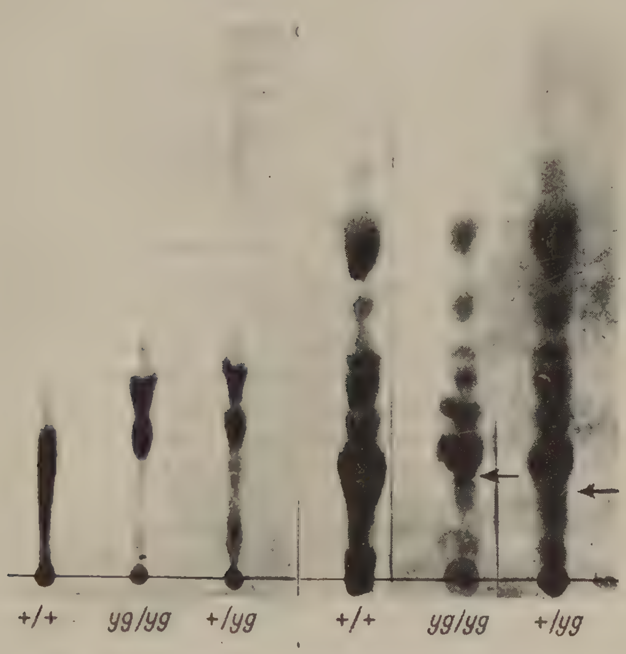

Fig. 4. Chromatographic patterns of ninhydrin-positive materials in muskmelon (*Cucumis melo*) tissues. A. Chromatograms from ground leaves. B. Chromatograms from mashed root tips. Genotypes: +/+ = homozygous wild type; +/*yg* = heterozygous; *yg*/*yg* = homozygous for the recessive *yellow-green* mutant. Arrows indicate whitish halo corresponding to very bright blue coloured fluorescing substance present in *yg*/*yg* and in the heterozygote (from Buzzati-Traverso, 12).

This technique has been profitably used for the study of other hereditary metabolic disorders. An extensive and clear review of this subject can be found in a paper by Harris [70]. Such investigations have revealed that in addition to pathological conditions, variations in amino-acid excretion occur within the range of normal variation in man. Thus Dent, Harris and others [21, 69] have found a hereditary condition occurring in about 10% of the English population in which large amounts of β-aminoisobutyric acid are present in the urine without producing, however, any abnormal symptom. Studies conducted at the Institute of Human Biology of the University of Michigan [106, 108, 28] indicate that there are racial differences in the occurrence of this biochemical peculiarity in Chinese and Caucasoids, and support the hypothesis of genetic determination of this trait. Other studies on amino-acid excretion in man have been carried out by this technique to discover genetically controlled anomalies within the range of normal variation [3, 4, 5, 47, 118, 119].

It may be of interest for those who are interested in human biology that Rogers [101, 102] has successfully applied the technique of squashing directly small quantities of mammalian tissues onto the filter paper for obtaining chromatograms. These showed constant differences between normal and pathological conditions. Differences were found between different mice tissues, between lymph nodes sampled from rabbits of different age, between lymph nodes of mice with lymphocitic leukaemia and of normal ones, between liver tissues of mice in which fulminating necrosis had developed as a result of the treatment with carbon tetrachloride or of infection with the hepatitis virus of Nelson, in liver tissues of mice made fatty by fasting or by treatment with aminopterin or ethionine, and also in liver tissues poisoned with several toxic agents. The author believes that this technique offers great promise for an understanding of the metabolic background of disease processes, now known for the most part through clinical effects and their gross microscopic appearance and also for discovering chemical compounds effective in blocking or bypassing the primary biochemical injury.

III. PAPER CHROMATOGRAPHY IN SYSTEMATICS

In 1953 two short notes were published indicating that paper partition chromatography as applied to fresh tissues of several species of fish [13] and in *Drosophila* [12] yielded results that seemed to have value for taxonomic studies. Since that time, a relatively large number of papers have appeared confirming the usefulness of this technique in problems of sytematics and population genetics of a variety of microorganisms and animals, and these will be reviewed now. In Table 1 is presented a list of the studied organisms. No similar attempts appear to have been made in the vegetable kingdom.

1. *Microorganisms*

A number of papers have recently appeared on the results obtained in the study of the taxonomy of lactobacilli [2, 8, 15, 50, 51], streptococci and micrococci, using acid extracts from bacterial cells. Even though the medium and the age of the culture influence the constancy of the chromatograms, this method of analysis seems to offer promise in this group of organisms. While these authors have used extracts from whole cells, Cummins and Harris [22] have analyzed by paper chromatography the hydrolysates of cell-wall preparations of more than 60 strains of corynebacteria, lactobacilli, streptococci, staphylococci and other gram-positive cocci. They found that the amino-acids present in the cell wall seem to be characteristic of the genus, while the sugars and amino sugars seem to characterize the species within the genus. It thus appears that cell wall composition possesses a definite taxonomic value.

Lee, Wahl and Barbu [86] concentrated their studies on the desoxyribonucleic acids of 60 strains of bacteria. They analyzed by paper chromatography the relative amounts of purine and pyrimidine bases present in DNA extracted by first treating with soda, cells which had been ground or lysed by lysozyme and then precipitated after hydrolysis at 175° in concentrated formic acid. The ratio of adenine plus thymine over guanine and cytosine varies through a range between 0.4 and 2.7 and seems to be characteristic of the species. In most species belonging to the same genus in Bergey's classification the ratio is about the same. No relationship was found between the relative amounts of these purine and pyrimidine bases, the Gram character and the aerobic or anaerobic requirements of the bacteria studied.

Different approaches have thus shown that paper chromatography can be of remarkable significance for taxonomic studies in bacteria.

Before leaving this group of organisms it seems worthwhile to mention an early paper which did not have any taxonomic aim but is pertinent to the subject under discussion. While studying the adsorptive behaviour of bacterial viruses Shepard [106] found that mixtures of the various members of the seven bacteriophages of the T series of *Escherichia coli* could be partially separated chromatographically in paper strips which had been treated with hydrochloric acid. The extent of movement up the paper strips of different T-phages has parallelled to a certain extent their other characteristics, such as their serological type. There is a possibility, therefore, that the technique could be extended to the study of other viruses.

Only one study has been made on protozoa. Lee [84] has found that the fluorescent and the ninhydrin-positive patterns of the hydrolysates of *Paramecium aurelia*, *caudatum* and *multimicronucleatum* differ consistently and thus offer a new tool for discriminating between species.

2. *Invertebrates other than insects*

An interesting observation was recently made by Chen and Baltzer [17] working on echinoderms. By paper chromatographic analysis constant differences were found in free amino-acids and peptides separated from homogenates of eggs from three species of urchins. In spite of their quantitative differences, in all three types of eggs, the chromatographic patterns remained largely constant during development. When, however, the protein precipitates of these species were hydrolyzed in 6N-hydrochloric acid, strikingly similar ninhydrin-positive chromatograms were found. The species-specific differences found in the free amino-acids are not reflected in the amino-acid composition of the proteins. This, according to the authors, may indicate that differences of specific proteins in the sea-urchin egg probably lie on the structural level, as serological studies had previously shown.

In order to test the validity of the procedure described by the writer when applied to an invertebrate phylum, Kirk, Main and Beyer [78] analyzed the fluorescent and absorption patterns under ultraviolet light, of chromatograms obtained from the foot muscle of seven species of Australian landsnails directly squashed on the paper. Chromatography was carried out by using circles of filter paper and feeding the solvent to the centre of the disc. They found clear-cut differences between the species, and these proved to be largely independent of feeding conditions, age and the locality of collection of the animal. These data were later confirmed using an improved chromatographic technique by British investigators [120] who also found this method useful in the study of aquatic snails.

A comparison between the polysaccharides present in aquatic *vs.* landsnails has recently been carried out [91] by chromatography of ethanol extracts of the hydrolyzed tissues. Seven species were studied, and it was found that the galactogen of aquatic forms is different from that of landsnails. In two species, *Lanistes boltenianus* and *Pomacea reteki*, a biochemical sexual dimorphism was found, in that males possessed glycogen while females had galactogen.

3. *Insects*

Since 1951 Micks and coworkers [88, 89, 90] have found constant differences in the free amino acids of mosquitoes. Using one- and two-dimensional chromatography and studying ninhydrin-positive as well as fluorescent patterns, these investigators have been able to show that this technique can be profitable when used not only with mosquitoes but also with three other orders of insects (see Table 1, p. 119). A comparison of density curves obtained from one-dimensional chromatograms proved the high degree of reproducibility of the amino-acid patterns of each species studied. Striking quantative differences were found between chromatograms representing different orders. Appreciable quantitative differences were also found in the comparison of different strains within three species, thus confirming the possibility of using this tool also for population genetic work, as demonstrated in *Drosophila* and fish [12, 13, 98]. Ball and Clark [1] found also similar differences between four species of mosquitoes.

Similarly Robertson [100] on the basis of the results obtained from the study of the fluorescent and ninhydrin-positive patterns of seventeen species of *Coleoptera*, *Lepidoptera*, *Diptera* and *Hymenoptera* concludes that this biochemical approach offers a promising means of elucidating problems in taxonomy and population genetics.

An example of such possibilities is given by a recent paper by Merker [87] in which he solves some problems of the taxonomy and distribution of pine mites of the genus *Dreyfusia* using the fluorescent chromatograms obtained by squashing these animals on the filter paper.

Mention should be made also of investigations on the occurrence of pteridines in *Bombyx mori*, *Colias croceus*, *Gonopteryx rhamni*, *Pieris rapae*, *Vespa crabo*, *Papilio machao*, *Opistographis luteolata*. By an association of chromatographic and electrophoretic techniques, interesting results were obtained by Polonovski, Jérome and Gonnard [94] on these insects.

The most complete attempt to evaluate the validity of the paper chromatographic technique for taxonomic studies was carried out by Inge Rasmussen, on the genus *Drosophila*. This seemed to offer an ideal test object because of the very advanced systematic knowledge reached in this group on the basis of morphological, cytological, distributional and genetic data. More than 600 species are known to belong to this genus, and their relative degree of affinity has been established in a very satisfactory way by several students of the subject and especially by A. H. Sturtevant and J. T. Patterson. Within the genus *Drosophila*, subgenera have been established and within some of these a number of "species groups". One can thus find examples within this genus of different levels of taxonomic and probably of phylogenetic relationship. Many living strains of species were available to Miss Rasmussen so that she had ample material available for carrying out such investigation. On the basis of the comparative study of the fluorescent patterns obtained from 19 *Drosophila* species, of *Zaprionus vittiger*, a member of a genus belonging to the *Drosophilidae* family and of *Aphiochaeta xanthina* of the *Phoridae* family, Rasmussen [95, 96] reached the conclusion that

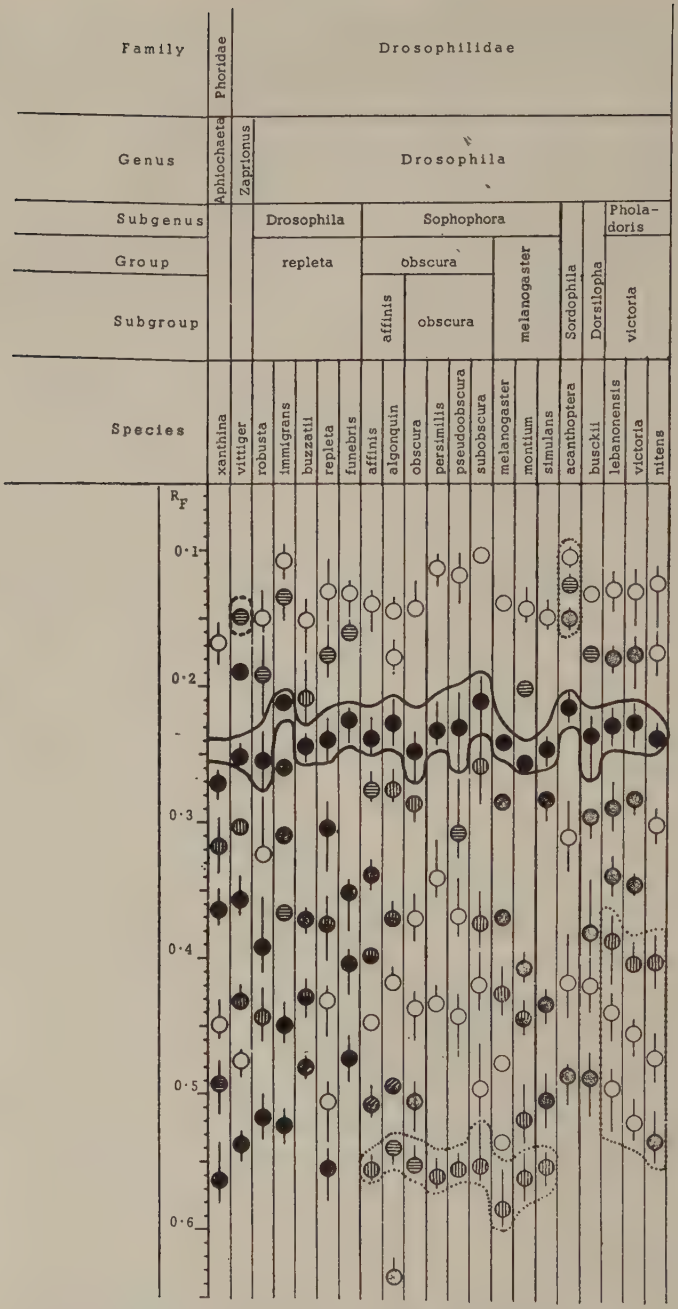

Fig. 5. Schematic representation of the fluorescent patterns obtained in one-dimensional chromatograms of fruit flies. R_F values are given as means of at least 12 readings from a corresponding number of samples of females squashed on the filter paper. Solvent used: 2 parts of n-propanol, 1 part of 1% ammonia. Stripings of the circles indicate different fluorescent colors. (from Rasmussen, 96).

there is a close parallelism between levels of taxonomic affinity as revealed by morphological and other criteria and of biochemical similarity as revealed by these chromatographic studies. Further, chemical compounds and groups of compounds possessing different levels of taxonomic specificity were isolated. Both one-dimensional and two-dimensional chromatographic analyse were used, but no attempt was made to identify the chemical structure of the spots, which have specific or genetic significance. Fig. 5 gives an example of the results obtained. In the only tested case comparable results were obtained using fresh and lyofilized material.

Results comparable to these in insects were also obtained from four species of spiders by Lee, Rene and Roddy [85].

4. *Vertebrates*

Preliminary data on fish [13] showed that: (1) Fluorescent and ninhydrin-positive patterns of the same tissue taken from various specimens of the same species are remarkably constant, irrespective of the size and age of fish; (2) Patterns obtained from muscle of different species show constant and easily recognizable differences; (3) The closer the taxonomic position of the species studied, the greater the similarity of their chromatographic patterns; (4) The same technique can be used to distinguish stocks of the same species belonging to populations geographically separated. These observations were later confirmed by Rechnitzer [98] and Dannevig [25, 26] on the California sardine (*Sardinops coerulea*), 10 *Gadidae*, 3 *Clupeidae* and 4 *Pleuronectidae* and on cod populations. Biochemical investigations by Jones [74] showed also that except for bacterial spoilage, very little change occurs in fish muscle after death, thus opening the possibility of using this technique for field work or market tests.

In 22 mammalian species, Datta and Harris [27] observed differences in the urinary amino-acid pattern. High concentrations of methyl-histidine were found in the urine of all the carnivores: of cystein-S-*iso*pentanol in the urine of several *Felidae;* of cystine in the urine of the Kenya genet (*Genetta tigrina erlangeri*) and of taurine in the mouse, rat, dog, binturong and puma. The observed differences result from complex interactions between dietary, physiological and genetical factors which require a more detailed study.

5. *Interspecific hybrids*

Fluorescent patterns of hybrids between five pairs of species of *Drosophila* and their reciprocal crosses were studied by Scossiroli and Rasmussen [104, 105]. It was found that hybrids show pattern revealing characteristics of both parental species. In some crosses the hybrids show the pattern of the species employed as the mother, but with some minor changes revealing the influence of the father. In some chromatograms of the hybrids a few spots were bigger and brighter than in the two parental species. These spots showed a phenomenon of exaggeration in terms of size and intensity of fluorescence. In three out of these five interspecific crosses, one or more spots not present in either parental species occurred in the chromatogram of the hybrid. It could not be decided whether these "hybrid substances" were already present in the patterns of the parental species at too low concentrations to be detected, or if they were really new and typical of the hybrids only.

Chen and Baltzer [17] report that the ninhydrin-positive chromatograms of the interspecific hybrids between the sea-urchins *Paracentrotus lividus* × *Arbacia lixula* and *Sphaerechinus granularis* × *Paracentrotus lividus* show an entirely maternal character.

IV. CONCLUSIONS

The experimental evidence reviewed in the preceding pages indicates without any doubt that the technique of paper partition chromatography is indeed a very useful tool for genetic and taxonomic research. As yet, very few attempts have been made to apply this method of analysis on a wide front and in a systematic way; the majority of the contributions have so far had a cursory character, with the very notable exception of the work of Hadorn and coworkers on the origin of *Drosophila* eye pigments. It appears worthwhile at this stage to extend in depth and in scope genetic and taxonomic research by taking advantage of this chemical tool. A few suggestions for future work will follow.

At the technical level it appears worthwhile to discuss the relative merits of (1) carrying out chromatographic analysis of organisms or tissues directly squashed onto the paper as compared with the study of tissue extracts, and of (2) using one-dimensional or two-dimensional chromatographic analysis. As for the first question, I think it is safe to state that the direct analysis of tissue squashes offers notable advantages in spite of its crudeness. It is simple and can be carried out without any complicated chemical equipment; as a matter of fact it can even be done in the field. It gives surprizingly constant results with a high degree of independence from environmental conditions. It may reveal biochemical relationships that would disappear if one studies extracts or products of hydrolysis of tissues. The case reported by Chen and Baltzer [17] for echinoderms where they found appreciable differences between species in the free amino-acids but not in the products of hydrolysis illustrates this point. Indeed one should keep in mind that in fresh tissues or body fluids there can be substances such as salts or proteins which may interfere with the attainment of clean chromatograms, and proper care should be taken in the choice of the solvents to be used. Sometimes, after a preliminary study of the chromatographic patterns obtained by squashing, it may become necessary to bring the analysis to a higher degree of accuracy and then extracts and hydrolysis products will have to be studied. But this technique can certainly not replace the apparently more crude one. To give only one example, two peptides or protein molecules may possess very different properties in spite of their being made of equal amounts of the same amino-acids. Paper chromatographic analysis of the free peptides as present in the tissues may reveal differences that would disappear if one were to study the hydrolysis product of such peptides.

As for the second question, somewhat similar considerations can be developed. Fox [45] has pointed out the advantages of two-dimensional chromatographic analysis over one-dimensional. The greater resolution obtained, this author maintains, insures better results. One can hardly disagree with this view in general terms, but it appears to me that one-dimensional analysis has its definite merits. For one-dimensional analysis a very small quantity of material is sufficient and in this way one may study single organisms with better results. Sometimes, as in the case reported by Fox, one-dimensional chromatograms fail to reveal differences that appear very evident with two-dimensional analysis, but sometimes things may work the other way around. Like in a kaleidoscope, the mutual interactions between the components of the figure may produce characteristic patterns which would disappear after separation of the parts. Here again, then, both methods of analysis should be used according to the varying requirements of the investigation.

At the genetic level of study a number of problems appear especially interesting for further analysis using this technique. In bacteria it would be very interesting to study how metabolic pathways that have been studied in detail may affect other cell components and how different biochemical conditions, which have been genetically determined, may alter the complex biochemical picture, which one may analyze with the crude technique of studying whole cells. In multicellular organisms the visual measurement of the degree of homozygosity of a strain may furnish useful information. The possibility offered by this technique of revealing genetic differences not evident in the phenotype, as in the case of heterozygotes for recessive mutants, opens new perspectives in the study of dominance relationships, of pleiotropic action of genes, and on the hypomorphic or hypermorphic nature of mutants. The comparison between biochemical differences in the course of development of two or more genotypes producing different morphological traits may give a clue for an understanding of differentiation in chemical terms. For applied genetic work the identification of heterozygotes offers promise, especially in some problems of animal breeding where the diagnosis of carriers of undesired traits gives appreciable economic reward.

At the taxonomic level it is no longer interesting to show that one species differs from another in some biochemical trait. This is what one would expect any way, and it has been abundantly shown that this technique makes this differentiation possible. But there certainly are at least two areas of investigation that appear to offer more fun. By comparing the chromatographic patterns of species belonging to different genera within a family or belonging to different families within a higher taxonomic category one may hope to discover degrees of taxonomic and phylogenetic relationships that are obscure to the morphologist or the cytologist. There are often cases where the systematist has no doubts in establishing relationships between species within a genus, but has no way of deciding whether a genus of a family is likely to be more closely related in phylogeny to this or that other genus or family: in such cases the discovery of common chemical traits may solve the question. Serological methods have also been used for studying the affinities between closely or less closely related forms, our paper chromatography is an alternative method which offers some advantages. Simplicity is the first, but more important is the fact that the zoologist or the botanist may conduct, with the aid of the biochemist, a more precise study of biochemical relationships than with the serological methods, owing to the smaller size of the molecules involved.

Clearly, the biochemical constitution of a cell and of an organism must be the result of the information provided by its desoxyribonucleic acid. One should expect therefore that biochemical analysis would reveal the kind of differences which have been reviewed. Paper chromatographic methods have rendered possible the identification of such differences by means of very simple manipulations, and thus has won their right of citizenship in the domains of genetics and taxonomy. J. B. S. Haldane once wrote [67]: "If I am right in believing that there is at least a correlation between morphological and biochemical diversity, the study of biochemical evolution, based as it must be almost wholly on living organisms, may not be as hopeless a task as has been sometimes assumed." Paper chromatography promises to make this prediction come true.

REFERENCES

1. BALL, G. H. and CLARK, E. W. *Syst. Zool.* **2**, 138 (1953).
2. BERRIDGE, N. J., CHEESEMAN, G. C., MATTICK, A. T. R. and BOTTAZZI, V. *J. Appl. Barteriol.* **20**, 205 (1957).

3. Berry, H. K., Cain, L. and Rogers, L. L. *Univ. Tex. Publ.* **5109**, 150 (1951).
4. Berry, H. K., Cain, L. and Rogers, L. L. *Univ. Tex. Publ.* **5109**, 157 (1951).
5. Berry, H. K., Dobzhansky, Th., Gartler, S. M., Levene, H. and Osborne, R. H. *Amer. J. Hum. Genet.* **7**, 93 (1955).
6. Block, J. R., Durrum, E. L. and Zweig, G. "A manual of paper chromatography and paper electrophoresis", p. 110. Academic Press, New York (1958).
7. Block, J. R., Le Strange, R. and Zweig, G. "Paper chromatography. A laboratory manual." p. 195, Academic Press, New York (1952).
8. Bottazzi, V. *Ann. Microbiol.* **7**, 3 (1957).
9. Brimley, R. C. and Barrett, F. C. "Practical chromatography." p. 128, Chapman and Hall, London (1953).
10. Butzel, H. M. and Martin, W. B. *Genetics* **40**, 565 (1955).
11. Buzzati-Traverso, A. A. *Nature Lond.* **171**, 575 (1953).
12. Buzzati-Traverso, A. A. *Proc. Nat. Acad. Sci. Wash.* **39**, 376 (1953).
13. Buzzati-Traverso, A. A. and Rechnitzer, A. B. *Science* **117**, 58 (1953).
14. Cassidy, H. G. "Fundamentals of Chromatography. Technique of Organic Chemistry," Vol. 10, p. 235, Interscience Publishers Inc., New York (1957).
15. Cheeseman, G. C., Berridge, N. J., Mattick, A. T. R., Bottazzi, V. and Sharpe, M. E. *J. Appl. Bacteriol.* **20**, 195 (1957).
16. Chen, P. S. *Rev. Suisse Zool.* **63**, 216 (1956).
17. Chen, P. S. and Baltzer, F. *Nature Lond.* **181**, 98 (1958).
18. Chen, P. S. and Hadorn, E. *Rev. Suisse Zool.* **62**, 338 (1955).
19. Consden, R., Gordon, A. A. and Martin, A. J. P. *Biochem. J.* **38**, 224 (1944).
20. Cramer, F. "Papierchromatographie." p. 135, Verlag Chemie, Weinheim Bergstr (1951).
21. Crumpler, H. R., Dent, C. E., Harris, H. and Westall, R. G. *Nature Lond.* **167**, 307 (1951).
22. Cummins, C. S. and Harris, H. *J. Gen. Microbiol.* **14**, 583 (1956).
23. Danneel, R. and Eschrich, B. *Z. Naturf.* **116**, 105 (1956).
24. Danneel, R. and Zimmermann, B. *Z. Naturf.* **9**, 12 (1954).
25. Dannevig, E. H. *Tidsskr. Hermetikind. No.* **3** (1955).
26. Dannevig, E. H. *Fiskeridir. Skr. Havundersøk.* Report on Norwegian fishery and Marine investigations. **11**, 1 (1956).
27. Datta, S. P. and Harris, H. *Eugenics* **18**, 107 (1953).
28. De Grouchy, J. and Sutton, H. E. *Amer. J. Hum. Genet.* **9**, 76 (1957).
29. De Lerma, B. *Boll. Soc. Ital. Biol. Sper.* **26**, 1 (1950).
30. De Lerma, B. and De Vincentiis, M. *Boll. Soc. Ital. Biol. Sper.* **31**, 1 (1955).
31. De Lerma, B. and De Vincentiis, M. *Boll. Zool.* **22**, 1 (1955).
32. De Lerma, B., Dupont-Raabe, M. and Knowles, M. F. *C. R. Acad. Sci. Paris*, **241**, 995 (1955).
33. Dent, C. E. *Biochem. J.* **41**, 240 (1947).
34. Dent. C. E. *Biochem. J.* **43**, 168 (1948).
35. Dent, C. E. and Harris, H. *Ann. Eugen, Lond.* **16**, 60 (1951).
36. Dent, C. E. and Rose, G. A. *Quart. J. Med.* N.S. **20**, 205 (1951).
37. Egelhaaf, A. *Z. Indukt. Abstamm. -u. Vererb. Lehre* **87**, 769 (1956).
38. Finley, H. E. and Williams, H. B. *J. Protozool.* **2**, 13 (1955).
39. Forrest, H. S. and Mitchell, H. K. *CIBA Symp.* **143** (1954).
40. Forrest, H. S. and Mitchell, H. K. *J. Amer. Chem. Soc.* **76**, 5656 (1954).
41. Forrest, H. S. and Mitchell, H. K. *J. Amer. Chem. Soc.* **76**, 5658 (1954).
42. Forrest, H. S. and Mitchell, H. K. *J. Amer. Chem. Soc.* **77**, 4865 (1955).
43. Fox, A. S. *Rec. Gen. Soc. Am.* **23**, 40 (1954) and *Genetics* **39**, 967 (1954).
44. Fox, A. S. *Physiol. Zoöl.* **29**, 288 (1956).
45. Fox, A. S. *Science* **123**, 143 (1956).

(397)

46. Fox, A. S. *Z. Indukt. Abstamm.-u. VererbLehre* **87**, 554 (1956).
47. Gartler, S. M., Dobzhansky, Th. and Berry, H. K. *Amer. J. Hum. Genet.* **7**, 108 (1955).
48. Goldschmidt, E. *Nature Lond.* **174**, 883 (1954).
49. Graf, G. E. *Experientia* **13**, 404 (1957).
50. Gregory, M. and Mabbit, L. A. *J. Appl. Bacteriol.* **20**, 226 (1957).
51. Gregory, M. and Mabbit, L. A. *J. Appl. Bacteriol.* **20**, 218 (1957).
52. Griffiths, L. A. *Nature Lond.* **180**, 286 (1957).
53. Hadorn, E. *Arch. Klaus-Stift. VererbForsch.* **26**, 470 (1951).
54. Hadorn, E. *Caryologia* suppl. **6**, 326 (1954).
55. Hadorn, E. *Experientia* **10**, 483 (1954).
56. Hadorn, E. "Letalfaktoren in ihrer Bedeutung für Erbpathologie und Genphysiologie der Entwicklung." p. 338. G. Thieme, Stuttgart (1955).
57. Hadorn, E. *Cold. Spr. Harb. Symp. Quant. Biol.* **21**, 363 (1956).
58. Hadorn, E. *Rev. Suisse Zool.* **64**, 338 (1957).
59. Hadorn, E. and Egelhaaf, A. *Z. Naturf.* **11**, 21 (1956).
60. Hadorn, E. and Kühn, A. *Z. Naturf.* **8**, 582 (1953).
61. Hadorn, E. and Kursteiner, R. *Arch. Klaus-Stift VererbForsch.* **30**, 494 (1956).
62. Hadorn, E. and Mitchell, H. K. *Proc. Nat. Acad. Sci.* **37**, 650 (1951).
63. Hadorn, E. and Schwinck, I. *Nature, Lond.* **177**, 940 (1956).
64. Hadorn, E. and Schwinck, I. *Z. Vererbung.* **87**, 528 (1956).
65. Hadorn, E. and Stumm-Zöllinger, E. *Rev. Suisse Zool.* **60**, 506 (1953).
66. Hadorn, E. and Ziegler-Günder, I. *Z. Vererbung.* **89**, 221 (1958).
67. Haldane, J. B. S. "The Biochemistry of Genetics." p. 144. G. Allen and Unwin, London (1954).
68. Hasborne, J. B. and Scherratt, H. S. A. *Nature, Lond.* **181**, 25 (1958).
69. Harris, H. *Ann. Eugen. Lond.* **18**, 43 (1953).
70. Harris, H. "An Introduction to Biochemical Genetics." Eugenics Laboratory mem. 37, p. 96, Cambridge University Press, London (1953).
71. Hoenigsberg, H. F. and Castiglioni, M. C. *Nature, Lond.* **181**, 1404 (1958).
72. Hoenigsberg, H. F. and Castiglioni, M. C. *R.C. Ist. Lombardo. B* **92**, 241 (1958).
73. Hoenigsberg, H. F. and Castiglioni, M. C. *R.C. Ist. Lombardo B* **92**, 249 (1958).
74. Jones, N. R. *Biochem. J.* **58**, 47 (1954).
75. Kaplan, W. D., Holden, J. T. and Hochman, B. *Science* **127**, 473 (1958).
76. Kikkawa, H. *Jap. J. Genet.* **30**, 46 (1955).
77. Kikkawa, H., Ogito, Z. and Fujito, S. *Proc. Jap. Acad.* **30**, 30 (1954).
78. Kirk, R. L., Main, A. R. and Beyer, F. G. *Biochem. J.* **57**, 440 (1954).
79. Koref, S. and Brncic, D. *Drosophila Inform. Serv.* **28**, 126 (1954).
80. Kühn, A. *Naturwissenschaften* **43**, 25 (1956).
81. Kühn, A. and Berg, B. *Z. Vererbung.* **87**, 25 (1955).
82. Kühn, A. and Egelhaaf, A. *Naturwissenschaften* **42**, 634 (1955).
83. Laven, H. and Chen Shen, P. *Z. Naturf.* **11**, 5 (1956).
84. Lee, J. W. *Trans. Amer. Micr. Soc.* **75**, 228 (1956).
85. Lee, J. W., Rene, A. A. and Roddy, L. R. *Trans. Amer. Micr. Soc.* **74**, 311 (1955).
86. Lee, K. Y., Wahl, R., and Barbu, E. *Ann. Inst. Pasteur* **91**, 212 (1956).
87. Merker, E. *Naturwissenschaften* **45**, 118 (1958).
88. Micks, D. W. *Ann. Ent. Soc. Amer.* **49**, 576 (1956).
89. Micks, D. W. and Ellis, J. P. *Proc. Soc. exp. Biol., N.Y.* **78**, 69 (1951).
90. Micks, D. W. and Gibson, F. J. *Ann. Ent. Soc. Amer.* **50**, 500 (1957).
91. McMahon, P. P., von Brant, T. and Nolan, M. D. *J. Comp. Physiol.* **50**, 219 (1957).
92. Nawa, S. and Taira, T. *Proc. Jap. Acad.* **30**, 632 (1954).
93. Neu, R. and Neuhoff, E. *Naturwissenschaften* **44**, 10 (1957).

94. Polonowski, M., Jérome, M. and Gonnard, P. *CIBA Symp.* **124** (1954).
95. Rasmussen, I. E. *Boll. Zool.* **21**, 339 (1954).
96. Rasmussen, I. E. *Ric. sci. Conv. gen. Suppl.* **25**, 59 (1955).
97. Rasmussen, I. E. and Scossiroli, R. E. *Boll. Zool.* **21**, 329 (1954).
98. Rechnitzer, A. B. *Proc. XIV Int. Congr. Zool. Copen. 1953*, 333 (1955).
99. Robertson, F. W. and Forrest, H. S. *Univ. Tex. Publ.* **5721**, 229 (1957).
100. Robertson, J. G. *Canad. J. Zool.* **35**, 411 (1957).
101. Rogers, S. *Amer. J. Clin. Path.* **25**, 1059 (1955).
102. Rogers, S. and Berton, W. M. *Lab. Invest.* **6**, 310 (1957).
103. Schütte, H. R., Langenbek, W. and Bohme, H. *Naturwissenschaften* **44**, 63 (1957).
104. Scossiroli, R. E. and Rasmussen, I. E. *Drosophila Inform. Serv.* **28**, 155 (1954).
105. Scossiroli, R. E. and Rasmussen, I. E. *Z. Indukt. Abstamm -u. Vererb.Lehre* **88**, 427 (1957).
106. Shepard, C. C. *J. Immunol.* **68**, 179 (1952).
107. Sutton, H. E. *Eugenics Quart.* **2**, 205 (1955).
108. Sutton, H. E. and Clark, P. J. *Amer. J. Phys. Anthrop.* **13**, 53 (1955).
109. Stumm-Zöllingher, E. *Z. Vererbung.* **86**, 126 (1954).
110. Turba, F. "Chromatographische Methoden in der Protein-Chemie." p. 358, Spring-Verlag, Berlin (1954).
111. Viscontini, M., Hadorn, E. and Karrer, P. *Helv. Chim. Acta* **40**, 579 (1957).
112. Viscontini, M., Kühn, A. and Egelhaaf, A. *Z. Naturf.* **11**, 501 (1956).
113. Viscontini, M., Loeser, E. and Egelhaaf, A. *Naturwissenschaften* **43**, 379 (1956).
114. Viscontini, M., Loeser, E. and Karrer, P. *Helv. Chim. Acta* **41**, 440 (1958).
115. Viscontini, M., Loeser, E., Karrer, P. and Hadorn, E. *Helv. Chim. Acta* **38**, 2034 (1955).
116. Viscontini, M., Loeser, E., Karrer, P. and Hadorn, E. *Helv. Chim. Acta* **38**, 1222 (1955).
117. Viscontini, M., Schoeller, M., Loeser, E., Karrer, P. and Hadorn, E. *Helv. Chim. Acta* **38**, 397 (1955).
118. Williams, R. J. "Biochemical Institute Studies. IV: Individual metabolic patterns and human disease: an exploratory study utilizing predominantly paper chromatographic methods." Univ. Texas Publ. 5109, Austin (1951).
119. Williams, R. J. "Biochemical Individuality." p. 254, J. Wiley and Sons, London (1956).
120. Wright, C. A., Harris, R. H. and Claugher, D. *Nature, Lond.* **180**, 1489 (1957).
121. Ziegler-Günder, I. *Z. Vergl. Physiol.* **39**, 163 (1956).
122. Ziegler-Günder, I. and Hadorn, E. *Z. Vererbung.* **89**, 235 (1958).

TABLE 1

Taxa	Authors and references
ARTROPODA	
BLATTOIDEA	
Blattidea	
Periplaneta americana	Micks, 88; Micks and Gibson, 90.
Periplaneta brunnea	Micks, 88; Micks and Gibson, 90.
Blattelidae	
Blattella germanica	Micks, 88; Micks and Gibson, 90.
Supella supellectilium	Micks, 88; Micks and Gibson, 90.

TABLE 1 (continued)

Taxa	Authors and references
LEPIDOPTERA	
Galleridae	
Galleria mellonella	Robertson, 100.
Tortricidae	
Archips cerasivora	Robertson, 100.
Pyralididae	
Plodia interpunctella	Robertson, 100.
Anagasta kühniella	Robertson, 100.
Lasiocampidae	
Malacosoma distria	Robertson, 100.
Malacosoma fluviale	Robertson, 100.
Ephestia kühniella	Robertson, 100.
COLEOPTERA	
Cucujidae	
Laemophloeus pusilloides	Robertson, 100.
Laemophloeus turcicus	Robertson, 100.
Laemophloeus pusillus	Robertson, 100.
Bruchidae	
Acanthoscelides obtectus	Robertson, 100.
HYMENOPTERA	
Braconidae	
Macrocentrus ancylivorus	Robertson, 100.
Tenthredinidae	
Pristiphora erichsonii	Robertson, 100.
Vespa erabro	Polonowski, Jérome and Gonnard, 94.
LEPIDOPTERA	
Bombyx mori	Polonowski, Jérome and Gonnard, 94.
Pieris rapae	Polonowski, Jérome and Gonnard, 94.
Papilio machao	Polonowski, Jérome and Gonnard, 94.
Opistographis luteolata	Polonowski, Jérome and Gonnard, 94.
Colias croceus	Polonowski, Jérome and Gonnard, 94.
Gonopteryx rhamni	Polonowski, Jérome and Gonnard, 94.
DIPTERA	
Culicidae	
Aedes aegypti	Robertson, 100; Micks and Ellis, 89, Micks 88; Micks and Gibson, 90.
Aedes sollicitans	Micks and Gibson, 90; Micks and Ellis 89.
Aedes quadrimaculatus	Micks and Ellis, 89.
Aedes taeniorhynchus	Micks and Gibson, 90.
Aedes polynesiensis	Micks and Gibson, 90.

TABLE 1 (continued)

Taxa	Authors and references
Aedes varipalpus	Ball and Clark, 1.
Anopheles quadrimaculatus	Micks, 88; Micks and Gibson, 90.
Anopheles albimanus	Micks and Gibson, 90.
Anopheles aztecus	Micks and Gibson, 90.
Culex molestus	Micks and Gibson, 90; Micks, 88.
Culex fatigans	Micks, 88; Micks and Gibson, 90.
Culex pipiens	Micks, 88; Micks and Gibson, 90; Micks and Ellis, 89.
Culex tarsalis	Micks, 88; Micks and Gibson, 90; Ball and Clark, 1.
Culex quinquefasciatus	Micks and Ellis, 89.
Culex salivarius	Micks and Ellis, 89.
Culex stigmatosoma	Ball and Clark, 1.
Culiseta incidens	Micks and Ellis, 89; Ball and Clark, 1.
Culiseta inornata	Micks and Gibson, 90.
Phoridae	
Aphiochaeta xantina	Rasmussen, 95.
Calliphoridae	
Sarchophaga kellyi	Robertson, 99.
Tachinidae	
Drino bohemica	Robertson 99.
Drosophilidae	
Zaprionus vittiger	Rasmussen, 96.
Drosophila robusta	Rasmussen, 96.
Drosophila immigrans	Rasmussen, 96.
Drosophila buzzatii	Rasmussen, 96.
Drosophila repleta	Rasmussen, 96.
Drosophila funebris	Rasmussen, 96.
Drosophila affinis	Rasmussen, 96.
Drosophila algonquin	Rasmussen, 96.
Drosophila obscura	Rasmussen, 96.
Drosophila persimilis	Rasmussen, 96; Scossiroli and Rasmussen, 105.
Drosophila pseudoobscura	Rasmussen, 96; Scossiroli and Rasmussen, 105.
Drosophila subobscura	Rasmussen, 96;
Drosophila melanogaster	Rasmussen, 96; Fox, 44.
Drosophila montium	Rasmussen, 96;
Drosophila simulans	Rasmussen, 96;
Drosphila acanthoptera	Rasmussen, 96; Scossiroli and Rasmussen, 105.
Drosophila busckii	Rasmussen, 96.
Drosophila lebanonensis	Rasmussen, 96; Scossiroli and Rasmussen, 105.
Drosophila victoria	Rasmussen, 96.

TABLE 1 (continued)

Taxa	Authors and references
Drosophila nitens	Rasmussen, 96; Scossiroli and Rasmussen, 105.
Drosophila spinofemora	Rasmussen, 96.
Drosophila setifemur	Scossiroli and Rasmussen, 105.
Drosophila helvetica	Rasmussen, 95.
Drosophila narragansett	Rasmussen, 95.
Drosophila willistoni	Rasmussen, 95.
Drosophila mirim	Rasmussen, 95.
Drosophila baeomyia	Rasmussen, 95.
Drosophila bifasciata	Rasmussen, 95.
Drosophila simulans	Rasmussen, 95.
Drosophila miranda	Scossiroli and Rasmussen, 105.
HEMIPTERA	
Reduvidae	
Triatoma gestaeckeri	Micks, 88; Micks and Gibson, 90.
Triatoma infestans	Micks, 88; Micks and Gibson, 90.
ACARA	
Ixodidae	
Dermacentor andersoni	Micks and Gibson, 90.
Dermacentor variabilis	Micks and Gibson, 90.
Dermacentor albipictus	Micks and Gibson, 90.
ARACNIDA	
Filistata hibernalis	Lee, Rene and Roddy, 85.
Pholcus phalangoides	Lee, Rene and Roddy, 85.
Plexippus paykulli	Lee, Rene and Roddy, 85.
Lacrodectus mactans	Lee, Rene and Roddy, 85.
ECHINODERMATA	
Echinoidea	
Arbacia lixula	Chen and Baltzer, 17.
Sphaerechinus granularis	Chen and Baltzer, 17.
Strongylocentrotus purpuratus	Chen and Baltzer, 17.
Paracentrotus lividus	Chen and Baltzer, 17.
MOLLUSCOIDEA	
Aplexa nitens	McMahon, Von Brant and Nolan, 91.
Australorbis glabratus	McMahon, Von Brant and Nolan, 91.
Austrosuccinia contenta	Kirk, Main and Beyer, 78.
Bothriembryon indutus	Kirk, Main and Beyer, 78.
Bothriembryon kingii	Kirk, Main and Beyer, 78.
Bothriembryon dux	Kirk, Main and Beyer, 78.
Bothriembryon leeuwinensis	Kirk, Main and Beyer, 78.
Helix aspersa	Kirk, Main and Beyer, 78. McMahon, Von Brant and Nolan, 91.
Lanistus baltenianus	McMahon, Von Brant and Nolan, 91.
Lymnaea stagnalis	McMahon, Von Brant and Nolan, 91.

TABLE 1 (continued)

Taxa	Authors and references
Olata lactea	McMahon, Von Brant and Nolan, 91.
Pomacea zeteki	McMahon, Von Brant and Nolan, 91.
Theba pisana	Kirk, Main and Beyer, 78.
FISHES	
Gadidae	
Gadus pollachius	Dannevig, 25.
Gadus eallarias	Dannevig, 25.
Gadus minutus	Dannevig, 25.
8 untold species	Dannevig, 25.
Pleuronectidae	
Pleuronectes platessa	Dannevig, 25 and 26.
Pleuronectes microcephalus	Dannevig, 26.
4 untold species	Dannevig, 25.
Clupeidae	
3 untold species	Dannevig, 25.
Hysterocarpus traski	Buzzati-Traverso and Rechnitzer, 13.
Paralobrax clatratus	Buzzati-Traverso and Rechnitzer, 13.
Paralobrax maculofasciatus	Buzzati-Traverso and Rechnitzer, 13.
Sardinops coerulea	Rechnitzer, 97.
MAMMALIA	
Felis catus	Datta and Harris, 27.
Felis leo	Datta and Harris, 27.
Felis tigris	Datta and Harris, 27.
Felis concolor	Datta and Harris, 27.
Felis pardus	Datta and Harris, 27.
Felis bengalensis	Datta and Harris, 27.
Felis serval	Datta and Harris, 27.
Felis pardinus	Datta and Harris, 27.
Felis vivarrina	Datta and Harris, 27.
Genetta tigrina erlangeri	Datta and Harris, 27.
Artictis binturong	Datta and Harris, 27.
Putorius putorius	Datta and Harris, 27.
Canis familiaris	Datta and Harris, 27.
Rattus norvegicus	Datta and Harris, 27.
Mus musculus	Datta and Harris, 27.
Orytolagus cuniculus	Datta and Harris, 27.
Cavia porcellus	Datta and Harris, 27.
Mesocricetus auratus	Datta and Harris, 27.
Macacus rhesus	Datta and Harris, 27.
Equus caballus	Datta and Harris, 27.
Bos taurus	Datta and Harris, 27.
Capra hircus	Datta and Harris, 27.

REPRINT FROM JOURNAL OF MARINE RESEARCH, VOLUME 19, 1, 1961

pp.40-56

(405)

A Multiple-Detector Irradiance Meter and Electronic Depth-Sensing Unit for Use in Biological Oceanography[1]

Robert W. Holmes and James M. Snodgrass[2]

Scripps Institution of Oceanography
University of California
La Jolla, California

ABSTRACT

The underwater irradiance meter or submarine photometer described here is designed to operate in the upper 100 to 150 m. It permits direct measurement of the downward blue-green irradiance (480 mμ) to a depth of 100–120 m on a clear day in water with an attenuation coefficient in the blue-green region of the spectrum of approximately 0.04/m. The meter can accommodate as many as five individual detector units as well as an associated depth-sensing element. The detectors are cosine flux collectors, equipped with a dry disk, self-generating, barrier layer cell. Any single detector unit may be readily oriented up, down, or horizontally. Selection among the detectors is made by energizing the switching mechanism with a push button. Their output is measured in the vessel's laboratory with a damped multirange microammeter of low internal resistance. The associated depth-sensing unit is transistorized and battery-powered and is capable of measuring depth down to 200 m with an accuracy of $\pm 2\%$ in the 50–200 m range. The unit is stable, rugged, and relatively insensitive to temperature changes in the range between 2° and 25°C. The detector and depth signals are carried by a two-conductor electrical cable, which also supports the instrument. A sea return is utilized in the detector unit switching assembly.

Introduction. The need for a versatile irradiance meter for use in connection with studies of phytoplankton ecology has been plain for some time. Marine biologists and biological oceanographers studying phytoplankton and littoral alga photosynthesis are now frequently measuring attenuation coefficients and light levels; they require more complex and precise information as their studies become more elaborate.

---

[1] Contribution from the Scripps Institution of Oceanography, New Series. This paper represents results of research carried out by the University of California under contract with the U.S. Bureau of Commercial Fisheries. No. 1273

[2] The authors wish to acknowledge the information received from John Tyler, research physicist of the Visibility Laboratory of the University of California, Scripps Institution of Oceanography, La Jolla, concerning the design and characteristics of the flat plate collectors used in the detector unit.

Reproduced by Permission

The meter described here is the result of the authors' experience over seven years in measuring attenuation coefficients and developing instrumentation. This particular instrument has been in intermittent use and under modification for two years. The present design has proved to be reliable and of general applicability for high seas research in which the objective is to study, in the field, the role of light in photosynthesis.

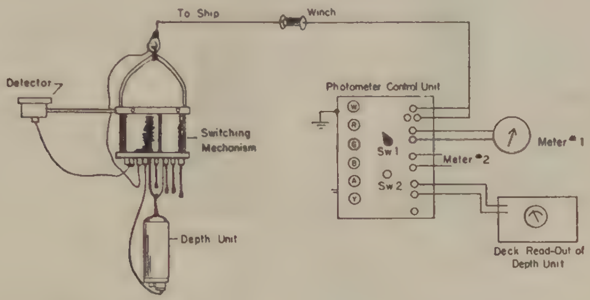

Figure 1. The irradiance meter and depth-sensing unit.

The meter (Fig. 1) is a single or multidetector unit capable of measuring the irradiance on a flat surface oriented at any desired angle. The individual flux collectors may be oriented in advance to measure the attenuation coefficient for downwelling or upwelling irradiance. By combining these two measurements it is possible to compute the reflectance at an imaginary horizontal plane in the sea, or to obtain the ratio of the irradiance on a plane facing the sun to that on a plane facing away from it. By proper selection of optical filters, the instrument can be set up to measure either the same optical property for a number of band widths nearly simultaneously or several optical properties for the same band width.

Irradiance is easily measured and by its use the results from different areas and regions can be standardized and compared. Furthermore, attenuation coefficients k calculated from the irradiance data using the following equation

$$k_\lambda = \frac{2.30}{L} (\log I_{\lambda,h} - \log I_{\lambda,h+L})$$

are useful in biological and physical oceanographic studies (Holmes, 1957 or Sverdrup, *et al.*, 1942).

The Detector Unit. Each detector unit (Fig. 2) consists of a photocell housing (i) and a threaded cap (c). The latter accommodates the Lambert or cosine collector (a), elevated about 1 mm above the cap and the lucite window (b). A watertight seal between these components is effected by rotating the threaded

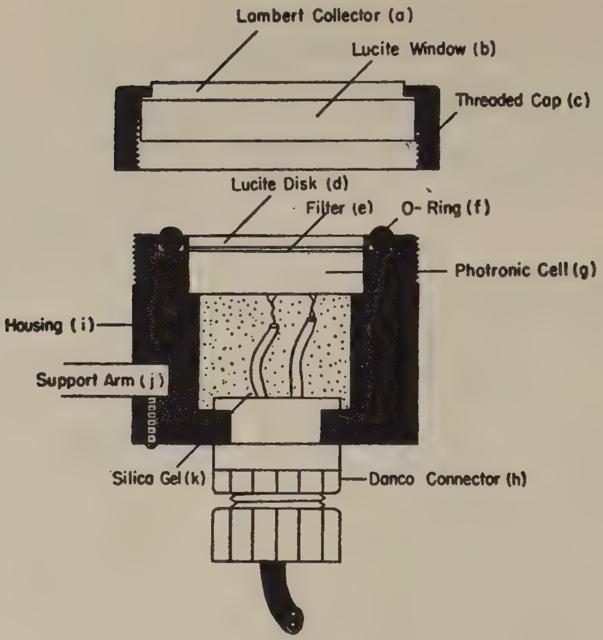

Figure 2. The detector unit.

cap until a seal is obtained between the O-ring (f) and the lucite window. The color and/or neutral filter (e) may be placed above the photocell (g); when gelatin filters are employed, they are held in contact with the photocell by a lucite disk (d). Silica gel (k) placed in the space below the photocell prevents window fogging and moisture damage to the gelatin filter. The electrical leads from the photocell are taken through the housing in a nylon stuffing tube (h) (Danco, Size 1, Danielson Mfg. Co., Danielson, Conn., packing assembly for the tube, Dorn Equip, Corp., Boston, Mass.); they terminate in a Joy plug (No. X8104–63, Joy Mfg. Co., Compton, Calif.).

The particular cosine collector used in this instrument is fabricated from milk-white translucent plastic (Rohm and Haas, Plexiglass 2333, Philadelphia, Pa.), the surface of which has been carefully abraded with carborundum (Grit No. 180) to give it cosine-collecting properties when submerged. There are of course other ways to build cosine collectors; the important thing to know is the properties of the flux collector.

Hermetically sealed barrier layer (dry disk) self-generating cells (Model 856RR), manufactured under the name Photronic Photoelectric Cell (Weston Electrical Instrument Corp., Newark, N.J.), have been employed in these detectors. These cells have proved stable and rugged enough for use in this type of work.

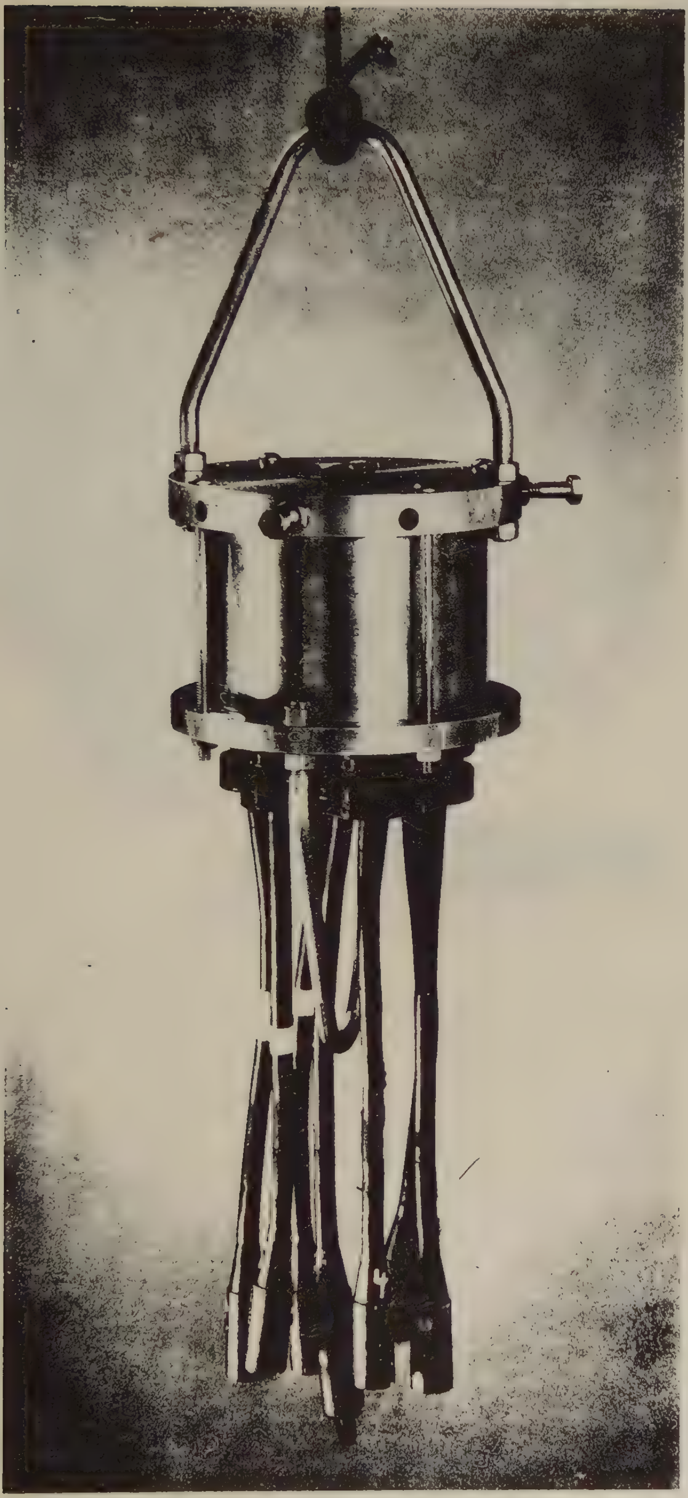

Figure 3. The underwater switching unit.

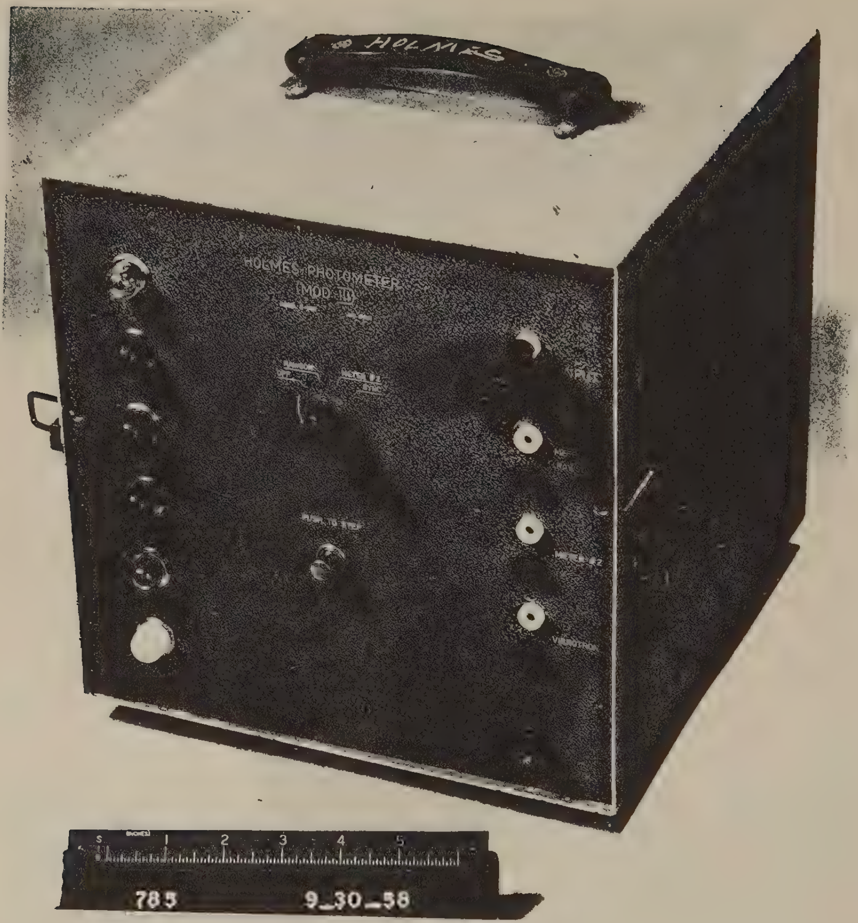
HOLMES
HOLMES PHOTOMETER
(MOD III)
PUSH TO STEP
INCHES
1
2
3
4
5
785
9_30_58

Figure 4. The deck control unit.

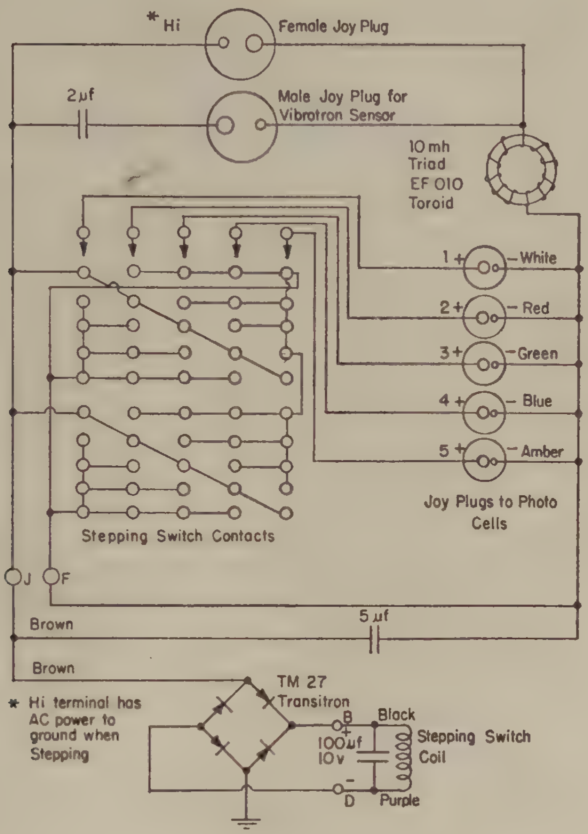
*Hi
Female Joy Plug
2μf
Male Joy Plug for Vibrotron Sensor
10 mh Triad EF 010 Toroid
1 +
– White
2 +
– Red
3 +
– Green
4 +
– Blue
5 +
– Amber
Joy Plugs to Photo Cells
Stepping Switch Contacts
J
F
Brown
5 μf
Brown
TM 27 Transitron
* Hi terminal has AC power to ground when Stepping
B
Black
+
100μf 10v
Stepping Switch Coil
–
D
Purple

Figure 5. The underwater switching unit. Schematic diagram.

Switching Mechanism and Deck Control Unit. The detector units are mounted on stainless steel rods, approximately 40 cm long, which are inserted into holes provided on the top plate of the underwater switching unit (Figs. 1, 3). The orientation of the detectors may be adjusted and maintained by utilizing the Allen set-screws mounted in either the detector or the switching mechanism. Electrical continuity from the detectors is achieved by means of connecting the Joy connectors (Fig. 3).

The underwater component of the switching mechanism consists of an oilfilled brass housing which contains a rotary stepping switch (Type 44, Automatic Electric Sales Corp., North Lake) and associated equipment (Figs. 3, 5). Seven outlets pass through the bottom of the housing; five for use with detectors, one to connect with the depth element, and one to connect to the cable that supports the instrument and carries the signal to the photo-

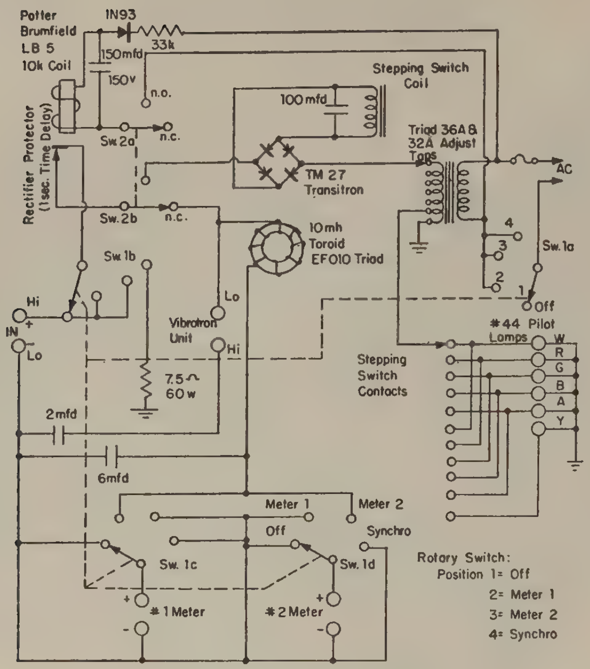
Potter Brumfield LB 5 10k Coil
IN93
33k
150mfd
150v
n.o.
Rectifier Protector (1sec. Time Delay)
Sw.2a
n.c.
Sw.2b
n.c.
Sw.1b
Hi
IN
Lo
100 mfd
Stepping Switch Coil
Triad 36A & 32A Adjust Taps
TM 27 Transitron
AC
10mh Toroid EFO10 Triad
Sw.1a
4
3
2
1
Off
Lo
Vibrotron Unit
Hi
7.5Ω 60w
2mfd
6mfd
Stepping Switch Contacts
#44 Pilot Lamps
W
R
G
B
A
Y
Meter 1
Meter 2
Off
Synchro
Sw. 1c
Sw. 1d
+
#1 Meter
-
+
#2 Meter
-
Rotary Switch:
Position 1= Off
2= Meter 1
3= Meter 2
4= Synchro

Figure 6. The deck control unit. Schematic diagram.

meter winch, whence the signal goes to the deck control unit. The selection of the particular detector is controlled by means of a push button on the deck control unit ("Push to Step", Sw. 2, Figs. 4, 6).

The deck control unit (Figs. 4, 6) is energized from 115-volt, 60-cycle, AC power. When the instrument is turned on, one of six panel lamps (the sixth has no detector associated with it) indicates which of the five detectors are connected to the meter or recorder jack located on the right-hand side of the instrument. Provision has been made for the use of two meters or of one meter and/or a meter-amplifier combination by the inclusion of a second outlet on the control unit. The selection of these outlets is controlled by a switch mounted in the middle of the control unit panel above the energizing (Push to Step) button.

There are several fundamental limitations to the mechanism as it is at present designed. First, a maximum of 4 ohms is all that can be tolerated per conductor between the deck and underwater units. If the resistance is increased above this limit, the photocell output becomes less linear at high light levels and effectively less sensitive. Further, since a sea return is used and is included in the 4-ohm limitation, the instrument is not designed to be used in fresh water. Because the sea return is normally less than ¹/₄ ohm, it is clear that the electrical conductor is essentially the limiting factor.

The circuitry is straightforward, as schematized Figs. 5 and 6 show. Two special features merit mention. The photocells not in use are shorted (as recommended by the manufacturer); and a specific control position is provided on the deck control unit to permit easy and rapid synchronization between the two units if they require rephasing. In addition, a simple filter system is used to prevent any interaction between the depth unit signal, which is AC, and the DC potentials from the photoelectric cells.

Performance of the Meter and Measurement of Attenuation Coefficients. The current generated by a Photronic cell in a constant light field is a function of cell sensitivity, external resistance, and temperature. During routine irradiance measurements, the first two of these factors are constant; only the temperature of the cell varies. Technical information supplied by the manufacturer shows that with an external resistance of about 105 ohms, the output of a cell in a constant light field of 200 foot-candles will vary from −2°/₀ to +3°/₀ in the temperature range 0–40°C, using 20°C as the reference point. The deviation is less in the temperature range 10–25° (*c* ±1.5°/₀); the data are not corrected to allow for this error.

TABLE I. LINEARITY OF RESPONSE OF TWO PHOTRONIC CELLS AS DETERMINED FROM OPTICAL BENCH MEASUREMENTS.

	μA Output at 105 ± 1 Ohms						
Log Flux	Cell No. 8				Cell No. 3		
(Theoretical)	4 Feb.	10 Mar.	21 Oct.	29 Dec.	3 Feb.	21 Oct.	26 Dec
0.0	1000	1000	1000	1000	1000	1000	1000
0.1	814	818	820	819	812	820	812
0.2	656	658	660	660	653	660	657
0.3	528	532	535	535	527	535	542
0.4	426	425	430	430	421	424	–
0.5	342	342	342	342	337	342	348
0.6	272	273	275	274	269	274	280
0.7	217	218	218	220	213	222	226
0.8	174	175	175	174	171	174	182
0.9	138	139	138	140	136	139	144
1.0	111	112	105	112	109	112	115
1.1	88.4	87.5	85	88	85.8	87.9	92
1.2	70.4	69.5	69.5	70.1	68.6	70.1	72.1
1.4	44.5	44.2	43	44.6	43	44.2	46.5
1.6	28.3	–	30	–	27.6	28.6	–
1.8	18.1	–	–	–	17.6	18.1	–
2.0	11.5	–	–	–	11.2	11.6	–
2.2	7.3	–	–	–	7.2	7.4	–
2.4	4.6	–	–	–	4.45	4.9	–

The type 856RR Photronic cells are stable in terms of linearity of response. However, since no two cells are identical, it is important if reliable measurements are to be made at high light levels to determine the linearity of response for each cell under the resistance load that will obtain during actual measurements. This may be done on an optical bench or with a series of neutral filters of known transmittance. In Table I, linearity-of-response data obtained at intervals over an 11-month period are given for two type 856RR cells. There is an indication of a slight increase in linearity over the time interval, but this may not be significant.

The flux sensitivity of one of these cells has remained virtually constant (*c* ± 5%) for two years.

During routine measurements at sea, the output of the detector unit(s) has been measured with a Rawson multimeter (Model 501, special slow response) possessing five scales (0–50, 100, 200, 500, and 1000 μA), each with an internal resistance of 100 ohms. The meter has been inductively damped so that its response time is on the order of 45 sec. It has been assumed that, under conditions of rapidly fluctuating light levels such as are frequently encountered in the upper 15 m, the damped meter gives an estimate of the average light levels.

Attenuation coefficients may be readily determined providing visible incident irradiance is measured simultaneously with the output of the detector(s) at a series of depths and providing the linearity of the detector element is known.

Under ideal field conditions this irradiance meter gives very reproducible

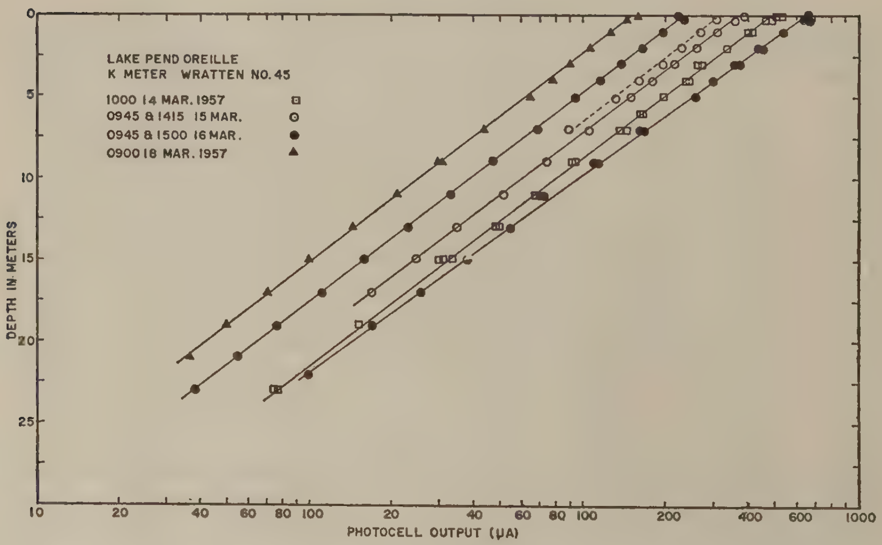

Figure 7. Relative irradiance at different depths. Lake Pend Oreille. Wratten No. 45 filter.

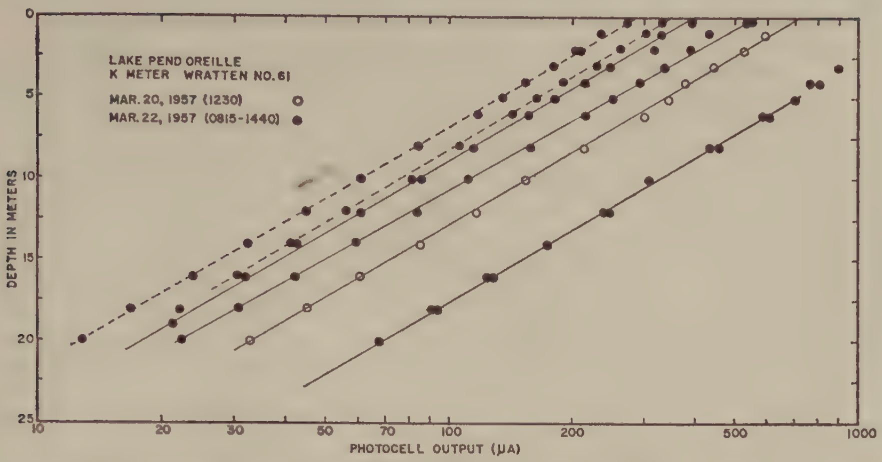

Figure 8. Relative irradiance at different depths. Lake Pend Oreille. Wratten No. 61 filter.

results, as the data presented in Figs. 7 and 8 demonstrate. These data were collected in Lake Pend Oreille, Idaho, in March 1957, with a different switching mechanism but with the same detector and galvanometer mentioned above. Correction for departure in linearity and for changes in incident solar radiation has been made. The corrections for incident radiation were made in such a way that the various curves are not superimposed. Thus the relatively minor departures in slope (the attenuation coefficient) between the eye-fitted curves may be readily seen. The Wratten No. 45 filter has its transmission peak at 480 mμ and the No. 61 at 520 mμ.

Comparable replicate measurement series obtained in the sea show that the *k* values are more variable than those obtained in Lake Pend Oreille. The vertical oscillations of the vessel and the high wire angles resulting from ship drift or subsurface currents make measurement more difficult and less certain. A typical series of measurements obtained on four separate lowerings of the irradiance meter in the Pacific Ocean about 20 miles west of La Jolla, California, on 1 May 1959 is illustrated in Fig. 9. Conditions were quite favorable during this set of observations: the sky was nearly uniformly overcast, sea and swell were moderate, and wire angles were less than 5 degrees. Corrections similar to those applied to the data in Figs. 7 and 8 were also made. The rather obvious differences in the slopes of these curves in the deeper layers probably are the result in part of inaccurate depth determinations. Had the depth element described in the next portion of this paper been employed, these curves might have become essentially parallel, as were the Pend Oreille profiles (Figs. 7, 8), where depth determinations had essentially no error.

While the sensitivity of the Photronic cell is not particularly high, measurements in the blue-green region (Wratten No. 45 filter) may be made to depths

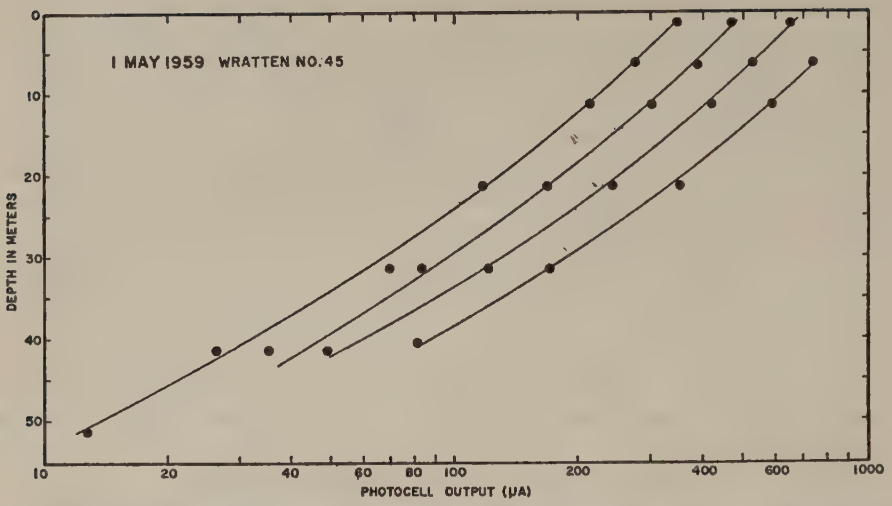

Figure 9. Relative irradiance at different depths. Pacific Ocean 20 miles west of La Jolla, California. Wratten No. 45 filter.

of approximately 100 to 120 m on clear days when the water possesses an attenuation coefficient (in this same spectral region) of approximately 0.04 per meter. Under these conditions about 1.8% of the blue-green light penetrating the sea surface will be found at 100 m depth. A considerable increase in sensitivity of the unit may be easily obtained by amplifying the photocell signal.

The Depth-sensing Unit. In order to measure attenuation coefficients with precision, instrument depth as well as light levels must be measured accurately. Experience gained from examining many irradiance-depth profiles has indicated that depths computed from wire length and wire angle measurements cease to be reliable with wire lengths exceeding 50–60 m if high wire angles (*i. e.*, 40–45°) are encountered. Thus if reliable light measurements deeper than approximately 60 m are desired, the photometer depth should be measured by some other technique. This requirement led to the development of the depth-sensing unit described below.

For convenience in describing it, the component parts of the depth unit are schematized in Fig. 10. The pressure-sensing element (Vibrotron Digital Pressure Gauge, Model 101-12-300, Borg-Warner Controlls Corp., Santa Ana, Calif.) consists of a vibrating wire maintained in a vacuum and driven by a transistorized, battery-powered amplifier. Pressure changes on the end of the wire that is attached to a pressure diaphragm alter the tension of the wire and hence its frequency.

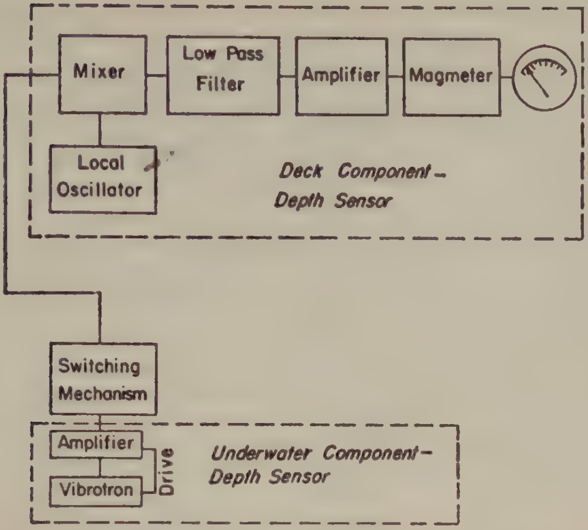
Mixer
Low Pass Filter
Amplifier
Magmeter
Local Oscillator
Deck Component–
Depth Sensor
Switching Mechanism
Amplifier
Vibrotron
Drive
Underwater Component–
Depth Sensor

Figure 10. Principal components of the depth-sensing unit. Diagrammatic.

The deck component of the depth-sensing unit is connected to the meter control panel (Fig. 1). The amplified signal from the vibrating wire, coupled into the irradiance meter's switching mechanism, feeds into a mixer, where the local oscillator produces a frequency which corresponds to the Vibrotron zero psia frequency. The resultant difference frequency is fed through a low-pass filter to remove unwanted components and then amplified. The amplified signal passes through a Magmeter (No. F-5161, Airpax Products Co., Balti-

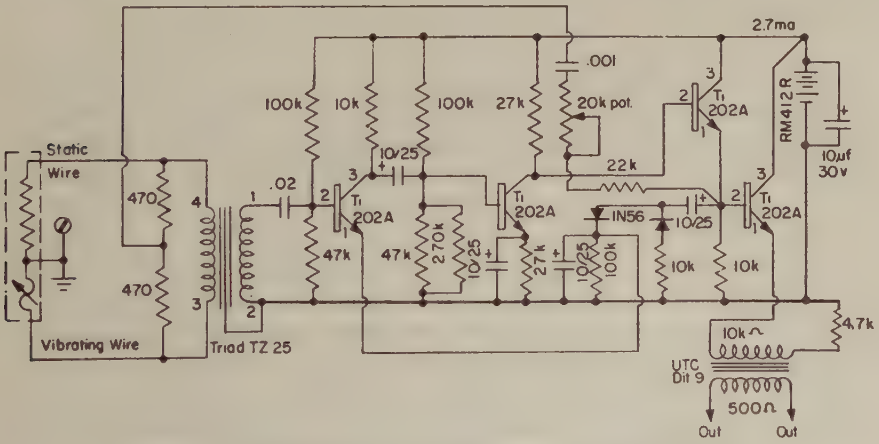
Static
Wire
Vibrating Wire
470
470
4
3
1
2
Triad TZ 25
.02
100k
10k
100k
27k
.001
20k pot.
2.7ma
10/25
47k
47k
270k
10/25
27k
10/25
100k
22k
IN56
10/25
10k
10k
T₁
202A
RM412R
10µf
30v
4.7k
10k
UTC
Dit 9
500Ω
Out
Out

Figure 11. Depth-sensing unit. Wiring diagram of underwater unit.

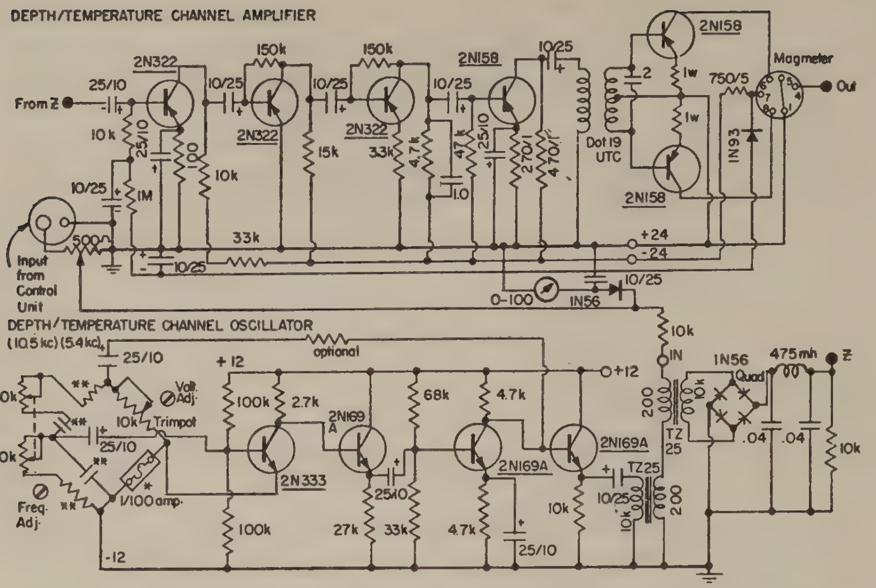
DEPTH/TEMPERATURE CHANNEL AMPLIFIER
2N322
25/10
From Z
10k
25/10
100
10/25
IM
10k
150k
10/25
2N322
15k
150k
10/25
2N322
33k
4.7k
10/25
2N158
47k
25/10
1.0
270Ω
470Ω
10/25
Dot 19
UTC
2
2N158
Iw
Iw
2N158
750/5
1N93
Magmeter
Out
33k
10/25
500
Input from Control Unit
+24
-24
0-100
1N56
10/25
DEPTH/TEMPERATURE CHANNEL OSCILLATOR
(10.5 kc) (5.4 kc)
25/10
optional
+12
50k
50k
Volt. Adj.
10k
Trimpot
25/10
Freq. Adj.
1/100 amp.
-12
100k
2.7k
2N333
100k
2N169 A
25/10
27k
33k
68k
4.7k
2N169A
4.7k
25/10
2N169A
10k
10/25
10k
TZ25
200
TZ 25
200
10k
1N
1N56
Quad
475mh
Z
.04
.04
10k

Figure 12. Depth-sensing unit. Wiring diagram of deck unit. * 8 AG Little fuse. ** Values depend on frequency. 904: Texas Instrument or 2N333 G.E. 2N169A; 2N322: G.E. 2N158 C.B.S.

more, Md.) and is then read on a 0–100 μA meter. Figs. 11 and 12 show the wiring diagrams of this circuitry.

Battery life in the deck component is of the order of several hundred hours. The depth component is somewhat underpowered, but battery life normally averages in excess of 10–11 hours with continuous operation at room temperature (18–24°C).

Calibration and Reproducibility of the Depth Unit. The depth unit was calibrated against an Aschcroft 0–600 psi dead weight gauge (type 1300) between 0 and 300 psia. During the test the Vibrotron frequency was also monitored with a Berkeley Eput Meter, Model 554-M. These data are presented in Table II and in part in Fig. 13.

A test of the reproducibility of the depth unit was made at room temperature (25°C) by taking 11 measurements at 5 pressures (50, 100, 150, 200, and 300 psia) after zeroing the instrument at atmospheric pressure. Each set of measurements between 0 and 300 psia was made by progressively increasing the pressure in the increments given above. After each series the pressure was released and the instrument was allowed to equilibrate at atmospheric pressure for a minute or two before beginning the next series. The Vibrotron frequency was also monitored directly with the Berkeley Eput Meter. The data obtained

TABLE II. Calibration of the Photometer Depth Unit (25°C).

	A		B	C
psia	Deck Unit Reading	Vibrotron Frequency	Vibrotron Frequency	Vibrotron Frequency
0	0.0	11108	–	11108
5	4.0	11067	11066	11066
10	5.0	11046	11045	11044
20	8.5	11004	11003	11002
30	11.5	10962	10961	10960
40	14.5	10919	10918	10918
50	17.5	10877	10876	10876
60	20.5	10834	10833	–
70	23.5	10791	–	–
80	27.0 –	10748	10747	10789(?)
90	30.0	10705	–	–
100	33.5	10661	10660	10659
110	36.5	10618	–	–
120	39.5	10574	10573	–
130	43.0 –	10530	–	–
140	46.5	10486	10484	–
150	50.5	10441	10440	10439
180	59.5	10306	10305	–
200	66.0+	10215	10214	10213
240	80.0	10031	10030	–
250	83.5	9984	–	9983
260	87.0 –	9937	–	–
280	93.5	9842	9842	–
300	100.5	9746	9746	9745

in this manner are given in Table III along with the mean value, standard deviation, and coefficient of variation for each pressure series.

A glance at the Vibrotron frequency at each pressure, as read on the Berkeley Meter, shows the high degree of consistency in the results. The deck component of the depth unit cannot be read as accurately as the frequency meter, nor is it as stable, but it is entirely adequate for the purpose for which it was designed. The coefficient of variation is not constant over the pressure range but averages somewhat less than 1 %. Thus, for 95 % confidence (±2 standard deviations) at room temperature, the depth estimate would be accurate to about ±2 %.

The underwater component of the depth unit was found during its design and assembly to be relatively insensitive to temperature changes between 0 and 25°C; and this matter was investigated further in the laboratory with the unit as a whole. In this test the pressure was measured with a 0–300 psi Heise Burdon gauge (No. H-1731) which was found subsequently to need recalibration, but relatively the readings are assumed to be satisfactory. The depth unit was allowed to equilibrate at room temperature (25°C) when readings

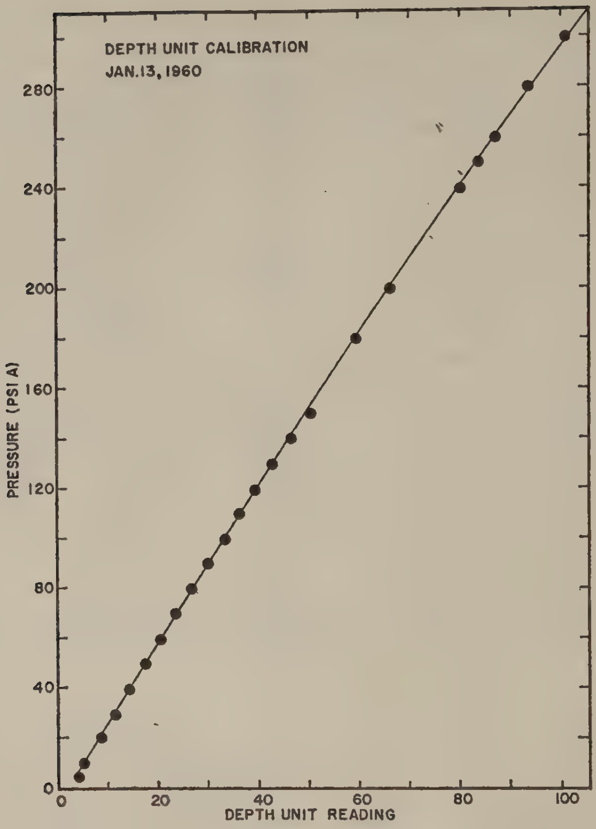

Figure 13. Depth unit calibration.

were taken, after which it was immersed in a water bath at 2–3°C for three hours before a second set of readings was taken. This procedure was repeated three times; the data are given in Table IV. The slight temperature effect observed should be taken into account if depth measurements are being made in arctic waters.

REFERENCES

Holmes, R. W.
1957. Solar radiation, submarine daylight, and photosythesis, *in*, Treatise on marine ecology and paleo-ecology. Mem. geol. Soc. Amer., 67; Editor Joel Hedgpeth; Zoology, Vol. 1: 109–128.

Sverdrup, H. U., M. W. Johnson and R. H. Fleming
1942. The oceans. Prentice Hall, Inc., New York, 1087 pp.

TABLE III. Reproducibility of the Depth Unit (25°C).

	Atmospheric Pressure		50 psia		100 psia		150 psia		200 psia		300 psia	
	Vibrotron Frequency	Unit Reading	Vibrotron Frequency	Unit Reading	Vibrotron Frequency	Unit Reading	Vibrotron Frequency	Unit Reading	Vibrotron Frequency	Unit Reading	Vibrotron Frequency	Unit Reading
	11107	0.0	10876	16.5	10660	32.5	10440	50.0	10214	66.0	09746	101.0
	11107	0.0	10876	16.5	10661	32.0	10440	50.0	10217	66.0	09746	100.5
	11107	0.0	10877	16.5	10661	32.0	10441	50.0	10214	66.5	09746	100.5
	11108	0.0	10876	16.0	10661	33.0	10440	50.0	10214	66.5	09746	101.0
	11106	0.0	10876	16.0	10661	32.0	10440	49.0	10214	65.0	09746	99.5
	11107	0.0	10876	16.5	10660	32.0	10440	49.5	10215	65.5	09746	100.0
	11107	0.0	10877	16.5	10661	32.5	10441	50.0	10215	66.0	09746	100.0
	11108	0.0	10876	16.5	10661	32.0	10440	49.5	10215	66.5	09746	100.0
	11106	0.0	10876	16.5	10662	32.0	10441	49.0	10214	65.0	09746	100.0
	11107	0.0	10876	16.5	10661	32.0	10441	49.5	10214	65.5	09746	100.0
	11107	0.0	10877	17.0	10662	32.5	10441	50.0	10215	66.0	09746	100.0
	11107	0.0	10877	16.5	10662	32.0	10440	49.5	10215	65.0	09746	100.0
Mean value	11107	0.0	10876	16.4	10661	32.2	10440	49.7	10215	65.8	09746	100.2
Standard deviation	0.6030	–	0.5222	0.257	0.454	0.335	0.522	0.390	0.904	0.582	–	0.451
Coefficient of variation (percent)	0.0054	–	0.0048	1.57	0.0063	1.04	0.00500	0.784	0.00885	0.885	–	0.450

TABLE IV. TEMPERATURE EFFECT ON THE DEPTH ELEMENT AT VARIOUS PRESSURES*.

	18 January 1960			19 January 1960			19 January 1960	
	Room Temp.	Cold	Room Temp.	Room Temp.	Cold	Room Temp.	Cold	Room Temp.
Pressure*	25°C	2–3°C	25°C	21°C	2–3°C	25°C	2–3°C	25°C
psia	1300 PST	1530 PST	1645 PST	1022 PST	1155 PST	1335 PST	1605 PST	
0........	0	0	0	0	0	0	0	0
50........	15.5	15.0+	15.5	15.5	15.0+	15.0+	15.0	15.0
100,........	30.5	30.5	30.5	30.5	30.5	30.5	30.5	30.5
150........	48.0 –	48.0 –	48.0 –	48.0 –	47.5	48.0	47.5	47.5
200........	64.0	64.0 –	64.0+	64.5 –	64.0 –	64.0 –	63.5	63.0+
290........	95.0	94.0+	95.0	95.0	94.0+	94.0+	94.0	94.0+

* The pressure gauge employed in this series was found to require recalibration, hence the pressure values given are not accurate.

(420)

Reprinted from the Journal of Marine
Research, v.19, no.1, 1961. pp.21-27.

Comparison of Norpac Temperature Sections with Average BT Sections along the same Tracks[1]

Margaret K. Robinson
Scripps Institution of Oceanography
University of California, La Jolla

The Norpac Atlas (Norpac Comm., 1960), now in press, contains horizontal and vertical charts of oceanographic data collected on the Norpac Expedition, the first multi-nation synoptic survey of the North Pacific Ocean. Vertical BT temperature sections, included in the Norpac Atlas, were prepared by the author. At that time the synoptic BT temperature observations were compared with the average BT temperature observations previously published by Robinson (1951, 1957) and by Pattullo, *et al.* (1950). These comparisons show the relationship of the August 1955 temperature distributions to average August conditions, based on BT data collected between the years 1941 and 1952. Such comparisons were possible only in the eastern Pacific, where available BT data had already been analyzed. Now that the Norpac Atlas will soon be available to all oceanographers, these comparative temperature sections appear to be of general interest.

There are two longitude sections and two latitude sections whose locations are as follows: 140°W Long., 20° to 59°N Lat. (Fig. 1); 158°W Long., 22° to 56°N Lat. (Fig. 2); 42° to 44°N Lat., 125° to 165°W Long. (Fig. 3); and 52°N Lat., 130°W Long. to 165°E Long. (Fig. 4). In these figures the vertical lines indicate individual BT observations. To simplify comparisons, only every fifth isotherm is shown except where gradients are small, in which case additional isotherms have been added. The average isotherms are shown as dashed lines while those isotherms based on Norpac BTs are solid lines.

Comparison of the average sections with the quasisynoptic Norpac sections show the following similarities:

(1) The isotherms, from their intersections with the surface to their location at 400 feet, have the same general trend in the longitude sections. In the

---

[1] Contribution from the Scripps Institution of Oceanography, New Series. This paper represents results of research carried out by the University of California under contract with the Office of Naval Research. Reproduction, in whole or in part, is permitted for any purpose of the U.S. Government so long as proper acknowledgement is made to the Journal of Marine Research.

Contributions from the Scripps Institution of Oceanography, New Series, 1274
Reproduced by Permission
REPRINT FROM JOURNAL OF MARINE RESEARCH, VOLUME 19, 1, 1961

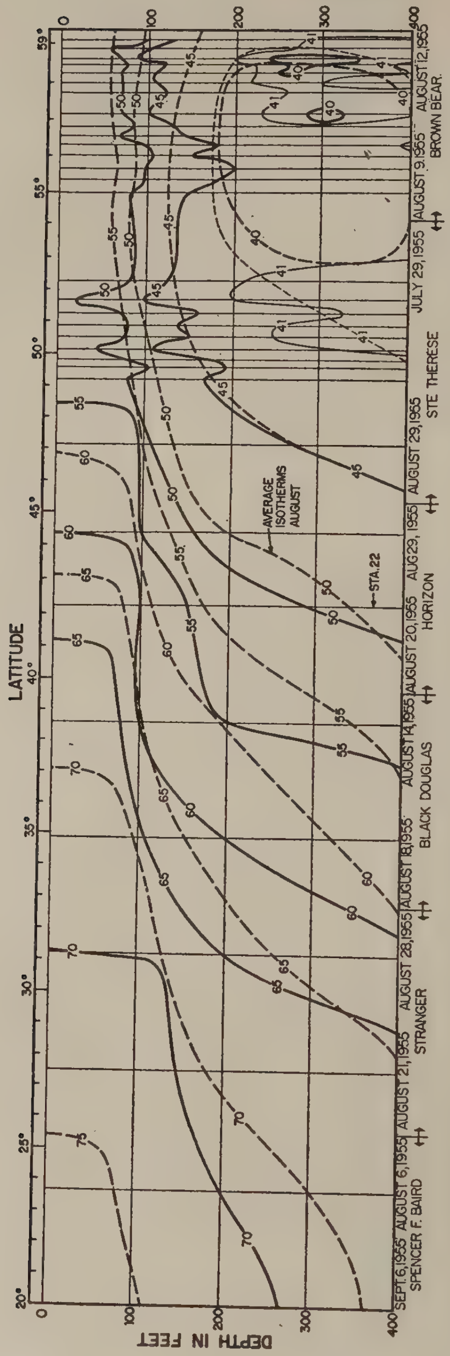

Figure 1. Comparison of vertical temperature sections at approximately 140° W Long. based on NORPAC BT observations with average BT temperature section along same track.

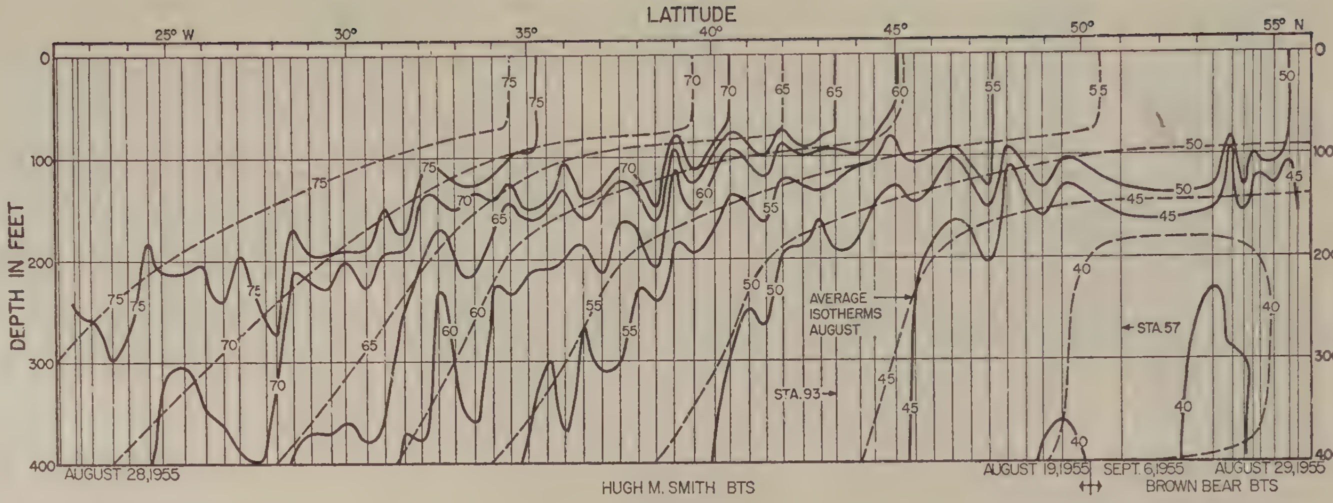

Figure 2. Comparison of vertical temperature section at 158° W Long. based on Norpac BT observations with average BT temperature section along same track.

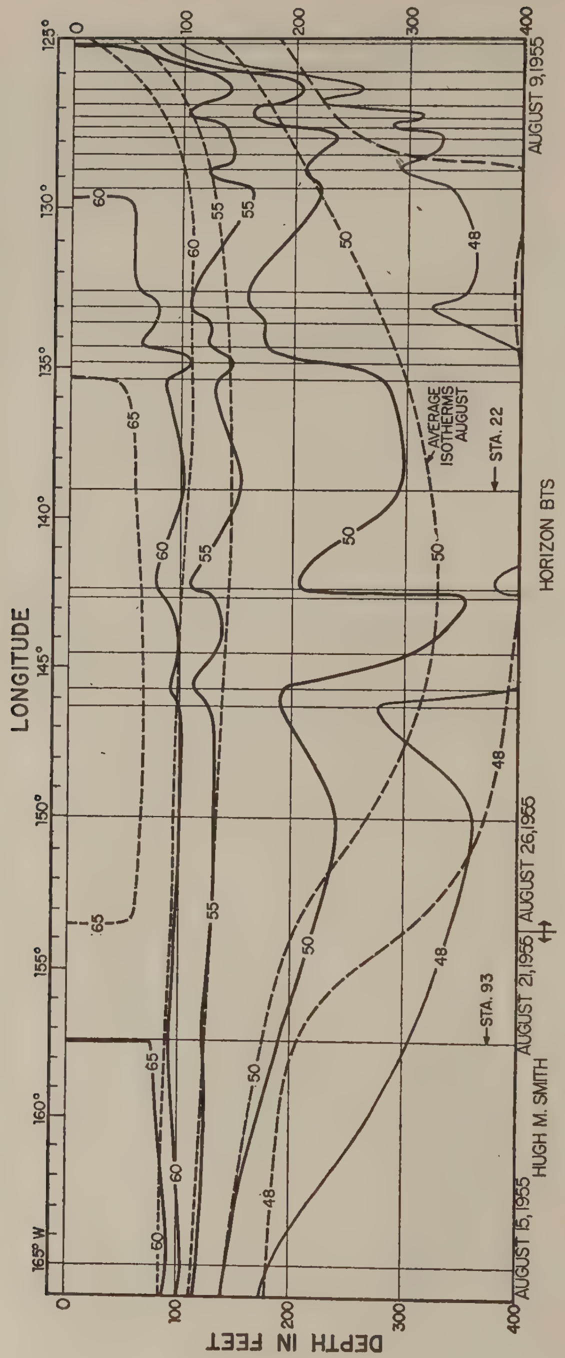

Figure 3. Comparison of vertical temperature section between 42° and 44° N Lat. based on Norpac BT observations with average BT temperature section along same track.

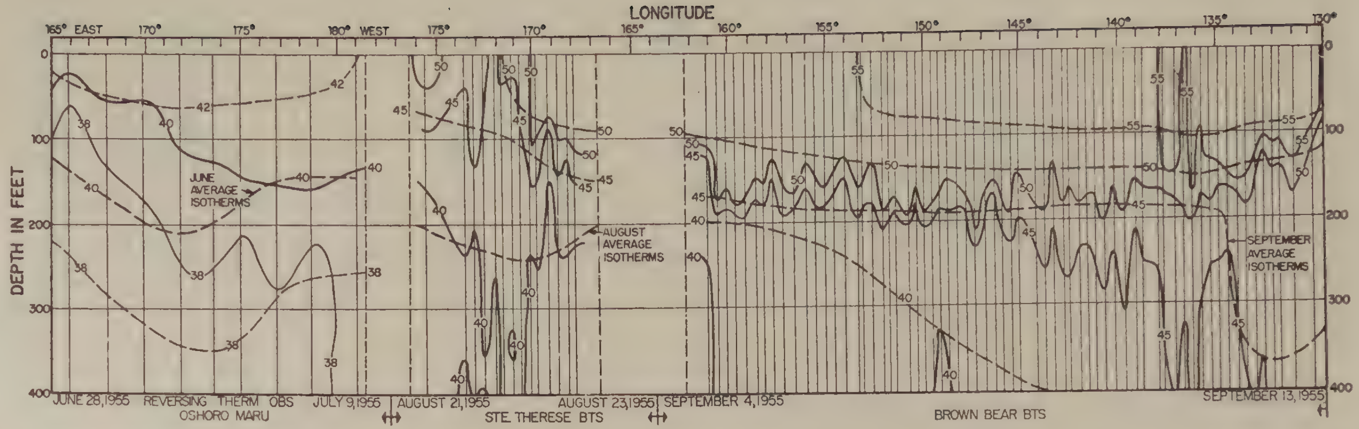

Figure 4. Comparison of vertical temperature section between 51° and 52°N Lat. based on Norpac BT and reversing thermometer observations with average BT temperature section along same track.

latitude sections there is disagreement above the thermocline but good agreement at depth.

(2) The average level of the thermocline derived from the NORPAC BTs agrees with the location of the thermocline in the average sections.

(3) The temperatures at 300 and 400 feet in the NORPAC sections are, in general, within 0.3°F of the temperatures shown by the average sections.

The differences between the average and quasisynoptic sections are as follows:

(1) In the surface mixed layer, the NORPAC 1955 temperatures were lower than the average temperatures with the following exceptions[2]: on the 158°W Long. section, south of 45°N Lat. (Fig. 2); on the 42°N Lat. section, west of 155°W (Fig. 3); in these two sections the 1955 temperatures were higher than average.

(2) The depth of any isotherm within the thermocline is extremely variable wherever the 1955 observations are closely spaced. Where observations are approximately 20 to 30 nautical miles apart, the displacements of the isotherms appear as irregular waves, with amplitudes averaging about 30 feet. The mean depth of the thermocline and isotherms, as noted above, agrees well with the average. However, in the 140°W Long. section south of 50°N (Fig. 1), where the observations are approximately 200 miles apart, the depth of the thermocline (or isotherms within the thermocline) appears as uniform as it does in the average section. This is merely a scale effect. The appearance of oscillations in the thermocline in any given section is a function of space and time between observations. Sections based on widely-spaced observations simply cannot reveal these oscillations, and the deceptive smoothness of the isotherms should not be construed as lack of variability. For this reason, if depths of isotherms, based on widely-spaced observations, differ by no more than 15 feet from the average, the difference should not be considered significant.

If predictions of temperature conditions had been made from the average charts, then in general they would have given: temperatures above the thermocline within 2°F; temperatures below the thermocline within 0.3°F; and thermocline depths within 15 feet.

The major difference between the 1955 observations and the averages is that the surface layer was colder than average everywhere except in the southwest quarter, where the surface layer was warmer than usual. In the cold surface mixed layer, the 1955 isotherms were displaced to the south from 60 to 360 miles relative to their average position; however, south of 45°N along

---

[2] See Hollister (1956) for additional evidence that the entire summer of 1955 was colder than average at Weather Station PAPA and along the British Columbia coast; see also Reid, *et al.* (1958) who showed that it was also colder than average in the California Current region in 1955.

158°W Long. the 1955 isotherms were displaced approximately 100 miles to the north. That is, the gradient between the two regimes was steepened. At 158°W Long. (Fig. 2), predicted temperatures and 1955 temperatures would have agreed at 45°N.

REFERENCES

HOLLISTER, H. J.

1956. The program of bathythermograph observations at the Canadian ocean weather station 'Papa', 50°N, 145°W. Pacific Oceanographic Group, Nanaimo, British Columbia. File N 6–18; 17 pp.

NORPAC COMMITTEE

1960. Oceanic observations of the Pacific: 1955, the NORPAC ATLAS. Univ. Calif. Press and Univ. Tokyo Press; 123 pls.

PATTULLO, JUNE G., J. D. COCHRANE and W. V. BURT

1950. Sea temperature in the Aleutian Island area. Oceanogr. Rep. Scripps Inst. Oceanogr., No. *24* (mimeo.); 6 pp.

REID, JR., J. L., G. I. RODEN and J. C. WYLLIE

1958. Studies of the California current system. Progr. Rep. Calif. Coop. Oceanic Fish. Invest., 1 July 1956 to 1 Jan. 1958; pp. 28–56.

ROBINSON, MARGARET K.

1951. Sea temperature in the North Pacific area, 20°–40°N, 125°–155°W. Univ. Calif. SIO Ref. *51–20* (mimeo.); 14 pp.

1957. Sea temperature in the Gulf of Alaska and in the Northeast Pacific Ocean, 1941–1952. Bull. Scripps Inst. Oceanogr., *7* (1): 1–98.

ABSTRACT

Evidence of the stratigraphic value of the fossil remains of an abundant and varied calcareous nannoplankton has been limited by little published data. Description of the species and tabulated distributions in 86 samples from a continuous sequence of Paleocene and Eocene strata of California permit recognition of six distinct biostratigraphic units. Available evidence on their extension as zones elsewhere and relations to type areas of some European stages are presented.

Coccolithophorids and related Nannoplankton of the early Tertiary in California

M. N. BRAMLETTE AND F. R. SULLIVAN
Scripps Institution of Oceanography
La Jolla, California

INTRODUCTION

The great variety of the tiny (2–30μ) fossil remains of the calcareous plankton which includes coccolithophorids has become apparent from recent studies. In rocks of Tertiary and late Mesozoic age, they form the major constituent of some chalks, are very abundant in many clay or shale formations, and may be found in some clayey sandstones. Wide geographic and restricted time distribution of many distinctive forms is now evident, although little of this information has yet been published. Much work is obviously required in the description of species, with records on their occurrence, for more general application of these microfossils promising to stratigraphy. Study of a sequence of many samples through a considerable part of the Tertiary seems a necessary task for any broader investigation. The local ranges of taxa may be of little significance elsewhere except as they are combined into broad stratigraphic zones by certain coincidences and partial overlaps of ranges and the succession of such zones established. The sequence of samples also offers evidence on the phylogeny of the few forms with lineages indicated by morphologic changes in the succession of strata of the one area.

Investigations of the coccolithophorids, which constitute a major element of the plankton in the present oceans, and especially of the taxonomic and related problems, have received considerable attention from marine biologists. The taxonomic problems are difficult, however, even with the living forms. Although the coccolithophorids are usually classed as unicellular algae, zoological nomenclature has been commonly applied and is followed here, as perhaps is justified by their protistid character, discussed later. Relations among many of the extinct forms are quite obscure, and the form species can only be placed in genera *incertae sedis*. Despite the artificial classification now necessary for the fossil species, delimitation of their character and distribution permits applications to biostratigraphy.

The type specimens, with their positions indicated on slides of the sample assemblages, are deposited in the U. S. National Museum, and their Museum numbers are included here. Sets of assemblage slides which include topotypes have been sent to the American Museum of Natural History in New York and the École Pratique des Hautes Études in Paris, and another set and part of the original samples remains at Scripps Institution of Oceanography.

ACKNOWLEDGMENTS

A part of each of the 110 samples collected from Lodo Canyon by the U. S. Geological Survey was generously supplied for this study. The measured section is also reproduced from U. S. Geological Survey Professional Paper 240A (1951). Samples from the stratigraphically higher strata of Oil City and Garza Creek were kindly supplied from measured sections of the Union Oil Company of California and the Texas Company of California. Our many samples from Europe and elsewhere were supplemented by additional ones from sources too numerous to enumerate here. Helpful information and discussion from G. Deflandre of Paris, E. Kamptner of Vienna, E. Martini of Frankfurt, and others are appreciated, and especially those of our colleague W. R. Riedel. A grant from the National Science Foundation helped to finance the investigation and is gratefully acknowledged.

Contributions from the Scripps Institution of Oceanography, New Series, 1275
Reproduced by Permission

(429)

micropaleontology, vol. 7, no. 2, pp. 129–188, pls. 1–14, april, 1961

PREVIOUS INVESTIGATIONS

The early investigations in this field have been summarized in other papers and need not be reviewed here, except for a few brief remarks. Fossil remains of some of the calcareous nannoplankton (including coccolithophorids and discoasters) were figured more than a century ago by Ehrenberg (1836, 1854). He considered them, however, as inorganic "crystalldrusen," and their true nature was recognized only through the work of Huxley (1858), Wallich (1860), and Sorby (1861).

Much systematic work on the major groups of living Coccolithophoridae began with Lohmann (1902), followed by Schiller (1930) and Kamptner (1941). Braarud and associates in Oslo are now most active in this field and have utilized the electron microscope for detailed study of many very small forms of the modern plankton.

Tan Sin Hok (1927) presented the first systematics on a fossil group of this calcareous nannoplankton, which he named *Discoaster.* Deflandre (Deflandre and Fert, 1954) has described a number of other genera *incertae sedis* and has given a general discussion and classification of the calcareous nannoplankton, including living and fossil forms (1952*a*, *b*).

Few workers have investigated the fossil forms from a stratigraphic viewpoint, but a preliminary paper by Bramlette and Riedel (1954) emphasized this aspect and their possible value for age assignments. Increasing interest is indicated by papers of Chamrai and Lazareva (1956), Noël (1956), Martini (1958, 1959), Stradner (1958, 1959), and others.

SAMPLES STUDIED AND THEIR STRATIGRAPHIC RELATIONS

The samples from the type section of the Lodo Formation are small parts of 110 samples collected at about 10-foot intervals by the U. S. Geological Survey, for study of the foraminiferal faunas by M. Israelsky. Part of his work has been published as Professional Paper 240A (1951) and 240B (1955), from which our columnar section (text-fig. 1) is reproduced to indicate the sampled intervals. The basal part of the formation was sampled from the better-exposed strata indicated as section B, which is about 200 feet south of the main section A. Correlation of the two parts of the section was based on similarities in lithology and foraminiferal faunas in some overlapping samples in the two sections. A very good correspondence of that correlation with the one indicated by this study is evident from the distribution of species shown in Table 1 in the overlapping samples of the two parts of the section.

This well-exposed section of the Lodo Formation is in northwestern Fresno County in central California, and the exact locality is shown on the geological map published in Professional Paper 240A. Foraminiferal

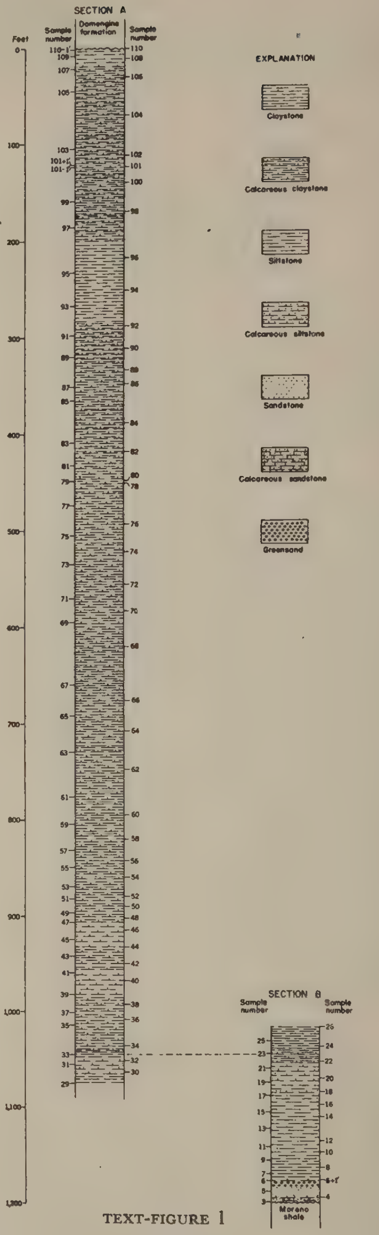

TEXT-FIGURE 1

COLUMNAR SECTIONS OF LODO FORMATION, SHOWING STRATIGRAPHIC POSITION OF SAMPLES

(from Geol. Surv. Prof. Paper 240A)

and other studies have indicated a Paleocene age for the lower 200 feet of strata, which are overlain by the much greater thickness of Lower and perhaps Middle Eocene strata of the formation. As interpretation of our data gave little evidence for a Middle Eocene age for the upper part of the Lodo Formation, a few additional samples were included as supplementary data from overlying formations of better-established Middle Eocene age.

The Domengine Formation, which immediately overlies the Lodo Formation, is generally assigned to the Middle Eocene from molluscan and foraminiferal faunas and other evidence. It is dominantly a sandstone in which fossil nannoplankton are rare or absent, but silty shale beds in the upper part contain many of these microfossils. Although they are present in the upper Domengine above the type Lodo section, the assemblage of these fossils is much better represented along the strike to the south, and the occurrences shown in Table 1 are from these more southern areas, indicated as follows:

Sample OC-1 is from a shale bed within the middle part of the Domengine Sandstone at Tumey Gulch, 4 miles southeast of the type Lodo section. Sample OC-2 is from a shale bed in the upper Domengine, 11 feet below the glauconite bed at the top of the formation, in the Oil City section located 9 miles north of Coalinga. Sample OC-3 is from this Oil City section, in the Canoas Member of the basal Kreyenhagen Formation, 30 feet above sample OC-2. Sample OC-4 is also from the Canoas Member in the Oil City section, only 4 feet above sample OC-3.

Samples GC-1, GC-2, and GC-3 are from the Canoas Member of the basal Kreyenhagen of the type region in Garza Canyon, 4 feet, 30 feet, and 52 feet, respectively, above the base of the Canoas. The base is poorly exposed here, but a sample from the basal bed along the strike southward indicates closer equivalence with OC-4 than with GC-1. A few additional samples which overlap these separated short sections were examined, but less thoroughly, and so are not included in Table 1. Samples from the intermediate Coal Mine Canyon section were also examined, and relations between the Canoas of different areas is considered in the discussion of correlations. Samples from many other parts of the world, including the type areas of some European stages, have had preliminary study, and the occurrences of species in these samples are indicated in the systematic descriptions.

METHODS OF STUDY

These very small fossils pose some special difficulties in their study, and techniques have not yet received adequate attention. Some simple and rapid methods were necessary for the examination of the many samples required to gain any idea of their distribution and value in biostratigraphy, and this procedure is briefly outlined. More elaborate studies, including examination with the electron microscope, will be needed in attempts at a more satisfactory classification.

Disintegration of the very small sample (less than 1 cc. is needed) commonly requires only soaking in water with some agitation, ultrasonic equipment being advantageous for indurated samples. More drastic treatment is seldom needed, as the tiny microfossils are apt to be poorly preserved and doubtfully identifiable when isolated by disintegration of much lithified shale or limestone.

Concentration of the fossils by some means of separating them from clastic particles of comparable size has not yet proved satisfactory. A pipette sample taken after an appropriate settling time will eliminate most particles above 30–40μ. Another settling within the pipette permits discarding a drop which includes other particles larger than about 30μ, and this is followed by placing two or three drops from the pipette on a large glass slide before much of the finest clay-size material (less than 2–3μ) has settled out. The material is spread on the slide and dried on an electric hot-plate; Canada balsam with xylene is then spread over it and a large cover glass pressed on to complete the simple preparation for microscopic examination. Before microscopic study it is usually desirable to dry the balsam by leaving the slide in an electric oven for several weeks, in order that specimens may become fixed in position if their coordinates from a mechanical stage are to be recorded.

Known species are usually identifiable in such a permanent Canada balsam slide, even though fixed in one orientation. For study and description of new forms, however, various orientations are necessary, and a second slide for this purpose may be prepared from additional drops from the same pipette sample. After being spread and dried on the slide, the fine material is scraped together from the tight adherence on the slide and dispersed in a few added drops of a viscous liquid such as the silicone Kel-F (Cargille Laboratories, New York). A large cover glass on such a preparation can be shifted around sufficiently to vary the orientation of the specimen under microscopic view. Advantages of the silicone over a viscous Canada balsam with xylene include its lower index of refraction, providing greater relief of calcite elements in most orientations, and the fact that this preparation will remain indefinitely viscous and inert to the calcite skeletal remains. Mounting media such as diaphane (Will Corp., Rochester, N. Y.), in which specimens show more relief than in Canada balsam and which will harden into permanent mounts, may prove useful for some purposes.

A magnification of about 500× is convenient and sufficient for most examination and photography, although double this magnification with an oil-immersion lens is necessary for the study of the smallest forms (less than about 5μ) and for details of some larger forms. A microscope with binocular head is obviously a great advantage, but this needs to be combined with polarizing equipment and a rotating stage, such as those now available in the Zeiss Standard WL Pol microscope.

The appearance under polarized light, and especially with crossed nicols, is very distinctive for many species and indicates the diagnostic microstructure of the large groups of heliolithid or ortholithid character (Deflandre, 1950) discussed under taxonomy. The extinction position of the calcite elements and the curvature of the extinction lines resulting from the crystallite arrangement in coccoliths and other forms of heliolithid character are important, not only for recognition of specific differences, but also for indicating whether the specimen under microscopic examination is oriented with the distal or proximal side up. Sinistral curvature of the crossed extinction lines consistently indicates the distal side of all coccoliths of the genus *Discolithus* examined, but dextral curvature of the extinction lines in distal view is usual for certain other groups, as indicated in the systematic descriptions. Questionable orientation in plan view of oval-shaped coccoliths, fixed in a permanent mount, can also be resolved by rotation of the stage to another position under crossed nicols. In this position, the two extinction-line arcs of the oval forms resemble those of the bisectrix interference figure of a biaxial mineral, and the position with the two arcs most separated relative to the orientation of a polarization plane indicates which side of the coccolith is oriented upward. Some of the forms photographed with crossed nicols are shown with the two arcs thus separated (pl. 2, fig. 9c), and others are photographed with orientations at 90 degrees to that position and thus show the curvature of the crossed extinction lines (pl. 2, fig. 5b). Study of the extinction lines in various positions of rotation of the stage, especially with the use of a universal stage, could provide other data on the crystallite arrangement or microstructure (Kamptner, 1954) otherwise evident only from electron microscope examination. Some species are more conspicuous and show a more distinctive character with crossed nicols than in normal transmitted light, as illustrated in plate 3, figures 1a, 1c, and plate 7, figures 11–12.

Some use has been made of a process for replacing the calcite of the skeletal remains with fluorite by treating a sample with dilute hydrofluoric acid. This treatment eliminates most of the clay and other fine clastic particles, thus concentrating the specimens, and the general form and even most details of specimens are surprisingly well replaced by the fluorite (see pl. 2, fig. 3). However, the important structural characters revealed by examination in polarized light cannot be determined after replacement by the isotropic fluorite.

Small forms (less than 4μ) are not distinctive unless studied with the electron microscope, and therefore have been neglected in this study. The electron microscope has shown quite distinctive characters for coccoliths only 2–3μ in size, and remarkable details appear, especially in carbon replicas from which the original calcite, opaque to the electron beam, has been dissolved. Although such detailed study is essential for an improved classification, it seems hardly practicable for obtaining much information in the near future on the distribution of fossil forms in space and time, which requires examination of the many forms in each of many samples. The form taxa recognizable otherwise may thus ultimately be subdivided by such detailed studies, but this should only refine and not seriously alter any previous biostratigraphic interpretations.

Not only the smallest forms have therefore been neglected here, but also some nondescript forms of larger size, which show little character for satisfactory specific definition and recognition elsewhere. The genus *Thoracosphaera* (pl. 9, fig. 11) is not recorded in the tabulation because most specimens of this large and robust form were eliminated in the settling separation. Their recovery by special treatment seemed of little value because it is doubtful that more than one species of *Thoracosphaera* is recognizable, similar forms ranging throughout the Tertiary and still living. Rare lopadoliths (pl. 5, figs. 19–20) likewise are not recorded.

Although the photographs of many specimens are not very satisfactory because high magnification gives little depth of focus, such reproductions are obviously more realistic and objective than the supplementary drawings. Refraction of light into some specimens may produce lines and effects that could be misleading unless the focus were varied, but the focus selected for the photographs is intended to minimize such effects. The depth of focus in side- and oblique-view orientations made drawings of these views seem advisable, especially as such orientations were obtained in the viscous mounting medium with specimens first identified in the usual plan view. However, a few specimens were successfully photographed in this viscous liquid, which indicates that this process might have been more commonly utilized. In order to resolve questions of orientation of specimens photographed in permanent slide preparations, sketches of the extinction lines between crossed nicols were made after the specimens had been oriented with their distal sides upward in the viscous medium.

The distribution shown in Table 1 is intended to indicate very approximately the order of relative abundance of the species listed. It is not based on counts, which seemed doubtfully justified for the purposes of this study. The symbols for common and abundant may therefore not be entirely consistent, and they undoubtedly overlap; the same is true of the symbols for common and few and for few and rare, but any greater discrepancies than these are improbable. The symbol for few is intended to indicate about 10 specimens out of perhaps a thousand noted among the many more that were included in most slides. Even the rough approximations should be significant, however, and may aid in the recognition of topotype specimens, although few species were described without a considerable number of specimens for examination.

PROBLEMS OF INTERPRETATION

Apart from the usual taxonomic problems and those related to the interpretation of age and other relations of the assemblages (discussed under special headings), two problems present greater difficulties than with most groups of fossils. The small size and delicacy of these forms results in poor preservation from diagenetic changes in some strata. Corrosion and secondary deposition of calcite thus may modify specimens so much that identification with any assurance is impossible. Another result of their very small size and great abundance is that fossil specimens are easily reworked from eroded strata and may be widely redistributed. Both of these problems require preliminary study and experience in the field of work, and critical observations and consideration of the evidence. Much confused and misleading data may thus appear in papers representing a first investigation with no consideration of these serious problems.

Partial or complete solution of such tiny calcareous forms is common on the deeper parts of the present ocean floor. Solution because of comparable conditions seems unlikely in the shallower-water accumulations of most strata, although solution is possible in accumulations associated with much organic matter. Many occurrences of marked corrosion and particularly of secondary growth seem, however, related to a diagenetic process after burial, generally increasing with greater burial and age and with deformation of strata. Secondary recrystallization may largely or completely obliterate recognizable remains in some fine-grained limestones, as was indicated for some of Cretaceous age (Bramlette, 1958). Unusually heavy specimens with abnormal amounts of calcite in some other occurrences, however, may be due to heavy growth of the nannoplankton in surface waters that were especially favorable for calcite deposition. This is suggested in samples where only certain species show an unusually heavy form and especially in such occurrences as Lodo samples 37 and 38, where specimens are generally heavier than those in samples immediately below or above and thus with no differences in depth of burial or other evident factors that might affect diagenetic processes.

Familiarity with distinctive species in various occurrences may permit identification with some assurance in an occurrence where specimens are considerably heavier than normal. However, identifications and descriptions of new species have been made by some workers from samples in which the specimens were too greatly modified by corrosion or secondary growth to be of any value.

These fossils, generally ranging between 2 and 20μ, may be easily transported after erosion from older strata. This reworking and redistribution is very important in some regions where such tiny fossils are common in the source rocks of later deposits and is especially striking in regions near the Pyrenees and Alps. Many other regions, however, show a succession of species ranges constituting zones without indications of the admixture of specimens from older strata, which were either barren of such fossils or were not then subject to nearby erosion. To recognize such redistribution where it has occurred and yet not to invoke this explanation to account for unexpected extensions of the life range of a species presents a serious problem requiring much critical attention.

The very marked difference between the large number of distinctive forms of the late Cretaceous (Maestrichtian) and those of the early Tertiary (including the Danian) is evident in many regions of Europe and America, in Egypt, Pakistan, and New Zealand (Bramlette, 1958). In southwestern France this marked difference is found with no admixture of the Maestrichtian forms in overlying Danian strata. Rare specimens of the abundant forms of the Upper Cretaceous appear in the Upper Paleocene and Lower Eocene (Ypresian or Cuisian) of this area, and a few occur in the lower Lutetian. As a result of the Middle Eocene deformation of the Pyrenees, however, a great abundance of Upper Cretaceous forms admixed with abundant specimens of many Paleocene and Lower Eocene species occurs in the late Middle Eocene and later strata of the region. The great number of reworked older specimens exceeds the many indigenous forms in the Upper Eocene of the Côte des Basques section at Biarritz, although they are much less common in equivalent strata at localities about 30 kilometers north of the Pyrenees. A nonmarine clay of Oligocene age in Provence, received from Deflandre, contains many specimens of Upper Cretaceous and early Tertiary forms (for locality see Deflandre, 1959, p. 133).

A comparable mixing of Cretaceous forms with those from various parts of the early Tertiary appears conspicuously in regions about the Alps in strata deposited after the mid-Tertiary deformation of the Alps. Obviously, any range chart from such a region which merely connects the earliest and latest occurrence of a species is meaningless if it does not indicate distribution in intermediate strata. Consideration of the relative abundance and conditions of preservation of specimens may assist in resolving problems of possible reworking. Data on distribution in many regions, however, are obviously necessary for interpreting the time range of a species; fortunately, the succession seems little affected by such reworking in many places. The possibility of redistribution nevertheless makes the earliest occurrence the most trustworthy part of the observed range in any interpretation of the actual life span of a species represented by such small fossil remains.

The Lodo section of California shows little evidence to suggest reworking of the material, except for rare specimens in the upper part of the Lower Eocene (Unit 3). The distributions shown in Table 1 indicate a remarkably abrupt termination of the range of many of the common species of the Paleocene, so abrupt as to suggest some discontinuity. All the common and easily recognizable species of the Paleocene, however, have been found sporadically but only as very rare specimens in samples from the upper part of the Lower Eocene strata (Unit 3). The only exception is that some of the Braarudosphaeridae reappear in considerable numbers in the Lower Eocene and are also known in the Eocene of other regions. Although these rare specimens may represent a sparse survival into the Eocene of species common only in the Paleocene, available evidence seems to favor the interpretation that they were reworked from the Paleocene.

This problem, as related to the actual life span of these particular species, seems especially important because of the wide geographic distribution known for most of them. Examination of other areas in California and additional ones elsewhere seems necessary, but the following considerations appear to indicate some redistribution into the Lower Eocene. None of these forms reappears in appreciable numbers in the Lower Eocene strata here, and none of them is as yet known in the Eocene elsewhere except where they are evidently reworked into distinctly later strata, as in the area north of the Pyrenees. Some redistribution is also indicated by the fact that these forms were apparently derived from two distinct biostratigraphic units, some of them occurring in Unit 1 but not in the latest Paleocene (Unit 2), and others occurring in the latest Paleocene (Unit 2) but not in Unit 1 nor in the lowest Eocene. Some reworking of underlying material into the Lower Eocene might be expected because the Cantua Member occurs as a large sandstone lens in the Lower Eocene part of the Lodo Formation a few miles to the south, indicating some uplift or increased erosion. This is also suggested by the absence of Paleocene strata at the base of the Lodo Formation farther south, as reported by Laiming (1940, p. 557).

Pending final resolution of this problem in the Lodo section, the rare and sporadic Lower Eocene occurrences of forms apparently redistributed from the Paleocene are recorded as "(reworked?)" in the discussions of distribution under the systematic descriptions.

BIOSTRATIGRAPHIC ZONES

The species distributions recorded in Table 1 indicate six biostratigraphic units, numbered from Unit 1, at the base and thus with its lower limit undefined, up to Unit 6, with its upper limit not defined here. Although the other units (2–5) are locally well defined by the range relations of many species, their delimitation as biostratigraphic zones with a designated species name seems best deferred until the sequence is similarly delimited in more than one area. The later discussion of correlations and age assignments indicates, however, that these local biostratigraphic units may be related to zones in similar succession that can be recognized widely, although they are not yet adequately delimited in the other regions.

The indicated range of any taxon may have only very local significance, except for the few taxa that show phylogenetic lineages in the local succession. The kind of biostratigraphic zone considered here, however, is a range zone based on the overlaps in the ranges of a considerable number of the species. Few of them are apt to be restricted to the zone, and the zone is recognized primarily by the association of those species having their highest (latest) occurrence in the zone with some others having their lowest (earliest) occurrence in the zone. On the other hand, a large number of coincident range limits, such as between Units 2 and 3, suggests a discontinuity either in the depositional record or of facies. Certain of the six biostratigraphic units may justifiably receive provisional zonal names, at least for the convenience of present discussion. The taxon used for a zonal name, however, is only one of those whose range seems significant in delimiting the zone, and the range of this taxon need not correspond even locally with the limits of the zone. Such a zone is thus quite different from the particular taxon's biozone, which is defined by the range of that taxon alone. *Discoaster tribrachiatus* is common in Unit 3 and happens to be locally limited to it. Because the species occurs also in other regions in strata in which the range relations of associated species are very similar, the name *Discoaster tribrachiatus* Zone appears to be appropriate for more than local or provincial use. Delimitation of the zone elsewhere, however, would be based primarily on the relations of the ranges of all associated taxa, and the range of *D. tribrachiatus* could extend into earlier or later strata of adjacent zones.

The six biostratigraphic units based on the calcareous nannoplankton, with provisional zonal names used for some, seem to correspond rather closely with the foraminiferal zones of Laiming (1940) that have been in common use in California. However, the strata included here in Unit 3 have been subdivided into several of these local foraminiferal zones, whereas Units 5 and 6 are not separated by the foraminiferal evidence. The biostratigraphic units are markedly unequal in terms of stratal thickness, as might be expected from varying rates of accumulation, and Unit 3 includes most of the Lodo Formation.

Biostratigraphic Unit 1 is represented in Table 1 by only two samples from the basal Lodo, as samples below and immediately above are barren of these fossils. The lower limit therefore cannot be delimited in this local section, and its upper limit is poorly defined because the sequence is interrupted by additional barren strata. Among distinctive forms not occurring in the overlying Unit 2 and known in similar association elsewhere are *Heliolithus riedeli*, *Discoaster helianthus*, and *Zygolithus junctus*. *Coccolithus bidens* and *C. eminens* are only locally restricted to this zone, and elsewhere their range extends up into the later Paleocene (Unit 2 equivalents).

Other species of the zone, but with known occurrences here and elsewhere in earlier or later strata, are indicated in the systematic discussions of species, and some also in the later discussion of correlations and age assignments. Although not well delimited locally, this biostratigraphic unit is apparently recognizable in a similar zonal succession in widely separated regions, and the name *Heliolithus riedeli* Zone seems appropriate for provisional use in the discussion of correlations. It appears to correspond closely with the local foraminiferal Zone E of Laiming (1940).

Biostratigraphic Unit 2 is quite distinct from Unit 1, although much of the abrupt change is doubtless related to factors involved in the intervening barren strata in this section. *Discoaster multiradiatus* s. l. is a conspicuous element of Unit 2. The more delicate varietal form (pl. 12, fig. 11) is locally dominant, but the typical form is the common one in equivalent strata of nearby localities of California and in most other occurrences. Although *D. multiradiatus* occurs rarely (possibly as reworked specimens) in the overlying Unit 3, its abundant and very widespread occurrence in strata having species range relations similar to those in Unit 2 suggests that the name *Discoaster multiradiatus* Zone may be appropriate for such strata. Among species with ranges now appearing particularly significant in delimiting the zone elsewhere are *Zygodiscus sigmoides*, *Zygrhablithus simplex*, *Zygolithus distentus*, *Rhomboaster cuspis*, and *Coccolithites distichus*. These common forms seem to have their latest known occurrence in the Paleocene elsewhere but occur locally as very rare specimens in Unit 3, although, as has been indicated, they may represent some local redistribution from Unit 2. Not questionable because of possible reworking, however, are the earliest known occurrences of many forms, which include *Lophodolithus nascens*, *Coccolithites delus*, *Clathrolithus ellipticus*, *Discoaster mediosus*, and *D. multiradiatus*. Unit 2 corresponds closely to the foraminiferal Zone D of Laiming (1940).

Biostratigraphic Unit 3 includes the upper 1050 feet, or most of the Lodo Formation. The assemblage is much the same throughout except for a general decrease in abundance of most species in the upper part. The change in the assemblage from that of Unit 2 is so marked and abrupt that it appears to indicate some considerable discontinuity either in recorded time or in facies. No conspicuous physical discontinuity is apparent, but it is perhaps significant that much glauconite is concentrated here. Similar general relations in the ranges of the species of Units 2 and 3 are known in other regions, but continuous sequences in these regions would presumably show more gradual change with more overlaps in species ranges than occurs in the Lodo section. Some transitional aspect is indicated only in the lower 40 feet of Unit 3 (samples 23 to 36 or 37). Although the similarities support its inclusion in Unit 3, this basal part has a somewhat larger number of species in common with Unit 2 than occur in the higher strata of Unit 3. The name *Discoaster tribrachiatus* Zone seems appropriate for the strata included in biostratigraphic Unit 3 and its equivalents elsewhere, as the species is locally restricted to the unit, although this is of less importance than its wide distribution with the associated species indicated in the later discussion of correlations and age assignments. Among many species locally restricted to Unit 3, those that are apparently equally restricted elsewhere include *Chiphragmalithus calathus*, *Discoaster diastypus*, and *Rhabdosphaera truncata*. Developments in a lineage involving *Lophodolithus nascens* also seem very significant, as this widespread species is nearly restricted to this zone. Many species have their earliest known occurrence in this zone, such as the common and widespread *Coccolithus grandis*, *Discolithus pulcher*, *Helicosphaera seminulum*, *Rhabdosphaera crebra*, *R. perlonga*, *R. scabrosa*, *Zygolithus dubius*, and *Discoaster lodoensis*. The lower part of Unit 3 corresponds to the foraminiferal Zone C of Laiming (1940), and the upper part to his less clearly defined Zones B4, B3, and B2. However, these upper subdivisions, based largely on benthonic foraminifera, are not apparent from the nannoplankton of the strata included in biostratigraphic Unit 3.

Biostratigraphic Unit 4 is represented in the finer-grained beds within and at the top of the otherwise barren Domengine Sandstone. Only two representative samples were thoroughly examined and are recorded in Table 1. Unit 4, for which the name *Chiphragmalithus acanthodes* Zone may prove appropriate, seems to be recognizable as a zonal unit in regions as distant as Europe. Although this species is not known to occur in large numbers, it appears to be significant because of a lineage indicating that it gave rise to *C. cristatus* in immediately overlying strata. Many of the species of Unit 3 have their latest occurrence in Unit 4, and among those which seem significant because of known occurrences elsewhere are *Coccolithus crassus*, *Rhabdosphaera crebra*, *R. morionum*, *R. perlonga*, *Coccolithites gammation*, *Clathrolithus ellipticus*, and *Discoasteroides kuepperi*. Among distinctive ones with their earliest known occurrence in Unit 4 are *Coccolithus expansus*, *Discolithus distinctus*, *D. panarium*, *Lophodolithus mochlophorus*, *Rhabdosphaera tenuis*, *Chiphragmalithus acanthodes*, *C. cristatus*, *Discoaster basquensis*, *D. nonaradiatus*, and *D. sublodoensis*. Unit 4 corresponds to the local foraminiferal Zone B1 of Laiming (1940).

Biostratigraphic Unit 5 is represented in the lower part of the "Canoas Member" of the basal Kreyenhagen Formation in the Oil City section and in the basal few feet of the Canoas Member near the type area on Garza Creek. Only three samples representing the unit were thoroughly examined and are recorded in Table 1. Most of the species of Unit 4 range up into this unit, although generally in lesser numbers. Among those having their latest known occurrence in this biostratigraphic unit are *Discolithus distinctus*, *D. panarium*, *Lophodolithus mochlophorus*, *Coccolithites delus*, *Chiphragmalithus acanthodes*, and *Discoaster sublodoensis*. Distinctive species with their earliest known occurrence in Unit 5 include *Discolithus exilis*, *D. fimbriatus*, and *Rhabdosphaera inflata*. Although this unit may not represent a very well defined one in other regions, similar range relations of most of the species even as far away as France, are indicated.

Biostratigraphic Unit 6 is represented by all but the basal few feet of the type Canoas Member of the basal Kreyenhagen Formation and extends upward in the Kreyenhagen to an upper limit not defined by the samples available for this study. Only two samples from the lower part of this unit on Garza Creek are recorded in Table 1. Although this unit is distinct from Unit 5 in the central California region, this may be largely a facies difference, and Unit 6 is not well characterized here by the appearance of many new species, except perhaps some small and nondescript forms. Further study of Unit 6 is therefore deferred until a better characterized equivalent from a sequence elsewhere may be examined and compared with Unit 6. *Chiphragmalithus*? *quadratus* is a distinctive form with wide geographic distribution, which is common in Unit 6, although a few specimens occur also in the uppermost part of the underlying unit. It seems to be one of the species of Unit 6 whose range may prove particularly significant.

CORRELATIONS AND AGE ASSIGNMENTS

The very widespread occurrence of many species of the calcareous nannoplankton is now evident; it is especially striking in the Cretaceous and early Tertiary, reflecting, like that of other fossils, the relative uniformity of the seas of that time. A comparatively short life span is indicated for many of these species by considerable (though still inadequate) data on their ranges, including a zonal sequence that is recognizable in widely separated regions. Much of the evidence bearing on correlations and age assignments cannot be reviewed because many species are still undescribed, and no evaluation of evidence from other groups of fossils can be attempted here.

Recognition with some assurance of a general succession similar to that of the biostratigraphic units delimited in the Lodo section seems possible in some regions as distant as the type areas of European stages. Although upper and lower limits will probably never be precise for any zones of such wide extent, further study of additional continuous sequences is obviously needed. Such sequences are not exposed, however, at most type localities of European stages, and the stage limits have remained undefined. The following discussion summarizes the evidence for correlating the local biostratigraphic units with those of some other areas, particularly with those closely related to the succession of early Tertiary stages in Europe, which thus offers some support to the age assignments.

Unit 1 (provisionally referred to as the *Heliolithus riedeli* Zone) includes strata which have been considered of Paleocene age from studies of the foraminifera and other fossils. The following considerations support this age assignment and suggest correlation with that part of the Paleocene represented by the type Thanetian Stage in England. The Strata underlying Unit 1 of the Lodo section are barren of nannoplankton fossils, but these lower strata have been assigned a Maestrichtian age from other evidence, and an unconformity is indicated at the base of Unit 1. However, at Borreguero Spring, about 13 miles to the southeast, strata correlating well with biostratigraphic Unit 1 are immediately underlain by strata containing species having range relations similar to those of the type Danian. Few of the many and distinctive species of the Maestrichtian have ranges extending up into the Danian of any known region (Bramlette, 1958). Forms such as *Zygrkablithus simplex*, *Zygodiscus sigmoides*, and *Zygolithus chiastus* are common in the type Danian but extend up into the Paleocene of Europe and likewise into Unit 1. The distinctive *Heliolithus riedeli* and *Discoaster helianthus* of Unit 1 occur in the type Thanetian and are as yet unknown in European strata of earlier or later ages. Except for a few poorly preserved and obviously reworked Cretaceous coccoliths, the species of the meager assemblage of the type Thanetian are all represented in the larger assemblage of Unit 1, including those forms which range either higher or lower in both regions. *Heliolithus riedeli* and others indicative of the zone occur in the Velasco Shale of Mexico, overlying strata assigned to the Danian and underlying strata with *Discoaster multiradiatus* and other species of Unit 2 in like association. A similar sequence is found in the lower Lizard Springs strata of Trinidad, with the *Heliolithus riedeli* Zone occurring in the *Globorotalia pseudomenardii* foraminiferal zone of Bolli (1957). The Nanafalia Formation of Alabama also includes *H. riedeli* and other species of Unit 1 and of the Paleocene elsewhere. Although the Nanafalia is commonly assigned to the Lower Eocene, the nannoplankton species of the basal Eocene elsewhere appear only in the stratigraphically higher Bashi Formation of Alabama. Loeblich and Tappan (1957) also presented evidence for considering the Nanafalia Formation of Paleocene age, based on a study of the pelagic foraminifera, and this problem thus seems to deserve more consideration.

Unit 2 (the provisional *Discoaster multiradiatus* Zone) is well represented in the Upper Paleocene of many regions, and the following considerations suggest equivalence with the largely nonmarine Sparnacian Stage of Europe. Many species identical with those of Unit 2, and with similar range relations, occur in the upper part of the Paleocene strata of southwestern France. These strata overlie those of the *Heliolithus riedeli* Zone (included in the type Thanetian) and underlie Cuisian strata considered to be of approximately the same age as the Ypresian and other Lower Eocene strata. The *Discoaster multiradiatus* Zone in France thus occurs in a similar stratigraphic position to that of the Sparnacian, which is generally considered the upper stage of the Paleocene. Similarly, *D. multiradiatus* and some of the

(436)

associated species of Unit 2 occur in Trinidad in the *Globorotalia velascoensis* Zone of Bolli, which is underlain by strata here assigned to the *Heliolithus riedeli* Zone and is overlain by the *Globorotalia rex* Zone of Bolli, which he assigns to the basal Eocene. Similar relations with the *Heliolithus riedeli* Zone in the Velasco Shale of Mexico were mentioned in the discussion of Unit 1. The *Discoaster multiradiatus* Zone seems to be recognizable in the Waipawan Stage of New Zealand and in the Paleocene of Algeria, but relations with other zones are not known in those regions. Nearly all the species in the Bashi Formation of Alabama are found in the Lodo, where their range relations result in a similar association in the uppermost part of Unit 2. However, some similarity of the Bashi assemblage to that of the basal part of Unit 3 suggests a more transitional aspect than appears in the Lodo section, where some discontinuity is indicated by the sharply marked difference between biostratigraphic Units 2 and 3. The following discussion of Unit 3 indicates the basis for its assignment to the Lower Eocene, and the Bashi Formation might thus be assigned to either the uppermost Paleocene or the basal Eocene from available evidence of the calcareous plankton. Unfortunately, the strata immediately overlying the Bashi are barren of these fossils.

Unit 3 (the *Discoaster tribrachiatus* Zone) includes strata that apparently correlate well with some part, at least, of the Ypresian Stage. Although none of the nannoplankton has been found in samples from the type Ypresian, relations with other Lower Eocene strata in Europe are indicated. The London Clay, which is a well-established equivalent of the Ypresian, seems to include few of these fossils, but the occurrence in it of *Discoaster tribrachiatus* and *Chiphragmalithus calathus* seems significant, as these forms are restricted to Unit 3. The Rösnaes clay of Rögle Klint, Denmark, also considered to be Ypresian, contains many species, and those which occur also in the Lodo section include forms that characterize Unit 3 by their range relations. *Discoaster tribrachiatus* is abundantly represented in the Rösnaes clay, as is *Lophodolithus nascens*, a species which appears to be especially significant because of a lineage recognizable in the Lodo succession, where the range of this form corresponds approximately to the limits of Unit 3. *Discoaster lodoensis* is also common, although in Europe, as in the Lodo, it ranges upward into strata assigned to the Middle Eocene, as do some of the other species in the Rösnaes clay. In Trinidad, the *Discoaster trichbrachiatus* Zone seems to be well represented in the *Globorotalia aragonensis* foraminiferal zone of Bolli, which he too assigns to the Lower Eocene. The Bashi Formation of Alabama may include the basal part of the *Discoaster tribrachiatus* Zone, but its greater similarity to the uppermost Paleocene Unit 2 is indicated in the preceding discussion of that unit.

Unit 4 is represented locally only in the Domengine Formation, which has been assigned to the Middle Eocene on the basis of various studies of the Mollusca, foraminifera, and other fossils. A zone similar to that delimited as Unit 4 is recognizable in strata generally assigned to the Middle Eocene in some widely separated regions. Although species restricted to the zone are not yet known, it seems clearly recognizable by the distinctive association of many species which have their earliest or their latest occurrences in Unit 4. Correlation with the type Lutetian is unsatisfactory as the strata of that stage represent a shallow-water facies, and very few of these or other planktonic fossils are present. However, the very large assemblage present in samples from the Tuilerie of Donzacq, southwestern France, many of which were described by Deflandre (1954), is from strata commonly assigned to the lower Lutetian. This assemblage is remarkably similar to that of Unit 4, although their correlation seems justified only because of the large number of associated forms which have range overlaps characteristic of the zone. Among the many species common to the two areas, *Lophodolithus mochlophorus* is especially significant because of the lineage showing the development of this species from *L. nascens* in Unit 4 of the California sequence. Higher strata of Lutetian age in southwestern France are discussed under Unit 5. Samples from the lower part of the Weches Formation (Middle Eocene) of southeastern Texas also contain an association of species very much like that of Unit 4, which likewise includes *L. mochlophorus* among the more significant elements. At least a part of the Tallahatta Formation of Alabama is apparently assignable to this zone, although the samples that are available have a rather meager assemblage.

Unit 5 is represented locally in the "Canoas Member" of the Kreyenhagen Formation in the Oil City section, and also in the basal part of the type area of the Canoas Member, on Garza Creek. The occurrence of this biostratigraphic unit in the 20 feet of clay beneath the Kreyenhagen Formation and overlying the "Avenal" Sandstone in Coal Mine Canyon, about 8 miles south of Oil City, is significant in connection with an interesting problem of local correlation. The basal one foot of this clay unit above the "Avenal" Sandstone can be assigned to Unit 4, but the remaining 19 feet, below a glauconite bed, seem to be clearly equivalent to Unit 5 in the "Canoas" overlying the Domengine Formation at Oil City. Unit 5 may not prove as well characterized as the underlying units for extension as a zone elsewhere, although strata of the middle Lutetian at Gibret in southwestern France have a surprisingly similar association of species. Among those in samples from Gibret now appearing particularly significant are abundant specimens of *Discoaster sublodoensis* and the peculiar and apparently quite restricted form *Rhabdosphaera inflata*. The upper part of the Weches Formation (Middle Eocene) in southeastern Texas appears to be equivalent to Unit 5, but available samples do not include a very large number of species.

Unit 6 was indicated in the preceding definitions of units as still inadequately characterized, and the upper limit has not yet been determined. Although it may prove to be of Upper Eocene age, the little evidence now available from this study suggests that it too should be included in the Middle Eocene.

TAXONOMIC PROBLEMS

Classification of most groups of the living nannoplankton is especially difficult, as reflected by the common use of the term Protista for many of them. The living coccolithophorids, which form the most important group of nannoplankton with calcareous skeletal elements, are usually classed with the unicellular algae because they photosynthesize food. However, they not only have a flagellate motile form, but Parke and Adams (1960) have observed ingestion and assimilation of foreign food particles (phagotrophy) among typical coccolithophorids. Their observations thus support the grouping as protists, and since the nomenclature of zoology rather than botany has commonly been applied, such usage is followed here.

Advantageously for paleontology, the classification of living coccolithophorids has been based largely on the calcareous skeletal elements (various forms of coccoliths, rhabdoliths, etc.). However, attempts at a natural classification remain very unsatisfactory. Details of form and microstructure of the coccoliths obtained from studies with the electron microscope are proving important in nomenclature, but cultures (Parke and Adams, 1960) indicate complications in at least one species, owing to the alternation of generations having quite different forms of coccoliths for the single species. Some living species also have skeletal elements surrounding the oral opening which are quite different from the rest of the coccoliths on the coccosphere, and these two forms of coccoliths are normally dissociated after the death and disintegration of the organism. The usual difficulties encountered in classifying fossil forms with little similarity to modern species are thus increased.

An artificial classification based on morphologic similarities characterizing form-genera and species thus seems necessary at this time and may prove serviceable in biostratigraphy. Even though two form-species may prove to represent only a single species having two different skeletal elements, this finding would not alter stratigraphic interpretations based on records of their distribution in space and time. This distribution, by indicating consistently associated forms and their numerical ratio, might afford some evidence for recognizing dimorphous coccoliths from one species. Although many form- or parataxa seem necessary, two groups (*Coccolithus* and *Rhabdosphaera*) of the fossil species may be assigned to living genera, with at least as much assurance as with most fossils. These two genera, defined by the distinctive character of skeletal parts of the living species, are therefore recognized here, but they are also rather artificial taxa at present, and the precise and marked distinction of parataxa from the usual taxa as applied in paleontology may not be particularly significant. This more objective but quite artificial classification does not seem to justify elaborate grouping into hierarchies, which is therefore not followed here to any great extent.

Two major groups, classed as the orders Heliolithae and Ortholithae by Deflandre (1950), suggest a useful subdivision, although the distinguishing character is not applicable to some genera, and the phylogenetic significance is not yet apparent. The Heliolithae include forms composed of many fibrous elements or crystallites in more or less radial arrangement, as is usual in the coccolithophorids proper, and the Ortholithae include forms composed of a single calcite crystal, or crystals of like orientation, as in *Discoaster* and many other genera *incertae sedis*. This difference in microstructure is evidently important and is an obvious one, despite certain forms in which these characters are combined. The heliolithid character (as in the new genus *Heliolithus*) or the ortholithid character is emphasized here, but genera are not here assigned to these formal orders.

Kamptner (1958) made the most recent attempt to classify the calcareous nannoplankton, applying form-genus names to fossil groups of doubtful relation to living genera. Deflandre (1952*b*) followed a somewhat similar classification; in Deflandre and Fert (1954), he described a number of new paragenera and genera *incertae sedis*. Their generic usage is followed here in large part but without Kamptner's elaboration of family, subfamily, tribe, and subtribe groupings. All the coccolithophorids proper are included here, as by Lohmann (1902), in his family Coccolithophoridae. The latter, however, includes groups that may raise it to a higher taxonomic level than Deflandre's family Braarudosphaeridae, which is the only other family name used here. The many remaining forms are unassigned other than to genera *incertae sedis*.

SYSTEMATIC DESCRIPTIONS

Family Coccolithophoridae Lohmann

Genus Coccolithus Schwarz, 1894

An inadequately defined genus commonly used for coccoliths consisting of two elliptical plates joined rather closely by a hollow stud or tube, with the opening continuous through tube and plates. Distal plate larger than proximal one; both curved, with their concave surfaces on the proximal side.

This genus is well represented in the modern plankton by such species as *Coccolithus pelagicus*. Coccoliths of this type have been termed placoliths, and some of the fossil forms have been assigned to the paragenus *Tremalithus* (Kamptner, 1948). A special form-genus seems unnecessary, however, as coccoliths of this form are the main basis for characterizing the living genus *Coccolithus*. Assignment of the isolated fossil coccoliths to the paragenus *Tremalithus* until the complete coccosphere has been observed seems equally unnecessary, as the considerable number of modern and fossil species now recognized show little of the dimorphism of coccoliths on individual coccospheres found in some other genera.

Coccolithus bidens Bramlette and Sullivan, new species
Plate 1, figure 1

Description: Distal plate of the coccoliths (placoliths) with a steep, slightly concave outer slope and a slightly wider, smooth inner slope. Small tooth-like projections into the central opening are vague or absent in the long axis but present though not prominent in the short axis. Central opening transversely spanned by a robust x-shaped structure consisting of one straight and one sigmoid bar. Length 6–13µ, usually about 10µ.

Remarks: This species is similar to *Coccolithus grandis* except in the much smaller size of the coccoliths and the vagueness of the tooth-like projections, though two of them are apparent, especially between crossed nicols. Similarities and range relations indicate that *C. grandis* developed from this small form.

Holotype: U.S.N.M. 564177, Lodo 6+1.

Distribution: Locally abundant in Unit 1 (Paleocene). Occurs in the Paleocene of many regions, including the Nanafalia Formation of Alabama, the type Thanetian of England, and 2.95 km. south of Gan, France.

Coccolithus consuetus Bramlette and Sullivan, new species
Plate 1, figure 2a–c

Description: Coccoliths (placoliths) with two plates closely appressed, the larger normally showing clearly the straight-radiating striae on the wide, convex outer slope. Inner slope narrow; small central opening transversely spanned by an x-shaped structure. Length 8–16µ, usually about 14µ.

Remarks: Placoliths of this species may be distinguished from those of the several other species of *Coccolithus* with a central x-shaped structure by the wide, convex outer slope, narrow inner slope, and relatively small central opening.

Holotype: U.S.N.M. 564178, Lodo 73.

Distribution: Locally present throughout Units 1, 2, and 3 (Paleocene to Lower Eocene). Occurs in the Weches Formation (Middle Eocene) of Sabine River, Texas, and in the Paleocene 2.95 km. south of Gan, France.

Coccolithus crassus Bramlette and Sullivan, new species
Plate 1, figure 4a–d

Description: Coccoliths (placoliths) subelliptical to elliptical and high, with plates not closely appressed; the larger plate thin and indistinct between crossed nicols but showing straight-radiating striae in transmitted light, commonly marked enough to appear as small petals. Connecting tube robust and conspicuous. Central opening small. Length 10–13µ.

Remarks: These placoliths differ from many rather similar but less distinctive undescribed forms of this genus in that the thinness of the upper plate contrasts strongly with the heavy connecting tube. The two plates are less closely appressed than in most described species.

Holotype: U.S.N.M. 564179, Lodo 71.

Distribution: Locally common in the middle part of Unit 3 (Lower Eocene) and extending upward in lesser numbers into Unit 4 (Middle Eocene). Occurs in the lower Lutetian (Middle Eocene) of Donzacq, France.

Coccolithus eminens Bramlette and Sullivan, new species
Plate 1, figure 3a–d

Description: Coccoliths (placoliths) subelliptical or nearly circular and very high, with the two plates very closely appressed and cupped together so that the smaller is barely visible in side view. The steep, concave outer slope of the larger plate usually shows striae running to the periphery. Small central opening spanned by cross bars, the transverse one of which is the more conspicuous. Length 9–11µ.

Remarks: This small, almost circular form differs from most other members of the genus studied here in its unusual height and in having its small central opening occupied by cross bars aligned with the axes of the ellipse.

Holotype: U.S.N.M. 564180, Lodo 6+1.

Distribution: Locally present in Unit 1 (Paleocene). Occurs in the Nanafalia Formation (Paleocene) of Alabama, in the type Thanetian of England, and in the Paleocene 2.95 km. south of Gan, France.

Coccolithus expansus Bramlette and Sullivan, new species
Plate 1, figure 5a–d

Description: Coccoliths (placoliths) large, with closely appressed plates. Both outer and inner slopes of the upper plate narrow, the outer slope steep and slightly concave. Relatively large central opening transversely spanned by a wide, arching x-shaped structure. Length 15–23µ.

Remarks: These placoliths are distinctive in their large central opening as contrasted with the narrow surrounding rim. They differ from those of *Coccolithus oamaruensis* (Deflandre) (Deflandre and Fert, 1954,

(439)

p. 154) in having a more widely spread x-shaped structure with curved bars, and in the larger proportion of the central opening.

Holotype: U.S.N.M. 564181, Canoas OC–4.

Distribution: Locally present in Units 4, 5, and 6 (Middle Eocene). Occurs in the Weches Formation (Middle Eocene) of Sabine River, Texas, and in the lower Lutetian (Middle Eocene) of Donzacq, France.

Cococlithus gigas Bramlette and Sullivan,
new species
Plate 1, figure 6a–d

Description: Coccoliths (placoliths) unusually large, with closely appressed plates, the larger of which shows fine radiating striae on its wide, convex outer slope, which have a slightly sigmoid curvature, sinistral at the periphery in distal view. These striae extend onto the outer part of the inner slope, which is relatively narrow. Central opening transversely spanned by an x-shaped structure. Length 19–27μ.

Remarks: The placoliths of this species differ from those of *Coccolithus consuetus* in their much larger size, in the fineness and somewhat sigmoid curvature of the radiating striae, and in having fine "teeth" along the margin of the inner slope. They are larger than other species here included in the genus.

Holotype: U.S.N.M. 564182, Canoas GC–3.

Distribution: Locally present in Unit 6 (Middle Eocene).

Coccolithus aff. C. gigas Bramlette and Sullivan
Plate 1, figure 7a–d

Remarks: This form occurs in only the two lowermost samples, and as it does not differ greatly from *Coccolithus gigas*, a distinct taxonomic unit is not proposed here. Differences from the typical species and from the somewhat similar *C. consuetus* include the obscurity of the striae on the distal plate, which is also more delicate and shows little relief in contrast to the heavy connecting tube; many specimens show the x-shaped structure broken out, suggesting a delicate attachment. It also differs in size, being intermediate between the other two forms. The rather variable radial lines that mark the outer part of the inner slope are similar to those in *C. gigas*, although they are fewer in number and tend to extend farther inward toward the central opening. However, these differences may be due, at least in part, to localized conditions of less available calcium carbonate in the surface waters, as many other forms in these two samples also appear abnormally delicate.

Hypotype: U.S.N.M. 564183, Lodo 7.

Distribution: Locally common in Unit 1 (Paleocene), with very rare and sporadic occurrences in the upper part of Unit 3 (Lower Eocene). Occurs in the Paleocene 2.95 km. south of Gan, France.

Coccolithus grandis Bramlette and Riedel
Plate 2, figures 1a–b, 2a–c, 3

"Coccolith," Jukes-Browne and Harrison, 1892, Quart. Jour. Geol. Soc., vol. 48, p. 178, text-fig. 7.

Coccolithus cretaceus Archangelsky. – Deflandre, 1952, Traité de Zoologie (ed. P. P. Grassé), vol. 1, fasc. 1, p. 463, text-fig. 360d.

Coccolithus grandis Bramlette and Riedel, 1954, Jour. Pal., vol. 28, no. 4, pp. 391–392, pl. 38, fig. 1a–b. – Deflandre, 1954, *in* Deflandre and Fert, Ann. Pal., vol. 40, p. 152, text-fig. 48.

Remarks: Material from the type locality has been restudied. The original description fails to indicate the distinctive, small tooth-like projections that extend into the central opening between the bars of the wide x-shaped structure. The side view of the holotype shows less height than the average and distinctly less than that of the Lodo specimens; it also fails to show the steep, concave outer slope of the upper plate. The Lodo specimens range in length from 13 to 27μ, usually about 17μ.

Hypotypes: U.S.N.M. 564184–85, Lodo 67; and 564186, Lodo 80.

Distribution: Locally common throughout Units 3–6 (Lower and Middle Eocene). Common and very widespread in the Lower and Middle Eocene. The many occurrences include the Weches Formation (Middle Eocene) of Sabine River, Texas, and the lower Lutetian (Middle Eocene) of Donzacq, France.

Coccolithus solitus Bramlette and Sullivan,
new species
Plate 2, figure 4a–c

Description: Coccoliths (placoliths) with closely appressed plates, the larger having a steep, slightly concave outer slope and a slightly wider inner slope. Diameter of inner slope approximately equal to that of the lower plate, so that in transmitted light the placolith appears rather similar on both sides. Relatively large central opening transversely spanned by a somewhat delicate x-shaped structure. Length 9–13μ.

Remarks: These placoliths are distinguished from those of *Coccolithus bidens* of similar size by the lack of tooth-like projections into the central opening and by the more delicate x-shaped structure. Although they are easily distinguished from *C. consuetus* in the Lodo strata by the narrower outer slope without apparent striae, this distinction may be more difficult to observe elsewhere.

Holotype: U.S.N.M. 564187, Lodo 62.

Distribution: Locally present in the upper part of Unit 3 (Lower Eocene) and common in Units 4, 5, and 6

(Middle Eocene). Common in the Weches Formation (Middle Eocene) of Sabine River, Texas.

Coccolithus staurion Bramlette and Sullivan, **new species**
Plate 2, figures 5a–b, 6a–c

Description: Coccoliths (placoliths) large, with closely appressed plates, the larger distal one having conspicuous straight-radiating striae on the wide outer slope. Central opening small, with a small cross, obscure in some specimens, aligned in the axes of the ellipse. Length usually 12–15μ.

Remarks: This species is distinguished from the many forms of rather similar character by its large size and very small central cross, and from the even larger *Coccolithus eopelagicus* (Bramlette and Riedel) primarily by having a central cross. The hypotype (pl. 2, fig. 5a–b) is from the Weches Formation, which has better preserved specimens than our California samples.

Holotype: U.S.N.M. 564188, Canoas GC–2.

Hypotype: U.S.N.M. 564189, Weches Formation, Sabine River, Texas (Feray sample T.U. 245).

Distribution: Locally present in Unit 6 (Middle Eocene). Common in the Weches Formation (Middle Eocene) of Sabine River, Texas, and at Gibret, France (Middle Eocene).

Genus **Cyclolithus** Kamptner, 1948

An inadequately defined genus generally used for coccoliths formed as a single ring with a large central opening. The genus may be represented by several species in our samples, but the small size of most, together with their nondescript character, makes recognition difficult and questionable. Electron microscope examination seems necessary for such forms, which are therefore neither described nor otherwise recorded here, except for an unusual form that is questionably assigned to the genus.

Cyclolithus? robustus Bramlette and Sullivan, **new species**
Plate 2, figure 7a–c

Description: Specimens large, circular, forming a thick ring, one side of which shows oblique striae. Ring grooved so as to resemble two closely appressed rings in side view. Open central area large and bordered by a narrow inner rim. Diameter 9–15μ.

Remarks: The large size and especially heavy or robust ring are distinctive features of the species but make the assignment to the genus *Cyclolithus* questionable.

Holotype: U.S.N.M. 564190, Lodo 7.

Distribution: Locally common in Unit 1 (Paleocene).

Genus **Discolithus** Kamptner, 1948

An inadequately defined genus commonly used for coccoliths consisting of a single elliptical plate, generally somewhat curved, with the proximal side concave and either with or without a marginal rim on the distal side.

The many California species assigned to this genus show a sinistral curvature of the extinction lines when viewed from the distal side between crossed nicols. The full interpretation and significance of this phenomenon must await electron microscope study, and it is not included in the generic characterization. The opposite curvature of the extinction lines is shown only on the outer flange of *Discolithus fimbriatus*, but this is the only species recorded here in the group with such a flange extending out from the rim.

Discolithus distinctus Bramlette and Sullivan, **new species**
Plate 2, figures 8a–b, 9a–c

Description: Discoliths with a high, very thick rim, but thickness varies greatly. Heavy basal plate about half as thick as the height of the rim and much reduced in area in specimens with a thicker rim. Basal plate irregularly perforated by conspicuous pores and with a longitudinal line, which is interrupted in the middle. Length 12–16μ.

Remarks: This unusually robust form is easily distinguished, despite marked variations, by its very heavy rim and basal plate and its conspicuously perforated central area. The appearance between crossed nicols is also distinctive, with the thickness producing birefringence in yellow and red and up to green in the thicker rim area.

Holotype: U.S.N.M. 564191, Domengine OC–1.

Paratype: U.S.N.M. 564192, Domengine OC–2.

Distribution: Locally present in Units 4 and 5 (Middle Eocene) but more common in Unit 4. Occurs in the Weches Formation (Middle Eocene) of Sabine River, Texas, in the Middle Eocene of Trinidad, in the lower Lutetian (Middle Eocene) of Donzacq, France, and in the somewhat later Middle Eocene of the Carriere de Nousse, France.

Discolithus duocavus Bramlette and Sullivan, **new species**
Plate 2, figure 11a–d

Description: Discoliths with a low, thin rim and a thin basal plate having two widely separated circular openings at the ends of a longitudinal line. Length 10–13μ.

Remarks: The widely separated circular openings in the basal plate of this relatively simple form characterize the species.

Holotype: U.S.N.M. 564193, Lodo 36.

Distribution: Locally present in Unit 3 (Lower Eocene).

Discolithus exilis Bramlette and Sullivan, new species

Plate 2, figure 10a–c

Description: Discoliths with a thin rim and two very large openings, leaving little of the basal plate other than a narrow transverse part. This bridge widens at opposite sides near the rim. Length 13–15μ.

Remarks: This species differs from *Discolithus* aff. *pulcher* Deflandre in having larger discoliths with larger openings and a somewhat sigmoid transverse bridge, and in the absence of even vague furrows on the rim.

Holotype: U.S.N.M. 564194, Canoas OC–4.

Distribution: Locally present in Unit 5 (Middle Eocene). Occurs in the Cane River Formation (Middle Eocene) of Louisiana.

Discolithus fimbriatus Bramlette and Sullivan, new species

Plate 3, figure 1a–d

Description: Discoliths with a high, thin rim with numerous vertical furrows or slits and a wide but thin striated flange extending outward from the top of the rim. Basal plate thin and pierced by two circular openings. Length 15–16μ.

Remarks: Except for the rim, this form is indistinct in Canada balsam, the wide, thin flange and the basal plate with its central openings being difficult to see except between crossed nicols. It differs from *Discolithus panarium* in the presence of the flange and in the longer slits in the rim.

Holotype: U.S.N.M. 564195, Canoas OC–4.

Distribution: Locally present in Unit 5 (Middle Eocene). Occurs in the Weches Formation (Middle Eocene) of Sabine River. Texas.

Discolithus ocellatus Bramlette and Sullivan, new species

Plate 3, figure 2a–c

Description: Discoliths consisting of a thick plate without rim but thinning slightly toward the center. Central area with two small openings and bisected by a longitudinal line ending near the periphery. Length 9–12μ.

Remarks: The discoliths of this species are nearly complanate but have some thickening of the margin rather than a distinct rim. The strong relief in Canada balsam and the birefringence up to red indicate the thickness of the plate shown in side view.

Holotype: U.S.N.M. 564196, Lodo 67

Distribution: Locally present in Units 3, 4, and 5 (Lower and Middle Eocene).

Discolithus panarium Deflandre

Plate 3, figure 3a–d

Discolithus panarium Deflandre, 1954, *in* Deflandre and Fert, Ann. Pal., vol. 40, p. 141, text-figs. 39–40.

Remarks: The Lodo specimens appear indistinct in Canada balsam except for the rim, as do the topotype specimens examined. The rim is thin but well defined, with a row of small perforations at its base. The thin basal plate normally has two circular openings, difficult to see except between crossed nicols, with a longitudinal line between them. The perforations and two larger openings are usually not as well developed in the topotype specimens, and the two larger openings are not mentioned in Deflandre's description. The Lodo specimens, however, seem to be properly included in his species. Specimens were found ranging in length from 11 to 19μ.

Hypotype: U.S.N.M. 564197, Canoas OC–4.

Distribution: Locally present in Units 4 and 5 (Middle Eocene). Occurs in the Weches Formation (Middle Eocene) of Sabine River, Texas; recorded from the lower Lutetian (Middle Eocene) of Donzacq, France.

Discolithus pectinatus Bramlette and Sullivan, new species

Plate 3, figures 4a–b, 5a–b

Description: Discoliths with a thin rim pierced by about 25 narrow vertical slits. Basal plate thin and bisected by a longitudinal line, interrupted toward the middle by two small circular openings. Length 9–13μ.

Remarks: As in *Discolithus pulcher*, the side view of this form clearly shows the vertical slits in the rim. It is distinct from *D. pulcher*, however, in that the central openings are circular rather than semicircular, it is smaller with more of the basal plate present, and the basal plate is bisected by a longitudinal line. Variants of *D. pectinatus* with shorter slits in the rim (pl. 3, fig. 5a–b) differ from *D. panarium*, which has the openings confined to the junction of rim and plate. *D. panarium* is also larger and appears vague in a Canada balsam mount except for the rim.

Holotype: U.S.N.M. 564198, Lodo 67.

Paratype: U.S.N.M. 564199, Lodo 80.

Distribution: Locally present in Units 3–6 (Lower and Middle Eocene). Occurs in the Weches Formation (Middle Eocene) of Sabine River, Texas.

Discolithus planus Bramlette and Sullivan, new species
Plate 3, figure 7a–c

Description: Discoliths consisting of a thick plate without rim, thinning only slightly toward the center. Central area smooth, bisected by a longitudinal line which is indistinct in the middle part. Length 7–11μ.

Remarks: This is another of the simple forms with nearly uniform thickness of the plate and without a rim. It differs from *Discolithus ocellatus* in not having the two openings in the plate.

Holotype: U.S.N.M. 564200, Lodo 70.

Distribution: Locally rare throughout Units 3, 4, and 5 (Lower and Middle Eocene). Occurs in the Weches Formation (Middle Eocene) of Sabine River, Texas, and in the lower Lutetian (Middle Eocene) of Donzacq, France.

Discolithus aff. D. planus Bramlette and Sullivan
Plate 3, figure 6a–b

Remarks: This very thin form is difficult to distinguish from especially thin specimens of the normally thick *Discolithus planus*. The typical form is absent, however, from the lower part of the section, where this thin form is most common. Recording it separately as *D.* aff. *planus* permits a provisional distinction, although this form may prove to be only locally significant.

Hypotype: U.S.N.M. 564201, Lodo 32.

Distribution: Locally common in Unit 2 (Paleocene) and rare in Unit 3 (Lower Eocene). Occurs in the Bashi Formation (Paleocene or Lower Eocene) of Alabama.

Discolithus pulcher Deflandre
Plate 3, figure 8a–c

Discolithus pulcher Deflandre, 1954, in Deflandre and Fert, Ann. Pal., vol. 40, p. 142, pl. 12, figs. 17–18.

Remarks: The California specimens appear identical with topotypes of the species. The species typically has a rim with distinct vertical slits and a basal plate with two semicircular openings, leaving a narrow bridge-like transverse portion between them.

Hypotype: U.S.N.M. 564202, Lodo 36

Distribution: Locally present in Units 3, 4, and 5 (Lower and Middle Eocene). Recorded from the lower Lutetian (Middle Eocene) of Donzacq, France.

Discolithus aff. D. pulcher Deflandre
Plate 3, figures 9a–b, 10

Remarks: This form with only vague or no slits or furrows in the rim grades into those with well-developed slits like the typical species. The transverse central part of the basal plate, however, is usually more oblique than in the typical species, and this form appears somewhat lower in the Lodo section.

Hypotypes: U.S.N.M. 564203–04, Lodo 67.

Distribution: Locally present throughout Units 2–5 (Paleocene to Middle Eocene). Occurs in the Weches Formation (Middle Eocene) of Sabine River, Texas, and in the lower Lutetian (Middle Eocene) of Donzacq, France.

Discolithus punctosus Bramlette and Sullivan, new species
Plate 3, figure 11a–c

Description: Discoliths consisting of a plate without rim but thinning slightly toward the center and irregularly perforated by many pores. Central area bisected by a longitudinal line, interrupted toward the middle by two openings only slightly larger than the pores. Length 9–11μ.

Remarks: The discoliths of this species are distinct in being nearly uniform in thickness, without the rim and thin basal plate common in the genus, and in having perforations over an unusually large part of the surface.

Holotype: U.S.N.M. 564205, Lodo 36.

Distribution: Locally rare in Unit 3 (Lower Eocene).

Discolithus rimosus Bramlette and Sullivan, new species
Plate 3, figures 12a–c, 13

Description: Discoliths consisting of a very thick plate, with thickness up to about one-half the length. Distinct rim lacking, but, plate thins toward the longitudinally elongate, irregular central opening, which varies greatly in width. Distal surface commonly shows irregular depressions extending into the central opening. Length 9–12μ.

Remarks: This species is distinct in the strong relief in Canada balsam due to its thickness and the orientation of the calcite crystallites, and also in the single, irregular, elongate central opening.

Holotype: U.S.N.M. 564206, Lodo 19.

Paratype: U.S.N.M. 564207, Lodo 22.

Distribution: Locally present in Units 1 and 2 (Paleocene), with rare occurrences in Units 3, 4, and 5 (Lower and Middle Eocene). Occurs in the lower Lutetian (Middle Eocene) of Donzacq, France, and in the Paleocene 2.95 km. south of Gan, France.

Discolithus solidus Deflandre
Plate 3, figures 14a–c, 15

Discolithus solidus Deflandre, 1954, *in* Deflandre and Fert, Ann. Pal., vol. 40, p. 141, pl. 12, figs. 14–16.

Remarks: These very small but thick forms appear identical with topotype specimens. A short spike in the middle of the distal side is commonly present, and more depression around the six small holes is evident on this side (pl. 3, fig. 14a). Other characters of this small species are difficult to determine, but the strong relief in Canada balsam also aids in specific identification. Retention in the genus *Discolithus*, however, is only provisional.

Hypotypes: U.S.N.M. 564208, Lodo 67, and 564209, Domengine OC–2.

Distribution: Locally present throughout Units 2, 3, and 4 (Paleocene to Middle Eocene). Occurs in the Weches Formation (Middle Eocene) of Sabine River, Texas; recorded from the lower Lutetian (Middle Eocene) of Donzacq, France.

Discolithus versus Bramlette and Sullivan, **new species**

Plate 3, figure 16a–d

Description: Discoliths with a low rim and thin basal plate, bisected by a longitudinal line, which is indistinct toward the middle. Length 8–12μ.

Remarks: The distinct rim is the only obvious difference between this species and *Discolithus planus.*

Holotype: U.S.N.M. 564210, Lodo 67.

Distribution: Locally present in Units 3 and 4 (Lower and Middle Eocene). Occurs in the lower Lutetian (Middle Eocene) of Donzacq, France.

Genus **Helicosphaera** Kamptner, 1954

This hitherto monotypic genus was originally characterized by coccoliths having two asymmetrical plates appearing as a helicoid form, with a bridge across the central opening.

Coccoliths here assigned provisionally to the genus show little of the helicoid form indicated by Kamptner (1954, pp. 21–23) for *Helicosphaera carteri.* However, our examination of that living species showed such a helicoid form only in an overlap on the larger (distal) plate, and revealed similarities to the Eocene form *H. seminulum* discussed below. Several species apparently intermediate in character and in age need further study for proper generic assignment and may reveal a phylogenetic sequence.

Helicosphaera seminulum Bramlette and Sullivan, **new species**

Description: Coccoliths consisting of two curved plates, both concave on the proximal side and somewhat asymmetrical in plan view, the distal plate larger. The two plates are closely joined at the small end and partly along one side but are distinctly separated at the large end. Small central opening spanned by a thick bar. Length 10–15μ.

Remarks: As mentioned in the discussion of this genus, the helicoid form is not evident in this species, but it seems less pronounced in *Helicosphaera carteri* than indicated by Kamptner (1954, pp. 21–23). Similarities in the two species include the same asymmetry in side view due to the plates being closely joined at their small end, and the arrangement of the crystallite components appear the same between crossed nicols.

Helicosphaera seminulum seminulum Bramlette and Sullivan, **new subspecies**

Plate 4, figures 1a–c, 2

Description: This subspecies has the oblique bar more nearly parallel to the transverse than the longitudinal axis. Length 10–13μ.

Remarks: The bar is usually more oblique to the transverse axis in specimens from the upper part of the Lodo section, and thus seems gradational into the later subspecies.

Holotype: U.S.N.M. 564211, Lodo 67.

Paratype: U.S.N.M. 564212, Lodo 67.

Distribution: Locally common through most of Unit 3 (Lower Eocene) and rare in Units 4 and 5 (Middle Eocene). Common in the Lower and Middle Eocene of many regions, including the lower Lutetian (Middle Eocene) of Donzacq, France.

Helicosphaera seminulum lophota Bramlette and Sullivan, **new subspecies**

Plate 4, figures 3a–b, 4

Description: Differs from the nominate subspecies in being wider, especially at one end, and in having more distinct striae on the large end of the distal plate. The central opening is smaller, and the bar is more nearly parallel to the longitudinal than the transverse axis. Length 10–15μ.

Remarks: This subspecies is somewhat more similar to *Helicosphaera carteri* than the nominate subspecies in the greater asymmetry of the plan view outline. Between crossed nicols it shows a peculiar and distinctive crenulation in the extinction line across the larger end, which appears to be related to the coarse striae of this part. This subspecies is the more common form in the upper strata and appears to have been derived from the nominate subspecies of the lower strata. The specimen shown in plate 4, figure 4, seems to represent the intermediate forms.

Holotype: U.S.N.M. 564213, Canoas OC–4.

Paratype: U.S.N.M. 564214, Lodo 67.

Distribution: Locally rare in the upper part of Unit 3 (Lower Eocene) and common in Units 4 and 5 (Middle Eocene). Occurs in the Weches Formation (Middle Eocene) of Sabine River, Texas, and in the Middle Eocene of Gibret and Donzacq, France.

Genus **Lophodolithus** Deflandre, 1954

"Coccolithe asymétrique, avec une différenciation par élargissement de l'un des pôles, dont la marge est généralement plus développée."

Additional study of the type species, *Lophodolithus mochlophorus*, from topotypic and California samples indicates that the characteristic asymmetry of the plan view has a corresponding asymmetry in side view, with the rim higher at the end with the wider flange. Polarized light reveals that the single transverse bar consists of at least two calcite segments with orientations differing from each other and from those of the elements in the adjacent part of the rim. This peculiar bar seems to be another significant feature of the genus, although it is not unique, as a similar one occurs in related forms lacking the asymmetry in shape, which are assigned to the new genus *Zygodiscus*.

Type species: Lophodolithus mochlophorus Deflandre, 1954.

Lophodolithus mochlophorus Deflandre
Plate 4, figure 6a–c

Lophodolithus mochlophorus DEFLANDRE, 1954, *in* DEFLANDRE AND FERT, Ann. Pal., vol. 40, p. 147, pl. 12, figs. 20–23; text-figs. 69–71.

Remarks: The Lodo specimens, as well as most topotype specimens, show the narrow end more rounded than the ogival or pointed shape indicated by Deflandre's holotype. However, the wide end of the rim is even more broadly rounded, and the species is distinctive in the degree of this asymmetry and in having developed fine crenulations within the wide flange. The side view (pl. 4, fig. 6b) also shows a conspicuous asymmetry, with the rim distinctly higher at the end with wide flange. Development from *Lophodolithus nascens* is indicated in the discussion of that species.

Hypotype: U.S.N.M. 564215, Canoas OC–4.

Distribution: Locally present in Units 4 and 5 (Middle Eocene). Recorded from the lower Lutetian (Middle Eocene) of Donzacq, France; present in the Weches Formation (Middle Eocene) of Sabine River, Texas.

Lophodolithus nascens Bramlette and Sullivan, new species
Plate 4, figures 7a–c, 8a–c

Description: Coccoliths with a thin rim higher at one end and turned out at the top to form a narrow flange, which is distincly wider at the high end of typical specimens. Central opening spanned by a basal transverse bar, with the component calcite in more than one orientation. Length 10–16μ.

Remarks: Specimens are more conspicuous between crossed nicols than in normal light, especially the thin flange and the bar. The early forms of this species, with less asymmetry in height of rim and width of flange (pl. 4, fig. 8a–c), are similar to *Zygodiscus adamas* (pl. 4, fig. 10a–c), and appear to have developed from it. Specimens with a conspicuously wider flange at one end are present throughout the local range of this species, although they are more common in the upper part, where they differ from *Lophodolithus mochlophorus* only in the lack of crenulations within the flange at the broader end and in the less ogival shape of the rim at the opposite end. A lineage involving these species seems clearly indicated.

Holotype: U.S.N.M. 564216, Lodo 33.

Paratype: U.S.N.M. 564217, Lodo 33.

Distribution: Locally present in Units 2, 3, and 4 (Paleocene to Middle Eocene). Present in the Lower Eocene of Pakistan, Denmark, and the Marnière de Sourbé, east of Doazit, France; rare in the lower Lutetian (Middle Eocene) of Donzacq, France.

Lophodolithus reniformis Bramlette and Sullivan, new species
Plate 4, figure 5a–c

Description: Specimens reniform, with the rim slightly higher at one end and arched upward at the inturned side. Rim turned out at top to form a narrow flange, which is wider at the high end of most specimens. Central opening spanned by a transverse bar. Length 10–15μ.

Remarks: Although this form is distinguished from *Lophodolithus nascens* by its reniform shape in plan view, it is nevertheless closely related to that species. It resembles the genus *Nephrolithus* Gorka (1957, p. 282) only in general outline.

Holotype: U.S.N.M. 564218, Lodo 67.

Distribution: Locally present in Units 3 and 4 (Lower and Middle Eocene).

Genus **Rhabdosphaera** Haeckel, 1894

This genus is well represented by living species, including the type species, *Rhabdosphaera claviger* Murray and Blackman (1898). The basal plate of the elongate rhabdolith has a central hole, continuous with a canal in the superimposed high stem.

The paragenus name *Rhabdolithus* for fossil rhabdoliths seems unnecessary here, as rhabdoliths with the abovementioned features constitute the main basis for characterizing the living genus. Similar fossil forms may thus be assigned here with as much assurance as are many other kinds of fossils. Dimorphic forms on individual rhabdospheres are not known in *Rhabdosphaera*,

(445)

and assignment to a paragenus until the complete rhabdosphere is recognized also seems unnecessary on such a basis. Similar reasons were mentioned for using the name *Coccolithus* rather than the form genus name *Tremalithus*.

A circular basal plate is normal for rhabdoliths assigned to *Rhabdosphaera* but is perhaps of less fundamental significance than assumed by Kamptner (1958, p. 75), and, as Deflandre (1959, p. 137) has indicated, to distinguish it from slightly elliptical plates requires exact orientation of specimens, which is difficult to achieve with elongate rhabdoliths. Only two of the rhabdolith-like forms described here, however, have other than circular basal plates, and these two are otherwise peculiar and are only provisionally assigned to *Rhabdosphaera*.

Rhabdosphaera crebra (Deflandre)

Plate 5, figures 1–3

Rhabdolithus creber Deflandre, 1954, *in* Deflandre and Fert, Ann. Pal., vol. 40, p. 157, pl. 12, figs. 31–33; text-figs. 81–82.

Remarks: This common Eocene form is identical with topotype specimens in the shape of the stem and the enlargement or collar at the junction with the basal plate. Variation is evident only in the height (length of stem).

Hypotypes: U.S.N.M. 564219–21, Lodo 52.

Distribution: Locally present in Units 3 and 4 (Lower and Middle Eocene). Recorded from the lower Lutetian (Middle Eocene) of Donzacq, France. Also present in the Lower Eocene of Gan, France, and in the Weches Formation (Middle Eocene) of Sabine River, Texas.

Rhabdosphaera inflata Bramlette and Sullivan, new species

Plate 5, figures 4a–b, 5

Description: Rhabdoliths much inflated in middle part of stem, having a small circular base with small central opening. Slightly rugose stem enlarges not far above the base to a diameter greater than the base, and then tapers gradually to a sharp tip. Height 16-20μ.

Remarks: This distinctive form shows variations in height corresponding to the length of the tapering tip.

Holotype: U.S.N.M. 564222, Canoas OC–3.

Paratype: U.S.N.M. 564223, Canoas OC–3.

Distribution: Locally common in Unit 5 (Middle Eocene). Common in the Middle Eocene of Gibret and Carrière de Nousse, in southwestern France.

Rhabdosphaera morionum (Deflandre)

Plate 5, figures 12a–b, 13

Calyptrolithus morionum Deflandre, 1954, *in* Deflandre and Fert, Ann. Pal., vol. 40, p. 147, pl. 12, figs. 7–8; text-figs. 63–64.

Remarks: This peculiar and variable species is represented in the California material by some specimens similar to the holotype and by others with a range of variation comparable with that shown by topotype material. The low and inflated or bulbous stem is distinctive, but specimens with somewhat higher stems and less inflation near the base (pl. 5, fig. 13) are more like the usual rhabdolith. Between crossed nicols, the indicated arrangement of component crystallites, especially in the base, is also like that in *Rhabdosphaera*, and the species is therefore assigned to that genus.

Hypotypes: U.S.N.M. 564224, Lodo 58, and 564225, Domengine OC–2.

Distribution: Locally rare and sporadic throughout Units 3 and 4 (Lower and Middle Eocene). Recorded from the lower Lutetian (Middle Eocene) of Donzacq France.

Rhabdosphaera perlonga (Deflandre)

Plate 5, figure 7a–c

Rhabdolithus perlongus Deflandre, 1954, *in* Deflandre and Fert, Ann. Pal., vol. 40, p. 158, pl. 12, figs. 34–35; text-fig. 86.

Remarks: The forms assigned to this species include some that are identical with *Rhabdolithus perlongus* Deflandre, but also may include his *R. pinguis*, as the distinguishing features of the two species commonly seem obscure.

Hypotype: U.S.N.M. 564226, Lodo 71.

Distribution: Locally common throughout Unit 3 (Lower Eocene) and rare in Unit 4 (Middle Eocene). Recorded from the lower Lutetian (Middle Eocene) of Donzacq, France. Also present in the Lower Eocene of Gan, France, and in the Weches Formation (Middle Eocene) of Sabine River, Texas.

Rhabdosphaera? rudis Bramlette and Sullivan, new species

Plate 5, figure 6a–b

Description: Rhabdoliths urn-shaped, large, robust, and rugose. Base elliptical; stem in the form of a large round tube, rapidly flaring to the diameter of the base and then gradually tapering to a truncate tip. Stem buttressed by four ridges, which extend upward along the sides of the narrow lower part and appear as an X in proximal view, where they join the base. Central canal very large in middle part. Height 13–15μ.

Remarks: This robust and rugose form has a very distinctive character and is questionably assigned to the genus. Forms of somewhat intermediate character between this species and the peculiar Cretaceous form *Lucianorhabdus cayeuxi* Deflandre (1959, pp. 142–143) occur in the Paleocene of France, which suggests a possible phylogenetic series.

Holotype: U.S.N.M. 564227, Lodo 66.

Distribution: Locally rare and sporadic in Unit 3 (Lower Eocene).

Rhabdosphaera scabrosa (Deflandre)
Plate 5, figure 11a–b

Rhabdolithus scabrosus Deflandre, 1954, *in* Deflandre and Fert, Ann. Pal., vol. 40, p. 158, pl. 12, fig. 30; text-fig. 85.

Remarks: The uniform taper from base to tip and the slight rugosity of the stem are distinctive features of these specimens and of topotypes of the species.

Hypotype: U.S.N.M. 564228, Domengine OC–2.

Distribution: Locally present in the middle of Unit 3 and in Unit 4 (Lower and Middle Eocene). Recorded from the lower Lutetian (Middle Eocene) of Donzacq, France; common in the Weches Formation (Middle Eocene) of Sabine River, Texas.

Rhabdosphaera? semiformis Bramlette and Sullivan, **new species**
Plate 5, figures 8–9, 10a–b

Description: Rhabdolith-like in general form but lacking some of the normal features. Base on one side of the stem, and stem like a longitudinal half of a tapering tube. Height about 19μ.

Remarks: This very peculiar form is assigned very questionably to the genus *Rhabdosphaera*, as it is unlike all other species of the genus. It appears similar to a longitudinally split half of *Zygrhablithus bijugatus*. The many specimens, however, show no evidence of such breakage, and their restricted occurrence is not consistent with such an interpretation.

Holotype: U.S.N.M. 564229, Canoas OC–3.

Paratypes: U.S.N.M. 564230–31, Canoas OC–3.

Distribution: Locally common in Units 4 and 5 (Middle Eocene).

Rhabdosphaera tenuis Bramlette and Sullivan, **new species**
Plate 5, figure 14a–b

Description: Rhabdoliths with relatively small circular base and high, slender stem uniformly tapering to a sharp tip. Central canal small. Height about 25μ.

Remarks: This very elongate but otherwise rather nondescript form may prove difficult to distinguish from some rhabdoliths in the Upper Eocene but appears to be stratigraphically significant because it is the common form above the range of the other rhabdoliths recorded here, and the same range relations appear in the Eocene elsewhere. It is slightly rugose like *Rhabdosphaera scabrosa*, but the lower part of the stem is smaller in diameter and thus has distinctly less taper.

Holotype: U.S.N.M. 564232, Canoas GC–2.

Distribution: Locally present in Units 4, 5, and 6 (Middle Eocene). Common in the upper part of the Middle Eocene and in the Upper Eocene of many regions.

Rhabdosphaera truncata Bramlette and Sullivan, **new species**
Plate 5, figure 15a–b

Description: Rhabdoliths with circular base and an enlargement or collar above the basal plate. Stem nearly parallel-sided, though typically somewhat constricted in the middle part, and with truncate tip. Central canal large. Height 9–12μ.

Remarks: If specimens were rare and poorly preserved they might be interpreted as broken, but where they occur abundantly they consistently have the truncate stem.

Holotype: U.S.N.M. 564233, Lodo 37.

Distribution: Locally present in Unit 3 (Lower Eocene). Present in the Lower Eocene of the Marnière de Sourbé, east of Doazit, France.

Rhabdosphaera vitrea (Deflandre)
Plate 5, figures 16–17

Rhabdolithus vitreus Deflandre, 1954, *in* Deflandre and Fert, Ann. Pal., vol. 40, pp. 157–158, pl. 12, figs. 28–29; text-figs. 83–84.

Remarks: Like topotypes of this species, these rhabdoliths are small and have so delicate a stem that a canal, if present, is obscure. The basal plate is thin and rather flat but with a thickened collar at the junction with the stem. Figure 16 on plate 5 shows a specimen replaced by fluorite, and therefore the stem appears more distinct in Canada balsam.

Hypotypes: U.S.N.M. 564234, Lodo 52, and 564235, Lodo 67.

Distribution: Locally sporadic and rare in Units 3 and 4 (Lower and Middle Eocene). Recorded from the lower Lutetian (Middle Eocene) of Donzacq, France. Also present in the Cane River Formation (Middle Eocene) of Louisiana.

Rhabdosphaera sp.
Plate 5, figure 18a–b

Remarks: This small, nondescript rhabdolith, which occurs only in the Paleocene, is different from the other recorded forms but lacks distinctive features for specific identification.

Hypotype: U.S.N.M. 564236, Lodo 32.

Distribution: Locally present throughout Unit 2 (Paleocene).

Genus **Zygodiscus** Bramlette and Sullivan, new genus

Coccoliths with an elliptical rim, a transverse bar with more than one segment of different calcite orientation, and some vestige, at least, of a basal plate.

The genus thus has some features of three other genera: *Zygolithus*, *Discolithus*, and *Lophodolithus*, and is characterized by the combination of these features. The elliptical rim spanned by the transverse bar is like *Zygolithus*, but similarity to *Discolithus* is indicated by some extension of a plate into the basal area. The peculiar internal structure of the bar is unlike that of *Zygolithus* but identical with that of *Lophodolithus*, although *Lophodolithus* is distinctive in its asymmetry. In the discussion of *L. nascens*, progressive increase of the asymmetry in that species and possible development from *Zygodiscus* were indicated.

Between crossed nicols in distal view, the extinction lines across the rim and plate show a dextral curvature, as in *Lophodolithus* and *Zygolithus*, unlike the sinistral curvature usual in *Discolithus*. Although the bar appears uniform in normal light, the Quartz Red 1 plate with crossed nicols indicates at least two segments of the bar having different crystallite orientation, and both orientations are more nearly perpendicular than parallel to the length of the bar. Precise interpretation of the arrangement of component crystallites in the bar seems possible only from electron microscope examination of a carbon replica of the coccolith.

Type species: Zygodiscus adamas Bramlette and Sullivan, n. sp.

Zygodiscus adamas Bramlette and Sullivan, new species
Plate 4, figures 9a–c, 10a–c

Description: Coccolith with a thin rim of uniform height, turned out at the top to form a very narrow flange. Basal plate with inconspicuous to large openings on each side of the diamond- or lozenge-shaped transverse bar. Length 11–13μ.

Remarks: In polarized light the transverse bar shows the peculiar difference in crystallite orientation within segments characteristic of this genus and of *Lophodolithus*, as shown in plate 4, figure 10a–b. The openings in the basal plate are inconspicuous in early forms of the species but are increasingly larger in later forms, which thus have little of the basal plate. The lozenge-shaped form of the bar (fig. 9a) is also modified in the specimens with large openings (fig. 10a). These later forms thus resemble those early forms of *Lophodolithus nascens* which show little of the asymmetry in height of rim and width of flange that is characteristic of that species. The development of *Lophodolithus* from *Zygodiscus* thus seems well supported by forms of these two species having characters transitional between the two genera.

Holotype: U.S.N.M. 564237, Lodo 32.

Paratype: U.S.N.M. 564238, Lodo 32.

Distribution: Locally present throughout Unit 2 (Paleocene) and in the basal part of Unit 3 (Lower Eocene).

Zygodiscus plectopons Bramlette and Sullivan, new species
Plate 4, figure 12a–d

Description: Coccoliths with a thick rim thinning toward the central opening, which is restricted to less than half the total width and is spanned by a thick transverse bar having the complex crystal orientations characteristic of the genus. Length 7–9μ.

Remarks: The concave slope of the rim on the distal side of specimens results in a thinning inward that is gradual, unlike the usual abrupt change from rim to basal plate of discoliths, although this is not very obvious in plan view. The bridging bar appears uniform in normal light but in polarized light it is seen to consist of two twisted longitudinal segments of different crystal orientation, although both orientations are more nearly perpendicular than parallel to the length of the bar. The bar is thus quite distinct from that of *Zygolithus*, which it resembles otherwise more than do the other species of *Zygodiscus*.

Holotype: U.S.N.M. 564239, Lodo 31.

Distribution: Locally common throughout Unit 2 (Paleocene) and very rare (reworked? specimens) in Unit 3 (Lower Eocene). Occurs in the Bashi Formation (Paleocene or Lower Eocene) of Alabama, and in the type Thanetian of England.

Zygodiscus aff. **Z. plectopons** Bramlette and Sullivan
Plate 4, figure 13a–e

Remarks: Perhaps subspecific distinction may prove desirable for this form, which is not only larger than normal for the species (9–13μ), but also shows somewhat more differentiation into rim and basal plate, although this is not apparent in plan view. It has a broader rim than is typical for the species, the central opening is restricted to one-third or less of the total width, and some specimens have the central area completely closed. Between crossed nicols, the extinction lines curve strongly as compared with the species, but this probably reflects their greater length because of the wider rim.

Hypotype: U.S.N.M. 564240, Lodo 6+1.

Distribution: Locally common in Unit 1 (Paleocene) and very rare (reworked?) in Unit 3 (Lower Eocene).

Zygodiscus sigmoides Bramlette and Sullivan, new species

Plate 4, figure 11a–e

Description: Coccoliths with a low rim and little of the basal plate except that which extends in from the rim along the sides of the transverse bar. This bar normally shows a sigmoid curvature, accentuated by the different orientation of the two calcite segments, which is apparent in polarized light. The bar is arched and commonly supports a central knob or very short stem. Length of base 9–11μ.

Remarks: Some extension from the rim of a partial basal plate, obscure in Canada balsam, is seen distinctly between crossed nicols (pl. 4, fig. 11d). It is unusual in that the orientation of component crystallites in the plate is quite different from that in the rim, as is evident with the addition of the Quartz Red 1 plate. This is an unusual feature for *Zygodiscus*, but otherwise the characters are similar to those of other species of the genus.

Holotype: U.S.N.M. 564241, Lodo 31.

Distribution: Locally common throughout Units 1 and 2 (Paleocene); a few very rare specimens (reworked?) in the upper part of Unit 3 (Lower Eocene). Occurs in the Nanafalia Formation (Paleocene) of Alabama, and in the type Thanetian of England. Common in the Paleocene 2.95 km. south of Gan, France, and in the upper part of the type Danian of Denmark.

Genus Zygolithus Kamptner, 1955 (1949?)

An inadequately defined generic name generally used for coccoliths consisting of an elliptical rim transversely spanned by one bar or two cross bars.

Species here assigned provisionally to this genus may require a new generic name following restudy after the designation of a genotype; none has yet been designated. The several species which were classed as *Zygolithus* by Kamptner (1956, p. 9) in the late Tertiary of Rotti appear different from ours in having cross bars attached at the top of the rim and apparently continuous in calcite orientation with the rim. These species were evidently represented by very rare forms, however, as similar specimens could not be found in our examination of a part of the type material.

Species here classified as *Zygolithus* show a dextral curvature of the extinction lines across the rim in distal view between crossed nicols, and different crystal orientation in the bar and adjacent rim, but the consistency and significance of these features remain doubtful, and are not considered definite generic characters.

Zygolithus chiastus Bramlette and Sullivan, new species

Plate 6, figures 1a–d, 2a–b, 3a–b

Description: Zygoliths with a thin rim and open central area transversely spanned by two straight bars crossing to form a narrow x-shaped structure or by one straight and one slightly to distinctly sigmoid bar crossing more nearly at right angles. Bars slightly enlarged at juncture with rim. Length 7–11μ.

Remarks: Several taxa were tentatively distinguished and recorded, based on the differences in the cross bars. However, the existence of intermediate forms and the doubtful significance of the dominance of any one form in a restricted part of the sequence caused the abandonment of this subdivision as apparently unjustified.

Holotype: U.S.N.M. 564242, Lodo 6+1.

Paratypes: U.S.N.M. 564243, Lodo 22, and 564244 Lodo 36.

Distribution: Locally common throughout Units 1 and 2 (Paleocene) and present throughout most of Unit 3 (Lower Eocene). Occurs in the Nanafalia Formation (Paleocene) of Alabama, in the type Thanetian of England, in the type Danian of Denmark, and is common in the Paleocene 2.95 km. south of Gan, France.

Zygolithus crux (Deflandre and Fert)

Plate 6, figures 8–10

Discolithus crux Deflandre and Fert, 1952, C. R. Acad. Sci., vol. 234, p. 2101, text-fig. 8; 1954, Ann. Pal., vol. 40, p. 143, pl. 14, fig. 4; text-fig. 55.

Remarks: The Lodo specimens of this small and delicate form differ from the species described by Deflandre and Fert (1952) in having the cross usually oriented very slightly off the axes of the ellipse, with a slight thickening at the center of the cross, and in being somewhat larger, ranging in length up to 9μ. However, they seem to be within the range of variation shown by topotype specimens of this species. The transverse bars are not like a rudimentary basal plate, and it thus seems best assigned to *Zygolithus*.

Hypotypes: U.S.N.M. 564245, Lodo 46, and 564246–47, Lodo 67.

Distribution: Locally rare in Units 3, 4, and 5 (Lower to Middle Eocene). Recorded from the lower Lutetian (Middle Eocene) of Donzacq, France.

Zygolithus distentus Bramlette and Sullivan, new species

Plate 6, figures 4a–c, 5, 6a–d, 7

Description: Specimens with a thick rim extending over most of the central area and a central opening, largely filled by a somewhat obscure transverse x-shaped structure varying in robustness. Distinct lines at each end extend from the inner margin across most of the rim. Length 5–9μ.

Remarks: This unique small form is characterized by its broad rim, marked by longitudinal lines, and by its unusual x-shaped structure, the bars of which vary from distinct ones, enlarged where they join the rim and only partially occupying the central opening, to very robust bars that form a four-leaf-clover-shaped structure (pl. 6, figs. 4–5), which completely fills the small central opening. It differs from the other species here assigned to *Zygolithus* in having very little central opening and in having longitudinal lines similar to several species of *Discolithus*. There is, however, no obvious differentiation of a distinct basal plate and a marginal rim as in *Discolithus*. The x-shaped structure of this species and the dextral curvature of the extinction lines in distal view between crossed nicols are usual in other species here classed as *Zygolithus* and give some additional basis for provisional assignment to this genus.

Holotype: U.S.N.M. 564248, Lodo 22.

Paratypes: U.S.N.M. 564249–50, Lodo 22, and 564251, Lodo 32.

Distribution: Locally common throughout Unit 2 (Paleocene); very rare (reworked?) specimens in Unit 3 (Lower Eocene). Occurs in the Bashi Formation (Paleocene or Lower Eocene) and the Nanafalia Formation (Paleocene) of Alabama, in the type Thanetian of England, and is common in the Paleocene 2.95 km. south of Gan, France.

Zygolithus dubius Deflandre

Plate 6, figures 12–13, 14a–b

Zygolithus dubius Deflandre, 1954, *in* Deflandre and Fert, Ann. Pal., vol. 40, p. 149, text-figs. 43–44, 68. – Martini, 1958 (part), Senckenbergiana leth., vol. 39, no. 5–6, pp. 369–370, pl. 1, figs. 1a, 1c (not fig. 1b).

Remarks: These common zygoliths are identical with topotypes of the species. The open central area is transversely spanned by an H-shaped rather than x-shaped structure, which extends higher than the rim. The side view shown in Deflandre's text-figure 68 evidently represents another form, as he indicated was probable. The bars of the central structure and the rim are higher than thick (pl. 6, fig. 14), and this feature, along with the nearly vertical orientation of the component crystallites, results in strong relief of the plan view in Canada balsam. The crystallite structure differs from that of the other species here assigned to *Zygolithus*, except the closely related *Z. protenus*, in that the extinction lines seen between crossed nicols on the rim are very vague. Both species, however, are similar to *Chiphragmalithus* in this respect and in having high septum-like bars. In addition, forms with weakly developed barbs around the periphery but otherwise like *Z. dubius* are known elsewhere. It thus appears that *Z. dubius* and *Z. protenus* are intermediate forms that gave rise to the distinctive species assigned to *Chiphragmalithus*.

Hypotypes: U.S.N.M. 564252, Lodo 58; 564253, Domengine OC-2; and 564254, Canoas OC-4.

Distribution: Locally present throughout Units 3–6 (Lower and Middle Eocene). Common in the Eocene of many regions; originally recorded from the lower Lutetian (Middle Eocene) of Donzacq, France.

Zygolithus junctus Bramlette and Sullivan, new species

Plate 6, figure 11a–b

Description: Zygoliths with a thin rim and open central area transversely spanned by a very delicate x-shaped structure, the bars of which cross at a very small angle and are distinctly enlarged where they join the rim. Length 11–15μ.

Remarks: This form is distinguished from *Zygolithus chiastus* by its distinctly larger size and more delicate x-shaped structure, the bars of which cross at such a small angle that they appear joined except toward the periphery.

Holotype: U.S.N.M. 564255, Lodo 6+1.

Distribution: Locally present in Unit 1 (Paleocene). Occurs in the Nanafalia Formation (Paleocene) of Alabama.

Zygolithus protenus Bramlette and Sullivan, new species

Plate 6, figure 15a–b

Description: Zygoliths elliptical, with a thin, steeply sloping rim. Open central area transversely spanned by an x-shaped structure consisting of two bars equal in height to the rim. Bars and rim are higher than thick. Length 7–9μ.

Remarks: This form, occurring lower in the Lodo section and appearing to give rise to *Zygolithus dubius*, differs from that species in having the central area transversely spanned by an x-shaped rather than H-shaped structure and in having a less elongate elliptical form. It differs from *Z. chiastus* in having a more nearly vertical rim, which thus appears narrower in plan view, and bars that do not enlarge where they join the rim, and in showing extinction lines only vaguely between crossed nicols. *Zygolithus dubius* Deflandre of Martini (1958 (part), p. 356, pl. 1, fig. 1b (not figs. 1a, 1c)) may be the same form.

Holotype: U.S.N.M. 564256, Lodo 32.

Distribution: Locally rare in Unit 2 (Paleocene). Occurs at the Tuilerie (Lower Eocene) of Gan, France.

Genus **Zygrhablithus** Deflandre, 1959

"Rhabdolithe combiné à un zygolithe, composé d'une embase elliptique ou subcirculaire, barrée par uncroisillon en x surmonté d'une hampe généralement complexe, celle-ci pouvant être le prolongement direct du croisillon."

Type species: *Zygrhablithus bijugatus* (Deflandre).

Zygrhablithus bijugatus (Deflandre)
Plate 6, figures 16a–b, 17a–c, 18

Rhabdolithus costatus Deflandre, 1954, *in* Deflandre and Fert, Ann. Pal., vol. 40, p. 157, pl. 11, figs. 8–11; text-figs. 41–42, 77–79.

Zygolithus bijugatus Deflandre, 1954 (part), *in* Deflandre and Fert, Ann. Pal., vol. 40, p. 148, pl. 11, fig. 21 (not text-fig. 59).

Zygrhablithus bijugatus (Deflandre). – Deflandre, 1959, Rev. Micropal., vol. 2, pp. 135–136.

Remarks: This common though peculiar form resembles a rhabdolith in side view and a zygolith in end view. Deflandre therefore applied this new generic name and gave much discussion of the type species. The size, especially the height, are very variable. The appearance is quite different in the various orientations illustrated, but recognition of the species is not difficult if this fact is taken into account. A general trend toward larger and heavier specimens upward from the Lower Eocene to the Oligocene is evident here and elsewhere. Very small specimens which may belong to this species occur in Unit 2 of the Paleocene but were not recorded.

Hypotypes: U.S.N.M. 564257, Domengine OC–1, and 564258–59, Domengine OC–2.

Distribution: Locally common in Units 3, 4, and 5 (Lower and Middle Eocene). Common in the Eocene of many regions; originally recorded from the Upper Eocene of Oamaru, New Zealand.

Zygrhablithus simplex Bramlette and Sullivan,
new species
Plate 6, figures 19, 20a–b, 21–22

Description: Specimens with elliptical rim slightly arched upward and bridged by an arching transverse bar which supports a long stem showing faint spiral lines and tapering near the tip to a blunt point. Central canal obscure in some specimens. Length of base 8–11μ. Height 13–18μ.

Remarks: This distinctive form is provisionally assigned to this genus although it has only one transverse bar. The stem with canal is like that of *Rhabdosphaera*, but the base resembles that of *Zygodiscus*. Extinction between crossed nicols for the stem is parallel to the polarization planes, with the crystallites arranged at right angles to the length of the stem, as indicated with the quartz wedge. Broken specimens occur rather commonly, in which the rim is broken away leaving the stem with forked remnants of the bar (pl. 6, fig. 20). The vague spiral arrangement in the stem is more apparent between crossed nicols (fig. 20b).

Holotype: U.S.N.M. 564260, Lodo 32.

Paratypes: U.S.N.M. 564261–62, Lodo 6+1, and 564263, Lodo 32.

Distribution: Locally present in Units 1 and 2 (Paleocene); very rare specimens (reworked?) in Unit 3 (Lower Eocene). Occurs in the Paleocene 2.95 km. south of Gan, France, and in the type Danian of Denmark.

Genus **Coccolithites** Kamptner, 1955

This generic designation is applied here, as by Kamptner, provisionally to some fossil coccoliths with characters that are either obscure or not sufficiently studied to warrant assignment to known genera or the establishment of new generic names. Some of the species here included in the one genus, however, are obviously not closely related and need further study.

Coccolithites cribellum Bramlette and Sullivan,
new species
Plate 7, figures 5a–b, 6a–b

Description: Coccoliths elliptical, consisting of two closely appressed plates. Distal plate with wide outer slope, straight, radiating fine striae, and very narrow inner slope. Central area perforated by several rows of fine pores, with a vague cross indicating division of a central plate into quadrants. Length 6–14μ, usually about 11μ.

Remarks: The structure of this peculiar and scarce form is difficult to determine, but it appears similar to a Cretaceous species which is discussed under the form provisionally recorded here as *Coccolithites* sp.

Holotype: U.S.N.M. 564268, Lodo 46.

Paratype: U.S.N.M. 564269, Lodo 63.

Distribution: Locally rare throughout most of Unit 3 (Lower Eocene).

Coccolithites delus Bramlette and Sullivan,
new species
Plate 7, figures 1a–c, 2a–b

Description: Coccoliths with subelliptical rim, which appears nearly rectangular in plan view due largely to the strong curvature evident in side view. A conspicuous groove in the rim produces a ridge along the inner margin of the proximal side, resulting in an appearance like two closely appressed plates. Bars span the central opening in the major and minor axes. Length 7–11μ.

Remarks: Between crossed nicols with the Quartz Red 1 plate, it is evident that the component crystallites of the rim are oriented more nearly parallel to the rim than radial, and that those of the cross bars are oriented at about 45° to the bar length. A consistently much smaller but otherwise apparently identical form is included here with the typical form. Only this much smaller form is known in the Paleocene here and elsewhere, however, and subspecific distinction may prove desirable.

Holotype: U.S.N.M. 564264, Lodo 80.

Paratype: U.S.N.M. 564265, Lodo 80.

Distribution: Locally common throughout Units 2–5 (Paleocene to Middle Eocene). Common in the Lower and Middle Eocene of many regions, including the Weches Formation (Middle Eocene) of Sabine River, Texas, the lower Lutetian (Middle Eocene) of Donzacq, France, and the Lower Eocene of Pakistan.

Coccolithites aff. C. delus Bramlette and Sullivan

Plate 7, figures 3–4

Remarks: This form appears to be identical with the typical species except for the lack of cross bars and the somewhat less conspicuous ridge in the rim. It is usually associated with the typical species but much less common. A very similar or identical form is common, however, to the exclusion of typical *Coccolithites delus* in an Eocene sample from the Mid-Pacific Mountains and was described and named by E. Kamptner in an unpublished manuscript. Additional study may justify subspecific distinction from *C. delus* s. s.

Hypotypes: U.S.N.M. 564266, Lodo 80, and 564267, Domengine OC–2.

Distribution: Locally present throughout Units 3–6 (Lower and Middle Eocene). Occurs in the Lower and Middle Eocene of many regions, including the lower Lutetian of Donzacq, France.

Coccolithites distichus Bramlette and Sullivan, **new species**

Plate 7, figure 8a–c

Description: Coccoliths elliptical, consisting of a very thin, flat plate with central openings bordered by a slight ridge. Central area with a grid consisting of 3–6, commonly 5, transverse bars which may vary in number on either side of the heavier, slightly raised longitudinal bar. Length 11–14μ.

Remarks: Except for the thick central grid, this distinctive form is difficult to see with transmitted light in Canada balsam, although the entire form is plainly visible between crossed nicols.

Holotype: U.S.N.M. 564270, Lodo 22.

Distribution: Locally present in Units 1 and 2 (Paleocene); very rare and sporadic (reworked?) specimens in Unit 3 (Lower Eocene). Common in the Paleocene 2.95 km. south of Gan and elsewhere in France, but consistently smaller than in California.

Coccolithites gammation Bramlette and Sullivan, **new species**

Plate 7, figures 7a–c, 14a–b

Description: Coccoliths circular and probably consisting of two very closely appressed plates of almost equal size, rather than a single plate. A somewhat depressed central area occupies less than half the total diameter, and a tiny central spot may represent a central opening. This form is especially distinctive between crossed nicols, as discussed below. Diameter 5–9μ.

Remarks: Between crossed nicols the outer part of the specimens is indistinct but the inner portion clearly shows the extinction cross, curving strongly in the form of a swastika. A large group of coccoliths with the original tight articulation is represented by the form illustrated in plate 7, figure 14a–b. The slight curvature in this group indicates an unusually large size for the complete coccosphere, apparently much more than 100μ, although some compression without breakage and disaggregation is possible. The marked change in size of the coccoliths is probably toward a buccal opening.

Holotype: U.S.N.M. 564271, Lodo 46.

Hypotype: From the Tuilerie de Donzacq, Landes, France.

Distribution: Locally present in Units 3 and 4 (Lower to Middle Eocene). Occurs in the Weches Formation (Middle Eocene) of Sabine River, Texas, and in the lower Lutetian (Middle Eocene) of Donzacq, France.

Coccolithites macellus Bramlette and Sullivan, **new species**

Plate 7, figures 11–12, 13a–d

Description: Coccoliths elliptical, consisting of a very thin, nearly flat plate with somewhat depressed central area bordered by a slightly raised ridge. Central area longitudinally bisected by a line commonly interrupted toward each end by a small round opening. Length 9–15μ.

Remarks: This delicate form is difficult to see in Canada balsam except with crossed nicols. Specimens in the two lowermost Lodo samples have a smaller central area with a less well developed bordering ridge than is typical (pl. 7, figs. 11–12). However, occasional specimens of this character were found along with the more typical forms, and they are not considered distinct enough to warrant taxonomic separation.

Holotype: U.S.N.M. 564273, Lodo 33.

Paratypes: U.S.N.M. 564274–75, Lodo 6+1.

Distribution: Locally present in Units 1, 2, and 3 (Paleocene and Lower Eocene), rare except in the lower part of its range. Occurs in the Paleocene of Trinidad and 2.95 km. south of Gan, France.

Coccolithites sp.

Plate 7, figures 9a–b, 10

Remarks: This form is similar to or identical with a common Cretaceous species, and its rare occurrence in the Lodo section may be due to reworking from the older strata. The Lodo specimens are elliptical, consisting of a single plate slightly grooved around the periphery or of two very closely appressed plates. The central area within a narrow rim is somewhat irregularly perforated and divided into quadrants with different optical orientations and with the dividing line appearing as a vague cross.

Determination of whether it is formed of one or of two closely appressed plates and interpretation of the anomalous appearance between crossed nicols of the four central segments can best be made in a study of the abundant larger specimens in the Upper Cretaceous. It may be the same as the poorly illustrated form described as *Arkhangelskiella specillata* by Vekschina (1959, p. 67). It differs from *Coccolithites cribellum* in the coarser, more irregular perforations of the central area and the distinctly narrower peripheral part.

Hypotypes: U.S.N.M. 564276, Lodo 58, and 564277, Lodo 80.

Distribution: Locally rare and sporadic in Units 3 and 5 (Lower and Middle Eocene).

Family Braarudosphaeridae Deflandre

Genus Braarudosphaera Deflandre, 1947

"Coque dodécaédrique; 12 pentalithes pentagonaux, formés de plaquettes trapézoïdales très difficilement dissociables" (Deflandre, 1952*b*, p. 112).

The extensive discussion of the genus by Deflandre (1947) and of the common species *Braarudosphaera bigelowi* by Gaarder (1954) is not reviewed here. It is one of the few genera, other than those of the coccolithophorids proper, occasionally retaining the skeletal elements intact, with the 12 pentaliths in a dodecahedral form (pl. 8, fig. 4). However, the usually isolated pentaliths are quite distinctive. Although the genus is most common in the Eocene, forms referable to the modern *B. bigelowi* have persisted for an unusually long time since the late Cretaceous.

Braarudosphaera bigelowi (Gran and Braarud)

Plate 8, figures 1a–b, 2–5

Pontosphaera bigelowi Gran and Braarud, 1935, Jour. Biol. Board Canada, vol. 1, p. 389, text-fig. 67.

Braarudosphaera bigelowi (Gran and Braarud). – Deflandre, 1947, C. R. Acad. Sci., vol. 225, p. 439, text-figs. 1–5. – Deflandre, 1954, *in* Deflandre and Fert, Ann. Pal., vol. 40, pp. 165–166, pl. 10, figs. 8–13; pl. 13, figs. 7–9. – Bramlette and Riedel, 1954, Jour. Pal., vol. 28, no. 4, pp. 393–394, pl. 38, fig. 6a–b. – Gaarder, 1954, Rept. Sci. Results "Michael Sars" North Atlantic Deep-Sea Exped. 1910, vol. 2, no. 4, pp. 5–6, text-fig. 2. – Martini, 1958, Senckenbergiana leth., vol. 39, no. 5–6, p. 355, pl. 2, fig. 6a–b.

Remarks: The pentaliths of this species are variable in thickness and range greatly in diameter, from 8 to 27μ. Their periphery also varies, both in plan and side view, from being sharply angled to more commonly rounded. The original description of this species, from a sample of living plankton, failed to indicate the division of the pentaliths into five segments, but Gaarders' (1954) later studies show such a division of the pentaliths in the modern form. An extraordinary life span is indicated for the species, in that it occurs as early as the late Cretaceous.

Hypotypes: U.S.N.M. 564278, Lodo 19; 564279, Lodo 31; 564280–81, Lodo 32; and 564282, Lodo 67.

Distribution: Locally abundant throughout Unit 2 (Paleocene) and sporadic in Units 3 and 4 (Lower and Middle Eocene). Widely distributed in Cretaceous to Recent sediments of many regions.

Braarudosphaera discula Bramlette and Riedel

Plate 8, figures 6a–b, 7

Braarudosphaera discula Bramlette and Riedel, 1954, Jour. Pal., vol. 28, no. 4, p. 394, pl. 38, fig. 7.

Remarks: These discoid pentaliths might be classed as *Micrantholithus*, but the segments commonly show (pl. 8, fig. 7) a suggestion of the basic trapezoidal form of the genus *Braarudosphaera*. Forms with outlines more similar to *B. bigelowi* are common in the Danian of Europe. This species differs from *Pemma rotundum* Klumpp (1953, p. 381) in not having a central opening in the segments. Reexamination of topotype specimens shows that they are nearly biconvex, with an average thickness approximately one-half the diameter. The few Lodo specimens examined in side view are planoconvex, but this difference does not seem to justify another taxonomic unit, as such differences are common in *B. bigelowi* and in many species of *Micrantholithus*. Diameter ranges widely, from 6 to 21μ.

Hypotypes: U.S.N.M. 564283, Lodo 21, and 564284, Lodo 46.

Distribution: Locally rare in Units 2, 3, and 4 (Paleocene to Middle Eocene). Common in the Eocene of Cuba, southwestern France, and elsewhere.

Genus **Micrantholithus** Deflandre, 1950

"Pentalithes étoilés, à pièces triangulaires peu cohérentes, souvent isolées" (Deflandre, 1952*b*, p. 112).

In the various species, deviations from the basically triangular shape of the five segments are produced by modification of their marginal sides. Only pentaliths with segments of trapezoidal form are here excluded from *Micrantholithus* and are considered characteristic of the closely related genus *Braarudosphaera*. Many species of *Micrantholithus* are thick, like *Braarudosphaera*, and thus are likewise usually preserved as complete pentaliths.

Type species: Micrantholithus flos Deflandre.

Micrantholithus attenuatus Bramlette and Sullivan, **new species**
Plate 8, figures 8a–b, 9–11

Description: Pentaliths star-shaped, large for the genus, consisting of five V-shaped segments, the adjacent sides of which form long tapering rays. The segments vary from having adjacent sides equal to having one side three times as long as the other (pl. 8, figs. 9–11), this feature being consistent, however, within any one pentalith. Deeply indented margin of segments sharply angular to somewhat rounded. Overall diameter 14–27μ, usually about 20μ.

Remarks: This species is commonly represented by isolated segments of the pentaliths. Its probable development is discussed under *Micrantholithus* aff. *attenuatus*. This species is probably the same as a species of *Micrantholithus* described in a paper (in press) of E. Martini, and his specific name therefore may have priority.

Holotype: U.S.N.M. 564285, Lodo 67.

Paratypes: U.S.N.M. 564286–88, Lodo 67.

Distribution: Locally present in Unit 3 (Lower Eocene). Occurs in the Bashi Formation (Paleocene or Lower Eocene) and in the Nanafalia Formation (Paleocene) of Alabama, in the London Clay (Lower Eocene) of England, and in the Lower Eocene of the Tuilerie of Gan, France.

Micrantholithus aff. **M. attenuatus**
Bramlette and Sullivan
Plate 8, figure 12a–b

Remarks: The pentaliths of this form differ from typical *Micrantholithus attenuatus* in being smaller, ranging in overall diameter from 9 to 14μ, and in having segments with adjacent sides consistently equal in length. High in its recorded range it is associated with and may have given rise to forms typical of the species. In this same interval, some specimens also show a small web between the rays suggesting development into *M. flos*, which makes its first appearance here. It differs from *M. pinguis* in having pentaliths which are not as thick but with much longer and narrower rays.

Hypotype: U.S.N.M. 564289, Lodo 21.

Distribution: Locally present throughout Unit 2 and in the lower part of Unit 3 (Paleocene and Lower Eocene).

Micrantholithus basquensis Martini
Plate 8, figures 14a–c, 15

Micrantholithus basquensis Martini, 1959, Senckenbergiana leth., vol. 40, no. 5–6, p. 417, pl. 1, figs. 9–12.

Remarks: Examination of numerous specimens from any one locality shows that this species is subject to considerable variation. The California specimens are not identical with either of the photographed specimens shown by Martini but appear to be within the range of variation noted for this species in other samples. Marked differences in thickness produce some of the variations in general appearance. The distinctly depressed central part of the segments and the indentation in the middle of their outer margins cause the outline of the thicker parts of the pentalith to resemble the general outline of *Discoaster deflandrei*. Overall diameter 7–12μ.

Hypotypes: U.S.N.M. 564290–91, Domengine OC–2.

Distribution: Locally present in Unit 4 (Middle Eocene). Occurs in the Weches Formation (Middle Eocene) and in the Cook Mountain Formation (Middle Eocene) of Sabine River, Texas, in the type Lutetian region at Grignon, France, and was recorded from near Biarritz, France.

Micrantholithus bramlettei Deflandre
Plate 9, figure 2a–b

Micrantholithus bramlettei Deflandre, 1954, *in* Deflandre and Fert, Ann. Pal., vol. 40, p. 167, pl. 13, fig. 22; text-fig. 117.

Remarks: Further study of the type material from the Lodo shows that the pentaliths of this species vary, some forms having segments with symmetrical trilobate outer margins, as figured by Deflandre (1954, text-fig. 117), but most having segments with asymmetrical bilobate outer margins, as illustrated by our figure 2 on plate 9. Various intermediate forms indicate that they represent a single species. Although the middle part of the segment margin is extended rather than indented as in most species of the genus, a thickening adjacent to the sutures, as in the type species, *Micrantholithus flos*, supports the generic assignment.

Hypotype: U.S.N.M. 564292, Lodo 31.

Distribution: Locally present throughout Unit 2 (Paleocene) and rare in the lower part of Unit 3 (Lower Eocene).

Micrantholithus concinnus Bramlette and Sullivan, new species

Plate 9, figure 1a–c

Description: Pentaliths consisting of five segments with asymmetrically bilobate outer margins. Major lobe of each segment broad, with sides paralleling the sutures and with rounded tip. Overall diameter 10–13μ.

Remarks: The pentaliths of this species are distinct from the bilobate variant of *Micrantholithus bramlettei* in that the outer margins of the segments show that the major lobe is wide and much less extended. No gradation between the two forms was observed, although they appear to be closely related. As in *M. bramlettei*, the thickening adjacent to the sutures supports the generic assignment.

Holotype: U.S.N.M. 564293, Lodo 32.

Distribution: Locally rare in Unit 2 (Paleocene).

Micrantholithus crenulatus Bramlette and Sullivan, new species

Plate 9, figures 3a–b, 4

Description: Pentaliths with thickness equal to about half the diameter. Segments triangular or with slightly concave outer margin, which is somewhat crenulate and commonly shows a depression or thinning at the middle. Overall diameter 7–12μ.

Remarks: This species differs from *Micrantholithus basquensis* in having pentaliths more clearly pentagonal in shape, with segments lacking a central depression. However, the general outline and the median depression of the outer margin of the segments (pl. 9, fig. 4) suggest that the two species may be closely related.

Holotype: U.S.N.M. 564294, Domengine OC–2.

Paratype: U.S.N.M. 564295, Domengine OC–2.

Distribution: Locally rare in Units 2 and 3 (Paleocene and Lower Eocene) and more common in Unit 4 (Middle Eocene).

Micrantholithus entaster Bramlette and Sullivan, new species

Plate 9, figures 5a–c, 6, 7a–b

Description: Pentaliths star-shaped, consisting of five V-shaped segments, the adjacent sides of which form tapering rays with blunt to acutely pointed tips. Indentation between rays only slightly rounded. Central area thickened on one side to form a superimposed star, smaller but as much as twice as thick, with the tips alternating with the marginal ones of the pentalith. Overall diameter 9–20μ.

Remarks: The pentaliths of this species are distinct in having a thick and conspicuous superimposed central star, although this development appears less conspicuously in some other members of the genus. Rare forms of somewhat smaller size, with a delicate web between the rays and showing the conspicuous central star (pl. 9, fig. 6), may be a variant of the species. The tendency to develop an intermediate web is noted in *Micrantholithus attenuatus* and others.

Holotype: U.S.N.M. 564296, Lodo 32.

Paratypes: U.S.N.M. 564297-98, Lodo 31.

Distribution: Locally present throughout Unit 2 (Paleocene).

Micrantholithus flos Deflandre

Plate 9, figure 8a–b

Micrantholithus flos Deflandre, 1950, C. R. Acad. Sci., vol. 231, p. 1157, text-figs. 8–11. – Deflandre, 1954, *in* Deflandre and Fert, Ann. Pal., vol. 40, p. 166, pl. 13, figs. 10–11; text-figs. 113–114. – Martini, 1958, Senckenbergiana leth., vol. 39, no. 5–6, p. 356, pl. 1, fig. 2a–c.

Remarks: The pentaliths recorded here are generally typical of the species. However, some variants are included which have the triangular segments more broadly thickened so that the normally thin central area is much reduced.

Hypotype: U.S.N.M. 564299, Lodo 67.

Distribution: Locally present in Units 3 and 4 (Lower and Middle Eocene). Originally recorded from the lower Lutetian (Middle Eocene) of Donzacq, France, and recorded from the Middle Eocene of Germany.

Micrantholithus pinguis Bramlette and Sullivan, new species

Plate 8, figure 13a–b

Description: Pentaliths star-shaped, small for the genus but ranging in thickness from one-third to almost equal the total diameter. Adjacent sides of the marginally concave segments form rather short rays. Overall diameter 7–12μ.

Remarks: The thickness of these relatively small pentaliths is one of the more distinctive features and is evident even in plan view, from the birefringence, relief, and depth in focusing.

Holotype: U.S.N.M. 564300, Lodo 31.

Distribution: Locally common throughout Unit 2 (Paleocene).

Micrantholithus truncus Bramlette and Sullivan, new species

Plate 9, figure 9a–b

Description: Pentaliths with some thickening of the central area on one side, forming a superimposed small star, the tips of which extend to near the middle of the cordate segments. The median part near the outer margin of the segments is usually thin. Overall diameter 12–18µ.

Remarks: The superimposed central star and general outline appearing as truncated rays of a star are characteristic of this species.

Holotype: U.S.N.M. 564301, Lodo 31.

Distribution: Locally present throughout Unit 2 (Paleocene).

Micrantholithus vesper Deflandre
Plate 9, figure 10a–b

Micrantholithus vesper Deflandre, 1950, C. R. Acad. Sci., vol. 231, p. 1157, text-figs. 5–7. – Deflandre, 1954, *in* Deflandre and Fert, Ann. Pal., vol. 40, p. 166, pl. 13, fig. 17; text-figs. 5, 115–116. – Martini, 1958, Senckenbergiana leth., vol. 39, no. 5–6, pp. 356–357, pl. 1, fig. 3a–c.

Remarks: The pentaliths recorded here appear typical of this large but thin species. They are seldom found except as the easily separated segments, and are partially separated in figure 10.

Hypotype: U.S.N.M. 564302, Lodo 67.

Distribution: Locally present in Units 3 and 4 (Lower and Middle Eocene). Originally recorded from the lower Lutetian (Middle Eocene) of Donzacq, France, and recorded from the Middle and Upper Eocene of Germany.

INCERTAE SEDIS

Genus **Chiphragmalithus** Bramlette and Sullivan, new genus

Form basket-like, with cross septa dividing it into quadrants. The septa, especially at the center, extend higher than the side wall, and this wall slopes down to an open basal area which is commonly closed in *C. cristatus.*

Although the exact form can be determined only by varying the orientation, the described species are easily recognized by distinctive features seen in side view or the more usual plan view. It appears somewhat like an ortholithid in polarized light; although this is evidently due to the crystallites being arranged nearly perpendicular to the plan view, with their optic C-axis nearly vertical, rather than being formed of a single unit of calcite.

Development from a form such as *Zygolithus dubius* or, more probably, *Z. protenus* seems indicated by similarities in side view (compare pl. 6, fig. 14a, and pl. 10, figs. 3, 9, and 10) and also by the peculiar orientation of component crystallites evident between crossed nicols.

Type species: Chiphragmalithus calathus Bramlette and Sullivan, n. sp.

Chiphragmalithus acanthodes Bramlette and Sullivan, new species
Plate 10, figures 1a–b, 2–6

Description: Specimens elliptical, height of rim equal to about one-quarter the greatest diameter, rim flaring distally, with the periphery in most specimens showing well-developed barbs hooking sinistrally in distal view. Central opening transversely spanned by septa forming an X-shaped structure. Septa higher than the rim, especially toward the center, and show through the rim conspicuously in side view. Length 9–13µ.

Remarks: Specimens that are typical of this species except for a higher and more flaring rim resemble *Chiphragmalithus cristatus* and indicate development into that species.

Holotype: U.S.N.M. 564303, Domengine OC-2.

Paratypes: U.S.N.M. 564304–08, Domengine OC–2.

Distribution: Locally present in Units 4 and 5 (Middle Eocene). Occurs in the Tyus member of the Weches Formation (Middle Eocene) of Sabine River, Texas, and in the Middle Eocene of the Carrière de Nousse, in southwestern France.

Chiphragmalithus calathus Bramlette and Sullivan, new species
Plate 10, figures 7a–b, 8–10

Description: Specimens ranging from circular or slightly quadrate to slightly elliptical in plan view. Rim thin, its height one-half to equal to the greatest diameter, flaring somewhat distally, with the periphery commonly showing slight barbs hooking sinistrally in distal view. Central opening transversely spanned by an X-shaped structure formed by septa, which are slightly higher than the rim and are conspicuous through the rim in side view. Length 6–9µ.

Remarks: This form differs from *Chiphragmalithus acanthodes* in being smaller but relatively higher and more nearly circular in plan view and in having less conspicuous peripheral barbs.

Holotype: U.S.N.M. 564309, Lodo 36.

Paratypes: U.S.N.M. 564310, Lodo 34, and 564311–12, Lodo 36.

Distribution: Locally present throughout Unit 3 (Lower Eocene), more common near the base. Occurs also in the London Clay (Lower Eocene) of England.

Chiphragmalithus cristatus (Martini)
Plate 10, figures 11a–c, 12–13

Trochoaster cristatus Martini, 1958, Senckenbergiana leth., vol. 39, no. 5–6, p. 368, pl. 5, fig. 26a–b. – Stradner, 1959, Erdoel-Zeitschr., no. 12, p. 481, text-figs. 56, 58.

(456)

Remarks: Specimens in a sample obtained from Martini appear identical with our form, but various orientations indicate the characters typical of *Chiphragmalithus* rather than of *Trochoaster* Klumpp (1953, pp. 384–385). The species is represented in the California samples by a large number of well-preserved specimens. It is circular to somewhat quadrate in plan view, with the rim greatly flaring distally. The rim is ornamented by two or three thickened ridges in each quadrant, extending into a lobate periphery. The central area is spanned by cross septa which tend to curve dextrally in distal view, and the central opening is small and commonly obscured by the septa in this view (pl. 10, fig. 11a) but apparent on the proximal side. In side view the septa are seen to be about twice as high in the center as at their junction with the rim. Evidence of development from *C. acanthodes* was mentioned in the discussion of that species. Diameter 8–16μ.

Hypotypes: U.S.N.M. 564313–15, Canoas OC–4.

Distribution: Locally present in Units 4, 5, and 6 (Middle Eocene). Recorded from the Middle Eocene of Germany and Austria. Also occurs in the Middle Eocene at Gibret, in southwestern France.

Chiphragmalithus? quadratus Bramlette and Sullivan, new species

Plate 10, figures 14a–b, 15

Description: Specimens large, with four long, acutely tipped rays, usually slightly offset at the center and not consistently equal in length. Webbing with thin and irregular margin connects the rays to form a base, although this may be poorly developed or lacking in some specimens. Side view shows rays tapering outward from thick central section. Diameter 11–23μ.

Remarks: This form appears closely related to "*Trochoaster*" *swasticoides* Martini (1958, pp. 368–369), differing only in having nearly straight rather than hook-ended rays as in his species. Neither form seems to be related to *Trochoaster* Klumpp (1953, pp. 384–385), although that genus was poorly described, and both are more similar to *Chiphragmalithus*, particularly to *C. cristatus*. The differences, however, will probably warrant a new generic assignment for this species after the type species of *Trochoaster* has been restudied.

Holotype: U.S.N.M. 564316, Canoas GC–2.

Paratype: U.S.N.M. 564317, Canoas GC–3.

Distribution: Locally present in the upper part of Unit 5 and common in Unit 6 (Middle Eocene). Occurs in the Middle Eocene of Trinidad and Germany.

Genus Clathrolithus Deflandre, 1954

"Corpuscules calcaires assez épais, de contour arrondi, percés de trous formant une sorte de réticulum à mailles hexagonales ou polygonales arrondies."

The side view shows an increase in height toward the center of the mesh of ridges on the distal side of the flat basal plate. As this is an ortholithid form consisting of a single unit of calcite, no birefringence is shown between crossed nicols in the usual flat orientation, the optic C-axis thus being perpendicular.

Type species: Clathrolithus ellipticus Deflandre, 1954.

Clathrolithus ellipticus Deflandre

Plate 10, figures 16a–b, 17

Clathrolithus ellipticus Deflandre, 1954, *in* Deflandre and Fert, Ann. Pal., vol. 40, p. 169, pl. 12, fig. 19; pl. 14, fig. 7; text-figs. 123–124.

Remarks: This species in the Lodo section appears to be identical with topotype specimens, except for being slightly larger (9–15μ in length). The specimens are planoconvex in side view (pl. 10, fig. 17), with the ridges that form the honeycomb-like reticulum not perpendicular to the flat, proximal surface but curving toward one end.

Hypotypes: U.S.N.M. 564318, Lodo 19, and 564319, Lodo 62.

Distribution: Locally common in Unit 2 (Paleocene) and sporadic in Units 3 and 4 (Lower and Middle Eocene). Occurs in the Weches Formation (Middle Eocene) of Sabine River, Texas, and in the Bashi Formation (Paleocene or Lower Eocene) of Alabama; originally recorded from the lower Lutetian (Middle Eocene) of Donzacq, France.

Clathrolithus minutus Bramlette and Sullivan, new species

Plate 10, figure 18

Description: Plates small, elliptical, planoconvex, with ridges forming a honeycomb-like reticulum of usually 16–20 hexagonal cellules. Length 6–7μ.

Remarks: This species is easily distinguished from *Clathrolithus ellipticus* by the distinctly smaller size of the plates and their much finer mesh. In side view the convex surface is not as highly arched as in the larger species.

Holotype: U.S.N.M. 564320, Lodo 67.

Distribution: Locally sporadic in Units 3 and 4 (Lower and Middle Eocene). Sparse in the Weches Formation (Middle Eocene) of Sabine River, Texas, and in the lower Lutetian (Middle Eocene) of Donzacq, France.

Genus Discoaster Tan Sin Hok, 1927

Various stellate to multiradiate discoidal forms (asteroliths) are assigned to this genus. The subdivision, apparently subgeneric, proposed by Tan Sin Hok (1927, p. 117) as *Heliodiscoaster* to distinguish the more discoidal

(457)

forms consisting of many closely joined rays is not followed here. An arbitrary delimitation based on such a difference is difficult to apply, as variations in some of the species would bridge any such subdivision.

The central area in many species bears a stem, usually on one side of the disc only, and in some species, a less prominent stem also occurs on the other side of the disc. In other species the stem is broad and less elongate, like a bulla. In still other species, no comparable central process is developed, and in some otherwise well characterized species, such as *Discoaster multiradiatus*, it is not present in all specimens. Species with curved rays have this curvature sinistral as viewed on the side with stem. The significance of this feature is not now apparent, but it seems consistent for all known species with curved rays.

The asteroliths have the typical ortholithid character of being formed as a single unit of calcite, including the stem. The optic C-axis of the calcite unit is consistently perpendicular to the plane (or curved surface) which includes the rays, and thus in plan view between crossed nicols the specimens lack birefringence but show the maximum relief or refringence.

Most species show some variation (usually about 25 per cent) in the number of rays but have features otherwise sufficiently constant to permit identification with assurance in widely separated regions. Certain other species or groups of closely related forms, especially some in the Middle Eocene, show much variation, and consistent specific characters are questionable and difficult to determine. A group of such forms is illustrated (pl. 13, figs. 1–5) but left undescribed. The similarities and differences are difficult to evaluate, even with many such specimens, because of the plexus of intergrading features. Unfortunately, new species have been described from among such variable forms without abundant specimens for study.

Discoaster barbadiensis Tan Sin Hok
Plate 11, figure 2

"Crystalloids," Jukes-Browne and Harrison, 1892, Quart. Jour. Geol. Soc. London, vol. 48, p. 178, text-figs. 4–6.
Discoaster barbadiensis Tan Sin Hok, 1927 (part), Jaarb. Mijnw. Ned. Oost-Indië, p. 119. – Bramlette and Riedel, 1954, Jour. Pal., vol. 28, no. 4, pp. 398–399, pl. 39, fig. 5a–b. – Martini, 1958, Senckenbergiana leth., vol. 39, no. 5–6, p. 366, pl. 5, fig. 24a–c.

Remarks: The specimens found here and elsewhere show that this species is quite variable in robustness. Because the robustness of associated species in the same sample is often similar, this variation seems to be due to the amount of calcium carbonate available in surface waters or to diagenetic additions of calcite. Asteroliths such as that illustrated here are near the average, but their features are more obscure in specimens heavy with excess calcite.

Hypotype: U.S.N.M. 564321, Lodo 76.

Distribution: Locally present in Unit 3 (Lower Eocene) and common in Units 4, 5, and 6 (Middle Eocene). Common throughout the Eocene of many regions.

Discoaster binodosus Martini
Plate 11, figure 1a–b

Discoaster binodosus binodosus Martini, 1958, Senckenbergiana leth., vol. 39, no. 5–6, p. 362, pl. 4, fig. 18a–b.

Remarks: Some specimens included here have some or all of their rays truncated, or even slightly bifurcated as in Martini's (1958) *Discoaster binodosus hirundinus*. The group as a whole, however, compares well with the nominate subspecies, and the subspecific distinction seems of doubtful value here.

Hypotype: U.S.N.M. 564322, Lodo 33.

Distribution: Locally present throughout most of Unit 3 (Lower Eocene). Recorded from the Eocene of Germany, and occurs in the London Clay (Lower Eocene) of England.

Discoaster cruciformis Martini
Plate 11, figure 5a–b

Discoaster cruciformis Martini, 1958, Senckenbergiana leth., vol. 39, no. 5–6, pp. 357–358, pl. 2, fig. 9a–b.

Remarks: This species seems to be constantly four-rayed, and it differs from *Discoaster tribrachiatus* not only in the number of rays but also in its smaller and more uniform size and in the usual slight enlargement at the tips of the rays.

Hypotype: U.S.N.M. 564323, Lodo 100.

Distribution: Locally present in Units 3 and 4 (Lower and Middle Eocene). Recorded from the Middle Eocene of Germany, and occurs in the lower Lutetian (Middle Eocene) of Donzacq, France.

Discoaster deflandrei Bramlette and Riedel
Plate 11, figure 4a–b

Discoaster deflandrei Bramlette and Riedel, 1954, Jour. Pal., vol. 28, no. 4, pp. 399–400, pl. 39, fig. 6; text-fig. 1a–c. – Martini, 1958, Senckenbergiana leth., vol. 39, no. 5–6, pp. 363–364, pl. 5, fig. 23a–c.

Remarks: Specimens such as that illustrated here, though not identical with the holotype, seem to belong to this variable species.

Hypotype: U.S.N.M. 564324, Lodo 45.

Distribution: Locally present in Unit 3 (Lower Eocene). Occurs in the Eocene and more commonly in the Oligocene of many regions.

Discoaster delicatus Bramlette and Sullivan, **new species**
Plate 11, figure 3

Description: Asteroliths discoidal, very thin and delicate, with 30–50 rays joined throughout their length, commonly obscure except near the margin. Central area normally somewhat raised on one side, forming a ring around a depressed center. Diameter 10–16μ.

Remarks: Although this species differs here from *Discoaster multiradiatus* s. l. in having a greater number of rays, it varies considerably and may be difficult to differentiate elsewhere.

Holotype: U S.N.M. 564325, Lodo 7.

Distribution: Locally common in Unit 1 (Paleocene), and sporadic and very rare in Units 2 and 3 (Paleocene and Lower Eocene).

Discoaster diastypus Bramlette and Sullivan, **new species**
Plate 11, figures 6–8

Description: Asteroliths with 9–16 sharply pointed rays, joined through most of their length and curving sinistrally as viewed from the side with the larger part of the stem. Rays asymmetric, with a ridge forming the thick or high part along the convex curving side. Central area pierced by a heavy column (stem) somewhat larger on one side, with both ends depressed or concave. Diameter 11–20μ.

Remarks: Some specimens with fewer rays than average and with the stem less developed on one side somewhat resemble *Discoaster lodoensis* and suggest relationship between the two species.

Holotype: U.S.N.M. 564326, Lodo 23.

Paratypes: U.S.N.M. 564327, Lodo 33, and 564328, Lodo 36.

Distribution: Locally common in the lower part and sporadic through the rest of Unit 3 (Lower Eocene). Occurs in Bolli's *Globorotalia rex* Zone (basal Eocene) of Trinidad, and in the Lower Eocene at Louer (Landes), France.

Discoaster aff. D. diastypus Bramlette and Sullivan
Plate 11, figures 9–10

Remarks: This form seems to differ from *Discoaster diastypus* only in having the rays nearly straight rather than distinctly curved. Although intermediate forms suggest that it is only a variant of the species, it is here recorded separately pending study of similar forms occurring elsewhere.

Hypotypes: U.S.N.M. 564329. Lodo 23, and 564330, Lodo 83.

Distribution: Locally common in the lower part of Unit 3 (Lower Eocene). Occurs in the Bashi Formation (Paleocene or Lower Eocene) of Alabama.

Discoaster distinctus Martini
Plate 11, figures 11–13

Discoaster distinctus MARTINI, 1958, Senckenbergiana leth., vol. 39, no. 5–6, p. 363, pl. 4, fig. 17a–b.

Remarks: The name of this species seems rather inappropriate for the California specimens as they are highly variable and difficult to delimit. Many of those included here, nevertheless, compare well with specimens in type material obtained from Martini. The paired nodes toward the tips of the rays are conspicuous on most specimens but much less so on some, as shown by a few of the rays in figure 11, plate 11. These nodes, however, together with the character of the bifurcating tips, help to distinguish this species from many somewhat similar forms.

Hypotypes: U.S.N.M. 564331–32, Lodo 77, and 564333, Domengine OC-1.

Distribution: Locally present in Units 3–6 (Lower and Middle Eocene). Common in the Eocene of many regions; recorded from the Middle Eocene of Germany.

Discoaster elegans Bramlette and Sullivan, **new species**
Plate 11, figure 16a–b

Description: Asteroliths with 11–15 pointed rays, joined through most of their length and concentrically lined. Central area with a pronounced stem on the concave side. Diameter 11–21μ.

Remarks: This more delicate and concentrically ornamented form commonly occurs with the more common and rather variable Eocene species *Discoaster barbadiensis*. When more heavily calcified, the concentric lines become less distinct, and the specimens are difficult to distinguish from that species. The intermediate forms are few, however, and two distinct groups seem to be represented.

Holotype: U.S.N.M. 564334, Lodo 68.

Distribution: Locally present in Units 3–6 (Lower and Middle Eocene). Occurs in the Eocene of many regions.

Discoaster falcatus Bramlette and Sullivan, **new species**
Plate 11, figures 14a–b, 15

Description: Asteroliths with 7–10, commonly 9, curving rays joined through half their length. Rays asymmetric, with a ridge near the convexly curving side and a slight thickening of the other edge of the ray, resulting in a thinner central part. Central boss small but higher on the side showing the sinistral curvature of the rays. Diameter 11–19μ.

(459)

Remarks: In the lowermost Lodo occurrence (Sample 7) of this species, the asteroliths are more delicate than normal, with 7 rather than 9 rays common and with a smaller central knob (pl. 11, fig. 15). Typical forms of this species show some similarity to *Discoaster limbatus*, especially to less ornate variants of that species. *D. lodoensis* may have evolved from this species, as similarities are evident and their range relations seem to suggest it.

Holotype: U.S.N.M. 564335, Lodo 22.

Paratype: U.S.N.M. 564336, Lodo 7.

Distribution: Locally common in Units 1 and 2 (Paleocene) and rare throughout Unit 3 (Lower Eocene). Occurs in the Bashi Formation (Paleocene or Lower Eocene) of Alabama, in Bolli's *Globorotalia rex* Zone (basal Eocene) of Trinidad, and in the Paleocene 2.95 km. south of Gan, France.

Discoaster germanicus Martini
Plate 11, figure 17

Discoaster germanicus Martini, 1958, Senckenbergiana leth., vol. 39, no. 5–6, pp. 360–361, pl. 3, fig. 15a–b.
Discoaster plebeius Martini, 1958, Senckenbergiana leth., vol. 39, no. 5–6, p. 361, pl. 3, fig. 16a–b.

Remarks: The tips of the rays of the specimens recorded here are variable, some with small nodes, some without, some slightly bifurcating, some truncate, and many intermediate. They seem, however, to represent only one species. Such variations occur also in topotype material of *Discoaster germanicus* and *D. plebeius*. Distinction between the two species is difficult and is not attempted here. Its smallness and almost parallel-sided rays help to distinguish it from similar forms.

Hypotype: U.S.N.M. 564337, Lodo 107.

Distribution: Locally present throughout Units 3 and 4 (Lower and Middle Eocene). Recorded from the Middle Eocene of Germany.

Discoaster helianthus Bramlette and Sullivan, new species
Plate 11, figure 18a–b

Description: Asteroliths sunflower-shaped, with 13–14 straight-radiating rays joined through more than half their length and having rounded to somewhat pointed tips. Rays have thickened borders and radiate from a central boss that is very little raised but of large diameter, especially on one side. Diameter 7–15μ.

Remarks: This rather distinctive form shows considerable variation in size, and the illustrated specimen, though otherwise typical, is larger than average.

Holotype: U.S.N.M. 564338, Lodo 6+1.

Distribution: Locally common in Unit 1 (Paleocene); sporadic and very rare (reworked?) specimens in Unit 3 (Lower Eocene). Occurs in the Nanafalia Formation (Paleocene) of Alabama, in the type Thanetian of England, and in the Paleocene 2.95 km. south of Gan, France.

Discoaster lenticularis Bramlette and Sullivan, new species
Plate 12, figures 1a–b, 2

Description: Asteroliths discoidal, small but centrally thick, with 20–26 rays joined throughout their length, curving sinistrally toward the periphery as viewed from the stem (boss) side and having bluntly rounded tips. Central area of one side with a small, low boss, depressed in the center. Diameter 8–12μ.

Remarks: This small species differs from other many-rayed discoasters in the relatively great increase in thickness toward the center and in the marked curvature of the rays, which are joined out to the periphery.

Holotype: U.S.N.M. 564339, Lodo 31.

Paratype: U.S.N.M. 564340, Lodo 31.

Distribution: Locally present in Unit 2 (Paleocene); sporadic and very rare (reworked?) specimens in Unit 3 (Lower Eocene). Occurs in the Bashi Formation (Paleocene or Lower Eocene) and in the Clayton formation (Paleocene) of Alabama, and in the Paleocene 2.95 km. south of Gan, France.

Discoaster limbatus Bramlette and Sullivan, new species
Plate 12, figure 3a–b

Description: Asteroliths with 8–11, usually 9, rays joined through about half their length, curving slightly and commonly ornamented by small nodes toward the tips. Rays thickened around the margin and along the ridge or high part of each ray, which is on the convex curving side. Ridges merge centrally into a boss of large diameter, which, however, is somewhat elevated on only one side of the asterolith. Diameter 11–15μ.

Remarks: This distinctive form differs from *Discoaster falcatus* in having a larger central boss, rays commonly ornamented with nodes toward the tips, and more thickened or limbate ridges and margins. Dark radiating lines appear within the central boss on focusing down into the specimen. These are apparently due to an inward continuation of ray structure beneath the surface boss. Some specimens show similarities to *D. helianthus*, but the latter has straight rays of more uniform width and with rounded tips.

Holotype: U.S.N.M. 564341, Lodo 31.

Distribution: Locally common throughout Unit 2 (Paleocene). Occurs in the Bashi Formation (Paleocene or Lower Eocene) of Alabama.

Discoaster lodoensis Bramlette and Riedel
Plate 12, figures 4a–b, 5

Discoaster lodoensis Bramlette and Riedel, 1954, Jour. Pal., vol. 28, no. 4, p. 398, pl. 39, fig. 3a–b. – Martini, 1958, Senckenbergiana leth., vol. 39, no. 5–6, pp. 366–367, pl. 6, fig. 28a–d. – Stradner, 1959, Erdoel-Zeitschr., no. 12, p. 478, text-figs. 14–16, 19–20.

Discoaster currens Stradner, 1959, Erdoel-Zeitschr., no. 12, pp. 477–478, text-figs. 12–13, 18.

Remarks: A restudy of type material shows a stem on both sides of most specimens, though distinctly more prominent on one side. The rays curve sinistrally when viewed from the side with the more prominent stem. Some forms with very short rays and little stem (pl. 12, fig. 5) appear to be only occasional variants of the species. Rare aberrant forms with only three rays and very little stem development are associated with normal specimens and were called *Discoaster currens* by Stradner (1959), although he mentioned their possible relationship to *D. lodoensis*. This widespread species is quite distinctive despite the range in size and number of rays.

Hypotypes: U.S.N.M. 564342, Domengine OC–2, and 564343, Lodo 41.

Distribution: Locally common throughout Units 3 and 4 (Lower and Middle Eocene) and rare in Units 5 and 6 (Middle Eocene). Common in the Lower and Middle Eocene of many regions.

Discoaster martinii Stradner
Plate 12, figure 12a–c

Discoaster pentaradiatus Tan Sin Hok. – Martini, 1958, Senckenbergiana leth., vol. 39, no. 5–6, p. 359, pl. 3, fig. 12a–b.

Discoaster martinii Stradner, 1959, Erdoel-Zeitschr., no. 12, pp. 479–480, text-figs. 45, 47.

Remarks: The California specimens are smaller but otherwise like those from the Aragon Formation of Mexico, from which Stradner (1959) described the species, and resemble his figure 47. His figure 45, however, seems to represent a bizarre and unusual variant, as only one such specimen was observed in our Aragon material among many specimens more like that illustrated here. The asteroliths have five or rarely four rays, with strongly bifurcated and turned-down tips, which extend out at nearly right angles to the rays. The central area is large, and the rays are normally parallel-sided and do not show nodes, nor are the bifurcated tips normally as extended as shown in Stradner's figure 45.

This species differs from *Discoaster pentaradiatus* in being much larger and more robust and in the character of the bifurcated tips of the rays. Examination of material from which Martini (1958) identified this form as *D. pentaradiatus* supports Stradner's view that Martini's form is synonymous with his new species. The California specimens are about 13 to 14μ in diameter.

Hypotype: U.S.N.M. 564344, Canoas GC–3.

Distribution: Locally present in Unit 6 (Middle Eocene). Recorded from the Middle Eocene of Germany.

Discoaster mediosus Bramlette and Sullivan, new species
Plate 12, figures 7a–b, 8

Description: Asteroliths large, having 8–10 small, nearly parallel-sided rays with rounded to somewhat pointed tips, radiating from a large central disk, one side of which has ridges intermediate to the rays and a low central knob. Diameter 11–21μ, usually about 17μ.

Remarks: This species is distinguished by its large central disk and small, nearly parallel-sided rays. The intermediate ridges on the disk are usually distinct, though less so when seen through the specimen from the opposite side.

Holotype: U.S.N.M. 564345, Lodo 22.

Paratype: U.S.N.M. 564346, Lodo 20.

Distribution: Locally common in Unit 2 (Paleocene) and rare in the base of Unit 3 (Lower Eocene).

Discoaster aff. D. mediosus Bramlette and Sullivan
Plate 12, figure 9

Remarks: Forms so designated are not typical in that they are distinctly smaller, ranging from 8 to 13μ in diameter, and have fewer rays, usually 7–9, which are longer in relation to the central disk than in *Discoaster mediosus*. Possibly these sparse forms are only immature specimens, but they are consistently smaller and their range is higher than that of the typical form.

Hypotype: U.S.N.M. 564347, Lodo 68.

Distribution: Locally present in Unit 3 (Lower Eocene). Occurs in the Bashi Formation (Paleocene or Lower Eocene) of Alabama.

Discoaster multiradiatus Bramlette and Riedel
Plate 12, figure 10

Discoaster multiradiatus Bramlette and Riedel, 1954, Jour. Pal., vol. 28, no. 4, p. 396, pl. 38, fig. 10.

Remarks: Relatively few specimens typical of this species were observed in the Lodo samples compared with abundant specimens of the associated varietal form provisionally recorded as *Discoaster multiradiatus* var. The knob on many specimens is indistinct or lacking, as in topotype material.

Hypotype: U.S.N.M. 564348, Lodo 30.

Distribution: Locally rare and sporadic in Units 2 and 3 (Paleocene and Lower Eocene) but very common in the Paleocene strata of the Lodo in nearby localities. Common in the Paleocene of many regions.

Discoaster multiradiatus Bramlette and Riedel var.
Plate 12, figure 11a–b

Remarks: This form differs from the typical species in being more delicate, with rays not thickened but rather thin along the middle and somewhat thicker at the borders, and showing a faint concentric ornamentation. The central knob varies in its degree of development and is lacking in some specimens, as in the typical form. *Discoaster multiradiatus* s. s. is rare in this Lodo section, and this more delicate form might be considered a subspecies. It seems probable, however, that it merely represents less heavily calcified specimens, as some gradation is evident and only the typical form is common in equivalent strata in the Lodo within a few miles. Both forms and intermediate ones commonly occur together in the Paleocene of France.

Hypotype: U.S.N.M. 564349, Lodo 30.

Distribution: Locally common in Unit 2 (Paleocene) and rare through most of Unit 3 (Lower Eocene). Occurs in the Bashi Formation (Paleocene or Lower Eocene) of Alabama.

Discoaster nonaradiatus Klumpp
Plate 12, figures 13–15

Discoaster nonaradiatus Klumpp, 1953, Palaeontographica, vol. 103, pt. A, p. 383, text-fig. 3 (5). – Martini, 1958, Senckenbergiana leth., vol. 39, no. 5–6, p. 364, pl. 4, fig. 21a–b.

Remarks: The California specimens compare well with those identified by Martini and seem to agree with Klumpp's diagrammatic figure. The tips of the rays bifurcate broadly, almost joining to form an entire margin. Strongly curving short ridges in the central area, as in *Discoaster mirus*, are rather common though somewhat obscure (pl. 12, fig. 13); some specimens show ornamentation similar to that of *D. septemradiatus* but differ from that species in the nearly closed margin. Specimens with eight rays are more common than those with nine.

Hypotypes: U.S.N.M. 564350–51, Canoas OC–3, and 564352, Canoas OC–4.

Distribution: Locally present in Units 4, 5, and 6 (Middle Eocene). Recorded from the Middle Eocene of Germany, and occurs in the Weches Formation (Middle Eocene) of Sabine River, Texas, and in the Middle Eocene of France.

Discoaster septemradiatus (Klumpp)
Plate 12, figures 16–17

Agalmatoaster septemradiatus Klumpp, 1953, Palaeontographica, vol. 103, pt. A, p. 384, text-fig. 4(1). – Martini, 1958, Senckenbergiana leth., vol. 39, no. 5–6, pp. 364–365, pl. 4, fig. 20a–b.

Remarks: Although the tips of the rays of this form vary in degree of bifurcation, the ornamentation in the form of ridges between and on the rays is distinctive. The California specimens compare well with those identified by Martini as this species, and seem to agree with Klumpp's figure and description.

Hypotypes: U.S.N.M. 564353, Lodo 58, and 564354, Lodo 71.

Distribution: Locally present in Units 3–6 (Lower and Middle Eocene). Recorded from the Middle Eocene of Germany.

Discoaster sublodoensis Bramlette and Sullivan, **new species**
Plate 12, figure 6a–b

Description: Asteroliths small, with 5 (or less commonly 6) sharply pointed rays joined through about half their length and straight-radiating in the separated outer part. High part of each ray forms a ridge along one side, which turns sharply counter-clockwise near the periphery, as viewed from the stem side, and is usually faint to obscure from there to the tip. Central area with a small stem on one side. Diameter 8–13μ.

Remarks: This species differs from the smallest specimens of *Discoaster lodoensis*, which approach the same size, in having straight-radiating rays with sharply angled ridges, obscure on the outer half, rather than the distinctly curved rays and ridges of the larger species. It commonly occurs in large numbers with few or no associated *D. lodoensis*.

Holotype: U.S.N.M. 564355, Canoas OC–4.

Distribution: Locally present in Units 4 and 5 (Middle Eocene) but abundant only in Unit 5. Occurs in the Weches Formation (Middle Eocene) of Sabine River, Texas, and in the Middle Eocene at Gibret, France.

Discoaster tribrachiatus Bramlette and Riedel
Plate 13, figures 6a–b, 7–13

Discoaster tribrachiatus Bramlette and Riedel, 1954, Jour. Pal., vol. 28, no. 4, p. 397, pl. 38, fig. 11. – Martini, 1958, Senckenbergiana leth., vol. 39, no. 5–6, p. 357, pl. 2, fig. 8a–b. – Stradner, 1959, Erdoel-Zeitschr., no. 12, p. 477, text-figs. 5–6, 10. – Deflandre, 1959, Rev. Micropal., vol. 2, no. 3, pp. 138–139, pl. 2, figs. 1–2.

Discoaster rotans Stradner, 1959, Erdoel-Zeitschr., no. 12, p. 477, text-figs. 7, 11.

Remarks: This consistently three-rayed species shows much variation in the curvature of the rays as seen in side view, in the taper of the rays, and in the character of the tips. Abundant specimens show all intermediate forms between those illustrated in plate 13, figures 6–13, and some of the differences in the rays are shown by one individual. Further subdivision seems of doubtful value, and assignment to more than one taxon becomes difficult. A topotype specimen illustrated by Deflandre (1959, pl. 2, fig. 1), and especially certain variants somewhat similar to it, resemble Deflandre's *Marthasterites*, as he has indicated. Though development from *Marthasterites* seems probable, inclusion of this whole group of variants in *Discoaster tribrachiatus* avoids difficult and apparently unnatural subdivision. Modification of the generic characterization of *Marthasterites* to include them all would eliminate its most important generic character and involve the triradiate variants of species such as *D. brouweri*.

Hypotypes: U.S.N.M. 564356–58, Lodo 33; 564359–62, Lodo 41; and 564363, Lodo 67.

Distribution: Locally common throughout Unit 3 (Lower Eocene), and especially common in the lower part. Common in the Lower Eocene of many regions, including the London Clay of England and the Ypresian of Denmark.

Discoaster spp.
Plate 13, figures 1–5

Remarks: The forms grouped together here show similarities, although the differences in certain features are such as to suggest that perhaps more than one species is represented. The intergradation among many specimens, however, makes any well-defined species difficult to recognize, and their associated stratigraphic occurrence further minimizes any value of subdivision within the group. Pending further study, one or more specific names are not proposed here.

Hypotypes: U.S.N.M. 564364, Lodo 36; 564365, Lodo 50; 564366, Lodo 54; 564367, Lodo 71; and 564368, Domengine OC–1.

Genus **Discoasteroides** Bramlette and Sullivan, **new genus**

Asteroliths having a large, terminally concave stem flaring out as radiate elements at the end.

Between crossed nicols, the difference is especially evident between the ortholithid discoasters, with stem included in the unit mass of calcite, and the heliolithid character of the large stem of *Discoasteroides*. A side view of the stem thus shows different extinction positions for its two sides, and the end view of the stem shows the extinction lines forming a cross.

Although this unusual character of the stem seems adequate as a basis for generic distinction from *Discoaster*, close relationship is indicated by forms such as *Discoaster diastypus*, the large stem of which is deeply depressed terminally, and, although not pronouncedly flaring, it also shows a slight difference in the extinction positions of the two sides.

Type species: Discoasteroides kuepperi (Stradner) = *Discoaster kuepperi* Stradner, 1959.

Discoasteroides kuepperi (Stradner)
Plate 13, figures 16a–b, 17, 18a–c, 19

Discoaster kuepperi Stradner, 1959, Erdoel-Zeitschr., no. 12, p. 478, text-figs. 17, 21.

Remarks: This distinctive and common form in the California section is evidently that described by Stradner. Specimens are mushroom-shaped and have 8 to 10 (usually 9) rays joined through most of their length, with bluntly pointed tips. The large flaring stem has an end diameter as great as half that of the asterolith and is strongly depressed toward the center. The crystallite arrangement in the large stem is characteristic of *Discoasteroides*. An especially large variant of this form (pl. 13, fig. 17) has a smaller stem than normal and rays showing concentric lines, and thus resembles and is perhaps related to *Discoaster elegans*.

Hypotypes: U.S.N.M. 564369, Lodo 41; 564370, Lodo 52; 564371, Lodo 67; and 564372, Lodo 80.

Distribution: Locally common throughout Units 3 and 4 (Lower and Middle Eocene). Recorded from the Paleocene of Austria, and common in the Eocene of many regions.

Discoasteroides megastypus Bramlette and Sullivan, **new species**
Plate 13, figures 14a–d, 15a–c

Description: Asteroliths mushroom-shaped, having about 30 delicate rays, joined throughout their length, with rounded to bluntly pointed tips. Large flaring central stem has a terminal diameter about half that of the asterolith, with end depressed or concave and depression continuing as a small hole down most of the stem. Diameter 8–12μ.

Remarks: In contrast to the heavy stem, the delicate rays of this form are very difficult to see in plan view in Canada balsam. Between crossed nicols, the plan and side views of the large stem show the radiate structure of heliolithids, whereas the petals, which are like the ortholithid discoasters, show no distinct birefringence in plan view. The plan view of *Heliolithus riedeli* appears much like this species, similarly oriented, in transmitted light, but between crossed nicols the radiate petals of *H. riedeli* are quite different in their distinct birefringence and extinction cross (pl. 14, fig. 9c). The rare specimens recorded in Unit 2 include variants rather similar to some specimens of the common *Discoaster multiradiatus* with abnormally large stem, and suggest the development of *D. multiradiatus* from this species.

Holotype: U.S.N.M. 564373, Lodo 22.

Paratype: U.S.N.M. 564374, Lodo 7.

Distribution: Locally present in Unit 1 (Paleocene); sporadic and very rare occurrences in Units 2 and 3 (Paleocene and Lower Eocene).

Genus **Fasciculithus** Bramlette and Sullivan, new genus

Forms of short cylindrical shape, appearing as a bundle of short rods with two or three encircling bands suggestive of a much shortened fascis. End view appearing as a rosette of about ten elements, with one end concave and the other protruding in the central area.

Although showing marked variations, especially in the compactness or solidity of the structure with varying degrees of calcification, which tends to obscure the surface features, this form-genus is distinctive, especially between crossed nicols. The side view shows extinction positions for each side at 25° to 30° from the central axis, and the end view shows an extinction cross indicating the radial arrangement of the heliolithid group.

Type species: Fasciculithus involutus Bramlette and Sullivan.

Fasciculithus involutus Bramlette and Sullivan, new species

Plate 14, figures 1a–c, 2a–b, 3a–b, 4a–b, 5a–b

Description: Specimens of short cylindrical form, with end view appearing as a rosette of about ten rounded petals, both ends somewhat concave but with a small central knob in one end. Commonly compact, with surface ridges on cylindrical sides rather obscure. Length 5–13μ.

Remarks: Much of the variation in appearance of this species seems to be largely related to the solidity of construction by varying amounts of calcite deposition. Specimens are typically like that shown in plate 14, figure 3. Less compact specimens, such as that shown in figure 1, and some of intermediate character are less common. However, subdivision of better characterized taxa within this genus elsewhere may permit their recognition among forms here included in the broadly defined species.

Holotype: U.S.N.M. 564375, Lodo 7.

Paratypes: U.S.N.M. 564376–77, Lodo 7; 564378, Lodo 31; and 564379, Lodo 32.

Distribution: Locally common in Units 1 and 2 (Paleocene); rare and sporadic (reworked?) specimens in Unit 3 (Lower Eocene). Common in the Paleocene of many regions, including France and the type Thanetian of England.

Genus **Heliolithus** Bramlette and Sullivan, new genus

Forms consisting of two partial cones joined at truncate apices and having concave basal ends. The larger of the conical parts is more appressed or flaring and shows more distinctly the many thin radiate elements of construction.

Specimens in Canada balsam are more apparent between crossed nicols than in normal transmitted light, and the heliolithid radial arrangement of component calcite elements is especially conspicuous in end view, which shows the sharply defined cross of the extinction lines.

Type species: Heliolithus riedeli Bramlette and Sullivan.

Heliolithus riedeli Bramlette and Sullivan, new species

Plate 14, figures 9a–c, 10–11

Description: Forms with two conical-shaped parts joined at truncate apices. Conical ends vary from being similar to having one distinctly more appressed and greater in diameter of base. Thin peripheral part of concave bases showing about 20 petal-like elements; small hole present in the thick central part. Diameter 7–11μ.

Remarks: The distinct extinction cross seen in end view between crossed nicols indicates the heliolithid construction, and specimens thus observed are more conspicuous than in ordinary transmitted light. Large specimens are usually more delicate than average ones, due to the deeper concave depression of the ends, especially the larger end.

Holotype: U.S.N.M. 564380, Lodo 6+1.

Paratypes: U.S.N.M. 564381–82, Lodo 6+1.

Distribution: Locally present in Unit 1 (Paleocene); sporadic and very rare (reworked?) specimens in Unit 3 (Lower Eocene). Widespread in the Paleocene, including occurrences in the Nanafalia and Salt Mountain Formations of Alabama, the Velasco shale of Mexico, the *Globorotalia pseudomenardii* Zone of Bolli in Trinidad, the type Thanetian of England, and in the Lower Paleocene 3.2 km. south of Gan, France.

Heliolithus aff. **H. riedeli** Bramlette and Sullivan

Plate 14, figure 12

Remarks: Forms so recorded have the larger end flaring to such a degree as to approach a nearly flat disk, and the number of petal-like elements is correspondingly great, nearly double the twenty usual in the typical form. The smaller end is much reduced in size, so as to appear as a small knob, nevertheless showing the central depression.

Despite the occurrence of specimens that are somewhat intermediate between this form and typical *Heliolithus riedeli*, a distinct taxon may be represented here because in some other occurrences, this is the common form or the only one of the two present.

Distribution: Locally sporadic and very rare (reworked?) in Unit 3 (Lower Eocene), but common in the Paleocene strata of the Lodo in nearby localities. Common in the Paleocene at Belus, France.

Genus **Isthmolithus** Deflandre, 1954

"Corpuscule calcaire à claire-voie, en forme des parallélogramme allongé curviligne, divisé par des barres transversales."

The peculiar shape of the rim seems to be the distinctive feature of this hitherto monotypic genus. Additional study of *Isthmolithus recurvus* indicates some similarities and a possible relationship to *Zygolithus dubius*. The rim of both is higher than it is thick, but the strong relief of their plan view in Canada balsam also seems due to the orientation of their component crystallites. Polarized light shows that the dominant orientation is nearly perpendicular to the plan (flat) view, and this view thus shows nearly the maximum relief or refringence of the calcite in these two species of different genera.

Type species: Isthmolithus recurvus Deflandre.

Isthmolithus unipons Bramlette and Sullivan, new species

Plate 14, figures 15, 16a–b

Description: Specimens in the form of a parallelogram with rounded corners, with central opening divided by a single transverse bar. The two open areas are normally bridged by a rather obscure longitudinal bar, difficult to see except in side view, which arches above the rim and is connected to it and to the transverse bar. Length 5–7μ.

Remarks: This distinctive species has the basic parallelogram form of the genus but differs from *Isthmolithus recurvus* in having only one transverse bar and in having a longitudinal bridge. It is, however, generally scarce and small, and therefore needs more study.

Holotype: U.S.N.M. 564383, Lodo 40.

Distribution: Locally rare and sporadic in Unit 3 (Lower Eocene).

Genus **Polycladolithus** Deflandre, 1954

"Corpuscule calcaire polyédrique arrondi, à contour sensiblement hexagonal, constitué par des sortes de branches émanant du centre, ramifiées et anastamosées, se terminant à la surface en formant des dépressions arrondies."

Variations and the consistent sparseness of specimens make specific and generic characterizations difficult. Most forms seem to have three ridges radiating from the center, each of which bifurcates outward one or more times, as indicated in Deflandre's figured plesiotype but not evident in the holotype. Similarities between *Polycladolithus* and *Lithostromation*, and the occurrence of forms with characters intermediate between these two, require further study. Both groups are ortholithids with the optic C-axis of the single calcite units perpendicular to the flat side.

Type species: Polycladolithus operosus Deflandre.

Polycladolithus operosus Deflandre

Plate 14, figure 13a–c

Polycladolithus operosus Deflandre, 1954, *in* Deflandre and Fert, Ann. Pal., vol. 40, p. 170, pl. 12, figs. 3–6; text-fig. 125.

Remarks: Each side of this discoidal form has three ridges radiating at equal angles from the center, each of which bifurcates twice toward the periphery. The structural patterns on each side of the disk are similar but are offset 60° from each other, as can be seen by focusing down through the specimens. The disk area between the ridges is normally thin and nearly transparent. Diameter 7–13μ.

The California specimens appear similar to Deflandre's (1954, pl. 12, fig. 6) plesiotype from Donzacq, and identical specimens were found in our Donzacq sample. The holotype, from New Zealand, appears, however, somewhat different, although the character is not entirely clear in the illustrations. Pending further study this form is recorded as *P. operosus*.

Hypotype: U.S.N.M. 564384, Lodo 67.

Distribution: Locally rare and sporadic in Units 3 and 4 (Lower and Middle Eocene). Recorded from the Upper Eocene of Oamaru, New Zealand, and the lower Lutetian (Middle Eocene) of Donzacq, France. Also present in the Weches Formation (Middle Eocene) of Sabine River, Texas.

Polycladolithus? sp.

Plate 14, figure 14

Remarks: This distinct form differs from the discoidal *Polycladolithus operosus* in having a trigonal outline and in having more complex outer bifurcation of the ridges. As in *P. operosus*, the radiating ridges on the two sides are offset and oriented at 60° to each other. Specimens are very rare here, however, and evident variations, along with some similarity to *Lithostromation*, make it seem desirable to defer a general description for the species.

Hypotype: U.S.N.M. 564385, Domengine OC–2.

Distribution: Locally rare in Unit 4 (Middle Eocene).

Genus **Rhomboaster** Bramlette and Sullivan, new genus

Forms with the basic symmetry of a rhombohedron but with the faces strongly depressed which, results in extended spine-like corners.

The ortholithid character, as a unit of calcite, is evident in polarized light. The edges of all sides are apparent in transmitted light, and in various orientations correspond to those of an oblate rhombohedron of calcite. This unusual form is perhaps more suggestive of an internal than an external skeletal element. The abundance of specimens and their occurrence only in association with abundant coccolithophorids, however, indicates derivation from some form of the nannoplankton, and their restricted occurrence in time and their associations disprove an inorganic origin even though the form is suggestive of some unusual habit of inorganic calcite crystal growth.

(465)

"*Discoaster*" *contortus* Stradner (1958) appears to be closely related to *Rhomboaster* but shows a peculiar contortion, as though twisted on an axis between opposite corners of the rhombic form. Topotype specimens of "*Trochoaster*" duplex Klumpp (1953) also appear to represent a related form, but the type species, *Trochoaster simplex* Klumpp (1953), is a complanate form and quite different from *Rhomboaster.*

Associated with an undescribed species of *Rhomboaster* in the Upper Cretaceous, there is a common form somewhat similar to the type species, particularly to that form illustrated in plate 14, figure 17, but differing fundamentally in being constructed of at least two units of differently oriented calcite, evident in polarized light.

Type species: Rhomboaster cuspis Bramlette and Sullivan.

Rhomboaster cuspis Bramlette and Sullivan, **new species**

Plate 14, figures 17–18, 19a–c

Description: Specimens with edges indicating a rhombohedral symmetry but with faces depressed, usually strongly concave, and cuspate corners extended like spines. Polarized light shows that it is composed of a unit mass of calcite.

Remarks: Normal Lodo specimens are shown in plate 14, figures 18–19. They appear in the usual orientation as one triradiate form superimposed on another. Figure 17 illustrates a form included in the species which has less depressed faces than usual and appears more like an ordinary rhomb of calcite. This variant is rare in the Lodo section but is the dominant form in equivalent strata in a nearby locality. Overall diameter 8–9μ, average 11μ.

Holotype: U.S.N.M. 564386, Lodo 22.

Paratypes: U.S.N.M. 564387, Lodo 22, and 564388, Lodo 32.

Distribution: Locally present throughout Unit 2 (Paleocene); very rare and sporadic occurrences in Unit 3 (Lower Eocene). Occurs in the Bashi Formation (Paleocene or Lower Eocene) of Alabama, and in the Paleocene of Trinidad.

Genus **Sphenolithus** Deflandre, 1952

"Sphénolithes à embase prismatique surmontée d'un cône allongé costulé; embase polygonale arrondie (en vue apicale), formée de bâtonnets calcaires rayonnant autour de son centre" (Deflandre, 1952*a*, p. 466).

Specimen in Canada balsam are distinctive and more obvious between crossed nicols than in normal light, and the elongate elements forming the spike also seem to be a part of the radiate arrangement of a heliolithid type.

Type species: Sphenolithus radians Deflandre.

Sphenolithus radians Deflandre

Plate 14, figures 6–7, 8a–b

Sphenolithus radians Deflandre, 1954, *in* Deflandre and Fert, Ann. Pal., vol. 40, p. 163, pl. 12, figs. 36–38; text-figs. 109–112.

Remarks: The specimens recorded here appear identical with those of topotype material and Deflandre's figures 36–38. His text-figures 109–112 seem to represent more heavily calcified specimens. The base is concave owing to the absence of the radiate "elements" there, and the stem consists of unusually large ones, but the basically radiate character of the heliolithids is evident.

Hypotypes: U.S.N.M. 564389, Lodo 52, and 564390–91, Lodo 80.

Distribution: Locally common throughout Unit 3 (Lower Eocene) and also present in Units 4 and 5 (Middle Eocene). Common in the Eocene of many regions; recorded from the lower Lutetian (Middle Eocene) of Donzacq, France.

Contribution from Scripps Institution of Oceanography, La Jolla, California. New Series.

BIBLIOGRAPHY

Bolli, H. M.
1957 – *The genera Globigerina and Globorotalia in the Paleocene—Lower Eocene Lizard Springs Formation of Trinidad, B.W.I.* U. S. Nat. Mus., Bull. 215, pp. 61–81.

Bramlette, M. N.
1958 – *Significance of coccolithophorids in calcium carbonate deposition.* Geol. Soc. Amer., Bull., vol. 69, pp. 121–126.

Bramlette, M. N., and Riedel, W. R.
1954 – *Stratigraphic value of discoasters and some other microfossils related to recent coccolithophores.* Jour. Pal., vol. 28, no. 4, pp. 385–403, pls. 38–39.

Chamrai, I. A., and Lazareva, E. P.
1956 – *Coccolithophoridae and their stratigraphic importance.* Akad. Nauk S.S.S.R., Doklady, vol. 108, pp. 711–714, 1 pl. (in Russian).

Deflandre, G.
1947 – *Braarudosphaera nov. gen., type d'une famille nouvelle de coccolithophoridées actuels à éléments composites.* Acad. Sci., C. R., vol. 225, pp. 439–441.
1950 – *Observations sur les coccolithophoridés, à propos d'un nouveau type de braarudosphaeridé, Micrantholithus, à éléments clastiques.* Acad. Sci., C. R., vol. 231, pp. 1156–1158.
1952*a* *Classe des Coccolithophoridés.* In: Grassé, P. P. (Ed.), *Traité de Zoologie.* Vol. 1, fasc. 1, pp. 439–470, text-figs. 339–364.
1952*b* *Sous-embranchement des flagellés.* In: Piveteau, J. (Ed.), *Traité de Paléontologie.* Vol. 1, pp. 99–130, text-figs. 1–150.
1959 – *Sur les nannofossiles calcaires et leur systématique.* Rev. Micropal., vol. 2, no. 3, pp. 127–152, pls. 1–4.

Deflandre, G., and Fert, C.
1952 – *Sur la structure fine de quelques coccolithes fossiles observés au microscope électronique; Signification morphogénétique et application à la systématique.* Acad. Sci., C. R., vol. 234, pp. 2100–2102, 8 text-figs.

1954 – *Observations sur les coccolithophoridés actuels et fossiles en microscopie ordinaire et électronique.* Ann. Pal., vol. 40, pp. 117–176, pls. 1–15.

Ehrenberg, C. G.
1836 – K. Preuss. Akad. Wiss. Verh., Berlin, pp. 84–85.
1854 – *Mikrogeologie.* Leipzig.

Gaarder, K. R.
1954 – *Coccolithineae, Silicoflagellatae, Pterospermataceae and other forms from the "Michael Sars" North Atlantic Deep-Sea Expedition 1910.* Rept. Sci. Results "Michael Sars" North Atlantic Deep-Sea Exped. 1910, vol. 2, no. 4, pp. 3–20.

Gorka, H.
1957 – *Coccolithophoridae z górnego mastrychtu Polski środkowej.* Acta Pal. Polonica, vol. 2, pp. 235–284, pls. 1–5.

Gran, H. H., and Braarud, T.
1935 – *A qualitative study of the phytoplankton in the Bay of Fundy and the Gulf of Maine.* Jour. Biol. Board Canada, vol. 1, pp. 279–467.

Haeckel, E.
1894 – *Systematische Phylogenie der Protisten und Pflanzen.* Leipzig: Vol. 1, p. 111.

Huxley, T. H.
1858 – *Appendix to Capt. Dayman's Admiralty Report "Deep-Sea soundings in the N. Atlantic Ocean made in H.M.S. Cyclops."*

Israelsky, M. C.
1951 – *Foraminifera of the Lodo Formation, central California: General introduction and Part 1, Arenaceous foraminifera.* U. S. Geol. Survey, Prof. Paper 240–A, pp. 1–29, pls. 2–11.
1955 – *Foraminifera of the Lodo Formation, Central California: Part 2, Calcareous foraminifera (Miliolidae and Lagenidae, part).* U. S. Geol. Survey, Prof. Paper 240–B, pp. 31–79, pls. 12–19.

Jukes-Browne, A. J., and Harrison, J. B.
1892 – *The geology of Barbados; Part II, The Oceanic deposits.* Geol. Soc. London, Quart. Jour., vol. 48, pp. 170–226.

Kamptner, E.
1941 – *Die Coccolithineen der Südwestküste von Istrien.* Ann. Naturhist. Mus. Wien, vol. 51, pp. 54–149, pls. 1–15.
1948 – *Coccolithen aus dem Torton des Inneralpinen Wiener Beckens.* Österr. Akad. Wiss., Math.-Naturwiss. Kl., Sitzber., Abt. 1, vol. 157, pp. 1–16.
1949 – *Fossile Coccolithineen-Skelettreste aus dem Molukken-Archipel.* Österr. Akad. Wiss., Math.-Naturwiss. Kl., Anz., vol. 86, pp. 77–80.
1954 – *Untersuchungen über den Feinbau der Coccolithen.* Archiv Protistenk., vol. 100, no. 1, pp. 1–90, text-figs. 1–50.
1955 – *Fossile Coccolithineen-Skelettreste aus Insulinde; Eine mikropaläontologische Untersuchung.* K. Nederl. Akad. Wetensch., Verh., ser. 2, vol. 50, no. 2, pp. 1–87, pls. 1–9.
1956 – *Zur Systematik und Nomenklatur der Coccolithineen.* Österr. Akad. Wiss., Math-Naturwiss. Kl., Anz., no. 1, pp. 4–11.
1958 – *Betrachtungen zur Systematik der Kalkflagellaten, nebst Versuch einer neuen Gruppierung der Chrysomonadales.* Archiv Protistenk., vol. 103, no. 1–2, pp. 54–116.

Klumpp, B.
1953 – *Beitrag zur Kenntnis der Mikrofossilien des Mittleren und Oberen Eozän.* Palaeontographica, vol. 103, pt. A, pp. 377–406, pls. 16–20.

Laiming, B.
1940 – *Some foraminiferal correlations in the Eocene of San Joaquin Valley, California.* Proc. Sixth Pacific Sci. Congr., 1939, vol. 2, pp. 535–568.

Loeblich, A. R., and Tappan, H.
1957 – *Planktonic foraminifera of Paleocene and early Eocene age from the Gulf and Atlantic Coastal Plains.* U. S. Nat. Mus., Bull. 215, pp. 173–198.

Lohmann, H.
1902 – *Die Coccolithophoridae, eine Monographie der coccolithenbildenden Flagellaten.* Archiv Protistenk., vol. 1, pp. 89–165, pls. 4–6.

Martini, E.
1958 – *Discoasteriden und verwandte Formen im NW-deutschen Eozän (Coccolithophorida).* Senckenbergiana Leth., vol. 39, no. 5–6, pp. 353–388, pls. 1–6.
1959 – *Pemma angulatum und Micrantholithus basquensis, zwei neue Coccolithophoriden-Arten aus dem Eozän.* Senckenbergiana Leth., vol. 40, no. 5–6, pp. 415–421, pl. 1.

Murray, G., and Blackman, V. H.
1898 – *On the nature of the coccospheres and rhabdospheres.* Roy. Soc. London, Phil. Trans., vol. 190, sec. B, pp. 427–441.

Noël, D.
1956 – *Coccolithes des terrains Jurassiques de l'Algérie.* Publ. Service Carte Géol. Algérie, new ser., Bull. 8, pp. 303–345.

Parke, M., and Adams, I.
1960 – *The motile (Crystallolithus hyalinus Gaarder & Markali) and nonmotile phases in the life history of Coccolithus pelagicus (Wallich) Schiller.* Jour. Marine Biol. Assoc. U. K., vol. 39, pp. 263–274, pls. 1–4.

Schiller, J.
1930 – *Coccolithineae.* In: Rabenhorst, L., *Kryptogamen-Flora.* Leipzig: Vol. 10, pt. 2, pp. 89–267.

Schwarz, E. H. L.
1894 – *Coccoliths.* Ann. Mag. Nat. Hist., ser. 6, vol. 14, pp. 341–346.

Sorby, H. C.
1861 – *On the organic origin of the so-called crystalloids of the Chalk.* Ann. Mag. Nat. Hist., ser. 3, vol. 8, pp. 193–200.

Stradner, H.
1958 – *Die fossilen Discoasteriden Österreichs; I.* Erdoel-Zeitschr., no. 6, pp. 178–188, text-figs. 1–38.
1959 – *Die fossilen Discoasteriden Österreichs; II.* Erdoel-Zeitschr., no. 12, pp. 472–488, text-figs. 1–77.

Tan Sin Hok
1927 – *Over de samenstelling en het ontstaan van krijt- en mergelgesteenten van de Molukken.* Mijnw. Ned. Oost-Indië, Jaarb. (1926), pp. 1–165, 16 pls.

Vekschina, V. N.
1959 – *Kokkolithoforidy maastrikhtskikh otlozhenii Zapadno-Sibirkoi Nizmennosti.* Trudy SNIIGGIMS, no. 2, pp. 56–77, pls. 1–2.

Wallich, G. C.
1860 – Ann. Mag. Nat. Hist., ser. 3, vol. 6, pp. 451–458.

EXPLANATION OF PLATES

PLATE 1

1 *Coccolithus bidens* Bramlette and Sullivan, n. sp.
Distal view; fluorite replacement.

2 *Coccolithus consuetus* Bramlette and Sullivan, n. sp.
a, proximal view; b, side view, drawing; c, proximal view, long axis 0° to x-nic*.

3 *Coccolithus eminens* Bramlette and Sullivan, n. sp.
a, proximal view; b, side view, drawing; c, proximal view, long axis 0° to x-nic*; d, distal view, drawing.

4 *Coccolithus crassus* Bramlette and Sullivan, n. sp.
a, proximal view; b, side view, drawing; c, proximal view, long axis 0° to x-nic*; d, distal view, drawing.

5 *Coccolithus expansus* Bramlette and Sullivan, n. sp.
a, distal view; b, oblique view, drawing; c, side view, drawing; d, distal view, long axis 17° to x-nic*.

6 *Coccolithus gigas* Bramlette and Sullivan, n. sp.
a, distal view; b, side view, drawing; c, distal view, long axis 80° to x-nic*; d, distal view, drawing.

7 *Coccolithus* aff. *C. gigas* Bramlette and Sullivan
a, distal view; b, side view section, drawing; c, distal view, long axis 50° to x-nic*; d, distal view, drawing.

PLATE 2

1 *Coccolithus grandis* Bramlette and Riedel
Hypotype no. 564185: a, proximal view; b, proximal view, long axis 0° to x-nic*.

2 *Coccolithus grandis* Bramlette and Riedel
Hypotype no. 564184: a, distal view, fluorite replacement; b, side view, drawing; c, end view, drawing.

3 *Coccolithus grandis* Bramlette and Riedel
Hypotype no. 564186, oblique view, fluorite replacement.

4 *Coccolithus solitus* Bramlette and Sullivan, n. sp.
a, proximal view; b, side view, drawing; c, proximal view, long axis 0° to x-nic*.

5 *Coccolithus staurion* Bramlette and Sullivan, n. sp.
Hypotype no. 564189: a, distal view; b, distal view, long axis 0° to x-nic*.

6 *Coccolithus staurion* Bramlette and Sullivan, n. sp.
Holotype, no. 564188: a, distal view; b, side view, drawing; c, distal view, long axis 0° to x-nic*.

7 *Cyclolithus? robustus* Bramlette and Sullivan, n. sp.
a, plan view; b, side view, drawing; c, plan view, drawing.

8 *Discolithus distinctus* Bramlette and Sullivan n. sp.
Paratype no. 564192: a, proximal view; b, proximal view, long axis 30° to x-nic*.

9 *Discolithus distinctus* Bramlette and Sullivan, n. sp.
Holotype, no. 564191: a, distal view; b, side view section, drawing; c, distal view, long axis 30° to x-nic*.

10 *Discolithus exilis* Bramlette and Sullivan, n. sp.
a, distal view; b, side view, drawing; c, distal view, long axis 0° to x-nic*.

11 *Discolithus duocavus* Bramlette and Sullivan, n. sp.
a, proximal view; b, side view, drawing; c, proximal view, long axis 12° to x-nic*; d, distal view, drawing.

PLATE 3

1 *Discolithus fimbriatus* Bramlette and Sullivan, n. sp.
a, proximal view; b, side view, drawing; c, proximal view, long axis 75° to x-nic*; d, distal view, drawing.

2 *Discolithus ocellatus* Bramlette and Sullivan, n. sp.
a, distal view; b, side view, drawing; c, distal view, long axis 10° to x-nic*.

3 *Discolithus panarium* Deflandre
a, distal view; b, side view, drawing; c, distal view, long axis 72° to x-nic*; d, distal view, drawing.

4 *Discolithus pectinatus* Bramlette and Sullivan, n. sp.
Holotype, no. 564198: a, distal view; b, distal view, long axis 20° to x-nic*.

5 *Discolithus pectinatus* Bramlette and Sullivan, n. sp.
Paratype no. 564199: a, distal view; b, distal view, long axis 15° to x-nic*.

6 *Discolithus* aff. *D. planus* Bramlette and Sullivan
a, distal view; b, distal view, long axis 10° to x-nic*.

7 *Discolithus planus* Bramlette and Sullivan, n. sp.
a, proximal view; b, side view section, drawing; c, proximal view, long axis 20° to x-nic*.

8 *Discolithus pulcher* Deflandre
a, distal view; b, side view, drawing; c, distal view, long axis 5° to x-nic*.

9 *Discolithus* aff. *D. pulcher* Deflandre
Hypotype no. 564203: a, distal view, fluorite replacement; b, side view, drawing.

---

*Measured clockwise from either plane of crossed nicols.

*Measured clockwise from either plane of crossed nicols.

10 *Discolithus* aff. *D. pulcher* Deflandre
Hypotype no. 564204, proximal view, long axis 75° to x-nic*.

11 *Discolithus punctosus* Bramlette and Sullivan, n. sp.
a, distal view; b, side view section, drawing; c, distal view, long axis 15° to x-nic*.

12 *Discolithus rimosus* Bramlette and Sullivan, n. sp.
Paratype no. 564207: a, distal view; b, side view section, drawing; c, distal view, long axis 60° to x-nic*.

13 *Discolithus rimosus* Bramlette and Sullivan, n. sp.
Holotype, no. 564206, distal view.

14 *Discolithus solidus* Deflandre
Hypotype no. 564208: a, distal view; b, side view, drawing; c, distal view, drawing.

15 *Discolithus solidus* Deflandre
Hypotype no. 564209, proximal view.

16 *Discolithus versus* Bramlette and Sullivan, n. sp.
a, distal view; b, side view, drawing; c, distal view, long axis 20° to x-nic*; d, distal view, drawing.

PLATE 4

1 *Helicosphaera seminulum seminulum* Bramlette and Sullivan, n. ssp.
Paratype no. 564212: a, proximal view, fluorite replacement; b, side view, drawing; c, end view, drawing.

2 *Helicosphaera seminulum seminulum* Bramlette and Sullivan, n. ssp.
Holotype, no. 564211, proximal view, long axis 0° to x-nic*.

3 *Helicosphaera seminulum lophota* Bramlette and Sullivan, n. ssp.
Holotype, no. 564213: a, proximal view; b, proximal view, long axis 0° to x-nic*.

4 *Helicosphaera seminulum lophota* Bramlette and Sullivan, n. ssp.
Paratype no. 564214, proximal view, fluorite replacement.

5 *Lophodolithus reniformis* Bramlette and Sullivan, n. sp.
a, distal view, fluorite replacement; b, side view, drawing; c, distal view, drawing.

6 *Lophodolithus mochlophorus* Deflandre
a, proximal view; b, side view, drawing; c, proximal view, long axis 70° to x-nic*.

7 *Lophodolithus nascens* Bramlette and Sullivan, n. sp.
Paratype no. 564217: a, proximal view; b, side view, drawing; c, proximal view, long axis 75° to x-nic*.

8 *Lophodolithus nascens* Bramlette and Sullivan, n. sp.
Holotype, no. 564216: a, distal view; b, side view section, drawing; c, distal view, long axis 0° to x-nic*.

9 *Zygodiscus adamas* Bramlette and Sullivan, n. sp.
Holotype, no. 564237: a, proximal view; b, side view, drawing; c, proximal view, long axis 85° to x-nic*.

10 *Zygodiscus adamas* Bramlette and Sullivan, n. sp.
Paratype no. 564238: a, proximal view, long axis 90° to polarizer, lower nicol only; b, proximal view, long axis 0° to polarizer, lower nicol only; c, proximal view, long axis 70° to x-nic*.

11 *Zygodiscus sigmoides* Bramlette and Sullivan, n. sp.
a, distal view; b, side view, drawing; c, end view, drawing; d, distal view, long axis 30° to x-nic*; e, distal view, drawing.

12 *Zygodiscus plectopons* Bramlette and Sullivan, n. sp.
a, distal view; b, side view, drawing; c, end view, drawing; d, distal view, long axis 12° to x-nic*.

13 *Zygodiscus* aff. *Z. plectopons* Bramlette and Sullivan
a, proximal view; b, side view, drawing; c, proximal view, long axis 25° to x-nic*; d, proximal view, long axis 65° to x-nic*; e, proximal view, long axis 40° to x-nic*.

PLATE 5

1 *Rhabdosphaera crebra* (Deflandre)
Hypotype no. 564219.

2 *Rhabdosphaera crebra* (Deflandre)
Hypotype no. 564221, long axis 45° to x-nic.*

3 *Rhabdosphaera crebra* (Deflandre)
Hypotype no. 564220, long axis 0° to x-nic*.

4 *Rhabdosphaera inflata* Bramlette and Sullivan, n. sp.
Holotype, no. 564222: a, side view; b, side view, long axis 0° to x-nic*.

5 *Rhabdosphaera inflata* Bramlette and Sullivan, n. sp.
Paratype no. 564223.

6 *Rhabdosphaera? rudis* Bramlette and Sullivan, n. sp.
a, side view; b, slightly oblique view, drawing.

---

*Measured clockwise from either plane of crossed nicols.

*Measured clockwise from either plane of crossed nicols.

7 *Rhabdosphaera perlonga* (Deflandre)
a, side view; b, side view, long axis 45° to x-nic*; c, side view, long axis 0° to x-nic*.

8 *Rhabdosphaera? semiformis* Bramlette and Sullivan, n. sp.
Holotype, no. 564229.

9 *Rhabdosphaera? semiformis* Bramlette and Sullivan, n. sp.
Paratype no. 564230.

10 *Rhabdosphaera? semiformis* Bramlette and Sullivan, n. sp.
Paratype no. 564231: a, side view; b, side view, long axis 45° to x-nic*.

11 *Rhabdosphaera scabrosa* (Deflandre)
a, side view; b, side view, long axis 0° to x-nic*.

12 *Rhabdosphaera morionum* (Deflandre)
Hypotype no. 564224: a, side view; b, side view, long axis 45° to x-nic*.

13 *Rhabdosphaera morionum* (Deflandre)
Hypotype no. 564225.

14 *Rhabdosphaera tenuis* Bramlette and Sullivan, n. sp.
a, side view; b, side view, long axis 0° to x-nic*.

15 *Rhabdosphaera truncata* Bramlette and Sullivan, n. sp.
a, side view; b, side view, long axis 0° to x-nic*.

16 *Rhabdosphaera vitrea* (Deflandre)
Hypotype no. 564235, side view, fluorite replacement.

17 *Rhabdosphaera vitrea* (Deflandre)
Hypotype no. 564234.

18 *Rhabdosphaera* sp.
a, side view; b, side view, long axis 45° to x-nic*.

19 Lopadolith from Lodo 39
Side view.

20 Lopadolith from Lodo 52.
Side view.

PLATE 6

1 *Zygolithus chiastus* Bramlette and Sullivan, n. sp.
Paratype no. 564243: a, distal view; b, side view, drawing; c, end view, drawing; d, distal view, long axis 65° to x-nic*.

2 *Zygolithus chiastus* Bramlette and Sullivan, n. sp.
Holotype, no. 564242: a, proximal view; b, proximal view, long axis 52° to x-nic*.

3 *Zygolithus chiastus* Bramlette and Sullivan, n. sp.
Paratype no. 564244: a, distal view; b, distal view, long axis 75° to x-nic*.

4 *Zygolithus distentus* Bramlette and Sullivan, n. sp.
Paratype no. 564249: a, proximal view; b, proximal view, long axis 20° to x-nic*; c, distal view, drawing.

5 *Zygolithus distentus* Bramlette and Sullivan, n. sp.
Paratype no. 564250, distal view.

6 *Zygolithus distentus* Bramlette and Sullivan, n. sp.
Holotype, no. 564248: a, distal view; b, side view, drawing; c, distal view, long axis 70° to x-nic*; d, distal view, drawing.

7 *Zygolithus distentus* Bramlette and Sullivan, n. sp.
Paratype no. 564251, distal view.

8 *Zygolithus crux* (Deflandre and Fert)
Hypotype no. 564246, plan view, fluorite replacement.

9 *Zygolithus crux* (Deflandre and Fert)
Hypotype no. 564245.

10 *Zygolithus crux* (Deflandre and Fert)
Hypotype no. 564247.

11 *Zygolithus junctus* Bramlette and Sullivan, n. sp.
a, distal view; b, distal view, long axis 20° to x-nic*.

12 *Zygolithus dubius* Deflandre
Hypotype no. 564252, distal view.

13 *Zygolithus dubius* Deflandre
Hypotype no. 564254, distal view.

14 *Zygolithus dubius* Deflandre
Hypotype no. 564253: a, side view; b, side view, long axis 45° to x-nic*.

15 *Zygolithus protenus* Bramlette and Sullivan, n. sp.
a, distal view; b, distal view, long axis 45° to x-nic*.

16 *Zygrhablithus bijugatus* (Deflandre)
Hypotypes no. 564258: a, side views of two specimens; b, long axis of specimen to right 0° to x-nic*.

17 *Zygrhablithus bijugatus* (Deflandre)
Hypotype no. 564257: a, distal view, long axis 0° to polarizer, lower nicol only; b, distal view, long axis 90° to polarizer, lower nicol only; c, distal view, long axis 45° to x-nic*.

18 *Zygrhablithus bijugatus* (Deflandre)
Hypotype no. 564259, oblique view.

19 *Zygrhablithus simplex* Bramlette and Sullivan, n. sp.
Holotype, no. 564260, side view.

---

*Measured clockwise from either plane of crossed nicols.

*Measured clockwise from either plane of crossed nicols.

20 *Zygrhablithus simplex* Bramlette and Sullivan, n. sp. Paratype no. 564263: a, side view, with rim broken off; b, side view, long axis 45° to x-nic*.

21 *Zygrhablithus simplex* Bramlette and Sullivan, n. sp. Paratype no. 564262, distal view, fluorite replacement.

22 *Zygrhablithus simplex* Bramlette and Sullivan, n. sp. Paratype no. 564261, oblique view, fluorite replacement.

PLATE 7

1 *Coccolithites delus* Bramlette and Sullivan, n. sp. Paratype no. 564265: a, proximal view, fluorite replacement; b, side view, drawing; c, end view, drawing.

2 *Coccolithites delus* Bramlette and Sullivan, n. sp. Holotype, no. 564264: a, proximal view, long axis 0° to x-nic*; b, proximal view, long axis 45° to x-nic*.

3 *Coccolithites* aff. *C. delus* Bramlette and Sullivan Hypotype no. 564266, proximal view, fluorite replacement.

4 *Coccolithites* aff. *C. delus* Bramlette and Sullivan Hypotype no. 564267, distal view, long axis 0° to x-nic*.

5 *Coccolithites cribellum* Bramlette and Sullivan, n. sp. Holotype, no. 564268: a, distal view, lower nicol only; b, distal view, long axis 75° to x-nic*.

6 *Coccolithites cribellum* Bramlette and Sullivan, n. sp. Paratype no. 564269: a, proximal view; b, side view, drawing.

7 *Coccolithites gammation* Bramlette and Sullivan, n. sp. Holotype, no. 564271: a, proximal view; b, side view, drawing; c, proximal view, crossed nicols.

8 *Coccolithites distichus* Bramlette and Sullivan, n. sp. a, distal view; b, side view, drawing; c, distal view, long axis 45° to x-nic*.

9 *Coccolithites* sp.
Hypotype no. 564277: a, distal view, fluorite replacement; b, side view, drawing.

10 *Coccolithites* sp.
Hypotype no. 564276, distal view, long axis 0° to x-nic*.

11 *Coccolithites macellus* Bramlette and Sullivan, n. sp. Paratype no. 564274, proximal view.

12 *Coccolithites macellus* Bramlette and Sullivan, n. sp. Paratype no. 564275, distal view, long axis 35° to x-nic*.

13 *Coccolithites macellus* Bramlette and Sullivan, n. sp. Holotype, no. 564273: a, distal view; b, side view, drawing; c, distal view, long axis 45° to x-nic*; d, distal view, drawing.

14 *Coccolithites gammation* Bramlette and Sullivan, n. sp. Specimens from Donzacq, France: a, proximal view of part of a coccosphere; b, proximal view, with crossed nicols, of part of a coccosphere.

PLATE 8

1 *Braarudosphaera bigelowi* (Gran and Braarud)
Hypotype no. 564280: a, distal view; b, side view, drawing.

2 *Braarudosphaera bigelowi* (Gran and Braarud)
Hypotype no. 564278, distal view of unusual specimen with large central opening, crossed nicols.

3 *Braarudosphaera bigelowi* (Gran and Braarud)
Hypotype no. 564279, side view.

4 *Braarudosphaera bigelowi* (Gran and Braarud)
Hypotype no. 564282, small complete specimen of 12 pentaliths.

5 *Braarudosphaera bigelowi* (Gran and Braarud)
Hypotype no. 564281, distal view of specimen with *Micrantholithus*-like central star, crossed nicols.

6 *Braarudosphaera discula* Bramlette and Riedel
Hypotype no. 564283: a, plan view; b, side view, drawing.

7 *Braarudosphaera discula* Bramlette and Riedel
Hypotype no. 564284, distal view.

8 *Micrantholithus attenuatus* Bramlette and Sullivan, n. sp.
Holotype, no. 564285: a, plan view; b, plan view, crossed nicols.

9 *Micrantholithus attenuatus* Bramlette and Sullivan, n. sp.
Paratype no. 564286, single segment.

10 *Micrantholithus attenuatus* Bramlette and Sullivan, n. sp.
Paratype no. 564287, single segment.

11 *Micrantholithus attenuatus* Bramlette and Sullivan, n. sp.
Paratype no. 564288, single segment.

---

*Measured clockwise from either plane of crossed nicols.

*Measured clockwise from either plane of crossed nicols.

12 *Micrantholithus* aff. *M. attenuatus* Bramlette and Sullivan
a, plan view; b, plan view, crossed nicols.

13 *Micrantholithus pinguis* Bramlette and Sullivan, n. sp.
a, plan view; b, side view, drawing.

14 *Micrantholithus basquensis* Martini
Hypotype no. 564290, a, plan view; b, side view, drawing; c, plan view, crossed nicols.

15 *Micrantholithus basquensis* Martini
Hypotype no. 564291, plan view, crossed nicols.

PLATE 9

1 *Micrantholithus concinnus* Bramlette and Sullivan, n. sp.
a, plan view; b, side view, drawing; c, plan view, crossed nicols.

2 *Micrantholithus bramlettei* Deflandre
a, plan view of common variant; b, plan view, crossed nicols.

3 *Micrantholithus crenulatus* Bramlette and Sullivan, n. sp.
Holotype, no. 564294: a, plan view; b, plan view, crossed nicols.

4 *Micrantholithus crenulatus* Bramlette and Sullivan, n. sp.
Paratype no. 564295.

5 *Micrantholithus entaster* Bramlette and Sullivan, n. sp.
Paratype no. 564297: a, plan view; b, side view, drawing; c, plan view, crossed nicols.

6 *Micrantholithus entaster* Bramlette and Sullivan, n. sp.
Paratype no. 564298.

7 *Micrantholithus entaster* Bramlette and Sullivan, n. sp.
Holotype, no. 564296: a, plan view, median focus; b, plan view, high focus.

8 *Micrantholithus flos* Deflandre
a, plan view; b, plan view, crossed nicols.

9 *Micrantholithus truncus* Bramlette and Sullivan, n. sp.
a, plan view; b, plan view, crossed nicols.

10 *Micrantholithus vesper* Deflandre
a, plan view, with segments partly separated; b, plan view, crossed nicols.

11 *Thoracosphaera* sp. from Lodo 32
Sphere oriented with buccal opening upward.

PLATE 10

1 *Chiphragmalithus acanthodes* Bramlette and Sullivan, n. sp.
Holotype, no. 564303: a, distal view; b, oblique view, drawing.

2 *Chiphragmalithus acanthodes* Bramlette and Sullivan, n. sp.
Paratype no. 564304, plan view.

3 *Chiphragmalithus acanthodes* Bramlette and Sullivan, n. sp.
Paratype no. 564306, side view.

4 *Chiphragmalithus acanthodes* Bramlette and Sullivan, n. sp.
Paratype no. 564307, proximal view, slightly oblique.

5 *Chiphragmalithus acanthodes* Bramlette and Sullivan, n. sp.
Paratype no. 564305, proximal view.

6 *Chiphragmalithus acanthodes* Bramlette and Sullivan, n. sp.
Paratype no. 564308, oblique view.

7 *Chiphragmalithus calathus* Bramlette and Sullivan, n. sp.
Holotype, no. 564309: a, distal view; b, oblique view, drawing.

8 *Chiphragmalithus calathus* Bramlette and Sullivan, n. sp.
Paratype no. 564310, plan view.

9 *Chiphragmalithus calathus* Bramlette and Sullivan, n. sp.
Paratype no. 564312, side view.

10 *Chiphragmalithus calathus* Bramlette and Sullivan, n. sp.
Paratype no. 564311, side view.

11 *Chiphragmalithus cristatus* (Martini)
Hypotype no. 564313: a, distal view; b, oblique view, drawing; c, proximal view, drawing.

12 *Chiphragmalithus cristatus* (Martini)
Hypotype no. 564315, side view, slightly oblique.

13 *Chiphragmalithus cristatus* (Martini)
Hypotype no. 564314, proximal view.

14 *Chiphragmalithus? quadratus* Bramlette and Sullivan, n. sp.
Holotype, no. 564316: a, distal view; b, side view, drawing.

15 *Chiphragmalithus? quadratus* Bramlette and Sullivan, n. sp.
Paratype no. 564317, plan view.

16 *Clathrolithus ellipticus* Deflandre
Hypotype no. 564319: a, distal view, low focus; b, distal view, high focus.

17 *Clathrolithus ellipticus* Deflandre
Hypotype no. 564318, side view.

18 *Clathrolithus minutus* Bramlette and Sullivan, n. sp.
Plan view, fluorite replacement.

PLATE 11

1 *Discoaster binodosus* Martini
a, plan view; b, side view, drawing.

2 *Discoaster barbadiensis* Tan Sin Hok

3 *Discoaster delicatus* Bramlette and Sullivan, n. sp.

4 *Discoaster deflandrei* Bramlette and Riedel
a, plan view; b, side view, drawing.

5 *Discoaster cruciformis* Martini
a, plan view; b, side view, drawing.

6 *Discoaster diastypus* Bramlette and Sullivan, n. sp.
Paratype no. 564328.

7 *Discoaster diastypus* Bramlette and Sullivan, n. sp.
Paratype no. 564327, side view.

8 *Discoaster diastypus* Bramlette and Sullivan, n. sp.
Holotype, no. 564326.

9 *Discoaster* aff. *D. diastypus* Bramlette and Sullivan
Hypotype no. 564330, side view.

10 *Discoaster* aff. *D. diastypus* Bramlette and Sullivan
Hypotype no. 564329.

11 *Discoaster distinctus* Martini
Hypotype no. 564333.

12 *Discoaster distinctus* Martini
Hypotype no. 564331.

13 *Discoaster distinctus* Martini
Hypotype no. 564332.

14 *Discoaster falcatus* Bramlette and Sullivan, n. sp.
Holotype, no. 564335: a, plan view; b, side view, drawing.

15 *Discoaster falcatus* Bramlette and Sullivan, n. sp.
Paratype no. 564336.

16 *Discoaster elegans* Bramlette and Sullivan, n. sp.
a, plan view; b, side view, drawing.

17 *Discoaster germanicus* Martini

18 *Discoaster helianthus* Bramlette and Sullivan, n. sp.
a, plan view; b, side view, drawing.

PLATE 12

1 *Discoaster lenticularis* Bramlette and Sullivan, n. sp.
Holotype, no. 564339: a, plan view; b, side view, drawing.

2 *Discoaster lenticularis* Bramlette and Sullivan, n. sp.
Paratype no. 564340.

3 *Discoaster limbatus* Bramlette and Sullivan, n. sp.
a, plan view; b, side view, drawing.

4 *Discoaster lodoensis* Bramlette and Riedel
Hypotype no. 564342: a, plan view; b, side view, drawing.

5 *Discoaster lodoensis* Bramlette and Riedel
Hypotype no. 564343, questionable short-rayed variant.

6 *Discoaster sublodoensis* Bramlette and Sullivan, n. sp.
a, plan view; b, side view, drawing.

7 *Discoaster mediosus* Bramlette and Sullivan, n. sp.
Holotype, no. 564345: a, plan view; b, side view, drawing.

8 *Discoaster mediosus* Bramlette and Sullivan, n. sp.
Paratype no. 564346.

9 *Discoaster* aff. *D. mediosus* Bramlette and Sullivan

10 *Discoaster multiradiatus* Bramlette and Riedel

11 *Discoaster multiradiatus* Bramlette and Riedel var.
a, plan view; b, side view, drawing.

12 *Discoaster martinii* Stradner
a, plan view; b, side view, drawing; c, plan view, drawing.

13 *Discoaster nonaradiatus* Klumpp
Hypotype no. 564351.

14 *Discoaster nonaradiatus* Klumpp
Hypotype no. 564352.

15 *Discoaster nonaradiatus* Klumpp
Hypotype no. 564350.

16 *Discoaster septemradiatus* (Klumpp)
Hypotype no. 564354.

17 *Discoaster septemradiatus* (Klumpp)
Hypotype no. 564353.

PLATE 13

1–5 *Discoaster* spp.
Hypotypes no. 564364, 564365, 564366, 564368, and 564367.

6 *Discoaster tribrachiatus* Bramlette and Riedel
Hypotype no. 564357: a, plan view; b, side view, drawing.

7 *Discoaster tribrachiatus* Bramlette and Riedel
Hypotype no. 564358.

8 *Discoaster tribrachiatus* Bramlette and Riedel
Hypotype no. 564359.

9 *Discoaster tribrachiatus* Bramlette and Riedel
Hypotype no. 564356.

10 *Discoaster tribrachiatus* Bramlette and Riedel
Hypotype no. 564360.

11 *Discoaster tribrachiatus* Bramlette and Riedel
Hypotype no. 564363, side view.

12 *Discoaster tribrachiatus* Bramlette and Riedel
Hypotype no. 564362, immature(?) specimen.

13 *Discoaster tribrachiatus* Bramlette and Riedel
Hypotype no. 564361, immature(?) specimen.

14 *Discoasteroides megastypus* Bramlette and Sullivan, n. sp.
Holotype, no. 564373: a, plan view; b, side view, drawing; c, plan view, crossed nicols; d, plan view, drawing.

15 *Discoasteroides megastypus* Bramlette and Sullivan, n. sp.
Paratype no. 564374: a, side view; b, side view, stem axis 0° to x-nic*; c, side view, stem axis 78° to x-nic*.

16 *Discoasteroides kuepperi* (Stradner)
Hypotype no. 564371: a, plan view; b, plan view, crossed nicols.

17 *Discoasteroides kuepperi* (Stradner)
Hypotype no. 564369, plan view.

18 *Discoasteroides kuepperi* (Stradner)
Hypotype no. 564370: a, side view; b, side view, stem axis 0° to x-nic*; c, side view, stem axis 25° to x-nic*.

19 *Discoasteroides kuepperi* (Stradner)
Hypotype no. 564372, oblique view, fluorite replacement.

PLATE 14

1 *Fasciculithus involutus* Bramlette and Sullivan, n. sp.
Paratype no. 564376: a, side view; b, side view, long axis 0° to x-nic*; c, side view, long axis 63° o x-nic*.

2 *Fasciculithus involutus* Bramlette and Sullivan, n. sp.
Paratype no. 564379: a, plan view; b, plan view, crossed nicols.

3 *Fasciculithus involutus* Bramlette and Sullivan, n. sp.
Holotype, no. 564375: a, side view; b, side view, long axis 0° to x-nic*.

4 *Fasciculithus involutus* Bramlette and Sullivan, n. sp.
Paratype no. 564377: a, plan view; b, plan view, crossed nicols.

5 *Fasciculithus involutus* Bramlette and Sullivan, n. sp.
Paratype no. 564378: a, plan view; b, plan view, crossed nicols.

6 *Sphenolithus radians* Deflandre
Hypotype no. 564390, side view, fluorite replacement.

7 *Sphenolithus radians* Deflandre
Hypotype no. 564391, side view, fluorite replacement.

8 *Sphenolithus radians* Deflandre
Hypotype no. 564389: a, side view; b, side view, long axis 0° to x-nic*.

9 *Heliolithus riedeli* Bramlette and Sullivan, n. sp.
Holotype, no. 564380: a, plan view, small side; b, oblique view, drawing; c, plan view, crossed nicols.

10 *Heliolithus riedeli* Bramlette and Sullivan, n. sp.
Paratype no. 564382, side view.

11 *Heliolithus riedeli* Bramlette and Sullivan, n. sp.
Paratype no. 564381, plan view, large side.

12 *Heliolithus* aff. *H. riedeli* Bramlette and Sullivan
Oblique view, drawing.

13 *Polycladolithus operosus* Deflandre
a, plan view; b, plan view, high focus; c, plan view, low focus; d, plan view, drawing.

14 *Polycladolithus?* sp.
Plan view.

15 *Isthmolithus unipons* Bramlette and Sullivan, n. sp.
Holotype, no. 564383, plan view.

16 *Isthmolithus unipons* Bramlette and Sullivan, n. sp.
a–b, side views of specimens from Lodo 43.

17 *Rhomboaster cuspis* Bramlette and Sullivan, n. sp.
Paratype no. 564388, oblique view.

18 *Rhomboaster cuspis* Bramlette and Sullivan, n. sp.
Paratype no. 564387, oblique view.

19 *Rhomboaster cuspis* Bramlette and Sullivan, n. sp.
Holotype, no. 564386: a, plan view with 3 edges of lower side showing through as the lighter ones; b, side view, drawing; c, plan view, drawing.

---

*Measured clockwise from either plane of crossed nicols.

*Measured clockwise from either plane of crossed nicols.

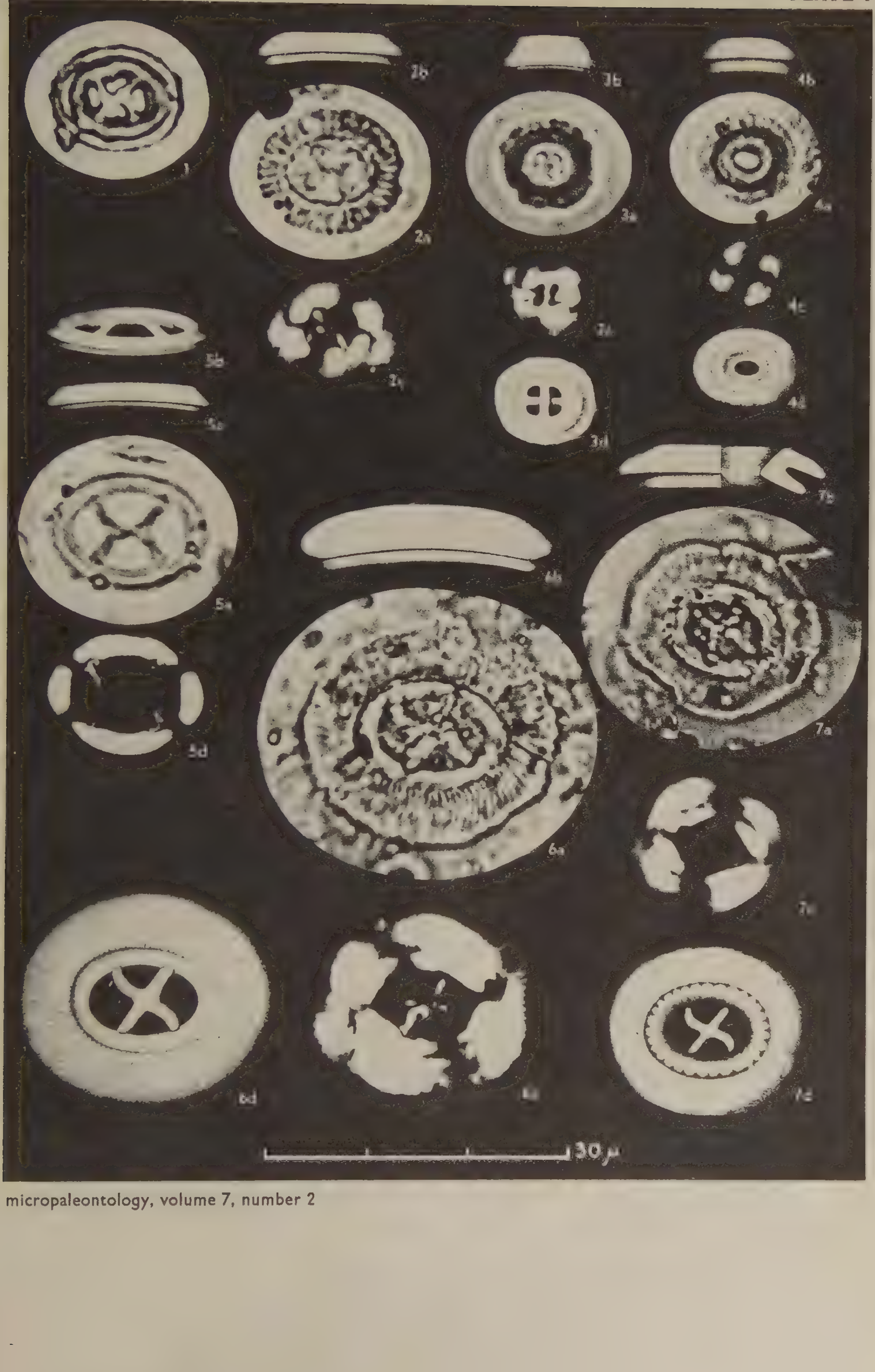
1
2b
3b
4b
2a
3a
4a
4c
3c
2c
5b
5c
4d
3d
7b
6b
5a
7a
5d
6a
7c
6d
6c
7d
30 μ

PLATE 2

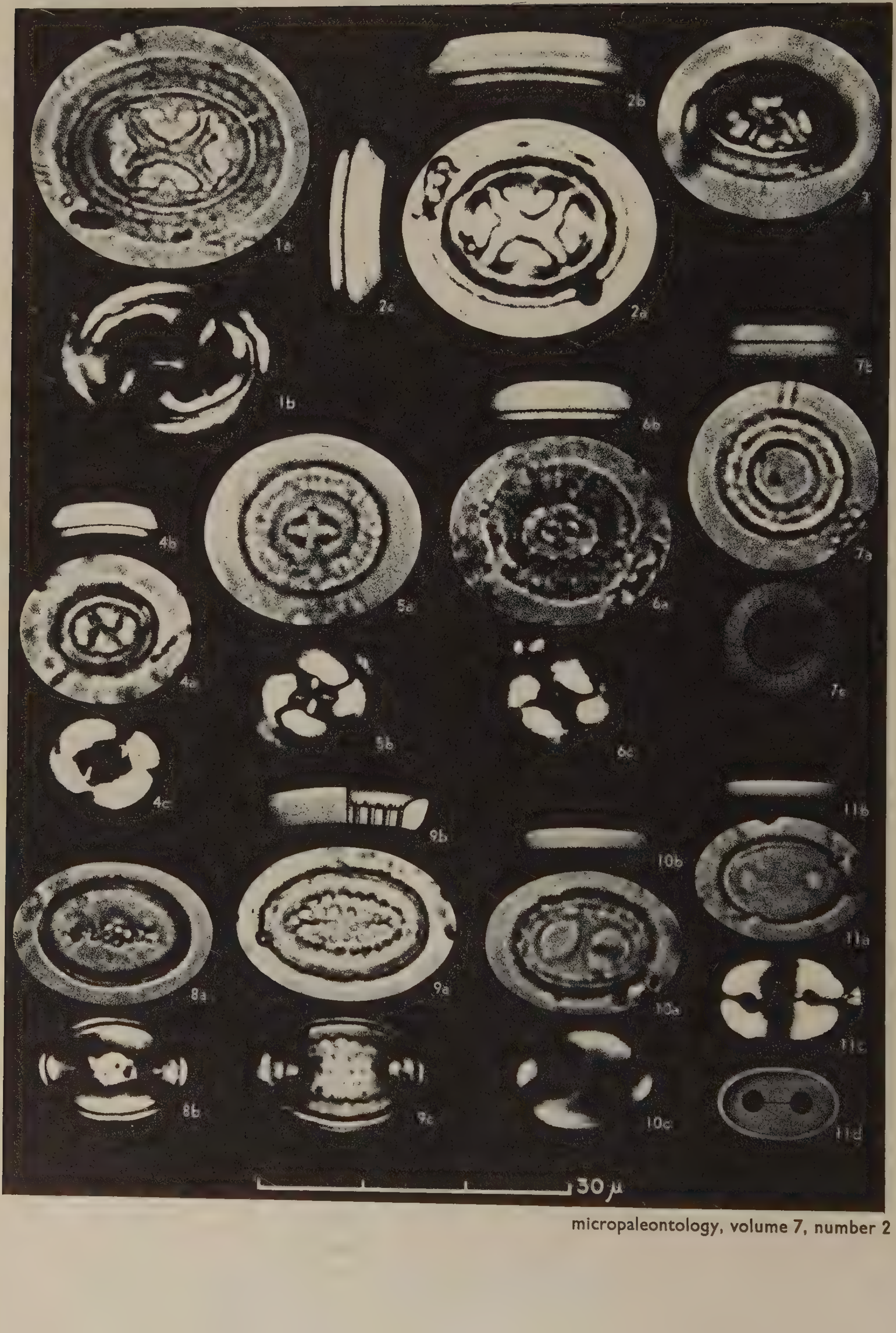
1a
2b
3
2c
2a
1b
7b
6b
7a
4b
5a
6a
4a
7c
5b
6c
4c
11b
9b
10b
11a
8a
9a
10a
11c
8b
9c
10c
11d
30 μ

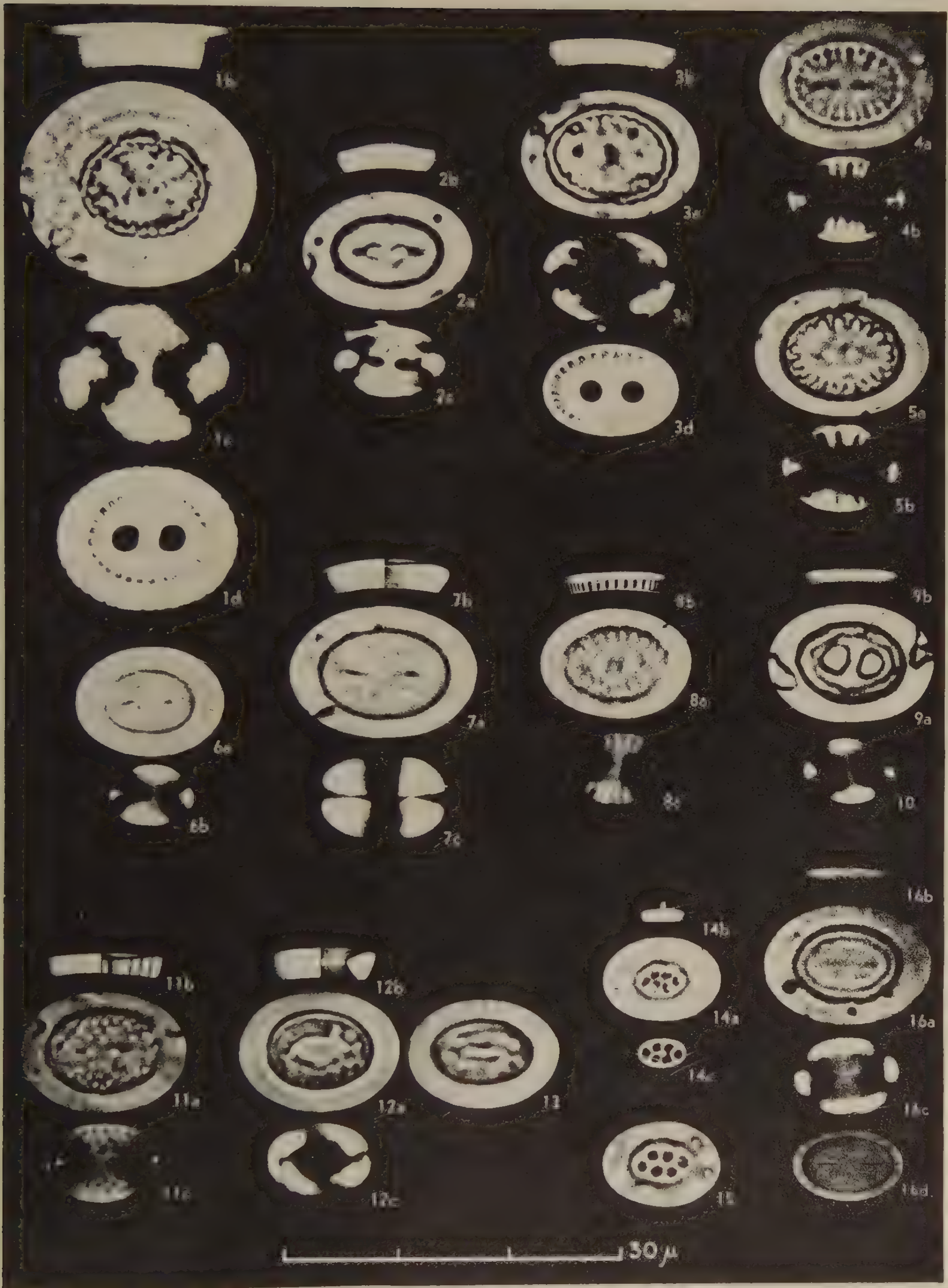
1b
1a
1c
1d
2b
2a
2c
3b
3a
3c
3d
4a
4b
5a
5b
6a
6b
7b
7a
7c
8b
8a
8c
9b
9a
10
11b
11a
11c
12b
12a
12c
13
14b
14a
14c
15
16b
16a
16c
16d
30μ

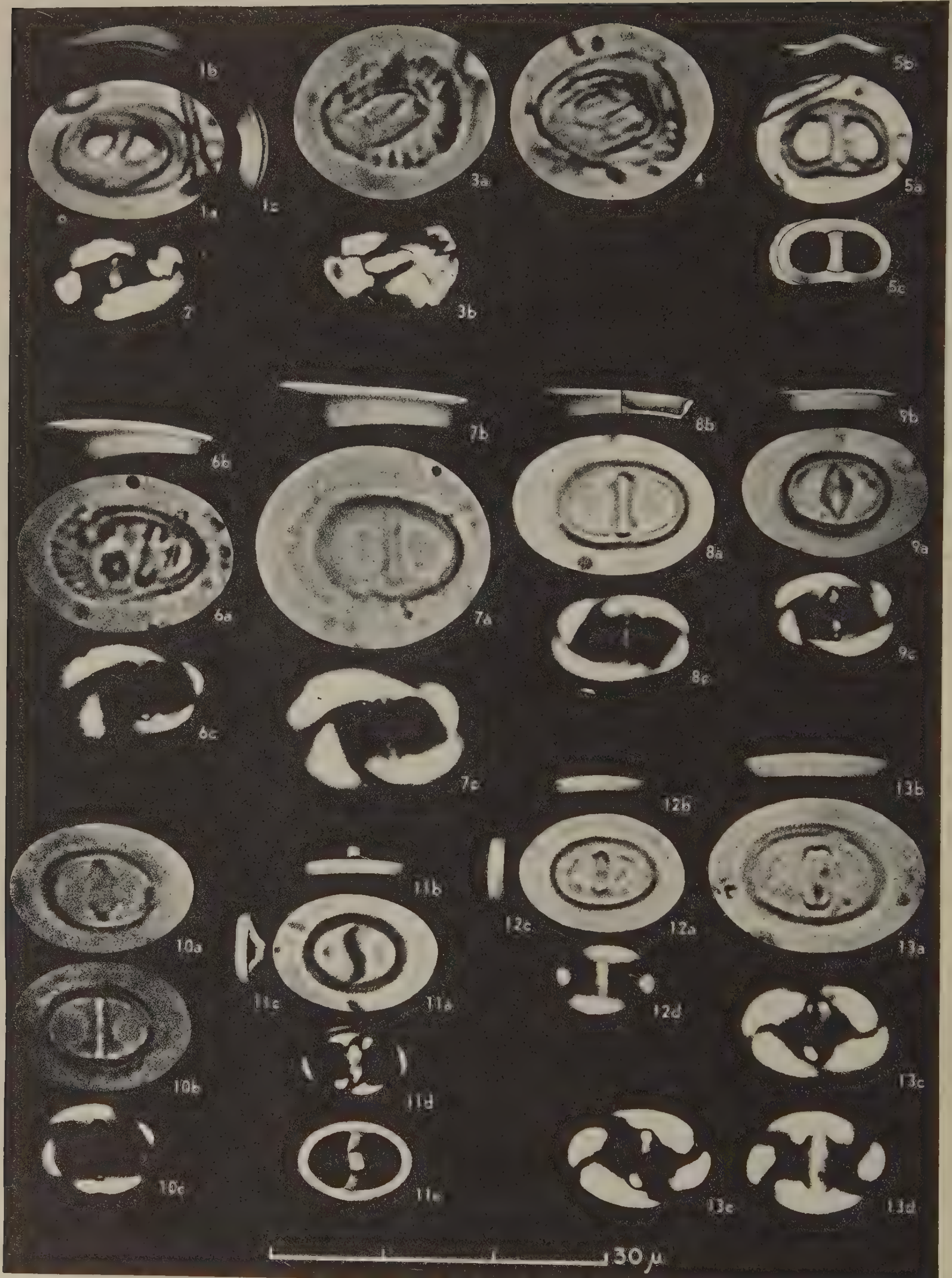
1b
1a
1c
3a
4
5b
5a
5c
2
3b
7b
8b
9b
6b
8a
9a
6a
7a
8c
9c
6c
7c
12b
13b
11b
12c
12a
13a
10a
11c
11a
12d
10b
11d
13c
10c
11e
13e
13d
30 μ

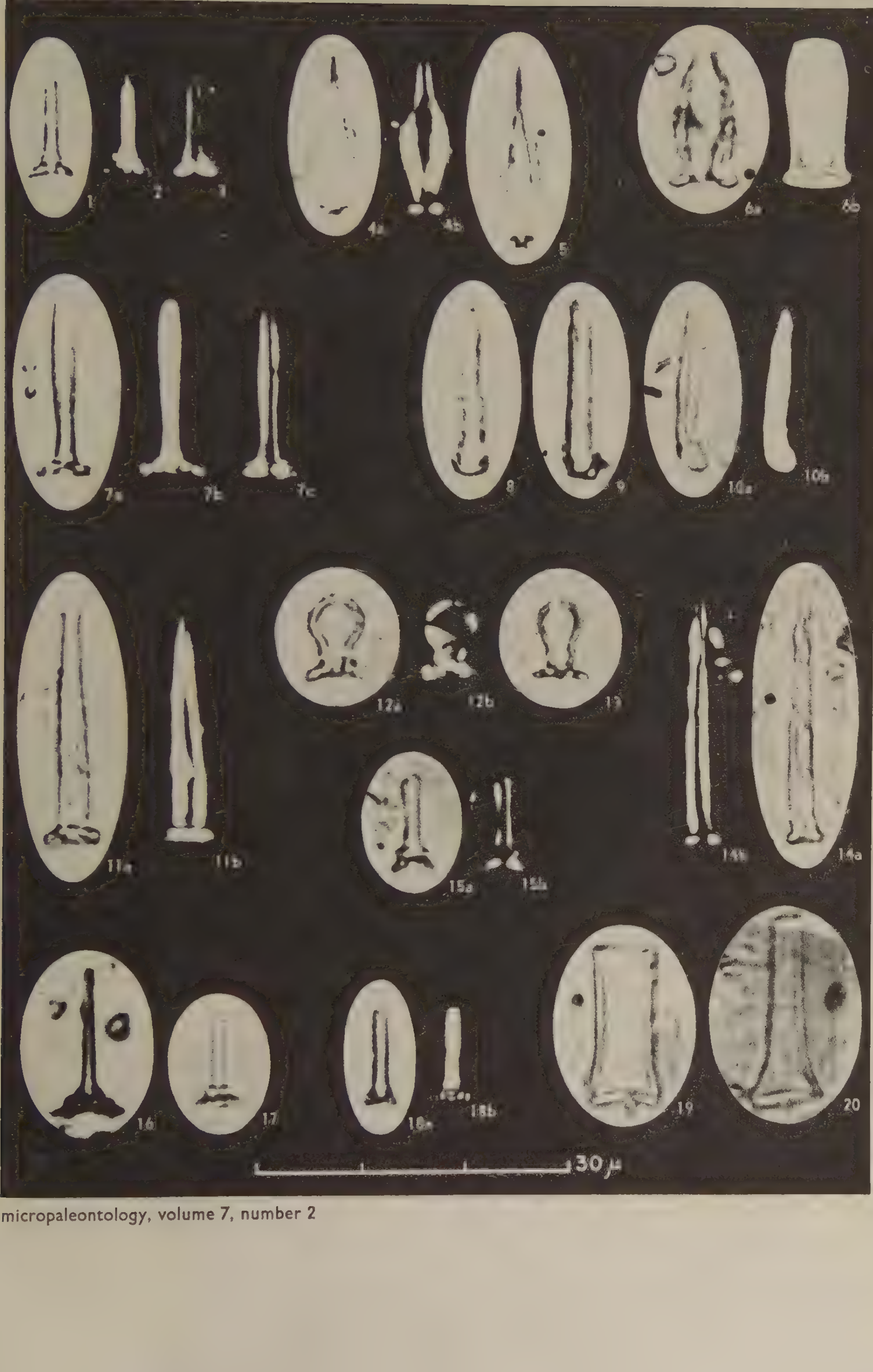
1
2
3
4a
4b
5
6a
6b
7a
7b
7c
8
9
10a
10b
11a
11b
12a
12b
13
14b
14a
15a
15b
16
17
18a
18b
19
20
30 µ

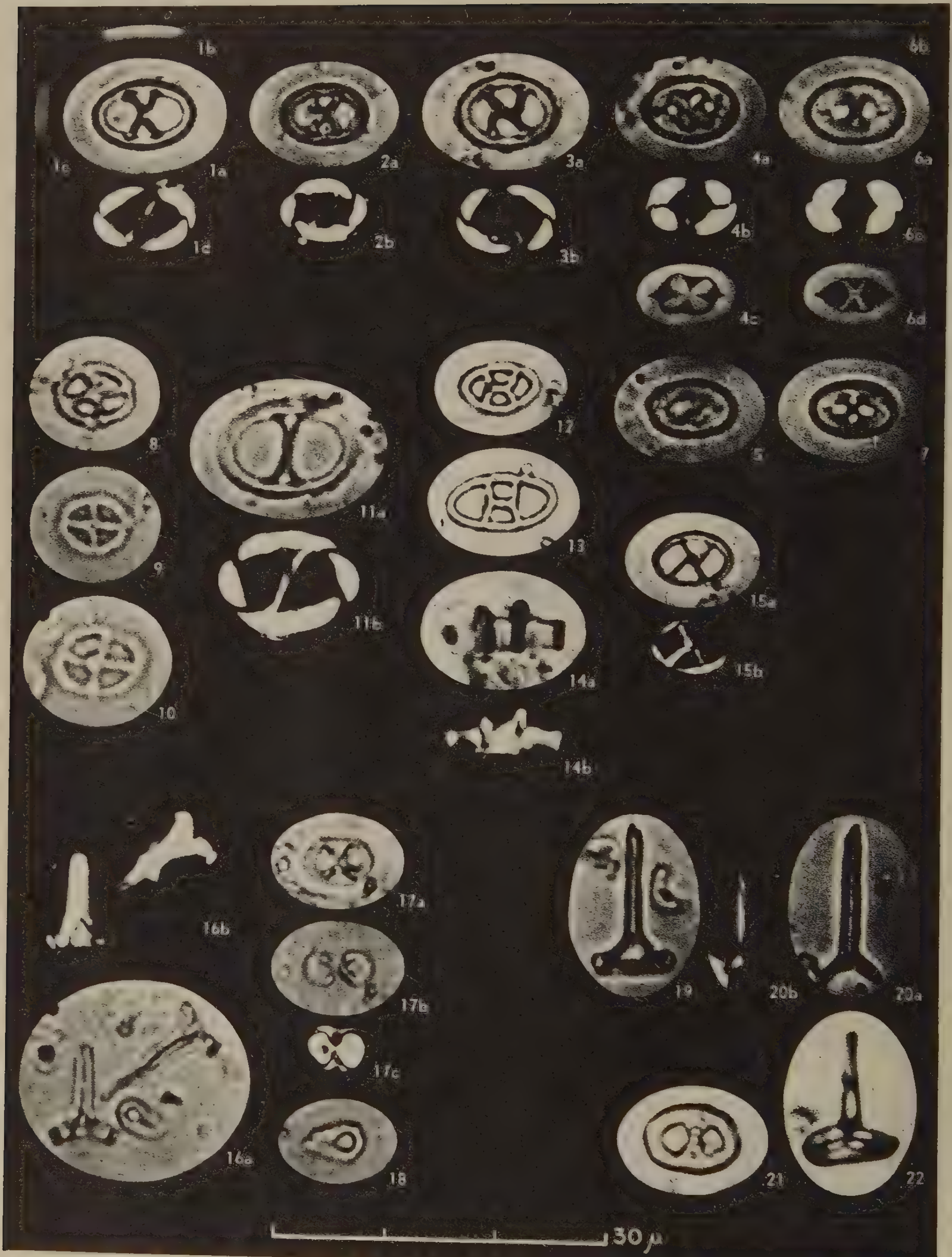
1b
6b
1c
1a
2a
3a
4a
6a
1d
2b
3b
4b
6c
4c
6d
8
12
5
7
11a
9
13
15a
11b
14a
15b
10
14b
16b
17a
19
20b
20a
17b
17c
16a
18
21
22
30 μ

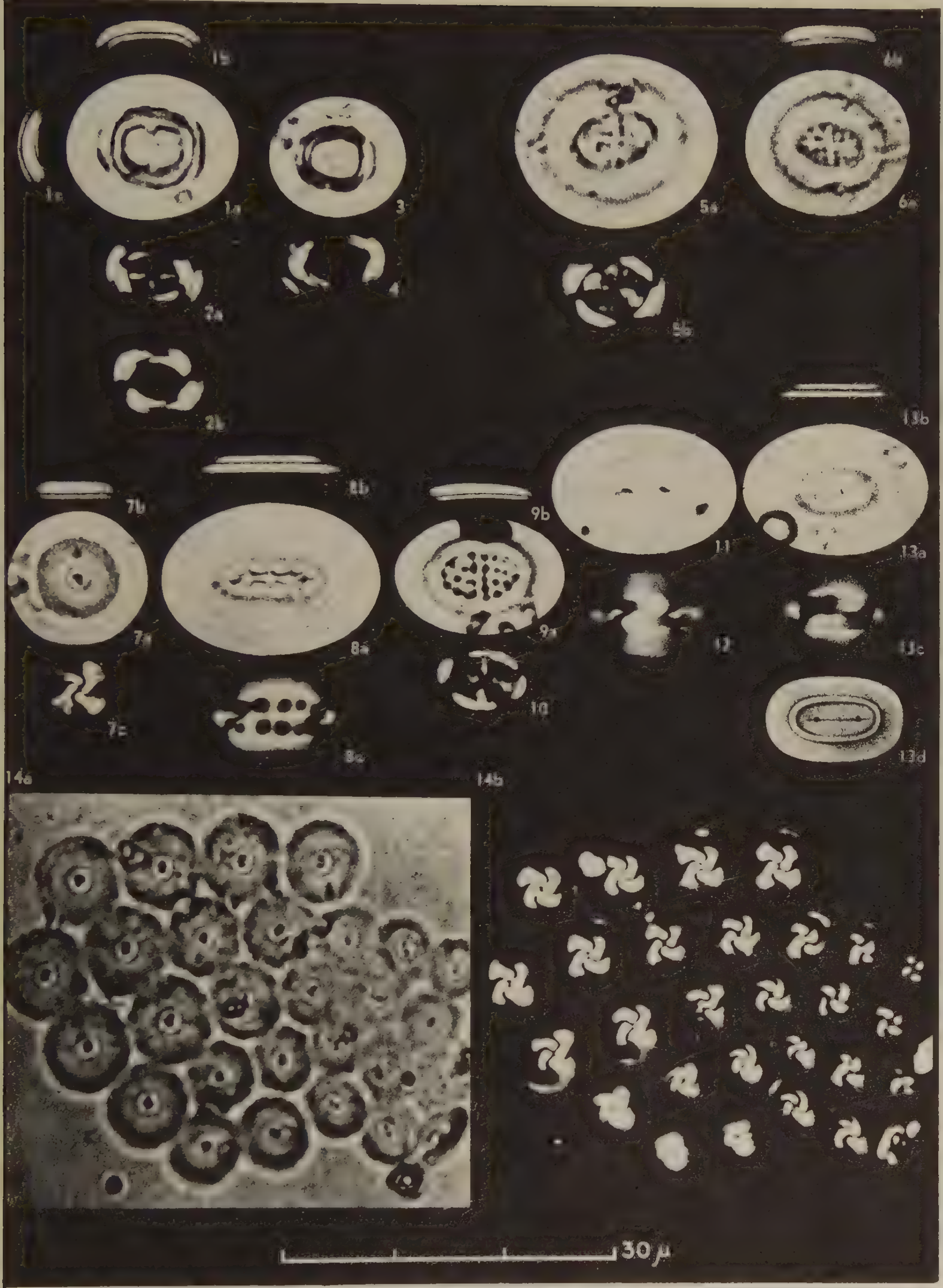
1b
1c
1a
3
5a
6b
6a
2a
4
5b
2b
13b
7b
8b
9b
11
13a
7a
8a
9a
12
13c
7c
8c
10
13d
14a
14b
30 μ

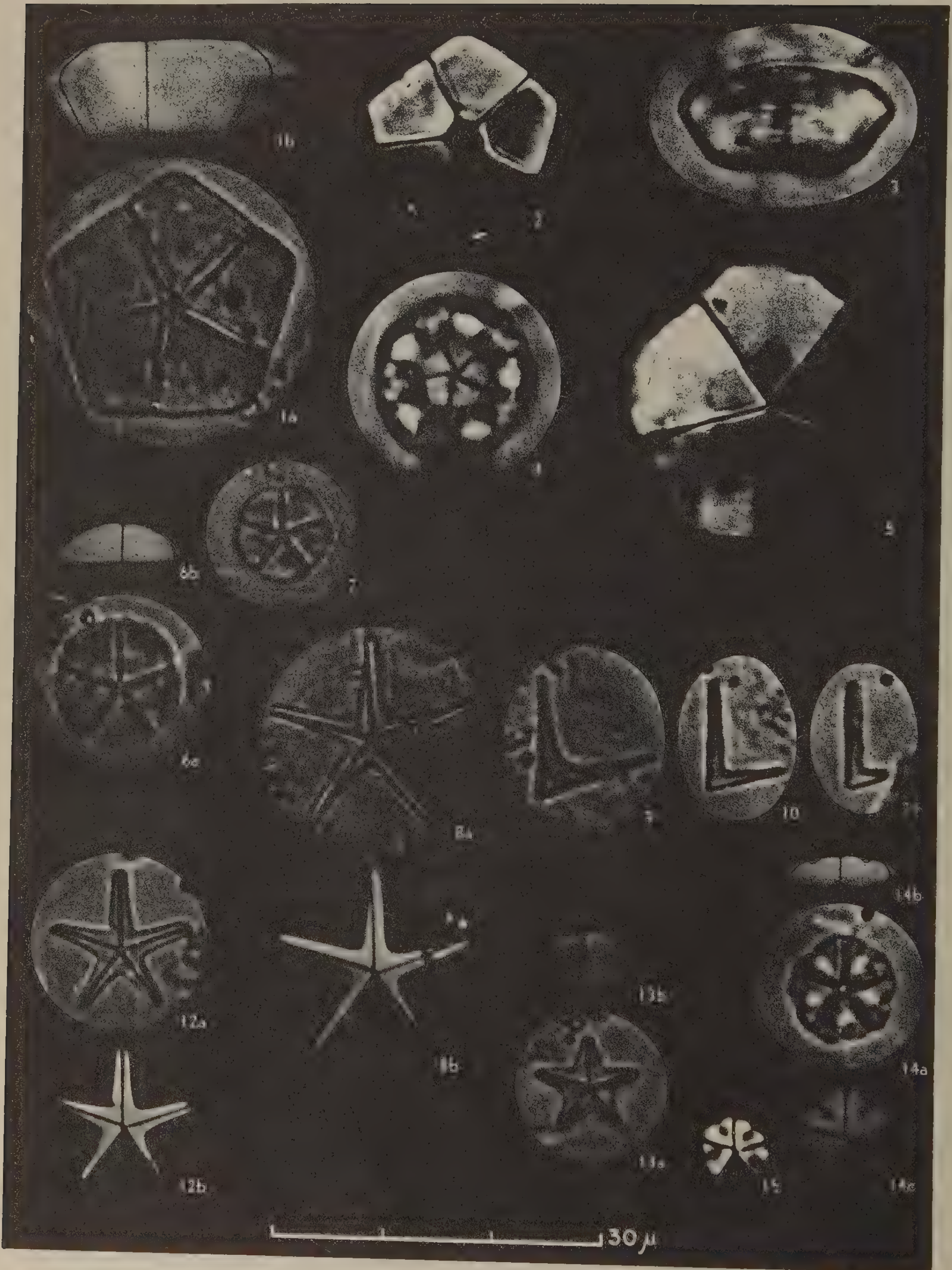
1b
2
3
1a
4
5
6b
7
6a
8a
9
10
11
14b
12a
8b
13b
14a
12b
13a
15
14c
30 μ

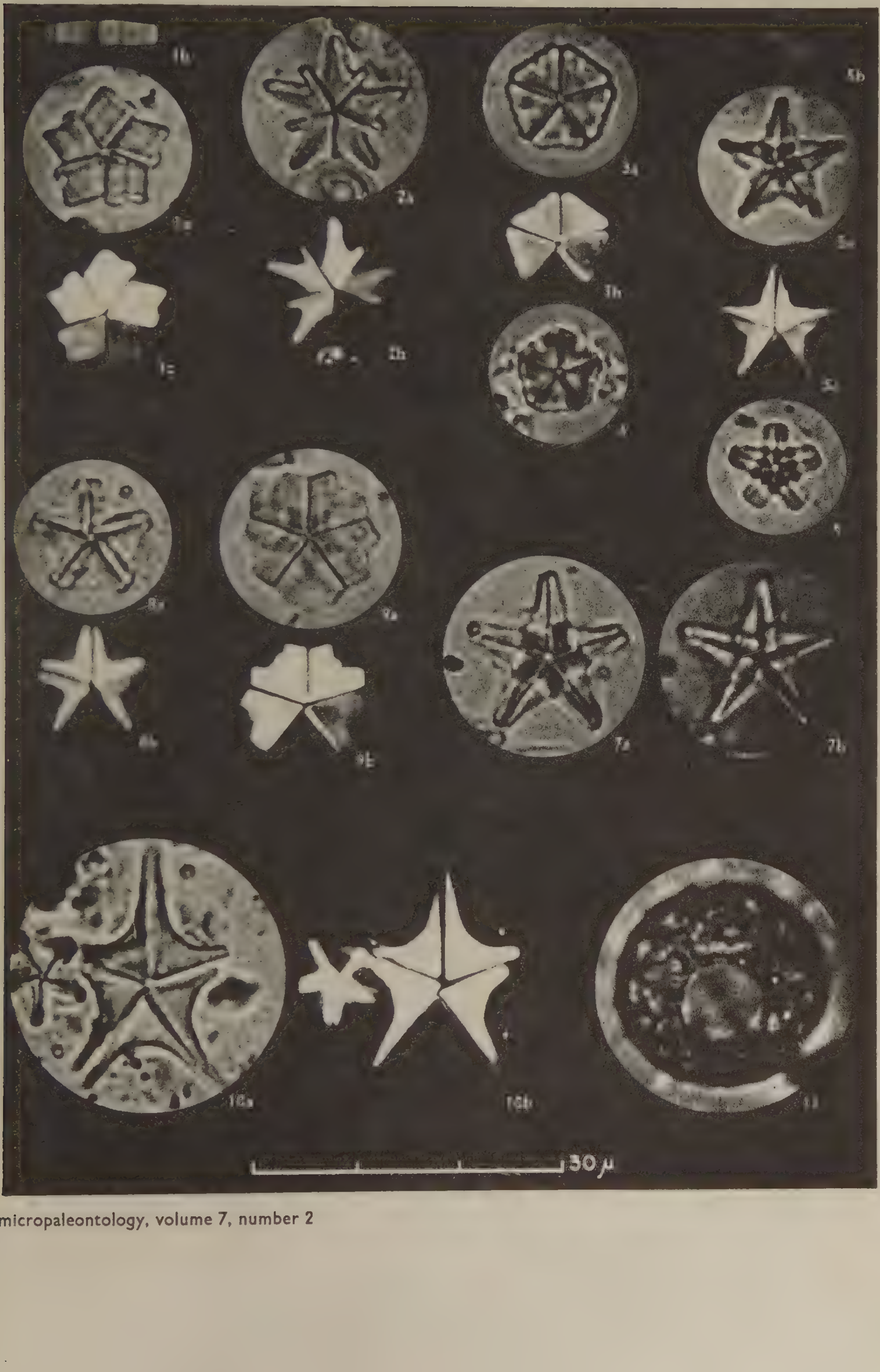
1b
1a
1c
2a
2b
3a
3b
4
5b
5a
5c
6
8a
8b
9a
9b
7a
7b
10a
10b
11
30 μ

PLATE 10

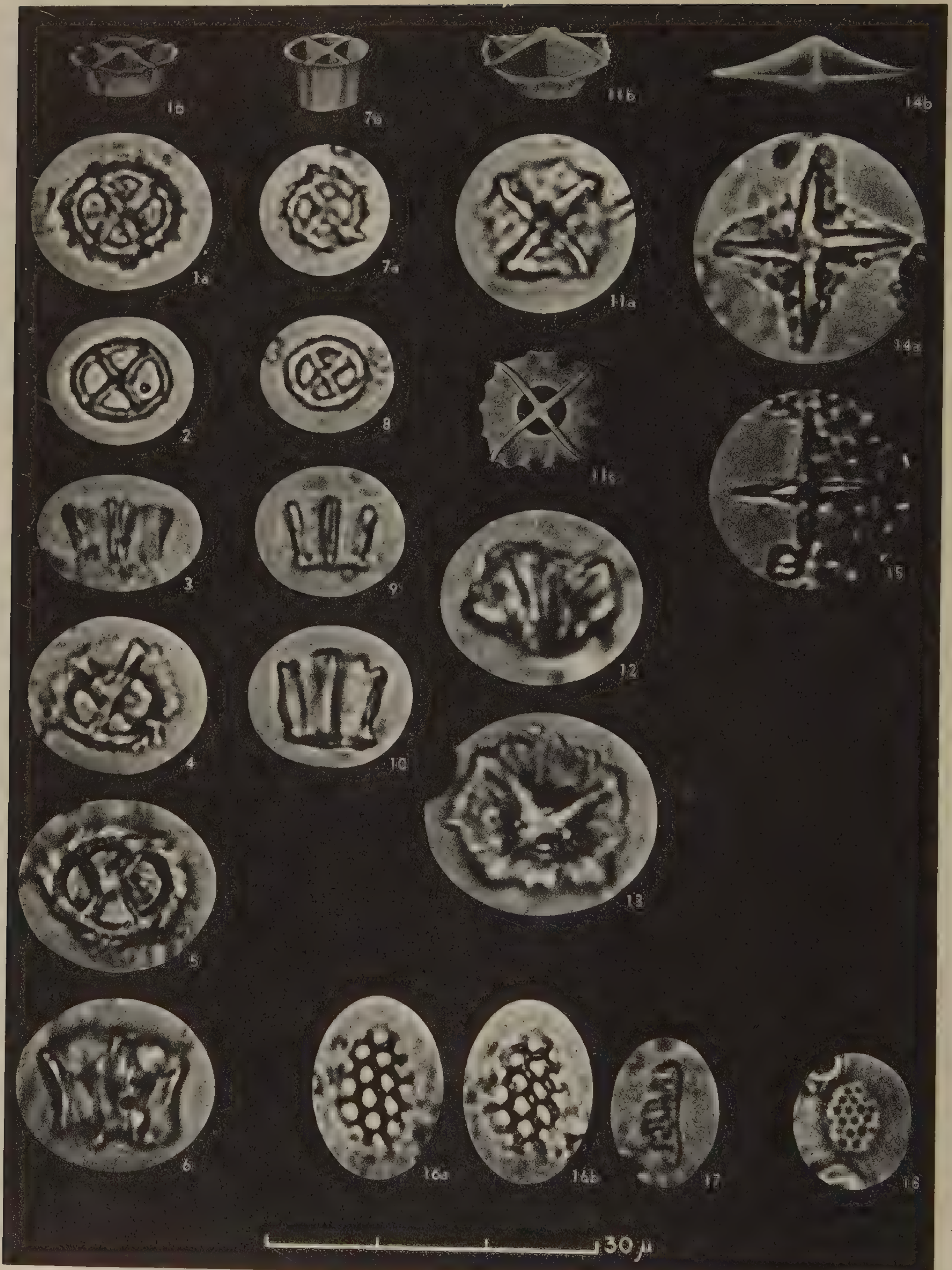
1b
7b
11b
14b
1a
7a
11a
14a
2
8
11c
15
3
9
12
4
10
13
5
6
16a
16b
17
18
30μ

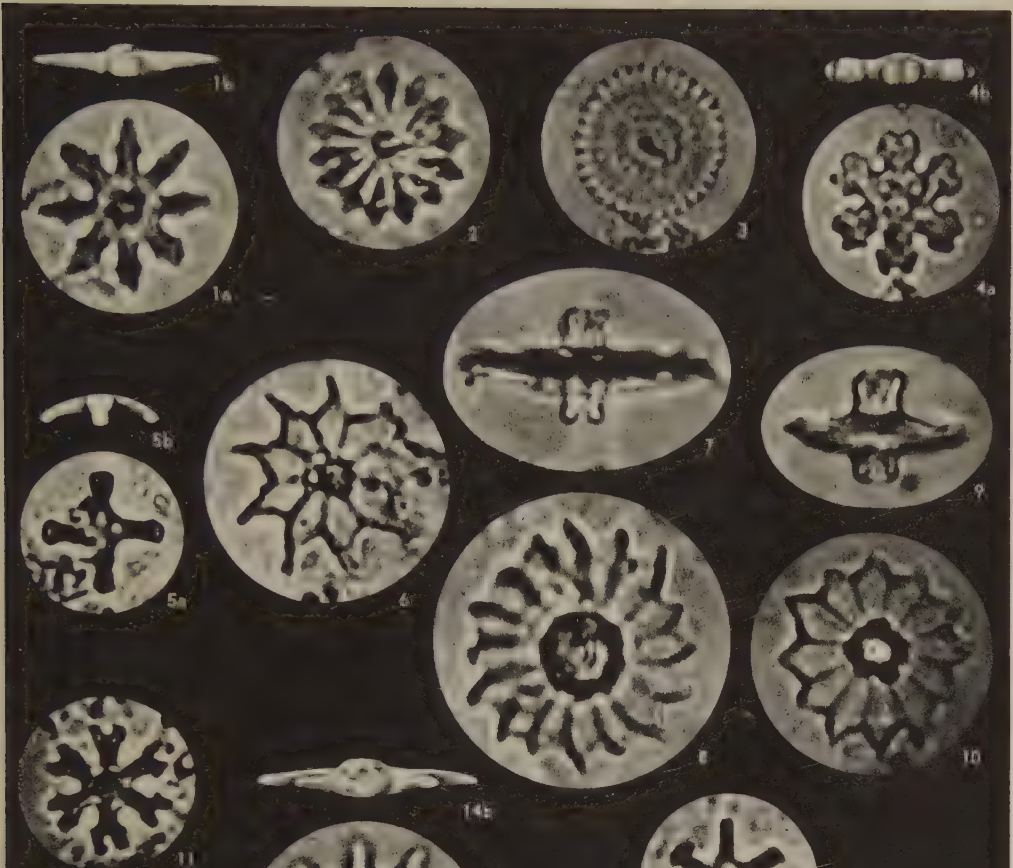
1b
2
3
4b
1a
4a
7
5b
9
5a
6
8
10
11
14b
17
12
14a
16b
18b
13
15
16a
18a
30 μ

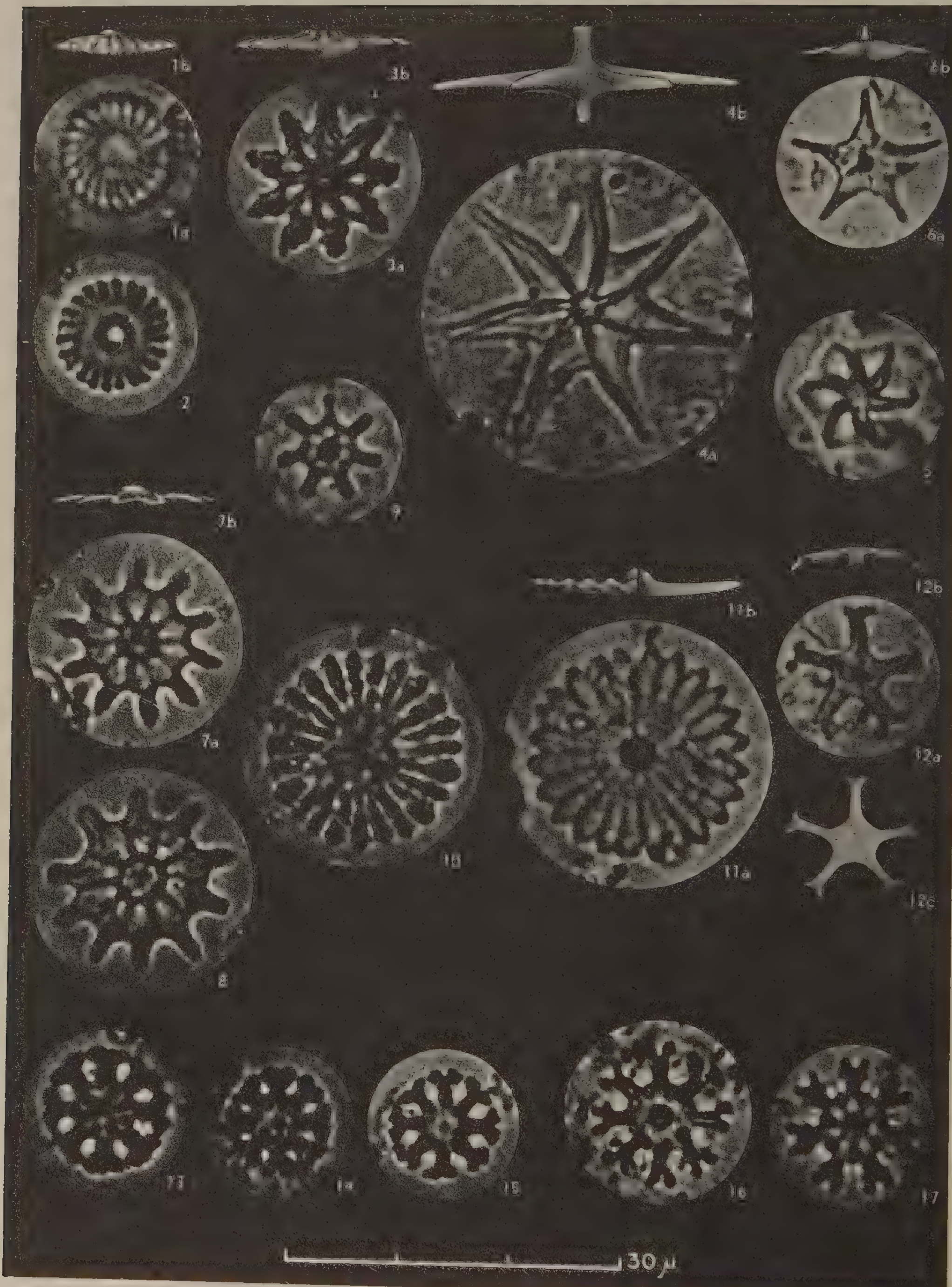
1b
3b
4b
6b
1a
3a
6a
2
4a
5
9
7b
12b
11b
7a
10
11a
12a
12c
8
13
14
15
16
17
30 μ

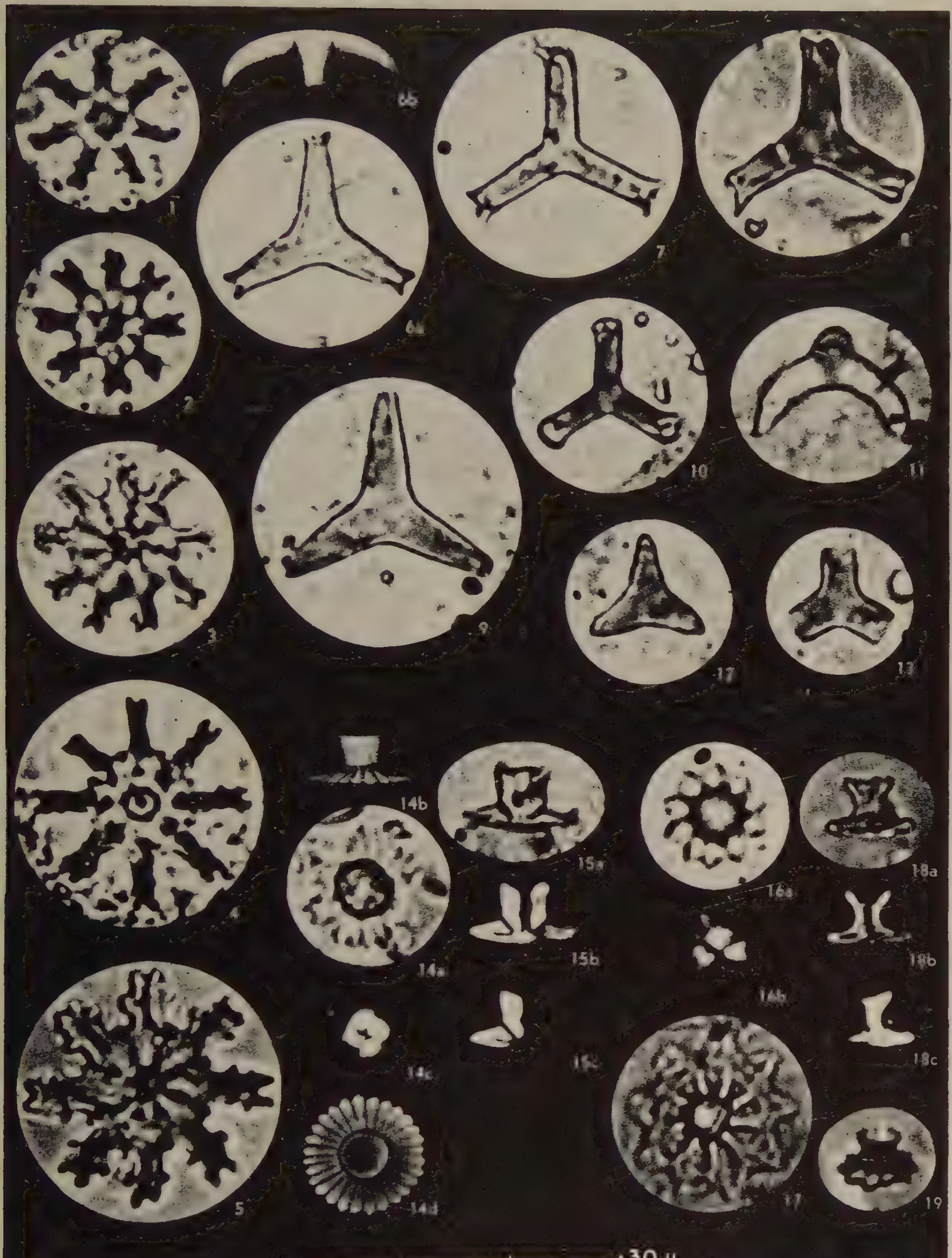
1
2
3
4
5
6a
6b
7
8
9
10
11
12
13
14a
14b
14c
14d
15a
15b
15c
16a
16b
17
18a
18b
18c
19
30 μ

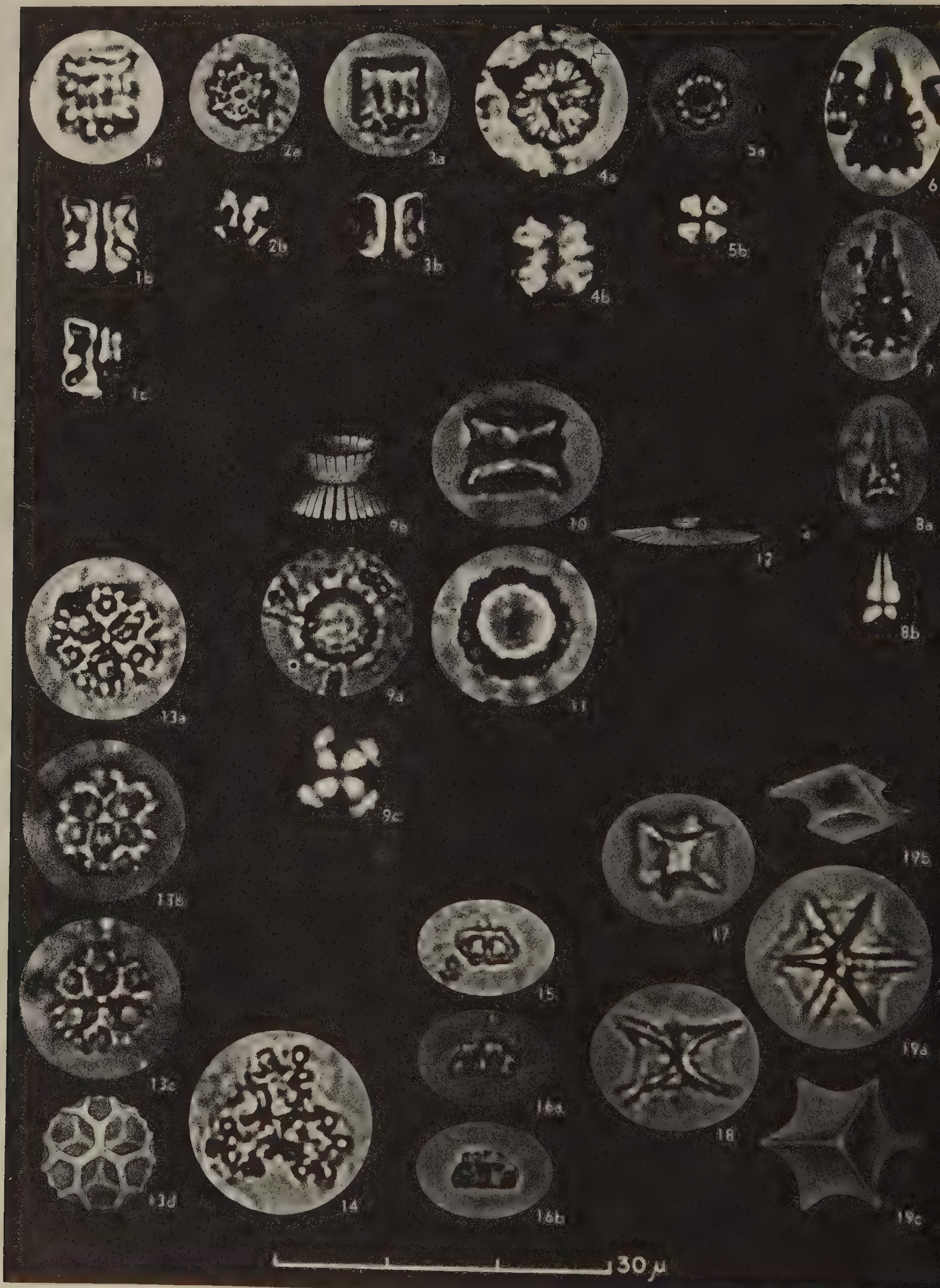
1a
2a
3a
4a
5a
6
1b
2b
3b
4b
5b
7
1c
9b
10
8a
12
13a
9a
11
8b
9c
19b
13b
17
15
19a
13c
16a
18
14
16b
13d
19c
30 μ

DISTRIBUTION OF EARLY TERTIARY COCCOLITHOPHORIDS AND RELATED NANNOPLANKTON IN THE LODO SECTION OF CALIFORNIA

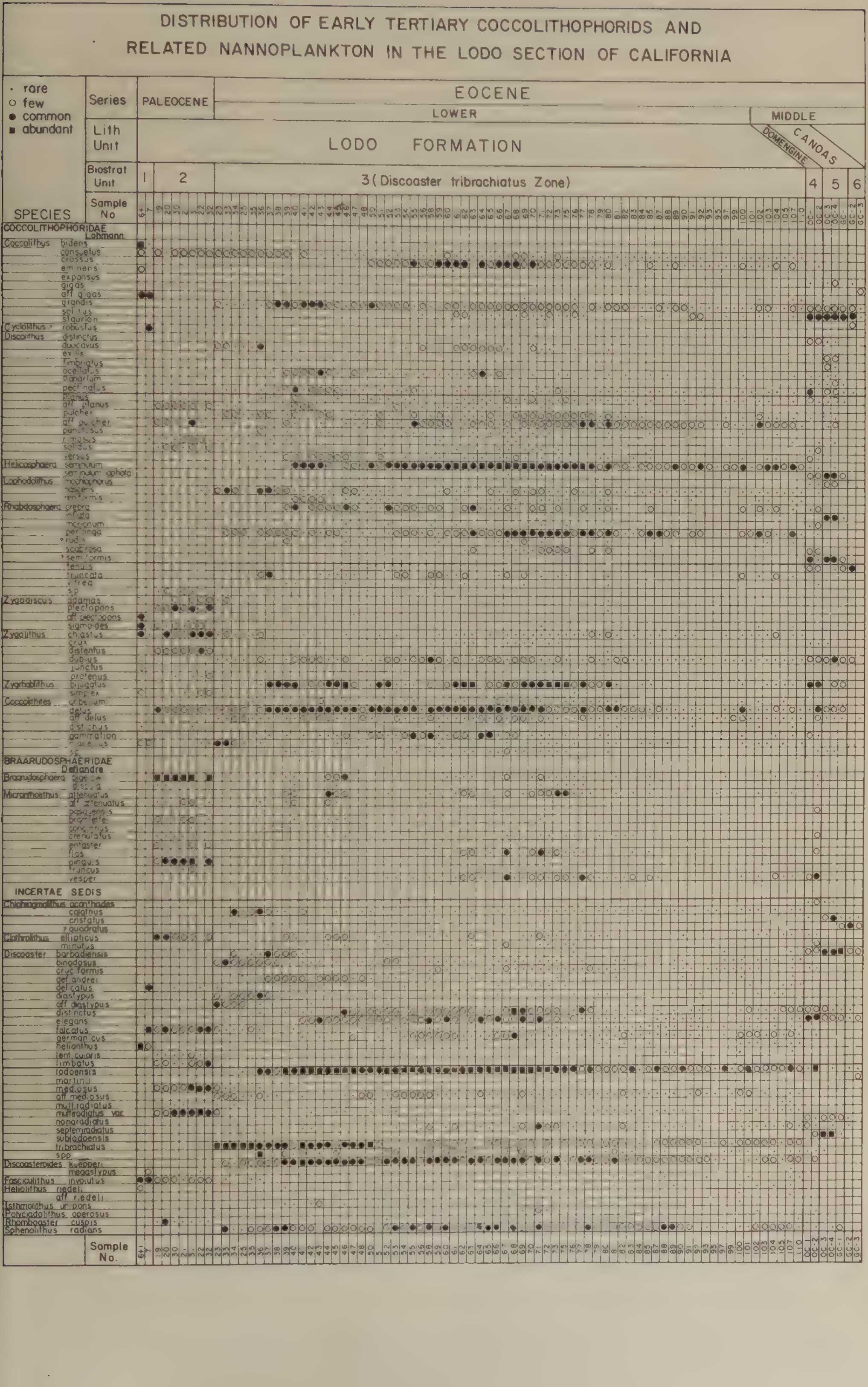

- · rare
- ○ few
- ● common
- ■ abundant

Series: PALEOCENE; EOCENE (LOWER; MIDDLE)

Lith Unit: LODO FORMATION; DOMENGINE; CANOAS

Biostrat Unit: 1; 2; 3 (Discoaster tribrachiatus Zone); 4; 5; 6

Sample No: 6+; 7; 19; 20; 30; 2; 3; 21; 22; 32; 33; 34; 35; 36; 37; 38; 39; 40; 41; 42; 43; 44; 45; 46; 47; 48; 50; 51; 52; 53; 54; 55; 56; 58; 59; 60; 61; 62; 63; 64; 65; 66; 67; 68; 69; 70; 71; 72; 73; 75; 76; 77; 78; 79; 80; 81; 82; 83; 84; 85; 87; 88; 89; 90; 91; 92; 93; 95; 97; 99; 100; 101; 102; 103; 104; 105; 107; 110; GC-1; GC-2; OC-3; OC-4; GC-1; GC-2; GC-3

SPECIES

COCCOLITHOPHORIDAE Lohmann

Coccolithus bidens
consuetus
crassus
eminens
expansus
gigas
aff. gigas
grandis
solitus
staurion
Cyclolithus ? robustus
Discolithus distinctus
duocavus
exilis
fimbriatus
ocellatus
panarium
pectinatus
planus
aff. planus
pulcher
aff. pulcher
punctosus
rimosus
solidus
versus
Helicosphaera seminulum
seminulum lophota
Lophodolithus mochlophorus
nascens
reniformis
Rhabdosphaera crebra
inflata
morionum
perlonga
? rudis
scabrosa
? semiformis
tenuis
truncata
vitrea
sp.
Zygodiscus adamas
plectopons
aff. plectopons
sigmoides
Zygolithus chiastus
crux
distentus
dubius
junctus
protenus
Zygrhablithus bijugatus
simplex
Coccolithites orbiculum
delus
aff. delus
distichus
gammation
macellus
sp.

BRAARUDOSPHAERIDAE Deflandre

Braarudosphaera bigelowi
discula
Micrantholithus attenuatus
aff. attenuatus
basquensis
bramlettei
concinnus
crenulatus
entaster
flos
pinguis
truncus
vesper

INCERTAE SEDIS

Chiphragmalithus acanthodes
calathus
cristatus
? quadratus
Clathrolithus ellipticus
minutus
Discoaster barbadiensis
binodosus
cruciformis
aff. andrei
delicatus
diastypus
aff. diastypus
distinctus
elegans
falcatus
germanicus
helianthus
lenticularis
limbatus
lodoensis
martinii
mediosus
aff. mediosus
multiradiatus
multiradiatus var.
nonaradiatus
septemradiatus
sublodoensis
tribrachiatus
spp.
Discoasteroides kuepperi
megastypus
Fasciculithus involutus
Heliolithus riedeli
aff. riedeli
Isthmolithus unipons
Polycladolithus operosus
Rhomboaster cuspis
Sphenolithus radians

TABLE 1

Reprinted from Oceanography
American Association for the Advancement of Science
Copyright 1961
pp.129-148

Geological Record on the Ocean Floor*

GUSTAF ARRHENIUS

Scripps Institution of Oceanography, University of California, La Jolla, California

GEOLOGICAL events with worldwide or large-regional effects such as climatic change, volcanic activity, evolution of the ocean, and interaction with outer space are often recorded on the deep ocean floor far away from the continents, in a manner that makes this record advantageous for quantitative interpretations. The Pacific basin (Fig. 1) has some characteristics that make it particularly well suited as a recipient of representative sedimentary sequences.

The marginal trenches and ridges effectively bar turbidity currents from the central basins; the lack of such protection in exceptional cases such as along the coast of the northern United States and Canada has resulted in widespread detrital deposits over adjacent areas of the deep ocean floor. On account of the approximately isometric shape and the large dimensions of the Pacific Ocean, several of its topographically protected basins are separated by several thousand kilometers from the continental sources of windborne detritus, and the eolian component of the sediment thus is largely attenuated.

Another important feature of the Pacific Ocean is that its vast open area extends into high latitudes both in the Northern and the Southern Hemispheres. This makes it possible for the wind-driven circulation to develop without interference from land masses in a far more pronounced way than in the Atlantic and Indian oceans. At the equator, the forces arising from the rotation of the earth, cause cold, deep water, rich in nutrients, to ascend to the surface where the sunlight makes photosynthesis possible (Fig. 2, middle graph). The resulting zone of highly increased organic productivity

---

* Contribution from Scripps Institution of Oceanography, New Series.

Contributions from the Scripps Institution of Oceanography, New Series, 1276
Reproduced by Permission

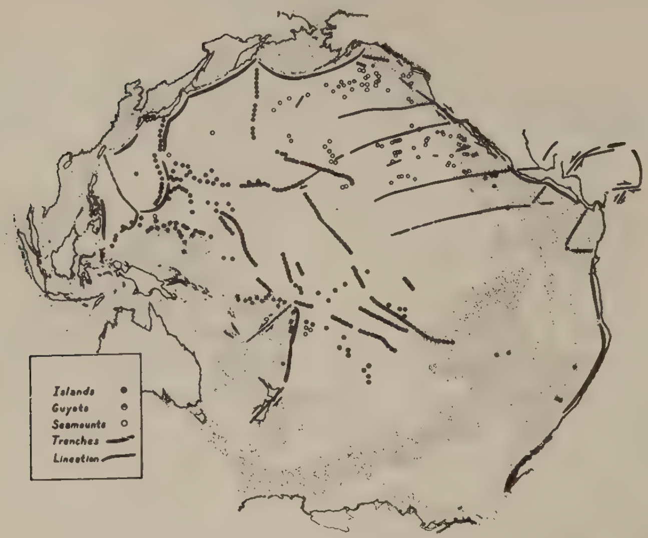

Fig. 1. Structural features of the Pacific Ocean (Menard and Fisher, 1958).

marks the position of the geographic equator on the surface of the sea, and the rain of organic remains which fall down on the ocean floor below makes a permanent record of the position of the equator at any given time.

The nature of this record is indicated in the lower graph of Fig. 2, a generalized meridional cross section through the top 5-m layer of the sediments, at about 125° W Long. Owing to the strongly increased production of calcareous and siliceous plankton, responsible for the bulk of the biogenous contribution to the sediment, the sedimentary strata attain a maximum thickness below the equator. It is obvious that we here have a means for determining its position in the past, inasmuch as any displacement of the geographic equator should be traceable as a corresponding displacement of the thickness maximum of the strata. Provided the position of the equator is determined in two places, preferably about ninety degrees apart, the position of the poles is also fully determined. Other parameters, which are still more useful for this purpose because of their larger gradients toward the equator, are the rates of accumulation of fossils, minerals, or chemical elements

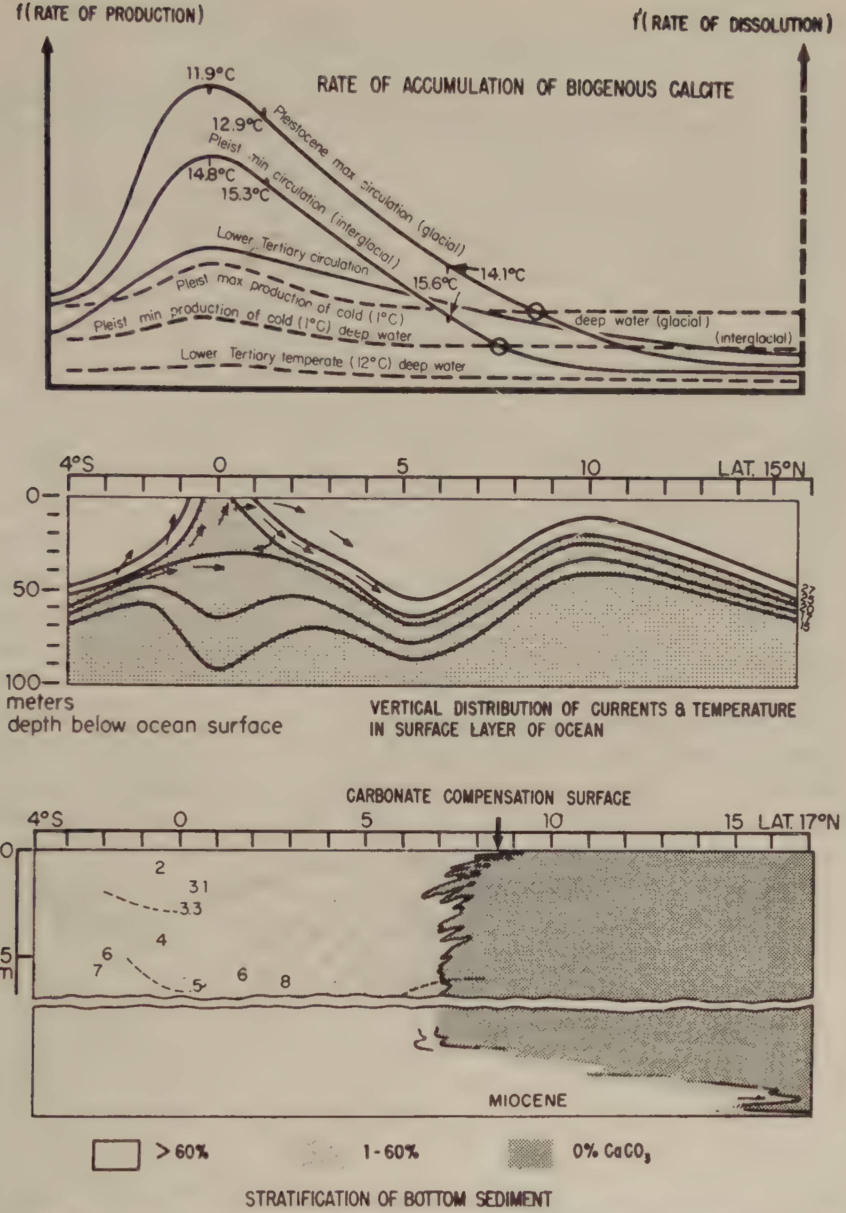

Fig. 2. Meridional profile at approximately 130°W Long showing the distribution of temperature and vertical motion in the surface layer of the ocean (middle graph), the stratification of the bottom sediment (lower graph), and the interpretation of the sedimentary record in terms of paleotemperature and rates of production and dissolution of calcium carbonate from planktonic organisms (upper graph) (Arrhenius, 1959a).

which are concentrated by the biological processes at the equator and which do not to the same extent as the major biogenous sedimentary component, calcite, suffer from dissolution (Fig. 2, top graph). These rates can be expressed in relative units as mass of the biologically concentrated component per unit mass of inorganic deposit. As a convenient measure of the latter have been employed elements like aluminum or titanium in such remote and protected basins where evidence for a reasonably low variability in the contribution of inorganic components has been obtained. In Fig. 3 are plotted the results by Goldberg on the rate of accumulation of barium in the Postglacial stratum in the east Pacific as a function of latitude, showing a sharp maximum under the equator with about twenty-five times the rate prevailing at higher latitudes, and a drop to 1/*e* of the maximum value at a distance of about 1½ degrees north and south of the equator. The rare earth elements and zirconium are still more promising than barium in this respect, as they are laid down in the form of highly insoluble phosphates which do not appear to migrate in the sediment.

In the sedimentary sequence available at the equator by present coring methods we do not reach further back in time than to the Middle Pleistocene, or roughly half a million years. During this time, the pole has remained constant within the resolution of the present sampling grid which is about four degrees of latitude. A 500-m long core in the equatorial sediment bulge would probably take us back at least into Middle Cretaceous strata, and to a time

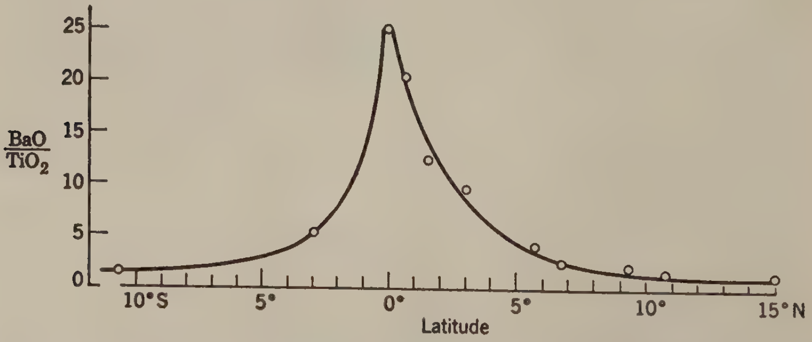

Fig. 3. Relative rate of accumulation of barium in the Postglacial stratum of the profile shown in Fig. 2 (Goldberg and Arrhenius, 1958).

during which a position of the North Pole in the North Pacific has been postulated. As Walter Munk has pointed out, this is one of the most interesting applications that can be thought of for some of the drilling tests planned to precede the ultimate attempt for penetration of the earth's crust.

So far the meridional cross section through the sedimentary strata under the equator, shown in Fig. 2, has been used to demonstrate the possibilities for accurate mapping of polar wandering; however, another interesting feature of the equatorial sedimentation mechanism should also be pointed out. If, instead of investigating the relation between latitude and accumulation, we focus our attention on the variation in time of accumulation of biologically produced materials such as skeletal material of carbonate, silica, or phosphate, or elements such as the rare earths, or zirconium, we find (Fig. 4) that there is a marked variation with time in the amount and kind of organic remains, in the cases shown here, of calcium carbonate and diatomaceous silica. This sequence is repeated in detail along the equatorial strip of high productivity; the section shown in the middle is from north of Marquesas; the one to the left shows the conditions found 5400 km further to the east at the Galápagos Islands. Westward this stratification can be followed to near the date line, and altogether it extends along the equator over nearly one-quarter of the earth's circumference.

The present time is characterized by a relatively low carbonate content in the sediment whereas during the preceding age, which coincides in time with the last glaciation in higher latitudes, the contribution of organic remains was high. Going downward in the sediment, four or five major maxima of this kind and a number of smaller ones are encountered before the Tertiary boundary is reached, identified by Emiliani on the basis of the markedly higher paleotemperature of planktonic Foraminifera. It has been demonstrated by Bramlette that this change in temperature coincides in time with an evolutionary change in the coccolithophorids, which is recognizable over the equatorial Pacific and probably also elsewhere. The Tertiary strata are characterized by smaller amplitude of the variations in the supply of organic remains to

(479)

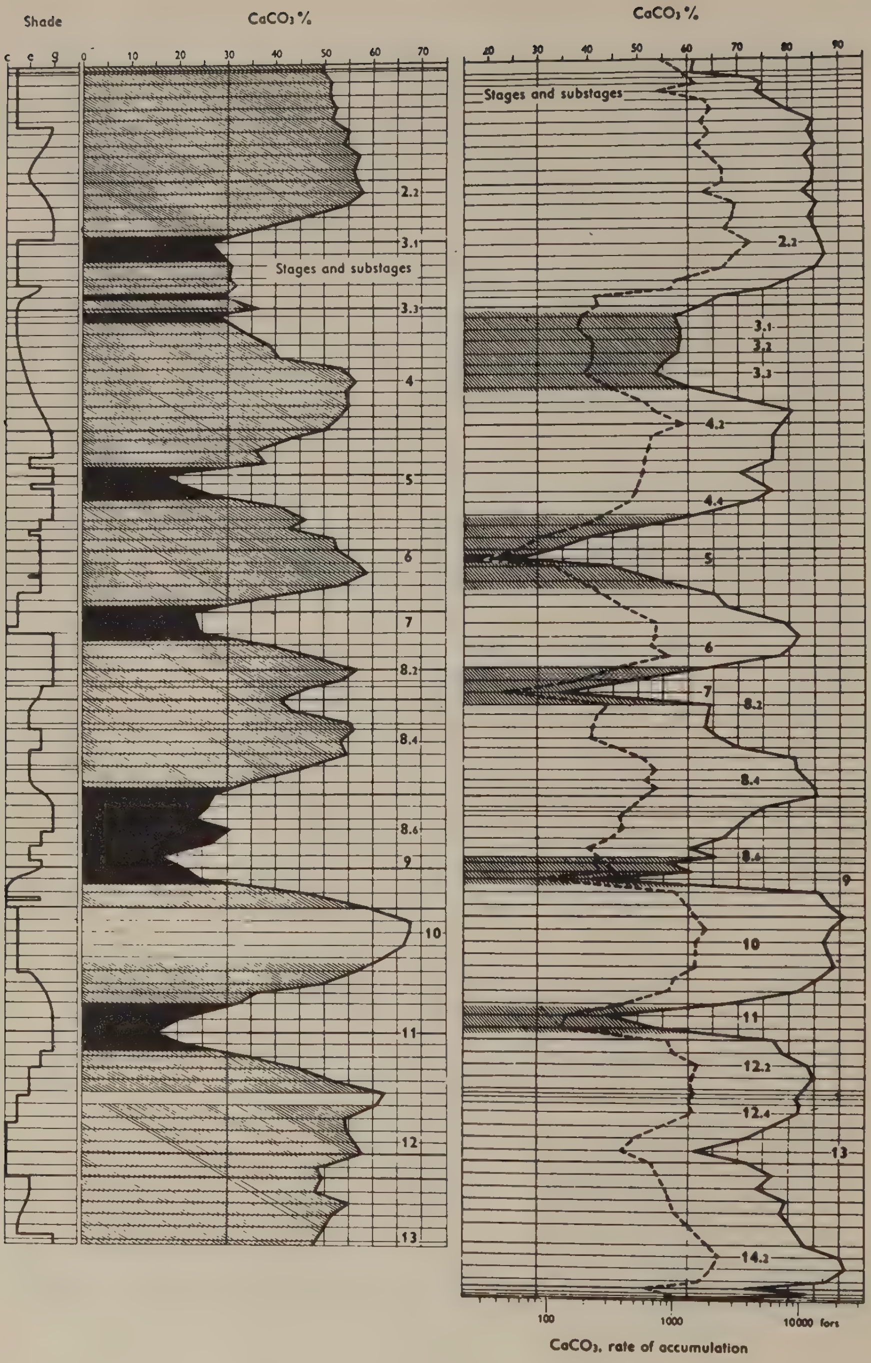

(a) (b)

Fig. 4. (*Continued on facing page.*)

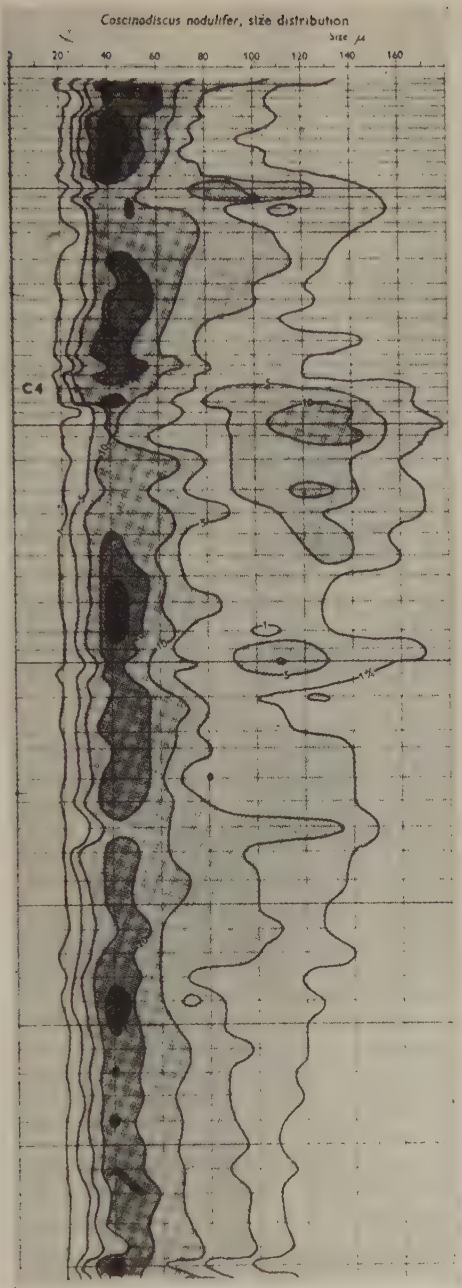

(*c*)

Fig. 4. Carbonate concentration as a function of depth in Equatorial Pacific sediment cores from (*a*) 106°W Long and (*b*) 135°W Long, and (*c*) size frequency distribution of the diatom *Coscinodiscus nodulifer* in the latter core (Arrhenius, 1952).

the sediment, and a lower average carbonate content, indicating a general decrease in the productivity.

It has been demonstrated by Emiliani that the strata formed at increased productivity in the equatorial Pacific are associated with colder surface water, as indicated by the oxygen isotope ratio in planktonic Foraminifera. He has also shown that during each given time period the surface temperature of the ocean drops toward the equator, consistent with the upwelling of cold deep water there, and that this temperature gradient becomes steeper during periods of high productivity (Fig. 2, top graph).

All these observations strongly suggest that the periods with a high rate of accumulation of organic remains were periods of increased rate of vertical water transport in the equatorial divergence, which ultimately appear to be caused by increase in the trade wind intensity. The ocean sediments thus provide us with a record not only of polar wandering but also of the intensity changes in the low-latitude atmospheric circulation, which is directly tied in with the great climatic changes that during the last geological period resulted in the ice ages.

The direct effect of cooling of the surface water at intermediate latitudes has also been traced over large areas in the Atlantic Ocean and in the Mediterranean through the original work by Schott (1935) on species of Foraminifera, sensitive to cold and warm water, followed by a number of similar studies by Cushman and Henbest, Phleger, Ovey, Ericson, and others. Quantitative information on the temperature development has been provided by Emiliani's (1955) extensive studies of the paleotemperature as indicated by the oxygen isotope ratio in tests of planktonic Foraminifera. Again it is here evident that the last period of cooling coincides in time with the last ice age, and by inductive reasoning it seems safe to assume that the previous low-temperature periods correspond to the older ice ages. The reason why this is difficult to prove directly is that the time scale of these events, as they are recorded on the continents, is only approximately known.

It should be mentioned in this connection that Emiliani (1955) has attempted to correlate the succession of cold and warm periods as reflected by the paleotemperature in Atlantic sediments, with the periodic changes in distribution of solar radiation over the earth, postulated by Milankovic as responsible for the glaciations. The time lag observed between temperature minima and the maximum extension of continental ice sheets has recently been explained by Emiliani and Geiss (1959) on the basis of plastic flow of the ice. With the more accurate measurements of geological age in the range of a few hundred thousand years that are promised by the ionium-thorium method which is now being perfected by Goldberg and co-workers, and by the protactinium method which is being developed by Rosholt, Sackett, and Koczy it should be possible to check Emiliani's theory accurately.

In spite of our still limited knowledge of the sediments covering the deep ocean floor and in spite of the ambiguities attached to the time scales, which so far have been extrapolated from carbon-14 measurements in the surface layer, it is probably right to say that our best quantitative information about the climatic evolution of the earth during the last million years comes from the oceanic record. An exception has to be made for the last 20,000 years, which are known in greatest detail from continental sediments, where the record has in this case not been disturbed by later catastrophic events.

Among recent geophysical hypotheses, inspired by observations on the deep ocean floor must also be mentioned the one proposed by Ewing and Donn (1956) attempting to explain the climatic oscillations in our geological period, and their commencement about a million years ago. Ewing and Donn were impressed by the indications in Atlantic cores of sudden transition from low surface water temperatures, typical of the glacial ages, to the conditions prevalent now and during interglacial ages. They assume that the location of the pole in the Arctic basin gives rise to a climatic instability and self-sustained oscillations. An originally ice-free Arctic Ocean, freely exchanging water with the Atlantic would be an efficient source of moisture in the Arctic region, causing growth of the continental ice sheets. The tying up of water in these ice sheets, however, would lower the sea level to near the sill depths of the Arctic basin, and the lowered influx of warm, Atlantic water together with the cooling from the inland ice over North America, northern Europe, and part of Siberia would lead to the sudden freezing over of the Arctic Ocean. The source of nourishment for the ice sheets and glaciers would thereby be sealed off, and they would start to wane and return their water to the ocean; the sea level would rise above the effective sill depth, the influx of warm water from the Atlantic would be increased, the ice cover over the Arctic Ocean would vanish, and the cycle could start over again.

Some authorities have questioned the assumption that there is really a lag effect in the system, causing it to overshoot, and leading to self-sustained oscillations rather than to a steady state. Also, it has been debated whether the heat effects involved would be sufficient. The hypothesis, however, possesses another interesting feature, namely, that it can be checked experimentally. To explain the start of the series of oscillations mentioned, Ewing and Donn (1956) assume that the North Pole in Tertiary time was in the Pacific Ocean, that is at least thirty degrees away from its present position, and that the first ice age occurred as a result of the motion of the pole into the Arctic basin. It must be said that such a motion is indicated neither by the numerous Tertiary sequences available from the Pacific Ocean floor, nor by paleomagnetic measurements, however, further evidence for or against the theory could probably be obtained from cores about 20 m long in the Pacific equatorial zone; this is within the reach of present coring methods.

The density of solid particles in the atmosphere and in the space between us and the sun has attracted great interest as possible variables in the past, responsible for climatic change and other phenomena, and again, the best record of worldwide or large-regional changes in source, path, and amount of such particles seems to be the ocean sediments. Singular events like volcanic eruptions are of special interest, as they provide us with useful stratigraphic marking horizons. The Late Glacial eruption in Laacher See in Germany is a famous example in which the ash spread over large parts of Northern Europe making it possible to recognize the Alleröd interstadial during which the eruption happened. In Iceland the archeological development is tagged by widespread ash layers, and in Patagonia the local records of the

Late Pleistocene climatic development in peat bogs have been correlated by interstratified ash layers from the Andean volcanoes. Correns (1937), in his work on equatorial Atlantic sediments, noted the variability in the volcanic components, and in the Mediterranean a great deal of interest has been devoted by Mellis, Pettersson, and Norin (1958) to identification of observed ash layers in the sediments with known historic or prehistoric volcanic events. The first and so far perhaps most successful attempt at oceanwide correlation of ash layers in long sediment sequences was made by Bramlette and Bradley (1942) in the cores raised by Piggot between Newfoundland and Ireland (Fig. 5). These results offer a powerful tool for correlation of the numerous long cores which since have been raised in the North Atlantic, and for reconstruction of the volcanic history of the whole region.

One of the most dramatic discoveries of this kind is the recent finding by Worzel (1959) of extensive ash beds in sediment cores near the South American coast (Fig. 6) all the way from Peru to Mexico. In their preliminary description of these strata, Ewing, Heezen, and Ericson (1959) interpret them as one continuous unit, which would represent a single gigantic eruption. One would, however, under these conditions expect to encounter the layer also in the more slowly accumulating sediments further out in the equatorial Pacific, reworked and spread vertically by bottom organisms (Fig. 7) and perhaps altered to montmorillonite but still mineralogically discernible. In these cores, including one from the Galápagos area, not far away from the Worzel ash in the Bight of Panama, however, several minor concentrations of unaltered ash of different types, and of montmorillonite are found, but nothing of the dimensions observed near the coast. It appears, therefore, that at the present time caution should be observed in the correlation of the coastal ash layers, that might well be derived from a series of eruptions from different volcanoes in the Cordillera.

While the volcanic dust appears as spikes in the sedimentary record, there is a fluctuating continuum of airborne detritus carried out over the oceans (Fig. 8) and deposited there, especially from the arid lands of the world. This dust has quite a varied mineral composition. One of the major components which is easily deter-

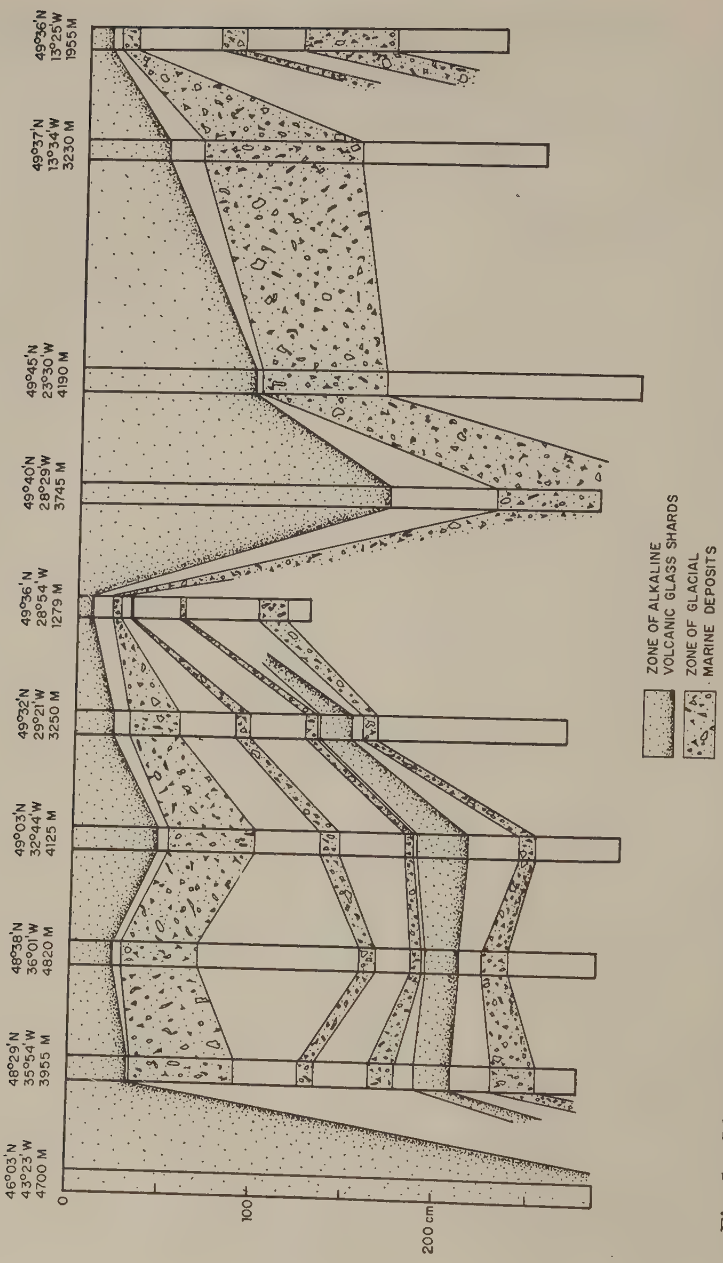
46°03'N 43°23'W 4700 M
48°29'N 35°54'W 3955 M
48°38'N 36°01'W 4820 M
49°03'N 32°44'W 4125 M
49°32'N 29°21'W 3250 M
49°36'N 28°54'W 1279 M
49°40'N 28°29'W 3745 M
49°45'N 23°30'W 4190 M
49°37'N 13°34'W 3230 M
49°36'N 13°25'W 1955 M
0
100
200 cm
ZONE OF ALKALINE VOLCANIC GLASS SHARDS
ZONE OF GLACIAL MARINE DEPOSITS

Fig. 5. Lithology of North Atlantic sediment cores, showing zones with glacial marine deposits and with alkalic volcanic glass (Bramlette and Bradley, 1942).

(486)

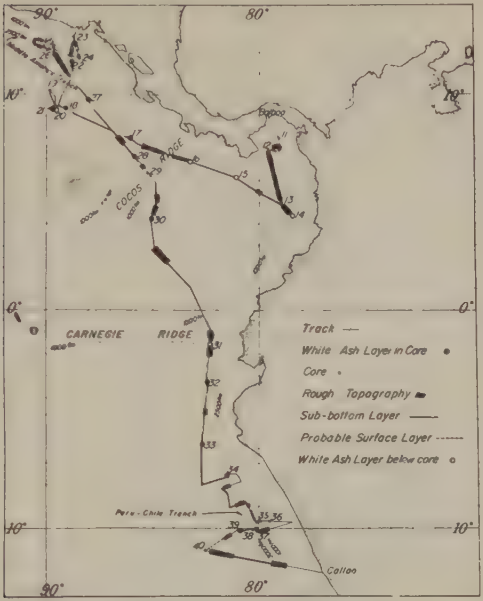
90°
80°
10°
0°
COCOS RIDGE
CARNEGIE RIDGE
Peru-Chile Trench
Callao
Track —
White Ash Layer in Core ●
Core •
Rough Topography ▬
Sub-bottom Layer ——
Probable Surface Layer ------
White Ash Layer below core ○

Fig. 6. Stations where an ash layer was sampled by the piston corer are shown by filled circles. Heavy lines indicate those parts of the track of the *Vema* along which a subbottom layer was recorded by the echo sounder. Ewing, Heezen, and Ericson have assumed that the subbottom reflection is caused by volcanic ash, and that this forms a continuous layer with a minimum extent over the area shown in the figure (Worzel, 1959).

mined, namely quartz, has been studied in some detail in the Pacific and shows a distribution of considerable interest.

Investigations of the size frequencies of the quartz particles in pelagic sediments (Fig. 9) showed a high degree of sorting, a mean diameter in fine silt, and an unusual cutoff of the very small particle sizes indicating an eolian origin of the material in several cases. Subsequent measurements by Goldberg and Rex (1958) support this view in several independent ways, and indicate the existence of two zonal maxima, in each hemisphere around 30° Lat, with a markedly increased content of quartz in the form of fine silt (Fig. 10). Goldberg and Rex have ascribed these maxima to fallout from the jetstreams which with high wind velocities circle the globe in these two latitudinal zones on the border between the stratosphere and the troposphere. The difference in intensity

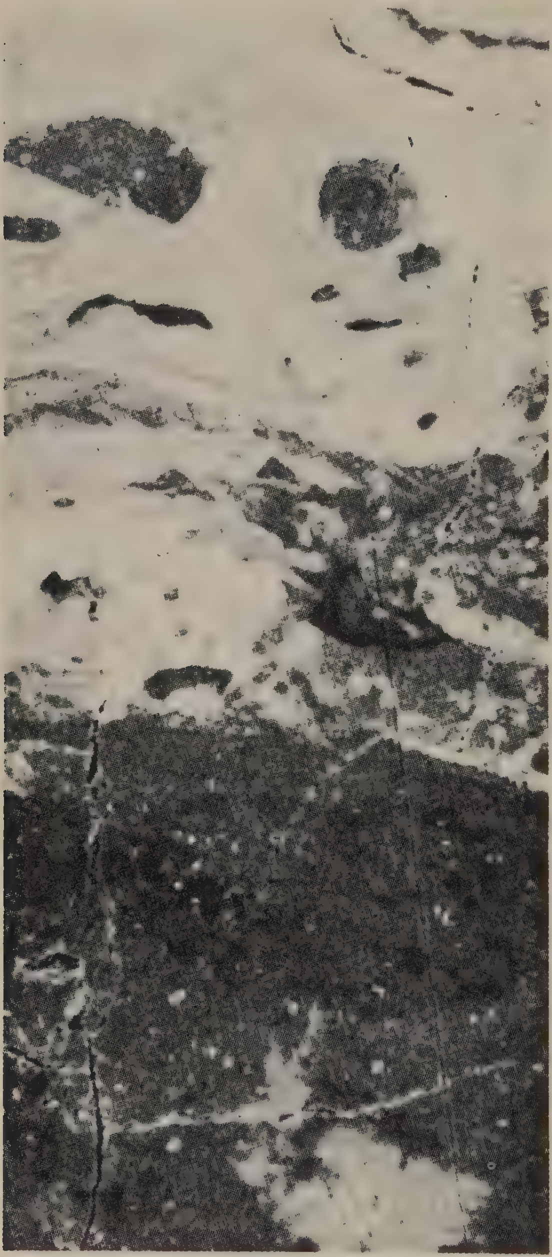

Fig. 7. Vertical section through the top eight centimeters of a sediment core from the East Equatorial Pacific, showing the mixing of material from adjacent strata by the activity of mud eating animals. Measurements of the amount of foreign material present at each level demonstrate that, assuming an originally sharp boundary between the light and dark sediment units, 2–3 cm thick layers below and above this boundary will ultimately contain 50 percent of material originating from the other side of the boundary. The drop of concentration of material originating from a given level with increasing vertical distance from this level is rapid; in only a few cases have single worm channels been observed to penetrate more than 20 cm (Picciotto and Arrhenius, unpublished).

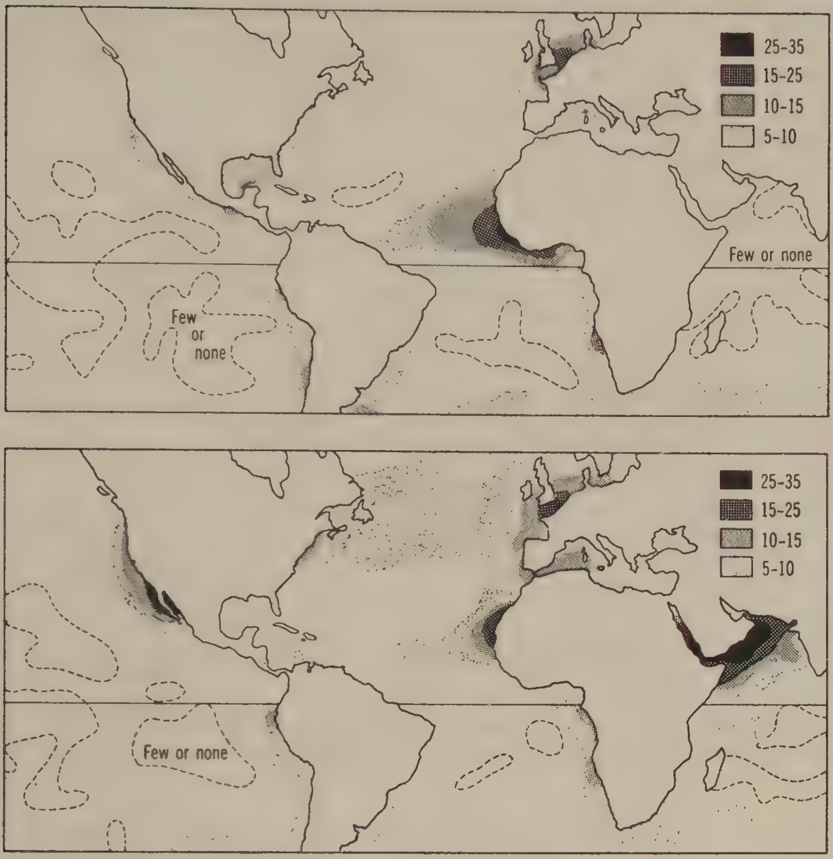

Fig. 8. Average frequency of haze (solid aerosol) during northern winter (upper graph) and summer season (lower graph). The extensive transport of dust from the African continent and the Arabian peninsula is clearly reflected, and the importance of the Sonoran and Andean deserts as supply areas for the Pacific sediments is indicated. The haze area in northwestern Europe is probably due to industrial smoke production (Arrhenius, 1959a).

of the quartz maxima in the Northern and Southern Hemispheres is, according to the same authors, due to the smaller areas of arid lands in the Southern Hemisphere. In addition, it appears that the distance from the coast has an important effect on the rate of fallout of quartz and other windborne minerals.

The concentration values of up to 20% quartz in the northern

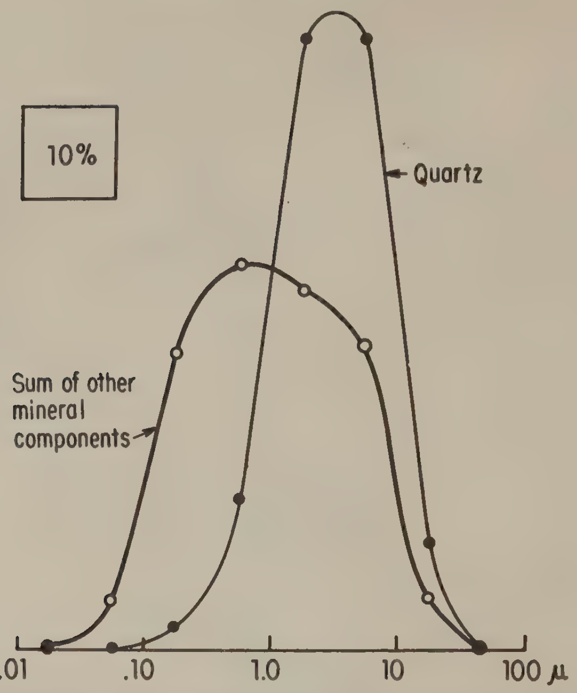

Fig. 9. Size frequency distribution of quartz and of the sum of other mineral components in a clay sediment from the north equatorial Pacific (Arrhenius, 1954, unpublished).

maximum suggest a total contribution of windborne minerals to the pelagic sediments in this zone of perhaps twice this value, and emphasize the quantitative importance of eolian components in some pelagic sediments. Strangely enough, no significant variations in this contribution have been found between the glacial and interglacial stages. The Tertiary sediments in the north equatorial Pacific, however, are low in quartz, indicating smaller arid source areas, or less efficient transport, and in the upper Pliocene a gradual transition is found from this situation to present-day conditions.

The importance of accretion of cosmic dust and micrometeorites was realized during the first extensive investigations of deep sea sediments by Murray and Renard (1891) after the *Challenger* expedition during the last century; however, it was left to the

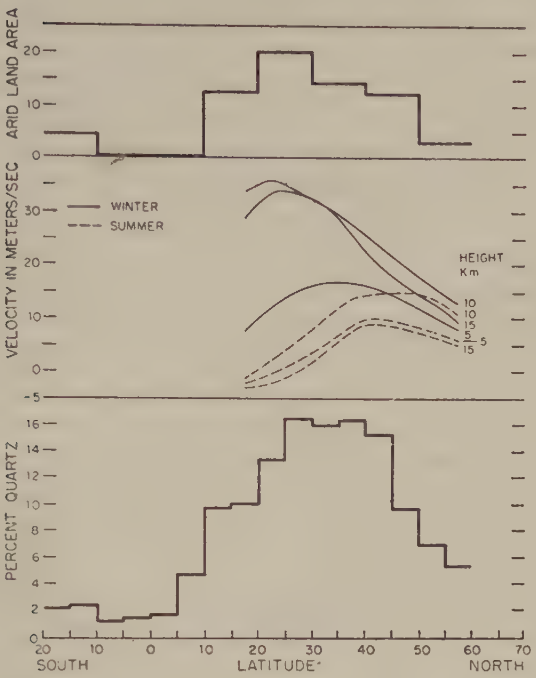

Fig. 10. Meridional distribution of quartz in east Pacific sediments (lower graph), velocities of high altitude winds (middle graph), and arid areas of the world (top graph) (Goldberg and Rex, 1958).

initiative of Hans Pettersson to start a quantitative study of the concentration and distribution in time of the microscopic spherules of nickel iron which form the perhaps most easily concentrated and identified component of cosmic material in deep sea sediments. Thanks to the technique developed by Kullenberg (1947) and employed by him during the Swedish Deep Sea Expedition large-diameter cores were available which permitted the collection of statistically significant numbers of spherules from sufficiently narrow depth intervals (Fig. 11). The results obtained by Pettersson, Fredriksson (1958), and Laevastu and Mellis (1955) indicate an increase in concentration of cosmic spherules in the Recent strata, which is interesting in view of the hypothesis that meteorites have started to reach the earth in increasing numbers in historic time. This distribution has been found both in the Pacific

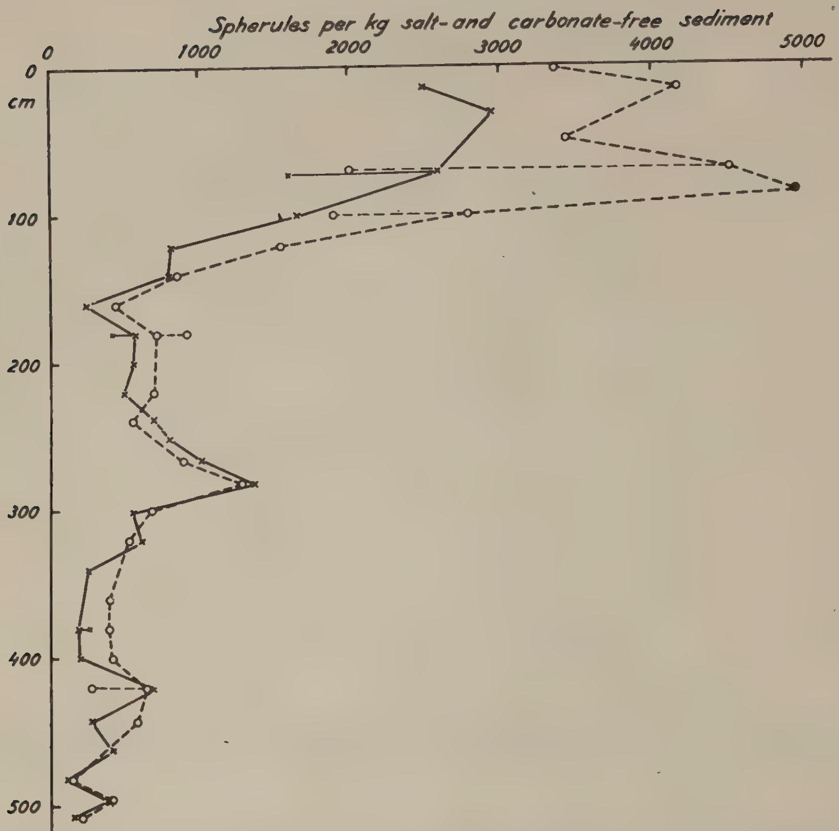

Fig. 11. Concentration of cosmic spherules in a sediment core from the West Pacific. The different curves represent results obtained by slightly different methods of assay (Pettersson and Fredriksson, 1958).

and the Indian oceans; in addition, several significant minor variations are found in older strata. Radiocarbon data, combined with stratigraphic measurements, appear to confirm that the recent increase in the concentration of cosmic spherules is due to an increase in their rate of accretion on the earth rather than to dilution with a larger amount of other sedimentary components.

The original idea by Murray and Renard (1891) that the spherules are solidified droplets of molten iron splashed off from meteorites entering the atmosphere has been further corroborated through elegant microradiographic analyses by Castaing and

Fredriksson (1958) and Fredriksson (1958). Still nobody has been able to establish the rate of accretion on the earth's surface of fine cosmic dust that might be of great geophysical significance. Silicate chondrules like those in meteorites have, however, been observed by Murray and Renard, and recently by Bramlette. An interesting possibility for estimating the amount of cosmic dust settling on the earth may be offered by the fact that the meteorites, in contrast to terrestrial rocks, are reported to contain considerable amounts of monoclinic magnesium-iron pyroxenes, clinoenstatite and clinohypersthene, which are relatively easy to concentrate, and which belong to a series of minerals which do not readily decompose on the ocean floor.

In a survey like this it has been necessary to limit the subject to an impressionistic account of a few topics. It is impossible to give justice, under such conditions, to all the interesting work that has been done in the field, and to point out all the fascinating possibilities that are now apparent. I hope, however, that I have been able to convey a general impression of the wealth of information that the pelagic sediments offer to those who devote themselves to quantitative study of the past history of the solid earth, its ocean and atmosphere, and its interrelation with outer space.

REFERENCES

Arrhenius, G. 1952. Sediment cores from the East Pacific. *Rept. Swed Deep Sea Expedition 5*, Göteborg, Sweden.

———. 1959a. Sedimentation on the ocean floor. *Researches in Geochemistry*, Ph. H. Abelson, Editor. John Wiley and Sons, New York, N.Y.

———. 1959b. Climatic records on the ocean floor. *Rossby Memorial Volume*, B. Bolin, Editor. Rockefeller Institute Press, New York, N.Y.

Bramlette, M., and W. Bradley. 1942. Geology and biology of North Atlantic deep sea cores between Newfoundland and Ireland. Lithology and geologic interpretations. *U.S. Geol. Survey Prof. Papers No. 196.*

Castaing, R., and K. Fredriksson. 1958. Analyses of cosmic spherules with an x-ray microanalyzer. *Geochim. et Cosmochim. Acta, 14,* 114.

Correns, C. W. 1937. Die Sedimente des Äquatorialen Atlantischen Ozeans. *Wiss. Ergeb. Deut. Atl. Exp. Meteor, 1925–27, 3*, 3, Leipzig.

Emiliani, C. 1955. Pleistocene temperatures. *J. Geol., 63*, 538–578.

Emiliani, C., and G. Edward. 1953. Tertiary ocean bottom temperatures. *Nature, 171*, 887–889.

Emiliani, C., and J. Geiss. 1959. On glaciations and their causes. *Geol. Rundschau, 46*, 576–601.

Ewing, M., and W. L. Donn. 1956. A theory of ice ages. I. *Science, 123*, 1061; II. *ibid., 127*, 1159.

Ewing, M., B. C. Heezen, and D. Ericson. 1959. Significance of the Worzel deep sea ash. *Proc. Natl. Acad. Sci. U.S., 45*, 355.

Fredriksson, K. 1958. A note on investigations of cosmic spherules and other small meteoritic particles. *Astronomical Notes*, University of Göteborg, Sweden, p. 21.

Goldberg, E. D., and G. Arrhenius. 1958. Chemistry of Pacific pelagic sediments. *Geochim. et Cosmochim. Acta, 13*, 153–212.

Goldberg, E., and M. Koide. 1958. Ionium-thorium chronology in deep sea sediments of the Pacific. *Science, 128*, 1003.

Goldberg, E. D., and R. W. Rex. 1958. Quartz contents of pelagic sediments of the Pacific Ocean. *Tellus, 10*, 153–159.

Kullenberg, B. 1947. *The Piston Core Sampler.* Svenska Hydrografisk-Biologiska Kommissionens Skrifter, Tredje Serien. Hydrografi. Vol. I, Book 2. Göteborg, Sweden.

Laevastu, T., and O. Mellis. 1955. Extraterrestrial material in deep sea deposits. *Trans. Am. Geophys. Union, 36*, 385–389.

McDonald, W. F. 1938. Atlas of climatic charts of the oceans. *U.S. Dept. of Agriculture, Weather Bureau, W. B. No. 1247.*

Menard, H. W., and R. L. Fisher. 1958. Clipperton fracture zone in the Northeastern Equatorial Pacific. *J. Geol., 66*, 239.

Murray, J., and A. Renard. 1891. *Challenger Reports*, London.

Norin, E. 1958. The sediments of the Central Tyrrhenian Sea. *Rept. Swed. Deep-Sea Expedition, 8*, 1.

Pettersson, H., and K. Fredriksson. 1958. Magnetic spherules in deep sea deposits. *Pacific Sci., 12*, 71.

Revelle, R., M. Bramlette, G. Arrhenius, and E. Goldberg. 1955. Pelagic sediments of the Pacific. *Geol. Soc. Am., Spec. Papers No. 62*, 221–236.

Schott, W. 1935. Die Foraminiferen in dem Äquatorialen Teil des Atlantischen Ozeans. *Wiss. Ergeb. Deut. Atl. Exp. Meteor, 1925–27, 3*, 3.

Worzel, J. L. 1959. Extensive deep sea sub-bottom reflections identified as white ash. *Proc. Natl. Acad. Sci. U.S., 45*, 349.

(494)

Reprinted from Oceanography
American Association for the Advancement of Science
Copyright 1961
pp.345–366

Pelagic Sediments

M. N. BRAMLETTE*

Scripps Institution of Oceanography, La Jolla, California

THE vast extent of pelagic deposits, covering about 70 per cent of the ocean floor, thus about half of the earth, makes them of obvious importance to all earth science. A record, more nearly complete than elsewhere, reflecting many major events of earth history will surely be found through examination of pelagic sediments, especially with their penetration to greater depths. Obviously only a few aspects of the subject, from a geological viewpoint, may be considered in this paper.

Pelagic sediments seems a useful term although it is not easily defined, as there is a considerable variety of such sediments and, naturally, gradations from pelagic to other sediments. Derivation from *pelagos* only implies "of the open ocean," but it has been restricted in usage by differentiating such sediments as the hemipelagic sediments bordering major land masses. All the pelagic (eupelagic) sediments, whether largely of plankton remains or fine inorganic particles, have certain distinctive characteristics to reflect their environment of accumulation. Pelagic sediment is precipitated and/or settled from the overlying ocean waters of regions where rates of accumulation are slow enough to cause little change in the great volume of circulating bottom waters, and the little sediment thus accumulates, and normally remains, in a highly oxidized state. This is reflected in their composition and more obviously in the colors of red, brown, and buff. Even the more nearly white oozes, composed largely of plankton remains, show only small parts of the sediment, and these are beneath the

---

* Contribution from the Scripps Institution of Oceanography, New Series. This paper is based in part on results of research carried out for the Office of Naval Research.

Contributions from the Scripps Institution of Oceanography, New Series, 1277
Reproduced by Permission

surface, of green gray color from locally developed reducing conditions.

Some deep-sea or abyssal deposits, even though distant from continents or islands, seem properly excluded from the pelagic type. These include the glacial-marine, and the turbidity current deposits. These are more rapidly accumulated and thus less oxidized, and are likewise more similar to the hemipelagic and continental sediments in lithology, mineralogy, and thus in chemical composition.

Some of the deposits composed largely of the remains of plankton may also be excluded, not only because these were accumulated near or even on the continents, but also normally accumulate more rapidly and lack the characteristic of highly oxidized components. These might be termed planktonic deposits except for confusion of such with those of the typical pelagic deposits composed largely of plankton remains. It is, however, this distinct kind of deposit of plankton remains, lacking the highly oxidized character of pelagic deposits, such as some in the Gulf of California, which form the usual and perhaps only plankton accumulations known in the ancient strata on the continents. Their much greater rate of accumulation is commonly reflected in their thickness relative to probable time,. and rather than being highly oxidized like pelagic sediments, these are normally high in organic matter content. A thick deposit, for the amount of upper Eocene time, is known as the Oceanic formation in Barbados, B.W.I., because of the abundance and variety of marine planktonic remains, including many Radiolaria. It lacks, however, the pelagic sediment feature of slow accumulation with the highly oxidized character of the iron minerals. The reported red clay in this formation has proved to be limited only to weathering of some present day exposures of the rocks.

Depth of water, though normally great, is not a factor of particular significance for pelagic deposits, as *Globigerina* ooze on guyots and banks shows the typical characteristics of pelagic sediments even where accumulated at hundreds rather than thousands of meters. Here it commonly shows better than average sorting in grain size, but a similar relation of sorting to topography is apparent in some pelagic sediments at great depths.

The most distinctive chemical and other characters of pelagic deposits thus seem related primarily to their slow accumulation and the resulting approach to chemical equilibrium with the normal open ocean bottom water environment. Even the comparatively rapid pelagic accumulation of some *Globigerind* ooze in the equatorial Pacific, at rates of several centimeters per thousand years, results in only the oxidized minerals of iron and tetravalent manganese. The gray diatomaceous sediments of the subarctic Pacific are not highly oxidized. Menard (1955, p. 240) has indicated, however, that this is largely glacial-marine and turbidity current deposition. Diatom remains are a distinctly minor element, and as indicated, these deposits also lack the slow accumulation and other features of typical pelagic deposits.

Many of the more interesting discoveries and advances in knowledge of pelagic sediments are coming from geochemistry, and the stratigraphic evidence of former conditions that is indicated in core samples. Much regarding the surface sediments, however, remains little changed from the pioneer work of Murray and Renard (1891). Not only is the *Challenger* volume on deep-sea deposits a great compilation of data, but much of the interpretations seem confirmed.

The classification and most of the terms of Murray and Renard, though not entirely satisfactory, are sufficiently descriptive and well known not to require time to discuss the original or any modified definitions here. Even their map of distribution covering most of the earth's surface presented much of the major features indicated on the map from Sverdrup *et al.* (1946, p. 975, Fig. 253). It will be indicated that though the pelagic clay includes great areas with different colors and other characters, the old term "red clay" still seems not entirely inappropriate as a general term, in that it implies the highly oxidized character of all pelagic clays.

The great volume of calcareous deposits in the oceans presents problems that have been much discussed. The present rate of supply of calcium from the rivers is sufficient to double the large amount in the oceans in about one million years if no calcium were removed, and Revelle and Fairbridge (1957, p. 244) calculated this should result in deposition equivalent to 0.66 g of carbonate per square centimeter per thousand years for an area equal to the whole ocean floor. A large but indeterminate part of this accumulates in hemipelagic deposits and locally, as in coral atolls, but most of it must go into the pelagic calcareous ooze. The noncalcareous "red" clay, where solution results in no carbonate accumulation, covers about one-third of the total area, and thus would not radically change the above estimate on rate for the areas of calcium carbonate accumulation. This rate based on influx from rivers corresponds approximately with the 1 cm per thousand years for *Globigerina* ooze accumulation, indicated by Kuenen (1950, p. 383).

The great excess of calcium carbonate deposits in the rocks of the continents, over the percentage to be expected from the original igneous rock sources, cannot represent a segregation there, through dominance of shallow water deposition of the calcium carbonate, if the present great percentage of calcareous deposition in the deep-sea persisted through much of the earth's history known in the sedimentary rocks.

This enigma is evident in all the attempts at a geochemical balance of the elements eroded from igneous rocks and accumulated in all sediments and ocean water. The various estimates and results cannot be summarized here. Results from various approaches and assumptions led Kuenen (1950, p. 389) to conclude that the present large segregation of calcium carbonate in pelagic sediments may have begun in Cretaceous time, with the advent of the planktonic Foraminifera. The coccoliths and other very small calcareous remains of planktonic algae appear to have been a more important carbonate component than the Foraminifera until late in the time since the Cretaceous. Present evidence, however, does not preclude the possibility that all such calcareous plankton were unimportant before the Cretaceous. This interpretation is inviting as it could account for a great dominance of shallow water deposition of the calcium carbonate, by the benthonic organisms, and perhaps inorganically, in pre-Cretaceous time.

An attempt at a geochemical balance by Goldberg and Arrhenius (1958, p. 207) resulted in a much smaller total volume of the noncalcareous pelagic clays than that of Kuenen's computations, but the same problem of a long-term lack of balance for calcium carbonate deposition is again evident in their results.

The following observations of the present extent and rate of accumulation of pelagic calcium carbonate deposits seem to offer little help to this problem, but rather emphasize it more.

The shells and their fragments from pelagic Foraminifera, including *Globigerina*, clearly form most of the calcium carbonate of modern pelagic deposits. The tiny coccoliths from certain planktonic algae form a minor part of the present day calcareous deposits. No inorganic crystals or other nonskeletal calcium carbonate is found in pelagic sediments.

Figure 1*a* shows an electron microscope photograph of the fine part of such sediment, which consists of coccoliths of a few microns that are also discernible with a light microscope, and their recognizable debris in the finer fraction of less than 0.1 micron, with no inorganic carbonate.

Figure 1*b* shows a core (Ch 40) of pelagic sediment of Miocene age, with only about 10 cm of Quaternary cover and small amounts of the upper part carried down in borings from benthonic organisms. The Miocene clay grades down into coccolith ooze. The shorter core (Ch 17), at different scale, is of Oligocene age that has almost no later sediment cover. It is a coccolith ooze with a few per cent of pelagic Foraminifera, and more than 80% calcium carbonate. A small manganese nodule is evident, and the dark upper surface is largely a surface residue from dissolution of the calcium carbonate. It contains the same Radiolaria as in the lower sediment, but here it is mixed with a few Recent ones.

Figure 2*a* shows the abundant calcareous remains known as discoasters and some of the larger coccoliths from the core of Oligocene age. The discoasters, though generally associated in occurrence with coccoliths, are only questionably related, as they are now largely or entirely extinct forms. These average about 10 microns in size. Figure 2*b* shows another such assemblage of Miocene age.

Much recent data by Bradshaw (1959, p. 53, Fig. 37) on the living populations of pelagic Foraminifera in the Pacific provide information here interpreted in terms of present rates of accumulation on the sea floor. Figure 3 shows his summarized total population values, with the highest productivity areas indicating more than 100 specimens per cubic meter of water. A large part of the subarctic Pacific is known to have high plankton productivity but it is perhaps surprising that this is indicated also for the calcareous Foraminifera. His data, however, indicate that the number of species is small here.

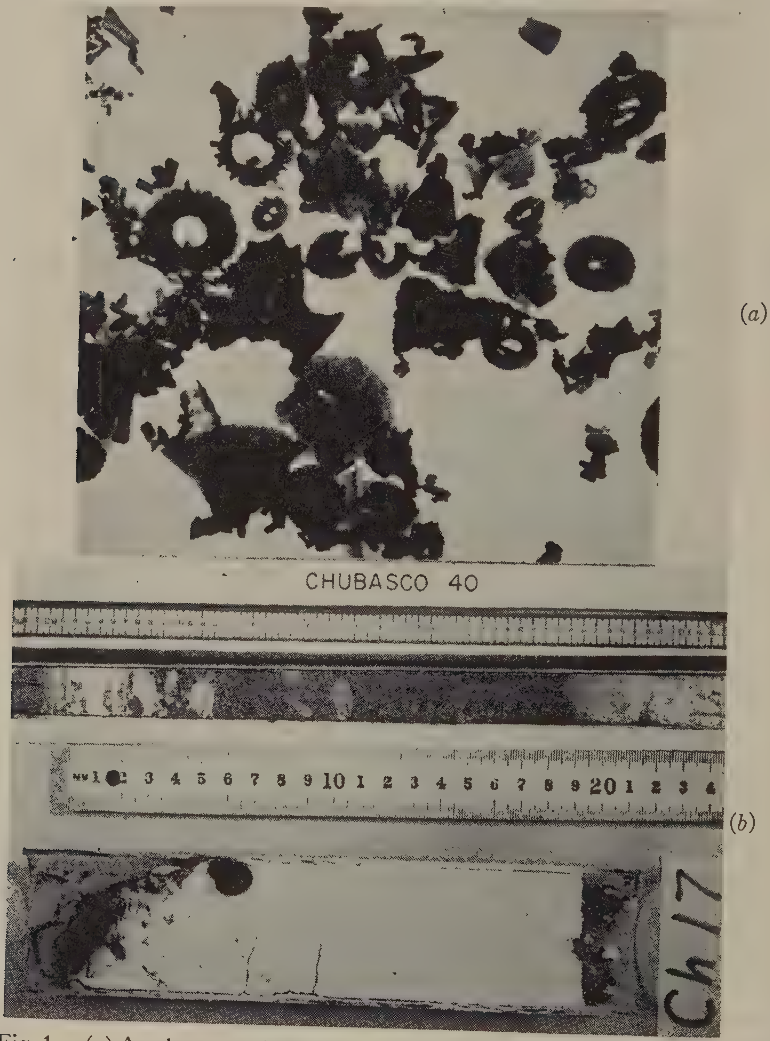

Fig. 1. (*a*) An electron microscope photograph of coccoliths and fragments of them from calcareous ooze of Quaternary age (× 3,000). (*b*) Core Ch. 40 of Miocene age, except upper 10 cm (at left) of Quaternary age. Core Ch. 17 is an Oligocene calcareous ooze. Different scales indicated.

(500)

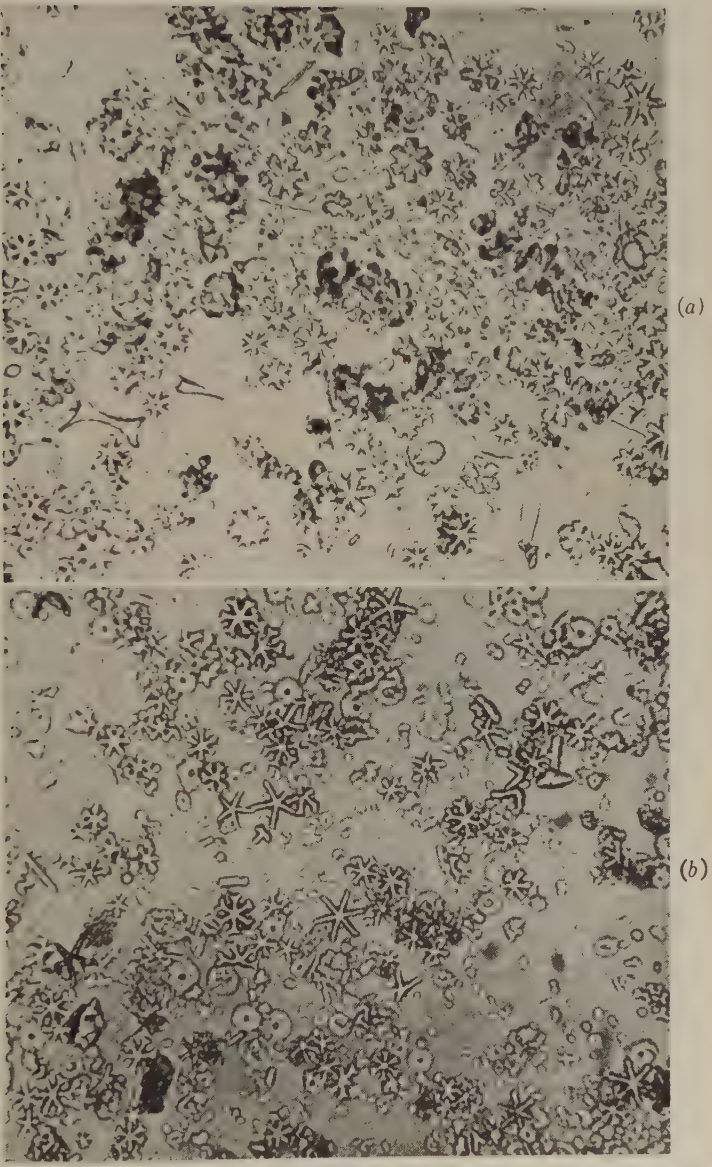

Fig. 2. (*a*) Constituents of core sample of Oligocene age, showing many discoasters (× 450). (*b*) Discoasters and coccoliths from core sample of Miocene age (× 450).

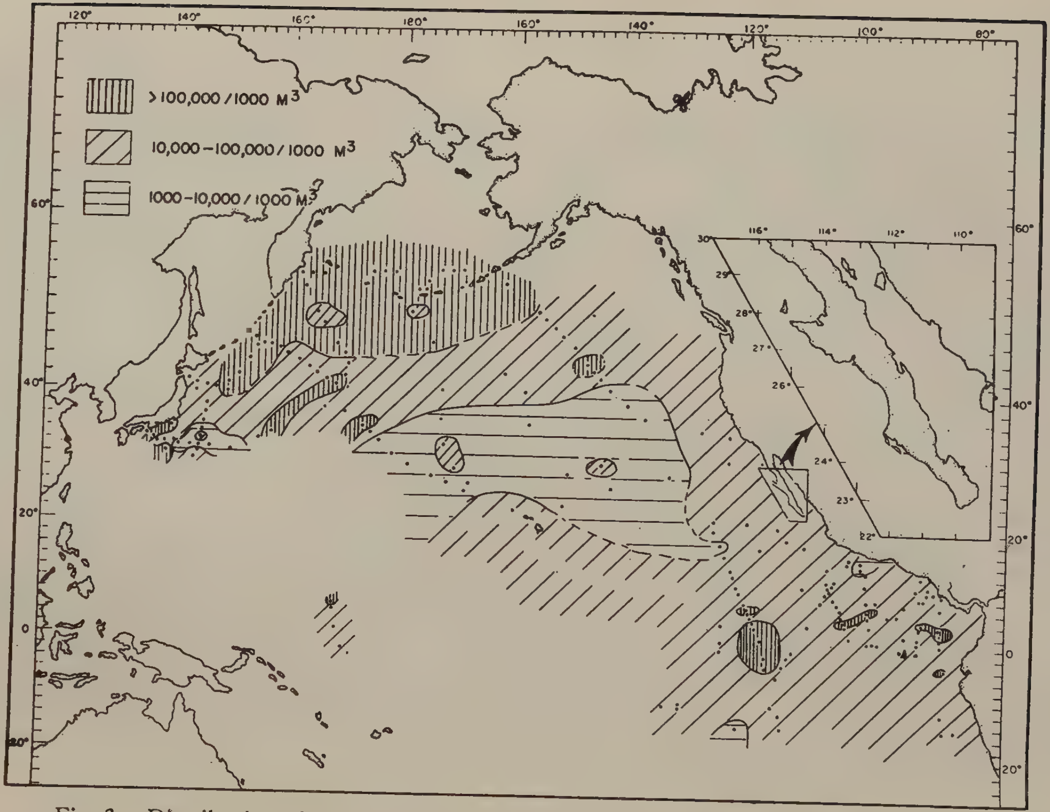
>100,000/1000 M^3
10,000–100,000/1000 M^3
1000–10,000/1000 M^3
120°
140°
160°
180°
160°
140°
120°
100°
80°
60°
40°
20°
0
20°
116°
114°
112°
110°
30°
29°
28°
27°
26°
24°
23°
22°

Fig. 3. Distribution of planktonic Foraminifera in the North Pacific (Bradshaw, 1959).

In the more productive areas, 100 specimens per cubic meter is near Bradshaw's average down to a depth of 100 m, with rapid decrease at greater depths. This would approximate 10,000 for the total water column above a square meter of ocean floor. With a life cycle or residence time of about one year probable, this indicates deposition of one calcareous test per square centimeter of the bottom per year. This rate would approximate only 1 mm of *Globigerina* ooze per thousand years.

This rate of accumulation would be only one-tenth of the 1 cm per thousand years indicated from other evidence as near an average rate of post-Tertiary accumulation, and expectable from rate of supply of calcium by rivers. The approximate balance indicated by saturated waters should be maintained in major part by *Globigerina* ooze deposition. Even smaller rates would be indicated for most of the North Pacific showing the much smaller standing crop. Solution with no net accumulation occurs over much of this region of 5000 m or more depth.

Some recent data by Bé (1959, p. 80, Table 2) indicates much smaller populations of planktonic Foraminifera in the North Atlantic than Bradshaw shows in the Pacific Ocean. The reverse would be expected from rates of post-Pleistocene accumulation in the two oceans. Differences and inadequacies of sampling methods would not seem to account for the difference that exceeds an order of magnitude of ten. Perhaps the residence time or life cycle is much less than one year, and the accumulation rate thus greater, but this would not affect the great difference indicated for the two oceans. Need for additional data on this problem is evident.

Over large areas of the ocean, such as that in the equatorial Pacific, calcareous tests (dominantly planktonic Foraminifera) constitute up to more than 80 per cent of the sediment. In this belt of high productivity in the equatorial current and countercurrents, the diatom and radiolarian remains commonly form 10% or more. The clay and other inorganic particles are less than 10%. This and following considerations indicate that in the more productive areas of the ocean the remains of calcareous organisms have accumulated at rates up to nearly 10 times that of other pelagic sediments.

Arrhenius' study (1952, p. 192) of the Swedish deep-sea cores in the equatorial belt shows a thickness up to more than 10 m of the Quaternary *Globigerina* ooze, with the minor amount of clay accumulation. His extrapolation from a rate determined by carbon-14 suggests an average rate near 1 cm per thousand years for this calcium carbonate accumulation. He indicates a distinctly lower Recent rate of carbonate accumulation than the average of Quaternary time for the equatorial belt of high productivity.

In contrast to some 10 m of Quaternary *Globigerina* ooze accumulation in the equatorial Pacific, the thickness for noncalcareous clay of this age to the north seems to average near 1 m, and rates here averaging 1 mm per thousand years from ionium-thorium ratios by Goldberg are in agreement. The fine clay suspension in the ocean waters that Kuenen termed the lutite veil is not apt to accumulate at uniform rates everywhere, especially in regions with marked differences in bottom topography and water movement. As measured by TiO_2 percentage, however, its accumulation does not seem to vary by more than a factor of 2 in the equatorial Pacific region and seems to serve as a very rough approximation for relative rates of accumulation over larger regions. Despite all the approximations and uncertainties, it seems evident from the area and rates of calcium carbonate accumulation that its total volume dominates that of Quaternary pelagic accumulations.

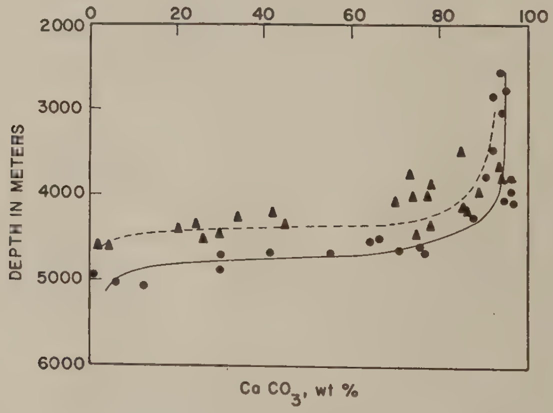

Fig. 4. Pelagic surface samples of the Pacific. – – – – Across Tuamotu Archipelago, 10°–27° S Lat, 128°–147° W Long. ——— Across east Pacific rise at approximately 45° S Lat (*Downwind* expedition).

Murray and Renard (1891), and all since, have recognized that solution of calcium carbonate is important on the deeper parts of the ocean floor, and is a factor in the decreasing carbonate content below depths of about 4000 m. What may be called a compensation condition, where supply does not exceed the solution, and thus with no net accumulation of calcium carbonate, includes obvious factors other than depth and rate of supply. Data presented here, however, appear to indicate that factors related to a rather narrow depth difference are more important than has previously been indicated, and largely control the pattern of carbonate percentages in pelagic sediments. Conditions related with marked deviations to unusually great depths, or rates of supply, or other factors will be apparent, but the depth of compensation remains surprisingly near limits between 4000 and 5000 m. The sharp decrease in $CaCO_2$ and compensation depth appears even more limited, within a range of about 500 m in localized regions where depth differences are greater than differences in the other factors. This poses a problem on the solubility conditions in the bottom waters that a depth below 4000 to 5000 m appears so important.

Figure 4 shows $CaCO_3$ per cent plotted against depth in meters for an area near 10–27° S Lat in the Pacific. The curve shows a

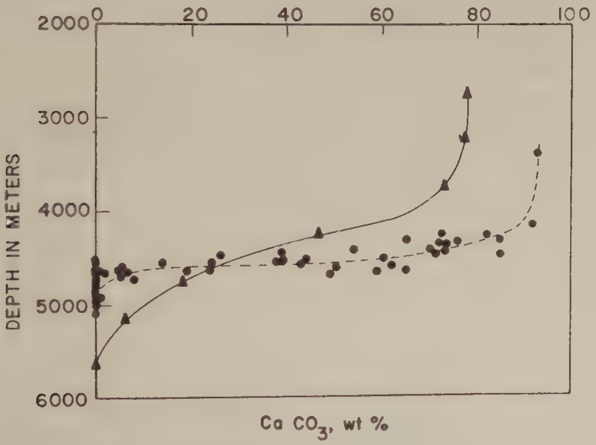

Fig. 5. Calcium carbonate versus depth of the Pacific. – – – – Central equatorial Pacific, 15° N to 5° S Lat, 120°–135° W Long. ——— Average for 500-meter intervals from all available data for top of core samples.

sharp decrease with depth, and a compensation depth near 4500 m. The lower curve is from a more southern area, between latitudes 40° and 50° S, where the compensation depth is greater (near 5000 m), and comparable with that common in the Atlantic Ocean.

Figure 5 represents an area at the north edge of the Pacific equatorial belt of high productivity and carbonate deposition. The carbonate percentage is here controlled more largely by the abrupt change northward in carbonate supply from the counter-current belt of very high productivity, and with little change in depth of water. Even here, however, the depth relation is also indicated, with a compensation depth near 4700 m. The other curve is an average of all available samples from the Pacific, affected by all the variable factors, but nevertheless showing a marked change between 4000 and 5000 m. The points are based on averages for all samples between 500-m intervals.

Figure 6 shows the distribution of calcium carbonate from all available data for the central and eastern Pacific, and its relation to the depth contours of 4000 and 5000 m. Despite the inadequate control on both, the relation of carbonate content and depth is apparent in the southern Pacific. It would be closer if additional depth contours, such as 4500 m, were shown, as indicated by individual core depths. Most of the North Pacific is below depths of 4000 m, but factors other than depth are apparent here. Productivity of calcareous plankton is relatively low over large areas, including part of that of less than 4000 m depth to the southwest of Mexico. Rapid clastic accumulation and high organic matter content have been indicated for the large region off Alaska. Increased supply of CO_2 to the bottom waters thus seems probable, and may influence the compensation depth above 4000 m here.

Statements commonly imply that the solution largely occurs during the descent of calcareous shells to great depth. This time, however, is insignificant compared with that possible on the ocean floor, with the slow rates of accumulation. Foraminiferal tests settle at rates requiring only a few days to reach 5000 m depth, but might remain near the sediment-water interface for hundreds of years in areas of no net accumulation of carbonate. Coccoliths, averaging 5 microns, would settle much more slowly (requiring

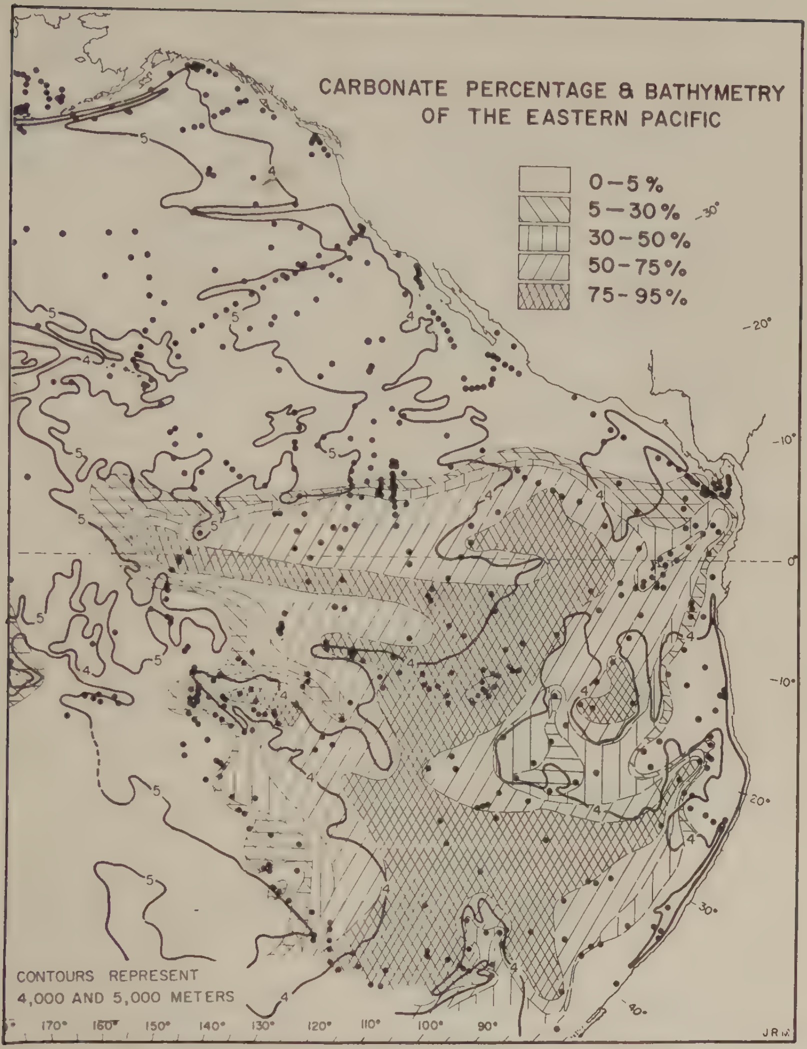
CARBONATE PERCENTAGE & BATHYMETRY OF THE EASTERN PACIFIC
0–5 %
5–30 %
30–50 %
50–75 %
75–95 %
CONTOURS REPRESENT 4,000 AND 5,000 METERS
170° 160° 150° 140° 130° 120° 110° 100° 90°
30° 20° 10° 0° 10° 20° 30° 40°
4
5
JRM

Fig. 6. Carbonate percentage and bathymetry of the eastern Pacific (data compiled by Mr. Donald Lynn).

more than 10 years), yet these normally reach the bottom, and accumulate with the Foraminifera above the compensation depth. Coccoliths are lacking only near and below this compensation depth, where any remains of Foraminifera consist only of fragments of the thicker shell parts.

The cold bottom waters of polar origin are known to be relatively high in carbon dioxide, and thus are able to dissolve more of the calcium carbonate. It seems improbable, however, that temperature stratification in the waters could be so marked that this factor alone could account for the sharp limits of the compensation depth that have been indicated. Most present consideration of increased solution from hydrostatic pressure does not suggest it as a major factor. It may seem worth additional investigation, however, for with pressures below about 4000 m becoming rather critical, it could explain the sharp limits indicated for the compensation depth.

Other interesting but quantitatively minor biogenous deposits can be mentioned only briefly.

As indicated, the diatomaceous belt of the North Pacific contains a minor part of diatoms, and lacks the features characteristic of pelagic deposits. Diatoms appear to average little more than 10 per cent of this sediment, as indicated by x-ray determinations of Goldberg, after converting the opaline silica of the diatoms to cristobalite by heating. Samples from the Antarctic belt are more highly diatomaceous, and in part, at least, show the more oxidized character of typical pelagic sediments.

The small size and shape of diatoms results in settling rates approximating 50 years or more to reach the bottom, and the more delicate ones are dissolved before reaching the ocean floor. Lateral distribution by currents appears to be less extensive, however, than has been suggested, as indicated by Fig. 7. These unpublished data from Kanaya indicate a few of the characteristic species, among more cosmopolitan ones, that are not mixed in the bottom sediment throughout the Pacific. The indicated distribution from north to south in the Pacific is only from the few samples studied to date.

The skeletal remains of Radiolaria are a conspicuous element of some pelagic sediment, though seldom amounting to more than about 10 per cent even in the so-called radiolarian ooze. Accumulation appears greatest in the equatorial belt of generally high productivity, but they dominate the biogenous component only in the north edge of this belt where solution of calcium carbonate has increased their proportion. Their value in age assignments has

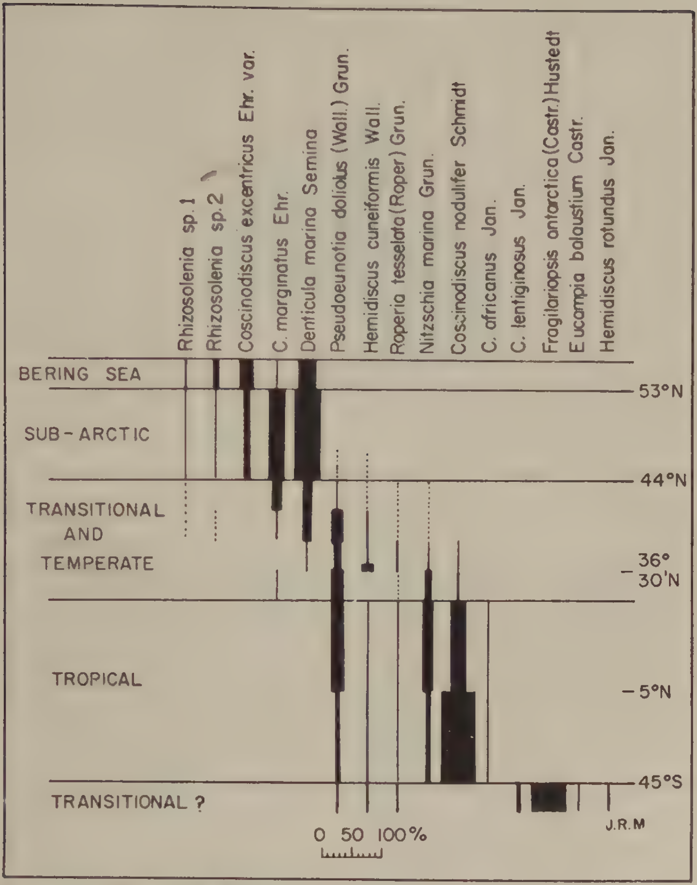

Fig. 7. Distribution of diatoms in Pacific sediments, few selected species (preliminary data from T. Kanaya, unpublished).

been demonstrated by Riedel (1959), especially in sediments where few other fossils have been preserved. Solution of the opaline remains occurs even within the sediment, however, under some conditions. (See Fig. 8*b*.)

Debris from pelagic fish is quite a minor element, but accounts for the relatively high phosphorus content of pelagic sediments. The scales are generally dissolved, but teeth and larger amounts of small skeletal fragments accumulate in the sediment. This material is of particular interest because of the surprising amounts of certain elements concentrated from the bottom waters. These include several per cent of rare earths, abnormal amounts of zinc, copper, tin, and lead, and radioactive elements such as thorium (Arrhenius *et al.*, 1957). Figure 8*a* shows the tracks, in a photographic emulsion, of alpha particles from such a fish fragment. The brown color from organic components in the fish fragments is gradually lost with time in the oxidizing environment, and appears more related to rate of sediment accumulation or burial than to age. This material in Tertiary pelagic deposits has generally lost the brown color, although this is not the case for many Tertiary and older sediments from environments less oxidizing and more rapidly accumulated than in the pelagic one.

The pelagic (red) clay still poses many problems, such as the proportion derived from pyroclastics and the various other sources. Much of this information may come with more reliable methods and knowledge on clay mineralogy. Occurring over the vast areas with water depths of 4000–5000 m or more, it contains little calcareous material, but commonly includes less than 1% of small rhombs of dolomite, apparently formed within the sediment as indicated by Correns (1939, p. 385) for the Atlantic Ocean. Even the opal tests of plankton, especially of the delicate diatoms, tend to be dissolved in the slowly accumulated clay, and at depth within it. Figure 8*b* shows in thin section one of the radiolarian tests that has been largely dissolved within Tertiary sediment at 8 m below the top of a core.

Although pelagic clay is generally highly oxidized, and high in manganese, there is much variation in some features, with a marked difference between some large regions. The pelagic clay of the South Pacific might seem a type area, as it is here most distant from major land sources of sediment. Accumulation in the area seems slower than average from several characters, including the exceptionally high manganese content with the resulting dark brown color. Goldberg's ionium-thorium ratios also indicate the slow rate, of about ½ mm per thousand years. Pyroclastic material of andesitic to basaltic composition is particularly abundant here, though the original glass component has completely disappeared, except in local areas of more rapid accumulation near some volcanic islands. The hydrated glass, with the iron converted to ferric state, known as palagonite is common. One of the zeolite

(508)

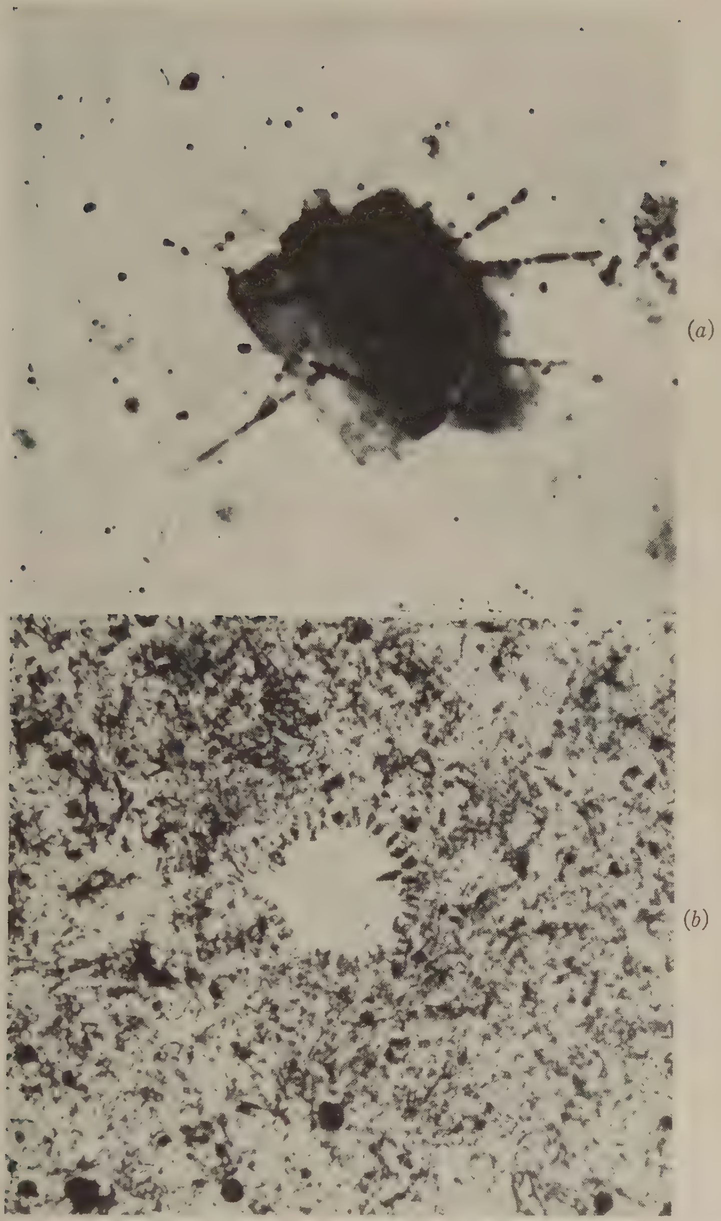

Fig. 8. (*a*) Small fragment of fish skeleton showing alpha tracks in the emulsion (Reprinted with permission from *Researches in Geochemistry*, P. H. Abelson, Editor, p. 17, John Wiley & Sons, New York, 1959.) (*b*) Partially dissolved radiolarian skeleton in thin section of Tertiary sediment at 8 m below top of core, Capricorn 49 BP (× 200).

minerals, phillipsite, is also especially common in the South Pacific, and forms up to nearly 50% of some pelagic clay. Figure 9*a* shows the abundant phillipsite crystals unseparated from other fine sediment. The associations, especially where the phillipsite is in concentric bands with palagonite around incompletely altered basaltic glass, support the conclusion of Murray and Renard (1891, pp. 405–411) that the phillipsite was derived from the alteration of pyroclastics. Arrhenius is investigating interesting features of phillipsite which include high concentration of certain elements, such as the radioactive ones that show alpha emissions like that illustrated from the fish debris (Fig. 8*a*). Derivation of such elements from the bottom water, however, does not preclude derivation of the essential constituents of phillipsite from alteration of the pyroclastics by the bottom water. Such derivation of the silica, alumina, calcium, and perhaps the potassium, rather than directly from the ocean water, seems probable, as the common association of zeolites with altered pyroclastics, even in nonmarine waters, is well known.

The pelagic clay of the North Pacific shows differences from that of the South Pacific that may be related in part to closer proximity to land sources; and other factors to be mentioned, which have increased the rate of accumulation. Goldberg's determinations here show rates between 1 and 2 mm per thousand years here compared with rates of ½ mm in the South Pacific. The iron and especially manganese content is distinctly less than in the South Pacific. Pyroclastics and their alteration products are also less important here, probably in part because more diluted with other material. The sparsely disseminated volcanic shards of alkalic glass are unaltered in the near surface sediment, and indicate much less susceptibility to alteration than a basaltic glass.

The quartz content, as particles averaging less than 10 microns, is relatively high, especially near 30° N Lat in the Pacific, and Rex and Goldberg (1958) relate these high percentages to dust fallout, mostly from the jet stream circling the globe near this latitude. Menard (1955, p. 240) indicated that turbidity current deposition is important in the northwest Pacific, and perhaps the finest of the suspended particles from this may also contribute

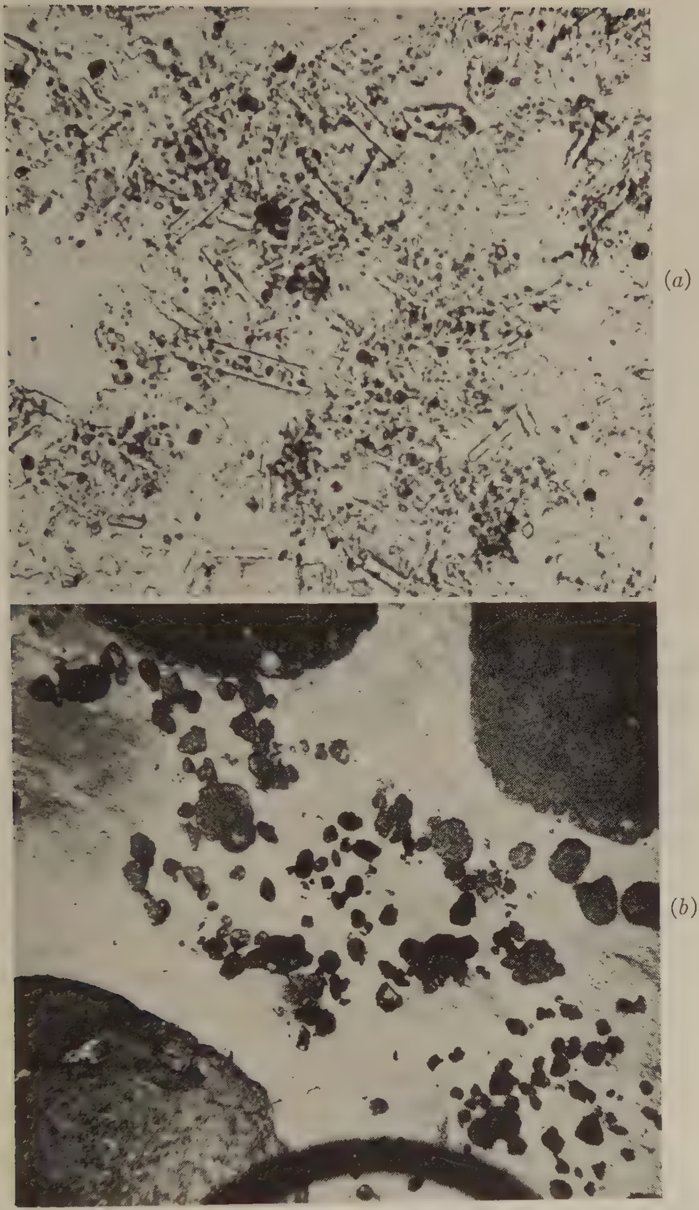

Fig. 9. (*a*) Crystals of phillipsite (elongate laths), unseparated from other particles of pelagic clay at 114 cm in core, Midpac 3 (× 200). (*b*) Manganese nodules at depth of 4560 m in southwestern Pacific (area about 6 m square). (Photo DWP–11 from Menard and Shipek, 1958.)

more to the pelagic sediments in the North Pacific than in the South Pacific.

Sources and rate of pelagic clay accumulation in the North Pacific thus seem more similar to those of the Atlantic Ocean than in the South Pacific, and these differences seem clearly reflected in the color and other features of the pelagic clays of the two regions.

A distinct discontinuity between this surface clay of the North Pacific and an underlying clay much like that in the South Pacific is encountered in many cores at depths of about 3 to less than 1 m, with the upper bed thinner on topographic highs. The upper clay shows the usual character of modern pelagic sediments of this region, including any remains of the plankton preserved, and is doubtless all of Quaternary age. The clay below the marked discontinuity is commonly dark brown, and similar in this color and other features to the surface clay of the South Pacific. Goldberg and Arrhenius (1958, p. 203) show the chemical composition of the lower clay is also more like that of the South Pacific.

All this sediment below the marked change is probably of Tertiary age, as indicated where evidence from fossils is adequate. Some of the differences in sources of sediment and rates of its accumulation that result in the marked differences of modern clay in the North Pacific from that beneath it, may thus indicate certain post-Tertiary influences greater in the North Pacific than in the South Pacific where no such difference in the later clay is evident. Goldberg has indicated that the windborne fine-grain quartz is much less common below the discontinuity. Both this, and any possible contributions from areas of turbidity current deposition in the northwest Pacific, might be more conspicuous with advent of the glacial times.

The great segregation of manganese in pelagic sediments presents many problems, but only one may be considered here. Vast amounts are disseminated as fine particles or micronodules in the slowly accumulated pelagic clay. Very great amounts are also obvious in the large nodules over large areas of the ocean floor.

Menard and Shipek (1958) have estimated, from such photographs as shown in Fig. 9*b* and many dredge and core samples, that these nodules cover from one-fourth to one-half of large areas of the floor, especially in the southwest Pacific. Their estimates of amounts are so great that, including the considerable percentage of cobalt and nickel, eventual recovery and utilization seem possible.

Coring generally indicates that finely disseminated manganese is in greater amounts in underlying sediments (of pre-Quaternary age in part, at least) than near the surface. The coring also indicates, however, that the nodules are more concentrated at the present sediment surface. A suggestion is offered that may account, in part at least, for the exceptional amounts occurring as nodules on the present ocean floor.

The large accretions as nodules from the low percentage of manganese in solution in ocean water are obviously in regions of slow sediment accumulation. Although the average of sediment accumulation has been indicated as now more rapid than in the pre-Quaternary, there is considerable evidence that the character and rates are now less uniform over the ocean floor than in the pre-Quaternary.

Water temperatures were higher and more uniform in the Tertiary, from data of Emiliani (1954) and others. This should result in a more uniform areal distribution of the supply of calcium carbonate from surface waters. The greater compensation depth with warmer water would greatly reduce the areas of solution of carbonate below this depth. Less cold polar bottom water with its higher carbon dioxide content, would also have less influence on the differences in solution related to topography and depth than followed the advent of glacial times. Sorting and grain size differences related to topography also appear greater in the recent sediments, and suggest stronger bottom water motion than that usual in Tertiary time. This also results in differences of accumulation rate between areas.

Summarizing this too brief consideration of evidence, it suggests that the high proportion of manganese accumulation as large nodules is now abnormal because rates of sediment accumulation, though now greater than average, also show much greater differences between areas. Those present day areas of relatively slow accumulation may thus permit deposition of more of the manganese as large nodules, rather than as the disseminated micronodules that are in larger proportion in the Tertiary.

Many interesting, even though minor, components of pelagic sediments cannot be mentioned here, such as the cosmic spherules discussed by Fredriksson (1959), and many geochemical and other aspects must be omitted.

REFERENCES

Arrhenius, G. 1952. Sediment cores from the East Pacific. *Repts. Swedish Deep-sea Expedition, 1947–1948, Göteborg, 5* (1), 192.

Arrhenius, G., M. N. Bramlette, and E. Picciotto. 1957. Localization of radioactive and stable heavy nuclides in ocean sediments. *Nature, 180*, 85–86.

Bé, Allan W. H. 1959. Ecology of Recent planktonic Foraminifera. *Micropaleontol., 5*, No. 1, 77–100.

Bradshaw, John S. 1959. Ecology of living planktonic Foraminifera in the north and equatorial Pacific Ocean. *Contribs. Cushman Foundation, 10*, Pt. 2, 25–64.

Correns, Carl W. 1939. Pelagic sediments of the North Atlantic Ocean. In *Recent Marine Sediments*, pp. 373–395. American Association Petroleum Geologists, Tulsa, Oklahoma.

Emiliani, C. 1954. Temperatures of Pacific bottom waters during the Tertiary. *Science, 119*, 853–855.

Fredriksson, K. 1959. On the origin, age and distribution of "Cosmic Spherules." *Preprints International Oceanographic Congress*, pp. 456–457. American Association for the Advancement of Science, Washington, D.C.

Goldberg, E. D., and G. O. S. Arrhenius. 1958. Chemistry of Pacific Pelagic sediments. *Geochim. et Cosmochim. Acta, 13*, 207.

Kuenen, Ph. H. 1950. *Marine Geology*, p. 383. John Wiley & Sons, New York.

Menard, H. W., Jr. 1955. Deep-sea channels, topography and sedimentation. *Bull. Am. Assoc. Petrol. Geologists, 39* (2), 240.

Menard, H. W., and C. J. Shipek. Surface concentrations of manganese nodules. *Nature, 182*, 1156–1158.

Murray, John, and A. F. Renard. 1891. Report on Deep-sea Deposits of *H.M.S. Challenger.*

Revelle, Roger, and Rhodes Fairbridge. 1957. Carbonates and carbon dioxide. *Bull. Geol. Soc. Am. Mem. No. 67, 1*, 244.

Rex, R., and E. D. Goldberg, 1958. Quartz content pelagic sediments of the Pacific Ocean. *Tellus, 10*, 153–159.

Riedel, William R. 1959. Oligocene and lower Miocene Radiolaria in tropical Pacific sediments. *Micropaleontol., 5*, No. 3, 285–302.

Sverdrup, H. U., M. W. Johnson, and R. H. Fleming. 1946. *The Oceans.* Prentice-Hall, Englewood Cliffs. New Jersey.

(514)

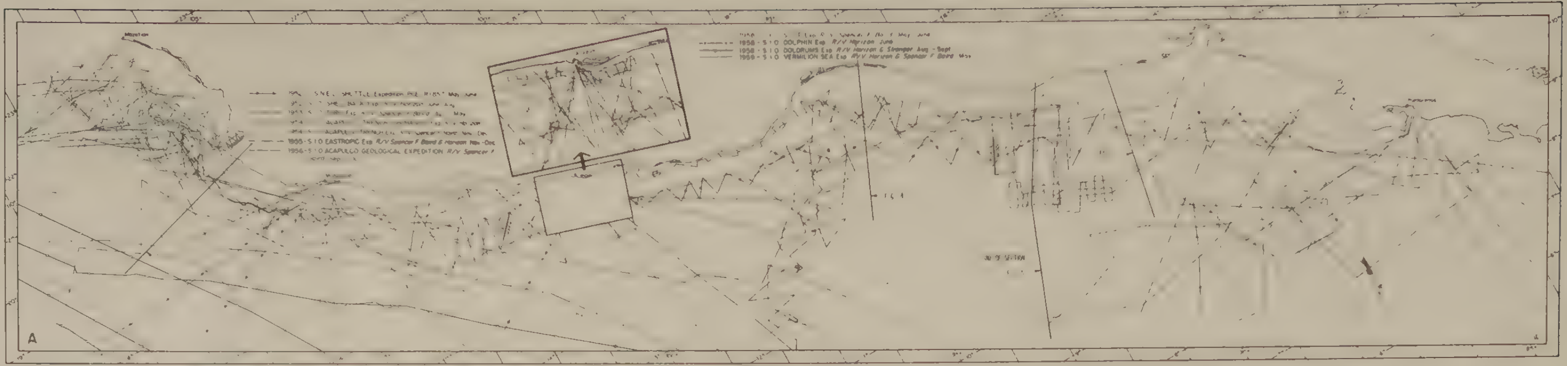
A
1958 - S I O DOLPHIN Exp R/V Horizon June
1958 - S I O DOLORUMS Exp R/V Horizon & Stranger Aug - Sept
1959 - S I O VERMILION SEA Exp R/V Horizon & Spencer F Baird May
1955 - S I O EASTROPIC Exp R/V Spencer F Baird & Horizon Nov - Dec
1956 - S I O ACAPULCO GEOLOGICAL EXPEDITION R/V Spencer F
Mazatlan

A. Index map: S.I.O. and N.E. L. exploration of the Middle America Trench

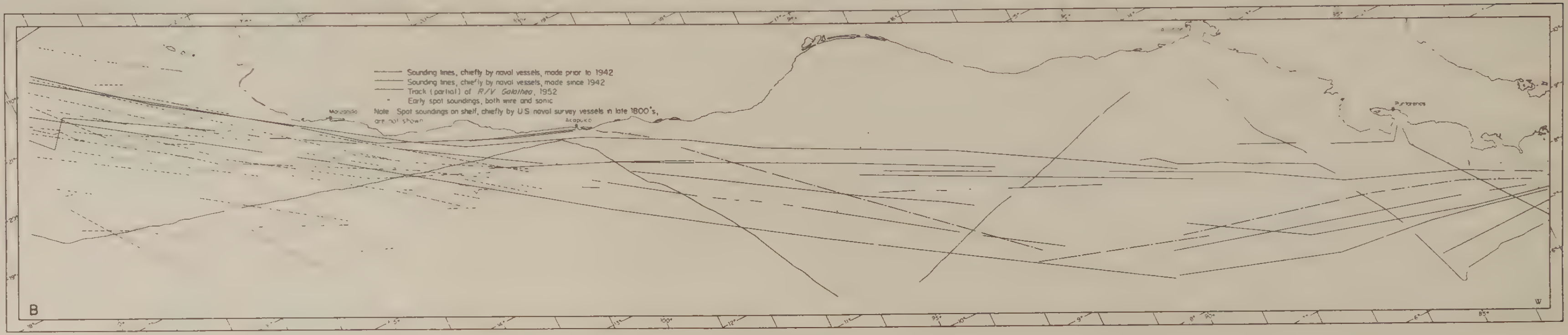
B
Sounding lines, chiefly by naval vessels, made prior to 1942
Sounding lines, chiefly by naval vessels, made since 1942
Track (partial) of R/V Galathea, 1952
Early spot soundings, both wire and sonic
Note Spot soundings on shelf, chiefly by U S naval survey vessels in late 1800's, are not shown
Acapulco
Puntarenas
100°
95°
85°
W

B. Index map: Sounding lines furnished by the U.S. Hydrographic Office

ECHO-SOUNDING LINES USED IN THE PREPARATION OF PLATES 2, 3, AND 6

FISHER, PLATE 1
Geological Society of America, volume 72

ROBERT L. FISHER *Scripps Institution of Oceanography, University of California, La Jolla, Calif.*

Middle America Trench: Topography and Structure

Abstract: From 1952 to 1959, during nine expeditions of the Scripps Institution of Oceanography and one of the U. S. Navy Electronics Laboratory, research vessels recorded 31,950 miles of echo-sounding traverses in and adjacent to the Middle America Trench, which extends from the Islas Tres Marías off western Mexico to the Cocos Ridge southwest of Costa Rica.

The Middle America Trench is continuous at depths greater than 2400 fathoms (4400 m) for 1260 miles, except off Manzanillo and Zihuatanejo, Mexico, where submarine mountains lie in the trench. It is deeper than 3000 fathoms (5500 m) for 380 miles as the Guatemala Deep. Northwest of Acapulco it is generally U-shaped in cross section, with a steeper shoreward flank and a flat bottom suggesting sedimentary fill. From Acapulco southeast to the west side of the Gulf of Tehuantepec, the trench shoals, in a series of basins, to 2700 fathoms (5000 m). To the southeast it widens and deepens abruptly to a maximum 3500 fathoms (6400 m) off western Guatemala, then shoals gradually to merge into the sea floor off Costa Rica. The southeast segment is also asymmetrical in cross section but is V-shaped with irregular bottom. A northeast-trending band of ridge-and-trough topography, 60 miles wide, separates the 1800- to 1900-fathom sea floor outside the trench off southern Mexico from the 2100- to 2200-fathom Guatemala Basin. This zone has been traced from several hundred miles offshore to an intersection with the trench near the west side of the Gulf of Tehuantepec.

Seismic-refraction studies reported in an accompanying paper (Shor and Fisher, 1961) were employed in determining the trench structure. Three refraction stations were taken along the axis of the trench west of Acapulco and two along its axis off Guatemala and El Salvador. Another station was shot on the shelf and one 60 miles seaward of the trench off Guatemala. Thick sediments were found in the Tres Marías Basin off Manzanillo and at the shelf station off Guatemala. Arrivals from rock with compressional wave velocity of 4–6 km/sec were observed at the Tres Marías Basin and Guatemala shelf stations. Off Guatemala, on a section normal to the trench, the depth below sea level to the M discontinuity is interpreted from these seismic data as about 9 km (Pacific Basin), 10 km (outer ridge), 16 km (trench), and 17 km (shelf). Below the sea floor the crust thickens from 5–7 to 10–17 km along this section. The M discontinuity is deeper and the crust below the sediments thicker under the two southern stations than under the two central trench stations. The mantle is deeper under the Tres Marías Basin, where thick (1½ km) sediments are found, than under the central stations.

The Gulf of Tehuantepec marks a major change in trench configuration and possibly in age. Northwest of Tehuantepec the flat trench bottom developed in most places suggests a greater age. Southeast of the gulf the deep V-shaped trench, with thicker crustal layers but very little fill, borders a volcanically active coast. The zone of ridge-and-trough topography trending southwest from Tehuantepec may be another evidence of this boundary.

CONTENTS

Introduction 704
  Regional relations 704
  Scope of the present study 704
Acknowledgments 706
Previous work 706
  Bathymetry 706
  Gravity measurements 706
Topography 707
  Preparation of the charts 707
  Topography within and shoreward of the Middle America Trench 708
  Topography seaward of the Middle America Trench 711
  Topography of the Gulf of Tehuantepec . . . 712
  Bathymetric evidence for sedimentary fill in the Middle America Trench 713
Discussion 714
References cited 717

Figure
1. Index map: seismic setting of the Middle America Trench 705
2. View to northwest from Banderas Bay 708
3. View to southeast from La Libertad, El Salvador 710
4. View to northwest from Gulf of Tehuantepec . 712
5. Schematic structure section off western Guatemala 715

Geological Society of America Bulletin, v. 72, p. 703–720, 5 figs., 6 pls., May 1961

(515)

Contributions from the Scripps Institution of Oceanography, New Series, 1278
Reproduced by Permission

Plate Facing
1. Echo-sounding lines used in the preparation of Plates 2, 3, and 6 703
2. Submarine topography, from Islas Tres Marías to Acapulco, Mexico 706
3. Submarine topography, from Acapulco, Mexico, to San José, Guatemala 710
4. Echogram of traverse along trench, near Manzanillo, Mexico 714
5. Echograms of three crossings of the Middle America Trench 715
6. Submarine topography, from San José, Guatemala, to Punta Burica, Panama 720

Table
1. Maximum depth of fill in the Middle America Trench, as deduced from bathymetric records 714
2. Velocities of refracting layers 717

INTRODUCTION

Regional Relations

A narrow depression, 20–100 miles offshore, extends 1550 miles along the west coasts of Mexico and Central America, from the Islas Tres Marías to the Golfo de Dulce (Fig. 1). This deep area includes the Acapulco Trench or Deep and the Guatemala Trench of various authors (*e.g.*, Agassiz, 1906; Whitcroft, 1944; Fisher and Revelle, 1955). Following Heacock and Worzel (1955), the writer now favors the name Middle America Trench for the entire structure.

Miocene to Recent volcanic rocks, folded and faulted Paleozoic, Mesozoic, and Cenozoic sedimentary and metamorphic rocks, and granitic rocks largely of late Cretaceous age, are exposed along the mountainous coasts of Jalisco, Colima, Michoacan, Guerrero, and Oaxaca (Schuchert, 1935, p. 129–131). Coastal mountains trend nearly parallel to the shore line. The east-west line of recently active Mexican volcanoes intersects the trench near 19° N. (Fig. 1). The Pacific coastal plain of Tehuantepec has a thin cover of undeformed Pleistocene marine sedimentary rocks lying on the pre-Carboniferous basement. The isthmus was downfaulted, probably in Late Miocene time, then raised slightly during late Pliocene and Pleistocene to its present low elevation (Webber and Ojeda R., 1956, p. 78). From southeastern Chiapas to Lake Nicaragua, the coastal plain is bordered on the east by late Cenozoic to Recent andesitic volcanoes. Rocks extruded by these young volcanoes have buried the western ends of east-trending mountain ranges of folded and faulted upper Paleozoic rocks (Schuchert, 1935, p. 314–320). The Pacific coasts of southern Nicaragua and Costa Rica are mountainous and composed chiefly of Tertiary and Quaternary volcanic rocks and igneous detritus. The recently active "Volcanic Range" of Costa Rica trends southeast, and passes inland from the Nicaragua-Costa Rica border (Schuchert, 1935, p. 592–600).

Along the trench axis and to the east of it, a very active zone of shallow earthquakes follows the Mexican coast from Jalisco to Oaxaca, crosses the Gulf of Tehuantepec, and continues, with reduced activity, to western Panama (Fig. 1). Outside the trench shallow activity is most frequent west of Colima, but several shocks have occurred off Oaxaca. Intermediate shocks follow the volcanic belts on land. No deep shocks are known from this area (Gutenberg and Richter, 1954, p. 36). The earthquake distribution has been studied by Benioff; he concluded that from the Islas Tres Marías to Panama a "marginal reverse fault complex," with an "intermediate component" extending to a depth of about 220 km, dips eastward beneath the continent (Benioff, 1954, p. 390).

Gunn (1947) attempted a quantitative treatment of the Middle America Trench–Coastal Mountain–Volcanic Chain relations. He assumes a strong elastic lithosphere supported on a weak magma and examines the mechanics of a "compressed shear thrust fault" formed in such a crust. From his calculations, Gunn states that shear faults resulting from horizontal compression would be localized at continental margins and that with continuing compression the higher continental mass would overthrust the ocean basin and simultaneously form a linear deep at the toe of the overriding block and a line of volcanoes, parallel to the deep, 50–90 km inland from the continental margin.

Scope of the Present Study

This work represents one of the results of research carried out under contracts with the Office of Naval Research and the Bureau of Ships, U. S. Navy.

The bathymetric studies were made during the 1952 U. S. Navy Electronics Laboratory Shuttle Expedition (bathymetry, bottom-sampling, hydrography) and the Scripps Institution of Oceanography expeditions: Shellback (1952; hydrography, bathymetry), Toro (1953; bathymetry, seismic-reflection studies, bottom-sampling), Acapulco Trench (1954; bathymetry, seismic-refraction studies, heat-flow and

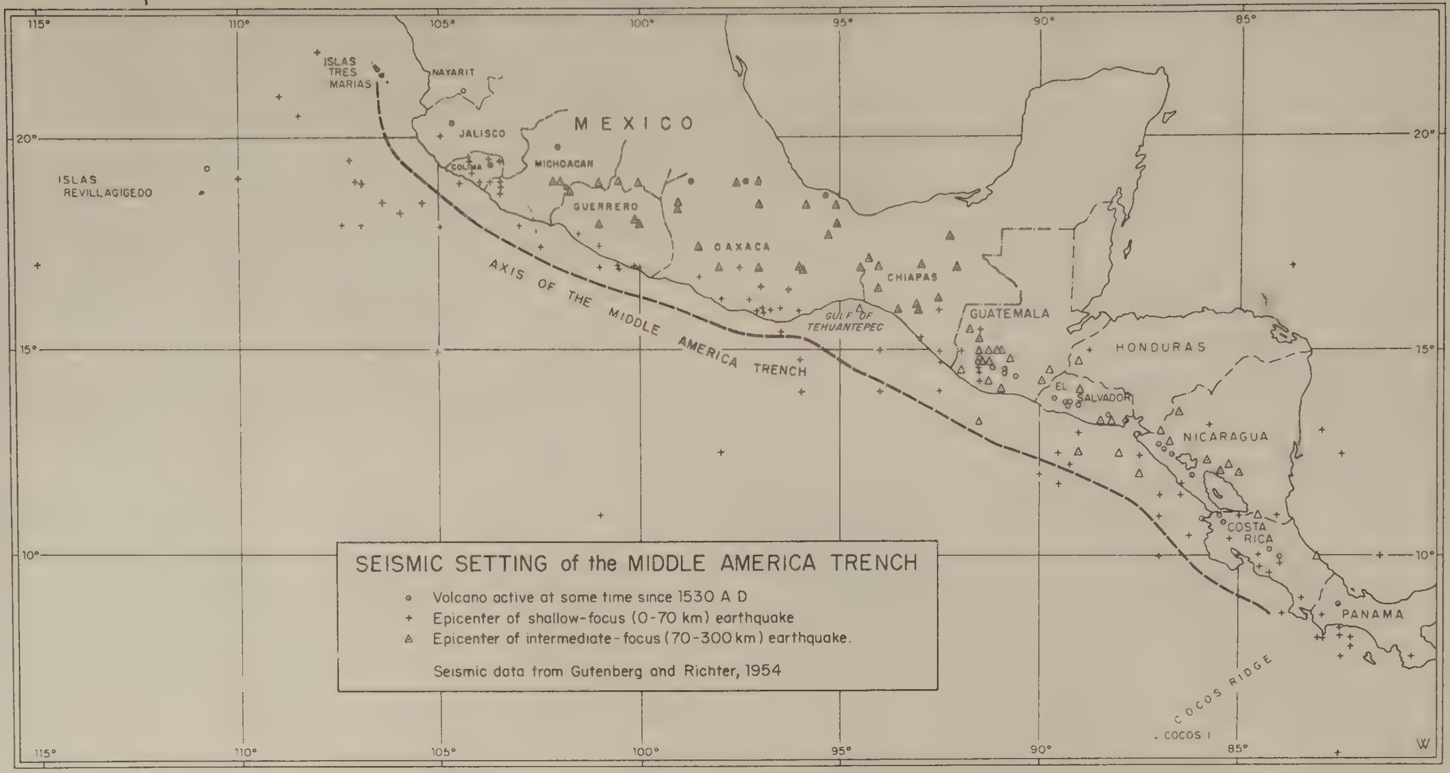
SEISMIC SETTING of the MIDDLE AMERICA TRENCH
○ Volcano active at some time since 1530 A D
+ Epicenter of shallow-focus (0-70 km) earthquake
△ Epicenter of intermediate-focus (70-300 km) earthquake.
Seismic data from Gutenberg and Richter, 1954
MEXICO
NAYARIT
JALISCO
COLIMA
MICHOACAN
GUERRERO
OAXACA
CHIAPAS
GUATEMALA
HONDURAS
EL SALVADOR
NICARAGUA
COSTA RICA
PANAMA
ISLAS TRES MARIAS
ISLAS REVILLAGIGEDO
GULF OF TEHUANTEPEC
AXIS OF THE MIDDLE AMERICA TRENCH
COCOS RIDGE
COCOS I
115°
110°
105°
100°
95°
90°
85°
20°
15°
10°
W

Figure 1. Index map: seismic setting of the Middle America Trench

magnetic measurements), Eastropic (1955; hydrography, bathymetry), Acapulco Geological (1956; bathymetry, bottom sampling), Dolphin (1958; magnetic measurements, hydrography), Scot (1958; biology, hydrography), Doldrums (1958; hydrography, biology), and Vermilion Sea (1959; bathymetry, seismic-refraction, and heat-flow studies, biology, bottom sampling). About 190 ship days were spent in the area.

Seismic-refraction data reported in an accompanying paper (Shor and Fisher, 1961) were collected on the 1954 Acapulco Trench Expedition. A short paper on the topography and structure of the Middle America Trench contains some discussion of the techniques and evaluation of the seismic-refraction data (Fisher and Shor, in press). On the 1954 cruise, other refraction data were taken in the homeward run, well seaward of the trench; one station of this later series lies on the seaward extension of the Champerico profile discussed below. An interpretation of the data from this station (Raitt, personal communication) has been included in the structural cross section (Fig. 5). Interpretation of the reflection records taken on the Toro Expedition in 1953 has not been completed, although preliminary results have been taken into account in following discussions of probable sediment thickness.

Similarly, bottom samples, taken both by gravity and piston corers, have not been studied microscopically but logged macroscopically in the field and stored for laboratory examinations. Statements regarding sedimentation in and bordering the trench are made on the basis of these field data.

Heat-flow and magnetic measurements were made by Arthur E. Maxwell and Ronald G. Mason, respectively. Their results, also bearing on inferred structure, will be reported elsewhere.

ACKNOWLEDGMENTS

The task of collecting sounding or seismic data on the nine Scripps expeditions was shared with 58 members of the scientific parties. On the N.E.L. Shuttle Expedition the author was assisted by Edwin L. Hamilton and Maxwell Silverman. The officers and men of the U. S. Navy Electronics Laboratory research vessel PCE(R) 857 and of the Scripps Institution of Oceanography research vessels Spencer F. Baird and Horizon and Stranger executed difficult ship operations and shared in the scientific program. Their help is gratefully acknowledged. Special thanks are due Maxwell Silverman, Alan C. Jones, M. Allan Beal, and Gene A. Rusnak. Warren Wooster, Townsend Cromwell, John Knauss, and Robert Holmes made available the echo-sounding data from the Shellback, Eastropic, Dolphin, Scot, and Doldrums expeditions.

Ing. Carlos Acosta del Campo of the Instituto Nacional de Recursos Minerales kindly provided copies of unpublished geological and structural maps of the Isthmus of Tehuantepec and of southern Chiapas, Mexico.

Robert C. Winsett, Howard Taylor, and James Moriarty prepared the illustrations. Russell Raitt, H. W. Menard, Roger Revelle, J. B. Hersey, and J. Lamar Worzel read and made suggestions in the manuscript.

PREVIOUS WORK

Bathymetry

The earliest systematic bathymetric observations, from Baja California to the Gulf of Panama, were the coastal surveys of the U.S.S. Narragansett (1873–1875), U.S.S. Tuscarora (1878–1879, 1880), and the U.S.S. Ranger (1882, 1884–1885). Deep soundings were taken by the U. S. Fish Commission Steamer Albatross in 1888, and especially during two expeditions (1891, 1904–1905) led by Alexander Agassiz, who noted (1906, p. 5) the very steep continental slope (Jalisco to Guerrero), the near-shore Tres Marías, Manzanilla (sic), and Acapulco Basins, and the Guatemala Basin lying 150–200 miles off San José, Guatemala.

In 1923 the Coast and Geodetic Survey Steamer Guide discovered the 3500-fathom Guatemala Deep at the base of the continental slope. Other survey vessels traversing the area include the Emden, the U.S.S. Chopper (1949), and the Galathea (1952). Thousands of soundings of varying quality have been reported by military and commercial vessels en route between Panama and the United States west coast or Hawaii; however, their courses generally lie well outside the trench area, except between long. 97° and 106° W.

Bathymetric charts and discussions of the topography have been published by Whitcroft (1944), Tamayo (1949), and Heacock and Worzel (1955).

Gravity Measurements

In 1926, aboard a Dutch submarine, F. A. Vening Meinesz made gravity observations

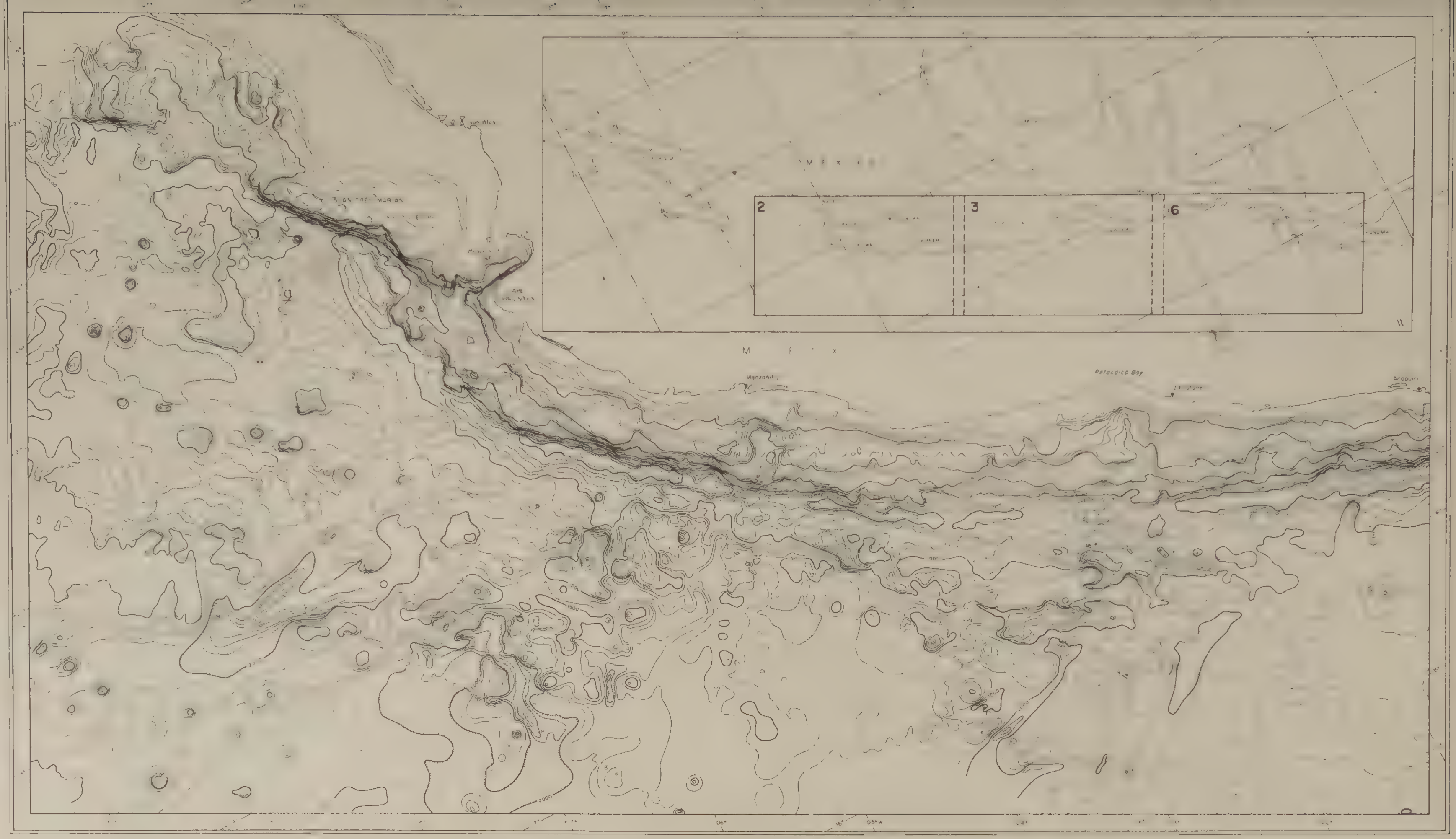
2
3
6
M E X I C O
Manzanillo
Petacalco Bay
Acapulco
05°W

SUBMARINE TOPOGRAPHY, FROM ISLAS TRES MARÍAS TO ACAPULCO, MEXICO

FISHER, PLATE 2
Geological Society of America, volume 72

west of Mexico and Central America. Two north-south profiles, totaling seven stations, cross the trench at 98°20′ W. and 103°25′ W. According to Vening Meinesz (1948, p. 116), adjusted values suggest that off this coast a landward crustal block is riding over a seaward block, depressing it to form the trench.

In 1949, John G. Heacock, Jr., made 41 stations aboard the U.S.S. CHOPPER, along 1750 miles of track, in this area (Worzel and Ewing, 1952, p. 455). Heacock's gravity observations and interpretations are not yet published.

TOPOGRAPHY

Preparation of the Charts

During Scripps and N.E.L. expeditions of 1952–1958, research vessels recorded 27,900 miles of echo-sounding traverses in and adjacent to the Middle America Trench (Pl. 1A). On the 1959 Vermilion Sea Expedition 4050 miles of track was run in the region bounded by Banderas Bay, Mazatlan (23°10′ N., 106°28′ W.), and the southern tip of Baja California (22°52′ N., 110° W.). Each ship was equipped with Edo echo sounder modified to permit shoal scale recording speed on all ranges and calibrated to correct for instrument errors. On six of the cruises, input to each sounder was held at 60 cycles per second by a constant-frequency unit. Soundings from these instruments are precise to ±5 fathoms. During the Shellback and Eastropic expeditions, line frequency was noted, and the sounding as recorded was corrected to its equivalent at the standard 60 cycles. On the 1956–1959 expeditions the ships were equipped with "Precision Depth Recorder" similar to that described by Luskin *et al.* (1953). This unit, a modified commercial facsimile printer, records the output of the Edo echo sounder on a greatly expanded scale, so that soundings can be read with a precision of ±1 fathom under all conditions when a recordable bottom echo is detected. However, the relatively precise values recorded are subject to the usual difficulties of interpretation of echo sounding: side-echo effects, slope corrections, and sweeping by the sound cone as the ship rolls. Soundings were recorded in fathoms, assuming a nominal sounding velocity of 4800 feet/second. With the temperature-pressure-salinity conditions prevailing at depths of more than 500 fathoms in the region of the Middle America Trench, the true sounding velocity ranges from 4880 to 4960 feet/second. Soundings recorded on the Edo echo sounder, from which Plates 2, 3, and 6 were constructed, are 1½–3½ per cent too shoal. In deep water the increase in sounding velocity with depth is about 1 per cent per 1500 fathoms, so that conclusions as to bottom slopes within a basin, for example, are relatively accurate. Ships' positions were established by visual bearings on land, or by star sights that have a probable error of about 2 miles.

Plates 2, 3, and 6, plots of sea-floor topography contoured at 100-fathom intervals, were prepared from Scripps data, published and unpublished U. S. Hydrographic Office sheets, and 1150 miles of sounding lines recorded by the R/V GALATHEA. Sounding lines that agreed within 10 fathoms at crossings were accepted without adjustment. Preference was given to Scripps and N.E.L. soundings, then to GALATHEA and recent Navy soundings, then to old H. O. lines which crossed well with recent traverses (Pl. 1B). Many additional older or stray soundings were rejected. Slope corrections have not been applied. At great depths and steep slopes, the usually accepted first arrival echo distance may be significantly less than the depth beneath the ship (*e.g.*, Fisher, 1954). Occasionally in this study when an especially clear echogram was obtained, and particularly when clear echoes from a narrow but flattish trench bottom returned later than echoes from the walls, the wave trains were analyzed and the nominal true depth—the probable distance to the trench bottom vertically beneath the ship— was noted.

Dredged bedrock from Pacific seamounts investigated to date has been volcanic, and bathymetric surveys of seamounts usually show the peak to be conical, or nearly conical (see Menard, 1955, for example). Therefore, for this study stray or isolated shoal soundings have been contoured as conical peaks unless data on nearby lines strongly indicate the presence of a ridge. This practice may cause an unreal abundance of contoured peaks, since some shoals must be slightly mislocated duplicated soundings. The ridges, presumably of volcanic rocks, are contoured as nearly conical peaks rising from a low swell, not as small peaks between fairly shallow saddles, such as might be expected along fault-bounded ridges.

In the descriptions that follow, topographic characteristics such as shelf-break depth, trench bottom, trench terminations, and the nature of the landward and seaward flanks, each is discussed proceeding along the trench from northwest to southeast. The sea-floor relief outside the seaward flank of the trench is discussed below under Topography Seaward of the Middle America Trench. Because the Gulf of Tehuantepec marks a boundary in the submarine topography, just as the Isthmus of Tehuantepec forms a boundary between two major structural provinces on land, the Tehuantepec region, both Isthmus and Gulf, is discussed in a separate section.

Topography Within and Shoreward of the Middle America Trench

Conclusions that may be drawn from Plates 2, 3, and 6 and study of Edo echograms are:

(1) The trench, sigmoid in plan, in general follows the Mexican-Central American shore line. The sharpest change in direction occurs just west of Tehuantepec, where it leaves the coast and trends nearly east-southeast for 400 miles. The change in trend is most marked at depth shallower than 1000 fathoms but persists to the bottom of the trench at 2600–2800 fathoms.

(2) At 2400 fathoms the trench is only 5–25 miles wide, but it is continuous at this depth for 1260 miles, except off Manzanillo and Zihuatenejo, where submarine mountain ranges intersect the axis. At 2700 fathoms it extends for 660 miles and at 3000 fathoms it continues for 380 miles as the Guatemala Deep.

(3) From configuration of the trench bottom, the Middle America Trench can be divided into two sections, with the boundary near 15° N., 95° 30′ W., off Tehuantepec.

From Islas Tres Marías to Tehuantepec, the bottom of the trench consists of flat-floored, elongate basins separated by ridges or seamounts (Pl. 2, 3). The bottom deepens, in a series of nearly horizontal steps, to a maximum depth of 2965 fathoms southwest of Acapulco. Such steps, especially well developed west and northwest of Manzanillo, suggest that sediment is being ponded behind hills or spurs of the trench flank (Pl. 4). Ponding in the Puerto Rico Trench has been reported by Ewing and Heezen (1955, p. 256). Similar basins, with much smaller flat floors at depths of 2780–2900 fathoms, continue to about 15° 15′ N., 96° W.

Southeast of 15° N., 95° W., the trench bottom drops steeply to a maximum of 3510 fathoms near 14° N., 93° 40′ W., continues deep in a series of very narrow elongated basins to 87° 30′ W., then shoals and widens gradually, with several basins, to end at about 84° W. (Pls. 3, 6).

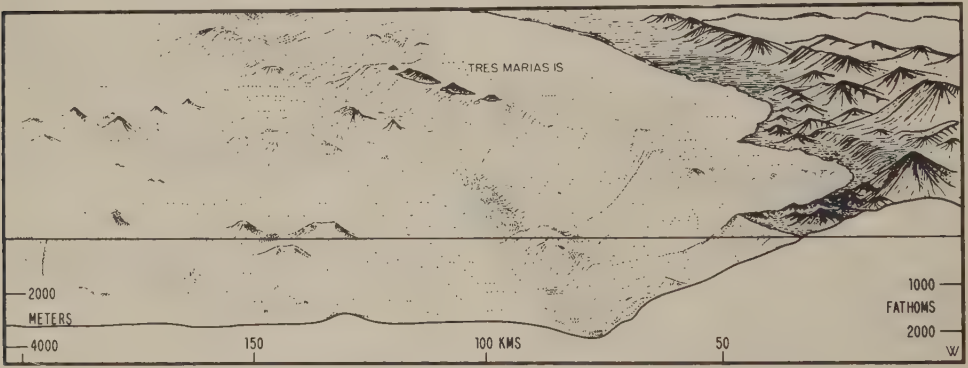

Figure 2. View to northwest from Banderas Bay. Vertical exaggeration 10 X. *See* Plate 1A for location of section.

(4) At 20° N. the trench axis bends northward and sharply intersects the Islas Tres Marías (Pl. 2). The north flank of the Tres Marías Basin, where the trench apparently ends, is a steep (>21°) slope. Several seamounts and a region shoaler than 1600 fathoms bound the basin on the northwest (Fig. 2). If projected, the axis of the rather straight Gulf of California would pass near 22° N., 108° W., about 60–75 miles west of the Islas Tres Marías. The present topographic study indicates that the Gulf probably is not a direct extension of the Middle America Trench.

To the southeast, the trench ends gradually against the northeast-trending Cocos Ridge (Pl. 6). Near 85° W., it is sharply constricted by a bulge in the continental slope and a group of seamounts on the trench south flank.

(5) Submarine canyons, like those off Cali-

fornia (Shepard and Emery, 1941), indent the shelf and upper continental slope, particularly along the narrow shelf northwest of Acapulco (Pl. 2). None of these canyons has been traced to the trench bottom; many, however, extend to depths of 600–800 fathoms. More detailed sounding may show that some of these canyons, V-shaped in cross section, continue to the bottom of the trench. Several canyons appear related in position to present-day river mouths.

Larger re-entrants, some branching and traversing the entire continental slope, occur off Banderas Bay (Fig. 2; Pl. 2), Manzanillo and Petacalco Bay (Pl. 2). Salina Cruz (Pl. 3), and San José and Puntarenas (Pl. 6). Banderas Bay is a structural trough, separating outcrop areas of middle Cenozoic intrusive rocks and early Cenozoic extrusive rocks on the north from Paleozoic metamorphic rocks on the south (Sanchez Mejorada, 1956). A very narrow, deep chasm extends along the south shore to the head of the bay. A shelf 5–7 miles wide borders the north shore of Banderas Bay and is developed west and south of Cape Corrientes. No shelf exists along the south shore of the bay; depths greater than 100 fathoms lie less than 1000 feet from shore. The trough near Manzanillo has slope reversals along the axis and several peaks bordering the broad valleys. Others are asymmetrical in cross section. Most have wide heads and steplike longitudinal profiles. Similar large sea valleys on the north flank of the Aleutian Trench have been described by Gates and Gibson (1956, p. 139–143). Those authors suggest a fault origin for the valleys and show that some of them lie along or near projected trends of faults mapped on the islands. Udintsev (1955, Fig. 4) reports such features bordering the Kuril-Kamchatka Trench. Unlike their possible counterparts in the Aleutian region, most of the Middle America Trench sea valleys are aligned nearly normal to the continental slope. However, the reversals in slope and the U-shaped cross sections commonly developed suggest a tectonic origin, at least in part, for these interlobate valleys; they are probably related to the unusually irregular topography, both within and just outside the trench, adjacent to most of them.

During the 1952–1959 cruises, 121 echo-sounding profiles were made across the Middle America Trench. Echograms of parts of three such profiles are reproduced in Plate 5. Additional conclusions from a study of all the echograms include:

(6) From Islas Tres Marías to Manzanillo, the shelf break is at 55–60 fathoms, where a nearly horizontal shelf is terminated rather sharply.[1] Possible evidence of local warping exists in two tilted benches, which deepen landward, cut on a submerged pinnacle southeast of María Cleopha Island.

Off Acapulco, the depth of the shelf break ranges from 55 to 140 fathoms within a distance of 20 miles, as determined from crossings nearly normal to the coast. The steeply dipping shelf shoreward of the deeper breaks suggests that here the shelf has been locally warped or faulted downward.

From 30 miles southeast of Acapulco to just west of Port Angeles, except for the somewhat anomalous shelf topography of Tartar Shoal, the shelf is very narrow to nonexistent. The shelf break ranges in depth from 65 to 100 fathoms; most normal crossings indicate depths of 70–90 fathoms. Here faulting is suggested; the depths do not increase or decrease progressively along the coast.

The depth of the shelf breaks south of the Isthmus of Tehuantepec was the subject of special study on the 1956 Acapulco Geological Expedition and is discussed below.

From Champerico to the Golfo de Nicoya the shelf break, at 59–90 fathoms, sharply terminates the wide shelf.

(7) Continental slope morphology differs east and west of the Gulf of Tehuantepec, although in both areas steepness generally increases with depth, and one or more deep breaks in slope occur in many places.

To the northwest, average slope of the landward wall of the trench is 10°–14°; some slopes are as low as 5° and, off María Cleopha Island (Fig. 2) and Acapulco, as great as 24°. The surface is irregular, and peaks rise 50–300 fathoms; there are many submarine canyons on the upper part of the slope.

Southeast of Tehuantepec the slope is more gentle, ranging from 4° to 8°, and smoother; its few pinnacles are only 20–50 fathoms high. Some large valleys traverse the slope (Fig. 3).

(8) Most profiles northwest of Acapulco show a broad, nearly flat trench bottom (Pl. 5, upper profile), except where mountain ranges intersect the axis, as near Manzanillo and Zihuatanejo. On these basin floors, the bottom

---

[1] In this discussion of the depth of the shelf break the writer assumes that along this coast the shelf break is due primarily to wave abrasion related to some past lowered sea level, as discussed by Dietz and Menard (1951).

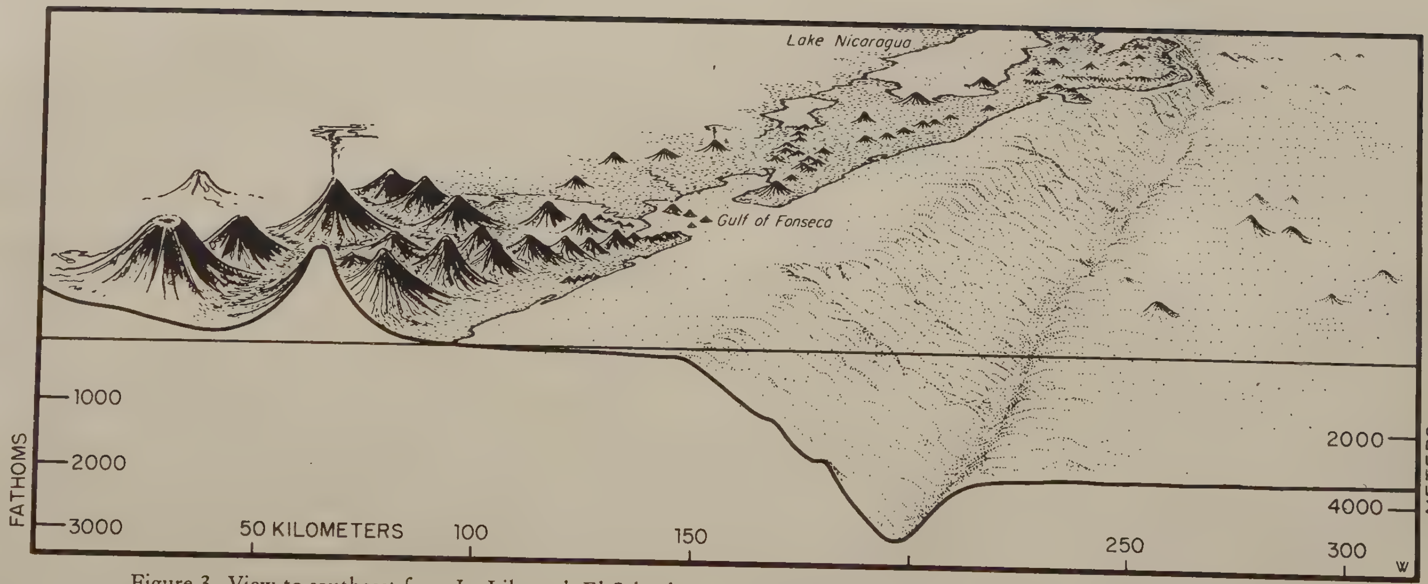
Lake Nicaragua
Gulf of Fonseca
FATHOMS
1000
2000
3000
50 KILOMETERS
100
150
250
300
W
METERS
2000
4000

Figure 3. View to southeast from La Libertad, El Salvador. Vertical exaggeration 10 X. *See* Plate 1A for location of section.

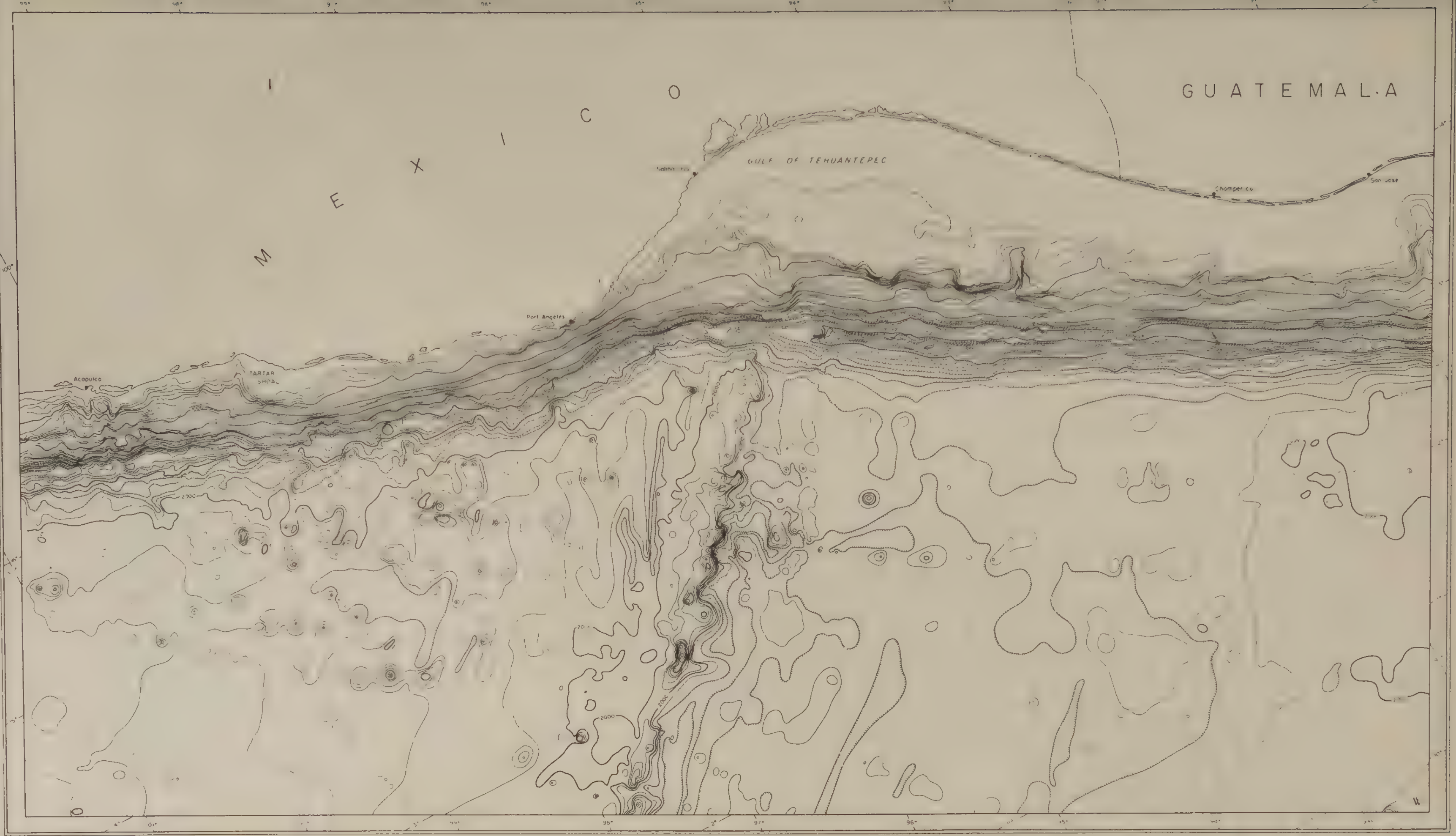
MEXICO
GUATEMALA
GULF OF TEHUANTEPEC
Salina Cruz
Champerico
San Jose
Port Angeles
Acapulco
TARTAR SHOAL
2000
98°
97°
96°

SUBMARINE TOPOGRAPHY, FROM ACAPULCO, MEXICO, TO SAN JOSÉ, GUATEMALA

FISHER, PLATE 3
Geological Society of America, volume 72

commonly rises 5–10 fathoms toward the land and seaward flanks, although sharp breaks in slope occur at the edges of the basin. Some echograms show knolls projecting 50–100 fathoms above the trench floor.

In the deepest portion of the trench, extending from the east side of the Gulf of Tehuantepec to the Gulf of Fonseca, the trench is V-shaped in profile, with little bathymetric evidence of sedimentary fill (Fig. 3; Pl. 5, middle profile). As the trench shoals toward the Cocos Ridge, its bottom widens, but the deepest portions are not quite flat (Pl. 5, lower profile).

(9) Off Jalisco, the seaward flank of the trench is smooth and rises gently (at ½°–2°); off Colima, Michoacan, and northwestern Guerrero it is steeper (3°–10°) and irregular, and peaks 150–300 fathoms high project from the slope. Off southeastern Guerrero and Oaxaca the outer slope rises smoothly, at 1°–3°, to depths of 1800–1900 fathoms.

Southeast of Tehuantepec, the seaward flank slopes upward at 2°–6° to a low swell or to nearly flat bottom, except southwest of Nicoya where isolated groups of seamounts locally constrict the trench, steepening the outer flank.

Topography Seaward of the Middle America Trench

Sea-floor topography west and south of the trench differs in character in four regions where rough bottom is best developed.

(1) West of 105° W., between 15° N. and 23° N. (Pl. 2), the sea floor is shallow (1500–1800 fathoms) with many seamounts, probably volcanoes, capping broad swells. The trends of some of the swells are real as shown; other trends merely follow ships' tracks. In this volcanic field a random distribution of peaks seems likely. Nearly all the earthquakes seaward of the trench occur in this region; all are shallow shocks, with computed epicenters plotting north of 17° N. and west of 105° W. (Gutenberg and Richter, 1954, p. 168–169; Coast and Geodetic Survey, 1948–1958). The only extensive deep areas within this region lie 100–250 miles east of the volcanic island of San Benedicto; they may be part of the east-trending Revillagigedo structure.

(2) Southwest of Zihuatanejo, two elongate deeps, separated from the trench axis and from each other by pinnacle-topped ridges, lie subparallel to the trench (Pl. 2). Steep-walled and flat-floored, at 2450 and 2800 fathoms, they are 150–450 fathoms deeper than the trench proper adjacent to them, where an irregular ridge intersects the axis. The writer suggests that such bordering deeps are fault troughs, and that formation of the deeps and ridges occurred as adjustments after the trench was formed. Generally off Mexico the trench cross section is regular, though asymmetrical; the sea floor drops steeply to a flat or nearly flat trench bottom, then rises more gently offshore. Near Zihuatanejo, however, the trench bottom is both shallow and irregular and has peaks several hundred fathoms high. Locally the offshore flank is the steeper, with one or more peaks apparently superposed on the more normal gentle offshore slope. The flat bottoms in the troughs mentioned above probably resulted from the sediment moving downslope from the neighboring peaks, though no aprons were detected.

(3) A band of irregular topography, 60–120 miles wide, separates the gently rolling, 1850- to 1950-fathom sea floor off southern Guerrero and Oaxaca from the even flatter 2100- to 2200-fathom Guatemala Basin off Chiapas and Guatemala. This zone, termed the Tehuantepec Ridge by Menard and Fisher (1958), extends at least 420 miles southwest from the seaward flank of the trench off southern Oaxaca. The best explored segment, between 12° N. 98° W. and the trench, is shown in Plate 3. Here 24 echo-sounding lines give very similar profiles. Along a northwest to southeast traverse, the zone begins in most places with a broad depression, 100–150 fathoms deeper than the regional depth to the west. The sea floor then rises gently to a swell or ridge with a depth along its axis that has been contoured on Plate 3 as less than 1700–1800 fathoms in most places. Because of the spacing of the soundings, possibly the 1600-fathom contour should be drawn more extensively, to indicate a shoaler ridge than has been shown in Plate 3. However, of the 11 accepted sounding lines that might be considered random in that the ships reporting them were just passing through the area, only five show soundings shoaler than 1750 fathoms. Several seamounts, one with a minimum depth of 990 fathoms, have been found along the ridge. The east flank descends sharply into one of a series of narrow, nearly flat-bottomed elongated depressions. The sea floor then rises 150–250 fathoms to the regional depth of 2100–2200 fathoms in the Guatemala Basin off Chiapas and Guatemala. A marginal depression 150–200 fathoms deep, lying 50–90 miles east

of the ridge and trending nearly east-west, has been contoured from an older, generally reliable line.

(4) The Guatemala Basin shoals to the southeast. West of Costa Rica, isolated seamounts rise from a smooth, 1700- to 1800-fathom bottom (Pl. 6). One notable group lies just outside the southeast end of the trench and another at 9° 30′ N. Guardian Bank, largest and shoalest of the shallow areas reported off Costa Rica, was not found by ships on the 1952, 1954, and 1955 cruises, despite special searches at and near its various reported positions.

Topography of the Gulf of Tehuantepec

A linear structure such as that described in the preceding section, an asymmetrical ridge with narrow flanking deeps, separating large areas with several hundred fathoms difference in regional depth, is characteristic of the "fracture zones" of the northeastern Pacific, as described by Menard (1955). The best-explored zones discussed by Menard have been traced several hundred miles seaward from the North American coast and projected landward across the continental margin. If the linear structure off Oaxaca is part of such a major zone, it might be expected to continue seaward for hundreds of miles and, in the landward direction, to cross the trench and shelf and affect the structure of the Isthmus of Tehuantepec (Pl. 3).

Three weeks of the scientific program of the 1956 Acapulco Geological Expedition consisted of making echo-sounding runs across the upper continental slope and the shelf in the Gulf of Tehuantepec, and in exploring the westward extension of the zone of ridge-and-trough topography. Plate 1A shows the track of the expedition. A detailed discussion of this "fracture zone" (?) has been published (Menard and Fisher, 1958): the northeast trend has been traced definitely from the south flank of the trench to 10° N., 100°–101° W., where it joins the nearly east-trending "Clipperton fracture zone" indicated by Menard. Apparently the northeast-southwest "fracture zone" (?) intersects the trench between 95° W. and 96° W., as suggested by (1) the shoal axial depth at that point, (2) constriction of the trench by peaks on the south flank and a bulge, to 1000 fathoms or greater, on the north side, (3) the peak lying along the trench axis just south of 15° N., 95° W., and, possibly, (4) by the irregularities in the 100-, 200-, and 300-

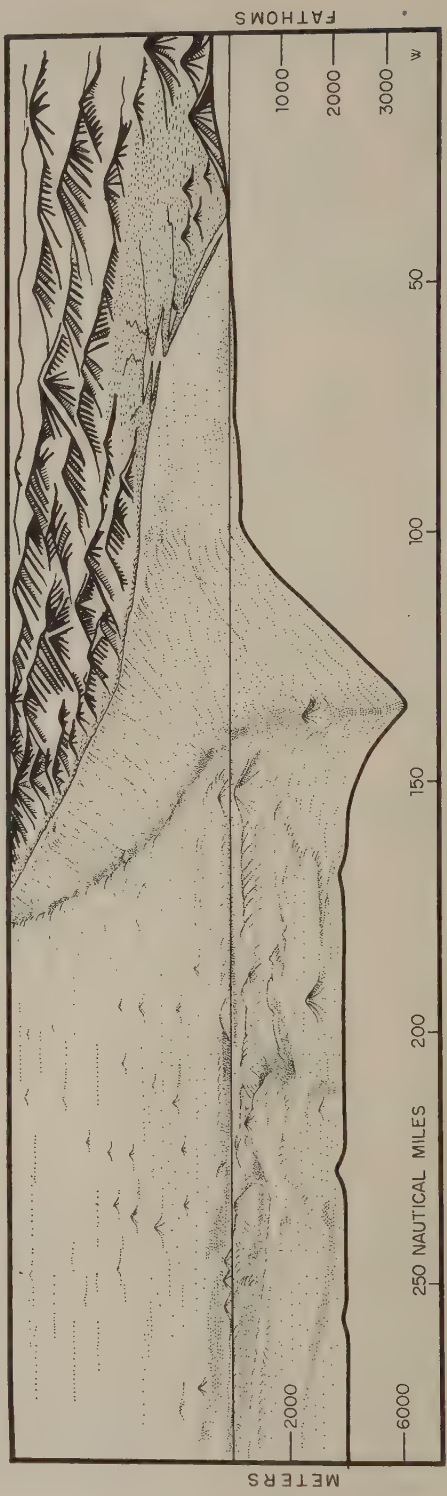

Figure 4. View to northwest from Gulf of Tehuantepec. Vertical exaggeration 10 X. *See* Plate 1A for location of section.

fathom contours south of Salina Cruz (Fig. 4).

On the 1956 cruise, 23 echo-sounding profiles nearly normal to the shelf break and upper slope were made between 97° W., near Port Angeles, and the Guatemala border. Eighteen of these lines show a deep shelf or terrace, with a drop-off at 155–200 fathoms, lying downslope from the more usual 70- to 90-fathom shelf break. The occurrence of this deep shelf detected farthest west is just east of Port Angeles, and it continues with a recognizable break in slope at about 200 fathoms to near 95° 15′ W., south of Salina Cruz. Between Salina Cruz and the large canyon near 93° 30′ W. the deep break lies at 165–175 fathoms, and the shallow shelf break is not well developed. It may represent warping rather than a stillstand at sea level. Southeast of Champerico only one shelf break, at 65–90 fathoms, was found. West of Salina Cruz both the shallow and deep shelves are narrow and thus steep in slope. East of Salina Cruz the shallow and deep parts of the shelf are wide; a steep-sided depression, 5–10 fathoms deeper than the adjacent shelf, was found shoreward of the possible shallow shelf break on four sounding lines. Apparently the canyon south of Salina Cruz forms a boundary for both shelves. The deeper part of the shelf begins to slope upward at about 95° W. Southeast of the canyon at 93° 30′ W. the deeper shelf slopes upward more sharply and narrows until it merges with the upper shelf.

The above description indicates that along the trench as explored to date a series of deep breaks in slope, suggesting a downwarped or downfaulted shelf below the more normal shallow shelf, is developed only in the Gulf of Tehuantepec. The variation laterally in vertical separation of the two breaks in slope and the depression shoreward of the shallower shelf break indicate that faulting across the shelf may have been important south of the Isthmus of Tehuantepec.

The most detailed recent survey of the geologic structure of the Pacific side of the Isthmus is summarized by Webber and Ojeda R. (1956). These authors conclude that Tertiary deformation in this region consisted of faulting, chiefly vertical, along two fault systems. The chief event was the dropping and slight tilting to southward of a triangular block with its base in the present gulf. This block, bounded on the west by northeast trending faults passing near 16° 30′ N., 96° W., and on the east by a north-trending fault system near 94° 20′ W., dropped 1500 feet in relation to the Chiapanecan block to the east. The motion had an unspecified lateral component. This faulting was Miocene, probably Late Miocene, as established by offset of dated volcanic flows.

Although this information from the nearby land establishes neither the date nor magnitude of possible faulting on the shelf, it shows that vertical movements of considerable extent have occurred very near the shelf. This faulting has taken place along fairly extensive fault systems, some members of which have been traced to the present shore line, and may represent a shoreward expression of the extensive linear structure seaward of the trench off the Tehuantepec region.

Bathymetric Evidence for Sedimentary Fill in the Middle America Trench

Most of the echograms recorded during the 1952–1959 explorations of the Middle America Trench are of sufficiently high quality to permit analysis in an attempt to learn the nature and the thickness of the material that constitutes the nearly flat floor of the trench over much of its length.

Several echograms have been studied to determine bottom slopes within three of the basins or ponds on the trench floor. The echogram shown in Plate 4 includes traverses along three steps in the trench bottom, finishing on the southeast with a crossing at about 50° to the trend of the trench. Since frequency input to the Edo echo sounder was held at 60 cycles per second and the records are clear, the soundings can be read to ±5 fathoms. In these basins the depths recorded vary in a consistent manner. Hence, the slight slopes indicated are believed real. Bottom slopes within one or another of the three ponds or basins range from nearly horizontal to as much as 0.01^{-}, the steepest slopes occur near the trench walls, and most slopes are 0.001–0.003.

In a discussion of deep-sea cores from the North Atlantic, Ericson, Ewing, and Heezen (1952) state that large quantities of sediment of shallow-water origin have been deposited in the deep basins by turbidity currents flowing down steep submarine slopes and out over the very gently sloping deep-sea floor. Their principal criteria for shallow-water origin of these sediments are graded sand and silt layers and tests of shallow-water benthonic organisms, chiefly Foraminifera. In the Atlantic, cores containing an abundance of such material have been taken in areas where bottom slopes are only 0.001–0.002. Foraminifera from the

Middle America Trench cores have not been examined in detail, but studies already made indicate the presence of displaced fauna. Piston cores from the trench bottom off Acapulco contain graded sand and silt layers and fragments of organic debris, possibly wood, at depths of 8–10 feet in the core. The writer suggests that the flat trench bottom results from deposition of sediments carried down the trench walls by turbidity currents on the nearshore flank and by slumps down the offshore flank. Such mass movements might be expected in a region of frequent earthquake activity, such as coastal Mexico. As these sediment-laden currents moved out from the trench walls they slowed and deposited their loads as the very gently sloping aprons now observed. Similar occurrences have been discussed by other authors (*e.g.*, Hersey and Rutstein, 1958).

TABLE 1. MAXIMUM DEPTH OF FILL IN THE MIDDLE AMERICA TRENCH, AS DEDUCED FROM BATHYMETRIC RECORDS

Region	Possible range of thickness (in km)	Probable thickness (in km)
Tres Marías Basin, near seismic station 1	0.2 –0.65	0.6+
Tres Marías Basin, near seismic station 1	0.5	0.5
Tres Marías Basin, near seismic station 1′	0.4+	0.4
Tres Marías Basin, near seismic station 1′	0.45	0.4
West of Manzanillo	0.45–1.0	1.0
Southwest of Manzanillo	0.2 –0.4	0.4
South of Manzanillo	0.08–0.2	0.2
Southwest of Petacalco Bay	0.45–0.9	0.7
Southwest of Acapulco	0.04–0.05	0.05
South of Acapulco	0.3 –0.4	0.35
Southwest of Champerico	0.01–0.02	0.02
South of Champerico	Not detected	
South of San José	0.02–0.04	0.035
South of Gulf of Fonseca	0.02–0.04	0.03
Southwest of San Juan del Sur	0.07	0.07
West of Gulf of Nicoya	0.03	0.03
South of Gulf of Nicoya	0.05	0.05

Echograms of most of the 121 trench crossings, such as those shown in Plate 5, have been examined to obtain data on the probable thickness of the material partially filling the trench and resulting in a nearly flat trench bottom off most of Mexico, Nicaragua, and Costa Rica (Pl. 5, upper and lower profiles). On each crossing, the apparent width of the flat bottom giving a strong echo was noted. The slopes of the trench walls were computed and, where necessary, slope corrections made. Several crossings were normal to the trench axis; others have been projected to normal crossings, in which apparent width of the flat bottom is at a minimum and slope of the trench walls is at a maximum. These corrections tend to balance one another, as far as computed fill is concerned. For each profile, the observed side slopes were projected to intersection, and the maximum value for possible fill noted. This operation was then repeated using the extreme values of side slope for each region in order to cover the probable range in thicknesses and to allow for changes in the wall slopes with depth.

Computations from these bathymetric data suggest that moderately thick fill is present only in the Tres Marías Basin and near Manzanillo and that there is almost no fill off Guatemala. They also indicate rapid changes in the amount of fill in short distances along the trench, as for example near Manzanillo. Representative values computed from bathymetric data are presented in Table 1.

A similar calculation was made to learn the thickness of fill in one of the suggested fault troughs offshore of the trench off Zihuatanejo; very tentatively, a value of 0.3–0.4 km seems likely.

DISCUSSION

The Middle America Trench, though bordering a continent and shallower than the western Pacific trenches, exhibits most of the phenomena associated with trench—island-arc systems (Gutenberg and Richter, 1954, p. 36). It has negative gravity anomalies and many shallow-focus earthquakes along its length and active vulcanism and intermediate-focus shocks landward of the Central American section. The abundance of seamounts and the shallow seismicity seaward of the trench west of Colima and Jalisco, and the irregular topography interrupting the trench off Michoacan, are considered indicative of tectonic activity that may postdate the early stages of the formation of the trench.

Echo sounding and seismic interpretations (Shor and Fisher, 1961) differ as to amount of sediment in the trench bottom, except that

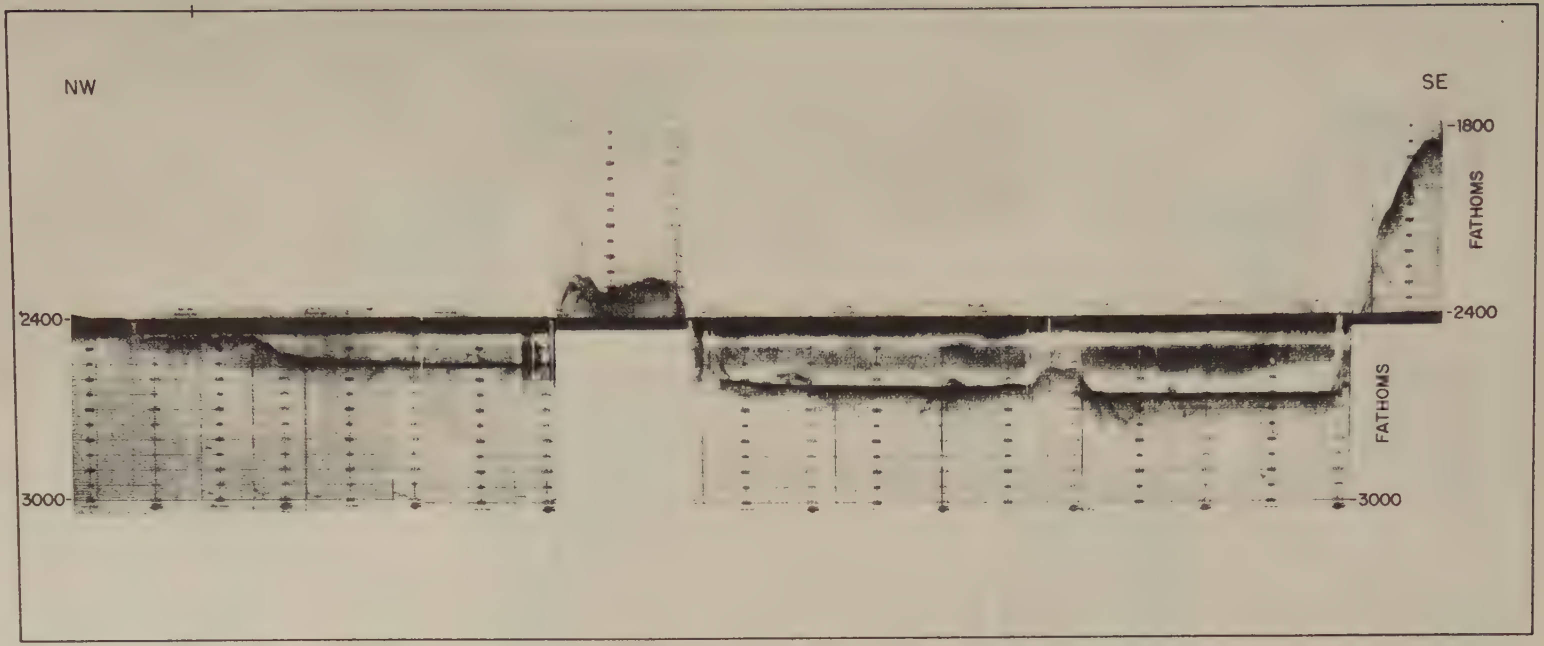

ECHOGRAM OF TRAVERSE ALONG TRENCH NORTHWEST OF MANZANILLO, MEXICO

Vertical exaggeration 15 X. *See* Plate 1A for track. The dark zone recorded at 2400–2450 fathoms is the outgoing signal. The slightly lighter zone at 2500–2600$^+$ fathoms on the tape is the corresponding return from the "deep scattering layer," which in this case actually lies at 100–200$^+$ fathoms.

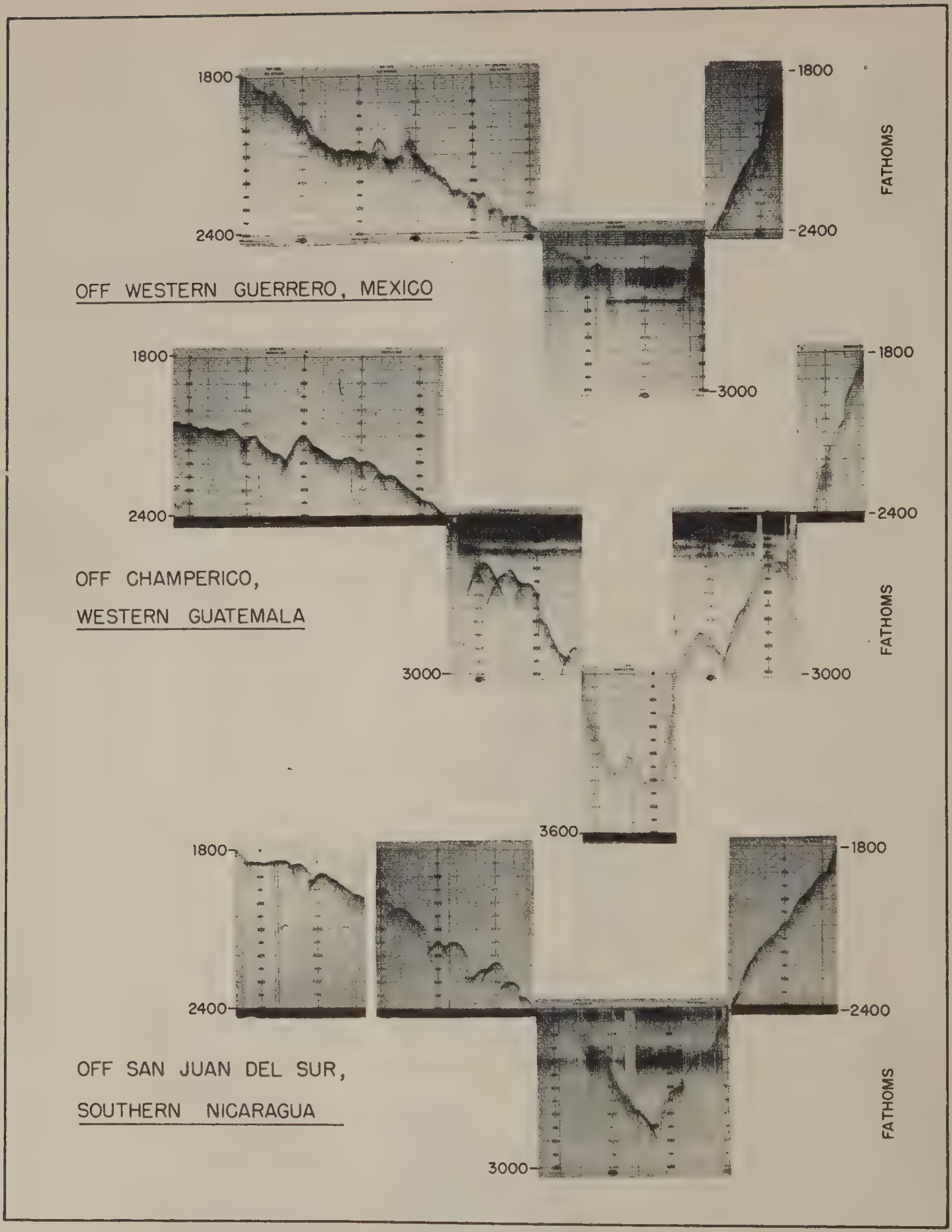

ECHOGRAMS OF TRAVERSES ACROSS THE MIDDLE AMERICA TRENCH

Vertical exaggeration about 15 X. *See* Plate 1A for tracks. Note the strong echo from the flat trench floor off Guerrero and from the narrow flat floor off Nicaragua.

sediments are considerably thicker in the Tres Marías Basin and near Manzanillo than elsewhere along the trench axis. Little significance is attached to apparent differences in sediment thickness found on other seismic lines. Inserting a totally masked layer of about 4 km/sec velocity below the 2.15 km/sec sedimentary layer reduces the computed thickness of sedimentary fill to agree more nearly with values obtained from interpretation of the echograms. Bathymetric profiles strongly suggest more fill off Central Mexico than off Chiapas, Guatemala, El Salvador, and Nicaragua, despite possible important contributions of ash from the Central American volcanoes to the southern part of the trench. The apparently thicker fill off Mexico may be due to a greater age of this portion of the trench, to a more ample source of sediment, or to the narrowness of the indented shelf northwest of Acapulco, which could allow land-derived material to move more readily across the shelf to the steep trench flank and thence downward by slumping to the bottom. Southeast of Tehuantepec, such material would more probably settle on the broad shelf; there trench-bottom deposits would be largely ash. The average thickness of sediments in the Middle America Trench appears intermediate between the very thin (<200 m) volcanic (?) detritus of the Tonga Trench (Raitt, Fisher and Mason, p. 249, 1955) and the reportedly 2- to 3-km-thick turbidity-current deposits of the Puerto Rico Trench (Ewing and Heezen, p. 265, 1955; Talwani *et al.*, 1959, p. 1550).

The crustal structure deduced for the Middle America Trench may be compared with that of the Tonga Trench reported by Raitt *et al.* (1955). The presence of a basement layer with velocity of 5.2±0.1 km/sec was observed beneath and landward of the Tonga Trench. The presence of layers with similar intermediate velocity several kilometers thick was detected beneath the continental shelf off Guatemala, and a layer perhaps 1 km to 2 km thick probably exists beneath the sediments in the Middle America Trench. Thickness of the lower crustal layer (velocity 6.5–7.0 km/sec) increases from 4.5, 5.0, and 5.2 km on the Tres Marías Basin, Manzanillo, and Acapulco trench-axis lines, respectively, to 7.6 and 7.7 km on the corresponding lines off Central America. The latter values are comparable to the thickness (more than 8 km) found for the corresponding layer beneath the Tonga Trench, which is 3.5–4 km deeper (Raitt *et al.*, 1955, p. 248).

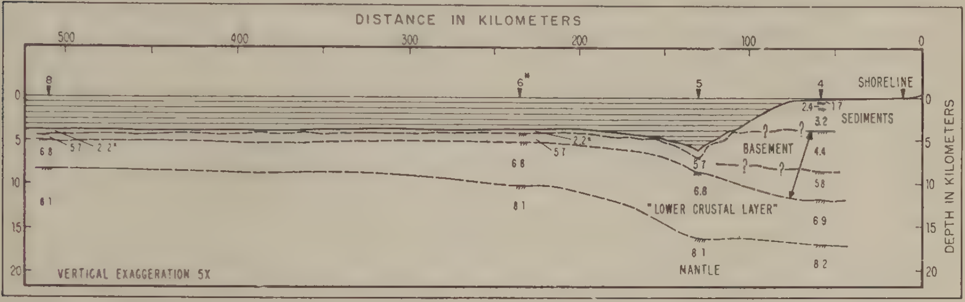

Figure 5. Schematic structure section off western Guatemala. *See* Plate 1A for location.

The mantle, with velocities of 7.7–8.5 km/sec, lies at about 10.8 km below sea level in the Tres Marías Basin, 11.7 and 12.2 km off Manzanillo and Acapulco, then deepens to 16.2 and 14.9 km off Guatemala and Nicaragua, respectively. By any method of interpretation tried, present travel-time data indicate that, along the trench axis, the crust is thicker off Guatemala and Nicaragua than off Central Mexico, notwithstanding the greater thickness of sediments in the Tres Marías Basin and near Manzanillo.

Figure 5 is a schematic structural cross section, normal to the trench off western Guatemala, based on interpreted travel-time data of seismic lines on the shelf, in the trench, and offshore. The section crosses near the midpoint of profile 4–4′ and of profile 5–5′ (Shor and Fisher, 1961, Fig. 1), and that of 8 well outside the trench; station 6 has been shifted westward to fall on the section. At the positions where seismic lines cross the section, depths of the various layers, computed using regional velocities, are indicated by hachured interfaces. The dashed lines are possible interpolations, if the upper three layers of the shelf lines are considered as sediments in different stages of compaction, and the fourth and fifth layers are combined as basement complex (volcanic rocks?, plutonic rocks?). Any sediment-basement and basement-lower crustal layer contacts are probably more irregular than shown here. Although the subsurface information is sparsely distributed, several conclusions can be made regarding trench structure off western Guatemala:

(1) Below the trench axis, the M discontinuity is 6 km deeper than in the Pacific Basin to the west, and less than 1 km shallower than beneath the outer shelf 70 km to the northeast. There is no indication of a tectogene-like bulge of crustal material into the mantle beneath the trench. At station 6 the estimated depth to the mantle, about 10 km, is shallower than its depth at the average Pacific Basin station (Shor and Fisher, 1961, Table 2). Thus the depth to the mantle beneath the trench is about 5 km greater than in the average of the Pacific stations.

(2) A thick section of material with velocity of 3.5–6 km/sec (volcanic rocks?, metamorphosed sedimentary rocks?, sialic intrusive rocks?) is present beneath the outer portion of the shelf. This section thins rapidly seaward, although it may persist as a thin basement layer beneath and outside the trench.

(3) Whether or not basement rocks are present beneath and outside the trench, the lower crust is about half again as thick beneath the trench as beneath the outer station or the average Pacific Basin station. Though of smaller dimensions, this Middle America Trench section more nearly resembles the Tonga Trench structure deduced by Raitt *et al.* (1955, p. 253) and the Peru-Chile Trench structure reported by Raitt (1958, p. 37) than the Mindanao or Puerto Rico trench sections as interpreted by Worzel and Shurbet (1955, p. 93–96) or the Tonga Trench reinterpretation offered by Talwani, Worzel, and Ewing (1959).

However, differences in crustal sections proposed may be more a matter of the kind of data available than of actual structure. For the Tonga, Peru-Chile, and Middle America trenches work, seismic-refraction data were used, with records from waves traveling in the layers down to and including the upper mantle beneath the trenches. Worzel and Shurbet constructed "standard" oceanic and continental crustal sections from gravity and averaged seismic data. Working from the standard sections, they based their schematic crustal structure of the Mindanao Trench on gravity computations and that of the Puerto Rico Trench on gravity computations supported by seismic data from the sediment layer in the trench proper and from some of the deeper layers outside the trench. Both computed sections contain a locally thinned (lower) crustal layer overlain by more or less sediment along the trench axis. According to Ewing and Heezen (1955, p. 266), "The fact that a local thinning of the crust can better explain the gravity results leads one to the conclusion that tension rather than compression may be the dominant force involved in the formation of the trenches." Without going more deeply into the question of forces forming trenches, the present writer wishes to point out that the interpreted results for the Middle America Trench off western Guatemala as here reported, and those from the Tonga and Peru-Chile trenches, apparently do not support this conclusion. Additional gravity and seismic observations in the Puerto Rico Trench, reported by Shurbet and Worzel (1957, p. 263–266), have been interpreted by those writers as indicating that sediments in that trench are not so thick as they previously supposed and that "Some thickening of the crustal rock section under the trench is shown by the seismic data and confirmed by the gravity calculations" (p. 266).

Talwani, Sutton, and Worzel (1959) give a detailed seismic and gravity section across the Puerto Rico Trench. They show (Fig. 3, p. 1550) a considerably greater depth to the M discontinuity under the trench axis from seismic- refraction observations than by gravity computations. They note that the difference could be due to structural variations transverse to the section. The refraction measurements reported in greater detail by Officer *et al.* (1957) indicate a crustal thickness there of about 10 km and a lower crustal-layer thickness of 7–8 km, very similar to those reported for the Middle America and Tonga trenches.

Heacock's gravity observations should prove of special significance in this connection. According to a published station chart (Worzel and Ewing, 1952, p. 455), five of Heacock's stations, numbers 960–964, lie within 60 miles of the Champerico section figured here; the two profiles cross at about 60° near station 6.

Since the depth below sea level to basement along the axis of the Middle America Trench, from the Islas Tres Marías to the Gulf of Fonseca, probably is of the order of only 5–7 km, and since the trench borders a continental structure rather than an island arc, perhaps it is more appropriate to compare its deduced structure to that found at, for example, the continental slope off southern California rather than the postulated structure of the classic deeps of the western Pacific or the Puerto Rico Trench.

A recent paper by Shor and Raitt (1958) describes their seismic-refraction studies in the southern California continental borderland. They include a schematic structure section (Fig. 2, p. 249) drawn from the deep sea across the slope and borderland to the mainland. The section is a composite, based on work during several years. The western 60 km of the section, with five stations included, passes from the deep Pacific across the continental rise and slope up to the 1-km-deep shoal known as Patton Ridge, the ridge directly shoreward of the Patton Escarpment (Shepard and Emery, 1941, Pl. 1), and may be compared with the structure section drawn off Guatemala (Fig. 5).

From the structure sections as drawn, the following comparisons seem valid:

(1) Velocities obtained and layer identifications are similar (Table 2).

(2) At the base of the continental slope, the depth from sea level to basement is 5–6 km, about 1 km shallower than in the trench off Guatemala.

(3) Off the borderland, the mantle lies at so-called "oceanic depth," 9–11 km, as close to the base of the continental slope as it can be measured. Beneath the trench, at the base of the slope, the depth below sea level to the mantle is 15–17 km.

(4) Beneath the 1-km-deep Patton Ridge, 30–35 km northeast of the base of the continental slope, the computed depth to the M discontinuity is 17 km, very similar to the 15–18 km depth to the mantle beneath the outer, 0.1-km-deep shelf 70 km northeast of the trench off Guatemala.

(5) A thick shallow mass, with velocity of about 5 km/sec, lies beneath Patton Ridge but thins rapidly at the continental slope. A possibly similar mass, with velocity of 4–6 km/sec, underlies the outer shelf off Guatemala but thins rapidly toward the trench.

TABLE 2. VELOCITIES OF REFRACTING LAYERS

Layer	California velocities (km/sec)	Guatemala velocities (km/sec)
Sediments	1.8–2.8	1.7–3.2
Basement complex, possibly volcanic rocks or consolidated sediments	4.6–5.1 5.9–6.2	4.4 5.7–5.9
"Lower crustal layer"	6.7–7.0	6.8–6.9
Mantle	8.1–8.2	8.1–8.2

(6) The "lower crustal layer" (velocity 6.7–7.0 km/sec) thickens in the landward direction from 4.5 to 8 km in a distance of 45 km in the schematic section off California. Off Guatemala (observations were more widely spaced here), it increases from 5 km at 6 to 7.6 km at 5, then thins to 5 km beneath the outer shelf, in a horizontal distance of 175 km.

The most striking difference in the two sections is that off the borderland the rapid transition to a deep mantle occurs landward of the base of the continental slope, and off Guatemala the deepening of the mantle occurs seaward of the trench. In this respect, the structure of the moderately deep trench off the continental margin of Central America more nearly resembles that of the very deep trench off the Tonga island arc than of the seaward margin of the southern California continental borderland.

REFERENCES CITED

Agassiz, A., 1906, Reports on the scientific results of the expedition to the eastern tropical Pacific . . . 1904–5 . . ., v. 5, General report of the expedition: Cambridge, Mass., Harvard Coll., Mus. Comp. Zool. Mem., v. 33, 75 p.

Benioff, Hugo, 1954, Orogenesis and deep crustal structure—additional evidence from seismology: Geol. Soc. America Bull., v. 65, p. 385–400

Coast and Geodetic Survey, 1948–1958, Preliminary determination of epicenters: Washington, D. C., U. S. Dept. Commerce

Dietz, R. S., and Menard, H. W., Jr., 1951, Origin of abrupt change in slope at continental shelf margin: Am. Assoc. Petroleum Geologists Bull., v. 35, p. 1994–2016

Ericson, D. B., Ewing, M., and Heezen, B. C., 1952, Turbidity currents and sediments in North Atlantic: Am. Assoc. Petroleum Geologists Bull., v. 36, p. 489–511

Ewing, M., and Heezen, B. C., 1955, Puerto Rico trench topographic and geophysical data, p. 255–267 *in* Poldervaart, A., *Editor*, Crust of the earth: Geol. Soc. America Special Paper 62, 762 p.

Fisher, R. L., 1954, On the sounding of trenches: Deep-Sea Research, v. 2, p. 48–58

Fisher, R. L., and Revelle, R., 1955, The trenches of the Pacific: Sci. Am., v. 193, no. 5, p. 36–41

Fisher, R. L., and Shor, G. G., Jr., in press, Topography and structure of the Middle America Trench: Mexico, 20th Intern. Geol. Cong. Proc.

Gates, O., and Gibson, W., 1956, Interpretation of the configuration of the Aleutian Ridge: Geol. Soc. America Bull., v. 67, p. 127–146

Gunn, Ross, 1947, Quantitative aspects of juxtaposed ocean deeps, mountain chains and volcanic ranges: Geophysics, v. 12, p. 238–255

Gutenberg, B., and Richter, C. F., 1954, Seismicity of the earth: Princeton, N. J., Princeton Univ. Press, 310 p.

Heacock, J. G., Jr., and Worzel, J. L., 1955, Submarine topography west of Mexico and Central America: Geol. Soc. America Bull., v. 66, p. 773–776

Hersey, J. B., and Rutstein, M. S., 1958, Reconnaissance survey of Oriente Deep (Caribbean Sea) with a precision echo sounder: Geol. Soc. America Bull., v. 69, p. 1297–1304

Luskin, B., Heezen, B. C., Ewing, M., and Landisman, M., 1953, Precision measurement of ocean depths: Deep-Sea Research, v. 1, p. 131–140

Menard, H. W., Jr., 1955, Deformation of the northeastern Pacific basin and the west coast of North America: Geol. Soc. America Bull., v. 66, p. 1149–1198

Menard, H. W., Jr., and Fisher, R. L., 1958, Clipperton fracture zone in the northeastern equatorial Pacific: Jour. Geology, v. 66, p. 239–253

Officer, C. B., Ewing, J., Edwards, R. S., and Johnson, H. R., 1957, Geophysical investigations in the Eastern Caribbean; Venezuelan Basin, Antilles Island Arc, and Puerto Rico Trench: Geol. Soc. America Bull., v. 68, p. 359–378

Raitt, R. W., 1958, Seismic surveys, p. 36–38 *in* Fisher, R. L., *Editor*, Preliminary report on Expedition Downwind: Washington, D. C., IGY World Data Center A, IGY Gen. Rept., Ser. 2, 58 p.

Raitt, R. W., Fisher, R. L., and Mason, R. G., 1955, Tonga Trench, p. 237–254 *in* Poldervaart, A., *Editor*, Crust of the earth: Geol. Soc. America Special Paper 62, 762 p.

Sanchez Mejorada, S. H., 1956, Carta geologica de la Republica Mexicana (1:2,000,000): Mexico, 20th Intern. Geol. Cong.

Schuchert, Charles, 1935, Historical geology of the Antillean-Caribbean region: New York, John Wiley & Sons, 811 p.

Shepard, F. P., and Emery, K. O., 1941, Submarine topography of the California coast; canyons and tectonic interpretation: Geol. Soc. America Special Paper 31, 171 p.

Shor, G. G., Jr., and Fisher, R. L., 1961, Middle America Trench: seismic-refraction studies: Geol. Soc. America Bull., v. 72, p. 721–730

Shor, G. G., Jr., and Raitt, R. W., 1958, Seismic studies in the southern California continental borderland: Mexico, 20th Intern. Geol. Cong. Proc. Section 9, Geofisica Aplicada, v. 2, p. 243–259

Shurbet, G. L., and Worzel, J. L., 1957, Gravity anomalies and structure of the West Indies, part III: Geol. Soc. America Bull., v. 68, p. 263–266

Talwani, M., Sutton, G. H., and Worzel, J. L., 1959, A crustal section across the Puerto Rico Trench: Jour. Geophys. Research, v. 64, p. 1545–1555

Talwani, M., Worzel, J. L., and Ewing, M., 1959, Gravity anomalies and crustal section across the Tonga Trench (Abstract): Jour. Geophys. Research, v. 64, p. 1126

Tamayo, J. L., 1949, Geografia general de Mexico, tome 2 (Geografia fisica): Mexico, Talleres Graficos de la Nacíon, 583 p.

Udintsev, G. B., 1955, Topography of the Kuril-Kamchatka Trench: Trud. Inst. Okeanology, v. 12, p. 16–61

Vening Meinesz, F. A., 1948, Gravity expeditions at sea, 1923–1938, v. 4: Delft, Netherlands Geod. Comm. Pub., 233 p.

Webber, B. N., and Ojeda R., J., 1956, Estructuras geologicas del sureste de Oaxaca y sur de Chiapas, Mexico: Mexico, 20th Intern. Geol. Cong. Guidebook to Excursion G-15, p. 75–82

Whitcroft, H. T., 1944, The bathymetry of the Central America region, west coast of Mexico and northern Central America: Am. Geophys. Union Trans., Pt. 4, p. 606–608

Worzel, J. L., and Ewing, M., 1952, Gravity measurements at sea, 1948 and 1949: Am. Geophys. Union Trans., v. 33, p. 453–460

Worzel, J. L., and Shurbet, G. L., 1955, Gravity interpretations from standard oceanic and continental crustal section, p. 87–100 *in* Poldervaart, A., *Editor*, Crust of the earth: Geol. Soc. America Special Paper 62, 762 p.

MANUSCRIPT RECEIVED BY THE SECRETARY OF THE SOCIETY, FEBRUARY 25, 1959
CONTRIBUTION FROM THE SCRIPPS INSTITUTION OF OCEANOGRAPHY, NEW SERIES

(531)

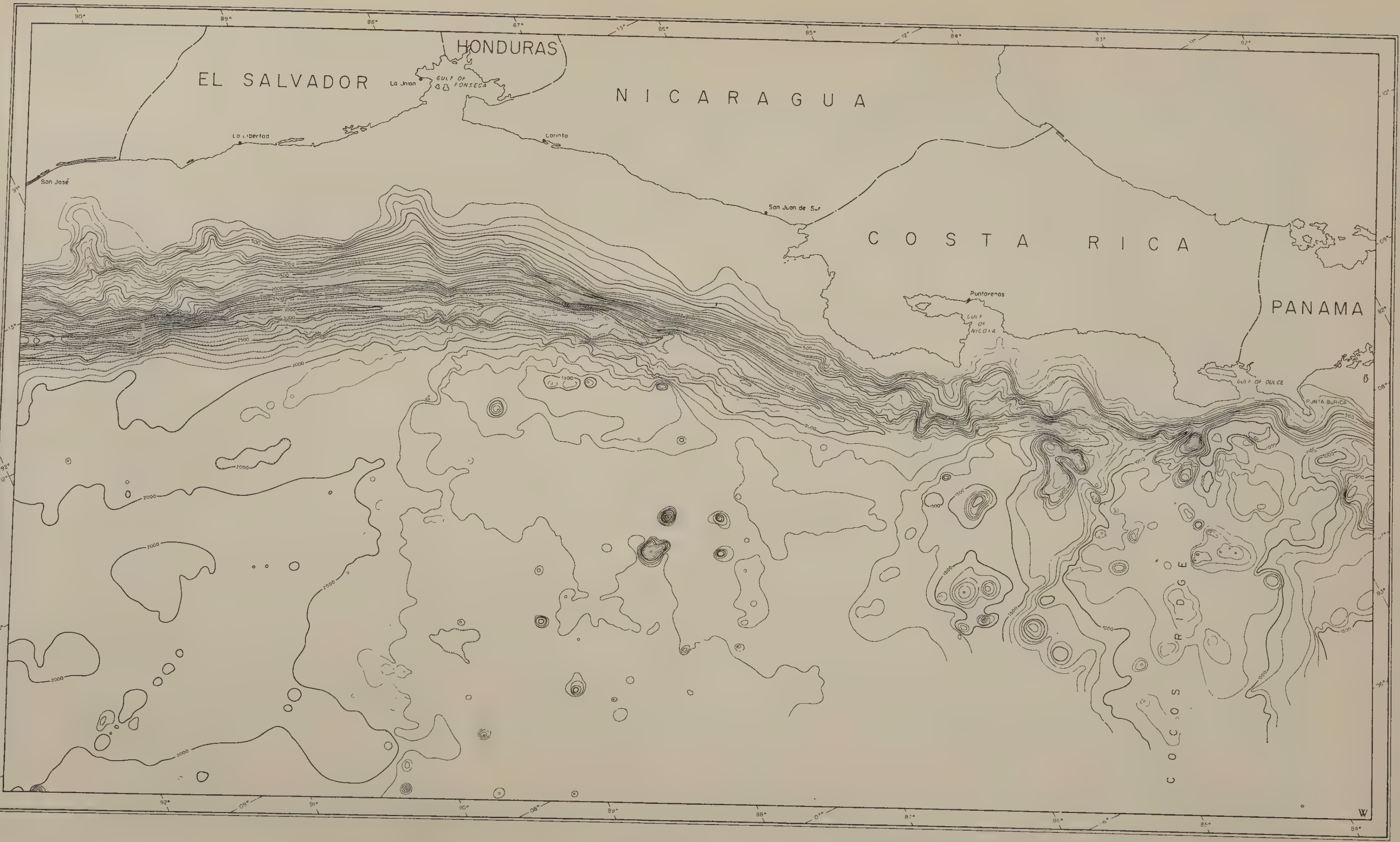
EL SALVADOR
HONDURAS
NICARAGUA
COSTA RICA
PANAMA
San José
La Libertad
La Union
GULF OF FONSECA
Corinto
San Juan de Sur
Puntarenas
GULF OF NICOYA
GULF OF DULCE
PUNTA BURICA
COCOS RIDGE
500
1000
1500
2000
2500
90°
89°
88°
87°
86°
85°
84°
83°
82°
91°
92°
13°
12°
11°
10°
09°
08°
07°
06°
W

SUBMARINE TOPOGRAPHY, FROM SAN JOSÉ, GUATEMALA, TO PUNTA BURICA, PANAMA

FISHER, PLATE 6
Geological Society of America, volume 72

GEORGE G. SHOR, JR. *University of California, The Scripps Institution of Oceanography, La Jolla,*
ROBERT L. FISHER *Calif.*

Middle America Trench: Seismic-Refraction Studies

Abstract: Seismic-refraction profiles in the Middle America Trench show that the main crustal layer ranges from normal oceanic thickness (about 5 km) to half again as thick. Sediments are thicker than in the Pacific Basin. Because of the increased depth of water and sediment at all stations and thickening of the main crustal layer at some stations, the M discontinuity bows down beneath the trench. At the outer edge of the continental shelf near Guatemala, the water is replaced by sediments and rocks which may be either consolidated sediments or volcanic rocks; the M discontinuity is at little greater depth than beneath the trench.

CONTENTS

Introduction 721
Acknowledgments 721
Field methods 722
Computation 723
Interpretation of results 726
  Sedimentary and basement layers 726
  Main crustal layer 728
  Mantle 729
  Structure 729
References cited 729

Figure
1. Locations of stations 722
2. Travel-time plots for stations 1 and 1′ (Tres Marias Basin) 722
3. Travel-time plots for stations 2 (near Manzanillo) and 3 (near Acapulco) 724
4. Travel-time plots for stations 4 and 4′ (on continental shelf near Champerico) 724
5. Travel-time plots for stations 5 and 5′ (on axis of trench near Champerico) 726
6. Travel-time plots for stations 6 (on outer ridge, near Champerico) and 7 (on axis of trench near La Union) 727
7. Structural sections based on individual station solutions 727
8. Structural sections based on the assumption of regionally uniform velocities 728

Table
1. Equations of arrival times 723
2. Seismic velocities and layer thicknesses 725
3. Layer thicknesses computed by assuming regional uniformity of velocities 726

INTRODUCTION

On the 1954 Acapulco Trench Expedition seismic-refraction work was done by the Scripps Institution of Oceanography ships Spencer F. Baird and Horizon at seven locations (Fig. 1) in and near the Middle America Trench. Five of the stations were along the trench axis, near Puerto Vallarta, Manzanillo, and Acapulco, Mexico; Champerico, Guatemala, and La Union, El Salvador. The other two were on the outer edge of the continental shelf and on the ridge seaward of the trench, both near Champerico. The choice of station positions was based on previous bathymetric studies by Fisher which, with bathymetry and structural interpretations from this and later trips, are reported separately (Fisher, 1961). The purpose of the seismic work was to measure the depth of the M discontinuity beneath the trench.

ACKNOWLEDGMENTS

In the work at sea the authors were aided greatly by Alan C. Jones and Maxwell Silverman; computational work ashore was assisted by Gloria Slack and Frieda James. The seismic-refraction program has been under the general direction of Prof. Russell W. Raitt. Illustrations have been prepared by Christine Baldwin. The authors are indebted to Russell Raitt and J. B. Hersey for critical reading of the manuscript, and to the officers, crews, and scientific parties of the vessels Spencer F. Baird and Horizon for their help.

This work represents results of research sponsored by the U. S. Navy, Bureau of Ships

---

Geological Society of America Bulletin, v. 72, p. 721-730, 8 figs., May 1961

Contributions from the Scripps Institution of Oceanography, New Series, 1279

Reproduced by Permission

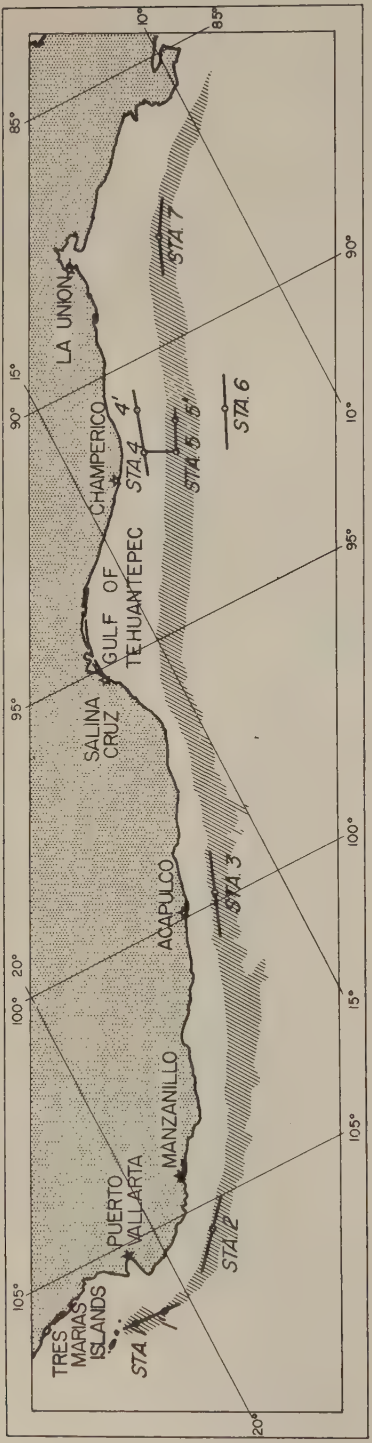
85°
10°
85°
90°
15°
90°
10°
95°
95°
100°
20°
100°
15°
105°
105°
20°
LA UNION
CHAMPERICO
GULF OF TEHUANTEPEC
SALINA CRUZ
ACAPULCO
MANZANILLO
PUERTO VALLARTA
TRES MARIAS ISLANDS
STA. 7
STA. 6
4'
STA. 4
5'
STA. 5
STA. 3
STA. 2
STA. 1

Figure 1. Locations of stations

under contract Nobsr 72512 and the Office of Naval Research under contract Nonr 2216(05).

FIELD METHODS

Recording was done aboard the Spencer F. Baird, while the Horizon, dropping charges, steamed toward the Baird, passed it close abeam, and continued onward. Stations 2, 3, 6, and 7 were split profiles. At stations 1, 4, and 5 two receiving positions were occupied; the outbound shooting track from the first position was followed on the inbound track to the second, so that each station consisted of a reversed profile with unreversed short profiles on the ends.

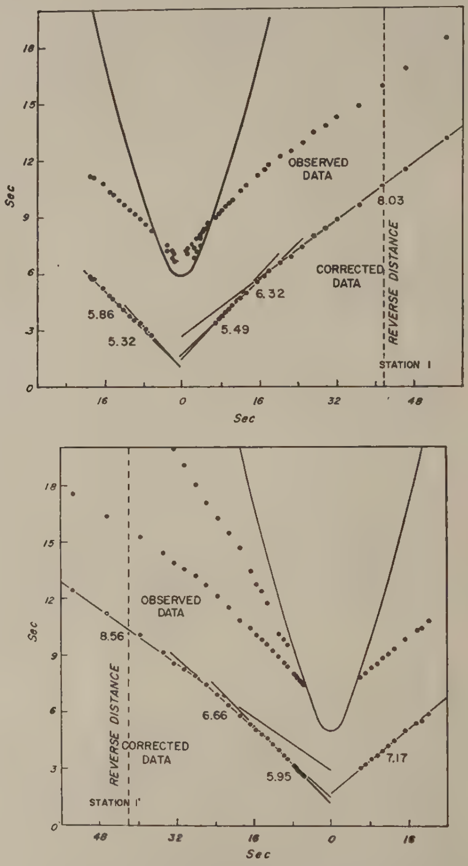

Figure 2. Travel-time plots for stations 1 and 1′ (Tres Marias Basin). Upper points are observed data; lower points are corrected to sea floor.

Both shipboard operations and data analysis are more difficult to execute for a narrow trench than for either a broad trench (such as the Puerto Rico Trench) or ocean-basin areas, because of the rapid changes in water depth and sediment thickness transverse to the trench, which require that both ships stay closely on the trench axis. On stations in the narrow portion of the trench (2, 3, 5, and 7) an attempt was made to have the shooting ship follow the trench axis as defined by prior exploration instead of following a straight track. The receiving ship moved back to the trench axis whenever it drifted appreciably toward the trench walls. Effects of structural variations along and across the trench are still probably large and have given difficulty in interpretation.

Receiving and shooting procedures otherwise were as described by Raitt (1952; 1956); signals from four hydrophones were recorded in three frequency bands at two levels. Shots were half a pound to 300 pounds of high explosives.

COMPUTATION

Travel times were corrected first for firing-mark delay and then for water delay to sea

TABLE 1. EQUATIONS OF ARRIVAL TIMES

Station	Northwest line	Southeast line
1	0.94 ± .04 + X/5.86 ± .07	1.41 ± .05 + X/5.49 ± .12
	0.91 ± .02 + X/5.32 ± .22	
		1.73 ± .08 + X/6.32 ± .13
		2.65 ± .07 + X/8.03 ± .09
1′	1.19 ± .01 + X/5.95 ± .02	
	1.51 ± .08 + X/6.66 ± .13	1.70 ± .03 + X/7.17 ± .10
	2.86 ± .12 + X/8.56 ± .15	
2	0.94 ± .08 + X/5.45 ± .24	
	1.08 ± .06 + X/6.18 ± .13	1.32 ± .10 + X/7.32 ± .24
	1.58 ± .07 + X/7.50 ± .07	1.67 ± .13 + X/7.77 ± .15
3	0.51 ± .03 + X/5.86 ± .09	0.15 ± .09 + X/4.75 ± .19
	1.19 ± .13 + X/7.00 ± .28	0.62 ± .09 + X/6.66 ± .21
	1.58 ± .17 + X/7.98 ± .19	1.77 ± .21 + X/8.52 ± .28
4	0.00* + X/1.78 ± .16	0.00* + X/1.78 ± .16†
	0.44 ± .07 + X/2.60 ± .10	0.42 ± .04 + X/2.55 ± .05
	0.84 ± .04 + X/3.16 ± .05	0.91 ± .05 + X/3.16 ± .06
	1.84 + X/4.64 **	1.82 ± .02 + X/4.41 ± .03
		3.20 ± .02 + X/5.76 ± .02
		4.21 ± .10 + X/6.78 ± .10
		5.66 ± .14 + X/8.27 ± .10
4′	0.00* + X/1.64 ± .07	0.00* + X/1.64 ± .07†
	0.48 ± .03 + X/2.29 ± .02	0.47 ± .09 + X/2.22 ± .07
	1.55 ± .04 + X/3.33 ± .05	1.44 ± .11 + X/3.21 ± .12
	2.32 ± .03 + X/4.39 ± .03	2.38 ± .04 + X/4.74 ± .05
	3.99 + X/5.90 **	3.55 ± .15 + X/6.09 ± .20
	4.79 ± .07 + X/6.97 ± .09	
	5.85 ± .19 + X/8.09 ± .14	
5		0.61 ± .30 + X/5.65 ± .82
		0.88 ± .08 + X/6.32 ± .11
		2.53 ± .25 + X/8.34 ± .27
5′	1.06 ± .04 + X/7.11 ± .07	0.99 ± .15 + X/6.69 ± .39
	1.97 ± .76 + X/7.76 ± .65	
6	0.74 ± .02 + X/6.91 ± .04	0.67 ± .03 + X/6.62 ± .06
	1.19 ± .04 + X/7.68 ± .04	1.31 ± .02 + X/7.85 ± .03
7	1.13 ± .12 + X/6.39 ± .33	
	0.97 ± .06 + X/6.77 ± .07	1.01 ± .04 + X/6.53 ± .06
	3.04 ± .27 + X/8.72 ± .27	2.69 ± .10 + X/8.47 ± .12

* Intercept assumed to be 0.00

† Solution for points on both sides of receiving position together

** Line fitted to 2 points; no least-squares solution

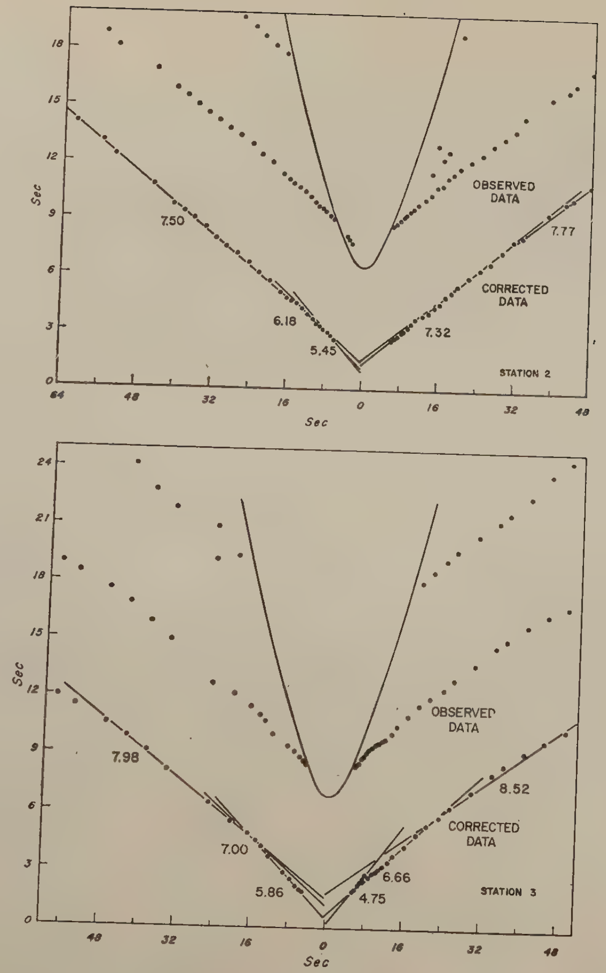

Figure 3. Travel-time plots for stations 2 (near Manzanillo) and 3 (near Acapulco). Both are along axis of trench.

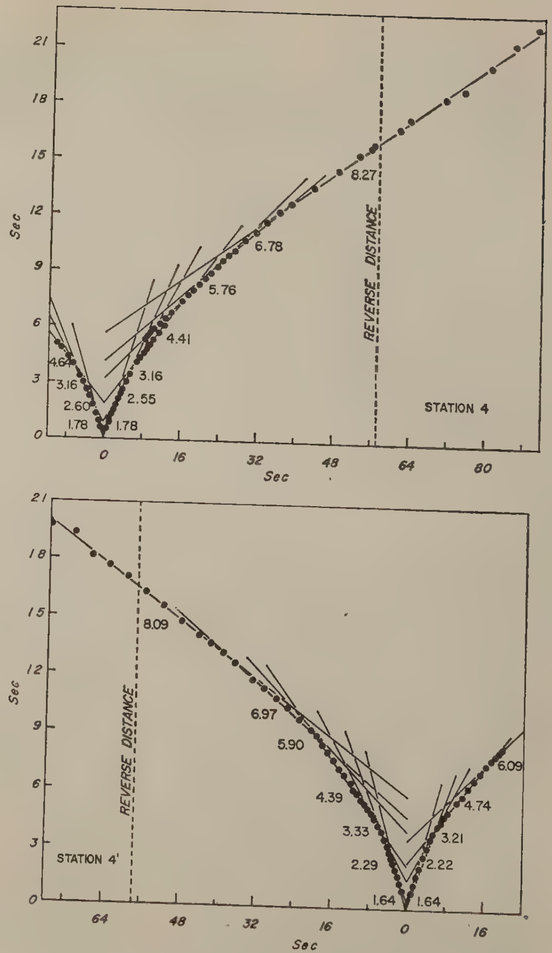

Figure 4. Travel-time plots for stations 4 and 4′ (on continental shelf near Champerico)

floor, by using correction cosines determined from the observed slopes of the uncorrected travel-time plots. Distances were determined from the travel time of the direct water wave and velocities of sound in water computed from hydrographic casts at each station by using Kuwahara's (1939) tables. If the direct water wave was not observed, its travel time was computed from that of the bottom-reflected waves by a method similar to that of Katz and Ewing (1956, p. 507).

Travel-time plots are shown in Figures 2–6. The upper points in each plot are the observed data; the lower points are refracted arrivals corrected for water delay. On station 4, the observed and corrected data coincided to the scale of the figure in most cases, so that only the corrected points are shown. Straight lines were fitted to the arrivals by least squares; equations of the lines are given in Table 1. The deviations listed are the standard deviations of the velocity and intercept time.

Structural computations by a number of methods are possible. The simplest method, in which a "horizontal layer" computation is made for each station independently, is presented in Table 2. In this method the harmonic mean of the velocities and the direct mean of the intercept times were taken from the least-squares solutions for the split profiles and a single section computed. For the reversed profiles only the data for the reversed pair were used; the velocities were again the harmonic mean, but the intercepts were used separately to obtain sections for each end of the reversed profile.

Difficulties arise in the computation and in comparison of the results because of the possible presence of a "basement layer" with velocity between 4 and 6 km/sec, intermediate between those of the sediments and the main crustal layer. This layer was recorded reliably on three of the four profiles of station 1 and on both profiles of station 3. Its presence is indicated, with very poor determination of velocity, on one of two profiles of station 2 and two of four profiles of station 5. On station 4, in shallow water, there are two well-observed layers with velocity in the 4–6 km/sec range. On stations 6 and 7 the layer was not indicated. The line with velocity 6.4 km/sec on station 7 has too high an intercept time to be a separate layer and is probably caused by variation in sediment thickness.

For solutions based only on the observed data from each station separately, the "basement" can be included only on stations 1, 3, and 4. The results of these computations are plotted in Figure 7. To make it easier to compare stations and to take account of the possi-

TABLE 2. SEISMIC VELOCITIES AND LAYER THICKNESSES
Data for each station were computed independently.

	Water		Sediment		Basement		Crust		Mantle	
Station	h_0	c_0	h_1	c_1	h_2	c_2	h_3	c_3	c_4	Σh
1	4.40	1.54	1.64	2.15	1.77	5.71	3.84	6.49	8.29	11.65
1′	3.76	1.54	1.38	2.15	1.79	5.71	6.05	6.49	8.29	12.98
2	4.91	1.54	1.36	2.15			2.86	6.70	7.64	9.13
3	5.14	1.54	0.39	2.15	2.31	5.25	3.93	6.82	8.24	11.77
4	0.12	1.50	0.50 0.74 1.83	1.71 2.41 3.25	3.84 4.03	4.40 5.83	6.53	6.88	8.18	17.59
4′	0.12	1.50	0.58 1.75 1.14	1.71 2.41 3.25	4.81 2.61	4.40 5.83	4.33	6.88	8.18	15.34
5	6.18	1.54	1.00	2.15			9.84	6.69	8.04	17.02
5′	6.02	1.54	1.20	2.15			5.36	6.69	8.04	12.58
6	3.62	1.53	0.80	2.15			3.69	6.76	7.76	8.11
7	5.13	1.53	1.13	2.15			9.71	6.65	8.60	15.97
Pacific average	4.34		0.30	2.15	1.18	5.23	4.78	6.81	8.20	10.60

bility that variations in velocity from station to station (and the resulting variations in structure computed) are due to changes in dip along the individual profiles, the stations have been reworked using regional velocities and a uniform number of layers (in all but the continental shelf station, number 4). In this computation the harmonic mean of all observed velocities for each layer was taken, and for each station the mean delay times were computed. Where no basement layer was observed it was assumed to be at the time of the first refracted arrival. The remainder of the solution was as before; the results appear in Table 3 and Figure 8.

INTERPRETATION OF RESULTS

Sedimentary and Basement Layers

Computations for all except station 4 were made using an assumed velocity of 2.15 km/sec for the sediments. No first arrivals were received from this layer, and second arrivals were indistinct. The velocity of 2.15 km/sec was obtained by Raitt (1956) from reflection studies on deep-water lines in the central Pacific. Reflection data for similar analysis on the trench stations were examined but had too large a scatter to determine a velocity; presumably this was caused by variations in sediment thickness. Wobbles in the refraction travel-time plots also indicate considerable variation in sediment thickness, as does a perceptible shift in the crust arrival line on the first profile of station 7. This latter occurred at the time of a relatively small shift of the receiving position during the course of the run. Bathymetric results (Fisher, 1961) indicate ponding of sediments in the low parts of the trench; this would mask rough topography and create a scatter of the refraction arrivals.

TABLE 3. LAYER THICKNESSES COMPUTED BY ASSUMING REGIONAL UNIFORMITY OF VELOCITIES

Station	Water depth	Layer 1 2.15 km/s	Layer 2 5.74 km/s	Layer 3 6.75 km/s	Depth below sea level to 8.11 km/sec (M discontinuity)
1	4.1	1.3	2.9	4.5	12.8
2	4.9	1.2	0.6	5.0	11.7
3	5.1	0.6	1.3	5.2	12.2
5	6.2	0.8	1.6	7.6	16.2
6	3.6	0.6	1.0	5.0	10.2
7	5.2	1.0	1.0	7.7	14.9

Sediment-thickness values in Table 2 for lines 2, 5, 6, and 7 are maxima because no basement layer has been introduced. If this layer is present but masked, the sediment thickness is decreased by some hundreds of meters, as shown in Table 3.

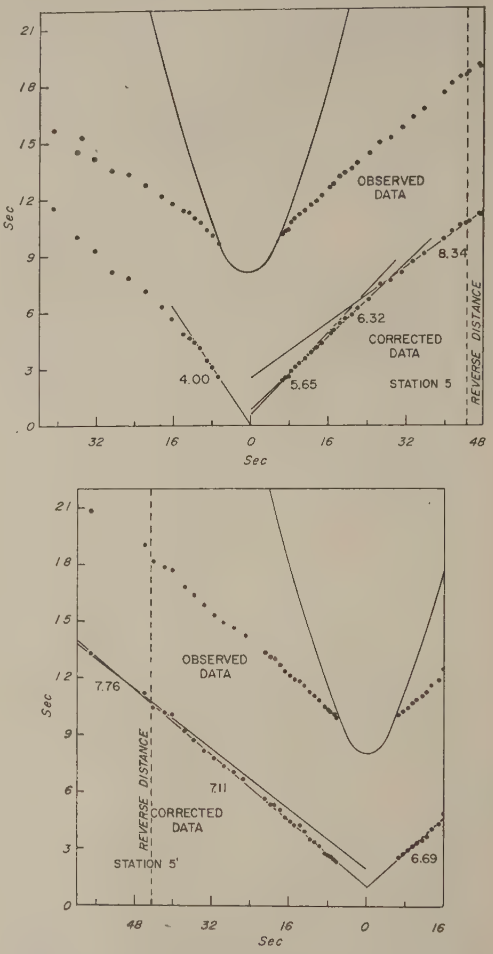

Figure 5. Travel-time plots for stations 5 and 5′ (on axis of trench near Champerico)

All observed early arrivals interpreted as being from the basement layer could be explained by deviations in the crustal arrival times caused by variations in sediment thickness of the order of 100 m. Some evidence for interpretation as an extra layer is found in subbottom reflections on stations 1, 2, and 6 and in the presence of arrivals with apparent veloc-

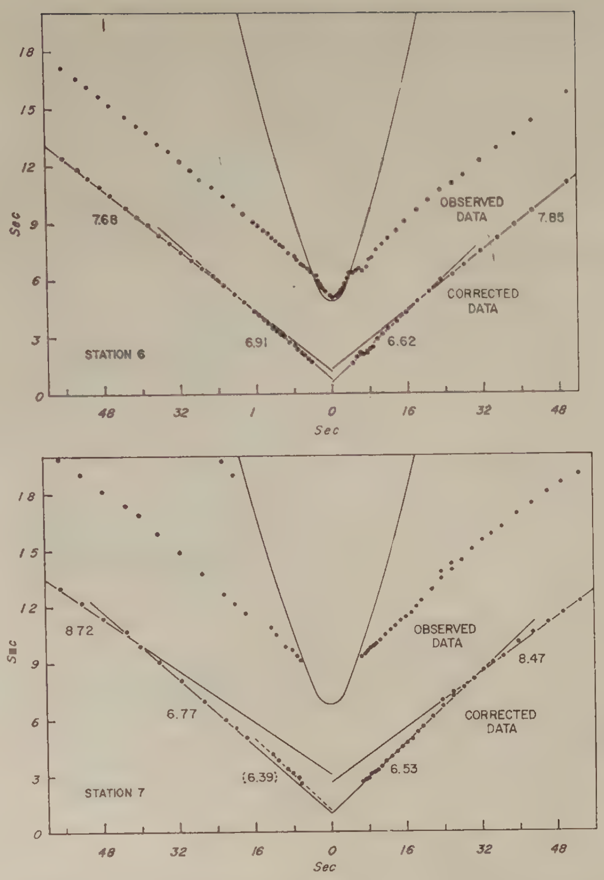

Figure 6. Travel-time plots for stations 6 (on outer ridge, near Champerico) and 7 (on axis of trench near La Union)

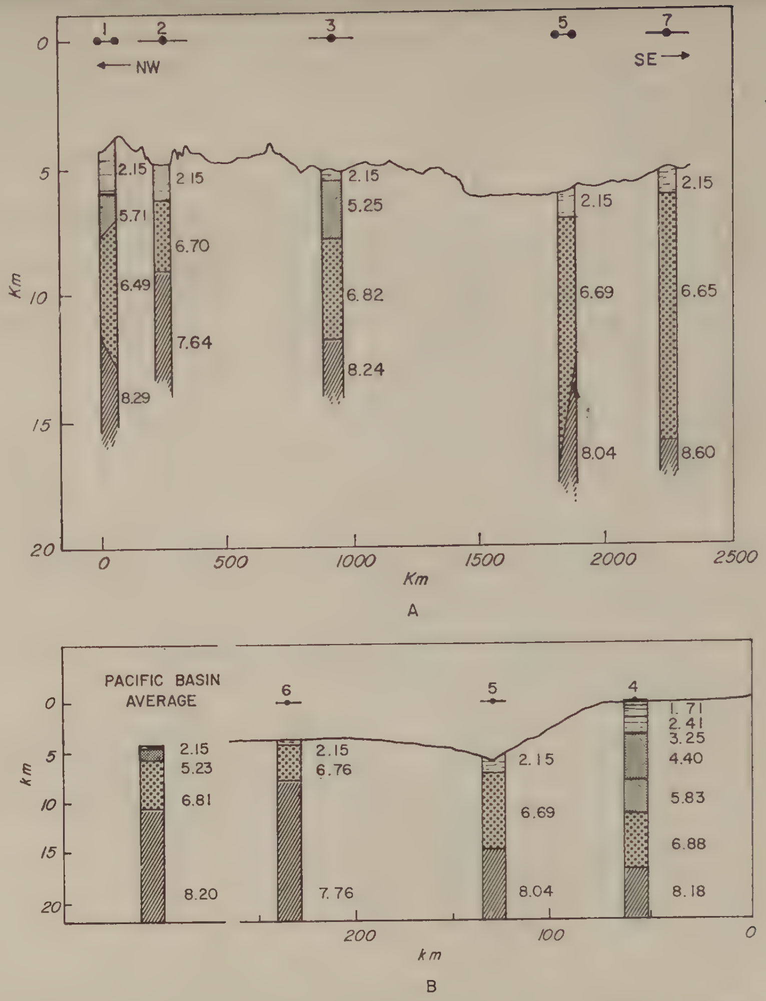
1
2
3
5
7
← NW
SE →
Km
0
5
10
15
20
2.15
5.71
6.49
8.29
2.15
6.70
7.64
2.15
5.25
6.82
8.24
2.15
6.69
8.04
2.15
6.65
8.60
0
500
1000
1500
2000
2500
Km
A
PACIFIC BASIN AVERAGE
2.15
5.23
6.81
8.20
6
2.15
6.76
7.76
5
2.15
6.69
8.04
4
1.71
2.41
3.25
4.40
5.83
6.88
8.18
km
0
5
10
15
20
200
100
0
km
B

Figure 7. Structural sections based on individual station solutions. A—along trench; B—transverse to trench

ity 4.0 km/sec and zero intercept on a line up the trench wall from station 5.

Station 4, on the shelf near Champerico, is a special case. Layers with velocities of 1.7, 2.4, 3.2, 4.4, and 5.8 km/sec were found above the main crustal layer. The first three layers could be interpreted equally as a single layer with a continuous increase of velocity with depth. The 4.4 km/sec layer is a definite entity as shown by a sharp break in travel-time slope and a long straight plot of arrivals. The 5.8 km/sec layer is strongly shown on one of the reversed lines and one of the unreversed lines but is masked on the other reversed line. The first three layers probably represent sediments of varying stages of compaction. The fourth and fifth layers could, lithologically, be sedimentary rocks or igneous intrusive or extrusive rocks, as could the corresponding basement layer in the deep-sea stations. Vulcanism in the neighboring area of Guatemala and southern Mexico suggests that they may be volcanic rocks.

Main Crustal Layer

Arrivals with velocity between 6 and 7 km/sec were found at every station; the "true velocity" ranged from 6.5 to 6.9 km/sec; the mean of all observations was 6.75 km/sec. This is almost the same as the mean for the main crustal layer in the central Pacific as found by

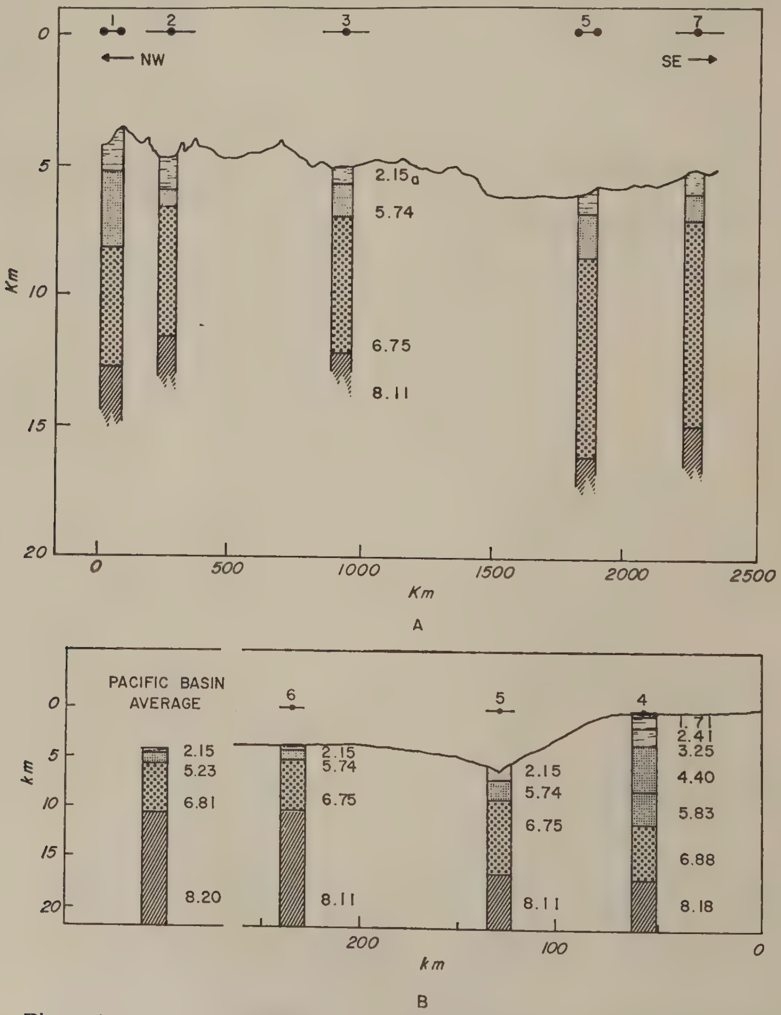
1
2
3
5
7
NW
SE
0
5
10
15
20
Km
2.15a
5.74
6.75
8.11
0
500
1000
1500
2000
2500
Km
A
PACIFIC BASIN AVERAGE
6
5
4
0
5
10
15
20
km
2.15
5.23
6.81
8.20
2.15
5.74
6.75
8.11
2.15
5.74
6.75
8.11
1.71
2.41
3.25
4.40
5.83
6.88
8.18
200
100
0
km
B

Figure 8. Structural sections based on the assumption of regionally uniform velocities. A—along trench; B—transverse to trench

Raitt (1956, p. 1634) and does not differ significantly from values obtained by Ewing and others in the Atlantic. The evidence indicates that this layer is continuous from the deep sea under the trench to at least the outer edge of the continental shelf.

Mantle

Arrivals with mantle velocity were obtained on all stations; computed "true velocity" scatters widely from 7.6 to 8.6 km/sec; the mean of all observations was 8.11 km/sec. This mean is not significantly different from values obtained on either oceanic or continental lines in the past. The scatter in velocities, although it may be real, could be explained by variations in structure along the length of each profile, as could the scatter in velocities in the crust.

Structure

The M discontinuity is depressed beneath the trench. In the central sector (stations 2 and 3) the main crustal layer is not significantly thickened; the depression corresponds only to the deepening of the water and the thickening of the sediments. At the southern trench stations (5 and 7) the crust is thickened. The thickening is not great, however, and does not approach that implied in the tectogene hypothesis. This thickening at the southern stations is independent of the form of layer solution, although regional velocity solutions smooth out the extremes. The section transverse to the trench shows the M discontinuity dipping beneath the trench and then descending only a little more beneath the edge of the shelf. The M discontinuity must be deeper landward.

The crustal thickness beneath the Middle America Trench is not less than that beneath the Pacific basin, and in places it is greater. This is essentially the same conclusion as that derived for the Tonga Trench by Raitt, Fisher, and Mason (1955) and for the Puerto Rico Trench by Officer *et al.* (1957) from seismic data; it does not agree with the interpretation from gravity data for the latter two trenches and others by Worzel and Shurbet (1955) and Talwani, Worzel, and Ewing (1959).

REFERENCES CITED

Fisher, Robert L., 1961, Middle America Trench: Topography and structure: Geol. Soc. America Bull., v. 72 p. 703–720

Katz, S., and Ewing, M., 1956, Seismic-refraction measurements in the Atlantic Ocean. Pt. VII, Atlantic Ocean basin west of Bermuda: Geol. Soc. America Bull., v. 67, p. 475–510

Kuwahara, Susumu, 1939, Velocity of sound in sea water and calculation of the velocity for use in sonic sounding: Hydrog. Rev., v. 16, no. 2, p. 123–140

Officer, C. B., Ewing, J., Edwards, R. S., and Johnson, H. R., 1957, Geophysical investigations in the Eastern Caribbean; Venezuelan Basin, Antilles Island Arc, and Puerto Rico Trench: Geol. Soc. America Bull., v. 68, p. 359–378

Raitt, R. W., 1952, Geophysical measurements in oceanographic instrumentation: Natl. Res. Council of Natl. Acad. Sci. Pub. 309, p. 233

—— 1956, Seismic-refraction studies of the Pacific Ocean Basin. Pt. I, Crustal thickness of the central equatorial Pacific: Geol. Soc. America Bull., v. 67, p. 1623–1640

Raitt, R. W., Fisher, R. L., and Mason, R. G., 1955, Tonga Trench, p. 237–254 *in* Poldervaart, A., *Editor,* Crust of the earth: Geol. Soc. America, Special Paper 62, 762 p.

Talwani, M., Worzel, J. L., and Ewing, M., 1959, Gravity anomalies and crustal section across the Tonga Trench (Abstract): Jour. Geophys. Research, v. 64, p. 1126

Worzel, J. L., and Shurbet, G. L., 1955, Gravity interpretations from standard oceanic and continental crustal sections, p. 87–100 *in* Poldervaart, A., *Editor*, Crust of the earth: Geol. Soc. America Special Paper 62, 762 p.

MANUSCRIPT RECEIVED BY THE SECRETARY OF THE SOCIETY, FEBRUARY 25, 1959
CONTRIBUTION FROM THE SCRIPPS INSTITUTION OF OCEANOGRAPHY, NEW SERIES

(542)

TYPE SPECIMENS OF NORTH AMERICAN PALEOZOIC RADIOLARIA

BY

WILLIAM R. RIEDEL AND HELEN P. FOREMAN

Reprinted from
JOURNAL OF PALEONTOLOGY
Vol. 35, No. 3, May, 1961

pp. 628-632

(543)

TYPE SPECIMENS OF NORTH AMERICAN PALEOZOIC RADIOLARIA

WILLIAM R. RIEDEL AND HELEN P. FOREMAN
Scripps Inst. Oceanography, La Jolla, Calif. and Oberlin College, Ohio

In connection with our current studies of Paleozoic radiolarian assemblages from the Devonian of Ohio (Foreman, 1959) and Western Australia (Glenister & Crespin, 1959) and the Silurian of the Canadian Arctic Archipelago, we have had occasion to examine type material of two assemblages of Paleozoic Radiolaria previously described in the United States (Ruedemann & Wilson, 1936; Aberdeen, 1940). Apart from direct comparisons of the species in these previously described assemblages with forms in our undescribed material, which will be discussed in subsequent papers, we have made certain incidental observations which it seems appropriate to report in this separate note. Our examination of Ruedemann and Wilson's material in the New York State Museum at Albany, N. Y. was made possible by the cooperation of Dr. Donald W. Fisher and his staff, and Aberdeen's material in the Walker Museum of Paleontology at the University of Chicago was kindly loaned to us by Dr. J. Marvin Weller and Matthew H. Nitecki. For one of us (H.P.F.), this represents part of a research project supported by a grant from the Geological Society of America.

At least some of the structures in the Ordovician Normanskill and Deepkill cherts of New York on which Ruedemann and Wilson based their radiolarian descriptions may well represent Radiolaria, but they are not sufficiently well defined to warrant the reconstructions and identifications which those authors made.

Aberdeen's Radiolaria from the Santiago chert member of the Caballos novaculite of Texas, on the other hand, are well preserved and must be taken into account for comparative studies. One of our principal objects in examining this type material was to determine whether certain structures which have recently been found commonly in a few widely separated Silurian to Carboniferous localities might have been overlooked during the original description—namely, members of the genera *Palaeoscenidium* Deflandre and *Ceratoikiscum* Deflandre, and the presence within many of the Sphaerellaria of spicular structures similar to those described by Hinde (1899) as occurring within several species from the Devonian of New South Wales including his *Staurosphaera pusilla* and *Acanthosphaera etheridgei.* We have confirmed that none of these occur in Aberdeen's material.

In searching for Aberdeen's type specimens, we have become aware of some discrepancies between the positions of the type specimens as given in her text, and those indicated in the legends to the plates. We therefore record, under the specific names below, the positions of type specimens as we have found them on the slides. The relative abundances of the species are also noted, together with observations which amplify the original descriptions.

The positions of type specimens were marked by Aberdeen in India ink on the cover glasses or lower surfaces of the slides. Although these markings have been preserved fairly well through the past twenty years, it seems desirable to supplement them by coordinates, the future reliability of which is not so dependent upon careful handling of the slides. For this purpose we have used an England Finder, made by Graticules Ltd., 57/60 Holborn Viaduct, London E.C.1, and distributed in the U. S. by Eric Sobotka Co., 110 West 40th Street, New York 18, N.Y. and Edmund Scientific Co., 101 Gloucester Pike, Barrington, New Jersey. This Finder is a 3″×1″ glass slide on which is centered a grid 73 mm.×24.5 mm. divided into approximately 1 mm. squares (75×25). The squares are marked in such a way that when viewed through a compound microscope the vertical rows are numbered 1 to 75 from left to right, and the horizontal rows are lettered A to Z (excluding 1) from top to bottom. Each square is subdivided

Reproduced by Permission

into five parts, four of which are labelled 1 to 4 and the fifth may be designated 0 (text-fig. 1). When it is wished to record the position of a specimen, the slide bearing the preparation is placed in the holder of a mechanical stage and the desired specimen centered in the field of view. The slide is then removed and replaced by the Finder. The position is recorded according to the numbered and lettered subdivisions of the grid: thus the location of a specimen in a position corresponding to X in text-fig. 1 would be recorded as R39/3. Two adjacent edges of the Finder and the corresponding edges of the slides bearing the specimens are reference edges, and these vary with different mechanical stages: for the purposes of the present work, the reference edges are the short edge of the slide on the observer's right hand, and the long edge nearer the observer. Both Finder and specimen slide are placed on the microscope stage so that their labels (viewed normally, not through the microscope) are in the normal reading position. In the following notes, the positions of specimens follow the slide numbers in parentheses.

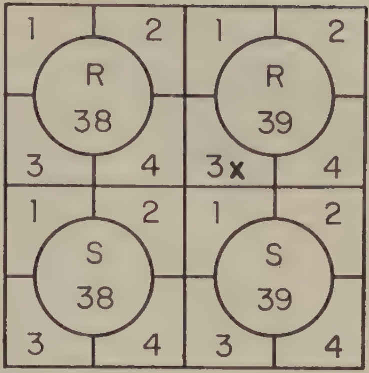

TEXT-FIG. *1*—Portion of the grid of an England Finder. X marks position R39/3.

TYPE SPECIMENS OF ABERDEEN'S RADIOLARIA

References to figures on plates are to those of Aberdeen (1940).

"Thallassicollidae."—Figured specimen (Pl. 20, fig. 1), slide 44537 (K26/0). Other figured specimens (Pl. 20, figs. 2 and 3) not found.

Cenosphaera variabilis.—Syntype (Pl. 20, fig. 17), slide 44496 (M30/3). Unfigured syntype on slide 44997 not found. The figured syntype has at least three spines, two of them broken off and one 60 μ long, arising from tent-like protuberances on the shell surface (text-fig. 2): the bases of the two broken spines are visible in Aberdeen's published figure. The species is apparently rare—the only specimen which we have been able to identify positively is the figured syntype.

Cenosphaera hexagonalis.—Holotype (Pl. 20, fig. 12), slide 44999 (T34/0). Paratype (Pl. 20, fig. 13) on slide 44995 not found. This species is not uncommon. Many specimens have short, acute spines arising from the lattice surface (text-fig. 3; slide 44494, H33/4). The specific name is preoccupied by *Cenosphaera hexagonalis* Haeckel, 1887.

Cenosphaera semiequalis.—Syntype (Pl. 20, fig. 7), slide 44538 (N22/4). Syntype (Pl. 20, fig. 8), slide 44998 (D33/2). The syntype on slide 44538 shows distinctly the bases of three rod-like spines originating from the lattice surface: the other syntype is not sufficiently well preserved to show presence or absence of external spines. Skeletal fragments which may belong to this species are rather common.

Carposphaera magna.—Syntype (Pl. 21, fig. 4), slide 44545 (R27/0). Syntype (Pl. 21, fig. 10), slide 44535 (T27/0). The remaining syntype (Pl. 20, fig. 18) is probably the specimen on slide 44493, at coordinates O43/2 when the slide is turned over so that the cover glass is downward. The ratio of the diameters of inner and outer lattice shells, on the basis of which this species is distinguished from *Carposphaera equalis*, grades to those proportions described as characteristic of the latter species. The specific name is preoccupied by *Carposphaera magna* Rüst, 1892.

Carposphaera equalis.—Syntype (Pl. 20, fig. 4), slide 44532 (F28/3). Syntype (Pl. 20, fig. 5), probably slide 44535 (E30/2). As indicated in the preceding paragraph, it is impossible to distinguish this species reliably from *Carposphaera magna*. Taken together, the two forms are common in the assemblage. Many specimens which apparently belong to this species have rod-like external

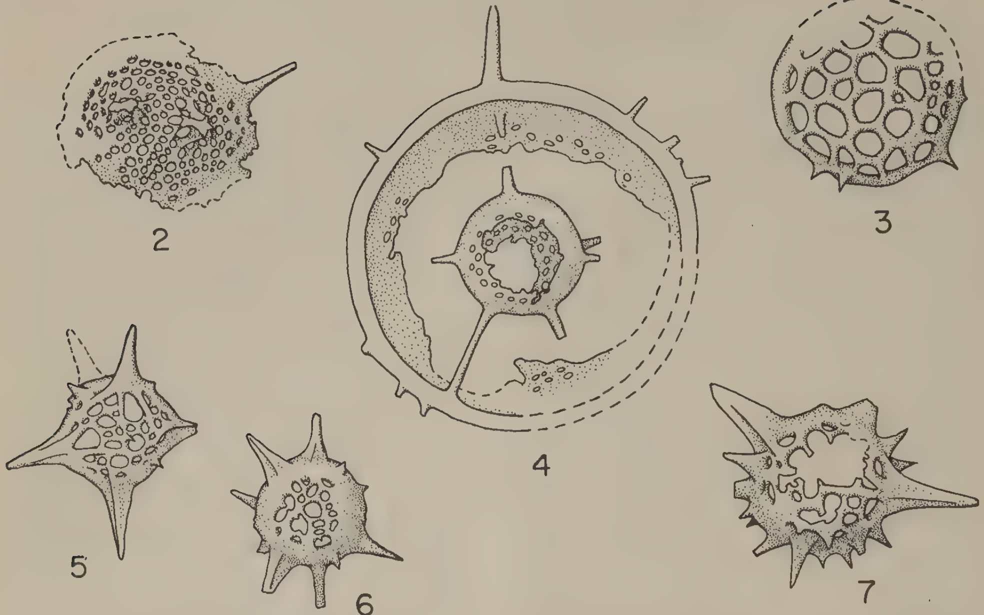

TEXT-FIGS. *2–7*—Radiolaria from Aberdeen's preparations of the Caballos novaculite. All figures ×150. 2, *Cenosphaera variabilis;* 3, *Cenosphaera hexagonalis;* 4, *Carposphaera equalis;* 5, *Hexastylus basiporosus;* 6, *Hexastylidium variatum;* 7, *Heliosphaera macrospinosa.*

spines (text-fig. 4; slide 44491, R22/0).

Thecosphaera hexpenetrata.—Holotype (Pl. 21, fig. 16), slide 44536 (M27/0). The holotype is the only specimen found.

Rhodosphaera sp.—Figured specimen (Pl. 20, fig. 10), slide 44547 (T28/3). It is doubtful that this species can be reliably distinguished from those described in the genus *Spongoplegma.*

Plegmosphaera spiculata.—Holotype (Pl. 21, fig. 3), slide 44532 (Q29/0). Unfigured paratype, probably slide 44497 (B38/0). Apart from the absence of a medullary shell and associated radial beams, this form resembles those described in the genus *Spongoplegma.* Specimens lacking these inner structures are common, but it is doubtful whether this is significant or whether it is due to vagaries of the type of preservation of the radiolarians in this material—coating or replacement of the original silica by iron oxide.

Spongoplegma brevisphaera.—Syntype (Pl. 21, fig. 17), slide 44542 (N32/4). Unfigured syntype, probably slide 44538 (L33/4). The specimen believed to be the unfigured syntype has distinct radial beams between the inner and outer surfaces of the spongy cortical region: these are shorter than those described for *Spongoplegma longispinosa,* but otherwise similar.

Spongoplegma longispinosa.—Syntype (Pl. 20, fig. 6), slide 44546 (H42/2). Syntype (Pl. 21, fig. 1), slide 44998 (R32/0). The width of the spongy region, and the length of the radial beams within it, are variable between those described for this species and for *Spongoplegma brevisphaera.* Taking these two species together, they are common in the assemblage.

Xiphostylus inclinatus.—Syntype (Pl. 21, fig. 7), slide 44548 (E43/1). Syntype (Pl. 21, fig. 8), slide 44494 (H36/0). This species is apparently not uncommon, though it is of course impossible to recognize except in those sections which are longitudinal.

Stylosphaera quasiobtusa.—Syntype (Pl. 21, fig. 5), slide 44544 (S34/4). Unfigured syntype, probably slide 44998 (M26/0). Besides the syntypes, three specimens were found.

Staurostylus varispinatus.—Holotype (Pl.

20, fig. 19), slide 44997 (P40/3). The holotype is the only specimen found. The classification of this specimen is regarded as quite doubtful, because the object which Aberdeen regarded as the short spine might equally well be a fortuitously apposed dark grain of inorganic origin.

Staurosphaera rotunda.—Holotype (Pl. 20, fig. 11), slide 44548 (P36/3). As the specimen is incomplete, its determination as a staurosphaerid rather than a cubosphaerid seems somewhat doubtful. The holotype is the only specimen found.

Staurodoras brevispinosa.—Holotype (Pl. 21, fig. 11), slide 44546 (M34/3). The lattice shell is thick-walled, but we see no evidence that it is spongy as described. Most of the pores of the lattice-shell are approximately 5 μ in diameter. The holotype is the only specimen found.

Hexastylus basiporosus.—Syntype (Pl. 21, fig. 6), slide 44546 (J42/3). Syntype (Pl. 21, fig. 9), slide 44542 (N37/2). Syntype (Pl. 21, fig. 13), slide 44495 (R24/3). Unfigured syntype, possibly slide 44549 (Q36/4). Unfigured syntype, probably slide 44537 (Q37/4). This species is common. Many specimens have by-spines arising from the lattice shell (text-fig. 5; syntype figured by Aberdeen on Pl. 21, fig. 13) and thus approach *Heliosphaera macrospinosa*. The number of main-spines is not constantly six, but may also be five or seven. Diameter of lattice shell generally 90–120 μ.

Hexastylidium variatum.—Holotype (Pl. 21, fig. 14), slide 44545 (S39/3). It is impossible to reconcile the description of this species with the specimen figured as its holotype. Examination of both sides of the holotype reveals that six or perhaps seven, almost complete spines (each approximately 35 μ long) are present, together with the bases of at least two others (text-fig. 6: the structure which may be a seventh complete spine is not visible in this figure, as it is on the side of the specimen away from the observer).

Hexalonche sp.—Figured specimen (Pl. 20, fig. 9), slide 44997 (N37/2). The figured specimen is the only one found. It is not sufficiently well preserved to permit its certain identification as *Hexalonche*.

Acanthosphaera dodecaspinosa.—Syntype (Pl. 21, fig. 2), slide 44538 (028/0). Syntype (Pl. 21, fig. 15), slide 44535 (P29/1). Syntype (Pl. 21, fig. 18), slide 44548 (L25/0). In many specimens, the lengths of the spines approximate or exceed the diameter of the lattice shell. This species is apparently common: most of the specimens are fragmentary.

Acanthosphaera microspinosa.—Holotype (Pl. 20, fig. 21), slide 44535 (M34/4). Spines on the holotype range up to 40 μ in length. The species is rather common.

Acanthosphaera hirsuta.—Holotype (Pl. 21, fig. 12), slide 44543 (T36/4). This species is rather common.

Acanthosphaera grandispinosa.—Holotype (Pl. 21, fig. 19), slide 44547 (J28/1). The holotype is the only specimen positively identified.

Heliosphaera macrospinosa.—Holotype (Pl. 20, fig. 14), slide 44498 (F36/2). Examination of the holotype, particularly the side opposite that from which Aberdeen's photograph was taken (text-fig. 7), shows that this species closely resembles *Hexastylus basiporosus* with strongly developed by-spines. This species, if it be distinguished from *H. basiporosus* by its strongly developed by-spines, is rather common. Diameter of the lattice shell generally 95–120 μ.

Heliosphaera alternata.—Holotype (Pl. 20, fig. 22), slide 44545 (N28/0). Two of the main-spines of the holotype are about 220 μ long. Several specimens of this species were found.

Haliomma perfecta.—Syntype (Pl. 20, fig. 20), slide 44546 (Q35/0). Syntype (Pl. 20, fig. 16) not found. Unfigured syntype on slide 44537 not found. Few specimens of this species were found.

Astrophacus cingulatus.—Holotype (Pl. 20, fig. 15), slide 44996 (C34/2). The holotype is the only specimen found. There is no strong evidence for the outer shell being lenticular rather than spherical: if it is spherical, this species may be the same as *Carposphaera equalis*.

LITERATURE CITED

ABERDEEN, ESTHER, 1940, Radiolarian fauna of the Caballos formation, Marathon Basin, Texas: Jour. Paleontology, v. 14, no. 2, p. 127–139, pls. 20, 21, 2 text-figs.

FOREMAN, H. P., 1959, A new occurrence of Devonian Radiolaria in calcareous concretions of the Huron member of the Ohio Shale: Jour.

(547)

Paleontology, v. 33, no. 1, p. 76–80, pl. 15.

Glenister, B. F., & Crespin, Irene, 1959, Upper Devonian microfaunas from the Fitzroy Basin, Western Australia: Australian Jour. Sci., v. 21, no. 7, p. 222–223.

Hinde, G. J., 1899, On the Radiolaria in the Devonian rocks of New South Wales: Geol. Soc. London, Quart. Jour., v. 55, p. 38–63, pls. 8, 9.

Ruedemann, Rudolf, & Wilson, T. Y., 1936, Eastern New York Ordovician cherts: Geol. Soc. America Bull., v. 47, p. 1535–1586, pls. 1–7, 2 text-figs.

Contribution from Scripps Institution of Oceanography.

Manuscript received June 9, 1960

(548)

Made in United States of America
Reprinted from Limnology and Oceanography
Vol. 6, No. 2, April, 1961
pp. 205–215

ON THE RESPONSE TO CHANGING TEMPERATURE OF THE TEMPERATURE-LIMITED PLANKTER *DOLIOLUM DENTICULATUM* QUOY AND GAIMARD 1835[1]

Leo D. Berner and Joseph L. Reid, Jr.
Scripps Institution of Oceanography, University of California

ABSTRACT

D. denticulatum is limited at the lower end of its temperature range by temperature values of about 14° to 15°C. In the Pacific it inhabits the subtropical anticyclonic gyres and the area between them. It is carried southeastward past California and Baja California and is spread into the California Current system by horizontal mixing. It survives where the water carries it if temperatures are suitable. The seasonal movements of the isotherms are so rapid that the organism does not at any time inhabit all favorable areas and it may be overtaken in some months by unfavorable environments. In the period from 1949 through 1955, its seasonal movement was to the north in summer and to the south in winter. Its range of spatial fluctuation was less than that of its critical temperature. In the warmer period beginning in 1957, it has lived closer to the coast in late fall and has been more generally distributed in the cooler part of its range than in the earlier years. It has been carried northward by the winter coastal countercurrents and southward again in late spring with the cold upwelled water. The direction of its seasonal fluctuation has thus been reversed in the warmer years.

INTRODUCTION

During the latter part of 1957, the temperature in the upper mixed layer of the California Current system rose approximately 1°C above the average of the previous 8 years and remained high through December of 1959 at least. This presented an opportunity to test the temperature responses of various organisms to a new environment. One of these organisms, *Doliolum denticulatum*, has proved especially interesting. It is the purpose of this paper to describe the general distribution of the species, its temperature limitations and its normal seasonal fluctuations in the earlier years and to discuss its peculiar responses during the latter period.

METHODS

The plankton samples and the hydrographic data used in this study were collected off the west coast of California and Baja California, Mexico, on cruises of the California Cooperative Oceanic Fisheries Investigations (CCOFI) and on other cruises in the region. The nets used in the collection of the plankton samples were made of No. 30 xxx grit gauze (0.65 mm mesh size), conical in shape, with a one-meter mouth opening. The last 40 cms and cod-end bags were made of No. 56 xxx grit gauze (0.31 mm mesh size). Tows were oblique from either 70-m depth (1949–50) or 140 m (after 1950). Each net was equipped with a flow meter, which allowed the amount of water filtered to be calculated. Detailed descriptions of the nets, methods used in making the plankton tows and generalized station patterns are given by Ahlstrom (1948, 1952 and 1954).

Extensive plankton sampling in the area under consideration was started in March of 1949. There were very few data or samples available previous to that time. The NORPAC Cruise (NORPAC Committee 1960) made in August and September 1955 has been used to establish the offshore distributions beyond the usual area sampled by CCOFI cruises.

All of the samples from 24 of the CCOFI cruises, alternate samples from 6 others, and samples from the pertinent areas from 10 others have been examined. In all, samples from 2,961 stations, not including the NORPAC material, have been examined. *D. denticulatum* was present at 1,230 of them.

---

[1] Contribution from the Scripps Institution of Oceanography: New Series, 1281.

(549)

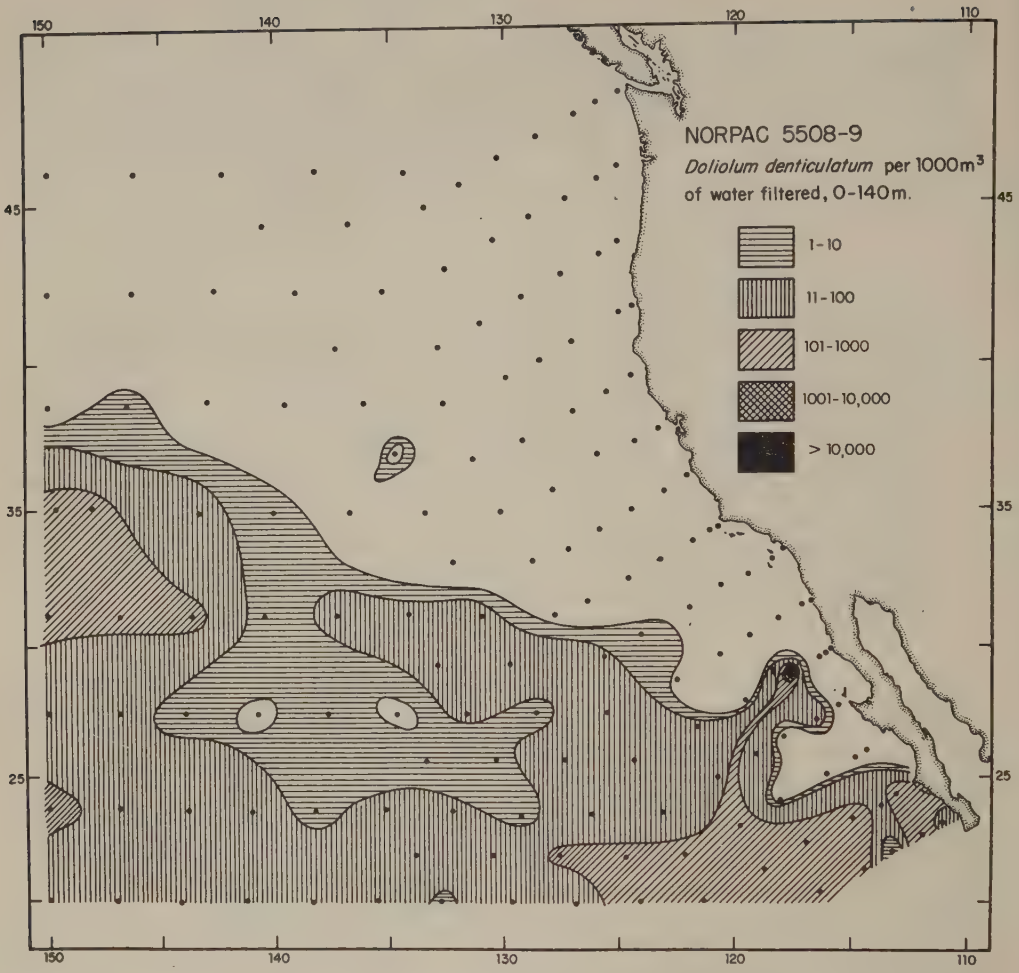

FIG. 1. Distribution of *Doliolum denticulatum* in August and September 1955 (the NORPAC expedition).

HORIZONTAL DISTRIBUTION

D. denticulatum has been found in subtropical waters near Australia (Thompson 1948), in the western equatorial Pacific by the Siboga expedition (Ihle 1910), in the Kuroshio (Tokioka 1937), north of Hawaii in the NORPAC collections of the Bureau of Commercial Fisheries Honolulu Biological Laboratory (unpublished data), in SHELLBACK sections across the equator (unpublished data) and in the area between the Californias and Hawaii (Fig. 1). These observations indicate that the species inhabits the subtropical anticyclonic gyres of the North Pacific (Kuroshio, Westwind Drift, California Current, and North Equatorial Current) and the South Pacific (East Australia Current, Westwind Drift, Peru Current, and South Equatorial Current) and the waters between these two gyres. *D. denticulatum* moves with these systems, constantly spreading outward from its permanent central concentrations. This study is limited to the California Current system; the NORPAC data (Fig. 1) are sufficient to describe the pertinent part of the general habitat of *D. denticulatum*. The long series of CCOFI data can be used to

TABLE 1. *Vertical distribution of* D. denticulatum *at 79 stations; numbers per 1000 m³ of water filtered*

Depth (m)	Min. number	Quartile based on 0–131 m			Max. number
		1st	2nd	3rd	
0–131	2	14	38	133	34,617
131–262	0	0	0	0	20

Whenever *D. denticulatum* was present in a deep tow it was also taken in the associated upper tow.

TABLE 2. *Vertical distribution of* D. denticulatum *(average of 6 stations)*

Depth (m)	No. of samples	No/1000 m³	Temp. (°C)
0–25	6	97	18.8
25–50	5	34	19.1
50–75	5	18	18.2
75–100	6	12	17.7
100–300	3	2	11.0

examine its temperature dependence in that area.

VERTICAL DISTRIBUTION

All data where depth range can be determined indicate that *D. denticulatum* is found primarily in the upper 100 m of the water column, with the major portion of the population in the upper 50 m. The vertical distribution of the species found during the NORPAC Cruise is given in Table 1.

The vertical distribution of the species is shown in more detail by an analysis of 6 stations taken on a cruise southwest of San Diego in May 1954. Three of these stations were occupied during daylight hours and three at night.

The species is small, ranging up to 8 mm, and its swimming movements at best can be described as weak. It is also restricted to the shallow depths (Tables 1 and 2), mostly above the depth of the winter thermocline, and as an indicator of surface flow may be better than those organisms which undergo extensive vertical migration or have a greater depth range.

THE LIMITING EFFECT OF TEMPERATURE

The subtropical and shallow distribution of *D. denticulatum* suggests that temperature may be limiting. Since the organism is most abundant in the upper mixed layer we have chosen the temperature at 10 m below the surface as an index of its environment. The value at 10 m differs from the value at the surface by small amounts near the coast in the late summer months. Later we shall refer to anomalies of surface temperature, since data in this form are more readily available and since these anomalies have been shown to extend throughout the mixed layer (Reid 1960).

The CCOFI cruises cover an area with a broad range of temperature, but the nature of the program is such that, at most of the stations taken, the 10-m temperature lies between 12 and 19°C (Fig. 2). In the cruises discussed here, the greatest numbers of stations were found in the 14–15°, 15–16° and 16–17° ranges, but the greatest percentages of stations at which *D. denticulatum* was found were at higher temperatures. If one considers the ratio of stations at which it was found to all stations in each 1°C-interval (Fig. 3) there is a rapid rise between 12 and 16°C and above 16°C the ratio is consistently high. *D. denticulatum* is found in much warmer water, and these

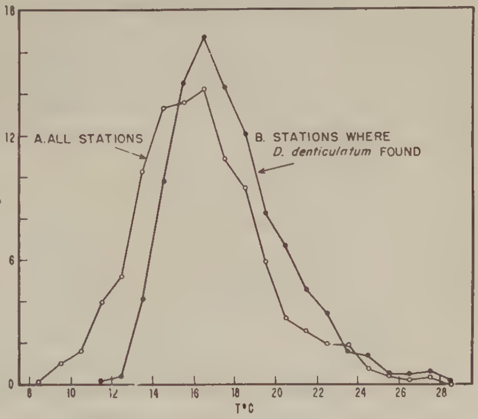

FIG. 2

A. Classification of the samples by the temperature at 10 m depth at the sampling position. The ordinate is the percentage of the 2,961 samples within the 1°C classes.

B. Classification of the 1,230 samples at which *D. denticulatum* was found.

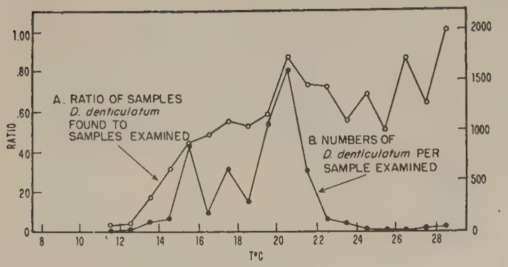

Fig. 3

A. Ratio of samples in which *D. denticulatum* was found to samples examined.

B. Average numbers of *D. denticulatum* per sample per 1,000 m^3.

data do not suggest an optimum or an upper limiting temperature.

The numbers of *D. denticulatum* per station in the 1°C-intervals, and the ratio of stations where the organism is found appear to be unrelated to temperature above 22°C. In that range the concentrations are low but the ratios are high. This may be taken to imply that the species, though generally distributed in the region of high temperatures (most of the high temperature data are from south of Punta Santa Eugenia), is limited in abundance there by other factors.

We believe, however, that the species is limited by temperatures less than about 14–15°C. The lowest 10-m temperature at which *D. denticulatum* was found was 11.8°C, but rather small numbers are found below 14–15°C (Fig. 3).

MOVEMENT OF THE ISOTHERMS

A planktonic organism moves with the water and survives where conditions are suitable. If one environmental factor alone limits an organism then the distribution of that factor will describe the areas favorable for its survival. Organisms, however, will not enter suitable areas if currents are adverse or if the favorable conditions appear and disappear too rapidly. The seasonal movements of isotherms in the mixed layer, for example, are in most cases very rapid compared to processes of advection and diffusion and may have a limiting effect on organisms.

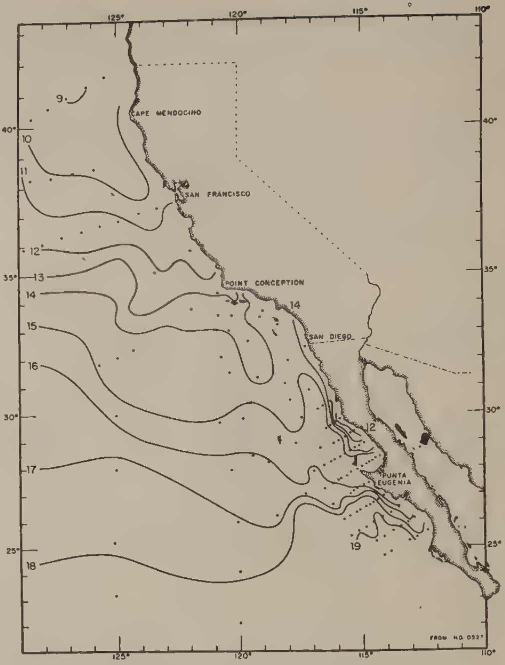

Fig. 4. Temperature at a depth of 10 m in March based on data from several years.

The California Current system offers certain curious illustrations of the combined effects of the seasonal changes of current and temperature. The currents well offshore generally flow southeastward and carry water colder and less saline than that to the west. Between 25° and 35°N a tongue of colder water is generally found extending southeastward (Figs. 4 and 5). The inshore currents flow southeastward from March through October and northwestward from November through February. Isotherms in these latitudes normally move northward during the period of high radiation from March through September and southward in the other months. Upwelling, which occurs north of 35°N in summer, reduces the coastal temperatures well below the latitudinal average. The coastal currents flow north during the period of falling temperatures and south during the period of rising temperatures. The 10-m temperatures in March and August are illustrated in Figures 4 and 5. A rapid northward movement of some iso-

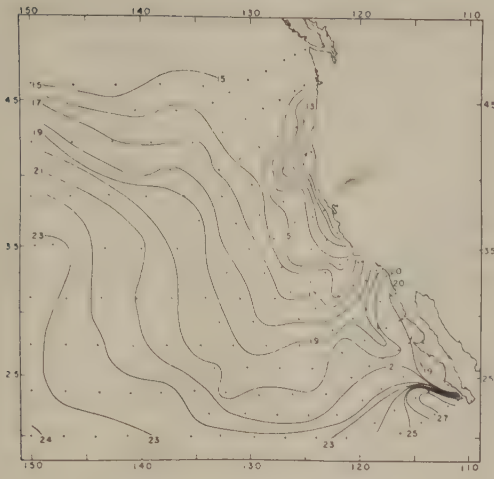

FIG. 5. Temperature at a depth of 10 m in August, 1955. Data are from the CCOFI part of the NORPAC expedition.

therms is indicated. That part of the change from May to August is faster still. The coastal end of the 18°C isotherm, for example, moves northward at about 6 miles per day. If the southerly flow of the water is taken conservatively as a quarter-knot, the average speed of the isotherm through the water is 12 miles per day during three months.

Conversely, the most rapid southerly movement of the 18°C isotherm occurs as the result of the winter cooling of the surface waters from November to February. This movement amounts to about 4 miles per day although the water is moving northward near shore at that time of year.

SEASONAL VARIATION OF *D. DENTICULATUM*

D. denticulatum normally lives in the southwestern part of the California Current system. It is continually supplied to the area from the northwest and swept away to the south by prevailing currents. As in any concentration the processes of horizontal mixing tend to spread the species outward from the permanent concentrations to the west. As inshore areas become favorable in temperature, for example, the species will tend to spread into them. If the areas change in temperature rapidly the rate of mixing and flow may not be able to keep up, so that at any time there may be uninhabited favorable areas or areas which have become unfavorable, but from which the species has not yet been entirely eliminated.

In such a regime the rapid seasonal movement of the isotherms may cause large monthly shifts in the boundaries of the favorable environment, and the seasonal adjustments of the species may lag.

In the period from 1949 through 1955, *D. denticulatum* showed fairly regular seasonal changes. In 1949, it was least abundant and farthest south in March and most abundant and farthest north in September (Fig. 6A, B, C,). If one compares the distributions with the position of the 14°C isotherm at a depth of 10 m in the various months it may be seen that in March (approximately the seasonal minimum of temperature) the northern limit of the species is aligned rather closely with this temperature but has been slightly over-run by the rapid southerly movement of the isotherm. (The position of the 14°C isotherm is determined not only from the hydrographic station data where the net tow was made but from the intermediate bathythermograph data as well. The isotherm therefore may have a more complex shape than the other isopleths.)

Between March and June upwelling begins with a strong offshore movement of the surface waters north of Point Conception. This opposes any rapid northward movement of *D. denticulatum*, although the increased radiation has raised the temperature and moved the 14°C isotherm well to the north. By September the processes of horizontal mixing have extended the northern distribution more than 200 miles closer to the coast where it takes advantage of part of the vast area of warmer water which has appeared since March. It is presumed that the upwelled water that continues to flow southward from the area above Point Conception represents both a velocity and low-temperature barrier, which the species usually cannot cross to reach the warmer inshore waters.

The most northward coastal observation of *D. denticulatum* in the period 1949–1955

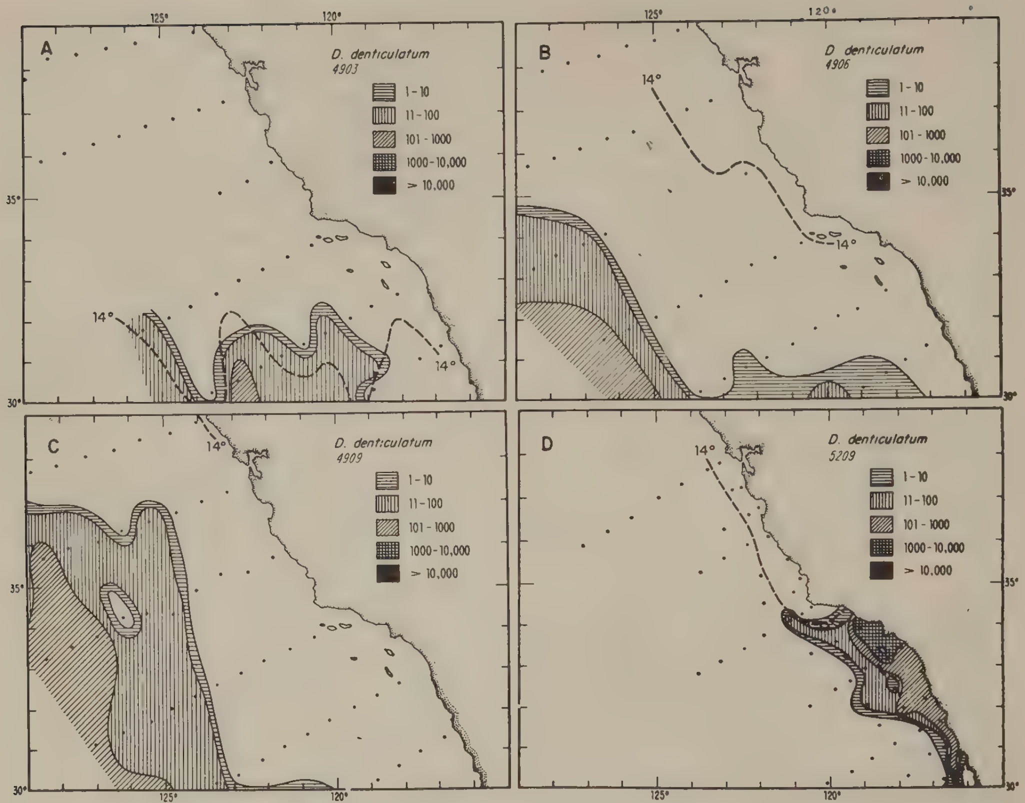

Fig. 6. Distribution of *D. denticulatum* in March (4903), June (4906) and September (4909) of 1949 and in September of 1952 (5209). Units are numbers per 1000 m^3 of water filtered. The dashed line represents the position of the 14°C isotherm at a depth of 10 m.

was in September of 1952, when it reached Point Conception (Fig. 6D). The temperature, however, was already falling at this time and no specimens were found in the October samples from that area.

The small extent of the seasonal fluctuations described by Figure 6 may be only the consequence of this particular system, in which seasonal fluctuations of coastal currents and temperature are in opposite phase. The species cannot adjust as rapidly as the changing environment and is constantly being overtaken by favorable or unfavorable conditions. Its northward movement in summer and its southward movement in winter are further retarded by the motion of the water, which is most strongly southward and offshore in summer and least so in winter.

NON-SEASONAL VARIATIONS OF TEMPERATURE

The years from 1949 through 1956 were of course not identical in temperature, in distribution of organisms or in perhaps any other item measured by CCOFI. Comparison with previous periods (mostly shore station data) and subsequent CCOFI measurements suggest that with regard to temperature these 8 years had certain common features which distinguished them from other years and from the long-term mean which was determined from the years 1920–1938 (Reid, Roden and Wyllie 1958). From 1949 through 1956 the spring temperatures were lower than the mean by about 0.5°C and the late fall values were higher than the mean by a smaller amount all along the coast between 25° and 40°N.

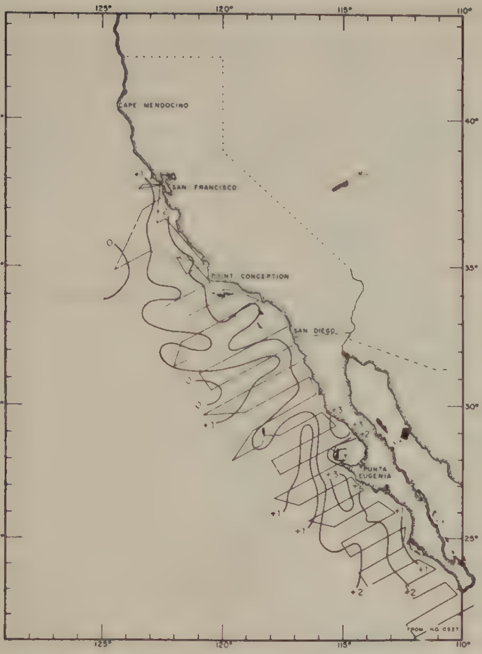
125°
120°
115°
110°
40°
35°
30°
25°
CAPE MENDOCINO
SAN FRANCISCO
POINT CONCEPTION
SAN DIEGO
PUNTA EUGENIA
0
+1
+2
+3
FROM H.O. 0527

FIG. 7. Surface temperature anomaly in January 1958. (Surface temperature in January 1958 less the mean January temperature 1949–1954.)

Since the mean values were from coastal data a new mean was defined from the CCOFI cruises for the years 1949 through 1954, and the years since 1956 have been compared with it, offshore as well as at the coast. Compared with this 1949–1954 mean, the late 1957 and earlier 1958 surface temperatures were found to be high by about 1°C (Reid 1960) and later unpublished data reveal that this period of high temperature has persisted at least through December 1959.

This anomaly is concurrent with certain changes in the circulation that might also be important to *D. denticulatum.* Upwelling north of Point Conception was reduced in the summers of 1958 and 1959 and the countercurrent was more strongly developed in winter (Reid 1960). The temperature anomaly from the 1949–1954 January mean and the geostrophic flow and drift bottle recoveries for January 1959 are shown in Figures 7, 8 and 9.

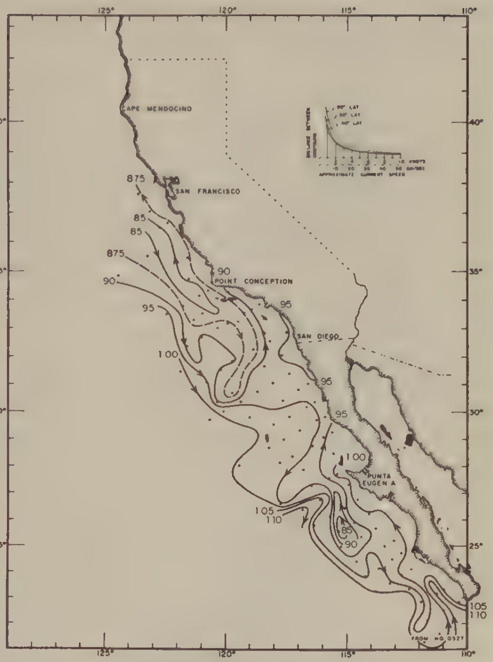
125°
120°
115°
110°
40°
35°
30°
25°
CAPE MENDOCINO
SAN FRANCISCO
POINT CONCEPTION
SAN DIEGO
PUNTA EUGENIA
875
85
90
95
100
105
110
APPROXIMATE CURRENT SPEED
FROM H.O. 0527

FIG. 8. Geostrophic current in January 1958. (Geopotential anomaly of the zero-decibar surface with respect to the 500-decibar surface, in dynamic meters. The velocity scale is drawn for a contour interval of 0.05 dynamic meters.)

NON-SEASONAL VARIATIONS OF *D. DENTICULATUM*

The effect of these changes in temperature and circulation in redefining the favorable environment has been not only to bring *D. denticulatum* farther inshore but to allow it to extend across the colder tongue and in to the coast at about 32°N. It not only survived inshore of the Channel Islands (Fig. 10) but advanced northward with the winter countercurrent as far as San Francisco Bay in January. It remained far north until the countercurrent ceased and then was swept slowly south and west as upwelling began (Figs. 10 and 11).

Among the March samples, the 4 innermost of the northern line included larvae of the intertidal sand crab *Emerita analoga*, which must have come from very close inshore. They indicate an offshore movement of water (Johnson 1939). The *D.*

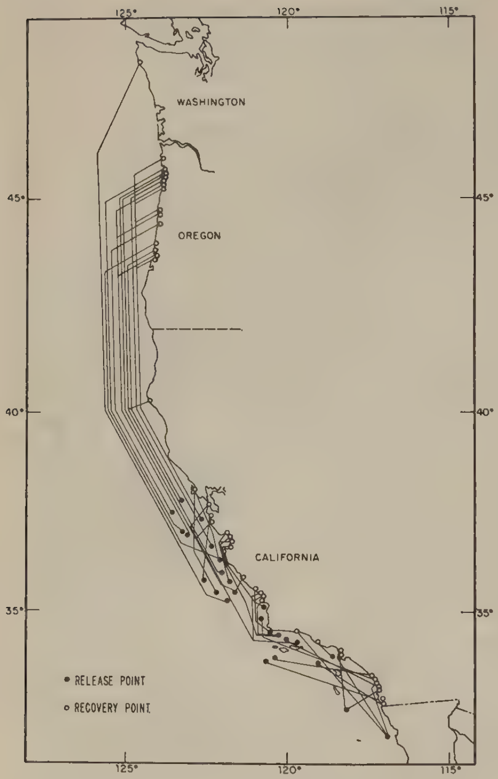

FIG. 9. Recovery points of drift bottles released in January 1958.

denticulatum specimens may have come either with these larvae from farther north (where they were found in January) or eastward by mixing from the offshore concentration.

Ordinarily it would seem curious that a temperature-limited plankter should move northward in winter, as temperatures fall, and southward as temperatures rise. In the earlier years (1949–1955) no such movements were observed. *D. denticulatum* was usually kept offshore by the current and the cold tongue; when it did cross the tongue, as in September of 1952, it could not survive more than a month.

In the presence of the warmer water of 1957–58, *D. denticulatum* crossed the area usually occupied by the cold tongue, survived and was later carried northward by the countercurrent. As upwelling began the northern part of the population did not retreat to the southwest but was swept away from the coast and to the south (Figs. 10 and 11). This same phenomenon may explain part of the offshore distribution found in March. The species was thus carried from the northern area in May and June even though the temperatures remained high.

The period of high temperature in the California Current persisted at least through December of 1959. This allowed the hypothetical relation between *D. denticulatum* and the temperature and currents to be tested twice more. Not all of the samples from every cruise since June of 1958 have been examined, but a check of samples taken in October 1958, January, October, and November of 1959 has found *D. denticulatum* in the inshore area north of Point Conception in each month.

Although temperatures north of Point Conception have risen in the latter period, they are still relatively low in terms of the animal's range. The northward movement of the animal has in fact changed its distribution with temperature. In Figure 12 the ratio of samples with *D. denticulatum* to total samples is plotted separately for the period 1949–1955 (2,207 samples, 747 with the animal present) and for 1957–1958 (754 stations, 483 with the animal present). A marked rise in the ratio is seen near the cooler part of the range in the latter period, but the range is not extended nor its previous limit reached. Curiously, the animal has been more generally distributed in the colder water in the warmer years. The authors suggest that this also is a consequence of the warming and weakening of the cold tongue south of Point Conception, which has allowed the animal to extend into the seasonally northward-flowing water, whose temperature, though low, is not beyond the range tolerable to the animal.

SUMMARY

D. denticulatum inhabits the central subtropical anitcyclonic gyre, which includes the outer part of the California Current. The species is maintained in the areas offshore from California and Baja California by this system, and is carried inshore by

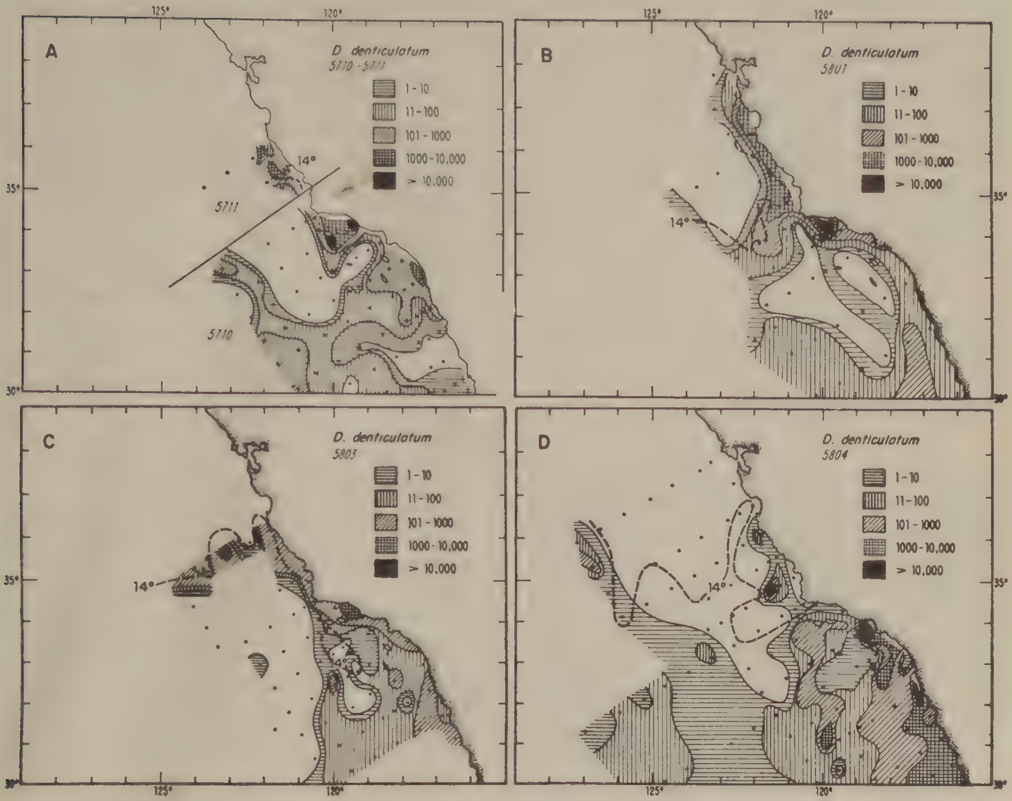
A
D denticulatum
5710 -5711
1-10
11-100
101-1000
1000-10,000
> 10,000
14°
5711
5710
B
D. denticulatum
5801
14°
C
D. denticulatum
5803
14°
D
D. denticulatum
5804
14°
125°
120°
35°
30°

FIG. 10. Distribution of *D. denticulatum* in October–November 1957 (5710–5711), January 1958 (5801), March 1958 (5803) and April 1958 (5804). Units are numbers per 1000 m^3 of water filtered. The dashed line represents the position of the 14°C isotherm at a depth of ten meters.

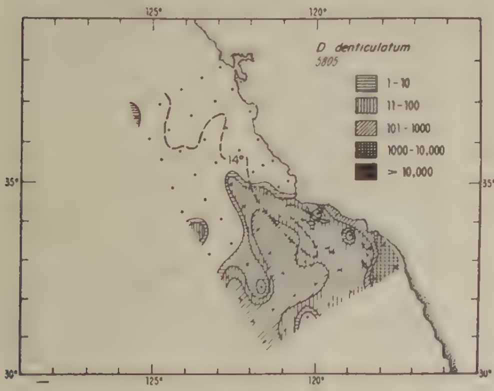
D denticulatum
5805
1-10
11-100
101-1000
1000-10,000
> 10,000
14°
125°
120°
35°
30°

FIG. 11. Distribution of *D. denticulatum* in May 1958 (5805). Units are numbers per 1000 m^3 of water filtered. The dashed line represents the position of the 14°C isotherm at a depth of ten meters.

horizontal mixing processes. It survives in such favorable areas as it enters, but the areas of favorable environment fluctuate so rapidly with season that at any time the organism may not inhabit all of the favorable areas. It may also be overtaken by unfavorable conditions. It is severely limited by low temperature (about 14° to 15°C) and it is the rapid movement of isotherms near these temperatures which accounts for the environmental changes. The species' limited ability to adjust its position with these changes probably accounts for its rather small seasonal fluctuation, since in the greater part of the year the coastal waters move in a direction opposite to the motion of the isotherms.

The species can, however, be distributed into regions that remain favorable for sev-

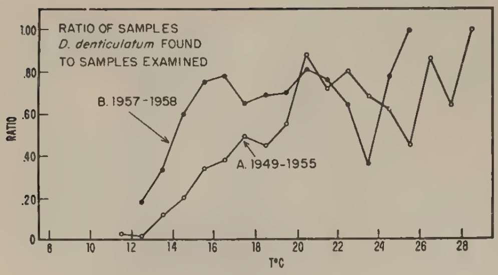

Fig. 12

A. Ratio of samples in which *D. denticulatum* was found to samples examined in the period 1949–1955.

B. The ratio in 1957–1958.

eral months, and the winter seasons of 1957–58, 1958–59 and 1959–60 represent longer period changes of environment to which the organism has more successfully adjusted. Its northward movement has not been into water colder than its previous range, but the northern water does represent the cooler part of its range. Its distribution in the warmer period has thus been shifted toward the cooler part of its range.

D. denticulatum is of particular interest as an example because of its critical temperature limit. Temperatures in the California Current system have changed in the period 1957–59 in such a fashion that inshore the seasonal fluctuation of the species has reversed, and it is farthest north in winter. Organisms critical to higher temperatures might not show this reversal; organisms critical to lower temperatures might show it every year.

ACKNOWLEDGMENTS

The research leading to the results described in this paper was conducted under the Marine Life Research Program, the Scripps Institution of Oceanography's component of the California Cooperative Oceanic Fisheries Investigations, a project sponsored by the Marine Research Committee of the State of California.

The authors are indebted to Mr. G. I. Murphy and to Dr. E. H. Ahlstrom for various suggestions and for the interest they have shown in discussing various points.

REFERENCES

Ahlstrom, E. H. 1948. A record of pilchard eggs and larvae collected during surveys made in 1939 to 1941. U. S. Dept. of Int., Fish and Wildl. Serv., Spec. Sci. Rept. Fish., **54**, 76 pp.

———. 1952. Pilchard eggs and larvae and other fish larvae, Pacific Coast 1950. U. S. Dept. of Int., Fish and Wildl. Serv., Spec. Sci. Rept. Fish., **80**, 58 pp.

———. 1954. Pacific sardine (Pilchard) eggs and larvae and other fish larvae, Pacific Coast 1952. U. S. Dept. of Int., Fish and Wildl. Serv., Spec. Sci. Rept. Fish., **123**, 76 pp.

Anonymous. 1958. 1957: The year of warm water and southern fish off California Coast. Comm. Fish. Rev., **20**(9): 15–24.

Fraser, J. H. 1949. The distribution of Thaliacea in Scottish waters 1920–1939. Scot. Home Dept., Fish. Div. Sci. Invest., **1**: 1–44.

Ihle, J. E. W. 1910. Die Thaliaceen (einschliesslich Pyrosomen) der Siboga-Expedition. (*In*) Siboga-Expeditie Monogr. 56d, pp. 1–55.

Johnson, M. W. 1939. The correlation of water movements and dispersal of pelagic larval stages of certain littoral animals, especially the sand crab, *Emerita*. J. Mar. Res., **2**: 236–245.

Krüger, H. 1939. Die Thaliaceans der "Meteor" Expedition. Wiss. Ergeb. Deuts. Atlantische. Exped. "Meteor" 1925–27, **12**(2): 111–152.

Newmann, G. 1906. Doliolum. Wiss. Ergeb. Deuts. Tiefsee-Exped., **12**(2): 93–243.

NORPAC Committee. 1960. Oceanic Observations of the Pacific: 1955, the NORPAC DATA; 1955, The NORPAC ATLAS. University of California Press and University of Tokyo Press.

Reid, J. L., Jr. 1960. Oceanography of the Northeastern Pacific Ocean during the last ten years. (*In*) The Changing Pacific Ocean in 1957 and 1958, O. E. Sette and J. D. Isaacs, (Eds.) pp. 77–90.

———, G. I. Roden and J. G. Wyllie. 1958. Studies of the California Current System. California Cooperative Ocean. Fish. Invest. Prog. Rept. 1 July 1956—1 January 1958. pp. 27–56.

Russell, F. S. and J. S. Colman. 1935. The Zooplankton IV. The occurrence and seasonal distribution of the Tunicata, Mollusca and Coelenterata. Brit. Mus. (Nat. Hist.) Gt. Barrier Reef Exped. 1928–29, Sci. Rept., **2**: 207–234.

SETTE, O. E. AND JOHN D. ISAACS. (ed.) The Changing Pacific Ocean in 1957 and 1958 (Rancho Santa Fe Symposium). Calif. Coop. Ocean. Fish. Invest., **7**: 14–217.

THOMPSON, HAROLD. 1948. Pelagic tunicates of Australia. Commonwealth Couns. for Sci. and Indus. Res. Australia, 196 pp.

TOKIOKA, T. 1937. Notes on the salpas and doliolums occurring on the Pacific Coast of Middle Japan. Annot. Zool. Japan, **16**(3): 219–232.

UNIVERSITY OF CALIFORNIA, SCRIPPS INSTITUTION OF OCEANOGRAPHY. 1958. Physical and Chemical Data Reports, Calif. Coop. Ocean. Fish. Invest. Cruises 5804 and 5805.

Made in United States of America
Reprinted from Limnology and Oceanography
Vol. 6, No. 2, April, 1961
pp. 222–226

YEARLY CHANGES IN THE PERU CURRENT

by Warren S. Wooster

YEARLY CHANGES IN THE PERU CURRENT[1]

The scientific investigation of the Peru Current in the past has been a sporadic effort, punctuated by the occasional visit of a British, American or other foreign research vessel, followed in a decade or two by a flurry of scientific reports. The systematic observation of changes in the current system, so essential to an eventual understanding of its normal and abnormal functioning, has been almost nonexistent. Fortunately, nearly 20 years ago, Dr. Erwin Schweigger of the Peruvian Compañia Administradora del Guano had the foresight to initiate the collection and compilation of sea-surface temperature and weather observations from Peruvian vessels, so that there exists, sparse though it may be, a record of ocean changes since the year 1939.

The accumulated data have been published (in the recently discontinued *Mapas Mensuales* of the Guano Administration) by half-degree squares, in most of which too few data are available to permit the calculation of meaningful averages. However, along the coastal shipping routes it is possible to select for each parallel of latitude a one-degree square containing the maximum number of observations (Fig. 1). I have calculated mean surface temperatures for these squares for each month of each year for the period 1939 through 1956. As shown by the inset, the annual range of temperature varies from about 4°C at 12°S to nearly 6°C at 4°S.

The grand averages of these data are shown in an isogram (Fig. 2) which illustrates the seasonal change of surface temperature along the Peruvian coast. Highest temperatures, up to more than 22°C, are found farthest north (*i.e.*, nearest to the

---

[1] Contribution from the Scripps Institution of Oceanography. Paper delivered at meeting of Pacific Section, American Society of Limnology and Oceanography, San Diego, 17 June 1959. The work was supported in part by the Peruvian Consejo de Investigaciones Hidrobiológicas, and by the Office of Naval Research and the Bureau of Commercial Fisheries through contracts with the University of California.

Contributions from the Scripps Institution of Oceanography, New Series, 1282.

Reproduced by Permission

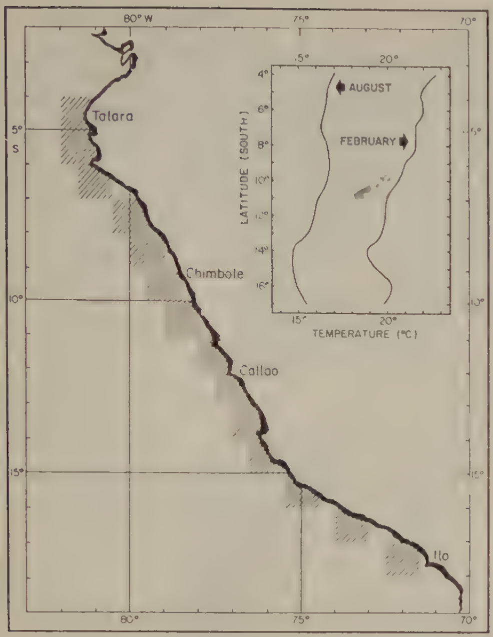

FIG. 1. One-degree squares used in analysis. Inset shows average February and August surface temperatures for period 1939–1956.

equator) in the summer, February and March being the months in which warm waters extend farthest south. The summer warming in southernmost Peru is separated from that in the north by colder water at 14° and 15°S. Indeed, during all months of the year lowest temperatures are found at those latitudes. Only there do average temperatures fall below 15°C during the winter cool period, which seems to be best developed in August, September and October. The most conspicuous event of the year appears to be the oncoming of summer, with temperature changes of several degrees per month, whereas during the rest of the year the average rate of change is one degree per month or less.

The detailed yearly isograms (Figs. 3 and 4), as one would expect, are much more irregular in appearance, primarily because of the much smaller number of observations involved (when less than 6 observations were available for a given square, the average was not used). The alternation of seasons is still plainly visible. Obviously not all years are the same, and the differences between years are often striking.

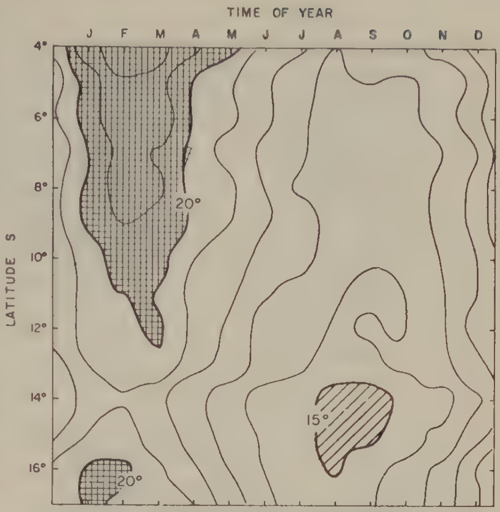

FIG. 2. Average surface temperature for one-degree squares for period 1939–1956, from Wooster (1960).

For example, waters warmer than 20°C were first observed off northern Peru as early as November, 1940, two months before usual, and by January, 1941, the warm region extended southward to at least 16°S, with temperatures from 2°C to nearly 5°C higher than normal. In February and March temperatures in excess of 25°C were observed north of 9°S, and the presence of water several degrees warmer than usual persisted through June.. Disappearance of the warm regime was abrupt, with surface temperatures dropping 2–3°C in a month to the north of 12°S.

This "El Niño" of 1941 has been described by several investigators (Schweigger 1942; Sears 1954; Lobell 1942; Vogt 1942). Its principal characteristic, as shown by these temperature charts, is the marked increase in southward penetration, duration and intensity of the annual summer warming off the Peruvian coast. Another year, 1953 (Fig. 4), which has been considered a Niño year (Posner 1957), shows some of the same features, although to a smaller extent.

Other years are clearly colder than usual, the period 1950–51 presenting an interest-

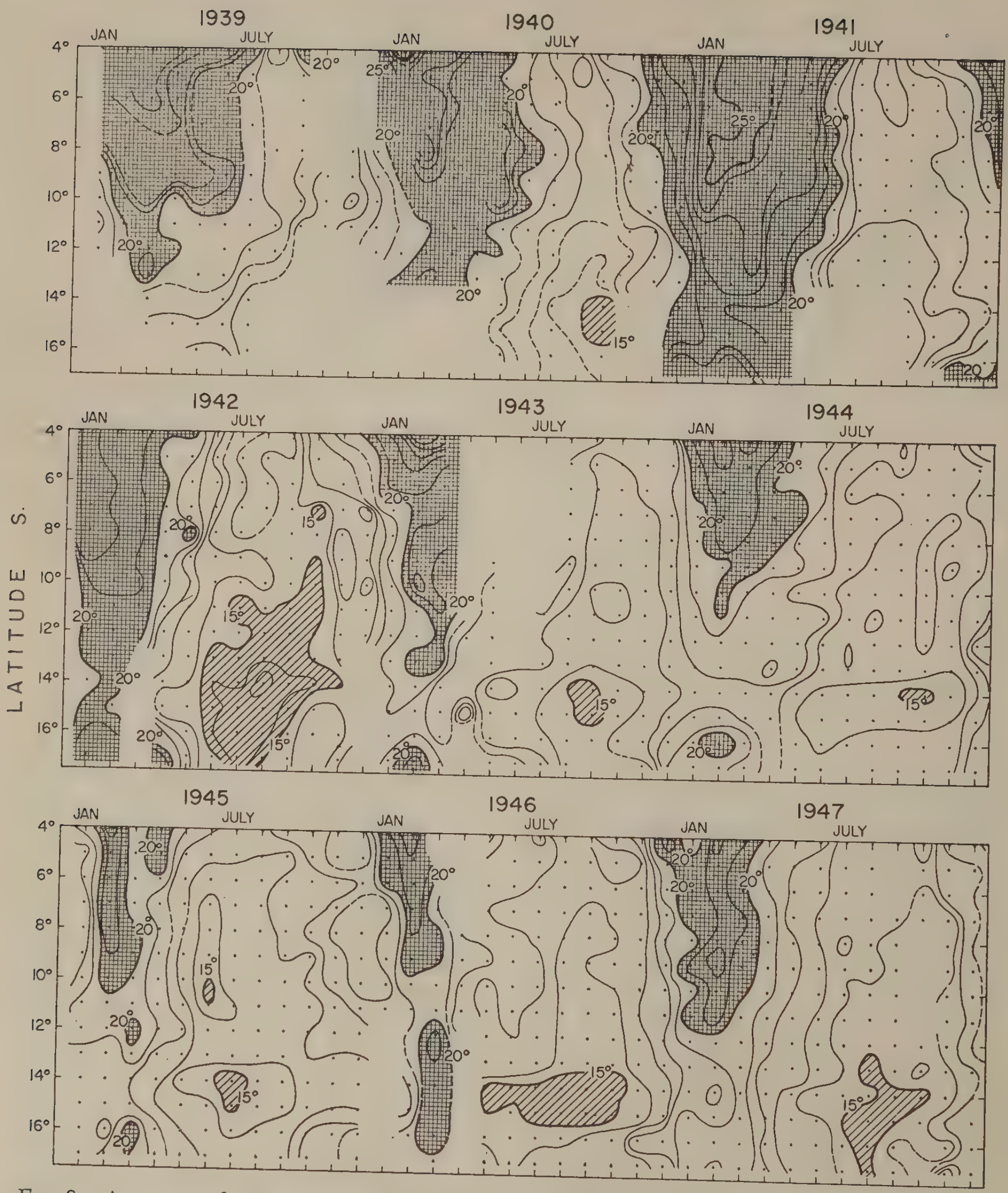

Fig. 3. Average surface temperature for one-degree squares, for individual years 1939 to 1947.

ing example. The summer warming of 1950 was notably reduced; even in northern Peru, surface temperatures remained below 20°C, from 2° to 3.5°C cooler than usual. The winter cold regime was well developed, and the warming of early 1951 was again weak. Then conditions changed rapidly in May, 1951, with a wintertime development of waters warmer than 20°C extending as far south as 13°S, a feature apparent nowhere else in the available record.

Although it is obviously impossible to account for all the features of these records,

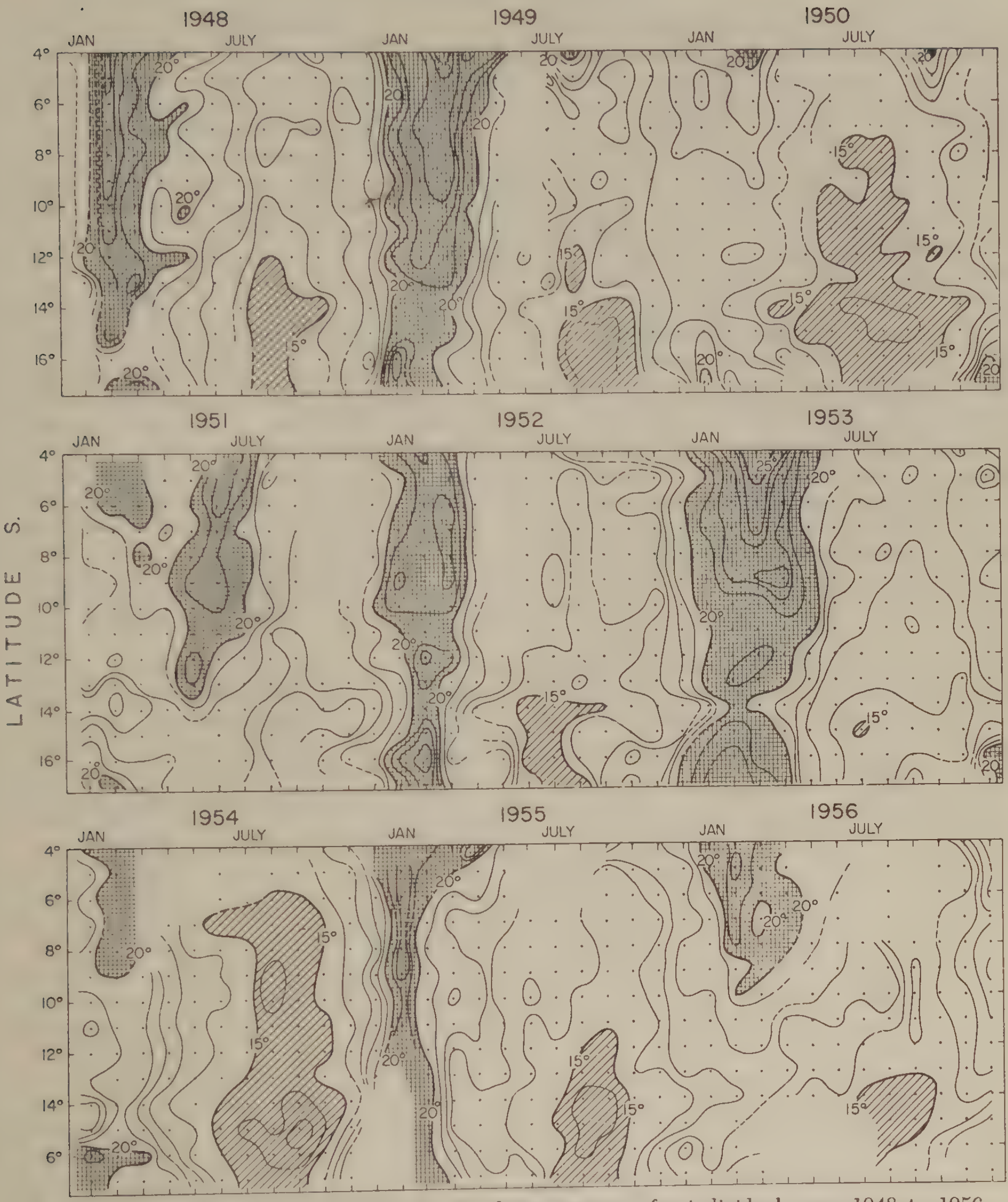

Fig. 4. Average surface temperature for one-degree squares, for individual years 1948 to 1956.

the general trends are not so inexplicable. During the winter the strongly developed southeast trades are responsible for the optimal development of upwelling, so that low temperatures prevail along the entire coast. The zone of lowest temperatures, at 14° to 15°S, is located where there occurs a 30° change in direction of the coast line relative to that of the average wind. During the summer the intertropical convergence is at its southernmost latitude, as is the north boundary of the Peru Current, and the weakened southeast trades are less effective in producing upwelling.

If this picture of seasonal change in the Peru Current region is essentially correct, it seems reasonable to expect that the major non-seasonal changes are linked to major variations in the surface wind circulation. The events of 1941 could be interpreted as indicating an abnormal weakening of the trade wind circulation (Wooster 1960). The low temperatures of 1950–51 could result from stronger than usual southerly winds along the Peruvian coast. The recent work of Bjerknes (1959), Roden and Groves (1960), Roden and Reid (in press) and others tends to support such an interpretation, although temperature-wind correlations do not yet give as clear-cut an answer as one might wish. Unfortunately in the southern hemisphere the supply of reliable historical weather data seems to be small. If usable data can be located, it seems likely that the picture of yearly change suggested by these surface temperature isograms will be relatively simple to explain.

FOOTNOTE

Since completion of this work, Schweigger (1959; Fig. 6 A, 6 B) has published surface temperature isograms for the period 1948–1956 based on a somewhat different interpretation of the same data.

WARREN S. WOOSTER

Scripps Institution of Oceanography,
La Jolla, California

REFERENCES

BJERKNES, J. 1959. The recent warming of the North Atlantic. *In* Bolin, B. (Ed.), The Atmosphere and the Sea in Motion. New York: Rockefeller Institute Press, pp. 65–73.

LOBELL, M. G. 1942. Some observations on the Peruvian Coastal Current. Trans. Amer. Geophys. Un., **2**: 332–336.

POSNER, G. S. 1957. The Peru Current. Bull. Bingham Oceanogr. Coll., **16**: 105–155.

RODEN, G. I. AND G. W. GROVES. 1960. On the statistical prediction of ocean temperatures. J. Geophys. Res., **65**: 249–263.

——— AND J. L. REID, JR. Sea surface temperature, radiation, and wind anomalies in the North Pacific Ocean. Rec. Oceanogr. Wks. Japan (in press).

SCHWEIGGER, E. 1942. Las irregularidades de la corriente de Humboldt en los años 1925 a 1941. Una tentativa de su explicación. Bol. Compañia Admin. Guano, **18**: 27–42.

———. 1959. Die Westküste Südamerikas im Bereich des Peru-Stroms. Heidelberg–München: Keysersche Verlagsbuchhandlung. 513 pp.

SEARS, M. 1954. Notes on the Peruvian coastal current. 1. An introduction to the ecology of Pisco Bay. Deep-Sea Res., **1**: 141–169.

VOGT, W. 1942. Informe elevado a la Compañia Adminstradora del Guano. Lima, Compañia Admin. Guano, **18**: 1–132.

WOOSTER, W. S. 1960. El Niño. Calif. Coop. Ocean. Fish. Invest., Rep., **7**: 43–45.

Reprinted from Biological Bulletin, Vol. 120, No. 2, pp. 148–156, April, 1961
Printed in U. S. A.

LUNAR ORIENTATION OF ORCHESTOIDEA CORNICULATA STOUT (AMPHIPODA)

J. T. ENRIGHT

Scripps Institution of Oceanography, La Jolla, California

Contributions from the Scripps Institution of Oceanography, New Series, 1283

Reproduced by Permission

LUNAR ORIENTATION OF ORCHESTOIDEA CORNICULATA STOUT (AMPHIPODA)

J. T. ENRIGHT

Scripps Institution of Oceanography, La Jolla, California

The celestial navigation accomplished by Talitridae (Amphipoda) was first reported by Pardi and Papi (1953) and Papi and Pardi (1953). These two papers contain numerous observations of the solar navigation of *Talitrus saltator* and, in the second paper, certain night-time observations suggested the existence of lunar navigation in this species, *i.e.*, appropriately time-shifted angles of orientation with the moon. The existence of solar navigation has been confirmed with several other species of Talitridae: *Talorchestia megalophthalma* and *Talorchestia longicornis* (Menaker, 1958); *Talorchestia deshayesei* (Pardi and Grassi, 1955); *Orchestoidea corniculata* and *Orchestoidea benedicti* (unpublished qualitative observations of the author). The existence of lunar navigation, however, had not been completely documented until the recent paper by Papi and Pardi (1959) which presents results supporting the contention that, under the experimental conditions described, *Talitrus saltator* oriented to moonlight with an angle that varied with lunar position. This resulted in a relatively constant and ecologically "correct" compass orientation. On the basis of this evidence, the authors conclude (p. 596) "dass zwei verschiedene physiologische Rhythmen die Sonnen- und die Mondorientierung von *Talitrus* bedingen." (Two different physiological rhythms are responsible for the solar and lunar orientation of *Talitrus.*)

Because of the significance of such a conclusion to the general theory of endogenous rhythms, the present study was undertaken to determine whether *Orchestoidea corniculata* Stout, a related amphipod which is capable of solar navigation, is similarly able to navigate by moonlight.

This work was performed during the tenure of a National Science Foundation predoctoral fellowship, and supported by N.S.F. grant G-7141 to Dr. E. W. Fager. The author wishes to express sincere thanks to his scientific advisor, Dr. E. W. Fager, for encouraging this study and greatly assisting with the manuscript. Appreciation is also due to: Mrs. D. L. Minis (Princeton University) for help with translation; to Mr. A. O. Flechsig, who aided with photography; and to Dr. Leo D. Berner, who demonstrated the calculation of lunar azimuths.

METHODS AND MATERIALS

The experimental animals were adult and sub-adult specimens of *Orchestoidea corniculata* Stout, collected usually on the morning before the experiment. In a few cases, as indicated in Table I, the animals were collected one or two weeks before the experiment and kept at constant temperature until the day of the experiment. Following collection, all animals were kept in light-tight, one-liter bottles containing moist sand. The animals can survive two weeks in such containers with no evidence of oxygen shortage. No control of the temperature was attempted on the day of the experiment, but the range was not greater than 16° to 28° C. Collections were made on the beach in front of the Scripps Institution of Oceanography, La Jolla, California. The shoreline there is oriented north 15° east; the "correct" azimuth orientation to return the animals to the water is thus 285° from north.

In order to avoid fog, city sky-glow, surf sounds, etc., the experiments were conducted in a level, open field about 40 km. northeast (inland) of San Diego.

TABLE I

Orientation of Orchestoidea corniculata with moon: animals kept in constant darkness

Date	Time	Lunar stage: days	Lunar azimuth	Orientation azimuth	Vector length	N	Angle with moon
1960							
*9 July	2241	16	137°	258°	0.74	26	121°
9 July	2306	16	141°	266°	0.77	32	125°
**9 July	2330	16	148°	277°	0.40	28	129°
***10 July	0055	16	171°	260°	0.62	29	89°
*10 July	0133	16	183°	280°	0.64	30	97°
10 July	0153	16	189°	307°	0.62	25	118°
*10 July	0330	16	216°	001°	0.64	26	145°
10 July	0355	16	222°	349°	0.65	29	127°
16 July	0144	22	093°	212°	0.59	30	119°
30 July	2003	8	228°	352°	0.53	31	124°
30 July	2055	8	239°	348°	0.56	25	109°
30 July	2105	8	241°	359°	0.62	23	118°
30 July	2147	8	248°	010°	0.58	26	122°
30 July	2158	8	250°	041°	0.65	13	151°
6 August	2201	15	144°	314°	0.72	24	170°
7 August	0005	15	181°	299°	0.85	25	118°
7 August	0017	15	185°	293°	0.61	26	108°
7 August	0240	15	224°	329°	0.65	25	105°
7 August	0252	15	226°	338°	0.79	29	112°

* Animals kept for one week at 20° C.
** Animals kept for one week at 10° C.
*** Animals kept for two weeks at 10° C.

The observation chamber was an opaque, white, circular plastic tray 25 cm. in diameter, 4 cm. deep, over which an unmarked sheet of glass was placed. No attempt was made to control the humidity within the chamber; Papi and Pardi (1959, p. 585) state that this is usually unimportant.[1]

The camera was mounted 1.4 meters above the chamber. Photographic lighting involved a single electronic photo-flash bulb ("strobe light") fixed 1.2 meters above the observation chamber, and at a constant position relative to it. The results suggest that the photographic equipment did not affect orientation. As later discussed, the flashes necessary for picture-taking did have an effect.

---

[1] See, however, Papi and Pardi (1953, p. 501, 502).

A compass and a clock, out of view of the animals, were included in each photograph.

Results are summarized by the method described by Pardi and Papi (1953, p. 463) : a vector sum of the positions of the individual animals is calculated (using 16 equal sectors), and this is divided by the number of animals. The orientation of the resultant vector gives the average orientation direction and its length gives an indication of the degree of scatter about the average. Such a vector can range in length from zero, indicating an even distribution of directions around the center, to unity, indicating all animals within the same sector. Random distributions will, of course, result in vectors larger than zero.

In order to determine the vector length which would result from random, independent orientation of the animals, 20 "experiments" were performed by assigning positions to 30 hypothetical "animals" by use of a table of random numbers. Eighty per cent of the resultant vectors were less than 0.30 in length and none was greater than 0.37. This suggests that a vector of length 0.35 or less based on the positions of 20 to 35 animals, the number usually used in the actual experiments, is of doubtful meaning. As there is clearly a lack of independence in the behavior of the individual animals, which predominantly cluster around the edge of the container, and often crowd and crawl over one another, a vector of greater length, perhaps 0.50 or more, is required to indicate definite orientation. No observations were used in the tests of the lunar navigation hypothesis (Tables I and II) if the calculated vector was less than 0.40 in length. The interaction invalidates conventional statistical techniques for more rigorously evaluating variability on the basis of an individual experimental result.

All angles are measured clockwise; azimuths are measured clockwise from north.

TABLE II

Orientation of Orchestoidea corniculata *with moon: animals not kept in constant darkness*

Date	Time	Lunar azimuth	Orientation azimuth	Vector length	N	Angle with moon
1960						
6 August	2015	122°	288°	0.59	25	166°
6 August	2025	124°	291°	0.87	21	167°
6 August	2225	151°	339°	0.77	25	188°
6 August	2235	153°	299°	0.72	25	146°
*6 August	2245	156°	319°	0.87	25	163°
*6 August	2255	159°	325°	0.86	30	166°
7 August	0025	187°	321°	0.68	22	134°
7 August	0045	193°	286°	0.47	31	93°
*7 August	0100	198°	325°	0.77	25	127°
*7 August	0110	201°	321°	0.75	26	120°
7 August	0305	229°	280°	0.44	27	51°
7 August	0315	231°	298°	0.64	28	67°
*7 August	0325	233°	341°	0.64	26	108°
*7 August	0335	235°	320°	0.52	25	85°

* "Redarkened" animals; all others "Natural Light."

Results

Moonlight as the orienting stimulus

In order to determine whether the observed orientations were due to moonlight, a group of amphipods, which had shown a given orientation relative to the moon, was shaded and an image of the moon was presented at about 180° from the actual position of the moon by means of a mirror. The results, shown in Figure 1, clearly demonstrate that the apparent lunar position is the dominant orienting stimulus for *Orchestoidea corniculata* under these experimental conditions.

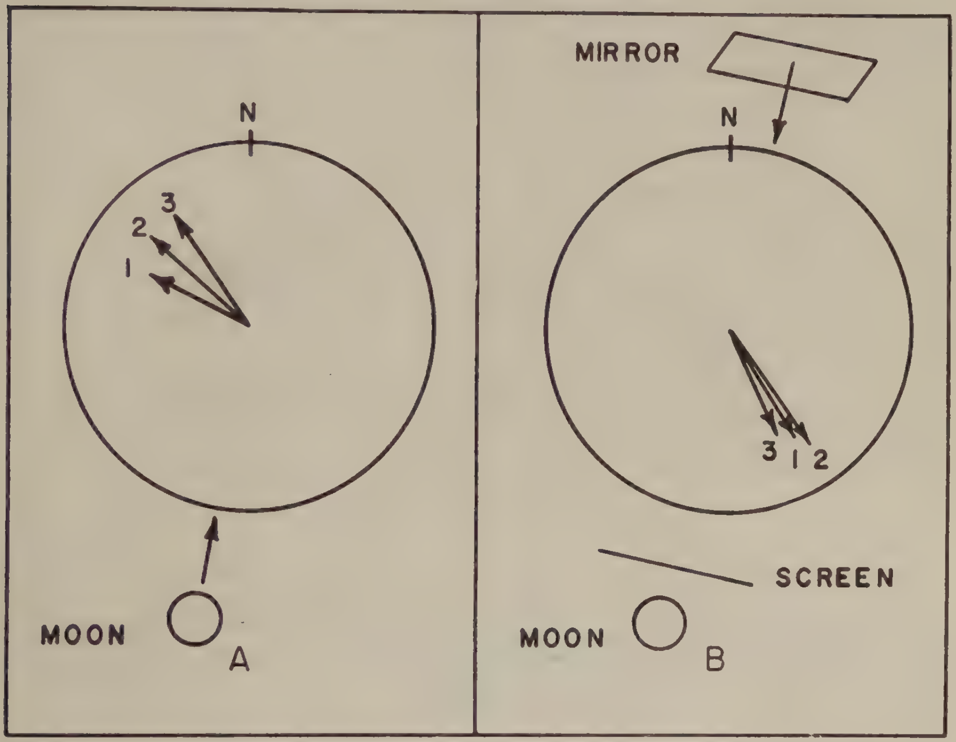

FIGURE 1. Orientation of a group of *Orchestoidea corniculata* to apparent lunar position. A: Initial orientation with the moon; B: orientation with moon reflected at about 180° from true position. Arrows within circle (which has unit radius) indicate average direction and scatter of orientation. Numbers adjacent to arrows indicate sequence in which pictures were taken. Observations made 10 July 1960, 0153–0209 hours, with 25 amphipods.

Serial observations with electronic flash

In initial experiments, a series of three photographs of each group of animals was taken. It was noted that groups of amphipods frequently showed a consistent shift in average direction of orientation, presumably as a reaction to the electronic flash. These results, while too few to be statistically significant, indicated a trend for the animals to orient with successively larger angles with the moon. (See, for example, Fig. 1A.) There was significant evidence of an increase in scatter from Photograph 1 to Photograph 3. For example, in 19 sets of 3 photographs, Photograph 1 showed least scatter in 14 cases and Photograph 3 showed most scatter in 12 cases.

Two series of ten photographs were taken to determine whether the shifts in direction and increase in scatter are cumulative (Fig. 2). In both cases, the ultimate angle of orientation with the moon after ten photographs was much smaller than the initial angle (contrary to the initial trend, over sets of only three photographs), with a net shift of 85° to 90°. In neither case is the final orientation more "correct" than the initial (although an average of the vectors of Figure 2B would be much closer to "correct" than either initial or final results). The short duration of the experiments, less than 15 minutes in each case, precludes the possibility that the shift is due to some normal compensation for changes in lunar position. Furthermore, the shift apparently does not take place without photography: qualitative continuous observation of a group of unphotographed amphipods, kept in the observation chamber for 15 minutes, indicated no noticeable orientation shift. (2 September 1960, 2315–2330 hours; lunar day 12; lunar azimuth 206°–210°; estimated orientation azimuth, initial and final, about 340°; angle with the moon, about 130°.)

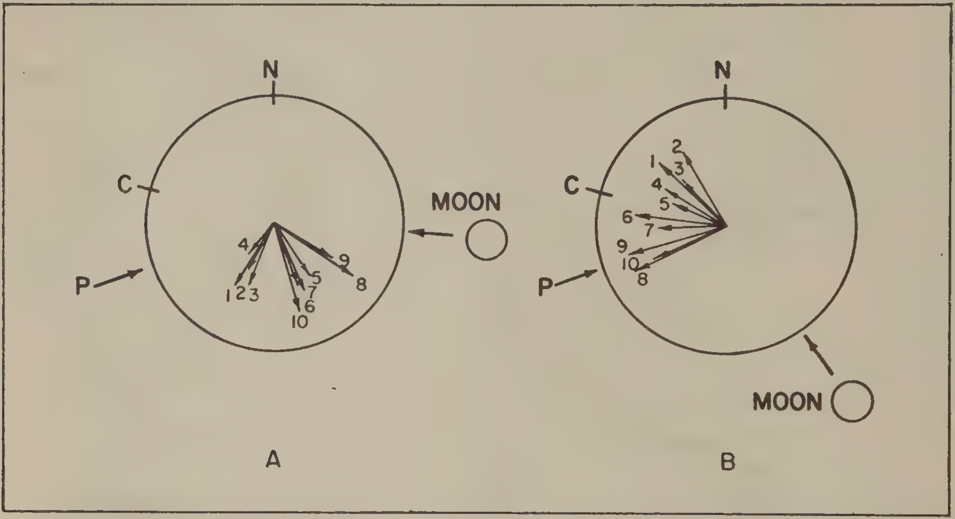

FIGURE 2. Orientation in sequential photographs of two groups of amphipods. A: 16 July 1960, 0144–0158 hours, with 30 amphipods; B: 6 August 1960, 2201–2214 hours, with 24 amphipods. Arrows within circle (unit radius) represent average direction and scatter of orientation; numbers associated with arrows indicate sequence. "P" indicates direction of photoflash; "C" indicates "correct" orientation direction relative to "N," north.

The results in Figure 2 seem best interpreted as a resetting effect of light on a rhythmic system, a phenomenon previously demonstrated using similar millisecond electronic flashes[2] (Pittendrigh, in press). The lengths of vectors in

---

[2] See Pardi and Papi (1953, pp. 466–467) for an alternative explanation of a superficially similar result with solar orientation.

Figure 2 indicate that, after an initial increase in scatter over the first three to five photographs, there is a recovery so that final orientation, after ten photoflashes, is strongly directed, but in a different direction from the initial.

Because of these complications with multiple photographic observations of the moonlight orientation of *Orchestoidea corniculata*, all data subsequently cited consist only of results from first photographs of the initial, unshifted orientation, and no group of amphipods was used twice.

Orientation of amphipods kept in constant darkness

Observations of the orientation of *Orchestoidea corniculata*, kept in complete darkness until just prior to observation, are summarized in Table I and Figure 3. As Figure 3 shows, the data can be explained by the hypothesis that this amphipod, when exposed after ten or more hours of constant darkness, orients to the moon

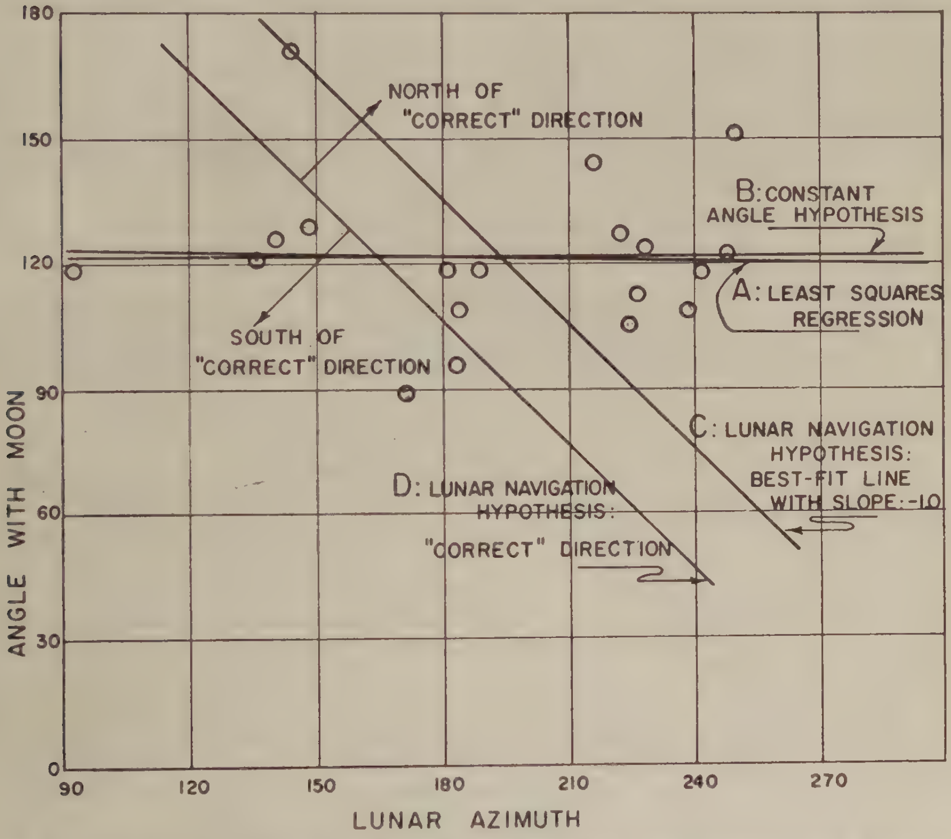

FIGURE 3. Orientation of *Orchestoidea corniculata* with moon, compared with three hypotheses: animals kept in constant darkness. The slope of the least-squares regression line (A) is −0.015. This is not significantly different from zero (line B); ($p > .50$). The probability that the slope of the regression line is as large as −0.50 is less than .001; steeper slopes (−1.0 for line C) are even less likely; and the departure from line D is even greater.

with an average angle of about 120°, regardless of lunar stage or position (Lines A and B). The hypothesis of a *continuously-operating* endogenous lunar physiological rhythm in this species, similar to that claimed for *Talitrus saltator*, appears unnecessary and is contradicted by the data (Lines C and D).

Orientation of amphipods exposed to sunset and moonrise

Additional observations were made with amphipods placed in constant darkness at the time of collection, and then re-exposed, in the sand-containing bottles, to

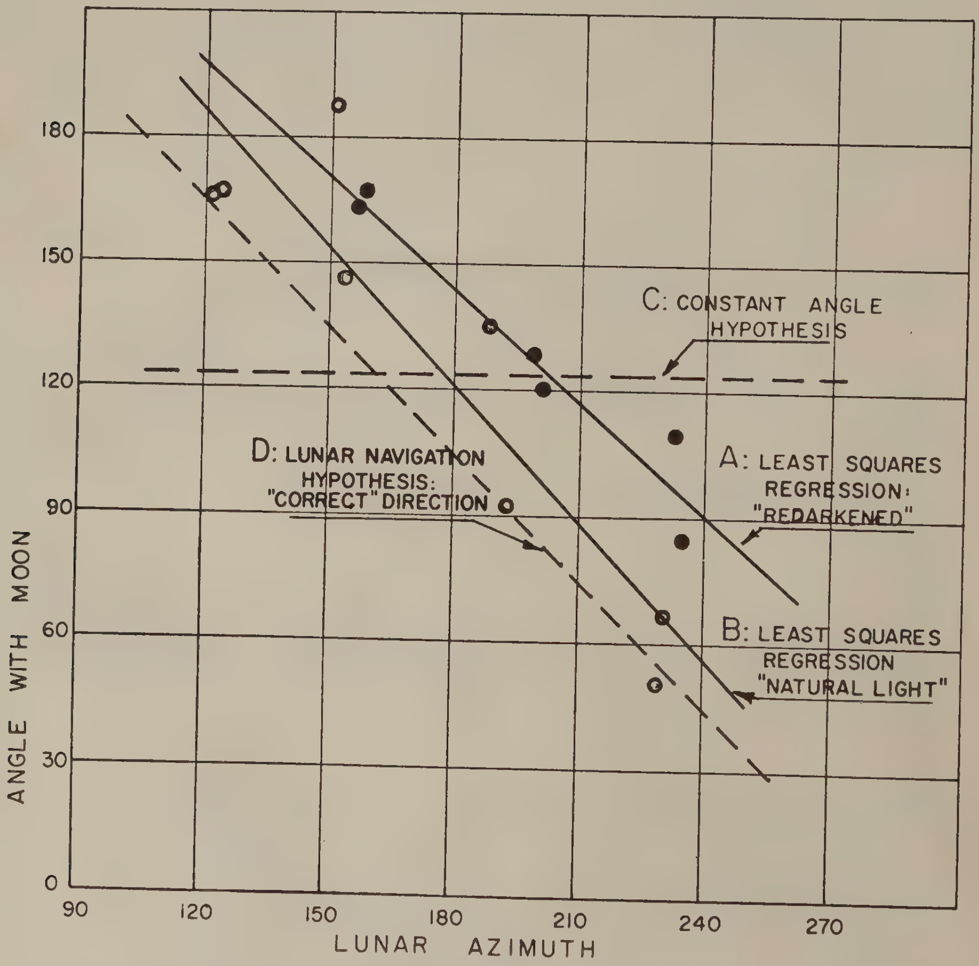

FIGURE 4. Orientation of *Orchestoidea corniculata* with moon as a function of lunar azimuth: animals not kept in constant darkness. Open circles represent orientation of "Natural Light" animals; solid circles represent orientation of "Redarkened" animals. The slope of line A is −0.888; and of line B is −1.078. The probability of the slope being −1.00 is > .20 for line A, and > .50 for line B. Points to the right of line D are north of "correct" orientation.

natural light about one hour prior to sunset. Those which were then continually exposed until observation are designated "Natural Light"; others which were replaced in constant darkness two hours after moonrise are designated "Redarkened." The observations, made August 6 and 7 (full moon), are summarized in Table II and Figure 4. The orientation resulting from this treatment of the animals does not seem adequately explained by the constant-angle hypothesis (Line C); the probability that the slope of the regression is 0 is extremely small in both cases ($p < .001$).

The directions of orientation, particularly those of the "Redarkened" animals, are generally somewhat north of the "correct" 285° azimuth, but the slopes of both regression lines are not significantly different from -1.0, the expected value if the animals compensated appropriately for shifts in lunar position.

A possible explanation is that sunset and/or moonrise (or perhaps removal from constant dark) can initiate a single cycle of appropriately time-compensated lunar orientation in these organisms. Such a system, with no information carry-over from the preceding nights, would afford the animals a crude but workable orientation mechanism (except at first quarter?). It would not require the organizational complexity and long-term precision necessary for the *continuously-operating* endogenous lunar periodicity claimed for *Talitrus saltator*. Further investigation may indicate that "night-sun" orientation (Pardi, 1953/54) or some other by-product of solar navigation is involved. No investigation of the effect of this treatment on the solar navigation of the amphipods was made.

SUMMARY

1. The orientation of *Orchestoidea corniculata* in direct moonlight, compared with the orientation when moonlight is reflected from a mirror, demonstrates that apparent lunar position is the dominant night-time orienting stimulus for this organism.

2. An analysis of the effects of repeated photographic recording of the orientation indicates that this species changes its angle of lunar orientation and the scatter about the average as a result of repeated electronic photo-bulb flashes.

3. Using only single observations of each group of animals, in order to avoid these artifacts, it was determined that this species, kept in total darkness for ten or more hours before observation, orients at a relatively constant angle with the moon, regardless of lunar stage or position. This result is not compatible with the hypothesis that *O. corniculata* possesses a *continuously-operating* lunar physiological rhythm similar to that claimed for *Talitrus saltator*.

4. When the amphipods were exposed to sunset and moonrise on the night of observation, there was an indication of subsequently time-shifted angles of orientation with the moon. The tentative hypothesis of a single-cycle night-time orientation rhythm, re-initiated by the appropriate stimuli each night, would explain such observations.

LITERATURE CITED

MENAKER, M., 1958. Celestial time compensated orientation of East Coast amphipods. *Anat. Rec.*, **132**: 476.

PAPI, F., AND L. PARDI, 1953. Ricerche sull'orientamento di *Talitrus saltator* (Montagu) (Crustacea-Amphipoda). II. *Zeitschr. vergl. Physiol.*, **35**: 490–518.

(575)

PAPI, F., AND L. PARDI, 1959. Nuovi Reperti sull'orientamento lunare di *Talitrus saltator* Montagu (Crustacea-Amphipoda). *Zeitschr. vergl. Physiol.,* **41**: 583–596.

PARDI, L., 1953–54. Esperienze sull'orientamento di *Talitrus saltator* (Montagu) (Crustacea-Amphipoda): l'orientamento al sole degli individui a ritmo nictiemerale invertito, durante la "loro notte." *Boll. Ist. Mus. Zool. Univ. Torino,* **4**: 127.

PARDI, L., AND M. GRASSI, 1955. Experimental modification of direction-finding in *Talitrus saltator* (Montagu) and *Talorchestia deshayesei* (Aud.). (Crustacea-Amphipoda). *Experientia,* **11**: 202–205.

PARDI, L., AND F. PAPI, 1953. Ricerche sull'orientamento di *Talitrus saltator* (Montagu) (Crustacea-Amphipoda). I. *Zeitschr. vergl. Physiol.,* **35**: 459–489.

PITTENDRIGH, C. S., in press. "Circadian Rhythms and the Circadian Organization of Living Systems," in Cold Spring Harbor Symposia on Quantitative Biology, Volume XXV, Biological Clocks.

JOURNAL OF MAMMALOGY, v.42, no.2. pp.271-273.

OBSERVATIONS ON THE CALIFORNIA SEA OTTER[1]

The major portion of these notes was collected from 4–15 September 1953, while filming the activities of the sea otter, *Enhydra lutris.* In part, these notes are supplemental to the accounts by Edna M. Fisher (J. Mamm., 20: 21–36, 1939; 21: 132–137, 1940). Observations were made on approximately 27 otters in the vicinity of Monterey Bay, Monterey County, California: at Yankee Point, Rocky Point, off Slates Hotsprings Baths, and at a point just north of Slates Hotsprings.

Food and feeding habits.—Sea otters were observed to feed on the red abalone (*Haliotis rufescens*), the sea urchin (*Strongylocentrotus franciscanus*), purple-hinged scallops (*Hinnites gigantea*)—a sessile scallop as an adult, the California mussel (*Mytilus californianus*) and various species of snails. It is possible that they also fed on the giant chiton or gumshoe (*Cryptochiton stelleri*). Numerous other unidentifiable animals were used as food.

All feeding was accomplished while the otters were lying on their backs, utilizing the chest and abdomen as a floating table. Females shared their food with juveniles and possibly with the males. The adults continually washed their food by rolling in the water,

---

[1] This paper, based on research notes maintained by the author prior to his death, has been organized by Howard M. Feder, Hartnell College, Salinas, California. Arthur Kelly, Scripps Institution of Oceanography, J. B. Phillips, California Department of Fish and Game, and Paul Johnson and Janet Stearn, Hartnell College, assisted in the preparation of the final draft.

Conrad Limbaugh, chief diving officer at Scripps Institution of Oceanography and one of the world's foremost underwater naturalists, had been working on numerous and diverse research projects before he met his untimely death in a diving accident in the Mediterranean, on 20 March 1960. Many of his projects, including this one, were left unfinished although his intention to finish this particular work has been indicated in a statement found among his papers. Because of the extensive field notes and photographic records he maintained, it is anticipated that the results of most of his studies can be assembled and eventually published so the vast wealth of his accumulated knowledge will not be lost. —H. M. F.

Contributions from the Scripps Institution of Oceanography, New Series, 1284

Reproduced by Permission

the food clasped tightly against them with their forepaws. Occasionally the food material was pounded against a rock balanced on the abdomen; this action fractured the hard parts and made the internal organs of sea urchins and scallops available. Apparently pounding and fracturing of abalone shells permitted the otters to feed on the soft parts more readily. Sometimes, prior to feeding on abalone, an otter would balance the foot of the mollusk on its chest while it licked the shell clean. The foot and internal organs were removed from the shell and eaten, generally in a leisurely fashion. Small abalones were eaten directly from the shell. When the otter was through with a shell, it was discarded by dropping it to one side or by rolling over.

Rocks used as feeding aids were 2½ to 3½ inches in diameter, but sometimes flat ones as large as 6 inches in diameter were observed. Most food items were pounded against this rock held on the chest or abdomen; possibly other objects were pounded with the rock. Sometimes the same rock was carried on a series of successive dives.

Dives lasted from 60 to 90 seconds, frequently being made in a quick series to obtain a large abalone. Feeding occurred in shallow water, usually less than 3 feet, but sometimes as deep as 15 feet. The food organisms were removed from the rocks with the forepaws, often with the hind legs protruding out of the water while the otter attempted to dislodge its food in shallow water.

General habits.—A dive always began with the otter raising its head high, diving forward, and thrusting its hind legs clear of the water. During the dive a large number of air bubbles would rise to the surface. The dives were completed in a small area while feeding. However, dives made while traveling from one place to another were performed in sea-lion fashion: swimming face down while ducking the head forward just beneath the surface, and arching the body in an "S."

Swimming was accomplished by the otters in several ways: by paddling their hind feet while floating on their backs, by paddling their hind feet while lying face down, or by undulating their bodies from side to side. Sometimes the slender tails protruded from the water while the otters were swimming. Most travel by groups or individuals was along the inner edges of the bull whip kelp (*Nereocystis*) beds, which were extremely thick during the period of observations.

The otters seemed to have rather definite feeding areas and paths. Resting areas also remained fairly constant. After morning feeding the otters retired in small, sociable groups to a patch of giant kelp (*Macrocystis pyrifera*) and fall asleep while floating on their backs. Young otters spent considerable time cleaning and preening their fur. One adult was observed cleaning himself with a piece of seaweed.

When the young were awake, they played with other young and occasionally with adult male otters. They appeared to derive great enjoyment from sneaking up behind an old male and pulling him underwater while he fed or slept. Playing consisted of ducking and wrestling. If a youngster was getting the worst of the play, he would emit a cry similar to that of a sea gull. At this sound, the mother otter grasped him by the shoulders and carried him away from the play area. One otter was observed playing with a floating stick.

Whenever a young otter became separated from its mother, it uttered the same type of cry emitted by a playing otter in trouble. When the female heard this cry, or when she was concerned by a long absence of her young one, she stretched her head out of the water and peered in all directions, finally located the youngster, and swam directly toward it.

At the time of these observations the young otters were probably still nursing, judging from the swollen and red appearance of the two mammary glands of the females with young. Mammary glands of the sea otter, incidentally, are almost human in placement, but proportionately smaller.

Sea otter vision appeared to be good; their hearing seemed exceptionally fine. They could hear and locate an operating motion-picture camera from a distance of 100 yards. Occasionally a female was seen to take a male by the shoulders and pull him underneath

(578)

the water when he moved too near the photographers. The male was possibly a juvenile or a mate.

Otters apparently were undisturbed by the presence of the harbor seal (*Phoca vitulina*), but were quite concerned with the appearance of a California sea lion (*Zalophus californianus*). They demonstrated their fear by actively looking above and beneath the water when a sea lion was swimming nearby.

Methods of locating these animals.—Several guides are helpful in locating active sea otters. (1) Watch for ripples or wake marks made by swimming animals. (2) Search for sea gulls that might be hovering over otters in hope of recovering food scraps dropped during the feeding ritual. (3) Listen for the sound of shells being pounded against rocks by feeding otters. (4) Listen for the gull-like cry of the young otters. (5) Watch for the unusual presence of large numbers of sea urchin (*Strongylocentrotus franciscanus*) tests on the shore, many containing fragments of fresh tissue and bearing spines still in motion. This is an indication of sea otters feeding nearby. (6) Examine areas in or near kelp beds. —CONRAD LIMBAUGH, *Scripps Institution of Oceanography, Univ. of California, La Jolla.* *Received 3 October 1960.*

[Publication of this paper was aided by a grant from The Permanent Science Fund of the American Academy of Arts and Sciences and by The Conrad Limbaugh Memorial Fund.]

(579

Reprinted from SCIENCE, November 11, 1960, Vol. 132, No. 3437, pages 1379-1381

Specific Transport of Oxygen Through Hemoglobin Solutions

Why is this transport abolished when opposed by a slight back pressure of oxygen?

E. Hemmingsen and P. F. Scholander

It has recently been shown that under certain steady-state conditions oxygen moves several times faster through hemoglobin solutions than through water. In these experiments the solution was held in a Millipore membrane, above which was air at varying pressures and below which was moist vacuum. It was found that the nitrogen flux in all cases was strictly proportional to the diffusion pressure, but that the oxygen flux was enhanced. At air pressure of 1 atmosphere the oxygen-nitrogen ratio was almost double that of water, and at 1/12 atmosphere it was eight times higher than that of water. The following simple numerical relation prevailed in each case: Total oxygen flux = oxygen diffusion + a constant. Or, to express it more empirically: Total oxygen flux = nitrogen diffusion × 0.56 + a constant, where 0.56 is the O_2/N_2 ratio in the hemoglobin-free solution.

This was interpreted to mean that the oxygen flux proceeds via two separate routes—namely, a simple Fick's diffusion through the solution and a specific transport which is mediated by the hemoglobin. The latter is constant over a wide pressure range, increases with the concentration of the hemoglobin until the viscosity becomes excessive, and is abolished when the pigment is oxidized to methemoglobin. Suspensions of intact red cells and solutions of myoglobin show a similar effect (*1*).

These results were obtained by a gasometric technique which required that a near-vacuum be maintained below the membrane; it could not be used to study gas flow into a system containing oxygen of various tensions. In a muscle, zero or near-zero oxygen tension is relevant enough, but this would very rarely apply to the blood. The question therefore presented itself: What happens to oxygen transport through hemoglobin when the low pressure is elevated? In order to answer this question a new approach was needed, and it was highly desirable, also, to determine the state of oxygen saturation in the membrane at various pressures.

The authors are members of the staff of the Scripps Institution of Oceanography, University of California, La Jolla.

Contributions from the Scripps Institution of Oceanography, New Series, 1285
Reproduced by Permission

Methods

Determination of gas flux against back pressure. A Millipore filter charged with hemoglobin solution was used to separate two large volumes of oxygen or nitrogen gas. When a pressure difference was applied, gas permeated the filter and the steady-state flux was determined.

Two 300-cm^3 gas chambers were moistened with a little water and interconnected through a capillary measuring device and a diffusion chamber (Fig. 1). The latter was divided into an upper and a lower half. The Millipore filter, resting on a rigid stainless steel screen, was clamped, airtight, between them. The graduated capillary, of 1- to 2-millimeter inside diameter, held a drop of kerosene for measuring the rate of gas flux. The drop could be reset at any time for repeated measurements by means of a three-way stopcock. Adequate sensitivity was obtained by keeping the gas volume between the drop and the membrane small (1 cubic centimeter). Change in the water content of the membrane by evaporation and condensation was the greatest source of error and was minimized by inserting a ring of wet filter paper in the lower diffusion compartment. The whole apparatus was immersed in a thermoregulated water bath.

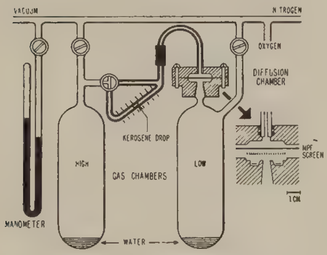

Fig. 1. Diffusion apparatus.

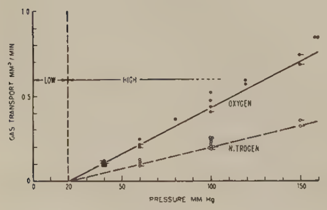

Fig. 2. Flux of oxygen and nitrogen through hemoglobin solution at an oxygen back pressure of 20 mm-Hg. Oxygen capacity, 20 to 21 vol percent. The marked points belong to sequences taken on two membranes. The other points are mostly single determinations from various membranes.

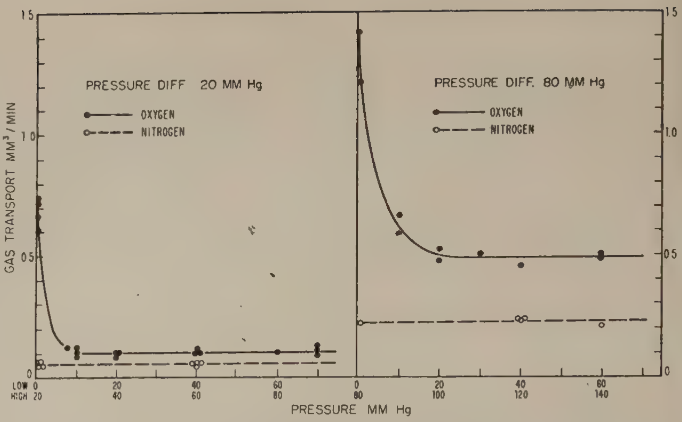

Fig. 3. Flux of oxygen and nitrogen through hemoglobin solution at constant pressure gradients but varying absolute pressures. Oxygen capacity of solutions, 20 to 21 vol percent. (Right) Two membranes at *p*H 7.2; (left) four membranes at *p*H 7.2, 7.3, 8.2, and 8.5, respectively.

Hemoglobin solutions were prepared from heparinized human blood, and the Millipore filter was charged with the solution, as previously described (*1*). With the membrane clamped, airtight, in the diffusion chamber, the system was evacuated and filled with purified oxygen (or nitrogen), evacuated again, and refilled. The desired pressure on the high and low sides of the membrane was obtained by means of the manometer. With the stopcock set as in Fig. 1, the rate of gas flux through the membrane was determined from the rate of movement of the kerosene drop. Final readings were taken when steady-state flux was reached. For each membrane the gas flow was determined at several different pressures, first with oxygen gas, then with nitrogen gas.

Determination of oxygen saturation in membrane. A membrane charged with hemoglobin solution was suspended in a flat plastic chamber which was kept moist with a strip of wet filter paper. The air spaces on each side of the membrane communicated with each other, and the air was maintained at various pressures. The state of oxygenation at each pressure was read on a reflectance spectrophotometer.

Two different series of experiments were performed in order to determine the effect of back pressure on the oxygen transport. In the first series the low pressure stayed constant at 20 mm-Hg, while the high pressure varied from 30 to 150 mm-Hg (Fig. 2). It may be seen that the transport of both nitrogen and oxygen proceeds exclusively by simple diffusion; that is, the rate is proportional to the gradient, and the oxygen moves nearly twice as fast as the nitrogen; there is no enhancement of the oxygen rate.

In the second series the total gas pressure varied while the pressure difference was maintained constant, either at 20 or at 80 mm-Hg (Fig. 3). It will be seen that the rate of *nitrogen* flux closely reflects the fourfold difference in gradient, and looking at each run separately, we find that the rates are constant all the way down to zero pressure; that is, the nitrogen moves by simple diffusion. In the case of *oxygen*, however, simple diffusion prevails only down to opposing oxygen pressure of 10 mm-Hg. Below this, the flux increases rapidly and reaches a maximum at zero back pressure; that is, the specific transport mediated by the hemoglobin is abolished when it is opposed by a slight back pressure of oxygen.

This blocking effect by oxygen is specific, for neither water-vapor pressure of 20 mm-Hg (moist vacuum) nor the addition of nitrogen to a pressure of 80 mm-Hg impedes the flux. The specific oxygen transport appears to be insensitive to temperature, for there was no clear difference in the oxygen-nitrogen ratio in runs made at 15° and 25°C. Likewise, there was no *p*H effect (compare Fig. 3, left), although such an effect becomes manifest at very low oxygen pressures (*1*).

The state of saturation of a membrane suspended in air at various pressures may be seen in Fig. 4. Full oxygenation occurs down to pressures of 30 to 25 mm-Hg, and one may therefore assume that our diffusion membranes were fully saturated, or nearly so, in the surface layer down to air pressure of ⅙ atmosphere. Similarly, it can be seen that the blocking pressure of 5 to 10 mm-Hg corresponds to less than half saturation of the lower surface. Evidently, therefore, a maximally accelerated oxygen transport requires full reduction pressure on one side of the membrane and full saturation pressure (or more) on the other.

When the hemoglobin solution in the membrane was solidified by gelatine, the nitrogen diffusion remained unchanged but the specific oxygen transport was cut in half (*1*). This suggests that the oxygen transport is linked with the kinetic motion of the hemoglobin molecules. One concept would assume that a certain exchange of oxygen takes place from one hemoglobin molecule to the next when these collide. At the vacuum end of the chain there is no more than one oxygen molecule attached to the hemoglobin. When this molecule is lost to the vacuum, the deficit or "hole" is filled in from above; that is, the disturbance is transmitted through the entire chain in a rate-limited "bucket-brigade" fashion (*1*).

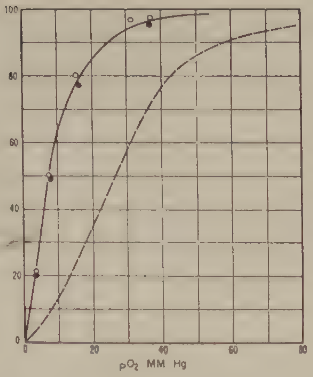

Fig. 4. Saturation of a membrane suspended in air at various pressures, measured by reflectance spectroscopy. (Left) Observed curve measured on two different membranes at 23°C, *p*H 7.3 and no carbon dioxide; (right) reference curve (37°C, *p*H 7.4, carbon-dioxide pressure, 40 mm-Hg) (*3*).

An alternative view would be that the transport is caused by oxyhemoglobin diffusing from one surface to the other. The porosity of the Millipore filter is much too fine for convection to take place, but hemoglobin readily diffuses into much finer structures, such as agar gels. Hence, some of the oxygenated molecules might carry oxygen downward and unload it to the vacuum, but if this is the case, an equal number of empty molecules would be moving upward, and one would expect these to receive oxygen from the loaded descending molecules. As in other countercurrent systems, such a cross exchange would strongly limit the net transfer. This concept is in line with the relatively low efficiency of our system. But neither of the proposed systems explains why a slight back pressure of oxygen should completely block further unloading.

What role does this hemoglobin transport system have in human beings? Presumably very little, if intact red cells are as sensitive to back pressure as is hemoglobin. If, however, the blocking pressure is related to degree of saturation rather than to absolute pressure, the transport might still be effective under tissue asphyxial conditions wherein the carbon dioxide tension and the presence of lactic acid have lessened the oxygen affinity (*2*).

References and Notes

1. P. F. Scholander, *Science*, **131**, 585 (1960).
2. This investigation was supported by a research grant (No. RG-5979) from the U.S. Department of Health, Education, and Welfare, Public Health Service. We wish to thank John Tyler for his help in making the reflectance measurements and Denis L. Fox for his stimulating suggestions.
3. F. J. W. Roughton and J. C. Kendrew, Eds., *Haemoglobin* (Interscience, New York, 1948).

(584)

DISTINGUISHING BETWEEN BEACH AND DUNE SANDS

BY

FRANCIS P. SHEPARD AND RUTH YOUNG

Reprinted from the Journal of Sedimentary Petrology for June, 1961
v.31, no.2. pp.196-214
Contributions from the Scripps Institution of Oceanography, New Series, 1286

(585)

Reproduced by Permission

JOURNAL OF SEDIMENTARY PETROLOGY, VOL. 31, NO. 2, PP. 196–214
FIGS. 1–17, JUNE, 1961

DISTINGUISHING BETWEEN BEACH AND DUNE SANDS[1]

FRANCIS P. SHEPARD AND RUTH YOUNG
Scripps Institution of Oceanography, University of California, La Jolla, California

ABSTRACT

The comparison of adjacent pairs of beach (largely foreshore) and dune sands from 74 localities of world-wide distribution has shown that it is generally possible to distinguish between the two, particularly if there are predominant onshore winds. The dune sands are usually rounder than the adjacent beach sands, have a larger silt content, and this silt has a higher content of heavy minerals. The beach foreshores, on the other hand, usually contain more shells and other calcareous organisms than the dunes. There is also some reason to believe that mica content is greater in beach foreshores than in adjacent dunes. The sand of beach berms appears to be intermediate in most respects between that of the foreshores and dunes.

The areas where beaches and dunes are most difficult to distinguish are those where there are longshore, extremely variable, or offshore winds. In such localities it is thought that the dune sands are blown back onto the beaches causing intermixture and that in some cases the dunes are derived from sources other than from the adjacent beach. The best results in separating the two environments have come from beaches of the west coast of the United States and Baja California where onshore winds predominate.

It is suggested that the chief reason for the differences between dune and beach sands is that the wind picks up from the beaches more of the rounder grains than of the flat and angular grains. There is no reason to believe that the grains are rounded appreciably by the wind in transit to the dunes. Nor does there appear to be any evidence from these comparisons that the dune grains become frosted. The greater quantity of heavy minerals in the dune silt fraction may be caused by removal by the wind of the light minerals.

INTRODUCTION

Distinguishing ancient beach and dune sands may serve to tell the direction and approximate position of the shore line in a stratigraphic sequence. Beaches and dunes are often buried and hence incorporated into a stratigraphic sequence by prograding coastal fans which build over the dunes without destroying them, whereas an encroaching seashore may destroy the dunes as the waves act at higher and higher levels. Beaches and dunes also may be incorporated into the stratigraphic column during subsidence, provided the beaches and the dunes inside grow upward apace with the coastal subsidence. Where bedding is present beaches and dunes can often be distinguished by the distinctive nature of the cross-bedding in the dunes. Many dune sands, however, lack this distinctive cross-bedding so that other criteria become necessary to distinguish them from bordering beaches. Among these criteria roundness has been referred to by a number of investigators as being greater in dune sands than in the beach from which the dune was derived (MacCarthy, 1935; Russell, 1939; Pettijohn, 1956, and Beal and Shepard, 1956).

Other investigators have questioned the authenticity of any actual difference in roundness between beaches and dunes (Mattox, 1955; Mason and Folk, 1958). Furthermore, a trip along the length of Padre Island, Texas, with the collection of beach and dune pairs at approximately 2-mile intervals, yielded samples which, when investigated by the present writers, showed a number of beach sands that were rounder than the adjacent dune sands. Accordingly, material was collected from a considerable number of other localities from various parts of the world, largely by the senior writer, and these have been subjected to tests.

---

[1] Acknowledgments: This work represents one of the results of research carried out under Contract Nonr-2216(01), Office of Naval Research. The writers wish to acknowledge the assistance which they received from M. A. Beal, G. V. Cohee, J. T. Enright, R. L. Folk, P. K. Hansen, D. L. Inman, R. R. Lankford, J. R. Moriarty, F. B Phleger, Tj. H. van Andel, and J. D. Waskom. Manuscript received April 25, 1960.

(586)

If the dune sands are more rounded than beach sands because of the abrasion between grains produced during wind transportation, as is a common impression, very little rounding would have occurred in transporting sand to the bordering dunes. That being the case it would be necessary to collect samples at considerable distances within the dunes in order to get appreciable differences from the parent beach sand. If, on the other hand, the principal difference comes from the sorting action of the wind in picking up rounder grains from the beach, an immediate difference should be found and a comparison be made by collecting dune sands at close propinquity to the beach where the parentage is more certain. The experiments of MacCarthy and Huddle (1938) indicated the importance of wind as a selector of round grains. As further indication, the comparison of sand dunes at varying distances from the beach (Beal and Shepard, 1956) showed that there was no progressive change at least over a distance of several miles, and studies by the present writers have given more confirming information. Furthermore, wind-blown sand collected from a wheel track across a beach was found to have as great a difference in roundness from the beach sand as was found in samples taken well within the adjacent dunes. Therefore, no hesitation was felt in comparing the nearby dune sands with those of the beach. In general, the dune samples were obtained on the windward slope well above the highest level reached by waves. In order to determine whether the roundness change occurred between foreshore and berm or between berm and dune, a considerable number of berm samples were compared with both dune and foreshore sands.

Suggestions have been made that beaches and dunes may be distinguished by their grain size parameters, particularly the sorting, skewness, and kurtosis (Mason and Folk, 1958). These factors have been checked between beach and dune samples in the present study from a large number of localities. Finally, the general composition of beach and dune constituents has been given some comparative study, and an attempt has been made to look for a difference between the frosting of grains of the beaches and the adjacent dunes.

ROUNDNESS ("PRIVOTABILITY") STUDIES

Methods and Purpose

There is a large volume of literature on the methods of determining roundness and sphericity. Roundness according to Wadell (1932) is the ratio of average radius of curvature of the several corners or edges of a solid to the radius of curvature of the maximum inscribed sphere, whereas sphericity is the degree in which the shape of a fragment approaches the form of a sphere. Realizing the great difficulty of measuring the diameters of sand grains along more than two axes, most methods have tested roundness of grain outline. Wadell, for example, compared the average radius of the corners and edges to the radius of the maximum inscribed circle. Krumbein (1941) used values determined by Wadell to set up a visual comparison chart based entirely on silhouettes. A well-constructed globe or ball represents a perfect sphere, if all diameters are equal, whereas (using the outline method) a coin may have the highest degree of roundness but very low sphericity. The scale developed by Powers (1953) is also based on Wadell's values, but it shows photographs of models which give the eye a sense of the third dimension. The "sphericity" method of Riley (1941) gives the ratio between inscribed and circumscribed circles on grain outlines and differs from the others in that it may give high values to grains of low sphericity and roundness as, for example, a 6-sided flake of mica.

In choosing a method for determining roundness or sphericity it is necessary to consider the purpose of the comparison. In the present study this purpose was not so much to determine the amount of wear which grains had undergone by long distance transportation, which as shown by Kuenen (1958, 1960) and Russell (1939) may or may not result in sphericity and roundness, but to distinguish the difference in shape of grains at or near the boundary between beaches and dunes that could be produced by selective choice of grains by the wind. If such selection takes place, there should be a means of determining the boundary between ancient dunes and beaches which lie contiguous to each other. It is evident that well-rounded grains can roll and, hence, be blown more easily than grains with flat surfaces and, furthermore, that grains with projecting points are more difficult to dislodge from a beach surface and are, therefore, somewhat less likely to be carried by the wind into the dune. On the other hand, thin platy grains like mica are more easily transported than spherical grains once they have been dislodged. Thus, there are two factors working against each other, making it necessary to find out from observations of many beaches and dunes the shape differences which actually exist.

To compare dune and beach roundness a somewhat modified version of Powers' scale was adopted by the writers. In this scale the idea of "pivotability" was given paramount importance so that the grains which could be most easily pivoted were given the highest values. Examples of typical grains in the six roundness grades used are shown in figure 1.

Technique Employed

In all cases in the present investigation beach sands were compared with those of adjacent dunes. To do this the samples were sieved and a split was taken from the same size for each pair. In most cases the .062 to .125 mm grade was used largely because this is usually present in beach and dune sands and constitutes a large proportion of the beaches and dunes of the Gulf of Mexico and the west coast of the United States where most of the samples for the work were collected.

The split was obtained by spreading the sample on a large tray and taking portions at random with a scoop. This was found from tests to be fully as representative of the entire sample as the split obtained by a much more time-consuming sample splitter.

The split was then spread on a gridded tray and examined under the binocular-microscope. Grains were chosen by following a grid pattern on the tray so as to avoid bias. A count of 100 grains was made and the types were recorded on a *Denominator* (a blood-cell counter) which stops at 100 and can be manipulated with one hand while the other hand moves the tray and adjusts the microscope. After a little practice, no trouble is found in using this counter by the touch system so that the eyes do not have to be moved from the microscope. Average time for a count appears to be about 10 minutes.

Results of such counts are made much more reliable when the operator is unaware of the nature of the sample being tested. Otherwise a certain bias can be introduced. At first, the present authors tested only one pair at a time, but it was found that it was difficult to avoid some bias if the second sample examined appeared on first sight to be either rounder or more angular than the other. As a result, six or more unknown samples were counted before using a check list to see what they represented. In this way no bias can be developed. Another important thing is to have more than one operator. This increases the number of grains examined and thus helps avoid the possibility of a chance spread of the roundest or the most angular grains on the tray which may develop occasionally in a count of 100. Furthermore, if one operator is having an off day or a temporary tendency to make the classes too high or too low it will show up in a striking difference between the counts of the two operators. Where such large differences existed, both operators repeated the counts again as unknowns, with almost always a satisfactory adjustment.

Only two operators were involved in this study, both of whom have become quite experienced in studying roundness during a period of more than two years, in which time each has measured more than 60,000 grains. This experience has resulted in a high degree of consistency in each operator's measurements.

Results of Roundness Counts

The result of examination by both writers of 74 pairs of beach and dune samples from many parts of the world is indicated in table 1 and in figure 2. At first sight it will be seen that there is by no means a consistent difference between the roundness of the beach sand and that of the adjacent dune, as had been indicated by the previous counts made on a much smaller group of pairs by Beal (Beal and Shepard, 1956). On the other hand, the dune sands are generally more round, and the averaging of a large number of samples from a locality showed a greater degree of roundness in almost all cases.

The most striking conclusion from the

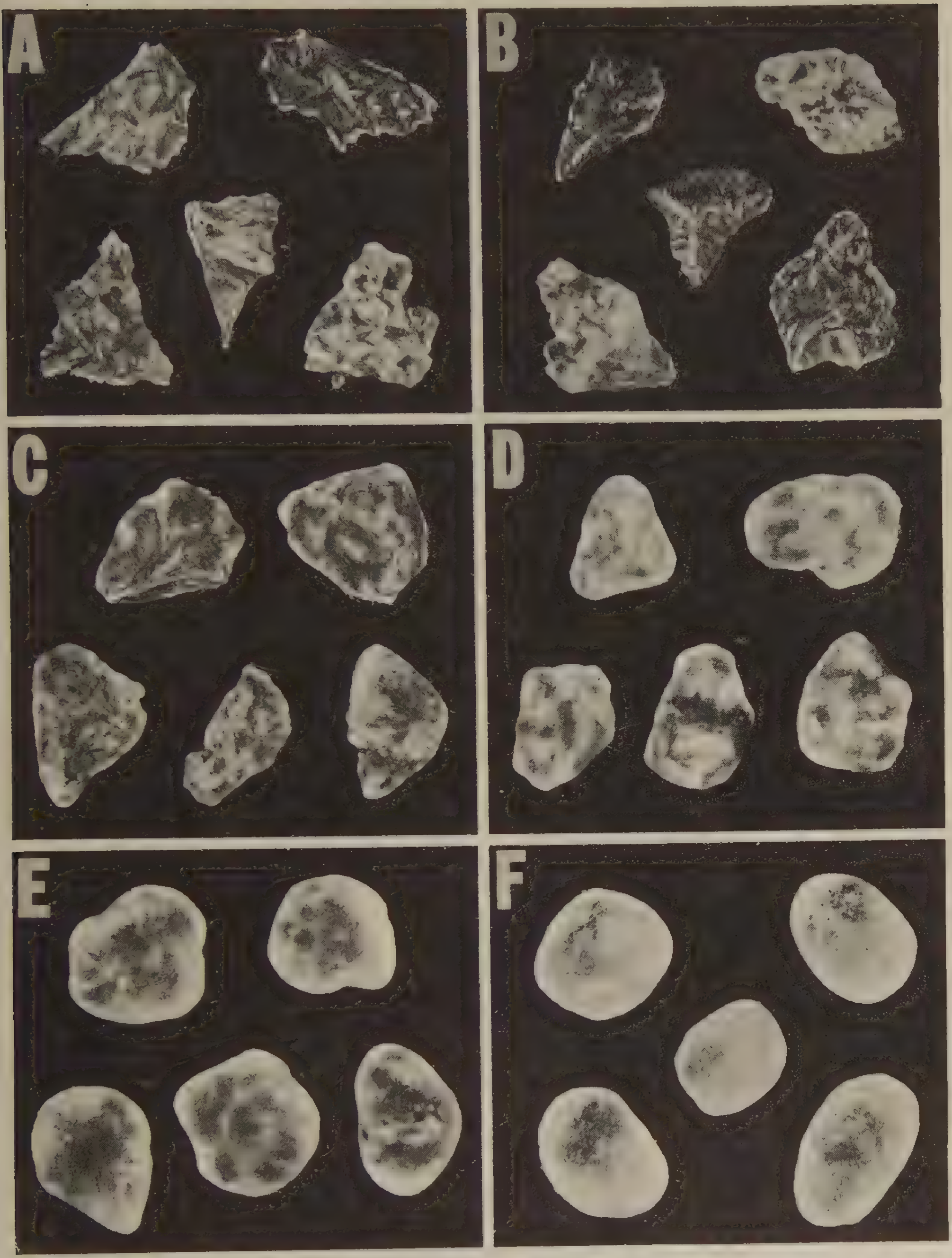

Fig. 1.—Examples of the six classes used for roundness (pivotability) determinations. Modified after Powers (1953). A = Very angular, B = Angular, C = Sub-angular, D = Sub-rounded, E = Rounded, F = Well-rounded. Photographs by junior author, retouching by J. R. Moriarty.

TABLE 1

Sample Location	Roundness		Percent Silt Content		Percent Black Minerals in Silt		Percent Crystals* in Silt		Percent Shells in .25 − .5 mm.		Mean Diameter, M_ϕ		Sorting, σ_ϕ		Skewness, $\alpha_{2\phi}$		Kurtosis, β_ϕ	
	Beach	Dune	Beach	Dune	Beach	Dune	Beach	Dune	Beach	Dune	Beach	Dune	Beach	Dune	Beach	Dune	Beach	Dune
ONSHORE WINDS (27 prs.)																		
U. S. West Coast (15)																		
La Push, Wash.	25.82	29.15	.02	.19	—	—	—	—	—	—	2.02	1.96	.44	.44	−.55	−.80	.73	1.07
Copalis, Wash	27.27	30.06	.04	.16	8	50	2	10	—	—	2.81	2.84	.25	.23	−.52	−.44	.64	.61
Westport, Wash.	28.84	29.56	.02	.03	4	4	—	—	—	—	2.71	2.48	.23	.37	−.57	−.43	.78	.57
Bay City, Wash	25.47	28.15	.14	.03	1	12	0	1	—	—	2.77	2.73	.23	.20	−.52	−.30	.57	.70
Coos Bay, Oregon	26.49	26.75	.02	.03	tr	2	0	1	—	—	2.27	2.54	.31	.29	−.19	−.28	.50	.59
Cresent City, Calif.	27.78	39.06	.03	.01	tr	18	0	2	20	4	2.77	2.43	.26	.29	−.54	−.28	.81	.62
Eureka, Calif.	29.94	31.20	.01	.03	6	13	—	—	—	—	2.14	2.18	.27	.29	−.15	−.21	.63	.66
Bodago, Calif.	29.73	30.17	.04	.10	3	5	—	—	3	tr	2.69	2.50	.30	.32	−.77	−.50	.93	.59
Moss Landing, Calif.	29.06	30.02	.02	.01	tr	1	0	2	—	—	1.96	2.17	.37	.34	−.35	−.35	.65	.68
Morro Bay, Calif.	31.06	34.23	.02	.18	2	20	0	4	5	2	2.56	2.74	.28	.24	−1.04	−.04	1.46	.58
Pismo Beach, Calif.	29.92	31.73	.20	.68	40	50	50	70	—	—	—	—	—	—	—	—	—	—
La Jolla, #1, Calif.	25.97	26.92	.03	.06	—	—	—	—	—	—	2.66	2.54	.28	.26	+.04	−.19	.71	.62
La Jolla, #2, Calif.	26.34	26.33	.03	.03	30	60	10	70	10	1	2.71	2.51	.28	.25	−.07	−.20	.57	.72
La Jolla, #3, Calif.	26.28	26.48	.04	.04	40	45	8	8	12	16	2.47	2.48	.29	.26	−.17	−.35	.62	.88
Coronado, Calif.	27.56	28.08	.22	.09	55	60	2	20	3	tr	2.81	2.38	.34	.32	−.12	−.41	.62	.69
Baja Calif. West Coast (5)																		
Rosarita Beach	24.56	27.71	.04	.11	3	25	tr	15	—	—	2.41	2.44	.22	.25	−.14	−.20	.73	.68
La Mission	25.79	28.69	.03	.12	10	23	tr	8	—	—	2.41	2.54	.27	.24	−.37	−.25	.63	.79
Ensenada #1	22.46	25.61	.03	.11	0	8	0	1	tr	2	0.99	2.78	.72	.26	−.32	−.46	.42	.54
Ensenada #2	23.41	26.76	.02	.08	1	12	0	1	1	0	0.96	2.72	.52	.30	0	−.50	.58	.77
Scammons	26.67	30.40	.03	.05	1	50	0	8	35	10	2.41	2.83	.45	.22	−.73	−.36	.80	.68
Miscellaneous (7)																		
Puerto Rico #1	25.99	26.84	—	—	—	—	—	—	59	16	3.19	2.29	.40	.47	−.08	−.62	.58	1.04
Puerto Rico #2	27.05	30.15	—	—	—	—	—	—	30	14	2.28	2.33	.45	.51	−.31	−.24	.69	.59
Puerto Rico #3	28.40	27.76	—	—	—	—	—	—	12	10	0.92	1.71	.81	.37	−.30	−.14	.69	.76
Fanø, Denmark	32.26	33.47	.05	.09	6	6	5	1	5	2	2.88	2.76	.34	.38	−.38	−.42	.79	.68
Skallingen, Denmark	29.81	32.43	.05	.01	5	3	2	1	7	tr	2.46	2.59	.46	.28	−.39	−.11	.76	.57
Sagami Bay, Japan	26.30	27.40	.02	.23	14	10	—	—	—	—	2.26	1.88	.44	.67	−.48	−.72	.68	.82
Eboshi, Japan	25.63	29.24	.12	.24	22	15	—	—	—	—	2.36	1.87	.41	.59	−.88	−.42	1.05	.61
OTHER (not onshore) (47)																		
Padre Island (27)																		
M-101	30.67	33.66	.13	.18	15	25	2	10	4	16	3.15	3.12	.31	.35	−.61	−.37	1.00	.69
M-103	33.03	34.07	.04	.15	21	31	3	25	9	7	2.92	3.05	.29	.28	−.24	−.79	.79	.86
M-106	31.30	33.57	.08	.03	30	24	18	13	2	11	2.69	2.89	.35	.27	−.37	−.22	.74	.78
M-107	31.25	30.26	.04	.08	17	27½	6	9	6	16	2.97	3.05	.31	.29	−.48	−.45	.90	.90
P-8	33.72	34.62	.08	.15	19	25	5	26	8	4	—	—	—	—	—	—	—	—
P-10	30.84	32.30	.02	.07	10	20	5	18	2	0	2.96	3.02	.33	.29	−.18	−.38	.64	.79
P-13	32.03	33.65	.12	.13	14	25	5	16	1	tr	2.99	3.19	.27	.23	−.41	−.48	.74	.91
P-14	34.22	34.61	.07	.06	15	30	9	27	—	—	3.06	2.97	.25	.26	−.48	−.31	.80	.69
P-16	34.73	35.08	.09	.06	10	30	—	—	—	—	3.03	3.16	.27	.19	−.33	−.32	.74	1.05

TABLE 1—*Continued*

Sample Location	Roundness		Percent Silt Content		Percent Black Minerals in Silt		Percent Crystals* in Silt		Percent Shells in .25 − .5 mm.		Mean Diameter, M_ϕ		Sorting, σ_ϕ		Skewness, $\alpha_{2\phi}$		Kurtosis, β_ϕ	
	Beach	Dune	Beach	Dune	Beach	Dune	Beach	Dune	Beach	Dune	Beach	Dune	Beach	Dune	Beach	Dune	Beach	Dune
P-18	30.31	34.20	.03	.05	25	35	7	11	2½	2	2.98	2.89	.25	25	−.18	−.40	.84	.76
P-20	32.25	33.70	.04	.07	8	25	5	10	10	1	3.03	3.03	27	.29	−.26	−.20	78	.72
P-22	29.76	32.82	.04	.05	8	15	8	19	34	15	2.79	2.83	.35	.36	−.83	−1.08	.83	1.36
P-25	33.25	32.39	.04	.07	12	8	1	4	tr	5	2.84	2.96	.33	.29	.79	−.83	.85	1.17
P-27	34.14	32.63	.03	.07	2	5	3	14	14	43	2.70	2.58	.42	66	.50	−.91	.62	.64
P-30	32.54	34.50	.01	.03	2	4	0	5	18	4	2.75	2.86	.39	.29	−.64	−.24	.74	.55
P-32	33.57	35.23	.02	.02	2	1	2	12	20	15	2.34	2.48	.59	.35	−2.30	−.14	1.09	.63
P-33	33.63	33.22	tr	tr	—	—	—	—	9	1	2.58	2.51	.39	.34	−.46	−.12	.87	.65
P-35	33.74	34.19	.02	.06	20	28	2	21	4	2	2.81	2.96	.33	30	−.12	−.33	.58	.80
P-37	33.59	32.06	.02	.04	10	45	15	8	1	5	2.77	2.73	.33	.36	−.09	+.17	.61	.61
P-39	32.90	32.33	tr	.05	—	—	—	-	12	4	2.49	2.80	.34	.23	−.35	−.13	.79	.74
P-42	33.90	32.37	.02	.01	25	32	5	19	tr	3	2.77	2.61	.29	.27	−.10	−.04	.59	.63
P-45	31.65	33.04	.03	.03	2	18	2	3	2	4	2.54	2.62	.28	.31	−.14	−.13	.64	.71
P-48	33.65	35.86	.02	.04	3	15	0	7	3	½	2.58	2.62	.31	.27	−.10	−.07	.81	.74
P-50	35.17	32.32	.10	.07	7	10	-	—	2	4	2.74	2.66	.23	.30	−.39	−.10	.83	.67
P-53	33.89	33.82	.02	.03	13	29	7	7	0	2	2.69	2.65	.25	.28	−.12	−.04	.56	.57
P-57	35.94	35.93	.15	.09	65	38	—	—	3	6	2.68	2.57	.21	.23	−.24	−.17	.76	.61
RG-4	31.73	32.92	—	—	—	—	—	—	1	8	—	—	—	—	—	—	—	—
Miscellaneous (20)																		
Kiel, Germany	34.93	31.95	.02	2.16	4	0	0	0	—	—	2.19	2.00	.31	.29	−.45	+.03	.97	1.04
Lake Geneva	29.69	27.10	.45	7.08	12	0	0	0	5	tr	2.73	2.36	.51	.44	−.33	—	75	—
Dhahran, Sandi Arabia	39.16	36.89	.03	.14	3	tr	0	0			1.36	2.60	.41	.48	−.81	−.13	.72	.50
Karachi, Pakistan	21.59	24.99	1.49	2.80	2	1	0	1	½	2	3.18	3.43	.31	.35	+.10	−.14	.87	.66
Kalutara, Ceylon	27.81	31.31	.34	.34	30	10	11	3	—	—	2.38	1.49	.30	.64	+.07	−.67	.80	67
Hambantota, Ceylon	26.91	26.17	.16	.04	35	10	6	0	½	tr	1.65	1.90	.79	.33	−.73	−.45	.66	1.27
Colombo, Ceylon	30.72	31.75	.20	.64	55	70	5	20	10	8	2.49	2.30	41	.55	−.34	−.31	.61	.58
Galle, Ceylon	32.28	31.69	.04	.01	1	15	0	0	60	60	1.57	2.25	.63	.33	−.29	−.45	.49	70
Waltair, India	32.01	29.70	.82	.03	70	25	3	tr	1	tr	2.80	1.95	.38	.49	−.24	−.39	.71	.69
Kakinada, India	31.14	29.34	.60	1.21	20	65	2	3			2.82	2.88	.37	.36	0	−.11	.70	.89
Seven Pagodas, India	34.85	30.96	.03	.03	20	8	8	tr		-	1.94	1.83	.39	.52	−.49	−1.04	.82	1.23
Thai #1	37.38	32.27	.02	.03	tr	tr	4	1	1	0	2.49	2.34	.31	.26	−.90	−.58	.97	.81
Thai #2	35.33	37.72	.03	.03	tr	tr	1	6	—	—	2.26	2.51	.32	.25	−.22	−.36	.56	.76
Okudi, Japan #1	29.21	28.56	.01	.03	1	3	0	0	16	12	1.35	1.36	.33	.35	−.61	−.46	.76	.49
Okudi, Japan #2	28.60	30.10	.12	.60	30	20	0	0	52	49	2.36	2.52	.42	.34	−.36	−.21	.67	.79
Oiso, Japan #1	23.95	27.03	.05	11	18	34	0	0	—	—	2.01	1.85	.61	.52	−1.18	−.56	1.33	.75
Oiso, Japan, #2	25.18	27.73	.01	.02	17	17	0	0	—		1.54	1.43	.65	.71	−.42	−.08	.83	.42
San Felipe, Baja California	29.25	30.32	.01	.90	1	3	tr	2		—	0.82	1.28	.78	.75	+.13	+.17	.46	.99
Magdalena Bay	29.25	29.85	.38	.36	40	61	11	9	12	tr	2.67	2.59	.27	.39	−.19	−.23	.74	.59
Las Cabras, Baja California	24.12	23.00	.02	.04	8	16	tr	3	—	—	1.48	1.74	.60	.46	−.25	−.41	.55	.76

* Probably all zircon.

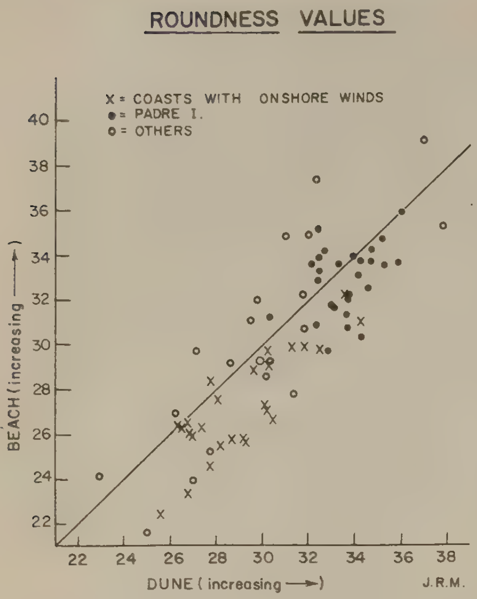

FIG. 2.—Comparison between roundness values of beach (foreshore) and dune pairs. All those above have rounder beach sands. Virtually all of the pairs from coasts with onshore winds have rounder dune sands, whereas there is little difference along other coasts. Scales are those of Powers (1953) times 100.

study has come from comparing the differences in areas where the prevailing winds are onshore with those where the winds are either longshore, variable, or ordinarily offshore. It was found that all but two samples of the former show greater dune roundness and one of the two showed a tie-count. Along the Texas coast the wind is ordinarily from the southeast and hence onshore. Therefore, the samples studied by Beal showed consistently greater roundness in the dunes. As the result of a trip made by G. A. Rusnak and the senior writer along Padre Island, 27 pairs of beach and dune sands were compared. These showed 17 with rounder dune sands, 1 tie, and 9 with rounder beach sands. This seemed to be out of line with the results obtained by Beal which came partly from the same island. Two factors probably contributed to the difference. One was that the more extensive suite of samples from Padre Island was collected during and shortly after a strong northwest wind had changed conditions from those of onshore to offshore winds; during much of this trip the sands were being blown onto the beach by the wind coming from the dunes (fig. 3). The other factor may be that the southern and central portion of Padre Island, where almost all of the rounder beach sands were found, has a beach which is largely a mass of shells without much terrigenous sand available. Although terrigenous sand was collected from the beach, it may not be representative of the sand which formed the dunes.

Many of the other exceptions to the rounder dune sands came from India, Ceylon, and Thailand. In these areas the monsoons cause alternate onshore and offshore winds. Similarly, an attempt to identify samples of the sands collected by Waskom (1958) from northwest Florida produced poor results, but rounder dune sands were found in the only line which extended in from a beach with onshore winds. Where the wind was either longshore or offshore, no difference was found.

On the other hand, numerous samples taken all along the west coast of the United States and in adjacent Baja California where the winds are almost entirely onshore showed remarkably consistent results, with the dunes rounder than the beaches.

Roundness and Grain Size

The best possible results of roundness studies should come from testing the roundness of the various grain sizes produced by sieving the sample. This, however, is very time-consuming, so that it was only done with a few selected samples. Taking 11 of the sample pairs from the west coast, all of which showed greater dune roundness than beach in the .062–.125 mm size, the roundness was also measured on both dune and beach samples taken from sievings having size limits of .125–.177 mm, .177–.25 mm, and .25–.5 mm. A plot of the results shows that the roundness varies irregularly with size in both dunes and beaches (fig. 4). Only four samples showed a progressive change. In the others the roundness alternately increased and decreased. Comparison of roundness in the pairs shows that five of the samples had greater roundness in all sizes of the dune sand. Only the largest size, .25–.5 mm, showed no difference between dunes

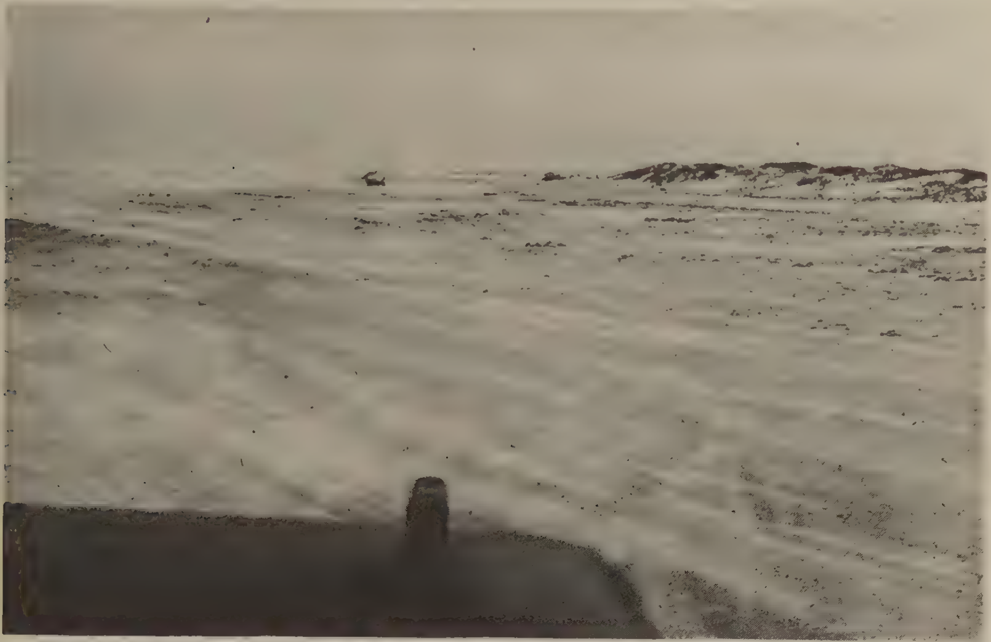

FIG. 3.—A photograph taken through jeep windshield during the collection of beach and dune pairs from Padre Island. The strong offshore wind is indicated by the streaks of sand moving diagonally seaward.

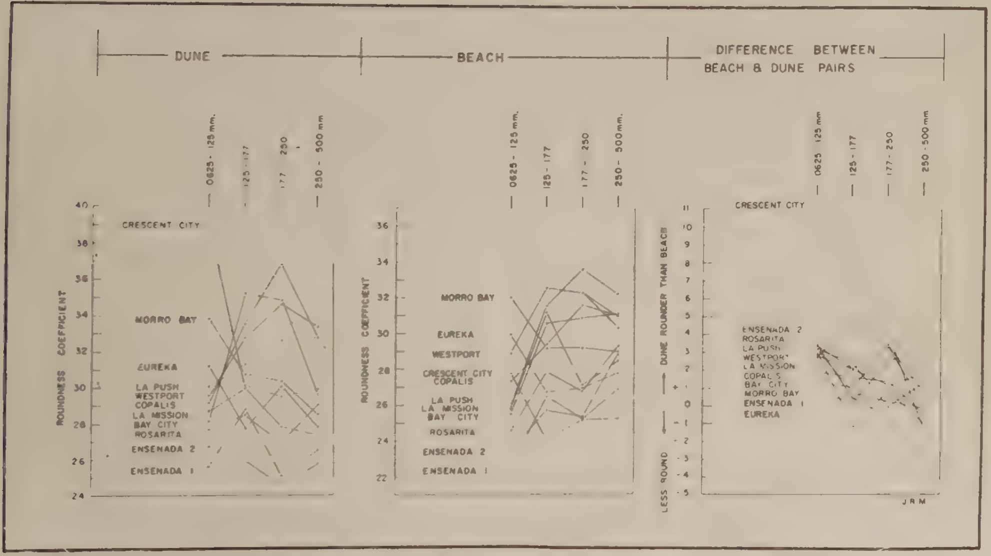

FIG. 4.—Showing the variation in roundness coefficient with grain size in a series of dune and beach (foreshore) sands from the west coast of North America. The difference between the beach and dune pairs in relation to grain size is indicated on the right.

and beaches. A few comparisons from other areas have also indicated that there is little consistent difference in the results obtained by using different grain sizes.

An attempt was made to try larger grain sizes for roundness comparisons in several of the samples from Padre Island where the .062 to .125 size did not show greater roundness in the dunes. No significant difference was found so that it appeared that the roundness was not a function of size in these cases.

Roundness in Sandstones

In order to compare the roundness values obtained in the study of beaches and dunes with those in some of the sandstones which have been described as unusually round, samples of sandstones from a number of formations said to have very round grains were obtained (through arrangements made by G. V. Cohee). Those from which the grains were easily separated included St. Peter Sandstone, Jordan Sandstone, Bromide Formation, Hickory Sandstone, Bidahochi Formation, and Carrizo Sandstone. From all of these, roundness was determined in two or more size grades. No trouble was found in making the roundness test of the coarser sizes, but the .062–.125 size proved somewhat difficult because of possible confusion of the original grains with quartz cement and incipient crystal growth along with what appeared to be artificially broken fragments. Neglecting these fine grains, the results show clearly that all but one of these sandstones have higher roundness values than those obtained in the dunes and beaches (table 2). The somewhat doubtful determination of roundness in the .062–.125 sizes shows much less contrast but indicates that even in the finest sizes these sandstones are probably rounder than typical beaches and dunes of the present day. A few samples of sands from Georges Bank off the New England coast and a sample from a turbidity current deposit in a submarine canyon outside Georges Bank are the only modern sediments tested by the writers with roundness comparable to the round-grained sandstones.

TABLE 2.—*Roundness values of sandstones*

	.062–.125 mm	.35–.71 mm	.71–2.0 mm
St. Peter Sandstone	45.87	57.46	68.40
Jordan Sandstone	47.77	59.12	72.17
Bromide Formation	39.65	71.24	78.84
Hickory Sandstone	34.09	54.12	61.19
Bidahochi Formation	39.77	49.04	67.45
Carrizo Sand	36.73	34.89	37.50

The sandstone samples also differed from the beach and dune sands in showing a decided decrease in roundness with decrease in size, as has been said to be the case for sand and sandstones in general (Pettijohn, 1956, p. 60–65).

Foreshore and Berm Roundness

Virtually all beach sands for the tests were collected from foreshores. Therefore, in order to determine whether the difference between the beach sands and the dunes might not actually be a difference between foreshore and berm (inner horizontal portion of a beach), a series of sample pairs were taken from these two environments and roundness tests were run, using the same methods. All 20 of the sample-pairs which were examined in this way were taken from areas where there were onshore winds and hence where the dune sands were rounder. The results are remarkably consistent. Eighty percent of the berms (fig. 5A) have rounder sand than that on the foreshores. Comparison of the berm and dune (where present) in the same areas shows that the roundness values in the berms are in general intermediate between those of the foreshore beach and the dune (fig. 5B).

Two possible explanations exist for greater roundness in the berm than on the foreshore. One is that the waves carrying the sand up onto the berm may select the rounder grains. The other is that the occasional offshore winds mix the dune sand in with the sand on the berm, whereas the active wave action on the foreshore inhibits such a mixing. Worthwhile experiments could be conducted with artificial beaches in wave tanks. These should help explain the difference.

DIFFERENCES IN SIZE PARAMETERS

Mean Diameter

One might anticipate that wind blowing over a beach would pick up the smaller grains and hence that a dune sand could be easily distinguished from a parent beach by

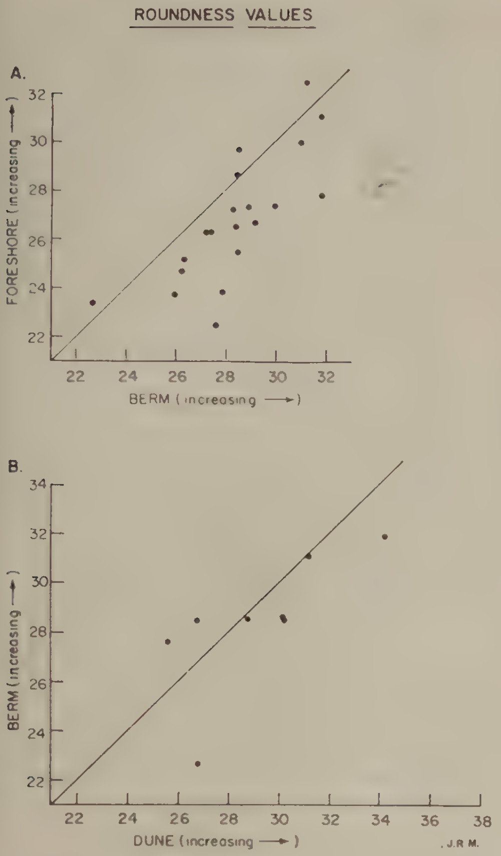

FIG. 5. A.—Comparison between roundness values of sample pairs taken from the foreshore and the adjacent berm (backshore). (Powers' scale times 100). B.—Comparison between roundness values of sample pairs taken from the berm and adjacent dune. (Powers' scale times 100.)

its smaller grain size. The exchange, however, is not as simple as that. In the first place, the beach is already well sorted and the wind is evidently capable of picking the larger grains almost as well as the smaller, since the shape of the grain appears to make more difference than the slight range in size. Furthermore, the smaller grains are carried farther and may entirely by-pass the dune, and after deposition the dune sand, being dry, is subject to more sorting from the wind than the relatively wet beach. This sorting may remove the finer grains.

A test of grain size may be made to best advantage by mean diameters, that is, the average of the 16th and 84th percentiles (Inman, 1952). The mean seems preferable to the median (the 50 percentile) because it gives a more representative measure of the average size of particles in the frequency distribution and is not merely the mid-point of the size distribution. Comparison of the mean diameters of each pair of beach-dune samples (fig. 6) shows that there is little difference between the two. In these comparisons, 48 are within 0.2 phi of each other; of the others, 14 show coarser beach sands and 9 coarser dune sands. Furthermore, no difference exists in the cases of onshore wind beaches from the others. From these results, therefore, it would appear that the mean diameters do not constitute a reliable means of distinguishing beach and dune sands.

Silt Content

All of the beach and dune sands were analyzed for silt and clay content. Actually, clay is a minor factor and the greater part of the fines proved to be relatively coarse silt. A comparison between the silt content of the beach and dune pairs has shown a strik-

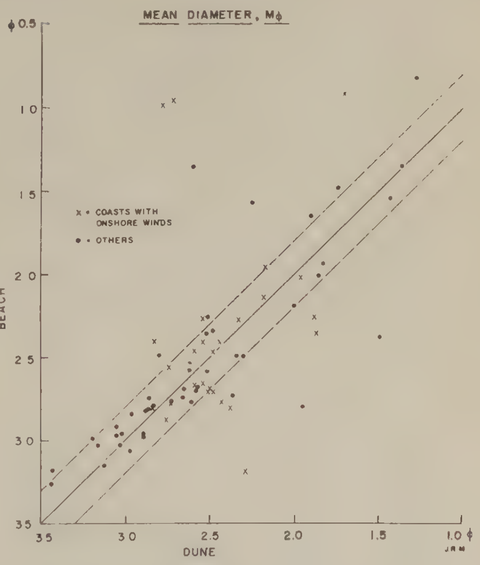

FIG. 6.—Comparison of mean diameter of pairs of beach (foreshore) and adjacent dune sands. The dashed lines are located within 0.2 ϕ of the line which indicates the same value for the pair.

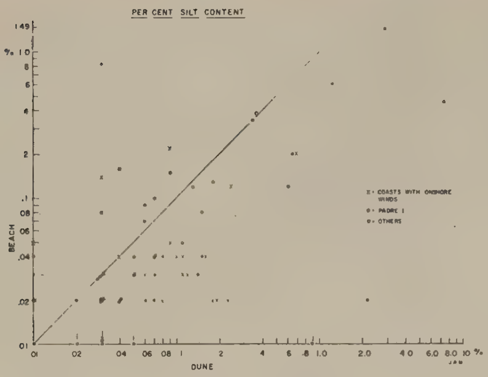

FIG. 7.—Comparison of the percent of silt for each of the beach-dune pairs. Note that here, as in the case of roundness, the coasts with onshore winds have considerably more silt in the dunes than in the beach foreshores.

ing contrast (table 1, fig. 7). Sixty-seven percent of the pairs have a higher silt content in the dune sands. Little, if any, relationship exists with wind direction since beaches with onshore winds have 71 percent with higher silt.

Comparison of the silt content between foreshore and berms shows more silt in 58 percent of the berms (fig. 8). Here also the dunes show more silt than the berms.

The explanation of the greater silt content in the dunes than beaches appears to be relatively simple. Wave action is much more likely to prevent deposition of fine sediments than wind action, because the waves are almost always sufficiently turbulent to keep silt in suspension whereas the wind is much more variable. On the berms the waves have less continuous effect than on the foreshore so that silt introduced by wind can settle on the sand between the occasional periods of wave inundation.

Sorting, Skewness, and Kurtosis

Studies of beaches and dunes from a single locality have suggested that other size parameters such as sorting, skewness, and kurtosis can serve to distinguish the two (Mason and Folk, 1958). In order to test these parameters more widely, cumulative curves were made from all of our size analyses using a combination of sieving and settling tube. From these curves sorting, skewness, and kurtosis were obtained using the formulas suggested by Inman (1952). The values of sorting, skewness, and kurtosis based on 25 and 75 percentiles used by some other investigators are statistically less representative as pointed out by Inman so that they were not used. The more comprehensive formulas used by Folk and Ward (1957) were applied to a few samples for comparative purposes, but as the results differed so slightly from those obtained using the simpler Inman formulas, the latter were used throughout.

Sorting (phi deviation) is here expressed as $\sigma_\phi = \frac{1}{2}(\phi_{84} - \phi_{16})$. Using this formula to compare the sorting of the beach and dune pairs it was found that there are only minor differences in the sorting of the pairs (fig. 9). Seventy-three percent of the pairs had a sorting value within 0.1_ϕ of each other. Little or no difference existed between areas with onshore winds and the others. These differences are only slightly favorable to better dune sorting and, therefore, while this agrees with the opinion of Mason and Folk (1958) for Mustang Island, Texas, it does not appear to offer a valid means for distinguishing dune and beach sands.

Skewness (second phi skewness), which measures the symmetry of the curve and particularly the distribution in the tails of the curve, is here expressed as

$$\alpha 2_\phi = \frac{1/2(\phi 5 + \phi 95) - Md_\phi}{\sigma_\phi} .$$

The skewness values we obtained appear to

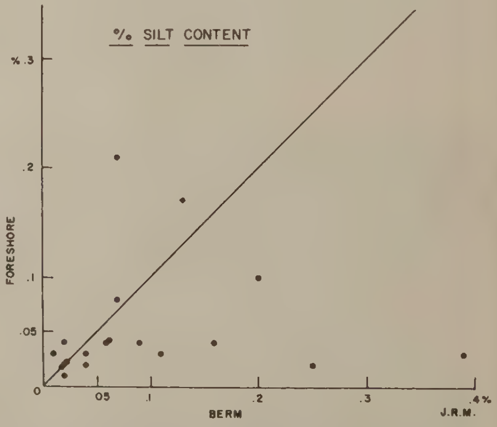

FIG. 8.—Showing comparison of the silt content between pairs of foreshore and berm samples.

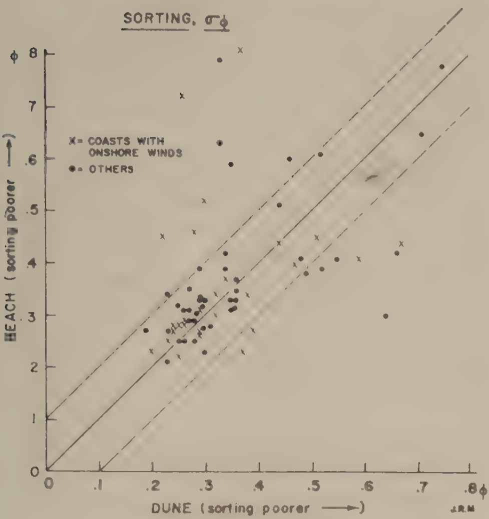

FIG. 9.—Comparing the sorting of the pairs of beach (foreshore) and dune sands. The dashed lines indicate a difference of 0.1ϕ from the condition of equal sorting for the pair.

be more negative than is entirely normal. This may be caused by the effect of the settling tube method as compared to that of sieves, but it affects the analysis of both beaches and dunes in the same manner so that a comparison is justified. Despite the fact that silt values are higher in dunes which tends to produce positive skewness, the difference in the skewness of dunes and beaches is very slight with 53 percent having a skewness value within 0.2_ϕ of the paired sample (fig. 10). Where the wind was onshore, only 46 percent of the samples showed the dunes with more positive skewness whereas 59 percent of the others had the dunes skewed more to the positive. This last may have some significance, but it is not evident to the writers. Here again the findings of Mason and Folk (1958) for Mustang Island indicating more positive skewness in dunes are favored by such a scant margin that the criterion as a means of distinguishing beaches and dunes does not appear to be practical.

The expression of kurtosis has not been used extensively by sedimentologists, but it has been suggested by Mason and Folk (1958) as offering some promise in differentiation of dunes and beaches particularly when skewness is plotted against kurtosis. Phi kurtosis, which measures peakedness of the curve by comparing sorting in the central portion with the average spread in the tails of the distribution, is here expressed as

$$\beta_\phi = \frac{1/2(\phi95 - \phi5) - \sigma_\phi}{\sigma_\phi}.$$

Plotting the difference in kurtosis between beach and adjacent dune (fig. 11) again shows that there is no trend in this parameter which will allow distinction between beaches and dunes. The comparison shows that 66 percent had values within 0.2_ϕ of each other. Plotting the skewness against the kurtosis for all of the dunes and beaches (fig. 12) also fails to show any significant trend which would differentiate the two environments.

Comparisons between mean diameter and sorting and between sorting and skewness for all beach and dune samples were attempted (figs. 13 and 14). These again failed to show any striking difference between the environments. Thus, it appears that differentiation of dunes and beaches by size parameters other than silt content is not possible.

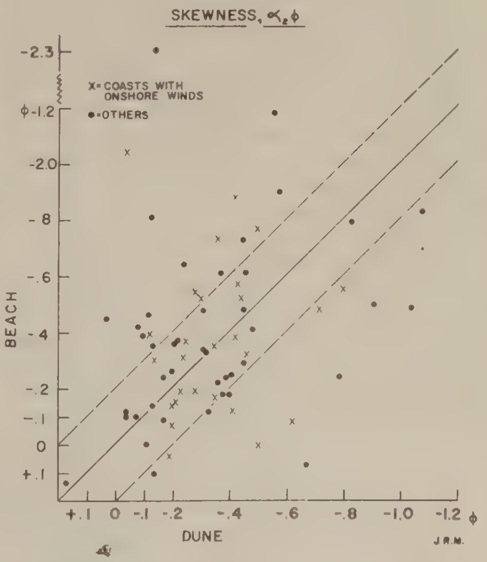

FIG. 10.—Comparing the skewness of the pairs of beach (foreshore) and dune sands. The dashed lines indicate a difference of 0.2ϕ from the condition of equal skewness for the pair.

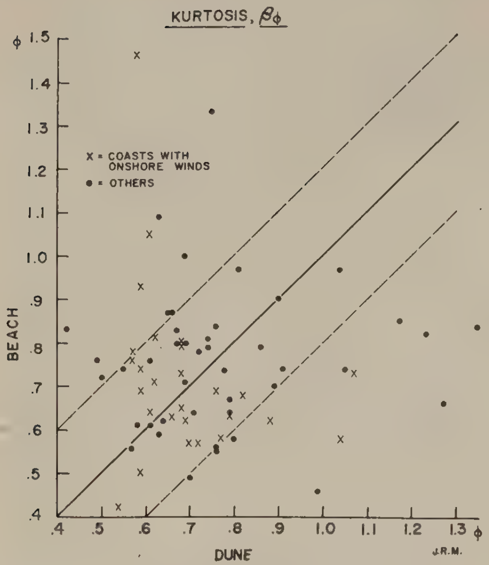

FIG. 11.—Comparing the kurtosis of the pairs of beach (foreshore) and dune sands. The dashed lines indicate a difference of 0.2ϕ from the condition of equal kurtosis for the pair.

DISTINCTION BY CONSTITUENT COMPOSITION

Black Minerals in the Silt Size

Investigations by Bradley (1957, p. 116), Stewart (1956), and von Englehardt (1940) have shown that heavy minerals in the .062–.125 mm size are more common in dunes than in beaches respectively on Mustang Island, at San Miguel Lagoon along the coast of Baja California, and on parts of the German coast. In studying the composition of the .062–.125 mm fraction of a considerable number of beach and dune samples along the Gulf Coast and the California coast the senior writer did not find any appreciable difference in the black minerals, the most easily identified heavies. It was observed, however, that these heavies are greatly concentrated in the coarse silt fraction. Accordingly, a check was made of the silt size fractions of all the beach and dune pairs used for the present study. Here a striking difference was found. Using the simplest test, which was counting the percentage of black minerals (omitting biotite which is very different from the others from a sedimentation viewpoint), it was found that the silt from 45 dunes had more black minerals than that of the corresponding beaches whereas 16 beaches had more than the dunes, and 3 were ties (table 1). Thus, this agrees in general with the findings of Bradley, Stewart, and von Englehardt. It will be seen from figure 15 that many of these differences are very considerable, amounting to as much as 50 times as many black minerals in one dune. The percentages of black minerals are surprisingly large, particularly since the samples were not collected from areas where an obvious concentration had taken place, such as in the black mineral lag concentrate left after the light minerals of a beach or dune have been largely removed.

The composition of the black minerals in four of the samples was determined by Tj. H. van Andel and found to be predominantly ilmenite and magnetite with some hornblende. It is thought that these minerals are also dominant in most other samples.

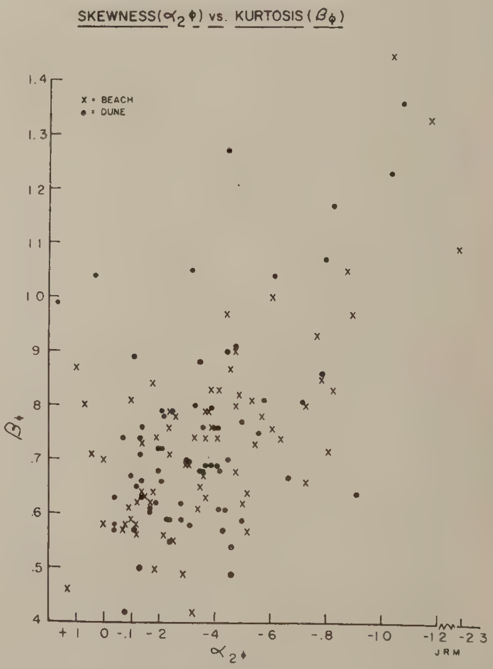

FIG. 12.—Comparison of skewness against kurtosis for individual samples of beach (foreshore) and dune sands. There is little difference between the two environments.

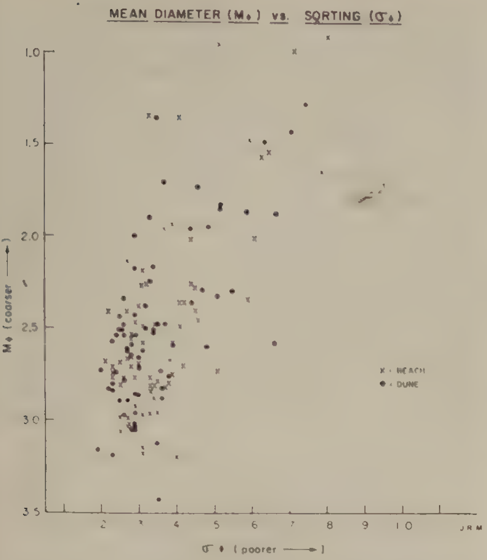

Fig. 13.—Comparison of mean diameter against sorting for individual samples of beach (foreshore) and dune sands. There is little difference between the two environments.

The most interesting discovery was that in the samples from the west coast of the United States and Baja California where the dunes showed a consistently greater roundness, the dunes had an equally consistent excess of black minerals of silt size. All but one west coast dune showed more black minerals than the corresponding beach, and this one had approximately the same number. The Mustang-Padre Island area in southern Texas where roundness was not particularly effective in distinguishing beaches and dunes proved to have 20 samples of silt with more black minerals in the dunes as compared to 4 with more in the beaches. On the other hand, the samples from Asia showed more black minerals in the beaches than in the dunes. Since most of the Asiatic beaches are located in zones lacking consistent onshore winds, the failure of the rule here may perhaps be related to the back and forth movement of the black minerals because of alternating onshore and offshore winds.

The explanation of greater content of black minerals in the silts of dunes than in the silts of beaches is not clearly evident. It is possible that the rather high degree of rounding shown in most of the black minerals, where the contrast was striking, may explain the greater concentration, provided that winds are more capable of picking up round grains. The greater weight of the heavy black minerals would not make as much difference in the case of silt size frac-

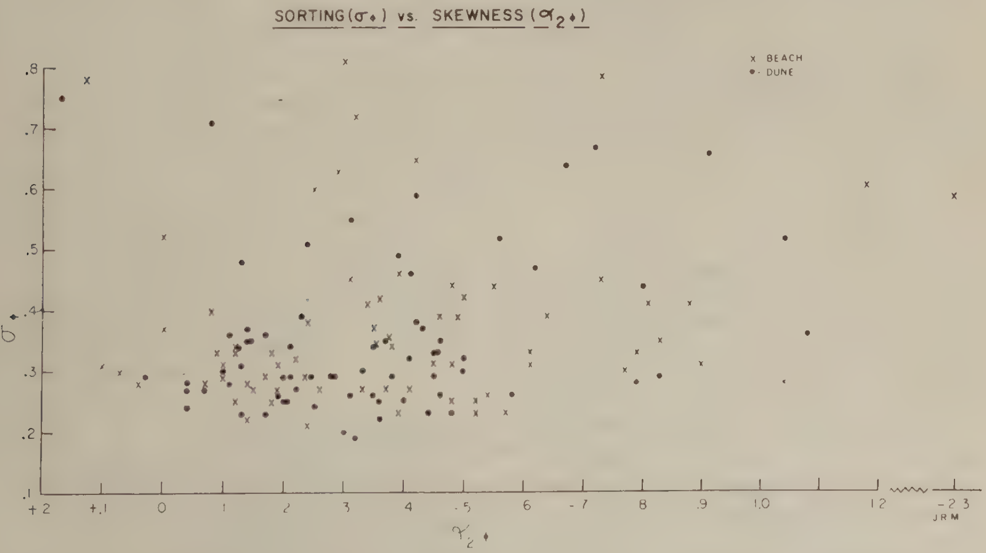

Fig. 14.—Comparison of sorting against skewness for individual samples of beach (foreshore) and dune sands. Again there is little difference between the two environments.

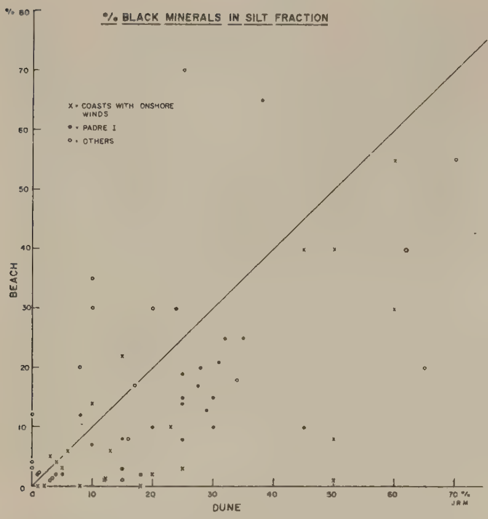

FIG. 15.—Comparison of black mineral percentages in the silt fraction of the beach (foreshore) and dune pairs. The higher content of black minerals in the dunes along coasts with onshore winds and on Padre Island is indicated.

tions as in coarser material. However, a few cases where black minerals were found in the .25 to .5 mm fractions indicated the same trend, although the number of occurrences and the amounts of black minerals were such that the case is not well established. Another possibility is that the black minerals represent the lag concentrate due to wind working over the dunes more than the foreshores of the beaches where wetness prevents much wind action. In this reworking the light mineral fraction of silt size may be largely removed.

Zircon Crystals in the Silt Sizes

In comparing the silt fractions of the dunes and beaches it was observed that crystals were surprisingly abundant although they are rare in the sand sizes. Examination of these crystals in a few samples by Tj. H. van Andel showed that they were all zircons and hence a heavy mineral. Van Andel found that an approximately equal number of zircons lacked crystal form or showed much abraded crystals. Since it is far easier to identify the crystals under binoculars than the other zircons, these were used as a test for environment. It is assumed that the crystals in the other samples are also zircon as they are all similar in appearance under the binoculars. Tabulation showed that the zircon crystals, like the black minerals, were also more abundant in the dunes than in the beaches (table 1 and fig. 16). The samples with abundant zircon crystals were almost entirely samples which also had a high content of black minerals.

Since the crystals have decidedly more rounding than the rest of the minerals, it can be suggested that their greater concentration in the dunes is caused by the selectivity of the wind. As in the case of the black minerals, a lag concentration is also possible.

Shells and Other Calcareous Fragments

No complete study has been made of the organisms found in the beach-dune pairs. Estimates of organisms were made, however, of the .25–.5 mm fraction in all of the pairs. Beaches would be expected to have more shells, since few shell animals live on the dunes and numerous shells are cast up on the beaches by the waves. Although the

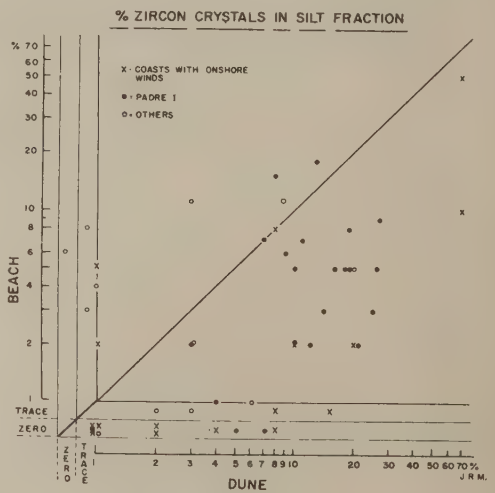

FIG. 16.—Comparing percentages of zircon (or similar appearing) crystals in the silt fractions of the beach (foreshore) and dune pairs. Included are cases where no crystals or only a trace of zircon crystals were found in one member of the pair. Here also the dune samples have more crystals than the beach foreshores on the coasts with onshore winds and on Padre Island.

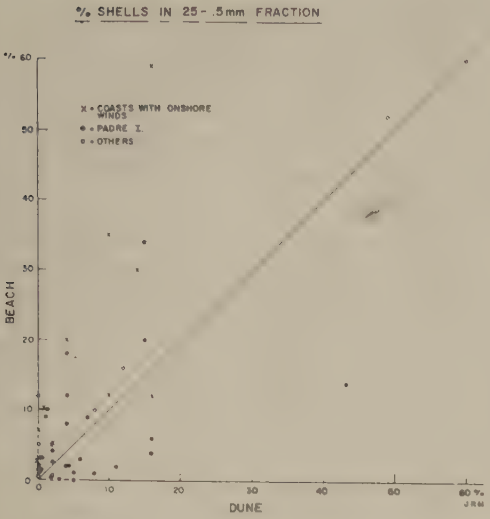

FIG. 17.—Comparison of percentages of shells in the .25–.5 mm fraction in the paired beach (foreshore) and dune samples. Here a greater quantity of shells is found in the beaches except on Padre Island where they are virtually the same in both environments.

wind does transport shells, they are usually larger than the sand grains and more angular so that they are not quite as easily picked up by the wind as the sand. Furthermore, the shells are more likely to be leached out of the dunes. The comparisons showed that 67 percent of the beach sands had more shells than the dune sands (table 1, fig. 17). The test worked well for onshore wind coasts, with 86 percent having more shells in the beach, and almost equally well for the other areas except Padre Island. In some cases the shell content in dunes may have been introduced by man because kitchen middens are quite common among coastal dunes. The sizes studied, however, should minimize the effect of man since small fragments are not commonly left by man although the shells might have been reduced in size by nature subsequent to man's activities.

Perhaps the most surprising thing about the shells is the large number of beaches which did not appear to have any shells at all. This scarcity was even discovered in many of the tropical beaches of India and Ceylon.

Foraminifera are very common in some tropical beaches, particularly in tropical islands. They were rare in most of the beaches investigated and even less common in the dunes. At Karachi, however, they constitute 15 percent in the .25–.5 mm size beach material but are scarce in the dunes. In some other beaches rounded calcareous grains probably represent eroded Foraminifera.

Other Constituents

Not many beaches or dunes were found to contain an appreciable content of mica although Karachi is predominantly a mica beach with about one half as much mica in the dunes. The comparison of 28 pairs containing mica showed that mica is more abundant in 17 beaches than in the adjacent dunes whereas 9 show more mica in the dune and 2 were ties. Here again there is some indication that the flat grains in contrast to the round are less subject to wind selection. Furthermore, once the flat mica grains are picked up by the wind they are transported grester distances, in many cases by-passing the dunes.

Plant fibers are found occasionally in beaches and dunes although most of the samples examined had only negligible quantities. In those pairs containing appreciable amounts, plant fibers were more abundant in seven dunes and in only one beach. Presumably the plant fibers come from the vegetation which partly covers many dunes. Plants are rare on beaches although driftwood is locally very abundant, for example in northwestern United States.

GRAIN FROSTING

The common statement that dune sands are more frosted than beach sands may be true, but frosting appeared to be very rare in the dunes bordering the beaches which we investigated. The frosting of sand grains by the wind is considered by Ph. H. Kuenen (1960) to be nonexistent. His experiments showed that frosting was a development of chemical action on the dunes rather than sand blast, although sand blast is well known to frost window panes and pieces of glass left on a beach. The coastal dunes are remarkably free of frosted grains, and in no

Table 3.—*Summaries of the nine tests*

("×" = Onshore)
("●" = Padre Is.)
("○" = Others, not onshore)

		Beach Higher		Tie		Dune Higher		Total No.	Sign Test (probability)
		No.	%	No.	%	No.	%		
Roundness Values (Fig. 2)	×	1	3.7	1	3.7	25	92.6	27	<.01
	●	9	33.3	1	3.7	17	63.0	27	.17
	○	11	55.0	0	0	9	45.0	20	>.25
Total		21	28.4	2	2.7	51	68.9	74	
% Silt Content (Fig. 7)	×	5	20.9	2	8.3	17	70.8	24	.02
	●	6	23.1	3	11.5	17	65.4	26	.03
	○	4	20.0	3	15.0	13	65.0	20	.05
Total		15	21.4	8	11.4	47	67.2	70	
% Black Minerals in Silt (Fig. 15)	×	3	13.6	2	9.1	17	77.3	22	<.01
	●	4	16.7	0	0	20	83.3	24	<.01
	○	9	50.0	1	5.6	8	44.4	18	>.25
Total		16	25.0	3	4.7	45	70.3	64	
% Zircon Crystals in Silt (Fig. 16)	×	2	11.8	1	5.9	14	82.3	17	<.01
	●	2	9.5	1	4.8	18	85.7	21	<.01
	○	6	50.0	0	0	6	50.0	12	>.25
Total		10	20.0	2	4.0	38	76.0	50	
% Shells in .25–.5 mm. size (Fig. 17)	×	12	85.7	0	0	2	14.3	14	.01
	●	13	52.0	0	0	12	48.0	25	>.25
	○	8	80.0	1	10.0	1	10.0	10	.04
Total		33	67.4	1	2.0	15	30.6	49	
Mean Diameter (Fig. 6)	×	13	50.0	0	0	13	50.0	26	>.25
	○	24	53.3	1	2.2	20	44.5	45	>.25
Total		37	52.1	1	1.4	33	46.5	71	
		Beach Poorer		Tie		Dune Poorer			
Sorting (Fig. 9)	×	15	57.7	1	3.8	10	38.5	26	>.25
	○	25	55.6	1	2.2	19	42.2	45	>.25
Total		40	56.3	2	2.8	29	40.9	71	
		Beach more neg.		Tie		Dune more neg.			
Skewness (Fig. 10)	×	12	46.2	1	3.8	13	50.0	26	>.25
	○	26	59.1	0	0	18	40.9	44	>.25
Total		38	54.3	1	1.4	31	44.3	70	
		Beach Higher		Tie		Dune Higher			
Kurtosis (Fig. 11)	×	12	46.2	0	0	14	53.8	26	>.25
	○	21	47.7	2	4.6	21	47.7	44	>.25
Total		33	47.1	2	2.9	35	50.0	70	

case could the difference between a beach and an adjacent dune be determined by degree of frosting.

CONCLUSIONS

Results of Combination of Tests

Comparing the tests for roundness, silt content, black minerals, zircon, and shells for each pair of beach and dune samples, it was found that of the 74 pairs 54 could be identified as having the majority of the tests favorable whereas 14 showed the majority unfavorable and six pairs had the same number of favorable and unfavorable tests. Of the beaches with onshore winds, 25 were favorable and only one unfavorable with one tie. It seems that in areas with onshore wind the tests should prove very reliable in distinguishing between beaches and dunes. Of the Padre Island samples from an area which ordinarily has onshore winds but which had just experienced a strong offshore wind before and during collections, the favorable cases numbered 18 and unfavorable six with three ties. In the northern 44 miles of Padre Island only one unfavorable case was found.

The other areas with offshore or longshore winds proved much less satisfactory, with only 11 favorable and seven opposed along with two ties. Thus it appears that little can be learned from the tests in these areas.

Statistical Significance of the Individual Tests

Table 3 summarizes the results of each of the nine tests. Since the distribution of differences between pairs is conspicuously non-normal, a non-parametric statistical comparison was used. The Sign Test (Dixon and Massey, 1957) indicates that on coasts with onshore winds, beach sand differs from dune sand in five characteristics (roundness, silt content, black minerals, zircon crystals, and shell content). These differences are significant at the .02 level (or less), implying that if there was, in fact, no difference between beach and dune sands in these characteristics, one would observe such a large apparent difference less than two times in a hundred. This is so unlikely that it is concluded that there is a real difference in this group of samples between these two types of sand.

In the Padre Island samples the Sign Test indicated a real difference between environments in three of the tests (silt content, black minerals, and zircon crystals), but not in the other characteristics. Samples from the other areas with offshore or longshore winds proved to differ significantly only in silt content and shell content.

All of the grain size parameter tests proved to be definitely not significant, regardless of area.

REFERENCES

Beal, M. A., and Shepard, F. P., 1956, A use of roundness to determine depositional environments. Jour. Sedimentary Petrology, v. 26, p. 49–60.

Bradley, J. S., 1957, Differentiation of marine and sub-aerial sedimentary environments by volume percentage of heavy minerals, Mustang Island, Texas. Jour. Sedimentary Petrology, v. 27, p. 116–125.

Dixon, W. J. and Massey, F. J., Jr., 1957, Introduction to Statistical Analysis (2nd ed.). McGraw-Hill Book Co., Inc., New York. 488 p.

Folk, R. L. and Ward, W. C., 1957, Brazos River Bar: a study in the significance of grain size parameters. Jour. Sedimentary Petrology, v. 27, p. 3–26.

Inman, D. L., 1952, Measures for describing the size distribution of sediments: Jour. Sedimentary Petrology, v. 22, p. 125–145.

Krumbein, W. C., 1941, Measurement and geological significance of shape and roundness of sedimentary particles: Jour. Sedimentary Petrology, v. 11, p. 64–72.

Kuenen, Ph. H., 1958, Some experiments on fluviatile rounding: Koninkl. Nederl. Akademie van Wetenschappen-Amsterdam, Proc., Series B, 61, No. 1, p. 47–53.

———, 1960, Sand: Scientific American, v. 202, no. 4, p. 94–113.

MacCarthy, G. R., 1935, Eolian sands, a comparison: Am. Jour. Sci., v. 30, no. 176, p. 81–95.

MacCarthy, G. R. and Huddle, J. W., 1938, Shape sorting of sand grains by wind action: Am. Jour. Sci., v. 35, no. 205, p. 64–73.

Mason, C. C. and Folk, R. L., 1958, Differentiation of beach, dune, and aeolian flat environments by size analysis, Mustang Island, Texas: Jour. Sedimentary Petrology, v. 28, p. 211–226.

Mattox, R. B., 1955, Eolian shape-sorting: Jour. Sedimentary Petrology, v. 25, p. 111–114.

Pettijohn, F. J., 1956, Sedimentary rocks (2nd ed.). Harper & Bros., New York, p. 60–65

POWERS, M. C., 1953, A new roundness scale for sedimentary particles: Jour. Sedimentary Petrology, v. 23, p. 117–119.

RILEY, N. A., 1941, Projection sphericity: Jour. Sedimentary Petrology, v. 11, p. 94–97.

RUSSELL, R. D., 1939, Effects of transportation on sedimentary particles: in Recent Marine Sediments, Trask, Ed., Am. Assoc. Petroleum Geologists. Tulsa, p. 32–47.

STEWART, H. B., JR., 1956, Sediments and the environments of deposition in a coastal lagoon: Ph.D. Thesis, Univ. of Calif., 355 p.

VON ENGLEHARDT, WOLF, 1940, Unterscheidung wasser- und windsortierter sande auf grund der korngrössenverteilung ihrer leichten und schweren gemengteile: Chemie der Erde, v. 12, p. 445–465.

WADDELL, HAKON, 1932, Volume, shape, and roundness of rock particles: Jour. Geology, v. 40, p. 443–451.

WASKOM, J. D., 1958, Roundness as an indicator of environment along the coast of panhandle Florida: Jour. Sedimentary Petrology, v. 28, p. 351–360.

(604)

July 1, 1961. pp.29-32.

Observations of the Effect of Diet on Shell Coloration in the Red Abalone, *Haliotis rufescens* SWAINSON

by

DAVID L. LEIGHTON

(Contribution from the Scripps Institution of Oceanography, New Series) 1287
University of California, La Jolla, California

(Plate 6)

The color of the ostracal shell layer of the red abalone, Haliotis rufescens Swainson, 1822, is typically a "dull brick red" (Cox, 1960). In many specimens the continuity of the general red aspect may be interrupted by zones of pink, white or green coinciding in position with the growth lines. Variation of shell color may be extreme; the writer has collected many specimens with predominantly or purely white shells. The feature of variable shell color occurs, to a greater or lesser degree, in all California abalones and has been reported to occur also in Japanese forms (Ino, 1952). Study has been made of the effect of diet on shell coloration in the topshell, Turbo cornutus (Solander, 1788), by the same investigator (Ino, 1949, 1958).

Coloration of shells in mollusks has in several other instances been linked with diet. Perhaps most notable of these is the demonstration that a diet of Mytilus edulis Linnaeus, 1758, is accompanied by secretion of brown shell in Purpura lapillus Linnaeus, 1758, and that feeding upon barnacles (Balanus balanoides and Chthamalus stellatus) results in deposition of white shell material (Moore, 1936). Purpura is, however, a carnivorous mollusk while the abalones and topshells are herbivores.

The red abalone was selected for the present study because the range of colors displayed in shells is appreciable. Also minute, juvenile and young adult individuals were easily obtained in the required numbers.

Valuable advice given by Dr. Denis L. Fox, Mr. John E. Fitch, and Dr. Wheeler J. North is gratefully acknowledged.

Materials & Methods

Specimens of Haliotis rufescens were collected, using SCUBA (Self Contained Underwater Breathing Apparatus), at depths ranging from 40 to 80 feet in waters near La Jolla, California. Greatest numbers of small specimens (1.1 to 25.0 mm. in length) were found within holdfasts of the giant kelp, Macrocystis pyrifera (Linnaeus) Agardh, 1771. Larger individuals were commonly taken from beneath rocks. Kelp plants torn from the bottom and washed ashore by storms often yielded minute abalones in large numbers. As many as 23 specimens were retrieved from a single beached holdfast. Interestingly, the abalones collected from holdfasts were largely of the species H. rufescens, though occasionally H. corrugata Gray, 1828, and H. assimilis Dall, 1878, were taken. Only among specimens less than 3 mm. long was there any confusion as to species. Identification of smaller individuals was made by comparison with a carefully graded series of juvenile shells of each locally occurring abalone species.

Sizes of experimental animals ranged from 4 to 120 mm. in shell length. The smallest were maintained in one-quart polyethylene containers perforated with numerous holes ⅛ inch in diameter and submerged in a wooden frame rack in circulating aerated sea water. The largest animals were held in 100-gallon concrete tanks similarly supplied with sea water. Low light intensities were maintained in the laboratory at all times precluding adventitious growth of algae.

Food consisted primarily of a variety of species of marine algae representing the brown, red and green algal classes. On several occasions such foreign materials as boiled potato, carrot, and yam were given.

Feeding experiments were conducted throughout one year during which time over 50 abalone were held for varying periods of time on restricted diets.

Results

Shells of juvenile Haliotis rufescens collected from holdfasts of Macrocystis were purely white, pale green or, when found in holdfasts with epiphytically growing red algae, were partially red. Predominantly red-shelled specimens were collected about rocks which supported red algae.

In the laboratory a wide variety of red algal species (Rhodophyta) were provided as food with the consistent result that red pigmented shell was deposited. Pink color appeared in newly deposited shell after red algae had been given together with brown algae (Phaeophyta). When brown algae, green algae (Chlorophyta), or a number of foreign foods (e. g., potato or yam) had been given, the shell formed was either white, cream, or green, but never red. Results of all feeding experiments are given tabular summary below (see Table I).

Diets of brown algae, Macrocystis and Laminaria, were found to result in either white or green color in the newly formed shell. Other brown algae (e.g., Egregia and Eisenia), when ingested, influenced the formation of cream colored shell. Pelvetia fastigiata (Agardh) De Toni, 1895, gave origin to olive-green shell coloration.

Individuals fed alternately red and brown algae for one-month periods displayed similar growth rates on either diet. Shells of these abalones show alternate banding of red and white. It is also noteworthy that growth was substantial in abalone fed either potato or yam. Light green shell was produced on occasions when those diets were provided.

The multiple-colored specimen shown in the accompanying plate (Lower, right) is one of nu-

Table 1: Coloration of shell (ostracum) secreted by *Haliotis rufescens* on restricted diets

Diet	Color of Shell Produced	Number of Observations
Rhodophyta (Red Algae)		
Pterocladia pyramidale	red	12
Plocamium pacificum	red	20
Gelidium purpurascens	red	6
Gelidium nudifrons	red	5
Gigartina spinosa	red	25
Gigartina californica	red	7
Gigartina canaliculata	red	8
Phaeophyta (Brown Algae)		
Macrocystis pyrifera	white or pale green	44
Laminaria farlowii	green	18
Egregia laevigata	white or cream	8
Eisenia arborea	cream	6
Pelvetia fastigiata	olive green	5
Chlorophyta (Green Algae)		
Ulva sp.	pale green	8
Miscellaneous		
Potato, boiled	pale green	6
Yam, boiled	pale green	6
Carrot, boiled	cream	4
Agar	cream	4

Explanation of Plate 6

Figure 1: "Normally" pigmented juvenile *Haliotis rufescens* collected from a kelp bed with a mixed benthic flora. Figure 2: White phase abalone collected from a holdfast of the giant kelp *Macrocystis pyrifera*. Figure 3: Multiple-colored specimen with bands formed as a result of restricted feeding in the laboratory. For convenience, diets and their respective color bands are listed in reverse order of their deposition: *Eisenia* (shell margin), cream; *Pterocladia*, red; Potato, green; Miscellaneous red algae, red; Potato, pale green; *Gigartina*, red; *Macrocystis*, pale green. For additional explanation of this specimen, see text.

(The scale adjacent to the specimens represents ten millimeters)

(606)

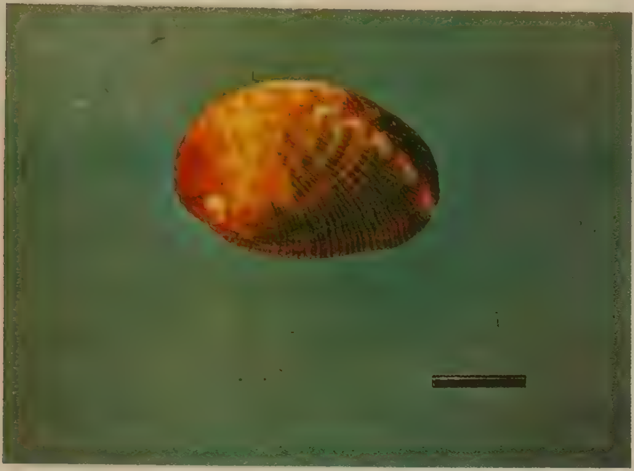

Figure 1

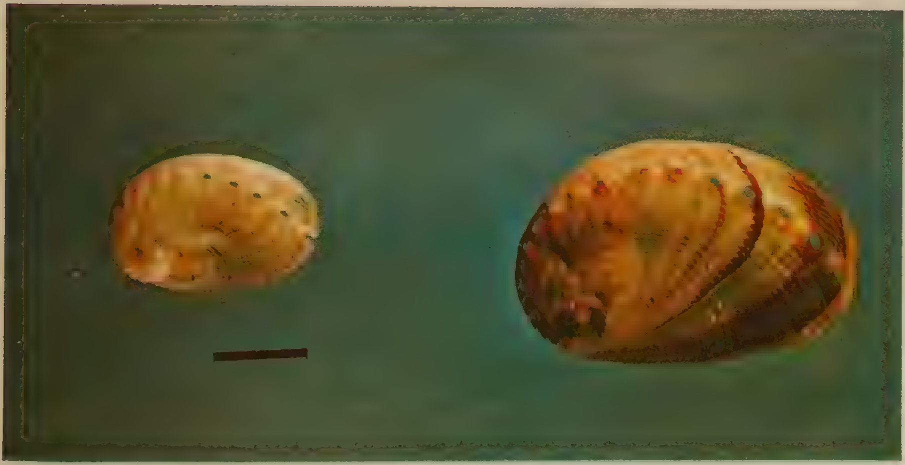

Figure 2 Figure 3

merous abalone which were maintained in the laboratory for as long as six months. When collected from beneath a rock on June 4, 1960, in the Point Loma Kelp Bed, it was 18.5 mm. long and had a predominantly red shell. When the animal was removed from the shell on January 15, 1961, it was 37.5 mm. long and its shell displayed bands of several colors. Initially, Macrocystis and Egregia were provided for a period of three months. The two minor red bands at the center of the shell were formed during brief feedings of Plocamium. Subsequently, it was supplied the foods listed in the explanation of the plate.

Microscopic epiphytes were found to contain substances influencing the formation of red shell. These small filamentous plants were probably red algae. A future study designed to demonstrate the effects of ingestion of sessile diatoms and other microflora on shell pigmentation will provide an answer to the question. In all feeding experiments of the present study care was taken to select fronds of algae which were free of epiphytic growths.

Discussion

White shell is secreted by Turbo cornutus, when restricted to a diet of the brown alga Eisenia bicyclis (Kjellman) Setchell, 1887, a Japanese form similar to our local E. arborea Areschoug, 1876, (Ino, 1949). Shell of "normal" color was secreted when both E. bicyclis and a coralline alga (Rhodophyta) were given. A diet consisting of a species of Sargassum influenced the production of white shell, while a species of Gelidium yielded a mixture of green-black and brown color. Haliotis rufescens, similarly, has been found in the present study to secrete cream colored shell when fed Eisenia and red shell when fed Gelidium.

The red pigment of shells of Haliotis rufescens has been given the name rufescine (Dhéré and Baumeler, 1930). Chemically it is a bilin, or member of a biochemical category of pigments including bilirubin and biliverdin, pigments of bile. The relationship of rufescine to phycoerythrin (the red pigment of red algae and also a bilin) has yet to be demonstrated. The nature of the other pigments of abalone shells must also be ascertained through careful biochemical analyses. These studies will be undertaken by the writer in the near future.

Ecologically there may exist a considerable utility in the type of study described in this paper, for a dietary history may be obtained from examination of the pigments in a given shell. Food habits may be indicated by the presence and arrangement of pigments. In abalones, which do not, as a rule, move about extensively (Cox, 1960) and which normally live in excess of a decade, the sequence of color bands in a number of specimens may indicate trends in floral succession occurring over periods of several years in their home area. A series of eight Haliotis rufescens was collected from the Point Loma Kelp Bed which shows impressive similarity of shell color arrangement and extent. The known kelp history of the area agrees well with the observed pigment patterns. Additional support is given this hypothesis by the findings of almost purely white adult H. rufescens by commercial abalone divers in areas rich in brown algae (primarily the giant kelp, Macrocystis) slightly south of Point Conception, and of "blood red" specimens from the red alga beds north of Point Conception (B. Owens, personal communication).

Conclusions

Pigmentation of the ostracum of the red abalone reflects the diet in nature. Feeding experiments performed in this study indicate that the source of red pigments may be found in the red algal foods. Shells lacking the typical red coloration are formed by abalone living in areas or niches with brown or green algae, but which lack red algae. A minor quantity of red algae in the diet may be detected as a diluted red pigment in the shell. Since red algae will usually form at least a minor portion of the diet of Haliotis rufescens in nature, the most prevalent color of the ostracum of H. rufescens is red. Color sequences in shells of this species may be used as a key to botanical succession in the home area of the respective animals.

Summary

Common collection of Haliotis rufescens with little or no red shell pigmentation from areas devoid of red algae, but rich in brown algae, suggested that shell pigmentation was related to the foods available. These observations prompted an investigation of the effect of restricted diet on shell pigmentation. Through controlled feeding in the laboratory it was consistently demonstrated that a primary source of red shell pigment is red algae. Feedings of brown or green algae resulted in secretion of shell of white or green color, but never red.

The ecological and biochemical significance of these observations is discussed.

Literature Cited

Cox, K. W.

1960. Review of the abalone of California. Calif. Fish and Game, 46: 381-406, 9 figs.

Dhéré, C., & C. Baumeler

1930. Recherches sur la rufescine, pigment de la coquille de l'Haliotis rufescens. Arch. Int. Physiol. 32: 55.

Ino, Takashi

1940. The effect of food on growth and coloration of the topshell, (Turbo cornutus Solander). J. Mar. Res. 8: 1-5.

——, ——

1952. Biological studies on propagation of Japanese abalone (Genus Haliotis). Tokai Reg. Fisheries Res. Lab. Tokyo, Japan.

——, ——

1958. Ecological studies of the topshell, Turbo cornutus (Solander). Bull. Tokai Reg. Fisheries Res. Lab. Tokyo, Japan, 22: 33-36.

Moore, H. B.

1936. The biology of Purpura lapillus. I. Shell variation in relation to environment. J. Mar. Biol. Ass. U. K. 21: 61-89.

Meteorological Monographs, v.4, no.24
(December, 1960), 40p.

FLUCTUATIONS IN THE ATMOSPHERIC INERTIA: 1873-1950

El Sayed Mohamed Hassan
Cairo University[1]

TABLE OF CONTENTS

1. INTRODUCTION 1
2. THE VARIABLE LOAD 1
3. OCEAN YIELDING 1
4. THE ATMOSPHERIC INERTIA 1
5. THE DISTRIBUTION OF STATIONS 2
6. DATA 4
7. TABULATED VALUES 5
8. HARMONIC EXPRESSIONS 27
APPENDIX 27
  A. List of all stations used in the computation 27
  B. Sea level correction 36
  C. The mean of the pressure record 39
  D. Rejected data 40

1. Introduction

In a study of the meteorological contribution toward irregularities in the rotation of the earth, Munk and Hassan (1961) have evaluated the seasonal terms in the moments and products of atmospheric inertia and the power spectrum of the non-seasonal products of inertia. For that purpose, mean monthly values were computed from all available station-level pressures since 1873. Calculations were extensive and performed on the IBM 709 computer at the University of California at Los Angeles. The resulting time series constitute a description of some integral properties of the global atmosphere—in particular, of the coefficients of the second spherical harmonic of the variable surface pressure. In publishing the computed values, we hope that this description of the atmosphere might be useful to other investigators.

2. The variable load

Let $q(\theta, \lambda; t)$ designate the departure, from the mean, of atmospheric load per unit surface area, as a function of colatitude θ, east longitude λ, and time t. Let $S = 4\pi a^2$ designate the surface area of the earth, and let $ds = a^2 \sin\theta d\theta d\lambda$ designate a differential surface element. Then

$$\int q(\theta, \lambda; t)ds = SV(t)$$

is the departure in total atmospheric mass, and this will vary because of the variable storage of atmospheric water vapor. Other effects are comparatively small. According to Bannon and Steele (1957), the seasonal variation is given by

$$V(t) = -0.17 \cos \odot - 0.08 \sin \odot \qquad (1)$$

where $\odot$ is the sun's longitude, varying from 0 deg on 1 January to 360 deg on 31 December.

3. Ocean yielding

In the frequency range under consideration here, it would appear that the ocean responds to atmospheric pressure as an inverted barometer (Munk and MacDonald, 1960; §9.3). Consequently, departures of the total load on the sea floor are everywhere the same at a fixed time, but the departures vary in time because of the variation in the fraction of the atmosphere that lies above oceans. Let $q_O(t)$ designate the value of $q(\theta, \lambda; t)$ for oceanic areas. Then

$$\begin{aligned} SV(t) &= \int_{Land} q(\theta, \lambda; t)ds + \int_{Oceans} q(\theta, \lambda; t)ds \\ &= SA_0^0(t) + Sa_0^0 q_O(t). \end{aligned} \qquad (2)$$

Here A_n^m, B_n^m designate the amplitudes of the spherical harmonics of an expansion of a function $F = q(\theta, \lambda; t)$ over *land* and $F = 0$ over oceans. Similarly, a_n^m, b_n^m refer to the expansion of a function equal to 1 over *oceans* and zero over land. The latter coefficients have been evaluated by Munk and MacDonald (1960, §A.1).

4. The atmospheric inertia

It is convenient to represent the inertial tensor in terms of the dimensionless quantities ψ_1, ψ_2, ψ_3. Here ψ_1, ψ_2 are components of the atmospheric products of inertia divided by $(C - A)$, where A, A, C are the three principal moments of inertia of the planet earth. ψ_1 is the component relative to an axis from the center of mass through the meridian of Greenwich; ψ_2 is the component relative to an axis 90 deg east of Greenwich. ψ_3 is the atmospheric moment of inertia divided by C. For further details, we refer to Munk and MacDonald (1960). We then have

---

[1] This work was done while the author was visiting the Scripps Institution of Oceanography.

Contributions from the Scripps Institution of Oceanography, New Series, 1288
Reproduced by Permission

$$\Delta = \left| \begin{array}{lllll}
\Sigma (p_o^o)^2 & \Sigma p_1^o p_o^o & \Sigma p_1^1 \cos \lambda_i p_o^o & \Sigma p_1^1 \sin \lambda_i p_o^o & \Sigma p_2^o p_o^o \\
\Sigma p_o^o p_1^o & \Sigma (p_1^o)^2 & \Sigma p_1^1 \cos \lambda_i p_1^o & \Sigma p_1^1 \sin \lambda_i p_1^o & \Sigma p_2^o p_1^o \\
\Sigma p_o^o p_1^1 \cos \lambda_i & \Sigma p_1^o p_1^1 \cos \lambda_i & \Sigma (p_1^1 \cos \lambda_i)^2 & \Sigma p_1^1 \sin \lambda_i p_1^1 \cos \lambda_i & \Sigma p_2^o p_1^1 \cos \lambda_i \\
\Sigma p_o^o p_1^1 \sin \lambda_i & \Sigma p_1^o p_1^1 \sin \lambda_i & \Sigma p_1^1 \cos \lambda_i p_1^1 \sin \lambda_i & \Sigma (p_1^1 \sin \lambda_i)^2 & \Sigma p_2^o p_1^1 \sin \lambda_i \\
\Sigma p_o^o p_2^o & \Sigma p_1^o p_2^o & \Sigma p_1^1 \cos \lambda_i p_2^o & \Sigma p_1^1 \sin \lambda_i p_2^o & \Sigma (p_2^o)^2 \\
\Sigma p_o^o p_2^1 \cos \lambda_i & \Sigma p_1^o p_2^1 \cos \lambda_i & \Sigma p_1^1 \cos \lambda_i p_2^1 \cos \lambda_i & \Sigma p_1^1 \sin \lambda_i p_2^1 \cos \lambda_i & \Sigma p_2^o p_2^1 \cos \lambda_i \\
\Sigma p_o^o p_2^1 \sin \lambda_i & \Sigma p_1^o p_2^1 \sin \lambda_i & \Sigma p_1^1 \cos \lambda_i p_2^1 \sin \lambda_i & \Sigma p_1^1 \sin \lambda_i p_2^1 \sin \lambda_i & \Sigma p_2^o p_2^1 \sin \lambda_i \\
\Sigma p_o^o p_2^2 \cos 2 \lambda_i & \Sigma p_1^o p_2^2 \cos 2 \lambda_i & \Sigma p_1^1 \cos \lambda_i p_2^2 \cos 2 \lambda_i & \Sigma p_1^1 \sin \lambda_i p_2^2 \cos 2 \lambda_i & \Sigma p_2^o p_2^2 \cos 2 \lambda_i \\
\Sigma p_o^o p_2^2 \sin 2 \lambda_i & \Sigma p_1^o p_2^2 \sin 2 \lambda_i & \Sigma p_1^1 \cos \lambda_i p_2^2 \sin 2 \lambda_i & \Sigma p_1^1 \sin \lambda_i p_2^2 \sin 2 \lambda_i & \Sigma p_2^o p_2^2 \sin 2 \lambda_i
\end{array} \right.$$

FIG. 1. Determinant Δ arising from the

$$(\Delta A)_2^1 = \left| \begin{array}{lllll}
\Sigma (p_o^o)^2 & \Sigma p_1^o p_o^o & \Sigma p_1^1 \cos \lambda_i p_o^o & \Sigma p_1^1 \sin \lambda_i p_o^o & \Sigma p_2^o p_o^o \\
\Sigma p_o^o p_1^o & \Sigma (p_1^o)^2 & \Sigma p_1^1 \cos \lambda_i p_1^o & \Sigma p_1^1 \sin \lambda_i p_1^o & \Sigma p_2^o p_1^o \\
\Sigma p_o^o p_1^1 \cos \lambda_i & \Sigma p_1^o p_1^1 \cos \lambda_i & \Sigma (p_1^1 \cos \lambda_i)^2 & \Sigma p_1^1 \sin \lambda_i p_1^1 \cos \lambda_i & \Sigma p_2^o p_1^1 \cos \lambda_i \\
\Sigma p_o^o p_1^1 \sin \lambda_i & \Sigma p_1^o p_1^1 \sin \lambda_i & \Sigma p_1^1 \cos \lambda_i p_1^1 \sin \lambda_i & \Sigma (p_1^1 \sin \lambda_i)^2 & \Sigma p_2^o p_1^1 \sin \lambda_i \\
\Sigma p_o^o p_2^o & \Sigma p_1^o p_2^o & \Sigma p_1^1 \cos \lambda_i p_2^o & \Sigma p_1^1 \sin \lambda_i p_2^o & \Sigma (p_2^o)^2 \\
\Sigma p_o^o p_2^1 \cos \lambda_i & \Sigma p_1^o p_2^1 \cos \lambda_i & \Sigma p_1^1 \cos \lambda_i p_2^1 \cos \lambda_i & \Sigma p_1^1 \sin \lambda_i p_2^1 \cos \lambda_i & \Sigma p_2^o p_2^1 \cos \lambda_i \\
\Sigma p_o^o p_2^1 \sin \lambda_i & \Sigma p_1^o p_2^1 \sin \lambda_i & \Sigma p_1^1 \cos \lambda_i p_2^1 \sin \lambda_i & \Sigma p_1^1 \sin \lambda_i p_2^1 \sin \lambda_i & \Sigma p_2^o p_2^1 \sin \lambda_i \\
\Sigma p_o^o p_2^2 \cos 2 \lambda_i & \Sigma p_1^o p_2^2 \cos 2 \lambda_i & \Sigma p_1^1 \cos \lambda_i p_2^2 \cos 2 \lambda_i & \Sigma p_1^1 \sin \lambda_i p_2^2 \cos 2 \lambda_i & \Sigma p_2^o p_2^2 \cos 2 \lambda_i \\
\Sigma p_o^o p_2^2 \sin 2 \lambda_i & \Sigma p_1^o p_2^2 \sin 2 \lambda_i & \Sigma p_1^1 \cos \lambda_i p_2^2 \sin 2 \lambda_i & \Sigma p_1^1 \sin \lambda_i p_2^2 \sin 2 \lambda_i & \Sigma p_2^o p_2^2 \sin 2 \lambda_i
\end{array} \right.$$

FIG. 2. Determinant $(\Delta A)_2^1$ arising from the

$$\begin{aligned}
\psi_1(t) &= -\frac{a^2}{C-A}\left\{\int_{Land} q(\theta, \lambda ; t) \sin\theta \cos\theta \cos\lambda \, ds \right. \\
&\qquad \left. + q_O(t) \int_{Oceans} \sin\theta \cos\theta \cos\lambda \, ds \right\} \\
&= -\frac{a^4}{C-A}\,\frac{2\pi}{5}\,\{A_2{}^1(t) + q_O(t) a_2{}^1\}.
\end{aligned}$$

We now substitute for $q_O(t)$ from (2), and this allows us to evaluate $\psi_1(t)$ from measurements over land only:

$$\psi_1(t) = -\frac{a^4}{C-A}\,\frac{2\pi}{5}\left\{A_2{}^1(t) + [V(t) - A_0{}^0(t)]\frac{a_2{}^1}{a_0{}^0}\right\}. \qquad (3)$$

Similarly,

$$\psi_2(t) = -\frac{a^4}{C-A}\,\frac{2\pi}{5}\left\{B_2{}^1(t) + [V(t) - A_0{}^0(t)]\frac{b_2{}^1}{a_0{}^0}\right\}, \qquad (4)$$

and

$$\psi_3(t) = +\frac{a^4}{C}\,\frac{8\pi}{15}\left\{A_2{}^0(t) + [V(t) - A_0{}^0(t)]\frac{a_2{}^0}{a_0{}^0}\right\}. \qquad (5)$$

5. The distribution of stations

The stations are not uniformly distributed (fig. 3). To evaluate surface integrals, the usual procedure is to contour the required quantities as well as possible, to read off representative values for each 5-deg square for example, multiply by sin θ, and sum. The procedure is subjective and not suitable for machine calculations. Assume a network of observation stations not uniformly distributed on the earth's surface. Denote the coordinates of station i by θ_i, λ_i, the total number of stations being I. Let $F_i(t)$ be the atmospheric-pressure departure for the continental station i ($F = 0$ over oceans). It is required to approximate $F_i(t)$ by a function

$$f_i(t) = \sum_{n=0}^{N} \sum_{m=0}^{n} \{[A_n{}^m(t) \cos(m\lambda_i) + B_n{}^m(t) \sin(m\lambda_i)] \times [p_n{}^m(\cos\theta_i)]\}$$

such that

$$\epsilon^2 = \sum (F_i(t) - f_i(t))^2 \qquad (6)$$

$\Sigma\ P_2^1 \cos\lambda_i\ P_0^0$	$\Sigma\ P_2^1 \sin\lambda_i\ P_0^0$	$\Sigma\ P_2^2 \cos 2\lambda_i\ P_0^0$	$\Sigma\ P_2^2 \sin 2\lambda_i\ P_0^0$
$\Sigma\ P_2^1 \cos\lambda_i\ P_1^0$	$\Sigma\ P_2^1 \sin\lambda_i\ P_1^0$	$\Sigma\ P_2^2 \cos 2\lambda_i\ P_1^0$	$\Sigma\ P_2^2 \sin 2\lambda_i\ P_1^0$
$\Sigma\ P_2^1 \cos\lambda_i\ P_1^1 \cos\lambda_i$	$\Sigma\ P_2^1 \sin\lambda_i\ P_1^1 \cos\lambda_i$	$\Sigma\ P_2^2 \cos 2\lambda_i\ P_1^1 \cos\lambda_i$	$\Sigma\ P_2^2 \sin 2\lambda_i\ P_1^1 \cos\lambda_i$
$\Sigma\ P_2^1 \cos\lambda_i\ P_1^1 \sin\lambda_i$	$\Sigma\ P_2^1 \sin\lambda_i\ P_1^1 \sin\lambda_i$	$\Sigma\ P_2^2 \cos 2\lambda_i\ P_1^1 \sin\lambda_i$	$\Sigma\ P_2^2 \sin 2\lambda_i\ P_1^1 \sin\lambda_i$
$\Sigma\ P_2^1 \cos\lambda_i\ P_2^0$	$\Sigma\ P_2^1 \sin\lambda_i\ P_2^0$	$\Sigma\ P_2^2 \cos 2\lambda_i\ P_2^0$	$\Sigma\ P_2^2 \sin 2\lambda_i\ P_2^0$
$\Sigma\ (P_2^1 \cos\lambda_i)^2$	$\Sigma\ P_2^1 \sin\lambda_i\ P_2^1 \cos\lambda_i$	$\Sigma\ P_2^2 \cos 2\lambda_i\ P_2^1 \cos\lambda_i$	$\Sigma\ P_2^2 \sin 2\lambda_i\ P_2^1 \cos\lambda_i$
$\Sigma\ P_2^1 \cos\lambda_i\ P_2^1 \sin\lambda_i$	$\Sigma\ (P_2^1 \sin\lambda_i)^2$	$\Sigma\ P_2^2 \cos 2\lambda_i\ P_2^1 \sin\lambda_i$	$\Sigma\ P_2^2 \sin 2\lambda_i\ P_2^1 \sin\lambda_i$
$\Sigma\ P_2^1 \cos\lambda_i\ P_2^2 \cos 2\lambda_i$	$\Sigma\ P_2^1 \sin\lambda_i\ P_2^2 \cos 2\lambda_i$	$\Sigma\ (P_2^2 \cos 2\lambda_i)^2$	$\Sigma\ P_2^2 \sin 2\lambda_i\ P_2^2 \cos 2\lambda_i$
$\Sigma\ P_2^1 \cos\lambda_i\ P_2^2 \sin 2\lambda_i$	$\Sigma\ P_2^1 \sin\lambda_i\ P_2^2 \sin 2\lambda_i$	$\Sigma\ P_2^2 \cos 2\lambda_i\ P_2^2 \sin 2\lambda_i$	$\Sigma\ (P_2^2 \sin 2\lambda_i)^2$

right-hand side of the system of eq (7).

$\Sigma\ F_i\ P_0^0$	$\Sigma\ P_2^1 \sin\lambda_i P_0^0$	$\Sigma\ P_2^2 \cos 2\lambda_i\ P_0^0$	$\Sigma\ P_2^2 \sin 2\lambda_i\ P_0^0$
$\Sigma\ F_i\ P_1^0$	$\Sigma\ P_2^1 \sin\lambda_i\ P_1^0$	$\Sigma\ P_2^2 \cos 2\lambda_i\ P_1^0$	$\Sigma\ P_2^2 \sin 2\lambda_i\ P_1^0$
$\Sigma\ F_i\ P_1^1 \cos\lambda_i$	$\Sigma\ P_2^1 \sin\lambda_i\ P_1^1 \cos\lambda_i$	$\Sigma\ P_2^2 \cos 2\lambda_i\ P_1^1 \cos\lambda_i$	$\Sigma\ P_2^2 \sin 2\lambda_i\ P_1^1 \cos\lambda_i$
$\Sigma\ F_i\ P_1^1 \sin\lambda_i$	$\Sigma\ P_2^1 \sin\lambda_i\ P_1^1 \sin\lambda_i$	$\Sigma\ P_2^2 \cos 2\lambda_i\ P_1^1 \sin\lambda_i$	$\Sigma\ P_2^2 \sin 2\lambda_i\ P_1^1 \sin\lambda_i$
$\Sigma\ F_i\ P_2^0$	$\Sigma\ P_2^1 \sin\lambda_i\ P_2^0$	$\Sigma\ P_2^2 \cos 2\lambda_i\ P_2^0$	$\Sigma\ P_2^2 \sin 2\lambda_i\ P_2^0$
$\Sigma\ F_i\ P_2^1 \cos\lambda_i$	$\Sigma\ P_2^1 \sin\lambda_i\ P_2^1 \cos\lambda_i$	$\Sigma\ P_2^2 \cos 2\lambda_i\ P_2^1 \cos\lambda_i$	$\Sigma\ P_2^2 \sin 2\lambda_i\ P_2^1 \cos\lambda_i$
$\Sigma\ F_i\ P_2^1 \sin\lambda_i$	$\Sigma\ (P_2^1 \sin\lambda_i)^2$	$\Sigma\ P_2^2 \cos 2\lambda_i\ P_2^1 \sin\lambda_i$	$\Sigma\ P_2^2 \sin 2\lambda_i\ P_2^1 \sin\lambda_i$
$\Sigma\ F_i\ P_2^2 \cos 2\lambda_i$	$\Sigma\ P_2^1 \sin\lambda_i\ P_2^2 \cos 2\lambda_i$	$\Sigma\ (P_2^2 \cos 2\lambda_i)^2$	$\Sigma\ P_2^2 \sin 2\lambda_i\ P_2^2 \cos\lambda_i$
$\Sigma\ F_i\ P_2^2 \sin 2\lambda_i$	$\Sigma\ P_2^1 \sin\lambda_i\ P_2^2 \sin 2\lambda_i$	$\Sigma\ P_2^2 \cos 2\lambda_i\ P_2^2 \sin 2\lambda_i$	$\Sigma\ (P_2^2 \sin 2\lambda_i)^2$

system of eq (7) when solving for A_2^1.

is a minimum. The calculation is carried out for one month at a time. To simplify the notation, we write F_i, f_i, A_n^m, B_n^m for $F_i(t)$, $f_i(t)$, $A_n^m(t)$, $B_n^m(t)$. Furthermore, $p_n^m(\cos\theta_i)$ is designated by $(p_n^m)_i$. By minimizing (6) with respect to $\left\{\begin{matrix} A_n^m \\ B_n^m \end{matrix}\right\}$, we obtain

$$\sum_i (F_i - f_i) \left\{\begin{matrix} \cos j\lambda_i \\ \sin j\lambda_i \end{matrix}\right\} (p_k^j)_i = 0$$

or

$$\sum_i (F_i) \begin{matrix} \cos j\lambda_i \\ \sin j\lambda_i \end{matrix} (p_k^j)_i$$

$$= \sum_i \sum_{n=0}^{N} \sum_{m=0}^{n} \{[A_n^m \cos(m\lambda_i) + B_n^m \sin(m\lambda_i)](p_n^m)\} \times \left[\left\{\begin{matrix} \cos j\lambda_i \\ \sin j\lambda_i \end{matrix}\right\} (p_k^j)_i \right].$$

For the case of uniformly distributed stations, the summation of terms containing $p_n^m p_k^j$ will vanish except when $n = k$ and $m = j$. In that case,

$$\sum_i (F_i) \left\{\begin{matrix} \cos j\lambda_i \\ \sin j\lambda_i \end{matrix}\right\} (p_k^j)_i = \sum_i \left\{\begin{matrix} A_k^j \cos^2(j\lambda_i) \\ B_k^j \sin^2(j\lambda_i) \end{matrix}\right\} (p_k^j)_i^2, \quad (7)$$

and the coefficients A_k^j, B_k^j are independent. Hence, the value of any one coefficient (A_2^1, say) does not depend on the number of terms to which the expansion is carried.

For the case of nonuniformly distributed stations, the *entire system* of eq (7) has to be solved. The value of any one coefficient (A_2^1, for example) now depends on the number of terms to which the expansion is carried.

We have chosen to evaluate all terms up to and including degree two. This involves the nine coefficients:

$$A_0^0;\ A_1^0,\ A_1^1;\ A_2^0,\ A_2^1,\ A_2^2.$$
$$B_1^1;\ B_2^1,\ B_2^2.$$

The coefficients A_0^0, A_2^0, A_2^1, B_2^1 are required in the expressions for ψ, and it seems reasonable to choose a system (7) that includes *all* terms up to degree two.

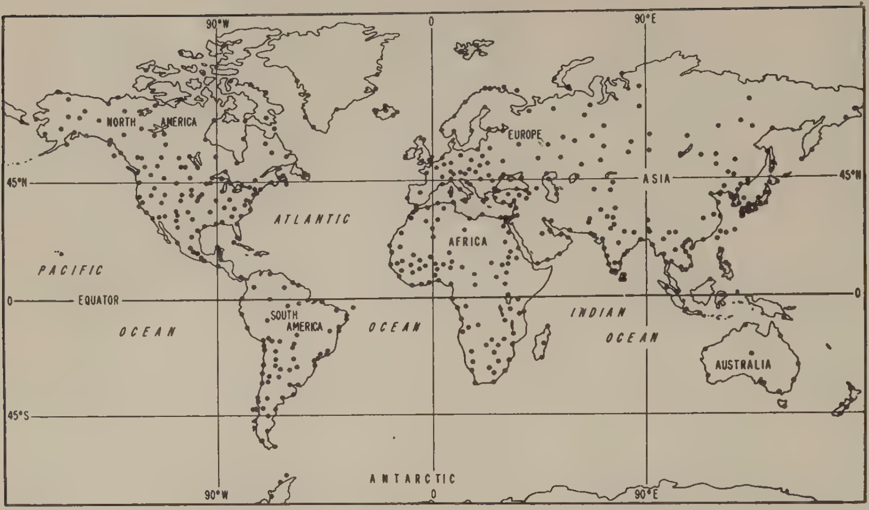

Fig. 3. Positions of stations used in the computation of excitation functions.

We find that

$$A_n^m = \frac{(\Delta A)_n^m}{\Delta}, \quad B_n^m = \frac{(\Delta B)_n^m}{\Delta} \qquad (8)$$

where Δ is a ninth order determinant given by fig. 1. The summation is all terms of the determinant over i. The terms of $(\Delta A)_n^m$ can be found from Δ by replacing the column $\sum (p_n^m \cos m\lambda_i)^2$ by the left-hand side of eq (7). As an example, $(\Delta A)_2^1$ is given by fig. 2.

6. Data

All the data have been taken from the Smithsonian Miscellaneous Collections, Vols. 79, 90, and 105, and from the World Weather Records published by the Weather Bureau. The latter publication is a continuation of the Smithsonian volumes. In the majority of the cases, the pressure in all these volumes has been published for the station level. All the data were accorded equal weight, even though there are large differences in precision. In spite of the obviously enormous effort to produce a homogeneous record for any one station, there are, in some cases, variations in the level of the instrument. In some cases, corrections are entered explicitly. In other cases, it is not clear whether corrections have been made. A list of the large number of minor decisions in the reduction of the observations are included in the appendix.

The following rules are followed in processing the data:

(1) Island stations were not used when the area of the island was less than ten degrees square, except for islands close to continents. The islands used are:

(a) Atlantic Ocean: Spitzbergen, Iceland, Greenland, Resolution Island, Baffin Island, Perrin Islands, The British Isles, Ireland, Cuba, Haiti and Trinidad.
(b) Indian Ocean: Ceylon and Madagascar.
(c) Pacific Ocean: The Japanese Islands, The East Indies, Indonesia, New Zealand, and Tasmania.

(2) Station-level pressure was used whenever reported.

(3) When only sea-level pressure was reported, the correction to bring it up to station level was calculated. The known station height and the mean monthly temperature were used, and the correction was calculated with the help of the Smithsonian Meteorological Tables (Fifth Revised Edition). The record was used only when the maximum seasonal variation of the correction term was less than 10 per cent of the maximum variation of the sea-level pressure. This criterion limits the use of sea-level pressure to stations rather near sea level. When the station level changed during the length of the record, the lowest value was taken for this calculation.

(4) Calculations were started for the year 1873, the first year when the number of stations exceeded 50 (fig. 4). A graph showing the growth of number of stations is shown in fig. 4, and a map showing the positions of all stations used in the computation is shown in fig. 3.

(5) The mean pressure was calculated on an IBM 650 for each station using all published monthly means whenever possible. In some instances, the homogeneity of the whole record could not be ascer-

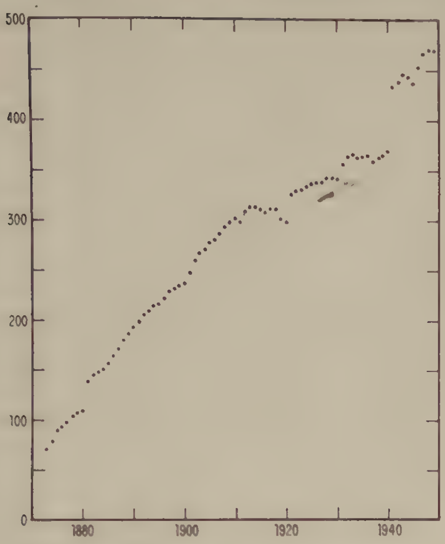

Fig. 4. Number of stations used in the computation of excitation functions.

tained, and the mean was calculated for different portions separately. In most cases, the mean was based on more than ten years of record. Only in 60 out of 567 stations was the record shorter than a decade.

(6) The reported data were used without corrections. Data were rejected only in cases of obvious errors. No attempts were made to smooth the records or to correct the data beyond the corrections that have already been published.

7. Tabulated values

The first two columns refer to year and month. Columns 3 to 10 give the number of stations used in the computation according to the following scheme:

	0		90E		180E		270E		0
Northern hemisphere		Col. 3		4		6		5	
Southern hemisphere		7		8		10		9	

Thus,

column	3	4	5	6	7	8	9	10
	1	2	3	4	5	6	7	8

means that in the northern hemisphere there is 1 station between 0 and 90E, there are 2 stations between 90E and 180E, 3 stations between 0 and 90W, and 4 stations between 90W and 180W; in the southern hemisphere there are 5 stations between 0 and 90E, 6 stations between 90E and 180E, 7 stations between 0 and 90W, and 8 stations between 90W and 180W.

The remaining columns give

$$10^9\ \psi_1,\qquad 10^9\ \psi_2,\qquad 10^{11}\ \psi_3.$$

These have been evaluated according to eq (3) and (5) for the following four models:

I.	Col. 11–13	A_n^m, B_n^m, from (7),	$V = 0$
II.	14–16	A_n^m, B_n^m, from (7),	$V \neq 0$
III.	17–19	A_n^m, B_n^m, from (8),	$V = 0$
IV.	20–22	A_n^m, B_n^m, from (8),	$V \neq 0.$

Thus, for Models I and II, no allowance is made for the uneven distribution of stations. In Models III and IV, this has been taken into account. For I and III, the variation in water vapor is neglected. The time series plotted in fig. 5 (pp. 26–27) correspond to Model IV.

The year 1999 at the end of the table gives ψ calculated from the means of all station records. For comparison, we include $\bar{\psi}$ calculated by taking the means of all $\psi(t)$. This mean has been taken over two periods, 1873 to 1950 and 1900 to 1950.

1873	1	22	1	24	11	1	6	5	0	12	-4	-4	10	-7	-3	12	-7	-3	10	-10	-2
	2	22	1	24	11	1	6	5	0	-18	-9	2	-20	-12	3	-22	-18	-0	-24	-21	0
	3	22	1	24	11	1	6	5	0	6	-2	-0	4	-4	0	8	-1	0	6	-3	1
	4	22	1	24	11	1	6	5	0	0	-5	1	0	-5	1	1	-2	2	1	-2	2
	5	22	1	24	11	1	6	5	0	2	-7	0	3	-6	0	3	-4	2	3	-2	2
	6	22	1	24	11	1	6	5	0	-5	1	1	-3	4	0	-3	8	2	-2	10	1
	7	22	1	25	11	1	6	5	0	0	10	1	2	13	0	2	17	2	5	20	1
	8	22	1	25	11	1	6	5	0	1	9	0	3	12	-0	3	15	0	5	18	-0
	9	22	1	26	11	1	6	5	0	2	6	0	3	9	-0	2	8	0	3	11	0
	10	22	1	26	11	1	6	5	0	17	5	-2	18	5	-3	20	9	-1	20	9	-1
	11	22	1	26	11	1	6	5	0	9	-1	-1	9	-2	-1	10	-2	-1	9	-3	-1
	12	22	1	26	11	1	6	5	0	-13	6	-1	-15	4	-0	-17	-1	-4	-19	-4	-3
1874	1	24	1	31	11	1	6	5	0	3	7	-5	1	4	-4	2	3	-6	0	0	-5
	2	23	1	31	11	1	6	5	0	-10	-0	-0	-12	-4	0	-13	-8	-2	-15	-11	-1
	3	23	1	31	11	1	6	5	0	-19	-13	0	-21	-15	1	-24	-21	-1	-26	-23	-0
	4	23	1	31	11	1	6	5	0	11	0	-2	11	-0	-2	14	6	-0	13	5	-0
	5	24	1	31	11	1	6	5	0	0	-3	2	1	-1	2	2	2	4	3	3	3
	6	24	1	31	11	1	6	5	0	-11	-2	3	-9	0	2	-12	-0	2	-10	1	2
	7	24	1	31	11	1	6	5	0	-0	4	2	1	7	0	0	10	2	2	13	1
	8	24	1	31	11	1	6	5	0	12	4	-0	14	7	-1	14	12	1	16	15	-0
	9	24	1	32	11	1	6	5	0	10	2	-0	11	5	-1	10	5	-0	11	7	-0
	10	24	1	32	11	1	6	5	0	14	6	-3	14	7	-3	15	10	-2	16	10	-2
	11	24	1	32	11	1	6	5	0	7	7	-1	6	6	-0	8	7	-1	8	6	-0
	12	24	1	32	11	1	6	5	0	17	17	-2	15	15	-1	21	20	-1	19	17	-0
1875	1	31	2	32	14	1	6	5	0	-7	10	-0	-9	7	0	-10	1	-4	-12	-1	-3
	2	31	2	32	14	1	6	5	0	-16	-1	3	-18	-4	4	-19	-12	0	-21	-15	1
	3	31	2	32	14	1	6	5	0	-22	-2	4	-23	-4	5	-25	-9	1	-26	-11	2
	4	31	2	32	14	1	6	5	0	-12	2	3	-12	2	3	-12	4	3	-12	4	3
	5	31	2	32	14	1	6	5	0	3	-8	0	4	-7	0	2	-5	2	3	-4	1
	6	31	2	32	14	1	6	5	0	8	10	-0	10	13	-0	12	24	3	14	27	2
	7	31	2	32	14	1	6	5	0	-2	19	4	-0	22	3	0	30	5	2	33	4
	8	31	2	32	14	1	6	5	0	-3	4	2	-1	7	1	-1	10	3	0	13	2
	9	31	2	32	14	1	6	5	0	-8	2	2	-7	4	1	-9	2	1	-8	4	0
	10	31	2	32	14	1	6	5	0	10	-7	0	10	-7	0	10	-9	0	10	-9	0
	11	31	2	32	14	1	6	5	0	7	-8	0	7	-9	0	6	-17	-0	5	-18	-0
	12	31	2	32	14	1	6	5	0	0	-29	-4	-0	-31	-3	-5	-41	-5	-7	-43	-4
1876	1	32	4	32	15	1	6	5	0	-35	-12	2	-37	-15	3	-44	-33	-5	-46	-36	-4
	2	32	4	32	15	1	6	4	0	5	4	-2	3	1	-1	5	0	-2	3	-2	-1
	3	32	4	32	15	1	6	5	0	35	6	-7	34	4	-6	41	17	-1	40	15	-0
	4	32	4	32	15	1	6	5	0	-0	4	3	-1	3	3	0	8	4	0	8	4
	5	31	4	32	15	1	6	5	0	-12	4	4	-12	5	4	-12	8	4	-11	9	4
	6	31	4	32	15	1	6	5	0	5	-1	1	7	1	0	7	8	4	9	10	3
	7	31	4	32	15	1	6	5	0	1	13	0	3	16	-0	6	27	3	8	31	2
	8	32	4	32	15	1	6	5	0	3	12	1	5	15	0	7	22	3	9	25	2
	9	32	4	32	15	1	6	5	0	14	7	0	16	10	-0	17	13	2	18	16	1
	10	32	4	32	15	1	6	5	0	-4	-25	-0	-3	-24	-0	-8	-31	-0	-7	-31	-0
	11	32	4	32	15	1	6	5	0	-3	-9	3	-4	-10	3	-6	-19	1	-7	-20	1
	12	32	4	32	15	1	6	5	0	30	-15	-6	29	-17	-5	31	-21	-5	29	-23	-4

1877	1	32	4	32	15	1	6	6	0	9	-11	-6	7	-14	-5	4	-25	-9	2	-28	-7
	2	32	4	32	15	1	6	6	0	11	9	-4	9	6	-3	12	5	-5	10	2	-4
	3	32	4	33	15	1	6	6	0	11	-1	-3	10	-3	-2	14	0	-1	12	-2	-0
	4	32	4	33	15	1	6	6	0	5	-2	3	4	-2	3	6	-1	4	6	-1	5
	5	32	4	33	15	1	6	6	0	4	-5	2	4	-4	2	4	-2	4	5	-1	3
	6	32	4	33	15	1	6	6	0	-6	-2	1	-4	0	1	-6	4	2	-4	6	2
	7	33	4	33	15	1	6	6	0	-3	9	0	-1	12	-0	-0	20	3	1	24	2
	8	33	4	33	15	1	6	6	0	2	9	3	4	12	2	4	16	4	6	20	3
	9	33	4	33	15	1	6	6	0	-4	-2	1	-2	-0	0	-4	-2	1	-3	-0	0
	10	33	4	33	15	1	6	6	0	-0	-10	-2	-0	-9	-2	-4	-18	-3	-3	-17	-3
	11	33	4	33	15	1	6	6	0	24	-4	-7	23	-5	-7	24	-7	-6	23	-8	-5
	12	33	4	33	15	1	6	6	0	-5	-1	-2	-7	-4	-1	-9	-13	-5	-10	-15	-4
1878	1	35	4	33	19	1	6	6	0	-14	-19	-1	-16	-22	-0	-22	-38	-6	-24	-41	-5
	2	34	4	33	19	1	6	6	0	-30	-39	-1	-32	-42	-0	-42	-60	-6	-43	-63	-5
	3	34	4	33	19	1	6	6	0	-0	-18	-2	-1	-20	-2	-2	-25	-2	-4	-27	-1
	4	34	4	33	19	1	6	6	0	3	-42	0	2	-43	1	-0	-47	3	-1	-47	3
	5	34	4	33	19	1	6	6	0	7	-8	-0	8	-6	-0	9	-1	2	10	-0	2
	6	34	4	33	19	1	6	6	0	11	-2	1	13	0	0	13	6	4	14	8	3
	7	35	4	33	19	1	6	6	0	18	6	-0	20	9	-1	23	21	4	25	24	3
	8	35	4	33	19	1	6	6	0	29	-7	-0	31	-4	-2	33	5	4	35	8	3
	9	35	4	33	19	1	6	6	0	6	15	0	7	17	-0	10	26	2	11	28	1
	10	35	4	33	19	1	6	6	0	10	-3	-1	11	-2	-1	11	-2	0	11	-1	0
	11	35	4	34	19	1	6	6	0	12	-3	-0	11	-4	0	12	-7	-0	11	-8	0
	12	35	4	34	19	1	6	6	0	17	8	-1	16	5	-0	19	5	-1	17	3	-0
1879	1	37	4	32	20	1	6	6	0	-19	-13	1	-21	-16	2	-25	-31	-3	-27	-34	-2
	2	36	4	34	20	1	6	6	0	36	4	-7	34	1	-6	40	8	-3	38	5	-2
	3	37	4	33	20	1	6	6	0	-1	3	0	-2	1	1	-1	-0	-1	-2	-2	-0
	4	37	4	34	20	1	6	6	0	14	-3	-0	14	-4	-0	19	4	3	18	4	3
	5	37	4	34	20	1	6	6	0	-4	8	4	-4	9	4	-2	16	5	-1	17	5
	6	36	4	34	20	1	6	6	0	13	5	0	15	7	-0	18	19	4	19	22	4
	7	36	4	34	20	1	6	6	0	15	13	0	17	16	-0	21	30	5	23	33	4
	8	36	4	34	20	1	6	6	0	4	-0	0	6	2	-0	8	14	5	10	17	4
	9	36	4	34	20	1	6	6	0	-0	7	0	1	9	-0	2	14	1	3	16	0
	10	37	4	34	20	1	6	6	0	-8	1	1	-8	2	1	-9	-2	-0	-9	-2	-1
	11	37	4	34	20	1	[illegible]	6	0	-15	4	3	-15	3	4	-18	-8	-0	-19	-9	-0
	12	37	4	34	20	1	6	6	0	-27	-0	0	-28	-3	1	-34	-16	-5	-35	-19	-4
1880	1	38	4	33	22	1	6	6	0	-42	-12	3	-44	-16	4	-52	-34	-4	-54	-37	-3
	2	38	4	34	22	1	6	6	0	6	-5	-6	4	-8	-5	4	-10	-6	2	-14	-5
	3	38	4	34	22	1	6	6	0	-24	-9	3	-25	-11	4	-28	-19	-0	-30	-21	0
	4	39	4	33	22	1	6	6	0	3	-8	-1	2	-9	-1	4	-4	0	4	-4	1
	5	38	4	33	22	1	6	6	0	2	0	3	3	1	2	4	6	5	5	7	4
	6	39	4	33	22	1	6	6	0	4	14	3	5	16	2	8	28	6	9	30	5
	7	39	4	33	22	1	6	6	0	3	20	2	5	24	1	8	35	6	10	38	4
	8	39	4	33	22	1	6	6	0	3	8	2	5	11	0	6	17	5	8	20	3
	9	38	4	33	22	1	6	6	0	-8	0	3	-6	2	2	-7	1	2	-6	3	1
	10	38	4	34	22	1	6	6	0	-2	12	3	-2	13	2	-2	8	1	-1	9	0
	11	38	4	33	22	1	6	6	0	1	14	-3	1	13	-3	0	5	-6	-0	4	-6
	12	38	4	34	22	1	6	6	0	2	-3	-4	1	-5	-3	-1	-15	-6	-2	-18	-5

1881	1	59	6	37	23	1	4	6	0	-1	15	1	-3	12	2	-1	6	-1	-3	2	-0
	2	60	6	37	23	1	4	6	0	-23	-13	6	-25	-16	8	-25	-29	0	-27	-32	1
	3	60	6	37	23	1	4	6	0	12	-41	-1	11	-43	-0	10	-48	-0	9	-50	-0
	4	61	6	37	24	1	4	6	0	0	-4	2	-0	-4	2	1	-1	3	0	-1	3
	5	62	6	37	24	1	4	6	0	-22	6	7	-21	7	6	-22	10	6	-21	11	6
	6	62	6	36	24	1	4	6	0	15	15	-1	16	17	-2	18	33	5	19	36	4
	7	62	6	37	24	1	4	6	0	15	38	-2	17	41	-3	19	59	4	21	62	3
	8	61	5	37	24	1	4	6	0	30	30	-3	32	33	-4	35	50	4	37	53	3
	9	61	5	37	24	1	4	6	0	-19	-5	5	-18	-3	4	-20	-4	4	-18	-2	3
	10	62	5	36	24	1	4	6	0	-18	-6	5	-18	-5	5	-19	-13	2	-19	-12	2
	11	62	5	36	24	1	4	6	0	-13	-13	-4	-13	-14	-3	-18	-24	-8	-18	-25	-8
	12	62	5	37	24	1	4	6	0	-30	-37	0	-32	-39	1	-37	-60	-8	-39	-62	-7
1882	1	63	6	38	25	1	5	6	0	-60	-36	1	-62	-39	2	-70	-62	-11	-72	-66	-10
	2	63	6	38	25	1	5	6	0	-32	-10	-1	-34	-13	-0	-38	-24	-8	-40	-27	-7
	3	63	5	38	25	1	5	6	0	6	-2	-7	5	-4	-6	5	-6	-7	3	-8	-6
	4	63	5	37	25	1	4	6	0	3	5	3	2	5	3	5	10	5	4	9	5
	5	63	5	37	25	1	5	6	0	-17	9	7	-17	10	6	-17	13	7	-16	15	6
	6	63	6	37	25	1	5	6	0	6	19	1	8	21	0	9	36	7	11	39	6
	7	64	6	37	25	1	5	6	0	32	48	-2	34	51	-3	39	71	5	41	74	4
	8	64	6	38	25	1	5	6	0	23	43	-1	25	46	-3	29	62	4	31	65	3
	9	64	6	37	25	1	5	6	0	-0	5	2	1	7	1	1	8	3	2	10	2
	10	64	6	37	25	1	5	6	0	-28	-38	5	-28	-37	5	-32	-48	1	-32	-47	1
	11	64	6	38	25	1	5	6	0	15	7	-3	14	6	-2	16	2	-3	16	1	-3
	12	64	6	38	25	1	5	6	0	-3	-23	3	-5	-25	4	-4	-38	-1	-6	-40	-0
1883	1	63	7	38	24	1	5	7	0	-3	-19	-2	-5	-22	-1	-7	-35	-8	-9	-38	-7
	2	64	7	38	24	1	5	7	0	-44	-26	5	-46	-29	6	-51	-50	-7	-53	-53	-5
	3	63	8	38	24	1	5	7	0	16	9	-0	15	7	0	19	12	2	18	10	3
	4	65	8	38	24	1	5	7	0	-12	-27	6	-12	-28	6	-13	-29	5	-13	-30	5
	5	64	8	38	24	1	5	7	0	7	14	1	7	15	1	10	26	6	10	27	5
	6	65	9	38	24	1	5	7	0	0	30	3	2	33	2	4	47	8	5	50	7
	7	66	9	38	24	1	5	7	0	23	51	-1	25	54	-2	29	74	6	31	77	5
	8	65	9	38	24	1	5	7	0	10	37	0	12	40	-0	14	53	4	16	56	3
	9	66	9	38	24	1	5	7	0	0	4	2	2	6	1	2	8	2	3	10	2
	10	65	9	38	24	1	5	6	0	-9	-16	-0	-9	-15	-1	-12	-25	-4	-11	-24	-4
	11	66	9	37	24	1	5	6	0	-7	-35	-1	-7	-36	-0	-11	-49	-6	-11	-51	-5
	12	65	9	37	24	1	5	6	0	-7	-18	-2	-8	-20	-1	-11	-34	-8	-12	-37	-7
1884	1	65	10	38	25	2	4	6	0	-4	-5	-6	-6	-8	-5	-8	-21	-12	-10	-24	-11
	2	65	10	38	25	2	4	6	0	-18	-32	-0	-20	-35	0	-22	-47	-6	-24	-50	-5
	3	66	10	38	25	2	4	6	0	-24	-46	3	-25	-48	4	-28	-58	-0	-29	-61	0
	4	66	10	38	25	2	5	6	0	14	-11	2	13	-11	2	16	-6	6	15	-7	6
	5	66	10	38	25	2	5	6	0	-8	7	3	-7	8	3	-7	14	5	-6	15	4
	6	66	10	38	25	2	5	6	0	13	40	-1	15	42	-2	18	59	5	19	62	4
	7	66	10	38	25	2	5	6	0	5	26	3	7	29	2	8	44	8	10	47	7
	8	67	10	37	25	2	5	6	0	-6	33	3	-4	36	2	-4	46	6	-2	49	5
	9	67	10	36	25	2	5	6	0	-17	-6	2	-16	-4	1	-19	-5	1	-17	-3	0
	10	67	10	38	25	2	5	6	0	-7	-21	-0	-7	-20	-0	-10	-31	-4	-9	-31	-4
	11	66	10	38	25	2	5	6	0	-44	-36	7	-44	-37	8	-49	-57	-2	-50	-59	-2
	12	66	10	37	25	2	5	6	0	12	-36	-7	11	-39	-6	9	-52	-9	7	-55	-8

1885	1	67	10	35	28	2	7	7	0	-18	-43	0	-20	-46	2	-23	-65	-6	-25	-68	-5
	2	68	10	37	28	2	7	7	0	-12	-52	3	-14	-55	4	-16	-68	-1	-18	-71	-0
	3	67	10	36	28	2	7	7	0	7	-3	-0	5	-5	0	7	-9	-1	6	-11	-0
	4	68	10	37	28	2	7	7	0	19	5	-0	19	4	-0	23	11	4	22	11	4
	5	67	10	36	28	2	7	7	0	7	1	-0	8	2	-0	9	8	4	10	9	3
	6	66	10	37	28	2	7	7	0	7	32	-1	9	35	-2	11	50	4	12	53	3
	7	65	10	36	28	2	7	7	0	-16	30	5	-14	33	4	-14	43	7	-12	46	6
	8	66	10	36	28	2	7	7	0	9	41	1	11	44	0	14	60	8	16	63	7
	9	67	10	36	28	2	7	7	0	8	5	-4	9	7	-5	8	11	-0	9	13	-1
	10	68	10	36	28	2	7	7	0	18	-10	-2	18	-9	-2	18	-11	-0	19	-11	-1
	11	69	10	37	28	2	7	7	0	-12	-50	-1	-13	-51	-1	-17	-66	-5	-18	-67	-4
	12	69	10	37	28	2	7	7	0	-15	-13	-4	-16	-15	-3	-19	-24	-9	-20	-27	-8
1886	1	67	10	40	32	2	7	7	0	23	-10	-4	21	-13	-3	24	-16	-3	22	-19	-1
	2	69	9	40	32	2	7	7	0	-72	-77	17	-74	-80	18	-79	-111	0	-81	-114	2
	3	69	10	40	32	2	7	7	0	-20	-42	3	-22	-44	4	-24	-52	-0	-25	-54	0
	4	69	11	39	32	2	7	7	0	-21	-17	6	-22	-18	6	-22	-21	3	-22	-22	4
	5	69	12	39	32	2	7	7	0	-10	8	5	-10	9	4	-9	15	6	-8	16	5
	6	69	12	39	32	3	7	7	0	27	43	-3	29	45	-4	32	67	6	34	69	5
	7	69	12	37	32	3	7	7	0	24	45	-3	26	48	-5	28	70	5	30	73	4
	8	66	11	37	32	3	7	7	0	26	20	-4	28	23	-5	30	39	3	32	42	2
	9	66	11	37	32	3	7	7	0	-7	11	1	-6	13	0	-7	15	1	-6	18	0
	10	67	11	38	32	3	7	7	0	-10	-5	3	-9	-4	3	-10	-13	-0	-10	-12	-1
	11	67	11	37	31	3	7	7	0	1	-30	-1	0	-31	-0	-1	-44	-5	-2	-45	-5
	12	67	11	38	32	3	7	7	0	33	-4	-8	31	-6	-7	34	-12	-8	32	-15	-7
1887	1	67	13	39	31	3	8	8	[illegible]	-14	-55	-1	-16	-58	-0	-20	-72	-6	-22	-75	-5
	2	68	13	39	31	3	8	8	0	-66	-35	7	-68	-38	8	-75	-61	-7	-77	-64	-5
	3	68	13	38	31	3	8	8	0	1	4	1	0	2	2	1	2	0	0	0	1
	4	68	13	40	32	3	8	8	0	-3	4	1	-3	4	1	-2	8	3	-2	8	3
	5	68	13	40	32	3	8	8	0	-0	10	3	0	11	2	1	17	4	2	18	4
	6	[illegible]	13	40	32	3	8	8	0	-12	29	3	-11	31	2	-11	43	6	-9	46	5
	7	[illegible]	13	39	32	3	8	8	0	8	40	0	10	43	-0	12	59	4	14	62	3
	8	69	13	40	32	3	8	8	0	2	32	0	4	35	-0	5	48	6	7	51	5
	9	69	13	39	32	3	8	8	0	6	17	1	8	19	1	8	22	3	9	24	2
	10	70	13	40	31	3	8	8	0	7	0	-1	8	1	-1	7	-2	-2	7	-1	-2
	11	72	13	39	31	3	8	8	0	30	-1	-6	29	-2	-5	31	-5	-4	30	-7	-4
	12	71	13	40	31	3	8	8	0	23	-0	-5	22	-2	-5	24	-5	-4	23	-8	-3
1888	1	75	13	41	32	3	8	8	0	-43	-8	7	-45	-11	8	-46	-30	-5	-42	-33	-4
	2	75	13	41	32	3	8	8	0	-5	-35	6	-7	-38	7	-5	-50	1	-7	-53	2
	3	75	13	41	32	3	8	8	0	51	21	-7	49	19	-6	55	26	-0	54	23	-0
	4	75	13	41	32	3	8	8	0	8	41	3	7	40	3	13	47	5	12	46	5
	5	74	13	41	32	3	8	8	0	-25	0	4	-25	2	3	-26	8	5	-25	9	5
	6	73	13	42	32	3	8	8	0	1	11	-1	3	14	-2	2	30	5	4	32	4
	7	72	14	42	32	3	8	8	0	39	71	-7	41	74	-8	46	97	3	40	100	2
	8	72	15	42	32	3	8	8	0	-6	37	0	-4	40	-0	-4	51	4	-2	54	3
	9	73	15	41	32	3	8	8	0	-44	2	7	-43	4	6	-47	-1	1	-46	0	1
	10	73	15	42	32	3	8	8	0	-10	-21	-0	-10	-20	-0	-14	-27	-2	-13	-27	-2
	11	74	15	42	32	3	8	8	0	14	-5	-5	13	-6	-5	13	-13	-7	12	-14	-7
	12	75	15	42	32	3	8	8	0	-20	-52	-1	-22	-55	-0	-26	-73	-9	-28	-75	-8

1889	1	74	17	42	31	4	8	9	0	-44	-85	9	-46	-88	10	-52	-115	-3	-54	-118	-2
	2	74	16	43	31	4	8	9	0	45	23	-5	43	20	-4	51	22	-2	49	19	-1
	3	74	17	43	31	4	8	9	0	5	-39	0	4	-41	1	3	-48	-0	2	-50	0
	4	74	17	43	31	4	8	9	0	34	7	-4	34	7	-3	38	16	2	37	15	3
	5	74	16	43	31	4	8	9	0	-4	-16	3	-3	-15	3	-4	-13	5	-3	-12	5
	6	75	17	42	31	5	8	9	0	12	44	-3	14	47	-3	15	64	4	17	67	3
	7	75	17	42	31	5	8	9	0	8	64	-1	10	67	-3	12	87	6	15	90	5
	8	75	17	43	31	5	8	9	0	19	59	-6	21	62	-7	23	80	1	25	83	0
	9	75	18	43	31	4	8	9	0	-2	3	4	-1	5	3	-1	7	4	-0	9	3
	10	76	18	43	31	5	8	9	0	-4	-7	4	-4	-7	4	-4	-13	1	-4	-13	1
	11	75	18	43	31	5	8	9	0	-58	-50	11	-59	-51	11	-65	-74	-3	-65	-75	-2
	12	75	18	43	31	5	8	9	0	-71	-80	9	-72	-82	10	-80	-111	-6	-82	-114	-5
1890	1	76	19	43	33	5	8	9	0	1	-23	-5	-0	-26	-4	-1	-37	-10	-3	-40	-9
	2	76	19	43	33	5	8	9	0	-69	-51	13	-71	-54	14	-75	-74	-0	-77	-77	0
	3	76	19	43	33	4	8	9	0	23	-26	-2	22	-28	-2	24	-29	-1	22	-31	-0
	4	75	19	43	33	4	8	9	0	18	29	-2	18	28	-1	23	37	2	22	36	2
	5	75	19	43	33	4	8	9	0	7	20	-0	7	21	-0	9	34	6	10	35	5
	6	76	22	43	33	4	8	9	0	5	58	-3	6	61	-4	8	79	4	10	82	3
	7	76	22	42	33	4	8	9	0	25	71	-7	27	74	-8	31	97	3	33	100	2
	8	77	22	43	33	4	8	9	0	8	57	-4	10	60	-5	12	74	2	14	77	1
	9	77	22	43	33	4	7	9	0	-37	9	8	-36	11	7	-38	8	3	-37	10	2
	10	77	23	43	33	4	7	9	0	10	-32	-1	10	-32	-2	7	-37	-2	7	-36	-2
	11	77	23	43	33	4	7	[illegible]	0	12	-31	0	12	-32	1	11	-44	-3	10	-46	-3
	12	76	23	43	33	4	7	9	0	-33	-36	5	-35	-38	6	-38	-55	-3	-40	-58	-2
1891	1	79	23	44	31	4	8	9	0	-42	-54	11	-45	-57	12	-47	-78	-1	-49	-81	-0
	2	79	24	44	31	4	8	9	0	-84	-80	8	-86	-83	9	-96	-107	-7	-98	-110	-6
	3	79	24	44	31	4	9	9	0	22	4	-3	21	2	-2	24	3	-0	23	1	-0
	4	79	23	44	31	4	9	9	0	-11	-18	5	-11	-18	6	-11	-21	4	-12	-21	4
	5	79	24	44	31	5	9	9	0	5	57	-2	6	58	-2	10	72	4	11	73	4
	6	80	24	44	31	5	9	9	0	-15	21	3	-13	23	2	-14	34	8	-13	37	7
	7	79	24	43	31	5	9	9	0	5	81	-3	7	84	-4	10	104	5	12	107	4
	8	80	23	43	31	5	9	9	0	20	58	-5	22	61	-7	23	76	1	25	79	0
	9	80	23	43	31	5	9	9	0	-14	29	-1	-13	31	-2	-14	34	-2	-12	36	-2
	10	79	23	42	31	5	9	9	0	7	1	-2	8	1	-2	7	-2	-3	7	-2	-3
	11	79	23	43	31	4	9	9	0	-9	-35	5	-10	-36	5	-11	-51	-1	-12	-52	-1
	12	79	23	43	31	5	9	9	0	-8	-58	-4	-10	-60	-3	-15	-78	-12	-16	-81	-11
1892	1	77	22	46	35	6	9	10	0	30	-17	-2	28	-20	-1	31	-27	-3	29	-30	-2
	2	78	22	46	35	6	9	10	0	16	5	4	14	2	5	20	1	5	18	-1	6
	3	78	24	46	35	6	9	10	0	-18	-52	12	-19	-54	13	-19	-63	7	-20	-65	8
	4	78	24	46	35	6	8	10	0	4	12	1	3	12	2	6	18	4	6	18	4
	5	78	22	45	35	6	8	10	0	-9	21	3	-8	22	3	-7	31	6	-6	32	6
	6	78	22	[illegible]	35	6	8	10	0	1	36	-1	2	38	-2	3	55	5	5	57	4
	7	79	22	46	35	6	9	10	0	12	86	-3	14	89	-4	18	110	4	20	113	3
	8	79	21	46	35	6	9	10	0	10	56	-3	12	59	-4	14	75	3	16	78	2
	9	79	23	46	35	6	9	10	0	-9	22	0	-8	24	-0	-8	26	0	-7	29	-0
	10	80	23	45	35	6	9	10	0	19	-11	-0	20	-11	-0	20	-12	1	20	-11	1
	11	80	23	45	35	6	9	10	0	-60	-67	13	-60	-68	14	-66	-91	0	-66	-92	0
	12	81	23	45	35	6	9	10	0	15	-54	0	14	-56	1	13	-71	-3	12	-73	-2

1893	1	82	22	45	34	6	9	10	0	-20	-75	14	-22	-79	16	-22	-94	6	-24	-97	7
	2	82	22	45	34	6	9	10	0	32	-36	-3	30	-39	-2	32	-46	-4	30	-49	-3
	3	82	22	45	34	6	9	11	0	4	-2	-6	2	-4	-5	3	-3	-5	1	-5	-4
	4	82	22	45	34	6	9	11	0	-14	-12	2	-14	-13	2	-15	-12	1	-16	-12	2
	5	82	22	46	34	6	9	11	0	-14	-17	6	-13	-16	6	-15	-12	7	-14	-11	7
	6	82	22	46	34	6	9	11	0	9	46	-2	11	49	-3	12	66	5	14	69	4
	7	82	22	46	34	6	9	11	0	25	60	-5	27	63	-7	29	84	5	31	87	3
	8	82	22	46	34	6	9	11	0	-4	37	-1	-2	40	-2	-3	52	3	-1	55	2
	9	82	22	46	34	6	9	11	0	33	9	-7	35	11	-8	35	22	0	36	25	-0
	10	82	22	46	34	6	9	11	0	6	-18	-0	7	-18	-0	6	-22	-1	6	-22	-2
	11	82	22	46	34	6	9	11	0	18	-16	-3	17	-18	-2	17	-25	-5	17	-26	-4
	12	81	21	46	34	6	9	11	0	-12	-32	-1	-14	-35	-0	-16	-52	-9	-18	-54	-8
1894	1	82	22	46	36	6	10	11	0	-22	-41	0	-24	-44	1	-26	-58	-7	-28	-61	-5
	2	81	24	46	36	6	10	11	0	29	-15	-10	27	-18	-9	27	-24	-11	25	-27	-10
	3	81	24	46	36	6	10	11	0	11	-31	-3	10	-33	-2	10	-36	-3	9	-38	-2
	4	82	24	46	36	6	10	11	0	-18	-18	8	-19	-19	8	-19	-22	4	-19	-22	4
	5	81	24	44	36	6	10	11	0	2	10	4	3	11	3	4	19	8	5	20	7
	6	81	24	46	36	6	10	11	0	20	57	-9	21	60	-10	23	82	1	25	84	0
	7	83	24	46	36	6	10	11	0	20	87	-7	22	90	-8	24	110	1	26	113	0
	8	82	24	45	36	6	10	11	0	15	70	-5	17	74	-6	20	91	2	22	94	1
	9	82	24	45	36	6	10	11	0	-12	21	3	-11	23	3	-11	28	4	-10	30	3
	10	81	24	46	36	6	10	11	0	0	-37	2	0	-37	1	-1	-41	1	-0	-40	0
	11	81	25	48	36	6	10	11	0	-15	-50	2	-16	-51	3	-20	-71	-7	-20	-72	-7
	12	81	24	48	36	6	10	11	0	-10	-30	-1	-12	-32	-0	-13	-46	-8	-15	-49	-7
1895	1	81	24	49	36	6	10	11	0	34	-58	2	32	-61	3	34	-70	2	32	-73	3
	2	79	24	49	36	6	10	11	0	17	-13	8	15	-16	9	20	-22	6	18	-25	7
	3	82	24	49	36	6	10	11	0	59	-11	-7	58	-13	-7	61	-7	0	60	-9	0
	4	83	24	48	36	6	10	11	0	7	7	-0	7	6	-0	9	11	2	8	10	2
	5	83	24	48	36	6	10	11	0	-31	9	5	-30	11	4	-31	13	4	-30	14	3
	6	83	24	48	36	6	10	11	0	-11	62	2	-9	65	1	-8	76	4	-7	79	3
	7	82	24	48	36	6	10	11	0	26	63	-6	28	66	-7	30	84	2	32	87	1
	8	84	23	47	36	6	10	12	0	6	44	-1	8	47	-3	8	62	5	10	66	4
	9	84	23	49	36	6	10	11	0	-18	-7	-0	-17	-5	-0	-21	-7	-1	-19	-5	-2
	10	84	23	48	36	6	10	11	0	23	-2	-1	23	-1	-1	24	-4	0	24	-3	-0
	11	84	22	49	36	6	10	11	0	-26	-27	1	-27	-28	1	-30	-45	-8	-30	-46	-7
	12	83	22	48	36	7	9	11	0	24	-32	-3	22	-34	-2	23	-43	-4	22	-46	-3
1896	1	83	21	48	38	8	10	13	0	-56	-14	7	-58	-17	8	-59	-34	-4	-62	-37	-3
	2	84	21	48	38	8	10	13	0	-42	-90	6	-44	-93	7	-50	-112	-5	-52	-115	-4
	3	84	22	48	38	8	10	13	0	29	-43	-0	28	-45	0	30	-49	0	28	-51	1
	4	84	22	48	38	7	10	13	0	-15	-5	4	-15	-6	4	-14	-7	2	-15	-7	2
	5	84	22	49	38	7	10	13	0	-12	3	3	-11	4	3	-11	9	5	-11	11	4
	6	83	22	49	38	7	10	12	0	11	51	-1	12	53	-2	14	72	6	16	74	5
	7	84	22	49	38	8	10	12	0	22	77	-5	25	80	-6	26	99	2	28	102	1
	8	85	22	49	39	8	10	13	0	2	57	1	4	60	0	5	70	5	7	73	4
	9	84	22	48	39	8	10	13	0	10	10	0	12	12	-0	11	16	3	13	18	2
	10	85	23	49	39	8	10	13	0	-12	-24	5	-12	-24	5	-13	-36	-0	-13	-35	-0
	11	84	23	48	39	8	10	13	0	-21	13	1	-22	12	2	-22	4	-3	-23	3	-3
	12	84	23	48	39	8	10	13	0	-5	-46	-0	-7	-48	0	-8	-69	-9	-10	-72	-8

1897	1	85	23	48	41	8	10	14	0	-10	-44	11	-12	-47	12	-10	-65	2	-13	-68	3
	2	86	24	48	41	8	10	14	0	-17	-47	0	-19	-50	1	-21	-61	-5	-23	-64	-4
	3	86	25	48	41	8	10	14	0	31	-51	1	30	-53	2	32	-57	2	30	-60	3
	4	85	25	48	41	8	10	14	0	20	3	-0	20	3	-0	22	3	0	21	3	0
	5	85	23	48	41	8	10	14	0	13	28	2	14	29	1	16	39	8	17	40	7
	6	85	25	48	41	8	10	14	0	-17	44	2	-15	47	1	-15	64	7	-13	66	6
	7	85	24	48	41	8	10	14	0	29	56	-6	31	59	-7	33	80	4	35	83	3
	8	85	24	47	41	8	10	14	0	15	59	-4	17	82	-5	18	79	3	20	82	2
	9	85	23	49	41	8	10	14	0	6	29	-1	8	31	-2	8	34	-1	9	36	-2
	10	84	25	48	41	8	10	14	0	-41	-23	8	-40	-22	7	-44	-35	-0	-44	-34	-0
	11	86	25	48	41	8	10	14	0	-48	-25	5	-48	-26	5	-52	-43	-6	-53	-44	-6
	12	86	24	48	41	8	10	14	0	-42	-80	9	-44	-83	10	-48	-109	-5	-50	-112	-4
1898	1	87	25	48	41	8	10	14	0	-51	-63	-2	-53	-66	-1	-60	-86	-15	-62	-89	-14
	2	87	25	48	41	8	10	13	0	-2	-19	7	-4	-22	8	-2	-30	2	-3	-33	3
	3	87	25	48	41	8	10	13	0	-2	-40	13	-4	-42	14	-0	-52	9	-1	-54	10
	4	87	25	47	41	8	10	13	0	-5	-11	4	-5	-11	4	-5	-12	3	-5	-13	3
	5	86	24	48	41	8	10	13	0	7	16	-0	8	18	-1	9	30	6	10	31	6
	6	86	24	48	41	8	10	13	0	-1	57	-2	0	59	-3	1	79	6	2	82	5
	7	86	24	48	41	8	10	13	0	17	78	-4	19	81	-5	22	101	4	24	104	3
	8	85	23	48	41	8	10	13	0	-12	33	-0	-10	36	-1	-11	48	3	-9	52	2
	9	86	25	48	41	8	10	13	0	-14	-18	2	-12	-16	1	-15	-16	2	-14	-14	1
	10	87	26	48	41	8	10	13	0	10	3	-0	10	3	-1	10	1	-1	10	2	-1
	11	87	26	48	41	8	10	13	0	2	-41	-2	1	-42	-2	-0	-52	-5	-1	-53	-5
	12	87	26	48	41	8	10	13	0	2	-1	-10	1	-4	-9	-0	-11	-14	-2	-14	-13
1899	1	88	25	48	43	8	10	13	0	24	-18	-8	22	-21	-7	22	-29	-9	20	-32	-8
	2	88	25	48	43	8	10	13	0	13	-41	0	11	-44	1	13	-50	-1	11	-54	-0
	3	88	24	47	43	8	10	13	0	-6	-17	0	-7	-19	0	-7	-20	0	-8	-22	0
	4	88	25	49	43	8	10	13	0	6	9	-1	6	8	-1	7	13	1	7	12	1
	5	88	23	49	43	8	10	12	0	-18	24	3	-18	25	3	-18	32	5	-17	33	4
	6	88	24	49	43	8	10	13	0	3	48	-0	5	51	-1	6	66	5	7	69	4
	7	88	24	49	43	8	10	13	0	-14	70	-0	-12	73	-1	-12	90	6	-10	93	5
	8	88	25	50	43	8	10	13	0	-20	46	-0	-18	49	-1	-19	63	5	-17	66	4
	9	86	24	50	43	8	10	13	0	24	19	-2	26	21	-3	26	23	-0	27	25	-1
	10	88	24	49	43	8	10	13	0	-30	-24	5	-29	-23	4	-32	-38	-3	-32	-38	-3
	11	88	25	50	43	8	10	13	0	-22	-40	-5	-23	-41	-5	-28	-55	-12	-29	-56	-12
	12	88	25	49	43	8	10	13	0	-30	-56	13	-32	-58	14	-32	-80	1	-34	-83	2
1900	1	89	23	50	43	8	10	14	0	-11	-84	7	-13	-87	8	-14	-110	-2	-16	-113	-1
	2	89	22	50	43	9	10	14	0	23	-39	6	21	-43	7	25	-51	4	23	-54	5
	3	89	23	50	43	9	10	14	0	-9	-12	7	-10	-15	8	-8	-20	4	-9	-22	5
	4	89	22	49	43	9	10	14	0	3	-17	-0	2	-18	-0	2	-16	1	2	-16	1
	5	89	23	50	43	9	10	14	0	-1	21	-2	-0	22	-2	-0	30	3	-0	32	2
	6	89	22	49	43	9	10	14	0	11	24	-2	12	27	-3	12	42	5	13	45	4
	7	90	21	49	43	9	10	14	0	11	72	-7	13	76	-9	12	97	3	14	100	2
	8	90	22	49	43	9	10	14	0	2	52	-2	4	55	-3	4	69	3	6	72	2
	9	90	22	50	42	9	9	15	0	-15	13	-2	-14	15	-3	-18	15	-4	-16	17	-4
	10	89	22	50	42	9	10	15	0	-16	-27	1	-16	-27	1	-18	-39	-4	-18	-38	-4
	11	89	22	50	43	9	10	15	0	-5	-42	4	-6	-43	4	-6	-58	-1	-7	-59	-1
	12	89	22	50	43	9	10	16	0	10	-22	-8	8	-25	-7	7	-35	-11	5	-38	-10

1901	1	89	23	49	43	12	12	19	0	-15	-52	-1	-17	-55	-0	-19	-70	-8	-21	-73	-7
	2	89	24	49	43	12	12	19	0	-7	-67	5	-9	-70	6	-9	-85	-0	-11	-88	0
	3	89	22	49	43	12	12	19	0	33	-45	-5	32	-47	-4	33	-49	-1	32	-51	-1
	4	89	22	49	43	12	12	19	0	-2	9	4	-2	8	4	-0	9	3	-0	9	3
	5	89	22	49	43	12	12	19	0	-29	-17	8	-29	-16	8	-31	-14	8	-30	-13	8
	6	89	23	49	43	12	12	19	0	-4	26	-1	-2	28	-2	-4	41	4	-2	44	3
	7	89	25	49	43	12	12	19	0	4	57	-4	6	60	-5	6	79	5	8	82	4
	8	89	25	49	43	12	12	19	0	4	66	-1	6	69	-2	7	85	4	9	88	3
	9	90	25	49	44	12	12	19	0	-10	-8	0	-9	-6	-0	-11	-5	0	-10	-3	0
	10	90	26	49	44	12	12	19	0	-23	-25	8	-22	-24	8	-24	-38	0	-24	-38	0
	11	90	25	49	44	12	12	19	0	-7	26	-4	-7	25	-3	-7	21	-7	-8	20	-6
	12	89	25	49	44	12	12	19	0	43	-34	-1	42	-37	-0	44	-48	-2	43	-51	-1
1902	1	90	25	50	45	12	12	20	0	-1	4	-2	-3	1	-1	-3	-7	-8	-3	-10	-7
	2	91	25	50	45	12	12	20	0	-10	-91	0	-12	-94	2	-16	-112	-5	-18	-115	-4
	3	90	26	50	45	12	12	21	0	16	-18	-5	14	-20	-4	16	-15	-0	15	-17	0
	4	90	26	49	45	12	12	21	0	-25	-21	7	-26	-22	7	-25	-23	7	-26	-24	7
	5	91	25	50	45	11	12	21	0	-6	24	0	-5	25	0	-5	33	5	-4	34	4
	6	91	26	50	45	11	12	21	0	-0	45	-0	0	48	-1	1	67	9	2	70	8
	7	91	27	49	45	11	13	21	0	-4	80	-2	-2	84	-4	-2	102	5	-0	106	4
	8	94	27	50	45	12	13	21	0	7	46	-1	9	49	-2	10	63	5	12	66	4
	9	94	28	50	45	12	13	21	0	-23	10	2	-21	12	2	-24	13	1	-22	15	1
	10	93	28	49	45	12	13	21	0	-0	-33	-2	0	-33	-3	-3	-44	-7	-3	-44	-7
	11	94	29	49	45	12	13	21	0	-19	-57	-0	-19	-58	-0	-23	-72	-6	-23	-73	-6
	12	94	29	50	45	12	13	21	0	-8	-26	-2	-10	-28	-1	-11	-39	-7	-13	-41	-6
1903	1	92	33	50	46	12	13	20	0	-15	-89	-3	-17	-93	-2	-22	-110	-11	-24	-113	-10
	2	93	33	50	46	12	13	21	0	13	-17	-19	11	-20	-17	7	-30	-23	5	-33	-22
	3	93	33	50	46	12	13	21	0	-20	-18	0	-21	-20	1	-22	-29	-5	-23	-31	-4
	4	93	32	50	46	12	13	21	0	34	-32	0	33	-32	0	36	-30	5	35	-30	5
	5	94	33	50	46	12	13	21	0	-1	24	-1	-0	25	-2	0	32	2	1	33	1
	6	94	32	50	46	12	13	21	0	-5	68	2	-3	71	1	-2	86	8	-0	88	8
	7	94	32	50	46	12	13	22	0	24	75	-4	26	78	-6	27	99	5	29	102	4
	8	91	32	50	46	12	13	22	0	21	61	-7	23	64	-8	24	80	1	26	84	0
	9	92	32	50	46	12	13	22	0	-28	21	3	-26	23	3	-29	22	0	-27	24	-0
	10	94	34	50	46	12	13	22	0	18	13	-1	18	14	-1	19	16	0	20	17	0
	11	94	34	49	46	12	13	22	0	-12	-38	1	-13	-39	2	-14	-53	-5	-15	-54	-5
	12	92	34	50	46	12	13	22	0	-0	-54	4	-2	-56	5	-3	-73	-2	-4	-76	-1
1904	1	92	34	50	45	12	13	22	0	-21	-66	3	-24	-69	4	-26	-88	-7	-28	-92	-6
	2	93	34	50	45	12	13	22	0	54	-8	-7	52	-11	-6	56	-12	-3	54	-15	-2
	3	92	34	50	45	12	13	22	0	-40	-68	12	-42	-70	13	-43	-81	6	-44	-83	6
	4	93	34	50	45	12	13	22	0	-2	-24	4	-2	-24	4	-2	-25	3	-2	-26	3
	5	94	34	50	45	12	13	21	0	-13	22	-0	-12	23	-1	-13	32	3	-12	33	2
	6	94	35	50	45	13	13	21	0	7	74	-5	8	77	-6	9	93	1	10	95	0
	7	95	35	50	45	13	13	22	0	-4	96	-6	-2	100	-7	-2	120	3	-0	123	2
	8	95	35	50	45	13	13	21	0	-0	86	-0	1	89	-1	2	101	3	4	105	2
	9	96	34	50	45	13	13	21	0	-31	20	7	-29	22	6	-32	17	2	-31	20	1
	10	97	34	50	45	13	13	21	0	-23	-49	7	-23	-49	7	-25	-63	-0	-25	-63	-0
	11	97	35	50	45	13	13	21	0	4	-7	-8	4	-8	-8	1	-17	-11	1	-18	-11
	12	96	34	50	45	13	13	21	0	29	-32	-11	27	-34	-10	26	-43	-13	24	-46	-12

1905	1	94	36	50	49	13	13	21	0	-30	32	-1	-32	29	-0	-33	16	-12	-35	13	-11
	2	94	37	50	49	13	13	21	0	-42	-28	6	-44	-31	7	-45	-50	-6	-47	-53	-5
	3	94	37	51	49	13	13	21	0	1	-76	4	0	-78	4	-0	-90	-0	-1	-92	-0
	4	94	36	51	49	13	13	22	0	12	-43	3	12	-43	3	12	-44	5	12	-44	5
	5	93	37	51	49	13	13	22	0	-25	-7	3	-24	-6	2	-26	-1	4	-25	-0	4
	6	95	38	51	49	13	13	23	0	-9	57	-2	-7	59	-3	-7	75	6	-6	77	5
	7	92	37	51	49	13	13	23	0	17	91	-6	19	94	-7	20	115	3	22	119	2
	8	90	37	51	49	13	13	23	0	2	65	-4	4	68	-5	5	84	3	7	87	2
	9	91	37	51	49	13	13	23	0	4	11	-2	6	13	-3	5	16	0	6	18	0
	10	93	37	51	49	13	13	23	0	13	6	2	14	7	1	15	2	0	15	3	0
	11	94	38	50	49	13	13	23	0	37	-61	-7	36	-62	-7	34	-74	-9	33	-75	-9
	12	93	38	51	49	13	13	23	0	-22	-36	-2	-24	-38	-1	-27	-53	-12	-29	-55	-11
1906	1	93	40	51	48	13	13	23	0	-4	-70	-1	-6	-73	-0	-9	-91	-11	-11	-95	-10
	2	94	40	51	48	13	13	23	0	29	-8	3	27	-11	4	32	-18	-0	30	-22	0
	3	95	39	51	47	13	13	23	0	35	27	-10	33	25	-9	36	27	-7	35	25	-6
	4	95	37	51	48	13	13	23	0	-19	1	2	-19	0	2	-20	-0	0	-20	-1	0
	5	94	37	51	47	13	13	23	0	-2	38	2	-1	39	2	0	50	8	0	51	8
	6	95	38	51	48	13	13	23	0	3	51	-4	4	53	-5	5	74	5	7	76	4
	7	94	38	51	48	13	13	23	0	16	105	-5	18	108	-6	20	132	6	22	135	5
	8	96	38	51	48	13	13	23	0	-7	77	-4	-5	80	-5	-4	96	3	-2	99	2
	9	96	38	51	48	13	13	23	0	-31	8	7	-30	10	6	-31	11	4	-30	13	4
	10	94	38	50	48	13	13	23	0	-15	-43	3	-15	-42	3	-18	-53	-2	-18	-53	-2
	11	94	38	51	48	13	13	22	0	-7	-59	9	-8	-61	9	-9	-81	-1	-10	-82	-1
	12	95	39	51	48	13	13	23	0	3	6	-5	1	4	-4	2	-4	-9	1	-6	-8
1907	1	95	44	51	48	13	13	23	0	-51	-36	12	-53	-39	13	-55	-60	-3	-57	-63	-2
	2	94	45	51	47	13	13	22	0	26	-35	0	24	-38	1	27	-46	-3	25	-50	-2
	3	94	45	51	47	13	13	23	0	-16	-45	-0	-17	-47	0	-19	-55	-5	-21	-57	-4
	4	93	45	51	47	13	13	23	0	43	-7	-2	43	-7	-2	47	1	4	47	0	4
	5	94	44	51	50	13	13	23	0	-19	56	-0	-18	57	-1	-16	69	4	-16	70	4
	6	95	45	51	49	13	13	23	0	-3	54	-4	-2	56	-5	-1	75	6	0	77	5
	7	94	44	51	49	13	13	22	0	3	74	0	5	77	-0	8	96	9	10	99	7
	8	94	45	51	50	13	13	22	0	5	80	-4	7	83	-5	9	100	3	11	103	2
	9	93	44	51	49	13	13	22	0	-19	1	6	-18	3	5	-20	1	3	-18	3	2
	10	94	45	51	50	13	13	22	0	4	-11	1	4	-10	1	3	-17	-2	4	-16	-2
	11	95	45	51	50	13	13	22	0	-38	-80	13	-39	-81	14	-42	-103	-0	-43	-104	-0
	12	94	44	51	49	13	13	22	0	-4	-83	-2	-5	-86	-1	-9	-101	-7	-11	-103	-7
1908	1	97	44	51	50	14	13	24	0	3	-71	-7	1	-74	-5	-2	-88	-14	-4	-91	-13
	2	96	46	51	50	14	13	23	0	3	-39	2	1	-42	3	2	-50	-3	0	-53	-2
	3	95	45	51	50	14	13	24	0	-11	-53	6	-12	-55	7	-13	-68	-0	-14	-70	0
	4	95	45	51	50	14	13	24	0	6	-18	3	6	-18	3	8	-14	7	7	-14	7
	5	96	45	51	50	14	13	24	0	-17	2	-1	-17	3	-1	-19	9	0	-19	10	0
	6	95	46	50	50	14	13	24	0	-21	56	-0	-19	58	-1	-19	70	4	-17	73	3
	7	94	45	51	51	14	13	24	0	5	121	-2	7	124	-3	11	144	5	13	147	4
	8	94	45	51	51	14	13	24	0	12	89	-4	14	92	-5	18	112	4	20	115	3
	9	94	43	51	52	14	13	23	0	-13	20	0	-11	22	-0	-13	23	0	-11	25	-0
	10	93	45	49	52	14	13	24	0	-60	-15	8	-59	-15	8	-63	-27	-1	-63	-27	-1
	11	95	45	51	52	14	13	24	0	-16	-29	-2	-16	-30	-2	-19	-40	-7	-20	-41	-7
	12	95	45	51	52	14	13	23	0	-10	-58	-1	-12	-61	-0	-15	-77	-9	-17	-79	-8

1909	1	95	48	51	51	14	14	24	0	-23	-60	3	-25	-63	4	-27	-79	-7	-29	-83	-6
	2	96	48	51	51	14	14	24	0	-17	-74	-0	-19	-77	1	-20	-83	-2	-22	-86	-1
	3	94	48	51	51	14	14	24	0	35	-92	8	34	-94	9	35	-97	10	34	-99	10
	4	94	48	51	51	14	14	24	0	1	9	3	1	8	3	3	12	4	3	12	4
	5	94	49	51	51	14	14	24	0	-38	-12	10	-37	-11	9	-38	-8	9	-37	-7	9
	[illegible]	93	49	51	51	14	14	24	0	4	84	-3	6	87	-4	10	105	5	11	107	4
	7	96	49	51	52	14	14	24	0	43	86	-14	45	90	-15	48	113	0	50	117	-0
	[illegible]	96	48	51	52	14	14	24	0	9	80	-9	11	83	-11	13	99	0	15	102	-0
	9	95	49	51	52	14	14	24	0	-22	37	7	-21	39	7	-19	42	7	-18	44	6
	10	95	48	51	52	14	14	24	0	-4	-46	6	-4	-45	6	-6	-55	0	-6	-55	0
	11	96	49	51	52	13	14	24	0	22	8	-3	21	7	-3	23	2	-4	22	1	-4
	12	97	48	51	52	14	14	23	0	40	-66	-3	39	-69	-2	38	-78	-4	37	-81	-4
1910	1	98	49	51	52	15	14	23	0	29	-9	-9	27	-13	-8	28	-18	-10	26	-21	-9
	2	98	50	51	52	15	14	23	0	8	-35	1	6	-38	2	7	-47	-3	5	-50	-2
	3	98	50	51	52	15	14	23	0	-31	-30	8	-32	-32	8	-31	-38	1	-33	-40	2
	4	99	50	51	52	15	14	23	0	19	3	0	19	2	0	21	8	4	21	8	4
	5	99	50	51	52	15	14	23	0	22	53	0	22	54	0	27	65	7	27	66	6
	6	99	49	51	52	15	14	23	0	3	100	-8	5	102	-8	8	123	4	10	125	4
	7	97	49	51	52	15	14	22	0	35	101	-10	37	104	-11	41	128	5	43	131	4
	8	96	48	51	52	15	14	22	0	0	105	1	2	108	0	6	125	9	8	128	8
	9	96	48	50	52	15	14	22	0	-31	37	10	-29	39	9	-29	41	7	-27	44	7
	10	97	48	50	52	15	14	22	0	-14	-46	3	-14	-46	3	-18	-55	-3	-17	-54	-3
	11	98	48	50	52	15	14	22	0	25	-75	6	24	-76	6	24	-86	3	23	-87	3
	12	98	48	50	52	15	14	22	0	27	-74	1	25	-76	1	24	-93	-6	22	-96	-6
1911	1	94	50	52	51	14	13	23	0	-38	-36	9	-40	-39	10	-41	-55	-3	-43	-58	-1
	2	95	50	52	51	14	13	23	0	0	-39	-1	-1	-42	-0	-2	-55	-10	-4	-58	-9
	3	94	50	52	50	14	13	23	[illegible]	12	-32	1	11	-34	2	13	-36	0	11	-38	0
	4	95	50	52	50	14	13	23	0	9	37	-2	8	37	-2	11	42	0	10	42	1
	5	94	50	52	50	14	13	23	0	-2	31	-2	-1	32	-2	0	43	4	0	44	3
	6	92	50	52	50	14	13	23	0	-11	57	-1	-9	60	-2	-8	72	3	-7	75	2
	7	94	51	52	50	14	13	23	0	-26	89	3	-24	92	2	-23	103	6	-21	107	4
	8	94	52	53	50	14	12	24	0	-1	96	-0	0	99	-2	4	116	7	6	119	6
	9	94	52	54	50	14	13	24	0	-6	27	1	-5	29	1	-5	33	2	-4	35	1
	10	94	52	54	50	14	13	24	0	-7	-16	1	-7	-15	1	-10	-24	-4	-9	-24	-4
	11	95	52	54	50	14	13	24	0	33	-43	-8	32	-44	-8	29	-54	-10	28	-55	-10
	12	96	52	54	50	14	13	24	0	-0	-96	4	-1	-98	5	-6	-120	-6	-7	-122	-5
1912	1	98	53	53	50	15	14	24	0	6	-82	2	4	-85	3	0	-103	-8	-1	-106	-7
	2	96	53	52	50	15	14	24	0	39	-25	-8	37	-28	-7	38	-28	-5	36	-31	-4
	3	97	53	53	50	15	14	25	0	6	-28	1	4	-30	2	4	-37	-2	3	-39	-1
	4	98	53	53	50	15	14	25	0	-12	-7	-5	-13	-8	-5	-14	-6	-3	-14	-7	-3
	5	98	53	52	50	15	14	25	0	-9	29	-2	-8	31	-3	-8	40	2	-7	41	2
	6	98	53	52	49	15	14	25	0	6	115	-6	8	118	-7	13	137	5	14	140	4
	7	99	53	52	49	15	14	26	0	4	117	-3	6	120	-4	11	140	6	13	143	5
	8	100	53	54	49	15	14	26	0	17	66	-3	19	69	-4	23	85	6	24	88	5
	9	100	53	54	48	15	14	25	0	-20	-6	11	-19	-4	10	-19	-8	7	-10	-6	6
	10	100	52	54	49	15	14	26	0	-12	-66	5	-12	-66	5	-16	-79	-2	-16	-79	-2
	11	99	52	54	49	15	14	26	0	6	-52	-1	6	-54	-0	3	-68	-8	2	-69	-7
	12	100	52	55	49	15	14	26	0	9	-123	-3	8	-125	-2	0	-146	-14	-0	-149	-13

1913	1	98	53	55	49	15	13	27	0	-1	-90	0	-3	-93	1	-8	-112	-10	-10	-115	-9
	2	98	53	55	50	15	13	27	0	-19	-72	2	-21	-76	3	-24	-89	-6	-26	-92	-5
	3	99	53	54	49	15	13	27	0	11	-1	-13	10	-3	-12	9	-4	-12	7	-6	-12
	4	99	54	55	49	15	13	27	0	0	16	-0	-0	15	0	2	19	3	2	18	3
	5	99	54	54	50	15	14	28	0	-9	65	-1	-8	66	-2	-5	77	4	-4	78	4
	6	100	54	54	49	15	14	28	0	-24	86	-5	-23	88	-6	-21	104	2	-19	106	1
	7	99	52	55	50	15	14	28	0	13	114	-4	15	118	-6	20	137	6	22	140	4
	8	98	54	55	50	15	14	28	0	-14	82	0	-12	85	-0	-9	95	5	-7	98	4
	9	99	54	55	51	15	14	27	0	-24	37	4	-23	39	4	-22	40	3	-21	42	3
	10	99	54	55	51	15	14	27	0	2	-18	-0	3	-17	-0	0	-23	-4	1	-23	-4
	11	98	55	55	51	15	14	27	0	13	-67	-10	12	-68	-9	7	-82	-15	6	-83	-15
	12	100	55	55	51	15	13	27	0	34	-42	-11	32	-45	-10	30	-56	-15	28	-58	-14
1914	1	97	55	54	50	15	13	29	0	6	-66	-19	4	-69	-18	-1	-78	-20	-3	-81	-19
	2	97	55	54	50	15	13	29	0	40	-11	-9	38	-14	-7	38	-20	-12	36	-24	-11
	3	97	55	54	50	15	13	28	0	51	12	-3	49	9	-2	54	13	-0	53	11	-0
	4	97	56	54	50	15	13	28	0	-8	3	-2	-8	2	-2	-9	2	-3	-9	2	-2
	5	97	56	54	50	15	13	28	0	-31	54	-0	-31	56	-0	-30	57	-1	-30	58	-1
	6	97	55	54	50	15	13	28	0	-12	106	-8	-11	109	-8	-8	126	2	-6	128	1
	7	96	55	54	50	15	13	28	0	9	146	-9	11	150	-10	18	174	5	20	178	4
	8	97	55	53	50	15	13	29	0	-18	91	-2	-16	94	-3	-14	108	4	-12	111	2
	9	97	54	54	50	15	13	29	0	-16	39	-0	-15	41	-1	-15	44	-0	-14	46	-0
	10	95	55	54	50	15	13	29	0	-25	-51	3	-25	-51	2	-30	-64	-4	-30	-63	-4
	11	96	55	54	49	15	13	29	0	29	-21	-6	28	-23	-5	28	-27	-6	27	-28	-6
	12	96	55	54	49	14	13	29	0	5	-48	-4	4	-50	-3	0	-66	-11	-1	-68	-10
1915	1	93	57	54	48	15	13	29	0	77	-80	-3	75	-83	-2	77	-88	-2	75	-92	-1
	2	93	56	55	48	15	13	29	0	-0	-57	4	-2	-60	5	-2	-71	-0	-4	-74	0
	3	93	57	55	48	15	13	29	0	41	-26	2	40	-28	3	42	-30	1	40	-32	2
	4	92	57	55	48	15	13	29	0	-16	-2	-2	-16	-2	-2	-17	-2	-0	-17	-3	-0
	5	94	57	55	48	15	13	29	0	-27	32	1	-26	33	1	-26	42	8	-25	43	7
	6	94	57	55	48	15	13	29	0	-11	85	-1	-9	88	-2	-5	102	6	-3	105	5
	7	95	57	55	48	15	13	29	0	0	108	-7	2	111	-9	8	131	4	10	134	3
	8	94	57	55	48	15	13	29	0	-8	114	-4	-6	117	-5	-1	134	6	0	137	5
	9	94	57	55	48	15	13	29	0	-8	20	0	-6	22	-0	-6	26	3	-4	28	2
	10	94	56	55	48	15	13	29	0	-32	-34	12	-31	-33	12	-34	-43	4	-34	-42	4
	11	94	56	55	48	15	13	29	0	29	-65	-0	29	-66	-0	26	-75	-4	25	-76	-3
	12	94	56	55	48	15	13	29	0	11	-42	-7	9	-44	-6	7	-51	-8	5	-54	-7
1916	1	91	58	54	48	15	13	29	0	-1	-45	-6	-3	-49	-5	-8	-63	-14	-10	-66	-13
	2	90	57	54	48	15	13	29	0	33	-29	3	31	-32	5	33	-37	0	31	-40	1
	3	91	56	54	48	15	13	29	0	29	-59	9	27	-61	10	30	-62	10	28	-64	11
	4	91	58	54	48	15	13	29	0	11	5	0	10	4	0	13	11	5	13	10	5
	5	90	58	54	48	15	13	29	0	-14	9	-0	-13	10	-1	-12	19	5	-11	20	5
	6	91	58	54	48	15	13	29	0	-8	63	-2	-6	65	-3	-0	87	9	0	89	8
	7	90	59	54	48	15	13	29	0	-0	84	-9	1	87	-10	7	108	1	9	111	0
	8	91	58	54	48	15	13	29	0	16	92	-12	18	95	-14	25	116	-0	27	119	-1
	9	93	58	54	48	15	13	29	0	-7	47	-1	-6	50	-2	-3	58	2	-2	60	2
	10	93	58	54	48	15	12	29	0	5	-40	1	5	-40	1	2	-48	-3	2	-47	-3
	11	91	57	54	48	15	12	29	0	24	-56	3	24	-57	3	20	-71	-3	20	-73	-3
	12	91	57	54	48	15	12	29	0	44	-106	4	43	-109	5	41	-115	4	40	-118	5

1917	1	91	55	55	52	15	12	29	0	49	-54	-0	47	-57	0	47	-64	-1	45	-68	-0
	2	91	56	55	53	15	12	29	0	12	-28	1	10	-31	2	10	-37	-2	8	-40	-1
	3	91	56	55	54	15	12	29	0	36	-26	-0	35	-28	0	38	-25	0	37	-27	1
	4	92	56	55	54	15	12	29	0	12	23	3	11	22	3	16	33	8	16	32	9
	5	92	56	55	54	15	12	29	0	-26	11	2	-25	12	2	-25	17	5	-24	18	4
	6	91	56	55	55	15	12	29	0	-36	90	1	-34	92	1	-29	106	6	-28	108	5
	7	91	55	55	55	15	12	29	0	-3	73	-2	-1	77	-3	3	95	6	5	99	5
	8	90	56	55	55	15	12	29	0	11	91	-3	13	94	-4	20	111	4	22	114	3
	9	89	56	55	55	15	12	29	0	-0	39	-5	1	42	-6	2	46	-3	3	49	-4
	10	91	56	54	55	15	12	29	0	14	-8	1	14	-8	1	14	-9	0	15	-9	-0
	11	90	55	55	55	15	13	28	0	5	-21	0	4	-22	0	3	-35	-8	2	-36	-7
	12	90	55	55	54	15	13	28	0	-29	-3	20	-31	-6	21	-30	-26	6	-32	-28	7
1918	1	91	57	55	55	15	13	29	0	-3	-86	-2	-5	-90	-1	-12	-102	-7	-14	-105	-6
	2	91	57	54	55	15	13	29	0	-37	-102	0	-39	-105	1	-49	-126	-12	-50	-129	-11
	3	91	57	55	55	15	13	29	0	-6	-35	-4	-7	-37	-3	-10	-40	-5	-11	-43	-4
	4	91	57	55	55	15	13	29	0	-14	1	6	-14	1	6	-14	0	6	-14	0	6
	5	91	56	55	55	15	13	29	0	-24	57	2	-24	58	1	-20	68	6	-19	70	5
	6	91	57	55	55	15	13	29	0	-2	79	-6	-0	82	-7	3	100	3	5	102	3
	7	90	55	55	55	15	13	29	0	-8	128	0	-6	131	-0	0	149	8	3	152	6
	8	89	55	55	55	15	13	29	0	6	79	-5	8	82	-6	12	96	0	14	99	-0
	9	89	55	55	55	15	13	28	0	16	62	-6	17	64	-7	21	73	-1	22	75	-2
	10	87	56	53	55	15	13	27	0	-18	-36	0	-17	-36	0	-22	-48	-4	-22	-47	-5
	11	87	56	52	55	15	13	27	0	-28	-83	2	-29	-84	3	-38	-104	-6	-39	-105	-6
	12	88	57	53	55	15	13	28	0	-8	-83	3	-10	-86	4	-17	-107	-7	-18	-110	-6
1919	1	87	55	54	54	14	13	29	0	-2	-113	5	-4	-116	6	-11	-139	-4	-13	-142	-3
	2	87	55	53	54	14	13	29	0	37	-55	-10	35	-58	-9	35	-56	-6	33	-59	-5
	3	85	54	54	54	14	13	29	0	12	20	0	11	18	0	14	17	-1	13	15	-0
	4	85	54	53	54	14	13	27	0	4	37	-5	3	36	-5	7	45	-0	7	44	-0
	5	85	53	54	54	14	13	28	0	-48	17	3	-47	18	3	-49	22	5	-48	23	5
	6	85	53	54	54	14	13	29	0	-25	111	0	-24	114	-0	-19	129	5	-17	131	4
	7	84	53	55	54	14	13	28	0	1	93	-3	3	96	-4	9	115	4	12	119	3
	8	84	54	54	54	13	13	27	0	2	76	-8	4	79	-9	9	96	-0	11	99	-1
	9	86	53	54	54	14	13	27	0	-6	10	-4	-5	12	-5	-7	14	-2	-5	16	-3
	10	86	53	54	54	14	13	27	0	-22	-8	8	-21	-7	8	-25	-18	0	-25	-17	0
	11	85	53	54	54	14	12	27	0	25	-0	-0	24	-1	0	25	-6	-1	24	-7	-1
	12	86	52	54	54	14	13	28	0	35	-31	-1	33	-34	-0	31	-46	-7	30	-49	-6
1920	1	85	51	53	53	14	13	29	0	28	2	-1	26	-0	0	27	-12	-8	24	-15	-6
	2	86	51	53	53	14	13	29	0	-9	-81	11	-11	-84	12	-18	-108	-3	-20	-111	-2
	3	88	51	53	53	14	13	29	0	20	-81	-13	18	-83	-12	13	-86	-11	12	-88	-10
	4	88	52	53	53	14	13	29	0	23	-53	0	22	-54	0	21	-51	4	20	-51	4
	5	88	52	51	53	14	13	29	0	-39	34	10	-38	35	9	-38	36	9	-37	37	8
	6	88	51	52	53	14	13	29	0	-13	73	-1	-12	76	-2	-7	94	6	-5	96	5
	7	88	50	52	53	14	13	29	0	11	103	-4	13	106	-6	19	128	3	21	131	1
	8	88	51	52	53	14	13	29	0	-24	82	-0	-22	85	-1	-19	95	3	-17	98	2
	9	87	51	52	53	14	13	29	0	-24	-9	1	-23	-7	0	-25	-7	1	-24	-5	0
	10	86	51	52	53	14	13	29	0	-28	-31	1	-27	-31	1	-32	-39	-3	-31	-39	-3
	11	86	49	53	53	14	13	28	0	-36	-31	2	-36	-32	3	-43	-53	-9	-44	-55	-8
	12	85	49	53	53	14	13	29	0	-40	-129	5	-41	-132	6	-53	-158	-4	-54	-161	-3

1921	1	91	59	56	59	14	16	29	0	26	-21	-14	24	-24	-13	22	-31	-18	20	-34	-17
	2	92	59	56	59	14	16	29	0	-53	-54	5	-55	-57	6	-61	-73	-5	-63	-76	-4
	3	93	58	55	59	14	16	29	0	-12	-23	-1	-13	-26	-0	-15	-31	-5	-16	-33	-4
	4	94	59	56	59	14	16	29	0	-22	-13	8	-22	-13	9	-22	-16	5	-22	-16	5
	5	94	59	55	59	14	16	29	0	-10	53	3	-10	54	3	-5	65	9	-4	66	8
	6	94	59	56	58	14	16	29	0	-16	71	-4	-15	74	-5	-9	94	6	-7	97	5
	7	93	58	55	59	14	16	29	0	11	85	-3	13	88	-5	19	105	3	21	109	1
	8	94	58	55	59	14	16	29	0	1	118	-5	3	121	-6	10	139	4	11	142	2
	9	95	58	56	59	14	16	29	0	-18	-15	-1	-16	-13	-2	-19	-12	-2	-18	-9	-2
	10	96	58	55	59	14	16	29	0	-1	-75	-5	-1	-75	-5	-8	-84	-9	-8	-83	-10
	11	96	58	56	59	14	16	29	0	-30	-80	11	-31	-81	12	-38	-105	-2	-39	-106	-2
	12	95	56	56	59	14	16	29	0	36	-50	-11	34	-52	-10	30	-62	-14	29	-64	-13
1922	1	96	59	55	59	15	16	29	0	34	-88	11	32	-91	12	31	-107	2	29	-110	3
	2	98	59	54	59	15	16	29	0	27	-36	2	25	-39	4	26	-43	-1	24	-46	0
	3	98	59	52	59	15	16	29	0	44	-5	-6	43	-7	-6	45	-4	-3	44	-7	-2
	4	98	59	52	59	15	16	29	0	31	7	0	30	7	0	34	13	3	34	12	3
	5	98	59	54	60	15	16	29	0	-27	29	3	-27	30	2	-26	35	4	-26	36	4
	6	97	59	55	60	15	16	29	0	-1	111	-5	0	113	-6	7	137	6	9	139	6
	7	97	59	54	60	15	16	29	0	10	139	-5	12	142	-6	19	162	4	22	165	3
	8	97	60	53	60	15	16	29	0	-12	94	-4	-10	98	-5	-4	114	5	-2	117	4
	9	97	60	53	59	15	16	29	0	-5	41	2	-3	43	2	-1	49	4	-0	51	3
	10	97	60	54	59	15	16	29	0	2	-36	-2	2	-35	-2	0	-38	-2	0	-37	-2
	11	98	60	55	59	15	16	29	0	8	-58	0	7	-59	1	3	-72	-6	3	-73	-6
	12	98	60	55	60	15	16	28	0	45	-51	-8	43	-54	-7	41	-63	-11	39	-65	-10
1923	1	95	60	56	60	15	16	28	0	8	-96	-1	6	-99	-0	0	-116	-10	-2	-119	-9
	2	94	60	56	60	15	16	28	0	67	-2	3	65	-5	4	70	-8	1	68	-11	2
	3	95	60	56	59	15	16	28	0	5	-44	4	3	-46	4	0	-54	-1	-0	-56	-1
	4	95	60	56	59	15	16	28	0	11	-2	-2	11	-3	-2	14	7	4	14	7	5
	5	94	60	56	59	15	16	28	0	-6	13	1	-5	14	1	-3	22	7	-3	24	6
	6	96	60	56	59	15	16	28	0	9	65	-10	11	68	-11	14	86	2	16	88	1
	7	96	60	56	60	15	16	28	0	-1	117	-4	0	120	-5	7	139	5	9	142	4
	8	96	60	56	60	15	16	28	0	9	114	-7	11	117	-8	18	137	3	20	140	2
	9	97	60	56	60	15	16	28	0	-28	24	1	-27	26	0	-28	23	0	-26	25	-0
	10	97	60	56	60	15	16	28	0	41	13	-13	41	13	-13	42	15	-9	42	16	-9
	11	97	60	56	60	15	16	28	0	19	-20	-5	18	-21	-5	18	-26	-6	17	-27	-6
	12	96	60	55	59	15	16	28	0	21	-80	-8	20	-82	-7	15	-94	-12	13	-96	-12
1924	1	96	61	58	60	15	16	28	0	8	-77	7	6	-80	8	1	-101	-6	-0	-104	-5
	2	96	61	57	60	15	16	28	0	21	-16	9	19	-20	10	22	-25	4	20	-28	6
	3	97	61	57	60	15	16	28	0	22	-110	6	21	-112	7	17	-117	5	16	-119	6
	4	97	61	56	60	15	16	28	0	15	13	1	15	12	1	19	21	6	18	21	6
	5	97	62	57	61	15	16	28	0	-22	20	2	-21	21	2	-20	28	7	-19	29	6
	6	97	62	57	60	15	16	28	0	-6	77	0	-4	80	-0	0	94	8	1	97	8
	7	97	62	57	60	15	16	27	0	27	117	-13	29	120	-14	37	146	1	39	149	0
	8	97	62	57	60	15	16	28	0	7	71	-8	9	74	-9	14	92	3	16	95	2
	9	97	61	58	61	15	16	28	0	6	19	-9	7	21	-9	7	27	-4	9	30	-5
	10	97	61	57	60	15	16	28	0	-18	-57	4	-17	-57	4	-22	-70	-3	-22	-69	-3
	11	96	61	58	61	15	16	28	0	-20	-40	-1	-21	-41	-1	-26	-55	-10	-27	-56	-10
	12	97	61	58	61	15	16	28	0	10	-53	1	8	-56	2	2	-77	-12	0	-79	-11

1925	1	100	62	57	61	15	16	28	0	-42	-38	-0	-44	-41	1	-50	-57	-14	-52	-60	-13
	2	100	61	57	61	15	16	28	0	33	-95	-3	31	-98	-2	27	-108	-8	25	-112	-7
	3	100	61	57	61	15	16	28	0	-14	-19	12	-16	-21	13	-14	-25	7	-15	-27	8
	4	100	61	57	61	15	16	28	0	10	-7	-5	10	-8	-5	10	-4	-1	9	-5	-1
	5	100	61	57	61	15	16	28	0	1	35	-0	1	36	-0	6	49	8	6	50	7
	6	100	61	57	60	15	16	28	0	-2	85	-6	-1	88	-7	5	109	6	6	111	6
	7	99	60	56	59	15	16	28	0	15	88	-3	17	91	-4	23	107	6	25	110	5
	8	100	61	55	61	15	16	28	0	7	114	-4	9	117	-5	15	132	4	17	135	3
	9	100	62	56	60	15	16	28	0	15	30	-4	16	33	-5	16	36	-0	18	38	-0
	10	100	63	56	60	15	16	28	0	31	-29	-9	32	-29	-9	29	-31	-8	29	-30	-8
	11	100	63	56	60	15	16	28	0	28	-8	-10	27	-9	-10	26	-12	-11	26	-13	-10
	12	99	63	56	60	15	16	28	0	49	-65	-11	47	-67	-10	43	-76	-12	41	-78	-11
1926	1	99	66	57	58	15	14	27	0	2	-108	-2	0	-111	-0	-7	-128	-11	-9	-131	-10
	2	99	66	57	59	15	15	26	0	5	-150	-1	3	-153	-0	-6	-168	-8	-8	-171	-7
	3	99	66	57	59	15	15	27	0	18	-22	-6	17	-24	-5	15	-26	-7	14	-28	-6
	4	99	66	57	58	15	15	27	0	-2	2	-4	-3	1	-4	-2	4	-1	-3	4	-1
	5	99	66	57	59	15	15	27	0	13	9	-1	14	10	-1	16	19	6	17	21	5
	6	99	66	57	59	15	15	27	0	3	74	-1	5	76	-2	9	92	8	11	94	8
	7	99	66	57	60	15	15	27	0	14	117	-15	16	120	-16	24	143	1	26	146	-0
	8	99	66	57	60	15	15	27	0	-5	95	-8	-3	98	-9	1	111	0	2	114	-0
	9	99	65	56	60	15	15	27	0	-35	34	6	-34	36	5	-34	36	5	-32	39	4
	10	99	65	56	60	15	15	27	0	19	-39	-4	20	-38	-4	18	-38	-0	18	-37	-0
	11	95	64	56	60	15	15	27	0	25	-59	-3	24	-60	-2	19	-73	-8	18	-74	-8
	12	100	65	55	60	15	15	27	0	-8	-76	3	-9	-78	4	-14	-92	-5	-16	-94	-5
1927	1	100	65	53	61	15	16	27	0	10	-37	4	8	-40	5	6	-53	-5	4	-56	-4
	2	100	65	53	61	15	16	27	0	-35	-111	9	-37	-114	10	-44	-132	-3	-46	-135	-1
	3	101	65	53	60	15	16	27	0	29	-31	-1	28	-33	-0	28	-33	-2	27	-35	-1
	4	101	66	53	60	15	16	27	0	47	22	-5	46	21	-5	50	31	1	50	31	1
	5	101	66	53	60	15	16	27	0	-16	8	3	-15	9	3	-14	14	6	-14	15	6
	6	101	67	53	60	15	16	27	0	-13	85	-8	-11	88	-9	-7	102	2	-6	104	1
	7	100	67	53	60	15	16	27	0	23	130	-6	25	133	-7	33	150	5	35	154	4
	8	100	67	53	60	15	16	27	0	-0	105	-5	1	108	-6	7	121	4	9	124	3
	9	101	67	54	60	15	16	26	0	10	36	-9	12	38	-10	13	48	-0	14	50	-1
	10	101	67	54	60	15	16	26	0	-6	-42	-4	-6	-42	-4	-10	-46	-6	-10	-46	-6
	11	102	67	54	60	16	16	25	0	-6	-39	4	-7	-40	4	-11	-53	-4	-12	-54	-4
	12	102	67	54	60	16	16	26	0	3	-60	10	2	-62	11	-0	-74	2	-1	-77	2
1928	1	101	67	55	60	16	16	26	0	14	-90	-5	12	-93	-4	5	-108	-15	3	-111	-14
	2	102	67	55	60	16	16	26	0	-4	-72	4	-6	-75	5	-11	-89	-8	-13	-92	-7
	3	101	66	55	60	16	16	26	0	-7	-83	6	-8	-85	7	-12	-90	2	-13	-92	3
	4	102	66	55	60	16	16	26	0	31	-8	-6	30	-8	-6	32	0	2	32	-0	2
	5	102	66	55	60	16	16	27	0	7	45	-1	8	46	-1	12	57	7	13	58	6
	6	102	67	55	60	15	16	27	0	-2	77	-8	-0	80	-9	4	100	7	6	103	6
	7	102	67	53	60	15	16	27	0	-2	99	-9	-0	102	-11	3	116	0	5	119	-1
	8	103	67	53	60	15	16	26	0	0	92	-4	2	95	-6	7	107	3	9	110	2
	9	104	66	54	59	16	16	27	0	-18	-5	3	-16	-3	2	-18	-6	2	-16	-3	1
	10	104	67	54	59	16	16	27	0	18	-50	-1	19	-50	-2	15	-58	-6	15	-57	-6
	11	103	67	54	59	16	16	27	0	42	-55	-11	41	-56	-11	38	-63	-13	37	-64	-12
	12	104	67	54	59	16	16	27	0	-11	-95	2	-13	-97	3	-19	-114	-8	-20	-117	-7

1929	1	101	66	56	60	17	16	27	0	-50	-125	31	-52	-129	32	-60	-155	9	-62	-158	11
	2	102	66	56	60	17	16	27	0	-29	-87	25	-31	-90	26	-33	-105	11	-35	-108	12
	3	102	66	56	60	17	16	27	0	-31	-81	-4	-32	-83	-3	-39	-89	-8	-40	-92	-7
	4	102	65	57	60	17	16	27	0	12	-7	-6	11	-7	-5	12	-1	0	11	-1	0
	5	102	65	56	60	17	16	27	0	-15	41	5	-14	42	4	-11	48	7	-11	49	6
	6	102	65	56	60	17	16	27	0	-5	89	-10	-4	92	-11	-0	108	2	1	111	1
	7	103	66	54	60	17	16	27	0	-5	121	-8	-3	124	-9	1	139	1	3	142	0
	8	103	65	57	60	17	16	27	0	-17	89	-2	-15	92	-3	-11	102	4	-9	105	3
	9	102	65	55	60	17	16	27	0	-23	24	3	-22	26	2	-23	26	2	-22	28	1
	10	102	64	56	60	17	15	27	0	17	-38	-9	17	-38	-9	14	-42	-9	14	-41	-9
	11	101	64	55	60	17	16	27	0	30	-63	0	29	-65	1	25	-79	-6	25	-80	-6
	12	101	64	54	59	17	16	27	0	30	-107	4	28	-110	5	22	-129	-6	20	-132	-5
1930	1	104	65	54	60	17	15	26	0	49	-47	6	47	-51	7	45	-66	-6	43	-69	-5
	2	104	66	54	60	17	16	26	0	-16	-102	4	-18	-106	5	-24	-118	-6	-26	-121	-5
	3	104	67	54	60	17	15	26	0	52	-65	-6	51	-67	-6	50	-61	-2	48	-63	-1
	4	104	67	54	60	17	16	27	0	20	-0	2	19	-0	2	23	6	7	23	5	7
	5	104	66	54	60	17	16	27	0	-5	30	-5	-5	31	-6	-4	39	-0	-3	40	-0
	6	104	67	54	60	17	16	27	0	-15	76	-10	-14	78	-11	-11	91	0	-10	94	0
	7	105	67	54	60	17	16	27	0	28	143	-14	30	146	-15	39	169	3	41	172	2
	8	105	66	54	59	17	16	26	0	-4	91	-1	-2	94	-2	2	105	5	4	108	4
	9	103	64	54	60	17	16	27	0	-0	-20	2	1	-18	1	-1	-20	1	0	-18	0
	10	104	64	53	60	17	16	26	0	22	-21	-3	22	-20	-3	20	-25	-5	20	-24	-5
	11	103	63	53	60	17	16	26	0	29	-47	-5	28	-48	-5	23	-61	-13	23	-62	-12
	12	104	62	53	60	17	16	26	0	-13	-90	1	-15	-93	2	-21	-112	-10	-23	-114	-9
1931	1	101	62	61	65	17	14	34	0	17	-94	-2	15	-97	-1	11	-109	-7	9	-112	-6
	2	101	62	61	65	17	15	34	0	-15	-130	12	-17	-133	13	-23	-151	1	-24	-154	2
	3	101	62	61	65	17	15	34	0	25	5	9	24	2	9	27	4	7	26	2	8
	4	102	62	60	66	17	15	33	0	2	-3	8	2	-4	8	5	-2	9	4	-3	9
	5	102	62	61	66	17	15	35	0	-2	9	5	-1	10	5	1	19	9	1	20	9
	6	101	62	61	66	17	15	34	0	-12	68	-4	-10	70	-5	-7	84	2	-6	86	1
	7	102	62	61	66	17	15	34	0	28	74	-10	30	78	-11	36	99	4	38	102	3
	8	102	62	61	66	17	15	34	0	29	119	-4	31	122	-6	40	143	6	42	146	5
	9	102	61	61	66	17	15	34	0	10	-1	-2	11	0	-3	13	7	2	14	9	1
	10	102	61	62	66	17	15	35	0	-6	-40	-8	-6	-39	-8	-11	-45	-10	-10	-45	-11
	11	102	61	62	66	17	15	35	0	-23	-103	6	-24	-104	6	-31	-123	-4	-32	-124	-4
	12	102	61	62	66	17	15	35	0	-15	-84	-6	-16	-87	-5	-23	-100	-14	-25	-102	-13
1932	1	99	61	62	67	18	15	37	0	-25	-83	-2	-27	-86	-1	-37	-109	-18	-39	-113	-16
	2	101	61	63	67	18	15	38	0	-18	-95	15	-20	-98	16	-24	-112	4	-26	-115	5
	3	102	61	62	67	18	15	38	0	1	-71	9	0	-73	9	-1	-77	7	-2	-79	8
	4	102	61	63	67	17	15	38	0	10	27	-1	10	27	-1	13	35	5	13	35	6
	5	104	62	63	67	17	15	38	0	-9	49	2	-8	50	2	-4	61	7	-3	62	7
	6	104	62	63	67	17	15	38	0	-0	56	-2	1	58	-3	4	74	8	6	76	7
	7	102	61	63	67	18	15	38	0	26	100	-13	28	103	-14	35	131	4	37	134	3
	8	104	62	62	67	18	15	37	0	-34	24	1	-32	27	0	-31	35	5	-29	38	4
	9	103	62	61	66	18	15	37	0	9	32	-4	10	34	-4	13	42	0	14	44	-0
	10	101	63	63	66	18	15	37	0	38	-18	-7	38	-18	-8	37	-15	-3	38	-15	-4
	11	103	62	64	67	18	15	37	0	-37	-17	7	-37	-18	7	-41	-34	-4	-42	-35	-4
	12	103	62	64	66	18	15	36	0	-36	-103	1	-38	-105	2	-48	-128	-13	-49	-131	-12

1933	1	102	64	64	67	17	15	39	0	-36	-214	10	-38	-217	12	-51	-245	-3	-53	-248	-2
	2	103	63	64	67	17	15	39	0	22	-70	17	20	-73	18	20	-84	10	18	-87	11
	3	102	64	64	67	17	15	39	0	3	-45	7	1	-47	8	0	-51	3	-0	-53	4
	4	103	64	63	67	17	15	39	0	-2	-7	5	-3	-8	5	-1	-4	6	-2	-5	7
	5	104	64	62	67	18	15	38	0	11	5	0	11	6	0	14	16	7	15	17	7
	6	103	64	64	67	18	15	38	0	25	87	-11	26	90	-12	34	114	4	35	117	3
	7	103	63	62	67	18	15	39	0	-6	80	-6	-4	83	-7	0	101	2	2	104	1
	8	103	63	62	67	18	15	38	0	-1	84	-12	0	87	-13	4	103	-1	6	106	-2
	9	103	63	61	67	18	15	39	0	-29	-47	1	-28	-45	0	-31	-41	4	-30	-39	3
	10	103	63	59	67	18	15	39	0	-4	-33	9	-4	-32	9	-5	-40	4	-5	-40	4
	11	104	63	61	67	18	15	37	0	29	-32	0	29	-33	1	20	-39	-1	27	-40	-1
	12	103	62	61	66	18	15	39	0	-1	-17	10	-3	-19	11	-2	-28	3	-4	-31	4
1934	1	106	64	61	64	17	14	38	0	-34	-98	5	-36	-101	6	-44	-124	-10	-46	-127	-9
	2	106	63	62	64	17	14	39	0	-30	4	1	-32	1	2	-31	-6	-7	-33	-9	-6
	3	106	64	62	64	17	14	39	0	25	13	6	23	11	6	28	12	6	26	10	7
	4	105	64	62	64	17	14	36	0	4	-7	2	3	-7	2	6	-1	5	5	-2	5
	5	104	63	62	64	17	14	37	0	-20	21	-1	-20	22	-1	-19	29	2	-18	30	2
	6	105	64	62	64	16	14	37	0	-3	71	-5	-1	74	-6	2	91	6	3	94	5
	7	104	64	62	64	16	14	38	0	16	92	-5	18	95	-6	25	115	7	27	118	6
	8	104	64	62	64	17	14	38	0	22	76	-3	24	79	-4	30	93	5	32	97	4
	9	103	64	63	64	17	14	38	0	-22	7	11	-20	9	10	-20	9	8	-18	11	7
	10	102	64	62	64	17	14	38	0	5	-68	-3	5	-68	-4	0	-76	-8	0	-75	-8
	11	101	64	63	64	17	14	38	0	-36	-74	4	-37	-76	4	-42	-90	-4	-43	-91	-3
	12	102	64	63	64	17	13	39	0	24	-72	1	23	-74	2	18	-87	-7	17	-90	-6
1935	1	102	65	62	65	18	15	39	0	-15	-41	9	-17	-44	10	-20	-61	-3	-22	-64	-2
	2	104	65	62	64	18	15	39	0	84	-0	-21	82	-3	-20	84	3	-15	82	0	-14
	3	102	65	63	65	18	15	39	0	-37	-38	8	-38	-40	9	-40	-46	3	-41	-49	4
	4	103	65	63	65	18	15	38	0	28	-8	10	28	-9	10	32	-2	14	31	-3	14
	5	102	63	63	64	18	15	38	0	-25	51	10	-25	52	10	-20	58	12	-20	59	12
	6	102	64	63	64	18	15	38	0	-11	70	-5	-10	72	-6	-6	86	4	-5	88	3
	7	102	65	62	65	18	15	38	0	4	110	-10	6	113	-11	12	134	2	14	137	0
	8	103	65	60	64	18	15	38	0	3	74	-6	5	77	-7	10	91	3	11	94	2
	9	103	65	62	64	18	15	38	0	9	41	-3	10	44	-3	14	54	3	15	56	2
	10	103	64	62	64	18	15	38	0	34	4	-0	35	5	-1	36	5	-0	37	5	-0
	11	103	65	62	64	18	15	38	0	6	-84	17	6	-85	17	0	-107	1	-0	-108	2
	12	104	65	62	64	18	14	39	0	23	-96	11	21	-98	11	17	-113	2	15	-116	3
1936	1	102	65	63	64	18	15	39	0	39	-82	1	37	-85	2	35	-93	-0	33	-96	0
	2	102	65	63	64	18	15	38	0	48	-51	16	46	-54	17	50	-55	15	48	-58	16
	3	102	65	63	64	18	15	38	0	11	-118	8	10	-120	8	5	-128	4	3	-130	4
	4	102	65	63	64	18	15	38	0	12	31	4	12	30	4	16	36	7	16	35	8
	5	103	65	63	62	18	15	39	0	-19	49	5	-19	50	4	-14	61	11	-13	62	10
	6	103	65	63	62	18	15	39	0	-8	70	-6	-6	72	-7	-3	88	3	-1	91	2
	7	103	64	62	63	18	15	39	0	11	93	-10	13	96	-11	18	116	2	20	119	1
	8	103	64	62	63	18	15	39	0	-6	62	0	-4	65	-1	-0	74	5	1	78	4
	9	103	64	63	63	18	15	38	0	-5	27	1	-4	29	0	-3	32	1	-2	34	0
	10	103	64	62	63	18	15	39	0	11	-5	-6	11	-4	-7	10	-7	-7	10	-6	-7
	11	102	64	63	63	18	15	39	0	24	-48	0	23	-49	1	20	-64	-7	19	-65	-7
	12	103	64	63	62	18	15	39	0	-41	-41	-3	-43	-44	-2	-49	-60	-14	-50	-62	-13

1937	1	105	62	61	62	18	15	36	0	-18	-97	17	-20	-100	18	-24	-122	1	-26	-125	2
	2	105	62	61	62	18	15	37	0	53	-60	-11	51	-63	-10	50	-62	-7	48	-65	-6
	3	105	62	61	62	18	15	37	0	18	-27	13	17	-29	14	20	-29	14	19	-31	15
	4	104	62	62	62	18	15	36	0	4	-36	1	3	-36	1	4	-33	3	3	-34	3
	5	105	61	61	62	18	15	36	0	-26	23	0	-25	24	0	-24	29	3	-23	30	3
	6	104	62	61	62	18	15	36	0	-9	56	-4	-8	59	-5	-5	72	3	-3	75	2
	7	105	62	60	62	18	15	36	0	9	124	-10	12	128	-11	19	151	4	21	154	2
	8	105	62	62	62	18	15	37	0	-1	71	-0	0	74	-1	4	87	6	6	91	5
	9	104	62	62	61	18	15	38	0	19	21	-3	21	24	-4	22	28	-1	23	30	-1
	10	103	62	63	62	18	15	38	0	-28	-52	2	-27	-52	2	-32	-61	-2	-31	-60	-3
	11	102	62	60	62	18	15	38	0	-23	-55	9	-24	-56	9	-27	-70	1	-28	-71	1
	12	101	61	62	62	18	15	38	0	-17	-45	16	-19	-47	17	-19	-62	7	-21	-64	8
1938	1	102	61	64	63	18	16	35	0	26	-85	-0	24	-88	0	21	-100	-6	19	-103	-5
	2	103	62	64	63	18	16	37	0	-39	9	13	-41	6	14	-40	-6	0	-42	-9	1
	3	102	62	64	64	18	16	38	0	-25	-48	-15	-26	-50	-14	-30	-47	-11	-31	-49	-11
	4	100	62	64	64	18	16	38	0	-24	30	-3	-25	30	-3	-21	38	1	-21	37	1
	5	100	62	64	64	18	16	38	0	-17	47	-1	-16	48	-1	-12	62	7	-12	63	6
	6	100	61	64	63	18	16	38	0	-4	93	-10	-2	96	-11	1	113	-0	3	115	-1
	7	100	63	64	64	18	16	38	0	5	96	-5	7	99	-6	12	115	4	14	119	3
	8	100	63	63	65	18	16	38	0	12	64	-2	14	67	-3	19	83	6	21	86	5
	9	99	64	65	65	18	16	38	0	-25	5	-0	-24	8	-1	-25	9	0	-23	11	-0
	10	99	64	64	66	18	16	38	0	0	-21	-10	0	-21	-11	-1	-23	-10	-1	-22	-10
	11	100	64	65	66	18	16	38	0	9	-68	-4	8	-69	-4	2	-81	-10	1	-83	-10
	12	100	64	62	66	18	16	38	0	-29	-132	17	-30	-135	18	-37	-159	4	-39	-161	5
1939	1	101	65	65	65	18	16	38	0	35	-107	-5	33	-110	-3	28	-120	-7	26	-123	-6
	2	100	65	65	65	18	16	38	0	11	-54	-2	9	-57	-1	6	-63	-7	5	-66	-6
	3	101	65	65	64	18	16	38	0	4	-8	11	3	-10	12	7	-9	10	6	-11	10
	4	101	65	64	64	18	16	38	0	10	-11	-1	10	-11	-0	12	-5	2	11	-6	2
	5	101	65	65	64	18	16	39	0	-12	30	3	-12	32	3	-8	42	10	-8	43	9
	6	101	65	66	64	18	16	39	0	10	86	-4	12	89	-5	17	105	6	19	108	5
	7	100	65	66	64	18	16	39	0	14	94	-9	16	97	-10	23	116	2	25	119	1
	8	100	65	64	64	18	16	39	0	-4	66	-1	-2	69	-2	1	79	6	3	82	5
	9	99	65	65	64	18	16	39	0	-8	20	-1	-7	22	-2	-6	26	0	-5	28	0
	10	99	65	65	63	18	16	38	0	6	-40	1	6	-39	1	4	-43	0	4	-42	0
	11	99	65	65	63	18	16	38	0	-9	-21	2	-10	-22	3	-12	-35	-5	-13	-36	-5
	12	98	64	64	64	17	14	38	0	3	-150	-11	2	-152	-10	-8	-168	-17	-9	-171	-16
1940	1	109	65	63	65	17	15	38	0	-14	-83	25	-16	-86	26	-16	-105	11	-18	-108	12
	2	109	65	63	65	17	15	38	0	26	-97	6	24	-100	8	22	-110	1	20	-113	2
	3	109	65	63	65	17	15	38	0	2	-30	3	1	-32	4	2	-31	4	1	-33	2
	4	109	66	63	65	17	16	38	0	-17	15	2	-17	15	2	-16	15	2	-17	15	2
	5	109	66	63	65	17	16	39	0	-13	54	4	-12	55	3	-9	63	9	-8	64	9
	6	106	66	60	63	17	16	39	0	3	74	-7	4	76	-8	8	93	3	10	95	2
	7	107	66	61	63	17	16	39	0	7	139	-10	9	142	-11	15	160	0	17	163	-0
	8	108	66	61	63	17	16	38	0	-17	64	-2	-15	67	-3	-13	76	1	-11	79	0
	9	108	64	59	62	17	16	39	0	-9	13	-2	-8	16	-2	-8	17	-0	-7	19	-0
	10	106	64	59	62	17	16	39	0	-8	-46	-2	-8	-45	-2	-11	-52	-6	-11	-51	-6
	11	107	64	58	62	17	16	39	0	36	-12	-1	35	-13	-1	35	-19	-5	34	-20	-4
	12	108	64	57	62	17	16	39	0	-36	-53	-2	-38	-55	-1	-43	-67	-10	-44	-69	-9

.1941	1	131	66	83	65	25	16	48	0	[illegible]	-6	3	16	-9	4	17	-17	-3	15	-20	-2
	2	132	66	82	66	25	16	48	0	67	-93	1	65	-96	2	62	-102	-0	60	-105	0
	3	133	66	84	[illegible]	25	16	48	0	20	-11	4	19	-14	5	20	-13	5	19	-15	5
	4	132	65	85	67	25	16	49	0	-13	33	5	-14	33	5	-11	38	9	-12	37	9
	5	131	65	85	67	25	16	48	0	12	42	-3	13	43	-3	15	55	5	15	56	5
	6	130	65	83	66	24	16	49	0	-2	80	-11	-0	83	-12	1	97	-3	3	99	-4
	7	131	65	84	66	25	16	49	0	2	102	-11	4	105	-12	6	121	-1	9	124	-2
	8	130	65	84	67	25	16	47	0	32	115	-8	34	119	-9	38	135	3	40	138	2
	9	129	65	83	66	25	16	46	0	-26	-6	4	-25	-4	3	-25	-4	3	-24	-2	2
	10	129	65	85	67	25	16	48	0	-19	-51	-3	-19	-50	-3	-23	-60	-9	-23	-59	-9
	11	130	65	84	67	26	16	48	0	-29	-86	7	-30	-87	7	-33	-101	-1	-34	-102	-0
	12	130	64	84	67	26	16	48	0	-31	-80	-5	-32	-82	-4	-37	-94	-13	-38	-97	-12
1942	1	131	62	85	68	25	16	51	0	-19	-62	3	-21	-65	5	-23	-80	-6	-25	-83	-8
	2	131	63	87	68	25	16	50	0	-10	-111	25	-12	-114	26	-13	-128	17	-15	-131	18
	3	131	63	86	66	24	16	51	0	2	-59	-0	1	-61	0	-0	-59	2	-1	-61	3
	4	132	62	85	67	26	15	50	0	-15	-13	-1	-16	-14	-1	-16	-12	0	-16	-12	0
	5	132	62	86	65	26	16	50	0	8	34	5	9	35	4	11	42	9	12	43	9
	6	133	62	86	67	25	15	49	0	-10	74	-4	-8	76	-5	-5	94	5	-3	97	4
	7	133	62	85	66	25	16	50	0	26	120	-15	28	124	-16	32	142	-4	34	145	-6
	8	133	64	84	67	25	16	51	0	-6	70	-7	-4	73	-8	-2	83	0	-0	86	-0
	9	132	64	85	67	25	16	50	0	11	23	-3	12	25	-4	12	28	-0	14	30	-1
	10	132	64	85	68	25	16	49	0	-4	-51	-5	-4	-50	-5	-7	-55	-7	-7	-54	-7
	11	132	63	86	68	26	16	49	0	-19	-68	3	-20	-69	4	-23	-79	-1	-23	-81	-1
	12	131	64	86	68	26	16	48	0	-16	-103	2	-18	-106	3	-22	-122	-8	-24	-125	-7
1943	1	136	63	87	69	26	16	49	0	22	-78	9	20	-81	10	19	-94	-0	17	-97	0
	2	135	63	[illegible]	69	26	16	49	0	-15	-60	-1	-17	-63	-0	-19	-77	-11	-21	-80	-10
	3	136	63	[illegible]	69	26	16	49	0	-23	6	14	-24	4	15	-22	-0	8	-23	-2	9
	4	136	63	88	69	26	16	50	0	20	-35	-10	20	-36	-10	18	-34	-9	17	-35	-9
	5	135	63	89	68	26	16	49	0	-19	64	6	-18	65	5	-15	71	8	-14	73	8
	6	135	63	88	69	26	16	49	0	-4	76	-3	-3	78	-4	-0	90	3	1	93	2
	7	137	63	88	69	26	16	50	0	31	87	-13	33	91	-15	35	107	-3	37	111	-4
	8	136	63	87	67	26	16	49	0	23	33	-10	25	36	-11	26	51	0	28	54	-1
	9	135	62	87	67	26	16	47	0	-2	23	-3	-0	25	-4	-0	27	-2	0	29	-3
	10	136	63	87	69	25	16	49	0	-37	-63	-2	-36	-62	-2	-40	-71	-5	-40	-70	-5
	11	136	63	87	69	26	16	50	0	-33	-42	5	-34	-43	6	-36	-59	-4	-37	-60	-4
	12	138	62	87	69	26	16	50	0	-31	-109	-3	-33	-112	-3	-38	-132	-16	-39	-134	-15
1944	1	137	59	88	71	25	15	49	0	-26	-97	-11	-28	-100	-10	-33	-117	-23	-35	-120	-22
	2	138	60	88	71	25	16	51	0	24	-36	2	22	-39	3	22	-45	-1	20	-48	-0
	3	139	60	[illegible]	69	25	16	51	0	39	-11	8	38	-13	9	39	-13	7	38	-15	8
	4	138	60	87	68	25	15	50	0	-7	-24	3	-7	-24	3	-7	-24	3	-7	-25	3
	5	138	60	87	69	25	16	52	0	-23	50	0	-23	51	0	-21	57	3	-20	58	3
	6	137	58	87	70	25	16	50	0	20	86	-9	21	88	-10	23	107	5	25	110	4
	7	137	58	88	69	25	16	52	0	28	113	-13	30	116	-14	32	138	-0	34	141	-1
	8	137	57	87	71	25	16	51	0	-1	56	-10	0	59	-11	0	70	-2	2	73	-3
	9	135	57	87	70	26	16	53	0	-28	0	2	-27	2	2	-28	1	2	-27	4	1
	10	134	57	87	71	26	16	52	0	3	-0	0	4	-0	0	2	-6	-1	3	-6	-1
	11	135	57	86	71	26	16	53	0	4	-60	12	4	-61	13	3	-71	7	2	-72	8
	12	133	57	85	67	26	15	51	0	-23	-86	20	-24	-88	21	-25	-111	6	-27	-113	7

1945	1	143	43	85	71	26	15	53	0	-4	-47	12	-6	-51	13	-4	-64	4	-6	-67	5
	2	140	43	85	71	26	15	51	0	-67	-83	17	-69	-86	19	-66	-103	5	-68	-106	6
	3	144	43	87	73	26	15	51	0	-79	-111	-6	-81	-113	-5	-81	-123	-11	-82	-125	-11
	4	143	43	88	71	26	15	53	0	9	32	6	9	32	6	10	34	7	10	34	7
	5	140	43	87	73	26	15	51	0	31	44	0	32	45	-0	32	57	8	33	58	7
	6	142	43	89	71	26	16	51	0	7	59	-4	9	62	-5	9	79	3	10	82	2
	7	140	43	89	68	26	16	51	0	24	113	-9	26	117	-10	25	136	1	27	139	0
	8	141	43	88	70	26	15	53	0	62	78	-8	64	82	-9	63	98	2	65	101	1
	9	144	43	89	71	27	16	51	0	0	34	1	2	36	0	2	40	1	3	42	0
	10	143	43	89	72	28	16	51	0	-32	-43	-12	-31	-43	-13	-34	-51	-15	-33	-50	-15
	11	144	43	91	73	28	16	51	0	-25	-44	1	-26	-45	1	-26	-54	-2	-27	-55	-2
	12	144	43	91	73	28	15	51	0	-13	-76	1	-15	-78	2	-14	-91	-3	-16	-93	-2
1946	1	141	47	91	74	27	14	51	0	-64	-88	-1	-66	-91	-0	-66	-110	-12	-68	-113	-11
	2	143	48	92	74	28	15	51	0	4	-30	-6	2	-33	-5	1	-38	-7	-0	-41	-6
	3	143	48	91	74	27	15	52	0	-16	-86	4	-17	-88	5	-17	-92	4	-18	-94	5
	4	143	48	92	72	28	14	53	0	-9	19	-8	-9	18	-8	-10	22	-4	-10	22	-4
	5	143	48	93	72	28	15	53	0	23	30	8	24	32	8	24	40	14	25	41	13
	6	144	49	93	73	28	14	53	0	20	97	-7	22	100	-8	22	116	-0	24	119	-1
	7	145	49	92	72	29	15	53	0	32	108	-7	34	111	-8	35	131	2	37	134	1
	8	146	49	92	74	28	14	52	0	44	93	-6	46	96	-7	45	112	2	47	115	1
	9	147	49	93	73	29	15	50	0	-11	22	-1	-9	24	-1	-10	26	0	-9	28	0
	10	144	49	94	73	28	15	52	0	-27	-29	-9	-27	-29	-9	-29	-33	-9	-29	-33	-9
	11	146	49	93	72	27	15	53	0	6	-29	3	5	-30	3	5	-42	-1	5	-43	-1
	12	147	47	94	73	27	14	52	0	-23	-92	16	-25	-95	17	-22	-113	6	-24	-116	7
1947	1	148	55	94	74	27	15	51	0	-14	-111	12	-16	-114	13	-15	-129	3	-17	-133	4
	2	149	55	95	74	28	15	53	0	23	-68	34	21	-71	35	25	-85	25	23	-88	27
	3	148	56	95	73	28	15	52	0	51	-44	2	49	-46	3	49	-47	2	47	-49	3
	4	149	56	93	72	28	14	52	0	-21	14	-0	-21	14	-0	-20	15	-1	-21	14	-1
	5	149	56	97	72	28	15	53	0	-11	27	2	-10	28	2	-10	37	7	-9	38	7
	6	150	57	96	72	28	15	50	0	12	64	-5	13	67	-6	14	82	4	15	84	3
	7	150	57	96	72	28	15	52	0	41	103	-13	43	106	-15	42	127	-1	44	130	-2
	8	148	56	95	72	28	15	53	0	20	62	0	22	65	-1	22	75	4	24	78	3
	9	149	57	96	72	28	15	52	0	-3	39	-4	-1	41	-5	-2	43	-4	-0	46	-5
	10	149	57	96	71	28	15	53	0	-62	-101	-8	-62	-100	-8	-65	-110	-13	-64	-110	-13
	11	148	57	96	73	28	15	53	0	10	-71	10	9	-72	10	9	-84	3	8	-85	3
	12	149	57	96	71	28	15	51	0	1	-84	3	-0	-87	4	-1	-99	-1	-3	-102	-1
1948	1	149	58	96	71	28	15	50	0	43	-22	-14	41	-25	-13	38	-32	-16	36	-35	-15
	2	149	57	97	73	29	15	51	0	-12	-8	14	-14	-11	15	-10	-24	2	-12	-27	4
	3	148	57	97	73	29	15	53	0	-52	-45	0	-54	-48	1	-53	-54	-6	-54	-56	-5
	4	146	57	96	73	29	15	54	0	32	35	4	32	35	5	33	40	8	32	40	8
	5	147	56	96	74	29	16	54	0	14	36	13	15	37	12	17	43	16	18	44	16
	6	146	58	97	73	29	16	51	0	19	108	-5	21	111	-6	22	129	3	24	131	3
	7	146	58	95	74	29	16	52	0	20	97	-11	22	100	-12	22	121	1	24	124	0
	8	146	60	94	74	29	16	53	0	36	70	-7	38	73	-8	39	92	3	41	95	2
	9	146	59	95	74	29	16	51	0	-1	18	-5	0	20	-6	-0	26	-0	0	29	-1
	10	145	59	95	74	29	16	52	0	-22	-49	-18	-22	-49	-18	-26	-54	-19	-25	-54	-19
	11	145	59	95	74	29	16	54	0	-54	-136	-2	-55	-137	-2	-58	-156	-13	-59	-157	-12
	12	145	57	95	73	29	16	53	0	-78	-73	-1	-79	-75	-0	-80	-92	-11	-81	-94	-10

. 1949	1	146	57	94	75	29	15	50	0	-18	-2	-0	-20	-5	0	-19	-20	-12	-21	-23	-10
	2	145	57	94	75	29	16	52	0	-49	-20	-1	-51	-23	0	-49	-33	-9	-51	-36	-7
	3	145	57	96	75	29	16	50	0	-33	-56	17	-34	-58	18	-33	-66	14	-34	-68	15
	4	146	57	95	75	29	15	51	0	2	-17	-4	2	-18	-4	1	-16	-2	0	-16	-2
	5	146	57	95	75	29	16	52	0	8	68	10	9	69	10	11	80	16	12	81	15
	6	146	57	96	75	29	16	52	0	3	63	-1	5	66	-2	6	80	6	7	83	5
	7	146	55	95	74	29	16	51	0	29	75	-5	31	79	-6	31	95	2	33	98	1
	8	146	56	95	75	29	16	53	0	-2	69	-3	-0	72	-4	-0	85	2	1	89	1
	9	145	57	96	75	29	16	52	0	-33	5	2	-31	7	1	-31	10	2	-30	13	1
	10	145	55	95	75	29	16	53	0	-24	-56	-4	-24	-55	-5	-25	-61	-8	-25	-60	-8
	11	145	57	95	74	28	16	53	0	-6	-130	-2	-7	-131	-2	-11	-146	-5	-11	-147	-5
	12	145	57	92	74	29	16	50	0	3	-35	10	1	-37	11	2	-51	3	1	-54	4
1950	1	144	54	96	75	29	16	50	0	-26	-4	22	-28	-7	23	-23	-19	11	-25	-23	12
	2	144	54	96	75	29	16	50	0	9	-2	5	7	-5	6	9	-14	-1	7	-17	-0
	3	144	54	96	76	29	16	51	0	-15	-50	2	-16	-52	2	-16	-55	1	-17	-57	2
	4	145	54	95	75	29	16	52	0	46	42	7	46	42	7	47	49	13	46	49	13
	5	145	53	95	76	29	16	51	0	-2	38	7	-2	40	7	-0	51	13	-0	52	13
	6	145	54	96	76	29	16	52	0	15	66	-8	17	68	-9	17	88	2	19	91	2
	7	145	52	95	75	29	16	49	0	26	122	-8	28	125	-9	29	149	3	31	152	2
	8	144	54	94	75	29	16	50	0	26	98	-5	28	101	-6	28	119	5	30	123	4
	9	144	53	96	75	29	16	51	0	27	23	-11	28	25	-12	27	36	-5	28	38	-6
	10	144	54	96	75	29	16	50	0	-44	-76	-0	-44	-76	-0	-45	-82	-3	-45	-82	-3
	11	144	54	96	74	29	16	49	0	11	-42	15	10	-43	15	11	-56	8	10	-58	9
	12	144	53	94	75	29	16	49	0	-3	-63	5	-4	-66	5	-5	-81	-0	-6	-83	0
1999	1	170	89	107	88	32	18	63	0	-11	-94	1	-13	-97	2	-14	-108	-9	-16	-111	-8
	2	170	89	107	88	32	18	63	0	-1	-69	7	-3	-72	8	-3	-80	-1	-5	-83	-0
	3	170	89	107	88	32	18	63	0	5	-48	5	3	-50	6	3	-52	3	1	-54	4
	4	170	89	107	88	32	18	63	0	8	12	5	7	12	5	7	14	7	7	14	8
	5	170	89	107	[illegible]	32	18	63	0	-1	57	9	-1	58	9	1	64	14	1	65	14
	6	170	89	107	88	32	18	63	0	5	106	-4	6	108	-5	9	120	6	10	122	5
	7	170	89	107	88	32	18	63	0	27	134	-9	29	137	-10	31	150	2	33	154	1
	8	170	89	107	88	32	18	63	0	18	105	-6	20	108	-7	21	118	3	23	121	2
	9	170	89	107	88	32	18	63	0	-7	21	-2	-5	23	-3	-5	25	-0	-4	27	-1
	10	170	89	107	88	32	18	63	0	-18	-55	-8	-18	-54	-8	-20	-59	-10	-20	-58	-10
	11	170	89	107	88	32	18	63	0	-10	-70	0	-10	-71	0	-12	-80	-7	-13	-81	-6
	12	170	89	107	88	32	18	63	0	-14	-98	0	-15	-100	1	-17	-111	-8	-18	-114	-8

Mean of	1									-12	-73	-5
(1873- 1950)	2									-5	-60	-1
	3									3	-39	1
	4									5	3	3
	5									-6	33	6
	6	91	40	54	48	13	12	24	0	5	79	4
	7									20	108	2
	8									12	84	2
	9									-6	21	1
	10									-6	-32	-3
	11									-6	-54	-4
	12									-8	-73	-5
Mean of	1									-8	-88	-6
(1900- 1950)	2									1	-69	-1
	3									2	-48	2
	4									7	4	3
	5									-8	42	6
	6	106	54	62	59	17	15	33	0	3	97	4
	7									21	128	2
	8									12	101	2
	9									-8	25	1
	10									-9	-41	-5
	11									-3	-65	-5
	12									-7	-88	-6

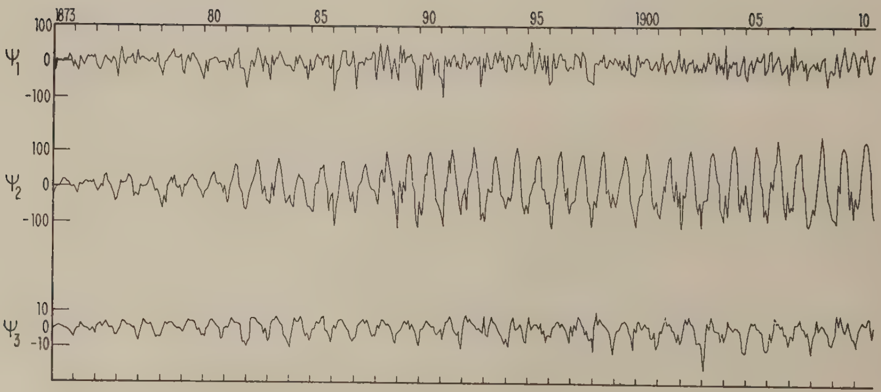

FIG. 5. The excitation functions ψ_1, ψ_2 are

8. Harmonic expressions

The Fourier coefficients for the annual and semiannual terms for the three types of averages are

(1999)	− 1.8 cos ⊙	+0.2 sin ⊙	+0.4 cos 2⊙	+0.8 sin 2⊙
(1900–1950)	− 0.7	+0.2	+0.2	+0.5
(1873–1950)	− 0.9	+0.04	+0.1	+0.4
(1999)	−12.9	−1.0	+1.8	+1.4
(1900–1950)	−10.2	−1.4	+1.7	+0.8
(1873–1950)	− 8.5	−1.2	+0.[illegible]	+0.7
(1999)	− 0.0028	+0.0085	−0.0017	−0.0006
(1900–1950)	− 0.0047	+0.0024	−0.0009	+0.00003
(1873–1950)	− 0.0045	+0.0020	−0.0009	+0.00003

All coefficients are in parts per 10^8 (these are not the units in the table).

Acknowledgments. The author wishes to express his deep thanks to Dr. Walter Munk of Scripps Institution of Oceanography. He suggested the point of research, and his help was frequently sought and generously given in every phase of the work. Mrs. Katherine Cromwell was a great help in the processing phase of the large amount of data that was involved. She performed a long and tedious task diligently and conscientiously. Mrs. Georgette Price and Mr. Soliman Lotayef gave appreciated help during different phases of the research. Mrs. Gretchen Chambers and Miss Helen Rehn have ably typed the manuscript.

This research has been supported, in part, through a grant from the Institute of Geophysics, University of California, and the computations have been carried out on an IBM 709 at the Western Data Processing Center, University of California, Los Angeles. Preparation of the data was performed on an IBM 650 at General Atomic.

REFERENCES

Bannon, J., and L. Steele, 1957: *Average water vapour content of the air.* Meteor. Res. Comm., London.

Munk, W., and E. M. Hassan, 1961: Atmospheric excitation of the earth's wobble. *Geophys. J.* (*in press*).

Munk, W., and G. J. F. MacDonald, 1960: *The rotation of the earth; a geophysical discussion.* Cambridge, Cambridge Univ. Press (in press).

Smithsonian Miscellaneous Collections Vol. 79, 1927: *World weather records*, 1199 pp.

Smithsonian Miscellaneous Collections Vol. 86, 1939: *Smithsonian meteorological tables* (fifth rev. ed.), 282 pp.

Smithsonian Miscellaneous Collections Vol. 90, 1934: *World weather records 1921–1930*, 616 pp.

Smithsonian Miscellaneous Collections Vol. 105, 1947: *World weather records 1931–1940*, 646 pp.

U. S. Weather Bureau, 1959: *World weather records 1941–1950*, 1361 pp.

APPENDIX

A. List of all stations used in the computation

The stations are arranged under twelve major divisions of the Earth and by countries or political divisions in alphabetical order within the major divisions. All stations appearing under one country then appear also in alphabetical order; *e.g.*; New Delhi appears under India which appears in the division Asia. One exception to this system is Alaska, which does not appear under the U.S.A. This makes numbering the stations more systematic. (List of stations begins on following page.)

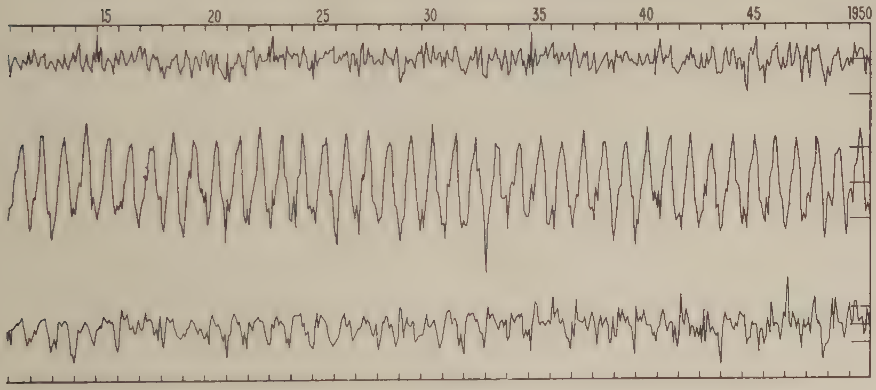

given in 10^{-9} radians, ψ_3 in 10^{-11} radians.

AFRICA

Algeria

Aoulef	1
Beni-Abbes	2
Biskra	3
Bouzareah	4
El Golea	5
Oran	6
Ouallen	7

British East Africa

Dar-Es-Salaan	8
Entebbe	9
Kampala	10
Nairobi	11
Tabora	12
Zanzibar	13

British West Africa

Calabar	14
Freetown	15
Kano	16
Lagos	17
Maiduguri	18

Federation of Rhodesia and Nyasaland

Bulawayo	19
Kasama	20
Livingstone	21
Salisbury	22
Zomba	23

French Equatorial Africa

Bangui	24
Brazzaville	25
Fort-Archambault	26
Pointe-Noire	27
Port-Gentil	28

French West Africa

Abidjan	29
Agadez	30
Atar	31
Bamako	32
Bobo-Dioulasso	33
Fort Trinquet	34
Gao	35
Kandi	36
Kayes	37
Mamou	38
Mopti	39
Nema	40
Niamey	41
Nouakchott	42
Odienne	43
Ouagadougou	44
Port Etienne	45
Tabou	46
Tambacounda	47
Tchaourou	48
Zinder	49

Gambia

Bathurst	50

Ghana

Accra	51

Libya

Cyrene	52
Sebha	53
Sirte	54

Morocco

Cape Spartel	55
Casablanca	56
Marrakech	57

Portuguese East Africa

Beira	58
Lourenco Marques	59

Portuguese West Africa

Luanda	60
Luso	61
Mocamedes	62
Nova Lisboa	63
Sa Da Bandeira	64

Sudan

Atbara	65
El Fasher	66
El Obeid	67
Juba	68
Kassala	69
Khartoum	70

Kosti 71
Malakal 72
Port Sudan 73
Wadi Halfa 74
Wau 75

Tunisia

Tunis 76

Union of South Africa

Aliwal North 77
Cape Town 78
Durban 79
Johannesburg 80
Keetmanshoop 81
Kimberley 82
Mahalapye 83
Maun 84
O'OKiep 85
Port Elizabeth 86
Windhoek 87

United Arab Republic

Alexandria 88
Cairo 89
Helwan 90
Kom El Nadura 91
Luxor 92
Minya 93
Port Said 94

ANTARCTICA

South Shetland Islands

Deception Island 95

Palmer Peninsula

Marguerite Bay 86
Port Lockroy 97

ASIA

British Malaya

Singapore 98

Burma

Akyab 99
Mandaley 100
Mergui 101
Rangoon 102

Cambodia

Phnom-Penh 103

Ceylon

Colombo 104
Hambantota 105
Nuwara Elija 106
Trincomalee 107

China

Anta 108
Fort Bayard 109
Hailar (Hulun) 110
Hankow 111
Harbin 112
Kunming 113
Mukden 114
Nanking 115
Port Arthur 116
Shanghai 117
Tientsin 118
Tsingtao 119
Wuhan 120
Yunnanfu 121

Hong Kong 122

India

Ahmedabad 123
Allahabad 124
Bangalore 125
Belgaum 126
Bombay 127
Calcutta 128
Cherraphunji 129
Cochin 130
Gauhati 131
Jaipur 132
Kodaikanal 133
Leh 134
Madras 135
Mangalore 136
Masulipatam 137
Nagpur 138

New Delhi 139
Patna 140
Shillong 141
Simla 142
Visakhapatnam 143

Iran

Bushire 144
Jask 145

Iraq

Baghdad 146
Basra 147

Israel

Jerusalem 148

Japan

Akita 149
Ashizuri 150
Fukuoka 151
Ishigaki 152
Kagoshima 153
Kyoto 154
Matsumoto 155
Miyako 156
Nagasaki 157
Naha 158
Nemuro 159
Ochiai 160
Sapporo 161
Shionomisaki 162
Syana 163
Tokyo 164
Wajima 165
Yonago 166

Jordan

Amman 167

Korea

Chemulpo 168
Inchon 169
Joshin 170
Mokpo 171
Pyongyang 172
Taegu 173
Ullung-Do 174
Unggi 175

Laos

Vientiane 176

Lebanon

Beirut 177

Pakistan

Hyderabad 178
Kalat 179
Karachi 180
Lahore 181
Peshawar 182
Quetta 183

Saudi Arabia

Aden 184
Bahrain 185
Muscat 186
Riadh 187
Riyan 188
Salalah 189
Sharjah 190

Taiwan

Tainan 191
Taipeh 192

Thailand

Bangkok 193

Tibet

Lhasa 194

Turkey

Adana 195
Ankara 196
Antalya 197
Diyarbakir 198
Edirne 199
Erzurum 200
Istanbul 201
Izmir 202
Rize 203
Samsun 204
Sivas 205

USSR

Akmolinsk 206
Alma-Ata 207
Anadir 208
Barnaul 209
Berezov 210
Blagovyeshtchensk 211
Dickson 212
Dolinsk (Ochiai) 160
Dudinka 213
Fort Shevtchenko 214
Horomushiro 215
Irkutsk 216
Kasalinsk 217
Kirensk 218
Krasnovodsk 219
Malye Karmakuly 220
Markovo on Anadyr 221
Minusinsk 222
Naryn 223
Nerchinsky Zavod 224
Nikolayevsk on Amur 225
Obdorsk 226
Okhotsk 227
Olekminsk 228
Omsk 229
Petropavlovsk 230
Primorskaja 231
Shikuka 232
Surgut 233
Tashkent 234
Tchita 235
Tobolsk 236
Tomsk 237
Turgai 238
Turukhansk 239
Ust Mayskoe 40
Verchoyansk 241
Vladivostok 242
Waigatz 243
Yakutsk 244
Yennisseysk 245

Viet Nam

Dong Hoi 246
Haiphong 247
Moncay 248
Nhatrang 249
Phu-lien 250
Saigon 251
Tourane 252

AUSTRALIA AND EAST INDIES

Adelaide 253
Alice Springs 254
Brisbane 255
Cairns 256
Darwin 257
Hobart 258
Melbourne 259
Onslow 260
Perth 261
Sydney 262

New Guinea

Port Moresby 263
Sandakan 264

Indonesia

Djakarta 265
Medan 266
Pasuruan 267

EUROPE

Austria

Obir 268
Sonnblick 269
Wien 270

Denmark

Copenhagen 271

Finland

Helsinki 279

France

Lyon 273
Marseille 274
Nantes 275
Paris 276

Germany

Berlin 277
Breslau 278
Frankfurt 279
Königsberg 280
Potsdam 281
Trier 282

Greece	
Athens	283
Hungary	
Budapest	284
Ireland	
Valentia	285
Italy	
Catania	286
Milano	287
Roma	288
Sassari	289
Netherlands	
De Bilt	290
Norway	
Bergen II	291
Bodø	292
Gjesvar	293
Ingøy	294
Oslo	295
Sletnes	296
Vardø	297
Poland	
Krynica	298
Warsaw	299
Wroclaw	278
Portugal	
Lisboa	300
Rumania	
Bucharest	301
Cernăuti	302
Sibin	303
Sulina	304
Spain	
Madrid	305
Sweden	
Haparanda	306
Uppsala	307
Switzerland	
Santis	308
Zurich	309
USSR	
Archangelsk	310
Astrachan	311
Kasan	312
Kiev	313
Leningrad	314
Lwow	315
Molotov	316
Moskva	317
Nikolaewskoe	318
Novorossisk	319
Odessa	320
Swerdlowsk	321
Tbilisi	322
Tchkalov	323
Ust-Zylma	324
Vilnjus	325
United Kingdom	
Aberdeen	326
Gibralter	327
Greenwich	328
Kew Observatory	329
Yugoslavia	
Beograd	330
Hvar Lesina	331
Split-Marjan	332
INDIAN OCEAN	
Madagascar	
Diego-Suarez	333
Fort-Dauphin	334
Tananarive	335

NORTH AMERICA

Alaska

Anchorage 336
Barrow 337
Bethel 338
Cordova 339
Eagle 340
Fairbanks 341
Fort Yukon 342
Gambell 343
Juneau 344
Kodiak 345
McGrath 346
Nome 347
Sitka 348
Tanana 349
Valdez 350

British Honduras

Belize 351
Tegucigalpa 352

Canada

Aklavik 353
Anticosti 354
Arctic Bay 355
Barkerville 356
Belle Isle 357
Calgary 358
Cambridge Bay 359
Cape Race 360
Charlottetown 361
Chesterfield Inlet 362
Churchill 363
Clyde 364
Coppermine 365
Dawson 366
Edmonton 367
Eureka 368
Father Point 369
Fort Good Hope 370
Port Harrison 388
Fort McKenzie 371
Fort McMurray 372
Fort Simpson 373
Fort Smith 374
Frobisher 375
Goose Bay 376
Grindstone Island 377
Hay River 378
Isachsen 379
Kamloops 380
Knob Lake 381
Langara 382
Montreal 383
Moose Factory 384
Moosonee 385
Mould Bay 386
Nottingham Island 387
Prince Albert 389
Prince George 390
Prince Rupert 391
Qu'Appelle 392
Regina 393
Resolute 394
Resolution Island 395
Sable Island 396
St. Johns 397
The Pas 398
Torbay 399
Toronto 400
Trout Lake 401
Victoria 402
Watson Lake 403
White River 404
Winnipeg 405

Canal Zone

Cristobal 406

El Salvador

San Salvador 407

Mexico

Chihuahua 408
Leon 409
Mazatlan 410
Merida 411
Mexico City 412
Monterrey 413
Oaxaca 414
Progreso 415
Puebla 416
Salina Cruz 417
Tacubaya 418

USA

Abilene 419
Albany 420
Alburquerque 421
Alpena 422
Amarillo 423

Asheville 424
Bismark 425
Blue Hill Obs. 426
Boise 427
Charleston 428
Cheyenne 429
Chicago 430
Cincinnati 431
Concordia 432
Corpus Christi 433
Denver 434
Detroit 435
Devils Lake 436
Duluth 437
Eastport 438
El Paso 439
Galveston 440
Hatteras 441
Helena 442
Jacksonville 443
Key West 444
Lincoln 445
Little Rock 446
Macon 447
Marquette 448
Minneapolis 449
Mobile 450
Modena 451
Nashville 452
New Haven 453
New Orleans 454
New York 455
North Platte 456
Omaha 457
Oswega 458
Phoenix 459
Portland 460
Red Bluff 461
Richmond 462
Sacramento 463
St. Louis 464
St. Paul 465
Salt Lake City 466
San Diego 467
San Francisco 468
San Luis Obispo 469
Santa Fe 460
Sheridan 471
Spokane 472
Valentine 473
Washington 474
Winnemucca 475
Yuma 476

NORTH ATLANTIC

Cuba

Habana 477

Greenland

Angmagssalik 478
Godthaab 479
Ivigtut 480
Jacobshavn 481
Myggbukta 482
Scoresbysund 483
Upernivik 484

Haiti

Port-au-Prince 485

Iceland

Akureyri 486
Grimsey 487
Stykkisholmur 488
Teigarhorn 489
Vestmannaeyjar 490

Spitsbergen

Isfjord Radio 491

Trinidad

Piarco 492

NORTH PACIFIC

Phillipines

Aparri 493
Iloilo City 494
Legaspi 495
Manila 496

SOUTH AMERICA

Argentina

Bahia Blanca 497
Buenos Aires 498
Catamarca 499
Cipolletti 500
Cordoba 501
Esquel 502
Goya 503

La Quiaca	504
Mar Del Plata	505
Mendoza	506
Puerto Santa Cruz	507
Salta	508
San Juan	509
Sarmiento	510
Trelew	511
Tucuman	512

Bolivia

Cochabamba	513
La Paz	514
Santa Cruz	515

Brazil

Brusque	516
Caetité	517
Corumba	518
Cuiaba	519
Curitiba	520
Fernando de Noronha	521
Iguape	522
Juiz de Fóra	523
Manaus	524
Olinda	525
Ondina	526
Quixeramobim	527
Recife	528
Rio de Janeiro	529
Salvador	530
Sao Paulo	531
Sena Madureira	532
Taperinha	533
Turiacu	534
Uaupes	535

British Guiana

Georgetown	536

Chile

Arica	537
Caldera	538
Coquimbo	539
Iquique	540
Isla Guafo	541
La Serena	542
Punta Arenas	543
Punta Galera	544
Santiago	545
Valdivia	546

Colombia

Bogota	547

Ecuador

Quito	548

Paraguay

Asuncion	549
Bahía Negra	550
Encarnación	551

Peru

Arequipa	552
Chiclayo	553
Lambayeque	554
Lima	555

Surinam

Paramaribo	556

Uruguay

Montevideo	557

Venezuela

Caracas	558
Santa Elena	559

SOUTH ATLANTIC

Año Nuevo	560

SOUTH PACIFIC

New Zealand

Auckland	561
Christchurch	562
Dunedin	563
Hokitika	564
Wellington	565

B. Sea-level correction

In some cases, only sea-level pressure was reported for a particular station during a particular perod. Correction had to be applied to bring it up to the station level. This correction was found in the following way:

1. for stations where the station-level pressure and the sea-level pressure simultaneously reported for a particular period of the record, the correction was found by the inspection of that period;
2. for stations where there was no period when both station level and sea-level pressures were reported, the correction was calculated by using the known station height and the mean monthly temperature, with the help of the Smithsonian Meteorological Tables (5th rev. ed.);
3. if the station level changed during the recorded period, the lowest station level was used for the calculation of the sea-level correction.

If the correction for the hottest month is C, then the correction for any month can be considered to consist of two parts $C + \gamma(t)$, and we have the relation

$$\text{sea-level pressure} - (C+\gamma(t)) = \text{station-level pressure}.$$

As the computation uses only the difference of the pressure from the mean, it is sufficient for our purposes to subtract γ from the reported sea-level pressure. When $\gamma_{\max}$ was greater than one tenth of the sea-level-pressure range, the correction was not attempted and the sea-level pressure was not used. When $\gamma_{\max}$ was less than 0.05 mb, no correction was considered necessary, and the sea-level pressure was used without correction.

Stations for which γ was applied are listed starting on opposite page, together with γ and the period for which it applied.

Station		J	F	M	A	M	J	J	A	S	O	N	D	Unit	Beginning & End of Period
54	Sirte	2	2	2	1	1	0	0	0	0	0	1	2	1/10mb	1946-1950
55	Cape Spartel	3	3	3	2	2	1	0	0	0	1	2	3	1/10mb	1894-1920
59	Laurenco Marques	0	0	0	0	1	2	2	2	1	1	0	0	1/10mb	1910-1950
86	Port Elizabeth	0	0	0	1	1	2	2	2	2	1	1	0	1/10mb	1941-1950
111	Hankow	4	4	3	2	1	0	0	0	0	2	3	4	1/10mm	1905-1942
114	Mukden	8	8	6	3	2	0	0	0	1	3	6	7	1/10mm	1905-1941
116	Port Arthur	2	2	2	1	1	0	0	0	0	1	1	2	1/10mm	1906-1944
118	Tientsin	1	1	1	0	0	0	0	0	0	0	1	1	1/10mm	1906-1944
119	Tsingtao	8	8	6	5	3	1	0	0	1	2	5	7	1/10mm	1916-1944
146	Baghdad	5	5	4	3	1	0	0	0	0	2	3	5	1/10mb	1941-1950
147	Basra	1	1	1	0	0	0	0	0	0	0	1	1	1/10mb	1941-1950
163	Syana	4	4	4	3	2	1	0	0	0	1	2	3	1/10mm	1903-1944
171	Mokpo	4	4	4	2	1	2	1	0	0	2	2	4	1/10mm	1904-1940
172	Pyongyang	4	4	3	2	1	0	0	0	0	1	3	4	1/10mm	1907-1944
173	Taegu	6	7	5	3	2	1	0	1	1	3	3	7	1/10mm	1907-1940
188	Riyan	1	1	1	1	0	0	0	0	0	1	1	1	1/10mb	1942-1950
160	Dolinsk (Ochiai)	6	6	7	5	4	3	3	0	1	3	6	7	1/10mb	1946-1950
253	Adelaide	0	0	1	2	4	5	5	5	4	3	2	0	1/1000inch	1873-1940
		0	0	0	1	2	2	2	2	2	1	1	0	1/10mb	1941-1950
255	Brisbane	0	0	1	3	4	6	6	6	4	3	1	0	1/1000inch	1887-1940
		0	0	0	1	2	2	2	2	2	1	0	0	1/10mb	1941-1950
258	Hobart	0	0	0	0	1	1	1	1	1	0	0	0	1/10mb	1896-1950
261	Perth	0	0	0	0	1	1	1	1	1	1	0	0	1/10mb	1885-1950

Station		J	F	M	A	M	J	J	A	S	O	N	D	Unit	Beginning & End of Period
262	Sydney	0	0	0	1	2	2	2	2	2	1	0	0	1/1000inch	1873-1940
		0	0	0	0	1	1	1	1	1	0	0	0	1/10mb	1941-1950
326	Aberdeen	4	4	4	3	2	1	0	0	1	2	3	4	1/1000inch	1873-1930
		1	1	1	1	1	0	0	0	0	1	1	1	1/10mb	1931-1940
329	Kew Observatory	1	1	1	1	1	0	0	0	0	1	1	1	1/10mb	1941-1950
337	Barrow	3	3	3	2	1	0	0	0	0	1	2	3	1/1000inch	1921-1940
		1	1	1	1	0	0	0	0	0	0	1	1	1/10mb	1941-1950
338	Bethel	5	5	5	3	1	0	0	0	1	3	4	5	1/10mm	1931-1940
339	Cordova	1	1	1	1	0	0	0	0	0	0	1	1	1/10mb	1942-1950
348	Sitka	1	1	1	1	0	0	0	0	0	0	1	1	1/1000inch	1881-1950
355	Arctic Bay	2	2	2	2	1	0	0	0	0	1	2	2	1/10mb	1937-1950
359	Cambridge Bay	4	4	4	3	2	0	0	0	1	2	3	4	1/10mb	1941-1950
360	Cape Race	3	3	3	2	2	1	0	0	0	1	2	3	1/10mb	1941-1950
361	Charlotte Town	2	2	2	2	1	0	0	0	0	0	1	2	1/10mb	1941-1950
364	Clyde	2	2	2	2	1	0	0	0	0	0	1	2	1/10mb	1943-1950
365	Coppermine	1	1	1	1	0	0	0	0	0	0	1	2	1/10mb	1941-1950
375	Frobisher	4	4	4	3	1	0	0	0	0	1	2	3	1/10mb	1947-1950
379	Isachsen	7	7	6	5	3	0	0	0	2	4	5	6	1/10mb	1948-1950
386	Mould Bay	4	4	3	3	1	0	0	0	1	2	3	4	1/10mb	1948-1950
388	Port Harrison	4	4	4	3	1	0	0	0	0	1	2	3	1/10mb	1941-1950
394	Resolute	5	5	4	4	2	0	0	0	1	3	4	4	1/10mb	1947-1950
397	St. Johns	1	1	1	1	1	0	0	0	0	0	1	1	1/100inch	1931-1940
478	Angmagssalik	2	2	2	2	1	0	0	0	0	1	2	2	1/10mm	1894-1940
483	Scoresby Sound	3	4	4	3	1	0	0	0	0	1	2	3	1/10mm	1948-1950
487	Grimsey	1	1	1	1	1	0	0	0	0	0	1	1	1/10mb	1940-1950

Station		J	F	M	A	M	J	J	A	S	O	N	D	Unit	Beginning & End of Period
488	Stykkysholmur	2	2	2	1	1	0	0	0	0	1	1	2	1/10mm	1873-1940
		2	2	2	2	1	0	0	0	1	1	2	2	1/10mb	1941-1950
489	Tiegarhorn	1	1	1	0	0	0	0	0	0	0	1	1	1/10mm	1873-1940
		1	1	1	1	0	0	0	0	0	1	1	1	1/10mb	1941-1944
490	Vestmanaeyjar	3	3	3	2	2	1	0	0	1	2	2	3	1/10mm	1881-1940
		4	4	4	3	2	1	0	0	1	2	3	4	1/10mb	1941-1950
505	MarDel Plata	0	0	0	0	1	1	1	1	1	1	0	0	1/10mb	1941-1950
507	Puerto Santa Cruz	0	0	0	1	1	1	1	1	1	0	0	0	1/10mb	1941-1950
541	Isla Guafo	0	0	1	2	2	2	3	3	3	3	2	1	1/10mm	1908-1940
561	Aukland	0	0	0	1	2	3	3	3	2	2	1	0	1/1000	1873-1930
		0	0	0	0	1	1	1	1	1	1	0	0	1/10mb	1931-1950

C. The mean of the pressure record

For obtaining the mean of monthly pressures, the whole record was used in most of the cases. In some cases, however, the level for which the pressure is reported changed during the reported period. Sometimes this was easy to take into account, as the change in level introduced a systematic change in the pressure, and the whole record could be made to represent the pressure at one level. In other cases, it was not obvious whether the whole record was reduced to one level or not. In these cases, the mean was calculated for different portions of the record separately. The following is a list of stations where such was the case:

Station No.	Station	End of period
4	Bauzareah	1940
9	Entebbe	1930
15	Freetown	1939
17	Lagos	1930, 1945
80	Johannesburg	1940
82	Kimberley	1940
85	O'Okiep	1940
86	Port Elizabeth	1940
89	Cairo	1922
107	Trincomalee	1940
113	Kunming	1946
117	Shanghai	1920
146	Baghdad	1920, 1930, 1940
156	Miyako	1938
160	Ochiai	1944
206	Akmolinsk	1930
207	Alma Ata	1928
211	Blagovyeshtchensk	1920
222	Minusinsk	1920, 1930
223	Narynskaye	1915, 1940
225	Nikalayevsk	1925
228	Olekminsk	1930
229	Omsk	1937
241	Verkhoyansk	1920, 1930
245	Yenisseysk	1915, 1940
248	Moncay	1930
251	Saigon	1930
266	Medan	1940
274	Marseille	1930
288	Roma	1920, 1930
292	Bodo	1940
295	Oslo	1940
303	Sibiu	1940
324	Ust-Zylma	1915
327	Gibraltar	1930
335	Tananarive	1939
338	Bethel	1940
345	Kodiak	1930
348	Sitka	1926
361	Charlottetown	1940
366	Dawson	1930
397	St. Johns	1930
410	Mazatlan	1914, 1940
411	Merida	1940
413	Monterrey	1938
439	El Paso	1925
442	Helena	1930
451	Modena	1926
478	Angmagssalik	1940
484	Upernivik	1936
492	Trinidad	1920
494	Iloilo City	1930
497	Bahia Blanca	1940
502	Esquel	1940
503	Goya	1930
505	Mar Del Plata	1940
506	Mendoza	1940
511	Trelew	1930, 1940
514	La Paz	1940
527	Quixeramobim	1930
529	Rio de Janeiro	1930, 1940
541	Isla Guafo	1940
549	Asuncion	1930
555	Lima	1940
557	Montevideo	1930
561	Auckland	1930

D. Rejected data

The following data were rejected for various reasons:

	Station	Period	Remarks
14	Calabar	Prior to 1946	The data were reported to be unreliable.
15	Freetown	Nov. 1948 Aug. 1950	Comparing the station-level pressure with the sea-level pressure reveals a mistake in these months.
108	Anta	1940 1941	Sea-level pressures for these years were reported instead of station-level pressures.
169	Inchon	April 1942	Comparing the station-level pressure with the sea-level pressure reveals a mistake in that month.
194	Lhasa	April 1941 to April 1942	Reported pressure remained constant for nine months. A mistake was suspected.
210	Berezov	1937	Data was not reliable.

CONTRIBUTIONS FROM THE CUSHMAN FOUNDATION
FOR FORAMINIFERAL RESEARCH
VOLUME XII, PART 3, JULY, 1961

228. LABORATORY EXPERIMENTS ON THE ECOLOGY OF FORAMINIFERA[1]

JOHN S. BRADSHAW
Scripps Institution of Oceanography, La Jolla, California

ABSTRACT

Laboratory experiments were conducted on **Ammonia beccarii tepida** (various strains), **Spirillina vivipara, Bolivina compacta, Massilina** sp., **Rosalina columbiensis**, and **Bolivina vaughani.** Lethal temperatures, based on five-minute exposures, varied from 37.5°C. for **Bolivina vaughani** to 45°C. for **Ammonia beccarii tepida.** Attempts to change the lethal temperatures by temperature acclimation failed but high salinity may have increased the lethal temperatures slightly. Increased temperatures resulted in higher growth and reproductive rates and a decrease in generation time. Temperatures of 25-30°C. were optimal for **A. beccarii tepida**; those below approximately 18-20°C. did not permit reproductive activity. Specimens grown at lower temperatures were larger than those grown at higher temperatures. **A. beccarii tepida** showed the greatest resistance to lowered salinity; **Spirillina vivipara** was least tolerant. At normal salinity (34 o/oo), growth and reproductive rates were highest for **Ammonia beccarii tepida**; at salinities below 15 o/oo growth rates were lower and there was no reproductive activity. Food concentrations (**Dunaliella** sp.) less than 112 cells/mm^2 did not permit growth or reproduction. Growth rate and reproductive activity increased with additional food. Addition of antibiotics to cultures inhibited growth and increased mortality. **A. beccarii tepida** tolerated extreme pH values; **Spirillina vivipara** was more sensitive. Hydrostatic pressures of more than approximately 400 atmospheres were fatal to **Ammonia beccarii tepida.** No mortality occurred in 3 days at 400 atmospheres. Rates of oxygen consumption of approximately 2500-8000 μμl O_2 per foraminifer per hour were determined for individual specimens using a micro-respirometer. Oxygen consumption for **A. beccarii tepida** increased with increase in temperature.

INTRODUCTION

The definition of marine environments for ecological purposes is a difficult and at times almost an impossible task largely owing to the complexity and interplay of environmental factors. In the laboratory, however, it is possible to single out from the complex natural environment some of those ecologic factors which appear to be of critical importance and to study the effect of these one at a time. It should be possible to determine which factor, or factors, limit the range of each species in the various natural environments, and ultimately, to assess the ecologic interactions of the entire fauna.

The present study describes a series of experiments designed to investigate the influence of temperature, salinity, and food on basic physiological processes, especially the growth rate and survival of some species of Foraminifera. In addition, preliminary observations on the effect of pH, hydrostatic pressure, and the rate of oxygen consumption under various environmental conditions have been made. A technique for the determination of critical oxygen tensions is described. This paper is a continuation and expansion of earlier studies (Bradshaw, 1955, 1957) initiated to evaluate ecologic factors by experimental procedures.

Many technical problems arise in laboratory experimentation of this kind. A somewhat artificial environment is set up and in most instances a relatively long time period has elapsed between field collection and the experiments. It is possible that short term acclimation processes may so alter basic physiological responses that experimental results may be misleading. Acclimation experiments have been conducted in an attempt to gain some insight into this problem.

Support for these studies has been given by American Petroleum Institute Project 51, the National Science Foundation and a contract of the Office of Naval Research with the Scripps Institution of Oceanography of the University of California. Fred B Phleger gave many helpful suggestions. Thanks are due to P. F. Scholander, B. M. Sweeney and W. H. Thomas for helpful advice and assistance.

MATERIAL AND METHODS

The Foraminifera were cultured from samples of surface sediment collected from localities listed in Table 1. The following species were used in the experiments: *Ammonia beccarii tepida* (Cushman), *Spirillina vivipara* Ehrenberg, *Bolivina compacta* Sidebottom, *Bolivina vaughani* Natland, *Massilina* sp., and *Rosalina columbiensis* (Cushman). For the sake of brevity, generic names will be indicated throughout by initials only. The individual species were isolated and cultured under optimal conditions. Routine culture and experimental techniques have been described previously (Bradshaw, 1955, 1957). It has not yet been possible to obtain bacteria-free cultures but bacterial effects have been kept to a minimum by transfer to fresh media at 3-4 day intervals.

The method used to assess the effect of changes in environmental factors has been to observe qualitative and quantitative changes that occur when a single given factor is altered, all the others being kept constant. This gives a measure of the importance of each factor. Environmental factors are assumed to act directly upon biochemical processes, affecting their extent and velocity. This is reflected by changes in metabolic rate and by other changes such as rate and

---

[1] Scripps Institution of Oceanography Contribution, New Series. Marine Foraminifera Laboratory Contribution No. 38

Reprinted from CONTRIBUTIONS FROM THE CUSHMAN FOUNDATION FOR FORAMINIFERAL RESEARCH
Volume XII, Part 3, July, 1961 pp.87-106.
Printed by Dorr's Print Shop, Bridgewater, Massachusetts, U. S. A.

(649)

tributions from the Scripps Institution of Oceanography, New Series, 1289
duced by Permission

extent of growth. Inhibitory effects and, in extreme situations, death occur when biochemical rate reactions become unbalanced. A convenient measure of assessing response is by comparing growth rates under different conditions. In the following experiments, growth has been estimated by measuring the maximum diameter of the test at 3-4 day intervals.

TEMPERATURE EXPERIMENTS

Temperature has long been known to be of great importance in affecting physiological processes but few experimental data are available concerning its effect upon different species of Foraminifera. It is of importance ecologically in at least two respects: (1) It may limit a species geographically by killing the individuals or by preventing the completion of certain vital activities, such as reproduction. (2) The quantitative effect of temperature on growth, reproductive rates and other vital functions may selectively favor one species more than another.

Temperature Tolerance

Figure 1 illustrates a series of ecologically important temperature ranges and their critical limits. Individuals of a species will survive in a relatively large temperature range, grow within a smaller range, and reproduce only within a relatively narrow range. The extreme survival range is limited by the maximum and minimum instantaneous lethal temperatures. In the following experiments, instantaneous lethal temperature is defined as that temperature which kills 50% of the specimens during a five-minute exposure.

Within the extreme range of lethal temperatures (as defined) there is a narrower range limited by the upper and lower incipient lethal temperatures. This is the temperature beyond which the organism cannot live for an indefinite period of time. It is an ecologically significant point, which effectively divides the entire survival range into two zones. Within the upper and lower incipient lethal temperatures there is a zone of tolerance in which the organism will never die from the effects of temperature alone. Beyond the incipient lethal temperatures there is a range of resistance in which the foraminifer will ultimately succumb but in which it can survive for a certain period of time.

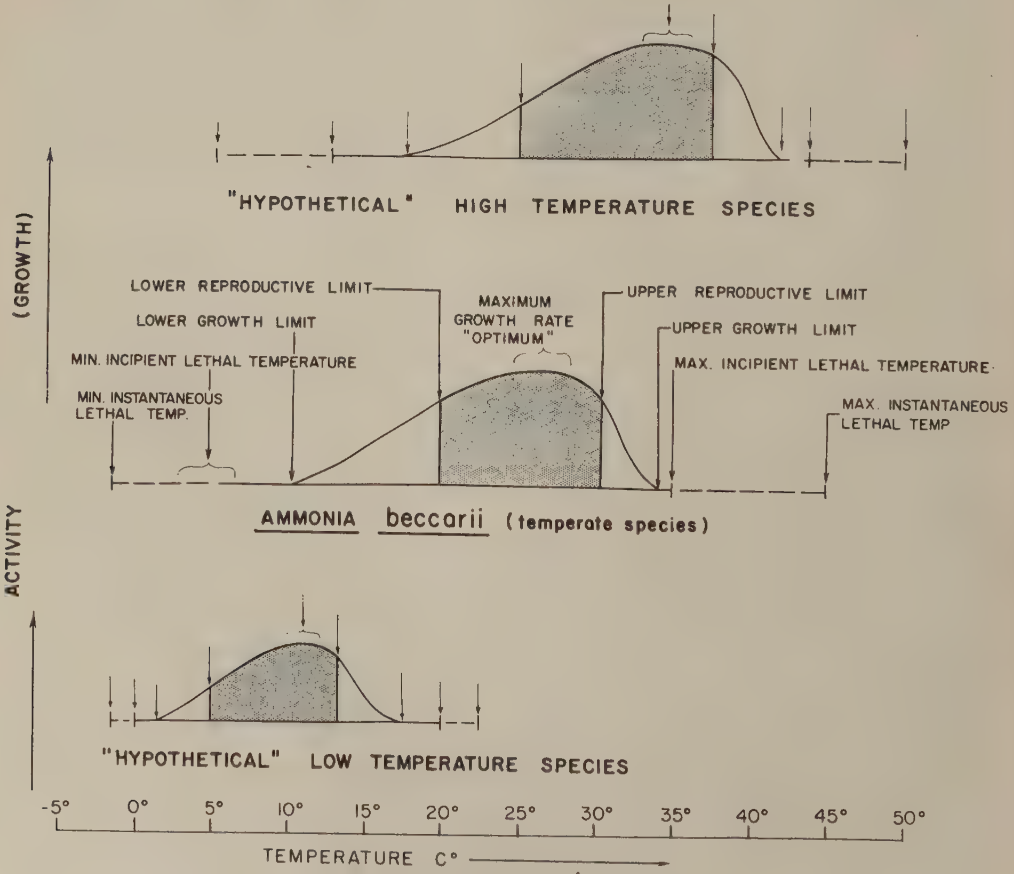
"HYPOTHETICAL" HIGH TEMPERATURE SPECIES
(GROWTH)
ACTIVITY
LOWER REPRODUCTIVE LIMIT
LOWER GROWTH LIMIT
MIN. INCIPIENT LETHAL TEMPERATURE
MIN. INSTANTANEOUS LETHAL TEMP.
MAXIMUM GROWTH RATE "OPTIMUM"
UPPER REPRODUCTIVE LIMIT
UPPER GROWTH LIMIT
MAX. INCIPIENT LETHAL TEMPERATURE
MAX. INSTANTANEOUS LETHAL TEMP
AMMONIA beccarii (temperate species)
"HYPOTHETICAL" LOW TEMPERATURE SPECIES
-5°
0°
5°
10°
15°
20°
25°
30°
35°
40°
45°
50°
TEMPERATURE C°

FIGURE 1
Significant temperature ranges showing critical limits.

Growth occurs only within a relatively narrow temperature range. The maximum, or optimum growth rate, is found near the middle of the zone but somewhat closer to the upper than to the lower limits. Near the extremes, the growth rate decreases.

The vital process having the narrowest range of tolerance is reproduction. Reproductive activity can only occur within this temperature zone; even though the animal may move about, feed, grow and exhibit otherwise normal behavior at higher or lower temperatures. The ability of many organisms to resist extreme temperatures varies greatly from species to species (Doudoroff, 1942; Southward, 1958). Such specific differences in the temperature tolerances of marine organisms may explain differences in their geographical distribution and breeding ranges (Orton, 1920). There appear to be characteristic critical temperature limits for each species, which may or may not be the same for others. Moreover, within the range the level of activity in question is not necessarily uniform; there may be an "optimum level," which in these studies is defined as "maximum rate of activity."

The present experiments and most of the tolerance experiments reported in the literature have been conducted under constant conditions. In nature, a non-uniform and often widely fluctuating environment is more often the rule, except in certain specialized habitats such as the deep sea. In correlating natural distributions of Foraminifera with temperature, for example, is it the occasional extreme temperatures that limit the Foraminifera, or are monthly, seasonal or annual sea temperature means more important? Hutchins (1947) has correlated the distribution of some intertidal animals with temperature by selecting those values of maximum and minimum mean monthly temperatures which best fit the distributions. In the Foraminifera there is little direct evidence for a causal relationship between temperature and distribution. Some observations and experiments have been reported on the effect of temperature on reproduction and rate of growth of a relatively few Foraminifera species (Arnold, 1951, 1954, 1955; Myers, 1935, 1936, 1937, 1940, 1943b; and Bradshaw, 1955, 1957) but little is known of the actual temperature extremes that can be tolerated.

Lethal Temperatures

Lethal temperatures were determined by placing a number of specimens (2-5) in a thinly drawn out pipette, plugging the end with putty, and inserting into sea water of the desired temperatures for specific periods of time. Prior to the test, the specimens were kept at their normal culture temperatures (see Table 1). For the instantaneous lethal points, the batches were immersed in sea water of the desired temperature for exactly 5 minutes. After preliminary trials had located the approximate lethal range, samples were exposed to temperatures at 0.5°C. or 1°C. intervals. After this exposure the Foraminifera were removed

TABLE 1. Species used in experiments and localities where collected.

Species	Environment	Locality collected	Temperature °C. Stock Culture
Ammonia beccarii tepida (Cushman)	Intertidal mud	Coos Bay, Oregon Lat. 43° 24.2′ N; Long. 124° 13.8′ W	25
Ammonia beccarii tepida (Cushman)	Intertidal mud	Carlsbad Slough, California Lat. 33° 08.7′ N; Long. 117° 19.4′ W	25
Ammonia beccarii tepida (Cushman)	Intertidal mud	La Paz, Baja California Lat. 24° 10′ N; Long. 110° 19′ W	25
Bolivina compacta Sidebottom	Dredge, sand 36 feet	VS-102, Gulf of California Lat. 26° 16.5′ N; Long. 111° 23.8′ W	20
B. vaughani Natland	Kelp holdfast 50 feet	Del Mar, California Lat. 32° 56′ N; Long. 117° 15.5′ W	20
Massilina sp.	Kelp holdfast 50 feet	Del Mar, California Lat. 32° 56′ N; Long. 117° 15.5′ W	20
Rosalina columbiensis (Cushman)	Sandy mud 50 feet	La Jolla, California Lat. 32° 52′ N; Long. 117° 15′ W	20
Spirillina vivipara Ehrenberg	Intertidal, rock	Carmine Island, Baja California Lat. 25° 59′ N; Long. 111° 06.5′ W	20

from the pipette and allowed to recover at their original culture temperature. That temperature at which one-half the batch was killed is considered to be the lethal point. After the specimens have been subjected to high sub-lethal temperatures, a considerable recovery period (up to 24 hours) often is required before it can be determined whether they are alive or dead.

There appears to be no general agreement on methods or criteria used in the determination of lethal temperatures. Some workers (Southward, 1958) slowly heat the vessel containing the specimens at a specified rate, e.g., 1°C. per 5 minutes, until the required temperature is reached. Slow heating, however, may allow gradual acclimation to successively higher temperatures and also introduces possible lethal effects due to prolonged heating at normally sublethal temperatures. Because of the unknown effect of these factors, it was considered preferable to immerse the specimens directly at the desired temperature and thus allow minimum opportunity for acclimation and other temperature-duration effects.

Death is not always easy to recognize in a relatively non-motile organism such as a foraminifer. Obvious criteria for living specimens are movement and/or pseudopodial activity. Life may still persist, however, in the absence of these obvious criteria, and it has been found necessary to examine the protoplasm within most tests for the streaming movements which are characteristic of living protoplasm. This final test of viability was made by using a 22× water-immersion lens inserted directly into the water above the specimen.

There is some disagreement about the percentage mortality necessary to provide an estimate of the lethal temperature of a population. Assuming a normal distribution of temperature tolerance, a large sample might be expected to yield a relatively wider range of tolerance before all the specimens were killed than a small sample. According to Andrewartha and Birch (1954), the most instructive figure is the dosage required to kill 50% of the population. This statistic has been used in the present study for comparison of different populations and species, but there was little difference in practice between the 50% and 100% lethal points (Table 2).

TABLE 2. Maximum lethal temperatures determined for various Foraminifera species.

Species	Strain	Lethal point (°C.)			No. of specimens at each temp.	Temp. interval °C.
		0%	50%	100%		
Ammonia beccarii tepida	La Paz	44.5	45	>45	10*	0.5
Ammonia beccarii tepida	Carlsbad	44	44.5	>45	10*	0.5
Ammonia beccarii tepida	Coos Bay	43.5	44.5	46	10*	0.5
Bolivina compacta	VS-102	40	40.5	41	4	0.5
Massilina sp.	Del Mar	39	39.5	40	3	0.5
Spirillina vivipara	Carmine Isl.	38	39	>39	10*	1
Rosalina columbiensis	La Jolla	38	38.5	39	4	1
Bolivina vaughani	Del Mar	37	37.5	38	2	1

*Two groups

After the determination of instantaneous lethal temperatures, the effect of duration at high sublethal temperatures was studied. This was done by immersing batches of specimens, as before, into a water bath held at different specified temperatures. At given time intervals, samples were removed, allowed to recover, and tested for viability.

The possibility that the prior temperature or salinity history of the specimens might have an effect on the lethal temperature was studied in several experiments. To test for temperature acclimation, several groups were kept at temperatures of 10, 15, 20, and 30°C. for periods up to two weeks before determination of the lethal point. The possibility of a salinity influence upon the lethal temperature was tested by keeping the specimens at salinities of 10, 17, 27, 34, 50 and 67 o/oo for one week before and during the actual test.

Results

Table 2 shows the maximum lethal temperatures determined for the various species and strains of Foraminifera tested. Different populations of *A. beccarii tepida,* even from widely separated localities, show approximately the same lethal temperature (45°C.), but the lethal temperature appears to be different for various species. Of the forms tested, *A. beccarii tepida* shows the greatest tolerance to high temperatures, while *B. vaughani* and *R. columbiensis* showed the greatest sensitivity.

Some species appear to have remarkable tolerance to cold, as shown by the fact that *A. beccarii tepida* withstood temperatures of −2°C. for at least 1 hr. 52 min. (not shown on Table 2). During this period, ice was crystallizing out on the water surface.

Longer periods of exposure will cause death at lower temperatures than the maximum instantaneous lethal points (Figure 2). The maximum lethal temperature decreases as the duration of exposure is increased.

Temperature history immediately prior to the experiments did not appear to have a significant effect upon the maximum instantaneous lethal temperature. Table 3 gives the results of three series of experiments

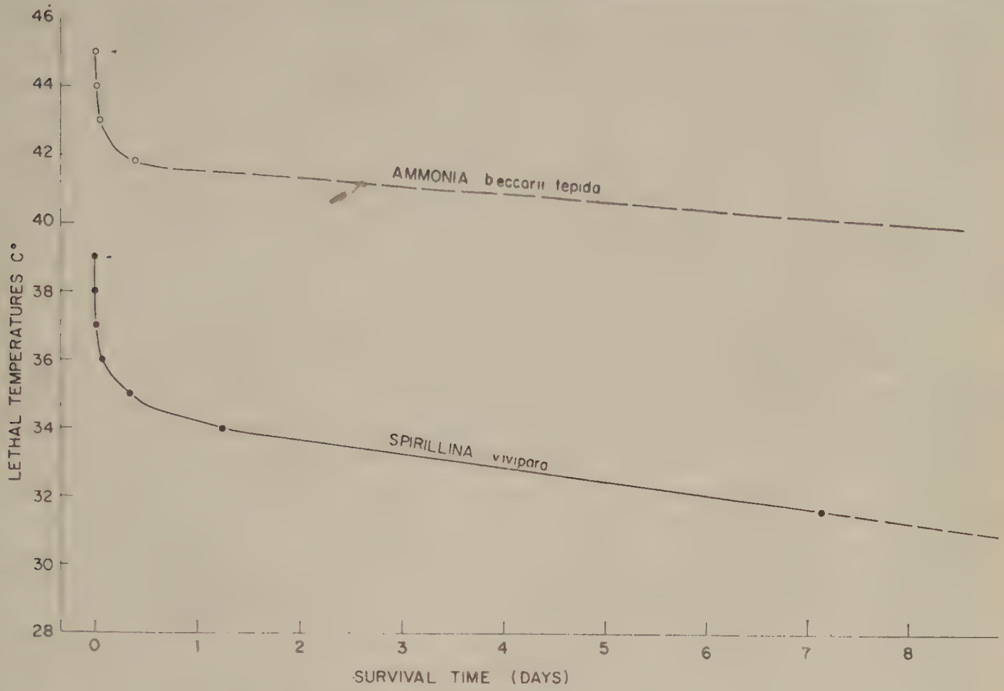

FIGURE 2

The relationship between temperature and duration of exposure in the determination of lethal temperatures. Each point represents the duration and temperature required to kill 50% of the specimens from each batch. The arrows indicate instantaneous lethal temperatures.

TABLE 3. The effect of previous temperature history (acclimation temperatures) upon the maximum lethal temperatures. *A. beccarii tepida* (Coos Bay strain).

Acclimation temperature (°C.)		Lethal point (°C.)			No. of specimens at each temp.	Temp. interval (°C.)
		0%	50%	100%		
Series I	15	<44	44	45	2	1
7-day acclimation	20	<43	43	44	2	1
	35	43	44	45	2	1
	15	42	42.5	43	2	1
Series II	20	<43.5	43.5	44	2	1
7-day acclimation	25	<42	42	43	2	1
	35	44	45	46	2	1
	15	43	43.5	44	2	1
Series III	20	<42	42	43	2	1
26-day acclimation	24-28	42	42.5	43	2	1
	35	<44	44	45	2	1

designed to determine whether temperature acclimation had occurred for cultures kept at temperatures of 15, 20, 25, 24-28 and 35°C. The Foraminifera were exposed for periods of from 7 to 26 days. Series II (Table 3) shows a difference of 3°C. in the maximum lethal temperatures of the highest and lowest of the acclimation temperature samples, but the irregularity of the data and the small number of specimens tested suggest that this is probably not a significant difference.

Salinity history (Table 4) prior to and during the test does not greatly influence the instantaneous lethal temperature, although minor differences are noted. The difference in the lethal point of 2.5°C. between specimens grown at 10 o/oo and 67 o/oo may be significant. The fact that 50 o/oo salinity appears to lower the lethal temperature is interesting but cannot be explained at present.

TABLE 4. Effect of salinity upon the maximum lethal temperatures for *A. beccarii tepida* (Coos Bay strain).

Salinity o/oo	Lethal point (°C.) 0%	50%	100%	No. of specimens at each temp.	Temp. interval (°C.)
10	<43	43-43.5	43.5	5	0.5
17	<43.5	43.5-44	45	5	0.5
27	<44.5-45	44.5-45	45	5	0.5
34	<44.5	44.5-45	45	5	0.5
50	<42.5-43	42.5-43	44	5	0.5
67	43.5	45.5-46	46	5	0.5

Reproductive Temperatures

A novel temperature gradient block for maintaining a wide range of temperatures has been designed by members of the microbiology department at the Scripps Institution of Oceanography. An adaptation suitable for Foraminifera cultures has been made. The device was constructed from a solid aluminum block with depressions bored at evenly spaced intervals to hold the culture dishes. By circulating water of different temperatures through channels at each end, a temperature gradient was set up across the entire block. In this way, eight different temperatures, with four cultures at each temperature, were obtained from only two constant temperature sources. Disposable plastic petri dishes 60 mm. in diameter were used as culture vessels. A small amount of water between the dishes and the aluminum block increased the heat flow.

In any one culture dish, the temperature was found to vary somewhat at various locations because the dish was of large enough diameter to permit temperature gradient across it also. The magnitude of this gradient and the constancy of the temperatures were determined by the use of a thermistor thermometer inserted at various locations in each dish and at various locations in the block. It was found that the temperature gradient across each dish usually amounted to less than 0.5°C. Similarly the extreme temperatures measured for the four equal temperature cultures did not vary more than ±0.5°C. from the value indicated by the central thermometer.

Reproductive temperatures were determined by culturing groups of specimens at closely spaced temperatures in the thermal gradient block and noting the percentage of individuals showing reproductive activity at each temperature. The reproductive temperatures for *A. beccarii tepida* are shown in Table 5. The lowest temperature at which reproduction occurred was 20°C., and the highest 32°C. Within this reproductive range (20-32°C.), temperatures from approximately 25 to 30°C. appear to allow a better chance for reproduction to occur, judging by the percentage of each batch undergoing reproduction. As their reproductive limits are approached, fewer and fewer of each batch appear able to reproduce. Generation time, or the time required from birth to the onset of a new generation,

TABLE 5. The influence of temperature upon growth and reproductive rate of *Ammonia beccarii tepida* (Coos Bay strain).

Temp. (°C.)	Mean growth rate (μ/10 day)	Generation time (days) Median	Range	Number Specimens	% Reproduction
15*	4	>280		8	0
15.2*	18	>68		10	0
16.7*	27	>55		10	0
18.0*	33	>50		10	0
19.0*	41	>44		10	0
20.0†	41	88	73-101	120	72
21.0*	48	>40		10	0
22.0	52	125	106-128	5	80
23.7	47	108	39-130	6	83
25.0†	72	38	35-49	10	88
25.2	37	76	44-99	5	100
26.6	41	65	56-109	5	80
27.9	49	44	37-87	5	80
29.7	41	47	47-56	5	100
30.0	84	33	26-35	19	67
30.6	21	121	86-121	5	80
32.0	22	121	121-121	5	20
35.0	0	∞		5	0

*Experiment terminated before occurrence of reproduction.
†Median values for more than one culture.

varies greatly within the reproductive range. Table 5 shows the median generation time to vary from a maximum of 88 days at a temperature of 20°C. to a minimum of 33 days at a temperature of 30°C. Median generation times of 125 and 108 days for temperatures of 22.0°C. and 23.7°C. respectively appear to be anomalous and, in view of the small number of specimens used, require verification. Above 30°C. the generation time again appears to show an increase until reproduction ceases entirely at temperatures above approximately 32°C.

Growth Rate

The effect of temperature upon individual rate of growth in *A. beccarii tepida* was determined by growing groups of specimens at standard temperatures of 15, 20, 25, 30 and 35°C. Additional data were obtained from the thermal gradient block set at narrower temperature intervals between 15 and 32°C. Since the growth rate is not uniform throughout the life of the individual, being fastest in young stages and slowing as maturity is reached, it is important to determine the growth rate in a standard manner. This was done by plotting the mean growth curve at each temperature and determining the slope during the steepest part of the growth curve.

The results of growth-temperature experiments for *A. beccarii tepida* are shown on Table 5. The mean growth rate (expressed in microns per 10 days) increased from a minimum value of approximately 4μ/10 days at 15°C. to a maximum of 84μ/10 days at 30°C. Above 30°C. there was a sharp decrease in rate until at temperatures above 32-35°C. growth ceased entirely.

Figure 3 illustrates selected growth curves for cultures of *A. beccarii tepida* from Coos Bay grown at various temperatures.

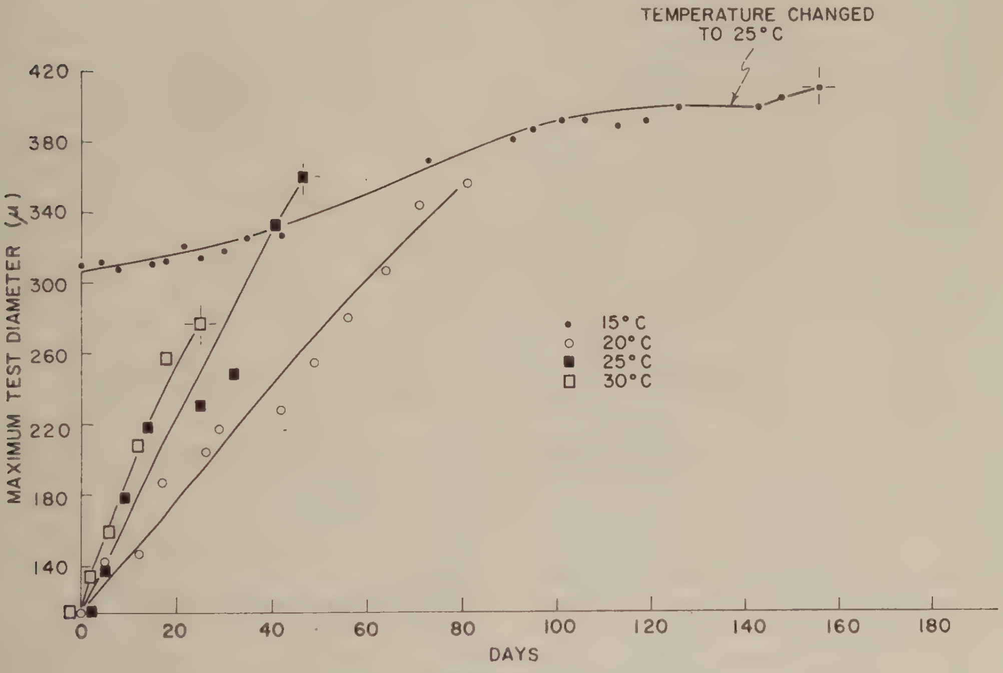

FIGURE 3

Growth of *Ammonia beccarii tepida* at different temperatures. The crosses indicate first occurrence of reproduction in culture.

Effect of Temperature upon Size

Figure 4 shows the effect of temperature upon the maximum diameter of tests at the time of reproduction. It will be noted that the largest tests were found at the lowest temperatures while the smallest occurred under the warmest conditions. A nonparametric method (Tate and Clelland, 1957, p. 78) of fitting the regression line and testing parameters showed a highly significant inverse relationship between temperature, at which the individuals had been living, and the maximum diameter of the test at the time of reproduction.

SALINITY EXPERIMENTS

General Statement

Relatively few species of Foraminifera are recorded from brackish and hypersaline water as compared to the large number found under normal marine condi-

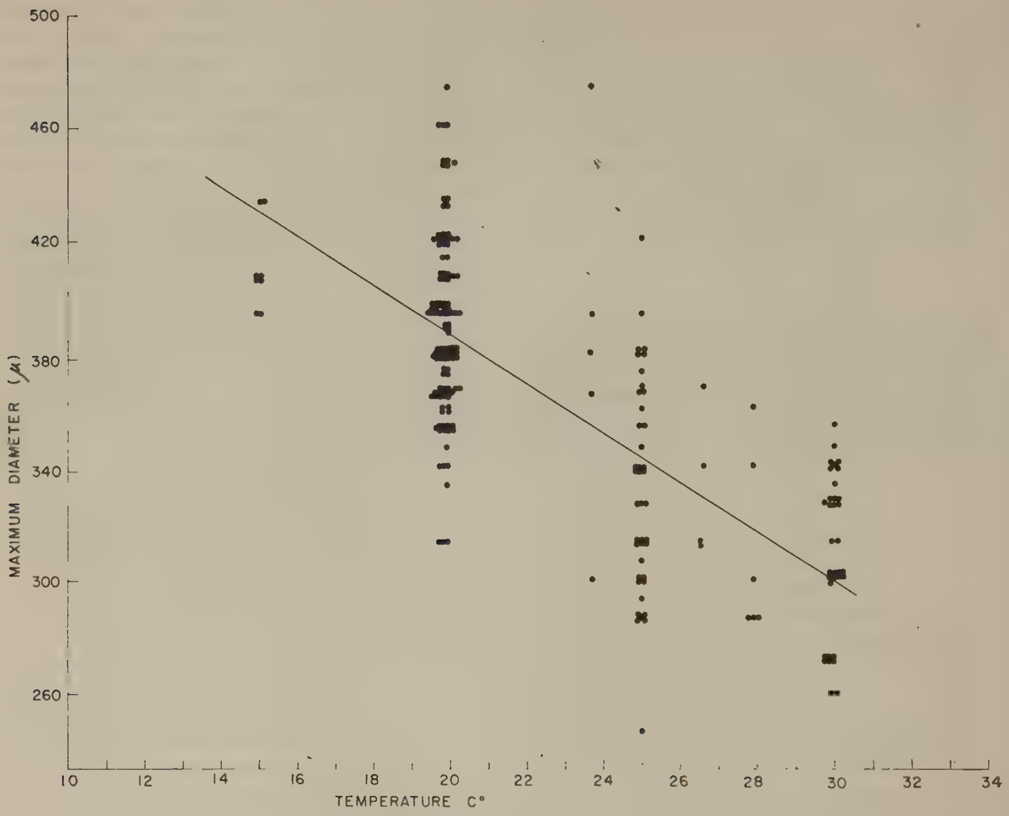

FIGURE 4

Relation between maximum test diameter and culture temperature for *Ammonia beccarii tepida* (Coos Bay population). Regression line drawn using nonparametric methods described in Tate and Clelland (1957, p. 78).

tions (Glaessner, 1947). This suggests that the salinity of the sea water may be a critical factor in limiting the distribution of many species. In the marine environment, lower than normal salinities are found in localities where fresh water from the land flows into the sea, such as river estuaries and polar seas. Land drainage is responsible for the slightly lower than normal salinities that are found along all except arid coasts.

Hypersalinities are uncommon in the ocean but are found in limited areas where evaporation exceeds precipitation. Thus, tropical seas tend to have slightly higher than normal salinities while some semi-enclosed lagoons have salinities of 50-80 o/oo and occasional values up to 155 o/oo (Pearse and Gunter, 1957). In addition, brackish and hypersaline environments commonly have widely fluctuating salinities.

Very few experimental data have been published on the ability of Foraminifera to survive either very high or very low salinities or on their ability to tolerate rapid salinity changes. Arnold (1954) stated that *Discorinopsis aguayoi* (Bermudez) could be grown in the laboratory in salinities from 20-57 o/oo but he did not note differences in growth rate within this range or determine lethal limits. Myers (1943b) found the upper limit of salinity tolerance for laboratory cultures of *Elphidium crispum* to be 48 o/oo but he also did not note whether this referred to inability to reproduce or to a direct lethal effect. Preliminary salinity studies have been published previously (Bradshaw, 1955, 1957). The following experiments were designed to furnish further evidence on the effect of different salinities upon growth rate and reproductive activity and also to develop new techniques for the study of salinity tolerance.

Salinities of less than 33.5 o/oo were prepared by diluting sea water with double-distilled water. Salinities greater than 33.5 o/oo were prepared by evaporating sea water to the desired concentration.

Lethal Salinities

Lethal salinities were determined by pipetting batches of Foraminifera directly from normal sea water to vessels containing 15 ml of sea water of the desired salinity. The specimens were kept at that salinity for specified time intervals, after which they were transferred back to normal sea water and allowed to recover. After allowing a time period for recovery (approximately 24 hours), the individuals from each sample were examined for evidence of life and the time required to kill one-half the batch was determined.

It was not possible to find an instantaneous lower lethal salinity for *A. beccarii tepida* on the same basis as was done for instantaneous lethal temperatures (e.g., 5-minute exposure) because this form was so tolerant of low salinities that it could even withstand direct transfer to distilled water for up to 32 minutes. For this reason, longer exposures were made. Table 6 shows the lower lethal salinities, determined on the basis of 12-hour exposures, required to kill one-half the batch of the forms listed.

TABLE 6. Minimum lethal salinities, determined on the basis of 12-hour exposures. Salinity interval is that interval between successive salinity values used for the experiment.

Species	Lethal point (o/oo)			No. of specimens at each salinity	Salinity interval (o/oo)
	0%	50%	100%		
Ammonia beccarii tepida (Coos Bay)	<2	<2	<2	2	2
Bolivina vaughani	13	7	3	4	3
Massilina sp.	10	10-7	7	4	3
Spirillina vivipara	17	7	7	4	3

Reproductive Salinities

The results of salinity experiments designed to determine the critical salinity for reproduction are shown in Table 7. Here it will be seen that reproduction has occurred at all salinities down to, and including, 15 o/oo. At the other extreme, earlier experiments (Bradshaw, 1957) on the same species from San Antonio Bay, Texas, showed no reproduction above salinities of 40 o/oo.

Within this reproductive range of approximately 15-40 o/oo, the length of time required for completion of each generation does not appear to be uniform. Table 7 shows the median generation time to be approximately 35 days at 34 o/oo, while at 15 o/oo 56 days were required.

Growth Rate

Figure 5 shows the rates of growth of *A. beccarii tepida* populations from Coos Bay, when cultured at different salinities. The highest rate of growth was found in cultures grown at normal salinities of 34 o/oo. Salinities of 8 o/oo allowed no growth. Slight growth was noted at 10 o/oo with gradually increasing rates of growth with increase of salinity up to 34 o/oo. The subsequent resumption of normal growth of the 8 o/oo and 10 o/oo cultures when returned to 34 o/oo sea water shows that there are no lethal effects at salinities of 8 o/oo over a two-week period.

Table 7 summarizes most of the data obtained on growth rate at different salinities. It will be noted that again, in general, the highest growth rates occur in cultures of normal salinity while the lowest rate is found where the salt content is least.

TABLE 7. Effect of salinity upon growth and reproductive rate of *A. beccarii tepida* (Coos Bay). Five specimens used at each salinity.

Salinity (o/oo)	Mean growth rate (μ/10 days)	Generation time (days) Median	Range	% specimens reproducing
34	90	35	29-56	100
25	32	82	56-96	80
17	51	47	43-56	60
15	41	56	43-87	80
13	14	∝		0
12	27	∝		0
10	4	∝		0
8	0	∝		0

Effect of Salinity on Size

Table 8 gives data on the effect of salinity upon the maximum size of tests of *A. beccarii tepida.* Salinity may influence size but the relationship is not as clear as it was for temperature. The largest specimens appear to have grown at the lowest salinities, while the smallest tests were produced under normal or slightly brackish conditions. A similar inverse relationship between size and salinity was found previously in specimens of *A. beccarii tepida* from San Antonio Bay, Texas (Bradshaw, 1957).

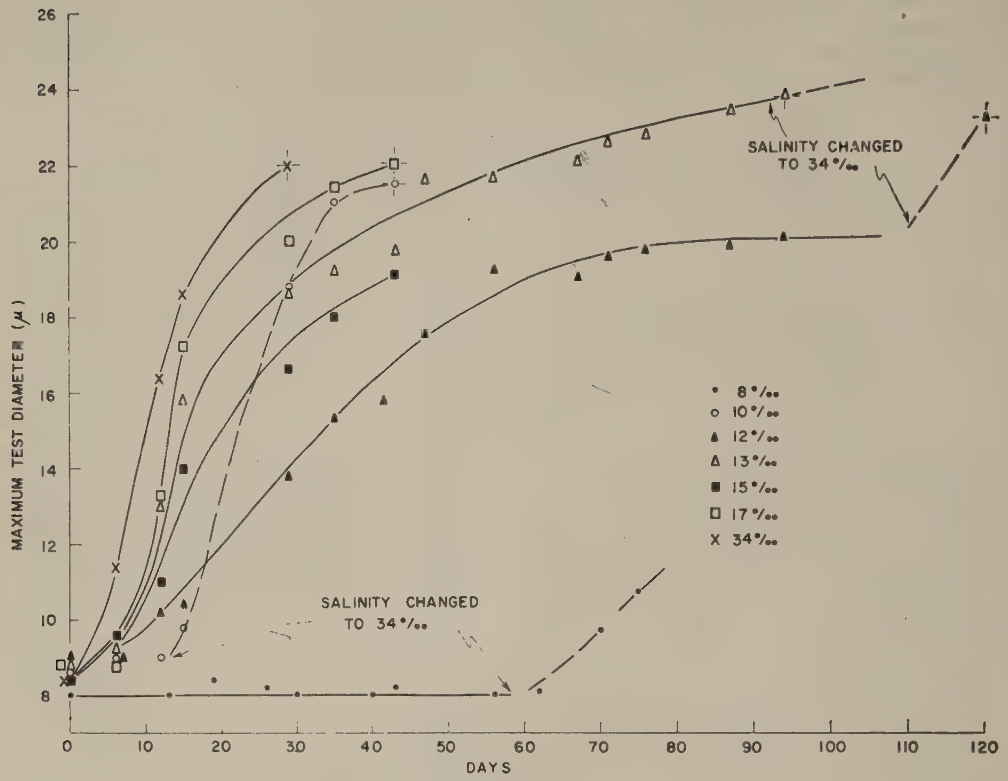

FIGURE 5

Growth of *Ammonia beccarii tepida* (Coos Bay population) at different salinities. The crosses indicate first occurrence of reproduction in culture.

TABLE 8. Effect of salinity upon mean test diameter at time of reproduction. *A. beccarii tepida* (Coos Bay).

Salinity (o/oo)	Max. test diameter (microns) Mean	Range	No. Specimens
34	305	280-340	9
25	290	260-340	4
17	340	230-400	35
15	340	250-392	4

FOOD EXPERIMENTS

General Statement

Food is obviously of importance for growth and maintenance of life, both for the individual and for the population. Very little is known of the food requirements of Foraminifera, either in nature or in the laboratory. They have been reported to feed upon a wide variety of food substances, including decaying vegetation, diatoms, flagellates, algal gametes, filamentous algae, organic debris, copepods and bacteria. The author knows of no field study comparing the natural distribution of a Foraminifera species with known food. Myers (1943b) studied the influence of food in localized natural populations of *Elphidium crispum*. Although he did not identify the particular food organisms or the amount utilized, growth and reproduction were found to parallel closely the phytoplankton cycle in the sea. Said's (1950) study comparing the concentration of Foraminifera with per cent nitrogen content of the sediments was an attempt to determine the role of food in Foraminifera distribution but the carbon or nitrogen content of the sediments will not necessarily indicate the amount of food available for Foraminifera. Many nitrogen compounds are highly refractory and cannot be considered as a food source. The food must be passive enough for the Foraminifera to catch with their relatively weak pseudopodia. Since the normal operation of the pseudopodia in benthonic Foraminifera is along a solid surface, suspended organic matter such as plankton or leptopel is of little value until it settles out. Bacteria undoubtedly play a role in nutrition but their relative importance is unknown.

The following experiments were designed to see if useful information could be obtained from laboratory food studies. A necessary condition for accurate nutritional studies is first to make the foraminiferal cultures bacteria free. Several attempts have been made by elaborate washing methods, whereby individual specimens are transferred through many dishes of sterile sea water. Apparently the numerous irregular surfaces on the Foraminifera provide shelter for bacteria so they cannot be washed off readily. Antibiotics have been used by some workers to rid protozoan cultures of associated bacteria. In the following food experiments the possibility of using antibiotics was tested in a parallel set of experiments.

Dunaliella sp., a green flagellate of approximately 8 μ diameter, was used for food. The algae were grown separately in 250-ml Erlenmeyer flasks in sea water enriched with earth extract, nitrate and phosphate. Twice weekly, approximately 25 ml of this stock food culture was centrifuged, and the cells resuspended in sterile sea water. In this way possible adverse effects of metabolites in the *Dunaliella* medium were avoided. The cells were killed by heating to 50°C. and the number per ml was determined by counting in a hemocytometer. Five specimens of *A. beccarii tepida* (Coos Bay) with an average diameter of 281 μ were placed in separate petri dishes (60 mm diameter) of sterile sea water containing 15 ml of media and kept at 25°C. throughout the course of the experiments. The following number of *Dunaliella* were added to each dish of one set of cultures: 0; 55,000; 110,000; 220,000; 440,000 and 880,000 cells. In a parallel experiment, 1400 units of penicillin G and 1.5 mg streptomycin were added in addition to the food. The resultant concentration of penicillin and streptomycin per ml of culture medium was 72 units and 83 μg respectively. Twice weekly, each specimen was transferred to fresh sea water medium, measured and fed.

Results

Figure 6 and Table 9 show the results of the food experiments. It will be noted (Table 9) that the specimens treated with penicillin showed a slightly higher rate of growth than the untreated specimens. The presence of penicillin, however, appeared to increase the time necessary to attain reproductive maturity. The median reproduction intervals (Table 9) show that in each instance where reproduction occurred the specimens that were not treated with antibiotic reproduced before the treated individuals.

When the effect of food apart from the influence of antibiotics is considered, it will be seen that the rate of growth is increased with additional food. Food concentrations below approximately 220,000 cells per culture do not allow any growth or reproduction. As the

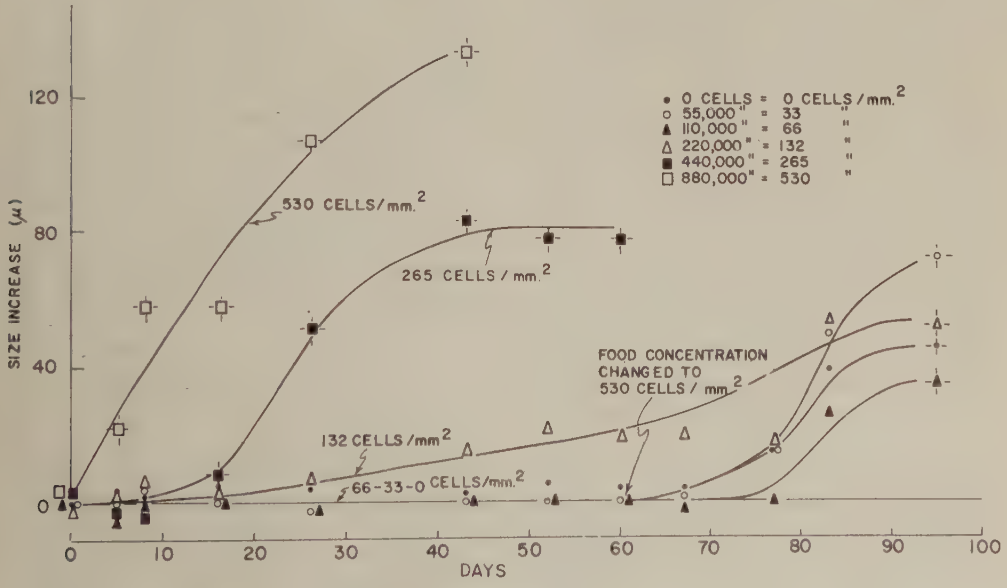

FIGURE 6

Growth of *Ammonia beccarii tepida* (Coos Bay population) fed different concentrations of food (*Dunaliella* sp.). The crosses indicate reproductive activity. Average size (maximum diameter) of specimens at beginning of experiment, 288 μ. mm² = surface area grazed.

TABLE 9. Effect of different concentrations of food (*Dunaliella* sp.) and treatment with antibiotics upon growth rate and reproductive interval of *A. beccarii tepida* (Coos Bay). Five specimens used for each experiment (average diameter 281 μ).

Food concentration No. cells per dish (15 cc)	Growth rate (μ/10 day)	Reproduction interval (days) Median	Range	% reproduction	% mortality
0	0	∝		0	20
0*	0	∝		0	100
55,000	0	∝		0	40
55,000*	0	∝		0	100
110,000	0	∝		0	0
110,000*	0	∝		0	80
220,000	4	95	43-122	60	40
220,000*	48	∝		0	80
440,000	8	34	16-60	80	20
440,000*	68	95	26-95	40	0
880,000	68	8	5-43	100	0
880,000*	82	43	16-95	100	0

*72 units penicillin and 83 μg streptomycin added per ml culture medium.

food supply was increased above this limiting value of 110,000 - 220,000 cells, the growth rate increased until the maximum food concentration given in this experiment (880,000 cells) was reached.

The results of the food experiments show that a food concentration of at least 220,000 cells per dish is necessary for minimal growth and reproduction. Assuming that all the food cells settle out on the dish bottom and sides, this is equivalent to approximately 112 cells/mm^2 of surface of the culture dish. Table 9 shows that a food concentration one-half this value (110,000 cells or 56 cells/mm^2) is apparently too low to support any growth or reproduction. Although this food concentration is too low for growth, it yields enough energy to keep the specimens alive for at least 60 days. Figure 6 shows that at the end of this time when a food concentration of 880,000 cells (450 cells/mm^2) was added, growth resumed and ultimately reproduction occurred. Even the complete withholding of food for a period of at least 60 days did not cause death, although growth was halted. When food was again added, growth did not occur immediately, but 1 to 2 weeks elapsed before normal growth resumed. At the end of 60 days of fasting, the protoplasm in each of the specimens had contracted into the earlier chambers leaving the last 4 to 6 chambers empty. One week after feeding, the protoplasm had resumed its normal size but a further period of approximately one week was needed to show renewed growth.

Growth rate and reproductive efficiency appear to increase with the continuous addition of food, at least to the maximum value of 880,000 cells or 530 cells/mm^2 supplied in the experiment. The effect of food concentrations higher than this was not determined. It is possible that a large excess of food might be deleterious because of the high bacterial concentrations that occur when food decomposes.

The effect of food upon reproductive activity may be estimated by the percentage of individuals completing reproduction at each food concentration and by the time period required for reproduction to occur. Table 9 shows that in both the penicillin-treated and the untreated cultures the percentage of inidividuals completing reproduction increased with the addition of food and that the reproduction interval decreased.

PRELIMINARY pH EXPERIMENTS

Although the range of pH in the open sea varies from approximately 7.5 to 8.5, in marine bottom deposits, tide pools, bays and estuaries the pH may exceed 8.5 or fall below 7.0 (ZoBell, 1946). Values of pH of 9.0 are common in localized regions of high plant production such as in tide pools or in dense phytoplankton blooms. Values as high as 10.0 have been noted by Moore (1958) resulting from the photosynthetic activity of *Ulva* in tide pools. Carpelan (1957) has reported pH values as high as 9.8 from salt ponds in San Francisco Bay. These recorded values suggest that under certain conditions, at least, the pH may have an effect upon the Foraminifera.

Solutions of different pH values were prepared by adding concentrated HCl or NaOH to sea water until the desired pH was reached. Individual specimens of *A. beccarii tepida* were pipetted from their normal media (pH 8.1) to the various pH solutions for specified periods of time. After exposure, the specimens were transferred back to their original media and allowed to recover.

The results of the pH experiments (Table 10) show that as the pH becomes increasingly basic or acidic the survival time is decreased. At a pH of 2.0, *A. beccarii tepida* can survive for a period of 25 minutes to 1 hour 15 minutes. A preliminary experiment on *Spirillina vivipara*, on the other hand, shows that it may be more sensitive to low pH, as is indicated by its much shorter survival time (2-6 minutes).

It was noted during the course of the pH experiments that it was possible under sublethal conditions to dissolve the $CaCO_3$ test and yet not kill the specimen. This observation was made on both *Spirillina vivipara* and *A. beccarii tepida*. Individuals of *A. beccarii tepida* that had been left in sea water with a pH of 2.0 for 5 minutes showed slight dissolution of the later chambers. Specimens left for 10 minutes under these conditions showed dissolution of their last 4 chambers, while 15 and 25-minute exposures resulted in dissolution of all the $CaCO_3$, with nothing but a thin chitinous membrane remaining to show the outline of the test. At the end of all these exposures, however, normal streaming of the protoplasm was still evident. Two days later all the individuals exhibited normal pseudopodial activity, except for the specimens exposed for 25 minutes. Here the only indication of life was a faint movement in the earlier chambers. Twenty-four hours later protoplasmic movement had extended throughout the entire cell. The three specimens with major shell solution showed no indication of recalcification by the second day, but 24 hours later the specimen which had lost its four distal chamber walls showed replacement of the calcareous covering. While the specimens were being transferred from the acid media, the later chambers were somewhat damaged in the process and consequently the chambers were recalcified in an abnormal manner. Three weeks later, of the three specimens which had showed signs of solution, all appeared to be in normal condition and two had reproduced.

TABLE 10. pH tolerance of *A. beccarii tepida*. Time required to reach 50% mortality at indicated pH levels.

pH	No. drops conc. HCl or NaOH per 100 ml medium	Survival time	No. Specimens
2.0	10		
2.0	8	25 min. - 1 hr. 15 min.	1
2.0	3	>5 min.	1
2.4	2	>1 min.	1
3.2	1	>25 min.	1
8.1	0		10
8.5	0.5	>13 hr. 15 min.	2
8.9	1	>13 hr. 15 min.	2
9.0	4	>64 hr. 45 min.	4
8.8	4	>14 hr.	4
9.1	5	>14 hr.	4
9.1	6	>37 hr. 30 min.	2
9.3	7	>42 hr. 30 min.	2
9.5	8	14 hr. - 37 hr.	8
9.9	9	<14 hr.	4
10.0	10	<14 hr.	2

PRELIMINARY HYDROSTATIC PRESSURE EXPERIMENTS

The presence of faunal depth zonation in the sea has stimulated much speculation as to its cause. The direct relationship that exists between depth and pressure suggests that hydrostatic pressure may be a limiting factor in this zonation. Since the range of pressure found in the sea varies up to 1000 atmospheres, it seems probable that there may be specific differences in pressure tolerance over such a wide range of values. Regnard (1891), Fontaine (1930), and Oppenheimer and ZoBell (1952) have studied pressure effects upon organisms ranging from crustaceans to bacteria. They found that marked physiological changes occurred with increased pressure, the effects depending upon the species studied. Some species, particularly shallow-water forms, are killed by pressures approaching those found in abyssal water. It appears likely that those species living at great depths must be especially adapted for life at high pressures and that their biochemistry may be very different from shallow-water forms.

There is no information concerning the effect of pressure upon the Foraminifera. In order to see if a pressure relationship exists for the Foraminifera similar to that found for other forms, a series of experiments was conducted on a nearshore species, *A. beccarii tepida* (Coos Bay) .The apparatus described by ZoBell and Morita (1959) was used to develop the required pressures. Five specimens were selected at random, measured, and transferred to small test tubes (10x50 mm) completely filled with sea water. The tubes were plugged with neoprene stoppers, care being taken to ensure the complete removal of air bubbles. Duplicate tubes were placed in cylinders at the following pressures: 1, 100, 200, 400, 500, 800, and 1000 atmospheres. Duplicate samples also were placed in 60-mm plastic petri dishes at one atmosphere and kept at 25°C. as a control. The cylinders were left at the indicated pressures for 3 and 8 days at a temperature of 25° ± 0.5°. After this period the specimens were removed from the test tubes, measured and allowed to recover at atmospheric pressure.

The results of the hydrostatic pressure experiments are shown in Table 11. All the *A. beccarii tepida* specimens withstood pressures as high as 400 atmospheres for 3 days, but pressures of 1000 atmospheres were sufficient to kill all individuals within this same time period. Specimens subjected to longer exposures (8 days) also showed lethal effects at pressures greater than approximately 400 atmospheres. The greater mortality shown for specimens at 8-day exposures as compared to those at 3-day exposures suggests the lethal effect of prolonged exposure to pressures which could be successfully withstood for shorter periods.

Growth was slowed considerably while the specimens were kept under these experimental conditions. It was not possible to attribute this decrease in growth entirely to pressure effects, however, since the specimens in the pressure cylinder at one atmosphere also showed negligible growth when compared to the control group. Upon removal from the cylinders, the growth rate of the survivors increased, the specimens which had been subjected to the lowest pressures growing faster than the individuals kept at higher pressures.

TABLE 11. Pressure tolerance of *A. beccarii tepida* (Coos Bay). A and B represent two different experiments; + represents relative growth.

Pressure (atmospheres)		3-day exposure			8-day exposure		
		% survival	Growth	No. Specimens	% survival	Growth	No. Specimens
0	(control)	100	+++	10	100	+++	10
0	A	100	+	10	80	0	5
0	B				90	0	10
100	A	100	+	10	100	0	10
200	A	100	0	10	60	+	10
200	B				100	+	10
400	A	100	+	10	65	0	10
500	B				0	0	10
800	B				0	0	10
1000	A	0	0	5	0	0	10

OXYGEN CONSUMPTION EXPERIMENTS

Respiration is a basic mechanism affected by environmental factors and the rate of oxygen consumption is a valuable index of growth and other activity. Rate of respiration provides another convenient measure of the quantitative effect of various environmental factors. Thus, oxygen consumption might be expected to correspond more or less closely to growth and hence provide a measure of the latter. In this way, information on the effects of environmental factors might be obtained in a short time that would take weeks with usual growth experiments. In addition, there is a possibility of obtaining ecological information from delicate species that so far have resisted attempts to culture in the laboratory.

A very sensitive micro-respirometer technique devised by Scholander *et al.* (1952) was used to measure the oxygen consumption of individual specimens of Foraminifera. The method is essentially a manometric technique that is based on the measurement of the pressure change required to keep an air bubble a constant volume while an organism is consuming oxygen from it. The general method and techniques described by Scholander *et al.* (1952, 1958) have been followed. Close temperature control in this technique is extremely important. In the following experiments, temperatures were kept to within ± 0.01°C. of the required value by the use of a specially designed water bath.

Because of the relationship of oxygen consumption to size, the maximum diameter of the test was measured prior to each experiment and the same individual was used when comparing the effect on respiration by any factor.

The effect of temperature upon respiration was studied by measuring the oxygen consumption of the same individual over a wide temperature range. In the following experiments the oxygen consumption was first determined for the lowest temperature (10°C.), after which the bath temperature was raised by successive 5° increments and the oxygen consumption measured at the end of each increment. Approximately 10 minutes were required after each temperature change for the system to equilibrate. After this equilibration period, 10 to 20 minutes were usually adequate to yield a reliable oxygen consumption curve.

Results

Figure 7 shows the pressure changes in the microrespirometer caused by the respiration of a single specimen of *A. beccarii tepida*. The straight line portion of the curve, representing a constant rate of oxygen consumption, was used for the determination of oxygen consumption. In most cases the oxygen consumption experiments were terminated while still in the linear portion of the graph. Figure 7 shows the situation that occurs when a specimen is left in the respirometer for a longer period of time. The pressure, which is proportional to the oxygen tension, first falls at a steady rate until it reaches a certain point, after which the rate of decrease becomes less until it finally ceases altogether at a particular oxygen tension. At a relatively high partial pressure the rate of consump-

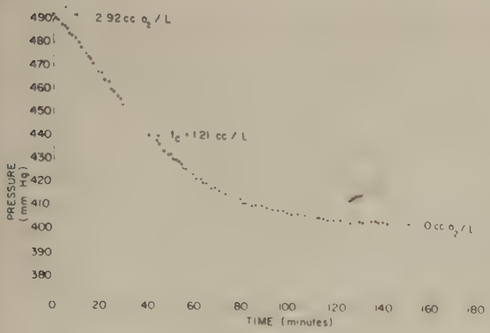

FIGURE 7

Pressure changes in micro-respirometer caused by respiration of a single specimen of *Ammonia beccarii tepida* (Carlsbad population). Maximum test diameter 288 μ; Salinity 25 o/oo; temperature 26.0°C. t_c represents critical oxygen tension. Change of 1 mm. pressure is equivalent to 23.8 μμl O_2.

tion was independent of the oxygen concentration but below a certain partial pressure the rate of consumption was in part dependent upon the oxygen concentration.

The point at which the curve begins to show oxygen dependence has been termed the "critical oxygen tension" (Bishop, 1950). The critical oxygen, t_c, is an important index of ability to survive in environments of low oxygen. A species with a low t_c may be able to survive indefinitely in water of low oxygen concentration, whereas a species with a high t_c requires a higher concentration. If it is assumed that the point of no oxygen consumption represents the point at which all the oxygen has been exhausted from the water, the oxygen concentration at any pressure during the experiment can be calculated, since the rate of oxygen uptake is known. In this manner the critical oxygen tension for the species portrayed in Figure 7 was found to be 1.21 cc oxygen/liter.

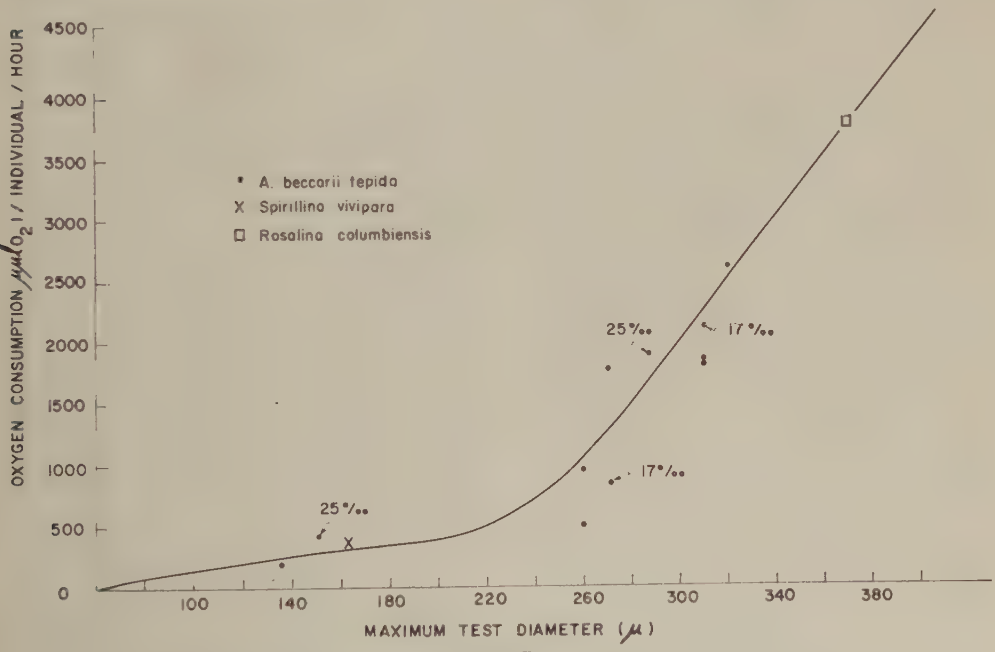

FIGURE 8

Effect of size (maximum diameter) upon oxygen consumption per individual. Temperature 26.0°C; salinity 33.5 o/oo unless otherwise indicated.

Figure 8 shows the relationship between maximum test diameter and oxygen consumption for the three species examined. It will be noted that under equivalent conditions there appeared to be a direct relationship between size and oxygen uptake with the result that the larger individuals (and species) consumed oxygen at a more rapid rate than did smaller individuals (or species).

Figure 9 shows the effect of temperature upon oxygen consumption in *A. beccarii tepida*. The oxygen consumption rose gradually from low values between 10-15°C. to a maximum between temperatures of 35-40°C. Above 40°C. oxygen consumption decreased rapidly until death at approximately 45°C.

The relationship between size and oxygen consumption found in the present study agrees with Zeuthen's (1947) study of the relationship between size and activity for many animal groups. The values obtained at 25°C. for oxygen consumption (2500 - 8000 μμl O_2

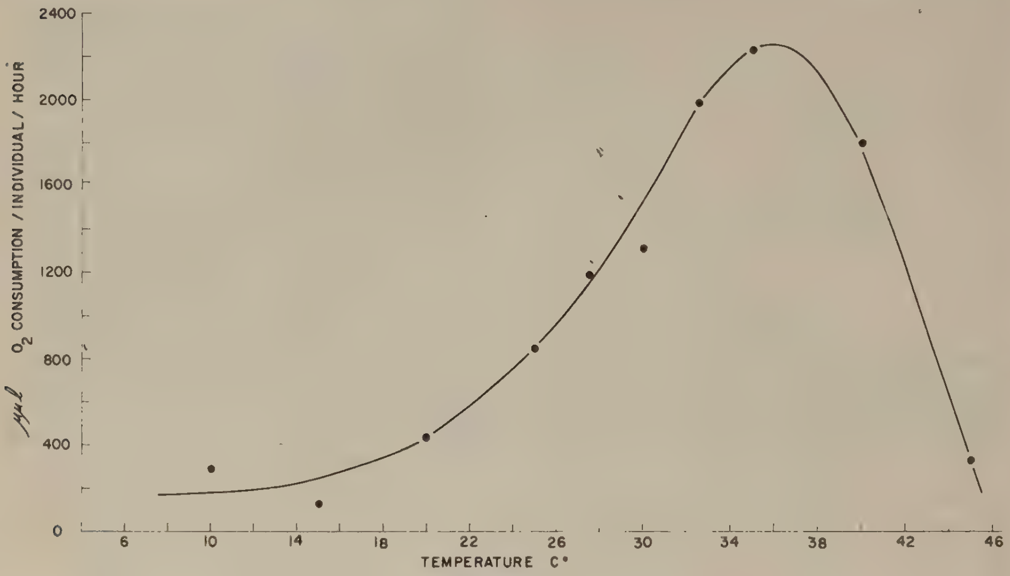

FIGURE 9

Effect of temperature upon oxygen consumption of one specimen of *Ammonia beccarii tepida* (Coos Bay Population). Maximum test diameter 245 μ; Salinity 33.5 o/oo.

per individual per hour) agree in general with values reported for other protozoan types (Bishop, 1950).

The increase of oxygen consumption with temperature is well known for many organisms and may be expressed in terms of a temperature coefficient, Q_{10}. This is the ratio of the rate of activity at any temperature to the rate at a temperature 10° lower. For most biological processes it varies from 2-4 over most of the biological temperature range (Bishop, 1950). The Q_{10} for the oxygen consumption of *A. beccarii tepida* over the range from 10-35°C. (figure 8) is approximately 3.2.

The maximum oxygen consumption occurred at approximately 35°C. This is approximately 5°C. higher than the temperature for maximum growth and reproductive rate for the same species, as shown in Table 5 and Figure 3. This type of discrepancy between maximum activity rates and maximum oxygen consumption was noted by Fry (1947). He found that metabolism, as measured by rate of oxygen consumption, does not give a direct measure of an activity, such as growth or reproductive rate. The important metabolic measure of activity is the difference between the maximum and minimum metabolic rates, but not any single rate. This is illustrated by data showing the temperature relationship between active and standard metabolism in the goldfish (Fry, *op. cit.*). Standard metabolism appears to increase with temperature right up to the lethal level, but the maximum oxygen consumption (active metabolism) shows a peak at about 30°C., apparently representing the extreme capacity of the system involved. Fry (*op. cit.*, fig. 24) believes the difference between the two oxygen consumption curves approximates the metabolism available for external work. If this is true, a temperature of approximately 28°C. should correspond to an optimum temperature for many activities of the goldfish. For this form, the relation of cruising speed to temperature does indeed show a maximum at about this point.

The concept of the optimum, derived from the relationship of metabolism to activity, advanced by Fry (1947), promises to be a useful tool in laboratory study of environmental relationships. A major difficulty to be overcome is the development of a method whereby the active metabolism of Foraminifera can be measured.

DISCUSSION

The results of the temperature experiments clearly show the effect of temperature upon such ecologically important characteristics as survival, growth and reproductive rates when other variables such as salinity, pH, etc., are held constant. The observation that acclimation to various temperatures did not cause highly significant changes in the lethal temperatures is of considerable interest. It indicates that the ability of Foraminifera to tolerate high temperatures may be an inherent genetic trait that is not subject to great environmental variation. This finding was surprising in view of the widespread evidence showing considerable temperature acclimation for many invertebrate species (Bullock, 1955). The variability of the data (Table 3), however, suggests that if more specimens had been used, a small amount of acclimation might have been noted. Further studies are needed to establish this point. The apparent ability of previous salinity history to influence the lethal temperature is also of ecologic significance. Similar observations showing that hypersaline conditions enable many organisms to tolerate high temperatures have been reported by Gunter (1957).

Although the concept of an instantaneous lethal temperature (or salinity, etc.) appears to offer a useful and reproducible index of ability to tolerate extreme conditions, it may have little direct application to nature. Temperatures of 45°C. acting for 5 minutes and even long exposures to temperatures slightly above the upper incipient lethal temperature, which have been shown to kill *A. beccarii tepida*, are probably rarely experienced by this species in its natural habitat. Probably of much greater importance to the survival of the species is the relationship of the more usually experienced environmental levels to vital activities such as reproduction and rates of development. Although *A. beccarii tepida* has been shown in the laboratory to have a wide range of tolerance to both temperature and salinity, it will reproduce only within a temperature range of approximately 18-30°C. and between salinities of approximately 13-40 o/oo.

In nature, this species is found throughout the tropic and temperate regions but does not occur in the cold water north of Bergen, Norway and the Faroe Islands (Nørvang, 1945), or in Alaska (Tappan, personal communication). Throughout this area, *A. beccarii tepida* appears to be a euryhaline, shallow-water species that has not been recorded *living* at depths where the temperature is usually below its lower reproductive limit. (Recorded occurrences in deeper water do not include specimens known to be living *in situ*.) The overall latitudinal distribution of this particular species, therefore, appears to be largely governed by prevailing temperature conditions. Within these wide limits, however, the influence of other factors such as salinity, pH, etc., or competition with other species may serve to exclude this form from localized areas.

The relationship of environmental factors to size is of considerable interest. Experiments with *A. beccarii tepida* have shown a greater increase in size for specimens grown under colder conditions 15-20°C. than for those grown under warmer temperatures 25-30°C. In nature, Nicol (1944) and Parker (personal communication) have reported finding larger specimens of other Foraminifera species from the colder higher latitudes of their ranges. The difference in size of the tests of *Elphidium crispum* throughout its range was so extreme that Nicol divided it into two subspecies, the northern group having larger tests. Gunter (1957) has summarized observations of many different organisms in the natural environment, showing a similar inverse relationship between size and temperature. The relationship between salinity and size (Table 8 and Bradshaw, 1957), while not so marked, nevertheless shows that the smallest tests were found under the optimal salinity. The above observations suggest that larger tests within the range of a species do not represent optimal environments, as commonly assumed, but possibly represent marginal environmental conditions. Under these marginal conditions reproductive maturity is delayed and the individuals continue to grow in size.

The effect of salinity upon such ecologically important factors as survival, reproduction rate, and rate of growth as determined in laboratory cultures suggest that a corresponding effect might be expected in natural environments. The fact that relatively few species have been recorded from natural brackish areas is apparently explained by the experimental results. The species that do occur and flourish in brackish situations are those that are adapted to survive, grow and reproduce under conditions that are adverse to other species. A comparison of *A. beccarii tepida* and *Massilina* sp. will illustrate this difference in adaptability. *A. beccarii tepida* survived salinities as low as 2 o/oo for periods of at least 12 hr (Table 6). *Massilina* sp., however, died when exposed to salinities of 7 o/oo for the same period. A similar lack of tolerance to decreased salinity has been observed in other open-ocean species (Table 6).

The results of the food experiments agree with the observations of Myers (1943b) and Bradshaw (1955) that when adequate food is available growth is continuous and rapid but is retarded when food is sparse. It has been assumed that all the energy for growth has come from the *Dunaliella* sp. supplied for food. At 25°C., the breakdown of algal cells was relatively rapid so that in the 3-4 day interval between feedings a certain percentage of the algae had already broken down. The percentage of material thus transformed into unusable, dissolved organic matter and/or into bacteria is unknown. Presumably some of the bacteria are ingested but proof of their value as food is lacking.

The presence of penicillin and streptomycin caused no apparent ill effects to *A. beccarii tepida*, at least for short periods of time. Long-continued use of antibiotic at these concentrations, however, coincided with a slackening of growth and increased mortality in some cultures (Table 9). Dense growths of fibrous molds surrounding the specimens were noted in the penicillin-treated cultures by the twenty-sixth day of the experiment. No molds were observed in the untreated dishes. Attempts to clean away the contaminant failed and the mold continued to persist as long as the antibiotics were present. When antibiotic treatment was discontinued, the mold eventually disappeared but most of the specimens did not recover. The eventual dominance of molds when the associated bacteria are inhibited is well known. It is possible that it was the direct or indirect influence of the mold and not the presence of antibiotics that contributed to the delayed maturity and death of the Foraminifera specimens.

The pH experiments indicate that the species of Foraminifera tested were relatively highly resistant to pH changes. Values of pH as low as 2.0, for example, are probably never found in the marine environment, yet *A. beccarii tepida* could withstand such an extreme value for more than 25 minutes. The ability to resist low pH values appears to vary between different species. *A. beccarii tepida* can tolerate the same pH (2.0) for a much longer period of time than can *Spirillina vivipara.* The normal habitat of *Spirillina* is reported to be in the open ocean from depths of 0 to 300 meters, where little change of pH is expected, whereas *A. beccarii tepida* is characteristic of near-shore areas and shallow bays and lagoons where it may occasionally experience low pH.

Reliable data on the distribution of pH in natural environments are meager. Stevenson and Emery (1958) report a series of pH values of water and surface sediment from their study of plant communities in the marsh at Newport Bay, California, as follows:

	Tidal Stage	
Zone	High	Low
Water	7.88	7.78
Tidal flat	7.24	7.64
Spartinetum	6.73	7.62
Salicornietum	6.88	7.10

The pH decreased with distance from the marsh edge and with an increase in percentage of organic matter. If pH values less than 7.8 do indeed dissolve calcareous tests (Krumbein and Garrels, 1952), the above observed pH values must be an important control upon the distribution of species living under such conditions. Parker and Athearn (1959), in a study of marsh Foraminifera in Poponesset Bay, Massachusetts, noted that the calcareous species from surface sediment were represented for the most part by living specimens and that very few empty tests were found. Stevenson and Emery (1958) found that the surface of the Newport marsh was littered with *Cerithidea californica,* both living and dead. These gastropods, however, were found only on the surface and in the upper 5 mm of the soil. No remains were found below this layer down to the underlying sand. These observations suggest that pH values sufficiently low for test solution occur below the sediment surface but that pH values in the living micro-environment of the species are within the normal range for existence of $CaCO_3$. The author knows of no measurements showing the detailed vertical distribution of pH for the uppermost layers of sediment and across the sediment-water interface. Values of pH derived in the usual manner by insertion of electrodes deep into the sediment and from sediment slurries may not be representative of those of the actual micro-environment of the Foraminifera.

It is of interest that the experiments showing complete lack of tolerance for hydrostatic pressures greater than approximately 400 atmospheres and lethal effects at lower pressures agree, in general, with reports of other workers studying other organisms.

Regnard (1891), the first to study effects of hydrostatic pressure on organisms, found that fermentation of sugar by yeast, while normal at 400 atmospheres, was stopped at 600 atmospheres and that trout eggs which hatched normally at pressures of 300 atmospheres were destroyed at pressures of 400-650 atmospheres. *Paramecia* and other ciliated protozoans withstood pressures to 300 atmospheres but became immotile at 400-600 atmospheres. Salmon eggs exposed for six hours to pressures of 200 atmospheres developed normally but were inhibited at 300 atmospheres and stopped development at 400 atmospheres.

Studies of the effect of hydrostatic pressure on *Amoeba* are of particular interest because of their similarities to Foraminifera. Marsland and Brown (1936), using a special pressure cylinder with a glass window, found that pseudopodial movement in *Amoeba* ceased at 250 atmospheres. With increase in pressure, no further effect was noted until 450 atmospheres when the pseudopodia suddenly retracted and the specimen became spherical. A one-hour exposure at pressures above 300 atmospheres was lethal.

From the evidence presented, it appears that the protoplasm of normally shallow-living forms is destroyed, or at least inhibited, by pressures found at abyssal depths. The protoplasm of Foraminifera found in deep water, therefore, must be especially adapted for life at high pressures. In this regard, Phleger (1960) has suggested that the Foraminifera faunal boundary existing at 2000 meters may be due to a "pressure threshold" at 200 atmospheres pressure. Oppenheimer and ZoBell (1952) found that many shallow-water bacteria were intolerant of pressures exceeding 200 atmospheres. They suggested that the physiological action of pressure was through its effect on solubilities and dissociation constants and on pH and Eh values. Nicol (1960, p. 24) summarizes present knowledge on the physiological effect of hydrostratic pressure as follows: "At high pressures protein molecules are compressed, denatured and altered in structure and chemical activity. In the ocean depths two factors, low temperatures and high pressures, both of which affect the rate of biological processes, are acting concomitantly, and the animals of the abyss must be genotypically modified to withstand the conditions obtaining there."

Experiments thus far have only concerned pressure tolerance and have not furnished information on more sensitive growth and reproductive activities. Nevertheless, the results with Foraminifera and other organisms show that hydrostatic pressure may be of the greatest importance in determining the faunal composition of the deep sea.

REFERENCES CITED

Andrewartha, H. G. and Birch, L. C., 1954, The distribution and abundance of animals: University of Chicago Press, Chicago, Ill., 782 pp.

Arnold, Z. M., 1951, Occurrence of *Gromia oviformis* Dujardin in California: Wasman Jour. Biology, vol. 9, pp. 351-353.

———, 1954, *Discorinopsis aguayoi* (Bermudez) and *Discorinopsis vadescens* Cushman and Bronnimann: A study of variation in cultures of living Foraminifera: Contr. Cushman Found. Foram. Research, vol. 5, no. 1, pp. 4-13.

———, 1955, Life history and cytology of the foraminiferan *Allogromia laticollaris:* Univ. Calif. Publications in Zoology, vol. 61, pp. 167-252.

Bishop, D. W., 1950, Respiration and metabolism, *in* Prosser *et al.*, Comparative animal physiology: N. B. Saunders Co., Philadelphia, pp. 209-289.

Bradshaw, J. S., 1955, Preliminary laboratory experiments on ecology of foraminiferal populations: Micropaleontology, vol. 1, pp. 351-358.

———, 1957, Laboratory studies on the rate of growth of the foraminifer "*Streblus beccarii* (Linné) var. *tepida* (Cushman)": Jour. Paleontology, vol. 31, no. 6, pp. 1138-1147.

Bullock, T. H., 1955, Compensation for temperature in the metabolism and activity of poikilotherms: Biol. Reviews, vol. 30, pp. 311-342.

Carpelan, L. H., 1957, Hydrobiology of the Alviso salt ponds: Ecology, vol. 38, no. 3, pp. 375-390.

Doudoroff, P., 1942, The resistance, reactions, and acclimatizations of some marine fishes to changes of temperature, Pt. I. Experiments with *Girella nigricans* (Ayres): Biol. Bull., vol. 83, pp. 219-244.

Fontaine, M., 1930, Recherches expérimentales sur les réactions des êtres vivants aux fortes pressions: Annal. Inst. Oceanogr., vol. 8, 100 pp., 16 figs.

Fry, F. E. J., 1947, Effects of the environment on animal activity: Publ. of Ontario Fisheries Research Laboratory, no. 55, Univ. of Toronto Press, Toronto, pp. 5-62.

Glaessner, M. F., 1947, Principles of micropaleontology: John Wiley & Sons, Inc., 296 pp.

Gunter, Gordon, 1957, Temperature, *in* Treatise on marine ecology and paleoecology: Geol. Soc. America Mem. 67, vol. 1, pp. 159-184.

Hutchins, L. W., 1947, The bases for temperature zonation in geographical distribution: Ecol. Monographs, vol. 17, pp. 325-335.

Krumbein, W. C., and Garrels, R. M., 1952, Origin and classification of chemical sediments in terms of pH and oxidation-reduction potentials: Jour. Geology, vol. 60, pp. 1-33.

Marsland, D. A., and Brown, D. E. S., 1936, Amoeboid movement at high hydrostatic pressure: Jour. Cell. and Comp. Physiol., vol. 8, pp. 167-177.

Moore, H. B., 1958, Marine ecology: John Wiley and Sons, Inc., New York, 493 pp.

Myers, E. H., 1935, The life history of *Patellina corrugata* Williamson, a foraminifer:: Bull. Scripps Inst. Oceanography, Tech. Ser., No. 3, pp. 355-392.

———, 1936, The life cycle of *Spirillina vivipara* Ehrenberg, with notes on morphogenesis, systematics and distribution of the Foraminifera: Jour. Roy. Micr. Soc., vol. 61, pp. 120-146.

———, 1937, Culture methods for marine Foraminifera of the littoral zone, *in* Culture methods for invertebrate animals, Ithaca, N.Y., pp. 93-96.

———, 1940, Observations on the origin and fate of flagellated gametes in multiple tests of *Discorbis* (Foraminifera): Jour. Mar. Biol. Assoc., vol. 24, pp. 201-226.

———, 1943a, Biology, ecology and morphogenesis of a pelagic foraminifer: Stanford Univ. Publ. in Biol. Sci., no. 9, pp. 1-30.

———, 1943b, Life activities of Foraminifera in relation to marine ecology: Proc. Amer. Philos. Soc., vol. 86, pp. 439-458.

Nicol, D., 1944, New west American species of the foraminiferal genus *Elphidium:* Jour. Paleontology, vol. 18, pp. 172-185.

Nicol, J. A. C., 1960, The biology of marine animals: Interscience Publishers Inc., New York, 707 pp.

Nørvang, Aksel, 1945, Foraminifera, vol. 2, pt. 2, *in* The zoology of Iceland: Ejnar Munksgaard, Copenhagen and Reykjavik.

Oppenheimer, C. H., and ZoBell, C. E., 1952, The growth and viability of sixty-three species of marine bacteria as influenced by hydrostatic pressure: Jour. Mar. Research, vol. 11, no. 1, pp. 10-17.

Orton, J. H., 1920, Sea-temperature, breeding and distribution in marine animals: Jour. Mar. Biol. Assoc., vol. 12, pp. 339-366.

Parker, F. L. and Athearn, W. D., 1959, Ecology of marsh Foraminifera in Poponesset Bay, Massachusetts: Jour. Paleontology, vol. 33, no. 2, pp. 333-343.

Pearse, A. S. and Gunter, G., 1957, Salinity, *in* Treatise on marine ecology and paleoecology: Geol. Soc. America Mem. 67, vol. 1, pp. 129-158.

Phleger, F. B, 1960, Ecology and distribution of Recent Foraminifera: Johns Hopkins Press, Baltimore, 297 pp.

Regnard, Paul, 1891, Recherches expérimentales sur les conditions physiques de la vie dans les eaux: G. Masson. Editeur, Paris, 501 pp.

Said, R., 1950, The distribution of Foraminifera in the northern Red Sea: Contr. Cushman Found. Foram. Research, vol. 1, pp. 9-29.

Scholander, P. F., Claff, C. L., and Sveinsson, S. L., 1952, Respiratory studies of single cells, I. Methods: Biol. Bull., vol. 102, pp. 157-177.

———, Leivestad, H., and Sundnes, G., 1958, Cycling in the oxygen consumption of cleaving eggs: Exper. Cell Research, vol. 15, no. 3, pp. 505-511.

Southward, A. J., 1958, Note on the temperature tolerances of some intertidal animals in relation to environmental temperatures and geographical distribution: Jour. Mar. Biol. Assoc., vol. 37, pp. 49-66.

Stevenson, R. E. and Emery, K. O., 1958, Marshlands at Newport Bay, California: Allan Hancock Found. Publ. Occas. Pap. no. 20, pp. 1-109.

Tate, M. W. and Clelland, R. C., 1957, Nonparametric and shortcut statistics: Interstate Printers and Publishers, Inc., Danville, Illinois, 171 pp.

Zeuthen, Erik, 1947, Body size and metabolic rate in the animal kingdom, with special regard to the marine micro-fauna: C. R. Lab. Carlsberg Ser. Chim., vol. 26, no. 3, pp. 17-161.

ZoBell, C. E., 1946, Marine microbiology: Chronica Botanica Co., Waltham, Mass., 240 pp.

———, and Morita, R. Y., 1959, Deep-sea bacteria: Galathea Report vol. 1, pp. 139-154.

INSTRUMENT SOCIETY of AMERICA

PREPRINT NUMBER
62-NY60

CONFERENCE Preprint

Other publications are encouraged to include abstracts or excerpts of this paper provided credits are given to authors, the meeting and the Society. For permission to publish complete papers write to ISA, 313 Sixth Avenue, Pittsburgh 22, Pa.
The responsibility for all statements in this paper rests with the authors.

FALL INSTRUMENT-AUTOMATION CONFERENCE AND EXHIBIT
NEW YORK CITY, NEW YORK • SEPTEMBER 26-30, 1960

A TELEMETERING OCEANOGRAPHIC CURRENT METER*

James M. Snodgrass
Special Developments Division
Scripps Institution of Oceanography
University of California
La Jolla, California

ABSTRACT

A telemetering deep sea oceanographic current meter designed to use IRIG standards for data transmission. The instrument covers four current velocity decades and transmits in addition both depth and current direction. The instrument supplies simultaneous outputs to a function plotter recorder and a magnetic tape recorder.

INTRODUCTION

Of all the sciences, perhaps the science of Oceanography has been most plagued with unsatisfactory and inadequate instruments. By and large, instruments for the measurement of oceanographic currents have been notably unsatisfactory. It was concluded that a major improvement in oceanographic current meters would be a significant step in the advancement of the science.

In order to avoid getting the cart before the horse, it was necessary to examine the desired end result. As a result, the design requirements were tailored from the standpoint of providing a readout system that would supply a "quick look" and at the same time record in suitable form to permit automatic data processing.

The current meter was also designed with the idea of providing an opportunity to evaluate novel ideas. Some of the requirements outlined for the current meter are as follows:

1. It must have a substantially improved sensitivity.
2. The current meter must be capable of ignoring current components perpendicular to the plane of interest.
3. The instrument must be designed to record and indicate on deck.
4. Instrument must measure velocity,

---

*Contributions from the Scripps Institution of Oceanography, New Series, No.000. This work was supported in part by funds from the Office of Naval Research and from the Bureau of Ships, U.S. Navy. Reproduction in part or entirety is permitted for any purposes of the United States Government.

Printed in U.S.A.

Contributions from the Scripps Institution of Oceanography, New Series, 1290
Reproduce: by Permission

depth, and direction.

5. Measurements must be concurrent and not sequential.
6. Instrument must telemeter the information using existing IRIG standards.
7. Instrument must supply output for magnetic tape recording.
8. Instrument must supply output to operate function plotter.

To a large extent the final design of the instrument reflects the state of the art of approximately six years ago and represents a combination of both solid state and electron tube techniques. However, since the design has proven out, it is felt that a detailed description presents much of technical interest.

GENERAL CONSIDERATION

The oceanographic current meter consists essentially of two major components. First, the underwater portion, which contains the transducers which respond to velocity, depth, and direction; and the on-deck portion of the equipment which actually consists of three parts, namely, the power supply, demodulator, and indicating section and the recording devices.

The underwater and deck portions of the instrument are connected together by means of conventional electric cable; in this case, a two-conductor cable such as BUORD #1178 was found to be acceptable. This cable has a breaking strength of approximately 825 lbs. and possesses a very tough insulation. In practice the cable is wound on a winch which is equipped with slip rings. Another accessory, which will not be described in detail, consists of an electric swivel which connects the underwater portion of the current meter to the electric cable, which also serves as the mechanical supporting element. The swivel is necessary so that the current meter can easily orient itself without twisting the supporting cable.

UNDERWATER SECTION

Velocity Sensor

The selection of a suitable velocity transducer presented one of the major problems in the design of the entire instrument. Since it was desired that the current-measuring instrument permit raising and lowering while measuring the horizontal component of velocity, it was obviously necessary to design the sensing transducer so that it would ignore perpendicular current components. The further necessity of designing a velocity sensor that would permit a substantial improvement in sensitivity over existing instruments further restricted possible methods. The simpliest solution to the problem seemed to be through the design of a mechanical velocity sensor. The most promising mechanical current sensor appeared to be that known as the S-Rotor designed by S. J. Savonius[1]. The basic Savonius rotor was found to be unsatisfactory, since it did not possess a uniform torque characteristic, with respect to the direction of current flow. However, it was found by horizontally sectioning the Savonius rotor, and rotating the two sections 90° with respect to each other, that a thoroughly satisfactory rotor could be produced. The modified Savonius rotor further possesses the desired characteristic of ignoring current flow parallel to its axis of rotation.

The problem of obtaining substantially improved sensitivity was solved by fabricating the rotor from a plastic known as Cycolac[2], which has a specific gravity actually less than that of sea water. The average density of sea water may be assumed to be 1.025, and the density of Cycolac is about 1.01, so that the Cycolac would actually float in sea water. The Cycolac has the added advantage of being easily formed, and possesses a minimum of cold flow and plastic memory. With this plastic it was actually feasible to build the entire velocity sensing rotor so that it possessed neutral buoyancy and was thus without weight in sea water. The rotor bearings required special consideration. The axles of the rotor consist of 5/32" diameter burnished stainless steel shafts. The stainless steel axles run in bearings that are bushed with sintered Teflon. The axial thrust is absorbed by means of 3/16" diameter sapphire balls bearing on 1/16" thick inserts of tungsten carbide in the ends of the stainless steel axles.

The pickoff system requires essentially no energy from the rotor, since it uses a low radio frequency of approximately 100 kc. The 100 kc oscillator is a simple transistorized unit which has its oscillating coil in close proximity to very thin brass shim stock disks mounted around the periphery of the underside of the plastic rotor. Each time one of the brass disks passes the oscillator coil, the eddy currents block the oscillator. The blocking of the 100 kc oscillator acts to gate a 5.5 kc transistor oscillator, which carries the velocity information on IRIG channel 10. There are twenty-four of the brass disks on the 6" diameter rotor; and the rotor turns at approximately 1.35 revolutions per second per knot. The velocity range of the completed instrument is from slightly less than 6 knots to below .006 or from approximately 308 centimeters per second to 0.3 centimeters per second. The lower limit of a well-built rotor has yet to be determined, but is known to be less than .005 knots.

Direction Transducer

Direction pickoff techniques have long proved troublesome and it is felt that the basic solution to the problem as incorporated in the oceanographic current meter represents a significant improvement in technique. A conventional 3" fluid-filled mariner's compass was modified by replacing the conventional compass card with an opaque spiral compass card possessing approximately a 3/16" offset for one revolution. A small incandescent light source was mounted above the spiral compass card so that the light passing the edge of the card varied as a function of the compass heading. Just beneath the compass card, and immediately below the light source, two cadmium sulphide photoconductive cells were mounted so that each received an approximately equal portion of light passing the edge of the spiral disk. Electrically each of the photoconductive cells made up the resistance arm of a Wien bridge oscillator. The photoconductive cells were each padded by identical resistors so that the frequency of the Wien bridge oscillator fell in channel 8 of the IRIG specifications. Somewhat less than the full bandwidth was utilized, and only a 400 cycle bandwidth was found to be necessary.

Depth Transducer

A Vibrotron[3] was selected as the most suitable transducer available, since it supplies an output directly compatible with the IRIG standards. The depth information is transmitted on IRIG channel 12.

Underwater Assembly

All of the electronic package is enclosed in a thin-walled brass case, and the entire assembly fluid filled. A relatively inexpensive filling fluid known as Ondina No. 17[4] is used. It is a water-white mineral oil possessing the required optical and lubricity characteristics. The volumetric changes of the filling fluid due to temperature are compensated by making one end of the cylindrical enclosure in the form of a loose piston fitted with O-rings. The static friction of the piston was found to be negligible; therefore, the depth transducer was designed to connect directly to the internal oil volume. This had the advantage of avoiding corrosion problems due to sea water attacking the pressure diaphragm. A major disadvantage of the fluid filling which perhaps should be pointed out, since it is of far reaching significance in oceanographic instrument design, where pressure equalization is employed, is the difficulty due to the behavior of various electronic components under hydrostatic pressure. This is a very extensive field of study, and beyond the scope of this paper. However, it should be pointed out that composition resistors, for instance, have relatively high pressure coefficients and tantalum electrolytic capacitors may often present erratic behavior under pressure. In any case, all components must be tested in excess of the design pressure. There is one very great advantage which accrues due to the oil filling, and this is the decided ease of removing heat from within the electronic assembly. Care must be given to the design so that convection currents may be easily set up to carry heat from the source to the brass instrument case. Since the ocean is essentially an infinite heat sink, the unwanted heat is quickly dissipated.

The output from each of the transducer electronic assemblies goes through an isolating amplifier, and thence to a power amplifier which couples the IRIG-FM signals to the cable for transmission to the surface.

A few illustrations will help to clarify the discussion. Figure 1 shows the current meter hanging just above the water and suspended on the electric swivel. The large white fin orients the current meter in azimuth in response to the direction of current flow. The fin is open top and bottom, and presents almost no resistance to vertical motion. The point of suspension of the current meter for attachment to the supporting yoke is such that the current meter is in dynamic equilibrium from essentially zero velocity up to its maximum operating velocity, and is thus held automatically in the vertical position. The illustration shows the instrument tilted slightly from vertical, but this is due to the weight in air of the Cycolac orienting fin. Once the instrument is underwater, the vertical position is attained. Figure 2 illustrates the arrangement of the electronic assembly and the method of pickoff from the rotor system. From right to left may be seen the toroidal power supply transformer housing, the compass direction element, and the electronic deck. Figure 3 is a simplified block diagram of the electronic assemblies. Figure 4 is a complete wiring diagram of the operational unit.

DECK EQUIPMENT

Power Supply

The power supply package is straightforward and to a large extent conventional. Since the equipment is designed for shipboard operation, it was considered advisable in the interest of safety to operate the underwater instrument on approximately 28 volts 60 cycle power. As an operating convenience, a monitor meter is installed in the power package which reads the FM composite signal level input to the system. The input for the magnetic tape recorder is also obtained from this unit, and is a direct composite signal from the transmitting telemetering cable.

Demodulator and Indicating Chassis

A. Velocity Readout. As may be seen from Figure 5, there are two velocity indicating instruments. The two velocity indicating instruments are necessary in order to cover the wide ranges of velocity which the instrument is capable of covering. It becomes obvious that a problem exists, since the current-sensing rotor requires approximately four minutes to complete one revolution in a .006 knot current, and since there are twenty-four pulses per revolution, this means that the interval between pulses is approximately ten seconds; hence, integration of some sort becomes imperative. The simplest solution to the problem of integration appeared to be in fluid filling of the indicating instrument with silicone oil of suitable viscosity. It was found in practice that oil of approximately 250 centistokes viscosity was quite adequate. The left indicating instrument is the fluid-filled one, and covers the range from 0 to 0.03 knots, and 0 to 0.3 knots. The other indicating velocity meter is not oil filled and covers the range from 0 to 3.0 knots. As a bit of experimentation, rather unconventional scales were selected for the velocity instruments. Center scale, for instance, was selected to be about 1/6 of the full scale value, and just above the center scale position, the range is rapidly compressed toward the full scale value. The scale below center position is approximately linear. With this type of scale it is quite easy to read ratios of somewhat better than 10 to 1 without the necessity of switching.

Though the indications of velocity are on a non-linear scale, the current supplied to the indicating instruments is, however, linear, and all of the non-linearity is achieved by specially shaped magnetic pole pieces in the indicating instrument. Since the signal to the indicating instrument is linear, this may be used directly with a suitable coupling circuit to drive one pen of the function plotter.

B. Depth Indicator. The third instrument from the left indicates depth in feet and is a dual-range instrument reading from 0 to 100 ft. and 0 to 1000 ft., depending upon position of the depth-selector switch. The indicating instrument for depth is also non-linear as in the case of the velocity instruments, but uses a different ratio. In this case the center scale position corresponds to about 1/4 of full scale with the linear scale over the first half of the scale and the rapidly compressed scale above the center scale position. Below thirty feet, the instrument divisions are in one-foot intervals, and it is quite easy to read to a fraction of one foot. However, above 50 feet the divisions are in five-foot intervals, and at very nearly 100 feet, it is only practical to read the instrument to an accuracy of about two and one-half feet. Since the transducer is far more accurate than the indicating instrument, the major errors occur at this point. Here again, a linear input is supplied to the depth indicating meter, and it too may be coupled with a suitable network to drive one axis of the function plotter.

C. Direction Indicator. The direction indicator is a linear instrument, and is calibrated linearly from 0 to 360°. In order to simplify the figuring dial, only the tens and hundred digits are shown. The signal supplied to the direction instrument may be used to operate the second pen of a two-point function plotter.

D. Circuit Characteristics. A somewhat simplified block diagram of the deck unit is shown in Figure 6. Each of the information channels is fed by an isolation amplifier, which is coupled to a bandpass filter matching the IRIG information channel from the underwater transmitting unit. In the case of the velocity channel, over the range from approximately 0.2 knots to 3 knots, a 0 to 500 cycle Magmeter[5] drives the indicating meter directly. However, at the lower velocities, a different technique is employed. In this case, a high speed, single-pole, single-throw mercury wetted contact relay is used to control the alternate charging to different polarities of a polystyrene film capacitor. The charging currents are made uni-directional as far as the indicating meter is concerned by means of a bridge silicon rectifier.

The depth and direction channels of the indicating units are essentially identical with the exception of the frequency ranges of the components employed. In order to obtain maximum advantage from the FM signal bandwidth, beat frequency oscillators of the Wien bridge type are used in conjunction with mixers to obtain a difference frequency which may be readily demodulated by means of the Magmeters. In the case of the depth channel the problems of operating near the zero beat condition are eliminated since the depth-sensing transducer reads absolute pressure. Therefore, at the sea surface the instrument sees a pressure corresponding to atmospheric, which in turn corresponds to a virtual depth of approximately 33 feet. Therefore, this depth of 33.1 feet is marked with a red line on the indicating meter and the beat frequency oscillator is adjusted in the proper direction with the underwater unit suspended in air until the pointer reaches the red index point. The the indicating meter is returned to zero on the depth scale by means of a high-resistance zero bias current of opposite polarity, which is inserted across the indicating meter. Thereafter the zero depth scale corresponds to a very definite difference frequency, which is other than zero. For instance, in one case, this frequency was approximately 35 cycles.

The direction channel is somewhat more awkward to properly align though this procedure is quite straightforward. In aligning the direction channel, it is necessary to use the beat frequency oscillator adjustment as well as the meter zero biasing circuit in conjunction with a span adjustment. The span adjustment is nothing more or less than a simple shunt across the indicating meter. The necessary inputs for the adjustment of this direction channel are obtained by rotating the underwater instrument case while it is hanging in air through an arc of about 5° to 8° so that the spiral compass card goes from maximum light to minimum light which corresponds to maximum frequency and minimum frequency while the controls are adjusted on the indicating deck.

SUMMARY

All of the major objectives set forth for the performance of the current meter have been achieved, as may be seen from the accompanying calibration curve, Figure 7, and in the analog plot, Figure 8. The sensitivity and performance are rather striking. New designs have eliminated the problems due to the low information rates supplied by the velocity pickoff system and the entire system is now transistorized. The rotors, or current-sensing portion, which were once laboriously made by hand are now made at high rates and very inexpensively by means of injection molding. Furthermore, the inconveniences of 60 cycle AC power have been eliminated, either by self-powering the units, or supplying DC power from the surface control unit. Either of the latter two systems permit the complete elimination of slip rings on the deck winch, since the signals may be rather easily picked off the cable by means of passing the cable through a toroid transformer. At the present writing the threshold of the current-sensing system seems to be below that of either direct measurements of velocity by means of acoustic means, or electromagnetic means.

Two excellent references[6,7] on current meters should not be neglected by those who wish to explore the subject further.

REFERENCES

1. "The S-Rotor and Its Applications" S.J. Savonius, Mechanical Engieering, May 1931, Vol. 53, No. 5, p. 333-338.
2. Product Marbon Corp. Available from Southern Plastics Co., 408 Pendelton St., Columbia, South Carolina.
3. Borg-Warner Controls, Borg-Warner Corp., 3300 Newport Blvd., Santa Ana, California.
4. Shell Oil Co., 50 West 50th St., New York 20, New York.
5. Airpax Electronics, Inc., Seminole Div., Fort Lauderdale, Florida.
6. "Investigation of Current Measurements in Estuarine and Coastal Waters" by J. W. Johnson and R. L. Wiegel.
7. "Prakticheskaya Okeanografiya" by V. A. Snezhinskii, p. 318-435.

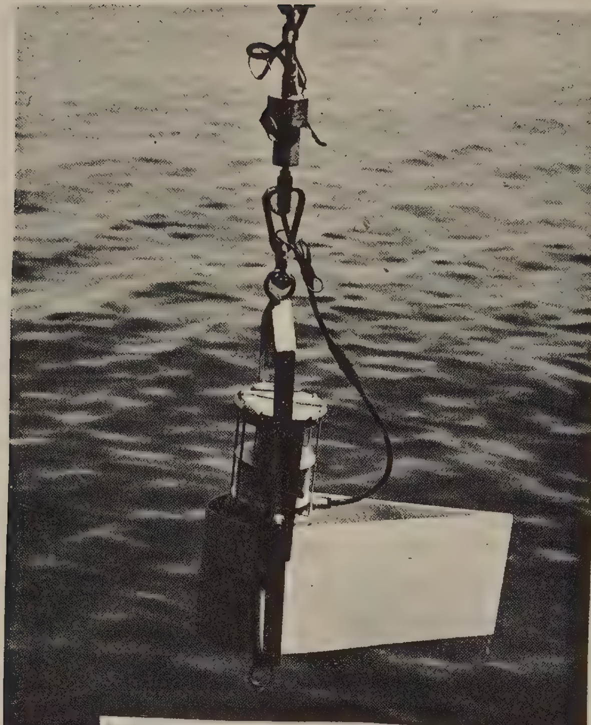

Figure 1. Current Meter with Electric Swivel.

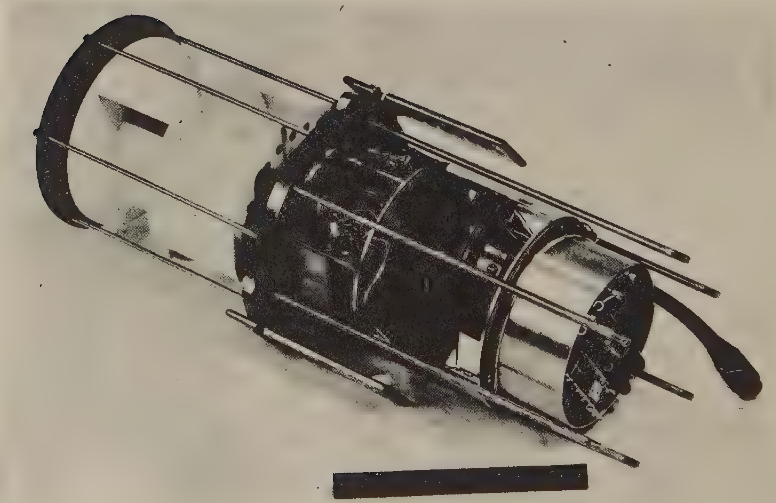

Figure 2. Current Meter with Cover Removed.

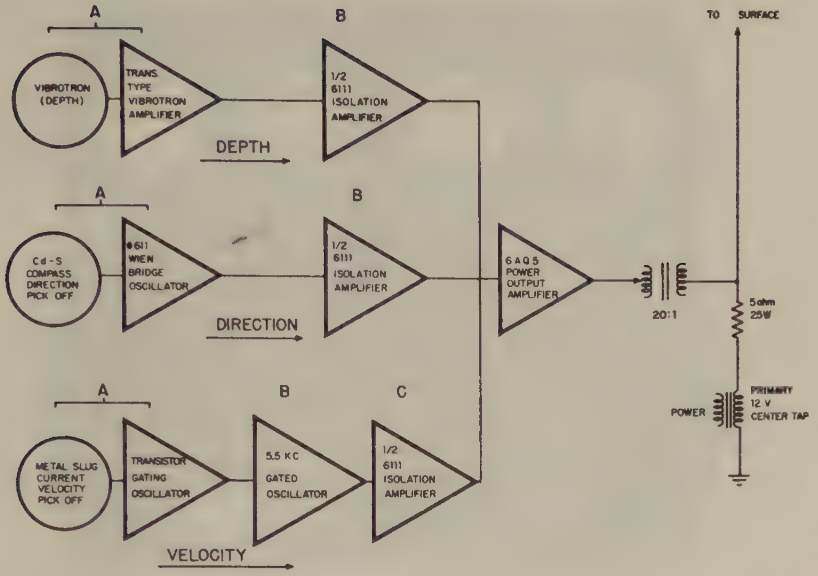
A
B
TO SURFACE
VIBROTRON (DEPTH)
TRANS. TYPE VIBROTRON AMPLIFIER
1/2 6111 ISOLATION AMPLIFIER
DEPTH
A
B
Cd-S COMPASS DIRECTION PICK OFF
6111 WIEN BRIDGE OSCILLATOR
1/2 6111 ISOLATION AMPLIFIER
DIRECTION
6AQ5 POWER OUTPUT AMPLIFIER
20:1
5 ohm 25W
POWER
PRIMARY 12 V CENTER TAP
A
B
C
METAL SLUG CURRENT VELOCITY PICK OFF
TRANSISTOR GATING OSCILLATOR
5.5 KC GATED OSCILLATOR
1/2 6111 ISOLATION AMPLIFIER
VELOCITY

Figure 3. Block Diagram of Underwater Unit.

62-NY60

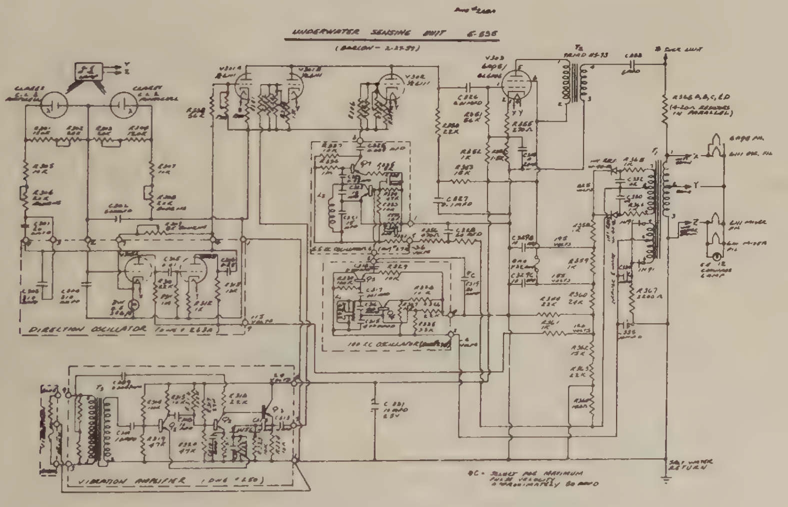
UNDERWATER SENSING UNIT
DIRECTION OSCILLATOR
VIBRATION AMPLIFIER

Figure 4. Wiring Diagram of Underwater Unit.

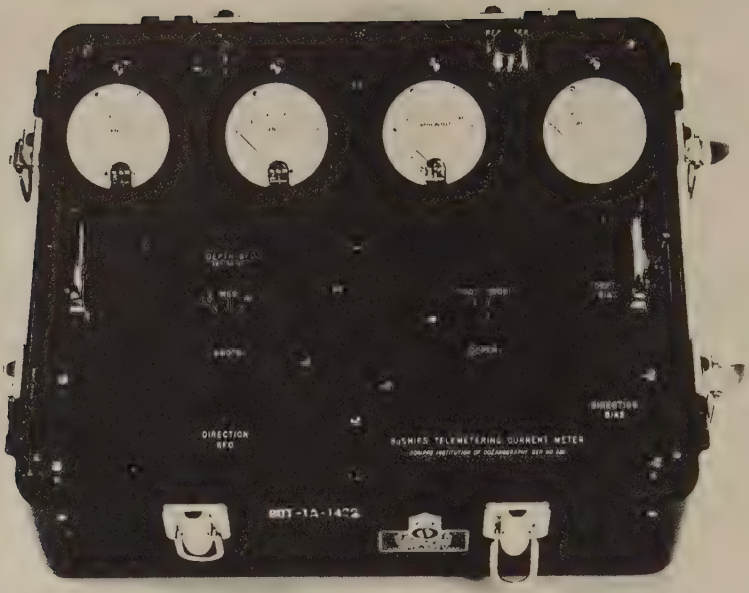
DIRECTION
BFO
BuSHIPS TELEMETERING CURRENT METER

Figure 5. Deck Demodulating and Indicating Unit.

62-NY60

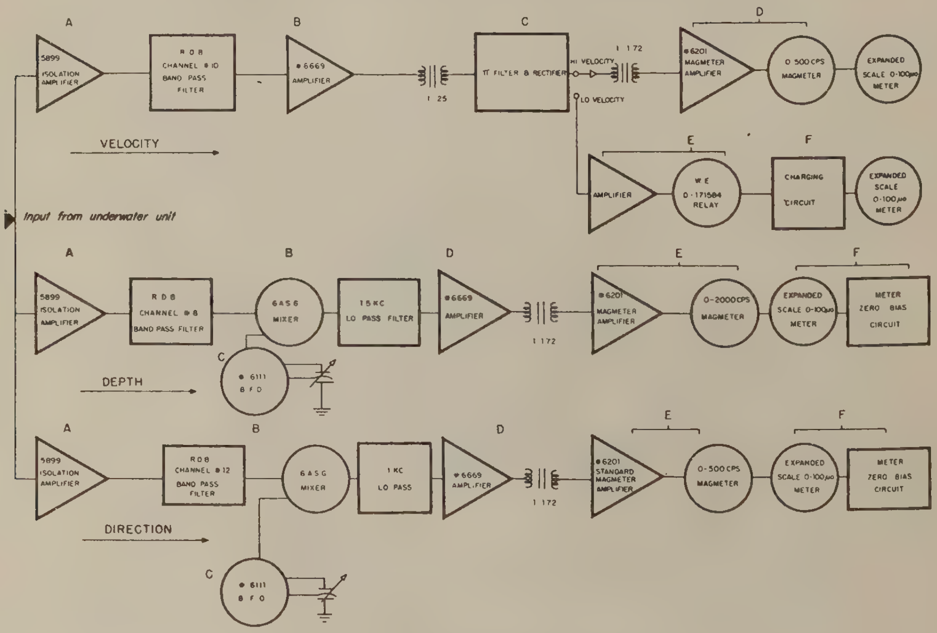
A
5899
ISOLATION AMPLIFIER
R D B
CHANNEL # 10
BAND PASS FILTER
B
# 6669
AMPLIFIER
1 25
C
π FILTER & RECTIFIER
HI VELOCITY
LO VELOCITY
1 172
D
#6201
MAGMETER AMPLIFIER
0 500 CPS
MAGMETER
EXPANDED SCALE 0-100μa METER
VELOCITY
E
AMPLIFIER
W E
0-171584
RELAY
F
CHARGING CIRCUIT
EXPANDED SCALE 0-100μa METER
Input from underwater unit
A
5899
ISOLATION AMPLIFIER
R D B
CHANNEL # 8
BAND PASS FILTER
B
6AS6
MIXER
1.5 KC
LO PASS FILTER
D
#6669
AMPLIFIER
1 172
E
#6201
MAGMETER AMPLIFIER
0-2000 CPS
MAGMETER
F
EXPANDED SCALE 0-100μa METER
METER ZERO BIAS CIRCUIT
C
# 6111
B F O
DEPTH
A
5899
ISOLATION AMPLIFIER
R D B
CHANNEL # 12
BAND PASS FILTER
B
6AS6
MIXER
1 KC
LO PASS
D
# 6669
AMPLIFIER
1 172
E
#6201
STANDARD MAGMETER AMPLIFIER
0-500 CPS
MAGMETER
F
EXPANDED SCALE 0-100μa METER
METER ZERO BIAS CIRCUIT
DIRECTION
C
# 6111
B F O

Figure 6. Block Diagram of Deck Unit.

62-NY60-8

62-NY-6(

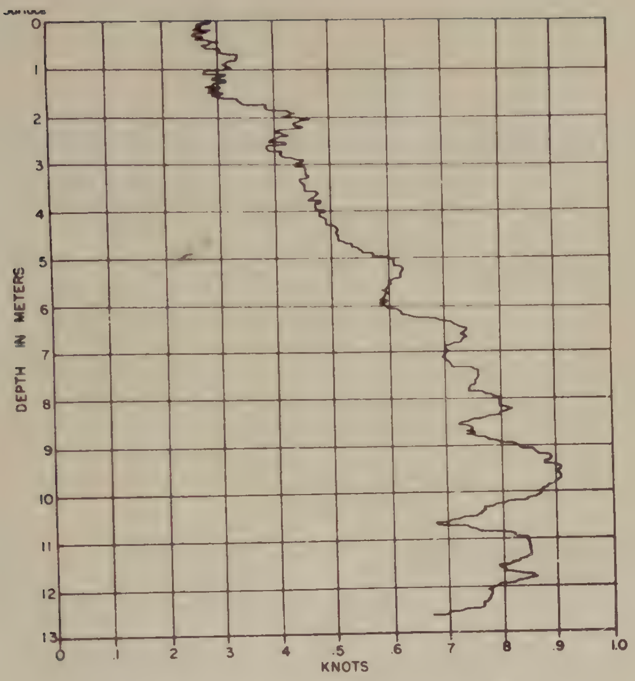

CURRENT METER - CURRENT PROFILE RECORD, 23 AUGUST 1957, TIME 1603

Figure 7. Current Meter Calibration Curve.

Figure 8. Function Plotter Record.

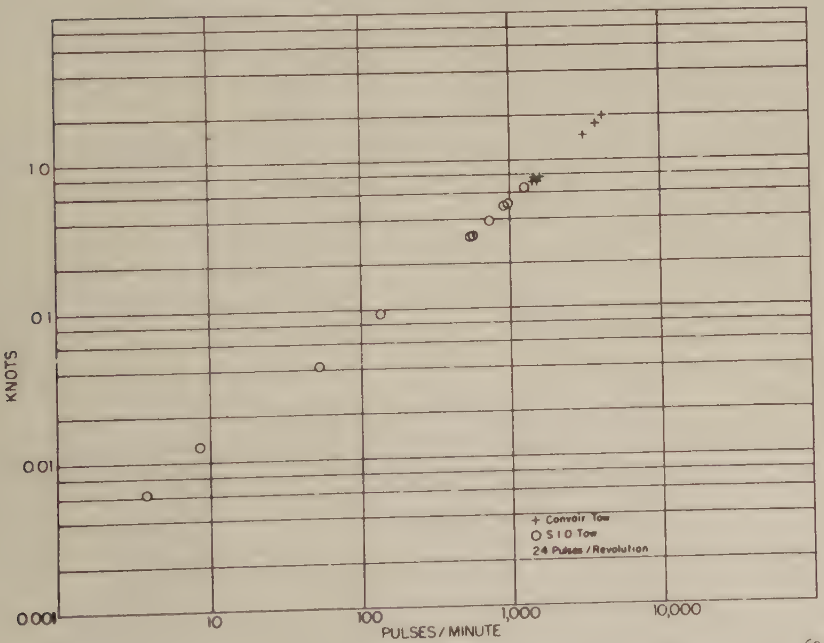

62-NY60-9

ON THE MARINE GEOCHEMISTRY OF BARIUM

by

Tsaihwa J. Chow and Edward D. Goldberg

Reprinted from Geochimica et Cosmochimica
Acta, v.20, 1960. pp.192-198.

Geochimica et Cosmochimica Acta, 1960, Vol. 20, pp. 192 to 198. Pergamon Press Ltd. Printed in Northern Ireland

On the marine geochemistry of barium

Tsaihwa J. Chow and E. D. Goldberg
Scripps Institution of Oceanography, University of California, La Jolla, California

(*Received* 16 *April* 1960)

A number of questions involving the geochemical behaviour of barium in the marine domains has prompted us to ascertain the barium content of sea water as a function of depth, inasmuch as previous analyses, which dealt mostly with surface Atlantic waters, have only revealed with one exception the upper limit of barium concentrations (Table 1).

Table 1. Previous investigations of the barium content of marine waters

Location	Depths (m)	Barium concentration (μg/l.)	Reference
English Channel	70	<200	Orton (1924)
Irminger Sea	2900	<(30–90)	von Englehardt (1936)
North Sea	0	<(30–90)	von Englehardt (1936)
West Scottish Coast	0	<100	Black and Mitchell (1952)
English Channel	0	6·2	Bowen (1956)

In the first place, is the depth distribution of barium in sea water similar to that of radium? On the basis of their chemical and physical characters, these two elements should follow each other in nature. Koczy (1958) has published an extensive study of depth profiles of radium in sea water which could be used as a basis of comparison. Secondly, how closely do barium concentrations approach a state of saturation in sea water with respect to precipitation of barium sulphate? Finally, it has been pointed out repeatedly that barium concentrations in pelagic sediments underlying biologically productive oceanic areas are unusually high (Revelle *et al.*, 1955; Goldberg and Arrhenius, 1958; Goldberg, 1960). If so, is there any correlation between the biological phenomena and the barium distribution in marine waters?

METHOD

The barium was assayed by isotope dilution technique using the 60° sector single focusing mass spectrometer with a 12 in. radius of curvature at the California Institute of Technology. An enriched barium-135 spike, obtained from the Oak Ridge National Laboratory, was dissolved in 5% nitric acid to make up a standard solution containing 0·45 mg of barium per ml. The isotopic compositions of the spike and of "common barium" were determined (Table 2).

Sea water (100 ml) was introduced into a 250 ml beaker, and 100 μl of the barium spike were then added. The combined solutions were taken to dryness. The

(680)

Contributions from the Scripps Institution of Oceanography, New Series, /29/
Reproduced by Permission

soluble alkali salts were leached from the precipitate with distilled water. The remaining solids, including barium in the form of sulphate, were transferred to a 1 ml centrifuge tube and washed several times with distilled water. About 5 μg of the barium sulphate were placed on the surface of a tantalum filament which had been carefully baked in a vacuum at elevated temperature to remove any barium initially present on the surface.

Table 2. Isotopic composition of common barium and the barium spike (Units in atom %.)

Isotope	130	132	134	135	136	137	138
Spike barium	0·02	0·03	1·48	67·32	12·35	5·63	13·17
Common barium	0·12	0·10	2·44	6·62	7·87	11·25	71·60

The spectrometric procedure has been described by CHOW and MCKINNEY (1958). The filament current was slowly raised to 2 A, corresponding to a temperature of about 1500°C. At this temperature only the Ba^+ spectrum was observed. The BaO^+ and the BaO_2^+ peaks occurred at much lower filament temperatures. The amount of barium in the sample was calculated from the following equation:

$$M = \frac{m(\mathrm{Ba}_s^{135} - N \times \mathrm{Ba}_s^{138})}{N \times \mathrm{Ba}_w^{138} - \mathrm{Ba}_w^{135}}$$

where M = barium in the sample (μg);
m = amount of spike added (μg);
N = observed $\mathrm{Ba}^{135}/\mathrm{Ba}^{138}$ ratio;
Ba_s^{135}, Ba_s^{138} = percentage of Ba^{135} and Ba^{138} in the spike, respectively;
Ba_w^{135}, Ba_w^{138} = percentage of Ba^{135} and Ba^{138} in the common barium, respectively.

RESULTS

The barium profiles for four Pacific Ocean stations are given in Table 3. The probable error of the analyses is about 3 per cent. It is quite clear that at all

Table 3. The barium concentrations in Pacific Ocean waters (Stations are from the Downwind Expedition of the Scripps Institution of Oceanography, October, 1957 to February, 1958.)

Station	Downwind 6		Downwind 7		Downwind 8		Downwind 17	
Latitude	11° 00′ N		07° 08′ N		03° 14′ N		34° 50′ S	
Longitude	128° 30′ W		129° 16′ W		130° 31′ W		135° 53′ W	
	Depth (m)	Ba (μg/l.)	Depth (m)	Ba (μg/l.)	Depth (m)	Ba (μg/l.)	Depth (m)	Ba (μg/l.)
	0	12	705	32	0	12	4	10
	2698	32	3107	43	517	16	518	12
	4752	46	4323	51	1051	31	865	12
					2167	29	1937	27
					3002	43	3470	28
					4392	63	4185	30

stations there is an increase in barium content with depth. The waters were unfiltered and had been stored in acid leached Pyrex bottles with wax-sealed polyethylene stoppers for a period of approximately 2 years at a temperature slightly above 5°C. Possible loss of barium from solution by sorption on the glass walls or dissolution from the glass, if any, would most probably introduce a small, constant and additive error to all of the results.

DISCUSSION

The depth distribution of barium is similar to that of radium (Fig. 1). KOCZY (1958) postulates that the radium originates from the radioactive decay of its parent ionium in the sediments and subsequently diffuses upward through the water column. However, where radium doubles its concentration from the surface to 4000 m, barium, in an adjacent station, shows a fivefold increase over the same depth range.

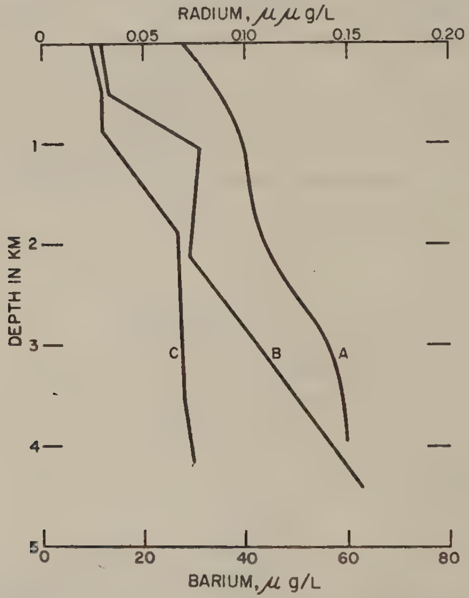

Fig. 1. Barium and radium profiles in sea water. (a) Radium from Swedish Deep Sea Expedition No. 102. Radium values from KOCZY, 1958. (b) Barium from Downwind Station 8. (c) Barium from Downwind Station 17.

The degree of saturation of barium in sea water can be approached in the following way. Barium in solution probably exists in two principle forms, divalent barium ion and the undissociated barium sulphate. The solubility product of barium sulphate at 25°C and a pressure of 1 atm is of the order of 10^{-10} (BJERRUM *et al.*, 1958). The dissociation constants of all divalent ions cluster about 0·005 for the undissociated soluble sulphates (ROBINSON and STOKES, 1955). The sulphate concentration in sea water is 28 mM, while the activity coefficients of di-divalent salts can be assigned the value of 0·1 for solutions with an ionic strength of 0·7, similar to that of sea water (LATIMER, 1952). An activity coefficient of 1·0 is taken for the undissociated barium sulphate. Thus,

$$[Ba^{2+}][SO_4{}^{2-}] = 10^{-10}$$

$$(Ba^{+2}) = 3{\cdot}6 \times 10^{-7}\ M$$

$$= 49\ \mu g/l.$$

and

$$\frac{[Ba^{+2}][SO_4{}^{2-}]}{[BaSO_4]_{undiss.}} = 5 \times 10^{-3}$$

$$(BaSO_4)_{undiss.} = 2 \times 10^{-8}\ M$$

$$Ba\ in\ (BaSO_4)_{undiss.} = 2{\cdot}7\ \mu g/l.$$

Hence, for a total soluble barium concentration of around 52 μg/l., 5 per cent is in the undissociated form.

Other possible ionic associations of barium with such anions as phosphate, bicarbonate, carbonate, hydroxide and silicate have been neglected for two reasons: (1) these anions are less abundant than sulphate and would have a consequentially smaller role in delimiting the total dissolved barium concentration in sea water; and (2) the stability constants of such ion pairs are yet to be determined.

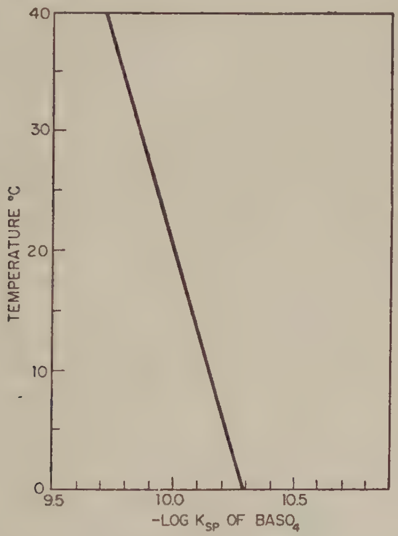

Fig. 2. The dependence of the solubility product of barium sulphate upon temperature.

More consequential to the saturation concentration of barium sulphate in sea water, however, is the pressure and temperature dependence of the solubility product. The temperature dependence of the solubility product is shown in Fig. 2 which is calculated from data in BJERRUM *et al.* (1958). It is readily seen that at one atmosphere, a change of temperature from 25°C to 0°C results in a decrease of the solubility product by over a factor of 2.

OWEN and BRINKLEY (1941) have tabulated the necessary data from which the effect of pressure on the barium sulphate solubility product in sea water can be considered. Neglecting the pressure effect upon partial molal volumes, which is a second-order term for pressure up to 500 atm

$$RT \ln K^P/K = -\Delta\bar{V}(P - 1)$$

where K^P and K are the solubility products at pressure P and 1 atm, respectively, and $\Delta\bar{V}$ is the difference in partial molal volumes at 1 atm between barium ion plus sulphate ion and barium sulphate. At a pressure of 500 atm, $\Delta\bar{V}$ has a value of -42 ml and hence K^P/K can be calculated from the above equation to have a value of 2·5, i.e. the pressure effect upon the saturation value of barium ion, assuming constant sulphate concentration, results in a value 2·5-fold greater at depths around 5000 m than at the surface.

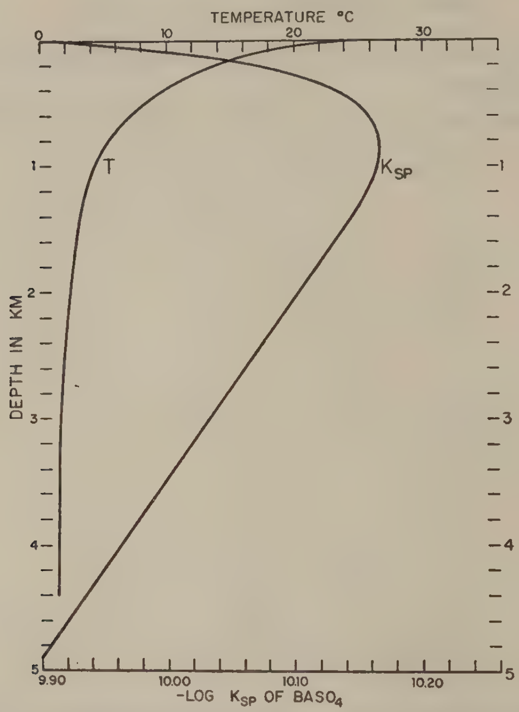

Fig. 3. The temperature profile of Downwind Station 8 and the corresponding depth profile of the solubility product of barium sulphate corrected for temperature and depth.

The pressure and temperature effects may be combined, as illustrated in Fig. 3 for the Downwind Station 8, to show a minimum in the saturation value of barium ion as a function of depth in the oceans. The initial decrease in barium ion concentration with depth reflects the temperature effect, while below the thermocline the subsequent increase mirrors the pressure effect. It should be pointed out that we have not taken into consideration changes in activity coefficients with either temperature or pressure and the pressure effect on the temperature dependence of K_{sp}.

Notwithstanding these uncertainties in the above computations, it is evident that the saturation values of barium are not approached in surface ocean waters but may be reached at greater depths. Note the value of 63 μg/l. at Downwind Station 8 at 4392 m and the predicted value of about 70 μg/l. from Fig. 3.

Finally, we may seek out the mechanisms governing the depth distribution of barium. The similarity of the barium curve with those of the nutrient species such as phosphate, silicate and nitrate suggests a correlation between barium and the biochemical cycles in the seas. Several possibilities exist.

During the oxidation of detrital organic matter as it falls from the surface to deeper layers of the oceans, high levels of sulphate ion can be presumed to exist in the organic microenvironment. Therefore a subsequent precipitation of barium sulphate could occur. As the organic matter is further oxidized, the microenvironment is destroyed. Then, the precipitated barium sulphate may dissolve and return to solution. The net effect of such processes is the transference of barium from surface to depths.

We may also consider a direct transfer of barium by organisms from surface to deeper waters. BOWEN (1956) has reported an enrichment of barium in the dry organisms over sea water by factors of from 450 to 4400 in a suite of specimens which includes brown, red and green algae, chiton shells, cephalopod bone, mollusc shells and corals. As organisms die or as plants fall out of the euphotic zone, the decaying remnants can furnish barium ions to the sea water. If such a mechanism is an important conveyor of barium to deeper waters, other ions such as copper, nickel, vanadium and cobalt, which are highly enriched in organisms, may show similar depth distributions to those of barium.

Finally, we can not completely disregard the regeneration of barium from the sea floor. As it decomposes, organic debris on the ocean bottom can supply barium to waters overlying the sediments. If barium is in such solid phases as barite (GOLDBERG and ARRHENIUS, 1958), contact of such materials with any undersaturated bottom waters may result in dissolution of the barium sulphate. However, at the present time it is extremely difficult to assess such contributions in relation to those transported downward by the marine biosphere.

Acknowledgements—We are indebted to Dr. CLAIRE PATTERSON of the California Institute of Technology who provided the stimulation for this work as well as the use of the mass spectrometer and to Mr. F. T. MANHEIM of the Geological Survey of Sweden whose refined spectrographic techniques confirmed the observed increase in barium with depth in seawater. This work was supported by the Division of Biology and Medicine, U.S. Atomic Energy Commission, under a contract with the University of California at La Jolla.

REFERENCES

BJERRUM J., SCHWARZENBACH G. and SILLEN L. (1958) *Stability Constants* Pt. II. *Inorganic Ligands.* Chemical Society, London.

BLACK W. A. P. and MITCHELL R. L. (1952) Trace elements in the common brown algae and sea water. *J. Mar. Biol. Ass., U.K.* **30,** 575–584.

BOWEN H. J. M. (1956) Strontium and barium in seawater and marine organisms. *J. Mar. Biol. Ass., U.K.* **35,** 451–460.

Chow T. J. and McKinney C. R. (1958) Mass spectrometric determination of lead in manganese nodules. *Analyt. Chem.* **30,** 1499–1503.

Goldberg E. D. (1960) The determination of opal in marine sediments. *J. Mar. Res.* In press.

Goldberg E. D. and Arrhenius G. O. S. (1958) Chemistry of Pacific pelagic sediments. *Geochim. et Cosmochim. Acta* **13,** 153–212.

Koczy F. F. (1958) Natural radium as a tracer in the ocean. *Proceedings of the Second International Conference on the Peaceful Uses of Atomic Energy, Geneva,* 1958 Vol. 18, pp. 351–357. United Nations, New York.

Latimer W. M. (1952) *Oxidation Potentials* (2nd Ed.). Prentice-Hall, New York.

Orton J. H. (1924) An account of investigations into the cause or causes of the unusual mortality among oysters in English oyster beds during 1920–1921. *Fishery Investigations London,* Series 2, **6,** Nos. 3 and 4.

Owen B. B. and Brinkley S. R. (1941) Calculation of the effect of pressure upon ionic equilibria in pure water and salt solutions. *Chem. Rev.* **29,** 461–474.

Revelle R. R., Bramlette M., Arrhenius G. O. S. and Goldberg E. D. (1955) Pelagic sediments of the Pacific. *Geol. Soc. Amer. Special Paper* **62,** 221–236.

Robinson R. A. and Stokes R. H. (1955) *Electrolyte Solutions.* Butterworths, London.

von Englehardt W. (1936) Die Geochemie des Barium. *Chem. Erde* **10,** 187–246.

Deep-Sea Research, 1961, Vol. 8, pp. 28 to 38. Pergamon Press Ltd., London. Printed in Great Britain

Geology of the Sea Floor East of Guadalupe Island

DALE C. KRAUSE
Scripps Institution of Oceanography, University of California, La Jolla, California

(*Received 9 December*, 1960)

Abstract—A gently rolling surface of very soft folded sediment lies at the anomalously shallow deep-sea depth of 1900 fathoms east of Guadalupe Island. Sub-bottom echoes occur at a uniform depth of 6-8 metres over most of the area and photographs reveal organisms vigorously reworking much of the upper ten centimetres of sediment. At present, the region is surrounded by a deeper sea floor and cannot receive bottom-transported sediment. The origin of this anticlinorium is indeterminate. Geomagnetic profiles reveal north-south anomalies which are typical of the oceanic crust of the northeastern Pacific Ocean basin and which parallel the folds though are not necessarily related to them. Large tectonic features surround the area such as volcanoes, ridges, basins and deeps. Compared to these features, it is relatively deformed and appears to have a normal oceanic crust because it has (1) a long depositional history, (2) north-south magnetic anomalies and (3) a normal thickness.

INTRODUCTION

AN ANOMALOUSLY shallow and smooth portion of the deep-sea floor lies east of Guadalupe Island in the northeast Pacific Ocean (FIGS. 1, 2, 3 and 4). The Fanfare Expedition under H. W. MENARD and R. W. RAITT spent several days in the area during July, 1959, engaged in seismic and gravity studies, bathymetric surveying and coring in order to determine its suitability as a site for obtaining drill cores of the oceanic crust. Since then, bathymetry, geomagnetism, gravity, heat flow, sonic measurements of sediment thickness, core and rock samples, photographs, and current measurements have been studied. This report is concerned with the bathymetric, geomagnetic surveys and the photography.

The first bathymetric maps of the area were prepared by SHEPARD and EMERY (1941) and SHEPARD (1950) from scanty soundings on U.S. Navy Hydrographic Office charts and from Scripps cruises. They showed several prominent features of the area but only in a very generalized way. Unpublished bathymetric charts of the Cedros Deep area (FISHER, 1953) and Pacific Ocean west of California and Baja California (MENARD, 1954, 1959) existed prior to the Fanfare Expedition and were based mostly on soundings taken by the Scripps Institution of Oceanography and the U.S. Navy. MENARD (1955) discussed the regional, bathymetric and structural picture.

RESULTS

The discussion of the sea floor of this region is divided into two sections: (1) the shallow, smooth, rolling area east of Guadalupe Island and (2) the sea floor surrounding this rolling area. In order to discuss the region intelligibly, *arrugado* has been coined to designate the rolling area. *Arrugado* comes from the spanish " la arruga " : corrugation, wrinkle (ROBB, 1949). An arrugado is the rolling equivalent of a plain.

Contributions from the Scripps Institution of Oceanography, New Series, 1292
Reproduced by Permission

THE ARRUGADO

Sub-bottom echoes

The Precision Depth Recorder (PDR) records show widely distributed sub-bottom echoes (FIG. 9) (echoes returned from an acoustic reflecting surface below the sea floor) indicating that a layer of soft sediment overlies another layer with different sound properties. Where sub-bottom echoes were found with well-tuned echo sounders, additional reflections were usually recorded below the first strongly recorded layer. Three and four echoes were common, but it is not known whether these additional echoes represent more layers or whether sometimes they merely record sound reverberation within the upper sediment layer. Gravity cores (up to 10ft.) show the sediment to be very soft. The distribution of the sub-bottom echoes

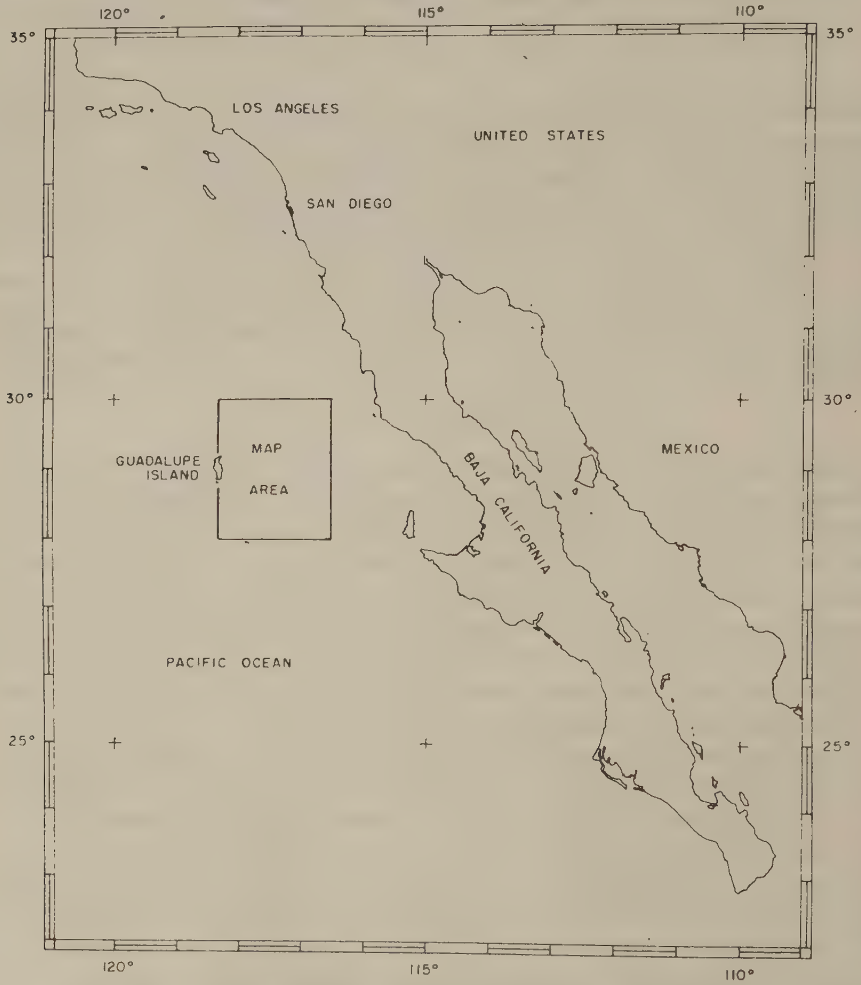
120°
115°
110°
35°
30°
25°
LOS ANGELES
UNITED STATES
SAN DIEGO
MAP
AREA
GUADALUPE
ISLAND
MEXICO
BAJA CALIFORNIA
PACIFIC OCEAN

FIG. 1. Index map. The area lies west of continental borderland, a region of submarine ridges and troughs which lies along the coast between Viscaino Bay (28°N) and Point Conception ($34\frac{1}{2}$°N).

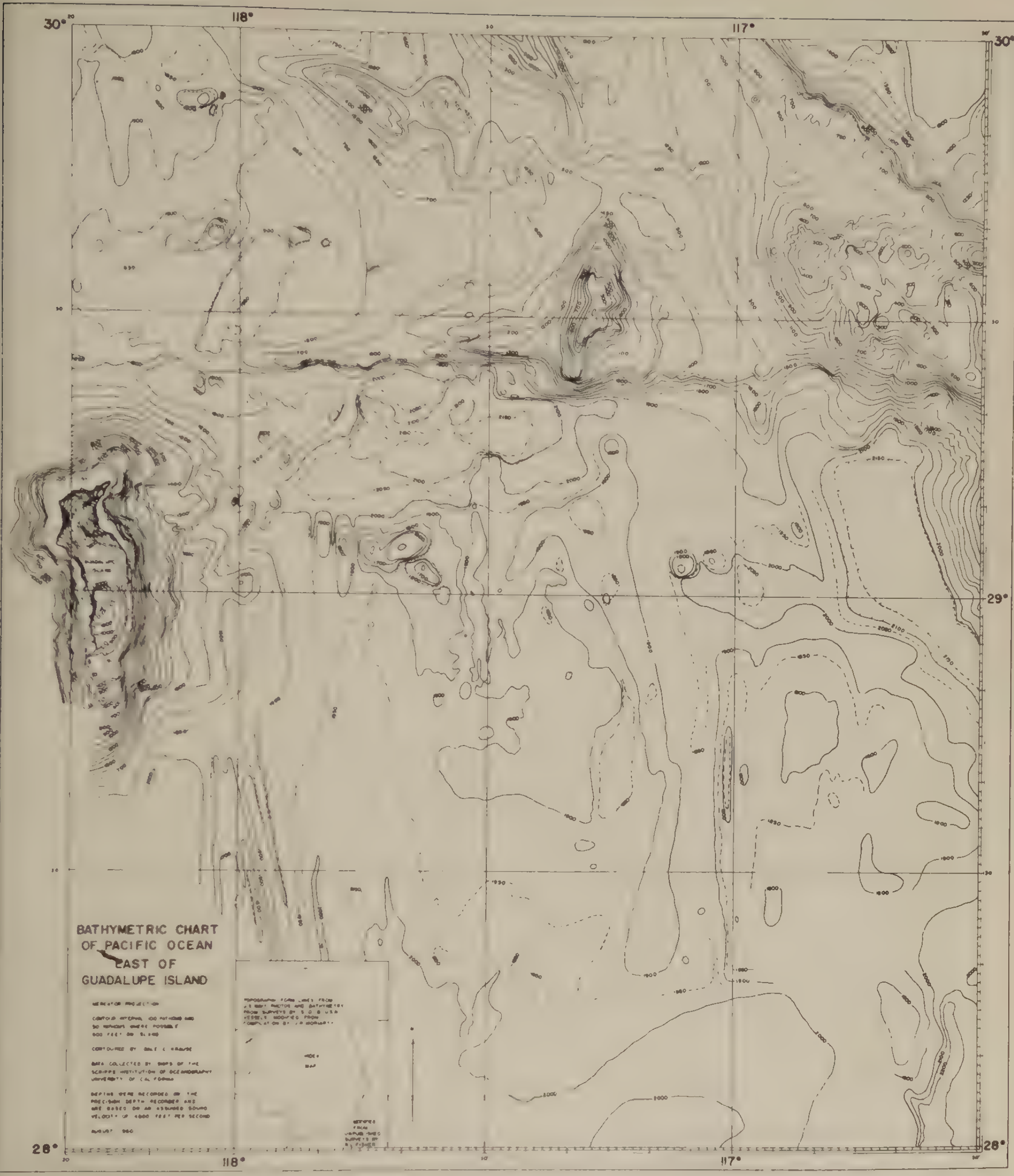
30°
118°
117°
30°
29°
28°
118°
117°
28°
BATHYMETRIC CHART OF PACIFIC OCEAN EAST OF GUADALUPE ISLAND
MERCATOR PROJECTION
CONTOUR INTERVAL 100 FATHOMS AND 50 FATHOMS WHERE POSSIBLE
500 FEET ON ISLAND
DATA COLLECTED BY SHIPS OF THE SCRIPPS INSTITUTION OF OCEANOGRAPHY UNIVERSITY OF CALIFORNIA
DEPTHS WERE RECORDED ON THE PRECISION DEPTH RECORDER AND ARE BASED ON AN ASSUMED SOUND VELOCITY OF 4800 FEET PER SECOND
AUGUST 1960
2000
2100
1900
1950
1800

FIG. 2. Bathymetric charts of the Pacific Ocean east of Guadalupe Island. The depths are in fms. which are based on an assumed sound velocity of 4800 ft per second. Most of the soundings were taken with a Precision Depth Recorder (PDR) and were obtained on expeditions since 1957 (FIG. 4) except for the work of MORIARY (1956) and FISHER (1953, 1955). Closed contours about depressions are hachured.

(FIG. 6) over the arrugado is suprisingly uniform with only changes that might be expected from the slumping of a very soft sediment : some of the depressions have deeper sub-bottom echoes, and several highs have no such echoes. Whether the sea floor was flat or rolling at the time of deposition of the material above the sub-bottom echo is not known because the surface material is pelagic in origin (E. D. GOLDBERG, 1960). At the present time, the arrugado is cut off from bottom-transported sediments, which may originate outside the area, by the deeper water on all sides (FIG. 2).

Photographs

The sea floor near 29°N l, 117½°W l was studied at two camera stations (FIG. 7) about 2 miles apart and at that locality is literally covered by the tracks of animals. Various animals occurring there are tentatively identified as holothurians, echinoids, an isopod, a sea pen and crinoids (fragments). The presence of holes in the bottom, the tentacles and sea pens projecting from the bottom and the holothurians ingesting the mud reveals that the upper centimetre or two of mud is continually being mixed and that perhaps as much as the upper ten centimetres is also in a state of slow flux. No evidence of ripplemarks was found although such evidence of rapid currents would be destroyed by the organisms if the event occurred rarely.

Abyssal hills

The arrugado is a province of abyssal hills about 60 miles square (FIG. 2 and 3). A special survey (FIG. 8) with the R/V *Orca* in July, 1960, definitely established the north-south elongation of the hills which was indicated by the more general surveys (FIG. 2). The hills vary in width from one to 20 miles but tend to fall into two sets : 1–3 miles (FIGS. 5 and 8) and 5–20 miles (FIGS. 2 and 9). The smaller set is generally less than 150 ft high while the larger set is up to 1000 ft high. The smaller group of hills is super-imposed on the larger group which trend across the entire arrugado as a system of broad ridges. The smaller hills are broad with relatively sharp margins. Occasionally the margins are so steep (FIG. 5) that they would seem to be produced by faulting.

A north-south zone of poorly reflecting irregular sea floor (FIGS. 8 and 9) was found during the detailed survey. Very little sound was reflected from it, and the normal layered structure of the surrounding sediment appears to be destroyed. This disturbed band runs more or less along a trough between two hills and probably represents a fault zone.

Interpretation of the abyssal hills

The even depth of the sub-bottom echoes over the elongate abyssal hills reveals that the hills are folds by geologic definition (HOWELL, 1957). It is immaterial to the definition whether the sediment was deposited in the present attitude or whether it was deformed into this position. Furthermore, the entire arrugado may be considered an anticlinorium by definition (HOWELL, 1957). The folding may have been developed in one or a combination of the following four processes which are pure types and are not expected to exist alone :

(1) Gentle pelagic deposition over a previously existing rough bottom gradually subduing the hills and filling the valleys but reflecting the underlying topography.

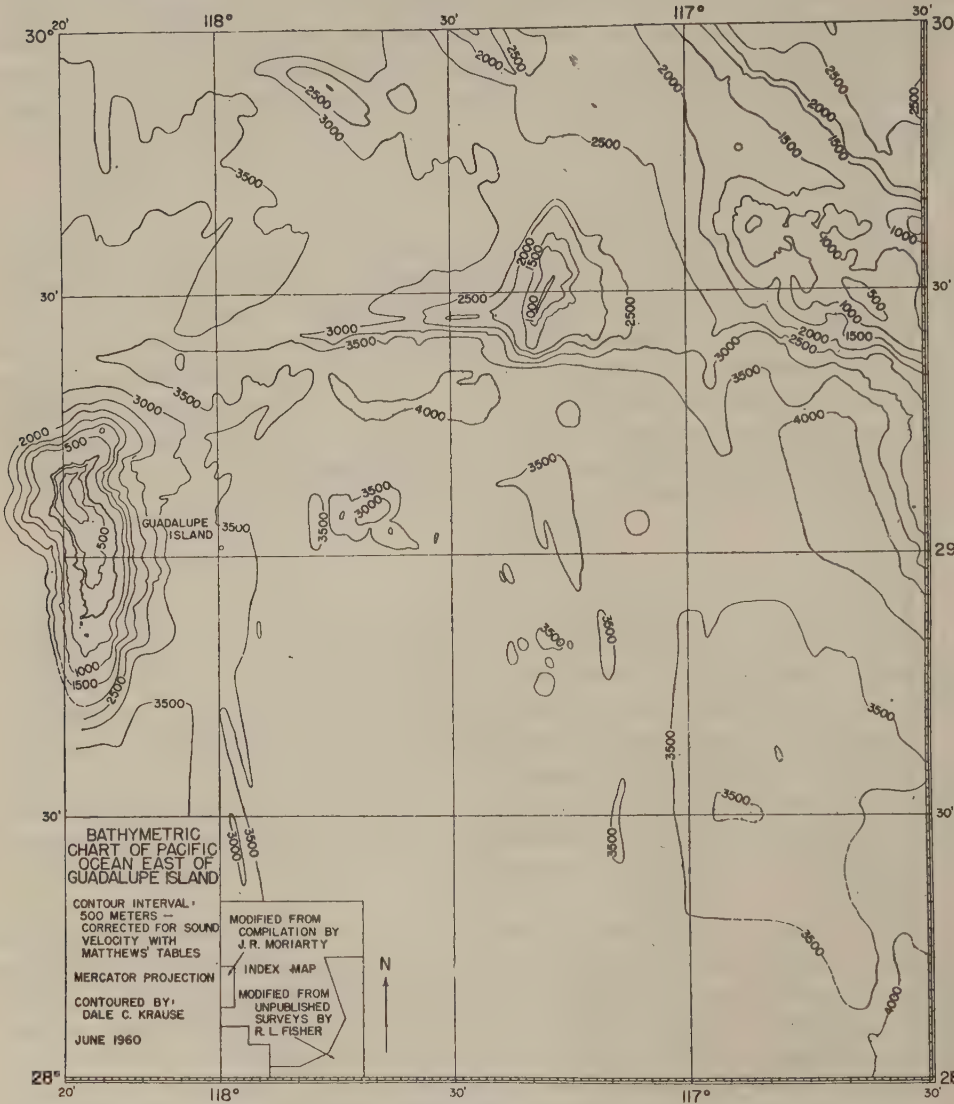
30°
20'
118°
30'
117°
30'
30°
30'
29°
30'
28°
20'
118°
30'
117°
30'
28°
2000
2500
3000
3500
4000
1500
1000
500
GUADALUPE ISLAND
BATHYMETRIC CHART OF PACIFIC OCEAN EAST OF GUADALUPE ISLAND
CONTOUR INTERVAL: 500 METERS — CORRECTED FOR SOUND VELOCITY WITH MATTHEWS' TABLES
MERCATOR PROJECTION
CONTOURED BY: DALE C. KRAUSE
JUNE 1960
MODIFIED FROM COMPILATION BY J. R. MORIARTY
INDEX MAP
MODIFIED FROM UNPUBLISHED SURVEYS BY R. L. FISHER
N

FIG. 3. Bathymetric chart of the Pacific Ocean east of Guadalupe Island based on depth in metres from soundings corrected for sound velocity (see caption to FIG. 2).

(2) Complete burial of a pre-existing rough topography with subsequent differential compaction of the sediment causing a subdued reflection of the underlying topography.

(3) Deformation of a flat sea floor with folds caused by compression or gentle normal faulting of the underlying crust.

(4) Instrusions of parallel dike swarms into the underlying crust.

At our present state of knowledge, we cannot distinguish between the various processes except that any previously existing topography (if it did exist) has been buried.

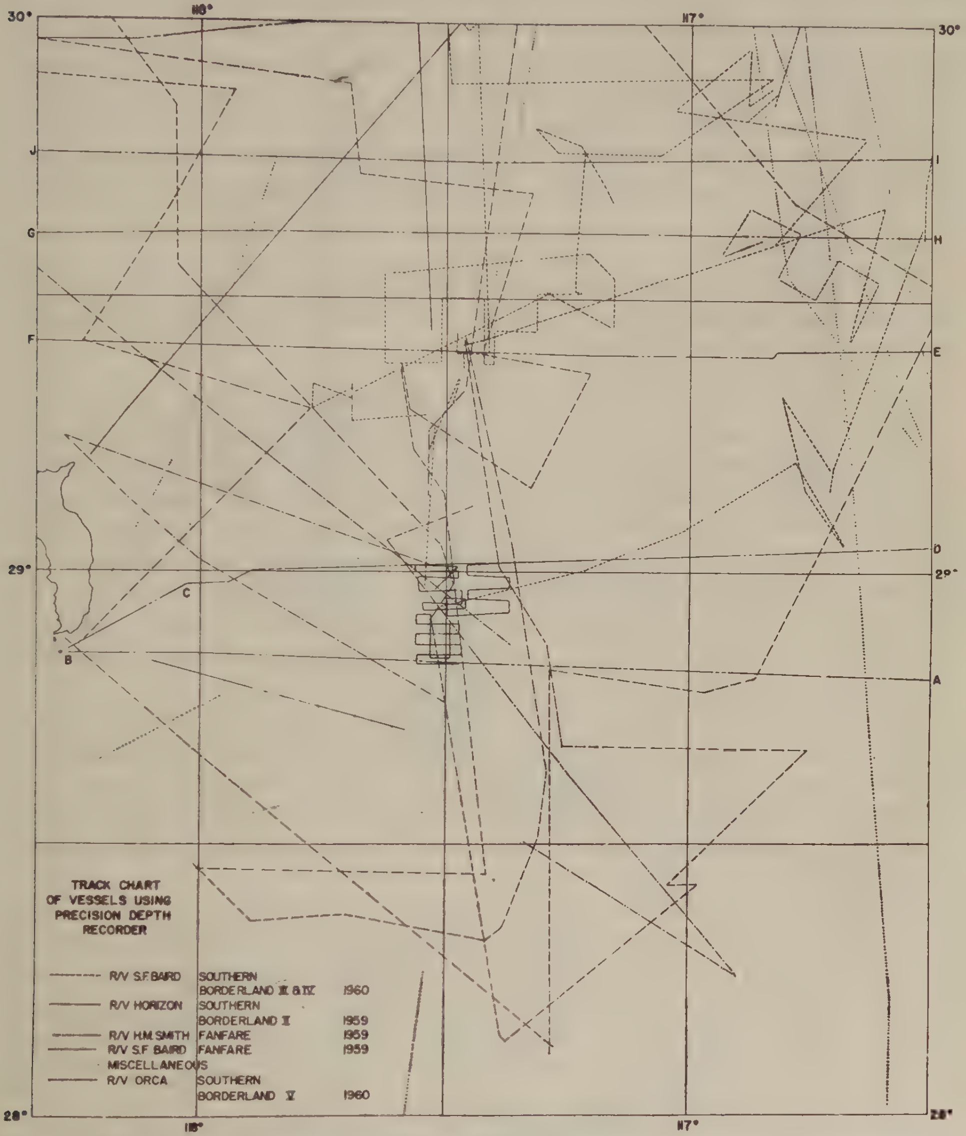
30°
118°
117°
30°
J
I
G
H
F
E
D
29°
29°
C
B
A
TRACK CHART OF VESSELS USING PRECISION DEPTH RECORDER
R/V S.F. BAIRD SOUTHERN BORDERLAND III & IV 1960
R/V HORIZON SOUTHERN BORDERLAND II 1959
R/V H.M. SMITH FANFARE 1959
R/V S.F. BAIRD FANFARE 1959
MISCELLANEOUS
R/V ORCA SOUTHERN BORDERLAND V 1960
28°
118°
117°
28°

FIG. 4. Track chart of vessels using Precision Depth Recorders from which the bathymetric charts (FIGS. 2 and 3) were made.

Geomagnetism

A magnetic survey was made on the cruise Southern Borderland II on the ship R/V *Horizon* with a ship-towed magnetometer which had been modified from an airborne model (ASQ-3A MAD). Not enough survey lines cross the area to construct a map of the total magnetic intensity but the similarity of profiles A–B and

B–C–D (FIGS. 4, 10 and 12) show that the magnetic anomalies are oriented north–south in the arrugado. This orientation is the same as found by MASON (1958), RAFF (1960) and VACQUIER (1960) to characterize the north-east Pacific Ocean basin. The size of the anomalies (10 miles wide and 250 gammas high) is somewhat smaller than many of the northern ones but not significantly so. In essence, these anomalies demonstrate that the oceanic crust of the arrugado is similar in structure to the rest of the northeast oceanic basin in so far as the origin of the anomalies and their preservation is concerned. MASON (1958) ably presented several possible origins for the magnetic anomalies without being able to find a firm conclusion, and the present study still emphasizes their enigmatic features.

Seismic refraction studies

R. W. RAITT (1960) found from seismic refraction studies of the Fanfare cruise that the crustal thickness of the sea floor east of Guadalupe Island is similar to that of the standard oceanic section.

ENVIRONS OF THE ARRUGADO

Guadalupe Island, an upper Cenozoic basaltic and andesitic volcano (JOHNSON, 1953) bounds the area to west. The recent undissected cinder cones on the south end indicate that the volcano may only be dormant and not extinct. The steep arcuate eastern shore on the north end of the island looks like the rim of a caldera because the beds are truncated at the cliff and often slope away from it. Two other possible origins exist which are compatible with the submarine contours : (1) a very large landslide scar, perhaps volcanically induced or (2) faulting unrelated to caldera formation. The island is flanked (FIG. 6) by a small archipelagic apron consisting of relatively smooth submarine slopes (MENARD, 1956).

An east-west graben-like basin bounds the arrugado (FIGS. 2 and 3) to the north by escarpments. Its floor varies in depth up to 4090 metres with areas of flat bottom of different depth separated by low escarpments or hills. Coring revealed very soft sediment, and sub-bottom echoes showed many layers to a depth of 25 metres. RAITT (1960) interprets the sediment to be about a kilometre thick, i.e. several times thicker than on the arrugado.

The basin is bordered by a very steep east-west escarpment (FIG. 2 and 3) almost a mile high which often attains an average slope of 30°. Rock dredged from the scrap consists of (1) a vesicular volcanic glass which was spontaneously disintegrating when brought on deck, (2) a slightly altered andesite and (3) andesite much altered to chlorite and veined by quartz. Magnetic profile E–F (FIGS. 11 and 12) runs along this long cliff and its character does not resemble either the profiles to the north or the profiles to the south.

The northwest corner of the chart (FIG. 2 and 3) is in the deep sea where the relief is on too small a scale to be accurately contoured from the widely spaced survey lines, but its character is similar to that of the arrugado east of Guadalupe Island. Magnetic profiles (FIGS. 11 and 12, profiles G–H and I–J) reveal north-south anomalies characteristic of the oceanic crust but which cannot be directly correlated with the anomalies of the arrugado to the south.

In the northeast corner of the map (FIGS. 2 and 3) just north of the east-west escarpment, there is a field of small volcanic peaks (as revealed by dredging and

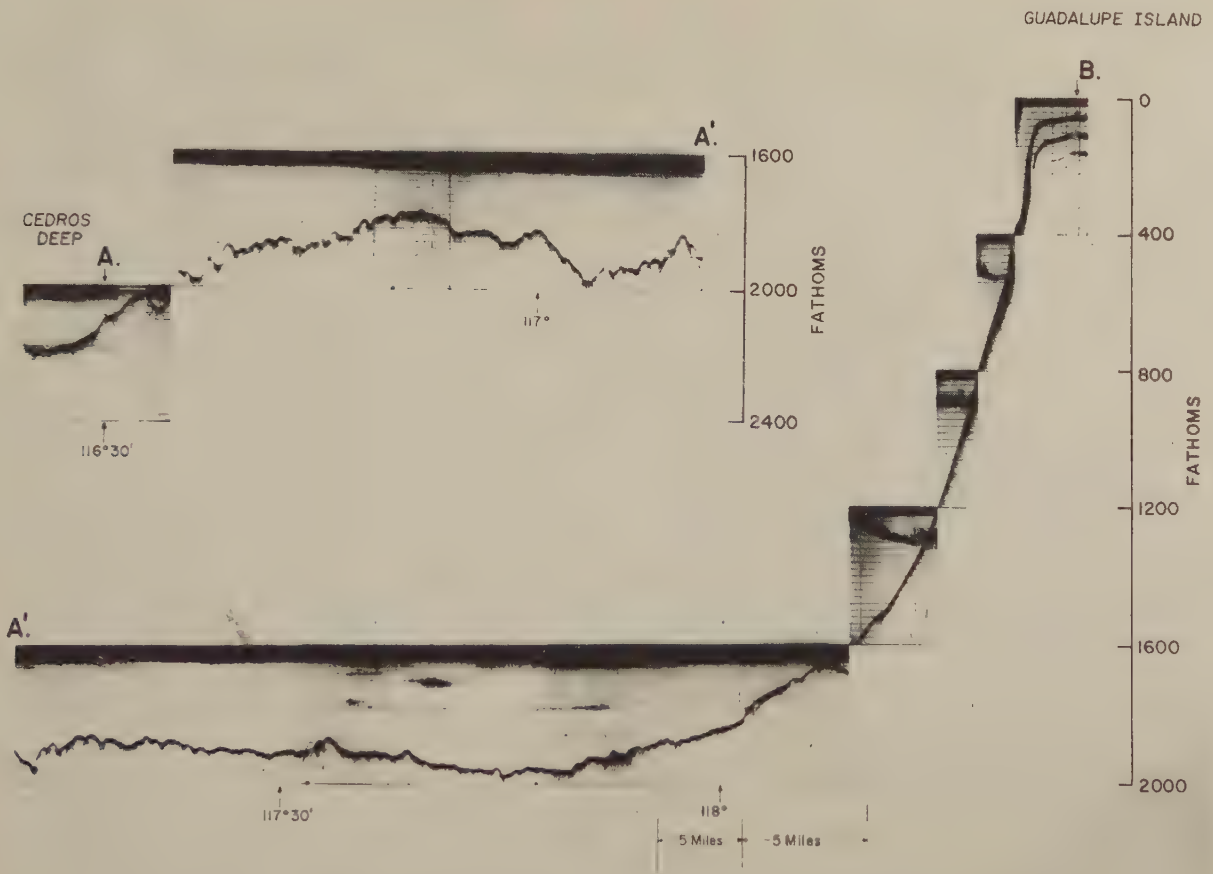

Fig. 5. Bathymetric profile along line AB of Fig. 4. Note the subdued and rolling character of the central part of the profile.

surveying) situated on the northwest end of a ridge which trends southeast to the San Benito Islands. Another volcano (andesite ?) lies 30 miles west of this field and just north of the escarpment.

The various seamounts and basins in the northeast part of the chart (FIGS. 2 and 3) mark the continental borderland, a province of sub-sea ridges and troughs similar in structure to the subaerial continent to the east (SHEPARD and EMERY, 1941). The continental margin therefore may be considered to run along the seaward edge of the borderland. The eastern ends of magnetic profiles (FIGS. 11 and 12, profiles G–H and I–J) show that the typical oceanic anomalies have disappeared and that smaller, more irregular anomalies occur which reflect the geologic structure of the borderland.

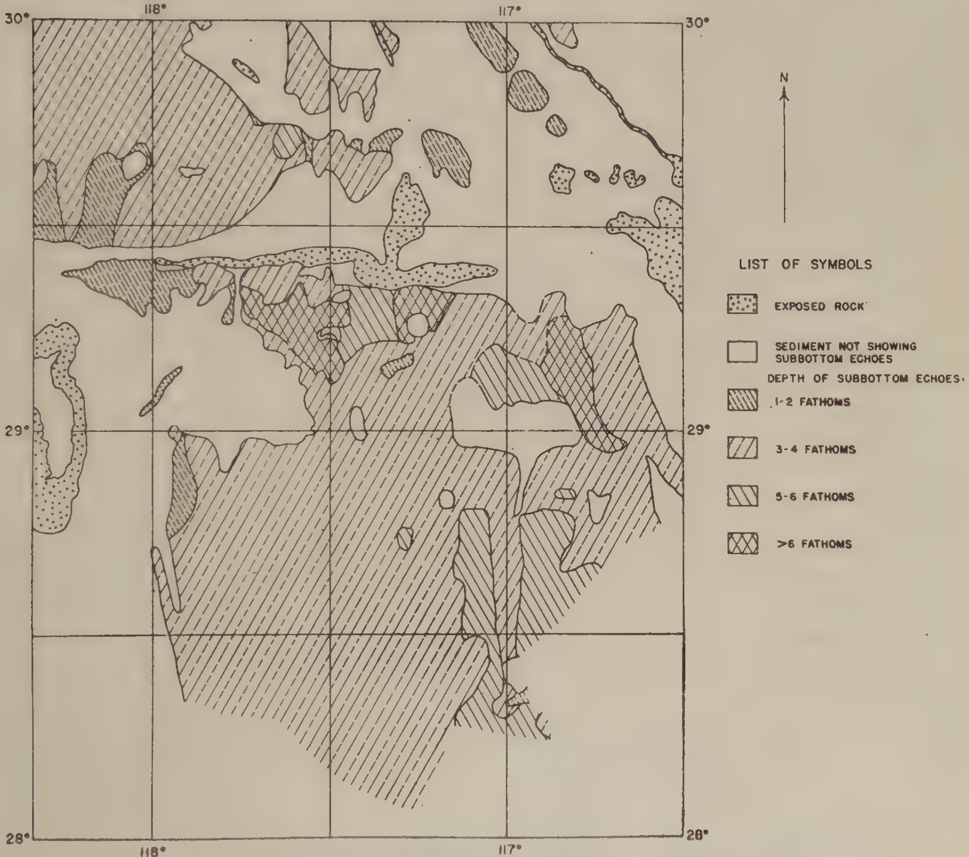
30°
118°
117°
30°
N
LIST OF SYMBOLS
EXPOSED ROCK
SEDIMENT NOT SHOWING SUBBOTTOM ECHOES
DEPTH OF SUBBOTTOM ECHOES
1-2 FATHOMS
3-4 FATHOMS
5-6 FATHOMS
>6 FATHOMS
29°
29°
28°
28°
118°
117°

FIG. 6. Map of depth distributions of the sub-bottom echoes. This Figure also shows regions where rock is known or is inferred to occur and where sediment occurs but shows no sub-bottom echoes.

The flat-floored Cedros Deep (FIGS. 2 and 3) marks the eastern margin of the arrugado as well as the seaward edge of the continental slope along much of Baja California. The sub-bottom echoes in the deep (FIG. 6) have a peculiar distribution that is in part due to the fact that bottom transported sediment, both volcanic and erosion products, can be deposited in the deep. The only other large source of such material in the area of FIG. 2, would be Guadalupe Island.

The arrugado changes to a deeper, perhaps more irregular sea floor near the south edge of the chart which may be related to an east–west bathymetric feature south of the area studied (CHASE, 1960).

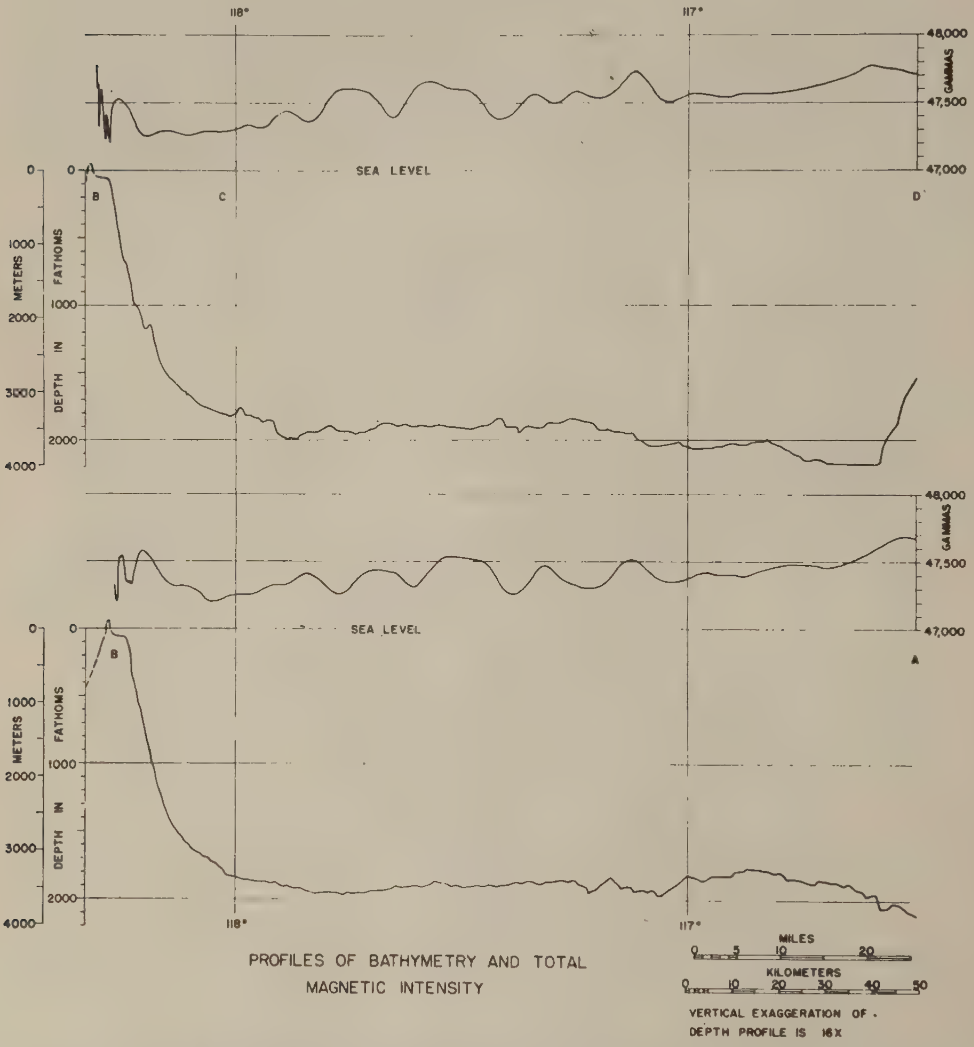

FIG. 10. Profiles AB and BD of the total magnetic intensity and the bathymetry. Location of the profiles are shown in FIG. 4. One gamma (γ) = 10^{-5} oerstads.

RELIABILITY OF CONTOURS

In general, much interpolation has gone into drawing the bathymetric contours (FIGS. 2, 3 and 8). The ship tracks are not spaced evenly (FIG. 4), and even where they are spaced closely on the arrugado, the relief is so low that it is not completely revealed. However, the interpretation gives a consistent picture and one that is close to reality.

The navigation, based on celestial and shore fixes, forms the largest uncertainty in the data. The navigational accuracy at best has an uncertainty of a mile in position and in most cases, it is only good to two or three miles. During long periods, the area was cloudy, and no celestial fixes were obtained. The uncertainty has been lessened by adjusting the ships' courses to the bathymetry whereby two tracks which cross must have the same depth. Independent checks such as later surveys indicate that adjustment by bathymetry brought the error back to a mile. Although larger local errors must exist, a feature on the bathymetric map generally should be within a mile of its true position.

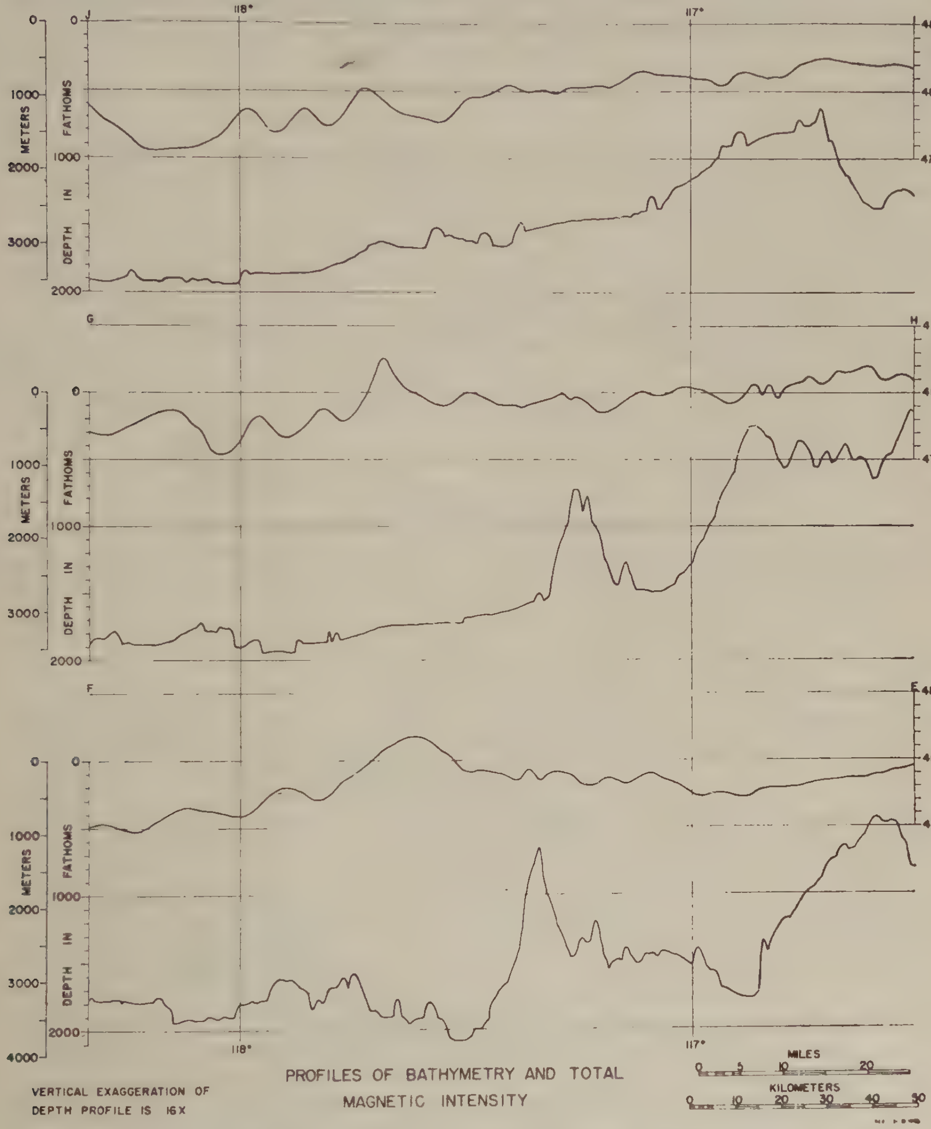

FIG. 11. Profiles EF, GH and IJ of the total magnetic intensity and bathymetry. Location of the profiles are shown in FIG. 4.

GEOLOGIC STRUCTURE

The interpretation of the geologic structure of the area depends on its regional relations, and these are being investigated at the present time so that a thorough discussion would be premature at the moment. Actually the available facts are very few, and any conclusions from them would have to be speculative. Any conclusions must take in these facts :

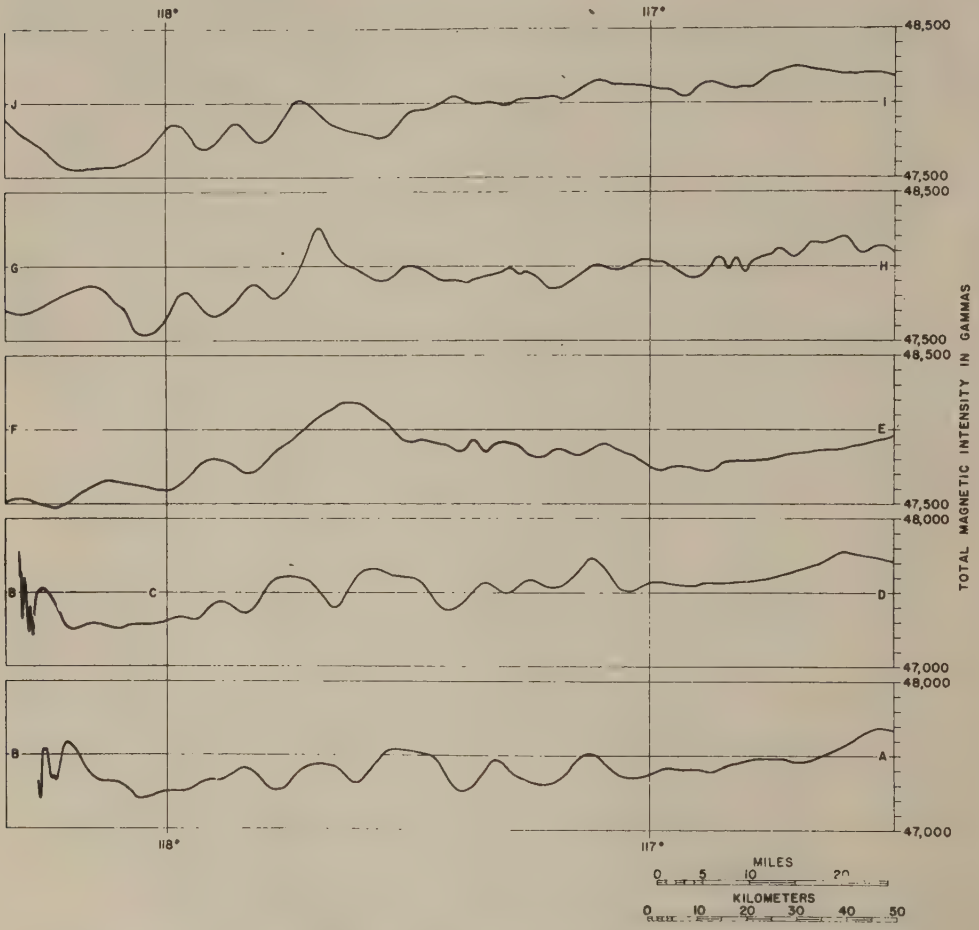

FIG. 12. Profiles of total magnetic intensity. Note the north–south alignment of the anomalies in profiles AB and BD and the west ends of profiles GH and IJ.

(1) the anomalous depth of the area

(2) the presence of the right lateral San Andreas fault system of California and Baja California.

(3) the presence of the borderland

(4) the volcanism

(5) the basin north of the arrugado.

MENARD (1960) suggests that the shallow depth is evidence of the area's position on the west flank of the East Pacific Rise. The elevation of the arrugado in part may be analogous to the Hawaiian Arch (HAMILTON, 1957) wherein the crust is bulging upward due to the isostatic load of Guadalupe Island and Baja California.

The author feels that a combination of regional northwest–southeast right lateral shear superimposed on a relative east–west tension would explain most of the features present in the area. Documentation must wait until the study to the north has been completed.

CONCLUSIONS

Although the region has been subjected to intense activity during Tertiary time, the deep-sea floor east of Guadalupe Island has been relatively little deformed compared to the surrounding regions. This is demonstrated by (1) the fact that the arrugado is smooth and rolling – it must have had a long history of quiet deposition of sediment, (2) it has a seismically normal oceanic crust and, (3) the north-south magnetic anomalies are typical of the rest of the northeast Pacific Ocean basin. The folding, if caused by structural movements, is mild deformation compared to the large tectonic features surrounding the arrugado.

Acknowledgments—H. W. MENARD and J. R. CURRAY were kind enough to review the paper, V. VACQUIER and A. RAFF made it possible to use the magnetometer. The Scripps Institution of Oceanography, University of California, generously furnished ships and support. J. R. MORIARTY and R. L. FISHER furnished unpublished surveys. The work was in part supported by the Office of Naval Research and the National Science Foundation. Finally, the author wishes to thank the officers and crews of the vessels and the scientists and technicians who stood the many watches that made possible the compilation of material.

REFERENCES

CHASE, T. E. and MENARD, H. W. (1960) Topographic Chart No. 1. U.S. Bureau of Commercial Fisheries and University of California, Institute of Marine Resources.
FISHER, R. L. (1953, 1955) Unpublished charts.
GOLDBERG, E. D. (1960) Personal communication.
HOWELL, J. V. (1957) *Glossary of Geology*. American Geological Institute, Washington, D.C., pp. 12, 113.
JOHNSON, C. W. (1953) Notes on the geology of Guadalupe Island, Mexico. *Amer. J. Science* **251**, 231–236.
MASON, R. G. (1958) A magnetic survey off the west coast of the United States between latitudes 32° and 36 °N, longitudes 121° and 128 °W. *Roy. Astronom. Soc. Geophys. J.* **1**, 320–329.
MENARD, H. W. (1955) Deformation of the northeastern Pacific basin and the west coast of North America. *Bull. Geol. Soc. Amer.* **66**, 1149–1198.
MENARD, H. W. (1956) Archipelagic aprons. *Amer. Assoc. Petroleum Bull.* **40**, 2195–2210.
MENARD, H. W. (1954, 1959) Unpublished charts.
MENARD, H. W. (1960) The East Pacific Rise. *Science*, **132**, No. 3441, 1737–1746.
MORIARTY, J. R. (1956) Unpublished chart.
RAFF, A. (1960) Personal communication.
RAITT, R. W. (1960) Personal communication.
ROBB, L. A. (1949) *Engineer's Dictionary, Spanish–English*. John Wiley, New York, 32.
SHEPARD, F. P. (1950) 1940 Scripps Cruise to the Gulf of California, Part III. *Geol. Soc. America, Memoir* **43**, Charts I, XI.
SHEPARD, F. P. and EMERY, K. O. (1941) Submarine topography off the Claifornia coast. *Geol. Soc. America, Special Paper* **31**, 1–49.
VACQUIER, A. (1960) Personal communication.

Printed in Great Britain by The Salisbury Press Ltd., Publicity House, Wilton Road, Salisbury, Wilts. (29170)

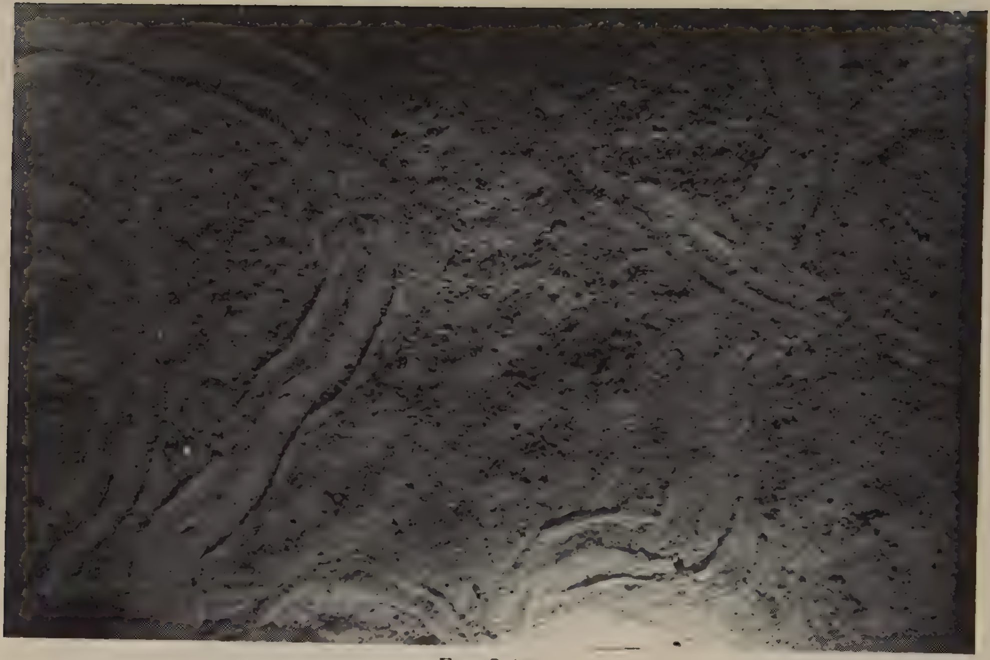

FIG. 7 (a)

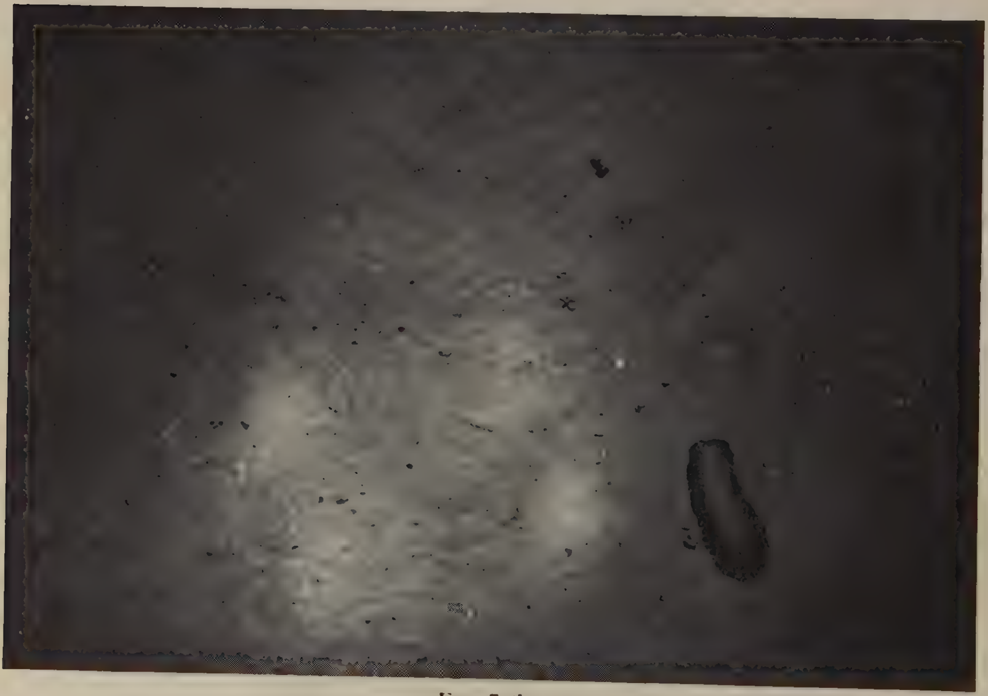

FIG. 7 (b)

FIG. 7. Photographs taken in about 1900 fms of water near 28° 57′N, 117° 30′W. The tracks in the photograph on the left are about 3 in. long. All of the photographs taken in the area show tracks criss-crossing the mud and various holes and tentacles in the mud. The holothurian (?) on the right is about nine inches long and is one of the animals which is reworking the mud. Other animals observed are tentatively identified as echinoids, an isopod, a sea pen and crinoid fragments. The pictures were taken with an Edgerton camera in conjunction with an Edgerton pinger.

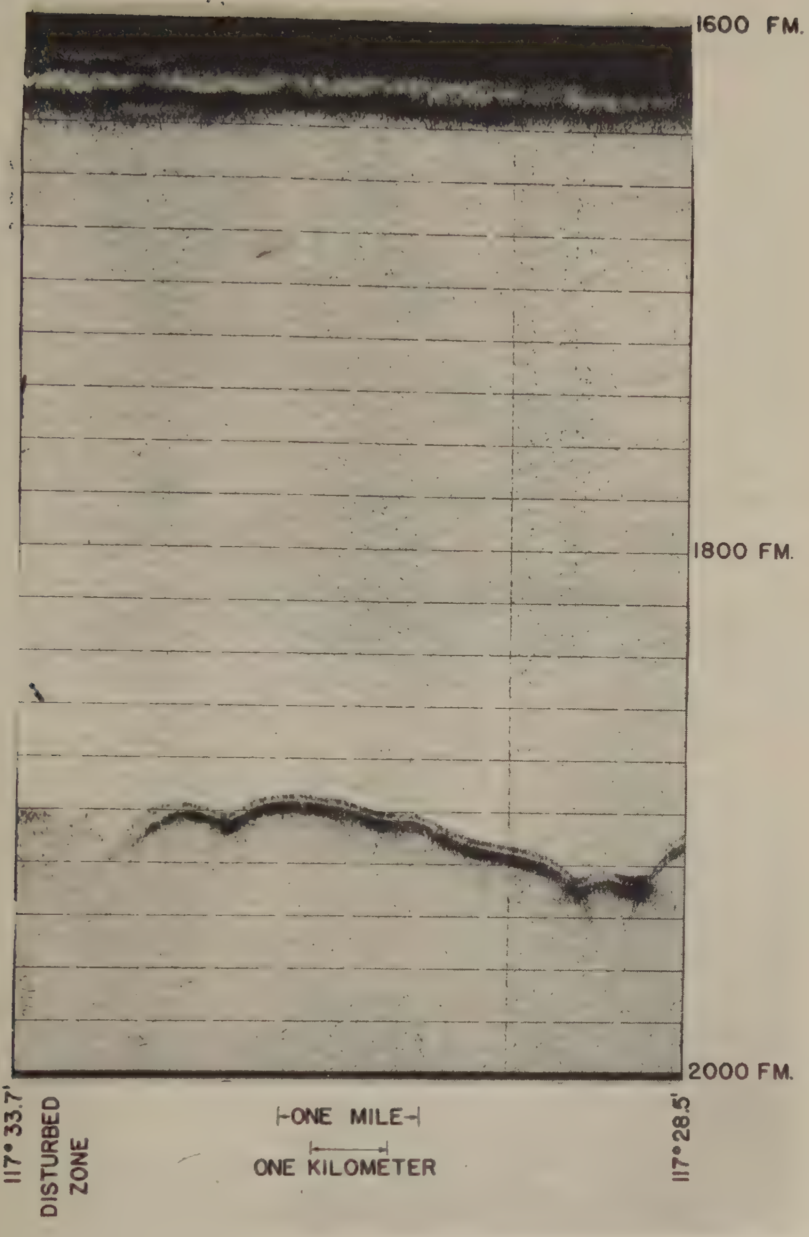

FIG. 9. East–west bathymetric record across part of the area of the detailed survey (FIG. 8). Note the smoothness of the sea floor and the sub-bottom echoes. The irregular disturbed zone of FIG. 8 is shown at the left.

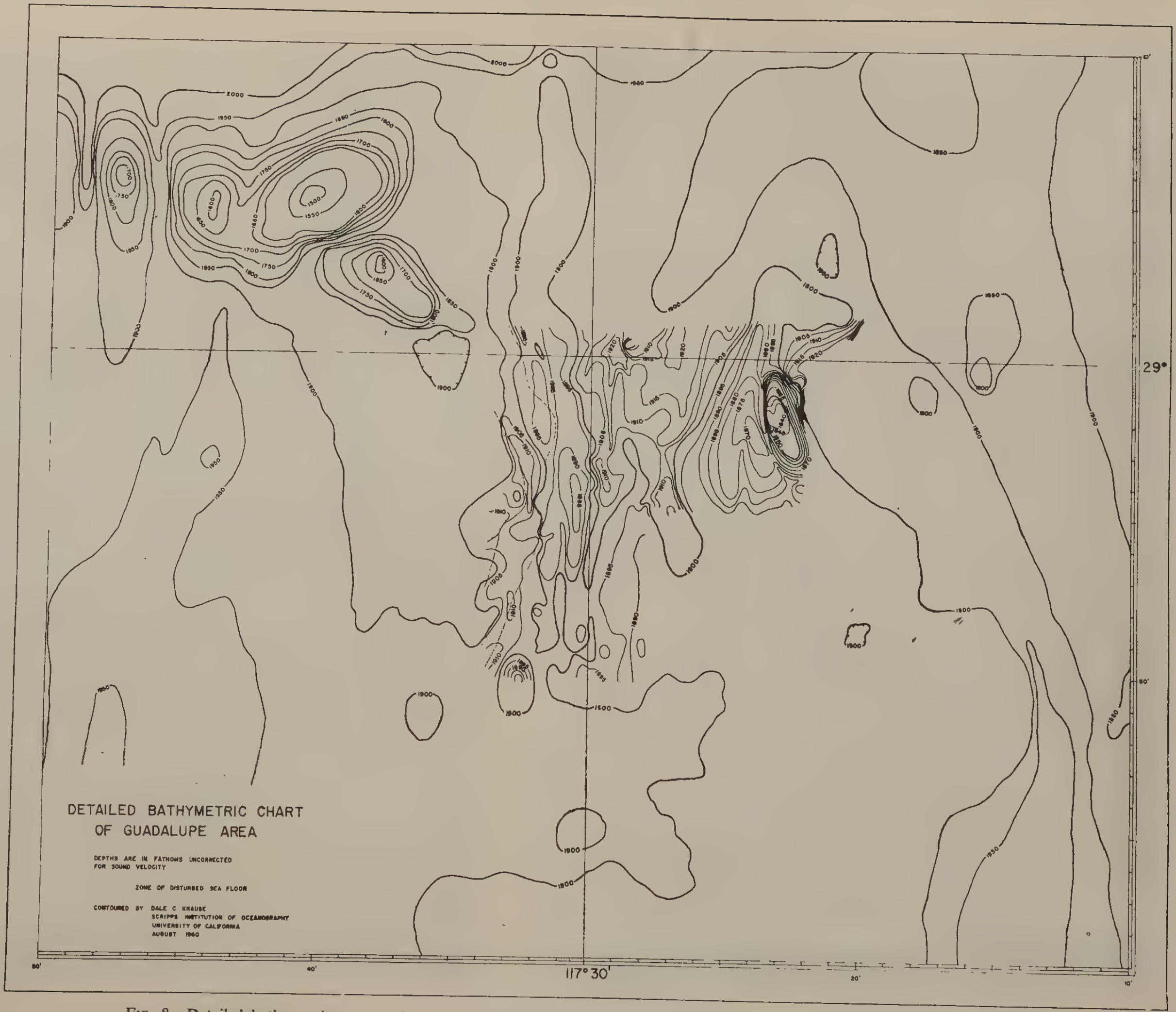
DETAILED BATHYMETRIC CHART
OF GUADALUPE AREA
DEPTHS ARE IN FATHOMS UNCORRECTED FOR SOUND VELOCITY
ZONE OF DISTURBED SEA FLOOR
CONTOURED BY DALE C KRAUSE
SCRIPPS INSTITUTION OF OCEANOGRAPHY
UNIVERSITY OF CALIFORNIA
AUGUST 1960
29°
117° 30'
40'
20'
10'
50'
2000
1950
1900
1850
1800
1750
1700
1650
1600
1550
1500

FIG. 8. Detailed bathymetric survey of a portion of the Guadalupe area. Note the north-south trend of the bathymetry and the disturbed belt just west of 117° 30′W.

Vol. 74, pp. 207–212 11 August 1961

PROCEEDINGS
OF THE
BIOLOGICAL SOCIETY OF WASHINGTON

A NEW PEARLFISH (FAMILY CARAPIDAE) FROM THE GULF OF CALIFORNIA[1]

By Richard H. Rosenblatt
Scripps Institution of Oceanography, University of California, La Jolla, California

Recent investigations of the shelf fauna of the Gulf of California, México, have revealed a number of novelties, among which is an undescribed species of pearlfish. Reference to the review by Arnold (1957) leaves little doubt that this new form is referable to the genus *Echiodon* Thompson 1837. This is somewhat surprising since one of the two species placed with certainty in *Echiodon* occurs in the North Atlantic, and the other in the Mediterranean. However, the Pacific specimen shares certain distinctive characters with *Echiodon drummondi* Thompson 1837 and *E. dentatum* (Cuvier, 1817): There is a diastema in the lower jaw, the teeth are arranged in bands, the transverse processes of the third, fourth, and fifth vertebrae are unfused, and the anus is posterior (for a carapid). These features indicate that the present specimen cannot be placed either in *Carapus*, in which the tooth rows of the jaws are continuous, the lateral processes of the third and fourth vertebrae are fused, and the anus is under the pectoral base, or in *Encheliophis*, in which the teeth in the lower jaw are in a single continuous row, the lateral processes of the third, fourth, and fifth vertebrae are fused, and the anus is anterior in position.

Echiodon exsilium, new species

Fig. 1

Holotype: Fish Collection, Scripps Institution of Oceanography, University of California, La Jolla, S.I.O. 60-97-61A, a 100 mm ♀ taken

---

[1] Contribution from the Scripps Institution of Oceanography, New Series. 1293

(699)

by Robert H. Parker on the R. V. "Spencer F. Baird" in 35–41 fathoms on a muddy sand bottom off Estero de Tasiota (from 28° 13.8′ N, 111° 46.7′ W to 28° 15′ N, 111° 48′ W), Golfo de California, Sonora, México, on 21 March 1960. The type was taken in a shrimp trawl and the host is unknown. The specimen may have been free-living, since the collection contained no holothurians, no large lamellibranchs or echinoids, and only two gastropods of moderate size.

Following are counts and measurements in millimeters of the type and single known specimen: Precaudal vertebrae 22; gill rakers 0 + 1 + 2 (+ six rudiments); branchiostegals 7; pectorals 20; dorsal and anal undeterminable. Total length 100.0; snout to dorsal origin 20.9; snout to anal origin 17.1; snout to center of anus 17.0; body depth at anus 7.9; head length 14.1; head depth 6.0; head width 5.9; snout 3.1; bony orbit diameter 3.2; eye diameter 2.9; interorbit 2.0; upper jaw 7.2; pectoral 8+ (tips of middle rays curled).

The body is elongate and tapering; the maximum depth is at the anus and is contained 13 times in the total length. The head is about one-seventh of the total length. The upper profile of the head is slightly convex from the nape to before a point above the middle of the eye, then shallowly concave to a point even with the posterior nostril. Anterior to the posterior nostril the profile descends abruptly to the upper lip. The short, obtuse snout is 5 in the head. Both nostrils are circular, but the anterior ends in a short tube. The nasal capsule is large, half as long as the orbit. The olfactory rosette has five pairs of simple, flattened lamellae. The bony orbit goes 8 times in the snout and 4.8 times in the head. The narrow interorbital is contained 1.7 times in the orbit.

The maxillary extends behind the orbit for a distance somewhat less than one-half an orbit diameter. The lower jaw is slightly shorter than the upper, which overhangs it by a distance about equal to the diameter of the pupil. A fang at the front of each upper jaw is separated by a pronounced diastema from a band of villiform teeth, which is about five rows wide anteriorly and two rows wide posteriorly. The dentition of the lower jaw is similar, except that the diastema is more pronounced, and the bone narrows at this point (see Arnold, 1957: 256, Fig. 3B). The vomer is covered by an oval patch of blunt, almost granular, teeth. The villiform palatine teeth are in a band about four rows wide. The vomerine and palatine tooth patches are well separated. There are two crescentic patches of tiny upper pharyngeal teeth on each side. The toothless tongue ends in a narrow free forward projection.

The anus is posterior for a carapid: 2.8 mm behind a vertical through the middle of the pectoral base. The body cavity extends far back of the anus. It ends 18.4 mm behind the center of the anus, and is empty of any organs for the last 11.8 mm. In *Carapus* a similar cavity is filled by the gas-bladder. In *E. exsilium*, however, the gas-bladder is elongate and tightly applied to the roof of the body cavity. In this respect it resembles the gas-bladder of *E. dentatum* as figured by Emery (1880: Pl. II, Fig. 15).

(700)

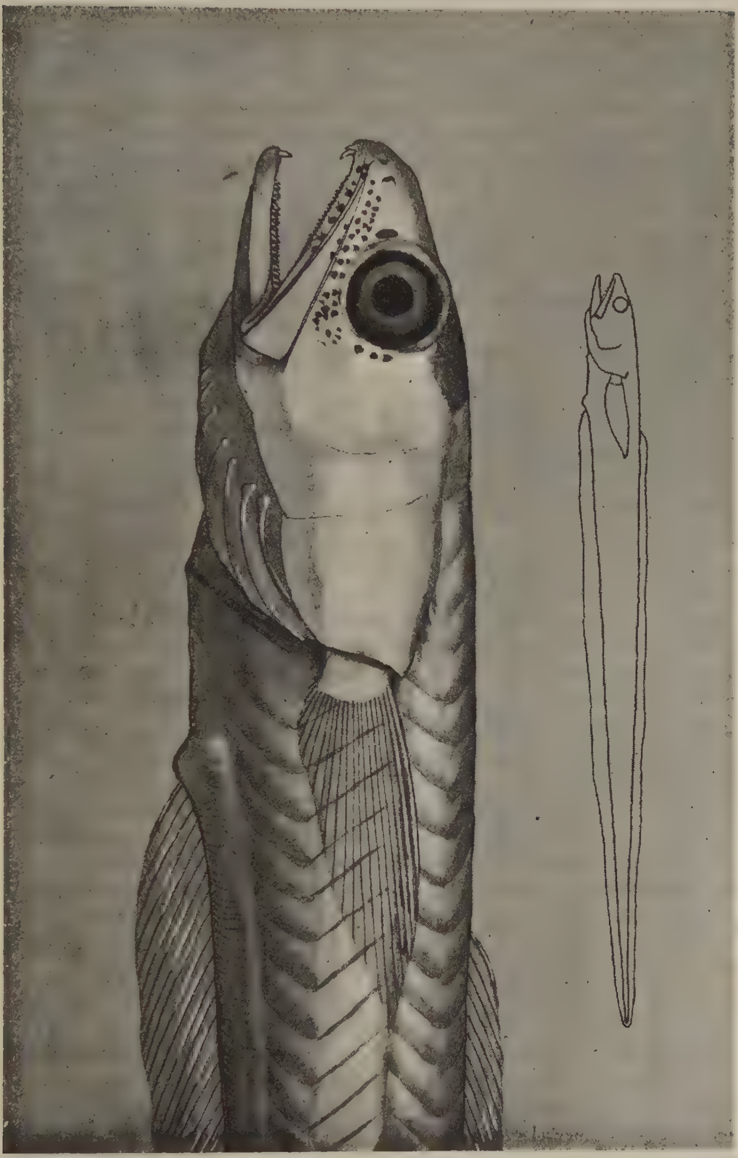

FIG. 1. *Echiodon exsilium* new species. Female holotype, SIO-60-97-61A. Total length, 100 mm.

There is a narrow slit behind the fourth gill arch. There appear to be no pseudobranchiae. The gill rakers are poorly developed. There are none on the upper limb of the first arch, and only the one at the angle and the two immediately below it are well developed. They are about half as long as the eye; the remaining six are developed as low rudiments only. The rakers of the posterior arches are all rudimentary.

I am unable to determine the position of the pores along the sensory canals of the head, nor can I observe any lateral-line pores.

The origin of the dorsal is over the posterior third of the pectoral, and above a vertical from the tenth or eleventh anal ray. The dorsal and anal are confluent with the very reduced caudal. The pectoral is long and almost filamentous at the posterior extremity.

The body is mostly pale. The skull is dark brown around the brain case, and some dark pigment runs down either side of the snout and continues back beneath the eye as a feeble bar. The anterior half of the body is completely colorless, but about halfway back there begins a series of dots along the bases of the vertical fins. There is a dusting of black pigment over the posterior third of the body, concentrated mostly along the fin bases and the edges of the myomeres. The peritoneum is mostly white, although there are a few melanophores ventrally, and a larger number dorsally.

The name is derived from the Latin *exsilium*, an exile, and refers to the geographic isolation of the species from other members of the genus.

Echiodon exsilium is not closely related to the carapids reported in the eastern Pacific, *Carapus dubius* (Putnam 1874), *Encheliophis jordani* Heller and Snodgrass, 1903, and *E. hancocki* (Reid, 1940). The characters which separate the genus *Echiodon* from the species of the above genera are discussed in the introduction.

Arnold placed two species in *Echiodon*, *E. drummondi* Thompson, 1837, and *E. dentatum* (Cuvier, 1817). On the basis of dentition, *E. exsilium* is closer to *dentatum* than to *drummondi*. As in *dentatum* the vomerine tooth patch is rounded posteriorly, and there is a distinct gap between the vomerine and palatine dentition. *E. exsilium* also agrees with *dentatum* in the relatively anterior insertion of the dorsal fin (see Arnold's Figs. 16 and 17). *E. dentatum* and *exsilium* differ markedly in head shape, however. In *E. dentatum* the major outline of the head is concave from the occiput to the snout, whereas in *E. exsilium* the major outline of the upper surface of the head is convex (there is a shallow concavity, just before the eyes). Also, the head is wider (width 42% of head length rather than 32%) and the pectoral fin longer (56% of head length rather than 42%) in *exsilium* than in *dentatum*. In addition there appears to be a difference in the number of precaudal vertebrae. According to Emery (1880: 26), *E. dentatum* has 95 vertebrae of which 26 are precaudal. Radiographs of the type of *E. exsilium*, however, indicate that only the first 22 vertebrae bear unfused haemal arches. In the 23rd vertebra the haemal arches are fused to form a haemal spine. This is not an apparent effect produced by the hiding of one haemal element by another in the picture, since three radiographs, each taken from a different angle, show only 22 precaudal vertebrae. Due to the attenuation of the body, the total number of vertebrae cannot be determined.

Arnold felt that two more species might prove to be referable to *Echiodon*. These are *Carapus rendahli* Whitley, 1940, and *C. cinereus* Smith, 1955. The sketchy description of *C. rendahli* indicates that in that species the pectoral fin is considerably shorter (4 in the head rather than 1.8) and the dorsal origin farther forward (predorsal about .9 in head rather than .66). *Carapus cinereus* differs from *E. exsilium* in a number of respects. The most important difference involves the vomerine dentition. In *C. cinereus* (as in a number of species of *Carapus*) the vomer bears a median row of enlarged teeth, while in *E. exsilium* none of the vomerine teeth is enlarged. Also in *C. cinereus* the dorsal and anal origins are farther forward (predorsal 15% of total length rather than 21%) and the head is somewhat shorter (10.8% of length rather than 14.1%). It is not likely that the observed difference in head length is due to the greater size of the type of *C. cinereus* (215 mm), since the observed tendency in the Carapidae is for the head to become proportionally larger with increasing size (Arnold, 1957).

The zoogeographic implications of the discovery of a species of *Echiodon* in the eastern tropical Pacific are difficult to assess. It is unfortunate that the generic affinities of the Indian Ocean and Pacific species *Carapus cinereus* and *C. rendahli* cannot be determined with certainty, although it seems probable that *rendahli* at least will prove to be referable to *Echiodon*. The available evidence suggests that the affinities of *E. exsilium* lie with the Atlantic species, especially *E. dentatum*. This would suggest that *E. exsilium* or a progenitor entered the eastern Pacific from the east, via a Tertiary Central American water gap (Durham and Allison, 1960: 66–68, Fig. 7), rather than from the west, across the eastern Pacific barrier (Ekman, 1953: 72–75). If this hypothesis is correct, it might reasonably be expected that the western Atlantic might harbor a species of *Echiodon*. That no such form has yet been captured is not surprising considering the rarity of carapids in collections.

LITERATURE CITED

Arnold, D. C. 1957. A systematic revision of the fishes of the teleost family Carapidae (Percomorphi, Blennioidea), with descriptions of two new species. Bull. Brit. Mus. Nat. Hist., Zool., 4(6): 247–307.

Cuvier, G. L. C. F. D. 1817. Le Règne Animal, Ed. 1, v. 2. Paris, Deterville: 532 pp.

Durham, J. W. and E. C. Allison. 1960. The biogeography of Baja California and adjacent seas. Pt. 1. Geologic History. The geologic history of Baja California and its marine faunas. Systematic Zool., 9(2): 47–91.

Ekman, S. 1953. The zoogeography of the sea. London, Sidgwick & Jackson: 417 pp.

EMERY, C. 1880. Le specie del genere Fierasfer nel Golfo di Napoli e regione limitrofe. Fauna U. Flora Golfes Neapel, 2: 1–76.

Heller, E. C. and R. E. Snodgrass. 1903. Papers from the Hopkins Stanford Galapagos Expedition, 1898–1899. 15. New fishes. Proc. Washington Acad Sci., 5: 189–229.

Putnam, F. W. 1874. Notes on Ophidiidae and Fierasferidae, with descriptions of new species from America and the Mediterranean. Proc. Boston Nat. Hist. Soc., 16: 339–348.

Reid, E. D. 1940. A new genus and species of pearl fish, family Carapidae, from off Gorgona Island, Colombia. U. Southern California, Allan Hancock Pacific Exp., 9(2): 47–50.

Smith, J. L. B. 1955. The fishes of the family Carapidae in the western Indian Ocean. Ann. Mag. Nat. Hist., (12) 8: 401–416.

Thompson, W. 1837. Notes relating to the natural history of Ireland, with a description of a new genus of fishes (*Echiodon*). Proc. Zool. Soc. London, 5: 52–63.

Whitley, G. P. 1941. Ichthyological notes and illustrations. Australian Zoologist, 10(1): 1–50.

(*Reprinted from Nature, Vol.* 190, *No.* 4782, *pp.* 1214–1215,
June 24, 1961)

Life-span of the Fronds of the Giant Kelp, *Macrocystis pyrifera*

THE large brown attached alga, *Macrocystis pyrifera*, member of a widespread genus, is of considerable importance as the direct and indirect source of food for a large number of near-shore animals; it is also gathered by man, to be used as fertilizer, food additives, and it is processed for certain of its chemical constituents. The fronds develop continuously from growing points located on the perennial hold-fast at the base of the plant[1]. Little information exists about the life-span of the fronds, although this is a factor of considerable importance in management of the resource and in computing the productivity of the kelp groves. Authors have estimated the life-span as several months[1,2]. Further information is now available as a by-product of work on rate of growth in several kelp-beds spread over a geographical range of about 150 km.

Individual fronds were tagged with numbered small white plastic squares, by divers using self-contained underwater breathing apparatus (SCUBA)[3]. Two tags were attached to each frond by a rubber band loosely encircling the stipe; thus if one marker disappeared, replacement could be effected without loss of the identity of the frond (in practice, however, few tags were lost). Two or more fronds per plant were always tagged. It has always been possible to relocate the plant on subsequent visits, except when the entire organism was removed by a storm or by concentrated grazing. Elimination of the parent plant was disregarded in the statistical calculations of the loss of fronds.

Results for eleven different time periods and three locations are presented in Table 1. For work on rate of growth, fronds were tagged when quite small, 30–100 cm. long; measurements of length were made at intervals as they developed. Experiments 1, 2, 4 and 5 show consecutive measurements on groups of fronds tagged at the beginning of each series. For experiments 2 and 3 many of these time-intervals are lumped in Table 1 and only a few of the visits are represented. In preparing Table 1, a frond was considered as being defunct when it had lost the distal growing tip from which all its blades originate. Measurements have shown that although elongation can occur after loss of this apical blade,

Contributions from the Scripps Institution of Oceanography, New Series, 1294

overall growth-rates quickly slow down and no more blades are produced (as was also observed in *Macrocystis integrifolia*[1]).

The first experiment in Table 1 summarizes a long-term investigation that began with a large number of young stipes. Experiment 4 in Table 1 was started at about the same time, at Pt. Loma, about 16 km. away. Both beds showed similar rates of mortality, but the Pt. Loma site was abandoned after the final observations shown in experiment 4*b* because of the encroachment of a horde of sea-urchins, *Strongylocentrotus franciscanus*, which destroyed all the plants at their bases. At La Jolla, in experiment 1, only 3 incomplete fronds remained after 162 days, and these bore evidences of heavy grazing and deterioration. Their lengths were 28, 32 and 35 m.; the stipes were so fragile and chewed that they broke in several places during recovery and measurement, although extreme care was used in handling. Had the fronds been complete, their lengths would probably have been increased by perhaps as much as 5–10 m. Growing conditions during the period of this experiment were favourable with respect to temperature and water clarity, throughout the water column, but a series of storms presumably took a considerable toll of both the Pt. Loma and the La Jolla fronds.

Experiments 2 and 3 describe late spring and summer observations on other groups of fronds when the ocean was comparatively calm. After 72 days, only 1 of the original 9 fronds in experiment 2 had broken, indicating a much slower rate of mortality than had been observed in the winter and spring in experiments 1 and 4. Subsequent to the final observation of this group, the fronds grew up into the warm water above the thermocline and rates of growth quickly decreased practically to nil. All the fronds took on an unhealthy appearance, involving loss of pigment, and became brittle. The mortality-rate increased markedly. A younger set of 14 fronds nearby, below the thermocline, constituting experiment 3, exhibited a very low rate of mortality and normal growth-rates during the period when the older fronds of experiment 2 were suffering heavy losses.

Experiments 5*a–d*, which were run consecutively in a very small bed in a cold upwelling area at Punta Banda, Baja California, illustrate a continuous attrition process, as was likewise demonstrated by experiments 1 and 4. The loss per unit of time was somewhat variable in this bed. The half-life expectation of the fronds ranged from 12 to 38 days (Table 1). These values compare with a

Table 1. MORTALITY OF *Macrocystis pyrifera* FRONDS AT DIFFERENT SEASONS AND LOCATIONS

Experiment	Dates of observations		No. of intact tagged fronds		Elapsed time (days)	Loss (per cent)	Half-life (days)	Depth (m.)
	Initial	Subsequent	Initial	Subsequent				
(1) (La Jolla)*								
a	6/12/59	7/1/60	66	25	32	62	23	20
b	7/1/60	16/5/60	25	0†	131	100	—	20
(2) (La Jolla)								
a	9/5/60	20/7/60	9	8	72	11	400	20
b	20/7/60	22/8/60	8	3‡	33	63	24	20
(3) (La Jolla)	23/7/60	27/8/60	14	13	35	7	340	20
(4) (Pt. Loma)								
a	28/12/60	22/1/60	106	74	25	30	47	15
b	22/1/60	18/2/60	34	23	27	32	48	15
(5) (Punta Banda)								
a	28/6/60	26/7/60	49	24	28	51	27	2–16
b	26/7/60	11/8/60	24	18	16	25	38	2–16
c	11/8/60	2/9/60	14	7	22	50	22	2–10
d	2/9/60	23/9/60	7	2	21	71	12	2–10

* A composite sample of plants along a straight transect line 125 m. long; experiments 2 and 3 were conducted on 2 groups of plants along this same line, separated by about 100 m.

† 3 incomplete fronds were found remaining.

‡ These 3 fronds, although complete, seemed unhealthy, fragile, and brittle, and were heavily grazed and encrusted.

winter half-life of 23 days at La Jolla (experiment 1) and of 47 to 48 days at Pt. Loma (experiment 4). The chief damaging factor in the Punta Banda bed was apparently an excessively thick and continuing encrustation of the bryozoan *Membranipora serrilamella*, which restricted growth, deformed the tissues, and induced brittleness and breakage by water movements.

It is apparent from the examples just cited that considerations of the life-span of kelp fronds can be quite complex. It is important to define accurately the terms used. In some circumstances the average age of a group may be considerably less than the maximum age. The age of our experimental fronds at the time of tagging may be safely estimated from our growth data as 1–2 months, hence the observations indicate that the maximum age of a frond in 20 m. of water under favourable growing conditions is about 6 months, confirming the values of Scagel[1] and Brandt[2]. The average age, however, may often be only 2–3 months.

If unfavourable conditions, such as the temperature destruction of the fronds in experiment 2, develop suddenly, the maximum age of a population of fronds may almost coincide with the average age, and may be substantially less than 6 months.

Support of this work by the California Department of Fish and Game and the State Water Pollution Control Board is gratefully acknowledged.

W. J. North

University of California
Institute of Marine Resources,
La Jolla, California.

---

[1] Scagel, R. F., *An Investigation on Marine Plants near Hardy Bay, B.C.* (Provincial Dept. of Fisheries, Victoria, British Columbia, 1947).

[2] Brandt, R. P., *Potash from Kelp* (U.S. Dept. Agric., Bull. No. 1191, 1923).

[3] North, W. J., *Yale Sci. Mag.*, **31** (1956).

[4] Cribb, A. B., *Austral. J. Mar. Freshwater Res.*, **5**, 1 (1954).

Contributions from the Scripps Institution of Oceanography, New Series, 1294
Reproduced by Permission

Printed in Great Britain by Fisher, Knight & Co., Ltd., St. Albans.

JULY 1961 PHYCOLOGICAL NEWS BULLETIN
v.14, no.2. p.11

PERSISTENCE OF A DIURNAL RHYTHM IN PHOTOSYNTHESIS IN ENUCLEATED ACETABULARIA

Beatrice M. Sweeney and Francis T. Haxo
University of California, La Jolla

The unicellular alga *Acetabularia* was found to show a diurnal rhythm in photosynthesis. This rhythm was observed to continue for at least three cycles in constant light and temperature, and hence can be considered endogenous. Plants from which the nucleus had been removed by severing the basal rhizoids showed no modification in the photosynthetic rhythm over a number of cycles. The nucleus is, therefore, not essential for the maintenance of rhythmicity in *Acetabularia*. Conversely, a mechanism for sustaining time-keeping must exist in the cytoplasm.

Contributions from the Scripps Institution of Oceanography, New Series, 1295

Reproduced by Permission

From:
ICSU REVIEW
v.3, no.4, October 1961.
pp. 164-169.

THE CHEMIST IN OCEANOGRAPHY*

NORRIS W. RAKESTRAW
Scripps Institution of Oceanography, University of California, La Jolla, Calif. (U.S.A.)

The first attempt to discover the nature of sea water was probably that of an obscure alchemist in early modern times. His observations have been largely lost and forgotten, however, because of the limited methods available to him and the inadequate ideas of those times about the nature of chemical constitution in general.

The first really productive efforts in this direction were those of two contemporaries in the late eighteenth century, BERGMANN and LAVOISIER, the latter often known as the father of modern chemistry. From different motives and independently, each isolated from sea water some of its principal constituents, by evaporation, crystallization and selective solubliity, methods which would occur to any modern chemist who might approach the same problem.

LAVOISIER was concerned with what would now be called geochemistry, the relationship of the dissolved constituents of natural waters to the composition of the surrounding terrain. BERGMANN, on the other hand was interested in biological matters, analyzed water from great depth (60 fathoms!), observed that products of putrefaction were more abundant in the surface, and was thus one of the first to investigate the marine biological cycle.

MURRAY, in the early nineteenth century, long before the advent of the ionic theory, precociously suggested that sea water does not contain a collection of dissolved salts as such, but rather an array of "acids and bases", ions or radicals in modern nomenclature, which combine to form various salts depending upon the conditions under which they are separated from the solution. His analytical methods were those of modern gravimetry.

Another well-known name in the history of chemistry, that of GAY-LUSSAC, figures also in the early development of oceanography. Although others had noted the variable amount of salt in sea water, he made a serious study of these variations and was led to the conclusion that differences in "salinity"—related to the processes of evaporation, precipitation and fresh water inflow—bring about differences in density, which in turn give rise to permanent currents and other movements in the sea.

From these early days to the present, in his study of the ocean the chemist has been busy answering certain questions, either simultaneously or successively.

---

* Contribution No. 1296 from the Scripps Institution of Oceanography, University of California.

Reproduced by Permission

ticle III du Traité, le SCAR devrait être encouragé à poursuivre cette tâche consultative qui a si effectivement facilité la coopération internationale en matière de recherche scientifique".

Cette résolution est évidemment de grande importance pour le SCAR et pour le Conseil International des Unions Scientifiques. Elle décevra sans doute ceux qui espéraient que le Traité établirait des relations formelles avec le SCAR et qui la trouveront peu constructive. On peut la juger inefficace aussi bien dans le contexte étroit de la recherche antarctique que dans celui plus large, de la politique scientifique internationale. Il faut cependant reconnaître qu'il était sage, alors que le Traité venait seulement d'entrer en vigueur, de ne pas établir de liens trop étroits entre le Traité et le SCAR. Les termes de la résolution n'interdisent d'ailleurs pas de rechercher dans l'avenir, à la lumière de l'expérience acquise, une formule concrète pour le développement de relations plus étroites entre la Science et les Gouvernements.

Sans entrer dans le détail des résolutions adoptées par la réunion de Canberra, il convient de noter que les principes suivants, qui sont ceux du Conseil International des Unions Scientifiques, ont été implicitement reconnus, à savoir, d'une part, que les programmes de recherches doivent être établis par des scientifiques éminents réunis à titre personnel sous les auspices d'organisations internationales, mais que l'éxécution de ces programmes revient à des organismes nationaux; et, d'autre part, que les programmes adoptés par les organisations internationales ne sauraient, en aucune façon, engager les gouvernements, et que ces organisations ne doivent ni entreprendre ni conduire elles mêmes l'exécution de programmes scientifiques.

Il n'est pas doûteux que l'action du SCAR a parfois été gênée par l'absence de convention internationale pour résoudre des problèmes techniques mettant en jeu une action inter-gouvernementale. Aussi la réunion a-t-elle considérée avec sagesse qu'elle devait résoudre ces difficultés. A cet effet diverses résolutions ont été adoptées remettant aux Gouvernements la responsabilité des questions relatives aux échanges de personnes, à la logistique, à la conservation de la nature et aux radio-communications, laissant ainsi le SCAR libre de se consacrer entièrement à la recherche scientifique.

Certains pourront craindre qu'une action inter-gouvernementale, dans le cadre d'un Traité pour lequel n'est prévu aucun secrétariat permanent, ne soit fort lente et ils redouteront le risque de voir les programmes scientifiques compromis dans l'attente d'accords concernant la logistique et les radio-communications. Les plus pessimistes iront sans doute jusqu'à présager les effets des tensions internationales dans un domaine qui en était jusqu'ici affranchi. De toute façon, le SCAR, qui se réunira à Wellington (Nouvelle Zélande) au mois d'octobre 1961 examinera les conclusions de la réunion de Canberra, et prendra avec tact les mesures nécessaires pour permettre à la machinerie inter-gouvernementale de se mettre en branle et de se roder.

Aussi bien dans les discours prononcés à la séance inaugurale qu'au cours des discussions, le rôle du SCAR et les résultats obtenus ont été abondamment loués, reconnaissant implicitement le rôle joué par le Conseil International des Unions Scientifiques dans la coopération internationale.

(1) What substances are contained in sea water and in what amounts?

The foundations of our knowledge of the composition of sea water were laid by GEORG FORCHHAMMER, who between 1843 and 1865 analysed an enormous number of water samples for their chief constituents and established the important basic principle that although the total quantity of dissolved salt in sea water may vary with conditions, nevertheless the relative proportions between the principal constituents are constant within narrow limits. This generalization was further confirmed by the careful analytical work of DITTMAR, who carried out extensive and exacting analyses of 77 samples collected from various depths during the cruise of the "Challenger". Until the present, no one has had the temerity to repeat such complete analyses, and the Law of Constant Proportions based upon this work is sometimes known as DITTMAR'S Law.

It was well recognized by the very early workers, however, that all elements found in terrestrial materials should very likely be present in the ocean. As better and more sensitive analytical methods have become available, more and more of the chemical elements have been found in sea water, until now there remain only a few which have not been identified. Without doubt, the whole periodic table will sometime be represented. Indeed, the sea has been the source of the first discovery of at least two of the important elements, iodine and bromine.

In very recent years the search has turned to organic substances, not living organisms, that is to say, but dissolved organic compounds. A number of these have been identified, decomposition products or compounds otherwise involved in biological processes.

After we have some knowledge of the dissolved material in sea water, our next question is:

(2) How are the physical properties of sea water determined by its dissolved constituents?

The most important physical property which determines the water's behavior is its density, and this is obviously a function of temperature and dissolved content. Because of the Law of Constant Proportions the total dissolved content of the water can be defined in terms of any *one* constituent. For this purpose chloride is most convenient because it can be both easily and accurately determined. Since we know very precisely the empirical relation of "chlorinity" to "salinity", which represents the total dissolved material, a simple chemical titration yields a clue to the total salt in a sample of sea water.

Other properties of the water are also influenced by the dissolved matter, such as optical characteristics and electrical conductivity. The accuracy with which the latter can be determined, and the application of the Law of Constant Proportions, have led to more sensitive and simpler methods of measuring the density of the water, conductimetrically.

(3) How does the composition of sea water affect the activities of living organisms, and vice versa?

In other words, how is the composition of sea water involved in the biological environment, how do the hydrosphere and the biosphere react upon each other?

One of the most striking observations of marine biology is the fact that some parts of the ocean are very fertile while other parts are quite barren. There must be chemical factors which determine fertility, and an explanation of this was perhaps the first serious question which oceanographers asked the chemist. In the year 1930 there were probably no more than a dozen professional chemists in the world who were actively interested in the ocean, and practically every one of them was trying to answer this question.

Much of the progress towards an answer was made by two men, HARVEY at Plymouth and WATTENBERG, the chemist whose work on the Meteor Expedition in 1925–27 was one of the most important milestones in the progress of marine or oceanographic chemistry.

It soon became apparent that the fundamental conditions of life in the sea were the same as those elsewhere. Photosynthesis is the same in the marine world, and growing marine plants require the same nutrient or fertilizing substances: nitrate, phosphate, silicate, etc. Where these substances are lacking the sea is barren; where they are abundant—notably in places where upwelling brings them up from deep water where they are plentiful—microscopic plants can grow and give rise to the whole chain of living creatures. Death, decomposition and decay complete the biological cycle, furnishing new material for regeneration and growth again.

It took some years to fill in the main details of this picture, but there are also minor requirements for nutrition and this part of the story is still being told. Trace substances, both organic and inorganic, are needed by growing organisms, and the part that these play in the marine world is not yet altogether clear.

For all living organisms, however, overshadowing the nutritional requirements, is the need for oxygen, and no other substance in the ocean has been studied with so much care and detail. From a knowledge of oxygen we can tell more about the chemical and biological characteristics and the previous history of a water mass than from any other one substance. Its determination is the one chemical analysis of sea water made most frequently in the field. Many chemical workers have contributed to our knowledge about it, but there are still mysteries connected with the distribution of oxygen in the sea.

As we have been able to apply more and more chemical methods of analysis, we have asked the question:

(4) Are there any chemical "tags" or indicators by which a water mass can be identified?

There is no general answer to this. We can sometimes follow the progress of a water mass by a series of chemical analyses. WATTENBERG, and in greater detail REDFIELD, followed the course of the Antarctic Intermediate Water up through the Atlantic basin by means of the oxygen distribution in it. Baltic waters from different sources were identified by STINA GRIPPENBERG from their alkalinity and other chemical characteristics. And of course if salinity can be considered a chemical parameter this is one of the most common means of identifying water masses.

But in many cases the search for a convenient chemical indicator has been in vain, or the interpretations have been so complicated as to be impracticable. Radiochemical indicators and fission-products were at one time thought promising but so far have been of limited value. However, the search goes on.

The question was at one time asked me, in all seriousness:

(5) Why is the sea full of sea water?

At first this seems altogether facetious, but not if it is properly translated: Why is the sea full of the stuff that is in it, how did it get there, and why does it remain as it is? And after all, this is perhaps the fundamental question of marine geochemistry.

In proportion to its mass the ocean is a relatively small part of the Planet Earth. But if one considers the superficial relations, the area covered, our earth might better be called Planet Ocean. Consequently, the ocean plays a large part in the various geophysical and geochemical processes. To understand the total earth one must consider lithosphere, hydrosphere, atmosphere and biosphere.

The origin of the ocean itself is a geological and geochemical question which is perhaps not completely answered, although the most widely held theory seems to be that it was virtually *squeezed* out of the earth's interior and that some of the dissolved constituents accompanied it. At any rate, it is not possible to account for the large quantities of such elements as chlorine, carbon and boron by the process of weathering of igneous rock and denudation of the land, by which means the remainder of the ocean's materials got there.

Although, in general, the ocean is the earth's big "sink hole", into which soluble material from the land areas is being washed, it is nevertheless easy to note that the solutes now in the sea are not representative of those which are being carried into it by the rivers. The discrepancy is evidently balanced by the process of sedimentation, by which insoluble combinations of elements are continually being removed from the ocean. The processes and results of sedimentation can therefore not be neglected by the oceanographic chemist, and work in this field is now a large part of his activity. The total geochemical cycle consists of weathering and solution by drainage waters, transportation to the sea, sedimentation and deposit on the sea bottom. The particulars of these processes are the concern of geochemists, and the marine specialist or oceanographic chemist studies the last part of the cycle particularly, residence in the ocean and formation of sediments.

Many interesting problems concern the history of particular elements, some of which indeed are involved in both biochemical and geochemical cycles. Copper, for example, owes its presence in sediments for the most part, apparently, to the role it plays in the metabolism of certain organisms. We may even designate a certain branch of the science as biogeochemistry.

This general field, which we may describe as marine geochemistry, is now probably the most productive area of activity for the chemist in oceanography. A large number of elements offer attractive opportunities for research. Our knowledge of the part that many of them play in the geochemical cycle is almost nil. Isotopic distributions and fractionations present many interesting problems. The distribution of natural radioactive isotopes and a number of unusual ones which are formed by cosmic ray action in the upper atmosphere and which eventually find their way into the ocean, is receiving close attention now.

Such research also involves an answer to our question No. 1, for new elements, or new isotopes of old ones, are continually being turned up in the sea. New, more powerful and more sensitive methods of chemical analysis, for example such radiochemical methods as neutron activation, enable us to go further and further down in the order of chemical concentration; 10^{-9} is no longer the limit, we are down into 10^{-11} and 10^{-12}.

And as a result, we are learning why the sea is full of sea water.

Because some of the material that gets into the ocean never gets out of it again, and because the ocean has been there a very long time, we wonder:

(6) Can the ocean serve as an archive of the past?

For this purpose we must consider not only the water itself, but more important, the sediments on the bottom. For there, in the sediments, is a large part of the story of the past. This the geologist has known for a long time and has built around this idea a whole science of paleontology. But the oceanographic chemist also contributes to this field and his ocean is the source of it all. For the story of the past is revealed not only by the gross structures, fossils, and skeletal material in the sediments, but also by such chemical parameters as isotopic ratios and trace element composition, even radioactivity.

Perhaps the best known examples of the work of the chemist here are in radiocarbon dating and determination of paleotemperatures from oxygen isotope distribution. As a result, we know that ocean temperatures have not always been as they are now, and we are able to correlate these changes with the occurrence and distribution of sedimentary remains of organisms affected by temperature changes.

The chemist, the geologist and the paleontologist form a team which, from the study of the ocean and ocean deposits will bring us more and more information about the past history of our earth.

A number of different kinds of chemical analysis have given us a measure of the rates of sedimentary deposit, a time constant which is important as an historical measure.

Much of our knowledge is based upon the phenomena of radioactivity. The rates of radioactive decay of many elements are now known with sufficient precision for us to fix accurate dates, if we have a good enough chemical analysis. We have "clocks" which will measure time in ranges between a few years and many millions. By both chemical and microscopic analysis of successive layers in sedimentary cores we can tell something of what has been going on physically, climatologically and biologically during thousands or even millions of years.

In many such ways as those just recounted, the chemist has contributed to the study of the ocean and its behavior. Sometimes the question occurs to him: *(7) Is there any way in which the study of the ocean can contribute to chemistry?*

As a chemical system, the ocean is not a very pure one, for the solution contains a great deal of "dirt", suspended matter of various sorts, which after all, is a pretty important part of the ocean, for it includes all the living material in it.

And if one removes all this, the clear remaining solution is still very complicated, and certainly not the kind of system which a chemist would choose for accurate work, for its composition is not altogether fixed and would vary, at least in minor respects, depending upon its source. It is a rather concentrated solution of a fair number of constituents, and at the same time an extremely dilute solution of an indefinitely large number of constituents. And unfortunately, these latter constituents are usually the ones of greatest interest.

One can certainly *apply* a lot of chemistry to the study of such a system, but what can the study of such a system contribute to chemistry itself?

I believe there is an important possibility and that it will sometime be developed.

All of our knowledge of physical chemistry, such fields as reaction kinetics, has been derived from the study of pure chemical systems prepared in the laboratory and which have a short history behind them. A solution which has been standing in the laboratory for a year would be thrown out as useless and a new one prepared. The result is that we have no knowledge of chemical kinetics in the time range anywhere approaching the geological. To be sure, most chemical reactions proceed in fractions of a second, or perhaps, minutes, a few even in years. But we have never had the opportunity to follow any longer ones, even if they exist. Therefore, we do not know if they *do* exist. But here is a chemical system prepared for us which has been standing on nature's laboratory shelf for millions of years, at least. What very slow chemical processes, of a nature unknown to us, may have gone on in it?

From the study of rocks and sediments we have learned of a few very slow processes that take place in the solid state, but here is an opportunity to look for very slow kinetic changes in solution. What can they be? This may be the ocean's contribution to chemistry.

(718)

Separatum of Supplement-Volume 3 of
Zeitschrift für Geomorphologie
Annals of Geomorphology — Annales de Géomorphologie

Herausgegeben von H. Mortensen, Göttingen
in Gemeinschaft mit J. P. Bakker, Amsterdam / A. Cailleux, Paris / D. L. Linton, Sheffield / N. Nielsen, København / R. J. Russell, Baton Rouge / H. Spreitzer, Wien F. E. Zeuner, London

Pacific Island Terraces: Eustatic?

P. 30—35
Verlag Gebrüder Borntraeger, Berlin-Nikolassee
1961

Contributions from the Scripps Institution of Oceanography, New Series, 1297

Reproduced by Permission

Sea Level Rise during the Past 20,000 Years

By

FRANCIS P. SHEPARD

Scripps Institution of Oceanography,
University of California, La Jolla, California

With 1 figure

INTRODUCTION

Since DALY (1920) first suggested that there had been a Holocene (postglacial) high stand of sea level, there has been a common impression that low terraces around oceanic islands like the Hawaiian group are the result of the high sea level episode. The discovery that land plants from a period of about 7,500 to 4,000 B.P. indicate a warmer climate than that of the present day (FLINT 1957, p. 377) appeared to confirm such a high stand. At first DALY (1920) referred to a six meter (19 foot) terrace level and several other authors pointed to recent-looking terraces at this level. The examination of raised reefs in reconnaissance studies of the Pacific Islands (WENTWORTH and PALMER 1925) appeared to favor a lower level for the high stand and a 10 foot high sea level was gradually substituted for the 19 foot. Somewhat later STEARNS (1935) called attention to a five foot terrace which is said to be particularly common in Hawaii and certainly exists at a variety of places around the island of Oahu.

On the other hand investigations of the Gulf Coast of the United States, particularly in Texas and Louisiana, failed to show evidence of these Holocene high levels (LEBLANC and BERNARD 1954). This was particularly surprising because the broad gently sloping coastal plains would have been widely inundated by a sea level rise and should have left records in the form of marine sediments and raised beaches of Holocene date. As a result of the Gulf Coast studies it has been widely held that the sea level has been constant for about 5,000 years (LEBLANC and BERNARD 1954; FISK 1956, 1959). The chief evidence for this contention has come from the abandoned beaches (cheniers) inland from the Cameron area west of the Mississippi Delta. These cheniers have been studied in great detail recently and many dates obtained. The conclusion has been reached that the stillstand here has been of the order of 3,000 years (GOULD and McFARLAN 1959). The area of study, however, is just outside the hinge line between submergence of the Mississippi Delta on one side and emergence on the other (FISK and McFARLAN 1955, fig. 11) so that it does not seem to be a particularly good place to use as an index of sea level. A somewhat similar conclusion concerning a constant sea level was reached by GODWIN et al. (1958) from European and Asiatic data, but many of the dates used are from unstable areas.

Different conclusions have been expressed by FAIRBRIDGE (1960) who has tackled the problem on a rather world-wide basis. He has called for a series of high stands of sea level during the Holocene between about 6,000 and 1,000 B. P. with intervening periods when the sea level was lower than the present.

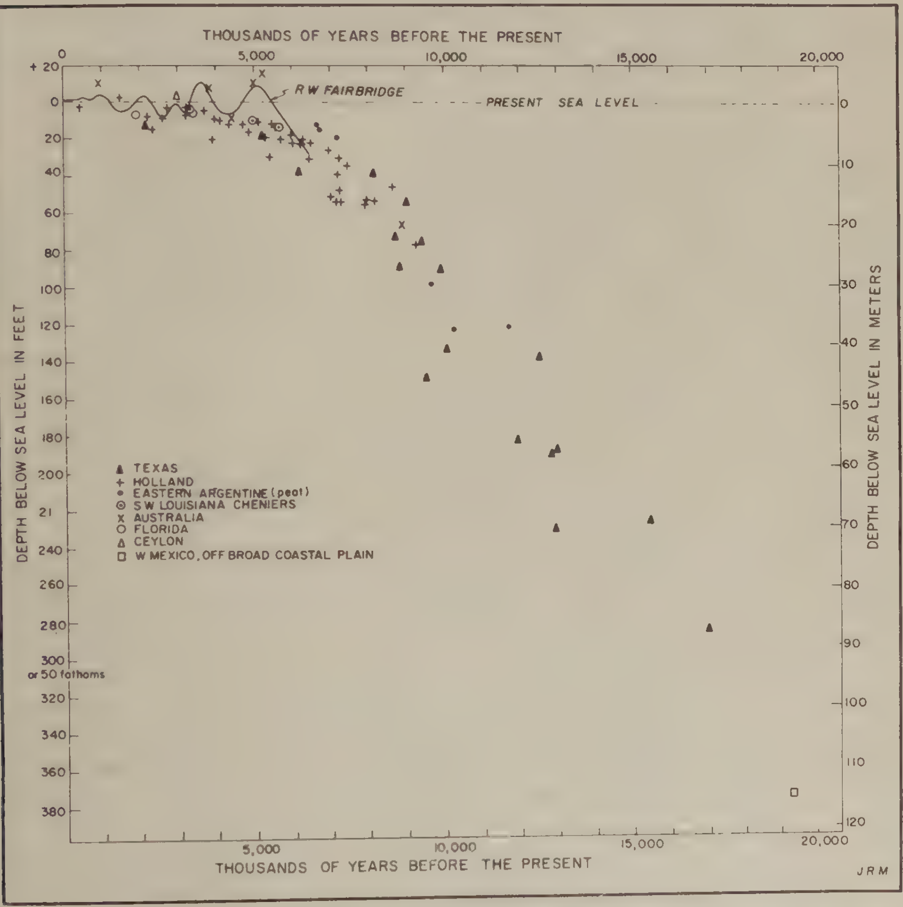

Fig. 1. The rise of sea level indicated by Carbon 14 dates of organisms and plants that lived close to sea level in relatively stable areas.

Opinions coming from the study of Carbon 14 dates in stable areas have suggested that the sea level rise was rapid up to 6,000 B. P. and has continued slowly since that period (SHEPARD and SUESS 1956; CURRAY 1960; SHEPARD 1960; and JELGERSMA and PANNEKOEK 1960). The data for this last conclusion come from the Carbon 14 analyses of samples from borings along the Texas coast in bays and on barrier islands; from borings along the coast of Holland; and from samples of beach and lagoonal sediments taken at various depths on the continental shelves off the Texas Coast and in various other relatively stable areas. To this information can be added dates from Australian raised terraces, and from shells in slightly raised reefs along the coast of Ceylon. Dates have also been obtained from the north coast of Oahu, where five-foot terraces and a 12-foot terrace are developed, although this may not be a stable area.

NATURE OF RELIABLE EVIDENCE

Dating sea level in the Holocene is complicated by many factors. If shells are used, it is important to determine whether the original shell material has been replaced, as for example, from aragonite to calcite. Original material is more reliable. Best results come from analyzing several types of shells to see if they give the same date. Analysis of modern shells from similar environments in the same general area may also make it possible to apply corrections.

The shells must be chosen with care since most marine shells have a considerable depth range, and therefore are not good indicators of sea level. Beach shells such as Donax that live commonly in the surf along the beach edge are quite satisfactory. Oyster shells, particularly oyster reefs along the Gulf Coast, are found largely in the shallow waters of bays and are, therefore, rather good but not perfect indicators of sea level.

Peat layers are likely to form at sea level, but it is important to study the plants and associated Foraminifera to make sure they represent salt water rather than fresh water conditions, since the latter could form at any level. Other types of wood are suspect although they may give a moderately good indication of sea level if they occur in the sediment directly over an unconformity, and are covered by a basal marine deposit. The danger of using wood in borings around a large river delta is that it may have been deposited as water-logged wood in the bottom of a channel cut deep below sea level by the river. For example, near the mouth of the Mississippi there are channel depths of over 100 feet and the Amazon and Congo have channel depths of several hundred feet. On the other hand, the great masses of wood deposited on the bars at river mouths or in the lower flood plains would be good indicators of sea level.

Compaction may play an important part in distorting evidence from borings. This would be particularly likely in cases where thick peat deposits exist and can have some effect where the dated deposit is overlain by clayey sediments of appreciable thickness. Better results come from areas where the sediments are sand or shell reef material since these do not compact to any great extent. The compaction of clay in the first 10 to 20 feet will, of course, be so slight as not to change the situation appreciably. Corrections can be applied where the stratigraphy is known and the compaction can be estimated.

An area used for information concerning past sea levels should be one where there is no evidence of present day diastrophism. This rules out many areas that have been used by writers in discussing sea level changes. For example, the Persian Gulf is diastrophically unstable. The Baltic coast, Scandinavia, and all but the southern end of Great Britain have been rising since the retreat of the ice caps so that they are of little use. The Mississippi Delta used by McFarlan (1961), is known to be sinking rather rapidly (Russell 1936) so that information from drillings into the delta should not be used except comparatively. Almost all areas are somewhat unstable but the movements appear to have been so slow in many that they have not particularly interfered with sea level observations of the past 10,000 to 20,000 years. For example, the sinking necessary to develop the great thicknesses of sediment along the Gulf Coast outside of the Mississippi Delta area has averaged only about one foot in two or three thousand years. Also along the Gulf Coast the edge of the continental shelf lies at 65 fathoms (Curray 1960), close to the average for the world. It can be assumed that this level was established at the time of the last major sea level lowering accompanying the Wisconsin. Similarly coastal Holland outside of the Würm glaciation has probably undergone slow sinking but not enough to prevent the use of Holocene dates from borings along this coast (Jelgersma and Pannekoek 1960).

EVALUATION OF THE DATED SAMPLES

A plot of the dates and depth below present sea level from samples of relatively stable areas is shown in Figure 1. The data appear to indicate a rather rapid rise between 17,000 years B. P. and about 6,000 B. P. when the sea had apparently reached about —20 feet. After that time the points show a slow rise with the sea some six feet below the present during most of the time from 3,500 to 2,000 B. P. This small amount could be explained by inaccuracies of the method so that it may equally well support a constant sea level since the time of Roman and Greek civilization. All but one of the dates that are above sea level in the past 5,000 years come from Australia, and the other is from a slightly raised reef in southwest Ceylon. The Australian dates may be erroneous. A sample of shells given to the writer by Harold Wanless was collected on the 12-foot terrace near Sydney. This appeared to be a part of the terrace deposit and was cemented into the underlying material but had a date of only 900 years. This raises the suspicion that the shells are kitchen middens and one cannot help wondering if the older shells from these Australian terraces were not also introduced by human occupation. Such an explanation would account for the three widely separated dates from this same terrace and the finding of shells more than 30,000 years old from another part of the Australian 12-foot terrace may indicate an interglacial age for terrace cutting. In other words, the terrace may have been formed during the high sea level of the last interglacial, as believed to be the case for a 10-foot terrace in Maryland (George F. Carter, personal communication), and the shells could have been introduced by man becoming consolidated into the terrace at various times during the Holocene. Before this question can be answered satisfactorily many more terraces should be dated to see if there is any uniformity to the dates of the shells on raised reefs and terraces. If introduced by man or by birds they should cover a wide range, but if introduced by sea level the range should be short unless, of course, the level has been bobbing up and down repeatedly during the last few thousand years as suggested by Fairbridge (1958, 1960).

EVIDENCE FROM OAHU

Collections of shells made by Gordon F. Macdonald and the writer in 1960 from the north coast of Oahu came from the tops of coral reefs with surfaces lying at respectively five feet and 12 feet above sea level. The shells collected were a species of Cyprea, a small Cowry shell that is too small for food. They were rather clearly a part of the elevated reef rather than recently introduced by birds or man. The ages determined were respectively 24,100 ± 700 from the five-foot terrace and 31,400 ± 1,200 from the 12-foot terrace. At least the five-foot terrace looks very much like the present sea level reef and, therefore, may represent growth rather than erosion although this is a difficult point to determine. In either case it becomes clear that the sea stood relatively higher in Oahu during what is usually interpreted as a low sea level glacial time. Therefore, one can conclude that Oahu is unstable and not a good island to test for sea level changes. If it is really true that there are five-foot terraces all around these islands, which I personally doubt, the islands must either have become stable quite recently or must have been elevated very uniformly. Certainly the matter must be given more study.

This evidence from Hawaii should give one considerable uncertainty about the reliability of volcanic islands as indicators of postglacial high stands of sea level. This is perhaps not surprising especially where vulcanism has been relatively recent. Lava movements beneath the islands could not fail to cause variations in level.

RAISED REEFS OF THE CORAL ATOLLS

The persistent report that coral atoll islands have raised reefs cannot be dismissed lightly. However, the most thorough studies of these reefs which have been made are in the Marshall Group (EMERY et al. 1954) and in Kapingamarangi (MCKEE 1958). In neither case have the investigators found anything but locally raised reefs of about three to four feet above sea level. Most of the elevation of the islands are the result of storm waves piling up debris. The writer observed an elevated reef at two feet above sea level at Aitutaki in the Cook Island group. None of these cases has been dated nor is there any available date on the other reported elevated tracts. One cannot avoid concluding that the evidence is very incomplete and that it will take future studies to determine whether or not the coral island terraces can be used in answering the question of postglacial high sea level stands.

HISTORICAL EVIDENCE

An extensive study of historical records might prove very helpful in determining the history of sea level rise especially during the past 6,000 years. If there had been any stand of sea level as much as 12 feet above the present the record should be very clear in all of the great delta areas such as the Nile, the Euphrates-Tigris, the Yellow River of China, and other great rivers of Asia. FAIRBRIDGE (1960) referred to the widespread legends of floods among ancient people as evidence for higher sea level in historical times, but this seems to be rather questionable evidence because any great river flood in a broad flood plain could lead primitive peoples to create legends that their whole world was engulfed. There is apparently no evidence that these floods were simultaneous. Nor is there evidence that they led to a long period abandonment of communities on deltas as would have happened if the sea stood higher for any length of time.

So far as the writer is aware of the historical aspects there appear to be no indications of the broad submergence of the great flood plains at least as far back as about 6,000 B. P. The occasional submergences of western Europe as, for example, the Holland coast, according to JELGERSMA and PANNEKOEK (1960), are quite clearly noncontemporaneous and indicate times when peat growth could not keep pace with the slow rise of sea level. Shifting of barriers also had no important effect.

References

CURRAY, J. R., 1960, Sediments and history of Holocene transgression, continental shelf, northwest Gulf of Mexico, in Recent Sediments, Northwest Gulf of Mexico, ed. by Shepard, F. P., Phleger, F. B., and van Andel, Tj. H., Amer. Assoc. Petrol. Geol., Tulsa, pp. 221—266.

DALY, R. A., 1920, A recent world-wide sinking of ocean level, Geol. Mag., **57**: 246—261.

EMERY, K. O., TRACEY, J. I., Jr. & LADD, H. S., 1954, Geology of Bikini and nearby atolls, Part. I, Geology, U. S. Geol. Surv. Prof. Paper **260-A**: 265.

FAIRBRIDGE, R. W., 1958, Dating the latest movements of the Quaternary sea level, Trans. N. Y. Acad. Sci., Ser. II, **20**, 6: 471—482.

—: 1960, The changing level of the sea, Scientific American 202, 5: 70—79.

FISK, H. N., 1956, Nearsurface sediments of the continental shelf off Louisiana, Proc. Eighth Texas Conf. on Soil Mechanics and Found. Engrg., pp. 1—36, Univ. of Texas, Bur. of Engrg. Research.

—: 1959, Padre Island and the Laguna Madre flats, coastal South Texas, 2nd Coastal Geography Conf., La. State Univ., Nat'l. Acad. Sci., pp. 103—151.

FISK, H. N. & MCFARLAN, E., Jr., 1955, Late Quaternary deltaic deposits of the Mississippi River, from The Crust of the Earth, Geol. Soc. Amer. Spec. Paper **62**: 279—302.

FLINT, R. F., 1957, Glacial and Pleistocene Geology, John Wiley & Sons, Inc. N. Y., 553 pp.

GODWIN, H., SUGGATE, R. P. & WILLIS, E. H., 1958, Radiocarbon dating of the eustatic rise in ocean-level, Nature, **181**: 1518—1519.

GOULD, H. R. & MCFARLAN, E., Jr., 1959, Geologic history of the chenier plain, southwestern Louisiana, Trans. Gulf Coast Assoc. Geol. Societies, **9**: 10.

JELGERSMA, S. & PANNEKOEK, A. J., 1960, Post-glacial rise of sea-level in the Netherlands (a preliminary report), Geol. en Mijnbouw, **39**, 6: 201—207.

LEBLANC, R. J. & BERNARD, H. A., 1954, Resume of late Recent geological history of the Gulf Coast, Geol. en Mijnbouw, **16**, 6, Nw. Ser.: 185—194.

MCFARLAN, E., Jr., 1961, Radiocarbon dating of Late Quaternary deposits, south Louisiana, Bull. Geol. Soc. Amer., **72**: 129—158.

MCKEE, E. D., 1958, Geology of Kapingamarangi Atoll, Caroline Islands, Bull. Geol. Soc. Amer., **69**: 241—277.

RUSSELL, R. J., 1936, Physiography of the Lower Mississippi River Delta, in Reports on the Geology of Plaquemines and St. Bernard Parishes, Louisiana Dept. Conserv. Geol. Bull. **8**: 3—199.

SHEPARD, F. P., 1960, Rise of sea level along northwest Gulf of Mexico, in Recent Sediments, Northwest Gulf of Mexico, ed. by Shepard, F. P., Phleger, F. B., and van Andel, Tj. H., Amer. Assoc. Petrol. Geol., Tulsa, pp. 338—344.

SHEPARD, F. P. & SUESS, H. E., 1956, Rate of postglacial rise of sea level, Science, **123**: 1082—1083.

STEARNS, H. T., 1935, Pleistocene shore lines on the islands of Oahu and Maui, Hawaii, Bull. Geol. Soc. Amer., **46**: 1927—1956.

WENTWORTH, C. K. & PALMER, H. S., 1925, Eustatic bench of islands of the North Pacific, Bull. Geol. Soc. Amer., **36**: 521—544.

Reprinted from Science, June 9, 1961, Vol. 133, No. 3467, pages 1833-1834

Copyright © 1961 by the American Association for the Advancement of Science

Standard for Reporting Concentrations of Deuterium and Oxygen-18 in Natural Waters

Abstract. A standard, based on the set of ocean water samples used by Epstein and Mayeda to obtain a reference standard for oxygen-18 data, but defined relative to the National Bureau of Standards isotopic reference water sample, is proposed for reporting both deuterium and oxygen-18 variations in natural waters relative to the same water. The range of absolute concentrations of both isotopes in meteoric waters is discussed.

In a previous report (*1*) the relationship between deuterium and oxygen-18 variations in meteoric waters throughout the world was shown. Many laboratories are measuring one or the other of these isotopes in various types of natural waters, and those workers studying O^{18} variations have more or less adopted, as a reference level for reporting enrichments, the "average ocean water" found by Epstein and Mayeda in the first precise work on O^{18}/O^{16} ratios in natural waters (*2*).

Deuterium analyses, however, occur in the literature relative to at least six different "working tap water" standards. In the previous report (*1*) the data presented for both isotopes showed how important it is to obtain data on both D and O^{18} variations in the same water samples, and it therefore seems that a common deuterium standard, preferably the same water as the O^{18} standard, should be adopted for consistency. The data shown previously (*1*) indicate that tap waters from various countries could easily differ by as much as 15 percent in the D/H ratio, and for many reasons it appears to be desirable to have an ocean water standard for reporting geochemical data.

For this purpose, the same set of ocean waters chosen by Epstein and Mayeda to give their "average ocean water" for O^{18} data was analyzed for the D/H ratio along with the samples described previously (*1*). These waters, taken from depths of 500 to 2000 m in open ocean areas where no direct dilution by continental runoff or glacial melt water could occur, were grouped by Atlantic, Pacific, and Indian Ocean samples, and equal volume composites were made from each set and analyzed relative to the laboratory working standard.

No single sample of "average ocean water" which could be circulated widely for analysis actually exists. Oxygen-18 data have generally been tied to the Epstein-Mayeda scale by analysis of various carbonate samples, requiring special techniques for preparation of 100 percent H_3PO_4, and so on. However, in the course of the present work it was found that both the D and O^{18} data on the set of ocean waters analyzed could be very simply specified in terms of the National Bureau of Standards isotopic reference sample No. 1, a distilled water sample of large volume intended for cross-check circulation to mass spectrometric laboratories (*3*). After consultation with various laboratories it was decided to define a "standard mean ocean water" (SMOW) in terms of the National Bureau of Standards reference sample 1, such that

$$\text{D/H (SMOW)} \equiv 1.050 \text{ D/H (NBS-1)}$$
$$O^{18}/O^{16} \text{ (SMOW)} \equiv 1.008\ O^{18}/O^{16} \text{ (NBS-1)}$$

and to report isotopic data for both isotopes as per mil enrichments relative to the defined SMOW (*4*), thus tying the standard to a sample readily available for world-wide distribution.

The isotopic analyses of the composite ocean water sets made from the samples used by Epstein and Mayeda are shown in Table 1, in which the O^{18} data are averages for each set taken from their paper (*2*) with slight corrections later found necessary (*5*). The deuterium analyses are those I made, and all data have been calculated relative to SMOW, so that

$$\delta = [(R_{\text{sample}}/R_{\text{SMOW}}) - 1] \times 1000$$

is the per millage enrichment in either isotopic ratio R, relative to SMOW. The analytical precision has been described (*1*).

These data indicate that, within the limits of analytical precision and geographical variation, SMOW as defined above provides a consistent and convenient zero reference level for reporting isotopic enrichments and is an adequate average for the Epstein-Mayeda O^{18} data on "average ocean water." Clearly it will be a long time before the actual mean ocean composition is known; the designation "standard" indicates that SMOW is an arbitrary mean value based on the Epstein-Mayeda oxygen scale but defined in terms of an actual water reference standard, the NBS-1. The δO^{18} value of the Chicago PDB-1 carbonate standard (CO_2 from reaction with 100 percent H_3PO_4 at 25°C) is +0.22 per mil on the SMOW scale (*6*).

Table 1. D/H and O^{18}/O^{16} enrichments of the Epstein-Mayeda "average ocean water" set and other samples, in per millage relative to SMOW. Numbers in parentheses after ocean names indicate number of samples in each set.

Sample	δD (per mil)	δO^{18} (per mil)
Atlantic (6)	− 0.7	+ 0.14
Pacific (11)	+ 0.9	+ 0.04
Indian (2)	+ 0.1	− 0.07
NBS-1	− 47.60	− 7.94
NBS-1A	−183.3	−24.33

Table 1 also shows the NBS-1 data as defined versus SMOW, and the value obtained for the NBS-1A secondary water standard. The D/H enrichment of NBS-1A relative to NBS-1 is found to be −142.5 ± 2.5 per mil (*3*). Horibe and Kobayakawa found a value of −141.3 ± 2.3 per mil (*3, 7*) in good agreement. Their data yield an absolute D concentration for SMOW of 157 ± 1 atomic parts per million (ppma), based on direct calibration with enriched standards. I analyzed five water samples which had been measured previously for absolute D content by Kirshenbaum (*8*); this comparison gives a D concentration of 159 ± 2 ppma for SMOW. We may therefore take the absolute D content of SMOW as 158 ± 2 ppma, corresponding to a D/H ratio of 1/6328.

Absolute O^{18} concentrations, based on data obtained by Nier and me, have been given for standards including the NBS-1 water (*5*). From these data the O^{18} concentration in SMOW is found to be 1989.5 ± 2.5 ppma, corresponding to an O^{18}/O^{16} ratio of $(1993.4 \pm 2.5) \times 10^{-6}$.

In the previous paper (*1*) the relation between δD and δO^{18}, expressed as per millage enrichments relative to SMOW, was found to be linear in the majority of meteoric waters, obeying the equation

$$\delta D = 8\, \delta O^{18} + 10$$

By using the absolute concentrations for SMOW as given above, the atom fractions of D and O^{18} are found to be related in meteoric waters by the expression

$$X_D = 0.6359\, X_O - 1105.6$$

when the atom fractions are given in atomic parts per million. This relation is approximately obeyed by ocean waters also, but does not hold for lakes having high ratios of evaporation to outflow.

The total variations in meteoric waters are about 360 per mil for deuterium and about 48 per mil for oxygen-18, relative to the concentrations in SMOW. This variation in D content corresponds to a variation of about 6 ppm in density, while the O^{18} variation corresponds to about 11 ppm in density. Thus the total density variation in meteoric waters produced by these isotopes is about 17 ppm, of which about 65 percent is due to O^{18}. The atomic weight variations in hydrogen and oxygen in these waters are about 5.7×10^{-6} and 1.9×10^{-4} atomic mass units respectively.

HARMON CRAIG

Department of Earth Sciences,
University of California, La Jolla

References and Notes

1. H. Craig, *Science* **133**, 1702 (1961).
2. S. Epstein and T. Mayeda, *Geochim. et Cosmochim. Acta* **4**, 213 (1953).
3. F. L. Mohler, *Natl. Bur. Standards* (*U.S.*) *Tech. Note No. 51* (1960), p. 8.
4. δD values have generally been reported in percentage, in contrast to all other stable isotope data which are given in per millage. However, as more laboratories begin to work on both isotopes, they will surely find it intolerable to work with enrichment ratios with two systems of units.
5. H. Craig, *Geochim. et Cosmochim. Acta* **12**, 133 (1957).
6. I am greatly indebted to I. Friedman, S. Epstein, Y. Horibe, N. Kokubu, and H. C. Urey for discussions and suggestions on a consistent isotopic reference scale.
7. Y. Horibe and M. Kobayakawa, *Bull. Chem. Soc. Japan* **33**, 116 (1959).
8. I. Kirshenbaum, *Physical Properties and Analysis of Heavy Water* (McGraw-Hill, New York, 1951), p. 398.

18 January 1961

Reprinted from Science, May 26, 1961, Vol. 133, No. 3465, pages 1702-1703

Copyright © 1961 by the American Association for the Advancement of Science

Isotopic Variations in Meteoric Waters

Abstract. The relationship between deuterium and oxygen-18 concentrations in natural meteoric waters from many parts of the world has been determined with a mass spectrometer. The isotopic enrichments, relative to ocean water, display a linear correlation over the entire range for waters which have not undergone excessive evaporation.

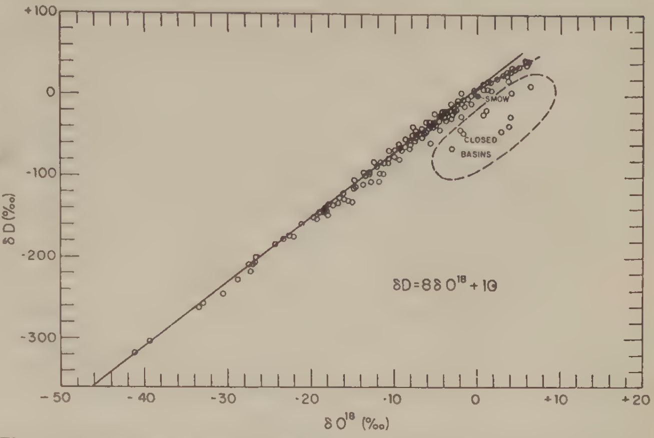

Fig. 1. Deuterium and oxygen-18 variations in rivers, lakes, rain, and snow, expressed as per millage enrichments relative to "standard mean ocean water" (SMOW). Points which fit the dashed line at upper end of the curve are rivers and lakes from East Africa.

Epstein and Mayeda (*1*) and Friedman (*2*) reported precise data for O^{18}/O^{16} and D/H ratios in nine nonmarine meteoric waters and found a rough linear correlation between the isotopic enrichments. In the course of research on isotopic variations in volcanic waters, I have analyzed mass spectrometrically some 400 samples of water from rivers, lakes, and precipitation in order to establish the exact nature of the isotopic relationship in meteoric waters. Gas samples were prepared by the standard CO_2-H_2O equilibration technique (*1*) and by reduction of H_2O to H_2 with uranium metal and analyzed on the McKinney-Nier type spectrometers used by the authors mentioned above as well as in my present laboratory.

The isotopic data for all samples analyzed for both isotopes (excluding detailed sets of data from Chicago and Steamboat Springs, Nev.) are shown in Fig. 1. About 40 percent of the samples are from North America, the rest being distributed all over the world. The data shown are per mil enrichments of the isotopic ratios D/H and O^{18}/O^{16} relative to a mean ocean water standard, that is,

$$\delta = [(R/R') - 1]\,1000$$

where R is either isotopic ratio and R' is the ratio in "standard mean ocean water" (SMOW) defined relative to the National Bureau of Standards isotopic water standard as described in a following report (*3*). The precision of the data is ±0.5 per mil, or ± 1 percent of δ, for D, and ± 0.1 per mil, or ± 0.5 percent of δ, for O^{18}, the larger error applying in each case and representing ±2 standard deviations.

The straight line in Fig. 1 represents the relationship

$$\delta D = 8\,\delta O^{18} + 10$$

(both δ values in per millage) and is seen to be an adequate fit to the data, except for waters from closed basins in which evaporation is a dominant factor governing the isotopic relationship. The samples which fit the dashed line at the high enrichment end of the curve represent rivers and lakes in East Africa. They fit a line with a slope of about 5, in contrast to the slope of 8 found for most of the data. Studies of evaporation in the laboratory, and in areas where seasonal data have been obtained, show that in free evaporation at ordinary temperatures the heavy isotope enrichment ratio $\delta D/\delta O^{18}$ consistently follows a slope of about 5 as observed in East African waters. Many of the points falling to the right of the line plotted in Fig. 1 have a similar slope of 5 when connected to points on the line which represent direct precipitation in the same area.

It can be shown (*4*) that for small enrichments the slopes in Fig. 1 are the ratios of the single-stage enrichments when the isotopic concentrations are governed by vaporization or precipitation under Rayleigh conditions at constant temperature. The isotopic vapor pressure data show that slopes of 8 and 5 correspond to Rayleigh processes at liquid-vapor equilibrium at temperatures of about −10°C and +100°C respectively. It seems, therefore, that atmospheric precipitation follows a Rayleigh process at liquid-vapor equilibrium, as first proposed by Kirshenbaum (*5*), but that the process of free evaporation at room temperature is governed by kinetic factors. The present studies have shown that this is so up to the boiling point, and that the disequilibrium occurs principally in the O^{18}/O^{16} separation (*4*). Some of the variability along the line in Fig. 1 is certainly due to evaporation effects as well as to variations in temperature of precipitation.

All points in Fig. 1 for δD and δO^{18} lighter than −160 and −22 per mil, respectively, represent snow and ice from the Arctic and Antarctic, while tropical samples show very small depletions relative to ocean water. This distribution is expected for an atmospheric Rayleigh process as vapor is removed from poleward moving tropospheric air. However, it is actually log (1 + δ) which should be plotted for such a process, and, in such a plot, the points in Fig. 1 fall on a curve with a continually increasing slope for lighter δ values, as would be expected (from the vapor pressure data) for precipitation at lower temperatures in high latitudes. The linear relation observed in Fig. 1 simply reflects a coincidence of the effect of the increasing difference in δ and log (1 + δ) at high enrichments with the effect on the slope of the average temperature decrease for precipitation along a meridian from equator to poles (*6*).

HARMON CRAIG

*Department of Earth Sciences,
University of California, La Jolla*

References and Notes

1. S. Epstein and T. Mayeda, *Geochim. et Cosmochim. Acta* 4, 213 (1953).
2. I. Friedman, *ibid.* 4, 89 (1953).
3. H. Craig, *Science*, in press.
4. H. Craig, G. Boato, D. E. White, "Nuclear Processes in Geologic Settings: Proceedings of the Second Conference," *Natl. Acad. Sci.–Natl. Research Council Publ. No. 400* (1956), pp. 29–38.
5. I. Kirshenbaum, *Physical Properties and Analysis of Heavy Water* (McGraw-Hill, New York, 1951), p. 398.
6. Detailed papers on isotopic variations in meteoric and volcanic waters of specific areas will be published elsewhere. It is a pleasure to acknowledge my gratitude to Harold C. Urey in whose laboratories at the Institute for Nuclear Studies, University of Chicago, most of this work was done, to Mrs. T. Mayeda for her excellent services in the Chicago laboratory, and to G. Boato for many interesting discussions. This research has been supported by the National Science Foundation, the University of California Water Resources Commission, the Office of Naval Research, and the Atomic Energy Commission.

18 January 1961

Contributions from the Scripps Institution of Oceanography, New Series, 1299

Reproduced by Permission

pp.2850-2857

Journal of the
POWER DIVISION
Proceedings of the American Society of Civil Engineers

POWER FROM THE SEA

By El Sayed Mohamed Hassan[1]

SYNOPSIS

Evaporation exceeds precipitation over the Red Sea by 1.5 x 10^6 cfs. All this amount is now supplied from the Indian Ocean through the narrow Straits of Bab El Mandeb. If these straits are dammed, the loss of water will result in lowering the Red Sea level by 12 ft per yr. A scheme is presented to utilize this drop to generate electricity at a very cheap cost.

INTRODUCTION

Among the great engineering projects contemplated, a proposal for what is probably the most ambitious of all will be presented herein. This is an oceanic hydroelectric power plant that dwarfs all existing plants and if constructed, will have far-reaching effect on Africa and the world.

THEORY

Evaporation exceeds precipitation[2] over the Red Sea (Fig. 1) by about 1.5 x 10^6 cfs. This amount is now replenished from the Indian Ocean through the Straits of Bab El Mandeb. If these Straits and the Suez Canal are dammed, this evaporation will lower the level of the Red Sea by about 12 ft per yr. By

---

Note.—Discussion open until December 1, 1961. To extend the closing date one month, a written request must be filed with the Executive Secretary, ASCE. This paper is part of the copyrighted Journal of the Power Division, Proceedings of the American Society of Civil Engineers, Vol. 87, No. PO 2, July, 1961.

[1] Lectr. in Oceanography, Univ. of Cairo, United Arab Republic, on loan as Research Scientist, Dept. of Meteorology and Oceanography, New York Univ., New York, N. Y.

[2] "The Oceans, Their Physics, Chemistry and General Biology," by H. U. Sverdrup, M. W. Johnson, and R. H. Fleming, Prentice Hall, Inc., Englewood Cliffs, N. J., 1942.

Contributions from the Scripps Institution of Oceanography, New Series, 1300
Reproduced by Permission

allowing a part of the evaporated water to be replaced, electricity can be generated. The difference in level between the Red Sea and the Indian Ocean will continue to increase as long as only part of the evaporated water is replaced. This can go on until the head reaches a desired amount. The maximum head depends on the site of the dam, but it need not be less than 500 ft. The maximum amount of electricity that can be produced with such a head is 70,000,000 kw. Other considerations will reduce this to about 50,000,000 kw, as will be seen later. This is about 1/5 of the electric energy generated in all

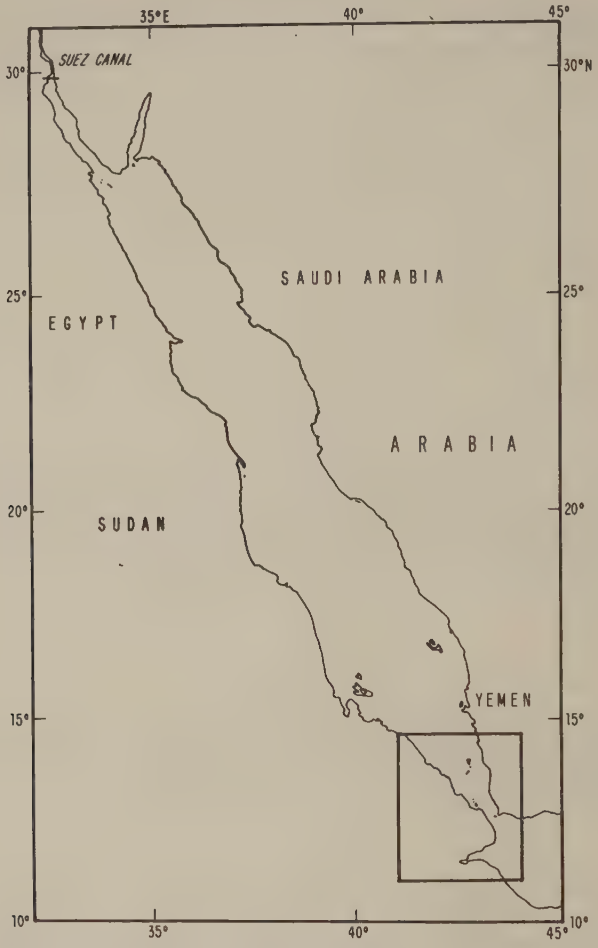
35°E
40°
45°
30°
30°N
SUEZ CANAL
SAUDI ARABIA
25°
25°
EGYPT
ARABIA
20°
20°
SUDAN
YEMEN
15°
15°
10°
35°
40°
45°
10°

FIG. 1.—THE RED SEA

the world in 1959, or more than the total energy from all sources used in the United Kingdom in 1948.

SITES FOR THE DAM

The geography and topography of the Bab El Mandeb Straits make the choice of a site for the dam arbitrary within a large area since the sill is situated inside the Red Sea, north of the Straits. Thus the narrowest section of the Straits is also the deepest, while the shallowest depth occurs in a section where the Straits are wider. The volume of the dam will be approximately the same if constructed anywhere between these two extremes. Other factors, such as the nature of the sea bottom, the availability of suitable materials, or the engineering difficulties, will have to be considered to choose one location from all the possible ones. Three sections of the Straits of Bab El Mandeb are shown in Figs. 2 and 3. Section AA' is the narrowest part where the width is about 12.5 miles, and the greatest depth is about 950 ft. Section BB' is 21 miles wide, but the maximum depth is about 600 ft. Further north the Straits become relatively shallow, and the maximum depth is about 500 ft, but the width becomes about 60 miles. The difficulties of damming the Straits at any of these places are certainly great, but they are not insurmountable.

GENERAL

The amount of evaporation is roughly proportional to the area of the sea. If the sea level is to be lowered by 600 ft, its area and consequently the evaporation will be reduced by one third of the present amount. This will occur 50 yr after damming the entrance if no water is allowed to come into the sea. If water flow is allowed to compensate for part of the evaporation, it will take longer for these conditions to be attained.

The effect of the increase of salinity on evaporation is small. If no water is allowed into the sea, the salinity will be doubled after 200 yr. This will decrease the evaporation by about 3%. The combined effect of decrease of area and increase of salinity will reduce the possible maximum of generated electricity from 70,000,000 kw to 50,000,000 kw for a 500-ft head.

A great variety of schemes is possible that would generate electricity at an attractive cost. The amount of electricity generated can be tailored to the demands through the control of the amount of water inflow to the Red Sea. As long as the inflow is less than the water evaporated, the generated electricity by a certain amount of water will continue to increase. One scheme will be computed to illustrate these points.

ASSUMPTIONS

1. Two dams will be built, one at the southern end of the Red Sea and another at the southern entrance of the Suez Canal. The southern dam will be built of rock, sand, and clay of local origin at a cost of $0.80 per cu yd. It will have a slope of 4:1 towards the Indian Ocean and a 3:1 towards the Red Sea. It will rise 30 ft above the sea level and be 30 ft wide at the top (Fig. 4). With these specifications the southern dam will cost a little less than $2,000,000,000.

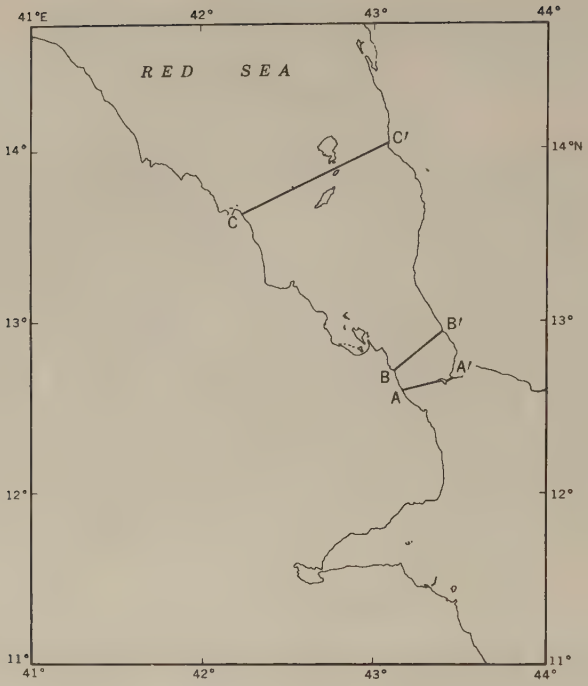
41°E
42°
43°
44°
RED SEA
14°
14°N
13°
13°
12°
12°
11°
11°
41°
42°
43°
44°
C
C′
B
B′
A
A′

FIG. 2.—THE STRAITS OF BAB EL MANDAB, SHOWING POSITIONS OF THE CROSS SECTIONS FOR WHICH THE PROFILES ARE GIVEN IN FIG. 3

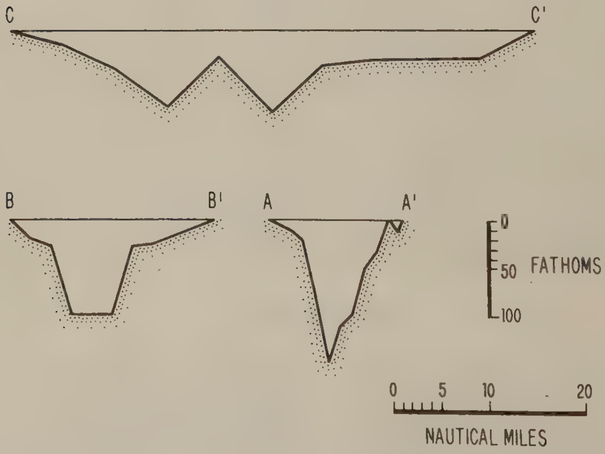
C
C'
B
B'
A
A'
0
50
100
FATHOMS
0
5
10
20
NAUTICAL MILES

FIG. 3.—PROFILES OF THE THREE CROSS SECTIONS SHOWN IN FIG. 2

The cost of the northern dam will be insignificant in comparison. The combined cost of construction will be taken therefore as $2,000,000,000.

2. The electric generating system will generate 75% of the maximum available power as computed from the water head. It will cost $200 per kw. It will need replacement of parts to the extent of 4% of its capital cost every year.

3. After the completion of the dams, 2 yr will pass without allowing any water from the Indian Ocean into the Red Sea except as necessary through navigational locks. After that, and throughout the period of this computation, half as much water as evaporates will be allowed into the sea. As a result of this the sea level will drop by 24 ft in the first 2 yr, and 6 ft per year from that time onwards.

4. After the 25th yr of operation, another dam will be built in the southern end of the Gulf of Suez. This dam will cost $1,000,000,000 and will be finished in 10 yr.

5. The rate of evaporation will continue to be the same throughout the period of the computation. This assumption simplifies the computation, although it is strictly not valid as evaporation will decrease with decrease of surface area. However, as long as the power generated is within the maximum possible limit, computations resulting from this assumption can still be realized.

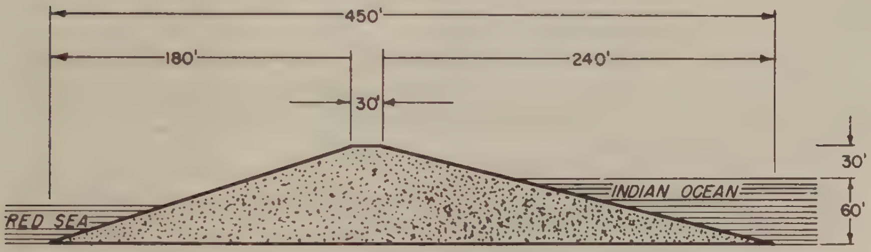

FIG. 4.—PROFILE OF THE PROPOSED DAM AT A PLACE 60 FT DEEP

6. The necessary loan to carry out the project will be available at 4% interest compounded annually.

REQUIREMENT

The price of electricity at the source should be 3.5 mills per kwh. In comparison, the price of electricity generated from atomic plants is predicted by the Atomic Energy Commission to be 6.57 mills per kwh in 1975. Also, any power plants producing electricity at 5 mills per kwh in the United States could capture 43% of the market, and any plant producing it at 4 mills per kwh could capture 71%.

RESULTS

A computation carried out according to the preceding assumptions and requirement gave the following results:

(735)

1. The cost of new equipment that has to be bought annually is 58,500,000.
2. The cost of renewing existing equipment will thus rise annually by $2,400,000.
3. The annual increase of income due to increased power is $8,900,000.
4. After 6 yr from the start of generating electricity the income will be sufficient to meet the annual cost of equipment and replacements.
5. After 46 yr, the debt reaches a maximum of $6,717,000,000.
6. By the 82nd yr the entire debt, with its interest charges, is liquidated.
7. The net revenue after the 82nd yr is about $500,000,000.

CHARACTERISTICS

This project has some new features that make it unique among existing hydroelectric projects. Because of their novelty they are enumerated here to bring them into sharper focus.

1. It makes use of direct evaporation due to solar energy.
2. Power is produced by lowering the level of the lower reservoir rather than raising the level of the higher one.
3. Only water that is needed for power generation needs to be allowed in the sea. There is no need to allow water flow for flood control as the water level in the upper reservoir is constant.
4. The power that is not produced is actually stored, and when it is needed, it will become available and with interest. The interest comes from the fact that due to the increase of head, the same amount of water will generate more electricity at a later time.
5. Because of the increasing salinity in the Red Sea, it can eventually be mined for different chemicals, and thus the project will be producing some of the raw materials that the new industries will need.
6. The problem of silting which plagues many river projects is nonexistent.
7. Because of the ever increasing head (at least during the first 50 yr of operation) special turbines will have to be designed to work efficiently over a wide range of heads.
8. The dam will be protected from the action of large waves because of the shape of the Gulf of Aden and the Bab El Mandeb Straits.
9. The project also offers the intriguing possibility of the first planned tapping of the nutrients stored in the deep water of the oceans. By restricting the water intake to certain depths in the Indian Ocean, it is possible to pump into the Red Sea more than 1,000,000 tons of fish nutrients per year. This could develop a major fishing industry in that area. Many problems have to be investigated, however, before such an extension of the project is made.[3]

PROBLEMS

Problems will, of course, arise. The most important are as follows:

1. Shipping which now passes through the Red Sea without any locks will have to be carried through systems of locks. These should be of adequate size to handle at least the volume of traffic that can pass through the Suez Canal.

---

[3] "Food from the Sea," by E. M. Hassan, Bulletin of the Oceanographic Inst., Univ. of Cairo, United Arab Republic, 1961 (in press).

2. Existing port facilities will be rendered useless, and new ports will have to be constructed as the sea level drops. This is a major expense to the countries concerned, but may well be a profitable investment considering the benefits expected to the whole area from industrialization.

GENERALIZATION

The same condition on which this project rests also exists in other marginal seas. This condition is the inherently unbalanced water budget of these seas. The deficit or the excess is taken care of by transporting water over the sill from or to the nearest ocean. Seas with a surplus budget are not suitable for the generation of electricity since, to produce a head there, the sea level has to be raised substantially. This will flood dry land which is very undesirable.

Example of seas with a deficit water budget are the Mediterranean Sea and the Persian Gulf. Other reasons make them not as suitable as the Red Sea for the generation of electricity.

CONCLUSIONS

1. Because of excess evaporation, the Red Sea will drop by about 12 ft per yr, if dammed.
2. A dam with the necessary installations for generating electricity and systems of locks for shipping will cost something like $33,000,000,000. The actual debt needed is less than $7,000,000,000, the rest being met by the revenue.
3. The system can be paid for in 82 yr while producing electricity at 3.5 mills per kwh. A conservative estimate of the amount of electricity possible to generate is that it will be more than 15 times that generated by the Grand Coulee Dam.
4. The advantages of getting that much electricity for industrialization greatly outweighs any foreseeable disadvantages.

ACKNOWLEDGMENTS

The writer wishes to thank Charles S. Cox and Robert S. Arthur of the Scripps Institution of Oceanography for many stimulating discussions and valuable suggestions, and David M. Garner of New York University for reading the manuscript.

Since the writing of this article, it has been brought to the writer's attention that the principle of this project has been suggested by M. R. Bigarre[4] in 1940. The writer has not been able to locate the original reference.

---

[4] "Engineers' Dreams," by W. Ley, The Viking Press, New York, N. Y., 1954.

INSTRUMENT SOCIETY of AMERICA

PREPRINT NUMBER
221-LA-61

CONFERENCE Preprint

Other publications are encouraged to include abstracts or excerpts of this paper provided credits are given to authors, the meeting and the Society. For permission to publish complete papers write to ISA, Penn-Sheraton Hotel, 530 William Penn Place, Pittsburgh 19, Pa.
The responsibility for all statements in this paper rests with the authors.

FALL INSTRUMENT-AUTOMATION CONFERENCE AND EXHIBIT
LOS ANGELES, CALIFORNIA • SEPTEMBER 11–15, 1961

LONG-RANGE OUTLOOK FOR OCEANOGRAPHIC TELEMETERING*

James M. Snodgrass
Head, Special Developments
Scripps Institution of Oceanography
University of California, San Diego
La Jolla, California

ABSTRACT

With expanding oceanographic research programs, communications promise to be a troublesome problem. Existing frequencies in the radio communications spectrum are almost completely absorbed by military, commercial and amateur interests. New means must be devised to communicate with research and survey ships. Circuits which will permit large amounts of data to be transmitted with high accuracy are needed.

Data telemetering over vast ocean areas will require many new techniques since present practice in the missile and flight test field is limited to line of sight. Conflicts with ocean missile ranges will need to be resolved, as well as devising suitable international agreements to permit long-range telemetering and the establishment of unattended deep-sea buoys and instrument stations.

Telemetering over ranges of several thousands of miles is necessary from unmanned floating instrument stations. Proposed communications types of satellites offer promising possibilities.

Communications, in one form or another, is inextricably linked with oceanographic research and oceanographically-oriented research projects. Unfortunately, it is only within comparatively recent time that the oceanographers have begun to become aware of their needs. The oceanographers' needs involve truly world-wide requirements.

Expanding oceanographic programs are planned which will require the use of instrumented buoys and the transmission of information by means of radio telemetering both to ship and shore based stations. It appears to be almost impossible to plan anything like a serious program involving the use of remote buoys or ocean stations, if we must count on presently available frequencies in the electromagnetic communications spectrum. The difficulties are complicated by the fact that available frequencies are already largely allocated and are used almost completely by the military, commercial and amateur interests. There do not appear to be any suitable frequencies for extensive reliable communications available to the oceanographically-oriented research program.

---

*Contribution from the Scripps Institution of Oceanography, New Series, No. ~~[illegible]~~ 1301 This work was supported in part by funds from the Office of Naval Research, U.S. Navy. Reproduction in part or entirety is permitted for any purposes of the United States Government.

Anticipating the general problems of the oceanographer, the Office of Naval Research sponsored a study contract on oceanographic telemetry (Contract Nonr-3062(00)) with the Convair Division of the General Dynamics Corporation. The first phase of the study has been completed, and an excellent report has been submitted to ONR. One of the purposes behind the study contract was to investigate various factors involved in telemetering data from remote oceanographic instrument buoys to shore based facilities. The factors which must be considered in this operation are tremendously involved and complicated. Some of the factors involve the behavior of specific radio frequencies in regard to radio propagation characteristics, such as skip distances, seasonal variations of noise with respect to latitude, solar induced radio propagation anomalies, power requirements, frequency bandwidths, etc. All of these variables have now been organized and collected together in the report submitted to ONR by Convair.

It appears that long-range communication may not be considered reliable using whatever frequencies may be available between a shore based receiving station and remote buoy or ocean station. This is assuming that dependable communication is required and that data be transmitted without objectionable error. It is quite true that one may obtain occasionally, and even for a limited period, transmission which might be considered acceptable. The difficulty is, however, that such conditions cannot be counted upon if reliable transmission is required. It is therefore necessary to seek modifications of the system whereby reliable communications may be established.

For somewhat over a decade Mr. E.F. Corwin, Mr. L.J. Allison and Mr. J.C. Appleby of the Meteorological Branch, Bureau of Naval Weapons,[1] and Mr. Hakkarinen of the Electronics Branch, National Bureau of Standards, have been carrying out highly significant work in the development of radio telemetering ocean buoys and instrument stations. It is interesting to note that, as time went on, each succeeding buoy design involved the use of larger amounts of radiated RF power. Later designs tended to evolve around the "squirt" techniques and used radiated power levels as high as 5kw.

The "squirt" system combined with knowledge gained in ionospheric research by the Canadian Defence Research Establishment may well prove to be valuable. The substance of the method developed involves the use of an interrogation technique between the shore based station and the remote buoy. In this technique the buoy would be equipped with a transponder system which would be interrogated by means of short pulses on a short duty cycle transmitted repetitively by the shore based station. When the radio propagation conditions are suitable, and the interrogation pulse is able to reach the buoy, the buoy transponder would send out a pulse to the shore station. The received pulse signifies that the communications path is for the time being open between the two stations. The shore based station then would send a coded request to the buoy to transmit its stored information. When this cycle is completed, the shore based station then seeks to interrogate another buoy, etc. This particular system is based upon the fact that when a given transmission channel becomes open between two stations it may be expected to remain open for a period of from four to five minutes. If suitable recording and memory systems are on board the buoy, it is quite practical to count on interrogating the buoy at some time during a given 24-hour period. However, it is quite apparent that one cannot establish over a long period of time precisely when it will be possible to interrogate the buoy, and the memory system must take such variables into account.

There is an additional alternative to the above-outlined system, which is recommended by the Canadian Defence Research group, and that is to have available a selection of a wide range of radio frequencies for such a communication system and that the shore based interrogation system transmit an interrogation pulse in sequence through the different assigned frequency bands. This means, of course, that the remote buoy must have a somewhat more sophisticated receiving system, i.e., one which can listen simultaneously on all of the expected frequency bands. However, if such a system is used, the assurance of being able to effect communication with the remote station when desired is tremendously improved. This latter method is the method which apparently receives the most favorable recommendation by the Canadian group.

It is quite possible if such a system as proposed were used that it would involve substantial modifications in methods of licensing. This is considered to be beyond the scope of this discussion and will not be further considered.

Whether we like it or not, the research institutions find themselves involved in the problem of obtaining space in the electromagnetic communications spectrum. Since we have not been notably successful in the past in obtaining suitable radio frequency assignments for research programs, it appears that we should turn our attention to methods of operation which will not be conflicting with existing operations.

The problem of non-interference with existing services is an extremely sticky one. An installation for the collection of oceanographic information now beinginstalled in the Gulf of Mexico by Mr. Roy D. Gaul of the Department of Oceanography and Meteorology, A. & M. College of Texas, has encountered an entirely new series of headaches from the standpoint of the oceanographer. It so happened that the area in which it was planned to locate the telemetering system was physically in an overlap area between Patrick Air Force Base Missile Range and Eglin Air Force Base Missile Range, and it appeared to be almost impossible to find a suitable means of using any radio frequencies which would be considered acceptable by the Air Force.

After considerable difficulty, Mr. Gaul has worked out a temporary arrangement for operation which meets with approval of the Air Force representatives concerned. A significant point which his operations raise, however, is the problem faced in major buoy programs in both the Atlantic and the Pacific Oceans which undoubtedly will run afoul the Atlantic Missile Range and the far more extensive Pacific Missile Range. We are already having problems in the San Diego area with respect to interference by transmitters in the San Diego area with the Pacific Missile Range operations. These are considered serious and they are by no means resolved at the present time.

Looking first at techniques which would permit buoy operation, we have considered the possibility of systems which would permit the use of relatively low-power transmitting systems in the buoys. Perhaps the most available method at present to begin to solve the buoy-shore communication problem, and evolve a method which could be put into effect with existing technical facilities, is the use of high flying aircraft to serve as an interrogation platform for communicating with floating buoys, etc. This would permit the use of relatively low-power radio transmitters in the buoys and a relatively simple information storage system. The high flying plane would transmit a suitable coded interrogation pulse which would insure the response of the desired buoy. Since the airplane would be carrying a suitable recording system, such as magnetic tape, the information transmitted by the buoy could be recorded as desired. In this system it would be planned to have the data processed at the conclusion of the flight. Difficulties with this system are not to be minimized since it requires the availability of suitable high flying long-range aircraft, as well as the necessary operating bases. However, it would be possible to carry out some fairly extensive programs with existing bases and aircraft. It should also be pointed out that suitable radio frequency assignments must be made if communications of this type are to be carried out. Unquestionably, a suitable long-range aircraft for our purposes would be the U-2, which satisfies many of our basic requirements. Whether the plane would actually prove adequate for such operations, remains to be seen.

Another and most promising system for long-term operation is to be found in the various types of communication satellites. For practical purposes we may discard the passive satellites of the ECHO type, since this involves very large high power and highly directive antenna systems which are quite impractical on buoys, and, for that matter, even on ships the size of oceanographic research vessels. The active satellites, however, would appear to be useful. The satellites which are planned on being programmed for orbits between 5,000 and 6,000 miles will undoubtedly require powers that are not readily available to small floating buoys and instrument stations. However, these satellites can be counted upon for communicating between ships and shore bases using stabilized dish-type antennas. It would thus be possible to transmit a very large amount of data with high reliability from ship-to-shore and vice versa using the satellite system. This would mean that it would be possible to send data directly ashore for data analysis as desired. The active satellites which are referred to for this type of data relaying operate in real time. Another type of satellite known as the COURIER type is perhaps the most adaptable under the present basis of operation. The COURIER type of satellite does not retransmit radio signals in real time, but involves a memory system. The COURIER satellite is planned on being programmed to a much lower orbit, namely, the range from 300 to 400 miles. Since it is much lower, it will require a great deal less power to effect reliable communication between buoy and satellite. At present the COURIER type of satellite is designed to record information received via radio and play it back on proper interrogation from the ground based station. It is considered practical to program the COURIER type of satellite to interrogate buoys as it passes over various portions of the ocean and then to playback the data obtained from the buoy when it passes over a suitable land based station. The land based station would be able to keep a longer contact with the satellite, since it would have a much superior antenna system than that possessed by the floating station.

In view of the many difficulties which are found in the use of the conventional portions of the electromagnetic communications spectrum, perhaps we should search out other regions.

A most significant problem presently exists with the proposed use of any of the satellites and this is the fact that there are now tremendous demands upon the electromagnetic communications spectrum that is expected to be available to the satellite systems, and unless the research groups interested in obtaining ocean data make a very strenuous effort to obtain proper frequency allocations, or time allocations, on the communications types of satellites, it is quite probable that none will be available when needed at some future date. It is almost impossible to overemphasize the amount of pressure being brought to bear to obtain communications frequencies in the satellite programs. Since groups interested in collecting data from the ocean are not in any way represented on the committees and boards making such studies, it is imperative that remedial steps be taken along this line as soon as possible.

Since the oceanographers' communication problems extend well beyond the continental limits of the United States, it is apparent that international relationships are involved. This would be true whether high flying aircraft or satellites are used in the solution of the communication problems.

Unfortunately, the groups interested in various aspects of marine research in this country are not organized from the standpoint of representation to the FCC for frequency assignments. Also, there is no voice from the oceanographers in the ICSU (International Council of Scientific Unions), which through the CCIR (International Radio Consultative Committee), reports directly to the ITU, or International Telecommunications Union, for ultimate international frequency allocations.

So much for the background. We have seen something of the problems confronting the oceanographer. We will now concern ourselves with the current status and what is being done. As of June 29, the National Academy of Sciences Committee on Oceanography, acting for the oceanographic and meteorological community, voted to initiate a formal study of the problem. The direct responsibility is placed with the Panel on New Devices which serves as a sub-committee.

An engineering firm has been retained to assist in delimiting the engineering requirements from the inputs supplied by oceanographers and meteorologists. After the preliminary study is complete, the report will be studied by the Panel on New Devices and plans developed to carry out the major program, which is the development of engineering requirements for the justification of a new type of service in the field of radio communication. It will be necessary to work up a complete case which may then be ultimately presented to the FCC.

The major engineering study will be worked up with the advice and assistance of the National Academy of Sciences Committee on Radio Frequency Assignments for Science. This committee was formed initially to justify the radio frequency requirements of the radio astronomers, and will now be fulfilling a somewhat broader purpose.

The National Academy of Sciences Committee on Oceanography will undertake to check the input requirements from the standpoint of oceanographers and meteorologists, and the National Academy of Sciences Committee on Radio Frequency Assignments for Science will check and evaluate the engineering considerations.

It should be apparent that the entire problem is one of a rather complex sort and that its ultimate, satisfactory solution is of direct interest to industry. Since industry has a definite stake in the field of oceanography and meteorology, it is hoped that representatives of industry will be interested in assisting directly in formulating and recommending possible systems which may assist in the solution of our communications problem.

The areas to be covered are essentially those of the oceans, so that in effect we require world-wide coverage. As an example of the numbers of unattended ocean instrument stations or buoys which may be required the figure of 100 buoys for the northeast Pacific, i.e., the area east of 180° and north of the Equator may be used. It is felt that this is a somewhat conservative figure. This does not, however, include special buoys and instrument stations for studying short-time projects, but rather represents the number which would be necessary for routine, relatively long-time programs. Integrated into this are also the requirements of the ship-to-shore communications, ship-to-ship, ship-to-buoy, buoy-to-ship, etc. It is quite probable that multiple solutions to the problem exist but major efforts will be centered toward determining what system, or systems, appear to be most suitable for the purpose. We earnestly solicit assistance from industry and research laboratories and will welcome serious recommendations and suggestions.

REFERENCES

1. "The Floating Automatic Weather Stations of the United States Navy," Weatherwise, Vol. 12, No. 5, October 1959.

From: International Union of Geodesy and Geophysics.
International Association of Physical Oceanography.
Symposium on radiant energy in the sea. Helsinki,
4-5 August 1960. Monograph No.10, June, 1961.
pp.91-95.

DAYLIGHT PENETRATION MEASUREMENTS IN THREE OCEANS

by

E. M. Kampa

The data presented here were collected as a part of a study of the environment of migratory sonic-scattering layers. Our interest was primarily in conditions immediately above the layers, but inasmuch as the photometers recorded continuously, the intensityof light throughout the water column above the layers was measured as well.

The photometers were designed and built by James M. Snodgrass with assistance and advice from John E. Tyler, both at the Scripps Institution of Oceanography. The optics and circuitry have been described by Boden, Kampa and Snodgrass (1960). Briefly, the optical system consists of an opal plastic window with the characteristics of a Lambert cosine collector, mounted flush with the end of a collimating tube which restricts the angle of light to a 5° cone. At the proximal end of the tube is a chamber to hold interference filters for which collimation is essential. The collimator and filter holder are free-flooding. This assembly is bolted to the head of the photometer, over a sapphire window through which the collimated, filtered light passes to the photocathode of a 931-A multiplier phototube. The water-tight, pressure-resistant unit of the photometer contains the photomultiplier, its power supply and amplifier, a depth sensor, and, in the Mark II instrument, a temperature sensor. Mar II is equipped with a three-position strip shutter (positions: closed, open, pinhole)which may be changed at will by the operator when the instrument is submerged. Commands to the underwater unit and signals from it are transmitted by a polyethylene-coated single-conductor stainless steel cable, which also supports the instrument in the water. The signals are recorded by a Leeds and Northrup Speedomax recorder. Balzers interference filters, sealed at the edges with Araldite resin, are used to define the wavelength of light. Calibration of these filters with a spectrophotometer shows that they transmit 35 to 45% of the light at the peak wavelength and that the wave bands at one-half maximum transmission are 8 to 12m μ wide.

The instrument measures irradiance. The values of irradiance, H, were obtained by

$$n = K H_{\lambda} = \int T_{\lambda} \cdot S_{\lambda} \cdot E_{\lambda} \, d\lambda$$

where H = irradiance in μ watts/cm^2, n = recorder reading in mv, $\int T_{\lambda} . S_{\lambda} . E_{\lambda}$ is the integral of the transmission of the filter , the sensitivity of the multiplier phototube and the energy of the source through the wavelength interval $d\lambda$ in mμ, and k, the relationship between intensity and recorder reading, is determined by calibration of the entire instrument against a thermopile and galvanometer, using a U.S. Bureau of Standards source.

Three widely separated areas were sampled in 1955: the 600-fathom trough between the Californian coast and the islands off San Diego (July), the northwest edge of the Sargasso Sea off Bermuda (August), and the Golf du Lion in the Mediterranean off Banyuls-sur-Mer (October). At that time we did not have an automatic filter changer, and individual casts were made with each of the interference filters in the light path. A cast took from 25 minutes to 1 hour, depending on the wavelength being measured.

Contributions from the Scripps Institution of Oceanography, New Series, 1302
Reproduced by Permission

All measurements were made between 1030 hrs and 1400 hrs., local standard time, when the sun was nearest its zenith.

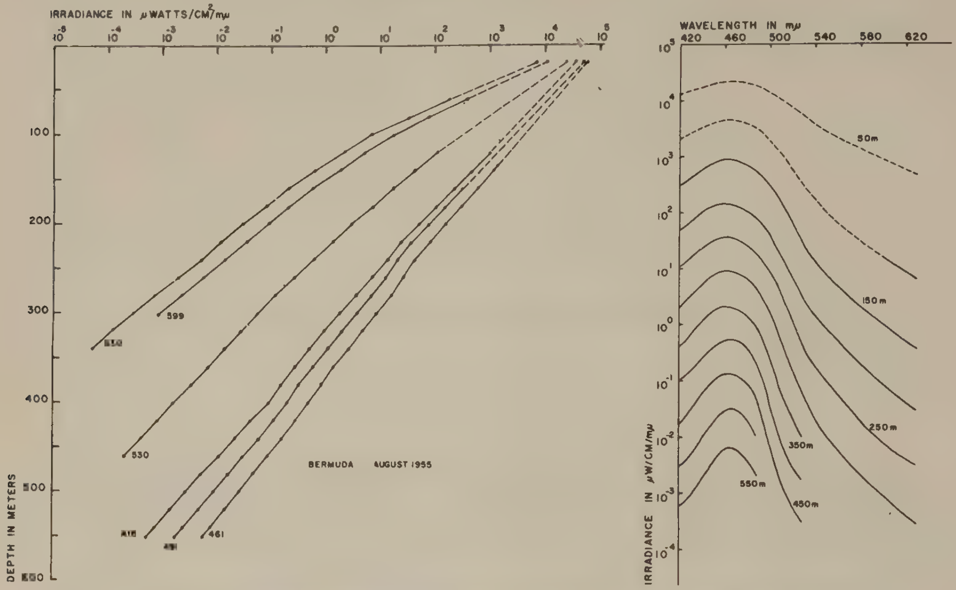

Fig. 1. Left. Relation between depth and irradiance at various wavelengths. The numbers at the ends of the curves indicate the wavelength in mµ of maximum transmission of the interference filters used.
Right. Spectra of transmitted daylight at 50-m intervals off Bermuda. The spectra were derived from the attenuation curves at the left.

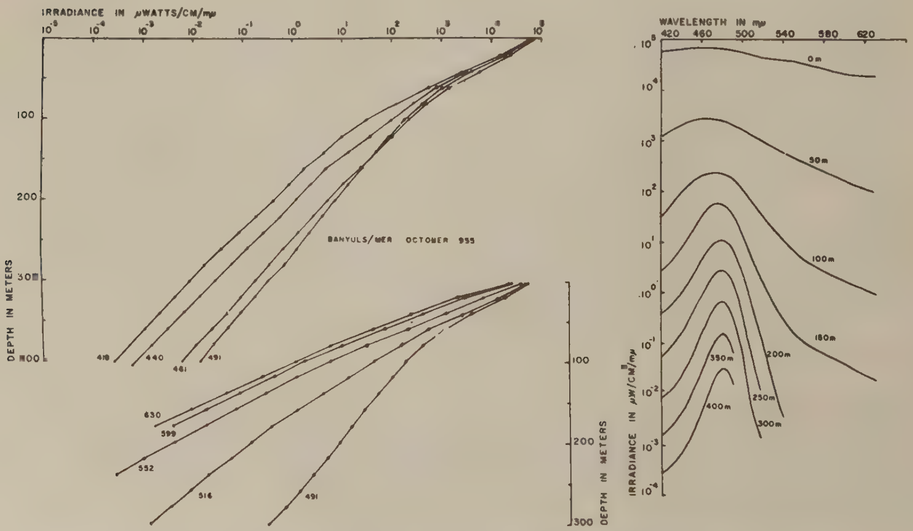

Fig. 2. Left. Relation between depth and irradiance at various wavelengths. The numbers at the ends of the curves indicate the wavelength in mµ of maximum transmission of the interference filters used.
Right. Spectra of transmitted daylight at 50-m intervals off Banyuls-sur-mer. The spectra were derived from the attenuation curves at the left.

The Mark I photometer without a pinhole shutter was used off California and Bermuda, and the intensity of transmitted daylight from the surface to considerable depth was too great to measure directly. To obtain an estimate of the color and intensity of light near the surface, a neutral density filter (transmission: 0.0001) was placed in the light path along with the particular interference filter, and the instrument was sent down again to 20 meters after each deep cast. The Mark II photometer was

Table 1. Extinction coefficient $k_\lambda = \ln H_{\lambda, z} - \ln H_{\lambda, (z+1)}$ where $H_{\lambda, z}$ and $H_{\lambda, (z+1)}$ are the irradiance of wavelength λ on horizontal surfaces at depths z and (z+1) m.

	Bermuda			Banyuls sur Mer			California		
λ(mμ)	Depth (m)	k	Oceanic water type (1)	Depth (m)	k	Oceanic water type	Depth (m)	k	Oceanic water type
418	120-220	.038	I-II	000-020	.068	I-II	040-060	.066	I-II
	220-550	.033	I-II	020-060	.085	I-II	070-250	.056	I-II
				060-100	.068	I-II			
				150-300	.038	I-II			
				300-400	.034	I-II			
440				000-020	.066	I-II			
				020-060	.074	I-II			
				060-100	.053	I-II			
				150-400	.035	I-II			
461	135-240	.033	I-II	000-020	.056	I-II	045-065	.058	I-II
	240-550	.028	I-II	020-060	.072	I-II	110-160	.052	I-II
				100-240	.037	I-II	180-350	.058	I-II
				250-400	.033	I-II			
491	160-220	.036	I-II	000-020	.064	I-II	040-060	.072	I-II
	220-550	.031	I-II	020-060	.074	I-II	080-160	.039	I-II
				060-100	.046	I-II	180-350	.058	I-II
				120-280	.031	I-II			
516				000-020	.067	I-II	040-065	.074	I-II
				020-060	.082	I-II	085-185	.046	I-II
				075-180	.057	I-II	200-310	.072	I-II
				180-300	.047	I-II			
530	120-200	.043	I-II				045-065	.061	I-II
	200-340	.039	I-II				070-150	.051	I-II
	340-460	.035	I-II						
552				000-020	.100	I-II	045-065	.074	I-II
				020-080	.088	I-II	070-125	.054	I-II
				125-140	.072	I-II	155-290	.064	I-II
572							045-065	.088	I-II
							070-175	.066	< I
							180-265	.060	< I
599	080-100	.073	< I	000-020	.128	< I	045-130	.077	< I
	120-180	.052	< I	040-100	.092	< I	130-200	.066	< I
	195-300	.046	< I	100-180	.077	< I			
630	060-100	.085	< I	000-020	.135	< I	045-130	.085	< I
	100-160	.056	< I	040-100	.092	< I	130-180	.062	< I
	180-340	.047	< I	100-180	.082	< I			

(1) According to Jerlov (1951).

(747)

used in the Mediterranean, and with the pinhole and open shutter positions it was possible to record light intensity continuously from the surface to the depth of the scattering layer.

Results of these observations are presented graphically in Figures 1 to 3. Although the Californian preceded them, it seems preferable to discuss the other regions first.

The transparency of the Sargasso Sea off Bermuda (Fig. 1) was measured from a buoy tender on three different days in August. The passage of two hurricanes interrupted the sequence of the casts, and we were finally evacuated from the islands after measuring midday attenuation at only 6 of 10 possible wavelengths. Despite the storms and the relative turbulence of the surface waters, this was the most transparent body of water that we have encountered. The photometer began to record reliably after it had reached depths of 75 to 150 m, and we had insufficient cable to reach the limit of sensitivity of the instrument at the shorter wavelengths.

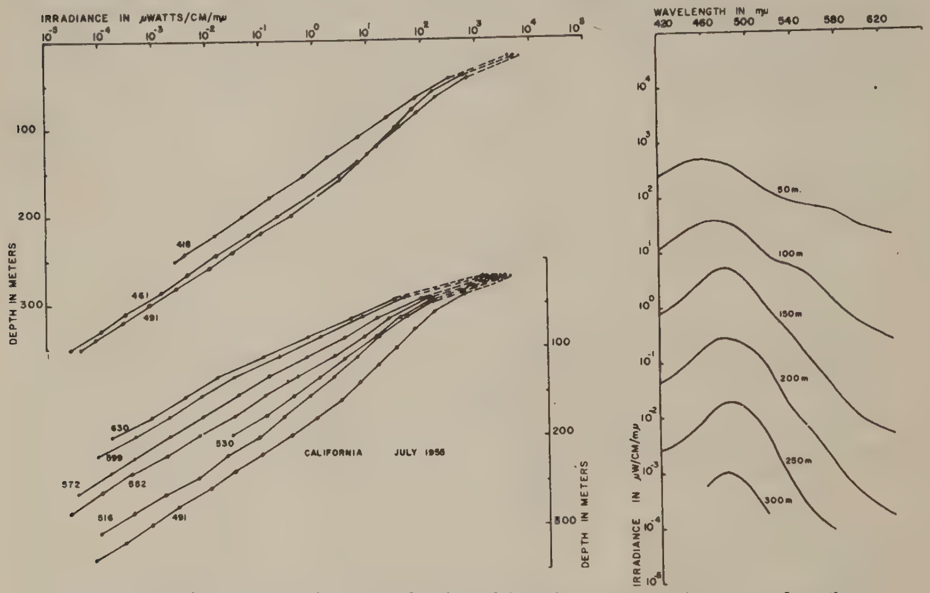

Fig. 3. Left. Relation between depth and irradiance at various wavelengths. The numbers at the ends of the curves indicate the wavelength in mµ of maximum transmission of the interference filters used.
Right. Spectra of transmitted daylight at 50-m intervals off San Diego, Calif. The spectra were derived from the attenuation curves at the left.

The extinction coefficients (Table 1) at 418, 461, 491, and 530 mµ are comparable with those for clearest oceanic water. At longer wavelengths we found the water more transparent than we had expected from an examination of the literature (Utterback, 1936; Clarke and James, 1939; Jerlov, 1951). The spectra of the light are fairly symmetrical, with energy decreasing regularly on either side of 465 mµ at all of the depths measured.

In the Mediterranean off Banyuls-sur-Mer, the surface water down to about 20 m. is relatively transparent, and at wavelengths shorter than 516 mµ, this layer could be classified as clear to average oceanic water. From about 20 to 75 m, the extinction becomes much greater at these shorter wavelengths and is well within the range of average oceanic water. Below about 75 m, the water is again more transparent, with extinction coefficients (Table 1) similar to those obtained off Bermuda. It is interesting to note that at this station water temperature was found to decrease gradually from 15.5 to 14.5°C between the surface and about 30 m. A sharp thermocline (from 14.5°C to 11°C) was present in the 30 to 70 m layer, and below 70 m the temperature was constant at 10.7°C. Such correlations between attenuation coefficients and thermoclines have been reported from the North Pacific (M. Koslyaninov, Acad. Sci., USSR-personal communication to J.E. Tyler) and from the Bay of Biscay (Boden, Kampa and Snodgrass, 1960).

At wavelengths longer than 530mμ, transparency increases regularly from the surface to about 100m, where the extinction coefficients stabilize and remain constant to depths of at least 200 m. The peak of the spectrum of transmitted daylight is at 460 m μ just below the surface. It is shifted to 465 mμ at 50 m , to 470 mμ at 100 m, and at greater depths it is constant near 478 mμ .

The study of daylight penetration in the coastal waters off California (Fig. 3) was more detailed than those at the other two stations. All ten of the interference filters were used on two consecutive days. The surface layers from 20 to about 60 m are less transparent than those in the Mediterranean, but their extinction coefficients (Table 1) are within the range of average oceanic waters. Below 100 m, the transparency increases greatly, and, at wavelengths shorter than 530 mμ , the extinction values are midway between those for average and those for clearest oceanic waters. At the Pacific station, as at the others, the water near the surface and at depth is unexpectedly transparent to wavelengths longer than 530 mμ .

In the water off California the peak of the spectrum of transmitted daylight is at about 460 mμ at 50 m , 470mμ at 100 m, and 475mμ at 150 m. Below 150 m, the position of the energy maximum is constant at 480mμ . There is a slight inflexion in the energy spectrum between 540 and 580mμ .

Conclusion

The shape of the spectrum of transmitted daylight at a depth of 50 m is nearly identical in the waters off Bermuda, Banyuls-sur-Mer and California, although the energy levels in the Mediterranean and the Pacific are only 15% and 2.5% respectively, of the levels in the Sargasso Sea.

Below 100 m the shape of the energy spectrum does not change appreciably off Bermuda. At the Mediterranean station below 100 m, the rate of attenuation at about 470 mμ is similar to that in the Bermudian water. On either side of this wavelength, extinction values are higher than those in the Sargasso Sea, and the spectrum at depth peaks sharply in the blue-blue green.

At the Pacific station below 100 m, extinction coefficients for wavelengths greater than 470mμ are lower than those in the Mediterranean, and the longer wavelengths make a greater contribution to the total energy at depth. For example, at 50 m the energy level at 520mμ off California is only 10% of that off Banyuls. At 200 m the energies at 520mμ are equal, and the energy at 540mμ is 4 times as great in the Pacific. In the region of the peak of the spectrum, of course, the light in the Mediterranean is nearly 100 times as intense as that in the Pacific at 200 m. While the minute differences in transparency to certain wavelengths in various water masses may seem inconsequential to the study of light penetration in the sea, they may have a very real significance to biological systems operating at depth.

We have no direct evidence to account for the observed differences in light transmission at the three stations. The Californian coast is an upwelling one, relatively rich in nutrients and in phytoplankton production. Collections of zooplankton from sonic-scattering layer depths made during these investigations indicate that biological activity is greater at both the Mediterranean and Pacific stations than in the relatively barren waters off Bermuda. Similarly, the Pacific and Mediterranean stations were near large land masses, and one would expect that the geological effects on water transparency would be greater than those near an oceanic island.

References

Boden, B.P., E.M. Kampa and J.M. Snodgrass., 1960. Underwater daylight measurements in the Bay of Biscay., J. Mar. Biol. Assn. U.K., 39: 227-238.

Clarke, G.L., and H.R. James., 1939. Laboratory analyses of the selective absorption of light by sea water., J. Opt. Soc. Amer., 29: 43-55.

Jerlov, N.G., 1951. Optical studies of ocean water., Rept. Swedish deep-sea Exped., 3: Physics and Chemistry., Fasc. 1, 1-59.

Utterback, C.L., 1936. Spectral bands of submarine solar radiation in the North Pacific and adjacent inshore waters. Rapp. Cons. Explor. Mer. 101 (2): 15 pp.

From: International Union of Geodesy and Geophysics.
International Association of Physical Oceanography.
Symposium on Radiant Energy in the Sea.
Helsinki, 4-5 August 1960. Monograph No. 10.
June 1961. pp. 96-101.

TWILIGHT IRRADIANCE IN THE SEA

by

Brian P. Boden

(751)

International Union of Geodesy and Geophysics.
INTERNATIONAL ASSOCIATION OF PHYSICAL OCEANOGRAPHY

Symposium on Radiant Energy in the Sea. Helsinki, 4-5 August 1960.

TWILIGHT IRRADIANCE IN THE SEA

by

B. P. Boden

Four experiments and their results are described here. These experiments were performed in an effort to determine some of the characteristics of the light (particularly its spectral characteristics) in the water column just above the sonic-scattering layer. We were especially interested in the changes occurring at sunset and sunrise, and the

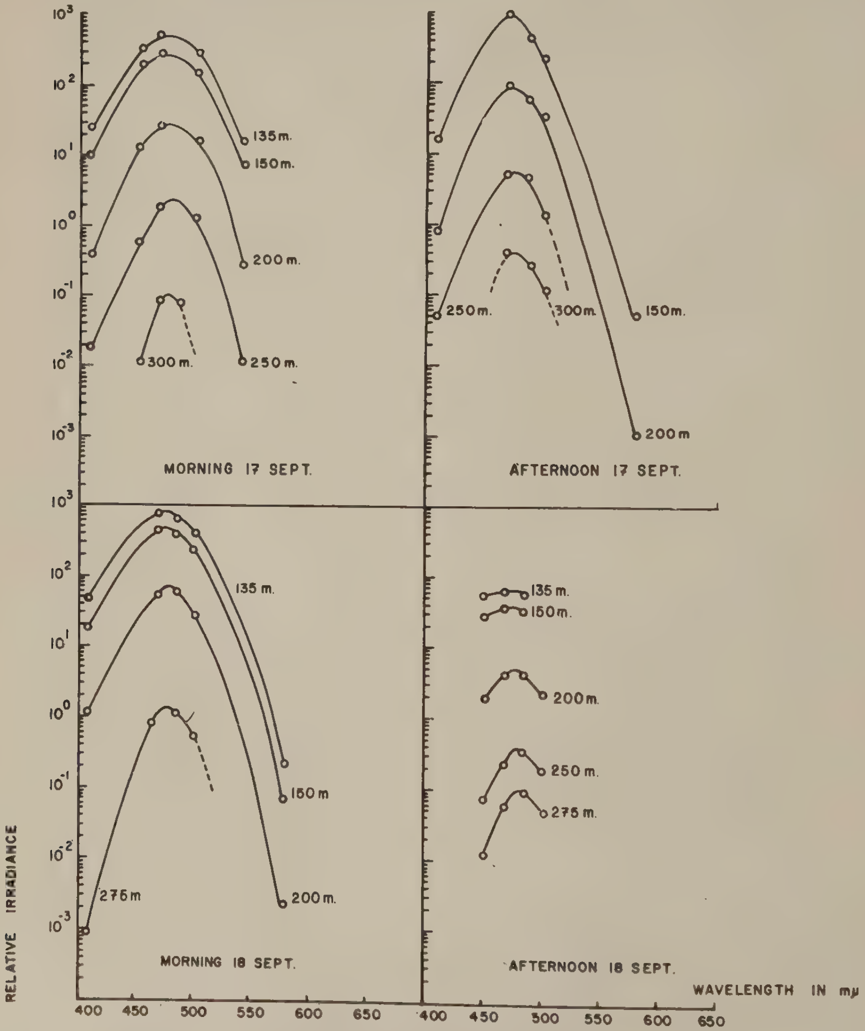

Fig. 1 . Relative irradiance spectra at indicated depths off San Diego in September.

Contributions from the Scripps Institution of Oceanography, New Series, 1303
Reproduced by Permission

twilight periods during which the scattering layer undertakes its vertical migrations toward and from the surface. It is our wish to duplicate the observed light conditions in the laboratory and ascertain the physiological reactions of animals captured in the layer by some objective method.

In the scattering layer off San Diego heavy concentrations of plankton occur and euphausiid crustaceans are dominant members of this plankton. They are concentrated in the upper part of the layer, particularly when the layer migrates toward the surface. At this time the layer usually splits into two or more components. The upper component, in which the auphausiids concentrate, reacts to a particular intensity of light (about $1x10^{-4}$ μ watts/cm^{2}). These contentions are supported by the work of Johnson (1948), Boden (1950), Tucker (1951), and Kampa & Boden (1954) as well as by much of our unpublished field work since then.

We have, therefore, selected the euphausiids as experimental animals and our first interest was to define the characteristics of their light environment, and the changes they encounter in the course of their vertical migrations to and from the surface.

The bathyphotometers used in these experiments have been described by Boden, Kampa and Snodgrass (1960). These employ multiplier phototubes and a series of interference filters placed in front of the tube by an automatic filter-changer. These filters permit the measurement of near-monochromatic light of low intensity. The window of the photometer is opal plastic with the characteristics of a Lambert cosine collector. A collimating tube restricts the angle of incidence on the 931-A photocathode to the useful 5° cone of the interference filters. The instrument measures irradiance.

The water column above the sonic-scattering layer

The first series of measurements reported here was made to determine midday conditions in the water column down to the depth of the scattering layer. The photometer looked upward and was lowered immediately before noon and immediately after noon on two consecutive days (Sept. 17 & 18, 1957). The filters used had transmission peaks at 410, 452, 470, 489, 503, 541, 581 and 634 mμ and were placed in position in different order in each cast. The instrument was lowered to depths indicated by the depth sensor and held in position while the filter changer completed a cycle.

At depths between 135 and 300 m the light was blue-green with a peak between 475 and 480 mμ , Fig. 1, whichever combination of filters was used. The instrument could not sense light through the red filter (634 mμ peak) below a depth of 105 m, whereas the light was too bright at this depth for measurement through the other filters.

The peaks of the curves become increasingly sharp with depth as the sea water acts as a natural monochromator (Tyler, 1958).

Values of the extinction coefficient (k) for each wavelength at different depths are shown in Table 1. The extinction coefficient at depth z is defined by

$$k_{\lambda} = \ln H_{\lambda,z} - \ln H_{\lambda,(z+1)}$$

where $H_{\lambda,z}$ and $H_{\lambda,(z+1)}$ represent irradiance values of wavelength λ on the horizontal surfaces at depths z and (z+1 m).

Table I. Extinction coefficients (k) or irradiance at wavelengths (λ) at depths (D). The extinction coefficient is defined as $k = \ln H_{\lambda,z} - \ln H_{\lambda,(z+1)}$

(D)	(λ)	(k)
150-250	410	.065
	452	.053
	470	.051
	489	.048
	503	.047
	541	.064
122-198	581	.081

where z and (z+1) represent 1m. intervals of depth (D)

The values presented were obtained in the water mass below the photic zone and above the scattering layer, where the decay curves were fairly straight and k was constant, which suggests that there was little interference from biological or geological sources.

Figure 2 shows extinction per meter for various wavelengths and it can be seen that the water was rather clear for shelf water. According to the data of Utterback (1936) and Jorgensen and Utterback (1939) it would be typified as average oceanic water.

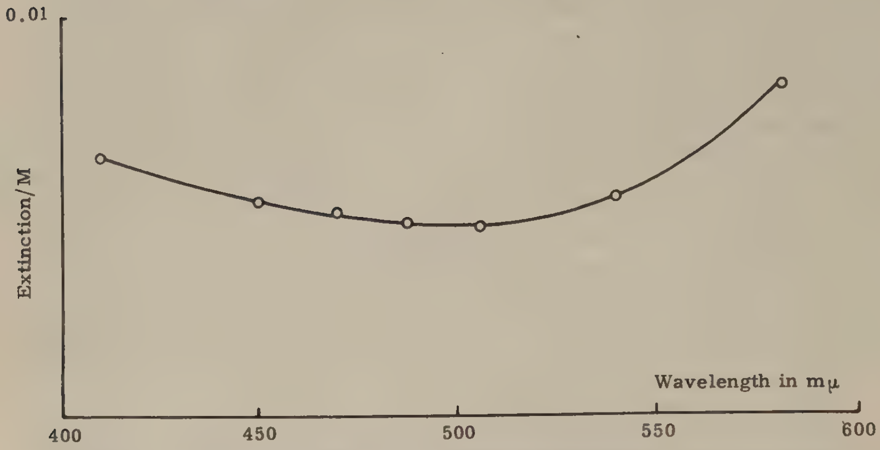

Fig. 2. Extinction coefficients at various wavelengths at depths between 150 and 250 m. off San Diego in September.

Rate of attenuation at the surface and at depth at sunset

For the purpose of determining the rates of decay simultaneously at two different depths two identical photometers were used.

One was suspended 10 m below the surface from a rubber float, the other was suspended 200 m directly below. No filter was used in either. Separate recorders were used and simultaneous recordings were made.

Figure 3 shows that the rate of extinction was very similar at both depths from 30 minutes before sunset until 50 minutes after sunset. From thereon the curves

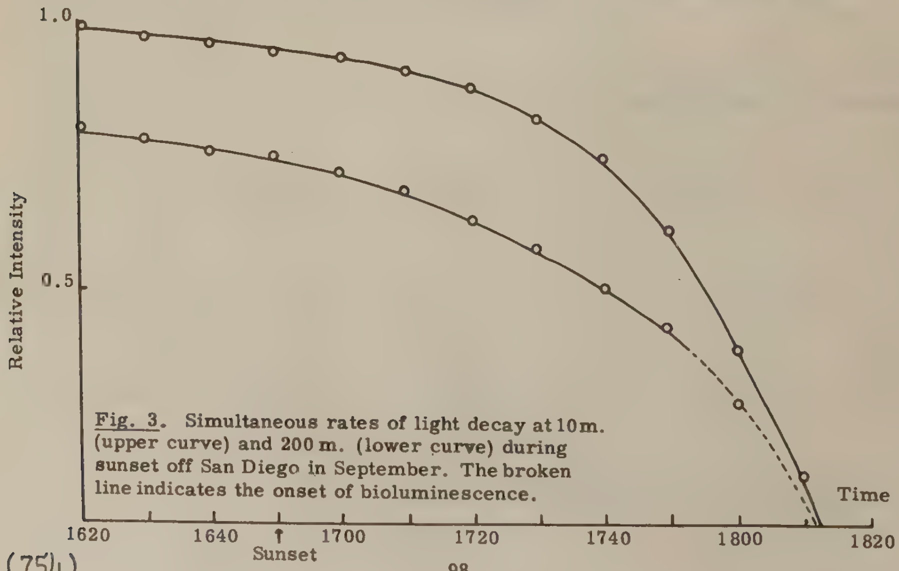

Fig. 3. Simultaneous rates of light decay at 10 m. (upper curve) and 200 m. (lower curve) during sunset off San Diego in September. The broken line indicates the onset of bioluminescence.

(754)

approach each other rather rapidly with the rate of extinction at the surface being apparently more rapid than at 200 m. We suggest that this deeper picture is obscured by bioluminescence.

A strong scattering layer was present on this evening and 50 minutes after sunset this layer was shoaler than 200 m. Shortly after 1750 hrs the bioluminescence was so marked and the flashes so large that it was not possible to obtain sky-light readings at that depth. These results were similar to those obtained in Hawaii by Boden and Kampa (1957). The experiment was terminated at 1810 hrs on this account.

Spectral distribution of light at a constant depth at noon, sunset and sunrise

The photometer was lowered on three successive days, at noon and sunset to a depth of 170 m. It was equipped with its automatic filter changer, and eight different filters were used in different orders. The values in Figure 4 have been equated to 1 at 470 mμ. They represent the average of the values obtained on each of the three days.

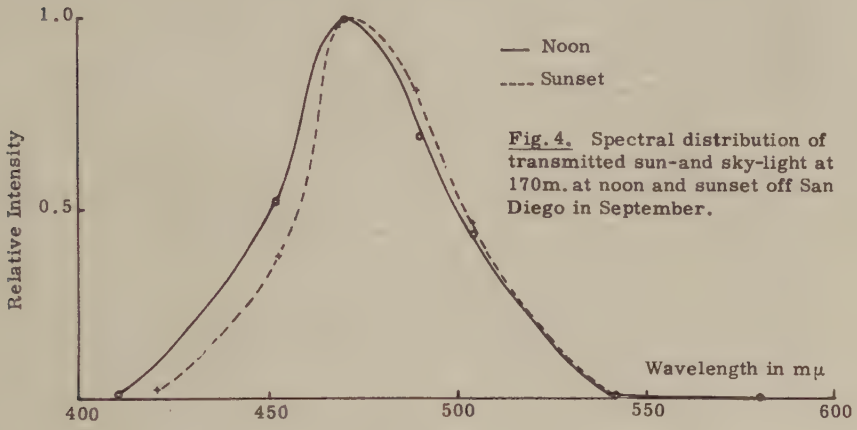

Fig. 4. Spectral distribution of transmitted sun-and sky-light at 170m. at noon and sunset off San Diego in September.

It can be seen that there is a shift away from the shorter wavelengths at sunset.

The data presented in this figure were taken in September and represent the sunset values obtained within a few minutes around sunset.

In Figure 5 we present the values obtained during an hour period around sunrise in January. It can be seen that before sunrise higher values are obtained for the longer wavelengths than for the shorter. As sunrise approaches the penetration of the shorter wavelengths becomes greater, until shortly after sunrise there is an actual crossing of the 410 and 515 mμ isolumes.

It must be remembered that these are measurements made just before sunrise, at sunrise, sunset, and conditions of very low sun, and are of both transmitted sun- and sky-light. Mr. JohnTyler, in a personal communication, has suggested that this shift is possibly due to selective refraction at the sea surface at such periods. There must be some critical point after twilight at which a reversal of these conditions occurs for the conditions observed in Figure 1 to pertain.

Spectral composition of transmitted sun- and sky-light just above the sonic-scattering layer during the twilight migration

The photometer was equipped with its automatic filter changer, and a variety of filters was used. The instrument was lowered to just above the sonic scattering layer, and the filter changer was allowed to rotate. The intensity observed at 470 mμ was selected as a reference value. During light decay at sunset the photometer was raised to follow this 470 mμ isolume.

The ship was far from shore and ship lights were doused. Only sky-light or possibly bioluminescence, although it was not recognizable as such, was being recorded.

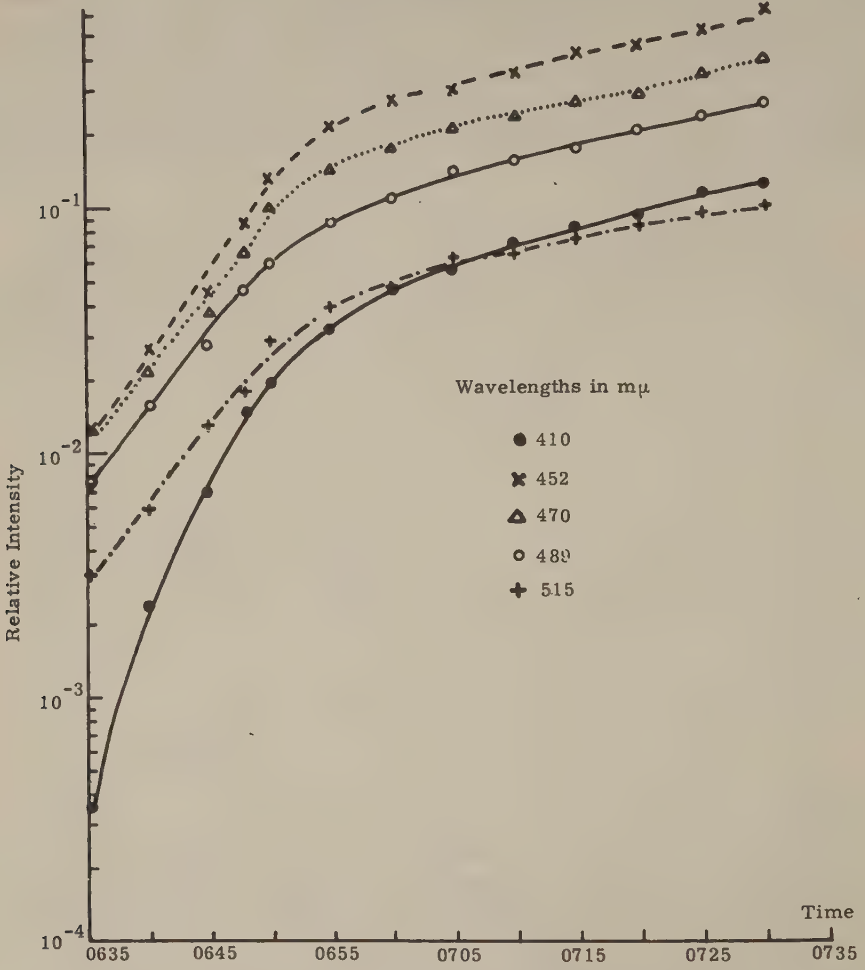

Fig. 5.- Spectral composition of transmitted sun- and sky-light at 100m. for the period of an hour around sunrise.

Figure 6 shows the average values obtained at similar depths, similar times and similar wavelengths during three successive twilight periods. It can be seen that the peak values shift from about 490 mμ at sunset toward shorter wavelengths to about 465 mμ at the end of official twilight.

References

Boden, B.P., 1950, Plankton organisms in the deep scattering layer USNEL Rept. 186, 1-29.

Boden, B.P. and E.M. Kampa. 1957, Records of bioluminescence in the ocean. Pacific Science, 11: 229-235.

Boden, B.P., E.M. Kampa and J.M. Snodgrass. 1960, Light measurements in the Bay of Biscay, J. Mar. Biol. Assoc. U.K. 39: (2): 227-238.

Johnson, M.W., 1948, Sound as a tool in marine ecology, J. Mar. Res. 7: 443-458.

Jorgensen, W. and C.L. Utterback, 1939, Periodic changes in spectral scattering and spectral transmission of daylight in tidal water. J.Mar. Res. 2:30-37.

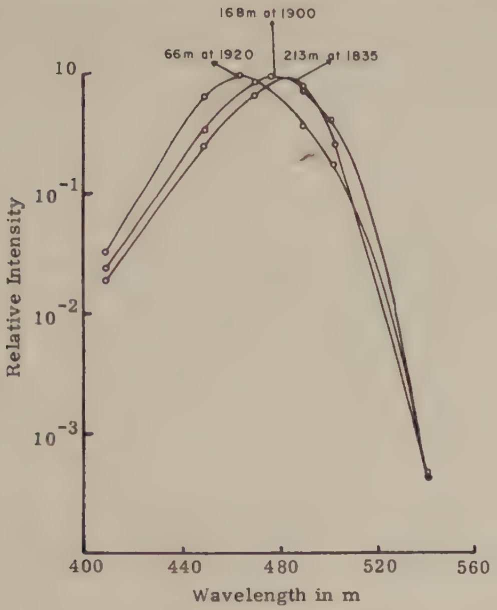

Fig. 6. Spectral composition of light just above the scattering layer during its twilight migration toward the surface off San Diego in September.

Kampa, E.M. and B.P. Boden, 1954, Submarine illumination and the twilight movements of a sonic scattering layer. Nature, 174:869

Kampa, E.M. and B.P. Boden, 1957, Light generation in a sonic scattering layer. Deep Sea Res. 4: 73-92.

Tucker, G.H., 1951, Relation of fishes and other organisms to the scattering of underwater sound. J.Mar. Res., 10(2): 215-238.

Tyler, J.E., 1958, Natural water as a monochromator. Limnol. Oceanogr. 4(1): 102-105.

Utterback, C.L., 1936, Spectral bands of submarine solar radiation in the North Pacific and adjacent inshore waters. Conseil Perm. Intern. p. l'Explor.de la Mer., Rapp. et Proc. Verb., 101 (2) N° 4, 15 pp.

Reprinted from PACIFIC SCIENCE, *vol. XV, no. 3, July, 1961*
pp.311-323

On Zooplankton of Some Arctic Coastal Lagoons of Northwestern Alaska, with Description of a New Species of *Eurytemora*

MARTIN W. JOHNSON[1]

A CHARACTERISTIC FEATURE of the low-lying Alaskan coast of the Chukchi Sea is the presence of a more or less broken beadlike series of "lagoons" extending from Cape Prince of Wales to Point Barrow. The general scientific interest in these lagoons is succinctly summarized by R. H. Fleming and staff in a preliminary report on the "Brown Bear" cruise no. 236 in 1959:

> The geological and oceanographic processes that have led to development and life history of these features are of major scientific interest. Because each of them may represent a variable but unique micro-environment, the biology of these lagoons is also of unusual interest because they represent a transitional series of marine to freshwater environments. At one extreme these lagoons are, in effect, the complex estuaries of rivers that flow only during the summer. At the other extreme the older lagoons, now permanently isolated from the sea and clogged with sediment and vegetation, are only distinguishable from aerial photographs. Between these two extremes are bodies of water, varying greatly in size, that must from time to time be flooded with sea water and then are closed off again and slowly diluted by the accumulation of precipitation and runoff.

During August 4–15, 1959, an opportunity was provided by the U. S. Atomic Energy Commission's Committee for Environmental Studies of Project Chariot and the University of Washington Department of Oceanography[2] to conduct a survey of the plankton in a number of these more or less landlocked lagoons situated at the immediate coast in the region of Cape Thompson, Alaska. The samples collected, being from various lagoons, are important in providing a broad picture of the deviations or similarities that characterize the populations of these bodies of water. The fauna encountered are of special interest in furthering our knowledge of the geographic distribution, biology, and taxonomic status of certain calanoid copepod species that are in varying degrees transitional between the purely marine and freshwater forms.

Prior to the initiation of this project, there had apparently been no study of the zooplankton of these remote and relatively inaccessible lagoons. Some studies that provide especially useful records for comparison have been made previously of the offshore plankton of the Alaskan coast of the Chukchi and Beaufort seas (Willey, 1920; Johnson, 1953, 1956), and in ponds situated at Point Barrow (Comita and Edmondson, 1953; Comita, 1956; Johnson, 1958). Coincident with the present restricted study, a general plankton survey was made in the offshore waters of portions of Chukchi and Bering seas by members of the University of Washington Oceanographic Department aboard the "Brown Bear" (R. H. Fleming and staff, 1959).

It is a pleasure to thank Dr. Richard H. Fleming for providing this opportunity to participate in the research expedition of the University of Washington oceanographic vessel "Brown Bear" to the Chukchi Sea area. The assistance of Dr. Norman J. Wilimovsky, Philip Buscemi, and Howard Smith in the field is gratefully acknowledged, as is also the cooperation of the administrators and contractors of the project site. The water samples were titrated for chlorinity by the Geological Survey laboratory at the project camp site.

PROCEDURE AND RESULTS

The plankton samples were collected with a 30-cm. net, 1 m. long, constructed of no. 6 bolting cloth. An inflated rubber boat was used

---

[1] Scripps Institution of Oceanography, University of California, La Jolla, and the University of Washington, Department of Oceanography, Seattle. Contribution from Scripps Institution of Oceanography, New Series. Manuscript received September 12, 1960.

[2] Contract AT-45-1-540 and Nonr-477 (10).

Contributions from the Scripps Institution of Oceanography, New Series, 1304
Reproduced by Permission

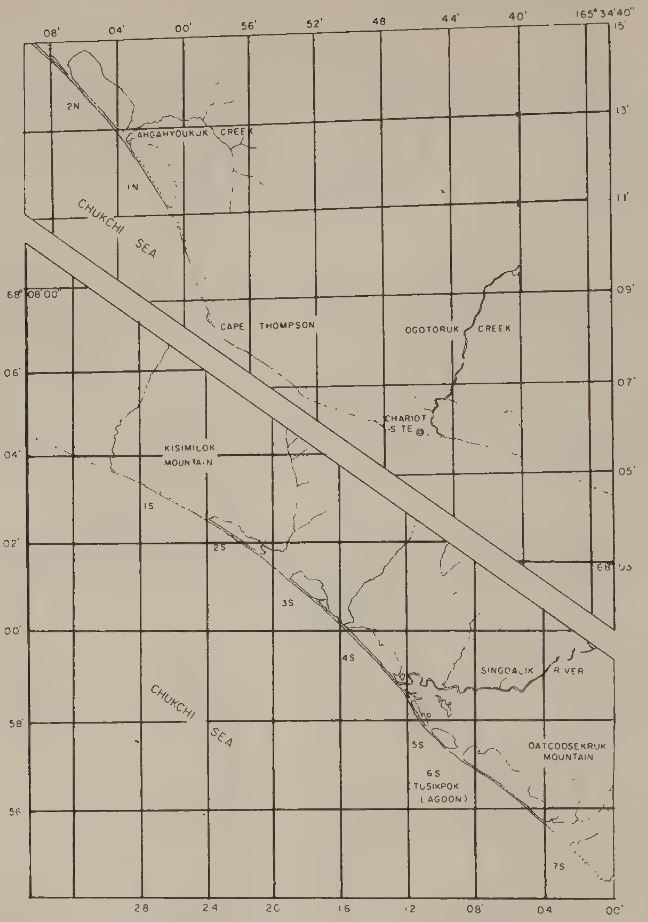
08'
04'
00'
56'
52'
48
44'
40'
165°34'40"
15'
13'
11'
09'
07'
05'
68°03
68°08'00"
06'
04'
02'
00'
58'
56
2N
AHGAHYOUKUK CREEK
1N
CHUKCHI SEA
CAPE THOMPSON
OGOTORUK CREEK
CHARIOT SITE
KISIMILOK MOUNTAIN
1S
2S
3S
4S
SINGOALIK RIVER
CHUKCHI SEA
5S
OATCOOSEKRUK MOUNTAIN
6S
TUSIKPOK LAGOON)
7S
28
24
20
16
12
08'
04
00'

FIG. 1. Numbered lagoons sampled in the Cape Thompson, Alaska area. Based on U. S. Coast and Geodetic Survey Topographic Map T-9425 Alaska.

while obtaining the deeper hauls and the water samples. Most surface hauls were made by wading along shore with the net attached to the end of a pole.

Lagoons

The position, approximate size, and identification of the lagoons sampled are shown in Figure 1. Cape Thompson divides them geographically into a northern and a southern group, as numbered in Figure 1. The only lagoon for which a name occurs on U.S.C. and G.S. Topographic Map T-9423, on which Figure 1 is based, is Tusikpok, which corresponds to no. 6 south. All of the lagoons are shallow; the depths at the positions of sampling (about one-half the distance across the lagoon) were from 1.3 to 3 m., and, as anticipated from wind conditions and shallowness, they showed only moderate or no thermal or haline stratification except in no. 2 south where the salinity at the bottom was 1.65 per mille higher than that at the surface (Table 1). It is clear that they are at times subject to invasion of salt water from the sea. This is evidenced by the brackish water of some, by high wave-washed channels on the gravel berms separating the lagoons from the sea, and, in several instances, by the presence of marine and brackish water animals found in the plankton of some lagoons. Lagoons no. 2

TABLE 1

WATER TEMPERATURE AND SALINITY IN COASTAL LAGOONS IMMEDIATELY SOUTH AND NORTH OF CAPE THOMPSON, ALASKA, AUG. 1959

(The lower sample was taken just above the bottom depth indicated)

LAGOON	TEMP. °C	SALINITY ‰
Lagoon no. 1 south, Aug. 12		
surface	11.0	0.83
bottom (1.5 m.)	11.0	0.83
Lagoon no. 2 south, Aug. 12		
surface	11.2	14.31
bottom (1.3 m.)	11.1	15.96
Lagoon no. 3 south, Aug. 12		
surface	11.0	0.16
bottom (2.1 m.)	10.4	0.17
Lagoon no. 4 south, Aug. 13		
surface	12.3	6.42
bottom (1.3 m.)	12.1	7.16
Lagoon no. 5 south, Aug. 13		
surface	13.6	0.83
bottom (1.3 m.)	13.6	0.83
Lagoon no. 6 south, Aug. 13		
surface	12.6	0.73
bottom (2.4 m.)	12.4	0.73
Lagoon no. 7 south, Aug. 13		
surface	12.6	3.58
bottom (2 m.)	12.1	3.58
Lagoon no. 1 north, Aug. 14		
surface	13.5	0.18
bottom (3 m.)	13.0	0.18
Lagoon no. 2 north, Aug. 15		
surface	13.8	0.46
bottom (2.5 m.)	13.0	0.55

and 4 south each have a narrow above-sea-level outlet that probably floods with sea water during high storms and undoubtedly accounts for the higher salinities observed there.

Judged by the composition of the contained zooplankton, the lagoons are strikingly dissimilar ecologically. How persistent this dissimilarity is cannot be said from this preliminary survey. Basically, the differences probably arise from the geographic position of each lagoon with respect to (1) extent of influx of fresh water in relation to the amount and frequency of that which spills over from the sea during high winds, (2) the height of the lagoon with respect to sea level, and (3) the effectiveness of the berm in serving as a barrier (reinforced by permafrost?) to water percolating out from the lagoon through the gravel. However, the environmental conditions characteristic of each lagoon have been sufficiently unique in the immediate past to permit selection and development of one or two species to a position of overwhelming dominance numerically, as shown by the analysis of the plankton fauna.

Zooplankton

The percentage composition of the fauna is shown in Table 2. Specific attention was given mainly to the calanoid copepods, because of the interest that some of the species hold as transitory forms or as permanent residents in the overlapping environmental conditions between the sea and fresh water. In all cases the populations were composed dominantly of fresh-water or brackish-water forms. But in lagoon no. 2 south, there was a conspicuous element of marine plankton, which was probably only recently recruited from the sea (Table 2). Although *Acartia bifilosa,* a brackish-water species, was overwhelmingly dominant in this lagoon, several marine copepods were also present, but no larval stages of any species were found that might indicate local production. However, if only one generation is produced each year in the lagoon, as is common in some Arctic lakes, the season of nauplii-hatching was probably about past. Most of the marine species found are considered typical of strongly neritic waters, but *Calanus finmarchicus, Pseudocalanus minutus,* and *Acartia longiremis* do also occur well offshore and are very common in the Chukchi Sea, especially off the eastern coast and well north into the Arctic.

Eurytemora pacifica is one of the more infrequent neritic species encountered. Rather little is known regarding its preferred habitat. Hitherto, on the Alaskan coast it has been taken only at Grantley Harbor, and in the region of Point Hope, where it was reported by Willey (1920) as *E. johanseni* n. sp. Excepting lagoon no. 2 south, it was not found in any of the present lagoons, but it was common in a tow taken immediately offshore from lagoon no. 1 north. It is also common in Kivalina Lagoon, where it constituted 7 per cent of the calanoids in a sample kindly provided by Mr. Robert W. Owen of

TABLE 2

Percentage Composition by Number of Plankton in Coastal Lagoons Immediately South and North of Cape Thompson, Alaska
(c = common; + = present, but neither in sufficiently large numbers to constitute 1 per cent of population)

	LAGOONS SOUTH														LAGOONS NORTH			
	1		2		3		4		5		6		7		1		2	
Date of sampling	6	12	6	12	6	12	6	13	6	13	6	13	6	13	14	15	5	15
Surface or bottom	S	B	S	B	S	B	S	B	S	B	S	B	S	B	S	B	S	B
Arcartia bifilosa			78	90			90	12	c									
A. clausi			2						+									
A. longiremis			18	8														
Calanus finmarchicus			+															
Centropages abdominalis			c	+														
Cyclops spp.	65	12				+	+	4	c	c	2	c	+	+	c	1	1	+
Eurytemora canadensis	3					1		+	+	+	3		c	3				
E. herdmani			c	c														
E. pacifica			+	+														
E. foveola, n. sp.											95	90			99	98	57	28
Limnocalanus grimaldi															c	c		
L. johanseni	28	81			c	1	+		96	38		+	14	17	c	c	1	15
Pseudocalanus minutus			1	+														
Tortanus discaudatus			c	c														
Harpacticoids			+	1	+	+	5	72	+	+								
Daphnia	2	6			99	97	+		c	37	+	85	80				40	57
Podon			+	+			1	12										
Evadne			+				+	+										
Clam shrimp	2	1			+				3	25								
Fairy shrimp (Anostraca)	c																	
Ostracods		+		+		+	+				+							+
Neomysis (juvenile)								+										
Sagitta			+															
Fish larvae (total found)				3				7										
Rotifer												9						

the University of Washington from collections made near the outlet on Aug. 22, 1959. These are the only known locality records for the American coast. Elsewhere the species occurs on the Asian coast.

The other neritic species encountered are quite common in small numbers on the Alaskan coast to Point Barrow and in diminishing numbers eastward (Johnson, 1953, 1956).

In lagoon no. 4 south, the plankton was sparse and *Acartia bifilosa* was the most numerous copepod in the surface water on Aug. 6, but an unidentified harpacticoid was the dominant form at the bottom on Aug. 13. It is probably a benthic species since the net contained much bottom debris. Intermingled in the plankton on both dates were the neritic cladocerans, *Podon* and *Evadne*, as the chief evidence of marine invasion.

The plankton fauna of all of the remaining lagoons in the numbered series was characteristically fresh-water. However, there was still a strange marine affinity evidenced by the presence of *Limnocalanus grimaldi* and *L. johanseni*. The former species was common in lagoon no. 1 north, and the latter in all other lagoons with the exception of no. 2 south. The species of this copepod genus have long been the subject of much speculation with respect to their geographic distribution and affinities to the sea. One species, *L. macrurus*, commonly occurs in deep fresh-water lakes, and is generally believed to be a marine relict of glacial times. *L. grimaldi* is an Arctic marine and brackish-water form occurring along the Arctic coast of the U.S.S.R. and is also considered to be a relict of Arctic fauna when found in such widely different isolated localities as the Caspian Sea, the Gulf of Bothnia, and the Baltic Sea. Aside from its present occurrence in lagoon no. 1 north, it has been reported from the Alaskan coast on two previous occasions, once from a collection taken about 100 yd. from the shore at Collinson Point (Willey, 1920), and once at a series of nine offshore stations in the same region, and off the mouth of the Colville River (Johnson, 1956). The present discovery is therefore of special interest in extending the known range of the species on the Alaskan coast, and in recording its occurrence in virtually fresh water, together with *Eurytemora foveola* n. sp. that apparently thrives best at very low salinities.

Less is known about the distribution of *Limnocalanus johanseni*. It was originally described by Marsh (1920) from a fresh-water pond at Collinson Point, just inland from, but not connected with, the shore where Willey recorded *L. grimaldi*. Subsequently, Comita and Edmondson (1953) reported it from Imikpuk Lake, a fresh-water lake near Point Barrow. In the present survey it was a conspicuous element ranging from small to dominant numbers in all lagoons except no. 2 south, the one which most nearly approaches marine conditions. In lagoon no. 5 south, it was extremely abundant, and although a considerable number of early copepodid stages occurred mingled with adults no nauplii were observed. This agrees in general with the observations of Comita (1956) in a more extensive analysis which indicated that the eggs of this species in Imikpuk Lake hatched early in spring, and only copepodid stages are to be found in late July and August. His data show no nauplii after Jul. 31 and the first appearance of adults (copepodid stage VI) was on Aug. 10. In the present collections from lagoon no. 5, adults already outnumbered the other stages on Aug. 6, when the first sampling was done. Comita concluded that *L. johanseni* in Imikpuk Lake produces only one generation a year and that the species winters over in the egg stage. This agrees with the known life cycle of another fresh-water species, *L. macrurus*, discussed by Gurney (1931). Another similarity between the populations of Imikpuk Lake and lagoon no. 5 south was the presence of at least two size groups. This bimodality was not so pronounced in the males as in the females, but some tendency is shown (Fig. 2). The present analysis of the population applies only to the standing crop at the time of sampling, and hence further comparisons cannot be made other than to note that the large-size group was the most abundant. But it cannot be said whether they were produced before or after the small-size group.

TAXONOMIC NOTES

The following observations can be made regarding a few of the species encountered.

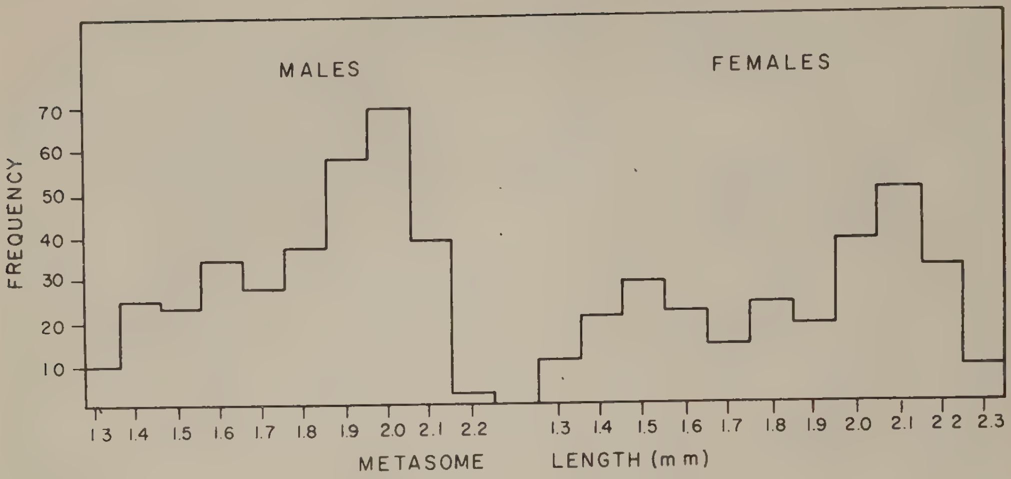

FIG. 2. Length frequency histogram for *Limnocalanus johanseni* adult (copepodid VI) population.

Limnocalanus grimaldi (de Guerne)

A total of 25 specimens was taken in lagoon no. 1 north, mostly near the bottom at a depth of only 3 m. Specimens were compared directly with *L. grimaldi* taken in 1950 in the Beaufort Sea at various stations offshore near Collinson Point and the Colville River. The fresh-water species *L. macrurus* Sars has not been seen for comparison. The Beaufort Sea specimens which were re-examined at this time agree well with the descriptions given in the literature for *L. grimaldi*. The head is not in the least vaulted as occurs in various degrees in *L. macrurus*, and there is only a slight cervical depression (Sars, 1897: pl. 4, figs. 2, 3, 17). The structure of the fifth feet also agrees. The first antennae of the female reach beyond the anterior margin of the anal segment. In the male there are five distinct segments in the distal end of the right antenna beyond the geniculation. The deviations from descriptions of *grimaldi* are mainly in the posterior margins of the fifth thoracic segment. These were smoothly rounded in some cases, but many specimens had the characteristic triangular or spine-like point, and this was sometimes present only on one side. The caudal rami were about eight times as long as broad and were slightly longer in relation to the urosome than given by Sars.

The specimens collected in lagoon no. 1 north are here also considered to be *L. grimaldi*, since they agree in nearly all respects with the Beaufort Sea material. The posterior margin of the fifth thoracic segment was acutely pointed in most specimens, but a few occurred with smoothly rounded margins (a characteristic of *L. macrurus*); there were, however, only four distinct segments in the distal end of the male right antenna beyond the geniculation. This is also a characteristic of *L. macrurus*, although Marsh (1933) states that in exceptional cases there may be five segments. The lagoon specimens were slightly smaller than those from the Beaufort Sea, namely 2.6 to 2.7 mm. as opposed to 2.9 to 3.3 mm. for females.

Since the condition of the fifth thoracic segment is obviously an unreliable character, one is left to choose between the relative specific value of the outline of the head, and the segmentation of the distal end of the male first antennae. Both of these are variable for *L. macrurus*. The habitat presented by lagoon no. 1 north is probably an important consideration, for although it was virtually fresh at the time and place of sampling, it is shallow and so near the sea that it may be reached by very high storm waves. This environmental situation may constitute an interesting natural experiment in which a landlocked population of *L. grimaldi* has assumed some characteristics of its freshwater counterpart, particularly in the fusion of two of the segments in the distal portion of the male right antenna.

Limnocalanus johanseni Marsh

A comparison of specimens of this species from the lagoons and from collections I made in Imikpuk Lake in 1957 shows only small variations in structure. Mention should be made, however, of some features that are not included in the original description. It was noted that in many specimens the fifth thoracic segment may be smoothly rounded or with only slightly angular outline. Marsh states that this segment is rounded on the sides, and each side is armed with a small spine which may be either sharp or blunt. Apparently inadvertently omitted from Marsh's drawings is a long, heavy seta that occurs on the inner anterior distal angle of the second basis of the first feet.

Centropages abdominalis Sato 1913

Centropages mcmurrichi Willey 1920

Willey (1920) was apparently unaware of Sato's (1913) publication, and described this species as new under the name *C. mcmurrichi* n. sp. His description is without figures, but he considered the species to be identical with a copepod reported and figured by McMurrich (1916), with some reservations, as *C. hamatus* Lilljeborg. Examination of Alaskan material and reference to McMurrich's figures, and to those of Sato (photostatic copies of which are at hand through the courtesy of Dr. Takasi Tokioka and Isamu Yamazi of the Seto Marine Biological Laboratory), and of Mori (1937) leaves little doubt that these species are identical.

Eurytemora pacifica Sato 1913

Eurytemora johanseni Willey 1920

This is a clearly defined species, principally on the basis of the fifth feet in the female (Figs. 7–10). In the female, the fifth thoracic segment is provided with broad triangular wings, but breeding females were also found with this segment smoothly rounded (Fig. 8). The hyaline wing apparently may be shed or fails to develop. In the present study both males and females were found in the same catches. Willey (1920) described the species under the name *E. johanseni* n. sp. Sato described only the adult male, but his figures agree especially with Willey's figures 11 and 12 of the fifth feet. Smirnov (1931) first pointed out the probable identity of the species.

Eurytemora foveola n. sp.

TYPES: Holotype, male, U. S. National Museum no. 105996; allotype, female, USNM no. 105997. Type locality, lagoon no. 6 south.

In lagoon no. 6 south and nos. 1 and 2 north the dominant copepod was this hitherto unknown species. It was present in these lagoons in vast numbers and despite its small size constituted 90 per cent or more of the biomass in the samples from lagoon no. 6 south and no. 1 north where it was actively reproducing and many females were found carrying eggs and spermatophores. In lagoon no. 2 north it was greatly surpassed in mass by the larger cladoceran *Daphnia.* It is closely allied to *Eurytemora gracilis,* both sexes of which were described by Sars (1898) from the lower Yana (Jana) River and, judging from Sars' figures and description, the females may be nearly indistinguishable. The chief differences separating the present species from that of Sars' are structural details in the fifth feet of the males. In view of these small but apparently persistent differences, as shown by examination of a great many specimens, it seems best to designate it a new species rather than a variety of *E. gracilis.*

FEMALE (Figs. 3, 4): Length 1.15–1.25 mm. The body is slender in both dorsal and lateral aspects with about the following linear proportions: metasome (anterior division) 67, genital segment 11, first abdominal segment 6, anal segment 11, caudal rami 17. The metasome is slightly widest in the region of the first pedigerous segment. There is a slight cephalic depression, but no medial knob on the posterodorsal margin of the cephalic segment. (In *E. gracilis* the greatest width appears to extend somewhat farther forward according to Sars' pl. 8, fig. 8; and in his fig. 9, the lateral profile also differs in that his species is relatively thicker through the midbody and the cephalic

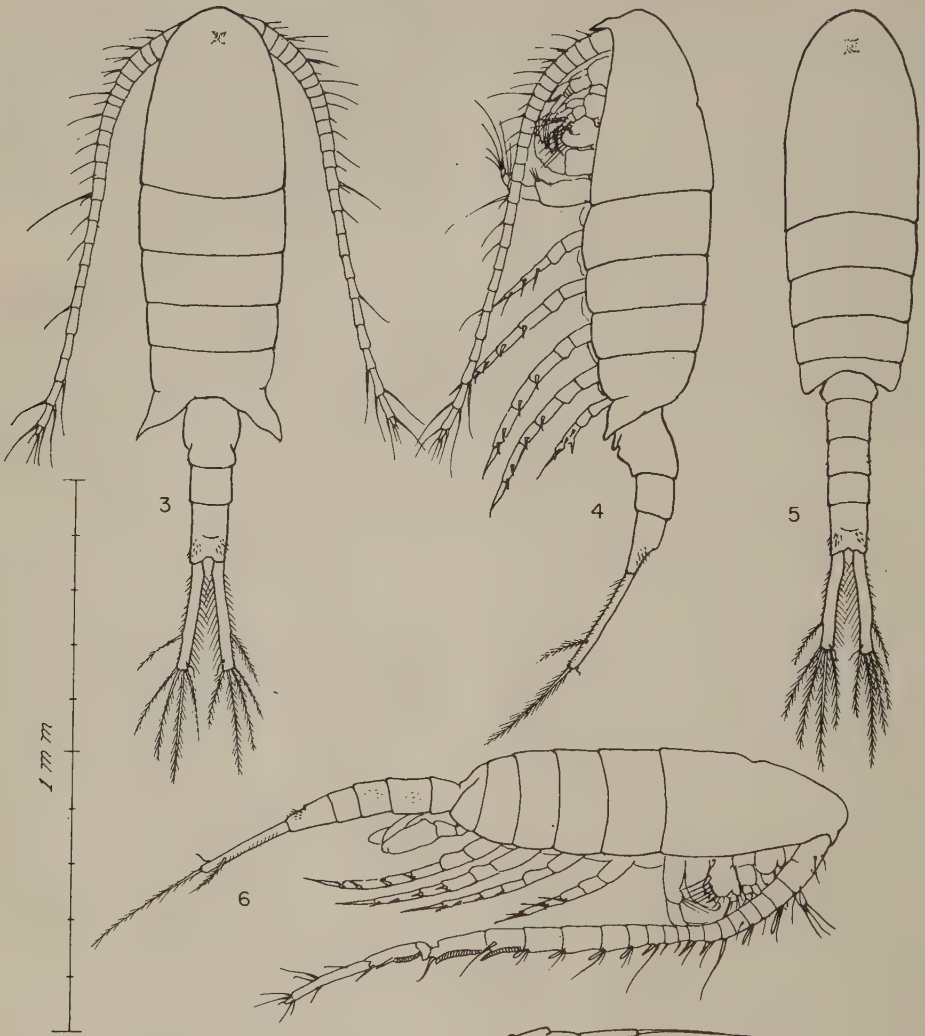

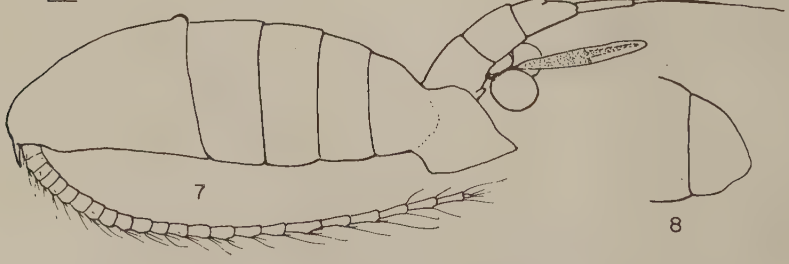

FIGS. 3–6. *Eurytemora foveola* n. sp. 3, Female, dorsal; 4, female, lateral; 5, male, dorsal; 6, male, lateral.

FIGS. 7–8. *Eurytemora pacifica.* 7, Female, lateral with eggs and spermatophore; 8, female, lateral outline of fifth thoracic segment occurring in some adults.

segment is slightly raised dorsally at the hind edge.) The fifth thoracic segment is extended into laterally projected "wings" that vary considerably in length and hyalinity. Many adult specimens were observed in which the left wing was only slightly developed, although the right wing was always well developed. The first antennae reach to, or slightly beyond, the fifth thoracic segment. The genital segment is nearly symmetrical and only slightly constricted laterally. It bears no lateral expansions but in lateral aspect has a rather conspicuous genital operculum. The anal segment is armed dorsolaterally with patches of fine spinules, best observed in aqueous media. (Sars states that in *E. gracilis* "the last caudal segment is perfectly smooth without any trace of the densely crowded spikes clothing the dorsal face of this segment in *T.* (*E.*) *hirundoides*.") The caudal rami are provided with fine "hairs" on both their inner and outer margins. The longest caudal setae are only slightly longer than the rami. The terminal spine of the exopod of the second, third, and fourth swimming feet (Fig. 11) is cultriform as in *E. gracilis*. The fifth feet (Fig. 13) are symmetrical as in *E. gracilis,* and the first exopod segment bears a heavy, slightly setose, unguiform process directed inward. There are two spines on the outer margin of this segment. The end segment is short and bears one long terminal spine and one short outer spine. The terminal spine of the exopod of the third and fourth feet is somewhat broadened in the middle and is shorter than the end segment. In the male this spine is longer and more slender. The genital operculum is rounded (Fig. 16) in contrast to the pointed operculum of the closely related species *E. affinis* as described and figured by Gurney (1931), and which he considers synonymous with *E. hirundoides*.

MALE (Figs. 5–6): Length 1.0–1.2 mm. The body is slender and nearly parallel-sided anteriorly but tapers posteriorly. The body proportions are about as follows: metasome 57, urosome (without caudal rami) 25, caudal rami 15. As in the female, the anal segment bears dorsal patches of tiny spinules. The caudal rami have fine "hairs" on the inner and outer margins. The right geniculated first antenna has 25 segments with moderately heavy spines on segments 8, 9, and 12. The fifth feet (Figs. 14, 15) are asymmetrical, uniramous, and each exopod consists of two segments. The specific characters separating the species from closely related forms are seen mainly in the basal segments and in the relative proportions of the segments of the rami. At the inner proximal margin of the second basipod of the right foot there is a well-defined rounded projection and associated smooth notchlike depression suggesting the specific name. The inner margin of the first basipod of the left foot projects downward, forming an irregular blunt process overlapping about one-third the length of the second basipod. The second basipod is broadened with an inward expanse forming a dull flange along the long axis of the segment. Sars' plate 8, figure 16, shows no trace of these three features for *E. gracilis*. Otherwise the exopod segments agree with that species which, however, appears to have a shorter first exopod segment on the left foot. The uncertain species described by Kiefer (1938) also differs in the absence of these characters and in the shape of the second basal segments of each foot. The second antennae and the mouth appendages of *E. foveola* are similar in the two sexes and appear to have no specific character except perhaps for the shape of the mandibular blade (Fig. 17). Few illustrations of other species are available with which to make comparisons, but the gap between the first and second tooth is considerably wider than that figured by Gurney (1931) for *E. affinis*, Sars (1903) for *E. velox*, and Wilson (1953) for *E. yukonensis* and *E. composita*.

It should be mentioned that a single damaged female specimen of a *Eurytemora* was collected by the Canadian Arctic Expedition offshore near Cape Thompson. Willey (1920) tentatively referred it to *E. gracilis*. It is not possible to conclude what species he dealt with but the proximity of the catch to the lagoons so richly populated by *E. foveola* makes it highly likely that it had been washed out from a nearby lagoon. Although there may be an intermittent present-day connection between the Yana River population and that in the Cape Thompson area, it must be a very tenuous one for a fresh- or brackish-water species, especially in view of the prevailing oceanic circulation northward through

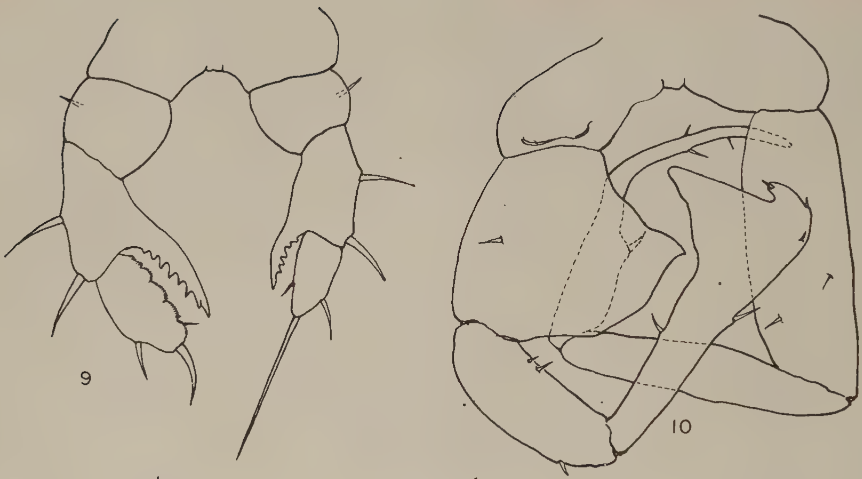

FIGS. 9–10. *Eurytemora pacifica.* 9, Female, fifth feet; 10, male, fifth feet.

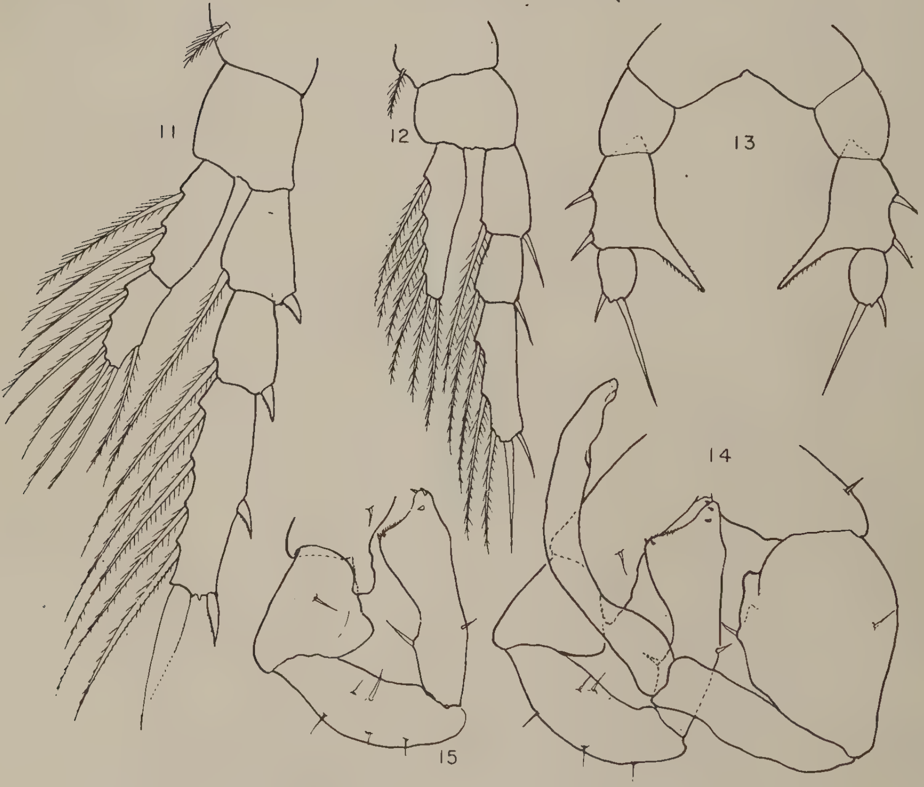

FIGS. 11–15. *Eurytemora foveola* n. sp. 11, Female, fourth foot; 12, female, first foot; 13, female, fifth feet; 14, male, fifth feet; 15, male, left fifth foot.

the Bering Strait and eastern Chukchi Sea. However, other studies indicate that plankton organisms may be transported across rather well-defined currents by eddy diffusion, and the prevailing currents along the Siberian coast might bring expatriates into the western portion of the Chukchi Sea. Brodskii (1950) does not include *E. gracilis* in his list of copepods of the Polar Basin.

Gurney (1931) has pointed out the specific variabilities that may occur in several species of *Eurytemora* living in different habitats in Europe. It remains to be shown to what extent *E. foveola* may also be morphologically variable in diverse environments. The great range of Alaskan lagoon and estuarian habitats and the seven or more species on the Alaskan coast should provide excellent material for such a study.

SALINITY RELATIONS

Although the data are too few to give more than a glimpse into the salinity tolerances observed for the various copepod species identified, still it is worthwhile to record such analyses as can be made from this area. Figure 19 appears to divide the copepods encountered into three groups with respect to salinity range and preference. (1) *Acartia bifilosa* and *A. clausi* occurred over nearly the whole range encountered but not below 0.83 ‰ at which value only relatively few specimens were found, especially *A. clausi*. The former was the dominant copepod in the two lagoons having highest salinities 6.42 to 15.96 ‰. (2) *Cyclops* spp., *Eurytemora canadensis*, and *Limnocalanus johanseni* ranged from 0.16 to about 7 ‰ but appeared to thrive best at 0.73 to 0.83 ‰. *Eurytemora foveola* n. sp. probably belongs to this group but stands somewhat alone in occurring only in ranges from 0.18 to 0.73 ‰ at which salinities it was dominant. *Limnocalanus grimaldi*, in this unique situation, occurred also at only a very low salinity, but elsewhere in the arctic it has a strong affinity for the sea. (3) The final group, into which *Acartia bifilosa* and *A. clausi* extended, are the characteristically marine forms occurring in lagoon no. 2 south with salinities of 14.31 to 15.96 ‰. Only in the more saline lagoons, nos. 2 and 4 south, was there any appreciable range in salinity from top to bottom. These two lagoons are also probably the ones most readily invaded by marine forms, but the influx of fresh water appears also to be quite high in these lagoons. Hence the communities are probably more or less transitory and fluctuate with repeated recolonizations.

Whittaker and Fairbanks (1958) have studied the occurrence of various nonmarine copepods in inland lakes and ponds of different salt content. The salinities and fauna they dealt with are of course not directly comparable with those of coastal lagoons, since the ratio of salts differ and their more saline species have different taxonomic relationships. But it is interesting to note that the transition between saline and fresh-water communities in their study was "somewhere between 425 and 875 ppm" for most bodies of water. If a comparison is justified it must be with the fresh-water fauna of the lagoons, then lagoons nos. 1, 3, 5, and 6 south and 1 and 2 north could be expected to foster truly fresh-water species and the occurrence of *Eurytemora canadensis* and *Limnocal-*

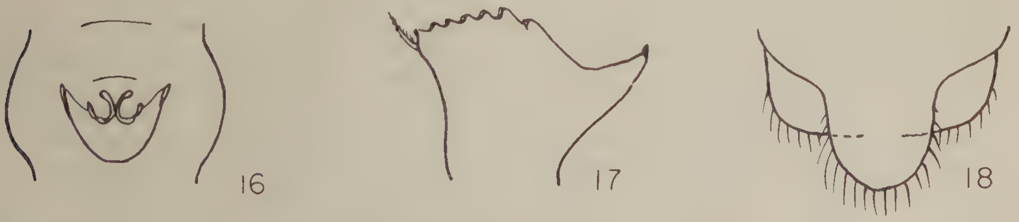

FIGS. 16–18. *Eurytemora foveola* n. sp. 16, Female, genital field and operculum, ventral; 17, male, mandibular blade; 18, male, labrum.

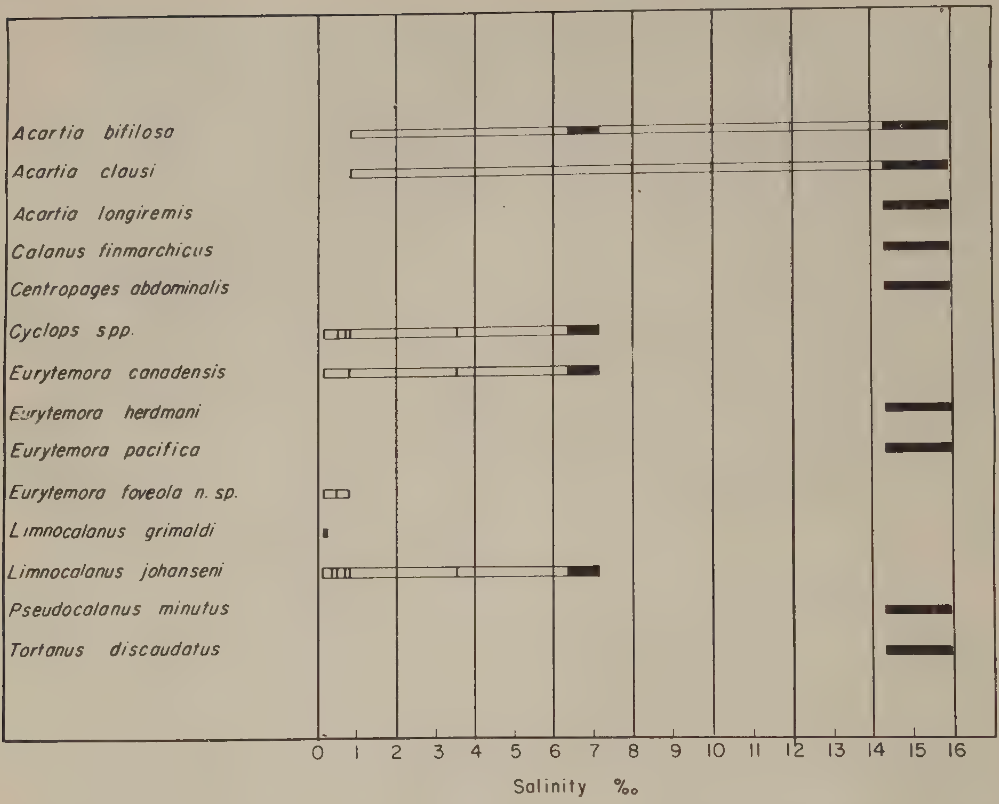

FIG. 19. Total salinity ranges over which certain copepod species occurred in nine coastal lagoons near Cape Thompson, Alaska, 1959. Cross bars denote salinity at stations of sampling.

anus johanseni in most of these and in lagoons nos. 4 and 7 south would mark them as quite euryhaline but with preferences for the lower salinities.

REFERENCES

BRODSKII, K. A. 1950. Copepoda, Calanoida, of the far-eastern waters of the USSR and the Polar Basin. Zool. Inst. Acad. Sci. USSR Mosc.: 441 pp. (In Russian.)

COMITA, G. W. 1956. A study of a calanoid copepod population in an arctic lake. Ecology 37(3): 576–591.

COMITA, G. W., and W. T. EDMONDSON. 1953. Some aspects of the limnology of an arctic lake. Stanf. Univ. Publ. Biol. Sci. 11: 7–13.

FLEMING, R. H., and STAFF. 1959. Oceanographic survey of the eastern Chukchi Sea, 1 August to 2 September 1959. Progress report as of 1 December 1959, BROWN BEAR Cruise No. 236. Dept. Oceanogr. Univ. Wash. Ref. 59–47: 17 pp.

GURNEY, R. 1931. British fresh-water Copepoda. Ray Soc. Publ. 1(118): 1–238.

JOHNSON, M. W. 1953. Studies on plankton of the Bering and Chukchi seas and adjacent areas. Proc. Seventh Sci. Congr. 4: 480–500.

——— 1956. The plankton of the Beaufort and Chukchi Sea areas of the arctic and its relation to the hydrography. Arct. Inst. N. Amer. Tech. Pap. No. 1: 32 pp.

——— 1958. Observations on inshore plankton collected during summer 1957 at Point Barrow, Alaska. J. Mar. Res.: 17: 272–281.

KIEFER, F. 1938. Freilebende Süsswassercopepoden von den Nordkurilen. Bull. Biogeogr. Soc. Japan 7(4): 75–94.

MARSH, C. D. 1920. Report of the Canadian Arctic Expedition, 1913-18. Southern Party, 1913-16. Vol. 7: Crustacea, pt. J: Freshwater Copepoda. 25 pp.

——— 1933. Synopsis of the calanoid crustaceans, exclusive of the Diaptomidae, found in fresh and brackish waters, chiefly of North America. Proc. U.S. Nat. Mus. 82, art. 18: 1–58.

MCMURRICH, J. P. 1916. Notes on plankton of British Columbia Coast. Trans. Roy. Soc. Can. Ser. III, 10, Sec. IV: 75–89.

MORI, T. 1937. The Pelagic Copepoda from the Neighbouring Waters of Japan. 150 pp.

SARS, G. O. 1897. Pelagic Entomostraca of the Caspian Sea. Ann. Zool. Mus. Imp. Acad. Sci. St. Petersb.: 1–73.

——— 1898. The Cladocera, Copepoda and Ostracoda of the Jana Expedition. Ann. Zool. Mus. Imp. Acad. Sci. St. Petersb. 3: 324–359.

SATO, T. 1913. Pelagic copepods. Rep. Fish. Res. Hokkaido Fish. Exp. Sta. No. 1: 79 pp. (In Japanese.)

SMIRNOV, S. 1931. Zur Kenntnis der Copepodengattung *Eurytemora* Giesbr. Zool. Anz. 94(5/8): 194–201.

WHITTAKER, R. H., and C. W. FAIRBANKS. 1958. A study of copepod communities in the Columbia Basin, Southeastern Washington. Ecology 39(1): 46–65.

WILLEY, A. A. 1920. Report of the Canadian Arctic Expedition, 1913-18. Vol. 7: Crustacea, pt. K: Marine Copepoda. 46 pp.

WILSON, M. 1953. New Alaskan records of *Eurytemora* (Crustacea, Copepoda). Pacif. Sci. 7: 504–512.

(772)

Atlantide Report No.6, May 20, 1961
pp.251-262.

Euphausiacea (Crustacea) from Tropical West Africa*

By

BRIAN P. BODEN

In his General Report on the 1945–46 Atlantide Expedition to tropical West Africa ANTON BRUUN (1950) mentions the extreme difficulties encountered, due to the war, in assembling proper collecting gear and general equipment. As a result the euphausiid crustaceans that form the subject of this report were collected by a wide variety of methods, ranging from deep hauls with a 200-centimetre stramin net to dip-netting with a light at night. Because of this unavoidable lack of consistency in procedure we have no quantitative data on distribution, and while the euphausiids taken in each haul were counted the numbers certainly do not reflect relative abundance of the species over the area of the survey.

The collection is interesting, however, since it was made in a region seldom visited by scientific expeditions and our knowledge of the representatives of this order here has been slight indeed.

While no new species was encountered, twenty species are reported and our comprehension of their distribution ranges is thus expanded. This is a gratifyingly large number of species of this small but widespread group, although more systematic collections will undoubtedly reveal more in time.

A partial track chart is shown in figure 1 and the stations at which euphausiids occurred are indicated. Further station data such as gear used, depth, time, date, etc., are to be found in the station list (BRUUN 1950). The occurrence of the species at the stations follows.

Thysanopoda tricuspidata Milne-Edwards, 1830.

Thysanopoda tricuspide Milne-Edwards, 1830: 454, pl. 19; *T. tricuspidata* MILNE-EDWARDS 1837: 466, pl. 26, figs. 1–6; G. O. SARS 1885: 98–102, 165–169, pls. 17, 31, figs. 1–22; HANSEN 1910: 82–84, pl. 12, fig. 3, a–b; 1912: 208, pl. 4, fig. 2, a; BODEN 1954: 188, fig. 4, a–b.

---

* Contribution from the Scripps Institution of Oceanography, University of California; New Series. 1305.

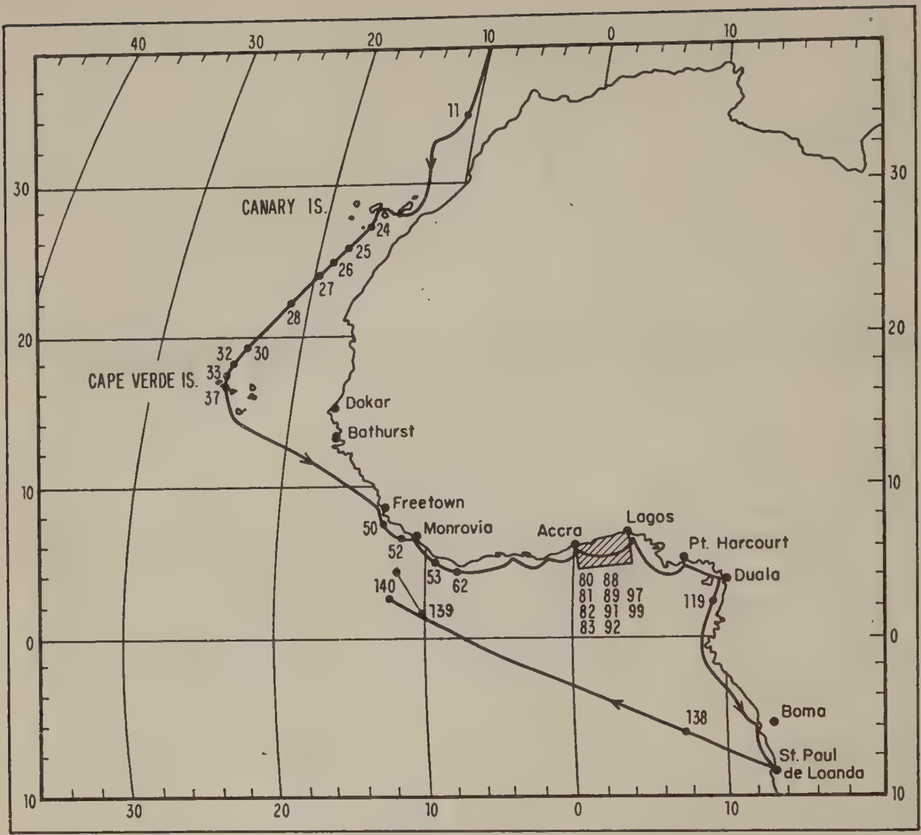
CANARY IS.
CAPE VERDE IS.
Dakar
Bathurst
Freetown
Monrovia
Accra
Lagos
Pt. Harcourt
Duala
Boma
St. Paul de Loanda
11
24
25
26
27
28
30
32
33
37
50
52
53
62
140
139
80 88
81 89 97
82 91 99
83 92
119
138
40
30
20
10
0
10

Fig. 1. Partial track-chart of "Atlantide" Expedition, showing stations at which euphausiids were collected.

Material:

St. 33. 7. XII. 45, 20.00 hrs., Cape Verde Is., 17°11′ N, 24°52′ W, surface. – 1 female.

St. 139. 2. IV. 46, 4.00 hrs., 1°30′ N, 10°10′ W, 1750 m wire. – 10 females.

Distribution elsewhere: This is a tropical, oceanic form in the Atlantic, Pacific and Indian oceans.

Depth: Adults, 1,000–200 m; larvae, 200–0 m.

Thysanopoda aequalis Hansen, 1905.

Thysanopoda aequalis Hansen, 1905: 18–20, pl. 12, fig. 4, a–c, pl. 13, fig. 1, a; 1912: 214, pl. 4, fig. 4, a; Boden 1954: 190, fig. 5, a–d; Boden and Brinton 1957: 337–341, figs. 1–2; *nec* Zimmer 1914; *nec* Tattersall 1924.

Material:

St. 24. 30. XI. 45, 11–12.00 hrs., S. of Canary Is., 27°23′ N, 16°36′ W, 500 m wire. – 1 larva.

Distribution elsewhere: Eastern and Central tropical and sub-tropical Pacific, tropical and sub-tropical Atlantic and Indian oceans.

Depth: Adults, 500–100 m; larvae, 150–0 m.

Euphausia recurva Hansen, 1905.

Euphausia recurva Hansen, 1905: 13–14; 1912: 233–235, pl. 7, fig. 3, a–n; Boden 1954: 201–202, fig. 8, e–i.

Material:

St. 25. 30. XI. 45, 21.30 hrs., 26°57′ N, 17°10′W, surface. – 4 females.
St. 26. 1. XII. 45, 20.00 hrs., 25°34′ N, 18°24′ W, surface – 40 males, 69 females.

Distribution elsewhere: This form is oceanic in the tropical and sub-tropical Pacific, Atlantic and Indian oceans.

Depth: Adults, 500–0 m; larvae, 150–0 m.

Euphausia mutica Hansen, 1905.

Euphausia mutica Hansen, 1905: 14–15 (*partim*); 1910: 93, pl. 14, fig. 1, a–d; Boden 1954: 202–205, fig. 9, a–d.

Material:

St. 30. 5. XII. 45, 21.15 hrs., 19°54′ N, 22°42′ W, surface. – 3 females.
St. 37. 9. XII. 45, S. of Porto Grande, St. Vincent, tidal zone. – 2 females.
St. 62. 10. I. 46, 20.10 hrs., 4°16′ N, 8°18′ W, 400 m wire. – 34 females.
St. 83. 29. I. 46, 21.30 hrs., 5°29′ N, 0°20′ E, surface. – 1 male, 1 female.
St. 92. 1. II. 46, 19.45 hrs., 6°01′ N, 2°21′ E, surface. – 1 male, 2 females.
St. 97. 14. II. 46, 21.00 hrs., 6°06′ N, 3°41′ E, surface. – 1 male, 3 females.
St. 119. 28. II. 46, 19.56 hrs., S. of Duala, 2°55′ N, 9°21′ E, surface. – 3 males, 18 females.

Distribution elsewhere: Found in the tropical and sub-tropical Atlantic, Pacific and Indian oceans.

Depth: Adults, 300–0 m; larvae, 150–0 m.

Euphausia brevis Hansen, 1905.

Euphausia gibbosa Streets, 1877: 122–123; *E. brevis* Hansen, 1905: 15–16; 1912: 239–241, pl. 8, fig. 1, a–g; Boden 1954: 205, fig. 9, e–h; Boden Johnson and Brinton 1955: 328–330, fig. 21, a–d.

Material:

St. 24. 30. XI. 45, 11–12.00 hrs., S. of Canary Is., 27°23′ N, 16°36′ W, 500 m wire. – 1 female.

St. 27. 2. XII. 45, 19.00 hrs., 24°30′ N, 19°11′ W, surface. – 6 males, 158 females, 58 larvae.

St. 30. 5. XII. 45, 21.15 hrs., 19°54′ N, 22°42′ W, surface. – 3 females.

Remarks: *E. gibbosa* is included in the synonymy here although it antedates *brevis* as a specific epithet. As pointed out by Boden, Johnson and Brinton (1955) this is thought to be consistent with the decisions of the Fourteenth International Congress of Zoology (1953).

Distribution elsewhere: This form is widespread in the tropics and subtropics of the Pacific, Atlantic and Indian oceans.

Depth: Adults, 300–0 m; larvae, 150–0 m.

Euphausia eximia Hansen, 1911.

Euphausia eximia Hansen, 1911: 23, fig. 5; 1912: 230–233, pl. 7. fig. 2, a–g; Boden, Johnson and Brinton 1955: 331–333, fig. 23, a–d.

Material:

St. 138. 24. III. 46, 20.30 hrs., 7°40′ S, 7°56′ E, surface. – 790 males, 2,280 females.

Remarks: Slight differences from the Pacific form were noted in the terminal process and the median lobe. These were very slight and probably do not warrant specific separation.

Distribution elsewhere: This form has been reported formerly only from the tropical eastern Pacific.

Depth: Adults, 500–0 m; larvae, 150–0 m.

Euphausia americana Hansen, 1911.

Euphausia americana Hansen, 1911: 23–24, fig. 6.

Material:

St. 27. 2. XII. 45, 19.00 hrs., 24°30′ N, 19°11′ W, surface. – 14 males, 88 females, 30 larvae.

St. 28. 3. XII. 45, 18.30 hrs., 22°59′ N, 20°30′ W, surface. – 2 females.

St. 30. 5. XII. 45, 21.15 hrs., 19°54′ N, 22°42′ W, surface. – 8 males, 19 females.

St. 32. 7. XII. 45, 0.00 hrs., N. of Cape Verde Is., 18°18′ N, 24°03′ W, surface. – 1 male, 3 females.

St. 33. 7. XII. 45, 20.00 hrs., Cape Verde Is., 17°11′ N, 24°52′ W, surface. – 22 males, 21 females, 4 larvae.

St. 92. 1. II. 46, 19.45 hrs., 6°01′ N, 2°21′ E, surface. – 1 male, 1 female, 9 larvae.

St. 97. 14. II. 46, 21.00 hrs., 6°06′ N, 3°41′ E, surface. – 7 males, 20 females.

St. 139. 2. IV. 46, 4.00 hrs., 1°30′ N, 10°10′ W, 1750 m wire. – 45 males, 98 females.

St. 139. 2. IV. 46, 6.00 hrs., 1°30′ N, 10°10′ W, surface. – 45 males, 85 females.

St. 140. 4. IV. 46, 0.05 hrs., 4°10′ N, 12°18′ W, surface. – 21 males, 14 females.

Distribution elsewhere: Western Atlantic and Cape Verde Islands.

Depth: Although taken occasionally at great depths this is essentially a surface form (see Tattersall 1926 and Moore 1952).

Euphausia tenera Hansen, 1905.

Euphausia gracilis G. O. Sars, 1885: 89–91, pl. 15, figs. 12–23, (*nec E. gracilis* Dana, 1852: 644); *E. tenera* Hansen, 1905: 9; 1910: 95–97, pl. 14, fig. 3, a–e; Boden, 1954: 206–208, fig. 10, d–f.

Material:

St. 30. 5. XII. 45, 21.15 hrs.; 19°54′ N, 22°42′ W, surface. – 10 males, 20 females.

St. 52. 2. I. 46, 20.00 hrs., off Monrovia, surface. – 1 male, 3 females, 13 larvae.

St. 92. 1. II. 46, 19.45 hrs., 6°01′ N, 2°21′ E, surface. – 5 males, 10 females, 12 larvae.

St. 97. 14. II. 46, 21.00 hrs., 6°06′ N, 3°41′ E, surface. – 1 female.

St. 119. 28. II. 46, 19.56 hrs., S. of Duala, 2°55′ N, 9°21′ E, surface. – 20 females.

St. 139. 2. IV. 46, 4.00 hrs., 1°30′ N, 10°10′ W, 1750 m wire. – 52 males, 112 females.

St. 139. 2. IV. 46, 6.00 hrs., 1°30′ N, 10°10′ W, surface. – 15 males, 58 females.

St. 140. 4. IV. 46, 0.05 hrs., 4°10′ N, 12°18′ W, surface. – 140 males, 889 females.

Distribution elsewhere: Widely distributed in the tropical and sub-tropical Pacific, Atlantic and Indian Oceans. Boden, Johnson and Brinton (1955) find it occupies the broadest belt of latitude of any of the euphausiids whose principal affinity is with equatorial waters.

Depth: Adults, 300–0 m; larvae, 150–0 m.

Euphausia hemigibba Hansen, 1910.

Euphausia hemigibba Hansen, 1910: 100, pl. 14, fig. 5, a–f; Boden, Johnson and Brinton 1955: 342–344, fig. 29, a–e.

Material:

St. 25. 30. XI. 45, 21.30 hrs., 26°57′ N, 17°10′ W, surface. – 1 male.

St. 26. 1. XII. 45, 20.00 hrs., 25°34′ N, 18°24′ W, surface. – 22 males, 13 females.

St. 27. 2. XII. 45, 19.00 hrs., 24°30′ N, 19°11′ W, surface. – 10 males, 4 females, 2 larvae.

St. 30. 5. XII. 45, 21.15 hrs., 19°54′ N, 22°42′ W, surface. – 9 males.

St. 138. 24. III. 46, 20.30 hrs., 7°40′ S, 7°56′ E, surface. – 10 males, 40 females.

Distribution elsewhere: Widely and generally distributed in the tropical and subtropical oceanic of the Pacific, Atlantic and Indian oceans.

Depth: Adults, 500–0 m (maximum about 100 m); larvae, 250–0 m.

Euphausia gibboides Ortmann, 1893.

Euphausia gibboides Ortmann, 1893: 12, taf. 1, fig. 5; HANSEN 1911: 33; 1912: 252–255, pl. 9, fig. 2, a–h; BODEN 1954: 213, fig. 13, d–e.

Material:

St. 50. 30. XII. 45, 19.30 hrs., off Freetown, 7°16′ N, 13°29′ W, surface. – 1 male.

St. 82. 29. I. 46, 15.00 hrs., 5°27′ N, 0°07′ E, 100–0 m wire. – 1 female.

St. 92. 1. II. 46, 19.45 hrs., 6°01′ N, 2°21′ E, surface. – 3 larvae.

St. 97. 14. II. 46, 21.00 hrs., 6°06′ N, 3°41′ E, surface. – 4 males, 6 females.

St. 139. 2. IV. 46, 4.00 hrs., 1°30′ N, 10°10′ W, 1750 m wire. – 9 males, 5 females.

St. 140. 4. IV. 46, 0.05 hrs., 4°10′ N, 12°18′ W, surface. 21 males, 35 females.

Distribution elsewhere: It occurs in the cooler tropical and temperate waters of the Pacific, Atlantic and Indian oceans.

Depth: Adults, 500–100 m (rarely at the surface); larvae, above 200 m.

Euphausia hanseni Zimmer, 1915.

Euphausia hanseni Zimmer, 1915: 180; BODEN 1954: 215, fig. 14, a–c.

Material:

St. 62. 10. I. 46, 20.10 hrs., 4°16′ N, 8°18′ W, 400 m wire. – 68 males, 1071 females.

St. 83. 29. I. 46, 21.30 hrs., 5°29′ N, 0°20′ E, surface. – 2 males.

Distribution elsewhere: Tropical and subtropical in the eastern Atlantic.

Depth: In this collection between 400 m and the surface.

Larval Stages

A number of larval forms belonging to the genus *Euphausia* were encountered. Although these were of various stages from calyptopis to late furcilia it was not possible to identify them to species. They certainly represent several different species.

Station	Larvae	Station	Larvae
11	20	87	1
25	10	89	1
28	1	97	9
50	13	99	1
53	2	119	11
80	6	139	14
83	14	140	126

Nematoscelis megalops G. O. Sars, 1885.

Nematoscelis megalops G. O. Sars, 1885: 127; Boden 1954: 224–225, fig. 17, a–c.

Material:

St. 139. 2. IV. 46, 4.00 hrs., 1°30′ N, 10°10′ W, 1750 m wire. – 49 females.

Distribution elsewhere: Common in temperate and tropical Atlantic and Indian oceans.

Depth: Adults, usually below 100 m; larvae, 200–0 m.

Nematoscelis tenella G. O. Sars, 1883.

Nematoscelis tenella G. O. Sars, 1883: 28; 1885: 133–134, pl. 15, figs. 5, 7; Hansen 1910: 110–112, pl. 15, fig. 4, a–m; 1912: 263–264, pl. 10, fig. 3, a–c; Boden 1954: 226, fig. 17, d–f; *N. mantis* Chun, 1896: 165.

Material:

St. 62. 10. I. 46, 20.10 hrs., 4°16′ N, 8°18′ W, 400 m wire. – 111 females.

Distribution elsewhere: This form is found in the tropical and subtropical waters of the Pacific, Atlantic and Indian oceans.

Depth: Adults, below 200 m; larvae, frequently above 100 m.

Nematoscelis microps G. O. Sars, 1883.

Nematoscelis microps G. O. Sars, 1883: 28; 1885: 131–133, pl. 15, figs. 1–4; Hansen 1910: 107–109, pl. 15, figs. 2, a–k; 1912: 259–261, pl. 9, fig. 4, a–d, pl. 10, fig. 1, a–b; Boden 1954: 226–227, fig. 18, a–c; *N. rostrata* G. O. Sars, 1885: 135–136, pl. 15, figs. 8–10 (subadults).

Material:
St. 11. 15. XI. 45, 20.10 hrs., 34°13′ N, 12°16′ W, 35 m wire. – 4 larvae.

Remarks: This identification was based on larval forms which were in rather poor shape. It should be treated with caution.

Distribution elsewhere: This is a tropical and subtropical species in the Pacific, Atlantic and Indian oceans.

Depth: Adults, below 150 m; larvae occasionally above 100 m.

Nematobrachion boöpis (Calman, 1896).

Nematodactylus boöpis Calman, 1896: 16; *Nematobrachion boöpis* Calman, 1905: 153–154, pl. 26; Hansen 1912: 267–269, pl. 10, fig. 5, a–m; Boden, Johnson and Brinton 1955: 377–379, fig. 47, a–b.

Material:
St. 82. 29. I. 46, 15.00 hrs., 5°27′ N, 0°07′ E, 100 m wire. – 1 male.
St. 139. 2. IV. 46, 4.00 hrs., 1°30′ N, 10°10′ W, 1750 m wire. – 2 males, 3 females.

Distribution elsewhere: Found in the tropical and subtropical waters of the Atlantic, Pacific and Indian oceans. It has not yet been reported from the tropical S.E. Pacific (Peru Current).

Depth: Adults, below 400 m; larvae, occasionally above 300 m.

Stylocheiron suhmii G. O. Sars, 1883.

Stylocheiron suhmii G. O. Sars, 1883: 31; 1885: 142, pl. 27, figs. 1–4; Hansen 1912: 277–278, pl. 11, fig. 3, a–b; *S. mastigophorum* Chun, 1896: 144, pl. 9 (*partim*); Boden, Johnson and Brinton 1955: 383–385, fig. 50, a–c.

Material:
St. 27. 2. XII. 45, 19.00 hrs., 24°30′ N, 19°11′ W, surface. – 4 females.
St. 140. 4. IV. 46, 0.05 hrs., 4°10′ N, 12°18′ W, surface. – 42 females.

Remarks: This species is closely related to *S. affine*, and they have a similar distribution and morphology. There are fewer crystalline cones in the adult eye of *S. suhmi*.

Distribution elsewhere: *S. suhmii* is widespread in the tropical, subtropical and temperate Atlantic, Pacific and Indian oceans.

Depth: Adults and larvae, above 300 m.

Stylocheiron affine Hansen, 1910.

Stylocheiron affine Hansen, 1910: 118–120, pl. 16, fig. 4, a–d; 1912: 278–279; Boden, Johnson and Brinton 1955: 382–383, fig. 49, a–c.

Material:

St. 24. 30. XI. 45, 11–12.00 hrs., S. of Canary Is., 27°23′ N, 16°36′ W, 500 m wire. – 1 female.

St. 26. 1. XII. 45, 20.00 hrs., 25°34′ N, 18°24′ W, surface. – 16 females.

St. 27. 2. XII. 45, 19.00 hrs., 24°30′ N, 19°11′ W, surface. – 6 females, 16 larvae.

St. 52. 2. I. 46, 20.00 hrs., off Monrovia, surface. – 1 female.

St. 91. 31. I. 46, 23.15 hrs., 5°44′ N, 1°02′ E, surface. – 1 female.

Distribution elsewhere: Tropical, subtropical and temperate Atlantic, Pacific and Indian oceans.

Depth: Adults and larvae, above 300 m.

Sylocheiron microphthalmum Hansen, 1910.

Stylocheiron microphthalma Hansen, 1910: 117–118, pl. 16, fig. 3, a–d; Boden, Johnson and Brinton 1955: 385–386, fig. 51, a–c.

Material:

St. 11. 15. XI. 45, 20.10 hrs., 34°13′ N, 12°16′ W, 35–0 m wire. – 7 larvae.

Remarks: Since only larvae were encountered this record is dubious. Young *S. suhmii* frequently have only two crystalline cones in the eye, which makes positive identification very difficult.

Distribution elsewhere: This form has been reported as an equatorial species in the Pacific and Indian oceans.

Depth: Adults and larvae above 300 m.

Stylocheiron elongatum G. O. Sars, 1883.

Stylocheiron elongatum G. O. Sars, 1883: 32; 1885: 146–147, pl. 27, figs. 6–10; Boden, Johnson and Brinton 1955: 386–388, fig. 52, a–c.

Material:

St. 26. 1. XII. 45, 20.00 hrs., 25°34′ N, 18°24′ W, surface. – 3 females.

Distribution elsewhere: This form occurs, but not very plentifully, in the tropical, subtropical and temperate Atlantic, Pacific and Indian oceans.

Depth: Adults and larvae usually below 300 m. In this collection they were taken in the upper 100 m at night.

Stylocheiron longicorne G. O. Sars, 1883.

Stylocheiron longicorne G. O. Sars, 1883: 32; 1885: 144–145, pl. 27, fig. 5; Hansen 1910: 120–121, pl. 16, fig. 5, a–b; 1912: 279–280, pl. 11, fig. 4, a–b; Banner 1949: 37–38, pl. 4, fig. 25, a; *S. mastigophorum* Chun, 1887: 30 (*partim*); Boden 1954: 234–236, fig. 21, a–c.

Material:

St. 24. 30. XI. 45, 11–12.00 hrs., S. of Canary Is., 27°23′ N, 16°36′ W, 500 m wire. – 1 female.
St. 28. 3. XII. 45, 18.30 hrs., 22°59′ N, 20°30′ W, surface. – 1 female.
St. 62. 10. I. 46, 20.10 hrs., 4°16′ N, 8°18′ W, 400 m wire. – 8 females.

Distribution elsewhere: Tropical, subtropical and temperate in the Pacific, Atlantic and Indian oceans.

Depth: Adults and larvae, 500–100 m.

Larval stages of this genus were encountered at three stations as follows: St. 25–12, St. 26–9, St. 81–2. It was not possible to assign these to species.

Finally a great number of specimens were mutilated beyond recognition during capture.

Station	Number	Station	Number
27	104	28	2
33	8	85	1
119	8	139 (deep)	281
139 (shallow)	165	140	126

The jar containing the euphausiid catch from St. 82 was broken in transit and the specimens were dried up, making it impossible either to count or identify them.

Acknowledgements

This report is based on a collection made available to me through the courtesy of Dr. Torben Wolff, Zoological Museum, Copenhagen and Dr. Marie Lebour, The Laboratory, Plymouth, both of whom I wish to thank. I wish to thank too, my colleagues Dr. Carl Hubbs and Dr. Edward Brinton for their assistance while the work was in progess and in manuscript.

References

Banner, A. H., 1949: A taxonomic study of the Mysidacea and Euphausiacea (Crustacea) of the North Pacific (Pt. III) Euphausiacea. — Trans. Royal Soc. Canadian Inst. **28** (58): 2–49.

Boden, B. P., 1954: The euphausiid crustaceans of southern African waters. — Trans. Royal Soc. S.A. **34** (1): 181–243.

— M. W. Johnson and E. Brinton, 1955: The Euphausiacea (Crustacea) of the North Pacific. — Bull. Scripps. Inst. Ocean. Univ. Calif. **6** (8): 287–400.

— and E. Brinton, 1957: The euphausiid crustaceans *Thysanopoda aequalis* Hansen and *Thysanopoda subaequalis* Boden, their taxonomy and distribution in the Pacific. — Limnol. & Oceanogr. **2** (4): 337–341.

Bruun, A. F., 1950: General Report and List of Stations. — Atlantide Rep. **1**: 10–47.

Calman, W. F., 1896: On deep-sea Crustacea from the south-west of Ireland. — Trans. Royal Irish Acad. **31** (1): 1–21.

— 1905: Note on a genus of euphausiid crustacean. — Fish., Ireland, Sci. Invest. 1902–03, **4** (II): 153–155.

Chun, C., 1887: Die pelagische Tierwelt in grösseren Meerestiefen und ihre Beziehungen zu der Oberflächenfauna. — Biblio. Zool. **1**: 1–66.

— 1896: Atlantis. Biologische Studien über pelagische Organismen. — Ibid. **7** (9): 1–262.

Dana, J. D., 1852: Conspectus of the Crustacea of the Exploring Expedition under Capt. C. Wilkes. — Silliman Jour., **13** (1): 1–685.

Hansen, H. J., 1905: Further notes on the Schizopoda. — Bull. Mus. Ocean. Monaco, **42**: 1–32.

— 1910: The schizopoda of the Siboga Expedition. — Siboga Exped., **37**: 1–123.

— 1911: The genera and species of the order Euphausiacea, with an account of remarkable variation. — Bull. Inst. Ocean. Monaco, **210**: 1–54.

— 1912: The Schizopoda. Repts. on Sci. Res. Exped. to Tropical Pacific. U.S. Fish. Comm. Steamer "Albatross" XVI & XXVII. — Mem. Mus. Comp. Zool. Harvard College **35**: 173–296.

Milne-Edwards, H., 1830: Mémoire sur une disposition particulière d'appareil branchial chez quelques Crustacea. — Ann. Sci. Nat. **19**: 451–460.

— 1837: Histoire naturelle des Crustacés, — Paris: Librarie Encyclopédique de Roret, **2**: 1–531.

Moore, H. B., 1952: Physical factors affecting the distribution of euphausids in the North Atlantic. — Bull. Mar. Sci. Gulf & Caribbean **1** (4): 278–305.

Ortmann, A. E., 1893: Decapoden und Schizopoden. — Ergebn. Plankton-Exped. **11**, G.b.: 1–120.

Sars, G. O., 1883: Preliminary notices on the Schizopoda of H.M.S. "Challenger" Expedition. — Forhandl. Vidensk. Selsk. Christiania **7**: 1–43.

— 1885: Report on the Schizopoda collected by H.M.S. "Challenger" during the years 1873–1876. — Challenger Rep. **13**: 1–228.

Streets, T. H., 1877: Contributions Nat. Hist. Hawaiian and Fanning Islands and Lower Calif., made in conn. U.S. North Pacific Survey Exped., 1873–75. — Bull. U.S. Nat. Mus. **7**: 3–172.

Tattersall, W. M., 1924: Euphausiacea. — Brit. Antarctic "Terra Nova" Exped. 1910. Nat. Hist. Rep. Zool. V., **13** (1), Crustacea, Pt. VIII: 1–36.

— 1926: Crustaceans of the orders Euphausiacea and Mysidacea from the western Atlantic. — Proc. U.S. Nat. Hist. Mus. **69** (8): 1–31.

Zimmer, C., 1914: Die Schizopoden der Deutschen Südpolar Exp. 1901–1903. — Deutsche Südpolar Exp. **15**, Zool. VII: 376–445.

— 1915: Schizopoden des Hamburger Naturhistorischen (Zoologischen) Museums. — Mitt. Naturh. Mus. Hamburg **32**: 159–182.

Särtryck ur Tellus nr 1, 1961

Tellus, v.13, no.1.
1961. pp.85-105.

The Production Rate of Natural Tritium

By HARMON CRAIG AND DEVENDRA LAL[1]

Scripps Institution of Oceanography, University of California, La Jolla

(Manuscript received July 5, 1960)

Abstract

A detailed evaluation is made of the production rate of natural tritium in the pre-thermonuclear epoch. Deuterium and tritium analyses on the same precipitation samples are used to establish the uncontaminated tritium levels in precipitation sampled before the Castle tests, and the tritium balance is calculated for the North American troposphere. The global mean production rate $\overline{Q}$, calculated from the geochemical inventory, is found to be 0.5 ± 0.3 atoms T/cm^2 sec. This value is three to four times smaller than values found previously by such calculations because of the following developments:

1. The deuterium and tritium data show that the increases in tritium content observed during early thermonuclear tests before Castle are due to addition of synthetic tritium rather than to random fluctuations. The deuterium-tritium relationships are used to establish the general pattern of tritium variations over the North American continent and to evaluate the uncontaminated tritium levels.
2. The mean stratospheric residence time for tritium is found to be about 1.6 years from studies on fission product fallout and from the latitudinal variation of stratospheric cosmic ray production.
3. Stratospheric tritium is preferentially injected into the troposphere at high latitudes, as shown by fallout observations. The tritium influx into the North American troposphere is therefore higher than the mean global value.

The predicted production rate is calculated from cosmic ray and nuclear cross section data using the star production rates in the atmosphere. The predicted mean global tritium production rate during an average solar cycle is found to be 0.25 ± 0.08 atoms T/cm^2 sec. The variation in the production rate over an average solar cycle is found to be ± 4.5 %.

Within the uncertainties of the data and calculations, the production rates calculated from the geochemical inventory and from the cosmic ray data are in agreement, and there is thus no observational evidence for accretion of tritium from an extra-terrestrial source.

Introduction

The geochemistry of tritium is a subject which has been much discussed during the decade since the discovery, by Faltings and Harteck and by Libby and his associates, that this isotope is continuously formed in the atmosphere by cosmic radiation. By 1956 Libby and his coworkers had analyzed a large number of natural waters and had found that there was general agreement between the global production rate computed from the natural inventory of tritium and that calculated from the cosmic ray flux and nuclear cross section data, namely about 0.14 atoms T/cm^2 sec. However in 1957 one of us showed that previous calculations of the production rate from observed tritium concentrations had neglected several essential factors, the most important of which was transport of water vapor out of North America, and that the most likely value was a production rate $\overline{Q}$ of about 1.3 atoms/cm^2 (Craig, 1957). It was also shown that with the observed concentrations in the atmosphere and sea, the mixing rates deduced from the better-known radiocarbon

---

[1] On leave from the Tata Institute of Fundamental Research, Bombay, India.

Contributions from the Scripps Institution of Oceanography, New Series, 1306 (785)

Reproduced by Permission

data required a figure of similar magnitude. Begemann and Libby (1957) calculated $\overline{Q} = 2$ from a study of the Mississippi valley water balance.

Since 1957 on the average of two papers per year have been published in which tritium production rates ranging from $\overline{Q} = 1$ to 2 have been calculated from data on natural concentrations, suggesting that the cosmic-ray production rate is too small by an order of magnitude to account for the pre-bomb tritium inventory. The present paper breaks the chain. Our treatment of the problem is essentially that given by Craig (*op. cit.*), modified however by consideration of several important factors and new data which have since been developed. Because the comparison of the cosmic ray production rate with observed natural concentrations, and the possibility of accretion of tritium from extraterrestrial sources as suggested by several authors, are important geophysical problems, we have attempted to evaluate as carefully as possible the production rate of natural tritium from the small amount of available data. In what follows, we first discuss the associated deuterium-tritium variations in precipitation samples and eliminate pre-Castle precipitation affected by thermonuclear contamination. We then calculate the natural production rate from the observed tritium concentrations, and finally compare this value with the most accurate calculation we can make based on the cosmic ray flux and cross section data.

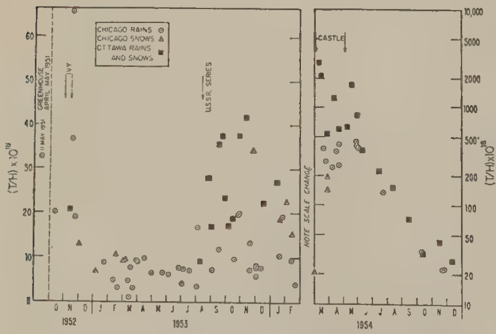

Fig. 1. Tritium concentration in Chicago and Ottawa precipitation up to the end of 1954. The dates of announced thermonuclear explosions are indicated. (Tritium data: Kaufman and Libby, 1954; von Buttlar and Libby, 1955; Brown and Grummitt, 1956; Begemann and Libby, 1957).

Deuterium and tritium analyses of precipitation

Tritium analyses of Chicago precipitation make up by far the major part of the data on natural waters and we therefore begin with an evaluation of these measurements (Kaufman and Libby, 1954; von Buttlar and Libby, 1955; Begemann and Libby, 1957).[1] The Chicago data, as well as the analyses of Ottawa precipitation (Brown and Grummitt, 1956) up to and including the year 1954 are shown in Figure 1.[2] The most prominent feature of these data is the large injection of artificial tritium as a result of the Castle tests in the spring of 1954 (Begemann, 1956).

Figure 1 also shows, however, that there are significant increases in the natural level associated with the thermonuclear tests carried out before Castle by U.S. and the U.S.S.R.[3] It is unfortunate that there are no Ottawa data for the period January 1 to August 1, 1953, but as we show below it does not seem possible that the natural uncontaminated level in Ottawa can have been anywhere near as high as the values of 20—40 T.U. found from August 1953 to the Castle tests. If these levels represent artificial injection, as we believe, they are significantly higher than those observed in Chicago during the same period, but this phenomenon is definitely observed during the Castle injection and the pattern is therefore significant. It should be noted that after the Castle shots the tritium level in Ottawa precipitation decayed to a level of about the same magnitude as observed in Chicago at that time.

Because the Chicago data do not for the most part show increases to levels as high as those seen in Ottawa during the seven months before Castle, and because of the lack of Ottawa data prior to this period, Figure 1 does not in itself constitute proof of pre-Castle artificial tritium injection and it is necessary to seek more definite evidence. This can be done by a method of "isotopic renormalization" based on the comparison of deuterium and tritium analyses on the same precipitation samples. Deuterium variations in precipitation are due to preferential concentration of HDO in the liquid phase because of its lower vapor pressure relative to H_2O, so that in atmospheric water vapor passing over a continent the ratio D/H decreases as moisture is removed by precipitation. The removal rate of HDO is greater at lower temperatures because of the increase in the isotopic vapor pressure difference with decreasing temperature. The precipitation process affects the HTO/H_2O ratio in the same way but to a greater extent because of the larger vapor pressure difference in the case of HTO.

---

[1] Hereafter these papers are referred to as K-L, VB-L, and B-L, respectively.

[2] We use the abbreviation 1 tritium unit (1 T.U.) = 1×10^{-18} atoms T/atom H hereafter.

[3] Our source of information on dates and locations of thermonuclear detonations is the paper by Telegadas (1959). We believe, however, that the tritium data indicate that the dates announced for some of these tests are not precisely accurate, as we note later on.

Figure 2 is an isohydrogram of Chicago, Greenland, and Pacific island precipitation, in which the tritium content in T.U. is plotted vs. the deuterium content of the same samples. The deuterium data were measured by one of us (H. C.) by mass spectrometric analysis of H_2 obtained by quantitative reduction of the original precipitation samples using zinc or uranium. The δ values plotted are the per cent deviations of the D/H ratio from that of an arbitrary "standard mean ocean water" (SMOW)[1] which is the composite of ocean water samples taken from 500—2,000 meters depth used as a standard for O^{18} measurements by EPSTEIN and MAYEDA (1953). That is,

$$\delta D\,(\%) = \left[\frac{D/H_{\text{sample}}}{D/H_{\text{SMOW}}} - 1\right] \times 100$$

The data plotted in Figure 2 are accurate to about ± 0.2 %.

A complete discussion of the isohydrogram and the deuterium, tritium, and oxygen data in these and other samples will be given elsewhere. At present, we wish only to compare the tritium-deuterium relationships during the possible periods of contamination indicated in Figure 1. However as we refer to various aspects of Figure 2 in later discussions in this paper, we shall briefly describe the properties of this diagram. The trajectories of points in the isohydrogram representing precipitation samples derived from an idealized air mass moving across a continent are in general governed by the following factors:

1. Preferential removal of the heavy isotopic species HDO and HTO relative to H_2O during precipitation because of the lower vapor pressures of the heavy isotopic species. These effects are given by the well-know Rayleigh distillation equations—see calculations and discussion for HDO and H_2O^{18} by CRAIG, BOATO, and WHITE (1956).
2. Continuous injection of cosmic ray produced tritium as HTO.
3. Injection of HTO from thermonuclear explosions.
4. Mixing with extraneous water vapor, addition of water from continental evaporation, etc.

In general, it has been found that the D and O^{18} content of Chicago precipitation reflects the dominant source and trajectory of the water vapor from which the precipitation is derived. Precipitation which can be identified as coming from polar air is relatively light, values of δD ranging down to $-16\ \%$, while precipitation from maritime tropical air which has suffered little loss of moisture prior to its arrival ranges up to $\delta D = 0$ or even somewhat higher. The distribution of deuterium in precipitation samples taken over the two-year period 1953—54 in Chicago is shown in Figure 3, in which the lower D concentrations in the winter snow samples are quite evident. These lower values also reflect to some extent the lower temperature of precipitation as described previously. Oxygen 18 measurements on these samples correlate with the D data according to the equation given above which seems to hold true for precipitation from all over the world, for climates ranging from the tropical Pacific Ocean to the Arctic and Antarctic.

Assuming no artificial injection of tritium, tropical maritime air should begin a trajectory

---

[1] On this scale the δ values for the NBS water standards vs. SMOW are:

$$\delta D\,(\text{NBS-1}) = -\ 4.76\ \% \pm 0.02$$
$$\delta D\,(\text{NBS-1A}) = -18.33\ \% \pm 0.20$$

The relative enrichment of NBS-1A vs. NBS-1 taken as the standard is then $-14.25\ \% \pm 0.25$.

Oxygen 18 analyses were also made on these samples and the O^{18} data correlate precisely with the D/H data according to the relationship: $\delta D = 8\,\delta O^{18} + 1$ (both δ's in per cent) in agreement with the general relationship which has been established for precipitation from all over the world (H. CRAIG, 1961).

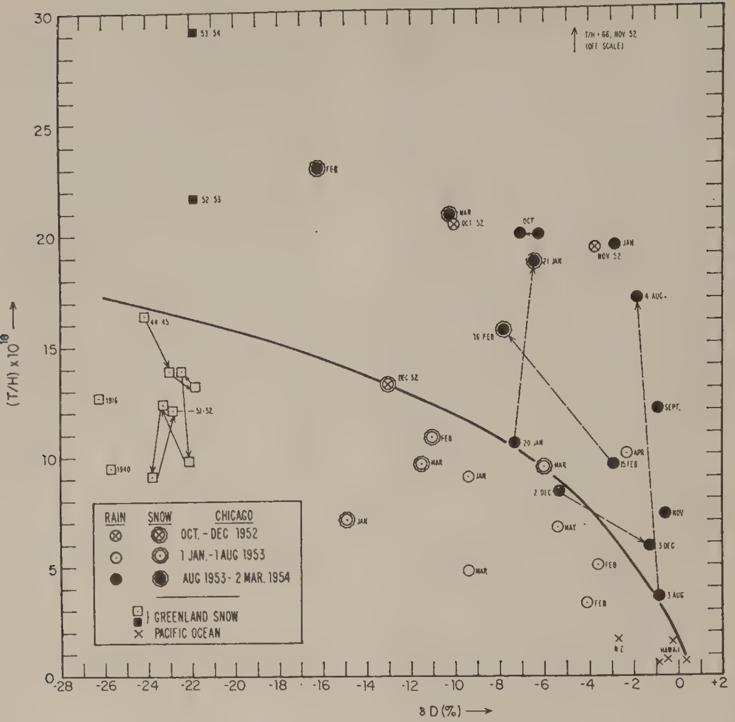

Fig. 2. Isohydrogram showing tritium and deuterium variations in Chicago, Greenland, and Pacific island precipation. Deuterium data (H. Craig, paper in preparation) are per cent deviation of D/H ratio from "standard mean ocean water" (SMOW). Tritium analyses by K-L, VB-L, and Begemann (1959). The Greenland core samples consist of yearly precipitation from summer to summer; the connecting arrows and indicated dates show the time sequence from 1944—52 according to Begemann. We believe the actual precipitation dates may be a year earlier than shown (see text).

at a point close to the origin of Figure 2, with a D/H ratio representing approximate isotopic equilibrium of the vapor with surface ocean water (which has a δ value of about + 1 due to evaporation) and a T/H ratio reflecting the approximate steady state balance between the tendency to reach isotopic equilibrium and the gradient imposed by continuous atmospheric production with a finite exchange rate with the sea. As the vapor moves to higher latitudes and inland over continents the factors (1) and (2) above will impose various slopes upon a trajectory of points plotted in the isohydrogram, depending on the varying importance of these two effects (we neglect the minor complications imposed by item 4 in this discussion). On the average, however, a rather continuous spread of discrete points may be expected as the vapor moves from the ocean, let us say, northward and/or eastward into and over continents.

In Figure 2 the following data have been plotted:

1. Chicago precipitation, identified as to the periods (see Figure 1) (a) prior to January, 1953; (b) 1 January to 1 August, 1953; and (c) from 1 August, 1953 to the Castle test series. The tritium data for these samples are given in K-L, VB-L, and B-L.

2. Samples of Greenland snow from a core taken about 320 km east of Thule at altitude 2,300 meters, by H. Bader and E. W. Marshall of SIPRE. These samples were divided by year of precipitation according to the summer melt layer, and each sample shown represents a year of precipitation from

summer to summer. Two additional samples from Thule, of summer snow from 1916 and winter snow from 1940—41 are also shown. Tritium analyses of these samples have been made by BEGEMANN (1959).

3. Several samples of rain from the Hawaiian Islands and one from New Zealand (tritium data given in K-L and VB-L).

The most prominent feature of the isohydrogram is the tendency toward a rather continuous trend from the Hawaiian samples, through the Chicago samples of group 1 (b) above, to the Greenland samples of pre-Ivy precipitation. On the other hand one sees that the samples of Chicago precipitation from groups 1 (a) and (c), taken during periods of possible artificial injection of tritium, have on the average much higher T concentrations compared to samples of the same D concentrations in group 1 (b) taken from 1 January to 1 August 1953 when no thermonuclear tests were made. We have drawn an arbitrary line in the isohydrogram as the approximate envelope of these latter samples. If we now compare the δ D values for Chicago precipitation from 1953 and from 1954, as shown in Figure 3, we see that there is no apparent tendency for a systematic difference in D content, either for rain or for snow, so that there is no reason to expect a systematic difference in the HDO-HTO relationship from one year to the next. Yet the T contents for samples of quite similar δD values may differ by as much as a factor of 5 and by much more in the case of one sample from November, 1952 which plots off the diagram.

In Figure 2 we have also shown the month in which the Chicago samples were collected, and one sees that even in samples from the same season of the year the T levels in the different periods can be quite different for the same δD values. Moreover, we have indicated by connecting arrows samples separated by not more than a day in time, and in two cases, August 3—4 and January 20—21, 1954, there is a striking sudden increase in tritium while the deuterium concentration remains practically constant. Such a phenomenon requires the existence of relatively large tritium gradients in moisture which is arriving with a homogeneous D (and O^{18}) concentration, and which would therefore be expected to have had a uniform history of precipitation and trajectory.

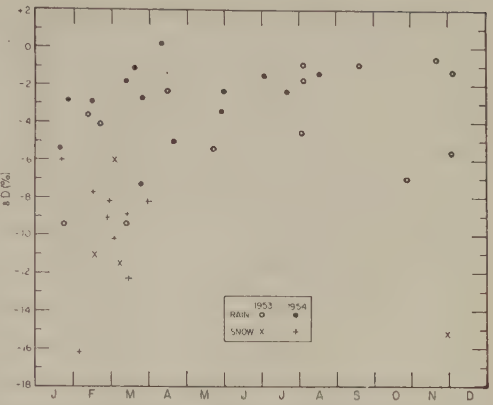

Fig. 3. Deuterium variations in Chicago precipitation for two years, showing δD relative to SMOW (cf. Figure 2). Not all precipitation was analyzed. (From a paper in preparation by H. Craig.)

By far the easiest way to achieve such gradients is by the sudden injection of tritium into a portion of a relatively uniform system. On the other hand, the points shown for December 2—3, 1954, represent the type of change which may well be entirely meteorological in origin, regardless of whether any artificial T is or is not present.

The U.S.S.R. thermonuclear test of August 12, 1953 was announced by the U.S. as "part of a series" (TELEGADAS, 1959) and if our interpretation is correct, the August 3—4 points indicate a shot somewhat earlier. We have no explanation for the point shown for October 14, 1952, just prior to the announced date of the Ivy shot.

Thermonuclear tritium in Ottawa and Greenland

The importance of the conclusions obtained from the isohydrogram lies in the strong evidence of appreciable contamination during the period of Ivy and the U.S.S.R. thermonuclear tests (and possibly during Greenhouse). The first Ivy shot (Mike) was a refrigerated fusion device which presumably contained a liquid deuterium-tritium mixture and thus released directly a relatively small amount of pre-synthesized tritium (CAMERON, 1959). The amount of artificial T injected into the atmosphere was much less than in the Castle and subsequent shots, which probably produced tritium by the Li^6 (n, α) T reaction. No information is available to us on the mechanism of the 1953 U.S.S.R. shots. The Greenhouse mechanism was presumbly even more primitive than Ivy, and it seems fair to conclude that Chicago precipitation levels from 1 January to 1 August 1953 can be taken as fairly representative of the natural level, especially when we consider the rapid removal of artificial tritium from the troposphere after Castle (Figure 1).

The Ottawa samples from 1 August 1953 to Castle show much higher values than the T levels observed in Greenland snow. The deuterium content of precipitation and river samples taken from British Columbia and Alaska through northern Canada to the east coast and into Greenland is very uniform at about the average value found in the Thule samples, or a little lower (H. Craig, paper in preparation). On the other hand, a sample from the Ottawa River, 4 August 1954, gave $\delta D = -7.9\ \%$, while the lightest sample found in this general area, from the Rivière à Claude on the Gaspé Peninsula, 25 June 1954, gave $\delta D = -10.4\ \%$. Since average Chicago precipitation will plot on the isohydrogram at about $\delta D = -5\ \%$, $T/H = 6$ T.U., Ottawa precipitation would normally be expected to plot somewhere between the Chicago and Greenland averages, whereas it actually contains about twice as much T as Greenland precipitation during the period in question. These data thus provide further evidence for pre-Castle contamination.

Tritium variations in the Greenland samples shown in Figure 2 have been discussed by Begemann (1959) who pointed out that the high value found for summer 1952—summer 1953 precipitation is most probably due to artifical contamination from the Ivy tests, so that the layers for the following years contain the tritium injected by Castle. In addition to the data shown in Figure 2, there were two more layers in the core which are not plotted; the dates and observed T concentrations for these are: 1954—55, 212 T.U.; and 1955—56, 101 T.U. (Begemann, 1959). Deuterium measurements on these two samples gave $\delta D = -23.6\ \%$ for each, very close to the values found for the samples plotted in Figure 2. Thus the D/H ratio is practically constant throughout the core, indicating that the high T concentrations from 1952 on are indeed due to artificial tritium. This evidence from the isohydrogram is further strengthened by the fact that the core data plotted cover a complete sunspot cycle from the minimum in 1944 to the following minimum in 1954.[1]

Pre-thermonuclear tritium levels

We conclude that the isohydrogram presents a reasonable picture of the pattern of tritium-deuterium variations in North America when injection of artificial tritium is not of major importance. The effect of contamination in Chicago precipitation from August 1953 to the Castle tests is shown in Table 1, in which we summarize the data for the period 1 January to 1 August, 1953, during which no tests were held and the Chicago level was relatively constant, together with the data from August 1953 to the Castle tests. Weighted means are not available for the latter period, but the unweighted means indicate that during this time the Chicago tritium levels were increased by about 1.7 in rain, 2.4 in snow, and by an overall average of about a factor of 2. The higher increase factor observed in snow is in agreement with the very low δ values often found in snow (see Figure 3) indicating the presence of vapor derived from high latitudes and therefore more subject to con-

---

[1] It appears, however, than the dating given by Begemann is incorrect by one year, at least in the upper part of the core. The observed value of 29.2 T.U. for summer 1953—54, a period which included both the U.S.S.R. and the Castle tests, seems much too low considering that Ottawa precipitation averaged about 30 T.U. during the eight months before Castle, and about 1 000 T.U. for the four months from Castle to summer, 1954, and that the Castle tritium appeared in Chicago and Ottawa almost immediately. The seasonal distribution of precipitation at the location of the core is not known to us, but Petterssen *et al.* (1956, Table 15) show that at Thule, about 80 % of the annual precipitation occurs from July through February. Taking the Ottawa levels as given above, weighted 80/20 for the two periods, we calculate an approximate mean value for this period as 200 T.U., which may be compared with the value 212 T.U. given by Begemann for the 1954—55 layer, a period in which no increases were observed in Chicago. We conclude that the dates shown in Figure 2 should be put back one year, and that the first observed increase, to 21.7 T.U., represents tritium from the Greenhouse test incorporated in a summer melt layer and showing up in the snow for 1951—52. The following layer with 29.2 T.U. would then contain the artificial tritium from Ivy. If our interpretation is not correct it is necessary to assume that Castle tritium arrived simultaneously and almost immediately at Chicago and Ottawa but took at least five months longer to get to Greenland, which seems improbable.

Table 1. Tritium assays (T.U.) of pre-Castle Chicago precipitation.
(Data from Kaufman and Libby, 1954, von Buttlar and Libby, 1955).

Period	Unweighted mean	Weighted mean
I. *1 January—1 August 1953*		
Summer rains...	7.3	7.3
Winter rains....	5.5	3.9
All rains.......	6.4	5.7
Snow..........	9.2	9.6
All precipitation	7.0	6.0
II. *3 August 1953—2 March 1954*	Unweighted mean	Ratio of means II/I, = increase factor
Rain...........	10.8	1.7
Snow..........	22.5	2.4
All precipitation	13.5	~2

tamination from the Russian tests. Humidity and total precipitation factors do not account for the difference; this point will be discussed elsewhere together with the details of the isotopic data.

The weighted mean of Chicago precipitation from 1 January to 1 August, 1953, is 6.0 T.U.; this should be a good annual average inasmuch as it includes both winter and summer precipitation covering almost the entire range of D/H variation (Figure 3). The extent of possible remnant contamination from Ivy can be answered approximately by comparison with data on two old samples of Illinois precipitation (K-L); water collected August, 1952 from a Decatur cistern gave 5.9 T.U., and water from a Sullivan cistern about 15 years old gave 6.3 T.U. extrapolated to time of origin. It seems likely therefore that the precipitation during this period was not significantly contaminated; we shall take the tritium content of average pre-thermonuclear era Chicago precipitation to be 6.0 T.U., and hereafter we refer to the period 1 January—1 August, 1953, as the "clean period".

The only other extensive set of precipitation data is that reported by Giletti, Bazan, and Kulp (1958) for New York rains. Unfortunately all their pre-Castle samples were taken after October, 1953, during the period of contamination from the U.S.S.R. thermonuclear tests. In order to make an approximate estimate of the natural level in N.Y. rain it is necessary to apply a correction factor to their data. There are enough data on Chicago precipitation to insure that the contamination factor estimated in Table I is statistically significant, and we assume that an approximately similar factor applies to the N.Y. data. Deuterium concentrations are quite similar in waters from the two areas; average Chicago precipitation is about—5 % relative to SMOW, while the following δD values have been obtained for N.Y. area waters:

Lake Erie (17 July, 1954)	− 5.3 %
Lake Ontario (19 Sept., 1948)	− 4.6 %
Lake Ontario (20 July, 1954)	− 5.0 %
Niagara River (12 March, 1954)	− 5.3 %
Hudson River (27 June 1954)	− 6.0 %

(H. Craig, paper in preparation). Considering the relationships shown in the isohydrogram, we conclude that the average moisture received by the two areas is similar enough in history that the Chicago correction can be applied to N.Y. data.

There are only three snow samples in the pre-Castle Lamont data and these analyses vary by a factor of three in T content, but there are eleven rain samples which fell between 25 October 1953 and 3 March 1954 with an unweighted average T content of 9.45 T.U. Dividing this by 1.68, the increase factor found in Chicago rain during this period, we obtain a value for the natural level of 5.6 T.U. which agrees well with the average of 5.9. T.U. obtained for three N.Y. wines (K-L), and therefore fixes an approximate figure for uncontaminated N.Y. precipitation.

In Table 2 we list all the available data for pre-thermonuclear era precipitation, including the approximately corrected N.Y. value and the average figure derived for Chicago precipitation during the clean period. The two Hawaiian samples listed are plotted in Figure 2 together with three other Hawaiian rains and one New Zealand rain taken during the period October—December, 1953. Two of the Hawaiian rains of this period contained 0.67 and 0.73 T.U. (VB-L) indicating that an average figure of 0.6 is not a bad average for the natural level in Hawaiian rain.

In our calculations of the natural tritium production rate we have not considered data from lakes, reservoirs, or wells, since the age

Table 2. Tritium levels in pre-thermonuclear precipitation.

Sample	Tritium content (T.U.)
Greenland snow (1944—52)	12.4 Begemann (1959)
Chicago precipitation (clean period)	6.0 (K-L, VB-L)
New York rain (Lamont data, corrected)	5.6 Giletti *et al.* (1958)
Three New York wines (1940—52)	5.9 (K-L)
Arkansas snow (January, 1953)	5.5 (K-L)
Arkansas rain (February, 1953)	2.25 (VB-L)
Four French wines, Bordeaux (1928—45)	4.4 (K-L)
Four French wines, Rhone Valley (1929—51)	3.8 (K-L)
Three Spanish wines, Jerez de la Frontera (1942—51)	3.1 (VB-L)
Philippine Islands rain (June, 1953)	0.9 (VB-L)
Two Hawaiian rains . . . . . . (March and July, 1953) .	0.61 (VB-L) 0.59

of such water at the time of collection is always in question. The only other data available refer to pre-Castle samples of surface ocean water. These data are shown in Table 3. It is obvious that not much can be said about the pre-Castle ocean from these measurements. For example, the analyses of GILETTI, BAZAN, and KULP (1958) are 1 T.U. higher for two samples, and 0.7 T.U. lower for a third, compared with measurements on identical samples by VB-L.[1]

Table 3. Pre-Castle oceanic mixed layer tritium analyses.

Sample	Tritium content (T.U.)
Pacific, off California, 6/6/53	0.54 ± .02 (K-L)
Atlantic, Gulf Stream, 9/11/53	0.19 ± .05 (VB-L)
Atlantic, 300 miles from N.Y	0.55 ± .04 (VB-L)
Same sample	1.31 (GBK)[1]
Atlantic, Sargasso Sea 9/10/53	0.29 ± .02 (VB-L)
Same sample	1.34 (GBK)
Atlantic, Sargasso Sea, 9/7/53	1.6 ± 0.1 (VB-L)
Same sample	0.92 (GBK)
Atlantic, 10/31/52	2.2 ± .25 (B-L) 1.8 ± .25
Atlantic, 10/22/52	1.3 ± .1 (B-L)
Pacific, 10/28/52	1.05 ± .1 (B-L) 1.0 ± .1
Pacific, 11/26/52	1.5 ± .2 (B-L)
Pacific, 11/18/52	10 ± 1 (B-L)
Pacific, 12/19/52	16.3 ± 1 (B-L)
Eleven Atlantic samples, 7/22 to 9/12/53	0.62 to 1.5 (GBK)

[1] Giletti, Bazan, and Kulp (1958)

The Lamont data are corrected for a blank of 0.3 T.U. found for dead water; Libby and his co-workers do not report any blanks. It is difficult to account for the generally high values found by B-L relative to the earlier data of VB-L and K-L except by assuming laboratory contamination due to the high atmospheric levels during the times of measurement. The average surface ocean water after Castle is about 2 T.U. as measured at Lamont and Chicago, and assuming that all of this is due to Castle production, we can estimate from Figure 1 that, considering atmospheric levels only, the Ivy and U.S.S.R. tests could not have produced more than about 10 % of the amount of T produced by Castle, which would therefore have raised the surface sea water level by possibly 0.2 T.U. as an upper limit. Of course this estimate does not include direct local introduction into the sea, and there is some evidence from the very high values obtained by B-L in the Pacific after Ivy that this may be significant, though one would still expect the effect to be considerably smaller than in the case of the Castle tests, and also that it would be completely diluted before reaching the Atlantic.

It is possible to calculate the rate of introduction of tritium into the troposphere by two basic methods (CRAIG, 1957). The first of these considers the balance in the oceanic mixed layer, assuming an oceanic mixing model with parameters given by radiocarbon data.[2] The introduction rate calculated by this method is a very sensitive function of the amount of tritium in the mixed layer. Considering the disparity between Lamont and Chicago data on the same samples, and the scatter of data in Table 3, we do not believe a meaningful calculation can be made by this method. A high upper limit of about 0.65 T.U. for the mixed layer T concentration can be derived from the Hawaiian rain trajectory in the isohydrogram, assuming no T enters the troposphere (Craig, in press), but no good lower limit can be estimated. The second method is based on the precipitation data and water balance for the North American continent, using the data in Table 2; we make this calculation in the following section.

---

[1] Lamont sample numbers are given by VB—L, but GILETTI, BAZAN, and KULP do not list their sample numbers so that comparisons cannot be made from their paper. We have looked up the sample numbers and descriptions in their original reports.

[2] The calculation cannot be made for the global tropospheric balance without making an assumption about the rate of molecular exchange of H_2O between the atmosphere and the sea. See discussion by CRAIG (in press).

Tritium balance in the North American troposphere

We now calculate the net introduction rate of tritium into the North American continental troposphere by direct tropospheric cosmic ray production and by downward mixing from the stratosphere. The flux of tritium from these two sources is termed the *gradient flux* into the North American troposphere, ϕ_i^* (NA) (cf. discussion of the similar term for the global troposphere in the following section). The overall water balance for North America is known from the data of Benton and Estoque (1954) who measured the net transport of water vapor at a series of stations around the continental border in 1949 (Figure 4). We shall make the balance in the troposphere over the continent, rather than for the system troposphere + continent, because we do not have sufficient data to estimate accurately the tritium removed from the continent in runoff. The vapor transport, precipitation, and evaporation fluxes into and out of the continental atmosphere are given in the first column of Table 4. The equation for the atmospheric tritium balance is:

$$4.73\,\phi_i^*(\text{NA}) = V_o\text{T}_o - V_i\text{T}_i + \\ + P\text{T}_p - E\text{T}_e + \lambda A\text{T}_a$$

in which the symbols are defined in Table 4, except for the last term which is the decay of tritium in the atmosphere, A being the standing water content and T_a its tritium content. This term can readily be shown to be of the order of 0.01 and can always be neglected. ϕ_i^* (NA) is the gradient flux of tritium into the North American troposphere by direct cosmic ray production and stratospheric injection, and 4.73 meters of water/year = 10^{18} H atoms/cm^2 sec.

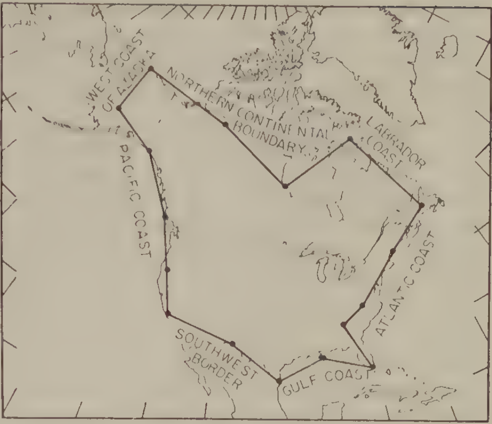

Fig. 4. North American continental boundaries used in the vapor transport study by Benton and Estoque (1954).

The tritium content of evaporating vapor on the continent can be obtained from the average precipitation value, as these concentrations must be quite similar (Bolin, 1958). The exposed area of lakes and rivers is so small that they cannot contribute significantly to the large amount of evaporation and transpiration which takes place in the soil before the precipitation reaches these storage units. Moreover, this evaporation will take place so soon after the precipitation falls that no tritium can be lost by decay, and the only effect on the tritium content of the evaporating vapor will be isotopic fractionation. If a small amount of water evaporates the single stage factor will apply, so that T_e is about 0.91 T_p (Sepall and Mason, 1960), whereas if it all evaporates $\text{T}_e = \text{T}_p$; moreover the effect in transpiration will be small if the plant transpires most of the water it takes in.[1] Therefore we may set $\text{T}_e = 0.95\ \text{T}_p$ as an average value for the continent.

Fortunately, it seems that Chicago and New York precipitation, the only extensive set of uncontaminated tritium data, should be a reasonably adequate approximation to the mean type of precipitation on the continent.

---

[1] The water in a tomato grown outside Chicago had $\delta D = -2.5$ %, about the same as mean Chicago rain. If we can extrapolate from tomatoes to grapes, this result indicates that the wine data in Table 2 have probably not been significantly affected by isotopic fractionation.

For example, the distribution of precipitation over the continent, as shown by Reed (1941), and the trend of D and T concentrations in the isohydrogram, indicate that the precipitation received at Chicago should be an approximate average both with regard to amount of precipitation and absolute tritium content. The southeastern U.S. receives the most precipitation, but its area is small and the T content of the incoming vapor is low because of recent derivation from the ocean. δD values of waters in this area range from -1 to -2%. The west and northwest sections of the continent receive less precipitation, but they make up more of the area. Rains along the U.S. Pacific coast show $\delta D = -4$ to -5%, while inland waters from the Canadian border to the Beaufort Sea, in the western half of Canada and in Alaska, show δD uniformly about -12 to -16%, so that the T content of the precipitation will be correspondingly high (cf. our discussion of trajectories in the isohydrogram).

This pattern can be correlated roughly with Figure 5, taken from Benton and Estoque (1954), which shows the average integrated water vapor transport for the year 1949. In this figure one can see that Chicago and New York lie approximately on a sort of median convergence line between the major vapor trajectories into the continent across the Gulf coast and the Pacific coast. The large δD variations in Chicago, shown in Figure 3, which have a range equal to that found over the whole continent, and the associated T/H variations shown in Figure 2, are a measure of the sampling of northern and southern air during the seasonal migration of the polar front between Manitoba and Florida. Considering these variations, the fact that the U.S. gets slightly over half the continental precipitation with the highest rate in the southeast U.S., and the indication from Figure 2 that the Greenland snow probably represents a maximum value for any precipitation on the continent, we do not believe that the mean tritium content of North American precipitation could possibly have been greater than 8 T.U. or less than 4 T.U. in the pre-thermonuclear epoch. Accordingly we conclude that we can take the Chicago and New York averages in Table 2 as the continental average, and we set $T_p = 6 \pm 2$ T.U.

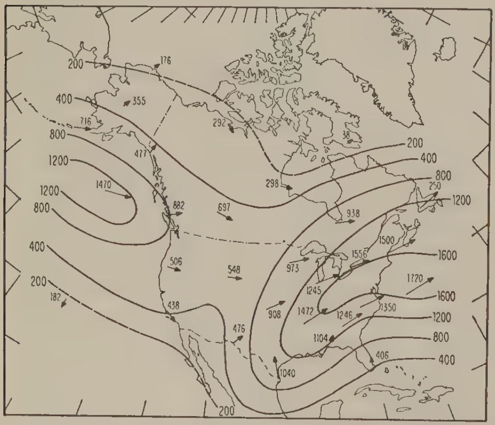

Fig. 5. The integrated water vapor transport (surface to 400 mb) for the North American continent, averaged for 1949. The figures are vapor transport in grams/cm sec (Benton and Estoque, 1954).

In order to estimate the amount of tritium transported by vapor, the liquid-vapor fractionation factor for HTO is needed. We have obtained this in the following way. The ratio between deuterium and oxygen 18 variations in worldwide precipitation samples is uniformly about 8, indicating an average temperature for precipitation-vapor equilibrium in the atmosphere of about $-10°$ C $\pm 10°$ (H. Craig, 1961). Extrapolation of the data of Sepall and Mason (1960) for minimum and maximum slopes shows that the liquid-vapor fractionation factor for HTO at —10° C may be taken as $\alpha = 1.1 \pm 0.1$. The actual relationship between the T/H ratios in mean vapor crossing a boundary and precipitation observed in storms will depend upon whether an open or closed system is assumed as a model, but in all cases the T/H ratio of mean vapor will vary between limits of the mean ratio in precipitation, or this ratio divided by α. Therefore α as given above, with the limits noted, can be taken as a mean value covering all possibilities.

According to Benton and Estoque (1954) about half the vapor entering the continent comes in along the Gulf coast and southwest border boundaries (Figure 4), and about half comes in along the Pacific coast, with a principal vector at about 50° of latitude (Figure 5). The precipitation characteristic of such vapor is estimated as follows. There is undoubtedly a latitude effect in the tritium content of marine vapor due to the occurrence of the

(794)

stratospheric injection site in high latitudes. For the Pacific coast vapor we use the French and Spanish wines in Table 2 (in which fractionation is probably not important; cf. our comment on the deuterium content of natural tomato juice) especially at Bordeaux, assuming an average of 4 T.U. for the characteristic precipitation. For the Gulf and southwest border, the Hawaiian and Philippine rains (Table 2) and our estimated upper limit for the mixed layer, indicate that average precipitation from such vapor will have about 1 T.U. Also, a measurement on a Puerto Rican river gave 1.1 T.U. (VB-L). Therefore we take the precipitation characteristic of the mean incoming vapor as about 2.5 T.U., and we assume for the incoming vapor $T_i = 2.3 \pm 0.5$ T.U.

About 32 % of the outgoing vapor leaves along the Labrador coast boundary, and about 68 % along the Atlantic coast border, according to the measurements of Benton and Estoque. The characteristic precipitation from Labrador coast vapor is taken as the mean of Greenland snow, and New York precipitation as estimated from rain and wine, or about 9.0 T.U. The Atlantic coast shows a fairly uniform outward flux (Figure 5); we have divided it in half, and taken New York precipitation as characteristic of the northern half, and the mean of New York and estimated Gulf coast precipitation for the southern half, for a mean Atlantic coast precipitation level of 4.75 T.U. Weighting these two means according to the proportions given by Benton and Estoque gives 6.1 T.U. for precipitation from outgoing vapor; and we take $T_o = 5.5 \pm 0.9$ T.U. for the outward vapor transport from the continent.

In Table 4 we summarize the water transport data, the estimated natural tritium concentrations, and the flux of T by each route. The limits of uncertainty indicated for the tritium flux data are those estimated from the tritium concentrations and the uncertainties in averaging and in α; these errors are believed to be much more important than the uncertainties in the Benton and Estoque transport values which probably tend, to some extent, to cancel each other, and which are, in any case, unknown. It should be remembered, however, that these values actually apply only to the year 1949. The removal of tritium by vapor transport is seen to be four times as great as removal by precipitation to the continent.

The net introduction of tritium into the North American troposphere, by tropospheric cosmic ray production and stratospheric mixing, is found to be ϕ_t^* (NA) $= 0.64 \pm .33$ atoms T/cm² sec, for the pre-thermonuclear epoch. We shall use this value to estimate the global tropospheric and total atmospheric production rates of natural tritium.

The gradient flux of tritium into the global troposphere

Prior to entrance into the sea, tritium is introduced into the troposphere by direct cosmic ray production and by stratospheric injection during the downward mixing of stratospheric air across the tropopause. We shall call the sum of these two introduction rates the *gradient flux*, ϕ_t^*, i.e. the mean

Table 4. Values of annual water transport, pre-thermonuclear titrium concentrations, and tritium flux, estimated for North American troposphere.

	Annual net flux H_2O (meters)[1]	Tritium content[2] (T.U.)	Tritium flux[2] (atmos T/cm² sec)
Vapor, sea to land.	$V_i = 0.87$	$T_i = 2.3 \pm 0.5$	$+ 0.42 \pm .08$
Vapor, land to sea.	$V_o = 0.72$	$T_o = 5.5 \pm 0.9$	$- 0.84 \pm .14$
Precipitation	$P = 0.68$	$\left.\begin{array}{l} T_p = 6 \pm 2 \\ T_e = 0.9\, T_p \end{array}\right\}$	$T_p(P - 0.95E) = - 0.22 \pm .07$
Evaporation	$E = 0.53$		
			$\phi^*(\mathrm{NA}) = 0.64 \pm .33$

[1] Data from Benton and Estoque (1954). Evaporation was calculated (a) as the difference between precipitation and estimated continental runoff, $E = 0.50$, and (b) from atmospheric transport data and estimated change of atmospheric reservoir, $E = 0.56$. We have taken the mean of these two values.

[2] Errors shown are calculated for $\alpha = 1.1$, except for the final value of the net T flux where the limits are the total range including the uncertainty in α.

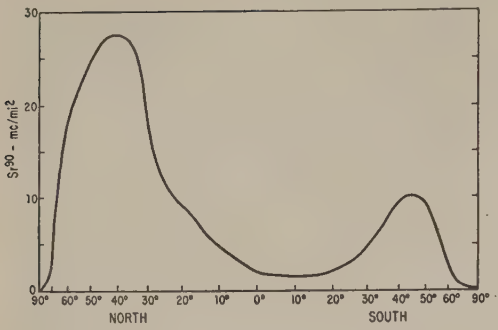

Fig. 6. Stratospheric Sr^{90} deposition through spring, 1958. From Machta and List (1959).

introduction rate exclusive of back mixing from reservoirs farther down the gradient (in this case the sea and the continental standing water).

The steady mixing fluxes of stable and radioactive isotopes from reservoir i to reservoir j are termed ϕ_{i-j} and ϕ^*_{i-j} respectively.

In order to calculate the global tritium production rate $\overline{Q}$, we first need to calculate the tropospheric gradient flux ϕ^*_t from the North American tropospheric gradient flux ϕ^*_t (NA) obtained in the previous section. To evaluate the ratio ϕ^*_t/ϕ^*_t (NA), the distribution of cosmic ray production between stratosphere and troposphere, and the distribution pattern of stratospheric injection into the troposphere, must be known.

In a later section of this paper we calculate $\overline{Q}$ directly from cosmic ray data. The relative production rates in the stratosphere and troposphere can be obtained from the relative star production ratios, independent of the normalization to absolute values, because the triton yield per star does not vary more than 15 % throughout the atmosphere. The tropospheric and total global triton production rates as a function of geomagnetic latitude, assuming constant triton/star ratio, are shown in Figure 9; the integrated fractions of total production in the troposphere and stratosphere are $\overline{Q}_t/\overline{Q} = 1/3$; $\overline{Q}_{st}/\overline{Q} = 2/3$.

The ratios of North American to global production rates are obtained by integrating the star production rates over the continent (30—65° latitude, using the area defined in Figure 4); this can be done with respect to latitude only, because the east-west continental dimension happens to be practically constant over the area considered.[1] The ratios of North American to global star production rates/cm² in the troposphere, stratosphere, and total atmosphere, are then found to be 0.97, 1.67, and 1.40 respectively. Thus the continental shape is such that the North American troposphere is almost a perfect average for global tropospheric production.

The general features of the distribution of stratospheric tritium can be evaluated from the studies on fission products injected into the stratosphere by nuclear weapons because the fission products are removed from the stratosphere by air circulation rather than by gravitational settling. Models for stratospheric-tropospheric mixing have been proposed by LIBBY (1959), MACHTA (MACHTA and LIST, 1959), and MARTELL (1959); a detailed discussion of these models and of the most recent data is given by Martell and reference is made to his paper for details. The minor differences between these models do not affect our discussion which is based on the following general characteristics:

1. The fallout pattern of stratospheric activity shows a pronounced peak at middle latitudes, regardless of the latitude of injection. Figure 6 from MACHTA and LIST (1959) shows the latitudinal distribution of Sr^{90} fallout; practically all of this material is of stratospheric origin (LIBBY, 1959; MARTELL, 1959).

2. The average residence time of material injected into the stratosphere is a function of the injection latitude. The residence time is of the order of 5 years for high altitude equatorial injection, but for middle and high latitude injection it is of the order of 6 months to a year (MARTELL, 1959).

From these observations, it is possible to calculate the approximate ratio of the global and North American tropospheric gradient fluxes for three limiting types of stratospheric tritium injection. For this purpose we may assume that there is no stratospheric decay (cf. the mean residence time derived in the next section) and we take the mean tropospheric production rate in North America as equal to $\bar{Q}_t$ as noted above. Then the tropospheric gradient flux ratio may be written:

---

[1] That is, we integrate $S(\Theta)\,d\Theta$, and compare with $S(\Theta)\cos\Theta\,d\Theta$, where S is the star production rate.

$$\phi_t^*/\phi_t^*\,(\text{NA}) = \bar{Q}/(\bar{Q}_t + F\bar{Q}_{st}) = 3/(1+2F)$$

where F is the ratio of the tritium flux from the stratosphere into the North American troposphere to $\bar{Q}_{st}$. The following limiting cases are readily derived from the parameters discussed above:

1. We assume all stratospheric tritium is injected into the troposphere between latitudes 30 and 90°. Then $F = 2$, and the gradient flux ratio as written above is 0.60.

2. We assume that stratospheric injection occurs at the tropopause at all latitudes with relative rates/cm^2 as given by the Sr^{90} stratospheric fallout curve in Figure 6. From this curve one can see that the mean fallout rate/cm^2 over North America is about three times the rate for the rest of the troposphere. Then $F = 1.5$ and the gradient flux ratio is 0.75.

3. We assume that only the tritium produced in the North American stratosphere is injected into the North American troposphere. Then, as given above, $F = 1.67$ and the gradient flux ratio is 0.69.

Case 1 is the most likely, but in order to have reasonable limits for $\bar{Q}$ we shall take a mean value of ϕ_t^*/ϕ_t^* (NA) $= 0.68 \pm 0.08$. From the value obtained previously for ϕ_t^* (NA), we find the mean flux of tritium into the global troposphere from production and stratospheric injection to be $\phi_t^* = 0.44 \pm .27$ atoms T/cm^2.

Calculation of $\bar{Q}$ from the geochemical inventory

Using the terminology defined at the beginning of the previous section, the steady state tritium balance in the stratosphere is given by:

$$\bar{Q}_{st} + \phi^*_{t-st} = \phi^*_{st-t} + \lambda N^*_{st}$$

The back flux from the troposphere, ϕ^*_{t-st}, is completely negligible because of the very small amount of water in the stratosphere. If internal mixing in the stratosphere is rapid enough, relative to the decay constant λ, so that significant tritium gradients are not present, then we may write $\phi^*_{st-t} = N^*_{st}\phi_{st-t}/N_{st}$, where the * signifies the radioactive, low concentration, isotope and the unstarred terms refer to the stable species. We also write $N_{st}/\phi_{st-t} = \tau_{st}$, the residence time or average life of a water molecule in the stratosphere relative to exchange into the troposphere. The stratospheric balance equation may then be written:

$$\bar{Q}_{st} = \phi^*_{st-t}(1 + \lambda\tau_{st})$$

in which we have only assumed that tritium obeys first order kinetics because of its low concentration and rapid internal mixing. The gradient flux of tritium into the troposphere is the sum of the tropospheric production rate and the mixing rate from the stratosphere, and remembering the proportionality factors between total, tropospheric, and stratospheric cosmic ray production rates deduced earlier, we have, finally:

$$\frac{\phi_t^*}{\bar{Q}} = \frac{1}{3} + \frac{2}{3}\left[\frac{\tau_r}{\tau_r + \tau_{st}}\right]$$

where ϕ_t^* is the mean global tropospheric gradient flux calculated in the last section, and we have written λ^{-1} as τ_r, the mean radioactive life (18.0 years).

As discussed in the previous section, the fallout studies indicate a variation of the stratospheric residence time with the latitude of injection into the stratosphere (MARTELL, 1959). We have therefore assumed a graded series of stratospheric residence times over four latitude intervals, based on Martell's work, and we apply these factors to the relative fractions of stratospheric tritium produced by cosmic rays in these intervals, as evaluated from the latitudinal production curves given in Figure 9 in a following section. The assumed intervals, residence times, and stratospheric production fractions are as follows:

Latitude Interval	Residence time, τ_{st}	Fraction of total Stratospheric Production
0—20°	6 ± 2 years	8 %
20—30°	3 ± 1 years	7 %
30—45°	1.5 ± .5 years	20 %
> 45°	1.0 ± .3 years	65 %

The mean residence time for stratospheric tritium, relative to removal to the troposphere, is then found to be 1.6 ±0.5 years, in which we have used the maximum limits given above. Therefore only 8 % of the tritium produced in the stratosphere decays in the stratosphere and 92 % is injected into the troposphere.

From the stratospheric balance equation and the mean residence time we then have $\overline{Q} = (1.06 \pm .02)\ \phi_t^*$, and with the gradient flux obtained in the last section we obtain: $\overline{Q} = 0.46^{+.34}_{-.26}$ atoms T/cm² sec as the mean global production rate calculated from the geochemical inventory. The errors assigned in the various stages have been kept as maximum deviations, rather than combined as statistical errors, and we take in round numbers $\overline{Q} = 0.5 \pm 0.3$.

The single most serious assumption in this calculation seems to us to be that the average North American precipitation tritium level can be taken as the Chicago and New York mean, plus or minus 2 T.U. Our study of the precipitation data and the isohydrogram leads us to believe these limits are justified.[1] We turn now to the calculation of $\overline{Q}$ from the cosmic ray and nuclear cross section data, independent of the inventory.

Calculation of $\overline{Q}$ from cosmic ray data

The cosmic ray production rate of tritium has been calculated directly by Fireman and Rowland (1955) and by Currie *et al.* (1956) who obtained values of 0.2 and 0.14 tritons/cm² sec. Benioff (1957) recalculated the tritium production rate using the theories of nucleonic cascade development in the atmosphere, and obtained a slightly higher value of 0.31 atoms/cm² sec. Simpson (1960) has estimated that the low energy (~ 100 Mev) solar protons incident at the polar regions following solar flares may produce about 3 times the global amount produced by cosmic rays. Wilson and Fergusson (1960) estimated the tritium production rate in the atmosphere from the observed T contents of stone meteorites, and also calculated the atmospheric production rate using the theoretical production rate of helium in iron meteorites (Martin, 1953) and nuclear evaporation theory. These calculations gave values of $.63^{+.40}_{-.20}$ and 1.3 ± 0.5 tritons/cm² sec. Their calculations require knowledge of several factors necessary to transform the production rate in a meteorite to that in the atmosphere; the choice of the parameters is quite arbitrary and with a reasonable set of numbers, one can easily obtain values smaller by a factor of five. A calculation of this type therefore turns out to be very inaccurate and not very meaningful.

Fireman and Rowland, and Currie *et al.* used the available cross sections for the formation of tritium in nitrogen and oxygen in bombardments by protons of 450 MeV and 2 Bev, and in nitrogen by fission neutrons above 4.4 Mev. Recently, tritium cross sections have become available for medium energy protons (Honda and Lal, 1960) as well as for very high energy protons (Currie, 1959). These values combined with cosmic ray data, particularly the recently studied neutron energy spectrum in the atmosphere, suffice to make fairly reliable estimates of tritium production in the atmosphere.

Tritium production takes place principally in the nuclear disintegrations of atmospheric nitrogen and oxygen. The nuclear interactions can be produced by the nucleonic component (neutrons and protons) and by the weakly interacting component consisting of fast and slow mesons, and photons. The abundance of μ mesons and photons is known fairly well for atmospheric depths greater than 100 gm cm⁻². No cross sections for tritium production in their interactions have been measured as yet, but we can estimate reasonable values for the total rates of all interactions caused by these particles in the atmosphere. With conservative estimates of the yield of tritium in stars produced by μ mesons and photons, it is found that tritium production by these particles is smaller by two orders of magnitude than the amount produced by the nucleonic component; thus the inherent large uncertainties in these calculations are not serious and we need only consider the production by neutrons and protons.

---

[1] Begemann (1959) has calculated $\overline{Q}$ from his Greenland snow data, assuming all tritium formed over Greenland in the troposphere precipitates there and none is carried in by vapor. It is impossible to estimate the reliability of this value since no vapor transport data are available and his samples are from only the northwest fringe of the continent. He has assumed $\tau_{st} = 10$ years, and we only wish to point out that the use of the residence time we assume would make his value of Q become 0.5.

Tritium production by the nuclear component

The rate of occurrence of nuclear disintegrations (stars) in the atmosphere has been calculated as a function of altitude and latitude by Lal *et al.* (1958) using only the experimentally determined cosmic ray data. The relative variations within the atmosphere are based on the extensive data on slow neutrons and stars. Absolute star production rates were obtained by normalization at the point 680 gm cm^{-2}, $\lambda = 50°$, where star production rates in a nitrogen and argon filled cloud chamber have been determined (Brown, 1954). Measurements of the Be^7 production rate in oxygen at Echo Lake ($\lambda = 50°$, 685 gm cm^{-2}) and the excitation function of Be^7 in nitrogen and oxygen (Honda and Lal, 1960) have now shown that the normalization value for stars as used by Lal *et al.* (1958) is correct within ± 20 %. We will use their calculated star production rate together with the tritium yield per star for different positions in the atmosphere. The star production rate refers primarily to nuclear disintegrations produced by nucleons of energy above 40 Mev. Appreciable tritium production also occurs by lower energy nucleons because the thresholds in nitrogen and oxygen are 4.4 Mev and 15 Mev respectively (Currie *et al.*, 1957). The tritium yield per star is calculated below using (a) the excitation function of tritium in air, and (b) the nucleon energy spectrum in the atmosphere.

The average cross sections, per atom, for tritium production in the bombardment of a mixture of nitrogen and oxygen having the composition of air are plotted in Figure 7. The errors in the cross sections are ~ 20 %. The cross section data are fairly well spaced above 225 MeV and permit a reasonable interpolation. Below 225 Mev the only available measurement is in nitrogen for fission neutrons above 4.4 Mev. The mean neutron energy is estimated to be 5.7 Mev (Currie *et al.*, 1957). At this energy the average cross section for air nuclei is obtained by multiplying the nitrogen cross section by 0.78 because tritium production does not occur in oxygen below 15 MeV. The dotted line in Figure 7 shows the interpolation made between 5.7 MeV and 225 MeV.

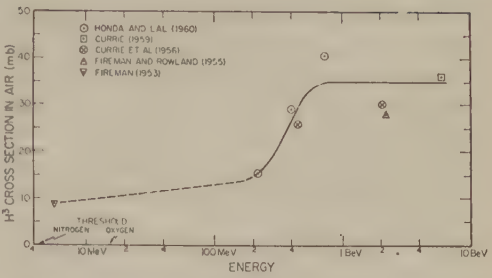

Fig. 7. Excitation function of tritium in air. Note: the value of Fireman and Rowland should be increased by about 20 % (to atomic values of 33 ± 4 mb for N and 39 ± 4 mb for O) because of recent revisions in the cross section for their monitor reaction Al^{27} $(p, 3pn)$ Na^{24} (Rowland, personal communication).

The differential energy spectrum of neutrons and protons has been measured at atmospheric depths greater than 200 gm cm^{-2}. Various measurements show that nucleons of energy below 500 MeV are in equilibrium for depths greater than 200 gm cm^{-2}; the shape of the energy spectrum below 500 MeV remains unaltered throughout the equilibrium region at all latitudes and altitudes. The relative variations in intensity can be obtained from the data on slow neutrons (Soberman, 1956; Hess *et al.*, 1959). The nucleon flux for $\lambda = 50°$, 680 gm cm^{-2}, is plotted in Figure 8. The ordinate shows the integrated flux, J, of nucleons passing through a unit sphere (particles/cm^2 MeV sec), i.e.

$$J = 2\pi \int_0^{\pi/2} J_\theta \sin\theta \; d\theta$$

where J_θ represents the intensity (cm^{-2} sec^{-1} sterad^{-1} MeV^{-1}) at azimuth angle θ. The number of interactions per gram is then given by $JN\sigma$, where N is the number of atoms/gm and σ is the cross section for the interaction.

The results of the vertical proton flux determinations agree within the experimental errors (Mylroi and Wilson, 1951; Filthuth, 1955; Puppi, 1956). The angular dependence of the flux is given by Conversi and Rothwell (1954). In the case of neutrons, the agreement between the various data is not as good. Curve I in Figure 8 shows the energy spectrum of neutrons from 1 MeV to 2 BeV as obtained

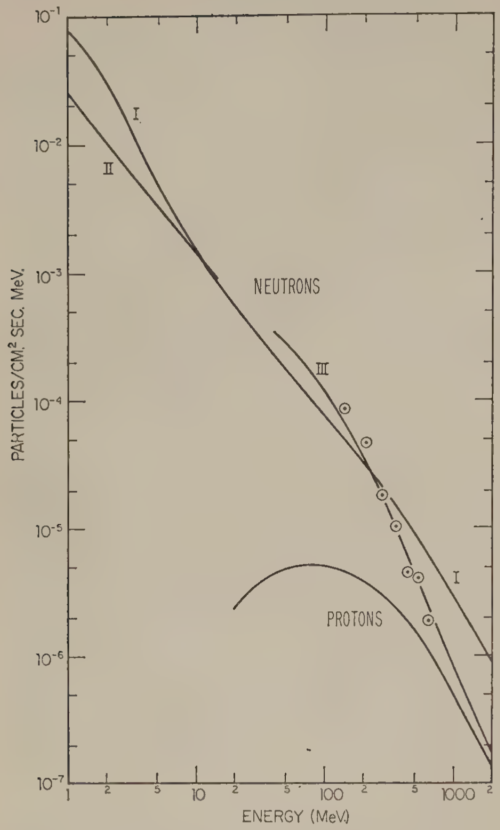

Fig. 8. Differential energy spectrum of nucleons in the atmosphere at $\lambda = 50°$, 680 gm cm^{-2}.

by Hess *et al.* (1959). These workers employed several calibrated detectors of varying sensitivity to neutron energies from thermal to few hundred MeV. The shape of the spectrum was determined by trial and error functions which matched the total counting rates of the detectors, and production rate of stars in nuclear emulsions. Curve II shows the neutron energy spectrum as measured by Miyake *et al.* (1957) using proton recoils in a high pressure hydrogen cloud chamber.

The circled points were obtained (Lal, 1958) using the proton energy spectrum and the relative frequency of neutron and proton induced stars of different sizes in nuclear emulsions (Brown *et al.*, 1949; Barford and Davis, 1952). The average energy $\bar{E}$, of nucleons producing a star of N prongs was calculated using the empirical relation $\bar{E} = 37N + 4N^2$ (Brown *et al.*, 1949). This relation holds for stars where the energy of no emitted particle exceeds 350 MeV. The solid curve III drawn through these points has been extended to 40 MeV using the data on the production spectrum of protons in stars (Camerini *et al.*, 1949; Lal, 1958). Curve III approaches the proton energy spectrum at $E > 1$ BeV, as anticipated, because the production spectra of neutrons and protons are expected to be identical for energies well above the coulomb barrier. Above 1 BeV absorption or loss of energy occurs only by nuclear interactions, while at the lower end of the spectrum neutrons are more abundant than protons as the latter are depleted by ionization losses. Curve I departs considerably from the expected behavior above 500 MeV.

The yield of tritium per star depends on the shape of the energy spectrum, and we have therefore calculated the tritium yields separately for these spectra in order to estimate the errors introduced. The average cross section for the formation of tritium in stars above 40 MeV was calculated by the relation:

$$\bar{\sigma}_T = \frac{\int_{40}^{\infty} \sigma_T(E)\, J(E)\, dE}{\int_{40}^{\infty} J(E)\, dE}$$

where $J(E)$ represents the differential energy spectrum of nucleons (particles/cm² sec MeV) as given in Figure 8. The total nucleon flux $J_{n+p}(>40)$, above 40 MeV and $\bar{\sigma}_T$ are tabulated separately for the neutron spectrum I and III in Table 5. In the same table, we also give the tritium yield in stars, Y_T, obtained by dividing $\bar{\sigma}_T$ by σ_S, the average cross section for star production. The value of σ_S in air is estimated[1] to be 225 ± 20 mb, by subtracting the cross sections for the nuclear reactions involving emission of neutrons only (which lead to zero pronged stars) from the total inelastic cross section in nitrogen and oxygen.

The ratio of the amounts of tritium produced

---

[1] Support for this value is obtained from the measurements of cross sections in C, N and O nuclei of emulsions by protons of energy 40 MeV—900 MeV (Lock and March, 1955, and references therein). The average cross sections for 45—100, 240, 600, and 950 MeV protons were found to be 170 ± 20, 230 ± 30, 222 ± 60 and 202 ± 50 mb respectively.

Table 5. Tritium production parameters (see text).

Neutron energy spectrum	J_{p+n} (> 40) (cm^{-2} sec^{-1})	$\bar{\sigma}_T$ (mb)	Y_T (> 40)	R	$Y_T(1 + R)$
Curve I....................	$27.6 \times 10^{-3*}$	21.3	9.5 %	0.52	14.4 %
Curve III..................	$27.5 \times 10^{-3*}$	16.3	7.2 %	0.66	12 %
Average....................	27.5×10^{-3}	18.8 ± 2.5	8.4 ± 1.2	0.59 ± .07	13.2 ± 1.2 %

* Though the shape of the energy spectra I and III differ significantly, the total fluxes above 40 MeV agree very well. The star production rate at 680 gm cm^{-2}, $\lambda = 50°$, is found to be 2.5×10^{-4} stars/gm air sec, which should be compared with the value of $2.3 \; 10^{-4}$ used in the calculations by Lal *et al.* (1958).

below and above 40 MeV, *R*, is given in the fifth column of Table 5. The spectrum used below 40 MeV for Curve III was obtained by extrapolating through the curves I and II. The total tritium production due to nucleons of $E > 5$ Mev, $Y_T(1 + R)$, is found to be 13.2 % ± 1.2 % in stars (Table 5).

As mentioned earlier, these calculations apply for all latitudes and altitudes in the equilibrium region of the atmosphere. No measurements of nucleon energy spectrum are available for depths < 200 gm cm^{-2}. The energy spectrum is expected to be flatter near the top, and the tritium yield per star will consequently be higher. For this region we have calculated the total tritium yield per star under the following assumptions:

(a) The ratio of the neutron flux, $5 < E < 40$ MeV to total remains constant throughout the atmosphere. The tritium cross section in this energy interval remains essentially constant and no error is introduced by using the same energy spectrum as in the equilibrium region.

(b) The shape of the energy spectrum in the non-equilibrium region can be obtained by comparing the star size distributions. Star size distributions at several latitudes and altitudes are available (Birnbaum *et al.*, 1952; Lal *et al.*, 1958).

We find that the total tritium produced per star at depths < 200 gm cm^{-2} is larger than the value for the equilibrium region of the atmosphere by 15 % and 7 % in low and medium latitudes respectively. Considering the absolute rates of star production in different regions of the atmosphere, the average tritium produced per star in the entire atmosphere is effectively 8 % higher than the calculated value for the equilibrium region.

The global star production rate in the atmosphere has been estimated to be 1.7 stars/cm^2 sec (Lal *et al.*, 1958). The corresponding rate of tritium production is therefore $1.7 \times 0.13 \times 1.08 = 0.24$. The uncertainty in this value[1] is probably less than ± 30 %, i.e. ± 0.07.

The approximate distribution between tropospheric and total atmospheric triton production as a function of geomagnetic latitude is shown in Figure 9, in which the T production rates have been plotted by assuming constant proportionality to the star production rates. Integration of these curves shows that about $^2/_3$ of the total global tritium production

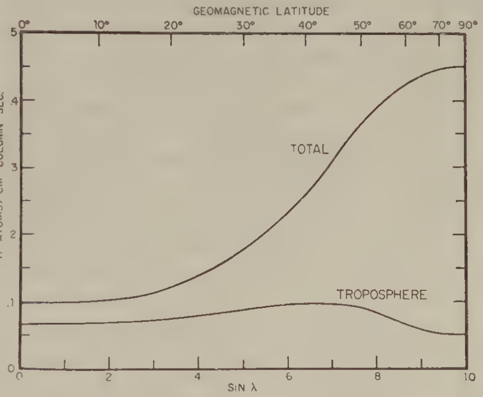

Fig. 9. Calculated tritium production rate in a cm^2 column to the top of the atmosphere ("total" curve) and up to the tropopause ("troposphere" curve), vs. geomagnetic latitude.

---

[1] It has so far been assumed that the star production rate obtained by Lal *et al.* (1958) refers to stars produced by nucleons above 40 MeV. The production rate of stars below 40 MeV is small since the star production cross section is expected to fall rapidly below 30—40 MeV. In order to estimate the uncertainty due to the cut off energy used in the calculation, we have made the unlikely extreme assumption that the star production cross section in air is 225 mb up to 25 MeV. This would lower the tritium per star value by 18 %.

Table 6. Comparison of $\bar{Q}$ values calculated from cosmic ray and nuclear data.

Energy Region (MeV)	Global production rate of T (atoms/cm² sec)			
	Present Work	Currie *et al.* (1956)	Fireman & Rowland (1955)	Benioff (1957)
< 10	0.04	0.05	0.1*	0.05**
10—40	0.05	0.01 (for 10—100 MeV)	0.1	0.26
> 40	0.15	0.082		
Total $\bar{Q}$	0.24 ± 0.07	$0.14^{0.22}_{0.09}$	0.2	$0.31^{0.45}_{0.15}$

* Fireman and Rowland estimated a value of 0.1 for slow neutrons without specifying the energy range considered. Part of this production belongs to neutrons of ~ 10 MeV.

** Benioff used the value of Currie *et al.* (1956) for < 10 MeV.

takes place in the stratosphere and $^1/_3$ in the troposphere. These data were used earlier to calculate $\bar{Q}$ from the gradient flux into the North American troposphere.

The value of $\bar{Q}$ obtained here is compared with previous calculations in Table 6. Within the calculation errors, the various estimates are seen to be in good agrement. The mean value of Currie *et al.* is the lowest and this can be ascribed to their underestimating the contribution to production by 10—100 MeV nucleons. Our calculations yield a value of 0.1 for this region compared to the value of 0.01 estimated by Currie *et al.* Taking this into account, their value becomes 0.23, in good agreement with ours.

Time variations in $\bar{Q}$, and the mean $\bar{Q}$ value over the solar cycle

The incident cosmic ray intensity varies with time due to solar modulations in space. The variation has been shown to be inversely correlated with the 11-year sunspot cycle. The changes brought about in the energy spectrum of primary cosmic rays, as well as those in the neutron counting rates at different depths in the atmosphere, have been studied fairly extensively between 1954 (sunspot minimum) and 1958 (sunspot maximum). The changes during 1956 and 1958 with respect to 1954, when cosmic ray intensity was maximum, are shown in Figure 10. For a detailed discussion see LAL and PETERS (1960).

The calculations of LAL *et al.* (1958) of the star production rate were based on the cosmic ray data obtained during 1948—1949, a period close to the maximum in a sunpot cycle. It can be seen from Figure 10 that during 1958 solar activity was unusually high and the cosmic ray intensity was therefore abnormally low. The mean yearly sunspot numbers in 1958 are in fact higher than observed in any year during the last 200 years for which measurements are available. The sunspot activity during 1948—49 and 1956 is nearly the same, and we have therefore assumed that the primary cosmic ray spectrum during these years was nearly the same. The changes with time in total tritium production rate in a 1 cm² atmospheric column, ΔI, can be calculated from the corresponding change ΔP in the primary cosmic ray flux:

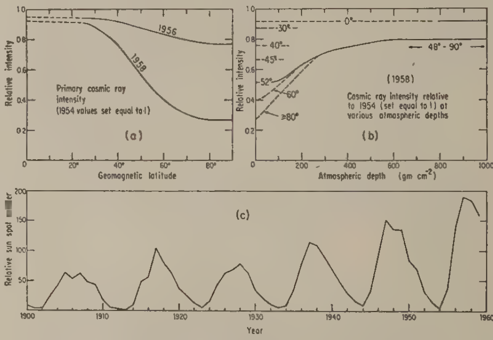

Fig. 10. (a) Primary cosmic ray intensity during 1956 and 1958, relative to 1954 values, vs. geomagnetic latitude. (b) Cosmic ray intensity during 1958 relative to 1954 values, plotted vs. atmospheric pressure for several latitudes. (c) Relative annual sunspot numbers from 1900—1959.

$$\Delta I = \frac{\left(\frac{\partial I}{\partial \lambda}\right)}{\left(\frac{\partial P}{\partial \lambda}\right)} \Delta P$$

The derivatives of the total tritium production rate and the primary cosmic ray intensity with respect to latitude, $\partial I/\partial\lambda$ and $\partial P/\partial\lambda$ are known (LAL *et al.*, 1958; MCDONALD, 1959). We find that the mean global production rates during 1958 and 1954 were respectively 22 % lower and 9 % higher than during 1948—49 (or 1956).

From the available solar data, we find that the maximum and minimum sunspot activities during a typical cycle are close to that observed during 1956 and 1954 respectively. Since we estimate that the global tritium production rate during 1954 was higher than in 1956 by 9 %, the average deviation amounts to ± 4.5 %. The calculated value of 0.24 for $\overline{Q}$ refers to 1948—1949 (or 1956) and the average value during a typical solar cycle becomes, $\overline{Q} = 0.24 \times 1.05 = 0.25 \pm 0.08$ T atoms/cm^2 sec

Tritium production by solar protons

Recently it has been found that the occurrence of solar flares which give rise to a substantial flux of low energy protons is quite frequent. The number of such flares has been estimated to be about 20 for the period May 1957—July 1959, based on the measurements of cosmic radio noise absorption in the polar regions. The proton flux in some events is believed to have reached levels of 10^6 times the normal cosmic ray level for a few hours. The average numbers of protons incident at the poles (cm^{-2}, yr^{-1}) have been estimated to be 10^{10} and 10^8 respectively for protons above 30 and 100 MeV respectively (K. A. ANDERSON, private communication). The zone of incidence of protons depends on their energy. For conservative estimates of tritium production by solar protons we have taken the flux of protons above 30 MeV and assumed that they arrive down to 60° geomagnetic latitude where the cut-off under normal conditions is 400 MeV. (FREIER *et al.*, 1959, have reported that over short periods, particles of lower rigidities than the cut-off values were incident at Minnesota following a solar flare.) The average T cross section was taken to be 10 mb and the average range of protons was estimated to be 1.5 gm cm^{-2}, taking for the differential energy spectrum of protons a slope of 4.5 (ANDERSON *et al.*, 1959).

The calculated solar flare production rate of tritium in the polar region is found to be 0.20 atoms/cm^2 sec. This corresponds to an increase of 45 % in the tritium production rate in the polar region (see Figure 9). The corresponding change in the global value is only about 10 % because of the small area involved. The uncertainty in this calculation is very large due to very limited knowledge of particles accelerated in solar flares. Furthermore, the data are based on observations during unusually high solar activity. The solar proton flux should probably exhibit a positive correlation with the solar activity, in which case the present calculations would not be typical of normal conditions. A 10 % increase in $\overline{Q}$ during say 4 years at the peak of a sunspot cycle would amount to only a 3 % increase in the mean production rate averaged over the solar cycle.

Two independent arguments lead to the conclusion that solar flares do not produce appreciable changes in the average production rate of tritium:

(a) BEGEMANN (1959) has measured T contents of dated Greenland snows covering approximately one solar cycle period. Within the errors of measurements (± 15 %) the tritium fall-out is found to be constant. A slight indication of negative correlation with the solar activity may be present.[1] The data at least rule out any large contributions by solar flares, in which case a positive correlation should be seen.

(b) The hypothesis of substantial tritium production by solar protons can be checked by studies of the C^{14} production rate, which must be affected more greatly. The polar flux of solar protons above 10 MeV has been estimated to be 10^{12}/cm^2 yr (K. A. ANDERSON, private communication). The production rate of C^{14} due to secondary neutrons produced by protons can be estimated from the behavior of (p, n) cross sections in light nuclei. We find that the global production rate of C^{14} due to solar protons is about the same as that calculated from cosmic ray neutrons. This seems extremely unlikely since the C^{14} inventory checks closely with the estimated cosmic ray production rate (CRAIG and LAL, in press).

---

[1] BEGEMANN calculated a yearly production rate from the specific activities obtained from the thickness of each annual snow layer. However, PETTERSSEN, JACOBS, and HAYNES (1956) have pointed out that in general the snow cover in Greenland at any place and time bears no fixed relation to the actual amount of precipitation because of extensive drifting. Their tables 17 and 18 show large deviations at Thule, both positive and negative, between monthly snowfall and mean monthly snow cover. A somewhat different plot of Begemann's data is obtained if one assumes constant annual precipitation; four layers before the sunspot peak are rather uniformly higher than four layers after the peak. The true situation can only be determined by a large number of such analyses from different sites.

Our present conclusion is that the mean global production rate of tritium over an average cycle is not significantly increased by solar flare activity relative to the limits of uncertainty assigned to the value calculated from cosmic ray data.

Summary and conclusions

1. Deuterium and tritium analyses of precipitation from Chicago, Greenland, and Pacific islands, indicate a rather consistent general relationship between these isotopes in fresh precipitation, when no synthetic tritium from thermonuclear explosions is present. The general relationship reflects the balance between continuous injection of cosmic ray tritium, discontinuous preferential removal of the heavy isotopes in precipitation, and mixing.

2. The global mean production rate of natural tritium, calculated from the tritium and water balance in the North American troposphere, is $\overline{Q} = 0.5 \pm 0.3$ atoms T/cm² sec. The principal assumption is that the tritium content of the mean continental precipitation is given by the Chicago and New York means (excluding contaminated samples) of 6 ± 2 T.U. Within these limits the assumption seems justified.

3. The present value is three to four times lower than values obtained previously by similar calculations. This is due to the following factors:

a) Pre-Castle tritium data have previously been assumed to represent uncontaminated natural conditions. Our present analysis, based on both deuterium and tritium analyses, indicates that fallout of artificial tritium was already important in 1953 when most of the pre-Castle data were obtained. The available uncontaminated tritium data reduce to three sets of precipitation, from Chicago, Greenland, and Pacific islands, two samples of Arkansas precipitation, and vintage wines from New York, France and Spain, excluding data from lakes and reservoirs. Except for the Greenland snow, the precipitation samples are confined to the seven month "clean period" from 1 January to 1 August, 1953.

b) The residence time of stratospheric air has previously been taken as about 10 years based on early estimates from Sr^{90} fallout. Recent studies by Martell, Libby, and Machta, indicate significantly lower times which thus decrease the calculated decay of tritium in the atmosphere. The stratospheric residence time is a function of latitude; in this paper we consider the latitudinal variation in both residence time and stratospheric production rate of tritium, and conclude that the mean stratospheric tritium residence time is about 1.6 years.

c) The recent discovery of preferential concentration of stratospheric fallout at medium and high latitudes shows that the North American average influx rate must be significantly higher than the global average.

4. A detailed calculation of the cosmic ray production rate based on cosmic ray and nuclear cross section data gives a predicted mean global production rate of 0.25 ± 0.08 atoms T/cm² sec. The variation in the production rate over a mean solar cycle, due to the effect of the solar activity maxima on the cosmic ray flux, is found to be ± about 5 %.

5. The production rate calculated from the observed tritium concentrations agrees with that predicted from cosmic ray data within the limits of uncertainty in the calculations and the data. We thus conclude that there is no observational evidence for accretion of tritium from extraterrestrial sources.

Acknowledgements

We are deeply indebted to Dr. B. Peters for detailed discussions of most of the material in this paper. Dr. Peters had independently concluded that the pre-Castle tritium data included significant contamination from thermonuclear testing and that the tritium concentrations observed during the "clean period" are consistent with the production rate calculated from cosmic ray data. Drs. Libby, Kaufman, von Buttlar, and Begemann provided the precipitation samples which they had analyzed for tritium content, and the senior author has had the benefit of many discussions with them. The research on deuterium variations was done in Dr. Harold C. Urey's laboratories at the University of Chicago and was supported by the National Science Foundation and the U.S. Atomic Energy Commission. We are grateful to Dr. A. Bainbridge and Dr. F. Begemann for criticism of the manuscript of this paper.

REFERENCES

Anderson, K. A., Arnoldy, R., Hoffman, R., Petterson, L. E., and Winckler, J. R., 1959: *Bull. Am. Phys. Soc.* **4**, p. 238.

Barford, N. C., and Davis, G., 1952: *Proc. Roy. Soc.* **A 214**, p. 225.

Begemann, F., 1956: Nuclear Processes in Geologic Settings, National Academy of Sciences — *National Research Council Publication* **400**, p. 166.

Begemann, F., 1959: *Z. Naturforsch.* **14a**, 334. Tritium analyses of the 1916 and 1940 Greenland snow are given in his Air Force Report of 31 December 1957, University of Chicago.

Begemann, F., and Libby, W. F., 1957: *Geochim. et Cosmochim. Acta* **12**, p. 277.

Beinoff, P. A., 1957: *Proceedings of Conference on Recent Research in Climatology*, Ed. H. Craig, Univ. Calif. La Jolla, p. 74.

Benton, G. S., and Estoque, M. A., 1954: *Jour. Meteorology* **11**, p. 462.

Birnbaum, M., Shapiro, M. M., Stiller, B., and O'Dell, F. W., 1952: *Phys. Rev.* **86**, p. 86.

Bolin, B., 1958: *Proc. Second U.N. Int. Conf. Peaceful Uses Atomic Energy* **18**, p. 336.

Brown, R. H., Camerini, V., Fowler, P. H., Heitler, H., King, D. T., and Powell, C. F., 1949: *Phil. Mag.* **40**, p. 862.

Brown, R. M., and Grummitt, W. E., 1956: *Can. Jour. Chem.* **34**, p. 220.

Brown, W. W., 1954: *Phys. Rev.* **93**, p. 528.

Camerini, V., Coor, T., Davies, J. H., Fowler, P. H., Lock, W. O., Muirhead, H., and Tobin, N., 1949: *Phil. Mag.* **40**, p. 1073.

Cameron, A. G. W., 1959: *Can. Jour. Phys.* **37**, p. 322.

Conversi, M., and Rothwell, P., 1954: *Nuovo Cimento* **12**, p. 191.

Craig, H., 1957: *Phys. Rev.* **105**, p. 1125.

— 1960: *Science* (in press).

— 1960: (in press)

Craig, H., White, D. E., and Boato, G., 1956: Nuclear Processes in Geologic Settings, *National Academy of Sciences — National Research Council Publication* **400**, p. 29.

Currie, L. A., 1959: *Phys. Rev.* **114**, p. 878.

Currie, L. A., Libby, W. F., and Wolfgang, R. L., 1956: *Phys. Rev.* **10**, p. 1557.

Epstein, S., and Mayeda, T., 1953: *Geochim. et Cosmochim. Acta* **4**, p. 213.

Filthuth, H., 1955: *Z. Naturforschg.* **10a**, p. 219.

Fireman, E. L., and Rowland, F. S., 1955: *Phys. Rev.* **97**, p. 780.

Freier, P. S., Ney, E. P., and Winckler, J. R., 1959: *Phys. Rev.* (letters) **3**, p. 183.

Giletti, B. J., Bazan, F., and Kulp, J. L., 1958: *Trans. Am. Geophys. Union* **39**, p. 807.

Hess, W. N., Petterson, H. W., Wallace, R., and Chupp, E. L., 1959: *Phys. Rev.* **116**, p. 445.

Honda, M., and Lal, D., 1960: *Phys. Rev.* (In press).

Kaufman, S., and Libby, W. F., 1954: *Phys. Rev.* **93**, p. 1337.

Lal, D., 1958: *Investigations of Nuclear Interactions produced by Cosmic Rays* (Thesis, unpublished), Tata Institute, Bombay.

Lal, D., Malhotra, P. K., and Peters, B., 1958: *Jour. Atm. Terrest. Phys.* **12**, p. 306.

Lal, D., and Peters, B., 1960: *Progress in Cosmic Ray Physics* (to be published).

Lal, D., Rama, and Zutshi, P. K., 1960: *Jour. Geophys. Res.* **65**, p. 669.

Libby, W. F., 1959: *Proc. Nat. Acad. Sci.* **45**, p. 959.

Lock, W. O., and March, P. V., 1955: *Proc. Roy. Soc.* **A 230**, p. 222.

Machta, L., and List, R. J., 1959: *Fallout from Nuclear Weapons Tests*, Hearings of Subcomm. Radiation, Joint Comm. Atomic Energy, U.S. Congress, May 5—8, 1959, U.S. Govt. Printing Office, Washington, D.C., p. 742.

Martell, E. A., 1959: *Science* **129**, p. 1197.

Martin, D., 1953: *Geochim. et Cosmochim. Acta* **3**, p. 288.

McDonald, F. B., 1959: *Phys. Rev.* **116**, p. 462.

Miyake, S., Hinotani, K., and Nunogaki, K., 1957: *Jour. Phys. Soc.* (Japan) **12**, p. 113.

Mylroi, M. G., and Wilson, J. G., 1951: *Proc. Phys. Soc.* **A 64**, p. 404.

Petterssen, S., Jacobs, W. C., and Haynes, B. C., 1956: *Meteorology of the Arctic*, U.S. Navy, Washington, D.C.

Puppi, G., 1956: *Progress in Cosmic Ray Physics III*, North Holland Publishing Co., p. 341.

Reed, W. W., 1941: *Climate and Man*, U.S. Dept. Agriculture, Washington, D. C., p. 665.

Sepall, O. and Mason, S. G., 1960: *Can. J. Chem.* **38**, p. 2024.

Simpson, J. A., 1960: *Jour. Geophys. Res.* **65**, p. 1615.

Soberman, R. K., 1956: *Phys. Rev.* **102**, p. 1399.

Telegadas, K., 1959: *Announced Nuclear Detonations*, Office of Meteorological Research, U.S. Weather Bureau, Washington, D.C., 16 pp.

Von Buttlar, H., and Libby, W. F., 1955: *Jour. Inorg. Nucl. Chem.* **1**, p. 75.

Wilson, A. T., and Fergusson, G. J., 1960: *Geochim. et Cosmochim. Acta* **18**, p. 273.

PRINTED IN SWEDEN
ESSELTE, STHLM 61

Reprinted from
B. Chr. Christensen and B. Buchmann (editors),
Progress in Photobiology
Proceedings of the 3rd International Congress on Photobiology, 1960. pp.189-196.

PHOTORECEPTION OF A PLANKTONIC CRUSTACEAN IN RELATION TO LIGHT PENETRATION IN THE SEA

BRIAN P. BODEN, ELIZABETH M. KAMPA AND BERNARD C. ABBOTT

Scripps Institution of Oceanography, University of California, La Jolla, Calif. (U.S.A.)

For several years we have been concerned with the ecology of the euphausiid crustaceans and, in particular, with their photobiology. This paper summarizes our findings and presents some of our thoughts on the subject at this time.

We need not elaborate again the arguments for using the migratory sonic-scattering layer in the coastal waters off San Diego as an indication of the depth at which euphausiids may be found. The works of Boden[1] and Tucker[12], as well as our collections from 1954 to 1960, have shown that when a scattering layer can be detected in the area, euphausiids will be in it, and that when the layer splits at sunset, euphausiids are present in the upper part of the layer.

The depth of this migratory scattering layer off San Diego is associated with the depth of an isolume (about $1 \cdot 10^{-4}$ μWatts/cm^2) as detected by a 931-A multiplier phototube (Kampa and Boden[2]). This association is especially close during the rapid migration of the layer at twilight.

In 1955, we first used our present bathyphotometers (Boden, Kampa and Snodgrass[3]), and the response of these is rapid enough that we have been able to show that the light within the scattering layer is modified by the luminescence of the animals themselves (Kampa and Boden[4]; Boden and Kampa[5]). The luminescence is greatest during the vertical migrations of the animals at twilight when their association with the constant level of transmitted sun- and sky-light is most marked. The luminescence appears on the bathyphotometer record as a mass of flashes, often of such frequency and intensity as to cause an apparent increase of ambient light with depth. The animal light is blue-green in color with an energy spectrum that peaks near 478 mμ.

In the laboratory we have measured the luminescence of three euphausiid species from separate genera: *Euphausia pacifica* (Kampa and Boden[4]), *Thysanoëssa raschii* (Boden and Kampa[6]), and *Meganyctiphanes norvegica* (unpublished results). The emission curve is bimodal in each species, with a sharp primary peak near 476 mμ and a second lower peak between 520 and 540 mμ. The intensity of the glow from an individual is about 20 times the intensity of transmitted skylight with which the scattering layer is associated.

A photosensitive pigment, which we have called euphausiopsin, has been extracted in aqueous solution from dark-adapted eyes of euphausiids from Californian coastal waters (Kampa[7]), and its presence in *Meganyctiphanes norvegica* has been reported by Dartnall (1957, personal communication) and Fisher and Goldie[8]. The pigment

References p. 196

Contributions from the Scripps Institution of Oceanography, New Series., 1307.

Reproduced by Permission

absorbs light maximally between 460 and 465 mμ, and it is bleached by light to release first retinene (Fisher and Goldie[8]) and then vitamin A (Kampa[7]).

The new material which we should like to present here is twofold. At sea, we have examined the spectral characteristics of the light in the water column above the sonic-scattering layer and the changes in this spectrum during the twilight migrations of the layer. In the laboratory, we have begun electrophysiological measurements of the sensitivity of the euphausiid eye.

PHYSICAL MEASUREMENTS AT SEA

The photometers used were of the type described by Boden, Kampa and Snodgrass[3]. Since these employ multiplier phototubes and a series of interference-type filters with peaks at intervals between 410 and 634 mμ, they permit measurement of near-monochromatic light of low intensity. An automatic filter changer places a succession of 5 filters in the light path. The window of the photometer is opal plastic with the characteristics of a Lambert cosine collector. A collimator restricts the angle of incidence on the photocathode to the useful 5° cone of the interference filters. The instrument measures irradiance.

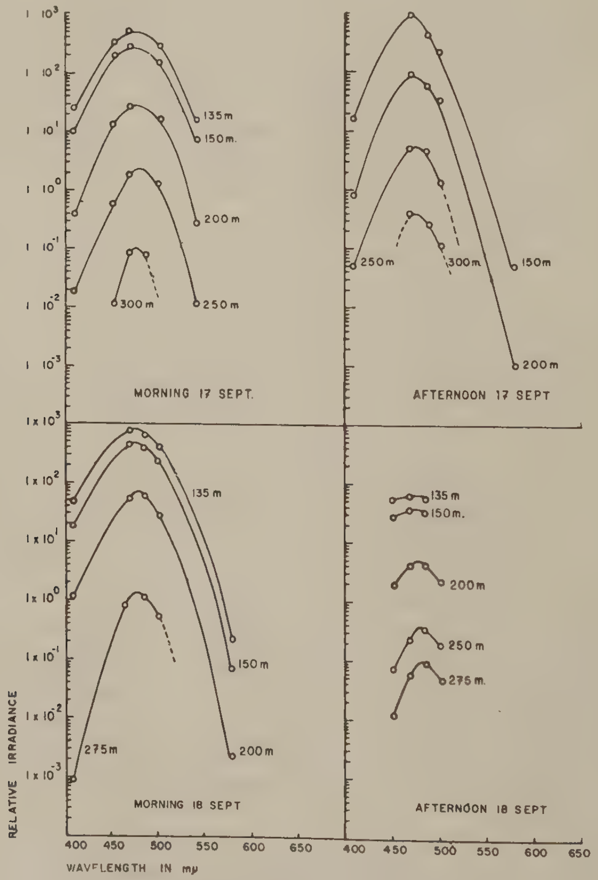

Fig. 1. Relative irradiance spectra at indicated depths off San Diego in September.

The water column above the sonic-scattering layer

The first series of measurements was made to determine midday conditions in the water column down to the depth of the scattering layer. The photometer was oriented to look upward. It was lowered immediately before and after noon on two consecutive days in September.

The light at depths between 135 and 300 m was blue-green and peaked between 475 and 480 mμ (Fig. 1) whichever combination of filters was used. The peaks of the curves obtained become increasingly sharp with depth as the sea water acts as a monochromator (Tyler[9]).

Values of the extinction coefficient (k) for each wavelength at different depths are shown in Table I. The extinction coefficient at depth z is defined by

$$k_\lambda = \ln H_{\lambda,z} - \ln H_{\lambda,(z+1)}$$

where $H_{\lambda,z}$ and $H_{\lambda,(z+1)}$ represent irradiance values of wavelength λ on horizontal surfaces at depths z and $(z + 1\ m)$.

TABLE I

EXTINCTION COEFFICIENTS (k) OF IRRADIANCE AT WAVELENGTHS (λ) AT DEPTHS (D)

D	λ	k
150–250	410	0.065
	452	0.053
	470	0.051
	489	0.048
	503	0.047
	541	0.064
122–198	581	0.081

The extinction coefficient is defined as $k_\lambda = \ln H_{\lambda,z} - \ln H_{\lambda,(z+1)}$ where z and $(z + 1)$ represent 1—m intervals of depth (D).

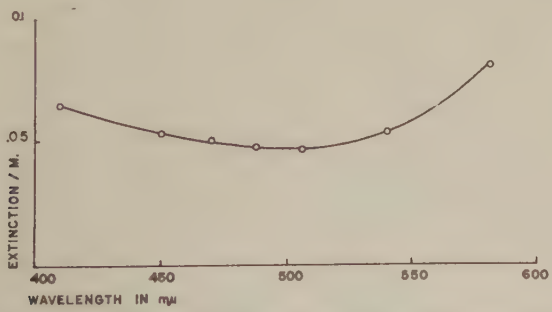

Fig. 2. Extinction coefficients at various wavelengths at depths between 150 and 250 m off San Diego in September.

The values presented were obtained in the water mass below the photic zone and above the scattering layer, where k was constant and the attenuation curves were fairly straight, which suggests that there was little interference from biological or geological sources.

Fig. 2 shows extinction per meter for various wavelengths, and it can be seen that

References p. 196

the water was rather clear for shelf water. According to the data of Utterback[10] and Jorgensen and Utterback[11], it would be typified as average oceanic water.

Rate of attenuation at the surface and at depth at sunset

To determine the difference in the rate of attenuation at two different depths two identical photometers were used. One was suspended 10 m below the surface from a rubber float, the other was suspended 200 m directly below. No filter was used in either. Separate recorders were used, and simultaneous recordings were made.

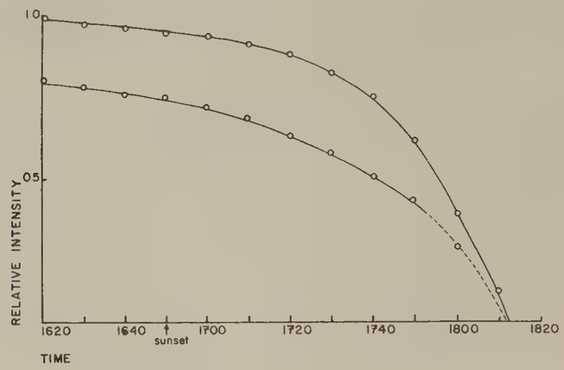

Fig. 3. Simultaneous rates of light decay at 10 m (upper curve) and 200 m (lower curve) during sunset off San Diego in September. The broken line indicates the onset of bioluminescence.

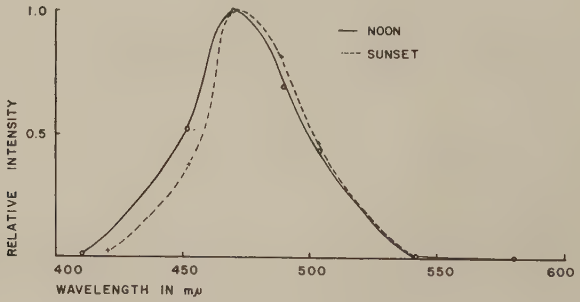

Fig. 4. Spectral distribution of transmitted sun- and sky-light at 170 m at noon and sunset off San Diego in September.

Fig. 3 shows that the rate of extinction was very similar at the two depths from 30 min before sunset until 50 min after sunset. From that time on the curves approach each other, with the rate of extinction at the surface being apparently more rapid than at 200 m. We suggest that this deeper picture is obscured by bioluminescence.

A strong scattering layer was present on this evening, and 50 min after sunset this layer was shoaler than 200 m. Shortly after 1750 h the bioluminescence at 200 m was so marked and the flashes so large that it was not possible to obtain sky-light readings at that depth.

Spectral distribution of light at a constant depth of 170 m at sunset

The photometer was lowered on three successive days, at noon and sunset, to a predetermined depth of 170 m. The values in Fig. 4 represent the average of the values obtained on each of the three days.

It can be seen that there is a strong shift to the longer wavelengths at sunset. The light being measured was, of course, a combination of sun- and sky-light, and this shift is possibly due to selective refraction at the sea surface at a critical point during sunset.

Spectral composition of transmitted sun- and sky-light just above the sonic-scattering layer during its twilight migration

The photometer was equipped with the automatic filter changer, and a variety of filters was used. The instrument was lowered to just above the sonic-scattering layer, and the changer was allowed to rotate. The intensity observed at 470 mμ was selected as a reference value. During light decay at sunset the photometer was raised to follow this 470-mμ isolume.

The ship was far from shore, and ship lights were doused. Only sky-light or possibly bioluminescence, although it was not recognizable as such, was being recorded.

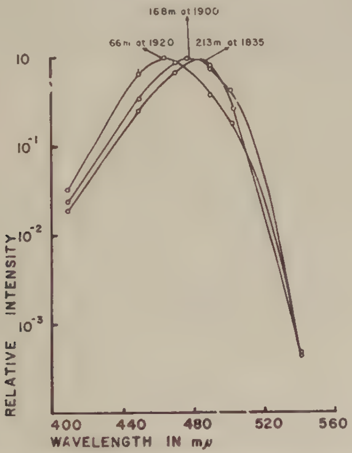

Fig. 5. Spectral composition of light just above the scattering layer during it twilight migration toward the surface off San Diego in September.

Fig. 5 shows the average values obtained at similar depths, similar times and similar wavelengths during three successive twilight periods. It can be seen that the peak values shift from about 490 mμ at sunset toward shorter wavelengths to about 465 mμ at the end of twilight.

ELECTROPHYSIOLOGICAL EXPERIMENTS IN THE LABORATORY

Rather than attempt to design valid laboratory behavioral studies for animals that may well never encounter an interface in their natural lives, we have depended on biochemical and electrophysiological experiments to determine the visual sensitivity of the euphausiids.

References p. 196

Electroretinograms have been obtained from the eyes of a number of species of euphausiids. A tungsten grid serves as the grounded neutral electrode, and the living animal rests on this in a shallow bath of sea water at 7–10°C. A tungsten microelectrode (diameter 2–3 μ), insulated to near the tip is inserted into the eye. The signal from the recording electrode is transmitted via a Grass P-6 preamplifier (with probe) to a Tektronix oscilloscope with a Polaroid Land camera.

The stimulating light is a uniform field, and flash duration is determined by a diaphragm shutter which also triggers the oscilloscope. Interference filters are used to select various wavelengths in color experiments, and neutral density filters modify intensity. Light intensities at the level of the euphausiid eye are determined directly with a thermopile and galvanometer calibrated against a U.S. Bureau of Standards source.

The structure of the euphausiid eye differs greatly from genus to genus. So far, we have worked with two species having spherical eyes *(Euphausia pacifica* and *Meganyctiphanes norvegica)* and two with bilobed eyes *(Thysanoëssa gregaria* and *Nematoscelis difficilis)*.

Responses from the upper and lower lobes of bilobed eyes are quite distinct. The main wave of the electroretinogram of the upper lobe is a fast response, lasting 20–30 msec. Its duration and amplitude are independent of the duration of the stimulus. The main wave of the ERG in the lower lobe is a slow response which varies in duration, but not in amplitude (through the range of shutter speeds we have used), with the duration of the stimulating flash.

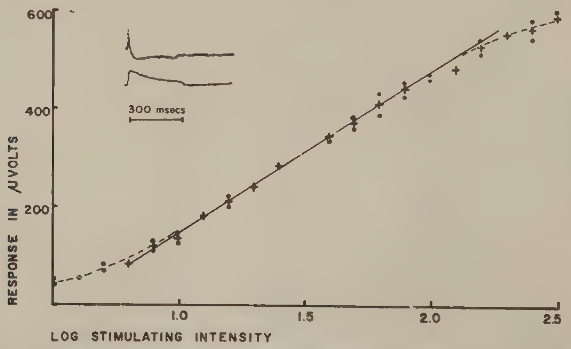

Fig. 6. Relationship of intensity of stimulus to degree of response in the eye of *Euphausia pacifica*. Inset: Upper, the fast, and Lower, the slow response of *E. pacifica* to a 300 msec flash.

Both fast and slow components are present in the spherical eye of *E. pacifica* (Fig. 6). The fast response, like that recorded from the upper lobe of a bilobed eye, is independent of flash duration, whereas the duration of the slow response varies directly with the duration of the stimulus. In some experiments with *E. pacifica* only the slow response has been detected, possibly because of differences in microelectrode placement.

The main wave of the ERG may be either a positive or a negative deflection in any one experiment. This is probably due to differences in depth of penetration by the microelectrode.

The amplitude of both fast and slow responses varies directly with the logarithm of the stimulating intensity through a range of 1 to 2 orders of magnitude (Fig. 6). The slope of the log I-response curve varies from animal to animal, but in any one experiment the linear relationship is consistent.

Our interest in the colors of the lights encountered and produced by euphausiids has led us naturally to studies of the relative sensitivity of their eyes at different wavelengths. Since the relationship between the logarithm of the stimulating intensity and the amplitude of response is linear, spectral sensitivity may be measured either be exposing the eye to restricted wave bands of an equal energy spectrum or by varying the intensity of the stimulus to produce an equal biological response at each wave band. Both approaches have been used, first on the spherical eyes of *E. pacifica* and *M. norvegica*, and more recently on the bilobed eye of *N. difficilis*. The results with spherical eyes were so confusing as to seem meaningless until the bilobed eye was examined.

The curves representing spectral sensitivity of the lower and upper lobes of *N. difficilis* are quite different. The lower lobe (Fig. 7, A) is almost uniformly sensitive to a wide band from 460–515 mμ, with a sharp peak near 490 mμ. The upper lobe (Fig. 7, B) is most sensitive between 460 and 470 mμ, with a secondary peak near 530 mμ. The response curve of the upper lobe is interesting, for its primary peak is in good accord with the difference spectrum of the photosensitive pigment euphausiopsin (Fig. 7, C). This is the first evidence that the pigment participates in the vision of euphausiids.

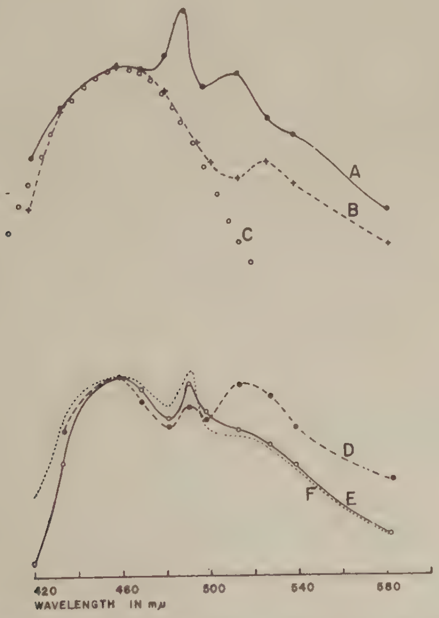

Fig. 7. Spectral sensitivities of: A, *N. difficilis* lower lobe; and B, *N. difficilis* upper lobe; C, Difference spectrum of euphausiopsin; D. *M. norvegica*; E, *E. pacifica*; F, Artificial curve obtained by adding spectral sensitivities of upper and lower lobes of *N. difficilis* at each wavelength. Values representing sensitivity and difference spectrum have been equated to 1 at 460 mμ and the two families of curves have been separated for clarity of presentation.

The spectral sensitivity curves of spherical eyes are unlike either of those from the bilobed eye. *M. norvegica* (Fig. 7, D) is about equally sensitive to lights of 460 and 515 mμ, with a third, lower peak of sensitivity near 490 mμ. *E. pacifica* (Fig. 7, E) is most sensitive to light near 460 mμ, with a second peak near 490 mμ.

When the responses of the upper and lower lobes are added at each wavelength, an artificial curve representing the total spectral sensitivity of *N. difficilis* results (Fig. 7, F). This curve is similar to the response curve of *E. pacifica.*

Either a peak or plateau is apparent near 460 mμ in each of the response curves, and euphausiopsin may be responsible for the sensitivity of all three species to the 420–480-mμ region of the spectrum. Euphausiopsin cannot account for the peaks of sensitivity near 490 and 515 mμ, however. We suggest that euphausiopsin and two additional light-sensitive substances may function in the vision of euphausiids, and that the ratios of their concentrations vary from species to species and from place to place in an individual eye.

ECOLOGICAL CONSIDERATIONS

Adult euphausiids of the Pacific species discussed here are intimately adapted to their photic environment, and this has helped solve certain of the problems confronting them. They are large, succulent animals, eagerly sought as food, and they must avoid predators. They achieve this, in part at least, by living at a light level so low that they must be invisible most of the time. During the day this light level is at a depth which is barren except for detrital fall-out. The complicated visual system of the euphausiids must permit them to detect very slight changes in light intensity, and they follow the isolume to which they are attuned to the phytoplankton-rich surface layers where they may feast at night.

Euphausiids must also remain in a community to avoid specific suicide. Here again, light sensitivity seems important, and luminescent flashing and the ability to detect and recognize such flashing may well serve to keep together like animals living at a light level too low to permit ordinary recognition of form.

Recognition of the relationship of the wavelengths between 460 and 490 mμ in the physical environment of these animals to their visual mechanisms — the fast response associated with 460 mμ, and the slow response associated with 490 mμ — and to their luminescence midway between these wavelengths is too recent to permit anything but speculation on its significance at this time.

REFERENCES

[1] B. P. Boden, *USNEL Rept.*, 186 (1950) 1.

[2] E. M. Kampa and B. P. Boden, *Nature*, 174 (1954) 869.

[3] B. P. Boden, E. M. Kampa and J. M. Snodgrass, *J. Marine Biol. Assoc. United Kingdom*, 39 [2] (1960) 227.

[4] E. M. Kampa and B. P. Boden, *Deep-Sea Research*, 4 (1957) 73.

[5] B. P. Boden and E. M. Kampa, *Pacific Sci.*, 11 (1957) 229.

[6] B. P. Boden and E. M. Kampa, *Nature*, 184 (1959) 1321.

[7] E. M. Kampa, *Nature*, 175 (1955) 996.

[8] L. R. Fisher and E. H. Goldie, *Proc. XVth Intern. Cong. Zool.*, 1958, p. 533.

[9] J. E. Tyler, *Limnol. Oceanog.*, 4 (1) (1959) 102.

[10] C. L. Utterback, *Conseil Perm. Intern. p. l'Explor. de la Mer, Rapp. et Proc.-Verb.*, 101 [2] No. 4 (1936) 15 pp.

[11] W. Jorgensen and C. L. Utterback, *J. Marine Research (Sears Foundation)*, 2 (1939) 30.

[12] G. H. Tucker, *J. Marine Research (Sears Foundation)*, 10 [2] (1951) 215.

Reprinted from
The Physics of Fluids
Volume 4, Number 7, July, 1961
pp.791-799

Internal Waves in the Ocean

Carl Eckart
University of California at San Diego, La Jolla, California
(Received March 22, 1961)

Salinity, temperature, and pressure gradients all cause the density of sea water to vary with depth in the ocean, and the density gradient affects the motion of the waters. A quantity N, having the units radians per second, can be defined using the density gradient, the velocity of sound, and the acceleration of gravity.

The simplest motions have the form of horizontally progressive waves of frequency ω, wave number κ, and velocity V. If h is the amplitude of the vertical displacement of the water and z the vertical coordinate, then $V^2(d^2h/dz^2) + [N^2(z) - \omega^2]h = 0$; this equation is formally identical with Schrödinger's wave equation. The stream function of these waves is $\phi = Vh(z) \sin(\kappa x - \omega t)$, and the variable part of the pressure is $-\rho\, d\phi/dz$, while the vorticity is $R = -N^2\phi/V^2$. The wave may be described as a lattice of vortices moving with velocity V. In the ocean $N(z)$ ordinarily has one or two maxima called thermoclines. The analogy with the quantum-mechanical problems of one and two potential minima is exploited to obtain semiquantitative solutions for the internal waves associated to thermoclines.

I. INTRODUCTION

INTERNAL waves occur both in the ocean and in the atmosphere. The best-known example is the cloud formation, called "mackerel sky," which consists of numerous rows of small clouds. Similar parallel rows of clouds are commonly less closely spaced and attract less attention. In all these cases, the clouds make the waves visible, and the waves have a more or less well-defined wavelength and velocity; less well-defined waves doubtless occur even more commonly.

Clouds associated with internal waves do not move with the wind, but with the phase velocity of the waves. This brings out the primary characteristic of the internal wave phenomenon; it transports energy without a corresponding transport of matter. The importance of this mechanism for energy transport has probably been underestimated in the past.

The reason is that it cannot occur in an incompressible fluid of constant density, and this has served as the primary object of study by the great hydrodynamicists of the nineteenth century. The internal waves are always associated with density gradients. The theory of such waves is somewhat simpler in the case of the oceans than in the atmospheric case. The reason is that certain approximations, permissible in the first, are not permissible in the second (see Sec. IX).

It is well known that, in the upper 4000 m of the deep ocean, the temperature usually decreases with depth. In the winter, there is an exception to this general rule: The upper 200–300 m may be nearly isothermal, or even show a slight increase of temperature with depth. Below 5000 m there is usually a small increase in temperature; this positive gradient may be as much as one degree centigrade per kilometer.

There are also salinity gradients, and of course the pressure increases with depth. These all combine to cause the density of sea water to vary, the water at 4000 m being about 2.5% more dense than at the surface. For comparison, it may be remarked that at atmospheric pressure and room temperature sea water is also about 2.5% denser than distilled water.

Although small by some standards, these density gradients are not negligible, even from an engineering point of view. The diving officer of a submarine must consider them, for they affect the stability of

Copyright © 1961 by the American Institute of Physics

(815)

Contributions from the Scripps Institution of Oceanography, New Series, 1308
Reproduced by Permission

his ship. It should therefore not be surprising to find them affecting the motion of the water itself.

II. STABILITY FREQUENCY

Most of the density gradient is caused by the compression of the water, at depth, by the weight of the overlying water. The remainder is caused by the variation of temperature and salinity with depth. Only this remainder influences the motion of the water. The following definitions give these remarks a precise meaning.

If the density of a fluid is changed adiabatically, then

$$dp = c^2\, d\rho, \tag{1}$$

dp and $d\rho$ being the changes in pressure and density, and c the velocity of sound. If dp is caused by changing the level of a bit of sea water by an amount dz, then

$$dp = -\rho g\, dz, \tag{2}$$

g being the acceleration of gravity.

Eliminating dp:

$$(1/\rho)(d\rho/dz) = -(g/c^2). \tag{3}$$

The quantity g/c^2 is the adiabatic density gradient and is the part of the actual density gradient loosely referred to as being "due to compressibility."

Except under unusual conditions in the sea, the quantity

$$E = -\left(\frac{1}{\rho}\frac{d\rho}{dz} + \frac{g}{c^2}\right) \tag{4}$$

is positive. It has the dimensions of a reciprocal length, and may be called Sverdrup's measure of stability. The meteorologists Väisälä and Brunt have introduced another quantity N defined by

$$N^2 = gE = -g\left(\frac{1}{\rho}\frac{d\rho}{dz} + \frac{g}{c^2}\right) \tag{5}$$

It has the dimensions of a frequency, and $T = 2\pi/N$ is therefore a period.

One is most easily led to this definition by considering the motion of a balloon in the atmosphere.[1,2] If it is constructed to float at a certain level, any disturbance will cause it to oscillate about that level. The period of this oscillation will depend on many things: the gas inside the envelope, the elastic properties of the envelope, the mass of the balloon, including payload, etc. In the limiting case of no mass and a flaccid envelope filled with the same fluid as its surrounding, this period approaches the one defined by Eq. (5). In this calculation, the differences between a gas and a liquid are, of course, irrelevant.

In the upper 4000 m of the ocean, T varies within wide limits, the extremes being 1 min and 3 or 4 hr. This is shown in Fig. 1, which is based on an actual hydrographic sounding made in August, 1928, in the mid-Atlantic.

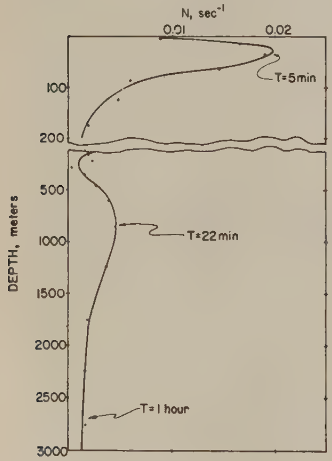

Fig. 1. Variation of T with depth in the upper 400 m of the ocean.

It is seen that, on this occasion, N had two pronounced maxima. These are called thermoclines. If the sounding had been made in late winter rather than in late summer, the upper thermocline, at about 25 m, would have been absent, and the lower one would have been at a somewhat shallower depth and have had a slightly higher maximum value. The lower one is called the permanent thermocline, the upper one, the seasonal or summer. In the winter, T would be 1 hr (or more) in the upper 200 m.

Below 5000 m, it is practically impossible to calculate N. The two terms of Eq. (5) are then very nearly equal, but opposite in sign. The calculation of the density gradient, at the pressures and temperatures concerned, is seriously in doubt because the coefficient of thermal expansion has not been measured and can only be estimated by extrapolation. Such estimates vary by more than a factor of 3 and this causes a large uncertainty in the value of N. A further contribution to this uncertainty arises from errors in the measurement of the very small salinity gradient. It has even been suggested that $N^2 < 0$ at these depths.

---

[1] V. Väisälä, Soc. Sci. Fennica, Commentationes Phys.-Math. 19, 37 (1925).

[2] C. Eckart, *Hydrodynamics of Oceans and Atmospheres* (Pergamon Press, New York, 1960), p. 59.

TABLE I. Data for Fig. 1.

Depth, meters	$10^7\rho^{-1}(d\rho/dz)$, cm^{-1}	$10^7g/c^2$, cm^{-1}	10^2N, sec^{-1}	$T = 2\pi/N$, min
37.5	−4.08	+0.44	1.9	5.5
125.	−0.68	+0.44	0.49	21.
850.	−0.66	+0.44	0.47	22.
2750.	−0.47	+0.44	0.17	60.

In order to illustrate the relative magnitude of the two terms of Eq. (5), numerical data for Fig. 1 given in Table I.

III. INTERNAL WAVES

The stability frequency N enters into the equations of motion of sea water. For simplicity, it will be supposed that N is practically independent of the horizontal coordinates. If the water were at rest, the surfaces of constant density (and of constant N) would then be horizontal. If the water is now set into motion, any of these horizontal surfaces is displaced from depth z to $z + \zeta(txyz)$.

There is a great variety of possible motions; the simplest have the form of harmonic waves:

$$\zeta = h(z) \sin (\kappa x - \omega t), \tag{6}$$

h being the amplitude of the wave at depth z, ω its frequency, and κ its wave number. Its phase velocity is

$$V = \omega/\kappa$$

and the amplitude h is determined (to a certain approximation) by the equations[3]

$$V^2(d^2h/dz^2) + [N^2(z) - \omega^2]h = 0 \tag{7}$$

and

$$h(0) = h(-D) = 0, \tag{8}$$

($z = 0$ and $-D$ are the coordinates of the surface and bottom of the ocean).

The analogy between Eq. (7) and Schrödinger's wave equation,[4]

$$\frac{\hbar^2}{2m}\frac{d^2\psi}{dq^2} + [W - V(q)]\psi = 0,$$

will be apparent, and makes it possible to use many known results of quantum mechanics for the present problem.

Once h has been determined as a function of z, the velocity of the water is readily calculated; its horizontal component is

$$u = -V(\partial\zeta/\partial z), \tag{9}$$

and its vertical component is

$$w = V(\partial\zeta/\partial x). \tag{10}$$

The orbits of the particles are thus ellipses in the x-z plane, whose vertical axis is $h(z)$, and whose horizontal axis is

$$(V/\omega)(dh/dz); \tag{11}$$

note that $2\pi V/\omega = \lambda$ is the wavelength. Since $|dh/dz|$ is much less than unity, the dimensions of the orbits will be much smaller than the wavelength. The streamlines must be clearly distinguished from the orbits; the streamlines are the curves $\zeta = \text{const}$, t being held constant as x and z vary.

Because of the motion, the pressure will differ from the hydrostatic by the amount

$$\Delta p = \rho V u.$$

The motion is not irrotational; its vorticity is in the y direction and has the magnitude

$$R = (\partial u/\partial z) - (\partial w/\partial x) = -N^2\zeta/V. \tag{12}$$

It is clear that R varies with time; the density gradients cause this failure of the law of conservation of vorticity.

IV. CASE OF A CONSTANT STABILITY FREQUENCY

Although it never occurs in the earth's oceans, the case of constant N is of importance for introductory purposes. The solution of Eqs. (7) and (8) is then (A is an arbitrary constant):

$$h = A \sin (n\pi z/D), \qquad n = 1, 2, 3 \tag{13}$$

and

$$(n\pi V/D)^2 + \omega^2 = N^2. \tag{14}$$

The integer n is the analog of the quantum number—it will be called the ordinal number. It is seen that h has $n - 1$ roots in $-D < z < 0$ [here and elsewhere, the two roots specified by Eq. (8) will not be counted]. This definition of the ordinal number in terms of the number of roots of h will persist even in more elaborate cases.[4] Referring to Eqs. (9) and (10), it is seen that the direction of the vertical motion reverses at the roots of h, while that of the horizontal motion reverses

---

[3] The present Eq. (7) is essentially the same as Eq. (4) of Sec. 72 of reference 2. Since the earth's rotation is here neglected, $\Omega = 0$; terms in V^2/c^2 have also been omitted in Eq. (7). The quantity Q that is used in reference 2 is proportional to h: $h = -Q/(\rho c)^{\frac{1}{2}}$. Derivatives of ρc are here neglected; this is justifiable in the ocean, but not in the atmosphere.

[4] E. U. Condon and P. M. Morse, *Quantum Mechanics* (McGraw-Hill Book Company, Inc., New York, 1929), Chap. II.

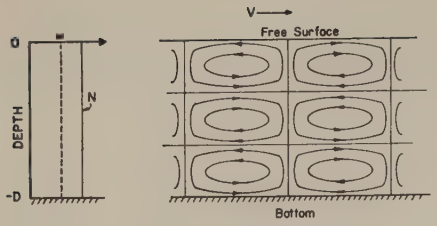

FIG. 2. The wave shown as a rectangular lattice of identical vortices, advancing with phase velocity V.

at its extrema. The direction also reverses at the roots of the sine and cosine factors in Eqs. (9) and (10). Thus the wave can be described as a rectangular lattice of identical vortices, that advances with the phase velocity V (see Fig. 2).

The ordinal number may also be described as the number of vortices in a vertical column of the lattice, or as the number of horizontal layers in the lattice.

To the present approximation, the surface disturbance consists only of horizontal motions. Actually, there is also a small vertical displacement of the free surface, but no attempt will be made to calculate this.

The Eq. (14) connects the phase velocity V to the frequency and ordinal number. Its graph is shown on Fig. 3, and consists of a family of ellipses, one for each value of the ordinal number. All of the ellipses intersect the ω axis at $\omega = N$; they intersect the V axis at the points $V = ND/n\pi = 2D/nT$. There are thus no internal waves with frequency greater than N, and none with velocity greater than $2D/T$. For a given frequency, the velocity is inversely proportional to the ordinal number; small, numerous vortices move more slowly than large, less numerous. For a given velocity, the frequency decreases with increasing ordinal number, and there are only a finite number of these waves that have a given velocity.

In addition to these simple harmonic waves (which are called eigensolutions), there are many other modes of free motion. These are all obtainable by the superposition of eigensolutions, each of the simple harmonic components having its own value of V, n, and ω, and also its own horizontal direction. The forced motions (e.g., forced by tidal attraction) can also be expressed in terms of the eigensolutions.

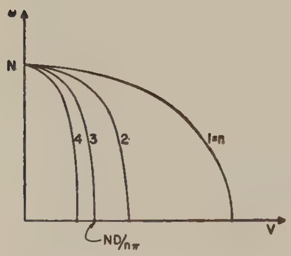

FIG. 3. Phase velocity V vs ω from Eq. (14).

Since $V = \omega/\kappa$, the Eq. (14) also can be plotted as a family of curves in the κ, ω plane, as has been done on Fig. 4. The curves all pass through the origin and become asymptotic to the horizontal line $\omega = N$. This diagram lends itself readily to a discussion of the relation between phase and group velocities; the phase velocity at a point such as A is the slope of the chord OA. The group velocity is the slope of the tangent to the curve at A.

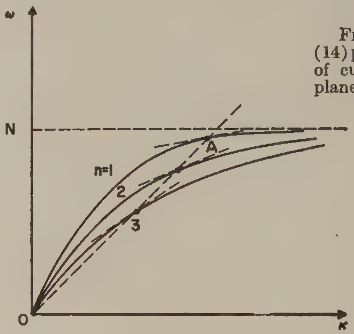

FIG. 4. Equation (14) plotted as a family of curves in the κ, ω plane.

It follows that waves with different ordinal number, but the same phase velocity, will have different group velocities. A wave packet containing waves of different ordinal numbers will therefore break up very rapidly—a fact that is probably of considerable importance for the theory of large-scale turbulence.

V. CASE OF A SINGLE THERMOCLINE

Even in the case of a single thermocline, the analytic form of the equations that correspond to Eqs. (13) and (14) is very complicated. However, a simiquantitative treatment of the problem establishes the results outlined below.

There are no eigensolutions for $\omega > N_M$, N_M being the maximum value of the stability frequency. For $\omega < N_M$, the equation

$$N(z) = \omega \tag{15}$$

has two roots, z_+ and z_-, as shown on the left of Fig. 5. The roots [2,4] of $h(z)$ all lie between z_- and z_+, and the graph of h has points of inflection at z_+ and z_-. The extrema of h also all lie in the interval

z_- to z_+ and there is a root between any two extrema. These remarks make it possible to sketch the graph of $h(z)$ for any n and ω.

It follows that all except two of the vortices in a vertical column of the lattice occur in the layer between z_- and z_+, as shown on the right of Fig. 5. Even these two, the uppermost and lowermost, are strongly asymmetric, and the motion in them diminishes with distance from the layer just mentioned. While the motion is not entirely confined to this "vortex layer" where $z_- < z < z_+$, the motion is less intense outside it.

The ordinal number retains its previous significance; it is still the number of vortices in a vertical column of the lattice. The above description has been worded for $n > 1$; the necessary modification for $n = 1$ should be obvious.

The graph corresponding to Fig. 3 can also be constructed semiquantitatively, as shown on Fig. 6. For each ordinal number, there is one $V-\omega$ curve, and it intersects the ω axis at $\omega = N_M$. However, the slope at this intersection is no longer zero, but can be approximately determined as follows: When ω is very close to N_M, the approximation

$$N^2 = N_M^2[1 - (z - z_M)^2/a^2] \tag{16}$$

is valid. With this expression for N, the analogous quantum-mechanical problem is that of the harmonic oscillator.[5] The well-known calculations for this problem lead to

$$N_M^2 - \omega^2 = (2n - 1)VN_M/a, \tag{17}$$

$$h = A(d/d\xi)^{n-1} \exp(-\tfrac{1}{2}\xi^2), \tag{18}$$

$$\xi = (N_M/aV)^{\frac{1}{2}}(z - z_M). \tag{19}$$

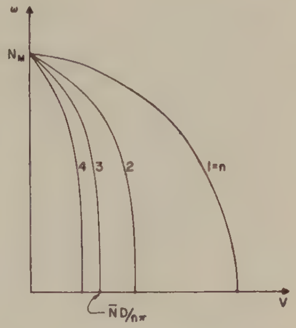

FIG. 6. Semiquantitative graph of V and ω for one thermocline.

This approximation is valid only when V is small and $\omega \sim N_M$. It can be proven that the $V-\omega$ curves always have a negative slope, and do not intersect except at $V = 0$. For small values of ω, they have a vertical tangent, and the WKB approximation[6] is

$$V = \bar{N}\ D/n\pi, \tag{20}$$

$$h = A \sin[\phi(z)/V], \tag{21}$$

$$\phi(z) = \int_{-D}^{z} N(z)\,dz, \tag{22}$$

$$\bar{N}\ D = \phi(0). \tag{23}$$

The Rayleigh-Ritz[7] method yields a somewhat different approximation for $\omega = 0$:

$$V^2 = [D/(n\pi)^2] \int_{-D}^{0} N^2[1 - \cos(2\pi nz/D)]\,dz, \tag{24}$$

$$h = A \sin(n\pi z/D). \tag{25}$$

It is impossible to say which approximation will be most accurate in a given case; more precise approximations are also available.

By using these results, semiquantitative estimates may be made concerning the eigensolutions associated with any empirically determined thermocline.

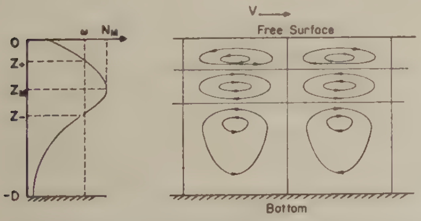

FIG. 5. The lattice of vortices for the case of a single thermocline and ordinal number $n = 3$. Comparison with Fig. 2 indicates that the thermocline distorts the vortices and concentrates the motion into the vortex layer $z_- < z < z_+$, where $N(z) > \omega$.

VI. CASE OF TWO THERMOCLINES

The quantum-mechanical analog of the two thermoclines shown on Fig. 1 is the problem of two potential minima and the penetration of the potential barrier between them. Since this problem is not often treated in introductory textbooks, it is outlined in the Appendix to this paper; however, the calculations are somewhat abbreviated, and not all the assertions that follow are given detailed proof.

Call the upper thermocline 1, the lower 2; it is supposed that the peak of 1 is higher and narrower

---

[5] Reference 4, pp. 47–52.

[6] Reference 4, pp. 111–116; reference 2, pp. 155, 193.

[7] J. W. S. Rayleigh, *Theory of Sound* (Dover Publications, New York, 1945), Vol. 1, pp. 109 *et seq.*

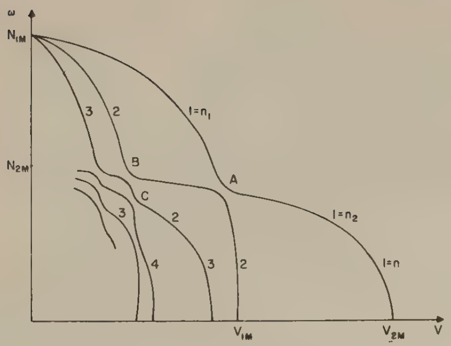

Fig. 7. Thermocline diagram.

than that of 2, and that the two peaks are well separated. Then one may write

$$N^2 = N_1^2 + N_2^2,$$

where N_1 and N_2 are functions that each have a single maximum, representing one of the thermoclines. Hence N_1 will be small where N_2 is large, and conversely. The maxima of N are essentially those of N_1 and N_2, and $N_{1M} > N_{2M}$. If 2 were absent, the maximum phase velocity (for $n = 1$, $\omega = 0$) would be V_{1M}, etc., and $V_{2M} > V_{1M}$.

It may at once be said that, if $N_{1M} > \omega > N_{2M}$, all effects of thermocline 2 are very minor, and only the presence of 1 need be considered. Similarly, if $V_{2M} \geq V > V_{1M}$, only the thermocline 2 need be drawn into calculation.

The $V - \omega$ diagram is the most convenient basis for discussing the remaining cases. This is constructed by first drawing the $V - \omega$ diagrams for N_1 and N_2 on the same sheet. Each will consist of curves that are distinguished by ordinal numbers n_1 and n_2, and the curves of the two families will intersect. These intersections may be called resonance points. In order to complete the diagram for the two thermoclines, the curves are broken at each resonance point and then rejoined as shown at A, B, C on Fig. 7. The result is a family of step-like curves, no two of which intersect except on the ω axis and which may be numbered $n = 1, 2, 3 \cdots$, beginning with the uppermost. This integer n is the ordinal number for the combined pair of thermoclines, and has the significance explained above.

The regions marked A, B, C will be called resonance regions. Two curves pass through each such region; the resonance is characterized, for practical purposes, by the separation of the two curves and by their curvature. Formulas for the approximate calculation of these parameters have been developed (see Appendix). For the present, it suffices to say that if the two thermoclines are well separated, the separation of the two curves is small and their curvature great. Correspondingly, the resonance regions will be small and often well separated from each other. Only for small values of V and $0 < \omega < N_{2M}$ will the resonance regions merge together; the formulas derived in the Appendix then cease to yield good numerical values.

The earlier remarks, about the possibility of ignoring one or the other of the two thermoclines, may now be extended. Both thermoclines need be considered only when the $V - \omega$ point is in one of the resonance regions. For points far removed from a resonance, one or other of the coefficients α, β in Eq. (A9) will be very small, and $h = h_1$ or $h = h_2$ as the case may be.

The Fig. 7 is in need of one correction; it shows that the curves for various values of n intersect the V axis at quite irregular intervals. The Eqs. (20) or (24), which apply equally to one or two thermoclines, show that this is probably wrong. However, the way to correct this error is not immediately obvious, and some numerical work would be needed to find it.

VIII. RESONANCE TRANSFER OF ENERGY

The justification for the use of the term *resonance* in the preceding section will now be given. Instead of the eigensolutions, consider a wave packet formed by superposition of the two eigensolutions of Eq. (A20):

$$\begin{aligned} \zeta &= \tfrac{1}{2}[h_+ \sin(\kappa_0 x - \omega_+ t) + h_- \sin(\kappa_0 x - \omega_- t)] \\ &= a_1 h_1 \cos(\tfrac{1}{2}t\,\Delta\omega) \sin(\kappa_0 x - \omega_0 t) \\ &\quad - a_2 h_2 \sin(\tfrac{1}{2}t\,\Delta\omega) \cos(\kappa_0 x - \omega_0 t). \end{aligned} \tag{26}$$

The trigonometric factors with the argument $\tfrac{1}{2}t\,\Delta\omega$ will vary slowly in comparison to those with the argument $\kappa_0 x - \omega_0 t$. Hence for small values of t, ζ will be essentially

$$\zeta = a_1 h_1 \sin(\kappa_0 x - \omega_0 t)$$

and the disturbance will be almost entirely confined to the upper thermocline. As t increases, however, the factor $\cos(\tfrac{1}{2}t\,\Delta\omega)$ will decrease and $\sin(\tfrac{1}{2}t\,\Delta\omega)$ will increase. That is, energy will be transferred from the upper thermocline to the lower. When $t\,\Delta\omega = \pi$, the transfer will be complete, and the disturbance will be almost entirely confined to the lower thermocline. Thereupon the transfer process is reversed, and when $t\,\Delta\omega = 2\pi$, the energy will again be in the upper layer. This is the essential characteristic of resonance.

It must at once be added that this complete transfer of energy between the two thermoclines occurs only when h_+ and h_- have a resonance value of κ [$= \kappa_0$; cf. the remarks preceding Eq. (A17)]. It is possible to construct wave packets similar to that of Eq. (26), but with other values of κ. The fraction of the energy that is interchanged between the thermoclines then diminishes rapidly as $|\kappa - \kappa_0|$ increases, and becomes practically zero outside the resonance regions. A detailed discussion of this matter can be deduced from Eq. (A16).

Still more elaborate motions are possible, obtained by superposing eigensolutions for many values of n, κ and their associated values of ω and V. If most of these are nonresonant, the motion in the two thermoclines will be statistically independent.[8] However, if any resonant pairs are included, some interchange of energy will occur.

The importance of this resonance transfer is not immediately obvious. If the nonlinear terms in the hydrodynamics equations are ignored (this has been done in all of the above discussion) one will be inclined to assess it as a minor effect. When the nonlinear terms are considered, it may be found to have a greater importance.

These terms modify the above theory; together with viscous and other dissipative effects, they cause a phenomenon that can best be described as a flow of energy in the $V-\omega$ diagram.[9] This flow will ultimately carry all of the energy through many resonance regions, and the integrated effect of the resonance phenomenon may be considerable.

The stability frequency N may also show a slow change with horizontal position; this would have a similar effect in enhancing the importance of resonance transfer. These suggestions require a more detailed study than is possible in this paper.

IX. ATMOSPHERIC THERMOCLINES

The earth's atmosphere also exhibits two thermoclines,[10] and the magnitude of the stability frequency is much the same as in the ocean. The vertical scale of the phenomenon is greater, however. The term "thermocline" is not used by meteorologists, however; instead, the two thermoclines are usually called the stratosphere and the thermosphere, respectively. The troposphere is the region of small stability below the stratosphere, and the mesosphere is the region between the stratosphere and the thermosphere.

The theory of the atmospheric thermoclines is similar to that of the oceanic, but more complicated. This complication arises primarily from the greater compressibility of the atmosphere, and the greater variation in its temperature at different levels. For these reasons, a number of approximations, that were justifiable above, are not valid in the atmospheric case. Those complications will not be considered here, but probably do not alter the general qualitative character of the internal waves.

Two other complicating factors, that affect both ocean and atmosphere, are the earth's rotation, and their steady circulation. These may be ignored only for waves whose length is a very small fraction of the earth's radius.

ACKNOWLEDGMENT

A considerable part of this paper was written while at The Institute for Advanced Study, Princeton, New Jersey. The hospitality of the Institute is gratefully acknowledged.

APPENDIX

In order to treat the two thermocline problem, even approximately, various general principles and methods must be used. Equation (7) is derivable from a variation principle; let

$$K = \int [(N^2/V^2)h^2 - (dh/dz)^2]\, dz, \qquad \text{(A1)}$$

$$J = \int h^2\, dz, \qquad \text{(A2)}$$

these, and all other integrals that will appear below, being extended from $z = -D$ to $z = 0$. Equation (7) is the condition that K shall be stationary subject to the conditions that

$$J = 1, \qquad h(0) = h(-D) = 0. \qquad \text{(A3)}$$

The second term in the integrand of K can be integrated by parts, yielding

$$K = \int h[(N^2/V^2)h + d^2h/dz^2]\, dz. \qquad \text{(A4)}$$

Hence the stationary value of K is, because of Eq. (7) and $J = 1$,

$$K = \omega^2/V^2 = \kappa^2. \qquad \text{(A5)}$$

---

[8] This statistical independence of the motions in the two thermoclines has been empirically established by B. Haurwitz, H. Stommel, and W. H. Munk, *On the Thermal Unrest in the Ocean* (Rockefeller Institute Press and Oxford University Press, New York, 1959), Rossby Memorial Volume, p. 74. Unfortunately, their interpretation of the results is marred by the use of an incorrect formula for N.

[9] G. K. Batchelor, *Homogeneous Turbulence* (Cambridge University Press, New York, 1953), p. 82.

[10] Reference 2, pp. 71–74.

The Rayleigh-Ritz method for the approximate solution of this variation problem is as follows: Let $f(z, \alpha, \beta \cdots)$ be a parametric family of functions. One attempts to find that one of this family of functions that is the "best" approximation to h; whether or not it is a "good" approximation will depend, of course, on the choice of the family of functions. When $f(z, \alpha, \beta \cdots)$ is substituted for h, K, and J will become functions of the parameters $\alpha, \beta \cdots$. The simplest form of the Rayleigh-Ritz method determines the best values of $\alpha, \beta, \cdots$ by requiring that $K(\alpha, \beta, \cdots)$ be stationary subject to the condition $J(\alpha, \beta, \cdots) = 1$.

These values are found by solving the equations

$$\begin{aligned} \partial K/\partial\alpha &= \kappa^2\, \partial J/\partial\alpha, \\ \partial K/\partial\beta &= \kappa^2\, \partial J/\partial\alpha, \end{aligned} \qquad \text{(A6)}$$

and the values of κ for which these equations have a solution are approximations to the eigenvalues defined by Eq. (A5).

This method will now be applied to the two thermocline problem, for which

$$N^2(z) = N_1^2(z) + N_2^2(z), \qquad \text{(A7)}$$

N_1 representing the upper thermocline and N_2 the lower, each of these functions having a single maximum and each having very small values in the region of the other's maximum. It is assumed that the eigenfunctions and $V-\omega$ curves for each of these one thermocline problems are known and that one of the resonance points is V_0, ω_0, κ_0; that is, functions h_1 and h_2 are known for which

$$\begin{gathered} d^2h_1/dz^2 + (N_1^2/V_0^2 - \kappa_0^2)h_1 = 0, \\ d^2h_2/dz^2 + (N_2^2/V_0^2 - \kappa_0^2)h_2 = 0, \\ h_1(0) = h_1(-D) = h_2(0) = h_2(-D) = 0, \\ \int h_1^2\, dz = \int h_2^2\, dz = 1. \end{gathered} \qquad \text{(A8)}$$

The function h_1 will then have large values only where N_1 is large, and will have quite small values where N_2 is large, etc.

As the family of comparison functions, one now takes

$$h = \alpha h_1(z) + \beta h_2(z); \qquad \text{(A9)}$$

there is reason to believe that one of these will be a good approximation to h, provided that the resonance point V_0, ω_0 is well separated from its nearest neighbors. After substituting this for h in Eq. (A4) and using Eq. (A8), it is found that

$$\begin{aligned} K - \kappa_0^2 J = \int \{&(\alpha h_1 + \beta h_2)^2(N_1^2 + N_2^2)/V^2 \\ &- (\alpha h_1 + \beta h_2)[\alpha h_1 N_1^2/V_0^2 + \beta h_2 N_2^2/V_0^2]\}\, dz, \end{aligned} \qquad \text{(A10)}$$

$$J = \alpha^2 + \beta^2 + 2\alpha\beta \int h_1 h_2\, dz. \qquad \text{(A11)}$$

Both K and J are thus homogeneous quadratic forms in α and β, and the Eq. (A6) are homogeneous linear equations determining α and β. The eigenvalue κ is fixed by the requirement that the determinant of the linear equations shall vanish.

In order to determine the coefficients of the quadratic forms K and J, the following seven integrals must be evaluated:

$$\begin{aligned} A_1 &= \int N_1^2 h_1^2\, dz, & A_2 &= \int N_2^2 h_2^2\, dz, \\ B_1 &= \int N_1^2 h_1 h_2\, dz, & B_2 &= \int N_2^2 h_1 h_2\, dz, \\ C_1 &= \int N_1^2 h_2^2\, dz, & C_2 &= \int N_2^2 h_1^2\, dz, \\ && D &= \int h_1 h_2\, dz. \end{aligned} \qquad \text{(A12)}$$

The B's will have considerably smaller values than the A's, and the C's, smaller than the B's; for in B_1, the factor h_2 will be small wherever the factor $N_1^2 h_1$ is large, and conversely. Similarly in C_1, either h_2^2 or N_1^2 will be small at all points. To a certain approximation the problem may therefore be simplified by setting $C_1 = C_2 = 0$.

The quantity D will be small compared to unity; a detailed examination shows that only a small error results from the approximation $D = 0$.

A further simplification results from the fact that $B_1 = B_2$, as will now be proven. For

$$\begin{aligned} \frac{d}{dz}\left[h_2 \frac{dh_1}{dz} - h_1 \frac{dh_2}{dz}\right] &= h_2 \frac{d^2h_1}{dz^2} - h_1 \frac{d^2h_2}{dz^2} \\ &= (N_2^2 - N_1^2)h_1h_2/V_0^2 \end{aligned} \qquad \text{(A13)}$$

by Eq. (A8); on integration, the required result follows because the square bracket vanishes at both limits.

With these simplifications, Eqs. (A10) and (A11) become

$$\begin{aligned} K - \kappa_0^2 J = (\alpha^2 A_1 + \beta^2 A_2)&[(1/V^2) - (1/V_0^2)] \\ &+ 2\alpha\beta B[(2/V^2) - (1/V_0^2)], \end{aligned} \qquad \text{(A14)}$$

$$J = \alpha^2 + \beta^2, \qquad \text{(A15)}$$

and the Eq. (A6),

$$\alpha\{A_1[(1/V^2) - (1/V_0^2)] + [\kappa_0^2 - \kappa^2]\} + \beta B[(2/V^2) - (1/V_0^2)] = 0, \qquad \text{(A16)}$$

$$\alpha B[(2/V^2) - (1/V_0^2)] + \beta\{A_2[(1/V^2) - (1/V_0^2)] + [\kappa_0^2 - \kappa^2]\} = 0.$$

In order that α and β shall not both be zero, the determinant of these equations must vanish; this yields a relation between V and κ and enables the $V-\omega$ diagram to be constructed in the neighborhood of the resonance point V_0, ω_0. The reader may verify that this relation is consistent with the discussion in Sec. VI.

For the present purpose, only the case $\kappa = \kappa_0$ will be discussed in detail, then the Eqs. (A16) become (recalling that $\omega = V\kappa$)

$$\alpha A_1(\omega_0^2 - \omega^2) + \beta B(2\omega_0^2 - \omega^2) = 0,$$

$$\alpha B(2\omega_0^2 - \omega^2) + \alpha A_2(\omega_0^2 - \omega^2) = 0.$$

Since B and $\omega_0 - \omega$ are both small, the approximations $2\omega_0^2 - \omega^2 = \omega_0^2$, $\omega_0^2 - \omega^2 = 2\omega_0(\omega - \omega_0)$ are justified, and the equations become

$$\begin{aligned} 2\alpha A_1(\omega_0 - \omega) + \beta B\omega_0 &= 0, \\ \alpha B\omega_0 + 2\beta A_2(\omega_0 - \omega) &= 0. \end{aligned} \qquad \text{(A17)}$$

The determinant of these equations must vanish:

$$4A_1A_2(\omega_0 - \omega)^2 - B^2\omega_0^2 = 0,$$

so that

$$\begin{aligned} \omega &= \omega_0 \pm \tfrac{1}{2}\,\Delta\omega, \\ \Delta\omega &= \omega_0 B/(A_1A_2)^{\frac{1}{2}} = \omega_0/Q. \end{aligned} \qquad \text{(A18)}$$

The quantity

$$Q = (A_1A_2)^{\frac{1}{2}}/B \qquad \text{(A19)}$$

is thus the sharpness measure of the resonance. The more completely the thermoclines are separated, the greater Q and the smaller $\Delta\omega/\omega_0$.

With the values of ω thus determined, Eq. (A17) is

$$\pm\,\alpha A_1^{\frac{1}{2}} + \beta A_2^{\frac{1}{2}} = 0,$$

and one obtains two solutions for h:

$$\begin{aligned} h_+ &= a_1h_1 + a_2h_2 \quad \text{for} \quad \omega_+ = \omega_0 + \tfrac{1}{2}\,\Delta\omega, \\ h_- &= a_1h_1 - a_2h_2 \quad \text{for} \quad \omega_- = \omega_0 - \tfrac{1}{2}\,\Delta\omega, \end{aligned} \qquad \text{(A20)}$$

where

$$a_1 = [A_2/(A_1 + A_2)]^{\frac{1}{2}}, \; a_2 = [A_1/(A_1 + A_2)]^{\frac{1}{2}}. \qquad \text{(A21)}$$

(824)

Reprinted from: California Cooperative Oceanic Fisheries Investigations.
Reports, v.8. 1 July 1959-30 June 1960. pp.75-82.

EVIDENCE OF A NORTHWARD MOVEMENT OF STOCKS OF THE PACIFIC SARDINE BASED ON THE NUMBER OF VERTEBRAE

ROBERT L. WISNER[1]

INTRODUCTION

Evidence on the movements of stocks of sardines along the Pacific Coast of the United States and Mexico has been derived from tagging, from counts of vertebrae, and from related data. The present study represents a second major attempt using numbers of vertebrae. Previous studies, reviewed below, have demonstrated an unknown but presumably significant amount of heterogeneity within the range of the sardine, as well as considerable intermingling of stocks between the regions of Punta Eugenia (in central Baja California), California, and the Pacific Northwest.

Tagging studies: An extensive tagging program, initiated in 1936 and carried on continuously until 1942, demonstrated that the sardine stocks intermingle considerably within the area from Pta. Eugenia to Central California and from Southern California to British Columbia (Hart, 1943; Clark and Janssen, 1945). Some fish tagged in Southern California were recovered along the west coast of British Columbia and some tagged in the latter region were recovered in Southern California. The tag-recoveries demonstrated a rather rapid migration: sardines tagged off Southern California in February and March were retaken off British Columbia in the following July; others, tagged off British Columbia in July and August, were caught off San Pedro, California, in the succeeding December and January (Hart, 1943). Associated with this rapidity of migration is a size relationship. Clark and Janssen (op. cit.) stated that, "The largest sardines may be expected to move quickly to distant fishing grounds whereas the smaller fish tend to remain longer in the locality where tagged or to make short migrations. These smaller fish reach distant grounds in later years when they have grown to larger sizes."

The one lot of sardines that was tagged south of Pta. Eugenia, in April, 1938, comprised 963 fish in Magdalena Bay. No recoveries were made from this lot, possibly because the number was too small to insure a return, or, as the authors suggested, because sardines from the area do not intermingle with the more northern fish.

Vertebral Studies: Clark (1947) compiled the results of vertebral counts made by previous investigators in the United States and Canada—Hubbs (1925), Thompson (1926), Hart (1933), and Clark (1936). The 1947 data, when grouped by latitude, showed a rather definite trend from north to south, particularly within the 0 and 1 age groups. No adults (2-year fish or older) were available from south of San Diego with the exception of a small sample of 31 fish from the Gulf of California. The areas treated ranged from Alaska to the Gulf of California and the years sampled from 1921 to 1941.

From the combined age-group data Clark (1947) reached a tentative conclusion that, "sardines found in southern Lower California and the Gulf of California constitute a separate population which rarely intermingles with the more northern population, but that a considerable, and perhaps variable, amount of interchange takes place throughout the range of the northern population from Alaska to Pta. Eugenia in central Lower California." The results of the tagging in the Magdalena Bay area, though somewhat inconclusive, recounted above, augmented Clark's interpretation of vertebral data from the area and strengthened the hypothesis that the stocks of fish in the area may well constitute a separate population that intermingles little if at all with the more northern stocks.

Growth Studies: Felin (1954) attempted to assay the heterogeneity of the sardine populations from the standpoint of growth characteristics, using age and length data gleaned from samples of the commercial landings in Southern and Central California during the years 1942-1950. The following excerpts from her conclusions appear to be pertinent to the present study:

> Complete intermixture and homogeneity in population of adult fish as sampled by the fishery in different regions is not evidenced from data on mean calculated lengths. The apparent cline in the growth characteristic . . . appears indicative of intraspecific populations in which there is limited intermingling, and suggests a series of overlapping coastal migrations of more than one stock.

Wolf and Daugherty (1960) have reported that two-year-old fish comprised the bulk of the Southern California catch in the 1958-59 season (to be discussed later). These fish were unique in that they averaged 191 mm. (7.7 inches) in standard length, 12 mm. (0.5 inches) smaller than the previous recent minimum (1954-55), but not much smaller (3 mm. or 0.1 inch) than the 1939 year-class as two-years-olds, an outstanding year-class. It has further been reported (Ibid., 1960) that the fish in Baja California averaged even smaller (162 mm., 6.4 inches)—so much smaller as to suggest that the fishery there was not utilizing the same stocks of fish as was the Southern California

---

[1] Contributions from the Scripps Institution of Oceanography. 1309

Reproduced by Permission

fishery. Also, the two-year-olds landed at Monterey were smaller than the San Pedro fish, indicating somewhat more population heterogeneity than usual (no samples from the Monterey landings were available for the present study).

These previous studies have all pointed either to a mixture of stocks, of phenotypic or genotypic origin, that intermingle more or less completely within the area from north and central Baja California to Southern California and from the latter area to British Columbia, or to more or less sporadic influxes of non-intermingling fish from other areas, presumably the south.

The present study attempts to cover essentially the same areas (Fig. 1) reported on by Clark, with the exception of Central and Northern California, and provides a body of data well separated in time from any previous similar data. No samples were available from these northern areas, as it was not until the 1958-59 season that the sardines reappeared there in sufficient numbers, since about 1950, to warrant a fishery or a sampling program (Marine Research Committee, 1960). No samples were available for study from the 1958-59 central California fishery, although about 25,000 tons were landed at Monterey and San Francisco (Ibid., 1960). In general, the present data agree with Clark's findings only for the areas south of Pta. Eugenia. From there northward to San Pedro, California, the data show that a major portion of the samples studied are characterized by a marked reduction in average number of vertebrae.

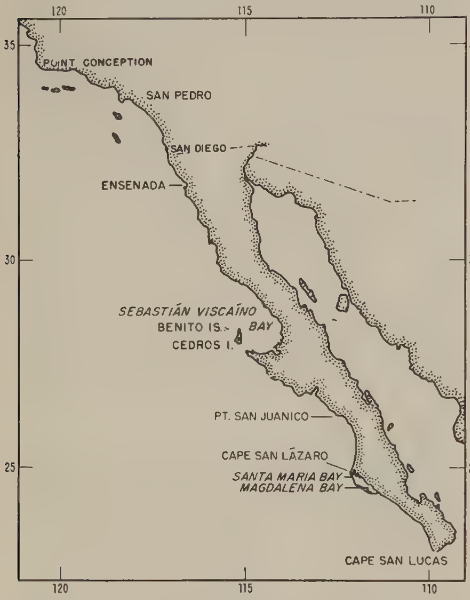

FIGURE 1. Chart of areas discussed, showing the localities from which samples were secured in the present investigation and in that of Clark (1947).

METHODS

As age determinations were not available for samples from most of the localities treated, all age-groups are combined. Only the 1957-58 Ensenada and San Pedro samples were aged (by CalCOFI personnel, employing a subsample amounting to approximately 20 percent of each sample studied). In the other areas studied, aging would have been possible only by arbitrarily assigning an age to any given length frequency. This was not attempted as age-length composition studies have shown that adult sardines (2 years or older) vary in length from 1.5 to 2.5 inches in each age-group. Thus, an arbitrarily assigned age may result in an error of two or three years.

All fish, except one sample of 500 postlarvae from the Gulf of California, were X-rayed for determination of vertebral numbers. The postlarvae were stained with alizarin and cleared in glycerin before counting. All vertebrae were counted by the author. The urostyle was included in the count.

The nature of the data does not warrant detailed statistical analyses, and the study is not intended as a purely racial one. The real significance lies in the differences in average values, both in individual and in grouped samples, between the present body of data and that presented by Clark (1947) for the region north of Pta. Eugenia, Baja California.

Because of the rather small range in total numbers of vertebrae the standard deviations about the mean do not differ markedly. For the region north of Pta. Eugenia the range of deviations, including both Clark's and the present data, is 0.5980 to 0.6719 (ave., 0.6191). The range of standard errors of the means is 0.0006 to 0.0225 (ave., 0.0149). This large range in standard error values is due to the quite large variation in numbers of specimens used (Table 1).

An indication of the significance of the difference between means of Clark's and the present data, for the northern region, is the average difference of 0.23, nearly one-fourth of a vertebra. In comparing this with the almost three-fourths of a vertebra that separates the Gulf of California fish (average mean, 51.00) from those reported by Clark for northern Baja California and northward (average mean, 51.70), elementary statistical treatment will provide odds of but one in hundreds of thousands of chances that the two sets of data comprise a single population or stock of fish. Such orders of significance do not, of course, pertain to the southern areas—from Pta. Eugenia southward and into the Gulf of California—because of the striking similarity of the two sets of data in this southern region.

RESULTS

Figure 2 is a plot of all samples embodied in the present data, arranged by area. Wherever the areas are closely comparable, Clark's 1947 data are also plotted. Each solid dot represents an individual sample of the present data, and each open circle repre-

TABLE I

VERTEBRAL NUMBERS—ALL AGE GROUPS

Locality	Year, Month	Number of Vertabrae						Number of Fish	Average Vertebrae
		49	50	51	52	53	54		
San Pedro	1951: I	----	1	33	40	3	----	77	51.58
	X	----	4	52	39	3	----	98	51.42
	XI	----	2	31	28	3	----	64	51.50
	XII	----	1	11	10	----	----	22	51.41
	1954: X	----	1	18	17	1	----	37	51.49
	1957: X	----	7	78	69	4	----	158	51.44
	XII	----	10	225	228	20	----	483	51.53
	1958. I	----	7	88	101	8	----	204	51.54
	II	1	5	87	74	12	----	179	51.51
	V	----	2	39	49	1	----	91	51.54
	VII	----	4	101	99	7	----	211	51.52
	VIII	----	----	40	35	5	----	80	51.56
	IX	1	7	68	78	6	----	160	51.51
San Pedro total		2	51	871	867	73	----	1,864	51.51
Clark total		4	119	3,039	5,802	677	11	9,652	51.73
San Diego	1950: VII	----	2	89	96	5	1	193	51.55
	1951 I	----	1	10	13	1	----	25	51.56
	1952. VII	----	1	11	22	2	----	36	51.69
	1957: III	----	2	4	7	2	----	15	51.60
	V	----	----	8	16	1	----	25	51.72
	1958. VI	1	1	26	26	1	----	55	51.45
	VII	----	1	32	21	4	----	58	51.48
	X	----	2	46	41	2	----	91	51.47
	XII	----	1	26	25	1	----	53	51.49
	1959 I	----	1	17	19	2	----	39	51.56
	XII	----	4	37	34	1	----	76	51.42
San Diego total		1	16	306	320	22	1	666	51.52
Clark total		2	86	2,085	3,923	452	5	6,553	51.73
Ensenada	1952: IV	----	----	8	18	----	----	26	51.69
	VIII	----	1	19	13	1	----	34	51.41
	XI	----	1	16	23	----	----	40	51.55
	XII	----	----	15	21	2	----	38	51.66
	1956: IX	----	1	33	26	----	----	60	51.42
Ensenada total prior to 1957		----	3	91	101	3	----	198	51.53
	1957: IX	----	5	83	102	8	----	198	51.57
	X	----	17	315	434	33	----	799	51.60
	XI	----	10	265	230	8	----	513	51.46
	XII	1	35	562	494	24	----	1,116	51.45
1957 total		1	67	1,225	1,260	73	----	2,626	51.51
	1958: I	----	2	22	23	2	----	49	51.51
	II	1	2	112	158	14	----	287	51.63
	III	----	16	383	435	42	----	876	51.57
	IV	----	12	197	240	17	----	466	51.56
	V	----	9	181	200	13	----	403	51.54
	VI	----	19	296	268	5	----	588	51.44
	VII	----	20	362	340	12	----	734	51.47
	VIII	1	27	346	299	18	----	691	51.44
	IX	----	24	497	422	17	1	961	51.45
	X	----	18	358	363	18	----	757	51.50
	XI	----	31	600	581	45	----	1,257	51.51
	XII	----	32	390	339	16	----	777	51.44
1958 total		2	212	3,744	3,668	219	1	7,846	51.50
Ensenada total		3	282	5,060	5,029	295	1	10,670	51.50
Cedros and San Benito Islands	1946: VIII	----	9	89	71	3	----	172	51.40
	1952: XI	----	1	10	11	1	----	23	51.52
	1955	----	----	31	99	13	----	143	51.87
	1958. VIII	----	2	21	27	----	----	50	51.50
	IX	----	1	107	85	5	----	198	51.47
	XI	----	1	44	48	4	----	97	51.54
	XII	----	5	45	44	6	----	100	51.51
Cedros and San Benito total		----	19	347	385	32	----	783	51.55

TABLE I—Continued

VERTEBRAL NUMBERS—ALL AGE GROUPS

Locality	Year, Month	Number of Vertabrae						Number of Fish	Average Vertebrae
		49	50	51	52	53	54		
Sebastián Viscaíno Bay	1953: IV	----	6	27	20	1	----	54	51.30
	1958: VIII	----	7	72	24	1	----	104	51.18
	VIII	----	7	19	24	----	----	50	51.34
	IX	1	2	11	17	----	----	31	51.42
	XII	----	3	70	58	1	----	132	51.43
	1959: I	----	2	36	35	----	----	73	51.45
	IV	----	8	54	53	----	----	115	51.39
Sebastián Viscaíno Bay total		1	35	289	231	3	----	559	51.36
Clark total		----	22	420	596	55	----	1,093	51.63
Pta. Eugenia to Cape San Lázaro	1951: V	1	18	146	141	----	----	306	51.40
	IX	----	14	105	130	6	1	256	51.51
	1952: II	----	----	7	11	----	----	18	51.61
	IX	2	8	39	25	----	----	74	51.18
	1953: II	----	2	5	5	----	----	12	51.25
	V	----	3	63	54	3	----	123	51.46
	VIII	----	----	15	18	1	----	34	51.59
	XI	----	21	178	117	5	----	321	51.33
	1956: VII	----	6	73	55	3	----	137	51.40
	VIII	----	3	51	87	3	----	144	51.63
	IX	----	3	22	23	1	1	50	51.50
	X	----	2	9	23	----	----	34	51.62
	1958: VIII	----	9	103	55	1	----	168	51.29
	IX	----	20	190	78	1	1	290	51.22
Pta. Eugenia Cape San Lázaro total		3	109	1,006	822	24	3	1,967	51.39
Clark: total Pta. Eugenia to Pt. San Juanico		----	32	417	248	13	----	710	51.34
Santa María Bay	1951: VII	----	----	27	17	1	----	45	51.42
	X	----	3	31	43	1	----	78	51.54
	XI	----	----	4	7	2	----	13	51.85
	1952: IV	----	1	8	3	1	----	13	51.31
	VII	----	7	57	6	----	----	70	50.99
	VIII	----	1	7	10	1	----	19	51.58
	1953: VII	----	5	68	51	----	----	124	51.37
	VIII	----	5	51	41	6	----	103	51.47
	1955: VIII	----	3	20	25	3	----	51	51.55
	IX	----	1	14	18	----	----	33	51.52
	X	----	1	11	9	----	----	21	51.38
	XI	----	2	23	24	2	----	51	51.51
	1956: VI-VII	----	9	10	----	----	----	19	50.53
	XI	----	----	33	22	----	----	55	51.40
	1959: II	----	19	107	21	----	----	147	51.01
Santa María Bay total		----	57	471	297	17	----	842	51.33
Magdalena Bay	1949: II	----	1	27	17	1	----	46	51.39
	1951: VI	----	1	8	10	3	----	22	51.68
	1952: VII	1	4	38	9	----	----	52	51.06
	VII	----	8	43	39	----	----	90	51.34
	VIII	----	5	41	13	----	----	59	51.14
	IX	----	----	32	35	1	----	68	51.54
	1953: VI	----	1	23	20	2	----	46	51.50
	1958: VI	----	7	105	27	----	----	139	51.14
	VI small	----	18	82	20	----	----	120	51.02
	VI larger	----	2	23	12	----	----	37	51.27
Magdalena Bay total		1	47	422	202	7	----	679	51.25
Clark total		1	44	500	243	7	----	795	51.27
Pt. Marquis	1952: X	----	6	38	18	3	----	65	51.28
Gulf of California	1953: VIII	----	15	71	25	----	----	111	51.09
	1956: XII (postlarvae)	4	84	315	97	----	----	500	51.01
Gulf of California total		4	99	386	122	----	----	611	51.02
Clark total		2	91	521	118	3	----	735	51.04

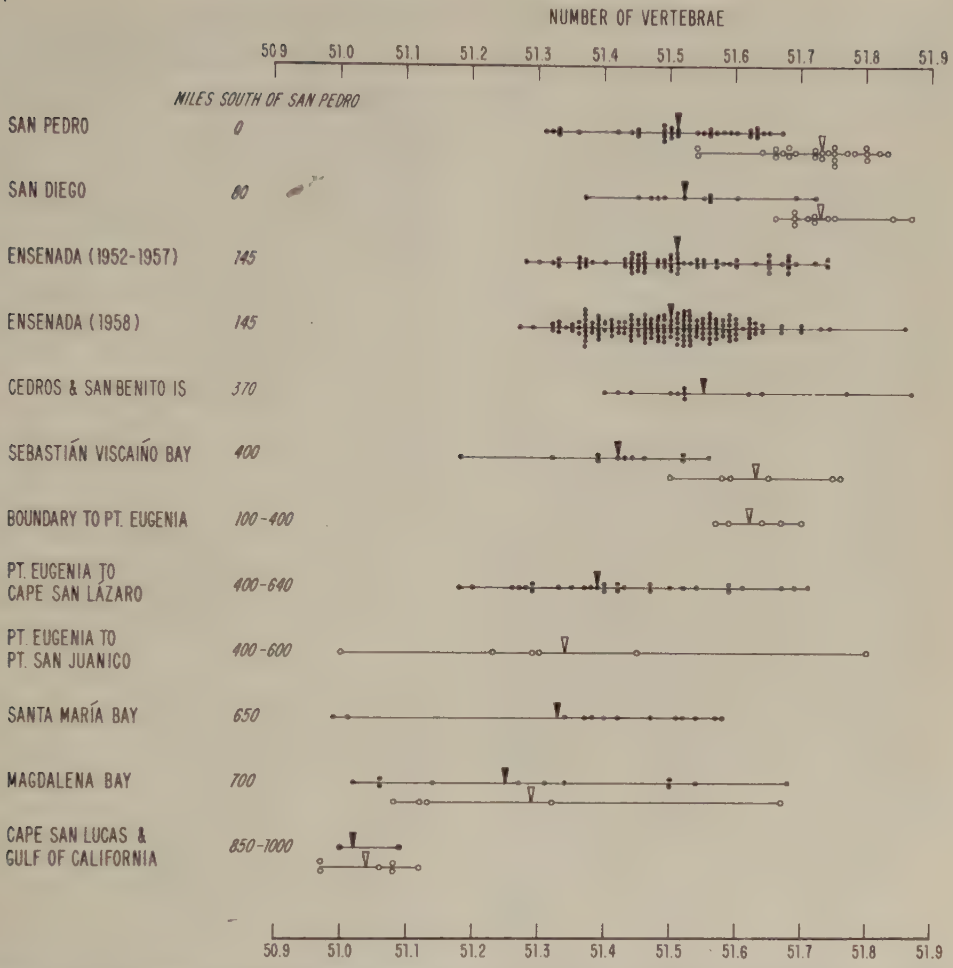

FIGURE 2. Frequency distribution of individual sample means and the mean of each area. Each solid dot (present data) or open circle (Clark's data) refers to an individual sample. The acute triangles represent the area means.

sents a sample listed by Clark (1947). Table 1 summarizes the present data in Fig. 2 by year and month.

Clark's 1947 data, with all age-groups combined, indicate that prior to 1942 the mean vertebral values changed abruptly in the vicinity of Pta. Eugenia, Baja California: average values south of this point were markedly lower than those to the northward. The higher values to the northward formed the basis for Clark's statement that "The average number of vertebrae is approximately 51.7 for all sardines north of southern Lower California and about 51.2 for sardines from southern Lower California." These numerical values have since been considered to be "standard" for sardines spawned under what has been thought to be "normal" oceanographic conditions. For Southern California alone Clark's average for all age groups combined was 51.73. She reported on only five samples with a combined mean value of 51.62, sampled from 1938 to 1940 from the Boundary to Pta. Eugenia—excluding Sebastián Viscaíno Bay samples, considered separately.

Whereas Clark's data from north of Pta. Eugenia comprised samples taken between 1921 and 1941, the present data stems from samples taken between 1950 and 1959. A distinct and significant change has taken place in the decade that separates the sampling efforts (Fig. 2). The plotted mean values of all samples from each area and the area means for the present data show a rather marked reduction in areal mean values as well as a very great number of sample mean values that fall well below the lowest reported by Clark. It will be noted that this reduction persists from Southern California to Pta. Eugenia. Both sets of data are in excellent agreement from Pta. Eugenia southward and into the Gulf of California.

It is unfortunate that very few samples from the region, "Boundary to Pt. Eugenio," were available to Clark, as compared with the much larger number from Ensenada that are used in the present study. Clark's five sample means from this region all fall within the range of those from Ensenada, though they are distinctly on the high side. Clark's data from Sebastián Viscaíno Bay alone correspond very closely with those for the broad areal grouping from the Boundary to Pta. Eugenia. The higher averages appear to have persisted further south in 1921-41 than in 1950-59.

It is of considerable interest that so many sample means from the northern region should fall well below those reported by Clark. For areas south of Pta. Eugenia, excluding those of Cape San Lucas and the Gulf of California, very few samples in the present body of data (only 21 percent) have lower vertebral mean values than do those from Ensenada and Southern California (Fig. 2). Clark's data alone show 82 percent of the samples from these southern areas to have appreciably lower values than do the samples from Southern California reported on in 1947. This difference of 61 percent is striking evidence of the reduction in mean numbers of vertebrae between the two time periods in the samples from Southern California and northern Baja California. The populations, or stocks, of fish from areas south of Pta. Eugenia may intermingle to at least a small degree with those from the Gulf of California: of all samples from south of Pta. Eugenia, excluding those from the Gulf, about 23 percent have vertebral mean values similar to those reported from the Gulf (Fig. 2).

In contrast to the expected lower mean values for the areas south of Pta. Eugenia are the several relatively high values. The value of 51.795 for 78 fish (0 age-group), listed by Clark for the "Pt. Eugenio to Pt. San Juanico" area, and the value of 51.669 for 127 fish (I age-group) from Magdalena Bay, are generally considered as typically "northern" or "high" means. The present data includes one sample of limited significance (comprising only 22 fish) from the same area with a high mean of 51.68. The reasons for these higher mean values are difficult to assess.

McHugh (1950) offered a possible explanation of these high values, which average 51.71. Postlarval sardines from southern Baja California, spawned in spring and summer, were found to have significantly different mean vertebral numbers of 51.54 and 51.21 respectively (as McHugh did not count the urostyle, his counts are increased by one to conform to those of the present study). The values of 51.79 and 51.17 for spring- and summer-spawned fish in samples from northern Baja California differ even more significantly. Whereas McHugh's high value of 51.54 for postlarvae spawned in the spring in southern Baja California falls well below the average figure of approximately 51.71 for the older fish under consideration from these southern areas, it does indicate the possibility that environmentally induced meristic differences may result in abnormally high mean vertebral numbers in at least some samples from these areas, and, possibly, for all areas throughout the range. Of course the reverse situation may also occur as is shown by two samples taken near the San Benito Islands, about 15 miles west of Cedros Island. In 1946, 172 0-year fish furnished a mean vertebral value of 51.40 and in 1955, 143 fish (estimated at nearly two years of age) provided a mean of 51.87 vertebrae. This is an area that was quite "northern" in the data presented by Clark, but considerably less so in the present data: the means are about 51.64 and 51.50, respectively.

Both Magdalena and Santa María Bays also show a tendency to produce some samples with relatively high mean vertebral numbers. Excluding the two low mean values, 50.99 and 51.01 (Fig. 2, Table 1), raises the Santa María Bay average to 51.44, a figure notably higher than the combined average for the Bay and one that would appear to fit the plotted distribution of sample means (Fig. 2). It is reasonable to assume that as Santa María Bay is entirely open to the sea any migrating northern stock may readily enter. In contrast, the relatively enclosed Magdalena Bay is presumably less accessible to coastal migration and may be expected to harbor a more indigenous population. The number of samples from each bay is hardly adequate to resolve the question. Actually the highest mean value recorded for Magdalena Bay in each set of data exceeds any of the means for Santa María Bay. However, the high value of 51.68 listed in the present data is derived from a sample of only 22 specimens and may not be of great significance. The next highest value, 51.54, is derived from 68 fish. It thus appears probable that higher values may occur in the Bay. Clark's 1947 data includes a sample of 127 I-year fish which furnished the more significant mean value of 51.669. Thus it is apparent that either migrations from the north may enter these bays or that local spawning conditions may occasionally be such that higher average vertebral numbers may result. It is also apparent that the same situation pertains to those samples having lower vertebral mean values comparable to those listed for the Gulf of California. From the standpoint of migration these bays may be considered to be more within the range of Gulf stock than those from more northern waters, particularly those from north of Pta. Eugenia.

As noted by Clark (1947) the Gulf of California may well harbor a separate population of sardines that intermingles little if at all with the northern populations, but that may mix to a degree with stocks occurring below Pta. Eugenia. The present data has strengthened Clark's conclusion, for the two sets of data are remarkably similar, considering both the time interval between the two sets of data and the total number of years involved. Whereas Gulf samples consist of O fish or postlarvae, except for the 31-fish sample of adults reported by Clark, affording a mean of 50.968, all samples have provided mean values of about 51.00.

Year Class Data and the "Warm" Years: The occurrence of abnormally high ocean temperatures in 1957 and 1958, and the observed reduction in average numbers of vertebrae in samples from northern Baja California and Southern California, requires that some consideration be given to year classes comprising the present data. As a major portion of the samples were taken in 1957-58, particularly in these two areas, the age data are considered for these areas only.

Daugherty and Wolf (1960) show that, for the 1957-58 season in Southern California, the 1957 year class contributed only 1.3 percent to the commercial catch. During the same period of the northern Baja California season (including Ensenada and Cedros Island landings) these authors show that the 1957 year classes contributed only 1.4 percent. The 1958-59 catch data for Southern California showed that 1957 fish comprised only 10.2 percent of the catch and in Baja California only 11.6 percent (Wolf and Daugherty, 1961).

Thus it is clear that the 1957 and 1958 year classes, presumably hatched in warmer water, were a minor constituent of the catches and the vertebral count samples. Therefore, the recent "warm water" can be almost completely discounted as contributing to the low vertebral numbers off Southern California and northern Baja California during the 1957-58 and 1958-59 fishing seasons.

DISCUSSION

If the effect of the warm years may be discounted as being a major cause for the observed reduction in average vertebral numbers in the area of northern Baja California and Southern California, other hypotheses may be erected: (1) The environment had begun to change as early as 1950 and the change was reflected in the reduced average number of vertebrae (but there is no oceanographic evidence of such a change); (2) Micro-environmental changes affected the vertebral numbers and morphometry of the individual spawnings that were later sampled (such an event is, of course, always possible; however, there are great odds against the chance that such spawnings and samples make up the bulk of the present data); (3) Stocks of fish migrated northward from the southern areas, which are characterized by lower average numbers of vertebrae, accompanied by a reduction in the numbers of northern-type fish. This is the most attractive hypothesis.

Ahlstrom (1959) has reported that such a northward movement did occur in early 1954. Associated with this northward movement was an appreciable rise in water temperatures, particularly in the early spring. Clothier and Greenhood (1956) reported that 67,258 tons of sardines were landed during the 1954-55 season in contrast to the slightly more than 3,000 tons in 1953-54 and some 4,500 tons in 1952-53.

Unfortunately, the present data are not adequate to test whether or not this observed migration of sardines into Southern California contributed to the lowering of the average number of vertebrae within the area in 1954, though they are suggestive. Only one sample of 37 fish, from San Pedro, was available for study. This sample afforded a mean of 51.49 (Table 1), quite characteristic of the recent period in the Southern California fishery, whereas the average for the earlier period reported on by Clark was 51.73.

That these 1954 fish, and those of subsequent and earlier samples to 1950, were probably not spawned in the area of capture during any warm period is evidenced by the following statement by Reid, Roden, and Wyllie (1958), "the period from 1949 to 1956 is distinguished from the previous 15 or 20 years by substantially colder waters in the first few months of the year."

The foregoing evidence of the period of 1949-1956 being colder than the previous 15 or 20 years adds further interest to the comparison of the two sets of data on vertebral numbers. If most specimens in the present study are presumed to have been spawned in waters colder than those in which Clark's must have been (all spawned prior to 1941), it could also be presumed that the average numbers of vertebrae would be higher than observed. This obviously is not the case in those samples studied from northern Baja California and Southern California; thus by every test the change in vertebral numbers is opposite that suggested by the environmental changes. There must, then, have been major changes in the stocks on the fishing grounds.

One question posed by the present body of data is, what happened to the "northern" type of sardine? Temperature data indicate that sufficiently cold water was available to have produced high vertebral numbers. The number of samples studied would appear to afford an adequate representation of the fish available to the sampling techniques. It may be that the northern types were "somewhere else" and not available to the fisherman or the sampling techniques. It may also be that the influx of southern fish in 1954 continued and that interbreeding with the northern types has resulted in lower average numbers of vertebrae, or that the northern types were still present but in considerably reduced numbers.

In review, south of Pta. Eugenia there was no change in vertebral numbers between the earlier and later period, all counts being low. North of Pta. Eugenia, vertebral counts during the recent decade are lower than the earlier period, the average being intermediate between the stable southern average and the earlier northern average. Further, the direction of the change, i.e., a decrease, has been contrary to that expected to have resulted from the cooler environment during the recent period. Thus, there is good evidence that there has been a change in the "racial" composition of the stocks taken by the fishery in Southern California and northern Baja California.

The precise nature of the change is not so clear. There has been a severe decline in the stocks available to those fisheries compared to the early period (Clark and Marr, 1955). This almost rules out the possibility that the lowering of the vertebral numbers was

(831)

caused only by an influx of southern fish. Rather, the change in vertebral numbers must have been associated with a reduction of the population of the northern, high vertebral number, ''race,'' possibly, but not necessarily, accompanied by additional influx from the south.

SUMMARY

1. The results of the summarized three widely differentiated earlier approaches to the problem of heterogeneity of sardine stocks throughout the range indicate the presence of more than one population, or stock, of sardines inhabiting the total range.

2. The present study demonstrates that a marked reduction in average numbers of vertebrae, for sardines sampled in northern Baja California and Southern California, has occurred throughout the period from about 1950 through 1958. This reduction results in a much lower average value than that reported by Clark (1947), the respective values being 51.50 and 51.73.

3. The plot of average numbers of vertebrae for each sample within a given area, and the area averages (Fig. 2), indicates that many of the samples taken in northern Baja California and Southern California, in the period from 1950 to 1959, have sufficiently low values to have originated in the waters off Central or Southern California.

4. Year-class data for a major portion of these fish with low values indicate that only a small percentage of the total catch could have been spawned in the area of capture during the abnormally high ocean temperatures that began in 1957.

5. For the areas of southern Baja California (Pta. Eugenia into the Gulf of California) the present data is in excellent agreement with that presented by Clark (1947). The two sampling efforts cover a period of time from 1926 to 1958 for this broad area. This fact indicates that these areas may harbor indigenous populations in that no apparent change in the average vertebral numbers has occurred in the 32-year period.

6. It is concluded that the sardines caught in northern Baja California between the years 1950 and 1959 were comprised of a different ''racial'' mixture than those taken prior to 1941, because the recent reduction in vertebral numbers is contrary to the phenotypic increases usually associated with cooler water. Concurrently, abundance has declined, so the change in vertebral number is most easily explained by postulating reduction in a northern ''race,'' possibly accompanied by an influx of additional southern fish.

ACKNOWLEDGMENTS

Numerous members of the various agencies comprising the California Cooperative Oceanic Fisheries Investigations (CalCOFI) have contributed time and effort toward collecting and preserving the samples used in this study. Particular thanks are due Anita B. Daugherty, of the California State Fisheries Laboratory, Terminal Island, and to Franklin G. Alverson of the Inter-American Tropical Tuna Commission, for making available samples respectively from the commercial landings in Southern California and from the bait samples taken by the tuna fleet in Mexican waters Especial thanks are due to A. M. Vrooman, J. S McGregor, and R. S. Wolf of the La Jolla Laboratory of the U.S. Bureau of Commercial Fisheries for making available the samples from the 1957-58 Ensenada commercial fishery and to E. H. Ahlstrom, Car L. Hubbs, and Garth I. Murphy for valuable criticism of the manuscript.

REFERENCES

Ahlstrom, E. H., 1959. Distribution and abundance of eggs of the Pacific sardine, 1952-1956. *U.S. Dept. of Int., Fish and Wildl. Serv., Fish Bull. No.* 165, **60** : 185-213.

Clark, F. N., 1936. Variations in the number of vertebrae of the sardine, *Sardinops caerulea* (Girard). *Copeia*, (3) : 147-150.

Clark, F. N., 1947. Analysis of populations of the Pacific sardine on the basis of vertebral counts. *California Division of Fish and Game, Fish. Bull. No.* 65 : 26.

Clark, F. N., and J. F. Janssen, Jr., 1945. Movements and abundance of the sardine as measured by tag returns. *California Division of Fish and Game, Fish Bull. No.* 61 : 7-42.

Clothier, C. R., and E. C. Greenhood, 1956. Jack mackerel and sardine yield per area from California waters, 1946-47 through 1954-55. In the marine fish catch of California for the years 1953 and 1954. *California Division of Fish and Game, Fish Bull. No.* 102 : 99.

Daugherty, A. E., and R. S. Wolf, 1960. Age and length composition of the sardine catch off the Pacific coast of the United States and Mexico in 1957-58. *California Fish and Game.* **46** (2) : 189-194.

Felin, F. E., 1954. Population heterogeneity of the Pacific pilchard. *U.S. Fish and Wildl. Serv., Fish Bull. No.* 86 : 201-225.

Hart, J. L., 1933. Statistical studies on the British Columbia pilchard: Vertebra counts. *Trans. Roy. Soc. Canada*, Sect. V : 79-85.

Hart, J. L., 1943. Tagging experiments on British Columbia pilchards. *Journ. Fish. Res. Bd., Canada,* **6** (2) : 164-182.

Hubbs, C. L., 1925. Racial and seasonal variation in the Pacific herring, California sardine, and California anchovy. *Calif. Fish and Game Comm., Fish Bull. No.* 8 : 23.

Marine Research Committee, 1955. *Progress Report, California Cooperative Oceanic Fisheries Investigations, 1 July, 1953 to 31 March, 1955* : 52.

Marine Research Committee, 1960. *Reports of the California Cooperative Oceanic Fisheries Investigations, Vol. VII, 1 January, 1958 to 30 June, 1959* : 217.

McHugh, J. L., 1950. Variations and populations in the clupeoid fishes of the North Pacific. *A Doctoral dissertation on file in the Scripps Institution of Oceanography, La Jolla, California* :116.

Reid, J. L., Jr., G. Roden, and J. Wyllie, 1958. Studies of the California Current System. *Progress Report, California Cooperative Oceanic Fisheries Investigations, 1 July, 1956 to 1 January, 1958* :57.

Thompson, W. F., 1926. The California sardine and the study of the available supply. *California Fish and Game Comm., Fish. Bull. No.* 11 : 8-17.

Wolf, R. S., and A. E. Daugherty. In press. Age and length composition of the sardine catch off the Pacific coast of the United States and Mexico in 1958-59. *California Fish and Game.*

[RADIOCARBON, VOL. 3, 1961, P. 1-3]

Radiocarbon

1961

MASS-SPECTROMETER ANALYSES OF RADIOCARBON STANDARDS

HARMON CRAIG

Department of Earth Sciences, University of California, La Jolla

Twenty-four samples of CO_2 from combustion of the NBS oxalic-acid radiocarbon standard, submitted from 13 radiocarbon laboratories, were analyzed for C^{13} content in this laboratory in order to provide comparative data for normalizing the counting results. The samples were analyzed on Samson, a 60° sector, six-inch radius, McKinney-Nier type mass-spectrometer with magnetic switching between sample and standard gas feed to the instrument.

The CO_2 samples were received in sealed breakoffski flasks containing on the order of 100 cc of gas, except for the Lamont, Yale, Isotopes Inc., and La Jolla samples which were in sample tubes with stopcocks. Aliquots of 10-15 cc were taken for analysis by direct expansion of the gas into an evacuated gas pipette on a vacuum line. The Lamont, Isotopes Inc., and Socony Mobil samples contained small amounts of an impurity not condensible in liquid N_2, and the wet combustion sample from the National Physical Laboratory contained some water; these samples were purified with liquid N_2 and dry-ice traps. The other samples contained no detectable impurities.

The samples were analyzed in series against a single gas standard which had previously been well calibrated against the PDB Chicago C^{13} standard. The following corrections were applied to the raw δC^{13} values:

a. Valve mixing: $f = 1.006$
b. Fraction of mass 44 tail falling on mass 45: $f = 1.0066$
c. CO_2 background in source: $f = 1.0033$
d. 0^{17} content of standard and sample gas: correction as given by Craig (1957).

The raw δC^{13} values are multiplied by the indicated factors; samples were also analyzed for O^{18} to obtain the corrections for 0^{17} in the individual samples. The instrumental corrections were minimized for inter-comparison of standards with each other by using a spectrometer gas standard chosen to have a C^{13} content close to the oxalic-acid value (–24.8‰ relative to PDB). The mass-spectrometer has been shown to be exactly linear (to 0.1‰) over a range of 0 to–50‰.

Table 1 presents the results in terms of C^{13} enrichment relative to the Chicago PDB standard ($\delta^{t}C^{13}$), and also as enrichments ($\delta_{w}C^{13}$) relative to

(833)

Contributions from the Scripps Institution of Oceanography, New Series, 1310
Reproduced by Permission

TABLE 1

Isotopic composition of CO_2 from NBS oxalic-acid-radiocarbon standards. All samples represent the CO_2 which was actually counted except for La Jolla and Socony Mobil who do not use CO_2 as counter gas.

Laboratory[1]	$\delta^{\dagger}C^{13}$	$\delta_{w}C^{13}$	$\delta^{\dagger}O^{18}$	Oxalic Acid Combustion
Copenhagen				
K-301	–19.41	+5.73	–15.09	direct
K-302	–19.73	+5.40	–15.92	direct
	–19.72	+5.42	—	—
K-303	–19.51	+5.63	–11.67	wet
Groningen				
1st series	–18.77	+6.39	–12.42	direct
Duplicate sample	–18.73	+6.43	–12.44	—
2nd series	–19.24	+5.91	–13.82	direct
Duplicate sample	–19.21	+5.94	–13.82	—
Isotopes, Inc.	–21.57	+3.52	–12.68	wet
La Jolla[2]				
170 A	–31.34	–6.50	–2.75	wet
170 B	–31.37	–6.53	—	—
145	–22.72	+2.34	(–5.3)	direct
197	–21.84	+3.24	(–5.3)	wet
Lamont				
L-456 D	–19.05	+6.10	–11.60	wet
National Physical Lab.				
A	–18.94	+6.21	–10.86	wet
B	–21.43	+3.66	–12.63	direct
New Zealand				
CR-929	–19.50	+5.64	–10.20	direct
Duplicate sample	–19.45	+5.69	–10.35	—
Pennsylvania				
P-263	–25.67	–0.67	–16.29	wet
	–25.70	–0.71	–16.36	—
Socony Mobil[3]	–19.28	+5.87	–16.30	direct
Stockholm				
ST 532	–17.15	+8.05	–17.26	direct
Duplicate sample	–17.26	+7.94	–17.28	—
Trondheim				
T-200	–18.37	+6.80	–19.35	wet
Uppsala				
Oxalic acid-1	–18.97	+6.18	–13.24	direct
Yale	–20.01	+5.12	–12.22	wet

NOTES

[1] All sample numbers or letters denote separate combustions. "Duplicate sample" means duplicate flasks of gas from one combustion were received and analyzed. An analysis with no notation is a repeat analysis of the same gas, made as a check after the series was analyzed (K-302 and P-263).

[2] The samples are CO_2 from recombustion of the C_2H_2 which was actually counted. The C_2H_2 samples were combusted with CuO and O_2 in a closed recycling system as described by Craig (1953), which prevents fractionation in this step. Samples 170A and 170B are duplicate recombustions of the same C_2H_2 from a single combustion. (The O^{18} value—5.3 is the average of several other combustions, as the last two samples were not analyzed for oxygen.)

[3] The sample represents CO_2 produced from the combustion of oxalic acid. The CO_2 was then hydrogenated to CH_4 for counting; the isotopic analysis does not include any fractionation which may occur in the preparation of the CH_4.

the C^{13} content of average wood which is taken as $\delta = -25‰$ relative to PDB (Craig, 1953). The delta values are defined by:

$$\delta^{\dagger} = 1000\,[(R/R_{PDB}) - 1];\ \delta_{w} = 1000\,[(R/R_{wood}) - 1]$$

where $R = C^{13}/C^{12}$, and $R_{wood} \equiv 0.975\ R_{PDB}$. The absolute values of the ratios are given by Craig (1957). The uncertainty in the δ values is ± 0.1‰.

Table 1 also shows the measured O^{18}/O^{16} enrichments in per mil ($\delta^{\dagger}O^{18}$) relative to PDB standard CO_2, as it may be of some interest to record the range and variation of O^{18} content in the different combustions. The observed data are quite typical of values observed for carbon combustion with CuO and tank O_2 (Craig, 1957, p. 141) except for the C_2H_2 combustions which were done with CuO and tank O_2 and deviate for an unknown reason.

Average values for both "direct" combustion (with O_2) and wet combustion were computed by using only one value for direct or wet combustion for each laboratory; when duplicates or samples from more than one combustion of the same type were analyzed the average of these was used as one analysis. In order to compare combustions directly, the La Jolla data were not included, as these values include the effect of the additional step of making C_2H_2 from the CO_2 obtained from the combustion.

The average direct combustion value thus obtained (7 laboratories) is $\delta^{\dagger}C^{13} = -19.3‰$. The average wet combustion value (excluding also the Pennsylvania value which seems clearly divergent; 6 laboratories) is −19.6‰, indicating that wet oxidation is probably about as reliable as direct combustion with O_2, at least for oxalic acid. A histogram of all the data appears markedly non-Gaussian, with a pronounced tendency for enrichment of C^{12} in the product CO_2, as might be expected if some combustions are less complete than others.

δC^{14} values relative to any standard are given by:

$$\delta_{14} = 2\delta_{13} + 10^{-3}\delta_{13}^{2} \qquad (\delta \text{ values in per mil})$$

assuming that for any separation process $\alpha_{14} = \alpha_{13}^{2}$ (Craig, 1954, p. 133). The total C^{13} range, excluding the one very light La Jolla wet combustion value and the Pennsylvania value, is 5.5‰, indicating that the probable spread among various laboratories for careful work will be of the order of only 1% variation in reported activity when fractionation is neglected, in the case of a single sample. The range of C^{13} variation in ancient and modern wood is of the order of 10‰ (Craig, 1953) and is thus a more important factor than most of the laboratory effects observed in the present study.

Thanks are due the Isotopes Inc., New Zealand, Socony Mobil, and Stockholm laboratories for their courtesy in indicating the pressures in their sample flasks. Construction and operation of Samson were supported by the Office of Naval Research, the Atomic Energy Commission, and the National Science Foundation.

REFERENCES

Craig, H., 1953, The geochemistry of the stable carbon isotopes: Geochim. et Cosmochim. Acta, v. 3, p. 53-92.

——— 1954, Carbon 13 in plants and the relationships between carbon 13 and carbon 14 variations in nature: Jour. Geology, v. 62, p. 115-149.

——— 1957, Isotopic standards for carbon and oxygen and correction factors for mass-spectrometric analysis of carbon dioxide: Geochim. et Cosmochim. Acta, v. 12, p. 133-149.

(836)

Records of Oceanographic Works
in Japan Vol. 6 No. 1
March 1961
pp. 36-52.

Sea Surface Temperature, Radiation, and Wind Anomalies in the North Pacific Ocean*

By

Gunnar I. Roden and Joseph L. Reid, Jr.

(Scripps Institution of Oceanography, University of California)

Abstract

Nonseasonal variations of sea surface temperature occur in many parts of the ocean. These anomalies cover large areas and have an average endurance of three to six months. Equally large scale, but less persistent, variations occur in the sea level atmospheric pressure which may be interpreted as geostrophic wind anomalies, and in radiation. An examination of the relation of temperature anomalies to those of wind and radiation is made by computing the crosscorrelations. Significant values were found in some cases, but are at best restricted to certain times of the year and to certain areas.

Introduction

Sea surface temperature anomalies in almost any part of the world are of some interest to oceanographers, meteorologists and fisheries biologists. Various authors have sought to relate to them such matters as the frequency of hurricane occurrence (Riehl, 1954), agricultural problems (Hanzawa and Inoue, 1952) and the anomalous distribution of organisms (Hubbs, 1948). Yet the extent and causes of sea surface temperature anomalies are only incompletely understood. Two possible causes are wind and radiation. The effect of wind upon temperature has received some attention, including studies by Helland-Hansen and Nansen (1920) and Rodewald (1953) in the Atlantic, and Hanzawa (1957), Hatanaka (1952), Hirano (1957) and Uda (1955) in the western Pacific. The influence of radiation has not been studied in detail owing ot the difficulty of obtaining reliable data from oceanic regions.

In this paper we shall consider the dependence of the temperature anomalies upon anomalies of radiation and also of wind acting through advection and mixing. The importance of mixing in influencing the surface temperatue depends critically upon the vertical temperature structure ; if the temperature

---

* Contribution from the Scripps Institution of Oceanography New Series. 1311.

Reproduced by Permission

does not decrease appreciably with depth, i.e., the mixed layer is quite deep, as is frequently the case in winter in higher latitudes, mixing is not likely to have an appreciable influence upon the surface temperature. The anomalies are then principally the result of horizontal advection. If, on the other hand, the thermocline is shallow, mixing becomes increasingly important in altering the surface temperature.

Since there are not sufficient data available to study the depth of the mixed layer and the intensity of the underlying gradient, it is not possible to go further into the vertical transport of heat. Instead, much of the following discussion is limited to the winter season in temperate and high latitudes where there is reason to assume that the surface temperature change due to vertical heat transport is small compared to that due to horizontal movement. The strongest temperature anomalies can then be expected in regions where the wind blows across strong horizontal temperature gradients such as off northern Japan and in the region of the North Pacific westerlies.

Data

Monthly mean sea surface temperature records from 1921-1938 for the North Pacific Ocean were obtained from the publications of the Imperial Marine Observatory, Kobe, Japan. Sea surface temperature for 1957 and 1958 for the North Pacific east of longitude 180 were obtained from the Bureau of Commercial Fisheries, Honolulu Biological Laboratory in Hawaii. Monthly mean sea level atmospheric pressure charts for the period 1899-1958 (prepared from daily maps) were obtained from the U.S. Weather Bureau. Where necessary, pressure differences were converted into geostrophic winds. Geostrophic winds were not determined for ocean areas south of latitude 20 N, owing to the scarcity of pressure observations and the doubtful application of the geostrophic assumption in those places. From the geostrophic wind components the vertical component of the curl of the wind stress was determined.

Incoming short wave radiation was computed from cloudiness data (Imperial Marine Observatory, Kobe, Japan, 1921-1938) making use of the relation $Q=(1-r)\,Q_0(1-kn)$ where Q is the incoming radiation with a cloudy sky, r the amount reflected from the sea surface, Q_0 the incoming radiation with a clear sky, k a constant and n cloudiness in tenths. Values for r, Q_0 and k are given by Budyko (1956).

In all cases differences were taken between the monthly mean and the long term mean for the same month in order to eliminate the seasonal variation.

Relation between pressure and temperature anomalies

A qualitative agreement between pressure (wind) and temperature anomalies is seen by comparing the pressure anomaly maps with the correspond-

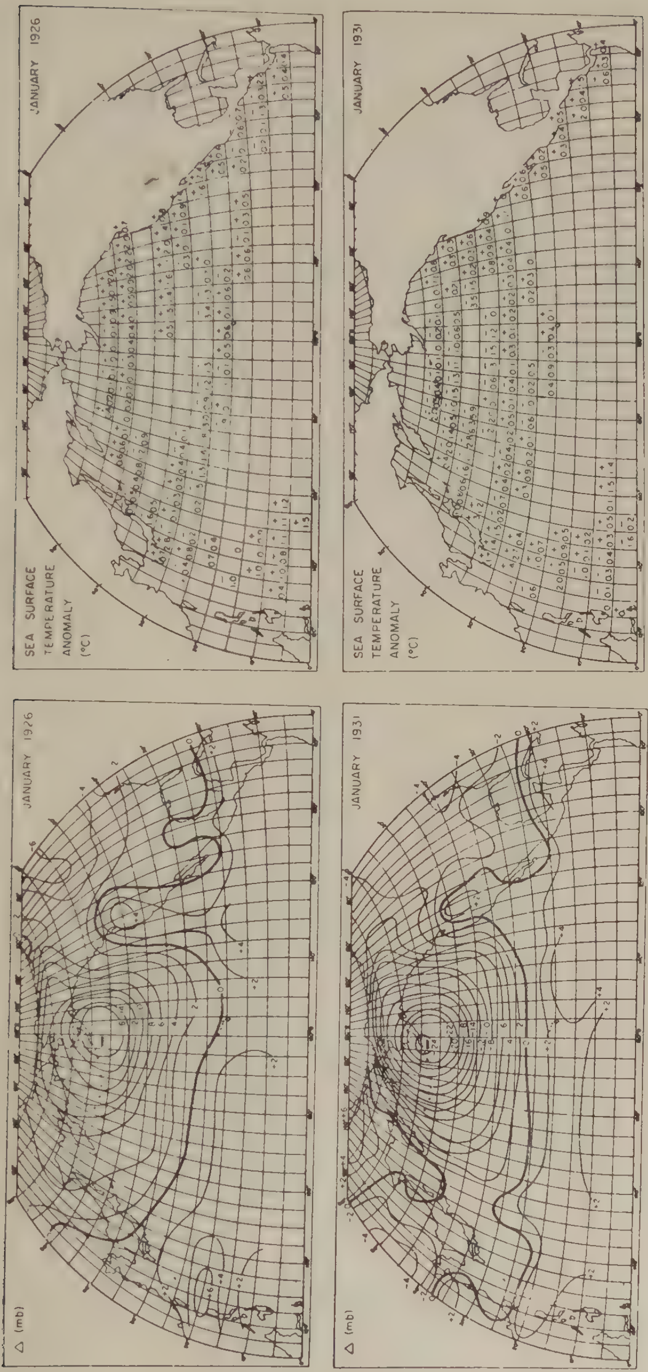
SEA SURFACE TEMPERATURE ANOMALY (°C)
JANUARY 1926
JANUARY 1931
Δ (mb)
JANUARY 1926
JANUARY 1931

Fig. 1. Pressure and temperature anomalies during January 1926 and January 1931.

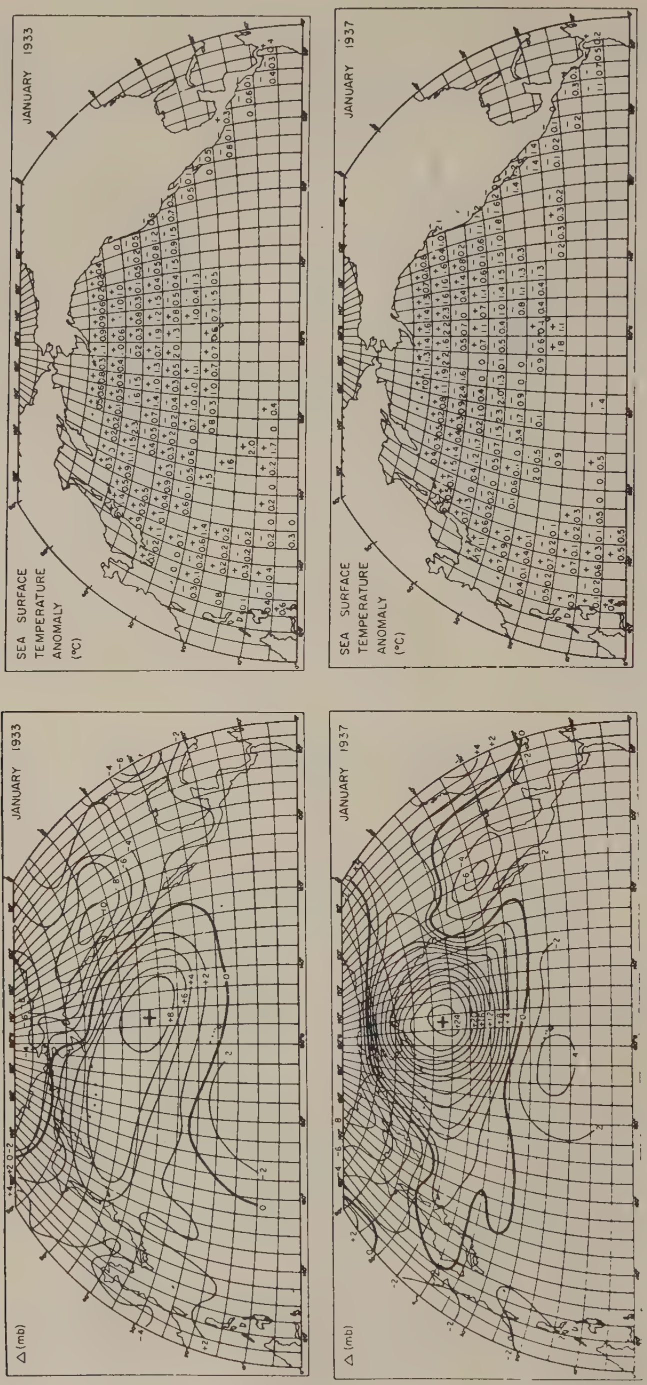
SEA SURFACE TEMPERATURE ANOMALY (°C)
JANUARY 1933
SEA SURFACE TEMPERATURE ANOMALY (°C)
JANUARY 1937
Δ (mb)
JANUARY 1933
Δ (mb)
JANUARY 1937

Fig. 2. Pressure and temperature anomalies during January 1933 and January 1937.

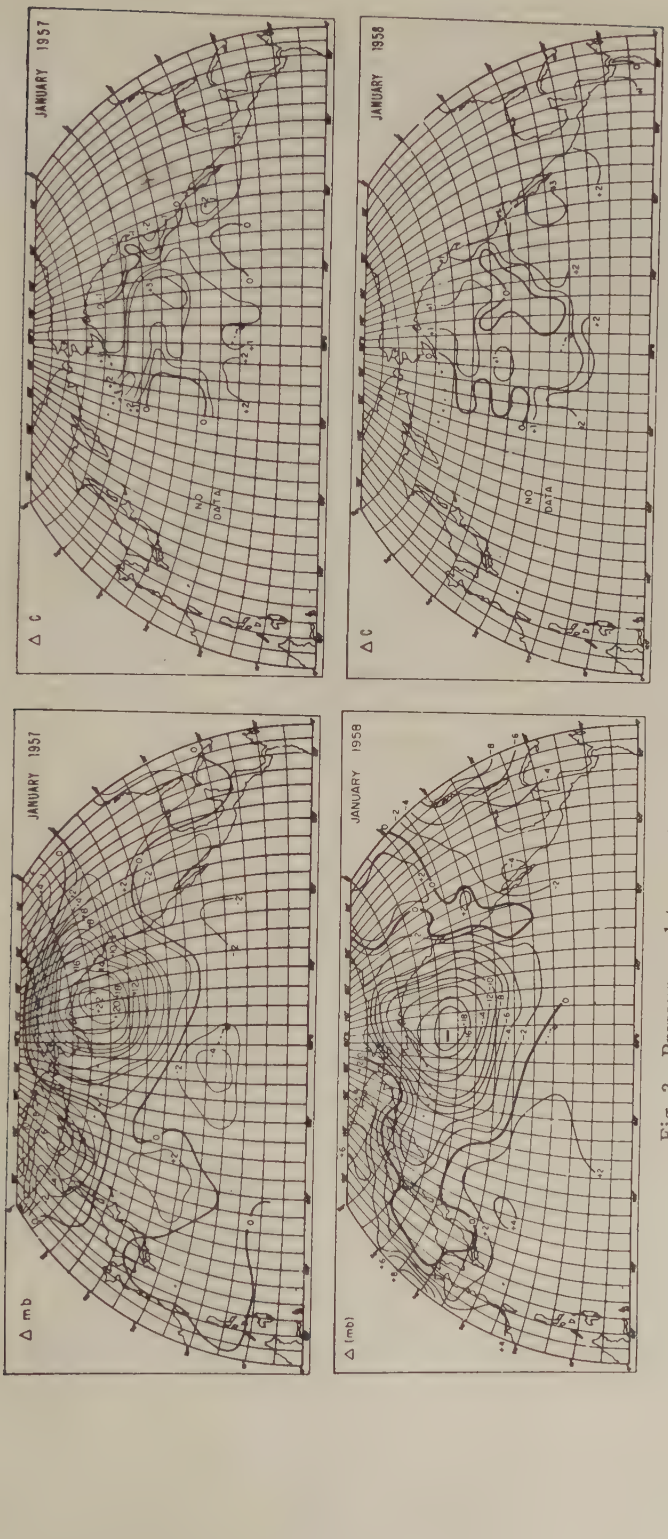
Δ C
JANUARY 1957
NO DATA
Δ C
JANUARY 1958
NO DATA
Δ mb
JANUARY 1957
Δ (mb)
JANUARY 1958

Fig. 3. Pressure and temperature anomalies during January 1957 and January 1958

ing temperature anomaly maps in Figs. 1, 2 and 3. Thus in January 1926, 1931 and 1958 the dominant feature in the central North Pacific was a large negative pressure anomaly. Since this anomaly occurs in the same region as the Aleutian Low, the circulation around this pressure cell was strengthened and consequently one could expect increased northerly winds in the northwestern and increased southerly winds in the Northeastern Pacific. If it is assumed that the surface waters move approximately in the direction of the wind or slightly to the right of it, one might anticipate negative temperature anomalies to the left and positive temperature anomalies to the right of the pressure anomaly. The observed temperature anomalies in January 1926, 1931 and 1958 show below average temperatures in the western central Pacific and above average temperatures in the eastern Pacific, as was expected from the above considerations. During January 1933, 1937 and 1957 the central North Pacific was occupied by a pronounced positive pressure anomaly. This anomaly was caused in 1933 by a strongly developed subtropical high pressure cell and in 1937 and 1957 by a southward extension of a polar anticyclone into regions normally occupied by the Aleutian Low. In the first case one could expect a reduced circulation around the Aleutian Low and in the last cases the atmospheric circulation was actually reversed. Thus, owing to the reduced northerly winds in the central and western Pacific, positive temperature anomalies could be expected there. In the eastern Pacific one would anticipate negative temperature anomalies owing to the reduced advection of warm water from the southwest. The observed temperature anomalies seem to confirm this.

The above examples shown were chosen to represent the strongest anomalies, but their large scale nature is a characteristic feature and not dependent upon the particular years selected. Notable negative pressure anomalies in the central Pacific occurred also in 1912 and 1941 and strong positive anomalies in 1911 and 1949. No temperature anomalies for the open ocean are available for these years but coastal records of air temperature (U. S. Weather Bureau) and sea surface temperature (U. S. Coast and Geodetic Survey, 1956) seem to indicate that 1912 and 1941 were warm and 1911 and 1949 cold winters along the shores of Alaska and the United States.

The increased or decreased circulation around the Aleutian Low can also be expressed in terms of anomalies in the curl of the geostrophic wind stress (Fig. 4), henceforth referred to as curl anomalies. Normally cyclonic (positive) curl prevails in the region of the Aleutian Low. Its magnitude is in the order of $3 \cdot 10^{-8}$ dynes cm^{-3}. (The mean January curl chart is remarkably similar to the chart of divergence and convergence areas in the Pacific Ocean in northern winter, prepared by Hidaka and Ogawa (1958)). In years when the circulation around the low is greatly increased the curl may be as high as $10 \cdot 10^{-8}$ dynes cm^{-3} and at times when a high pressure occupies the area of

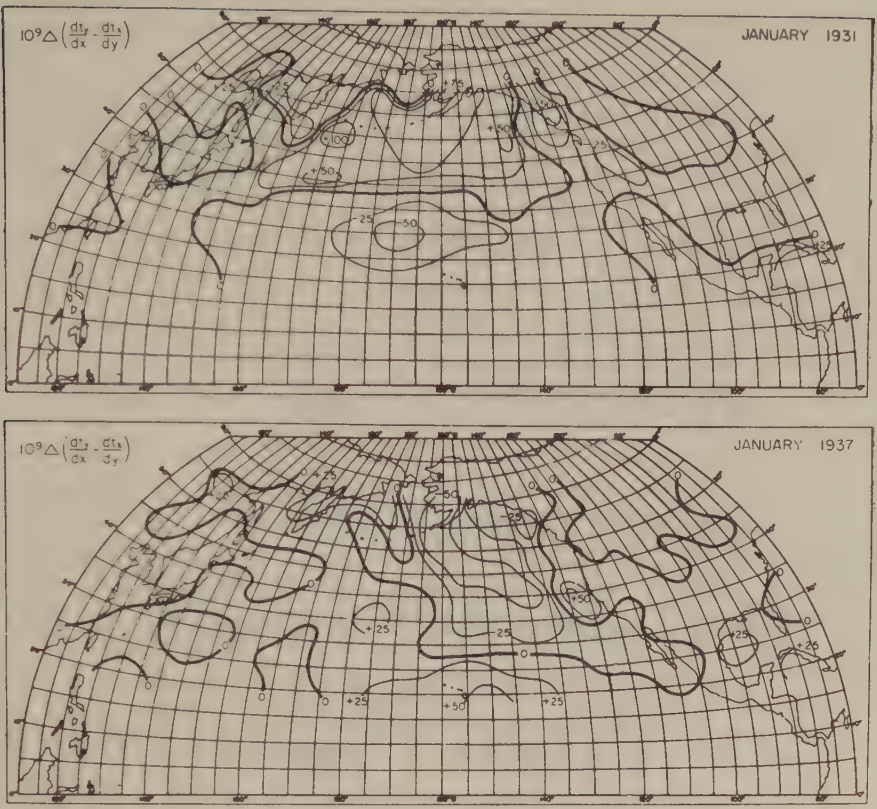
$10^9\Delta\left(\frac{d\tau_y}{dx}-\frac{d\tau_x}{dy}\right)$
JANUARY 1931
+75
+100
+50
-25
-50
$10^9\Delta\left(\frac{d\tau_y}{dx}-\frac{d\tau_x}{dy}\right)$
JANUARY 1937
+25
-50
+50
-25
+25
+50
0

Fig. 4. Geostrophic wind stress vorticity anomalies for January 1931 and January 1937.

the Aleutian Low anticyclonic (negative) curl of the order of $2 \cdot 10^{-8}$ dynes cm^{-3} is found. The notable feature is the large scale nature of the anomalies and the fact that the anomaly is frequently larger than the mean. There is a very rough agreement between the respective areas of curl anomalies and temperature anomalies. If the respective charts for 1931 and 1937 are compared to each other, it is seen that cyclonic curl anomalies are accompanied by negative temperature anomalies in approximately the same region and that areas of anticyclonic curl anomalies correspond roughly to areas of positive temperature anomalies. Since both the cyclonic curl (through upwelling) and horizontal advection anomalies could have produced the negative temperature anomalies in the central Pacific, it is not clear which factor is the more important one. However, the small vertical temperature gradients normally observed in winter in high latitudes are suggestive that horizontal advection probably has the greater effect upon changing the surface temperatures there.

Areal coherence, persistence and variance of temperature, wind and radiation anomalies

The areal coherence of temperature anomalies is illustrated for the California Current region in Fig. 5. It is seen that anomalies of the same sign and approximately of the same magnitude occur almost simultaneously between latitudes 20 N and 40 N.

The persistence of these anomalies can be calculated from the autocorrelation function:

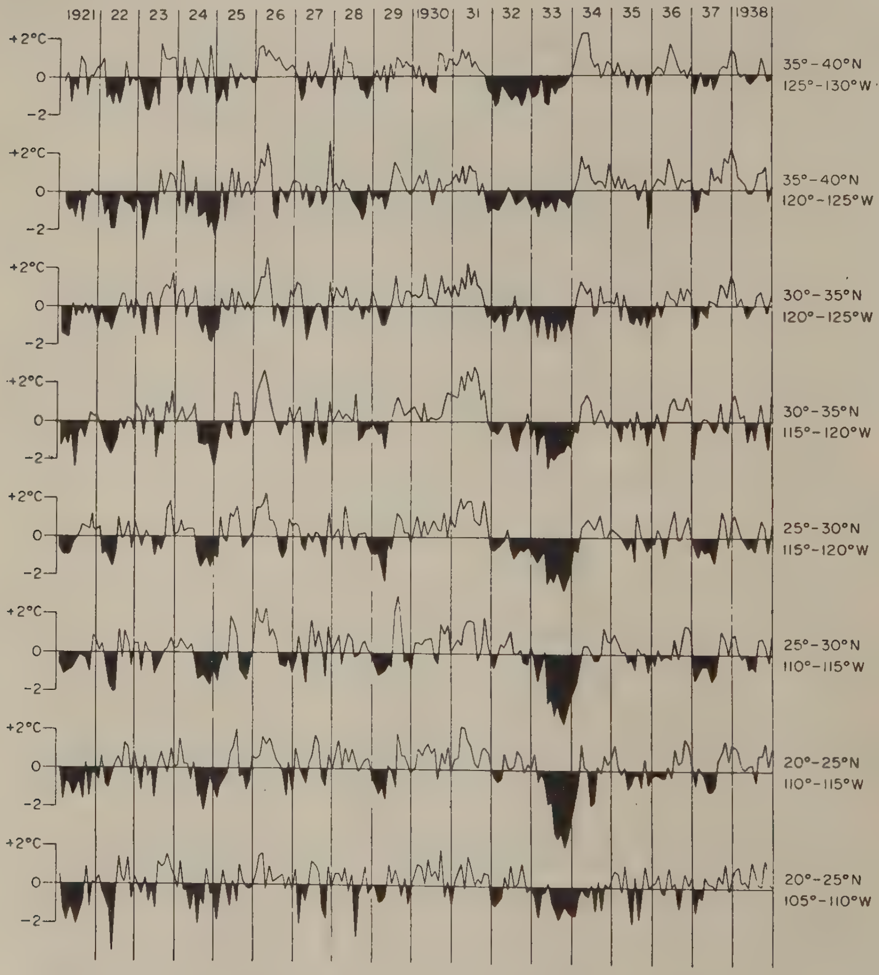

Fig. 5. Time series of temperature anomalies 1921-1938 for eight adjacent five degree squares in the California Current region.

$$\phi_{XX}(\tau)=\frac{<X(t)\,X(t+\tau)>}{<X^2>}$$

where $< >$ denotes the average taken over the record length and τ denotes the time lag in months. The standard deviation (σ) of the autocorrelation function (ϕ_{XX}) over the record length T can be estimated foom the variance (σ^2) inequality (Laning and Battin, 1956).

$$\sigma^2 \leqq \frac{4}{T}\sum^{\tau}\phi^2{}_{XX}(\tau)$$

The autocorrelation of temperature in the California Current region and several other regions in the North Pacific is shown in Fig. 6. The dashed line indicates the standard deviation defined above. It is seen that in widely different places the decay rates of the autocorrelations are similar and that temperature anomalies appear to be persistent, on an average, from three to six months. A notable exception is found east of Hokkaido in the Oyashio region where the temperature anomalies are slightly more persistent than elsewhere.

This particular period of persistence (three to six months) suggests at first that the anomalies might be expressed as minor variations of amplitude or phase from the mean annual curve. A shift in phase or amplitude of a sine curve of 12-month period would certainly result in an anomaly lasting six months followed by another six-month anomaly of opposite sign, that is, if we assume the anomaly during a given year could be written

$$X(t)=(a_0+a\sin\omega t)-(b_0+b\sin(\omega t+\varphi)$$

where a_0 is the mean of all months of all years, a the mean amplitude of seasonal variation, b_0 and b the corresponding values for a given year, and φ the phase shift from the mean during that year. The autocorrelation of the above expression is

$$\phi_{XX}(\tau)=(a_0-b_0)^2+\tfrac{1}{2}(a^2+b^2-2ab\cos\varphi)\cos\omega t$$

The first term is a constant and, if considered alone, would give a persistence of a year. Anomalies of a year's duration are occasionally seen, but do not appear to be the dominating type of anomaly. From the second term one can see that an amplitude shift alone or phase shift alone lead to cosine curves with maxima and minima six months apart. If the autocorrelations are normalized and compared with those of Fig. 6, two striking differences are noted. First the cosine autocorrelation (which is a cosine curve of unity and period 12 months) does not decay so rapidly in the first two months as the observed autocorrelations; then the cosine autocorrelations have a minimum at six months and a maximum at twelve months, which the observed autocorrelations do not show. From these differences one may conclude that no systematic variations in phase and amplitude (large enough to be discerni-

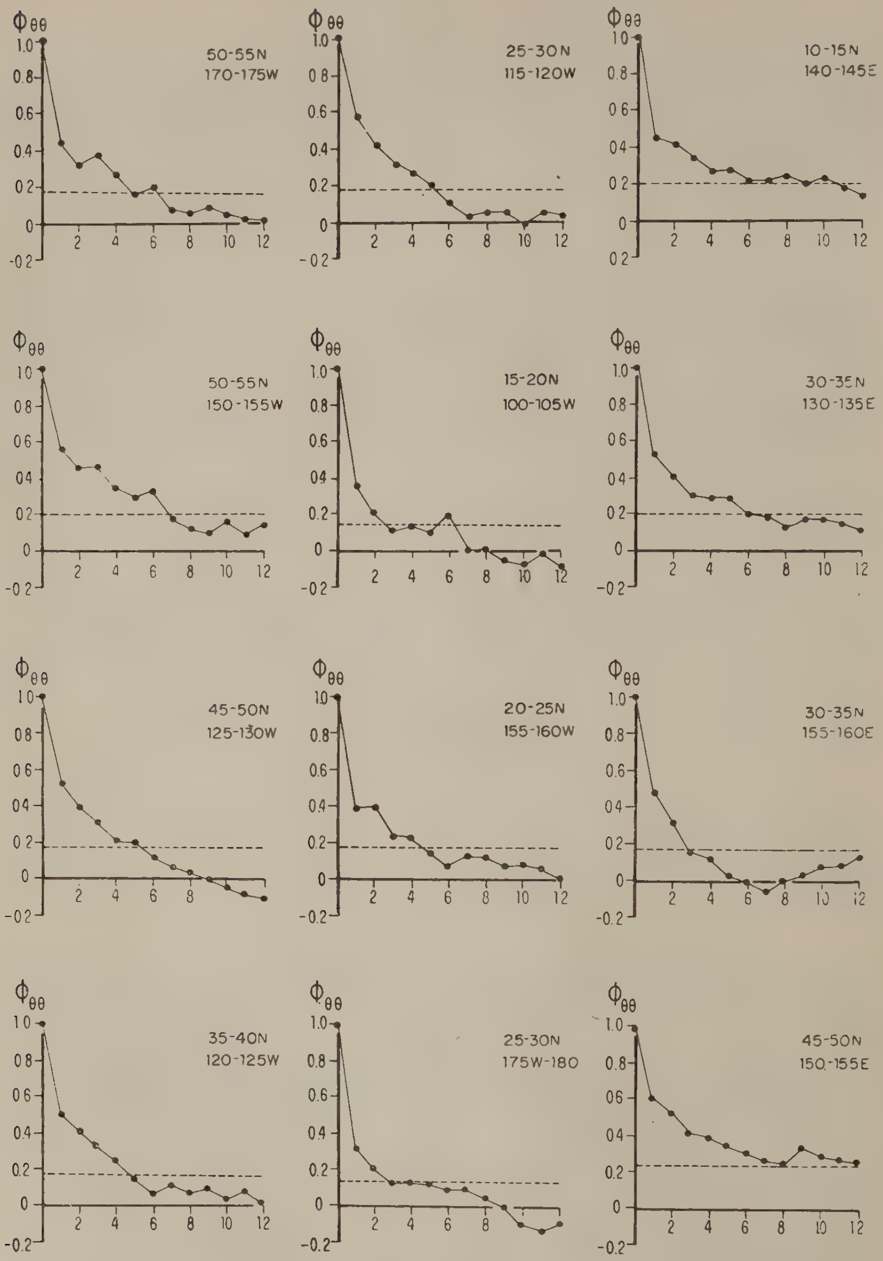

Fig. 6. Autocorrelations of temperature anomalies over the period 1921–1938 for lags from zero to twelve months. The dashed line indicates the standard deviation.

ble in the data over more than six months) have contributed substantially to the autocorrelations.

It is of interest to examine how the yearly mean, amplitude and phase have varied at a particular place. In Table 1 these variations are shown for a five degree square off the coast of Baja California. It is seen that the standard deviation of phase is only nine degrees (days). The standard deviations of amplitude and annual mean are 0.6°C. Thus it appears very unlikely that the observed shifts in the seasons have any important effect upon the autocorrelations.

Table 1. Amplitude (A), phase (φ) and yearly mean (m) of sea surface temperatures (°C) in area C 25-30N, 115-120W. σ denotes standard deviation.

Year	A °C	φ deg.	m °C
1921	2.8	214	17.5
1922	2.8	208	17.3
1923	2.3	202	17.6
1924	1.2	236	17.2
1925	2.1	233	17.8
1926	0.9	232	18.2
1927	2.0	218	17.5
1928	1.7	216	17.5
1929	3.0	221	17.3
1930	2.2	213	18.2
1931	2.0	232	18.6
1932	2.0	220	17.1
1933	1.7	213	15.9
1934	2.4	221	17.8
1935	2.2	215	17.4
1936	2.3	223	17.7
1937	2.9	209	17.2
1938	1.2	221	17.6
mean	2.1	219	17.5
σ	±0.6	±9	±0.6

Similar investigations of the autocorrelations of radiation and wind anomalies led to the result that they were rarely persistent for more than a month (Roden and Groves, 1960).

The above autocorrelations were determined over the entire record length. If, on the other hand, the month to month variations of the autocorrelations are investigated, a different picture results. Nine ocean areas were chosen (Fig. 7) to study the month to month variations of temperature, wind and radiation anomalies. The ocean areas are designated by capital letters and represent five degree squares of latitude and longitude for which temperature and radiation records were used. The east-west wind component (u) and the north-south wind component (v) where selected adjacent to each area and were computed from the pressures at the end points of the dotted lines shown in Fig. 7. For areas D and F winds were not available.

The monthly variation of the persistence of the anomalies is indicated by the variation of the autocorrelation between two adjacent months in Table 2. Significant values are in heavy print. The general impression gained from this table is that only for temperature anomalies is there a significant correlation from one month to the next. The few meaningful values in the autocorrelations of radiation and wind anomalies do not follow any simple pattern.

The variance of the anomalies is given in Table 3. It is seen that the variance of temperature anomalies varies very little with month. Over most

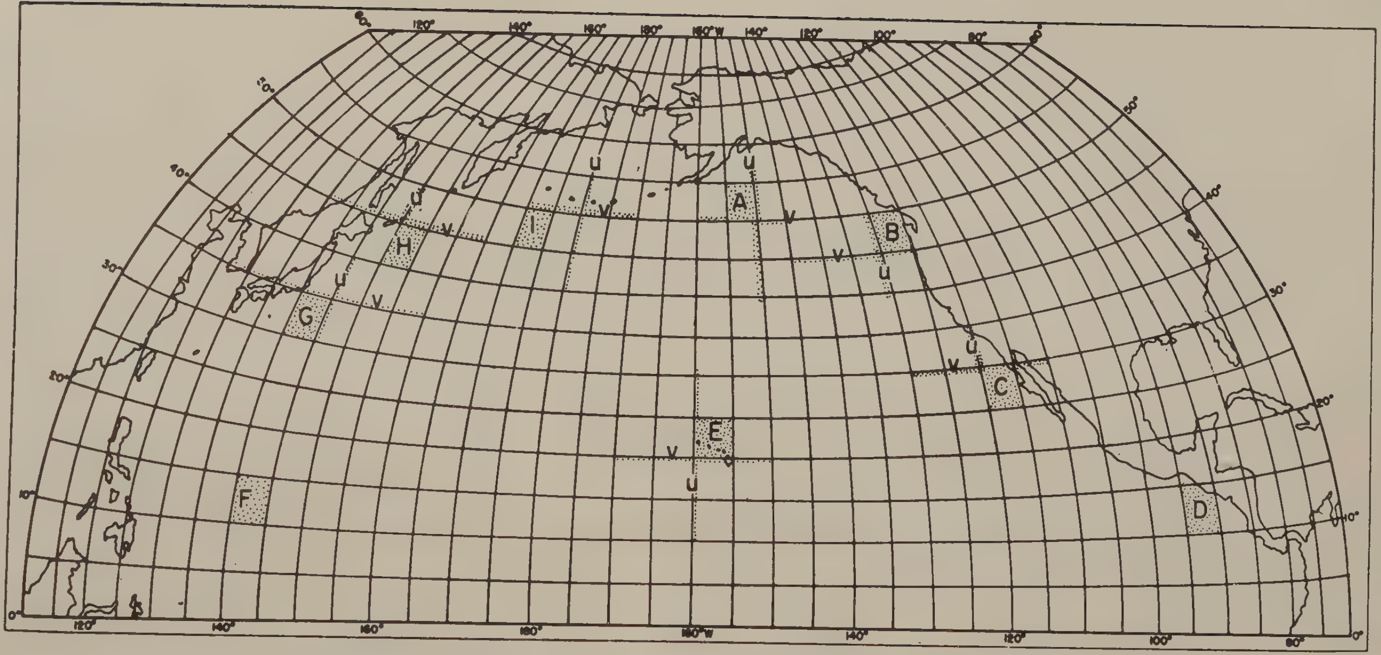
A
B
C
D
E
F
G
H
I
u
v
120°
140°
160°
180°
160°W
140°
120°
100°
80°
60°
50°
40°
30°
20°
10°
0°

Fig. 7. Location of five-degree squares (A to I) in which temperature and radiation and corresponding east-west (u) and north-south (v) wind components are compared.

Table 2. Autocorrelation of temperature $\phi_{\theta\theta}$, radiation ϕ_{qq} and wind component ϕ_{uu}, ϕ_{vv} (u east, v north) anomalies between the present and next following month.

95% confidence limits are at ±0.47. Significant values are in heavy print.

	I	II	III	IV	V	VI	VII	VIII	IX	X	XI	XII	mean annual
							$\phi_{\theta\theta}$						
A	**0.54**	−0.12	0.34	0.31	**0.95**	**0.86**	**0.72**	**0.52**	**0.64**	**0.66**	**0.48**	0.66	**0.55**
B	**0.59**	**0.83**	**0.54**	0.45	**0.63**	**0.79**	0.36	0.44	0.07	0.44	**0.68**	−0.03	**0.48**
C	**0.78**	**0.60**	**0.89**	**0.52**	**0.80**	**0.67**	0.34	**0.80**	**0.74**	0.24	0.25	**0.60**	**0.60**
D	**0.47**	0.44	0.05	**−0.57**	−0.36	0.31	0.34	**0.82**	0.38	**0.52**	**0.54**	0.41	0.27
E	0.30	0.09	**0.55**	0.42	0.20	**0.67**	0.36	**0.54**	0.30	0.40	**0.49**	**0.47**	0.40
F	**0.59**	0.23	**0.47**	0.34	**0.89**	**0.46**	**0.58**	0.27	**0.54**	0.46	0.41	0.05	0.44
G	0.27	**0.94**	0.28	**0.81**	**0.75**	0.42	0.31	−0.04	0.02	0.37	**0.58**	0.42	0.42
H	**0.53**	**0.69**	**0.53**	**0.86**	**0.51**	**0.60**	**0.70**	**0.74**	**0.53**	**0.58**	**0.50**	**0.56**	**0.61**
I	**0.69**	0.30	**0.80**	0.44	**0.73**	**0.53**	**0.69**	**0.59**	**0.69**	0.34	0.37	**0.60**	**0.56**
							ϕ_{qq}						
A	0.13	**0.65**	**0.53**	**−0.47**	−0.19	0.17	−0.25	0.34	0.26	0.20	−0.12	0.37	0.14
B	−0.17	**−0.55**	0.33	0.08	0.08	−0.03	0.06	**−0.55**	−0.10	0.06	−0.02	−0.02	−0.07
C	−0.23	−0.03	**0.88**	**−0.61**	0.17	0.20	0.03	**0.85**	0.04	0.01	0.20	−0.26	0.10
D	0.16	−0.21	0.36	**−0.56**	−0.38	0.00	0.22	−0.02	**−0.47**	−0.11	0.02	0.08	−0.07
E	**0.78**	0.03	0.44	0.21	**0.67**	**0.71**	−0.18	0.08	−0.05	−0.22	0.11	**−0.67**	0.16
F	0.22	0.18	−0.14	−0.34	0.16	0.34	−0.32	−0.21	−0.11	−0.39	−0.08	0.26	−0.04
G	0.16	−0.16	**0.76**	0.09	**0.52**	0.05	0.14	−0.12	0.10	0.12	−0.17	**0.49**	0.17
H	0.28	−0.21	0.19	−0.28	−0.28	0.12	0.30	0.18	0.12	−0.06	0.00	0.38	0.06
I	−0.01	−0.25	**0.47**	0.16	−0.01	−0.25	−0.20	−0.34	0.08	0.02	−0.02	−0.09	−0.05
							ϕ_{uu}						
A	−0.16	−0.13	0.05	0.05	**0.69**	−0.14	**0.63**	−0.17	**0.60**	0.21	0.10	0.00	0.14
B	−0.02	−0.27	0.33	0.02	0.04	−0.15	0.12	0.00	0.22	**0.50**	−0.14	0.26	0.08
C	−0.07	−0.17	−0.41	−0.15	0.11	0.30	0.00	**−0.84**	0.18	0.14	0.00	−0.31	−0.10
E	0.14	0.03	0.40	0.20	0.16	0.05	0.20	**0.61**	0.06	0.16	0.46	0.45	0.24
G	0.12	−0.15	0.26	−0.16	−0.15	−0.22	0.19	0.54	−0.04	−0.43	0.18	−0.18	−0.03
H	−0.23	−0.06	0.07	−0.03	−0.43	−0.02	−0.20	0.11	0.09	−0.06	−0.01	−0.15	−0.08
I	0.25	−0.37	0.01	0.03	0.14	−0.18	0.24	**0.87**	0.44	**0.70**	0.02	0.02	0.20
							ϕ_{vv}						
A	0.03	−0.02	0.06	−0.35	0.07	**0.58**	−0.05	−0.22	0.27	0.18	−0.29	−0.30	0.00
B	0.33	0.09	0.36	0.32	−0.32	0.20	0.26	−0.30	−0.08	0.09	0.11	**0.82**	0.16
C	−0.13	0.36	0.30	0.41	0.30	0.25	−0.40	**−0.50**	**0.47**	−0.43	**−0.80**	−0.32	−0.04
E	0.22	0.19	0.45	0.22	0.23	0.27	0.20	0.17	0.46	0.06	0.05	0.23	0.23
G	**−0.80**	−0.02	0.05	−0.20	**0.56**	**0.50**	−0.06	−0.14	0.14	0.27	0.30	0.23	0.20
H	0.09	−0.24	−0.26	0.00	0.18	−0.31	−0.18	−0.27	0.25	0.31	−0.05	−0.12	−0.05
I	0.05	−0.01	−0.20	**−0.58**	0.11	0.33	0.11	−0.28	**−0.49**	0.10	0.28	0.36	−0.18

Table 3. Variance of temperature θ, radiation q and wind component (u east, v north) anomalies.

	I	II	III	VI	V	VI	VII	VIII	IX	X	XI	XII	mean annual
$\langle\theta^2\rangle$ (°C)^2													
A	0.8	0.7	0.3	0.5	0.2	0.6	0.8	1.0	0.7	1.1	0.8	0.7	0.7
B	0.5	0.6	0.8	1.1	0.6	0.6	0.6	0.4	0.4	0.4	0.4	0.6	0.6
C	0.6	0.8	0.8	1.0	0.9	0.8	0.1	0.6	0.8	1.0	0.9	0.5	0.8
D	0.5	0.6	0.7	0.7	0.4	0.5	0.4	0.3	0.3	0.3	0.2	0.3	0.4
E	0.9	0.4	0.8	0.3	0.4	0.7	0.8	0.3	0.2	0.4	0.6	0.6	0.5
F	0.5	0.6	0.7	0.7	0.4	0.5	0.4	0.3	0.3	0.3	0.2	0.3	0.4
G	0.9	0.4	0.8	0.3	0.4	0.7	0.8	0.3	0.2	0.4	0.6	0.6	0.5
H	2.0	2.2	2.1	1.3	1.4	1.0	1.5	2.4	2.6	1.3	2.0	2.1	1.8
I	0.3	0.4	0.4	0.3	0.3	0.5	0.6	0.7	0.7	0.7	0.5	0.4	0.5
$\langle q^2\rangle$ (k cal cm^{-2} mo^{-1})^2													
A	0.1	0.1	0.3	0.9	2.4	0.8	0.5	0.8	0.5	0.3	0.1	0.1	0.6
B	0.1	0.2	0.7	1.8	1.6	1.1	1.9	1.1	1.2	0.2	0.2	0.1	0.9
C	1.1	2.4	2.4	3.8	5.6	4.0	2.0	1.1	5.7	3.4	1.0	0.6	2.8
D	0.4	0.6	1.0	1.2	2.7	2.5	1.7	1.3	1.7	2.2	1.0	0.4	1.4
E	1.2	3.2	4.2	3.9	1.2	1.0	2.6	3.6	2.2	0.8	1.7	0.7	2.1
F	0.9	0.6	0.8	0.9	1.1	1.0	1.7	1.9	2.0	0.6	1.0	0.4	1.1
G	1.0	0.6	1.4	3.1	1.9	2.3	3.4	2.3	2.1	1.3	0.8	0.4	1.7
H	0.1	0.1	0.3	0.8	0.9	0.8	0.3	0.8	0.4	0.2	0.2	0.1	0.4
I	0.1	0.2	0.5	0.6	0.4	0.3	0.4	0.3	0.5	0.2	0.1	0.1	0.3
$\langle u^2\rangle$ (m/s)^2													
A	6.0	4.4	5.0	2.1	1.1	2.1	0.4	0.9	2.1	3.8	2.8	10.3	3.4
B	7.2	6.3	4.8	3.4	2.7	1.1	1.9	0.7	2.8	2.2	4.3	4.3	3.5
C	2.4	6.4	2.1	2.2	0.5	0.6	0.9	0.3	1.2	2.3	2.7	1.8	2.0
E	8.2	7.2	5.0	3.1	1.4	1.1	0.6	1.0	2.8	3.1	2.6	8.2	3.7
G	3.2	2.6	3.0	5.0	2.3	3.1	5.6	3.8	3.1	1.6	4.0	5.3	3.6
H	4.1	5.1	3.3	3.8	2.1	2.9	2.8	1.9	3.7	3.6	3.7	3.4	3.4
I	5.6	5.8	4.9	5.6	1.9	1.2	2.1	1.2	2.3	1.4	3.1	10.2	3.8
$\langle v^2\rangle$ (m/s)^2													
A	9.5	10.5	9.7	4.6	4.1	2.5	3.2	3.5	4.6	8.5	5.4	6.4	6.0
B	17.6	8.4	5.8	2.6	2.3	3.0	1.1	1.8	2.0	2.4	4.1	7.9	4.9
C	1.3	2.6	1.1	2.2	1.7	1.1	0.3	0.3	0.8	0.8	0.5	1.7	1.2
E	1.0	1.2	0.5	1.3	0.7	0.6	0.6	0.3	0.6	0.9	0.1	1.9	0.9
G	0.8	2.3	1.1	0.6	0.5	0.4	0.9	0.8	0.8	0.6	0.6	0.7	0.8
H	3.6	2.1	1.5	1.3	0.9	0.7	1.2	0.6	0.7	0.9	2.2	3.2	1.6
I	9.7	4.7	6.1	2.9	3.2	3.2	2.7	3.9	3.4	5.0	2.8	5.2	4.4

of the ocean it is less than 1 C^2, but a notable exception occurs off northern Japan in the boundary region between the Kuroshio and Oyashio where the variance is about twice as large.

The variance of radiation anomalies shows a characteristic maximum in summer and a minimum in winter. In areas with a semipermanent cloud-cover, such as in the region of the North Pacific westerlies, the variance is smaller than in areas where the sky is only partly obscured by clouds, such as off the coast of Baja California. The mean value of the radiation variance is about 1.5 (kcal cm^{-2} $\mathrm{mo}^{-1})^2$.

The variance of wind anomalies shows a very pronounced seasonal variation with maximum values occurring in winter and minimum values in summer. The seasonal variation is particularly conspicuous in high latitudes and appears to be larger for the north-south components than for the east-west components. In middle latitudes, however, the east-west component is more variable. On an annual average the variance of the east-west component is not far from 3 m^2 sec^{-2}, but for the north-south component it varies between 1 m^2 sec^{-2} and 6 m^2 sec^{-2}.

Crosscorrelations between temperature, wind and rediation anomalies

The crosscorrelations between temperature and radiation and temperature and the two wind component anomalies are given in Table 4. The crosscorrelations were computed from the expression

$$\varphi_{XY}(\tau) = \frac{<X(t)\,Y(t+\tau)>}{\sqrt{<X^2><Y^2>}}$$

for zero lag. Consideration of lag times other than zero was not possible owing to the short record length available.

It is seen that a few significant correlations between temperature and radiation anomalies do exist and that they are found mainly in the summer and early fall months. The summer and fall correlations are positive meaning that increased radiation leads to higher temperatures. The negative winter correlations in areas *D* and *F*, if real, are difficult to explain.

The crosscorrelations between wind and temperature show significant values mostly in the colder half of the year. It is noteworthy that an increased east to west component of the wind in the region of the North Pacific westerlies decreases the temperature in all significant cases. In the northeastern Pacific, off the coast of Washington, increased southerly winds in winter are related to higher temperatures (probably through an increase in the Davidson Current). Off the coast of Baja California increased northerly winds are related to lower temperatures owing to increased upwelling and advection of cold water from the north (REID, RODEN, WYLLIE, 1958). In the Japanese region significact correlations between wind and temperature occur only in winter where stronger north winds lead to lower temperatures, as can be expected. In the Hawaiian region there appears to be no meaningful relation between the wind and temperature anomalies, possibly because of the doubtful application of the geostrophic relationship between pressure gradient and wind.

Table 4. Crosscorrelations between temperature and radiation $\phi_{\theta q}$ anomalies, temperature and east wind $\phi_{\theta u}$ anomalies and temperature and north wind anomalies $\phi_{\theta v}$. 95% confidence limites arc at ±0.47.
Significant values are in heavy print.

	I	II	III	IV	V	VI	VII	VIII	IX	X	XI	XII	mean annual
							$\phi_{\theta q}$						
A	−0.08	−0.06	0.46	−0.07	0.16	0.25	**0.48**	−0.10	−0.04	0.27	0.31	0.24	0.15
B	0.34	0.25	0.11	0.09	0.34	0.24	0.07	0.28	−0.08	0.05	0.19	−0.27	0.13
C	0.36	0.22	0.12	0.18	0.22	0.42	0.33	**0.49**	**0.60**	**0.48**	0.12	0.19	0.30
D	−0.32	−0.21	−0.46	−0.27	0.40	0.34	**0.56**	**0.63**	**0.62**	0.27	−0.22	−0.40	0.08
E	0.41	**0.81**	−0.03	−0.32	0.13	0.32	0.14	0.38	−0.44	0.10	0.33	0.15	0.16
F	0.24	−0.18	**−0.59**	0.45	−0.45	−0.01	0.28	−0.11	−0.05	0.20	0.11	−0.06	0.02
G	0.01	−0.34	0.25	0.08	−0.03	−0.33	−0.25	0.10	−0.04	**−0.48**	0.15	0.20	−0.06
H	0.04	0.04	−0.05	−0.13	0.02	0.15	**0.56**	0.28	0.00	0.22	0.29	−0.31	−0.09
I	0.19	−0.19	−0.10	−0.20	0.13	0.02	−0.01	**0.58**	−0.12	−0.17	−0.28	0.07	−0.01
							$\phi_{\theta u}$						
A	−0.04	−0.46	**−0.61**	−0.25	−0.34	**−0.66**	−0.05	−0.19	−0.38	−0.40	0.03	0.30	−0.25
B	−0.09	0.08	**−0.55**	**−0.48**	−0.29	−0.05	0.35	−0.08	0.04	−0.19	0.08	0.25	−0.08
C	0.21	0.33	**−0.53**	0.22	0.11	−0.09	−0.24	−0.13	0.06	−0.31	0.10	−0.07	−0.03
E	0.13	−0.20	−0.08	0.34	0.28	−0.38	−0.34	0.33	0.18	−0.06	0.08	−0.26	0.00
G	−0.44	0.18	−0.14	−0.16	0.12	0.44	−0.21	0.04	−0.39	0.11	−0.35	−0.31	−0.09
H	−0.05	−0.17	−0.14	−0.16	−0.29	−0.28	0.01	**−0.50**	0.04	−0.31	0.21	0.00	−0.14
I	−0.16	−0.31	0.20	−0.45	−0.06	0.07	0.06	−0.14	−0.39	−0.31	**−0.58**	**−0.48**	−0.21
							$\phi_{\theta v}$						
A	−0.03	0.13	0.24	0.30	0.24	−0.45	−0.06	−0.12	0.20	0.39	0.30	0.14	0.11
B	**0.57**	**0.82**	**0.55**	**0.47**	0.44	−0.32	−0.31	−0.12	0.01	0.44	0.26	0.31	0.26
C	**0.50**	−0.20	−0.28	**−0.49**	**−0.65**	−0.13	−0.19	−0.06	−0.26	0.08	−0.27	0.02	−0.22
E	0.29	0.36	−0.05	0.37	−0.02	0.17	0.11	−0.07	0.09	0.16	0.28	0.33	0.17
G	−0.33	−0.20	**−0.48**	0.25	−0.04	0.00	0.18	−0.05	0.31	0.19	−0.07	**−0.55**	−0.07
H	**−0.52**	−0.38	−0.43	−0.03	0.30	0.04	0.11	0.14	−0.10	0.17	−0.40	−0.15	−0.10
I	−0.21	0.03	0.06	−0.13	0.14	−0.08	**−0.47**	−0.12	0.07	−0.45	−0.38	0.06	−0.12

Acknowledgments

The authors are indebted to Drs. R. S. Arthur, G. W. Groves, June Pattullo, O. E. Sette, W. S. Wooster, K. Yoshida, Prof. J. D. Isaacs and Mr. J. F. T. Saur for valuable suggestions.

The research carried out in this paper was conducted under the Marine Life Research Program, the Scripps Institution of Oceanography's component of the California Cooperative Oceanic Fisheries Investigations, a project sponsored by the Marine Research Committee of the State of California.

References

Budyko, M. I. 1956: Teplovoi balans zemnoĭ poverkhosti. Gimiz. Leningrad. 254 pp.
Bureau of Commercial Fisheries, Honolulu Biological Laboratory, Hawaii 1958: Ten

day mean sea surface temperature charts for the eastern North Pacific. (unpublished)

HANZAWA, M. and T. INOUE 1952: Relation between oceanic and atmospheric states in the North Pacific for the year of bad and good rice crop. Ocean. Rep. Japan, Vol. 2. No. 3, pp 283-289.

HANZAWA, M. 1957: Studies between the interrelationship between the sea and the atmosphere (Part 2). Oceanogr. Mag., Japan, Vol. 9 No. 1, pp 87-94.

HATANAKA, M. 1952: Studies on the fluctuation of hydrographic conditions and its effect on the pelagic fishery resources. Bull. Tohoku Reg. Fish. Res. Lab., No. 1, pp 87-120.

HELLAND-HANSEN, Bj. and F. NANSEN 1920: Temperature variations in the North Atlantic Ocean and in the atmosphere. Smithsonian Misc. Coll. Vol. 70 No. 4, 408 pp.

HIDAKA, K. and K. OGAWA 1958: Records of Oceanog. works, Japan, Vol. 4 No. 2 (New Series) pp 124-169.

HIRANO, T. 1957: On the durability of surface temperature at hydrographic stations of the Pacific Coast. Bull. Tokai Reg. Fish. Res. Lab. No. 16, pp 23-38; No. 17, pp 65-72.

HUBBS, C. 1948: Changes in the fish fauna of western North America with changes in Ocean temperatures. J. Mar. Res. Vol. 7, No. 3, pp 459-482.

Imperial Marine Observatory, Kobe, Japan 1911-38: The mean atmospheric pressure, cloudiness, air and sea surface temperature of the North Pacific Ocean and neighboring seas.

LANING, J. and R. H. BATTIN 1956: Random process in automatic control. McGraw Hill, New York, 434 pp.

REID' J. L., Jr., G. I. RODEN and J. G. WYLLIE 1958: Studies of the California Current System. State of California Marine Research Committee. Calif. Coop. Ocean. Fish. Invest. Prog. Rep. 1 July 1956-1 January 1958. Sacramento State Printer, pp 27-56.

RIEHL, H. 1954: Tropical Meteorology. McGraw Hill. New York, 392 pp.

RODEN, G. I. and G. W. GROVES 1960: On the statistical prediction of ocean temperatures. Jour. of Geophy. Res., Vol. 65, No. 1 pp 249-263.

RODEWALD, M. 1953: Die Abweichungen der Oberflächentemperatur des Ozeans bei nordatlantischen Wetterschiffen. Deutsche Hydr. Zeit. Vol. 6, Nos. 4, 5, 6.

TAKENOUTI, Y. 1957: Long range oceanographic forecast. Historical review and future problem. Ocean. Mag. Japan Vol. 9, No. 2, pp. 1-12.

UDA, M. 1955: Researches on the fluctuation of the North Pacific circulation. Res. Ocean. Works Japan, Vol. 2, No. 2, pp 43-55.

U. S. Coast and Geodetic Survey 1956: Surface Water temperature at tide stations. Pacific Coast North and South America and Pacific Islands. Spec. Pub. No. 280, 74, pp.

U. S. Weather Bureau 1952: Normal weather charts for the northern hemisphere. Tech. Pap. No. 21, 74 pp.

(mimeographed) Monthly mean sea level pressure charts for the northern hemisphere for the period 1899-1959.

——— 1959: Local climatological data for 1958 with comparative data for Yakutat, Tatoosh Island, Seattle, Eureka and San Diego.

(854)

Reprinted from: California Cooperative Oceanic Fisheries Investigations.
Reports, v.8, 1 July 1959-30 June 1960. pp.95-119.

ON NONSEASONAL TEMPERATURE AND SALINITY VARIATIONS ALONG THE WEST COAST OF THE UNITED STATES AND CANADA

GUNNAR I. RODEN[1]

ABSTRACT

Power spectra of sea surface temperature and salinity anomalies are investigated for the frequency range between zero and six cycles per year. It is found that the power of these anomalies is concentrated at low frequencies and that high frequencies contribute almost nothing to it. The power spectra of temperature anomalies are similar for all 20 stations investigated here, but large regional differences exist in the salinity spectra. The coherence between sea and air temperature anomalies is moderate to good for well exposed stations, and there exists a direct relationship between them. The coherence between salinity and precipitation anomalies is good only for stations along the open coast where there is little river discharge, the anomalies being related inversely to each other. The coherence between salinity and river discharge anomalies is moderate to good for stations at the boundary between river and oceanic water and poor elsewhere. The coherence between surface temperature and salinity anomalies is moderate for light ship and island stations and poor along the continent. The relation between them is mostly an inverse one, as is characteristic of upwelling regions.

INTRODUCTION

For many years careful records have been kept of sea surface temperature and salinity at various stations along the west coast of the United States and Canada. If these records are plotted against time, seasonal as well as nonseasonal variations are obtained. The seasonal variations have been studied by McEwen (1912, 1919, 1929, 1938), and Pickard (1953) and the nonseasonal variations by Hubbs (1948), Reid (1960) and Roden (1958). The particular relation between temperatures and tides was investigated by Herlinveaux (1957), and between salinity and river discharge by Tully (1952).

In this paper the regular seasonal variation is eliminated by taking differences between the monthly mean and the long term mean of the same month. The resulting anomalies are then used to compute the average power contained in each record and also the power spectral density, coherence and phase as defined below. In performing the calculations it has been assumed that the anomaly records are stationary, at least in the wide sense, so that the functions derived depend only upon the sampling interval, and are independent of any origin in time.

The location of tide gage and lighthouse stations is shown on figure 1. Most of them are located in harbors and bays and only few of them are well exposed. Blunts Reef represents a light-ship, anchored a few miles off Cape Mendocino, in the heart of the upwelling region. For meteorological records the nearest meteorological station was chosen. In most cases the tide gage an meteorological stations are located within a radius of 20 km, but in a few instances stations further apart had to be combined. Where the nearest meteorological station was more than 50 km away, no comparisons between oceanographic and meteorological variables were made.

DATA

Sea surface temperatures and salinities were obtained from the U.S. Coast and Geodetic Survey (1956), the Fisheries Research Board of Canada (1958) and the Scripps Institution of Oceanography of the University of California (unpublished). At the Canadian stations the monthly means were computed from daily observations made one hour before the daytime high water. The individual temperature readings are estimated to be accurate within 0.2 C and the individual salinities, determined by a modified Mohr titration, are reported to have an accuracy of $\pm 0.06^0/_{00}$. At the United States stations the observations are made at a random hour during each week day, and in many cases the monthly means are computed from less than 20 daily values. The accuracy of individual temperature readings is estimated to be within 0.2 C except for stations in Southern California where the accuracy is somewhat greater, because better thermometers were used. The accuracy there is estimated to be within 0.05 C. The surface salinities up to July 1954 were obtained from density observations by hygrometer at all stations. The accuracy of a single hygrometer reading is not very great, and must very with the individual skill of the observer. In some cases the salinities so determined are probably accurate only within $0.3^0/_{00}$. Since July 1954 the salinities at La Jolla, Balboa, Hueneme, Pacific Grove, SE Farallon Island, and Blunts Reef Lightship are determined by a Knudsen titration, the accuracy of which is about $\pm 0.05^0/_{00}$.

Air Temperature and precipitation records were obtained from the U.S. Weather Bureau (1872-1949, 1950-1960, and 1916-1960) and the Canadian Department of Transport (personal communication). The monthly averages of air temperatures are computed from four equidistant daily readings at 0000, 0600, 1200 and 1800 GMT. The accuracy of an individual reading is estimated to be within 0.1 C. The accuracy of rainfall is estimated to be 1% of the total or about 0.3 cm, whichever is the greater.

---

[1] Contribution from the Scripps Institution of Oceanography, 1312

Reproduced by Permission

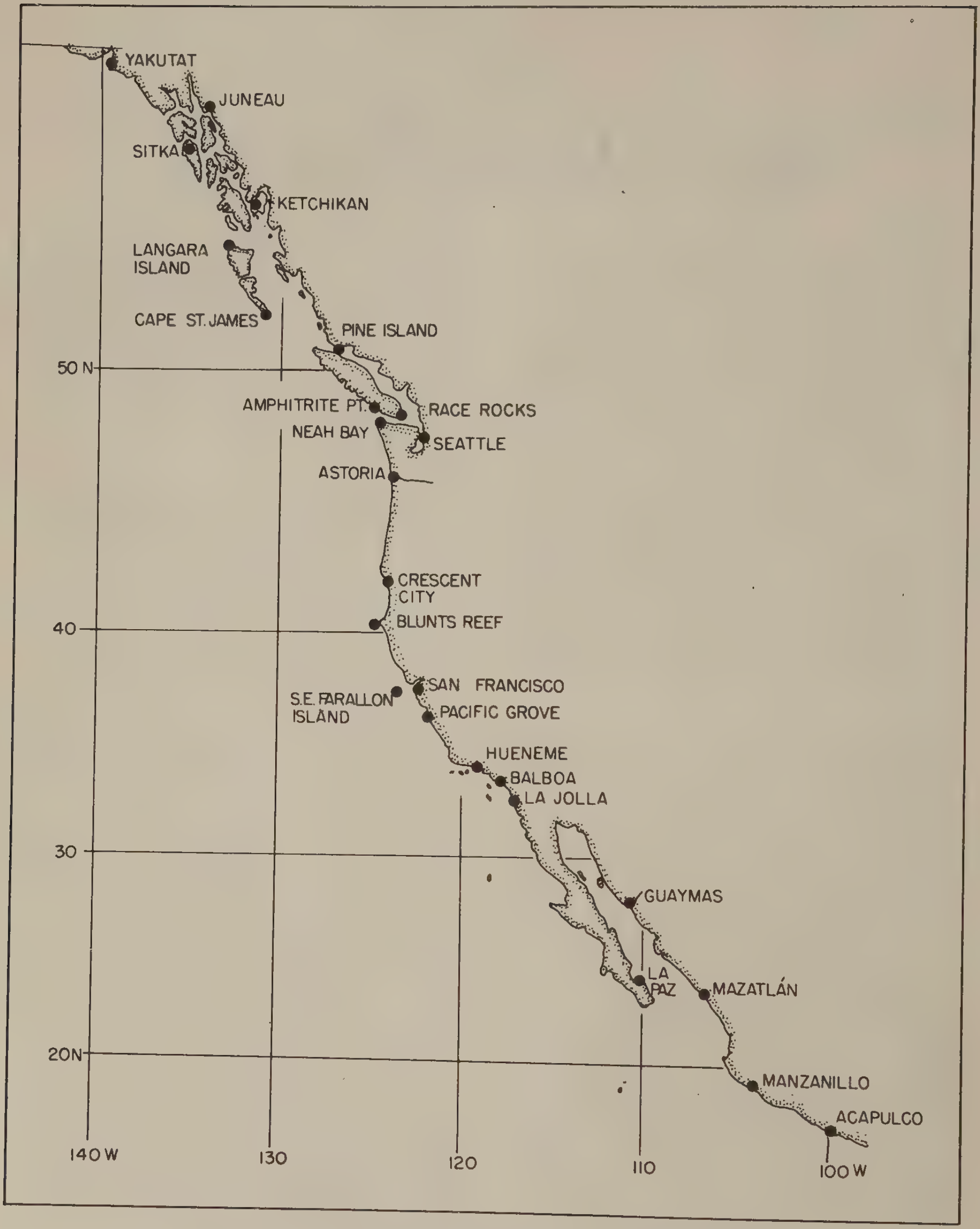
YAKUTAT
JUNEAU
SITKA
KETCHIKAN
LANGARA ISLAND
CAPE ST. JAMES
PINE ISLAND
50 N
AMPHITRITE PT.
RACE ROCKS
NEAH BAY
SEATTLE
ASTORIA
CRESCENT CITY
BLUNTS REEF
40
SAN FRANCISCO
S.E. FARALLON ISLAND
PACIFIC GROVE
HUENEME
BALBOA
LA JOLLA
30
GUAYMAS
LA PAZ
MAZATLÁN
20N
MANZANILLO
ACAPULCO
140 W
130
120
110
100 W

FIGURE 1. Location of stations where temperature and salinity observations are made.

(856)

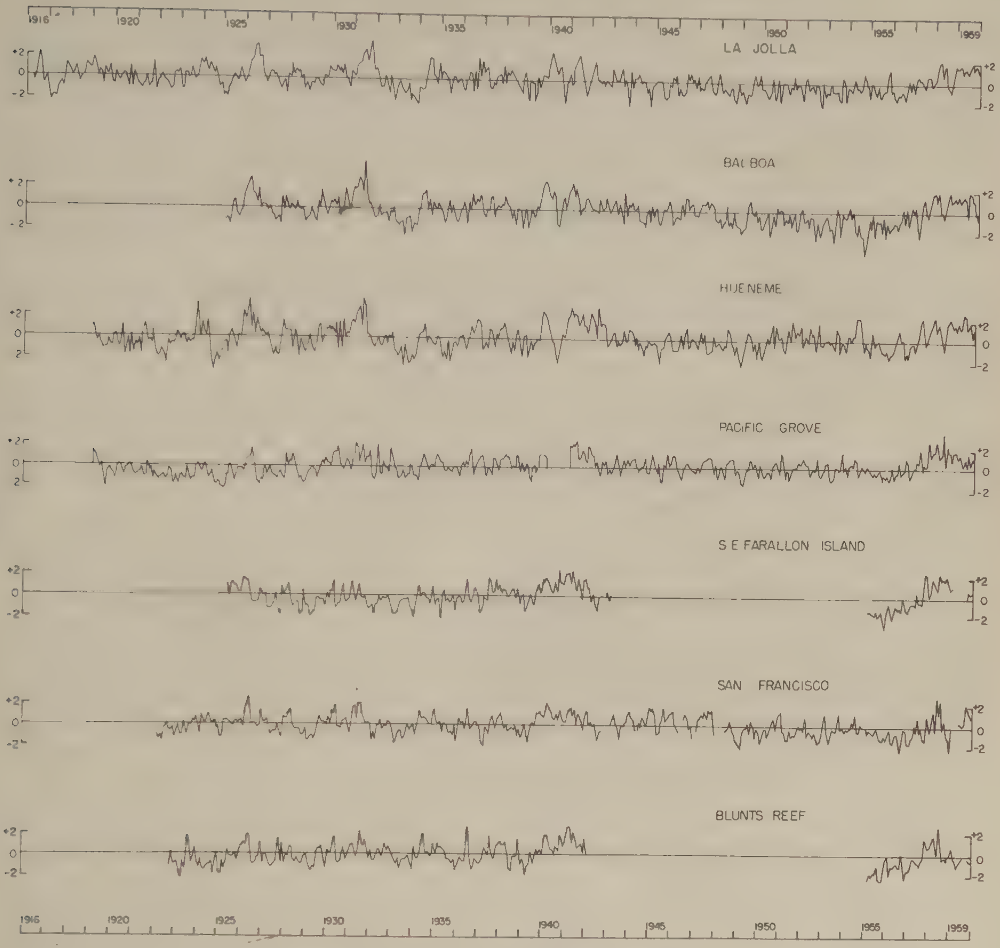

FIGURE 2. Sea surface temperature anomalies at California stations. .

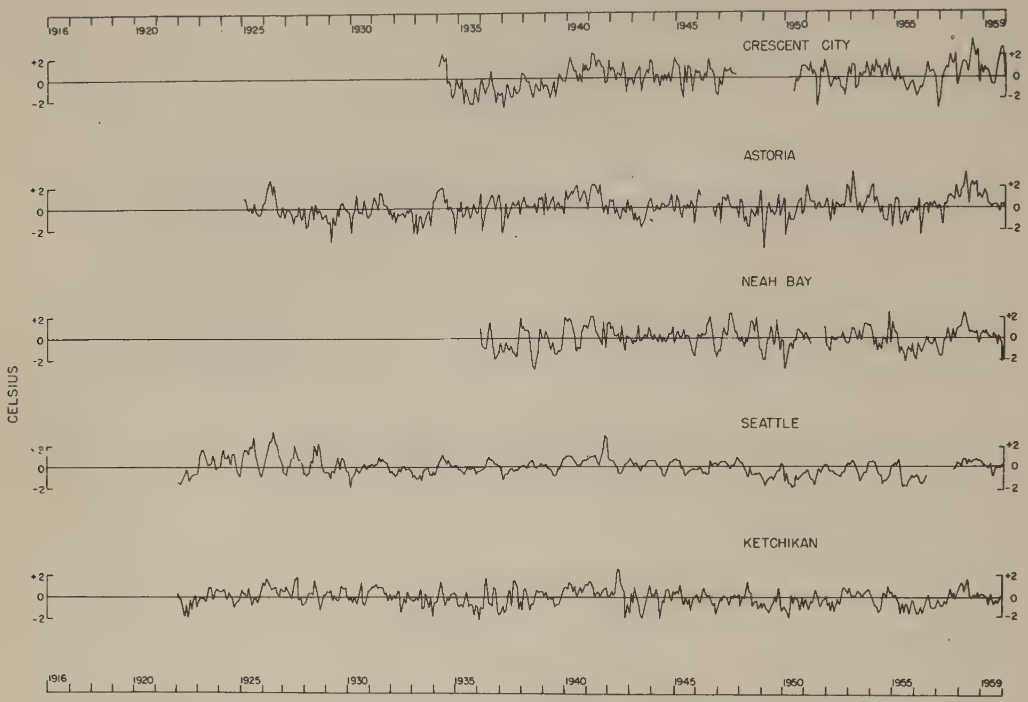

FIGURE 3. Sea surface temperature anomalies at Oregon and Washington stations and at Ketchikan, Alaska.

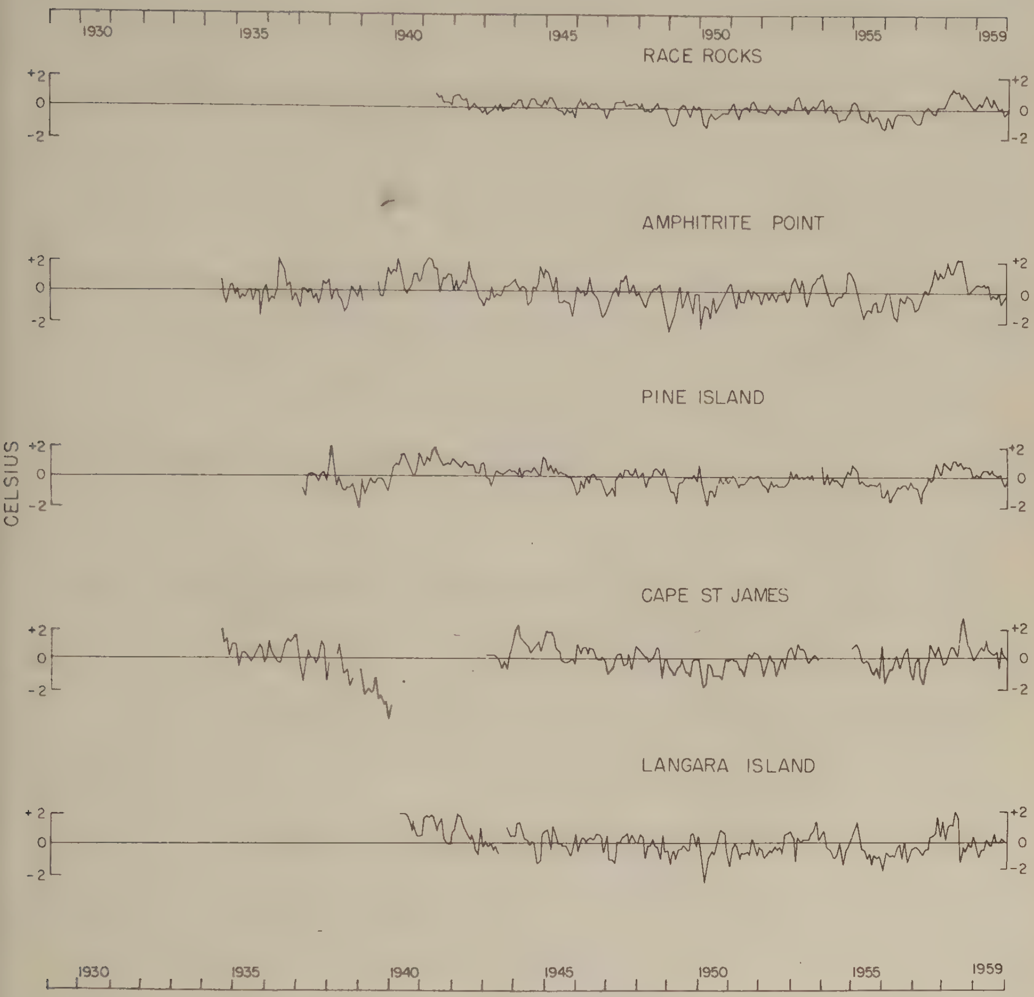

FIGURE 4. Sea surface temperature anomalies at British Columbia stations.

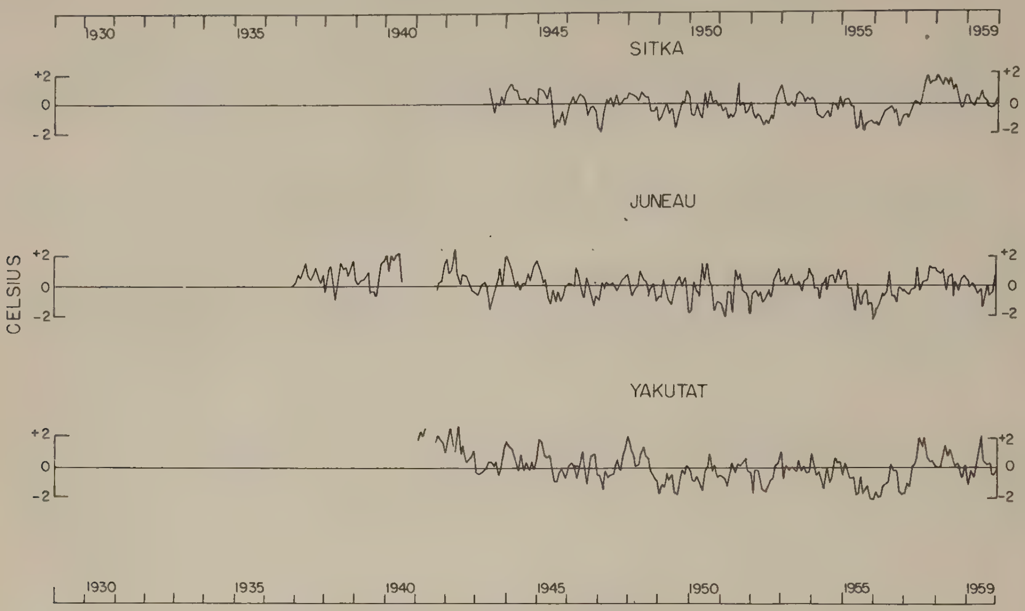

FIGURE 5. Sea surface temperature anomalies at Alaskan stations.

860)

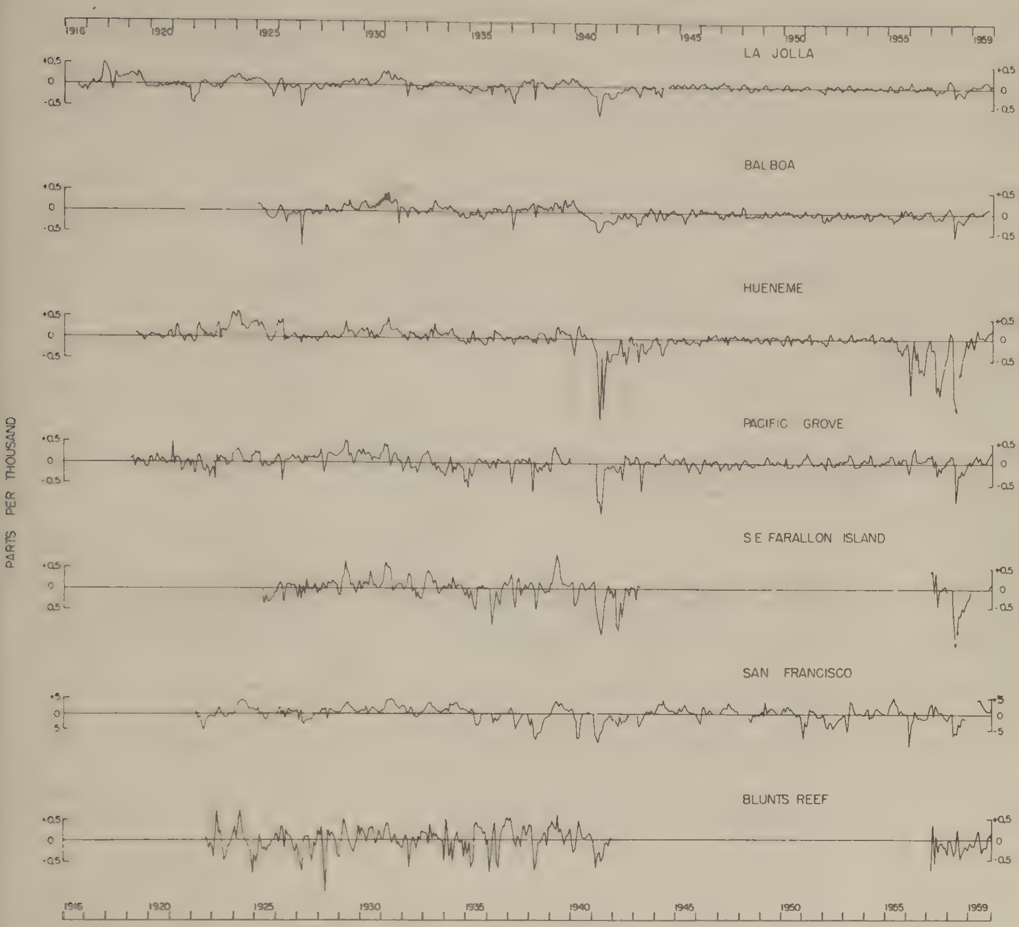

FIGURE 6. Salinity anomalies at California stations. The records for La Jolla, Balboa, Hueneme and Pacific Grove are questionable between 1944 and 1955.

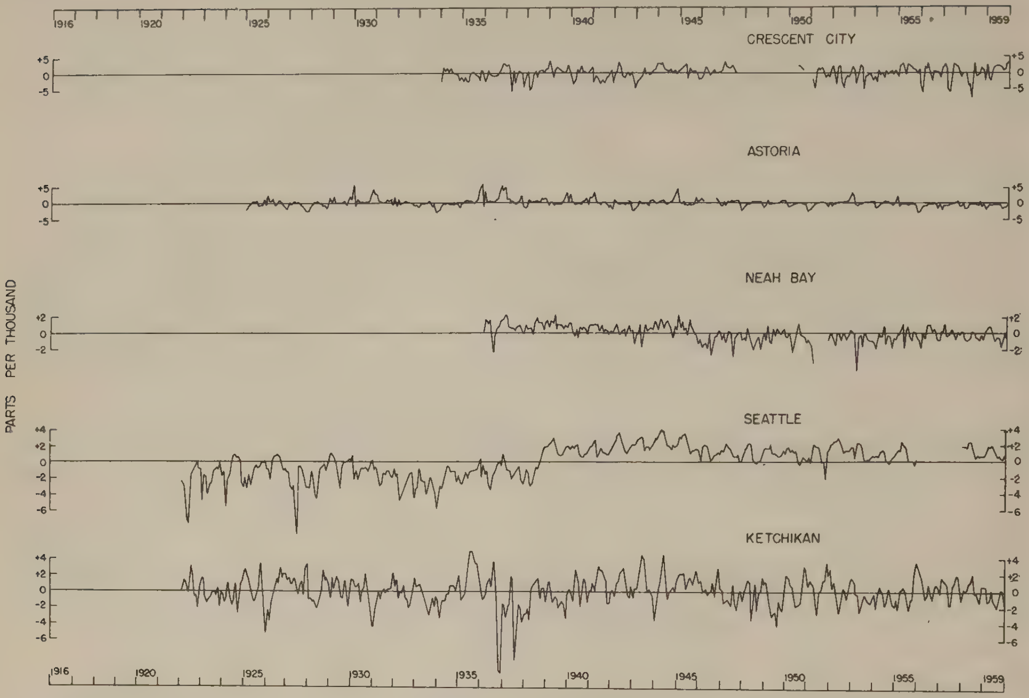

FIGURE 7. Salinity anomalies at Oregon and Washington stations and at Ketchikan, Alaska. The Seattle record is questionable.

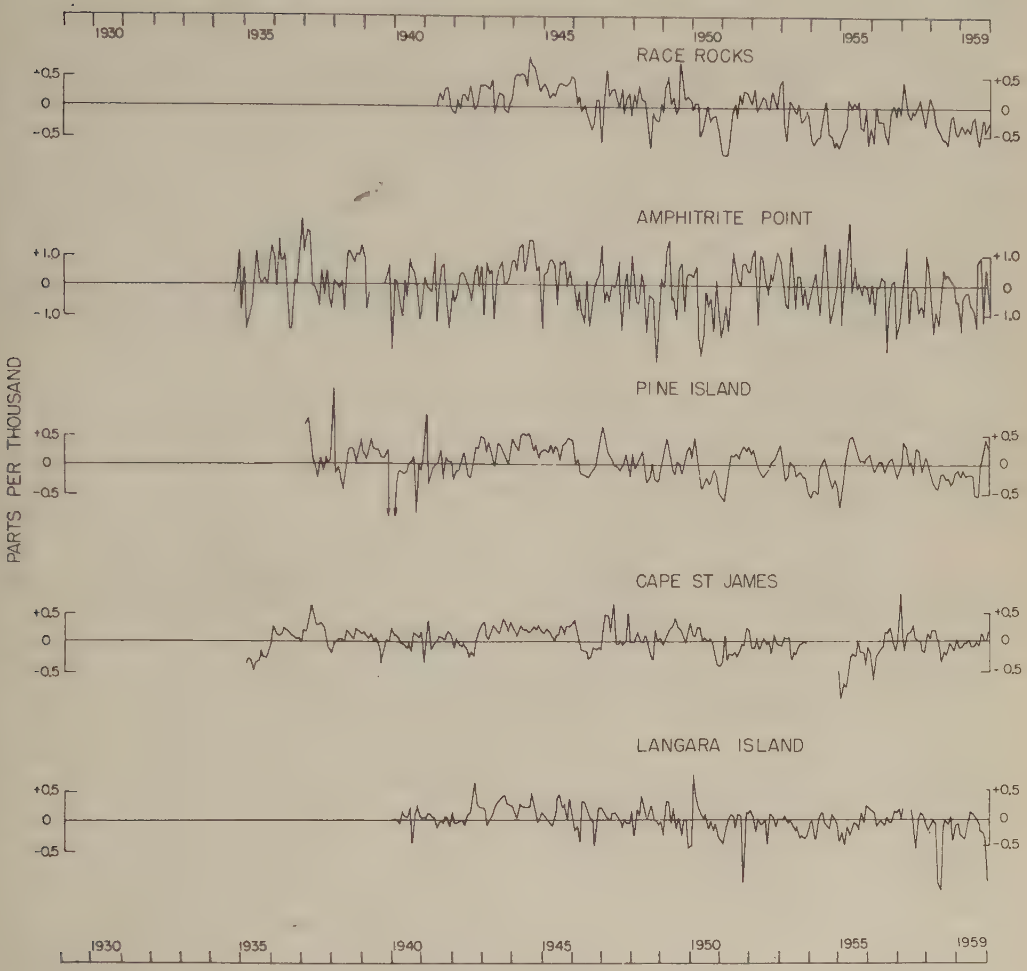

FIGURE 8. Salinity anomalies at British Columbia stations.

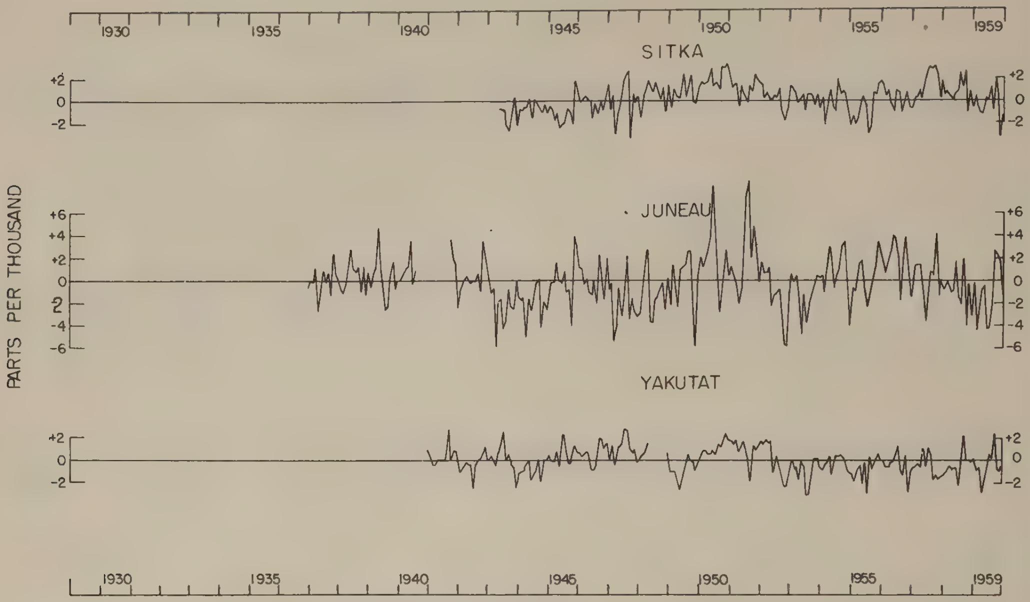

FIGURE 9. Salinity anomalies at Alaskan stations.

Runoff records were obtained from the U.S. Geological Survey (1958) and the Surface Water Branches in Menlo Park, California, and Sacramento, California. They are considered to be accurate within 5% of the individual flow.

The sea surface temperature records are shown in figures 2 to 5. Although the details of the records vary, a few preliminary results can be obtained from a visual inspection of them; (a) the magnitude of the anomalies is about the same for all stations, (b) the maximum amplitude of the anomalies appears to be 4C, (3) there are no obvious periodicities discernible, (d) the anomalies are similar over distances of several hundred kilometers and (e) for the majority of stations the mean of the record does not change appreciably, indicating stationary conditions.

The surface salinity records are shown in figures 6 to 9. A visual examination of them leads to the following preliminary conclusions: (a) the magnitude of the salinity anomalies varies greatly from one station to another, (b) the smallest anomalies are found at stations in Southern California where rainfall is scarce and at stations in straits where tidal mixing is considerable, (c) the largest anomalies occur at stations where there is considerable influence by both runoff and oceanic water, (d) there are no obvious periodicities. The salinity anomalies at La Jolla, Balboa, Hueneme and Pacific Grove show a sharp discontinuity in magnitude and general character about 1944. Although there was some reduction of the magnitude of other anomalies at this time (Isaacs 1960), no sharp discontinuities of the type shown here were observed.

The salinity determinations of the above mentioned stations were all done by the same observer, and it is possible that the discontinuity is due to a change in instrument, or to some other reason. Since the cause is not known, the records between 1944 and 1955 should be regarded with suspicion. Similarly the Seattle record suggests some radical change, and should be questioned.

The probability distribution of sea surface temperature and salinity anomalies is shown in figure 10. It is seen that the temperature anomalies are normally distributed, and that their probabilities vary very little from one station to another. The salinity anomalies are generally not normally distributed, and tend to be negatively skew. This is particularly the case where there is considerable influence of runoff (San Francisco).

The standard deviations and extreme ranges for each of the stations are given in Table 1. For sea surface temperature anomalies there is no dependence upon latitude; the anomalies appear, however, to be larger for stations situated in shallow bays and harbors than for those situated in straits and sounds, suggesting that tidal mixing may be important in reducing the amplitude of the temperature variation. For air temperature anomalies there is a slight dependence upon latitude, the anomalies being somewhat larger at high than at low latitudes. The salinity and precipitation anomalies are dependent upon the particular environment of the station and do not suggest a relation to latitude.

TABLE 1

Standard Deviations (σ) and Extreme Ranges (r) of Monthly Sea Surface Temperature (θ), Salinity (S), Air Temperature (A) and Precipitation (p) Anomalies

STATION*	σ_θ °C	σ_s °/₀₀	σ_A °C	σ_p cm	r_θ °C	r_s °/₀₀	r_A °C	r_p cm
La Jolla-San Diego	0.9	0.1	1.1	2.8	6	1	7	24
Balboa-Los Angeles	1.0	0.1	1.3	4.1	7	1	7	24
Hueneme-Sta. Barbara	1.1	0.2	1.2	4.4	7	3	7	34
Pacific Grove-Sta. Cruz	0.9	0.2	1.2	6.0	6	2	7	36
SE. Farallon Isl.-Pt. Reyes	0.9	0.3	..	2.9	5	4	..	24
San Francisco	0.8	2.3	1.0	3.9	5	13	7	33
Blunts Reef-Eureka	0.9	0.3	1.2	5.6	4	3	8	41
Crescent City	1.1	1.7	1.2	11.5	6	10	8	61
Astoria-North Head	1.0	1.1	1.2	..	7	8	9	
Neah Bay-Tatoosh Isl.	1.0	1.0	1.2	7.3	5	7	10	43
Seattle	0.8	1.9	1.4	4.0	5	11	10	26
Race Rocks-Victoria**	0.5	0.3	1.2	3.4	3	2	10	21
Amphitrite Point**	0.9	0.8	..	..	4	4		
Pine Island-Port Hardy**	0.5	0.2	1.3	5.8	4	4	8	37
Cape St. James**	0.8	0.2	..	..	7	2	..	
Langara Island-Masset**	0.8	0.2	1.5	4.2	4	2	11	24
Ketchikan	0.8	1.8	..	13.5	4	14		65
Sitka	0.8	1.3	1.6	9.0	4	6	11	58
Juneau	0.8	2.3	2.0	8.4	4	11	10	42
Yakutat	1.0	1.1	1.9	13.1	5	5	11	107

* Where two names occur, the first refers to the oceanographic, the second to the meteorological station.

** Salinity determined by titration.

COMPUTATIONAL PROCEDURES

Let $\theta\ (t)$ and $A\ (t)$ denote anomalies of sea surface temperature and air temperature, respectively. Then the autocorrelations and crosscorrelations are defined by

$$(1)\qquad \begin{aligned} \phi_{\theta\theta}(\tau) &= <\theta(t)\theta(t+\tau)>; \\ \phi_{AA}(\tau) &= <A(\mathrm{t})A(t+\tau)>; \\ \phi_{\theta A}(\tau) &= <\theta(t)A(t+\tau)> \end{aligned}$$

provided the records are stationary. Here $< >$ denotes the time average over the entire record length, and τ is the time lag in months.

The power spectral densities and cross power spectral densities are obtained from a Fourier transform of the correlation functions

$$(2)\quad E_{\theta\theta}(\omega) = \frac{2}{\pi}\int_0^\infty \phi_{\theta\theta}(\tau)\cos\omega\tau d\tau;$$

$$E_{AA}(\omega) = \frac{2}{\pi}\int_0^\infty \phi_{AA}(\tau)\cos\omega\tau d\tau;$$

$$E_{\theta A}(\omega) = \frac{1}{\pi}\int_{\infty}^{\infty} \phi_{\theta A}(\tau)e^{-i\omega\tau}d\tau$$

Practical methods for evaluating the power spectra are given by Munk, Snodgrass and Tucker (1959).

The coherence between $\theta\ (t)$ and $A\ (t)$ is defined by

$$(3)\quad \mathrm{R}_{\theta A}(\omega) = \frac{E_{\theta A}(\omega)}{[E_{\theta\theta}(\omega)\ E_{AA}(\omega)]^{1/2}}$$

and must lie between the values zero and one. If $R = 1$ the coherence is perfect, if $R = 0$ there is no coherence between the two variables. The phase lag of θ (t) over A (t) is defined by

$$(4) \quad \pi_{\theta A}(\omega) = \text{arc tan}\, \frac{E_{\theta A}(\omega) - E_{A\theta}(\omega)}{E_{\theta A}(\omega) + E_{A\theta}(\omega)}$$

provided that for a positive numerator $0 \leq \pi \leq 180$ and for a negative numerator $180 \leq \pi \leq 360$. If $\pi = 0$ degrees, the two variables are related directly to each other, if $\pi = 180$ degrees there exists an inverse relationship between them.

Similar relations can be established for any other pair of variables. The length of the records used varies from 163 months at Crescent City to 444 months at Ketchikan. The length of the record at each station, n, the number of lags used, m, and the resulting *degrees of freedon*, ν, defined by

$$(5) \quad \nu = \frac{2n}{m}$$

are given in Table 2. Also shown in this table are the 95% confidence limits for the power spectra, provided the variables are normally distributed.

TABLE 2

Total Length of Record (n), Number of Spectral Estimates Used (m), and Resulting Degrees of Freedom (ν). Also Given Are the 95 Percent Confidence Limits for the Power Spectra (P)

STATION	n month	m month	ν	P (unit)²/c.p.y.
La Jolla-San Diego	504	24	42	0.67–1.62
Balboa-Los Angeles	348	24	29	0.63–1.81
Hueneme-Sta. Barbara	420	24	35	0.66–1.69
Pacific Grove-Sta. Cruz	480	24	40	0.67–1.64
SE. Farallon Isl.-Point Reyes	204	24	17	0.56–2.25
San Francisco	336	24	28	0.63–1.83
Blunts Reef-Eureka	228	24	19	0.58–2.13
Crescent City	163	24	14	0.53–2.54
Astoria-North Head	372	24	31	0.64–1.78
Neah Bay-Tatoosh Isl.	276	84	23	0.60–1.97
Seattle	408	24	34	0.65–1.71
Race Rocks-Victoria	192	24	16	0.56–2.73
Amphitrite Point	276	24	23	0.60–1.19
Pine Island-Port Hardy	174	24	15	0.55–2.40
Cape St. James	192	24	16	0.56–2.31
Langara Island-Masset	228	24	19	0.58–2.13
Ketchikan	444	24	37	0.66–1.67
Sitka	192	24	16	0.56–2.31
Juneau	204	24	17	0.56–2.25
Yakutat	216	24	18	0.57–2.19

It should be pointed out that the power spectral densities depend upon the amount of averaging done upon the original data (Munk 1960); if the monthly means were obtained from hourly readings, the power spectrum will be different from one where the monthly means were obtained from daily readings. In case of a simple Markov process the power is decreased by an increased amount of averaging.

The computations of the power spectra, coherence and phase were performed on a IBM 709 electronic calculator at the Western Data Processing Center in Los Angeles.

POWER SPECTRA OF TEMPERATURE AND SALINITY ANOMALIES

The power spectra of sea surface temperature anomalies are shown in figure 11 for the frequency range between zero and 6 cycles per year (c.p.y.). It is seen that most of the power is concentrated at low frequencies, mainly between 0 and 1.5 c.p.y. and that the high frequency end of the spectrum contains relatively little power. This suggests that there is very little contamination from frequencies beyond 6. c.p.y. in the spectra shown here. Most of the spectra indicate an exponential decrease of the power with frequency, suggesting a Markov type process, for which prediction is not very effective (Roden and Groves 1960). The spectra for Neah Bay, Washington, and Seattle, Washington, show peaks near 1 c.p.y., which, when real, would indicate an annual periodicity. The peaks are, however, barely significant (upon applying the confidence limits shown in Table 2), and the periodicity is therefore not well established.

The power spectra of surface salinity anomalies are shown in figures 12 and 13. Most of the power is concentrated between 0 and 2 c.p.y., and for the majority of stations the spectra do not contain any power for frequencies higher than about 4 c.p.y. There is a large variation from station to station of the power contained in each spectrum; the Canadian stations located on small islands and the Californian island stations contain a hundred times less power than those along the mainland coast, excepting the Southern California stations. There are no significant peaks, or periodicities, contained in spectra of the salinity anomalies.

COHERENCE AND PHASE BETWEEN SEA SURFACE AND AIR TEMPERATURE ANOMALIES

The coherence (Fig 14) between sea and air temperature anomalies is moderate to good for stations along the open coast and for island stations, and is relatively poor for stations located considerable distances from the open coast along inland sounds. Thus for Blunts Reef, Neah Bay and Yakutat the coherence varies around 0.7 whereas for Seattle and Juneau it is only 0.4 or less. The maximum values of coherence vary around 0.9, indicating that in the most favorable cases about 80% of the anomalies can be related to each other. The phase (Fig. 15) between sea and air temperature anomalies varies around zero degrees and is at most stations independent of frequency, which suggests a direct relation between sea and air temperature anomalies, for all frequencies between 0 and 6 c.p.y. The considerable scatter at Juneau together with the low coherence indicates the absence of any significant relationship there.

The ratio of the power of sea surface to air temperature anomalies is shown in Table 3. For the Californian stations and Yakutat the ratio is somewhat larger at low than at high frequencies suggesting that a certain time is required for the anomalies to respond to each other. For Neah Bay and Langara Island there is no simple dependence upon frequency.

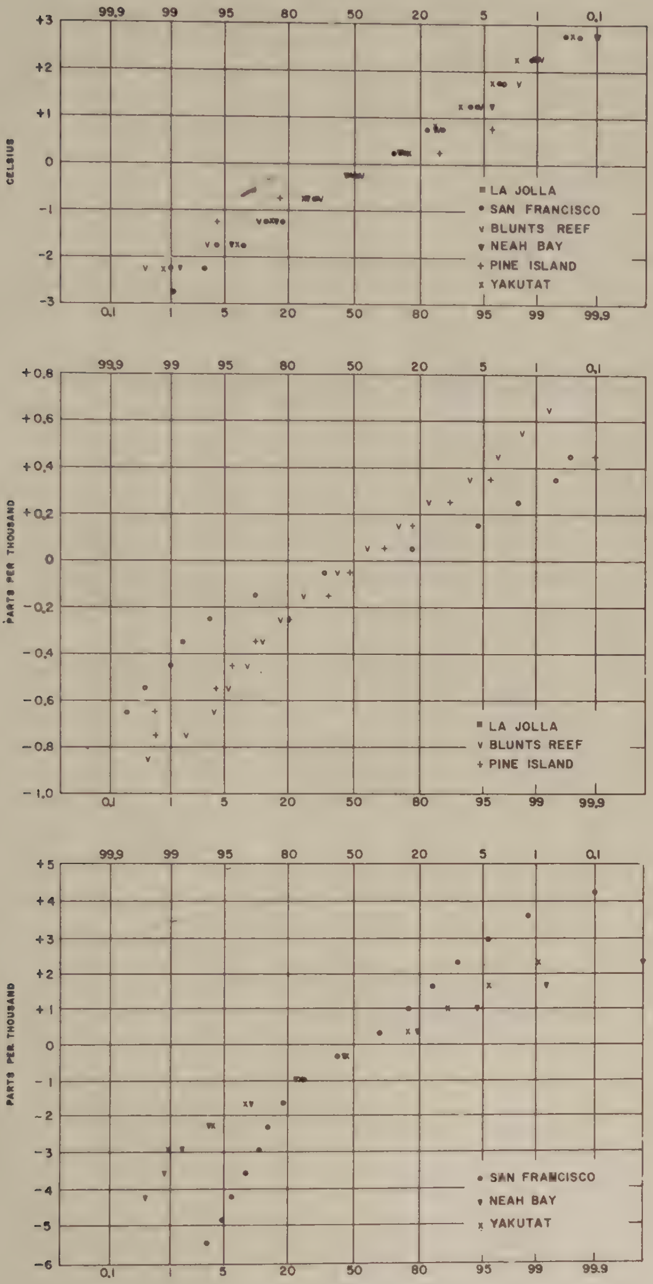

FIGURE 10. Probability distribution of sea surface temperature and salinity anomalies.

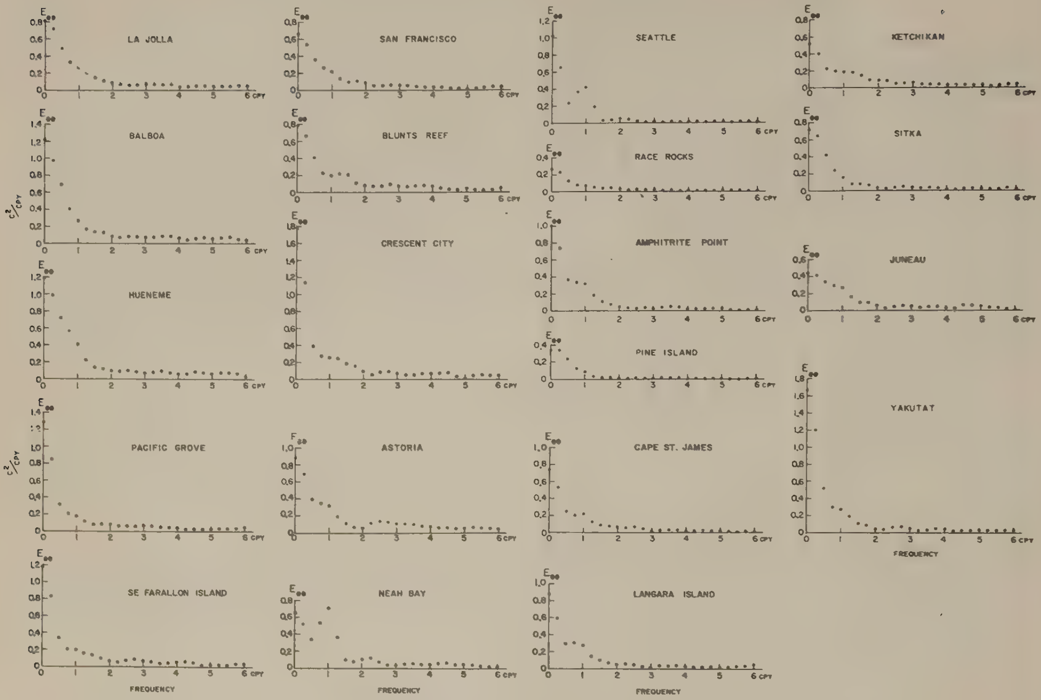

FIGURE 11. Power spectra of sea surface temperature anomalies.

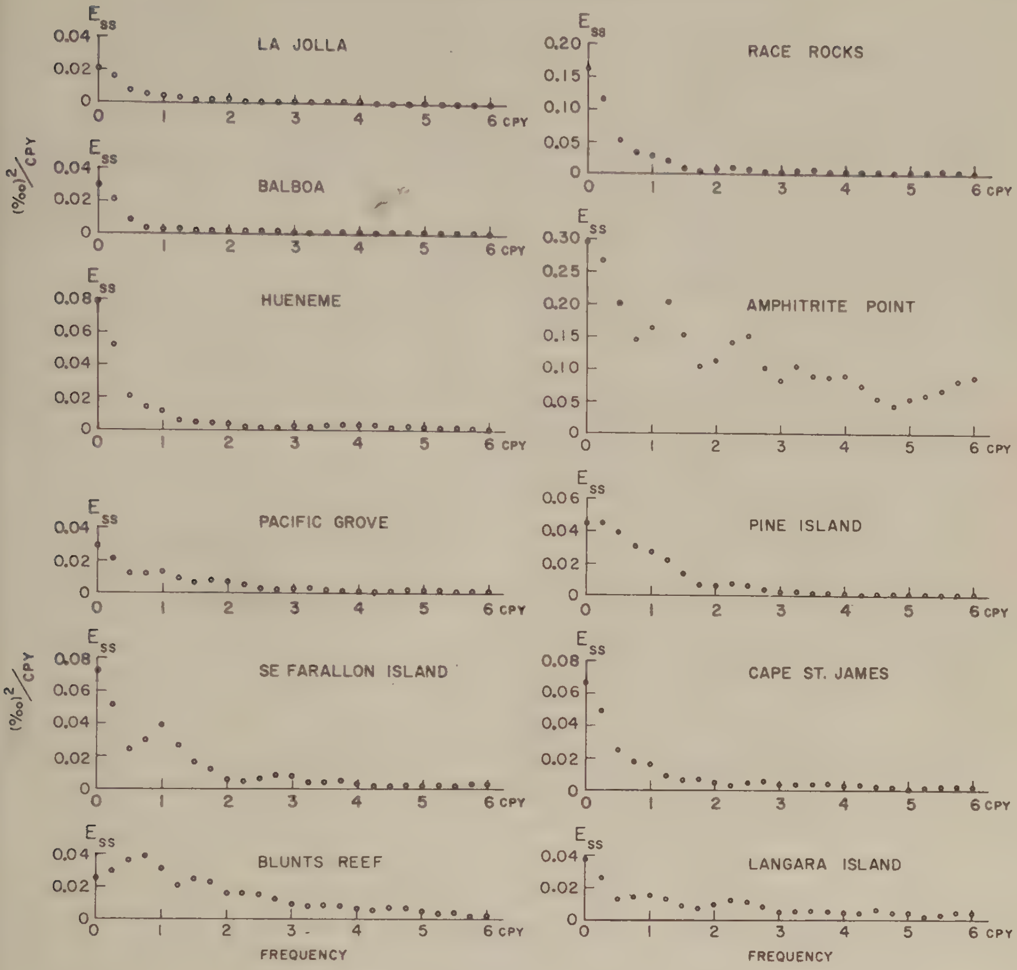

FIGURE 12. Power spectra of salinity anomalies.

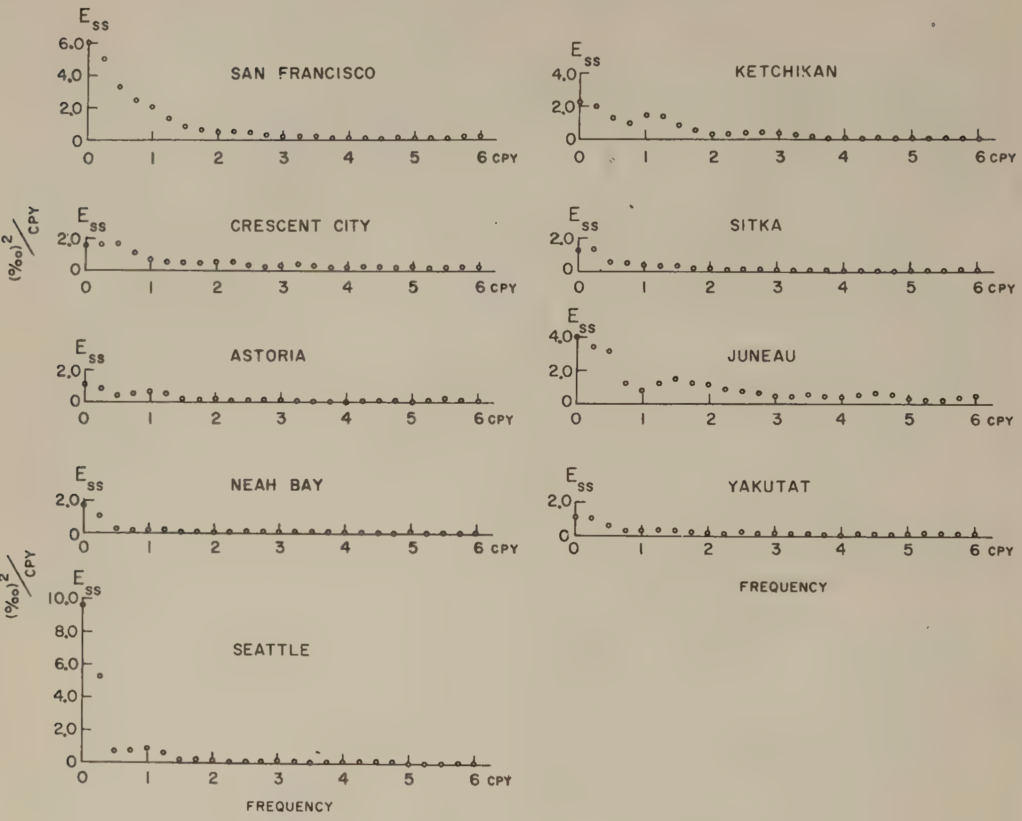

FIGURE 13. Power spectra of salinity anomalies.

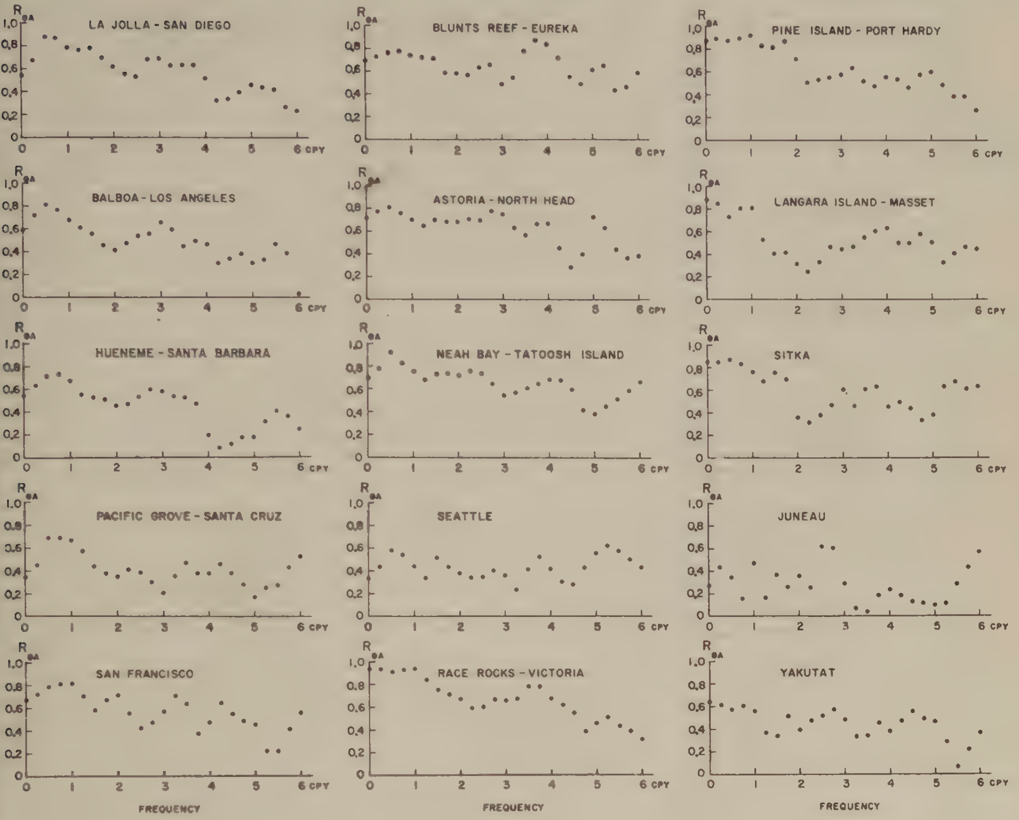

FIGURE 14. Coherence between sea surface temperature and air temperature anomalies

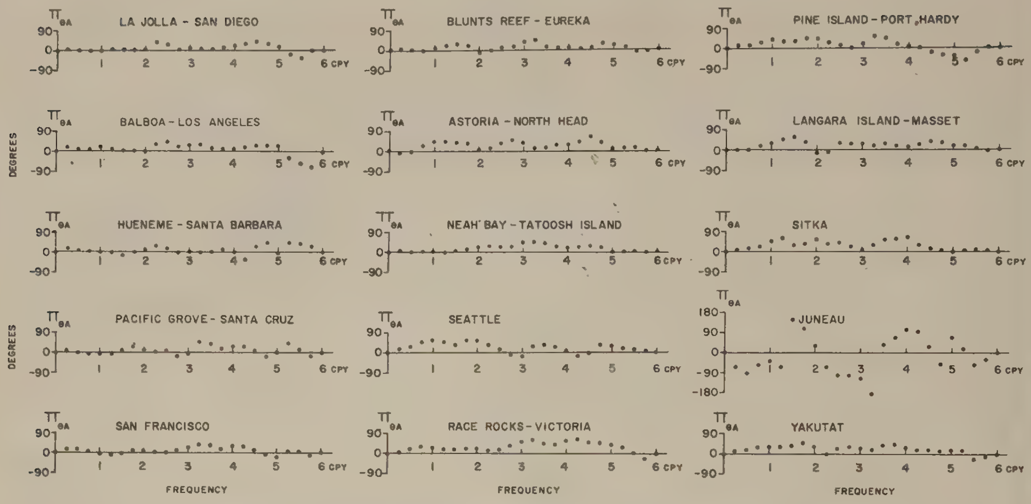

FIGURE 15. Phase between sea surface temperature and air temperature anomalies.

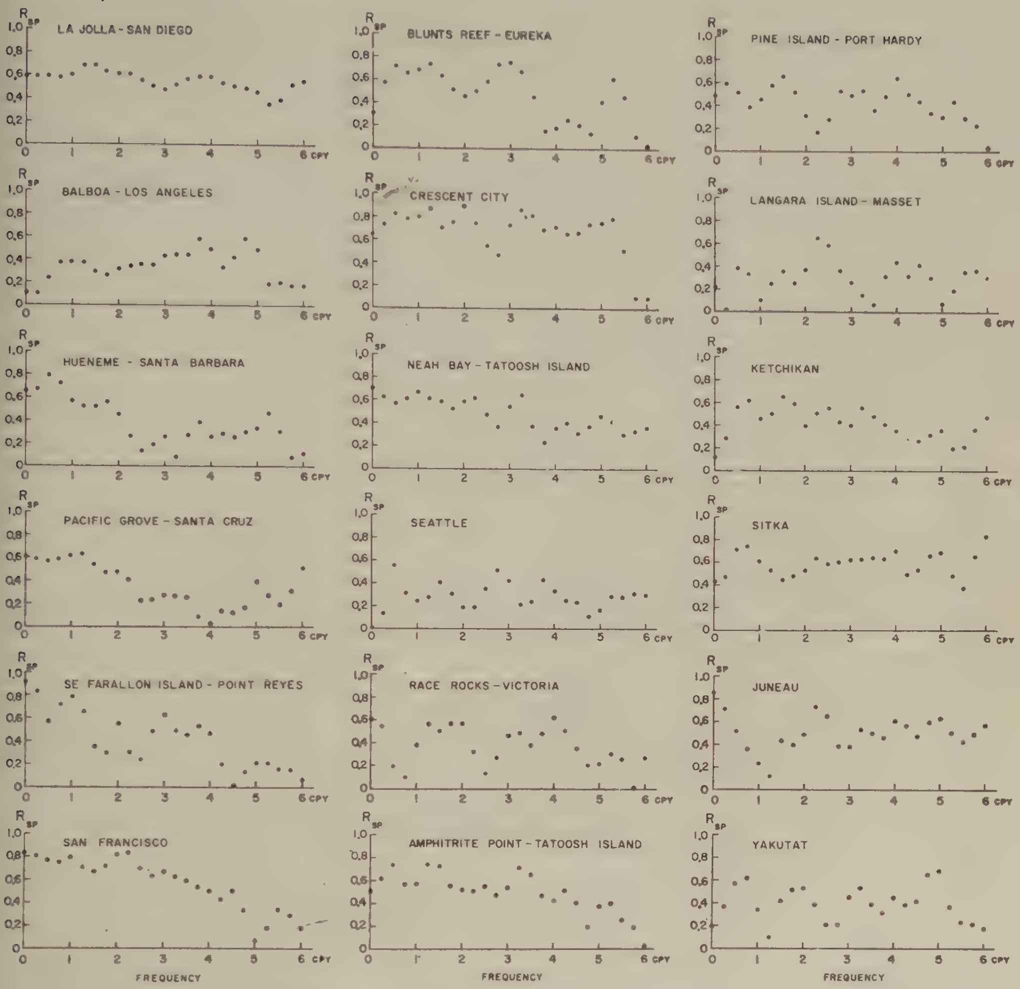

FIGURE 16. Coherence between salinity and precipitation anomalies.

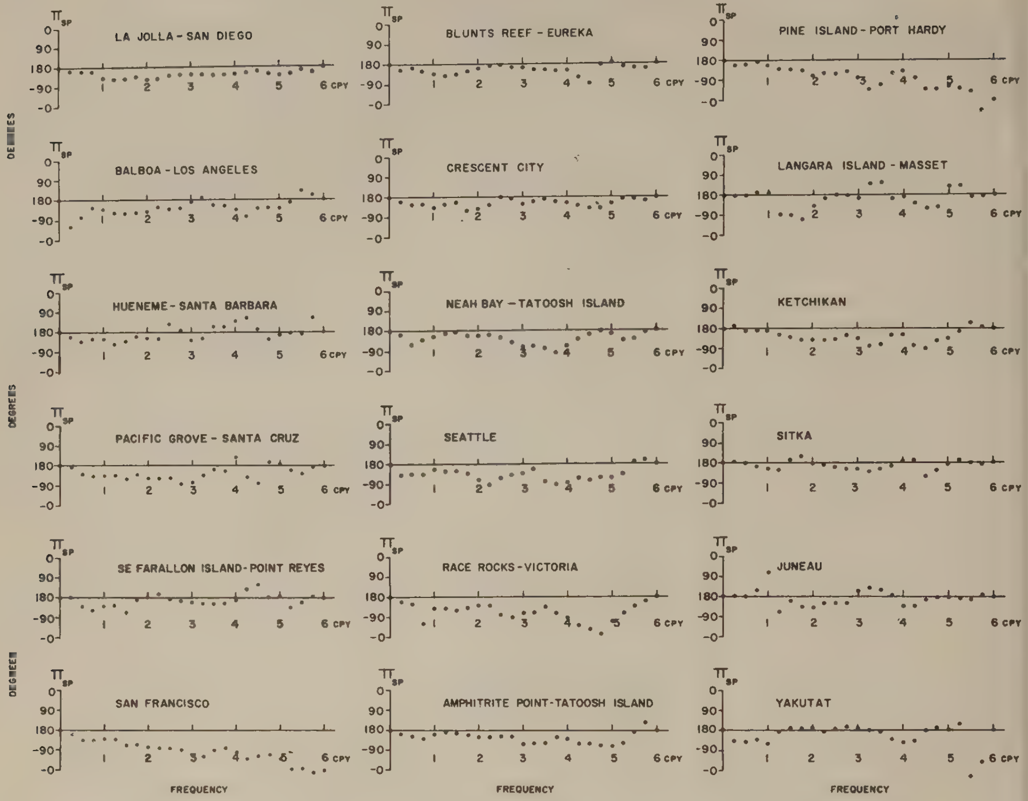

FIGURE 17. Phase between salinity and precipitation anomalies.

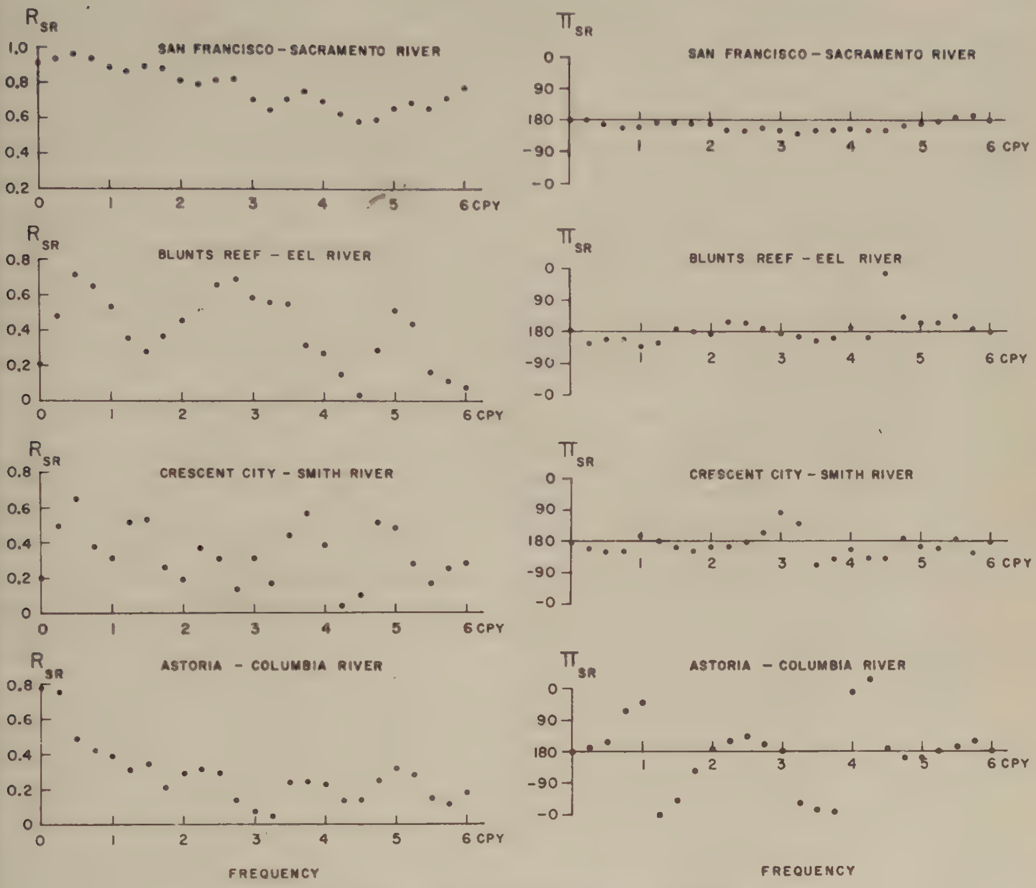

FIGURE 18. Coherence and phase between salinity and river discharge anomalies.

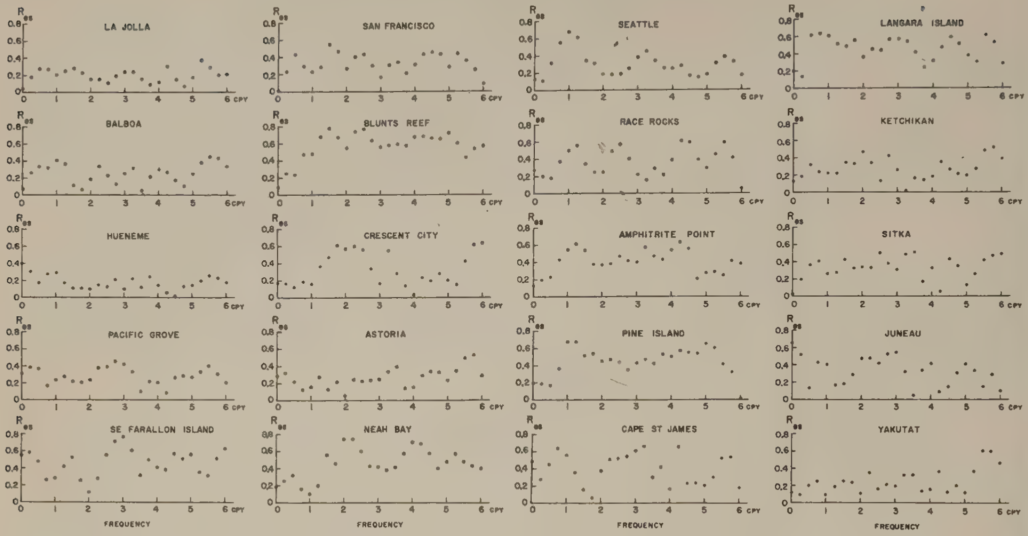

FIGURE 19. Coherence between sea surface temperature and salinity anomalies.

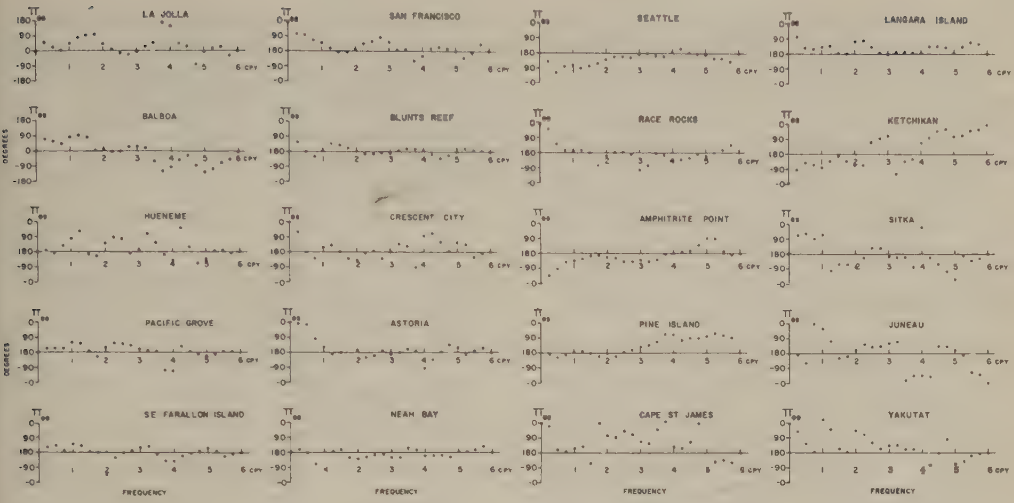

FIGURE 20. Phase between sea surface temperature and salinity anomalies.

TABLE 3

The Ratio $E_{\theta\theta}/E_{AA}$ As a Function of Frequency

f c.p.y.	La Jolla	San Francisco	Blunts Reef	Neah Bay	Langara Isl.	Yakutat
0	0.70	0.73	1.01	0.45	0.36	0.65
1	0.84	0.69	0.67	1.39	0.68	0.30
2	0.67	0.64	0.57	0.54	0.25	0.10
3	0.44	0.70	0.42	0.28	0.11	0.14
4	0.40	0.50	0.47	0.39	0.15	0.16
5	0.50	0.50	0.31	0.83	0.13	0.10
6	0.56	0.50	0.37	0.50	0.45	0.06

COHERENCE AND PHASE BETWEEN SALINITY AND PRECIPITATION ANOMALIES

The coherence (Fig. 16) between salinity and precipitation anomalies varies widely from station to station, because of the very local character of rainfall. For La Jolla, Crescent City, Neah Bay, Amphitrite Point and Sitka the coherence is relatively high and does not vary much with frequency. About 40% to 60% of the salinity anomalies at these stations can be related to anomalies in precipitation. At San Francisco and SE Farallon Island the coherence is high at low frequencies (0 to 3 c.p.y.) and low at high frequencies, which suggests that short period salinity variations are related to some other factor than rainfall. At Blunts Reef the coherence scatters widely, which is probably due to the influence of upwelling, in addition to precipitation, upon the surface salinity. The phase (Fig. 17) between the anomalies is generally 180 degrees, which shows that salinity and precipitation anomalies are related inversely to each other. At San Francisco and a few other places there is a phase drift from 180 degrees at low frequencies to 0 degrees at high frequencies; this is, however, not significant in view of the low values of coherence at higher frequencies.

COHERENCE AND PHASE BETWEEN SALINITY AND RUNOFF ANOMALIES

At stations located near rivers, the variation in the discharge of the river can be expected to have considerable influence upon the surface salinity. This is particularly true of stations located near the boundary of oceanic and river water. In figure 18 are shown the coherence and phase between the salinity anomalies at Fort Point, San Francisco and the discharge of the Sacramento River at Verona, and other cases. It is seen that about 70% of the San Francisco salinity anomalies can be accounted for in terms of anomalies of river discharge. The relatively low coherence between the salinity anomalies at Astoria and the discharge of the Columbia River at The Dalles is not surprising in view of the fact that Astoria is located right at the river and is seldom influenced by oceanic water. The coherence between the Blunts Reef salinity and the Eel River discharge at Scotia is moderate, and is better at certain frequencies than at others, which is probably due to the additional influence of upwelling upon the salinity. In the best cases about 50% of the salinity anomaly can be related to discharge anomalies. The coherence between the Crescent City salinity anomalies and the discharge of the Smith River near Crescent City is not particularly good. The phase between salinity and runoff anomalies is 180 degrees where the coherence is high.

COHERENCE AND PHASE BETWEEN SEA SURFACE TEMPERATURE AND SALINITY ANOMALIES

The coherence between surface temperature and salinity anomalies (Fig. 19) is moderate for stations on islands and on well exposed capes and points, and relatively poor elsewhere. The best coherence is found for Blunts Reef Lightship, where for frequencies between 1.5 and 6 c.p.y. about 50% of the variations can be related to each other. The phase (Fig. 20) is 180 degrees indicating that an inverse relation exists between the anomalies. This is not surprising, since in summer low temperatures are associated with high salinities, owing to upwelling, and in winter relatively high temperatures are connected with low salinities due to abundant precipitation. A similar but poorer relation is also found at SE Farallon Island. Several northern stations, particularly Race Rocks, B.C., and Seattle, Washington, show an oscillation of the coherence with frequency; the cause for this remarkable feature is not known. The phase between temperature and salinity anomalies scatters about 180 degrees at many stations which suggests that high temperatures are associated with low salinities and vice versa; this is not an unexpected result in view of the extensive upwelling occuring during summer months.

CONCLUSION

The following results were obtained from a statistical analysis of the various oceanographic and meteorological records:

(1) At most well exposed stations air temperature anomalies can be used as an indicator of sea surface temperature anomalies. The relation between these anomalies is direct and instantaneous.

(2) At most stations not affected by river discharge local precipitation anomalies can be used as an indicator of salinity anomalies. The relation between these anomalies is an inverse one.

(3) The relation between river discharge and salinity anomalies is good at stations located at the boundary between oceanic and river water. It is not good upstream. The anomalies are related inversely to each other.

(4) Temperatures and salinity anomalies at most coastal stations are not related to each other. At island stations and on lightships there is a moderate and inverse relation between these anomalies. The inverse relation between temperature and salinity anomalies is characteristic of upwelling regions off the west coast of the United States.

(5) Sea surface and air temperature anomalies occur more or less simultaneously over very large areas. Salinity and precipitation anomalies are very local phenomena.

ACKNOWLEDGMENTS

The author is indebted for valuable discussions and advice to J. D. Isaacs, G. R. Miller, W. H. Munk, and J. L. Reid, Jr. The research reported herein was partly financed by the Marine Life Research Program of the Scripps Institution of Oceanography of the University of California, La Jolla.

The computations were carried out at the Western Data Processing Center of the University of California in Los Angeles.

REFERENCES

Fisheries Research Board, Canada, 1958. Observations of Seawater Temperature and Salinity on the Pacific Coast of Canada. Manuscript Report Series 23. Pacific Oceanographic Group, Nanaimo, B.C. 100 pp.

Herlinveaux, R. H., 1957. On tidal currents and properties of the sea water along the British Columbia Coast. *Prog. Rep. Pac. Coast St. Fish. Res. Bd, Canada* Issue 108, 7-9.

Hubbs, C. L., 1948. Changes in the Fish Fauna of Western North America with Changes in temperature. J. Mar. Res. 7 (3) : 460-482.

Isaacs, J. D., 1960. Introductory Statement, Symposium on the Changing Pacific Ocean in 1957 and 1958. *Calif. Coop. Oceanic Fish. Invest. Rept.* 7:27.

McEwen, G. F., 1912. The distribution of ocean temperatures along the west coast of North America deduced from Ekman's theory of upwelling of cold water from the adjacent ocean depths. *Internationale Revue der gesamten Hydrobiologie and Hydrographie.* Werner Klinkardt, Leipzig : 243-286.

1916. Summary and interpretation of the hydrographic observations made by the Scripps Institution for Biological Research 1908-1915. *Univ. Calif. Publ. Zool.* 15 (3) : 255-356.

1929. A mathematical theory of the vertical distribution of temperature and salinity of water under the action of radiation, conduction, evaporation, and mixing due to the resulting convection. *Bull. Scripps Inst. Ocean, Univ. Calif. Tech. Ser.* 2(6) : 197-306.

1938. Some energy relations between the sea surface temperature and the atmosphere. *J. Mar. Res.* 1(3) : 217-238.

Munk, W. H., F. E. Snodgrass, and M. J. Tucker, 1959. Spectra of low frequency ocean waves. *Bull. Scripps Inst. Oceanogr. Univ. Calif.* 7(4) : 283-362.

Munk, W. H., 1960. Smoothing and persistence. *J. Met.* 17(1) : 92-93.

Pickard, G. L., and D. C. McLeod, 1953. Seasonal variation of temperature and salinity of surface waters of the British Columbia Coast. *J. Fish. Res. Bd. Canada* 10 (3) : 125-145.

Reid, J. L., Jr., 1960. Oceanography of the northeastern Pacific during the last ten years. *Calif. Coop Oceanic Fish. Rep.* 7: 77-90.

Roden, G. I., 1958. Spectral analysis of a sea surface temperature and atmospheric pressure record off Southern California. *J. Mar. Res.* 16 (2) : 90-95.

Roden, G. I., and G. W. Groves, 1960. On the statistical prediction of ocean temperatures, *J. Geophys. Res.* 65 (1) : 250-263.

Tully, J. P., 1952. Notes on the behavior of fresh water entering the sea. *Seventh Pac. Sci. Congr.* 3 : 1-22.

U. S. Geological Survey, 1958. Compilation of Records of Surface Waters of the United States through September 1950. Part 14 Pacific slope basins in Oregon and lower Columbia River basin. *Geol. Surv. Water Supply Pap.* 1318, Washington, D. C. : 550.

U. S. Weather Bureau, 1872 1949. *Monthly Weather Review* 1-77, Washington, D. C.

1950-1960. *Climatological Data. National Summary* 1-11, Washington, D. C.

1916-1960. *Climatological Data California* 20-64, Washington, D. C.

Reprinted from: California Cooperative Oceanic Fisheries Investigations. Reports, v.8, 1 July 1959-30 June 1960. pp.33-39.

FISHERIES OCEANOGRAPHY IN EUROPE

MAURICE BLACKBURN[1]
Scripps Institution of Oceanography, University of California, La Jolla

Any review of the status and accomplishments of fisheries oceanography would be incomplete without an account of fisheries oceanography in Europe, where the science began and is still vigorous after more than 50 years.

Fisheries oceanography may be said to have begun with the establishment in 1902 of the International Council for the Exploration of the Sea, by representatives of north-west European governments. The form that fisheries oceanography was to take was foreseen and described by the Council in its first Administrative Report (1903), in the following words:

"It was thereby shown that the research work might best be divided into two main divisions, of which the one had in view the physical conditions of the sea, the other the biological—more especially in regard to the animals most useful as human food. Naturally it was seen from the beginning that the study of the physical conditions, of the chemical nature of the ocean waters, of the currents, etc., was of the greatest importance for the investigation of the problems connected with life, that on the other hand, the study of the floating organisms had particular worth for the solution of hydrographic problems, and consequently that a sharp line should never be drawn between these two main divisions . . ."

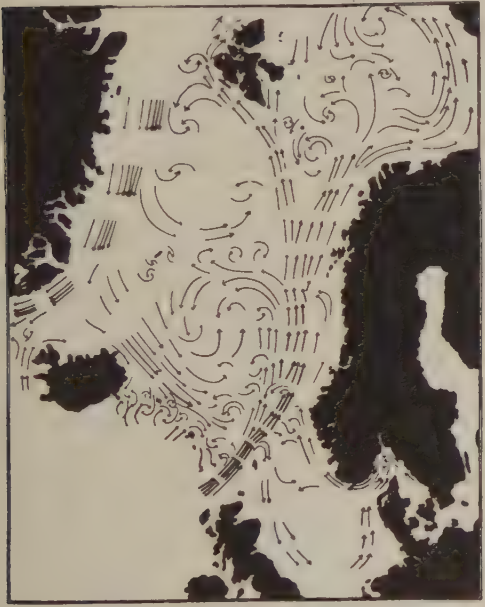

FIGURE 1. Surface currents in the Norwegian Sea (from Helland-Hansen and Nansen 1909).

Most marine scientists know in a general way how, mainly under the aegis of this Council, the north-west European countries have co-operatively and individually planned, performed, discussed, and published an immense amount of oceanographic work which was, or was hoped to be, pertinent to fisheries problems. The remarks in this paper will be confined to the investigations in the region between the English Channel, the Barents Sea, and Greenland. There has, of course, been much work also off the Atlantic coasts of France, Spain, and Portugal, which are in the International Council's area, and in the Mediterranean and Black Seas, which are not.

Figure 1, the well-known surface current chart of Helland-Hansen and Nansen (1909), shows how the warmer more saline North Atlantic water enters the region, mainly through the Faroe-Shetland Channel, as the Norwegian Current, while colder less saline Arctic water flows out, between Greenland and Iceland, as the East Greenland Current. An outflow of low-salinity water from the Baltic contributes to the Norwegian Current. The shallow North Sea receives Atlantic water from the north, around Shetland; and to a less extent from the south, through the English Channel, as indicated in Figure 3.

Another kind of summary of the hydrography of part of this region is the chart of Dietrich (1950) showing natural regions based on distribution of salinity and temperature (Fig. 2).

These figures demonstrate the great differences in the environment of the fishes of the region. Much of the early fisheries oceanographic work consisted of collection, description, and analysis of material in sufficient mass to show what species or populations of fish reacted to what properties of the environment and in what ways. The results have been summarized by Tait (1952, Chapters 1, 2). They gave rise, among other things, to a few rather useful, though not entirely dependable, rules; e.g. that fish populations breed at particular temperatures (Orton 1920) and that breeding migrations are contranatant (E. S. Russell 1937). Mention must be made at this point of the aquarium experiments of Bull (1952), which demonstrated the ability of fishes to perceive and act purposively to changes as low as 0.03° C., 0.2 $^0/_{00}$ of salinity, and 0.05 units of pH, in the water around them; this made the conclusions from the field work more acceptable.

---

[1] Contribution from the Scripps Institution of Oceanography. 1313

Reproduced by Permission

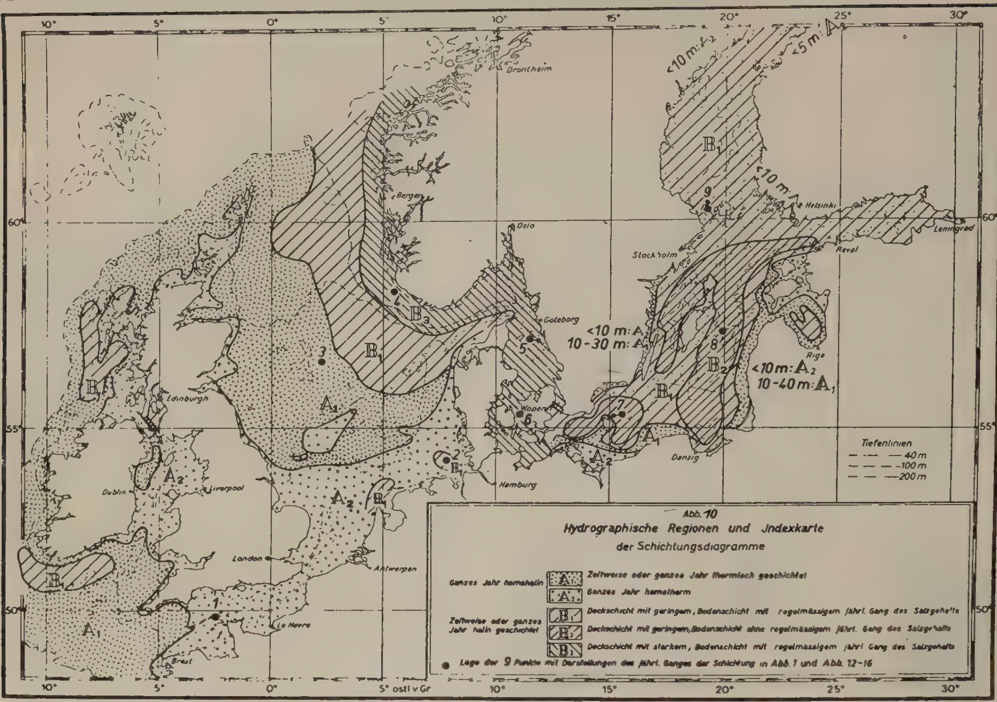
Drontheim
Bergen
Oslo
Stockholm
Helsinki
Leningrad
Reval
Goteborg
Riga
Edinburgh
Dublin
Liverpool
London
Antwerpen
Le Havre
Brest
Kopenhagen
Hamburg
Danzig
<10 m: A
10-30 m: A
<10 m: A₂
10-40 m: A₁
<10 m
<5 m
Tiefenlinien
40 m
-100 m
200 m
Abb. 10
Hydrographische Regionen und Jndexkarte
der Schichtungsdiagramme
Ganzes Jahr homohalin
A₁ Zeitweise oder ganzes Jahr thermisch geschichtet
A₂ Ganzes Jahr homotherm
Zeitweise oder ganzes Jahr halin geschichtet
B₁ Deckschicht mit geringem, Bodenschicht mit regelmässigem jährl. Gang des Salzgehalts
B₂ Deckschicht mit geringem, Bodenschicht ohne regelmässigem jährl. Gang des Salzgehalts
B₃ Deckschicht mit starkem, Bodenschicht mit regelmässigem jährl. Gang des Salzgehalts
Lage der 9 Punkte mit Darstellungen des jährl. Ganges der Schichtung in Abb. 1 und Abb. 12-16
5° östl v Gr

FIGURE 2. Hydrographic regions in the North and Baltic Seas (from Dietrich 1950).

This kind of work was more straightforward than that which came later. In the period between the wars several lines of fisheries work were progressing in a way that seemed to leave the hydrographers and planktologists with a minor role to play as far as practical fisheries problems were concerned. The hydrographers and planktologists found plenty to do on their own account, but their connection with fisheries biology was temporarily weakened.

One reason was that it had become clear that the condition of many important fish populations, especially demersal populations, could be improved by restricting man's fishing (E. S. Russell 1942). This meant: that there was no need of oceanography to help fishermen find these fish, since the fishermen were already too efficient at that for their own good; and that oceanography's promise to understand and predict changes, nothing more, seemed less attractive than the promise of fisheries biology to control changes by regulating fishing. This affected the work on plaice, haddock, hake and other species, and the programs of the countries concerned—especially England, Holland, Belgium, Denmark, and Germany—and continues to do so. The work on the pelagic herring and the semi-pelagic cod was not greatly affected.

Another reason was the well-merited popularity of the theory of natural fluctuations in fish populations according to Hjort (1914). The essential points of the theory were: that year-classes may vary greatly in size because of differing natalities and mortalities of young from year to year; that the progression of these rich, medium, and poor year-classes through the older fishable part of the population has a decisive effect upon the numbers present and catchable each year; and that this effect is predictable in detail if the initial year-class strengths, and average growth-rate of the fish, are known. Although Hjort perceived the probable significance of environmental factors in causing the differences in the year-classes, he pointed out that the causes would have no great importance for practical forecasting if one could measure the differences themselves before the year-classes became important in the fishable segment of the population. It turned out that the differences could be so measured in several populations, by study of age-composition of numerous samples of fish taken before or just at their entry into the fishery, and that useful predictions could be made. This was done particularly for herring, in south-east England (Hodgson 1932) and elsewhere.

In proposing his theory of natural fluctuations, Hjort (1914) had considered and virtually rejected the idea that the coastal food-fish penetrate the ocean waters. Coastal fishermen everywhere tend to believe that fish must be offshore when they cannot be found inshore, and persistently ask their scientists to investigate these waters for them. We will see later that the

Norwegian fishermen were partly right in this belief, and that Hjort was wrong when he disagreed with it. However his conclusion was reasonable in the light of the evidence available to him, and it is salutary to give his words:

"In the course of the Norwegian fishery investigations carried out under my supervision, I have endeavoured in various ways to discover whether any fish move out beyond the coastal banks . . . Numerous experiments have been made with drift net and floating lines, for the most part, however, with negative result."

He then explains that he did find *Sebastes*, the redfish, in many places; some herring in deep water between the North Sea and the Faroe area, but virtually none in the main part of the Norwegian Sea; and little or nothing in the way of cod, haddock, coalfish, and catfish; and he continues:

"Experiments of this nature are, however, by no means easy to carry out, and negative or mainly negative results are scarcely sufficient to warrant the conclusion that the species in question do not occur in any quantity in the waters investigated; there is always the possibility that the fish might occur in shoals, which it would be a matter of merest chance to encounter in so great an expanse of sea. One thing at least is certain; we have no other grounds for supposing the existence, in any considerable numbers, of coastal fish in the deeper parts of the Norwegian Sea, beyond (occurrences of *Sebastes* and restricted occurrences of herring noted above)."

This helped to divert attention from the ocean waters, and was another disservice to the kind of fisheries oceanography that the founders of the International Council had envisaged.

We now turn to what some fisheries oceanographers, physical and biological, did while some fisheries biologists were specializing in the above-mentioned ways; and how some common ground has now been reached again, especially in herring and cod research.

There were workers in England and Scotland who believed that the varying influx of Atlantic water to the North Sea and English Channel was the key to many fluctuations in fish populations.

Plymouth, in the western English Channel, had a herring fishery until about 1938; its extinction began in 1931 when the first of an unbroken series of poor year-classes appeared. The same year marked the beginning of a fall in the standing crop of planktonic young fish generally, and the beginning of a large drop in the winter maximum of inorganic phosphate. It was also the period at which *Sagitta elegans* was replaced in the plankton by *S. setosa*. It was concluded that the influence of Atlantic ocean water upon the Channel, and with it the possibility of renewal of nutrients to the levels of the nineteen-twenties, had receded (F. S. Russell 1939). There has been no definite improvement since that time.

Cooper (1955), noting no evidence that Atlantic surface waters have ever been rich enough to account for the phosphate levels found off Plymouth before 1931, considered various possibilities by which deeper nutrient-rich Atlantic water could have been carried or mixed upwards, in the Channel approaches, during the nineteen-twenties. Observing that this would be facilitated by the elevation of a layer fairly rich in phosphate by a few hundred metres, he supposed the arrival of a suitably large body of water at greater depth, formed by cooling and sinking of water between Faroe and Greenland. Winter temperatures in those regions were particularly low in several years ending about 1921, a year before the beginning of the phosphate record at Plymouth. The effect of the heavy water in keeping the nutrient-rich water elevated in the mouth of the English Channel is supposed to have continued for some years after the recruitment of the heavy water ceased.

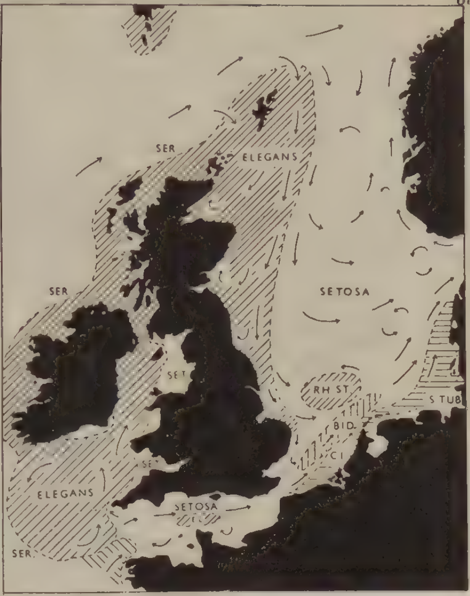

FIGURE 3. Generalized picture of distribution of plankton indicators in the North Sea area: showing occurrence of *Sagitta elegans*, *S. setosa* (SET.), and other species; arrows indicate general water circulation (from F. S. Russell 1939).

Figure 3 shows that *Sagitta elegans*, the plankton-indicator of good conditions for fish in the English Channel, is also distributed in the North Sea in a way that suggests an association with Atlantic water entering through the Faroe-Shetland Channel (F. S. Russell 1939). The idea of plankton organisms as indicators of hydrographic conditions has been so popular in England and Scotland that plankton has been routinely collected, along regular steamship and weathership tracks radiating out from Britain, in most peace-time years since 1932. The convenient Hardy Continuous Plankton Recorder is used. Figure 4 shows the coverage now being obtained (Hardy 1956).

The surface currents of the Northern North Sea region are shown, from the drift-bottle work of Tait (1937), in figure 5. Tait (1955) has also studied vol-

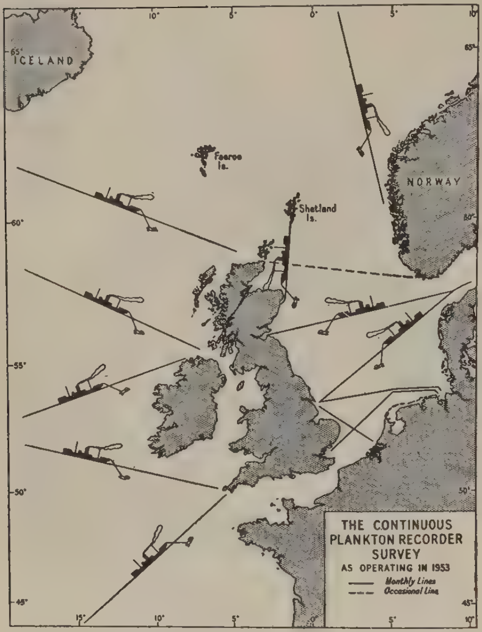

FIGURE 4. Scope of Continuous Plankton Recorder survey in 1953 (from Hardy 1956).

ume transport of oceanic water (salinity >34.99 $^0/_{00}$) through 68 sections made across the Faroe-Shetland Channel from 1927 through 1952, noting various seasonal and annual changes. Scottish biologists have been trying to link such changes with fluctuations in distribution of plankton organisms on the above-mentioned sampling lines around the north of Britain, and with events in the herring fishery off the northeast coasts of Scotland (Glover 1955).

Another aspect of plankton work related to herring must be mentioned, the aggregation of the herring on to the plankton, especially the copepod *Calanus,* which it eats. This has been investigated several times in different areas, frequently in the hope that the relationship would prove sufficiently close to enable fishermen to locate herring from their own plankton surveys with simple collecting instruments. This has happened sometimes but not always (e.g. Hardy, Lucas, Henderson, and Fraser 1936, in the North Sea). It is now clear that a close positive relationship between herring and food is much more likely to occur in some situations than in others, as shown for example from the work of Manteufel (1941) in the Barents Sea, where the study was simplified by the fact that only one brood of *Calanus* occurs per year. The relationships between this brood and the herring are summarized diagrammatically in figure 6.

Finally, for the herring, we must note the appearance in the last decade of an important herring fishery and herring-oceanography program in the middle of the Norwegian Sea, from Iceland to Spitzbergen (Fig. 1), in the very region where Hjort (1914) thought no appreciable amount of herring existed. Location of the resource was primarily the result of equipping a new research ship with asdic (sonar) and using it in regions where a new generation of Norwegian and Icelandic biologists had concluded, from tagging experiments, that herring must occur. But oceanographic work accompanied these surveys from the start, and is producing a picture of herring shoals concentrated, in summer, along the eastern boundary of the cold East Iceland and East Greenland Currents (Devold 1952, Marty 1956). Plankton and productivity (C^{14} method) observations indicate that this is the best part of the region for production of herring food (Berge 1958). Much has been added to our knowledge of currents in the region (Alekseev and Istoshin 1956).

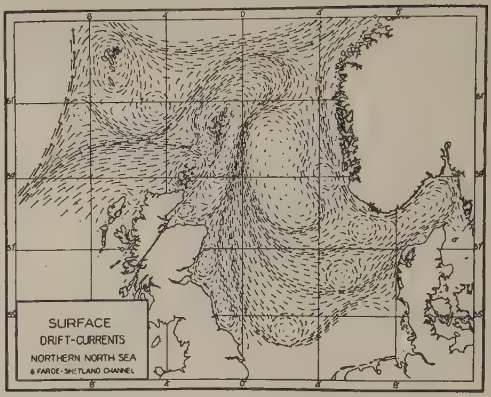

FIGURE 5. Surface currents in the northern North Sea (from Tait 1937).

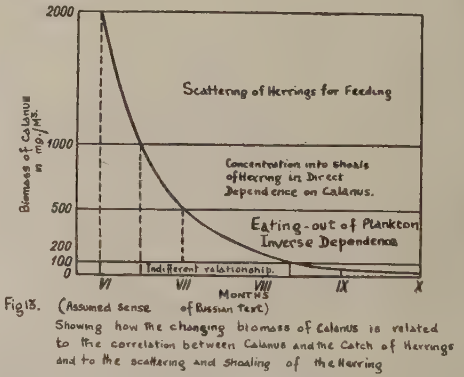

FIGURE 6. Summary of *Calanus*-herring relationships in the Barents Sea (from Manteufel 1941).

The amount of work done on oceanography in relation to cod has likewise been large. Much of it has been planned around the belief that cod are particularly selective about temperature, which arose in part through the work of Thompson (1943) at Newfoundland. The fact that the cod extended its range northwards, from Iceland well into Greenland waters, after the middle nineteen-twenties when the waters of this region were warming, gave further support to the general idea and encouraged the expansion of cod research generally. Biological and hydrographic observations regarding this extension of the cod's range were given by Hansen (1949). Fishery records of the early nineteenth century suggest previous invasions and retreats of cod in Greenland waters. Sea temperature data do not go back quite so far, only to 1876; they show the recent warming very well, of course, and also the preceding cold period about 1920 to which reference has been made (Smed 1949).

There was an unexpected increase in the abundance of cod in the Baltic Sea in the nineteen-forties which Alander (1952) has explained in terms of a series of rich year-classes associated with increased salinity of Baltic water.

Returning to Arctic cod, we note an important investigation by England, commencing in 1949, of the distribution of cod in relation to the environment around Bear Island, between Norway and Spitzbergen. Bear Island lies in the region where the warm Norwegian Current divides and cold water penetrates from the north-east (Fig. 1). The intention was to study relationships of cod to temperature, not so much to predict abundance changes of the whole population through year-class strengths as to predict the location of any payable concentrations of the fish (i.e., similar in motive to some of the herring studies).

The results of this work are still appearing. The results available are somewhat inconclusive on the value of temperature observations to fishermen in the area as a whole, but they point to some situations in which measurement of bottom temperatures would facilitate location of fish (Lee 1952). It was shown that paying quantities are rarely caught in water colder than 1.75°C, except in summer when the fish are feeding heavily to the east of Bear Island and may be found down to –0.5°C. Another finding was that on grounds west of Bear Island, in early summer and in autumn, Atlantic water touching the Bear Island bank can give good catches with bottom temperature between 3° and 5°C. For the area as a whole the range of temperature associated with cod is wide —about –0.5° to 5°C—in the summer feeding season, and narrow—about 2° to 4°C—in the winter nonfeeding season. Even in the winter there may be waters of "suitable" temperature without fish.

Another member of the Bear Island research team has attempted to explain the distribution of cod in the area in a different and more comprehensive way (Trout 1957). The hypothesis, derived from tagging experiments and other biological observations on the cod, is that cod are carried along with currents during summer when they leave the bottom in response to light, and work back against currents in the dark of winter when they have resumed a bottom-living existence.

The report of the first two years of this program provides interesting reading for those interested in European fisheries oceanography from the point of view of outlook, organization, facilities, and methods (Graham *et al.* 1954).

There have been many other investigations on the effects of oceanographic variables on European fish, some conclusive and some not. Much of the work has been done in the "Transition Area" at the entrance of the Baltic (Jensen 1952), on many species. Other references to such work, and to oceanographic work less intimately connected with fisheries at the present time, may be found in papers in the International Council's "Rapport Jubilaire" (1952), and in reviews by F. S. Russell (1952) and Fleming and Laevastu (1956). It is proper also to mention the immense contribution made over about 20 years by Britain, to the fisheries oceanography and general oceanography of the Antarctic Ocean, through the "Discovery Committee". The fisheries in this case were for whales, whose relationships to environment have been summarized by Hardy and Gunther (1935). The effort continued as a general oceanographic survey of the Antarctic and adjacent seas, including the Peru and Benguela Currents, and the ships and personnel finally became the nucleus of the National Institute of Oceanography (Mackintosh 1950).

We may return to the matter of whether or not it is important to understand the causes of year-class fluctuations. It is now generally held that they should be known, if only because it is not always possible to measure the changes properly by sampling juvenile fish. Carruthers has for some years approached this problem *ex hypothesi;* he has assumed that the differences are mainly differences in mortality of young and that they occur in the North Sea because of the vagaries of currents that may carry the young into favorable or unfavorable situations; and he has examined the relationships between year-class sizes and measurements of the winds held responsible for the currents, and has found some satisfactory agreements. The idea is shown in figure 7 which is from one of his earlier papers (1938), showing the correspondence over a series of years between the relative size of haddock year-class and sum of east components in the wind, in the North Sea. Since the war he and his colleagues have produced similar arrays

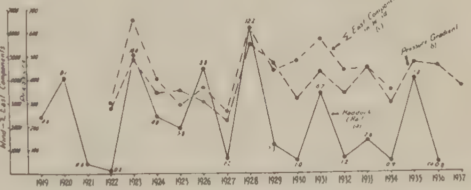

FIGURE 7. Comparison of annual changes in haddock year-class size, pressure gradient, and sum of east components in wind; North Sea data (from Carruthers 1938).

of data, regarding year-class strength and wind, for other species including herring, plaice, cod, and sprat (Carruthers, Lawford, and Veley 1951; other references in Carruthers 1954).

As a result of this work Carruthers (1951) has taken what he calls "An attitude on fishery hydrography", which amounts to this: oceanographers who are not obliged to produce practical results may study what they like, but fisheries oceanographers should study winds. Wind data, he emphasizes, are cheap. Warming to this theme in other papers (1953, with Lawford and Veley; 1954) Carruthers asks whether the complex kind of work now thought of as fisheries oceanography, the kind we have been considering, can do the fisheries any good within reasonable time, or ever. He says (1953) of Tait's work:

"Tait is well known of course for the meticulous detail of his work carried out over many years on water movements in the sea areas to which attention has to be paid by those whose task it is to study the fish of the North Sea. Unless the reviewer has got quite a wrong impression, Tait wants more detail still . . . If so, we must wait a goodly time yet before 'Fisheries Hydrography' can pay the dividends which the biologists seem to expect. There is at least the chance, however, that fruitful associations of the kind needed may be worked out between fish fortunes and environmental conditions in a more simple way involving less industry and less cost."

However, the pattern of fisheries oceanography in Europe has not yet changed much. The work of the last decade has reflected the following recommendation made by the Consultative Committee of the International Council in 1951, after a special scientific meeting on "Fisheries Hydrography" which featured many of the above-mentioned papers.

"As the proceedings of this meeting have shown that a combination of biological, hydrographical, meteorological, physiological or statistical researches has furthered our knowledge of biological productivity, of the habits of the fish stocks, and also the fisheries themselves, it is recommended that researches along these lines should be continued."

REFERENCES

Alander, H., 1952. Fisheries hydrography in the Baltic. *Rapp. Cons. Perm. Internat. Explor. Mer*, **131**: 61-2.

Alekseev, A. P., and B. V. Istoshin, 1956. Chart of constant currents in the Norwegian and Greenland Seas. *Trudy Polar Sci. Res. Inst. Sea Fish. Oceanog. Murmansk*, 9, in Russian: English transl. in *U.S. Fish Wildl. Serv., Spec. Sci. Rept., Fish.* 327 (1959) : 69-76.

Berge, G., 1958. The primary production in the Norwegian Sea in June 1954, measured by an adapted ^{14}C Technique. *Rapp. Cons. Perm. Internat. Explor. Mer*, **144**: 85-91.

Bull, H. O., 1952. An evaluation of our knowledge of fish behaviour in relation to hydrography. *Rapp. Cons. Perm. Internat. Explor. Mer*, **131**: 8-23.

Carruthers, J. N., 1938. Fluctuations in the herrings of the East Anglian autumn fishery, the yield of the Ostend spent herring fishery, and the haddock of the North Sea—in the light of relevant wind conditions. *Rapp. Cons. Perm. Internat. Explor. Mer*, **107**: 10-15.

1951. An attitude on "fishery hydrography." *J. Mar. Res.* **10**: 101-18.

1953. Review of Tait, J. B., 1952 *(q.v.)*. *J. Cons. Perm. Internat. Explor. Mer*, **19**: 211-3.

1954. Some inter-relationships of oceanography and fisheries. *Arch. Meteorol. Geophys. Bioklimatol.* B., **6**: 167-89.

Carruthers, J. N., A. L. Lawford, and V. F. C. Veley, 1951. Fishery hydrography: brood-strength fluctuations in various North Sea fish, with suggested methods of prediction. *Kiel. Meeresforsch.* **8**: 5-15.

1953. Winds and fish fortunes. *J. Cons. Perm. Internat. Explor. Mer*, **18**: 354-8.

Conseil Permanent International pour l'Exploration de la Mer. 1952. Rapport Jubilaire. *Rapp. Cons. Perm. Internat. Explor. Mer*, **132**: 85.

Cooper, L. H. N., 1955. Hypotheses connecting fluctuations in Arctic climate with biological productivity of the English Channel. *Pap. Mar. Biol. Oceanog., Deep-Sea Research*, **3**, suppl.: 212-23.

Devold, F., 1952. A contribution to the study of the migrations of the Atlanto-Scandian herring. *Rapp. Cons. Perm. Internat. Explor. Mer*, **131**: 103-7.

Dietrich, G., 1950. Die natürlichen Regionen von Nord- und Ostsee auf hydrographischer Grundlage. *Kiel. Meeresforsch.* **7**: 35-69.

Fleming, R. H., and T. Laevastu, 1956. The influence of hydrographic conditions on the behavior of fish. *F. A. O. Fish. Bull.* **9**: 181-96.

Glover, R. S., 1955. Science and the herring fishery. *Advancement of Science*, **44**: 426-34.

Graham, M., G. C. Trout, R. J. H. Beverton, J. Corlett, A. J. Lee, and R. W. Blacker, 1954. Report on research from the *Ernest Holt* into the fishery near Bear Island, 1949 and 1950. *Ministry Agric. Fish., London, Fish. Invest. II*, **18** (3), 87.

Hansen, P. M., 1949. Studies on the biology of the cod in Greenland waters. *Rapp. Cons. Perm. Internat. Explor. Mer*, **123**: 1-77.

Hardy, A. C., 1956. "The open sea—its natural history: the world of plankton." Houghton Mifflin Co., Boston: 335.

Hardy, A. C., and E. R. Gunther, 1935. The plankton of the South Georgia whaling grounds and adjacent waters, 1926-1927. "Discovery" Rep. **11**: 1-456.

Hardy, A. C., C. E. Lucas, G. T. D. Henderson, and J. H. Fraser, 1936. The ecological relations between the herring and the plankton investigated with the plankton indicator. *J. Mar. Biol. Assn. U. K.* **21**: 147-291.

Helland-Hansen, B., and F. Nansen, 1909. The Norwegian Sea. Its physical oceanography based upon the Norwegian researches 1900-1904. *Rep. Norw. Fish. Mar. Invest.* **2** (2) : 390.

Hjort, J., 1914. Fluctuations in the great fisheries of northern Europe viewed in the light of biological research. *Rapp. Cons. Perm. Internat. Explor. Mer*, **20**: 1-228.

Hodgson, W. C., 1932. The forecasting of the East Anglian herring fishery. *J. Anim. Ecol.* **1**: 108-18.

Jensen, A. J. C., 1952. The influence of hydrographical factors on fish stocks and fisheries in the transition area, especially on their fluctuations from year to year. *Rapp. Cons. Perm. Internat. Explor. Mer*, **131**: 51-60.

Lee, A. J., 1952. The influence of hydrography on the Bear Island cod fishery. *Rapp. Cons. Perm. Internat. Explor. Mer*, **131**: 74-102.

Mackintosh, N. A., 1950. The work of the Discovery Committee. *Proc. Roy. Soc. London*, B, **137**: 137-52.

Manteufel, B. P., 1941. Plankton and herring in the Barents Sea. *Trans. Knipovich Polar Sci. Inst. Sea Fish. Oceanog. Murmansk*, **7**: 125-218, in Russian.

Marty, J. J., 1956. The fundamental stages of the life-cycle of the Atlantic-Scandinavian herring. *Trudy Polar Sci. Res. Inst. Sea Fish. Oceanog. Murmansk*, 9, in Russian: English transl. in *U.S. Fish Wildl. Serv., Spec. Sci. Rept., Fish.* 327 (1959) : 5-68a.

Orton, J. H., 1920. Sea-temperature, breeding and distribution of marine animals. *J. Mar. Biol. Assn. U. K.* 12: 339-66.

Russell, E. S., 1937. Fish migrations. *Biol. Rev., Camb. Phil. Soc.* 12: 320-37.

1942. "The overfishing problem." University Press, Cambridge: 130.

Russell, F. S., 1939. Hydrographical and biological conditions in the North Sea as indicated by plankton organisms. *J. Cons. Perm. Internat. Explor. Mer*, 14: 171-92.

1952. The relation of plankton research to fisheries hydrography. *Rapp. Cons. Perm. Internat. Explor. Mer*, 131: 28-34.

Smed, J., 1949. The increase in the sea temperature in northern waters during recent years. *Rapp. Cons. Perm. Internat. Explor. Mer*, 125: 21-5.

Tait, J. B., 1937. The surface water drift in the northern and middle areas of the North Sea and in the Faroe-Shetland Channel. *Fish. Bd., Scotland, Sci. Invest.* 1937 (1) : 1-60.

1952. "Hydrography in relation to fisheries." Edward Arnold, London : 106.

1955. Long-term trends and changes in the hydrography of the Faroe-Shetland Channel region. *Pap. Mar. Biol. Oceanog., Deep-Sea Research*, 3, suppl. : 482-98.

Thompson, H., 1943. A biological and economic study of cod (*Gadus callarias*, L.) in the Newfoundland area, including Labrador. *Newfoundld. Res. Bull., Fish.* 14: 160.

Trout, G. C., 1957. The Bear Island cod: migrations and movements. *Ministry Agric. Fish., London, Fish. Invest.*, II, 21 (6) : 51.

Reprinted from Science, October 27, 1961, Vol. 134, No. 3487, pages 1366-1368

Copyright © 1961 by the American Association for the Advancement of Science

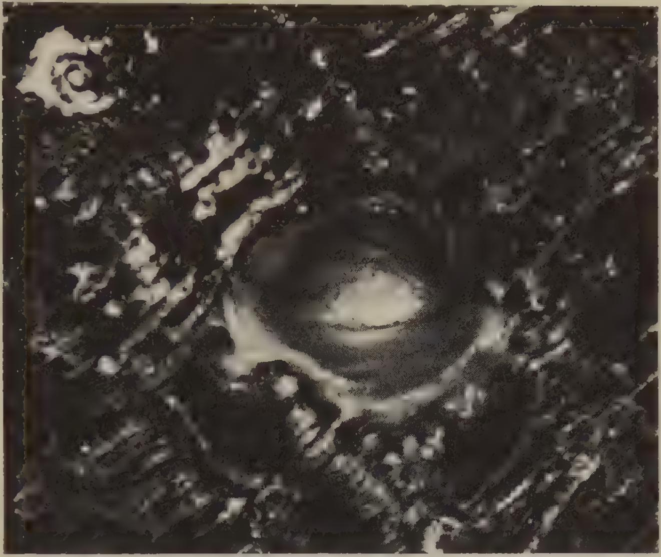

Fig. 1. Hole drilled in an abalone shell (*Haliotis fulgens*) by a large *Octopus bimaculatus* (arm spread, 1.5 m) (about × 18). [A. O. Flechsig]

Hole Drilling by Octopus

Abstract. *Octopus bimaculoides* and *O. bimaculatus* can drill holes in the shells of their molluscan prey, through which they appear to inject a paralyzing venom.

Octopuses are found among the marine littoral fauna throughout most of the world. Because of their appearance, edibility, and behavior, they are well known to maritime peoples. It has long been known that a large part of the food of the octopus consists of shelled mollusks (*1*). The suggestion has been made that the octopus obtains this food by exerting greater force than the prey can withstand. Bartsch (*2*), writing of *Octopus vulgaris* Lam., says, "Presumably he opens a mussel by attaching some of his suckers to the two valves of the shells and then applying pressure until the valves give way." Phillips (*3*), discussing California species of octopus, states that "abalone divers tell of occasionally finding an octopus patiently exerting pressure on an abalone. The abalone eventually tires, even as an oyster gives in to a starfish. The octopus can also open mussels in this manner."

The investigation reported here was prompted by the observation that the empty shells of small abalones appearing in an aquarium tank, which contained abalones and an octopus, had in them small holes of an unusual nature. This octopus, probably *Octopus bimaculoides* Pickford and McConnaughey (*4*), and three others—one certainly *O. bimaculatus* Verrill, one certainly *O. bimaculoides*, and a juvenile which might have been either of the two species—were isolated in large jars supplied with running sea water. Various shelled mollusks were introduced, and after the octopus had eaten the shellfish, the empty shells were removed and examined. The octopus ate individuals of the following species: *Haliotis fulgens* Philippi, *H. cracherodii* Leach, *Tegula funebralis* Adams, *Chione fluctifraga* Sby., *C. undatella* Sby., *Mytilus edulis* L., *M. californianus* Conrad., *Nassarius fossatus* Gould, and *Ischnochiton conspicuus* Carpenter. In most cases there was a hole of characteristic, somewhat oval, shape in the shell (Fig. 1). The hole drilled through a shell 1.4 mm thick by a 48-g octopus was 0.8 mm long and 0.6 mm wide at the top, narrowing at the bottom to an opening which was 0.3 mm long and 0.2 mm wide. The size of the hole is somewhat dependent upon the thickness of the shell and on the size of the octopus, but even a very large octopus produces a hole which is generally smaller than those typically drilled by carnivorous snails, and clearly distinguishable in shape. A boring snail consumes its prey by inserting its proboscis through the hole and rasping the flesh of the prey. The minute size of the octopus hole makes it impossible for the prey to be eaten in this manner. We believe that the octopus injects venom through the hole, causing an abalone or chiton to release its hold on the substrate, a bivalve to relax the adductor muscles, or a gastropod to weaken the closure of its operculum.

Microscopic examination of the hole, beak, and radula indicated that the beak was not of the necessary shape or sharpness to drill the hole. It appeared that this drilling was done by the radula. The following quotation is relevant: ". . . the line of centrals [teeth of the radula] seen through the open beaks [of *Octopus vulgaris*] resemble the teeth of a circular saw, and doubtless its purpose is that of finishing the work begun by the beaks of carving crustaceans. . . . When we examine the extracted radula we find signs of very hard wear in the front portion, greatest in the central teeth, which are often worn flat, but also severe on the laterals" (*5*).

Once we were fortunate enough to see an octopus in the act of drilling a hole in an abalone (*Haliotis fulgens*). The octopus weighed 48 g, the abalone 19 g. The entire process, from initial attack by the octopus to detachment of the abalone from the aquarium wall, took just 3 hours. The abalone was immediately taken from the octopus. There was a typical hole in the shell. The abalone was placed in another aquarium, where it readily attached itself to the wall and crawled away actively but was unable to hold on strongly. It is almost impossible to detach normal abalone of

Reproduced by Permission

this size with the fingers, but this individual could be readily detached. Three days later it could still be detached easily, but 2 weeks later it was normal.

It has long been known that the octopus has a venom elaborated chiefly by the posterior salivary glands (*6*), the duct from which opens just beneath the radula (*7*). The use of this venom for paralyzing crabs is also well known (*8*).

An extract was prepared (*6*) of the combined posterior salivary glands (0.8 g, fresh weight) which had been excised from two freshly killed *Octopus bimaculoides;* frozen and stored at −18°C. In a room at 6°C the glands were ground with sand in a mortar, sea water (9 parts) being added in increments to the homogenate. The suspension was centrifuged, and the opalescent supernatant, kept in ice water, was injected into crabs and abalones. In the crab *Pachygrapsus crassipes* Randall the injections produced death and paralytic symptoms similar to those described elsewhere for octopus venom (*8*); such symptoms were not produced by sea water, nor were they produced by a similarly prepared extract of octopus muscle tissue. Three abalones, *Haliotis fulgens* (19, 20, and 33 g, fresh weight, respectively) each received an injection into the foot muscle of 0.025 ml of extract per gram of abalone. Three other abalones (22, 25, and 31 g, respectively) were similarly injected with sea water. The latter three animals retained their ability to adhere tightly to the aquarium wall and to right themselves when placed on their backs. The abalones injected with salivary extract were easily removed from the aquarium wall and did not right themselves when turned over. They died within 2 days.

Sometimes the octopus does not drill a hole. In such cases it appears to open the bivalve or to pull an abalone off the substrate by force. We are not certain what factors are involved in the choice of the method of feeding, but it seems reasonable to assume that the octopus may try force first and, failing in this, may then drill a hole.

These observations suggest that *Octopus bimaculoides* and *O. bimaculatus* may prey naturally on shelled mollusks by drilling a hole and injecting venom. We have found in nature numerous empty shells of the species *Tegula funebralis* Adams, *Chione undatella* Sby., *Protothaca staminea* Conrad, and *Haliotis* spp. with holes identical in shape to those made by *Octopus* in the aquarium (*9*).

Note added in proof: Dr. S. Stillman Berry has brought a paper by Fujita (*10*) to our attention. Fujita discovered that *O. vulgaris* on the coast of Japan bored holes into the shells of the pearl oyster, and he suggested that venom was injected to weaken the adductor muscle.

M. E. Q. Pilson
P. B. Taylor

*Scripps Institution of Oceanography,
University of California, La Jolla*

References and Notes

1. Aristotle, *Historia Animalium* [about 340 B.C.; trans. by D. W. Thompson (Clarendon, Oxford, 1910)]; F. W. Lane, *The Kingdom of the Octopus* (Jarrolds, London, 1957); T. A. Stephenson, *J. Marine Biol. Assoc. United Kingdom* **13**, 480 (1924); P. H. Fischer, *Bull. lab. maritime Dinard* **20**, 92 (1938).
2. P. Bartsch, *Smithsonian Inst. Publ. Sci. Ser.* **10**, 325 (1931).
3. J. B. Phillips, *Calif. Fish Game* **20**, 20 (1934).
4. G. E. Pickford and B. H. McConnaughey, *Bull. Bingham Oceanog. Colloq.* **12**, 1 (1949).
5. A. J. Peile, *J. conchyliol.* **20**, 292 (1937)
6. E. de Rouville, *Compt. rend. soc. biol.* **68**, 834 (1910).
7. B. W. Halstead, *Dangerous Marine Animals* (Cornell Maritime Press, Cambridge, Md., 1959), p. 45.
8. F. Ghiretti, *Ann. N.Y. Acad. Sci.* **90**, 726 (1960).
9. This work was carried out in the laboratory of Dr. Denis L. Fox, to whom we are most grateful for advice and discussion. Drs. E. W. Fager and John A. M. McGowan gave helpful advice and criticism.
10. S. Fujita, *Dobytsugaku Zasshi* **28**, 250 (1916).

19 June 1961

VICTOR VACQUIER
ARTHUR D. RAFF
ROBERT E. WARREN

HORIZONTAL DISPLACEMENTS IN THE FLOOR OF THE NORTHEASTERN PACIFIC OCEAN

Abstract: A total magnetic intensity survey in the northeastern Pacific Ocean revealed a north-south pattern of magnetic anomalies, which is cut through by the Murray, the Pioneer, and the Mendocino faults. The amount of slip along these faults is measured by fitting the magnetic anomaly pattern across the faults. The combined left-lateral displacement across the Mendocino and the Pioneer faults is 1420 km.

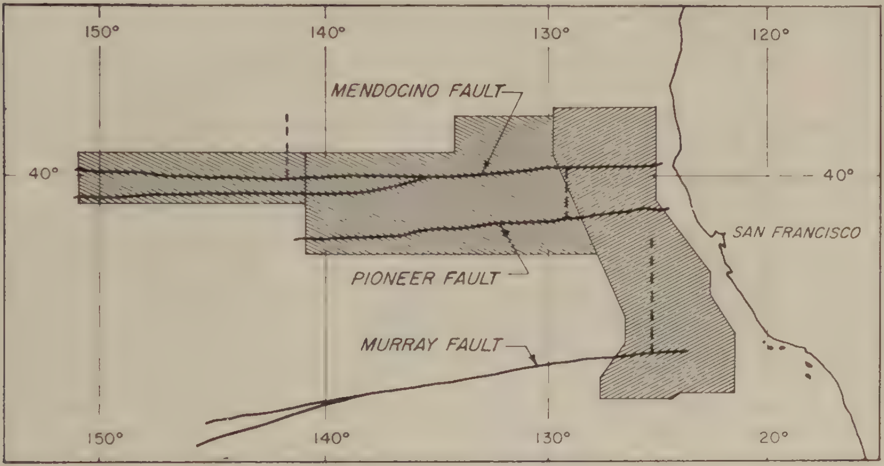

Figure 1. Location of the magnetic survey relative to the Mendocino, Pioneer, and Murray fractures. The dashed vertical line represents the axis of a north–south magnetic anomaly which was continuous before slipping started.

Displacements along strike-slip faults on land have been discussed in the literature. Kennedy (1946) has demonstrated a strike-slip displacement of 65 miles (104km) on the Great Glen fault in Scotland. According to Wellman 1952 the Alpine fault in New Zealand may have slipped 300 miles (480 km). The work of Hill and Dibblee (1953) suggests a right-lateral displacement of 175 miles (320 km) along the San Andreas fault in California since early Miocene time, and 350 miles (640 km) since the Jurassic.

This note presents evidence for displacements of comparable magnitude along some of the transcurrent faults of the northeastern Pacific Ocean.

The geomagnetic surveys first conducted by the Scripps Institution of Oceanography aboard the Coast and Geodetic Survey ship Pioneer and later extended by cruises of Scripps ships have revealed in the eastern Pacific Ocean magnetic anomalies with north–south lineation which are cut by the transcurrent east–west striking faults described by Menard (1959).

Geological Society of America Bulletin, v. 72, p. 1251–1258, 4 figs., 1 pl., August 1961

Contributions from the Scripps Institution of Oceanography, New Series, 1315

Reproduced by Permission

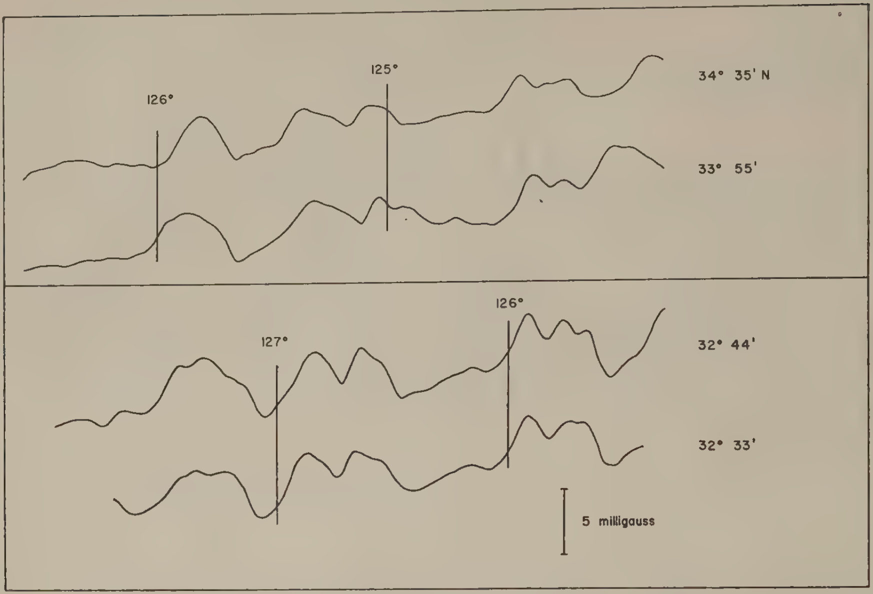

Figure 2. Profiles of anomalous total magnetic intensity north and south of the Murray fault suggesting a right-lateral slip of 84 nautical miles (154 km)

The surveyed area is shown on Figure 1. By matching the magnetic grain north and south of a fault the direction and magnitude of horizontal slip can be measured. This was first done across the Murray fracture zone (Menard and Vacquier, 1958; Mason, 1958) where a right-lateral displacement of 84 nautical miles (154 km) was interpreted (Fig. 2). The displacement along the Murray fault zone suggested an investigation of a possible displacement across the Pioneer fault 300 nautical miles to the north. The cruise of the R/V Horizon in December 1958, undertaken for the express purpose of looking for this displacement, found a left-lateral slip of roughly 3° in longitude (Vacquier, 1959). The cruises of the R/V Spencer F. Baird in August 1959 and April 1960 extended the magnetic survey to the west on both sides of the Pioneer and the Mendocino faults.

The fluxgate ASQ-3A magnetometer was used on all cruises except the last, which employed a proton free-precession magnetometer. The original data are plotted as a magnetic contour chart on Plate 1. Its eastern edge joins the western edge of the contour chart of Mason and Raff (1961, Pl. 1). The normal geographic change of the total magnetic intensity was estimated by smoothing Magnetic Chart No. 1703 published by the Hydrographic Office of the U. S. Navy. Ground-wave Loran positions taken every half hour supplemented by astronomic sights were used for locating the ship. West of 134° W. long., the reception of the ground wave becomes uncertain at night because of the interference of the sky wave. The dead-reckoned course during the night was corrected in the morning as soon as Loran signals became identifiable again. West of 140° W. long. astronomic sights and dead reckoning were the only means of establishing the ship's position. From the spread of the fixes parallel to the track, it is estimated that the average departure of the fixes from the true positions was between 1 and 2 miles. Since short-time fluctuations of the geomagnetic field were not removed from the data, fluctuations of 0.5 milligauss, the contour interval, can originate from this cause during daylight hours. Throughout the two expeditions the ship's average speed was 11 knots.

On Figure 3 profiles of the total magnetic intensity are plotted along the long east-west tracks. The profiles are drawn in their actual positions on the map. Their eastern portion extends across the map of Plate 1 of Mason and Raff (1961). The locations of the Pioneer and Mendocino faults are indicated on Figure 3. The magnetic pattern in the fault zones is too complex to permit contouring with the sparse data. In fact, the contouring of the western portion of the map of Plate 1 depends on the assumption that the magnetic trends are directed north–south as they are on the eastern half of the map where the control is adequate.

East–west magnetic intensity profiles will now be examined for fit of the magnetic grain across the faults without speculation as to origin of the anomalies. The chart of Plate 1 and the profiles of Figure 3 show that as a rule the anomalies strike N.–S. ± 10°. Occasionally a northwest–southeast trend is observed as well as circular anomalies in the fault zones. The correlation for the measurement of slip depends on the continuity of the north–south trending anomalies. Because the elongate anomalies occasionally terminate where there is no major fault, correlations across the faults cannot be perfect everywhere.

Figure 4 represents our interpretation of the magnetic data as slips along the Pioneer and Mendocino faults. The profiles north of Lat. 38°45′ N. have been translated eastward 3°05′, which amounts to 145 nautical miles (265 km). The profiles north of Lat. 40° N. have been translated eastward by an additional 13°42′ (640 nautical miles or 1160 km). The total displacement across both faults is thus 780 nautical miles (1425 km). The correlation of some of the magnetic features across the faults is shown on Figure 4 by dashed lines. To make the goodness of fit more obvious, the northernmost profile of Figure 4 has been drawn again as a dotted line between the profiles south of the Pioneer fault.

Possible origins for the observed magnetic-anomaly pattern are discussed by Mason (1958) and by Mason and Raff (1961). There is of course an infinity of possible distributions of magnetic rocks that will yield the same magnetic anomaly. However, certain types of distributions can be excluded because they would require the presence of rocks possessing unreasonable magnetic properties. To have a reasonable magnetic-polarization contrast, the bodies of rock causing the north-south trending anomalies should be at least 2 km thick. Some of these anomalies are sufficiently sharp to place the top of the magnetic rock no deeper than 6 km from sea level (1.5 km below the sea floor). A likely origin of the magnetic pattern is the intrusion of more strongly magnetic material into the basaltic crust. That the large magnetic anomalies are not directly related to the known topography is demonstrated by the anomaly caused by the 200-fathom relief of the Pioneer Ridge which is no more than one-tenth of the anomalies due to intrusives or extrusives in this fault zone, some of which are as large as 8 milligauss. Plate 1 shows a crossing of the Pioneer Ridge centering at 38°40′N. lat., 130°25′W. long., where no large magnetic anomaly was encountered.

Evidence of the extension of the oceanic faults into the continent is weak and contradictory. Its lack of definiteness compared to that of the magnetic data in the ocean suggests that the geotectonics of the continental crust are influenced by the slips along the transcurrent oceanic faults without directly taking part in these displacements. Thus, the geologic expression of the Mendocino fault is that it lines up with the southern termination of the Cascades Range. From the geophysical point of view, James Affleck of the Gulf Research and Development Company (Personal communication) writes:

> "There is evidence from magnetics that the Mendocino feature may extend eastward from the coast for at least 100 statute miles (160 km). There is no direct evidence of horizontal displacements, but strong lineaments and changes of magnetic character are present."

Nothing on land corresponds to the Pioneer fault. This fault may be regarded as a sliver of the Mendocino fault zone.

The Murray fault to the south marks the northern boundary of the drowned Basin and Range topography of the continental borderland (Shepard and Emery, 1941). South of the Murray fault the continental borderland shows evidence of right-lateral strike-slip faults parallel to the San Andreas fault, suggesting that the latter belongs to a fault zone a part of which is under water. On the continent the Murray fault lines up with the Channel Islands and the Transverse Ranges of California, where all horizontal displacements measured by geological methods are left lateral. This direction is opposite to the 154-km right-lateral slip found in the deep ocean by the magnetic survey. However, all magnetic and bathymetric evidence of the Murray fault stops east of 124°W. long., making a gap of 4° between the eastern end of this fault at sea and the Channel Islands.

The presence of this gap makes it possible to reconcile the opposite directions of displacement by assuming an absence of genetic relationship between the displacements at sea and on land. This explanation may be unlikely, but it follows directly from the assumption,

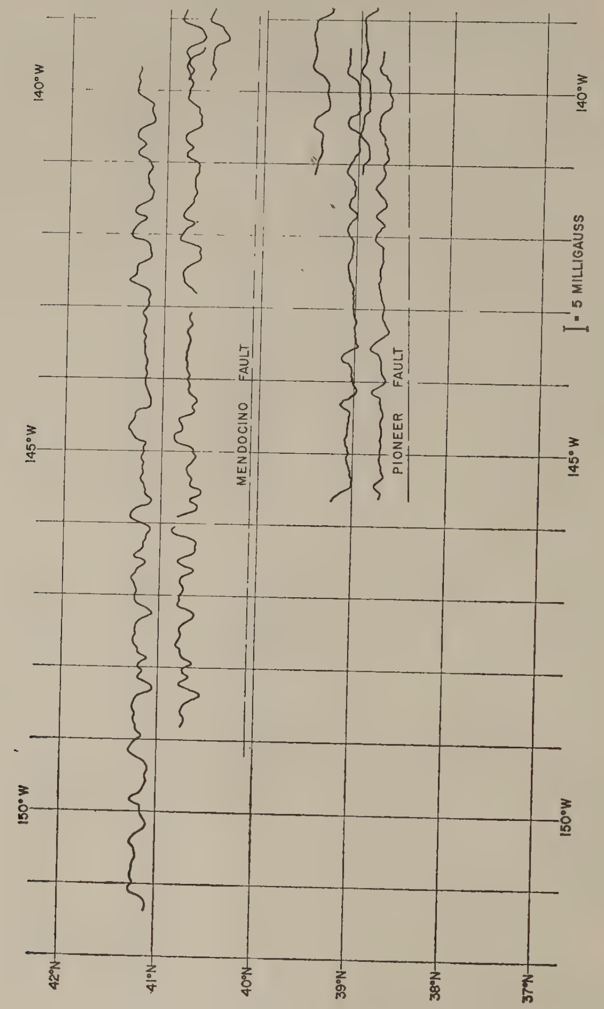
140°W
145°W
150°W
140°W
145° W
150°W
42°N
41°N
40°N
39°N
38°N
37°N
MENDOCINO FAULT
PIONEER FAULT
= 5 MILLIGAUSS

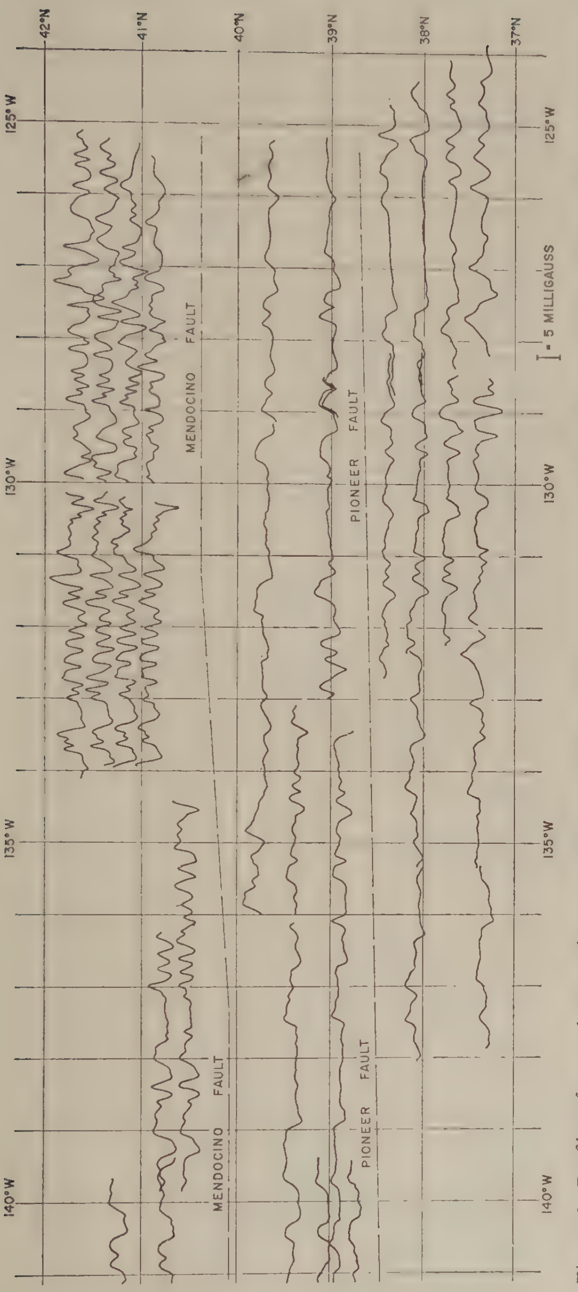

Figure 3. Profiles of anomalous total magnetic intensity along the long east-west tracks. The location of the profiles is approximately that of the corresponding tracks of Plate 1

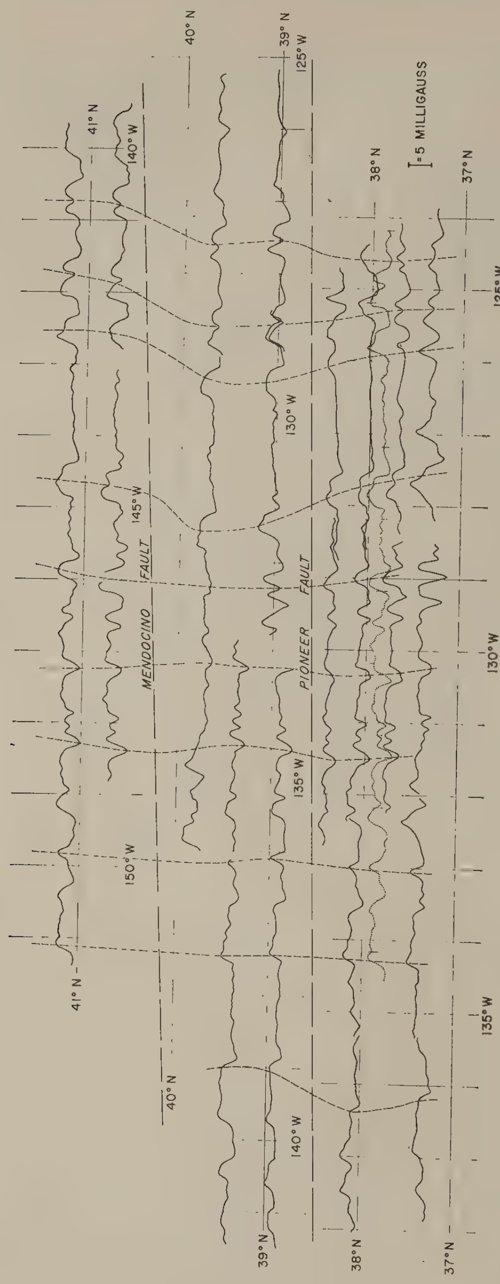

Figure 4. Interpretation of the anomalous total magnetic intensity profiles of Figure 3 in terms of left-lateral displacement of 265 km along the Pioneer fault and 1150 km along the Mendocino fault.

which again may be unlikely although still possible, that the displacements along oceanic faults propagate into the continent at the time they happen. If this time is ancient, both magnetic and geologic evidence for the slips gets largely wiped out on the continent. Furthermore, geologists do not usually look for slips of 1400 km. The absence of definite extension of the oceanic faults into the continent can be explained by the motion along the San Andreas fault zone which separates the ocean from the continent. The land east of the San Andreas fault is now slipping to the south at the rate of 5 cm per year. Since the Jurassic it has moved 560 km (Hill and Dibblee, 1953), roughly the distance between the Mendocino and the Murray faults. There is no need to be disturbed about the discrepancy between the displacements of the Murray fault at sea and the faults on land at about the same latitude unless one insists that the oceanic faults are younger than the San Andreas fault. This is contrary to present-day evidence; the San Andreas fault is seismically active, whereas the oceanic faults are seismically dead west of 130° W. long. Also, mild heat-flow anomalies seem to cross the Mendocino escarpment as though it did not exist (R. P. Von Herzen, personal communication), indicating quiescent conditions in the last 100,000 years at least.

Recalling again that the present discussion has postulated without proof the extension of the oceanic displacements into the continent at the time of their formation, a limit to their age is set by the age of the San Andreas fault—namely, they must have stopped moving some time in the Cretaceous. At 1 cm per year, the average rate of motion along the San Andreas fault, the slip along the Mendocino fault must have taken another 100 million years. The rocks that give us the magnetic lineations that permit us to measure the lateral displacements along the transcurrent faults are thus still older and must have been laid down in Paleozoic time or earlier. They have not been disturbed appreciably since that time either mechanically or by intrusions or extrusions, or we would not have been able to read the magnetic record of the motions. Thus, except for the motions along the transcurrent faults, it is likely that the floor of the eastern Pacific Ocean between 30° and 45°N. lat. has been relatively quiescent since some time in the Paleozoic. This interpretation could be directly confirmed by dating paleontologically and geochemically the material from a deep boring in the ocean floor.

If the motions along oceanic faults do not propagate into the continent at the time of their occurrence, then nothing can be said about their age, and the preceding discussion is discarded. It can be imagined that somehow the oceanic crust carrying the magnetic pattern can slip under the continental mass without disturbing appreciably the continent's geology and isostasy. The oceanic crust would be depressed under the continent, which would cause smoothing out of the geomagnetic field as noted by Heezen (Heezen and Tharp, 1959) in the Atlantic Ocean as one proceeds shoreward over the continental slope and shelf. The same happens along the west coast of North America as shown by unpublished observations by workers at the Scripps Institution of Oceanography, except that the band of smooth field is much narrower along the Pacific margin, as one would expect it to be.

The discovery of slips of the order of 1000 km in the ocean floor suggests looking for such displacements on the continents by reviewing geological and geophysical evidence. As a start, James Affleck (Personal communication) has examined for that purpose over 1 million square miles of aeromagnetic surveys. He found that there are numerous magnetic trends related to major tectonic features. Some of these can be followed for several hundred miles. In addition, offsets in anomaly-trend systems commonly suggest horizontal displacements but generally only of the order of 10 miles. In general, geomagnetic measurements indicate that the crust is more complex in continental areas than under the oceans. In evaluating the evidence from land magnetic surveys one should remember that surveys for oil exploration are confined to sedimentary basins.

The displacements along strike-slip faults in the ocean floor are thus of the same magnitude as the distances through which continents have been presumed to drift to accommodate physiographic and paleomagnetic data. Except for Carey (1958), who invokes a several-fold expansion of the whole Earth, continents are pictured in the literature as rigid plates drifting without distortion through the viscous ocean floor. Now we have evidence for the rigidity of the upper part of the oceanic crust that carries the magnetic pattern, which is just as good as the evidence for the rigidity of continents exemplified by the fit obtained by Carey (1958) between the coasts of Africa and South America along the 2000-m isobath. Since it is most unlikely that the magnetic or the physiographic correlations are accidental, the resolution of this paradox will be an important advance in geophysics.

This work was wholly supported by the Office of Naval Research Contract 2216(05). Thanks are due the Sperry Gyroscope Company, Inc., for the loan of their excellent Mark II, Model 2A Loran set used for locating the ship on the last two cruises.

References Cited

Carey, S. Warren, 1958, Continental drift: A Symposium: Univ. Tasmania, Hobart, Tasmania, p. 177–355

Heezen, B. C., and Tharp, M., 1959, Floors of the oceans I: North Atlantic; Geol. Soc. America Special Paper 65, 122 p., map

Hill, M. L., and Dibblee, T. W., Jr., 1953, San Andreas, Garlock, and Big Pine faults, California: Geol. Soc. America Bull., v. 64, p. 443–458

Kennedy, W. Q., 1946, The Great Glen fault: Geol. Soc. London Quart. Jour., v. 102, p. 41–76

Mason, R. G., 1958, A magnetic survey off the west coast of the United States between Latitudes 32° and 36°N and Longitudes 121° and 128°W: Geophys. Jour., v. 1, p. 320–329

Mason, R. G., and Raff, A. D., 1961, Magnetic survey off the west coast of North America, 32° N. to 42° N.: Geol. Soc. America Bull., v. 72, p. 1259–1266

Menard, H. W., 1959, Minor lineations in the Pacific Basin: Geol. Soc. America Bull., v. 70, p. 1491–1496

Menard, H. W., and Vacquier, V., 1958, Magnetic survey of part of the deep sea floor off the coast of California: Office of Naval Research, Research Reviews, June, p. 1–5

Shepard, F. P., and Emery, K. O., 1941, Submarine topography off the California Coast: Geol. Soc. America Special Paper 31, 171 p.

Vacquier, V., 1959, Measurement of horizontal displacement along faults in the ocean floor: Nature, v, 183, p. 452–453

Wellman, H. W., 1952, The Alpine fault in detail: New Zealand Jour. Science and Technology, sec B. v. 33, no. 5, p. 409–414

UNIVERSITY OF CALIFORNIA, MARINE PHYSICAL LABORATORY OF THE SCRIPPS INSTITUTION OF OCEANOGRAPHY, SAN DIEGO, CALIF.

MANUSCRIPT RECEIVED BY THE SECRETARY OF THE SOCIETY, OCTOBER 3, 1960

(898)

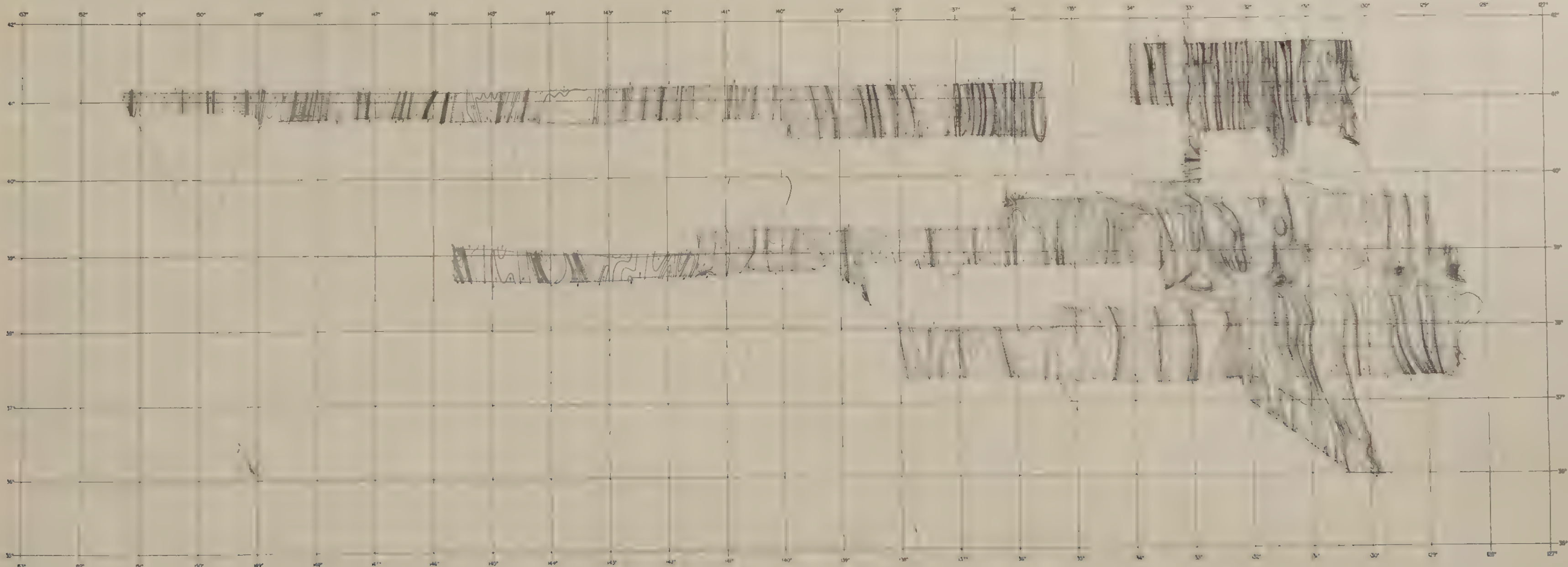

[illegible]

The [illegible] plotted [illegible]. The [illegible] are shown with light lines. The [illegible] largely [illegible]

[illegible] PLATE
[illegible] Society of America Bulletin, volume

RONALD G. MASON
ARTHUR D. RAFF

MAGNETIC SURVEY OFF THE WEST COAST OF NORTH AMERICA, 32° N. LATITUDE TO 42° N. LATITUDE

Abstract: A ship-towed magnetometer survey of an area 250–300 miles wide off the foot of the continental slope along the coast of California has revealed a narrow pattern of anomalies of about 400 gammas magnitude trending north-south for more than 500 miles. The pattern is interrupted at the known faults and elsewhere; offset of the pattern at the Murray fault suggests a right-lateral displacement of about 84 nautical miles. The anomalies are such as might be expected of slablike structures underlying the ocean floor; geological possibilities include basic lava flows, topography of the main crustal layer, and intrusion of ultrabasic material from the mantle.

While making detailed hydrographic surveys off the west coast of North America, the Coast and Geodetic Survey ship PIONEER towed a total-field magnetometer and enabled us to survey an area 250–300 miles in width off the foot of the continental slope between latitudes 32° and 52° N., to a standard approaching that of air-borne magnetometer surveys over land.

A map of the section between latitudes 32° and 36° N., which includes part of the Murray fault, has already been published (Mason, 1958). This note presents a map of the area from latitude 32° N. to latitude 42° N., a little north of the Mendocino fault, and includes the section published previously. The geographical location and major physiographic features of the area are shown in Figure 1.

The area surveyed was covered with a regular grid of lines, normally about 5 miles apart (about twice the average depth of the water). Except in the vicinity of the Mendocino fault, where intersecting lines were run north–south and east–west, the lines were mostly east–west —*i.e.*, across the grain of the anomalous magnetic field. Sufficient lines were run in the other direction, however, to resolve any ambiguities that might otherwise have arisen in the contouring process. A radio-navigation system, using fixed beacons ashore, enabled positions to be determined about every 8 miles with a probable error of the order of 0.1 mile.

The magnetometer was a highly stabilized, self-orienting, total-field fluxgate. To reduce the effect of the ship's magnetism, the fluxgate mechanism was mounted in a streamlined fish and towed 500 feet behind the ship. The instrument was calibrated ashore, at approximately monthly intervals, by comparison with a proton-precession magnetometer. Taking into account the principal sources of error, namely inherent drift, inaccuracy of adjustment, and the effect of the ship, the standard deviation of a single observation from the absolute value is about 15 gammas. Provided that the instrument is kept in proper adjustment, the relative error between any two points on the same line is negligible.

The magnetic anomaly map (Pl. 1) is a plot of the observed field from which the regional magnetic field has been subtracted. The latter was derived from the map of the observed field by a smoothing process. No attempt was made to remove the effects of diurnal variation and magnetic storms. The daily range in hourly values of the total field at these latitudes is usually of the order of 30 gammas, and seldom exceeds 50 gammas, except during magnetic storms. It is unlikely, therefore, that the normal diurnal variation will have any significant effect on the positions and magnitudes of the more important anomalies, although individual contours may be distorted, particularly in areas of shallow magnetic relief. There were several magnetic storms during the survey, but the contours did not appear to be significantly affected by them. Long-term changes in the earth's magnetic field are automatically removed in the smoothing process for deriving the regional field.

The regional bathymetry has been described by Menard and Dietz (1952) and by Menard (1955). The area is crossed by two of the great east–west fault zones of the northeast Pacific,

---

Geological Society of America Bulletin, v. 72, p. 1259–1266, 4 figs., 1 pl., August 1961

Contributions from the Scripps Institution of Oceanography, New Series, 1316

Reproduced by Permission

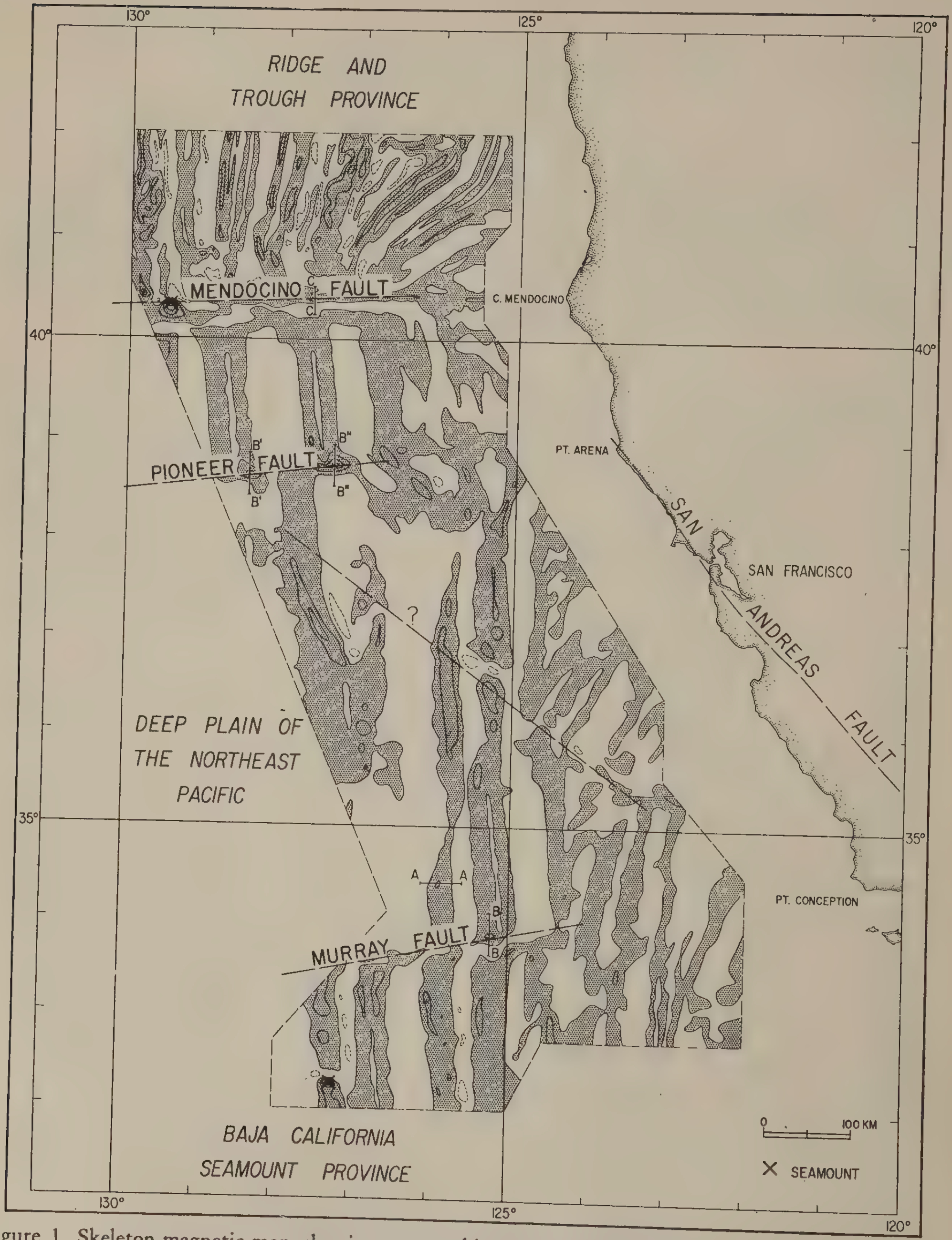
130°
125°
120°
RIDGE AND TROUGH PROVINCE
MENDOCINO FAULT
C
C
C. MENDOCINO
40°
40°
PT. ARENA
B'
B'
B"
B"
PIONEER FAULT
SAN ANDREAS FAULT
SAN FRANCISCO
?
DEEP PLAIN OF THE NORTHEAST PACIFIC
35°
35°
PT. CONCEPTION
A
A
B
B
MURRAY FAULT
0
100 KM
× SEAMOUNT
BAJA CALIFORNIA SEAMOUNT PROVINCE

Figure 1. Skeleton magnetic map, showing geomorphic provinces, principal known faults, and locations of profiles. The contour interval is 250 gammas. Areas of positive anomaly are stippled. Negative contour lines are broken.

the Mendocino and the Murray. The former is by far the most spectacular topographic feature of the area; the bottom rises about 800 fathoms (1½ km) from south to north across it, and across most of the map it forms an asymmetrical ridge with a south-facing escarpment 5000–10,000 feet (1½–3 km) high. It marks the boundary between the Deep Plain of the Northeast Pacific, a comparatively smooth abyssal plain 2100–2600 fathoms (4–5 km) deep, to the south, and the shallower Ridge and Trough province, an area of narrow north or northeast trending ridges and troughs, to the north. The Murray fault, about 6° south of the Mendocino, divides the Deep Plain from the slightly shallower Baja California seamount province. A recently discovered topographic feature, the Pioneer Ridge, crosses the Deep Plain about 100 nautical miles (185 km) south of the Mendocino fault, marking the line of another major east–west fault.

Seismic-refraction measurements have been made at points widely distributed throughout the area. Results for stations south of the Mendocino fault are consistent with a normal oceanic crust (R. W. Raitt, personal communication). Thus at A–A (Fig. 1) the structure consists of 4.6 km of water, 0.3 ± 0.1 km of unconsolidated sediments, 1.4 ± 0.3 km of a second layer of velocity 5.4 ± 0.4 km/sec and commonly believed to be either volcanic rocks or consolidated sediments, and the main crustal layer 4.8 ± 0.5 km thick and of velocity 6.9 ± 0.1 km/sec. The M discontinuity is at a depth of 11.1 ± 0.6 km. North of the Mendocino fault, where the bottom is shallower, the structure appears to be distinctly different, but the exact nature of the difference has not yet been established.

The magnetic map is unusual in many respects. Although some correlation might have been expected between the magnetic field and the linear topography of the Ridge and Trough province, there were no grounds for anticipating either the strongly lineated character of the map over the Baja California seamount province and the relatively featureless Deep Plain, or the large horizontal displacements of the magnetic pattern that occur at the known faults and elsewhere. These lineations, and the horizontal displacements, far exceed in scale any that have been observed over the continents.

At the Murray fault, a 200-km section of the pattern on the north side can be matched against a similar section on the south side in a way that suggests a right-lateral displacement of about 84 nautical miles (155 km) (Mason, 1958). There is no obvious match of the pattern across either the Pioneer or the Mendocino fault, within the limits of the map. The survey has recently been extended westward on both sides of these faults, by ships of the Scripps Institution of Oceanography, to look for such a match and hence to determine the strike-slip movement along them. The results are reported elsewhere (Vacquier, 1959; Vacquier *et al.*, 1961). They are interpreted as indicating a left-lateral slip of about 140 nautical miles (265 km) across the Pioneer fault and about 640 nautical miles (1185 km) across the Mendocino.

At the Mendocino fault the character of the map changes abruptly. Some of the anomalies on the north side are so sharp as to place the top of the magnetic rocks no deeper than 3½ km (1900 fms) below sea level, which is shallower than the sea floor on the south side of the fault, and shallower therefore than the magnetic structures on that side. The change in character of the map is undoubtedly due in part to this factor. However, the seismic results, the change in elevation, and the fact that the line of the Mendocino fault marks the approximate boundary between various physiographic provinces of the neighboring continent (Eardley, 1951, p. 430) all point to a more general change in crustal structure. There is no significant change in the character of the map across either the Pioneer or the Murray fault.

The lineations of the anomalous magnetic field are remarkably straight. The principal north–south trending anomalies, for example, strike almost exactly N.5° W. from the southern edge of the map to the Mendocino fault, a distance of 500 nautical miles (900 km). This is surprising, in view of the very large relative displacements that have taken place at the intervening faults. They are also remarkably uniform in magnitude and width. Over most of the area they show little correlation with topography, and there is no indication of any systematic difference between seismic velocities in the anomalous areas and in the areas between, although the amount of data is not yet sufficient to demonstrate this point conclusively.

As to their immediate cause, the anomalies are such as might be expected of flat slablike structures approximately underlying the areas of positive anomaly. Figure 2 shows the observed anomalies along lines A–A and B–B of Figure 1, and superimposed on them theoretical anomalies computed respectively for an east–west line across an infinite north–south striking slab, and for a north–south line across the southern edge of a semi-infinite slab, both immediately underlying the ocean floor. The agreement is striking.

Two factors restrict the theoretically infinite range of possible depths and thicknesses of these slabs: (1) the sharpness of the anomalies places a limit on the depth to the magnetic rocks; and (2) since there is an upper limit to the polarization contrast that can reasonably be assumed, the bodies must be of a certain minimum thickness to produce anomalies of the observed magnitude.

The effect of these restrictions was investigated by comparing profiles from various parts of the map with theoretical anomalies computed for slabs of various depths and thicknesses. This investigation showed that the anomalies can be closely matched by slabs lying in the "second layer," and by slabs extending through the whole depth of the crust, but that, in general, anomalies computed for

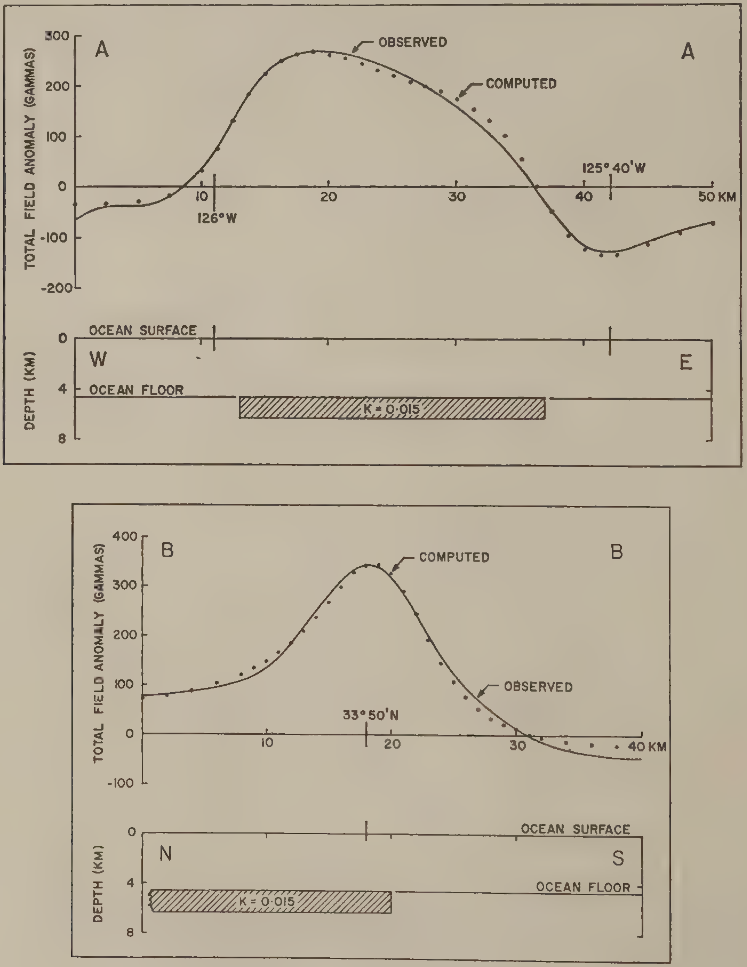

Figure 2. Observed anomalies along lines A–B and B–B of Figure 1. Superimposed on them are theoretical anomalies computed respectively for an east-west line across an infinite north-south striking slab, and north-south line across the southern edge of a semi-infinite slab.

slabs confined to the main crustal layer do not match the sharpness of the observed anomalies. Polarization contrasts corresponding to susceptibilities in the range 0.005–0.015 are necessary, which are values appropriate to the contrast between highly magnetic basalts and relatively nonmagnetic sediments.

The geological possibilities fall into three categories: (1) isolated bodies of magnetically anomalous material, for example basic lava flows, within the "second layer"; (2) elevated folds or fault blocks of the main crustal layer; and (3) zones of intrusion of highly magnetic material from the mantle, extending from top to bottom of the crust. Category (1) would fit in well with current views about the somewhat enigmatic "second layer." Such lavas would constitute 10 per cent of the local crustal volume. For (2), a parallel might be drawn with the fault-block topography of the neighboring Basin and Range province. For (3), the anomalies might arise from magnetic contrasts within both the second and the main crustal layers. Objection might be raised to all three on the grounds of lack of topographic and seismic expression. Figure 3 illustrates the three cases in terms of infinite north–south structures each of which has been adjusted by trial and error to fit the anomaly exactly (Mason, 1958).

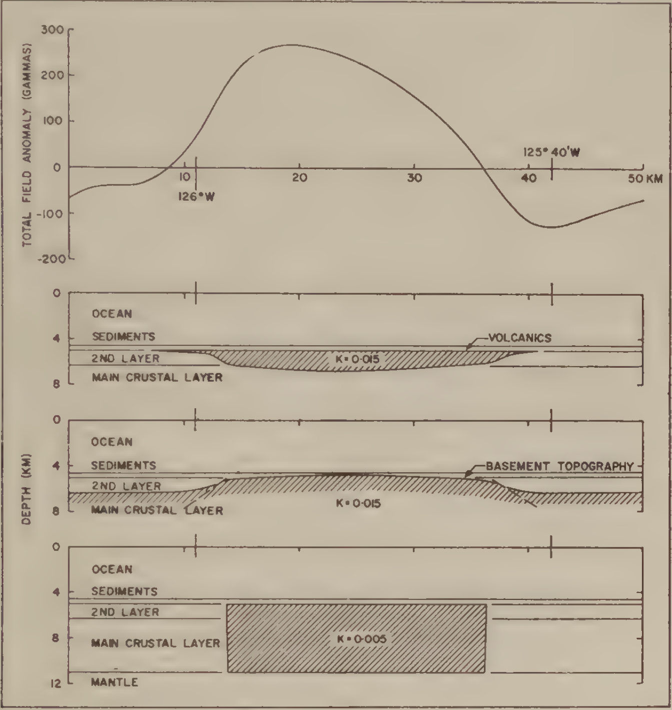

Figure 3. Possible interpretations of magnetic profile A–A. The theoretical anomaly computed for each of the three infinite north-south striking structures fits the observed anomaly almost exactly.

On the magnetic map the Mendocino fault is marked by a narrow east–west anomaly of 300–500 gammas, almost symmetrical about the crest of the ridge. Figure 4 shows a typical section across the fault, along line C–C of Figure 1, and the observed anomaly along the same line. The question arises as to whether the anomaly is directly related to the ridge—*i.e.*, whether the magnetic rocks conform to the surface topography. Figure 4 shows a theoretical anomaly computed for uniform magnetization of the topographic section, assumed infinite in the east–west direction. The discrepancy between observed and computed anomalies suggests a deficiency of magnetic material on the south side of the fault. The stepped section, which has been adjusted by trial and error to approximately fit the anomaly, and which agrees closely with a possible interpretation of a nearby gravity profile (J. C. Harrison, personal communication), suggests a steeper and more abrupt discontinuity than might be expected from the topographic profile. For a polarization contrast of 0.007, a vertical displacement of about 3 km is indicated, or proportionately more or less for smaller or larger polarization contrasts.

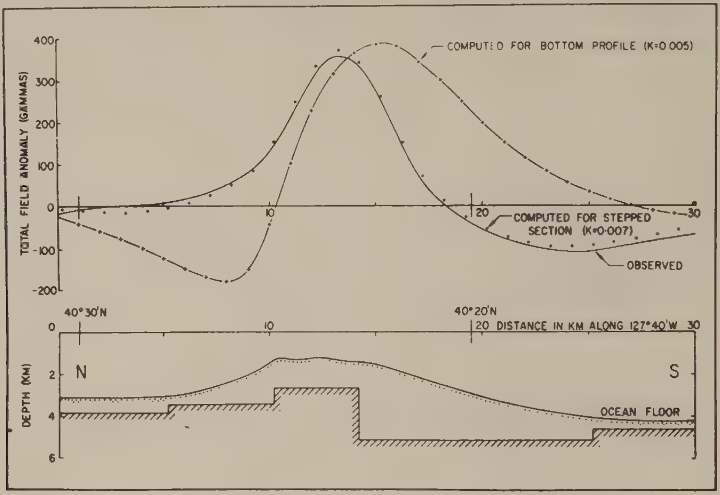

Figure 4. North-south profile across the Mendocino fault along line C–C of Figure 1, showing theoretical anomalies computed for uniform magnetization of topographic and stepped sections respectively, assumed infinite in the east-west direction

The vertical relief across the Pioneer and Murray faults averages only a few hundred fathoms; the Pioneer fault forms a shallow ridge with a south-facing scarp, the Murray rises irregularly from north to south. On the magnetic map these faults are marked more by the effects of the transcurrent movements than by any persistent feature that could be ascribed to vertical displacements. The elliptical pattern of contours at B–B of Figure 1 on the line of the Murray fault, and the similar patterns at B′–B′ and B″–B″ on the line of the Pioneer fault, can be interpreted as the effects of south-facing ends of blocks intersected by the faults. The negative anomaly under the "A" of Murray in Figure 1 indicates a north-facing end.

This discussion has necessarily been based on very simple models. Not only are individual structures likely to be complex, but considerable heterogeneity of magnetic polarization is to be expected also. However, from their overall uniformity, the anomalous trends must clearly be considered part of a single homogeneous pattern. In the absence of any magnetic structures cutting across them, except neat the foot of the continental slope, where there is evidence for complex faulting with north–south components of slip, it must be concluded that the faults are more recent than the structures. Possibly the latter are relatively ancient features of the crust. A more significant discussion of both pattern and faults will be possible when the rest of the map, and projected extensions westward and over the continental shelf, have been completed, and when samples of the rocks have been obtained.

Acknowledgments

The authors gratefully acknowledge the cooperation of the Coast and Geodetic Survey and particularly wish to place on record their appreciation of the interest taken in the work by Captain (now Admiral) Charles Pierce, who was in command of the PIONEER during the early stages of the survey. They also wish to acknowledge the facilities for calibrating the magnetometer generously made available by the Varian Associates of Palo Alto, California, and the interest taken in the work by Drs. L. L. Nettleton and N. C. Steenland of the Gravity Meter Exploration Company of Houston, Texas. They are indebted to colleagues at Scripps for helpful discussion of the results, and to Dr. R. W. Raitt, in particular, for supplying the seismic data. Dr. J. C. Harrison of the Institute of Geophysics supplied unpublished gravity data. The work was supported by the U.S. Office of Naval Research under contract Nonr–233(04).

References Cited

Eardley, A. J., 1951, Structural geology of North America: Harper, New York, 624 p.

Mason, R. G., 1958, A magnetic survey off the west coast of the United States: Geophys. Jour., v. 1, p. 320–329

Menard, H. W., 1955, Deformation of the northeastern Pacific basin and the west coast of North America: Geol. Soc. America Bull., v. 66, p. 1149–1198

Menard, H. W., and Dietz, R. S., 1952, Mendocino submarine escarpment: Jour. Geology, v. 60, p. 266–278

Vacquier, V., 1959, Measurement of horizontal displacement along faults in the ocean floor: Nature, v. 183, p. 452–453

Vacquier, V., Raff, A. D., and Warren, R. E., 1961, Horizontal displacements in the floor of the northeastern Pacific Ocean: Geol. Soc. America Bull., v. 72, p. 1251–1258

University of California, Marine Physical Laboratory of the Scripps Institution of Oceanography, San Diego, Calif.

Manuscript Received by the Secretary of the Society, June 3, 1960

(905)

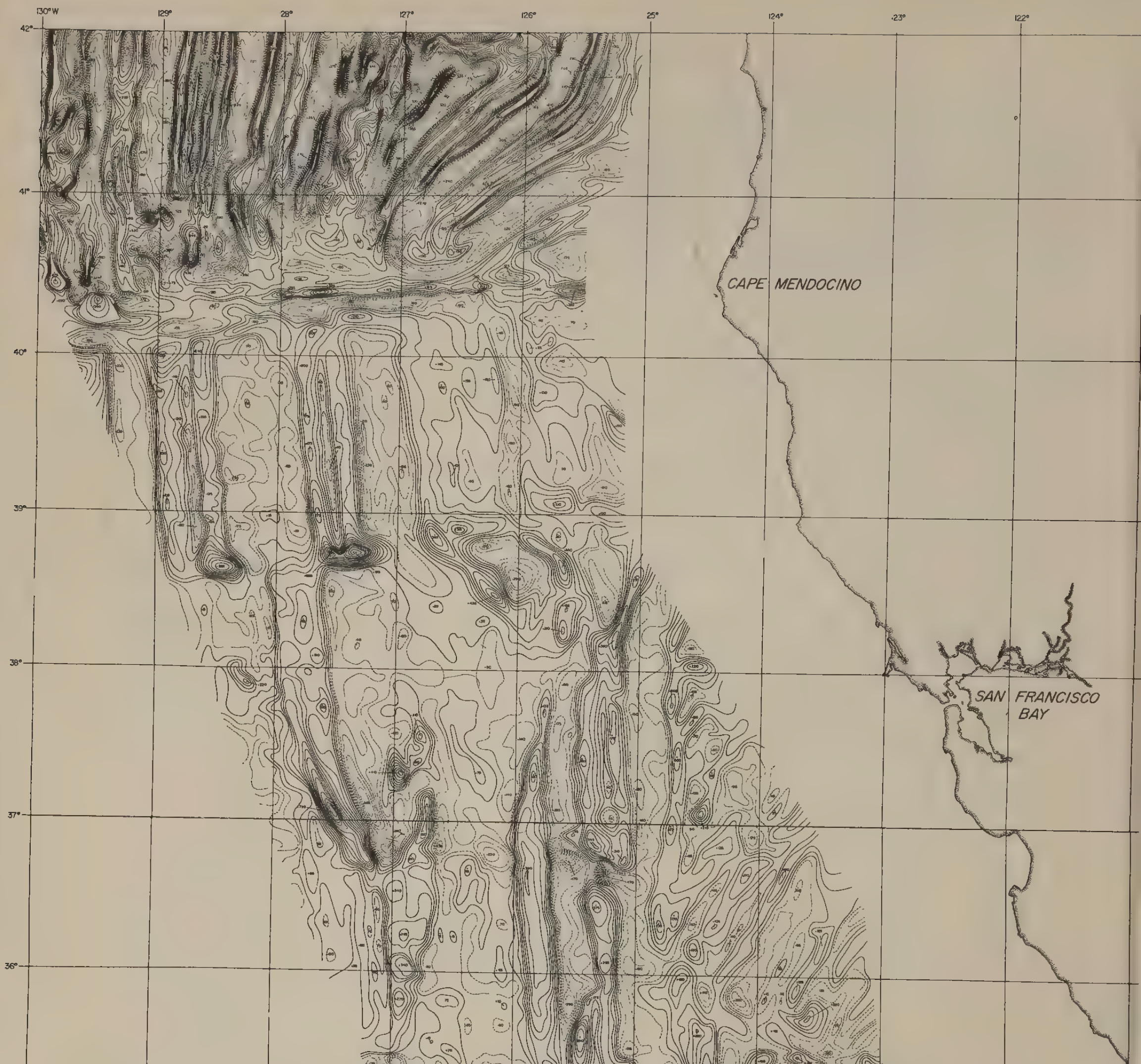
130°W
129°
28°
127°
126°
25°
124°
23°
122°
42°
41°
40°
39°
38°
37°
36°
35°
34°
33°
32°
CAPE MENDOCINO
SAN FRANCISCO BAY
130°W
129°
128°
127°
126°
125°
124°
123°
122°
121°

MAP OF THE TOTAL MAGNETIC INTENSITY AFTER REMOVAL OF THE REGIONAL FIELD

The contour interval is 50 gammas, and spot values are rounded off to the nearest 5 gammas beyond the extreme values recorded.

MASON AND RAFF, PLATE 1
Geological Society of America Bulletin, volume 72

Reprinted from: California Cooperative Oceanic Fisheries Investigations.
Reports, v.8, 1 July 1959-30 June 1960. pp.83-93.

THE WATER MASSES OF SEBASTIAN VIZCAINO BAY

JOHN G. WYLLIE[1]

INTRODUCTION

This report is a descriptive analysis of the water masses and certain processes, which combine to produce the major changes in the physical environment observed throughout the year in Sebastian Vizcaino Bay. No effort is made to explain the forces involved or mechanics of the changes described. A discussion of the currents of the bay has been avoided since it is felt sufficient measurements for such a discussion have not yet been obtained.

GENERAL AREAL DESCRIPTION

Sebastian Vizcaino Bay is located 350 miles (all distances are expressed in nautical miles) south-southwest of San Diego on the Pacific Coast of Baja California (Fig. 1). The bay has the shape of a fishhook completely exposed to the sea toward the northwest. The distance from the northern end of Cedros Is. due north to Punta Canoas on the mainland measures 63 miles; the distance from Punta Canoas to the southernmost shore of the bay is about 115 miles. The narrowest dimension of the bay measures 48 miles from the northern end of Cedros Is. to Punta Maria. The inset in Figure 1 shows Monterey Bay of central California for a size comparison. Two channels, separated by Natividad Is., open to the sea in the southwestern portion of the bay: they are Kellett Channel, which is 8 miles wide and 40 to 45 meters deep, and Dewey Channel, which is 4 miles wide and 25 to 30 meters deep. Three very shallow lagoons are found along the southeastern boundary: Scammon, Black Warrior and Manuela. The San Benitos Islands lie approximately 15 miles west of Cedros Is. Ranger Bank, about 100 meters deep, lies 15 miles northwest of Cedros Is. There is little rainfall in this area and no rivers empty into the bay.

DESCRIPTION OF WATER MASSES[2]

For purposes of identification, seven water-mass sources are defined. The term "water-mass source" is a misnomer in some cases since some of the areas mentioned as source regions are not sources of water having definite reproducible characteristics, but rather areas where more or less permanent processes occur which result in water types which differ strikingly from neighboring water.

The seven water sources (Fig. 2) are:

1. California Current water, which is a water mass with very characteristic physical parameters. It is the source of low-salinity water for the bay. It is relatively cool, but not the coldest water in the bay; it has a high oxygen and PO_4-P content. It is present in large quantities and often dominates the bay waters.

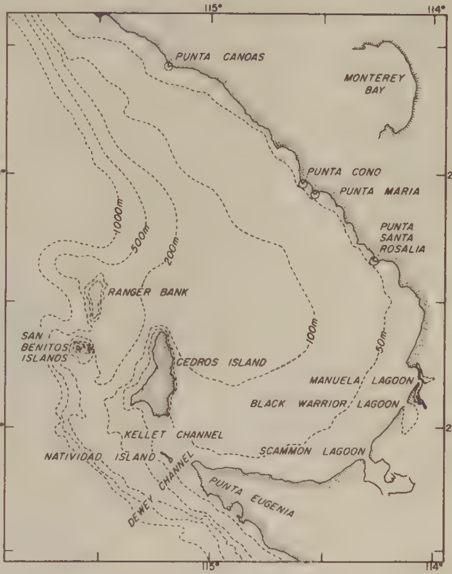

FIGURE 1. Geography of Sebastian Vizcaino Bay.

2. Upwelled water from the Punta Canoas region. Water of definite physical characteristics cannot be assigned to this region since upwelling is a process which brings to the surface layer whatever type of water happens to be present below the surface at a particular time. Usually the upwelling process, coastal

---

[1] Contribution from the Scripps Institution of Oceanography. 1317

[2] The water masses described in this report should not be confused with the major water masses as defined by Sverdrup in "The Oceans". They are used for convenience only in identifying and separating the local conditions found within, and in the immediate vicinity, of the Bay.

Reproduced by Permission

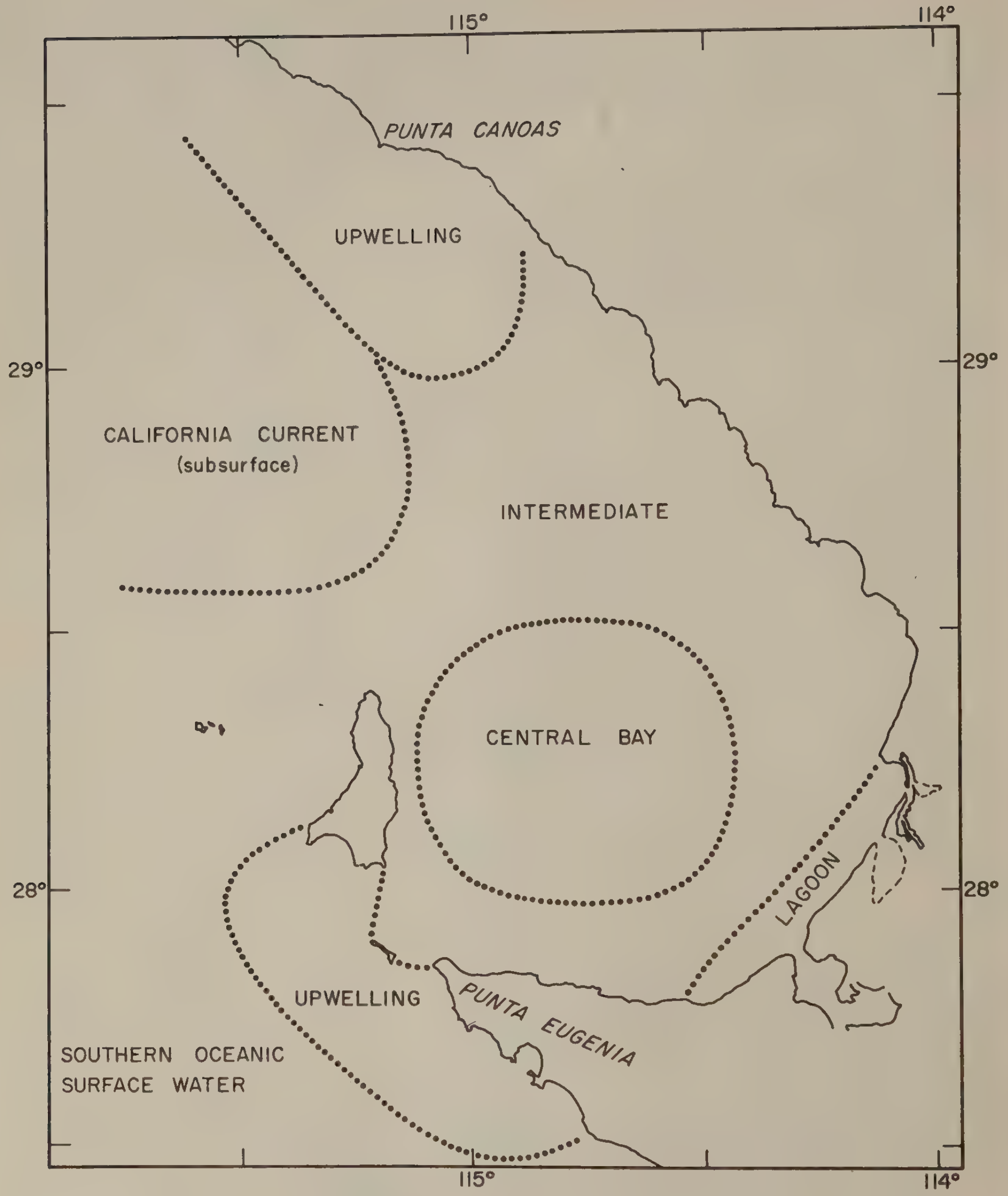
115°
114°
PUNTA CANOAS
UPWELLING
29°
29°
CALIFORNIA CURRENT
(subsurface)
INTERMEDIATE
CENTRAL BAY
LAGOON
28°
28°
UPWELLING
PUNTA EUGENIA
SOUTHERN OCEANIC
SURFACE WATER
115°
114°

FIGURE 2. Water masses of Sebastian Vizcaino Bay.

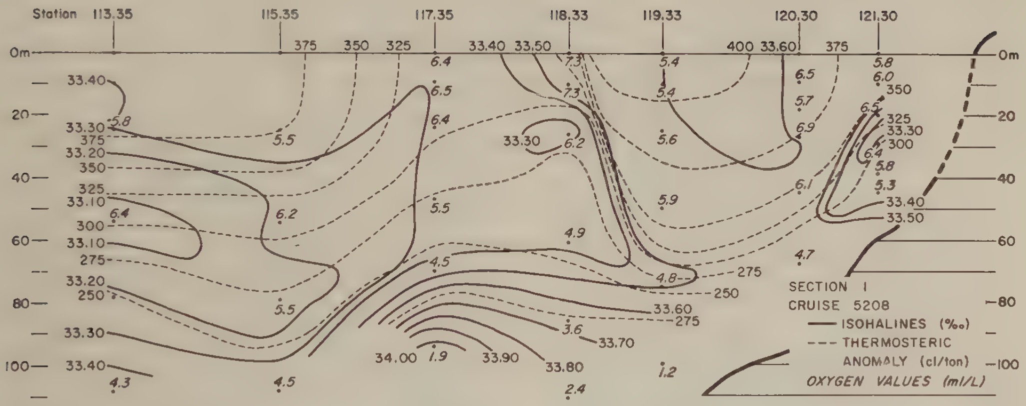

FIGURE 3. Section 1, Cruise 5208. Vertical section from the surface to 110 meters showing distribution of salinity (isohaline lines), thermosteric anomaly (lines of equal Δ′ or δ_T) with oxygen values (ml/L) entered.

in this region, results in the coldest water because the vertical temperature gradient is normally negative. Whether or not this water will have a high or low salinity value depends upon what water is being upwelled. In the Punta Canoas area higher-salinity water is most frequently upwelled.

3. Central Bay water is also the result of a local condition and cannot be described as having definite characteristic values. There appears to be a permanent or semi-permanent clockwise rotating eddy in the bay. Its position and size vary considerably. It is definable because it is characteristically delineated from the

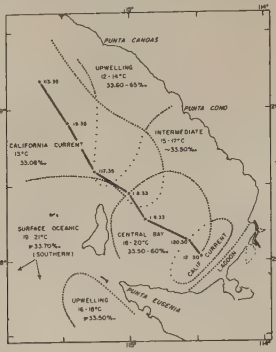

FIGURE 4. Cruise 5208. Block Diagram showing general characteristics and locations of water masses in August 1952 (5208).

surrounding water by a very sharp thermocline and oftentimes by "fronts" (Cromwell and Reid 1956). This pocket of water is usually found to be well mixed and relatively warm. It is usually warmer than the surrounding water indicating it is probably held for a longer time in the surface layers.

4. Lagoon water appears to be of minor importance in the regime of the bay, but it often has extremely different characteristic values. High temperatures and salinities are found. This water is probably mixed into the bay water somewhere along its southern periphery. It can be called a true source region since water of definite characteristics forms there.

5. Upwelled water from the Punta Eugenia area can be described in the same manner as the water from the Punta Canoas region. The main difference is in the importance of the two areas in relation to the bay. Punta Eugenia water is probably the least important of any of the water-mass sources described. Some of this water may enter through the southwestern channels and affect some of the southern coast of the bay, as evidenced by certain cold water algae found there (Dawson 1952).

6. Southern oceanic surface water is characterized by high temperatures and salinity. This water is found along the coast to the south of Punta Eugenia and influences the bay mainly during the late summer and fall months.

7. Water from the deep coastal salinity maximum is a subsurface mass (usually found at 200-300 meter depth) which is characterized by relatively high temperatures and salinities, a very low oxygen content and a relatively high phosphate content. It is actually an extension of Equatorial Pacific water northward along the coast. It enters the bay circulation from below by moving up over the continental slope and shelf.

In addition to the types of water just described other water is sometimes found which does not fit any of these classifications. This is, of course, to be expected when two or more of the above water types mix. We will call this intermediate water.

A general descriptive analysis of certain special cruises into the bay will be made in terms of the above-mentioned water-mass source regions.

SPECIAL CRUISE, AUGUST, 1952 (CR 5208)

In August, 1952, the first special CalCOFI cruise was made into Sebastian Vizcaino Bay. At this time low salinity California Current water was found within the upper 100 meters. (Fig. 3 and Fig. 4). This appears as a tongue of water to the west and northwest of the bay entrance, north of Cedros Island. Salinities as low as 33.08 ‰ and temperatures of about 13°C were observed in the core of the tongue at a depth of 50 to 55 meters immediately west of the bay entrance (Fig. 3). A patch of similar water is found along the southern shore at a depth of 20 meters or more. It may be a continuation of the present invasion or the remnants of an earlier invasion.

Punta Canoas upwelled water has a temperature range of 12 to 14°C and a salinity range from 33.60 to 33.65 ‰ in the surface layers. It is found as a crescent shaped ridge opening to the west, extending south from Punta Canoas, reaching to within 10 miles of Cedros Is. (Fig. 4 and 5). This water is found at the surface in the northern one-third of this distance only. It apparently upwells from depths of less than 100 meters. A relatively strong "front" is found between the California Current water and this upwelled water. The entrance of upwelled water into the bay circulation probably accounts for the depression of the bay temperatures as compared to the neighboring surface oceanic waters (Fig. 4).

Central bay water is restricted to a prominent clockwise rotating eddy occupying the main part of the bay east of Cedros Island (See the isobaths and isothermes of the $\Delta' = 300$ surface on Figure 6). The $\Delta' = 300$ surface has been chosen as a reference surface because it coincides closely with the core of the low salinity California current water in this region and usually delineates the bottom of the central bay eddy. A sharp thermocline separates this water from the colder less saline water below. The central bay

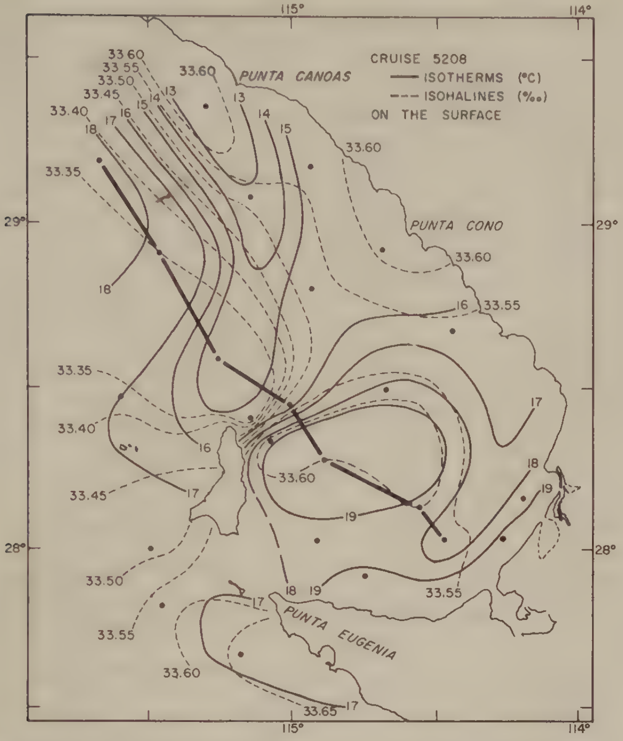

FIGURE 5. Cruise 5208. Surface temperature and salinity distribution (Isotherms in °C, isohalines in ‰).

water is well mixed from the surface to the thermocline, which has a maximum depth of 60 to 70 meters. The surface temperatures range from 18 to 20°C and the salinities from 33.50 to 33.60 ‰. A strong "front" is found along the northwestern boundary of the eddy. The southern end of the cold Punta Canoas upwelled water is found adjacent to the central water and helps to intensify the "front" (Fig. 5). Another weaker "front" can be traced between the central bay and the intermediate water found to the east and northeast. Along the southeastern edge of the eddy the intermediate and central water becomes homogeneous and the "front" disappears.

Lagoon water is found immediately offshore of the lagoons along the southeastern edge of the bay. We have little data but we do know the water is very warm and saline.

Upwelled water from the Punta Eugenia area had surface temperatures from 16 to 18°C and salinities of 33.50 ‰ or greater (Fig. 4). Apparently some of this water is carried into the bay on the incoming tide and gives evidence of being found along the northern shore of Punta Eugenia (Dawson, 1952).

Southern surface oceanic water is found southwest of the bay beyond the Punta Eugenia upwelled water with temperatures, at the surface, from 19 to 21°C or greater (Fig. 4). None of this water seems to have been in the bay at this time.

Intermediate water was found as a very shallow layer (less than 20 meters thick) immediately west of Punto Cono (Fig. 4 and 5). It extends along the eastern and southeastern shoreline of the bay where it blends with the central water. Temperatures range from 15 to 17°C and salinities are near 33.50 ‰. This water appears to be a mixture of California Current, Punta Canoas upwelled and central bay waters. The thermocline separating it from the cooler water below comes to the surface just southeast of Punta Canoas forming another front. This front between the upwelled and intermediate water becomes diffuse to the south.

Underlying most of the water in the bay is water from the deep coastal salinity maximum. This water may slide up the continental shelf south and west of Kellett and Dewey Channels and continue over the sill between Cedros Island and the San Benitos Is-

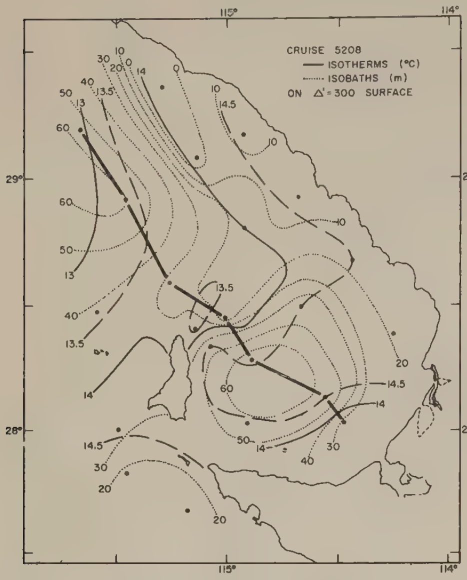

FIGURE 6. Cruise 5208. The depth of, and temperature distribution on, the thermosteric anomaly surface $\Delta' = 300$. (Isobaths in meters, isotherms in °C.)

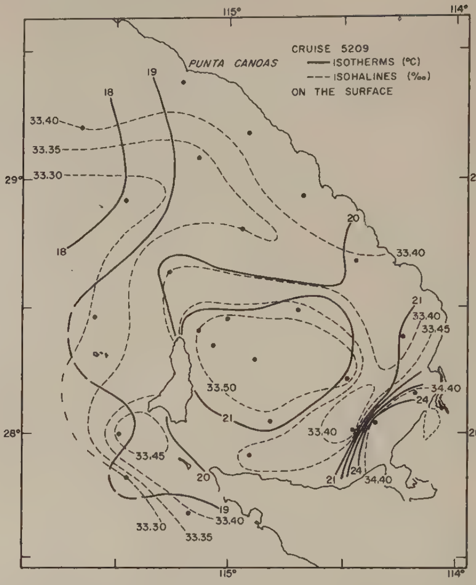

FIGURE 7. Cruise 5209. Surface temperature and salinity distribution. (Isotherms in °C, isohalines in ‰.)

lands and then around the northern end of Cedros Island into the bay (Fig. 1). The presence of this water is clearly seen at station 117.35 in Sect. 1. Evidently water of this type is often upwelled into the surface layers.

The weather situation at the time of this cruise should have resulted in a moderately strong flow of air from the northwest. This fits in well with the observed conditions, since evidence of coastal upwelling certainly was found.

COMPARISON WITH OTHER CRUISES

The special cruise made in August, 1952, (CR 5208) was followed by a second special cruise, the next month, September, 1952, (CR 5209) which is of interest since it gives some idea as to how conditions can change at least within four or five weeks.

A list of the most obvious changes are given below:

1. No upwelling was in evidence at either Punta Canoas or Punta Eugenia.

2. California Current water had invaded most of the bay as well as the area immediately outside the bay.

3. The central bay eddy shifted northward.

4. No strong fronts were found.

5. There was marked warming of the entire bay.

In general, these changes brought about more homogeneous conditions between the water masses in the bay. (Fig. 7) California Current water dominated the scene. The core of this relatively cool, low salinity water enters the bay midway between Punta Canoas and Cedros Island spreads to the east and southeast along the coast, then underruns and mixes with the central bay water along the southern and southeastern coast.

The central bay water has been diluted with California Current water. The average salinities dropped from 33.50 to 33.60 ‰ to 33.40 to 33.45 ‰, except at the very surface with salinities continuing at about 33.50 ‰. On the average the temperatures are about 2°C higher in the mixed layer than in August. With the cessation of upwelling off Punta Canoas and the spread of the central bay water northward, the surface fronts along the northern edge of the eddy appear to have been eliminated. (Compare Figures 5 and 7.)

Lagoon water is evident along the southern shore. It is very warm (23 to 24°C) and saline (34.20 to 34.40 ‰). This water apparently remains along the southern coastline.

Surface oceanic water outside the bay in the upper few meters is a degree or two warmer than in August, but it is otherwise not much changed.

The intermediate water of the August cruise is difficult to find. The region where it was found during August now has water with salinities from 0.20 to 0.35 ‰ lower and temperatures from 19 to 21° C, an average of 3 to 4° higher.

Deep coastal salinity maximum water is found at Stations 117.35 and 118.35. In figures 8 and 9 this is

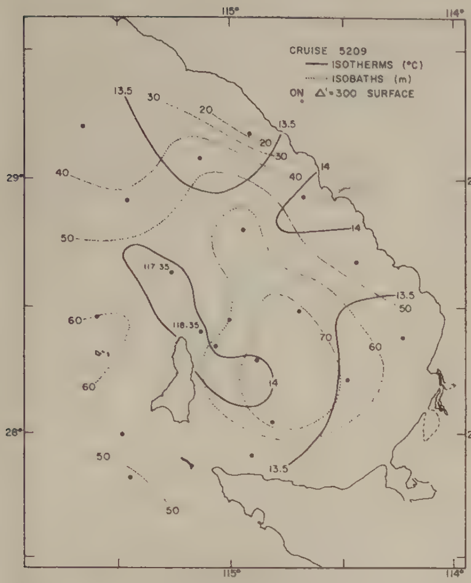
CRUISE 5209
ISOTHERMS (°C)
ISOBATHS (m)
ON Δ'=300 SURFACE
115°
114°
29°
28°
13.5
30
20
13.5
20
30
14
40
40
50
14
117.35
13.5
50
60
118.35
70
60
60
14
50
13.5
50

FIGURE 8. Cruise 5309. The depth of, and temperature distribution on, the thermosteric anomaly surface Δ' = 300. (Isobaths in meters, isotherms in °C.)

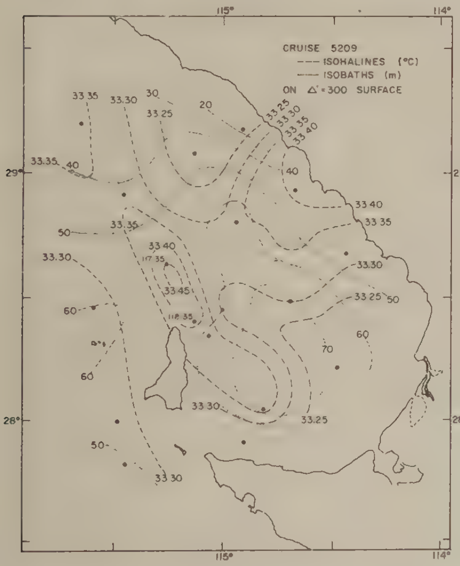
CRUISE 5209
ISOHALINES (°C)
ISOBATHS (m)
ON Δ'=300 SURFACE
115°
114°
29°
28°
33.35
33.30
30
33.25
20
33.25
33.30
33.35
33.40
33.35
40
40
33.40
33.35
50
33.35
33.40
33.30
117.35
33.30
33.45
33.25
50
60
118.35
60
70
60
33.30
33.25
50
33.30

FIGURE 9. Cruise 5309. The depth of, and salinity distribution on, the thermosteric anomaly surface Δ' = 300. (Isobaths in meters, isotherms in °C.)

clearly seen as a warmer, more saline zone on the Δ' = 300 surface. This water is about 1°C warmer than during August.

The general meteorological conditions over the Pacific should have resulted in a relatively weak flow of air from the northwest. This could account for the absence of coastal upwelling at this time.

Reference has been made to surface oceanic water originating to the south and southwest as playing a part in the water-mass sequence in the bay. Neither cruise in 1952 offered any definite evidence of this. We were fortunate, however, in obtaining direct evidence during a special bay cruise in September, 1953, (CR 5309, see Fig. 10). At this time conditions were found to be similar to those in September, 1952, (CR 5209). No upwelling was in evidence at either Punta Canoas or Punta Eugenia. California Current water dominated the scene, being found along the entire northeastern shore of the bay to a depth of 50 meters. It was also found beneath the central bay water as a layer 10 meters or more thick. It could be traced as a subsurface layer 20 to 30 meters thick seaward from the northern half of the bay and as a thin sheet to the northern end of Cedros Island.

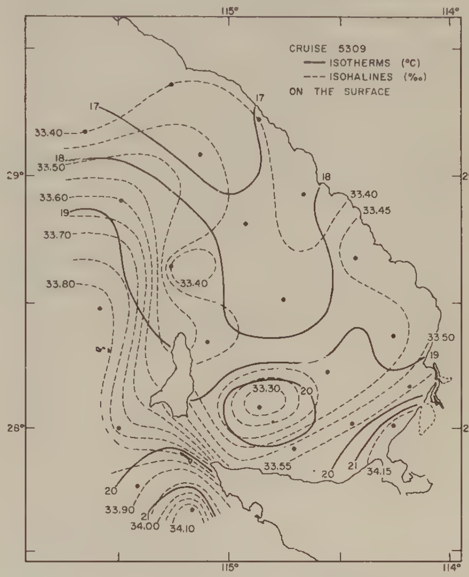
CRUISE 5309
ISOTHERMS (°C)
ISOHALINES (‰)
ON THE SURFACE
115°
114°
29°
28°
17
17
33.40
18
33.50
18
33.40
33.45
33.60
19
33.70
33.40
33.80
33.50
19
33.30
20
33.55
20
21
34.15
20
33.90
21
34.00
34.10

FIGURE 10. Cruise 5309. Surface temperature and salinity distribution. (Isotherms in °C, isohalines in ‰.)

The central bay water was diluted with California Current water. It had uniform salinity values of 33.35 to 33.40 ‰, and surface temperatures near 20°C. The eddy was displaced to the southern portion of the bay (Figure 10) as contrasted to September, 1952, when it was found to the north (Figure 7). A weak front can be found along its northern edge.

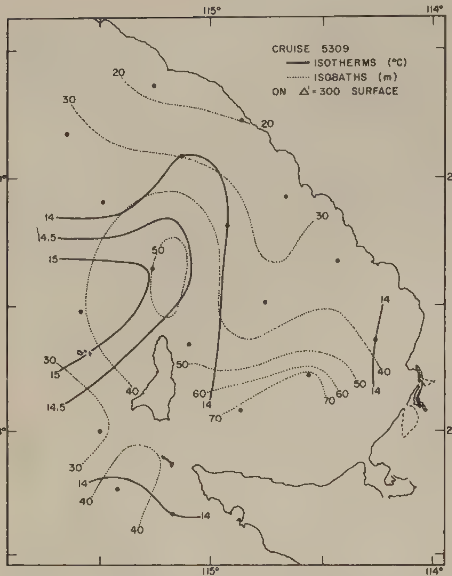
115°
114°
CRUISE 5309
ISOTHERMS (°C)
ISOBATHS (m)
ON Δ'=300 SURFACE
29°
28°
20
30
14
14.5
15
50
40
60
70
14
30
15
14.5
30
14
40
14
40

FIGURE 11. Cruise 5309. The depth of, and temperature distribution on, the thermosteric anomaly surface Δ' = 300. (Isobaths in meters, isotherms in °C.)

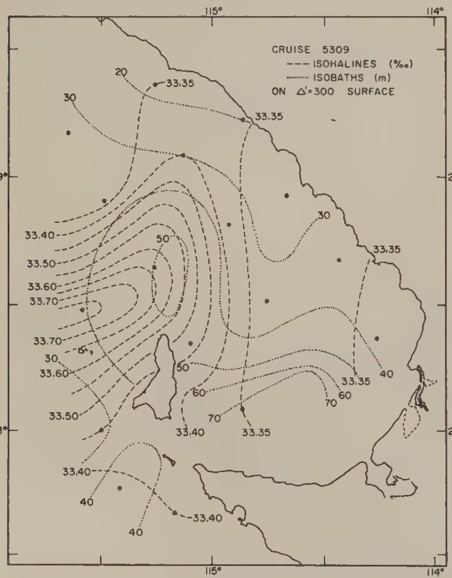
115°
114°
CRUISE 5309
ISOHALINES (‰)
ISOBATHS (m)
ON Δ'=300 SURFACE
29°
28°
20
33.35
30
33.35
33.40
33.50
33.60
33.70
33.70
30
33.60
33.50
50
30
33.35
40
33.35
60
70
60
70
33.40
33.35
33.40
40
33.40
40

FIGURE 12. Cruise 5309. The depth of, and salinity distribution on, the thermosteric anomaly surface Δ' = 300. (Isobaths in meters, isohalines in ‰.)

As in the 1952 cruises, lagoon water was found along the southern shore line. Temperatures of at least 22°C and salinities greater than 34.00 ‰ are found.

The most interesting feature, however, is the southern surface oceanic water found immediately west of the channels and Cedros Island in the upper 30 to 50 meters. As can be clearly seen on Figures 11 and 12, this warm saline water extends into the bay around the northern end of Cedros Island. Invasion of the bay by water of this type and in this amount could certainly account for any sudden increase in the temperature and salinity values, especially in the surface layers.

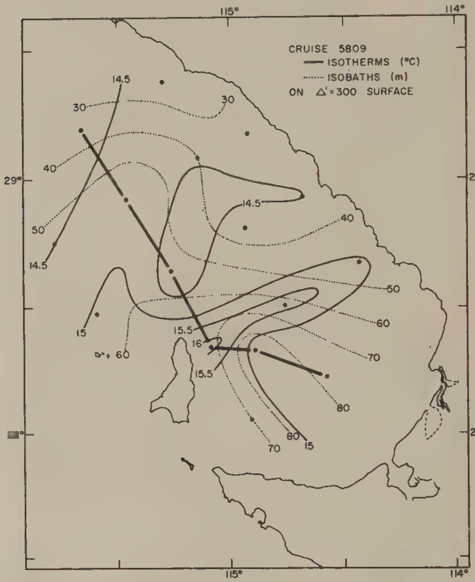
115°
114°
CRUISE 5809
ISOTHERMS (°C)
ISOBATHS (m)
ON Δ'=300 SURFACE
29°
28°
14.5
30
30
40
50
14.5
14.5
40
50
60
70
80
15
60
15.5
16
15.5
80
70
15

FIGURE 13. Cruise 5809. The depth of, and temperature distribution on, the thermosteric anomaly surface Δ' = 300. (Isobaths in meters, isotherms in °C.)

In September, 1958, (CR 5809), a good example of the influx of deep coastal salinity maximum water into the bay circulation is found (Figures 13, 14 and 15). This is of special interest since it shows this deeper water being injected into the upper (shallow) levels of the bay water and therefore being made available for rapid inclusion in the surface circulation. As is evident from the figures, this water is relatively warm and saline with an exceptionally low oxygen content.

Other special cruises have been made into the bay but the above mentioned cruises give examples and support the hypothesis that the sequence of events of the physical environment, both seasonally and year to year changes can, in part, be explained and described in terms of these water masses and processes.

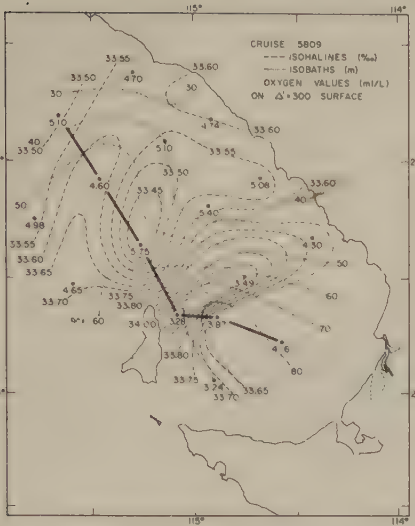

FIGURE 14. Cruise 5809. The depth of, salinity distribution and oxygen values on the thermosteric anomaly surface Δ' = 300. (Isobaths in meters, isohalines in °/₀₀, oxygen values in ml/L.)

SEASONAL VARIATION

In discussing seasonal patterns at any particular point, we wish to delineate between variations which are easily predictable, such as the effect of incoming radiation from the sun and sky, and those which are not. The less predictable events which cause variations throughout the year are the replacement of one water mass by another, plus all the degrees of mixing which attend these changes. The changes we observe are a result of a combination of all these phenomena.

In the upper layers each water mass undergoes its own seasonal changes which can vary to some extent from year to year. These year by year variations can change the characteristics of a water mass, but these changes are not usually so great that the water mass loses its identity. Therefore, even though water mass characteristics may vary, they can still be distinguished from other water masses.

An examination of a monthly plot of surface temperatures for Station 120.30 in the bay, shows the coldest months to be March and April and the warmest, September and October (Fig. 16). This follows closely the 10 year averages for neighboring inshore oceanic stations not in the bay. These stations also show March-April as the coldest period and September-October, the warmest. The bay tends to be 1° or 2°C cooler than the oceanic water outside the bay most of the year. This is probably due to its proximity

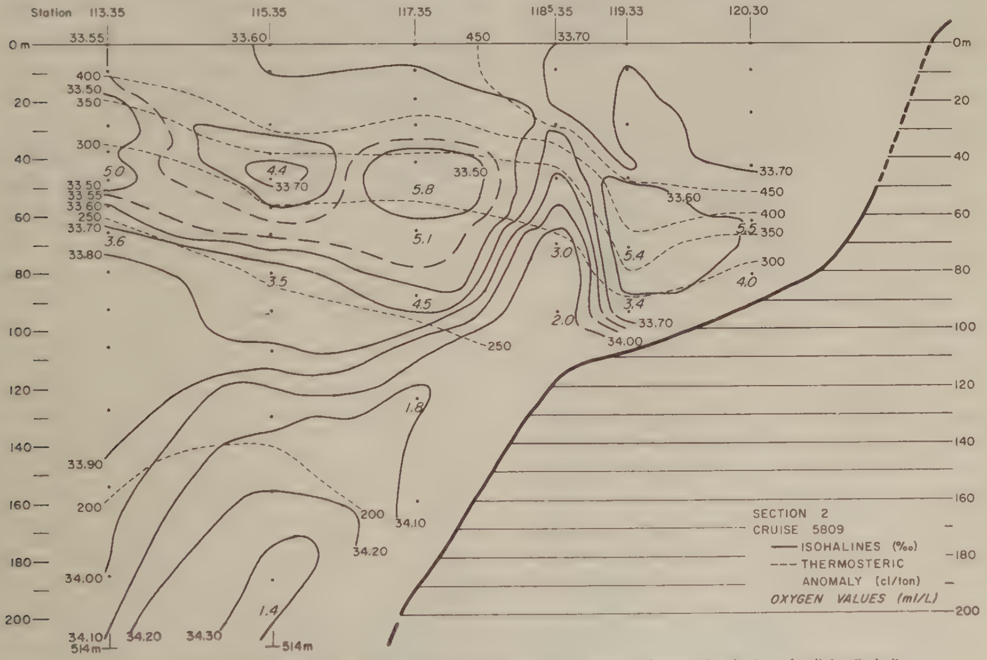

FIGURE 15. Section 2, Cruise 5809. Vertical section from the surface to 210 meters showing distribution of salinity (isohaline lines), thermosteric anomaly (lines of equal Δ' or δτ) with oxygen values (ml/L) entered.

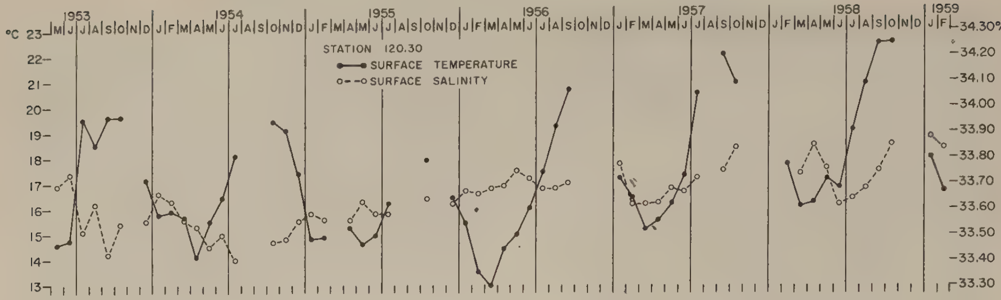

FIGURE 16. Plot of surface temperature and salinity values for each month observed from May 1953 to February 1959 for station 120.30.

to the coastal upwelling area near Punta Canoas. The annual temperature range for the surface layers in the bay is normally 5° to 7°C.

A plot of the salinities for each month does not show any such simple pattern on the average (Fig. 16). If we keep in mind the relative temperature and salinity conditions at any particular location and within a period of time of a few months, at most, so as to eliminate from the discussion longer trends, the presence of a more or less predictable cycle is found.

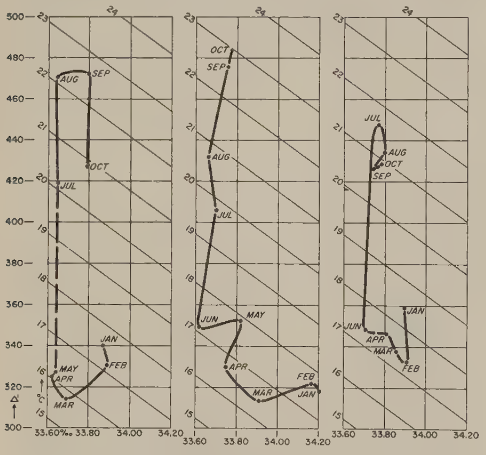

FIGURE 17. Monthly values of the surface temperature and salinity at station 119.33 plotted on a special chart used in the processing of hydrographic data (Klein, MS).

Figure 17 gives some examples of the surface temperature and salinity values plotted on a special chart developed by Klein (Klein, MS). Each point represents the observed value at station 119.33 for a given month. This station was chosen for the illustration since it is centrally located and is usually under the influence of the central bay eddy which in turn seems to reflect the characteristics of the water masses which are dominating the bay at any particular time. Considering the lower points on this graph to be relatively cold, the upper points relatively warm, the points farthest left as having relatively low salinity and the ones to the right relatively high salinity, we can regroup the data into a table showing the relative values, as defined above, from month to month (Fig. 18). This table also includes results from station 120.30. A pattern emerges which can be explained in terms of the water masses and processes defined as available for the bay.

In general, the bay waters are relatively cool from January through June. At the same time the salinity can be either high or low. The water is cold at this time because of two factors. The first is the predictable normal temperature pattern for all waters of similar latitude due to the incoming radiation. The second factor is the presence of coastal upwelling which tends to keep the water cold. Upwelling can and does occur at any time of the year but seems to be most persistent during this period. The salinity variation can be explained by the presence or absence of upwelling or California Current water, or both. With upwelling in progress, a source of higher salinity water is available. Although all upwelled water is not necessarily of high salinity, it usually appears to be in this area. With California Current water present, a readily available source of low-salinity water is found. Therefore these are the dominating factors controlling conditions in the bay from January through June.

The months of July and August tend to be somewhat warmer with low-salinity values continuing. Detailed weather data throughout the year would clarify the picture, but it is proposed that the upwelling process usually weakens at this time, owing to lighter winds. This, in addition to the normal increasing solar radiation, would allow more rapid warming of the mixed layer. The main source of water available to the bay would most likely be low-salinity California Current water. This would account for the relatively warm low-salinity water usually found at this time.

During the months of September through December the bay waters tend to be warmest and most saline, although the warm water is normally in the process of cooling later during this period, especially during December. The higher salinities are most likely the result of advection of water from the coastal regions

Relatively	J	F	M	A	M	J	J	A	S	O	N	D	J	F	M	A	M	J	J	A	S	O	N	D
LOW SALINITY	○	○	○	○	○	○	○	○	○				○	○	○	○	○	○	○	○	○			
HIGH SALINITY	●	●	●	●	●	●			●	●	●	●	●	●	●	●	●	●			●	●	●	●
LOW TEMPERATURE	△	△	△	△	△	△							△	△	△	△	△	△						
HIGH TEMPERATURE							▲	▲	▲	▲	▲	▲							▲	▲	▲	▲	▲	▲

FIGURE 18. Tabulation showing the relative seasonal values obtained from Fig. 17. The data are repeated through a two-year period to show the pattern more clearly.

south of the bay. An example of this type of invasion was described earlier in this report (September 1953, CR 5309).

The cycle begins again with the onset of more wind and consequent upwelling in late December or early January along with normally cooler weather. This sequence is probably oversimplified and may be interrupted but the available data indicate the presence of a basic pattern. If this is the case, a combination of monitoring certain water masses and a good coverage of wind and weather for the bay may be sufficient to follow satisfactorily the changes in the physical environment.

ACKNOWLEDGMENT

The author is indebted to Mr. H. S. Shirley for the preparation of all the figures. This work was supported by the Marine Life Research Program of the Scripps Institution of Oceanography, a part of the California Cooperative Oceanic Fisheries Investigations.

REFERENCES

1. Cromwell, T., and J. L. Reid, Jr., 1956. A study of oceanic fronts. *Tellus*, **8** (1) : 94-101.
2. Dawson, E. Y., 1952. Circulation within Bahia Vizcaino, Baja California, and its effects on marine vegetation. *Jour. Bot.* 39 (7) : 425-432.
3. Klein, H. T. A new technique for processing physical oceanographic data. (MS.)

Reprinted from: California Cooperative Oceanic Fisheries Investigations.
Reports, v.8, 1 July 1959-30 June 1960. pp. 73-74.

FISHERIES OCEANOGRAPHY

WARREN S. WOOSTER [1]
Scripps Institution of Oceanography
University of California, La Jolla, California

In considering how to summarize the oceanographic aspects of the papers we have just heard, I found my thoughts falling into several distinct categories—the definition and goals of fisheries oceanography, current practice in this field, and the success of this approach.

Some may feel that fisheries oceanography is nothing more specific than the broad assemblage of problems being studied by oceanographers working for fishery laboratories. The interests of marine fisheries scientists and those of oceanographers overlap in so many areas that almost any marine research can be included in a suitably broad definition. But unfortunately such broad definitions have little operational value.

One might speak, however, of a somewhat restricted area of marine research which could be called ecological oceanography. This deals with the relationship between the ocean as a physico-chemical environment and the populations of organisms inhabiting it. A special case exists in which the populations consist of species of commercial interest. This point of view leads to the following definition:

Fisheries Oceanography—the study of oceanic processes affecting the abundance and availability of commercial fishes.

Obviously populations of commercial fishes are affected by other than oceanic processes. In particular they are subject to the pressure of an aggressive nonenvironmental factor, the fisherman. Much of fisheries research has resulted from the fear that this pressure was excessive and would soon lead to decimation of the stock; thus it has concentrated primarily on the dynamics of the populations involved. The working hypothesis of the fisheries oceanographer, on the other hand, is that variations in apparent abundance are due primarily to changes in the environment. These changes must be described and understood before the role of man can be properly evaluated.

The relationship is traced out in a model which starts with the observation that significant changes in the atmospheric pressure field occur from place to place and from time to time. These changes lead to variations in the stress applied to the sea surface by the wind. It is now generally believed that the major near-surface circulation of the ocean is wind driven, so that the changing wind stress causes changes in the velocity, depth, breadth, transport or other characteristics of the surface currents. Furthermore, the processes whereby the surface layer is refertilized with nutrient elements from below appear to be either directly wind-produced (for example, wind stirring and coastal upwelling) or secondary effects of the wind-driven circulation (for example, doming or ridging).

The near surface circulation may affect directly the distribution or abundance of organisms at all trophic levels. In addition, changes in the intensity of the refertilizing processes are reflected in the time and space distribution of primary production. This in turn affects production in the next higher trophic level, and so on, with assorted time and space lags, to the desired fish. At each step in this line of reasoning, refinements and complications are involved, but the basic theme of the model remains:

"Changes in the wind field lead eventually to changes in the success of fishing."

The goal of investigation of this model is often considered to be prediction. Certainly if one could forecast accurately the changes in abundance, distribution and availability of fish, this would be of great economic significance. But, conceivably, a useful prediction could result from the blind statistical treatment of a large number of variables, rather than from a fundamental understanding of the interplay of the pertinent atmospheric, oceanic, and biospheric processes. It is the acquisition of this fundamental knowledge which is the scientific goal of fisheries oceanography.

Current practice in fisheries oceanography has concentrated on documenting and trying to interpret the changes in the marine environment. One of the leaders in this field in the United States was the late Townsend Cromwell, who originally proposed this symposium. His first important work, in Honolulu, was a study of wind-induced upwelling along the equator. Subsequently, the Honolulu group has examined the mechanisms of surface enrichment near the Hawaiian Islands and to the north. At Scripps Institution and the Tuna Commission, there have been studies of coastal upwelling, oceanic fronts, and of processes such as those Cromwell labelled "doming" or "ridging". Dr. Sette and his colleagues have been examining past weather and the marine climate, looking for long-term changes related to those in the fisheries. All of these investigations have been facilitated by the presence of certain conspicuous features or discontinuities. As Henry Stommel has suggested, studying the oceans resembles dissecting a lobster—it is easier to do at the joints.

What has been the success of fishery oceanography in recent years? Certainly in the Pacific it has had no dramatic impact on the commercial fisheries. And if the goal be considered prediction, very little success can be recorded. Yet the fund of basic knowledge of

---

[1] Contribution from the Scripps Institution of Oceanography. 1318

Reproduced by Permission

the ocean has increased tremendously. The near surface circulation and the distributions of properties such as temperature, salt and oxygen have been much more adequately described. The theory of wind-driven circulation is well established. The variations in time and space of coastal upwelling are recognized, and other important surface-enriching mechanisms are known. In short, the general scheme by which atmosphere, ocean and biosphere are interrelated is taking form, and we are ready to formulate and test hypotheses having bearing on important and specific problems in fisheries science.

Reprinted from Limnology and Oceanogr
vol.6, no.4 (October, 1961)
pp.451-456

SCATTERING PROPERTIES OF DISTILLED AND NATURAL WATERS[1]

John E. Tyler
Visibility Laboratory
Scripps Institution of Oceanography, La Jolla

ABSTRACT

Measurements of the volume scattering function and other optical properties are presented for distilled water, Pacific coastal and offshore water, and lake water. The depth and time variability of Pacific water at one station is given and the effect of a wind storm on the optical properties of the lake water is demonstrated.

INSTRUMENTATION

The scattering meter used in this work was originally described by Tyler and Richardson (1958). It has recently been critically tested for performance by comparing the results of measurements on prepared stable hydrosols by two independent methods, one of which employed the scattering meter, the other employed an optical integration method described by Tyler (1957). The results of these tests are reported elsewhere.

In order to maintain the accuracy of the data obtained with the scattering meter it has been necessary to maintain its calibration in several respects as follows:

1. *Angle calibration*—The scattering angle θ is related to the output of a voltage divider circuit supplied by a highly stable power source. The phototube arm is geared directly to the potentiometer of the voltage divider which governs the position of the pen of a Brown synchronously driven strip-chart recorder. The performance of this circuit and power supply has been checked at the beginning of every series of measurements and can be post checked for each individual run if desired. The voltage divider has proved to be very precise. The indication of angle is accurate to ± .25° at 180°, ± .13° at 90° and smaller fractions of an angle at 0°, the forward scattering direction. The error in the indication of angular position is generally no larger than the error encountered in reading the data.

2. *Circuit calibration*—The output of the multiplier phototube circuit is designed to be proportional to the log of the light input to the phototube. The circuit used is not quite linear over its 5-log range. Data obtained with this circuit is read by means of a scale which is made by exposing the multiplier phototube to known steps in light

TABLE 1. *Scattering properties of commercial "distilled" water samples. Bandwidth limited by a Wratten No. 57 filter*

Sample	A	B
Total attenuation coefficient α/m	.062	.047
Total scattering coefficient s/m	.00845	.00457
Absorption coefficient a/m	.0536	.0424
Forward scattering coefficient f/m	.00763	.00396
Backward scattering coefficient b/m	.00082	.000620
Ratio f/s	.900	.870
Volume scattering function $\sigma(\theta)$		
$\theta =$ 0°		
10		
20	.00648	.00316
30	.00223	.00107
40	.000941	.000520
50	.000473	.000294
60	.000271	.000191
70	.000181	.000128
80	.000140	.000096
90	.000117	.000083
100	.000110	.000079
110	.000118	.000082
120	.000126	.000092
130	.000134	.000102
140	.000139	.000112
150	.000146	.000119
160	.000171	.000141
170	.000193	.000161
180	.000201	.000169

---

[1] This research was supported by a grant from the National Science Foundation, Earth Sciences Division. The α-meter, scattering meter, and other instrumentation used in this research were developed by the Visibility Laboratory under a Bureau of Ships contract. The loan of these instruments for the present measurements is gratefully acknowledged.

Contributions from the Scripps Institution of Oceanography, New Series, 1319

Reproduced by Permission

TABLE 2. *Scattering properties of Pacific Coastal and offshore water at the Stations shown in Figure 1. Bandwidth limited by a Wratten No. 57 filter*

Station number		1	2	3	4
Total attenuation coefficient α/m		.736	.129	.118	.111
Total scattering coefficient s/m		.125	.01094	.01420	.0120
Absorption coefficient a/m		.611	.1181	.1038	.099
Forward scattering coeficient f/m		.119	.01010	.01321	.0110
Backward scattering coefficient b/m		.00630	.000847	.000982	.000984
Ratio f/s		.950	.925	.930	.915
Volume scattering function $\sigma(\theta)$					
	$\theta = 0°$				
	10				
	20	.1014	.00881	.01192	.00959
	30	.0360	.00268	.00358	.00313
	40	.0152	.00117	.00145	.00129
	50	.00739	.000616	.000698	.000661
	60	.00419	.000356	.000396	.000388
	70	.00266	.000232	.000253	.000249
	80	.00181	.000164	.000179	.000175
	90	.00134	.000132	.000145	.000142
	100	.00109	.000120	.000134	.000130
	110	.000940	.000120	.000135	.000135
	120	.000903	.000124	.000146	.000146
	130	.000912	.000134	.000158	.000159
	140	.000944	.000145	.000175	.000176
	150	.001003	.000156	.000192	.000193
	160	.001028	.000175	.000202	.000208
	170	.001036	.000191	.000206	.000219
	180	.001037	.000197	.000207	.000223

level, using the inverse square law to establish the steps. Scales of this kind have been made on the average of every two months during the work, usually just before or just after a series of measurements.

The circuit has ben found to vary ± 2.5%

TABLE 3. *Variability in the optical properties of coastal water at Station 4. Data taken in November 1960. Bandwidth limited by a Wratten No. 57 filter*

Depth (m)	α (per m)	s (per m)	a (per m)	f/s	Time	Tide (ft)
20	.218	.0205	.197	.935	1850	
10	.162	.0176	.144	.940	1910	
1	.148	.0156	.132	.928	1925	4.4
20	.183	.0200	.163	.940	2200	
10	.153	.0173	.136	.935	2213	
1	.161	.0186	.142	.935	2225	
20	.148	.0189	.129	.935	0100	
10	.132	.0167	.115	.935	0110	
1	.111	.0120	.099	.917	0123	1.1
20	.139	.0151	.124	.929	0405	
10	.133	.0131	.120	.944	0420	
1	.133	.0130	.120	.944	0430	
Averages						
20m	.172	.0186	.153	.934		
10m	.145	.0161	.129	.938		
1m	.138	.0148	.123	.931		
Overall	.152	.01653	.1343	.9347		
Variability	± 35%	± 25%	± 35%	± 1.5%		

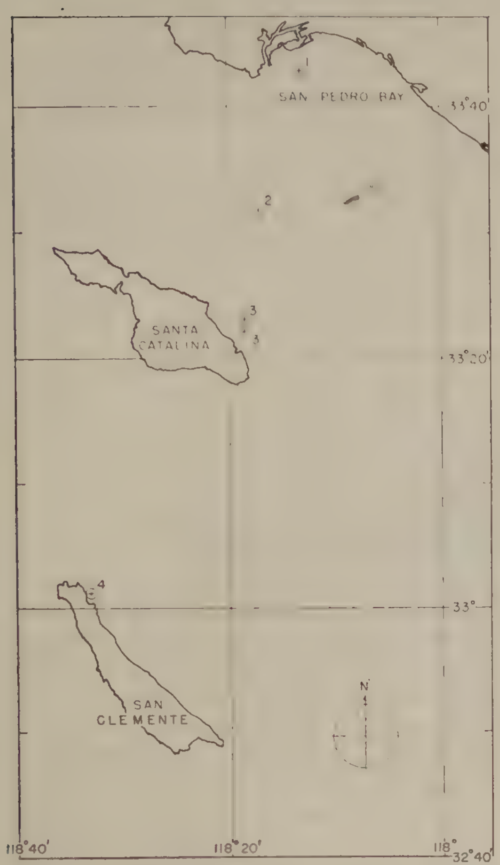

FIG. 1. Chart showing location of coastal and offshore stations where the volume scattering function has been measured.

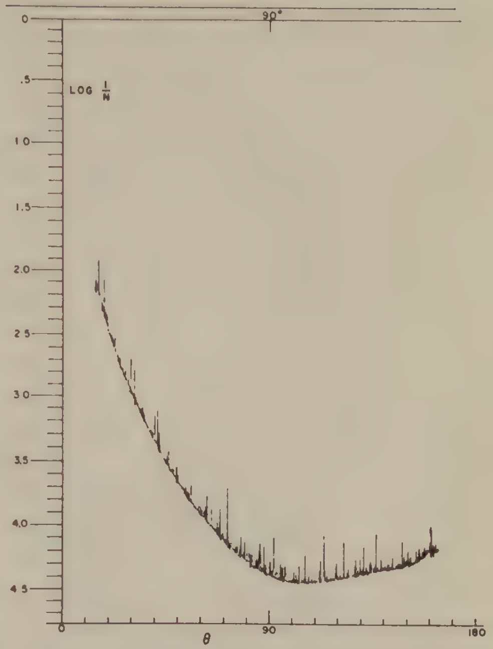

FIG. 2. Data record from a depth of 20 m at Station 4, showing bioluminescent flashing superimposed on the scattering data. This record is uncorrected for changes in the sample volume.

at high light levels, ± 10% at the extreme low light levels.

3. *Volume calibration*—The sample volume has been determined by a method very similar to that described by Pritchard and Elliott (1960). Since the volume is defined by optical and mechanical components, which do not change their characteristics as readily as electrical components, a volume calibration, made near the beginning of these measurements in 1959, was used throughout. The volume calibration consisted of 59 determinations of the sample volume at 15 different angular settings. Maximum uncertainty in the determination of the sample volume is ± 12%.

4. *Irradiance input calibration*—Irradiance input has been determined from measurements on the beam itself using the instrument's own multiplier phototube in order to cancel out optical and circuit gain factors. The calibration procedure has been repeated 5 times during the course of this work and, in between these calibrations, the irradiance input has been controlled by regulation and control of the lamp voltage to ¼%. The accuracy of the irradiance input calibration is estimated to be ± 10%.

The sources of inaccuracy in these measurements do not characteristically vary during short periods of time. Thus, values of the volume scattering function in a single determination can be expected to describe accurately the shape of the curve but there is a high degree of probability that the values reported will collectively be too high, or too low, by 10%. Similarly there is a high degree of probability that data taken during one month will be inconsistent with data taken during another month by ±10%.

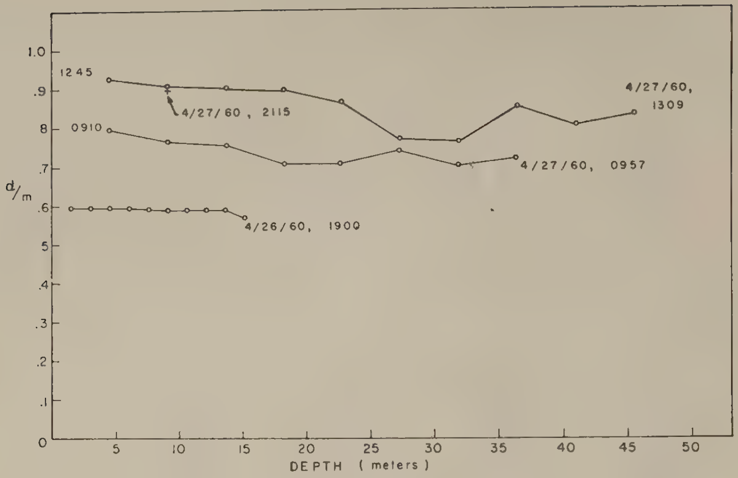

FIG. 3. Showing the variation of α with depth at Lake Pend Oreille on a calm day (April 26, 1960) and at various times during the following day, which was very windy. Bandwidth limited by a Wratten No. 45 filter.

Because of the circuitry employed the lake and ocean data presented here have been obtained at night and the distilled water data has been obtained in a darkened tank.

RESULTS

Table 1 gives the volume scattering function and other optical data for two samples which were purchased as distilled water. Neither sample is regarded as being distilled in the strict sense of the word. The two samples do, however, provide a convenient base for comparison. The filter used has its maximum transmittance at about 522 mμ and has a halfband width of about 80 mμ. Sample B compares favorably

TABLE 4. *Variability in the optical properties of coastal water at Station 4. Data taken in January, 1961. Bandwidth limited by a Wratten No. 57 filter*

Depth (m)	α (per m)	s (per m)	a (per m)	f/s	Time	Tide (ft)
20	.153	.0154	.138	.938	0230	
10	.162	.0149	.147	.935	0245	1.4
1	.159	.0123	.147	.935	0255	
20	.176	.0157	.160	.943	1920	
10	.186	.0163	.170	.945	1935	
1	.170	.0131	.157	.939	1945	
20	.165	.0154	.150	.936	2210	
10	.152	.0141	.138	.943	2230	4.6
1	.139	.0108	.128	.924	2240	
20	.167	.0157	.151	.937	0100	
10	.162	.0166	.145	.935	0110	
1	.162	.0143	.148	.930	0125	
					0850	6.9
					1558	–1.7
Averages						
20m	.165	.0156	.150	.939		
10m	.166	.0155	.150	.940		
1m	.158	.0126	.145	.932		
Overall	.163	.0146	.148	.937		
Variability	± 10%	± 20%	± 11%	± 1.1%		

TABLE 5. *Volume scattering function for Lake Pend Oreille before and after a high wind. Bandwidth limited by a Wratten No. 45 filter*

Sample date	April 26	April 27
Total attentuation coefficient α/m	.589	.909
Total scattering coefficient s/m	.258	.585
Absorption coefficient a/m	.331	.324
Forward scattering coefficient f/m	.248	.559
Backward scattering coefficient b/m	.00976	.0256
Ratio f/s	.960	.955
Volume scattering function $\sigma(\theta)$		
$\theta =$ 0°		
10		
20	.222	.470
30	.0715	.166
40	.0291	.0758
50	.0137	.0380
60	.00712	.0206
70	.00416	.0121
80	.00271	.00780
90	.00198	.00559
100	.00162	.00448
110	.00147	.00394
120	.00143	.00379
130	.00145	.00372
140	.00149	.00371
150	.00156	.00383
160	.00163	.00396
170	.00168	.00406
180	.00170	.00410

with the distilled water described by Hulburt (1945). The ratio of f/s for distilled water is lower than it is for the lake and ocean samples. This would be expected as a consequence of predominately smaller particle size in the cleaner water. The minimum value of the volume scattering function occurs at 100° in both samples.

Table 2 gives the volume scattering function and other data for coastal and off-shore water in the Los Angeles—San Diego area. Station locations are shown in Figure 1. Station 1 is in the outfall area of a sewage disposal plant. The water at Station 1 was full of phosphorescent microorganisms. However, the relative motion between the scattering meter and the water was very slow at this station and phosphorescense was not seen during the measurements. It is unlikely that the relative motion between instrument and water caused enough phosphorescence to affect the measurement.

TABLE 6. *Variability in the optical properties of Lake Pend Oreille as a function of depth before and during a high wind. Bandwidth limited by a Wratten No. 45 filter*

Depth (m)	α (per m)	s (per m)	a (per m)	f/s	Date
4.6	.594	.236	.348	96.4	
9.2	.589	.258	.331	96.6	April 26, 1960
13.8	.589	.245	.344	96.1	
9.2	.909	.585	.324	95.5	
18.2	.897	.559	.338	95.2	April 27, 1960
24.7	.865	.585	.280	95.7	

Stations 2, 3, and 4 were outside the sewage outfall area but were full of flashing bioluminescent organisms. A typical record from Station 4 at 20-m depth is shown in Figure 2. Relative motion between instrument and the water was fairly rapid at Station 4 and the organisms could be seen flashing as they bumped into the various parts of the scattering meter. The same Wratten No. 57 filter was used in these measurements. Note that the angular position of the minimum value of the volume scattering function varies from 100° to 120° in these data.

Tables 3 and 4 show the principle features of the time and depth variability of the water at Station 4 — again using the Wratten No. 57 filter. In Table 3 the water appears to become more absorbing and more scattering with depth and exhibits a high degree of variability. In Table 4, the water is much less variable with time and depth. The ratio of f/s is substantially constant for both days and for all depths and times, indicating that the particle shape is not varying significantly.

Table 5 gives the volume scattering function for lake water at the southern end of Lake Pend Oreille, Idaho, just before (April 26) and after (April 27) a strong north wind. These data were taken with a Wratten No. 45 filter which has a peak transmittance at 480 mμ and a half bandwidth of about 60 mμ. Minimum scattering here occurs at 120° and 140° and the ratio f/s is the highest reported.

There has been an obvious increase in scattering following the high wind. The changes in α are followed in a little more detail in Figure 3 which shows α as a function of depth on April 26 at 1900 and for two periods during April 28 with one check point taken at 2115. The slopes of the two curves for the 28th suggest that wave action along the shores is introducing scattering material into the surface water which is being carried away from shore by the wind and mixed by wave action. Disturbing of bottom sediments at the station seems unlikely because of the 750 ft of depth.

Table 4 gives additional data on the variability of the lake water with depth on these two days.

REFERENCES

HULBURT, E. O. 1945. Optics of distilled and natural water. J. Opt. Soc. Am., **35**: 698–705.

PRITCHARD, B. S., AND W. G. ELLIOTT. 1960. Two instruments for atmospheric optics measurements. J. Opt. Soc. Am., **50**: 191–202.

TYLER, J. E. 1957. Monochromatic measurement of the volume scattering of natural waters. J. Opt. Soc. Am., **47**: 745–747.

———, AND W. H. RICHARDSON. 1958. Nephelometer for the measurement of volume scattering function in situ. J. Opt. Soc. Am., **48**: 354–357.

(926)

Reprinted from JOURNAL OF THE OPTICAL SOCIETY OF AMERICA, Vol. 51, No. 11, 1289–1293, November, 1961
Printed in U. S. A.

Measurement of the Scattering Properties of Hydrosols*

JOHN E. TYLER
Visibility Laboratory, Scripps Institution of Oceanography, University of California, La Jolla, California

(Received February 8, 1961)

The scattering properties of prepared stable hydrosols have been obtained by two independent methods, by integration of volume scattering function data, and by direct measurement of the total scattering. The correlation coefficient between the two methods has been determined to be 0.99. Data are given for the total attenuation coefficient, the total-scattering coefficient, the forward- and backward-scattering coefficients, and the volume-scattering function for two samples of water and one prepared hydrosol consisting of 40 cc of skim milk in 600 gallons of water. For the prepared hydrosols a correlation coefficient of 0.999 was found between the total scattering coefficient and the volume-scattering function at 45°. A comparison is made between the present data for distilled water and data published by Hulbert in 1945.

INTRODUCTION

DATA for the scattering properties of hydrosols have been found useful in at least three forms: *directional scattering*, which gives the flux scattered from a beam of light, as a function of the angle of observation, by a volume which varies with the angle of observation; *relative volume-scattering function*, which gives the flux scattered from a beam of light, as a function of the angle of observation, by a *constant* volume of hydrosol; and the *volume-scattering function* $\sigma(\theta)$, which gives the flux per unit solid angle scattered in each direction θ, per unit volume, per unit irradiance input. That is

$$\sigma(\theta)=dJ(\theta)/Hdv, \tag{1}$$

where $dJ(\theta)$ represents the watts per unit solid angle scattered in the direction θ, H represents the irradiance in watts/unit area at the volume, and dv represents the experimental volume.

The existence of these three forms of the data is largely a matter of instrument calibration and intended application. *Directional scattering* is useful for intralaboratory correlations, *relative volume-scattering function* exhibits the form of the function and can be integrated to yield the *relative* total scattering coefficient, *volume-scattering function* gives the real value of the optical property, and when integrated yields the real value of the total scattering coefficient, i.e.,

$$s=2\pi\int_0^\pi \sigma(\theta)\sin\theta d\theta. \tag{2}$$

This paper is concerned with the correlation between two methods for determining the total-scattering coefficient; first, the classical method, by integration [using Eq. (2)] from experimental values of the volume-scattering function $\sigma(\theta)$, and second, by computation from the direct measurement of the total scattering by an optical-integration technique described by Tyler.[1] A similar comparison of the total scattering of "solutes" was made by Carr and Zimm[2] using small sample volumes contained in special glass cells.

The present work is directed towards the measurement of the volume-scattering function and the total-scattering coefficient of natural hydrosols, such as ocean and lake waters.

EXPERIMENTAL

The experiment made use of prepared stable hydrosols having a wide range of scattering properties. Since the work was directed towards the ultimate goal of *in situ* measurements of the scattering properties of the sea, a scattering agent was chosen which provided irregular particles and which exhibited low absorption in the region of high transmittance for water.

With the instrumentation on hand, it was not possible to make simultaneous measurements, and so it was also important that the prepared hydrosols each be stable for the duration of the measurements. Skim milk seemed to fulfill all of these requirements quite well. Dilute solutions of skim milk are stable scattering agents for an hour or more although they are not stable overnight.

Hydrosol samples were prepared in a large tank, the procedure being to purchase 600 gallons of commercial "distilled" water and make consecutive additions of skim milk, usually in amounts increasing in geometric progression. A mixing technique was worked out which assured a homogeneous sample throughout the tank. The volume-scattering functions were measured with the scattering meter shown in Fig. 1 immersed in the sample. The basic optical design of this instrument has been described by Tyler and Richardson.[3] The source, which is unpolarized, consists of a uniformly irradiated field stop which is imaged on the sample volume so that the stop image is the same size and shape as the exit pupil of the projection lens. The beam is thus cylindrically restricted between the projection lens and the Waldram stop (see Fig. 1). The maximum angular divergence between limiting rays in the beam was

---

* This research was supported by a grant from the National Science Foundation, Earth Sciences Division.

[1] J. E. Tyler, J. Opt. Soc. Am. 47, 745 (1957).

[2] C. I. Carr, and B. H. Zimm, J. Chem. Phys. 18, 1616–1626 (1950).

[3] J. E. Tyler and W. H. Richardson, J. Opt. Soc. Am. 48, 354 (1958).

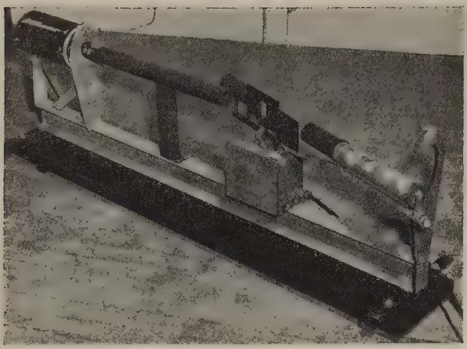

FIG. 1. Scattering meter for measuring the volume-scattering function of hydrosols. The light source is on the left, the detector is on the arm at the right. The Waldram stop in the center, with an oblong aperture, rotates with the detector arm, but on a different axis, and is designed to make the observed volume of hydrosol independent of its angle of observation. (See Fig. 3).

approximately 2°. The detector on the right is an end-on multiplier phototube (a selected Dumont No. 6291—K1242) which was insensitive to changes in the orientation of the plane of polarization of polarized light and which was mounted inside a μ-metal shield to prevent deflection of the electron beam in the dynode stages as a result of changes in orientation with respect to the earth's magnetic field. An optical system similar to that used for the light source was used to restrict the beam of detection. Its maximum angular divergence was approximately 6°.

In order to control stray light (see Fig. 1) an internally baffled tube was provided between the source housing and the Waldram stop, an internally baffled shade was provided for the multiplier phototube, a light trap was provided for the beam of detection and for the light beam (not shown in Fig. 1) and an additional baffle was mounted on the Waldram stop. All baffles had to be provided with vents so that they could be properly drained and flushed with each new sample.

The total attenuation coefficient was also measured by immersion by using the instrument shown in Fig. 2.

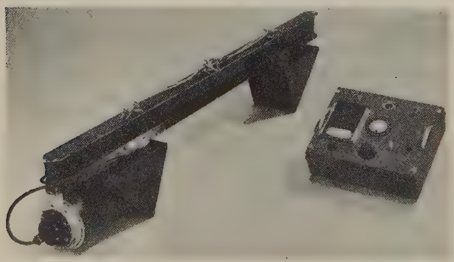

FIG. 2. The α meter for determining the total-attenuation coefficient of hydrosols. The instrument has a monitor cell in the lamp housing at the left to maintain the flux output of the lamp constant.

This instrument also employs a cylindrically restricted beam of light, as described above, and has an angular divergence of less than 1°.

Nearly simultaneously with the immersion measurements, a sample was carefully siphoned into a 5-liter glass sphere described in reference 1 and measured on a Hardy[4] spectrophotometer to obtain data for determining the total scattering coefficient by the optical integration method.

The bandwidth of the immersion measurements was restricted by means of a Wratten filter No. 61 which has a peak transmittance at 522 mμ and half-bandwidth of 56 mμ. By using an independent tungsten source and a Wratten No. 61 filter to illuminate the exit slit of the monochromator of the Hardy instrument, it was demonstrated that the data obtained were the same as data obtained with the monochromator as a source, set at 522-mμ and 10-mμ bandwidth. Spectrophotometric data were taken at this latter wavelength and bandwidth setting.

RESULTS

The results reported here are for unpolarized light. Both the scattering meter and the attenuation meter were insensitive to changes in orientation of the plane of polarization of polarized light. Measurements made on the Hardy spectrophotometer were made insensitive to polarization effects by means of a Buc-Stearns[5] plate.

The volume calibration of the scattering meter has been described in detail in an earlier publication.[3] Recent data for volume calibration which were obtained in air are shown in Fig. 3. The procedure used gives relative volume in air as a function of angle, but can be made absolute for volume in water by computing the real volume at one point ($\theta=90°$) from measurements on the intersecting beams in water.

Computation of the volume-scattering function from the ratio of directional scattering data to volume calibration data, suggested by Pritchard[6] could not be employed in the present measurements. Instead the input irradiance was determined by means of measurements of the direct beam by using the same multiplier phototube assembly that was used to obtain the scattering data. Measurements were made in air and corrected for a water environment. Measurements were also made directly in a water environment. For reasons that could not be determined these two measurements of the input irradiance to the sample volume could not be reconciled to better than 10%, and to this extent, the values reported here should be regarded as those of relative volume scattering function.

For any one series of measurements, the total-scattering coefficient reported by one method, plotted against the total-scattering coefficient obtained by the other

---

[4] A. C. Hardy, J. Opt. Soc. Am. 25, 305 (1935).

[5] G. L. Buc and E. I. Stearns, J. Opt. Soc. Am. 35, 521 (1945).

[6] B. S. Pritchard and W. G. Elliott, J. Opt. Soc. Am. 50, 191 (1960).

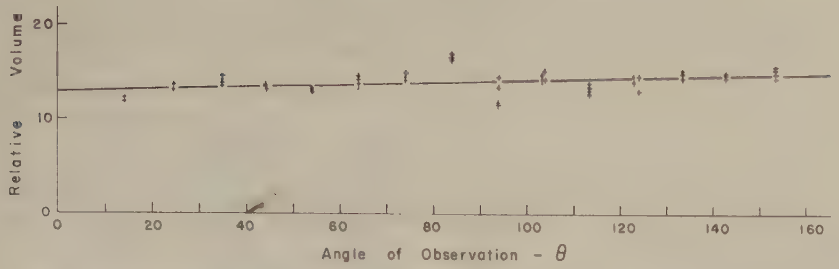

Fig. 3. Volume calibration data for the scattering meter. Data at 84° and 94° are subject to greater error because of the rapid change in reflectance of the calibration screen with θ at and near 90°.

method resulted in a straight line. Because of variation in flux from the lamp of the scattering meter from one series to the next, together with the uncertainty in the determination of the input irradiance, the slopes of the plots for the various series were not all quite the same. If these slopes are not averaged, the correlation coefficient for all runs combined is 0.99. Variability in the input irradiance can be smoothed, of course, by determining the best straight line for each series of runs independently and normalizing all runs to the average slope. When this is done the correlation coefficient is also found to be 0.99. Figure 4 is a graphical representation of the correlation between the two methods. About 100 experimental determinations of the total-scattering coefficient are plotted.

The volume-scattering function is itself of very great interest. Table I gives the volume-scattering functions and other data for two samples of water (in columns A and B) and one prepared hydrosol (in column C). Sample A, called "distilled" water in Table I was of commercial quality. Its optical purity was adequate for the work, but was by no means perfect. Sample A represents the cleanest water measured during the course of this work. Sample B was visibly contaminated in 600-gallon lots.

Skim milk was added to the "distilled" water in small volumes starting with 5 cc per 600 gallons. There is some evidence of solubility, but for additions of 20 cc to 640 cc per 600 gallons, the plot of log T vs concentration is very nearly linear. Column C of Table I gives data for a hydrosol consisting of 40 cc skim milk in 600 gallons of distilled water.

In Table I the total attenuation coefficient α has been obtained experimentally from transmittance measurements made with the α meter illustrated in Fig. 2, using the equation

$$T=e^{-\alpha r}. \tag{3}$$

The definition of α, viz.,

$$\alpha=s+a, \tag{4}$$

where s is the total-scattering coefficient and a is the absorption coefficient, requires that none of the scattered light be included in the transmittance measurement. The question therefore arises as to the effect of the forward scattered light within the beam on the accuracy of α obtained in this way. This problem has been investigated recently by Preisendorfer.[7] From his work the error in the value of α is computed to be less than 0.3%.

In the measurement of the volume-scattering function experimental values could be obtained only between 20° and 160° (due to mechanical interference). Values at 170° and 180° were interpolated and are given in the table. Values were also interpolated for 0° and 10° in order to complete the data for the computation of s. These latter values are, of course, multiplied by the

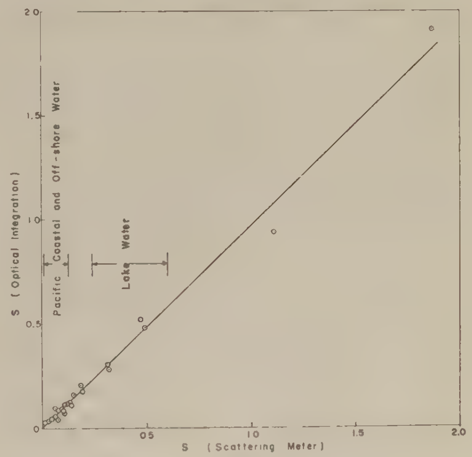

Fig. 4. Plot showing the correlation between the total-scattering coefficient s, obtained by optical integration and from the scattering-meter data. Each point represents between 2 and 6 experimental determinations of s by the two methods. The slopes of the various runs have not been averaged in this plot. The range of values recently obtained for the total-scattering coefficient of lake and ocean waters is indicated. Since the slope of the line is a function of the input irradiance, it is subject to the inaccuracy already noted in the text.

---

[7] R. W. Preisendorfer, "A general theory of perturbed light fields, with applications to forward scattering effects in beam transmittance measurements," Visibility Laboratory, SIO, SIO Ref. 58-37, 23 pp., (1958).

TABLE I. Volume-scattering functions and other data for two samples of water and one prepared hydrosol.

Column	"Distilled" water A Per meter	Water sample B Per meter	Hydrosol 40 cc/600 gal C Per meter	1945 Hulburt distilled water D Per meter	1941 Dawson and Hulburt theoretical water E Per meter
Total-attenuation coeff	0.047	0.162	0.264	0.04	
Total-scattering coeff	0.00457	0.0159	0.137	0.00931	0.00194
Absorption coeff (by difference)	0.0424	0.146	0.127	0.0307	
Forward-scattering coeff	0.00396	0.0147	0.112		
Backward-scattering coeff	0.00062	0.00118	0.0255		
% Forward scattering	86.5	92.5	82.0	86.4	50.0
Volume-scattering function					
0°	Interpolated for the computation of total scattering coefficient only.				0.000222
10					0.000219
20	0.00316	0.0125	0.0623		0.000210
30	0.00107	0.00454	0.0330		0.000197
40	0.000520	0.00189	0.0205		0.000180
50	0.000294	0.000883	0.0142		0.000163
60	0.000191	0.000487	0.00982		0.000146
70	0.000128	0.000307	0.00718		0.000133
80	0.000096	0.000228	0.00543		0.000124
90	0.000083	0.000191	0.00448	0.000144	0.000121
100	0.000079	0.000177	0.00408		0.000124
110	0.000082	0.000173	0.00390		0.000133
120	0.000092	0.000179	0.00386		0.000146
130	0.000102	0.000185	0.00403		0.000163
140	0.000112	0.000193	0.00402		0.000180
150	0.000119	0.000204	0.00407		0.000197
160	0.000141	0.000217	0.00421		0.000210
170	0.000161	0.000227	0.00433		0.000219
180	0.000169	0.000230	0.00438		0.000222

sine of 0° and 10°, respectively, in the computation and can vary by a factor of 10 without affecting the total-scattering coefficient significantly. However, the interpolated values of $\sigma(\theta)$ could be very misleading and consequently are not given.

Jerlov,[8] in his paper on "Particle distribution in the ocean," has pointed out that the ratio of the total-scattering coefficient to the scattering at 45° is a constant for the ocean. This is an important observation since it permits the use of simple instrumentation for generating descriptive charts of particle distributions.

TABLE II. Ratio of the forward-scattering coefficient to total-scattering coefficient.

Sample	% Forward scattering
Water sample B	92.5
Distilled water A	86.5
A+5 cc skim milk	83.0
10	82.0
20	82.0
40	82.0
80	81.5
80 (stood 12 hr)	83.0
160	81.5
320	81.0
640	81.0

Figure 5 gives a plot of the volume-scattering function at 45° against the total-scattering coefficient for the same samples reported in Fig. 4. The correlation coefficient here is 0.999.

This does not mean, of course, that the ratio of volume-scattering function at 45° to total-scattering coefficient is independent of particle shape or size. Rather, it means that in hydrosols containing the same type of particles, the value of the volume-scattering function at some fixed angle can be used as a measure of the total-scattering coefficient.

Evidence of the effect of particle shape or size can be found in Table II which gives the ratio of the forward-scattering coefficient to total-scattering coefficient for a series of measurements. For the two samples marked A & B, in which the particle size or shape might be significantly different from those of fresh skim milk, this ratio is significantly higher. Also in the two samples marked 80, although the total scattering remained the same to within 1%, the forward-scattering coefficient increased significantly for the sample in which the particles had 12 hr to aggregate. It is of interest to compare the present data on distilled water, column A of Table I, with data published by Hulbert[9] (column D) and with a theoretical water (column E) calculated from equations given by Dawson and Hulbert.[10] The distilled waters of columns A and D are very similar as far as the data go, but both are a long way from being the theoretical water of column E.

---

[8] N. G. Jerlov, *Reports of the Swedish Deep-Sea Expedition* (Wettergren and Kerbers Forlag, Göteborg, Sweden, 1953), Vol. III, Physics and Chemistry, No. 3.

[9] E. O. Hulbert, J. Opt Soc. Am. **35**, 698 (1945).

[10] L. H. Dawson and E. O. Hulbert, J. Opt. Soc. Am. **31**, 554 (1941).

DISCUSSION

It is well known that the terminology of photometry has been abused. This paper employs terminology which is currently under consideration for adoption by the International Association of Physical Oceanography.

The term volume-scattering function, which has been defined for an arbitrary angle θ in Eq. (1), includes all scattered flux at that angle regardless of the shape or size of the scattering particle or the homogeneity or purity of the scattering medium. It should not be confused with Rayleigh ratio which under special circumstances may be numerically equal to the volume scattering function at 90°. See, for example, Carr and Zimm.[2] The term, total-scattering coefficient, defined in Eq. (2), is derived from the volume-scattering function and should not be confused with turbidity although again under special circumstances the two may be numerically equal.

Values for the volume-scattering function at 0°, 10°, 170°, and 180° were obtained by means of the Gregory-Newton divided-difference interpolation method. This interpolation has no physical significance. It is believed to yield low values of $\sigma(0)$ and $\sigma(10)$.

In the study of the effect of scattering and absorption on image-forming systems underwater it is important to know the gross scattering properties of the existing hydrosol. The methods of measurement do not, therefore, make comparison between the hydrosol and a standard, which may be the practice for other purposes, but simply measure the gross scattering from the mixture of particles that are present.

It is also important in optical studies of ocean water to make the measurements *in situ* since rapid changes take place in a sample removed from its natural environment.

At the present time no instrument exists which is capable of making direct measurements of the total scattering coefficient of the ocean *in situ*. Such an instrument would be very useful and, although the present work has not clarified all of the problems, the results presented in Fig. 4 indicate the potential usefulness of the principle of the Hardy spectrophotometer for this purpose.

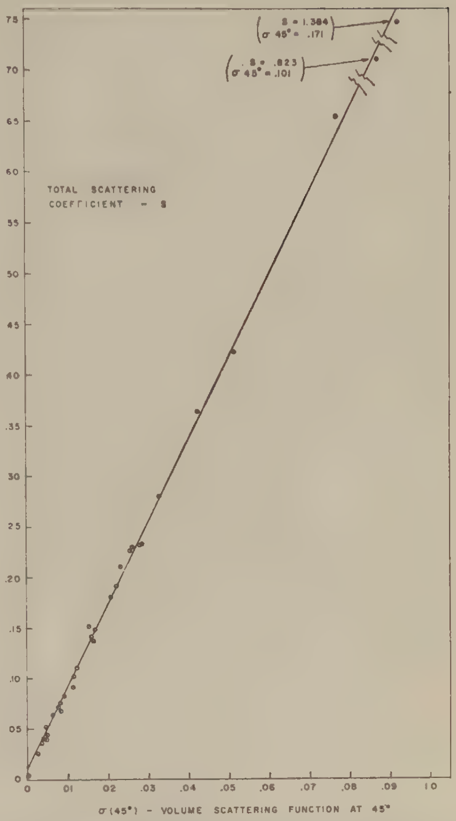

FIG. 5. Graphical representation of the correlation between the total scattering coefficient and the volume-scattering function at 45°. The line represents the "best straight line fit" to the data.

(932)

JOSEPH R. CURRAY

LATE QUATERNARY SEA LEVEL: A DISCUSSION

Abstract: Recent literature and new evidence on the position of sea level during the late Quaternary are reviewed critically. Some evidence suggests a glacial interstadial and stand of sea level at about −8 fathoms 30,000 years ago. Sea level then dropped to perhaps −65 fathoms. The rapid rise of sea level and warming of climate covered a period of time from 15,000 to 7,000 B.P. (Before Present) and consisted of a period of climatic and sea-level fluctuations rather than a single abrupt warming as proposed for 11,000 B.P.

McFarlan (1961) has presented a stimulating and extremely well-documented study of the position of sea level relative to the late Quaternary alluvial deposits of the Mississippi River. Broecker (1961, p. 159) has debated McFarlan's conclusions. It seems appropriate to test the hypotheses of these writers with data from the continental shelf off Texas (Curray, 1960) and with other pertinent new evidence.

McFarlan has attempted to date the position of sea level during the late Quaternary by means of radiocarbon dates of material from known environments of deposition. His task has been greatly complicated by the rapid deposition and subsidence in the Mississippi delta, thereby necessitating the application of corrections to most of the dates lying outside the "hinge-line" area of the delta. Despite the obvious difficulties and dangers of the determination of sea level from an unstable area, the general trend of dates from 6000 to 17,000 years B.P. reported by McFarlan is remarkably similar to the trends reported by other investigators (Bennema, 1954; van Straaten, 1954; Shepard and Suess, 1956; Godwin *et al.*, 1958; Fairbridge, 1958; 1960; Curray, 1960; Shepard, 1960; Jelgersma and Pannekoek, 1960). The agreement of the general trend of the dates from many parts of the world suggests that McFarlan has been essentially correct in the difficult task of applying corrections to dates from the rapidly subsiding Mississippi delta.

7000 B.P. to 15,000 B.P.

Broecker (1961) suggests that we should observe an acceleration in the rise of sea level correlating with an abrupt warming of climate about 11,000 years ago. This appears to be based on the assumption that the rise of sea level is a simple, one-way event, without allowing for the probable complexity of events around this general period of time. Broecker and Orr (1958) have shown the rapid climatic fluctuations affecting lake level in the Great Basin of western United States (Fig. 1). The levels of Lakes Lahontan and Bonneville lowered until approximately 12,000 to 13,000 years B.P., rose sharply at 11,000 to 12,000 years B.P., dropped, possibly rose again at about 10,000 years, and dropped immediately afterward to remain low until the present day. Meteorological events must certainly have been complex during the period of time from about 13,000 B.P. to 9000 B.P., so let us not assume simplicity in the position of sea level. Lake level presumably responds rather rapidly to local climatic events, while sea level responds more slowly to the net integrated effects of climate in all glaciated areas.

A comparison is made (Fig. 1) between the standard European pollen profile (Barendson *et al.*, 1957, as modified by Broecker, *et al.*, 1960), the levels of Lakes Lahontan and Bonneville (Broecker and Orr, 1958), and the position of sea level (Curray, 1960). The coincidence of peaks is striking. The pollen represents a very quick reaction to climatic changes. Lake levels were high during cold periods and low during warm periods, showing possibly a very slight time lag behind the pollen profile. Sea level, on the other hand, rises during warm periods and falls during cold periods, very probably showing considerably more time lag as a second-order effect caused by the growth and shrinkage of glaciers. The general trend of the sea-level curve of Figure 1 was postulated on the basis of radiocarbon dates; the fluctuations in the curve were postulated on the basis of distribution of sediment characteristics reflecting current directions and the morphology

Geological Society of America Bulletin, v. 72, p. 1707–1712, 2 figs., November 1961

Contributions from the Scripps Institution of Oceanography, New Series, 1321

Reproduced by Permission

of the areas of the Texas shelf covered with the basal sands of the Holocene transgression. Assuming that the interpretation is correct (Curray, 1960, p. 256–258), the relict shoreline deposits can determine fairly precisely the heights of sea level at the beginnings and ends of the brief regressions, but the dates are much less certain. The comparisons of Figure 1 cannot, therefore, be used to estimate the amount of time lag of sea level behind the causative climatic changes. The comparison is made only to demonstrate that a correlation may exist between climatic fluctuations and sea-level fluctuations.

Broecker *et al.* (1960) have attempted to demonstrate evidence for an abrupt change in climate about 11,000 years ago. Examination of their evidence shows two things: (1) A rather abrupt change in climate (*i.e.*, Atlantic surface-water temperature) occurred between about 15,000 B.P. and 7000 B.P. It is perhaps an unnecessary oversimplification to average the occurrence of this change to a single date such as 11,000 years. (2) The details of this

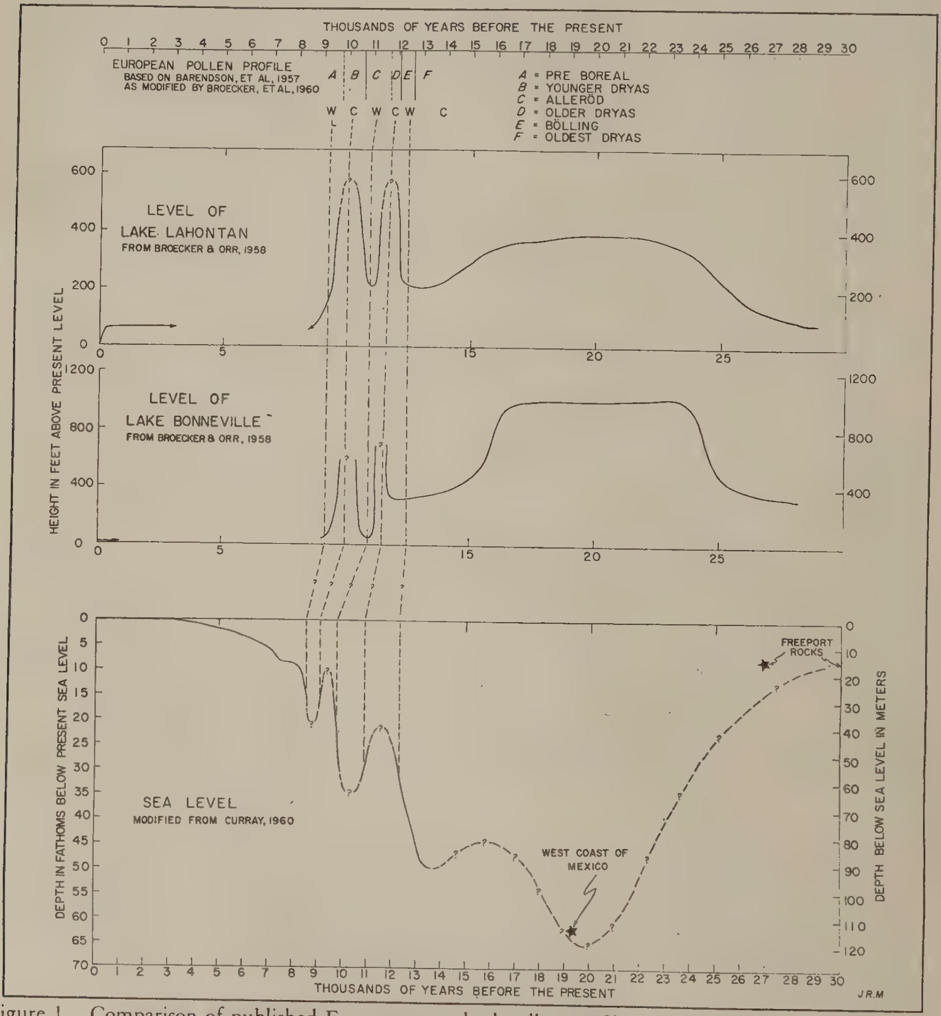

Figure 1. Comparison of published European standard pollen profile with curves for Great Basin lake levels and sea level. Curve for sea level modified to hit present level at 3000 B. P. on basis of Gould and McFarlan (1959), Byrne, LeRoy, and Riley (1959), and Jelgersma and Pannekoek (1960)

climatic change, as revealed by Great Basin lake levels and the European pollen profile, show a complex sequence of fluctuations. These fluctuations are not at all incompatible with the change in ocean-surface temperature and have been damped out of the record. The fluctuations appear to be present, however, in the record of sea level during approximately the period of time of most rapid rise, from about 15,000 to 7000 B.P. It would seem appropriate to re-examine the records of this period of time. We are probably attaching undue significance to the date 11,000 when we should be referring to a period of transition covering several thousand years, still rather abrupt in terms of the length of time involved in the Wisconsin.

Use of the time 11,000 B.P. seems particularly inappropriate in referring to the time of triggering the end of the glaciation by freezing over the Arctic Ocean (Ewing and Donn, 1956). Most of the published estimates of the position of sea level for this time agree that approximately half the water had been returned to the oceans from the late Wisconsin glaciers. Events at 11,000 could not, then, have triggered the end of the glaciation, but may instead have helped to complete a process already well started.

Prior to 15,000 B.P.

Broecker (1961) has rejected the negative argument by McFarlan that sea level was constant at a level of − 250 feet from sometime prior to 35,000 B.P. until about 18,500 B.P. He suggested the alternative hypothesis that sea level dropped between 25,000 B.P. and 18,000 B.P., citing as evidence the Great Basin lake levels (Broecker and Orr, 1958), studies of ice-sheet advances in the Lake Erie to southern Ohio area (Flint and Rubin, 1955), pollen sequences of northern Europe and the Paudorf interstadial (deVries, 1958), and oxygen-isotope and coarse-fraction studies of deep-sea cores (Emiliani, 1955; Broecker *et al.*, 1958). The study of the continental shelf off Texas further corroborates Broecker's suggestion of lowering of sea level following an interstadial prior to 25,000 B.P.

There is no evidence from the shelf off Texas of a long-continued stillstand of sea level at − 250 feet (42 fathoms). Such a stillstand would have had a profound effect on the continental shelves of the world and particularly on the areas such as parts of the eastern Texas shelf where present deposition is negligible. Extensive terraces and submerged deltas would have been formed at this depth; shore-line features and deposits would be widespread; and the banks in the Gulf of Mexico would show pronounced terraces cut into their sides, or else they would have been planed off to this level. Detailed bathymetry of the eastern Texas shelf (Curray, 1960, p. 226–227) shows marked changes in gradient at 35 fathoms (215 feet) and 65 fathoms (390 feet), but nothing at 250 or 300 feet. These latter depths lie on the slightly steeper outer shelf, devoid of significant escarpments or shore-line features. Although relict shore-line deposits are rather widespread on the sandy part of the shelf, there is no evidence of especially extensive development of such deposits in the 250- to 300-foot depth range.

The bathymetry of the rock, shell, coral, and Lithothamnion banks on this shelf was studied by Parker and Curray (1956) by plotting a histogram of the depths to the tops of 130 banks. The most frequent occurrences of bank tops are at about 9, 32, and 48 fathoms (54,192 and 288 feet), suggesting periods of erosion at or near sea level at these depths. Terraces observed in the sides of the better surveyed banks fall at approximately these same depths. If sea level had stayed at − 250 feet (42 fathoms) for more than 15,000 years, many of the banks would show flat tops or terraces at this level. The 48-fathom mode of the histogram of bank tops, and the occasional low escarpments in the sediments on the shelf at 45 to 50 fathoms (Curray, 1960, p. 259) do not suggest a long-continued stand of sea level.

A very recently obtained date from the continental shelf south of Mazatlan, Mexico, corroborates the suggestion (Curray, 1960, p. 258–259) that sea level was at about − 65 fathoms between 18,000 and 20,000 B.P. A sample (C-331) dredged by the writer from near the shelf edge at 62½ fathoms about 60 nautical miles south of Mazatlan (22° 06.7′ N. Lat., 106° 17.8′ W. Long.) consists of shells identified by Robert H. Parker (personal communication) as predominantly shallow-water organisms. A sample of *Strombus grannulatus*, with living depth range of 1 to 10 fathoms (Parker, personal communication), gave a C^{14} date of 19,300 ± 300 B.P.

Little is known of the stability of this Mexican shelf except from an uncompleted study of the morphology and sediments by the writer. Both the development of the wide strand plain along the coast and the depths of

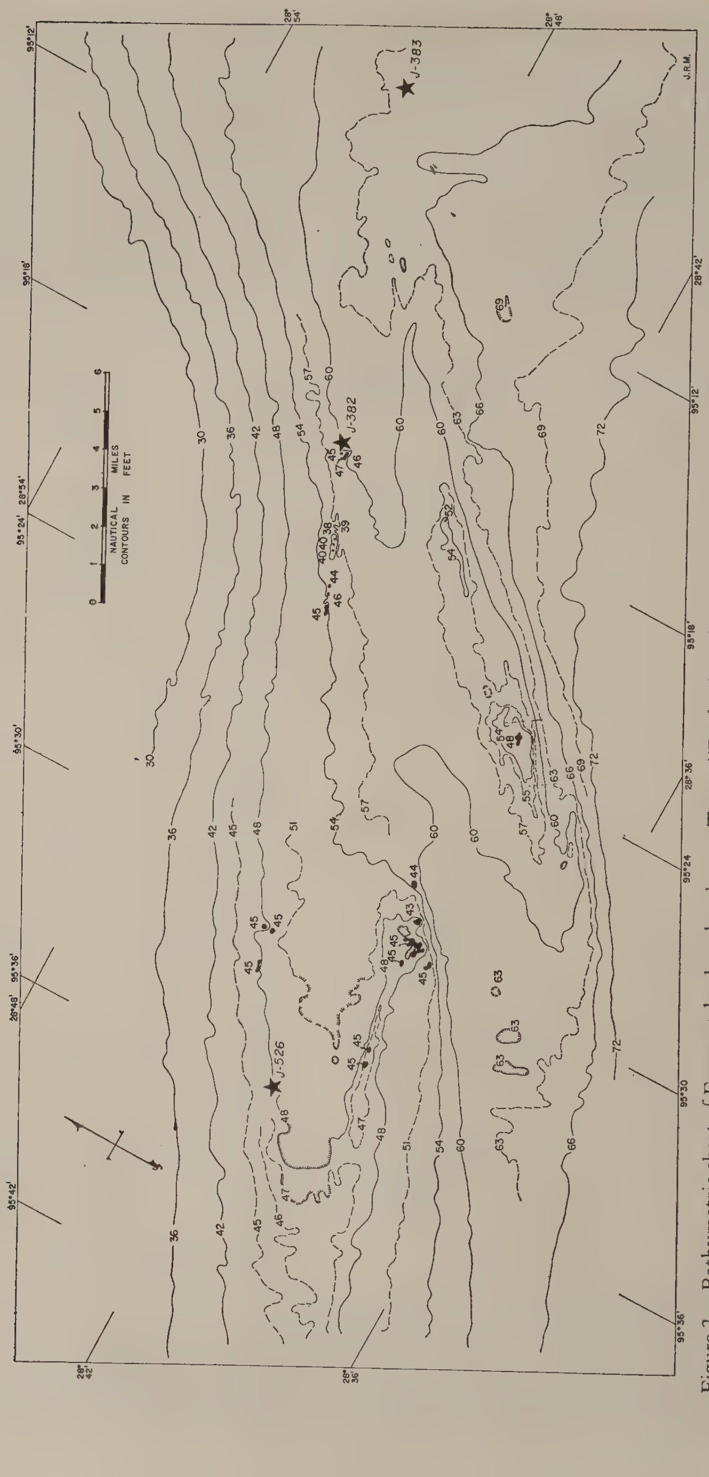
95°12'
28° 54'
28° 48'
95°18'
95°24'
28°54'
95°30'
95°36'
28°48'
95°42'
28° 42'
28° 36'
28°42'
95°12'
95°18'
28°36'
95°24
95°30
95°36'
0
1
2
3
4
5
6
NAUTICAL MILES
CONTOURS IN FEET
J-383
J-382
J-526
J.R.M.
30
36
42
45
48
51
54
57
60
63
66
69
72
38
39
40
44
46
47
43
52
55
64

Figure 2. Bathymetric chart of Freeport bank and rock area, Texas. "Rock Pinnacles" shown in black with depths to tops in feet. Samples and observations at locations indicated with stars. Soundings from unpublished plotting sheets, Coast and Geodetic Survey

relict shore-line deposits on the shelf suggest, but certainly do not prove, that the area has been relatively stable during this time.

Some additional evidence on the position of sea level prior to 20,000 B.P. comes from dates from the shallow shelf off Freeport, Texas (Curray, 1960, p. 225, 255, 256). Two pre-Tazewell dates were obtained from a line of isolated rock pinnacles at about 8 fathoms in this area. The rocks on two pinnacles (J-382 and J-383) were examined by SCUBA diving and found to be calcareous-cemented beachrock and coquina. A radiocarbon date of 26,900 ± 1800 years was obtained on *Crassostrea virginica* selected by Robert H. Parker (sample J-383, Fig. 2). In line with these rocks and farther west is rough bottom of shells and coquina (J-526), which give a date of 32,500 ± 3500 B.P. from *Rangia cuniata* and *Crassostrea virginicia*, also selected by Parker.

The low sediment bank in the 60-foot contour off Freeport (Fig. 2) is probably a Holocene feature formed during the transgression. The rock pinnacles, rising to 15 feet above the adjacent bottom, are arranged in a line at an angle to the sediment bank. These rocks probably represent the few remaining remnants of a beach-line development from an interstadial approximately 30,000 years ago. Parts of the beach were cemented to form hard beachrock and coquina and survived the long subaerial exposure. The nature of the other "rocks" shown in Figure 2 has not been investigated, but they probably hold some of the record of a complex sequence of climatic and sea-level fluctuations.

Francis P. Shepard (personal communication) reports new dates on shells from 5- and 12-foot elevated terraces on Hawaii of 24,000 ± 700 and 31,400 ± 1200 B.P. respectively. The stability of Hawaii is certainly questionable, but these dates may indicate an approximation of the position of sea level at that time.

None of this evidence has any bearing on the probability of stands of sea level lower than − 65 fathoms, but no dates are yet available to determine when these low stands occurred. It is suggested here that these low stands may have occurred in the early Wisconsin, prior to the 25,000 to 30,000 year interstadial.

Conclusions

(1) The general trend of dates for the last 17,000 years presented by McFarlan agrees with published results of many other investigators.

(2) The sequence of climatic events "at about 11,000 years ago" was not a simple unidirectional change, but was instead a complex sequence of fluctuations in climate occurring between about 15,000 and 7000 B.P., which also affected sea level. Warming at 11,000 B.P. could not have triggered the end of the glaciation because by that time approximately half the water had been returned to the oceans by the glaciers. We should not refer to the end of glaciation as 11,000 B.P. because it was more probably a period of transition and fluctuation lasting several thousand years. The Holocene/Pleistocene sedimentary contact along our continental shelves and coastal plains is a time-transgressive unconformity, older than 11,000 on the outer shelves, and younger inside of approximately 25 to 35 fathoms.

(3) There is no corroborating evidence from the rather densely sampled and very well-sounded shelf off Texas of a stillstand of the sea at −250 feet (42 fathoms) for a duration of many thousands of years.

(4) Preliminary studies of the continental shelf off the west coast of Mexico corroborate previous suggestions that sea level was at about −65 fathoms between 18,000 and 20,000 years ago, at the height of the Tazewell glaciation.

(5) Isolated remnants of a shore-line deposit at a depth of 8 fathoms off Freeport, Texas, give radiocarbon dates suggesting an interstadial somewhere around 30,000 years ago.

Acknowledgments

This work was sponsored by the American Petroleum Institute Project 51. Francis P. Shepard, Robert H. Parker, and Tj. H. van Andel have contributed significantly to this study and to reviewing the manuscript.

References Cited

Barendson, G. W., Deevey, E. S., and Gialenski, L. J., 1957, Yale radiocarbon measurements III: Science, v. 126, p. 908–919

Bennema, J., 1954, Holocene movements of land and sea-level in the coastal area of the Netherlands: Geologie en Mijnbouw, v. 16e, (n. ser.), p. 254–264

Broecker, W., 1961, Radiocarbon dating of Late Quaternary deposits, south Louisiana: A discussion: Geol. Soc. America Bull., v. 72, p. 159–162

Broecker, W. S., and Orr, P. C., 1958, The radiocarbon chronologies of Lake Lahontan and Lake Bonneville: Geol. Soc. America Bull., v. 69, p. 1009–1032

Broecker, W. S., Ewing, M., and Heezen, B. C., 1960, Evidence for an abrupt change in climate close to 11,000 years ago: Am. Jour. Sci., v. 258, p. 429–448

Broecker, W. S., Turekian, K. K., and Heezen, B. C., 1958, The relation of deep sea sedimentation rates to variations in climate: Am. Jour. Sci., v. 256, p. 503–517

Byrne, J. V., LeRoy, D. O., and Riley, C. M., 1959, The chenier plain and its stratigraphy, southwestern Louisiana: Gulf Coast Assoc. Geol. Socs. Trans., v. 9, p. 237–260

Curray, J. R., 1960, Sediments and history of Holocene transgression, continental shelf, northwest Gulf of Mexico, p. 221–266 *in* Shepard, F. P., *et al.*, *Editors*, Recent sediments, northwest Gulf of Mexico, 1951–1958: Am. Assoc. Petroleum Geologists, 394 p.

deVries, Hl., 1958, Radiocarbon dates for upper Eeem and Wurm-interstadial samples: Eiszeitalter und Gegenmark, Band 9, p. 10–17

Emiliani, C., 1955, Pleistocene temperatures: Jour. Geology, v. 63, p. 538–578

Ericson, D. B., Broecker, W. S., Kulp, J. L., and Wollin, G., 1956, Late-Pleistocene climates and deep-sea sediments: Science, v. 124, p. 385–389

Ewing, M., and Donn, W. L., 1956, A theory of the ice ages: Science, v. 123, p. 1061–1066

Fairbridge, R. W., 1958, Dating the latest movements of the Quaternary sea level: N. Y. Acad. Sci. Trans., ser. 2, v. 20, p. 471–482

—— 1960, The changing level of the sea: Scientific American, v. 202, p. 70–79

Flint, R. F., and Rubin, Meyer, 1955, Radiocarbon dates of pre-Mankato events in eastern and central North America: Science, v. 121, p. 649–658

Godwin, H., Suggate, R. P., and Willis, E. H., 1958, Radiocarbon dating of the eustatic rise in ocean-level: Nature, v. 181, p. 1518–1519

Gould, H. R., and McFarlan, E., Jr., 1959, Geologic history of the chenier plain, southwestern Louisiana: Gulf Coast Assoc. Geol. Socs. Trans., v. 9, p. 261–270

Jelgersma, S., and Pannekoek, A. J., 1960, Post-glacial rise of sea level in the Netherlands (A preliminary report): Geologie en Mijnbouw, v. 39, p. 201–207

McFarlan, E., Jr., 1961, Radiocarbon dating of Late Quaternary deposits, south Louisiana: Geol. Soc. America Bull., v. 72, p. 129–158

Parker, R. H., and Curray, J. R., 1956, Fauna and bathymetry of banks on continental shelf, northwest Gulf of Mexico: Am. Assoc. Petroleum Geologists Bull., v. 40, p. 2428–2439

Shepard, F. P., 1960, Rise of sea level along northwest Gulf of Mexico: p. 338–344 *in* Shepard, F. P., *et al.*, *Editors*, Recent sediments, northwest Gulf of Mexico, 1951–1958: Am. Assoc. Petroleum Geologists, 394 p.

Shepard, F. P., and Suess, H. E., 1956, Rate of postglacial rise of sea level: Science, v. 123, p. 1082–1083

van Straaten, L. M. J. U., 1954, Radiocarbon dating and changes of sea level at Velzen (Netherlands): Geologie en Mijnbouw, n. ser., v. 16, p. 247–253

SCRIPPS INSTITUTION OF OCEANOGRAPHY, LA JOLLA, CALIF.

MANUSCRIPT RECEIVED BY THE SECRETARY OF THE SOCIETY, APRIL 24, 1961

Addendum

After this note was submitted, the following papers appeared or were called to the writer's attention:

Flint, R. F., and Brandtner, F., 1961, Climatic changes since the last interglacial: Am. Jour. Sci., v. 259, p. 321–328

Frye, J. C., and Willman, H. B., 1960, Classification of the Wisconsinian Stage in the Lake Michigan glacial lobe: Ill. Geol. Survey Circ. 285, 16 p.

—— 1961, Continental glaciation in relation to McFarlan's sea-level curves for Louisiana: Geol. Soc. America Bull., v. 72, p. 991–992

Each of these papers shows warmer climate or glacial retreat between approximately 25,000 and 30,000 years ago, colder climate or glacial maximum approximately 18,000 to 20,000 years ago, and short-period fluctuations between 15,000 and 7000 years ago, corroborating the sea-level curve proposed in this note.

(938)

Reprinted from the Proceedings of the NATIONAL ACADEMY OF SCIENCES
Vol. 47. No. 11, pp. 1726–1733. November, 1961.

*IN SITU DETECTION AND ESTIMATION OF CHLOROPHYLL AND OTHER PIGMENTS IN THE OCEAN**

BY JOHN E. TYLER

VISIBILITY LABORATORY, SCRIPPS INSTITUTION OF OCEANOGRAPHY, LA JOLLA,
CALIFORNIA

Communicated by Roger Revelle, September 25, 1961

The scattering centers in ocean water and in other natural scattering-absorbing media give rise to space light in the medium. This space light contains quantitative information about the absorption spectra of the components of the medium. By appropriate spectral measurements this information can be obtained in a form which may be useful for estimating the standing crop of phytoplankton in the ocean as a function of location or time, for *in situ* identification of plankton communities, for comparing and classifying waters with respect to clarity and productivity, for measuring the absorption spectra of living marine organisms in their natural environment, and for studying various other aspects of optically extensive scattering-absorbing media.

Theory.—In a source-free homogeneous scattering-absorbing medium, the change in field radiance, N_r, as a function of position, r, at some point along any path of sight, is given by the equation of transfer for radiance.[1]

$$\frac{dN_r}{dr} = -\alpha N_r + N_* \qquad (1)$$

Contributions from the Scripps Institution of Oceanography, New Series, 1322
Reproduced by Permission

The constant α in this equation is the total attenuation coefficient commonly determined from transmittance measurements by means of equation (2),

$$T = e^{-\alpha r} \tag{2}$$

and is equal to the sum of the absorption coefficient and the scattering coefficient. N_* is the radiance per unit length at the point r on the path, generated by scattered light. N_* is called the path function and is defined by Preisendorfer[1] as follows:

$$N_* = \frac{N_l^*}{l} \tag{3}$$

N_l^* being the recorded radiance for a path of length l. All quantities in equations (1)–(3), of course, express the conditions along a particular path.

In environmental optics a situation is commonly found for which N_r is substantially a constant over distances that are long compared to the path that contributes significantly to the value of N_r at the point of measurement. In ocean water, for example, N_r is substantially constant for great distances along any specified horizontal direction if the lighting on the surface of the water is uniform and the water is homogeneous. A similar situation can be found in lakes, in the atmosphere, and in large bodies of ice. For these situations

$$\frac{dN_r}{dr} = 0$$

and equation (1) can be written (4)

$$\alpha = \frac{N_*}{N_r}$$

All three quantities in equation (4) will vary with the concentration of scattering particles and with the concentration of absorbing material. For constant conditions of scattering and absorption the quantities also will vary with wavelength.

Measurements of space light, in accordance with equation (4), can be used together with appropriate calibration curves as a basis for *in situ* spectroscopy of natural scattering-absorbing media.

In order to conform strictly with the assumptions employed in obtaining equation (4), measurements of N_r and N_* must be made in a horizontal direction under lighting conditions which are uniform over relatively large areas of the surface of the hydrosol. Such conditions are commonly provided by natural sun and sky light. Since natural light is variable with respect to both time and wavelength, and especially because of the presence of Fraunhofer lines, it is essential to use a measuring technique which makes both measurements, (N_r and N_*), with an identical bandwidth and in a short time. This is no real hardship since many flicker techniques have been developed which record a ratio such as that required by equation (4).

Experimental.—Before proceeding to measurements at sea, it was considered important to ascertain the sensitivity of the method, called "spacelight spectroscopy," in the laboratory; that is, to determine the capability of the method to describe the absorption spectra of a dilute scattering-absorbing medium. To accomplish this in the limited volume of water available in even a large tank, it was necessary to proceed in a somewhat different fashion. The experimental work, described below, demonstrates the essential capability of the method, but does not demonstrate its capability to determine the absolute values of all the quantities in equation (4).

The scattering-absorbing medium (hydrosol) was contained outdoors in a 1300-gallon open-top tank with a window installed in the side so that observations could be made horizontally through the hydrosol about 2.5 feet below the water surface. A minus-green dye, having a maximum absorption coefficient at 550 mμ of 3.098 per cm at a concentration of 0.237×10^{-4} gms/cc. was added in varying amounts to a full tank of filtered tap water containing a fixed amount of scattering agent.

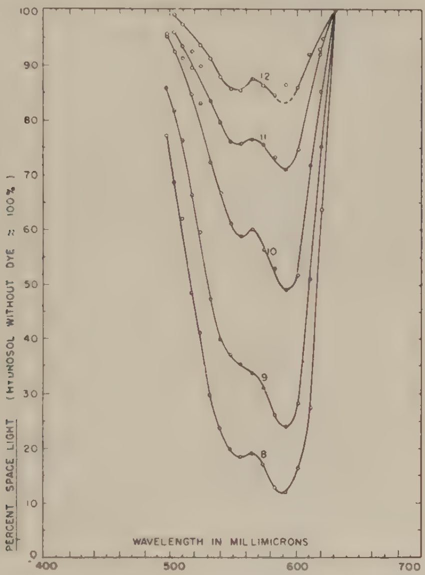

FIG. 1.—The ratio of the spacelight radiance from the dyed solution to the spacelight radiance from the original water-base scattering medium without dye is shown as a function of wavelength for the region of the major absorption bands of the dye. To compensate partially for variation in natural lighting, the curves have been normalized at 630 mμ and are consequently not quantitatively arranged.

The ratio of the space light generated by the sample to that generated by the hydrosol without dye was determined. The spectral distribution of the space light in a horizontal direction generated under sun and sky light was recorded by means of a small prism spectrograph. The maximum path length through the hydrosol was 7 feet and at the smaller concentrations the far wall of the tank was not entirely hidden at all wavelengths by the space light. Since the wall of the tank was painted gloss black, it had the effect of returning to the spectrograph too little light in the region of high transmittance of the dye, and it thus reduced the sensitivity of the experiment to some extent.

Figure 1 shows a series of curves obtained from spacelight measurements using the hydrosol without dye as a standard. Because of small differences in exposure for the different concentrations, the curves are normalized at 630 mμ. The bandwidth for these measurements was set at 10 mμ in the green region of the spectrum but varied elsewhere in accordance with the dispersion of the prism. Table 1 gives the measured dye concentrations for each curve.

TABLE 1

Concentration of Dye in the Solution Used to Obtain the Spectrophotometric Curves of Figure 2 and the Spacelight Measurements in Figure 1

Curve No.	Concentration, gms/cc	
	Spectrophotometry	Spacelight measurements
1	0.237×10^{-4}	
2	0.136×10^{-4}	
3	0.0682×10^{-4}	
4	0.0341×10^{-4}	
5	0.0170×10^{-4}	
6	0.0085×10^{-4}	
7	0.00425×10^{-4}	
8		0.0006×10^{-4}
9		0.000384×10^{-4}
10		0.000192×10^{-4}
11		0.000096×10^{-4}
12		0.000048×10^{-4}

If curve 11 of Figure 1 is taken to represent positive identification of the absorption band at 550 mμ, then the technique of spacelight spectroscopy has made the identification at a concentration level of 0.96×10^{-8} gms/cc (0.0096 mg/liter). Lower levels of concentration should be detectable with an unobstructed path of sight.

Figure 2 shows a series of spectrophotometric curves run at various concentrations of the same dye in a 1-cm. cell, using a 10-mμ bandwidth throughout the spectrum. A 1-cm cell of distilled water was used for comparison. It will be

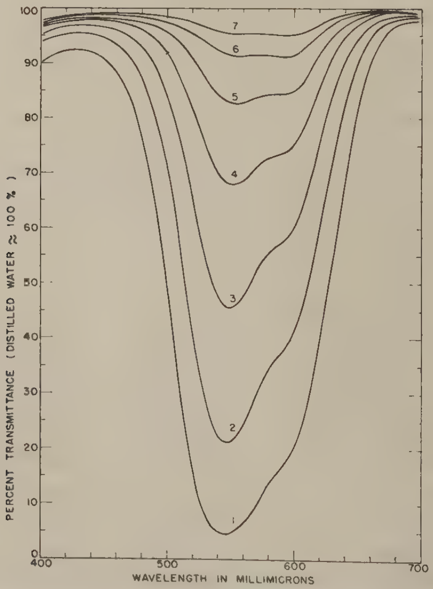

Fig. 2.—Spectrophotometric curves made on a G.E.-type spectrophotometer of various concentrations of the minus-green dye in a 1-cm cell.

observed from Figure 2 that the minus-green dye exhibits departures from Beer's law; in particular, the relative strength of the two absorption minima reverses with dilution. This is barely discernable in curve 7 of Figure 2 and has been confirmed by using a 10-cm cell. In Figure 1 these two bands appear in the relative strength characteristic of great dilution, thus demonstrating one of the characteristics of spacelight measurements.

An experiment in which the particles (rather than the water) contained the dye is perhaps of greater interest to marine biologists. In this experiment, suitable nutrients for the growth of the fresh-water plant *Scenedesmus* were added to a tank of filtered tap water, and the tank was then seeded with a pure culture of this plant. Mirrors were installed in the tank in such a way that the path length was increased to about 21 feet. Spectroradiometric measurements of the space light were made daily. In order to remove the wavelength variability of the natural sun and sky light, spectral data from the *Scenedesmus* cultures were divided at

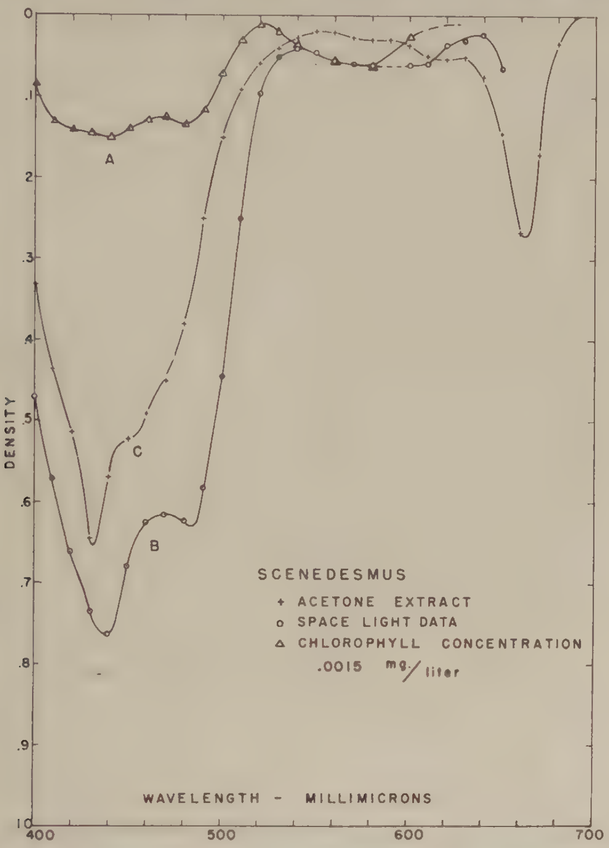

FIG. 3.—Curve A is the spectrum of *Scenedesmus* obtained *in situ*. The chlorophyll concentration was determined to be 0.0015 mg/liter. Curve B is the spectrum of *Scenedesmus* obtained *in situ*. The chlorophyll concentration is estimated to be 0.06 mg/liter. Curve C is the spectrum of the acetone extract of *Scenedesmus* given for comparison with curve B.

each wavelength by spectral measurements made on the space light from the nutrient solution without the *Scenedesmus.*

In addition to spacelight measurements, the chlorophyll concentration was determined daily by standard techniques used for biological studies of the ocean. These techniques yield spectrophotometric data on an acetone extract of the chlorophyll from a sample of known volume. Comparison of the two methods reveals that detection of the chlorophyll by spacelight spectroscopy was achieved with the present method at a chlorophyll concentration of about 0.0015 mg/liter.

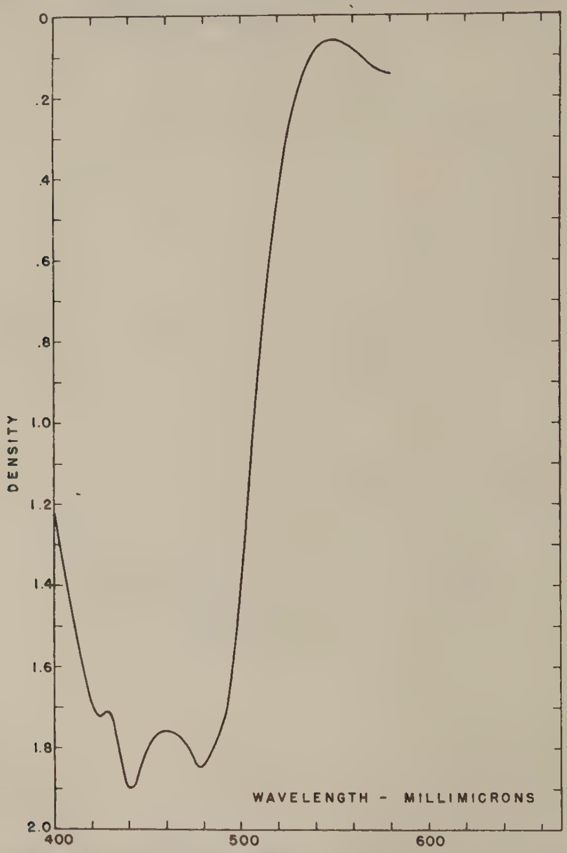

Fig. 4.—A more detailed spectrum of *Scenedesmus in situ* obtained from a highly concentrated culture. The chlorophyll concentration is estimated to be over 0.08 mg/liter.

The spectrum obtained at this concentration is shown in curve A of Figure 3. Also in Figure 3 the spectrum of the living organism at a concentration of about 0.06 mg/liter (curve B) is compared with the absorption spectrum obtained from an acetone extract of the chlorophyll (curve C). For ease of comparison, two curves have been chosen that exhibit approximately the same density differences between maximum and minimum values. It would be expected that curve B would show some differences from curve C since other pigments, in addition to chlorophyll, contribute to the absorption spectrum of the living plant. In addition to this,

(944)

the spectrum of chlorophyll may be different at the great dilutions present in the culture tank from that in acetone in the spectrophotometric cell. The spectrum of a still more concentrated culture of the living plant showing more detail than curve B is shown in Figure 4. The cultures represented by curve B of Figure 3 and by Figure 4 were very concentrated and overtaxed the normal extraction methods. The values given for chlorophyll concentration for these two curves are estimated.

Discussion.—Spacelight spectroscopy is based on the total attenuation coefficient α and in this respect differs from other spectrophotometric techniques which are generally based on the absorption coefficient, a. For biological oceanography there may be an important advantage in using the total attenuation coefficient. Phytoplankton and the particulate matter associated with them are generally large enough so that the scattering from them is nonselective with respect to wavelength. Ideally, therefore, one can assume that variations of α versus wavelength are due to absorption only. In principle it follows that the minimum spectral value of α, minus the absorption of H_2O at this minimum, must most nearly represent the total scattering coefficient and that the difference between the minimum value of α and its maximum value at some other wavelength must represent, at that wavelength, the absorption coefficient of the absorbing constituents other than the water. Thus the curve of α versus wavelength can be used to estimate both the scattering and the absorbing coefficients of the medium.

The normal ratio of scattering coefficient to absorption coefficient for a specific organism should soon become apparent and departures from this normal may have important biological significance.

There is, of course, some choice in the selection of a "standard" with which to compare N_r. The choice of N_* as a standard leads to the determination of α, as we have seen, but it may not always be necessary or advantageous to determine α. For example, the data of Figure 1 are not values of α and yet they adequately identify the dye, as previously discussed.

Similarly, one might wish to make a laboratory study of a pure strain of phytoplankton using an equivalent path of water with scattering agent but no plankton as a standard. This technique would have the advantage of cancelling out the absorption characteristics of the water. The measurements on *Scenedesmus* indicate that the method can be expected to provide useful detection of plant pigments in the ocean at concentrations down to at least 1.5 micrograms/liter. It is likely that this detection level will be improved, perhaps by a factor of 2, in ocean measurements where there are no mechanical limits to the path length. Holmes[2] has measured surface chlorophyll a in the Pacific and has found values ranging from 10.2 to 0.719 micrograms/liter in rich areas with lower values down to 0.037 micrograms/liter in poor areas. Thus spacelight spectroscopy should be a useful tool in areas of high standing crop. Its application to areas of low standing crop remains to be tested.

The author wishes to express thanks and appreciation to Ralph A. Lewin, Division of Marine Biology at Scripps Institution of Oceanography for his help in isolating and growing the pure strains of *Scenedesmus* and for his counsel in growing this plant experimentally in large volumes; and to Robert W. Holmes and Mrs. Anne N. Dodson, also of the Division of Marine Biology, for their help in determining chlorophyll concentration.

(945)

The experimental tank and other equipment used in this research was loaned by the Bureau of Ships. The small spectrograph was loaned by Waldo K. Lyon of the U. S. Navy Electronic Laboratory. The loan of this equipment is gratefully acknowledged.

---

* This research was supported by a grant from the National Science Foundation, Earth Science Division.

[1] Radiative transfer theory has been applied extensively to problems in hydrologic optics by R. W. Preisendorfer. See, for example, *Jour. Mar. Res.*, **18**, 1–9 (1959); also U. S. Govt. Reports PB 153995, PB 153994, PB 153993, PB 153987, PB 153992, and PB 153990.

[2] Holmes, R. W., "Surface Chlorophyll 'A,' Surface Primary Production, and Zooplankton Volumes in the Eastern Pacific Ocean," in *Rapp et Proc.-Verb., Cons. Internat. Explor. de la Mer.*, 144, 109–116 (1958).

(946)

October 1, 19
pp.64-69.

A Distributional List of Southern California Opisthobranchs

by

JAMES R. LANCE

Scripps Institution of Oceanography, La Jolla, California

The opisthobranch fauna inhabiting the intertidal regions along the coast of California has become comparatively well known. The early species descriptions of Cooper (1862, 1863), Bergh (1879, 1894), and Cockerell (1901-1915), while of a rather cursory nature, form the basis upon which more precise investigations by later workers have been carried out. Outstanding among these reports are the excellent anatomical accounts by MacFarland (1905-1929) of Central California forms. The publication of a distributional list of all the known species from the Pacific Coast of North America up to 1926 (O'Donoghue) has also contributed greatly to our knowledge of these mollusks. Of more recent date is a list by Smith and Gordon (1948) of species from the Monterey area, and a key by Steinberg (1954) to the Central California forms. Marcus (1961) has described 12 new species from this coast and provided anatomical details for 38 others.

In view of additional data obtained by various observers and from my own collections along the coasts of California and Baja California, Mexico, during the past several years, it seems appropriate to offer a synopsis of the bathymetric and geographic ranges of Southern California opisthobranchs as they are now known. Miss Joan Steinberg has kindly provided me with information regarding the northern ranges of many species, and for bathymetric observations I am indebted to the late Conrad Limbaugh, to Mrs. Limbaugh, and to Mrs. Homer Rydell.

The marine province of Southern California is here geographically defined as that region between Point Conception and the Mexican border. Excluding the cephalaspideans and pteropods, all the regional species for which there exist descriptions sufficient to permit identification are included. In view of the chaotic taxonomic state of the genus Triopha, it was deemed advisable to include the names of all the species reported from Southern California although probably only two distinct forms occur.

The systematic arrangement here followed is that of Odhner (1939). For convenience, the habitats are divided into (1) bays, lagoons, and estuaries with their associated boat landings, pilings, wharfs, buoys, etc.; (2) intertidal; (3) subtidal; and (4) the kelp canopy which, within the limits of these observations, consists exclusively of the giant brown kelp, Macrocystis pyrifera, and grows in 20-100 feet of water. The quantitative observations are based on some 140 field trips over the past 10 years, principally to Mission and San Diego Bays, Point Loma, the Coronados Islands, and the kelp beds off La Jolla and San Diego.

The degrees of abundance are arbitrarily designated as (1) common, which, for example, in the case of Corambella sp., may number as many as 140 individuals per square foot of kelp surface; (2) uncommon, such as Crimora coneja, one or two specimens of which may be observed every second or third trip to Point Loma; and (3) rare, indicating that very few individuals have ever been collected.

Examples of prey-predator associations such as that which exists between Armina californica and the sea pansy, Renilla koellikeri, are noted. The substrata for the intertidal and subtidal habitats are rocky unless stated otherwise.

The new ranges are followed by the old in parentheses. A species name preceded by a single asterisk (*) indicates that I have never collected that form. Two asterisks (**) are used to signify new species whose descriptions will shortly appear in this journal. A list of positions for the geographic points mentioned is included.

Contributions from the Scripps Institution of Oceanography, New Series, 1323

Reproduced by Permission

(948)

ALASKA		
Sitka	57° 03' N	135° 20' W
BRITISH COLUMBIA		
Nanaimo, Vancouver Island	49° 10' N	123° 56' W
CALIFORNIA		
Humboldt Bay	40° 45' N	124° 14' W
Gualala	38° 48' N	123° 30' W
Bodega Bay	38° 18' N	123° 03' W
Dillon Beach	38° 14' N	122° 58' W
Tomales Bay	38° 14' N	122° 59' W
San Francisco Bay	37° 47' N	122° 27' W
Moss Beach	37° 32' N	122° 31' W
Santa Cruz	36° 58' N	122° 01' W
Pacific Grove	36° 38' N	121° 55' W
Monterey	36° 37' N	121° 53' W
Cayucos	35° 26' N	120° 54' W
Pismo Beach	35° 09' N	120° 38' W
Point Conception	34° 27' N	120° 28' W
Santa Barbara	34° 25' N	119° 41' W
Santa Cruz Island	34° 01' N	119° 41' W
San Pedro	33° 44' N	118° 16' W
Corona del Mar	33° 36' N	117° 54' W
Newport Bay	33° 36' N	117° 54' W
Laguna Beach	33° 32' N	117° 44' W
Catalina Island	33° 29' N	118° 36' W
Doheny Beach	33° 27' N	117° 39' W
La Jolla	32° 52' N	117° 15' W
San Diego	32° 42' N	117° 11' W
Point Loma	32° 40' N	117° 14' W
MEXICO		
Los Coronados Islands	32° 24' N	117° 14' W
Bahia Todos Santos	31° 52' N	116° 38' W
Bahia de Los Angeles	28° 55' N	113° 32' W
Isla Cedros	28° 22' N	115° 12' W
Punta Eugenia	27° 51' N	115° 05' W
La Paz	24° 10' N	110° 19' W
Cabo San Lucas	22° 52' N	109° 53' W
FLORIDA		
Manatee Bay	27° 30' N	82° 35' W
CHILE		
Islà de Chiloé	41° 52' S	73° 50' W

ANASPIDEA

Aplysiidae

Aplysiinae

Aplysia californica Cooper, 1863.

Common intertidally and subtidally to 40 feet. Bodega Bay to the Gulf of California.

* *Aplysia juliana* Quoy & Gaimard, 1832.

Cosmopolitan in warm seas. Coast of California.

Aplysia vaccaria Winkler, 1955.

Common intertidally. San Pedro to Point Loma (San Pedro to Doheny Beach).

Dolabriferinae

Phyllaplysia zostericola McCauley, 1960.

Common in bays and lagoons on the eelgrass, Zostera marina. San Juan Island to San Diego Bay (San Juan Island to Newport Bay).

NOTASPIDEA

Umbraculacea

Tylodinidae

Tylodina fungina Gabb, 1865.

Locally abundant intertidally and in bays on the yellow sponge, Verongia thiona. Cayucos to Todos Santos Bay (Santa Barbara Island to San Diego).

Pleurobranchacea

Pleurobranchidae

* *Pleurobranchus californicus* Dall, 1900.

Crescent City to San Diego (San Pedro to San Diego).

* *Pleurobranchus digueti* Rochebrune, 1895.

San Pedro to the Gulf of California.

SACOGLOSSA

Elysiacea

Elysiidae

Elysia hedgpethi Marcus, 1961.

Seasonally common intertidally, July through September. Tomales Bay to La Jolla.

Hermaeidae

Hermaeinae

Hermaeina smithi Marcus, 1961.

Seasonally common intertidally, January through June. San Juan Island to San Diego (Tomales Bay).

NUDIBRANCHIA

Doridacea

EUDORIDACEA

Cryptobranchia

Dorididae

Glossodoridinae

Cadlina flavomaculata MacFarland, 1905.

Uncommon intertidally and subtidally to 65 feet. Vancouver Island to Point Eugenia (Vancouver Island to San Diego).

Cadlina marginata MacFarland, 1905.

Common subtidally to 150 feet; not known from the intertidal. Vancouver Island to Point Eugenia (Vancouver Island to San Diego).

Cadlina sparsa (Odhner, 1921).

Rare intertidally and subtidally to 131 feet. San Diego to the Juan Fernandez Islands, Chile.

** *Cadlina sp.*

Rare subtidally to 140 feet. La Jolla to the Coronados Islands.

Glossodoris californiensis (Bergh, 1879).

Uncommon intertidally and subtidally to 100 feet. Monterey to the Coronados Islands (Monterey to San Diego).

Glossodoris macfarlandi (Cockerell 1902),

Uncommon intertidally at the southern end of its range; rare subtidally to 30 feet in the north. Monterey to the Coronados Islands (San Pedro to San Diego).

Glossodoris porterae (Cockerell, 1902).

Uncommon intertidally. Monterey to Cedros Island (Monterey to San Diego).

SUBFAMILY *incertae sedis*

* *Glossodoridiformia alba* O'Donoghue, 1927.

Intertidal. Laguna Beach.

Thorunninae

Rostanga pulchra MacFarland, 1905.

Uncommon intertidally and subtidally to 60 feet. Vancouver Island to Chile; Japan.

* *Aldisa sanguinea* (Cooper, 1862).

Rare intertidally. Bodega Bay to San Diego; Japan.

Archidoridinae

Archidoris montereyensis (Cooper, 1862).

Rare intertidally and uncommon subtidally to 150 feet. Alaska to San Diego.

Discodoridinae

Anisodoris nobilis (MacFarland, 1905).

Common on bay boat landings and pilings and subtidally to 100 feet; rare intertidally. Vancouver Island to the Coronados Islands (Vancouver Island to Laguna Beach).

Diaulula sandiegensis (Cooper, 1862).

Uncommon intertidally; common subtidally to 120 feet. Japan to Cape San Lucas (Japan to San Diego).

* *Discodoris heathi* MacFarland, 1905.

Rare intertidally. Vancouver Island to Laguna Beach.

PLATYDORIDINAE

* *Platydoris macfarlandi* Hanna, 1951.

Subtidal to about 516 feet. Pismo Beach.

Phanerobranchia

NONSUCTORIA

NOTODORIDIDAE

Aegires albopunctatus MacFarland, 1905

Seasonally common intertidally, March through August; common subtidally to 100 feet. Vancouver Island to the Coronados Islands (Vancouver Island to San Diego).

POLYCERIDAE

Polycera atra MacFarland, 1905.

Seasonally common in bays on boat landings and pilings, April through August; rare intertidally and subtidally. San Francisco Bay to the Coronados Islands (Monterey to San Diego).

** *Polycera sp.*

Seasonally common on offshore kelp, June through September. Laguna Beach to the Coronados Islands.

Laila cockerelli MacFarland, 1905.

Sporadically common intertidally in the spring, at other times absent; uncommon subtidally to 110 feet. Vancouver Island to Cape San Lucas (Vancouver Island to San Diego).

TRIOPHIDAE

* *Triopha aurantiaca* Cockerell, 1908.

Laguna Beach to La Jolla.

Triopha carpenteri (Stearns, 1873).

Rare subtidally to 80 feet. Dillon Beach to San Diego; Japan (Dillon Beach to Laguna Beach; Japan).

* *Triopha catalinae* (Cooper, 1863).

Santa Cruz to Catalina Island.

* *Triopha grandis* MacFarland, 1905.

Monterey to Laguna Beach.

Triopha maculata MacFarland, 1905.

Seasonally common intertidally; rare subtidally to 60 feet. Bodega Bay to San Diego.

* *Triopha scrippsiana* Cockerell, 1915.

La Jolla.

Crimora coneja Marcus, 1961.
Uncommon intertidally. Point Loma.

SUCTORIA

Onchidorididae

Acanthodoris lutea MacFarland, 1925.

Very rare intertidally in the southern part of its range; seasonally abundant at Moss Beach. Moss Beach to Point Loma (Moss Beach to Cayucos).

Acanthodoris rhodoceras Cockerell & Eliot, 1905.

Seasonally common intertidally, April through July; rare subtidally to 60 feet. Dillon Beach to the Coronados Islands (Dillon Beach to San Diego).

Goniodorididae

Hopkinsia rosacea MacFarland, 1905.

Common intertidally; rare subtidally to 20 feet. Eureka to Point Loma (Gualala to Point Loma).

Ancula pacifica MacFarland, 1905.

Very rare intertidally. Moss Beach to Point Loma (Monterey to La Jolla).

Trapania velox (Cockerell, 1901).

Seasonally common on bay boat landings and pilings, July through October. San Francisco Bay to San Diego Bay (La Jolla).

Corambidae

Corambe pacifica MacFarland & O'Donoghue, 1929.

Seasonally common on colonies of the bryozoan, Membranipora serrilamella, growing on offshore kelp, January through September; at other times absent. Vancouver Island to Point Eugenia (Vancouver Island to Monterey).

***Corambella sp.*

This species shares the same habitat with the above form. Although their seasonal appearance coincides, Corambe pacifica seems to reach its maximum population density in March and April while Corambella sp. is most abundant during June and July. Vancouver Island to the Coronados Islands.

POROSTOMATA

Dendrodorididae

Dendrodoris albopunctata (Cooper, 1863).

Common intertidally and subtidally to 150 feet. Monterey to Point Eugenia (Monterey to Point Loma).

Dendronotacea

Tritoniidae

* *Tritonia exsulans* Bergh, 1894.

Intertidal and subtidal to 1'020 feet. Coast of Japan to Baja California (26° 14' N; 113° 13' W); Manatee Bay, Florida.

Tritonia festiva (Stearns, 1873).

Uncommon intertidally and subtidally to 80 feet. Vancouver Island to the Coronados Islands (Tomales Point to Corona del Mar).

* *Tritonia palmeri* Cooper, 1862.

San Pedro.

**Tritoniopsis aurantia* Mattox, 1955.

Catalina Island.

Hancockiidae

Hancockia californica MacFarland, 1923.

Uncommon intertidally at the northern end of its range, rare on floating kelp at the southern extremity; unknown from any intermediate point south of Monterey. Dillon Beach to Baja California (26° 43' N; 114° 29.5' W) (Monterey).

Dendronotidae

Dendronotus frondosus (Ascanius, 1774).

Rare intertidally and subtidally to 1'312 feet; uncommon on offshore kelp. Cosmopolitan in the Northern Hemisphere.

Dendronotus iris Cooper, 1863.

Rare subtidally to 85 feet. Vancouver Island to the Coronados Islands (Vancouver Island to Santa Barbara).

Phylliroidae

Cephalopyge trematoides (Chunn, 1889).

Rare; pelagic. Usually collected accidentally in plankton tows. Cosmopolitan.

Tethyidae

Melibe leonina (Gould, 1853).

Seasonally common on offshore kelp, March through September; at other times rare or absent. Alaska to La Paz Bay (Alaska to La Jolla).

Arminacea

EUARMINACEA

Arminidae

Armina californica (Cooper, 1862).

Locally common subtidally on sandy and muddy bottoms to 289 feet in association with the sea pansy, Renilla koellikeri, upon which it feeds; rare intertidally. Vancouver Island to Panama.

PACHYGNATHA

Antiopellidae

Janolus barbarensis (Cooper, 1863).

Seasonally common intertidally and in bays and lagoons, May through August. Santa Barbara to Point Loma (Santa Barbara to La Jolla).

Dironidae

* *Dirona albolineata* Cockerell & Eliot, 1905.

Rare intertidally and subtidally to 115 feet. Vancouver Island to Laguna Beach.

Dirona picta Cockerell & Eliot, 1905.

Seasonally common intertidally, June through August; at other times absent. Dillon Beach to Point Loma (Dillon Beach to La Jolla).

Eolidacea

PLEUROPROCTA

Coryphellidae

* *Coryphella cooperi* Cockerell, 1901.

San Pedro.

Coryphella piunca Marcus, 1961.

Uncommon intertidally and on boat landings; seasonally common on offshore kelp, April through June. Dillon Beach to the Coronados Islands (Dillon Beach to Point Pinos).

Flabellinidae

Flabellina iodinea (Cooper, 1862).

Uncommon intertidally; common subtidally to 120 feet. Vancouver Island to the Coronados Islands (Vancouver Island to San Diego).

ACLEIOPROCTA

Eubranchidae

Capellinia rustya Marcus, 1961.

Seasonally common on offshore kelp, February through August. San Francisco Bay to Bahia de Los Angeles (Monterey).

Fionidae

Fiona pinnata Eschscholtz, 1831.

Seasonally uncommon on floating wood, algae, buoys, etc., April through August. If present at all, there are often large numbers of individuals on the floating object. Cosmopolitan.

CLEIOPROCTA

Facelinidae

Hermissenda crassicornis (Eschscholtz, 1831).

The most common nudibranch in Southern California, intertidal and subtidal to 120 feet. Also common in bays and lagoons on mud flats, boat landings, and pilings. Sitka, Alaska, to Point Eugenia (Sitka, Alaska, to San Diego).

Phidianidae

** *Phidiana sp.*

Uncommon intertidally; common subtidally to 120 feet. Monterey to the Coronados Islands.

Aeolidiidae

Aeolidia papillosa (Linnaeus, 1761).

Seasonally rare intertidally and subtidally to 2'493 feet, February through May. Cosmopolitan.

Spurillidae

* *Spurilla chromosoma* Cockerell & Eliot, 1905.

Rare intertidally. San Pedro to Point Loma.

Literature Cited

Bergh, (Ludwig S.) Rudolph

1879. On the nudibranchiate gasteropod mollusca of the North Pacific ocean. Part I. Proc. Acad. Nat. Sci. Phila. 71-132, pls. 1-8.

——, ——

1894. Die Opisthobranchien. Bull. Mus. Comp. Zool. Harvard, 25 (10): 125-233, pls. 1-12.

Cockerell, Theodore Dru Alison

1901a. Three new nudibranchs from California. Jour. Malacol. 8 (3): 85-87.

——, ——

1901b. Notes on two Californian nudibranchs. Jour. Malacol. 8 (3): 121-122.

——, ——

1901c. A new *Tethys* (*ritteri*) from California. Nautilus, 15: 90-91.

——, ——

1908. Mollusca of La Jolla, California. Nautilus 21 (9): 106-107.

——, ——

1915. The nudibranchiate genus *Triopha* in California. Jour. Ent. Zool. Pomona Coll. 7 (4): 228-229, 2 textfigs.

Cockerell, T. D. A., & Charles Eliot

1905. Notes on a collection of Californian nudibranchs. Jour. Malacol. 12 (3): 31-53. pls. 7-8.

MacFarland, Frank Mace

1905. A preliminary account of the Doriidae of Monterey Bay, California. Proc. Biol. Soc. Washington 18: 35-54.

——, ——

1906. Opisthobranchiate mollusca from Monterey Bay, California, and vicinity. Bull. U. S. Bur. Fish. for 1905, 25: 109-151.

——, ——

1912. The nudibranch family Dironidae. Zool. Jahrb. Suppl., 15: 515-536, pls. 30-32.

——, ——

1923. The morphology of the nudibranch genus *Hancockia*. Jour. Morphol. 38: 65-104, pls. 1-6.

——, ——
1924. Expedition of the California Academy of Sciences to the Gulf of California in 1921. Opisthobranchiate mollusca. Proc. Calif. Acad. Sci., ser. 4, 13 (25): 389-420, pls. 10-12.

——, ——
1925-1926. The Acanthodorididae of the California coast. Nautilus 39 (2, 3): 49-65, 94-103, pls. 2, 3.

Marcus, Ernst
1961. Opisthobranch mollusks from California. Veliger 3 (Suppl., pt. I): 1-84, pls. 1-10.

Odhner, Nils
1939. Opisthobranchiate mollusca from the western and northern coasts of Norway. Kgl. Norske Vidensk. Selsk. Skr. No. 1, 93 pp.

O'Donoghue, Charles H.
1926. A list of the nudibranchiate mollusca recorded from the Pacific coast of North America, with notes on their distribution. Trans. Roy. Canad. Inst. 15 (2): 199-247.

Smith, Allyn G., & MacKenzie Gordon, Jr.
1948. The marine mollusks and brachiopods of Monterey Bay, California, and vicinity. Proc. Calif. Acad. Sci., ser. 4, 26 (8): 147-245, pls. 3, 4.

Steinberg, Joan E.
1954. Key to the more common opisthobranchs. In: Light, S. F., Ralph I. Smith, et. al. Intertidal Invertebrates of the central California coast. Univ. Calif. Press, Berkeley. pp. 264-270.

(954)

From: International Union of Geodesy and Geophysics.
International Association of Physical Oceanography.
Symposium on radiant energy in the sea. Helsinki,
4-5 August 1960. Monograph No.10, June 1961.
pp.83-91.

SOME RECENT DEVELOPMENTS IN OCEANOGRAPHIC INSTRUMENTATION 1)

by

J. M. Snodgrass

A method of instrumentation, which is proving to be quite successful in the field of missile and flight testing, known as the "systems concept" may well be of value to the field of oceanography. The "systems concept" is designed to consider all aspects of the instrumentation problem from data acquisition and recording through processing and analysis. A major advantage of this concept is that the instrument used for the data acquisition is designed with the end result in mind. For the sake of convenience, we will limit our interest in the "systems concept" to the first two portions; namely, data acquisition and recording.

Another technological development in the missile and flight test field known as **telemetering** offers a great deal of interest and value to the oceanographer. Perhaps it is advisable to pause briefly to explain what is meant by telemetering. Of the many definitions proposed, the one by Borden and Mayo-Wells is probably the best: "Essentially, electric telemetering involves the conversion of a measurand, or measured magnitude, into a representative electrical signal, the transmission of that signal over a significant path, and its reconversion into a quantitative display which may be viewed or graphically recorded, processed into a form which may be temporarily stored, incorporated into a computation, or utilized as a function of an automation process." While it is quite practical for the oceanographer in some applications to use radio for the information transmitting length, wire-connected systems will serve our present purpose. Fortunately, suitable electric wires or cables are now available, and these will be discussed later. There are major advantages in the use of telemetering techniques, to a large extent due to the tremendous amount of effort which has been expended in the telemetering field by the missile and flight test programs. Fortunately, a great deal of the necessary equipment can be purchased in an already suitable form, particularly that which may be used for recording and demodulation purposes. Another by-product of the telemetering systems, if adapted to oceanography, is the fact that this would mean, to a large extent, that recorded data would be in a compatible system which would permit ready exchange of data between laboratories. Furthermore, much of the data would then be in a form which would be suitable for automatic data processing and subsequent analysis.

Magnetic tape is a most valuable adjunct to any data telemetering system, since it makes possible the accurate high speed recording of tremendous quantities of oceanographic data in a compact available form. Data recorded properly on magnetic

(955)

Contributions from the Scripps Institution of Oceanography, New Series, 1324
Reproduced by Permission

tape may be fed directly into computers and automatic high-speed data processing systems for reduction and analysis. It should be explained that the use of magnetic tape recording does not in any wise restrict the type of records which the experimenter would like to have in order to gain knowledge of moment-to-moment changes in information. The so-called "quick look" systems which give an immediate analog supply this much needed pertinent information. Since the information rate of much oceanographic data is comparatively low, it is feasible to use relatively low-speed tape recording and play back, or analyse, at much higher speeds. This has the distinct advantage in economical operation over long periods of time.

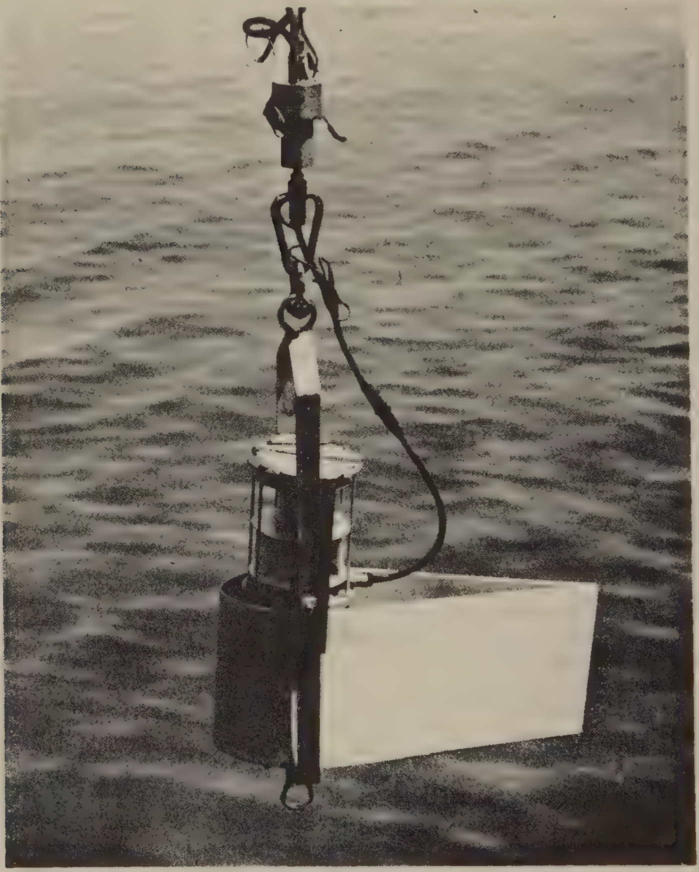

Fig.1. Current meter hanging from electric swivel. Rotor visible just above large protective fin. Fin is open top and bottom to facilitate rapid raising and lowering. Note electrical connectors between swivel and current motor.

An instrument known as a telemetering current meter has been designed from the standpoint of the previously-mentioned "systems concept" and possesses features of general interest. Since it is considerably beyond the scope of this paper to adequately describe the current meter, we will limit our consideration to some of its most interesting features. The current meter is designed to permit raising and lowering while at the same time sensing the horizontal current components. The instrument ignores the vertical components, and transmits continuously depth, current magnitude, and direction. The instrument is cable suspended or it may be bottom

(956)

mounted. It is designed to record and indicate on deck, or at a remote point. The sensitivity of the instrument permits operation to from below .005 knots to very nearly 6 knots. The current sensing system is mechanical, and consists of a modified Savonius type rotor (2). The basic Savonius rotor design has been modified by sectioning it horizontally and rotating the two resulting sections 90° with respect to each other. Fig. 1 shows the current meter hanging in the air just above water. The instrument is suspended on a freely rotating electric swivel. The rotor is visible just above the large white direction orienting fin. Fig. 2 illustrates the type of record which it is possible to obtain with this type of current meter. It is an analog plot made by an XY function plotter, and shows the variation of velocity in some relatively shallow water from the surface down to a depth of approximately 13 meters. The horizontal scale is in tenths of knots.

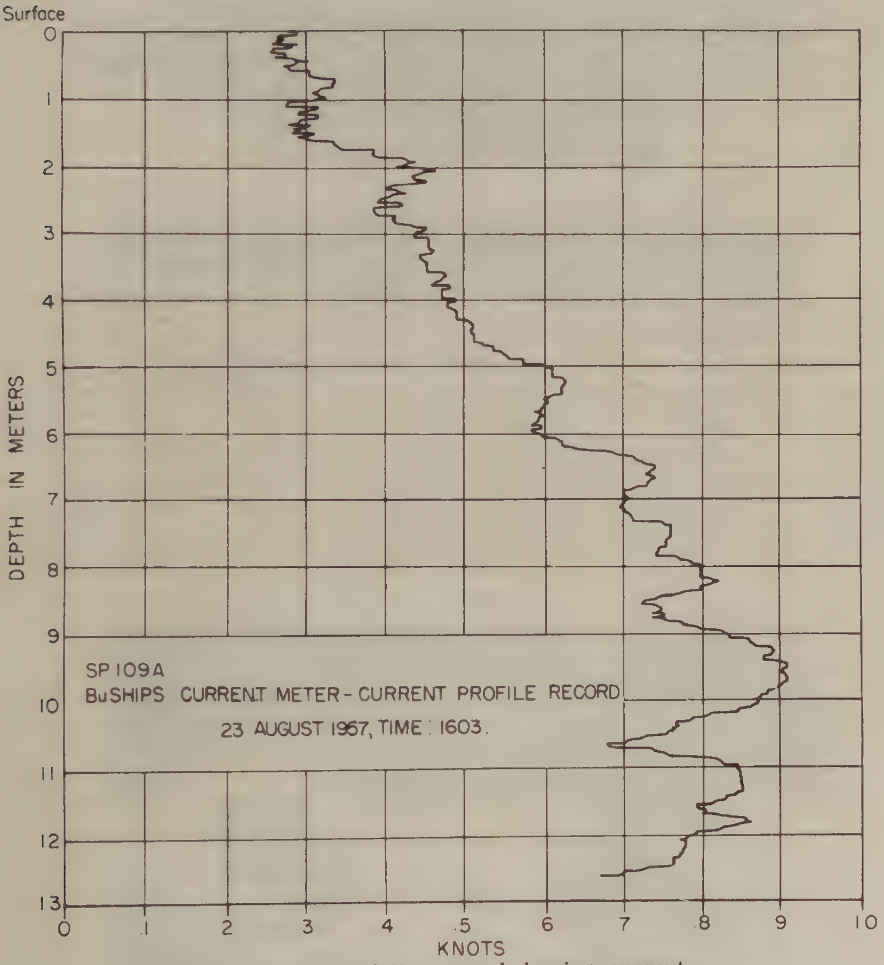

Fig. 2. Function plotter record showing current velocity as a function of depth. Note fine detail.

A further refinement of the "systems concept" which furnishes much needed flexibility to the oceanographer is one which we have called the "module concept". In the course of our instrument work it became apparent that we were building pressure, or depth-sensing, transducers into most of our instruments. This seemed to be an unnecessary waste of equipment and further reduced the over-all instrument reliability by virtue of adding unnecessary complexity to a given instrument. It was apparent that we could fulfill the depth measuring requirement by means of separate self-contained depth sensing transducers and their own power supply, providing there was a practical way of electrically interconnecting the necessary function modules. A depth sensing module is shown in Fig. 3. In its present form it is designed to operate down to a depth of approximately 6,000 meters. The pressure sensing transducer is known as a Vibrotron (3), which converts hydrostatic pressure directly into an FM signal which may be readily telemetered. To use the modules one simply selects the necessary function measuring assemblies, such as depth, current magnitude, etc., assembles them in a suitable package, makes the necessary electric connections to the suspending cable, and one has a completed and functioning instrument. This has a major advantage that, if one wishes to change the depth range over which the instrument is expected to perfom, one can select the necessary depth transducer to correspond.

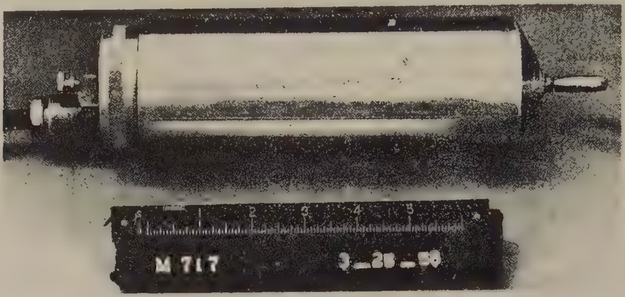

Fig. 3. Self-contained Depth Sensing and Telemetering Module. Case may be opened without assistance of tools. Designed for operation to 6,000 meters.

A most essential part of the above module system are the electric connectors. The electric connectors which we use are very simple and may be mated without the assistance of any tools whatsoever. They are watertight and will operate at any oceanic depth (4). Fig. 4 illustrates a pair of the connectors with a scale for ready determination

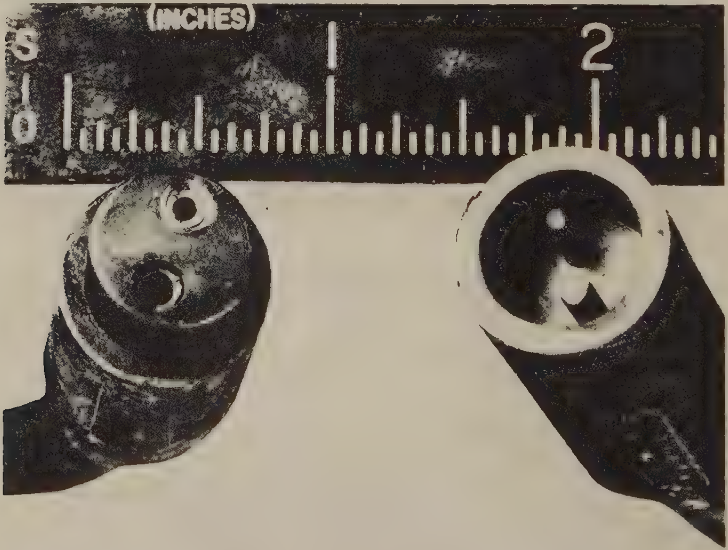

Fig. 4. Electric Connectors showing terminals. The long water sealed skirt on male plugs gives mechanical protection.

of size. The terminals themselves are of stainless steel, and successfully resist corrosion. It is recommended that just before the connectors are mated that a small amount of silicone grease or Vaseline be inserted into the male cavity. Then on mating the excess grease is extruded, leaving no air space. Fig. 5 illustrates the connectors in the closed position. It is apparent that these connectors are not designed to withstand an appreciable amount of mechanical tension. It is therefore necessary to make the mechanical tensions by other means.

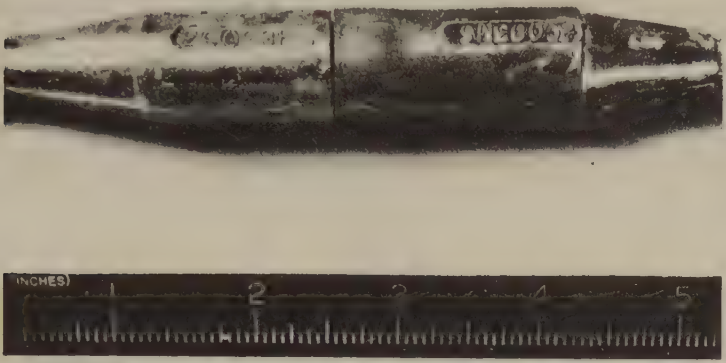

Fig. 5. Electrical Connectors in Mated Position.

The use of a modified Roberts current meter is a good example of one of the uses of the modular system. Fig. 6 shows the method of using a modified Roberts current meter with a depth module attached to the supporting yoke. Cross or "T" types of connectors are available which permit paralleling any number of sensing transducer mechanisms. As mentioned previously, the mechanical tensions are taken up independent of the electric connectors. This may be clearly seen in the use of the shackles which connect the current meter to the electric swivel.

There are two major categories of oceanographic instruments which we may select for our convenience; namely, the fluid-filled, or pressure-equalized types, and the pressure-protected types. The latter category, of course, are the most common, and these require heavy walled cases to resist the operating pressures. Since the components inside the cases are operating under essentially atmospheric pressure, no untoward problems exist in the selection of components. However, in the case of the fluid-filled and pressure-equalized instruments all components must operate under the hydrostatic pressure corresponding to the operating depth. These instruments often possess substantial advantages over the pressure-protected types, but at the same time, major problems are often incorporated from the standpoint of the operation of electronic components. For instance, composition types of resistors have a very high pressure coefficient and are often useless. Fortunately, small resistors utilizing metallic films, or even the wire-wound types, are available which operate quite successfully. Electrolytic capacitors often undergo rather interesting changes, as hydrostatic pressure is increased. For instance, leakage may increase rather substantially up to approximately 70 to 140 kg/cm^2, but then as the pressure is increased, may decrease to respectably low values; and after the pressure is returned to atmospheric, may actually have substantially lower leakage than they had initially at atmospheric pressure. This is by no means true of all electrolytic capacitors, since some never do recover from bad leakage characteristics at high pressures. In general, the electrolytic capacitors do not suffer a significant change of capacity due to high pressure. Electron tubes, particularly those employing the T 3½ envelope, may be operated under pressures up to 1400 kg/cm^2 providing thoroughly dehydrated silicone oil is used as the fluid coming in contact with the tube envelope. It has been reported that transistors may be used without any measurable changes in characteristics under high pressures, if they are first filled with dehydrated silicone oil.

An integrating radiant energy recorder and indicator was built to obtain information relative to incident radiant energy for use in a biological productivity study based on photosynthesis (Fig. 7). Aside from supplying a direct indication of the instantaneous value of radiant energy, the instrument also supplies a direct readout proportional to the total integrated incident radiant energy. In use the pyroheliometer is mounted on top of the ship's mast, and the small DC signal output from the pyroheliometer is chopped amplified and used to drive the two indicating instruments. The instantaneous dial reads 2 Gm.Cal/Cm^2/Min. The integrating instrument reads directly in gram calories per square centimeter. The integrating instrument is a conventional domestic electric watt hour meter, which has a special gear train designed to improve the resolution of the system. In reality the watt hour meter, of course, is an elementary computer, and calculates continuously the time function of the radiant energy. The basic circuitry of the instrument may of course be used to integrate essentially any small, direct current potential, such as a thermocouple output or a photocell output, as a function of time. The instrument is phase sensitive, and is capable of both adding and subtracting.

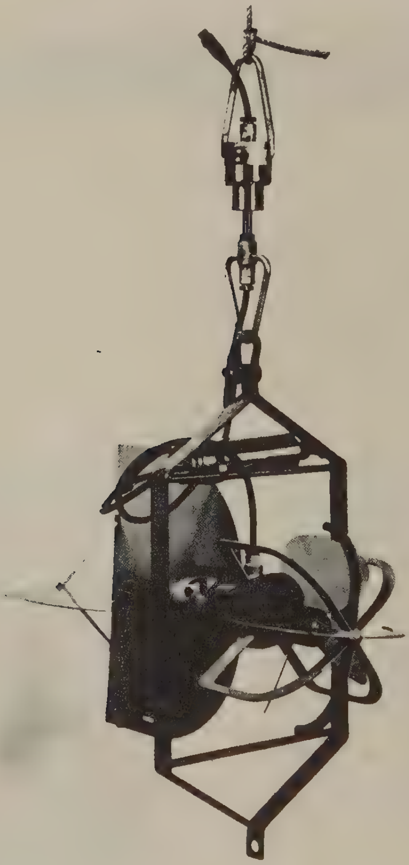

Figure 6

A somewhat simpler technique for integrating small electric potentials, or low currents, uses a modification of the classical silver-voltameter (5), to facilitate the measurement of temperature. Since a photovoltanic self-generating type of photocell generates its own electric current, it is capable of supplying the current directly to a silver-voltameter where the weight of the plated silver is a precision measurement of the total current, and hence the total incident radiant energy converted by the photocell. This particular scheme has been packaged for shallow submarine operations in the study of light penetration in sea water over prolonged periods of time. By equipping the photocell with various filters, information relative to the filtered wave lengths is also obtained. The volume of the small silver-voltameter cell is only about 5 cc. enabling the entire integrating device to be packaged in a fairly neat package. Since the package is quite small, it is quite practical to have the light integrating cell serviced by SCUBA divers. Depending upon the filters used, and the depth of water, it is quite practical to design the device to integrate light intensities over periods of from one to five weeks. The entire system is designed to be rather easily disassembled, making it suite easy for laboratory technicians to weigh out the electrodes on an analytical laboratory balance, and so obtain the necessary figures for calculating the integrated spectral energy over the total period under observation.

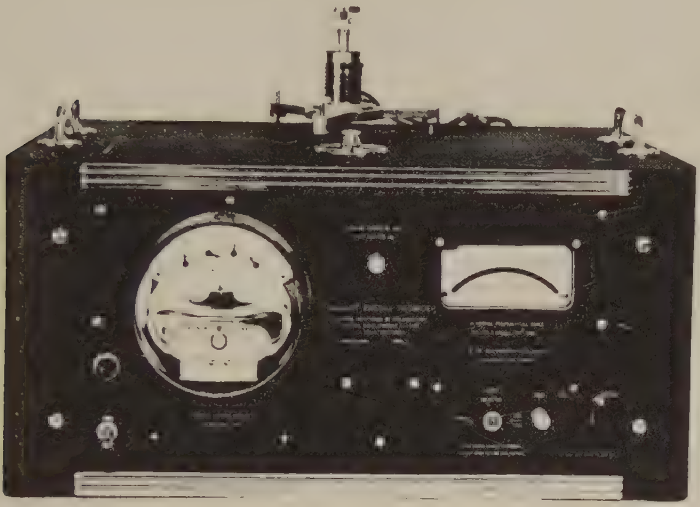

Fig. 7. Integrating Radiant Energy Recorder. Pyroheliometer shown on top of instrument normally used on top of ship mast.

Inevitably in the fabrication of oceanographic instruments the problems of selecting suitable materials to perform various functions must be decided. In the case of the current sensing rotor of the current meter which was described earlier, the fact that there existed a plastic which had a density less than sea water made the entire system feasible. Among the materials considered for the fabrication of the rotor was polyethylene. Though this has a very desirable density, namely, about .93, it proved to be wholly unsuitable as it lacked dimensional stability and distorted seriously if molded due to plastic memory. However, a modified polystyrene known as Cycolac (6), which is rigid, has a density of about 1.01. It has negligible cold flow, no plastic memory, and is easily cemented. The rotor system of the same current meter required bearings of very low friction. Materials satisfaying the requirements were stainless steel for the axle, and sintered Teflon for the bushings. These bearing materials are capable of operating indefinitely with simply water lubrication, and will also operate for protracted periods of time completely dry without damage. Perhaps one of the most successful materials for current meter fins, as well as instrument housings, particularly in the cylindrical shapes, is fiberglass-reinforced epoxy (epon) resins. This material is very tough, and is able to withstand the rigors of the marine environment indefinitely. Other forms of the epoxy resins which are designed for casting purposes lend themselves to the function of supplying protective cases for instruments with a minimum number of man-hours necessary for their fabrication. For instance, in the case of photoelectric cells they may be successfully cast in the resin with their electric leads, and do not require any junction boxes or electric stuffing tubes.

(961)

A material development in a class quite by itself is the development of a polyethylene-jacketed steel cable, which is capable of performing both the function of instrument support and transmission of electrical energy for powering instruments, as well as the transmission back from the instrument to the ship from the transducers contained in the instrument. We have been using a polyethylene-jacketed cable, which has a breaking strength of 1,270 kg, with an over-all diameter of 7.6 mm. The polyethylene jacket adds sufficient buoyancy to the cable so that it may be used to reach any depth in the ocean, and still possess a useful working tension. The electrical resistance is reasonably low for such a cable, and is of the order of 7 ohms per 300 meter length. Since in most of the telemetering work the ocean is used as a sea return, and has only a fraction of an ohm resistance, this, to a large extent, offsets the loss in the conductor, if it was necessary to use a metallic circuit for the return electrical circuit. The special polyethylene jacket (7). proves to be much tougher than neoprene or polyvinyl chloride. Furthermore, the polyethylene is a so-called weldable polyethylene, and may be rather easily repaired in case of damage. For certain special work another electric conductor, using also steel electric leads for strength and the same type of polyethylene as mentioned above, is designed to be almost exactly neutral in sea water of average density. This cable is also 7.6 mm in diameter, but its breaking strength is only 147 kg. Another electric wire development is one which has led to the procurement of wire which is considered to be expendable, due to its small cost. The combined strength and electric conductor is made from N° 24 gauge copperweld steel (8) with a thin extruded jacket of the above type of polyethylene. The wire itself is quite strong, having a breaking strength of approximately 29.5 kg. However, the length of this cable reaching to the bottom in approximately 10,000 meters of water will still have a useful residual breaking strength of about 11 kg.

Perhaps it is proper at this point to insert a word of warning about the use of many of the plastics for use in instrument cases or various shapes which are exposed to temperatures encountered in the ocean. In particular, this concerns temperatures below 8°C. The danger is due to what is known as plastic embrittlement. Plastic embrittlement causes the complete failure of many of the plastics when they are subjected to mechanical shock at temperatures of the order of 8°C and below. The failure does not, however, occur unless there exists a fine scratch or imperfection in the surface of the plastic. However, a scratch so fine as to be almost invisible is quite capable of triggering the failure. The failure of plastic under these conditions might be likened to the fracturing of glass when it is scratched with a diamond point. The Cycolac mentioned earlier, as well as Lucite (perspex), are quite sensitive to plastic embrittlement. Fortunately, fiberglass-reinforced epoxy resins and polyethylene are almost wholly insensitive to this difficulty.

One of the most interesting developments presently underway is the fabrication of a constant tension winch system for oceanographic instrumentation (9). The winch possesses a very sensitive tension-sensing servo system, and operates at all times to maintain tension in the cable independent of ship motion. The winch is expected to be capable of paying out and hauling in cable at uniform rates, also independent of the ship and wave motions. It should be apparent that a winch of this type will make it possible to suspend instruments from ships which actually behave as though they are suspended from stable platforms. Where it is necessary to make instrument attachments to the cable, it is possible to disable the servo feature by simply flipping a lever, which converts the winch to what has been considered conventional operation, so that the cable will not then experience differential motion with respect to the rolling and pitching ship. The winch is designed with easily interchangeable spools so that it may accommodate any type of electric telemetering wire, or conventional steel cable, within the limits of its spooling capacity.

References

(1) F.A. Borden and W.J. Mayo-Wells, "Telemetering Systems" Reinhold Publishing Co., New York, Chapman & Hall, Ltd., London, 1959; p. 1.

(2) S.J. Savonius, "The S-Rotor and Its Applications" Mechanical Engineering, May 1931, Vol. 53, N° 5, P. 333-338.

(3) Borg-Warner Controls Division, Borg-Warner Corporation, 3300 Newport Boulevard, Santa Ana, California.

(4) Joy Manufacturing Company, 1201 Macklind Avenue, St. Louis 10, Missouri.

(5) A. Macradyen, "A Simple Device for Recording Mean Temperature in Confined Spaces", Nature, Vol. 104, p. 965-966, December 3, 1949.

(6). Product of the Marbon Corporation. Available from Southern Plastics Company, 408 Pendelton Street, Columbia, South Carolina.

(7) Bakelite Company, Division of Union Carbide & Carbon Company, 30 E. 42nd Street, New York 17, New York.

(8) Copperweld Corporation, Flexo Wire Division, 70 West First Street, Oswego, New York.

(9) Clearing, Division of U.S. Industries, Inc., Research and Development, 3901 N.E. Twelfth Avenue, Pompano Beach, Florida.

Contributions from the Scripps Institution of Oceanography, New Series, [redacted]. This work was supported in part by funds from the Office of Naval Research and from the Bureau of Ships, U. S. Navy. Reproduction in part or entirety is permitted for any purposes of the United States Government.

(964)

From: International Union of Geodesy and Geophysics.
International Association of Physical Oceanography.
Symposium on Radiant Energy in the Sea. Helsinki,
4-5 August 1960. Monograph No.10, June 1961.
pp.83-91.

APPLICATION OF RADIATIVE TRANSFER THEORY TO LIGHT MEASUREMENTS IN THE SEA

by

R. W. Preisendorfer

Introduction

The equation of transfer for radiance N:

$$\frac{n^2}{v}\frac{D[N/n^2]}{Dt} = -\alpha N + N_* + N\eta \ , \qquad (1)$$

where

$$N_* = \int_{\Xi} N\sigma d\Omega \ ,$$

forms the heart of modern radiative transfer theory. For many years the equation of transfer in various simpler forms has been an extremely powerful tool in the hands of the theorists working in the fields of astrophysical and geophysical optics. The purpose of this discussion is to develop the thesis that the general equation of transfer may be used with equal incisiveness and to great practical advantage by the practicing experimenter to help him understand and collate with precision the results of his radiometric measurements of the light fields in the sea. In particular, I shall show how the equation may serve as a basis for the systematic classification of the principal optical properties of the sea, and of how the beginning of an exact theory of these properties may be achieved.

To understand the basic motivation for the formulations presented below, it is necessary first to understand the natural and fundamentally different ways in which the equation of transfer is viewed by theorists and experimenters: The theorist on the one hand, sees the equation of transfer as a set of mathematical operations on the radiance function. By means of the equation and various solution procedures, he

Contributions from the Scripps Institution of Oceanography, New Series, 1325

Reproduced by Permission

strives to determine the function N throughout a subregion of the optical medium of interest once he is given the values of N on its boundary along with the values of α, σ and other pertinent information throughout the region. The experimenter, on the other hand, sees the equation as a symbolic summary of certain basic operations with actual light measuring instruments. By means of the equation in various rearranged forms, he strives to determine the values of the functions α and σ in a given subregion of the medium once he has measured the function N in that region.

Since the equation of transfer in the experimenter's viewpoint is a symbolic representation of radiometric phenomena observed on a macroscopic scale, the resultant classification of optical properties will thus be phenomenological in nature (relative to such classifications as may be developed by means of, say, the maxwellian or quantum theories).

As the phenomenological classification proceeds, we shall see that the optical properties of the sea can quite naturally be divided into two mutually exclusive and exhaustive classes: The class consisting of the inherent optical properties, and the class consisting of the apparent optical properties. Now from the viewpoint of either the theorist or experimenter, an optical property of a medium is simply a function (defined by a certain sequence of realizable operations) which assigns to a given point in the medium a number representing the magnitude of the property at that point. With this in mind the two classes may be broadly defined as follows: An optical property is inherent if its operational value at a given point in a given medium is invariant under all changes of the radiance distribution at that point. An optical property is apparent if its operational value at a given point in a given medium is not invariant under all changes of the radiance distribution at that point. A practical test for these properties is the following: Suppose that a small element of volume of the medium about the given point were in imagination excised from the medium and placed in a new radiometric environment. Then apply the operational definition of the optical property to the element of volume in its new setting. If the operation remains meaningful and its value does not change, then the concept belongs to the class of inherent optical properties. If the operation becomes meaningless or the value of the function changes, then the concept belongs to the class of apparent optical properties.

By applying the preceding criterion to various cases, it becomes evident that the apparent optical properties depend in a rather complicated way on the inherent optical properties and on the ephemeral light field throughout the medium. This is the case for such well-known apparent optical properties as the logarithmic derivatives, with respect to depth, of upwelling and downwelling irradiances, and the reflectance functions of the sea. However, these concepts and the others classified below are worthy of the appellation "optical property" because: (i) their gross behavior with depth exhibits striking regularities, which are reproducible in medium after medium; (ii) it is possible to formulate exact mathematical interrelationships between these concepts and the inherent optical properties which hold in all practical cases; and finally (iii) the use of apparent optical properties reduces to a practical level the solution of underwater visibility problems and pertinent problems of marine biology. By experimentally determining the apparent optical properties of real media one is in effect solving on a practical level certain particularly difficult problems in the theoretical-analytical aspects of the radiative transfer theory.

INHERENT OPTICAL PROPERTIES

Preliminary Definitions

The equation of transfer (1) forms the basis of all the deductions of the present discussion: From the equation or the various terms appearing in it we deduce the operational definitions of the inherent and apparent optical properties and some of their principal interrelations. It is, therefore, essential to make clear the definitions of the various terms appearing in the equation; this will now be done.

The radiometric quantity which is the most basic from the viewpoint of either the theorist or experimenter is that of radiance: The amount of radiant flux of a given wave-length crossing a unit area within a unit solid angle about the normal to the plane of the area. This concept is denoted by the symbol N which stands for the function with the following property: Let $\underline{x}$ be a vector denoting position of a point in an optical medium and let $\underline{\xi}$ denote a unit vector at $\underline{x}$. Let radiant flux of wave-length λ exist at x at time t. Then $N(\underline{x}, \underline{\xi}, t, \lambda)$ denotes the radiance of wave-length λ at $\underline{x}$ flowing in the direction $\underline{\xi}$ at time t. Here and below, N will be associated with an arbitrary fixed wave-length λ. Thus the symbol λ may, without loss of generality, be dropped from the notation.

To see the physical significance of the equation of transfer's various terms, we follow in imagination a packet of photons as it traverses a path through the neighborhood of a point in a scattering-absorbing medium. First of all, from geometrical optics we know that the quotient N/n^2, where n is the index of refraction, is invariant along a path through a region which exhibits no scattering, absorption, or sources of radiant flux. In such a case the equation of transfer is simply

$$\frac{1}{v}\frac{D[N/n^2]}{Dt} = 0 , \qquad (2)$$

where v is the speed of light at the point instantaneously occupied by the packet. If the path were now directed through a region in which there was pure absorption -that is, no scattering mechanisms present, and no sources of flux, then (2) becomes

$$\frac{1}{v}\frac{D[N/n^2]}{Dt} = -a\frac{N}{n^2} , \qquad (3)$$

where a is the volume absorption function.
In reality, scattering mechanisms are coexistent with absorbing mechanisms. In this case there is, in addition to the absorption-loss term $a(N/n^2)$, a scattering-loss term $s(N/n^2)$ in the equation:

$$\frac{1}{v}\frac{D[N/n^2]}{Dt} = -(a+s)\frac{N}{n^2} , \qquad (4)$$

where s is the volume total scattering function. However, the scattering mechanism simultaneously increases the population of the streaming packet of photons by having photons scattered into the direction of its travel. Hence, the equation, when taking this into account, becomes:

$$\frac{1}{v}\frac{D[N/n^2]}{Dt} = -\alpha\frac{N}{n^2} + \frac{N_*}{n^2} , \qquad (5)$$

where we have set

$$\alpha = a + s \qquad (6)$$

which is the volume attenuation function,
and where

$$N_*(\underline{x},\underline{\xi},t) = \int_{\Xi} N(\underline{x},\underline{\xi}',t)\,\sigma(\underline{x},\underline{\xi}';\underline{\xi},t)\,d\Omega(\underline{\xi}') \qquad (7)$$

defines the path function N_*, and introduces the volume scattering function σ. The symbol Ω stands for the solid angle measure, and Ξ is the set of all unit vectors (the unit sphere) in space. Finally, if sources are present, we add to (5) the emission (source) function N_η, to obtain (1). Both $N_*(\underline{x}, \underline{\xi}, t)$ and $N_\eta(\underline{x}, \underline{\xi}, t)$ have units of radiance per unit length, the unit of length being in the direction of $\underline{\xi}$. The functions γ, α, σ, a, and s have dimensions of inverse length. For a rigorous derivation of the equation of transfer from first principles, see reference (1.)

The Steady-State, Emission-Free Equation of Transfer

Light fields in the sea are in the steady state or, more precisely, in the quasi-steady state. Furthermore, the values of the emission function, except for some cases which are for the present purposes only of academic interest, are all zero. Finally, the index of refraction function n is essentially constant within the body of the sea: the domain of present interest. Thus, I shall at present adopt the form of the equation of transfer which results from the introduction of these conditions into (1); the result is:

$$\frac{dN}{dr} = -\alpha N + N_* , \tag{8}$$

where d/dr is the steady state Lagrangian derivative:

$$\frac{d}{dr} = \frac{dx}{dr}\frac{\partial}{\partial x} + \frac{dy}{dr}\frac{\partial}{\partial y} + \frac{dz}{dr}\frac{\partial}{\partial z} ,$$

i.e.

$$\frac{d}{dr} = \underline{\xi}\cdot\nabla , \tag{9}$$

where

$$\nabla = \left(\frac{\partial}{\partial x}, \frac{\partial}{\partial y}, \frac{\partial}{\partial z}\right), \qquad \text{and} \qquad \underline{\xi} = \left(\frac{dx}{dr}, \frac{dy}{dr}, \frac{dz}{dr}\right), \tag{10}$$

in the usual cartesian coordinate system for space.
The physical significance of d/dr is simply that of a rate of change with distance r along a path with direction $\underline{\xi}$ at the point of interest. Equation (8) will form the basis of all the deductions below. It may be of interest to note that all of the results below may be generalized to the transient emission case. However, it is quite clear that such a case transcends present day interests, and will thus be reserved for subsequent study. However, the case of polarized radiance is of fundamental and immediate interest. The classification of the optical properties outlined below is easily extended to this case, but since this would introduce certain inessential complications, we omit it from the present discussion.

Enumeration of the Inherent Optical Properties

The inherent optical properties are:

α : the volume attenuation function
σ : the volume scattering function
a : the volume absorption function
s : the volume total scattering function

These properties are inherent in the sense described in the introduction. Their interrelations are very simple:

$$s(\underline{x}) = \int_{\Xi} \sigma(\underline{x}, \underline{\xi}, \underline{\xi}')\, d\Omega(\underline{\xi}') \tag{11}$$

$$\alpha(\underline{x}) = a(\underline{x}) + s(\underline{x}) \tag{12}$$

at each point $\underline{x}$ of the optical medium.

Thus either the pair (α, σ), or (a, σ) may be considered as the fundamental pair of inherent optical properties. That is, there are essentially two fundamental inherent optical properties; which two are considered as the fundamental pair is principally a matter of personal taste. As we shall see below, the equation of transfer provides operational definitions of comparable simplicity for either choice of α or a. Before leaving the enumeration of the inherent optical properties, we append two auxiliary inherent optical properties of comparatively minor importance:

$$f(\underline{x}, \underline{n}) = \int_{\underline{\xi}\cdot\underline{n} \geq 0} \sigma(\underline{x}, \underline{\xi}, \underline{\xi}')\, d\Omega(\underline{\xi}') \tag{13}$$

and

$$b(\underline{x}, \underline{n}) = \int_{\underline{\xi}\cdot\underline{n} \leq 0} \sigma(\underline{x}, \underline{\xi}, \underline{\xi}')\, d\Omega(\underline{\xi}') \tag{14}$$

which define the volume forward and volume backward scattering functions f and b respectively at $\underline{x}$ for the direction $\underline{n}$. If the medium is isotropic, then f and b are independent of $\underline{n}$. Furthermore,

$$s(\underline{x}) = f(\underline{x}) + b(\underline{x}) \tag{15}$$

We shall, henceforth, assume the sea to be an isotropic medium, so that $\underline{n}$ in (13), (14) may be dropped from the notation. This was already done in (11), (12), and (15) above.

Operational Definitions of the Inherent Optical Properties

The inherent optical properties will now be given operational definitions, i.e., definitions which show how the properties may be obtained by actual operations in natural or artificial light fields with a radiance meter and related radiometric equipment. Some of these operational definitions (for α and σ) are well-known. However, we are concerned, as stated above, with the attempt to unify and classify the optical properties by means of physically realizable operations with light-measuring apparatus guided by the equation of transfer. While the procedures described below will be idealized, it should be emphasized that they outline realizable operations which may be followed in obtaining their numerical values. I shall leave to the experimenters the necessary precautions that must be taken in actual practice in order to avoid the obvious pitfalls accompanying non-ideal instruments, perturbations of light fields by measuring equipment, etc.

An examination of the equation of transfer (8) shows that, in order to solve it for the volume attenuation function, one must generally know dN/dr, N_* and N:

$$\alpha = \frac{N_*}{N} - \frac{1}{N}\frac{dN}{dr} \tag{16}$$

However, by judiciously choosing a natural light field, or by generating an appropriate artificial light field, (16) may be simplified by causing, in turn, each of the two terms to be zero, thus yielding two basic methods of defining α. Recall that the function N_* represents radiance generated per unit length by the scattering of radiant flux into the direction of motion of the photons. Hence, if N_* can be made zero -or essentially negligible compared with the term $\frac{1}{N}\frac{dN}{dr}$, (16) reduces to

$$\alpha = -\frac{1}{N}\frac{dN}{dr} \tag{17}$$

This is the basic operational definition of α in local (differential) form. Formula (17) is the basis of the well-known beam-transmittance method of measuring α, wherein a radiance meter looks across an optically short path of length r within the medium at a controlled known source of flux of inherent radiance N_0. If N_r is the radiance measured at distance r, and α is known to be constant along the path, then (17) implies

$$\alpha = -\frac{1}{r}\ln\left(\frac{N_r}{N_0}\right) \tag{18}$$

which is the operational definition of α in global form. An analysis of the perturbations of the light field engendered by this method may be found in reference 2.

A less general, but quite interesting alternative operational definition of α is based on the generally valid fact that in the sea, the radiance along a horizontal path is invariant with respect to distance r along the path. It follows that, in this instance, (16) reduces to

$$\alpha = \frac{N_*}{N} \tag{19}$$

Now suppose that a radiance meter is built in such a way as to look across a horizontal path of small unit length at a black target (i.e., a target of zero inherent radiance in the wave-length in question). Then, this device will in principle record N_*. Another radiance meter, simultaneously records the actual horizontal radiance N at the same depth and in the same direction. Then (19) yields α by combining these readings as shown. This procedure was originated by Duntley in his studies of atmospheric optics and is quite successful in that context. In view of the excellent techniques now available by means of the more general definitions (17), (18), the definition summarized by (19) is perhaps only of academic interest for the case of light measurements in the sea.

The operational definition of the volume scattering function σ is based not on the entire equation of transfer, but only its path function term (7) now written for the steady state case. Suppose that the radiance function in the integrand were zero for all directions $\underline{\xi}'$ in Ξ except over a subset Ξ_0 of small solid angle measure $\Delta\Omega_0$ about $\underline{\xi}_0$ a representative direction for Ξ_0. Furthermore, suppose that N over Ξ_0 is uniform of magnitude $N_0(\underline{x}, \underline{\xi}_0)$. Then the corresponding path function value $\Delta N_*(\underline{x}, \underline{\xi})$ at $\underline{x}$ in an arbitrary direction $\underline{\xi}$ is related to $\Delta\Omega_0$ and $N_0(\underline{x}, \underline{\xi}_0)$ by the following special case of (7):

$$\Delta N_*(\underline{x}, \underline{\xi}) = N_0(\underline{x}, \underline{\xi}_0)\,\sigma(\underline{x}, \underline{\xi}_0, \underline{\xi})\,\Delta\Omega_0$$

From this follows the basic operational definition of σ at $\underline{x}$, for the pair of directions $\underline{\xi}_0\,\underline{\xi}$:

$$\sigma(\underline{x}, \underline{\xi}_0, \underline{\xi}) = \frac{\Delta N_*(\underline{x}, \underline{\xi})}{N_0(\underline{x}, \underline{\xi}_0)\,\Delta\Omega_0} \qquad (20)$$

Recall that $\Delta N_*(\underline{x}, \underline{\xi})$ is the radiance generated by flux at $\underline{x}$ moving in the direction ξ_0 within a small solid angle about $\underline{\xi}_0$ which is subsequently scattered in the direction $\underline{\xi}$.

An alternate form of (20) is obtained if one notes first of all that $N_0(\underline{x}, \underline{\xi}_0)\Delta\Omega_0$ is simply the irradiance $\Delta H_0(\underline{x}, \underline{\xi}_0)$ at $\underline{x}$ generated by flux in the direction $\underline{\xi}_0$, and secondly that $\Delta N_*(\underline{x}, \underline{\xi})\,\Delta V(\underline{x})$ is the radiant intensity $\Delta^2 J_*(\underline{x}, \underline{\xi})$ at $\underline{x}$ in the direction $\underline{\xi}$ generated by an element of volume of scattering matter at $\underline{x}$. Thus (20) may be written as:

$$\sigma(\underline{x}, \underline{\xi}_0, \underline{\xi}) = \frac{\Delta^2 J_*(\underline{x}, \underline{\xi})}{\Delta H_0(\underline{x}, \underline{\xi}_0)\,\Delta V(\underline{x})} \qquad (21)$$

where $\Delta V(\underline{x})$ is the actual volume irradiated.

This form of the definition, in the last analysis, is less operationally meaningful than (20), since the concept of radiant intensity is definable operationally only in terms of radiances and measurable areas, thus returning to (20). For further details concerning (20), see reference 3.

A straight-forward determination of the inherent optical property s follows from knowledge of σ and use of (11). However, the basic operational definition of the volume total scattering function s follows from (7) by the simple expedient of integrating (7) over Ξ. The result is

$$h_*(\underline{x}) \equiv \int_{\Xi} N_*(\underline{x}, \underline{\xi})\,d\Omega(\underline{\xi}) = h(\underline{x})\,s(\underline{x}) \qquad (22)$$

where

$$h(\underline{x}) = \int_{\Xi} N(\underline{x}, \underline{\xi})\,d\Omega(\underline{\xi}) \qquad (23)$$

is the scalar irradiance at $\underline{x}$. $h(\underline{x})$ is related to the radiant density (radiant energy per unit volume) $u(\underline{x})$ at $\underline{x}$ by: $h(\underline{x}) = u(\underline{x})\,v(\underline{x})$, where $v(\underline{x})$ is the speed of light at $\underline{x}$. Thus, from (22), we have:

$$s(\underline{x}) = \frac{h_*(\underline{x})}{h(\underline{x})} \qquad (24)$$

In order to determine $s(\underline{x})$ in accordance with (24) we need only integrate, either manually or automatically, the unit path radiance readings N_* over Ξ at $\underline{x}$. The scalar irradiance at $\underline{x}$ is measurable by suitably designed collecting spheres (see, e.g., reference 3). Observe the interesting similarity of structure between the operational definitions (19) and (24). For further details about (24) and other measurement procedures, see reference 4.

A straight-forward determination of the inherent optical property a from knowledge of s and α is made by means of (12). However, the basic operational definition of the volume absorption function a follows immediately from (8) in the form:

$$\underline{\xi}\cdot\nabla N = -\alpha N + N_* \tag{25}$$

after defining the concept of vector irradiance $\underline{H}$:

$$\underline{H}(\underline{x}) = \int_{\Xi} \underline{\xi} N(\underline{x},\underline{\xi})\, d\Omega(\underline{\xi}) \tag{26}$$

which is the radiometric counterpart to Gershun's light vector $\underline{D}$. Integrating (25) over Ξ, we have :

$$\nabla\cdot\underline{H}(\underline{x}) = -\alpha(\underline{x})h(\underline{x}) + s(\underline{x})h(\underline{x})$$

by using (22) and (26). This, in view of (12), reduces to:

$$\nabla\cdot\underline{H}(\underline{x}) = -a(\underline{x})h(\underline{x}) \tag{27}$$

which yields the basic operational definition of a($\underline{x}$) (local form) :

$$a(\underline{x}) = -\frac{\nabla\cdot\underline{H}(\underline{x})}{h(\underline{x})} \tag{28}$$

For further details concerning this definition, see reference 5. To illustrate the use of (28) for the case of the sea, we once again make use of the generally valid fact that the light field in the sea is stratified, i.e., that it depends spatially only on depth z below the surface. Suppose then that z represents depth measured with positive sense downward, and that $\underline{n}$ represents the unit outward normal to the surface of the sea (Fig. 1).

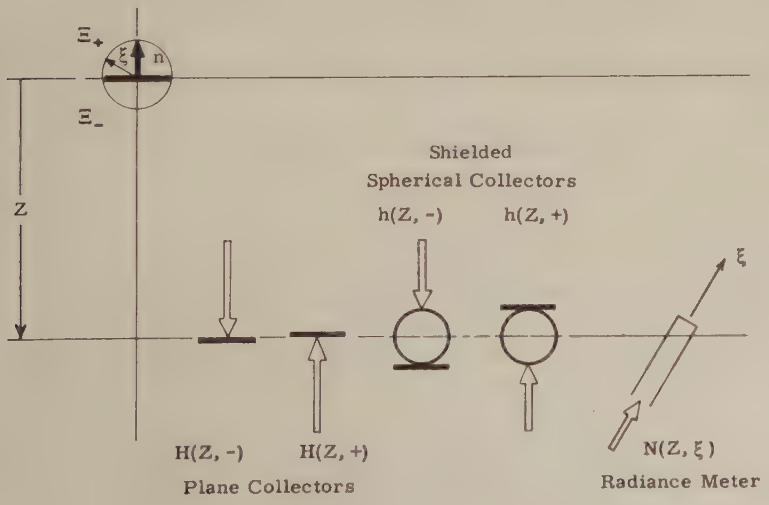

Fig. 1 . Two-flow analysis of light field.

Then the divergence of the irradiance vector $\underline{H}(\underline{x})$ is

$$\nabla \cdot \underline{H}(\underline{x}) = \frac{d}{dz}\left[H(z,-) - H(z,+)\right]$$

where H(z, +) is the upwelling irradiance at depth z across a horizontal surface, and H(z, -) is the downwelling irradiance at that depth across the same surface. Then (28) becomes

$$a(z) = \frac{1}{h(z)} \quad \frac{d\bar{H}(z,+)}{dz} \tag{29}$$

Here I have set

$$\bar{H}(z,+) = H(z,+) - H(z,-) \tag{30}$$

Each term on the right side of (29) is directly measurable. The irradiances H(z, ±) are related to the radiance distribution at depth z by the formulas:

$$H(z,\pm) = \int_{\Xi_{\pm}} |\underline{\xi} \cdot \underline{n}|\, N(z,\underline{\xi})\, d\Omega(\underline{\xi}) \tag{31}$$

where Ξ_+ is the subset of Ξ consisting of all $\underline{\xi}$ such that $\underline{\xi} \, . \, n \geqslant 0$; and Ξ_- consists of all $\underline{\xi}$ such that $\underline{\xi} \, . \, n \leqslant 0$.

A global form of the definition of the volume absorption function is obtained by assuming the function a to be constant over an arbitrary sub-region X of the medium and then applying the divergence theorem to (27). The result is:

$$a = \frac{\bar{P}(S,-)}{vU(X)} \tag{32}$$

where a is the (constant) value of the volume absorption function throughout X, U(X) is the radiant energy content of X, $\bar{P}(S,-)$ is the net inward flux across the simple closed surface S bounding X, and v is the speed of light throughout X. This form may be of some practical interest in laboratory procedures for determining a. The numerator of (32) may be obtained by traversing the boundary of X with flat plate (irradiance) collectors. The denominator is obtained by probing the interior of X with a spherical (scalar irradiance) collector and integrating the values over X. By suitably adjusting the light field within X to attain maximum (e.g., spherical) symmetry, the number of probing operations can be reduced to a minimum. It should be clear that this method is independent of the structure of the light field within X.

This completes the present discussion of inherent optical properties. We now go on to discuss the second main group of optical properties of the sea.

APPARENT OPTICAL PROPERTIES

Introduction and Preliminary Definitions

The total set of apparent optical properties of natural waters consists at present of twenty quantities. The properties are apparent in the sense explained in the introduction. However, for the reasons also touched on in the introduction, these properties have been found to possess striking regularities and to be extremely useful in the experimental study of the light fields in natural hydrosols. Over recent years, at least five of them (the K-functions for irradiance and the reflectance functions) have found a permanent place in the experimentalist's stock in trade in his study of the optics of the sea.

Historically, the apparent optical properties (with the exception of $K(z, \underline{\xi})$) are traceable (at least in their most rudimentary form) to the classical two-flow analysis of the light field in plane-parallel media. In this context they were truly "optical properties" and fixed in magnitude throughout the media. Thus, the present day apparent optical properties are outgrowths of man's conceptual decomposition of the light fields in such media into two counter-moving streams: An "upwelling" and a "downwelling" stream. An outline of the salient history of this concept and its evolution over the past fifty-five years may be found in references 6 and 7. I might venture to say that a complete understanding of the classical theory is indispensible for a thorough appreciation of the role of the apparent optical properties in the general modern theory given below.

It has been found possible to characterize nine of the basic optical properties by means of a basic quartet of directly observable irradiances. These irradiances require less effort to be determined than the radiance distribution and of course contain less information than the latter. However, the quartet supplies enough information about the depth dependence of the light field, its directional structure, and overall flux transmitting and reflecting properties of the medium to allow many practical problems to be solved with satisfactory precision and completeness. These facts along with their regularity features hold the secret of the utility of the apparent optical properties.

The basic irradiance quartet is:

$$\begin{matrix} H(z,+) & h(z,+) \\ H(z,-) & h(z,-) \end{matrix} \qquad (33)$$

where the $H(z,\pm)$ have already been defined in (31), and

$$h(z,\pm) = \int_{\Xi\pm} N(z,\underline{\xi})\, d\Omega(\underline{\xi}) . \qquad (34)$$

Observe that the notation reflects our standing assumption about the optical structure of the sea: It is horizontally stratified; the character of the stratification is, however, arbitrary. The quantities $h(z,\pm)$ are the upwelling (+) and downwelling (-) scalar irradiances at depth z (Fig. 1). They are related to the scalar irradiance $h(z)$ (Eq.(23)) by:

$$h(z,+) + h(z,-) = h(z)$$

Methods of measurement of $h(z,\pm)$ other than by means of integrated N-values are discussed in reference 3. The quantities $H(z,\pm)$ are measured by horizontal flat plate collectors or from N by integration.

Operational Definitions of the Apparent Optical Properties

The apparent optical properties along with their operational definitions are:

$$R(z,\pm) = \frac{H(z,\mp)}{H(z,\pm)} \qquad (35)$$

$$K(z,\underline{\xi}) = \frac{-1}{N(z,\underline{\xi})} \frac{dN(z,\underline{\xi})}{dz} \qquad (36)$$

$$K(z,\pm) = \frac{-1}{H(z,\pm)} \frac{dH(z,\pm)}{dz} \qquad (37)$$

$$k(z,\pm) = \frac{-1}{h(z,\pm)} \frac{dh(z,\pm)}{dz} \qquad (38)$$

$$k(z) = \frac{-1}{h(z)} \frac{dh(z)}{dz} \qquad (39)$$

$$D(z,\pm) = \frac{h(z,\pm)}{H(z,\pm)} \qquad (40)$$

In these formulas read all upper signs together and all lower signs together. For example:

$$R(z,-) = \frac{H(z,+)}{H(z,-)}$$

is the reflectance of the sea at depth z, with respect to the downwelling flux at that level. Since

$$R(z,+) = \frac{1}{R(z,-)} ,$$

it is sufficient to discuss only R(z, -).

The quantity $K(z, \underset{\sim}{\xi})$ is the diffuse attenuation function for radiance.
The quantities $K(z,\pm)$ are the values of the diffuse attenuation functions for irradiance at depth z. Knowledge of these functions over a depth interval from z_1 to z_2, $0 \leqslant z_1 \leqslant z_2$ is tantamount to knowledge of $H(z,\pm)$ over the same interval; for knowing $H(z,\pm)$ over this interval yields $K(z,\pm)$ by means of (37). On the other hand, (37) implies :

$$H(z_2,\pm) = H(z_1,\pm)\exp\left\{-\int_{z_1}^{z_2} K(z',\pm)\,dz'\right\} , \qquad (41)$$

Observe that if $K(z,\pm) = K$ a given value over $[z_1, z_2]$ then from (41),

$$H(z_2,\pm) = H(z_1,\pm)\exp\left\{-K(z_2 - z_1)\right\} ,$$

which shows that $K(z,\pm)$ are the exact generalizations of the classical diffuse attenuation function.

The $k(z,\pm)$ are the values of the diffuse attenuation functions for upwelling (+), downwelling (-) scalar irradiance. The subtle distinction required between the little k's and the big K's is a direct consequence of the increasing demands for accuracy by modern experimentalists in their basic determinations of the structure of light fields in natural hydrosols. k(z) is the value of the diffuse attenuation function for scalar irradiance. The interrelations among these K-functions will be illustrated below in the theoretical section.

Finally, $D(z,\pm)$ is the value of the distribution function for upwelling (+) downwelling (-) flux, at depth z. These numbers are indicators of the directional structure of the radiance distribution at depth z. For example, if N were collimated within Ξ_- and the collimated beam was in the direction defined by $\underset{\sim}{\xi}$, then

$$D(z,-) = \frac{1}{|\underset{\sim}{\xi}\cdot\underset{\sim}{n}|}$$

If, on the other hand, N were uniform over Ξ_- , then

$$D(z,-) = 2$$

The distribution functions, besides being simple conceptual indicators of the structure of the radiance distribution, are indispensible analytical links between the various optical properties, as shall be seen in detail below.

Examples of Values of D, K, a, R

Table I exhibits values of some of the apparent optical properties. Depths and units are in meters. Data were associated with wave-length 480 mμ and were derived from radiance information summarized in reference 8. The optical medium (Lake Pend Oreille, Idaho, U.S.A.) was found to be essentially homogeneous with $\alpha = 0.402$/meter. The sky was clear and sunny with sun at about 40° from zenith.
The values a(z) were obtained by means of (29).

(974)

Table I. Examples of the Values of $D(Z,\pm)$, $K(Z,\pm)$, $a(Z)$, $R(Z,-)$

Z (Meters)	D(Z, -)	D(Z, +)	K(Z, -)	K(Z, +)	a (Z)	R(Z, -)
4.24	1.247	2.704				0.0215
7.33			0.129	0.126		
10.42	1.288	2.727	0.153	0.150	0.115	0.0184
13.50			0.178	0.174		
16.58	1.291	2.778	0.174	0.172	0.118	0.0204
22.77			0.171	0.170		
28.96	1.313	2.781	0.169	0.169	0.117	0.0227
35.13			0.167	0.167		
41.30	1.315	2.757	0.165	0.165	0.117	0.0235
47.50			0.162	0.163		
53.71	1.307	2.763	0.158	0.158	0.112	0.0234
59.90			0.154	0.154		

Hybrid Optical Properties

The classification of the optical properties of the sea would not be complete without some provision for describing the direct scattering and absorbing counterparts to α, a, s, f and b which belong exclusively to the upwelling and downwelling streams. These descriptions are supplied by the set of hybrid optical properties which form a subset of the class of apparent optical properties. They receive their name from the fact that they escape any simple operational definitions of the kind described so far, and because their natural definitions are achieved by mating inherent optical properties with apparent optical properties by means of certain well defined analytical bonds. Thus, the volume attenuation functions for the two streams are:

$$\alpha(z,\pm) = \alpha(z)\, D(z,\pm); \tag{42}$$

the volume absorption functions for the two streams are:

$$a(z,\pm) = a(z)\, D(z,\pm); \tag{43}$$

the volume total scattering functions for the two streams are :

$$s(z,\pm) = s(z)\, D(z,\pm); \tag{44}$$

and, finally, the forward scattering functions for each stream are:

$$f(z,\pm) = \frac{1}{H(z,\pm)} \int_{\Xi\pm} \left[\int_{\Xi\pm} N(z,\underline{\xi}')\,\sigma(z,\underline{\xi}';\underline{\xi})\, d\Omega(\underline{\xi}') \right] d\Omega(\underline{\xi}) \tag{45}$$

and the backward scattering functions for each stream are:

$$b(z,\pm) = \frac{1}{H(z,\pm)} \int_{\Xi\mp} \left[\int_{\Xi\pm} N(z,\underline{\xi}')\,\sigma(z,\underline{\xi}';\underline{\xi})\, d\Omega(\underline{\xi}') \right] d\Omega(\underline{\xi}) \tag{46}$$

Clearly,

$$s(z,\pm) = f(z,\pm) + b(z,\pm) , \tag{47}$$

where we continue to read upper signs together for the upwelling stream and lower signs together for the downwelling stream;
and furthermore

$$\alpha(z,\pm) = a(z,\pm) + s(z,\pm) , \tag{48}$$

in complete analogy to (12) and (15).

The list of optical properties as it stands at present is summarized in Table II below:

CLASSIFICATION OF OPTICAL PROPERTIES OF THE SEA

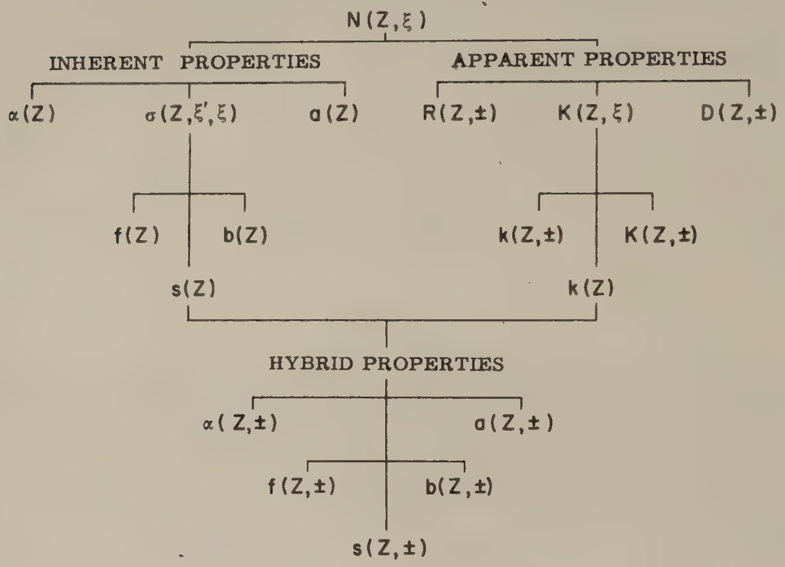

GENERAL THEORY OF OPTICAL PROPERTIES

I shall now briefly outline a theory, based on the exact equation of transfer, which ties together the various inherent and apparent optical properties discussed above. The theory in its present form is not intended to be exhaustive; rather, it is intended to illustrate the basic thesis of the present discussion, namely: That the equation of transfer can be turned into a useful, incisive tool in the hands of the experimental investigator who, having the light field of the sea at his finger-tips, so to speak, is concerned with the experimental documentation of the salient optical properties of the sea. Other than the generally valid assumption of the predominantly horizontal stratification of the light field in natural waters, the theory incorporates no further assumptions about such intricate features as the depth and directional dependence of the submarine radiance distribution, nor of the nature of the stratification of the optical structure of the sea. In short, the theory proposed below is generally applicable to any arbitrary stratified plane-parallel optical medium, of arbitrary depth, with arbitrary reflecting upper and lower boundaries, and with arbitrary incident radiance distribution at its upper boundary.

The theory of the optical properties of the sea is perhaps best expounded in the limited space at hand by attempting to answer some of the more fundamental questions that may be raised by the practicing optical oceanographer. The paragraphs below, it is hoped, will supply answers to some of these questions, and show by example how further questions of similar natures may be resolved once they are formulated.

The General Transport Equations for Irradiance

The core of the theory of optical properties resides in a pair of general equations which govern the depth behavior of the upwelling and downwelling irradiance $H(z,\pm)$. The starting point of their derivation is the equation of transfer in the form:

$$\underline{\xi}\cdot\nabla N(z,\underline{\xi}) = -\alpha(z)\,N(z,\underline{\xi}) + N_*(z,\underline{\xi}) \tag{49}$$

If each term of (49) is integrated over Ξ_-, we shall obtain the equation governing $H(z,-)$ as follows:

First,

$$\int_{\Xi_-}\xi\cdot\nabla N(z,\underline{\xi})\,d\Omega(\underline{\xi}) = \nabla\cdot\int_{\Xi_-}\xi\,N(z,\underline{\xi})\,d\Omega(\underline{\xi}) = \frac{dH(z,-)}{dz}$$

since the sea is stratified.

Second,

$$\int_{\Xi_-}\alpha(z)\,N(z,\underline{\xi})\,d\Omega(\underline{\xi}) = \alpha(z)\,h(z,-) = \alpha(z,-)\,H(z,-)$$

which follows from (34) and (40).

Finally,

$$\int_{\Xi_-}N_*(z,\underline{\xi})\,d\Omega(\underline{\xi}) = \int_{\Xi_-}\left[\int_{\Xi}N(z,\underline{\xi}')\,\sigma(z,\underline{\xi}';\underline{\xi})\,d\Omega(\underline{\xi}')\right]d\Omega(\underline{\xi})$$

$$= \int_{\Xi_-}\left[\left(\int_{\Xi_+}+\int_{\Xi_-}\right)N(z,\underline{\xi}')\,\sigma(z,\underline{\xi}';\underline{\xi})\,d\Omega(\underline{\xi}')\right]d\Omega(\underline{\xi})$$

$$= b(z,+)\,H(z,+) + f(z,-)\,H(z,-)\ ,$$

where the first equality follows from the definition of N_*, the second from the definition of Ξ, and the third from the interchange of the order of integrations, and use of (45), (46).

Assembling these results, we have, making use of (47) and (48):

$$\frac{dH(z,-)}{dz} = -\left[a(z,-) + b(z,-)\right]H(z,-) + b(z,+)\,H(z,+)\ ; \tag{50}$$

and in a similar manner we deduce:

$$-\frac{dH(z,+)}{dz} = -\left[a(z,+) + b(z,+)\right]H(z,+) + b(z,-)\,H(z,-)\ , \tag{51}$$

which are the desired, exact, transport equations for $H(z,\pm)$. For a more general derivation within the time dependent, emission context, see reference 6. For the relationship between (50), (51) and the classical Schuster two-flow equations, see references 6 and 7. The present equations are simultaneously more exact, more general, and operationally more meaningful than the classical two-flow equations; nevertheless, they are identical in spirit, and the historical indebtedness of the present set with respect to the classical set is most certainly acknowledged. The remainder of the discussion will be devoted to a brief survey of some of the fundamental interrelations between optical properties which may be deduced from the transport equations for $H(z,\pm)$.

Formulas for K (z, ±) and R (z, ±) in Terms of Hybrid Optical Properties

Dividing through (50) by H(z, -) and applying the operational definitions of K(z, -) and R(z, -) we have:

$$K(z,-) = a(z,-) + b(z,-) - b(z,+) R(z,-) \,, \tag{52}$$

Similarly, from (51):

$$-K(z,+) = a(z,+) + b(z,+) - b(z,-) R(z,+) \,. \tag{53}$$

These equations show how the experimental K-functions are linked to the absorption and scattering properties of the optical medium. From these, we immediately deduce the exact counterparts to some well-known classical equations for R(z, -):

$$R(z,-) = \frac{a(z,-) + b(z,-) - K(z,-)}{b(z,+)} \tag{54}$$

and

$$R(z,-) = \frac{b(z,-)}{a(z,+) + b(z,+) + K(z,+)} \tag{55}$$

By making use of (47) and (48) these may be cast into the alternate forms:

$$R(z,-) = \frac{\alpha(z,-) - f(z,-) - K(z,-)}{b(z,+)} \tag{56}$$

$$R(z,-) = \frac{b(z,-)}{\alpha(z,+) - f(z,+) + K(z,+)} \tag{57}$$

The Basic Reflectance Relation

The preceding formulas are simple, immediate consequences of the transport equations for H(z, ±). A more fundamental relation exists and is singled out for special attention because it relates the six direct observables of principal interest : The two K-functions for irradiance, the two distribution functions, the volume absorption function and the reflectance function.

This relation is:

$$R(z,-) = \frac{K(z,-) - a(z,-)}{K(z,+) + a(z,+)} \tag{58}$$

and follows from (52), (53) by performing the operations on them indicated in (58), and simplifying the result.

The Characteristic Equation for the Pair K(z, ±)

The classical theory gives a convenient expression for k (the classical diffuse absorption coefficient of which, as we have seen, K(z, ±) are the immediate generalizations) in terms of the volume absorption coefficient a and the backward scattering coefficient b* for diffuse flux. This classical relation is:

$$k = 2\left[a(a + b^*)\right]^{1/2} \tag{59}$$

(978)

The modern exact theory yields the following counterpart to (59):

$$1 = \frac{b(z,-)}{K(z,-) - a(z,-)} - \frac{b(z,+)}{K(z,+) + a(z,+)} \qquad (60)$$

which is the characteristic equation for the pair $K(z,\pm)$. It may be deduced from (52) and (58).

The characteristic equation reduces to (59) by setting

$$b(z,-) = b(z,+) = b^* \;, \quad a(z,-) = a(z,+) = 2a \;, \text{ and } \; K(z,+) = K(z,-) = k$$

The Basic Inequalities

What relation does the magnitude of, say, $K(z,-)$ have to α (z) and a(z)? Can one rigorously show that the well-known "fact" $R(z,-) \leqslant 1$ is really true, and under what conceivable conditions can one have $R(z,-) > 1$? Is there some invariable relation between the relative depth rates of change of $H(z,+)$ and $H(z,-)$ which is sufficiently sensitive to provide a check of empirical determinations of these quantities?

To answer these questions and to prepare the ground work for answering more of this general kind, consider once again equation (50) now written in the form

$$K(z,-) = \alpha(z,-) - \frac{1}{H(z,-)} \int_{\Xi_-} N_*(z,\xi)\, d\Omega(\xi) \,. \qquad (61)$$

Since the substracted number on the right is never negative, we deduce that

$$K(z,-) \leq \alpha(z,-)$$

for all z.

Furthermore, whenever $K(z,+) \geq 0$ we have from (58)

$$a(z,-) \leq K(z,-) \,.$$

Combining these two inequalities, we answer the first question in the form.

$$a(z) \leq \frac{K(z,-)}{D(z,-)} \leq \alpha(z) \qquad (62)$$

These are the sharpest possible inequalities, since examples can be found for which equality holds on either side. A similar inequality holds for the upwelling stream:

$$a(z) \leq \frac{-K(z,+)}{D(z,+)} \leq \alpha(z) \qquad (63)$$

For a detailed discussion of these inequalities and those below, see reference 7.

To answer the second question, we return to (29) which, upon integration over a depth interval $[z_1, z_2]$ yields:

$$\bar{H}(z_1,-) + \bar{H}(z_2,+) = \int_{z_1}^{z_2} a(z)\,h(z)\,dz \geq 0 \,,$$

where

$$\bar{H}(z,\pm) = H(z,\pm) - H(z,\mp) \;;$$

hence

$$\bar{H}(z_2,-) \leq \bar{H}(z_1,-) \tag{64}$$

from which we conclude that in source-free media, the net downward irradiance never increases. If the medium is finitely deep with a bottom of reflectance r, $0 \leqslant r \leqslant 1$, then (64) clearly implies

$$0 \leq R(z,-) \leq 1$$

for all depths z. If the sea is optically infinitely deep, then again, since $\bar{H}(\infty,+)=0$,

$$\bar{H}(z,-) = \int_z^\infty a(z')\,h(z')\,dz' \geq 0$$

so that:

$$0 \leq H(z,+) \leq H(z,-) \qquad \text{i.e.} \qquad 0 \leq R(z,-) \leq 1 \tag{65}$$

once again for all depths z.

To answer the third question, one may start with (58) to find

$$K(z,-) - K(z,+)\,R(z,-) = a(z,-) + a(z,+)\,R(z,-) \geq 0$$

whence:

$$K(z,-) \geq K(z,+)\,R(z,-) \tag{66}$$

or, equivalently

$$\frac{dH(z,-)}{dz} \leq \frac{dH(z,+)}{dz} \tag{67}$$

for all depths in an arbitrarily stratified source-free sea. These inequalities should by now show the versatility of the exact two-flow theory, so we may go on to consider further questions.

The Relation Between the Depth Behavior of R(z, -) and the K-Functions

It is of interest to characterize the variation of the reflectance function in terms of the experimental K-functions. The desired formula follows immediately from the definition of R(z, -) upon differentiation:

$$\frac{dR(z,-)}{dz} = R(z,-)\left[K(z,-) - K(z,+)\right] . \tag{68}$$

From this we see that the constancy of R(z, -) over an interval is equivalent to the equality of K(z, +) and K(z, -) over that interval. If, on the other hand, K(z, -) exceeds K(z, +) at some depth z then R(z, -) is increasing at depth z; and so on.

The Basic Relations Among the Various K-Functions

The K-functions for the irradiances and the K- functions for the scalar irradiances are related by the formulas:

$$k(z,\pm) = K(z,\pm) - \frac{1}{D(z,\pm)}\,\frac{dD(z,\pm)}{dz} \tag{69}$$

Thus, the little k's and the big K's coincide at a certain level when and only when the directional structure of the radiance distribution does not change in a vertical neighborhood of that level.

For the purposes of unifying all of the K-functions, we may use $K(z, \underline{\xi})$, perhaps the most fundamental of them all. This is the K-function associated with the radiance function:

$$K(z, \underline{\xi}) = \frac{-1}{N(z, \underline{\xi})} \, \frac{dN(z, \underline{\xi})}{dz} \tag{70}$$

From this and the preceding definitions, it may be deduced that:

$$K(z, \pm) = \frac{\int_{\Xi_\pm} N(z, \underline{\xi})\, K(z, \underline{\xi})\, \underline{\xi} \cdot \underline{n} \; d\Omega(\underline{\xi})}{\int_{\Xi_\pm} N(z, \underline{\xi})\, \underline{\xi} \cdot \underline{n} \; d\Omega(\underline{\xi})} \tag{71}$$

$$k(z, \pm) = \frac{\int_{\Xi_\pm} N(z, \underline{\xi})\, K(z, \underline{\xi})\, d\Omega(\underline{\xi})}{\int_{\Xi_\pm} N(z, \underline{\xi})\, d\Omega(\underline{\xi})} \tag{72}$$

$$k(z) = \frac{\int_{\Xi} N(z, \underline{\xi})\, K(z, \underline{\xi})\, d\Omega(\underline{\xi})}{\int_{\Xi} N(z, \underline{\xi})\, d\Omega(\underline{\xi})} \tag{73}$$

These representations will form a basis for the important conclusions about the asymptotic values of the K-functions in optically deep seas, which appear in the closing paragraph below.

The Covariation of K(z, -) and D(z, -)

If measurements of K(z, -) are made within a small depth interval about a fixed depth in the sea over a period of time during which only the external lighting conditions change, how does this change manifest itself in the recorded values of K(z, -)? Alternatively, how does K(z, -) depend on the shape of the radiance distribution at depth z, assuming the inherent optical properties do not change?

An answer to this question may be made by appealing once again to (61). Let

$$h_*(z, -) = \int_{\Xi_-} N_*(z, \underline{\xi})\, d\Omega(\underline{\xi}) \tag{74}$$

The physical significance of this concept is readily discerned: $h_*(z, -)$ is the downwelling scalar irradiance generated by radiant flux scattered by a unit volume at depth z. With this definition (61) becomes

$$K(z, -) = \left[\alpha(z) - \frac{h_*(z, -)}{h(z, -)} \right] D(z, -) \tag{75}$$

On the basis of this formula it may be shown that in all forward scattering media, of which the sea is an outstanding example, K(z, -) varies directly (but not necessarily linearly) with D(z, -). Thus, if D(z, -) increases, remains the same, decreases over a period of time, the inherent optical properties remaining unchanged, then K(z, -) likewise increases; remains the same, decreases over the same time period. For further details on this and related matters, along with some useful rules of thumb deduced from (75), see reference 9.

The Asymptotic Light Field

I have mentioned several times throughout this discussion that the apparent optical properties of the sea, despite their dependence on highly variable lighting conditions, nevertheless, exhibit certain striking regularities in both time and space. In this, the concluding part of the discussion, I wish to bring to your attention perhaps one of the most remarkable of all these regularities and its manifold consequences. This concerns the asymptotic (or limiting) behavior of the light field as great depths are approached in deep natural waters. The experimental evidence for this phenomenon is by now well established. The pioneering experiments by Whitney are perhaps the best known and best documented early instances in this matter (reference 10).

I wish now to formulate this phenomenon in terms of the apparent optical properties defined above and to draw out some of its practical consequences. For further consequences see reference 11. Proofs of the asymptotic radiance theorem will be omitted; they may be found in references 12 (the general case) and 13 (the case of the sea).

Briefly and simply the asymptotic radiance theorem states that, regardless of the external lighting conditions, the directional (ξ) and depth dependences (z) of the radiance distribution N(z, ξ) multiplicatively uncouple at great depths in all homogeneous, or eventually homogeneous waters. That is, at great depths we may write:

$$N(z,\underline{\xi}) = N(z_0,\underline{\xi})\, e^{-k_\infty (z-z_0)} \qquad (76)$$

where z_0 is some depth below which

$$K(z,\underline{\xi}) = k_\infty \qquad (77)$$

Here k_∞ is a fixed magnitude independent of direction ξ and which depends only on the inherent optical properties of the sea. Thus the shape of the radiance distribution eventually settles down to some fixed form which is independent of the external lighting conditions and dependent only on α and σ. More precisely, if

$$\lim_{z\to\infty} \sigma(z,\underline{\xi},\underline{\xi}') \equiv \sigma(\xi,\xi') \quad \text{exists}$$

and

$$\lim_{z\to\infty} \alpha(z) \equiv \alpha \quad \text{exists}$$

in an infinitely deep sea, then

$$\lim_{z\to\infty} K(z,\underline{\xi}) = \lim_{z\to\infty} k(z) = k_\infty \qquad (78)$$

exists for each ξ in Ξ. This is the content of the asymptotic radiance theorem in terms of inherent and apparent optical properties. The two versions of the theorem (76) and (78) are equivalent. From this we may deduce manifold consequences. For example:

(i) $$\lim_{z\to\infty} K(z,\pm) = \lim_{z\to\infty} k(z,\pm) = k_\infty \qquad (79)$$

which follows from (78) and (71), (72).

(ii) $$\lim_{z\to\infty} D(z,\pm) \equiv D(\pm) \quad \text{exists} \qquad (80)$$

which follows from (78) using (76) and (40)

(iii) $$\lim_{z\to\infty} R(z,-) = \frac{k_\infty - D(-)a}{k_\infty + D(+)a} \qquad (81)$$

which follows from (58), (78), (79) and (80).

From these few examples we see the vast simplifications, implied by the asymptotic radiance theorem, which are in store for the experimental study of light fields at great depths in essentially homogeneous media.

(982)

More generally, from these examples and the arguments presented above it is hoped that the main point of the present discussion has been made: By taking a strictly operational point of view of the general equation of transfer, it may be used without once solving it, or subjecting it to vitiating assumptions about the structure of of either the medium or the light field within the medium to erect a systematic classification of the optical properties of the sea and the attendant theory for these properties.

References

1. Preisendorfer, R.W., A Mathematical Foundation for Radiative Transfer Theory, J. Math. and Mech., 6, 685-730 (1957).
2. Preisendorfer, R.W., A General Theory of Perturbed Light Fields, with Applications to Forward Scattering Effects in Beam Transmittance Measurements. Scripps Institution of Oceanography, La Jolla, California, S10 Ref. 58-37 (1958).
3. Preisendorfer, R.W., and J.E. Tyler, The Measurement of Light in Natural Waters: Radiometric Concepts and Optical Properties, Scripps Institution of Oceanography, La Jolla, California, S10 Ref. 58-69 (1958).
4. Preisendorfer, R.W., On the Direct Measurement of the Total Scattering Function, Scripps Institution of Oceanography, La Jolla, California, S10 Ref. 59-41 (1959).
5. Preisendorfer, R.W., The Divergence of the Light Field in Optical Media, Scripps Institution of Oceanography, La Jolla, California, S10 Ref. 58-41 (1957).
6. Preisendorfer, R.W., Unified Irradiance Equations, Scripps Institution of Oceanography, La Jolla, California, S10 Ref. 58-43 (1957).
7. Preisendorfer, R.W., Directly Observable Quantities for Light Fields in Natural Hydrosols, Scripps Institution of Oceanography, La Jolla, California, S10 Ref. 58-46 (1958).
8. Tyler, J.E., Radiance Distribution as a Function of Depth in the Submarine Environment, Scripps Institution of Oceanography, La Jolla. California, S10 Ref. 58-25 (1958).
9. Preisendorfer, R.W., The Covariation of the Diffuse Attenuation and Distribution Functions in Plane Parallel Media, Scripps Institution of Oceanography, La Jolla, California, S10 Ref. 59-52 (1959).
10. Whitney, L.V. , The Angular Distribution of Characteristic Diffuse Light in Natural Waters, J. Mar. Res. 4, 122-131 (1941).
11. Preisendorfer, R.W., Some Practical Consequences of the Asymptotic Radiance Hypothesis, Scripps Institution of Oceanography, La Jolla, California, S10 Ref. 58-60 (1958).
12. Preisendorfer, R.W., A Proof of the Asymptotic Radiance Hypothesis, Scripps Institution of Oceanography, La Jolla, California, S10 Ref. 58-57 (1958).
13. Preisendorfer, R.W., A Theoretical Proof of the Existence of Characteristic Diffuse Light in Natural Waters, J. Mar. Res., 18, 1-9 (1959).

DISCUSSION

Prof. Ivanoff: Je voudrais remarquer que, étant donné que l'équation de base de la "radiative transfer theory" traduit le principe de conservation de l'énergie, certains résultats obtenus à l'aide de ce mode de calcul peuvent être obtenus très rapidement en appliquant directement le principe de conservation de l'énergie. Ainsi, en écrivant que l'énergie pénétrant dans une couche d'eau de mer d'épaisseur dZ est égale à l'énergie qui en ressort plus celle qui s'y trouve absorbée, on obtient la relation établie par le Dr. Preisendorfer entre le coefficient d'absorption, les éclairements sur les deux plans limitant la couche considérée, et l'éclairement dit "sphérique".

Dr. Preisendorfer: This view complements very nicely the statement I made at the outset of my talk, namely: "The equation of transfer may be viewed by the experimenter as a symbolic summary of operations with actual instruments in the sea". In particular, the empirically based law of conservation of energy as regards radiative transfer phenomena is already contained in the equation of transfer. Thus, as I had shown in 1957 (Preisendorfer, R.W. "The Divergence of the Light Field" S.I.O. Ref.

58-41, Scripps Inst. Oceanogr. 1957) by simply integrating the equation at a point in the sea over all directions, one deduces immediately that the divergence $\nabla . H (Z)$ of the vector irradiance is zero if

$$a (Z) = 0$$

and the radiant energy is conserved.

If

$$a (Z) \neq 0$$

then we may deduce how to measure directly the volume absorption function a (Z).

International Union of Geodesy and Geophysics.
INTERNATIONAL ASSOCIATION OF PHYSICAL OCEANOGRAPHY

Symposium on Radiant Energy in the Sea.
Helsinki, 4-5 August 1960. Monograph No.10
June 1961. pp. 40-45.

ON THE MEASUREMENT OF THE SCATTERING FUNCTION OF THE SEA

by

J.E. Tyler (*)

The most common form of the operational definition for the volume scattering function $\sigma(\theta)$ is given in equation 1).

$$\sigma(\theta)=\frac{J(\theta)}{H\ V} \qquad 1)$$

where $J(\theta)$ is the intensity of the scattered light in the direction θ, and H is the flux per unit area incident on the sample volume V. This equation is based on two important assumptions, first, it applies to monochromatic light and second, it applies only when the sample volume is so small that the magnitude of $J(\theta)$ is linear with changes in volume, regardless of the scattering and absorbing properties of the sample.

In determining the volume scattering function of the sea it is frequently important to make in situ measurements because of the changes that can take place in the sea water if it is pumped or if its environment is changed.

Two instruments have been described recently which have been specifically designed for in situ measurements of the volume scattering function of sea water. Most recently (1960) Dr. Jerlov (1) has described an exceedingly clever yet inexpensive scattering meter for oceanic exploration. The other instrument described by Tyler (2) was designed for scattering research but can also be used for oceanic measurements. Several instruments and methods have also been described which utilize a captive sample. An earlier instrument described by Jerlov (3), an instrument of unusual design described by Koslyaninov (4), and a method described by Tyler (5) all fall in this latter category.

One of the difficulties associated with instruments that measure directional scattering by varying the angle of observation, is that the maximum and minimum angles of observation are usually limited by the dimensions of the instrument. Thus important values of the volume scattering function in the forward direction may not be measurable or may be in doubt. Important and interesting values in the backward direction may also escape measurement. As a result, the value of the total scattering coefficient S computed from equation 2)

$$S = 2\pi\int_0^{180}\sigma(\theta)\sin\theta\, d\theta \qquad 2)$$

will be in error by an amount which depends on the method used for extrapolating $\sigma(\theta)$ to 0° and 180°.

In order to obtain a better knowledge of the magnitude of the error from this source, check the method of extrapolation, and improve the instruments and techniques for measuring scattering, two independent measurements have been applied to a variety of stable hydrosols.

Experimental Procedure

Hydrosol samples of varying properties were prepared in a large tank, shown in Figure 1, by mixing a scattering agent with distilled water. Enough sample was prepared to permit the measurement of its volume scattering function using the instrument shown in Figure 2. Some of the details of this instrument and its calibration have been given in a previous publication (2).

(*) This research has been performed as part of the Scripps Institution of Oceanography Hydrologic Optics program and has been supported by the National Science Foundation.

(985)

Contributions from the Scripps Institution of Oceanography, New Series, 1326
Reproduced by Permission

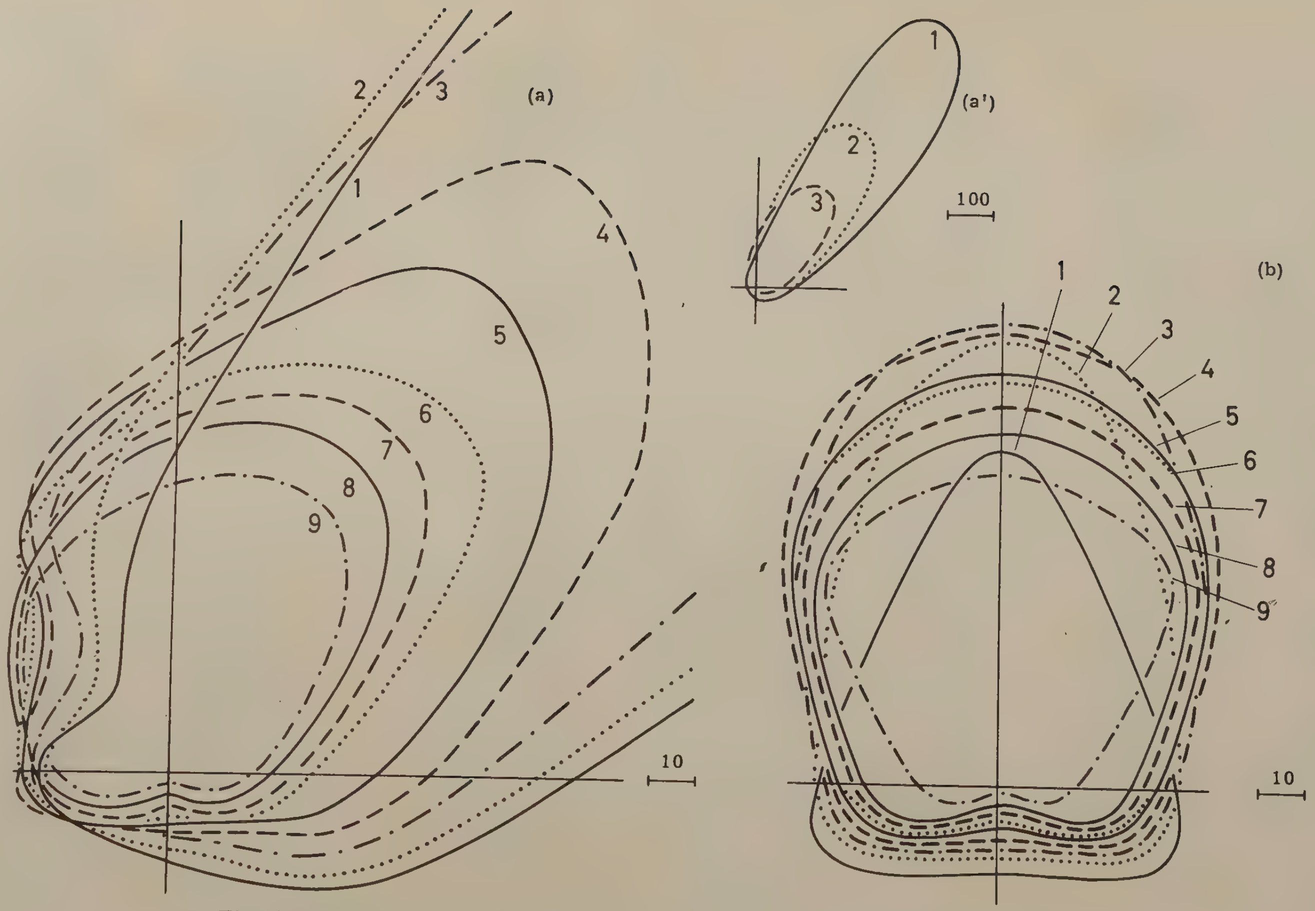

Fig. 8. Polar Diagrams of the luminance at different depths $\tau_1 = 27.6$, $\bar{\omega}_o = 1$. Curves 1 : $\tau = 3.18$; 2 : $\tau = 5.7$; 3 : $\tau = 8.2$; 4 : $\tau = 10.7$; 5 : $\tau = 13.2$; 6 : $\tau = 16.1$; 7 : $\tau = 18.2$; 8 : $\tau = 20.7$; 9 : $\tau = 24.0$

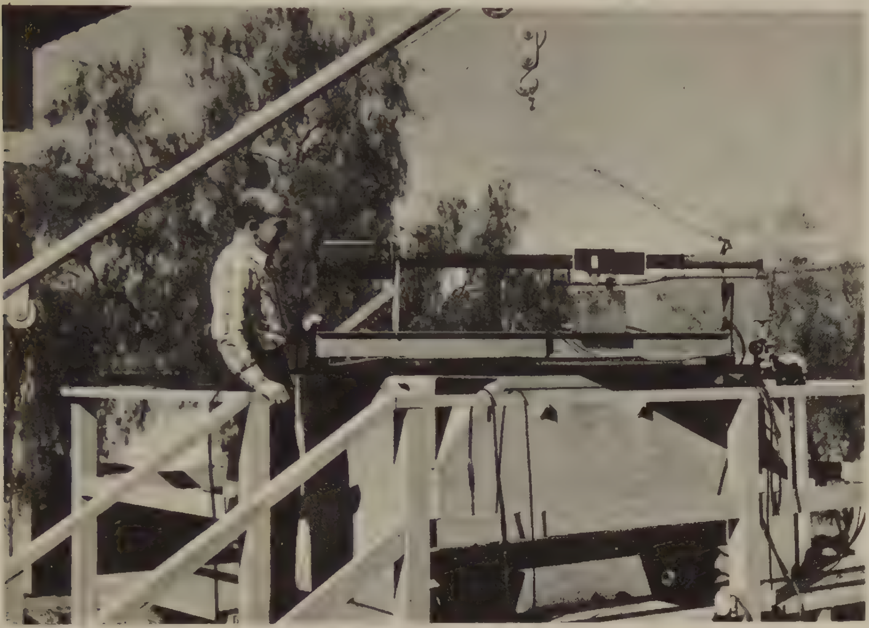

Fig. 1. The 1300 gallon tanks used for preparing hydrosol samples. The scattering meter and α - meter used for measuring the samples can also be seen.

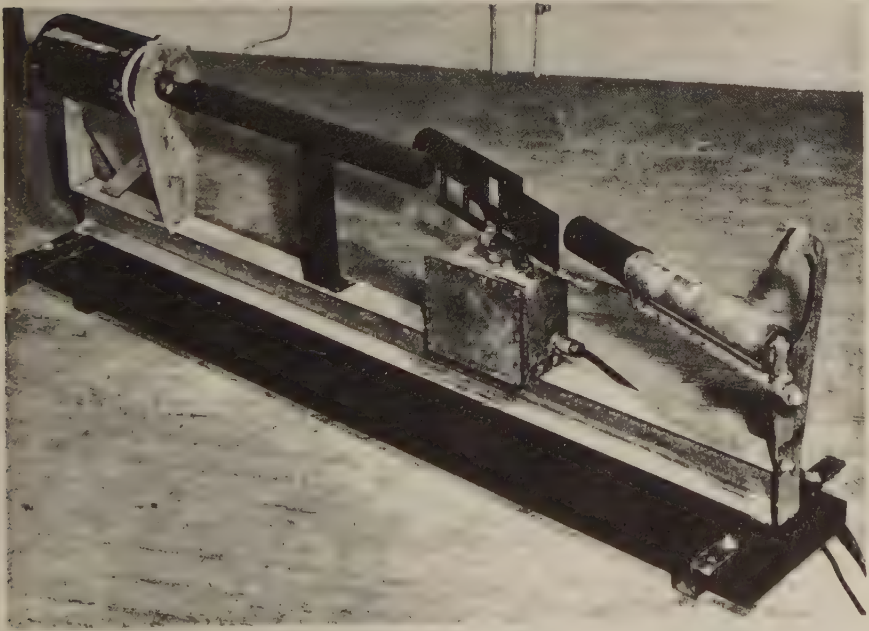

Fig. 2. Scattering meter used to measure the volume scattering function of the hydrosols.

The method of computing volume scattering function from instrumental data has also been given (2) and for various hydrosols yields the information illustrated in Figures 3 (solid lines), and 3a.

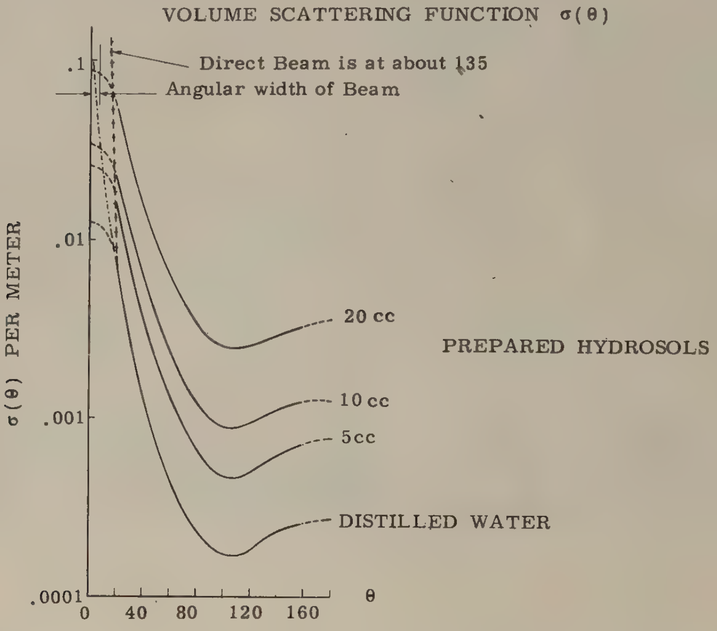

Fig. 3. Volume scattering functions for prepared hydrosols. Dashed portions of curves are extrapolated by the divided differences method. Dot and dashed extension of the curve for distilled water indicates another possible extrapolation. The magnitude of the direct beam is also indicated by the line of crosses.

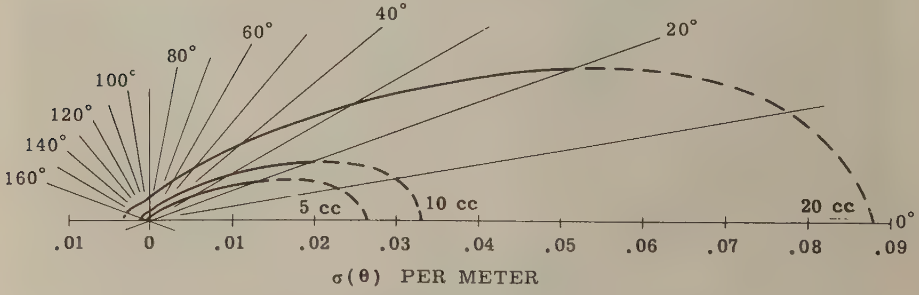

Fig. 3a. Three samples from Fig. 3 replotted in polar coordinates with linear scale for σ(θ).

The data was extrapolated to 0° and 180° by means of Newton's "divided differences" method (6). Extrapolated portions of the function are shown by dashed lines.

Equation 8 of reference (2) requires a measurement of the total attenuation coefficient α which in this experiment was measured for each hydrosol using the instrument shown in Figure 4.

As nearly simultaneously as possible with the scattering measurement a five liter sample was carefully siphoned from the tank into a special measuring cell shown in Figure 5 for measurement of the total fractional scattering in a null-type spectrophotometer. The details of this method have also been published (5).

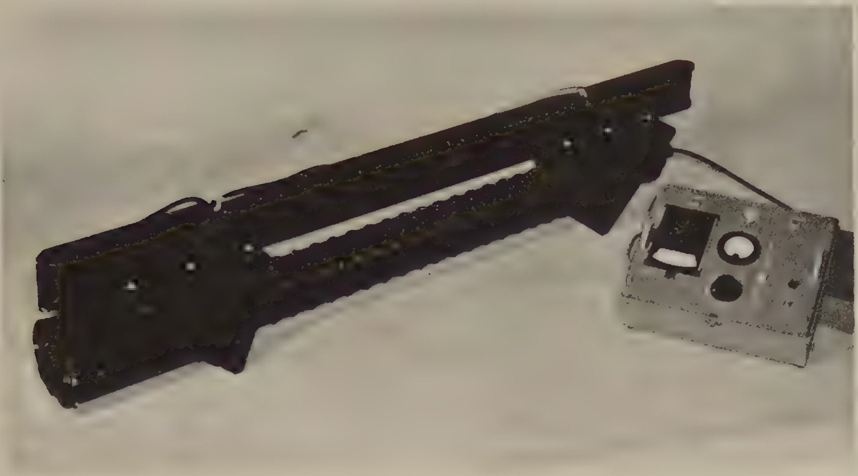

Fig. 4. α - meter

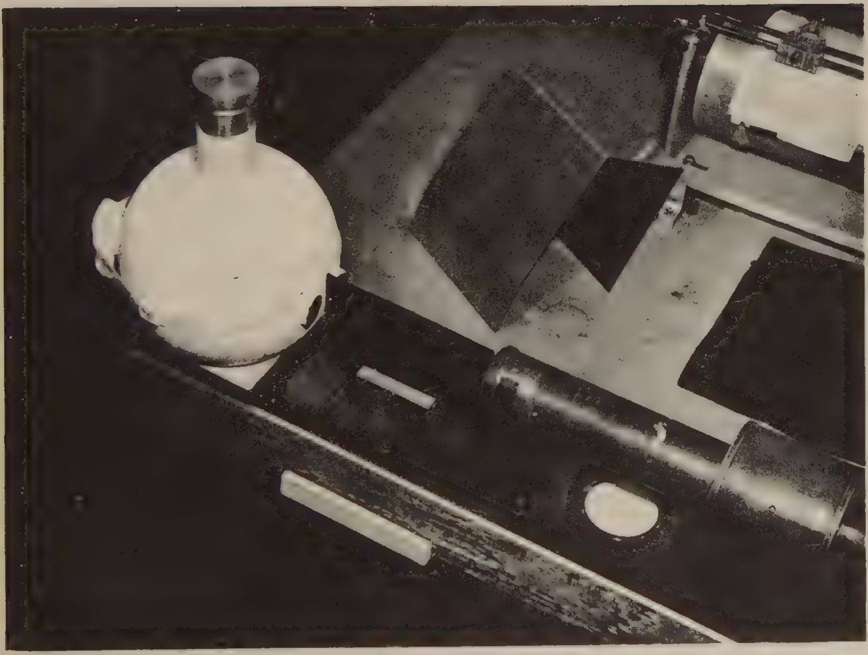

Fig. 5. Spherical measuring cell shown in place on an automatic recording spectrophotometer.

(989)

In order to obtain an idea of the correlation between these two methods a series of measurements was made on prepared hydrosols having absorption coefficients not much greater than water. The range in total attenuation coefficient, however, was from .685 to 1.897 per meter, a considerably greater range than would be expected in the ocean. Within this range the ratios of the total scattering coefficients obtained by the two methods varied by ± 10% of the ratio and was statistically judged to be a constant. The correlation coefficient between the two methods was computed to be .992.

Figure 6 gives the results of a series of measurements on prepared hydrosols having a range in total attenuation coefficient from .086 to .660 per meter. This series contained samples in which the absorption coefficient had been deliberately increased by the addition of a dye. The dashed line in Figure 6 represents the locus of points exhibiting perfect correlation.

The close correlation between the two methods and the fact that they give substantially the same answer would indicate that the extrapolation procedure is a realistic one, at least for the type of hydrosol employed in the experiment.

The question remains, of course, whether or not this extrapolation is satisfactory for ocean water. No data is yet available but some light may be thrown on the problem by comparing the ratios of the light scattered at 45° to the total scattering coefficient. This ratio has been found to be a constant for the ocean (Jerlov (3)) and would be expected to be constant for these prepared samples if they were like ocean water. Table I gives this ratio together with the total attenuation coefficient for each sample.

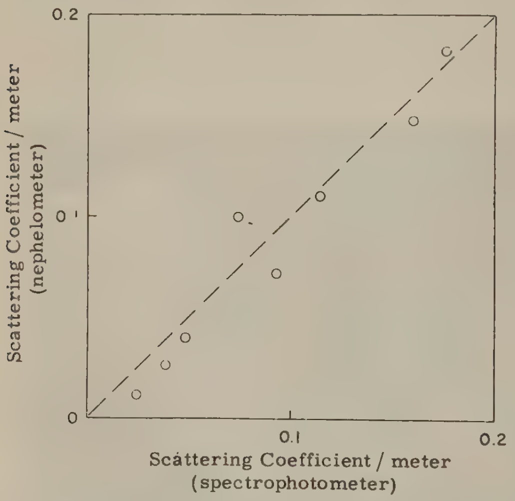

Fig.6. Plot showing correlation between the two methods for measuring the total scattering coefficient.

TABLE I

Sample	α	$^S/_\sigma$ (45°)
1	.0861/m	10.35
2	.1107	7.89
3	.1403	8.23
4	.1659	8.44
5	.2195	8.85
6	.2696	8.35
7	.3021	8.38
8	.3581	8.35
9	.3672	8.35
10	.4309	8.43
11	.5864	8.35
12	.6354	8.06
13	.6604	8.98

References

1. Jerlov, N.G., Unpublished.
2. Tyler, J.E., Nephelometer for the measurement of volume scattering function in situ. JOSA, 48, pp. 354-357 (1958).
3. Jerlov, N.G., Particle distribution in the ocean. Reports of the Swedish deep-sea expedition 1947-1948. Vol. III, Physics and Chemistry N° 3, Göteborg (1953).
4. Kozlyaninov, M.V., New instrument for measuring the optical properties of sea water, Trudy Instituta Okeanologie, Akademii Nauk SSSR Vol. XXV, pp. 134-142 (1957).
5. Tyler, J.E., Monochromatic measurement of the volume scattering of natural waters, JOSA, Vol. 47, 745-747, (1957).
6. Eshbach, O.W., Handbook of Engineering Fundamentals, John Wiley and Sons. New York, 2nd Ed. pp 2-31.

DISCUSSION

Prof. Sekara: The forward scattering in the atmosphere can be followed by rather simple theory and this theory agrees quite well with the measurements for very small scattering angles. This theory and measurements indicate much sharper increase of the radiance for smaller scattering angles. The curved part appears for scattering angles $< 1°$.

The direct application of the theory may be thought difficult for liquid medium, because it requires the knowledge of the relative index of refraction for the scattering centers.

Dr. Tyler: Acknowledged.

Dr. Preisendorfer: I presume that Prof. Sekera is referring to the Mie theory of scattering of dielectric spheres. Is this guess correct? Furthermore, is multiple scattering between the particles taken into account before applying the theory to find the appropriate extrapolation?

Prof. Sekera: The guess is correct. It is based on the electromagnetic theory with analytical approximation allowing the integration over size distribution. Since the measured volumes are small, the effect of multiple scattering which was neglected is small.

Dr. Jerlov: The constancy of the relation between total scattering and scattering through 45° obviously proves that the volume scattering function shows small fluctuations which is also indicated by actual measurements in the sea.

(992)

Reprinted from OCEANOGRAPHY
AMERICAN ASSOCIATION FOR THE ADVANCEMENT OF SCIENCE
Copyright 1961
pp. 583–597

Chemistry in the Oceans

EDWARD D. GOLDBERG

Scripps Institution of Oceanography, University of California, La Jolla, California

STUDIES in marine chemistry have gone through several phases since its birth with the first quantitative assays of sea water by Torbern Bergman, the famed Swedish scientist, and Antoine Lavoisier, the father of modern chemistry, at the turn of the eighteenth century. The seas were depicted as arising from the washings of the surface of the earth by natural waters, and investigations on both its chemistry and that of the organisms had a significant role in the development of chemistry. As you are well aware, the elements bromine and iodine were discovered in sea salt and marine algal ash, respectively.

When the rather dramatic effects of primary plant production on the distribution of some chemical species in the oceans were established during the first several decades of the twentieth century, impetus was given to work on the fertility of surface waters and the results of the combustion of the organic material in the deeper waters.

In the mid-twentieth century some attention again has been focused on the inorganic chemistries in the oceans, work paralleling and reflecting advances made in the mother science, chemistry. The geochemical behavior of elements during their residence in the sea, subsequent to their introduction from the continents and atmosphere, has provided the background for many recent investigations.

Although the discovery of new elements is apparently limited to a small group of people working in the foothills of Berkeley, California, two naturally produced radioisotopes have been initially found in the marine domain. Both of these isotopes, Be^{10} and Si^{32} are produced in the upper atmosphere by the cosmic ray fragmentation of the earth's enveloping gases, Be^{10} from nitrogen

Contributions from the Scripps Institution of Oceanography, New Series. 1327
Reproduced by Permission

and Si^{32} from argon. The beryllium isotope with a half-life of 2.7 million years was simultaneously found by groups led by Dr. James Arnold (1956) of Princeton and Dr. B. Peters (Goel *et al.*, 1957) of Bombay in the deep-sea sediments of the Pacific Ocean. Dr. Lal of Bombay and I (1959) have sought and observed Si^{32} in siliceous sponges taken from waters of the mixed layers.

In both cases the marine realm provides the unique sites for the accumulation of these radioactive species in amounts that are readily extractable for quantitative assay. These cosmic ray-produced isotopes come down to the land and sea surfaces in atmospheric precipitation but are heavily diluted in the relatively large amounts of stable silicon and beryllium contained in the continental surfaces, whereas in the oceans, the quantities of stable beryllium and silicon, at least in surface waters, are small and allow the specific activity, the disintegrations of the isotope per weight of its stable form per unit time, to attain reasonably high values.

The beryllium concentration in sea water (Merrill *et al.*, 1960) is of the order of 6×10^{-4} of a part per billion by weight. Hence, a 4000-m water column, representing the average oceanic depth, contains per square centimeter about the same amount of beryllium as a millimeter depth of average earth's crust which has for all practical purposes a uniform beryllium content of a few parts per million. Thus, two effects tend to reduce continental specific activities of Be^{10} to values lower than those of the marine environment: (*a*) mixing of the radioisotope with stable beryllium to levels on land greater than a millimeter; and (*b*) the runoff into the oceans of any of the isotopes taken up by the rivers. Hence, the authigenic minerals on the sea floor, solid phases that derive their components from the chemical species in sea water, readily revealed measurable quantities of Be^{10}.

Similarly, the low concentrations of silicon in surface sea waters, resulting from the assimilation of monomeric silicic acid and/or its ions by the photosynthesizing diatoms, suggest a promising medium for the attainment of high specific activities of Si^{32}. If we assume the depth of the mixed layer to be 100 m and to contain 15 micromoles of silicon per liter, a 1-cm² column of such waters contains about the same amount of inert silicon as 0.01 cm of

(994)

earth's surface. We have found that a disintegration rate of one per minute, readily measurable, necessitates the extraction of roughly 100 g of opal or silicon dioxide. Such quantities are available from siliceous sponges living in environments of the mixed layer waters. For every 100 g of sponge-produced opal, the equivalent of 100 tons of sea water must have had its silicon depleted to zero by the activity of these animals. Deep-sea sponges require the equivalent of 10 tons of sea water to obtain a corresponding amount of silicon inasmuch as these waters contain on the average 10 times more silicon.

Let us now turn to the more general problem of chemical processes in the oceans. Chemical reactions take place at phase discontinuities, i.e., the atmosphere-hydrosphere, biosphere-hydrosphere, and sediment-hydrosphere interfaces. We shall focus our attention mainly on the reactions of sea water with the solid components of the sea floor.

We can reasonably expect that most inorganic species correspond closely to those predicted from complete equilibration between all reacting substances. Such thermodynamically unstable species as iodide and manganous ions probably exist because the waters that contain them have been inaccessible to surfaces at which reactions to stable substances might occur. We shall return to this concept in considerations of the formation of ferromanganese minerals on the sea floor.

Insight into the *relative reactivities* of elements in the marine hydrosphere has been obtained from considerations of the average time an element spends in the oceans. An extremely simple model of the ocean is used in which it is assumed that the presently observed chemical composition represents a steady state system in which the amount of material introduced per unit time is compensated by an equal amount deposited as sediments. A further assumption is that there is a complete mixing of materials introduced into the oceans in times that are short with respect to the residence times. We can then define the residence time of an element as the total amount of the element in sea water divided by the amount of the given element introduced by the rivers or precipitated to the sediments per unit time.

About seven years ago Barth (1952), on the basis of rive influxes of the elements, initiated such calculations, and his data are shown in Table I. An alternate approach has been made upon the basis of the total amount of sedimentation in the marine environment (Goldberg and Arrhenius, 1958), and the residence times so derived also are shown in Table I. A remarkable agreement is observed between these sets of data. The only striking discrepancy is found for the case of calcium. The many difficulties in trying to obtain a geochemical balance for this element are well known, and we certainly have not been able to resolve this difficulty, at least within a factor of 8.

Although many independent assumptions are involved in the calculations, both the absolute and relative values for most of the residence times appear reasonable. Sodium has a residence time within an order of magnitude of the age of the oceans, several billion years. This lack of reactivity is in accord with its aqueous chemistry. The alkali and alkaline earth metals have residence times in the range of 10^6 to 10^8 years. Manganese shows a remarkably low value, 7000 years, especially in comparison with the metals nickel and zinc, which probably have similar chemistries

TABLE I. Residence Times of Elements in the Oceans

Element	Amount in Oceans, g	Residence Time, Years	
		Goldberg and Arrhenius (1958)	Barth (1952)
Na	1.47×10^{22}	2.6×10^8	2.1×10^8
Mg	1.8×10^{21}	4.5×10^7	2.2×10^7
Li	2.8×10^{17}	2.2×10^7	
Sr	9.8×10^{18}	1.6×10^7	
K	5.3×10^{20}	1.1×10^7	1.0×10^7
Ca	5.6×10^{20}	8.0×10^6	1.0×10^6
U	5.2×10^{15}	6.5×10^5	
Zn	1.4×10^{16}	1.8×10^5	
Cu	5.2×10^{15}	6.5×10^4	
Co	7.0×10^{14}	1.8×10^4	
Si	5.2×10^{18}	1.0×10^4	3.5×10^4
Pb	$<4.0 \times 10^{14}$	$<1.0 \times 10^4$	
Mn	1.4×10^{15}	7.0×10^3	
Th	$<2.8 \times 10^{13}$	$<1.4 \times 10^3$	
Fe	1.4×10^{16}	1.4×10^2	
Ti	1.4×10^{15}	1.6×10^2	
Al	1.4×10^{16}	1.0×10^2	

in the divalent state and are associated with manganese in marine deposits. The residence times of these latter elements are about 500 times higher. This reactivity of manganese is apparently related to the removal of this element from solution by oxidation to the tetravalent state to form the ferromanganese deposits, a subject we shall discuss subsequently. The sorption of the associated metals like zinc and nickel to the precipitated manganese requires a relatively larger amount of manganese. This results in longer residence times, compared to manganese, for these metals.

Silicon and aluminum are among the elements with the shortest calculated residence times. Both elements enter the oceans in both solid and dissolved phases; the solid phases, such as quartz, feldspars, and clay minerals, rapidly settle to the bottom. Iron and titanium which also quickly pass through the hydrosphere, prevail as solid phases during the major part of their residence. The absolute values for the residence times of these elements are somewhat tenuous as the assumption that such times are small in comparison with the mixing times of oceanic water masses, say of the order of hundreds to thousands of years, is invalid. It may be worthwhile in the future, when values exist for the contribution of solid and dissolved phases of these elements to the total concentrations, to calculate more accurately the residence times of the components.

The utility of such computations, the derivation of residence times, arose recently in our laboratory in the study of thorium isotopes as a dating tool for marine sediments. We were concerned primarily with two isotopes, normally occurring thorium, Th^{232}, and ionium, Th^{230}, which is one of the daughter products of the most abundant isotope of uranium, U^{238}. The residence of thorium can only be given in terms of an upper limit inasmuch as the thorium concentration in sea water has never been determined. A value of a life in sea water of less than one thousand years, probably closer to one hundred years, is derived for thorium on the basis of a maximum concentration in sea water of 10^{-8} g/liter.

The extremely short residence time of thorium suggests the possibility of ocean to ocean variations in its concentration. Those bodies of water exposed to the introduction of large amounts of continental runoff may very well be enriched in normally occurring thorium compared to sea waters which are isolated from land drainage for times comparable to the residence time of thorium.

The uranium-derived isotope of thorium, Th^{230}, provides a convenient normalization for intraocean comparisons of thorium contents. Uranium has a residence time of the order of a million years, a time that is long with respect to oceanic mixing processes. Hence, one would expect and one does find a uniform content of uranium in sea water, a value around 3.5 μg/liter. Thus, the rate of production of its daughter ionium per unit volume of sea water is constant in all oceans. The ionium input from land is less than one-fourth of this oceanic production value and is unimportant in our considerations. Since the aqueous chemistry of thorium involves only one valence state, we can make the initial assumption that both thorium and ionium will be present in the oceans in similar chemical forms. Thus, we shall seek out the ratio of ionium to thorium as a measure of possible thorium variations in the ocean.

Although the thorium content of sea water is so low that its actual value so far has escaped detection by modern analytical techniques, some surface minerals on the sea floor, which accumulate thorium in measurable amounts from the over-lying sea waters, should provide a convenient index of the sea water concentrations. The thorium isotopic ratios given in Table II were obtained from the authigenic minerals in the upper 2 or upper 4 cm of deep-sea sediments. The lowest values of thorium compared to ionium are found in the South Pacific Ocean whereas the highest numbers occur in the Atlantic Ocean. Intermediate values are found in the North Pacific.

These values are reasonable when one looks at the relative

TABLE II. Values of Ionium/Thorium Ratio in Hydrogenous Minerals from Surface Sediment Samples

Area	Io/Th, Units of Disintegrations of Ionium/ Disintegration of Thorium/Unit Time
Atlantic	12
North Pacific	25
South Pacific	150

contribution of land runoff waters to these oceanic areas. Table III gives the areas of the oceans and the respective areas of land that are drained into the oceans. The Pacific receives but one-sixth of the amount of drainage waters that enter the Atlantic on an areal basis, which apparently accounts for the higher values of thorium, normalized to ionium, in the Pacific sediments. Similarly, the well-known observation that more and larger rivers drain into northern hemispheric marine areas is reflected in the higher ionium/thorium ratios in southern Pacific deposits as compared to their northern counterparts. Thus, the concentration of thorium in the deeper parts of the ocean is seen to have an ocean to ocean variation, explainable, on the basis of our simple thesis of the residence time of thorium being small with respect to the times of oceanic mixing, coupled with the yearly contributions of thorium draining into the world's oceans.

Let us now turn to a rather dramatic example of chemistry occurring on the sea floor, the formation of the ferromanganese minerals, the major components of the manganese nodules. These minerals represent the most nearly unique and possibly the most abundant, and for these reasons, the most studied of the marine authigenic minerals. They exist in the form of nodular concretions which range in size from millimeters to about a meter, coatings about rocks and shells, and as components of the unconsolidated sediments. The two principal metals, iron and manganese, which occur as oxides or hydroxides, are normally present in similar amounts, although, less generally, either of these two elements can be dominant. They are found on all oceanic floors and normally occur in localities where the total rate of accumulation of sediments

TABLE III. Oceanic Areas and Complimentary Land Areas Draining into Them (in thousands of square kilometers) (Lyman, 1958)

Ocean	Area	Land Area Drained	Percentage
Atlantic	98,000	67,000	68.5
Indian	65,500	17,000	26.0
Antarctic	32,000	14,000	44.0
Pacific	165,000	18,000	11.0

is low. Menard and Shipek (1958) estimate that between 20% and 50% of the deep-sea floor in the southwestern Pacific is covered with nodules on the basis of the photographs of the bottom and the occurrence of nodules in cores. Phillipsite, barite, and fish debris, phases which are strongly diluted in rapidly amassing deposits, are found in high concentrations in areas associated with ferromanganese minerals.

The ferromanganese minerals act as hosts for a suite of elements which include copper, nickel, cobalt, zinc, lead, thorium, and the rare earths. These guest metals, which are enriched in the ferromanganese minerals, as well as the manganese, exist in sea water in states of undersaturation (Goldberg, 1958), and their assimilation by these minerals has been postulated to account at least in part for this situation.

Their unique chemical composition, unlike that of any terrestrial mineral has strongly indicated the authigenic character of the ferromanganese accumulations (Table IV). Further support comes from the lead isotopic analyses of Chow and Patterson (1959), who point out that the distinctive values of the radiogenic lead isotopes suggest a derivation of the lead from sea water.

TABLE IV. Average Composition of Manganese Nodules from the Pacific Ocean

Element	Weight %
Fe	14
Mn	19
Ni	0.4
Co	0.3
Cu	0.5
Ti	0.8
Zn	0.04
Pb	0.1
P	0.5
Al	0.7
Zr	0.006

Structural investigations by Buser and Grütter (1956) by x-ray and electron microscopic techniques indicate the minerals are composed of the crystalline iron and manganese compounds, δ-MnO_2, manganites and goethite, as well as some amorphous fractions. δ-MnO_2 is composed of disordered sheets of manganese dioxide, whereas the manganite crystals possess a double layer-lattice structure in which ordered layers of manganese dioxide alternate with disordered layers of manganous or ferric hydroxides or basic salts. The disordered layer is the site for the accumulation of the metal ions whose enrichment in these materials has been pointed out previously. In nodules with amounts of iron, greater than can be accommodated in the disordered layer, the mineral goethite appears. Buser (personal communication) points out that the appearance of goethite in the minerals suggests that particles of fresh iron hydroxide, or oxides of lower molecular weight, are initially deposited, which possess the potentiality of transformation to goethite.

The rates of accretion of these minerals on surfaces or during formation of the nodules is extremely slow. The "Horizon" nodule, a large concretion dredged from the North Pacific with a longest dimension of about 1 m, was analyzed by the ionium-thorium method and was found to amass its solid phases at a rate of somewhat less than 0.01 mm per thousand years or a rate of about one atomic layer per day. This is probably one of the slowest reactions occurring in nature in which a measure of the rate of the reaction can be ascertained. It should be emphasized that such rates are not necessarily continuous, as often layers of clay or detrital materials are found between the slowly accreting ferromanganese lamina.

The rather exotic nature of these minerals has inspired a number of hypotheses as to their mode of formation. The early workers were more concerned with the immediate origin of the manganese and associated elements, rather than any physicochemical considerations. Such sources of manganese as Foraminifera, volcanic debris, and subsurface springs were postulated. Further, both biochemical and inorganic mechanisms to deposit the manganese and iron oxides were invoked. Of special interest today is the thesis of biological oxidation, first proposed by Dieulafait (1883), taken up again by Dorff (1935), and recently revived by Graham (1959). I shall return to this problem somewhat later.

A satisfactory hypothesis must account not only for the chemical and physical characteristics of the materials, but also for the geological observations concerning their occurrences. Thus, whereas manganese is in a reduced, dissolved state in sea water, in the ferromanganese minerals it is in both the divalent and tetravalent forms, although mainly the latter. The only nonbiological species in the ocean in sufficient amounts capable of oxidizing manganese is dissolved gaseous oxygen and the reaction

$$2OH^- + Mn^{++} + \tfrac{1}{2}O_2 = MnO_2 + H_2O$$

has a free energy of -9 kcal at a pH of 8, a manganous ion concentration of $10^{-9}M$, and a partial pressure of oxygen of 0.25 atmosphere. All these concentrations are similar to those in near-bottom sea waters.

Since tetravalent manganese is not found in sea water, although from the above data it is the thermodynamically stable form, a reaction site or surface is probably necessary for the reaction to proceed. The well-known catalytic properties of iron oxide surfaces suggest the association of such material in the formation of the nodules. Iron exists in sea water dominantly in particulate phases, partly collodial. The accumulation of iron oxides on surfaces, where either the bottom topography or the lack of sediment source material does not allow any appreciable accumulation of solid phases, would initiate formation of the ferromanganese minerals. In areas of rapid deposition, where nodules or accretions are not found, the burial of any iron oxide surface by other sediment components minimizes any mineral formation.

The catalytic oxidation of manganese on the oxide surfaces leads directly to the formation of the ferromanganese minerals. Where an excess of iron is accommodated, the mineral goethite appears. The scavenging of the reactive, high charge density ions from sea water, those previously described as having relatively short residence times, and their incorporation into the disordered layer follow. The formation of the new mineral surface, allowing sites for further oxidation of manganese, i.e., the reaction becomes autocatalytic, completes the picture.

The recent and significant observation by Graham (1959) that these nodular materials contain appreciable amounts of organic matter has resulted in the revival of the hypothesis of biological origin. Although bacteria and other organisms have been sought on the nodules by previous investigators, possibly with not enough elegance, and not found, the enthusiasm of the adherents of biochemical theories has not been dampened.

The alternate hypothesis that the organic matter in the nodules was adsorbed from sea water appears plausible. The ferromanganese minerals possess rather high specific surface areas, ranging from 6 to 190 m^2/g (Buser and Grütter, 1956), reactive sites capable of the uptake and retention of organic phases. Further, it is conceivable that bacterial activity does take place at such surfaces and that benthic organisms might not be attracted to such material. But an extension of such thought to a direct biological deposition at the present time seems unwarranted.

On a biochemical basis, it is very difficult to account for the relative proportions of certain metals in these minerals, two in particular, cobalt and cerium. Cobalt exists in sea water at a concentration of about one-seventh that of nickel (Taivo Laevestu, personal communication) on the basis of recent, refined analyses. Although cobalt and nickel show a strong geochemical coherence in behavior during the major sedimentary cycle, the ferromanganese phases contain nearly as much cobalt as nickel on the average (Table IV). Cobalt shows a wider spectrum of concentrations in nodules than does nickel.

An explanation for these abundances may well be found in the greater ease of oxidation of cobalt from the divalent to the trivalent state. The oxidation potential of cobalt for such a reaction is slightly higher than that for manganese and the free energy of the reaction, using typical marine concentrations, appears to be positive, i.e., the reaction should not proceed. However, a combination of the cobalt and manganese oxidation reactions to form a solid solution of the cobalt oxides in the manganese dioxides gives a thermodynamically possible reaction, which could result in a fractionation of cobalt over nickel. Where the redox potential of the environment is relatively low, the cobalt/nickel ratios of sea water would be expected in the nodules, as only the divalent ions are involved. Thus, the cobalt/nickel ratios may well be a sensitive indicator of the oxidation environment in the vicinity of ferromanganese mineral formation.

Cerium, one of the rare earths susceptible to oxidation to a higher state than the normal plus three, is enriched in these minerals relative to its periodic table neighbor lanthanum, which exists solely in the trivalent state. In ferromanganese minerals, in which cerium is apparently oxidized in part to the plus four valence state, the cerium/lanthanum ratio normally is of the order of six, although this value was over an order of magnitude higher in the case of a Triassic nodule from Timor. Whereas in crustal rocks on the earth's surface, the cerium/lanthanum ratio is about three. Hence, it is proposed that the oxidation of cerium, which like that of cobalt is not evident from thermodynamic considerations, proceeds through the incorporation of ceric oxides into the manganese dioxide lattice with a coupling of the manganous and cerous oxidation reactions. The high concentrations of metals susceptible to oxidation offer a dilemma to any biological hypotheses. Are we to have not only manganese oxidizing capabilities in the organisms but also cerium and cobalt oxidizing capacities?

I do not wish to leave a picture of chemical reactions on the sea floor not influenced by the large biomass of the oceans. The plants and animals of the seas are responsible for the most dramatic compositional changes in the oceans. In the surface waters where plant production occurs, carbon dioxide and oxygen, the intake and release gases of photosynthesis, respond to this biological activity. Depletion of the former and supersaturation of the latter are often observed in waters near the surface. Also, the plant nutrients, chemical species of phosphorus, nitrogen, and silicon vary over wide ranges of concentrations both in time and space.

Barium is one non-nutrient element which shows very positive correlations between concentrations in sediments and biological activity. Concentrations of this element are markedly higher in pelagic sediments below productive oceanic areas than in bottom samples below the more barren seas (Goldberg and Arrhenius, 1958; Goldberg, 1958). The high barium contents are associated with both siliceous and calcareous deposits, although the concentration of this element is not markedly high in the siliceous or calcareous hard parts of organisms. The barium is probably accumulated in the sediments through chemical reactions involving the organic debris.

A clue to the marine geochemical behavior of barium may be found in its distribution in sea water. Dr. T. Chow and I have recently found barium existing in sea water in a state of undersaturation with respect to precipitation of the sulfate and with concentrations ranging between 10 and 70 μg/liter. The lower values are found in surface waters, and there is a consistent increase in barium content with depth. The depth profiles are somewhat similar to those previously reported for radium.

Possibly, the release of high concentrations of sulfate ion, resulting from the oxidation of organically bound sulfur in biological debris in the oceans, can result in a consequential precipitation of barium sulfate in the microenvironment of this organic material. As simultaneous sinking and combustion of this organic matter occurs in the oceans, part of the incorporated barium may be returned to the sea water through dissolution of the barium sulfate. Part of the barium may end up in the sediments. Further, one can conceive that any oxidation of organic matter in the sediment may result in the uptake of barium by the mechanism illustrated above. Such processes would result in an increase in barium with depth and its accumulation on the sea floor.

Early German and Russian workers pointed out the striking accumulation of heavy metals over sea water by a whole spectrum of marine organisms. Iron, vanadium, zinc, and nickel were amassed by the biosphere to average enrichments over sea water by factors of tens of thousands. Recently, a wealth of values on the heavy metal contents of members of the marine biosphere has resulted from problems involving the disposal of radioactive wastes and bomb fallout. Such work has strengthened the observation of the concentration of heavy metals in organisms of the sea. These metals are retained by strong chemical bonds and cannot be eluted (washed out) by repeated rinsings with fresh or sea waters.

The relative concentration factors of metals in the marine biosphere as compared with those of sea water closely parallel the order of stability of metal ions with a variety of organic complexing agents (Goldberg, 1957). If one takes the stability constants of metals forming organic complexes with a large suite of organic complexing agents, independent of the functional group, the increasing order of stability for the metals shows a covariance with the relative enrichment of the metals in marine organisms. The animals and plants of the sea provide a huge reaction area for the uptake of dissolved metallic ions. One governing factor for the uptake of specific ions in competition with other ions is the equilibrium constants of the chelating reactions.

Concepts in modern chemistry should provide an entry into the resolution of the host of problems confronting the marine chemist. Why, for example, do manganese nodules close to coastal areas contain extremely high amounts of manganese compared to iron? A nodule recently dredged from the Gulf of California contained essentially pure MnO_2 and was devoid of the normally associated metals such as nickel, cobalt, zinc, and copper.

What is the intimate chemistry involved in the formation of phosphorites and glauconites on the sea floor? What redox conditions are required for their buildup and what associations with the biochemistry of the seas, if any, are involved?

The distinction between detrital and authigenic clay minerals is not clear-cut, if it can ever be. It has been known since the early thirties, after the work of Goldschmidt, that boron is enriched in marine, compared to continental, clays. Marine sediments contain hundreds of parts per million of boron whereas continental clays contain but one-tenth to one-twentieth of this amount. The boron is strongly held in the clay lattice, not removed by various washing or chelating elements. Where does it sit in the clay lattice? Boron, much more abundant in the oceans than in terrestrial waters, may well enter the clay structure or additions to the already existing minerals resulting in higher contents of this element in marine clays. Any continental clays introduced into the oceans would obtain their boron on the sea floor rather than during their passage to the sea floor because of the much longer time periods. The problem of detrital versus authigenic marine clays in the extreme reverts to the classical conundrum of the sock which is repeatedly darned until none of the original material is left. Is this a new sock or not? A continental clay rearranges on the sea floor. Is this a new clay or not?

(1006)

These are but a few of the problems that may be found in the chemistries at the sea floor-sea water interface. Solutions will be found not solely in the bases provided by modern chemistry, but only in the coupling of such knowledge with the physical, biochemical, and geological processes in the oceans.

REFERENCES

Arnold, J. R. 1956. Beryllium-10 produced by cosmic rays. *Science*, *124*, 584–585.

Barth, T. W. F. 1952. *Theoretical Petrology*. John Wiley and Sons, New York.

Buser, W., and A. Grütter. 1956. Über die Natur der Mangen Knollen. *Schweiz. mineral. petrog. Mitt.*, *36*, 49–62.

Chow, T. J., and C. C. Patterson. 1959. Lead isotopes in manganese nodules, 1959. *Geochim. Cosmochim. Acta*, *17*, 21–31.

Dieulafait, L. 1883. Le manganese dans les eaux de mers actuelles et dans certains de leur depots. *Compt. rend.*, *96*, 718–721.

Dorff, F. 1935. *Biologie des Eisens und Mangan Kreislaufes*. Berlin.

Goel, P. S., D. P. Kharkar, D. Lal, N. Narsappaya, B. Peters, and V. Yatirajam. 1957. The beryllium-10 concentration in deep-sea sediments. *Deep-Sea Research*, *4*, 202–210.

Goldberg, Edward D. 1957. Biogeochemistry of trace elements. *Geol. Soc. Am.*, *Mem.*, *67* (1), 345–358.

———. 1958. The processes regulating the composition of sea water. *J. Chem. Education*, *35*, 116–119.

———. 1958. Determination of opal in marine sediments. *J. Marine Research*, *17*, 178–182.

Goldberg, Edward D., and G. O. S. Arrhenius. 1958. Chemistry of Pacific pelagic sediments. *Geochim. Cosmochim. Acta*, *13*, 153–212.

Graham, John. 1959. Metabolically induced precipitation of elements from sea water. *Science*, *129*, 1428–1429.

Lal, Devendra, Edward D. Goldberg, and Min Koide. 1959. Cosmic-ray produced Si^{32} in nature. *Phys. Rev. Letters*, *3*, 380.

Lyman, John. 1958. Chemical considerations. In "Physical and chemical properties of sea water." *Natl. Acad. Sci.-Natl. Research Council*, *Publ. No. 600*, 89.

Menard, H. W., and C. J. Shipek. 1958. Surface concentrations of manganese nodules. *Nature*, *182*, 1156–1158.

Merrill, John R., Edward F. X. Lyden, Masatake Honda, and James R. Arnold. 1960. The sedimentary geochemistry of the beryllium isotopes. *Geochim. Cosmochim. Acta*, *18*, 108–129.

Reprinted from Gray, Peter, ed.,
Encyclopedia of the Biological
Sciences
New York, Reinhold, 1961. pp.254-
261.

COLORATION OF ANIMALS

All opaque objects are seen by reflection of incident light from their surfaces, while transparent substances are viewed partly by reflection and in part by transmitted light, i.e., shining through them to the eye. White substances reflect, by simple random scattering, all components of the visible spectrum equally, while black objects absorb light of all wavelengths equally and entirely; they are therefore seen only by contrast with their surroundings. Various degrees of equivalent but incomplete absorption of light throughout the visible spectrum yield corresponding shades of grey. In a strict sense. however, black, white and grey are not defined among the true colors.

Contributions from the Scripps Institution of Oceanography, New Series, 1328
Reproduced by Permission

The manifestation of colors in animals depends upon the spectrally selective absorption of incident light before reflection of the residual components to the eye. But this fractionating process occurs at two distinct levels of morphology. The true *biochromes* owe their chemical or pigmentary colors to the absorption of one or more fractions of white light through the electron activities of their various special molecular types. The summation or integration of a set of electronic vibrational frequencies within any molecule evokes a resultant resonance throughout the whole molecule; the particular frequency of this resonance determines whether or not visible color is to be manifest. Should a compound's resonance frequency happen to match the wavelength of certain components of the visible light-spectrum, e.g., whether in the violet, blue, green, yellow, orange, red, or perhaps in more than one of these regions, then that portion of the incident light is quenched, being absorbed by internal frictional processes and converted into heat energy, while the transmitted beam of light, now lacking the absorbed component, appears to the eye as of complementary color. Thus the absorption of the *blue* component of incident white light confers upon the object the prominent color of *yellow*, and *vice versa*. These emergent colors are not spectrally pure, since they include other portions of the visible spectrum, save for the fractions absorbed; a yellow pigment, for example, will transmit all or much of the visible light save violet and blue. The perceived color of a substance is this an integrated result, and depends upon the wavelength of the predominating or maximally transmitted fraction of visible light.

In contradistinction to the true biochromes, which express color arising from molecular resonance, there are the so-called *schemochromes*; these are physical or structural colors evoked by materials which, although without any pigmentary coloration, are disposed into extremely small, ultramicroscopic states of subdivision. Their architectural dimensions lie within the range of wavelengths of ordinary visible light, just as do the resonance-frequencies of colored molecules, i.e., within limits close to 0.4 and 0.7 μ, thus disintegrating the component light-rays usually expressed as lying between about 400 and 700 mμ, or 4000 to 7000 Ångstrom units (between approximately 1/62,500 and 1/35,700 inch).

In the animal world there are two outstanding classes of schemochromic expression, each of widespread occurrence: the iridescent colors and the scattered blues. The iridescent spectral colors arise neither from prismatic refraction of light, e.g., as in water droplets, producing a rainbow, nor commonly through the kind of diffraction effected by finely spaced gratings, although there are a few examples of this among certain insects viewed in a direct beam of light. Rather, the basis of these so-called changeable and "metallic" colors lies in the *interference* between light rays reflected from an object, i.e., through alternating reenforcement and quenching of the returning spectral components by respective synchrony or asynchrony of matching fractions returning from different reflecting strata within a translucent object such as a pearl.

The basic phenomenon, discussed by Sir Isaac Newton in the late 1600's and early 1700's, followed upon his studies of the iridescence of soap bubbles, thin layers of transparent glass, oil films, peacock feathers and the like, and was pursued much later through careful experiments, chiefly on colored lepidopteran wing-scales and beetle elytra, by the elder Lord Rayleigh in 1919, by his son the younger Lord Rayleigh in 1923 and by other investigators, notably C. W. Mason, who, between 1923 and 1929, published critical studies on the iridescent colors of feathers and of insect structures.

The manifestations of changeable iridescent colors depends upon the disposition of transparent or translucent materials in extremely thin layers, which themselves or the interstices between them do not exceed in thickness the wavelength of visible light to which reference has been made (ca. 0.4 to 0.7 μ). Moreover, the finely attenuated interstices between successive layers or films of solid or fluid material must contain or be constituted of some substance differing from the latter in refractive index, else the system will appear homogeneous, i.e., either transparent, white, or of some fortuitous pigmentary color involved in the material.

A few glass microscope slides, tightly pressed together between the (softened) jaws of a clamp will, through the imposed thinness of the air-spaces intervening between the glass surfaces, manifest Newton's interference zones. And this effect is greatly accentuated by having an absorbing layer of dark pigment at the bottom of the stack; cf. the accentuation of light-interference colors by thin oil films lying on a black pavement, which serves as an absorbing screen, thus preventing the reflection of white light, which would obscure or weaken the observed effects. An oyster pearl involves very thin films of water between the concentric, attenuated layers of calcium carbonate. If the water be driven out of the interstitial layers of a pearl, or of other nacreous material, the object now assumes a "dead" whitish appearance, arising from mere random scattering of incident white light.

The brilliant colors of certain butterflies' wings, e.g., *Morpho menelaus*, predominantly blue but changeable with angle of incidence, arise from the presence, in the minute wing-scales, of ultra-thin air-layers between the keratinaceous lamellae. Substitution of the enclosed air by a fluid, such as carbon disulfide, of refractive index close to that of keratin (*ca.* 1.6) immediately renders the whole structure transparent down to the ventral surface, giving the wing the brown color of its underlying melanin deposits (see below). Evaporation of the foreign fluid now quickly restores the displaced air and thus the original coloration.

Unlike some biological products such as nacre or pearl, which enclose water, or certain lepidopteran or coleopteran wing-scales containing air in the interlamellar spaces, the iridescent feathers of

(1009

many birds, such as the peacock, hummingbird, pigeon, turkey, birds of Paradise, and certain ducks, apparently do not enclose either gaseous or aqueous films between their thin keratinaceous laminations, but instead some substance of sufficiently different refractive index to manifest the interference colors. This applies also to the horny coverings of many scale-less beetles, wasps and flies, whose metallic lustre arises from the presence of much underlying melanin pigment, accompanied by highly specular reflectivity of the surfaces. The fine order of spacing between these multiple thin lamellae, and the cross-dimensions of the layers themselves, determine whether the predominant reflected color shall be of the relatively shorter or longer wavelengths. For example, a pile of twelve transparent plates, each of refractive index = 1.5, a thickness of 0.05 μ, and separated from its neighbor by an air-space of 0.15 μ, will appear violet at an incident angle of 60° and blue-violet at 90°, whereas if the dimensions of the lamellae and those of their interlamellar air-spaces should be the reverse of the above, the predominant colors at the respective angles will be green and yellow-green. In such manner, and provided with an underlying deposit of dark melanin, the integumentary surfaces, wing-covers and other structures of insects, as well as the feathers of some birds, may exhibit steel-blue, red, coppery, golden or even silvery metallic colors. Removal of the underlying pigment layer by chemical or mechanical means greatly diminishes or abolishes the chromatic effects, while substitution of the original melanin by black ink then restores the colorful appearance of the structure.

Changes may be induced in these iridescent interference-colors in many instances by great mechanical pressures, whereby the diminution in thickness in the interlamellar layers shifts the predominant color toward those of shorter wavelengths (blue or violet), whereas increased thickening of laminations in structures possessing no internal air-spaces (e.g., the integument of certain scale-less beetles) by exposure to swelling agents such as steam, ammonia, alcohol or phenol yields changes of color in the opposite direction, from blue or blue-green through green to brassy or coppery hues. These changes are reversible. Certain chrysomelid beetles of the genus *Coptocycla* exhibit pronounced iridescent changes in their elytra by extensive dehydration of the interlamellar spaces, resulting in a general attenuation of the whole structure. Such changes occur on the death of the insect, and reversibly from golden through green, blue and violet to brownish orange when the living animal is disturbed.

The manifestation of *non-iridescent, structural blue colors,* discussed by John Tyndall in 1869, and subsequently referred to as Tyndall scattering, depends upon the presence of minute, ultramicroscopic micelles or other entities 0.6 μ or less in diameter and having a refractive index different from that of the containing medium. The longer rays of the spectrum pass through such systems, which therefore appear yellowish, reddish, brown or grey by *transmitted light,* while the blue colors of scattering are seen as the *reflected* portion (cf. the bluish colors of woodsmoke versus the ruddy brown *shadows* cast by it).

Blue eyes contain no pigment in the iris, which allows the green, yellow, orange and red rays to penetrate to the underlying dark, light-absorbing uvea, while the ultramicroscopic colloidal micelles in the iridial stroma reflect the scattered blue component. This scattering effect is precluded by the presence of dark melanin, which, in the stroma of the iris, confers any of several shades of brown or black. Minor quantities of pale yellow melanin, superimposed upon the blue colors of Tyndall scattering, are responsible for green eye-colors.

The conspicuous blue colors of skin areas arise from similar basic factors, i.e., a pale colloidal layer of epidermis overlying deposits of dark melanin pigment, e.g., in the corium. Examples of this are seen in the naked blue skin about the face and neck of turkeys, cassowaries, guinea fowl, certain psittacine birds and the like; also on the muzzle and buttocks of some baboons, notably the male *Mandrillus sphinx,* the face and scrotum of certain guenon monkeys, and integumental areas of numerous fishes and reptiles. The presence of super- or juxtaposed areas of rich blood supplies yields purple regions intermediately between the bright blue and the bright red patches; this is particularly noticeable in the naked haunches of the mandrill *M. sphinx,* and in the neck-skin of the double-wattled cassowary.

Turning from these examples of Tyndall blues evoked by solid-in-liquid or liquid-in-liquid colloidal systems, we find conspicuous instances of the same basic phenomenon in the feathers of countless species of birds, such as blue jays, some South American macaws and many others of the parrot group. In feathers, however, the blue-scattering entities are not solid or liquid, but are ultramicroscopic air-spaces, occurring as minute "bubbles" within the so-called alveolar or box-cells of pale keratinaceous material, lying beneath the horny sheath of the feather-barb and surrounding dorsally and in part laterally a mass of hollow medullary cells carrying dark granular melanin adsorbed to or embedded within their walls. The box-cells in the jay's feather-barbs are about 3 to 4 μ thick, and surround a central spheroid cavity 4 to 5 μ in diameter. The innumerable minute air-vesicles within the box-cells of some feathers are of the order of 100 to 250 mμ in diameter, separated one from another by horny walls only 15 to 20 μ thick.

The physical nature of these blue feather colors may be appreciated by (a) the fact that no blue pigment is recoverable by chemical means; (b) high mechanical pressures or a hammer-blow against the feather-barbs flattens the minute air-vesicles within, now rendering the area black from the quenching of Tyndall scattering; (c) replacement of the air within the barbs by a fluid of refractive index equal to that of feather keratin *(ca.* 1.6) renders the box-cells homogeneously translucent, and the feather therefore exhibits the dark or black appearance of the underlying melanin screen. This effect is readily reversible on evaporating or leaching out the foreign fluid.

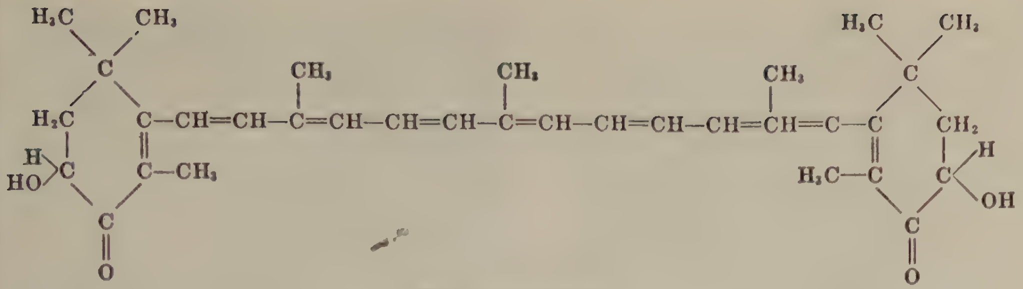

Fig. 1. Astaxanthin

Removal of the underlying black pigment causes the Tyndall blue feature to disappear or suffer great diminution, while restoration of a black under-surface restores the optical effect. The presence of a *yellow* pigment in the cuticle overlying the feather-barb renders its color *green* instead of blue, while mechanical or chemical removal of the yellow cuticle permits the expression of the Tyndall blue alone. The scattered blue colors of eyes or skin patches are readily imitable in some degree by placing cloudy, translucent (yellow-to-red transmitting) disks of agar gel upon black surfaces. Blue tattoo marks are made by injection of a black ink into the dermis underlying a white or very pale epidermal area.

Of the colored molecules displayed as true biochromes by animals, reference will be restricted here to those which impart conspicuous colors to the intact organisms or to products thereof, such as pelages, scales, feathers or certain secretions.

Carotenoids (Figure 1) are yellow, orange or red pigments of nearly universal distribution. Insoluble in water but readily soluble in various fat-solvents, they are characterized by definite crystalline habits and, in solution, by well defined spectral absorption bands in the violet, blue, and sometimes in the green regions. Closely similar carotenoids are resolvable by chromatographic separation, whether on paper or on columns of chemically inert powders, such as chalk, lime, magnesia or alumina. Synthesized *de novo* by many bacterial and fungal species, and by all green plants, carotenoids are thus acquired, directly or indirectly, by animals only through their food; hence the yellow colors of body-fat in horses, cattle and many birds, and in the egg-yolk of countless birds, fishes and invertebrates. The hydrocarbon (or carotene) type is selectively absorbed by relatively few animals, e.g., the horse, and to a great extent by cattle, whereas the oxygenated or xanthophyllic class of carotenoid, e.g., hydroxyl, ketonic, or combinations of such derivatives, are selectively assimilated by the domestic fowl and innumerable other birds, fishes and invertebrates, while a few animals such as man and some frogs and cephalopods absorb and store both kinds equally readily; numerous other animals, including swine, goats, sheep, carnivorous mammals and raptorial birds, store no colored carotenoids but only varying supplies of vitamin A, derived metabolically from certain members of this class of compounds (notably from β-carotene), and important in vision, reproduction and anti-xerosis.

The feathers, eyes, naked facial or shank skin and in some instances the bills of many herbivorous, fructivorous or omnivorous birds exhibit brilliant pigmentation due to the presence of xanthophyllic carotenoids (e.g., toucans, roseate spoonbills, flamingos). Some green feathers, but not all, exhibit their color through the combined effects of Tyndall-blue scattering from the internal box-cells of the barbs and the xanthophyllic yellow outer cuticle through which the reflected light must pass (see above).

Marine animals are particularly rich in carotenoids, notably in astaxanthin or closely similar oxygenated, acidogenic derivatives; these appear in the integument of crustaceans, sea-stars, nudibranch mollusks, or in the chitinous carapace and the eggs of many crustaceans, wherein the chromogen often is conjugated chemically with protein to yield green, blue, purple, brownish, grey or other colored complexes. These chromoproteins, upon boiling or treatment with alcohol, acetone or other protein coagulants, immediately turn red or orange with the release of the carotenoid.

Quinone biochromes (Figures 2, 3) are of two classes in animals; the polyhydroxynaphthoquinones and the polyhydroxyanthraquinones. In each

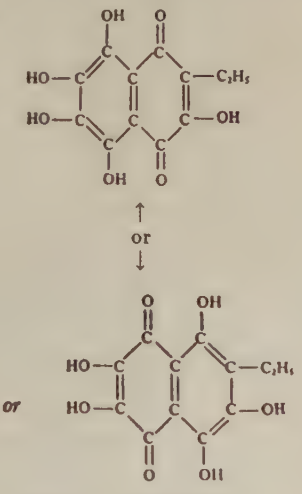

Fig. 2. Echinochrome.

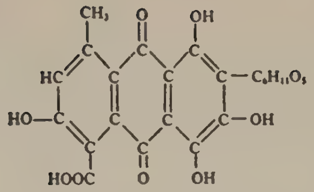

Fig. 3. Carminic acid.

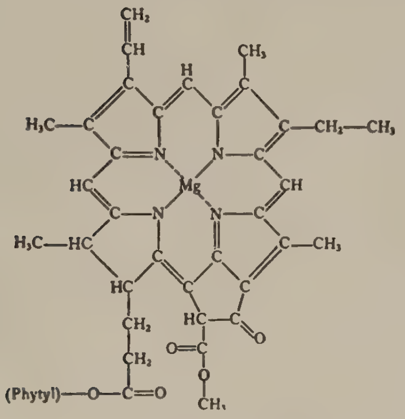

Fig. 4. Chlorophyll-a.

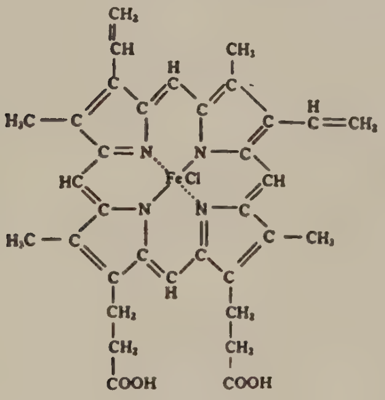

Fig. 5. Hemin.

instance the oxidized $\gt C{=}O$ or quinoid groups at *p*-positions on one of the phenyl rings are responsible for the color. The chemically reduced, corresponding hydroxy derivatives are without color. These quinones occur in countless plant species as yellow, orange, red or purple pigments, soluble in numerous organic solvents and have been used extensively as dyes for fabrics.

Chemical studies have revealed the existence of a number of different naturally-occurring, so-called echinochromes. These red, purple or sometimes green compounds are naphthoquinone derivatives encountered in two echinoderm classes, the echinoids (sea-urchins and sand-dollars) and the crinoids (sea-lillies or feather-stars). Red masses of echinochrome can be seen in the lining of the gut and of the shell, in the body-fluid, and in some echinoid species within the egg-jelly. The calcareous shell and spines incorporate the red or purple pigments as well, presumably as insoluble calcium salts. Echinochromes have been recovered from certain fossil species of crinoid, as well as from the soft parts of a free-swimming species, *Antedon bifida*, presumably a particulate feeder.

The sea otter, *Enhydra lutris*, gradually develops, as a consequence of consuming large numbers of sea urchins, pink to purple colors in its teeth, skull and other skeletal parts due to the deposition of insoluble echinochrome salts.

Like the naphthoquinones, the related anthraquinone biochromes comprise a number of brightly colored compounds which have long found wide use in the dyeing industry. They exhibit color changes in acids and bases and are chemically reducible by certain reagents. Cochineal is recovered as the red potassium salt of carminic acid from the fat-body and eggs of scale-insects of the genus *Dactylopius*, while kermesic acid, another red dye popular in ancient times, is a chemically similar pigment extractable from the females of the kermes scale-insect *Lacanium ilicis*; and laccaic acid is a component of lac-lac, a solid excrescence covering the female bodies of several species of lac insects. All of these insects are parasitic upon plants, whence they doubtless derive the anthraquinone pigments which, so far as we know at present, fulfill no essential physiological role in the insect's metabolism. Red anthraquinones are prominent pigments in crinoids of the genus *Comatula*, a particulate feeder which doubtless assimilates much marine plant material bearing the dye or its chemical precursors.

Tetrapyrroles (Figures 4, 5, 6) include both the closed ring class, or porphins, and the open chain variety or bilins, chemically and metabolically related to the porphins. The kinds and numbers of side-chains, as well as the relative degree of chemical unsaturation (double bonds), determine the character and functions of the endogenous tetrapyrroles. The so-called phaeophorbides, when binding a central atom of magnesium and bearing a molecule of the long, unsaturated alcohol phytol as a specifically placed side-chain to give the corresponding ester, constitute the photosynthesis-catalyzing chlorophylls of green plants. Similar quartets of substituted pyrrole nuclei, linked each to its neighbor by the same unsaturated methene (—CH=) bonds, but lacking the isocyclic ring

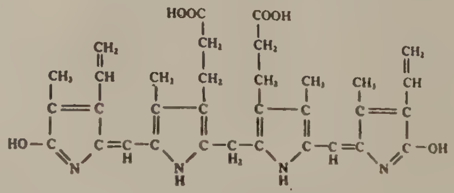

Fig. 6. Bilirubin.

condensed in chlorophyll to one of the pyrrole groups, and binding, through the pyrrolic nitrogen atoms, a central atom of ferrous iron instead of magnesium, characterize the unesterified haems; these, when conjugated with a globin protein, constitute the familiar red pigment haemoglobin in the bloods of vertebrates and of many invertebrates, particularly among the polychaete worms and to a limited degree in certain gastropod mollusks and a few crustacean and holothurian species. The capacity of haemoglobin to combine reversibly with atmospheric oxygen and thus to serve the animal's respiratory needs varies considerably, and notably between vertebrate and invertebrate forms, in accordance with the type and molecular weight of the protein moiety involved. The red oxyhaemerythrin in the blood of certain sipunculid worms and the green chlorocruorin in that of chlorhaemid worms involve porphyrins conjugated with protein and iron, and serving as oxygen carriers (see below).

The haemoglobin present in the root-nodules of leguminous plants supporting vigorous populations of symbiotic *Rhizobium* bacteria, is associated with the extraordinary catalytic function of fixing atmospheric nitrogen.

Characteristic pink to bright red colors arise from the presence of haemoglobin and oxyhaemoglobin within the capillaries beneath the relatively thin skin of lips and other facial or specific body-surfaces of man and other primates, the wattles and combs of birds and the muscles of all vertebrates and of many invertebrates. Various porphyrins confer ruddy, brownish or greenish colors to the shells of many gastropods and to the egg-shells of numerous species of birds, while feathers of the African turaco, a fruit-eating bird, contain the red copper uroporphyrin salt turacin and a green oxidized derivative of this called turacoverdin.

Yellow, green, bluish or brown, open-chained non-metallic tetrapyrroles, known collectively as bilins or bilichromes, occur in certain marine red and blue-green algae, wherein they are conjugated with proteins, and in the blood, skeletal parts, integument, excretory material, secretory products and eggshells of many animal forms.

Bilirubin ($C_{33}H_{36}O_6N_4$), red-brown when concentrated, confers orange or yellow colors to the blood plasma, sclera and skin of patients with jaundice, a condition involving disorders in the secretion of bile through the duct of the gall bladder. Its green oxidation product (actually a dehydrogenation derivative) biliverdin ($C_{33}H_{34}O_6N_4$) characterizes the color of bile and occurs also in the blue or blue-green eggshells of certain gulls and of some other wild birds, such as the emu, as well as in the bones and scales of several species of fish. Violet, red, blue or blue-green bilichromes confer their colors to the wings and integument of some insects, the integumentary tissues of some anemones and mollusks, the shells and inky secretions of some gastropods and the skeletons of some corals, e.g., helioporobilin, the blue bilichrome from the skeleton of the coral *Heliopora caerulea*. The bilichromes very probably are derived principally from the breakdown of haems or other porphyrins, but may play some role in the synthesis of new haemoglobin in vertebrates.

Of the *indole* biochromes, the *melanins* (Figure 7) are endogenous yellowish, orange, brown or black end-products of the oxidative metabolism of aromatic amino acids, principally tyrosine, accompanied by polymerization of the resulting derivatives. It is this class of compounds, relatively ill-defined in a stoichiometric sense, that controls the pigmentation of eyes, mammalian hair or fur, many feathers, scales of fishes and reptiles, ink secreted by cephalopods and by some fishes, and the integument itself of countless vertebrate and invertebrate animals.

Dark-skinned human races bear large, concentrated aggregates of so-called melanocytes in the corium, as well as dispersed melanin in the epidermis, while pale skin contains but little melanin, which may be yellowish, tan or other light brown hues rather than black. Many fishes, crustaceans, cephalopods and lizards are able to vary greatly their chromatic appearance by aggregating or dis-

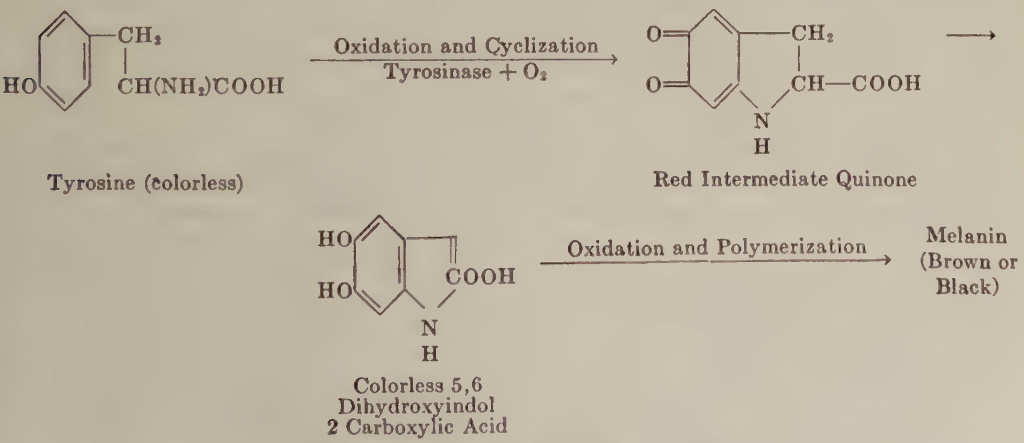

Fig. 7. Melanin formation from tyrosine.

persing the pigment microgranules within the melanophores of their skin.

The oxidation of tyrosine or similar phenolic compounds and their derivatives toward the ultimate production of melanin is catalyzed by a copper-containing enzyme tyrosinase. Copper is known to be a limiting factor in the ability of some animals to produce melanin.

Melanic pigmentation of the skin, resulting from "tanning" after exposure to unfiltered sunrays, doubtless affords to sensitive underlying tissues a degree of protection against injury from erythemogenic ultraviolet fractions, although most of the protection probably is effected by thickening of the outer, keratinized layers of skin.

The *indigoid* derivatives in this same general class (Figure 8), like the melanins, are among the excretory end-products of amino acid metabolism, but here tryptophan is involved, rather than tyrosine; moreover the indigoids are far more limited in their distribution among animals. And while the melanins are sombre, dark pigments, the indigoids exhibit blue, green, red or purple colors, and, for this reason, have sometimes been confused with the bilichromes. Indigo itself (indigo-blue or indigotin) occurs as glucocide derivatives in many plants, and was long employed as a dye, conspicuously by the ancient Britons, who smeared their naked skins with woad, a fermented blue paste of crushed cruciferous plants such as *Isatis tinctoria*. Caesar's soldiers encountered native British warriors so painted, while Pliny reported that their women similarly covered their nude bodies before participating in certain rites.

Indigoid biochromes are relatively inconspicuous, commonly of excretory occurrence and often of pathological significance in man and other mammals, but derivatives of the class found in purple secretions of certain marine gastropods, including *Murex, Purpura* and *Mitra* spp., were known in Biblical and Phoenician times, and have been referred to as Purple of the Ancients or Tyrian Purple. The chief representative, 6-6′-dibromindigo, is derived from a colorless precursor in the pale hypobranchial or adrectal gland of these snails. When the gland is crushed and exposed to light, the red-violet dye is generated, presumably through the action of an accompanying enzyme. No physiological role has yet been assignable to dibromindigo or its precursors, all of which probably are of excretory character, somewhat reminiscent of the bilichromes aplysiopurpurin and aplysiorhodin, secreted from the ink-gland of the sea-slug *Aplysia*, save that the latter are in all probability endogenous products, while one thinks of dibromindigo as deriving more or less directly from some plant source.

The *pterins* (Figure 9) are close chemical endogenous relatives of the colorless purines, and were formerly classed among them. They are white, yellow, orange or red insoluble deposits encountered commonly in butterflies' wings, and give rise to the yellow body-colors of many wasps. Xanthopterin is a common example, appearing as a yellow pigment in the wings of *Gonepterix rhamni* and other lepidopterans, in the abdominal integument of *Vespa* and other wasps, and in human urine, whence its alternative name, uropterin. This compound has been shown to prevent nutritional anemia in young salmon and in rats.

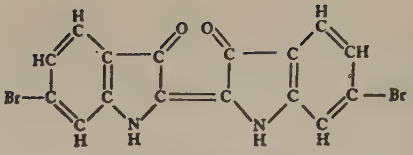
Fig. 8. Dibromindigo.

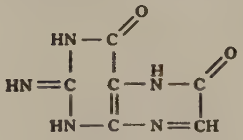
Fig. 9. Xanthopterin.

Fluorescyanin, a blue-fluorescing pterin occurring as a chromoprotein in fishes' scales, exhibits interesting chemical and physiological properties, being easily reducible by dithionite (hyposulphite) as is riboflavin, and apparently contributing to the respiratory processes, e.g., oxygen consumption, in the living scales, besides exhibiting some similarities to vitamins B_1 and B_2 when administered to experimental animals.

Among miscellaneous pigments of currently unknown chemical structure, many could be mentioned, but only a few will be listed here.

Chromolipoids, sometimes mistaken for melanins because of their yellowish, reddish or brown colors and their insolubility in water, or for carotenoids because of their colors and fat-soluble properties, are found in the fat-droplets of lipid-rich tissues and certain other cells, as well as in eggs. They are commonly regarded as oxidized derivatives of fatty acids, phospholipids or allied compounds, and perhaps bear some relationship to stored fuel. They are differentiable from the carotenoids chiefly through general failure to exhibit discrete absorption bands in the visible spectrum, while their variable solubility in organic solvents, the exhibition, in some instances, of blue to green fluorescence, occasionally with an absorption band in the far violet, and their stability in dilute acids rather than precipitability therewith, all contrast them with the melanins.

The *haemocyanins* serve as oxygen-transporting agents in the blood of gastropod, cephalopod and some amphineuran mollusks and of crustaceans and certain other arthropods, such as the "horse-shoe crab," *Limulus polyphemus*, and some scorpions and spiders. This is a copper-protein complex, colorless in the reduced condition and blue when oxygenated. The reversible condition is believed to involve changes in the valency of the copper, i.e., between the cuprous (Cu^+) and cupric (Cu^{++}) states, unlike the condition of iron in haemoglobin, which remains in the ferrous (Fe^{++}) valency save when oxidized to the trivalent ferric state as in methaemoglobin under abnormal conditions.

The haemocyanins involve no porphyrin moiety as a link between the metallic ion and the protein; instead, the copper is bound in some other fashion, and to large protein molecules, conferring upon the whole biochrome very high molecular weights, e.g., from about 1.3×10^6 in *Limulus* to 2×10^6 in *Octopus*, or even 5×10^6 in *Helix*, the land snail, thus comparing with some of the invertebrate haemoglobins, which may reach molecular weights of 3×10^6, in contrast with vertebrate myoglobins (17,000) or haemoglobins (68,000). The oxygen-combining capacity of the haemocyanins is considerably lower than that of typical haemoglobins.

Haemerythrin, the iron-containing respiratory protein of some sipunculid worms and of the brachiopod *Lingula*, turns from colorless to red when oxygenated and involves a porphyrin, as does chlorocruorin, the green iron-protein oxygen carrier of some serpulimorphid worms. But the porphyrin of haemerythrin is not believed to be a haem, and that of chlorocruorin appears to differ from the protohaem of haemoglobins.

Vanadium chromogen refers to the pale green biochrome contained within the blood cells, or vanadocytes, of some ascidians or tunicates, which are primitive chordates. The vanadocytes may constitute 1% or slightly more of the total blood volume, and enclose, along with the vanadium-rich pigment, sulfuric acid in concentrations approaching 9%. Cytolyzed vanadocytes release the pigment, which immediately turns red or brownish in color. This so-called haemovanadin, when alkalized, separates as a blue precipitate and, on oxidation, as a dark blue-green, insoluble compound bearing 5 to 10% of vanadium. No conjugated protein seems to be present in the raw pigment after cytolysis. Nor have purines or porphyrins been detected in the chromogen, which is a dialyzable molecule involving a considerable proportion of pyrrole material, suggesting a possible conjugation with an open-chained bilin-like compound. The free trivalent vanadium ion (V^{+++}) in the cytolyzate, however, would suggest that any chemical bonds between the metal and the organic radicals within the cells must be rather tenuous. The vanadium biochrome, while exhibiting strong chemical reducing properties, seems not to be a respiratory catalyst, and its physiological role, if any, remains a challenging enigma.

Denis L. Fox

Reference: Fox, D. L. "Animal Biochromes and Structural Colours," Cambridge, The University Press, 1953.

Reprinted from Gray, Peter, ed.
Encyclopedia of the Biological Sciences
New York, Reinhold, 1961. pp.593-595.

MARINE BACTERIA

The sea is the natural habitat of many kinds of BACTERIA. Morphologically marine bacteria are much like their better known terrestrial or freshwater counterparts. Although movements of water, air, and certain animals carry terrestrial bacteria into the sea, most of the bacteria found in the ocean appear to be specifically indigenous to the marine environment, except in coastal waters.

Upon initial isolation from the sea, most marine bacteria grow best or only in nutrient media having a salt content of from 2 to 4 per cent. The average salinity of sea water is approximately 3.5 per cent, about 68 per cent of which is accounted for by sodium chloride. The growth-promoting property of natural sea water is attributed to many minerals and trace elements as well as to certain organic accessory growth factors.

Most marine bacteria are thermosensitive and psychotolerant. Not only do they tolerate refrigeration temperatures; many species grow and are otherwise physiologically active at near 0°C. By water volume and bottom area, approximately 80 per cent of the sea is always colder than 3°C. Sea water of average salinity freezes at around 1.9°C. Excepting a few anomalous thermophilic species found in the sea, nearly all marine bacteria grow best between 15 and 25°C. A good many species are killed by 10 minutes' exposure to temperatures exceeding 25°C. Some of the more thermosensitive species are killed by being flooded or mixed with molten nutrient agar cooled to 42°C as in routine plating procedures.

The temperature tolerance of bacteria is influenced by the hydrostatic pressure, which increases with water depth by about 0.1 atmosphere per meter. In general, the temperature tolerance of bacteria is increased by compression, provided that the increased pressure is not injurious. A good many bacteria, taken from depths of 7000 to 10,000 meters, grow only when compressed to 700 to 1000 atm. Such bacteria are characterized as being *barophilic*. In this respect deep-sea bacteria differ from surface-dwelling organisms, most of which are slowly killed by such pressures.

On the average, marine bacteria are somewhat smaller than those living in soil, sewage, and other terrestrial materials. In general, marine bacteria grow more slowly and they form smaller colonies than their terrestrial counterparts. Facultative anaerobes predominate in the sea, there being relatively few strict aerobes. As a class, marine bacteria are actively proteolytic, more than half of the species being able to liquefy gelatin. Likewise more than half of the species produce pigments when grown in appropriate nutrient media. Nonsporulating, gram-negative rods predominate. Although both agar-liquefying and bioluminescent bacteria are commonly encountered in marine materials, only a small fraction of the bacteria isolated from the sea have the ability either to digest agar or to generate light.

Cultural procedures reveal the presence of from nil to millions of viable bacteria per gram of sea water or marine mud. Throughout the euphotic zone (i.e., the topmost hundred or so meters penetrated by sufficient light for photosynthesis by green plants), the bacterial population of sea water ranges roughly from 10 to 10^6 per ml, the mean density being about 10^3 bacteria per ml. Bacteria have been found in the sea at all latitudes, in all seasons, and at all distances from land wherever water samples from the euphotic zone have been examined. The largest bacterial populations are found associated with phytoplankton. It is not uncommon to find 10^6 viable bacteria per ml of water during or immediately following a plankton bloom. In certain polluted estuaries, bays, harbors, and areas around sewage outfalls, from 10^6 to 10^8 bacteria have been found per ml of water or bottom ooze, but such conditions are not typically marine.

Below the euphotic zone the bacterial population decreases with depth. Although appreciable numbers of bacteria have been recovered from all depths, at many oceanic stations sometimes a liter of more of water must be examined to detect any bacteria. In such water masses, the low organic content and not depth or the resultant hydrostatic pressure limits the bacterial population. From 10^3 to 10^8 viable bacteria per gram wet weight have been found in many samples of bottom sediments taken from depths exceeding 10,000 meters.

Based upon the results from analyzing several hundred samples, it seems that the mean bacterial population of the topmost two or three centimeters of bottom sediments is about 10^5 viable cells per gram wet weight. The abundance as well as the kinds of bacteria in such sediments is primarly a function of the organic content; secondarily of particle size, predators, pH, oxygen tension, and other environmental factors. Although the organic content of shallow bottoms is generally higher than that on the floor of deep trenches, there seems to be little correlation between the bacterial population of marine sediments and water depth. The distribution of bacteria in bottom sediments is even more sporadic than in water. Throughout extensive areas of red clays and other highly oxidized pelagic sediments, the bacterial population is very low. In most sediments, the bacterial population falls off rapidly below the mud-water interface with increasing core depth. However, a few living bacteria have been found in deep-sea deposits buried under several meters of bottom deposits. Most of these deeply buried bacteria are strictly anaerobic sulfate reducers, which utilize either organic matter or molecular hydrogen as an energy source.

Contributions from the Scripps Institution of Oceanography, New Series, 1329
Reproduced by Permission

By virtue of their action on organic matter and certain inorganic substances as well, bacteria influence chemical and physicochemical conditions in marine sediments. For example, the gradual diminution in the amounts of organic carbon and sulfate in bottom deposits with age or depth of burial is attributable to bacterial activities. The precipitation of calcium carbonate in shallow tropical seas has been attributed in part to bacteria which tend to increase the pH of sea water. This they may do by reducing either nitrates or sulfates, by forming ammonia from nitrogenous compounds, and by the oxidation of organic acids. Other kinds of bacteria may tend to decrease the pH under certain environmental conditoins by producing either carbon dioxide or organic acids, by oxidizing ammonium to nitrate, and by oxidizing either hydrogen sulfied or elemental sulfur to sulfate. Bacteria are believed to be the principal dynamic agents affecting the Eh or redox potential of marine sediments. This they may do by consuming free or dissolved oxygen, by producing hydrogen sulfide, and by destroying organic substances having a high electron-escaping capacity.

Besides being important as geochemical agents in the sea, bacteria influence the well-being of marine plants and animals in many ways. A few varieties cause infectious diseases. In localized environments, bacteria may vitiate the water by consuming all of the free oxygen and by producing hydrogen sulfide or toxic amines. Their beneficial activities, however, greatly exceed their harmful activities. Their most important beneficial function is the decomposition of waste organic matter and the conservation of carbon. Bacteria attack and mineralize virtually all kinds and classes of organic materials—sugars, starches, celluloses, proteins, lipids, hydrocarbons, carotenoids, chitins, keratins, etc. They quickly decompose the organic remains of both plants and animals and they are able to utilize dissolved and colloidal compounds of carbon. So effective are bacteria in decomposing organic materials that the sea has been characterized as being the world's largest and most efficient septic tank. In the vicinity of solid surfaces, which favor bacterial activity in dilute nutrient solutions, bacteria or their enzymes continue to act on organic matter in sea water until its content is reduced to less than 1 mg per liter. Ordinarily the organic carbon content of sea water ranges from 1 to 10 mg per liter.

On the average, approximately two-thirds of the carbon in organic compounds assimilated by marine bacteria is liberated as carbon dioxide and the remaining one-third is converted into bacterial cell substance or protoplasm. The conversion efficiency for various bacteria utilizing various kinds of organic matter ranges from 5 to 75 per cent. The conversion of soluble, colloidal, and waste organic materials into bacterial cell substance is of greater importance in the economy of the sea, because these bacterial cells constitute an important source of food for many kinds of marine animals. Quantitatively the standing crop of bacteria—the bacterial biomass—ranges from 0.001 to nearly 500 mg per cubic meter of sea water, the average throughout the euphotic zone being about 1 mg per cubic meter. There may be from 10 to 100 bacterial crops (cell divisions) per year, meaning an annual yield of from 10 to 100 mg of nutritious bacterial protoplasm per cubic meter of water.

Besides forming bacterial cell substances and producing carbon dioxide from the organic remains of plants and animals, bacteria liberate sulfate or hydrogen sulfide, ammonium, phosphate, and certain other substances. The ammonium and phosphate are important as plant nutrients. Bacteria which liberate ammonium from proteins or amino acids are spoken of as ammonifiers. Many species of marine bacteria are endowed with this ability. There are also many species which produce the enzyme urease, which acts upon urea in aquatic environments to yield ammonium. Ammonium as such may be assimilated by photosynthetic plants or it may be oxidized by nitrifying bacteria to nitrite and subsequently to nitrate, another plant nutrient. Although nitrogen-fixing bacteria have been found in the sea, the extent to which they contribute to the fertility of sea water is not known.

Under certain conditions (perhaps highly reducing sediments where large quantities of organic matter are being rapidly buried) there appears to be a tendency for anaerobic bacteria selectively to reduce the oxygen, sulfur, phosphorus, and nitrogen content of organic compounds, leaving a residue that is relatively richer in hydrogen and carbon—more petroleum-like in chemical composition. Methane is a common product of bacterial activity and small quantities of more complex petroleum hydrocarbons are produced by marine bacteria. There are several ways in which bacteria may contribute to the origin of oil, but whether they play an essential part in the process has yet to be proved.

Most marine bacteria are heterotrophs dependent upon organic matter to satisfy their carbon and energy requirements. However, the sea is also the home of numerous species of autotrophic bacteria, including both photosynthetic and chemosynthetic varieties whose carbon requirements are satisfied by either bicarbonate or carbon dioxide. Photosynthetic autotrophs, dependent upon radiant energy, are confined to shallow coastal waters penetrated by sunlight. These are the purple sulfur and green bacteria having bacteriochlorophyll and certain accessory photosynthetic pigments. They differ from higher green plants by not liberating free oxygen during the photosynthetic process; instead the oxygen is consumed in the oxidation of hydrogen sulfide and/or elemental sulfur. Among the chemosynthetic autotrophs are those that obtain their energy by oxidizing either molecular hydrogen, hydrogen sulfide, elemental sulfur, methane, ammonium, or nitrite. Such bacteria are widely distributed in the sea, but not in great abundance.

Large numbers of saprophytic bacteria are ordinarily associated with fin fish, shellfish, and other marine animals. As in terresterial animals, the intestinal tracts of marine animals have a typical microflora. *Escherichia coli* is generally absent except in the gut of animals inhabiting polluted coastal waters. Despite the large numbers of *E. coli* and allied coliform bacteria discharged into the sea with sewage, such bacteria of sanitary significance are rarely found in the sea except near the source of terrigenous or human contamination. These as well as other freshwater or terrestrial bacteria entering the sea rapidly disappear as a result of flocculation and sedimentation. Death is attributed to predation, starvation, and the germicidal properties of natural sea water. A good many species of marine bacteria as well as certain phytoplankton produce potent antibiotic substances.

The bacterial flora found in the gut of marine animals appears to depend in part upon the animal species and in part upon the food habits of the animal. Surface slime on the integuments and gills of fish is usually a veritable bacterial garden. Predominating are species of *Achromobacter, Pseudomonas, Flavobacterium, Proteus, Bacillus, Serratia,* and *Micrococcus.* The muscle tissue of living and recently killed fish is generally sterile. The bacterial population of improperly handled dead fish increases rapidly at a rate that is influenced primarily by handling and temperature. Spoilage is best controlled by careful handling to minimize the contamination of fish flesh, fast freezing, refrigeration, and by the use of appropriate antibiotics.

Claude E. Zobell

References: Wood, E. J. F., "The significance of marine microbiology." Bacteriological Reviews, **22:** 1–19, 1958; Zobell, C. E., "Marine Microbiology." Waltham, Mass., Chronica Botanica, 1946.

Reprinted from Gray, Peter, ed.
Encyclopedia of the Biological Sciences
New York, Reinhold, 1961. pp.150-151.

BIOLUMINESCENCE

Bioluminescence is the production of light by living organisms. This light results from an oxidative reaction in which the light-emitting molecule is called luciferin and the ENZYME, luciferase.

Luminescent organisms are much more numerous in the marine environment than on land and are notably rare in fresh water. They are especially abundant in the deeper layers of the ocean. Species displaying luminescence are extremely diverse. Simplest among these are the BACTERIA, which account for the glow observed on decaying fish or meat. Several species, in particular *Achromobacter fischeri*, have been used extensively in laboratory studies of bioluminescence. The hyphae and fruiting bodies of a number of FUNGI, *e.g.* the basidiomycete *Armillaria mellea*, glow continuously. The unicellular plants and animals include many marine luminous species, particularly among dinoflagellates (see MASTIGOPHORA) and radiolarians (see ACTINOPODA). The occurrence in abundance of luminescent dinoflagellates, for example *Gonyaulax* and *Noctiluca*, is the most common cause of the occasional brilliant displays of "phosphorescence" in the sea.

The COELENTERATES include a large number of luminescent species, especially striking being the sea pansies and the sea pens. Examples of luminous species from other animal groups are the comb jelly *Mnemiopsis*, the polychaet worm *Achloë*, the clam *Pholas*, the millipede *Luminodesmus*, the crustacean *Cypridina*, and among the insects, the fireflies and the glow-worms. Luminosity in fish is of common occurrence, but in many cases is due to symbiotic luminous bacteria. No luminous amphibians, reptiles, birds or mammals are known.

In bioluminescence, the light may be produced within the cell, or enzyme and substrate may be extruded and react outside the organism. Intracellular luminescence may be continuous, as in bacteria, or may be of very short duration, as in the flash of fireflies or dinoflagellates. In the single-celled protozoans, luminescence appears to arise from discrete granules distributed throughout the protoplasm. In multicellular animals, luminescence is often restricted to special light-emitting cells or photocytes which are distributed in characteristic patterns over the body. Luminous organs quite comparable in structure to the eye have evolved in some forms. The photophore of the euphausid *Meganyctiphanes norvegica* comprises a cornea, a lens, and a retina-like cup of photocytes, backed by a reflective material. In animals which show extracellular luminescence, the luminous secretion arises from special glands. The secretory cells within the photogenic gland of *Cypridina* contain distinguishable yellow granules of luciferin and colorless granules of luciferase, both of which dissolve when discharged into sea water. Luminescence in multicellular animals is under nervous control, and shows fatigue, facilitation and other phenomena characteristic of nervous responses in general.

Although the significance of luminescence in many organisms is not apparent, the ability to luminesce clearly serves a useful function in others. It can provide a means for recognition and attraction between members of the same species, as in some fireflies, the females of which flash in response to the spontaneous flashing of the males in the proximity. Luminous secretions in certain deep-sea squids are believed to aid in concealment from predators. The luminous organs of deep-water fishes may function as lures for attracting prey, or by illuminating the surroundings, facilitate the search for food.

All of the energy emitted in bioluminescence falls within the visible spectrum, typically giving blue or blue-green colors. The wave lengths of maximum emission for some of the luminescent forms mentioned above are as follows: *Achromobacter fischeri*, 495 $m\mu$; *Armillaria mellea*, 525

Contributions from the Scripps Institution of Oceanography, New Series, 1330
Reproduced by Permission

mμ *Gonyaulax polyedra*, 478 mμ; *Cypridina hilgendorfii*, 495mμ; *Luminodesmus sequoiae*, 495 mμ; and the firefly *Photinus pyralis*, 567 mμ. In living animals, the color of bioluminescence may be modified by pigmented screens external to the photophores. Such screens probably account for the red luminescence in the shrimp *Lycoteuthis diadema*. The intensity of luminescence varies widely, that of the ctenophore *Mnemiopsis leidyi* being among the brightest recorded for marine animals (0.3 millilamberts).

Bioluminescence is a special case of chemiluminescence, since light emission results from the decay of a molecule brought to the excited state by a chemical reaction. The general reaction for bioluminescence may be written:

$$LH_2 + \tfrac{1}{2}\, O_2 \xrightarrow{\text{luciferase}} L^* + H_2O$$

$$L^* \rightarrow L + \text{light}$$

where L stands for luciferin, and the asterisk denoted the excited state. Luciferin and luciferase are general terms, since the chemical nature of these substances is different in different organisms.

Best known from a biochemical point of view is the bacterial luciferin-luciferase system, Here, reduced flavin mononucleotide (FMNH), in the presence of the enzyme, oxygen, and an aliphatic aldehyde containing more than seven carbon atoms, yields the light-emitting complex. Only the enzyme need be of bacterial origin.

Both the luciferin and the luciferase of firefly have been crystallized. In this system, adenosine triphosphate (ATP) is necessary for the activation of luciferin (LH_2), forming an adenyl-luciferin complex as follows:

$$LH_2 + \text{ATP} + \text{enzyme} \xrightarrow{\text{Mg}} LH_2\text{-AMP-enzyme} + \text{pyrophosphate}$$

$$LH_2\text{-AMP-enzyme} + 1/2\ O_2 \rightarrow \text{L-AMP-enzyme} + H_2O + \text{light}$$

Adenyl-oxyluciferin (L-AMP) strongly inhibits light production, having a stronger affinity for luciferase than has reduced luciferin. Coenzyme A reverses this inhibition, forming a complex with oxy-luciferin and freeing the luciferase.

Other luminescent systems which are understood to a more limited extent are those of *Cypridina, Gonyaulax* and *Luminodesmus*. All these systems differ biochemically from one another and from those of firefly and bacteria. The low bioluminescence detectable in algae and higher plants immediately following exposure to light is believed to represent a reversal of photochemical reactions involved in photosynthesis.

Luminescence has been used as a tool in a number of ways. The luminescence of bacteria provides a very sensitive method for the detection of oxygen. The firefly may be used as an assay for ATP, DPN or coenzyme A. Since the intensity of luminescence provides an instantaneous measure of the rate of the luminescent reaction, luminescent bacteria have been used in kinetic studies of temperature and pressure effects. In *Gonyaulax polyedra*, luminescence shows diurnal rhythmicity and so has been used in studies of physiological clocks.

FRANCIS T. HAXO
BEATRICE M. SWEENEY

References: HARVEY, E. N. "Bioluminescence." New York, Academic Press, 1952; MCELROY, W. D. AND B. L. STREHLER. "Bioluminescence." Bact. Rev. **18:** 177–194, 1954; NICOL, J. A. C. *in* NICOL, J. A. C. "The Biology of Marine Animals." London, Pitman, 1960.

Reprinted from: Crustaceana,
vol.2, pt.4, 1961, pp.313-324.

A GIANT SPECIMEN OF *GNATHOPHAUSIA INGENS* (DOHRN, 1870) (MYSIDACEA) AND REMARKS ON THE ASYMMETRY OF THE PARAGNATHS IN THE SUBORDER LOPHOGASTRIDA

BY

WILLIAM D. CLARKE
Scripps Institution of Oceanography, La Jolla, California, U.S.A.

INTRODUCTION

During the "East Tropic" Expedition of Scripps Institution of Oceanography, an exceptionally large mysid was collected in the deep waters of the Eastern Equatorial Pacific (Lat. 7°50′ N., Long. 120°13′ W. to Lat. 8°12′ N., Long. 119°54′ W.). This specimen (fig. 1), a female measuring thirty-five centimeters from the tip of the rostrum to the end of the telson, is over 1½ times as large as the next largest specimen known and constitutes a record size for the Mysidacea. Comparison of this specimen with a considerable series of specimens in Scripps' collections leaves no doubt that it belongs to the species *Gnathophausia ingens* (Dohrn, 1870).

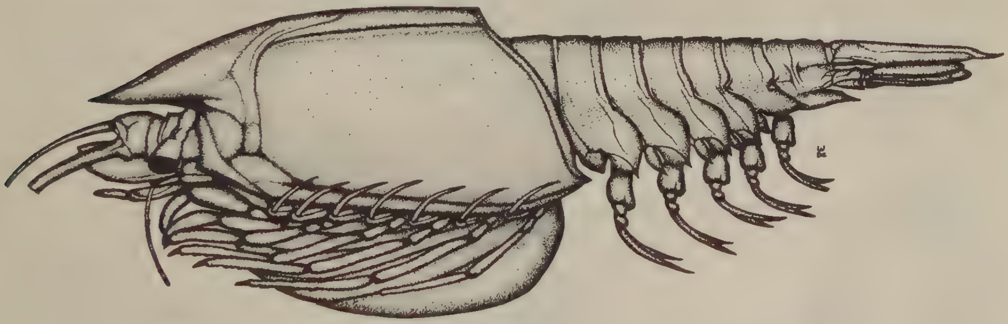

Fig. 1. Lateral view of large female of *Gnathophausia ingens* (Dohrn).

CONDITIONS OF CAPTURE

This large specimen was taken in a ten foot beam Isaacs-Kidd midwater trawl which was calculated to have operated at depths between 2,159 meters and 2,654 meters for seven hours. A mechanical failure of the trawl during its operation bears mentioning, since it may have contributed to the capture of this animal. When the trawl reached the surface the bridle on one side was broken and the

Contributions from the Scripps Institution of Oceanography, New Series, 1331
Reproduced by Permission

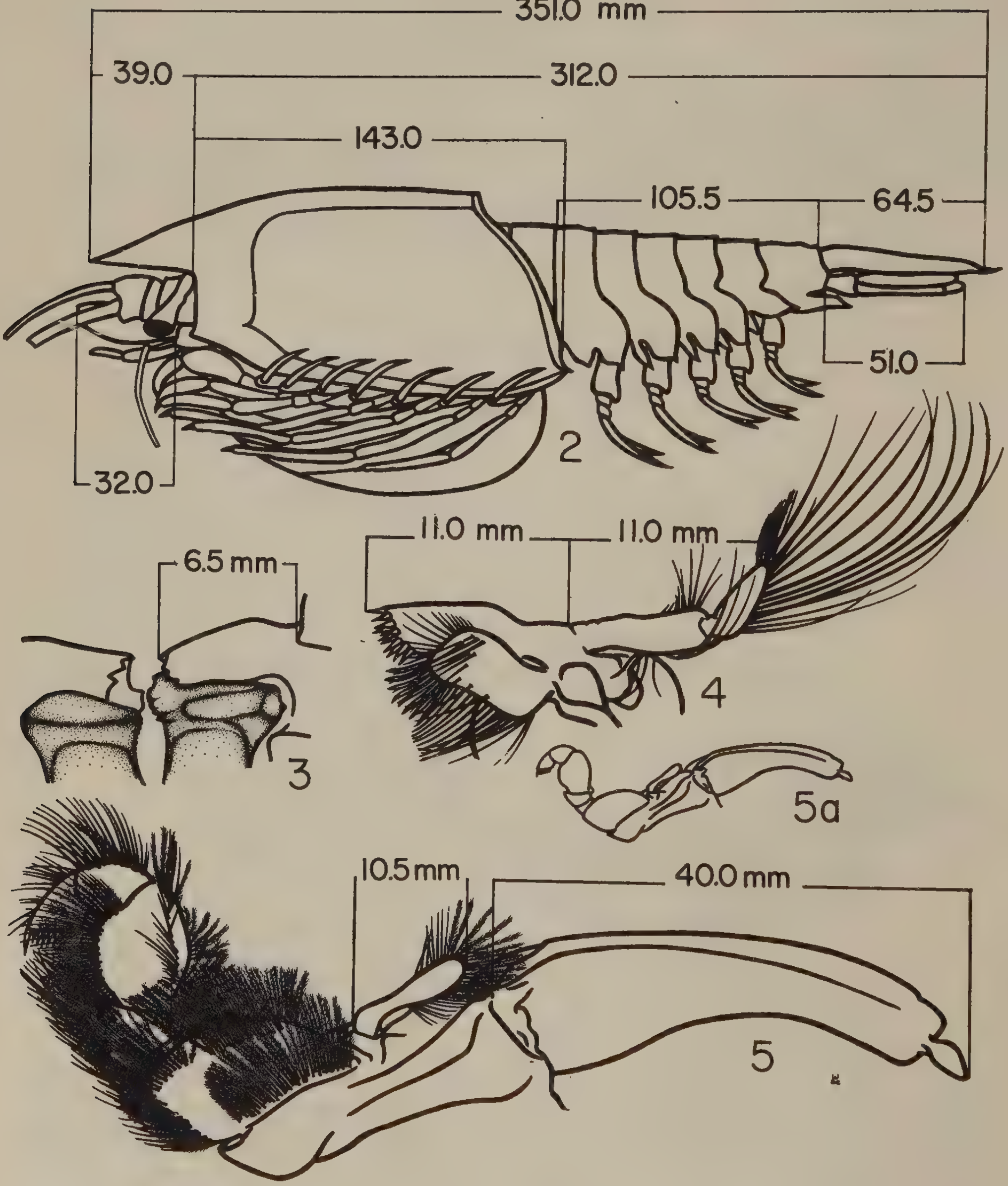
351.0 mm
39.0
312.0
143.0
105.5
64.5
51.0
32.0
2
11.0 mm
11.0 mm
6.5 mm
4
3
5a
10.5 mm
40.0 mm
5

Fig. 2-5. Measurements of large female of *Gnathophausia ingens* (Dohrn). 2, female in lateral view; 3, mandibles and paragnaths (stippled) in postero-ventral view; 4, left first maxilla in posterior view; 5, left maxilliped (first thoracic leg) in posterior view; 5a, same as 5, only with setae removed.

net had twisted so that it was closed. Since both deep water and near-surface species of fish were present, it seems probable that the bridle broke while the trawl was being towed at depth or else during its ascent to the surface. The closing of the net was possibly an important factor in the capture of the mysid, for large specimens of this species are seldom taken (Tables II and III). This may be because the larger individuals can successfully avoid conventional trawls and nets or even, if momentarily caught, can often escape from them. By way of comparison, adults of the shallow water mysid, *Neomysis kadiakensis* Ortmann, usually successfully avoided a small, hand operated dredge, but I have seen them occasionally escape even after being caught by the dredge while it was pushed along the bottom (these observations were made while diving with SCUBA). The age distribution in collections of *Neomysis kadiakensis* made with this hand operated dredge are much like those of *Gnathophausia ingens* obtained with deep water trawls and nets; larger numbers of juveniles and immatures but very few adults.

This large mysid appears to have moulted recently, another factor which may have contributed to its capture since the softened exoskeleton would have impaired its swimming ability.

DESCRIPTION OF THE LARGE SPECIMEN

The exoskeleton of this mysid is in a softened, pliable condition. Because of this lack of rigidity, some structures of the animal do not hold their shape well and a few measurements may unavoidably contain small errors. All measurements given in this paper have been made to the nearest half millimeter. (See Table I and figure 2).

TABLE I

Measurements of large female Gnathophausia ingens (*Dohrn*)

Total length	351.0 mm	see fig. 2
Body length	312.0 mm	
Rostral length	39.0 mm	
Carapace length	143.0 mm	
Abdominal length	105.5 mm	
Telson length	64.5 mm	
Uropod length	51.0 mm	
Antennal scale length	32.0 mm	
width	18.5 mm at widest point	
Antennular peduncle length	22.0 mm from base to distal end	
Eye length	29.0 mm from base to distal end	
Labrum		
length	14.5 from apex to posterior margin	
width	12.0 mm at widest point	
Mandible		
incisor process length	6.5 mm	see fig. 3

palp length	31.0 mm from base to distal end	
First maxilla		
second endite length	11.0 mm	see fig. 4
palp length	11.0 mm	
Second maxilla palp length	11.5 mm	see fig. 6
Maxilliped (first thoracic leg)		
exopod length	10.5 mm	see fig. 5
scaphopod length	40.0 mm	
Second thoracic leg		
endopod length	58.0 mm from base to distal end	
exopod length	24.5 mm from base to distal end	
oostegite length	37.0 mm from base to distal end	

The carapace is thin and membranous probably due to recent moulting. Several of the carapace spines (fig. 1), so greatly developed in young specimens, are completely lacking in this large specimen; e.g., there are no indications of the branchiostegal spines or posterior median spine. The ocular spines are absent also. These last mentioned spines, however, are always small even in very small specimens of *Gnathophausia ingens*. The antennal spines of this specimen are very weakly developed, their apices projecting only slightly from the anterior angles of the carapace. The posterior lateral spines are also greatly reduced forming small triangular projections at the posterior angles of the carapace.

The abdomen, unlike the carapace of this specimen, has a fairly rigid integument and holds its shape relatively well. The abdominal pleura, in particular the second (fig. 8) through the fourth, have the typical configuration of the species and the epimera of the sixth abdominal segment are fused ventrally in the manner usual for this species.

The seventh abdominal segment is still discernible in this giant specimen. It is delimited anteriorly by a faint suture on the sides and upper surface of the fused sixth and seventh segments (fig. 1).

The paired structures and appendages of this mysid are morphologically typical of the species, and, except for size, do not differ materially from those of smaller specimens. The antennal scales have the usual ovoid configuration but bear very weakly developed teeth along their outer margins. There are nine teeth, not counting the tooth which forms the apex of the scale, and their arrangement is somewhat different from that of smaller specimens. The four distal teeth appear to be grouped in pairs; i.e., the first tooth, commencing with the one nearest the apex, is slightly closer to the second than the second is to the third, and the third tooth is again slightly closer to the fourth than the fourth is to the fifth. Beyond this point the teeth are fairly evenly spaced along the margin as they are throughout in smaller individuals. Unlike those of smaller specimens of this species, the antennal scales project slightly beyond the end of the rostrum. This should be expected, however, in a specimen of this size because of the negative allometric growth of the rostrum.

The mouthparts are of exceptional interest, since their large size permits a more detailed description of the finer points of their morphology.

The labrum consists of a large triangular, ventrally projecting mass, the apex of which is directed forward between the bases of the antennae. The two sides extending down from the apex are framed laterally by the proximal portions of the large mandibular palps, while the base of the labrum closes off the area immediately in front of the mandibles and thus forms the anterior wall of the masticatory chamber. The right half of the base of the labrum bears a small tooth-like projection which occludes with part of the left mandible (see Nouvel, 1943, pl. 1 fig. 4).

The mandibles (fig. 3), unlike the other paired appendages, are asymmetrical. The smaller left mandible is hollowed out on its posterior surface to receive the large, left paragnath. There is a molariform protuberance at its base which occludes with a similar structure on the right mandible. The lacinia mobilis, located on the left mandible, lies on a gently curving ridge extending from the molariform protuberance to the incisor process which is merely a continuation of this ridge. The incisor process is armed with four strongly developed teeth. The larger right mandible, in contrast to the left, is not hollowed out posteriorly and presents a blunt tuberculate surface that occludes with the left mandible and left paragnath.

The paragnaths (fig. 3), though paired structures, are not true appendages, and may be best compared with the labrum since both represent structural modifications of the lip region of the mouth. They are asymmetrical in a manner opposite to that of the mandibles. The stout tubercles and ridges developed on the occlusal surface of the left paragnath, which is the larger of the two, indicate that it functions in connection with the mandibles as a chewing organ. It is completely cradled on its anterior surface and the lateral portion of its base by the left mandible which is hollowed out to receive it. Since the paragnaths apparently possess little musculature, the incorporation of the left paragnath as an organ of mastication has necessitated that it be held by the mandible and operated by the musculature of that structure through the apposition of the mandible against the paragnath. The distal portion of the left paragnath which bears the occlusal surface is enlarged and maleiform in shape. The right paragnath by contrast is a thin leaflike structure and is in no way coupled to the right mandible. There is no expansion of the distal part as in the left paragnath. Its chief function appears to be to close off the right rear portion of the masticatory chamber. A very weakly developed toothed ridge is present along its inner edge.

The asymmetry of the paragnaths in the genus *Gnathophausia* has apparently been overlooked by all previous authors. In fact, the paragnaths in general have been ignored almost completely by taxonomists in all sections of the mysidacean group. Only Gordon (1960) has examined critically the paragnaths of a number of genera of mysidaceans. She cites in her paper most of the previous works where the paragnaths have been illustrated and figures in addition the paragnaths of seven widely differing genera. These are *Stygiomysis, Boreomysis, Petalophthalmus, Lepidops* (= *Lepidomysis*), *Hansenomysis, Indomysis,* and *Eucopia.* I have examined specimens of the following species: *Gnathophausia ingens* (Dohrn), *G. gigas* Willemoes-Suhm, *G. gracilis* Willemoes-Suhm, *G. zoea* Willemoes-Suhm and *G. longispina* G. O. Sars. All of them possess asymmetrical paragnaths as described in the section above. I have not been able to examine specimens of *G. affinis* G. O. Sars and *G. elegans* G. O. Sars, but I suspect that they too have asymmetrical paragnaths. Sars (1885), for some strange reason, illustrated the paragnaths of *G. longispina* as being symmetrical in his report on the "Schizopoda" of the "Challenger" Expedition. The description in the text agrees also in giving the impression that these structures are symmetrical. However, his figure of the mandibles of *G. longispina* agrees so closely in every detail with the mandibles of the specimens that I have examined, that it would seem certain that he accidentally overlooked the asymmetry of the paragnaths, since the concavity of the posterior surface of the left mandible, which is clearly indicated in Sars' figure of the mandibles, reflects the enlarged condition of the left paragnath.

Other genera of the family Lophogastridae were investigated to ascertain whether asymmetrical paragnaths were a generic or family character. Specimens of *Chalaraspidium alatum* (Willemoes-Suhm), *Parachalaraspis vitjazi* Birstein and Tchindonova, *Lophogaster longirostris* Faxon, and *Paralophogaster atlanticus* Tattersall, were examined and found to have asymmetrical paragnaths like those of *Gnathophausia.* Thus it would appear that asymmetrical paragnaths of the type in which the left paragnath is larger and coupled with the left mandible are characteristic of the family Lophogastridae in general, though it must be pointed out that other species of the genera *Lophogaster* and *Paralophogaster* and the monotypic genus *Ceratolepis* have not been investigated by the author.

Asymmetrical paragnaths of this type, however, are not limited to the family Lophogastridae, I have found them also in species of the genus *Eucopia.* Thus this character may prove, upon further investigation, to be distinctive for the whole suborder Lophogastrida. Sars (1885) again figures these structures in his "Challenger" Report as symmetrical but the true condition of the paragnaths is the same as found in the genus *Gnathophausia*: the left paragnath is enlarged distally and cupped by the left mandible, while the right paragnath is a thin leaflike structure, independent of the right mandible. In view of the many other similarities found between the families Lophogastridae and Eucopiidae, it is not surprising that the mouth structures should so closely resemble one another.

Nouvel (1943) found that the mandibles were often reversed in species belonging to the genus *Eucopia* so that the lacinia mobilis was found on the right mandible rather than the left. In such cases, I would imagine that the paragnaths are also reversed, but I have been unable to check this point.

Since the same type of paragnaths occurred in both families of the suborder Lophogastrida, I also investigated seven species of the family Mysidae belonging to the suborder Mysida. I selected widely differing genera so as to have a representative from most of the subfamilies as well as most of the tribes of the subfamily Mysinae. The following species were examined: *Boreomysis californica* Ortmann (subfamily Boreomysinae), *Siriella pacifica* Holmes (subfamily Siriellinae), *Gastrosaccus johnsoni* Tattersall (subfamily Gastrosaccinae), *Erythrops erythrophthalma* (Goës) (subfamily Mysinae, tribe Erythropini), *Metamysidopsis elongata* (Holmes) (subfamily Mysinae, tribe Leptomysini), *Mysis oculata* (Fabricius) and *Neomysis kadiakensis* Ortmann (subfamily Mysinae, tribe Mysini). All of these species had essentially symmetrical paragnaths when viewed in ventral aspect (i.e. the surface facing the first maxillae). There were, however, slight differences in outline of the right and left member. Needless to say, there was no distal expansion of either one or the other paragnath as in species belonging to the suborder Lophogastrida, and there was no coupling of either paragnath to the mandibles. The paragnaths in these species are flat leaflike structures. When viewed in dorsal aspect (i.e. the surface facing the mandibles) there are more noticeable differences between right and left paragnath. In the region of the lacina mobilis of the left mandible, where there is a slight concavity, there is often a corresponding thickening of the left paragnath in the same region. As mentioned above, though, the paragnath is not coupled to the mandible. A sample of seven species selected from a family containing hundreds of species cannot provide proof that the trait occurs universally throughout the family, but it is possible that paragnaths of this sort will prove, upon further investigation, to be characteristic of species belonging to the family Mysidae.

The highly aberrant subfamily Thalassomysinae of the family Mysidae bears special mention. Nouvel (1943) found that the paragnaths of *Thalassomysis tattersalli* H. Nouvel were markedly asymmetrical and that the left one bore a cavity in which the tooth of the labrum lodged. This is very different from the situation found in the members of the suborder Lophogastrida and probably represents a highly specialized condition. (In the Lophogastrida the left paragnath occludes with the right mandible, not the labrum).

There are two other small families of mysidaceans which I was able to investigate, the Petalophthalmidae and the Lepidopidae (= Lepidomysidae). *Petalophthalmus armiger* Willemoes-Suhm, which belongs to the former family, has symmetrical paragnaths. *Typhlolepidomysis quinterensis* Villalobos (= *Spelaeomysis quinterensis*), which belongs to the latter family, has essentially symmetrical paragnaths, although there are slight differences in outline between right and left members. These paragnaths are quite similar to those found in the family Mysidae.

Continuing with the description of the mouth parts of the large specimen of *Gnathophausia ingens*, the first maxilla (fig. 4) bears a leaflike first endite, the margin of which is provided with long setae. Near its tip are found some heavier spines. There are also some setae on the surface of the endite, particularly its distal portion. The second endite is armed with stout spines arranged more or less in three rows on its distal end. The palp of this appendage is two-segmented.

The second maxilla (figs. 6 and 6a) is a leaflike organ which is divided into several lobes. The first endite like its counterpart on the first maxilla is fringed with long setae some of which are plumose. The second endite is cleft and forms two elongate lobes the distal ends of which are provided with densely set setae. Along the mid-portions of both the first and second endites are additional setae which form a more or less continuous band across the endites. The second maxilla unlike the first is provided with an epipod the margins of which are densely set with plumose setae. This structure pumps water out of the cavity under the carapace. It functions as an impeller which operates in a tubular opening formed by the edge of the carapace. This opening in turn leads into the branchial cavity beneath the carapace.

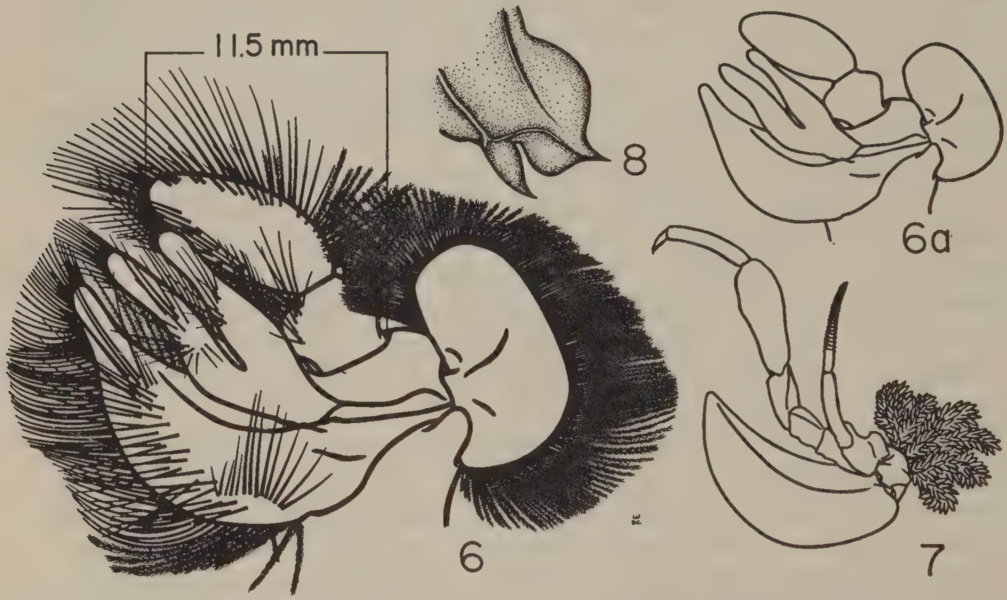

Fig. 6-8. *Gnathophausia ingens* (Dohrn). 6, left second maxilla in posterior view; 6a, same as 6, only with setae removed; 7, left second thoracic leg in posterior view (setae not indicated); 8, second abdominal pleurite.

The maxillipeds (figs. 5 and 5a) are the last appendages intimately associated with the mouth parts. They represent the first of eight thoracic pairs of appendages and are homologous with the first maxillipeds of decapods.

The maxilliped in its normal position extends forward covering the first and second maxillae as well as portions of the paragnath and mandible. The stout six-segmented endopod resembles those of the following thoracic legs, but is much shorter by comparison. Its segments are densely covered with setae and the distalmost is armed with a row of ten strong spines.

The exopod consists of a single segment. The scaphopod of this appendage

TABLE II

Total length and body length measurements of larger specimens of 550 Gnathophausia ingens *(Dohrn) reported in the literature*

Total length	Body length *	Sex	Latitude	Longitude	Authority
157 mm	—	female	5°41′ S.	134°04.5′ E.	G. O. Sars (1885)
165 mm	—	female	29°42′ S.	31°35′10″ E.	W. W. Tattersall (1925)
183 mm	—	male	33°27′ S.	16°38′ E.	”
210 mm	185 mm	male	36°11′ N. 36°12′ N.	34°21′ W. to 34°14′ W.	Hansen (1927)
—	121-140 mm	female	13°07′ N.	57°20′ W.	Fage (1942)
—	”	female	18°50′ N.	29°07′ W.	”
—	”	female	33°36.5′ S.	179°10′ W.	”
—	”	male	3°40.5′ N.	137°53′ E.	”
—	”	female	1°20′ S.	138°42′ E.	”
—	”	male	4°03′ N.	123°26′ E.	”
—	”	male	1°45′ N.	71°05′ E.	”
168 mm	142 mm	female	5°21′ N.	80°38′ E.	”
159 mm	132 mm	female	33°20′ S. 33°46′ S.	15°18′ E. to 15°08′ E.	O. Tattersall (1955)
—	148 mm	male	33°50′ S. 34°13′ S.	16°04′ E. to 15°49′ E.	”
146 mm	118 mm	female	18°33.2′ S.	41°35.4′ E.	”
156 mm	130 mm	female	18°33.2′ S.	41°35.4′ E.	”
173 mm	145 mm	male	32°03.5′ S.	40°35.2′ E.	”
155 mm	—	female	off west coast of Africa (Lagos)		Dohrn (1870)
145 mm	—	female	Kii Channel, Honshu, Japan		Shiino (1937)

* Total length minus rostral length.

TABLE III

Total length and body length measurements of larger specimens of Gnathophausia ingens *(Dohrn) in collections of Scripps Institution of Oceanography*

Total length	Body length	Sex	Latitude	Longitude	Collection No.
351.0 mm	312.0 mm	female	7°50′ N. 8°12′ N.	120°13′ W. to 119°54′ W.	SIO - 55-221
—	147.0 mm	female	28°50.2′ N. 29°06.5′ N.	118°11.2′ W. to 118°10.9′ W.	SIO - 56-79
169.0 mm	144.5 mm	female			
—	(144±)* mm	female	29°35′ N. 29°33′ N.	121°06′ W. to 121°15′ W.	H - 51-162
—	134.0 mm	male	25°34′ N. 25°31.3′ N.	115°05′ W. to 115°16.2′ W.	H - 51-85
—	129.0 mm	female	29°35′ N. 29°33′ N.	121°06′ W. to 121°15′ W.	H - 51-162
150.5 mm	128.5 mm	female	28°46.5′ N. 29°03.4′ N.	118°11′ W. to 118°11.3′ W.	SIO - 56-83
146.5 mm	124.5 mm	female			
—	(124±)* mm	female	32°17′ N. 32°37′ N.	117°37′ W. to 117°37′ W.	H - 52-15

* Estimated body length based on measurements of other structures.

TABLE IV

Comparison of measurements and proportions in different size groups of smaller specimens with large specimen of Gnathophausia ingens *(Dohrn)*

Median lengths for 15 mm size groups, ranges in ()	Number of specimens	Median carapace length (mm)	Carapace length % of body length	Median abdomen length (mm)	Abdomen length % of body length	Median telson length (mm)	Telson length % of body length	Median uropod length (mm)	Uropod length % of body length	Median antennal scale length (mm)	Antennal scale length % of body length	Median rostral length (mm)	Rostral length % of body length
30 (23-37)	10	12.8	43	—	—	—	—	—	—	—	—	13.0 (4)*	43
45 (38-52)	20	20.0 (19)*	45	19.0	42	10.5	23	8.0	18	5.8	13	16.0 (13)	36
60 (53-67)	35	28.0 (34)	47	23.5	39	15.0 (34)*	25	11.0	18	8.0	13	17.0 (20)	28
75 (68-82)	37	34.5 (35)	46	29.5	39	18.0 (35)	24	13.0	17	10.0	13	18.0 (21)	24
90 (83-97)	29	42.5	47	35.0	39	21.5	24	16.0	18	11.5	12	20.0 (21)	22
105 (98-112)	23	46.5	44	39.0	37	23.0	22	17.5	17	13.0	12	20.0 (13)	19
120 (113-127)	6	53.0	44	41.8	35	25.8	21	19.8	16	14.3	12	21.0 (5)	18
135 (128-142)	3	62.5	46	50.5	37	30.0	22	23.5	17	16.5	12	22.0 (1)	16
150 (143-157)	3	68.0	45	50.0	33	32.0	21	25.5	17	16.5	11	24.0 (1)	16
Large specimen													
312	1	143.0	46	105.5	34	64.5	21	51.0	16	32.0	10	39.0	13

* Numbers in parentheses indicate the number of specimens when less than number in second column.

is elongate and bears a small leaflike flap on its distal end. It normally extends back under the carapace into the brachial cavity.

The second through eighth thoracic legs have the same structure except for minor differences in proportions. Proceeding with a description of the second thoracic appendage (fig. 7), the endopod consists of six segments. It is much longer than the endopod of the maxilliped and heavier in build than those of the following thoracic limbs. The exopod is made up of a long proximal segment and a flexible whiplike distal piece. Both the endopod and exopod arise from a common basal segment (coxa) which also bears a small epipod on its outer edge. The oöstegite arises from the inner side of the body projection (precoxa) with which the coxa articulates, while the gills arise from the outer side of this projection. The epipod is thus located near the gills.

The pleopods and uropods of the abdomen are the same as those of smaller specimens.

DISCUSSION

To date only one other specimen has approached the size of the present large mysid. This specimen was collected in the Atlantic and was mentioned very briefly by Hansen (1927) in his report on the "Schizopods" collected by the "Travailleur" and "Talisman". Hansen reported this specimen to have a total length of 210 mm compared to the total length of 351 mm for the present specimen. Although Hansen gave no other measurements, Fage (1942) in his earlier "Dana" Report gave the body length of this specimen as 185 mm which would indicate a rostral length of 25 mm compared to a body length of 312 mm and a rostral length of 39 mm in the present specimen. Few other specimens reported in the literature have even approached this second large specimen in size. A compilation of all specimens having a body length of 121 mm or over, or a total length of 145 mm or over is given in Tables II and III. These tables include not only specimens previously reported in the literature but additional specimens from collections of Scripps Institution of Oceanography. Over 550 specimens of *Gnathophausia ingens* have been reported in the literature to date and I have examined more than 300 additional specimens of this species. Although large specimens are rare and there is only one intermediate specimen (185 mm body length) between the common upper limit of collections (147-148 mm body length) and this exceptionally large specimen (312 mm body length), it is possible to show by comparison of the proportions of various body structures that this specimen agrees perfectly with smaller specimens of the species *Gnathophausia ingens*. It is only structures such as the rostrum and spines of the carapace which demonstrate negative allometric growth that cause this large specimen to appear different from smaller specimens. However, even these characters show a linear relationship when plotted. A summary of these comparisons based on 166 specimens is given in Table IV. From the above comparisons and the morphological characters discussed earlier in this paper there is no question that this specimen belongs to the species *Gnathophausia ingens* (Dohrn, 1870).

ACKNOWLEDGEMENTS

I wish to express my thanks to Dr. Alfred Ebeling, who initially recognized the uniqueness of this specimen and kindly sent it on to me. I would also like to thank Dr. M. W. Johnson and Dr. E. W. Fager for their helpful suggestions during the preparation of this paper.

RÉSUMÉ

Un Mysidacé de dimensions exceptionnelles, de l'espèce *Gnathophausia ingens* (Dohrn, 1870) a été trouvé dans les eaux profondes de l'est de l'Océan Pacifique tropical (Lat. 7° 50′ N. Long 120° 13′ W. à Lat. 8° 12′ N. Long. 119° 54′ W.). La comparaison de ce spécimen avec une série de spécimens plus petits montre qu'il appartient sans aucun doute à la même espèce. Une étude détaillée des pièces buccales a révélé que les paragnathes sont asymétriques et que celui de gauche est couplé avec la mandibule gauche pour former un organe de mastication. Une recherche plus profonde a montré que l'on trouve des paragnathes asymétriques de cette sorte chez d'autres membres de la famille des Lophogastridae, de même que chez les espèces de la famille des Eucopiidae. Il est possible que ce trait se révèle comme caractéristique du sous-ordre des Lophogastrida. Toutes les espèces du sous-ordre des Mysida étudiées jusqu'à présent ont des paragnathes presque symétriques, à l'exception du genre *Thalassomysis.*

BIBLIOGRAPHY

Dohrn, Anton, 1870. Untersuchungen über Bau und Entwicklung der Arthropoden. 10. Beiträge zur Kenntnis der Malacostraken und ihrer Larven. Zeitschr. Wiss. Zool., **20**: 607-625, pls. 30-32.

Fage, Louis, 1941. Mysidacea Lophogastrida-I. The Carlsberg Foundations's oceanographical expedition round the world 1928-30 and previous "Dana"-expeditions under the leadership of Prof. Johannes Schmidt. Dana Report, **19**: 1-52, figs. 1-51.

Gordon, I., 1960. On a Stygiomysis from the West Indies, with a note on Spelaeogriphus (Crustacea, Peracarida). Bull. Brit. Mus. (Nat. Hist.), **6** (5): 285-324, text-figs. 1-34, pls. 3, 4.

Hansen, Hans Jacob, 1927. Sergestides et Schizopodes. Expédition scientifique "Travailleur" et "Talisman" 1880-3: 1-27, pl. 1 (Masson, Paris).

Manton, S. M., 1928. On some points in the anatomy of the lophogastrid Crustacea. Trans. Roy. Soc. Edinburgh, **56**: 103-119, text-figs. 1, 2, pls. 1-3.

Nouvel, H., 1943. Mysidacés provenant des campagnes du Prince Albert Ier de Monaco. Rés. Camp. Sci. Monaco, **105**: 1-128, pls. 1-3.

Sars, Georg Ossian, 1885. Report on the Schizopoda collected by H. M. S. "Challenger" during the years 1873-76. Challenger Rep., **13** (37): 1-228, text-figs. 1-3, pls. 1-38.

Shiino, Sueo M., 1937. Two species of the gigantic mysidacean Gnathophausia found in Japan. Annot. Zool. Japon., **16**: 181-187, figs. 1, 2.

Tattersall, Olive S., 1955. Mysidacea. Discovery Rep., **28**: 1-190, figs. 1-46.

Tattersall, W. W., 1925. Mysidacea and Euphausiacea of Marine Survey, South Africa. Rep. Fisher. mar. biol. Surv. S. Afr. **4** (5): 1-12, pls. 1, 2.

Received for publication: February 20, 1961

Reprinted from the Geophysical Journal of the
Royal Astronomical Society, v.4, 1961.
pp. 339-358.

Atmospheric Excitation of the Earth's Wobble*

Walter Munk and El Sayed Mohamed Hassan

"'Tis here! 'Tis here! 'Tis gone!"—*Shakespeare, Hamlet*, I, 2.

Summary

Hassan (1960) has computed mean monthly values of the atmosphere's moments and products of inertia for the period 1873 to 1950, using all available station-level pressures. On the basis of these time series the excitation of the seasonal and 14-month (Chandler) wobble is discussed.

With respect to the seasonal wobble, our calculations confirm the conclusion by Jeffreys and others that it is due largely to atmospheric excitation. By working directly with station-level pressures we have avoided the procedure followed previously of removing the sea-level correction from sea-level pressure charts (thus "uncorrecting" for a large and undesirable correction). Our amplitudes are 25 per cent smaller than those given by Jeffreys (1959).

With respect to the Chandler wobble, it has been suggested by Jeffreys (1940), Rudnick (1956), and by Munk & MacDonald (1960) that this represents a resonance amplification of the irregular (non-seasonal) variation in atmospheric inertia. The computed spectral density of the atmospheric variation at the Chandler frequency falls short by one to two orders of magnitude to meet the requirement of this hypothesis. Excitation by irregular motion in the core is briefly considered. Here the electromagnetic coupling (limited by conductivity in the lower mantle) appears to be far too weak to account for the observed wobble. The excitation of the Chandler wobble must be considered an unsolved problem.

1. Introduction

A discussion of the Chandler wobble involves three principal topics: frequency, dissipation, generation. The observed frequency of 0·85 cycles per year (cpy) has been interpreted since the time of Kelvin and Newcomb as the Earth's Eulerian frequency of mutation (1·20 cpy) diminished by about 0·25 cpy due to the elastic yield of the Earth and by about 0·1 cpy due to the fluid yield of the oceans. The dissipation (damping time $\sim$ 1 decade) has been attributed at one time or another to the Earth's fluid core, to the oceans, and to an elastic response of the mantle. The situation is confused. For a review we refer to Jeffreys (1959, Ch. 7) and to Munk & MacDonald (1960, Ch. 10).

One may regard the Chandler wobble as a resonance amplification of some (unknown) excitation; in this sense it is like playing a relatively broad-band noise

---

* This study was supported by a grant from the National Science Foundation.

through a moderately narrow pass-band filter. The fiter characteristics (its peak frequency, f_0, and relative band width, Q^{-1}) can be discussed without reference to input, and this is essentially what has been done in the literature (Rudnick 1956; Fellgett 1961). In this paper, on the other hand, our concern is with the input problem.

It has been known since the investigation of Spitaler (1901) that the seasonal wobble (a spectral "line" at 1 cpy) is due largely to seasonal variations in the distribution of air mass; one is then tempted to ascribe the peak at 0·85 cpy to the *irregular* variation in the distribution of air mass. This was first done by Jeffreys (1940). Rudnick (1956) put the argument into the language of communications engineering: If the annual "carrier" is modulated in the sense that some winters (say) are more severe than others (amplitude-modulation) or earlier than others (frequency modulation), then sum- and difference-frequencies between modulation and carrier are generated. The difference frequencies form a band around the annual line. The Chandler wobble is then interpreted as a resonance amplification of the side-band energy at 0·85 cpy. Rudnick's argument is illustrated in Figure 1.

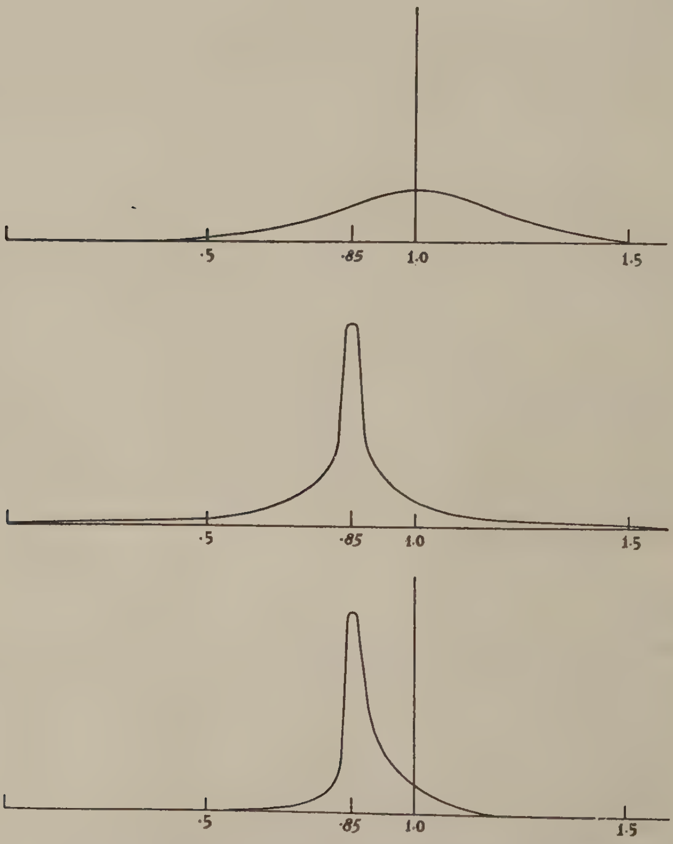

FIG. 1.—*Top:* the input spectrum is schematically presented by an annual line plus side bands. *Middle:* The power transmission of the Earth, peaked at the Chandler frequency, 0·85 cpy. *Bottom:* The power spectrum of the pole of rotation; this curve is the product of the upper two (adapted from Rudnick 1956).

The obvious procedure to test this hypothesis is to measure directly the atmospheric excitation spectrum at 0·85 cpy.

2. Atmospheric inertia

Let m_i, $(i = 1, 2)$, designate the angular displacements of the rotation pole toward Greenwich and 90° east of Greenwich, respectively. We wish to derive $m_i(t)$ arising from a variable distribution of surface load, $q(\theta, \lambda; t)\,\mathrm{g\,cm^{-2}}$, where θ is colatitude and λ east longitude. The equations of motion are

$$\psi_1 = m_1 - \dot{m}_2/\sigma_0, \qquad \psi_2 = m_2 + \dot{m}_1/\sigma_0, \tag{1}$$

where $\dot{m}_i = dm_i/dt$, and where

$$\begin{aligned} \psi_1(t) &= -\frac{a^4}{C-A}\int q(\theta,\lambda;\,t)\sin\theta\cos\theta\cos\lambda\,ds \\ \psi_2(t) &= -\frac{a^4}{C-A}\int q(\theta,\lambda;\,t)\sin\theta\cos\theta\sin\lambda\,ds \end{aligned} \tag{2}$$

designate the position of the *principal pole* (where the principal axis pierces the Earth's surface). Accordingly ψ_i equals the atmospheric products of inertia divided by $C-A$, where A, A, C are the Earth's principal moments of inertia. In the above equations

$$\sigma_0/2\pi = F_0 \tag{3}$$

designates the central frequency of the Chandler wobble (0·85 cpy), a the Earth's radius; $ds = \sin\theta\,d\theta\,d\lambda$ is an elementary area on the unit sphere.

Here $q(\theta, \lambda; t)$ is to be interpreted as the *departure* from the mean local load $\bar{q}(\theta, \lambda)$. This is derived from the departure, $p(\theta, \lambda; t)$, of the surface pressure from its local mean $\bar{p}(\theta, \lambda)$ according to $q = p/g$. Hassan (1960) has computed month by month values of $\psi_i(t)$ from published monthly pressures in accordance with equations (2) and subject to the following considerations:

(i) In deriving $\psi_i(t)$ there is no need to allow for the yield of the Earth under the superficial load. Equations (1), as written, allow for the cancellation between the effects of load deformation and rotational deformation (Munk & MacDonald 1960, Section 6.4).

(ii) There is observational and theoretical evidence that the ocean yields to the seasonable variation in air mass in the sense of an inverted barometer. The ocean then moves so as to annul horizontal pressure gradients on the sea bottom, but the bottom pressure varies in time because of the variable fraction of the atmosphere that is over the oceans.

(iii) The total mass of the atmosphere varies slightly on account of the variable content of water vapour, and we have prescribed an empirically determined seasonal variation in atmospheric mass.

(iv) With the yield of the oceans and the total mass of the atmosphere prescribed in accordance with (ii) and (iii), the equations (2) can be modified to give the excitation $\psi_i(t)$ in terms of continental observations only.

(v) The evaluation of $\psi_i(t)$ was done by fitting (in a least square sense) spherical surface harmonics to the observed values of $q(\theta, \lambda; t)$. Inasmuch as the stations are unevenly distributed, the orthogonality relations do not hold, and the amplitude of any one harmonic depends on the number of terms to which the expansion is carried. In the present discussion all nine terms up to and including harmonics of degree 2 were evaluated.

All calculations were performed on an IBM 709 computer. Monthly values of $\psi_i(t)$ are tabulated in Hassan's paper.*

3. The observations

The monthly pressure values used in the calculations were taken from Volumes 29, 90, and 105 of the Smithsonian Miscellaneous Collections and from the World Weather Records published by the U.S. Weather Bureau. Figure 2 shows the position of *all* stations. Not all of these stations are available for any one year, and for the early part of the record only a small fraction is available. Figure 3 gives the number of stations used for any one year.

4. The seasonal variation

The seasonal variation is summarized in Tables 1 and 2. Two methods have been used for extracting the seasonal variation from the time series: (i) forming the average excitation, $\overline{\psi_i}(q)$, of all January values of ψ_i, then of all February values, etc.; (ii) computing the average load departure, $\bar{q}$, for all Januaries at each station and then computing the excitation $\psi_i(\bar{q})$ associated with the mean January departure, etc. Amplitudes of the annual and semi-annual terms are given in Table 2. $\odot$ is the longitude of the "mean Sun" measured from the beginning of the year (not from March 21). Allowance has been made for the fact that January values correspond to $\odot = 15^\circ$ and not $\odot = 0^\circ$, etc. The discrepancy between $\overline{\psi_i}(q)$ and $\psi_i(\bar{q})$ probably reflects the variation of station density during the time series. In 1900 there were 237 stations, mostly in Europe and North America. In 1950 there were 463 stations, and these were distributed more uniformly. We consider the values for $\psi_i(\bar{q})$ to give the best description of the atmospheric excitation.

Jeffreys's values (as adjusted by Rosenhead) are also given in Table 2. The largest coefficients are those in cos $\odot$ for ψ_2, and in removing the unwanted sea-level correction the coefficient is reduced from $-25{\cdot}4\times 10^{-8}$ to $-16{\cdot}3\times 10^{-8}$. The magnitude of this adjustment points to the desirability of working directly with the uncorrected station-level pressure, as we have done. It is encouraging that Jeffreys's coefficients agree with ours as closely as they do.

For comparison we have included the excitation inferred in accordance with equation (1) from the astronomical observations of $m_i(t)$. The reduction by Jeffreys (1959) and by Walker & Young (1952) lead to results which differ considerably in phase. In all events the numerical values are roughly the same as those derived from the meteorological observations, and there is agreement concerning the predominance of ψ_2. A precise comparison is out of place because the effects of ground water and snow have not been considered. A rough estimate for these effects is (Munk & MacDonald 1960, Table 9.10)

$$\psi_1 = -0{\cdot}7\cos - \odot 0{\cdot}1\sin\odot, \qquad \psi_2 = 6{\cdot}4\cos\odot + 5{\cdot}9\sin\odot,$$

---

* R. Cowan has estimated the mean monthly atmospheric mass over four quadrants of the northern hemisphere for the period 1921 to 1930 (unpublished Master's Thesis, Mass. Inst. of Tech., 1950). The values are based on 80 monthly northern hemisphere station-level pressures. Cowan plots the difference in mass between opposite quadrants and finds these to bear a strong relation to the variable position of the pole.

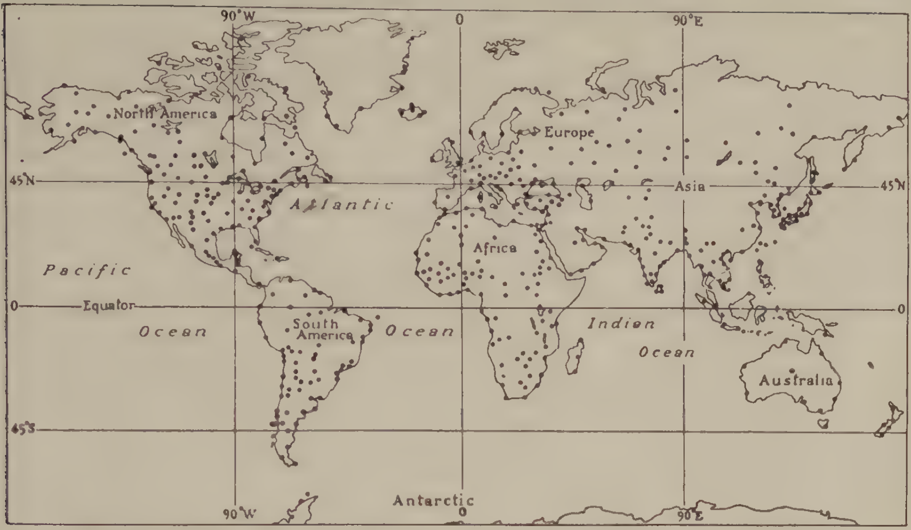
90°W
0
90°E
North America
Europe
Asia
45°N
45°N
Atlantic
Africa
Pacific
0
Equator
0
Ocean
South America
Ocean
Indian
Ocean
Australia
45°S
Antarctic
90°W
0
90°E

FIG. 2.—Position of stations used in the computation of excitation functions.

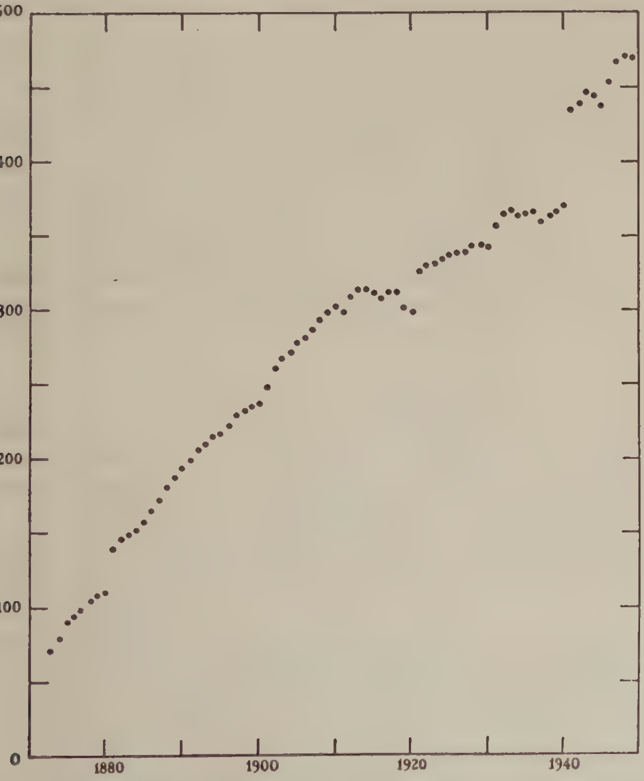

FIG. 3.—Number of stations used in the computation of excitation functions. The increments in 1921, 1931 and 1941 correspond to the publication of new summary volumes.

Table 1

Normal monthly values of ψ_1, ψ_2 *in* 10^{-8} *radians*

		Jan.	Feb.	Mar.	Apr.	May	June	July	Aug.	Sept.	Oct.	Nov.	Dec.
$\bar{\psi}_1$ (q)	1873–1950	−1·2	−0·5	+0·3	+0·5	−0·6	+0·5	+2·0	+1·2	−0·6	−0·6	−0·6	−0·8
$\bar{\psi}_1$ (q)	1900–1950	−0·8	+0·1	+0·2	+0·7	−0·8	+0·3	+2·1	+1·2	−0·8	−0·9	−0·3	−0·7
ψ_1 ($\bar{q}$)	1873–1950	−1·6	−0·5	+0·1	+0·7	+0·1	+1·0	+3·3	+2·3	−0·4	−2·0	−1·3	−1·8
$\bar{\psi}_2$ (q)	1873–1950	−7·3	−6·0	−3·9	+0·3	+3·3	+7·9	+10·8	+8·4	+2·1	−3·2	−5·4	−7·3
$\bar{\psi}_2$ (q)	1900–1950	−8·8	−6·9	−4·8	+0·4	+4·2	+9·7	+12·8	+10·1	+2·4	−4·1	−6·5	−8·8
ψ_2 ($\bar{q}$)	1873–1950	−11·1	−8·3	−5·4	+1·4	+6·5	+12·2	+15·4	+12·1	+2·7	−5·8	−8·1	−11·4

Table 2

Harmonic coefficients of ψ_i in 10^{-8} radians

Meteorological Observations

$\bar{\psi}_1(q)$	1900–1950	$-0\cdot7\cos\odot$	$+0\cdot2\sin\odot$	$+0\cdot2\cos2\odot$	$+0\cdot5\sin2\odot$
$\psi_1(\bar{q})$	1873–1950	$-1\cdot8$	$+0\cdot2$	$+0\cdot4$	$+0\cdot8$
$\bar{\psi}_2(q)$	1900–1950	$-10\cdot2$	$-1\cdot4$	$+1\cdot7$	$+0\cdot8$
$\psi_2(\bar{q})$	1873–1950	$-12\cdot9$	$-1\cdot0$	$+1\cdot8$	$+1\cdot4$

Jeffreys–Rosenhead (before and after removal of sea-level correction)

ψ_1	before correction	$-1\cdot6$	$-1\cdot6$
	after	$-1\cdot7$	$-0\cdot9$
ψ_2	before	$-25\cdot4$	$-6\cdot8$
	after	$-16\cdot3$	$-1\cdot6$

Astronomical Observations

ψ_1	Jeffreys	$-0\cdot5$	$-0\cdot5$
ψ_2	Jeffreys	$-15\cdot5$	$+6\cdot8$
ψ_1	Walker & Young	$-4\cdot8$	$+6\cdot3$
ψ_2	Walker & Young	$-7\cdot3$	$+15\cdot0$

which together with our values for $\psi_i(\bar{q})$ gives

$$\psi_1 = -2\cdot5\cos\odot + 0\cdot1\sin\odot, \qquad \psi_2 = -6\cdot5\cos\odot + 4\cdot9\sin\odot$$

for the geophysical estimates of the excitation. The good agreement with astronomical observations is now destroyed, and one wonders about the validity of the hydrological estimates.

5. Comparison of meteorological and astronomical time series

The most straightforward procedure for inquiring into the causes of the wobble is to compare the astronomically inferred excitation with the meteorologically derived excitation. Figure 4 shows the two functions for the last 12 years of observations. The result is disappointing. The curves bear no resemblance. Furthermore the astronomically derived values show much larger fluctuations (note difference in scale).

The seasonal variation has been removed from both time series by subtracting from each January value the mean of all Januaries, from each February value the mean of all Februaries, etc. Furthermore the operation involved in applying equation (1) acts as a rejection filter against the Chandler frequencies which are so prominent in the $m_i(t)$ observations (compare, for example, with Munk & MacDonald, Figure 7.4). Equation (1) as it stands does not allow for any dissipation. To allow for dissipation, the terms

$$-\tfrac{1}{2}Q^{-1}m_2, \qquad +\tfrac{1}{2}Q^{-1}m_1 \tag{4}$$

must be added on the right sides of equations (1). Here Q^{-1} is the usual dimensionless description of the width of the spectral peak, and the assumption of no dissipation corresponds to $Q = \infty$. Taking $Q = 30$ for a reasonable estimate, we have calculated the astronomically inferred excitation and find it not to differ significantly from the curve plotted in Figure 4 for $Q = \infty$.

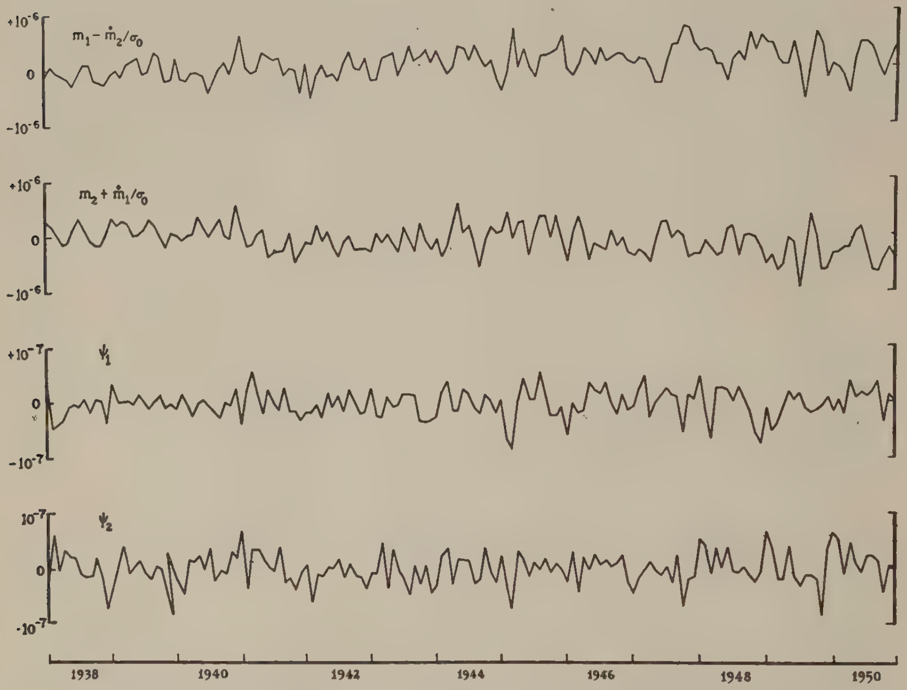

FIG. 4.—Components of the non-seasonal excitation function inferred from the astronomical observations (upper curves), and derived from meteorological observations (lower curves). The units are in radians; the scale for the meteorological excitation is magnified tenfold relative to astronomically inferred excitation. The position of January means is indicated on the time axis.

6. The spectra

Figure 5 shows the spectra and all possible cross-spectra between the astronomical and meteorological time series, after removal of the seasonal terms. The spectra are to be interpreted as the contribution, per unit frequency band (in cpy), toward the mean square value of the record (in radians^2). The ordinates represent then a "power density", and the units are radians^2/cpy. The central and bottom parts of the figure give coherence, R, and phase, ϕ, to be interpreted as follows: if any two records, $x(t)$ and $y(t)$ are played through identical narrow frequency filters centred at some frequency f, and the filtered $x(t)$ is lagged relative to the filtered $y(t)$ by various amounts until maximum correlation is achieved, then $R(f)$ is this maximum correlation and $\phi(f)$ the corresponding phase lag. The calculation is actually performed digitally by computing auto- and cross-correlations and forming Fourier transforms. The computing parameters are summarized in Table 3. For further details we must refer to an account by Blackman & Tukey

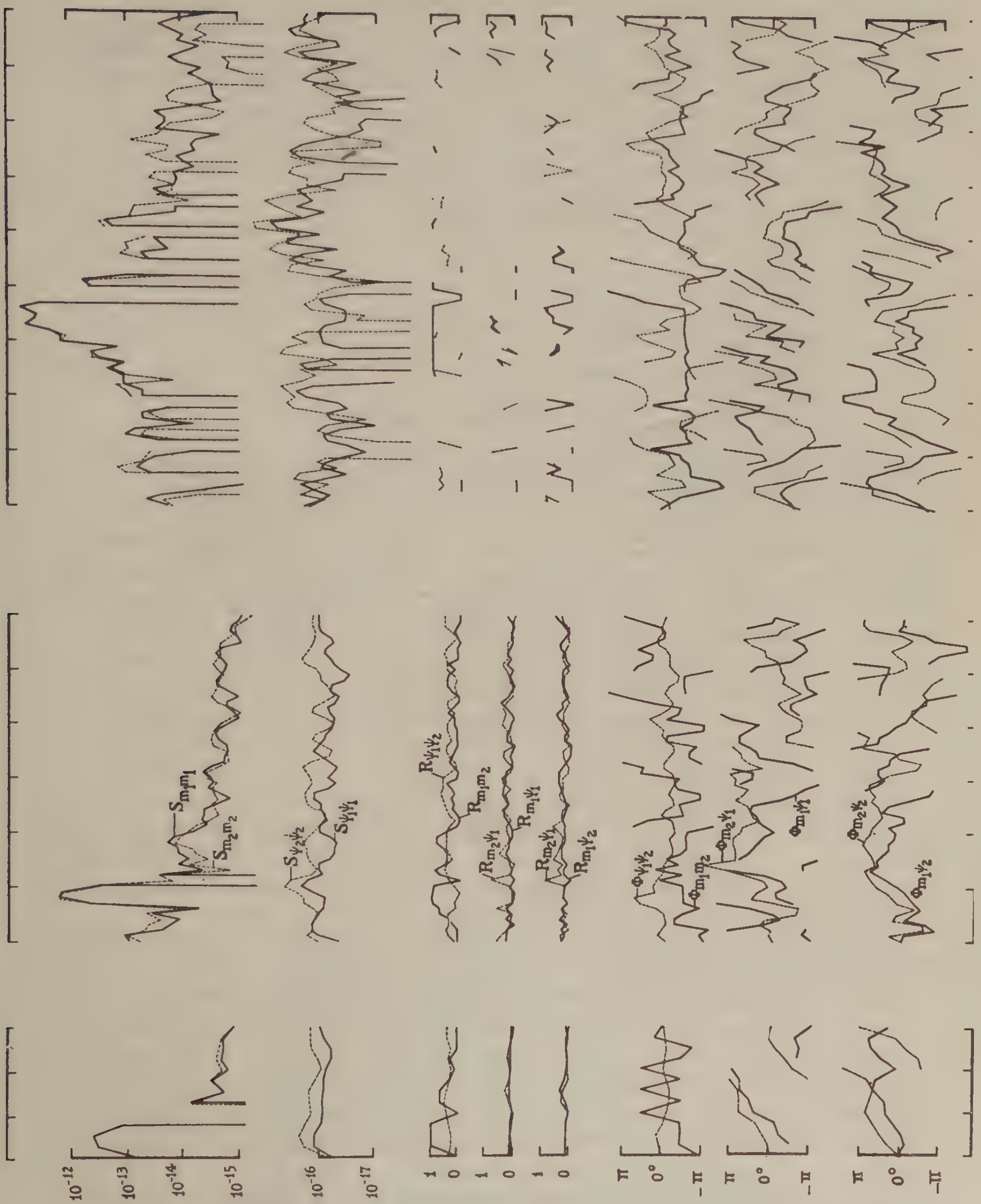

FIG. 5.—Spectra and cross-spectra of the astronomical and meteorological observations. The three displays correspond (from left to right) to increasing frequency resolution, at the expense of an increasing uncertainty in the spectral estimates. The upper curves show the power spectra in radians²/cpy); the central curves give coherence, and the lower curves phase relations between all pairs of time series.

(1958) and to Appendix A.2 of Munk & MacDonald (1960). The gaps in the spectra (particularly severe at high resolution) are the result of negative values for the spectra. It is the expected result when working with small degrees of freedom that an appreciable fraction of the computed values are outside the physically permissible range of values.

Table 3

*Computing parameters**

	N	m	Δf cpy	ν
Low resolution	613	12	0·5	101
Intermediate resolution	613	60	0·1	20
High resolution	613	600	0·01	1·5

* N is the total number of values in the time series, taken at intervals of $\Delta t = 1$ month $= (1/12)$ year. m is the number of spectral estimates, and $\Delta f = (2m\,\Delta t)^{-1}$ is the frequency resolution. The degrees of freedom, $\nu = (2N/m) - \frac{1}{2}$, determine the uncertainty in the spectral estimates.

The power spectra of m show a pronounced peak centred at 0·85 cpy. This is the Chandler wobble. Near this frequency the two components are perfectly coherent ($R = 1$) and m_1 leads m_2 by 90°. All this is as it should be, and has been previously discussed (see Munk & MacDonald, 1960, Section 10.1). The peak is narrow, and resolved only in the high resolution spectrum.* At higher frequencies the spectra flatten at roughly 4×10^{-15} radians^2/cpy.† If this density is applied throughout the entire frequency range, from 0 to 6 cpy, the corresponding power would be $4 \times 10^{-15} \times 6 \approx 2{\cdot}4 \times 10^{-14}$ radians^2, and the r.m.s. value is about $1{\cdot}5 \times 10^{-7}$ radians, or $0''{\cdot}03$. The conclusions is that uncorrelated errors of $0''{\cdot}03$ in the monthly values of $m_i(t)$ could account for the high-frequency asymptote of the spectrum. This is just about the precision claimed by the astronomers. Thus the spectrum is not significant above 2 cpy. At frequencies below the Chandler frequency the spectral density lies between 10^{-14} and 10^{-13} radians^2/cpy, and is apparently significant and related to the motion of the "mean pole".

With regard to the excitation spectrum, this is nearly "white" at 10^{-16} radians^2/cpy, thus corresponding to uncorrelated errors of $(10^{-16} \times 6)^{\frac{1}{2}} \approx 2{\cdot}5 \times 10^{-8}$ radians in the monthly values. For comparison, the amplitude of the annual term is 13×10^{-8} radians. Without further evidence we accept 10^{-16} radians^2/cpy as the observational noise level.‡ A significant rise occurs only near the annual frequency, and this is just the behaviour expected from a modulation in the sense discussed by Rudnick (see Figure 1). Here the ψ_2 spectrum lies above the ψ_1 spectrum, and this too is to be expected because the annual line is also stronger in ψ_2 than in ψ_1.

As an additional indication of error we have divided the time series into two portions. The dividing line at 1920 was selected on the basis of the station-time plot (Figure 3). We expected a lower noise level for the modern observations, but this is not the case.

---

* The negative values to either side of a peak are of no physical significance; for a sharp peak the Tukey method gives negative side bands between $2\Delta f$ and $3\Delta f$ to either side of the peak.

† The high-frequency spectrum shows weak but significant peaks centred at 1·7 and 1·84 cpy (outside the range of Figure 5). These correspond to $(2 \times 0{\cdot}85)$ cpy and $(0{\cdot}85 + 1)$ cpy and thus raise the intriguing possibility of a nonlinear interaction between the Chandler peak and the annual line.

‡ The coherence between ψ_1 and ψ_2 at higher frequencies may be interpreted as evidence to the contrary.

7. Cross-spectral analysis

Equation (1) expresses a relationship between two (vector) time series, and this then leads to a comparison between the astronomically inferred and meteorologically determined excitations. Figure 4 is an illustration of such a comparison in the *time domain*. For our purposes it is more convenient to make the comparison in the *frequency domain*. Accordingly we shall transform equation (1) as a relation between spectra.

The following discussion represents a generalization of the method of "multiple regression" and of "path analysis" in statistics (for example, Bartlett 1956, Chapter 14). The problem is to determine the relative contribution of $y_1(t)$, $y_2(t)$, ..., to $x(t)$. In the classical formulation one assumes $x(t) = a_1y_1(t)+a_2y_2(t)+ + \ldots$ as if there were no phase lag and as if the admittance did not vary with frequency. These are impossible restriction to geophysical problems, and the cross-spectral analysis removes the restrictions. Unfortunately the needed formulae are not readily available (see Kendall 1956, Section 9.3). Some of the needed relations will be developed below. The discussion is sketchy, particularly with regard to significance levels. We shall have to rely on future investigations for an adequate discussion of the numerical results.

First we need to summarize a few rules. Consider any two time series, $x(t)$, $y(t)$, and let correlation be defined by

$$R_{xy}(\tau) = \langle x(t)y(t-\tau)\rangle$$

where $\langle\ \rangle$ designates an average over time. It follows that

$$R_{xy}(\tau) = R_{yx}(-\tau).$$

Now let $\dot{R} = dR/d\tau$ and $\dot{x} = dx/dt$. Then

$$\dot{R}_{xy}(\tau) = R_{\dot{x}y}(\tau) = -R_{x\dot{y}}(\tau) = +R_{y\dot{x}}(-\tau) = -R_{\dot{y}x}(-\tau).$$

In the present exercise we assume no friction and no noise in either the astronomical or the meteorological time series. Equations (1) then predict certain relations between the spectra plotted in Figure 5. For example, multiply $m_1(t)$ by $\psi_1(t-\tau)$ and average each term with respect to time:

$$R_{m_1\psi_1}(\tau) = R_{m_1m_1}(\tau)+\sigma_0{}^{-1}\dot{R}_{m_1m_2}(\tau). \tag{5}$$

The spectra are related to the correlations according to

$$R_{xy}(\tau) = \int_0^\infty [S_{xy}(f)\cos 2\pi f\tau + T_{xy}(f)\sin 2\pi f\tau]\,df \tag{6}$$

where $S_{xy}(f)$ is termed the co-spectrum and $T_{xy}(f)$ the quadrature spectrum. It follows that

$$S_{xy}(f) = S_{yx}(f), \qquad T_{xy}(f) = -T_{yx}(f).$$

For ordinary power spectra, $x = y$ and hence $T_{xy}(f) = T_{yx}(f) = 0$. Note that

$$\sigma_0^{-1}\dot{R}_{xy}(\tau) = \int_0^\infty r[-S_{xy}(f)\sin 2\pi f\tau + T_{xy}(f)\cos 2\pi f\tau]\,df$$

where

$$r = \sigma/\sigma_0 = f/f_0.$$

Substituting (6) into (5) we obtain a relation between three integrals, and this is certainly satisfied if it is satisfied at each frequency. Equating cosine and sine terms leads to the equation in the first line of the following summary formulae. The others have been derived in a similar manner. The dependence of all spectra on f is to be understood.

$$\left.\begin{aligned}
S_{m_1\psi_1} &= S_{m_1m_1} + rT_{m_1m_1} & T_{m_1\psi_1} &= -rS_{m_1m_2} \\
S_{m_1\psi_2} &= S_{m_1m_2} & T_{m_1\psi_2} &= T_{m_1m_2} + rS_{m_1m_1} \\
S_{m_2\psi_1} &= S_{m_1m_2} & T_{m_2\psi_1} &= -T_{m_1m_2} - rS_{m_2m_2} \\
S_{m_2\psi_2} &= S_{m_2m_2} + rT_{m_1m_2} & T_{m_2\psi_2} &= rS_{m_1m_2} \\
S_{\psi_1\psi_2} &= |1-r^2|S_{m_1m_2} & T_{\psi_1\psi_2} &= (1+r^2)T_{m_1m_2} + \\
& & &\quad + r(S_{m_1m_1} + S_{m_2m_2}) \\
S_{\psi_1\psi_1} &= S_{m_1m_1} + 2rT_{m_1m_2} + r^2S_{m_2m_2} & S_{\psi_2\psi_2} &= S_{m_2m_2} + 2rT_{m_1m_2} + r^2S_{m_1m_1}.
\end{aligned}\right\} \quad (6)$$

It is sometimes more convenient to express all results as functions of the excitation spectrum. By proper elimination of terms between equations (6) we find

$$\left.\begin{aligned}
S_{m_1\psi_1} &= \frac{S_{\psi_1\psi_1} - rT_{\psi_1\psi_2}}{|1-r^2|} & T_{m_1\psi_1} &= \frac{-rS_{\psi_1\psi_2}}{|1-r^2|} \\
S_{m_1\psi_2} &= \frac{S_{\psi_1\psi_2}}{|1-r^2|} & T_{m_1\psi_2} &= \frac{-rS_{\psi_2\psi_2} + T_{\psi_1\psi_2}}{|1-r^2|} \\
S_{m_2\psi_1} &= \frac{S_{\psi_1\psi_2}}{|1-r^2|} & T_{m_2\psi_1} &= \frac{rS_{\psi_1\psi_1} - T_{\psi_1\psi_2}}{|1-r^2|} \\
S_{m_2\psi_2} &= \frac{S_{\psi_2\psi_2} - rT_{\psi_1\psi_2}}{|1-r^2|} & T_{m_2\psi_2} &= \frac{rS_{\psi_1\psi_2}}{|1-r^2|} \\
S_{m_1m_2} &= \frac{S_{\psi_1\psi_2}}{|1-r^2|} & T_{m_1m_2} & \\
& & &= \frac{-r(S_{\psi_1\psi_1} + S_{\psi_2\psi_2}) + (1+r^2)T_{\psi_1\psi_2}}{(1-r^2)^2} \\
S_{m_1m_1} &= \frac{S_{\psi_1\psi_1} + r^2S_{\psi_2\psi_2} - 2rT_{\psi_1\psi_2}}{(1-r^2)^2} & S_{m_2m_2} &= \frac{r^2S_{\psi_1\psi_1} + S_{\psi_2\psi_2} - 2rT_{\psi_1\psi_2}}{(1-r^2)^2}
\end{aligned}\right\} \quad (7)$$

Coherence and phase follow from the definitions

$$R_{xy}^2 = \frac{S_{xy}^2 + T_{xy}^2}{S_{xx}S_{yy}}, \qquad \tan\phi_{xy} = \frac{T_{xy}}{S_{xy}}. \tag{8}$$

8. Comparison of observed and computed power

If the excitation spectrum were known, then the wobble spectrum could be computed in accordance with the relations on the last line of equation (7). Note that $S_{m_i m_i}$ becomes infinite at $r = 1$, and so does the total Chandler power $\int S_{m_i m_i}\, df$. This follows because the formulae were developed neglecting dissipation, but very near resonance it is necessary to take the dissipation into account. This is done adding the terms (4) to equation (1) and proceeding as previously. The results are

$$\begin{aligned} S_{\psi_1\psi_1} &= S_{m_1m_1} + r^2 S_{m_2m_2} + 2rT_{m_1m_2} - Q^{-1}S_{m_1m_2} + \tfrac{1}{4}Q^{-2}S_{m_2m_2} \\ S_{\psi_2\psi_2} &= S_{m_2m_2} + r^2 S_{m_1m_1} + 2rT_{m_1m_2} + Q^{-1}S_{m_1m_2} + \tfrac{1}{4}Q^{-2}S_{m_1m_1} \\ S_{\psi_1\psi_2} &= (1-r^2)S_{m_1m_2} + \tfrac{1}{2}Q^{-1}(S_{m_1m_1} - S_{m_2m_2}) - \tfrac{1}{4}Q^{-2}S_{m_1m_2} \\ T_{\psi_1\psi_2} &= (1+r^2)T_{m_1m_2} + r(S_{m_1m_1} + S_{m_2m_2}) + \tfrac{1}{4}Q^{-2}T_{m_1m_2}. \end{aligned} \tag{9}$$

To proceed further it is convenient to separate the motion of the pole into positive (west-to-east) and negative motion. At a fixed frequency the relations are

$$\mathbf{m} = m_1 + im_2 = \mathbf{m}^+ \exp(2\pi i f\tau) + \mathbf{m}^- \exp(-2\pi i f\tau)$$

and this defines $\mathbf{m}^+(t)$ and $\mathbf{m}^-(t)$. Let $S_m{}^+$ designate the spectrum of $|\mathbf{m}^+|$. It can be shown (Munk & MacDonald 1960, Sections 6.7, 10.1) that for the continuous spectra

$$S_m{}^+ = \tfrac{1}{4}(S_{m_1m_1} + S_{m_2m_2} - 2T_{m_1m_2})$$

and similarly for $S_\psi{}^+$. Substituting from equation (9) we find that

$$S_m{}^+(f) = \frac{S_\psi{}^+(f)}{(1-r)^2 + \frac{1}{4}Q^{-2}}, \qquad r = \frac{f}{f_0}. \tag{10}$$

The expression $[(1-r)^2 + \frac{1}{4}Q^{-2}]$ is the quadratic impedance of a linear damped resonator.

It is reasonable to assume that $S_\psi{}^+(f)$ is fairly uniform over the narrow range of frequencies contained in the Chandler wobble, so that we can replace it by $S_\psi{}^+(f_0)$. The total power of the Chandler wobble then equals

$$S_\psi{}^+(f_0)\int_{-\infty}^{\infty} \frac{df}{(1-f/f_0)^2 + \frac{1}{4}Q^{-2}} = 2\pi f_0 Q S_\psi{}^+(f_0).$$

From a fit of the observed spectra, $S_m{}^+(f)$, one finds $f_0 = 0{\cdot}85$ cpy and Q between 10 and 100. The meteorological observations give (in radians²/cpy)

$$S_{\psi_1\psi_1}(f_0) = 1{\cdot}5\times 10^{-16}, \quad S_{\psi_2\psi_2}(f_0) = 0{\cdot}3\times 10^{-16}, \quad T_{\psi_1\psi_2}(f_0) = 0{\cdot}06\times 10^{-16}$$

for the excitation above the assumed noise level. Thus

$$S_\psi{}^+ = 0{\cdot}4\times 10^{-16} \text{ radians}^2/\text{cpy}$$

and the expected Chandler power from meteorologic excitation equals (in radians²)

Q	10	30	100
Chandler power	$0{\cdot}2\times 10^{-14}$	$0{\cdot}6\times 10^{-14}$	$2{\cdot}1\times 10^{-14}$

as compared to the measured power of $(0''.1)^2 = 24\times 10^{-14}$ radians². Thus the meteorologic excitation fails by one or two orders of magnitude to produce the observed power of the Chandler wobble. The argument can be put in another form. By choosing a sufficiently high value of Q (order 1 000) it is possible to match computed and observed Chandler power. But in that case the required sharpness of the peak exceeds the measured sharpness; other geophysical considerations also speak against a dissipation as small as is implied by a Q of the order 10^3 (Munk & MacDonald 1960, Section 10.7).

The objection might be raised here that the significance of the excitation spectrum is marginal; this is certainly the case. But then we should expect the computed spectral density to be too high, not too low! In this sense the discrepancy here derived between the computed and observed wobble may be regarded as a lower limit.

9. Coherence and phase

As an independent check we shall consider the coherence and phase relations between the astronomical and meteorological time series. Take, for example, m_1 and ψ_1. All we need to do is to substitute the expressions (7) into the definitions (8). For the case of no friction we find

$$R^2{}_{m_1\psi_1} = 1 - \frac{r^2 S_{\psi_2\psi_2}(1 - R^2{}_{\psi_1\psi_2})}{S_{\psi_1\psi_1} + r^2 S_{\psi_2\psi_2} - 2r T_{\psi_1\psi_2}}, \qquad \tan\phi_{m_1\psi_1} = \frac{r S_{\psi_1\psi_2}}{r T_{\psi_1\psi_2} - S_{\psi_1\psi_1}} \tag{11}$$

Thus the predicted coherence diminishes from $R_{m_1\psi_1} = 1$ at $r = 0$ to $R_{m_1\psi_1} = R_{\psi_1\psi_2}$ at $r \gg 1$. The phase varies from $\phi_{m_1\psi_1} = 0^\circ$ at $r = 0$ to $\phi_{m_1\psi_1} = 90^\circ - \phi_{\psi_1\psi_2}$ at large r.

The coherence implied by (11) far exceeds the computed amounts (Figure 5), particularly at small r. The reason for this lies in the present unrealistic model, according to which the loss of coherence is due entirely to imperfect coherence between the components ψ_1 and ψ_2 (if $R_{\psi_1\psi_2} = 1$ then $R_{m_1\psi_1} = 1$ for all r). There are other, much more important, sources for destroying coherence:

(i) Noise in the astronomical observations; but this cannot be a major factor for otherwise coherence would be peaked near f_0 where the noise level is *relatively* low.

(ii) Noise in the meteorologic observations; again this appears not to be the primary source of coherence loss, for otherwise the coherence would be peaked near 1 cpy where the noise level is again relatively small.

(iii) Multiple causes of the Chandler wobble; in fact the comparison of computed and observed spectra demonstrates that this is so and that meteorologic excitation is a rather minor factor.

To pursue (iii) we set

$$\psi_i = \psi_i' + \psi_i'', \qquad R_{\psi'\psi''} = 0$$

where ψ_i' designates the meteorological excitation and ψ_i'' the excitation by some other process uncorrelated with the meteorological excitation. As an example we consider

$$S_{m_1\psi_2} = \frac{S_{\psi_1\psi_2}}{1 - r^2}$$

according to (7). Suppose we define

$$S_{m_1\psi_2'} = \frac{S_{\psi_1'\psi_2'}}{1 - r^2}, \qquad S_{m_1\psi_2''} = \frac{S_{\psi_1''\psi_2''}}{1 - r^2}$$

as the co-spectra of m_1 with ψ_2' and ψ_2'', respectively. Then it follows by the rules in section (7) that $S_{m_1\psi_2} = S_{m_1\psi_2'} + S_{m_1\psi_2''}$ and similarly for other correlations. In particular, $S_{m_im_i} = S_{m_i'm_i'} + S_{m_i''m_i''}$, where $S_{m_i'm_i'}$ is spectrum of m_i due to ψ' and $S_{m_i''m_i''}$ that due to ψ''. The curves in Figure 5 represent functions such as $R_{m_1\psi_1'}$ and $\phi_{m_1\psi_1'}$. If the excitation had been due entirely to meteorological factors $\psi_i = \psi_i'$, $m_i = m_i'$, then equations (11) and other similar expressions apply; if there is an additional, uncorrelated excitation, ψ_i'', then

$$R^2_{m_1\psi_1'} = \frac{S^2_{m_1'\psi_1'} + T^2_{m_1\psi_1'}}{S_{m_1m_1}S_{\psi_1'\psi_1'}}$$

$$= \frac{S^2_{m_1\psi_1'} + T^2_{m_1\psi_1'}}{S_{m_1'm_1'}S_{\psi_1'\psi_1'}} \, \frac{S_{m_1'm_1'}}{S_{m_1m_1}}$$

so that $R^2_{m_1\psi_1'}$ is reduced in the ratio $S_{m_1'm_1'}/S_{m_1m_1}$ as compared to the case of atmospheric excitation only. Our previous result that atmospheric excitation accounts for only 1 per cent to 10 per cent of the wobble power then implies a reduction in R by a factor 10 to $\sqrt{10}$. The observed coherence is consistent with such a reduction.*

On the other hand, the computed phase

$$\phi_{m_1\psi_1'} = \arctan(T_{m_1\psi_1'}/S_{m_1\psi_1'})$$

does not depend on whether or not ψ_i'' vanishes, except that its precision rapidly deteriorates with diminishing coherence. According to Goodman (1957) the 95 per cent uncertainty of the computed phase is given by

$$\sin^2\Delta\phi = \frac{1-R^2}{R^2}\,\frac{6}{\nu}$$

provided $\nu \gg 1$. Even at low resolution the scatter is then very large. Setting $\nu = 100$ (Table 3) and $R = 0{\cdot}1$ gives $\Delta\phi = 50°$. In spite of the unfavourable statistics one is tempted to compare computed and observed phase. The result is disappointing (Figure 7).

The high coherence of m_1 with m_2 at resonance carries no implication concerning the nature of the excitation. Starting with equations (7) it can be shown that

$$R^2_{m_1m_2} = 1 - \frac{(1-r^2)^2 S_{\psi_1\psi_1} S_{\psi_2\psi_2}(1-R^2_{\psi_1\psi_2})}{(S_{\psi_1\psi_1} + r^2 S_{\psi_2\psi_2} - 2rT_{\psi_1\psi_2})(r^2 S_{\psi_1\psi_1} + S_{\psi_2\psi_2} - 2rT_{\psi_1\psi_2})}$$

and this has a parabolic peak of $R_{m_1m_2} = 1$ at $r = 1$ regardless of whether there are single or multiple causes. The normalized co-spectrum vanishes at resonance, and the quadrature-spectrum is negative. Hence $\phi_{m_1m_2}$ is nearly $-\frac{1}{2}\pi$ at frequencies adjoining f_0, and again this result is independent of excitation.

10. The astronomically inferred excitation spectrum

Figure 8 shows the excitation function as inferred from the astronomical observations in accordance with equations (9). The numerical contributions of the terms in Q^{-1} and Q^{-2} toward the computed excitation is small throughout.

---

* We have assumed ψ_i'' as completely uncorrelated with ψ_i'. On the other extreme we might contemplate ψ_i'' to be completely coherent with ψ_i'. In that case $R_{m_1\psi_1'}$, would not be reduced, but the computed power would still fail by one to two orders of magnitude to account for the observed power. The present result then implies that the source of the Chandler wobble is not only far more potent than shifts in atmospheric mass but also uncorrelated to it.

z

The rise of the inferred excitation spectrum at high frequencies is not significant, but merely reflects amplification by a factor $1+r^2$ of the astronomical noise level. At the Chandler frequency the inferred excitation is 3×10^{-14} radians²/cpy as compared to $1{\cdot}5\times10^{-16}$ from meteorological observations. In Section (8) we compared the computed and observed power of *wobble* and concluded that the meteorological excitation is negligible. The present comparison between the inferred and observed *excitation* leads to the same conclusion, but is subject to far greater statistical uncertainty. The reason is that we are dealing with a small difference between two large numbers. Thus at frequencies of 0·8 and 0·9 cpy, straddling the Chandler frequency, we have

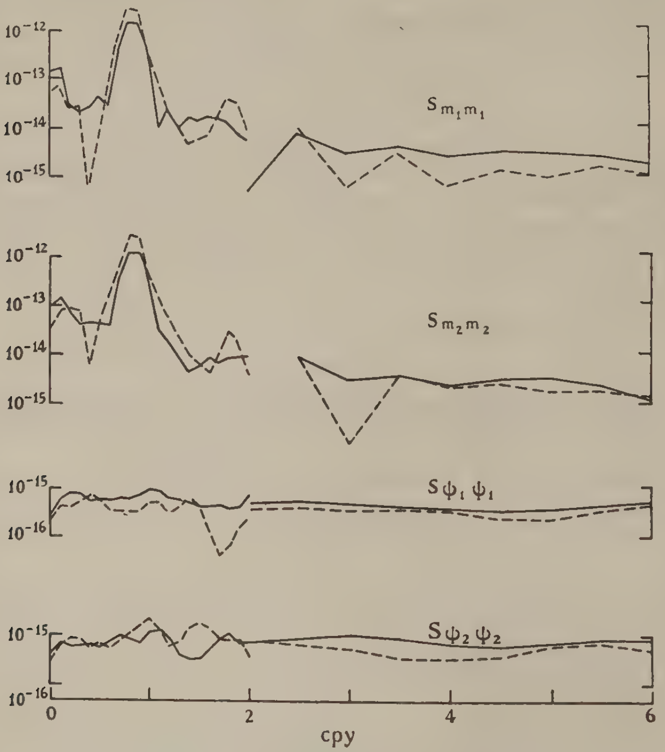

FIG. 6.—The spectra for the periods 1900 to 1920 (dashed) and 1921 to 1950 (solid). Spectra of intermediate resolution were plotted for frequencies below 2 cpy; those of low resolution for frequencies above 2 cpy.

$$S_{m_1m_1}+r^2S_{m_2m_2}-2r(-T_{m_1m_2}) = S_{\psi_1\psi_1}$$

$$r = 0{\cdot}941 : 4503 + r^2(4495) - 2r(4477) = 58$$

$$r = 1{\cdot}059 : 4903 + r^2(4100) - 2r(4064) = 83$$

respectively (all power densities in arbitrary units). In these calculations there are $\nu = 20$ degrees of freedom, and the proportional variance is accordingly $2/\nu = 0{\cdot}1$. Note that the values of $S_{m_1m_1}$ and $S_{m_2m_2}$ are within 0·002 of one another and hence clearly not statistically independent. This makes it a difficult matter to estimate the significance limits of the inferred excitation spectrum especially near resonance.

For frequencies of less than 2 cpy the coherence between the astronomically inferred ψ_1 and ψ_2 is very high, with ψ_2 leading by close to 90°. But note that $T_{\psi_1\psi_2}$ is a difference between two large numbers; whereas $S_{\psi_1\psi_2}$ is not. Thus the ratio $2_{\psi_1\psi_2}/S_{\psi_1\psi_2}$ is bound to be large in the presence of statistical scatter, especially near resonance, and $\phi_{\psi_1\psi_2} = \arctan(T_{\psi_1\psi_2}/S_{\psi_1\psi_2})$ is likely to be near $\pm 90°$. The preference for $+90°$ in Figure 8 is not understood. It follows from (6) that $S_{\psi_1\psi_1}$, $S_{\psi_2\psi_2}$ and $-T_{\psi_1\psi_2}$ approach identical limits as $r \to 1$, whereas $S_{\psi_1\psi_2} \to 0$. As a consequence $R_{\psi\ \psi_2} \to 1$ in the presence of errors.

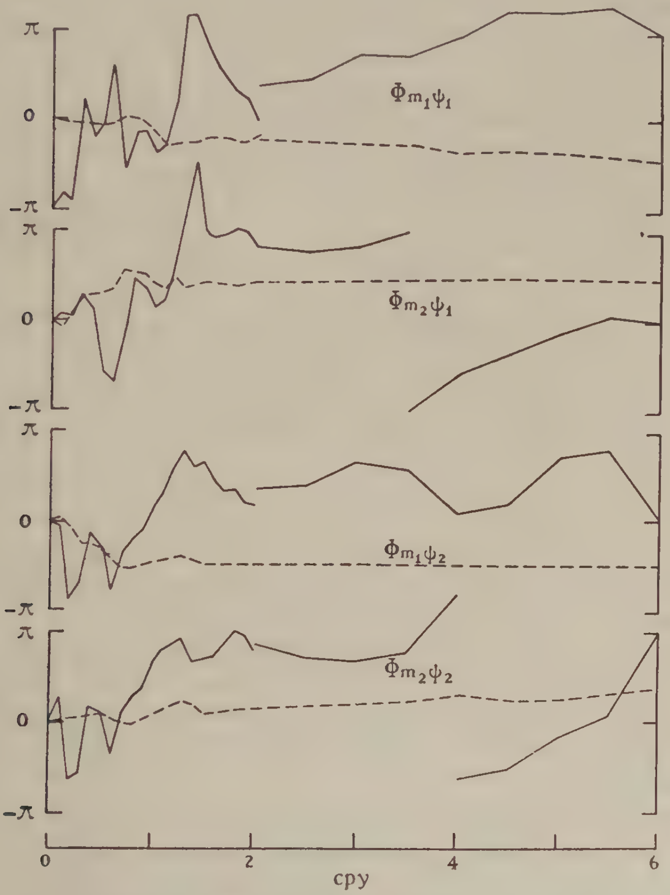

FIG. 7.—Comparison between observed (solid) and computed (dashed) phases. Spectra of intermediate resolution were used for frequencies below 2 cpy; those of low resolution for frequencies above 2 cpy.

A careful analysis of the significance of the inferred excitation would be highly desirable, for it could provide a clue to the nature of the excitation. For example, for a single coherent source we can factor $q(\theta, \lambda; t)$ into $f(\theta, \lambda)g(t)$ in equations (2) so that $\psi_1 = ag(t)$, $\psi_2 = bg(t)$, and hence $R_{\psi_1\psi_2} = 1$. For *two* incoherent sources

$R < 1$. In the case of *randomly* distributed sources the temporal-spacial correlation between $Q(\lambda, t) = \int q(\theta, \lambda;\ t) \sin^2\theta \cos\theta\, d\theta$ and $Q(\lambda-\delta,\ t-\tau)$ can be determined (at least in principle) from a knowledge of the excitation spectrum.

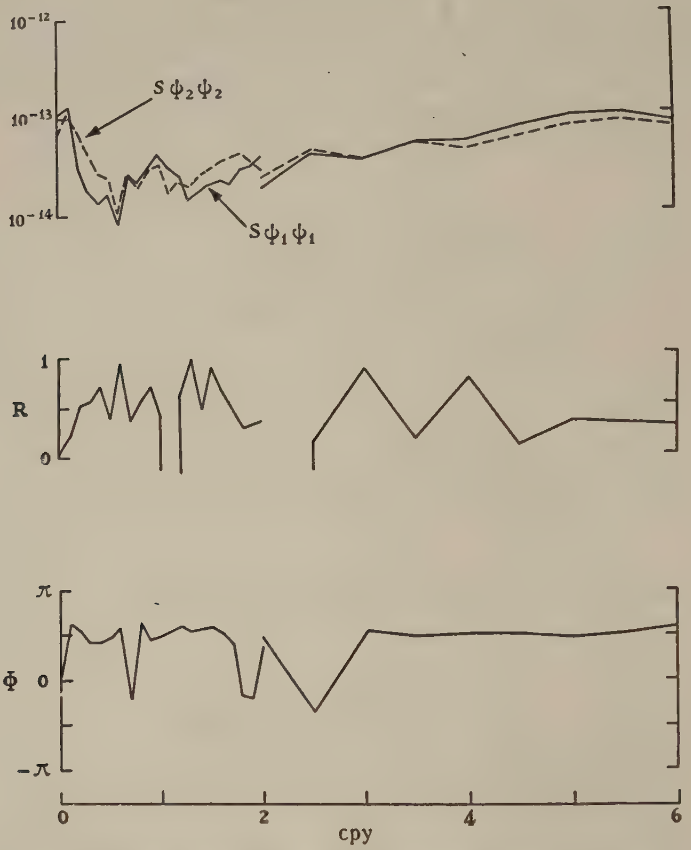

FIG. 8.—The astronomically inferred excitation spectra, according to equations (9).

11. Discussion

The smallness of the ratio of computed to observed wobble power implies that the variable distribution of air mass plays a minor role in the excitation of the Chandler wobble. Other variations in the hydrosphere are relatively unimportant to the *annual* wobble, and can hardly be expected to predominate at 0·85 cpy. Moreover, the low coherence between computed and observed wobble suggests that no other factors in the hydrosphere are of importance. One is tempted (as always) to look to the core.

Equations (1) govern the displacements of the rotation vector, m_i, parallel to the equatorial plane. The third component,

$$m_3 = \frac{\Delta\Omega}{\Omega} = -\frac{\Delta(\text{length of day})}{\text{length of day}}$$

designates the fractional variation in the diurnal rotation. The equation of motion is $\dot{m}_3 = \psi_3$, where ψ_3 is a suitably defined excitation function. Values of ψ_3 can be inferred from astronomical measurements of time, just as ψ_1 and ψ_2 were inferred from measurements of latitude. From comparisons of sidereal and ephemeris time (Munk & MacDonald 1960, Figure 11.10) we estimate

$$\begin{aligned} S_{\psi_3\psi_3} &= 3\times 10^{-15}\,\text{radians}^2/\text{cpy at } f = 0{\cdot}01 \text{ cpy} \\ S_{\psi_3\psi_3} &= 3\times 10^{-17}\,\text{radians}^2/\text{cpy at } f = 0{\cdot}1 \text{ cpy.} \end{aligned} \tag{13}$$

To go further we need to make some geophysical hypothesis concerning ψ_3. The only hypothesis that has survived so far is that it is due to electromagnetic coupling of the mantle with a turbulent core. To check this hypothesis we need to know either the variable angular momentum of the core or the variable flux of angular momentum across the core–mantle boundary (i.e. the torque). The momentum approach and torque approach are of course equivalent, and the choice depends on which quantity can be more readily estimated. Apparently this is the torque, and this is severely limited by the conductivity in the lower mantle. Rochester (1960) has placed an upper limit of 9×10^{24} dyn/cm on the component L_3. The excitation function and the torque are connected by the relations

$$\psi_1 = -\frac{L_2}{\Omega^2(C-A)}, \qquad \psi_2 = \frac{L_1}{\Omega^2(C-A)}, \qquad \dot{\psi}_3 = \frac{L_3}{\Omega C} \tag{14}$$

and the corresponding spectra are related according to

$$\begin{aligned} S_{\psi_1\psi_1}(f) &= \left[\frac{1}{\Omega^2(C-A)}\right]^2 S_{L_2L_2}(f), \quad \text{and similarly for } S_{\psi_2\psi_2} \\ S_{\psi_3\psi_3}(f) &= \left[\frac{1}{2\pi f}\right]^2 S_{\dot{\psi}_3\dot{\psi}_3}(f) = \left[\frac{1}{2\pi f\,\Omega C}\right]^2 S_{L_3L_3}(f). \end{aligned} \tag{15}$$

Taking Rochester's upper limit of 9×10^{24} dyn/cm and assuming a uniform spectrum between 0 and 1 cpy we obtain $S_{L_3L_3}(f) = 0{\cdot}81\times 10^{50}$ (dyn cm)^2/cpy and $S_{\psi_3\psi_3} = 6\times 10^{-19} f^{-2}$ radians^2/cpy, which is twice the estimate in equation (13). This satisfactory agreement is hardly an accident inasmuch as Rochester's estimate is based on the same astronomic observations as the spectra (13). Moreover the atomic frequency standards have provided some detailed information concerning the angular acceleration in recent times. Between July 1955 and January 1958 the length of day has increased at a rate of 0·43 milli-seconds per year. The requisite torque is

$$L_3 = I_m \frac{\Delta\Omega}{\Delta t} = \frac{2\pi I_m}{T^2}\frac{\Delta T}{\Delta t} = 8{\cdot}2\times 10^{24} \text{ dyn cm}$$

in excellent agreement with the previous estimate. Here I_m is the mantle's moment of inertia and T the length of day.

Suppose we accept $S_{L_3L_3} = 4\times 10^{49}$ (dyn cm)^2/cpy as determined by the length-of-day variations and found not to be inconsistent with electromagnetic theory. From the observed wobble we have estimated $S_{\psi_1\psi_1}$ and $S_{\psi_2\psi_2}$ to be of the order 10^{-15} to 10^{-14} radians^2/cpy. According to (15) the required torque spectra,

$S_{L_1L_1}$ or $S_{L_2L_2}$, then equal 2×10^{53} to 2×10^{54} (dyne cm)^2/cpy. Thus if the core were responsible for both the wobble and the changes in diurnal rotation, the equatorial torque components would have to be several hundred times larger than the axial torque, whereas one expects the equatorial components to be, if anything, less than the axial component. The conclusion is that the core is a negligible source of the Chandler wobble.

Scripps Institution of Oceanography,
University of California,
La Jolla, Calif.,
U.S.A.:
1960 *July* 26.

References

Bartlett, M. S., 1956. *An Introduction to Stochastic Processes* (Cambridge University Press).

Blackman, R. and Tukey, J., 1958. *Bell System Technical Journal*, **37**, 185.

Bullard, E., 1950. *The Observatory*, **70**, 139.

Fellgett, Peter, 1961. (In preparation).

Goodman, N. R., 1957. *New York University, Scientific Paper No. 10*, Engineering Statistics Laboratory.

Hassan, E. S. M., 1960. *Meteorological Monographs* (in press).

Jeffreys, H., 1940. The variation of latitude. *Mon. Not. R. Astr. Soc.*, **100**, 139.

Jeffreys, H., 1959. *The Earth* (Cambridge University Press).

Kempthorne, O., 1957. *An Introduction to Genetic Statistics* (John Wiley & Sons).

Munk, W. H. & MacDonald, G. J. F., 1960. *The Rotation of the Earth* (Cambridge University Press).

Rochester, M. G., 1960. *Phil. Trans. A*, **252**, 531.

Rudnick, P., 1956. *Trans. Amer. Geophys. Un.*, **37**, 137.

Spitaler, R., 1901. *Petermanns Mitteilungen, Erganzungsband*, **29**, 137.

Walker, A. & Young, A., 1957. Further results on the analysis of the observations of the variation of latitude. *Mon. Not. R. Astr. Soc.*, **117**, 119.

Reprinted from
BULLETIN OF MARINE SCIENCE
OF THE GULF AND CARIBBEAN
Vol. 11, No. 2, pp. 237-257
JUNE, 1961

SHRIMPS THAT CLEAN FISHES[1]

CONRAD LIMBAUGH
Scripps Institution of Oceanography, University of California
HARRY PEDERSON
McAllen, Texas
AND
FENNER A. CHACE, JR.
Smithsonian Institution

ABSTRACT

The symbiotic habits and color patterns of six species of caridean and stenopodidean shrimps that remove external parasites from fishes are described and discussed.

INTRODUCTION

Certain species of small, brightly colored shrimps have been observed to remove and eat parasites, injured tissue, and possibly undesirable food particles from a large variety of coöperating reef fishes. This symbiotic behavior is so well developed in some cases that the shrimps are invited to enter the mouths and gill cavities of their hosts, apparently with complete immunity from being eaten.

In many areas these shrimps, which are seldom abundant, seem to be the key organisms in small ecosystems. They are, together with certain fishes that also clean, seemingly responsible for the control of gill, oral, and external parasites of the various reef fishes. These reef fishes, in turn, to a large extent control directly or indirectly the biological environment surrounding reefs. In a field experiment conducted in the Bahamas by the senior author, the cleaner shrimps and fishes were removed from two isolated coral heads in the area under investigation. The observed result within a few weeks was a reduced number of reef fishes and a high incidence of fishes with frayed fins and ulcerated sores. Admittedly, the experiments because of their gross nature were not well controlled, but the observed

---

[1] This study developed from observations made and recorded on motion-picture film in the Bahamas by one of the authors (Pederson), beginning in 1952. In the following year, that author and his brother, Verne, determined that fishes frequent established cleaning stations to have their parasites removed, and, in 1954, he first observed and recorded the cleaning of fishes by a shrimp, *Periclimenes pedersoni*. In 1956, the senior author undertook an extensive investigation of cleaning relationships in the Bahamas, as well as at Manzanillo, Mexico; Clipperton Island; and off San Diego, California. The observations recorded here were made almost exclusively by the senior author, and the paper has been only slightly revised, posthumously, from a manuscript prepared by him. Many of those who have generously contributed to the final draft are mentioned at the end of the paper, but special acknowledgment must be made of the enthusiastic and tireless assistance received from Howard M. Feder of Hartnell College, Salinas, California; without his help and encouragement, the publication of the paper would certainly have been greatly delayed and possibly neglected.

(Publication of this paper was aided by a grant from The Permanent Science Fund of the American Academy of Arts and Sciences and by The Conrad Limbaugh Memorial Fund.)

Contributions from the Scripps Institution of Oceanography, New Series, 1333
Reproduced by Permission

contrast with the fish populations of the nearby coral heads was very striking.

Most cleaning shrimps locate in areas that are most likely to be utilized or observed by the majority of fishes on a small reef or section of a larger reef. Often they associate with fishes that clean. The reef fishes in turn frequent these particular areas or make special trips to these shrimp cleaning stations. The latter behavior is particularly characteristic of heavily parasitized or injured fishes.

Various behavior displays and mannerisms are often utilized by both the shrimps and the fishes to attract one another. The bright colored shrimps lash their conspicuous antennae and sway back and forth on prominent points of coral or rock. The fishes display color changes, move slowly to the shrimps, and gently extend fins and gill covers, open their mouths, and in some cases elevate their barbels.

This interesting cleaning behavior must be widespread in the marine environment judging from the known distribution of the shrimps involved. It occurs in both the Atlantic and Pacific Oceans, particularly in the tropical regions. Two species of cleaning shrimps are common to both the tropical Atlantic and the Indo-Pacific. Three species are known only from the tropical western Atlantic, and a single species is endemic to the temperate waters of the Southern California Province, where none of the other five species occur.

The shrimps thus far identified as cleaners belong to six species, two in each of three genera which are placed in three families and superfamilies and in two distinct sections of the decapod suborder Natantia (Figure 1). The similar behavior patterns and the similar prominent antennae of the various species suggest that cleaning, at least at the family level, is probably the result of convergent evolution. The similarity of the behavior patterns to those of fishes, such as territoriality and the tendency to pair, may also represent convergence.

The known cleaner shrimps may conveniently be divided into two groups on the basis of behavior, habitat and color. The five species comprising one group are usually solitary or paired (although *Periclimenes yucatanicus* and *P. pedersoni* are occasionally found in small aggregations of five or six). All five species are territorial and remain for weeks and, in some cases, months or possibly years within a meter or less of the same spot. They are omniverous to a slight extent but seem to be highly dependent upon their hosts for food. This group is tropical, and the individuals are brightly marked. They

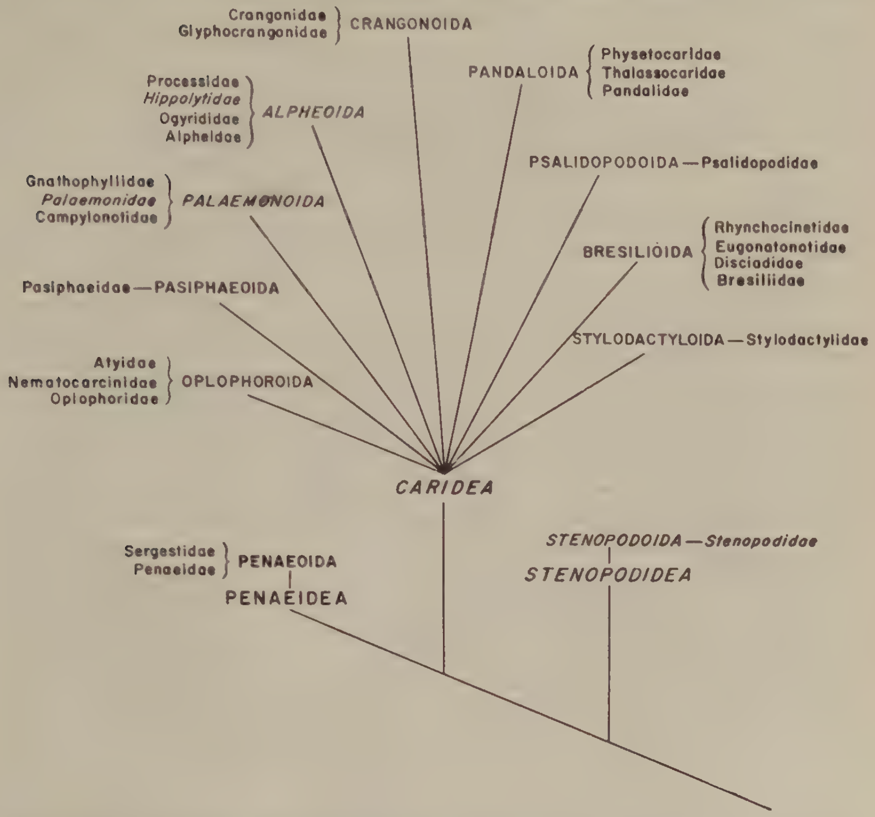
Crangonidae
Glyphocrangonidae
CRANGONOIDA
PANDALOIDA
Physetocaridae
Thalassocaridae
Pandalidae
Processidae
Hippolytidae
Ogyrididae
Alpheidae
ALPHEOIDA
PSALIDOPODOIDA—Psalidopodidae
Gnathophyllidae
Palaemonidae
Campylonotidae
PALAEMONOIDA
BRESILIOIDA
Rhynchocinetidae
Eugonatonotidae
Disciadidae
Bresiliidae
Pasiphaeidae—PASIPHAEOIDA
STYLODACTYLOIDA—Stylodactylidae
Atyidae
Nematocarcinidae
Oplophoridae
OPLOPHOROIDA
CARIDEA
Sergestidae
Penaeidae
PENAEOIDA
PENAEIDEA
STENOPODOIDA—Stenopodidae
STENOPODIDEA

FIGURE 1. Schematic arrangement of the sections, superfamilies, and families of shrimps (Natantia) showing the relationship between the groups (in italics) containing species that clean fishes.

display themselves to their hosts in a conspicuous manner. They probably rarely serve as prey for fishes. A single species, *Hippolysmata californica*, comprises the second group. The imperfect relationship with one of the host species, in which the shrimp is sometimes eaten, suggests that this is a primitive type of cleaning behavior. This species is a gregarious, wandering, omniverous animal which occurs in cooler waters and is not highly dependent upon its host for survival. So far as is known, it does not display itself to attract fishes.

Among these cleaner shrimps there exist considerable differences in behavior, morphology, and habitat even within a genus. These differences make it necessary to consider each species separately.

INDIVIDUAL SPECIES

Family PALAEMONIDAE

Subfamily Palaemoninae

Periclimenes (Periclimenes) yucatanicus (Ives, 1891)

Figure 2

This is a small species, usually less than three centimeters in body length. The antennae are longer than the body. The body and legs are smooth.

The body is transparent except for several distinct, large, white and tan saddles and spots. There is a large saddle of light tan bordered with white on the carapace. A pair of smaller light tan spots is situated on the dorsal surface of the second abdominal somite; a similar, smaller spot on each lateral surface of that somite; and one or two white spots anterior to the lateral spot. There is a large dorsal saddle on the third somite at the bend of the abdomen, and a smaller saddle on the fifth somite. At the base of the telson, a white saddle blends into a purple spot on either side. A row of white dots marks the ventral midline of the abdomen. The eyes are white, tipped with red. The eyestalks have a fine stippling of red and white dots which extends over the rostrum and the anterior part of the carapace and onto the antennular and antennal peduncles. The outer flagella of the antennules are white with an extended orange saddle at their bases. The inner flagella of the antennules are transparent with bands of red. The antennal flagella are usually banded with red and white, but the red bands may be absent. The third maxillipeds are white banded with purple. The smaller chelipeds are banded with purple and white. The larger chelipeds are banded with white, purple, red, and orange. The walking legs are purple banded with white. The uropods are tipped with reddish violet bordered proximally with white. The eggs are translucent brown. In general, this shrimp is somewhat less conspicuous in its normal habitat than are the other tropical cleaners.

This species is apparently widely distributed between southern Florida and Colombia (Holthuis, 1951). We observed it off the Bahamas, Virgin Islands, and Puerto Rico. Females with eggs were seen in July and August.

We always found it associated with either of two common Caribbean anemones, *Bartholomea annulata* (Lesueur) and *Condylactis gigantea* (Weinland), either resting on the anemones or occupying the

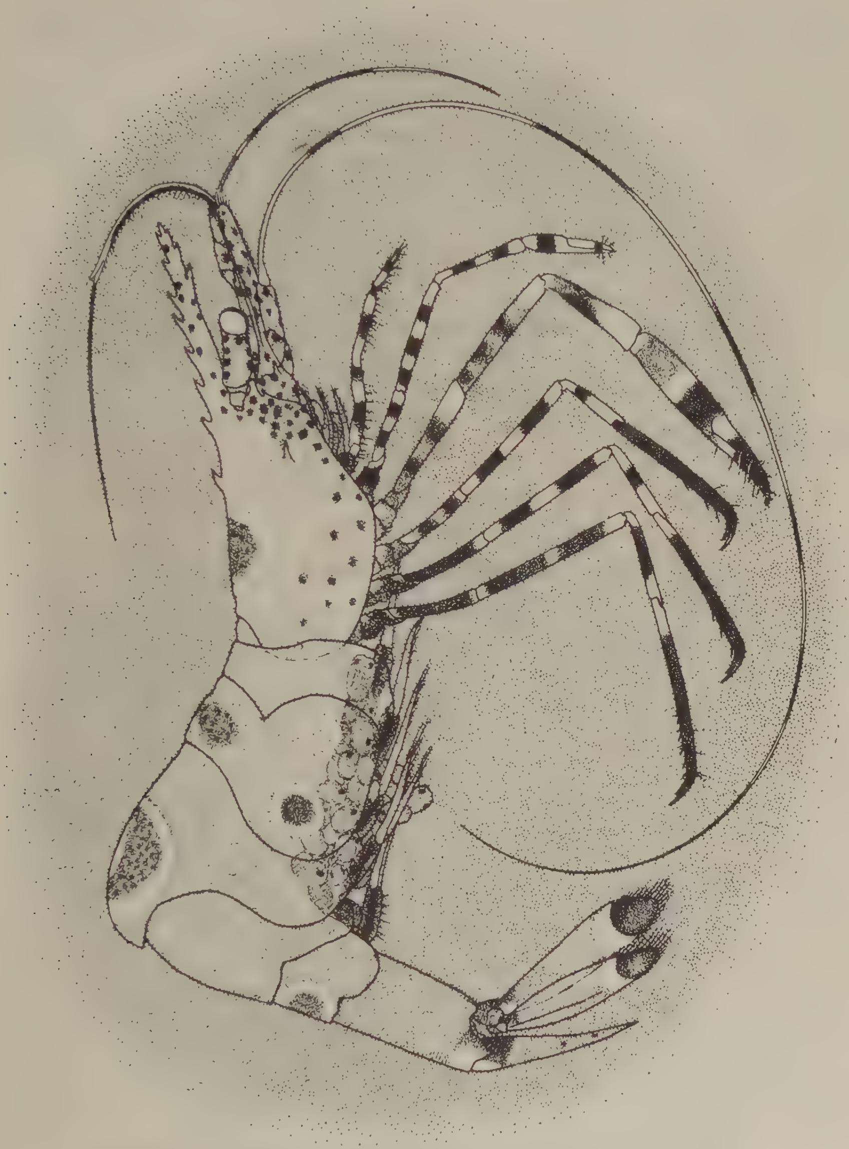

FIGURE 2. *Periclimenes* (*Periclimenes*) *yucatanicus* (Ives).

same crevice. As many as six of these shrimps may be found on a single anemone. The anemones are usually, but not always, attached to hard substrate buried in fine sand or mud at depths ranging from just below low tide line to at least 23 meters (Holthuis, 1951).

In the presence of fishes, and sometimes just in the presence of the observer, these shrimps may lash their antennae together and sway back and forth. On two separate occasions they were observed with juvenile fishes, including three-spot goatfishes *Upeneus maculatus* (Bloch); filefishes (Monacanthidae); and yellowtail snappers, *Ocyurus chrysurus* (Bloch). The contacts between fish and shrimp were momentary, and the shrimp did not leave the substrate.

These shrimps may possibly be examples of clever mimicry and not cleaners. The senior author has observed fishes that mimic cleaner fishes only to take bites out of would-be hosts. The victims were invariably juvenile fishes.

Periclimenes (Periclimenes) pedersoni Chace, 1958

Figures 3-4

The Pederson cleaning shrimp is another small species with a maximum body length of not more than four centimeters. The antennal flagella are longer than the body and, with the antennular flagella, seem to form a protective cage over the body. The shrimp is smooth. It is sexually dimorphic, especially in the form of the rostrum; females and young males closely resemble *P. yucatanicus* except for the color pattern.

The body is transparent with longitudinal white lines running posteriorly from the bases of the third maxillipeds and converging dorsally near the posterior margin of the third abdominal somite. Between the white lines on the dorsal surface of the abdomen are a variable number of violet spots of irregular sizes. Outside of the white lines on either side of the posterior half of the third abdominal somite are two or three similar small spots of violet followed by a large, triangular, violet patch bordered with white. There are usually two violet spots in the dorsal midline of each of the fourth and fifth somites, a few smaller lateral spots on those somites, and four or five spots in a longitudinal row on each side of the sixth somite. There may or may not be a white stripe in the dorsal midline of the sixth somite, as well as near the posterior margins of the two preceding somites. The telson bears two or three violet spots in the midline and a transverse bar of the same color proximad to the white tip. An opaque white line marks the ventral midline of the body from the posterior part of the thorax to the middle of the sixth abdominal somite. The eyes are opaque pink. The eyestalks are transparent with a purple and, sometimes, a white line below. The outer antennular flagella are entirely white; the inner ones are transparent. The antennal flagella are mostly opaque white, but transparent at their bases. The third maxillipeds are opaque white at the base and tip, banded with violet elsewhere. The smaller chelipeds are banded with purple, and the fingers are tipped with brown. The larger chelipeds are banded with purple on the distal half of the fingers, distal half of the palm, and distal part of the carpus or proximal part of the palm; there are brown saddles on the inner surface near the base of the palm and on the carpus, and purple saddles on the inner surfaces of the ischium and merus. The walking legs are translucent. The uropods are tipped with

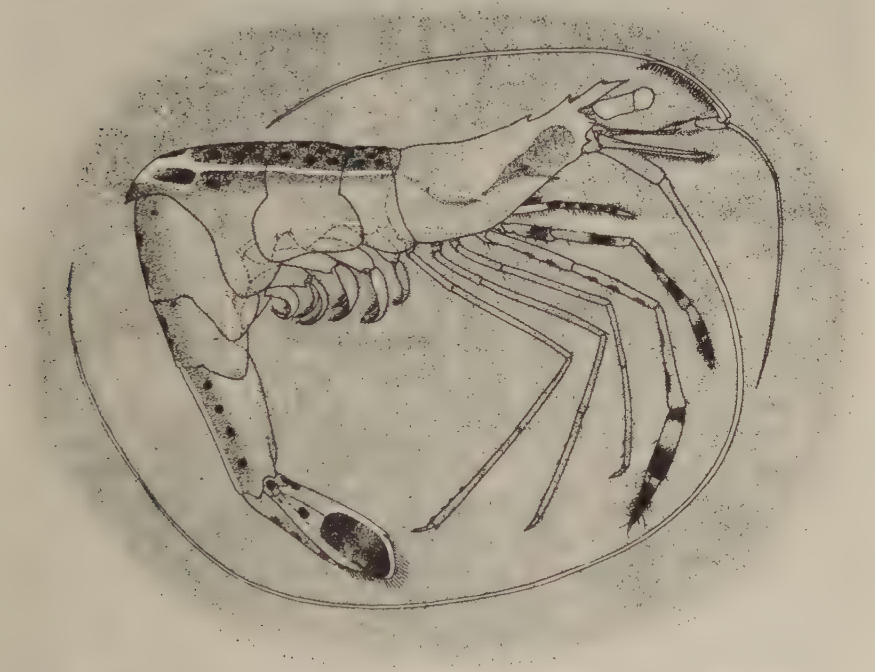

FIGURE 3. *Periclimenes* (*Periclimenes*) *pedersoni* Chace. (Modified from Chace, 1958.)

blue violet, outlined proximally and laterally with white, and there are a few violet spots near the bases of the uropods. Although the general color pattern of this species is constant and characteristic, the details of the pattern are subject to considerable variation. Specimens collected off the west coast of Florida that agree morphologically with *P. pedersoni,* although they were not associated with sea anemones and were not observed cleaning fishes, have fewer and redder spots on the abdominal somites and telson, reddish markings on the antennular peduncles and basal parts of the inner antennular flagella, a pair of red bands on the otherwise white antennal flagella, yellow bands on the chelipeds, and blue, violet, red and yellow bands on the walking legs, especially the posterior pair.

We have taken this species in the Bahamas and the Virgin Islands. It has also been collected at Antigua, British West Indies, and the color variety described above is reported to be common in 17 meters of water off West Florida.

In general, these shrimps seem to be found in areas protected from violent surge. In all cases, except off West Florida, they have been observed associated with the anemone, *Bartholomea annulata* (Lesueur), usually hanging directly to the anemone or occupying the same hole. We have observed them at depths ranging from 1.5 to 9 meters in the Bahamas and Virgin Islands. The species frequently occurs in pairs, but it is often solitary or, in rare cases, it is found in groups of up to five. The individuals may remain from one to three weeks on the same anemone and possibly even longer. They may on occasion completely disappear, however, or show up on a new anemone a short distance away.

The Pederson shrimp attracts the attention of a great variety of reef fishes by whipping its antennae and by swaying back and forth from a prominent position on or near the anemone. Fishes often line up or crowd around waiting their turn to be cleaned. When we removed the shrimp, fishes continued to visit the same anemone for over a week. Fishes cleaned include: three-spot goatfish, *Upeneus maculatus* (Bloch); squirrel fishes, *Holocentrus,* spp.; yellow grunt, *Haemulon flavolineatum* (Desmarest); Nassau grouper, *Epinephelus striatus* (Bloch); rock hind, *Epinephelus adscensionis* (Osbeck); parrot fish, *Sparisoma viride* (Bonnaterre); yellow-backed porgy, *Calamus calamus* (Valenciennes); filefishes, Monacanthidae; queen triggerfish, *Balistes vetula* Linnaeus; and peacock flounder, *Bothus*

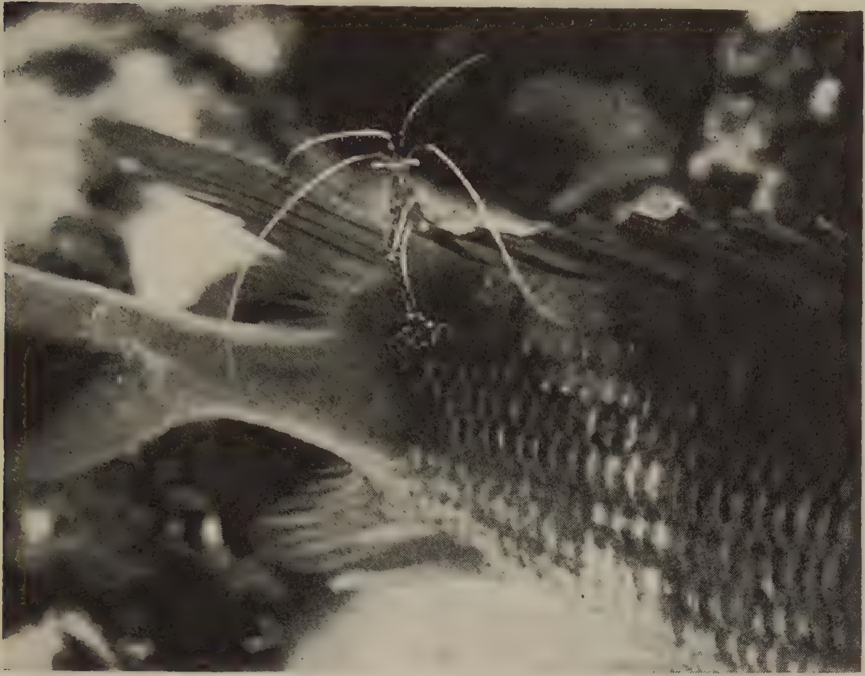

FIGURE 4. *Periclimenes pedersoni* cleaning a squirrelfish, *Holocentrus,* sp. (Photograph courtesy of Walt Disney Productions.)

lunatus (Linnaeus). The shrimp boards the fish as soon as the latter comes close enough and quiets down. It swims head first or crawls to the fish. Parasites are removed as the shrimp moves rapidly over the fish. In this operation, it pulls directly at the parasite or opens the tissue surrounding it. If the shrimp encounters a wound, it will spend considerable time picking at the injured flesh. As the shrimp approaches the gill region, the fish opens the gill cover and allows the shrimp to enter. The action is repeated on the opposite side The shrimp is also allowed to enter, and leave, the mouth. If the observer gets too close to a large fish, the shrimp either swims out or is ejected from the fish's mouth before the fish retreats. It is suspected that this shrimp includes, as part of its diet, undesirable food particles taken from the gills and teeth of the fish. When the shrimp is apparently satiated, it retires to the anemone, often with many fishes still waiting to be cleaned. At some cleaning stations, the shrimps' activities are joined by the cleaning fish, *Elacatinus,* sp.

The sea anemone, *Bartholomea annulata,* with which *P. pedersoni* is associated has several other interesting companions. Clarke (1955) described the red mysid, *Heteromysis actiniae,* which commonly swims among its tentacles. He also mentioned the snapping shrimp, *Alpheus armatus* Rathbun, which lives in pairs with the anemone. This snapping shrimp is apparently dependent upon the anemone for protection and vice versa. The snapping shrimp digs a burrow for both of them. It spends most of its time at the burrow entrance with its banded antennae mixed with the banded tentacles of the anemone. If danger comes near, the shrimp withdraws quickly, causing the anemone to contract and plug the entrance of the burrow. The shrimp was often observed to chase small blue damsel fishes, *Pomacentrus,* with its trigger claw. The snapping shrimp was invariably associated with the anemone off New Providence Island, Bahamas, but William Clarke (personal communication) maintains that this was not the case off Bimini. In a simple experiment, we removed the snapping

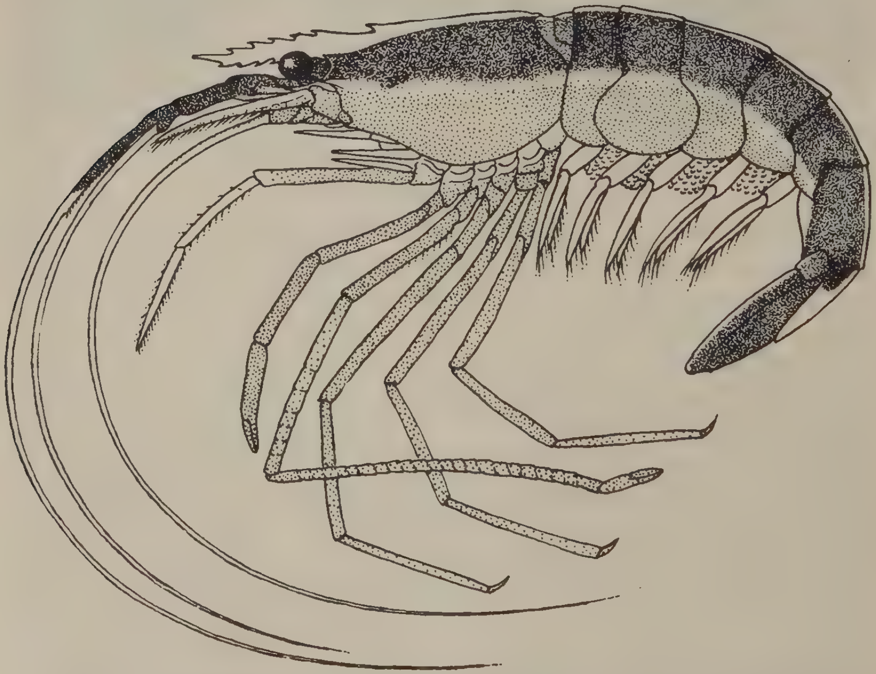

FIGURE 5. *Hippolysmata* (*Hippolysmata*) *grabhami* Gordon. (Modified from Gordon, 1935.)

shrimps from one anemone. Within a few days, only pieces of the anemone could be located, and they had obviously been preyed upon; subjective suspicion points to the stomatopods which are abundant in the same area. These same snapping shrimps in an aquarium seek out the anemones very quickly. In addition to this shrimp, there are other associates of this anemone which should be briefly mentioned: juvenile arrow crabs, *Stenorynchus seticornis* (Herbst); various small hermit crabs; a finspot fish, *Paraclinus grandicomis* (Rosén); and a cardinal fish, Apogonidae.

Family HIPPOLYTIDAE

Hippolysmata (Hippolysmata) grabhami Gordon, 1935

Figures 5-6

The red-backed cleaner shrimp is intermediate in size. The body lengths of those observed were estimated to be five centimeters or less, but the species is known to reach a length of at least 68 mm (Gordon, 1935). The antennae are longer than the body. The body and appendages are smooth.

The color is yellow ochre with a broad, red, longitudinal band extending from the basal part of the outer antennular flagella, along the carapace and abdomen, to the uropods. The red band is bisected for its entire length in the dorsal midline by an opaque white stripe. Most of the outer antennular flagella, the inner antennular flagella, the antennal flagella, the two distal segments of the third maxillipeds, and most of the telson are also white. The eyes are brown. The coloration of this shrimp seems to be very constant. The white of the antennae, tail, and back are conspicuous in the crevices in which the shrimps are found, but the antennae were not observed being displayed in the sunlight. It may be more than coincidental that the color pattern of this shrimp, although not necessarily the actual colors, is very similar to the patterns of at least three of the cleaner fishes: *Labroides dimidiatus* (Cuvier and Valenciennes), *Aspidontus taeniatus* Quoy and Gaimard, and *Elacatinus oceanops* Jordan.

H. grabhami has been recorded from Madeira (Gordon, 1935) and the Society Islands (Randall, 1958). It has also been found off southeastern Florida and in the Hawaiian Islands. Two pairs were observed off New Providence Island, Bahamas: one pair at Lyford Bay at a depth of two meters; the other off Hog Island under a small coral head at a depth of three meters.

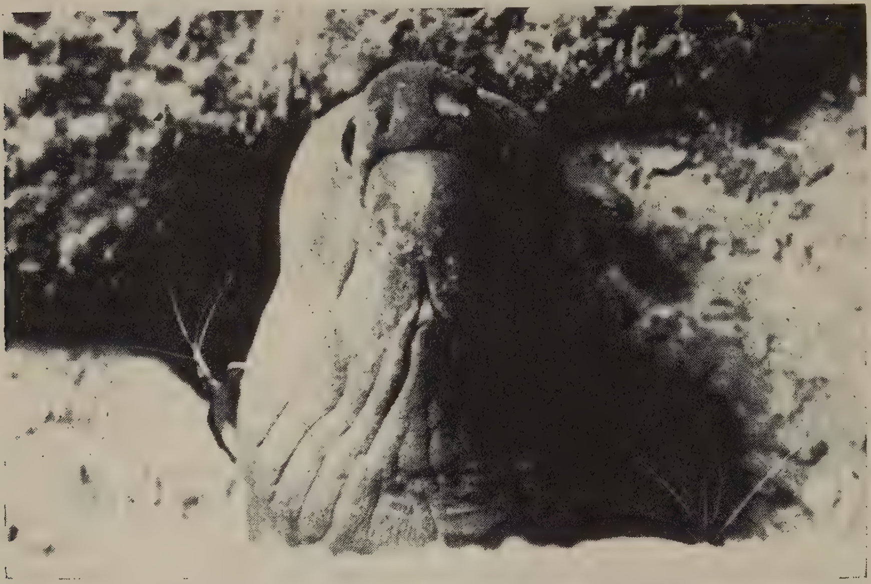

FIGURE 6. *Hippolysmata grabhami* cleaning a moray, *Gymnothorax*, sp., in Florida. Nearly hidden in the right foreground is a *Stenopus hispidus*. (Photograph by E. L. Fisher, Marine Laboratory, University of Miami.)

Those seen in the Bahamas were in large, shaded coral crevices on small, isolated coral heads in protected waters. Those crevices were occupied by unusually large numbers of fishes. In the more open and larger crevice off Hog Island, a pair of *Stenopus hispidus* shared a different area of the same crevice; it is interesting that the specimen photographed off Florida (Figure 6) was also accompanied by *S. hispidus*. Like the two species of *Stenopus, H. grabhami* does not seem to wander but restricts its movements to a certain small area of a crevice. The pair at Lyford Bay was observed in the same part of the same crevice from April through August, 1956. The individuals of a pair attempt to stay together. They lived on the walls of the crevice at Lyford Bay, on the roof of the crevice off Hog Island, and were observed by Randall (1958) in the open on coral blocks at a depth of 21 meters in the Society Islands.

In the Bahamas, they lashed their antennae vigorously in the presence of fishes and sometimes at the observer. Unfortunately the configuration of the crevices made it difficult to observe the cleaning activities of these shrimps; on one occasion a blue tang, *Acanthurus* *caeruleus* Bloch and Schneider, was observed being cleaned. The crevice at Lyford was invariably crowded with medium-sized fishes. In particular, they crowded around the shrimps which reached from the substrate and picked at the various fishes. Randall (1958) records the cleaning activities of this species in the Pacific. He identified the following fishes as having "entered into a symbiotic association" with the shrimp: *Apogon exostigma* (Jordan and Stark); *Apogon,* sp.; *Anthias,* sp.; juvenile *Acanthurus mata* (Cuvier), and *Gymnothorax flavomarginata* (Rüppell). He noted that the shrimp climbed onto the head of the latter moray.

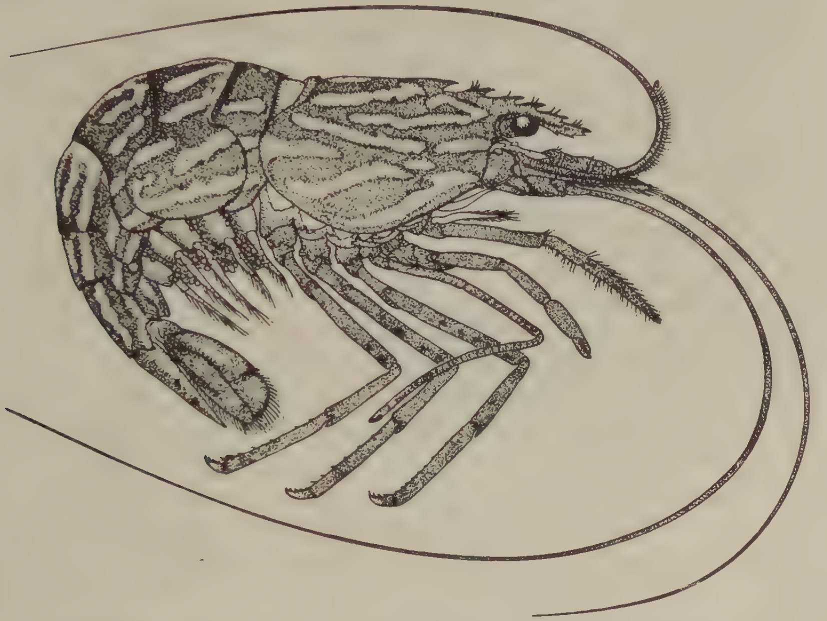

FIGURE 7. *Hippolysmata* (*Hippolysmata*) *californica* Stimpson.

Hippolysmata (Hippolysmata) californica Stimpson, 1866
Figure 7

Hippolysmata californica is one of the larger and heavier-bodied cleaning shrimps. The body may attain a length of up to seven centimeters or slightly more in the northern part of its distribution. The antennae are longer than the body but, because they are red, they are not as conspicuous as those of the other cleaning shrimps.

(1065)

The body and legs are smooth.

The color is translucent red, striped with rows of pink. The eyes are brown but the stalks have a white line down the front or lower surfaces which continues onto the body and converges to form a Y on the ventral side of the shrimp. In their own environment under natural light conditions, they are not conspicuous except for the white Y which is seen when the shrimp faces the observer. At night when these shrimps are most active, their eyes reflect artificial light as orange.

They have been reported from Santa Barbara, California, to Ensenada, Baja California (Ricketts and Calvin, 1952). Observations of the senior author confirm this distribution and extend it south to Sebastion Viscaino Bay and Guadalupe Island.

These shrimps are found in protected, rocky crevices and human artifacts from the back bays to the open coast and from tide pools to depths of at least 61 meters. They are highly gregarious and sometimes are found in groups of several hundred. They wander at night, but retire to cover during the day. The individuals quarrel a great deal with one another, particularly about food.

The three heavily integumented forms that are known to be cleaned by this shrimp under natural conditions are all part of the Southern California fauna, with distributions similar to that of the shrimp. They include the California moray, *Gymnothorax mordax* (Ayres); the garibaldi, *Hypsypops rubicunda* (Girard); and the California spiny lobster, *Panulirus interruptus* (Randall). These shrimps continually feed on the epibiose of the rocky substrate on which they occur, and they are probably not greatly dependent upon cleaning for food. They do not seem to try to attract fishes, but simply occupy holes where certain fishes and lobsters are found. When a suitable fish or lobster enters a crevice occupied by these shrimps, the latter will crawl or swim to the invader and clamber rapidly over the entire outside surface of the animal, stopping and picking at favorable areas. A diver's hand will receive the same attention, particularly the finger nails. The fishes do not seem to be bothered, although the moray may occasionally jerk its head as if annoyed. In some cases the shrimps may enter the mouths of these eels, but apparently not without some risk, for the stomachs of California morays examined at Guadalupe Island yielded a considerable number of these shrimps. On the other hand, in an aquarium where a fish cannot escape, the shrimps will clean it to the bone.

Hippolysmata californica therefore exhibits a rather simple and imperfect relationship with its hosts, sometimes eating them and sometimes being eaten itself. During the cleaning process, the shrimps seem only to seek food on a new substrate. From this simple and hazardous relationship, it is easy to visualize an evolutionary path by which the more complex cleaning behavior could have developed. We do not mean to imply that *H. californica* or its close relatives were the first cleaner shrimps. We merely offer its behavior as a model of how cleaning may have begun.

Family STENOPODIDAE
Stenopus hispidus (Olivier, 1811)
Figure 8

This species is the largest of the known cleaner shrimps. The body may attain a length of more than seven and a half centimeters. The

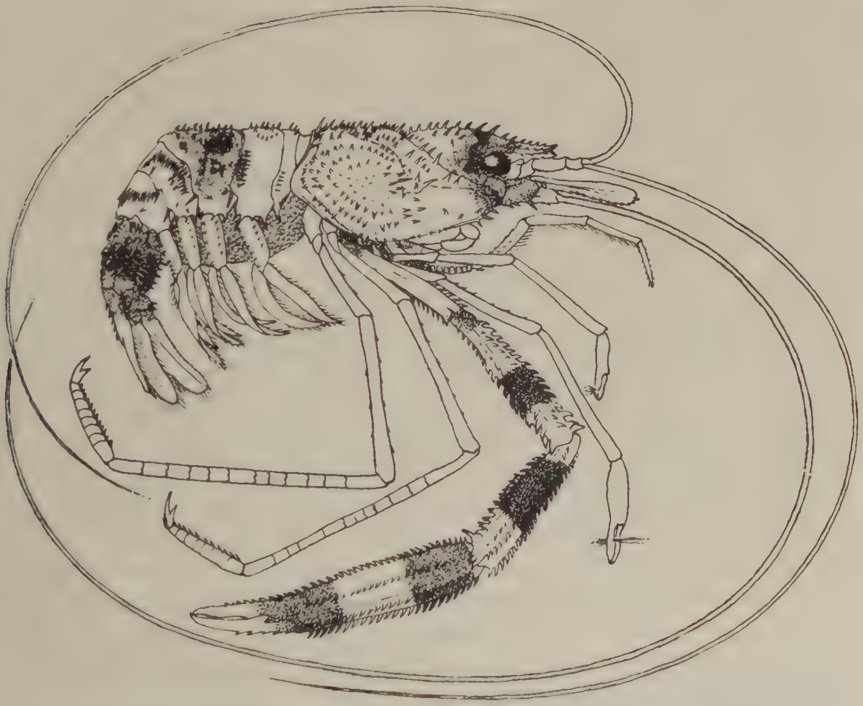

FIGURE 8. *Stenopus hispidus* (Olivier). (Modified from Bate, 1888.)

antennae and antennules are considerably longer than the body. The body and larger chelipeds are spiny.

The striking color of this shrimp has attracted considerable attention (Roughly, 1936, and Utinomi, 1956) and some speculation (Herrick, 1893). The body and legs are white with bands of red. A blotch of red is located on the anterior part of the carapace. The bases of the legs of large adults are blue. The antennae and antennules are white. The eyes are brown, and the large cluster of eggs carried by the female are turquoise. The color brilliance usually contrasts sharply with the generally dull background of gray coral rock. In the shaded environment, the red is dulled, but the white remains conspicuous. The antennae, which are usually displayed in the sunlight, are clearly visible.

Stenopus hispidus occurs throughout the Indo-Pacific region from the Red Sea and South Africa to the Hawaiian and Tuamotu Islands; in the western Atlantic, it is found from Bermuda and southern Florida to the north coast of South America (Holthuis, 1946). It is not known from the eastern Pacific or eastern Atlantic. The senior author was unable to find it during expeditions along the coast of Mexico and around Clipperton Island but, in the Atlantic, we found it to be common off the Bahamas, Puerto Rico and Virgin Islands.

Pairs were observed in quiet, shallow water where fishes were abundant. The pairs were most commonly located in shaded coral crevices or caves, usually on the ceiling near the entrance where the antennae could be displayed in the sunlight. Occasionally they were found in large holes or undercut mats of rhizomes of the turtle grass, *Thalassia*. Frequently they occupied discarded man-made objects such as auto tires, buckets and the like. In less protected areas, such as the seaward sides of islands, they do not commonly inhabit the very shallow, turbulent water. They usually occur at depths of two to four meters. A few, however, have been observed just below the low tide line in areas where the water is very calm, and the species has been recorded from a depth of 210 meters (Holthuis, 1946). Juveniles appear to pair and grow up together. Adults, as well as juveniles, were never observed to move more than half a meter except when disturbed by the investigator. They probably remain in an area of less than a square meter many months, possibly years. The pairs attempt to stay together even when disturbed.

The caves occupied by *S. hispidus* are frequented by a large variety of reef fishes, particularly morays, tangs, grunts and groupers. Unfortunately, the presence of a diver at the entrance of their retreat disturbs the cleaning activity and makes observations almost impossible. One of the authors (Pederson) observed one of these shrimps cleaning a white-spotted moray. The shrimp approached the moray, placed its large chelipeds around the eel, and proceeded to clean with its smaller claws. The shrimp was not observed to leave the substrate but only reached out to clean. On another occasion, the senior author observed a juvenile shrimp of this species picking at the side of a blue tang, *Acanthurus caeruleus* Bloch and Schneider. The tang was resting near the base of a coral boulder in which there was a small crevice into which the fish partially curved its body. All that could be seen of the small shrimp was its large chelae which were against the fish, its antennae, and the small claws which were presumably picking parasites. The fish finally became alarmed at the presence of the observer and swam away. In many instances, fishes in awkward positions were observed beside these shrimps, but they were disturbed by the presence of the observer before any cleaning activity ensued. There is no doubt, however, that these fishes were being cleaned.

No natural predators of this shrimp were found by us. In a simple experiment, an octopus was caged with a pair of these shrimps. The shrimps were not eaten until the octopus had gone without food for several weeks; usually octopuses will feed readily on crustaceans on the second or third day of captivity. Possibly the octopus had difficulty catching the shrimps, which are quite agile. That *S. hispidus* is not entirely immune from predators is indicated by Randall and Brock (1960) who found two complete specimens of this shrimp in the stomach of a grouper, *Epinephalus merra* Bloch, and a chela in the stomach of another grouper, *Cephalopholis miniatus* (Forskal).

The wide distribution, plus the background life-history work that has been done on this shrimp (Herrick, 1893), suggest that it would be an excellent subject for further research.

Stenopus scutellatus Rankin, 1898
Figure 9

This species is smaller than *S. hispidus* but similarly proportioned. It attains a body length of about three and a half centimeters. The antennae and antennules are considerably longer than the body. The body and larger claws are spiny.

The general color pattern and structure of this species are similar to those of *S. hispidus,* but the back is lemon yellow. The yellow may be an advantage in advertising the presence of this shrimp, which lives in smaller and usually darker crevices than those occupied by *S. hispidus.*

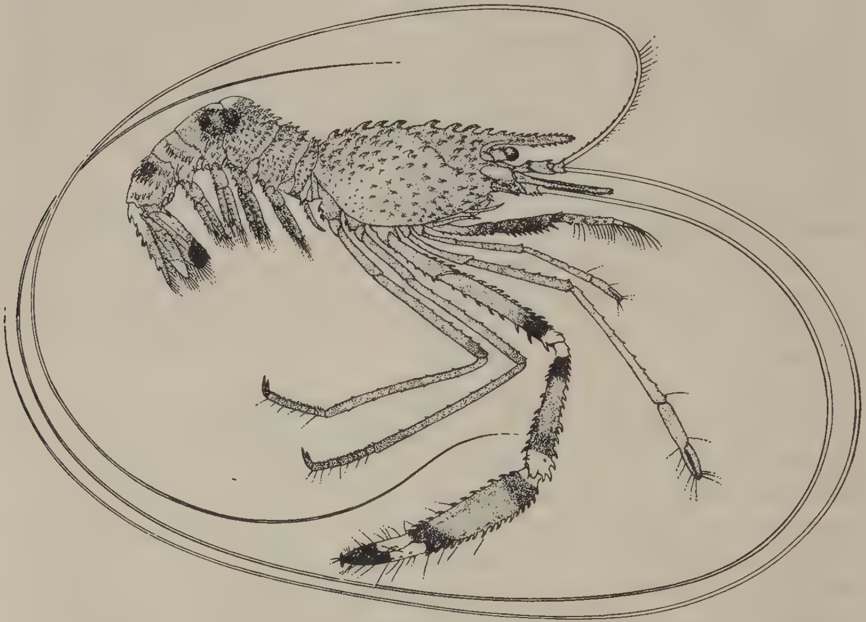

FIGURE 9. *Stenopus scutellatus* Rankin.

The recorded distribution of *S. scutellatus* is from Bermuda to Fernando de Noronha, Brazil, from shallow water to 55 meters. (Holthuis, 1946). We have found it to be common off New Providence Island in the Bahamas in depths ranging from just below low tide to six meters or more. All were observed on isolated solid substrates in or near large beds of turtle grass (*Thalassia*) in protected, quiet waters. They always occurred in pairs, often in discarded human artifacts, and commonly in coral boulders.

It is believed that they remain within centimeters of the same spot. One pair was observed in the same football-sized coral boulder from May through August 1956. During that period, we changed the position and orientation of the boulder several times within a radius of approximately seven meters without disturbing the shrimps. Visiting fishes were momentarily disturbed by the changes, but they soon relocated the shrimps.

These shrimps also whip their antennae in the sun in front of the dark hole in which they live in order to attract fishes. To clean a fish thus signaled, they simply reach out of their hole and pick at their host. On rare occasions, they were observed to leave their holes to clean, but they never climbed onto the fish. The most common visitors to these shrimps were the three-spot goatfish, *Upeneus maculatus* (Bloch), and the yellowtail snapper, *Ocyurus chrysurus* (Bloch). In addition to the visitors, the crevices inhabited by these shrimps often housed unusually large numbers of small fishes, such as apogonids. The goatfishes often placed their barbels inside the hole in order to have them worked on.

The two species of *Stenopus* that inhabit the same general area in the Bahamas have somewhat similar markings and habits. They do, however, have significant differences, particularly in their habits and habitats. *S. hispidus* prefers large, open crevices or caves and cleans larger fishes, while *S. scutellatus* prefers small holes or crevices and cleans only small fishes.

Discussion

Among the various degrees of specific interdependence demonstrated by these few cleaning shrimp examples, we can see some interesting patterns in several fields of biology. The bright markings that advertise the presence of these shrimps suggests a new significance for color in the marine environment. The interesting similarities in morphology and behavior suggest convergent evolution. The behavior itself, with its complex interaction between cleaners and hosts, provides an area for study by behaviorists. The wide distribution of two species of cleaners is subject matter for the zoogeographer to explore in more detail. The parasitologist should find answers to some of his questions, such as a reasonable explanation for parasites to blend well with their background on the host and an explanation of the natural control of some fish diseases. The implications for the economic biologist involved in fisheries work are obvious. The importance of these shrimps in controlling the external parasites of the associated reef fishes must be considerable. They must, then, be responsible for higher fish populations, and consequently exert a profound influence on the ecology of the nearby areas.

ACKNOWLEDGMENTS

Rarely have so many contributed so much to a study of this scope. We wish to express our gratitude to all of those mentioned below who responded most unselfishly to our requests for specimens, photographs, observations, identifications, or perusal of manuscript drafts: Cadet Hand of the University of California, Berkeley; W. J. North and James Stewart of the Institute of Marine Resources, University of California, La Jolla; William D. Clarke, Gifford Ewing, Raymond Ghelardi, Carl L. Hubbs and Nan Limbaugh of the Scripps Institution of Oceanography, University of California, La Jolla; R. B. Cowles of the University of California, Los Angeles; Demorest Davenport of the University of California, Santa Barbara; William H. Amos of the University of Delaware; Erwin Verity of the Disney Studios; Bonnie Eldred and Robert F. Hutton of the Florida State Board of Conservation Marine Laboratory, St. Petersburg; L. B. Holthuis of the Rijksmuseum van Natuurlijke Historie, Leiden, The Netherlands; E. L. Fisher, Raymond B. Manning, Anthony J. Provenzano, Jr., John E. Randall and Gilbert L. Voss of the University of Miami Marine Laboratory; James E. Böhlke and Charles C. G. Chaplin of the Academy of Natural Sciences of Philadelphia; Ron Church and Bev Morgan of Scientific Diving Consultants; Frederick M. Bayer, Thomas E. Bowman, Charles E. Cutress, Ernest A. Lachner and Waldo L. Schmitt of the U. S. National Museum, Smithsonian Institution; Dr. Richard Kirk of Madeira Beach, Florida; Desmond V. Nicholson of St. Johns, Antigua, British West Indies, and Verne Pederson of La Jolla, California.

LITERATURE CITED

BATE, C. S.
1888. Report on the Crustacea Macrura collected by H. M. S. Challenger during the years 1873-76. Rep. Voy. Challenger, Zool., *24:* xc + 942 pp.

CHACE, F. A., JR.
1958. A new shrimp of the genus Periclimenes from the West Indies. Proc. biol. Soc. Wash., *71:* 125-130.

Clarke, W. D.

1955. A new species of the genus *Heteromysis* (Crustacea, Mysidacea) from the Bahama Islands, commensal with a sea-anemone. Amer. Mus. Novit., 1716: 1-13.

Gordon, Isabella

1935. On new or imperfectly known species of Crustacea Macrura. J. Linn. Soc. (Zool.), *39:* 307-351.

Herrick, F. H.

1893. The life history of Stenopus. In: Brooks, W. K., and F. H. Herrick, The embryology and metamorphosis of the Macroura. Mem. nat. Acad. Sci., *5:* 339-352.

Holthuis, L. B.

1946. The Stenopodidae, Nephropsidae, Scyllaridae and Palinuridae. The Decapoda Macrura of the Snellius Expedition. I. Temminckia, *7:* 1-178.

1951. The subfamilies Euryrhynchinae and Pontoniinae. A general revision of the Palaemonidae (Crustacea Decapoda Natantia) of the Americas. I. Occ. Pap. Allan Hancock Fdn., 11: 1-332.

Ives, J. E.

1891. Crustacea from the northern coast of Yucatan, the harbor of Vera Cruz, the west coast of Florida and the Bermuda Islands. Proc. Acad. nat. Sci. Philad.: 176-207.

Olivier, A. G.

1811. Palémon. Palaemon. In: Olivier, A. G., Encyclopédie méthodique. Histoire naturelle. Insectes, *8:* 652-667.

Randall, J. E.

1958. A review of the labrid fish genus *Labroides*, with descriptions of two new species and notes on ecology. Pacif. Sci., *12* (4): 327-347.

Randall, J. E. and V. E. Brock

1960. Observations on the ecology of epinepheline and lutjanid fishes of the Society Islands, with emphasis on food habits. Trans. Amer. Fish. Soc., *89* (1): 9-16.

Rankin, W. M.

1898. The Northrop collection of Crustacea from the Bahamas. Ann. N. Y. Acad. Sci., *11:* 225-254.

Ricketts, E. F. and Jack Calvin

1952. Between Pacific tides. Stanford University Press, Stanford, California. xiii + 502 pp.

Roughley, T. C.

1936. Wonders of the Great Barrier Reef. Angus & Robertson, Ltd., Sydney and London. xiii + 282 pp.

Stimpson, W.

1866. Descriptions of new genera and species of macrurous Crustacea from the coasts of North America. Proc. Chicago Acad. Sci., *1:* 46-48.

Utinomi, Huzio

1956. Coloured illustrations of sea shore animals of Japan. Hoikusha, Osaka, Japan. xviii + 167 pp.

(1073)

Reprinted from Vertebrate Speciation.
A University of Texas Symposium, 1961.
pp.5-23.

Isolating Mechanisms in the Speciation of Fishes[1]

CARL L. HUBBS
Scripps Institution of Oceanography,
University of California

THAT THE PROBLEM of segregation versus integration is one of long standing will be obvious from the fact that I treat it as it is exemplified among the lowest of the vertebrates. Speciation in its early stages obviously results from the ascendancy of segregation, as integration is reduced and eventually eliminated. (I hasten to add that I derive no moral from this concept, and draw no comparison with any current social problem.)

We may visualize speciation as a long-continued and often fluctuating conflict between forces that tend to unify the gene pool and those that tend to diversify populations genetically. The prime unifying force is interbreeding. The opposing factors, which lead to genetic isolation and speciation, are, I believe, numerous and complex; they are both intrinsic, in genetic mechanisms, and extrinsic, in ecological relations.

I belong to the school that stresses what may be called the environ-

---

[1] Contributions from the Scripps Institution of Oceanography, University o California, New Series, No.1334

Reproduced by Permission

mental potential as a central factor in speciation, hence as a major force determining the rate of genetic isolation. I shall, therefore, place more emphasis on the ecological factors than on the genetic mechanisms as such.

Blocks to Interspecific Hybridization in Nature

Discrepancy between genetic potential and the facts of life is dramatically exemplified by the extreme infrequency of hybridization in nature between species that can readily be cross-fertilized or that interbreed freely on isolated pairing in aquaria.

In the perch family, Percidae, for example, interspecific hybridization in nature is rare, in fact, extremely rare except among some of the more primitive darters, such as *Hadropterus maculatus* and *Percina caprodes.* Yet Clark Hubbs has produced numerous hybrid combinations, almost at will, by appropriate juggling of gametes. Many of the darters live together on the same riffles, and breed in similar fashion and at the same time. We can only assume that minor but effective behavioral differences—habitudinal and psychic—segregate the breeding fish. That a parallel situation holds for the oviparous cyprinodonts has just been indicated by Clark Hubbs. He is also vigorously attacking the problem of reduced interspecific fecundity in regions of sympatry.

The same phenomenon is exemplified by viviparous fishes, with complicated intromissive organs, that pair in highly evolved patterns. Thus the two best-known species of *Xiphophorus, hellerii* and *maculatus* (until recently referred to distinct genera), have been crossed by forced isolated cohabitation thousands of times in the aquaria of fish geneticists and fish hobbyists, and the other species referred to the same tribe and now to the same genus often interbreed freely and produce fertile offspring under such conditions. Although many thousand specimens of *Xiphophorus* have been collected and critically examined from many localities, so far as I know not a single natural hybrid has appeared. Gordon (1957) came to the same conclusions. To be sure, some of the species of *Xiphophorus* are geographically isolated, but the ranges of *maculatus* and *hellerii* overlap very widely, and these species often occur in the same pond or same stream section (though they are more often isolated ecologically).

In the extensively studied genus *Mollienisia*—or if you wish, spell it *Mollienesia*, or lump the genus with *Poecilia*—we have found natural interspecific hybrids, but in extraordinary rarity. Thus between species of the *Mollienisia sphenops* and the *M. latipinna* species groups, fewer than ten hybrids have been encountered in nature, though the species pair and hybridize freely in isolated aquarium matings. These natural hybrids have involved *M. mexicana* of the short-finned *sphenops* group and the long-finned species *velifera* and *petenensis*. Hybridization in the past between these two species groups was presumably involved in the origin of the renowned all-female, matroclinous Amazon molly, *Mollienisia formosa* (Hubbs and Hubbs, 1932). (Clark Hubbs and associates [1959] have recently taken in nature a few genetically female, phenotypic males of this peculiar, genetically isolated type.)

The factors that so effectively block miscegenation between related poeciliid species must be subtle. The highly complicated copulatory apparatus is sufficiently similar among the species of *Xiphophorus* (Gordon and Rosen, 1951) to provide, in my opinion, no plausible block to cross-fertilization, and the gonopodial structure is virtually identical among the species of *Mollienisia*. Within each group the mating behavior is very similar, though not wholly identical, as Clark, Aronson, and Gordon (1954) showed in commendable detail for *Xiphophorus* and as we have observed in *Mollienisia*. Whether the matings be between isolated pairs or between pairs in mass matings involving both sexes of both species, sexual inhibitions seem to be of limited effect.

In one experiment, in which we kept together ten males and ten females of *Mollienisia latipinna* and ten males and ten females of a species of the *sphenops* group, counts of the ever-occurring copulatory thrusts showed no preference of intraspecific over interspecific. Yet all the young produced were from matings within the *sphenops* type. Some physiological advantage may accrue in the mating of intraspecific gametes or in the development of the nonhybrid embryo—but the advantage is certainly not complete in the sense that normal germ-cell mating and development precludes the hybrid, for we have had single broods of mixed male parentage, one of which was produced by a female collected in nature in a pregnant condition. (The one negative experiment in mass miscegenation just mentioned was somewhat abortive and needs to be repeated.)

Even more striking than this contrast between natural and aquarium hybridization between species of the long-finned and short-finned groups in *Mollienisia* is that between two species that have been confused under the name *Mollienisia sphenops.* I now have found that over the middle of the vast range of the *sphenops* group, from the region of Veracruz to Costa Rica, two species occur, each in an almost endless array of local differentiates. One species, which I have just checked as the true *sphenops,* has the inner teeth tricuspid; the other, which may take the name *M. mexicana,* has these teeth unicuspid. This sounds like a generic difference, but the two types, though they seem very seldom to hybridize where they occur together in nature (as they frequently do), cross without restraint in aquaria to produce apparently perfectly fertile offspring.

The hybrids between species of the *sphenops* and *latipinna* series, in contrast, are characterized by reduced fertility in the female. Hybrids between species of *Mollienisia* and those of related genera in the tribe Poeciliini, occasionally obtainable by aquarium matings, produce offspring in which the females are infertile and the males are apparently always incompetent. We might assume that somehow selection has operated to prevent such miscegenation, but this concept is difficult to apply to crossings within the *sphenops* complex.

Behavioral Blocks to Hybridization

Some factors, presumably behavioral, block interspecific hybridization in nature between species that are quite capable of miscegenation. I suspect that these factors are in part genetic, the result of selection against the varied inefficiencies of cross-mating, and in part nongenetic, perhaps also as a result of selection, in that advantageous patterns of behavior without a special genetic basis may become established continuously.

We have found that the blocks to hybridization are often broken down when fresh-water fish species previously separated geographically (or microgeographically) are brought into cohabitation. Thus, we have found hybridization to be unusually frequent where one species of sucker was led for the first time into habitation with another species through a spillway in the Owens Valley aqueduct in California, and where species of the Mississippi drainage have become established, presumably through escape of bait, in the Colorado River system (Hubbs, Hubbs, and Johnson, 1943). Here another factor, that of the great scarcity of one species in an abundance of another, decreasing the chance for homogeny, may be a contributing or even the controlling basis for the miscegenation. To the degree that this factor of relative numbers operates, we may regard reasonable numbers of both cohabiting species as a factor blocking undue interspecific hybridization.

The reality of this factor of unbalanced abundance seems to be further indicated by the very high incidence of hybridization characteristic of some species, like *Clinostomus elongatus*, that seem to be approaching extirpation in the disjunct populations now remaining.

Somehow it seems almost as if species through experience learn how to behave so as to avoid miscegenation, for the members of a given species pair may seldom hybridize where they have lived in contact for a long time, but break down the barrier to miscegenation where they have just been thrown together. Thus, we have encountered unusually high incidences of hybridization where one sunfish species was stocked in a lake previously populated only by other species, but here again the factor of unbalanced population numbers may have played a role (Hubbs and Hubbs, 1933). Clark Hubbs is attacking experimentally the problem of behavioral blocks to hybridization.

Very striking is the picture of natural hybridization between carp and goldfish. These representatives of quite distinct, though related, genera live together over much of eastern Asia, including Japan, in a wide spectrum of relative abundance and in a wide range of habitats, with virtually no natural crossing. Cross-fertilization, however, is readily accomplished in artificial settings, and in the Lake Erie drainage these species interbreed in great profusion. After its introduction about seventy-five years ago, the carp found the waters about Lake Erie so agreeable that a large population developed and has continuously maintained itself. Later goldfish were flushed into a Lake Erie tributary by floodwaters and they likewise built up a large population. Here the two species hybridize very freely. In places the hybrids, though at least normally infertile, actually outnumber the parental species. (The same situation has been found among the sunfishes, and seems to be explainable on the hypothesis that the heterotic hybrids stem currents more freely than do either parental species, and thus tend to segregate themselves.) At the start the few goldfish may have encountered an overwhelming abundance of carp, thus greatly increasing the chance of heterogeny; but for many years both species have been abundant, existing in relative numbers that surely could be duplicated in many places in Asia, where the species have somehow learned not to cross, or have developed genetical bases for homogeny. But if the bases for homogeny had become ingrained into the species, they must have become lost or rendered ineffectual during at most a few centuries of man-induced isolation.

The possibility that carp and goldfish once hybridized in China (and perhaps occasionally still do) and the possibility that the hybrids are occasionally fertile are indicated by the occurrence there of the genus *Carassiops,* with intermediate characters largely matching those of the carp × goldfish hybrid. Other characters, however, indicate that *Carassiops,* though possibly of ancient hybrid origin, is not in itself a hybrid.

Hybridization between fish species in nature is frequent, so far as is known, only among fresh-water species in northern regions, where ecological conditions and species associations have fluctuated greatly in response to Glacial and Pluvial events (Hubbs, 1955). This situation is comparable to that in plants, between which hybridization has been shown by Edgar Anderson (1949) and others to be particularly frequent where the ecological conditions have been markedly altered by natural or artificial activities. In tropical regions and especially in the tropical seas, interspecific hybridization seems almost unknown, despite (or perhaps because of) the great multiplication of species and the great diversity of habitat. In this connection I would like to express the opinion that Gordon (1957) and others have been unduly cautious about accepting any interpretation of fish hybrids not yet verified by experiments or by study of gonads. Clark Hubbs is finding some indications that the duration of sperm activity may be one of the factors affecting the frequency of hybridization.

Blocks to Hybridization and to Viability and Fertility of Hybrids

Genetic isolations are effected to varying degrees by the development of various blocks to the act of cross-mating and to the viability and fertility of such hybrids as may be produced.

Such blocks have been noted in certain fish hybrids. Heterogenetic crosses, as between families, may produce embryos, either with or without indications of paternal gene contribution, but normal young do not eventuate.

Among the rather freely hybridizing centrarchid fishes, particularly among sunfishes (*Lepomis* in the broad sense), the hybrids are almost invariably sterile and are predominantly males with abnormal spermatogenesis (Hubbs and Hubbs, 1933). Occasional sunfish hybrids, however, appear to be somewhat fertile. In other groups the incidence of hybridization varies, and the hybrids show varying degrees of viability and fertility. No sharp line can be drawn between more or less free gene flow within species and complete blocks between species. Under appropriate stimulus and favorable conditions species and even genera of fishes produce fertile offspring.

I have already spoken of the seemingly acquired blocks to hybridization in nature between species and between genera, such as *Carassius* and *Cyprinus*, in regions where they have long been sympatric. *Carassius* × *Cyprinus* hybrids seem to be normally infertile, because their characters are consistently intermediate, but there are some suggestions of occasional fertility.

Other well-defined species seem to produce quite fertile offspring, for all gradations between them are found in nature. Such gradation characterizes the frequently produced hybrids between *Chrosomus eos* and *Chrosomus neogaeus* (the latter until recently regarded as generically distinct), as also the hybrids between *Notropis cornuta* and *N. rubella*, which very often interbreed as a result of a chance meeting of sperm and egg when *rubella* is spawning in midwater over a breeding group of *cornuta* (Raney, 1940). The creek and lake forms of *Siphateles obesus*, though formerly regarded as generically distinct, often hybridize and in some lakes have fused (Hubbs and Miller, 1946). Where the appropriate habitats of the two parental types are available hybridization is limited, but under intermediate conditions they intermate freely.

Differential habits and habitats are commonly the isolating factors. By such means, no doubt, the Californian minnows *Hesperoleucus* and *Lavinia* ordinarily maintain their full distinctness in breeding and in morphology, seldom hybridizing. In one desiccating section of the San Juan River of the Salinas system, however, where they had been thrown into cohabitation in dwindling pools, they fused to form a hybrid swarm, much like those observed sporadically between plant species. In working over a very large series Dr. Robert Rush Miller and I thought we could recognize about five per cent as *Hesperoleucus* and about an equal minimal number as *Lavinia*, but on more thorough study even these few fish showed some evidence of introgression.

In general, the various effective blocks to hybridization are developed roughly in proportion to the degree of systematic divergence (Hubbs, 1955). This relationship was nicely illustrated in our long-continued but still largely unreported experimental studies of hybridization in the poeciliid fishes of the tribe Poeciliini. The various forms of *Mollienisia mexicana* and of *M. sphenops* cross freely and produce fully fertile offspring, in matings both within and between these closely allied species. Species of the *M. sphenops* group (including *mexicana*) rather readily cross in aquaria with members of the *M. latipinna* group (*latipinna*, *petenensis*, *velifera*), but the hybrids are not completely fertile: the male hybrids are almost fully fertile, but the females are ordinarily sterile. Species of *Mollienisia* and *Limia* occasionally produce hybrids, of which the males are sometimes fertile, the females apparently never. *Mollienisia* very rarely crosses with the less closely related genus *Lebistes*, and both sexes of the hybrids seem infertile. No hybridization whatever could be effected between any member of the tribe Poeciliini and any species of any other tribe. Aquarists often report such heterogenetic crossings, but on frequent checking I have never verified such a report. In general, I have found that natural hybrids are produced only among closely related genera, such as may be classed in one tribe (Hubbs, 1955).

Within limits there seem to be some exceptions to the rule that the incidence of hybridization is positively correlated with degree of relationship. Some very closely related species that are largely sympatric appear to have developed effective blocks to hybridization, whereas one or both may hybridize rather freely with a less closely related form with which it is much more restrictively sympatric. Thus, *Notropis spiloptera* seems virtually never to cross with its very near relative *N. whipplii*, with which it widely occurs, but does cross, at times, with the less similar species *N. lutrensis*, the range of which it overlaps much less widely.

Resistance to Genetic Swamping

A considerable body of evidence indicates that various factors minimize the swamping effects of hybridization and thus retard or even circumvent this major block to genetic isolation and speciation. These factors seem to exert a force that maintains taxa, as though pulling them apart, despite the force of interbreeding that tends to break down the differentiation of these taxa, by causing them to fuse. No doubt these opposing forces interact variously, so that the trend toward integration at times and at places is dominant, whereas on other occasions and elsewhere the trend toward segregation takes over. Let us consider some cases that seem to illustrate this grand interplay.

In the Lahontan Basin two minnows now referred to the genus *Siphateles* behave quite variously in respect to their mutual genetic relationships (Hubbs and Miller, 1946). One form, *obesus*, is characteristic of streams, where it feeds on insect larvae and other bottom invertebrates and gets along with fewer than twenty stubby gill-rakers. The other form, *pectinifer*, is adapted to lacustrine conditions and presumably evolved in the vast Pluvial Lake Lahontan. Its large size, strong build, upturned mouth, and its very numerous and long rakers fit it for life in open waters and for feeding on plankton (which is much richer in lakes than in streams). The differences are so great that a conservative ichthyologist (Snyder, 1917) erected a distinct genus (*Leucidius*) for the lacustrine form. However, in line with our finding that adaptations to differential feeding are apt to be terminal phenomena of no great phylogenetic significance, we now know that these two very diverse forms frequently interbreed—hybridize or intergrade depending on one's point of view. (We now put them not only in the same genus but also in the same species, *Siphateles obesus.*) In some now confined waters, like Eagle Lake, the two forms have completely fused to produce a strictly intermediate type. In the larger and more diverse Lake Tahoe intermediate stocks as well as populations of each type exist. Various degrees of intermediacy are exhibited by local populations. In Walker Lake near the mouth of Walker River a population essentially uniform in the characters of the lake form includes a small proportion aberrant only in the gill-raker character, in which respect some are like *obesus* and others are variously intermediate (indicating past introgression, exhibited only in the gill-raker character probably because relatively few genetic factors are involved). Yet over the basin as a whole the two forms maintain their distinctness in character and habitat, though there are in general no impassable barriers to gene flow. Moreover, the hybridization seems to have been proceeding for many centuries, because some of the mummies from ancient, dated Indian caches appear to be hybrids. Some factors, here as elsewhere, must counter gene interflow in this complex, in which the intergrades (or hybrids) must be fertile.

Another case of resistance to gene interflow, worked out first by Boyd W. Walker and me and more recently by Caryl P. Haskins, is that of the two northern subspecies of *Gambusia affinis*, which in many respects other than geographical intergradation are more distinct that many good species in the Poeciliidae. *G. a. holbrookii* inhabits the Atlantic Coast and peninsular Florida. *G. a. affinis* ranges through the Mississippi Valley to the Rio Grande. Between the Mississippi Delta and peninsular Florida the two forms have been brought into cohabitation by connecting waters near the coast, and here they intergrade. The intergrades, like most interspecific hybrids (and one could call them such if he wished), are intermediate in nearly all characters, including several trenchant peculiarities in gonopodial characters and in the sensory canals and pores of the head. But in the fin-ray formulas they combine the numbers of the two species in about equal frequency, apparently because in this species the fin-ray number, unlike almost all systematic characters, seems to depend on a single genetic factor: the dorsal fin has either six rays as in *affinis* or seven as in *holbrookii*, and the anal fin has either nine rays as in *affinis* or ten as in *holbrookii*. The reality of the interbreeding and the type of inheritance has been verified by experiment. The intergradation has doubtless existed in this limited area for many centuries, without evidence of extensive gene flow either into the Florida Peninsula or into the delta region of the Mississippi Valley. And, more dramatically, the headwater populations of certain streams, some only a few miles long, have remained essentially pure—of *affinis* to the westward and of *holbrookii* to the eastward.

Something has blocked the gene flow, even within very short distances, between the pure subspecies stocks and the intergrades. It is almost certain that no gross sterility factors are involved. The fact that the pure populations of each subspecies occupy headwaters argues against any special adaptation of either to headwaters. Seemingly there must be some inherent advantage that allows the pure subspecies to outbreed the intermediates and to build up populations large enough to block the spread of the intermediates. The extreme restriction of the population of hybrids between *Gambusia affinis* and *G. heterochir*, so nicely demonstrated by another and now more productive Hubbs (1957), bears out this interpretation.

The force that resists swamping (and even probably reconstitutes taxa after fusion), as well as the power of the ecological potential, seems to be illustrated dramatically by the complex, mosaic interrelationships between two subspecies of the darter *Etheostoma* (formerly *Boleosoma*) *nigrum* in the Great Lakes and upper Mississippi regions. One form, *E. n. nigrum*, much the more widespread and ubiquitous, inhabits chiefly terrigenous bottoms of open sand and mud, whereas the other, *E. n. eulepis*, is more typical of vegetated habitats. The open-water form, in apparent adaptation to its need for very abrupt darts to avoid capture, is usually slenderer and has rather smooth scales except on the head and adjacent regions, which are largely scaleless. The other form, *eulepis*, is generally more robust and has more strongly armed scales, which extend farther than those of the open-water form in that they largely cover the nape, breast, and cheek regions—suggesting that this roughness has adaptive value, probably in limiting predation by some small, though significant, amount. Experiments by Lagler and Bailey (1947) show that the differences are genetic. Each pattern of squamation has, we may assume, some advantages and some disadvantages, but the advantages of smoothness seem to dominate on the more open bottoms, while spininess seems to play the chief adaptive role in the more vegetated habitats. In Glacial lakes that are predominantly free of vegetation typical *nigrum* holds forth. A considerable number of lakes that are well vegetated, scattered far and wide within the general range of *B. n. nigrum*, harbor *B. n. eulepis* exclusively. Each subspecies, in waters that it exclusively occupies, tends to wander rather freely into habitats characteristic of the other. Regions with varied habitats and free passage, like the upper Mississippi River proper, are occupied by intergrades, and probably have been so populated through Postglacial time. During Postglacial redispersal the ancestors of lake populations now occupied by the respective forms presumably passed through and constituted part of this intergrade population. On their re-establishment in Glacial lakes, selection apparently reconstituted some into the *eulepis* type, others into the typical *nigrum* type. Lake St. Clair, the adjacent Detroit River, and the western part of Lake Erie now constitute a major and appropriate habitat of *eulepis*, as they probably have through much of the time when, during Postglacial redispersal, populations of *Boleosoma* were funneled through this area. On this assumption the individuals that moved on northward (and the genes for vagility may be associated with those for *nigrum* characters) became at once subject in the barren waters of Lake Huron to adaptation for *nigrum* characters, which in time became reconstituted in the population. But where habitat conditions favored the characters of *eulepis*, selection led toward, or to, that form.

Resistance to swamping may be effective even within a single lake. Thus, I found that two subspecies of *Mollienisia mexicana* occur in the large Laguna de Petén in Guatemala. They are segregated ecologically or microgeographically. One form occupies the definite marshy shallows; the other is semipelagic in the open waters (to which it is well adapted by its slender form, pale colors, and other characters). Along the outer fringe of the marsh, between the habitats of the two forms, I found a band of intergrades. The two forms freely produce fertile offspring in aquaria. Since they do intergrade when they come into contact in nature, one wonders why they have not gradually amalgamated. Obviously some force has countered the tendency to fuse. I interpret the force to be the effective adaptation of each subspecies to its own habitat, so that a high breeding potential is realized and the appropriate habitats are saturated with their respective pure stocks.

In still larger lakes, for example in Lake Nyasa, where essentially sympatric speciation seems to have been rife, hybrids may be eliminated while the process of geographic and systematic divergence progresses (Fryer, 1959).

Some of these hypothetical speciational interplays may not have been enacted in quite the way suggested, but there seems to be little reason to doubt that differential selection has led to the build-up of populations—such as those of *Boleosoma n. nigrum*, *B. n. eulepis*, and intergrades—that have resisted the inflow of genes of other types, perhaps by sheer reproductive potential and competition. Although inherent genetic barriers to gene flow are few there has been no such complete gene spread that many have insisted must eventuate wherever and whenever gene flow is made possible by topographic conditions and by the fertility of offspring. Opposing tendencies may be stronger—and probably often are.

Must Segregation Be Geographic?

A major question is whether genetic isolation can be accomplished without strict geographic segregation. The Chairman has championed the view that it cannot and he has a wide following. Perhaps I am a bit lonesome in disagreement. No one, of course, doubts that geographic isolation is a major factor in speciation, and if one uses glasses with sufficiently high magnifying power, even microhabitats or niches may be termed distinct geographic entities.

But in practice we are dealing with more than semantics, as we may see from two examples. The first concerns the plethora of cichlids in the great lakes of Africa. The usual view has been that this abundance indicates multiple speciation in one body of water. Greenwood (1958), inspired by Mayr, interprets the events that led to such profuse speciation as the formation, during the less pluvial periods, of several very shallow lakes, in which populations became isolated long enough to allow speciation to proceed to the level of mating incompatibility on the subsequent fusion of these ponds. The second example concerns the chars in Windermere. Dr. Frost has interpreted spring-spawning and fall-spawning stocks of chars in Windermere as the product of speciation *in situ*, and the deep-water dwarf type she has begun to study should fit into the same potential explanation. Dr. Svärdson, a distinguished disciple of the Chairman, has taken the view that the seasonal races are distinct species that arose somewhere else in geographic isolation, and independently reached Windermere in their dispersal, and I suppose he would follow the same reasoning for the deep-water dwarf.

These alternative explanations stand in bold contrast. For the moment, at least, I do not see how we can submit either view to experimental test, nor have we unearthed as yet fossil records of sufficiently assured completeness to be critical. We are, however, not totally lacking in pertinent indications.

Let us first consider the case of explosive evolution in lakes. To me, Greenwood's explanation seems inherently implausible and forced. In general, shallow ponds are not scenes of extensive speciation, and we can hardly conceive that differentiation proceeded so far in several such ponds in one lake basin as to have yielded the vast diversity that exists in the lake today. Nor can we conceive its having proceeded so far that fusion would not have occurred when the pond segregates were brought together by the reunion of the ponds to form Lake Victoria. No great diversity has arisen within small lakes and ponds over Africa.

Can Greenwood's explanation be applied to other supposed scenes of explosive lacustrine evolution? I doubt that Lake Tanganyika went through a history of disruption and unification that would adequately explain the numerous genera and the multitude of species that appear to have arisen there from a very few ancestors. Fryer (1959) gave cogent reasons why and how radiative adaptation has taken place within Lake Nyasa. He presented very plausible models to illustrate sympatric speciation in this lake.

It also seems unlikely that such a concept could explain the origin in the Lake Lanao Basin in Mindanao of several genera and a considerable number of species of minnows from the single plausible ancestor, *Barbus* (or *Puntius*) *binotatus* (Herre, 1933; Myers, 1959), though here, as elsewhere, an effort should be made to reconstruct the lake history by limnological and paleoclimatological data. In Lake Lanao, as in the large African lakes, the explosive evolution has gone to excessive extremes, nowhere attained outside these lakes (Myers, 1960).

Comparable to the diversity of cichlids in African lakes is the diversity of the genus *Orestias* in Lake Titicaca (Tchernavin, 1944). A few rather ordinary species occur in other high Andean lakes, but the great bulk of the species and all of the extreme variants occur only in Lake Titicaca, just as the more extreme cichlids are confined to Lake Tanganyika and other large African lakes. That they ever occurred elsewhere seems to me inherently improbable.

Suggested Pathways for Essentially Sympatric Speciation

The genetic segregation that is an essential antecedent to speciation may be accomplished sympatrically by any of a number of changes in the germ plasm that render some sets of individuals interfertile among themselves but intersterile with other individuals in the population—but it seems doubtful that such segregation has been at all common or effective among vertebrates.

Some degree of spatial or temporal segregation may be assumed. The simplest form of such segregation is that of allopatry, which may arise either through the dispersal of segregates of a population or through such environmental modifications as stream capture; disruption of drainage systems; isolation of marine populations through the closure of straits (as by the elevation of the Isthmus of Panamá); antitropical separation through the warming of the tropics (see, for example, Hubbs, 1952); local survivals, for example on mountaintops or in bogs, of populations that otherwise moved out of the region in the course of Postglacial redispersal; separation on islands as a result of elevations of the sea or of depressions of land masses; analogous isolations on land through climatic or other changes that render uninhabitable a reticulum between habitable island-like remnants of the former range. Such segregations have no doubt been frequent, and very probably the usual, antecedents to differentiation. I know of no serious student of speciation who questions that such enforced regional segregations set the stage for differentiation which in due course leads to genetic incompatibility.

Despite strong argumentation to the contrary, the possibilities of essentially sympatric speciation pose a timely and worth-while problem for consideration. I insert the attributive "essentially" because I am still thinking of assortive mating, within two or more groups of individuals, induced to some degree by the close association of mating pairs. The question is in part one of semantics. That all degrees of segregation exist—in terms of distance, time, and the amount of interbreeding—is obvious. The question may be put in this way: did the ecologically or temporally segregated and often adapted races that occupy essentially the same area (*patria*)—or in the case of some temporal segregates the identical habitat—originate *in situ,* or did they first differentiate in areas that are definitely separated geographically, and then come into essential cohabitation after genetic isolation had more or less developed? Some examples from fishes may be cited to clarify the question: two races of salmon (*Oncorhynchus* sp.) that breed in adjacent tributaries; two types of trout (*Salmo* sp.) that run into one stream to breed in successive periods; the two shallow-water races of *Salvelinus alpinus* that breed at different times on different shores of Windermere in England, as well as a deep-water race in the same lake (data from Dr. Winifred Frost); normal and neotenic types of smelt (*Osmerus* sp.) that occupy the same lake; three types of perch (*Perca flavescens*) that I observed in Douglas Lake, Michigan—two in different parts of the main lake and an extreme form in a marshy delta; shallow-water and deep-water races of various fresh-water and marine fishes; littoral and pelagic races of various marine fishes, or the marsh and open-water races of *Mollienisia mexicana* in Laguna de Petén, referred to above; the bay, littoral, and island subspecies of topsmelt (*Atherinops affinis*) of the Pacific Coast; ecologically segregated species of pipefish (*Syngnathus*) in the same region; and ecosubspecies of cyprinid and other fishes within one river system that are specifically adapted to different current conditions. Examples could be multiplied (and some might need be deleted if the observed differences should prove to be wholly phenotypic). I grant that it seldom will be possible on any present evidence to answer these questions with full assurance, but the weight of evidence seems to me to indicate that gradual speciation *in situ,* by increasing segregation, may often have been the process.

That ecologically and temporally segregated fish taxa may often have developed within single areas is strongly suggested by the varying degree of subspecific intergradation that often persists or of interspecific hybridization (the distinction is often arbitrary—Hubbs, 1943). Thus the bay and ocean races of topsmelt (*Atherinops affinis*) intergrade in the bay entrances, and in the intermediate stream habitats of various fresh-water fishes there are intergrades, or even a series of definable intergrading races, between the small, chunky-bodied, large-scaled, fewer-rayed, smaller- and rounder-finned, deep-peduncled headwater types of pool-and-riffle habitats, on the one hand, and, on the other, the larger, slenderer, and finer-scaled types, with larger and more falcate fins and a slender caudal peduncle, that inhabit constantly swift creeks and rivers in the same stream system, within which the populations are more or less continuously distributed (Hubbs, 1941).

The initial step in segregation that may allow the gradual onset of differentiation, particularly where selectional pressure is high, is probably often provided by homing behavior, which has been found to be highly developed in many fishes. Raciation is particularly well marked in those fishes, such as the salmonids, in which homing is most sharply developed; but both raciation and homing have been demonstrated to be characteristic, to varying degrees, of many other fishes of streams, lakes, and marine habitats. At first the homing is often, and probably is typically, nongenetic, as it must be in transferred salmon stocks. Gradually, however, genetic responses involved in the location of the spawning areas doubtless come into play, and concurrently morphological differences develop. Increased segregation and increased adaptation are mutually advantageous and, therefore, subject to selection. In time, speciation may become complete.

As the segregated stocks become increasingly restricted to diverse niches and increasingly specialized to the local conditions the high breeding potential will undoubtedly produce large and distinctive populations. Intergrades or hybrids will be outnumbered and will tend to be overwhelmed by competition. It seems obvious that the gradually lessened fecundity and viability characteristic of hybrids will further reduce their numbers.That the pure stocks will more or less completely replace the intermediates may be assumed, since even small differences in selection are eventually effective.

Certain specialized habits, notably oral gestation in the cichlids, apparently favor sympatric differentiation (Fryer, 1959).

Summary

Speciation is visualized as a fluctuating conflict between the unifying effects of crossbreeding and the trend toward genetic isolation. Intrinsic genetic mechanisms are involved in genetic isolation, but extrinsic factors are often more important. Many species that may be crossed readily by artificial fertilization or by enforced cohabitation in aquaria seldom, if ever, hybridize in nature. Behavioral and habitudinal factors are no doubt often effective. Blocks to interbreeding develop in sympatry, but may be lost by isolated stocks within centuries. Hybridization often occurs when two species or stocks previously separated are brought together in nature. Unbalanced numbers favor hybridization, but other factors are involved. Disturbances of habitats, either natural or artificial, often lead to crossbreeding. Some factors that lead to genetic isolation seem to be genetic; others, not. In general, with some minor exceptions, genetic isolation increases with phyletic differentiation.

Various factors resist genetic swamping, even of closely approximated types. Prominent among these factors are the high breeding potential of the pure stocks, especially when well adapted to a particular environment. The intergrades or hybrids tend to be swamped out by population pressure and competition, and are often reduced by reason of some small degree of lowered viability or lowered fertility. Selection may continue to sort out genetic types, even after fusion.

Although isolation is undoubtedly a common and probably the usual antecedent of differentiation, segregation and speciation apparently may often be effected in essential sympatry. This seems to be particularly true in lacustrine loci of explosive evolution. Homing behavior, at first wholly or largely unfixed genetically, may be a prime factor in sympatric speciation. Specialized habits, such as oral gestation, may well favor such differentiation.

REFERENCES CITED

Anderson, Edgar. 1949. *Introgressive Hybridization.* New York, John Wiley & Sons, Inc.

Clark, Eugenie, Lester R. Aronson, and Myron Gordon. 1954. Mating behavior patterns in two sympatric species of xiphophorin fishes: their inheritance and significance in sexual isolation. *Bull. Amer. Mus. Nat. Hist.*, 103: 135–226, figs. 1–10, pls. 1–9.

Fryer, Geoffrey. 1959. Some aspects of evolution in Lake Nyasa. *Evolution,* 13: 440–451, figs. 1–3.

Gordon, Myron. 1957. Physiological genetics of fishes, Chap. X, pp. 431–501, figs. 1–16, *Behavior,* Vol. 2 in *The Physiology of Fishes.* Margaret E. Brown, Ed. New York, Academic Press, Inc.

Gordon, Myron, and Donn Eric Rosen. 1951. Genetics of species differences in the morphology of the male genitalia of xiphophorin fishes. *Bull. Amer. Mus. Nat. Hist.*, 95: 409–464, figs. 1–23, pls. 17–18.

Greenwood, P. H. 1959 (preprint, 1958). Evolution and speciation in the Haplochromis fauna (Pisces, Cichlidae) of Lake Victoria. *Proc. XVth Intern. Cong. Zool.*, London, July, 1958, pp. 147–150.

Herre, Albert W. C. T. 1933. The fishes of Lake Lanao: a problem in evolution. *Amer. Nat.*, 67: 154–162.

Hubbs, Carl L. 1941. Relation of hydrological conditions to speciation in fishes, pp. 182–195, *A Symposium on Hydrobiology,* Madison, University of Wisconsin Press.

———. 1943. Criteria for subspecies, species, and genera, as determined by researches on fishes. *Ann. New York Acad. Sci.*, 44: 109–121.

———. 1952. Antitropical distribution of fishes and other organisms. *Proc. 7th Pac. Sci. Cong.*, 3: 324–329.

———. 1955. Hybridization between fish species in nature. *Syst. Zool.*, 4: 1–20, figs. 1–8.

Hubbs, Carl L., and Laura C. Hubbs. 1932. Apparent parthenogenesis in nature, in a form of fish of hybrid origin. *Science*, 76: 628–630.

———. 1933. The increased growth, predominant maleness and apparent infertility of hybrid sunfishes. *Pap. Mich. Acad. Sci., Arts and Letters*, 17 (1932): 613–641, figs. 69–71, pls. 64–65.

Hubbs, Carl L., Laura C. Hubbs, and Raymond E. Johnson. 1943. Hybridization in nature between species of catostomid fishes. *Contr. Lab. Vert. Biol., University of Michigan*, 22: 1–76, figs. 1–8, pls. 1–7.

Hubbs, Carl L., and Robert R. Miller. 1946. Correlation between fish distribution and hydrographic history in the desert basins of western United States, pp. 17–166, Chap. II, The Zoological Evidence, *The Great Basin, with Emphasis on Glacial and Postglacial Times. Bull. Univ. Utah*, 38 (No. 20), *Biol. Ser.*, 10 (No. 7).

Hubbs, Clark. 1957. *Gambusia heterochir*, a new poeciliid fish from Texas, with an account of its hybridization with *G. affinis*. *Tulane Stud. Zool.*, 5: 1–16, figs. 1–7.

Hubbs, Clark, George E. Drewry, and Barbara Warburton. 1959. Occurrence and morphology of a phenotypic male of a gynogenetic fish. *Science*, 129: 1227–1229, fig. 1.

Lagler, Karl F., and Reeve M. Bailey. 1947. The genetic fixity of differential characters in subspecies of the percid fish, *Boleosoma nigrum*. *Copeia*, 1947: 50–59.

Myers, George S. 1959 (preprint, 1958). The endemic fish-fauna of Lake Lanao and the evolution of higher categories. *Proc. XVth Intern. Congr. Zool.*, London, July, 1958, pp. 151–152.

———. 1960. The endemic fish fauna of Lake Lanao, and the evolution of higher taxonomic categories. *Evolution*, 14: 323–333.

Raney, Edward C. 1940. Reproductive activities of a hybrid minnow, *Notropis cornutus* × *Notropis rubellus*. *Zoologica*, 25: 361–367.

Snyder, John Otterbein. 1917. The fishes of the Lahontan system of Nevada and northeastern California. *Bull. U.S. Bur. Fish.*, 35 (1915–16): 33–86, figs. 1–9, pls. 3–5.

Tchernavin, V. V. 1944. A revision of the subfamily Orestiinae. *Proc. Zool. Soc., London*, 114: 140–233, figs. 1–27.

(1094)

Reprinted from ANNALS OF THE NEW YORK ACADEMY OF SCIENCES
v.93, art.3, December 4, 1961.
pp.37-132.

SCRIPPS ESTATES SITE, SAN DIEGO, CALIFORNIA: A LA JOLLA SITE DATED 5460 TO 7370 YEARS BEFORE THE PRESENT*

George Shumway,* Carl L. Hubbs,† James R. Moriarty†

**San Diego Science Foundation, La Jolla, Calif.*

†*Scripps Institution of Oceanography, University of California, La Jolla, Calif.*

INTRODUCTION

Shell middens abound along the coasts of southern California and Baja California and on all the offshore islands except for remote Guadalupe Island which, on repeated visits, has yielded no sign of aboriginal discovery. Signs of ancient habitation are almost continuous for long stretches of the mainland shore. A few of the coastal sites have been excavated, a number have been dated, and others currently are being dated by the La Jolla Radiocarbon Laboratory, La Jolla, Calif., but literally hundreds remain to be studied. The wide spread of dates, from only a few hundred years to more than 7000 years B.P. (before present), indicates that the coast has been occupied, probably continuously, by seafood-gathering people for more than seven millenia (Hubbs *et al.*, 1960). The intensity of population no doubt waxed and waned (for reasons that someday may come to light), and the cultures have varied somewhat.

Although shell middens are numerous along the California coasts, middens with burials are not abundant. Scripps Estates Site, described in this report, is of special significance because of its antiquity and because of the concentration of burials. Forty-six burials have been located on the site, and evidences of a number of others have been found. It is estimated that the site originally held more than 100 burials; some of these have been destroyed in the hurried advance of civilization and, undoubtedly, many others remain to be found.

Scripps Estates Site has been known for decades, but essentially nothing has been published concerning it. Early archeological work was done on the site by Malcolm J. Rogers of the San Diego Museum of Man in the late 1930s and again during World War II, as burials became exposed during the removal of topsoil and the construction of military fortifications. For the next 10 years the site remained essentially un-

---

*The work described in this article was supported in part by Contribution 1 from the San Diego Foundation, San Diego, Calif., and by contributions, new series, from the Scripps Institution of Oceanography. Much of the research, particularly the radiocarbon datings, the midden-shell analyses, and the environmental studies, was supported by National Science Foundation Grants 1250 and 10,733, issued to one of the authors (C.L.H.).

Contributions from the Scripps Institution of Oceanography, New Series, 1335
Reproduced by Permission

touched. In 1952 the land on which the site lies became part of a subdivision, Scripps Estates Associates, Inc. Some skeletal fragments were salvaged when a road was built in the subdivision in 1953. In December 1958, while digging in his front lawn, located on the midden, one of us (GS) struck the skull of what here is numbered Burial 7 (TABLE 1). This led to a flurry of digging in the spring of 1959 by ourselves, and by Claude N. Warren of the University of California, Los Angeles Archaeogical Survey, and resulted in a preliminary account of the work (Moriarty *et al.*, 1959) and in the present report.

About 300 m. southeast of Scripps Estate Site is a second site of similar nature in which 13 burials have been found by Moriarty. This site, the subject of a separate report by him (in preparation), and Scripps Estates Site presumably were once a single extensive site, but this cannot now be ascertained because a road and an area of cultivation have existed for many decades in the region between the two sites. This second site was referred to as Scripps Estate Site 2 by Moriarty *et al.* (1959). However, because the second site lies on land of the University of California, San Diego, it appears more appropriate to refer to it as the UCLJ-M1 Site and to drop the former designation. Thus there is only one site named Scripps Estates Site; the number "I" designation can be dropped from use.

SITE LOCATION

Scripps Estates Site is in western San Diego County, Calif., at 32°, 52' 16 to 23'' N. Lat, 117° 14' 53 to 56'' W. Long. The site lies along the seaward edge of the mesa complex that farther inland is called Kearney Mesa and Linda Vista Mesa. This mesa complex, comprising the Linda Vista Terrace (Hertlein and Grant, 1939, 1944, and 1954), is dissected (especially near the coast) by numerous canyons and valleys. Three of these—Soledad Valley to the north, Hidden Valley to the south, and Rose Canyon to the east—together with the high and steep seacliffs on the west, almost completely isolate a portion of the mesa surface called Torrey Pines Mesa (FIGURE 1). The elevation of the surface of this mesa generally is between 110 and 120 m. Small canyons cut the western edge of Torrey Pines Mesa, and it is along the south rim of one of these—Sumner Canyon—that Scripps Estates Site is located (FIGURES 1 and 2). The area of concentrated burials is about 3.1 km. northeast of Point La Jolla, 0.6 km. north of the Scripps Institution of Oceanography Pier, and about 100 m. north of the boundary between the Scripps Estates Associates subdivision and the University of California grounds.

TABLE 1

DESCRIPTIONS OF BURIALS EXCAVATED IN 1958 AND 1959 IN SCRIPPS ESTATES SITE

Burial No.	Sex	Age	Skull depth (cm.*)	Flexure	Azimuth†	Skeletal condition	Measurable bones	Remarks
1	Undetermined	Adult	12	Flexed, probably on right side	0° (±)	Poor; one femur, tibia, and fibula; a few ribs; fragmentary skull	None	Section of upper portion of skull, part of parietal and frontal, 2/3 of right zygomatic arch; metate over skull
2	Undetermined	Adult	22	Unknown	—	Poor	Left femur	Left femur, badly fragmented tibia and fibula, a section of two thoracic vertebrae, and a piece of jaw were only parts recovered
3	Male	Adult	25	Flexed, on right side	345°	Good; nearly complete, except for small bones of hands and feet; long bones articulated, including patella	Almost all	One of the most complete and undisturbed burials of the group; excavation incomplete (FIGURE 8)
4	Undetermined	Adult	6	Flexed, on right side	350°	Skull good; skeleton nearly complete	Skull; possibly other parts	Excavation incomplete

TABLE 1 (Continued)

Burial No.	Sex	Age	Skull depth (cm.*)	Flexure	Azimuth†	Skeletal condition	Measurable bones	Remarks
5	Undetermined	Child	21	Flexed, on left side	030°	Fair; skull and long bones of right side remain	Skull and femur	Teeth unground, showing little wear; excavation incomplete (FIGURE 11)
6	Undetermined	Adult	22	Flexed, but not lying on side	040°	Fair; skull missing, as well as atlas and axis; long bones poor	Tibia and fibula	Lying with upper part of spinal column nearly vertical
7	Male	Adult	20	Flexed, on right side	275°	Skull good, but deformed; long bones and small foot bones partly articulated	Skull, radius, femur, tibia, and fibula	Teeth show only moderate grinding; shellbeads of necklace in place with bones; large shell (*Laevicardium elatum*) (FIGURE 12)
8	Undetermined	Child	18	Flexed, on left side	095°	Poor; long bones fragmented, with badly deformed pelvis; skull much deformed	None	Large cobble and scraperlike flake with burial
9	Undetermined	Adult	9	Flexed, on left side	315° (±)	Poor; skull; long bones fragmentary	Skull	Skull protruded into soil horizon A
10	Female (?)	Adult	25	Flexed, on right side	113° (±)	Fair; nearly complete	Nearly all	Protruded into soil horizon A

TABLE 1 (Continued)

Burial No.	Sex	Age	Skull depth (cm.*)	Flexure	Azimuth†	Skeletal condition	Measurable bones	Remarks
11	Undetermined	Undetermined	32	Undetermined	180° (±)	Poor; fragmented skull; tibia and femur; others (?)	None (?)	Excavation incomplete
12	Undetermined	Undetermined	25	Undetermined	Unknown	—	Unknown	Portion of skull exposed, but not excavated
13	Female	Adult	20	Flexed, on right side	345°	Fair; skull badly crushed, with lower jaw and front teeth missing	None without reconstruction	See FIGURE 9
14	Undetermined	Adult	23	Unknown	Unknown	Unknown	Unknown	This burial underlies 3 and is unexcavated
15	Undetermined	Adult	20	Flexed, on right side	010°	Fair	Unknown	Underlies a metate; excavation incomplete
16	Undetermined	Adolescent	23	Flexed, on right side	027°	Good; skull crushed, fair dentition	Right femur, both radii	Removed in a block for museum display
17	Undetermined	Undetermined	10	Unknown	Unknown	Unknown	Unknown	Excavation incomplete; top of skull only has been uncovered

---

* Depth below present surface of ground.

† Direction from pelvis through skull.

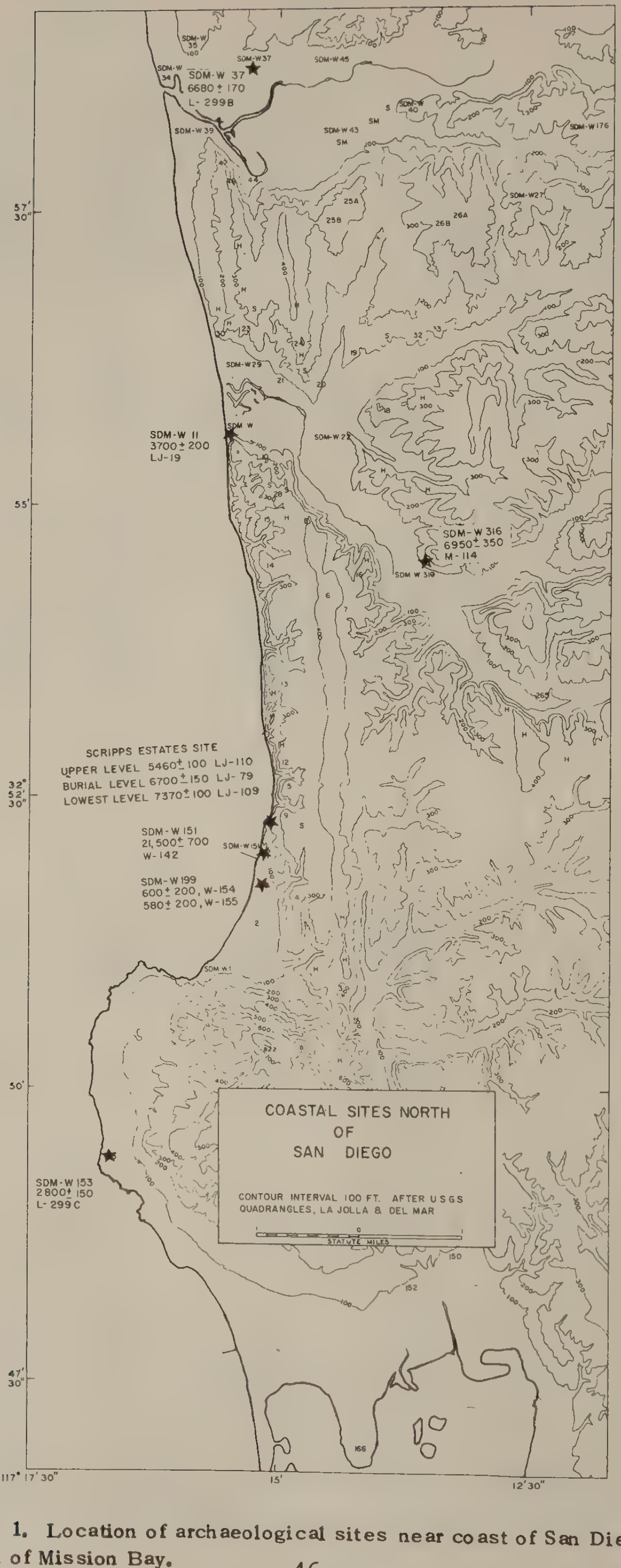
SDM-W 35
SDM-W37
SDM-W 45
SDM-W 34
SDM-W 37
6680 ± 170
L-299B
SDM-W 39
SDM-W 43
SDM-W 40
SDM-W 176
SDM-W 27
SDM-W 29
SDM-W 11
3700 ± 200
LJ-19
SDM-W 22
SDM-W 316
6950 ± 350
M-114
SCRIPPS ESTATES SITE
UPPER LEVEL 5460 ± 100 LJ-110
BURIAL LEVEL 6700 ± 150 LJ-79
LOWEST LEVEL 7370 ± 100 LJ-109
SDM-W 151
21,500 ± 700
W-142
SDM-W 199
600 ± 200, W-154
580 ± 200, W-155
SDM-W 1
SDM-W 153
2800 ± 150
L-299C
COASTAL SITES NORTH
OF
SAN DIEGO
CONTOUR INTERVAL 100 FT. AFTER USGS
QUADRANGLES, LA JOLLA & DEL MAR
STATUTE MILES
57′ 30″
55′
32° 52′ 30″
50′
47′ 30″
117° 17′ 30″
15′
12′30″

(1100) FIGURE 1. Location of archaeological sites near coast of San Diego County, Calif., north of Mission Bay.

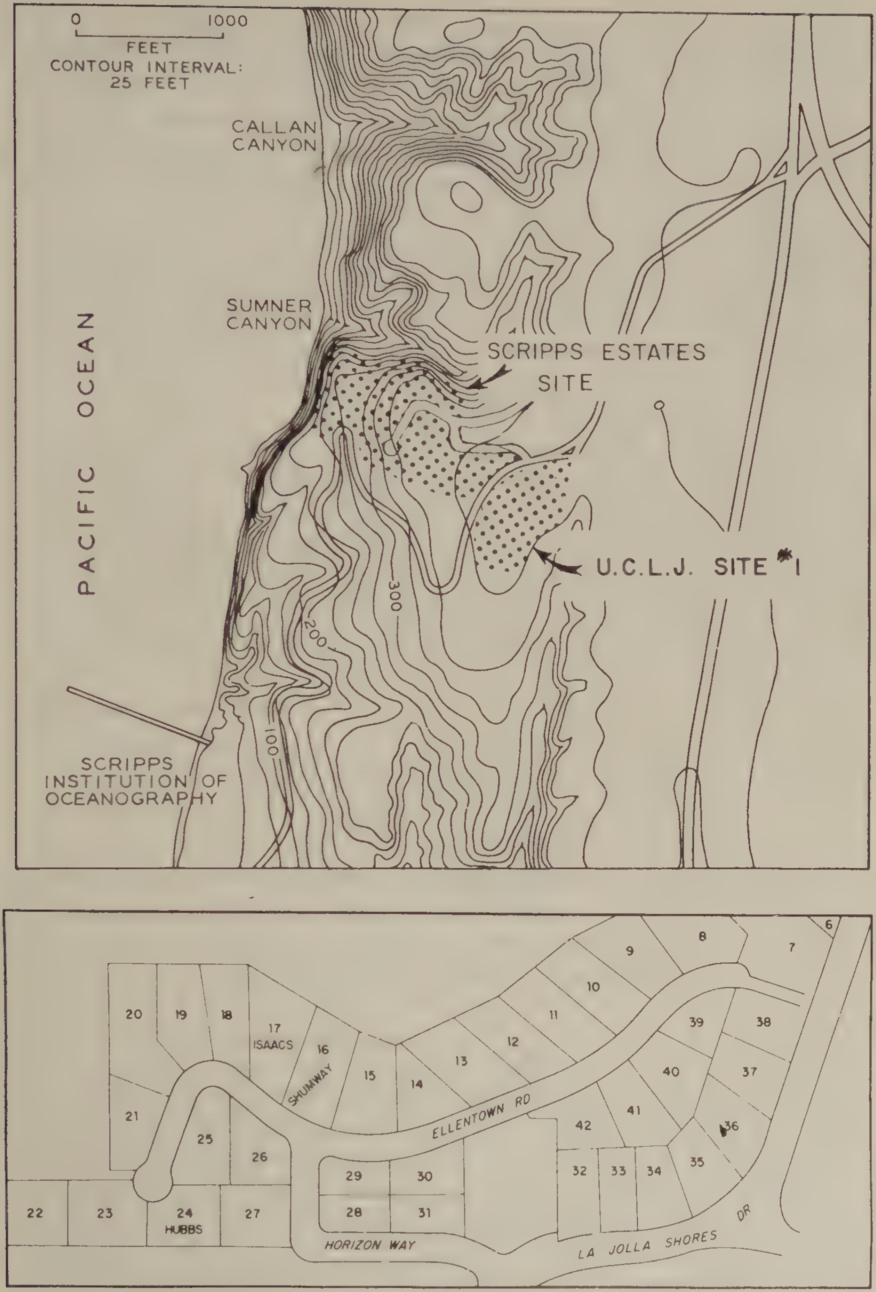
0
1000
FEET
CONTOUR INTERVAL: 25 FEET
CALLAN CANYON
SUMNER CANYON
PACIFIC OCEAN
SCRIPPS ESTATES SITE
U.C.L.J. SITE *1
300
200
100
SCRIPPS INSTITUTION OF OCEANOGRAPHY
6
7
8
9
10
11
12
13
14
15
16
17
ISAACS
18
19
20
21
22
23
24
HUBBS
25
26
27
28
29
30
31
32
33
34
35
36
37
38
39
40
41
42
SHUMWAY
ELLENTOWN RD
HORIZON WAY
LA JOLLA SHORES DR

FIGURE 2. Scripps Estates Site and environs (for location see FIGURE 1) with detail of part of S. E. A. subdivision to show location and numbers of lots.

The site provides a sweeping view to the north, west, and southwest. On a clear day it is possible to see San Clemente Island (110 km. distant), Santa Catalina Island (120 km. distant), and the peninsula of Palos Verdes Hill (140 km. distant)—all of which display much evidence of ancient occupation. Access to the seashore from the site area on the mesa is provided by the canyons mentioned above and by the gentle slope of the low area to the south-southwest.

The site lies largely within the western half of the Scripps Estates Associates (S.E.A.) subdivision from which it takes its name. The midden covers lots 14 to 21, which lie along the south rim of Sumner Canyon and front on Ellentown Road, and continues onto the western slope of the mesa and southward across lots 23 to 27 and onto the property of the University of California (FIGURE 2).

Scripps Estates Site is designated SDM-W9 in the records of the San Diego Museum of Man, and is listed as SDi-525 by the University of California Archeological Survey. The Smithsonian number is SDC-525. Carter (1957) mentions this site under the name of Scripps Faculty Site. The map of the site in the preliminary report (Moriarty *et al.*, 1959) shows only the northern half and extends too far into Sumner Canyon and over the sea cliff; the midden area is more correctly shown on a map in the present report (FIGURE 2).

Other sites, which in part or *in toto* also may have been sections of the same occupation, lie along the rims of a number of the canyons that dissect the western edge of Torrey Pines Mesa at intervening distances of less than 1 km. (FIGURE 1). In places the occupation may have been continuous around the heads of the canyons. Some signs of occupation extend across the mesa surfaces, roughly 0.5 km. wide, between the canyon rims. Archeological material similar to that at Scripps Estates Site and including burials was found by Malcolm J. Rogers and others (personal communication) along the north rim of Sumner Canyon.

GEOMORPHIC, GEOLOGIC, AND ECOLOGIC SETTING

The elevated block that constitutes Torrey Pines Mesa is composed chiefly of Eocene sandstone (Hanna, 1926; Hertlein and Grant, 1939, 1944, and 1954). In the region of Sumner Canyon and of Callan Canyon (the first canyon north of Sumner Canyon) only the Middle Eocene Rose Canyon Formation is exposed beneath the Quaternary veneer. Farther north, the Torrey Sand of Lower or Middle Eocene age and the Del Mar Sand of Lower Eocene age are present. A basalt dike is exposed on and just off the beach about 0.6 km. south of Sumner Canyon.

Conglomerate lenses are exposed on the sea cliffs in the vicinity of

Sumner and Callan Canyons. The clasts in these conglomerates are chiefly greenish and reddish rhyolites, largely prophyritic, but other volcanics and crystalline rocks are included. Boulders and cobbles weathered from these conglomerates collect at the foot of the sea cliff and pave the wave-cut terrace that underlies the beach sand. This cobble pavement often is exposed in the winter when the beach sands are removed by the strong wave action of that season. Thus an ample source of cobbles is present now; undoubtedly it was there at the time Scripps Estates Site was occupied. From such cobbles, manos, hammerstones, scrapers, and other implements could be made. Slabs of Eocene sandstone, from which metates could be fashioned, are found abundantly along the beach, and also along the canyon rim.

The surface of Torrey Pines Mesa and the other parts of the Linda Vista Terrace (or Mesa), were cut late in the Tertiary period. Parts of the Terrace are thinly capped by the conglomerate Sweitzer Formation, which commonly has been interpreted as of Pliocene age (Hertlein and Grant, 1939, 1944, and 1954), but by some as Plio-Pleistocene or early Pleistocene. Sand ridges, considerably consolidated and rather intensely reddened, raise the terrace level in lines paralleling the north-south coastline. These ridges may correlate with the Sweitzer Formation or or may be later, but almost certainly they are no later than early Pleistocene. Examination of these ridges has disclosed no signs of human occupation.

One of these ridges lies about 0.6 km. east of the site and has its top about 25 m. higher than the elevation of the site. A prominent feature of these ridges is the abundance of ironstone concretions of about 1 or 2 cm. diameter that they contain (Emery, 1950). A thin flank or an outwash from this ridge extends into the region of the UCLJ-M1 site. The concretions are found in the soil of the Scripps Estates Site, probably as a result of down-slope migration from the sand ridge.

Prior to the recent mass incursion of the area by white men, Scripps Estates Site and most of the rest of Torrey Pines Mesa was vegetated by semiarid shrubs and herbs. The narrowing north end, however, is covered—along with the adjacent slopes—by the main extant grove of the Torrey Pine, *Pinus torreyana*. Only two other, smaller native groves of this distinct and picturesque relict remain, one on the south-facing slope on the opposite side of Soledad Valley, and one on the northern slope of Santa Rosa Island. It is probable that these groves were considerably larger in the past and provided a source of pine nuts for the early inhabitants of the region.

The surface of Torrey Pines Mesa is relatively smooth and level except where it is incised by canyons. All of the canyons carry water after the occasional winter rains, and some of them retain water throughout much if not all of the year. The north side of Scripps Estates Site lies within 100 m. of the bottom of Sumner Canyon, where even today water sufficient to sustain a few dozen people is present throughout the entire year. Standing water also can be found today in the canyon southeast of site UCLJ-M1 (FIGURE 2). Rose Canyon, a few kilometers to the southeast, which is fed in lattice pattern by side canyons from the east, carries an intermittent stream now rendered almost permanent by the outflow of a septic system from a nearby military reservation. Local testimony indicates that this stream carried some water throughout much of the year, prior to the recent, severe, long-continued drought.

To the north and northeast of Torrey Pines Mesa lies the flat-bottomed Soledad or Penisquitos Valley, with a narrow lagoon that fluctuates greatly in area, depth, and salinity, and that at times nearly disappears. This valley is in part occupied by a low terrace that is not subject to flooding.

To the south of Torrey Pines Mesa is a lowland area known as La Jolla Shores, where a cliff cut in Eocene sandstone, possibly of Sangamon age, arches inward from the high cliffs north of Scripps Institution to return to the presently eroding sandstone cliffs where the coastline turns abruptly westward to form Point La Jolla. At the southern end of this lowland area there existed, until a few decades ago, a salt-water lagoon (now modified into a restricted fresh-water pond). Near the former entrance, the intertidal beach is underlain with peat, indicative of an older lagoon that existed when the rectified sandy shoreline stood somewhat farther west. Recent borings in the beach by Robert W. Thompson of Scripps Institution indicate a buried lagoon salt-flat deposit at a depth of about 8 m. below the present surface.

At the two ends of the La Jolla Shores lowland the terrace-fill forms exposures about 15 m. thick. Charcoal collected at about one third the depth downward on Scripps Institution property has yielded a date (W-142) of 21,500±700 years B.P. (Rubin and Suess, 1955). Another date, recently obtained by the La Jolla Radiocarbon Laboratory (LJ-217) for a mass of charcoal about two thirds the depth downward, is greater than 32,000 years B.P. A Pleistocene horse tooth has been found at about that level in the same fill. These and other considerations have led one of us (C.L.H.) to date the terrace-fill as encompassing the entire Wisconsin epoch. Apparent hearth sites throughout the terrace-fill—along ancient land surfaces—suggest human occupation, as do similar signs in terrace-fills elsewhere along the coast, notably on the north shore of Santa Rosa Island (Orr, 1952, 1956). Immediately north of Scripps Institution pier the alluvium grades downward into the Pleistocene (possibly Sangamon) beach, but this beach rapidly slopes to below sealevel to reappear at the southern end of the La Jolla Shores lowland.

Along La Jolla Shores there is a fine sand beach 2.1 km. long flanked on either side by rocky reefs. To the south, except for pocket beaches, reefs of varying width extend to Mission Beach. The reef north of Scripps pier, extending 1.0 km. nearly to the mouth of Sumner Canyon, has deteriorated during the past 30 or 40 years, and much of it now is intermittently covered with sand or cobbles. Within historic time, however, it hardly has been a major source of seafood. Farther north, the shore is composed of a sand beach almost continuously for many miles.

SOIL PROFILE

The soil that has imbedded and preserved the midden of Scripps Estates Site accumulated throughout the long period of ancient occupation and in the time since. The portion of the site in which most of the burials have been found, that is, near the south rim of Sumner Canyon, is on the flank of a small topographic rise; here too soil has accumulated over the years. Three distinctly different processes seem to account for the aggradation:

The first, but not necessarily the most important, is water action during freshets. There is a continuous gentle slope from the sand ridge lying 0.6 km. east of the site to the midden area and a gradual downslope movement of sand and ironstone concretions is the natural consequence.

The second process is the deposition of wind-blown sand and silt. Shrubs have grown in abundance over the site in historic times and, presumably, they existed at the time of occupation. These shrubs have caught sand and silt blown there from the cliffs immediately west of the site by the prevailing westerly winds and, at times, from the east during Santana conditions. Currently, shrubs (chiefly *Rhus integrifolia* with *Heteromeles arbutifolia* in secondary abundance) form a heavy growth along the north edge of the site, but formerly they covered a considerable portion of the site. According to M. J. Rogers (personal communication), the shrubs extended into the area south of Ellentown Road before the removal of topsoil from the site during World War II.

The third process is the direct activity of man. A significant portion of the soil consists of shells and shell fragments, rock artifacts, pebbles, cobbles, rock fragments, chips and spalls, and bone (human burials and food material), all of which could have been introduced only by human activity.

The accumulation of the soil apparently has been limited largely to post-Pleistocene time. The radiocarbon dates indicate a history of between 6000 and 8000 years for all but the lowermost part of the soil profile. During the undoubtedly cold as well as wet Pluvial period, which lasted until about 10,000 years ago, whatever soil had accumulated on the mesa in the vicinity of the site during Pleistocene time probably was eroded into the sea. Much of the soil at the site presumable accumulated during the long period of occupation.

The soil profile and the relation of midden shell and artifact levels to the soil profile can be discussed with the aid of a profile diagram, which is a generalized interpretation for the site (FIGURE 3). The soil profile is of composite origin, being definitely related both to the original ground surface and to the midden shell and artifact zone. The profile comprises a series of soil horizons that are difficult to classify not only because of the varying nomenclature and the diversity of criteria in pedology but also, particularly, because this soil does not consist of a horizon of mother material (C) and other horizons (B and A) derived therefrom by pedogenesis. Rather, the material has accumulated through millenia with concurrent eluviation and illuviation.

The lowest zone of the profile is the Eocene sandstone designated D*, which underlies the site and which outcrops in places throughout the site. In the vicinity of the site the sandstone is uniform in appearance, having a yellow color. The grains are chiefly of medium sand size. The upper surface of the sandstone is irregular. The soil produced by weathering of the upper surface of the sandstone bedrock and thinly overlying it is only in part the mother material of the overlying horizons.

Overlying the bedrock is a well-developed horizon consisting essentially of sand weathered from the bedrock but containing a considerable accumulation of clay and iron salts. This is a classic B horizon herein designated B_1. The upper 5 to 10 cm. of this zone are particularly rich in clay, hence the top of the zone is distinct. Intermixed with the clay are sand concentrations bound with a deep-red ferruginous cement. Iron oxide streaks are abundant in the clay. Ironstone concretions (discussed above) occur in this horizon as well as in upper layers. The presence of the ferruginous cement in the sand concentrations and the iron oxide streaks in the clay suggests that some of the ironstone concretions may have been, or are being, formed *in situ*. The concretions are found throughout the whole soil profile, however, so it seems most

---

*The letter designations of various soil horizons, as used here, differ somewhat from those used in the preliminary report (Moriarty *et al.*, 1959); a revision is made here to conform better to the usage of Carter (1957), Hubbs *et al.* (1960), and others.

probable that the majority of them have washed in from the sand ridge to the east where these concretions, along with seemingly developmental stages, abound. If this is true, this horizon is at least in part of alluvial origin. There is scarcely a trace of shell and, apparently, no artifacts in this horizon.

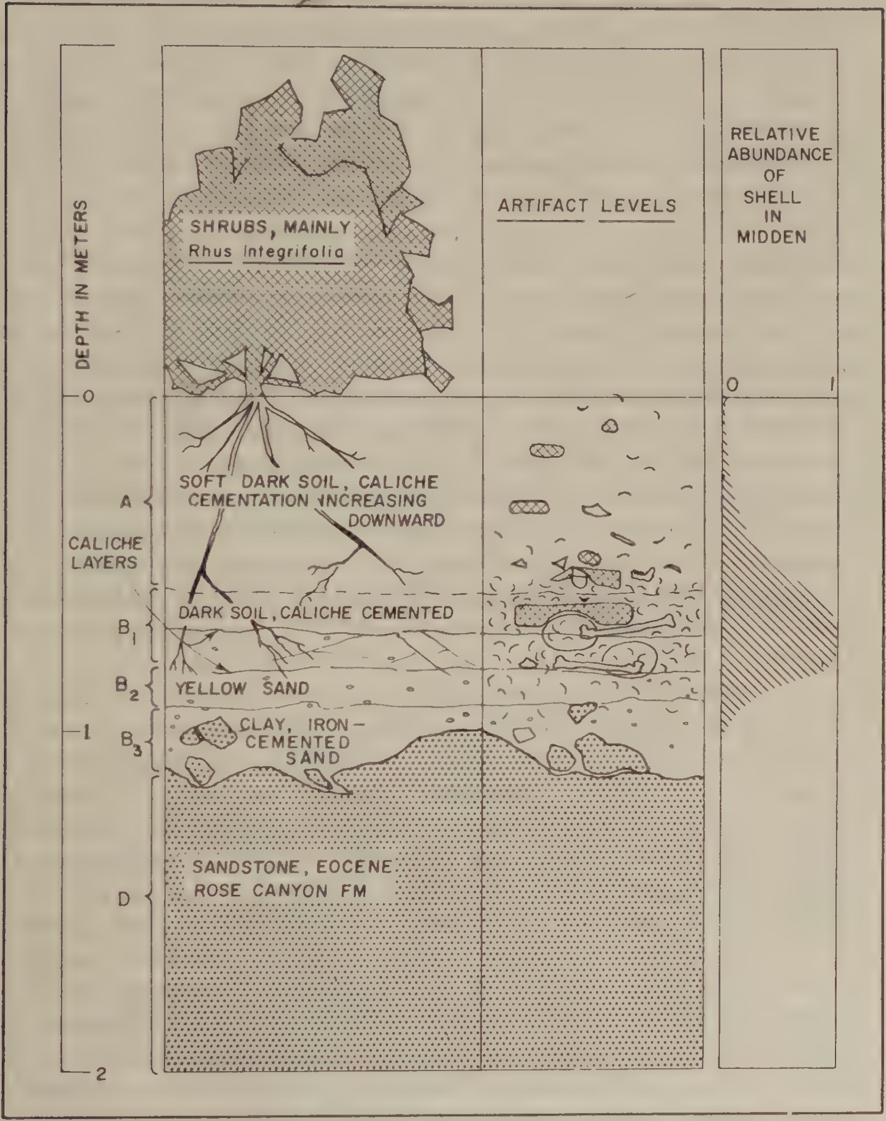
DEPTH IN METERS
0
1
2
SHRUBS, MAINLY
Rhus integrifolia
ARTIFACT LEVELS
RELATIVE ABUNDANCE OF SHELL IN MIDDEN
0
1
A
CALICHE LAYERS
SOFT DARK SOIL, CALICHE CEMENTATION INCREASING DOWNWARD
B1
DARK SOIL, CALICHE CEMENTED
B2
YELLOW SAND
B3
CLAY, IRON-CEMENTED SAND
D
SANDSTONE, EOCENE ROSE CANYON FM

FIGURE 3. Generalized soil profile in the area of concentrated burials at Scripps Estates Site (S.E.A. lots 16 and 17), showing also the relation of artifacts and relative shell abundance to the soil.

A zone of yellow sand designated B_2 lies above the clay zone. In this layer, as in the overlying B_1 horizon, caliche binds the sand into a rocklike mass when dry but has little binding effect when the soil is wet. Ironstone concretions are present but sparse. Midden shells, skeletal material, and artifacts occur in this horizon.

The yellow sand (B_2) is overlain by a dark, caliche-cemented soil designated B_1. Generally the transition from yellow to dark soil is gradational, and the transition region has a mottled appearance, largely as a result of the darker soil having dropped downward into holes produced by the decay of roots and by the burrowing of animals. Less extensively, a caliche layer abruptly separates the yellow and darker soils.

Proceeding upward as the abundance of caliche cement decreases and as the amount of organic matter increases, zone B_1 grades into the dark, friable topsoil designated zone A. In some parts of the site the A zone may be subdivided into an upper, more or less shell-less zone, and a lower zone with a small to moderate amount of shell. The upward decrease in shell now seems to be most plausibly attributable to post-occupational accumulation of soil and to the more rapid solution of shell in the upper layers, resulting from the higher content of organic matter and from the lower content of lime; farther down, an actual coating of lime prevents further weathering. Such processes probably would have led to the almost complete elimination of shell in the uppermost levels had it not been for the counteraction of other agencies, including rodents, roots, and man. These and other natural processes brought much shell to lie on the surface until the area recently was picked over heavily.

The roots of shrubs presently growing on the site extend into the zone of clay accumulation B_3. It is likely that vegetation has grown on the site continually since the time of occupation. Small bits of charcoal are sparsely scattered in horizons A, B_1 and B_2, and both living and charred roots occur (calling for caution in the collecting of charcoal for dating). Saucerlike depressions of burned clay often associated with charcoal, such as are common at lower (earlier) horizons in the same general region, were not recognized in Scripps Estates Site (whether such fire signs actually represent hearths is a much-debated question).

An outstanding feature of the soil profile, as in many of the older middens along the coasts of southern California and Baja California, is the caliche, in zones B_1 and B_2. Some of the caliche impregnates and indurates the sandy soil. Some occurs in thin and in places very firm layers and sheets, particularly along cracks, which may be horizontal, oblique, or vertical. Caliche also often fills the cavities of shells and other objects and tends to encase shells, artifacts, bone, and any other hard material. In general, the most prominent caliche layer lies within the B_1 zone and roughly parallels the original ground level. Where the topsoil was removed during World War II, this prominent caliche layer generally lies only about 10 cm. below the present ground level but, where the soil is intact, it is much deeper. This and other caliche streaks cut through burials and occasionally are abruptly displaced by soil movements of seismic or other origin.

These and other circumstances lead us, as they did Warren (Moriarty *et al.*, 1959) to the definite conclusion that the caliche formed subsequent to the occupation, that is, within the last 5000 years or so. Such caliche, either indurating the soil or forming discrete streaks, layers, or masses, commonly and perhaps usually underlies shell middens in the generally dry area along the coasts of southern California and Baja California. It is well formed below some middens of high shell concentration dating between 2000 and 3000 years B.P. It seems highly probable that lime leached from the overlying shell is redeposited in some form of caliche where the soil water usually evaporates. David R. Schink made for us a brief analysis of a layer of caliche 2 to 3 mm. thick that coated the skull of burial 3, which lay in the B_1 zone. X-ray diffractometry indicated pronounced calcite peaks, with secondary quartz and feldspar peaks. By weight, 67 per cent of the caliche—presumably, for the most part, calcite—dissolved in 2 molar HCl.

Considerable variance exists regarding the designation by letters of caliche-impregnated soil horizons in arid regions. Some authorities, including Robinson(1937) and Lyon and Buckman (1943), place the caliche-rich soil horizons of arid regions in the B series, but the Soil Survey Staff of the United States Department of Agriculture (1951) considers such layers as typical for the C series (but they admit that the caliche may accumulate in other horizons; sheets of calcite often form in the relatively unmodified C horizon and even in cracks deep down in the underlying bedrock, D). In the soil profile of the Scripps Estates it seems reasonable to treat the heavily illuviated yellow sand (B_2) and the dark, caliche-cemented soil (B_1) as parts of the B horizon, as also the underlying clay-rich, iron-cemented basal soil (B_3). Thus no C layer is included.

Rock fragments occur throughout the soil profile of the site, locally in marked concentration (but nowhere, in so far as observed, in paved hearths). Some of these fragments are pieces of the Eocene sandstone country rock that may have originated *in situ*. Seemingly unworked slabs of sandstone of varying size and thickness occur. Most of the pieces, however, are volcanic, metamorphic, or crystalline rocks. A rather high proportion shows evidence of having been discolored or cracked by fire, or having been battered, rubbed, or flaked. Nevertheless, whether they seem to have been modified by man, most of these fragments and cobbles seem foreign to the soil, and in all probability were transported to the site by man. They are interpreted, therefore, as part of the midden deposit.

EARLY EXPLORATION OF THE SITE

Scripps Estates Site has been known for decades, but essentially nothing was published concerning it until the appearance of the initial reports by Moriarty *et al.* (1959). Archaeological work was initiated on the site in the late 1930s by Malcolm J. Rogers, then director of the San Diego Museum of Man and long the mentor of local archaeology. Rogers' field work was intensified from 1940 to 1943 as a salvage project during the early years of World War II when many burials (FIGURE 4) came to light as topsoil was removed from a large part of the site in the construction of nearby Camp Callan. Thirty-three burials were located and leveled by transit, and the salvaged material was stored in the Museum of Man for future study. It is most regrettable that a report on the extensive collection was not then prepared, because in the meantime, after Rogers left the Museum in 1945, almost all of the material became lost or misplaced. Fortunately, before his recent, lamented death, Rogers recovered his transit-survey data, which he very kindly made available for our plot of burial locations (FIGURE 4). In his survey, Rogers used as a reference benchmark a sandstone outcrop that subsequently has been altered or eroded away. However, on accompanying us to the location (on S.E.A. Lot 17), he picked out a spot that he estimated to be within 2 or 3 m. of the original location. This spot was used in locating the burials that he had surveyed.

We have reason to believe that a considerable number of artifacts were removed from the surface of the site during the 1930's and perhaps even earlier. Subsequently, during the war, other material was taken by military personnel during the excavation for and occupation of gun emplacements and during the removal of topsoil. Since that time additional material has been removed by various persons, most of whom have not been engaged in serious research.

In 1953, after a 10-year lapse in the scientific exploration of the site, one of us (J.R.M.) took advantage of the opportunity for archaeological observation and collecting when the S.E.A. subdivision was being developed, especially when the streets were being graded. As a cut about 1 m. deep was made during the construction of Ellentown Road near the south side of the burial ground (FIGURE 4), remnants were found in the loosened soil of two rather severely disturbed burials. From the few

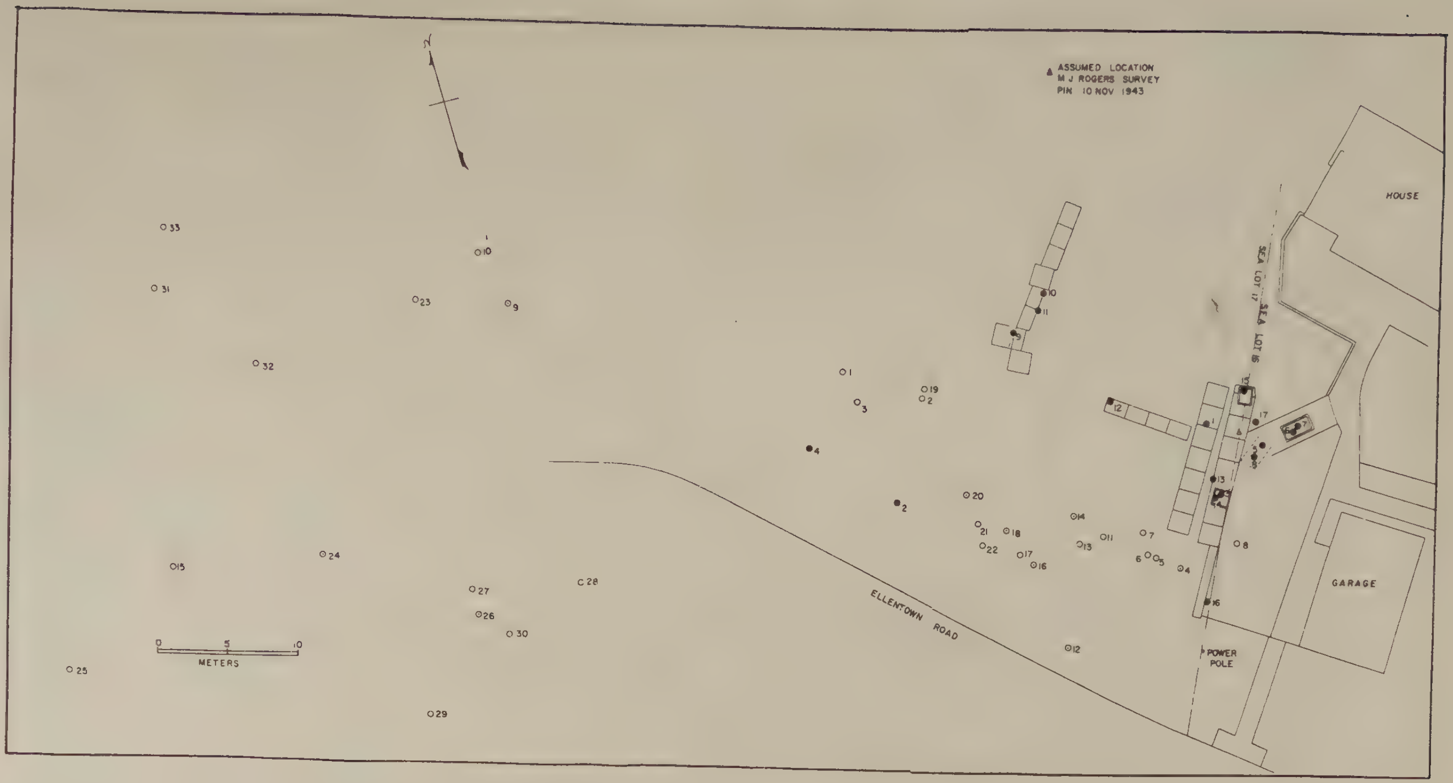
▲ ASSUMED LOCATION
M J ROGERS SURVEY
PIN 10 NOV 1943
HOUSE
GARAGE
SEA LOT 17
SEA LOT 16
POWER POLE
ELLENTOWN ROAD
N
0
5
10
METERS
1
2
3
4
5
6
7
8
9
10
11
12
13
14
15
16
17
18
19
20
21
22
23
24
25
26
27
28
29
30
31
32
33

FIGURE 4. Main burial ground in Scripps Estates Site. Open circles locate burials recorded by M. J. Rogers prior to 1944. Black dots locate burials discovered during 1958 and 1959.

bones that were salvaged a few measurements were obtained. An intact portion of one of the burials yielded about 25 shell beads, which had been fabricated from the thick part of heavy shell, presumably of pismo clams. These beads were remarkably consistent in shape and size; each was approximately spherical in shape, with a well-centered, drilled hole.

In the same year, in a reconnaissance of the undisturbed areas of the site, Moriarty found a number of manos and four or five fragments of sandstone metates. Food material was represented by an abundance of shell at the surface, but very little food-bone material was noted. The lower jaw of a sheephead *(Pimelometopon pulchrum)* and some fish vertebrae were found.

Among the miscellaneous rock pieces found at this time were 8 almost perfectly spherical sandstone balls, with diameters of 6 to 10 cm. Their high sphericity and presence in numbers suggests that they are artifacts, possibly gamestones. These balls, and the shell beads mentioned above, were deposited with the San Diego Museum of Man and cannot now be located.

Since 1954 two of us (C.L.H. and G.S.) have had houses built in the S.E.A. subdivision and within the site area. We have taken advantage of the soil disturbance during construction, and in the development of gardens, to collect artifacts. Hubbs has accumulated a large collection of shells and artifacts on and about Lot 24 and has found one burial (incomplete skeleton) in the A soil horizon on the University of California property a few meters southeast of the line between S.E.A. lots 24 and 27. Shumway also has made surface collections, supplemented by finds while gardening, on lots 15, 16, and 17. After the preliminary report was published he worked over the soil to a depth of about one-half meter. in a 20-m.^{2} area designated trench S-M-3 on lot 16 (FIGURES 4 and 5). The entire volume of soil in this trench was screened by a mechanical shaker, using a mesh with openings about 6 mm. square.

Almost all of the surface collections seem to pertain to the La Jolla Culture, for it agrees well with the buried material. At least three projectile points ascribable to the Yuman Culture have been picked up in the site area (two on lot 25, one on lot 17), but no other artifacts of Yuman origin have been found; not a single shard has been found on the site. The projectile points easily could have been lost by Yuman hunters wandering over but not living on the site. Except for a small decomposing pile of adobe bricks on lot 25 there has been found no evidence of any permanent residence on the western part of the S.E.A. subdivision since the La Jollans abandoned the ground about five millenia ago. Nor is there any evidence of underlying San Dieguito material on the site; however, Malcolm J. Rogers mentioned (personal communication) that he

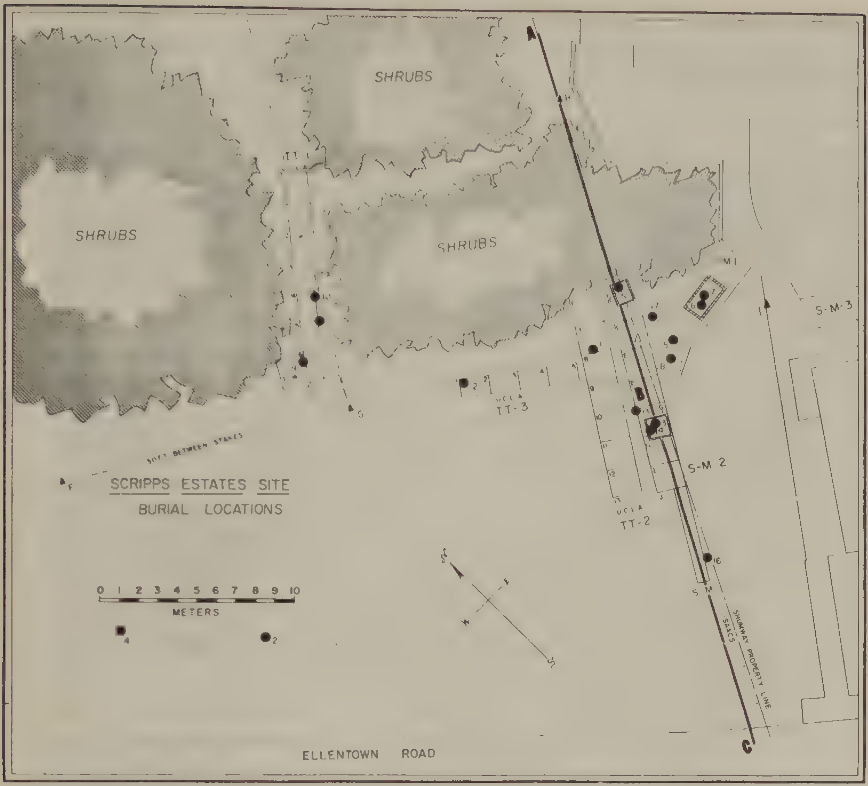
SHRUBS
SHRUBS
SHRUBS
SCRIPPS ESTATES SITE
BURIAL LOCATIONS
0 1 2 3 4 5 6 7 8 9 10
METERS
U.C.L.A. TT-3
U.C.L.A. TT-2
S-M-3
S-M 2
S M
SHUMWAY PROPERTY LINE
ELLENTOWN ROAD

Figure 5. Excavations of 1958 and 1959 at Scripps Estates Site. Numbered burials are shown as black dots. Shown also are the three concrete vaults preserving, respectively, skeletons 6 and 7, 3 and 14, and 15. Trenches labeled U.C.L.A. and TT-1, TT-2, and TT-3 were excavated by Warren; those labeled S-M-1, S-M-2, and S-M-3 by Shumway and Moriarty.

found San Dieguito material stratigraphically below the La Jolla on the north side of Sumner Canyon. Excavations in numerous places in the S.E.A. subdivision have been made to Eocene bedrock without disclosing any culture underlying the La Jolla. With the possible exception of the projectile points, all aboriginal material in the site seems attributable to the La Jolla people.

EXCAVATIONS OF 1958-1959

Introduction

At twilight on December 12, 1958, Shumway was spading up lawn in his front yard (S.E.A. lot 16) and struck the skull of what is herein numbered burial 7 (TABLE 1). Moriarty was notified and trenching began the next day. It soon was revealed that burial 6 also had been struck in the lawn spading. The trend of the two burials, the presence of a fence to the north, and the desire to provide drainage in case of rain prior to removal of the skeletons, determined that the trench should extend to the southwest, where burials 5 and 8 were discovered later. The tops of burials 6 and 7 were within 25 cm. of the surface of the lawn. In the development of the lawn the soil had been disturbed to a depth of about 10 cm. No grading was done at this location prior to planting of the lawn. Skeleton 6 was buried in an atypical position, with the upper part of the spinal column vertical. The skull from this burial was missing; it probably had been at about the level of the present sod and may have been demolished during the preparation of the lawn; or, it may have disintegrated previously in the loose upper soil.

Shortly after these discoveries, arrangements were made with Clement W. Meighan for the participation of the University of California, Los Angeles, Archaeological Survey, in this study, with local field work for the university in charge of Claude N. Warren. With the help of assistants, Warren dug three trenches (labeled U.C.L.A. on FIGURE 5). Three other trenches (labeled S-M on FIGURE 5) were excavated by Moriarty and Shumway with help from local volunteers. In this combined work 14 burials were located in the trenches, and two more (2 and 4) were found on the road-cut slope about 15 m. southwest of U.C.L.A. trench TT-1. In addition, many isolated bone fragments were found during the digging. A fragment of a child's jaw was found about 1 m. northwest of burial 8, and one half of an adult's jaw was found 2 m. north of burial 6. In 1960 the top of a skull was located about 2 m. north of burial 5. It has not been excavated but probably should be considered as burial 17.

A transit survey was carried out during the combined digging operations.

Seven burials (3, 5, 6, 7, 8, 14, and 15) are being preserved *in situ* by Shumway as permanent exhibits (FIGURES 5 and 6). Four of these burials fall entirely on his property (lot 16); the other three on the boundary between lots 16 and 17. Concrete boxes with walls 10 to 15 cm. thick were poured around the burials and waterproof lids were installed. Trench S-M-2 is notable in that it contained five burials, 3, 13, 14, 15, and 16 (FIGURES 5, 6, 7).

Burial Descriptions

At this time 10 of the 17 recently discovered skeletons remain in the ground, including 7 that are being preserved *in situ*. Because the excavation of these 10 specimens remains incomplete, only preliminary

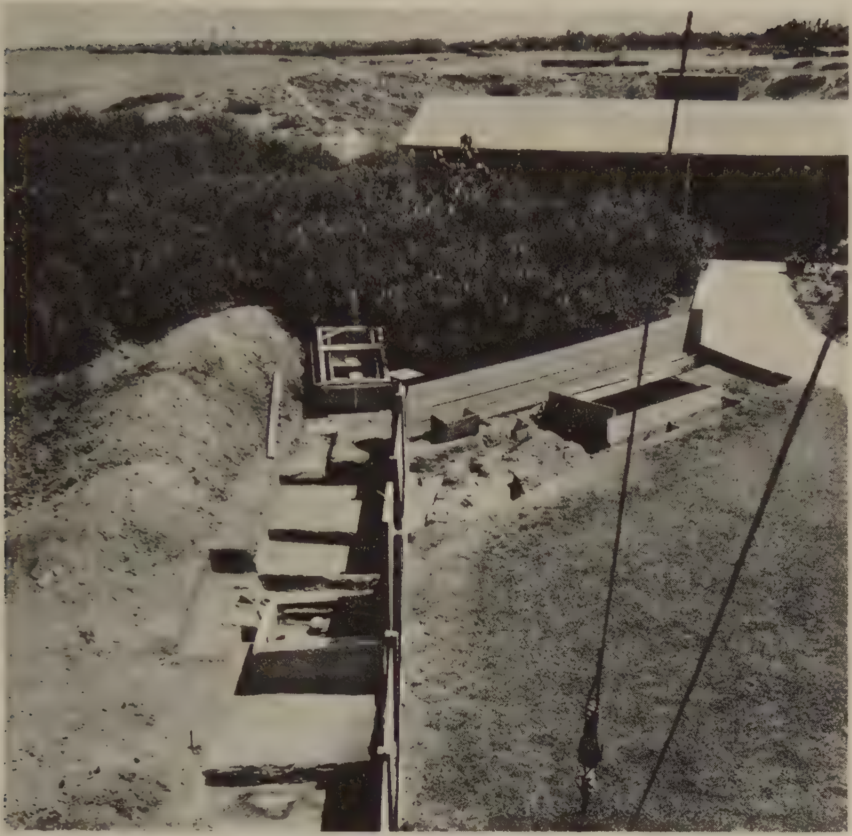

FIGURE 6. Excavation of trench S-M-2 at Scripps Estates Site, looking north along S.E.A. lot line 16-17 and showing also the three vaults (for orientation see FIGURE 5).

field measurements of the bones have been possible. Twelve of these burials are described briefly in TABLE 1. One of these also was treated by Warren (Moriarty *et al.*, 1959), who described four other burials. The field measurements of the skeletal material are not presented here because the bones can be measured more completely and accurately after further excavation.

All skeletons found in place in this site were in flexed position, as were those discovered earlier by Rogers (personal communication). In most but not all of the burials a line from the pelvis to the skull points toward the northerly quadrant, within 45° of true north (TABLE 1), as it does in other burials identified as La Jolla. The significance of the azimuthal bearing needs further statistical support from additional burials.

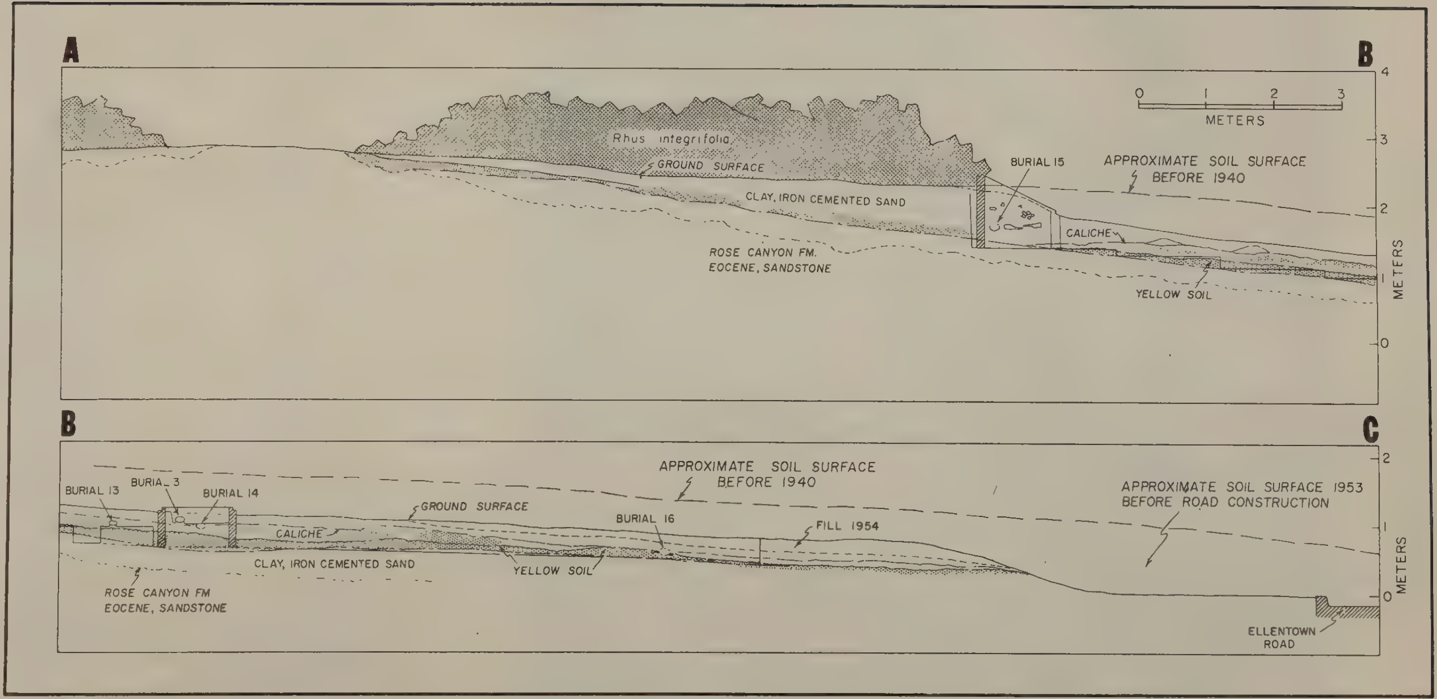
A
B
0
1
2
3
METERS
4
3
2
1
0
METERS
Rhus integrifolia
GROUND SURFACE
CLAY, IRON CEMENTED SAND
ROSE CANYON FM.
EOCENE, SANDSTONE
BURIAL 15
APPROXIMATE SOIL SURFACE
BEFORE 1940
CALICHE
YELLOW SOIL
B
C
BURIAL 13
BURIA_3
BURIAL 14
GROUND SURFACE
CALICHE
CLAY, IRON CEMENTED SAND
ROSE CANYON FM
EOCENE, SANDSTONE
APPROXIMATE SOIL SURFACE
BEFORE 1940
BURIAL 16
YELLOW SOIL
FILL 1954
APPROXIMATE SOIL SURFACE 1953
BEFORE ROAD CONSTRUCTION
ELLENTOWN
ROAD
2
1
0
METERS

FIGURE 7. Soil-profile section through trench S-M-2, showing relation of burials to soil horizons (for location see points A, B, C, and D on FIGURE 5) and approximate level of soil surface prior to 1940.

In all burials, midden shells occur in the spaces between bones as well as in the surrounding ground. In none of the burial excavations was there noticed any change in the soil surrounding the skeleton that might delineate the limits of the hole in which the body originally had been interred.

A metate lay in place over each of two burials (1 and 15). The burial-1 metate, which is the "variant C-basin metate" figured by Warren (Moriarty *et al.*, 1959), was directly over the skull. The burial-15 metate (FIGURE 10), which is broken in the middle, with one of the halves turned over, lay over the middle of the body. A cluster of about 6 pieces of rock, 10 to 20 cm. above the metate, appears to have been placed as grave marker.

The condition of the skeletal material in the several burials varied considerably. At best, a nearly complete skeleton (burial 10) was found

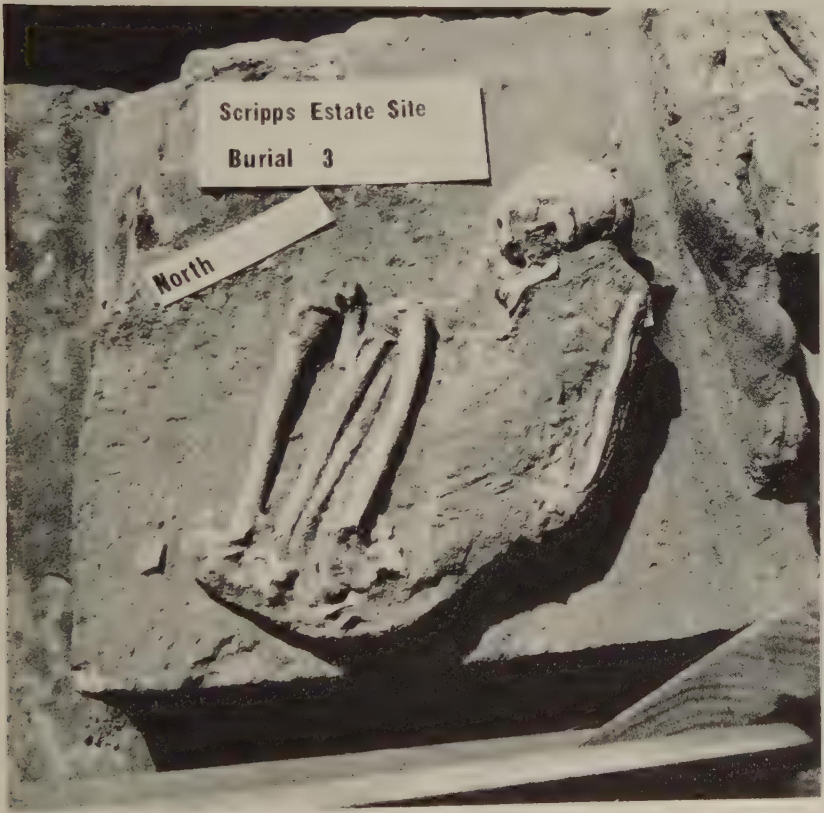

FIGURE 8. Burial 3, Scripps Estates Site, a relatively well preserved, typically flexed, La Jolla burial, incompletely excavated.

(1117)

that was measured, figured, and described by Warren (Moriarty *et al.*, 1959). A second burial, 3 (FIGURE 8), probably will yield a useful set of measurements when (and if) it is removed from the ground. It is one of the burials being preserved *in situ,* and its present condition is as shown in the figure. More typically, part of a skeleton was in fair condition and the remainder was either badly fragmented, or missing (FIGURES 9 and 11). Skulls usually were in a distorted or crushed condition (FIGURE 11). A particularly well-preserved skull was found with burial 7 (FIGURE 12), and some of its features are noteworthy. It was the discovery of this skull that initiated the 1958 and 1959 excavations, and the missing portion (recovered) was knocked off by shovel blade.

Most of the burials are devoid of ornaments or offerings. Burial 7 was an exception, however, for near the robust skull (FIGURE 12) a cluster of about 90 shell beads was found. These presumably formed the necklace

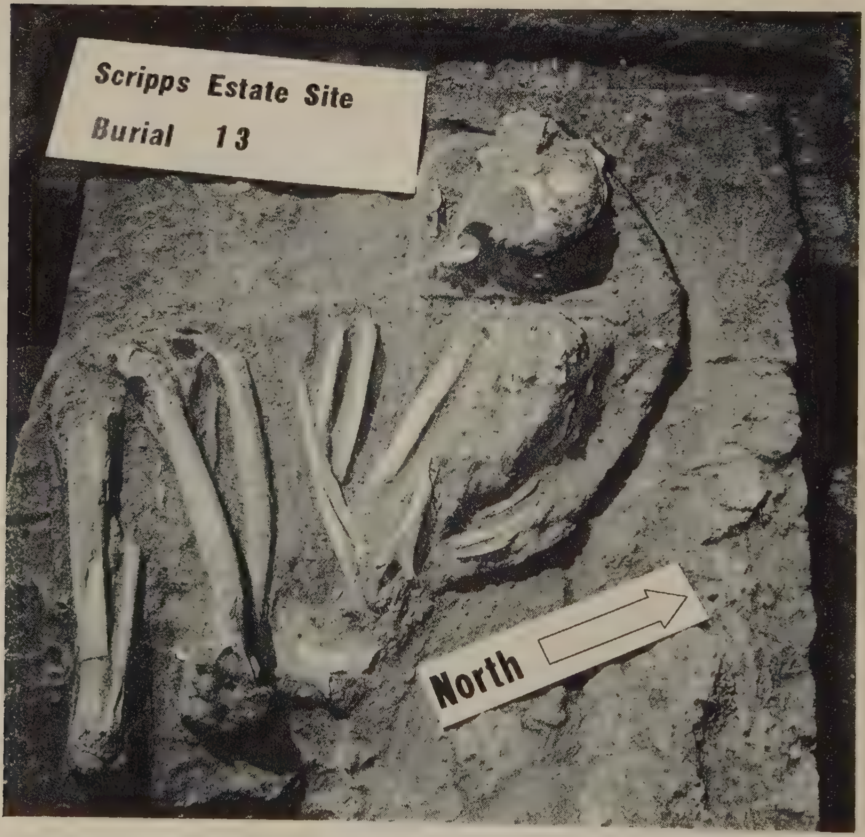

FIGURE 9. Burial 13, Scripps Estates Site, a typically flexed, La Jolla burial, in a fair state of preservation with crushed and incomplete skull.

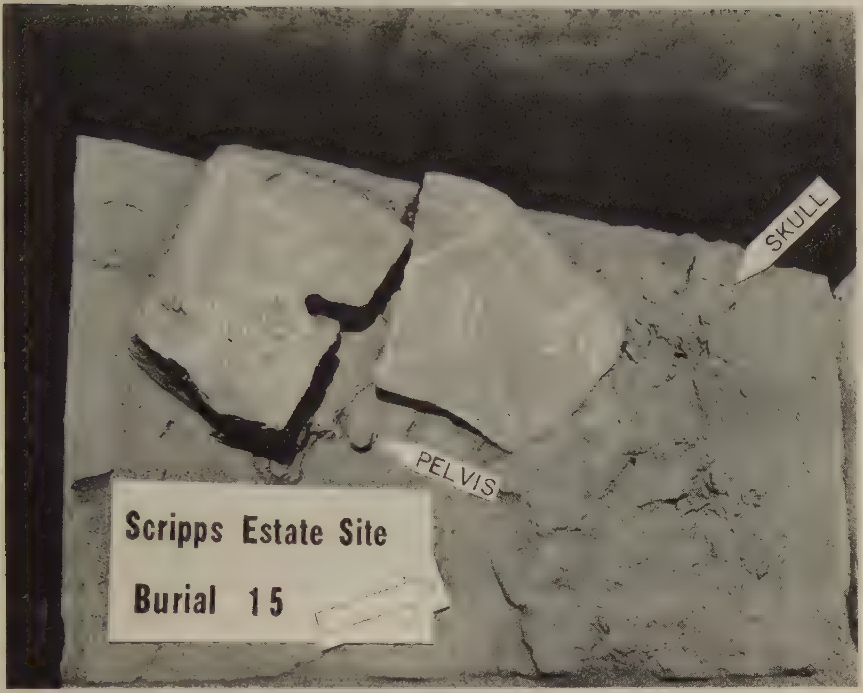

FIGURE 10. Broken metate overlying middle of skeleton of burial 15, Scripps Estates Site.

that is described and illustrated below. A few similar shell beads were found in association with burials 8 and 13, and a few others have been found in the site without any burial association.

Another object that probably was associated with burial 7 was a single large valve of *Laevicardium elatum*, measuring 145 × 132 mm., which lay with the convex surface upward—within 20 cm. of the skeleton—at the same level. Possibly it was a mortuary offering (the valves of this large clam are usable as a cup or dipper). Another specimen of this clam has been found on the site (which was not recognized when the preliminary report was published although available in a collection), and others have appeared during excavations on the adjacent site UCLJ-M1.

One of the three doughnut stones found at the site, and the only one made of steatite, was reported by Warren (in Moriarty *et al.*, 1959) as having been found close to burial 9. A cobble and a scraperlike flake were associated with burial 8. No other artifacts appear definitely to have been associated with burials 1 to 16, nor with the one partial skeleton found near lot 24.

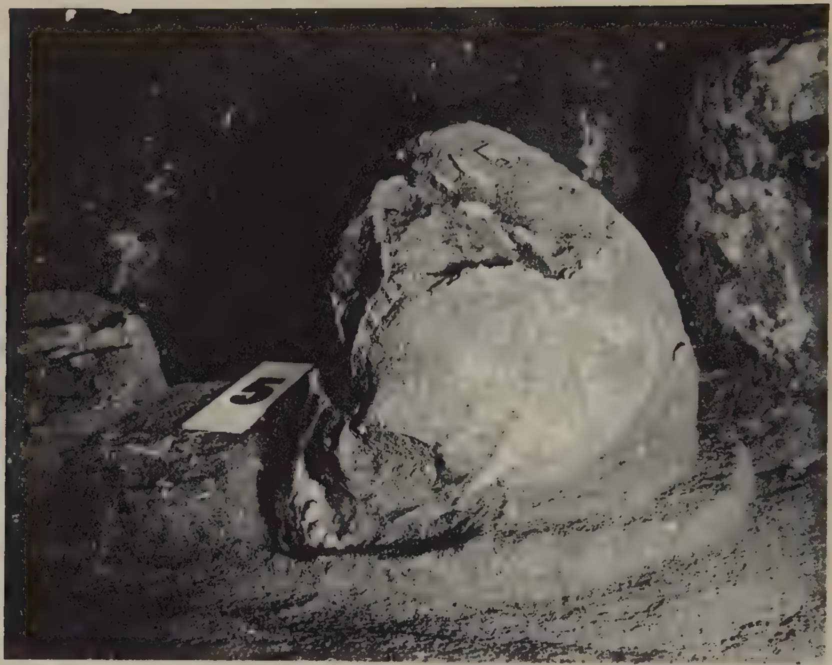

FIGURE 11. Crushed skull of a child, burial 5, Scripps Estates Site.

FIGURE 12. Skull of adult male, burial 7, Scripps Estates Site; note thickness of calvarium, the prognathism, and the heavy, little-worn, and sound teeth.

(1120)

Skeletal and Dental Features

As noted above, a detailed description of the skeletal remains is being deferred, pending more complete excavation and preparation. It already is obvious, however, that wide variance characterizes the skeletons already partially exhumed. The first skull encountered during the excavations of 1958 and 1959, that of burial 7 (FIGURE 12), exhibits a number of extreme characteristics. It is relatively narrow across the forehead, has a much thicker calvarium (the portion knocked off by shovel is 5 to 6 mm. thick) than any of the other skulls of the site that have been examined, is rather strongly prognathous, and has unusually massive and sound teeth as compared with most of the other skulls. The teeth show relatively little wear, whereas in most of the other skulls the teeth show the heavy wear to be expected of people who used sandstone metates.

The skulls so far examined show a range from dolichocephalic to brachycephalic. It would be premature to consider the possibility of racial mixture during the probably more than 2000 years of site occupation. The rather extreme skull of burial 7 has been dated at 6700 years B.P., which was near the middle of the long period of occupation. Pending a detailed morphological and morphometric study of the skeletons, it seems wise to hold in abeyance—as well as in strong doubt—the occasionally heard suggestions (Dixon, 1913; Count, 1938) that the La Jolla people, of seemingly simple culture, may have been of Australoid (or of other non-Mongoloid) stock.

Whatever their race (or races) may have been, the La Jolla people were of moderate stature and apparently were reasonably free of vitamin-deficiency or food-deficiency diseases. There is little, if any, sign of poor nutrition. Robert K. Murphy, who has studied the skeletal material from Scripps Estates Site for evidences of pathology, found no indication of dietary deficiency. Some dental caries appears in the adult specimens, and there are indications of arthritic lesions on adult femurs in burials 3 and 13. Apparently the abundance of seafood, supplemented by land vegetation, insured relatively straight and sturdy bones.

The variation in the extent of abrasive tooth wear suggests the possibility of changes or variation in food habits, and it might be postulated that seafood became relatively less important and metate-ground food more important as time progressed; but the vertical variation of the abundance of grinding tools and shells does not strongly support this idea.

Artifacts

Introduction. Consistent with the apparent occupation of the site for more than two millenia, nearly all of the innumerable pieces of rock in the midden soil show some indication of having been affected by human activity. A significant proportion shows signs of percussive flaking, either as cores or flakes, and further evidence of secondary working such as pecking, or grinding. Among the pieces not easily identifiable as purposely worked artifacts are numerous fragments with irregular, sharp, freshly-broken corners and edges, which the geological history of the site could account for only as the result of introduction to the site by man in relatively recent time. Numerous other rocks appear to be fire-reddened and cracked.

Because the site area appears to have been largely denuded of soil in early Recent time, because the mesa surface is largely isolated from upland rock sources, and because the immediately underlying Eocene sandstone is devoid of cobbles and pebbles, even the unworked pieces showing no specific sign of human activity give evidence of human occupation, for it is unreasonable to assume that they reached the site area by other than human agency. Included in the rock assemblage are a number of rounded and polished pebbles with attractive color that we imagine were brought in for some reason other than utilitarian.

Warren (Moriarty *et al.*, 1959) listed and attempted to classify 158 rock artifacts from the site. Moriarty and Shumway, in the same preliminary report, indicated a considerable variety, without counts and with limited classification. The collection by Hubbs from and near S.E.A. lot 24 contains numerous definitive tools and many other flakes, cores, and suggestive rock fragments in a collection of several thousand pieces. No attempt is made here toward a complete inventory, due in large part to the indefiniteness of the types and to the extensive intergradation between such types as might be recognized, as well as to the difficulty of deciding which pieces are and which are not definitive artifacts. Nearly all, however, are artifacts, if we define the term to cover products of human activity rather than as definitive tools.

It generally has been assumed that all, or nearly all, rock flaking by the La Jolla people was of the percussive rather than the more advanced pressure type (Rogers, 1945). In the preliminary report on this site (Moriarty *et al.*, 1959) Moriarty and Shumway accepted this view, having found nothing to contradict it in the artifact assemblage they had studied, including most of the Warren collection and a number of the better pieces from the Hubbs collection. Each of the three artifact collections, however, contains a number of flaked hand tools that show evidence of secondary flaking. Warren indicated that some of this relatively refined flaking was done by a pressure technique. We feel that some type of refined percussion technique would have served adequately to produce the observed results. However, because such tools, representing the most refined flaked instruments of the site are few, pressure methods (if used at all) were of little importance.

The vast majority of the flaked hand tools were made from pebbles or cobbles of fine-grained volcanic rock. Rhyolites, in large part slightly to heavily porphyritic, predominate. Many of the more finely worked pieces are of a greenish felsite. Other rocks, largely volcanics, are represented. A considerable number were made from quartzite cobbles. Manos were made of granites, volcanics, and sandstone (both quartzose and arkosic). Most of the metates were formed from quartzose sandstone, although some are granitic. Warren (Moriarty *et al.*, 1959) reported finding a single chip of obsidian and a single artifact, a doughnut stone, made from steatite. The only artifacts found thus far that were made from shells are beads. Only a very few bone tools have been discovered at the site.

An outstanding feature of the large artifact assemblage from the Scripps Estates Site is the abundance of utilitarian objects and the extreme paucity of specimens interpretable as of ceremonial or recreational significance. Nevertheless, among the few seemingly nonutilitarian artifacts are included a number of diverse and distinctive types, but generally these are represented by only one specimen, or by very few.

Manos. Among the ground artifacts in the S.E.A. site the most abundant are the manos. These occur throughout the site, in both the A and B soil horizons. They may be more common in the upper part of the soil profile, but this has not been determined quantitatively. In the preliminary report (Moriarty *et al.*, 1959) Moriarty and Shumway recorded the collection of 55 manos on the site over a period of years, chiefly from the vicinity of S.E.A. lots 15, 16, and 17 and Warren reported on 21 manos and mano fragments. Hubbs has collected more than 300 manos and mano fragments, nearly all from S.E.A. lot 24 and the adjacent University of California property, over an area of about 0.5 acre.

All the manos appear to have been made from naturally rounded cobbles chosen to be of suitable size for holding with one hand. One or two faces of each mano cobble exhibit flattening by abrasive grinding action. The range in shape and size of typical manos is illustrated (FIGURE 13). Of 159 manos from the Hubbs collection examined in detail, only 8 are of ordinary, rather readily abraded sandstone; others are of hard arkosic sandstone. However, because many of the sandstone artifacts in the site are largely decomposed, it is possible that some made of this ephemeral material have been lost. Most of the manos are

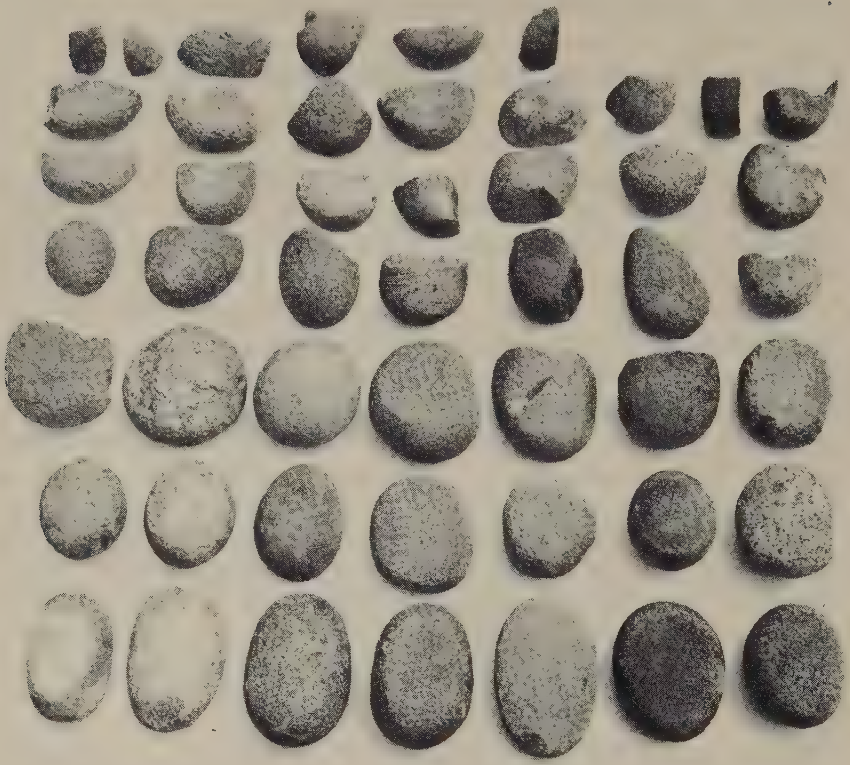

FIGURE 13. Representative manos and mano fragments from the main burial region (S.E.A. lots 16 and 17), Scripps Estates Site.

composed of various types of volcanic rocks, but pieces of a granitic nature are included. Among the volcanic rocks, fine- and coarse-grained rhyolites are particularly abundant.

The sandstone manos tend to be ground flatter and to be more sharply shouldered than the others. Those of the finest grained and hardest volcanics tend to have the abraded surface well polished and rounded. The rounded abraded surfaces of the two opposite sides occasionally meet along one or even both edges. A few specimens have one or, very rarely, both abraded surfaces ridged, so that they approach a trifacial or quadrifacial aspect. A few show grinding on one or more edges, in addition to the two flatter surfaces.

Many of the manos have one grinding face, and sometimes two, that exhibit purposeful roughening or pecking, which apparently made them more effective for food-grinding uses after having been worn too smooth. A few seem to have been pecked on the edges or ends, but there is little evidence of definitive shaping.

Most of the 159 particularly studied manos were heavily abraded: only 25 are listed as slightly ground, 33 as ground to a medium degree. The great majority are bifacially ground: only 22 are listed as unifacial, and 19 as well-ground on one face but only lightly ground on the other side. With very few exceptions these unifacial and intermediate manos have some fracture, concavity, flaking, or other irregularity on the unground or weakly ground side. Such irregularities presumably discouraged use of that side. The norm obviously was a bifacially ground, more or less oval, volcanic cobble.

In size, measured to the nearest millimeter but tabulated to the nearest 0.5 cm., the 159 specially studied manos grade in length from 6.5 to 18.5 cm. (of 105 measurements, 91 range between 8.5 and 14.0 cm.); in width from 6.5 to 13.5 cm. (120 of 122 measurements range between 7.0 and 11.0 cm.); and in thickness, from 2.5 to 7.0 cm. (with the great majority thicker than 3.5 cm.). Computed to the nearest 5 per cent, the width in 97 specimens varies from 70 to 100 per cent of the length and, in more than nine tenths of the manos, from 70 to 90 per cent; the thickness in 104 specimens varies from 25 to 70 per cent of the length, and in more than nine tenths of the manos, from 35 to 65 per cent.

An analysis of the detailed measurements (FIGURE 14) shows that the general form of the mano is to a large degree a function of its length: the shorter the mano, the more nearly rounded; the longer the mano, the narrower and thinner. Of the manos measured, nearly all

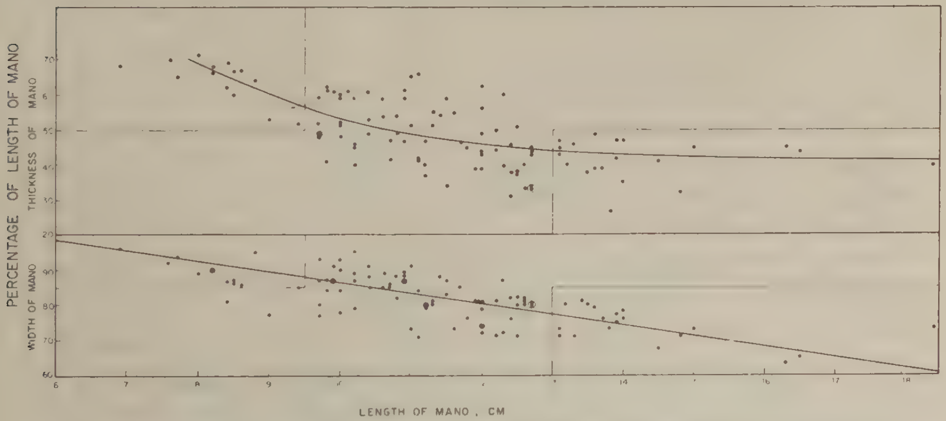

FIGURE 14. Relation of proportional width and proportional thickness to length among manos from Scripps Estates Site.

shorter than 9.5 cm. have a width:length ratio between 0.85 and 0.98, whereas all those longer than 13.0 cm. have a width:length ratio between 0.63 and 0.80; all shorter than 9.5 cm. are more than one half as thick as long, whereas all longer than 13.0 cm. are less than one half as thick as long.

The length, width, and thickness relationships suggest that bulk and mass were factors in the selection of cobbles for manos. Hand grip was presumably the controlling factor, because the longer the mano, the narrower it would need be proportionally to be held securely. A mano of small length would need sufficient width and thickness to be held readily and to have sufficient mass.

In general, the smaller the mano, the less well abraded are its faces. Nearly one tenth of the manos show evidence on one or both ends of having been used for pounding. Such use of a single tool for two purposes seems to have been rather common in the simple cultures along the California coast.

Because many of the characteristics of the manos, including the curvature, ridging, and polish of the grinding surface, appear to be a function of the kind of rock specimen used, because their general shape is largely a function of the size of the original cobble, and because the unifacial grinding of a minority of the manos seems to have been generally determined by irregularities on one face, it is concluded that the varied forms of manos utilized over the long period of occupation represent a single as well as a relatively simple cultural tradition.

Metates. Metates or milling stones are, oddly, much less common in the Scripps Estates Site than are the manos. One might expect the reverse, for the metates, generally made of the Eocene sandstone country-rock, presumably wore through rather rapidly or broke, so that rims or rim pieces should have accumulated along with the harder manos in roughly the same numbers. Yet manos now greatly outnumber the metates. In the collection from and near lot 24 there are more than 300 manos (largely whole) and only about 60 metates (largely represented by fragments). Typical metate fragments from the vicinity of lot 16 are illustrated in FIGURE 15.

Mention already has been made of two metates found, respectively, over burials 1 and 15. Other metates have been found in place over burials at the nearby site UCLJ-M1 by Moriarty. The sandstone metate over burial 1 of the Scripps Estates Site (Moriarty *et al.*, 1959) measured 459 × 356 × 115 mm. It was a well-used metate and presumably worn out; where it had been worn thin at the bottom of the bowl, concentric cracks have appeared. The sandstone metate over burial 15 (FIGURE 10) measured 56 × 36 × 15 cm., and it too probably had lasted out its usefulness before being placed in the burial. The minimum thickness at the center of the bowl was about 1 cm.

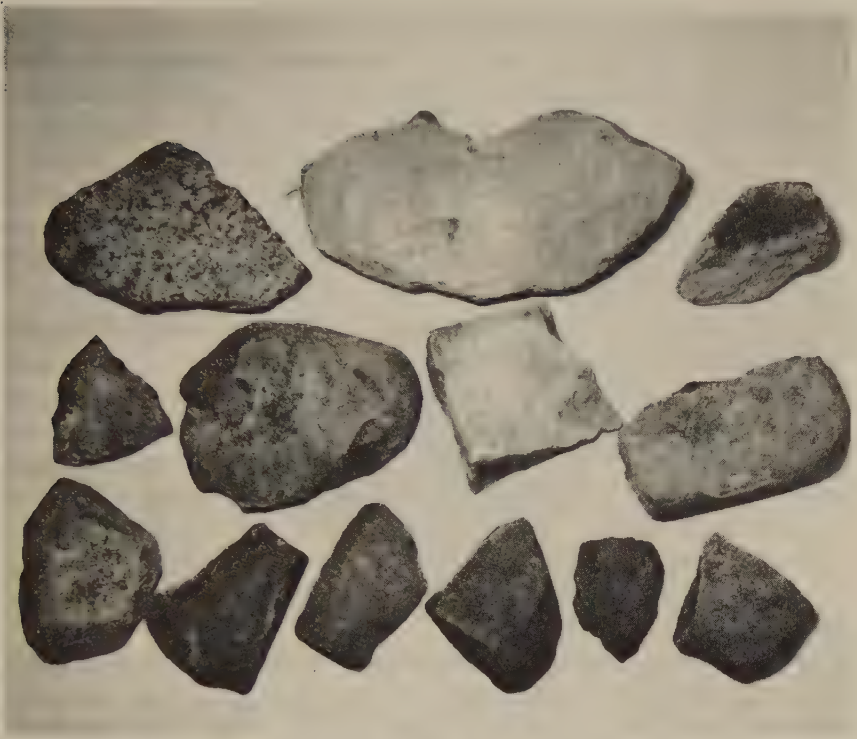

FIGURE 15. Metate fragments found in the main burial region (S.E.A. lots 16 and 17), Scripps Estates Site; piece in upper left is a granitic rock, all others are sandstone.

Warren recognized from his findings (Moriarty *et al.*, 1959) three variations of basin metates: (*A*) a slab unshaped except by use; (*B*) a shaped rounded exterior and a rounded lip; (*C*) a shaped exterior and an abrupt break around the edge of the upper surface giving it a sharper lip than variation B. Among the approximately 60 metate and metate pieces in the Hubbs collection are all variations from a thin, flat, scarcely cupped slab to deep basins. More than one half were shaped on the lower and outer surface, as well as in the bowl, by pecking or grinding. The sharpness of the lip varies, so that variants B and C grade together.

Very few metates from the Scripps Estates Site are complete and intact. The whole metates and the fragments show varying degrees of weathering. Many pieces of sandstone dug from S.E.A. lots 16, 17, and 24 are barely recognizable as weathered metate fragments. Probably a much higher proportion of the metates than of the manos have been lost through weathering. Nearly all of the metates and metate fragments are of sandstone, but one piece from lot 24 and one from lot 16 is granitic. The granitic fragment from lot 24 is flat-bottomed (apparently by natural fracture), has sides shaped by natural or artificial fracture, has the bowl polished (with some pecking medially), and has the remaining portion of the lip grading—through 11 cm.—between the forms rated as variants B and C; the maximum dimension of the piece is 25 cm., the thickness at the lip 10.5 cm. The granitic fragment from lot 16 (FIGURE 15) also has a maximum dimension of 25 cm.; the bowl surface is only slightly dished, and is well polished with some pecking.

The exterior shape of the metates, in plan, grades from rectangular to oval. One of the few that is intact is heavy and square with rounded corners; it is almost flat above, exclusive of the bowl; its sides were shaped by pecking to curve into the flat bottom; its maximum dimensions are 33 × 32 × 8 cm. Another is roughly rectangular with an almost perfectly flat bottom; it has been worn through at the bottom of the bowl; it is 45.5 cm. long and 10 cm. in maximum height at one end. A third specimen, still intact although riven with cracks, is roughly triangular in plan and has a maximum dimension of 19.5 cm. It was obtained from the lower part of the midden.

Mortars. Among the many hundreds of worked rock pieces found in the Scripps Estates Site only three are mortars, and all of these are broken remnants about half the original size (FIGURE 16). A few additional small edge pieces that we have classed as metate fragments might have been derived from flat mortars. A few mortars are reported to have been found by others on or near the site. The ones described here are from the collection made on and about S.E.A. lot 24. Two of these in particular are quite unlike the great majority of bowls that occur locally in abundance on the sea bottom off the La Jolla Shores region and elsewhere (Tuthill and Allanson, 1955) and, to this extent, suggest that the submarine artifacts have not been derived, either directly or indirectly, from La Jolla sites.

Two of the specimens were made of medium-grained granites, one (*a*) yellowish and one (*b*) purplish. They are very shallow, with the pit depressed only 17 mm. in each. Specimen *a* has a secondary, off-center, shallow pit that seems to have been made in a renewed use of the bowl subsequent to the breakage. The remaining part measures 154 × 84 × 59 mm. in *a* and 141 × 66 × 58 mm. in *b*, with minimum (central) and maximum (peripheral) widths of the broken edges respectively 42 to 49 and 43 to 47 mm. In each, the bottom, sides, and lip had been nicely rounded by pecking and grinding, and the edge of the depression is rather even and sharp.

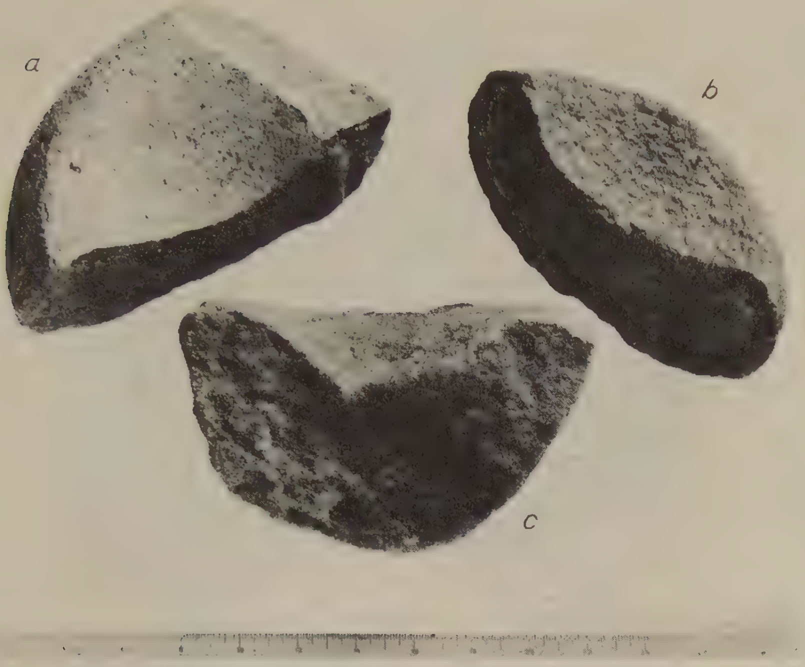

FIGURE 16. The three mortars from Scripps Estates Site.

The third mortar (c) is distinctly different from the other two. It was made from fine-grained arkosic sandstone, with the pit depressed about 23 mm. Present dimensions are 144 mm. long, 94 mm. wide, and 80 mm. thick, with the width of the broken edge 59 mm. centrally, and regularly decreasing peripherally. The angular lower-outer face has been irregularly and angularly shaped by percussion and pecking, and the bowl has been pecked.

Stone pestle. Only a single pestle has been recovered from the site (from the S.E.A. lot 24 accumulation). It was made from a small elongate-oval cobble of fine-grained granite. The oval cross-section measures 59 × 48 mm., the length 71 mm.; both ends are rounded-truncate as a result of grinding (FIGURE 17). The evidence is fresh and distinct. Either end fits nicely into the secondary pit in one of the bowls (specimen *a*, FIGURE 16, described above). The flatter surfaces show evidence, by their polish and grooves, that the artifact may also have served as a mano. Similar specimens have been found by one of us (J.R.M.) in other La Jolla sites.

Hammerstones. Cobbles or pieces of cobble well-battered at one or both ends, or around a partial or complete circumference, are plentiful

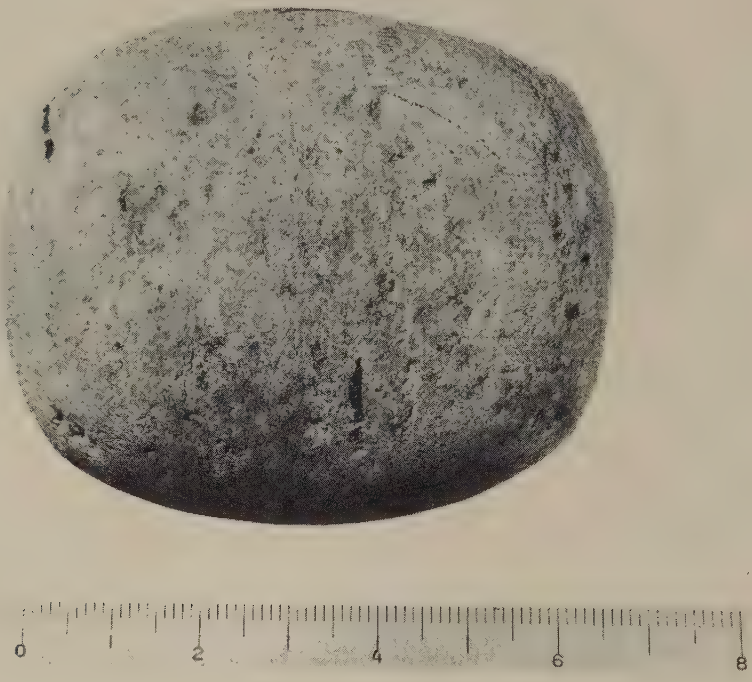

FIGURE 17. Double-ended pestle from Scripps Estates Site.

in the site. The nature of the battering with relation to the remainder of the rock is such that natural processes cannot be called upon for an explanation but rather indicates that these pieces were purposely used by the site occupants.

In some of the more definitive types of hammerstones the cobble has been flaked to form an acute to obtuse angle around the piece, either above a flat base or around the entire circumference, with partial secondary edges in some specimens. One such specimen, example 1 (FIGURES 18*a* and *b*), of deep bluish and olive porphyritic rhyolite, has a flat fractured base and a well-battered semicircular edge; it measures 68 mm. long, 43 mm. wide, and 54 mm. high. One side retains part of the cortex of the original beach cobble. Example 2 (FIGURES 18c and *d*) was made from a cobble of fine-grained greenish felsite, with one edge very extensively battered and the opposite edge flaked, in part bifacially but largely unifacially, into a chopping tool. This may be interpreted as an example of a multipurpose tool. As noted in other descriptions, various other tools also were used as, or were converted into, hammerstones, sometimes after having been broken. Examples are noted among manos, scrapers, choppers, and one probable gamestone. The pitted rocks probably also were used as pounding tools, but pre-

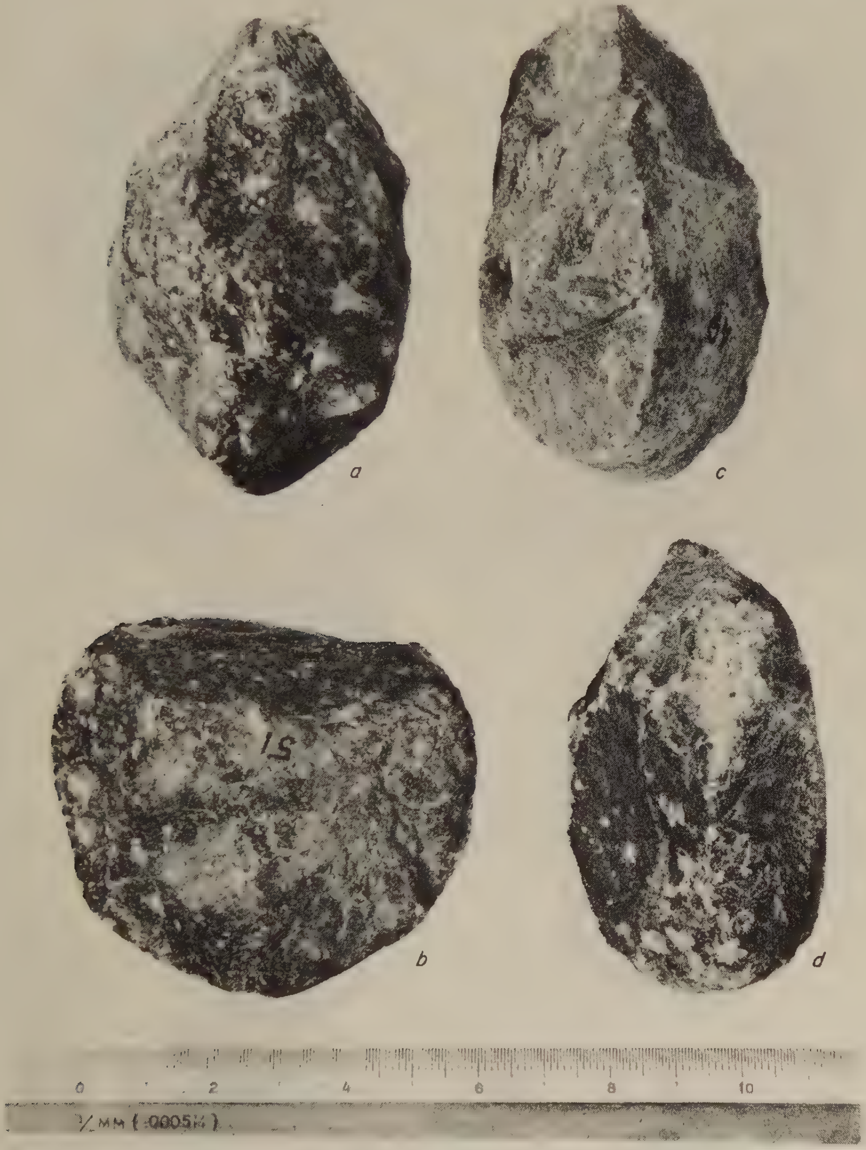

FIGURE 18. *(a)* Battered edge and *(b)* water-worn cobble cortex of one side of a hammerstone (example 1); *(c)* flaked edge and *(d)* battered edge of an artifact serving both as chopper and hammerstone (example 2).

sumably were not accorded such hard usage as the hammerstones. Example 3 (FIGURES 19*a* and *b*), of deep bluish-black quartzite branded with tan, has the complete circumferential edge battered, and several partial

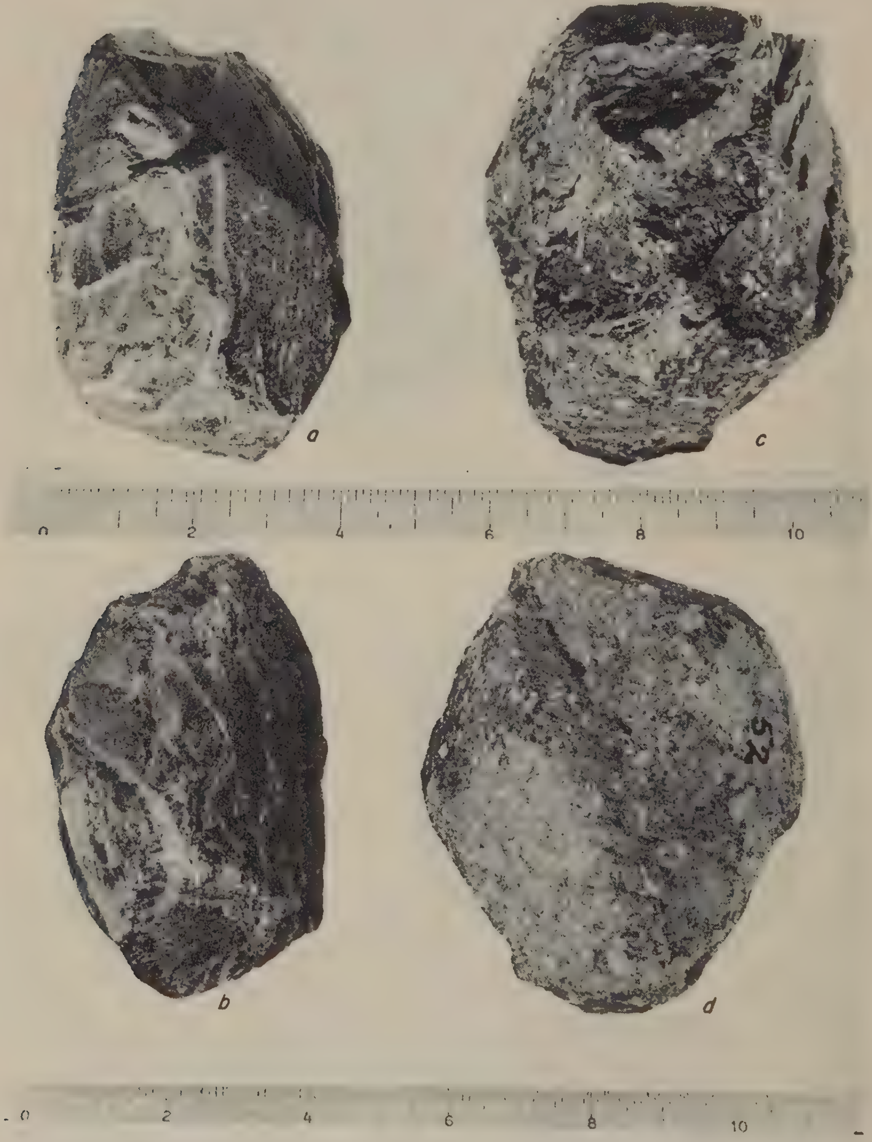

FIGURE 19. (*a* and *b*) The two edges, both battered, of a hammerstone (example 3), (*c* and *d*) battered edge and residual beach-cobble cortex of hammerstone (example 4).

edges also battered. It retains a few remnants of the cobble cortex, and measures 71 × 63 × 41 mm. Example 4 (FIGURES 19*c* and *d*) was made from a dark porphyritic rhyolite cobble. It retains, as its rounded base, a chatter-marked cortex. Most of the battering is at the opposite, bluntly pointed end, but there has been some pounding along various edges. Its dimensions are 71 × 66 × 53 mm.

A very different type, the fifth example (FIGURES 20*a* and *b*), was fabricated from a marginal flake rather than made from the main part of a cobble. It may be described as a planoconvex flake hammerstone. It is battered around more than one half the edge. The rock is a deep purplish, slightly porphyritic acid volcanic, and measures 64 × 56 × 22 mm. Other similar specimens were obtained.

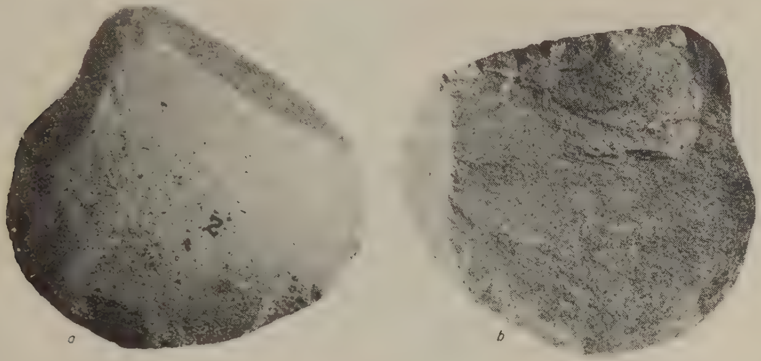

FIGURE 20. *(a)* Cortical and *(b)* fractured faces of planoconvex flake hammerstone (example 5).

Other hammerstones from the site were illustrated and described in the preliminary report (Moriarty *et al.*, 1959). Warren named three types of hammerstones from the burial area: "*Pebble hammerstones*" (usually flat ovoid pebbles battered on the edges); "*core hammerstones*" (regarded as multifacial cores subsequently used for pounding); and "*pestle-like hammerstones*" (elongate cobbles with an end, or both ends, battered). These and other types, along with intergrades, occur in our collections. As with manos, the form of the hammerstone often seems to be more a function of the size, shape, and kind of cobble that was used, than a different tradition.

Many of the core hammerstones seem to have been fractured only by use in pounding, or to have been prepared for pounding along an edge where two planes intersected, rather than being old cores put to a new use, although some do seem to fit the latter interpretation. Various shapes of hard cobbles were utilized for hammerstones. Generally only a portion of the hammerstone has a battered nature, and the opposite side is smooth and rounded for comfortable holding.

Pitted stones. Three bifacially pitted rocks found on S.E.A. lots 24 and 25 are, apparently, the only examples of this problematical type of artifact from the site (FIGURES 21*a* to *c*). All were fabricated from cobbles of fine-grained arkosic sandstone; all had been broken transversely before, during, or after fabrication to leave one original half edge. Two (*a* and *c*) show signs of battering at the end of this edge, and it seems rather probable that these half cobbles were used as tools for grinding and for gentle pounding; for these purposes the shallow pits would have served effectively as thumb-and-finger holds. The third pitted stone (*b*) is quite different. Its intact edge has been pecked into the shape of a small rounded mortar; the rather deep pit on the bottom is off-center and is in contact with the broken edge; the incipient pit on the opposite side is fresher. There is some sign of battering on the lip edge. It is thought that possibly this artifact was started as a mortar, then broke, and was fabricated into a pitted stone. The dimensions of this complex artifact are 104 × 87 × 65 mm. The other two measure 123 × 83 × 56 mm., and 81 × 101 × 53 mm.

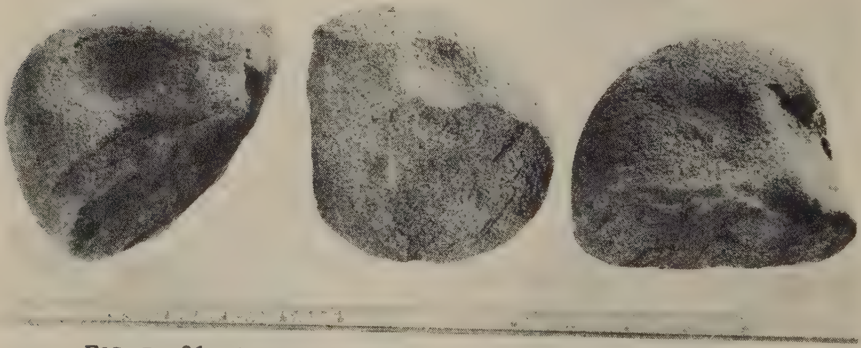

FIGURE 21. Pitted sandstone artifacts from Scripps Estates Site.

Doughnut stones. The extensive collecting at the site has yielded only three doughnut stones, each of which is a broken half of the original specimen. One, a beautiful steatite specimen measuring 48 mm. in diameter and 35 mm. high, was found in association with burial 9; it was illustrated and described by Warren (Moriarty *et al.*, 1959). Another specimen, somewhat smaller (35 mm. in diameter, 23 mm. high) and very symmetrically made and polished, was found on the surface; it was made from a light-colored, finely crystalline, igneous rock. Warren illustrated and discussed it also. Both have completed, biconical central holes, retaining circular grooves from the drilling process. Warren indicated that. . .“due to the small size of these doughnut stones the usual interpretation as digging stick weights does not appear to be valid in this instance. Interpretation as ornaments, possibly large beads, seems more reasonable.”

A third specimen (FIGURES 22*a* and *b*), found on the surface of S.E.A. lot 21, is interpreted as a doughnut stone that broke in half through the

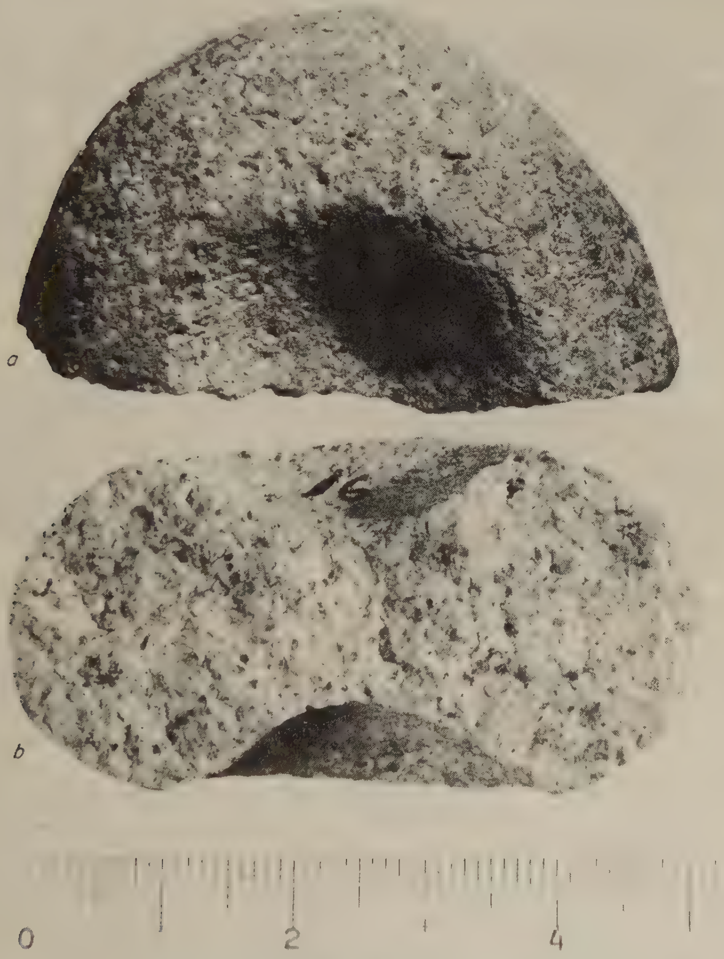

FIGURE 22. A possible uncompleted, broken, doughnut stone from Scripps Estates Site in *(a)* plan and *(b)* broken-edge views.

uncompleted hole during fabrication. It also is small (53 mm. in diameter and 25 mm. in height). It is a hard, fine-grained volcanic rock with conspicuous phenocrysts of quartz and feldspar. The pits appear to have been ground by a hard blunt point, which left no circumferential grooving such as appears on the two other specimens. In cross-section the artifact is everywhere approximately semicircular beyond the limits of the uncompleted hole. In plan, the piece is approximately semicricular.

Perforated slabs. Two problematical artifacts in this category have been found in the site. Warren (Moriarty *et al.*, 1959) briefly described and figured a perforated sandstone fragment that "is irregular in outline, roughly rectangular in cross section, and has a single conical hole drilled through the center." He suggested that "it may represent a fragment of a large ornament." Its dimensions were given as 63 × 42 × 18 mm.

A larger perforated object (FIGURE 23) found on S.E.A. lot 24, is 204 mm. long, 71 mm. from the hole to the remaining edge and 95 and 98 mm. from the hole to the respective ends; the greatest thickness along the longitudinally and transversely broken face, near the hole, is 30 mm. The hole, which appears to have been circular originally, is about 50 mm. in diameter on the entire, outer face and 33 mm. wide on the broken face. In cross-section the intact face is evenly curved, probably as the result of shaping the gently curved edge. The hole obviously was formed by grinding. The material is a coarse-grained arkosic sandstone.

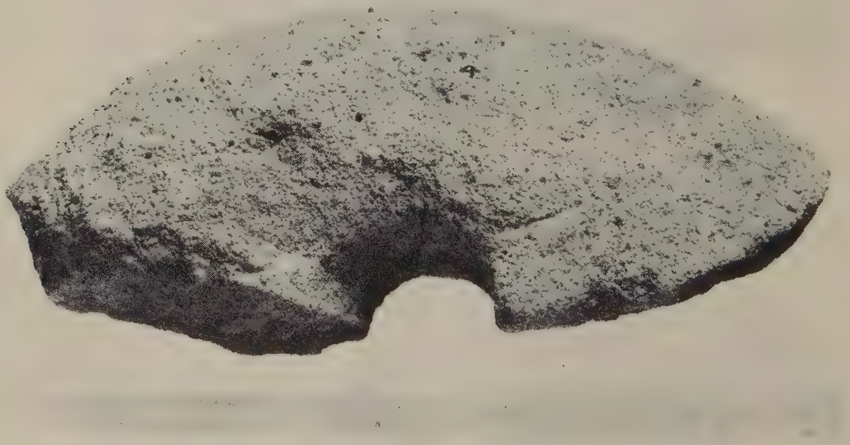

FIGURE 23. Large perforated sandstone slab from Scripps Estates Site.

It is suggested that one or both of these objects might have been used as weights on digging sticks.

Conical reamer (?). A blunt but regularly conical tool of greenish, medium-grained quartz diorite (FIGURE 24) was found in the vicinity of S.E.A. lot 24. No similar object has been found elsewhere on the site. It is 70 mm. long from the apparent transverse break to the end; at the break the almost perfectly circular cross-sectional diameter is 25 mm. The surface of the cone shows evidence of grinding. It is speculated that it possibly was used as a reamer for starting or making holes such as were found in the perforated slabs or in the artifact interpreted as an uncompleted doughnut stone.

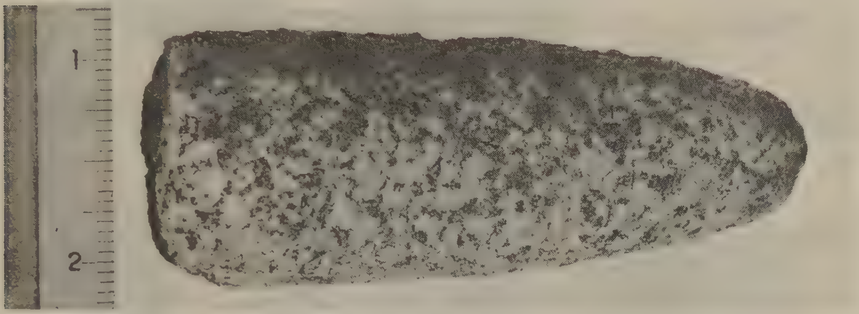

FIGURE 24. Conical reamer(?) of quartz-diorite from Scripps Estates Site.

Gamestones (?). Several artifacts found in the site appear to have had no specific utilitarian purpose and seem interpretable as possible gamestones. The most convincing are two highly polished discoidals (FIGURES 25*a* and *b*), which can be rolled on edge for 10 m. with barely perceptible deviation.

The larger discoidal, found on the surface about 30 m. south of S.E.A. lot 24, was fabricated from a cobble of fine-grained, compact, purplish quartzite. Its diameter varies less than 0.5 mm. from 93.5 mm.; the maximum thickness of 54 mm. decreases to 50 ± 1 mm. halfway to the rounded-truncate outer edge. Numerous fine grooves (circumferential around the edge) and high polish give evidence of much rubbing.

The smaller discoidal was found, with caliche coating, buried in S.E.A. lot 24. It was made from a flat, rounded cobble of very fine-grained, vari-colored granite. Its diameter varies from 73 to 75 mm. between the edges, which—around the complete circumference over a width of approximately 1 cm.—has been thoroughly pecked or ground, presumably to increase the roundness. The thickness is 23 mm. and the sides, which show evidence of much polishing and rubbing, are very gently and evenly curved.

A third artifact may represent the broken half of another discoidal

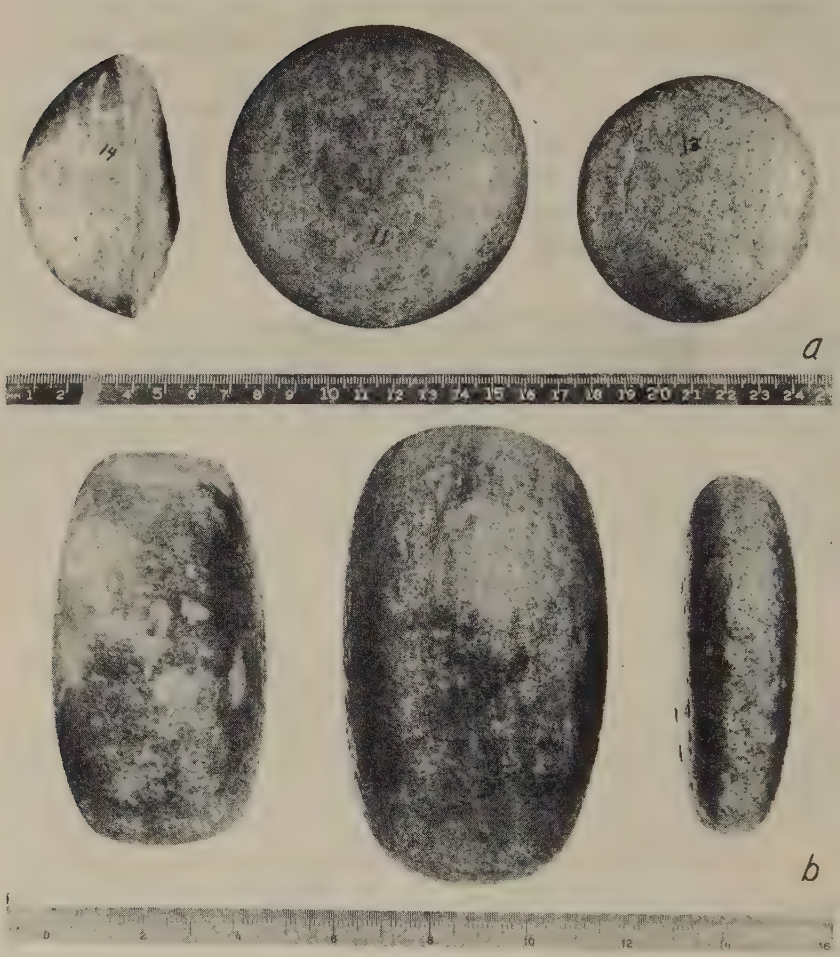

FIGURE 25. Discoidal gamestones from Scripps Estates Site in *(a)* plan and *(b)* profile.

gamestone, or possibly an excessively smooth and polished mano. Its remaining outline approximately coincides with that of the quartzite discoidal. It is made of very compact and fine-grained whitish granite-aplite. It is 81 mm. in diameter (not quite complete?) and it is 45 mm. thick. The cross-section, like that of the quartzite specimen, is rounded-rectangular, and the distance between the outer corners is 31 mm. Extensive evidence of battering at one end indicates that the broken artifact was used as a hammerstone.

Certain sandstone balls of high sphericity already have been mentioned as having been found in preliminary collecting on the site and as possibly having been gamestones of another type. Another such sphere, of quartzitic sandstone (FIGURE 26), was found recently on the surface of S.E.A. lot 25 (near where the others were found). It measures 75 mm. in shortest diameter and 79 to 81 mm. where the circumference is greatest (the ones found earlier were roughly of this size; the estimate of 10 to 15 cm. given in the preliminary report was too high). The surface shows suggestion of pecking and grinding.

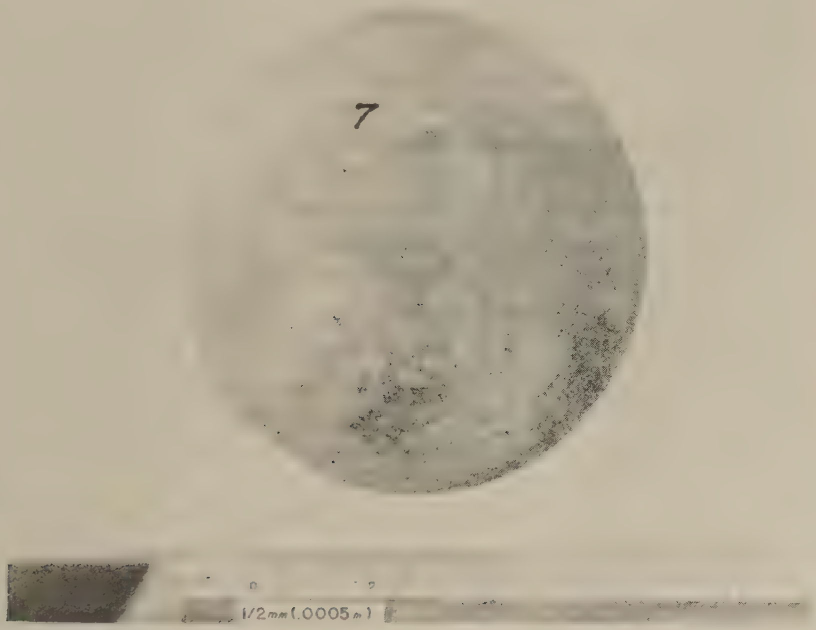

FIGURE 26. Spherical sandstone artifact—possibly a gamestone—from Scripps Estates Site.

Flaked hand tools. A bewildering array of core and flake implements has been collected from the Scripps Estates Site. Although the better specimens seem to be classifiable into a few categories suitable for description, their intergradation between types and their range from definitely flaked artifacts to irregularly broken pieces of rock seems to defy complete sorting into useful tools and discards, or into definitive nameable types. In the preliminary report (Moriarty *et al.*, 1959) Warren attempted a complete breakdown of 158 specimens. Among these he distinguished 15 types, with two variants for each of three types, and left only three "miscellaneous scrapers" that did not fit any of the types.

The flaked hand tools from this site, like those from many other similar sites along the coasts of the Californias, are not readily classifiable into the conventional paleolithic categories of pebble tools, core tools, and flake tools.

One of the more distinguishable categories into which some specimens can be placed is that of a whole, naturally rounded, flattened, unsplit cobble, or large pebble, percussively flaked at one end or side (FIGURE 27, specimens *n, o,* and *p).* The proportion of corticular to flaked surface in this category varies greatly and no doubt decreased as the tools were reflaked. Some (such as *o* and *p*) are unifacially flaked; others, such as specimen *n*, bifacially. The extreme case is a specimen in which almost the entire edge had been flaked, so that only a small section of cortex remains near the center of each side.

A second category of flaked tools, with more numerous specimens, was made from an originally rounded cobble or large pebble that had been longitudinally split or broken. If the split divided the cobble into two thick pieces, each (when reworked) would appear as a core tool. If the split was marginal or if the cobble originally was thin, the tool might be considered as a flake. The flakelike and corelike types completely intergrade. The amount of cortex on the split-cobble tools varies from a full one half of the total surface to a bare trace or, not infrequently, to none at all (in which case it cannot be ascertained that the piece was a split, rounded rock initially; however, the local abundant supply of rounded cobbles and the almost complete absence of local bedrock sources leave little doubt in most cases). Two specimens that are complexly and irregularly flaked all around, with very little cortex retained, are illustrated in FIGURES 27*a* and c.

The split-cobble tools usually were flaked with the fractured face as the striking platform, although occasionally a relatively flat cortex face served as the striking platform. One specimen *(x* in FIGURE 27) was flaked along the broad end from the fractured face but around the rest of the periphery from the cortical face. Commonly found are pieces in which the face opposite the original fracture is complexly flaked over all, or nearly all, of the surface, both coarse and fine flakes having been removed (FIGURES 27c to *k* and *w, y,* and *z).* Variations in the amount of cortex remaining, from most of the face to nothing, are illustrated in FIGURES 27*r* to *z.* Specimens *r* to *u* illustrate the rectangular type of split-cobble tool that is unifacially flaked by coarse percussion at both ends and along both sides; this type constitutes a definite minor mode in the variable complex. The fractured face of these often shows conchoidal fracture or may be irregularly fractured with two or more slopes.

The flaking varies from slight marginal retouching in teshoa flakes to coarse or fine chipping. These tools commonly are termed "scraper planes."

Some of the thicker split-cobble pieces have the flakes removed at high angles, occasionally approaching 90°. The extent of the high-angle flake-scars varies from all to not more than one half the periphery of the fractured face; the base varies from circular to subtriangular, subquadrate, or diamond-shaped; some have a flat or oblique top (cortex or flake scar); others have been so flaked as to form a lengthwise ridge over the whole top, or over only part of the top. Some variations of of these "pulping planes" (as they have been called) are shown in FIGURES 27*j* to *m*. Warren (Moriarty *et al.*, 1959), who had two specimens of this type, called them "platform cores."

The most sophisticated "scraper" from the S.E.A. lot 24 collection (FIGURES 27*h* and 28*b)* is finely chipped, especially around the steep-angled periphery. It would appear to have been finely pressure-flaked, but a similar yet larger example (FIGURES 27*i* and 28*a)* that is coarser and less domed, gives the impression of having been made by fine percussion flaking; hence possibly the more refined specimen was made by still finer percussion flaking. Warren (Moriarty *et al.*, 1959) listed three of these "small domed scrapers" and figured two of them; he wrote that "they are steeply flaked with well-controlled percussion and pressure flaking around ¾ of the periphery." Those illustrated here are flaked all around, more steeply at one end than at the other. Additional tools of this type, variously refined, were found within the main burial area.

A few of the tools are longitudinally flaked, apparently produced by the anvil technique. Four examples illustrated here (FIGURES 27*bb* to *ee)* grade from a type often called "blades" or "knives" to the type represented by what Warren called a "pick." Specimen *bb* is irregularly triangular in cross-section at the butt, with a longitudinal flake eliminating the apical two thirds of the primary ridge; its rounded end shows effects of battering. A second example *(cc)* is larger and flatter. A third specimen *(dd)* has a trace of cortex at one end and a thin flake scar along most of the ridge; the oppostie end shows effects of use. A fourth specimen *(ee)* seems somewhat intermediate between a "scraper" and a "blade."

One peculiar slate specimen (FIGURE 27*aa)* is problematical. It is coarsely flaked and has two nearly parallel edges, of which the one 30 mm. long shows signs of extensive grinding, whereas the sinuous edge 70 mm. long remains sharp.

The specimens that are illustrated here (FIGURE 27) were selected

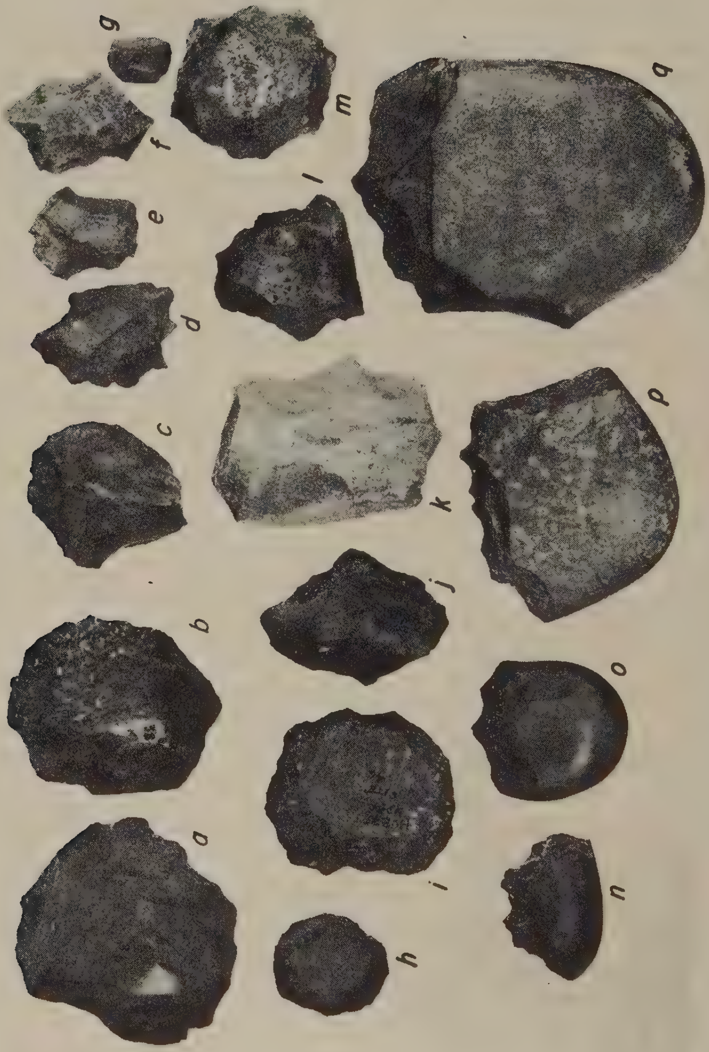
a
b
c
d
e
f
g
h
i
j
k
l
m
n
o
p
q

(1142)

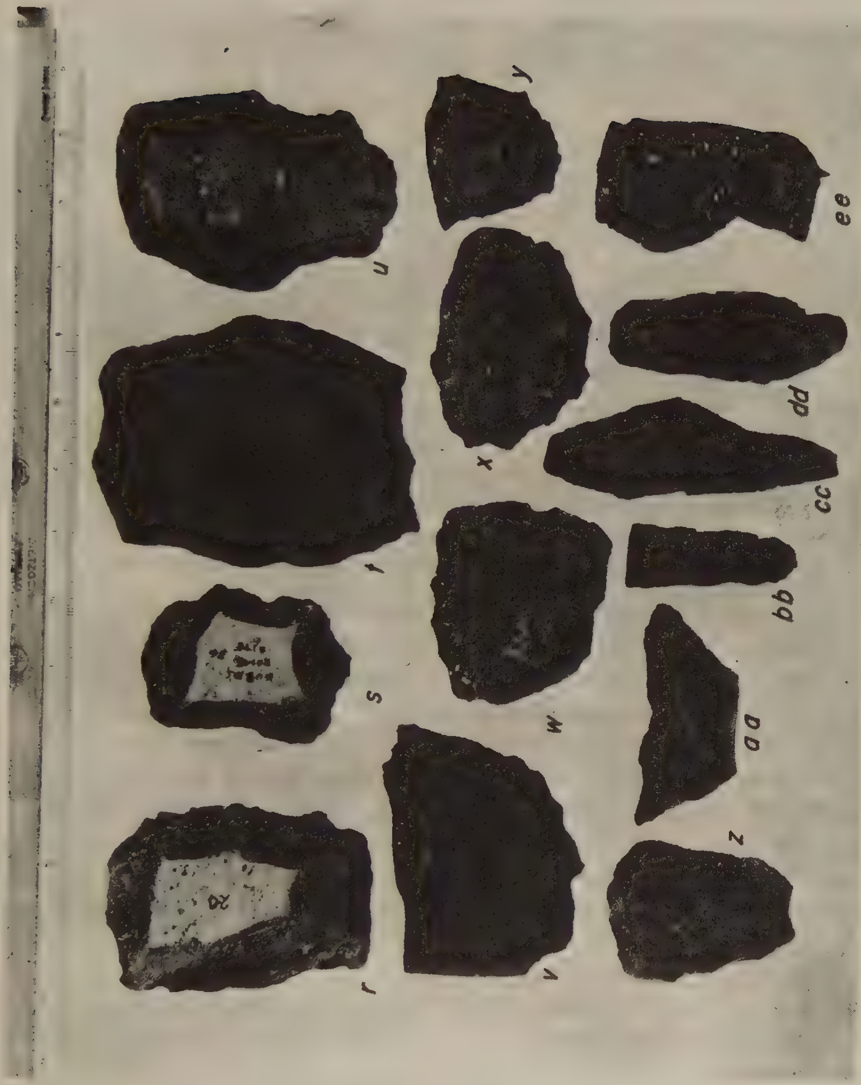
r
s
t
u
v
w
x
y
z
aa
bb
cc
dd
ee

FIGURE 27. A selection of flaked hand tools from Scripps Estates Site (described in text and in TABLE 2).

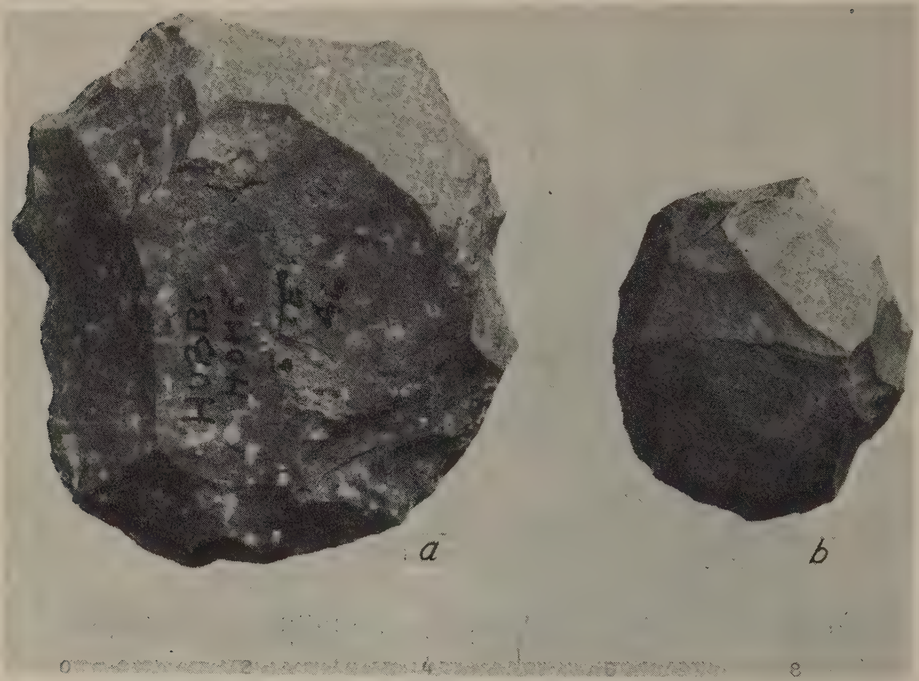

FIGURE 28. Domed scrapers, among the most sophisticated of the artifacts from Scripps Estates Site. The same specimens are shown in FIGURE 27*h* and *i*.

from an assemblage of several hundred pieces taken at the surface and at various levels of S.E.A. lot 24 and the immediate vicinity; they are typical for the site as a whole. They were chosen to illustrate certain types, which are scarcely more than modes in a complexly intergrading system. The vast majority are less definitely shaped, and to classify them into many additional categories and subcategories would require more skill than we possess. Furthermore, intergradation occurs between "choppers" and hammerstones. Many of the obvious tools of the scraper-chopper complex show evidence of having been used to some extent as hammerstones. Details concerning the scraping, chopping, and cutting tools illustrated in FIGURE 27 are listed in TABLE 2.

Beads. Rather uniformly small shells of *Olivella*, obviously representing a complete necklace, were closely associated with burial 7. The apex of each shell was ground off to facilitate stringing. Eighty such beads were recovered (FIGURE 29) and it is estimated that about 10 more probably remain in the ground, for this burial has not been completely excavated. In addition to the *Olivella* beads, a central pendant bead (FIGURE 29) was found during the excavation of burial 7, but its original location with respect to the burial cannot be given, as it was found in loosened earth. The pendant bead is a disc about 3 cm. in diameter and 1 cm. thick, probably made from the thick part of the shell of *Tivela stultorum*, the pismo clam. The bead has a central hole countersunk on each side. Similar but thicker beads were found during the earlier exploration of the site.

A few additional *Olivella* beads were found with burials 8 and 13, and a few more have been found unassociated with burials, on and about S.E.A. lot 24.

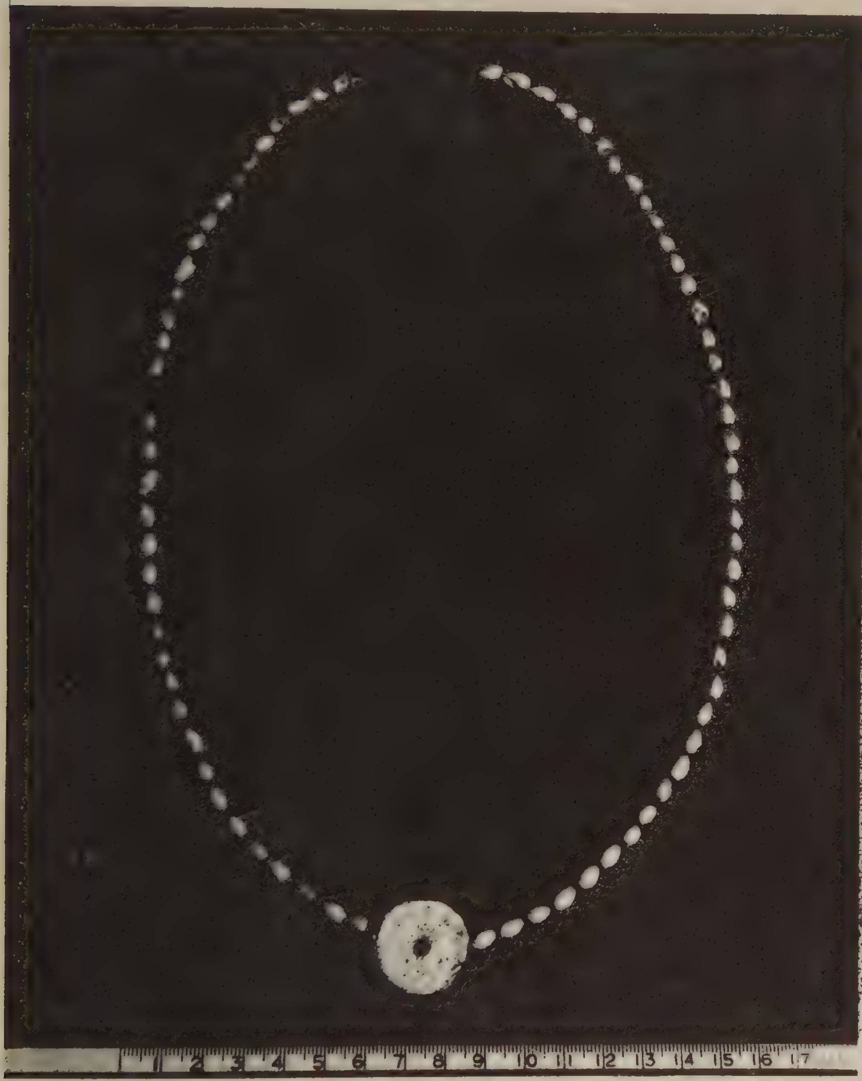

FIGURE 29. Reconstruction of *Olivella* shell-bead necklace found in burial 7.

TABLE 2

DATA ON SELECTED FLAKED HAND TOOLS SHOWN IN FIGURE 27*

Figure and specimen	Kind of rock	Ground color	Extent of cortex†	Length (mm.)	Width (mm.)	Thickness (mm.)
Figure 27						
a	Rhyolite	Slate	0+	77	76	45
b	Porphyritic rhyolite	Greenish-slate	<1	69	61	44
c	Rhyolite	Slaty-green	2	54	46	35
d	Felsite	Slaty-green	6	48	34	20
e	Rhyolite	Greenish-gray	<1	37	31	13
f	Quartzite	Whitish with rusty stain	<1	50	33	13
g	Rhyolite	Slaty-green	0	21	16	4
h	Microcrystalline rhyolite	Greenish-slate	0	37	33	20
i	Porphyritic rhyolite	Olive-slate	0	61	56	25
j	Rhyolite	Brownish-slate	0	61	47	40
k	Quartzite	Whitish with buffish stains	1	77	53	38
l	Porphyritic rhyolite	Reddish	3	47	43	25
m	Porphyritic rhyolite	Purplish-gray	1	57	50	37
n	Rhyolite	Greenish-slate	4	49	32	30
o	Felsite	Greenish-slate	8	50	46	21
p	Porphyritic rhyolite	Tan-gray	8	85	71	31
q	Rhyolite	Bluish-slate	5	112	85	36
r	Fine-grained cherty volcanic	Olive-gray, with rusty streaks	1	78	55	33
s	Porphyritic rhyolite	Slate, with rusty stains	1+	62	45	21
t	Fine-grained volcanic (andesite?)	Gray	3	95	78	28
u	Quartzite	Reddish with irregular olive streaks	2.5	83	61	21

TABLE 2 (Continued)

Figure and specimen	Kind of rock	Ground color	Extent of cortex†	Length (mm.)	Width (mm.)	Thickness (mm.)
Figure 27 (cont'd.)						
v	Rhyolite	Slate	2	76	58	26
w	Porphyritic rhyolite	Olive-slate	1	62	54	17
x	Slightly porphyritic rhyolite	Light greenish-gray	3	68	49	18
y	Slightly porphyritic rhyolite	Greenish-slate	2	46	42	19
z	Felsite	Buff and olive	<1	57	43	18
aa	Quartzite	Purple	0	69	29	15
bb	Andesite or dacite	Slate	<1	52	20	10
cc	Slightly porphyritic, probably rhyolite	Olive-slate	0+	89	30	11
dd	Felsite	Slaty-brown	0+	71	28	18
ee	Porphyritic felsite	Olive-green	1	60	41	14

* Dimensions are measured on the longest line parallel with the stated axis.

† Amount of cortex is estimated in classes, 0 to 10, with 10 complete on both sides.

The *Olivella* shell beads are, by nature, thin and fragile. The fact that a few beads have been found in each of two other burials in addition to burial 7 and the decomposed nature of much of the midden shell at the site suggest that many beads have probably disintegrated.

Bone tools. Bone tools are extremely scarce among the artifacts of Scripps Estates Site, as they are in other similar sites of comparable age. Warren (Moriarty *et al.*, 1959) reported: "Three fragmentary pieces of worked bone were recovered. A flat rectangular splinter has a partially ground edge and probably represents a piece of bone detritus removed from a larger piece by grooving and breaking. The second piece is a flat, ground, object, in fragmentary condition, with two ground faces and a rounded edge. The third piece is a tip fragment of a pointed object, possible a projectile point or fish gorge."

In a major soil-screening project conducted subsequent to the initial report and described in a later section of this report, a "tip fragment of a pointed object" almost identical in size and shape to the third piece described by Warren was found. Its length is 25 mm. In the extensive collecting on S.E.A. lot 24 not a single bone tool has been found.

Bone tools apparently are scarce, but whether truly scarce, as are many types of artifacts, or only apparently so by reason of decay, is not now certain. It seems probable that a considerable amount of bone originally in the midden has been destroyed by weathering, to judge from the condition of skeletal material.

Projectile points. A few well executed, finely pressure-flaked projectile points have been found at the surface or at relatively shallow depth at the Scripps Estates Site. None has been found in the extensive digging there at sufficient depth and in such appropriate relationship to other artifacts and to soil horizons as confidently to be considered part of the artifact assemblage of the La Jolla culture. Five points have been found by one of us (J.R.M.) in the loose upper soil at the UCLJ-M1 Site, which well may be continuous with the Scripps Estates Site; but none were in undisturbed soil at significant depth to be included without question in the La Jolla culture. Warren (Moriarty *et al.*, 1959) illustrated the outlines of five projectile points, procured from the late B. E. McCown that had been found, according to McCown, in the upper levels of the excavations of the La Jolla site in Sorrento Valley (SDM-W316); here too, apparently, is the possibility (if not probability) of an intrusive origin. Some authorities (such as Meighan, 1959), however, present evidence indicating that projectile points may be included, although rarely, in the cultural complex that includes the La Jolla.

In the area of Scripps Estates Site, two small, finely-flaked points were picked up on the surface on S.E.A. lot 25. A well-made triangular tip of a chalcedony point measuring 37 mm. long and 23 mm. wide where broken was found on the surface of S.E.A. lot 18. All of these are considered to be of the Yuman (Diegueño) type. In the burial area on lot 17 Warren (Moriarty *et al.*, 1959) found a finely pressure-flaked quartz point 27 mm. long and 3 mm. thick. It was obtained in the loose upper soil, and Warren interpreted it as intrusive from a more recent culture. A second quartz point (FIGURE 30) is included in the very large assemblage of artifacts from lot 24 and vicinity. It was finely but irregularly chipped from translucent-white quartz; the remaining length of the tip is 31 mm.; the width (apparently complete) is 31 mm. and the thickness is 15 mm.

FIGURE 30. Quartz projectile point from Scripps Estates Site.

Fossil shark tooth. A fossilized shark tooth *(Isurus* sp.) 21 mm. long to the broken tip seems most appropriately treated among the artifacts, although it shows no signs of having been worked. Local conditions make it seem almost certain to us (and to Dean Milow of San Diego State College, San Diego, Calif., who is making an extensive study of the local Eocene) that the specimen had not been eroded out of the Eocene underlying the site and had not been deposited there by natural down-wash. It seems most probable that it was transported to the site, perhaps from the San Diego Pliocene, where it was exposed along the coast at Pacific Beach to the southward. This needlelike tooth may have served some utilitarian purpose or may have been a curiosity. The tooth was found about 10 cm. down in the upper soil horizon of excavation C-D.

Possible charm stones. Throughout the site are found numerous pebbles and small cobbles, usually ellipsoidal in shape and relatively thin, that seem to be more abundant, more regular in form, better polished, and more attractively colored than would be expected from a random assortment. Furthermore, the soil of the site does not naturally contain these pebbles, and their presence must be attributable to man. They do not seem to be pieces that would have been usable for tools. It seems probable that they were brought to the site for some purpose, possibly as charm stones, or for some ceremonial or esthetic reason. The lengths range from 14 to 91 mm. None seem to have been worked into pendants or other ornaments.

RADIOCARBON DATES

The antiquity of the site is established by four critical radiocarbon dates, run by the La Jolla Radiocarbon Laboratory of the Scripps Institution of Oceanography through the courtesy of Hans E. Suess, who has been assisted by George S. Bien and Paula Sandoval (Hubbs *et al.*, 1960). The material utilized for all four dates was sound shell of the California mussel, *Mytilus californianus*, a species that lives chiefly in the intertidal zone of the rocky foreshore. This point is of significance, because it is to be expected that the available carbon in this superficial habitat is very largely of recent atmospheric origin, with a C^{14} content approximately in equilibrium with that of the atmosphere. The validity of radiocarbon datings from the shell of this mussel has been verified by other tests run under the direction of Suess by the same acetylene method. One pair of tests for a Baja California coastal midden (W-26 and 27) yielded a calculation of 2540 ± 200 years for mussel shell and of 2500 ± 200 years for charcoal taken in close association. Another pair of datings (W-154 and 155), from a very narrow occupation streak on the cliff about one kilometer south of Scripps Estates, yielded calculations of 600 ± 200 years for mussel shell and of 580 ± 200 years for charcoal. A more recent pair of tests (LJ-84 and 85) from an occupation streak in Valle de Rosario, Baja California, gave a date of 1060 B.P. for mussel shell and of 960 years for charcoal (see also Hubbs *et al.*, 1960, p. 200). Although an inadequate quantity of charcoal has been recoverable from the Scripps Estates Site for age determination, it seems safe to assume that the datings obtained from mussel shell are approximately correct.

Mussel shell taken in the soil immediately about the skeleton of burial 7 and at a comparable level, in which a considerable amount of caliche had been deposited, yielded a date estimate of 6700 ± 150 years B.P. (LJ-79). The level seems to be comparable with that of the other burials in the lower portion of the soil but not at the lowest level.

An initial estimate of the range of dates for this site was obtained from tests on mussel shell from S.E.A. lot 24, approximately 100 m.

south of burial 7. Shell from the uppermost, or A, horizon has been dated at 5460 ± 100 years B.P. (LJ-110), and shell from the B_1 horizon (filled by and encased in caliche) at 7370 ± 100 years B.P. (LJ-109). Mussel shell from trench fl-M-3, on lot 16, largely from the B_1 horizons, has been dated at 5740±140 years B.P. (LJ-221).

Because shell and artifacts of rather consistent type occur throughout the soil horizons designated A, B_1, and B_2, and because the dates were obtained from composite shell samples presumably not representing the extreme times of the establishment and abandonment of the site, we may assume that the site was occupied continuously or nearly so for a period of more than 2 millenia, from roughly 7500 to about 5000 years ago.

Additional dates for more or less similar middens in San Diego County and elsewhere in southern California and in Baja California are listed later in this report in a discussion of the coastal occupation and cultures.

ANALYSIS OF FOOD REMAINS

A study of the food remains in the Scripps Estates Site has provided a basis for several inferences regarding the environment and culture as well as the food habits of the aboriginal population. We indicate in following sections how the food remains suggest that the La Jolla people lived during a period of rising sea level, when the shoreline was sufficiently rocky to produce an abundance of seafood, when the valley-mouth lagoons were deep enough and in sufficient contact with the sea to support a plentiful supply of bay molluscs, and when the sand beaches were probably poorly developed. The faunal relationships of the 56 species of pelecypod and gastropod molluscs found on the site indicate, on detailed analysis, that the temperatures were as warm as at present and very probably somewhat warmer; the remains of animals in other groups confirm this indication. The shells provided material for isotope analyses, which yielded not only radiocarbon estimates of the age of the habitation but also paleo-temperature measurements that confirm the deductions stated above.

The type of molluscs eaten, the abundance of tools for grinding plant food, and the great scarcity of vertebrate remains all indicate a simple food-gathering culture, with little or no hunting for larger animals, either on land or on the high sea. Some of the fish remains, as indicated below, suggest however that boats or rafts were used.

The shells and the few bones in the midden include the remains not only of organisms that were eaten, but also of various invertebrates that happened to settle on the shells of molluscs that were gathered for food; other shells may have been carried in for utilitarian purposes or as curiosities. Probably most if not all of the barnacles arrived incidentally on the shells of mussels, as did minute snails, small limpets (*Acmaea* spp.), and others. For many of the remains there is no way of ascertaining which were taken purposefully, which incidentally. For faunal analysis this differentiation hardly is significant.

The fragmentation and solution of many of the animal remains renders the computation of numbers of organisms eaten too uncertain to be very meaningful. The irregular strata of almost coquinalike, shell-rich caliche in the lower part of the shell-bearing level in one part of the site further confuse the issue. The relative masses of the shell and bone remains obviously provide only rough indices of the relative importance of the various foods used but at present seem to be the soundest parameter to measure.

Most of the food remains were obtained by hand picking, with an effort toward obtaining random sampling that, however, undoubtedly favored the collection of the larger pieces. The material analyzed in TABLE 3 was obtained by hand screening, as was most of the material listed in the second column of TABLE 4. The large sample listed in the first column of TABLE 4 was obtained from trench S-M-3 (FIGURE 4) in with the aid of a motor-driven shaker with a mesh size of about 6 mm. (square); in this sieving a volume of 8 m.^{3} of soil was used. The sieving in trench S-M-3 constitutes the only excavation carried on in that trench, for no burials were found there; the surface area of the trench S-M-3 was 20 m.^{2} Most of the shell samples from the various collections were cleaned in a very effective motor-driven, baffled cylinder developed by Jacquelin N. Miller.

The large shell sample from trench S-M-3 was handled by the aliquot method. The whole sample was washed clean, weighed, mixed well, and spread, so that a fraction could be selected at random (in this case, about one eighth). All shells and fragments in this lot were identified (with a small residuum). The relative abundances of the commoner species in this aliquot were assumed to represent the proportions in the whole lot, so that the total weight estimates were obtained by proportion. The remaining, major part then was picked over to secure all specimens of rare species. To a limited extent this aliquot method was used on other series. It is unlikely that any serious errors were introduced by aliquot procedures, and the complete selection of the rarer species from the whole sample increased the species list and the accuracy of the estimates for the less common species.

TABLE 3

PERMILLAGE DISTRIBUTION OF FOOD REMAINS (AS A FUNCTION OF DEPTH): SCRIPPS ESTATES SITE MAIN BURIAL AREA, TRENCH U.C.L.A. TT-1*

Pit	Pit 5				Pit 6			
Depth (cm.)	61-46	46-30.5	30.5-15	15-0	61-46	46-30.5	30.5-15	15-0
Total weight (gm.)	1438.3	900.3	201.2	188.7	521.7	1221.2	1134.3	327.1
Rocky-shore molluscs								
Mytilus	689	710	662	715	691	741	808	778
Pseudochama	50	38	51	64	45	26	21	6
Haliotis	0.3	6	106	7	2	4	2	—
Astraea	9	3	—	11	7	1	6	3
Others	28	28	15	23	34	51	47	26
Total	776(16)	786(10)	834(5)	820(10)	779(13)	822(9)	884(10)	812(8)
Sand-beach molluscs								
Total	2(2)	4(2)	3(1)	5(1)	3(2)	5(2)	2(2)	9(4)
Bay molluscs								
Pecten	138	156	78	63	156	92	57	64
Chione	23	12	5	35	7	9	11	18
Ostrea	6	4	5	5	2	10	5	2
Others	1	4	5	5	1	0.3	0.3	—
Total	168(6)	172(4)	83(2)	109(4)	116(5)	111(5)	73(4)	84(3)
Unidentified shell fragments	9	8	45	30	4	19	7	33
Miscellaneous invertebrates	32(5)	15(3)	7(3)	18(2)	37(2)	29(4)	22(3)	34(2)
Invertebrates (total)	987(29)	985(19)	974(11)	981(17)	990(22)	986(20)	988(19)	972(17)
Vertebrate remains	13	16	26	19	11	14	12	28

*Number of genera shown in parentheses.

TABLE 4

PERMILLAGE DISTRIBUTION OF FOOD REMAINS FROM SCRIPPS ESTATES SITE*

	Screened		Hand-picked	Hand-picked		
	Trench S-M-3 Lot 16	Trench TT-1 Lot 17	Lots 16 & 17	Lot 24 and vicinity		
	Soil horizons A & B	Soil horizons A & B	Soil horizons A & B	Encrusted in caliche	Intermediate & doubtful	Soil horizon A
Total mass (gm.)	6733	296	2385	2438	16806	38418
Rocky-shore molluscs						
Mytilus	597	677	209	106	61	34
Pseudochama	76	50	472	190	270	514
Haliotis	23	—	10	—	2	8
Astraea	18	12	11	—	6	23
Tegula	16	17	2	0.3	0.4	0.4
Others	10	26	6	3	2	5
Total	740(16)	782(10)	710(13)	299(9)	341(14)	584(18)
Sand-beach molluscs						
Tivela	3	0.7	8	—	5	10
Donax	1	—	0.1	tr.	0.4	0.2
Olivella	1	—	0.4	77†	tr.	tr.
Total	5(3)	0.7(1)	8.5(3)	77†(2)	5(3)	10(3)
Bay molluscs						
Pecten	140	87	189	468	515	278
Chione	37	4	37	110	127	109
Ostrea	9	31	13	11	6	5
Polinices	3	—	—	2	2	3
Laevicardium	tr.	—	—	12	—	0.6
Others	2	0.2	7	0.7	0.5	.1
Total	191(9)	122(4)	246(6)	604(6)	650(6)	397(8)

TABLE 4 (Continued)

	Screened		Hand-picked	Hand-picked		
	Trench S-M-3 Lot 16	Trench TT-1 Lot 17	Lots 16 & 17	Lot 24 and vicinity		
	Soil horizons A & B	Soil horizons A & B	Soil horizons A & B	Encrusted in caliche	Intermediate & doubtful	Soil horizon A
Total mass (gm.)	6733	296	2385	2438	16806	38418
Unidentified shell fragments	14	5	13	15	0.5	6
Miscellaneous invertebrates						
Cirripedia (barnacles)	44	42	12	3	1	1
Others	1	—	—	—	—	1
Total	45(4)	42(2)	12(3)	3(3)	1(2)	2(3)
Invertebrates (total)	995(32)	952(17)	989(25)	998(20)	998(25)	999(32)
Vertebrate remains	6	49	11	1	0.7	0.7

*Number of genera in parentheses.

† Value too high, due to inclusion of embedding lime.

The most significant series of samples bearing on the ratios of different food items at various levels in the site were the quantitative samples secured by C. N. Warren at four 6-inch levels in pits 5 and 6 of U.C.L.A. TT-1 (TABLE 3, FIGURE 31). These levels extended through the A and B_1 soil horizons and represent much of the prolonged history of the prolonged history of the site. Throughout the series the proportion of major species and of both systematic and ecological groups showed rather remarkable consistency. Among the molluscs, those from the rocky foreshore constituted about eight tenths of the total shell, the mussels alone amounting to about two thirds to three fifths of the grand total shell content. The sand-beach molluscs contributed hardly more than an inconsequential amount. The bay molluscs contributed about 6 to 16 per cent, with an indication of a drop in relative quantity with time.

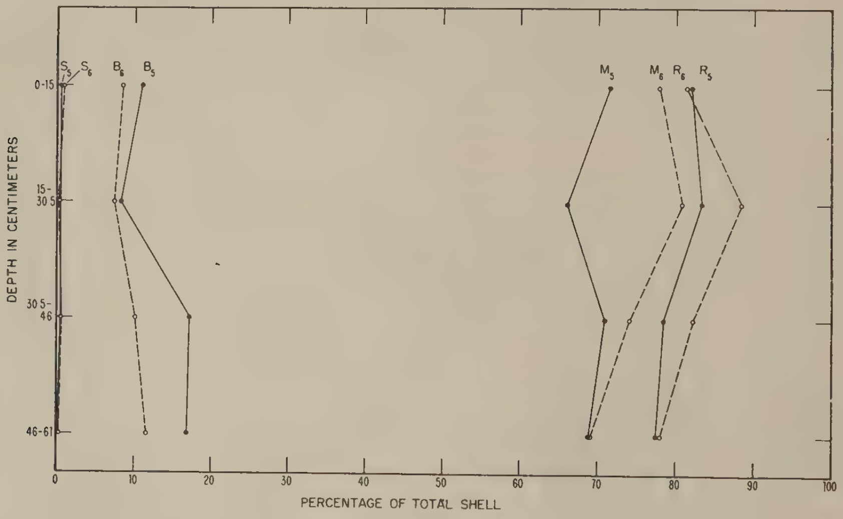

FIGURE 31. Distribution of food remains, with depth, on S.E.A. lot 17 in main burial area of Scripps Estates Site.

Among the rocky-shore molluscs the California mussel vastly predominated at all levels in these two sets of quantitative samples. In each of the eight samples the rock oyster *Pseudochama exogyra* constituted less than one tenth the weight of the mussels. Similarly, among the bay molluscs, *Pecten* greatly outweighed either *Chione* or the *Ostrea*.

These quantitative samples probably represent rather well the original shell composition, for they came from a topographical rise where water drains off rapidly, where the shells are relatively well preserved, and where the redeposited lime in the lower soil horizon is much more limited than in some other parts of the site.

The sample from S.E.A. lot 17 obtained from the immediate vicinity of burial 3, largely by screening, yielded values remarkably similar to those obtained from the screened sample from trench S-M-3 (compare TABLE 4, first and second columns). The miscellaneous, largely hand-picked samples from lots 16 and 17—lumped and represented by the third column in TABLE 4—show similar proportions for the molluscs of the ecological assemblages, but they also show, as would be expected, a much larger proportion of the larger species with heavier shells, particularly *Pseudochama, Pecten,* and *Tivela.*

The very large hand-picked collections from S.E.A. lot 24 and vicinity (last three columns in TABLE 4) show distinctly different ratios. In these samples the proportion of rocky-shore species is much lower. The mussels are relatively scarce from the lower (earlier) levels to the top, while the proportion of the rock oyster climbs from about 20 per cent to about 50 per cent of the grand total. Bay molluscs predominate in the lower and middle levels of the midden and remain high throughout. The scallops constitute about one half the total sample in the lower and middle levels, more than one fourth even in soil horizon A. The vast difference in relative weights of the different genera between these samples and those from the burial area about 100 m. distant probably is due less to an original discrepancy than to circumstances of preservation. The fact that these shells were hand-picked, largely during gardening, accounts only in part for the increased proportion of large and heavy shells, for real effort was made to obtain a random sample. The smaller and more delicate shells largely have disappeared in this area. Most of the mussels are represented by little more than a fragment near the umbone. Obviously the dissolution of the shells in the soil has been much more rapid here than on the topographic rise of the burial area (on lots 16 and 17). In wet seasons the ground becomes much soggier and retains moisture longer than in the burial area and, in rainy periods of the past, probably stood wet for long periods during which the weathering of the shell would have been accelerated. The very thick, shell-rich caliche in the lower soil layers in the region of lot 24 presumably resulted from the less optimal drainage and the increased weathering. The heavy shells, especially *Pseudochama,* we may assume to have become proportionally more abundant by reason of their resistance to weathering. This is particularly true in the upper soil layers, in which the solution of shell apparently has been more rapid than in lower layers, where the shell is protected by a coating of caliche.

Vertebrate remains (other than human) constitute a very small proportion of the midden material (TABLES 3 and 4), although we include some mammal material that is probably intrusive. The bird and mammal bones, largely fragmentary, have not yet been identified. Conspicuously lacking are remains of pinnipeds, sea otters *(Enhydra lutris)*, and cetaceans such as occur (often plentifully) in some younger middens along the coasts of southern California and Baja California. Nor have any traces been found of large pelagic fishes, such as swordfish *(Xiphias gladius)* and tunas (Thunnidae), that are well represented in some of the other sites. Obviously the La Jolla people were no more active as hunters at sea than ashore.

Fish remains, however, do indicate that the people who occupied the site supplemented their food, at least occasionally, by fish. The few fish remains thus far identified indicate that the fishing was done along the shore, probably in several habitats.

The sheephead *(Pimelometopon pulchrum)* is represented by a number of jaws and pharyngeals with the characteristic canine and molar teeth. These were largely from the upper soil horizon, but in part were from the B_1 horizon. This rock-inhabiting fish could have been caught either from rocks along the shore or from rafts or boats.

The only other fish remains thus far identified are five otoliths. These have been authoritatively determined by John E. Fitch of the California State Fisheries Laboratory who has, by means of proportional sizes, estimated the total length or weight of the fish represented. Two otoliths from trench S-M-3 represent adult spotfin croakers, *Roncador stearnsii*, each weighing 1.8 to 2.7 kg. approximately. Two other otoliths, identifiable as adult white croakers *(Genyonemus lineatus)* about 16 cm. long, came from the quantitative midden-food samples from pit 5 of trench TT-1 on lot 17, respectively in the levels 15 to 30.5 and 30.5 to 46 cm. These two species, as well as a small shark represented by one vertebra from trench S-M-3, could have been caught either along or off a sandy beach, in a bay, or in a slough. The fifth otolith represents a species of rockfish *(Sebastodes)* that is almost surely *S. miniatus*. The fish, which was about 51 cm. long, was almost caught on a rocky bottom at a depth that would have required the use of a raft or boat.

The gear used in capturing these fish is not indicated by any of the artifacts, with the possible exception of the two small worked-bone pieces. The rockfish probably was not taken by spear or by poison. Either hooks or gill nets might have been used. Among the relatively few fish vertebrae that have been found in the A soil horizon and the upper part of B_1 are a number that came from fish so small as to suggest capture in tide pools along the rocky foreshore, by poisoning or by hand capture, perhaps facilitated by bailing out the water.

We present in TABLE 5 a list of all animals that have been identified to date from the midden of Scripps Estates Site.

TABLE 5

ANIMALS IDENTIFIED FROM THE MIDDEN OF SCRIPPS ESTATES SITE*

MOLLUSCA

Pelecypoda

Anomia peruviana d'Orbigny: R (20)
Chama pellucida Broderip: B (19)
Chione californiensis Broderip: B (21)
Chione fluctifraga (Sowerby): B (28)
Chione undatella (Sowerby) †: B (16)
Donax gouldii Dall: S (26)
Hormomya adamsiana (Dunker): R (16)
Laevicardium elatum (Sowerby): B (21)
Mytilus californianus Conrad: R (36)
Ostrea lurida Carpenter: B (40)
Pecten circularis aequisulcatus Carpenter: B (30)
Protothaca staminea (Conrad): R‡ (48)
Pseudochama exogyra (Conrad): R (26)
Sanguinolaria nuttallii Conrad: B (31)
Septifer bifurcatus (Conrad): R (32)
Tagelus californianus (Conrad): B (26)
Tivela stultorum (Mawe): S (28)
Trachycardium quadragenarium (Conrad): B (34)

Gastropoda

Acanthina spirata (Blainville): R (33)
Acmaea asmi (Middendorf): R (42)
Acmaea digitalis Eschscholtz: R (37)
Acmaea limatula Carpenter: R (34)
Acmaea pelta Eschscholtz: R (39)
Acmaea scabra (Gould): R (35)
Aletes squamigerus Carpenter: R (27)
Amphissa versicolor Dall: R (36)
Astraea undosa (Wood): R (31)
Bulla gouldiana Pilsbry: B (28)
Cerithidea californica (Haldeman): B (32)
Conus californicus Hinds: R (32)
Crepidula lingulata Gould: R (34)
Crepidula onyx Sowerby: B (22)
Crucibulum spinosum (Sowerby): B (18)
Diodora aspera (Eschscholtz): R (42)
Fissurella volcano Reeve: R (25)
Haliotis cracherodii Leach: R (35)
Haliotis fulgens Philippi: R (30)
Haliotis rufescens (Swainson): R (32)

---

* Usual habitat is indicated for each species of mollusc by: B (bay or slough); R (rocky shore); S (sand beach). The number in parentheses, for all Pelecypoda and Gastropoda, is the median of the present latitudinal range (data from Keen, 1937).

† Commonly and perhaps correctly regarded as a mere variant of *C. californiensis.*

‡ Commonest on cobble beaches of open coast; too rare in site to confound the ecological classification.

TABLE 5 (Continued)

- Gastropoda (continued)
  - *Littorina planaxis* Nuttall: R (33)
  - *Littorina scutulata* Gould: R (38)
  - *Lottia gigantea* (Gray): R (35)
  - *Mitrella carinata* (Hinds): R (30)
  - *Moniliopsis ophioderma* Dall: S (32)
  - *Norrisia norrisi* (Sowerby): R (32)
  - *Ocinebra poulsoni* Carpenter: R (29)
  - *Olivella biplicata* (Sowerby): S (37)
  - *Olivella pycna* Berry: S (39)
  - *Opalia crenimarginata* (Dall): R (27)
  - *Polinices lewisii* (Gould): B (42)
  - *Polinices reclusianus* (Deshayes): B (31)
  - *Purpura nuttalli* (Conrad): R (32)
  - *Tegula aureotincta* (Forbes): R (29)
  - *Tegula funebralis* (Adams): R (38)
  - *Tegula gallina* (Forbes): R (30)
  - *Tegula ligulata* (Menke): R (27)
  - *Thais emarginata* (Deshayes): R (37)
- Amphineura
  - *Ischnochiton conspicua* (Carpenter): R
  - *Mopalia muscosa* (Gould): R

MISCELLANEOUS INVERTEBRATES

- Bryozoa (not identified)
- Annelida
  - Tube worms (not identified)
- Cirripedia
  - *Balanus glandula* Darwin
  - *Balanus tintinnabulum* Linnaeus
  - *Mitella polymerus* (Sowerby)
  - *Tetraclita squamosa* (Bruguière)
- Brachyura
  - Crab fragments
- Echinodermata
  - *Dendraster excentricus* (Eschscholtz)
  - *Strongylocentrotus purpuratus* (Stimpson)

VERTEBRATA

- Elasmobranchii
  - Shark vertebra (not further identified)
- Teleostei
  - *Genyonemus lineatus* (Ayres)
  - *Pimelometopon pulchrum* (Ayers)
  - *Roncador stearnsii* (Steindachner)
  - *Sebastodes miniatus* (Jordan & Gilbert)
- Aves and Mammalia
  - Miscellaneous bones (not identified)

SPECULATIONS ON THE POPULATION OF THE SITE

We already have suggested that the number of people occupying the Scripps Estates Site and similar nearby sites must have been considerable, but this does little except to set the limits somewhere safely between a few and a horde. If, as the radiocarbon dates suggest, the site was more or less continually occupied for 2 millenia, the standing crop of occupants probably varied by a factor of 10 or more and, at times perhaps, disappeared. In an attempt to gain some insight into the number of people typically living on Scripps Estates Site, the following order-of-magnitude calculations were made.

The Scripps Estates Site is only one of a complex of La Jolla sites on Torrey Pines Mesa and, most likely, there was free intercourse between the occupants of the various sites. It is not strictly correct to treat the site as an isolated unit, as is done here for the sake of the following arguments. However, the site is a major La Jolla site and is semi-isolated from other nearby sites; thus the assumption is not unreasonable. For the sake of argument we consider the portion of the site lying mainly within the western portion of the S.E.A. subdivision and designate it as area A. If the portion of the site lying on University of California grounds south of the S.E.A. subdivision and the adjacent site UCLJ-M1 are considered, along with area A, to be one contiguous site (as we believe likely), then data for area A could be multiplied by approximately three to apply to the entire site.

The major screening operation in trench S-M-3 on S.E.A. lot 16 yielded 6727 gm. of washed shell, and this does not account for fragmented shell that fell through the finest screen used or was missed in the separation process. We shall assume a total of 7000 gm., and this was obtained from a midden area of 20 $m.^2$ The soil that was sifted was largely from the A and B_1 horizons, where the greatest part of the midden shell remains. The shell mass for the total soil profile shilling in the area sifted can be estimated at 10,000 gm., equivalent to 500 gm./$m.^2$. Assuming that area A has an area of 20,000 $m.^2$, this yields a total shell content of 10^7 gm. for the area.

Consider an "average" value to be a specimen of *Chione* 4 cm. long with a mass of 12 gm. This yields a count of about 42 values/$m.^2$, and for area A a total count of about 8.4×10^5 shells.

Another estimate of the shell content of area A can be obtained by assuming a population for this area and estimating the number of shells left from a typical meal of shellfish. In the present period of drought, Sumner Canyon holds enough fresh water to sustain a population of perhaps 30. In the interests of conservatism, assume that the mean population of area A was 30 and that this continued for a period of 2000 years. Assume that each person had two meals per day and consumed 15 "average" shellfish, leaving a total of 60 shells in the area per day. Over the 2000-year period 1.314×10^9 shells would have been left on area A.

Thus, even with a conservative estimate of the population, the number of shells that might be expected to have been left on area A exceeds the amount presently found by a factor of 1577. This discrepancy suggests, as does the weathered nature of shell found in the site and the considerable content of caliche in the soil, that a vast amount of shell probably has been lost from the stie through weathering. Indeed it is not improbable that during moist periods most of the carbonate was washed through the soil and into the sea (caliche accumulates only under arid conditions). Yet it hardly seems reasonable to assume that the shell content of the site could have been reduced by a factor of several hundred by weathering. Other explanations need consideration.

It is possible that the mean daily shellfish consumption was overestimated, but if, as we believe, shellfish constituted a major part of the diet this estimate could not reasonably be reduced by a factor of more than about 3. It is possible that the period of occupation did not extend throughout the entire 2000-year period lying between the extreme radiocarbon dates, but at the very most this probably would not change the estimate by more than a factor of four. Thus the discrepancy remains in need of clarification; to postulate either a longer period of occupation or a larger population would only make the discrepancy greater.

Another population estimate can be made from the abundance of manos in the site. Collections mainly in area A have produced at least 350 of these implements. Many others undoubtedly have been removed over the years and much of the site is unexcavated. An order-of-magnitude guess at the total number in area A is 5000. Using the previous conservative estimate of 30 persons in residence on area A continually, an estimate of 10 adult women using manos at any one time seems reasonable. Assume that each woman created but 4 manos in her lifetime and that her life expectancy was about 20 years so that the occupation period represents 100 generations. Assuming that all manos created were lost in the soil eventually, 400 manos should have been left in the site. The agreement is reasonably close.

The above calculations are merely suggestive, but they serve a useful purpose by establishing some numerical values where none existed previously. Considering as a unit the entire Scripps Estates Site and the UCLJ-M1 Site, the calculations suggest that the mean population may have been between 100 and 200 individuals.

INFERENCES REGARDING THE FORMER ENVIRONMENT

By taking into consideration all the available facts and indications, it is possible to erect and to support a number of hypotheses regarding the environmental conditions that prevailed during the more than two millenia that the Scripps Estates Site appears to have been populated by La Jolla people.

Inferred Climatic Conditions

By the time the first La Jolla peoples arrived to establish the site, the cold weather of the Wisconsin Ice Age had ameliorated. The change in temperature almost certainly had been very great. For a variety of reasons it seems highly probable that the weather during the Wisconsin, until about 10,000 years ago, had been very cold at least as far south as San Diego. The transition from glacial to altithermal conditions was apparently abrupt and world-wide.

It seems highly probable that during the occupation of the site, from about 7500 to 5000 years ago, the sea temperatures near La Jolla were as warm as now or probably somewhat warmer and—except for Bahía Todos Santos—the surface shore-water temperatures near La Jolla are the warmest of any north of Bahia Sebastián Vizcaíno in central Baja California (Hubbs, 1960*b*). If the sea temperatures were as warm then as now, or warmer, the air temperatures probably were also, for the sea and air temperatures are very closely correlated (Hubbs, 1948).

Reasons for postulating warm sea (and air) temperatures in La Jolla times are several. First and most direct are two mass spectometric paleotemperature determinations made for one of us (C.L.H.) by Robert N. C. Bowen at Scripps Institution of Oceanography on two intertidal molluscs that constituted the chief ocean-shore species consumed by the inhabitants. The estimates are 21.3° C. for the California mussel, *Mytilus californianus*, and 20.6° C. for the rock oyster, *Pseudochama exogyra*. These temperatures approach the present upper monthly averages and far exceed the yearly average. The mussel, at least, grows and lays down shell locally throughout the year (Coe and Fox, 1942).

The shell assemblage in the midden confirms the view that the temperatures were probably a little higher than at present. Notably absent is the giant chiton *Cryptochiton stelleri*, which is an excellent indicator of the cold period that extended from about 1600 years B.P. or earlier to about 600 years ago along the northwestern coast of Baja California (Hubbs *et al.*, 1960). No distinctively northern types are included in the molluscan assemblage (a few fragments that seem to represent the red abalone *Haliotis rufescens* provide the nearest suggestion of cooler waters, but the abalone shell could well have been picked up on the beach).

The most distinctively southern mollusc represented is the giant clam *Laevicardium elatum*, one specimen of which was associated with burial 7, but other specimens of which occur in various soil horizons. This species now occurs northward into Golfo de California and southwestern Baja California, with only one small offshore population known in southern California (Fitch, 1953). It occurred in San Diego Bay during the last century when temperatures were high (Hubbs, 1948), but none seem to live there now, although dead shells are dredged in considerable numbers from the bottom of the bay.

Another suggestion of warmer temperatures is furnished by the species ot *Tegula*. The intertidal species of this genus, which were extensively used for food, are among the better temperature indicators. At present the local intertidal population is composed almost entirely of the more northerly of two abundant species, namely *Tegula funebralis*, whereas in the Scripps Estates Site midden—as also very definitely in the midden to the south, UCLJ-M1—the more southern species, *T. gallina*, is strongly dominant.

Another approach toward an estimate of the past temperatures of the inshore waters (and hence of the past air temperatures) is a statistical evaluation of the latitude inhabited by the organisms, following the index method developed by Schenk and Keen (1937, 1940) and Schenk (1945). The mid-points of the ranges of the 56 species of pelecypods and gastropods thus far identified from the site, taking the north-latitude figures for each species from the compilation of Keen (1937), are as follows: for the 35 rocky-shore species, 16° to 48° (mean, 32.5°); for the 5 sand beach forms, 26° to 39° (mean, 32.4°); and for the 16 bay species, 16° to 42° (mean, 27.4°). The value for each species is entered in the species list in TABLE 5. The more northerly (cooler-water) indication for the rock-shore species and the more southerly indication for the bay forms is a natural expectation related to the upwelling of water on the open coast and to the insolation on the bays (Hubbs, 1960*b*). The grand average of 31.0° N. lat. for the 56 species is further suggestive of temperatures probably slightly warmer than at present, for the site is close to 33°N. lat. Schenk (1945) indicated a median latitudinal value for all inshore molluscs at San Diego of 32° at present, which corresponds very closely to the actual latitude.

The fishes thus far identified, like the molluscs, represent either warm-temperate southern Californian types *(Roncador stearnsii* and *Pimelometopon pulchrum)* that range into much warmer waters or species *(Genyonemus lineatus* and *Sebastodes miniatus)* that presently range both northward and southward from southern California.

Another reason for thinking that the temperatures were very mild is the extreme paucity of charcoal in the midden (although heavier rainfall may have been a factor). A quantity sufficiently large for a radiocarbon test has not been readily obtainable (it is possible, however, that a few small fragments collected less than one-half meter north of burial

15 may prove sufficient for a date, but this remains to be determined). A few flecks of charcoal have been found in the soil inside shells, which indicates autochthony. Still another reason for inferring warmth is the extreme scarcity of remains of fur-bearing animals.

Because cold ocean (and air) temperatures are induced along the adjacent coasts principally by upwelling, due to the predominantly northwesterly winds, and because the temperatures during the occupation period probably were warmer than now, such winds probably were light. The weather probably was calm as well as warm. Life may have been easy in respects other than an ample supply of food from the sea.

It commonly is thought that the Altithermal period was relatively dry as well as warm. It almost certainly was drier than it had been during the Pluvial period, which came to an end about 10,000 years ago. The extensive development of lakes throughout the arid southwest is indicated (Hubbs and Miller, 1948). Radiocarbon dates are confirming the evidence. For example, a new date (LJ-200) from the La Jolla Laboratory indicates that the freshwater mussels of Lake Mohave were stranded by the probably last recession of the lake 9640 ± 120 years ago.

Although the period between 7500 and 5000 years ago was almost certainly much drier than it had been before about 10,000 years ago, the climate in all probability was more moist than at present (Hubbs, 1960a). The extensive populations that existed along the now semidesert coast, in both southern California and Baja California, could hardly have been supported by the amount of surface water that exists now in the area (disregarding the supplies brought in by aqueduct and by deep wells). The nearest natural surface-water supply extant in the vicinity of the Scripps Estates Site is in a few small, but apparently always present, pools in the lower portion of Sumner Canyon: a supply inadequate for an extensive population but sufficient, even in the present period of relative drought, to support at a subsistence level a few dozen people. No permanent stream approaches the usually saline lagoons at the mouth of Soledad Canyon, and there is no surface water in the region of Hidden Valley or La Jolla. It is conceivable that Rose Canyon Creek could have supplied water to be hauled several kilometers, but this seems improbable.

Physiographic evidence leads to the inference of heavy rainfall during the Pluvial (Periglacial) period and moderate rainfall, but greater than at present, in the La Jolla period. The Torrey Pines Mesa near the coast, including the Scripps Estates Site, seems to have been eroded to, or nearly to, the Eocene bedrock. During the La Jolla period the soil was aggraded, both by outwash from the sand ridge to the east and by wind-borne deposits.

Another reason for assuming moderately greater rainfall than at present is the indication that the coastal lagoons maintained connection with the ocean so that they kept producing a large supply of bay molluscs. Moderate rainfall would tend to maintain the favorable conditions, but too much rainfall would have rendered the estuaries too fresh to support the molluscs. The great paucity of charcoal in the site also suggests run-off greater than at present.

During La Jolla times the rainfall, although probably greater than at present, presumably was inadequate to produce permanent flow in all but the larger canyons and valleys. Some of the larger midden sites are located close to potential water supplies. The Scripps Estates Site supply has been mentioned; the Del Mar Race Track site adjoins a depression that still holds some stagnant water most of the year; the extensive habitations on the south side of Batiquitos Lagoon are beside a cattail marsh, where even today some water probably could be obtained.

In conclusion, the La Jolla people presumably enjoyed warm, almost certainly frost-free, temperatures, generally calm winds, and conditions somewhat more moist than prevail at the present time.

Inferred Physiographic Conditions

Evidence concerning the physiographic conditions under which the La Jollans lived is supplied by the type of seafood they were able to gather and by the known and inferred changes in sea level, in silting of estuaries, and in other processes.

From La Jolla Shores northward to Batiquitos Lagoon or beyond (the coastal region of known concentrations of people of La Jolla type), a distance of 20 km. or more, the shore features must have been greatly altered since the seafood-gatherers thrived there. The present coast does not have sufficient rocky foreshore to support molluscs in any approach to the quantities that were harvested in ancient times in the region. Great quantities of California mussels, *Mytilus californianus,* and rock oysters, *Pseudochama exogyra,* were consumed, and the supply must have been gathered along the adjacent rocky foreshore. However, at present, this shoreline is almost entirely sandy, with occasional cobble stretches (especially in winter) and, locally, some smooth intertidal rock, but with only a very few rocks of the type that support mussels and rock oysters. A similar predominantly sandy beach continues for about 55 km. to the northwest (to Dana Point). Toward the south largely rocky shores are present around La Jolla Point for a distance of about 9 km., but even here the supply of mussels and rock oysters would not supply more than a few hundred people at most, and the next rocky shore, along Point Loma, is too far away to be considered. The small reef near Scripps Institution of Oceanography could have supplied part of the mussels and rock oysters for the Scripps Estates Site but could not have yielded the vast quantities consumed there and farther north. During the dated period of seafood eaters along this shore, from 7400 to 3700 years ago, the shoreline must have been much rockier than at present to have produced the quantities of rock-inhabiting molluscs consumed.

The estuarine conditions also must have been different during the La Jolla occupation than at present. Not only in the Scripps Estates Site but also in the Sorrento Valley, Del Mar Race Track, and Batiquitos Lagoon sites (also dated as La Jolla) bay molluscs constituted a large proportion of the food of the thriving populations. These molluscs were predominantly *Pecten circularis* and species of *Chione* but included *Ostrea (lurida), Polynices,* and other genera. Similar middens exist along both sides of most if not all the estuaries in San Diego County from La Jolla northward. Today these estuaries, except the one at Carlsbad, which is kept open artificially, do not maintain conditions proper for the development of populations of *Pecten* and *Chione*. They are subject to filling with fresh water after the heavier winter rains and with sea water in storms. After being filled with sea water and then being cut off from the ocean by a rectification of the shoreline as a result of longshore sand drift, very high salinities develop. Studies by Jacqueline N. Miller show that the population of adults of *Pecten* and *Chione* develop only in the one lagoon (at Carlsbad) that has been dredged and kept open to the sea. Large populations do develop there, showing that these estuaries, if deeper and open to the sea, could produce a relatively large crop of these estuarine scallops and clams.

Thus we are confronted with good indications that, during the period from 7300 years ago or earlier until at least 3700 years ago, the shore north of La Jolla was considerably more rocky than at present with estuaries sufficiently deep and in sufficient contact with the sea to maintain, in baylike conditions, flourishing populations of *Pecten* and *Chione*. These conditions would be met by a rapidly rising sea level, during which the accumulation of shore sand would be kept low.

The rising of sea level also would tend to keep the estuaries deep and in contact with the ocean.

The concept of a relatively rapid eustatic rise in sea level concomitant with the waning of continental ice sheets at the close of Wisconsin time and the concept of a sea level 100 or more meters below present sea level during Wisconsin time are supported by so many lines of evidence as to warrant acceptance for present purposes. During the times of glacially lowered sea level, the coastal terraces of the San Diego region no doubt were dissected deeply by canyons and valleys. The conditions just mentioned doubtless long prevented or greatly delayed the filling in of the sloughs and valley floors with sediment during the Holocene transgression. The concept of deep bays existing as a consequence of the rapid rise in sea level is mentioned by Carter (1957).

It is now rather well established that the ice waned rapidly about 10,000 years ago, causing a rapid rise in sea level. There are indications that the rise slackened about 7000 years ago, but some authorities, notably Shepard and Suess (1956), suggest a continued rise to the present. Fairbridge (1958) disagrees, postulating certain late Postglacial higher-than-present sea stands.

Possibly the most complete picture of the Holocene transgression was obtained by Curray (1960), who secured radiocarbon dates on shells of shallow-water molluscs that were dredged from various depths on the relatively stable continental shelf west of 93° West longitude in the Gulf of Mexico. Curray assumed, with good reason, that these organisms had lived in shallow water and that their shells were left behind on the sea floor as the shoreline advanced. With his permission, Curray's figures are reproduced here (FIGURE 32), to illustrate some of the evidence that sea level rose rapidly during the period just preceding the La Jolla occupation and that it then still was below the present sea level.

That the sea level probably continued to rise during the period of La Jolla occupation and even later is indicated by an increasing body of evidence derived from middens near present sea level, some now dated, in California. Nowhere in southern California or in northwestern Baja California have we been able to find convincing evidence of what would appear to be a high Postglacial sea stand, but this does not rule out the possibility that it may have occurred. In a few places along the shore, notably on North Coronado Island, there are wave-cut notches a a meter or so above present high-tide level, but these possible could have been formed in the Pleistocene, or recently, by extreme storms; no shell deposits seem to occur. In extensive searches along the mainland seashore we have found no shell deposits that do not appear to be either of middens or of Pleistocene or earlier age. The nearest location where there appears to be evidence of a high Holocene sea stand is in the Colorado River delta region (Hubbs and Miller, 1948), but this is a region of tectonic instability. Of two samples tested by the La Jolla Radiocarbon Laboratory as bearing on possible raised beaches in the southern part of Golfo de California, one (LJ-131) proved to be Pleistocene and the other (LJ-132) seems to be midden (Hubbs *et al.*, 1960).

Several middens in California extend downward to below the present high-tide level, indicating a relatively lower sea level during the time

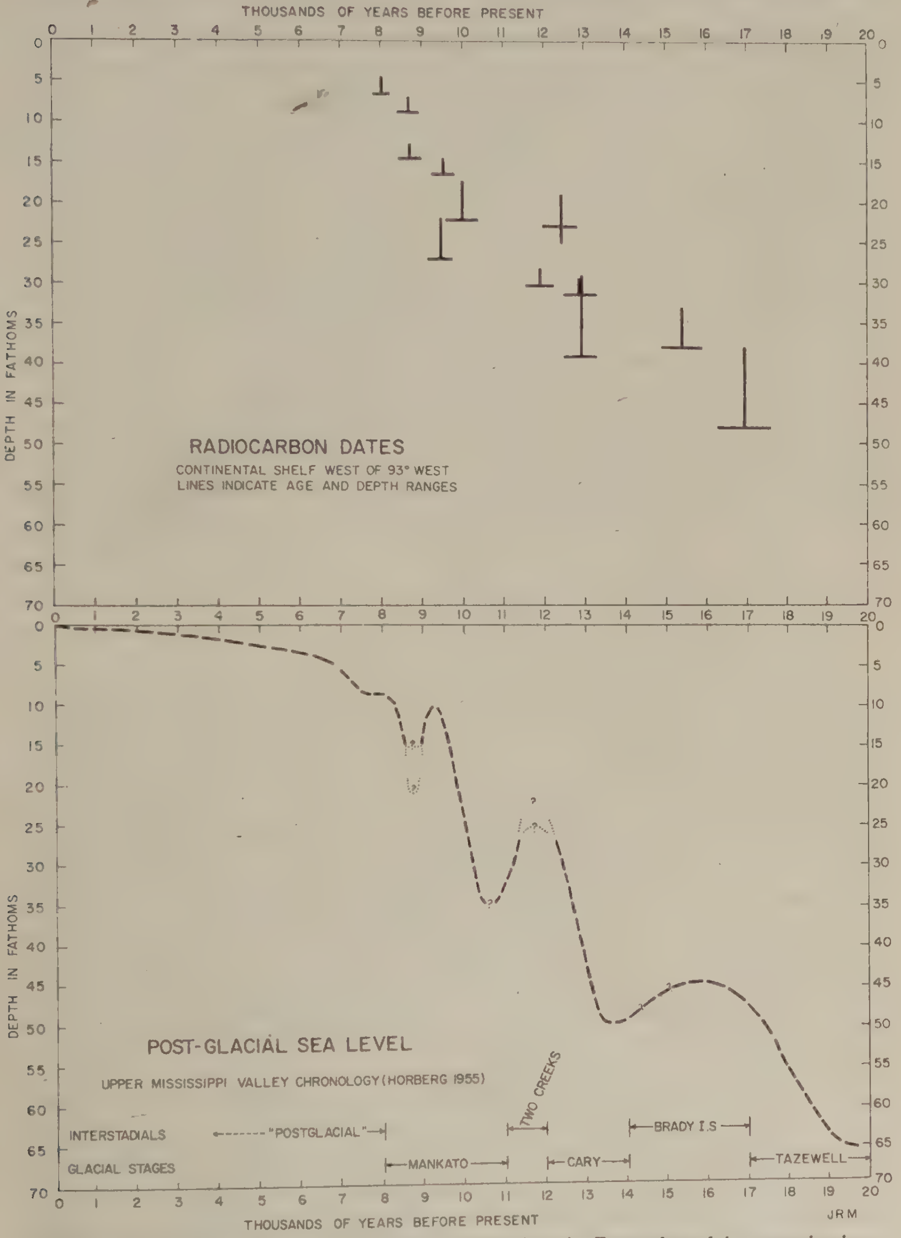

FIGURE 32. The Postglacial rise of sea level. Reproduced by permission of the *American Association of Petroleum Geologists, Special Publications* (Curray, 1960).

of occupation. One such midden is on the north side of Sorrento Valley near the mouth where, within the area of La Jolla occupation, Malcolm J. Rogers (personal communication) dug a midden to below sea level, ceasonly when seepage from the sea-level lagoon prevented further excavation. Of the several middens in central California that extend to below sea level, we now have a radiocarbon date of 2310 ± 120 years B.P. for the 244- to 267-cm. level, which is below sea level, of the Emeryville Shellmound (Site Ala-309). This site, however, is on San Francisco Bay, an area of suspected depression. The lower midden at the mouth of Willow Creek, Monterey County, Calif., which is buried to below sea level beneath more than 3 m. of waterlaid gravel (Site Mnt-282) has been dated by the Chicago Laboratory (C-628, C-695) at 1879 ± 250 and 1840 ± 400 years B.P. (Libby, 1951, 1952; Heizer, 1958). Various recently dated middens, along the coast on either side of the Mexican border, slope, or are inferred from physiographic indications to have sloped, to below present high-tide level (Hubbs *et al.*, 1960); three of the dates (LJ-34, 37, 38), of 950 to 1450 years B.P., refer to levels along Chollas Creek near the shore of San Diego Bay; other dates (LJ-19, 20, 78(?), 83, and 98), ranging from 1170 to 3700 years B.P., are from open-coastal sites. Subtidal peat from the beach at the La Jolla Beach and Tennis Club, lying above an apparent salt-flat level at 8 m. depth, has been dated (LJ-208) at 4230 ± 100 years B.P.

At least for southern California and northwestern Baja California it seems probable that sea level rose rapidly from the termination of Wisconsin time, about 10,000 years ago, until the beginning of La Jolla occupation, and has continued to rise (at a slackened rate) since about 7000 years ago. During the period of rapid rise the rocky foreshore was maintained to a greater degree than at present, so as to furnish a plentiful supply of such seafood as the California mussel and the rock oyster. During this period the valley-mouth estuaries were maintained with sufficient depth and with sufficient connections to the sea to provide an abundance of such bay molluscs as the scallop and the *Chione* clams. These conditions seem to have persisted in southern California, more or less, until about 1000 years ago.

As the rise in sea level slackened (to become slight in recent centuries) the rocky foreshore became largely replaced north of La Jolla by sandy beaches as sand accumulated. At the same time sedimentation in the stream mouths came to exceed the effects of the slackened rise in sea level, so that the former baylike estuaries became the more or less ephemeral and ecologically highly variable lagoons no longer suited for significant shellfish production. The shellfish-gathering populations seem eventually to have largely abandoned the coast north of La Jolla, although they persisted in southernmost California and northern Baja California where bays and rocky shores remained.

The changing ecological conditions seem to have affected the food and life of the shellfish-gathering people along the coast of northern San Diego County. To the southward, where lagoons apparently were less developed, the bay shellfish supply seems to have been depleted early through changes in the habitat. The Scripps Estates Site seems to have been abandoned by La Jolla people about 5000 years ago, although some shellfish-gatherers lived nearby as late as about 600 years ago but nearer the remaining rocky shore of the La Jolla region; they fed largely on mussels and other rocky-foreshore molluscs. Near some of the larger lagoons, such as Batiquitos Lagoon, the consumption of bay molluscs in large numbers persisted until about 1000 years ago.

Within the Scripps Estates Site, in line with the hypothesis that rocky shores predominated during the occupation, sand-beach molluscs, primarily pismo clams, *Tivela stultorum*, and bean clams, *Donax gouldii*, are extremely rare and never attain an abundance here commensurate with that shown for middens dating from recent centuries.

TEMPORAL, SPATIAL, AND CULTURAL POSITION OF THE LA JOLLA CULTURE

The Scripps Estates Site, as indicated by Warren's discussion (Moriarty *et al.*, 1959), bears very significantly on the rather ill-defined La Jolla Culture of San Diego County, Calif., as well as on similar but different, cultures that more or less contemporaneously existed along the mainland and islands of southern California north of this county. The temporal and cultural position of the early shellfish-gathering peoples along and within a few miles of the coast of southern California has recently been considered by Meighan (1959) and by Hubbs *et al.* (1960). The latter group of investigators showed that simple cultures of shellfish gatherers occurred contemporaneously along the coasts of southern Baja California.

The late Malcolm J. Rogers briefly described the La Jolla culture in 1929 as that of the "Shell-Midden" peoples, but did not name it until 1945. In his earlier paper (1929) he recognized a second, old, or "Scraper-Maker culture," which he named San Dieguito in 1939.

Originally Rogers indicated that what he later called La Jolla preceded the San Dieguito. On cultural grounds this was a logical deduction, for the San Dieguito artifacts are more advanced than those of the La Jolla people. In his 1945 contribution, however, Rogers concluded that "immediately after the disappearance of the San Dieguito peoples with their excellent stone-flaking technique, a new stock with a seafood-seed-gathering complex and no ability to work stone moved in" and, further, that "from this time on down until historic time the archaeological history is well recorded in a succession of numerous shell middens."

Rogers held that his revised sequence was based on stratigraphic evidence but failed to substantiate the evidence in published reports. As indicated below, his revised sequence in the opinion of some seems to have been verified on the basis of some new evidence. Whether the San Dieguitans were replaced by the La Jollans as he stated in 1945 or degenerated into the La Jollans remains an unsolved and significant problem.

The basic simplicity (or the degree of retrogression) of the La Jolla culture was consistently somewhat exaggerated by Rogers, even in a personal communication shortly before his death. Rogers seems to have overlooked or to have underestimated the significance of the occurrence of a few relatively refined artifacts of several types in La Jolla and related sites.

Rogers (1945) divided the La Jolla culture into two "developmental phases": La Jolla I and La Jolla II. The earlier culture he characterized by the use of basin metates, unshaped manos, a few primary flakes of rock, and even fewer crude cobble choppers; by the absence of rock projectile points: and by random interment without mortuary offerings. La Jolla II he characterized by frequent rock flaking, increased use of metates, burials in cemetaries, and evidence of contact with the peoples of the Channel Islands. The cultural features of the Scripps Estates Site hardly confirm the separation into such substages, for this is one of the earliest of such sites, yet it has concentrated burials, abundance of flaked-rock implements (a few of which are rather refined), and some inclusion of ornaments in burials.

Harding's (1951) discussion of the work done by the San Diego Museum of Man, obviously in the Sorrento Site (SDM-W316), recently dated as 6950 ± 350 years B.P., indicated a transition from La Jolla I to La Jolla II but, from an examination of several such sites, we believe it probable that the apparent early simplicity may merely reflect the gradual build-up and stabilization of a village population.

As Warren indicated, the dating of the La Jolla cultures before radiocarbon dates were available has been extremely varied. Rogers (1945) placed the origin of La Jolla I at about the beginning of the first century, following the first invasion of the area by man about four millenia ago. Carter (1957), going to the other extreme, had the La Jolla industry encompassed in a continuous dating from the last Interglacial to the recent introduction of the Yuman complex. Carter's conclusions have been severely criticized by Johnson and Miller (1958), Krieger (1958), and Oakley (1959).

In a general survey of the California cultures and the concept of an Archaic Stage, Meighan (1959) placed the San Dieguito earlier than the simpler La Jolla, in very early Recent time. The first dating of what Rogers, in submitting the shell sample, thought to be of San Dieguito age, gave an age of only 4720 ± 160 years B.P. (LJ-136; Hubbs *et al.*, 1960). Rogers indicated that these shells were unique in a San Dieguito site but that they were found in the same stratum with artifacts regarded by him as characteristic of "San Dieguito III." The site was below a caliche layer in the bottom of the San Dieguito stream bed. Taking this date at its face value as pertaining to the San Dieguito culture, one of us (C.L.H.) took the view that the San Dieguito probably followed the La Jolla but added that "the problem needs further elucidation, especially because stratigraphic relations in reworked flood-plain deposits like those at SDMM-W-198 are suspect, and because migrations, cultural deterioration, and independent developments and acquisitions may often affect the apparent cultural sequence."

The "further elucidation" now seems to be at hand. Claude N. Warren (personal communication) recently has found artifacts of La Jolla type clearly overlying the San Dieguito at the same locality near the bed of the San Dieguito River at a distance of about 12.5 km. inland from the sea, and a recent dating (LJ-202) of charcoal from a firepit (sweat house?) in the upper level gives a typical La Jolla date of 6300 ± 200 years B.P. The earlier date of 4720 years for shell reputedly of San Dieguito age possibly was based on shell from a La Jolla site mixed by stream flow with San Dieguito artifacts in a channel that has since been refilled. Midden shell often occurs this far (12.5 km.) and farther inland.

The problem is complicated by True's (1958) finding of an early complex (as yet undated) in the Pauma Valley area, farther inland in San Diego County, that shows resemblances to both the San Dieguito and the La Jolla. Possibly it represents a transition between the cultures of a hunting people (San Dieguito) and a food-gathering people (La Jolla).

Present evidence suggests that the coastal food-gathering culture(s) of which the La Jolla is representative were evolved between 7500 and 8000 years ago, presumably from some preceding hunting culture(s), San Dieguito or other.

How far northward and southward the La Jolla Culture extended has not been determined, but the current program of radiocarbon dating bears on this question. Other dates from the same general region, pertaining to at least generally similar, simple culture, are of comparable age. Several of these dates are for the sites in the coastal region of San Diego County north of the Scripps Estates Site. Other apparently similar sites remain to be dated.

Midden remains, seemingly of the La Jolla Culture, continue northward from the Scripps Estates Site, not only in the adjacent sea-cliff canyons but also much farther north on Torrey Pines Mesa and on the terrace along the Sorrento Valley side of Torrey Pines Park. Extensive middens of a similar type are now being studied by one of us (J.R.M.) on the grounds of the United States Department of Agriculture Horticultural Station east of Highway 101. Others continue along the sand ridge in Torrey Pines Park.

Other La Jolla middens occur in Sorrento Valley. The Sorrento Valley Site that obviously was the one studied by Harding (1951) and the one from which the projectile points discussed earlier were obtained has now been dated (M-114) by Crane and Griffin (1958) as 6950 ± 350 years B.P. The sample, of unrecorded shell species, was submitted by C. Carr Tuthill; the site number is SDM-W316 (also SDi-531). The location, shown in FIGURE 1, was misplaced about one-third mile north-northeast on the corresponding map of the preliminary report (Moriarty *et al.*, 1959, FIGURE 1). Recently the entire site was bulldozed into oblivion in the process of suburban development.

The next dated site northward is in the lower part of the next valley, that of the San Dieguito River. This midden caps a low island of terrace material near the north edge of the valley close to the mouth of Eden Valley, on the east side of the parking lot of the Del Mar Race Track. The radiocarbon date of 6680 ± 170 years was determined from unidentified shell species for George F. Carter by Broecker and Kulp (1957). In the preliminary report (Moriarty *et al.*, 1959), as a result of an erroneous verbal communication, the date was inadvertently given as 7300 ± 300 years B.P., and it was stated that it was obtained by the San Diego Museum of Man for site SDM-W45. The correct site number is SDM-W37 (see FIGURE 1).

Other middens of a seemingly similar type occur farther north on either side of the lagoon mouths of most, and probably all, of the valleys. An early La Jolla site on the south side of Batiquitos Lagoon near Leucadia has been dated (LJ-36) at 7300 ± 200 years B.P. It is overlain by a younger midden with simple cultural features dated (LJ-31) at 3900 ± 200 years B.P.; another date (LJ-35) for a nearby midden is 3500 ± 200 years B.P. (Hubbs *et al.*, 1960). These sites now are being excavated by Claude N. Warren and party of the Archaeological Survey, University of California, Los Angeles.

Still farther north in southern California two dates in the same general time range have been obtained by the La Jolla Radiocarbon Laboratory on shell from the lower levels of coastal middens (Hubbs *et al.*, 1960). Clam shell *(Chione californiensis)* from the thick zone of lime-indurated coarse sand at the base of the Malaga Cove Site near Redondo tested 6510 ± 200 years B.P. (LJ-3). Black-abalone shell *(Haliotis cracherodii)* from a low level in the Zuma Beach Site (Peck, 1955; Ascher, 1959) in northern Los Angeles County, submitted by Clement W. Meighan, tested 4950 ± 200 years B.P. (LJ-77).

Similar dates have been obtained for early middens of rather similar composition along the north shore of Santa Rosa Island off Santa Barbara. Two of these dates were run for Phil C. Orr (1956) by the Lamont Radiocarbon Laboratory (Broecker *et al.*, 1956; Broecker and Kulp, 1957). Red-abalone shell *(Haliotis rufescens)* from a midden layer 3 m. deep in a sand dune tested 6820 ± 160 years B.P. (LJ-257). Red-abalone shell from a midden level about 4 m. deep in terrace fill tested 7050 ± 300 years B.P. (L-290 D). An even older date of 7400 ± 200 years B.P. (LJ-27) has been obtained by the La Jolla Radiocarbon Laboratory, also on red-abalone shell, from a depth of nearly 5 m. nearby in the terrace fill (Hubbs *et al.*, 1960).

Warren (Moriarty *et al.*, 1959) conservatively stated that the detailed relationship between the La Jolla Culture and that of other coastal complexes (if different), "cannot now be defined because of lack of data." He continued: "Wallace (1955), however, has placed the La Jolla Complex in Horizon II of his four broad temporal divisions for the Southern California Coast. The data obtained from the Scripps Estates Site I support the placement of the La Jolla Complex in the same horizon as the Topanga sites (LAn-1 and LAn-2), Little Sycamore, Zuma Creek, Malaga Cove, and the Oak Grove culture. With the exception of Malaga Cove and the Oak Grove culture all show a rather large series of crude core and flake tools as well as manos and metates in numbers. The La Jolla Complex on the other hand lacks the number of points and blades and the few mortars and pestles reported from the northern sites. Wallace estimates the milling stone assemblages to be 2000 to 5000 years old. The C-14 dates now available from San Diego sites would extend the initial date back to about 7000 years in that area, and it seems reasonable to assume that an initial date of 5000 years is too conservative for this horizon throughout the southern coast."

The finding of three mortars and of one pestle in the Scripps Estates Site would seem to strengthen the hypothesis that all or most of these early coastal seafood-gathering peoples may have been closely related.

Meighan (1959) referred such cultures to the "Archaic stage," but argued that this stage continued into very recent time in southern California.

Three dates within the same time range have been obtained by the La Jolla Radiocarbon Laboratory for shell from coastal middens in northern Baja California as follows: 6400±200 years B.P. (LJ-107) on rock scallop *(Hinnites multirugosus)* from the surface of a midden at the tip of Punta Cabras on the west coast of the peninsula; 5020±200 years B.P. (LJ-6) on mussel *(Mytilus californianus)* from a past generation of the sand dune at the base of Punta Cabras; 6100±200 years B.P. (LJ-26) on clam *(Glycymeris* cf. *maculata)* from a coquinalike deposit about the large spring at Bahía de los Ángeles on Golfo de California (Hubbs *et al.*, 1960).

In all these early occupations, in the time range 4950 to 7400 years B.P., the culture appeared to be one of food-gathering, largely from the seashore, and the extant artifacts are almost all crude. Pressure-flaked rock is totally lacking or extremely scarce, and there is no trace of pottery.

Seemingly, not greatly dissimilar cultures of seafood-gathering peoples persisted throughout most of the subsequent five millenia until the Yumans appeared with their pottery and small well-worked projectile points a few hundred years ago; and the Yumans themselves partook extensively of seafood.

From north to south the datings on shellfish-gatherers along the coasts of southern California and of Baja California are given in TABLE 6.

TABLE 6

DATES ON SHELLFISH-GATHERERS ALONG SOUTHERN CALIFORNIA AND BAJA CALIFORNIA COASTS*

Southern California			
San Miguel Island	LJ-218	(shell)	2120 ± 140
San Miguel Island	LJ-25	(charcoal)	1750 ± 200
Santa Rosa Island	CT-38	(surfgrass)	1860 ± 340
Santa Rosa Island	CT-40	(charcoal)	2590 ± 360
Santa Rosa Island	L-257	(shell)	6820 ± 160
Santa Rosa Island	L-290D	(shell)	7050 ± 300
Santa Rosa Island	LJ-27	(shell)	7400 ± 200
Zuma Creek Site	LJ-77	(shell)	4950 ± 200
Near Malibu Beach	LJ-78	(shell)	3460 ± 200
Malaga Cove Site	LJ-3	(shell)	6510 ± 200

* Most of the dates listed above have been reported or discussed in the following publications: Broecker and Kulp (1957), Broecker *et al.* (1956), Carter (1957), Crane and Griffin (1958), Heizer (1958), Hubbs *et al.* (1960), Libby (1951, 1952, 1955), Meighan (1959), Orr (1956), Rubin and Suess (1955), and Suess (1954).

TABLE 6 (Continued)

Little Harbor, Santa Catalina Id.	M-434	(shell)	3880 ± 250
Batiquitos Lagoon 1	LJ-31	(shell)	3900 ± 200
Batiquitos Lagoon 2	LJ-35	(shell)	3500 ± 200
Batiquitos Lagoon 3	LJ-36	(shell)	7300 ± 200
San Dieguito River Valley	L-299B	(shell)	6680 ± 170
San Dieguito River Valley	LJ-136	(shell)	4720 ± 160
San Dieguito River Valley	LJ-202	(charcoal)	6300 ± 200
Sorrento Valley	M-114	(shell)	6950 ± 350
Torrey Pines Park	LJ-19	(shell)	3700 ± 200
Scripps Estates Site 1	LJ-79	(shell)	6700 ± 150
Scripps Estates Site 2	LJ-109	(shell)	7370 ± 100
Scripps Estates Site 3	LJ-110	(shell)	5460 ± 100
Scripps Estates Site 4	LJ-221	(shell)	5740 ± 170
Near Scripps Institution	W-154	(shell)	580 ± 200
Near Scripps Institution	W-155	(charcoal)	600 ± 200
Near Scripps Institution	L-299A	(shell)	4400 ± 150
La Jolla	L-299C	(charcoal)	2800 ± 150
Chollas Creek 1	LJ-34	(shell)	1450 ± 200
Chollas Creek 2	LJ-37	(shell)	950 ± 200
Chollas Creek 3	LJ-38	(shell)	2100 ± 200
Sweetwater River	LJ-103	(charcoal)	760 ± 100
Baja California (west coast)			
Rancho Cuevas rockshelter	LJ-33	(charcoal)	400 ± 200
Estero Beach	LJ-20	(shell)	1170 ± 200
Estero de Punta Banda	LJ-98	(charcoal)	1820 ± 200
Punta Clara	LJ-108	(shell)	1580 ± 100
South of Punta Clara	LJ-75	(charcoal)	1150 ± 150
Punta Cabras	LJ-107	(shell)	6400 ± 200
Punta Cabras	LJ-6	(shell)	5020 ± 200
Punta Minitas Site	W-26	(shell)	2540 ± 200
Punta Minitas Site	W-27	(charcoal)	2500 ± 200
Punta Minitas Site	LJ-5	(charcoal)	3100 ± 300
San Antonio del Mar	W-31	(shell)	300 ± 160
South of San Quintin	W-29	(shell)	300 ± 160
South of Cañon Rosario	W-32	(shell)	650 ± 200
Valle de Rosario	LJ-84	(shell)	1060 ± 150
Valle de Rosario	LJ-85	(charcoal)	960 ± 150
Punta Baja	W-30	(shell)	4030 ± 200
Near Punta Baja	LJ-83	(shell)	1600 ± 150
Colina Coyote 1	LJ-28	(charcoal)	1000 ± 250
Colina Coyote 2	LJ-30	(charcoal)	600 ± 150
Baja California (Golfo de California)			
San Felipe	LJ-96	(shell)	1370 ± 200
San Felipe	LJ-100	(charcoal)	200 ± 100
Bahia de los Angeles	LJ-26	(shell)	6100 ± 200
Bahia de los Angeles	LJ-29	(charcoal)	2500 ± 300
Isla Pescadero	LJ-132	(shell)	1700 ± 150

These data show the essential continuity of the shellfish-gathering habit along this coast for more than seven millenia. Thick middens now have been dated within each of the eight millenia. The hypothesis in the preliminary report on the Scripps Estates Site, based upon relatively few radiocarbon dates, and those mainly in the vicinity of San Diego, "that in the past few thousand years this shell midden activity diminished to minor importance" holds to some degree locally for certain periods but, for the whole coast and for the whole period for which dates now are available, it does not hold. Reliance on the free-and-easy food source from the littoral zone seems to have been persistent, and the supply, although no doubt fluctuating in time and space, maintained itself; but, as already discussed, it is probable that the supply of some types of shellfish was greater during the early period of La Jolla occupation than at present.

This is not to say that all the shellfish-gatherers up and down the coast were genetically or socially continuous, either in space or time. Much research will be needed to determine the spatial and temporal extent of the La Jolla Culture or even to estimate whether it had unity in any one place such as the Scripps Estates Site. It is highly probable that new stocks arriving on the coast, including the recent Yumans, absorbed the shellfish-gathering customs. This concept is contrary to the hypothesis of Rogers (1945) and others, that the "La Jolla II" culture, and presumably people also, developed directly into the Yuman Culture (and people) throughout a long period.

It seems to be a plausible assumption that the La Jolla people not only degenerated in habits and in tool-making ability butalso, after such early retrogression, stagnated. The Scripps Estates Site seems to have been inhabited for more than two millenia with little evidence of change in culture. The same general type of food and the great paucity of sophisticated tools or weapons argues for a long-continued, unprogressive existence. The comparatively very long persistence in southern California of simple culture, which he has equated with the "Archaic stage," has recently been forcefully stressed by Meighan (1959).

Most of the artifacts seem to have been concerned with the procurement and preparation of food. However, a few pieces of evidence indicate that the La Jolla people(s) had not degenerated into purely animal existence, as some have intimated. The inclusion in the artifact assemblage of a very few objects, of several types, that were not associated with food gathering and preparation show that they retained at least a trace of higher culture or absorbed such culture to a limited extent through contacts with other people. In this connection we may recall the relatively few shell beads, mostly associated with burials; the very few possible gamestones; the three doughnut stones that seem too small to have served as digging-stick weights; and the pretty little stones interpreted as possibly charm stones.

Although rock workmanship at Scripps Estates Site had degenerated into, or possibly retained, a state of extreme crudity in a period long subsequent to considerably more advanced cultures elsewhere in western North America, we do find a few artifacts that indicate some measure of skill and pride in fabrication. Outstanding among these are the very few well-made domed scrapers, the three doughnut stones and, if these are not all intrusive, a few projectile points.

It is possible, of course, that the few articles of more refined manufacture in the Scripps Estates Site may have stemmed from contacts with other peoples with higher culture. On this hypothesis, the rarity of such objects would reflect infrequency of such contacts or resistance to the adoption of better ways and things. Evidence for such contacts has been adduced by Warren (Moriarty *et al.*, 1959) from his studies of the main burial area, as follows: "A single flake of obsidian found in Stratum A_2 [soil horizon B_1] and the presence of a few flakes and artifacts of jasper suggest contact with the interior, while a steatite doughnut-shaped stone suggests contact with Santa Catalina Island."

SUMMARY

Shell from a recently investigated, extensive coastal midden designated as Scripps Estates Site at La Jolla, Calif., closely associated with a human burial, has been radiocarbon-dated at 6700 ± 150 years B.P. Three other datings for the same site, including one of 5460 ± 100 years for shell from the uppermost soil horizon and one of 7370 ± 100 years for shell encased in caliche from the lower layers, suggest, along with other circumstances, that the site was continuously occupied while the soil accumulated and weathered for at least two millenia. More than 50 burials have been uncovered in one small area during partial excavations of the site; many others no doubt remain to be discovered. A number undoubtedly have been lost in the removal of soil and many probably have been eliminated by weathering.

The skeletons, in so far as could be determined, all were buried in flexed position, usually on the side and with the head directed more or less toward the north. Large sandstone metates overlay two of the recently exhumed skeletons. Most of the shell beads found, consisting either of *Olivella* shells with the apex ground off or of drilled discs of pismo clams, were associated with burials. About 90 *Olivella* beads were found near the neck of one skeleton together with one heavy disc bead.

Relatively simple culture is suggested by the numerous artifacts, the vast majority of which seem to have been for simple utilitarian use. Crude core and flake hand tools, in considerable diversity and in large part not readily typeable, abound. A few less crudely flaked scrapers occur. Manos also abound. Basin metates (mostly broken), various types of hammerstones, and smooth, oval, often well-colored pebbles (unworked charmstones?) are common. The few finely pressure-flaked projectile points that lie on or near the surface of this and of similar nearby middens appear to be largely or wholly intrusive. Among the many hundred artifacts recovered are three doughnut stones, three broken shallow bowls, one double-ended rubbing pestle, two or three objects interpreted as discoidal gamestones, a number of almost perfectly spherical stones (gamestones?), two perforated pieces of sandstone, one granite reamer (?), three pitted stones, a crude quartz point, and a few fragments of worked bone. A fossil shark tooth seems to have been brought into the site, either for use or as a curiosity. The variety and scarcity of these artifact types is a characteristic of the site. No trace of pottery was found and, except for a few shards at the surface, none has been recovered from similar nearby sites. The culture of this site is identified as the rather vaguely characterized La Jolla. The artifactual complex does not conform with the tantalizingly brief and indefinite distinction between "La Jolla I" and "La Jolla II" and lends little or no support to such a division.

A considerable number of such sites, all lacking pottery and lacking or extremely deficient in finely pressure-flaked artifacts, constitute the earliest wholly definitive evidence of seafood-gathering and seed-grinding peoples in southern California and northern Baja California. These sites extend over a wide area from the northern Channel Islands to northwestern Baja California and to Bahia de Los Angeles on Golfo de California. Radiocarbon dates, which have been published recently for a number of these sites, lie within the period 7400 to 4950 years B.P. Apparently similar shell middens in the same area have been dated between 4950 and about 1000 years ago. Available dates for shellfish-gathering sites in southern California and northern Baja California are listed.

It seems plausible to assume that the crude culture indicated for the La Jolla people, for other people of the same general time and region (if different), and for their descendents or other people who followed them in this region, is attributable not to primitiveness but rather to degeneration, because of the ease of existence in a salubrious climate with an abundance of nutritious seafood supplemented by edible land plants. To call such cultures "preprojectile" seems much less reasonable than to assume that the people made few or no projectile weapons because they had little or no need for hunting or fighting. Some vertebrates were included in the food, but there are no indications that large game was captured either on land or at sea. The fishes that were captured are in part species that would seem to require the use of a boat or raft. No evidence was obtained at this site to indicate a rapid change in seafood diet that might be correlated with the depletion of a favored species.

There is evidence of only minimal contact with populations on the Channel Islands and in the desert. A second ancient culture in southern California termed San Dieguito, rather ill-defined but characterized by well-worked projectile points, has been held to antedate the La Jolla. The first radiocarbon date attributed to this culture (from shell at the type locality) is 4720 ± 160 years B.P. However, it now appears that this shell may have been erosionally intrusive and that the San Dieguito is indeed older than the La Jolla, as a date of 6300 ± 200 years B.P. recently was obtained for Claude N. Warren on charcoal from a firepit identified as La Jolla overlying the San Dieguito at the same locality.

Skeletal remains indicate considerable variation in skull types in the Scripps Estates Site. Both brachycephalic and dolichocephalic types occur. Some skulls have thick bones, but others have more typically thin bones. At least one skull is strongly prognathous in comparison with others. Pending a detailed morphological and morphometric study of the skeletons, it seems wise to hold in abeyance and in strong doubt suggestions that the La Jolla people were Australoids or of any other non-Mongoloid race. The people, whatever their race, were of moderate stature and apparently were reasonably free of vitamin-deficiency diseases. Variation in the extent of tooth grinding and in the distribution with depth of midden shells and grinding equipment suggests the possibility of a change in diet from a preponderance of seafood to a higher proportion of ground vegetable material. However, the apparent decrease of shell in the uppermost soil horizon may be due to postoccupational accumulation of soil, to disturbance of the soil, and to the greater weathering of shell in the A horizon as contrasted with the lime-enriched lower (B) layers.

The amount of shell in the middens is far less than would be expected from the indicated long period of occupation. Much dissolution of shell is suggested, and most of the lime may have been washed out of the site during moist periods. Indications of a long-continuing population at the site suggests a climate more humid than it is now. At the present time there is surface fresh water adjacent to the site sufficient to support only a few dozen people. If the site population was greater, the available water supply must have been greater than at present as a result of greater rainfall. A variety of other leads are consistent with the idea that the La Jolla region and other parts of the Southwest were better watered than at present throughout most, if not all, of Postglacial time.

Extreme scarcity of charcoal in this and other La Jolla sites suggests relatively little fire use, hence that temperatures were at least as warm as at present. On statistical analysis, the present latitudinal range of the molluscs represented in the midden of Scripps Estates Site confirms the hypothesis that the temperatures were somewhat warmer than at present. Paleo-temperature measurements definitely confirm this idea. Bay-inhabiting shells at this and nearby sites indicate that the adjacent canyon mouths were occupied by salt-water inlets, the existence of which can be interpreted as due to a rapid rise in sea level. Abundant use of rocky-foreshore molluscs testifies to the extensive development of intertidal rock, such as would have been exposed by a rising sea. Extreme scarcity of sand-beach molluscs suggests that sandy beaches were poorly developed during the La Jolla period. Recent studies on eustatic changes in sea level, especially along the coast of Texas, support the evidence from this and other California coastal sites that sea level was still rising during this period.

That relative sea level along the Californian coasts continued to rise somewhat during the past few millenia is indicated by the apparent retention of bay conditions until about 1000 years ago, evidenced by the circumstance that several middens of no great antiquity descend to below present sea level and by the vast abundance of deep bowls and other artifacts beyond the present low-tide line.

ACKNOWLEDGMENTS

Many professional and amateur archaeologists and others have contributed to the site investigations. Claude N. Warren of the Archeological Survey of the University of California, Los Angeles, and several associates participated extensively in the research. The late Malcolm J. Rogers very generously supplied data from the records of the San Diego Museum of Man, San Diego, Calif. on his earlier unpublished exploration of the site and participated in many stimulating discussions with us concerning this and other local sites. Assistance and advice was furnished by numerous colleagues of the Scripps Institution of Oceanography, particularly Hans E. Suess and George S. Bien, for radiocarbon measurements; Robert N. C. Bowen for paleo-temperature determinations;

Joseph R. Curray for use of his data on the recent rise in sea level; David R. Schink for analysis of caliche; Albert E. J. Engel for identification of rocks; and, particularly, Jacquelin N. Miller for analysis of shell material and other assistance. Emory P. Chace of the San Diego Museum of Natural History checked the identification of molluscs and some were referred to S. Stillman Berry. John E. Fitch of the California Department of Fish and Game identified the fish otoliths. Robert K. Murphy helped in cleaning and studying the skeletal material. Volunteers who helped us in the excavations include Bernice and John A. Beagles, Priscilla W. Field, David Folsom, Susan McKinley, and Georgina C. Peyton.

References

ASCHER, R. 1959. A prehistoric population estimate using midden analysis and two population models. Southwestern J. Anthropol. 15: 168-178.

BROECKER, W. S. & J. L. KULP. 1957. Lamont natural radiocarbon measurements IV. Science. 126: 1324-1334.

BROECKER, W. S., J. L. KULP & C. S. TUCER. 1956. Lamont natural radiocarbon measurements III. Science. 124: 154-165.

CARTER, G. F. 1957. Pleistocene Man in San Diego. Johns Hopkins Press. Baltimore, Md.

COE, W. R. & D. L. FOX. 1942. Biology of the California sea-mussel *(Mytilus californianus).* I. Influence of temperature, food supply, sex and age on the rate of growth. J. Exptl. Zool. 90: 1-30.

COUNT, E. W. 1938. The "Australoid" in California. Zeitsch. Rassenkunde. 8: 62-95.

CRANE, H. R. & J. B. GRIFFIN. 1958. University of Michigan radiocarbon dates III. Science. 128: 1117-1123.

CURRAY, J. R. 1960. Sediments and history of the Holocene Transgression/Continental Shelf, northwest Gulf of Mexico. *In* Sediments of the Northern Gulf of Mexico. Francis P. Shepard, Ed. Am. Assoc. Petrol. Geol., Spec. Publ. : 221-266.

DIXON, R. B. 1913. Some aspects of North American archaeology. Am. Anthropol. 15: 549-577.

EMERY, K. O. 1950. Ironstone concretions and beach ridges of San Diego, California. Calif. J. Mines and Geol. 46: 213-221.

FAIRBRIDGE, R. W. 1958. Dating the latest movements of the Quaternary sea level. Trans. N. Y. Acad. Sci., Ser. II. 20(6): 471-482.

FITCH, J. E. 1953. Common marine bivalves. Calif. Dept. Fish and Game, Fish Bull. No. 90: 1-102.

HANNA, M. A. 1926. Geology of the La Jolla Quadrangle, California. Univ. Calif. Publ., Bull. Dept. Geol. Sci. 16: 187-246.

HARDING, M. 1951. La Jollan Culture. El Museo 1:.

HEIZER, R. F. 1958. Radiocarbon dates from California of archaeological interest. Univ. Calif. Archaeol. Surv. Rept. No. 44: 1-16.

HERTLEIN, L. G. & U. S. GRANT, IV. 1939. Geology and oil possibilities of southwestern San Diego County. Calif. J. Mines and Geol. 35: 57-78.

HERTLEIN, L. G. & U. S. GRANT, IV. 1944. The geology and paleontology of the marine Pliocene of San Diego, California. San Diego Soc. Nat. Hist. Mem 2, Pt. 1, Geology.: 1-72.

HERTLEIN, L. G. & U. S. GRANT, IV. 1954. Geology of the Oceanside-San Diego coastal area, southern California. Calif. Div. Mines Bull. **170**: 53-63.

HUBBS, C. L. 1948. Changes in the fish fauna of western North America correlated with changes in ocean temperatures. J. Marine Research. 7: 459-482.

HUBBS, C. L. 1960*a*. Quaternary paleoclimatology of the Pacific Coast of North America. Calif. Coop. Oceanic Fish. Invest. Reports. 7: 105-112.

HUBBS, C. L. 1960*b*. The biogeography of Baja California and adjacent areas: The marine vertebrates of the outer coast. Syst. Zool. **9**: 134-147.

HUBBS, C. L., G. S. BIEN & H. E. SUESS. 1960. La Jolla natural radiocarbon measurements I. Am. J. Sci., Radiocarbon Suppl. 2: 197-223.

HUBBS, C. L. & R. R. MILLER. 1948. The zoological evidence: II. Correlation between fish distribution and hydrographic history in the desert basins of western United States. *In* The Great Basin, with Emphasis on Glacial and Postglacial Times. Bull. Univ. Utah (Biol. Ser.). **10**: 17-166.

JOHNSON, F. & J. P. MILLER. 1958. Review, Pleistocene Man at San Diego. Am. Antiquity. **24**: 206-210.

KEEN, A. M. 1937. An abridged check list of west North American marine Mollusca. Pp. 1-87. Stanford Univ. Press. Stanford, Calif.

KRIEGER, A. D. 1958. Review, Pleistocene Man at San Diego. Am. Anthropol. **60**: 974-978.

LIBBY, W. F. 1951. Radiocarbon dates, II. Science. **114**: 291-296.

LIBBY, W. F. 1952. Chicago radiocarbon dates, III. Science. **116**: 673-681.

LIBBY, W. F. 1955. Radiocarbon Dating 2nd. ed. Univ. Chicago Press, Chicago, Ill.

LYON, T. L. & H. O. BUCKMAN. 1943. The nature and properties of soils. A college text of edaphology. Macmillan Co., N.Y.

MEIGHAN, C. W. 1959. California cultures and the concept of an Archaic Stage. Am. Antiquity. **24**: 289-305.

MORIARTY, J. R., G. SHUMWAY & C. N. WARREN. 1959. Scripps Estates Site I (SDi-525): A preliminary report on an early site on the San Diego coast. Archaeol. Surv. Ann. Rept. 1958-1959. Dept. Anthropol. and Sociol. Univ. Calif., Los Angeles.: 185-216.

OAKLEY, K. P. 1959. Review, Pleistocene Man at San Diego. Man. 59(183).

ORR, P. C. 1952. Report on Santa Rosa Island. Sixth Santa Rosa Island Expedition. Santa Barbara Mus. Nat. Hist. Santa Barbara, Calif.

ORR, P. C. 1956. Radiocarbon dates from Santa Rosa Island I. Bull. Dept. Anthropol., Santa Barbara Mus. Nat. Hist. 2: 1-10.

PECK, S. L. 1955. An archaeological report on the excavation of a prehistoric site at Zuma Creek, Los Angeles County, California. Archaeol. Surv. Assoc. So. Calif. Paper. No. 2: 1-87.

ROBINSON, G. W. 1937. Soils. Their origin, constitution, and classification. An introduction to pedology. 2nd Ed. Thomas Murby & Co. Londong, England.

ROGERS, M. J. 1929. The stone art of the San Dieguito Plateau. Am. Anthropol. **31**: 454-467.

ROGERS, M. J. 1939. Early lithic industries of the lower basin of the Colorado River and adjacent desert areas. San Diego Museum Paper, No. 3: 1-75.

ROGERS, M. J. 1945. An outline of Yuman prehistory. Southwestern J. Anthropol. **1**: 167-198.

RUBIN, M. & H. E. SUESS. 1955. U. S. Geological Survey radiocarbon dates II. Science. 121: 481-488.

SCHENCK, H. G. 1945. Geologic application of biometrical analysis of molluscan assemblages. J. Paleontol. 40: 504-523.

SCHENK, H. G. & A. M. KEEN. 1937. An index-method for comparing molluscan faunules. Proc. Am. Philos. Soc. 77: 161-182.

SCHENK, H. G. & A. M. KEEN. 1940. Biometrical analysis of molluscan assemblages. Soc. Biogeograph. 7: 379-392.

SHEPARD, F. P. & H. E. SUESS. 1956. Rate of Postglacial rise of sea level. Science. 123: 1082-1083.

SOIL SURVEY STAFF. 1951. Soil Survey Manual. United States Dept. Agriculture Handbook No. 18: Washington, D. C.

SUESS, H. E. 1954. United States Geological Survey radiocarbon dates I. Science. 120: 467-473.

TRUE, D. L. 1958. An early complex in San Diego County, California. Am. Antiquity. 23: 255-263.

TUTHILL, C. & A. A. ALLANSON. 1955. Ocean bottom artifacts. Masterkev. 26: 222-232.

WALKER, E. F. 1951. Five prehistoric archaeological sites in Los Angeles County, California. Publ. Frederick Webb Hodge Anniversary Publication Fund. 6: 1-116.

WALLACE, W. J. 1955. A suggested chronology from southern California coastal archaeology. Southwestern J. Anthropol. 11: 214-230.

Printed in the United States of America

(1185)

(1186)

Reprinted from SYMPOSIUM: THE BIOGEOGRAPHY OF BAJA CALIFORNIA AND ADJACENT SEAS — PART II. MARINE BIOTAS. *Systematic Zoology*, Vol. 9, Nos. 3 & 4, Sept. - Dec. 1960, pp. 134 - 147.

The Marine Vertebrates of the Outer Coast[1]

CARL L. HUBBS

IT IS ONLY a first, in fact a very crude approximation, to include the Gulf coast of Baja California and the tip of the peninsula in the tropical Panamic Province and the rest of the outer coast in the warm-temperate (San Diegan) division of the Californian Province. The faunal changes along the outer coast of Baja California, in particular, are neither so abrupt nor so regular as to justify drawing definite boundaries to such provinces. The facts of the distribution of life along this coast emphasize the serious doubts that may be entertained regarding the wisdom of attempting a definite areal zoogeographic classification along an hierarchic system. It may well be more meaningful and dynamic to treat each areal faunal assemblage as a complex of faunal elements of diverse provenance, as Mayr (1946) and Parkes (1958) have done for the birds of North America.

General Distributional Pattern

The marine vertebrates of the outer coast of the Baja California peninsula—the prime subject of this paper—change irregularly from almost strictly tropical (Panamic) at Cabo San Lucas to largely warm-temperate (San Diegan) just north of the political boundary between Baja California Norte and California.

Though basically tropical, the marine vertebrate fauna of the Cape region lacks many of the species characteristic of the Central American coasts, and includes a number of San Diegan types, such as the California yellowtail, *Seriola dorsalis* (Gill), which also occurs in the Gulf, and the opaleye, *Girella nigricans* (Ayres), which is represented by a cognate species in the Gulf. Another San Diegan type, which occurs in shallower water to the northward, on both sides of the peninsula, namely the sheephead, *Pimelometopon pulchrum* (Ayres), rounds the Cape in relatively deep water. Included also are a number of Indo-Pacific fishes, including the Moorish idol, *Zanclus cornutus* (Linnaeus). In fact, as a result of recent explorations, Boyd W. Walker and Richard H. Rosenblatt regard the fauna of the Cape region as having insular characteristics. Indeed, it is very probable that the Cape mountains at no very great geological antiquity did constitute an island mass.

In conformity with the oceanographic conditions (Roden, 1958; Roden and Groves, 1959), the tropical elements in the Cape fauna extend much farther northward, and dominate the fauna much farther, on the Gulf side of the peninsula than on the ocean-exposed western shore. Along the western coast the marine vertebrate fauna, like the surface temperature, changes abruptly between the Cape and the region about Bahía Magdalena. The alteration in the fauna is most abrupt along the open coast, where the coastal water is subject to upwelling. Cooling of the shore water by upwelling is apparent as far south at least as the region of Cabo San Lázaro, near the offing of Bahía Magdalena. In this region of upwelling such typical Californian intertidal fishes as *Clinocottus analis* (Girard) and *Gibbonsia elegans* (Cooper) reach their southern limit.

---

[1] Contributions from the Scripps Institution of Oceanography, New Series, no. 1336

Within the Bahía Magdalena complex, where the waters are less affected by upwelling and are more subject to insolation, and are hence warmer, a more tropical fauna persists. This is especially true of Bahía Almejas, the warm, shallow, southern extension of Bahía Magdalena, in which the anchoveta, *Cetengraulis mysticetus* (Günther), finds its northernmost locality of abundance.

Farther north, in the lagoons and largely enclosed bays, and in the gentler coastal recesses (bahías Sebastián Vizcaíno and Todos Santos), the fauna also remains more nearly tropical than along the intervening coasts, where upwelling dominates insolation. In the enclosed waters tropical fishes occur incongruously far northward. Surveys are incomplete, but conspicuous examples among the fishes have come to light. To mention a few: *Ophioblennius* occurs in Bahía Tortuga; *Pareques viola* (Gilbert) and representatives of tropical blennioid genera (*Malacoctenus, Labrisomus, Enneanectes,* and *Ogilbia*) in the very warm southern shore of Bahía Sebastián Vizcaíno (Dawson, 1952); *Exerpes* in Bahía Tortuga and in Scammon and San Ignacio lagoons (Hubbs, 1952: 94–95); the tropical goby genus *Microgobius* also in Laguna San Ignacio; and *Cynoscion parvipinnis* Ayres in Bahía Todos Santos. Obviously, it would violate the facts either for the upwelling waters of the outer coast or for the insolated waters of the bays and lagoons to draw a faunal boundary line at any one latitude along the western coast of Baja California.

The temperature surveys now in progress, expanding the pioneering work by McEwen (1916) (see reports by Dawson, 1945–1953, his paper in this symposium, and preliminary statements by Hubbs, 1948, 1959a), offer a ready explanation for the incongruity between the biotic affinities along the open coast and in the bays and lagoons. Great discrepancies exist between the surface temperatures in these habitats during the warmer months (the temperatures are more uniform during the colder months). The conservative water masses of the lagoons and enclosed bays become warmed by insolation. The open "bays" (Sebastián Vizcaíno and Todos Santos) receive inflowing currents that tend to elevate the surface level, and hence inhibit upwelling, because they open to the northwest and are enclosed on the northeast, east, south, and, in part, on the southwest. Not only the prevailing northwesterly winds, but nearly all northerly and westerly winds induce flow into the open bays. Along the open coast, which generally trends from northwest to southeast, most winds, ranging from westerly through northerly to easterly, supplemented by Corioli's force, induce movement of the surface water away from the shore, to be replaced by cooler water from below. The upwelling and cooling is particularly striking on the southern and southwestern, and occasionally southeastern, sides of points, where one can actually watch the surface waters move offshore, when brisk winds, sweeping down the coastal slopes, induce catspaws that flick seaward. The surface temperatures on the northern and southern sides of points usually contrast sharply during the warmer months. The greatest contrasts have been observed at Punta Banda, which forms the southern border of Bahía Todos Santos. Here, at stations only two miles apart (across the base of the point), the surface temperatures along the coast have differed by as much as 12° C, commonly by 3° to 9° C. On the rare occasions when the temperature in summer is higher on the southern side of a point, the wind is from a southern sector, piling water up on the south side and driving it out on the north side.

The shallow-water fishes, along with the littoral algae (Dawson, 1945–1953) and the invertebrates (see the paper in this symposium by Garth), reflect the irregular temperature differentials. Dawson has documented the evidence extensively, and I have been accumulating physical and faunal data since 1945, with monthly temperature surveys since 1948. The whole aspect of the inshore fish fauna in the areas of strong upwelling along the northwestern coast of Baja California is reminiscent of that in the region of Monterey, California, where there is also much upwelling, inducing temperatures far below those in southern California. Some northern fishes, including the intertidal genera (or subgenera) *Amphigonopterus, Allocottus,* and *Epigeichthys,* occur disjunctly in areas of intense upwelling in Baja California, as about Puerto Santo Tomás, after skipping the warm waters of the southern part of southern California. The names of these species in different systematic appraisal are: *Amphigonopterus* (or *Micrometrus*) *aurora* (Jordan and Gilbert), *Allocottus* (or *Clinocottus*) *embryum* (Jordan and Starks), and *Epigeichthys* (or *Xiphister*) *atropurpureus* (Kittlitz). Another fish that seems to skip southern California south of the northern Channel Islands, to occur in the upwelling area of Baja California, is *Cebidichthys violaceus* (Girard) (the record from Point Loma, California, by Hubbs and Barnhart, 1944, proves to have been based on an unnamed genus and species). Other inshore species that are rare in the warm waters of southern California, but commoner on either side, are *Artedius lateralis* (Girard) and *Artedius notospilotus* Girard.

Nearly all northern fishes that reach as far south as San Diego, California, have by now been recorded, or have been taken by us, in the cooler waters of northwestern Baja California. The same relation holds for other marine vertebrates (as also for algae and invertebrates). Thus, I have found the black scoter, *Oidemia nigra americana* Swainson, and the rock sandpiper, *Erolia ptilocnemis* (Coues), in northwestern Baja California (Hubbs, 1955, 1956, 1960), and I have seen in waters off that coast two northern sea mammals long thought not to occur south of California, namely the northern fur seal, *Callorhinus ursinus* (Linnaeus), and the Dall porpoise, *Phocoenoides dalli* (True). It will probably prove to be a general rule, for all groups of littoral organisms, that the biota of northwestern Baja California includes the northern types that penetrate into the relatively warm water in the region of San Diego, California, plus a few species that skip those warm waters.

Other fishes (and invertebrates), which range continuously from the cold waters north of Point Conception through southern California to the upwelling areas of Baja California, follow a more or less isothermal path by submerging to greater depths in southern California and then coming into shallower water again in Baja California. Thus, species of *Sebastodes* that occupy depths of 30 to 80 meters about San Diego occur at about 10 to 30 meters near Santo Tomás. Species that occur between tides in central California but infratidally in southern California, such as *Sebastodes chrysomelas* (Jordan and Gilbert) and *Liparis mucosus* Ayres, reappear between tides in Baja California. This is no doubt a general phenomenon, which is illustrated among invertebrates by the red abalone, *Haliotis rufescens* Swainson, and by the large sea urchin, *Strongylocentrotus franciscanus* (Agassiz). Similarly, the whole community of the giant kelp, *Macrocystis,* extends into the shore rocks in central California and in the upwelling areas of Baja California, but near San Diego grows in about 10 to 30 meters of water.

The present pattern in the distribution of temperatures and of organisms along the outer coast of Baja California appears from recently gathered evidence to be of long standing, though modified by marked latitudinal shifts. Such shifts were no doubt accentuated during the Pleistocene. It was probably during the periods of continental ice sheets—the last ending about 10,000 years ago—that the ocean waters of the tropical eastern Pacific were sufficiently cooled to allow the transgres-

(1189)

sion of the equator by such now antitropical organisms (species or species groups) as now approach or barely reach the limits of the tropical fauna—in the Cabo San Lucas region from the north and in Peru from the south (Hubbs, 1952). Among the vertebrates, cognate pairs now flanking the tropics on either side include various sharks, and teleosts referred to the genera *Sardinops, Engraulis, Xenistius, Sebastodes* (the *rosaceus* species group only), and *Agonopsis;* also marine mammals of the pinniped genera *Mirounga, Zalophus,* and *Arctocephalus* (of the group *Arctophoca,* embracing the species *philippii* and *townsendi*) and the cetacean genera *Phocoena* and *Berardius.* Some marine birds may also be involved, as are also various invertebrates and a few algae, particularly the giant kelp, *Macrocystis.*

It may be assumed: (1) that the warm-temperate (San Diegan) and cool-temperate (Montereyan) vertebrate faunas were displaced southward, as the invertebrate faunas surely were, during the Wisconsin and earlier ice periods; (2) that some cool-temperate species were displaced so far southward that they were able to round Cabo San Lucas, where the tropical waters now interpose a barrier for such forms; (3) that anadromous trout then reached streams of western Mexico on the east side of Golfo de California; and (4) that the Gulf became populated by various organisms now characteristic of the fauna of southern California and northwestern Baja California. Some of these San Diegan types have survived in the Gulf, despite the high summer temperatures, probably because the cool winter temperatures (Roden, 1958; Roden and Groves, 1959) provide tolerable conditions for spawning and early development. They are thus able to survive alongside tropical forms that tolerate the cool winter temperatures (such types of temperature tolerance were discussed by Hutchins, 1947). The California spiny lobster, *Panulirus interruptus* (Randall), is a fine example among the invertebrates, along with several crabs that are being treated in a companion paper by John S. Garth. Among fishes in this category are representatives of the genera *Cetorhinus, Urolophus, Gymnura, Paralichthys, Hypsopsetta, Pleuronichthys, Xystreurys, Paralabrax* (*maculatofasciatus*), *Atherinops, Leuresthes, Anisotremus, Cheilotrema* (and probably other sciaenids), *Girella, Sebastodes, Gillichthys, Quietula, Ilypnus, Syngnathus,* and *Porichthys.* As a whole, these types are absent or very scarce in the Cape region. They are trapped in Golfo de California, just a many Pleistocene relicts are trapped i the geographically and zoogeographicall analogous Gulf of Mexico (Hedgpeth 1953). As in the Gulf of Mexico, many o the Pleistocene relicts in Golfo de California have undergone varying degrees of differentiation during their isolation.

During interglacial times the vertebrate fauna of the Baja California outer coast was no doubt displaced northward, but little evidence of such displacement can be cited. Some of the most tropical elements in the bays may be interglacial relicts, but they may merely be populations derived from immigrants that ranged northward in recent warm years. There is some paleontological evidence of northward dispersals during the Pleistocene. Perhaps the most spectacular example is that of a subtropical fauna, seemingly of Pleistocene age, that I have discovered on Guadalupe Island, and am analyzing with the collaboration of Emery P. Chace and others. This presumably interglacial fauna comprises a mixture of San Diegan species with a reef-building coral and with various mollusks that are now characteristic of the Panamic Province.

About 100 years ago the ocean temperatures of northwestern Baja California were no doubt sufficiently warmed to have allowed the transgression of this upwelling area by the tropical and subtropical types that then occurred at San Diego, California, but that are now wholly or largely confined to more southern waters, in Baja California Sur, and southward (Hubbs, 1948). Fishes illustrating this type of distribution include:

- *Anchoviella miarcha* (Jordan and Gilbert) (see Hubbs, 1953).
- *Chaetodon humeralis* Günther (see Hubbs and Rechnitzer, 1958).
- *Chaetodipterus zonatus* (Girard).
- *Eucinostomus argenteus* Baird and Girard.
- *Caranx caballus* Günther.
- *Dermatostethus punctipinnis* Gill (known only from the original description, but doubtless of southern origin).
- *Hippocampus ingens* Girard.
- *Sphoeroides annulatus* (Jenyns).

Other fishes of southern origin, which were reported from California in 1880, may have been holdovers from this warm period. This northward dispersal about the middle of the last century extended as far north as Monterey, California, where San Diegan types were encountered (Hubbs, 1948). Meteorological data confirmed the faunal indications of warmer temperatures at San Diego and at Monterey, with a decline until the early years of the twentieth century. There are indications that various other animals ranged farther north 100 years ago. In this connection we may list a clam, *Laevicardium elatum* (Sowerby), a crustacean, *Pleuroncodes planipes* Stimpson, and a porpoise, *Tursiops gillii* Dall.

Currently, in warm years, such as 1957 through 1959, the cold barrier of northwestern Baja California has been sufficiently weakened to have allowed the incursion into southern California, or even into more northern regions, of fishes that ordinarily live only farther south; or to induce in northern Baja California and in southern California a great increase in the numbers of types that are common southward, such as the yellowtail, *Seriola dorsalis* (Gill), the dolphinfish, *Coryphaena hippurus* Linnaeus, and the bonito, *Sarda lineolata* (Girard). The fish evidence for 1957–1959 is being reviewed by John Radovich. The northward movement of southern types in these warm years across and beyond the northwestern coast of Baja California involves not only fishes, which seem to be remarkably reactive to temperature changes, but also other marine vertebrates, such as the sea turtles *Chelonia, Caretta,* and *Lepidochelys;* also tropical seabirds, such as the red-billed tropicbird, *Phaethon aethereus mesonauta* Peters, and the magnificent frigatebird, *Fregata magnificens rothschildi* Mathews, and even the skua, *Catharacta skua* Brünnich (Small, 1959), which has not yet been reported from Mexico. Various marine invertebrates, including *Pleuroncodes planipes,* also moved northward in the warm period of 1957–1959, reappearing in numbers in Monterey Bay for the first time in decades.

The bathybial demersal fauna of the continental slope off Baja California is yielding a number of fishes, such as the hagfish, *Myxine circifrons* Garman, and the hake, *Merluccius angustimanus* Garman, that also occur in deep water off Panama and that exemplify, along with species of other genera, including *Lycodes,* the submergence in the tropics of types that occur antitropically in shallower water. Other bathybial bottom fishes of western Baja California, like the littoral fishes, are of either southern or northern origin.

The bathypelagic fish fauna off Baja California is yielding a considerable assortment of tropical forms that are presumably carried northward by a deep-lying current that is under study by Joseph L. Reid, Jr. Included among these are some of the bizarre genera of the black mid-depths, such as *Derichthys, Saccopharynx, Dysalotus, Kali,* and *Gigantactis.*

The epipelagic and the shallower bathypelagic fish faunas along the peninsula exhibit changes with latitude that somewhat parallel the changes in the littoral fauna. These changes involve geminate pairs as well as altered assemblages.

(1191)

Endemism

In view of the great latitudinal spread of Baja California and of the wide variety of habitats and oceanographic conditions, it is remarkable that so very few species of fish are confined to the outer coast of the peninsula. Excluding for the moment the fauna of the offshore islands, principally Guadalupe, the west-coast fauna of Baja California includes only a minimal number of forms that have been indicated as restricted endemics. A few littoral clinids are slightly differentiated (Hubbs, 1952, 1953; Springer, 1958); namely, *Paraclinus integripinnis zacae* Hubbs, in west-central Baja California and the offshore islands; *Paraclinus walkeri* Hubbs, from Bahía San Quintín; *Exerpes asper magdalenensis* Hubbs, from Bahía Magdalena; *Exerpes asper earli* Hubbs, from bays in central Baja California; and *Labrisomus wigginsi* Hubbs, from southwestern and west-central Baja California, *Labrisomus xanti* Gill, *Malacoctenus gigas* Springer, and two subspecies in *Malacoctenus* are confined to the same region plus the Golfo de California area. The nominal atherinid species *Leuresthes crameri* Jordan and Evermann appears to be invalid. The one gobiesocid indicated as confined to the mainland west coast of the peninsula, namely *Rimicola dimorpha* Briggs (1955), I have found also on the Channel Islands of California. Three deep-sea bottom fishes have been described only from off western Baja California, namely: (1) *Raja microtrachys* Osburn and Nichols (1916: 142–143, Fig. 1; see also Townsend and Nichols, 1925: 6); (2) *Harriotta curtissjamesi* Townsend and Nichols (1925: 6–8, Fig. 2); and (3) *Coryphaenoides albatrossus* Townsend and Nichols (1925: 17, Pl. 4, Fig. 2), a representative of a group in need of revision in North America. It is extremely improbable that any of these is confined to waters off the peninsula; the distinctness of the chimaeroid from *Harriotta raleighana* Goode and Bean of the Atlantic has been questioned by Bigelow and Schroeder (1953: 551). It seems highly probable that only a few forms of fishes are confined to the outer coast of Baja California, and that these are only slightly differentiated.

Greater local differentiation is exhibited by the fishes of the offshore islands—Guadalupe (oceanic) and the San Benitos (continental). No endemic fishes are known from the islands closer to shore. Some may be found about Rocas Alijos when the fish fauna of these offshore pinnacles (off southern Baja California) is explored. Some of the offshore banks and seamounts may also yield endemics, but their faunas have scarcely been touched (Hubbs, 1959b).

Two well-defined species that seem to be absent along the mainland occur on Guadalupe and the San Benitos, and nowhere else, so far as known. These are a clinid blenny, *Gibbonsia norae* Hubbs (1952), and a relatively deep-water butterflyfish, *Chaetodon falcifer* Hubbs and Rechnitzer (1958) (soon to be reported from Islas San Benito by me).

Several littoral fishes have been described from and appear to be restricted to Isla Guadalupe, which rises out of deep water more than 100 miles off Baja California Norte, and a considerable number of others (see list in Hubbs and Rechnitzer, 1958) exhibit varying degrees of differentiation and will in due time be distinguished. The forms already named as endemic from Guadalupe are:

Raja microtrachys Osburn and Nichols (1916:142–143, Fig. 1), originally ascribed to Guadalupe Island, but shown by Townsend and Nichols (1925: 6) to have come from deep water near Lat. 31° N.

Apogon guadalupensis (Osburn and Nichols, 1916: 160, Fig. 9). This species has been reported also from Cabo San Lucas (Breder, 1936: 18), but material recently collected there seems different.

Atherinops affinis guadalupae Hubbs (1918: 435–437), a well-defined subspecies. The local form of Islas San Benito is quite different, and much closer to *A. a. cedroscensis* of Cedros Island and the open coast thence northward to southern California (except for the two species shared with Isla Guadalupe, this local atherinid is the only fish on the San Benitos that shows evidence of endemicity).

Brachyistius aletes (Tarp, 1952: 89–90), a valid species.

Azurina hirundo Jordan and McGregor (in Jordan and Evermann, 1898: 1544–1545). This species was described as alone representing a district genus, but *Azurina* has since been found on other islands. Critical comparisons are needed to determine endemicity.

Scorpaena guadalupae Fowler (1944: 429–430, Figs. 217–218). This nominally endemic form proves to occur also in Golfo de California and to be merely the southern subspecies of *Scorpaena guttata* Girard.

Rimicola sila Briggs (1955:79–80, Figs. 5, 96). This distinct species and the next I discovered and distinguished, and supplied to Briggs for description in his monograph of the clingfishes.

Gobiesox eugrammus Briggs (1955: 100–101).

Heterostichus rostratus guadalupensis Hubbs (1952: 115–116, Fig. 43), a rather weakly defined subspecies based on lower meristic counts.

Gibbonsia elegans erroli Hubbs (1952: 151–152, Fig. 63), a subspecies verging on specific distinctness from the mainland subspecies.

Gibbonsia elegans rubrior Hubbs (1952: 152, Fig. 64), a deep-water differentiate (several fishes of the depleted fauna on Guadalupe appear to be in the process of bathymetric speciation).

Most of the Guadalupe endemics seem to be the descendents of waifs that reached this oceanic island from either the north or the south, mostly from the north. The higher incidence of endemism of forms of northern origin may have been due to the elimination during Wisconsin time of endemics of southern origin. The varying degree of differentiation may have resulted either from the length of isolation or from the rate of change. The island is notable also for endemism among the marine algae and some endemics have been discovered among the marine invertebrates. The terrestrial plants, gastropods, and birds exhibit a high incidence of endemism, in part autochthonous, in part of a relict nature.

The marine birds of Guadalupe and other islands off western Baja California also exhibit considerable endemism, as is indicated below. They seem, like most of the endemic fishes of Isla Guadalupe, to be of northern origin.

The almost complete lack of endemism among the marine fishes of the outer coast of Baja California, except on the offshore islands, is attributable in large part to an artificial circumstance, namely, the location of the international boundary. If the boundary had been set near Point Conception, only 2° farther north (about one-fifth of the latitude subtended by the peninsula), the west coast of Baja California would have ranked very high as an area of endemism. The warm-temperate San Diegan fish fauna is rich in endemic genera and species, very largely of remote southern origin.

The Elements in the Fish Fauna of Northwestern Baja California

Most members of the San Diegan fauna occur only south of Point Conception, though a few extend northward beyond this point: some, for example *Otophidium scrippsae* Hubbs, for a short distance; others, as strays or occasionally even in mass movements, in warm years, for longer distances, sometimes as far as Puget Sound; still others, for example *Girella nigricans* (Ayres), as waifs wafted north, in young stages, into cool, rich waters where reproduction is inhibited though good growth occurs; a few others, as residual populations in the warmer bays, particularly Morro and Tomales.

Nearly all fishes here listed as San Diegan have been recorded from northwestern Baja California, and probably all occur for varying distances down the Baja California coast. The two San Diegan species not yet reported from western Baja California are *Argentina sialis* Gilbert, which also occurs in Golfo de California, and *Rimicola muscarum* (Meek and Pierson; see Briggs, 1955), which we have recently taken in Baja California. A small proportion occurs or, as noted above is represented by geminate variants, in the cooler parts of Golfo de California (see also the accompanying paper by Boyd W. Walker).

Not included in the preceding and following tallies of the San Diegan species is a rare species, representing a monotypic genus, that is known only from southern California, but is probably tropical or subtropical. This is the peculiar pipefish, *Dermatostethus punctipinnis* Gill, already mentioned.

A tally of the distinctively San Diegan fish fauna indicates 76 genera and 96 species. Of the 96 species, 21 might almost as well be categorized as members of the fauna of Golfo de California and southward that reach northwestern Baja California and southern California, and at least eight approach the Californian category discussed below; on the other hand, several species attributed to each of these other categories might have been included on the San Diegan list. In addition, the San Diegan list includes two subspecies of southern and two of northern relationships. Twenty-two of the genera listed as San Diegan are endemic, in the sense of being essentially confined to southern California and adjacent Baja California, with or without representation in Golfo de California.

Most of the San Diegan fishes are confined in Mexico to Baja California Norte north of the warmish Bahía Sebastián Vizcaíno, but some extend farther, particularly in the areas of moderate upwelling south of Punta Eugenia and on the open coast opposite Bahía Magdalena. The following discussion is based largely on the fauna of northwestern Baja California north of Bahía Sebastián Vizcaíno, for which the data are more complete than for the more southern coast.

A considerable proportion of the fish fauna of the shores and ocean bottoms of northwestern Baja California (north of Bahía Sebastián Vizcaíno) can be classed as a Panamic element, as the forms involved are chiefly characteristic of Golfo de California and more southern waters. A tally of these forms, including a very few known from the Panamic region and California but not yet from anywhere on the outer coast of Baja California, discloses 58 genera and 65 species. As might be expected, from the circumstances that the waters of southern California are warmer than those of northwestern Baja California, except locally, nearly all of these warm-water fishes also occur in southern California, either regularly or sporadically, or did so during the warm period of the nineteenth century. The three definite exceptions encountered are *Achirus mazatlanus* (Steindachner), which is known north of Bahía Sebastián Vizcaíno from a single specimen collected barely south of the international border; *Moebia promelas* (Gilbert), a deep-water brotulid; and *Mugil curema* Valenciennes, the wide-ranging tropical American white mullet, which rarely ranges northward in the prejuvenile querimana stage.

Another large element in the shore and deep-bottom fishes of Baja California north of Bahía Sebastián Vizcaíno are members of what we may call the Californian fauna, in that its members commonly inhabit both the warm-temperate San Diegan and the cool-temperate Montereyan regions (some of the decisions as to placement in this as contrasted with the San Diegan element are somewhat dubious or arbitrary). A tally of this category totals 35 genera (19 endemic) and 62 species. The whole family Embiotocidae is largely characteristic of this fauna. A few species of this list occur also in the cooler parts of Golfo de California, but concerning only one, *Myliobatis californica* Gill, is there any question of a possibly sounder allocation in the subtropical and tropical element. Other species designated Californian range at times as far north as Puget Sound, but are hardly to be included in the Californian-Vancouveran faunal element.

Still other shore and deep-bottom fishes of northwestern Baja California can be allocated in what may be termed Californian-Vancouveran and Californian-Alaskan elements. A tally of these categories totals 50 genera (27 endemic) and 60 species, of which eight are rare enough, as immigrants or wanderers from the south, to be perhaps more reasonably classed as Californian. One of the species included, the deep-water alepocephalid *Narcetes stomias* (Gilbert), was described from off Washington, and has since been definitely recorded only from off northern Baja California (by Townsend and Nichols, 1925: 10, who question its possible identity with a Panamanian species).

Still more northern in affinity, among the fishes of northwestern Baja California, are the following Pacific amphiboreal fishes:

Squalus suckleyi (Girard), the Pacific spiny dogfish, by some now synonymized with *S. acanthias* Linnaeus of the North Atlantic.

Oncorhynchus kisutch (Walbaum), silver salmon, a rare stray below the California border.

Cololabis saira (Brevoort), the Pacific saury, essentially pelagic (genus endemic).

Coryphaenoides acrolepis (Bean), a deep-water macrourid, of a species group requiring revision.

Icichthys lockingtoni Jordan and Gilbert, the medusafish (genus endemic).

Icosteus aenigmaticus Lockington, the ragfish (genus endemic).

Pneumatophorus japonicus (Houttuyn), the Pacific mackerel, as a species.

Zesticelus profundorum (Gilbert), a deep-sea sculpin (genus endemic).

A summary by faunal elements of the genera, endemic genera, and species of the inshore and deep-bottom fishes of Baja California north of Bahía Sebastián Vizcaíno (Table I) indicates the essentially northern character of the fauna, particularly in respect to endemic genera (most of the species are endemic to each specified element). The high endemicity of the genera in the northern elements reflects the enormous richness and high distinctiveness of the North Pacific temperate-to-boreal fauna. The lack of endemic genera in the Panamic element that is represented in the fauna of northwestern Baja California reflects not only the low degree of generic endemism in that element but also its relative impoverishment, except in a few families, most notably in certain groups inhabiting inshore sandy and muddy waters, such as Engraulididae, Ariidae, and Sciaenidae. Very few of the tropical species of these families range north of the southern margin of Bahía Sebastián Vizcaíno. The low generic endemism in the Panamic fauna is due in considerable part to the circumstance that the Panamic fauna is largely a part of the common Atlantic-Pacific tropical fauna of the New World, with a few Indo-Pacific intrusions.

TABLE I—TALLY OF GENERA, ENDEMIC GENERA, AND SPECIES IN EACH OF THE ELEMENTS IN THE INSHORE AND DEEP-BOTTOM FISH FAUNA OF NORTHWESTERN BAJA CALIFORNIA.

ELEMENT	GENERA	GENERA ENDEMIC TO STATED ELEMENT	SPECIES
Panamic	58	0	65
San Diegan	76	21	96
Californian	35	19	62
Californian-Vancouveran Californian-Alaskan	50	29	60
Pacific Amphiboreal	8	4	8

The notable admixture of tropical and subtropical as well as San Diegan, Montereyan, Californian, and Vancouveran fishes in the fauna of western Baja California is attributable to the striking local differences in present surface temperatures, to the marked seasonal and annual fluctuations, and to extensive latitudinal shifts during Pleistocene and Holocene times.

The Marine Reptile Fauna

I have no certain record of the sea snake *Pelamis platurus* (Linnaeus) from the west coast of Baja California, but it probably occurs along that coast for some distance north of the Cape. At times it is extraordinarily common as far north as Puerto Vallarta on the mainland coast of Mexico.

All sea turtles of the eastern Pacific probably occur at least occasionally along the west coast of the peninsula. The eastern Pacific green turtle, *Chelonia mydas agassizii* Bocourt, supports a fishery as far northward as Bahía Sebastián Vizcaíno, is said to have occurred in Bahía San Quintín, and wanders occasionally, in warm years in some numbers, as far as southern California. The Pacific hawksbill turtle, *Eretmochelys imbricata squamata* Agassiz, occurs about La Paz and no doubt at times wanders into southwestern Baja California. The Pacific loggerhead turtle, *Caretta caretta gigas* Deraniyagala, occasionally reaches southern California, though much less frequently than the green turtle. The Pacific ridley, *Lepidochelys olivacea* (Eschscholtz), has not been recorded from the west side of the peninsula, but must have transgressed that side, for during the recent warm period one appeared in northern California (Houck and Joseph, 1958). The Pacific leatherback turtle, *Dermochelys coriacea schlegelii* (Garman), has been taken along the northwestern coast of Baja California, and occasionally wanders much farther, even to British Columbia (Carr, 1952).

The Marine Bird Fauna

As already indicated nearly all marine birds that breed or migrate as far south as the San Diego region at least occasionally occur along the cooler coast of northwestern Baja California. Similarly, most of the sea birds of southern affinity that occur along that area of upwelling transgress the international border. A number of species that occur northward only to southern or (a few) to central Baja California, appear to be wholly or largely blocked in their northward dispersal by the conditions that are associated with this upwelling. Most of the species that are limited in northward dispersal are definitely tropical, and add to the tropical stamp of southwestern Baja California.

The distributional relations involved are briefly presented in the following statements, derived largely from the data of Grinnell (1928), Friedman, Griscom, and Moore (1950), and Blake (1953).

The least grebe, *Colymbus dominicus bangsi* van Rossem and Hachisuka, a species of brackish and fresh waters, has been reported from the Cabo San Lucas region but not farther north on the outer coast.

The Pacific shearwater, *Puffinus pacificus chlororhynchus* Lesson, is a tropical species recorded in the Cape region but not farther north on the outer coast.

The Revillagigedo shearwater, *Puffinus auricularis* Townsend, is recorded with some doubt north to the Cape region.

The blue-footed petrel, *Pterodroma cookii orientalis* Murphy, has been reported northward only to off Cabo San Lucas.

The storm petrel, *Oceanodroma tethys tethys* (Bonaparte), wanders north to off Baja California, and has once been found breeding on Guadalupe Island (Huey, 1952).

The red-billed tropicbird, *Phaethon aethereus mesonauta* Peters, is fairly common north to the Cape region, but rare north to California.

The red-tailed tropicbird, *P. rubricauda rothschildi* (Mathews), is rare off northwestern Baja California, but is unknown from California.

Two of the three boobies, *Sula dactylatra californica* Rothschild and *S. leucogaster brewsteri* Goss, that occur occasionally along the western coast of Baja California have not been found north along the coast as far as California, unless, as seems likely to me, the old reports discredited by Grinnell and Miller (1944: 558) represent authentic records at a time when the southern fauna was dispersed far northward (Hubbs, 1948).

The magnificent frigatebird, *Fregata magnificens rothschildi* Mathews, and the thick-billed plover, *Charadrius wilsonius beldingi* Ridgway, are common along the southwestern coast of Baja California, but are rare farther north (as far as California).

The sooty tern, *Sterna fuscata crissalis* (Lawrence), is another tropical species that is known northward only to off southwestern Baja California.

The elegant tern, *Thalasseus comatus* (Philippi and Landbeck), is resident north to west-central Baja California, and is a post-breeding visitant into California.

Considerable insular endemism characterizes the marine avifauna of Baja California.

The now extinct Guadalupe petrel, *Oceanodroma macrodactyla* Bryant, apparently bred only on the forested mountain top of Isla Guadalupe.

The Baja California breeding populations of the Leach petrel, *Oceanodroma leucorhoa* (Vieillot), all confined to islands, have distinctive characters. *Oceanodroma l. willetti* van Rossem of Islas Los Coronados and *O. l. chapmani* Berlepsch of Islas San Benito may comprise a single form not known to breed elsewhere. On Guadalupe Island there are two separable forms, of similar size, smaller than any of the other subspecies. One, probably to be identified with *O. l. socorroensis* Townsend, which has the rump largely dark, and thus approaches the subspecies of the Coronados and the San Benitos, breeds in the summer. The other Guadalupe subspecies, *O. l. kaedingi* Anthony, breeds in the same places, even in the same burrows, but disjunctively in the winter. The segregation is temporal, not spatial.

The Heermann gull, *Larus heermanni* Cassin, is confined during breeding to only one island, San Roque, along the west coast of Baja California, and to several islands in Golfo de California.

The resident western gulls, *Larus occidentalis* Audubon, of Guadalupe Island contrast with the migrants from the north, *L. o. wymani* Dickey and van Rossem, in having feet very pale (whitish, yellowish, or barely pink), rather than distinctly pink, but not definitely yellow as in the Gulf form, *L. o. livens* Dwight. However, since western gulls from the central and southern parts of the west coast of Baja California are also in part light-footed, the problem is not yet settled.

The three forms of the alcid genus *Endomychura,* commonly assigned subspecific rank but perhaps better regarded as full species, are all insular endemics, largely of Baja California. *Endomychura hypoleuca hypoleuca* (Xantus) apparently breeds only on Isla Guadalupe; *E. h. scrippsi* Green and Arnold reproduces on several islands nearer to the mainland, from the Channel Islands of California to Islas San Benito off central Baja California; *E. craverii* (Salvadori) breeds only on islands in Golfo de California.

Another insular endemic alcid has been described from Baja California. This is *Ptychoramphus aleuticus australis* van Rossem, which breeds on islas San Benito and San Roque. The typical subspecies of the Cassin auklet breeds as far south as islas San Gerónimo and Guadalupe.

The Marine Mammal Fauna

The marine mammals furnish some of the most interesting and significant data bearing on the zoogeography of the outer coast of Baja California.

Five northern species reach their southern limit of distribution in the cool waters off northwestern Baja California. These include: (1) the southern sea otter, *Enhydra lutris nereis* (Merriam), which formerly ranged to Isla Cedros (but is now extinct south of San Miguel Island, California); (2) the northern fur seal, *Callorhinus ursinus* (Linnaeus), which migrates as far south as between islas Guadalupe and San Benito (personal observation); (3) the California harbor seal, *Phoca vitulina geronimensis* Allen, which occurs on the rocky reefs and in bays north of Bahía Sebastián Vizcaíno; (4) the striped porpoise, *Lagenorhynchus obliquidens* Gill; and (5) the Dall porpoise, *Phocoenoides dalli* True, both of which range well into the cool waters of northwestern Baja California, but no farther.

Three pinnipeds find their center of abundance off the northern half of the west coast of Baja California, but range, or primitively did range, beyond the limits of Baja California, both north and south. These are: (1) the California sea-lion, *Zalophus californianus* Lesson, which still ranges far north of Baja California, has a very small disjunct remnant population in the Sea of Japan (probably dating from Interglacial dispersal), originally ranged south of its present limit in the regions of Cabo San Lucas and Islas Tres Marías, and is represented in the Galápagos by a subspecies, *Z. c. wollebaeki* Sivertsen; (2) the Guadalupe fur seal, *Arctocephalus townsendi* Merriam, which seems always to have had its center of abundance on Isla Guadalupe, to which it now is restricted; and (3) the northern elephant seal, *Mirounga angustirostris* (Gill), which has rebuilt its population on Guadalupe to about 13,000 and is reestablishing colonies on other islands off northern Baja California and southern California, wanders north to southeastern Alaska, and is reported to have occurred on Clipperton Island. The Pacific bottlenose porpoise, *Tursiops gillii* Dall, seems also to have its center of abundance along the west coast of Baja California.

Of outstanding interest is the almost complete restriction of the east Pacific population of the gray whale, *Eschrichtius gibbosus* (Erxleben), during the calving season, to the lagoons along the west coast of Baja California. This unique species is here a relict, for the species existed prehistorically in northern Europe and in early historic time in the western North Atlantic, and still persists in limited numbers in the northwestern Pacific. Very limited breeding populations occur on the mainland coast of Mexico near the mouth of Golfo de California, and occasionally calves are born about Isla Guadalupe and along the coast of southern California, though San Diego Bay has been abandoned as a breeding locale.

Most of the wide-spread cetaceans of the North Pacific—ziphiids, delphinids, physeterids, and balaenopterids—either are known to occur off western Baja California or may be expected there. A recent addition to the list is the grampus, *Grampidelphis griseus* (Cuvier), which we recently observed in company with sperm whales at Isla Guadalupe.

Summary

As a first, crude approximation the Gulf coast and Cape region of Baja California may be included in the Panamic Province and the rest of the outer coast in the warm-temperate San Diegan division of the Californian Province. The transition is neither abrupt nor regular. The Cape region has a reduced tropical fauna, with some Indo-Pacific types, and insular characteristics. In conformity with oceanographic conditions, the tropical elements of the fauna persist much farther northward in the Gulf than on the outer coast, where they decline abruptly between the Cape and Bahía Magdalena. Northward, tropical elements tend to persist in bays, whereas northern types extend southward along the open coast, where temperatures are lowered by upwelling; any definite faunal boundary lines would violate some facts of distribution. Many tropical forms reach the southern shore of Bahía Sebastián Vizcaíno, a few extend farther, especially in warm years (as 1957–1959). Northward dispersal and warm temperatures were especially pronounced about a century ago. Warm-temperate (San Diegan) types persist in upwelling areas to near Bahía Magdalena (a few at the Cape); cool-temperate (Montereyan) types occur, some after skipping southern California, in the very cool open shores of northwestern Baja California. Differences are notable between the temperatures and the biota on the two sides of headlands.

The general pattern of distribution, though conservative, has been much modified by latitudinal shifts, most notably during the Pleistocene. During Glacial periods the fauna was displaced southward, to yield Pleistocene relicts in the upper Gulf. Interglacially, there were northward dispersals, indicated, for example, by a warm-water Pleistocene fauna on Guadalupe Island.

Endemism is remarkably slight among the fishes of the outer coast of Baja California, but would have been high if the international border had been fixed 2° of latitude farther north, near Point Conception (roughly the northern limit of the very distinctive San Diegan fauna). Endemism is noteworthy among the marine vertebrates of Isla Guadalupe, which is oceanic and more than 100 miles offshore.

The fauna of the northwestern coast of Baja California, which is cooled by upwelling, contains a limited number of Panamic types, almost none of which are Panamic endemics, and almost all of which occur at least occasionally in the waters of southern California, which are warmer. There is a much larger representation of northern elements, San

Diegan, Californian, Californian-Vancouveran, and Californian-Alaskan, with a few Pacific amphiboreal forms. In each of these elements, a considerable proportion of the genera are endemic to the given element. These circumstances reflect the immense richness and distinctness of the North Pacific fauna.

The notable admixture of tropical and subtropical as well as San Diegan, Montereyan, Californian, and Vancouveran fishes in the fauna of western Baja California is attributable to the striking local differences in surface temperatures, the marked seasonal and annual fluctuations, and the extensive latitudinal shifts during Pleistocene and Holocene times.

REFERENCES

Bigelow, Henry B., and William C. Schroeder. 1953. Chimaeroids. *In* Fishes of the western North Atlantic. Part Two. Mem. Sears Foundation Marine Research, 1:515–562.

Blake Emmet Reid. 1953. Birds of Mexico. A guide for field identification. Univ. Chicago Press, Chicago, 644 pp.

Breder, C. M., Jr. 1936. Scientific results of the Second Oceanographic Expedition of the "Pawnee" 1926. Heterosomata to Pediculati from Panama to Lower California. Bull. Bingham Oceanogr. Collection, 2(3): 1–56.

Briggs, John C. 1955. A monograph of the clingfishes (order Xenopterygii). Stanford Ichthyol. Bull., 6:1–224.

Carr, Archie. 1952. Handbook of turtles. The turtles of the United States, Canada, and Baja California. Comstock Publishing Associates, Cornell Univ. Press, Ithaca, New York, 542 pp.

Dawson, E. Yale. 1945. Marine algae associated with upwelling along the northwestern coast of Baja California, Mexico. Bull. Southern California Acad. Sci., 44:57–71.

1950. A note on the vegetation of a new coastal upwelling area of Baja California. Jour. Marine Research, 9:65–68.

1951. A further study of upwelling and associated vegetation along Pacific Baja California, Mexico. Jour. Marine Research, 10:39–58.

1952. Circulation within Bahia Vizcaino, Baja California, and its effects on marine vegetation. Amer. Jour. Botany, 39:425–432.

1953. Preliminary results of a marine algal reconnaissance of the Pacific Mexican coast. Proc. 7 Pacific Sci. Congr., 5:43–47.

Fowler, Henry W. 1944. Results of the Fifth George Vanderbilt Expedition (1941) (Bahamas, Caribbean Sea, Panama, Galápagos Archipelago and Mexican Pacific islands). The fishes. Acad. Natur. Sci. Philadelphia, Monogr. 6:57–529, 583.

Friedman, Herbert, Ludlow Griscom, and Robert T. Moore. 1950. Distributional check-list of the birds of Mexico. Part I. Cooper Ornithol. Club, Pacific Coast Avifauna, 29:1–202.

Grinnell, Joseph. 1928. A distributional summation of the ornithology of Lower California. Univ. California Publ. Zool., 32:1–300.

Grinnell, Joseph, and Alden H. Miller. 1944. The distribution of the birds of California. Cooper Ornithol. Club, Pacific Coast Avifauna, 27:1–608.

Hedgpeth, Joel W. 1953. An introduction to the zoogeography of the northwestern Gulf of Mexico with reference to the invertebrate fauna. Publ. Inst. Marine Sci., Univ. Texas, 3:107–224.

Houck, Warren J., and James G. Joseph. 1958. A northern record for the Pacific ridley, *Lepidochelys olivacea*. Copeia:219–220.

Hubbs, Carl L. 1918. The fishes of the genus *Atherinops,* their variation, distribution, relationships, and history. Bull. Amer. Mus. Natur. Hist., 38:409–440.

1948. Changes in the fish fauna of western North America correlated with changes in ocean temperature. Jour. Marine Research, 7:459–482.

1952. Antitropical distribution of fishes and other organisms. Proc. 7 Pacific Sci. Congr., 3:324–329.

1953. Identification and relationships of the anchovy described from California as *Anchovia scitula*. Copeia:193–194.

1955. Black scoters reported from Baja California. Condor, 57:121–122.

1956. Off-season, southern occurrence of the black scoter on the Pacific coast. Condor, 58:448–449.

1959a. Influence of land masses on the distribution and speciation in fishes and other organisms in the eastern Pacific. Internat. Oceanogr. Congr. Preprints, Amer. Assoc. Advanc. Sci., Washington:580–582.

1959b. Initial discoveries of fish faunas on seamounts and offshore banks in the eastern Pacific. Pacific Science, 13:311–316.

1960. The Rock Sandpiper, another northern bird recorded from the cool coast of northwestern Baja California. Condor, 62: 68–69.

Hubbs, Carl L., and Percy S. Barnhart. 1944. Extensions of range for blennioid fishes in southern California. California Fish and Game, 30:49–51.

(1199)

HUBBS, CARL L., and ANDREAS B. RECHNITZER. 1958. A new fish, *Chaetodon falcifer*, from Guadalupe Island, Baja California, with notes on related species. Proc. California Acad. Sci., (4) 29:273–313.

HUBBS, CLARK. 1952. A contribution to the classification of the blennioid fishes of the family Clinidae, with a partial revision of the eastern Pacific forms. Stanford Ichthyol. Bull., 4:41–165.

1953. Revision of the eastern Pacific fishes of the clinid genus *Labrisomus*. Zoologica, New York, 38:113–135.

HUEY, LAURENCE M. 1952. *Oceanodroma tethys tethys*, a petrel new to the North American avifauna. Auk, 69:460–461.

HUTCHINS, LOUIS W. 1947. The basis for temperature zonation in geographical distribution. Ecol. Monogr., 17:325–335.

JORDAN, DAVID STARR, and BARTON WARREN EVERMANN. 1898. Fishes of North and Middle America. Part II. Bull. U. S. Nation. Mus., 47:1241–2183.

MAYR, ERNST. 1946. History of the North American bird fauna. Wilson Bull., 58:1–41.

MCEWEN, GEORGE F. 1916. Summary and interpretation of the hydrographic observations made by the Scripps Institution for Biological Research of the University of California 1908 to 1915. Univ. California Publ. Zool., 15:255–356.

OSBURN, RAYMOND C., and JOHN T. NICHOLS. 1916. Shore fishes collected by the 'Albatross' Expedition to Lower California with descriptions of new species. Bull. Amer. Mus. Natur. Hist., 35:139–181.

PARKES, KENNETH C. 1958. The Palaearctic element in the New World avifauna. *In* Zoogeography, Publ. 51, Amer. Assoc. Advanc. Sci.:421–432.

RODEN, GUNNAR I. 1958. Oceanographic and meteorological aspects of the Gulf of California. Pacific Science, 12:21–45.

RODEN, G. I., and G. W. GROVES. 1959. Recent oceanographic investigations in the Gulf of California. Jour. Marine Research, 18:10–35.

SMALL, ARNOLD. 1959. Some additional records of the skua from California. Condor, 61:437.

SPRINGER, VICTOR G. 1958. Systematics and zoogeography of the clinid fishes of the subtribe Labrisomini Hubbs. Publ. Inst. Marine Science, Univ. Texas, 5:417–492.

TARP, FRED H. 1952. A revision of the family Embiotocidae (the surf perches). California Dept. Fish and Game, Fish. Bull., 88:1–99.

TOWNSEND, CHARLES H., and JOHN T. NICHOLS. 1925. Deep sea fishes of the 'Albatross' Lower California Expedition. Bull. Amer. Mus. Natur. Hist., 52:1–20.

CARL L. HUBBS is Professor of Biology, Scripps Institution of Oceanography, University of California, La Jolla.

(1200)

GEOKHIMIYA
pp.1124-1125

КРАТКИЕ СООБЩЕНИЯ

On the primordial lead of the Canyon Diablo meteorite

О ПЕРВИЧНОМ СВИНЦЕ МЕТЕОРИТА КАНЬОН ДЬЯВОЛА

Т. Дж. ШОУ и *К. К. ПАТТЕРСОН*
J. Tsaiwha Chow and C. C. Patterson
Океанографический институт Скриппса Калифорнийского университета
и Отделение геологических наук Калифорнийского технологического института

Первичный свинец, используемый для определения возраста Земли и метеоритов, был впервые выделен Паттерсоном, Тилтоном, Брауном и Ингрэмом [1] из троилита метеорита Каньон Дьявола. Масс-спектрометрический анализ образца был выполнен в лаборатории проф. Ингрэма в Чикагском университете. Полученные значения были впоследствии скорректированы на дискриминацию масс-спектрометра [2]. Еще позднее Старик и др. [3] определили изотопный состав первичного свинца, выделенного из металлической фазы метеорита Каньон Дьявола.

Так как изотопный состав первичного свинца является одной из основных величин в космохронологии, представлялось желательным провести повторный анализ на 12-дюймовом калиброванном масс-спектрометре в Калифорнийском технологическом институте [4]. Химическая подготовка образца заключалась в следующем: навеску (~ 8 *г*) троилита из метеорита Каньона Дьявола подвергали очистке разбавленной кислотой и затем растворяли в 6,5 *М* соляной кислоте. Железо удаляли эфирной экстракцией. Свинец отделяли от примесей других металлов экстракцией дитизоном и переводили в сульфид свинца, который наносили на танталовую ленту масс-спектрометра.

Содержание свинца в троилите было определено методом изотопного разбавления в $4{,}6 \cdot 10^{-4}\%$. Это значение отличается от опубликованного ранее содержания $18 \cdot 10^{-4}\%$ [2], что указывает на возможность присутствия в одном метеорите включения троилита с различными содержаниями свинца; такое же явление Чодос и Ничипорук [5] наблюдали в отношении других элементов-примесей в троилите. На том же образце троилита был выполнен параллельный анализ изотопного состава. Для каждого анализа было получено около 40 отсчетов. В изотопные отношения свинца вносились три поправки: 1) поправка на калибровку электрометрической шкалы; 2) поправка на квадратный корень из отношения масс и 3) поправка на относительное изменение магнитного поля, установленная по эталонным урановым образцам

Поправки имели следующие значения:

Скорректированное отношение		Наблюдаемое отношение	Поправочные коэффициенты. (1)	(2)	(3)
Pb^{206}/Pb^{204}	=	Pb^{206}/Pb^{204}	× 0,9996	× 1,0049	× 1,0069
Pb^{206}/Pb^{207}	=	Pb^{206}/Pb^{207}	× 1,0000	× 0,0076	× 0,9966
Pb^{206}/Pb^{208}	=	Pb^{206}/Pb^{208}	× 1,0007	× 0,9952	× 0,9932

В полученные отношения вносили также поправку на загрязнение обычным свинцом в количестве 0,2 *мкг* на 35 *мкг* свинца троилита. Точность определения изотопных отношений свинца в 90% случаев находилась в следующих пределах: ±0,3% для отношения Pb^{206}/Pb^{204}; ± 0,4% для отношения Pb^{207}/Pb^{204} и ±0,5% для отношения Pb^{208}/Pb^{204}.

Изотопные отношения свинца в метеорите Каньон Дьявола

Автор	Материал	Pb, $n \cdot 10^{-4}$, %	Pb^{206}/Pb^{204}	Pb^{207}/Pb^{204}	Pb^{208}/Pb^{204}
Паттерсон	Троилит	18	9,46	10,34	29,44
Старик и др.	Металлическая фаза	0,14	9,43	10,58	29,80
Данная работа	Троилит	4,6	9,61	10,38	29,87

Contributions from the Scripps Institution of Oceanography, New Series, 1337

Reproduced by Permission

Полученные результаты приведены в таблице вместе с результатами, полученными Паттерсоном [2] и Стариком [3]. Наблюдаемая здесь разница изотопных составов может лежать за пределами экспериментальной ошибки. В метеоритах, не содержащих урана, могут иметь место вариации изотопного состава свинца. Этот вопрос рассмотрен Мерти и Паттерсоном (рукопись готовится к печати).

Поступила в редакцию
4 августа 1961 г.

ЛИТЕРАТУРА

1. C. C. Patterson, G. Tilton, H. Brown, M. Ingram. Phys. Rev. 92, 1234, 1953
2. C. C. Patterson. Geochim. et Cosmochim. Acta 10, 230, 1956.
3. И. Е. Старик, Э. В. Соботович, Г. П. Ловцюс, А. В. Ловцюс, М. М. Шац. Радиохимия, 1, 596, 1959.
4. T. J. Chow, C. C. Patterson. Geochim. et Cosmochim. Acta 17, 21, 1959.
5. A. A. Chodos, W. Nichiporuk. An application of the mutual standards concept to X-ray fluorescence spectroscopy. The analysis of meteoritic sulphide nodules for eight elements. Proc. Conf. Ind. Appl. X-ray Anal., 7th Denver, 247, 1958.

From: Geofisica Internacional, v.1, no.3
July 1961. pp.55-72.

SOBRE LA CIRCULACION PRODUCIDA POR EL VIENTO EN EL GOLFO DE TEHUANTEPEC Y SUS EFECTOS SOBRE LAS TEMPERATURAS SUPERFICIALES *

G. I. Roden

RESUMEN

Se investiga la relación entre los vientos y las temperaturas de la superficie del mar en el Golfo de Tehuantepec. Se encuentra que las bajas temperaturas de invierno están relacionadas con la divergencia inducida por el viento en el transporte de las masas, cuya magnitud es de unos 0.02 g cm^{-2} seg^{-1} durante una galerna de invierno. Un análisis espectral de las anomalías de vientos y temperaturas en períodos de 10 días, indica que las anomalías en cuadrados adyacentes de 2 grados de latitud y longitud, son coherentes y casi simultáneas. Existe una relación más bien débil e inversa entre las anomalías del viento y la temperatura.

INTRODUCCION

El Golfo de Tehuantepec está situado directamente al sur del Istmo de Tehuantepec, una interrupción importante en la cordillera llamada Sierra Madre en el sur de México. En su punto más estrecho, el Istmo tiene unos 220 Km de un lado al otro. Hay aquí una interrupción de unos 40 Km en la cordillera; la máxima elevación en este lugar es de unos 250 m. Las ondas frías del norte que pasan a través del Istmo y llegan a una atmósfera más cálida, producen vientos "de descenso" de violencia particular. Esos vientos, conocidos de ordinario como "*Tehuantepequeros*" son más frecuentes en invierno y se sienten a varios centenares de kilómetros hacia el sur. El efecto de esos vientos sobre la superficie del océano es doble: mueven el agua hacia el sur, originando un arrastre de ella desde los lados y desde abajo y causan una mezcla considerable a lo largo del eje del viento. Estos últimos dos procesos llevan a un abatimiento considerable de la temperatura superficial del Golfo de Tehuantepec, que puede ser varios grados más baja que la observada en cualquier parte de la región mar afuera del sur de México y América Central.

ON THE WIND DRIVEN CIRCULATION IN THE GULF OF TEHUANTEPEC AND ITS EFFECT UPON SURFACE TEMPERATURES *

G. I. Roden

ABSTRACT

The relation between winds and sea surface temperatures in the Gulf of Tehuantepec is investigated. The low winter temperatures are found to be related to the wind induced mass transport divergence, the magnitude of which is about 0.02 g cm^{-2}sec^{-1} during a winter gale. A spectral analysis of ten-day temperature and wind anomalies indicates that anomalies in adjacent two degree squares of latitude and longitude are coherent and almost simultaneous. There exists a rather weak and inverse relation between temperature and wind anomalies.

INTRODUCTION

The Gulf of Tehuantepec lies directly south of the Isthmus of Tehuantepec, a major break in the Sierra Madre mountain range of Southern Mexico. At the narrowest point the Isthmus is about 220 Km across. Here, there is a gap of about 40 Km in the cordillera, the maximum elevation at this point being roughly 250 m. Cold waves from the north which pass through the Isthmus into the warmer atmosphere beyond produce *fall* winds of particular violence. These winds, commonly known as *Tehuantepecers*, occur most frequently in winter and are felt several hundred kilometers to the southward. The effect of these winds upon the ocean surface is twofold; they move the water to the southward causing entrainment of the water from the sides and from below, and they cause considerable mixing along the wind axis. The last two processes lead to a substantial lowering of the surface temperatures in the Gulf of Tehuantepec which may be several degrees lower than observed elsewhere in the region off southern Mexico and Central America.

---

* *Contribución de la Institución de Oceanografía Scripps. Nueva Serie.*

* *Contribution from the Scripps Institution of Oceanography. New Series,* 1338

Apenas existen investigaciones que se refieran a las condiciones meteorológicas y oceanográficas del Golfo de Tehuantepec. Hurd (1929) dio una descripción bastante detallada de los vientos. Las corrientes superficiales durante un “*Tehuantepequero*” fueron descritas vívidamente por la U. S. Hydrographic Office (1951): “La furia del norte arroja el agua fuera del Golfo hacia el sureste y cuando el agua baja en la parte superior, hay una corriente violenta a lo largo de cada ribera, hacia el norte, para llenar el vacío. Cuando el norte amaina o cesa de soplar, el agua que se ha represado fluye hacia atrás golfo arriba y una cantidad extra se precipita hacia el sur a lo largo de cada ribera. Este hecho se ha observado hacia el oeste hasta el Río Verde y hacia el este tan lejos como Champerico...” La descripción citada muestra claramente que el arrastre del agua tiene lugar durante el período de vientos fuertes y que después que el viento ha dejado de soplar, hay un reajuste al estado inicial. Se ha informado que la corriente costera hacia el norte durante la galerna adquiere una velocidad de 2 nudos y que la velocidad de la corriente costera hacia el sur después de aquella, es de 0.6 nudos; ambos datos vienen de Sacrificios. La distribución de las variables hidrográficas en el Golfo, según expediciones recientes, fue estudiada por Blackburn (MS). Una de las características interesantes fue que las temperaturas superficiales más bajas no ocurrieron en las cabeceras del Golfo, sino a alguna distancia hacia el sur.

Cuando las condiciones que producen un “*Tehuantepequero*” se extienden suficientemente hacia el sur en el Golfo de México, se encuentran también otras áreas de vientos de alta velocidad mar afuera de las costas de América Central, notablemente en el Golfo de Papagayo y en el Golfo de Fonseca. Los vientos en esas regiones, conocidos localmente como “*Papagayos*”, ocurren en una escala relativamente pequeña y tienen sobre la temperatura superficial un efecto similar a los “*Tehuantepequeros*”.

DATOS

Los datos de vientos y temperaturas superficiales en las estaciones costeras se obtuvieron del Servicio Meteorológico Mexicano (1928-1941) y del U. S. Coast and Geodetic Survey (1956, 1960) respectivamente. La exactitud de las observaciones individuales de temperatura en la costa se acerca a 0.3° C y de las observaciones individuales del viento a casi un 10% de la velocidad del viento. Las observaciones de temperatura y de velocidad del viento tomadas mar afuera a bordo de barcos mercantes, se obtuvieron del U. S. Weather Bureau (datos no publicados) para el período entre Enero de 1949 y Junio de 1957. La exactitud de las observaciones individuales no es muy grande: probablemente de ± 0.5° C para la temperatura y de ± 20% de la velocidad para las observaciones del viento. Una inspección cuidadosa de los registros lleva a la conclusión de que la calidad de las observaciones de temperatura es razonablemente buena, mientras que la calidad de

There are only few investigations dealing with the meteorological and oceanographical conditions in the Gulf of Tehuantepec. A rather detailed description of the winds is given by Hurd (1929). The surface currents during a *Tehuantepecer* are quite vividly described by the U. S. Hydrographic Office (1951); “The fury of the norther blows the water out of the gulf to the southward and, as the waters lower at the head, there is a rush along each shore to the northward to supply or fill the vacancy. When the norther moderates or ceases to blow, the water that was banked up, as it were, flows back up the gulf, and an extra amount rushes out along each shore to the southward. This fact has been observed as far west as Rio Verde and eastward as far as Champerico...” The above description clearly shows that entrainment of water takes place during the period of high winds and, after the wind has ceased to blow, there is readjustment to the initial state. The speed of the coastal nortward setting current during the gale is reported to be 2 knots and the speed of the coastal southward setting current after the gale 0.6 knots; both reported off Sacrificios. The distribution of hydrographic variables in the Gulf, based on recent cruises, was studied by Blackburn (MS). One of the interesting features was that the lowest surface temperatures did not occur at the head of the Gulf, but some distance to the southward.

When the conditions inducing the *Tehuantepecer* extend sufficiently far southward into the Gulf of Mexico, other areas of high wind velocity are found off the coast of Central America, notably in the Gulf of Papagayo and in the Gulf of Fonseca. The winds in these regions, locally known as *Papagayos* occur on a relatively small scale and have a similar effect upon the surface temperature as the *Tehuantepecers.*

DATA

Winds and sea surface temperatures at coastal stations were obtained from the Servicio Meteorologico Mexicano (1928-1941) and the U. S. Coast and Geodetic Survey (1956, 1960), respectively. The accuracy of individual coastal temperature observations is about ± 0.3 C and of individual wind observations about ± 10% of the wind speed. Offshore sea surface temperature and wind observations, taken aboard merchant ships, were obtained from the U. S. Weather Bureau (unpublished) for the period January 1949 to June 1957. The accuracy of individual observations is not great, probably ± 0.5 C for temperature and ± 20% of the wind speed for wind observations. A careful inspection of the records leads to the conclusion that the quality of temperature observations is reasonably good, whereas the quality of the wind observations is only moderate. The individual observations were combined and

las observaciones de viento es solamente moderada. Las observaciones individuales se combinaron y promediaron en cuadros de dos grados de latitud y longitud y en períodos de diez días y de un mes. El número de observaciones incluido en cada promedio de diez días varía generalmente entre 10 y 30. Las medias para cuadros de un grado de las temperaturas de superficie en Enero y Agosto se obtuvieron de la U. S. Hydrographic Office (datos no publicados) y del U. S. Bureau of Commercial Fisheries (1960).

Los datos de temperatura mensuales para cuadros de cinco grados, tomadas mar afuera de las costas de México y América Central, se obtuvieron de las publicaciones del Observatorio de Kobe, de la Marina Imperial (1921-1938). Las medias de las corrientes de deriva de barcos para el período 1885-1933, se obtuvieron de la U. S. Hydrographic Office (1947). Es de notar que los promedios que allí se reportan se basan en observaciones de corrientes hechas a velocidades del viento menores de 12 m sec^{-1}.

averaged over two degree squares of latitude and longitude and over periods of ten days and one month. The number of observations entering each ten-day average varies generally between 10 and 30. Mean one degree square sea surface temperatures for February and August were obtained from the U. S. Hydrographic Office (unpublished) and the U. S. Bureau of Commercial Fisheries (1960). Monthly five degree sea surface temperatures off southern Mexico and Central America were taken from publications by the Imperial Marine Observatory Kobe (1921-1938). Mean one degree ship drift currents for the period 1885-1933 were obtained from the U. S. Hydrographic Office (1947). It is noteworthy that the averages reported therein are based on current observations made at wind speeds less than 12 m sec^{-1}.

TABLA I

Velocidades máximas y medias mensuales del viento en Coatzacoalcos, Ver., Salina Cruz, Oax. y en el Golfo de Tehuantepec, según el Servicio Meteorológico Mexicano (1928-1947) y el U. S. Weather Bureau (inéditos).

TABLE I

Monthly mean and maximum wind velocities at Coatzacoalcos, Ver., Salina Cruz, Oax., and in the Gulf of Tehuantepec, after Servicio Meteorológico Mexicano (1928-1947) and U. S. Weather Bureau (unpublished).

Unidades en / All units in m sec^{-1}

Mes Month	I	II	III	IV	V	VI	VII	VIII	IX	X	XI	XII	Años de registro Years of record
						Coatzacoalcos, Ver.							
V media mean	8.6	7.7	5.7	5.5	5.0	4.5	6.2	3.5	4.3	4.0	9.7	9.5	3
V max	29.5	28.5	21.3	17.3	20.0	16.7	22.0	17.3	19.0	19.0	29.0	30.0	3
						Salina Cruz, Oax.							
V media mean	8.7	8.7	8.3	7.8	6.7	3.9	5.2	4.9	4.1	6.0	8.3	8.4	12
V max	28.2	26.3	27.2	26.5	21.7	18.1	19.8	19.9	19.6	24.5	27.0	26.4	12
	Golfo de Tehuantepec (Norte)					14-16 N 94-96 W			(North) Gulf of Tehuantepec				
V media mean	7.6	6.3	4.8	4.2	4.4	4.4	5.0	4.6	4.	7.6	8.4	8.1	8
V max	18.6	22.2	18.6	16.6	13.6	15.2	12.4	11.2	14.7	16.8	20.0	25.4	6
	Golfo de Tehuantepec (Sur)					12-14 N 94-96 W			(South) Gulf of Tehuantepec				
V media mean	6.2	5.4	3.7	3.8	3.4	4.2	4.4	3.7	4.6	6.5	7.1	6.4	8
V max	15.2	13.9	13.4	13.0	11.2	13.1	11.3	9.7	12.9	13.9	15.7	16.9	6
	Golfo de Tehuantepec (Oeste)					14-16 N 96-98 W			(West) Gulf of Tehuantepec				
V media mean	4.2	3.5	3.4	3.4	3.7	4.1	4.3	4.0	4.5	4.3	4.0	3.7	8
V max	15.6	9.8	13.2	10.1	12.9	12.4	12.6	10.2	13.1	14.7	15.9	15.4	6
	Golfo de Tehuantepec (Este)					12-14 N 92-94 W			(East) Gulf of Tehuantepec				
V media mean	3.4	2.7	2.7	2.8	3.2	3.8	4.1	3.4	3.8	4.5	3.4	3.4	8
V max	9.1	8.7	10.9	10.6	10.2	10.7	11.6	11.6	13.0	14.4	12.7	11.3	6

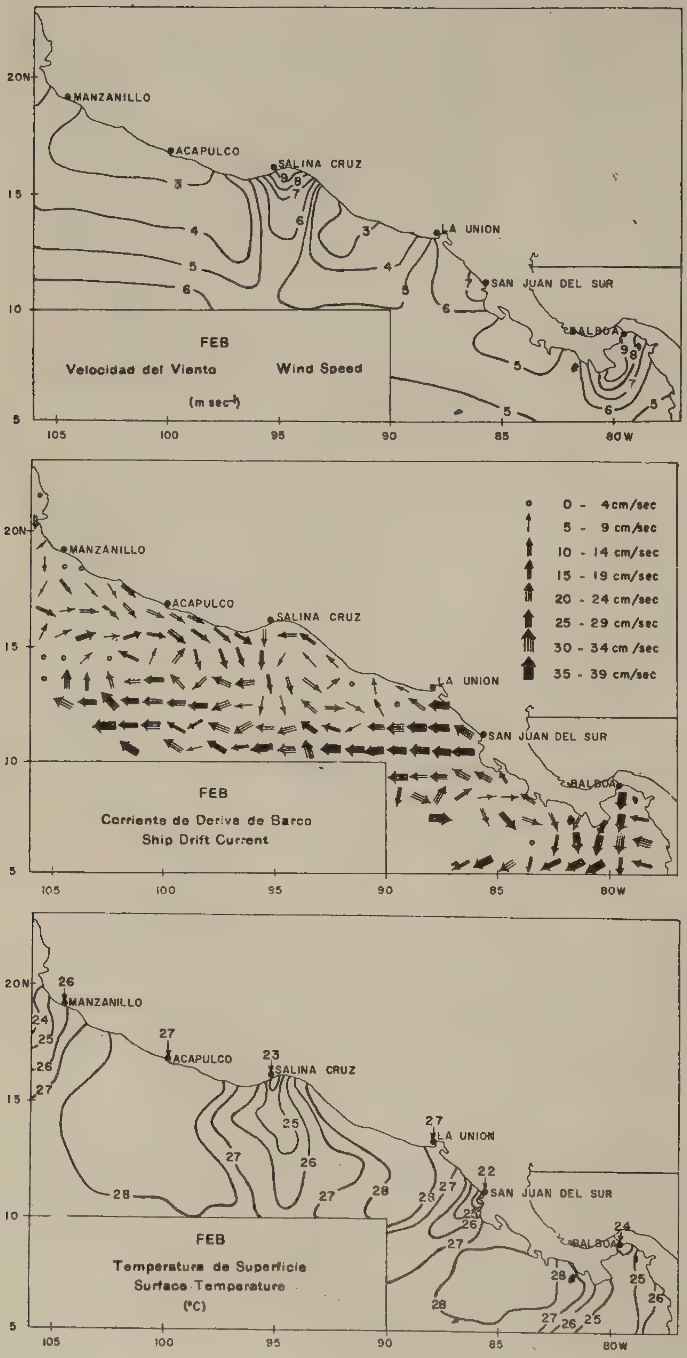
20N
15
10
5
105
100
95
90
85
80W
MANZANILLO
ACAPULCO
SALINA CRUZ
LA UNION
SAN JUAN DEL SUR
BALBOA
3
4
5
6
7
8
9
FEB
Velocidad del Viento
Wind Speed
(m sec⁻¹)
0 - 4 cm/sec
5 - 9 cm/sec
10 - 14 cm/sec
15 - 19 cm/sec
20 - 24 cm/sec
25 - 29 cm/sec
30 - 34 cm/sec
35 - 39 cm/sec
FEB
Corriente de Deriva de Barco
Ship Drift Current
22
23
24
25
26
27
28
FEB
Temperatura de Superficie
Surface Temperature
(°C)

Fig. 1a. Velocidad media del viento, corrientes de deriva de barcos y temperaturas de la superficie del mar para el mes de Febrero, basadas en datos del U. S. Weather Bureau (inéditos), U. S. Hydrographic Office (1947 e inéditos) y Bureau of Commercial Fisheries (inéditos).

Fig. 1a. Mean wind speed, ship drift currents and sea surface temperatures for the month of February, based on material from the U. S. Weather Bureau (unpublished), the U. S. Hydrographic Office (1947 and unpublished) and the Bureau of Commercial Fisheries (unpublished).

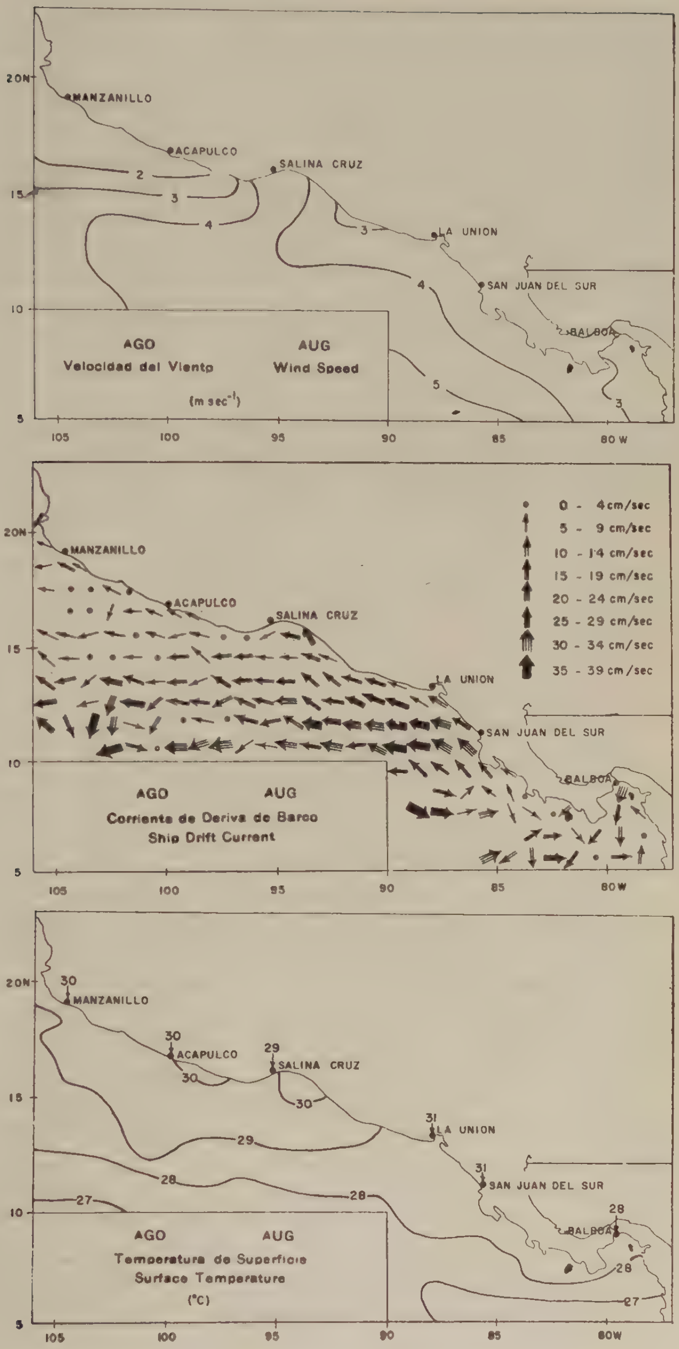
20N
15
10
5
105
100
95
90
85
80 W
MANZANILLO
ACAPULCO
SALINA CRUZ
LA UNION
SAN JUAN DEL SUR
BALBOA
2
3
4
5
AGO
AUG
Velocidad del Viento
Wind Speed
(m sec⁻¹)
0 - 4 cm/sec
5 - 9 cm/sec
10 - 14 cm/sec
15 - 19 cm/sec
20 - 24 cm/sec
25 - 29 cm/sec
30 - 34 cm/sec
35 - 39 cm/sec
Corriente de Deriva de Barco
Ship Drift Current
30
29
31
28
27
Temperatura de Superficie
Surface Temperature
(°C)

Fig. 1b. Velocidad media del viento, corrientes de deriva de barcos y temperaturas de la superficie del mar para el mes de Agosto, basadas en datos del U. S. Weather Bureau (inéditos), U. S. Hydrographic Office (1947 e inéditos).

Fig. 1b. Mean wind speed, ship drift currents and sea surface temperatures for the month of August, based on material from the U. S. Weather Bureau (unpublished), and the U. S. Hydrographic Office (1947 and unpublished).

VARIACIONES ESTACIONALES DE LAS CONDICIONES OCEANOGRAFICAS Y METEOROLOGICAS

Las estaciones en el Golfo de Tehuantepec pueden dividirse en una seca y generalmente ventosa de Noviembre a Abril y una lluviosa y usualmente en calma desde Mayo hasta Octubre. Durante la estación ventosa (Figs. 1a y 1b) una faja de vientos de alta velocidad se extiende hacia el sur desde el Istmo de Tehuantepec, en una longitud de unos 500 Km; su anchura es de unos 200 Km y las velocidades mayores tienen lugar en la extremidad norte del Golfo. Ahí la dirección del viento no se desvía mucho del norte. En la región de los vientos fuertes se ve que la corriente va hacia el sur con una velocidad media de unos 20 cm seg^{-1}.

THE SEASONAL VARIATION OF OCEANOGRAPHIC AND METEOROLOGICAL CONDITIONS

The seasons in the Gulf of Tehuantepec can be devided into a dry and generally windy season from November to April and a rainy and usually calm season from May to October. During the windy season (Figs. 1a and 1b) a belt of high wind speeds extends southward from the Isthmus of Tehuantepec for about 500 Km; its width is about 200 Km and the highest speeds occur at the northern end of the Gulf. The wind direction there does not vary much from north. In the region of strong winds the current is seen to set toward the south with an average speed of about 20 cm sec^{-1}. Along the coast the mean currents set toward Salina

TABLA 2

Temperaturas medias mensuales y medias máximas y mínimas de la superficie del mar en Coatzacoalcos, Ver., Salina Cruz, Oax., San Juan del Sur, Nicaragua y en el Golfo de Tehuantepec, según el U. S. Coast and Geodetic Survey (1956, 1960) y el U. S. Weather Bureau (inéditos).

TABLE 2

Monthly mean and mean maximum and minimum sea surface temperatures at Coatzacoalcos, Ver., Salina Cruz, Oax., San Juan del Sur, Nicaragua and in the Gulf of Tehuantepec, after U. S. Coast and Geodetic Survey (1956, 1960) and U. S. Weather Bureau (unpublished).

Unidades en
All units in °C

Month Mes	I	II	III	IV	V	VI	VII	VIII	IX	X	XI	XII	Años de registro. Years of record
Coatzacoalcos, Ver.													
media mean	23.1	24.2	26.2	27.9	29.0	29.0	27.5	28.0	27.1	25.6	24.7	23.3	13
max	25.1	26.7	28.9	30.0	31.2	31.1	29.8	29.3	29.1	27.4	22.8	25.9	13
min	21.2	22.2	23.6	25.3	26.5	26.9	25.8	26.2	24.9	24.9	22.4	21.2	13
Salina Cruz, Oax.													
media mean	23.0	22.7	24.8	26.2	27.9	28.4	28.6	28.8	28.1	26.4	24.1	23.3	4
max	26.1	25.4	28.1	28.8	30.2	29.7	30.3	30.3	30.4	30.0	29.2	28.1	4
min	18.9	20.0	18.9	22.4	23.9	25.8	26.8	27.2	27.0	22.8	18.1	18.7	4
San Juan del Sur, Nicaragua													
media mean	24.3	21.9	22.4	25.0	27.0	28.5	27.7	28.8	30.8	29.9	27.8	25.9	4
max	27.3	26.8	27.3	29.6	30.4	31.0	30.4	32.9	33.8	34.9	32.3	31.5	4
min	19.6	18.2	19.3	21.1	21.1	24.9	24.3	24.6	26.0	23.5	22.7	21.1	4
Golfo de Tehuantepec (Norte) 14-16 N 94-96 W (North) Gulf of Tehuantepec													
media mean	25.5	25.9	27.2	28.9	29.7	29.6	29.3	29.8	29.4	28.0	26.3	26.0	8
max	28.7	29.3	29.8	31.4	31.4	31.2	30.8	31.5	31.3	30.7	30.6	29.8	6
min	19.0	21.3	22.8	25.6	27.4	27.2	27.3	27.8	27.6	22.7	19.0	19.8	6
Golfo de Tehuantepec (Sur) 12-14 N 94-96 W (South) Gulf of Tehantepec													
media mean	25.3	26.4	28.1	29.9	30.0	29.6	29.1	29.5	29.2	27.6	26.6	25.9	8
max	28.3	28.5	30.3	31.1	31.8	30.8	30.4	30.9	30.8	30.2	29.7	29.3	6
min	21.6	22.2	24.8	26.0	27.1	27.7	27.1	27.9	27.0	24.0	21.8	21.3	6
Golfo de Tehuantepec (Oeste) 14-16 N 96-98 W (West) Gulf of Tehuantepec													
media mean	27.3	27.4	28.2	28.8	29.6	29.5	29.3	29.9	29.5	28.8	28.4	27.3	8
max	30.3	29.7	30.2	30.9	31.6	31.3	30.9	31.5	31.5	30.2	31.0	30.0	6
min	20.7	22.1	25.0	25.3	27.8	26.2	27.7	27.7	26.9	24.2	24.1	21.9	6
Golfo de Tehuantepec (Este) 12-14 N 92-94 W (East) Gulf of Tehuantepec													
media mean	26.7	27.4	28.5	29.5	29.9	29.5	29.2	29.4	29.3	28.1	28.1	27.7	8
max	29.4	29.8	30.1	31.8	31.7	31.1	30.9	31.3	31.5	30.3	30.4	29.8	6
min	23.2	22.8	25.4	27.1	28.0	27.5	26.4	27.4	27.0	24.9	23.2	23.7	6

A lo largo de la costa las corrientes medias van hacia Salina Cruz para reemplazar el agua que se ha movido. La circulación local de Tehuantepec se observa hacia el sur hasta las latitudes 12° N o 13° N, donde encuentra la Corriente Ecuatorial del Norte. Las temperaturas superficiales del mar son bajas donde las velocidades del viento son altas y también en las regiones inmediatamente adyacentes, lo cual indica que hay una difusión de agua fría hacia las áreas vecinas. Es de notar que la anchura del área de agua fría es algo mayor al sur del Golfo de Tehuantepec que dentro del mismo; esta característica sugiere que el efecto de surgencia en el Golfo está contrarrestado parcialmente por arrastres laterales de agua caliente.

Durante el verano los vientos son generalmente débiles y soplan de una dirección oriental. Ocasionalmente se observan vientos de alta velocidad durante el paso de huracanes, que ocurren con una frecuencia de unos dos por mes en el punto culminante de la estación en Septiembre. Las corrientes superficiales se establecen hacia el oeste y el noroeste, con velocidades de unos 15 cm seg^{-1}. Las temperaturas superficiales varían mayormente entre 28° C y 30° C y son las más altas en el Pacífico tropical oriental, excepto el Golfo de California (Roden y Groves, 1959).

Cruz to replace the water that has been moved away. The local Tehuantepec circulation is felt southward as far as latitude 12 N or 13 N, where it meets the North Equatorial Current. The sea surface temperatures are low everywhere the wind speeds are high and also in immediately adjacent regions, which indicates that outward diffusion of cold water into neighboring areas takes place. It is noteworthy that the width of the cold water area is somewhat larger south of the Gulf of Tehuantepec than inside the Gulf; this feature suggests that the upwelling effect in the Gulf is partly counteracted by lateral entrainment of warm water.

During the summer season the winds are generally weak and blow from an easterly direction. High wind speeds are occasionally observed during the passage of hurricanes which occur with a frequency of about two per month at the height of the season in September. The surface currents set toward the west and northwest with speeds of about 15 cm sec^{-1}. The sea surface temperatures vary mostly between 28° C and 30° C and are the highest in the eastern tropical Pacific, excepting the Gulf of California (Roden and Groves, 1959).

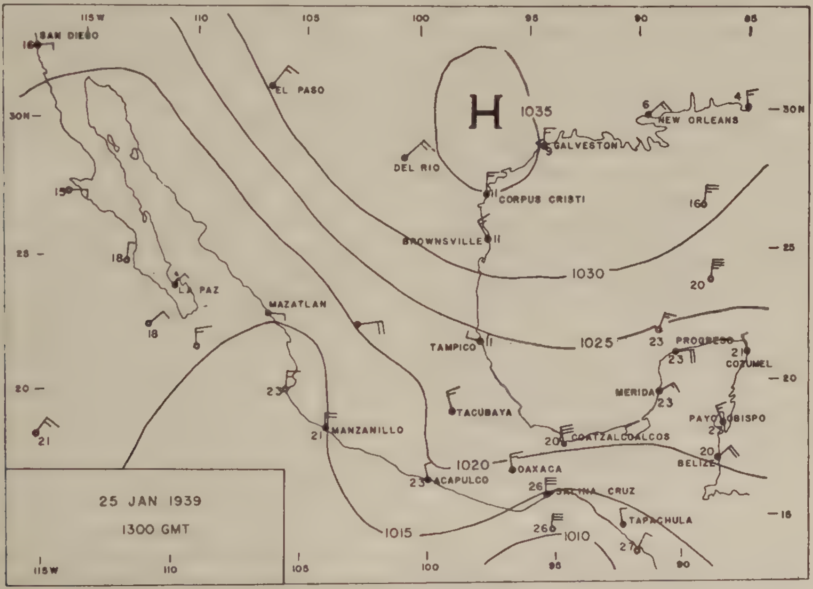
115W
110
105
100
95
90
85
SAN DIEGO
16
EL PASO
H
1035
NEW ORLEANS
6
4
30N
GALVESTON
DEL RIO
CORPUS CRISTI
11
16
15
25
18
BROWNSVILLE
1030
20
LA PAZ
MAZATLAN
18
TAMPICO
1025
23
PROGRESO
21
COZUMEL
20
23
MERIDA
TACUBAYA
PAYO OBISPO
21
MANZANILLO
20
COATZALCOALCOS
20
BELIZE
1020
OAXACA
23
ACAPULCO
26
SALINA CRUZ
TAPACHULA
15
1015
26
1010
27
25 JAN 1939
1300 GMT

Fig. 2. Una situación típica del tiempo que produce vientos fuertes en los Golfos de México y Tehuantepec. Las isobaras están representadas por líneas continuas y otros números indican las temperaturas del aire en la superficie del mar (según U. S. Weather Bureau, 1939).

Fig 2. A typical weather situation leading to strong winds in the Gulfs of Mexico and Tehuantepec. Isobars are represented by solid lines, other numbers refer to air temperatures at the sea surface (after U. S. Weather Bureau, 1939).

La variación anual de vientos y temperaturas se muestra en las Tablas 1 y 2. Se observa que el promedio de las velocidades máximas durante la estación de "*Tehuantepequeros*" varía alrededor de 25 m seg^{-1} y que los vientos en Coatzacoalcos, en el extremo norte del Istmo, no difieren mucho de los de Salina Cruz, en el extremo sur. La más alta velocidad del viento observada en Salina Cruz fue de 36 m seg^{-1} en Marzo de 1931. En el Golfo de Tehuantepec la velocidad del viento disminuye lentamente hacia el sur y rápidamente hacia el oriente y el occidente. La media de las mínimas de las temperaturas superficiales del mar en el punto culminante de la estación ventosa es de unos 18° C y a 19° C en la parte norte del Golfo y algo más alta en otros lugares. La temperatura más baja registrada en Salina Cruz es de 16.7° C y valores igualmente bajos han sido reportados por barcos mercantes. Es interesante hacer notar que las temperaturas mínimas en Coatzacoalcos, en el extremo norte del Istmo, están entre 20° C y 21° C o sea unos cuatro grados más altas que en Salina Cruz. Las temperaturas máximas en mar abierto en el Golfo varían entre 29° C y 30° C y en algunas áreas costeras entre 31° C y 43° C.

Una situación meteorológica típica que lleva a la producción de vientos fuertes en el área de Tehuantepec, se muestra en la Fig. 2. La característica más saliente del mapa meteorológico es un anticiclón continental bien desarrollado con su centro sobre la parte media de Texas que se extiende bastante hacia el sur dentro del Golfo de México. Esto conduce a un influjo de aire frío que viene desde las llanuras centrales y del noreste de los Estados Unidos. El desbordamiento del aire frío hacia el sur es detenido usualmente por las altas montañas del México meridional. Las ondas frías pasan al Océano Pacífico únicamente a través del Istmo de Tehuantepec y de la región del Lago de Nicaragua. Los vientos en esas regiones son fuertes, en parte debido a la tendencia que tienen las corrientes de aire de fluir alrededor de las montañas y amontonarse a través de sus interrupciones y en parte debido a la energía liberada cuando el aire frío fluye por sobre el aire caliente, más allá de la interrupción en la montaña (Godske *et al.*, 1957). Los "*Tehuantepequeros*" y "*Papagayos*" pertenecen a la clase de *Vientos de descenso*, cuya teoría ha sido desarrollada recientemente por Gutman y Frankl (1960). La intensidad de esos vientos depende de la elevación del Istmo, del espesor del frente frío y de la diferencia en los gradientes del lapso entre el aire frío y el aire caliente desplazado.

ALGUNOS ASPECTOS HIDRODINAMICOS DE LA CIRCULACION DE TEHUANTEPEC PRODUCIDA POR EL VIENTO

Para investigar la circulación producida por el viento en el Golfo de Tehuantepec, supóngase un sistema de coordenadas rectas y exprésense las ecuaciones de movimiento y continuidad según

The annual variation of winds and temperatures is shown in Tables 1 and 2. It is seen that the mean maximum wind velocities during the *Tehuantepecer* season vary around 25 m sec^{-1} and that the winds at Coatzacoalcos at the northern end of the Isthmus are not very different from those at Salina Cruz at the southern end. The highest wind speed observed at Salina Cruz was 36 m sec^{-1} in March 1931. In the Gulf of Tehuantepec the wind speeds diminish slowly toward the south and rapidly toward the east and west. The mean minimum sea surface temperatures at the height of the windy season are about 18° C to 19° C in the northern part of the Gulf and somewhat higher elsewhere. The lowest temperature recorded at Salina Cruz is 16.7° C; similar low values have been reported from merchant ships. It is of interest to note that the minimum temperatures at Coatzacoalcos at the northern end of the Isthmus are between 20° C and 21° C, or about 4° C higher than at Salina Cruz. The maximum temperatures in the open Gulf vary between 29° C and 30° C and in localized coastal areas between 31° C and 34° C.

A typical weather situation leading to strong winds in the Tehuantepec area is shown in Fig. 2. The outstanding feature on the weather map is a well developed continental anticyclone with its center over central Texas and extending far southward into the Gulf of Mexico. This leads to an influx of cold air from the plain states and from the northeast. The southward spread of the cold air is usually halted by the high mountains of southern Mexico. Only across the Isthmus of Tehuantepec and the Nicaragua lake district do cold waves pass into the Pacific Ocean. The winds in these regions are strong partly because of the tendency of air currents to flow around mountains and to crowd through mountain gaps, and partly because of the energy released when cold air overflows the warm air beyond the mountain gap (Godske *et al.*, 1957). The *Tehuantepecers* and *Papagayos* belong to the class of *fall winds*, the theory of which has recently been developed by Gutman and Frankl (1960). The intensity of these winds is dependent upon the elevation of the isthmus, the thickness of the cold front and the difference in lapse rates between the cold air and the displaced warm air.

SOME HYDRODINAMIC ASPECTS OF THE WIND DRIVEN TEHUANTEPEC CIRCULATION

In order to investigate the wind driven circulation in the Gulf of Tehuantepec assume a right-handed coordinate system, and let the equations of motion and continuity be given by

$$0 = -\frac{\partial p}{\partial x} + f\rho v + \frac{\partial \tau_{zx}}{\partial z}$$

$$0 = -\frac{\partial p}{\partial y} - f\rho u + \frac{\partial \tau_{zy}}{\partial z} \qquad (1)$$

$$0 = \frac{\partial \rho u}{\partial x} + \frac{\partial \rho v}{\partial y} + \frac{\partial \rho w}{\partial z}$$

En ellas p significa la presión, ρ es la densidad, f es la componente vertical del parámetro de Coriolis, u, v y w son las componentes de la velocidad y τ_{zx} y τ_{zy} se refieren a las componentes de los esfuerzos tangenciales sobre las superficies z. Las ecuaciones (1) son válidas para un océano baroclínico donde las variaciones del tiempo y las aceleraciones del campo sean pequeñas comparadas con los términos aquí considerados.

Integrando las dos primeras ecuaciones desde la superficie del mar hasta una profundidad donde se suponga que las componentes de los esfuerzos se desvanecen y efectuando la operación rotacional, tenemos:

Here p denotes pressure, ρ is density, f is the vertical component of the Coriolis' parameter, u, v and w are the velocity components, and τ_{ZX} and τ_{ZY} refer to the tangential stress components on the z-surfaces. Equations (1) are valid for a baroclinic ocean in which the time variations and field accelerations are small compared to the terms considered here.

Integrating the first two equations from the sea surface to a depth where the stress components are supposed to vanish, and performing the curl operation, gives

$$-f\ \mathrm{div}_h\ \mathbf{M} - \beta M_y + \mathrm{curl}_z \vec{\tau}_{zo} = 0 \qquad (2)$$

donde $\beta = \frac{\partial f}{\partial y}$, $\vec{\tau}_{zo}$ se refiere al esfuerzo del viento en la superficie del mar y donde

where $\beta = \frac{\partial f}{\partial y}$, $\vec{\tau}_{zo}$ refers to the wind stress at the sea surface and where

$$M_Y = \int_{-d}^{0} \rho v dz,\ M_X = \int_{-d}^{0} \rho u dz,\ \mathrm{div}_h\ \mathbf{M} = \frac{\partial M_X}{\partial x} + \frac{\partial M_Y}{\partial y}$$

son las componentes horizontales del transporte de masa (Sverdrup, 1946). La ecuación (2) es muy similar a la bien conocida de Sverdrup (1947), excepto que contiene el término adicional que comprende la divergencia horizontal del transporte de masa.

En el límite septentrional que es la costa sur de México, el transporte meridional de masas debe desvanecerse y la divergencia del transporte de masa es proporcional al rotacional del esfuerzo del viento. La divergencia del transporte de masa puede exceder en algún lugar al rotacional del esfuerzo del viento ya que el movimiento es generalmente hacia el sur y el término que contiene β, la vorticidad planetaria, se vuelve positivo.

Puede estimarse la divergencia horizontal del transporte de masa despejando $\mathrm{div}_h\ \mathbf{M}$ en la ecuación (2) y suponiendo que $\beta = 2.2 \cdot 10^{-13}$ cm^{-1} seg^{-1}; $f^{-1} = 2.5 \cdot 10^4$ seg y
Tendremos finalmente:
un rotacional medio $\vec{\tau}_{zo} = 5 \cdot 10^{-7}$ dinas cm^{-3} (ver Fig. 3).

are the horizontal mass transport components (Sverdrup, 1946). Equation (2) is very similar to that of Sverdrup, (1947) except that it contains the additional term involving the horizontal mass transport divergence.

At the northern boundary, which is the southern coast of Mexico, the meridional mass transport must vanish, and the mass transport divergence is proportional to the curl of the wind stress. Elsewhere the mass transport divergence is likely to exceed the curl of the wind stress, since the motion is generally to the southward, and the term containing β, the planetary vorticity, becomes positive.

An estimate of the horizontal mass transport divergence can be made by solving equation (2) for $\mathrm{div}_h\ \mathbf{M}$ and by assuming $\beta = 2.2 \cdot 10^{-13}$ cm^{-1} sec^{-1}, $f^{-1} = 2.5 \cdot 10^4$ sec and an average curl $\vec{\tau}_{zo} = 5 \cdot 10^{-7}$ dynes cm^{-3} (see Fig. 3). As a result we get:

$$\mathrm{div}_h\ \mathbf{M} = -5.5 \cdot 10^{-9} M_y + 1.25 \cdot 10^{-2} \qquad (3)$$

donde M_y (g cm^{-1} seg^{-}) es el transporte de masa hacia el sur. Aun cuando M_y no se conoce exactamente, puede demostrarse que la contribución del término que incluye M_y hacia la divergencia del transporte horizontal de masa es pequeña, comparada con el término que contiene el rotacional del esfuerzo del viento. Para apreciar esto supongamos una velocidad arbitraria de la corriente hacia el sur de 50 cm seg^{-1}, uniforme desde la superficie del mar hasta una profundidad de 100 m. Entonces, $M_y = 5 \cdot 10^5$ g cm^{-1} sec^{-1} y $\text{div}_h \, \mathbf{M} = 2.75 \cdot 10^{-3} + 1.25 \cdot 10^{-2}$. El primer término de la derecha es un orden de magnitud más pequeño que el segundo y puede despreciarse en primera aproximación. Así, el valor medio de la divergencia del transporte de masa es de unos $1.25 \cdot 10^{-2}$ g cm^{-2} seg^{-1}, o 1000 g cm^{-2} día^{-1}. El valor máximo es aproximadamente el doble de esta cantidad (Fig. 3).

La velocidad vertical puede estimarse integrando la ecuación de continuidad y haciendo notar que la velocidad vertical en la superficie del mar es cero. Tenemos

where M_y (g cm^{-1} sec^{-1}) is the southward mass transport. Although M_y is not accurately known, it can be demonstrated that the contribution of the term involving M_y toward the horizontal mass transport divergence is small compared to the term containing the curl of the wind stress. To see this, assume an arbitrary southward current speed of 50 cm sec^{-1} uniform from the sea surface to a depth of 100 m. Then $M_y = 5 \cdot 10^5$ g cm^{-1} sec^{-1} and $\text{div}_h \, \mathbf{M} = 2.75 \cdot 10^{-3} + 1.25 \cdot 10^{-2}$; the first term on the right hand side is thus an order of magnitude smaller than the second and can be neglected to a first approximation. Thus the average value of the mass transport divergence is about $1.25 \cdot 10^{-2}$ g cm^{-2} sec^{-1} or 1 000 g cm^{-2} day^{-1}. The maximum value is about twice as large (Fig. 3).

The vertical velocity can be estimated from an integration of the equation of continuity, noting that the vertical velocity at the sea surface is zero. We have

$$(\rho w)_z = \text{div}_h \, \mathbf{M} \approx f^{-1} \, \text{curl}_z \overrightarrow{\tau}_{zo} \tag{4}$$

donde el signo $\approx$ indica igualdad aproximada. Una ecuación similar a la (4) ha sido desarrollada por Yoshida y Mao (1957). Suponiendo que $\text{div}_h \, \mathbf{M} = 1000$ g cm^{-2} día^{-1} y que $\rho = 1$ g cm^{-3}, tenemos para la velocidad media de la surgencia durante un "*Tehuantepequero*" 10 m día^{-1}.

where the sign $\approx$ indicates approximate equality. An equation similar to (4) has been derived by Yoshida and Mao (1957). Assuming $\text{div}_h \, \mathbf{M} = 1000$ g cm^{-2} day^{-1} and $\rho = 1$ g cm^{-3} we get for the mean upwelling speed during a *Tehuantepecer* 10 m day^{-1}.

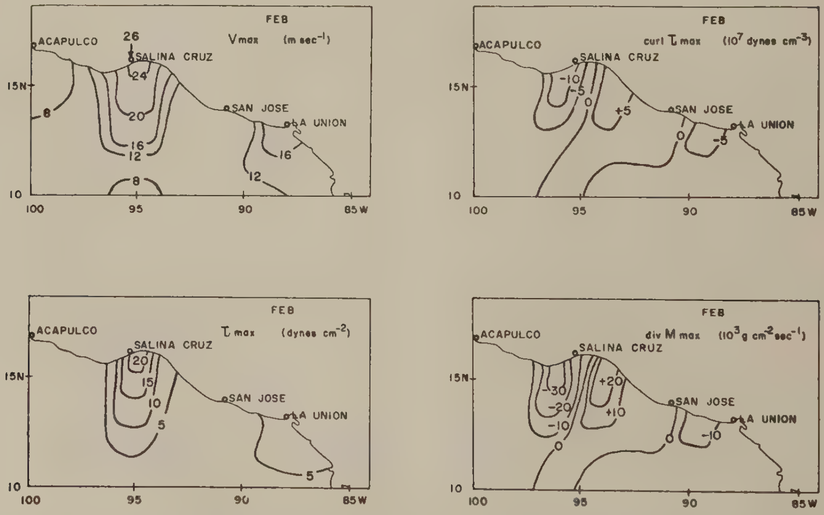

Fig. 3. Divergencia de la velocidad media máxima del viento, del esfuerzo rotacional del viento y del transporte de masa para los meses de Febrero.

Fig. 3. Mean maximum wind speed, wind stress curl and mass transport divergence for the months of February.

Un ejemplo típico de la velocidad máxima del viento en el Golfo de Tehuantepec se muestra en la Fig. 3, para el mes de Febrero. Aun cuando los valores se refieren a la velocidad escalar también representan la componente norte del viento porque su dirección durante una galerna de invierno se desvía muy poco del norte. A partir del viento se calcularon los valores de los esfuerzos y su efecto rotacional, así como de la divergencia del transporte de masa. Se observa que hacia el este de la región de grandes velocidades del viento existe una área de divergencia positiva con valores máximos de unos 0.02 g cm^{-2} seg^{-1}. Esto corresponde a una velocidad de surgencia de 17 m $día^{-1}$ aproximadamente, en el caso máximo. Ya que la divergencia positiva está asociada con movimientos hacia arriba y la divergencia negativa con movimientos hacia abajo, las temperaturas de la superficie del mar deben ser bajas en la primera área y altas en la segunda. De modo similar, el termoclinal en el área de divergencia positiva debería ser menos profundo que en el área de divergencia negativa. Las observaciones (Blackburn, MS) lo indican casi así.

La dificultad principal que encontramos con el modelo ya descrito es que no permite calcular el tiempo de reacción entre el viento y la circulación superficial. Si se agregan a las ecuaciones (1) las derivadas locales con respecto al tiempo y se llevan a cabo las operaciones efectuadas previamente, se obtiene el siguiente resultado:

A typical example of the maximum wind speed in the Gulf of Tehuantepec is shown in Fig. 3 for the month of February. Although the values refer to the scalar speed, they also represent the magnitude of the northerly wind component, because the wind direction during a winter gale deviates very little from north. From the wind were computed the wind stress, the curl of the wind stress and the mass transport divergence. It is seen that to the east of the region of high wind speeds there is an area of positive divergence with maximum values of about 0.02 g cm^{-2} sec^{-1}. This corresponds to an upwelling velocity of roughly 17 m day^{-1} in the maximum case· Since positive divergence is associated with upward motion and negative divergence with downward motion, the sea surface temperatures in the former area should be low and in the latter high. Similarly the thermocline in the area of positive divergence should be shallower than in the area of negative divergence. The actual observations (Blackburn, MS) roughly indicate this pattern.

The chief difficulty with the above described model is that it does not permit one to calculate the response time between the wind and the surface circulation. If the local time derivatives are added to equations (1) and the same operations as previously carried out, the following result is obtained:

$$\frac{\partial}{\partial t}\,\mathrm{curl}_z\,\mathbf{M} = -\frac{\partial}{\partial y}\int_{-d}^{0} u\,\frac{\partial\rho}{\partial t}\,d_z + \frac{\partial}{\partial x}\int_{-d}^{0} v\,\frac{\partial\rho}{\partial t}\,d_z - \beta M_y - f\,\mathrm{div}_h\,\mathbf{M} + \mathrm{curl}_z\,\overrightarrow{\tau_{zo}} \qquad (5)$$

que contienen tanto el efecto rotacional como la divergencia del transporte de masa. Esta ecuación es difícil de manejar. Si despreciamos la divergencia y las variaciones de ρ con el tiempo e introducimos la función de corriente del transporte de masa definida por

involving the curl as well as the divergence of the mass transport. This equation is difficult to treat. If one neglects he divergence and the time variation of ρ, and introduces the mass transport stream function, defined by

$$M_x = -\frac{\partial\psi}{\partial y} \qquad M_y = \frac{\partial\psi}{\partial x}$$

se obtiene una ecuación más simple:

a simpler equation is obtained:

$$\frac{\partial}{\partial t}\,\nabla^2\psi = -\beta\,\overset{\frac{\partial\psi}{\partial x}}{\cancel{\frac{\partial x}{\partial\psi}}} + \mathrm{curl}_z\overrightarrow{\tau_{zo}} \qquad (6)$$

El tiempo de reacción de este sistema ha sido dado por Welander (1959) como:

The time response of this system is given by Welander (1959) as

$$T = \beta^{-1}L^{-1} \qquad (7)$$

donde T es el tiempo de reaccion y L una longitud característica del movimiento. En el caso del Golfo de Tehuantepec, L es del orden de 300 Km y el tiempo de reacción es del orden de $1.5 \cdot 10^5$ seg o sea casi un día y medio.

where T is the time response and L a characteristic length of the motion. In case of the Gulf of Tehuantepec, L is of the order of 300 Km and the time response is in the order of $1.5 \cdot 10^5$ sec, or about a day and a half.

ANALISIS DE SERIES DEL TIEMPO DE LA TEMPERATURA SUPERFICIAL DEL MAR Y DE LOS REGISTROS DEL VIENTO

Un ejemplo típico de variaciones no estacionales de la temperatura a lo largo de la costa sur de México y América Central se muestra en la Fig. 4. La variación estacional fue eliminada tomando las diferencias entre la media men-

TIME SERIES ANALYSIS OF SEA SURFACE TEMPERATURE AND WIND RECORDS

A typical example of nonseasonal temperature variations along the southern coast of Mexico and Central America is shown in Fig. 4. The seasonal variation was eliminated by taking differences between the monthly mean and the long

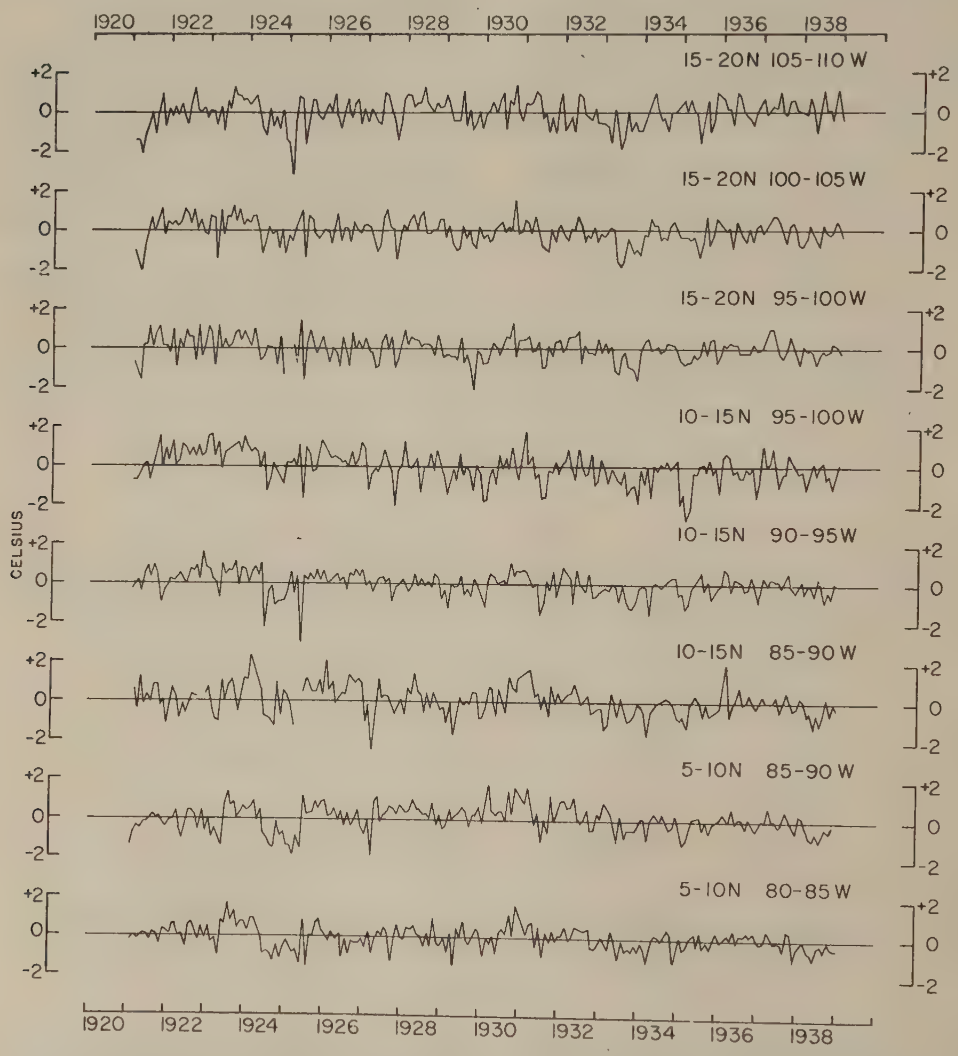

Fig. 4. Anomalías mensuales de la temperatura de la superficie del mar aguas afuera del sur de México y América Central (según Observatorio de Kobe de la Marina Imperial, 1921-1938).

Fig. 4. Monthly sea surface temperature anomalies off southern Mexico and Central America (after Imp. Marine Observatory, Kobe 1921-1938).

sual y la media de largo período para el mismo mes. Se ve que las anomalías resultantes se encuentran principalmente entre + 2° C y son de signo similar en los cuadrados de cinco grados adyacentes.

En la Fig. 5 se muestran registros de variaciones no estacionales de viento y temperatura para el área del Golfo de Tehuantepec. El intervalo de tiempo entre valores adyacentes es de diez días y cada valor representa el promedio sobre un cuadro de dos grados de latitud y longitud. Los cuadrados 14-16 N, 94-96 W y 12-14 N, 94-96 W están influenciados por fuertes galernas del norte en el invierno;

term mean for the same month. The resulting anomalies are seen to lie mostly between + 2° C and to be of similar sign in adjacent five degree squares.

More detailed records of nonseasonal temperature and wind variations are shown in Fig. 5 for the Gulf of Tehuantepec area. The time interval between adjacent values is ten days, and each value represents the average over a two degree square of latitude and longitude. The squares 14-16 N 94-96 W and 12-14 N 94-96 W are influenced by strong northerly gales in winter, the remaining two are not. Al-

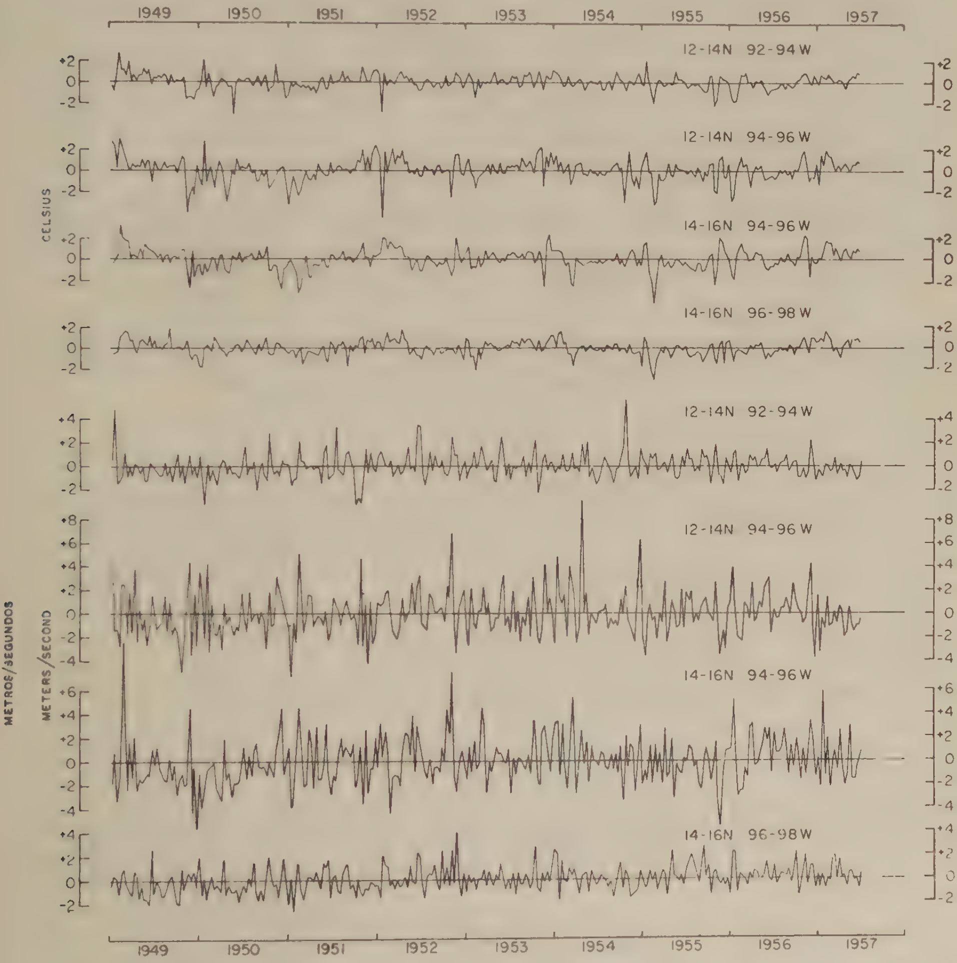

Fig. 5. Anomalías de la temperatura de la superficie del mar y de la velocidad del viento de diez días en el Golfo de Tehuantepec (según U. S. Weather Bureau, inéditas).

Fig. 5. Ten-day sea surface temperature and wind speed anomalies in the Gulf of Tehuantepec (after U. S. Weather Bureau, unpublished).

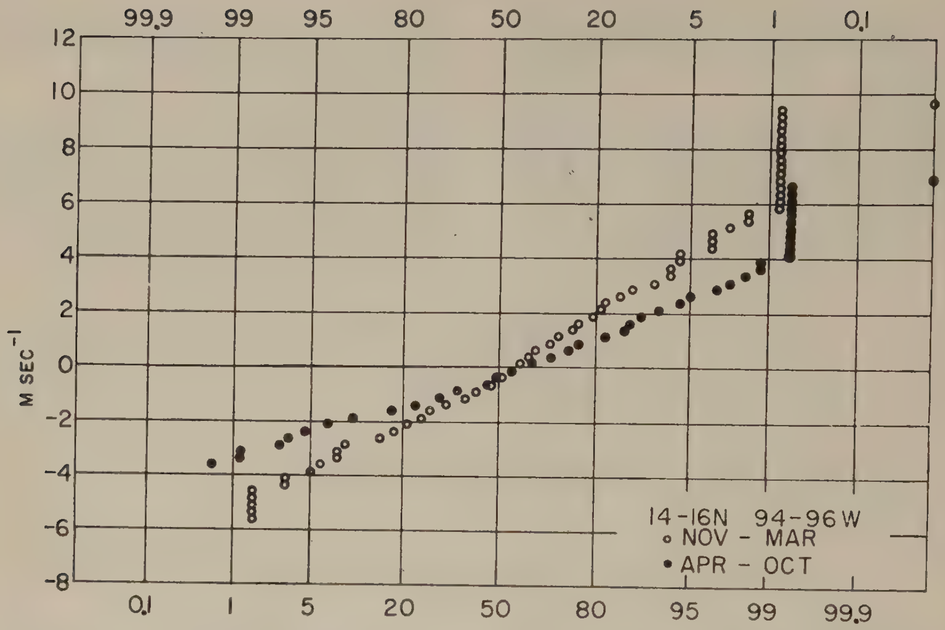

Fig. 6. Anomalías de la probabilidad de distribución de la velocidad del viento (arriba) y de la temperatura de la superficie del mar (abajo) de diez días en el Golfo de Tehuantepec.

Fig. 6. Probability distribution of ten-day wind speed (top) and sea surface temperature (bottom) anomalies in the Gulf of Tehuantepec.

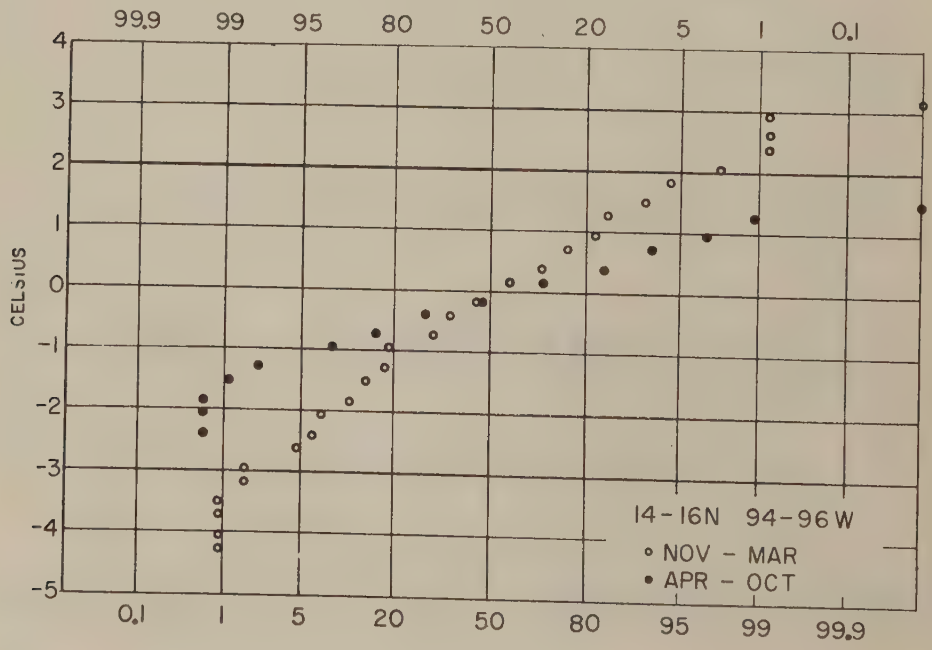

los otros dos restantes no lo están. A pesar de que los detalles de esos registros varían, pueden obtenerse algunos resultados preliminares mediante su inspección visual: (1) las anomalías de las temperaturas de la superficie del mar fluctúan mucho menos que las anomalías del viento; (2) las anomalías de temperatura y del viento son mayores en los cuadrados afectados por las galernas de invierno que en los no afectados; (3) las anomalías de temperatura y del viento en cuadrados adyacentes son de signo similar; (4) parece que no hay relación significativa entre las anomalías del viento y de la temperatura. La distribución probabilística de las anomalías de temperatura y viento se muestran en la Fig. 6. Se ve que las anomalías de la temperatura están distribuidas normalmente dentro de una amplitud de – 2° C a + 2° C y que las anomalías del viento lo están dentro de una amplitud de – 4 m seg^{-1} hasta + 4 m seg^{-1}. Los extremos no están distribuidos normalmente, sino que parecen acercarse a un valor asintótico.

Para investigar hasta dónde existe una relación estadística significativa entre las anomalías de 10 días de la temperatura y el viento, se aplicaron métodos de análisis espectral. Los procedimientos de cómputo son los siguientes: si $\theta(t)$ y $v(t)$ se refieren a las anomalías de temperatura y de viento, entonces las funciones de correlación están dadas por

though the details of these records vary, a few preliminary results can be obtained from a visual inspection of them: (1) the sea surface temperature anomalies fluctuate much less than the wind anomalies, (2) both the temperature and wind anomalies are larger in the squares affected by the winter gales than in those not affected by them, (3) temperature and wind anomalies in adjacent squares are of similar sign, (4) there appears to be no significant relation between temperature and wind anomalies. The probability distribution of temperature and wind anomalies is shown in Fig. 6. It is seen that the temperature anomalies are normally distributed within the range of – 2° C and + 2° C and the wind anomalies within the range of – 4 m sec^{-1} to + 4 m sec^{-1}. The extremes are not normally distributed, but seem to approach an asymptotic value.

In order to investigate whether any statistically significant relation exists between the ten-day temperature and wind anomalies, methods of spectral analysis were applied. The computational procedures are as follows: Let $\theta(t)$ and $v(t)$ refer to the temperature and wind anomalies, respectively. Then the correlation functions are given by

$$\begin{aligned} \phi_{\theta\theta}(\tau) &= <\theta(t)\theta(t+\tau)>, \text{ etc.} \\ \phi_{\theta v}(\tau) &= <\theta(t)v(t+\tau)> \end{aligned} \tag{8}$$

siempre que los registros sean estacionarios y < > denote el promedio en el tiempo sobre toda la longitud de los registros y τ se refiera al retraso en el tiempo. Las potencias de las densidades espectrales son las transformadas de Fourier de las funciones de correlación citadas y están dadas por:

provided the records are stationary and < > denotes the time average over the entire record length and τ refers to the time lag. The power spectral densities are the Fourier transforms of the above correlation functions and are given by:

$$\begin{aligned} E_{\theta\theta}(\omega) &= \frac{2}{\pi}\int_0^\infty \phi_{\theta v}(\tau)\cos\omega\tau\, d\tau, \quad \text{etc.} \\ E_{\theta v}(\omega) &= \frac{1}{\pi}\int_{-\infty}^{\infty} \phi_{\theta v}(\tau)\, e^{-i\omega\tau} d\tau \end{aligned} \tag{9}$$

La coherencia entre los registros de temperatura y de viento está definida por

The coherence between temperature and wind records is defined by

$$R_{\theta v}(\omega) = \frac{E_{\theta v}(\omega)}{[E_{\theta\theta}(\omega)\, E_{vv}(\omega)]^{1/2}} \tag{10}$$

y deben encontrarse entre los valores 0 y 1. Si R = 1 la coherencia es perfecta; si R = 0 no hay coherencia. La

and must lie between the values zero and one. If R = 1 the coherence is perfect, if R = 0 there is no coherence.

fase entre las anomalías de temperatura y de viento está definida por

The phase between the temperature and wind anomalies is defined by

$$\pi_{\theta v}(\omega) = \arctan \frac{E_{v\theta}(\omega) - E_{\theta v}(\omega)}{E_{v\theta}(\omega) + E_{\theta v}(\omega)} \qquad (11)$$

Si $\pi = 0$ los registros están relacionados directamente uno con otro; si $\pi = 180°$ existirá una relación inversa entre los registros.

Blackman y Tukey (1958) y Munk, Snodgrass y Tucker (1959) han dado métodos prácticos para calcular las ecuaciones (8) a (11). El análisis fue llevado a cabo en una computadora electrónica IBM 709 en el Western Data Pro-

If $\pi = 0$ the records are related directly to each other; if $\pi = 180$ degrees there exists an inverse relation between the records.

Practical methods for evaluating equations (8) to (11) are given by Blackman and Tukey (1958) and Munk, Snodgrass and Tucker (1959). The analysis was carried out on an IBM 709 electronic computer at the Western

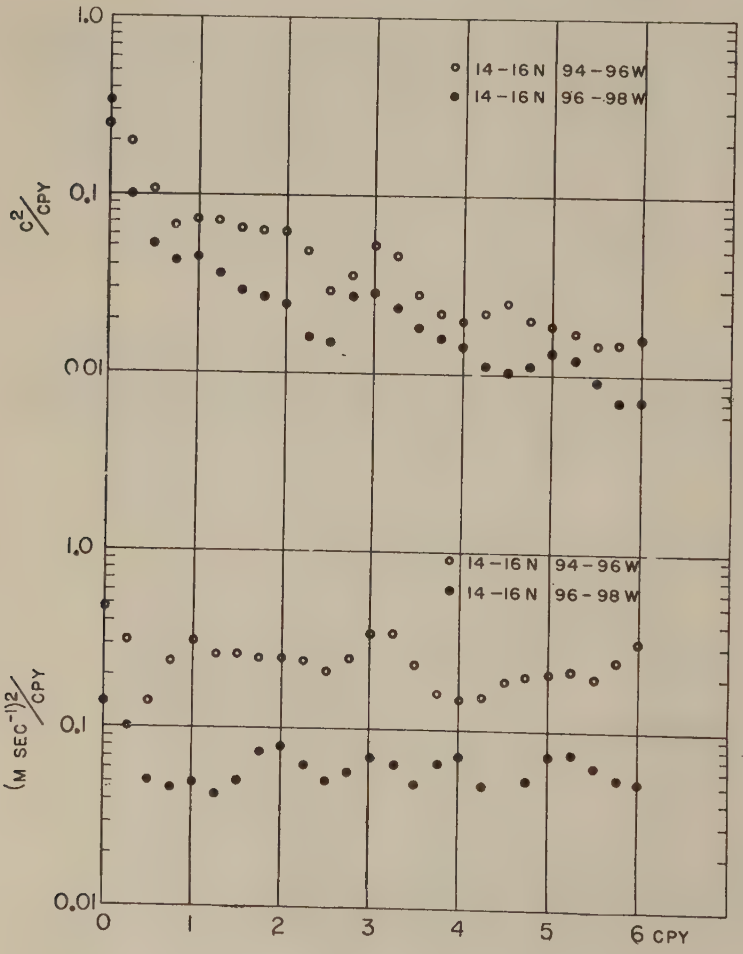

Fig. 7. Anomalías de la densidad espectral de la temperatura de la superficie del mar (izq.) y de la velocidad del viento (der.) de diez días en el Golfo de Tehuantepec.

cessing Center en Los Angeles para n = 306 observaciones y m = 24 estimaciones espectrales. Los *grados de libertad*, v, resultantes definidos por

Data Processing Center in Los Angeles for n = 306 observations and m = 24 spectral estimates. The resulting *degrees of freedom*, v, defined by

$$v = 2n/m \tag{12}$$

fueron 25.5 (Tabla 3).

was 25.5. (Table 3.)

Las densidades espectrales de las anomalías de la temperatura y el viento se ilustran en la Fig. 7. Se observa que la mayor parte está concentrada en frecuencias bajas y que no hay sino una muy pequeña contribución de parte de las frecuencias más altas. Las anomalías en los cuadrados influenciados por las galernas de invierno contienen considerablemente más fuerza que las no influenciadas por ellas. La fuerza de las anomalías del viento está concentrada más

The power spectral densities of temperature and wind anomalies are illustrated in Fig. 7. It is seen that most of the power of the temperature anomalies is concentrated at low frequencies and that there is very little contribution from higher frequencies. The anomalies in the squares influenced by the winter gales contain considerably more power than those not influenced by them. The power of the wind anomalies is concentrated rather evenly over the

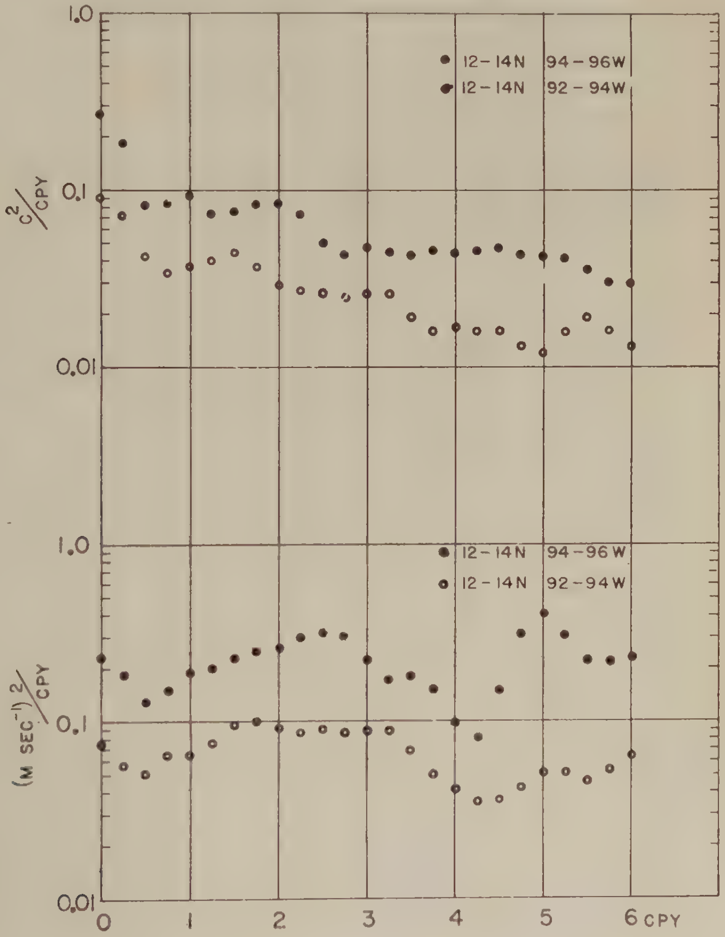

Fig. 7. Power spectral density of ten-day sea surface temperature (left) and wind speed (right) anomalies in the Gulf of Tehuantepec.

bien uniformemente sobre la gama entera de frecuencia, indicando que las componentes de alta frecuencia son tan importantes como las componentes de baja frecuencia. Debido a ello puede esperarse que las frecuencias de más de 6 ciclos por año (c.p.a.) contengan también una cantidad de fuerza considerable y que parte de esta fuerza haya contaminado el espectro del viento aquí mostrado.

La relación entre la fuerza de las anomalías de la temperatura y la fuerza de las anomalías del viento, como función de la frecuencia, se da en la Tabla 4. Se ve que la relación a bajas frecuencias es varias veces mayor que a frecuencias altas.

La coherencia por áreas entre cuadrados de dos grados adyacentes se muestra en la Fig. 8. La coherencia para anomalías de temperatura es ligeramente mejor a bajas frecuencias que a frecuencias altas, indicando que se requiere algún tiempo para que la anomalía de la temperatura se difunda a los cuadrados adyacentes. La fase de las anoma-

entire frequency range, indicating that high frequency components are as important as low frequency components. Because of this, it can be expected that frequencies beyond 6 cycles per year (c.p.y.) will also contain a considerable amount of power, and that part of this power has contaminated (aliased) the wind spectrum shown here.

The ratio of the power of the temperature anomalies to the power of wind anomalies as a function of frequency is given in table 4. It is seen that the ratio at low frequencies is several times larger than at high frequencies.

The areal coherence between adjacent two degree squares is shown in Fig. 8. The coherence for temperature anomalies appears to be slightly better at low than at high frequencies, indicating that some time is required for the temperature anomaly to spread into adjacent squares. The phase of the wind anomalies lies near zero and does not

TABLA 3

Número total de observaciones (n), número de retrasos usados (m), grados de libertad (ν), desviación standard (σ) y variación máxima (r) de la temperatura del mar (θ) y anomalías del viento (v). También se indica el 95% de límites de confianza (E) para la densidad espectral.

TABLE 3

Total number of observations (n), number of lags used (m), degrees of freedom (ν), standard deviation (σ) and extreme range (r) of sea surface temperature (θ) and wind (v) anomalies. Also shown are 95% confidence limits, (E), for the power spectra.

2° cuadrado 2° square	n	m	ν	σ_θ	σ_v	r_θ	r_v	E
	meses months	meses months		°C	m/s	°C	m/s	(°C)² c.p.a. o (m/s)²c.p.a. c.p.y. or (m/s)²c.p.y.
14-16 N 96-98 W	306	24	25.5	0.7	1.0	5.0	6.8	0.62 – 1.89
14-16 N 94-96 W	306	24	25.5	1.0	2.1	7.5	15.8	0.62 – 1.89
12-14 N 94-96 W	306	24	25.5	1.1	2.0	7.5	14.8	0.62 – 1.89
12-14 N 92-94 W	306	24	25.5	0.7	1.1	5.8	9.1	0.62 – 1.89

TABLA 4

El cociente $E_{\theta\theta}/E_{vv}$ como función de frecuencia.

TABLE 4

The ratio $E_{\theta\theta}/E_{vv}$ as a function of frequency.

Frec. Freq.	12-14N 92-94W	12-14N 94-96W	14-16N 14-16W	14-16N 14-16NW
c.p.y. c.p.a.	(°C/m sec⁻¹)²	(°C/m sec⁻¹)²	(°C/m sec⁻¹)²	(°C/m sec⁻¹)²
0	1.22	1.17	0.51	0.96
1	0.57	0.49	0.24	0.90
2	0.32	0.33	0.26	0.30
3	0.30	0.22	0.14	0.41
4	0.42	0.45	0.14	0.20
5	0.24	0.10	0.09	0.18
6	0.20	0.13	0.03	0.13

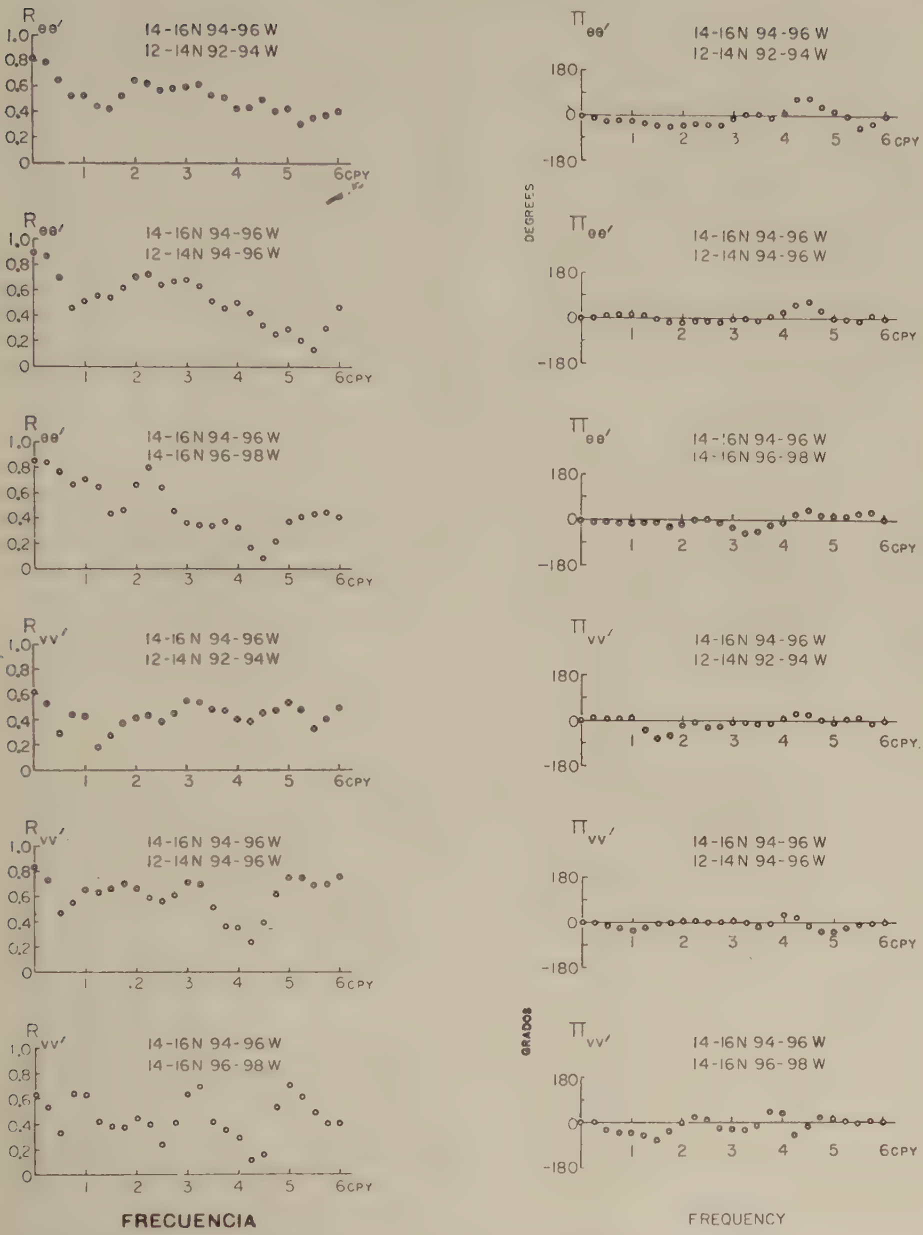

Fig. 8. Coherencia (R) y fase (π) entre anomalías en cuadrados adyacentes de dos grados. $R_{\theta\theta'}$ y $\pi_{\theta\theta'}$ referidas a las anomalías de la temperatura de la superficie del mar. Rvv' y $\pi_{vv'}$ a las anomalías de la velocidad del viento.

Fig. 8. Coherence (R) and phase (π) between anomalies in adjacent two degree squares. $R_{\theta\theta'}$ and $\pi_{\theta\theta'}$ refer to sea surface temperature anomalies, Rvv' and $\pi_{vv'}$ to wind speed anomalies.

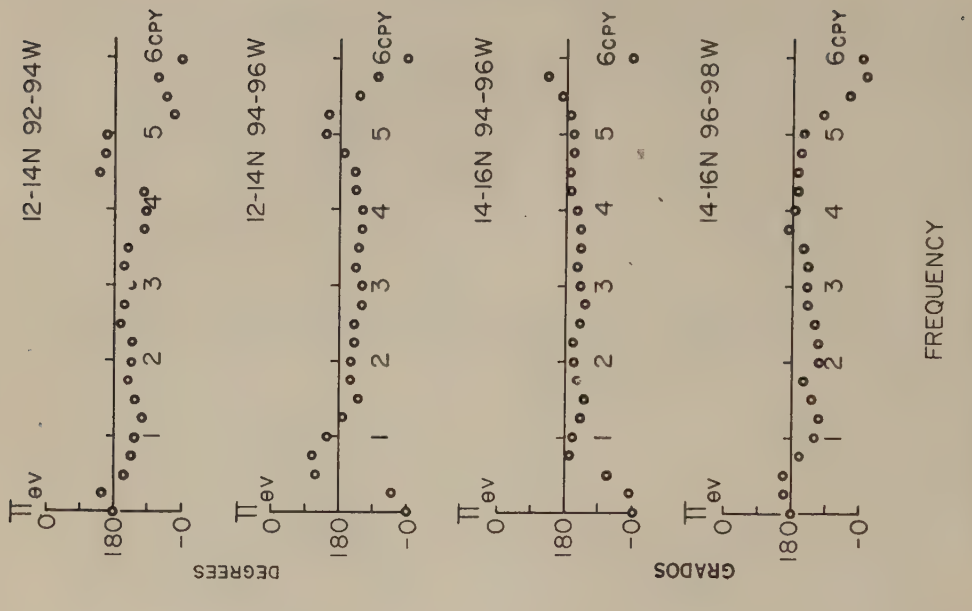

Fig. 9. Coherence ($R_{\theta v'}$) and phase ($\pi_{\theta v'}$) between sea surface temperature and wind speed anomalies.

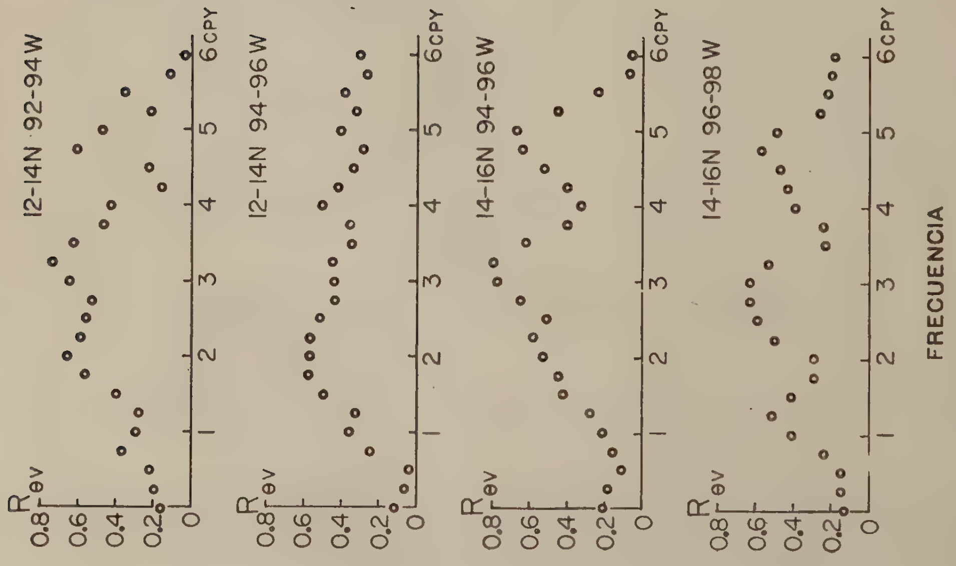

Fig. 9. Coherencia ($R_{\theta v'}$) y fase ($\pi_{\theta v'}$) entre las anomalías de la temperatura de la superficie del mar y de la velocidad del viento.

lías del viento se encuentra cerca de cero y no depende mucho de la frecuencia, lo cual sugiere que el viento actúa simultáneamente sobre el área entera.

La coherencia y la fase entre las anomalías de temperatura y las del viento se muestra en la Fig. 9. La coherencia fluctúa ampliamente con la frecuencia y varía entre 0 y 0.8. Es baja en ambos extremos del espectro y muestra algunos máximos mal definidos alrededor de 3 c.p.a. y 5 c.p.a. La fase se dispersa alrededor de 180° para frecuencias entre 2 c.p.a. y 5 c.p.a. e indica una relación inversa entre las anomalías de la temperatura y el viento. Si se supone una coherencia media para el espectro de 0.4, no más del 16% de las anomalías están relacionadas unas con otras. Esto puede ser debido parcialmente a la imperfección de los datos, pero es más seguro que la surgencia representa un fenómeno mucho más complejo que lo que puede describirse con solamente los datos de vientos.

CONCLUSION

El Golfo de Tehuantepec es notable por fuertes surgencias en el invierno, las cuales llevan a temperaturas superficiales del mar varios grados más bajas que en otras partes a lo largo de la costa del sur de México. La causa primaria de la surgencia es el viento con fuerza de galerna que sopla a veces desde el norte a través del Istmo de Tehuantepec sobre el Océano Pacífico. El efecto del viento se observa a varios centenares de kilómetros hacia el sur. Se investigó la relación entre los vientos y las temperaturas desde un punto de vista dinámico y desde un punto de vista estadístico.

El tratamiento dinámico llevó al resultado de que la surgencia en el Golfo de Tehuantepec está relacionada con el rotacional de los esfuerzos del viento y que se pueden esperar durante los nortes surgencias de 10 m día^{-1}. El tratamiento estadístico mostró que hay una relación inversa pero débil entre las temperaturas de la superficie del mar tomadas cada 10 días y las anomalías del viento.

AGRADECIMIENTOS

El autor derivó grandes beneficios de las discusiones con Gordon W. Groves. Deben darse las gracias igualmente a Blackburn, C. S. Cox, J. A. Knauss, J. D. Isaacs, G. Miller, W. H. Munk y J. L. Reid, Jr., por sus valiosas sugestiones y discusiones.

Los cálculos de espectros se llevaron a cabo en el Western Data Processing Center de la Universidad de California y las ilustraciones fueron hechas con todo cuidado, así como el resto de los cálculos, por la Sra. Joan Connell.

Las investigaciones de las cuales se informa aquí fueron financiadas en parte por el Comité de Investigaciones de Vida Marina, de la Scripps Institution of Oceanography de la Universidad de California y en parte por la Marine Life Research Committee de la Scripps Institution

depend much upon frequency, which suggests that the wind acts simultaneously over the entire area.

The coherenece and phase between temperature and wind anomalies are shown in Fig. 9. The coherence fluctuates widely with frequency and varies between 0 and 0.8. It is low at both ends of the spectrum and shows some ill defined maxima around 3 c.p.y. and 5 c.p.y. The phase scatters around 180 degrees for frequencies between 2 c.p.y. and 5 c.p.y. and indicates an inverse relationship between temperature and wind anomalies. If an average coherence of 0.4 is assumed for the spectra, not more than 16% of the anomalies are related to each other. This may be partly due to the crudeness of the data, but it is more likely that upwelling represents a much more complex phenomenon than can be described by the wind data alone.

CONCLUSION

The Gulf of Tehuantepec is noted for strong upwelling in winter which leads to sea surface temperatures several degrees lower than elsewhere along the coast of southern Mexico. The primary cause of upwelling is the gale force wind blowing at times from the north across the Isthmus of Tehuantepec into the Pacific Ocean. The wind effect is felt several hundred kilometers to the southward. The relation between winds and temperatures was investigated from a dynamical point of view and a statistical point of view.

The dynamical approach led to the result that upwelling in the Gulf is related to the curl of the wind stress, and that upwelling speeds of 10 m day^{-1} can be expected during northers. The statistical approach showed that there is an inverse, but rather weak relation between ten-day sea surface temperature and wind anomalies.

ACKNOWLEDGEMENTS

The author has benefitted considerably from many fruitful discussions with Gordon W. Groves. Thanks are also due to M. Blackburn, C. S. Cox, J. A. Knauss, J. D. Isaacs, G. Miller, W. H. Munk and J. L. Reid, Jr., for valuable suggestions and discussion.

The computations of the spectra were carried out at the Western Data Processing Center of the University of California at Los Angeles. The remaining desk calculations and illustrations were painstakingly done by Mrs. Joan Connell.

The research reported herein was supported in part by the Marine Life Research Committee of the Scripps Institution of Oceanography of the University of California and partly financed by the Bureau of Commercial Fisheries

of Oceanography de la Universidad de California y el Bureau of Commercial Fisheries según Contrato No. 14-19-008-9354, con fondos disponibles según la Ley del 1o. de Julio de 1954 (68 Stat. 376) conocida como el Saltonstall-Kennedy Act.

under Contract No. 14-19-008-9354, with funds made available under the Act of 1 July 1954 (68 Stat. 376), commonly known as the Saltonstall-Kennedy Act.

BIBLIOGRAFIA — *BIBLIOGRAPHY*

BLACKBURN, M. Oceanographic studies in the Gulf of Tehuantepec (Ms.).

BLACKMAN, R. B. and J. W. TUKEY. 1958. The Measurement of Power Spectra from the point of view of Communications Engineering. *The Bell System Technical Journal*, 37:185-282, 485-576.

GODSKE, C. L., T. BERGERON, J. BJERKNES and R. C. BUNDGAARD. 1957. *Dynamic Meteorology and Weather Forecasting*. Boston (American Meteor. Soc.), 800 p., il.

GUTMAN, L. N. and F. I. FRANKL. 1960. Termo-gidrodinamicheskaya model' bory. *Doklady Akad. Nauk USSR*, 130(3):533-536 (en Ruso) (in Russian).

HURD, W. E. 1929. Northers of the Gulf of Tehuantepec. *Monthly Weather Rev.*, 57(5):

IMPERIAL MARINE OPSERVATORY. The mean atmospheric pressure, cloudiness, air temperature and sea surface temperature of the North Pacific Ocean and neighboring seas. Kobe, 1921-1938.

MUNK, W. H., F. E. SNODGRASS and M. J. TUCKER. 1959. Spectra of Low frequency Ocean Waves. *Bull. Scripps Inst. Ocean., Univ. Calif.* (La Jolla), 7(4):283-362.

RODEN, G. I. and G. W. GROVES. 1959. Recent Oceanographic Investigations in the Gulf of California. *Jour. Marine Res.*, 18(1):10-35.

SERVICIO METEOROLÓGICO MEXICANO. 1928-1941. *Boletín Anual.* Tacubaya, D. F., México.

SVERDRUP, H. U., M. W. JOHNSON and R. H. FLEMING. 1946. *The Oceans.* New York (Prentice-Hall), 1 vol., il.

SVERDRUP, H. U. 1947. Wind driven currents in a baroclinic ocean. *Proc. Nat. Acad. Sci.* (Washington, D. C.), 33:318-326.

U. S. BUREAU OF COMMERCIAL FISHERIES. Sea surface temperature charts; Eastern Pacific Ocean, San Diego Laboratory, 1960 and unpublished.

U. S. COAST AND GEODETIC SURVEY. 1956. Surface water temperatures at tide stations. Pacific Coast of North and South America and Pacific Ocean Islands. *Spec. Pub.* 280, 60 p.

——————— 1960. Surface water temperature and salinity. Atlantic Coast of North and South America. *Coast and Geod. Surv.*, Pub. 31-1, 76 p.

U. S. HYDROGRAPHIC OFFICE. 1947. Atlas of surface currents Northeastern Pacific Ocean. *Hydrogr. Office Pub.* 570, 12 sheets, il.

——————— 1951. Sailing Directions. West Coasts of Mexico and Central America. *Hydrogr. Off. Pub.* 84, 306 p., il.

——————— Sea surface temperature in one degree squares of latitude and longitude North Pacific Ocean (inédito) (unpublished).

U. S. WEATHER BUREAU. Historical Weather Maps, Northern Hemisphere sea level. Daily synoptic series for January 1939.

——————— 10-day period listings of individual observations, 1949-1957. Marsden square 046 National Weather Records Center, Asheville, N. C. (inédito) (unpublished).

WELANDER, P. 1959. On the vertically integrated mass transport in the oceans. The atmosphere and sea in motion. *The Rossby Memorial Volume*, New York (Rockefeller Institute Press), p. 95-101.

YOSHIDA, K. and H. L. MAO. 1957. A theory of upwelling of large horizontal extent. *Jour. Marine Res.*, 16(1):40-54.

ARTHUR D. RAFF
RONALD G. MASON

MAGNETIC SURVEY OFF THE WEST COAST OF NORTH AMERICA, 40° N. LATITUDE TO 52° N. LATITUDE

Abstract: An extensive high-resolution magnetic survey of total field at sea level reveals unusual north-south lineations and much crustal faulting. Computations indicate that the linear pattern is due to strongly magnetized mafic rocks beneath the sediments.

A magnetic survey was made off the west coast of the United States and Canada, 40° N. lat. to 52° N. lat. as a continuation of work reported by Mason (1958) and Mason and Raff (1961). The total field at sea level was measured by a fluxgate magnetometer towed by a ship that ran east–west track lines spaced 5 nautical miles apart except for highly anomalous areas where the spacing was about 1 mile. The accuracy of navigation was 0.1 mile. The area surveyed is mostly over deep water (1500–1700 fathoms) and covers 230,000 square miles. Since the diurnal variation is small compared to the value of the anomalies, its effect was not removed. The map (Pl. 1) was contoured with intervals of 100 gammas, whereas the map by Mason and Raff (1961) has an interval of 50 gammas.

The unique north–south trends of the magnetic contours of Plate 1 make it possible to see many faults in the ocean's crust even though this area is covered with deep continental sediment (Menard, 1960). In locating and measuring these faults we assumed that the north–south trend was originally continuous and predated the faults. The faults are observed as a line of anomalous features, as a discontinuity of contour density, or as a shear of the north–south lineations.

At about 40° N. lat. (Fig. 1; Pl. 1) the strong east–west feature is the Mendocino fault, which Vacquier and others (1961), by extending the survey of this fault to the west, have shown to have a left-lateral slip of approximately 600 nautical miles. Two subsequent magnetometer lines run between the eastern limit of the present survey and the coast show that the Mendocino anomaly continues to the coast. This great fault is here a boundary between provinces of different ocean depth and different magnetic anomaly density. North of the Mendocino fault (41° N. lat.) and near the eastern limit of the survey, the lineations turn to the northeast as though the crust had been rotated by the action of the several large faults that converge in this area. Along the line A–A (Fig. 1) the linear structures bend smoothly, which is unusual. The anomalous interruption just northwest of line A–A has associated with it a small basin 400 fathoms deeper than the surrounding area.

The anomalous feature along line B-B has no topographic counterpart. The angular and curved line C-C-C marks a boundary of gradient density similar to that usually found along the continental shelf, but the continental shelf does not show any such departure here. Line D-D marks a row of three seamounts. Lines E-E, G-G, and H-H mark a boundary of magnetic gradient-density change that is not indicated by the topography. The area between these lines appears from the magentics to be either smoothed or depressed with respect to adjacent aras. The area enclosed by the B, E, G, and H lines looks like a dilated section with the motion hinged at the western corner. Lines J-J and K-K mark a fault of the magnetic linear trend. These two lines may be parts of the same fault that has disturbed a wide area. There is a suggestion from the map that the magnetic lineations L-L, M-M, and N-N are all the same feature with the center section having slipped to the east. Most of the area on the map from 41° N. lat. to 49° N. lat. looks like angular pieces of crust that have slipped and rotated with respect to neighboring pieces. The anomaly along Q-Q is associated with a trough that is 800 fathoms deeper than the surrounding area. Along the line R-R there is a 500-fathom ridge that has little or no magnetic counterpart.

Along the line S-S-S there is a suggestion of a fault, but nothing is indicated from the bottom

Geological Society of America Bulletin, v. 72, p. 1267–1270, 1 fig., 1 pl., August 1961

Contributions from the Scripps Institution of Oceanography, New Series, 1339
Reproduced by Permission

topography. In the general region west of this line there are many seamounts, some of which cause strong magnetic anomalies, while others do not. It is not at all clear why volcanic seamounts in the same area should give magnetic anomalies of such different magnitudes. Farther north the irregular line T-T encloses an area of apparent magnetic depression similar to the one to the south. There are a number of other partial breaks in the linear pattern such as along lines U-U, V-V, and W-W.

By far the largest topographic feature in the area of the survey is the continental shelf, and it shows little magnetic anomaly, as would be expected from its shape in cross section at the places where the magnetometer has crossed it. It appears to give a slight negative anomaly, suggesting that the material of the oceanic

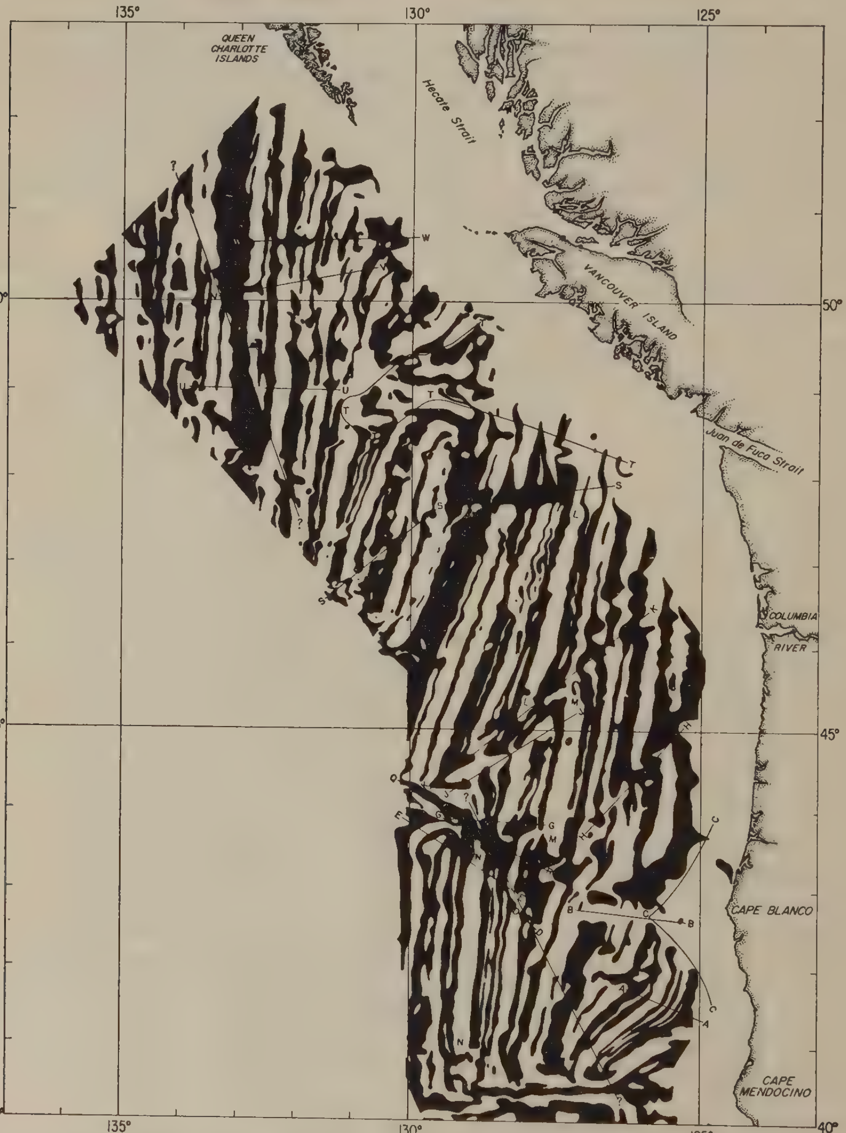
135°
130°
125°
QUEEN CHARLOTTE ISLANDS
Hecate Strait
VANCOUVER ISLAND
Juan de Fuca Strait
COLUMBIA RIVER
CAPE BLANCO
CAPE MENDOCINO
50°
45°
40°
W
V
U
T
S
L
K
M
H
Q
E
G
N
C
B
A
D
?

Figure 1. Index anomaly map of the total magnetic field. The positive area of the anomalies is shown in black.

crust is much more magnetic than that of the continental crust.

These north-south linear features have aroused considerable interest and speculation. They disappear over the areas where the continental crust extends into the ocean. The layer containing these magnetic structures may dip under the continental crust much as the M discontinuity does; this is supported by the changes in slope width and gradient of the magnetic ridges where they occur closer to the shore line. Using rules of thumb to find the depth of burial of the structures the structures are placed about 3 times deeper at the continental shelf than they are farther out to sea. The apparent deepening of these structures near the coast could be an illusion, however, caused by their having a wider thinning edge near the shelf.

There is as yet no satisfactory explanation of what sort of material bodies or physical configurations exist to give the very long magnetic anomalies. It has been suggested that they are troughs and ridges buried under sediment, platelike lava flows that filled older troughs, unique groupings of vertical dikes, high iron-content derivatives of weathering that filled older troughs, or a thermal pattern that has "highs" and "lows" about the Curie point of ocean rocks. Two of the principal difficulties in imagining a body that could cause these north-south features are that the measured magnetic anomalies and computations about them require that the upper surface of the body be within 1 km of the sedimentary layer and that the body have what is considered an unusually strong magentic moment. Such features were not revealed on the basis of topography nor have they been detected by seismic methods (R. W. Raitt, personal communication).

Magnetic measurements now being made of all the rocks collected in the Scripps dredge hauls indicate that most oceanic igneous rocks have a remanent magnetization and susceptibility several times greater than the median value for continental igneous rocks. Thus, a predominance of oceanic igneous rocks are similar magnetically to the less common mafic rocks of the continents. Magnetic patterns over the oceans should then show greater magnetic anomaly than generally is observed on land, and possibly, although masses of rock may be too thin to be detected seismically, they may have sufficient magnetic moment to give a strong anomaly.

If there originally had been a trough and ridge system, these troughs and ridges should show at least slightly in the topography of the heavily sedimented ocean floor. If the magnetic bodies are the original ridges, the magnetic "highs" should correspond with the slight topographic ridges; but if the magnetic bodies are accumulated material in the valleys, then the magnetic "highs" should be over the slight topographic valleys. A statistical correlation analysis made of the magnetic and topographic relief for some of this area showed that the topographic ridges and magnetic "highs" correspond in about 65 per cent of the cases as against 35 per cent of negative correspondence. This is certainly not conclusive, but does suggest that the magnetic bodies are the original igneous ridges or elevated areas that survive in a modified, perhaps flattened, form.

As to the notion that this is a thermal pattern about the Curie point, heat-flow measurements (Von Herzen, 1959) give values that make it almost impossible for such temperatures and thermal gradients to exist close to the sedimentary layer.

Acknowledgements

The success of this survey was made possible by the interest and help of many people: the officers and men of the Coast and Geodetic Survey aboard the ship Pioneer, a number of people at Scripps Institution of Oceanography who traveled with the field instruments or worked at reducing and presenting the data, and Varian Associates who helpfully furnished absolute calibration for the fluxgate magnetometer used at sea. About 5 per cent of the track data was collected by ships of the Scripps Institution of Oceanography, and another 4 per cent of the track data was obtained aboard the Rehoboth, sailing for the U.S. Hydrographic Office.

References Cited

Mason, R. G., 1958, A magnetic survey off the west coast of the United States between latitudes 32° and 36° N. and longitudes 121° and 128° W.: Royal Astronom. Society Geophys. Jour., v. 1, p. 320–329

Mason, R. C., and Raff, A. D., 1961, Magnetic survey off the west coast of the United States, 32° N. latitude to 42° N. latitude: Geol. Soc. America Bull., v. 72, p. 1259–1266

Vacquier, V., Raff, A. D., and Warren, R. E., 1961, Horizontal displacements in the floor of the northeastern Pacific Ocean: Geol. Soc. America Bull., v. 72, p. 1251–1258

Von Herzen, R. P., 1959, Heat-flow values from the southeastern Pacific: Nature, v. 183, p. 882–883

Menard, H. W., 1960, Possible pre-Pleistocene deep-sea fans off central California: Geol. Soc. America Bull., v. 71, p. 1271–1278

University of California, Marine Physical Laboratory of the Scripps Institution of Oceanography, San Diego, Calif.

Manuscript Received by the Secretary of the Society, December 16, 1960

Health Physics Pergamon Press 1961. Vol. 6, pp. 97–102. Printed in Northern Ireland

SOME FUNDAMENTAL ASPECTS OF MARINE ECOLOGY IN RELATION TO RADIOACTIVE WASTES*

MILNER B. SCHAEFER
Inter-American Tropical Tuna Commission, Scripps Institution
of Oceanography, LaJolla, California

(*Received* 10 *October* 1960)

THE MARINE ENVIRONMENT AND ITS SUBDIVISIONS

THE oceans of the world cover about 71 per cent of the earth's surface to an average depth of 3800 m. The ocean basins are characteristically bordered by a continental shelf which slopes out gently to a depth of about 200 m. Beyond the shelf, the continental terrace slopes much more abruptly to the deep sea floor at depths of 4000 m or more. The average width of the shelf is about 30 miles, varying from practically nothing off mountainous coasts to several hundred miles in such places as the China Sea. The shelf is not always smooth, but it is often intersected by submarine valleys and canyons. In the deep ocean there are high mountains and deep trenches, larger than any on land. Some of the mountains rise to the surface, forming islands, or to near the surface, forming "banks" and "shoals".

The waters of the ocean form, essentially, a two-layer system. The relatively thin upper layer varies from a few meters to about 200 m in thickness, averaging about 75 m. In this layer, vertical mixing caused by winds is relatively rapid and complete, so that temperature, salinity, and density are nearly uniform from top to bottom. In it are found the fast, wind-driven currents which are the "surface" currents shown on many charts. Below the mixed layer is a zone, extending down to 500 m in some places, within which the temperature decreases and density increases rapidly with depth. This thermocline, or pycnocline, separates the upper mixed layer from the layer of intermediate and deep water extending to the bottom, where the vertical gradients of decreasing temperature and increasing salinity and density are very gentle. Both vertical and horizontal movements in the deep layer are much slower, in general, than in the upper layer. The strong density gradient across the thermocline inhibits physical transport across it, thus there is a partial barrier between the upper mixed layer and the lower layers. There is, however, some interchange of water and its dissolved nutrient salts across the thermocline. Indeed, if there were not, the upper layer could not continue to support much life.

The energy that drives the whole life cycle in the sea, as on the land, is sunlight. This energy is bound chemically in organic compounds by the photosynthesis of plants, and is passed along through the food web in the food of all higher organisms. The zone of the sea to which sufficient light penetrates to support photosynthesis is only about 100 m deep, even in very clear waters, and is often less. Thus most of the photosynthesis takes place in the upper mixed layer, and mostly by microscopic floating plants,

---

* Presented at the Symposium on Waste Disposal, Fifth Annual Meeting of the Health Physics Society, Boston, Massachusetts, June, 1960 Contribution from the Scripps Institution of Oceanography, New Series, 1340

Reproduced by Permission

the phytoplankton. Only along the shallow margins of the sea are there large algae, and other plants analogous in size to plants on land. In order to grow, plants require, in addition to sunlight and water (of which there is of course plenty in the sea), certain chemical nutrients such as phosphates, nitrates, etc. Now, due to gravity effects on the dead plants and animals and their excreta, there is a continual rain of organic material from the upper layer to the deeper layers of the sea. Some of this material arrives at the very bottom of the ocean, even in its deepest parts, since living organisms, which depend ultimately on the plants near the surface, are found at all depths. This fallout of organic matter continually removes the plant nutrients, which are, by bacterial action, regenerated as inorganic compounds in the deep water, and must be returned to the sunlit zone to fertilize it.

Although there is probably some upward mixing of the water across the thermocline almost everywhere, the restoration of nutrient-rich water from below is most intense where the sea is "plowed" by certain physical processes. In some places winds drive the surface water away from the coast or an internal boundary and nutrient-rich waters well up from mid depths. At high latitudes, surface waters in winter are cooled to near freezing, sink, and mix with deeper waters. At boundaries of ocean currents, violent mixing brings up deeper waters. Over the continental shelf, the materials from the upper layer fall on to the bottom not far below, and are thus readily accessible to upward mixing. Such regions are the green pastures of the sea, supporting abundant life and major sea fisheries. Other regions, where the surface waters have been depleted of nutrients are biological deserts, supporting only very sparse populations.

Man's food harvest from the sea, which is the important route by which radioactive nutrients are returned to him, is taken almost entirely from the upper mixed layer of the open sea or from inshore and coastal waters out to the edge of the continental shelf, although some fisheries extend to depths of 500 fathoms, and some of the harvested fish populations perform migrations to deeper waters.

From the viewpoint of the physical and biological processes involved in returning to man radioactive materials introduced into the sea, there are several important sub-divisions of the marine environment.

(1) *Near-shore areas*, including the close in-shore zone of the open coast and areas which are partially enclosed by land, i.e. harbors, bays, estuaries and lagoons. In these areas dispersion of wastes by physical processes is often restricted, and, since they are shallow, the material that falls out on the bottom does not become inaccessible to the organisms. In this environment occur the large sedentary populations of oysters, clams, and seaweeds used by man, and it is an essential nursery ground for shrimp, menhaden and many other offshore commercial species, as well as the habitat of many fishes taken for food by man.

(2) *Continental shelf and the overlying waters.* Removal of waste materials by diffusion and current transport is generally greater here than in near-shore areas, but less than in the open sea off-shore. Sedimentation to the bottom may not remove elements from the biosphere in this region, since food organisms taken by man live all the way to the bottom. On the bottom are scallops, shrimp, crabs, and lobsters and also populations of both moving and sedentary invertebrates which are food for important commercial fish populations such as flounders, cod and haddock which live on or near the bottom. Some of the commerical species are fairly sedentary, but some perform extensive seasonal migrations to and from deeper waters. Some commercial species are found out along the continental terrace to depths as great as 1000 fathoms, or more.

(3) *The deep sea beyond the continental shelf.* Radioisotopes return to man from this region through the seafood harvest which depends almost entirely on organisms inhabiting the upper mixed layer or the region of the thermocline. Thus isotopes which are introduced into the deep water, or which are removed to the deep water from the surface, are mostly removed from the domain of man's food. The mean time for interchange between deep water and the surface layer is long, being of the order of at least several decades and probably several

hundred years, so that there is much time for dispersion and decay. Elements which sediment out on the bottom are removed for even longer periods, perhaps permanently. Dispersion in the upper layer is also rapid, leading to quick dilution. However, there is some additional interchange between the deep and surface layers due to migration of organisms, and this can be in some circumstances more important than the physical exchange.

The food web in the sea

One of the important differences between life in the sea and on land is the much greater length of most food chains in the former. On land the chains are mostly short, such as grass to cows to men. In the sea, particularly in the pelagic realm, food chains are much longer. The plants are mostly microscopic phytoplankton, which is eaten by tiny herbivorous animals which are eaten by small carnivores that are consumed by larger ones. Although man consumes some organisms low in the food chain, most of our seafish harvests is from animals two or more steps above the primary plant producers. At the same time, however, some of the animals take up minerals, both dissolved and particulate, directly from the sea water, so that radioisotopes can return to man by a shorter route than that starting with the plants. These complexities, and our lack of knowledge concerning them, are among the principal handicaps in precise evaluation of methods of sea disposal of radioactive wastes.

More detailed discussion of the foregoing matters, which I have reviewed very briefly, can be found in REVELLE *et al.*(1), BROWN *et al.*(2), CARRITT *et al.*(3), PRITCHARD *et al.*(4), REVELLE and SCHAEFER(5), SCHAEFER(6), KETCHUM and BOWEN(7).

With this general background, I would now like to discuss in a little more detail some of the processes in the ecosystem which are of importance in relation to radioactive wastes.

Uptake and retention of radioisotopes by organisms used as food for man, and the evaluation of permissible concentrations in the environment

Radioactive isotopes in the sea affect man primarily through his ingestion of marine organisms in his food. Thus, quantities of radioactive materials that can be safely introduced into the sea depend on the amounts that come to lodge in such marine organisms, and the permissible rate of intake by man. The last can be determined from the permissible rates of ingestion and body burdens of various radioisotopes published by the national and international committees on radiation protection. In making estimates of permissible concentrations in sea water, account must be taken of the facts that sea water is a solution of almost all the elements; that concentrations of many elements are known and that some of them are very nearly in constant proportions; and that marine animals concentrate, often by very large factors, some isotope both radioactive and non-radioactive. It should also be noted that organisms do not significantly distinguish between the radioactive and non-radioactive isotopes of a particular element, so long, at least, as the radioactive and non-radioactive species are in the same chemical form.

Various elements, in addition to the major organic constituents carbon, hydrogen, and oxygen, are essential to life processes, such as nitrogen, phosphorus, calcium, strontium, copper, zinc, cobalt and iron. These may be obtained by organisms above the plants in the food chain either from their food or by direct uptake from the water. Since the chemical requirements and concentrating ability differ for different kinds of organisms, the fluxes of various elements differ from species to species and at different parts of the food web. The concentrations of various elements in sea water and in different kinds of organisms, to the extent they are known, have been tabulated by REVELLE *et al.*(1), PRITCHARD *et al.*(4) and REVELLE *et al.*(8). Some elements which are abundant in sea water, for example sodium, occur in organisms at lower concentrations than in the water; they are selected against. On the other hand, elements such as phosphorus, that are essential to the organisms, but are scarce in the sea, are concentrated by several orders of magnitude.

The length of time an organism retains the average atom of a given element varies greatly from one element to another and with different organisms; this is often given as the "biological half-life". Much is known about the retention times of various elements in man(9), but there are few data for marine organisms.

Hazards to humans from radionuclides result from radiation to the gastro-intestinal tract as the food passes through it, and from radiation to other organs in which they accumulate. As indicated in NBS Handbook 69(9), the limiting factors for many isotopes, such as Cr^{51}, Fe^{59}, Co^{60}, Zr^{95}, Nb^{95}, Ru^{106}, Ce^{144} and Ta^{182}, is the dose to the gastrointestinal tract; for these we need to limit the concentration per unit volume in the seafood. For others, such as P^{32}, S^{35}, Fe^{55}, Zn^{65}, Sr^{90}, I^{131} and Cs^{137} the body burden is limiting; for these the specific activity of the seafood is of primary interest.

We may formulate some of these matters quantitatively following REVELLE *et al.*(8)

Designating by I_r and I_n the concentrations of radioactive and non-radioactive isotopes, it may be shown, that at equilibrium, a man getting all of the elements from seafood, will have a specific activity related to the specific activity in the seafood by

$$\frac{I_{rb}}{I_{nb}} = \frac{I_{rf}}{I_{nf}}\left(\frac{B}{K+B}\right) \qquad (1)$$

where b denotes the human and f the seafood, while B is the rate constant for biological elimination of the element in man and K is the radioactive decay constant.

Similarly, when the marine food organism accumulates an element directly from seawater, in equilibrium,

$$\frac{I_{rf}}{I_{nf}} = \frac{I_{re}}{I_{ne}}\left(\frac{B_f}{K+B_f}\right) \qquad (2)$$

where e denotes the sea water environment and B_f is the rate constant for biological elimination of the element in the fish. Then,

$$\frac{I_{rb}}{I_{nb}} = \frac{I_{re}}{I_{ne}}\left(\frac{BB_f}{K^2+KB_f+KB+BB_f}\right) \qquad (3)$$

For elements which reach man following several steps in the food chain an analogous expression with more terms within the parenthesis can be written, but we know yet so little about the biological half-lives and mode of accumulation in marine organisms of most elements that this is only an exercise without much useful 'application.

In the absence of knowledge, we make the conservative assumption that B_f is large with respect to B or K, or that the hold-up time in the marine organisms is short. Thus, for elements of long radioactive half life, where $K \ll B < B_f$, approaches

$$\frac{I_{re}}{I_{ne}} \doteq \frac{I_{rb}}{I_{nb}} \qquad (4)$$

so that the permissible specific activity in the ocean is about equal to that in the critical human body organ for isotopes of long radioactive half-life. Where $B_f \gg K \gg B$, we obtain from equation (3)

$$\frac{I_{re}}{I_{ne}} \doteq \frac{I_{rb}}{I_{nb}}\left(1+\frac{K}{B}\right) \qquad (5)$$

Thus, for isotopes of short radioactive half-life and long biological half-life in the human body, the permissible specific activity in the ocean is much greater than in the body. If the biological half-life in the marine food organisms is also known, the estimate of permissible specific activity in sea water can be further increased.

Where radiation to the gastrointestinal tract is critical, we are concerned with the concentration per unit volume of seafood or I_{rf}. It may be seen from equation (2) that taking I_{nf}/I_{ne} as the concentration factor (F) from sea water to seafood, we have

$$I_{rf} = F \, . \, I_{re}\left(\frac{B_f}{K+B_f}\right) \qquad (6)$$

I_{rf} is comparable to the maximum permissible value for drinking water for the gastrointestinal tract given in Handbook 69. Given an estimate of seafood eaten, per man per day, and taking the assumption of 15 l. of drinking water a week on which the MPC's for water were based, one may then calculate I_{re}, the permissible activity in the seawater.

REVELLE *et al.*(8) have tabulated for a number of isotopes the specific activity in sea water, and concentration factors in marine organisms, and the resulting permissible concentrations in sea water, both for cases where the gastrointestinal tract is critical and where the body burden for some organ is critical.

It should be noted that the concentration factors tabulated in this and other references earlier cited have usually been the highest observed in seafood; furthermore, in some cases they have been based on the observed concentrations of radioisotopes in sea water and organisms rather than on the non-radioactive species, and thus (as may be seen from equation (2)) may be overestimated. This is, again, a conservative approach made necessary by our lack of knowledge of the marine ecological systems.

Effects of organisms on the distribution of elements in the sea

The foregoing type of approach can provide estimates of permissible concentrations of radioisotopes in the sea water environment of the marine food organisms, but to relate this to waste disposal practices we must also know about the transport and dispersion of the material put in the sea. This is not a function only of physical parameters, but can also be significantly influenced by the marine biosphere. Those elements of which a large proportion is cycled through organisms can have their spatial distributions profoundly modified by the biosphere, so that they are quite differently distributed in the sea than those elements whose distributions are determined only by physical and inorganic chemical processes.

The marine biosphere acts as a reservoir for those elements that are selectively removed from sea water by organisms. In the case of sedentary populations this can provide local concentrations of elements. For example sessile invertebrates are a fixed reservoir for such elements as copper, zinc and cobalt which they concentrate by large factors. This will hold up the circulation of these elements, thus making their flushing rate from estuaries, for example, slower than that of the water.

Invertebrates growing on waste disposal containers, on the bottom, out of which radioactive elements are leaching may take up essentially all of such materials, the radioisotopes being effectively diluted only by the corresponding non-radioactive species in the water moving past the containers on the bottom. Such invertebrates can be eaten by commercial fishes and thus enter man's food. Calculations for at least some situations on the Pacific Coast indicate that the concentration of radioactive materials in foodfish under these circumstances can be much greater than if the material had been rapidly liberated into the overlying waters where quicker dilution by physical processes takes place.

As noted by KETCHUM(10), the combination of uptake by organisms in surface waters, and gravity effects on their excreta and dead bodies, will, in areas with positive estuarine type circulation, and regions of coastal upwelling, result in local concentrations of elements selectively taken up by such organisms. Even in the open sea, uptake by organisms may greatly impede the transfer to deep water of elements in particulate form which would be expected to settle out by sedimentation. For example HARLEY(11) found that cerium-144, which occurs in sea water in particulate form, and its daughter Pr^{144}, constituted from 80 to 90 per cent of fission product activity in plankton samples in the Western Pacific, after a considerable time following introduction into the sea.

Migrations of organisms can also have important effects in transporting elements from areas of high concentration to areas of low concentration. Vertical migrations of organisms, many of which readily cross the pycnocline, could readily transfer radioactive materials from the deep to surface waters. KETCHUM and BOWEN(7) have shown that this transport may in some circumstances be greater than that by physical means. Horizontal migrations can also transfer materials from the site of introduction to other areas. More important, however, is the fact that organisms used for food can be contaminated in one area and caught in distant uncontaminated areas. Some of the commercial fish species on our Pacific Coast, for example, make regular seasonal migrations to off-shore deeper waters and back to the shallower areas where they are caught. The sperm whale, which feeds on squids in the deep sea, but comes to the surface to breathe is an extreme example of a vertical migrant.

Present state of knowledge

Although our knowledge of most of these things is incomplete and fragmentary, we know enough about the ecology of the sea to be able to make useful estimates of the quantities of radioactive materials that can be placed in various marine environments without hazard. This involves, however, making the most conservative (safest) assumptions wherever information is incomplete. The necessity of doing this means that waste disposal practices must be more restrictive than would be the case if we knew more. This, of course, entails economic costs which can in the future be very large, and which may be reduced by the results of further research. Research requirements have been outlined in several recent publications, including BROWN *et al.*(2), REVELLE and SCHAEFER(5) and SCHAEFER(6).

REFERENCES

1. R. REVELLE *et al*, *The Effects of Atomic Radiation on Oceanography and Fisheries.* Publication 551, National Academy of Sciences–National Research Council (1957).
2. H. BROWN *et al*, Oceanography 1960 to 1970. *Artificial Radioactivity in the Marine Environment* Chap. 5, pp. 1–31. National Academy of Sciences–National Research Council (1959).
3. D. F. CARRITT *et al*, *Radioactive Waste Disposal into Atlantic and Gulf Coastal Waters.* Publication 655, National Academy of Sciences–National Research Council (1959).
4. D. W. PRITCHARD *et al*, *Radioactive Waste Disposal from Nuclear Powered Ships.* Publication 658, National Academy of Sciences–National Research Council (1959).
5. R. REVELLE and M. B. SCHAEFER, *Proceedings of the Second International Conference on the Peaceful Uses of Atomic Energy, Geneva,* 1958 Vol. 18, pp. 364–370. United Nations, New York (1958).
6. M. B. SCHAEFER, New research required in support of radioactive waste disposal. *Proceedings of the International Conference on Radioactive Waste Disposal* (*Monaco*), *IAEA* (1960).
7. B. H. KETCHUM and V. T. BOWEN, *Proceedings of the Second International Conference on the Peaceful Uses of Atomic Energy, Geneva,* 1958 Vol. 18, pp. 429–433. United Nations, New York (1958).
8. R. REVELLE *et al*, *Report of the Committee on Oceanography and Fisheries.* The Biological Effects of Atomic Radiation, Summary Reports, pp. 69–90. National Academy of Sciences–National Research Council (1960).
9. *Report of the National Committee on Radiation Protection and Measurements, Maximum Permissible Body Burdens and Maximum Permissible Concentrations of Radionuclides in Air and Water for Occupational Exposures,* National Bureau of Standards, Handbook 69 (1959). Superintendent of Documents, Washington 25, D.C.
10. B. H. KETCHUM, *The Effects of the Ecological System on the Transport of Elements in the Sea.* Effects of Atomic Radiation on Oceanography and Fisheries, Publ. 551, pp. 52–57 (1957).
11. J. E. HARLEY (Editor), *Operation Troll.* U.S. Atomic Energy Commission, New York Operations Office, N.Y. (1956).

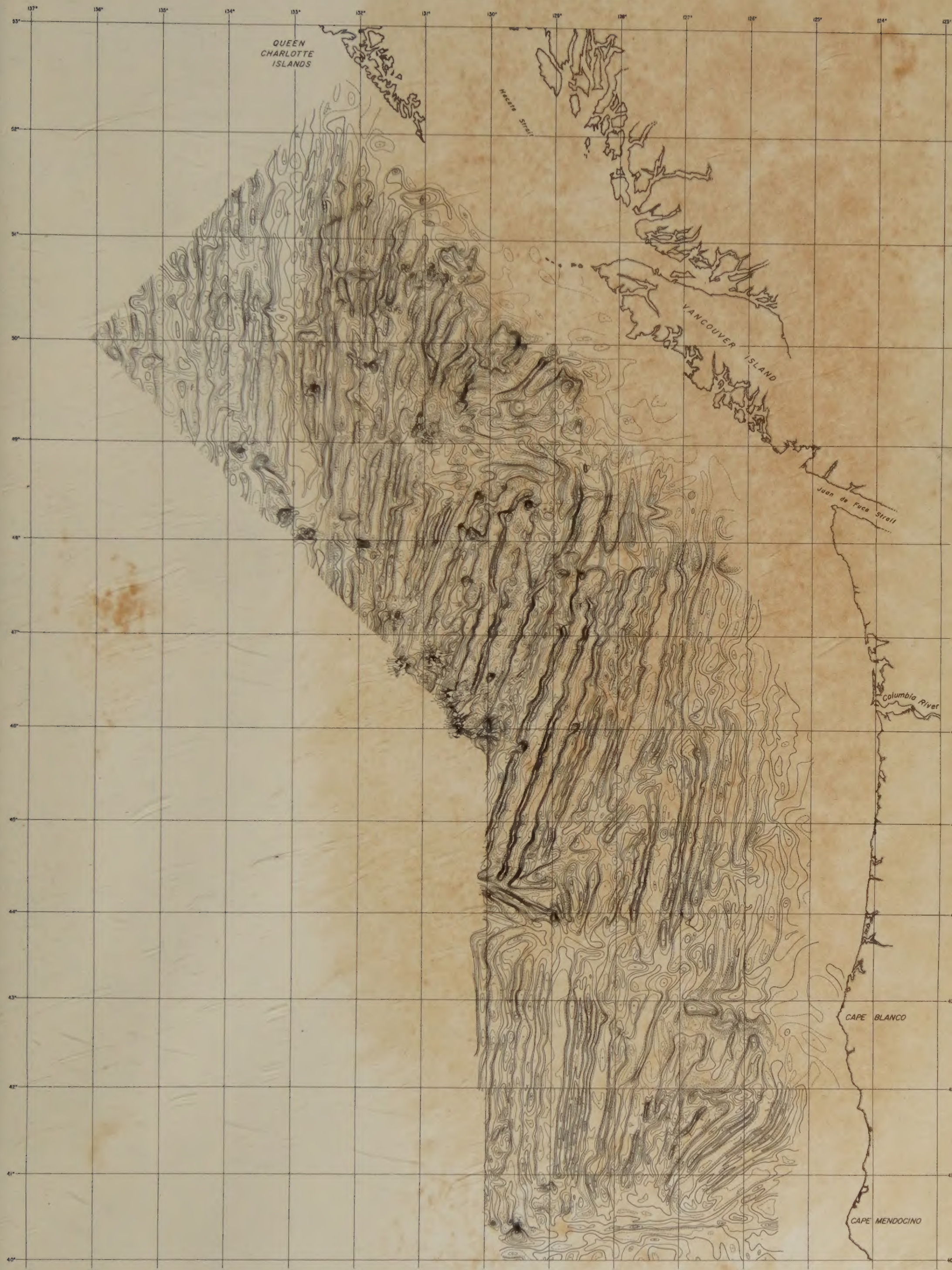

QUEEN CHARLOTTE ISLANDS
Hecate Strait
VANCOUVER ISLAND
Juan de Fuca Strait
Columbia River
CAPE BLANCO
CAPE MENDOCINO
137°
136°
135°
134°
133°
132°
131°
130°
129°
128°
127°
126°
125°
124°
123°
53°
52°
51°
50°
49°
48°
47°
46°
45°
44°
43°
42°
41°
40°

ANOMALY MAP OF THE TOTAL MAGNETIC FIELD

The contour interval is 100 gammas.

RAFF AND MASON, PLATE 1
Geological Society of America Bulletin, volume 72

LIBRARY
BUREAU OF COMMERCIAL FISHERIES
U. S. FISH AND WILDLIFE SERVICE
P. O. BOX 3830
HONOLULU 12, HAWAII